GEOLOGY OF WYOMING

Editors

Arthur W. Snoke
James R. Steidtmann
Sheila M. Roberts

Memoir No. 5
The Geological Survey of Wyoming
Gary B. Glass, State Geologist

Geology of Wyoming

Dedicated to

Donald L. Blackstone, Jr.

and

J. David Love

Volume 1

Editors

Arthur W. Snoke

James R. Steidtmann

Sheila M. Roberts

Geological Survey of Wyoming Memoir No. 5

Gary B. Glass, State Geologist

Laramie, Wyoming

1993

WYOMING STATE GEOLOGICAL SURVEY

Lance Cook, *State Geologist*

GEOLOGICAL SURVEY BOARD

Ex Officio

Jim Geringer, *Governor*
Randi S. Martinsen, *University of Wyoming*
Don J. Likwartz, *Oil and Gas Supervisor*
Lance Cook, *State Geologist*

Appointed

Ronald A. Baugh, *Casper*
Nancy M. Doelger, *Casper*
Charles M. Love, *Rock Springs*
Stephen L. Payne, *Casper*
John E. Trummel, *Gillette*

STAFF

Computer Services Unit

Susan McClendon - *Manager*

Geologic Sections

James C. Case, *Staff Geologist - Geologic Hazards*
Rodney H. De Bruin, *Staff Geologist - Oil and Gas*
Ray E. Harris, *Staff Geologist - Industrial Minerals and Uranium*
W. Dan Hausel, *Senior Economic Geologist - Metals and Precious Stones*
Alan J. Ver Ploeg, *Senior Staff Geologist - Geologic Mapping*
Robert M. Lyman, *Staff Geologist - Coal*

Publications Section

Richard W. Jones - *Editor*
Jaime R. Bogaard - *Editorial Assistant*
Lisa J. Alexander - *Sales Manager*
Fred H. Porter - *Cartographer*
Phyllis A. Ranz - *Cartographer*
Joseph M. Huss - *GIS Specialist*

Supportive Services Unit

Susanne G. Bruhnke - *Office Manager*
Joan E. Binder - *Administrative Assistant*

People with disabilities who require an alternative form of communication in order to use this publication should contact the Editor, Wyoming State Geological Survey at (307) 766-2286. TDD Relay operator 1(800) 877-9975.

This and other publications available from: Wyoming State Geological Survey
P.O. Box 3008
Laramie, Wyoming 82071-3008
(307) 766-2286

First edition, second printing of 1,000 copies by Pioneer Printing and Stationery Company, Cheyenne, Wyoming.

Geology of Wyoming: edited by Arthur W. Snoke, James R. Steidtmann, and Sheila M. Roberts
ISBN 1-884589-00-6 (volume 1)
ISBN 1-884589-01-4 (volume 2)
ISBN 1-884589-02-2 (2 volume set)

A cooperative project of the Wyoming State Geological Survey and the Department of Geology and Geophysics, University of Wyoming.

Table of Contents

page

Volume 1

Preface and acknowledgments ..... *Arthur W. Snoke, James R. Steidtmann, and Sheila M. Roberts* v

Dedication to Donald L. Blackstone, Jr. ..... *Robert S. Houston* vii

Dedication to J. David Love ..... *William R. Keefer* xi

"Geologists' Camp" ..... *Phyllis Ranz* xiv

Part I: Overview

Geologic history of Wyoming within the tectonic framework of the North American Cordillera ..... *Arthur W. Snoke* 2

Part II: Precambrian history

The Archean history of the Wyoming province ..... *Carol D. Frost and B. Ronald Frost* 58

Late Archean and Early Proterozoic geology of southeastern Wyoming ..... *Robert S. Houston* 78

The Laramie Anorthosite Complex and the Sherman batholith: geology, evolution, and theories of origin ..... *B. Ronald Frost, Carol D. Frost, Donald H. Lindsley, James S. Scoates, and Jeremy N. Mitchell* 118

Part III: Paleozoic history

Paleozoic history of Wyoming ..... *Donald W. Boyd* 164

The Ancestral Rocky Mountains in Wyoming ..... *Edwin K. Maughan* 188

Part IV: Mesozoic history

The early Mesozoic history of Wyoming ..... *M. Dane Picard* 210

The Cretaceous foreland basin and its sedimentary record ..... *James R. Steidtmann* 250

An overview of the geologic structure of the thrust belt in Wyoming, northern Utah, and eastern Idaho ..... *Frank Royse, Jr.* 272

Structural style of Laramide basement-cored uplifts and associated folds ..... *William G. Brown* 312

Part V: Cenozoic history

Laramide evolution of the Black Hills uplift ..... *Alvis L. Lisenbee and Ed DeWitt* 374

Correlation of Paleogene strata across Wyoming—a users' guide ..... *Jason A. Lillegraven* 414

Volume 2

Part V: Cenozoic history *(continued)*

A geologic overview of the Absaroka volcanic province ..... *Kent A. Sundell* 480

Petrographic and geochemical characteristics of mid-Tertiary igneous rocks in the Rattlesnake Hills, central Wyoming, with a comparison to the Bear Lodge intrusive suite of northeastern Wyoming ..... *Anthony R. Hoch and Carol D. Frost* 508

page

The Heart Mountain detachment, northwestern Wyoming: 100 years of controversy ..... *Thomas A. Hauge* 530

Neogene stratigraphy and tectonics of Wyoming ..... *Kathryn M. Flanagan and John Montagne* 572

Geomorphic history of Wyoming and high-level erosion surfaces ..... *Brainerd Mears, Jr.* 608

The Teton fault, Wyoming: seismotectonics, Quaternary history, and earthquake hazards ..... *Robert B. Smith, John O.D. Byrd, and David D. Susong* 628

Seismic surveys and Quaternary history of Jackson Lake, Wyoming ..... *Robert B. Smith , Kenneth L. Pierce, and Richard J. Wold* 668

Topographic signature, space-time evolution, and physical properties of the Yellowstone-Snake River Plain volcanic system: the Yellowstone hotspot ..... *Robert B. Smith and Lawrence W. Braile* 694

Part VI: Topical aspects

The influence of Laramide foreland structures on modern ground-water circulation in Wyoming artesian basins ..... *Peter W. Huntoon* 756

Geologic applications of remote sensing and GIS: A Wyoming landscape perspective ..... *Ronald W. Marrs and Dennis N. Grasso* 790

Metal and gemstone deposits of Wyoming ..... *W. Dan Hausel* 816

Overview of oil and gas geology of Wyoming ..... *Rodney H. De Bruin* 836

Processes and possible analogues in the formation of Wyoming's coal deposits ..... *T.A. Moore and J.C. Shearer* 874

Geologic classification and origin of radioactive mineralization in Wyoming ..... *Ray E. Harris and Jon K. King* 898

Industrial minerals and construction materials of Wyoming ..... *Ray E. Harris* 918

Map pocket (CD-ROM in Vol. 2, second printing)

Geologic map of Precambrian rocks of the Wyoming province (Sheet 1, Robert S. Houston)

Eight regional structural cross sections in the Wyoming-Utah-Idaho thrust belt (Sheet 1, Frank Royse, Jr.)

Restored structural cross section along latitude 41° 15' Wyoming-Utah thrust belt (Sheet 2, Frank Royse, Jr.)

Generalized geologic map of the Heart Mountain detachment, northwestern Wyoming (Sheet 1, Thomas A. Hauge)

Map of the Quaternary trace of the Teton fault (Sheet 1, R.B. Smith, J.O.D. Byrd, and D.D. Susong)

Bathymetric map of Jackson Lake, Wyoming (Sheet 1, R.B. Smith, K.L. Pierce, and R.J. Wold)

Seismic reflection profiles of Jackson Lake (Sheet 2, R.B. Smith, K.L. Pierce, and R.J. Wold)

Stratigraphic chart showing Phanerozoic nomenclature for the State of Wyoming (J.D. Love, Ann Coe Christiansen, Alan J. Ver Ploeg)

Revised Precambrian basement map of Wyoming: outcrop and structural configuration (D.L. Blackstone, Jr.)

Wyoming geologic highway map (1:1,000,000)

Preface and acknowledgments

This project evolved with a two-fold purpose: (1) to provide a volume on the geology of Wyoming as a tribute to Donald L. Blackstone, Jr., and J. David Love who have made numerous fundamental contributions to the geologic knowledge of Wyoming during their remarkable careers; and (2) to assemble a summary of the current knowledge of the geology of Wyoming that would provide a baseline for future research. From the inception of this project, it was a joint effort by the Department of Geology and Geophysics, University of Wyoming, and the Geological Survey of Wyoming. In this light, the majority of the authors of the chapters are presently associated with one of these organizations. However, some experts outside of these groups were also invited to participate in the project, and these scientists' contributions were critical in achieving the coverage we desired. Several of these individuals are alumni of the University of Wyoming.

The first manuscripts were received in Spring, 1990, with Peter W. Huntoon, W. Dan Hausel, Donald W. Boyd, Frank Royse, Jr., and Thomas A. Hauge submitting completed manuscripts at this time. Manuscripts from the other contributors gradually trickled in — even up to Summer 1993. All the manuscripts received at least two peer reviews as well as the detailed technical and editorial review of at least two of the editors. Authors were instructed to follow the format and style of the *Geological Society of America Bulletin* (as of 1989). Publications by the State of Wyoming typically use the English measurement system. We have generally used this system in many of the papers, but have also included metric system units, which is preferred for scientific publications.

The production of these volumes required the work and assistance of many individuals. As the editors, we first thank all the contributors to the volume, whose enthusiasm and hard work are demonstrated in their excellent syntheses. Certainly, the technical reviewers played a major role in making this project a scientifically sound venture; specific individuals are acknowledged in the articles that they reviewed. The work of several individuals at the Geological Survey of Wyoming was absolutely critical in the completion of the volumes. Our original layout artist and typesetter was Teresa L. Beck; Kim Mehring completed the job of bringing together this complex and lengthy manuscript. The drafting skills of Phyllis A. Ranz are manifested throughout this volume, and we thank her for her consistently superb work. Editor Richard W. Jones played an essential role in the final production of the volumes, and his help was indispensable in bringing this project to completion. Finally, the support and enthusiasm for the project by Gary B. Glass, State Geologist of Wyoming, was critical in bringing a concept into a two-volume reality.

Financial contributions to help defray some of the production costs of these volumes were supplied by: BHP Petroleum Company, Chevron U.S.A. Inc., Enron Oil and Gas Company, Exxon Company, Meridian Oil Company, Presidio Exploration, Inc., and the Wyoming Geological Association.

The geology of Wyoming is a fascinating, multifaceted story that provides a superb opportunity to understand the history of a large tract of the Earth's crust through a substantial part of geologic time. Our hope for these volumes is that some of the material summarized here will stimulate others to further investigate a part of this history. Several of the authors have presented specific challenges to future researchers. We are certain that in 10, 15, or 20 years the present story will have evolved; and new concepts and ideas will have replaced some, if not many, of the hypotheses of these volumes. However, this is the essence of science—a constantly evolving discipline.

Arthur W. Snoke and
James R. Steidtmann,
Laramie, Wyoming

Sheila M. Roberts,
Calgary, Alberta, Canada

Don Blackstone (center in white hat) surrounded by students on a structural geology field trip near Woods Landing, Wyoming, in 1948.

Bill Brearley and Don Blackstone at Princeton University in 1934.

Don Blackstone in the field about 1954.

Dedication to Donald L. Blackstone, Jr.

Robert S. Houston
Department of Geology and Geophysics
University of Wyoming
Laramie, Wyoming 82071

Donald L. Blackstone, Jr., was born in 1909 in Chinook, Montana, where his father was a lawyer, his uncle the town pharmacist, and his favorite uncle John a horse rancher. In this rural setting, Don mastered the western code—a code of honesty and hard work that has characterized his career.

Don attended the University of Washington, where he received his B.S. in geology in 1931, and the University of Montana, where he completed his M.S. in 1934. Don received his Ph. D. from Princeton University in 1936. He specialized in structural geology and has become the "authority" on Rocky Mountain foreland tectonics. The concepts of contractional tectonics that he has advocated in a lifetime of geologic mapping and interpretation have withstood the test of time and have been verified by deep seismic reflection profiling.

Before coming to the University of Wyoming in 1946 as an Associate Professor of Geology, Don taught at the University of Missouri, Columbia, and was a geologist for Carter Oil Company from 1942 to 1945. His experience in the oil industry which included periodic summer consulting was transmitted to generations of students who benefited from his first-hand expertise. As a teacher, Don chiefly focussed on structural geology, although he also taught courses in regional geology and hydrogeology. For many years, he offered an outstanding undergraduate course in the principles of structural geology that prepared students for careers in industry and for graduate study. Don was a demanding teacher who expected students to meet high standards in the classroom. Although tough at the time, many of his students have stated that these high standards were instrumental in their later success in professional careers. For a period of almost 10 years, Don Blackstone was one of the field directors of the University of Wyoming Science Camp, and from 1963 to 1967 he was Director. His expectations were as high in the field as in the classroom. Don's energy in the field was boundless. Students leaning on a plane table or mapping under a shade tree were in constant jeopardy when Don was in the field.

In addition to teaching and research, Don served as Head of the Department of Geology from 1963 to 1968. From 1967 to 1969 he served as State Geologist (to complete the term of H.D. Thomas) and was instrumental in setting up the Survey as an independent agency. Although he did not wish to continue as State Geologist, he has been a member of the advisory board of the State Survey from 1969 to the present.

Don has been active in the American Association of Petroleum Geologists as a committee member and distinguished lecturer and is a honorary member of the association. He has always been active in the Wyoming Geological Association (WGA). He edited three annual guidebooks and was and is a major contributor to the publication series of the WGA. In 1954, he received the Morgan award for distinguished service, and became an honorary life member of the WGA in 1956.

In 1971, Don's long and continuing service to the University of Wyoming was recognized when he was awarded the George Duke Humphrey Award for teaching and research. He also received an Honorary Doctor of Laws (LL.D.) from the University in 1985.

Don's devotion to teaching was illustrated by his willingness to teach structural geology on a part-time basis after his retirement, a task done with modest remuneration.

Houston, R.S., 1993, Dedication to Donald L. Blackstone, Jr., *in* Snoke, A.W., Steidtmann, J.R., and Roberts, S.M., editors, Geology of Wyoming: Geological Survey of Wyoming Memoir No. 5, p. vi-ix.

The State of Wyoming, the University of Wyoming, and the geology profession have benefited tremendously from Don's service. Few people have served in as many capacities and left as permanent an imprint. As a friend and colleague for 40 years, I continue to be amazed by Don's devotion to his chosen profession. He works almost as hard in retirement as he did at the peak of his career. He is more productive in research than ever and is constantly assisting staff and students. I hope to be around when he publishes a series of cross sections on his 100th birthday.

The geologists standing are (left to right): Ralph Holmes (Columbia University), Brainerd Mears, Jr., Don Blackstone, and Samuel H. ("Doc") Knight. John Montagne is kneeling in the front. Photograph taken about 1956.

University of Wyoming field camp instructors north of the Shirley Mountains, Wyoming, about 1954. From left to right: Robert S. Houston, Paul O. McGrew (seated), Horace D. Thomas (seated in front), Don Blackstone.

The geologists from left to right are: Paul W. Richards (U.S. Geological Survey), John R. Fanshawe (independent consultant, Billings, Montana), Don Blackstone, and C.E. Carlson (Socony-Vacuum, Pegasus Division) at the fairgrounds, Billings, Montana, September 10, 1954. This photograph was taken during the Fifth Annual Field Conference of the Billings Geological Society which focussed on the geology of the Pryor Mountains-northern Bighorn Basin, Montana.

Don Blackstone on field trip in 1954.

Don Blackstone at Geological Society of America Penrose Conference on Laramide deformation of the Rocky Mountains in 1982.

Love Ranch, Wind River Basin, *circa* 1910

Dave Love excavating camel skull from Miocene strata southeast of Wheatland, Wyoming, in August, 1933.

Dave Love surveying for the Sunshine Dam site, south of Cody, Wyoming, March-April, 1935.

Dedication to J. David Love

William R. Keefer
Geologist, U.S. Geological Survey
Denver, Colorado

Dr. J. David Love ("Dave" to all of his friends and colleagues), a research geologist with the U. S. Geological Survey for 45 years prior to his retirement in 1987, is an acknowledged authority on the geology of Wyoming and adjacent areas of the Rocky Mountains. Through more than 200 publications and numerous lectures and talks given before academic institutions and professional and scientific societies, he has shared the wealth of his scientific findings and broad geologic knowledge to the lasting benefit of the Rocky Mountain Earth science community. It is most appropriate for Dave's illustrious career to be acknowledged and honored in these important volumes on the geology of Wyoming, for it covers a state and region in which he has played a key role in the solution of extremely complex geologic problems.

J. David Love is a native of Wyoming, the son of pioneer parents who homesteaded a ranch in the Wind River Basin, southeast of Riverton, in the late 1800s. He was educated at the University of Wyoming (B.A., 1933; M.A., 1934) and Yale University (Ph.D., 1938). Following four years with Shell Oil Company in the mid-continent and southeastern parts of the U. S., he joined the U. S. Geological Survey in 1942 as a party chief for the Mineral Deposits Branch to conduct field studies of mineral occurrences in central and western Wyoming. The following year he established a field office for the Survey's Fuel Branch in Laramie, where he began a major assignment as supervisor of that branch's geological investigations in Wyoming as part of the national effort to enhance domestic petroleum exploration and production during and after World War II. In this capacity he planned, directed, and actively participated in a comprehensive, far-reaching program of basic stratigraphic and structural studies which resulted in new and fundamental concepts regarding depositional and tectonic histories of Wyoming's resource-rich sedimentary basins. Many of the maps and reports based on these investigations became, and are still considered to be, standards of reference, proving to be of inestimable value in the search for oil, gas, coal, uranium, phosphate, gold, and other resources during the past nearly half century. Although an effective leader and supervisor of scientific programs throughout his professional career, Dave is perhaps known best for his exceptional abilities as a field geologist and as a keen observer and thoughtful interpreter of complex regional geologic relationships — pursuits in which he has few peers as exemplified by his unraveling of the geologic history and tectonic evolution of Jackson Hole and surrounding regions in northwestern Wyoming. Especially worthy of mention, also, are the two versions of the *Geologic map of Wyoming* which bear his name as principal author (1955, 1985).

In addition to Dr. Love's outstanding scientific accomplishments and the application of his research results toward the advancement of the knowledge of the geology of Wyoming, he has long demonstrated a strong interest in applying Earth science information to environmental and human needs as indicated by lectures on such topics as "Relation of geology to human health and diseases and land use planning" delivered at the University of Washington in 1978. Held in the very highest esteem by his colleagues, he has been the recipient of several prestigious honors and awards by scientific and professional organizations and academic institutions, including an Honorary Doctor of Laws (LL.D.) in 1961 from the University of Wyoming, Meritorious and Distinguished Service Awards from the U. S. Department of Interior (1977, 1987), honorary life membership in the Wyoming Geological Association, Public Service Award from the American Association of Petroleum Geolo-

Keefer, W.R., 1993, Dedication to J. David Love *in* Snoke, A.W., Steidtmann, J.R., and Roberts, S.M., editors, Geology of Wyoming: Geological Survey of Wyoming Memoir No. 5, p.x-xiii.

gists, and Scientist-of-the-Year Award from the Rocky Mountain Association of Geologists (1986).

J. David Love has provided encouragement and inspiration to professional geologists and students of geology alike during his remarkable career. The high standards that he maintains in the conduct of his own scientific endeavors serve as a guide to other geologists. Furthermore, many individuals have greatly benefited from his helpful advice and counsel — but, famous also for having a wry and subtle sense of humor, he might, when asked for advice in what to look for while mapping an area of complex geology, simply challenge one to *get the meat out of the area.*

Dave Love at field camp in 1933 in Wyoming.

Dave Love during field work southeast of Carbondale, Illinois, in the summer of 1939.

Dave Love (on left) and Robert S. Houston (on right) collecting tuff in the Jackson Hole area, Wyoming, June 18, 1954.

John and Yolanda McPhee and Dave Love, October 10, 1990, Jackson, Wyoming. Photo by Bill Wilcox, *Jackson Hole News*.

Dave Love on field trip associated with the National Outdoor Leadership School (NOLS) in 1990. The site of the photograph was at Table Mountain on the eastern flank of the Wind River Range.

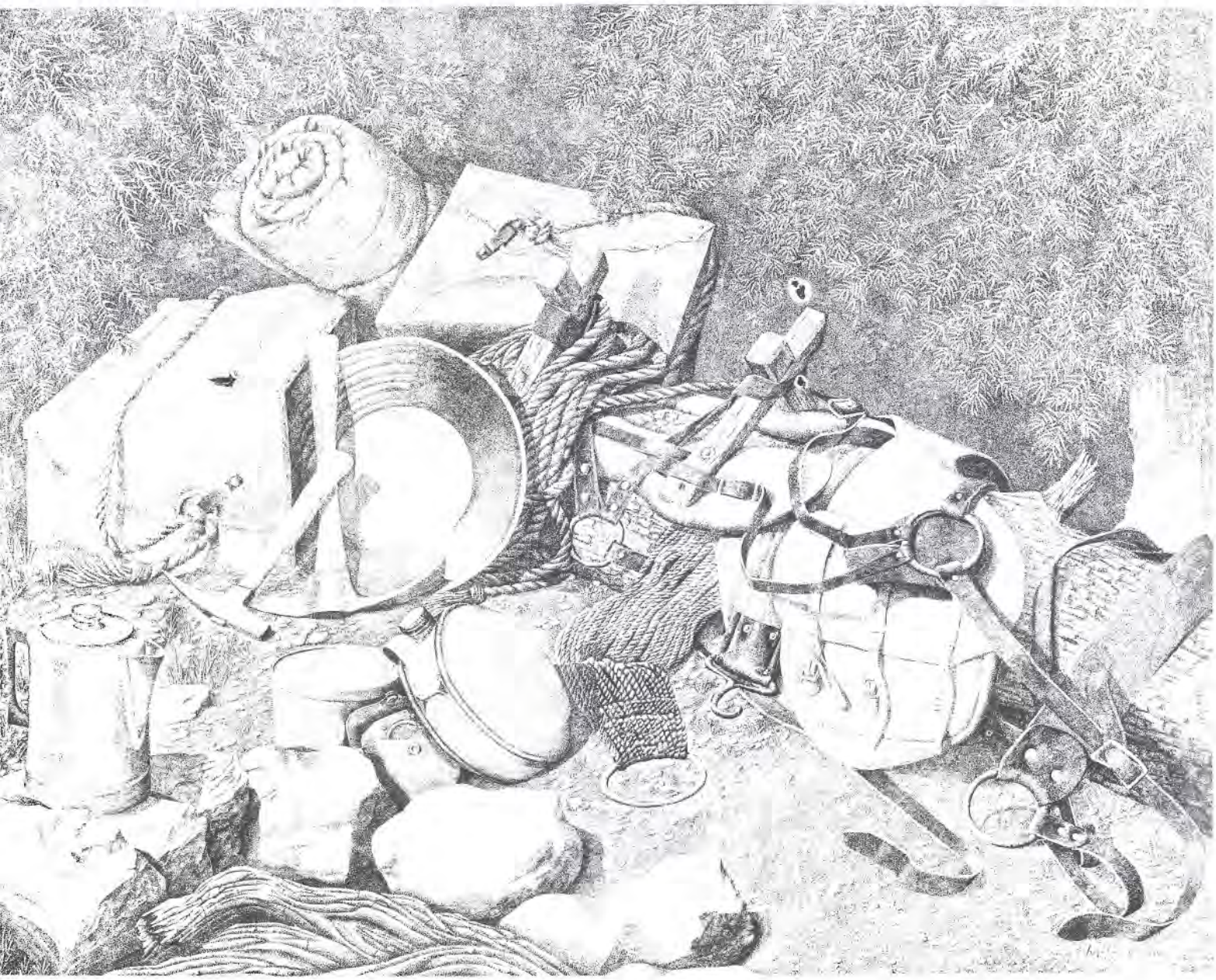

"Geologists' Camp"

Phyllis Ranz

Most of "Geologists' Camp" gear was graciously lent by Dr. J. David Love as a model for this still life. Dr. Love was born on a ranch outside Riverton and has spent a lifetime exploring Wyoming's geology. The packsaddle and U.S. Cavalry leather saddlebags had been stored by the U.S. Geological Survey in Miles City, Montana in 1904 (possibly they had been used on the Hague Survey of Yellowstone, 1886-1903). The saddlebags have waterproof canvas liners to hold wild game. The U.S. Geological Survey retrieved the camp equipment in 1938 and used it until 1981. Constructed of rawhide nailed to hardwood, the panniers were made by Sid Reynolds, who packed for Dr. Love from 1945 to 1957. The gold pan belonged to Dr. Love's father, who homesteaded in central Wyoming in 1896. The canteen dates from at least World War I. Other items include the Brunton compass (*circa* 1915) used by Anaconda Mining Company geologists for underground mine mapping in the Butte, Montana, area (loaned by Thomas Satterly) and the pick and rock hammer, used by Laura W. McGrew, U.S. Geological Survey geologist, from 1952 to 1979.

Part I

Overview

Frontispiece. Wyoming from 570 miles high. A mosaic of false-color Landsat images compiled by U.S. Department of Agriculture, Aerial Photography Field Office.

Geologic history of Wyoming within the tectonic framework of the North American Cordillera

Arthur W. Snoke
Department of Geology and Geophysics
University of Wyoming
Laramie, WY 82071

Abstract

Wyoming, a mountainous highland, is situated along the eastern margin of the U.S. Cordillera. A portion of the northern Great Plains forms the eastern part of the state, and much of the Wyoming basin and parts of the Southern and Central Rocky Mountains comprise the rest of the state. The early geologic history of Wyoming involved complex accretion and subsequent rifting of an Archean craton, commonly referred to as the Wyoming province. Late in the Early Proterozoic, an oceanic-arc terrane was accreted to the southern margin of the Wyoming province during an oblique collision. The Proterozoic suture, called the Cheyenne belt for exposures in southeastern Wyoming, is a zone of penetrative deformation. Middle Proterozoic anorthositic and associated monzosyenitic to granitic rocks intruded this tectonic zone.

After the mid-Proterozoic, a nearly billion-year gap exists in the geologic record of Wyoming. Lower and middle Paleozoic shelf-facies strata, commonly separated by disconformities, form a veneer upon Precambrian basement rocks. Uplifts of the late Paleozoic Ancestral Rocky Mountains extended northward into southeastern Wyoming and locally were eroded to Precambrian rocks; Pennsylvanian rocks therefore lie directly on the basement in parts of these uplifts. Late Paleozoic and early Mesozoic strata record diverse paleoenvironments, including paralic, eolian, and fluvial settings. Beginning in the mid-Cretaceous, a persistent interior seaway extended from the Arctic Ocean to the Gulf of Mexico. A nearly coeval, thin-skinned, fold-and-thrust belt (Sevier orogenic belt) evolved west of this seaway and remained active into the early Eocene. East of the fold-and-thrust belt, during the Late Cretaceous through early Eocene, deep-rooted reverse and thrust faults fractured the craton, forming basement-cored uplifts separated by deep, actively subsiding basins. These juxtaposed structures are the classic features of the Laramide orogeny.

Locally important magmatism, including both alkaline and subalkaline rocks, formed volcanic piles and subvolcanic intrusive complexes during the middle to late Eocene. The Heart Mountain detachment fault evolved during the middle Eocene, and allochthonous Paleozoic sedimentary and Tertiary volcanic rocks spread southeastward into the Bighorn Basin from a steep breakaway fault along the northeastern flank of the northern Absaroka Range. Extensive lakes also developed during the middle Eocene in southwestern, central, and northern Wyoming. During the latest Eocene through middle Miocene, airborne volcaniclastic debris, chiefly derived from the Great Basin,

Snoke, A. W., 1993, Geologic history of Wyoming within the tectonic framework of the North American Cordillera, *in* Snoke, A.W., Steidtmann, J.R., and Roberts, S.M., editors, Geology of Wyoming: Geological Survey of Wyoming Memoir No. 5, p. 2-56.

fell over the entire Wyoming foreland. The aggradational cycle continued intermittently throughout much of the Neogene, gradually burying all but the highest parts of the Laramide tectonic landscape.

Although late Neogene normal faulting occurred throughout Wyoming, only modest extension resulted. During the last 5 million years, the uplifts have been exhumed, exposing the Laramide skeleton as the present mountainous topography. Debate focuses on the relative importance of the roles of tectonic uplift versus climatic change in this exhumation. High-level erosional surfaces are common in the Rocky Mountains. Most of the high-level surfaces in Wyoming formed late in the Cenozoic, as erosional remnants of previously much more extensive pediments.

The massive Yellowstone Plateau is the product of dominantly rhyolitic volcanic eruptions that occurred during the past 2.2 million years associated with uplift above an inferred mantle hotspot. Recent seismic activity is common near the western border of Wyoming (Intermountain seismic belt); historic seismic events have been comparatively infrequent elsewhere in the state.

Introduction

A remarkably diverse and complex geologic history is preserved in the parallel-sided political unit called Wyoming. Its geologic history is vividly portrayed in color and form on the *Geologic map of Wyoming* by Love and Christiansen (1985). Wyoming provides rich slices of Earth history, preserved as the various rock units and structures that have formed the subjects of countless geological studies. An objective of this chapter is to put this long, multi-stage geologic history into a continental perspective by integrating the geology of Wyoming into the tectonic evolution of the North American Cordillera (**Figure 1**). Such a complex and broad-ranging task is destined to be an incomplete analysis. Nevertheless, this overview is designed as a framework for the evaluation of the many detailed syntheses included in this volume.

The State of Wyoming includes a large part of the Central Rocky Mountains (or Middle Rocky Mountains; Fenneman, 1931), much of the Wyoming basin province, three prongs of the Southern Rocky Mountains, and a part of the northern Great Plains (**Frontispiece**). Wyoming is therefore situated in an important Phanerozoic tectonic transition zone, extending from the essentially flat-lying rocks of the continental interior to the folded and faulted strata of the Rocky Mountains. However, this history is superposed on a staggeringly long Precambrian history that can be traced back to remnants of some of the oldest known rocks in North America (see Frost and Frost, this volume).

The present physiography of Wyoming provides important clues to past events that shaped the geologic evolution of the state (**Frontispiece**). The mean elevation of Wyoming is high (about 6,700 ft), second only to Colorado among the fifty states (Larson, 1978). The highest elevations in Wyoming are in the Wind River Range, where several peaks are over 13,000 ft; Gannett Peak, the highest in the state, reaches 13,804 ft. The lowest elevation, 3,125 ft, is along the Wyoming-South Dakota border. Much of Wyoming is characterized by broad intermontane basins surrounded by massive uplifts with Precambrian rocks exposed in their cores. Along the western margin of the state, Precambrian rocks are not exposed at the surface, and long linear color bands on the geologic map chiefly represent Paleozoic and Mesozoic rocks imbricated by thrust faults. In the northwestern corner of the state, a great plateau of Cenozoic volcanic rocks is the prominent physiographic feature, whereas in northeast Wyoming the margin of a regional domal uplift, centered in western South Dakota, is the dominant large-scale geologic feature.

Wyoming therefore can be subdivided into several distinct geologic provinces, which include: the fold-and-thrust belt, the uplifts and basins of the Rocky Mountain foreland, the Yellowstone Plateau, the Absaroka volcanic field, the Black Hills, and the Denver-Julesburg Basin (**Figure 2**). My approach to this complex geologic framework is to develop, chronologically, the main tectonic events preserved in the rock record (**Figure 3**).

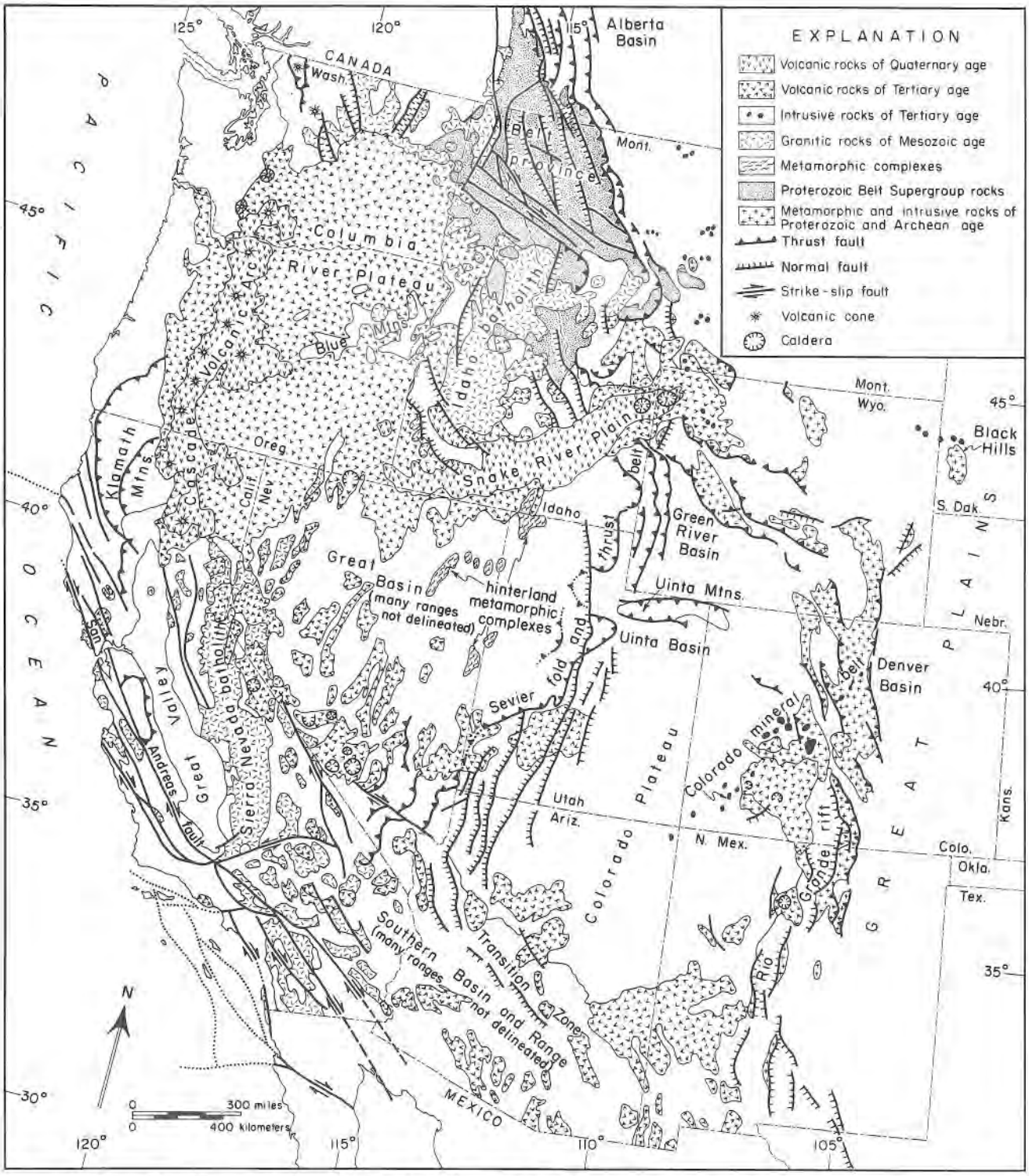

Figure 1. Generalized map of selected tectonic and geologic features of the conterminous U.S. showing Wyoming's location within this regional setting (adapted from King, [1967] 1970).

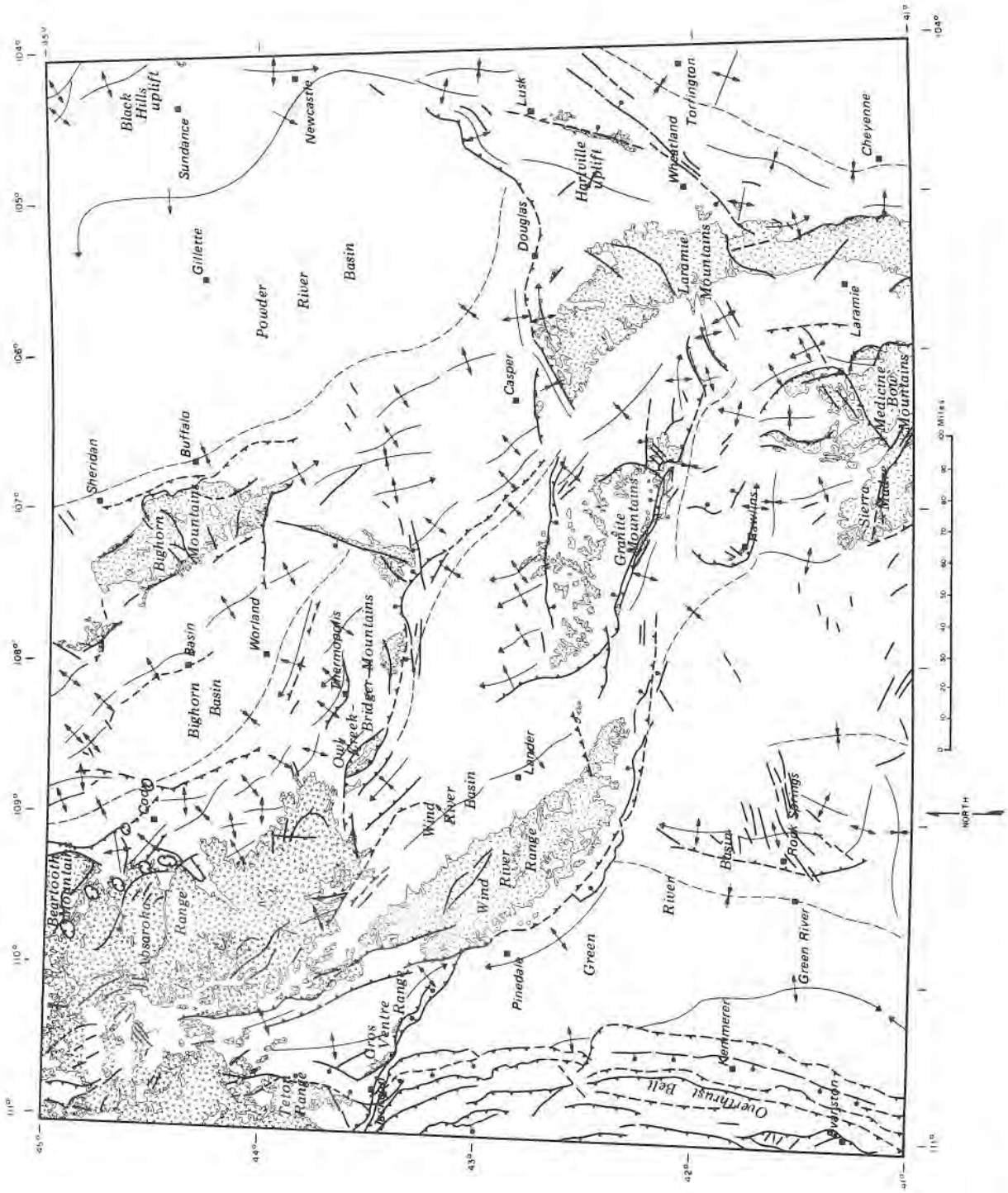

Figure 2. Generalized structural map of Wyoming, showing positions of basement-cored uplifts and main structural features (from Blackstone *in* Roberts, 1989).

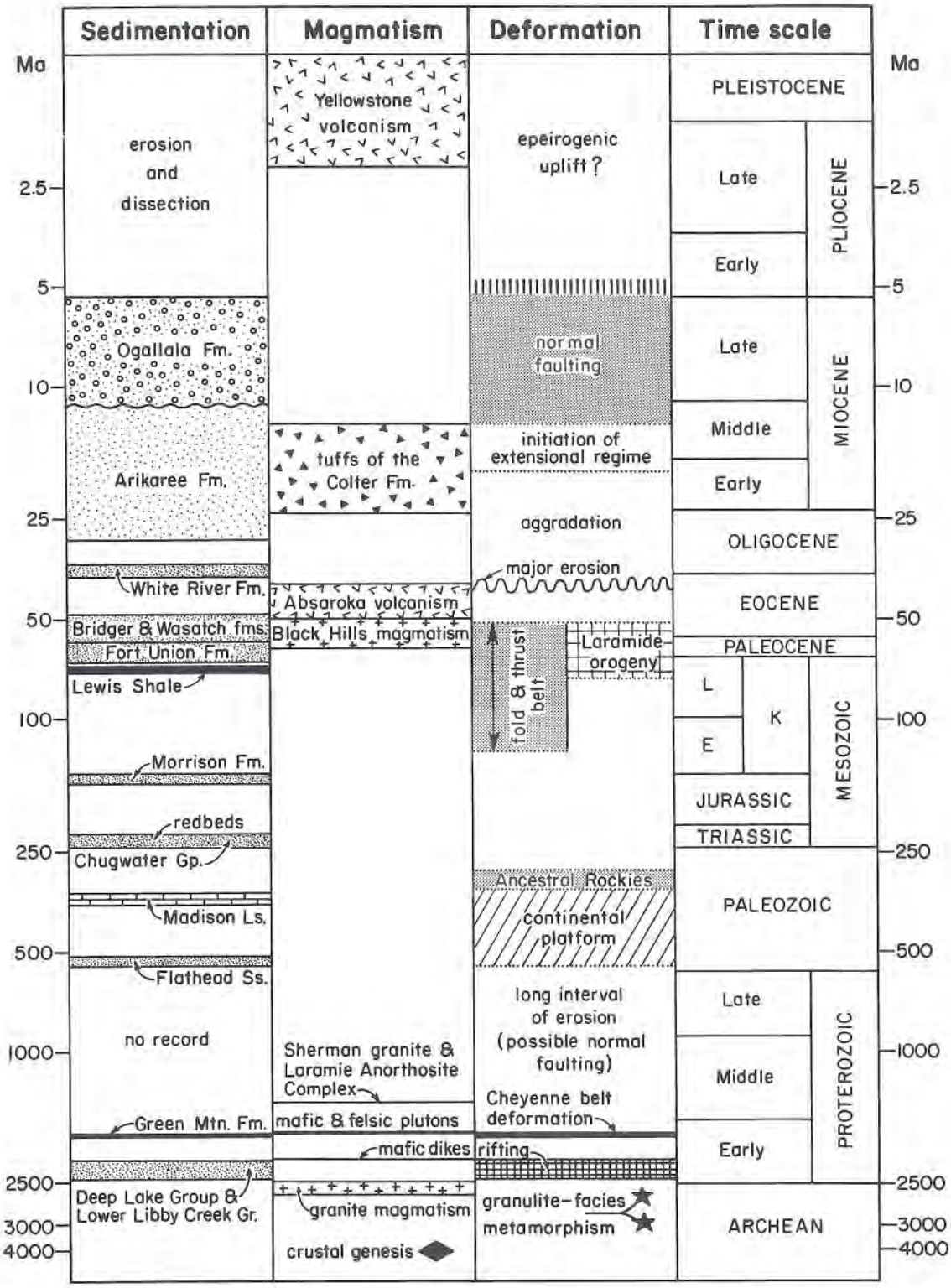

Figure 3. Salient aspects of the geologic history of Wyoming, including sedimentation, magmatism, and deformation. Only selected stratigraphic units are delineated in the sedimentation column. Logarithmic time scale in Ma; geologic time scale after Palmer (1983). This diagram was designed after Dickinson (1991, figure 5). The age range of Late Archean granitic rocks is derived from Peterman and Hildreth (1978) and Stuckless and others (1985). The age range of the Colter Formation and initiation of normal faulting is from Barnosky (1984). Other dates are derived from various publications cited in the text.

The Wyoming province: accretion of an Archean microcontinent

In Wyoming, Archean rocks are extensively exposed in the Laramide basement-cored uplifts of the Rocky Mountain foreland (**Figure 2**). These uplifts provide an important window into the Archean crust that underlies much of Wyoming, a terrane appropriately referred to as the Wyoming province (Engel, 1963; Condie, 1969). The Wyoming province is flanked by Proterozoic orogens on its northern, eastern, and southern margins (**Figure 4**). Its western margin, which extends into northeastern Nevada

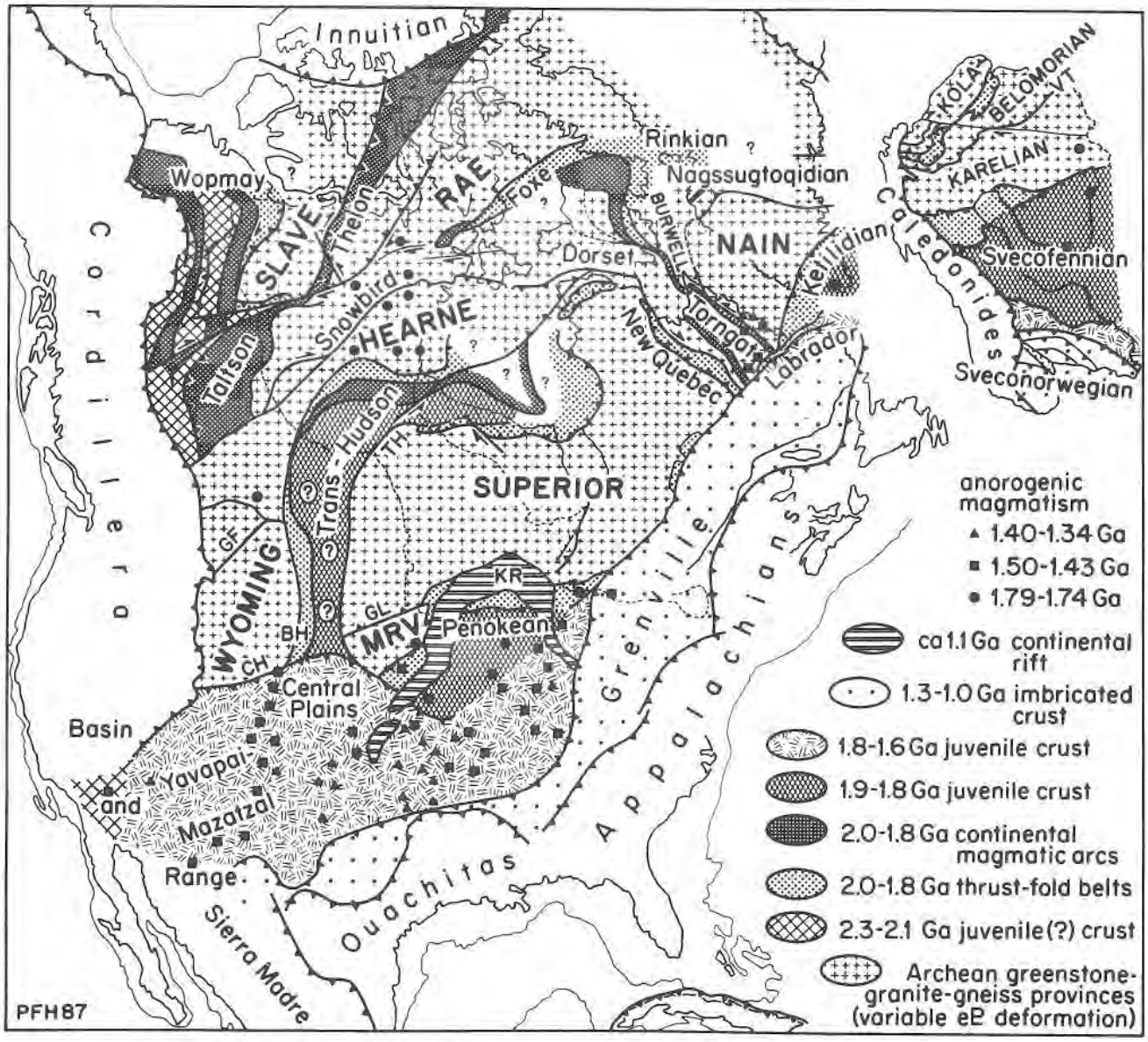

Figure 4. Position of the Archean Wyoming province relative to other Precambrian-age belts and 1.4 to 1.5 Ga magmatism (modified from Hoffman, 1989b, figure 13; used with permission). The platform cover of the North American craton has been removed. Upper-case names are Archean provinces; lower-case names are Proterozoic and Phanerozoic orogens. BH, Black Hills inlier; CH, Cheyenne belt; GF, Great Falls tectonic zone; GL, Great Lakes tectonic zone; KR, Keweenawan rift; MRV, Minnesota foreland.

(Lush and others, 1988) and under the Snake River Plain (Leeman and others, 1985), formed in the late Precambrian during breakup of the Proterozoic supercontinent (Stewart, 1976; Hoffman, 1991).

The Wyoming province is a complex aggregate of various Archean components chiefly including: Early(?) Archean to Middle Archean migmatitic gneisses, commonly containing enclaves of older supracrustal rocks; late Archean supracrustal sequences; widespread late Archean granitic rocks; and various ultramafic to mafic intrusive rocks. Zircons from a granulite-facies, migmatitic gneiss exposed in the central Wind River Range have yielded an Early Archean age component of >3.6 Ga (Aleinikoff and others, 1989). The supracrustal enclaves, a common component of the migmatitic gneisses, therefore probably constitute the oldest known element of Earth history preserved in Wyoming. This dismembered ancient stratigraphy includes metamorphosed igneous rocks (metabasite and metaperidotite) as well as a diverse original sedimentary succession now metamorphosed to pelitic paragneiss, iron formation, and scarce calc-silicate paragneiss and quartzite. Metamorphic and geochronometric studies suggest an early history of granulite-facies metamorphism for some of these rocks prior to incorporation into the migmatitic gneiss. The ages of most of the migmatitic gneisses are uncertain or poorly constrained, but most geochronometric studies yield dates within the interval 2.8 to 3.1 Ga (Frost and Frost, this volume). In the Beartooth Mountains, Montana, zircons from a Middle Archean quartzite indicate that an older crustal component (about 3.96 Ga) also exists or did exist in the northern Wyoming province (Mueller and others, 1992).

Late Archean supracrustal sequences are preserved locally in the Wyoming province. Some of these successions are metavolcanic rich and exhibit characteristics of classic greenstone belts of other Archean terranes (e.g., Superior province of the Canadian shield or Kaapvaal craton of South Africa). However, the limited areal distribution and generally higher metamorphic grade of Wyoming province rocks are major dissimilarities. Nevertheless, some mafic metavolcanic rocks in Wyoming's supracrustal sequences are magnesian, with geochemical characteristics of komatiitic basaltic rocks (Snyder and others, 1990). Spinifex-textured mafic metavolcanic rocks have been reported from the Seminoe Mountains in south-central Wyoming (Klein, 1980; Snyder and others, 1989). Still other late Archean successions are characterized by stromatolitic metadolomite, mafic metavolcanic rocks, quartzite, and metapsammite/schist (e.g., Hartville uplift, Snyder and others, 1989). This mixed sedimentary-volcanic association suggests that marine deposition (including very shallow water for the dolomite) in proximity to volcanic centers characterized at least part of the margin of the newly amalgamated Wyoming province during the late Archean (see Frost and Frost, this volume; Houston, this volume).

The Wyoming province is one of seven Archean provinces that presently form Laurentia, the North American craton (Hoffman, 1988, 1989b). These Archean provinces could have been originally independent microcontinents, subsequently amalgamated in the Proterozoic. Alternately, they could have been part of an original Archean protocraton subsequently both rifted and reassembled during the Proterozoic (Hoffman, 1988). Consequently, relationships of the Wyoming province to its more extensive Canadian equivalents (e.g., Hearn and Superior provinces) are poorly known. Hoffman (1989b) noted that the Wyoming province differs from the Superior province by the presence, in the former, of abundant shelf-type metasedimentary rocks and isotopic data suggesting widespread continental crust older than 3.1 Ga (e.g., Wooden and others, 1988).

The Late Archean Wyoming province must have been larger than its present extent. Its present southern boundary, in part, reflects Early Proterozoic rifting and spreading that led to establishment of an Early Proterozoic passive margin (Houston, this volume). Some mafic dike swarms within the Archean Wyoming province no doubt reflect this episode of crustal extension, although systematic geochronometric dating of mafic dike swarms in the Wyoming province is still in its infancy (Snyder and others, 1990).

An early Proterozoic continental margin and its destruction

A fundamental Precambrian boundary is exposed in southeastern Wyoming, where the Early Proterozoic Colorado province of probable island-arc affinity was accreted to the Archean Wyoming craton and its Early Proterozoic passive margin cover (Hills and Houston, 1979; Karlstrom and Houston, 1984). This important tectonic boundary zone, originally referred to as the Mullen Creek-Nash Fork shear zone (Houston and McCallum, 1961), was renamed the Cheyenne belt by Houston and others (1979). This well-exposed geosuture consists of a system of mylonite zones and varies in overall width from about 4.3 mi(7 km) to 0.4 mi(0.7 km) (Duebendorfer and Houston, 1986, 1987). In Wyoming, the event associated with the development of the Cheyenne belt is the oldest (ca. 1.75 Ga) in a complex Early Proterozoic crustal accretion history that added an enormous girth (>800 mi wide) of juvenile crustal material to the southwestern flank of nuclear North America during the interval 1,790 to 1,660 Ma (Condie, 1982; Nelson and DePaolo, 1985; Reed and others, 1987; Karlstrom and Bowring, 1988). The Cheyenne belt includes lenses of rocks of variable province affinity. The Bear Lake block of Duebendorfer and Houston (1987) includes orthogneiss of Archean affinity, whereas the Barber Lake block is composed of mixed provenance sediments yielding 2.0 to 2.4 Ga Nd model ages (Ball and Farmer, 1991). Nevertheless, south of the Barber Lake block no Archean rocks or components have been recognized in the extensive isotopic data reported by various workers (e.g., Nelson and DePaolo, 1985; Bennett and DePaolo, 1987; Ball and Farmer, 1991).

In the Medicine Bow Mountains, an exceptionally diverse and complete Early Proterozoic stratigraphic sequence is exposed north of the Cheyenne belt (Karlstrom and others, 1983). This sequence apparently records the rifting and eventual foundering of the Archean craton and the development of an Early Proterozoic passive margin. Rifting is suggested by thick conglomeratic units of the Deep Lake Group in inferred fault troughs floored by Archean basement (Houston, this volume). Intrusive mafic rocks in the Deep Lake Group have yielded a U-Pb zircon age of 2,092 ± 9 Ma (Premo and Van Schmus, 1989), providing the only geochronometric control for the inferred Early Proterozoic rifting event. The overlying Libby Creek Group consists, in part, of an approximately 15,000-foot-thick (4.6-km-thick) clastic succession, which is overlain by a 6,500-foot-thick (2-km-thick) stromatolitic dolomite unit (Nash Fork Formation). Together, these units constitute a passive margin sequence, suggesting the classic transition from fluvial to shallow-marine clastic rocks to carbonate bank. The uppermost part of the Libby Creek Group, more problematic in origin, is characterized by locally pillowed basaltic rocks and graphitic slate. Such rocks clearly indicate a major change in the overall depositional framework and may signal the proximity of an allochthonous oceanic-arc terrane, as suggested by Houston (this volume).

Rocks south of the Cheyenne belt are part of the Early Proterozoic Colorado province. They consist chiefly of various metamorphosed volcanogenic rocks, including both lavas and volcaniclastic rocks, complexly intruded by a variety of Proterozoic plutonic rocks ranging from mafic to felsic. In Wyoming, these rocks are exposed in the Sierra Madre, Medicine Bow Mountains, and Laramie Mountains (**Figure 2**). The best preserved volcanogenic rocks occur in the Sierra Madre, where they form part of the Green Mountain Formation of Divis (1976). Relict volcanic textures are preserved locally, allowing recognition of original lapilli tuff, volcanic breccia, and porphyritic phases. Geochemical studies of rocks from the Green Mountain Formation indicate an essentially bimodal basalt-dacite/rhyolite suite, with only sparse andesite, although an overall calc-alkaline trend is indicated (Schmidt, 1983; Condie and Shadel, 1984).

Zircons from a quartz-feldspar-mica gneiss (metadacite porphyry) of the Green Mountain Formation have yielded a U-Pb age of 1,792 ± 15 Ma, representing the best constraint on the age of volcanism in the accreted arc terrane (Premo and Van Schmus, 1989). Some plutonic bodies south of the Cheyenne belt may be comagmatic with the metavolcanic rocks, whereas other Proterozoic plutons clearly are younger. The Sierra Madre Granite forms an important younger pluton, three phases of which have been dated as 1,763 ± 6 Ma, 1,749 ± 8 Ma, and 1,744 ± 14 Ma by U-Pb zircon techniques (Premo and Van Schmus, 1989). This pluton intruded a

mylonite zone related to the plastic deformational history of the Cheyenne belt but is itself cut by a brittle cataclastic fault zone. Houston (this volume) argues that this granitoid constrains the final stages of the suturing process between the Colorado and Wyoming provinces as manifested in the Sierra Madre. Therefore, the deformational age of the Cheyenne belt is broadly defined as post-1,790 Ma but pre-1,750 Ma.

The northern boundary of the Wyoming province is still poorly understood but apparently is manifested by the reactivated Great Falls tectonic zone of east-central Idaho and west-central Montana (O'Neill and Lopez, 1985; O'Neill and Harlan, 1992). The buried Precambrian rocks north of this subsurface crustal discontinuity have been referred to as the Medicine Hat block (Hoffman, 1989b, figure 12).

1.4 to 1.5 Ga magmatism - anorogenic or syntectonic?

A transcontinental magmatic event that occurred about 1.4 to 1.5 Ga has been recognized from Labrador to southern California (Silver and others, 1977; Anderson, 1983). In southeastern Wyoming, this magmatism is well represented by the Laramie Anorthosite Complex (LAC) and Sherman batholith (see Frost and others, this volume). The LAC was emplaced across the inferred projection of the Cheyenne belt into the south-central Laramie Mountains (**Figures 2** and **4**). The youngest pluton of the complex (Red Mountain pluton) has yielded a U-Pb zircon age of 1,439 +7/-6 Ma (Frost and others, 1990). Geochronometric studies on granitic rocks from the Sherman batholith indicate a crystallization age of about 1.43 Ga (Zielinski and others, 1981; Aleinikoff, 1983), thereby suggesting the broadly coeval nature of these plutonic suites. Field relationships, however, indicate that anorthositic rocks of the LAC predate the granitic rocks of the Sherman batholith, whereas the late monzosyenitic rocks of the LAC locally grade into granitic rocks of the Sherman batholith (Frost and others, this volume).

The LAC is a multi-stage, lithologically heterogeneous plutonic complex. Anorthositic rocks ranging from pure anorthosite to plagioclase-rich gabbro, norite, and troctolite are the main components of the complex (see Frost and others, this volume, for exact petrographic nomenclature). Four domical structures, as defined by distribution and attitude of foliation, are present in the anorthositic rocks. Foliations in the anorthositic rocks range from primary igneous layering and plagioclase lamination to subsolidus flow layering, probably related to the forceful upward emplacement of a hot, but nearly solidified, aggregate of crystals (see Frost and others, this volume, for specific details). Various monzosyenitic to granitic rocks form discrete younger plutons along the margins of the composite anorthositic body.

The Sherman batholith is composed chiefly of potassic, iron-rich (relative to MgO) granitic rocks. The dominant granitic rock is massive megacrystic, biotite-hornblende granite. Other granitic rocks comprising the batholith (see Frost and others, this volume) have not been delineated systematically on a geologic map. A suite of fine-grained granitoids forms part of the Sherman batholith, and Frost and others (this volume) suggest that these rocks may be chilled equivalents of the granite. Near Virginia Dale, Colorado, Eggler (1968) documented a ring-dike complex as part of the Sherman batholith, suggesting an overall epizonal emplacement history for this mid-Proterozoic pluton.

The widespread 1.4 to 1.5 Ga magmatism of North America commonly is referred to as anorogenic (e.g., Anderson, 1983), implying that pluton emplacement was not associated with a specific orogenic event such as subduction or collision. This petrotectonic classification is based principally on the observation that Proterozoic deformation and metamorphism younger than 1.65 Ga has not been found associated with the transcontinental belt (Anderson and Bender, 1989). Furthermore, various levels of emplacement are exposed along the belt, so that the anorogenic characterization is not simply an artifact of epizonal plutonic emplacement (Anderson and Bender, 1989). Nevertheless, recent field studies in the Wyoming-Colorado segment of the belt have suggested that some tectonic events may be associated with emplacement of the plutonic complexes. Frost and others (this volume) note a significant geobarometric variation from north to south in the LAC, and suggest that the plutonic complex may be tilted northward. Furthermore, the coeval to younger Sherman batholith has subvolcanic characteristics such as a ring-dike complex and possible chilled phases, suggesting lower pressures of crystallization

than the LAC. These relationships suggest that the LAC may have been tilted prior to emplacement of the high-level Sherman batholith; however, no structural features associated with the inferred tilting have been identified. Graubard (1991) argued that the approximately 1,440-Ma Mt. Evans batholith in the Colorado Front Range was emplaced syntectonically into a pre-existing but reactivated, northeast-striking shear zone. During Middle Proterozoic transpression, plutonism apparently was localized in a dilational zone associated with a 6.2-mi-wide (10-km-wide), left-lateral shear system.

Various tectonic models involving extension, crustal thickening, or subduction have been proposed to explain the origin of the transcontinental, Middle Proterozoic magmatic belt (see Anderson and Bender, 1989, for review). However, none of these models has been supported enthusiastically by recent workers, and each model has shortcomings. Hoffman (1989a) proposed a bold, new idea of a "mantle superswell" — convective upwelling, thousands of kilometers in diameter, beneath a stationary supercontinent that aggregated previously in the late Early Proterozoic. According to this concept, mantle magmas invaded and ponded in the lower crust, causing partial melting and uplift. Rifting, if it occurred, would have been a consequence, not the cause, of the mantle upwelling (Hoffman, 1989a). Regardless of the tectonic setting of 1.4 to 1.5 Ga magmatism, a remarkable continent-wide event occurred during the Middle Proterozoic. Juvenile Proterozoic crust experienced deep-seated crustal melting, eventually leading to widespread distribution of potassic (rapakivi-type) granitic complexes with the local association, especially in Canada but also in Wyoming, of anorthosite and monzosyenitic rocks.

Missing Proterozoic record

Between the Middle Proterozoic magmatic event and the beginning of Paleozoic sedimentation on the Wyoming craton, there is no record of nearly 1 billion years of Earth history within the confines of the state. A few mafic dikes have yielded radiometric dates within this time span (see Snyder and others, 1990, figure 9.15) and may constitute an exception. Nevertheless, the long interval presumably represents emergence and erosion of this part of Laurentia prior to the Late Proterozoic breakup of the supercontinent (Hoffman, 1991).

Some evidence for the general Proterozoic tectonic framework of the region, however, is preserved in areas adjacent to Wyoming. During the Middle Proterozoic, the Belt-Purcell Supergroup of the Northern Rocky Mountains accumulated in the "Belt basin" as a thick stratigraphic unit [perhaps up to 52,500 ft (16 km), Winston, 1989] consisting chiefly of siltite, argillite, quartzite, and carbonate rocks (Harrison, 1972). The tectonic setting of the Belt basin is controversial, but one model suggests an intracratonic rift (Winston, 1986). Northwest-striking normal faults related to development of the Belt basin have been recognized in southwestern Montana and similar faults probably extended into northwestern Wyoming (Schmidt and Garihan, 1986b, figure 7). During deposition of the Belt-Purcell Supergroup, Wyoming apparently was a faulted upland. Nd-Sm isotopic data (Frost and Winston, 1987), however, suggest that rocks of the Archean Wyoming province were not the prime source of the terrigenous sediment that accumulated in the Belt basin.

Immediately south of the southwestern border of Wyoming, in northeast Utah and adjacent Colorado, the approximately 24,000 foot-thick Uinta Mountain Group of terrigenous sandstone (and quartzite), shale, and conglomerate was deposited in an east-west striking, fault-bounded basin (inferred aulacogen; e.g., Burke and Dewey, 1973) during the Middle to Late Proterozoic (Hansen, 1965). The maximum age range of the Uinta Mountain Group is 770 to 1,110 Ma, which is generally younger than the inferred age range of the Belt and Purcell Supergroups of the Northern Rocky Mountains (Bressler, 1981; see Winston, 1989, for a summary of the age of the Belt). Localization of the inferred Uinta aulacogen along the extended trace of the Cheyenne belt (Sears and others, 1982) suggests tectonic heredity and the importance of this suture zone to the post-Early Proterozoic structural development of the Rocky Mountain region (Bryant, 1985). Furthermore, similar east-west structural trends in the Wyoming foreland may reflect a Precambrian structural grain that was established in Archean basement rocks dur-

ing the Proterozoic and reactivated during later tectonism (Bryant, 1985).

The rifting that eventually led to the breakup of the supercontinent Laurentia was part of a protracted rift history that began about 730 to 770 Ma (Devlin and Bond, 1988). Deposition of the Upper Proterozoic Windermere Supergroup (or equivalents) represents early manifestations of this rift history, and these sedimentary rocks occur as thick stratigraphic sequences west of Wyoming. Although structures related to this long history of crustal extension may exist in Precambrian basement rocks of Wyoming, no such feature has been definitely recognized. However, Mitra and Frost (1981) argued that retrograde deformation zones containing chlorite and actinolite, formed between 900 and 600 Ma, are common throughout Precambrian rocks of the Wind River Range.

In summary, between the Middle Proterozoic and the beginning of the Phanerozoic, Wyoming apparently was a positive area that may have periodically experienced extensional faulting. Large areas adjacent to Wyoming were significantly extended, eventually leading to the development of deep basins and the accumulation of thick sedimentary successions. In some cases, the area of paleo-Wyoming served as a significant source area for terrigenous sediments that accumulated in these basins.

Early and middle Paleozoic shelf-facies sedimentation

At the dawn of the Paleozoic Era, Wyoming was situated on the west-central flank of rifted Laurentia (Hoffman, 1988). The complex Precambrian basement of Wyoming served as a low-relief platform for accumulation of a thin cratonic sedimentary cover during the early to middle Paleozoic (see Boyd, this volume) (**Figure 5**). The Transcontinental arch was a major paleotectonic feature that influenced the depositional history on the Rocky Mountain shelf especially during the Paleozoic Era. This feature was a broad, somewhat sprawling, southwest-northeast-trending basement high that extended from present-day northeastern Arizona to southern Minnesota and perhaps across the Canadian shield. Wyoming's Phanerozoic depositional record therefore accumulated on the northwestern flank of this large-scale basement arch. Influence of the Transcontinental arch is indicated by stratigraphic thickness and facies variations associated with the progressive west-to-east marine transgression that deposited the Sauk sequence during the Cambrian and Early Ordovician (Sloss, 1963; Lochman-Balk, 1972). However, its role as a long-lived (reactivated) paleotectonic feature is especially obvious in the absence of Silurian beds over a broad area of the west-central United States (Gibbs, 1972; Peterson and Smith, 1986). Paleogeographic reconstructions suggest that marine Middle Silurian strata covered the craton (Dott and Batten, 1981). However, their present distribution suggests broad-scale Late Silurian to Early Devonian uplift of the Transcontinental arch, associated with widespread erosion (the development of the pre-Kaskaskia unconformity).

The oldest known Phanerozoic stratigraphic unit in Wyoming is a quartz-rich sandstone (Flathead Sandstone) that formed an eastward-transgressive sheet across Wyoming during the Middle to Late Cambrian. The basal contact of this unit is the fundamental "great unconformity" seen between Precambrian and Phanerozoic rocks (base of the Sauk sequence of Sloss, 1963). Farther to the west, in the site of the developing Cordilleran miogeocline, an enormous thickness of Upper Precambrian and Lower Cambrian strata had accumulated along the rifted continental margin (Stewart, 1972). Wyoming, however, lay east of a regional hinge line (the so-called Wasatch line of Utah) and correlative deposits are absent on the Wyoming shelf. An enormous discrepancy in thicknesses of broadly coeval units originally deposited east and west of the Wasatch line continued as an essential characteristic of the Paleozoic depositional history.

On the Wyoming craton, the Flathead Sandstone is chiefly overlain by various thin, shallow-water marine deposits; and disconformities are common within this stratigraphic succession. However, during the Early Devonian, much of Wyoming was emergent, and only lenticular estuarine deposits are preserved locally (e.g., Beartooth Butte Formation in the Beartooth Mountains of northwest Wyoming and

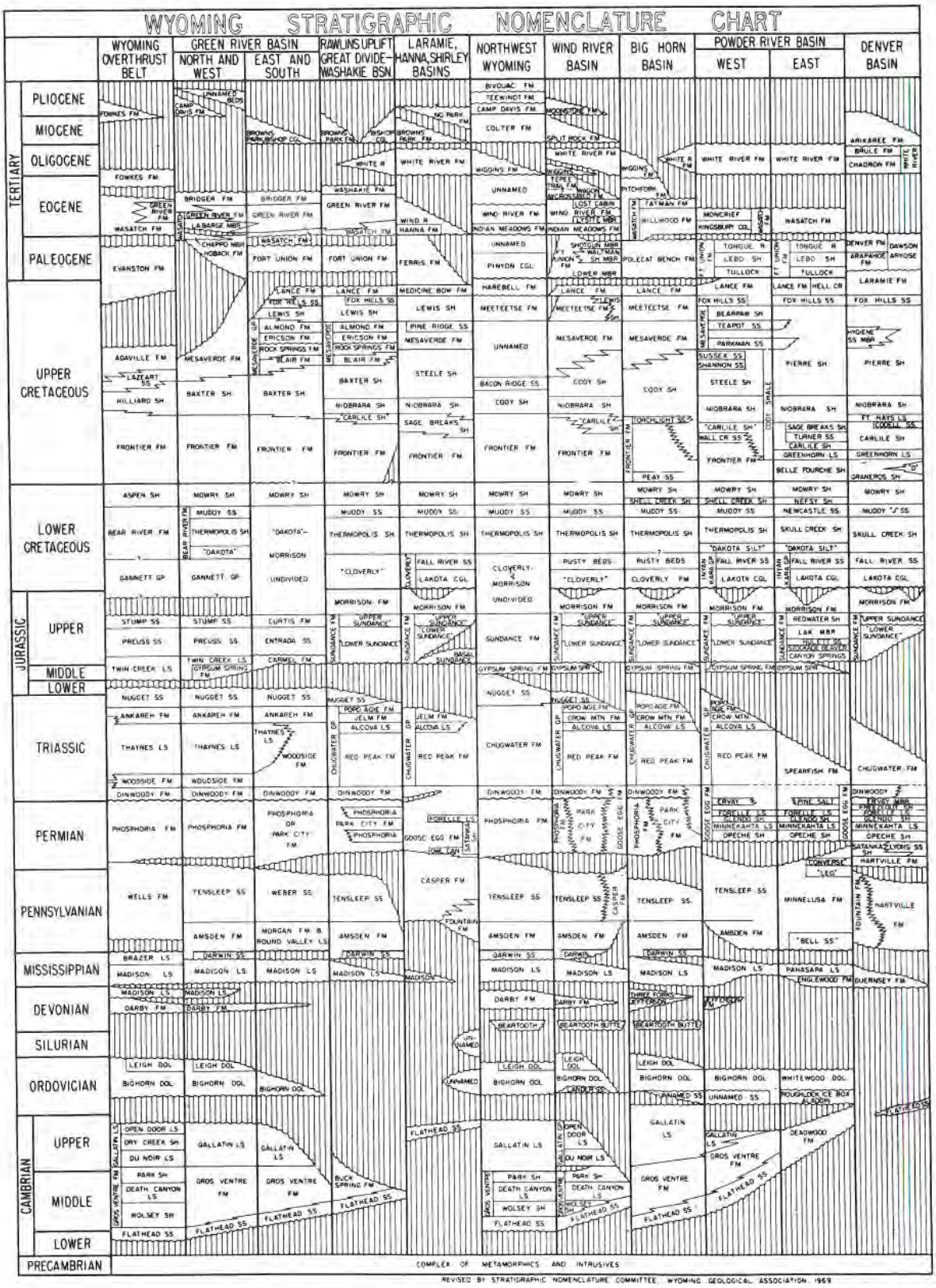

Figure 5. Wyoming stratigraphic nomenclature chart prepared by the Stratigraphic Nomenclature Committee, Wyoming Geological Association, 1969 (reprinted by permission). Please note that some significant changes in stratigraphic nomenclature as depicted on this classic chart are presented on the 1993 *Stratigraphic chart showing Phanerozoic nomenclature for the State of Wyoming* compiled by Love and others (map pocket).

southwest Montana). The Mississippian was a time of extensive carbonate deposition throughout Wyoming as well as over a large part of interior North America (Dott and Batten, 1981). In Wyoming these carbonate rocks are frequently dolomitic. Various stratigraphic names have been applied around the state (see Boyd, this volume); throughout central Wyoming, these rocks are called the Madison Limestone (Lageson and others, 1979). The Mississippian carbonate strata vary from a zero edge in southeastern Wyoming to more than 1,000 feet (305 m) thick along the western and northern borders of the state (Peterson and Smith, 1986).

Widespread emergence of much of the continental interior at the close of deposition of the Madison Limestone caused extensive erosion and dissolution of its upper surface. As a result, solution-breccia beds and paleokarst features are common in upper parts of the Madison Limestone (see Huntoon, this volume, for a discussion of the hydrologic significance). This unconformity coincides with the top of the Kaskaskia sequence of Sloss (1963). Overlying units such as the Amsden and Tensleep formations are primarily clastic rocks, indicating fundamental changes in depositional and tectonic conditions of the western North American craton (Peterson, 1988).

Late Paleozoic and early Mesozoic depositional basins

During Pennsylvanian through Permian time, the southern margin of North America experienced a major collisional event that is in part manifested by the Ouachita-Marathon orogenic belt. An aspect of this orogeny was reactivation of pre-existing zones of weakness and uplift of large crustal blocks in the foreland of the orogenic belt (Kluth and Coney, 1981). This intraplate deformation can be traced across a broad belt that extends west-northwest from the structural front of the Ouachita-Marathon orogenic belt to the continental margin of late Paleozoic North America as seen in Nevada and Utah (Kluth, 1986). Tectonic development of the Ancestral Rocky Mountains is a manifestation of this foreland deformation. Associated uplifts and their basins formed principally in Colorado, but important extensions affected parts of southeastern Wyoming (see Maughan, this volume).

In southeastern Wyoming, the Ancestral Rocky Mountains were manifested principally by the Pathfinder uplift, originally delineated by Mallory (1963). However, the extreme northern end of the Ancestral Front Range uplift also extended into Wyoming near the present site of the southwestern Medicine Bow Mountains and Sierra Madre (Mallory, 1963; Maughan, this volume). Delineation of uplifts associated with the Ancestral Rocky Mountains in Wyoming is based on: (1) stratigraphic relationships presently preserved on the flanks of younger, superposed Laramide uplifts such as the Laramie Mountains and Sweetwater arch, and (2) subsurface data from adjacent Laramide basins (especially see Mallory, 1967). An important unit in the delineation of these ancient uplifts is the widespread Amsden Formation, which ranges in age from Late Mississippian to Middle Pennsylvanian (Sando and others, 1975; but see Boyd, this volume). Mallory (1963) used the absence of Amsden Formation in southeastern Wyoming to define the extent of the Pathfinder uplift. In this area, the Amsden Formation probably was chiefly Morrowan and Atokan (Mallory, 1967) and, consequently, its absence indicates syn- or post-Atokan erosion.

Mallory (1963, 1967) also demonstrated that upper parts of the Amsden Formation (Atokan age) systematically thicken away from the inferred uplift, suggesting that the uplift was of Atokan age. Southern parts of the Pathfinder uplift apparently were eroded to Precambrian basement during the Middle Pennsylvanian. For example, along the west flank of the southern Laramie Mountains, south and east of Laramie, Precambrian basement rocks are immediately overlain by red sandstone, conglomerate, and arkose of the Fountain Formation (Knight, 1929), which ranges in age from Atokan to Virgilian. Lower Paleozoic rocks are absent in the southern Laramie Mountains, although regional paleogeographic reconstructions and fossiliferous blocks of Ordovician and Silurian rocks in diatremes near the Wyoming-Colorado border suggest their former presence in the area (see Boyd, this volume).

During the Permian, Wyoming was part of the western margin of the supercontinent Pangaea, and was situated near the equator (Smith and others, 1981). A regional disconformity in central Wyoming

separates Pennsylvanian and Permian strata. In contrast, along the western and eastern margins of the state, a more continuous Upper Pennsylvanian to Lower Permian record is preserved (e.g., the Wells Formation in the west and Casper and Minnelusa formations in the east). Permian stratigraphy in Wyoming is characterized by the intertonguing of numerous lithologic units that has fostered a bewilderingly complex stratigraphic nomenclature (Peterson, 1984; Boyd, this volume).

In the eastern part of the state, a redbed and evaporite facies, the Goose Egg Formation, is common, whereas shelf carbonates are important components of the Phosphoria (Park City) Formation in the central to western parts of the state. Phosphatic shale, phosphorite, and bedded chert are distinctive components of the Phosphoria Formation of western Wyoming. The organic-rich members of the Phosphoria Formation are especially significant as source rocks for hydrocarbons and as a phosphate reserve. The top of the Permian System exhibits an erosional surface across the Cordilleran miogeocline; Pipiringos and O'Sullivan (1978) suggested development of a general unconformity (their Tr-1 unconformity) at the Permian-Triassic boundary on the stable shelf of the Western Interior.

Red colors are commonly associated with Triassic strata in Wyoming. As Picard (this volume) vividly describes, the redbeds of the Chugwater Group (of Pipiringos, 1968) are visually the most spectacular stratigraphic units in Wyoming. During Chugwater deposition, much of the state was a virtually featureless, muddy coastal plain. However, coeval marine siltstones and limestones accumulated in western Wyoming, in the form of the Dinwoody and Thaynes formations. The Alcova Limestone is a distinctive marker unit in the Chugwater Group. This laminated, purplish gray, resistant limestone has been interpreted as a marine tongue extending eastward from upper parts of the Thaynes Formation into the redbed sequence (Picard and others, 1969).

After the Early Triassic, marine waters temporarily withdrew from the U.S. Cordilleran miogeocline (Carr and Paull, 1983). Regional emergence and erosion occurred, manifested by the widespread Tr-3 unconformity of Pipiringos and O'Sullivan (1978). For example, on the Colorado Plateau, the Tr-3 unconformity separates the Upper Triassic Chinle Formation from the underlying Lower Triassic Moenkopi Formation. However, in Wyoming the unconformity is much more subtle; according to Pipiringos and O'Sullivan (1978), Tr-3 occurs within the Crow Mountain Sandstone and Jelm Formation of the Chugwater Group. The Popo Agie Formation of Wyoming's Chugwater Group (see Picard, this volume) is temporally equivalent to continental beds of Arizona's Chinle Formation.

The eolian Nugget Sandstone, which is widespread in western and south-central Wyoming, is a distinctive and paleoenvironmentally significant Lower Jurassic unit. The regional J-0 unconformity of Pipiringos and O'Sullivan (1978) is at the base of the Nugget Sandstone. The Nugget Sandstone was part of an enormous Early Jurassic coastal to inland dune field that stretched from central Wyoming to southern Arizona (Kocurek and Dott, 1983). Other formations that were part of this great eolian sand sea include the scenic Navajo Sandstone of southern Utah and northern Arizona and the Aztec Sandstone of southern Nevada and adjacent California. In southern Arizona and southeastern California, equivalent eolian deposits intertongue with volcanic rocks of an Early Jurassic magmatic arc (Busby-Spera, 1988). The Nugget Sandstone is a profilic reservoir for hydrocarbons in the Wyoming-Utah part of the Cordilleran fold-and-thrust belt (see Picard, this volume).

Marine waters returned to Wyoming and the craton region in the Middle Jurassic with establishment of a shallow sea (Sundance Sea) that apparently extended from Canada to northern Arizona (Kocurek and Dott, 1983). This transgression was an early stage of a gradual worldwide rise in sea level that eventually would reach its zenith in the Late Cretaceous (Vail and others, 1977). In Wyoming, various rock units manifest this major transgression, including the Gypsum Spring Formation, Twin Creek Limestone, and Sundance Formation. These units represent the initial deposits of the classic Zuni sequence of Sloss (1963). The J-2 unconformity of Pipiringos and O'Sullivan (1978), which extends throughout the Western Interior, is at the base of this transgressive sequence.

During the Late Jurassic, a major interruption of the Jurassic transgressive sequence occurred throughout the Rocky Mountain region. Beginning approximately in the mid-Oxfordian, the Rocky Mountain shelf was transformed into a nonmarine environment, with deposition of the widespread,

chiefly fluvial, Morrison Formation. Although global sea level was continuing to rise at this time (Vail and others, 1977), a significant increase in siliciclastic debris in the Rocky Mountain region, probably related to increased orogenic activity to the west (e.g., Allmendinger and others, 1984; Thorman and others, 1990), filled the Jurassic seaway (Brenner, 1983). The Rocky Mountain shelf gradually became covered with varicolored continental deposits characterized by complex intertonguing of mud, sand, gravel, and lenses of lacustrine limestone. Volcanic ash, derived from distant volcanic centers to the west, is a conspicuous detrital component in these nonmarine rocks. Spectacular dinosaur fossils have been collected from the Morrison Formation at several localities in the Rocky Mountains; but at Como Bluff, Albany County, southeastern Wyoming, this paleontologically significant unit has also yielded the greatest diversity of Mesozoic mammals in the world (Clemens and others, 1979). The Morrison Formation throughout the Rocky Mountain region is bounded at its base by the J-5 unconformity of Pipiringos and O'Sullivan (1978), and its top is usually beveled by another unconformity.

Western Interior Cretaceous basin

At its maximum development, the Western Interior Cretaceous basin extended from the Arctic Ocean to the Gulf of Mexico (Kauffman, 1977). This epicontinental sea was separated from the Pacific Ocean by Cordilleran highlands, which also served as the main provenance of sediment shed eastward into the basin. In the Rocky Mountains, a regional unconformity of uncertain duration usually separates middle Cretaceous rocks, including widespread conglomerates (Heller and Paola, 1989), from the Upper Jurassic fluvial deposits of the Morrison Formation. This hiatus is synchronous with the Early Cretaceous magmatic lull that is well documented throughout the western North American Cordillera (Armstrong and Ward, 1993). By contrast, synchronous with the culmination of seaway advancement was widespread mid-Cretaceous magmatism (Armstrong and Ward, 1993) as well as the complex shortening history of the foreland fold-and-thrust belt. Thicknesses of late Lower to Upper Cretaceous strata increase dramatically across Wyoming, from about 6,000 to 7,000 feet (1.8 to 2.1 km) in northeastern Wyoming to more than 15,000 feet (4.6 km) in the southwest (Peterson and Smith, 1986) (**Figure 6**). Evolution of the Western Interior Cretaceous basin is chronologically linked with orogenesis along its western margin (Jordan, 1981; Steidtmann, this volume). Coincident with tectonic loading of the foreland fold-and-thrust belt during the mid-Cretaceous was a worldwide rise of sea level (Vail and others, 1977; Hallam, 1984), which amplified the development of this broad seaway.

Rocks of the Cretaceous Western Interior basin have been major sources of oil, gas, and coal in the Rocky Mountain region. These economic aspects, coupled with excellent exposures along the margins of many Laramide basins, have encouraged detailed analysis of these rocks. Correlation between isolated exposures is made possible by the presence of widespread and distinctive fossil assemblages (especially ammonites) and abundant subsurface data. These Cretaceous rocks are chiefly shale, siltstone, and sandstone. Conglomerate is also important along western margins of the basin, and limestone is generally restricted to the east (see McGookey and others, 1972, for various detailed stratigraphic sections). An important component of the fine-grained sedimentary rocks of the Western Interior Cretaceous basin is volcanic ash (now mostly bentonite). The abundance of bentonitic beds in these deposits is a byproduct of extensive, coeval arc magmatism along the western margin of North America throughout the middle to Late Cretaceous (Kauffman, 1977; Hamilton, 1988a).

Complex facies relationships exist between these various Cretaceous rocks, including intertonguing of nonmarine and marine deposits as the shoreline transgressed and regressed (Steidtmann, this volume). The geological significance of the migration of the shoreline is controversial. Some authors interpret these variations as chiefly related to global sea-level changes (Hancock and Kauffman, 1979), whereas others argue that local or subregional tectonic events were the principal causes (Lillegraven and Ostresh, 1990). Recognizing and dating intrabasinal unconformities are aspects in evaluating the relative importance of global sea-level changes versus localized tectonics in the evolution of depositional systems of the Western Interior basin. At least nine regional unconformities have been identified. These unconformities are completely

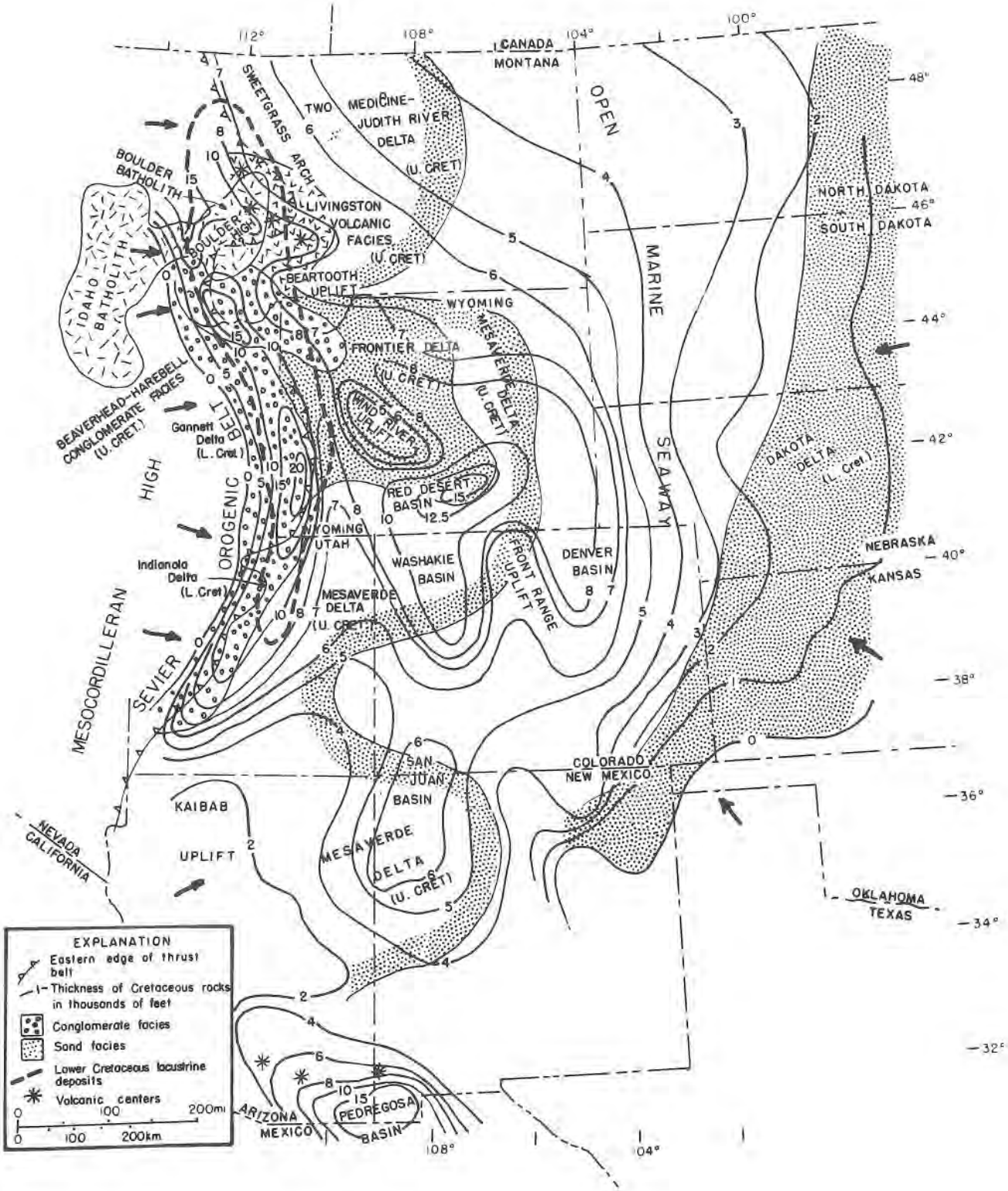

Figure 6. Cretaceous System, showing approximate thickness, general sedimentary facies, and main paleotectonic elements. Arrows indicate probable transport direction of terrigenous clastic sediments (from Peterson and Smith, 1986, figure 12; reprinted by permission).

within nonmarine strata, involve both marine and nonmarine rocks, or are totally within marine strata (Weimer, 1984). At least three of these unconformities (at 97, 90, and 80 Ma) appear to be primarily related to drops in sea level; however, either sea-level changes or tectonics could have been reponsible for the other unconformities (Weimer, 1984). Many minor, short-term variations in strandline position, especially along the western margin of the basin, undoubtedly were influenced by local tectonic events.

Fold-and-thrust belt of the Sevier orogeny

Paleogeographic setting

Late Cretaceous paleogeography of western North America was dominated by three sinuous mountain belts that extended virtually the length of the Cordillera: (1) a thin-skinned fold-and-thrust belt on the east; (2) a central hinterland; and (3) an Andean-type, volcanic-plutonic magmatic arc on the west (see Miller and others, 1992, for a regional summary). The fold-and-thrust belt on the east was localized at the miogeocline-to-craton hinge line. Initial eastward thrusting of thicker miogeoclinal strata over thinner cratonic strata was followed by progressively more eastward-propagating thrusts (Armstrong and Oriel, 1965; Royse and others, 1975). The roots of this thrust belt pass westward into the hinterland, where extensive tracts of metamorphic rocks and even Precambrian basement rocks are involved in the Mesozoic deformation (Lush and others, 1988). The hinterland is a zone of Mesozoic crustal thickening, manifested by its Jurassic and Cretaceous metamorphic, magmatic, and deformational features (Coney and Harms, 1984; Snoke and Miller, 1988). Some geologists have suggested that the Late Cretaceous hinterland was analogous to the Cenozoic Andean Altiplano (e.g., Allmendinger, 1986), which is a high arid plateau situated between the magmatic arc of the western Cordillera and the fold-and-thrust belt of the eastern Cordillera. The Mesozoic magmatic arc is characterized by an extensive batholithic belt extending from Baja California to the Coast Plutonic complex of western British Columbia and southeastern Alaska. Magmatism in this batholithic belt spanned the interval from about 225 Ma to 55 Ma, but reached a culmination during the mid-Cretaceous (125-85 Ma, Armstrong and Ward, in press).

Timing and structural style

The imbricate thrust belt exposed in western Wyoming, southeastern Idaho, and northern Utah is a major salient in the Cordilleran fold-and-thrust belt (**Figure 1**). This salient of the fold-and-thrust belt has been the site of classic geologic studies (e.g., Veatch, 1907; Schultz, 1914; Rubey and Hubbert, 1959; Armstrong and Oriel, 1965; Royse and others, 1975) and extensive hydrocarbon exploration. The thrust belt is generally not deeply eroded and thus provides excellent exposures of contractile structures at a shallow level in the crust. This segment of the Cordilleran fold-and-thrust belt is one of the best understood thin-skinned, foreland fold-and-thrust belts in the world (see Royse, this volume).

The Wyoming-Idaho-Utah fold-and-thrust belt, part of the Sevier orogenic belt (Armstrong, 1968), is a classic example of an intraplate, retro-arc fold-thrust belt. Contractile deformation manifested in this belt apparently began during the Early Cretaceous (Heller and others, 1986), although earlier studies (e.g., Armstrong and Oriel, 1965; Wiltschko and Dorr, 1983) suggested a possible Late Jurassic initiation. The Wyoming-Idaho-Utah fold-thrust belt also includes an exceptional record of synorogenic sedimentary rocks that date progressive thrust fault development and displacement during sedimentation (e.g., Armstrong and Oriel, 1965; Royse and others, 1975; Wiltschko and Dorr, 1983; Steidtmann and Schmitt, 1988). Progressive incorporation of early synorogenic sedimentary strata into the advancing thrust wedge, coupled with the overlap of fault traces by younger sedimentary deposits, bracket the timing of motion on many individual thrust sheets (e.g., Armstrong and Oriel, 1965).

The geometry and style of major structures in the Wyoming-Utah-Idaho fold-and-thrust belt are well documented (Royse and others, 1975; Lamerson, 1982; Royse, this volume). Structures characteristic of the Wyoming portion of the fold-and-thrust belt are basically analogous to the "Foothills family" of structures, as recognized by Dahlstrom (1970) for the Canadian Rocky Mountains. The thrusts are thin-

skinned, affecting only sedimentary rocks and merging into a décollement near the top of crystalline basement. They dip to the west, are listric in shape, and cut up-section in the direction of transport in a stair-step trajectory. Glide planes are long and flat and localized within weak layers such as Cambrian shale, Jurassic salt, and Cretaceous shale. Ramps are short and cut across more competent rocks such as Mississippian carbonate or Jurassic sandstone (Platt and Royse, 1989). Folds are generated chiefly by bending above ramps and commonly are kink-like in style (Boyer, 1986). Mylonitic rocks generally are absent along the thrust surfaces. Bedding-parallel shortening features (e.g., solution cleavage) are characteristic of parts of the thicker western thrust sheets (Mitra and others, 1988).

Models for the Sevier orogeny

Tectonic models for the Sevier orogeny (the retro-arc or foreland fold-and-thrust belt) are numerous and controversial. Early models for parts of the Cordilleran fold-and-thrust belt that involve gravitational gliding (e.g., Crosby, 1968; Mudge, 1970; Scholten, 1973) have been demonstrated to be untenable. Principal problems involve the requirement for significant slope; the downward rooting of the thrust faults, as indicated by detailed, regional cross sections; and the absence of a synchronously denuded area that could have compensated for imbrication in the thrust wedge (Price, 1971). Lateral gravitational spreading related to buoyant upwelling of metamorphic infrastructure, as envisioned by Price and Mountjoy (1970), has been abandoned by many workers because of problems related to detailed timing of metamorphism in the infrastructure and shortening in the foreland.

Hamilton (1978) and Smith (1981) argued for a close connection between arc magmatism and thrusting. They envisioned that thickening and uplift of the crust during arc magmatism developed a topographic high, which served to drive foreland thrusting. This model fails to explain development of the easternmost thrusts in the U.S. Cordillera, which are significantly younger than the youngest plutons in the batholithic belt at similar latitudes. Finally, intracontinental subduction (so-called Ampferer or A-type subduction, Bally, 1975; see also Scholten, 1982; **Figure 7**) involves westward subduction or shortening of cratonic crust with concomitant imbrication of the sedimentary cover along a décollement system that deepens westward. Various forms of this model have been proposed (e.g., Misch, 1960; Sales, 1968; Burchfiel and Davis, 1968, 1975; Campbell, 1973). Documentation and timing of significant Mesozoic shortening in the hinterland, however, have persistently been obstacles to correlation of tectonic histories between the hinterland internal zone and the shortening manifested in the flanking foreland fold-and-thrust belt.

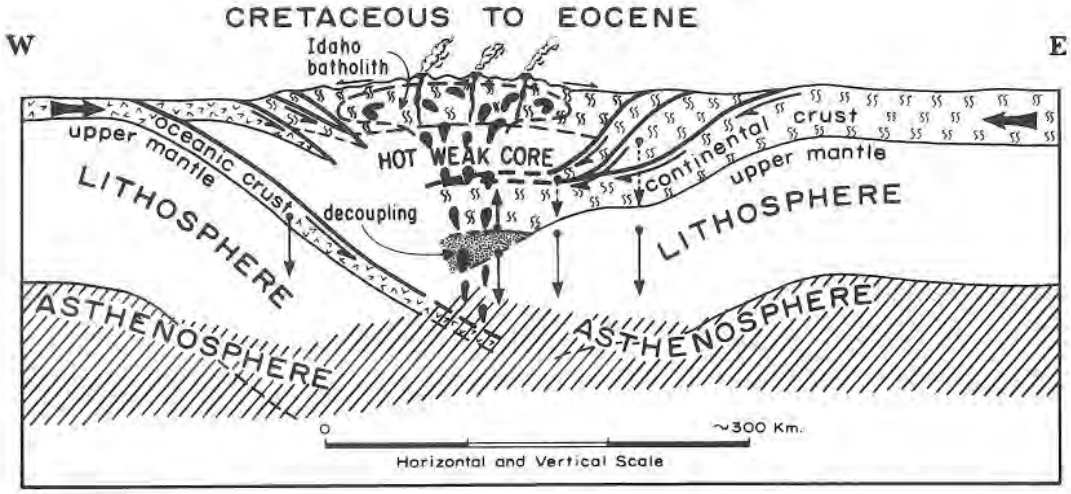

Figure 7. Diagrammatic model of intracontinental subduction from Cretaceous to Eocene in the western U.S. Cordillera (from Scholten, 1982, figure 8; reprinted by permission).

Detailed geochronometric and geothermobarometric studies, coupled with structural analysis in the hinterland, finally are beginning to reconcile the controversy. A complex, polyphase magmatic-metamorphic-deformational history is manifested in the hinterland, and part of that history was synchronous with foreland thrusting (Miller and Gans, 1989). Other parts of that history predated the shortening structures of the foreland (Snoke and Miller, 1988), and may be unrelated to the evolution of the Sevier orogenic belt. One outgrowth of the intracontinental subduction model is the concept of the "orogenic float," which assumes a fundamental decoupling between the complex structures of the crust and simpler lithospheric roots (Oldow and others, 1989a, 1990). This hypothesis argues for complete allochthoneity of crust across the whole of the Cordillera orogen.

Laramide orogeny

During the Late Cretaceous and early Tertiary, the Rocky Mountain foreland was fractured by deep-rooted, reverse and thrust faults that uplifted broad blocks of Precambrian basement rocks, separated by deep basins (**Figure 8**). This thick-skinned style of deformation is characteristic of the classic "Laramide orogeny" of specific tracts within the Rocky Mountain region. Considerable debate continues on precise timing of this fracturing and crustal shortening of the foreland , but recent studies suggest the interval 75 to 45 Ma (Cross, 1986; Dickinson and others, 1988). In Wyoming, however, stratigraphic and structural data indicate that the Laramide orogeny ended by 51 Ma (see Lillegraven, this volume). Some authors argue that Laramide-related orogenic events in Wyoming began earlier (e.g., Steidtmann and Middleton, 1991) and continued later (e.g., Steidtmann and others, 1989) than this time span.

The term "Laramide" apparently was first used by J.D. Dana (1895, p. 359) to refer to the Rocky Mountain system, which forms an eastern cordillera in western North America from Canada to Mexico (Tweto, 1975). The name was derived from the poorly defined "Laramie series," a lithostratigraphic term used in Dana's time in reference to coal-bearing, nonmarine strata (Hayden's "Lignitic series") that lie above fossiliferous marine Cretaceous rocks in the Rocky Mountain region (so-called "Montana group"). The series, in turn, is unconformably overlain by Eocene Wasatch Formation or equivalents. Subsequently, the U.S. Geological Survey restricted use of the term "Laramie Formation" to the Denver basin and designated this formation as entirely Cretaceous in age (Tweto, 1975). Perhaps in part because of its ambiguous initial definition, the term "Laramide" has been used to refer to various orogenic events that occurred during the late Mesozoic and early Tertiary. In fact, some authors have exported the term "Laramide" to beyond the confines of the North American Cordillera and have used it to refer to any orogenic event near the Mesozoic-Cenozoic boundary. In contrast, the recent tendency is to use "Laramide" in a geographically much more restricted and defined sense, limiting it to refer to orogenic events in the eastern Rocky Mountains that occurred during the Late Cretaceous through mid-Eocene (Cross, 1986; Dickinson and others, 1988). Debate continues, however, on specific chronologic boundaries.

Yet another use of "Laramide" is to employ the term to describe the distinctive basement-cored uplifts in the U.S. eastern Rocky Mountains. In this usage, "Laramide-style" deformation denotes thick-skinned, thrust and reverse faulting that has involved Precambrian basement rocks of the Rocky Mountain foreland. As documented by Brown (this volume), dips and orientations of these faults are variable; and in many cases, Laramide uplifts are bounded by conjugate, bivergent fault systems that form wedge-like, blocks of crystalline rock mantled by a thin cover of sedimentary rocks. True-scale representations of this distinctive style, in contrast to the thin-skinned deformation of the fold-and-thrust belt, are clearly depicted in Transect C-1 (Blake and others, 1989) or in cross section G (Oldow and others, 1989b, plate 7).

Basement-cored uplifts of the Rocky Mountain region are truly anomalous in comparison with typical foreland deformation along the Cordilleran structural front. For example, in Canada, the Precambrian basement slopes gently westward and forms an unfaulted, west-dipping 2 to 3° ramp beneath various faulted and folded supracrustal rocks (Bally and others, 1966; Price and Mountjoy, 1970). At the begin-

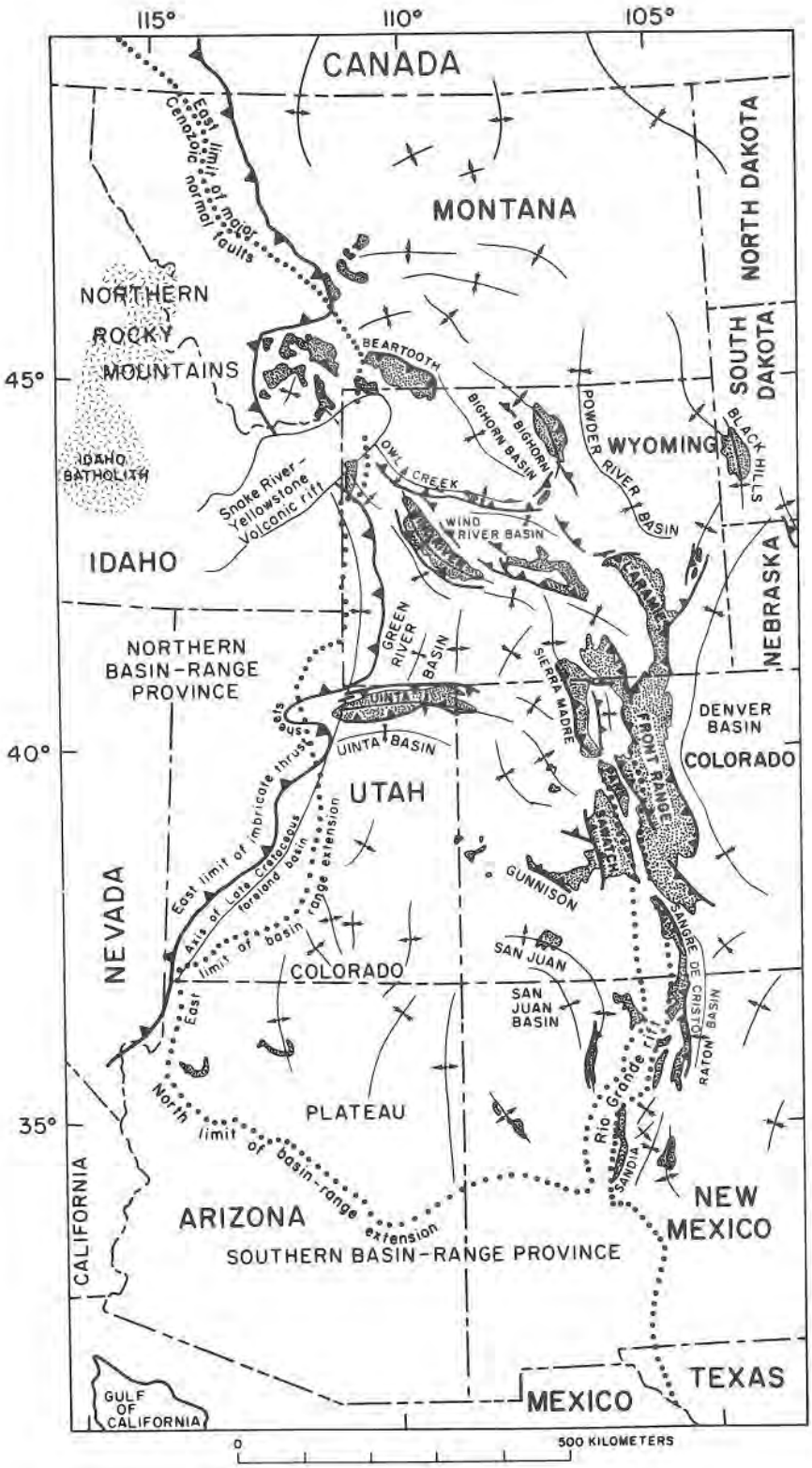

Figure 8. Basement-cored uplifts and basins of Laramide age in the U.S. Rocky Mountains. Precambrian basement rocks east of the foreland fold-and-thrust belt and north of the southern Basin and Range province are stippled (from Hamilton, 1988b, figure 1; used with permission).

ning of the Laramide orogeny (Late Cretaceous) in Wyoming, the Precambrian-Paleozoic unconformity, east of the zero isopach of Late Precambrian sedimentary rocks, lay at -8,000 to -10,000 feet (-2.4 to -3.0 km) (sea level) below a Paleozoic and Mesozoic sedimentary sequence (Stearns, 1971). A structure contour map of the present top of Precambrian basement indicates variations ranging from a restored, pre-erosion level of over 15,000 feet (4.6 km) above sea level in the Wind River Range to a level more than 30,000 feet (9.2 km) below sea level in the immediately adjacent northern Green River Basin (Blackstone, this volume, **map pocket**). This staggering structural relief was achieved chiefly by displacement along the Laramide, basement-rooted Wind River thrust in the early Tertiary (see Steidtmann and Middleton, 1991, for a detailed chronology of this faulting).

Structural style

The eastern Rocky Mountains, including the Wyoming foreland, is the "type" example of the uplift of basement rocks within a craton marginal to a thin-skinned, external zone of an orogen (see Rodgers, 1987, for a worldwide summary). Furthermore, fault zones associated with these basement-involved uplifts provide unparalleled opportunities to study the behavior of basement rocks during upper crustal deformation.

Controversy and debate has surrounded structural interpretation of the Rocky Mountain basement-involved

foreland uplifts, particularly as applied to subsurface geometries of the faults and deformational styles of basement rocks associated with the uplifts. Brown (1988, this volume) traces the history of thought and controversy concerning these structures, so my comments will be brief and can focus on the most recent debate concerning vertical uplift models vs. horizontal contractile models. The concept that Rocky Mountain basement-involved uplifts were principally vertical uplifts that occurred along steeply dipping faults evolved gradually, but probably is best summarized in a series of papers by David W. Stearns and coworkers (Stearns, 1971, 1978; Stearns and Weinberg, 1975; Stearns and Stearns, 1978). Their conceptual bases involve the following:

1. Basement-rooted fault zones are steep to subvertical;
2. Basement rocks, considered relatively homogeneous mechanically as contrasted to the overlying sedimentary cover, deformed by brittle fracture and did not fold; and
3. Uplift in the basement was partially compensated in the sedimentary cover as "forced folds," the so-called "drape folds" of Thom (1947).

During the 1970s, this school of thought dominated structural interpretations of basement-involved structures in the Rocky Mountain foreland. However, near the end of the 1970s, high-quality seismic reflection studies (e.g., Smithson and others, 1978, 1979) clearly demonstrated the actual thrust-fault geometry which, for example, involves substantial overhang of the Wind River thrust. This dramatic discovery underscored the importance of horizontal crustal shortening in the structural evolution of the Wyoming foreland (Kanter and others, 1981). Such shortening had been implied previously in the fold-thrust model of Berg (1962) as well as in some earlier cross sections (e.g., Anonymous, 1951). Subsequent systematic structural analysis of many of the Wyoming basement-involved uplifts by D.L. Blackstone, Jr., employing extensive use of well data, has clarified the importance of horizontal crustal shortening during the structural evolution of the Wyoming foreland (e.g., Blackstone, 1980, 1983, 1986, 1990, 1991).

Even though crustal shortening now has been demonstrated as a fundamental feature of the basement-involved structures in the Wyoming foreland, the role of basement deformation is still highly controversial and represents the focus of much recent research (e.g., a symposium at the 1990 Geological Society of America Rocky Mountain sectional meeting, Jackson, Wyoming). A fundamental problem in this regard involves the following question: Does the basement actually fold during foreland shortening? This is not a new problem and has been discussed in respect to foreland tectonics for many years (e.g., Lees, 1952; Hudson, 1955). In a short essay on this subject, Matthews (1986, p. 5) concluded *...that structural basement did not fold during the Laramide.* He contended that a planar unfolded contact typically exists between basement and the overlying sedimentary rocks, wherever such a contact is well exposed. Furthermore, he argued that the basement experienced rigid-body rotation during uplift (rather than folding), an interpretation that Erslev (1986) favored in order to balance the basement in cross sections of foreland uplifts.

Recently, the focus of this debate has changed. The question is not if the basement rocks actually fold, but rather what is the magnitude of folding (E.A. Erslev, personal communication, 1991). In his trishear model, Erslev (1991) argued that the style of folding in the sedimentary cover rocks would not have to be mimicked by underlying basement rocks if this folding had been focussed downward into a basement-rooted, brittle shear zone. Folding in the sedimentary cover therefore converges downward into a strain-compatible, propagating fault, and the entire system is modeled as a triangular shear zone in profile (i.e., Erslev's, 1991, "trishear" model for fault-propagation folding). Such fault-propagation fold models for Laramide basement-cored uplifts provide new approaches, which allow construction of balanced cross sections that account for both the uplift of the Precambrian crystalline basement and the deformation of sedimentary cover rocks. It is interesting to note that Blackstone's (1940) interpretative cross sections of the Pryor Mountains, Montana, are startlingly similar. His sections represent early examples of modern thinking regarding evolution of Laramide basement-involved uplifts.

Synorogenic sedimentary rocks

A broad foreland basin east of an active fold-and-thrust belt occupied much of the Central Rocky Mountain region prior to initiation of the Laramide orogeny in the Late Cretaceous (Jordan, 1981). Al-

though isopach studies across this basin indicate differential rates of subsidence, marine strata are laterally continuous for long distances. This depositional pattern was terminated with the onset of the Laramide orogeny (Love and others, 1963). As individual basement-cored mountain blocks evolved in response to Laramide crustal shortening, the Rocky Mountain foreland was transformed into a complex system of structurally separated nonmarine basins (e.g., see Dickinson and others, 1988; Lillegraven and Ostresh, 1988; and the numerous earlier papers cited in these review articles). Consequently, throughout the eastern Rockies, marine rocks of the Late Cretaceous (e.g., Lewis Shale in Wyoming) are succeeded by continental deposits of latest Cretaceous age (e.g., Lance Formation). These nonmarine rocks, in turn, are overlain by similar, commonly coal-bearing deposits of Paleocene age (e.g., Fort Union Formation).

Correlation of these nonmarine units throughout the Great Plains and Rocky Mountain region has been controversial. A complex lithostratigraphic terminology has been developed to replace the simple broad subdivisions first recognized by the early geologic explorers of the region. This terminology, in part, reflects the variety of depositional environments established in the evolving Laramide basins during the latest Cretaceous and Paleocene.

The early Laramide synorogenic sedimentary rocks are commonly overlain by nonvolcanogenic, arkosic, Lower Eocene continental rocks (e.g., the Wind River Formation of Wasatchian age) that reflect the continual erosion of mountain ranges formed during the Laramide orogeny. These Laramide deposits may be coarse bouldery facies deposited near rapidly eroding Laramide mountain fronts or fine-grained varicolored facies, commonly red-banded (Van Houten, 1948), interpreted as deposits of warm, humid lowlands that existed farther out into the Laramide basins. The Wind River Formation and equivalents were locally deformed during late-stage displacement along Laramide contractile faults. This sedimentary succession can also be unconformably overlain by still later Laramide or post-Laramide deposits (e.g., Steidtmann and Middleton, 1991), indicating continued erosion of Laramide highlands and commonly the input of detritus from new source areas (e.g., Absaroka volcanic field). The structural and stratigraphic relationships of Lower Eocene rocks with regard to younger contractile features and superjacent strata therefore can provide important constraints on establishing the end of the Laramide orogeny.

Orogenic timing in the eastern Rocky Mountains

During the development of Cordilleran plate-tectonic models in the late 1970s and early 1980s, the bracket 80 to 40 Ma was applied commonly to the Laramide orogeny (e.g., Coney, 1978; Dickinson and Snyder, 1978; Cross and Pilger, 1978b; Hamilton, 1981). Recent structural (Cross, 1986) and stratigraphic (Dickinson and others, 1988) syntheses have refined the timing, as well as investigated interregional variations. An important conclusion that comes from these studies, especially from Dickinson and others (1988), is that the Laramide orogeny was diachronous in the eastern Rocky Mountains. Using a variety of criteria, Dickinson and others (1988) argued that the orogeny ended near the close of the Wasatchian (about 51 Ma) in Wyoming. In contrast, the end of the Laramide orogeny in the southern Rocky Mountains (Colorado and New Mexico) was distinctly younger, perhaps between 35 and 40 Ma.

The time of initiation of the Laramide orogeny has always been more controversial. Plate-tectonic models favor initiation at about 80 to 75 Ma based on patterns of igneous activity and variations in convergence rates between the North American and eastern Pacific plates (e.g., Coney, 1978). According to Dickinson and others (1988), the sedimentary record indicates that Laramide deformation began in the Maastrichtian (75-66 Ma) and suggests no systematic areal diachroneity. In contrast, recent studies by Perry and others (1991) suggest a southeastward migration of Rocky Mountain foreland deformation beginning in southwestern Montana earlier than 80 Ma and reaching the Colorado Front Range in the late Maastrichtian. Furthermore, these authors argue for a younger, northeastward-advancing deformational front across Wyoming. The migration of these deformational fronts is inferred to be related to an advancing and laterally spreading deep crustal detachment (Perry and others, 1991).

A mid-Cretaceous or older initiation of the Laramide orogeny has been suggested by some authors (e.g., Steidtmann and Middleton, 1991) to explain various sedimentological patterns in rock units of the Western Interior basin (e.g., sandstone chan-

nels in the Muddy Sandstone). However, these subtle variations in sedimentation do not necessarily require significant tectonic uplift. Dickinson and others (1988) outlined a series of criteria useful in recognizing the initiation of the Laramide orogeny. Of the dozen specific points enumerated by Dickinson and others (1988), initial development of local depocenters defined by isopachs and recognition of locally derived clasts within the basin fill are especially valuable constraining clues. Consequently, the conclusion by Love and others (1963) that the Laramide orogeny must postdate the last major marine Cretaceous transgression (i.e., Upper Campanian - Lower Maastrichtian Lewis Shale) is still the most logical upper limit of the initiation of regional deformation.

Plate-tectonic setting

During the late Cretaceous through early Tertiary, virtually the entire western North American Cordillera was involved in a complex orogeny that included variable structural styles (**Figure 9**). In Alaska and northern Canada, the orogeny was manifested by large-scale strike-slip faults, which record hundreds of kilometers of dextral translation and associated transpressional deformation (Eisbacher, 1985). Farther south, in Canada and the U.S. Northern Rocky Mountains, thin-skinned thrusting formed an impressive fold-and-thrust belt east of the Rocky Mountain trench (Price and Mountjoy, 1970; Price, 1981). In the Central and Southern Rockies, the cratonic crust of the foreland was tectonically shortened by deep-rooted, thick-skinned thrust and reverse faults that uplifted the basement rocks as adjacent intermontane basins developed. In the Colorado Plateau, enormous monoclines developed along reactivated basement faults (Huntoon, 1990). In southern California, the base of the continental crust was truncated as quartzo-feldspathic metasedimentary rocks and associated oceanic rocks (Pelona-Orocopia-Rand schists) were thrust beneath crystalline basement rocks (Jacobson, 1983; Hamilton, 1989). In Mexico, a late Mesozoic to early Eocene fold-and-thrust belt, developed chiefly in late Mesozoic carbonate and clastic rocks, forms the Sierra Madre Oriental (Suter, 1987; de Cserna, 1989).

In an interpretation based principally on regional geologic arguments, Lowell (1974) and Dickinson and Snyder (1978) favored shallow-dipping subduction to explain the classic Laramide orogeny of the Rocky Mountain region in the western U.S. This "unfamiliar mode" of subduction, as characterized by Dickinson and Snyder (1978), was compared to segments of the modern Andean orogen. There, the subduction mode is amagmatic, with a diffuse, subhorizontal seismic zone. This analogue was further developed by Jordan and Allmendinger (1986), who demonstrated that the Laramide-style, basement uplifts of the Sierras Pampeanas of Argentina are coincident with a segment of subhorizontal subduction of the Nazca plate.

During latest Cretaceous and early Paleogene time, the rate of plate convergence between the North American and eastern Pacific plates increased markedly (Coney, 1972, 1978; Jurdy, 1984; Engebretson and others, 1984) (**Figure 10**). This change in relative plate motions led some tectonicists to postulate that the rapid overriding of subducting Pacific lithosphere by the North American plate was the fundamental cause of the shallow-dipping subduction mode (e.g., Coney and Reynolds, 1977; Cross and Pilger, 1978b). However, the increased convergence rate between the North American and eastern Pacific plates was not regionally restricted. Rather, it probably characterized the entire western North American continental margin (Henderson and others, 1984). Therefore, the cause of the shallow-dipping subduction mode must be more complex. If the subducting oceanic lithosphere was young and hot (Engebretson and others, 1984) (**Figure 10**), a shallow-dipping or flat-slab subduction geometry could have resulted. The age of the Farallon plate's eastern edge became progressively younger throughout the Laramide orogenic interval (**Figure 10**). Furthermore, Engebretson and others (1984) suggested that the gradual slowing of Farallon-North American convergence during the mid-Tertiary was also related to increased buoyancy of the subducting oceanic crust.

Livaccari and others (1981) and Henderson and others (1984) also used arguments involving buoyancy to account for the flat-slab subduction mode, as well as for the restricted basement-involved crustal shortening of the Rocky Mountain region. These authors suggested the subduction of unusually thick oceanic crust within the Farallon plate. Such anomalous crust could have been an aseismic ridge or oceanic plateau on the Farallon plate. If the feature was elongated, such as an aseismic ridge, its subduction, and consequently the locus of shallow subduction,

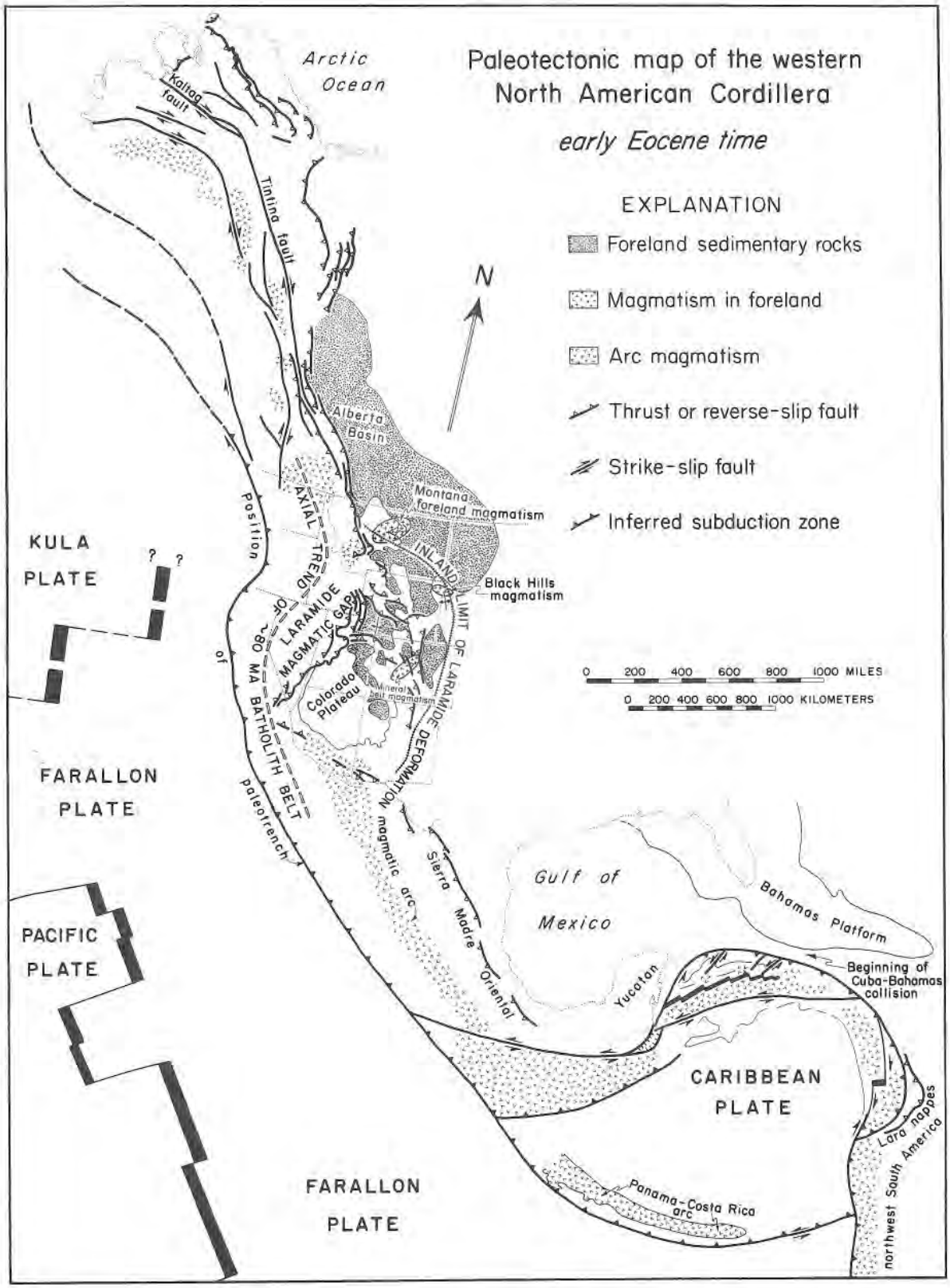

Figure 9. Generalized paleotectonic map of the western North American Cordillera at early Eocene time showing representative features that developed from Late Cretaceous through early Tertiary. Note that the shapes of some states have been modified (after Dickinson, 1991, figures 10A, B) to account for Tertiary extension that occurred after the early Eocene. This map is a compilation of features derived from King and Edmonston (1972), Pindell and Barrett (1990, plate 12 of volume H), Dickinson (1991, figures 10A, B), Coney (1987, figure 3), and Engebretson and others (1985, figure 3d).

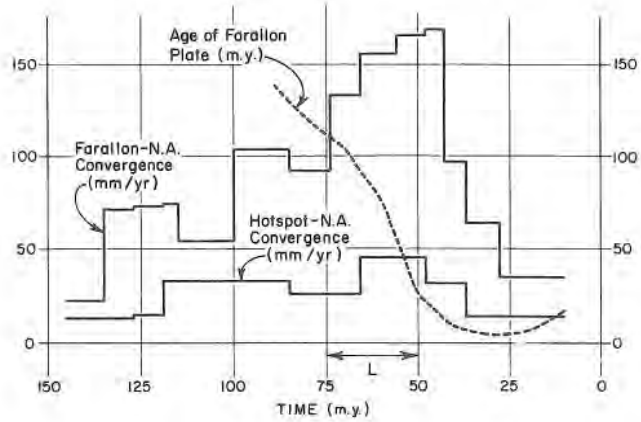

Figure 10. Components of motion of Farallon plate relative to North America and of North America over hotspots, perpendicular to an assumed coastline trend of N40°W near present San Francisco. Dashed curve is approximate age of Farallon plate that was subducted near the latitude of San Francisco (adapted from Engebretson and others, 1982). L denotes the Laramide orogeny, double-barbed arrow is the inferred length of orogenic activity in Wyoming (after Dickinson and others, 1988).

would have migrated with time. Henderson and others (1984) suggested that an aseismic ridge, oriented north-northeast, was subducted during the Laramide orogeny, thereby causing the well-documented, southward migration of the Laramide magmatic null or gap. Their model also predicts a southward migration of inland deformation as recently suggested by Perry and others (1991) but, as yet, not demonstrated in detail.

A different, but fundamentally related, argument concerns the role of crustal thickening in the Rocky Mountains. Bird (1984, 1988) noted that estimates of upper crustal shortening across the Rocky Mountain foreland, typically about 5 to 15 % (e.g., Kanter and others, 1981; Brown, 1988), are not sufficient to explain the magnitude of inferred crustal thickening that occurred during the Laramide orogeny. Bird (1984, 1988) postulated that this crustal thickening occurred by massive transport of deep crust and mantle lithosphere from southwest to northeast into the Rocky Mountain foreland, thereby substantially thickening the crust over a large region. This model requires a deep-crustal, high-strain zone (i.e., a zone of large-magnitude simple shear) that accommodated the massive transfer of lower crustal rocks beneath a huge area. Bird (1988) estimated that such a shear zone was 2 to 3 km thick, and recorded shear strains on the order of 1000. The shear tractions developed along this deep-crustal shear zone were transferred to the upper crust by basement-rooted faults that characterize the Rocky Mountain foreland structural style.

A fundamental problem with Bird's model (1984, 1988) is that geophysical studies in southeastern Wyoming (e.g., Johnson and others, 1984) indicate that variation in crustal thickness is directly related to the boundary between Precambrian provinces (i.e., the Cheyenne belt). Seismic refraction studies by the U.S. Geological Survey, show that crust beneath the Wyoming province is substantially thinner (37-41 km) than crust beneath the Colorado province (48-54 km). In a review of crustal structure of the Rocky Mountains, Prodehl and Lipman (1989) generalized variations in crustal thickness to conclude that it is thickest in southern Montana and Colorado and is 10 to 15 km thinner in the Central Rocky Mountains (i.e., chiefly Wyoming). These observations are difficult to reconcile with massive transport of lower crustal rocks from southwest to northeast during the Laramide orogeny, as postulated by Bird (1984, 1988).

The role of the Colorado Plateau in the Laramide orogeny has been a subject of much speculation. On virtually any small-scale geologic map of the Rocky Mountain region (e.g., **Figure 8**), the Laramide basement-cored uplifts appear to wrap partially around the Colorado Plateau along its eastern and northern margins (Hamilton, 1981, 1988b). This geographic and geometric relationship led Hamilton (1981, 1988b) to suggest that rotation of the Colorado Plateau was a key to basement-involved shortening of the Rocky Mountain foreland. His model involves the clockwise rotation of the plateau simultaneous with flat-slab subduction. He speculated that the Euler pole of rotation was near central New Mexico, and the rotation was about 4° clockwise (Hamilton, 1988b). Detailed comparative paleomagnetic data from correlative upper Paleozoic and Triassic strata from the Colorado Plateau and craton support a clockwise rotation of 11° +/-4° for the plateau relative to the craton (Steiner, 1986). Other investigators (Bryan and Gordon, 1990), using a larger but perhaps less reliable data set, have also found evidence of systematic differences between plateau poles and stable North America, but favored a more modest clockwise rotation of 5° +2.4°/-2.3°. In either case, paleomagnetic data support a clockwise rotation of the Colorado Plateau, as originally hypothesized by Hamilton (1981).

Another aspect of the Laramide orogeny in regard to plate-tectonic models is the orientation and possible variation of the maximum shortening direction during the Late Cretaceous to early Tertiary structural evolution of the Rocky Mountain foreland. Based on Coney's (1978) vector summations of relative motion of the North American and Farallon plates, Brown (1988) assumed a consistent convergence vector between the plates as oriented N 40° E for the Laramide orogeny. However, a previous analysis of structural development and timing by Gries (1983) had argued for a systematic counterclockwise rotation of the direction of maximum shortening during the Laramide orogeny, as manifested generally in the Rocky Mountain foreland. In contrast, the study of the evolution of Laramide basins by Dickinson and others (1988) suggested the broadly synchronous initiation of the complex pattern of Laramide uplifts and basins. Likewise, Cross' (1986) general inventory of dated structures in the Rocky Mountain foreland also did not support the chronology of structural development proposed by Gries (1983). Nonetheless, systematic overprinting relationships that developed during the Laramide structural evolution are well documented in the Wyoming foreland (e.g., Wise, 1983; Wise and Obi, 1992; Bergh and Snoke, 1992), suggesting that a complex, perhaps heterogeneous, strain field may be an important aspect of this history.

In summary, numerous plate-tectonic models and variants of these models have been proposed to explain the anomalous intraplate deformation of the Rocky Mountain foreland during the Laramide orogeny. The concept of shallow-dipping subduction has been the centerpiece for virtually all plate-tectonic models. Nevertheless, many important problems remain unresolved concerning the timing and nature of progessive deformation, variation in maximum shortening direction, importance of regional deep-crustal detachment, and role of the Colorado Plateau in foreland shortening.

Paleogene magmatism

Regional overview

About 80 million years ago, significant changes in the pattern of arc magmatism developed in the U.S. Cordillera (Armstrong, 1974; Snyder and others, 1976). During this episode of "Laramide" magmatism (about 80 to 55 Ma), an eastward sweep of magmatic activity is well documented from California across southern Arizona to New Mexico (Coney and Reynolds, 1977). In the northern Rockies, arc magmatism advanced from the Idaho batholith into southwestern Montana (e.g., Boulder batholith and associated volcanic rocks). A zone of northeastward-advancing magmatic activity along the Colorado mineral belt dates between 72 and 60 Ma (Mutscher and others, 1987). Isolated magmatism occurred in the Black Hills between 62 and 50 Ma (DeWitt and others, 1986; Lisenbee and DeWitt, this volume) and at various localities in central Montana during approximately the same time interval (Hearn, 1989). A distinct magmatic gap developed over a large region including parts of California, Nevada, and Utah (Armstrong, 1974).

The 225 to 80 Ma phase of Cordilleran magmatic activity is commonly attributed to effects of steep-dipping subduction, the "familiar mode" of Dickinson and Snyder (1978). In contrast, the overall sweep inboard of magmatic activity during the Late Cretaceous to early Tertiary (80-55 Ma) and development of a magmatic lull has been explained as caused by flat-slab subduction beneath a broad area of the U.S. Cordillera (Dickinson and Snyder, 1978). Evolution of the thin-skinned Sevier fold-and-thrust belt overlapped both this magmatic transition and the crustal shortening associated with the development of Laramide basement-cored uplifts.

At approximately 55 Ma (near the beginning of the Eocene), this complex Mesozoic - early Cenozoic magmatic activity terminated, as did the shortening associated with A-type subduction, in both the Northern and Central Rocky Mountains. However, a major new magmatic and tectonic episode was initiated over a broad region of the Rocky Mountains north of present latitude 42° N during the mid-Eocene (Armstrong, 1978). The igneous rocks of this magmatic episode are particularly well developed in the Absaroka-Gallatin (Wyoming-Montana), Challis (Idaho), and Kamloops (British Columbia) volcanic regions. Furthermore, broad-scale crustal extension developed in many regions, apparently genetically

associated with this renewed magmatism. Evolution of metamorphic core complexes in southern British Columbia, northeastern Washington, and central Idaho was closely associated with this Eocene magmatism (e.g., Wernicke and others, 1987; Armstrong and Ward, 1991).

Paleogene magmatic suites

In Wyoming, the igneous rocks of the Black Hills, Rattlesnake Hills, and Absaroka volcanic province are isolated remnants of Paleogene magmatism (**Figure 11**). As a group, these magmatic centers include a great diversity of igneous rock types, ranging in composition from calc-alkalic to alkali-calcic to alkalic. How these various igneous rocks are related, if at all, is uncertain. Petrographic and some geochemical data are included in several papers in this volume (see Lisenbee and DeWitt for the Black Hills, Hoch and Frost for the Rattlesnake Hills, and Sundell for the Absaroka volcanic province). Furthermore, geochronometric data from these various magmatic suites indicate a considerable age span, extending from ca. 62 to 38 Ma. The Absaroka volcanic province and the Rattlesnake Hills are dominantly post-Laramide, whereas the Black Hills magmatism is more difficult to classify in this regard. Lisenbee and DeWitt (this volume) conclude that the main phase of magmatism basically postdated initiation of Laramide uplift of the Black Hills (ca. 64 Ma), but these authors also note that the uplift may have continued with a second pulse extending into the late Paleocene and early Eocene. Furthermore, the magmatism in the Black Hills is probably part of a regional event that extended to the northwest into central Montana (**Figure 11**). In this light, the Black Hills magmatism is best considered syntectonic with the Laramide orogeny.

Igneous rocks of the Black Hills occur as various shallow-level intrusions and minor extrusive phases along a west-northwest-striking zone that transects the South Dakota-Wyoming border (**Figure 11**). Lisenbee and DeWitt (this volume) speculate that an ancient Precambrian zone of structural weakness (a strike-slip fault zone?) controlled distribution of these igneous rocks. This igneous activity has been bracketed between 50 and 62 Ma (DeWitt and others, 1986), although some younger dates have been reported (McDowell, 1971; Staatz, 1983). These rocks are chiefly alkaline, locally including alkali-calcic rocks; many rocks are iron rich. The rock types of this igneous suite vary from mafic (relatively minor) to silicic and range from silica oversaturated to highly undersaturated, although the extremes are related to extensive subsolidus alteration (Shearer, 1990). Some unusual rock types, such as carbonatite, occur locally.

The Rattlesnake Hills igneous complex consists of about 50 plugs, dikes, and various small masses of extrusive volcanic rock exposed in central Wyoming on the northeast flank of the Sweetwater arch, just north of the North Granite Mountains fault system (see Hoch and Frost, this volume). The igneous rocks that constitute this complex include both alkaline (sodium-rich) and subalkaline rocks. Two samples from this suite have yielded K-Ar feldspar dates of about 44 Ma (Pekarek and others, 1974). Magma emplacement postdated local Laramide folding and was probably controlled by a reactivated zone of crustal weakness in Archean basement. Various magmas were emplaced high into the crust in this area, and magma mixing was an important process in the development of the diversity of igneous rocks in the Rattlesnake Hills (Hoch and Frost, this volume). Scarce clinopyroxene-mica cognate inclusions (cumulates) also suggest the importance of crystal fractionation during the differentiation of this igneous suite. These rocks are petrographically and chemically most similar to the Eocene igneous rock suite exposed in the Bear Lodge Mountains area, northeastern Wyoming (Hoch and Frost, this volume).

The Absaroka volcanic province is exposed in the rugged Absaroka Range of northwest Wyoming (see Sundell, this volume), with a northwestern extension into the Gallatin Range of southwestern Montana (Chadwick, 1969). This volcanic province covers an area of 10,000 square miles (2,500 km^2) and constitutes a volume of approximately 7,000 cubic miles (29,000 km^3) of volcanogenic rocks (King and Beikman, 1978). It is the largest, least-studied volcanic province in the conterminous western United States.

Chadwick (1970) recognized two northwest-trending, subparallel belts of eruptive centers in the Absaroka-Gallatin volcanic province; an older eastern Absaroka belt and a younger western Absaroka belt. Igneous rocks as old as 92 Ma have been recognized in the eastern Absaroka belt of Montana (Meen

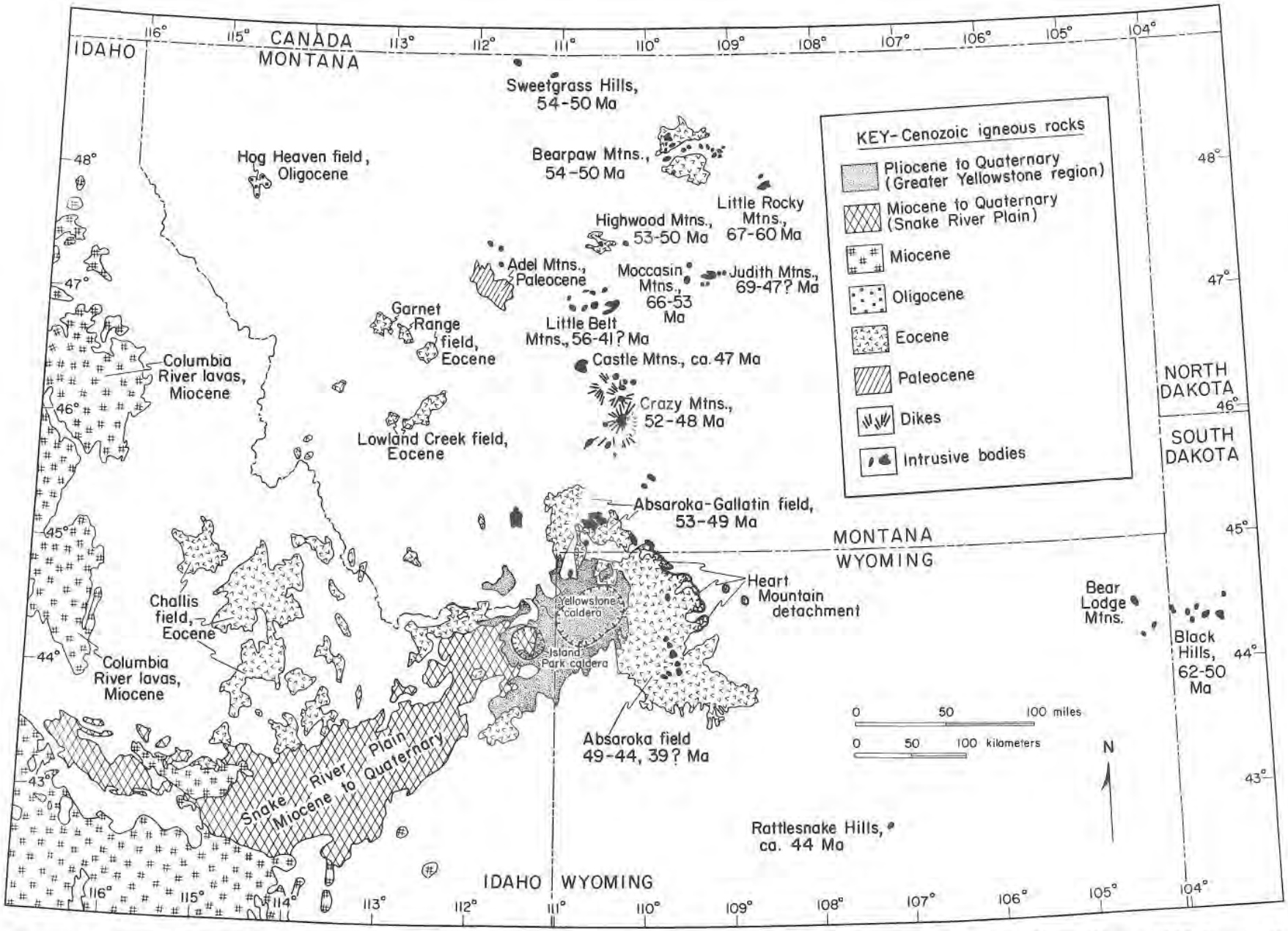

Figure 11. Cenozoic magmatism in the northern Rocky Mountains, U.S. (after Chadwick, 1985, figure 2; King and Beikman, 1974; and Hearn, 1989, figure 1.1).

and Eggler, 1987), although the bulk of the Absaroka volcanic province is Paleogene. These belts perhaps reflect ancient zones of crustal weakness, which could date back to the Precambrian (e.g., the northwest-striking Precambrian faults of Schmidt and Garihan, 1986b).

The pioneering geologists of Yellowstone Park and the northern Absaroka Range, under the direction of Arnold Hague, developed a six-part stratigraphic nomenclature for the Eocene volcanic rocks of the region (oldest to youngest): early acid breccia, early basic breccia, early basalt sheets, late acid breccia, late basic breccia, and late basalt sheets (Hague and others, 1896; Hague and others, 1899). Subsequent studies found various difficulties with this stratigraphic scheme, and gradually numerous other lithostratigraphic units were locally recognized and mapped. A modern reassessment of the volcanic stratigraphy of the Absaroka volcanic province was summarized by Smedes and Proskta (1972), who grouped all the Eocene volcanic rocks as the Absaroka Volcanic Supergroup. This supergroup is subdivided into three groups (oldest to youngest): the Washburn Group, Sunlight Group, and Thorofare Creek Group. In turn, each group contains various formations and members (Smedes and Prostka, 1972; see Sundell, this volume). Coupled with the stratigraphic studies of Smedes and Prostka (1972) were new K-Ar radiometric age determinations (see figure 8, Smedes and Prostka, 1972) that indicated an age range from about 49 to 44 Ma for the Absaroka Volcanic Supergroup. An older age range from about 53 to 49 Ma has been reported in the Gallatin Range, southwestern Montana, for rocks of the Absaroka Volcanic Supergroup (Chadwick, 1970). In contrast, L.L. Love and others (1976) reported a fission-track sphene age of 38.8±1.6 Ma from the southernmost plug (Washakie Needles) of the western Absaroka belt. The sum of these various age determinations perhaps suggests an overall pattern of progressively younger volcanism transgressing from northwest to southeast in the Absaroka volcanic province (L.L. Love and others, 1976; see also Armstrong and Ward, 1991, plate 1).

The Absaroka volcanic rocks are chiefly calc-alkalic andesitic and dacitic extrusive rocks, with subordinate potassic alkalic mafic lavas and rhyodacitic ash-flow tuffs (Smedes and Prostka, 1972). Small intrusive bodies are associated with these extrusive volcanic rocks. Complex facies relationships exist among various lithologies of the Absaroka Volcanic Supergroup, and two basic facies have been recognized: vent facies and alluvial facies deposits. The vent facies deposits are composed of autoclastic flow breccias, lava flows, mudflows, avalanche debris, and tuff. Stocks, plugs, laccoliths, and radial dike swarms also are common features of the vent facies. The alluvial facies deposits consist of aprons of well-bedded, reworked volcanic sedimentary rocks (see Smedes and Prostka, 1972, figures 6 and 7).

The Absaroka volcanic field is a series of deeply dissected Eocene stratovolcanoes that provide a remarkable window into evolution of the upper parts of a continental magmatic arc. In this light, it is important to emphasize that the Absaroka volcanic field was deposited unconformably across a complex paleotopography at the end of the Laramide orogeny (e.g., see Rouse, 1937). The subjacent rocks range in age from Precambrian to Tertiary, and some were strongly deformed during the Laramide orogeny (e.g., Love, 1939). In contrast, the volcanogenic rocks of the Absaroka volcanic province are only weakly deformed, if at all (Sundell, this volume).

An exception to the generally undeformed nature of the Absaroka volcanic rocks is the evolution of the Heart Mountain detachment fault, an enigmatic structure of virtually continuous controversy since its discovery (see Hauge, this volume). A key aspect of the present controversy regarding the evolution of the Heart Mountain detachment fault concerns the involvement of Eocene volcanic rocks during faulting. One model — long advocated by W.G. Pierce (e.g., 1963, 1973, 1987) — suggests that only older Absaroka volcanic rocks were involved in the faulting and that younger volcanic rocks were deposited on a denuded detachment surface in spaces between distended blocks of Paleozoic rocks. The "continuous-allochthon" model of Hauge (1985, 1990), however, argues that all the Eocene volcanic rocks associated with the Heart Mountain detachment fault are allochthonous and were part of an enormous, continuous allochthon that spread southeastward from a "break-away fault" (Pierce, 1960, 1980) in the northern Absaroka Range during the middle Eocene (Bridgerian). As outlined by Hauge (this volume), this controversy has yet to be resolved among the principal protagonists.

Petrotectonic setting of Paleogene magmatism within the Wyoming province craton

Petrogenesis of Paleogene igneous rocks within the Wyoming province craton is poorly understood, but it is the subject of several recent, detailed petrochemical studies (e.g., Dudás, 1991; O'Brien and others, 1991). Dickinson and Snyder (1978) related magmatism in central Montana and the Black Hills region to flat-slab subduction, thereby representing some of the most inland arc magmatism recognized in the western Cordillera. If Dickinson and Snyder's (1978) interpretation is correct, these igneous rocks were intruded and erupted approximately 750 to 930 mi (1,200-1,500 km), respectively, from their coeval Paleogene trench (see Heller and others, 1987, figure 5).

Some geochemical data, principally from central Montana, have been cited as evidence of a subduction-related, arc component within the Paleogene igneous suites (e.g., O'Brien and others, 1991). The initial stage of this petrogenetic model was the development of a metasomatized carapace of phlogopite- and amphibole-bearing peridotite above a low-angle subducted slab (i.e., Farallon Plate lithosphere) at a relatively shallow depth (**Figure 12A**). Subsequently, this metasomatized carapace of asthenospheric mantle was dragged to greater depths by induced asthenospheric flow, where it broke down, forming melts that interacted during ascent with a lithospheric mantle keel beneath the Wyoming province craton (**Figure 12A**).

In contrast, Eggler and others (1988) argued that the overall geochemical characteristics of the Late Cretaceous and Paleogene magmatism within the Wyoming province craton does not indicate arc magmatism; and consequently, subducted material has not contributed chemical components to the magmatism. These authors suggested that the geographically widespread magmatism of the Wyoming province craton is back-arc in character, probably related to partial melting of a postulated mantle keel during extension and thinning of lithosphere and induced flow of asthenosphere (**Figure 12B**). This keel presumably consisted largely of depleted peridotite, locally modified by metasomatic enrichment. Detailed arguments against a subduction-related origin for the Paleogene magmatism of the Wyoming province craton were also presented by Dudás (1991), who favored the heating of lithospheric mantle either by upwelling asthenosphere or during regional decompression. O'Brien and others (1991) questioned if sufficient heat would be generated during advection in the asthenosphere to melt mantle lithosphere or if sufficient decompression occurred to cause melting by lithospheric extension. The tectonic setting of Paleogene magmatism within the Wyoming province craton is therefore still both enigmatic and controversial, despite substantial new chemical, isotopic, and geochronometric data.

Green River Formation - A Middle Eocene lake system

During the Middle Eocene, extensive lakes were developed in southwestern, central, and northern Wyoming (see e.g., Lillegraven and Ostresh, 1988, figure 10) as well as in parts of Colorado and Utah. Love and others (1963) argued that the development of these lakes probably was related to a significant reversal in drainage, when the east-flowing drainage systems established in the Paleocene and early Eocene were cut off by an overall westward tilting of the Wyoming foreland. Synchronous with lake development in Wyoming was the initiation of extensive volcanism in the Absaroka Range, northwestern Wyoming, and in regions to the west (Chadwick, 1985). Lillegraven and Ostresh (1988) suggested that regional thermogenic upwarping may have been an important factor in the development of the extensive lake basin system.

Perhaps the best-studied ancient lake system in the North American Cordillera, or for that matter in the world, is Lake Gosiute, southwestern Wyoming. These ancient lake deposits have had a long history of scrutiny by a variety of geologists beginning with early explorations of the West (see Bradley, 1964, for early references). Their economic potential as the world's largest known trona reserve and as a source of oil shale have virtually guaranteed continuing analysis.

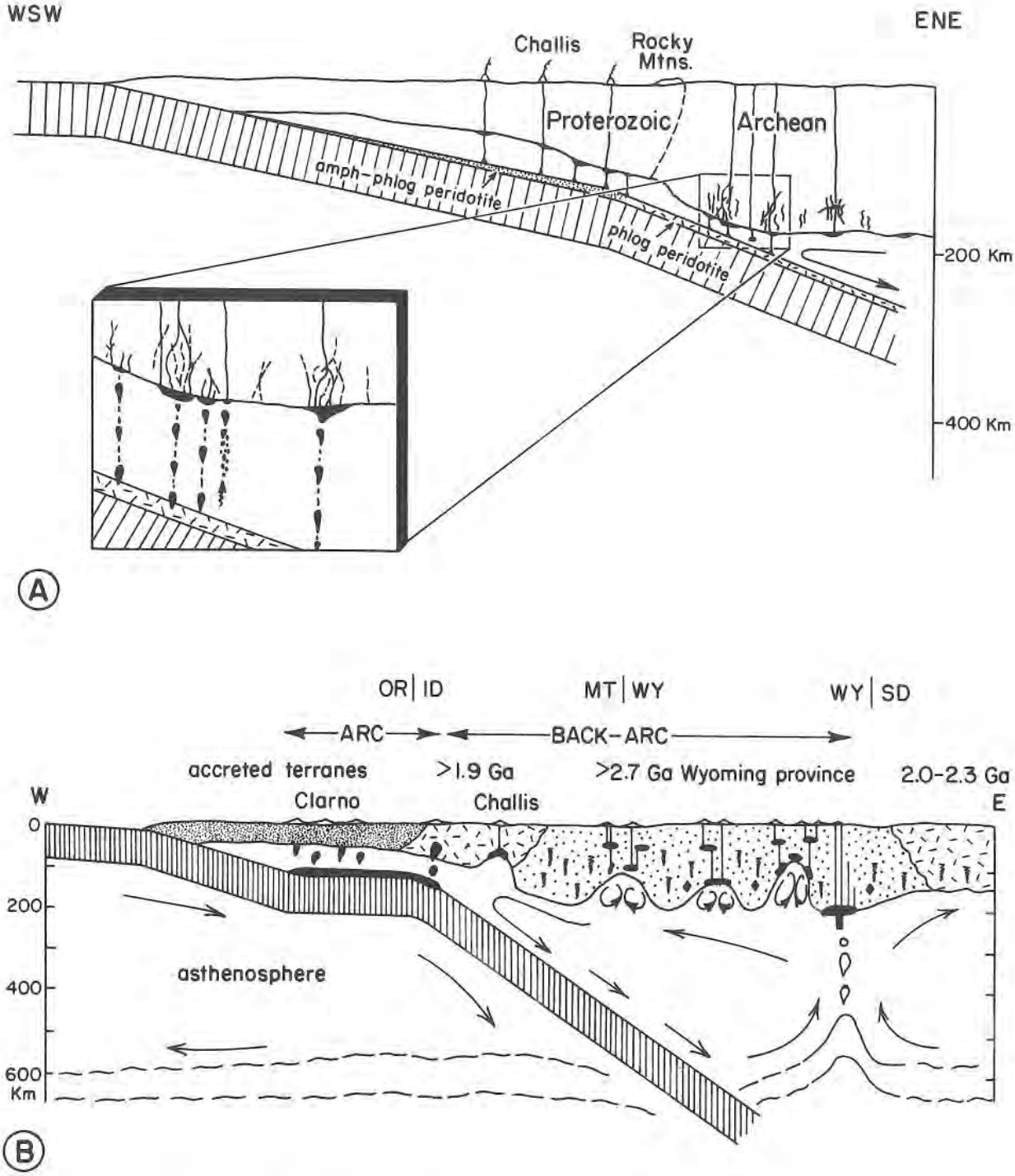

Figure 12. Contrasting petrogenetic models for Paleogene magmatism within the Wyoming province: (A) subduction-related arc magmatism associated with partial melting of asthenospheric mantle triggered by the infiltration of melts released from a metasomatized carapace formed above the low-angle slab of Farallon Plate lithosphere (after O'Brien and others, 1991); and (B) back-arc magmatism associated with asthenospheric upwelling (after Eggler and others, 1988). Some details and criticisms of these models are discussed in the text.

The Eocene lacustrine rocks are collectively referred to as the Green River Formation. These rocks form a gigantic lens between an enormous volume of fluviatile sediments divided into the Wasatch Formation below and Bridger Formation above (Bradley, 1964). Green River rocks are fine grained and generally calcareous. Rocks of both the Wasatch and Bridger formations are chiefly sandy mudstones with interbeds or lenses of sandstone; however, the Bridger Formation contains much more volcanogenic debris.

The history of Lake Gosiute is reflected in rocks of the Green River Formation (see Bradley, 1964, for detailed stratigraphic descriptions). The lake existed for about 4 to 8 million years and was characterized by two main high stands separated by a major constriction (Surdam and Stanley, 1979). These various stages in the evolution of Lake Gosiute are recorded in the Tipton, Wilkins Peak, and Laney members of the Green River Formation. The classic interpretation of Lake Gosiute as an open-drainage, chemically and thermally stratified, meromictic lake was developed in a series of papers by W.H. Bradley (e.g., Bradley, 1948, 1964; Bradley and Eugster, 1969). In contrast, R.C. Surdam, H.P. Eugster, and coworkers argued that the depositional environment of the Green River Formation was, until late in its history, a shallow, closed-basin lake surrounded by broad playa flats (e.g., Eugster and Surdam, 1973; Surdam and Wolfbauer, 1975; Surdam and Stanley, 1979).

The Wilkins Peak Member of the Green River Formation is a distinctive unit in this ancient lake complex because it contains abundant saline minerals. These beds constitute an important economic resource, especially for trona ($Na_2CO_3 \bullet NaHCO_3 \bullet 2H_20$). Bradley (1959, 1964) recognized the significance of the Wilkins Peak Member in the depositional history of Lake Gosiute and reasoned that the lake had dramatically shrunk to about one-third the area of its maximum extent and had no outlet during this stage. In a detailed analysis of the Wilkins Peak Member, Eugster and Hardie (1975) described at least 50 major alternations of wet and dry periods during its deposition. When the climate was wet, the lake expanded and oil shale accumulated. During arid times, the lake shrank, and trona and halite precipitated in its central depths. Furthermore, Eugster and Hardie (1975) argued that flat-pebble conglomerates and mudcracks, characteristic of some rocks in the Wilkins Peak Member, indicate the importance of local desiccation. They envisioned extensive mud flats surrounding a shallow lake; the desiccated mud flats repeatedly were transgressed by the lake during wetter periods. Although deposition of the Wilkins Peak Member represents the most evaporative conditions in the history of the Green River Formation, the overall depositional framework outlined by Eugster and Hardie (1975, figure 19) for the Wilkins Peak Member is perhaps broadly applicable to the Tipton Shale Member (Surdam and Wolfbauer, 1975) and Laney Shale Member (Surdam and Stanley, 1979) as well. However, during deposition of upper parts of the Laney Shale Member, the extent and depth of the lake were considerably greater (Bradley, 1964; Surdam and Stanley, 1979), and thereby a meromictic depositional environment could have played a more significant role (e.g., Boyer, 1982).

Lake Gosiute was part of a large middle Eocene lake system that was an important late Laramide geomorphic feature in the west-central United States. Another large lake in this system was ancient Lake Uinta, which during times of maximum expansion occupied most of the Uinta and Piceance Creek basins in northeastern Utah and northwestern Colorado, respectively. These lake basins were connected by transitory outlets that, during high-water stands, allowed Lake Gosiute to overflow into Lake Uinta around the eastern end of the Uinta Mountains uplift (Surdam and Stanley, 1980). Hanson (1985) noted that the fossil fish fauna from the Eocene lakes had Mississippi River affinities, and therefore suggested that the Continental Divide in Eocene time was west of the lakes. In contrast, Dickinson and others (1988) speculated that an Eocene river from Lake Uinta led westward through the extinct thrust belt, draining to the Pacific Ocean.

A flood of volcaniclastic debris

Uppermost Eocene and lower Oligocene clastic rocks (i.e., White River Formation), rich in airfall tephra but surprisingly poor in crystalline basement debris, are widespread in southeastern Wyoming and

adjacent states (Blackstone, 1975; Seeland, 1985). Deposition of these rocks marked the end of a period of intense late Eocene erosion that affected most of Wyoming (Lillegraven, this volume). Deposition of the White River Formation thereby signaled initiation of a new depositional cycle that occurred in a period of relative tectonic stability during the late Paleogene and most of the Neogene. The oldest rocks in the White River Formation contain mammalian remains of the Chadronian North American Land Mammal Age, which correlates approximately with an age of about 37 Ma on the geochronologic time scale (see Lillegraven, this volume).

Although various lithotypes comprise these Chadronian and younger volcaniclastic deposits, fine-grained, off-white siltstone and bentonitic claystone are most characteristic (Denson and Bergendahl, 1961). Abundant volcanic debris that inundated the Great Plains and adjacent mountains in the late Paleogene and through the early Neogene were derived from remote sources; no evidence for Oligocene magmatism is known in Wyoming. Andesitic volcaniclastic rocks exposed in the Absaroka Range, once considered early Oligocene (e.g., Love, 1939; Love and others, 1963), have been shown to be Eocene by radiometric dating techniques (Smedes and Prostka, 1972; J.D. Love and others, 1976). Therefore, probably much of the volcanic debris was derived from voluminous mid-Tertiary pyroclastic volcanic activity to the west, the so-called "ignimbrite flare-up" of the Great Basin.

Rocks of the White River Formation form extensive, low-dipping exposures and commonly rest with marked unconformity on older rocks. A late Eocene unconformity also is well developed in the Southern Rocky Mountains (e.g., Epis and Chapin, 1975), and is part of a widespread Cordilleran hiatus formed prior to extensive mid-Tertiary volcanism (Gresens, 1981). The depositional environment of these latest Eocene and Oligocene rocks was principally fluvial, and a complex east-flowing drainage network existed in the early Oligocene (Seeland, 1985). This paleodrainage system distributed an extensive blanket of tuffaceous sediments from central Wyoming to the High Plains of western Nebraska and into adjacent South Dakota and Colorado. Denson and Bergendahl (1961) demonstrated that the thickness of the White River Formation varies from about 300 feet in southeastern Wyoming to 850 feet in northwestern Nebraska. At the close of the Oligocene, only the upper 1,000 to 4,000 feet of the highest peaks in the major mountain ranges of the Wyoming foreland protruded above an extensive aggradational plain (Love, 1960).

An important aspect of the Oligocene depositional history is that strata of the White River Formation were deposited across a region of locally marked relief. Although post-Laramide erosion created a regional unconformity (Gresens, 1981), local relief at the end of the Eocene in the Wyoming foreland was as great, if not greater, than at present. In southern and central Wyoming, large late Eocene to early Oligocene paleovalleys apparently existed, because undeformed White River rocks extend into the Precambrian crystalline cores of the Medicine Bow Mountains, Laramie Mountains, and southeastern Wind River Range (Evanoff, 1990).

The depositional cycle that began in the Chadronian continued throughout much of the Neogene, and large thicknesses of Miocene rocks are preserved in some Wyoming basins (see Love, 1960, Table 1). Nevertheless, just prior to the deposition of basal Neogene sequences, yet another major erosional event affected broad areas of Wyoming (Lillegraven, this volume). This erosional interval is marked by a disconformity that typically occurs near the base of Arikareean sedimentary rocks (Denson and Chisholm, 1971; Trimble, 1980).

The lithostratigraphic terminology of the Neogene rocks of Wyoming is complex and controversial (see Flanagan and Montagne, this volume). The name Arikaree Formation was first used by Darton (1899) for a series of gray sands characterized by layers of dark-gray concretions and exposed in northwestern Nebraska. These rocks are overlain unconformably by the more heterogeneous and locally gravelly Ogallala Formation (Swinehart and others, 1985). These units were deposited during the period from early to late Miocene; a previously used Pliocene designation for the Ogallala Formation has been discontinued because of recent corrections to the geologic time scale as used in North America (e.g., Berggren and others, 1985). The names Arikaree and Ogallala at first were restricted in usage to areas east of the Laramie Mountains. However, Denson (1965) suggested extension of the Arikaree-Ogallala nomenclature into central Wyoming, where a widespread succession of fine-grained sandstone, tuffaceous silt-

stone, and shale with subordinate interbeds of conglomerate, tuff, and limestone had been designated the Split Rock and Moonstone formations by Love (1961). This nomenclatural controversy remains unresolved, leading to various designations on published geologic maps and unfortunate confusion to all users. Flanagan and Montagne (this volume) suggest that use of the names Arikaree and Ogallala formations be restricted to latest Oligocene and Miocene rocks east of the Laramie Mountains, in accord with their original geographic use.

In summary, the latest Paleogene and Neogene rocks of southeastern Wyoming are part of a great sheet of outwash that spread along the eastern slope of the Rocky Mountains chiefly during the Oligocene and Miocene (see King and Beikman, 1978, figures 2, 3, and 4). In Wyoming, this sedimentary sheet was deposited across a late Eocene landscape that developed during extensive post-Laramide erosion. An important regional change is manifested by the transition from the humid climate of the early Tertiary to the semiarid climate of the middle Tertiary, marked by changes in floras and faunas of the intermontane basins (e.g., Dorf, 1959; McGrew, 1971). This fundamental climactic change has been cited as a principal factor contributing to mid-Tertiary aggradation (Mackin, 1947). Synchronous with this transition in climate was the inundation of the region with volcanic tephra principally derived from remote sources to the west. The existing streams consequently steepened their gradients in response to the increased load but decreased discharge, and a broad aggradational plain gradually formed that stretched across the Rocky Mountains and into the High Plains (see Love and others, 1963, figure 9). However, in the last 5 million years, erosion has greatly exceeded deposition (Trimble, 1980), and only a scant record of Pliocene deposition is preserved in western Nebraska (Swinehart and others, 1985). The various stratigraphic units that constitute the Miocene part of this outwash sheet are invariably bounded by unconformities, with channeling of underlying deposits during deposition of the younger strata (Skinner and others, 1977; Swinehart and others, 1985). The preservation of significant thicknesses of Miocene strata westward within the Rocky Mountains (e.g., Love, 1961) suggests that this great sedimentary sheet probably was widespread throughout most basins, and even across some of the ranges, of the Wyoming foreland.

Neogene extension

Neogene normal faulting is manifested locally throughout Wyoming. An episode of late Neogene extension has been long recognized in the fold-and-thrust belt (Armstrong and Oriel, 1965). Many of the broad, linear north-south valleys in the thrust belt are half-grabens, bounded on the east by listric normal faults. Some of these faults have reactivated segments of the thrust faults. An example is the relationship between the Hoback normal fault and the Prospect thrust as indicated by surface geologic mapping and a seismic reflection profile (Royse and others, 1975). Detailed structural cross sections by Royse (this volume) indicate that ramps in the thrust fault trajectory localized the surface traces of the normal faults.

The most impressive manifestation of Neogene normal faulting in Wyoming is the spectacular, west-tilted Teton Range bounded on its east flank by the Teton normal fault (Smith, Byrd, and Susong, this volume). The Teton fault extends for about 44 miles (70 km) along the base of the eastern slope of the Teton Range, and exhibits stratigraphic separation, estimated locally, of at least 30,000 feet (Love and Reed, 1971; Love and others, 1973). The Teton fault is considered to be active, and an extensive set of adjacent Quaternary scarps suggests seismicity in the recent past (Smith, Byrd, and Susong, this volume). Although the north-striking Teton fault intersects northwest-striking, Laramide contractile structures at a high angle, Lageson (1987, 1992) argued that the Neogene normal fault may have reactivated the ramp of the Cache Creek thrust and was also controlled by pre-existing Precambrian shear zones.

Late normal faulting, although widespread in the Wyoming foreland (e.g., Love, 1970), is poorly understood in regard to its tectonic setting and regional significance. Some of these faults may not be of Neogene age and perhaps do not even indicate regional extensional deformation. Rather, these normal faults may have developed during, or shortly after, the

Laramide orogeny in association with complex space problems created during crustal shortening or the relaxation of regional compressive stresses (e.g., Wise, 1963; also see Brown, this volume). Nevertheless, important normal-fault systems are well documented at several localities in the Wyoming foreland and suggest that an episode of Neogene regional crustal extension affected this area (Hall and Chase, 1989). Three of the more important normal-fault systems of the Wyoming foreland include: the Continental fault system of the southern Wind River Range, the South Granite Mountains fault system, and the Whalen and Wheatland fault system of southeastern Wyoming.

The Continental fault is a major normal-fault system that extends for at least 50 miles (80 km) along the southwest flank of the Wind River Range (Zeller and Stephens, 1969). It was originally delineated and named by Nace (1939). This fault system apparently occurs in the hanging wall of the Wind River thrust (Blackstone, 1991). The Continental fault system consists of anastomosing normal faults, both sinuous and planar, that generally dip steeply to the north and northeast (Steidtmann and Middleton, 1991). There has been considerable discrepancy among reports of displacement along the Continental normal-fault system. Nace (1939) estimated a minimum throw of 1,450 feet (442 m); Berg (1962) cited a throw of 250-1,000 feet (76 to 305 m); and Love (1970) stated that the mountain block was downdropped about 2,000 feet (610 m) along the Continental normal fault. Recent analysis by D.L. Blackstone, Jr. (1991 and personal communication, 1992) suggests that this normal-fault system does <u>not</u> cut the plane of the Wind River thrust, and thereby caused only modest, late, normal-sense slip along the thrust. Steidtmann and Middleton (1991) suggested that displacement along the Continental normal fault system occurred about 13 Ma.

The South Granite Mountains fault system refers to various normal-fault strands that occur along the northern margins of the Seminoe, Ferris, and Green mountains. The fault system, which strikes approximately N70°W, consists of steep, northward-dipping normal faults. Love (1970) estimated a minimum displacement of 2,000 feet (610 m) along the fault system. Sales (1983) referred to this fault system as a major foreland collapse zone. Recent cross sections by Blackstone (1991), which cross the South Granite Mountains fault system and the Emigrant Trail thrust fault, suggest that the amount of late normal-sense displacement along the South Granite Mountains fault system was only a small fraction (perhaps 7% of total displacement) of the reverse-sense displacement along the Emigrant Trail thrust that occurred during the Laramide orogeny.

The Whalen and Wheatland faults of southeastern Wyoming are examples of northeast-striking normal faults. The Whalen fault strikes N43°E and dips steeply (74-77°) to the southeast (McGrew, 1963). This fault cuts the Upper Oligocene-Lower Miocene Arikaree Formation and exhibits about 600 feet (183 m) of stratigraphic separation. The Wheatland fault occurs northwest of the Whalen fault, strikes subparallel to it, but dips to the northwest. The Wheatland exhibits about 650 feet (198 m) of vertical separation (McGrew, 1963). These faults do not appear to be related to Laramide thrust faults, but they do parallel the inferred strike of the Cheyenne belt, again suggesting the importance of tectonic heredity in the evolution of foreland normal-fault systems.

Although late Cenozoic normal faults are relatively common in the Wyoming foreland, typically they record only modest displacements and represent only a few percent extension. Commonly these normal faults appear to reactivate older structures. The exact regional tectonic regime responsible for this late Cenozoic extension is uncertain. Similar structural relationships involving reactivation of older Laramide thrusts have been well documented in southwestern Montana (Schmidt and Garihan, 1986a; Lageson, 1989), but in this region the extensional deformation is attributed to the overprinting of Basin and Range structure onto a part of the Rocky Mountain foreland (Reynolds, 1979). In the Southern Rocky Mountains, normal faulting also is widespread (e.g., Taylor, 1975), and many authors have suggested that the effects of the Rio Grande rift system extend at least to central Colorado (e.g., Tweto, 1979). The Wyoming foreland is therefore a region of anomalous Neogene crustal extension, located north of obvious effects of the Rio Grande rift system and east of the Basin and Range structural province. Neogene extensional history of the Wyoming foreland suggests a zone of tectonic transition situated between areas of significant crustal extension and the unextended northern Great Plains.

The great exhumation

The late Neogene paleogeographic map of Love and others (1963, figure 9) depicts Wyoming as a broad aggraded plain characterized by volcanism in the northwest corner (Yellowstone area) and Leucite Hills (northeastern Rock Springs uplift, southwestern Wyoming). According to their reconstruction, only scattered knobs of exposed Precambrian basement rocks, surrounded by Neogene sedimentary rocks, existed across the state. If this picture accurately represents late Neogene topography, fundamental changes had to have occurred to provide the mountainous scenery that now characterizes Wyoming.

The cause of this great exhumation of Neogene and older sedimentary rocks from the basins of Wyoming is a matter of considerable debate. Some workers argue that the erosion is evidence for epeirogenic uplift of the Rocky Mountains (e.g., Trimble, 1980). Others suggest that the exhumation can be explained by climactic deterioration (Molnar and England, 1990), and that the region has been near its present elevation since the mid-Eocene (the end of the Laramide orogeny). Regardless of the exact role of tectonic uplift and climate, an enormous volume of sediment was stripped from the area now known as the eastern Rocky Mountains during the late Cenozoic. Much of this sediment was transported to the Gulf of Mexico, where thousands of feet of Pliocene and Pleistocene deposits accumulated (e.g., Woodbury and others, 1973).

If the great exhumation was driven by tectonic uplift, then the mantle lithosphere beneath the Rocky Mountains may have thinned significantly during the past 5 million years to compensate for the uplift (Suppe and others, 1975; Eaton, 1986). Results from seismic studies (e.g., Herrin and Taggart, 1968; Grand, 1987) are consistent with the presence of thin or hot mantle lithosphere under the western United States, but the spatial resolution of such studies is low. Nevertheless, analyses of lithospheric flexure (Sahagian, 1987; Angevine and Flanagan, 1987; Mitrovica and others, 1989) suggest that as much as one-half of the modern elevation of the Rocky Mountains is compensated by thick accumulations of late Cretaceous and early Tertiary sedimentary rocks (Cross and Pilger, 1978a; Cross, 1986) and Laramide crustal thickening.

To settle the debate about the relative roles of climate and tectonism in the great exhumation, reliable estimates of the absolute elevation history of the Earth's surface are needed. One approach may be to determine paleoaltitudes using estimates of paleotemperature that are derived from physiognomic analyses of fossil flora. Studies of this type (e.g., Wolfe and Schorn, 1989; Gregory and Chase, 1992) suggest that the mountains of Colorado reached their present elevations by the early Oligocene. Similar studies of paleoflora in Wyoming would be of value, but fundamental questions regarding the large corrections and poorly known parameters used in computing paleoaltitudes must be addressed.

High-level erosional surfaces

Many mountain ranges in Wyoming exhibit an extensive subsummit surface, above which peaks project and below which streams and rivers have cut valleys and gorges to depths of several thousand feet. Recognition of high-level erosional surfaces in the Rocky Mountain region goes back to early geologic explorers (e.g., A.R. Marvine of the Hayden Survey). An interesting summary of various ideas concerning the number of recognized surfaces, their inferred ages, and their origins in regard to the Colorado Front Range was presented by Bradley (1987). In this review, he emphasized that accurate dating is the key to understanding the significance of these erosion surfaces. In this light, the apparently best dated erosion surface in the Rocky Mountains is the so-called "late Eocene" surface of the southern Rocky Mountains (Epis and Chapin, 1975). Epis and Chapin based the age designation on recognition that an ancient surface, similar to exhumed surfaces, is overlain by radiometrically dated Oligocene volcanic rocks. Some Colorado workers (as cited in Bradley, 1987) argue that the famous Sherman surface of southeastern

Wyoming is of similar age, although no Oligocene volcanic rocks are deposited upon it. Knight (1953) also concluded that the subsummit erosion surface of the Medicine Bow Mountains [his Libby Flats surface; but called Medicine Bow surface by Steven (1956)] was of late Eocene age and represented post-Laramide, regional planation. In contrast, Steven (1956) noted that a major paleovalley in the Medicine Bow Mountains (Kings Canyon), filled chiefly with early Oligocene White River Formation and locally with Miocene sedimentary rocks, is truncated by the subsummit erosional surface (see his figure 2), suggesting that the age of this surface is late Tertiary. Knight (1953) had previously suggested that the paleovalleys were relicts preserved despite extensive late Eocene planation and subsequently filled with Oligocene and younger sedimentary deposits.

Interpretations of the age and developmental history of various high-level erosional surfaces in the Rocky Mountains are still very controversial after many years of study and numerous published reports (see Mears, this volume). Nevertheless, many past and recent workers concur that significant relief existed in the late Eocene (e.g., Knight, 1974, his figure 4) despite extensive post-Laramide erosion (see also Love, 1941, for a clear statement of this interpretation as well as Evanoff, 1990). Furthermore, many erosional surfaces in Wyoming may be of late Tertiary age. Mears (this volume) concludes his review of high-level erosional surfaces in Wyoming with this interpretation, citing the preservation in the Laramie Mountains of a planar surface of deposition, upon which the Upper Miocene Ogallala Formation was deposited. This erosional surface and the Miocene sedimentary rocks deposited upon it form the famous "Gangplank", which connects the late Miocene depositional surface of the High Plains with the Sherman erosional surface in the Laramie Mountains (Mackin, 1947; Moore, 1959). Mears also supports Mackin's (1947) hypothesis that these surfaces are pediments. According to this interpretation, the high regional slopes of the subsummit erosional surfaces are more compatible with the semiarid climate of the late Tertiary than the inferred humid climate of the late Eocene. Consequently, the subsummit pediment could have formed at a high elevation.

Yellowstone Volcanic Plateau

The Quaternary Yellowstone Volcanic Plateau is at the northeastern end of the eastern Snake River Plain, a volcano-tectonic feature in the U.S. Cordillera that developed across the Basin and Range province (**Figure 1**). The Yellowstone Plateau stands at about 8,200 ft (2,500 m), although flanked by mountains that rise to nearly 13,000 ft (4,000 m). To the southwest along the eastern Snake River Plain, the terrain drops gradually to a region of lower relief at about 3,300 to 5,000 ft (1,000 to 1,500 m) elevation. One widely-cited hypothesis attributes the development of the Snake River Plain to the southwestern migration of the North America plate across a hotspot fixed in the mantle and presently beneath the Yellowstone region (e.g., Morgan, 1972; Smith and others, 1974; Eaton and others, 1975; Smith and Christiansen, 1980; Pierce and Morgan, 1992; Smith and Braile, this volume). The vector of motion of the North America plate, inferred from other methods, is parallel to the azimuth of the eastern Snake River Plain (Minster and Jordan, 1978), and Leeman (1982) suggested that the hotspot trace can be extended to the ca. 16 Ma McDermitt volcanic field in north-central Nevada (also see Pierce and Morgan, 1992). However, Hamilton (1989) argued that magmatism in the eastern Snake River Plain was erratic, and an orderly progression of magmatism to the northeast, as predicted by the hotspot model, cannot be demonstrated in detail. Hamilton (1989) concluded that the eastern Snake River Plain is a wedge-shaped extensional rift that has propagated northeastward with time, resulting in volcanic activity.

Regardless of the exact origin of the Snake River Plain, the Yellowstone Plateau is the product of voluminous volcanic eruptions during the past 2.2 million years (e.g., Christiansen, 1984). Three cycles are recognized in the magmatic history of the Yellowstone Plateau, with climactic eruptions at about 2.0, 1.3, and 0.6 Ma. (Christiansen and Blank, 1972). The rhyolitic ash-flow sheets that formed during these pyroclastic eruptions constitute the major stratigraphic units of the volcanic plateau, and are called (oldest to youngest): Huckleberry Ridge, Mesa Falls, and Lava Creek Tuffs of the Yellowstone Group (Christiansen and Blank, 1972).

The three cycles evolved in a basically similar fashion. Each cycle began and ended with a protracted period of intermittent lava eruptions of rhyolite and subordinate basalt but climaxed with an explosive, caldera-forming pyroclastic eruption of rhyolitic ash flows (Christiansen, 1984). Voluminous ash flows spread out over hundreds of square miles, and volcanic debris from these eruptions rose high into the atmosphere and was carried for thousands of miles. Deposits of Yellowstone ash are widespread throughout the western U.S. and southern Canada (Izett and Wilcox, 1981).

The record of the third volcanic cycle is most complete and that cycle accounts for much of the volcanic landscape in present-day Yellowstone National Park (Christiansen and Blank, 1972). This cycle began about 1.2 Ma. Rhyolitic lava intermittently erupted from arcute fracture systems, gradually outlining a large area of the roof of the subjacent magma chamber. This faulted carapace subsequently collapsed during a climactic pyroclastic eruption 630,000 years ago, forming an enormous caldera (Christiansen, 1984). During the formation of the Yellowstone caldera, more than 1,000 km^3 of Lava Creek Tuff were so rapidly erupted (in hours or days) that there is no evidence of erosion, aqueous reworking, or the deposition of extraneous materials within the tuff sequence (Christiansen, 1984). However, detailed stratigraphic data indicate that the tuff consists of two sheetlike deposits that erupted so close in time that they welded and crystallized as a single cooling unit. Furthermore, the caldera is actually two overlapping ringlike fracture systems that form a compound feature about 47 mi (75 km) long and 28 mi (45 km) across (Christiansen, 1984). Resurgence of magma into the subjacent chamber caused uplift of the caldera floor, forming two structural domes (Smith and Christiansen, 1980). During the past 630,000 years, sediments and postcaldera rhyolitic lavas have covered much of the compound caldera basin. Furthermore, during the past 150,000 years, rhyolitic lavas have covered the western resurgent dome and completely buried the western rim of the caldera (Christiansen, 1984). Although no eruptions have occurred in the Yellowstone region in the past 70,000 years, the vigorously active hydrothermal systems manifested as geyers, hot springs, and fumaroles reflect the presence of a major, still-molten magma body beneath a large part of the Yellowstone Plateau (Eaton and others, 1975; Smith and Braile, this volume).

Holocene seismic activity in Wyoming

Although seismic activity is not common throughout much of Wyoming (Case, 1986), the Intermountain seismic belt crosses westernmost Wyoming, where it is defined by a zone of numerous earthquake epicenters (Smith and Sbar, 1974). Several active fault systems are part of this belt, including the Teton fault, which has been assigned a maximum credible earthquake (MCE) of magnitude 7.5 (Gilbert and others, 1983). The largest historic seismic event (M_S=7.5) of the Intermountain region occurred on August 17, 1959, at Hebgen Lake, Montana, located only a few miles west of the northwestern boundary of Yellowstone National Park. The shock was felt over an area of 600,000 square miles (Murphy and Brazee, 1964). Twenty-eight people were killed — the disastrous quake-caused Madison Slide accounted for all but two of these deaths (Hadley, 1964).

Several large fault scarps, and many smaller ones, formed during the Hebgen Lake earthquake. The most spectacular scarp-fissure system could be traced for 14 miles (22.5 km), defining the Red Canyon fault scarp (Witkind, 1964). This set of scarps and fissures appeared in surficial material along or near the trace of a Tertiary normal fault (Red Canyon fault). The scarp had an average height of 10 feet (3 m), but locally it increased to about 20 feet (~6 m) (Witkind, 1964). The close association of earthquake-related scarps and Tertiary normal faults with thrust faults suggests that the recent displacement was normal-sense along reactivated thrust faults (Myers and Hamilton, 1964; Doser, 1985).

A summary of the distribution of historic earthquake epicenters across Wyoming (Case, 1986) indicates only scattered events throughout much of the state as compared to the concentration of seismicity along the western margin of the state. Furthermore, many seismic events in Wyoming east of the Intermountain seismic belt do not correlate well with

mapped traces of known faults. However, such summaries of seismicity in Wyoming are based upon a historic record only compiled since 1871 (Case, 1986). The long-term frequency of seismic events throughout Wyoming is therefore very poorly known.

Concluding remarks

The geology of Wyoming includes many representative features of the general tectonic evolution of the North American Cordillera. During the past twenty or more years, models and syntheses of the geological evolution of the Cordillera have been based principally upon the paradigm of plate tectonics. To understand the geologic evolution of Wyoming in this perspective has proven to be a formidable challenge. Although inferred Proterozoic and younger tectonic settings seem to have many actualistic examples (i.e., passive margins, magmatic arcs, and so forth), plate-tectonic models for the Archean are still controversial and probably oversimplified. Furthermore, the great distance of Wyoming from the plate margin since early Mesozoic time has impeded the correlation of events recorded at the western continental margin. Many future insights into the geological evolution of Wyoming will be based upon carefully designed studies that challenge the "conventional wisdom" espoused within this chapter.

In this light, I conclude my overview of the geology of Wyoming with a list of unsolved problems (chiefly tectonic in scope) that could evolve into important research topics:

1. Accretion history of the Archean Wyoming province;
2. Regional extent of deformation and metamorphism associated with Early Proterozoic accretion along the southern margin of the Wyoming province;
3. Tectonic setting of the Laramie Anorthosite Complex and Sherman batholith;
4. The role of the middle and lower crust during Laramide crustal shortening;
5. Cause(s) of regional variation in orientation of Laramide uplifts and basins;
6. Kinematic history of basement-cored uplifts and the role of an evolving or heterogeneous stress field;
7. Petrotectonic setting of Laramide and post-Laramide magmatism in the Rocky Mountain foreland;
8. Tertiary mean-elevation history;
9. Cause of crustal extension in central Wyoming;
10. Cause(s) of late Cenozoic exhumation.

Acknowledgments

This summary is a synthesis based on the combined work of hundreds of geologists who have worked in Wyoming and the North American Cordillera. However, I owe an especially great debt of gratitude to the contributing authors of this volume. They provided up-to-date manuscripts on various aspects of Wyoming geology that I used extensively as intermediate summaries in my compilation. Furthermore, my knowledge of Wyoming geology has been enhanced continually by discussions with colleagues at The University of Wyoming: C.L. Angevine, D.L. Blackstone, Jr., D.W. Boyd, C.D. Frost, B.R. Frost, P.L. Heller, R.S. Houston, J.A. Lillegraven, B. Mears, Jr., and J.R. Steidtmann. Many of these colleagues provided me with written comments on parts of earlier versions of this manuscript. Emmett Evanoff commented on the late Paleogene and Neogene parts of the manuscript and pointed out several important references that I had overlooked. C.L. Angevine helped me understand the fundamental problems concerning the late Cenozoic exhumation of the Rocky Mountains. The detailed critical comments on an early version of the manuscript by D.L. Blackstone, Jr. and J.A. Lillegraven were especially useful in preparing a more readable text. The critical review comments of the penultimate version of the manuscript by D.R. Lageson, D.M. Miller, S.M. Roberts, and D.U. Wise provided numerous valuable

suggestions, many of which were incorporated into the final version. To all these reviewers, I express my sincere appreciation for their efforts to improve a complex and wide-ranging manuscript. Finally, I thank Phyllis A. Ranz for her help in preparing the final figures to accompany the text of the manuscript.

References cited

Aleinikoff, J.N., 1983, U-Th-Pb systematics of zircon inclusions in rock-forming minerals: a study of armoring against isotopic loss using the Sherman Granite of Colorado-Wyoming, USA: Contributions to Mineralogy and Petrology, v. 83, p. 259-269.

Aleinikoff, J.N., Williams, I.S., Compston, W., Stuckless, J.S., and Worl, R.G., 1989, Evidence for an Early Archean component in the Middle to Late Archean gneisses of the Wind River Range, west-central Wyoming: conventional and ion microprobe U-Pb data: Contributions to Mineralogy and Petrology, v. 101, p. 198-206.

Allmendinger, R.W., 1986, Tectonic development, southwestern border of the Puna Plateau, northwestern Argentine Andes: Geological Society of America Bulletin, v. 97, p. 1070-1082.

Allmendinger, R.W., Miller, D.M., and Jordan, T.E., 1984, Known and inferred Mesozoic deformation in the hinterland of the Sevier belt, northwest Utah, *in* Geology of northwest Utah, southern Idaho and northeast Nevada: Utah Geological Association Publication 13, p. 21-34.

Anderson, J.L., 1983, Proterozoic anorogenic granite plutonism of North America, *in* Medaris, L.G., Jr., Byers, C.W., Mickelson, D.M., and Shanks, W.C., editors, Proterozoic geology: selected papers from an international Proterozoic symposium: Geological Society of America Memoir 161, p. 133-154.

Anderson, J.L., and Bender, E.E., 1989, Nature and origin of Proterozoic A-type granitic magmatism in the southwestern United States of America: Lithos, v. 23, p. 19-52.

Angevine, C.L., and Flanagan, K.M., 1987, Buoyant subsurface loading of the lithosphere in the Great Plains foreland basin: Nature, v. 237, p. 137-139.

Anonymous, 1951, North-south cross section through the Carter Oil Co. no. 1 Immigrant Trail unit, Fremont County, Wyoming: Wyoming Geological Association 6th Annual Field Conference Guidebook, p. 122.

Armstrong, F.C., and Oriel, S.S., 1965, Tectonic development of Idaho-Wyoming thrust belt: American Association of Petroleum Geologists Bulletin, v. 49, p. 1847-1866.

Armstrong, R.L., 1968, Sevier orogenic belt in Nevada and Utah: Geological Society of America Bulletin, v. 79, p. 429-458.

_____ 1974, Magmatism, orogenic timing, and orogenic diachronism in the Cordillera from Mexico to Canada: Nature, v. 247, p. 348-351.

_____ 1978, Cenozoic igneous history of the U.S. Cordillera from lat 42° to 49°N, *in* Smith, R.B., and Eaton, G.P., editors, Cenozoic tectonics and regional geophysics of the western Cordillera: Geological Society of America Memoir 152, p. 265-282.

Armstrong, R.L., and Ward, P., 1991, Evolving geographic patterns of Cenozoic magmatism in the North American Cordillera: the temporal and spatial association of magmatism and metamorphic core complexes: Journal of Geophysical Research, v. 96, p. 13,201-13,224.

_____ in press, Late Triassic to earliest Eocene magmatism in the North American Cordillera: implications for the Western Interior Basin, *in* Geological Association of Canada Special Paper.

Ball, T.T., and Farmer, G.L., 1991, Identification of 2.0 to 2.4 Ga Nd model age crustal material in the Cheyenne belt, southeastern Wyoming: implications for Proterozoic accretionary tectonics at the southern margin of the Wyoming craton: Geology, v. 19, p. 360-363.

Bally, A.W., 1975, A geodynamic scenario for hydrocarbon occurrences: Tokyo, 9th World Petroleum Congress, v. 2, p. 23-44.

Bally, A.W., Gordy, P.L., and Stewart, G.A., 1966, Structure, seismic data and orogenic evolution of southern Canadian Rocky Mountains: Bulletin of Canadian Petroleum Geology, v. 14, p. 337-381.

Barnosky, A.D., 1984, The Colter Formation: evidence for Miocene volcanism in Jackson Hole, Teton County, Wyoming: Wyoming Geological Association Earth Science Bulletin, v. 17, p. 49-97.

Bennett, V.C., and DePaolo, D.J., 1987, Proterozoic crustal history of the western United States as determined by neodymium isotopic mapping: Geological Society of America Bulletin, v. 99, p. 674-685.

Berg, R.R., 1962, Mountain flank thrusting in Rocky Mountain foreland, Wyoming and Colorado: American Association of Petroleum Geologists Bulletin, v. 46, p. 2019-2032.

Berggren, W.A., Kent, D.V., Flynn, J.J., and Van Couvering, J.A., 1985, Cenozoic geochronology: Geological Society of America Bulletin, v. 96, p. 1407-1418.

Bergh, S.G., and Snoke, A.W., 1992, Polyphase Laramide deformation in the Shirley Mountains, south-central Wyoming foreland: The Mountain Geologist, v. 29, p. 85-100.

Bird, P., 1984, Laramide crustal thickening event in the Rocky Mountain foreland and Great Plains: Tectonics, v. 3, p. 741-758.

_____ 1988, Formation of the Rocky Mountains, western United States: a continuum computer model: Science, v. 239, p. 1501-1507.

Blackstone, D.L., Jr., 1940, Structure of the Pryor Mountains, Montana: Journal of Geology, v. 48, p. 590-618.

_____ 1975, Late Cretaceous and Cenozoic history of the Laramie Basin region, southeast Wyoming, *in* Geological Society of America Memoir 144, p. 249-279.

_____ 1980, Foreland deformation: compression as a cause: University of Wyoming Contributions to Geology, v. 18, no. 2, p. 83-100.

_____ 1983, Laramide compressional tectonics, southeastern Wyoming: University of Wyoming Contributions to Geology, v. 22, no. 1, p. 1-38.

_____ 1986, Foreland compressional tectonics: southern Bighorn Basin and adjacent areas, Wyoming: Geological Survey of Wyoming Report of Investigations no. 34, 32 p.

_____ 1990, Rocky Mountain foreland structure exemplified by the Owl Creek Mountains, Bridger Range and Casper arch, central Wyoming, *in* Specht, R.W., editor, Wyoming Geological Association 41st Annual Field Conference Guidebook, p. 151-166.

_____ 1991, Tectonic relationships of the southeastern Wind River Range, southwestern Sweetwater uplift, and Rawlins uplift, Wyoming: Geological Survey of Wyoming Report of Investigations no. 47, 24 p.

Blake, M.C., Jr., Bruhn, R.L., Miller, E.L., Moores, E.M., Smithson, S.B., and Speed, R.C., 1989, C-1 Mendocino triple junction to North American craton: Geological Society of America, Centennial Continent/Ocean Transect #12.

Boyer, B.W., 1982, Green River laminites: Does the playa-lake model really invalidate the stratified-lake model?: Geology, v. 10, p. 321-324.

Boyer, S.E., 1986, Styles of folding within thrust sheets: examples from the Appalachian and Rocky Mountains of the U.S.A. and Canada: Journal of Structural Geology, v. 8, p. 325-339.

Bradley, W.C., 1987, Erosion surfaces of the Colorado Front Range: a review, *in* Graf, W.L., editor, Geomorphic systems of North America: Boulder, Colorado, Geological Society of America Centennial Special Volume 2, p. 215-220.

Bradley, W.H., 1948, Limnology and the Eocene lakes of the Rocky Mountain region: Geological Society of America Bulletin, v. 59, p. 635-648.

_____ 1959, Revision of stratigraphic nomenclature of Green River formation of Wyoming: American Association of Petroleum Geologists Bulletin, v. 43, p. 1072-1075.

_____ 1964, Geology of Green River Formation and associated Eocene rocks in southwestern Wyoming and adjacent parts of Colorado and Utah: U.S. Geological Survey Professional Paper 496-A, 86 p.

Bradley, W.H., and Eugster, H.P., 1969, Geochemistry and paleolimnology of the trona deposits and associated authigenic minerals of the Green River Formation of Wyoming: U.S. Geological Survey Professional Paper 496-B, 71 p.

Brenner, R.L., 1983, Late Jurassic tectonic setting and paleogeography of western interior, North America, *in* Reynolds, M.W., and Dolly, E.D., editors, Mesozoic paleogeography of the west-central United States, Rocky Mountain Paleogeography Symposium 2: Denver, Colorado, The Rocky Mountain Section, Society of Economic Paleontologists and Mineralogists, p. 119-132.

Bressler, S.L., 1981, Preliminary paleomagnetic poles and correlation of the Proterozoic Uinta Mountain Group, Utah and Colorado: Earth and Planetary Science Letters, v. 55, p. 53-64.

Brown, W.G., 1988, Deformational style of Laramide uplifts in the Wyoming foreland, *in* Schmidt, C.J., and Perry, W.J., Jr., editors, Interaction of the Rocky

Mountain foreland and the Cordilleran thrust belt: Geological Society of America Memoir 171, p. 1-25.

Bryan, P., and Gordon, R.G., 1990, Rotation of the Colorado Plateau: an updated analysis of paleomagnetic poles: Geophysical Research Letters, v. 17, p. 1501-1504.

Bryant, B., 1985, Structural ancestry of the Uinta Mountains, *in* Picard, M.D., editor, Geology and energy resources, Uinta basin of Utah: Salt Lake City, Utah, Utah Geological Association, p. 115-120.

Burchfiel, B.C., and Davis, G.A., 1968, Two-sided nature of the Cordilleran orogen and its tectonic implications: XXIII International Geological Congress, v. 3, p. 175-184.

_____ 1975, Nature and controls of Cordilleran orogenesis, western United States: extensions of an earlier synthesis: American Journal of Science, v. 275-A, p. 363-396.

Burke, K., and Dewey, J.F., 1973, Plume-generated triple junctions: key indicators in applying plate tectonics to old rocks: Journal of Geology, v. 81, p. 406-433.

Busby-Spera, C.J., 1988, Speculative tectonic model for the early Mesozoic arc of the southwest Cordilleran United States: Geology, v. 16, p. 1121-1125.

Campbell, R.B., 1973, Structural cross-section and tectonic model of the southeastern Canadian Cordillera: Canadian Journal of Earth Sciences, v. 10, p. 1607-1620.

Carr, T.R., and Paull, R.K., 1983, Early Triassic stratigraphy and paleogeography of the Cordilleran miogeocline, *in* Reynolds, M.W., and Dolly, E.D., editors, Mesozoic paleogeography of the west-central United States, Rocky Mountain Paleogeography Symposium 2: Denver, Colorado, The Rocky Mountain Section, Society of Economic Paleontologists and Mineralogists, p. 39-55.

Case, J.C., 1986, Earthquakes and related geologic hazards in Wyoming: Geological Survey of Wyoming Public Information Circular no. 26, 22 p.

Chadwick, R.A., 1969, The northern Gallatin Range, Montana: northwestern part of the Absaroka-Gallatin volcanic field: University of Wyoming Contributions to Geology, v. 8, no. 2, pt. 2, p. 150-166.

_____ 1970, Belts of eruptive centers in the Absaroka-Gallatin volcanic province, Wyoming-Montana: Geological Society of America Bulletin, v. 81, p. 267-274.

_____ 1985, Overview of Cenozoic volcanism in the west-central United States, *in* Flores, R.M., and Kaplan, S.S., editors, Cenozoic paleogeography of west-central United States, Rocky Mountain Paleogeography Symposium 3: Denver, Colorado, The Rocky Mountain section, Society of Economic Paleontologists and Mineralogists, p. 359-382.

Christiansen, R.L., 1984, Yellowstone magmatic evolution: its bearing on understanding large-volume explosive volcanism, *in* Explosive volcanisn: inception, evolution, and hazards: National Academy Press, p. 84-95.

Christiansen, R.L., and Blank, H.R., Jr., 1972, Volcanic stratigraphy of the Quaternary rhyolite plateau in Yellowstone National Park: U.S. Geological Survey Professional Paper 729-B, 18 p.

Clemens, W.A., Lillegraven, J.A., Lindsay, E.H., and Simpson, G.G., 1979, Where, when, and what—a survey of known Mesozoic mammal distribution, *in* Lillegraven, J.A., Kielan-Jaworowska, Z., and Clemens, W.A., editors, Mesozoic mammals: the first two-thirds of mammalian history: Berkeley, University of California Press, p. 7-58.

Condie, K.C., 1969, Geologic evolution of the Precambrian rocks in northern Utah and adjacent areas: Utah Geologic Survey Bulletin 82, p. 71-95.

_____ 1982, Plate-tectonics model for Proterozoic continental accretion in the southwestern United States: Geology, v. 10, p. 37-42.

Condie, K.C., and Shadel, G.A., 1984, An Early Proterozoic volcanic arc succession in southeastern Wyoming: Canadian Journal of Earth Science, v. 21, p. 415-427.

Coney, P.J., 1972, Cordilleran tectonics and North American plate motion: American Journal of Science, v. 272, p. 603-628.

_____ 1978, Mesozoic-Cenozoic Cordilleran plate tectonics, *in* Smith, R.B., and Eaton, G.P., editors, Cenozoic tectonics and regional geophysics of the western Cordillera: Geological Society of America Memoir 152, p. 33-50.

_____ 1987, Circum-Pacific tectogenesis in the North America Cordillera, *in* Monger, J.W.H., and Francheteau, J., editors, Circum-Pacific orogenic belts and evolution of the Pacific Ocean Basin: American Geophysical Union Geodynamics Series, volume 18, p. 59-69.

Coney, P.J., and Harms, T.A., 1984, Cordilleran metamorphic core complexes: Cenozoic extensional

relics of Mesozoic compression: Geology, v. 12, p. 550-554.

Coney, P.J., and Reynolds, S.J., 1977, Cordilleran Benioff zones: Nature, v. 270, p. 403-406.

Crosby, G.W., 1968, Vertical movement and isostasy in western Wyoming overbelt belt: American Association of Petroleum Geologists Bulletin, v. 52, p. 2000-2015.

Cross, T.A., 1986, Tectonic controls of foreland basin subsidence and Laramide style deformation, western United States, *in* Allen, P.A., and Homewood, P., editors, Foreland basins: International Association of Sedimentologists Special Publication no. 8, p. 15-39.

Cross, T.A., and Pilger, R.H., Jr., 1978a, Tectonic controls of Late Cretaceous sedimentation, western interior, USA: Nature, v. 274, p. 653-657.

_____ 1978b, Constraints on absolute motion and plate interaction inferred from Cenozoic igneous activity in the western United States: American Journal of Science, v. 278, p. 865-902.

Dahlstrom, C.D.A., 1970, Structural geology in the eastern margin of the Canadian Rocky Mountains: Bulletin of Canadian Petroleum Geology, v. 18, p. 332-406.

Dana, J.D., 1895, Manual of geology [4th edition]: New York, American Book Company, 1087 p.

Darton, N.H., 1899, Geology and water resources of Nebraska west of the one hundred and third meridian: U.S. Geological Survey 19th Annual Report, part 4, p. 719-785.

de Cserna, Z., 1989, An outline of the geology of Mexico, *in* Bally, A.W., and Palmer, A.R., editors, The Geology of North America—An overview: Boulder, Colorado, Geological Society of America, The Geology of North America, v. A, p. 233-264.

Denson, N.M., 1965, Miocene and Pliocene rocks of central Wyoming, *in* Cohee, G.V., and West, W.S., editors, Changes in stratigraphic nomenclature by the U.S. Geological Survey, 1964: U.S. Geological Survey Bulletin 1224-A, p. A70-A74.

Denson, N.M., and Bergendahl, M.H., 1961, Middle and upper Tertiary rocks in southeastern Wyoming and adjoining areas: U.S. Geological Professional Paper 424-C, p. C168-C172.

Denson, N.M., and Chisholm, W.A., 1971, Summary of mineralogic and lithologic characteristics of Tertiary sedimentary rocks in the middle Rocky Mountains and the northern Great Plains: U.S. Geological Survey Professional Paper 750-C, p. C117-C126.

Devlin, W.J., and Bond, G.C., 1988, The initiation of the early Paleozoic Cordilleran miogeocline: evidence from the uppermost Proterozoic - Lower Cambrian Hamill Group of southeastern British Columbia: Canadian Journal of Earth Sciences, v. 25, p. 1-19.

DeWitt, E., Redden, J.A., Wilson, A.B., and Buscher, D., 1986, Mineral resource potential and geology of the Black Hills National Forest, South Dakota and Wyoming: U.S. Geological Survey Bulletin 1580, 135 p.

Dickinson, W.R., 1991, Tectonic setting of faulted Tertiary strata associated with the Catalina core complex in southern Arizona: Geological Society of America Special Paper 264, 106 p.

Dickinson, W.R., and Snyder, W.S., 1978, Plate tectonics of the Laramide orogeny, *in* Matthews, V., III, editor, Laramide folding associated with basement block faulting in the western United States: Geological Society of America Memoir 151, p. 355-366.

Dickinson, W.R., Klute, M.A., Hayes, M.J., Janecke, S.U., Lundin, E.R., McKittrick, M.A., and Olivares, M.D., 1988, Paleogeographic and paleotectonic setting of Laramide sedimentary basins in the Central Rocky Mountain region: Geological Society of America Bulletin, v. 100, p. 1023-1039.

Divis, A.F., 1976, Geology and geochemistry of the Sierra Madre Range [*sic*], Wyoming: Colorado School of Mines Quarterly, v. 71, no. 3, 127 p.

Dorf, E., 1959, Climatic changes of the past and present: University of Michigan Museum Paleontology Contributions, v. 13, no. 8, p. 181-210.

Doser, D.I., 1985, Source parameters and faulting processes of the 1959 Hebgen Lake, Montana, earthquake sequence: Journal of Geophysical Research, v. 90, p. 4537-4555.

Dott, R.H., Jr., and Batten, R.L., 1981, Evolution of the Earth (3rd edition): New York, McGraw-Hill Book Company, 573 p.

Dudás, F.Ö., 1991, Geochemistry of igneous rocks from the Crazy Mountains, Montana, and tectonic models for the Montana alkalic province: Journal of Geophysical Research, v. 96, p. 13,261-13,277.

Duebendorfer, E.M., and Houston, R.S., 1986, Kinematic history of the Cheyenne belt, Medicine Bow Mountains, southeastern Wyoming: Geology, v. 14, p. 171-174.

_____ 1987, Proterozoic accretionary tectonics at the southern margin of the Archean Wyoming craton: Geological Society of America Bulletin, v. 98, p. 554-568.

Eaton, G.P., 1986, A tectonic redefinition of the Southern Rocky Mountains: Tectonophysics, v. 132, p. 163-193.

Eaton, G.P., Christiansen, R.L., Iyer, H.M., Pitt, A.M., Mabey, D.R., Blank, H.R., Jr., Zietz, I., and Gettings, M.E., 1975, Magma beneath Yellowstone National Park: Science, v. 188, p. 787-796.

Eggler, D.H., 1968, Virginia Dale Precambrian ring-dike complex, Colorado-Wyoming: Geological Society of America Bulletin, v. 79, p. 1545-1564.

Eggler, D.H., Meen, J.K., Welt, F., Dudás, F.Ö., Furlong, K.P., McCallum, M.E., and Carlson, R.W., 1988, Tectonomagmatism of the Wyoming Province, *in* Drexler, J.W., and Larson, E.E., editors, Cenozoic volcanism in the Southern Rocky Mountains revisited: a tribute to Rudy C. Epis - Part 3: Colorado School of Mines Quarterly, v. 83, no. 2, p. 25-40.

Eisbacher, G.H., 1985, Pericollisional strike-slip faults and synorogenic basins, Canadian Cordillera, *in* Biddle, K.T., and Christie-Blick, N., editors, Strike-slip deformation, basin formation, and sedimentation: Society of Economic Paleontologists and Mineralogists Special Publication No. 37, p. 265-282.

Engebretson, D.C., Cox, A., and Gordon, R.G., 1985, Relative motions between oceanic and continental plates in the Pacific Basin: Geological Society of America Special Paper 206, 59 p.

Engebretson, D.C., Cox, A.V., and Thompson, G.A., 1982, Convergence and tectonics: Laramide to Basin and Range, EOS, v. 63, p. 911.

_____ 1984, Correlation of plate motions with continental tectonics: Laramide to Basin-Range: Tectonics, v. 3, p. 115-119.

Engel, A.E.J., 1963, Geologic evolution of North America: Science, v. 140, p. 143-152.

Epis, R.C., and Chapin, C.E., 1975, Geomorphic and tectonic implications of the post-Laramide, late Eocene erosion surface in the southern Rocky Mountains, *in* Curtis, B.F., editor, Cenozoic history of the southern Rocky Mountains: Geological Society of America Memoir 144, p. 45-74.

Erslev, E.A., 1986, Basement balancing of Rocky Mountain foreland uplifts: Geology, v. 14, p. 259-262.

_____ 1991, Trishear fault-propagation folding: Geology, v. 19, p. 617-620.

Eugster, H.P., and Hardie, L.A., 1975, Sedimentation in an ancient playa-lake complex: the Wilkins Peak Member of the Green River Formation of Wyoming: Geological Society of America Bulletin, v. 86, p. 319-334.

Eugster, H.P., and Surdam, R.C., 1973, Depositional environment of the Green River Formation of Wyoming: a preliminary report: Geological Society of America Bulletin, v. 84, p. 1115-1120.

Evanoff, E., 1990, Early Oligocene paleovalleys in southern and central Wyoming: evidence of high local relief on the late Eocene unconformity: Geology, v. 18, p. 443-446.

Fenneman, N.M., 1931, Physiography of western United States: New York, McGraw-Hill Book Company, 534 p.

Frost, C.D., Meier, M., and Oberli, F., 1990, Single zircon U-Pb age determination of the Red Mountain pluton, Laramie Anorthosite Complex, Wyoming: American Mineralogist, v. 75, p. 21-26.

Frost, C.D., and Winston, D., 1987, Nd isotope systematics of coarse- and fine-grained sediments: examples from the Middle Proterozoic Belt-Purcell Supergroup: Journal of Geology, v. 95, p. 309-327.

Gibbs, F.K., 1972, Silurian System, *in* Mallory, W.W., and others, editors, Geologic atlas of the Rocky Mountain region: Rocky Mountain Association of Geologists, Denver, Colorado, p. 86-89.

Gilbert, J.D., Ostenaa, D., and Wood, C., 1983, Seismotectonic study; Jackson Lake Dam and Reservoir, Minidoka Project, Idaho-Wyoming: U.S. Bureau of Reclamation Seismotectonic Report 83-8, 123 p.

Grand, S.P., 1987, Tomographic inversion for shear velocity beneath the North American plate: Journal of Geophysical Research, v. 92, p. 14,065-14,090.

Graubard, C.M., 1991, Extension in a transpressional setting: emplacement of the mid-Proterozoic Mt. Evans batholith, central Front Range, Colorado: Geological Society of America Abstracts with Programs, v. 23, no. 4, p. 27.

Gregory, K.M., and Chase, C.G., 1992, Tectonic significance of paleobotanically estimated climate and altitude of the late Eocene erosion surface, Colorado: Geology, v. 20, p. 581-585.

Gresens, R.L., 1981, Extension of the Telluride erosion surface to Washington State, and its regional and tectonic significance: Tectonophysics, v. 79, p. 145-164.

Gries, R.R., 1983, North-south compression of Rocky Mountain foreland structures, *in* Lowell, J.D., editor, Rocky Mountain foreland basins and uplifts: Rocky Mountain Association of Geologists, p. 9-32.

Hadley, J.B., 1964, Landslides and related phenomena accompanying the Hebgen Lake earthquake of August 17, 1959: U.S. Geological Survey Professional Paper 435-K, p. 107-138.

Hague, A., Iddings, J.P., Weed, W.H., Walcott, C.D., Girty, G.H., Stanton, T.W., and Knowlton, F.H., 1899, Descriptive geology, petrography, and paleontology, Part II of Geology of the Yellowstone National Park: U.S. Geological Survey Monograph 32, 893 p. and atlas of 27 sheets folio.

Hague, A., Weed, W.H., and Iddings, J.P., 1896, Description of the Yellowstone National Park quadrangle [Wyoming]: U. S. Geological Survey Geologic Atlas, Folio 30.

Hall, M.K., and Chase, C.G., 1989, Uplift, unbuckling, and collapse: flexural history and isostasy of the Wind River Range and Granite Mountains, Wyoming: Journal of Geophysical Research, v. 94, p. 17,581-17,593.

Hallam, A., 1984, Pre-Quaternary sea-level changes: Annual Review of Earth and Planetary Sciences, v. 12, p. 205-243.

Hamilton, W., 1978, Mesozoic tectonics of the western United States, *in* Howell, D.G., and McDougall, K.A., editors, Mesozoic paleogeography of the western United States, Pacific Coast Paleogeography Symposium 2, Los Angeles, California, The Pacific Section, Society of Economic Paleontologists and Mineralogists, p. 33-70.

_____ 1981, Plate-tectonic mechanism of Laramide deformation: University of Wyoming Contributions to Geology, v. 19, no. 2, p. 87-92.

_____ 1988a, Tectonic setting and variations with depth of some Cretaceous and Cenozoic structural and magmatic systems of the western United States, *in* Ernst, W.G., editor, Metamorphism and crustal evolution of the western United States, Rubey Volume VII: Englewood Cliffs, New Jersey, Prentice Hall, p. 1-40.

_____ 1988b, Laramide crustal shortening, *in* Schmidt, C.J., and Perry, W.J., Jr., editors, Interaction of the Rocky Mountain foreland and the Cordilleran thrust belt: Geological Society of America Memoir 171, p. 27-39.

_____ 1989, Crustal geologic processes of the United States, *in* Pakiser, L.C., and Mooney, W.D., editors, Geophysical framework of the continental United States: Boulder, Colorado, Geological Society of America Memoir 172, p. 743-781.

Hancock, J.M., and Kauffman, E.G., 1979, The great transgressions of the Late Cretaceous: Journal of the Geological Society, London: v. 136, p. 175-186.

Hansen, W.R., 1965, Geology of the Flaming Gorge area, Utah-Colorado-Wyoming: U. S. Geological Survey Professional Paper 490, 196 p.

_____ 1985, Drainage development of the Green River Basin in southwestern Wyoming and its bearing on fish biogeography, neotectonics, and paleoclimates: The Mountain Geologist, v. 22, p. 192-204.

Harrison, J.E., 1972, Precambrian Belt basin of northwestern United States: its geometry, sedimentation, and copper occurrences: Geological Society of America Bulletin, v. 83, p. 1215-1240.

Hauge, T.A., 1985, Gravity-spreading origin of the Heart Mountain allochthon, northwestern Wyoming: Geological Society of America Bulletin, v. 96, p. 1440-1456.

_____ 1990, Kinematic model of a continuous Heart Mountain allochthon: Geological Society of America Bulletin, v. 102, p. 1174-1188.

Hearn, B.C., Jr., 1989, Introduction - T346 Montana high-potassium igneous province, *in* Montana high-potassium igneous province, 28th International Geological Congress Field Trip Guidebook T346: Washington, D.C., American Geophysical Union, p. 1-5.

Heller, P.L., Bowdler, S.S., Chambers, H.P., Coogan, J.C., Hagen, E.S., Shuster, M.W., and Winslow, N.S., 1986, Time of initial thrusting in the Sevier orogenic belt, Idaho-Wyoming and Utah: Geology, v. 14, p. 388-391.

Heller, P.L., and Paola, C., 1989, The paradox of Lower Cretaceous gravels and the initiation of thrusting in the Sevier orogenic belt, United States Western Interior: Geological Society of America Bulletin, v. 101, p. 864-875.

Heller, P.L., Tabor, R.W., and Suczek, C.A., 1987, Paleogeographic evolution of the United States Pacific Northwest during Paleogene time: Canadian Journal of Earth Sciences, v. 24, p. 1652-1667.

Henderson, L.J., Gordon, R.G., and Engebretson, D.C., 1984, Mesozoic aseismic ridges on the Farallon plate and southward migration of shallow subduction during the Laramide orogeny: Tectonics, v. 3, p. 121-132.

Herrin, E., and Taggart, J., 1968, Regional variations in *P* travel times: Seismological Society of America Bulletin, v. 58, p. 1325-1337.

Hills, F.A., and Houston, R.S., 1979, Early Proterozoic tectonics of the central Rocky Mountains, North America: University of Wyoming Contributions to Geology, v. 17, p. 89-109.

Hoffman, P.F., 1988, United plates of America, the birth of a craton: Early Proterozoic assembly and growth of Laurentia: Annual Reviews of Earth and Planetary Science, v. 16, p. 543-603.

_____ 1989a, Speculations on Laurentia's first gigayear (2.0 to 1.0 Ga): Geology, v. 17, p. 135-138.

_____ 1989b, Precambrian geology and tectonic history of North America, *in* Bally, A.W., and Palmer, A.R., editors, The Geology of North America—An overview: Boulder, Colorado, Geological Society of America, The Geology of North America, v. A, p. 447-512.

_____ 1991, Did the breakout of Laurentia turn Gondwanaland inside-out?: Science, v. 252, p. 1409-1412.

Houston, R.S., and McCallum, M.E., 1961, Mullen Creek-Nash Fork shear zone, Medicine Bow Mountains, southeastern Wyoming [abstract]: Geological Society of America Special Paper 68, p. 91.

Houston, R.S., Karlstrom, K.E., Hills, F.A., and Smithson, S.B., 1979, The Cheyenne belt: a major Precambrian crustal boundary in the western United States: Geological Society of America Abstracts with Programs, v. 11, p. 446.

Hudson, F.S., 1955, Folding of unmetamorphosed strata superjacent to massive basement rocks: American Association of Petroleum Geologists Bulletin, v. 39, p. 2038-2052.

Huntoon, P.W., 1990, Phanerozoic structural geology of the Grand Canyon, *in* Beus, S.S., and Morales, M., editors, Grand Canyon geology: New York, Oxford University Press, p. 261-309.

Izett, G.A., and Wilcox, R.E., 1981, Map showing localities and inferred distributions of the Huckleberry Ridge, Mesa Falls, and Lava Creek ash beds (Pearlette family ash beds) of Pliocene and Pleistocene age in the western United States and southern Canada: U.S. Geological Survey Miscellaneous Investigations Map I-1325, scale 1:4,000,000.

Jacobson, C.E., 1983, Structural geology of the Pelona Schist and Vincent thrust, San Gabriel Mountains, California: Geological Society of America Bulletin, v. 94, p. 753-767.

Johnson, R.A., Karlstrom, K.E., Smithson, S.B., and Houston, R.S., 1984, Gravity profiles across the Cheyenne belt: a Precambrian crustal suture in southeastern Wyoming: Journal of Geodynamics, v. 1, p. 445-472.

Jordan, T.E., 1981, Thrust loads and foreland basin evolution, Cretaceous, western United States: American Association of Petroleum Geologists Bulletin, v. 65, p. 291-329.

Jordan, T.E., and Allmendinger, R.W., 1986, The Sierras Pampeanas of Argentina—a modern analog of Rocky Mountain foreland deformation: American Journal of Science, v. 286, p. 737-764.

Jurdy, D.M., 1984, The subduction of the Farallon plate beneath North America as derived from relative plate motions: Tectonics, v. 3, p. 107-113.

Kanter, L.R., Dyer, R., and Dohmen, T.E., 1981, Laramide crustal shortening in the northern Wyoming province: University of Wyoming Contributions to Geology, v. 19, no. 2, p. 135-142.

Karlstrom, K.E., Flurkey, A.J., and Houston, R.S., 1983, Stratigraphy and depositional setting of Proterozoic metasedimentary rocks in southeastern Wyoming: record of an Early Proterozoic Atlantic-type cratonic margin: Geological Society of America Bulletin, v. 94, p. 1257-1294.

Karlstrom, K.E., and Houston, R.S., 1984, The Cheyenne belt: analysis of a Proterozoic suture in southern Wyoming: Precambrian Research, v. 25, p. 415-446.

Karlstrom, K.E., and Bowring, S.A., 1988, Early Proterozoic assembly of tectonostratigraphic terranes in southwestern North America: Journal of Geology, v. 96, p. 561-576.

Kauffman, E.G., 1977, Geological and biological overview: Western Interior Cretaceous basin, *in* Kauffman, E.G., editor, Cretaceous facies, faunas, and paleoenvironments across the Western Interior basin: The Mountain Geologist, v. 14, p. 75-99.

King, P.B., [1967] 1970, Tectonic features, *in* The national atlas of the United States: United States Department of Interior, Geological Survey, p. 70-71, scale 1:7,500,000.

King, P.B., compiler, 1969, Tectonic map of North America: U.S. Geological Survey, scale 1:5,000,000.

King, P.B., and Beikman, H.M., 1974, Geologic map of the United States (exclusive of Alaska and Hawaii): U.S. Geological Survey, scale 1:2,500,000.

_____ 1978, The Cenozoic rocks; a discussion to accompany the Geologic map of the United States: U.S. Geological Survey Professional Paper 904, 82 p.

King, P.B., and Edmonston, G.J., 1972, Generalized tectonic map of North America: U.S. Geological Survey Miscellaneous Geologic Investigations Map I-688, scale 1:15,000,000.

Klein, T.L., 1980, The geology and geochemistry of the sulfide deposits of the Seminoe District, Carbon County, Wyoming [Ph.D. dissertation]: Golden, Colorado School of Mines, 232 p.

Kluth, C.F., 1986, Plate tectonics of the Ancestral Rocky Mountains, *in* Peterson, J.A., editor, Paleotectonics and sedimentation in the Rocky Mountain region, United States: American Association of Petroleum Geologists Memoir 41, p. 353-369.

Kluth, C.F., and Coney, P.J., 1981, Plate tectonics of the Ancestral Rocky Mountains: Geology, v. 9, p. 10-15.

Knight, S.H., 1929, The Fountain and the Casper formations of the Laramie Basin: University of Wyoming Publications in Science, Geology, v. 1, no. 1, 82 p.

_____ 1953, Summary of the Cenozoic history of the Medicine Bow Mountains, Wyoming: Wyoming Geological Association 8th Annual Field Conference Guidebook, p. 65-76.

_____ 1974, Geologic history of Wyoming landscapes, *in* Wilson, M., editor, Applied geology and archaeology: the Holocene history of Wyoming: Wyoming Geological Survey Report of Investigations 10, p. 1-7.

Kocurek, G., and Dott, R.H., Jr., 1983, Jurassic paleogeography and paleoclimate of the central and southern Rocky Mountains region, *in* Reynolds, M.W., and Dolly, E.D., editors, Mesozoic paleogeography of the west-central United States, Rocky Mountain Paleogeography Symposium 2: Denver, Colorado, The Rocky Mountain Section, Society of Economic Paleontologists and Mineralogists, p. 101-116.

Lageson, D.R., 1987, Laramide uplift of the Gros Ventre Range and implications for the origin of the Teton fault, Wyoming, *in* Miller, W.R., editor, The thrust belt revisited: Wyoming Geological Association 38th Annual Field Conference Guidebook, p. 79-89.

_____ 1989, Reactivation of a Proterozoic continental margin, Bridger Range, southwestern Montana, *in* French, D.E., and Grabb, R.F., editors, Geological resources of Montana, vol. 1: Montana Geological Society Field Conference Guidebook, p. 279-298.

_____ 1992, Possible Laramide influence on the Teton normal fault, western Wyoming, *in* Link, P.K., Kuntz, M.A., and Platt, L.B., editors, Regional geology of eastern Idaho and western Wyoming: Geological Society of America Memoir 179, p. 183-196.

Lageson, D.R., Maughan, E.K., and Sando, W.J., 1979, The Mississippian and Pennsylvanian (Carboniferous) Systems in the United States—Wyoming: U.S. Geological Survey Professional Paper 1110-U, p. U1-U38.

Lamerson, P.R., 1982, The Fossil basin and its relationship to the Absaroka thrust system, Wyoming and Utah, *in* Powers, R.B., editor, Geologic studies of the Cordilleran thrust belt: Denver, Colorado, Rocky Mountain Association of Geologists, p. 279-340.

Larson, T.A., 1978, History of Wyoming (2nd edition, revised): Lincoln, Nebraska, University of Nebraska Press, 663 p.

Leeman, W.P., 1982, Development of the Snake River Plain - Yellowstone Plateau Province, Idaho and Wyoming: an overview and petrologic model, *in* Bonnichsen, B., and Breckenridge, R.M., editors, Cenozoic geology of Idaho: Idaho Bureau of Mines and Geology Bulletin 26, p. 155-177.

Leeman, W.P., Menzies, M.A., Matty, D.J., and Embree, G.F., 1985, Strontium, neodymium and lead isotopic compositions of deep crustal xenoliths from the Snake River Plain: evidence for Archean basement: Earth and Planetary Science Letters, v. 75, p. 354-368.

Lees, G.M., 1952, Foreland folding: The Quarterly Journal of the Geological Society of London, v. 108, p. 1-34.

Lillegraven, J.A., and Ostresh, L.M., Jr., 1988, Evolution of Wyoming's early Cenozoic topography and drainage patterns: National Geographic Research, v. 4, p. 303-327.

_____ 1990, Late Cretaceous (earliest Campanian/Maastrichtian) evolution of western shorelines of the North American Western Interior Seaway in relation to known mammalian faunas, *in* Bown, T.M., and Rose, K.D., editors, Dawn of the Age of Mammals in the northern part of the Rocky Mountain Interior,

North America: Geological Society of America Special Paper 243, p. 1-30.

Livaccari, R.F., Burke, K., and Sengör, A.M.C., 1981, Was the Laramide orogeny related to subduction of an oceanic plateau?: Nature, v. 289, p. 276-278.

Lochman-Balk, C., 1972, Cambrian System, *in* Mallory, W.W., and others, editors, Geologic atlas of the Rocky Mountain region: Denver, Colorado, Rocky Mountain Association of Geologists, p. 60-75.

Love, J.D., 1939, Geology along the southern margin of the Absaroka Range, Wyoming: Geological Society of America Special Paper 20, 134 p.

_____ 1941, Geology along the southern margin of the Absaroka Range, Wyoming: Journal of Geology, v. 49, p. 101-106.

_____ 1960, Cenozoic sedimentation and crustal movement in Wyoming: American Journal of Science, v. 258-A, p. 204-214.

_____ 1961, Split Rock Formation (Miocene) and Moonstone Formation (Pliocene) in central Wyoming: U.S. Geological Survey Bulletin 1121-I, 39 p.

_____ 1970, Cenozoic geology of the Granite Mountains area, central Wyoming: U.S. Geological Survey Professional Paper 495-C, 154 p.

Love, J.D., McGrew, P.O., and Thomas, H.D., 1963, Relationship of latest Cretaceous and Tertiary deposition and deformation to oil and gas in Wyoming, *in* Childs, O.E., and Beebe, B.W., editors, Backbone of the Americas—tectonic history from pole to pole, a symposium: American Association of Petroleum Geologists Memoir 2, p. 196-208.

Love, J.D., and Reed, J.C., Jr., 1971, Creation of the Teton landscape—the geologic story of Grand Teton National Park: Grand Teton Natural History Association, 120 p.

Love, J.D., Reed, J.C., Jr., Christiansen, R.L., and Stacy, J.R., 1973, Geologic block diagram and tectonic history of the Teton region, Wyoming-Idaho: U.S. Geological Survey Miscellaneous Geological Investigations Map I-730.

Love, J.D., McKenna, M.C., and Dawson, M.R., 1976, Eocene, Oligocene, and Miocene rocks and vertebrate fossils at the Emerald Lake locality, 3 miles south of Yellowstone National Park, Wyoming: U.S. Geological Survey Professional Paper 932-A, 28 p.

Love, J.D., and Christiansen, A.C., 1985, Geologic map of Wyoming: U.S. Geological Survey, scale 1:500,000.

Love, L.L., Kudo, A.M., and Love, D.W., 1976, Dacites of Bunsen Peak, the Birch Hills, and the Washakie Needles, northwestern Wyoming, and their relationship to the Absaroka volcanic field, Wyoming and Montana: Geological Society of America Bulletin, v. 87, p. 1455-1462.

Lowell, J.D., 1974, Plate tectonics and foreland basement deformation: Geology, v. 2, p. 275-278.

Lush, A.P., McGrew, A.J., Snoke, A.W., and Wright, J.E., 1988, Allochthonous Archean basement in the northern East Humboldt Range, Nevada: Geology, v. 16, p. 349-353.

Mackin, J.H., 1947, Altitude and local relief of the Bighorn area during the Cenozoic: University of Wyoming - Wyoming Geological Association - Yellowstone-Bighorn Research Association Field Conference in the Bighorn Basin, p. 103-120.

Mallory, W.W., 1963, Pathfinder uplift of Pennsylvanian age in southern Wyoming: U.S. Geological Survey Professional Paper 450-E, p. E57-E60.

_____ 1967, Pennsylvanian and associated rocks in Wyoming: U.S. Geological Survey Professional Paper 554-G, 31 p.

Matthews, V., III, 1986, A case for brittle deformation of the basement during the Laramide revolution in the Rocky Mountain foreland province: The Mountain Geologist, v. 23, p. 1-5.

McDowell, F.W., 1971, K-Ar ages of igneous rocks from the western United States: Isochron/West, v. 2, p. 1-16.

McGookey, D.P., Haun, J.D., Hale, L.A., Goodell, H.G., McCubbin, D.G., Weimer, R.J., and Wulf, G.R., 1972, Cretaceous system, *in* Mallory, W.W., and others, editors, Geologic atlas of the Rocky Mountain region: Denver, Colorado, Rocky Mountain Association of Geologists, p. 190-228.

McGrew, L.W., 1963, Geology of the Fort Laramie area, Platte and Goshen Counties, Wyoming: U.S. Geological Survey Bulletin 1141-F, 39 p.

McGrew, P.O., 1971, The Tertiary history of Wyoming, *in* Renfro, A.R., editor, Symposium on Wyoming tectonics and their economic significance: Wyoming Geological Association 23rd Annual Field Conference Guidebook, p. 29-33.

Meen, J.K., and Eggler, D.H., 1987, Petrology and geochemistry of the Cretaceous Independence volcanic suite, Absaroka Mountains, Montana: Clues to the composition of the Archean sub-Montanan

mantle: Geological Society of America Bulletin, v. 98, p. 238-247.

Miller, D.M., Nilsen, T.H., and Bilodeau, W.L., 1992, Late Cretaceous to early Eocene geologic evolution of the U.S. Cordillera, *in* Burchfiel, B.C., Lipman, P.W., and Zoback, M.L., editors, The Cordilleran Orogen: Conterminous U. S.: Boulder, Colorado, Geological Society of America, The Geology of North America, v. G-3, p. 205-260.

Miller, E.L., and Gans, P.B., 1989, Cretaceous crustal structure and metamorphism in the hinterland of the Sevier thrust belt, western U.S. Cordillera: Geology, v. 17, p. 59-62.

Misch, P., 1960, Regional structural reconnaissance in central-northeast Nevada and some adjacent areas: Observations and interpretations, *in* Guidebook to the geology of east central Nevada: Intermountain Association of Petroleum Geologists 11th Annual Field Conference, p. 17-42.

Minster, J.B., and Jordan, T.H., 1978, Present-day plate motions: Journal of Geophysical Research, v. 83, p. 5331-5354.

Mitra, G., and Frost, B.R., 1981, Mechanisms of deformation within Laramide and Precambrian deformation zones in basement rocks of the Wind River Mountains: University of Wyoming Contributions to Geology, v. 19, no. 2, p. 161-173.

Mitra, G., Hull, J.M., Yonkee, W.A., and Protzman, G.M., 1988, Comparison of mesoscopic and microscopic deformational styles in the Idaho-Wyoming thrust belt and the Rocky Mountain foreland, *in* Schmidt, C.J., and Perry, W.J., Jr., editors, Interaction of the Rocky Mountain foreland and the Cordilleran thrust belt: Geological Society of America Memoir 171, p. 119-141.

Mitrovica, J.X., Beaumont, C., and Jarvis, G.T., 1989, Tilting of continental interiors by the dynamical effects of subduction: Tectonics, v. 8, p. 1079-1094.

Molnar, P., and England, P., 1990, Late Cenozoic uplift of mountain ranges and global climate change: chicken or egg?: Nature, v. 346, p. 29-34.

Moore, F.E., 1959, The geomorphic evolution of the east flank of the Laramie Range, Colorado and Wyoming [Ph.D. dissertation]: Laramie, University of Wyoming, 123 p.

Morgan, W.J., 1972, Plate motions and deep mantle convection: Geological Society of America Memoir 132, p. 7-22.

Mudge, M.R., 1970, Origin of the disturbed belt in northwestern Montana: Geological Society of America Bulletin, v. 81, p. 377-392.

Mueller, P.A., Wooden, J.L., and Nutman, A.P., 1992, 3.96 Ga zircons from an Archean quartzite, Beartooth Mountains, Montana: Geology, v. 20, p. 327-330.

Murphy, L.M., and Brazee, R.J., 1964, Seismological investigations of the Hebgen Lake earthquake: U. S. Geological Survey Professional Paper 435-C, p. 13-17.

Mutschler, F.E., Larson, E.E., and Bruce, R.M., 1987, Laramide and younger magmatism in Colorado—new petrologic and tectonic variations on old themes, *in* Drexler, J.W., and Larson, E.E., editors, Cenozoic volcanism on the Southern Rocky Mountains updated: a tribute to Rudy C. Epis - Part 1: Colorado School of Mines Quarterly, v. 82, no. 4, p. 1-47.

Myers, W.B., and Hamilton, W., 1964, Deformation accompanying the Hebgen Lake earthquake of August 17, 1959: U.S. Geological Survey Professional Paper 435-I, p. 55-98.

Nace, R.L., 1939, Geology of the northwest part of the Red Desert, Sweetwater and Fremont Counties, Wyoming: Geological Survey of Wyoming Bulletin 27, 51 p.

Nelson, B.K., and DePaolo, D.J., 1985, Rapid production of continental crust 1.7 to 1.9 b.y. ago: Nd isotopic evidence from the basement of the North American mid-continent: Geological Society of America Bulletin, v. 96, p. 746-754.

O'Brien, H.E., Irving, A.J., and McCallum, I.S., 1991, Eocene potassic magmatism in the Highwood Mountains, Montana: petrology, geochemistry, and tectonic implications: Journal of Geophysical Research, v. 96, p. 13,237-13,260.

Oldow, J.S., Bally, A.W., Avé Lallemant, H.G., and Leeman, W.P., 1989a, Phanerozoic evolution of the North American Cordillera; United States and Canada, *in* Bally, A.W., and Palmer, A.R., editors, The Geology of North America—An overview: Boulder, Colorado, Geological Society of America, The Geology of North America, v. A, p. 139-232.

_____ 1989b, Structural cross-sections of the Cordillera, *in* Bally, A.W., and Palmer, A.R., editors, The Geology of North America—An overview: Boulder, Colorado, Geological Society of America, v. A, plate 7.

Oldow, J.S., Bally, A.W., and Avé Lallemant, H.G., 1990, Transpression, orogenic float, and lithospheric balance: Geology, v. 18, p. 991-994.

O'Neill, J.M., and Lopez, D.A., 1985, Character and regional significance of Great Falls tectonic zone, east-central Idaho and west-central Montana: American Association of Petroleum Geologists Bulletin, v. 69, p. 437-447.

O'Neill, J.M., and Harlan, S.S., 1992, Montana has an Early Proterozoic history: Geological Society of America Abstracts with Programs, v. 24, no. 6, p. 56.

Palmer, A.R., 1983, Decade of North American Geology 1983 geologic time scale: Geology, v. 11, p. 503-504.

Pekarek, A.H., Marvin, R.F., and Mehnert, H.H., 1974, K-Ar ages of the volcanics in the Rattlesnake Hills, central Wyoming: Geology, v. 2, p. 283-285.

Perry, W.J., Jr., Weaver, J.N., Flores, R.M., Roberts, S.B., and Nichols, D.J., 1991, Sequential Laramide deformation in Montana and Wyoming: Geological Society of America Abstracts with Programs, v. 23, no. 4, p. 56.

Peterman, Z.E., and Hildreth, R.A., 1978, Reconnaissance geology and geochronology of the Precambrian of the Granite Mountains, Wyoming: U.S. Geological Survey Professional Paper 1055, 22 p.

Peterson, J.A., 1984, Permian stratigraphy, sedimentary facies, and petroleum geology, Wyoming and adjacent area: Wyoming Geological Association 35th Annual Field Conference Guidebook, p. 25-64.

_____ 1988, Phanerozoic stratigraphy of the northern Rocky Mountain region, *in* Sloss, L.L., editor, Sedimentary cover—North American craton; U.S.: Boulder, Colorado, Geological Society of America, The Geology of North America, v. D-2, p. 83-107.

Peterson, J.A., and Smith, D.L., 1986, Rocky Mountain paleogeography through geologic time, *in* Peterson, J.A., editor, Paleotectonics and sedimentation in the Rocky Mountain region, United States: American Association of Petroleum Geologists Memoir 41, p. 3-19.

Picard, M.D., Aadland, R., and High, L.R., Jr., 1969, Correlation and stratigraphy of Triassic Red Peak and Thaynes formations, western Wyoming and adjacent Idaho: American Association of Petroleum Geologists Bulletin, v. 53, p. 2274-2289.

Pierce, K.L., and Morgan, L.A., 1992, The track of the Yellowstone hot spot: volcanism, faulting, and uplift, *in* Link, P.K., Kuntz, M.A., and Platt, L.B., editors, Regional geology of eastern Idaho and western Wyoming: Geological Society of America Memoir 179, p. 1-53.

Pierce, W.G., 1960, The "break-away" point of the Heart Mountain detachment fault in northwestern Wyoming, *in* Geological Survey Research 1960, Short papers in the geological sciences: U.S. Geological Survey Professional Paper 400-B, B236-B237.

_____ 1963, Reef Creek detachment fault, northwestern Wyoming: Geological Society of America Bulletin, v. 74, p. 1225-1236.

_____ 1973, Principal features of the Heart Mountain fault and the mechanism problem, *in* DeJong, K.A., and Scholten, R., editors, Gravity and tectonics: New York, John Wiley & Sons, p. 457-471.

_____ 1980, The Heart Mountain break-away fault northwestern Wyoming: Geological Society of America Bulletin, Part 1, v. 91, p. 272-281.

_____ 1987, The case for tectonic denudation by the Heart Mountain fault—a response: Geological Society of America Bulletin, v. 99, p. 552-568.

Pindell, J.L., and Barrett, S.F., 1990, Plate 12. Caribbean plate tectonic history, *in* Dengo, G., and Case, J.E., editors, The Caribbean region: Boulder, Colorado, Geological Society of America, The Geology of North America, v. H.

Pipiringos, G.N., 1968, Correlation and nomenclature of some Triassic and Jurassic rocks in south-central Wyoming: U.S. Geological Survey Professional Paper 594-D, 26 p.

Pipiringos, G.N., and O'Sullivan, R.B., 1978, Principal unconformities in Triassic and Jurassic rocks, Western Interior United States—a preliminary survey: U.S. Geological Survey Professional Paper 1035-A, 29 p.

Platt, L.B., and Royse, F., Jr., 1989, The Idaho-Wyoming thrust belt: 28th International Geological Congress field trip guidebook T135, American Geophysical Union, Washington, D.C., 34 p.

Premo, W.R., and Van Schmus, W.R., 1989, Zircon geochronology of Precambrian rocks in southeastern Wyoming and northern Colorado, *in* Grambling, J.A., and Tewksbury, B.J., editors, Proterozoic geology of the southern Rocky Mountains: Boulder, Colorado, Geological Society of America Special Paper 235, p. 13-32.

Price, R.A., 1971, Gravitational sliding and the foreland thrust and fold belt of the North American Cordillera—discussion: Geological Society of America Bulletin, v. 82, p. 1133-1138.

_____ 1981, The Cordilleran foreland thrust and fold belt in the southern Canadian Rocky Mountains, *in*

McClay, K., and Price, N.J., editors, Thrust and nappe tectonics: The Geological Society of London Special Publication no. 9, Blackwell Scientific Publications, p. 427-448.

Price, R.A., and Mountjoy, E.W., 1970, Geologic structure of the Canadian Rocky Mountains between Bow and Athabasca Rivers—a progress report: Geological Association of Canada, Special Paper 6, p. 7-25.

Prodehl, C., and Lipman, P.W., 1989, Crustal structure of the Rocky Mountain region, *in* Pakiser, L.C., and Mooney, W.D., editors, Geophysical framework of the continental United States: Geological Society of America Memoir 172, p. 249-284.

Reed, J.C., Jr., Bickford, M.E., Premo, W.R., Aleinikoff, J.N., and Pallister, J.S., 1987, Evolution of the Early Proterozoic Colorado province: constraints from U-Pb geochronology: Geology, v. 15, p. 861-865.

Reynolds, M.W., 1979, Character and extent of Basin-Range faulting, western Montana and east-central Idaho, *in* Newman, G.W., and Goode, H.D., editors, Basin and Range symposium and Great Basin field conference: Rocky Mountain Association of Geologists and Utah Geological Association, p. 185-193.

Roberts, S., 1989, Wyoming geomaps: Geological Survey of Wyoming Educational Series 1, 42 p.

Rodgers, J., 1987, Chains of basement uplifts within cratons marginal to orogenic belts: American Journal of Science, v. 287, p. 661-692.

Rouse, J.T., 1937, Genesis and structural relationships of the Absaroka volcanic rocks, Wyoming: Geological Society of America Bulletin, v. 48, p. 1257-1296.

Royse, F., Jr., Warner, M.A., and Reese, D.L., 1975, Thrust belt structural geometry and related stratigraphic problems, Wyoming-Idaho-northern Utah, *in* Symposium on Deep Drilling Frontiers in Central Rocky Mountains: Rocky Mountain Association of Geologists, p. 41-54.

Rubey W.W., and Hubbert, M.K., 1959, Role of fluid pressure in mechanics of overthrust faulting, part II. Overthrust belt in geosynclinal area of western Wyoming in light of fluid-pressure hypothesis: Geological Society of America Bulletin, v. 70, p. 115-206.

Sahagian, D., 1987, Epeirogeny and eustatic sea level changes as inferred from Cretaceous shoreline deposits: Applications to the central and western United States: Journal of Geophysical Research, v. 92, p. 4895-4904.

Sales, J.K., 1968, Crustal mechanics of Cordilleran foreland deformation: a regional and scale-model approach: American Association of Petroleum Geologists Bulletin, v. 52, p. 2016-2044.

_____ 1983, Collapse of Rocky Mountain basement uplifts, *in* Lowell, J.D., editor, Rocky Mountain foreland basins and uplifts: Denver, Colorado, Rocky Mountain Association of Geologists, p. 79-97.

Sando, W.J., Gordon, M., Jr., and Dutro, J.T., 1975, Stratigraphy and geologic history of the Amsden Formation (Mississippian and Pennsylvanian) of Wyoming: U.S. Geological Survey Professional Paper 848-A, 83 p.

Schmidt, C.J., and Garihan, J.M., 1986a, Role of recurrent movement of northwest-trending basement faults in the tectonic evolution of southwestern Montana, *in* Proceedings of the 6th International Conference on Basement Tectonics, p. 1-15.

_____ 1986b, Middle Proterozoic and Laramide tectonic activity along the southern margin of the Belt basin, *in* Roberts, S.M., editor, Belt Supergroup: Montana Bureau of Mines and Geology Special Publication 94, p. 217-235.

Schmidt, T.G., 1983, Precambrian metavolcanic rocks and associated volcanogenic mineral deposits of the Fletcher Park and Green Mountain areas, Sierra Madre, Wyoming [M.S. thesis]: Laramie, University of Wyoming, 113 p.

Scholten, R., 1973, Gravitational mechanisms in the northern Rocky Mountains of the United States, *in* Jong, K.A., and Scholten, R., editors, Gravity and tectonics: New York, Wiley-Interscience, p. 473-489.

_____ 1982, Continental subduction in the northern U.S. Rockies—a model for back-arc thrusting in the western Cordillera, *in* Powers, R.B., editor, Geologic studies of the Cordilleran thrust belt: Denver, Colorado, Rocky Mountain Association of Geologists, p. 123-136.

Schultz, A.R., 1914, Geology and geography of a portion of Lincoln County, Wyoming: U.S. Geological Survey Bulletin 543, 139 p.

Sears, J.W., Graff, P.J., and Holden, G.S., 1982, Tectonic evolution of lower Proterozoic rocks, Uinta Mountains, Utah and Colorado: Geological Society of America Bulletin, v. 93, p. 990-997.

Seeland, D., 1985, Oligocene paleogeography of the northern Great Plains and adjacent mountains, *in* Flores, R.M., and Kaplan, S.S., editors, Cenozoic paleogeography of west-central United States, Rocky Mountain Paleogeography Symposium 3: Denver, Colorado, The Rocky Mountain Section, Society of Economic Paleontologists and Mineralogists, p. 187-205.

Shearer, C.K., 1990, Geochemistry of Laramide igneous intrusions, northern Black Hills, with implications for petrogenetic relationships and magma sources, *in* Paterson, C.J., and Lisenbee, A.L., editors, Metallogeny of gold in the Black Hills: Society of Economic Geologists Guidebook Series Volume 7, p. 35-42.

Silver, L.T., Bickford, M.E., Van Schmus, W.R., Anderson, J.L., Anderson, T.H., and Medaris, L.G., 1977, The 1.4-1.5 b.y. transcontinental anorogenic plutonic perforation of North America: Geological Society of America Abstracts with Programs, v. 9, no. 7, p. 1176-1177.

Skinner, M.F., Skinner, S.M., and Gooris, R.J., 1977, Stratigraphy and biostratigraphy of late Cenozoic deposits in central Sioux County, western Nebraska: Bulletin of American Museum of Natural History, art. 3, v. 158, p. 263-371.

Sloss, L.L., 1963, Sequences in the cratonic interior of North America: Geological Society of America Bulletin, v. 74, p. 93-114.

Smedes, H.W., and Prostka, H.J., 1972, Stratigraphic framework of the Absaroka Volcanic Supergroup in the Yellowstone National Park Region: U.S. Geological Survey Professional Paper 729-C, 33 p.

Smith, A.G., 1981, Subduction and coeval thrust belts, with particular reference to North America, *in* McClay, K., and Price, N.J., editors, Thrust and nappe tectonics: The Geological Society of London Special Publication no. 9, Blackwell Scientific Publications, p. 111-124.

Smith, A.G., Hurley, A.M., and Briden, J.C., 1981, Phanerozoic paleocontinental world maps: New York, Cambridge Press, 102 p.

Smith, R.B., and Sbar, M.L., 1974, Contemporary tectonics and seismicity of the western United States with emphasis on the Intermountain seismic belt: Geological Society of America Bulletin, v. 85, p. 1205-1218.

Smith, R.B., Shuey, R.T., Freidline, R.O., Otis, R.M., and Alley, L.B., 1974, Yellowstone hot spot: new magnetic and seismic evidence: Geology, v. 2, p. 451-455.

Smith, R.B., and Christiansen, R.L., 1980, Yellowstone Park as a window on the Earth's interior: Scientific American, v. 242, p. 104-117.

Smithson, S.B., Brewer, J.A., Kaufman, S., Oliver, J.E., and Hurich, C.A., 1978, Nature of the Wind River thrust, Wyoming, from COCORP deep reflection data and from gravity data: Geology, v. 6, p. 648-652.

_____ 1979, Structure of the Laramide Wind River uplift, Wyoming, from COCORP deep reflection data and from gravity data: Journal of Geophysical Research, v. 84, p. 5955-5972.

Snoke, A.W., and Miller, D.M., 1988, Metamorphic and tectonic history of the northeastern Great Basin, *in* Ernst, W.G., editor, Metamorphism and crustal evolution of the western United States, Rubey volume VII: Englewood Cliffs, New Jersey, Prentice Hall, p. 606-648.

Snyder, G.L., Hausel, W.D., Klein, T.L., Houston, R.S., and Graff, P.J., 1989, Precambrian rocks and mineralization, southern Wyoming Province: 28th International Geological Congress, Field Trip Guidebook T332, American Geophysical Union, Washington, D.C., 48 p.

Snyder, G.L., Hall, R.P., Hughes, D.J., and Ludwig, K.R., 1990, Early Precambrian rocks in the USA, *in* Hall, R.P., and Hughes, D.J., editors, Early Precambrian basic magmatism: Glasgow, Blackie, p. 191-220.

Snyder, W.S., Dickinson, W.R., and Silberman, M.L., 1976, Tectonic implications of space-time patterns of Cenozoic magmatism in the western United States: Earth and Planetary Science Letters, v. 32, p. 91-106.

Staatz, M.H., 1983, Geology and description of thorium and rare-earth deposits in the southern Bear Lodge Mountains, northeastern Wyoming: U.S. Geological Survey Professional Paper 1049-D, 52 p.

Stearns, D.W., 1971, Mechanisms of drape folding in the Wyoming province: Wyoming Geological Association 23rd Annual Field Conference Guidebook, p. 125-143.

_____ 1978, Faulting and forced folding in the Rocky Mountains foreland, *in* Matthews, V., III, editor, Laramide folding associated with basement block faulting in the western United States: Geological Society of America Memoir 151, p. 1-37.

Stearns, D.W., and Weinberg, D.M., 1975, A comparison of experimentally created and naturally formed drape folds: Wyoming Geological Association 27th Annual Field Conference Guidebook, p. 159-166.

Stearns, D.W., and Stearns, M.T., 1978, Geometric analysis of multiple drape folds along the northwest Bighorn Mountains front, Wyoming, *in* Matthews, V., III, editor, Laramide folding associated with basement block faulting in the western United States: Geological Society of America Memoir 151, p. 139-156.

Steidtmann, J.R., and Schmitt, J.G., 1988, Provenance and dispersal of tectogenic sediments in thin-skinned thrusted terranes, *in* Kleinspehn, K., and Paola, C., editors, New perspectives in sedimentary basin analysis: New York, Elsevier, p. 353-366.

Steidtmann, J.R., Middleton, L.T., and Shuster, M.W., 1989, Post-Laramide (Oligocene) uplift in the Wind River Range, Wyoming: Geology, v. 17, p. 38-41.

Steidtmann, J.R., and Middleton, L.T., 1991, Fault chronology and uplift history of the southern Wind River Range, Wyoming: implications for Laramide and post-Laramide deformation in the Rocky Mountain foreland: Geological Society of America Bulletin, v. 103, p. 472-485.

Steiner, M.B., 1986, Rotation of the Colorado Plateau: Tectonics, v. 5, p. 649-660.

Steven, T.A., 1956, Cenozoic geomorphic history of the Medicine Bow Mountains near the Northgate fluorspar district, Colorado: Colorado Scientific Society Proceedings, v. 17, no. 2, p. 35-55.

Stewart, J.H., 1972, Initial deposits in the Cordilleran geosyncline: evidence of a Late Precambrian (<850 m.y.) continental separation: Geological Society of America Bulletin, v. 83, p. 1345-1360.

_____ 1976, Late Precambrian evolution of North America: plate tectonics implications: Geology, v. 4, p. 11-15.

Stuckless, J.S., Hedge, C.E., Worl, R.G., Simmons, K.R., Nkomo. I.T., and Wenner, D.B., 1985, Isotopic studies of the Late Archean plutonic rocks of the Wind River Range, Wyoming: Geological Society of America Bulletin, v. 96, p. 850-860.

Suppe, J., Powell, C., and Berry, R., 1975, Regional topography, seismicity, Quaternary volcanism, and the present-day tectonics of the western United States: American Journal of Science, v. 275-A, p. 397-436.

Surdam, R.C., and Stanley, K.O., 1979, Lacustrine sedimentation during the culminating phase of Eocene Lake Gosiute, Wyoming (Green River Formation): Geological Society of America Bulletin, v. 90, p. 93-110.

_____ 1980, Effects of changes in drainage-basin boundaries on sedimentation in Eocene Lakes Gosiute and Uinta of Wyoming, Utah, and Colorado: Geology, v. 8, p. 135-139.

Surdam, R.C., and Wolfbauer, C.A., 1975, Green River Formation, Wyoming: A playa-lake complex: Geological Society of America Bulletin, v. 86, p. 335-345.

Suter, M., 1987, Structural traverse across the Sierra Madre Oriental fold-thrust belt in east-central Mexico: Geological Society of America Bulletin, v. 98, p. 249-264.

Swinehart, J.B., Souders, V.L., DeGraw, H.M., and Diffendal, R.F., Jr., 1985, Cenozoic paleogeography of western Nebraska, *in* Flores, R.M., and Kaplan, S.S., editors, Cenozoic paleogeography of the west-central United States, Rocky Mountain Paleogeography Symposium 3: Denver, Colorado, The Rocky Mountain Section, Society of Economic Paleontologists and Mineralogists, p. 209-229.

Taylor, R.B., 1975, Neogene tectonism in south-central Colorado, *in* Curtis, B.F., editor, Cenozoic history of the Southern Rocky Mountains: Geological Society of America Memoir 144, p. 211-226.

Thom, W.T., Jr., 1947, Structural features of the Bighorn Basin rim: University of Wyoming - Wyoming Geological Association - Yellowstone-Bighorn Research Association, Field Conference in the Bighorn Basin, p. 173-177.

Thorman, C.H., Ketner, K.B., and Peterson, F., 1990, The Elko orogeny - Late Jurassic orogenesis in the Cordilleran miogeocline: Geological Society of America Abstracts with Programs, v. 22, no. 3, p. 88.

Trimble, D.E., 1980, Cenozoic tectonic history of the Great Plains contrasted with that of the Southern Rocky Mountains: a synthesis: The Mountain Geologist, v. 17, p. 59-69.

Tweto, O., 1975, Laramide (Late Cretaceous-Early Tertiary orogeny in the Southern Rocky Mountains, *in* Curtis, B.F., editor, Cenozoic history of the Southern Rocky Mountains: Geological Society of America Memoir 144, p. 1-44.

_____ 1979, The Rio Grande rift system in Colorado, *in* Riecker, R.E., editor, Rio Grande rift: tectonics and magmatism: Washington, D.C., American Geophysical Union, p. 33-56.

Vail, P.R., Mitchum, R.M., Jr., and Thompson, S., III, 1977, Global cycles of relative sea level, *in* Payton, C.E., editor, Seismic stratigraphy - applications to hydrocarbon exploration: American Association of Petroleum Geologists Memoir 26, p. 83-97.

Van Houten, F.B., 1948, Origin of red-banded early Cenozoic deposits in Rocky Mountain region: American Association of Petroleum Geologists Bulletin, v. 32, p. 2083-2126.

Veatch, A.C., 1907, Geography and geology of a portion of southwestern Wyoming with special reference to coal and oil: U.S. Geological Survey Professional Paper 56, 178 p.

Weimer, R.J., 1984, Relation of unconformities, tectonics, and sea-level changes, Cretaceous of Western Interior, U.S.A., *in* Schlee, J.C., editor, Interregional unconformities and hydrocarbon accumulation: American Association of Petroleum Geologists Memoir 36, p. 7-35.

Wernicke, B.P., Christiansen, R.L., England, P.C., and Sonder, L.J., 1987, Tectonomagmatic evolution of Cenozoic extension in the North American Cordillera, *in* Coward, M.P., Dewey, J.F., and Hancock, P.L., editors, Continental extensional tectonics: Geological Society Special Publication no. 28, p. 203-221.

Wiltschko, D.V., and Dorr, J.A., Jr., 1983, Timing of deformation in overthrust belt and foreland of Idaho, Wyoming, and Utah: American Association of Petroleum Geologists Bulletin, v. 67, p. 1304-1322.

Winston, D., 1986, Sedimentation and tectonics of the Middle Proterozoic Belt basin and their influence on Phanerozoic compression and extension in western Montana and northern Idaho, *in* Peterson, J.A., editor, Paleotectonics and sedimentation in the Rocky Mountain region, United States: Tulsa, Oklahoma American Association of Petroleum Geologists Memoir 41, p. 87-118.

_____ 1989, Introduction to the Belt, *in* Middle Proterozoic Belt Supergroup, western Montana, 28th International Geological Congress Field Trip Guidebook T334: Washington, D.C., American Geophysical Union, p. 1-6.

Wise, D.U., 1963, Keystone faulting and gravity sliding driven by basement uplift of Owl Creek Mountains, Wyoming: American Association of Petroleum Geologists, v. 47, p. 586-598.

_____ 1983, Overprinting of Laramide structural grains in the Clarks Fork Canyon area and eastern Beartooth Mountains of Wyoming: Wyoming Geological Association 34th Annual Field Conference Guidebook, p. 77-87.

Wise, D.U., and Obi, C.M., 1992, Laramide basement deformation in an evolving stress field, Bighorn mountain front, Five Springs area, Wyoming: American Association of Petroleum Geologists Bulletin, v. 76, p. 1586-1600.

Witkind, I.J., 1964, Reactivated faults north of Hebgen Lake: U.S. Geological Survey Professional Paper 435-G, p. 37-54.

Wolfe, J.A., and Schorn, H.E., 1989, Paleoecologic, paleoclimatic, and evolutionary significance of the Oligocene Creede flora: Paleobiology, v. 15, p. 180-198.

Woodbury, H.O., Murray, I.B., Jr., Pickford, P.J., and Akers, W.H., 1973, Pliocene and Pleistocene depocenters, outer continental shelf, Louisiana and Texas: American Association of Petroleum Geologists Bulletin, v. 57, p. 2428-2439.

Wooden, J.L., Mueller, P.A., and Mogk, D., 1988, A review of the geochemistry and geochronology of the Archean rocks of the northern part of the Wyoming province, *in* Ernst, W.G., editor, Metamorphism and crustal evolution in the western United States, Rubey volume VII: Englewood Cliffs, New Jersey, Prentice-Hall, p. 383-410.

Zeller, H.D., and Stephens, E.V., 1969, Geology of the Oregon Buttes area, Sweetwater and Fremont counties, southwestern Wyoming: U.S. Geological Survey Bulletin 1256, 60 p.

Zielinski, R.A., Peterman, Z.E., Stuckless, J.S., Rosholt, J.N., and Nkomo, I.T., 1981, The chemical and isotopic record of rock-water interaction in the Sherman Granite, Wyoming and Colorado: Contributions to Mineralogy and Petrology, v. 78, p. 209-219.

Part II

Precambrian history

Frontispiece. Intensely eroded glacial topography of the southern Wind River Mountains looking southwest towards Atlantic Peak. In the foreground is Leg Lake in the upper Roaring Fork Creek valley. The area is underlain by the 2.63 Ga Louis Lake granodiorite. Photograph by Austin S. Post.

The Archean history of the Wyoming province

Carol D. Frost and B. Ronald Frost
Department of Geology and Geophysics
University of Wyoming
Laramie, Wyoming 82071

Abstract

The Archean-cored uplifts of the Wyoming province record a broadly similar geologic history. This is evidenced by (1) Early and Middle Archean gneisses and supracrustal rocks, that commonly preserve amphibolite- or granulite-facies assemblages; (2) Late Archean supracrustal sequences of greenstone belt or continental platform affinity; and (3) Late Archean postkinematic granitoid plutons. Exposed basement gneisses consist of tonalitic to granitic gneisses that contain enclaves of supracrustal rocks. Where dated, these gneisses are 2.8 Ga or older. The supracrustal rocks and some of the surrounding gneisses in several uplifts have been metamorphosed to granulite facies. At least two and possibly three different Late Archean supracrustal sequences occur in the Wyoming province. Both continental platform-type and greenstone-type sedimentary successions are found, but in both, pelitic rocks have Nd-isotopic characteristics typical of sediments that are derived from continental sources. Postkinematic granitoids help constrain the age of the last penetrative deformation and metamorphism and indicate that this last deformational phase shifted from the northern part of the Wyoming province, where deformation ceased before 2.7 Ga, to the south, where deformation continued to 2.6 Ga.

Although the Archean history of the Wyoming province is not yet known in detail, several generalizations about its evolution are possible. The province contains evidence for some of the oldest rocks in North America; detrital zircon ages indicate that continental crust was established as early as 3.6 to 3.8 Ga. Because of the lithologic similarities in the older gneisses and the uniform Early to Middle Archean Nd model ages for Archean metasediments throughout the province, it is likely that the Wyoming province was assembled by Middle Archean time. Plutonism and deposition of supracrustal rocks took place during the Late Archean. Incomplete mapping and limited geochronological and geochemical data preclude the construction of detailed tectonic models for Late Archean evolution of the province, but no feature is inconsistent with present-day plate tectonic processes.

Introduction

The Wyoming province, an Archean craton located in present-day Wyoming and parts of adjacent states, is the most southwestern of the Archean provinces of North America (**Figure 1**). Because Precambrian rocks of the Wyoming province are exposed only in the cores of Late Mesozoic-early Tertiary Laramide uplifts (sheet 1, Houston, map pocket), outcrops of Archean rocks are limited to around 10% of the total area underlain by Archean basement. Exposure within the basement uplifts is

Frost, C.D., and Frost, B.R., 1993, The Archean history of the Wyoming province, *in* Snoke, A.W., Steidtmann, J.R., and Roberts, S.M., editors, Geology of Wyoming: Geological Survey of Wyoming Memoir No. 5, p. 58-76.

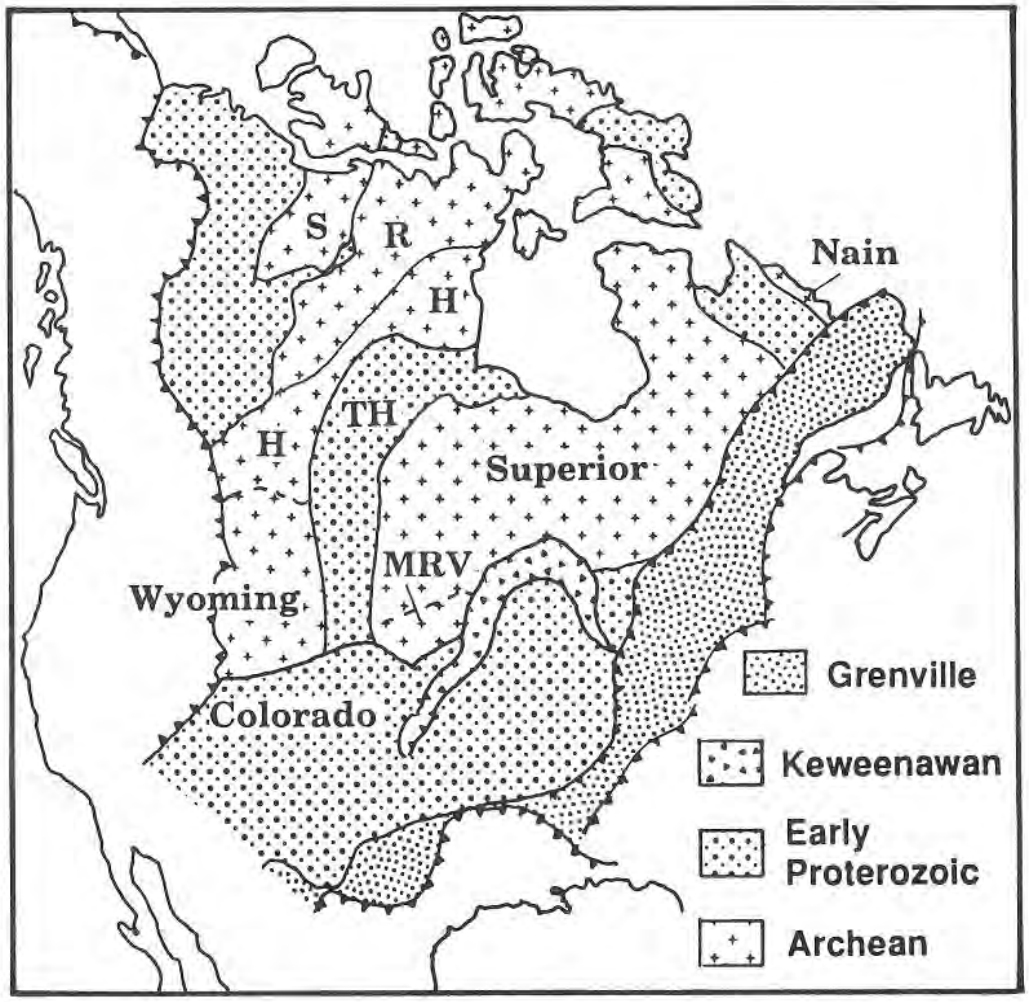

Figure 1. Map showing the relationship between the Wyoming province and other Archean provinces of North America. H = Hearn province, MRV = Minnesota River province, R = Rae province, S = Slave province. Also shown are the Proterozoic orogens that border the Archean provinces. TH = Trans-Hudson orogen (adapted from Hoffman, 1988).

generally very good, but extrapolation between uplifts is extremely tenuous. Even determination of the extent of the Wyoming province is difficult because only the southeastern margin is exposed. The southern boundary extends from southeastern Wyoming, where it is defined by the Cheyenne belt [the suture of the Wyoming province with the younger Colorado province (Houston and others, 1979)], westward to include the northeastern Uinta Mountains, the Wasatch Range, and the East Humboldt Range of Nevada (Lush and others, 1988). Archean rocks are also found in southwest Montana in the Ruby, Madison, Tobacco Root, and Little Belt Mountains. The Wyoming province may extend northward and be contiguous with the Hearne province of Canada (Hoffman, 1988). The Early Proterozoic Trans-Hudson orogen apparently defines the eastern margin of the Wyoming province. Archean rocks in the Black Hills of South Dakota, which have been affected by Trans-Hudson deformation, are the most easternmost exposures of the Wyoming province (Gosselin and others, 1988).

As recently as 1955, the geologic map of Wyoming showed the Precambrian as undivided (Love and others, 1955). Significant progress has been made since that time in subdividing and describing the Precambrian rocks of Wyoming, as summarized by Houston and others (in press) and shown on the most recent map of the state (Love and Christiansen, 1985). Although geological, geochronological, and petrogenetic descriptions of the old-

est rocks are still incomplete, some generalizations can now be made about the formation and evolution of the Archean rocks of the Wyoming province.

Geochronometric studies of the Wyoming province

Much progress has been made in establishing geochronological constraints on the evolution of the rocks of the Wyoming province since 1958, when Gast and others first reported Archean K-Ar ages from several of the Precambrian-cored Laramide uplifts. Houston and others (in press) and Wooden and others (1988) provide excellent summaries of the geochronological data presently available. Nevertheless, many of the age determinations are difficult to interpret; for example, the geologic significance of some of the early K-Ar ages is not known. In some cases it is difficult to determine whether Rb-Sr whole-rock isochrons from metasedimentary successions give depositional or metamorphic ages or whether they have no geological significance. Some zircon populations have proven so discordant that only a minimum age can be determined.

Despite such challenging problems, it is now possible to use the geochronological evidence to outline certain correlations and common sequences between uplifts. A summary of the best constrained radiometric ages for the Archean-cored uplifts of the Wyoming province is presented schematically in **Figure 2.** In this figure and the following discussion, we focus primarily upon U-Pb zircon age determinations, which in general give the most precise and easily interpreted dates, and only refer to those obtained by other methods where zircon ages are unavailable. Some of the uplifts, including the Teton Range and

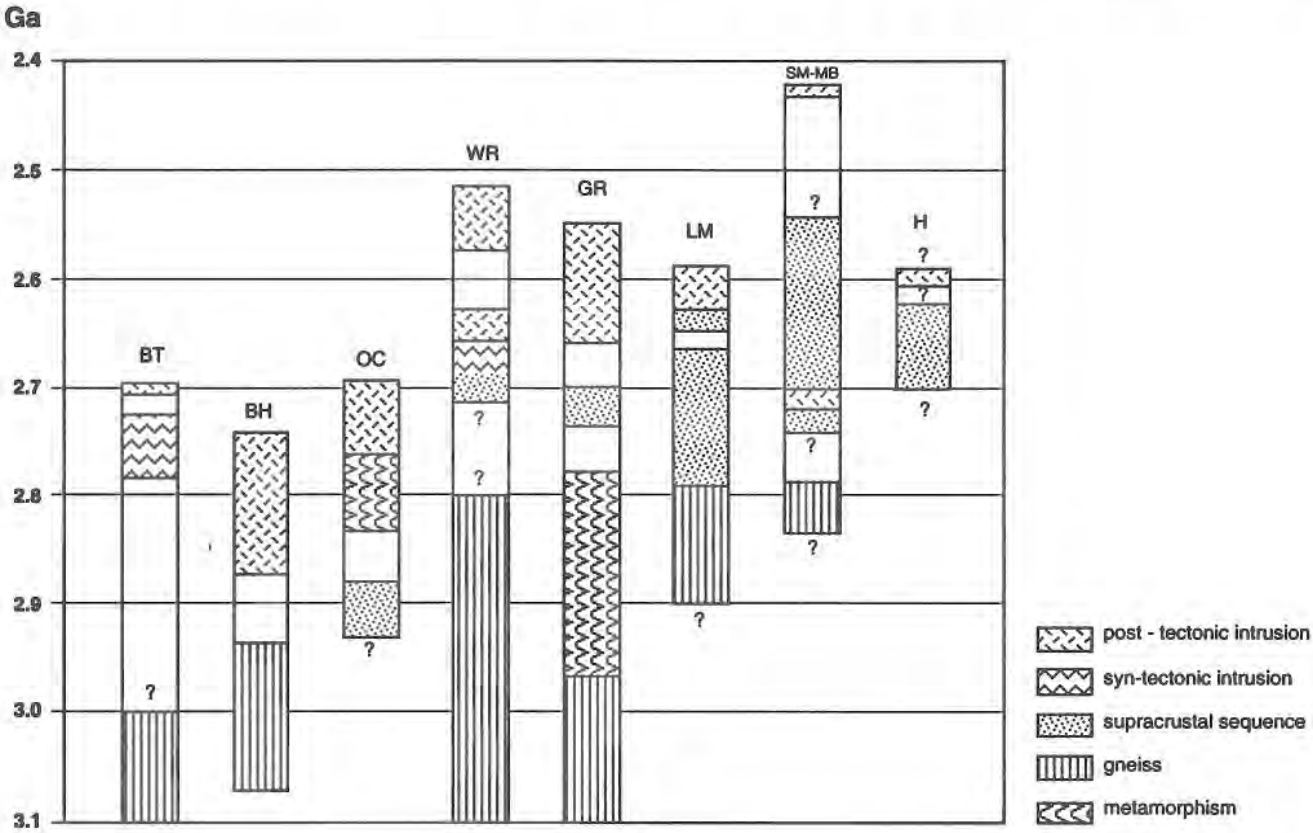

Figure 2. Comparison of the geochronology of the Precambrian uplifts in Wyoming. BT = Beartooth Mountains, BH = Bighorn Mountains, OC = Owl Creek Mountains, WR = Wind River Range, GR = Granite Mountains, LM = Laramie Mountains, SM-MB = Sierra Madre-Medicine Bow Mountains, H = Hartville uplift. Data sources are given in the text.

the mountains of southwest Montana, are not shown on **Figure 2** because age data are sparse and are associated with large errors. Where errors associated with radiometric ages are less than 100 Ma, dates are expressed in Ma, and where errors are in excess of 100 Ma, dates are given in Ga.

Beartooth Mountains

U-Pb ages of up to 3.96 Ga have been reported for detrital zircons from a Middle Archean quartzite in the eastern Beartooth Mountains (Mueller and others, 1992), and U-Pb ages of 3.10 ± 0.11 Ga and 3,065 ± 53 Ma have been obtained for detrital zircons from metasedimentary rocks intruded by the Late Archean Stillwater Complex in the northern part of the range (Nunes and Tilton, 1971). Both studies demonstrate that the zircons incorporated into these sediments were derived from Early to Middle Archean crust. Although it has proven difficult to obtain unambiguous ages on the oldest rocks from the eastern Beartooth Mountains, U-Pb, Rb-Sr, and Sm-Nd data from a variety of lithologies are compatible with the presence of rocks 3.3 Ga or older (Wooden and others, 1988). In the eastern Beartooth Mountains, amphibolites have been dated at 2,789 ± 5 Ma, the Long Lake granodiorite at 2,782 ± 3 Ma, and the Long Lake granite at 2,748 ± 25 Ma (Wooden and others, 1988). These ages are similar to a U-Pb zircon age reported by the same authors of 2,752 ± 14 Ma for a granitoid from the northern Beartooth Mountains. The last Archean events in the Beartooth Mountains were the emplacement of the Stillwater igneous complex (2,701 ± 8 Ma; DePaolo and Wasserburg, 1979) and the Mouat quartz monzonite, which intrudes the Stillwater complex (2,695 ± 10 Ma; data of Nunes and Tilton as reported in Wooden and others, 1988).

Bighorn Mountains

The Bighorn Mountains are one of the few uplifts in the Wyoming province for which Archean crystallization ages younger than 2.7 Ga are not known. The oldest rocks identified are gneisses from the southern half of the range, dated at 3,007 ± 68 Ma by whole-rock Rb-Sr method and 2.95 ± 0.10 Ga by U-Pb zircon method (Arth and others, 1980). Intrusion of trondhjemite, granite, and granodiorite followed in this area at 2,801 ± 62 (Rb-Sr whole-rock, Arth and others, 1980). In the northern end of the range, a granite has been dated at 2,850 ± 25 Ma (U-Pb zircon, Heimlich and Banks, 1968). Even K-Ar cooling ages give Archean dates: K-Ar biotite ages range from 2.73 Ga for tonalites and granites in the northern half of the range to 2.50 Ga for gneisses in the southern half (Heimlich and Armstrong, 1972). Peterman (1982) suggested that the difference reflects differential uplift through the biotite blocking temperature in the northern and southern parts of the range. Late Archean diabase dikes, dated at 2,766 ± 58 Ma by the Rb-Sr whole-rock method (Stueber and others, 1976), may have been intruded upon cooling and uplift of the northern Bighorn Mountains.

Owl Creek Mountains

Two units have been dated in the Owl Creek Mountains. The first is the supracrustal sequence of the Wind River Canyon in the central part of the range. Mueller and others (1985) obtained a U-Pb zircon age of 2,905 ± 25 Ma for a layered dacite, which they interpreted as the depositional age, and a Rb-Sr whole-rock age of 2,779 ± 55 Ma from basaltic andesites and basalts, which they suggested is a metamorphic age for the sequence. The second is a Late Archean granite to the east of Wind River Canyon, which intrudes an older metamorphic sequence that may be correlative with the Wind River Canyon sequence. Postkinematic granite from the Owl Creek Mountains has been dated at 2,730 ± 35 Ma by the U-Pb whole-rock method (Stuckless and others, 1986).

Wind River Range

Evidence for some of the oldest material in the Wyoming province comes from an ion microprobe study of zircons from the central Wind River Range by Aleinikoff and others (1989). A granulite-facies migmatitic gneiss contains zircons that are probably xenocrystic, which yield U-Pb ages of ~3.8, 3.65, and 3.35 Ga. Populations of zircons with morphology characteristic of zircon growth at granulite facies gave ages of ~3.2 and 2.7 Ga. Other zircons yielded concordia ages of ~2.85 Ga. Conventional U-Pb zircon dating of populations of grains from the migmatitic gneiss gave an age, interpreted to be the time of granulite facies metamorphism, of 2,698 ± 8 Ma.

Age determination of the "older orthogneiss" of Worl and others (1986), which forms the basement into which younger granitoids were intruded, has been attempted by us using the single-grain U-Pb zircon method. The zircons were quite discordant and yielded only minimum $^{207}Pb/^{206}Pb$ ages of 2.80 to 2.83 Ga (**Table 1** and **Figure 3**).

The oldest of the well-dated Late Archean plutons is the synkinematic Bridger batholith, which has been dated at 2,670 ± 13 Ma (Aleinikoff and others, 1989). Postkinematic granitoids include granodiorite and granite. In some areas these two lithologies are gradational, but in general the granite appears younger. The Louis Lake granodiorite has been dated at its type locality at 2,642 ± 13 Ma by Naylor and others (1970). The Bears Ears porphyritic granite has proven difficult to date precisely by the U-Pb zircon method because of inherited components. Stuckless and others (1985) examined all geochronological data for the Bears Ears and suggested a best estimate of 2,545 ± 30 Ma.

Granite Mountains and Seminoe Mountains

U-Pb data for zircons separated from the metamorphic basement complex of the Granite Mountains demonstrate that these gneisses include rocks of several different ages, some of which are 3.2 Ga or older (Fischer and Stacey, 1986). Peterman and Hildreth (1978) interpreted a Rb-Sr whole-rock date for the metamorphic complex of 2,860 ± 80 Ma as a metamorphic age, an hypothesis which was endorsed by Fischer and Stacey (1986) on the basis of an apparent U-Pb zircon age of 2,880 ± 90 Ma from the same massive gneiss samples examined by Peterman and Hildreth (1978). The postkinematic granites of the Granite Mountains have been dated at 2,640 ± 20 Ma for the Long Creek Mountain granite and 2,590 ± 40 Ma for the Lankin Dome granite, respectively (Ludwig and Stuckless, 1978).

In the Bradley Peak area of the Seminoe Mountains, a rhyodacite interbedded with other metavolcanic and metasedimentary rocks of a greenstone-type association has been dated at 2,718 ± 18 Ma (S.S. Goldich, *in* Houston and others, in press).

Laramie Mountains

Few geochronological data are available on the oldest gneisses of the Laramie Mountains, although Rb-Sr whole-rock dating of migmatite in the northern Laramie Mountains suggests the presence of rocks of Middle Archean age (Johnson and Hills, 1976). A U-Pb zircon date of 2,729 ± 62 Ma for a rhyolite in the Sellers Mountain supracrustal sequence of the west-central Laramie Mountains suggests that this succession predates the Elmers Rock supracrustal sequence in the central Laramie Mountains, which includes a rhyolite of 2,637 ± 10 Ma (K.R. Ludwig, *in* Snyder and others, 1988). Of the same age or slightly younger is the Squaw Mountain granite gneiss, possibly a phase of the Laramie batholith, which yielded a U-Pb zircon age of 2,620 ± 30 Ma (Z.E. Peterman, *in* Snyder and others, 1988).

Sierra Madre and Medicine Bow Mountains

The age of the basement gneisses in the Sierra Madre and Medicine Bow Mountains is poorly known. A quartzo-feldspathic orthogneiss in the northern Sierra Madre yielded an age of 2,683 ± 6 Ma (Premo and Van Schmus, 1989), but its field relationships are uncertain (Houston and others, in press). The Spring Lake granodiorite gneiss (2,710 ± 10 Ma) intrudes both basement gneisses and the lower part of the Phantom Lake metamorphic suite in the central Sierra Madre, thus providing a minimum age for these metasedimentary rocks. The Baggot Rocks granite post-dates deformation of the Phantom Lake metamorphic suite. Its age is 2,429 ± 4 Ma, earliest Proterozoic (Premo and Van Schmus, 1989).

Hartville uplift

The metasedimentary rocks of the Hartville uplift belong to the Whalen Group, a nearly 4-km-thick succession of clastic sediments, carbonates, and mafic lavas and volcaniclastic sediments. The age of the Whalen Group has not been determined directly and hinges on the relationship of these sediments with the 2.58 Ga Rawhide Buttes granite (Peterman, 1982). Snyder and others (1988) suggested that the Whalen Group predates the Rawhide Buttes granite. They

proposed that the Silver Springs schist in the upper part of the succession correlates with the Archean metasediments in the Elmers Rock greenstone belt of the central Laramie Mountains.

Common lithological elements of the Wyoming province

Despite the incomplete state of geochronological knowledge of the Wyoming province, some general observations about the evolution of the province are possible. Most ranges exhibit similar lithologies, including Early to Middle Archean gneisses, which incorporate older supracrustal rocks; Late Archean supracrustal sequences locally intruded by syn-kinematic granitoids; postkinematic intrusions; and mafic dikes. A detailed examination of geochronological data shows that these units did not form simultaneously in all parts of the province.

Early to Middle Archean rocks

In most of the uplifts, the oldest rocks exposed are complexly deformed, commonly migmatitic, gneisses. In only a few localities are these gneisses well dated. In the Bighorn Mountains, the early gneisses are approximately 3.0 Ga (Arth and others, 1980), whereas in the Wind River Range they are at least 2.8 Ga (**Figure 3**). Other evidence for the presence of Early Archean crust in the Wyoming province is obtained from detrital zircons in metasedimentary sequences, including those of the Beartooth Mountains (3.10 and 3.07 Ga: Nunes and Tilton, 1971; Wooden and others, 1988), the Wind River Range (as old as 3.8 Ga: Aleinikoff and others, 1989), and the Granite Mountains (3.2 Ga: Fischer and Stacey, 1986). In the Medicine Bow, Sierra Madre, and Laramie mountains, Archean gneisses are exposed but are poorly dated.

In almost all instances, these ancient gneisses contain supracrustal inclusions consisting of pelitic paragneiss, iron formation, metabasite, metaperidotite, and more rarely, calc-silicate paragneiss and quartzite. In the central Wind River Range, the supracrustal inclusions exhibit fabric elements that are absent in the surrounding gneisses, indicating the supracrustal rocks have experienced a longer, more complex history than their host gneisses (Koesterer and others, 1987).

In many of the Laramide uplifts, the older gneisses have undergone granulite-facies metamorphism. In the Wind River Range, evidence of granulite metamorphism survives in both the supracrustal rocks and the surrounding gneisses (Koesterer and others, 1987). On the basis of U-Pb ion microprobe data from zircons, Aleinikoff and others (1989) concluded that this granulite-facies event occurred at about 3.2 Ga. In the Teton Range, granulite-facies assemblages are found in the oldest rocks preserved, a layered gneiss supracrustal sequence (Miller and others, 1986). Inclusions of supracrustal rocks in the felsic gneisses and migmatites of the eastern Beartooth Mountains also preserve evidence of granulite-facies metamorphism (Mogk and Henry, 1988).

Table 1. U-Pb isotopic data for single zircon crystals from older orthogneiss of the central Wind River Range.[a]

Sample	Size (μm)	mass (μg)	U (ppm)	Pb_{rad} (ppm)	Pb_{com} (ppm)	^{238}U	^{208}Pb	^{207}Pb	^{206}Pb	^{204}Pb	$^{206}Pb/^{204}Pb$[b] (observed)
						(10^{-12} mol corrected for analytical blank)					
B	200x50	1.0	824.1	475.3	3.7	3.437	0.3129	0.3343	1.673	.00024	1207
E	230x125	7.8	526.3	244.7	3.9	17.122	0.9506	1.4250	1.019	.00237	2967
H	190x75	2.9	686.8	369.1	1.9	8.307	0.4989	0.7785	3.937	.00042	9311
L	215x75	3.0	559.9	326.4	1.0	7.006	7.006	0.7142	3.485	.00135	2588

[a]Granitic gneiss from Ink Wells Quadrangle described by Hulsebosch (in preparation). Analyses performed at ETH-Zurich; C. Frost, M. Meier, and F. Oberli, analysts.

[b]Measured ratio corrected for mass fractionation and tracer contributions.

[c]Analytical uncertainties (95% confidence level) refer to last significant digits of corresponding ratio.

[d]Correlation coefficient $^{207}Pb/^{235}U$ versus $^{206}Pb/^{238}U$.

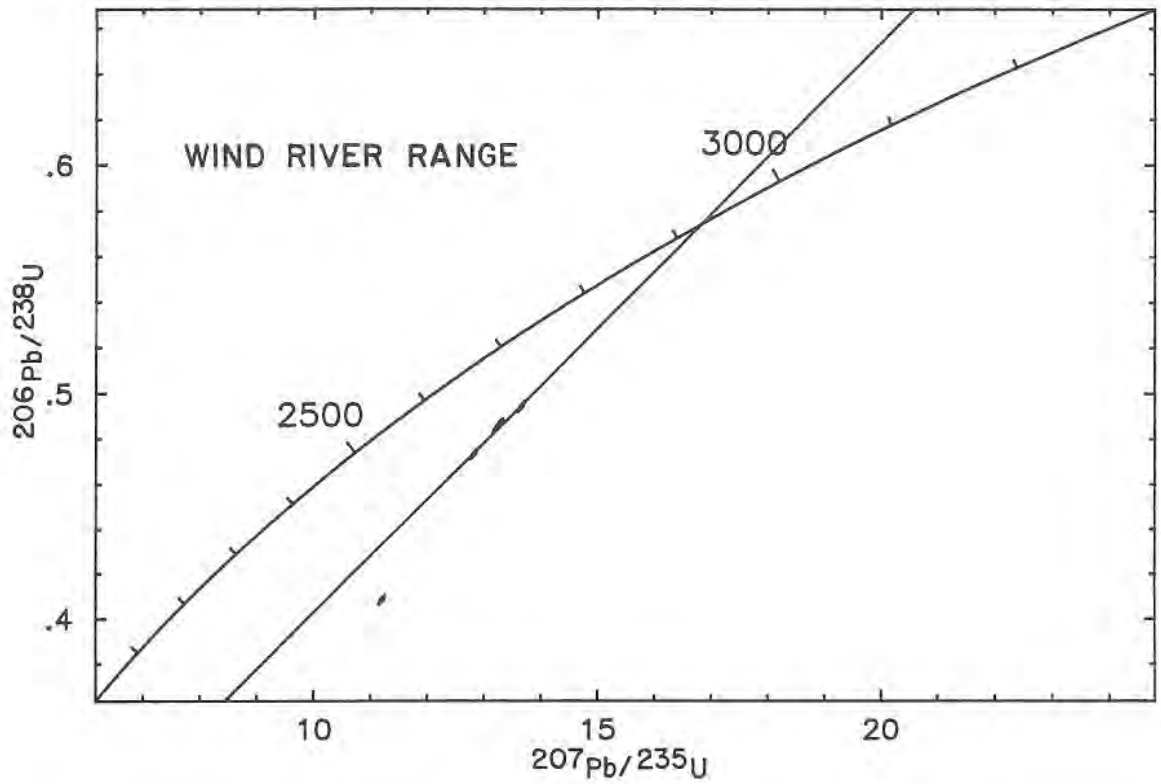

Figure 3. Concordia diagram for four zircon crystals from the older orthogneiss from the Wind River Range. Error ellipses are at the 95% confidence level. $^{207}Pb/^{206}Pb$ ages of 2.80 to 2.83 Ga provide a minimum age for the gneiss.

Late Archean supracrustal sequences

As is evident from **Figure 2**, there appear to be at least three different periods of Late Archean sedimentation and volcanism in the Wyoming province. The oldest dated supracrustal sequence is that of Wind River Canyon in the Owl Creek Mountains, which was deposited at 2.9 Ga (Mueller and others, 1985). Rhyolites from the volcanic sequences in the Seminoe Mountains and in the Sellers Mountain area of the Laramie Mountains are around 2.72 Ga (Houston and others, in press; Snyder and others, 1988). The Elmers Rock greenstone belt sequence is still younger, dated at 2.64 Ga (Snyder and others, 1988).

Table 1. *(continued)*

$^{208}Pb/^{206}Pb$	$^{207}Pb/^{206}Pb$	$^{207}Pb/^{235}U$	$^{206}Pb/^{238}U$	rho[d]
(isotopic ratios corrected for blank and common Pb[c])				
0.1818(6)	0.1977(2)	13.243(35)	0.4857(12)	0.96
0.1248(2)	0.1990(8)	11.197(22)	0.4081(8)	0.98
0.1234(2)	0.1965(1)	12.819(25)	0.4733(9)	0.98
0.1703(3)	0.2003(1)	13.647(27)	0.4941(10)	0.98

The deposition of some of the best geologically described supracrustal sequences, including those in the South Pass area of the Wind River Range, in the Sierra Madre and Medicine Bow Mountains, and in the Hartville uplift, can only be constrained by minimum ages. The South Pass supracrustal rocks have been intruded and metamorphosed by the Louis Lake batholith and therefore must be older than 2.67 Ga. It is not known whether these rocks are more appropriately correlated with the supracrustal rocks of the Wind River Canyon in the Owl Creek Mountains or with those in the Bradley Peak area of the Seminoe Mountains, but they apparently predate the supracrustal rocks of the Elmers Rock succession in the Laramie Mountains.

The age of the Phantom Lake metamorphic suite in the Medicine Bow Mountains and Sierra Madre is

also poorly known. The Phantom Lake metamorphic suite can be divided into three parts. The base of the succession is composed of a fluvial conglomerate, which grades upwards into a marine quartzite with interbedded metacarbonate. The middle part consists of metavolcanic rocks, metagraywacke, metapelites, and conglomerate containing granite and mafic volcanic clasts. The upper part of the Phantom Lake suite is quartzite. The lower part of the Phantom Lake metamorphic suite is intruded by a 2.71 Ga granodiorite gneiss in the Sierra Madre (Premo and Van Schmus, 1989), but the age of the upper portions of the sequence is unknown.

The Hartville uplift contains a similar succession. The base of the Whalen Group is composed of quartzite and dolomite; the middle part is composed of basaltic volcanic rocks, graywacke, and pelitic rocks; and the upper part consists of siliceous dolomite. Houston (personal communcation, 1990) has suggested, on the basis of similar stratigraphy, that the Phantom Lake metamorphic suite may be tentatively correlated with the Whalen Group of the Hartville uplift. It is unknown whether these successions are correlative with either the Elmers Rock or the Sellers Mountain supracrustal successions of the Laramie Mountains, although Snyder and others (1988) suggested they are best correlated with the Elmers Rock sequence.

Another well-described Precambrian supracrustal sequence, also poorly dated, is the Cherry Creek metamorphic suite of southwest Montana. The type section of the Cherry Creek suite, in the Gravelly Range, is composed of pelitic schist, dolomite marble, quartzite, hornblende gneiss, iron formation, phyllite, and anthophyllite gneiss. These rocks can be correlated by lithology and stratigraphic sequence to the metasediments of the southern Madison Range. Erslev (*in* Houston and others, in press) suggests that marble-bearing sequences in the Ruby and Tobacco Root ranges also can be correlated with the Cherry Creek metamorphic suite. Lithologic and geochemical characteristics of the Cherry Creek metamorphic suite suggest passive-margin deposition (Gibbs and others, 1986; Mogk and Henry, 1988). Mogk and Henry (1988) suggested that these sediments were accreted to the gneisses, migmatites, and granitoids of the eastern Beartooth Mountains, presumably during the Late Archean.

Late Archean deformation and postkinematic plutonism

Although postkinematic granites are present in all Archean-cored Laramide uplifts in Wyoming, they were not emplaced during a single, province-wide magmatic event (**Figure 2**). Their emplacement ages are significant because they provide the time of the latest penetrative deformation and metamorphism in each area. The postkinematic plutons are the oldest in the Bighorn Mountains, Beartooth Mountains, and Owl Creek Mountains, where they range in age from 2.8 to 2.7 Ga. Deformation apparently ceased in these areas while it continued farther south in the province. The waning phases of the last deformation in the Wind River Range are recorded by the foliated Bridger batholith (2,670 ± 13 Ma, Aleinikoff and others, 1989), after which the 2.50 to 2.65 Ga postkinematic granites were emplaced. In the Teton Range, a similar pair of syn- and postkinematic granitoids have been described (Reed and Zartman, 1973) — the Webb Canyon Gneiss and Mount Owen Quartz Monzonite respectively — but their ages are too poorly known to determine whether they are age correlative with the granitoids of the Wind River Range. Deformation in the Granite Mountains preceded intrusion of the Lankin Dome granite at 2.59 ± .04 Ga, on the basis of U-Pb zircon and Rb-Sr dates, it is inferred to have taken place much earlier, at around 2,860 Ma (Peterman and Hildreth, 1978). The synkinematic Squaw Mountain granite gneiss in the central Laramie Mountains records yet a younger deformation at 2.62 ± .03 Ga (Snyder and others, 1988). In the Medicine Bow Mountains and Sierra Madre, deformation of the Phantom Lake metamorphic suite preceded intrusion of the Early Proterozoic Baggot Rocks granite.

Mafic inclusions and dikes

Mafic inclusions and dikes are found within and cutting surface exposures of Archean rocks in all of the Laramide uplifts of the Wyoming province. Few are dated directly and, with the exception of amphibolite inclusions in younger granitoid rocks in the eastern Beartooth Mountains, none are dated with precisions of a few million years. Nevertheless, it is often possible to define a number of Archean events involving the intrusion of mafic magma within a

given Laramide uplift based upon crosscutting relationships and the degree of deformation exhibited by mafic rocks. Snyder and others (1990) noted the apparent contrast between the ages of mafic dikes from the Wyoming province and those of the Superior province. Whereas mafic dikes in the Superior province are predominately of Matachewan age (2.6 Ga), mafic dikes in Wyoming span a range of ages from greater than 3.0 Ga to latest Archean.

Geochemical and isotopic evidence of early establishment of the Wyoming province

Although there is considerable debate about the pattern of continental growth in the Archean, it is clear that at least some parts of the Earth's continental crust were present in the Early Archean. The first crust to form from partial melts of Archean mantle may have been tonalitic, and only upon further intracrustal melting may the crust have differentiated, producing a large-ion-lithophile enriched upper crust (Barker and Peterman, 1974). A number of lines of evidence suggest that the Wyoming province may be among the earliest portions of the continental crust to achieve this evolved state. As observed above, the Archean rocks of the province record a long and complex history, which, from ion microprobe dating of zircons, seems to have extended back at least as far as 3.8 Ga. The geochemical and isotopic characteristics of the gneisses, granitoids, and metasediments also provide evidence that continental crust was established and geochemically differentiated within the Wyoming province by Middle Archean time.

Evidence from gneisses and intrusive rocks

A striking feature of the Archean rocks of the Wyoming province is the paucity of tonalites and trondhjemites. The best studied low-potassium rocks are the Lake Helen E1 gneiss and the E2 trondhjemite, tonalite, and granodiorite pluton of the southern Bighorn Mountains. As is characteristic of the tonalitic rocks, the rare-earth patterns of the Bighorn gneiss and intrusion have no Eu anomaly (Barker and others, 1979a). The Wilson Creek area of the Wind River Range also contains quartzo-feldspathic gneisses with no pronounced Eu anomalies (Barker and others, 1979b). Small volumes of tonalitic rocks also have been observed in the southern Madison Range and elsewhere in southwest Montana (Erslev, 1983; Houston and others, in press), the northwest Beartooth Mountains (Mogk and Henry, 1988), and the Teton Range (Miller and others, 1986), but they are rarely the dominant rock type.

Moderately potassic rocks are much more volumetrically significant than tonalites in the Wyoming province. They are found both as prekinematic and synkinematic gneisses and as postkinematic granites. Potassic gneisses are found in the eastern Beartooth Mountains (Mogk and Henry, 1988; Wooden and others, 1988), and they compose the Webb Canyon gneiss of the Teton Range (Miller and others, 1986) and the Bridger batholith of the Wind River Range (Koesterer and others, 1987). Except in the southern Bighorn Mountains, where trondhjemite is more voluminous than granodiorite, the postkinematic granitoids are potassic granites and granodiorites. Although they have a wide range of light rare-earth element (LREE) enrichment [$(La/Yb)_n$= 8-100; Gosselin and others, 1988], almost all have slightly to strongly negative Eu anomalies (Gosselin and others, 1988; Stuckless and others, 1986; Koesterer and others, 1987). The negative Eu anomaly distinguishes these granitoids from typical Archean tonalites and trondhjemites (e.g., Taylor and McLennan, 1985, p. 210).

Several of the Late Archean granitoids of the province have geochemical characteristics that indicate they were source rocks for uranium deposits. The high uranium and other incompatible element contents of these granitoids suggests they were derived from sources that had undergone intracrustal recycling, during which an enrichment in incompatible elements occurred. Studies of the granites of the Granite Mountains have shown that uranium was lost from the intrusions during Tertiary exposure to the near-surface environment and is now found in nearby sedimentary uranium deposits (Stuckless and

Nkomo, 1978, 1980). Uranium in the granite of the Owl Creek Mountains was similarly mobilized during Laramide time, although no economic uranium deposits are associated with this source rock (Stuckless and others, 1986). The S-type chemical characteristics of the Bears Ears pluton in the Wind River Range suggest that it may have contained similar amounts of uranium, but Stuckless (1989) concluded that uranium may have been lost from the protolith prior to generation of this granite.

Evidence for early establishment of evolved continental crust in the Wyoming province is also provided by lead isotopic data. Wooden and Mueller (1988) compiled initial Pb isotopic compositions for the Wind River and Granite mountains granitoids and for amphibolites and granitoids of the eastern Beartooth Mountains. They observed that all of these rocks have Pb isotopic compositions that are more radiogenic than the mantle. Wooden and Mueller proposed that a component of evolved Early Archean crust must be involved in order to produce igneous rocks with these characteristics. This crust would attain the required radiogenic Pb isotopic signature so long as no uranium was lost through high-grade metamorphism for several hundred million years after it was formed.

The initial Sr isotopic ratios for the gneisses and granites of the Wyoming province also suggest the presence of old, evolved continental crust. Only the oldest gneisses in the Beartooth and Bighorn mountains have initial Sr isotopic ratios similar to or less radiogenic than the bulk earth, indicating that these rocks were derived either from mantle or young continental sources. All other initial Sr isotopic ratios are higher, and lie within the range typical of continental crustal rocks (**Figure 4**). These rocks must have been formed at least in part from sources in the upper continental crust that had evolved fairly radiogenic compositions. Taken together, the initial Sr data suggests that continental crust was established and was being recycled into granitoids and their extrusive equivalents by 2.9 Ga.

Evidence from metasedimentary rocks

The supracrustal sequences throughout the Wyoming province contain moderate amounts of pelitic schist. The sedimentary precursor, mature mudstone, suggests a continent with a long history of one or more cycles of erosion, transport, and deposition of sediments. In southwest Montana, geochemical data from pelitic metasediments corroborates this supposition. Pelitic schists from the South Snowy block of the Beartooth Mountains and from the southern Madison Range were found to have LREE-enriched patterns [$(La/Lu)_n = 2$)] and negative Eu anomalies (Gibbs and others, 1986). These rare-earth patterns are indistinguishable from those of the North American Shale Composite (NASC) and the post-Archean Australian shale of Taylor and McLennan (1985). Present-day mudstones with these rare-earth characteristics are derived from geochemically evolved crust. By analogy, Gibbs and others (1986) suggested that the source area for the Archean pelitic schist in southwest Montana was similarly differentiated.

Nd isotopic evidence of early establishment of the Wyoming province

Sm-Nd model "crustal residence" ages of various Archean lithologies are a relatively new, effective technique for overcoming some of the limitations geologists face in studying the Archean history of the Wyoming province. These limitations include the inaccessibility of nearly 90% of the Archean basement, which is overlain by Phanerozoic sediments and sedimentary rocks, and also the obliteration of much of the Archean crust by the intrusion of Late Archean granites.

Model crustal residence ages calculated from Sm-Nd isotopic measurements represent estimates of the average periods of residence in the continental crust of the rare-earth component of a sediment. The crustal residence age can be construed as the length of time elapsed since the sample possessed the same $^{143}Nd/^{144}Nd$ ratio as the mantle from which its precursors were extracted. Because igneous bodies and sedimentary rocks are rarely derived from a single source, but rather are mixtures of different mantle

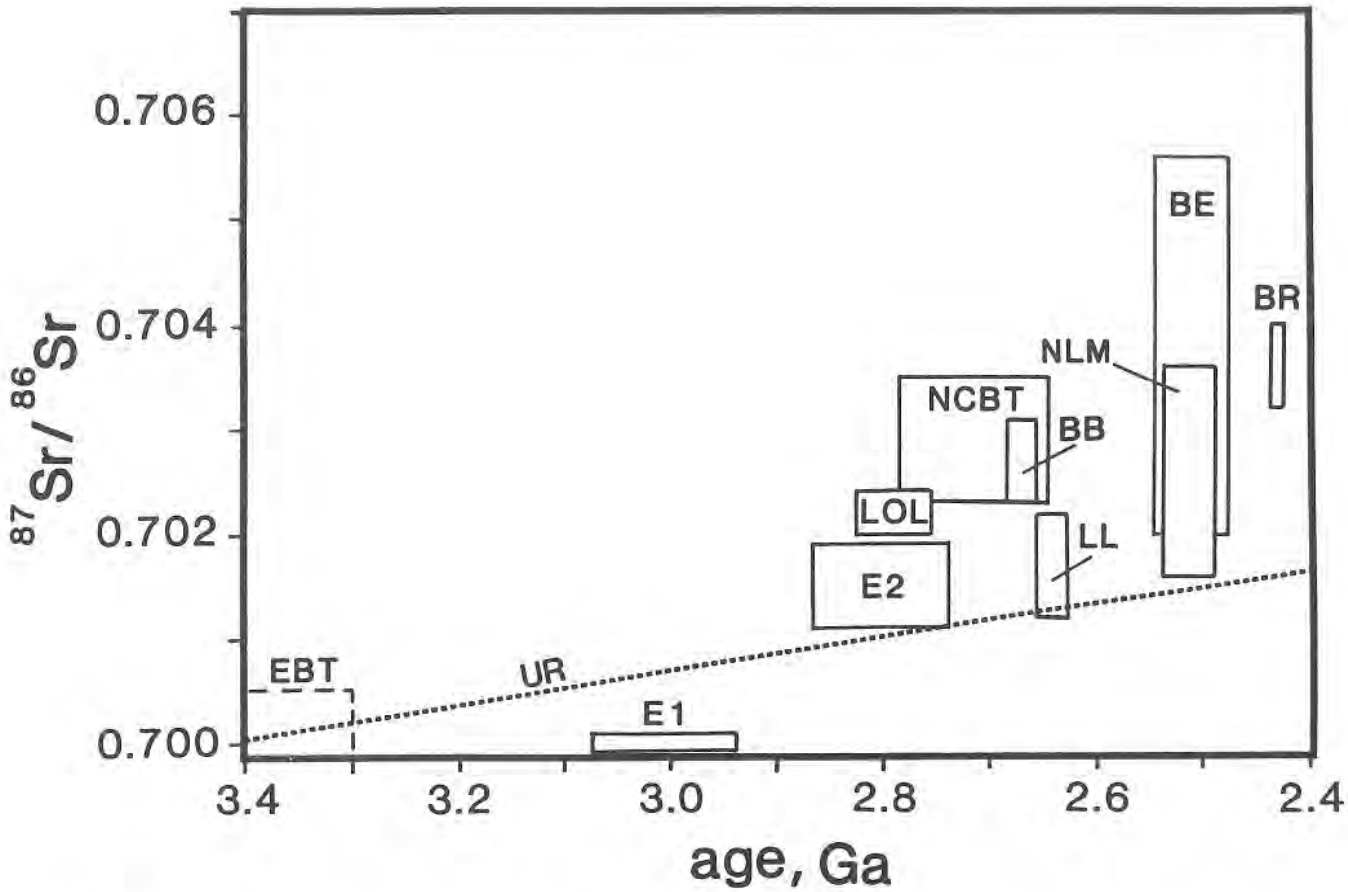

Figure 4. Variation of initial Sr isotopic ratio with age (determined using either U-Pb or Rb-Sr methods) for plutons from the Wyoming province. BB = Bridger batholith (Koesterer and others, 1987; Aleinikoff and others, 1989); BE = Bears Ears (Stuckless and others, 1985); BR = Baggot Rocks (Johnson and Hills, 1976); EBT = eastern Beartooth Mountains (Henry and others, 1982); E1 = early gneiss and E2 = postkinematic trondjhemite, both of the Bighorn Mountains (Arth, and others, 1980); LL = Louis Lake (Naylor and others, 1970; Stuckless and others, 1985); LOL = Long Lake (Wooden and others, 1982); NCBT = north-central Beartooth Mountains (Wooden and others, 1988); NLM = northern Laramie Mountains granite (Johnson and Hills, 1976). Dashed line shows the way the initial Sr ratio would evolve with age in a uniform reservoir (UR).

and crustal materials, the crustal residence age rarely identifies the time when a particular magma was extracted from the mantle and incorporated into the crust. Rather, the model age represents an average time, weighted according to the amount of Nd from different sources.

Nd model ages for sedimentary and igneous rocks provide information about different parts of the continental crust. Because clastic sedimentary rocks are mixtures of erosional products, crustal residence ages for sediments reflect the age of the exposed crust that was being eroded. Therefore, they can provide information about the average age of the rocks at the Earth's surface at the time the sediment was deposited. In contrast, igneous rocks form from mantle- and crust-derived magmas. They reflect to some degree the types of material that are available in a vertical profile beneath the level at which the magma crystallizes. Thus, model ages from igneous rocks give an indication of the mean age of rocks beneath the surface.

Nd isotopic data from Wyoming province metasedimentary rocks

Nd isotopic analyses are available for Archean metasedimentary rocks from the Beartooth, Madison, and Gravelly ranges in the northwestern Wyoming province, and from the Wind River, Owl Creek, Granite, Laramie, and Hartville uplifts in the central and

southern part of the province (**Table 2; Figure 5**). The samples described by C.D. Frost (unpublished data) are mainly pelitic schists. These metamorphosed mudstones were probably produced by repeated cycles of erosion and deposition in large drainages, and hence may provide a good average crustal residence age for large tracts of exposed Archean crust. The depositional ages of these samples are poorly known; however, most are thought to be Late Archean. Thus their model crustal residence ages provide an indication of the average age of the crust exposed at about this time. Model ages from the Archean metasediments, calculated relative to the depleted mantle model of Goldstein and others (1984), range from 3.8 to 2.7, but most are between 3.0 and 3.4 Ga. The oldest model ages are from the Granite, Owl Creek, and Beartooth mountains, but the average model age from each range is similar. Model ages calculated relative to a chondritic mantle reported for metasediments from the Beartooth Mountains likewise suggest the availability of Middle Archean sediment sources (Wooden and others, 1988).

Table 2. Location, rock type, and Nd crustal residence ages of Archean metasediment samples from the Wyoming province.

Sample	Description	Nd crustal residence age (Ga)
WIND RIVER RANGE		
WP1	cordierite schist	3.29
4CF8	garnet-biotite schist	3.41
4CF37	garnet-biotite schist	2.94
4CF53	garnet-biotite schist	3.40
FPN81-3	garnet-cordierite schist	3.39
FPN81-11b	garnet schist	3.17
DM83-28	garnet-cordierite schist	3.34
SOUTH PASS		
AR-7	biotite schist	3.15
GRANITE MOUNTAINS		
WP3	cordierite schist	2.95
WP7	sillimanite schist	3.68
WP15	garnet-biotite schist	3.78
BEARTOOTH MOUNTAINS		
4-44	garnet-biotite schist	3.20
WS84	garnet-biotite schist	2.70
WS86	garnet-biotite schist	3.42
AV14	biotite schist	3.41
CM79-3	biotite schist	3.37
CM79-6b	silicate iron formation	3.81
CM80-20	biotite schist	3.25
OWL CREEK MOUNTAINS		
OC-1	garnet-biotite schist	3.48
LARAMIE MOUNTAINS AND HARTVILLE UPLIFT		
WP35	sillimanite-biotite schist	3.16
WP36	sillimanite-staurolite schist	3.32
WP38	sillimanite-kyanite schist	2.97

In general, metasediment samples analyzed can be divided into three types. The first are those associated with the greenstone successions at South Pass and the Owl Creek, Seminoe, and Laramie mountains. The South Pass succession has been interpreted as a dismembered ophiolite sequence (Harper, 1985), based on the presence of metagabbros, pillow lavas, and metasedimentary rocks including iron formation. Similar lithologies are found within the sequences in the Seminoe and Laramie mountains (Snyder and others, 1988). The second metasediment type appears to represent continental platform deposits such as those in the Beartooth Mountains, the ranges of southwest Montana, and the Hartville uplift, where metacarbonates and fluvial clastic sediments predominate. The third type of meta-sediments, whose depositional environment is indeterminate, are found as inclusions and disrupted belts within high-grade gneisses. Both continental platform sediments and greenstone-type sediments give similar model ages, suggesting that they were derived from crust of similar average age. This result argues against the formation of greenstone belt rocks in a wide ocean basin away from continental influences. Instead, these metasedimentary rocks must have been deposited in narrow oceanic troughs or upon continental crust itself, where a supply of terriginous material was readily available.

Nd isotopic data from Wyoming province granitoids

Published Nd isotopic data (other than that summarized graphically or in abstracts) from Wyoming province granitoids are restricted to the Wind River Range (Koesterer and others, 1987; Grisham, 1987;

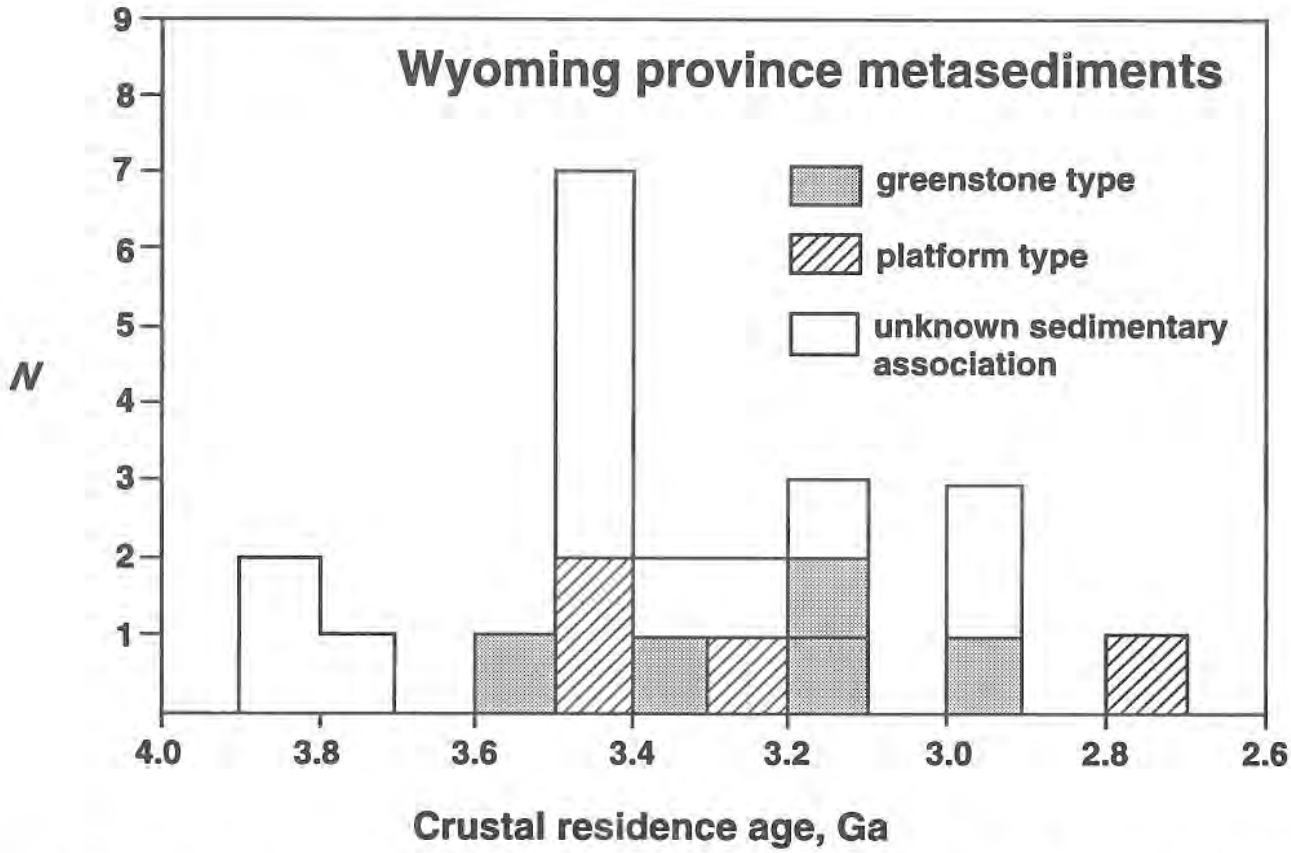

Figure 5. Nd model crustal residence ages for metasedimentary rocks from the Wyoming province. Metasediments from the Owl Creek Mountains, Laramie Mountains, and South Pass are classified as greenstone type, those of the Beartooth Mountains are identified as platform type, and samples from the other ranges are of unknown association (unpublished data from C.D. Frost).

Lawrence, 1987; Hulsebosch, unpublished data) and the Beartooth Mountains (Wooden and Mueller, 1988; Mogk and others, 1988). The crustal residence ages for granitoids from the Wind River Range are on average several hundred million years younger than those for the metasediments (**Figure 6**). Similar relationships exist between model ages for metasedimentary and granitoid rocks in the Beartooth Mountains, where chondritic Nd model ages for intrusive rocks from the Beartooth Mountains overlap but are on average younger than those reported for metasediment and gneiss samples (Wooden and Mueller, 1988; Wooden and others, 1988; Mogk and others, 1988).

This disparity can be explained in two ways. The granitoids may have been derived entirely from Archean continental crust, but this crust had become age stratified through thrusting or magmatic underplating, with the result that exposed portions of the crust were considerably older than lower portions. As a result, metasedimentary rocks derived from the surface of the Late Archean continent would not be typical of the whole crust. Alternatively, the metasedimentary rocks provide a good estimate of the average age of Archean continental crust in this area, but the granitoids incorporated a mixture of continental crust and juvenile mantle magmas, resulting in a Nd model age intermediate between that of the metasedimentary rocks and the emplacement age.

Nd crustal residence ages for granitoids in the Wind River Range depend upon their emplacement ages. The older orthogneiss, which is 2.8 Ga or older (**Figure 3**), yields the oldest model ages of 3.19 to 3.37 Ga. The 2.7 Ga Bridger batholith and the postkine-

matic 2.65 Ga Louis Lake and Bears Ears granitoids yield overlapping Nd model ages of 3.05 and 3.00 Ga, respectively. The model ages for all these granitoids show a considerable range (**Figure 6**), indicating either that different portions of the batholiths sampled different portions of a heterogeneous crust, or that they are composed of different proportions of crustal and mantle melts. The older orthogneiss magmas either sampled continental crust that was on average older than that available to syn- and postkinematic granitoids, or the older orthogneiss magmas incorporated a smaller mantle component.

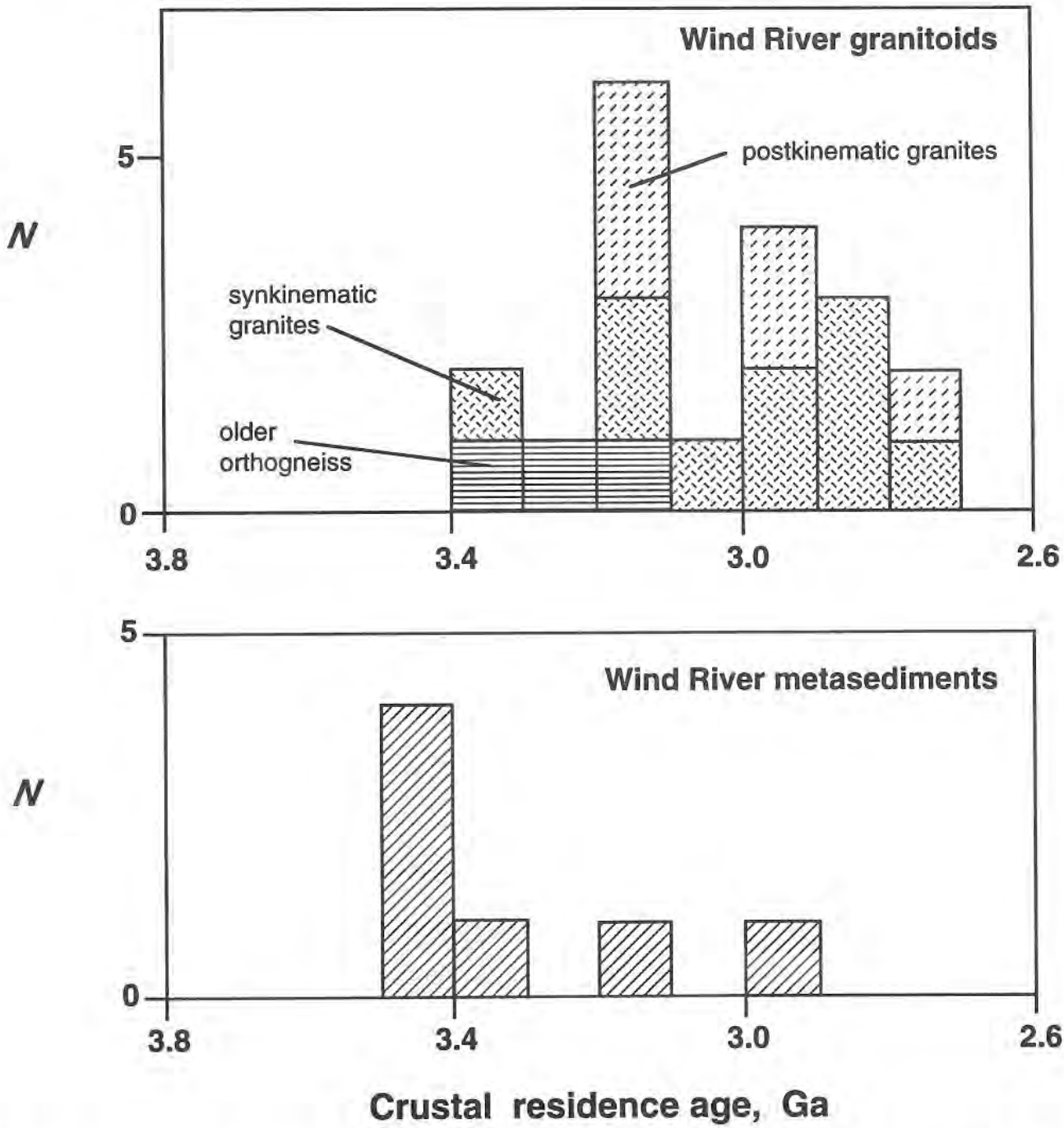

Figure 6. Comparison of Nd model crustal residence ages for metasedimentary rocks and granites from the Wind River Range. Data from Koesterer and others (1987) and C.D. Frost (unpublished data).

Discussion and conclusions

When considering models of the tectonic history of the Wyoming province, it is important to recall the incomplete state of geologic information upon which any model must be built. The Archean rocks of the province have been mapped mainly at the reconnaissance level; only a small percentage of Archean outcrop is mapped in detail. In addition, the ages of only a few units within the province are known precisely enough to reconstruct detailed histories. From a consideration of Phanerozoic orogenies, we recognize that significant tectonic events can be encompassed in a period of time as short as a few tens of millions of years, a time interval that is typical of the uncertainties on many Archean age determinations. Thus, until there is a large enough population of precise dates and detailed enough mapping to constrain the tectonic environment of any unit that is being dated, tectonic models for the Archean of Wyoming must necessarily remain generalized. Despite these qualifications, there are still enough data available to identify significant characteristics of the Archean evolution of the Wyoming province.

Perhaps the most important conclusion that can be drawn from the data described above is that *the Wyoming province represents one of the oldest portions of continental crust in North America.* Indeed, with individual zircon dates of 3.8 Ga, *it preserves evidence of some of the oldest continental crust in the world.* In North America, similarly old crust is found in the Slave province of the Northwest Territories (Bowring and others, 1989) and in the Nain province of Labrador and west Greenland (Bridgwater and others, 1978). As in the Wyoming province, the oldest rocks in these localities are gneisses containing inclusions of older supracrustal rocks.

One consequence of this antiquity is the early geochemical differentiation of the Wyoming province. Most of the Archean gneisses and granitoids are moderately potassic, geochemically and isotopically evolved rocks. Evidently, the early establishment of continental crust allowed for enough intracrustal recycling and differentiation that by the Late Archean granodiorites and granites predominated over tonalitic rocks. The fine-grained sediments formed by erosion of this continental surface were likewise mature shales. The evolved character of the Wyoming province contrasts with the Superior province, where greenstone belts predominate. Much of the Superior province was formed in the Late Archean (Card, 1990) and is less evolved geochemically (Wooden and Mueller, 1988). *The Archean rocks of the Wyoming province cannot be laterally correlative with those of the Superior province.*

The Superior province was assembled, at least in part, by the amalgamation of a series of island arcs (Hoffman, 1989; Card, 1990). Likewise, the Proterozoic Colorado province is composed of progressively younger arcs that were sutured to the southern boundary of the Wyoming province (Reed and others, 1987). In both areas, volcanic and plutonic rocks formed during the collision have Nd model ages that do not differ greatly from crystallization ages (Nelson and DePaolo, 1984; Peterman and Futa, 1987), confirming the absence of significant volumes of Middle and Early Archean continental crust. In contrast, the assembly history of the Wyoming province appears to have followed a very different pattern. There is a common early history across the province as suggested by Early and Middle Archean ages from zircons in metasedimentary rocks and gneisses. Late Archean granitoids provide Nd model ages that may differ significantly from their crystallization ages, indicating that the granitic magmas were derived from much older continental protoliths. Sedimentary belts within the province yield Nd model ages that are Early to Middle Archean, demonstrating that old continental rocks were exposed at the Earth's surface in Late Archean time. Mafic dikes were emplaced throughout the Archean and were not more voluminous at any particular time, which might date the occurrence of a fundamental province-wide tectonic process. Together, these data suggest that the *Wyoming province was assembled in the Early or Middle Archean.* Subsequent plutonic and tectonic events appear to have been concentrated on the margins of this continent. Conversely, if the Wyoming province had been amalgamated in the Late Archean, it had to be assembled from continental microplates with similar Early and Middle Archean histories and with evidence of intervening oceanic basins obliterated.

If we assume that the Wyoming province was established early, then the diachroneity of Late Archean deformation and plutonism cannot be related to the initial assembly of the province. The postkinematic intrusions

have a calc-alkaline affinity similar to Phanerozoic subduction-related plutons, and therefore could be the product of plate-tectonic processes. The Late Archean sedimentary successions are also compatible with plate-tectonic interpretations of deposition in back-arc rift or Tethyan-type narrow oceanic environments. The latest Archean sedimentation and plutonism appears to have taken place around the southern margins of the Wyoming province. Although such a model is not detailed, it describes the geologic framework of the Late Archean in terms of plate-tectonic processes. We envision that future work will verify and greatly expand upon this tectonic framework.

References cited

Aleinikoff, J.N., Williams, I.S., Compston, W., Stuckless, J.S., and Worl, R.G., 1989, Evidence for an Early Archean component in the Middle to Late Archean gneisses of the Wind River Range, west-central Wyoming: conventional and ion microprobe U-Pb data: Contributions to Mineralogy and Petrology, v. 101, p. 198-206.

Arth, J.G., Barker, F., and Stern, T.W., 1980, Geochronology of Archean gneisses in the Lake Helen area, southwestern Bighorn Mountains, Wyoming: Precambrian Research, v. 11, p. 11-22.

Barker, F., and Peterman, Z.E., 1974, Bimodal tholeiitic-dacitic magmatism and the early Precambrian crust: Precambrian Research, v. 1, p. 1-12.

Barker, F., Arth, J.G., and Millard, H.T., 1979a, Archean trondhjemites of the southwestern Bighorn Mountains, Wyoming: a preliminary report, *in* Barker, F., editor, Developments in petrology 6: Trondhjemites, dacites and related rocks: Elsevier Scientific Publishing Company, Amsterdam, p. 401-414.

Barker, F., Millard, H.T., and Lipman, P.W., 1979b, Four low-K siliceous rocks of the western U.S, *in* Barker, F., editor, Developments in petrology 6: Trondhje-mites, dacites and related rocks: Elsevier Scientific Publishing Company, Amsterdam, p. 415-433.

Bowring, S.A., Williams, I.S., and Compston, W., 1989, 3.96 Ga gneisses from the Slave province, Northwest Territories, Canada: Geology, v. 17, p. 971-975.

Bridgwater, D., Collerson, K.D., and Myers, J.S., 1978, The development of Archaean gneiss complex of the North Atlantic region, *in* Tarling, D.H., editor, Evolution of the Earth's crust: Academic Press, London, p. 19-69.

Card, K., 1990, A review of the Superior province of the Canadian Shield, a product of Archean accretion: Precambrian Research, v. 48, p. 99-156.

DePaolo, D.J., and Wasserburg, G.J., 1979, Sm-Nd age of the Stillwater Complex and the mantle evolution curve for neodymium: Geochimica et Cosmochimica Acta, v. 43, p. 999-1008.

Erslev, E.A., 1983, Pre-Beltian geology of the southern Madison Range, southwestern Montana: Montana Bureau of Mines and Geology Memoir 55, 26 p.

Fischer, L.B., and Stacey, J.S., 1986, Uranium-lead zircon ages and common lead measurements for the Archean gneisses of the Granite Mountains, Wyoming: U.S. Geological Survey Bulletin, 1622, p. 13-23.

Gast, P.W., Kulp, J.L., and Long, L.E., 1958, Absolute age of early Precambrian rocks in the Bighorn Basin of Wyoming and Montana, and southeastern Manitoba: Transactions of the American Geophysical Union, v. 39, p. 322-334.

Gibbs, A.K., Montgomery, C.W., O'Day, P.A., and Erslev, E.A., 1986, The Archean-Proterozoic transition: evidence from the geochemistry of metasedimentary rocks of Guyana and Montana: Geochimica et Cosmochimica Acta, v. 50, p. 2125-2141.

Goldstein, S.L., O'Nions, R.K., and Hamilton, P.J., 1984, A Sm-Nd isotopic study of atmospheric dusts and particulates from major river systems: Earth and Planetary Science Letters, v. 70, p. 221-236.

Gosselin, D.C., Papike, J.J., Zartman, R.E., Peterman, Z.E., and Laul, J.C., 1988, Archean rocks of the Black Hills, South Dakota: reworked basement from the southern extension of the Trans-Hudson orogen: Geological Society of America Bulletin, v. 100, p. 1244-1259.

Grisham, D. K., 1987, Rb-Sr and Sm-Nd geochronology of a Late Archean granite, central Wind River Mountains, Wyoming [B.S. honors thesis]: Laramie, University of Wyoming, 27 p.

Harper, G.D., 1985, Dismembered Archean ophiolite, Wind River Mountains, Wyoming (U.S.A.): Ofioliti, v. 10, p. 297-306.

Heimlich, R.A., and Armstrong, R.L., 1972, Variance of Precambrian K-Ar biotite dates, Bighorn Mountains, Wyoming: Earth and Planetary Science Letters, v. 14, p. 75-78.

Heimlich, R.A., and Banks, P.O., 1968, Radiometric age determinations, Bighorn Mountains, Wyoming: American Journal of Science, v. 266, p. 180-192.

Henry, D.J., Mueller, P.A., Wooden, J.L., Warner, J.L., and Lee-Berman, R., 1982, Granulite grade supracrustal assemblages of the Quad Creek area, eastern Beartooth Mountains, Montana, *in* Mueller, P.A., and Wooden, J.L., editors, Precambrian geology of the Beartooth Mountains, Montana and Wyoming: Montana Bureau of Mines and Geology Special Publication 84, p. 147-158.

Hoffman, P.F., 1988, United Plates of America, the birth of a craton: Early Proterozoic assembly and growth of Laurentia: Annual Reviews of Earth and Planetary Science, v. 16, p. 543-603.

_____ 1989, Precambrian geology and tectonic history of North America, *in* Bally, A.W., editor, The geology of North America: an overview: Geological Society of America, The Geology of North America, v. A, p. 447-512.

Houston, R.S., Karlstrom, K.E., Hills, F.A., and Smithson, S.B., 1979, The Cheyenne belt; the major Precambrian crustal boundary in the western United States: Geological Society of America Abstracts with Programs, v. 11, p. 446.

Houston, R.S., Reed, J.C. Jr., Karlstrom, K.E., Erslev, E.A., Snyder, G.L., Worl, R.G., Bryant, B., Reynolds, M.W., Peterman, Z.E., Page, N.J., Zientek, M.L., and Frost, C.D., in press, The Wyoming province, *in* Reed, J.C. Jr., Silver, L.T., Sims, P.K., Rankin, D.W., Houston, R.S., and Reynolds, M.W., editors, Precambrian, conterminous U.S.: Geological Society of America, The Geology of North America, v. C2.

Johnson, R.C., and Hills, A.F., 1976, Precambrian geochronology and geology of the Boxelder Canyon area, northern Laramie Range, Wyoming: Geological Society of America Bulletin, v. 87, p. 809-817.

Koesterer, M.E., Frost, C.D., Frost, B.R., Hulsebosch, T.P., Bridgwater, D., and Worl, R.G., 1987, Development of the Archean crust in the Medina Mountain area, Wind River Range, Wyoming (U.S.A.): Precambrian Research, v. 37, p. 287-304.

Lawrence, S.W., 1987, Sm-Nd and Rb-Sr isotope geochemistry of a Late Archean supracrustal belt, central Wind River Mountains, Wyoming [B.S. honors thesis]: Laramie, University of Wyoming, 48 p.

Love, J.D. and Christiansen, A.C., 1985, Geologic map of Wyoming: U.S. Geological Survey, scale 1:500,000.

Love, J.D., Weitz, J., and Hose, R.K., 1955, Geologic map of Wyoming: U.S. Geological Survey, scale 1:500,000.

Ludwig, K.R., and Stuckless, J.S., 1978, Uranium-lead isotope systematics and apparent ages of zircons and other minerals in Precambrian granitic rocks, Granite Mountains, Wyoming: Contributions to Mineralogy and Petrology, v. 65, p. 243-254.

Lush, A.P., McGrew, A.J., Snoke, A.W., and Wright, J.E., 1988, Allochthonous Archean basement in the northern East Humboldt Range, Nevada: Geology, v. 16, p. 349-353.

Miller, S.H., Hildebrandt, P.K., Erslev, E.A., and Reed, J.C., Jr., 1986, Metamorphic and deformation history of the gneiss complex in the northern Teton Range, Wyoming: 1986 Montana Geological Society - Yellowstone-Beartooth Research Association Field Conference, p. 91-109.

Mogk, D.M., and Henry, D., 1988, Metamorphic petrology of the northern Archean Wyoming province, southwestern Montana: evidence for Archean collisional tectonics, *in* Ernst, W.G., editor, Metamorphism and crustal evolution of the western United States, Rubey Volume VII: Englewood Cliffs, New Jersey, Prentice Hall, p. 362-382.

Mogk, D.W., Mueller, P.A., and Wooden, J.L., 1988, Archean tectonics of the North Snowy block, Beartooth Mountains, Montana: Journal of Geology, v. 96, p. 125-141.

Mueller, P.A., Peterman, Z.E., and Granath, J.W., 1985, A bimodal Archean volcanic series, Owl Creek Mountains, Wyoming: Journal of Geology, v. 93, p. 701-712.

Mueller, P.A., Wooden, J.L., and Nutman, A.P., 1992, 3.96 Ga zircons from an Archean quartzite, Beartooth Mountains, Montana: Geology, v. 20., p. 327-330.

Naylor, R.S., Steiger, R.H., and Wasserburg, G.J., 1970, U-Th-Pb and Rb-Sr systematics in 2700 x 10^6-year-old plutons from the southern Wind River Range, Wyoming: Geochimica et Cosmochimica Acta, v. 34, p. 1133-1159.

Nelson, B.K., and DePaolo, D.J., 1984, 1,700 Myr greenstone volcanic successions in southwestern North American and isotopic evolution of the Proterozoic mantle: Nature, v. 312, p. 143-146.

Nunes, P.D., and Tilton, G.R., 1971, Uranium-lead ages of minerals from the Stillwater igneous complex and

associated rocks, Montana: Geological Society of America Bulletin, v. 82, p. 2231-2250.

Peterman, Z.E., 1982, Geochronology of the southern Wyoming age province, a summary, *in* Goldich, S.S., Chairman, 1982 Archean Geochemistry Field Conference, August 15-19, 1982, Guide to field trips, pt. 1, Seminoe Mountains and Hartville uplift, Wyoming: IGCP Archean Geochemistry Project, U.S. Working Group, p. 1-23.

Peterman, Z.E., and Futa, K., 1987, Is the Archean Wyoming province exotic to the Superior craton? Evidence from Sm-Nd model ages of basement cores: Geological Society of America Abstracts with Programs, v. 19, p. 803.

Peterman, Z.E., and Hildreth, R.A., 1978, Reconnaissance geology and geochronology of the Precambrian of the Granite Mountains, Wyoming: U.S. Geological Survey Professional Paper 1055, 22 p.

Premo, W.R., and Van Schmus, W.R., 1989, Zircon geochronology of Precambrian rocks in southeastern Wyoming and northern Colorado, *in* Proterozoic geology of the Southern Rockies: Geological Society of America Special Paper 235, p. 13-32.

Reed, J.C., Jr., Bickford, M.E., Premo, W.R., Aleinikoff, J.N., and Pallister, J.S., 1987, Evolution of the Early Proterozoic Colorado province: constraints from U-Pb geochronology: Geology, v. 15, p. 861-865.

Reed, J.C., Jr., and Zartman, R.E., 1973, Geochronology of Precambrian rocks of the Teton Range, Wyoming: Geological Society of America Bulletin, v. 84, p. 561-582.

Snyder, G.L., Frost, B.R., Grant, J.A., Lindsley, D.H., and Peterman, Z.E., 1988, The crust of a young Earth—guide to the Precambrian continental core of southeastern Wyoming, *in* Holden, G.S., editor, Geological Society of America Field Trip Guidebook 1988: Colorado School of Mines Professional Contributions No. 12, p. 1-34.

Snyder, G.L., Hall, R.P., Hughes, D.J., and Ludwig, K.R., 1990, Early Precambrian rocks of the USA, *in* Hall, R.P., and Hughes, D.J., editors, Early Precambrian basic magmatism: Blackie, Glasgow, p. 191-220.

Stuckless, J.S., 1989, Petrogenesis of two contrasting, Late Archean granitoids, Wind River Range, Wyoming: U.S. Geological Survey Professional Paper 1491, 38 p.

Stuckless, J.S., and Nkomo, I.T., 1978, Uranium-lead isotope systematics in uraniferous alkali-rich granites from the Granite Mountains, Wyoming: implications for uranium source rocks: Economic Geology, v. 73, p. 427-441.

_____ 1980, Preliminary investigations of U-Th-Pb systematics in uranium-bearing minerals from two granitic rocks from the Granite Mountains, Wyoming: Economic Geology, v. 75, p. 289-295.

Stuckless, J.S., Hedge, C.E., Worl, R.G., Simmons, K.R., Nkomo, I.T., and Wenner, D.B., 1985, Isotopic studies of the Late Archean plutonic rocks of the Wind River Range, Wyoming: Geological Society of America Bulletin, v. 96, p. 850-860.

Stuckless, J.S., Nkomo, I.T., and Butt, K.A., 1986, Uranium-thorium-lead systematics of an Archean granite from the Owl Creek Mountains, Wyoming: U.S. Geological Survey Professional Paper 1388C, p. 39-48.

Stueber, A.M., Heimlich, R.A., and Ikramuddin, M., 1976, Rb-Sr ages of Precambrian mafic dikes, Bighorn Mountains, Wyoming: Geological Society of America Bulletin, v. 87, p. 909-914.

Taylor, S.R., and McLennan, S.M., 1985, The continental crust: its composition and evolution: Oxford, Blackwell Scientific Publications, 312 p.

Wooden, J.L., and Mueller, P.A., 1988, Pb, Sr, and Nd isotopic compositions of a suite of Late Archean igneous rocks, eastern Beartooth Mountains: implications for crust-mantle evolution: Earth and Planetary Science Letters, v. 87, p. 59-72.

Wooden, J.L., Mueller, P.A., Hunt, D.K., and Bowes, D.R., 1982, Geochemistry and Rb-Sr geochronology of the Archean rocks from the interior of the southeastern Beartooth Mountains, Montana and Wyoming, *in* Mueller, P.A., and Wooden, J.L., editors, Precambrian geology of the Beartooth Mountains, Montana and Wyoming: Montana Bureau of Mines and Geology Special Publication 84, p. 45-56.

Wooden, J.L., Mueller, P.A., and Mogk, D.W., 1988, A review of the geochemistry and geochronology of the Archean rocks of the northern part of the Wyoming province, *in* Ernst, W.G., editor, Metamorphism and crustal evolution of the western United States: Rubey Volume VII, Englewood Cliffs, New Jersey, Prentice Hall, p. 383-410.

Worl, R.G., Koesterer, M.E., and Hulsebosch, T.P., 1986, Geologic map of the Bridger Wilderness and the Green-Sweetwater Roadless Area, Sublette and Fremont counties, Wyoming: U.S. Geological Survey Miscellaneous Field Studies Map MF-1636-B, scale 1:250,000.

Frontispiece. View of cliff-forming Medicine Peak Quartzite (Proterozoic lower Libby Creek Group), central Medicine Bow Mountains, Wyoming.

Late Archean and Early Proterozoic geology of southeastern Wyoming

Robert S. Houston
Department of Geology and Geophysics
University of Wyoming
Laramie, Wyoming 82071

Abstract

Metamorphic rocks of Late Archean and Early Proterozoic age are exposed near the margin of the Archean Wyoming province in the Hartville uplift, southern Laramie Mountains, Medicine Bow Mountains, and Sierra Madre of southeastern and southern Wyoming. These metamorphic rocks are infolded with, lie unconformably on, or are in fault contact with gneisses and schists of Middle Archean age. Late Archean successions are approximately 2,700 Ma old and include a greenstone-belt type dominated by metavolcanic rocks or three-fold units consisting of metaconglomerate, quartzite, and metadolomite at the base; metavolcanic rocks and coarse clastic metasedimentary rocks in the middle; and quartzite or stromatolitic metadolomite at the top. The three-fold successions are located at the margin of the Archean Wyoming province and the greenstone-type successions are located on the landward side. The basal quartzite, metaconglomerate, and metadolomite of the three-fold succession are interpreted as shelf deposits; the middle volcaniclastic unit is interpreted as having been derived from an Andean-type arc that developed by north-directed subduction at the Wyoming province margin; and the upper quartzite or stromatolitic metadolomite may represent a return to marine deposition at the craton margin. The greenstone-belt successions landward of the craton margin may have been deposited in back-arc basins.

At the margin of the Wyoming province, in the Medicine Bow Mountains and Sierra Madre of southern Wyoming, a major fault system, the Cheyenne belt, is exposed. The Cheyenne belt is a northeast-striking series of fault blocks separated by zones of intense mylonitization. North of the Cheyenne belt, Early Proterozoic miogeoclinal metasedimentary rocks consisting of quartzite, metadolomite, and slate were deposited on Archean basement. South of the Cheyenne belt, Early Proterozoic metavolcanic and volcanogenic metasedimentary rocks are exposed in association with a complex suite of igneous intrusive rocks; and there is no evidence of Archean basement.

The Early Proterozoic (about 2.4 through 1.9 Ga) miogeoclinial rocks have a fluvial succession at the base (Deep Lake Group) that is thought to have developed during rifting. This fluvial succession is in fault contact with a glaciomarine succession that grades up-section into quartzite and schist (lower Libby Creek Group) interpreted as deltaic. The quartzite and schist of the lower Libby Creek Group are also interpreted as having developed during a rifting stage as a hypothetical southern continent separated from the Archean craton. Stromatolitic metadolomite (upper Libby Creek Group) that is in fault contact with the quartzites and schists of the lower Libby Creek Group is interpreted as a remnant of an Early Proterozoic carbonate platform. Metavolcanic rocks (pillow basalt) and black

Houston, R. S., 1993, Late Archean and Early Proterozoic geology of southeastern Wyoming, *in* Snoke, A.W., Steidtmann, J.R., and Roberts, S.M., editors, Geology of Wyoming: Geological Survey of Wyoming Memoir No. 5, p. 78-116.

graphitic slate (upper Libby Creek Group) that overly the stromatolitic dolomite may be remnants of foredeep basin deposits that developed as a volcanic arc collided with the rifted continental margin.

The Early Proterozoic (about 1.8 Ga) metavolcanic rocks and volcanogenic metasedimentary rocks south of the Cheyenne belt along with intermediate and mafic intrusive rocks of approximately the same age are interpreted as remnants of a magmatic arc. There is no isotope or geologic evidence indicating that these arc-related rocks are underlain by basement rocks older than 1.8 Ga, so they are considered juvenile crust.

Kinematic indicators in mylonitic rocks of the Cheyenne belt show a predominant south-side-up movement. If we include fault blocks within the Libby Creek Group, individual fault blocks within the Cheyenne belt show a distinct increase in metamorphic grade from north to south. The Cheyenne belt is interpreted as a Proterozoic suture, where the various allocthonous fault blocks of the Cheyenne belt and Libby Creek Group were thrust over autochthonous Deep Lake Group and underlying rocks of Archean age during arc-continent collision. Subsequent deformation rotated these various fault blocks to their present near-vertical orientation.

In the southern Sierra Madre, a series of cataclastic northwest-striking, right-lateral faults offset the volcanic arc succession and the Cheyenne belt. These right-lateral faults are related to an east-west zone of intense cataclasis in the central Sierra Madre that truncated and dismembered the Cheyenne belt. Kinematic analysis within the cataclastic zone suggests that it formed during north-directed thrusting.

South of the Cheyenne belt, syntectonic quartz monzonite and granite intrude metavolcanic rocks and associated mafic and intermediate intrusive rocks. These felsic intrusive rocks make up nearly 50% of the outcrop area in the Sierra Madre and more than 20% in the Medicine Bow Mountains. The felsic intrusive rocks were emplaced about 1.75 Ga, that is about 30 million years after the arc volcanism. They were probably emplaced during later stages of the deformational episode of the arc-continent collision and may have formed by melting at or near the base of a thickened crust.

This review of Late Archean and Early Proterozoic geology of the Wyoming province is an oversimplification, due in part to an incomplete record and in part to the need for additional detailed geologic and geochronologic studies. Problems associated with this and other interpretations of Late Archean and Early Proterozoic geology of this area are described in the text along with regional relationships that need to be clarified before a more satisfactory geologic history can be determined.

Regional framework

The Late Archean and Early Proterozoic history of Wyoming is closely tied to that of the Archean Wyoming province as a whole. Therefore, it is necessary to establish the regional setting before we examine the Proterozoic rocks of Wyoming. The Wyoming province is an Archean crustal plate largely covered by Phanerozoic sedimentary rocks, that is bordered on the east by a Proterozoic fold belt referred to as the Trans-Hudson orogenic belt and on the south by the Colorado Proterozoic province, where Proterozoic island-arc rocks were accreted to the rifted margin of the Archean plate (**Sheet 1**, Houston, map pocket; and **Figure 1**). The western margin of the Archean Wyoming province extends at least to the East Humboldt Range of northeastern Nevada (Lush and others, 1988), but its configuration can only be estimated from various geochemical and isotopic characteristics. The northern margin may coincide with a geophysical anomaly in Alberta that has been interpreted as a graben or possible suture between the Wyoming province and the Hearne province of Canada (Hoffman, 1988) (**Figure 1**), or with the Great Falls tectonic zone (Hoffman, 1989, figures 12 and 13).

The only rocks of Proterozoic age in the interior of the Wyoming province are mafic dikes and sills that range in age from about 2.2 Ga to 1.45 Ga. Early Proterozoic miogeoclinal metasedimentary and metavolcanic rocks overlie Archean basement at the margin of the Wyoming province in the Medicine Bow Mountains and Sierra Madre of southeastern Wyoming. The metasedimentary and metavolcanic

rocks border domes that expose Archean rocks in their cores on the east and west flanks of the Black Hills of South Dakota (**Sheet 1**, Houston, map pocket). The Red Creek Quartzite of the northeastern Uinta Mountains of Utah (**Sheet 1**, Houston, map pocket) may correlate with Proterozoic successions in the Medicine Bow Mountains (Graff and others, 1980). Metasedimentary rocks of the Little Willow Formation, located at the margin of the Wyoming province between Salt Lake City and Provo, Utah, may also be Early Proterozoic miogeoclinal rocks (Bryant, 1988). Middle and Late Proterozoic metasedimentary rocks overlie the Archean basement at its northwest margin in southwestern Montana, along its western margin in Idaho, and in a major reentrant in Utah and Colorado along the southwest margin. Early Proterozoic oceanic metavolcanic rocks of the Colorado Proterozoic province lie south of the Cheyenne belt in a series of fault blocks that

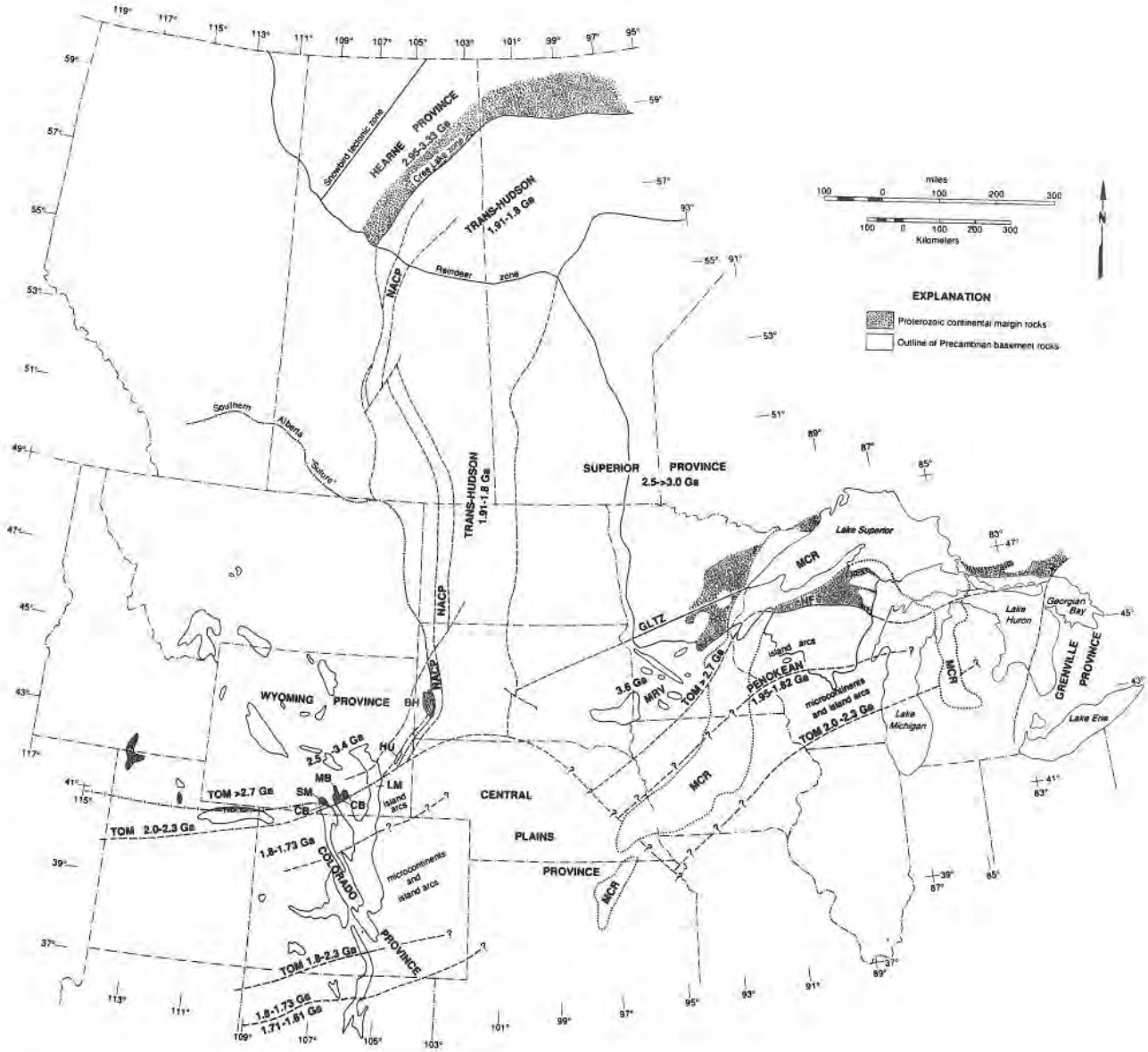

Figure 1. Regional setting of the Wyoming province.
Key: BH=Black Hills, CB=Cheyenne belt, GLTZ=Great Lakes tectonic zone, HU=Hartville uplift, LM=Laramie Mountains, MB=Medicine Bow Mountains, MCR=mid-continent rift, MRV=Minnesota River Valley, NACP=North American Central Plains anomaly, SM=Sierra Madre (sources are Bennett and DePaolo, 1987; Hoffman, 1988; Sims and Peterman, 1986; Reed and others, 1987). Dotted pattern=shelf-foredeep prisms.

mark the Archean continental margin of southern Wyoming (**Sheet 1**, Houston, map pocket).

Early Proterozoic metasedimentary and metavolcanic rocks are preserved at the inferred Archean plate margin, which is located in the Sierra Madre and Medicine Bow Mountains of southeastern Wyoming (**Figure 2**). These successions are in contact with, or are deformed and truncated by, a fundamental crustal discontinuity, named the Cheyenne belt by Houston and others (1979). The Medicine Bow Mountains, in particular, offer remarkable exposures of this zone of deformation, where Proterozoic island-arc rocks, once located well south of the belt of deformation, were accreted to the Archean plate margin. This zone of deformation projects northeast to the Laramie Mountains, where it is obscured by younger intrusions. East of the Laramie Mountains, the belt projects south of the Hartville uplift, where it appears to mark the northern limit of the Central Plains orogeny (Sims and Peterman, 1986).

Two contrasting successions of Early Proterozoic rocks are present along the plate margin of southeastern Wyoming. North of the Cheyenne belt, miogeoclinal metasedimentary rocks consisting of quartzite, metadolomite, and slate were deposited on Archean basement. South of the belt, metavolcanic and volcanogenic metasedimentary rocks are exposed in association with a complex suite of igneous intrusive rocks, and there is no evidence of Archean basement (Bennett and DePaolo, 1987; Ball and Farmer, 1991).

Rocks at the southeastern margin of the Wyoming province

Late Archean rocks and history

Archean crystalline rocks are exposed in the northern and eastern Sierra Madre, northwestern and northeastern Medicine Bow Mountains, central Laramie Mountains, and Hartville uplift (**Figure 3**). The oldest rocks are gneisses and migmatites that yield Rb-Sr model ages of about 3,200 Ma in the central Laramie Mountains (Snyder and Peterman, 1982). In the Sierra Madre and Medicine Bow Mountains, metavolcanic rocks (Vulcan Mountain metamorphic suite, **Figure 4**) that are probably fragments of greenstone belts are infolded with these gneisses.

Two types of late Archean successions overlie Archean crystalline basement. These include supracrustal rocks dominated by metavolcanic rocks similar to classic greenstone belt rock types, and three-fold sequences that contain (from base to top) fluvial and marine quartzites or stromatolitic dolomite, metavolcanic rocks, and quartzites or stromatolitic dolomite (**Figure 5**). Rhyolites of the greenstone-type successions range in age from about 2,729 to 2,637 Ma (Snyder and others, 1989) (**Figure 5**) and the lower quartzite of one of the three-fold successions is cut by a 2,700 Ma granodiorite. Thus, these successions appear coeval and may represent the southernmost elements of a collage of terranes that were assembled during final stages of development of the Wyoming province in the Late Archean.

In the Sierra Madre and Medicine Bow Mountains, the basal unit of the three-fold succession (Phantom Lake metamorphic suite, **Figure 4**) is a conglomeratic unit that lies on weathered gneiss. The lower part of the Phantom Lake suite is intruded by a 2,710-Ma granodiorite (Premo and Van Schmus, 1989) in the Sierra Madre; however, there are currently no firm age constraints on the upper part of the Phantom Lake suite. In the Hartville uplift, the basal unit is a quartzite that interfingers with and is overlain by stromatolitic dolomite. I interpret these lower units of the three-fold successions as shelf-type deposits near the margin of a microplate.

The middle of the three-fold succession of all three areas is dominated by metavolcanic rocks. In the Hartville uplift, these rocks are mafic metavolcanic rocks (including pillow lavas) interbedded and overlain by metagraywacke and schist. In the Medicine Bow Mountains, mafic and felsic tuffs are more abundant, and thick conglomerate beds with large clasts of mafic volcanic rocks and granite are also present. In the Sierra Madre, metavolcanic rocks are largely tuffs, and interbeds of arkosic quartzite and phyllite are common. Spectacular thick beds of boulder conglomerate with large clasts of gray granite in an arkosic quartzite matrix occur within the unit (**Figure 6**). This mixed volcanic-sedimentary succession is believed to have been derived from an Andean-type arc that developed along the margin of the

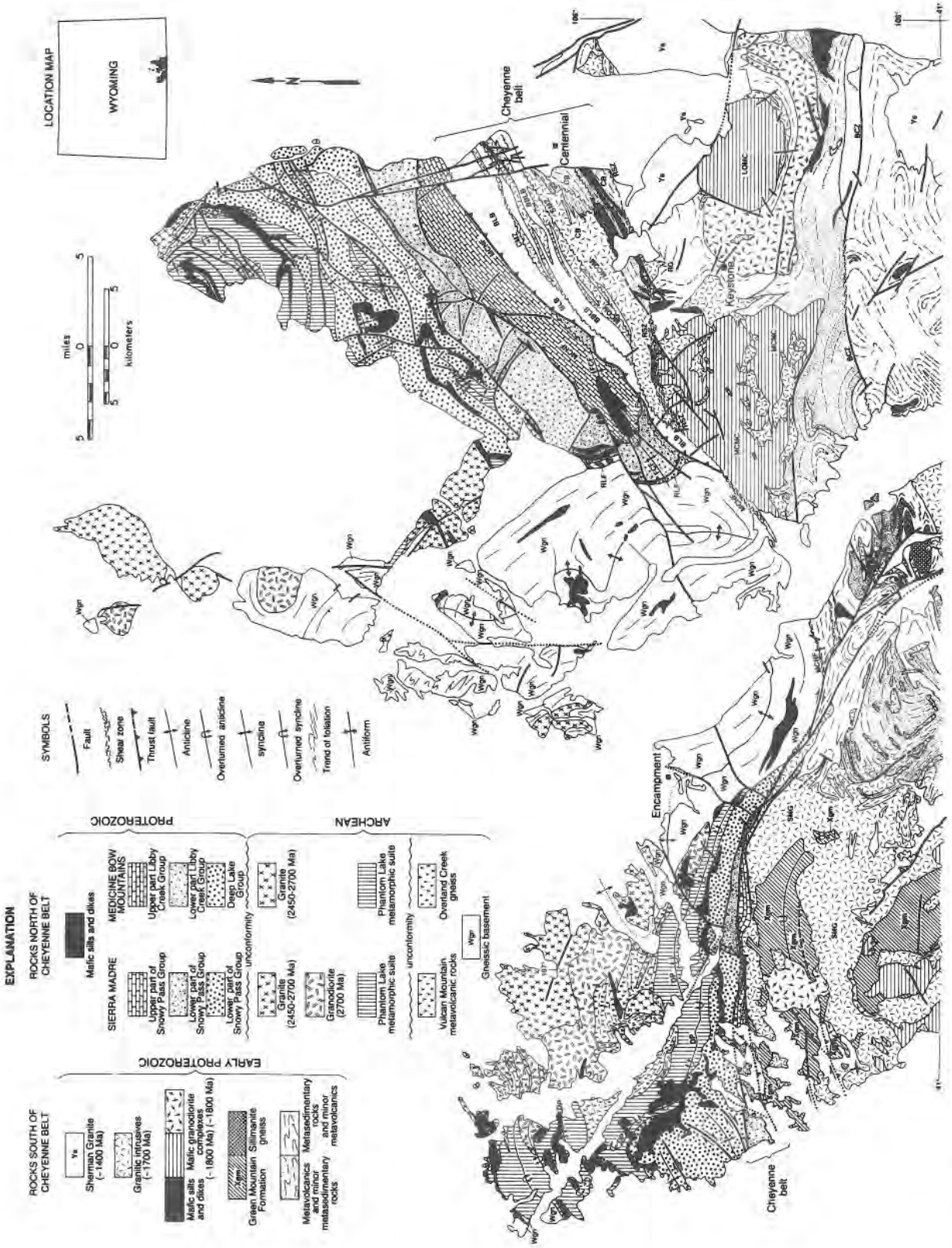

Figure 2. Geologic map of the Sierra Madre and Medicine Bow Mountains, southeastern Wyoming.
Key: BBLB-Barber Lake block, BCZ=Bear Creek shear zone, BLB=Bear Lake block, CB=Centennial block, CMZ=central mylonite zone, DP=Divide Peak synclinorium, FCF=French Creek fold, LLF-Lewis Lake fault, LOMC=Lake Owen mafic complex, MCMC=Mullen Creek mafic complex, MCNF=Mullen Creek-Nash Fork shear zone, MCQM=Mullen Creek Quartz Monzonite, RG=Rambler Granite, RLF=Reservoir Lake fault, RSZ=Rambler shear zone, SMZ=southern mylonite zone, RS=Rudefeha syncline, SMG=Sierra Madre Granite.

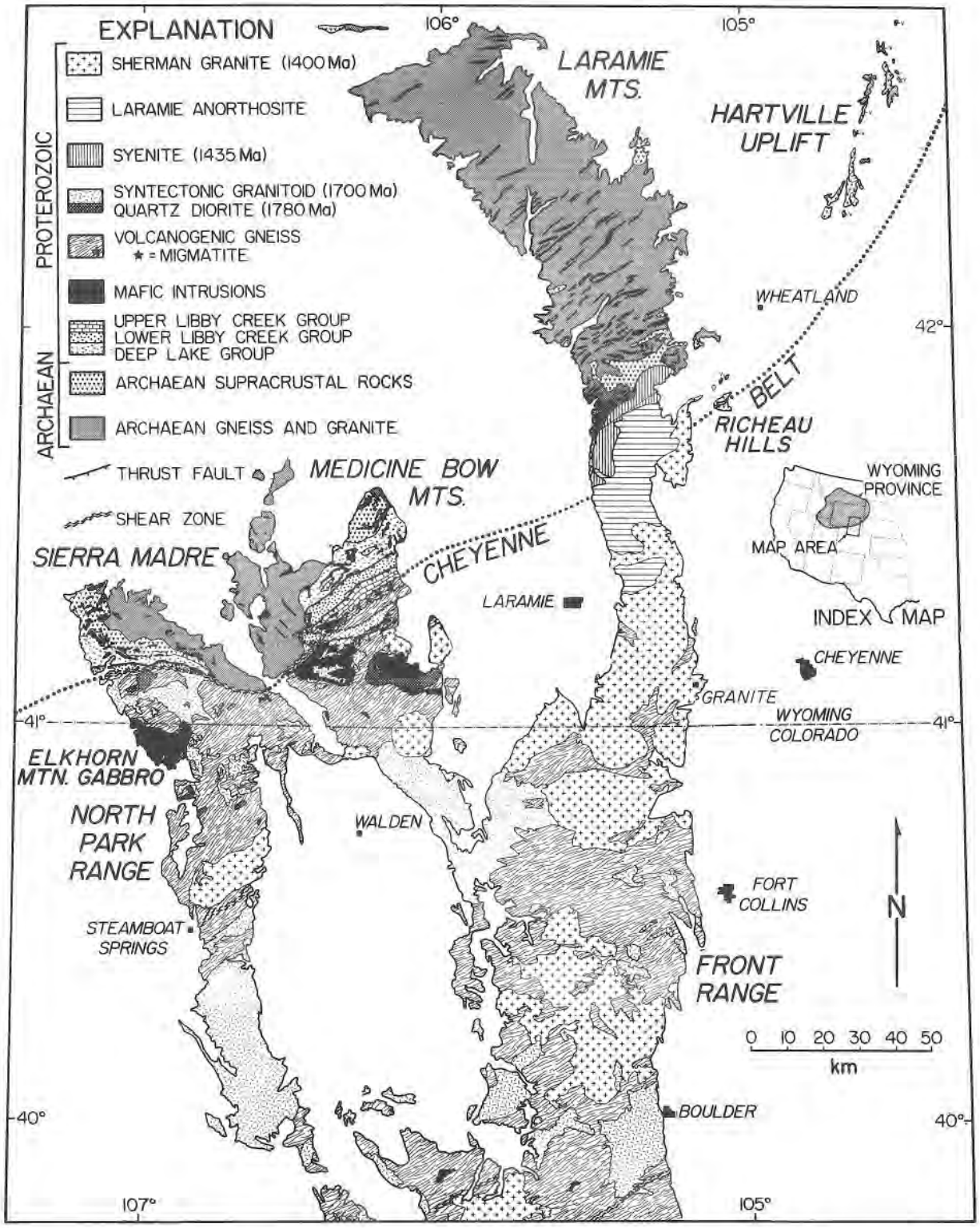

Figure 3. Geologic map of Precambrian rocks of southern Wyoming and northern Colorado (from Karlstrom and Houston, 1984).

Archean plate, the roots of which are represented by the 2,700-Ma granodiorite.

The upper parts of the three-fold successions, which are chiefly marine quartzites in the Medicine Bow Mountains and Sierra Madre (Houston and others, 1992) and stromatolitic metadolomite in the Hartville uplift (Snyder and others, 1989), may indicate a return to normal marine deposition at the plate margin.

If the greenstone belt rocks of the central Laramie Mountains are chronologically equivalent to the three-fold successions exposed in the other ranges, they may represent a *Rocas Verde*-type back-arc basin (Tarney and others, 1976) deposited on Middle Archean basement.

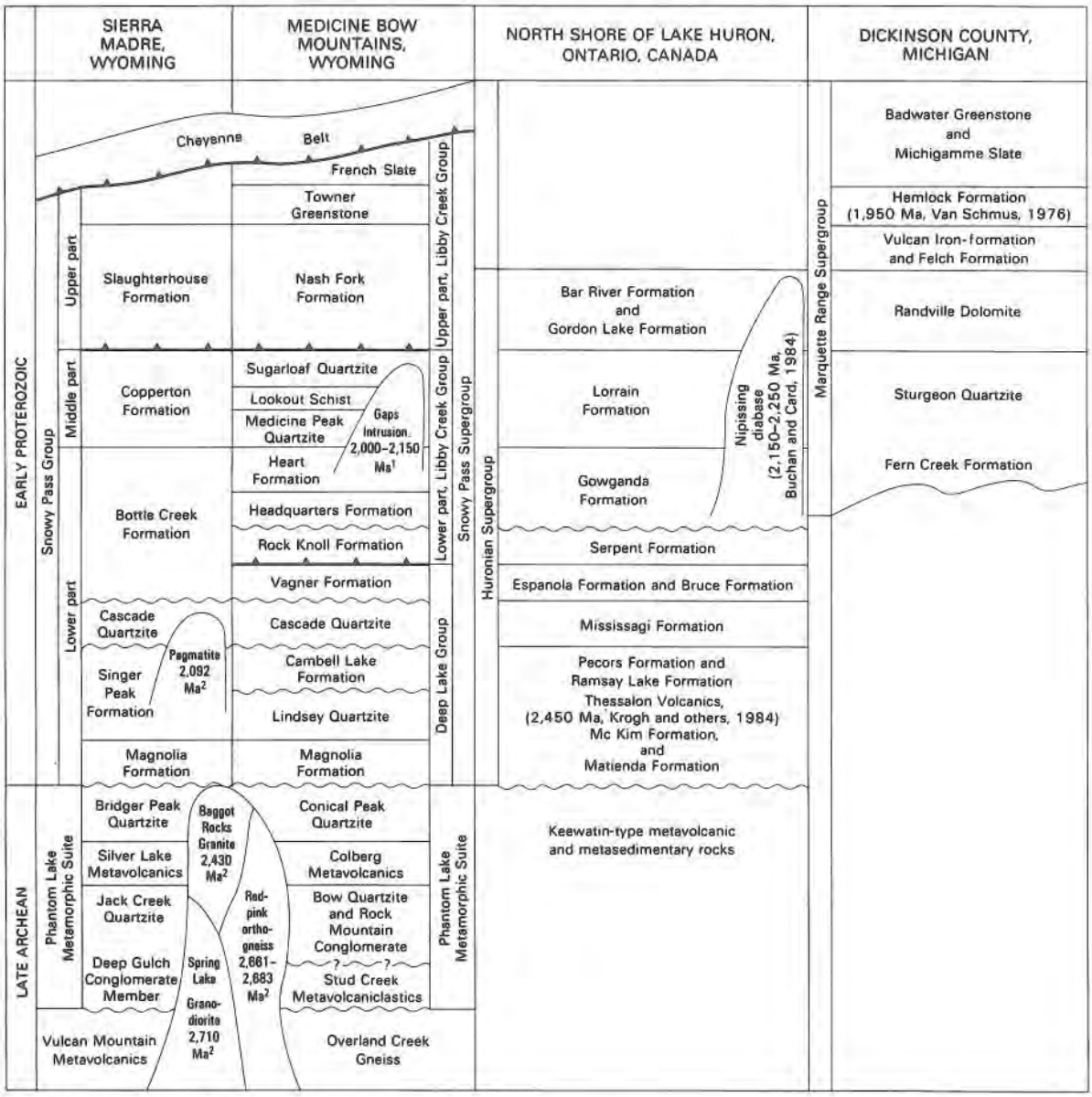

[1] C.E. Hedge (written communication, 1982)
[2] Premo (1983)

Figure 4. Correlation chart showing the stratigraphy of Precambrian rocks of the Sierra Madre and Medicine Bow Mountains, Wyoming province, and possible correlations with Proterozoic rocks on the north shore of Lake Huron, Ontario, Canada, and in Dickinson County, Michigan (from Houston and others, 1992).

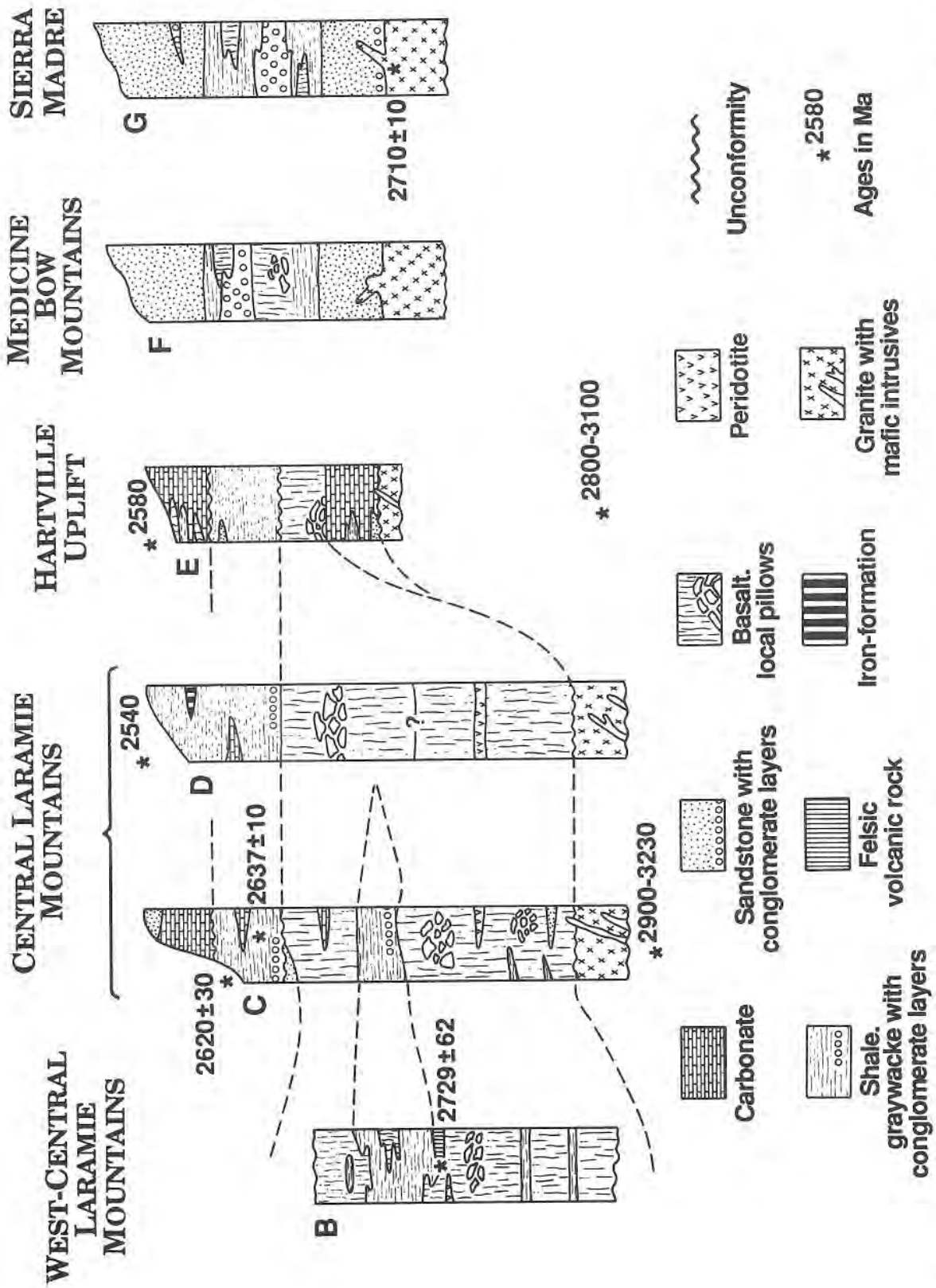

Figure 5. Chart showing possible correlations of Late Archean successions in central and southern Wyoming (modified from Snyder and others, 1989).

In the Medicine Bow Mountains, the three-fold succession was severely deformed prior to deposition of Early Proterozoic metasedimentary rocks (Karlstrom and others, 1981). This Archean to earliest Proterozoic deformation is interpreted as evidence that during the Early Proterozoic the Wyoming province was larger than it is today. The deformation requires either the collision of an allochthonous terrane, or the reassembly of a larger Middle Archean Wyoming province that had been previously rifted.

The final stage of crustal development during the Late Archean to earliest Proterozoic is represented by the intrusion of pink to red K_2O-rich granite, with high Th/U ratios. In the Sierra Madre and Medicine Bow Mountains, these granites range in age from about 2,683 Ma to 2,429 Ma, i.e., from latest Archean to earliest Proterozoic (Premo and Van Schmus, 1989). The granites were probably formed by melting near the base of the assembled and thickened Archean crust of the Wyoming province.

Early Proterozoic miogeoclinal succession

The Early Proterozoic miogeoclinal succession that lies unconformably on Archean rocks in the Sierra Madre and Medicine Bow Mountains consists of the Deep Lake Group and the upper and lower Libby Creek groups (**Figure 4**). The Deep Lake Group of the Medicine Bow Mountains is chiefly fluvial conglomerate and quartzite, although diamictites and laminated phyllites occur near the middle (Campbell Lake Formation, **Figure 4**) and top (Vagner Formation, **Figure 4**) of the Deep Lake Group and probably represent continental and glaciomarine deposits, respectively. In the Sierra Madre, the Deep Lake Group equivalents are fluvial quartzite at the base, but overlying formations contain a higher proportion of phyllite and slate and probably represent a more distal facies. The basal conglomerates of the Deep Lake Group are paraconglomerates with arkosic matrices that contain clasts of a variety of underlying rocks along with abundant granite. These paraconglomerates are interbedded with and grade into thick uranium- and thorium-bearing, quartz-pebble conglomerates that grade laterally and upsection into trough-crossbedded quartzites. The conglomerates are considered to be alluvial fan and braided stream sediments, which were deposited along faults that represent the early stages of rifting of the continental margin about 2.0 to 2.1 Ga (Karlstrom and others, 1981). The metasedimentary rocks of the Deep Lake Group are intruded by numerous thick and extensive sills of tholeiitic basalt, diabase, and norite. A pegmatitic phase of one of these sills that intruded the upper part of the Deep Lake Group equivalents exposed in the Sierra Madre (Cascade Quartzite, **Figure 4**) has been dated at 2,092±9 Ma (U-Pb zircon)

Figure 6. Graded bedding in conglomerate of the Silver Lake volcaniclastic rocks of the Late Archean Phantom Lake metamorphic suite, central Sierra Madre (photo by P.J. Graff).

(Premo and Van Schmus, 1989). Dikes and sills within the Deep Lake Group have been interpreted as products of rifting that occurred about 2,100 to 2,000 Ma (Karlstrom and others, 1981).

In the Sierra Madre, the basal quartz-pebble conglomerate of the Deep Lake Group (Magnolia Formation, **Figure 4**) contains a suite of morphologically homogenous detrital zircons that yielded an age of 2,451±9 Ma (U-Pb zircon) (Premo and Van Schmus (1989). These authors interpret the 2,451 Ma age as the maximum age of the Magnolia Formation. Consequently, the deposition of the Deep Lake Group is bracketed as between 2,451 and 2,092 Ma.

The upper beds of the Deep Lake Group of the Medicine Bow Mountains are glaciomarine (Vagner Formation, **Figure 4**) and are in fault contact with similar glaciomarine deposits (Rock Knoll and Headquarters formations, **Figure 4**) of the lower Libby Creek Group. The glaciomarine deposits of the lower Libby Creek Group are overlain by a clastic succession, chiefly quartzite, which is approximately 15,000 feet thick. This clastic succession has been interpreted as representing different facies of deltaic deposits laid down in a northeast-trending trough that developed during Early Proterozoic rifting of the Wyoming craton (Karlstrom and others, 1981; Flurkey, 1983).

The upper Libby Creek Group is separated from the lower Libby Creek Group by the Lewis Lake fault, a major structural discontinuity that has been interpreted as a thrust fault rotated to near vertical dip during late Early Proterozoic collision and accreton (Karlstrom and others, 1981). The upper Libby Creek Group consists of a lower stromatolitic dolomite (Nash Fork Formation, **Figures 4** and **7**), which is approximately 6,500 feet thick, overlain by pillow lavas (Towner Greenstone, **Figures 4** and **8**) and black slate (French Slate, **Figure 4**).

The Nash Fork Formation is predominantly tan siliceous metadolomite with thick lenses of black graphitic phyllite, thin beds of quartzite, metachert, flat-pebble conglomerate, and local sulphide-facies iron formation. It contains numerous altered gabbroic sills. The most striking sedimentary feature of the metadolomite is stromatolitic bioherms, which occur in a variety of shapes and sizes (Knight and Keefer, 1966; Knight, 1968) (**Figure 7**).

The stromatolites of the Nash Fork Formation are similar to those of approximately the same age in the Great Slave Supergroup of Canada (Hoffman, 1976). Hoffman interpreted the Pethei Group of the Great Slave Supergroup as a carbonate platform with five facies. The Nash Fork stromatolites of the Medicine Bow Mountains are very similar to two platform facies of Hoffman, whereas metalimestones of the Slaughterhouse Formation of the Sierra Madre, which are correlated with the Nash Fork, are considered equivalent to Hoffman's basin-slope facies (Houston and Karlstrom, 1992) (**Figure 4**). Both the

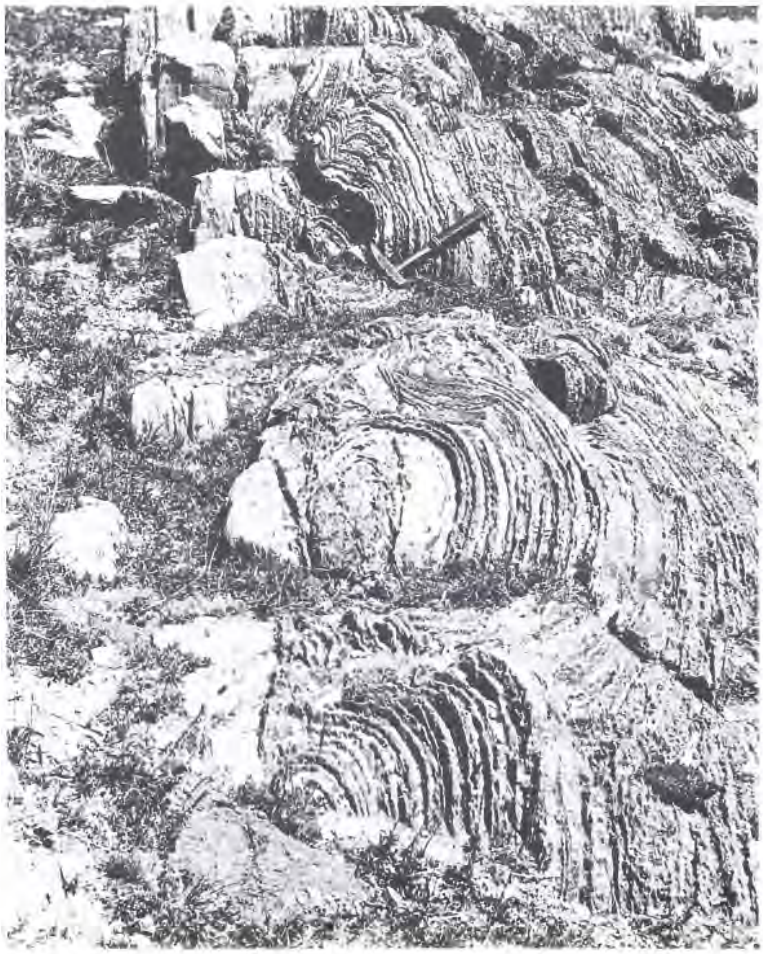

Figure 7. Stromatolites of the Nash Fork Formation, central Medicine Bow Mountains, Wyoming.

Figure 8. Pillow structure in the Towner Greenstone, central Medicine Bow Mountains, Wyoming.

Slaughterhouse Formation and Hoffman's basin-slope facies of the Pethei Group consist of light gray limestone with dark gray shale partings. Houston and Karlstrom (1992) interpreted the Nash Fork Formation as a carbonate platform that was probably deposited in a more seaward environment than the underlying beds and was brought into contact with them by thrust faults.

The Towner Greenstone, which conformably overlies the Nash Fork Formation, is a dark chlorite-actinolite-albite rock with both massive and schistose varieties. This lithology is interbedded with chert. Much of the Towner was subaqueously deposited basalt, as demonstrated by locally preserved pillow lava structures (**Figure 8**).

The Towner is overlain by the 2,000-foot-thick French Slate. The upper part of the French Slate is truncated by the Cheyenne belt. The French Slate is primarily a laminated, black, ferruginous and graphitic slate, which is locally phyllitic. It contains beds of poorly developed oxide-facies iron formation near its base. The stratigraphic position and composition of the French Slate are typical of Early Proterozoic foredeeps as discussed by Hoffman (1987).

The foredeep depositional setting was suggested by Hills and Houston (1979), who compared the Proterozoic continental margin of this area with the Phanerozoic Appalachian trailing margin and suggested that the Towner Greenstone and French Slate were deposited as an island arc approached the passive continental margin from the south. Recent models of Phanerozoic foredeep basins propose that they develop as a result of attempted subduction of a stable shelf of a trailing margin beneath approaching volcanic arcs of microplates (Shanmugan and Lash, 1982). The foredeep develops between the continental margin and a fold-and-thrust belt that progrades towards the continent as the arc or microplate approaches (Shanmugan and Lash, 1982). Crustal thinning beneath the basin accompanied by normal faulting (Hoffman, 1987) promotes basaltic magmatism and could explain the mafic volcanic rocks of the Towner Greenstone as well as gabbroic sills that are common in the French Slate. Sills that intrude the Libby Creek Group differ in composition from those of the Deep Lake Group (Karlstrom and others, 1981); they are typically more alkalic and are closer in composition to arc tholeiites than those of the Deep Lake Group. There are presently no age determinations from the suite of alkalic mafic sills.

In the Medicine Bow Mountains, the Early Proterozoic miogeoclinal suite is well preserved, especially in the north-central part of the mountains where Highway 130 crosses the range. In the Sierra Madre, late thrust faults have severely disrupted Early Proterozoic equivalents of the Deep Lake and Libby Creek groups and only partial sections are preserved. The Sierra Madre section contains a higher proportion of phyllite and slate in the quartzites. Although these facies changes to a more distal suite of rocks make correlation difficult, there are useful marker horizons that allow reasonable correlation between the two ranges (**Figure 4**). The Magnolia Formation of the Deep Lake Group has a distinctive radioactive conglomerate at its base in both ranges, although it is less well developed in the Sierra Madre. There are diamictite equivalents of the Campbell Lake, Vagner, Rock Knoll, and Headquarters formations of the Medicine Bow Mountains in the Singer Peak and Bottle Creek formations of the Sierra Madre. It is clear, however, that the Sierra Madre section includes more distal facies than the Medicine Bow section and may represent a time equivalent succession of rocks deposited a significant distance south and/or west of the Medicine Bow section.

Cheyenne belt

The Cheyenne belt is a series of fault blocks separated by mylonite zones. The Cheyenne belt separates rocks of the Archean Wyoming craton to the north from Proterozoic rocks of the Colorado Front Range to the south. It has been variously interpreted as a transform fault (Warner, 1978) or a Proterozoic suture associated with island arc-continent collision (Hills and Houston, 1979; Karlstrom and Houston, 1984).

The Cheyenne belt contains four major mylonite zones. From north to south, they are the Mullen Creek-Nash Fork shear zone (Houston and McCallum, 1961), central mylonite zone, southern mylonite zone, and Rambler shear zone (**Figure 2**). All of these mylonite zones converge to the southwest into one major fault (**Figure 2**).

Duebendorfer and Houston (1987) distinguished two blocks within the Cheyenne belt, the Bear Lake block (bordered on the north by the Mullen Creek-Nash Fork shear zone and on the south by the central mylonite zone) and the Barber Lake block (bordered on the north by the central mylonite zone and on the south by the southern mylonite zone) (**Figure 2**). An additional unnamed block mapped by McCallum (1964) is bordered on the north by the southern mylonite zone and on the south by the east-northeast trending Rambler shear zone. This block is here named the Centennial block (**Figure 2**).

To the southwest, the Bear Lake block is a bimodal sequence of amphibolite and granite gneiss; to the northeast it is granodiorite-tonalite laminated gneiss, biotite-granodiorite augen gneiss, and amphibolite. Amphibolite-facies mineral assemblages dominate. Texture, modal composition, and major-element chemistry suggest that the gneisses were intermediate plutonic rocks of a calc-alkaline suite (Duebendorfer, 1986).

The Barber Lake block is composed of metasedimentary and metavolcanic rocks, metaperidotite, migmatitic augen gneiss, and garnet-biotite granite. Duebendorfer (1986) interpreted the origin of the metasedimentary-volcanic sequence as a succession of volcanogenic and lithic sandstone, siltstone, and shale and intermediate to mafic volcanic rocks, based on mineral assemblages, major-element chemistry, and textural features. Mineral assemblages are characteristic of the sillimanite-K feldspar zone of the upper amphibolite facies (Duebendorfer and Houston, 1987). The garnet-biotite granite is peraluminous, corundum-normative, and may have formed by partial melting of the associated pelitic rocks.

The Centennial block is a complex succession of highly deformed metavolcanic and metasedimentary rocks with abundant sills of mafic and felsic igneous rocks that are also deformed and metamorphosed. In the northern and eastern parts of the Centennial block, felsic and mafic schists with fragmental textures are interlayered with fine-grained felsic and mafic gneisses. These rocks are interpreted as tuffs and flows. At the western and southern margins of the Centennial block, metasedimentary rocks including pelitic schist, diopside paragneiss, and siliceous marble are interlayered with the metavolcanic rocks (McCallum, 1964). Sills of mafic igneous rock are abundant and include orthoamphibolite, metagabbro, metapyroxenite, and metadiorite. Sills of felsic igneous rocks and pegmatite are present throughout the succession, and intrusions of quartz monzonite make up much of the western part of the block.

If we include deformed rocks of the Libby Creek Group within the Cheyenne belt, a distinct increase in metamorphic grade from north to south is evident (i.e., from greenschist to amphibolite to upper amphibolite facies).

Proterozoic supercrustal rocks south of the Cheyenne belt

Medicine Bow Mountains

In the Medicine Bow Mountains, all the blocks within the Cheyenne belt except the Bear Lake block are lithologically part of the southern province. In one of several interpretations, the Bear Lake block is considered to be a piece of rifted Archean basement by Duebendorfer and Houston (1987). That interpretation explains the abundance of mafic intrusive rocks in the Bear Lake block compared to the other

blocks of the Cheyenne belt. McCallum and Kluender (1983) also considered this block as possible Archean basement. These lithological interpretations are supported by Nd isotope data (Ball and Farmer, 1991) that demonstrated a low initial ε_{Nd} and an old Nd model age for the Bear Lake block that are similar to the range measured for Archean basement. Metavolcanic rocks of the Centennial block yielded initial ε_{Nd} values that indicate younger Nd model ages than the Bear Lake block, and these data were interpreted by Ball and Farmer (1991) to indicate the lack of any Archean component in the Centennial block. Paragneiss and peraluminous granite of the Barber Lake block had initial ε_{Nd} values and Nd model ages that fall between those of the Bear Lake and Centennial blocks and are interpreted to indicate a mixing of Archean and Proterozoic source detritus (Ball and Farmer, 1991).

Rocks south of the Centennial block are largely quartz-andesine gneiss (metagraywacke?) with interlayered marble, diopside paragneiss, and metavolcanic rocks. Southward, a heterogeneous succession of mafic, pelitic, and calcareous gneisses crops out in an east-west band some 3 to 5 miles wide that extends across the entire southern Medicine Bow Mountains (**Figure 2**). This unit is interpreted as a mixed volcanic and sedimentary sequence (Houston and others, 1968). The southernmost Medicine Bow Mountains are underlain by felsic gneiss (orthogneiss) that contains layers and irregularly shaped bodies of mafic and pelitic gneisses similar to those of the east-west-striking band to the north. The felsic orthogneiss also contains numerous sills and dikes of amphibolite, suggesting a possible comagmatic felsic and mafic intrusive suite (Houston and others, 1968).

Sierra Madre

The southeastern Sierra Madre is a continuation of the geology of the Medicine Bow Mountains. South of the main shear zone, which is the Sierra Madre equivalent of the Mullen Creek-Nash Fork shear zone, a metavolcanic succession crops out that is similar to the succession in the Centennial block. South of this, there is a block of felsic gneiss bordered by mylonite zones, and farther south the succession is similar to that of the southern Medicine Bow Mountains, except that in the southeast corner of the Sierra Madre there is a younger succession of sillimanite gneisses infolded with older rocks (**Figure 2**) (Houston and Graff, in press).

The Sierra Madre segment of the Cheyenne belt is disrupted by a series of northwest-striking, dextral strike-slip faults that may be kinematically coupled to tear faults associated with east-west-striking, north-directed thrust faults in the central Sierra Madre. These fault systems operated in concert with thrusts now exposed in the south-central and southwestern Sierra Madre, which involve rocks of both the Cheyenne belt and miogeoclinal Proterozoic successions (Duebendorfer and Houston, 1990) (**Figure 2**). The dextral strike-slip faults are largely brittle and post-date movement in the Cheyenne belt; the displacement on the thrust faults is unknown.

The south-central Sierra Madre is made up of a large, roughly circular amphibolite body about 2.5 miles in diameter (**Figure 2**). Some layers within the body have fragmental textures, suggesting original volcaniclastic rocks; others are massive and may have been intrusive. Pillow structures have been reported in the eastern part of the mafic succession (Condie and Shadel, 1984). This mafic succession is interpreted as a center of basaltic volcanism. The mafic rocks interfinger with and grade into a mixed volcanic-sedimentary succession to the north, east, and west.

Northwest and west of the mafic succession and its flanking metasedimentary and metavolcanic rocks is a folded and faulted synclinorium that contains a remarkably well-preserved succession of greenschist-facies metavolcanic rocks (**Figure 2**), the Green Mountain Formation of Divis (1976). Two or three basalt-rhyolite cycles overlain by chert, carbonate rocks, and graywacke are present (Houston and others, 1984). Breccias, agglomerate, and lapilli tuff are well preserved; some rhyolites have textures suggestive of welded tuffs. The Green Mountain Formation of this area is interpreted as a proximal, bimodal volcanic succession containing both subaerial and marine deposits. Whole-rock and trace-element analyses of basalt, dacite, rhyolite, and sparse andesite indicate that they are calc-alkaline volcanic rocks (Schmidt, 1983; Condie and Shadel, 1984). Premo and Van Schmus (1989) obtained a U-Pb age of 1,792±15 Ma on zircon separated from a metadacite porphyry from the east side of Green Mountain.

In the southwest Sierra Madre, the Green Mountain Formation increases in metamorphic grade to amphibolite facies, is more highly deformed, and has less well-preserved primary textures. Pillow structures, however, are still common in the metabasalt of

this area, and the abundance of metasedimentary rocks suggests that this sequence is a more distal marine facies.

The Sierra Madre has the most complete and best preserved volcanic-sedimentary suite of any of the mountain ranges of southern Wyoming. The structural interpretation of Houston and Graff (in press) indicates that the metavolcanic and metasedimentary rocks of the Medicine Bow Mountains and southeastern and south-central Sierra Madre are older than the rocks of the Green Mountain Formation. This interpretation is consistent with existing isotope and chemical studies (Ware, 1982; Condie and Shadel, 1984; Premo and Van Schmus, 1989) but has not yet been directly verified. It is also possible that these rocks, which are certainly more deformed and of higher metamorphic rank than rocks of the Green Mountain Formation, simply represent a deeper level of the crust.

Laramie Mountains

Metasedimentary and metavolcanic rocks are widely distributed in the Laramie Mountains south of the projected position of the Cheyenne belt (**Figure 3**). The largest exposure of these rocks makes a northeast-striking discontinuous strip in the eastern Laramie Mountains, north and southwest of the village of Granite (**Figure 3**). These metavolcanic rocks contain well-preserved textures and structures and constitute a bimodal succession that is similar to the Green Mountain Formation of the Sierra Madre. These rocks range in composition from basalt to rhyodacite and contain a higher proportion of felsic volcanic rocks than volcanic sequences of the Sierra Madre and Medicine Bow Mountains. The metavolcanic rocks extend to within 2 to 3 miles of the Colorado border, where they interfinger with quartz-biotite-plagioclase gneiss that may represent a mixed volcanic and sedimentary succession.

Areas of metasedimentary rocks, chiefly felsic gneiss and pelitic schist, are present in the southwest and south-central Laramie Mountains and in the Richeau Hills (**Figure 3**). In the Richeau Hills, a complex suite of metasedimentary rocks is exposed including quartzite and marble (Mueller, 1982). These rocks may be Archean according to G.L. Snyder (personal communication, 1985).

The metavolcanic and metasedimentary rocks of the southern Laramie Mountains have not been dated, but are considered to be Proterozoic based on lithology and their position with respect to the Cheyenne belt. Isotopic and chemical evidence suggests that part of the felsic volcanic suite near Granite may be genetically related to the 1.4 Ga Sherman Granite (Geist and others, 1989; Marlett, 1989), but the majority of the rocks are interpreted here as Early Proterozoic.

Proterozoic plutonic rocks south of the Cheyenne belt

About 50% of the rocks exposed in the southern Sierra Madre, 30% of those in the southern Medicine Bow Mountains, and 80% of those in the southern Laramie Mountains are Proterozoic intrusive rocks (**Figure 3**). These intrusive rocks fall into three categories: (1) Early Proterozoic mafic intrusions that are believed to be comagmatic with the Early Proterozoic metavolcanic rocks; (2) Syntectonic felsic intrusions that are about 30 million years younger than the metavolcanic suite but still Early Proterozoic; and (3) post-tectonic, Middle Proterozoic intrusions emplaced about 300 million years after development of the collision zone. These post-tectonic rocks, which appear to be unrelated to late Early Proterozoic accretion at the southern margin of the Wyoming craton, are discussed in detail by Frost and others (this volume).

Plutonic rocks comagmatic with metavolcanic rocks

In the southern Medicine Bow Mountains, two layered mafic complexes (Lake Owen and Mullen Creek), were emplaced into the metavolcanic succession (**Figure 2**). The 20-square-mile Lake Owen mafic complex of the eastern Medicine Bow Mountains has been tilted to expose 3 miles of interlayered norite, gabbro, troctolite, and anorthosite (**Figure 9**). The complex is divided into three major cycles defined by differences in lithology, igneous structure, and major-element compositional trends (Houston and Orback, 1976). The 60-square mile Mullen Creek mafic complex of the western Medicine Bow Mountains is compositionally similar to the Lake Owens complex, but

is highly disrupted and invaded by granitic sills, dikes, and irregularly shaped masses (**Figure 2**). A diorite within the Mullen Creek complex yielded a U-Pb zircon age of 1,778±2 Ma (Loucks and others, 1988) and the Horse Creek Granite that intrudes the complex yielded a U-Pb zircon age of 1,777±4 Ma (Premo and Van Schmus, 1989). Sm-Nd data have been interpreted to suggest that the Lake Owen mafic complex is younger than the Mullen Creek; augite from the Lake Owen complex yielded an ε_{Nd} of +2 at 1500 Ma (Fram and Rubenstone, 1988). If this model age dates the timing of petrogenesis, then the Lake Owen complex may be related to the younger anorthositic suite of the Laramie Mountains (i.e., Laramie Anorthosite Complex of Frost and others, this volume) rather than the about 1.8 Ga arc volcanic suite.

A body of unlayered gabbro, the Elkhorn Mountain Gabbro (Snyder, 1980), crops out in a 50-square-mile area in the southern Sierra Madre and adjacent parts of the Park Range of northern Colorado (**Figure 4**). Snyder reported a U-Pb zircon age of 1,781 Ma (C.E. Hedge, *in* Synder, 1980) for this intrusion and Pallister and Aleinikoff (1987) reported overlapping U-Pb zircon ages of 1,774±2 Ma, 1,769±6 Ma, and 1,768±8 Ma for intrusive rocks that cut the Elkhorn Mountain Gabbro as well as inclusions within the gabbro. The Elkhorn Mountain Gabbro is compositionally more homogeneous than either of the layered complexes discussed previously. Medium grain size and diabasic texture suggest emplacement at a relatively shallow depth.

Figure 9. Pseudo - graded bedding in gabbroic rock of the Lake Owens mafic complex, resulting from late growth of orthopyroxene, southern Medicine Bow Mountains, Wyoming.

Smaller bodies of mafic intrusive rock ranging in width from 10 feet to 3,000 feet are common south of the Cheyenne belt in all three mountain ranges. Metagabbro dominates, although olivine metagabbro, metapyroxenite, and metadiorite are also present. Most of these smaller mafic bodies have been largely or completely converted to amphibolite.

In earlier papers, the mafic complexes have been considered tectonically emplaced remnants of the lower parts of magmatic arcs (Hills and Houston, 1979; Karlstrom and Houston, 1984; Pallister and Aleinikoff, 1987), and this interpretation still appears reasonable for the Mullen Creek complex and Elkhorn Mountain gabbro, which are approximately the same age as the arc volcanic rocks. However, the Lake Owen Mafic complex may have different origin if the age inferred from Sm-Nd data approximates the crystallization age.

The Encampment River Granodiorite of the Sierra Madre and the Keystone Quartz Diorite of the Medicine Bow Mountains are distinctive intermediate intrusions with similar mineralogic and chemical characteristics. The Encampment River Granodiorite intrudes metavolcanic rocks of the Green Mountain Formation of the central Sierra Madre and contains abundant inclusions of volcanic rocks from the Green Mountain Formation. The Keystone Quartz Diorite is more highly deformed and metamorphosed than the Encampment River Granodiorite, but it is also marked by numerous inclusions. Inclusions within the Keystone are amphibolite, probably derived from mafic volcanic rocks. The two plutons yielded nearly identical U-Pb zircon ages: 1,779±5 Ma for the Encampment River Granodiorite and 1,781±7 Ma for the Keystone

Quartz Diorite (Premo and Van Schmus, 1989). The two plutons may be genetically linked and probably represent the intermediate component of a calc-alkaline suite whose volcanic equivalents were eroded.

Smaller intermediate plutonic bodies containing abundant metavolcanic inclusions are present in the Laramie Mountains south of Granite, Wyoming. These may have an origin like the Encampment Grandiorite and Keystone Quartz Diorite, inasmuch as they intrude metavolcanic rocks. Currently, there are no radiometric age constraints on these intrusions.

The complex cross-cutting relationships between the metavolcanic rocks and mafic and intermediate plutonic rocks, and geochronologic dates that indicate ages of about 1.8 Ga for all members, suggests that these rocks represent a broadly coeval and comagmatic suite, perhaps of an arc massif or of several volcanic arcs. The higher proportion of mafic rocks and the greater intensity of deformation and metamorphism in the southern Medicine Bow Mountains and southeastern Sierra Madre suggest that this area exposes a deeper level of the crust than the central and western Sierra Madre.

Syntectonic felsic intrusions

Quartz monzonite and granite intrude metavolcanic and metasedimentary rocks, mafic plutonic rocks, and rocks of the granodiorite-tonalite suite. These felsic intrusive rocks make up about 50% of the outcrop area of the Sierra Madre, where a large pluton, the Sierra Madre Granite of Divis (1976), completely surrounds the Green Mountain Formation. Facies of the Sierra Madre Granite have been dated by the U-Pb zircon methods as 1,749±8 Ma, 1,744±14 Ma, and 1,763±15 Ma (Premo and Van Schmus, 1989). Smaller granitic intrusions that are probably related to the Sierra Madre Granite intrude metavolcanic and metasedimentary rocks in the southeastern Sierra Madre (**Figure 2**). The Sierra Madre Granite intruded remnants of an earlier mylonite zone, but is itself cut by a cataclastic fault zone. These relationships suggest that the granite was emplaced during the final stages of the late Early Proterozoic accretion. Similar felsic intrusions have been recognized in the Medicine Bow and Laramie mountains.

In the Medicine Bow Mountains, the two-mica peraluminous granite and leucogranite of Mullen Creek extend northeast-southwest in a discontinuous band south of the central mylonite zone of the Cheyenne belt. Like the Sierra Madre Granite, these rocks intrude mylonites of the Cheyenne belt (**Figure 3**) and in turn are cut by mylonitic shear zones associated with a later phase of dextral strike-slip faulting. Several smaller granitic intrusions, including a distinctive tin-bearing tourmaline granite, the Rambler Granite, which crops out about 3 miles north of the village of Keystone (**Figure 2**), cut the metavolcanic and metasedimentary successions of the Medicine Bow Mountains. The Rambler Granite yielded a Rb-Sr whole-rock age of 1,730±15 Ma (Hills and Houston, 1979).

In the southern Laramie Mountains, granitic rocks older than the 1.4 Ga Sherman granite intrude the metavolcanic and metasedimentary successions south of Granite. These intrusions may correlate with those of the Sierra Madre and Medicine Bow Mountains, but are undated.

Syntectonic felsic intrusive bodies in all three ranges generally have sharp, but locally highly transposed, contacts with the country rock. The larger intrusives are massive to faintly foliated in the center and have better developed foliation near contacts. The smaller intrusions generally have well-developed foliation that parallels that of the country rock. Some felsic intrusions contain xenoliths that have an early deformational fabric, indicating that their intrusion postdates a major deformational event. These intrusions may have been emplaced in the terminal stage of the main deformational episode (similar to the scenario proposed for the Buffalo Pass pluton of northern Colorado by Snyder and Hedge, 1978).

Thus, the felsic intrusive bodies were emplaced about 1,750 Ma, some 30 million years after the arc volcanism. They were probably emplaced during the latter stages of the deformational episode involving arc-continent collision.

Gravity and seismic studies of the arc-continent boundary indicate that the crust south of the Cheyenne belt is thicker than that north of the belt [48 to 54 km in the south and 37 to 41 km in the north (Johnson and others, 1984)]. Perhaps the felsic intrusions

formed by melting at or near the base of this thickened crust. There is some chemical evidence to support this idea. Divis (1976) suggested that the dispersed Rb/Sr, Ba/Sr, and Ti/Zr, along with systematically decreasing K/Rb patterns of the Sierra Madre Granite, are indicative of a derivation by anatexis. The peraluminous composition of some intrusive bodies and the tin-bearing tourmaline Rambler Granite of the Medicine Bow Mountains is also suggestive of formation by crustal anatexis.

Structure north of Cheyenne belt

Medicine Bow Mountains

Archean

Structural analyses of the Archean of the Medicine Bow Mountains has revealed multiple phases of deformation, as shown by successive emplacement and deformation of mafic dikes (Houston and others, 1968). The dominant structural element in the Archean crystalline rocks is a northwest-striking foliation that is particularly well developed in the Overland Creek Gneiss (Houston and Karlstrom, 1992). This structural fabric is not well developed in the metasedimentary rocks and probably developed prior to deposition of rocks of the Phantom Lake metamorphic suite (**Figure 2**). Foliation in the Archean gneisses is locally warped around east-west axes, perhaps in response to Proterozoic deformation.

The Archean (?) Phantom Lake suite records several deformational events, as shown by the multiple S-surfaces and fold plunges. Folds are commonly tight and overturned, with axial surfaces vertical or dipping steeply northwest (Houston and Karlstrom, 1992).

Faults in the Phantom Lake metamorphic suite parallel the major foliation and show both vertical and horizontal displacement. Vertical movement on these faults may have been in response to the same stress that developed the major folds. Horizontal movement (left-lateral) may be related to a later fold system that developed about an east-west axis (**Figure 2**) (Houston and Karlstrom, 1992).

Proterozoic

Deep Lake Group

The earliest Proterozoic deformation was recorded in rocks of the Deep Lake Group and produced upright, northeast- to east-trending folds that are approximately coaxial with the more tightly appressed folds of the Phantom Lake metamorphic suite. A single anticline-syncline system in the Deep Lake Group transverses the entire northern Medicine Bow Mountains (**Figure 2**). The hinge lines vary in trend from east-west to north-northeast; and plunges are shallow—less than 30° to the southwest and northeast. The relationship between the folds of the Deep Lake Group and Phantom Lake suite can be seen in the Crater Lake area (sec. 35, T18N, R79W), where open folds in the Deep Lake Group are coaxial with tight to isoclinal folds in the unconformably underlying Phantom Lake suite (Houston and Karlstrom, 1992).

The timing of the development of the open folds of the Deep Lake Group can be constrained by U-Pb radiometric dating of zircon fractions from the Magnolia Formation, Rb-Sr whole-rock dating, and U-Pb dating of zircons from pegmatitic phases of gabbroic sills and dikes that cut the Deep Lake Group. Zircons from the Magnolia Formation in the Sierra Madre yielded an age of 2,451±12 Ma (Premo, 1984), whereas zircons from a pegmatitic metagabbro sill that cuts the Cascade Quartzite in the Sierra Madre was dated at 2,092±4 Ma (Premo, 1984). A differentiate of a gabbroic dike that intrudes the Lookout Schist of the Medicine Bow Mountains yielded an age of approximately 2,100 Ma (Rb-Sr whole-rock; Hedge, *in* Houston and others, 1993). The deformation is thus bracketed between about 2,500 and 2,100 Ma.

Two additional fold systems can be observed in the Deep Lake Group and underlying Phantom Lake metamorphic suite. In the northeastern Medicine Bow Mountains, the generally east- to northeast-trending folds of the Deep Lake Group and Phantom Lake metamorphic suite are rotated counterclockwise. The deformation was intense enough locally to overprint earlier structures of the metasedimentary-volcanic successions and to develop a strong foliation in gabbroic sills. Plots of poles to bedding and foliation in both the Phantom Lake suite and Deep Lake Group form a great circle girdle that defines a west-

plunging fold axis (Karlstrom and others, 1981, p. 321). This same east-west fold system is well developed in the Phantom Lake suite of the Sierra Madre, although the field data are insufficient to determine if the Deep Lake Group is involved in this deformation (Houston and Graff, in press). If the gabbroic sills of this northeast area are the same age as those noted above (i.e., about 2,100 Ma), this deformation took place after 2,100 Ma and may have involved the lower Libby Creek Group.

In several areas in the northern Medicine Bow Mountains, mesoscopic folds exhibit a northwest-striking axial-planar foliation that crenulated folds associated with the west-plunging fold axis. Similar northwest-trending folds and foliation are present locally in incompetent beds of the central Medicine Bow Mountains, especially near Twin Lakes (secs. 14 and 23, T16N, R80W; Houston and Karlstrom, 1992). In addition, folds and gabbroic intrusions are gently warped about the northwest axes. This is probably a Proterozoic event, however, there are no time constraints for this event except that it postdated the intrusion of the gabbroic sills (Houston and Karlstrom, 1992).

Libby Creek Group

The structural style of the Libby Creek Group differs from the older successions, and, in fact, resembles the rocks south of the Mullen Creek-Nash Fork shear zone more than it does those to the north. Rocks of the Libby Creek Group strike northeast and dip steeply southeast. They have characteristics of the steep limb of a south-facing monoclinal flexure, in which cleavage is generally parallel to bedding. Sedimentary structures are common in the Libby Creek Group, and they show a consistent top to the southeast orientation. Several major reverse faults have been recognized in the Libby Creek Group. One reverse fault follows the contact between the Libby Creek and Deep Lake groups and another, the Lewis Lake fault of Houston and others (1968), roughly follows the contact between lower and upper Libby Creek Group successions. The evidence for such faults, in addition to breccias and fault-line scarps along their trace, is that massive quartzite sections of both the Medicine Peak and Sugarloaf abruptly pinch to zero thickness, then reappear in normal thickness along strike. In addition, major transverse faults in the lower Libby Creek Group terminate at the inferred thrusts and are not present either in footwall rocks of the Deep Lake Group or younger hanging-wall rocks of the upper Deep Lake Group. Tectonic attenuation of this magnitude, as well as differing structural styles between hanging wall and footwall, suggest major movement. These faults are interpreted as thrust faults that have been subsequently rotated to steep attitudes (Karlstrom and others, 1981).

Rocks and major faults of the Libby Creek Group are folded at the southwest limit of outcrop, where they define a steeply plunging syncline, the French Creek fold of Houston and Parker (1963) (**Figure 2**). This fold was interpreted as a late flexural slip fold related to sinistral displacement along the Mullen Creek-Nash Fork shear zone (Houston and Parker, 1963). However, this interpretation is now questionable in light of new evidence that will be discussed in the section on the Cheyenne belt.

Sierra Madre

Archean

Between Encampment, Wyoming, and the Cheyenne belt of the eastern Sierra Madre, the major structure of the Archean basement gneiss is a northwest-trending antiform that roughly parallels the strike of Archean rocks in the Medicine Bow Mountains (**Figure 2**). North of Encampment, the antiform trends more to the west and at approximately half the distance between Encampment and the northern limit of exposure this antiform is folded about an east-west axis (**Figure 2**).

The Vulcan Mountain metamorphic suite is interlayered with and folded with the gneissic basement. Mesoscopic folds in the Vulcan Mountain suite exhibit recumbent geometries that are believed to represent an early stage of deformation of these rocks. In the north-central Sierra Madre, the Vulcan Mountain suite is warped about the same east-west axes as the gneissic basement (**Figure 2**).

The Phantom Lake metamorphic suite exhibits both mesoscopic and macroscopic recumbent folds that have axial surfaces that dip approximately 30° south in the central Sierra Madre (**Figure 10**). From available topping criteria in the Phantom Lake suite, major synclines and anticlines have been recognized, the most important being the Divide Peak

outcrop of the Phantom Lake suite (**Figure 2**) (Karlstrom and others, 1981; Houston and Graff, in press). These recumbent isoclinal folds of the Phantom Lake suite are interpreted as a nappe system (Karlstrom and others, 1981). The Phantom Lake nappe system trends roughly east-west and exhibits a northward vergence in the central and eastern Sierra Madre. In the western Sierra Madre, the Phantom Lake nappe system is folded about the same east-west axis as the gneissic basement and Vulcan Mountain metamorphic suite (**Figure 2**).

Proterozoic

The Deep Lake Group equivalents of the Medicine Bow section in the Sierra Madre unconformably overlie Archean rocks and dip generally 70 to 80° south. In the west-central Sierra Madre, rocks equivalent to the Deep Lake Group contain a large-scale "Z" fold and associated faults that strike northeast and show right-lateral separation (**Figure 2**) (Houston and Graff, in press).

Rocks equivalent to the Libby Creek Group are complexly folded and faulted and only partial sections appear to be preserved. These sections are nearly absent in the eastern Sierra Madre; somewhat more complete sections are preserved in the west (**Figure 2**). These rocks are believed to have been part of a major syncline that closed to the east, and was fragmented and thrust over older rocks in much the same manner as the Libby Creek Group was thrust over older rocks in the Medicine Bow Mountains. The sections are more highly dismembered in the Sierra Madre because of a late cataclastic event that ruptured the Cheyenne belt and thrust much of the southwest Sierra Madre over the Archean basement and its overlying miogeoclinal rocks (Duebendorfer and Houston, 1990) (**Figure 2**).

Figure 10. Recumbent folds in the Phantom Lake metamorphic suite, central Sierra Madre, Wyoming.

Structure of the Cheyenne belt

The earliest structure recognized in the Cheyenne belt is preserved in the Bear Lake and Barber Lake blocks in zones that were not strongly overprinted by later events. Isoclinal folds with subhorizontal axial surfaces that deform compositional layering of unknown origin are present in the Bear Lake and Barber Lake blocks. Subhorizontal lineations defined by elongate microcline megacrysts are present locally in the Bear Lake block. Duebendorfer and Houston (1987) suggested that these early structures may have resulted from combined low-angle thrusting (of unknown transport direction) and dextral strike-slip shear, perhaps reflecting a transpressional tectonic setting or oblique convergence between blocks.

The most pervasive and widely developed structures of the Cheyenne belt are folds and lineations that define the northeast-striking, subvertical fabric of the belt and overprint the structures described above. In the Libby Creek Group (primarily in the Lookout Schist and French Slate), bedding is transposed to a northeast-striking, subvertical schistosity that is axial planar to a set of generally intrafolial, isoclinal folds. Fold hinges plunge steeply northeast. In the Bear Lake block, the transition from folds that plunge gently northeast to southwest and verge northwest to steeply plunging folds can be seen in outcrop; in some outcrops steeply plunging sheath folds (**Figure 11**) have been observed (Duebendorfer

and Houston, 1987). Penetrative, down-dip, mineral lineations that parallel the more steeply plunging hinge lines are defined by elongation of hornblende, biotite, and microboudinaged staurolite. Macroscopic to microscopic kinematic indicators from these rocks demonstrate a consistent south-side-up sense of shear (Duebendorfer, 1986).

Figure 11. Sheath folds in the east Bear Lake Block south-central Medicine Bow Mountains (photo by E.M. Duebendorfer).

The mylonite zones (including the Mullen Creek-Nash Fork shear zone and Rambler shear zone) consist of mylonite, ultramylonite, and protomylonite (**Figure 12**). They dip from 60° S to vertical, range in width from 160 to 1,300 feet, and exhibit both sharp and gradational boundaries with nonmylonitic country rock. Blocks adjacent to the mylonite zones usually exhibit a tightening of folds, dismemberment of folds due to limb alteration, hinge arcuation, and steepening of fold hinge lines (Duebendorfer and Houston, 1987).

The French Creek fold of the Libby Creek Group plunges steeply northeast, approximately parallel to the hinge lines and lineations discussed above. Karlstrom and Houston (1984, p. 433-434) suggested that the French Creek fold developed in the same manner as the related folds and lineations, i.e., *by kinematic conditions characterized by subvertical extension (present orientation) related to dip-slip movements on the shear zone.*

The last unequivocal Precambrian event documented in the Cheyenne belt is the development of semipenetrative, subhorizontal lineations that are defined by chlorite and epidote fibers on the mylonitic foliation (Duebendorfer and Houston, 1987). Mesoscopic and microscopic kinematic indicators suggest right-lateral (dextral) shear. Related steeply plunging angular folds that deform the northeast foliation of slates of the Upper Libby Creek Group, rocks of the Bear Lake block, and mylonitic rocks of the Mullen Creek-Nash Fork shear zone show a consistent Z-shaped, down-plunge profile and further corroborate a dextral sense of shear.

The proposed thrusting of Libby Creek Group rocks and blocks of the Cheyenne belt over autochthonous Deep Lake Group and older successions probably took place during the development of a fold-and-thrust belt as the island-arc terrane collided with the passive margin. The rocks of the Libby Creek

Figure 12. Mylonite in the Mullen Creek - Nash Fork shear zone, south-central Medicine Bow Mountains, Wyoming (photo by M.E. McCallum).

Group were probably metamorphosed at this time; Hills and others (1968) attempted to date this metamorphic event using samples from the Medicine Bow Mountains. Whole-rock Rb-Sr dates on the Lookout Schist (1,710±60 Ma) and French Slate (1,620±425 Ma) suggest an age of metamorphism between 1,700 and 1,800 Ma. Timing of deformation is more tightly constrained in the Sierra Madre, where the about 1,750-Ma Sierra Madre Granite intrudes the shear zone and is in turn cut by late cataclastic faults. These observation suggest a minimum age of 1,750 Ma for collision.

Structure south of the Cheyenne belt

Medicine Bow Mountains

The Rambler shear zone consists of a series of anastomosing mylonite zones within the granite of Mullen Creek that exhibit both a penetrative subvertical mineral lineation and nonpenetrative slickenside lineations. These fabrics are consistent with fabrics in the Cheyenne belt proper that record early south-side up displacement and later right-lateral shear. Within and near the south margin of the Rambler shear zone, a belt of intense cataclasis and metamorphic retrogression was identified by Duebendorfer (1986). This fault, which Duebendorfer named the Rambler fault, can be traced to the western margin of the Medicine Bow Mountains and east to the western part of R79W, where it is covered. It may be a Precambrian fault that developed at shallower crustal levels, or it may be a Phanerozoic feature (Houston and Karlstrom, 1992).

An area some 8 to 10 miles wide, located south of the Rambler shear zone, is dominated by large plutons—the Mullen Creek and Lake Owen mafic complexes and the Keystone Quartz Diorite (**Figure 2**). The Mullen Creek and Lake Owen mafic complexes probably originated deeper in the volcanic massif than volcanic rocks of the Centennial block (Karlstrom and Houston, 1984). The presence of these mafic complexes suggests that the area south of the Rambler shear zone may represent another of the successively deeper levels of crust exposed in and south of the Cheyenne belt. South of this area, an east-west striking belt of hornblende gneiss and amphibolite 31 miles long and 3.5 miles wide extends entirely across the Medicine Bow Mountains (**Figure 2**). Foliation in this belt generally strikes east-west, but mesoscopic and macroscopic interference folds are common, especially in the western segment of the belt (Houston and others, 1968) (**Figure 2**). This belt is bounded on the south by the poorly exposed Bear Creek mylonite zone of Houston and others (1968). Mylonitic shear zones at Six Mile Gap (Sec. 4, T12N, R80W) parallel the Bear Creek shear zone and have the same subvertical lineation noted in the fault systems of the Cheyenne belt.

The area south of the Bear Creek shear zone is characterized by interference between northwest- and northeast-striking structures (Houston and others, 1968, plate 1). The steep plunge of lineations and the oval shape of some of the orthogneiss bodies suggest diapiric movement.

Sierra Madre

The structure of the southeast Sierra Madre is similar to that of the southern Medicine Bow Mountains. Both the Mullen Creek-Nash Fork shear zone and Bear Creek shear zone can be traced into the southeast Sierra Madre where they are offset by right-lateral faults (**Figure 2**). Lithologies between the Mullen Creek and Bear Creek shear zones are chiefly mafic and felsic gneiss that are interpreted as having primarily volcanic protoliths but with subordinate metasedimentary rocks. Two large bodies of orthoamphibolite are present in this succession. All of these rocks are intensely deformed and exhibit mesoscopic and macroscopic interference folds (**Figure 13**). South of the Bear Creek fault, metavolcanic and metasedimentary rocks are exposed that are similar to those to the north. In addition, a distinctive sillimanite gneiss unit may lie unconformably on the older volcanic-metasedimentary succession and is infolded with the older rocks. The sillimanite gneiss body exhibits the typical crescent shape of a folded fold (**Figure 2**).

Approximately 17 miles west of the southeastern margin of the Sierra Madre, a series of cataclastic northwest-striking right-lateral faults offset the metavolcanic-metasedimentary succession and the Chey-

enne belt (**Figure 2**). These right-lateral faults are related to an east-west zone of intense cataclasis in the central Sierra Madre that truncated and dismembered the Cheyenne belt. Kinematic analysis within the cataclastic zone suggests that it formed during north-directed thrusting (Duebendorfer and Houston, 1990). The two principal right-lateral faults of the southeastern Sierra Madre have a wedge of metamorphic rocks between them that consists primarily of felsic gneisses (orthogneiss?) with inclusions of hornblende-plagioclase gneiss and garnet-hornblende-plagioclase gneiss. These felsic and mafic rocks are intruded by pink granite of the Sierra Madre which is, in turn, sheared near the fault traces. Lithologically and structurally the wedge is more like rocks west of the right-lateral faults than those to the east.

These cataclastic fault systems have displaced a large mass of metamorphic rocks of the south-central and southwestern Sierra Madre (**Figure 2**) some distance north of its previous position. This deformation was accompanied by the development of a north-directed set of thrust faults in the Libby Creek Group equivalents north of the east-west cataclastic fault zone. Similar east-west faults that may be thrust faults cut the volcanic succession south of the cataclastic belt (**Figure 2**). Right-lateral faults and Z-shaped folds in the Libby Creek and Deep Lake group equivalents (Snowy Pass Group) north of the cataclastic belt suggest that movement of the block was directed both north and west.

This cataclastic deformation was accomplished by disrupting and bending mylonites of the Cheyenne belt in the east and overriding the belt in the central Sierra Madre (**Figure 3**). Facies of the Sierra Madre Granite invade the fault system and the granite is itself sheared, suggesting emplacement of the granite during this stage of faulting. The relationship of the cataclastic fault system to the Sierra Madre Granite suggests that the faults are Precambrian (about 1.75 Ga), but the right-lateral faults also show evidence of both Laramide and Cenozoic reactivation (Houston and Graff, in press).

This large displaced block of metamorphic rocks of the south-central and southwestern Sierra Madre is significantly different than metamorphic rocks of the southeast Sierra Madre and southern Medicine Bow Mountains. It consists of two terranes: (1) a terrane of metavolcanic rocks in the northern and western part of the block that is a folded syncline and (2) an older terrane in the eastern part of the block that has a core primarily of mafic volcanic rocks and associated mafic intrusions. The core of the older terrane is surrounded by and interfingers with felsic gneisses that are chiefly metasediments. These two terranes are separated from one another by the main body of the Sierra Madre Granite (**Figure 2**). Granite also cuts the metamorphic rocks of both terranes (**Figure 2**).

If foliations in metavolcanic rocks, metasedimentary rocks, and Sierra Madre Granite are plotted as in **Figure 2**, the structure of the eastern terrane resembles large-scale interference folds. However, this is difficult to interpret without good stratigraphic control. In R84W, T12N, near the confluence of Hog Park Creek and the Encampment River, recumbent isoclinal folds are present that plunge gently northeast, perpendicular to the general northwest strike of foliation in this area. These folds may represent an early stage of deformation that preceded development of the large-scale interference folds. The northern and western terrane (Green Mountain Formation) consists of metavolcanic and metasedimentary rocks of lower metamorphic grade (greenschist vs. amphibolite facies) that retain stratigraphic facing criteria. This terrain is a folded and faulted syncline that is interpreted as having been infolded into a basement of the eastern terrane and subsequently refolded about an east-west axis (**Figure 2**). The Sierra Madre

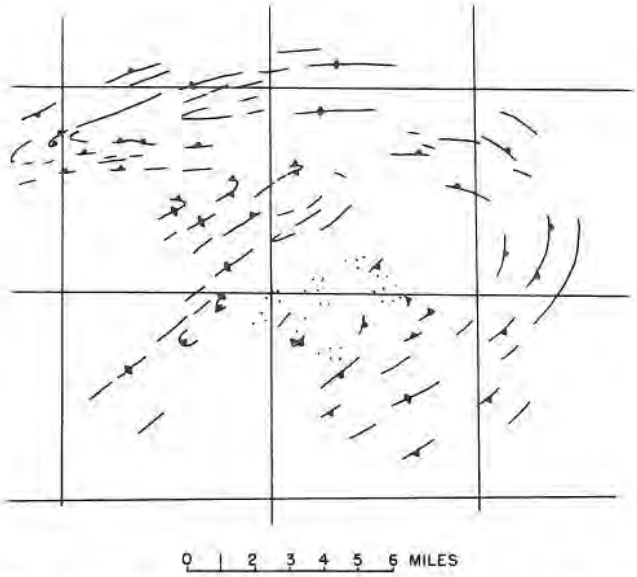

Figure 13. Sketch map of foliation trends in gneiss of the southwest Medicine Bow Mountains showing interference fold. Dotted area indicates more massive gneiss [from Houston and others (1968)].

Granite splits this folded syncline into two parts, a northern part that is largely greenschist facies and a southern part that ranges from upper greenschist to amphibolite facies. The plunging nose of the syncline in the south-central Sierra Madre is folded about an east-northeast axis and is cut by east-northeast-striking sills (**Figure 2**). This latter structure is thought to post-date the development of the refolded syncline and may be related to an east-northeast fault system that had south-side-up movement (as in the Medicine Bow Mountains), but is now completely obscured by granite.

Laramie Mountains

The structure of the metavolcanic and metasedimentary rocks of the southeastern Laramie Mountains is poorly known. The primary belt of metavolcanic and metasedimentary rocks strikes northeast (**Figure 3**), but the bedding and foliation within the belt strikes east to east-northeast, comparable to the general strike of the foliation in the southern Medicine Bow Mountains and Sierra Madre. A major east-west striking mylonite zone is located approximately halfway between Granite, Wyoming, and the Wyoming-Colorado State Line. This mylonite zone may represent the same type of structure as the Bear Creek shear zone of the Medicine Bow Mountains (Marlett, 1989). Good kinematic indicators have not been recognized in this shear zone, but the abundance of pegmatites on the south side of the fault suggests a deeper level of the crust than the pegmatite-free north side.

Late Archean and Early Proterozoic evolution of southeastern Wyoming

The following brief review of the Late Archean and Early Proterozic evolution of southern Wyoming relies heavily on earlier work, especially the detailed analyses in Karlstrom and others (1981). An emphasis is placed on critical problems that still exist in our attempts to understand the history of this complex area.

Gneissic basement, with remnants of Middle Archean (>3.2 Ga) metavolcanic and metasedimentary rock, extends south to the Wyoming province margin in southern Wyoming. The genesis of these basement rocks is uncertain; however, they are considered basement to Late Archean supracrustal successions (i.e., Phantom Lake metamorphic suite) that were deposited either near or at the margin of the Wyoming province or at the margin of an Archean microplate that was eventually accreted to the Wyoming province. By 2.7 Ga, the Wyoming province was assembled by the aggregation of microplates. Late Archean supracrustal rocks nearest the province margin are three-fold successions with a basal quartzite or stromatolitic dolomite interpreted as shelf deposits, a middle volcaniclastic member interpreted as having been derived from an Andean-type arc that developed by north-directed subduction at a microplate margin, and finally a quartzite or stromatolitic dolomite that represents a return to marine deposition at the plate margin. Supracrustal rocks landward of the plate margin are greenstone-belt type successions that may have been deposited in back-arc basins. The approximately 2.7 Ga age on both the greenstone belt volcanic rocks and arc-related granodiorite suggest that a plate margin existed in this area in Late Archean.

Archean to earliest Proterozoic deformation of the Late Archean successions and evidence of rifting in the Early Proterozoic suggest that an additional Archean body or microplate existed south of this margin and that the Wyoming province was more extensive in the Archean than today.

The final stage of assembly of the Archean Wyoming province was the emplacement in southern Wyoming of pink potassium-rich granites with high Th/U ratios that range in age from about 2.6 Ga to 2.45 Ga. These granites were probably generated by melting at or near the base of the Archean plate (**Figure 14A**).

Early Proterozoic successions at the margin of the Wyoming province in the eastern Black Hills and in southern Wyoming contain basal braided stream deposits (**Sheet 1**, Houston, map pocket). In southern Wyoming, the 2.4 to 2.1 Ga Deep Lake Group, which

lies unconformably on Archean basement, is primarily fluvial conglomerate and quartzite. The thick fanglomerates and braided stream deposits of the Deep Lake Group developed during an early stage of rifting that was accompanied by introduction of tholeiitic basalt at 2.1 to 2.0 Ga. The Deep Lake Group was mildly deformed into open folds and the underlying Late Archean supracrustal rocks were refolded.

The rifting stage must have continued or a second rifting event may have occurred during deposition of the lower Libby Creek Group of the Medicine Bow Mountains, which is a clastic succession some 14,000 feet thick. The metasedimentary rocks at the base of the lower Libby Creek Group are glaciomarine and indicate a period of glaciation probably near the end of deposition of the Deep Lake Group and in the initial stages of deposition of the lower Libby Creek Group. The bulk of the lower Libby Creek Group is interpreted as deltaic deposits formed in a northeast-striking trough that developed as a hypothetical southern block separated from the Wyoming province (Karlstrom and others, 1981; Flurkey, 1983).

Rocks of the upper Libby Creek Group of the Medicine Bow Mountains were deposited on the continental platform during and after separation of the southern block (**Figure 14D**). The lower 6,500 feet of the lower Libby Creek Group is stromatolitic dolomite that represents a carbonate bank deposited near the shelf margin (**Figure 14**). Pillow lava and graphitic slate that overlie the dolomite are interpreted as having been laid down in a foredeep basin that developed as an island arc approached from the south (**Figure 14**). Libby Creek Group equivalents in the Sierra Madre are partial sections disrupted severely by a late cataclastic event. They are a more distal facies of the Medicine Bow Mountains rocks and were deposited south or southwest of their Medicine Bow equivalents.

Unfortunately, we have been unable to date these various successions precisely enough to determine which rocks are time equivalents. The glacial deposits of both mountain ranges are good marker horizons, but are not useful in determining facies except to indicate that the Sierra Madre successions are distal facies of the Medicine Bow section. The glacial deposits of the upper Deep Lake and lower Libby Creek groups are considered part of a widespread episode of glaciation that can be correlated over much of the North American Lower Proterozoic rocks (Young, 1970). The development and deformation of the trailing margin can only be bracketed between about 2.4 and 1.75 Ga. If rifting spanned this entire interval, a longer period for development and deformation of the Early Proterozoic margin is indicated than for modern analogues.

The present-day contact between the Wyoming Archean and Colorado Proterozoic provinces may not resemble the original shape of the rifted Archean plate. Southwest-directed paleocurrents measured in the lower Libby Creek Group of the Medicine Bow Mountains suggest that a northeast-southwest trending trough developed during rifting (Flurkey, 1983). The northwest trend of the Archean-Proterozoic contact in the Sierra Madre (**Figure 2**) was originally interpreted to be a second arm of a triple junction rift system (Karlstrom and others, 1983). Our more recent detailed studies of the fault system in the Sierra Madre (Duebendorfer and Houston, 1990) demonstrate that Sierra Madre continuation of the northeast-striking fault system exposed in the Medicine Bow Mountains was disrupted and overridden, at approximately 1.75 Ga, by a later northwest-directed fault system. However, the Cheyenne belt of the easternmost Sierra Madre, which is unaffected by later faulting, does have more of an east-northeast strike, suggesting that the original margin may have changed strike in the Sierra Madre. Scant evidence from regional isotopic studies have been interpreted to indicate that the Archean-Proterozoic boundary trends roughly east-west west of the Sierra Madre (Bennett and DePaolo, 1987). This transition in trend of the original boundary from northeast to east-west may have occurred in the region of the Sierra Madre.

The Proterozoic arc terrane south of the Cheyenne belt was probably a composite arc or series of arcs that approached the Wyoming province from the south. The volcano-sedimentary successions directly south of the Cheyenne belt extend over an area some 60 miles wide from north to south (Reed and others, 1987), suggesting that this terrane is probably too wide to be a single arc. Structure in the metavolcanic-metasedimentary successions south of the Cheyenne belt exhibit complex interference folds, but the final fold orientation is east-west. Major shears that mark boundaries between crustal segments also strike east-west, as does the southernmost fault, the Rambler shear zone, of the Cheyenne belt. The present attitude of the shear zones separating the various blocks

in the Medicine Bow Mountains and Sierra Madre is steep south-dipping to vertical. The same is true of the two major faults within the Libby Creek Group of the Medicine Bow Mountains. If these faults represent thrust faults, then they must have been rotated during the later stages of the collisional event. To explain this phenomena, we (Karlstrom and others, 1981) suggested that there was a reversal in the direction of subduction because of the difficulty encountered in the attempted subduction of continental crust (**Figure 14G**).

The northeast-striking shear zones of the Medicine Bow Mountains and eastern Sierra Madre are more likely candidates for strike-slip displacement from north-south convergence than the east-west shear zones that may have existed in the western Sierra Madre. Left-lateral strike-slip movement could have displaced the rifted Archean basement south of the Mullen Creek-Nash Fork shear zone to the northeast, which would explain the apparent absence of Archean basement in the southern Medicine Bow Mountains.

The only evidence for left-lateral displacement in the Medicine Bow Mountains is the rotation of the French Creek fold axes and associated thrust faults in the southwest exposure. This can be explained in two ways, either as a product of left-lateral displacement (Houston and Parker, 1963) or as a result of progressive ductile deformation over a fairly wide zone along both sides of the shear zone (Karlstrom and Houston, 1984). Despite a careful search, no kinematic evidence has been found to indicate left-lateral displacement along the Mullen Creek-Nash Fork shear zone of the Medicine Bow Mountains (Duebendorfer, 1986). A late phase of low-grade dextral shear is recorded in mylonitic shear zones south of the Mullen Creek-Nash Fork shear zone of the Medicine Bow Mountains (Duebendorfer, 1986). Similar right-lateral structures are poorly preserved in the dismembered shear zones of the eastern Sierra Madre (Duebendorfer and Houston, 1990).

Refinement in geochronology is desperately needed if we are to further develop the geologic history of this area. Deposition of the rift-related Deep Lake and lower Libby Creek groups is constrained between about 2.4 and 2.1 Ga. No Phanerozoic rift sequence approaches a duration of 300 million years. The upper Libby Creek Group cannot be constrained in age except to say that it is older than about 1.75 Ga. The metavolcanic rocks south of the Cheyenne belt have yielded only one firm radiometric date, the ~1.8 Ga age of a metadacite in the Green Mountain Formation (Premo and Van Schmus, 1989). Despite numerous attempts, no other reliable age determination is available for this succession (Hills and Houston, 1979; Premo and Van Schmus, 1989). If 1.8 Ga is the approximate age of all the various successions in the arcs south of the Cheyenne belt, it is clear that collision could not have occurred before 1.8 Ga.

The final event of the closure is the cataclastic deformation in the Sierra Madre. As noted by Reed and others (1987), the oldest rocks of the arc predate suturing by 40 million years or less (actually the collisional event may have begun prior to 1.75 Ga). They calculate that, with a conservative convergence rate of about 5 cm/year, the arc or arcs may have originated some 1,250 miles south of the craton margin.

Possible regional stratigraphic and tectonic correlations

In our initial studies, the Early Proterozoic orogenic events of southern Wyoming were correlated with the better known Penokean orogeny of the Lake Superior area of the United States (Houston and others, 1968; Hills and others, 1968), and we postulated that southeastern Wyoming might be part of a fold belt that extended from the Lake Superior area into Wyoming (**Figure 1**). A north-northwest-striking fold belt that was called the Black Hills orogenic belt by Goldich and others (1966) was defined in the north-central U.S. A major problem was the relationship between these two fold belts, which were thought to be coeval even though they intersect at right angles (Houston and others, 1968). One early solution was to view the Black Hills fold belt as an aulacogen. This seems untenable today, as the Black Hills orogenic belt is now considered to be part of the extensive Trans-Hudson orogen. The Trans-Hudson orogen extends from Greenland through central Canada into the north-central U.S. (**Figure 1**). According to Bickford and others (1990), it is the most extensively preserved Early Proterozoic orogenic belt on Earth, and it dwarfs the Penokean.

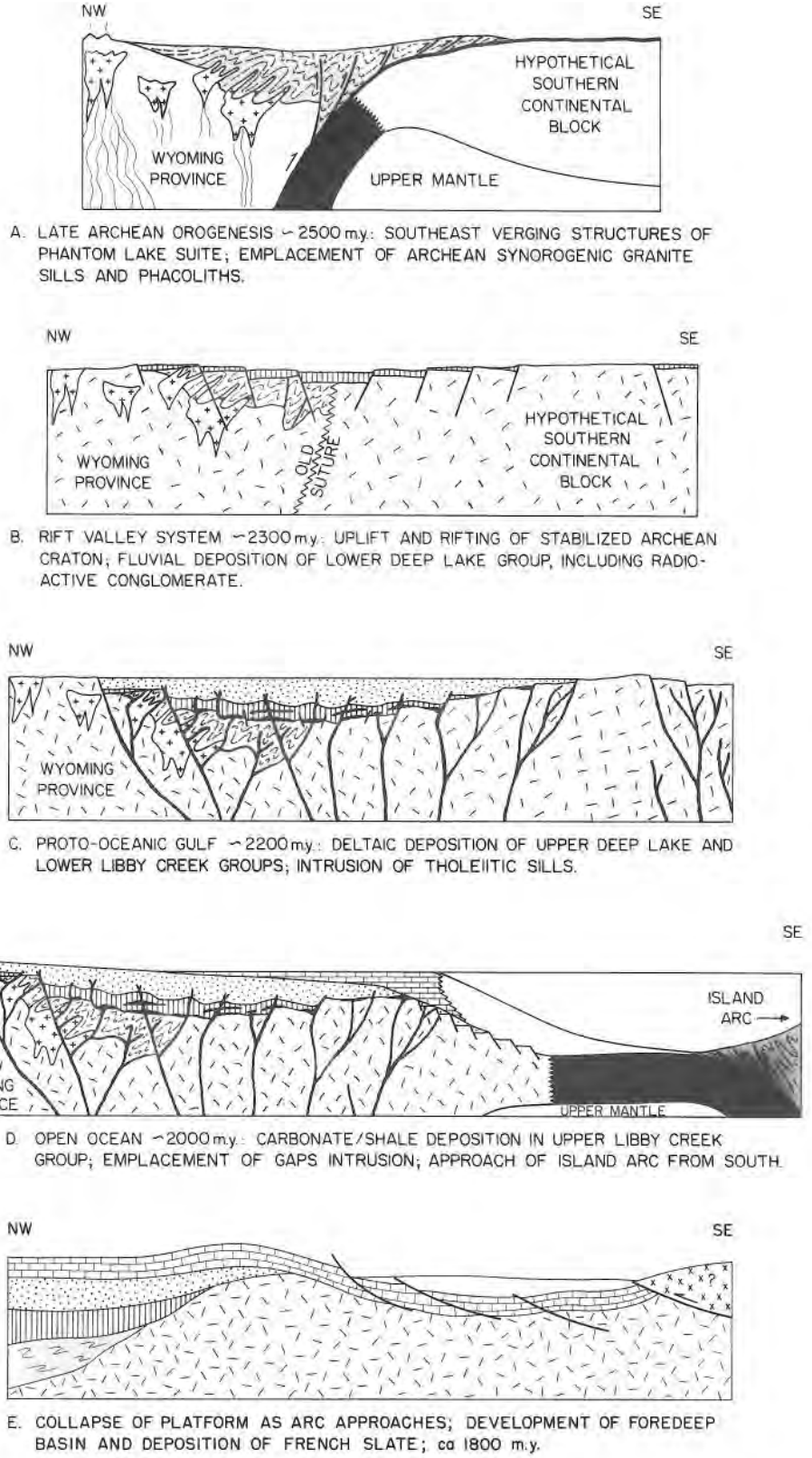

Figure 14. Diagrammatic cross sections showing possible sequence of events during Late Archean and Early Proterozoic, Medicine Bow Mountains, Wyoming (modified from Karlstrom and others, 1981 and Karlstrom and Houston, 1984).

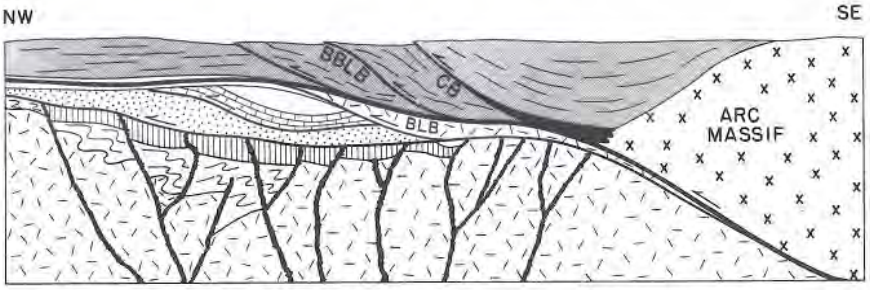

F. CONTINENT-ISLAND ARC COLLISION - ca 1780 m.y.; OBDUCTION OF ARC, THRUSTING IN LIBBY CREEK GROUP AND FOREARC VOLCANOGENIC ROCKS.

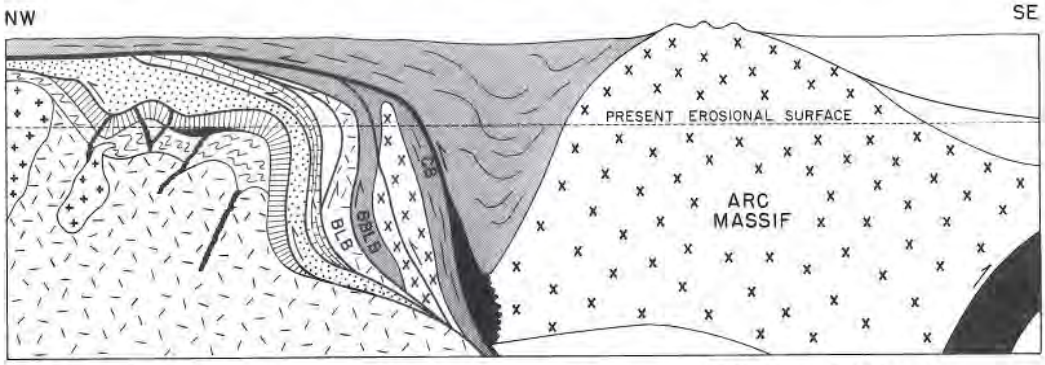

G. FLIP IN DIRECTION OF SUBDUCTION ca 1760 m.y.; ROTATION OF BEDS AND THRUSTS; CONTINUED DEFORMATION AND FOLDING.

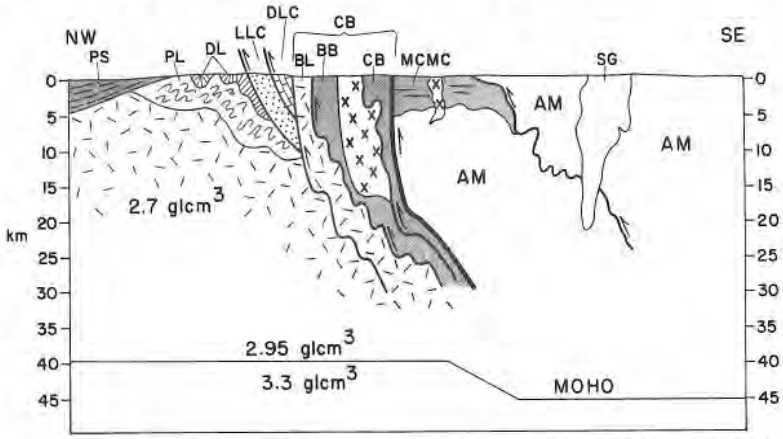

H. SKETCH SHOWING PRESENT GEOLOGIC SETTING AND DEPTH TO MOHO. PS=PHANEROZOIC SEDIMENTARY ROCKS; PL=PHANTOM LAKE SUITE; DL=DEEP LAKE GROUP; LLC=LOWER LIBBY CREEK GROUP; ULC=UPPER LIBBY CREEK GROUP; CB=CHEYENNE BELT; BL=BEAR LAKE BLOCK; BB=BARBER LAKE BLOCK; CB=CENTENNIAL BLOCK; MCMC=MULLEN CREEK MAFIC COMPLEX; SG=SHERMAN GRANITE; AM=ARC MASSIF.

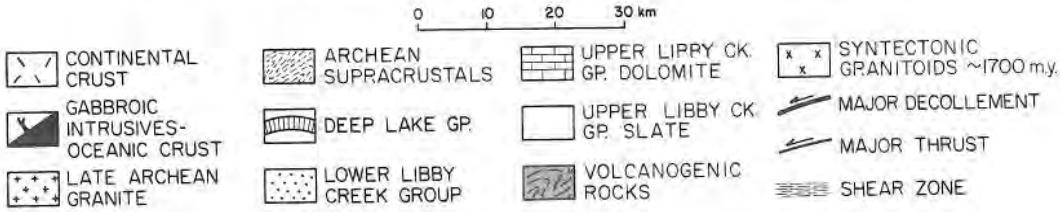

Figure 14. *Continued*

The problem posed by the intersection of the north-striking Trans-Hudson and the northeast-striking Penokean orogen and Cheyenne belt is one of timing. Current thinking is that both the Trans-Hudson and the Penokean orogenies occurred at approximately 1,800 to 1,900 Ma, whereas the Cheyenne belt developed later (1,700 to 1,800 Ma) as part of the Central Plains orogeny (Sims and Peterman, 1986; Hoffman, 1989). This is a reasonable solution to the problem, but I consider it a necessary oversimplification based on the current state of our geochronometric data. Based primarily on stratigraphic evidence, I suspect that the Cheyenne belt rocks preserve a history of sedimentation and deformation that is older than the arc collision (at 1,700 to 1,800 Ma). The arc collision was the last but perhaps not the most significant Early Proterozoic event that occurred in the area. In order to evaluate this concept, it is necessary to review the regional geology in more detail. I will first consider the Trans-Hudson and its relationship to the Wyoming province.

The best exposed part of the Trans-Hudson orogen is an arcuate area in Saskatchewan and Manitoba, the Reindeer zone, where the orogenic belt lies between the Archean Superior and Hearne provinces of Canada (**Figure 1**). The Reindeer zone is a complex assemblage of domains consisting chiefly of Early Proterozoic arc-related rocks with windows of Archean basement (Stauffer, 1984; Lewry and Stauffer, 1990). The Reindeer zone developed by rifting during the Early Proterozoic, as evidenced by the southeast margin of the Hearne province, where coarse clastic deposits at the base of an Early Proterozoic miogeoclinal succession are interpreted to be rift-related (Stauffer, 1984). An ocean developed, the Manikewan ocean of Stauffer (1984), probably between the Superior province and Hearne province, although there is no proof that it was the Superior province to the southeast. The timing of this rifting event is poorly documented in Canada (Green and others, 1985), but if it occurred at about the same time as rifting in the Hudsonian arm of the north-central U.S., it was >2.1 Ga (Redden, 1980).

Whether or not the Superior province was the plate that rifted from the Hearne, it was the plate that collided with it. Closure of the Manikewan ocean was accompanied by subduction, the development of island-arc volcanic and related sedimentary rocks, and magmatic arcs that make up the bulk of the Reindeer zone. Description and timing of the events that accompanied convergence are much better documented than the events of rifting. According to Bickford and others (1990), volcanism began by or before, 1,910 Ma, and was widespread by 1,885 Ma; related arc plutons were emplaced between 1,865 and 1,830 Ma. Bickford and others (1990) state that regional high-grade thermotectonism persisted until approximately 1,810 Ma and that late granites were emplaced into the Reindeer zone as late as 1,800 Ma; some 100 million years of subduction and tectonism during ocean closure. The recognition of folded mylonite in many areas of the Reindeer zone have led Lewry and Stauffer (1990) to interpret the Reindeer zone to be composed of deformed large-scale nappe sheets. They proposed that the later stages of deformation involved the emplacement of large-scale southeast-directed thrust sheets over the Superior plate, followed by folding of the thrust sheets or nappes. The presence of windows of Archean crust beneath these thrust sheets in the central Reindeer zone suggests that the Superior province extends a great distance beneath the Reindeer zone and implies northwest subduction of the Superior province during closure (**Figure 15**). As noted by Bickford and others (1990), it is conceivable that the Hearne province might be an upper plate hinterland if the Superior province extends that far northwest.

The only surface exposure of the Trans-Hudson orogen in the north-central U.S. is in the Black Hills of South Dakota, a north-northwest striking Laramide uplift cored by Precambrian rocks. Detailed mapping by Redden (1980, 1981) and geochemical and geochronological studies by Gosselin and others (1988) are interpreted to indicate that the Archean exposures in the Black Hills are the easternmost extension of the Wyoming province (**Sheet 1**, Houston, map pocket and **Figure 1**). In the Black Hills, Archean metasedimentary rocks are intruded by Archean granite and overlain by Early Proterozoic miogeoclinal successions. The bulk of the Black Hills Precambrian rocks are metamorphosed and multiply folded eugeoclinal volcanic and associated metasedimentary rocks. Two volcanic horizons in the eugeoclinal succession have been dated at 1.97 and 1.87 Ga (Peterman and Sims, 1993). The Early Proterozoic miogeoclinal successions resemble the miogeoclinal rocks on the Snowy Pass Supergroup of the Medicine Bow Mountains (Gosselin and others, 1988) and are approximately the same age. The Early Proterozoic miogeoclinal succession was probably deposited in an intracratonic rift (Redden, *in* Gosselin and others, 1988). The

clastic succession contains a metagabbro sill dated at 2,090±10 Ma by R.E. Zartman (Redden, 1980). This sill is the same age as tholeiitic sills and dikes that intrude the Deep Lake Group of the Medicine Bow Mountains and is probably related to the same rifting event. A marine succession that overlies the clastic succession is similar to the Libby Creek Group of the Medicine Bow Mountains.

There are three major deformational events recorded in the Black Hills, an Archean event that resulted in the development of northeast-striking foliation, a later Archean event that resulted in north-northwest-trending folds, and a profound Early Proterozoic event that caused the north-northwest-trending structure that characterizes the uplift (Redden, 1980; Gosselin and others, 1988). The timing of the last tectonic event may coincide with resetting of the Rb-Sr age of the easternmost Archean granite at about 1,850 Ma (Gosselin and others, 1988). The last major Precambrian event recorded in the Black Hills is the emplacement of the Harney Peak Granite in the south-central Black Hills at about 1,740 Ma. The Black Hills Precambrian crust was clearly involved in the Trans-Hudson orogeny, as

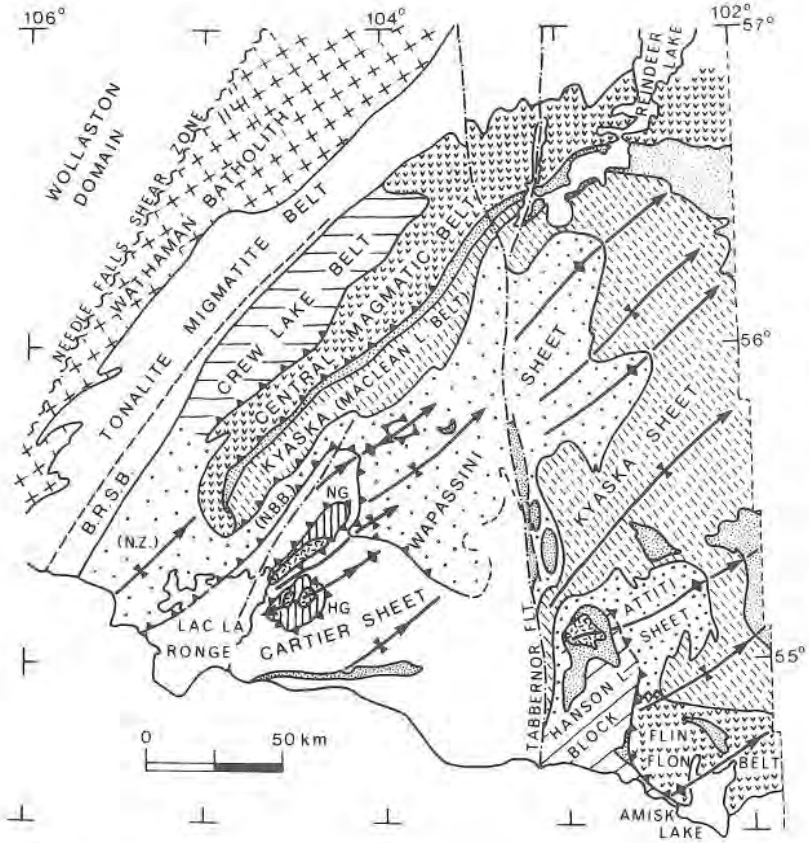

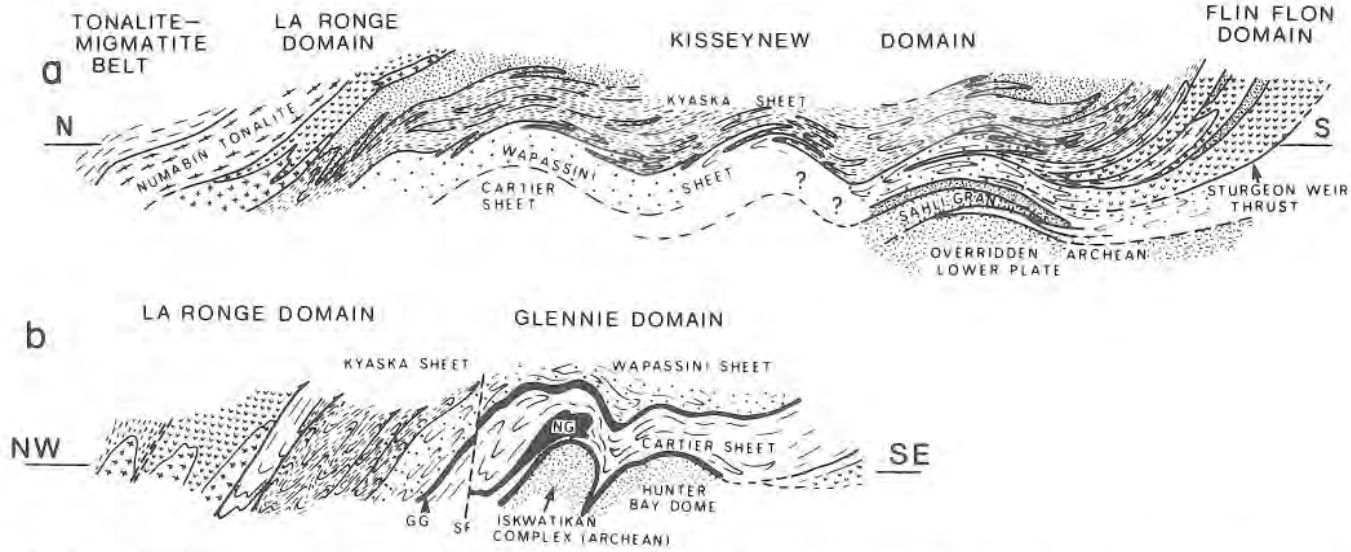

Figure 15. Reindeer zone in northern Saskatchewan showing Archean lower plate (Superior province) overridden by nappe sheets(from Bickford and others, 1990, figure 2). After Bickford and others (1990): *varying patterns emphasize different structural levels or early nappe sheets. Small areas of random - line pattern in northern Hanson Lake block (Sahli Granite) and northeast of Lac La Ronge (Iskwatikan and Hunter Bay windows) show documented Archean basement beneath allochthonous Early Proterozoic nappes. Major F_3 regional fold axial traces are also shown. Sections a and b show general interpretation of crustal structure.*

shown by the close correlation in the age of deformation and the striking parallelism in structure with that of geophysical trends in the buried basement to the east that is considered the U.S. continuation of the Trans-Hudson (Green and others, 1985). If the Black Hills is a southern equivalent of the Cree Lake province (Hearne margin), as suggested by Gosselin and others (1988), is it an upper plate hinterland underthrust by the Superior province or a plate margin deformed by collision? Is the eugeoclinal succession that overlies the miogeoclinal metasedimentary rocks a foredeep basin? A partial answer may be found in the Hartville uplift and eastern Laramie Mountains of Wyoming.

The Hartville uplift lies approximately 65 miles southwest of the Black Hills and is composed of Archean metasedimentary and metavolcanic rocks (the three-fold succession described previously). The rocks are intruded by two Proterozoic plutons, the diorite of Twin Hills (1,740±40 Ma) and the granite of Flattop Butte (1,980±10 Ma) (Snyder and others, 1989). According to Snyder and Peterman (1982), the granite of Flattop Butte is remobilized Archean granite and pelite (interpretation based on $^{87}Sr/^{86}Sr$ ratios, Sm-Nd model ages, and a S-type granite mineral assemblage). Snyder and others (1989) stated that the Archean succession developed north-northeast-trending, open to isoclinal folds that were tightly refolded about east-west axes between 1.98 and 1.74 Ga. Snyder and others (1989) also indicated that the Proterozoic diorite of Twin Hills and granite of Flattop Butte were intruded after deformation.

The central Laramie Mountains is underlain by middle Archean gneissic basement and infolded Archean greenstone belts, both of which exhibit complex interference folds with axes that trend generally east-northeast. In the east-central Laramie Mountains, K.R. Ludwig (*in* Snyder and others, 1989) reported the presence of small bodies of granitic to granodioritic rocks with U-Pb ages ranging from 1.74 to 2.05 Ga.

Proterozoic intrusive rocks of approximately 1.74 Ga are not present in Archean or Early Proterozoic rocks north of the Cheyenne belt in either the Medicine Bow Mountains or Sierra Madre. Is their presence in the Hartville uplift and eastern Laramie Mountains related to the Trans-Hudson orogeny? Certainly the north-northeast-trending structural grain of the Hartville uplift is more compatible with the Trans-Hudson orogen than with the Medicine Bow and Sierra Madre Mountains. If these events are indeed related to the Trans-Hudson orogeny, how much of the eastern Wyoming province was affected?

Isotopic studies of rocks from the Laramie Mountains and Black Hills may shed some light on this problem. Geist and others (1989) reported a Sm-Nd isotopic contrast between Early Proterozoic granites that intrude the Hartville uplift and Middle Proterozoic granites of the western Laramie Mountains. According to Geist and others (1989), the Early Proterozoic intrusions of the Hartville uplift are similar to the Harney Peak Granite of the Black Hills, exhibiting Nd model ages of 2.73±2.95 Ga. These workers further stated that the Hartville uplift and Black Hills granitoids contain some Proterozoic material (because their Nd model ages are younger than the rocks that they intrude). However, the volume of Proterozoic material required by the data of Geist and others (1989) is relatively small compared to granitoids of the Laramie Mountains. The Early Proterozoic granites of the east-central Laramie Mountains, which may be similar to those of the Hartville uplift, have not yet been analyzed isotopically, so the western extent of the Trans-Hudson orogeny in the Wyoming province is not yet known.

The implication of these studies is that the Hartville uplift and possibly the eastern Laramie Mountains were involved in the Trans-Hudson event. Furthermore, there may have been underplating of the Archean province by Proterozoic crust if these 1.74 Ga granites were derived by melting at or near the base of the crust.

Sims and Peterman (1986) proposed the Central Plains orogeny as the eastern extension in Nebraska, Kansas, and Missouri of the deformation zone represented by the Cheyenne belt (**Figure 1**). The concept was developed by considering gravity and magnetic anomalies in conjunction with examination of isotopic ages and rock types in some 1,500 drill holes that penetrated basement. According to this model, the orogenic belt strikes northeasterly from southeast Wyoming into southern South Dakota where it makes an abrupt right-angle turn to the southeast. The Penokean foldbelt is terminated by the Central Plain's southeast-northwest-striking segment in northeastern Nebraska (**Figure 1**). What happens to the Penokean?

Most of the recent geological research on the Penokean orogeny indicates a remarkable similarity to the Cheyenne belt. The Niagara fault zone of northern Wisconsin divides the Penokean into a northern domain (where Early Proterozoic metasedimentary and subordinate volcanic rocks were deposited on Archean basement) and a southern domain (composed of Early Proterozoic volcanic and plutonic rocks of probable island-arc origin) (Greenberg and Brown, 1983; Hoffman, 1988). The Niagara fault zone is an arcuate, generally east-west series of steeply dipping faults that exhibit down-dip stretching lineations (Sedlock and Larue, 1985). There are no Early Proterozoic Andean-type igneous rocks north of the Niagara fault. This observation suggests a history of south-dipping subduction followed by collision of island arcs with the continental margin (Schulz and others, 1984). One primary difference between the Penokean and Cheyenne belts is that a plate of Archean rocks was accreted during the Penokean south of the volcanic arc (Schultz and others, 1984). The Penokean fold belt extends in an east-northeast direction into Canada, where Penokean deformation has been recorded in Early Proterozoic miogeoclinal rocks that crop out on the north shore of Lake Huron (Roscoe, 1968; Brocoum and Dalziel, 1974). Further east, the Penokean may have been overprinted by the Grenville orogen.

In addition to the obvious parallels between the Niagara fault zone and the Cheyenne belt, the sedimentary successions north of these fault systems are strikingly similar (Houston and others, 1979; Houston and Karlstrom, 1992). The Huronian Supergroup of Lake Huron can be correlated with the Snowy Pass Supergroup of the Medicine Bow Mountains from the base of the Deep Lake Group to near the top of the Nash Fork Formation (**Figure 4**), an observation that led Roscoe (1989) to refer to the Snowy Pass Supergroup as the reappearance of the Huronian in Wyoming. The miogeoclinal successions in the Lake Superior area are more difficult to correlate with the Wyoming succession than the Huronian Supergroup because it has been difficult to establish the age of the base of the Marquette Range Supergroup (Van Schmus, 1976) of the Lake Superior area. One solution to this problem is to correlate unique lithologies such as diamictites and aluminous quartzites (Young, 1983, figure 2) (**Figure 4**). If these lithologies represent correlatable climatic events, the Marquette Range Supergroup would be in part younger and in part correlative with the upper part of the Huronian Supergroup, and the Snowy Pass Supergroup would have a nearly complete section representative of both areas (**Figure 4**). The correlation of part of the Snowy Pass Supergroup to the Huronian Supergroup is reasonable geochronologically, but the correlation with the Marquette Range Supergroup may not be. The Hemlock Formation of the Marquette Range Supergroup has been dated as 1,950 Ma (Van Schmus, 1976). If the Towner Greenstone of the Medicine Bow Mountains is the same age as the Hemlock and is in part of a foredeep succession, deformation in southern Wyoming would have had to be some 200 Ma older than the volcanic and granitic rocks south of the Cheyenne belt.

The timing of the Penokean orogeny is generally considered to range from about 1.9 to 1.83 Ga. If the upper successions of the Marquette Range Supergroup (Vulcan Iron Formation and overlying rocks shown on **Figure 4**) represent a fore-arc basin, as suggested by Hoffman (1987), then the 1.95 Ga Hemlock formation would provide a minimum date for early stages of closure. The 1.86 to 1.82 Ga volcanic rocks south of the Niagara fault zone (Peterman and others, 1985) constrain the timing of the latter stages of closure in that area.

Regional tectonic model

If the arc volcanic rocks south of the Cheyenne belt are no older than 1.8 Ga, we are required to postulate a separate event in Wyoming that imitates the Penokean in almost all characteristics except time. In addition, the Penokean must terminate abruptly in Nebraska (**Figure 1**). If the northwest segment of the Central Plains was a transform fault in the initial stage of rifting, an ocean may have developed with a margin similar to the present shape of the Central Plains orogeny (**Figure 16**). If closure was generally in a northwest direction, the transform may have been reactivated about 1.75 Ga and deformation in the Hudsonian rift and along the Penokean margin may have occurred at approximately the same time. The southern Wyoming margin may have been unaffected. The Superior province may have been driven beneath the Hudsonian Proterozoic domains, dragging some Proterozoic crust with it (**Figure 16**). This

scenario could explain the mixture of Archean and a modest amount of Proterozoic in the Nd-Sm signatures of the granitoids of the Black Hills and Hartville uplift. If the transform reactivated in a right-lateral sense during deformation of the southern Wyoming margin at about 1.75 Ga, the eastern Wyoming province may be an area where Proterozoic crust underthrust the Archean margin which accounts for the larger Proterozoic contribution to granitoids in the Laramie Mountains versus the Medicine Bow and Sierra Madre (**Figure 16**).

This transform hypothesis allows a connection between the Penokean orogeny and the events in southern Wyoming, but does not imply a continuous trailing margin. There are many similarities between sedimentary successions and orogenic events that took place along the southern margin of the Archean craton from southern Wyoming to southern Greenland and perhaps to Scandinavia (see Hoffman, 1988, figure 1, for a pre-rift reconstruction of this margin). Hoffman (1988, 1989) suggested that the Archean heart of North America was assembled from Archean continents in a remarkably short period of time (1.96 to 1.81 Ga). If Hoffman is correct, the margins of individual continents may have had similar Early Proterozoic sedimentary sequences, but there would have been no continuous trailing southern margin of the Archean protocraton until the final assembly (i.e., about 1.8 Ga). The post-assembly margin of the Wyoming-Hearne province from the Cree Lake zone (**Figure 1**) to southern Wyoming should have similar sedimentary successions. However, the southern Wyoming successions are more like those of the Lake Superior area than the Cree Lake zone.

The lithologic similarities (Karlstrom and others, 1981; Roscoe, 1989) between the Lake Superior area and Wyoming may relate to depositional environment rather than time, despite the possible glacial time line. Perhaps the history of the region will become clearer with further refinement in geochronology. Nonetheless, we have entertained the possibility (Karlstrom and others, 1981; Houston and others, 1993) that a large continent, like Hoffman's Archean protocraton, existed in Late Archean or Early Proterozoic, broke up, and reassembled. Such a concept implies that the Wyoming and Superior provinces were joined prior to about 2.1 Ga, but we emphasize that this was a joining of two separate Archean masses with different histories (Houston and others, 1993). The prime evidence for the early amalgamation is the strong similarity of metasedimentary prisms (about 2.4 to 2.1 Ga) that may be remnants of successions deposited in early rifted basins prior to complete break-up (i.e., Deep Lake and lower Libby Creek Groups of the Medicine Bow Mountains and lower part of the Huronian Supergroup).

If such a continent existed, our evidence suggests it was larger than Hoffman's Archean protocontinent with additional Archean south of the Cheyenne belt and probably south of the Penokean fold belt (**Figure 16**). Under this circumstance, the actual continental margin of the supercontinent would have been south of both the Niagara fault and Cheyenne belt. A new margin for Hoffman's Archean protocontinent would then have formed near the Cheyenne belt and Niagara fault. The sedimentary successions north of these fault systems preserve evidence of deposition in basins or troughs developed during early stages of rifting and deposition along the later rifted margin.

The earliest depositional prisms in this area are the Huronian Supergroup of the north shore of Lake Huron (2.48-2.22 Ga) (Krogh and others, 1984 and Corfu and Andrews, 1986, as cited *in* Hoffman, 1988), the Deep Lake and lower Libby groups of the Medicine Bow Mountains (ca. 2.4 to 2.1 Ga), and the lower part of the Black Hills succession (where clastic rocks were deposited prior to about 2.1 Ga) (Redden, 1980). In both the Black Hills and Medicine Bow Mountains, the early successions are interpreted as having been deposited during rifting (Karlstrom and Houston, 1984; Redden, 1980). Similar suggestions have been made for the lower part of the Huronian Supergroup (Young, 1983). Perhaps these successions represent the earliest stage of break-up of a supercontinent. A second stage or continued rifting is postulated during deposition of the Chocolay Group (lower part of the Marquette Range Supergroup) of the Lake Superior area by Larue (1981). In the Medicine Bow Mountains, Karlstrom and Houston (1984) have suggested that the Nash Fork Formation, which is correlated with the dolomites of the Chocolay Group (Kona, Randville, Bad River), represents a carbonate bank. Larue (1983) cited Bayley and others (1966) and Larue (1979, 1981) as indicating that the Randville Dolomite was deposited on a carbonate platform that had local exposures of Archean basement to supply siliciclastic detritus. If these inferences are correct, then an actual continental margin must have existed south of the Cheyenne belt and Niagara fault from about 2.3 to 2.0 Ga. How was this margin related to the Trans-

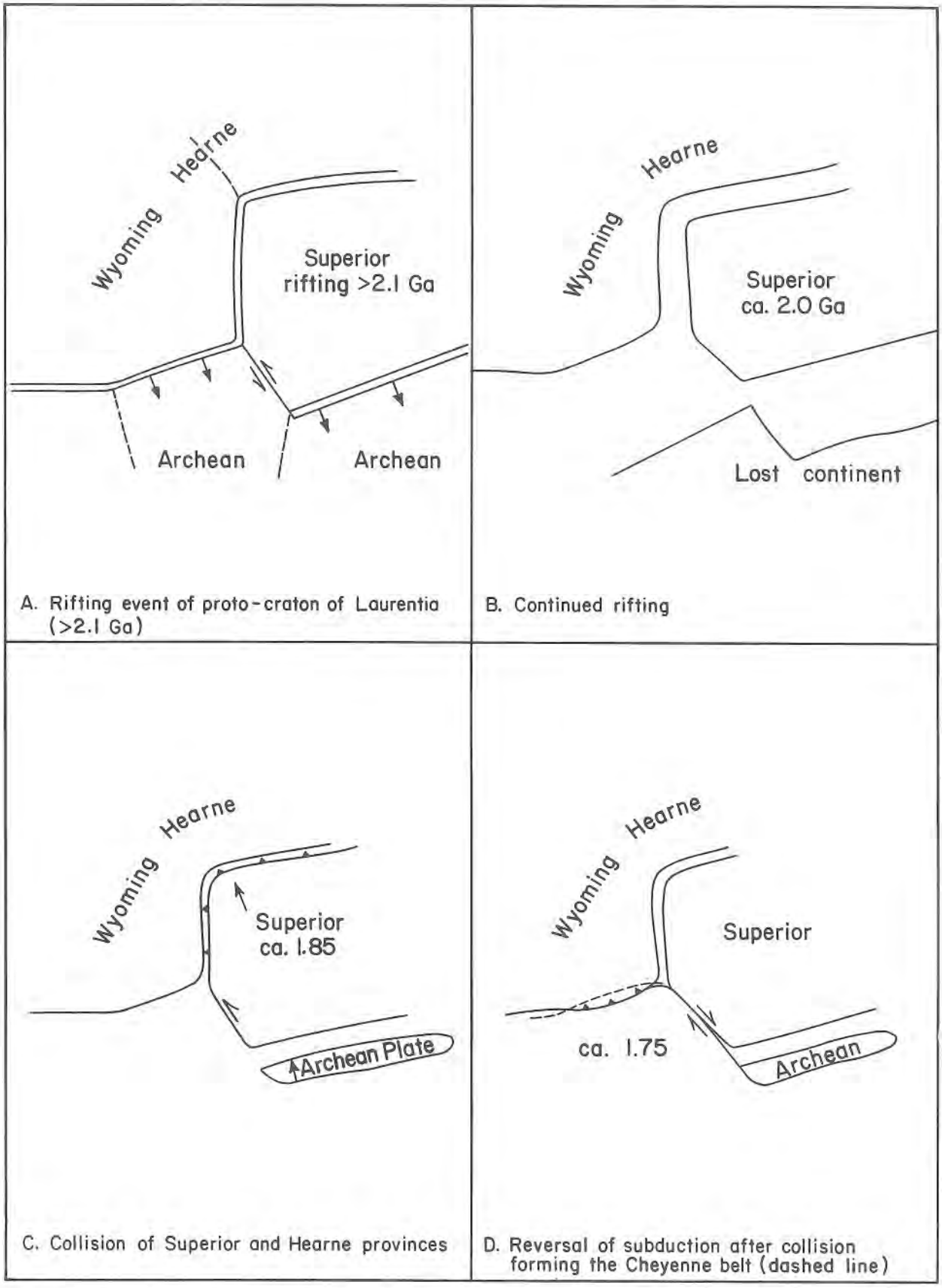

Figure 16. Diagrammatic sketches showing possible events during opening and closing of the Superior, Wyoming, and Hearne provinces.

Hudson? Perhaps refinement in geochronology will allow an opening of the Trans-Hudson after the initial development of the margin or perhaps each Archean province had its own margin.

These last two sections are not meant to offer solutions as much as they are to suggest problems that require attention by geologists, geochemists, and geochronologists. The most pressing need is for additional geochronology. For example, if the Phantom Lake metamorphic suite is indeed Late Archean and if the Towner Greenstone is about 1.90 to 1.95, then the history of the Medicine Bow Mountains can be interpreted quite differently. The Archean margin may have had Wilson cycles in the Late Archean (about 2.7 Ga) and Early Proterozoic (about 1.90 Ga), and the 1.8 Ga volcanic rocks may be exotic terranes added at a later date.

Advances in our understanding of the Precambrian have been remarkable in the last two decades, and in North America have been greatly accelerated by work on the DNAG volumes of the Geological Society of America. Nevertheless, I hope that I have demonstrated that we still have as many problems as solutions, even in areas that have been studied in some detail.

Acknowledgments

Geologic studies of the Proterozoic of southern Wyoming have involved numerous individuals, beginning with the pioneering studies by Blackwelder (1926) in the Medicine Bow Mountains and Spencer (1904) in the Sierra Madre. Major contributors to Medicine Bow Mountains geologic interpretations include: M.E. McCallum, K.E. Karlstrom, and E.M. Duebendorfer; additional workers are listed in Houston and others (1968) and Karlstrom and others (1981). Significant contributions to our understanding of Sierra Madre geology have been made by P.J. Graff and B.E. Ebbett; other workers are listed in Houston and Graff (in press). The primary geochronological studies used here were by F.A. Hills (Hills and Houston, 1979) and by W.R. Premo (Premo and Van Schmus, 1989). This manuscript has been significantly improved through careful editing by Kevin Chamberlain, Arthur Snoke, Sheila Roberts, and Ernie Duebendorfer. I am especially grateful to Ernie Duebendorfer, who has a great talent for reducing redundancy in my "deathless prose."

References cited

Bayley, R.W., Dutton, L.E., Lamey, C.A., and Treves, S.B., 1966, Geology of the Menominee iron-bearing district, Dickinson County, Michigan and Florence and Marinette Counties, Wisconsin: U.S. Geological Survey Professional Paper 513, 96p.

Ball, T.T., and Farmer, G.L., 1991, Identification of 2.0 to 2.4 Ga Nd model age crustal material in the Cheyenne belt, northeastern Wyoming: implications for Proterozoic accretionary tectonics at the southern margin of the Wyoming craton: Geology, v. 19, p. 360-363.

Bennett, V.C., and DePaolo, D.J., 1987, Proterozoic crustal history of the western United States as determined by neodymium isotopic mapping: Geological Society of America Bulletin, v. 99, p. 674-685.

Bickford, M.E., Collerson, K.D., Lewry, J.F., Van Schmus, W.R., and Chiarenzelli, J.R., 1990, Proterozoic collisional tectonism in the Trans-Hudson orogen, Saskatchewan: Geology, v. 18, p. 14-18.

Blackwelder, E., 1926, Precambrian geology of the Medicine Bow Mountains: Geological Society of America Bulletin v. 37, p. 615-658.

_____ 1935, Summary of the Precambrian rocks of Utah and Wyoming: Utah Academy of Sciences, Arts and Letters, v. 12, p. 153-157.

Brocoum, S.J., and Dalziel, I.W.D., 1974, The Sudbury Basin, the southern Province, the Grenville front, and the Penokean orogeny: Geological Society of America Bulletin, v. 85, p. 1571-1580.

Bryant, B., 1988, Geology of the Farmington Canyon Complex, Wasatch Mountains, Utah: U.S. Geological Survey Professional Paper 1476, 54 p.

Buchan, K.L., and Card, K.D., 1984, Preliminary comparison of petrographic and paleomagnetic characteristics of Nipissing Diabase intrusions in northeastern Ontario, *in* Current research, part A: Geological Survey of Canada Paper 85-1A, p.131-140

Condie, K.C., and Shadel, G.A., 1984, An Early Proterozoic volcanic arc succession in southeastern Wyoming: Canadian Journal of Earth Sciences, v. 21, p. 415-427.

Divis, A.F., 1976, Geology and geochemistry of the Sierra Madre Range [sic.], Wyoming: Colorado School of Mines Quarterly, v. 71, 127 p.

Duebendorfer, E.M., 1986, Structure, metamorphism, and kinematic history of the Cheyenne belt, Medicine Bow Mountains, southeastern Wyoming [Ph.D. dissertation]: Laramie, University of Wyoming, 323 p.

Duebendorfer, E.M., and Houston, R.S., 1987, Proterozoic accretionary tectonics at the southern margin of the Archean Wyoming craton: Geological Society of America Bulletin, v. 98, p. 554-568.

_____ 1990, Structural analysis of a ductile-brittle Precambrian shear zone in the Sierra Madre, Wyoming: western extension of the Cheyenne belt: Precambrian Research, v. 48, p. 21-39.

Flurkey, A.J., 1983, Depositional environment and petrology of the Medicine Peak Quartzite (Early Proterozoic), southern Wyoming [Ph.D. dissertation]: Laramie, University of Wyoming, 124 p.

Fram, M.S., and Rubenstone, J.R., 1988, Petrologic and isotopic constraints on the origin of the Proterozoic Lake Owen mafic complex, Wyoming: EOS, v. 69, no. 16., p. 521.

Geist, D.J., Frost, C.D., Kolker, A., and Frost, B.R., 1989, A geochemical study of magmatism across a major terrane boundary: Sr and Nd isotopes in Laramie Range granitoids: Journal of Geology, v. 97, p. 331-342.

Goldich, S.S., Likiak, E.G., Hedge, C.E., and Walthall, F.G., 1966, Geochronology of the midcontinent region, United States; part 2, northern area: Journal of Geophysical Research, v. 71, p. 5,389-5,408.

Gosselin, D.C., Papike, J.J., Zartman, R.E., Peterman, Z.E., and Laul, J.C., 1988, Archean rocks of the Black Hills, South Dakota: reworked basement from the southern extension of the Trans-Hudson orogen: Geological Society of America Bulletin, v. 100, p. 1244-1259.

Graff, P.J., Sears, J.W., and Holden, G.S., 1980, The Unita arch project, investigations of uranium potential in Precambrian X and older metasedimentary rocks in the Uinta and Wasatch Range, Utah and Colorado: U.S. Department of Energy Open File Report GJBX-170(80), 180 p.

Green, A.G., Weber, W., and Hajnal, Z., 1985, Evolution of Proterozoic terrains beneath the Williston Basin: Geology, v. 13, p. 624-628.

Greenberg, J.K., and Brown, B.A., 1983, Lower Proterozoic volcanic rocks and their setting in the southern Lake Superior district, *in* Medaris, L.G., Jr., editor, Early Proterozoic geology of the Great Lakes region: Geological Society of America Memoir 160, p. 67-84.

Hills, F.A., Gast, P.W., Houston, R.S., and Swainbank, I., 1968, Precambrian geochronology of the Medicine Bow Mountains of southeastern Wyoming: Geological Society of America Bulletin v. 79, p. 1757-1984.

Hills, F.A., and Houston, R.S., 1979, Early Proterozoic tectonics of the central Rocky Mountains, North American: University of Wyoming Contributions to Geology, v. 17, p. 89-109.

Hoffman, P.F., 1976, Shallow and deep water stromatolites in Lower Proterozoic platform to basin facies change, Great Slave Lake, Canada: American Association of Petroleum Geologists Bulletin, v. 58, p. 856-867.

_____ 1987, Early Proterozoic foredeeps, foredeep magmatism, and Superior-type iron formations of the Canadian Shield: *in* Kroner, A., editor, Proterozoic lithospheric evolution: American Geophysical Union Geodynamics Series, v. 17, p. 85-97.

_____ 1988, United plates of America, the birth of a craton: Early Protezoic assembly and growth of Laurentia: Annual Reviews of Earth and Planetary Science, v. 16, p. 543.

_____ 1989, Precambrian geology and tectonic history of North American, *in* Bally, A.W., and Palmer, A.R., editors, The Geology of North America - an overview: Geological Society of America, The Geology of North America, v. A, p. 447-512.

Houston, R.S., and McCallum, M.E., 1961, Mullen Creek-Nash Fork shear zone, Medicine Bow Mountains, southeastern Wyoming [abstract]: Geological Society of America Special Paper 68, p. 91.

Houston, R.S., and Parker, R.B., 1963, Structural analysis of a folded quartzite, Medicine Bow Mountains, Wyoming: Geological Society of America Bulletin, v. 74, p. 197-202.

Houston, R.S., and others, 1968, A regional study of rocks of Precambrian age in that part of the Medicine Bow Mountains lying in southeastern Wyoming, with a chapter on the relationship between Precambrian and

Laramide structure: Geological Survey of Wyoming Memoir no. 1, 167 p.

Houston, R.S., and Orback, 1976, Geologic map of the Lake Owen Quadrangle, Albany County, Wyoming: U.S. Geological Survey Geologic Quadrangle Map GQ-1034, scale 1:24, 000.

Houston, R.S., Karlstrom, K.E., Hills, F.A., and Smithson, S.B., 1979, The Cheyenne belt; the major Precambrian crustal boundary in the western United States: Geological Society of America Abstracts with Programs, v. 11, p. 446.

Houston, R.S., Schmidt, T., and Lane, M.E., 1984, Mineral resource potential and geologic map of Huston Park roadless area, Carbon County, Wyoming: U.S. Geological Survey Miscellaneous Field Studies Map MF-1637, scale 1:24,000.

Houston, R.S., and Karlstrom, K.E., 1992, Geologic map of Precambrian metasedimentary rocks of the Medicine Bow Mountains, Albany and Carbon Counties, Wyoming: U.S. Geological Survey Miscellaneous Investigations Map I-2280, scale 1:50,000.

Houston, R.S., Karlstrom, K.E., Graff, P.J., and Flurkey, A.J., 1992, New stratigraphic subdivisions and redefinition of subdivisions of Late Archean and Early Proterozoic metasedimentary and metavolcanic rocks of the Sierra Madre and Medicine Bow Mountains, southern Wyoming: U.S. Geological Survey Professional Paper No. 1520, 50 p.

Houston, R.S, Reed, J.C., Jr., Karlstrom, K.E., Erslev, E.A., Snyder, G.L., Worl, R.G., Bryant, B., Reynolds, M.W., Peterman, Z.E., Page, N.J., Zientek, M.L., and Frost, C.D., 1993, The Wyoming province, *in* Reed, J.C., Jr., Silver, L.T., Sims, P.K., Rankin, D.W., Houston, R.S., and Reynolds, M.W., editors, Precambrian, conterminous United States: Boulder, Colorado, Geological Society of America, The Geology of North America, v. C-2, in press.

Houston, R.S., and Graff, P.J., in press, Geologic map of the Sierra Madre, Carbon County Wyoming: U.S. Geological Survey Miscellaneous Investigation Map, scale 1:50,000.

Johnson, R.A., Karlstrom, K.E., Smithson, S.B., and Houston, R.S., 1984, Gravity profiles across the Cheyenne belt, a Precambrian crustal suture in southeastern Wyoming: Journal of Geodynamics, v. 1, p. 445-472.

Karlstrom, K.E., Houston, R.S., Flurkey, A.J., Coolidge, C.M., Kratochvil, A.L., and Serer, C.K., 1981, A summary of the geology and uranium potential of Precambrian conglomerates in southeastern Wyoming: U.S. Department of Energy Open File Report DJBX-139-81, 541 p.

Karlstrom, K.E., Flurkey, A.J., and Houston, R.S., 1983, Stratigraphy and depositional setting of Proterozoic metasedimentary in southeastern Wyoming: Record of an Early Proterozoic Atlantic-type cratonic margin: Geological Society of America Bulletin, v. 94, p. 1257-1294.

Karlstrom, K.E., and Houston, R.S., 1984, The Cheyenne belt: analysis of a Proterozoic suture in southern Wyoming: Precambrian Research, v. 25, p. 415-446.

Knight, S.H., 1968, Precambrian stromatolites, bioherms, and reefs in the lower half of the Nash Formation, Medicine Bow Mountains, Wyoming: University of Wyoming, Contributions to Geology, v. 7, p. 73-116.

Knight, S.H., and Keefer, D.K., 1966, Preliminary report on the Precambrian stromatolites in the Nash Fork Formation, Medicine Bow Mountains, Wyoming: University of Wyoming, Contributions to Geology, v. 5, p. 1-11.

Krogh, T.E., Davis, D.W., and Corfu, F., 1984, Precise U-Pb zircon and baddeleyite ages for the Sudbury area, *in* Pye, E.G., and others, editors, The geology and ore deposits of the Sudbury structure: Ontario Geological Survey Special Volume 1, p. 431-446.

Larue, D.K., 1979, Sedimentary history prior to chemical iron sedimentation of the Precambrian X Chocolay and Menominee Groups (Lake Superior region) [Ph.D. dissertation]: Evanston, Illinois, Northwestern University, 173 p.

_____ 1981, The Chocolay Group, Lake Superior region, U.S.A.; sedimentologic evidence for deposition in basinal and platform settings on an early Proterzoic craton: Geological Society of America Bulletin, V. 92, p. 417-435.

_____ 1983, Early Proterozoic tectonics of the Lake Superior region; Tectonostratigraphic terrances near the purported collision zone, *in* Medaris, L.G., Jr., editors, Early Proterozoic geology of the Great Lakes region: Geolocial Society of America Memoir 160, p. 33-48.

Lewry, J.F., and Stauffer, M.R., editors, 1990, The Early Proterozoic Trans-Hudson orogen: lithotectonic correlations and evolution: Geological Association of Canada Special Paper 37, 505 p.

Loucks, R.R., Premo, W.R., and Snyder, G.L., 1988, Petrology, structure, and age of the Mullen Creek layered mafic complex and age of arc accretion, Medicine Bow Mountains: Geological Society of America Abstracts with Programs, v. 20, no. 7, p. 73.

Lush, A.P., McGrew, A.J., Snoke, A.W., and Wright, J.E., 1988, Allochthonous Archean basement in the north-

ern East Humboldt Range, Nevada: Geology, v. 16, p. 349-353.

Marlett, G., 1989, Geology of the Precambrian igneous/metamorphic sequence, Laramie Range, Wyoming [M.S. thesis]: Laramie, University of Wyoming, 80 p.

McCallum, M.E., 1964, Petrology and structure of the Precambrian and post-Mississippian rocks of the east-central portions of the Medicine Bow Mountains, Albany and Carbon Counties, Wyoming [Ph.D. dissertation]: Laramie, University of Wyoming, 164 p.

McCallum, M.E., and Kluender, S.E., 1983, Mineral resource potential map of the Savage Run Wilderness, Carbon and Albany Counties, Wyoming: U.S. Geological Survey Miscellaneous Field Studies Map MF-1638 A, scale 1:24,000.

Mueller, R.E., 1982, The Cheyenne belt, southeastern Wyoming: part 1, descriptive geology and petrography [M.S. thesis]: Laramie, University of Wyoming, 98 p.

Pallister, J.S., and Aleinikoff, J.N., 1987, Gabbroic plutons south of the Cheyenne belt: Underpinnings of an Early Proterozoic continental margin arc: Geological Society of America Abstracts with Programs, v. 19, no. 5, p. 325.

Peterman, Z.E., Sims, P.K., Zartman, R.E., and Schultz, K.J., 1985, Middle Proterozoic uplift events in the Dunbar dome of northeastern Wisconsin, U.S.A.: Contributions to Mineralogy and Petrology, v. 91, p. 138-150.

Peterman, Z.E., and Sims, P.K., 1993, Geochronology of the Trans-Hudson orogen, *in* Reed, J.C., Jr., and others, editors, Precambrian, conterminous United States: Boulder, Colorado, Geological Society of America, The Geology of North America, v. C-2, in press.

Premo, W.R, 1984, U-Pb zircon geochronology of some Precambrian rocks in the Sierra Madre Range [sic.], Wyoming [M.S. thesis]: Lawrence, University of Kansas, 106 p.

Premo, W.R., and Van Schmus, W.R., 1989, Zircon geochronology of Precambrian rocks in southeastern Wyoming and northern Colorado: Geological Society of America Special Paper 235, p. 13-32.

Redden, J.A., 1980, Geology and uranium resources in Precambrian conglomerates of the Nemo area, Black Hills, South Dakota: U.S. Department of Energy Open File Report, GJBX 127(80), 147 p.

_____ 1981, Summary of the geology of the Nemo area, *in* Rich, F.J., editor, Geology of the Black Hills, South Dakota and Wyoming: Geological Society of America Rocky Mountain Section and American Geological Institute Guidebook, p. 193-210.

Reed, J.C., Jr., Bickford, M.E., Premo, W.R., Aleinikoff, J.N., and Pallister, J.S., 1987, Evolution of the Early Proterozoic Colorado province: constraints from U-Pb geochronology: Geology, v. 15, p. 861-865.

Roscoe, S.M., 1968, Huronian rocks and uraniferous conglomerates in the Canadian Shield: Geological Survey of Canada Paper 68-40, 205 p.

_____ 1989, The reappearance of the Huronian in Wyoming: Geological Society of America Abstracts with Programs, v. 21, no. 6, p. A373.

Schmidt, T.G., 1983, Precambrian metavolcanic rocks and associated volcanogenic mineral deposits of the Fletcher Park and Green Mountain areas, Sierra Madre, Wyoming [M.S. thesis]: Laramie, University of Wyoming, 113 p.

Schultz, K.J., LaBerge, G.L., Sims, P.K., Peterman, Z.E., and Klasner, J.S., 1984, The volcanic-plutonic terrane of northern Wisconsin: implications for Early Proterozoic tectonism, Lake Superior region: Geological Association of Canada Programs with Abstracts, v. 9, p. 103.

Sears, J.W., Graff, P.J., and Holden, G.S., 1982, Tectonic evolution of lower Proterozoic rocks, Uinta Mountains, Utah and Colorado: Geological Society of America Bulletin, v. 93, p. 990-997.

Sedlock, R.L., and Larue, D.K., 1985, Fold axes oblique to the regional plunge and Proterozoic terrane accretion in the southern Lake Superior region: Precambrian Research, v. 30, p. 249-262.

Shanmugan, G., and Lash, G., 1982, Analogous tectonic evolution of the Ordovician foredeeps, southern and central Appalachians: Geology, v. 10, p. 562-566.

Sims, P.K., and Peterman, Z.E., 1986, Early Proterozoic Central Plains orogen; major buried structure in the north-central United States: Geology, v. 14, p. 488-491.

Snyder, G.L., 1980, Geologic map of the northernmost Park Range and southernmost Sierra Madre, Jackson and Routt counties, Colorado: U.S. Geological Survey Miscellaneous Investigations Map I-1113, scale 1:48,000.

Snyder, G.L., and Hedge, G.E., 1978, Intrusive rocks northeast of Steamboat Springs, Park Range, Colorado: U.S. Geological Survey Professional Paper 1041, 42 p.

Snyder, G.L., and Peterman, Z.E., 1982, Precambrian geology and geochronology of the Hartville uplift, Wyo-

ming, *in* Goldich, S.S., chairman, 1982 Archean Geochemistry Field Conference, August 15-19, 1982, guide to field trips, part 1, Seminoe Mountains and Hartville uplift, Wyoming: IGGP, Archean Geochemistry Project, U.S. Working Group, p. 64-94.

Snyder, G.L., Hausel, W.D., Klein, T.L., Houston, R.S., and Graff, P.J., 1989, Precambrian rocks and mineralization, southern Wyoming province: 28th International Geological Congress Field Trip Guidebook T332, American Geophysical Union, Washington, D.C., 48 p.

Spencer, A.C., 1904, Copper deposits of the Encampment District: U.S. Geological Survey Professional Paper 25, 107 p.

Stauffer, M.R., 1984, Manikewan: an Early Proterozoic ocean in central Canada, its igneous history and orogenic closure: Precambrian Research, v. 25, p. 257-281.

Tarney, J., Dalziel, I.W.D., and DeWit, M.J., 1976, Marginal basin 'Rocas Verdes' complex from S. Chile: a model for Archean greenstone belt formation, *in* Windley, B.F., editor, The early history of the Earth: London, Wiley-Interscience, p. 131-146.

Van Schmus, W.R., 1976, Early and Middle Proterozoic history of the Great Lakes area, North American: Philosophical Transactions of the Royal Society of London, v. A280, p. 605-628.

Ware, D.C., 1982, Amphibolite complex of the Blackhall Mountain area, southeastern Sierra Madre, Wyoming [M.S. thesis]: Laramie, University of Wyoming, 71 p.

Warner, L.A., 1978, The Colorado lineament: a middle Precambrian wrench-fault system: Geological Society of America Bulletin, v. 89, p. 161-171.

Young, G.M., 1970, An extensive Early Proterozoic glaciation in North America?: Palaeogeography, Palaeoclimatology, Palaeoecology: v. 7, p. 85-101.

_____ 1983, Tectono-sedimentary history of Early Proterozoic rocks of the northern Great Lakes region, *in* Medaris, L.G., Jr., editor, Early Proterozic geology of the Great Lakes region: Geological Society of America Memoir 160, p. 15-32.

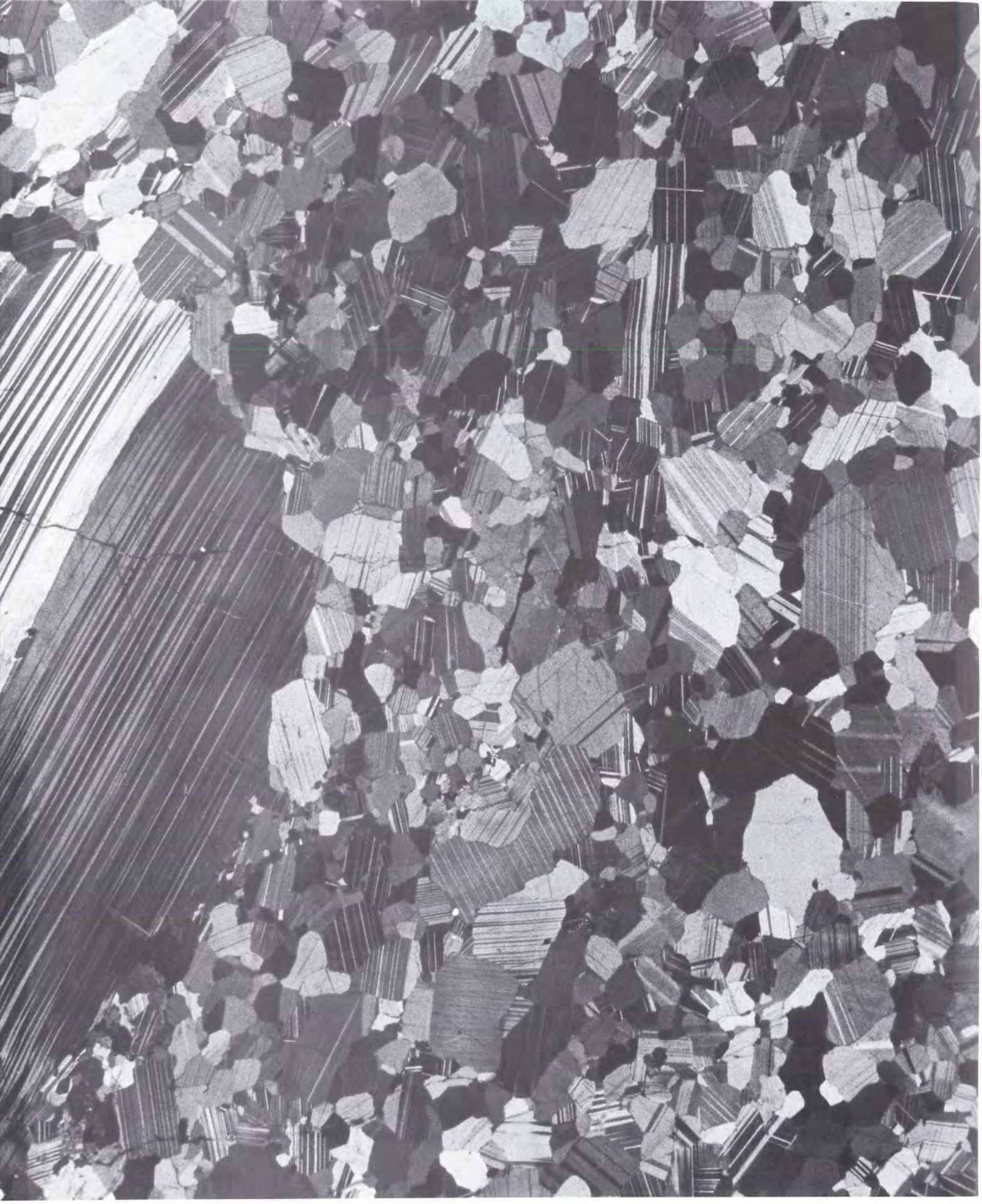

Frontispiece. Recrystallized and annealed anorthosite from the northern dome of the Laramie Anorthosite Complex. The rock is nearly 100% plagioclase. The coarser grains show evidence of strain such as bent albite twins, but the finer grains are relatively strain-free and meet at 120° grain boundaries, a texture typically indicative of high-temperature annealing. The horizontal field of view is 2.5 cm across.

The Laramie Anorthosite Complex and Sherman batholith: geology, evolution, and theories of origin

B. Ronald Frost and Carol D. Frost
Department of Geology and Geophysics
University of Wyoming
Laramie, Wyoming 82071

Donald H. Lindsley
Department of Earth and Space Sciences
State University of New York at Stony Brook
Stony Brook, New York 11794

James S. Scoates and Jeremy N. Mitchell
Department of Geology and Geophysics
University of Wyoming
Laramie, Wyoming 82071

Abstract

The Laramie Anorthosite Complex (LAC) and Sherman batholith are the northernmost components of widespread 1.4 Ga magmatism in the western United States. The LAC was emplaced across the Cheyenne belt, a major crustal suture that separates Archean rocks of the Wyoming province to the north from Proterozoic rocks to the south. Four domical structures have been recognized in the anorthositic rocks of the LAC, and are referred to as the northern, central, Snow Creek, and southern anorthosite domes.

The anorthositic rocks contain a wide range of structures and textures that formed both during the magmatic phase of crystallization and during high-temperature post-cumulus to subsolidus deformation and recrystallization. Leucotroctolite, leucogabbro, and anorthosite in the outermost and stratigraphically highest zones of the northern and central anorthosite domes contain abundant examples of well-developed igneous layering and a pervasive plagioclase lamination. The core of the northern anorthosite dome is dominated by pure anorthosite that has been strongly recrystallized, resulting in the destruction of most primary igneous features. In contrast, the core of the central anorthosite dome contains numerous lens-shaped bodies of leucotroctolite, leucogabbro, or mafic anorthosite interlayered with anorthosite. Massive Fe-Ti oxide deposits occur along the long axis of the central dome and are spatially associated with the mafic anorthositic rocks.

Frost, B.R., Frost, C.D., Lindsley, D.H., Scoates, J.S., and Mitchell, J.N., 1993, The Laramie Anorthosite Complex and Sherman batholith: geology, evolution, and theories of origin, *in* Snoke, A.W., Steidtmann, J.R., and Roberts, S.M., editors, Geology of Wyoming: Geological Survey of Wyoming Memoir No. 5, p. 118-161.

Three later intrusive complexes, the Strong Creek complex, Sybille monzosyenite, and Maloin Ranch pluton, were intruded along the flanks of the anorthosite domes. The Strong Creek complex was emplaced between the central and Snow Creek anorthosite domes. It consists of the Greaser layered intrusion, Strong Creek gabbro, Buttes granite, and a variety of dikes ranging in composition from granite to ferrodiorite. The Maloin Ranch pluton and Sybille monzosyenite are evolved monzonitic intrusions that were emplaced adjacent to anorthosite in the southeastern and northwestern portions of the LAC, respectively. Both of these intrusions have Fe/(Fe+Mg) contents that bridge the values where iron-rich pigeonite becomes unstable with respect to fayalite, hedenbergite, and quartz. This constrains the pressure at which the LAC was emplaced to 2.5-3 kilobars for the north and near 4 kilobars for the south. The Red Mountain pluton is the youngest pluton in the LAC. It intruded the Sybille monzosyenite in the northeastern part of the complex. It is a zoned stock consisting of hornblende syenite and minor amounts of fayalite-hedenbergite monzonite, hedenbergite monzonite, and granite.

The Sherman batholith was emplaced along the eastern and southern margins of the LAC. Rocks similar in composition to granites of the Sherman batholith are gradational with the upper portions of the Maloin Ranch pluton, Red Mountain pluton, and Sybille monzosyenite. The major rock unit in the Sherman batholith is geochemically a typical rapikivi-type granite: potassic, subalkaline, and enriched in iron relative to magnesium. In many respects, it is similar in composition to other rapikivi-type granites that formed between 1.4 and 1.5 Ga in the southwestern United States.

Our preferred interpretation for the origin of the LAC is that it was formed from magma of mantle origin, most likely basaltic in composition. This interpretation requires the existence of an initial magma chamber at or near the base of the crust, within which extensive fractionation of olivine, and probably pyroxene, occurred. A feldspathic, Fe-enriched residual magma was produced in this chamber and periodically injected into a second mid-crustal level magma chamber. Accumulation of plagioclase crystals on the floor of this second chamber, trapping variable amounts of interstitial liquid, resulted in thick sequences of layered anorthositic cumulate rocks. The plagioclase-rich cumulates were deformed during or shortly after crystallization producing large-scale domical structures. Deformation was accommodated by varying degrees of recrystallization of plagioclase and may have led to local mobilization of interstitial melt. Some of the interstitial melt and residual melt produced during extensive fractionation of plagioclase is present in the form of Fe-Ti oxide bodies and dioritic and gabbroic dikes. The massive Fe-Ti oxide bodies may have formed by unmixing from an Fe-rich leucotroctolitic melt. The origin of the monzonitic rocks is enigmatic. Clearly, they are not products of simple differentiation from the anorthosites. Some of their mass may represent a portion of residual liquids produced during crystallization of the anorthositic cumulates, which was then mixed with variable amounts of crustal-derived melt. The Sherman batholith is a product of this same magmatic event. It probably represents partial melting of the crust adjacent to mafic magma that was intruded at some lower crustal depth, possibly the deep initial chamber inferred for the parent magma of the anorthosite.

Introduction

The youngest rocks of Precambrian age in Wyoming are those of a mid-Proterozoic intrusive event consisting of the Laramie Anorthosite Complex (LAC) and Sherman batholith. The LAC occurs over an area of about 300 square miles (800 km^2) in the south-central Laramie Mountains, and the Sherman batholith is exposed over an equivalent area in the southern Laramie Mountains, Boulder Ridge, Sheep Mountain, locally within the southern Medicine Bow Mountains, and in portions of northern Colorado (**Figures 1** and **2**). These intrusive complexes are the northernmost plutons of 1.4 Ga magmatism that produced numerous granitic plutons throughout Colorado, New Mexico, Arizona, and parts of southern California (Anderson, 1983). Field relationships show that anorthosite of the LAC pre-dates the Sherman batholith, but that the late-stage monzonitic rocks of the LAC locally grade into granites that are

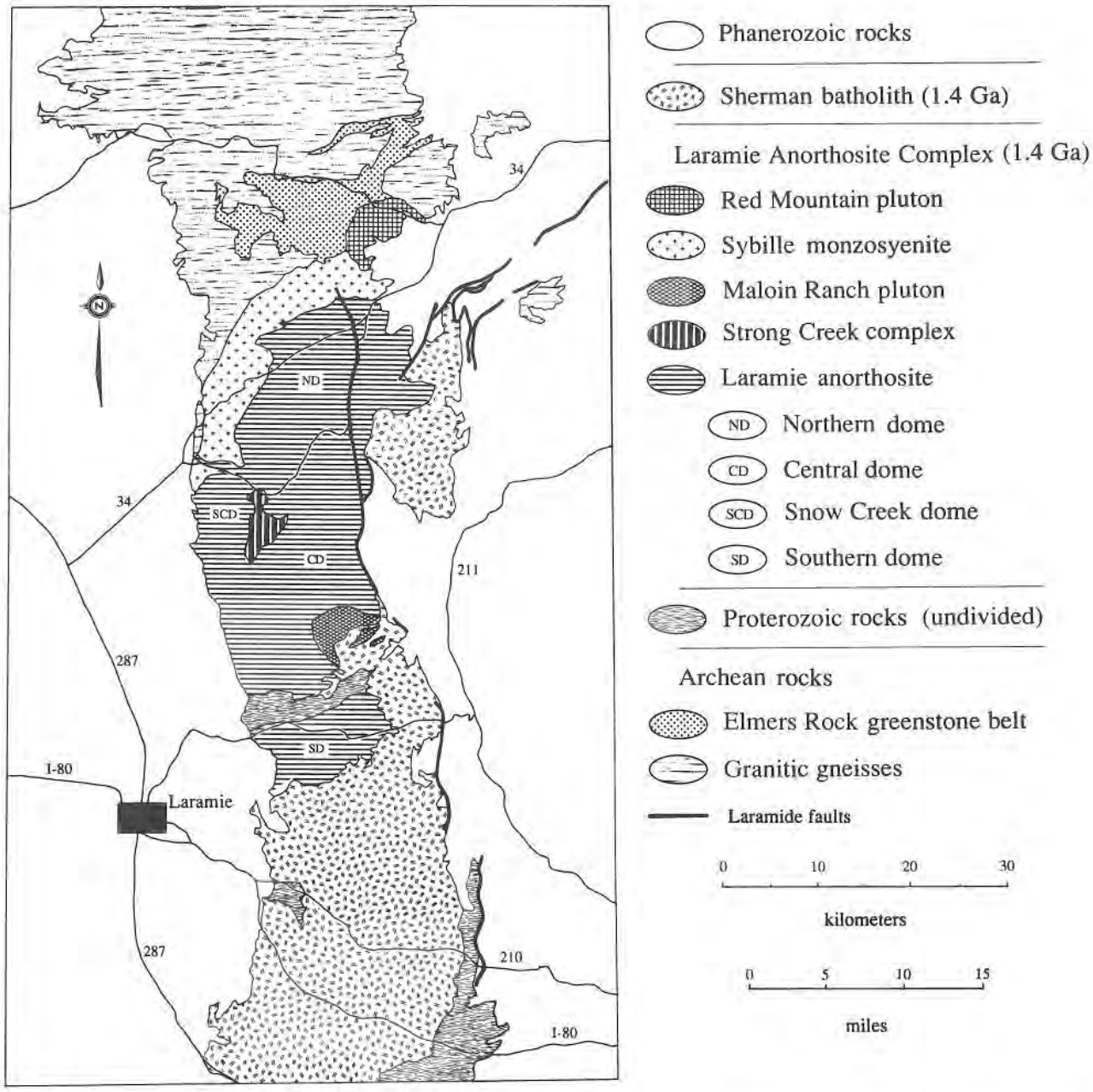

Figure 1. Regional geology of the south-central Laramie Mountains showing the location of 1.4 Ga intrusions.

petrographically indistinguishable from granites of the Sherman batholith. The coeval nature of the LAC with the Sherman batholith is confirmed by U-Pb dating of zircons, which yield 1,439 +7/-6 Ma for the Red Mountain pluton (Frost and others, 1990), the youngest pluton of the LAC, and about 1.43 Ga for the Sherman batholith (Aleinikoff, 1983). The LAC was emplaced across the Cheyenne belt, which is the boundary between Archean rocks of the Wyoming province to the north and 1.6 to 1.8 Ga Proterozoic supracrustal sequences to the south (Karlstrom and Houston, 1984; Duebendorfer and Houston, 1987) (**Figure 1**).

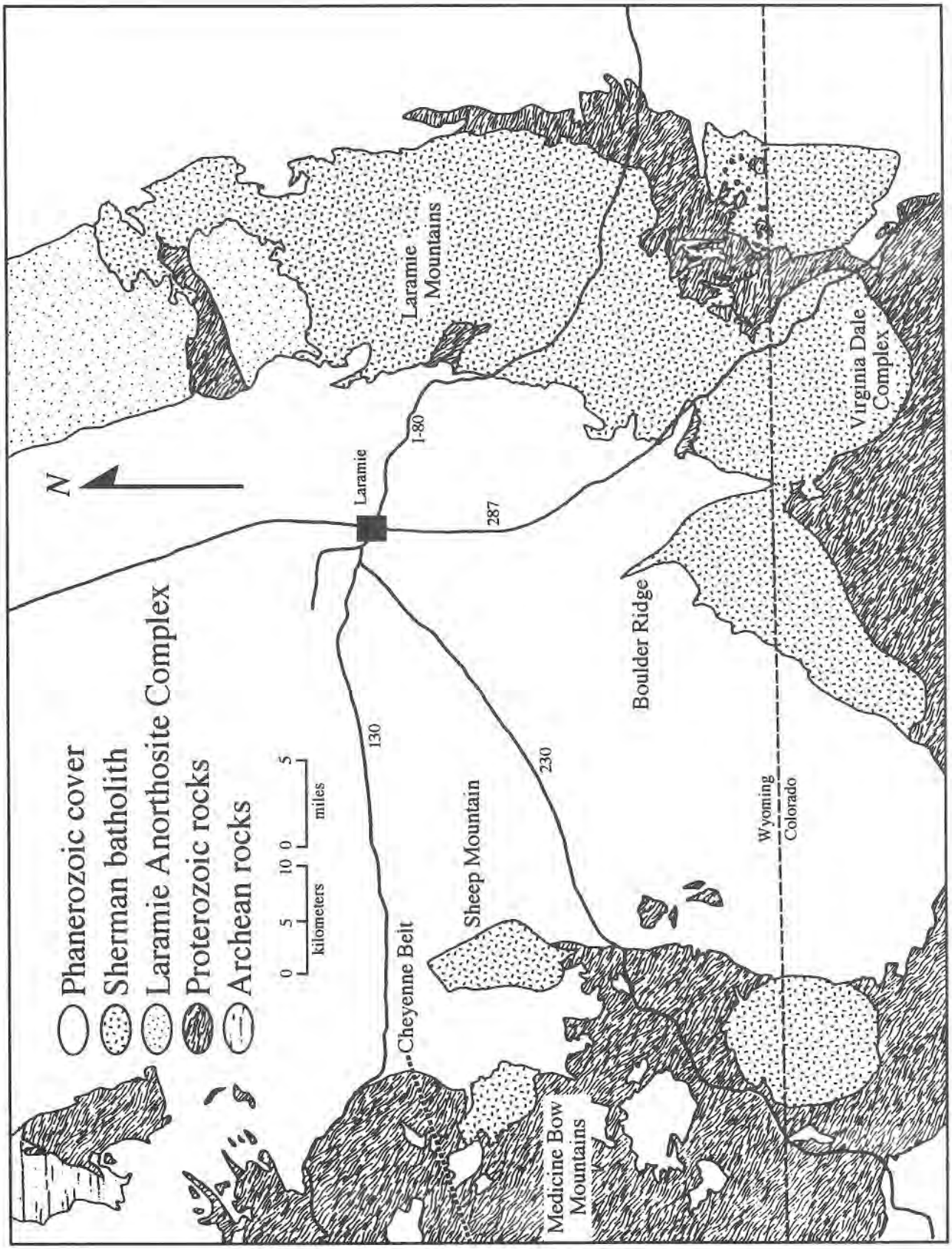

Figure 2. Regional geology of the southern Laramie Mountains and southern Medicine Bow Mountains showing the location of 1.4 Ga intrusions.

Laramie Anorthosite Complex

The occurrence of anorthositic rocks in the Laramie Mountains was first recognized by Darton and others (1910), who mapped the southern portion of the LAC. The formal name, Laramie Anorthosite Complex, was introduced by Hodge and others (1973). In the first detailed map of the entire complex, Fowler (1930) delineated most of the major units that are recognized today. One important difference between Fowler's map and those of later workers was her inclusion of the monzonitic and syenitic rocks as part of the Sherman batholith. Newhouse and Hagner (1957) defined two major units within the anorthositic rocks: anorthosite and gabbroic (or noritic) anorthosite, plus minor amounts of olivine anorthosite. They mapped two units of syenitic rocks: hypersthene syenite (despite the absence of orthopyroxene) and hornblende syenite. Newhouse and Hagner also mapped some units as norite which have subsequently been identified as porphyritic monzonite, fine monzonite, or simply gabbro (Fuhrman and others, 1988; Kolker and Lindsley, 1989; Mitchell and others, 1990). The mapping and designation of units by Newhouse and Hagner have served as an important basis for much of the later work on the complex, including our own. Whereas Newhouse and Hagner, and later DeVore (1975), proposed a metasomatic origin for the LAC, Klugman (1966) and most other subsequent workers have argued that all the major units are of an igneous origin. Recently, as part of a regional 1:24,000-scale mapping project of the central Laramie Mountains, Snyder (1984) mapped the northern portions of the LAC and the Archean rocks in contact with the complex.

Geochemical studies of the LAC were conducted by Fountain and others (1981) and Goldberg (1984). On the basis of rare earth element geochemistry, Fountain and others (1981) concluded that if the monzonitic rocks were samples of melts, rather than cumulates, they could not be simple differentiates from the anorthosite. Rb-Sr isotopic studies of the LAC were made by Subbarayudu (1975) and Subbarayudu and others (1975). Early geophysical studies of the LAC were conducted by Hodge and others (1970), Smith and others (1970), and Hodge and others (1973). Their gravity measurements indicate that the LAC is a relatively thin body, 2.5 miles (4 km) thick, without extensive roots of mafic rock beneath it, and that the monzonitic rocks in the northern portion of the complex are underlain by denser rock. More recently, seismic reflection profiles across the LAC have imaged the base of the anorthosite at depths ranging from 1 to 2.5 miles (1.5 to 4 km) (Allmendinger and others, 1982; Brewer and others, 1982; Speece and others, in review).

The present report is the result of detailed mapping of the LAC begun in 1981 by faculty and students from the University of Wyoming and from the State University of New York at Stony Brook. To date, approximately 150 square miles (384 km^2) of the complex have been mapped at a scale of 1:24,000. We have used the mapping as the basis for a number of petrologic, geochemical, and isotopic studies; these studies include: Frost and others (1990), Fuhrman (1986), Fuhrman and others (1988), Geist and others (1990), Kolker (1989), Kolker and Lindsley (1989), Kolker and others (1990), and Kolker and others (1991), mostly concentrating on the late-stage monzonitic rocks. Work is still in progress on the anorthositic and gabbroic to dioritic rocks. The units described below are those defined during this project.

Nomenclature

The rock types formally recognized by Streckeisen (1967) do not permit some important distinctions to be made within rocks of the LAC. For example, in his classification rocks with 90 to 100% plagioclase are defined as anorthosite, whereas those with as little as 11% ferromagnesian minerals are defined as leucogabbro (clinopyroxene-plagioclase), leuconorite (orthopyroxene-plagioclase), or leucotroctolite (olivine-plagioclase). In our opinion, adherence to this classification would disguise the fact that the majority of anorthositic rocks in the LAC contain between 67 and 90% plagioclase and are clearly related to the true anorthosites. In this paper, we retain anorthosite to refer to rocks with ≥90% plagioclase. Those rocks with 80 to 90% plagioclase are mafic anorthosite (ferromagnesian minerals not specified), gabbroic anorthosite (clinopyroxene dominant), noritic anorthosite (orthopyroxene dominant), gabbronoritic anorthosite (subequal amounts of clinopyroxene and orthopyroxene) or troctolitic anorthosite (olivine dominant). We use the prefix "leuco" to designate rocks containing 67 to 80%

plagioclase: leucogabbro, leuconorite, leucogabbronorite, or leucotroctolite, depending on the dominant ferromagnesian mineral(s). The reader should bear in mind that the principal mineral in these rocks is plagioclase. In this context, a rock containing 20 to 30% olivine and/or pyroxene is "mafic-rich" relative to anorthosite.

We have also found it useful to resurrect the old term "monzosyenite" to name some rocks that previous workers have called syenites because they are dominated by megacrysts of alkali feldspar. As these rocks also contain plagioclase (An_{30}) in roughly equal proportions to alkali feldspar, under the Streckeisen classification they should be called monzonites (Fountain and others, 1981). However, on textural grounds we have interpreted that some of these rocks originally contained strongly ternary feldspar, with the albite, anorthite, and orthoclase components all greater than 10% (Fuhrman and others, 1988). This mineralogy was not considered by Streckeisen. Like the rocks themselves, the name monzosyenite is intermediate between monzonite and syenite, but is mainly used to imply the original presence of ternary feldspar.

Laramie Anorthosite

The anorthositic rocks of the LAC are crosscut by all other lithologies and are presumed to be the oldest rocks in the complex. The anorthosite suite includes true anorthosite, various types of mafic anorthosite, leucogabbro, leuconorite, leucogabbronorite and leucotroctolite. Igneous layering is well developed in the outermost margin of the various anorthositic domes. Layer contacts may be modal changes (relative proportions of phases), grain size changes, or textural changes (other than grain size, such as tabular/granular plagioclase or oikocrystic/granular ferromagnesian minerals). A strong preferred orientation of tabular plagioclase is characteristic of many anorthositic rocks. Igneous layering described above is distinct from layering found in the lower stratigraphic levels of the domical structures. There one finds planar zones that are the product of high strain and are distinguished by grain-size reduction, neoblastic plagioclase growth, and strong preferred crystallographic orientation of plagioclase neoblasts. The orientation of igneous layering and of the planar zones of high strain define four major domical structures (**Figure 1**): the northern, central, Snow Creek, and southern anorthosite domes, each of which contains distinctive lithologies.

The LAC has not undergone the pervasive granulite metamorphism that is commonly associated with anorthosite complexes in the Grenvillian and Sveconorwegian terranes, although the deeper portions of the anorthosite have clearly undergone dynamic recrystallization at extremely high temperature. Because the higher structural levels of the anorthosite have not undergone penetrative deformation, they preserve primary structures, textures, and compositions that document the emplacement and crystallization history within an anorthositic magma chamber. The lack of regional metamorphism is particularly important because significant igneous features such as layering are preserved. Igneous layering was recognized by Newhouse and Hagner (1957) and Fountain and others (1981), but the potential for layering to provide important information on the crystallization of the anorthositic rocks was not addressed. Thus, like the large unmetamorphosed anorthosite bodies north of the Grenville front tectonic zone in Canada (e.g., Nain, Harp Lake, Michikamau), the Laramie anorthosites may shed important light on the origin of other anorthosite complexes that have undergone granulite-facies metamorphism.

Northern anorthosite dome

The northern anorthosite dome is the best studied anorthosite in the LAC to date (Scoates and Lindsley, 1989; Scoates, 1990) and is therefore described in greatest detail. The northern dome is well exposed in the deeply incised canyons in the drainage of Sybille Creek (**Figure 3**). The orientations of igneous layering and plagioclase lamination in the northern dome outline a large domical structure covering nearly 100 square miles (256 km^2). This structure exposes an outer layered series containing 20,000 feet (6,000 m) of anorthositic cumulate rocks that envelopes a core of heterogeneously strained and recrystallized anorthosite. Dip attitudes vary from near vertical on the margins to less than 30° near the core.

The layered series is subdivided into the upper layered zone (ULZ) and main layered zone (MLZ). The ULZ consists of steep (70 to 90°), outward-dipping, rhythmically alternating units of leucotroctolite, leucogabbro, and anorthosite. The ULZ conformably overlies rhythmically alternating units of anorthosite and troctolitic anorthosite of the

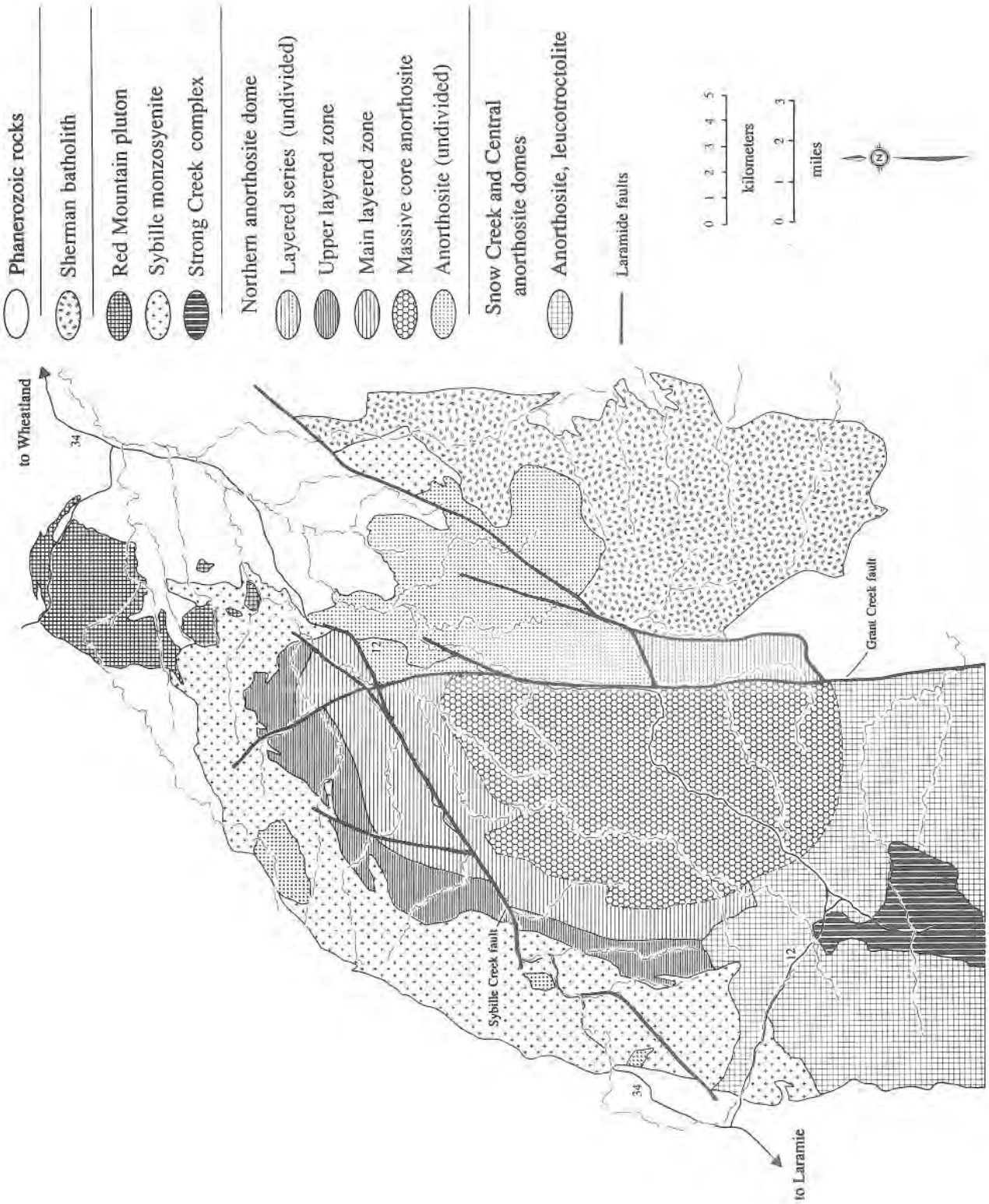

Figure 3. Geologic map of the northern anorthosite dome.

MLZ. The uppermost portions of the ULZ are in contact with Archean granitic gneisses of the country rock only along one short interval in the north. The vast majority of the top of the stratigraphic section has been truncated by the intrusion of the Sybille monzosyenite. Abundant inclusions of anorthosite, ranging in size from feet to miles (meters to kilometers) are found within the Sybille monzosyenite. The base of the section (the lowermost reaches of the MLZ) has not yet been defined and probably is not exposed.

Olivine leucogabbronorite and leucotroctolite layers dominate the composition of the ULZ and may represent the arrivals and disappearances of olivine and pyroxene with plagioclase as cumulus phases. True anorthosite is relatively rare in the ULZ, but becomes increasingly abundant inwards (downwards) from the ULZ/MLZ contact. The contact between the ULZ and MLZ is recognized as the first appearance of a thick [160 to 200 feet (50 to 60 m)] anorthosite layer as one moves inward from the margin of the intrusion. This marks the uppermost horizon of the MLZ. The base of the ULZ is occupied by a single, finely layered, leucotroctolitic unit 400 to 750 feet (125 to 230 m) thick. Although the MLZ/ULZ contact is offset distances of 300 feet to 1.2 miles (100 m to 2 km) by numerous small-scale faults of Laramide age, it can be mapped over a strike length of 12 miles (20 km). It is the single most prominent map feature in the northern dome and appears to represent a fundamental change in composition and layer structures within an evolving magma chamber. To the northeast, the contact is lost in an intensely brecciated and fault-blocked region formed by the intersection of fault zones striking along Middle Sybille Canyon and Grant Creek Valley, and is then buried beneath Tertiary sediments (**Figure 3**).

Both the MLZ and ULZ are composed of alternating units of anorthosite and olivine leucogabbronorite or leucotroctolite. Typical thicknesses of units are on the order of 200 feet (60 m) and they may range in thickness from 50 to 1000 feet (15 to 300 m). These alternating units impose a topographic effect on the landscape of the area. Resistant anorthosite units form ribs along hillsides separated by gullies occupied by more readily weathered mafic-rich units. Each unit is typically layered on scales varying from several inches to tens of feet (decimeters to decameters). In relatively unrecrystallized layers, a variety of primary igneous structures provide important information on the formation of the anorthositic rocks.

Primary structures. The most distinctive textural feature in the northern dome is the alignment of tabular plagioclase crystals subparallel to layering. The size of plagioclase laths varies greatly, but is typically 2 x 2 x 0.2 cm. Some layers also contain plagioclase megacrysts several times this size. In unrecrystallized layers, the plagioclase laths and especially the megacrysts are black, the result of small but abundant oriented inclusions of Fe-Ti oxides. The matrix surrounding the laths and megacrysts is composed of finer grained plagioclase and ferromagnesian minerals - olivine, orthopyroxene, clinopyroxene, and Fe-Ti oxides. The matrix ranges from poikilitic to interstitial, as detailed below. We interpret the laminar orientation of plagioclase to be mainly the result of primary igneous deposition on the magma chamber floor, but also partly the result of maturation of the cumulate pile accompanying expulsion of interstitial liquid by compaction.

Oikocrystic (or mottled) anorthosite is the predominant lithology in the northern dome. Within unrecrystallized anorthosite, spherical oikocrysts 2 to 3 cm in diameter of olivine, clinopyroxene, orthopyroxene, and/or Fe-Ti oxide minerals are regularly dispersed within the anorthosite host, which consists of strongly laminated tabular cumulate plagioclase (**Figure 4**). Each oikocryst encases abundant randomly oriented, small (5 x 5 x 1 mm), plagioclase chadacrysts. Some spherical oikocrysts also enclose strongly aligned plagioclase laths, suggesting that those oikocrysts nucleated and grew episodically during the textural and compositional maturation of the cumulate pile. Post-cumulus deformational processes locally resulted in flattening and elongation of primary spherical oikocrysts, as detailed in the following sections. Spotted anorthosite, defined by the presence of individual clots of mafic minerals randomly dispersed in a plagioclase matrix, is also a common rock type in the northern dome.

Rhythmically alternating compositional, grain-size, and textural layering is typical of both the ULZ and MLZ (**Figure 5**), although recrystallization has destroyed nearly all primary structures in the lower (inner) portions of the MLZ. The dominant layer type is one in which relative increases or decreases of interstitial ferromagnesian minerals define alternate

Figure 4. Photograph of mottled anorthosite, main layered zone, layered series, northern anorthosite dome. Diameter of lens cap is 1.8 in (5.5 cm).

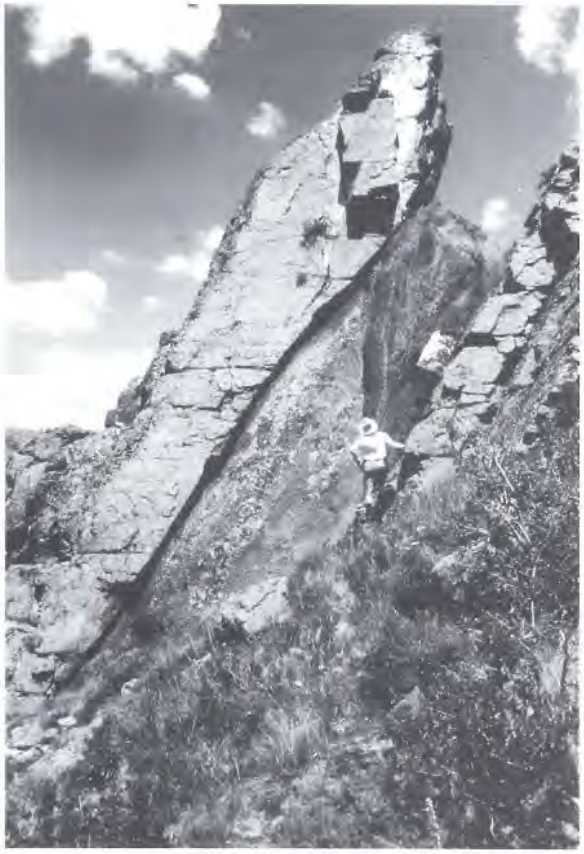

Figure 5. Photograph of foot-scale (meter-scale) compositional layering in anorthosite, upper layered zone, layered series, northern anorthosite dome.

layers (**Figure 6**). Reverse mineral grading, where plagioclase-rich basal zones grade upwards into olivine- (and pyroxene-, Fe-Ti oxide-) enriched uppermost zones (**Figure 7**), has been noted at several localities. Megacrystic layers alternating with oikocrystic layers are significant layer types in the MLZ. The basal layer of these couplets is megacrystic anorthosite consisting of black plagioclase (locally iridescent) in a finer grained olivine leucogabbronoritic matrix. Locally, the basal megacrystic layers extend down into the underlying anorthosite layer, truncating the laminar fabric in these layers. These features are interpreted to be scours produced on the floor of the magma chamber in response to current activity. The upper layer of each couplet is typically oikocrystic anorthosite. Megacrysts may be plagioclase crystals that evolved over extended residence times within the magma chamber at the level of emplacement. Alternatively, they could be samples of plagioclase that grew at a different pressure and temperature in a deeper seated chamber, which were transferred to the floor of the crystallizing magma chamber during a replenishment event. Most importantly, the arrangement of the layered couplets and the local presence of basal scours are strong indicators of accumulation and crystallization on a chamber floor.

Disruption of primary layering and lamination by cognate xenoliths, ranging in composition from anorthosite to olivine gabbro, has been identified at many locations and at different stratigraphic positions within the northern dome. In several localities, compositional layering and plagioclase lamination are strongly disrupted and convoluted beneath the xenolith blocks (**Figure 8**). Apparently, discrete blocks of previously crystalline material were periodically injected or spalled off from chamber walls or ceilings, settled through resident magma, and collected on the chamber floor. Individual blocks are rounded and they may be fractured as if they had broken upon impact. At some localities, both layering and lamination in the overlying cumulates drape over the blocks, thinning and tapering towards the

Figure 6. Photograph of modal layering in anorthosite defined by variable amounts of interstitial ferromagnesian minerals, main layered zone, layered series, northern anorthosite dome. Length of map tube is approximately 2 feet (0.6 m).

Figure 7. Photograph of reversely graded layering in anorthosite, main layered zone, layered series, northern anorthosite dome. The bulge in the lower central part of the exposure is caused by the presence of an olivine gabbro block that impacted downward (from left to right in the photograph). Stratigraphic top is to the left. Rocks are exposed on a cliff face along Johnson Creek. Width of view at base of cliff is approximately 25 feet (8 meters).

tops of blocks. These structures are strikingly similar to those observed associated with ultramafic blocks in the Duke Island intrusion (Irvine, 1974, 1987) and anorthositic blocks in the Skaergaard intrusion (Wager and Brown, 1967; Irvine, 1987). These relationships are of particular importance as they provide further evidence of the existence of a chamber floor (all block structures indicate accumulation and crystallization from the core upwards and outwards) and they bracket the timing of the formation of layering and lamination. Both the latter structures must have formed in the underlying layers prior to deposition of the blocks.

The erosional actions of density-driven magmatic currents or slumping of portions of a semi-consolidated cumulate pile are indicated by the presence of scour structures. The trough portions of the scour structures are consistently oriented inwards, again suggesting the presence of a chamber floor where crystals accumulated.

It appears that the formation of the northern dome was essentially coeval with its crystallization. Quite likely, crystallization and accumulation occurred on a sloping floor. Deformation associated with the doming event produced a variety of late-magmatic and subsolidus deformation structures within the northern dome.

Post-cumulus structures. The modification of structures and textures during late-magmatic stages has been recognized in the form of layer disruption

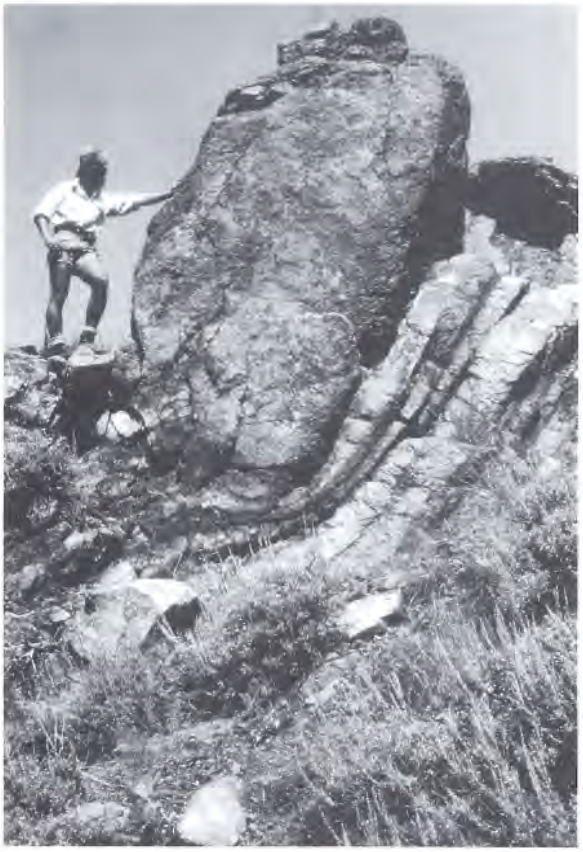

Figure 8. Photograph of an olivine leucogabbro xenolith, main layered zone, layered series, northern anorthosite dome. Note the compaction of layering beneath the block.

and in the production of pegmatoids. Layer disruption is represented by complex zones of convoluted, dismembered layering (**Figure 9**). Disruption of once continuous mafic-rich and anorthosite layers produced isolated mafic-rich pods within anorthosite, which retain chaotic remnants of a planar lamination. The near-absence of mechanical straining of crystals and the segregation of mafic-rich material indicates that interstitial liquid was present as a lubricating agent during this stage of deformation. This type of disruption probably occurred at high levels in the cumulate pile and may be related to such mechanisms as slope instability on an inclined floor, the force of impacting blocks, or large-scale movement within the cumulate pile in response to strain.

Pegmatoids are evidence of the accumulation and movement of interstitial liquids during the post-cumulus stage of consolidation. They range in size from several inches to tens of feet (centimeters to meters) in diameter. Although they typically cross-cut layering, pegmatoids rarely show evidence of forceful emplacement. Rather, they appear to create space by digesting or corroding surrounding anorthositic rocks. Coarse-grained olivine, orthopyroxene, Fe-Ti oxides and apatite, and giant elongate laths of plagioclase, many of which exceed 8 inches (20 cm) in length, are the typical mineral constituents of a pegmatoid (**Figure 10**). Clinopyroxene is noticeably absent from pegmatoids. Several small pegmatoids appear to display evidence of gravity stratification. Within a single pegmatoid, Fe-Ti oxides may occupy the base, apatite the middle, and olivine or orthopyroxene plus plagioclase the top. Vapor cavities occur in the uppermost portions of pegmatoids and are commonly lined with euhedral crystals of calcite and/or quartz. The distribution of pegmatoids is apparently controlled by the intensity of deformation and recrystallization. They are rare to absent in both the core and ULZ and are generally concentrated in the upper levels of the MLZ.

Figure 9. Photograph of disrupted layering, main layered zone, layered series, northern anorthosite dome. Exposure is in a road cut on Wyoming Highway 34 in Sybille Canyon.

Figure 10. Photograph of a portion of a pegmatoid, main layered zone, layered series, northern anorthosite dome. Pegmatoid consists of large, elongate plagioclase crystals with interstitial olivine. Length of pen in upper right corner is 5.5 inches (14 cm).

Subsolidus structures. Little subsolidus reorganization or recrystallization is recognized in the ULZ. The intensity of deformation increases sharply below the ULZ/MLZ contact. Isolated portions of the upper MLZ show the effects of strain: recrystallization of grain margins to fine-grained neoblastic mosaics around primary plagioclase laths, deformation twinning in plagioclase laths, flattening and elongation of oikocrysts, pull-apart structures and boudinage in compositional layering, and local development of secondary fabrics (**Figure 11**). The distribution and appearance of these zones suggests that they represent the effects of small-scale, high-temperature strain zones at some depth in the cumulate pile that developed subsequent to the crystallization of most or all of the interstitial melt.

Several miles (km) in structural depth beneath the ULZ/MLZ contact, primary structures are preserved only as isolated remnants in a mass of deformed anorthosite. All primary magmatic plagioclase laths are strongly recrystallized. This has produced a massive anorthosite consisting of annealed, equigranular, 2 to 3 cm diameter neoblasts of plagioclase. The fine-grained oxide inclusions that produce the black color typical of magmatic plagioclase in the northern dome are no longer present in the neoblasts. Consequently, the recrystallized rocks have a white or pale gray color. Plagioclase megacrysts, 2 to 10 cm in diameter, remained relatively intact throughout the early stages of deformation-associated recrystallization. In the most strongly recrystallized rocks,

Figure 11. Photograph of deformed layering in anorthosite, main layered zone, layered series, northern anorthosite dome. Layers have been strongly attenuated with the development of incipient boudinage. A thin shear zone transects the lower portion of the photograph. Hammer handle is 12 inches (30 cm) long.

however, megacrysts are also broken and are reduced in size to a mosaic of annealed grains identical in texture to the recrystallized matrix.

The intensity of recrystallization is variable over large distances. In some localities, zones of strong recrystallization occur well up to the ULZ/MLZ contact, whereas in other areas, relatively undeformed rocks are present even within lower portions of the MLZ. The intensity of recrystallization and the modal composition of rocks in the northern dome are directly correlative. Rocks at deep levels in the MLZ show evidence of extreme deformation and are in most cases virtually pure anorthosite. In zones of strong and heterogenous strain, an anastomosing "gneissic" fabric is imposed upon the anorthosite (**Figure 12**). The development of "gneissic" fabric and other deformation features observed in the rocks is the result of the subsolidus history of the intrusion (probably associated with the deformation that produced the domical structures) and has not been produced by penetrative regional deformation, as is the case for many Grenvillian anorthosites.

Low-temperature alteration. In addition to the high-temperature recrystallization and reorganization of primary structures and textures described above, some of the anorthositic rocks show the effects of low-temperature alteration. Primary ferromagnesian minerals may be replaced to different degrees by a variety of amphiboles, biotite, and chlorite. Plagioclase may be altered to epidote minerals, calcite, muscovite, quartz, and locally, to prehnite and pumpellyite. The extent of alteration is variable, but tends to be greatest in lower stratigraphic levels and in the most highly deformed rocks. Thus, much of the low-temperature alteration may have occurred during the latest stages of igneous cooling.

Central anorthosite dome

The central anorthosite dome is a suite of anorthosite, troctolitic anorthosite, and leucotroctolite, together with minor leucogabbro, that is exposed in a tight, southwest-plunging anticlinal structure in the central LAC (**Figures 1** and **13**). To the northeast, the fold axis is truncated by Laramide faults in Grant Creek valley. The western limb of the dome can be traced north and northwestward to where it grades into deformed rocks in the core of the northern dome. It is likely, therefore, that the central dome and the northern dome are manifestations of the same structure. Nevertheless, we will consider the central anorthosite dome and northern anorthosite dome as separate bodies in this paper. We do this for two reasons. First, the rocks of the central dome have characteristics distinctive from those of the northern dome—they tend to be more olivine-rich and rarely contain oikiocrystic anorthosite, the dominant rock of the northern dome. Second, the layering in much of the central dome is due to deformation, rather than being a primary igneous feature, particularly in the deeper structural portions of the dome. The dome exposes a minimum structural thickness of 2 miles (3.2 km).

Figure 12. Photograph of "gneissic anorthosite", massive series, northern anorthosite dome. A light matrix of intensely recrystallized anorthosite (white) envelopes lozenges of anorthosite that have seen slightly less deformation (gray). Ferromagnesian minerals are concentrated preferentially in the dark lozenges.

Much like the ULZ of the northern dome, the upper (outer) portions of the central dome are moderately mafic and show distinct igneous layering. The inner portion, which consists of significant amounts of mafic anorthosite and leucogabbro (**Figure 13**) contains deformation-induced pla-

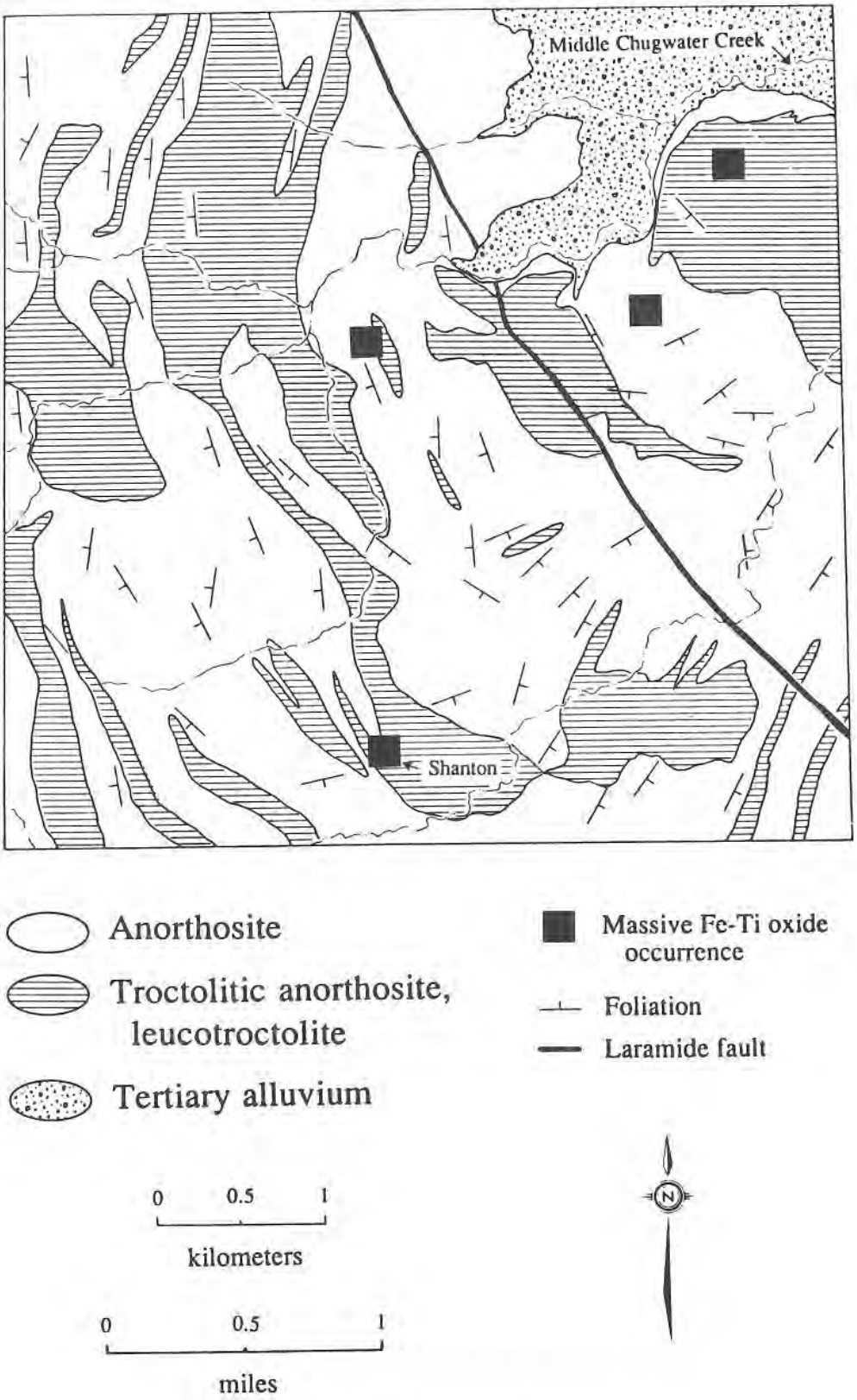

Figure 13. Geologic map of the central anorthosite dome.

nar fabrics. Mottled anorthosite, which is the major rock type in the northern dome, is rare in the upper stratigraphic horizons of the central dome and does not occur at all in the lower portions. Olivine-bearing mafic anorthosite and leucogabbro with olivine present as red-brown, interstitial grains 0.25 to 0.75 cm long, is the dominant rock type in the central dome. Black plagioclase megacrysts occur in a fine-grained plagioclase matrix. Megacrysts are commonly 5 x 2.5 x 0.75 cm, although some are as large as 10 to 13 cm across. The matrix plagioclase is much more equant in shape and has a wide range in grain sizes, typically 1 x 0.75 x 0.5 cm. Iridescent plagioclase is much more common in the central dome than in the northern dome.

There are several features indicating that anorthositic horizons in the lower portion of the central dome are a product of deformation, rather than being simply igneous layers. One of the most important is the fact that anorthositic horizons are always more intensely deformed than surrounding mafic anorthosite or leucotroctolite. The deformation is seen in grain-size reduction, growth of neoblastic white-to-grey plagioclase, and clear evidence for disaggregation of megacrystic plagioclase. Furthermore the anorthositic "layers" in the lower portions of the central dome are locally anastomosing and commonly grade into mafic anorthosite or leucotroctolite over short distances.

The age relationships between the anorthositic horizons and leucogabbro in the central dome is ambiguous. In some localities the anorthositic rocks form horizons that clearly crosscut the fabric of the leucogabbro. In other localities, the leucogabbro is gradational with the deformed anorthosite and contains megacrysts of deformed plagioclase, indicating that it post-dates the anorthosite horizons. In the structurally lower portions of the central dome, lens-shaped bodies, ranging in composition from olivine-bearing mafic anorthosite to leucogabbro, are interlayered with anorthosite. These lenses, which are up to 2 miles (3.2 km) long and 0.75 miles (1.2 km) wide, terminate laterally by interfingering with anorthosite (**Figure 13**). Both layering and lamination in the anorthositic rocks wrap around the leucogabbro lenses, which are commonly massive. Rare occurrences of plagioclase lamination in leucogabbro are subparallel to lamination and layering in the surrounding anorthosite. Some of the leucogabbro bodies crosscut anorthosite, but most are broadly conformable. Petrographically, the only difference between the rock types is the modal abundance of olivine and pyroxene. We believe that the lens-shaped leucogabbro bodies may represent some component of residual melt that was squeezed out or crystal mushes that were mobilized during deformation of the cumulate pile, whereas the anorthositic horizons represent the highly deformed crystalline portions of that cumulate. Southeast of the anticlinal axis, where granite dikes are relatively more abundant than elsewhere in the central dome, much of the olivine has been replaced by pseudomorphs of hornblende and green amphibole. The proportion of amphibole in anorthosite increases with proximity to the granite dikes, which suggests that these dikes may have been the source of water for the hydration of olivine. Newhouse and Hagner (1957) apparently mapped most of the amphibole-bearing rocks as anorthosite, regardless of the abundance of ferromagnesian minerals. Where there is good evidence that amphibole is pseudomorphic after olivine, the rocks were mapped as troctolitic anorthosite and/or leucogabbro.

Massive Fe-Ti oxide bodies are particularly abundant in the central dome. They occur as dike-like bodies that range in dimension from 1 foot x 300 feet (1 x 100 m) to 15 feet x 1 mile (4.5 m x 1.6 km). These bodies are concentrated near the axis of the fold structure and are spatially associated with mafic anorthosite and leucogabbro. The larger bodies at Iron Mountain and Shanton Creek have been extensively prospected and developed [see Frost and Simons, (1991) for details on these deposits].

Snow Creek anorthosite dome

The Snow Creek dome is a gently arched series of anorthosites and troctolitic anorthosites that occur in the west-central portion of the LAC (**Figure 1**). To date, this body has been virtually unstudied. The rocks of the Snow Creek dome are compositionally similar to those of the central dome; troctolitic anorthosite is common and mottled anorthosite is rare. Like the inner portions of the central dome, most of the layers in the Snow Creek dome are a product of deformation, rather than being due solely to igneous processes. Because of the shallow dip, this structure exposes a stratigraphic thickness of no more than 3,000 feet (1 km).

Southern anorthosite dome

The southern anorthosite dome (**Figure 1**) is an isolated body of anorthosite south of the main anorthosite complex covering an area of about 28 square miles (72 km^2) (**Figure 1**). In a mapping study of the southern dome, Ramarathnam (1962) described a fine-grained margin of anorthosite around the coarser grained core of the dome. Most of the ferromagnesian minerals in the southern dome have been altered to hornblende. Despite this alteration, the southern dome has many similarities to the northern dome. In many places, hornblende occurs as pseudomorphic oikocrysts after pyroxene, producing a mottled anorthosite that is similar in appearance to the most common lithology of the northern dome. Hydration of pyroxene to hornblende may be related to emplacement and crystallization of the nearby Sherman batholith. Like the northern dome, the southern dome contains compositional layering defined by alternating layers of anorthosite and mafic anorthosite. Layering is present on the scale of tens of feet to hundreds of feet (meters to decameters). The larger layers form prominent features on aerial photographs. Newhouse and Hagner (1957) showed that the large-scale structure is an elongate dome. The axis of the dome trends northeast to southwest, with a closure plunging to the northeast. If a southward closure to the structure exists, it is hidden beneath Phanerozoic cover rocks. The stratigraphic thickness exposed in this structure is approximately 2 miles (3.5 km). Compositional layering in the southern dome has been traced seismically to depths of about 2.5 miles (4 km) (Speece and others, in press).

Post-anorthosite intrusions

Strong Creek complex

The Strong Creek complex, located in the west-central portion of the LAC (**Figure 1**), consists of three major intrusions, as well as a number of dikes of diverse compositions (**Figure 14**). These intrusions occupy a region between the anorthositic rocks of the central and Snow Creek domes. These bodies include: the Greaser layered intrusion, Strong Creek gabbro (Kling, 1986), and Buttes granite.

Greaser layered intrusion. The Greaser layered intrusion is a composite mafic intrusion covering 3 square miles (7.7 km^2). It was first mapped by Newhouse and Hagner (1957) as norite and later named the Baldy Mountain norite by Nowak (1970). The name Greaser is used here in reference to the abundant exposures on the old Greaser Ranch, which is now the Strong Creek Ranch. It is composed of two dominant lithologies: gabbronorite to olivine gabbronorite and ferrogabbro (Mitchell and others, 1990). Three distinct sections have been identified in the Greaser intrusion. The northern section contains north-south striking, eastward dipping ferrogabbro layers with minor layers of olivine gabbronorite. The central section consists of interlayered olivine gabbronorite and ferrogabbro striking predominantly north-south, but which gradually curve to the southeast in the south. The southern section contains almost exclusively olivine gabbronorite layers striking east-west.

The central section of the Greaser intrusion has characteristics of both the northern and southern sections. It is bimodal in composition and contains alternating layers of olivine gabbronorite and ferrogabbro, 16 to 50 feet (5 to 15 m) thick. Olivine gabbronorite is composed of plagioclase, olivine, orthopyroxene, clinopyroxene, biotite, magnetite with lesser amounts of ilmenite, and sulfide (pyrrhotite with minor blebs of chalcopyrite). Plagioclase laths and biotite clusters are oriented subparallel to layering. Some horizons within the olivine gabbronorite have a distinctive dark-spotted appearance. This reflects the presence of relatively large augite grains, 3 to 4 mm in diameter, with abundant tabular oxide inclusions. The ferrogabbros are composed of plagioclase that is locally antiperthitic, inverted pigeonite, clinopyroxene, ilmenite with lesser amounts of magnetite, and rare olivine. These rocks are isotropic, and large plagioclase grains are commonly bent. Contacts between the olivine gabbronorite and ferrogabbro layers are sharp. Stratigraphic variations within individual layers are gradational and usually expressed by slight grain-size and modal variations.

Strong Creek gabbro. The Strong Creek gabbro is a coarse-grained gabbro located east of the Greaser intrusion, and covering 4 square miles (10 km^2). The stratigraphy and mineralogy of several drill cores from an oxide-rich portion of the Strong Creek gabbro have been described by Kling (1986). Discrete blocks of Strong Creek gabbro occur within the uppermost layers of the Greaser intrusion, indicating that the Strong Creek gabbro is the older of the two intrusions. Grain sizes coarsen from a relatively fine-grained phase in contact with the Greaser intrusion to

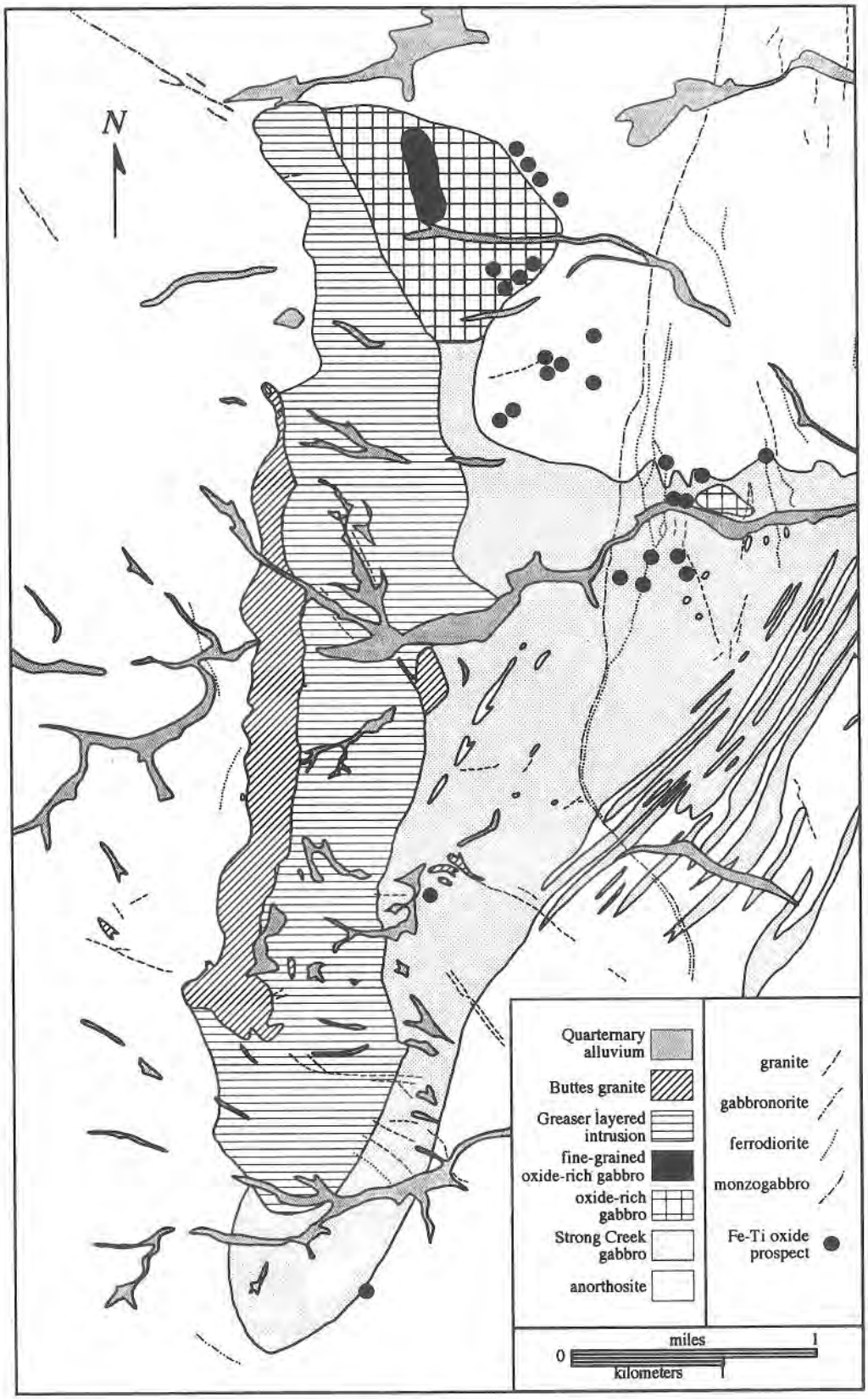

Figure 14. Geologic map of the Strong Creek complex.

a coarse-grained phase typical of most of the Strong Creek gabbro. Laminated, medium-grained, oxide-rich gabbro crops out in the northern portion of the Strong Creek complex. This unit may be an oxide-rich phase of the Strong Creek gabbro similar to that studied by Kling (1986). Field relationships reveal that the Strong Creek gabbro is gradational with leucogabbros of the central anorthosite dome to the east. The western Strong Creek gabbro is typically homogeneous and isotropic. Anorthosite layers occur about 1.2 miles (2 km) from the Greaser/Strong Creek gabbro contact. These layers are 15 to 30 feet (5 to 10 m) thick, dip 30 to 60° to the west, and strike northeast-southwest. The anorthosite consists of a fine-grained matrix of plagioclase with plagioclase megacrysts oriented parallel to the strike of layering. Anorthosite becomes increasingly abundant to the east, until it becomes the dominant lithology.

Buttes granite. The Buttes granite is the youngest unit in the Strong Creek complex, covering 0.75 square miles (1.9 km^2). It was mapped by Newhouse and Hagner (1957) as Sherman granite, but the Buttes granite contains fewer ferromagnesian minerals than granite typical of the Sherman batholith. The Buttes granite is a layered body striking north-south, dipping to the east. It contains two lithologies: a coarse-grained, quartz-poor granite (or quartz syenite) that consists almost entirely of alkali feldspar megacrysts and a fine-grained granite with abundant quartz. At its western or lowermost contact with anorthosite of the Snow Creek dome, the Buttes granite contains large xenoliths and xenocrysts of iridescent plagioclase and anorthosite. Augen-shaped alkali feldspar megacrysts found along the eastern or uppermost contact with the Greaser intrusion suggest that the Buttes granite was deformed at high temperature during or subsequent to emplacement.

Monzonitic plutons

There are three major late-stage plutons in the LAC. These include the Sybille monzosyenite (Fuhrman, 1986; Fuhrman and others, 1988), the Red Mountain pluton (Anderson and others, 1987; 1988), and the Maloin Ranch pluton (Kolker, 1989; Kolker and Lindsley, 1989; Kolker and others, 1990; Kolker and others, 1991) (**Figure 1**). These plutons each contain highly evolved rocks of monzonitic, syenitic, and granitic composition. However, in detail each pluton is distinct. Early workers recognized that on the northern margin of the LAC there are two types of syenitic rocks. Newhouse and Hagner (1957) subdivided the syenitic rocks into hypersthene syenite on the south and west and hornblende syenite on the northeast. Smith and others (1970) called the northeastern body the Red Mountain syenite, but Anderson and others (1987) renamed it the Red Mountain pluton to emphasize the variable rock types it contains. The pyroxene-bearing, southwestern portion was called hypersthene monzonite by Fountain and others (1981) in recognition of its high modal plagioclase content. This was renamed the Sybille monzosyenite by Fuhrman and others (1988), who noted that the pluton contains both monzonitic and monzosyenitic units. Crosscutting relationships indicate that the Red Mountain pluton is younger than the Sybille monzosyenite. The relative age between these plutons and the Maloin Ranch pluton is not known, since they are nowhere in mutual contact. It is assumed that they are essentially coeval, based upon unpublished U-Pb zircon data of Robert Zartman (Kolker and Lindsley, 1989).

Sybille monzosyenite. The Sybille monzosyenite consists of three units (**Figure 15**), including fine-grained monzonite, porphyritic monzonite, and monzosyenite (Fuhrman and others, 1988), which cover an area of 40 square miles (102 km^2). Fine-grained monzonite has an average grain size of 1 mm in diameter. It is dark red-brown on weathered surfaces, but dark olive-green on a fresh surface. With the increasing abundance of alkali feldspar megacrysts, 1 x 2 cm, fine-grained monzonite grades into porphyritic monzonite, which then grades into monzosyenite. A rock is considered to be monzosyenite rather than porphyritic monzonite when the alkali feldspar megacrysts are in mutual contact. Ferromagnesian minerals in the monzosyenite are approximately the same size as in the fine monzonite, but they occur in clusters, 0.5 cm in diameter, interstitial to the megacrysts. Monzosyenite is light red-brown on a weathered surface and, like both the fine monzonite and porphyritic monzonite, is dark olive-green on the fresh surface.

In many localities, fine-grained monzonite and porphyritic monzonite form a distinct border facies up to 900 feet (300 m) wide at the contact between the Sybille monzosyenite and the anorthositic rocks. Fine-grained monzonite is usually in direct contact with anorthosite and gradational through porphyritic monzonite to monzosyenite. However, at some locations, fine-grained monzonite and porphyritic mon-

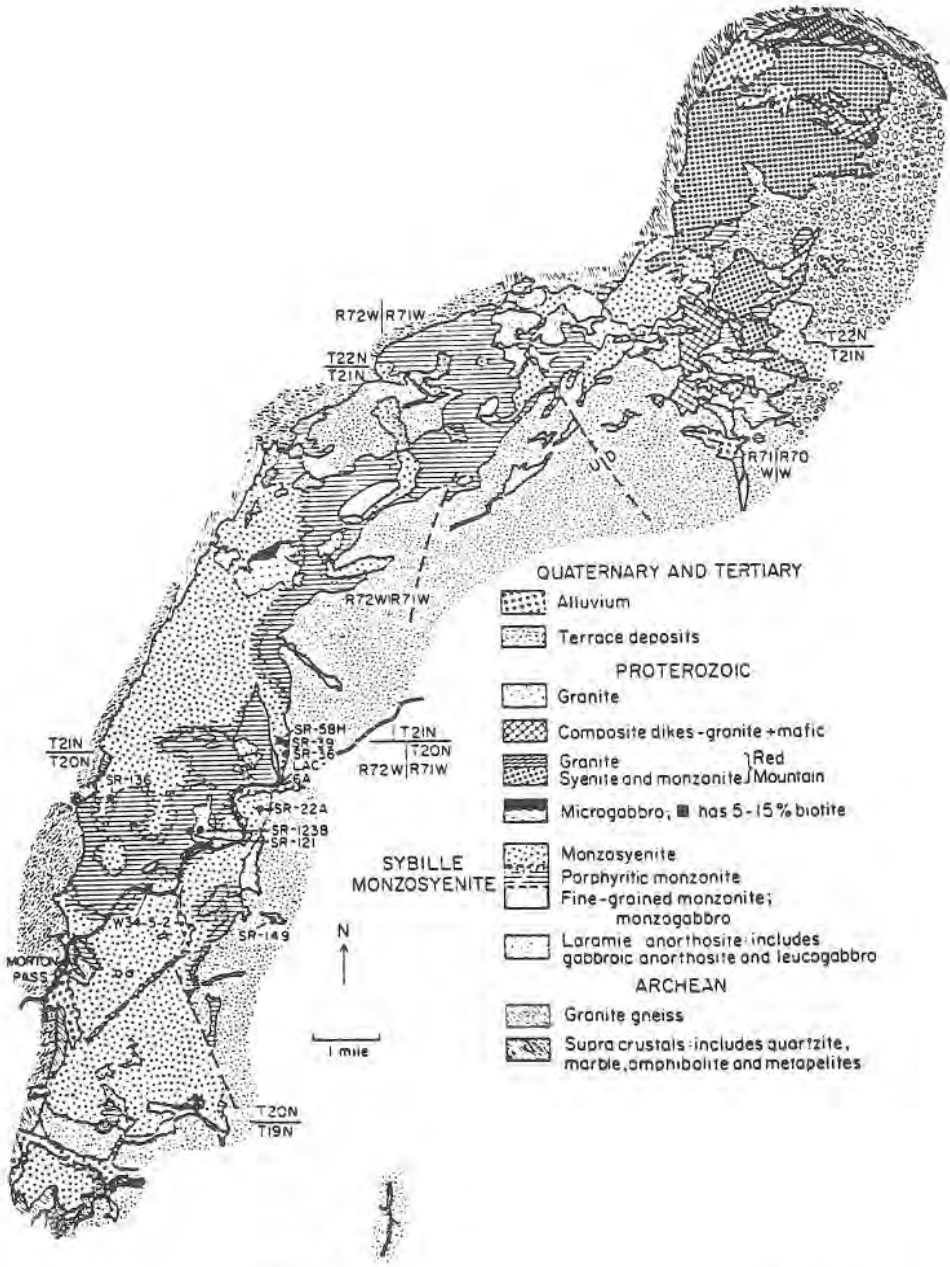

Figure 15. Geologic map of the Sybille monzosyenite and Red Mountain pluton (after Fuhrman and others, 1988).

zonite occur as inclusions in monzosyenite. In most outcrops of porphyritic monzonite and monzosyenite the fabric is isotropic, but locally alkali feldspar megacrysts show a preferred orientation.

Map relations indicate that the present exposure level is near the top of the intrusion (**Figure 15**). Not only does the Sybille monzosyenite contain numerous inclusions of country rock, but there are localities where the contact between the Sybille monzosyenite and the country rock is relatively shallow, with monzosyenite dipping beneath country rock. These relations, in addition to the weak fabric in the rock, indicate that the Sybille monzosyenite was emplaced mainly by stoping of country rock, rather than by forceful injection.

Maloin Ranch pluton. The Maloin Ranch pluton is a half-bowl shaped composite intrusion exposed over an area of about 20 square miles (50 km^2) (**Figure 16**). It contains a succession of rock types with ferrodiorite at the base, overlain sequentially by fine-grained and porphyritic monzonite, monzosyenite, and at the top, porphyritic granite. It was mapped in detail and named by Kolker (1989). In many respects, the rock types are similar to those of the Sybille monzosyenite. The Maloin Ranch pluton contains a distinctive layered horizon. Biotite gabbro or fine-grained monzonite are interlayered with monzosyenite over an 825 foot (250 m) section. Fine-grained margins in both the biotite gabbro and fine-grained monzonite layers suggest that these rocks were apparently injected onto the floor of the magma chamber, which was crystallizing monzosyenite, and subsequently chilled against the host monzosyenite. Geobarometry suggests a pressure of crystallization of 4 kilobars for the Maloin Ranch pluton (Kolker and Lindsley, 1989), as compared to 2.5 to 3 kilobars for the Sybille monzosyenite (Fuhrman and others, 1988).

Red Mountain pluton. The Red Mountain pluton is a zoned stock covering an area of about 8 square miles (20 km^2) in the northeastern portion of the LAC (**Figures 1** and **15**). It intrudes a small portion of the Sybille monzosyenite, but most of the pluton is in contact with Archean granitic gneisses, migmatites, and pelites. Strong penetrative deformation is present in the Archean host rocks around the Red Mountain pluton. The Red Mountain pluton is somewhat more mafic than the previously described monzonitic rocks of the Sybille and Maloin Ranch plutons. Unlike the irregular distribution of mafic minerals in the Sybille monzosyenite, mafic minerals in the Red Mountain pluton are distributed evenly throughout the various rock types. Four rock types were recognized petrographically by Anderson and others (1987). The dominant rock is a hornblende-biotite syenite. Minor amounts of fayalite-hedenbergite monzonite and hedenbergite monzonite occur locally at low elevations and along the southern contact. Distinguishing the rocks in the field is difficult, so their distribution is not indicated on **Figure 15**. Along the northern contact of the pluton, adjacent to Archean gneisses and metasediments of the Elmers Rock greenstone belt, rocks of the Red Mountain pluton contain significant amounts of quartz and are mapped separately as Red Mountain granite on **Figure 15**.

Minor intrusions

Numerous small intrusions and dikes occur within the major intrusions of the LAC. Many of these rocks are fine grained and may represent chilled melts. They could provide information about various liquid lines of descent for magmas present during the crystallization history of the LAC. Thus, they may have an importance that is far greater than their small volume might suggest. These rocks include gabbro (olivine gabbro, biotite gabbro, and monzogabbro), diorite (ferrodiorite and monzodiorite), Fe-Ti oxide bodies, composite dikes, and granites. Similar rocks occur in Proterozoic anorthosite complexes throughout the world (Ashwal, 1982; Wilmart and others, 1989; Dushesne, 1990; Wiebe, 1990a).

Gabbroic and dioritic rocks. Small intrusions and dikes of olivine gabbro, biotite gabbro, and monzogabbro occur throughout the complex. They are also found in the contact aureole, where they are strongly recrystallized and foliated. Olivine gabbros are typically composed of plagioclase, olivine, augite, locally orthopyroxene, and ilmenite. Some of the these olivine gabbros are very similar to the olivine gabbronorites of the Greaser layered intrusion. Biotite gabbros may contain up to 10% biotite, which is inferred to be primary. Iron-rich monzogabbro and monzodiorite, both containing abundant normative potassium feldspar, occur in the upper portions of the northern anorthosite dome, at or near the margins of the Sybille monzosyenite and Maloin Ranch pluton, and within the Strong Creek complex. These rocks contain mesoperthitic plagioclase (originally ternary feldspar), hedenbergite, fayalitic olivine and/or inverted pigeonite, ilmenite, magnetite, and apatite. Monzogabbros contain olivine and monzodiorites contain inverted pigeonite without olivine. These rocks form irregular masses or dike-like bodies that intruded anorthositic rocks. The relative age between these rocks and the monzonitic rocks is less clear. In some localities, they occur marginal to the monzonites and appear to be part of the border facies for these intrusions. In rare instances, the monzogabbros occur as inclusions in the monzonites. These inclusions may represent pieces of border facies that were ripped up by magma flowing along the margins of the chamber.

A single monzogabbro dike, 5 miles (8 km) long and striking N-S, transects both the central anorthosite dome and the Strong Creek gabbro (**Figure 14**).

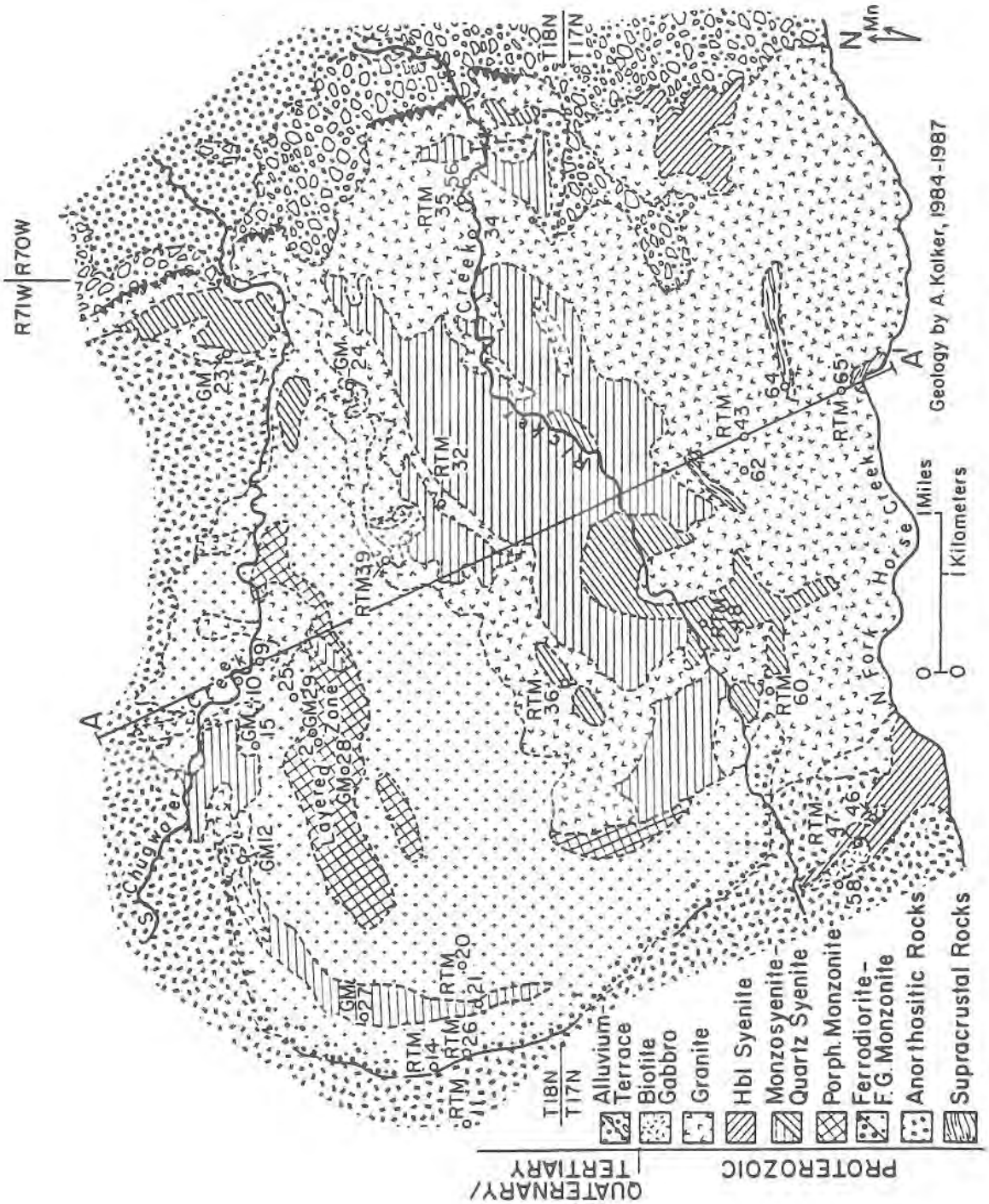

Figure 16. Geologic map of the Maloin Ranch pluton (after Kolker and Lindsley, 1989).

An anastomosing series of ferrodiorite dikes occurs subparallel to this dike. The monzogabbro contains fayalitic olivine, clinopyroxene, and strongly antiperthitic plagioclase. The ferrodiorite contains inverted pigeonite, plagioclase, and Fe-Ti oxides. Ferrodiorite dikes of similar composition occur at several other localities within the Strong Creek complex. Compositional similarities between some of the gabbroic and dioritic dikes with rocks of the Greaser intrusion suggest a possible complementary liquid/cumulate relationship.

Fe-Ti oxide bodies. Massive Fe-Ti oxide bodies occur within both the northern and central anorthosite domes. Their existence has been known since the earliest geologic investigations in Wyoming (Hayden, 1871). The best known occurrences are Iron Mountain (Frey, 1946; Eberle, 1983) and Shanton (Hild, 1953) in the central dome, and the Sybille pit (Bolsover, 1986; Epler, 1987) in the northern dome. In most Fe-Ti oxide bodies, the mineralogy is dominated by ilmenite and magnetite, but other minerals, such as apatite, olivine, or plagioclase may be present. Some of the occurrences have an irregular shape, but most, such as at Iron Mountain (Frey, 1946) and at Shanton (Hild, 1953), are distinctly tabular and dike-like. In the northern dome, the oxide bodies appear to be broadly stratabound, occurring in a band several hundred feet (meters) wide near the top of the main layered zone. The abundant oxide bodies within the central dome appear to reflect structural rather than stratigraphic control, as almost all occur along or close to the anticlinal fold axis.

In many occurrences, only massive Fe-Ti oxides are present. At the Sybille pit (Bolsover, 1986) and at Iron Mountain, Fe-Ti oxides are gradational with a pegmatitic iron-rich leucotroctolite containing iron-rich olivine. Gravity separation appears to have aided in the formation of these bodies. At both localities, oxide-poor leucotroctolite occurs near the top of the body. Oxides increase and silicates decrease in abundance downward. Massive Fe-Ti oxides occur near the bottom. The occurrence of an anorthosite xenolith with a cap of oxides within leucotroctolite at the Sybille pit is further evidence of the importance of gravity separation in the formation of these bodies. Small leucotroctolite bodies occur throughout much of the northern dome and are commonly associated with minor concentrations of Fe-Ti oxides. Large bodies of leucotroctolite are common in the central dome, where numerous massive oxide bodies occur. Thus, there appears to be a genetic relationship between leucotroctolite and Fe-Ti oxide bodies. Furthermore, both the geochemical data of Goldberg (1984) and our mapping suggest that leucotroctolite is closely related to anorthosite, probably as a late-stage or residual liquid.

We suggest that the Fe-Ti oxide bodies formed from a leucotroctolitic melt, either as crystal cumulates or through the process of magma unmixing (Lindsley and Frost, 1990). Experimental work of Epler (1987) on leucotroctolite from the Sybille pit suggests that this rock can produce two melts, one oxide-rich and one whose composition is similar to that of the monzogabbros. The identical Nd and Sr isotopic compositions of leucotroctolite and oxide-rich monzogabbro provide further permissive evidence of a genetic relationship between these rock types (Geist and others, 1990). Thus, there is abundant evidence that both the Fe-Ti oxide bodies and the monzogabbro dikes may represent some portion of the residual liquid inferred to have formed during crystallization of the anorthosite.

Composite dikes. Composite dikes in the LAC show evidence of the interaction of contemporaneous mafic and felsic melts in the same magma conduit (Nealon, 1988; Meurer, 1990). Similar relationships have been described in other Proterozoic anorthosite complexes throughout the world (Wiebe, 1979, 1980a, 1984; Wiebe and Wild, 1983). The majority of the composite dikes in the LAC occur in the upper layered zone of the northern anorthosite dome, north of Wyoming Highway 34 and east of the northernmost extension of the Grant Creek Valley fault. In this area, they represent between 20 and 30% of the outcrop surface. A detailed study of the physical processes of magma mixing showed that all composite dikes result from the intrusion of a mafic melt into a conduit occupied by a felsic melt (Meurer, 1990). The principal textural feature that results from the interaction of such compositionally and thermally contrasted melts is the occurrence of rounded, chilled "pillows" of mafic melt in felsic melt. Small amounts of hybrid material can be generated by magma mixing.

The felsic portions of composite dikes are dominantly granitic in composition, composed of phenocrysts of plagioclase and alkali feldspar in a finer grained matrix of plagioclase, alkali feldspar, quartz, biotite, hornblende, and minor Fe-Ti oxides, apatite, zircon, and allanite. The majority of these granites

may be related to granites of the Sherman batholith. The mafic portions of the composite dikes are variable in composition, ranging from diorite to quartz monzonite. The diorites contain plagioclase and differing amounts of augite, orthopyroxene, biotite, hornblende, Fe-Ti oxides, and apatite. The more evolved quartz monzonites contain phenocrysts of alkali feldspar, accessory zircon and allanite, and rare pyroxene. The variability in the composition of the mafic melts suggests that they may be the products of several different sources and fractionation histories. Both Nealon and Meurer suggest that some of the diorites may represent some component of residual liquids related to crystallization of the anorthosites. Field relationships indicate that most of the composite dikes were emplaced into the anorthosite prior to intrusion of the Red Mountain pluton. Only a few composite dikes clearly cut the Red Mountain pluton.

Granites. All the major intrusions of the LAC are cut by numerous granitic dikes. These dikes range in thickness from several feet to tens of feet (meters to decameters), and they may be traced along strike for distances up to 0.5 miles (1 km). They are conspicuous topographic features forming high-relief ribs or ridges in more easily weathered anorthositic or monzonitic rocks. There is a wide range of compositions of granitic dikes, from porphyritic granite to quartz monzonite to granodiorite. Although generally massive, some granitic dikes are strongly layered. Coarse-grained granitic dikes are associated with the Buttes granite of the Strong Creek complex and consist almost exclusively of alkali feldspar megacrysts. The largest concentration of granitic dikes is in the northeast portion of the northern anorthosite dome (Snyder, 1984).

Phanerozoic structures

Extensive fault systems were developed throughout the LAC during the Phanerozoic. Many of these are demonstrably Laramide in age, for they cut the Mesozoic cover rocks. However, a pre-Laramide age, possibly related to the uplift of the Ancestral Rockies, cannot be ruled out for those faults that lie entirely within the Precambrian rocks. Several faults produced significant offsets.

The dominant break is a north-south trending low-angle reverse fault/thrust dipping to the west, near the eastern margin of the complex (**Figure 1**). In its northern reaches, it strikes through Grant Creek Valley and therefore we call it the Grant Creek fault. South of the Iron Mountain area, this fault is a thrust forming the eastern margin of the complex. It places the anorthositic rocks of the LAC above Paleozoic and Mesozoic rocks. North of Iron Mountain, the fault steepens and cuts through the LAC. Displacement on the Grant Creek fault probably decreases northward until it dies out (or is simply lost) within the Sybille monzosyenite. The thrust system was clearly defined on a COCORP seismic reflection profile over this portion of the Laramie Mountains (Allmendinger and others, 1982; Brewer and others, 1982).

In addition to the north-south striking faults, there are a series of northeast-southwest striking faults that occur in the northern portion of the LAC. This includes the Middle Sybille Canyon fault, Long Canyon fault, and Hallack Canyon fault. All of these have a component of dextral strike-slip offset that is one mile (1.6 km) or less. Along fault traces, anorthosite has been strongly deformed by cataclasis and reduced to a fine-grained white powdery rubble.

In the southern area, where the Grant Creek fault is a thrust, the LAC seems to have moved as a coherent block with little additional deformation in the hanging wall. Although lineaments are present on aerial photographs, these lineaments seldom displace compositional layering of the central dome by more than a few feet (meters). In the northern area, where the Grant Creek fault is steeper, accommodation of Laramide deformation by the anorthositic basement was far more complex. Here, northeast-southwest striking faults, with a significant component of strike-slip offset, are common. A set of subsidiary faults displaces layering of the northern dome by distances on the order of tens to hundreds of feet (meters to decameters) (**Figure 3**).

Mineral chemistry

Ferromagnesian silicates

The compositions of ferromagnesian minerals from the LAC mimic many of the trends observed in layered mafic intrusions. Pyroxene and olivine compositions show a distinct iron-enrichment trend through the gabbroic and anorthositic rocks to the monzonitic rocks (**Figure 17**). Anorthositic and gabbroic rocks contain calcic pyroxenes with X_{Fe} = Fe/

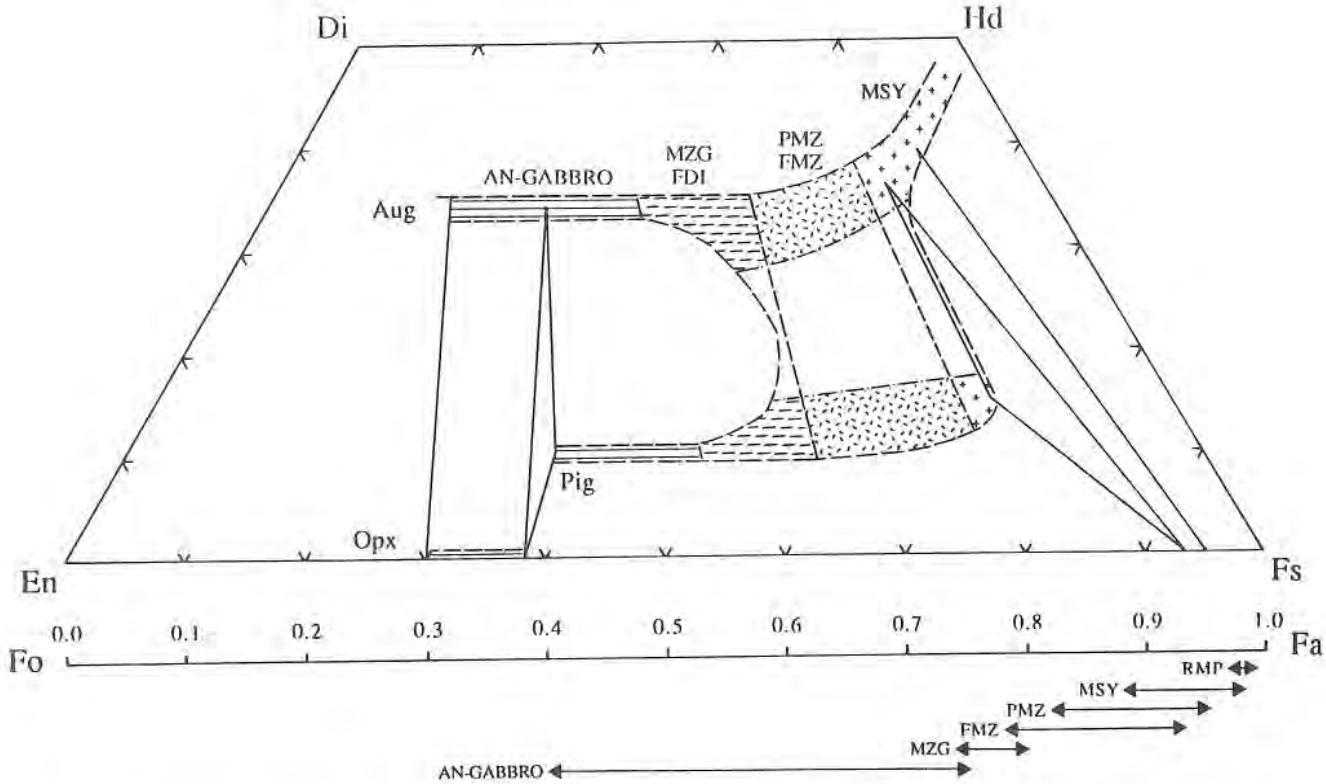

Figure 17. Compositional trends for olivine and pyroxenes from the LAC. Mineral abbreviations are: Aug - augite, Di - diopside, En - enstatite, Fs - ferrosilite, Hd - hedenbergite, Opx - orthopyroxene, Pig - pigeonite. Rock abbreviations are: AN-GABBRO - anorthosite and gabbro, FDI - ferrodiorite, MZG - monzogabbro, FMZ - fine-grained monzonite, PMZ - porphyritic monzonite, MSY - monzosyenite, RMP - Red Mountain pluton.

(Fe+Mg) ratios that range from less than 0.25 to near 0.50. The more magnesian augites coexist with orthopyroxene, whereas those with intermediate compositions occur with inverted pigeonite. Olivine (Fa_{40}), orthopyroxene (X_{Fe} = 0.32), and augite (X_{Fe} = 0.50 to 0.57) coexist in the olivine gabbronorite layers of the Greaser intrusion. Ferrogabbro layers in the Greaser intrusion contain inverted pigeonite (X_{Fe} = 0.65 to 0.70), augite (X_{Fe} = 0.70), and rare olivine (Fa_{75}). Ferrodiorite and monzogabbro dikes have augite with X_{Fe} = 0.45 to 0.60. Some ferrodiorites and monzogabbros contain pigeonite as well as augite, but most contain only one pyroxene. Fe-rich leucotroctolite of the Sybille pit contains olivine with Fa_{60} to Fa_{70}. Within the Sybille monzosyenite, augite in fine-grained monzonite and porphyritic monzonite ranges in composition from X_{Fe} = 0.60 to 0.75, whereas augite in monzosyenite has X_{Fe} > 0.90. In the most iron-rich rocks, augite (X_{Fe} > 0.80) coexists with fayalite and quartz rather than with pigeonite. Augite in fine-grained monzonite is markedly sub-calcic (Fuhrman and others, 1988), indicating that the rocks were hot enough to see the closure of the pigeonite-augite solvus. A similar phenomenon occurs in some monzosyenites from the Maloin Ranch pluton (Kolker and Lindsley, 1989). The iron-enrichment in pyroxene compositions is mirrored in olivine as well, with compositions ranging from Fa_{40} to Fa_{75} in gabbroic and anorthositic rocks, Fa_{74} to Fa_{86} in monzogabbros, and Fa_{78} to Fa_{96} in the monzonitic and monzosyenitic rocks.

It is important to note that **Figure 17** includes all the various rock types in the LAC. The magnesian portion of the diagram is defined by rocks of the northern anorthosite dome and the Strong Creek complex. The iron-rich end is defined by compositional trends in the Sybille monzosyenite (Fuhrman and others, 1988), the Maloin Ranch pluton (Kolker and Lindsley, 1989) and, to a lesser degree, in the Red Mountain pluton. However, in no individual pluton is the whole compositional range found. Indeed, to

some extent, **Figure 17** masks much of the compositional complexity presented by the LAC.

There is a wide range of silica activity within the various intrusive phases of the LAC. Some of the gabbroic rocks contain low-Ca pyroxene without olivine, whereas others contain olivine without low-Ca pyroxene. Similarly, monzogabbros with olivine and inverted pigeonite, and ferrodiorites with pigeonite and without olivine are equally well represented in the complex. Clearly, the Fe-enrichment trend observed in **Figure 17** is a product of several processes and not one of simple igneous differentiation.

Feldspars

Feldspars show a distinct trend toward sodium and potassium enrichment (**Figure 18**). Plagioclase in the anorthositic rocks ranges in composition from An_{60} to An_{40}. On average, the Greaser intrusion contains the most anorthitic plagioclase in the LAC. Plagioclase averages An_{60} in olivine gabbronorite layers, and ranges from An_{30} to An_{50} in ferrogabbro layers. A few small plagioclase grains from oxide-rich layers in the Strong Creek gabbro have compositions greater than An_{90}. Ternary feldspars (now exsolved) are found in rocks of the Sybille monzosyenite, some ferrogabbro layers of the Greaser intrusion, and in monzogabbro dikes. Feldspars of the porphyritic monzonite and monzosyenites of the Sybille monzosyenite are more potassic than those of the monzogabbros. These ternary feldspars occur as strongly exsolved perthites that are distinctive because of the large difference in refractive index between the moderately calcic plagioclase lamellae and the alkali feldspar host. Unlike the Sybille monzosyenite, direct evidence for ternary feldspars is

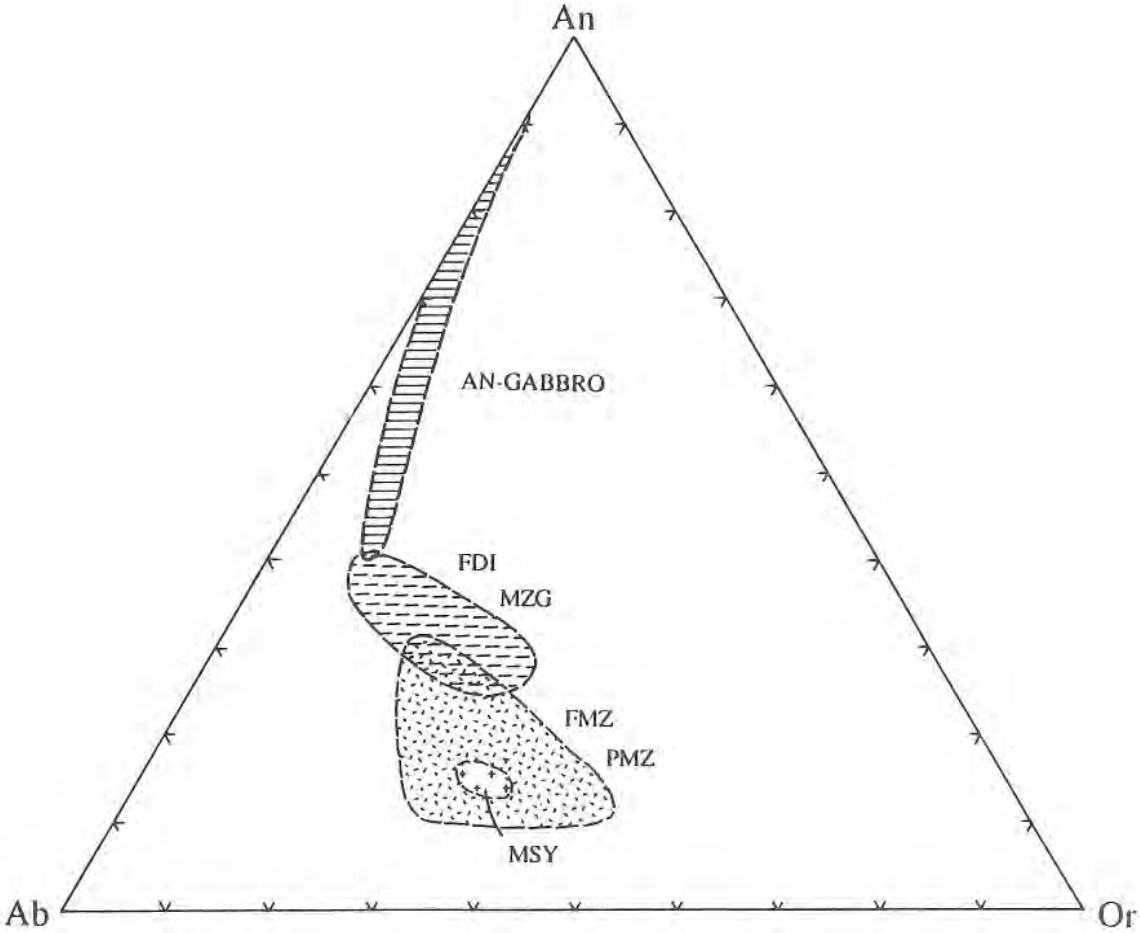

Figure 18. Compositional trends for feldspars from the Laramie Anorthosite Complex. Mineral abbreviations are: Ab - albite, An - anorthite, Or - orthoclase. Other abbreviations as in Figure 17.

lacking from the Maloin Ranch pluton. However, because inferred temperatures of crystallization for the Maloin Ranch pluton are similar to those for the Sybille monzosyenite (see following section), we suggest that early feldspars in the Maloin Ranch pluton were also ternary (Kolker and Lindsley, 1989). Ternary intergrowths may have been removed by re-equilibration during slow cooling or upon intrusion of the nearby Sherman batholith.

Conditions of emplacement and crystallization

Temperature

All the intrusions within the LAC were emplaced and crystallized at high temperatures. From the composition of coexisting pyroxenes, Kling (1986) estimated temperatures of 1,100 °C or higher for the Strong Creek gabbro. Crystallization temperatures of the anorthositic units were certainly in that range also, as indicated by the Fe/Mg ratio at which pigeonite appears (Lindsley, 1983). The late monzonitic plutons were all extremely hot for such evolved rocks. The Sybille monzosyenite crystallized in the range of 1,030 °C for fine-grained monzonite to ≥950 °C for monzosyenite (Fuhrman and others, 1988; Livi, 1987). The Maloin Ranch pluton shows more extensive mineral re-equilibration than does the Sybille monzosyenite and consequently the pyroxene thermometer records temperatures of 900 to 970 °C. These may be closure temperatures because the quartz-magnetite-ilmenite-fayalite (QUIlF) thermometer of Frost and others (1988) indicates that the oxides and silicates in the Maloin Ranch pluton equilibrated at 1,000 ± 50 °C (Kolker and Lindsley, 1989). A temperature of 950 °C is also estimated for the fayalite monzonite of the Red Mountain pluton (Anderson and others, 1987). The more hydrous units of the Red Mountain pluton probably crystallized at somewhat lower temperatures, but there are no thermometers available to constrain their crystallization temperatures.

Pressure

The composition of the most iron-rich pigeonite in the Sybille monzosyenite and the Maloin Ranch pluton establishes the pressures at which these plutons were emplaced. Although the full assemblage fayalite-pigeonite-hedenbergite-quartz is not present in the Sybille monzosyenite, the Fe/Mg range between fayalite coexisting with the most iron-rich pigeonite and fayalite coexisting with quartz is small (see above). These values establish that the Sybille monzosyenite crystallized at pressures between 2.5 and 3.0 kilobars (Fuhrman and others, 1988). The Maloin Ranch pluton does contain the critical assemblage with pigeonite more iron-rich than pigeonite in the Sybille monzosyenite. The pressure of crystallization for the Maloin Ranch pluton has been estimated to be 4 kilobars (Kolker and Lindsley, 1989).

Oxygen fugacity

All the intrusions within the LAC crystallized under relatively reduced oxygen fugacities. Preliminary studies indicate that crystallization of most gabbroic and anorthositic units of the complex occurred near or below oxygen fugacities of the fayalite-magnetite-quartz (FMQ) buffer. For example, Kling (1986) found that the more primitive portions of the Strong Creek gabbro equilibrated about 0.25 log units below the FMQ buffer. Other gabbroic units of the LAC certainly crystallized at lower oxygen fugacities because the gabbros studied by Kling (1986) had relatively high silica activity, as indicated by the absence of olivine. Two-oxide gabbros with pyroxenes of the same composition, and also containing olivine, must have formed at lower oxygen fugacities (Lindsley and others, 1990). A relatively evolved leucotroctolite from just north of the Strong Creek complex is estimated to have equilibrated at oxygen fugacities around 1 log unit below FMQ (Frost and others, 1989a). Similarly reducing conditions are inferred for the formation of massive Fe-Ti oxide bodies at the Sybille pit (Bolsover, 1986).

The oxygen fugacity of the monzonitic rocks is well determined because they contain the QUIlF assemblage (Frost and others, 1988). This assemblage constrains the oxygen fugacity to lie 1.75 ± 0.5 log units below FMQ for both the Sybille monzosyenite and the Maloin Ranch pluton. Somewhat more oxidizing conditions (1.2 ± 0.4 log units below FMQ) are indicated for the fayalite-bearing portions of the Red Mountain pluton (Anderson and others, 1987).

Fluid composition

A distinctive feature of the LAC is the evidence for a CO_2-rich fluid phase throughout the complex. One type of evidence is the widespread occurrence of graphite throughout the various intrusions. Graphite is found as a primary igneous phase in the Sybille

monzosyenite (Frost and Touret, 1989) and as a secondary phase in leucotroctolite from north of the Strong Creek complex (Frost and others, 1989a), from the massive Fe-Ti oxide body of the Sybille pit (Bolsover, 1986), and from the Sybille monzosyenite (Frost and others, 1989a). A further indication of the CO_2-rich nature of the fluids comes from the presence of CO_2-rich fluid inclusions in rocks throughout the complex. These fluid inclusions occur in apatite in both anorthositic rocks and massive Fe-Ti oxide - apatite rocks. They are also present in quartz in the Sybille monzosyenite and the Maloin Ranch pluton (Frost and Touret, 1989). A detailed study of the fluid inclusions from the Sybille monzosyenite indicates that they are probably magmatic in origin. In addition to CO_2 fluid inclusions, Frost and Touret (1989) found abundant solid salt ((Na, K) Cl) inclusions in feldspars and postulated that the magma of the Sybille monzosyenite crystallized in the presence of two fluids, a CO_2 fluid and a saline melt.

The nature of fluids is also indicated by the relative rarity of primary hydrous minerals throughout much of the complex. Up to 10% biotite occurs in biotite gabbros. The OH content of these biotites may be relatively low as they contain up to 8% TiO_2 and more than 1% F (Kling, 1986). Apart from this, primary hydrous phases are scarce in most rocks except for the later units of the Red Mountain pluton.

Hydration of the silicates is well recorded in the Red Mountain pluton. The least evolved phase of the Red Mountain contains fayalite, but it is usually rimmed by hornblende. With progressive crystallization of the Red Mountain pluton, first fayalite, and then hedenbergite, react to produce hornblende. Preliminary studies indicate that fluid inclusions in these rocks contain mixtures of CO_2 and H_2O. For all other rock types in the LAC (except those of the southern anorthosite dome), amphibole pseudomorphs after pyroxene and olivine are rare and localized. They commonly occur adjacent to granitic dikes or intrusions.

Sherman batholith

The Sherman batholith was one of the first rock units of Precambrian age to be documented in Wyoming (Hayden, 1871). It was formally named the Sherman granite by Darton and others (1910), who mapped its extent in the southern Laramie Mountains and Sheep Mountain. Many writers have used the term Sherman granite and Sherman batholith interchangeably (e.g. Fowler, 1930; Eggler, 1968). The dominant rock in the batholith is a pink biotite-hornblende granite. For this reason, we will use the designation Sherman batholith when describing the suite of rocks, and Sherman granite when describing the biotite-hornblende granite. Despite its early recognition, the Sherman batholith has received only minimal attention. Fowler (1930), Harrison (1951), Newhouse and Hagner (1957), and Smith (1977) mapped the northern extent of the batholith in the Laramie Mountains; Houston and others (1968) mapped its occurrence in the southern Medicine Bow Mountains; Eggler (1968) delineated the southern limits of the batholith where it is represented by the Virginia Dale ring dike complex; and Marlatt (1989) mapped its eastern limits near Interstate 80 in the Laramie Mountains. There have been some isotopic studies of the Sherman batholith (Zielinski and others, 1981; Aleinikoff, 1983; Geist and others, 1989), but to date, no comprehensive petrologic study has been undertaken.

Petrologic units

Various workers have recognized different rock types within the Sherman batholith, but the batholith itself has not been subdivided. Four major units have been identified including red-weathering biotite-hornblende granite, gray to red biotite quartz monzonite, fine-grained granitoids, and mafic rocks.

Biotite-hornblende granite

Biotite-hornblende granite is the dominant rock type of the Sherman batholith. It occurs widely in the Laramie Mountains (**Figure 1**) and is the major rock type of the Sherman batholith found on Sheep Mountain and in the Medicine Bow Mountains (**Figure 2**) (Houston and others, 1968). It is composed of alkali feldspar megacrysts and scattered clots of quartz and ferromagnesian minerals. This type of granite was called the Trail Creek granite by Eggler (1968), but we will use the term Sherman granite, which predates

the designation of Eggler by nearly 50 years. The main ferromagnesian minerals in this unit are hornblende and biotite. Fayalite has been reported in the northernmost extent of this unit in the Laramie Mountains (Geist and others, 1989) and near the summit of Interstate 80, east of Laramie.

Biotite quartz monzonite

Gray biotite quartz monzonite is much less abundant than the main Sherman granite. It is different in that it lacks hornblende and contains more plagioclase. It occurs in the Virginia Dale ring dike complex, where it was named the Cap Rock quartz monzonite (Eggler, 1968), and locally elsewhere in the Sherman batholith (Harrison, 1951). The distribution of biotite quartz monzonite outside of the Virginia Dale region is not well known.

Fine-grained granitoids

A suite of fine-grained granitoids, microgranite to porphyritic microgranite, has been described as closely associated with the Sherman granite (Smith, 1977). Smith (1977) described the microgranite and porphyritic microgranite from an area near Iron Mountain, close to the northern extremity of the Sherman batholith. He found complex relationships between these rocks and the main Sherman granite. In some places, the microgranite is intrusive into the Sherman granite, but in others the microgranite occurs as inclusions in the Sherman granite.

Fine-grained granitoids, ranging from hypabyssal rhyolite to microgranite, occur at two localities near Interstate 80. One is in the village of Granite, where a quarry from the Union Pacific Railroad provides an unusually good exposure. The other is in the ridge just east of the summit on Interstate 80. A microgranite porphyry with alkali feldspar phenocrysts in a matrix of microgranite occurs near the summit. In areas of high relief near the summit, the microgranite and porphyritic microgranite occur on ridge tops and appear to be underlain by coarse-grained Sherman granite. Both the porphyritic and the non-porphyritic variety of microgranite can be found as inclusions within the Sherman granite in many localities along the Interstate 80 transect. These fine-grained rocks were mapped as part of a unit called "earlier gneisses" by Darton and others (1910). On the basis of similar chemistry to the main biotite-hornblende granite (Geist and others, 1989), we consider these microgranites to be chilled equivalents of this granite.

Mafic rocks

Eggler (1968) described a suite of mafic rocks associated with the Sherman batholith, including andesite, diorite, hornblende gabbro, and olivine gabbro. These rocks are minor in volume, but they show important field relationships with the granites. At one locality near Virginia Dale, the occurrence of pillows of mafic rock in a granitic host indicates that the mafic melts were intruded into the batholith when the granitic rocks were partially molten. The biotite-bearing olivine gabbro described by Ferris and Krueger (1964) and Eggler (1968) is of particular interest because it is similar to the biotite gabbros of the LAC.

Metamorphism

The rocks of the LAC and Sherman batholith have not undergone regional metamorphism, but they have produced strong contact effects in some of the rocks they intrude. The thermal effects are not obvious where Archean granites are in contact with the complex, but where the LAC has intruded supracrustal rocks it is surrounded by a marked contact aureole. High-grade contact metamorphism is recognized in four areas around the LAC: at Morton Pass, along the northern contact of the Red Mountain pluton, within the septum of Proterozoic rocks that separates the central anorthosite dome from the southern anorthosite dome, and along the eastern margin of the southern dome. In addition, contact metamorphic effects may be present around the Sherman batholith.

Contact metamorphism

Morton Pass contact aureole

At Morton Pass, a supracrustal sequence of quartzite, mafic, pelitic, and calcareous rocks occurs adjacent to the Sybille monzosyenite. Metamorphism has led to dehydration of the metabasites, producing pyroxene hornfelses (Russ-Nabelek, 1989)

and extensive melting in the pelitic hornfelses (Bochensky, 1982; Grant and Frost, 1990). Dehydration of the metabasites lead first to the assemblage hornblende(hb)-augite(cpx)-plagioclase (plag)-quartz, then to hb-cpx-plag-orthopyroxene(opx), and finally to hb-cpx-plag-opx-olivine (Russ-Nabelek, 1989; Frost and Frost, 1989).

The mineral assemblages formed with progressive metamorphism of the pelitic hornfelses are shown in **Figure 19**. In the lowest grade assemblages, sillimanite and biotite coexist with alkali feldspar and quartz (other phases are cordierite, garnet, and spinel). Cordierite from these assemblages is iron rich, in accordance with the relatively low pressure of the contact aureole (see below). With progressive metamorphism, cordierite from the low-variance assemblages becomes enriched in Mg relative to Fe, recording both the increase in temperature and the tendency for iron to be preferentially extracted from the pelitic rocks during melting. A detailed study of pyroxene compositions indicates that contact metamorphism attained temperatures of 900° C (Russ-Nabelek, 1989). Mineral assemblages in the pelites indicate that pressure was near 3 kilobars (Grant and Frost, 1990), a pressure similar to that obtained for the Sybille monzosyenite from pyroxene-olivine-quartz relations.

Red Mountain pluton contact aureole

The Red Mountain pluton intruded the supracrustal rocks of the Elmers Rock greenstone belt and produced contact metamorphism in a sequence of metabasites, metapelites, and marbles similar to those at Morton Pass (Spicuzza, 1990). The major difference in this area is that the contact effects can be traced outward into the regional metamorphism of the Elmers Rock greenstone belt (Grant and Frost, 1986). At Morton Pass, where only about 1 mile (1.6 km) of the aureole is exposed, the lowest recorded contact temperature is near 700° C.

Contact metamorphism between the central and southern anorthosite domes

Isolated blocks of partially melted pelitic rocks occur in a sliver of gneisses covering 16 square miles (40 km²) between the central and southern an-

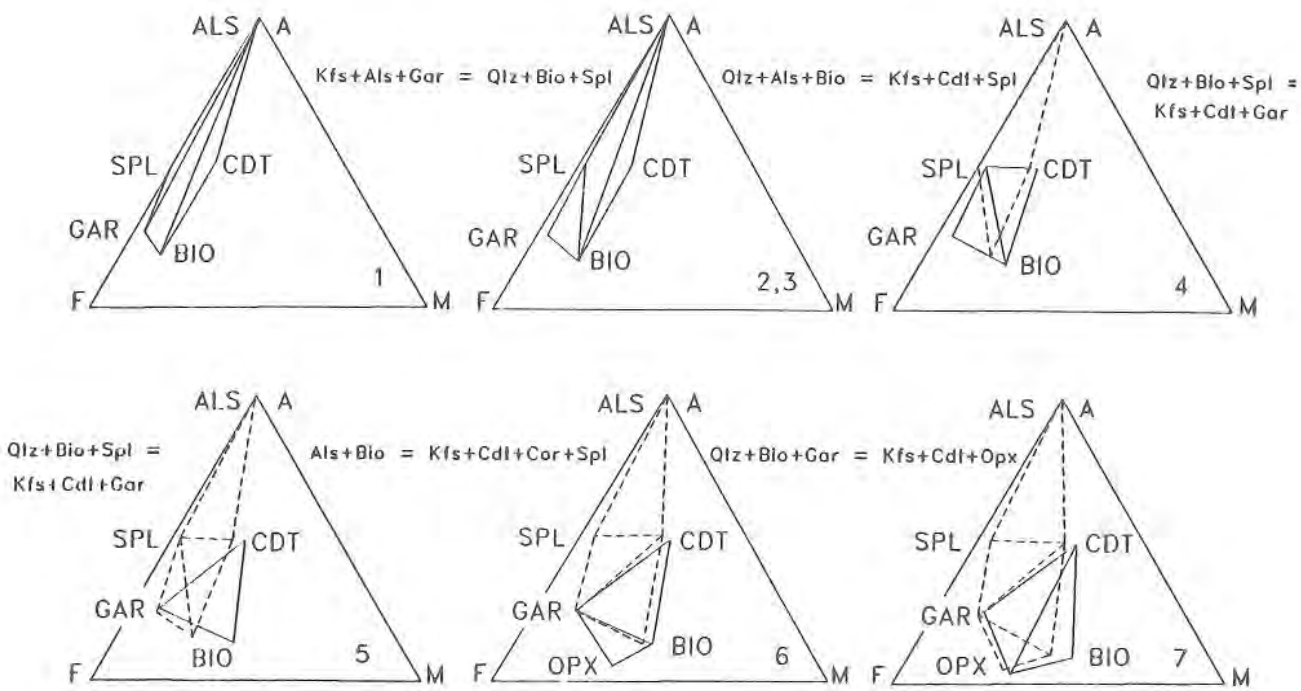

Figure 19. AFM projections from alkali feldspar, quartz, and water showing changes in assemblages at Morton Pass with increasing metamorphic grade. Mineral abbreviations are: ALS - aluminum silicate (sillimanite), BIO - biotite, CDT - cordierite, GAR - garnet, KFS - K-feldspar, OPX - orthopyroxene, SPL - spinel (after Grant and Frost, 1990).

orthosite domes. The gneisses were studied by McCullough (1974), who mapped several different units of gneiss. The pelitic rocks were studied in detail by Xirouchakis (1991). Based upon the high-temperature assemblage of hypersthene-sillimanite-cordierite-spinel, he estimated the pressure in this area to have been 3.5 (± 0.5) kilobars.

Southern anorthosite dome contact aureole

Early workers noted unusual rocks in the Horse Mountain area (Darton and others, 1910; Fowler, 1930), which were given the rather bizarre name of quartzite anorthosite by Newhouse and Hagner (1957). These rocks are a highly disrupted supracrustal sequence that includes mafic rocks, quartzite, rare metapelites, and probably calcareous rocks. It is likely that the plagioclase and quartz-rich rocks to which Newhouse and Hagner referred are metamorphosed calc-silicates, rather than a unit related to the anorthosite itself. This is one of the few places around the LAC where supracrustal rocks are in direct contact with anorthosite. Thermobarometry of the assemblage diopside-plagioclase-garnet-quartz from this area indicates pressures of around 3.2 kilobars (± 1.9 kbar) (Xirouchakis, 1991).

Sherman batholith contact aureole

Intrusion of the Sherman granite into the pelitic hornfelses on the southern portion of the aureole of the Laramie Anorthosite Complex caused marked retrogression, with andalusite-biotite-quartz replacing the high-temperature assemblage of alkali feldspar-cordierite-spinel and biotite-muscovite-quartz replacing cordierite + alkali feldspar (Xirouchakis, 1991). It is estimated that this retrogression took place at temperatures of around 600°C and pressures of 1 to 3 kilobars.

There are only a few other localities where reactive rocks such as pelitic schists are in contact with the Sherman batholith. Isolated inclusions of pyroxene-bearing metabasite are found on the ridge east of the summit on Interstate 80. Eggler (1968) reported that there were no contact effects at all around the Virginia Dale ring dike complex. However, he did describe the association of sillimanite and alkali feldspar in pelitic gneisses, indicating that a further petrologic study of contact relations in this area is warranted. This is particularly important since it might provide a pressure estimate for the depth of emplacement at the southern limits of the Sherman batholith.

Geochemistry of the LAC and Sherman batholith

Whole-rock geochemistry

Major- and trace-element data from the LAC have been presented by Hodge and others (1970), Fountain and others (1981), Goldberg (1984), Fuhrman and others (1988), and Kolker and others (1990). The anorthosites have geochemical signatures that, in part, reflect their plagioclase-rich compositions: high Al_2O_3, CaO, Na_2O, and Sr abundances. Mafic-rich anorthosites have higher FeO_{Total}, TiO_2, and MgO contents, reflecting their larger amounts of modal olivine, pyroxene, and Fe-Ti oxide. Leucotroctolites, rich in olivine, are characterized by relatively high MgO and lower SiO_2, Al_2O_3, and Na_2O contents. From geochemical and Sr isotopic characteristics, Goldberg (1984) determined that the anorthositic rocks and the oxide bodies are comagmatic, and that the gabbros represent the products of early differentiation of a high-Al parent magma. He suggested that large volumes of plagioclase could have crystallized from this high-Al parent magma to produce anorthosite. Fountain and others (1981) recognized on the basis of REE and Sr isotopic data that the anorthosites and monzonitic rocks could not be related by simple closed-system differentiation. They documented a regular variation in geochemical characteristics with distance from the monzonite-country rock contact and suggested that this variation is due to increasing amounts of wall-rock contamination as the contact is approached. The presence of country rock xenoliths in the Sybille and Red Mountain plutons, documented by Fuhrman and others (1988) and Anderson and others (1987, 1988), supports this hypothesis.

The Sherman batholith shares many geochemical features with other 1.4 to 1.5 Ga granite batholiths, which occur in a northeast- to southwest-trending belt from Labrador to southern California. These so-called "anorogenic" batholiths are potassic, subalkaline, and enriched in iron relative to magnesium (Anderson, 1983). According to the classifica-

tion scheme of Irvine and Baragar (1971), the Sherman batholith is predominantly subalkalic, although the most mafic members fall in the alkalic field (**Figure 20**). The Sherman batholith bridges the peraluminous-metaluminous boundary, defined in terms of $Al_2O_3/(CaO+K_2O+Na_2O)$ on a molecular basis (Shand, 1927), with the more mafic and intermediate rocks falling in the metaluminous field, and the most felsic samples lying in the peraluminous field (**Figure 21**). Most anorogenic granites are similarly marginally perealuminous, although the neighboring two-mica Silver Plume granite of Colorado, a phase of which intrudes the Sherman batholith in the Virginia Dale area (Eggler, 1968), is entirely peraluminous (Anderson and Thomas, 1985). The iron-enrichment trend typical of anorogenic granites is especially pronounced in the Sherman batholith (**Figure 22**), where the majority of analyses yield values of $FeO_T/(FeO_T+MgO) > 0.85$. High Fe/Mg ratios are also typical of the monzonitic and anorthositic rocks of the LAC (**Figure 22**).

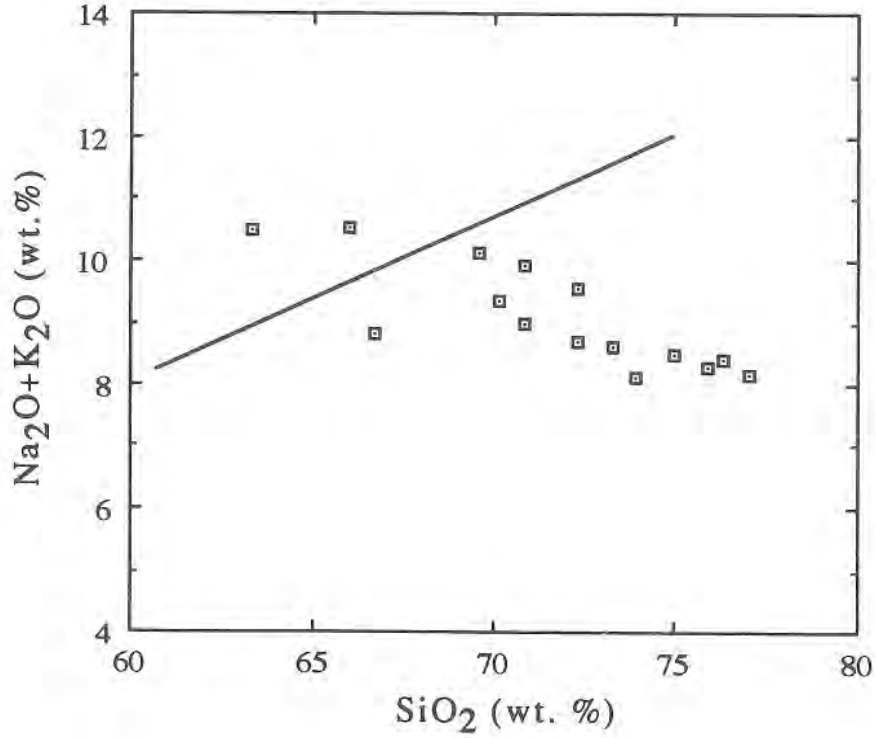

Figure 20. $K_2O + Na_2O$ plotted against SiO_2 for samples of the Sherman batholith. Heavy line separates alkalic field above from subalkalic field below (Irvine and Baragar, 1971). (Data from Eggler, 1968; Geist and others, 1989; Hodge and others, 1970; Kolker and others, 1990; and Zielinski and others, 1981.)

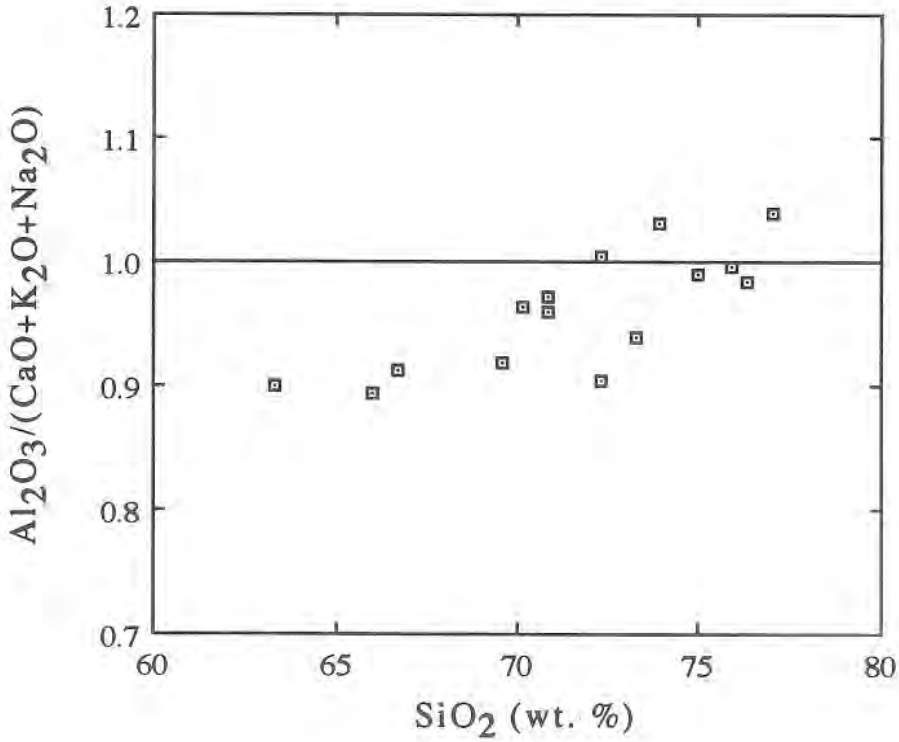

Figure 21. $Al_2O_3/(CaO+K_2O+Na_2O)$ (molecular) plotted against weight % SiO_2 for samples of the Sherman batholith. Heavy line separates field of peraluminous compositions above from metaluminous compositions below (Shand, 1927). (Data sources as in Figure 19.)

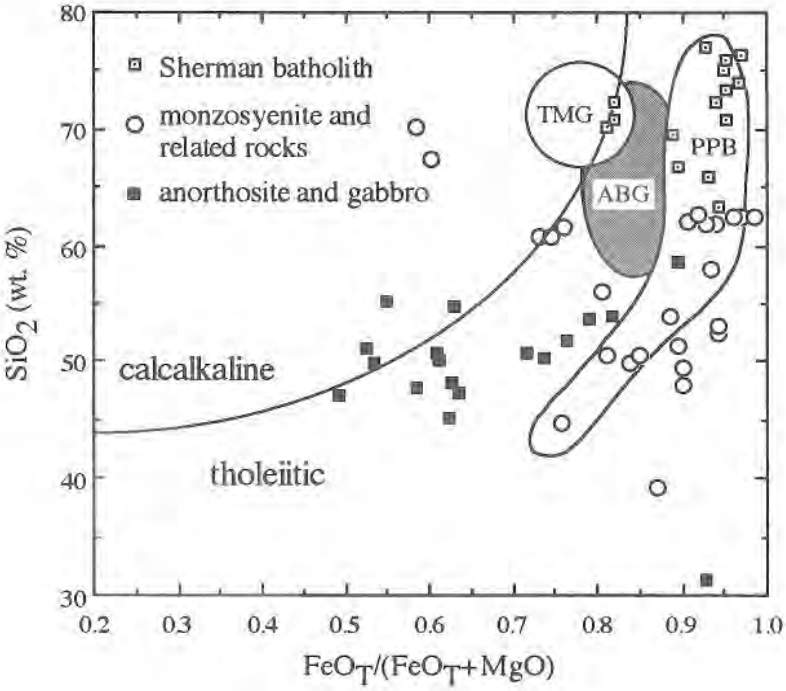

Figure 22. SiO_2 plotted against $FeO_T/(FeO_T+MgO)$ for samples of the Sherman batholith and the LAC. Heavy line separates field of calc-alkaline compositions (upper left) from tholeiitic compositions (lower right) (Anderson, 1983). (Data for Sherman granite samples as in Figure 19; representative LAC data from Fountain and others, 1981; Fuhrman and others, 1988; Goldberg, 1984; and Kolker and others, 1989.) For comparison, fields representing two-mica granites (TMG) and anorogenic biotite granites (ABG) from the southwest United States, and the Pikes Peak batholith (PPB) in Colorado are outlined (data from Anderson, 1983).

The anorthositic rocks are characterized by rare earth element (REE) patterns with strongly positive Eu anomalies (**Figure 23A**). In addition, the monzonites of the Sybille monzosyenite and Maloin Ranch pluton typically have positive, rather than negative, Eu anomalies (**Figure 23B**). Rare earth element contents of the Red Mountain pluton monzonites are higher than for the Sherman batholith or other LAC bodies (**Figure 23B**). This reflects the accumulation of REE-bearing accessory phases (Anderson and others, 1988). A chondrite-normalized light-REE/heavy-REE ratio of 10 is common for rocks of the LAC. The REE characteristics of the Sherman batholith, including light-REE-enrichment and a moderate negative Eu anomaly, are likewise typical of Proterozoic anorogenic granites (**Figure 23C**).

Isotope geochemistry

Whole-rock samples from the anorthositic rocks, the monzonitic plutons, and the Sherman batholith have been analyzed for Nd and Sr isotopic compositions in order to help determine whether the different intrusions of the complex were generated from a common source or from magmas of different origins, and to assess the degree of crustal assimilation (Geist and others, 1989; 1990; Kolker, 1989; Kolker and others, 1991). **Figure 24A** shows data for anorthositic rocks, including anorthosite, biotite gabbronorite, leucotroctolite, oxide-rich monzogabbro, and ferrodiorites. All these rocks span a restricted range in initial Sr isotope ratios of 0.7033 to 0.7058. These ratios are similar to, or slightly higher than, that of the contemporary bulk earth. In contrast, initial ϵ_{Nd} values for the anorthositic rocks span a wide range from +2.1 to -4.8, although most samples cluster between 0 and -2. Two biotite gabbros with Mg-rich olivine (Fa_{35}) and calcic plagioclase (An_{64}) have relatively radiogenic Nd isotopic ratios (ϵ_{Nd} = -1.3 to -1.6) whereas a biotite gabbro intruded into the Sybille monzosyenite has the least radiogenic ratio (ϵ_{Nd} = -4.8). The radiogenic initial Nd isotopic ratios of the first two biotite gabbros suggest a substantial mantle component in the magmas that produced these rocks. The biotite gabbros, being relatively fine grained and primitive in composition, may represent liquids. As such, they may be compositionally similar to parental melts from which some rocks of the LAC crystallized.

If batches of low-REE magmas were differentially contaminated with continental crust early in their evolution, then their Nd isotopic ratios could be substantially changed and the vertical trend on the Nd-Sr

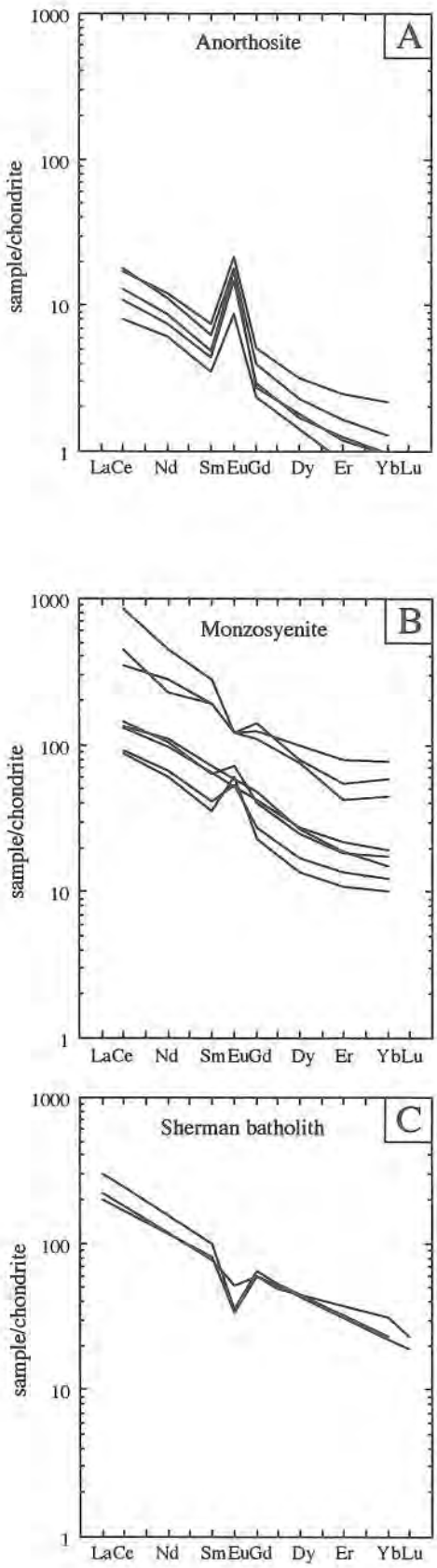

diagram would result (**Figure 24A**). At this early stage of evolution, the parental magmas would also be very Sr-rich. Thus, the effects of contamination would cause only small shifts in initial Sr ratio from values just above bulk-earth values to the range typical of continental crust.

Samples of the monzonitic bodies include monzosyenites, fine-grained monzonites, syenites, and monzogabbros. Samples from the Sybille monzosyenite form a horizontal array on a Nd-Sr diagram. Initial Sr ranges from values typical of the anorthositic rocks to much higher values (**Figure 24B**). This trend almost certainly reflects country rock assimilation, which is consistent with the occurrence of abundant country rock xenoliths in the Sybille monzosyenite. Monzonitic rocks that incorporated greater amounts of radiogenic Sr from the country rocks would be displaced further to the right (**Figure 24B**). At this stage of evolution, the monzonitic rocks had evolved to sufficiently high REE abundances that assimilation had less effect on ϵ_{Nd} than on Sr ratios. Rocks from the Maloin Ranch and Red Mountain plutons have more-radiogenic Nd values than the Sybille monzosyenite. This suggests that these plutons evolved from a magma that was less contaminated early in its history, perhaps from a magma similar to those that produced the relatively primitive biotite gabbros. The more evolved Maloin Ranch and Red Mountain monzosyenites and syenites show greater Sr and Nd isotopic evidence of upper-level crustal assimilation than do the monzonites from these plutons.

The monzonitic rocks grade into granite in the Maloin Ranch and Red Mountain plutons. Samples of these granites, as well as samples of Sherman granite, exhibit a wide range in initial Nd and Sr characteristics. Initial Sr ratios are generally higher than those of the anorthositic rocks, and no ϵ_{Nd} values are as radiogenic as the Maloin Ranch biotite gabbros and Red Mountain fayalite monzonite. If we assume that the granites of the Sherman batholith are predomi-

Figure 23. Chondrite-normalized rare earth element data for selected samples of the LAC and Sherman batholith. A: Anorthositic rocks and gabbros. B: Monzosyenite from the Sybille monzosyenite and Maloin Ranch pluton and monzonite from the Red Mountain pluton. C: Granite from the Sherman batholith. (Data from Geist and others, 1989; Kolker and others, 1990; and Mitchell, unpublished analyses.)

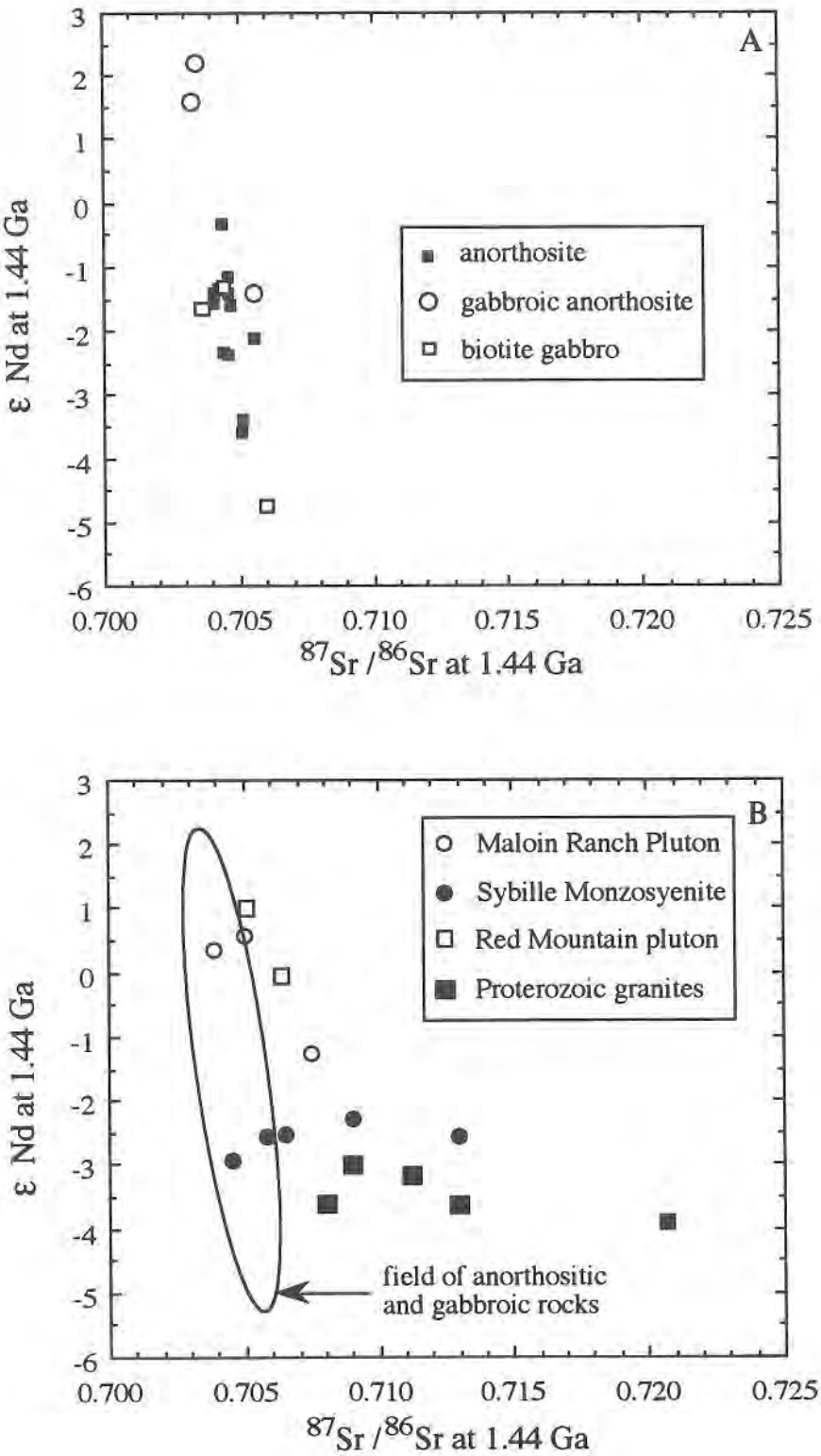

Figure 24. Selected Sr and Nd isotope data from the Laramie Anorthosite Complex and Sherman batholith. A. Data for biotite gabbros and an olivine gabbro, anorthosites and gabbroic anorthosites, and troctolite from the northern and central anorthosite domes and the Strong Creek complex. B. Data from the Maloin Ranch, Sybille, and Red Mountain plutons plus Sherman granite. Data from anorthositic rocks and gabbros is outlined. (Data from Geist and others, 1989, 1990; Kolker, and others, 1991; and C. Frost, unpublished.)

nantly crustal melts, then their crustal sources had, in general, more radiogenic Sr compositions and similar to or less radiogenic Nd compositions than did the magma sources of the anorthosites. The data for the monzonitic rocks are compatible with the hypothesis that they were derived from sources similar to those that produced the anorthosites. However, the monzonites were variably contaminated by granitic crustal melts like those that formed the granites of the Sherman batholith (**Figure 24B**).

Although a mantle source for anorogenic granites has been proposed (Higgins, 1981), the large volume of these batholiths and the absence of significant amounts of mafic differentiates suggests that a dominantly crustal source is likely (Anderson, 1983). Nd model ages for rocks of the Sherman batholith are mainly 1.9 to 2.0 Ga, suggesting that the sources of the Sherman batholith had an average residence time in the continental crust of around 500 Ma before being incorporated into Sherman-type magmas (Geist and others, 1989). Similar model ages are obtained for the LAC (calculated from data in Geist and others, 1990). Thus, the anorthosites, syenites, and granites of the Laramie Mountains exhibit a continuum in several major and trace element and isotopic compositional features, yet their genetic relationship is complex. As developed further below, this triad of rock types seems to have originated by the interaction of mantle melts with the crust.

Origin and evolution of the LAC and the Sherman batholith

Petrogenetic relations between rock units

A key problem to be resolved in understanding 1.4 Ga magmatism in southeastern Wyoming is determining how the various magmatic units are related. This has been a major controversy in the origin of Proterozoic anorthosite complexes for decades and is one that is far from settled (Morse, 1982; Duchesne, 1984; Frost and others, 1989b). For the purpose of discussion we consider the petrogenesis of the rock units in three groups: the gabbroic and anorthositic rocks, the monzonitic and syenitic rocks, and the granitic rocks. We are relatively certain of the origin of the first and third groups, but there remains considerable uncertainty about the second group. A complete petrogenetic model should explain the origin of the anorthositic rocks and of the associated gabbros, diorites, and Fe-Ti oxide bodies, and monzonitic, syenitic, and granitic rocks that are typical of Proterozoic anorthosite complexes. We are not at that stage, but can draw some strong inferences at this time.

Gabbroic and anorthositic rocks

There seems little question that the compositional range observed in the gabbroic rocks of the LAC is dominantly a product of magmatic differentiation, although crustal assimilation and post-cumulus re-equilibration have also played a significant role. The relationships described above indicate that the anorthositic rocks formed mainly by cumulus processes from a leucogabbroic or gabbroic parent. The parent may have been similar in composition to rocks of the gabbro suite (olivine gabbro, olivine gabbronorite, biotite gabbro) that were injected as small bodies throughout the history of the complex. The parental magma for the anorthositic rocks was not a pristine undepleted mantle melt. The range in Sr initial ratios in the anorthositic and gabbroic rocks indicates that the melts that formed these rocks had assimilated various amounts of crustal material.

The major features to be explained for the anorthositic rocks of the LAC, as for any Proterozoic anorthosite, are the high content of intermediate-composition plagioclase, the relatively low Mg number, and the absence of a thick sequence of complementary mafic to ultramafic cumulate rocks. To explain these features, we infer, in common with many workers (Emslie, 1978, 1985; Phinney, 1982; Longhi and Ashwal, 1985; Miller and Weiblen, 1990), that a basaltic melt ponded at or near the base of the crust, where it began crystallizing. The possibility that plagioclase supersaturation can be caused by crystallization of basalt at depth on a plagioclase-pyroxene cotectic has been suggested by Lindsley and Emslie (1968) and by Morse (1982). Olivine, and probably pyroxene, sank to the bottom of this initial deep magma chamber, depleting the magma in Mg and Ni, enriching it in Fe, and driving it towards plagioclase saturation. The fractionated ferromagnesian minerals would remain in the mantle or at the base of the crust, and be undetectable by geo-

physical methods. At this stage, our interpretation departs from those of the workers cited above, who inferred that the anorthositic bodies were intruded diapirically through the crust as crystal mushes of plagioclase that had crystallized and floated to the top of the initial magma chamber.

Textural evidence presented in this paper, including layering, impact structures related to blocks, and magmatic scours, suggests the operation of a vigorous and active magma chamber at the level of emplacement. Plagioclase crystallized in this chamber and accumulated on the chamber floor. The relatively low pressures (2.5 to 4 kilobars) inferred for final emplacement requires the existence of this second magma chamber at a depth of 6 to 7 miles (10 to 12 km). Plagioclase- and Fe-enriched residual magma from the initial deep chamber was repeatedly injected into this chamber. Some, and possibly all, of this magma contained plagioclase megacrysts, but the melt itself may also have been hyperfeldspathic. The existence of hyperfeldspathic liquids in the Nain anorthosite complex in Labrador was suggested by Wiebe (1980b, 1990b). Plagioclase was the only primary mineral to crystallize in the main layered zone of the northern anorthosite dome (and probably in the lower portions of the other anorthositic units as well). Repeated introduction of a hyperfeldspathic magma into the higher-level chamber and subsequent mixing with the resident magma could have maintained plagioclase as the liquidus phase during much of the crystallization history of the northern dome. Some anorthosite may have been formed directly from deposition of plagioclase coupled with adcumulus growth. Where the removal of interstitial liquid was slower, layers containing a greater proportion of interstitial ferromagnesian components developed. Post-cumulus processes, such as filter-pressing associated with deformation during doming, may have driven out some interstitial liquid, leaving mainly anorthosite and mafic anorthosite in the main layered zone. Some of this residual liquid may have migrated to the overlying magma chamber where, increasingly, olivine and/or pyroxene joined plagioclase as cumulus phases. Other portions of the liquid, possibly saturated with CO_2-rich vapor, remained trapped within the cumulate pile and crystallized as pegmatoids. Fe-Ti oxide-rich portions, probably immiscible melts, separated and settled from these residual liquids to form Fe-Ti oxide bodies, while the complementary liquids formed monzogabbroic and dioritic rocks. The number of Fe-Ti oxide, monzogabbro, and ferrodiorite bodies presently exposed represent only a small fraction of the inferred residual melt expelled from the anorthosites. As outlined in the next section, it is possible that the monzonitic and syenitic rocks may also have been derived in part from these residual liquids.

The secondary structural features in the northern dome indicate that deformation within the cumulate pile and the resultant domical shape of the intrusion was a high-temperature process, essentially coeval with crystallization and accumulation at higher levels on the chamber floor. The scarcity of recrystallization and related deformation products in the upper layered zone is particularly strong evidence for contemporaneous crystallization and deformation in the other units. Strain was most likely accommodated by the movement of interstitial melt out of the plagioclase-rich cumulates and by extensive grain-boundary rotation and recrystallization of plagioclase crystals. The occurrence of both pristine and strongly recrystallized anorthositic xenoliths in later intrusions (Greaser intrusion, Sybille monzosyenite) and the lack of high-temperature deformation in these intrusions places a strong limit on when deformation occurred. Deformation must have ceased prior to the emplacement and crystallization of the later-stage intrusions. The strong textural evidence that much of the northern dome underwent post-cumulus deformation suggests that the chemical trends displayed by the gabbroic and anorthositic rocks are likely to be very complex and may not reflect simple igneous differentiation.

The mechanism responsible for producing the final domical shapes of the anorthositic intrusions is far from clear. It is possible that the density contrast between the plagioclase-rich cumulate pile and the surrounding host rocks was sufficient to initiate diapiric uprising of the anorthositic cumulates. Whatever the cause of the doming, there is abundant evidence that it was essentially coeval with the late-stage crystallization of the anorthositic rocks.

Monzonitic and syenitic rocks

The monzonitic and syenitic rocks are the truly enigmatic rocks of the LAC. Fuhrman and others (1988) observed that mineral compositions are continuous from the anorthosites and gabbros through the chemically evolved rocks (monzogabbros, diorites, monzonites, and monzosyenites). One hypothesis is that the monzonitic and syenitic rocks are late-

stage residual liquids from the anorthositic magmas that were contaminated during crystal fractionation. However, Fountain and others (1981) argued that if the monzonitic rocks represent melts (rather than cumulates), they cannot be simple differentiates of the magma that formed the anorthositic rocks because they lack the large negative Eu anomaly that is expected in a residual melt from which massive amounts of plagioclase had been extracted. Morse and Nolan (1985) have shown that this argument may not be completely valid, given that extraction of minor phases may dramatically affect the magnitude of the Eu anomaly of residual liquids. The Nd and Sr isotopic data of Geist and others (1990) also indicate that if the monzonitic rocks are derived from gabbroic magmas it was by open-system processes. Despite these difficulties, the need to identify residual liquids from the anorthosite encourages us to consider the hypothesis that much of the mass of the monzonitic rocks was derived from residual liquids of the anorthosite, although significant aspects of their geochemical signature may have come from assimilated crustal material.

Alternatively, the monzonitic rocks may have been derived entirely from crustal melts. Kolker and others (1990) proposed that many of the monzonitic rocks are not comagmatic with each other and probably resulted from melting of different crustal sources. At present, there are no data that discriminate between these two hypotheses. It should be noted, however, that the monzonitic melts were emplaced at temperatures above 1,000 °C. These are extremely high temperatures for felsic melts. Thus, the monzonitic melts are unlikely to be products of partial melting at the relatively high level of emplacement of the LAC. Kolker and others (1990) suggested that the heat source for the monzonitic rocks may have been the deep initial magma chamber inferred for the parent magma to the anorthosite.

Granitic rocks

The Sherman batholith is almost certainly the product of a crustal melt. The variation in initial Sr ratio indicates that there is likely to have been considerable compositional variation in the source. Almost all of the Sherman batholith lies south of the inferred position of the Cheyenne belt. Thus, most of the crust that could have undergone partial melting was no more than 500 Ma older than the granite itself. This relatively short time interval allowed very little isotopic contrast to develop between mantle and crust. Hence, Nd model ages for the crustal-derived granites of the Sherman batholith and (at least in part) mantle-derived anorthosites and gabbros are very similar.

As noted above, our working hypothesis calls for the LAC to have been formed from mantle melts that underwent a period of crystallization at or near the base of the crust. The heat released by crystallization of melt in this deep chamber may have led to melting of the surrounding crust, producing granitic plutonism. This model for the origin of rapakivi-type granites has been postulated by many authors (Bridgwater and Windley, 1973; Barker and others, 1975; Emslie, 1978; Barker, 1981). These granites are represented in southeastern Wyoming by the Sherman batholith. Rocks similar to those of the Sherman granite are found on the margin of the Red Mountain and Maloin Ranch plutons. However, the LAC was emplaced at too shallow a depth to have produced extensive crustal melting. Minor amounts of melts were produced only within 1 mile (1.6 km) of the contact with the complex (Grant and Frost, 1990). Furthermore, the Sherman batholith extends much farther south than does the LAC. The presence of the Virginia Dale ring dike complex indicates that at least some of the Sherman batholith came from sources that were as much as 20 miles (32 km) south of the southernmost exposure of anorthosite. Either the first magma chamber extended farther south than the present-day exposures of anorthositic rocks, or the heat source for the Sherman batholith was different. However, partial melts of country rock surrounding the second (upper) magma chamber may have provided some of the mass and much of the geochemical signature of the monzonitic and syenitic rocks.

Implications for crustal structure

There are two important questions related to 1.4 Ga magmatism that are immediately evident from a geologic map of the western United States: (1) why are there no other occurrences of 1.4 Ga intrusions in the Wyoming province north and west of the LAC?, and (2) why is the LAC the only 1.4 Ga anorthosite complex exposed in the western United States despite the voluminous nature of the magmatism produced at this time?

Perhaps the absence of 1.4 Ga granites from the Wyoming province and the location of the LAC are

not coincidental. Instead, they may be closely related to crustal structure. It has been argued that mantle temperatures were significantly greater during the Archean (Bickle, 1986). This would result in thick lithospheric roots that had been melted and depleted relative to the rest of the mantle. These roots may have affected the later tectonic evolution of the Archean cratons (Groves and others, 1987). We suggest that 1.4 Ga igneous rocks are not seen in the Wyoming province because either the Archean craton was resistant to the tectonic processes that were operating at 1.4 Ga, or the lithosphere under the Archean craton was more resistant to melting.

There are two possible reasons why 1.4 Ga anorthositic rocks are exposed in southeastern Wyoming and not elsewhere in the western United States. One possibility is that the area in southeastern Wyoming has been eroded to greater depths, allowing the exposure of anorthosite that was emplaced at mid-crustal levels. It is equally possible that the presence of a major crustal weakness in southeastern Wyoming, the Cheyenne belt, allowed the mafic magmas of the LAC to ascend to shallower depths in the crust than elsewhere in the 1.4 Ga magmatic province.

Tectonic significance

The geobarometric results from both the contact metamorphic aureoles around the LAC and the evolved rocks of the complex raise some very interesting questions. In traversing from the northern contact of the Red Mountain pluton to the Maloin Ranch pluton, there is an apparent increase in pressure from about 3 kilobars to more than 4 kilobars. This implies that the LAC has been tilted and that the southern portions are more deeply eroded than the northern portions. In contrast, the ring dike complex at Virginia Dale is interpreted to be subvolcanic in nature (Eggler, 1968), although the exact pressure is not known. Furthermore, there is some indication that the hornfelses at the southern margin of the LAC have been overprinted by lower pressure assemblages that where produced by contact metamorphism from the Sherman batholith (Xirouchakis, 1991). The apparent difference in pressure, and hence depth, between the LAC and the Sherman batholith may have great significance with regard to the tectonic environment in which these intrusive bodies formed.

The barometry suggests that there may have been a tectonic denudation event that brought the LAC up to shallow crustal levels during the short time interval between the emplacement of the LAC and Sherman batholith. Structural features reflecting this inferred denudation have not yet been identified, although they may have been completely obliterated by the intrusion of the Sherman batholith. These observations, along with structural evidence of strike-slip deformation in central Colorado at 1.4 Ga (Graubard, 1990), suggest that the crust may have been tectonically active at the time of emplacement of the LAC and Sherman batholith.

Acknowledgments

We are indebted to many people who have contributed to this project. George Snyder generously made his maps, his knowledge, and his Scotch available to us. James Grant contributed greatly to the mapping of the contact aureoles. Carl Anderson, Leslie Bolsover, Mimi Fuhrman, Rosamund Kinzler, Allan Kolker, Bill Meurer, Jean Nealon, and Carol Russ-Nabelek all assisted with the mapping. We thank them all. We are especially grateful to the Earth Sciences Division, National Science Foundation, for a series of grants that made this work possible: EAR 8207433, 8409663, 8617812, and 8816604 to BRF and CDF; EAR 8207423, 8409665, 8614840, and 8816040 to DHL. We thank Fred Barker and Tony Morse for thorough and perceptive reviews.

References cited

Aleinikoff, J.N., 1983, U-Th-Pb systematics of zircon inclusions in rock-forming minerals: a study of armoring against isotopic loss using the Sherman granite of Colorado-Wyoming, USA: Contributions to Mineralogy and Petrology, v. 83, p. 259-269.

Allmendinger, R.W., Brewer, J.A., Brown, L.D., Kaufman, S. Oliver, J.E., and Houston, R.S., 1982, COCORP profiling across the Rocky Mountain Front in southern Wyoming, Part 2: Precambrian basement structure and its influence on Laramide deformation: Geological Society of America Bulletin, v. 93, p. 1253-1263.

Anderson, I.C., Frost, B.R., and Lindsley, D.H., 1987, Crystallization conditions of the Red Mountain syenite: EOS, v. 68, p. 442-443.

Anderson, I.C., Geist, D.J., Frost, B. R., and Lindsley, D.H., 1988, Rare earth depletion during late-stage fractionation, Red Mountain Pluton, Laramie Anorthosite Complex, Wyoming: EOS, v. 69, p. 524.

Anderson, J.L., 1983, Proterozoic anorogenic granite plutonism of North America, *in* Medaris, L.G., Jr., Byers, C.W., and others, editors, Proterozoic geology: selected papers from an international Proterozoic symposium: Geological Society of America Memoir 161, p. 133-154.

Anderson, J.L., and Thomas, W.M., 1985, Proterozoic anorogenic two-mica granites: Silver Plume and St. Vrain batholiths of Colorado: Geology, v. 13, p. 177-180.

Ashwal, L.D., 1982, Mineralogy of mafic and Fe-Ti oxide-rich differentiates of the Marcy anorthosite massif, Adirondacks, New York: American Mineralogist, v. 67, p. 14-27.

Barker, F., 1981, Introduction to special issue on granites and rhyolites: A commentary for the nonspecialist: Journal of Geophysical Research, v. 86, p. 10,131-10,135.

Barker, F., Wones, D.R., Sharp, W.N., and Desborough, G.A., 1975, The Pikes Peak batholith, Colorado Front Range, and a model for the origin of the gabbro-anorthosite-syenite-potassic granite suite: Precambrian Research, v. 2, p. 97-160.

Bickle, M.J., 1986, Implications of melting for stabilisation of the lithosphere and heat loss in the Archean: Earth and Planetary Science Letters, v. 80, p. 314-324.

Bochensky, P., 1982, Contact metamorphic effects of the Laramie Anorthosite Complex at Morton Pass, Wyoming [M.S. thesis]: Laramie, University of Wyoming, 58 p.

Bolsover, L.R., 1986, Petrogenesis of the Sybille iron-titanium oxide deposit, Laramie Anorthosite Complex, Laramie Mountains, Wyoming [M.S. thesis]: Stony Brook, State University of New York at Stony Brook, 78 p.

Brewer, J.A., Allmendinger, R.W., Brown, L.D., Kaufman, S., and Oliver, J.E., 1982, COCORP profiling across the Rocky Mountain Front in southern Wyoming, Part 1: Laramide structure: Geological Society of America Bulletin, v. 93, p. 1242-1252.

Bridgwater, D., and Windley, B.F., 1973, Anorthosites, post-orogenic granites, acid volcanic rocks and crustal development in the North Atlantic shield during the mid-Proterozoic: Geological Society of South Africa Special Publication 3, p. 307-317.

Darton, N.H., Blackwelder, E., and Siebenthal, C.E., 1910, Laramie-Sherman folio: U.S. Geological Survey Geologic Atlas of The United States, Folio 173.

DeVore, G.W., 1975, The role of partial melting of metasediments in the formation of the anorthosite-norite-syenite complex, Laramie Range, Wyoming: Journal of Geology, v. 83, p. 749-762.

Duchesne, J.C., 1984, Massif anorthosites: another partisan review, *in* Brown, W.L., editor, Feldspars and feldspathoids: D. Reidel Publishing Company, p. 411-433.

_____ 1990, Origin and evolution of monzonorites related to anorthosites: Schweizerische Mineralogische und Petrographische Mitteilungen, v. 70, p. 189-198.

Duebendorfer, E.M., and Houston, R.S., 1987, Proterozoic accretionary tectonics at the southern margin of the Archean Wyoming craton: Geological Society of America Bulletin, v. 98, p. 554-568.

Eberle, M.M.C., 1983, Genesis of the magnetite-ilmenite deposit at Iron Mountain, Laramie Anorthosite Complex, Wyoming [M.S. thesis]: Boulder, University of Colorado, 114 p.

Eggler, D.H., 1968, Virginia Dale Precambrian ring-dike complex, Colorado-Wyoming: Geological Society of America Bulletin, v. 79, p. 1545-1564.

Emslie, R.F., 1978, Anorthosite massifs, rapakivi granites, and late Proterozoic rifting in North America: Precambrian Research, v. 7, p. 61-98.

_____ 1985, Proterozoic anorthosite massifs, *in* Tobi, A.C., and Touret, J.L.R., editors, The deep Proterozoic crust in the North Atlantic provinces: D. Reidel Publishing Company, p. 39-60.

Epler, N.A., 1987, Experimental study of Fe-Ti oxide ores from the Sybille pit in the Laramie anorthosite, Wyoming [M.S. thesis]: Stony Brook, State University of New York at Stony Brook, 67 p.

Ferris, C.S., and Krueger, H.W., 1964, New radiogenic dates on igneous rocks from the southern Laramie Range, Wyoming: Geological Society of America Bulletin, v. 75, p. 1051-1054.

Fountain, J.C., Hodge, D.S., and Hills, F.A., 1981, Geochemistry and petrogenesis of the Laramie Anorthosite Complex, Wyoming: Lithos, v. 14, p. 112-132.

Fowler, K.S., 1930, The anorthositic area of the Laramie Mountains: American Journal of Science, v. 219, p. 373-405.

Frey, E., 1946, Exploration of Iron Mountain titaniferous magnetite deposits, Albany County, Wyoming: U.S. Bureau of Mines Report of Investigations 3968, 37 p.

Frost, B.R., Lindsley, D.H., and Andersen, D.J., 1988, Fe-Ti oxide - silicate equilibria: Assemblages with fayalitic olivine: American Mineralogist, v. 73, p. 727-74.

Frost, B.R., and Touret, J.L.R., 1989, Magmatic CO_2 and saline melts from the Sybille monzosyenite, Laramie Anorthosite Complex, Wyoming: Contributions to Mineralogy and Petrology, v. 103, p. 178-186.

Frost, B.R., Fyfe, W.S., Tazaki, K., and Chan, T., 1989a, Grain-boundary graphite in rocks and implications for high electrical conductivity in the lower crust: Nature, v. 340, p. 134-136.

Frost, B.R., Lindsley, D.H., and Simmons, C., 1989b, Origin and evolution of anorthosites and related rocks: Geology, v. 17, p. 474-475.

Frost, B.R., and Simons, J.P., 1991, Fe-Ti oxide deposits of the Laramie Anorthosite Complex: their geology and proposed economic utilization, *in* Frost, B.R., and Roberts S., editors, Wyoming Geological Association, 42nd Annual Field Conference Guidebook, p. 41-48.

Frost, C.D., and Frost, B.R., 1989, Sr and Nd isotopic effects of CO_2-streaming in dehydrated amphibolite, Morton Pass, Wyoming: Geological Society of America Abstracts with Programs, v.21, p. A85-A86.

Frost, C.D., Meier, M., and Oberli, F., 1990, Single zircon U-Pb age determination of the Red Mountain Pluton, Laramie Anorthosite Complex, Wyoming: American Mineralogist, v. 75, p. 21-26.

Fuhrman, M.L., 1986, The petrology and mineral chemistry of the Sybille monzosyenite and the role of ternary feldspars [Ph.D. dissertation]: Stony Brook, State University of New York at Stony Brook, 214 p.

Fuhrman, M.L., Frost, B.R., and Lindsley, D.H., 1988, Crystallization conditions of the Sybille monzosyenite, Laramie Anorthosite Complex, Wyoming: Journal of Petrology, v. 29, p. 699-729.

Geist, D.J., Frost, C.D., Kolker, A., and Frost, B.R., 1989, A geochemical study of magmatism across a major terrane boundary: Sr and Nd isotopes in Proterozoic granitoids of the southern Laramie Range, Wyoming: Journal of Geology, v. 97, p. 331-342.

Geist, D.J., Frost, C.D., and Kolker, A., 1990, Sr and Nd isotopic constraints on the origin of the Laramie Anorthosite Complex, Wyoming: American Mineralogist, v. 75, p. 13-20.

Goldberg, S.A., 1984, Geochemical relationships between anorthosite and associated iron-rich rocks, Laramie Range, Wyoming: Contributions to Mineralogy and Petrology, v. 87, p. 376-387.

Grant, J.A., and Frost, B.R., 1986, Decompression, metamorphism and melting in the aureole of the Laramie Anorthosite Complex: Geological Society of America Abstracts with Programs, v. 18, p. 620.

_____ 1990, Contact metamorphism and partial melting of pelitic rocks in the aureole of the Laramie Anorthosite Complex, Morton Pass, Wyoming: American Journal of Science, v. 290, p. 425-472.

Graubard, C.M., 1990, Tectonic control of internal structure and differentiation of the 1,440 Ma Mt. Evans batholith, central Front Range, Colorado: Geological Society of America Abstracts with Programs, v. 23, no. 4, p. A245.

Groves, D.I., Ho, S.E., Rock, N.M.S., Barley, M.E., and Muggeridge, M.T., 1987, Archean cratons, diamond, and platinum: Evidence for coupled long-lived crust-mantle systems: Geology, v. 15, p. 801-805.

Harrison, J.E., 1951, Relationship between structure and mineralogy of the Sherman granite, southern part of the Laramie Range, Wyoming-Colorado [Ph.D. dissertation]: Urbana, Illinois University, 79 p.

Hayden, F., 1871, Preliminary report of the United States Geological Survey of Wyoming and portions of contiguous Territories, 511 p.

Higgins, M.D., 1981, Origin of acidic anorogenic rocks, crust or mantle?: EOS, v. 62, p. 437.

Hild, J.H., 1953, Diamond drilling on the Shanton magnetite-ilmenite deposits, Albany County, Wyoming: U.S. Bureau of Mines Report of Investigations 5012, 17 p.

Hodge, D.S., Smith, B.S., and Smithson, S.B., 1970, Quantitative geophysical study of petrogenesis of syenites related to Laramie Anorthosite, Wyoming, U.S.A.: Lithos, v. 3, p. 237-250.

Hodge, D.S., Owen, L.B., and Smithson, S.B., 1973, Gravity interpretation of the Laramie Anorthosite Complex, Wyoming: Geological Society of America Bulletin, v. 84, p. 1451-1464.

Houston, R.S., and others, 1968, A regional study of rocks of Precambrian age in that part of the Medicine Bow Mountains lying in southeastern Wyoming—with a chapter on the relationship between Precambrian and Laramide structure: Geological Survey of Wyoming Memoir No. 1, 167 p.

Irvine, T.N., 1974, Petrology of the Duke Island ultramafic complex, southeastern Alaska: Geological Society of America Memoir 138, 240 p.

_____ 1987, Layering and related structures in the Duke Island and Skaergaard intrusions: Similarities, differences, and origins, *in* Parsons, I., editor, Origins of igneous layering: D. Reidel Publishing Company, p. 185-245.

Irvine, T.N., and Baragar, W.R.A., 1971, A guide to the chemical composition of the common volcanic rocks: Canadian Journal of Earth Sciences v. 8, p. 523-548.

Karlstrom, K.E., and Houston, R.S., 1984, The Cheyenne belt: analysis of a Proterozoic suture in southern Wyoming: Precambrian Research, v. 25, p. 415-446.

Kling, J.F., 1986, Petrology of the Strong Creek prospect, Albany County, Wyoming and in the system Fe-Ti-Si-O-S [M.S. thesis]: Laramie, University of Wyoming, 109 p.

Klugman, M.A., 1966, Resume of the geology of the Laramie anorthosite mass: The Mountain Geologist, v. 3, p. 75-84.

Kolker, A., 1989, Petrology and geochemical evolution of the Maloin Ranch pluton, Laramie Anorthosite Complex, Wyoming [Ph.D. dissertation]: Stony Brook, State University of New York at Stony Brook, 211 p.

Kolker, A., and Lindsley, D.H., 1989, Geochemical evolution of the Maloin Ranch pluton, Laramie Anorthosite Complex, Wyoming: petrology and mixing relations: American Mineralogist, v. 74, p. 307-324.

Kolker, A., Lindsley, D.H., and Hanson, G.N., 1990, Geochemical evolution of the Maloin Ranch pluton, Laramie Anorthosite Complex, Wyoming: trace elements and petrogenetic models: American Mineralogist, v. 75, p. 572-588.

Kolker, A., Frost, C.D., Hanson, G.N., and Geist, D.J., 1991, Nd, Sr and Pb isotopes in the Maloin Ranch pluton, Wyoming: implications for the origin of evolved rocks at anorthosite margins. Geochimica et Cosmochimica Acta, v. 55, p. 2285-2297.

Lindsley, D.H., 1983, Pyroxene thermometry: American Mineralogist, v. 68, p. 477-493.

Lindsley, D.H., and Emslie, R.F., 1968, Effect of pressure on the boundary curve in the system diopside-albite-anorthite: Carnegie Institute of Washington Yearbook, v. 66, p. 479-480.

Lindsley, D.H., Frost, B.R., Andersen, D.J., and Davidson, P.M., 1990, Fe-Ti oxide - silicate equilibria: assemblages with orthopyroxene, *in* Spencer, R. J., and Chou, I. -M., editors., Fluid-mineral interactions: a tribute to H.P. Eugster: The Geochemical Society, Special Publication No. 2, p. 103-119.

Lindsley, D.H., and Frost, B.R., 1990, Fe-Ti oxide deposits: A part of the "missing" residual liquid from the Laramie Anorthosite Complex: Geological Society of America Abstracts with Programs, v. 22, no. 7, p. A300.

Livi, K.J.T., 1987, Geothermometry of exsolved augites from the Laramie Anorthosite Complex, Wyoming: Contributions to Mineralogy and Petrology, v. 96, p. 371-380.

Longhi, J., and Ashwal, L.D., 1985, Two-stage model for lunar and terrestrial anorthosites: petrogenesis without a magma ocean, *in* Proceedings of the 15th Lunar and Planetary Science Conference, part 2; Journal of Geophysical Research, v. 90, supplement, p. C571-C584.

Marlatt, G., 1989, Geology of a Precambrian igneous/metamorphic sequence, Laramie Range, Wyoming [M.S. thesis]: Laramie, University of Wyoming, 80 p.

McCullough, P.T.P., 1974, Origin of the Ragged Top gneisses, Laramie Range, Wyoming [Ph.D. dis-

sertation]: Urbana, University of Illinois at Urbana-Champaign, 139 p.

Meurer, W.P., 1990, Magma mixing in the composite dikes of the Laramie Anorthosite Complex, Wyoming [M.S. thesis]: Stony Brook, State University of New York at Stony Brook, 252 p.

Miller, J.D. Jr., and Weiblen, P.W., 1990, Anorthositic rocks of the Duluth Complex: examples of rocks formed from plagioclase crystal mush: Journal of Petrology, v. 31, p. 295-339.

Mitchell, J.N., Frost, B.R., and Frost, C.D., 1990, Petrogenesis of the Greaser gabbro, Laramie Anorthosite Complex, Wyoming: Geological Society of America Abstracts with Programs, v. 22, no. 7, p. A300.

Morse, S.A., 1982, A partisan review of Proterozoic anorthosites: American Mineralogist, v. 67, p. 1082-1100.

Morse, S.A., and Nolan, K.M., 1985, Kiglapait geochemistry VII: yttrium and the rare earth elements: Geochimica et Cosmochimica Acta, v. 49, p. 1621-1644.

Nealon, J.M., 1988, Composite dikes in the Poe Mountain Quadrangle, Laramie Anorthosite Complex, Laramie Mountains, Wyoming [M.S. thesis]: Stony Brook, State University of New York at Stony Brook, 125 p.

Newhouse, W.H., and Hagner, A.F., 1957, Geologic map of anorthosite areas, southern part of the Laramie Range, Wyoming: U.S. Geological Survey, Mineral Investigations Field Studies MF-119, scale 1:63,360.

Nowak, F.J., 1970, Geology of the Baldy Mountain norite, Albany County, Wyoming [M.S. thesis]: Urbana, University of Illinois, 50 p.

Phinney, W.C., 1982, Petrogenesis of Archean anorthosites, *in* Walker, D., and McCallum, I.S., editors, Workshop on magmatic processes of early planetary crusts: magma oceans and stratiform layered intrusions: Lunar and Planetary Institute Technical Report 82-01, p. 121-124.

Ramarathnam, S., 1962, Geology and petrology of the southern portion of the Laramie anorthosite mass [Ph.D. dissertation]: Golden, Colorado School of Mines, 131 p.

Russ-Nabelek, C.A., 1989, Isochemical contact metamorphism of mafic schist, Laramie Anorthosite Complex, Wyoming: American Mineralogist, v. 73, p. 530-548.

Scoates, J.S., 1990, Syn-magmatic deformation of anorthosite: an assessment of the subsolidus evolution of anorthositic rocks in the 1.4 Ga Laramie Anorthosite Complex, Wyoming: Geological Society of America Abstracts with Programs, v. 22, no. 7, p. A300.

Scoates, J.S., and Lindsley, D.H., 1989, Primary layering and structures within a ca. 1.43 Ga massif anorthosite, Laramie Anorthosite Complex, S.E. Wyoming: Geological Association of Canada - Mineralogical Association of Canada Program with Abstracts, v. 14, p. A5.

Shand, S.J., 1927, The eruptive rocks: New York, John Wiley and Sons, 488 p.

Smith, B.D., Hodge, D.S., and Smithson, S.B., 1970, Geology and geophysics of syenites associated with the Laramie Anorthosite, Wyoming: University of Wyoming Contributions to Geology, v. 9, p. 27-38.

Smith, C.B., 1977, Kimberlite and mantle derived xenoliths at Iron Mountain, Wyoming [M.S. thesis]: Fort Collins, Colorado State University, 218 p.

Snyder, G.L., 1984, Preliminary geologic maps of the central Laramie Mountains, Albany and Platte Counties, Wyoming: United States Geological Survey Open-File Report 84-358, scale 1:24,000.

Speece, M.A., Frost, B.R., and Smithson, S.B., in review, Precambrian basement structure and Laramide deformation revealed by seismic reflection profiling in the Laramie Mountains, Wyoming: Tectonics.

Spicuzza, M.J., 1990, High-grade metamorphism and partial melting in the Bluegrass Creek suite, central Laramie Mountains, Wyoming [M.S. thesis]: Duluth, University of Minnesota-Duluth, 115 p.

Streckeisen, A.L., 1967, Classification and nomenclature of igneous rocks: Neues Jahrbuch fur Mineralogie Abhandlungen, v. 107, p. 144-240.

Subbarayudu, G.V., 1975, The Rb-Sr isotopic composition and origin of the Laramie anorthosite-mangerite complex, Laramie Range, Wyoming [Ph.D. dis-sertation]: Buffalo, State University of New York at Buffalo, 109 p.

Subbarayudu, G.V., Hills, F.A., and Zartman, R.E., 1975, Age and Sr isotopic evidence for the origin of the Laramie anorthosite-syenite complex, Laramie Range, Wyoming: Geological Society of America Abstracts with Programs, v. 7, p. 1287.

Wager, L.R., and Brown, G.M., 1967, Layered igneous rocks: Oliver and Boyd, Edinburgh and London, 588 p.

Wiebe, R.A., 1979, Fractionation and liquid immiscibility in an anorthositic pluton of the Nain complex, Labrador: Journal of Petrology, v. 20, p. 239-269.

Wiebe, R.A., 1980a, Commingling of contrasted magmas in the plutonic environment: examples from the Nain anorthosite complex: Journal of Geology, v. 88, p. 197-209.

_____ 1980b, Anorthositic magmas and the origin of Proterozoic anorthosite massifs: Nature, v. 286, p. 564-567.

_____ 1984, Commingling of magmas in the Bjerkrem-Sogndal lopolith (southwest Norway): evidence for the compositions of residual liquids: Lithos, v. 17, p. 171-188.

_____ 1990a, Dioritic rocks in the Nain complex, Labrador: Schweizerische Mineralogische und Petrographische Mitteilungen, v. 70, p. 199-208.

_____ 1990b, Evidence for unusually feldspathic liquids in the Nain Complex, Labrador: American Mineralogist, v. 75, p. 1-12.

Wiebe, R.A. and Wild, T., 1983, Fractional crystallization and magma mixing in the Tigalak layered intrusion, the Nain anorthosite complex, Labrador: Contributions to Mineralogy and Petrology, v. 84, p. 327-344.

Wilmart, E., DeMaiffe, D., and Duchesne, J.C., 1989, Geochemical constraints on the genesis of the Tellnes ilmenite deposit, southwest Norway: Economic Geology, v. 84, p. 1047-1056.

Xirouchakis, D., 1991, Contact metamorphism adjacent to the Laramie Anorthosite Complex, Albany County, Wyoming [M.S. thesis]: Duluth, University of Minnesota, Duluth, 100 p.

Zielinski, R.A., Peterman, Z.E., Stuckless, J.S., Rosholt, J.N., and Nkomo, I.T., 1981, The chemical and isotopic record of rock-water interaction in the Sherman Granite, Wyoming and Colorado: Contributions to Mineralogy and Petrology, v. 78, p. 209-219.

Part III

Paleozoic history

Frontispiece. Paleozoic section in Canyon Mouth anticline, a southeast-plunging fold north of Cody, Wyoming. To the right of the lower Triassic redbeds (Red Peak Formation), the skyline is formed by Pennsylvanian Tensleep Sandstone. To the right of the notch which coincides with the less resistant Amsden Formation, Mississippian limestone of the Madison Group forms the skyline to the right edge of the photograph. Below the Madison strata in the upper right, Devonian Three Forks and Jefferson formations are covered by forest. Below the forested slope are bright cliffs of Ordovician Bighorn Dolomite. Vegetated slopes below the cliffs are formed on the Upper Cambrian Gallatin Group and Middle Cambrian Gros Ventre Formation and Flathead Sandstone. The nonconformity between the Flathead Sandstone and Precambrian crystalline basement rocks is blocked from view by the promontory in the right foreground.

Paleozoic history of Wyoming

Donald W. Boyd
Department of Geology and Geophysics
University of Wyoming
Laramie, Wyoming 82071

Abstract

The Paleozoic Era began with Wyoming at the craton margin, above sea level, and near the equator. During the last half of the Cambrian Period, the sea advanced sporadically across the state, blanketing Precambrian rocks with sand and gravel. By the end of the period, when siliciclastic sediment finally covered the ancient crystalline rocks in northeastern Wyoming, the equivalent Cambrian facies in western Wyoming were buried under hundreds of feet of shale and limestone.

The state preserves little evidence of Early and Middle Ordovician deposition, but a Late Ordovician clear-water sea produced thick carbonate accumulations now represented by prominent cliffs of dolomite in northern and western Wyoming. Post-Ordovician erosion beveled the thick carbonate sequence from north to south, completely removing it from the southeastern area except for foundered blocks in small kimberlite diatremes near the Colorado border. Inclusions of Silurian marine fossils in a few diatremes prove that a sea covered the area sometime during the period.

By the time a Devonian sea invaded Wyoming, Silurian strata were lost to erosion and drainage systems had developed on older bedrock. Paleovalleys filled with estuarine strata record Early and Late Devonian transgressions. At the height of the Late Devonian transgression, marine deposition throughout the northern and western part of the state resulted in several hundred feet of Upper Devonian strata. Following a major regression, the sea returned to parts of Wyoming shortly before the Devonian Period ended and spread over most of the state in the ensuing period.

Wyoming's heritage from the warm, clear-water Mississippian sea is a wedge of carbonate strata thickening west and north from a zero edge in the southeast to more than 1,000 feet at the western border. Carbonate production on the Wyoming shelf was halted by a major regression that moved the shoreline to the western border of the state, and a prominent karst topography developed. The overlying Amsden Formation includes Mississippian and Pennsylvanian marine strata; it has been the center of a long controversy over lateral and vertical relations of its members.

Wind played a major role in distributing a thick blanket of Pennsylvanian sand over the Wyoming shelf, although some of it was reworked during occasional incursions of shallow seas. In eastern Wyoming, marine conditions were more continuous and carbonate environments more frequent. Meanwhile, arkosic fluviatile sediments spread into southeastern Wyoming from the north end of the ancestral Front Range.

Subaerial erosion that affected the central part of the state during the Pennsylvanian-Permian transition expanded to include the marginal areas where deposition had continued into Early Permian time. The state-wide erosion surface was subjected to aggradation as several contrasting depositional environments migrated back and forth over the region. This resulted in complex intertonguing of redbeds (east), carbonates (central), sandstone (northwest), and phos-

Boyd, D.W., 1993, Paleozoic history of Wyoming, *in* Snoke, A.W., Steidtmann, J.R., and Roberts, S.M., editors, Geology of Wyoming: Geological Survey of Wyoming Memoir No. 5, p. 164-187.

phatic and cherty strata (west). The absence of a prominent disconformity between Permian strata and overlying Triassic mudstones contrasts sharply with paleontological evidence of missing record at the close of the era.

Introduction

Humans have been examining Paleozoic rocks of the area we now call Wyoming for at least 10,000 years. For almost 99% of that time, investigations were limited to work by a few prospectors seeking to maintain or improve their quality of life in terms of projectile points, pigments, cave sites, and spring locations. Although these people published nothing aside from a few petroglyphs, the immigrants who followed them have, in the last century, produced an immense written record of observations and ideas about the rocks of interest here. The evidence they have interpreted represents all seven Paleozoic periods, albeit by no means equally (**Figure 1**). The following synthesis will not satisfy those who have mastered and(or) generated any significant part of that record, but it should be of use to those preparing to join that group and to those who are mildly interested in the topic but don't want to take their coats off.

The title should be taken literally; this is not an article on Paleozoic stratigraphy of the state. Although many important formations are mentioned by name, no attempt is made to review the many complexities of nomenclature that reflect different preferences on the part of stratigraphers separated by gen-

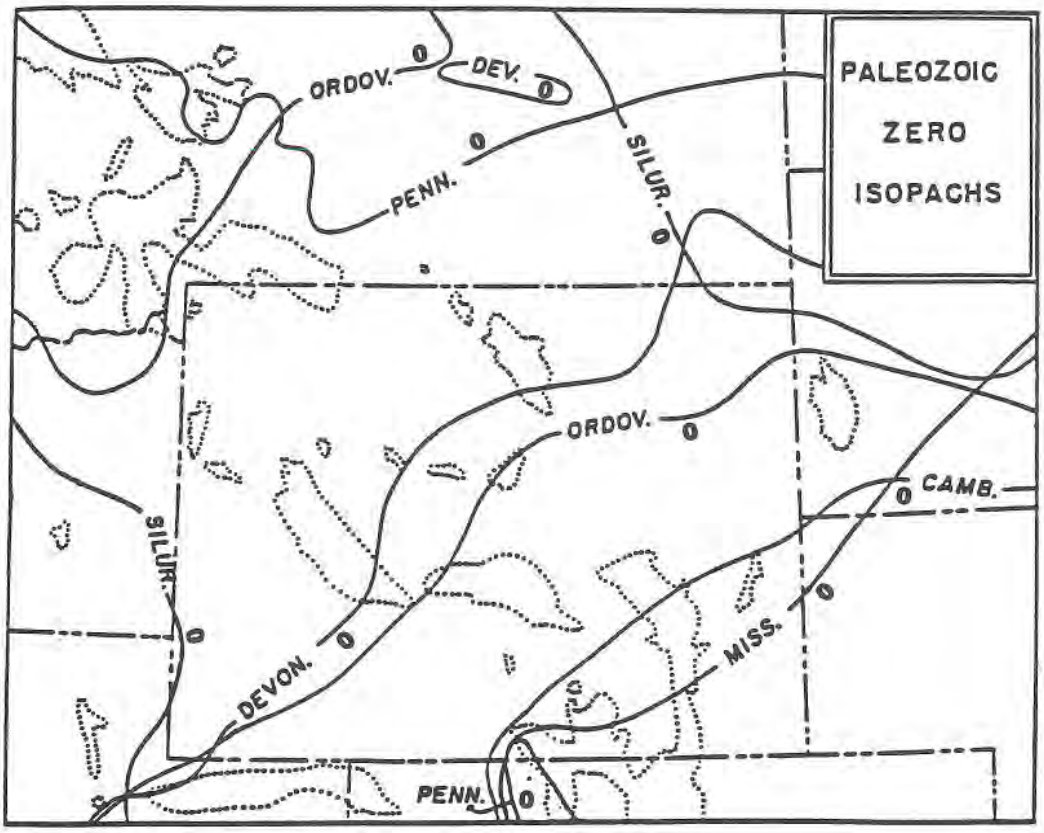

Figure 1. Distribution of Paleozoic zero isopachs in the Wyoming region. Permian strata were present throughout Wyoming at the close of the Paleozoic Era. [Reproduced from a paper by D.L. Blackstone, Jr.(1963), with addition of a zero on the side of each line where rocks of that age are absent. Incorporation of post-1963 information would change details, but not the basic pattern.]

eration, geographic location, and(or) philosophy. Likewise, little or no mention is made of many unresolved questions concerning correlation and detailed age assignment of individual stratigraphic units. Readers interested in these topics will find help in the bibliographies of the papers cited and from the correlation chart by Love and others included in the map pocket of this volume.

Although the references noted in this review represent only the tip of the iceberg, they provide entry to the wealth of literature on the Paleozoic geology of Wyoming. Some references not limited to a single geologic period can be mentioned at the beginning. The *Geologic Map of Wyoming* (Love and Christiansen, 1985) is accompanied by a description of stratigraphic units (sheet 2) and an extensive list of references (sheet 3). The large atlas published by the Rocky Mountain Association of Geologists (Mallory, 1972) provides several thickness and lithofacies maps for each system. Of several general surveys of regional Paleozoic history, recent ones by Peterson and Smith (1986) and Peterson (1987) are especially useful for the citations of previous literature. An interpretation of the Paleozoic history of southeastern Wyoming was provided by Sando and Sandberg (1987). The Paleozoic nomenclature and correlations shown in the 15 Wyoming columns of the American Association of Petroleum Geologists correlation chart for the central and southern Rockies region (Kent and others, 1988) differ only slightly from the terminology and age assignments utilized by Love and Christiansen (1985).

The annual guidebooks published by the Wyoming Geological Association since 1947 are a major source of information for those interested in the detailed geology of each Wyoming basin. For the regional picture outside Wyoming, the Rocky Mountain Association of Geologists' atlas cited above (Mallory, 1972) and volumes edited by Fouch and Megathan (1980) and Stewart and others (1980) are especially useful.

Cambrian Period

If we consider the Paleozoic record to have begun when the sea floor was first littered with tiny shells, then the place we call Wyoming was entirely above sea level at that time—a mosaic of ancient igneous and metamorphic rocks destined to remain in the erosional regime for another 30 million years. The terrain would have appeared desolate and inhospitable to a human eye, but there is no reason to believe it was lifeless. A microbial ecosystem involving photosynthetic and anaerobic bacteria no doubt flourished in the upper few millimeters of sediment, where the surface was not bare rock. Members of this microbiota functioned as binders of surface sediment as well as producers of various gases before the advent of more complex terrestrial communities.

Given its early Paleozoic location on the craton but near a passive continental margin, Wyoming differed greatly from the region now west of it in relative subsidence and in thickness of accumulating sediments. The Cambrian record demonstrates the hinge-like behavior of the western margin of the state, which separated the Wyoming platform from the developing miogeocline of Utah and Idaho. There, a thick record of Lower Cambrian marine strata accumulated while the transgressing sea moved toward Wyoming. Although the basal Cambrian strata lack age-diagnostic fossils, circumstantial evidence indicates that the shoreline had not reached Wyoming before Middle Cambrian time.

For the next 30 million years, the remainder of the Cambrian Period, the sea advanced sporadically eastward while the shoreline maintained a general north-south trend. These directional terms refer, of course, to present geography. This frame of reference is attractive because of its familiarity and because the Paleozoic geography is so imperfectly known. It must be remembered, however, that interpretations of Cambrian geography typically picture Wyoming near the equator and rotated 60° or more dextrally from its present orientation (Scotese and McKerrow, 1990).

By the end of the period, the Precambrian rocks were blanketed by siliciclastic deposits (**Figure 2**) whose progressive decrease in age from west to east reflects their transgressive origin. The surface across which they spread was dimpled with low hills—a few stood as much as 300 feet above the deepest valleys—so at any one time the advancing strandline formed an irregular border to a seascape dotted with islands.

Figure 2. Nonconformity between Middle Cambrian crossbedded sandstone (Flathead Sandstone) and Precambrian granite, Wind River Canyon, north-central Wyoming. Hammerhead for scale on contact at left center.

The blanket of pebbles, granules, and sand reached a maximum thickness of between 500 and 600 feet. Lateral variation in thickness of the Flathead Sandstone, as these deposits are termed in most of the state, reflect both the irregular surface on which it accumulated and its intertonguing relationship with the dominantly shale sequence above it. Typical Flathead outcrops are reddish brown conglomerates and sandstone with abundant cross stratification in various styles. Most of these rocks are compositionally and texturally mature, but arkosic beds are present. Skeletal material is rare, although trilobite parts and inarticulate brachiopods have been found. Vertical dwelling burrows are abundant in some units.

A detailed analysis of bedding and lithology of Flathead strata (Middleton and others, 1980) indicates that most of the formation originated in nearshore and shallow shelf depositional environments. Common bedforms imply origin as subtidal sand-wave complexes migrating offshore under the influence of storm-surge and tidal currents. Other forms and orientations of cross stratification represent local preservation of beach and intertidal sandflat deposits. By contrast, the sedimentological immaturity and bedding geometry of basal strata in south-central Wyoming suggest an origin as transverse bars and channel deposits in braided streams.

Precambrian rocks in northeastern Wyoming were finally covered by sand in Late Cambrian time. These deposits are referred to the Deadwood Formation, a name that originated during early work on the stratigraphic sequence flanking the Black Hills. By the time the Deadwood siliciclastic deposits were accumulating, the Flathead Sandstone of western Wyoming was buried beneath hundreds of feet of shale and limestone (**Figure 3**). Just as grain size typically decreases from bottom to top in Flathead strata at any one locality, so the overall Cambrian record in western Wyoming is a fining-upward sequence. Two hundred or more feet of coarse clastic rocks of the Flathead are overlain by an 800-foot section dominated by shale (Gros Ventre Formation). The succeeding 300-foot interval, representing the rest of the Cambrian record in this area, consists mainly of limestone (Gallatin Formation).

The simple picture of a transgressive sequence, in which superposed lithologies represent deposition successively farther from shore, is valid as a generalization, but stratigraphic details dictate a more complicated story. Limestones interrupting the Gros Ventre shales imply recurrent changes in pace of the transgression; shales in the Gallatin Limestone interval and minor disconformities record temporary retreats of the sea.

Although western Wyoming was farther and farther seaward during successive transgressive maxima, the Cambrian record there is not one of progressively deeper marine environments. At times when the advancing shoreline placed this area beyond reach of land-derived sediment, carbonate pro-

Figure 3. West side of Wind River Canyon, north-central Wyoming. Precambrian metamorphic rocks and granitic dike (railroad cut) overlain by Cambrian sandstone, shale, and limestone (tree-covered slope); white cliffs at top are Ordovician Bighorn Dolomite overlain by Mississippian Madison Limestone.

duction in the clear, warm water could more than compensate for the loss of siliciclastic material. Such times were increasingly common during the Late Cambrian, and carbonate shoals and intertidal flats veneered with algal mats occasionally developed seaward of the shallow subtidal seafloor undergoing mixed carbonate-siliciclastic sedimentation.

The record of the carbonate buildups is in the limestone ledges and cliffs that dominate Upper Cambrian outcrops in western Wyoming. These rocks are composed mainly of micrite and disarticulated parts of trilobites, echinoderms, and brachiopods. Grains of glauconite are common, and form the bulk of some beds. Prominent stromatolites cap a limestone member of the Gros Ventre Formation and these distinctive structures reappear in the Gallatin limestones. In both formations, beds of flat limestone pebbles are common and conspicuous.

The intraformational limestone conglomerates deserve special mention as perhaps the most distinctive rock in the Cambrian sequence. The tabular clasts of laminated micrite are typically an inch or less thick and several inches in maximum length. They form discontinuous beds, commonly less than a foot thick, interbedded with bioclastic limestone, calcareous siltstone, and green shale. Two generations of clasts, distinguishable by degree of rounding and oxidation, are present in some layers. Clast orientation varies from random to strongly imbricate—the edgewise conglomerates of some authors. Interpretations of origin typically invoke early hardening of thin layers of lime mud by desiccation on tidal flats or by subaqueous cementation. In either case, the brittle layers were susceptible to fragmentation by storm-generated currents that tumbled the pieces and finally concentrated them in a layer as hydraulic energy waned.

Stratigraphic nomenclature for Wyoming's Cambrian strata consists mainly of names that originated in southwestern Montana (e.g., Gallatin Group) and northwestern Wyoming (e.g., Gros Ventre Formation). In these areas, the basal coarse-clastic section (Flathead Sandstone) is overlain by a succession of thick units, each of which represents a period when either clay and silt deposition or carbonate sedimentation prevailed. Over the years, names have been proposed for each major unit and for combinations thereof. Thus, the Gros Ventre Formation overlying the Flathead is a package of three members (shale-limestone-shale) followed stratigraphically by two predominantly carbonate formations comprising the Gallatin Group.

The body of literature dealing with these rocks presents a kaleidoscopic scene, in which familiar names repeatedly change in rank (member, formation, or group) or undergo expansion or contraction in stratigraphic and geographic limits. The nomenclature problem is exacerbated by the fact that the limestone intervals give way to shale and siltstone to the east and south. As the carbonate units lose their identity in these directions their names become inapplicable, and placement of formation and group boundaries that is easily done in northwestern Wyoming becomes very subjective. As might be expected, several names have been introduced for parts of the

post-Flathead sequence of central Wyoming. Their lack of general acceptance is symbolized by their absence from the explanation sheet accompanying the latest geological map of Wyoming (Love and Christiansen, 1985).

Cambrian biostratigraphy is based on a succession of trilobite assemblages, of which certain genera have proven to be more valuable than others. Although they are in no sense evenly distributed in Wyoming Cambrian strata, trilobites have provided the basis for relating the mosaic of lithostratigraphic units to the series and stages of the standard Cambrian time scale. For example, the first appearance of certain taxa in the upper Gros Ventre Formation dictates placement of the boundary between Middle and Upper Cambrian within the formation rather than at its base or top.

A search for trilobites produces only frustration at many outcrops, whereas their skeletal debris is a major component of the rocks elsewhere. Complete skeletons are rare; the components typically came apart during molting or, to a greater extent, through postmortem action of scavengers and currents. Fortunately, many genera can be recognized by the morphology of one part of the original skeleton, typically the cranidium.

The succession of trilobite zones recognized in the Cambrian of the western U.S. has been established empirically, but the reason for recurrent extinctions is not understood. A few of these biostratigraphic boundaries are especially dramatic, in that a preexisting assemblage is replaced by a new one within a stratigraphic interval of inches. A detailed study of one of these boundaries in central Wyoming (Chronic, 1988) indicates that the extinctions and first appearances of trilobite taxa coincided with a modest increase in overall faunal abundance and diversity. This suggests that a subtle change in water temperature or chemistry was fatal to the preexisting trilobite assemblage, while favoring other species that were adapted to the new conditions.

By the end of the period, Cambrian strata formed a continuous cover over Wyoming with the possible exception of the southeastern area that borders the Transcontinental arch. This term is commonly used for a broad belt, characterized by positive crustal behavior, extending between Minnesota and the New Mexico-Arizona area. Although its relief was always subdued and its borders ill defined, the feature influenced lithofacies, biofacies, and thicknesses of stratigraphic units to varying degrees during much of the Paleozoic Era.

Maps showing lithofacies and paleogeography of the Wyoming region at various times in the Cambrian are featured in several publications by Lochman-Balk (e.g., 1972). Middleton and others (1980) provided an excellent review of Wyoming Cambrian sedimentology, with emphasis on the siliciclastic rocks. An example of detailed interpretation of Cambrian carbonates is that of Martin and others (1980), whereas Chronic's (1988) documentation of faunal changes bracketing one extinction event illustrates the type of detailed work needed in Cambrian biostratigraphy.

Ordovician Period

A hypothetical geologist whose knowledge of lower Paleozoic stratigraphy was limited to the Wyoming record might be excused for questioning the applicability of Sloss' (1963) sequence scheme. That seminal paper, based on craton-wide analysis, emphasized the separate identities of two major packages of lower Paleozoic strata termed the Sauk and Tippecanoe sequences. The former includes Cambrian and Lower Ordovician beds, whereas the latter consists of Middle Ordovician through Lower Devonian strata. The two are bounded, as are the other sequences in Sloss' stratigraphic synthesis, by craton-wide unconformities.

The only places in Wyoming where one can find a record of continuous deposition across the Cambrian-Ordovician boundary are in the northeastern and north-central parts of the state. There, a minimal record of Lower Ordovician strata is present in the upper parts of the Deadwood and Gallatin formations. The sandstones and limestones that yield Lower Ordovician conodonts are lithologically like those comprising the lower parts of the two formations; the systemic boundary is intraformational and conformable. Elsewhere in Wyoming where the two systems are in contact, a disconformity separates Upper Ordovician strata (typically) or Middle Ordovi-

cian strata (less commonly) from the underlying Cambrian.

Although the Lower Ordovician evidence in the upper Deadwood and Gallatin formations is inconspicuous and geographically localized, it contributes to the regional paleogeographic picture dictated by evidence from surrounding states. The combined evidence supports the concept of continuous marine sedimentation from Late Cambrian through Early Ordovician time over much of Wyoming.

The state preserves little evidence of the sand that spread southward over much of the central and western U.S. (e.g., St. Peter Sandstone) in Middle Ordovician time. A 25-foot thickness of red and white sandstone unconformably overlying the Gallatin Formation in northern Wyoming is correlated with the Winnipeg Sandstone of the Williston basin and the Harding Sandstone of Colorado. It resembles the latter unit in yielding abundant small fragments of dermal plates of primitive fish. There is no way to know how much of this sandstone was eroded before deposition of the Bighorn Dolomite, which unconformably overlies it and extends far beyond its southern limit.

The new depositional phase, represented by the Bighorn Dolomite, was associated with the Late Ordovician transgression generally regarded as the greatest inundation in North American history. With the sand supply effectively stopped, the tropical sea covering Wyoming was floored by carbonate sediments. The mud was littered with skeletal material produced by diverse communities of brachiopods, rugose and tabulate corals, large orthocone nautiloids, gastropods as much as half a foot in diameter, and the picturesque receptaculitids currently interpreted as skeleton-building algae.

The Bighorn Dolomite forms nearly all of the 500 feet of Ordovician strata preserved in northern Wyoming. The formation is fairly uniform in degree of dolomitization, but four members have been differentiated on other characteristics. Toward the bottom of the formation, the dolomite commonly grades downward into a few feet of sandstone. This basal member, known as the Lander Sandstone, contains fossils that place it with the rest of the Bighorn as Upper Ordovician. It can, however, be confused with the Winnipeg, from which it was probably derived. The two sandstones are separated by a disconformity, but the Lander is present in some parts of northern and western Wyoming beyond the limit of Winnipeg preservation.

The prominent cliffs formed by the Bighorn Dolomite (**Figure 3**) in northern and western Wyoming

Figure 4. Part of Bighorn Dolomite (Ordovician) exposed in northwest Bighorn Mountains. Jacob staff in left foreground rests against typical fretted weathered surface.

reflect the massive character of the thick (250 feet) carbonate member overlying the Lander. Weathered faces (**Figure 4**) of this distinctive unit, the lowest of three carbonate members, exhibit a complex network of ridges. Of various theories proposed to explain the distinctive relief, the most likely one invokes different resistance to weathering on the part of abundant burrow fillings and intervening matrix.

Significant intercrystalline porosity makes the formation a reservoir in several oil fields of the thrust belt and the Bighorn Basin. The present areal extent in Wyoming of the several carbonate members of the Bighorn Dolomite is the result of post-Ordovician erosion, which beveled the thick carbonate sequence from north to south. Ordovician rocks were completely removed from southeastern Wyoming except for carbonate blocks that foundered in small kimberlite diatremes near the Colorado border.

The fossils reported by Chronic and others (1969) from the diatreme blocks include a diverse, normal-marine, Late Ordovician fauna dominated by brachiopods and corals. The faunal lists are less conclusive in supporting the theory that older Ordovician sediments also covered the area. Diatreme fossils with affinities to known Early Ordovician taxa include hyoliths, a small nautiloid, a gastropod, and a trilobite segment. A piece of sandstone yielded a fragment of a fish plate like those found in Middle Ordovician rocks.

The reader will find more detailed regional reviews of Ordovician history in publications by Foster (1972) and Ross (1976).

Silurian Period

On a pleasant summer day in 1954, Clinton (Nick) Ferris, Jr. stepped out of a southern Wyoming hay meadow and into the lore of Rocky Mountain paleontology. Taking a break from the haying operation on his family's ranch, young Ferris, then a geology student at Colorado College, indulged his interest in rocks by collecting fossils from a boulder-strewn slope near the meadow (**Figure 5**). The site

Figure 5. Ferris diatreme and surroundings, south of Laramie. Diatreme rocks form the sagebrush-covered knoll immediately beyond the pond, extending from the hay meadow (left) to the right edge of the picture. Hills in the upper half of photo and the steep slope between camera and pond are Precambrian granite.

subsequently gained renown among regional paleontologists and stratigraphers as the Ferris outlier, the only Silurian rocks for 300 miles in any direction.

The circle of professional interest broadened dramatically when evidence of ultramafic rock caused the fault-block explanation for the site to be replaced by the kimberlite diatreme theory now accepted without question. With diamonds as an added incentive for prospecting, over 100 diatremes have been found in the Laramie Mountains of southeastern Wyoming and the Front Range of northeastern Colorado (Hausel, 1985). Very few of them have sedimentary inclusions, so one of the great ironies in the story is that discovery of the only diamond-bearing localities in the western U.S. was triggered by a fossil collection.

Before Ferris' discovery and the subsequent fossil identifications by John Chronic and other paleontologists, paleogeographic maps for the Silurian showed Wyoming and Colorado as part of an extensive area not covered by the sea (**Figures 1** and **6**). One could not ask for a better example of how a dramatic change in conventional paleogeographic wisdom can be required by a discovery at a single locality.

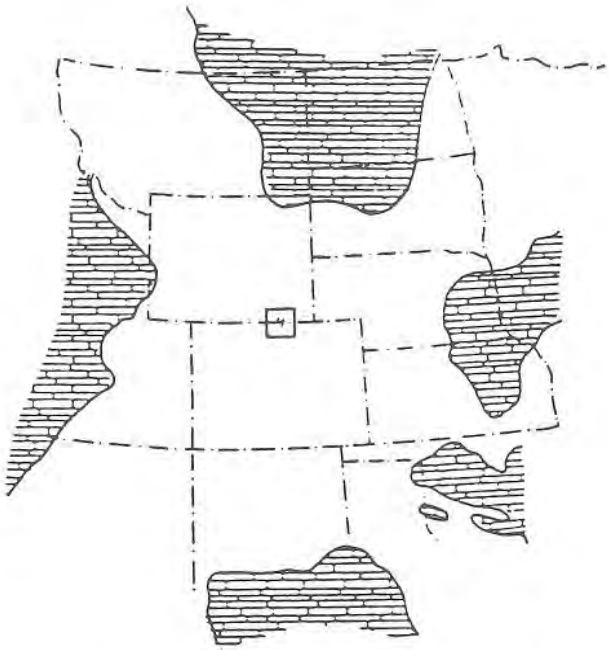

Figure 6. Regional distribution of Silurian rocks as known before diatreme discovery (brick pattern). The small rectangle on the Wyoming-Colorado border shows the location of the first diatremes discovered. (Reproduced from Chronic and others, 1969.)

The Silurian brachiopods and corals reported by Chronic and others (1969) from the Ferris diatreme and a smaller one nearby represent at least two ages (late Llandoverian and late Wenlockian or Ludlovian). This fact, together with the environmental significance of the fossils and their carbonate host rock, leaves no doubt that this area was beneath clear-water seas for a significant part of Silurian time. It follows that the same was probably true for much or all of Wyoming.

Figure 7. Largest outcrop of sedimentary rock in the Ferris diatreme (visible at right center of Figure 5). Hay meadow (upper left) and hay crib (upper right) are also shown in Figure 5. This outcrop contains Ordovician fossils, whereas nearby boulders yield Silurian brachiopods. (Hat and camera bag for scale.)

In map view, the Ferris diatreme occupies an oval area with maxi-

mum length of about 250 feet. Like all those subsequently discovered in the Front Range, it is surrounded by Precambrian crystalline rocks. The closest outcrops of in situ strata are about 2 miles away, where Pennsylvanian arkoses cover the granite. In contrast to the absence of sedimentary rock at the vast majority of the diatremes, the Ferris outcrops consist of the foundered blocks of Ordovician and Silurian carbonates (**Figure 7**). Cuttings from the bottom half of a 230-foot borehole drilled at its center indicate that ultramafic matrix dominates over inclusions at that depth (Chronic and others, 1969).

It is not known whether the diatreme intrusions reached the Earth's surface, nor is it certain when they occurred during the window of opportunity bracketed by origin of the youngest fossiliferous blocks and deposition of the Pennsylvanian arkose. Absence of undoubted Devonian and Mississippian inclusions favors late Silurian or early Devonian as the most likely time of intrusion. Other than the diatreme material, the only certain Silurian rocks in Wyoming are along the western border in the form of the easternmost record of the Laketown Dolomite.

Devonian Period

Wyoming's position on the craton margin was not favorable for a detailed recording of the numerous rises and falls of Devonian sea level now being documented by stratigraphic studies farther west. Only the major transgressive pulses affected the state, and long regressive intervals resulted in loss of strata deposited not long before. Those units that were preserved typically change thickness laterally because of both depositional thinning in the direction of transgression (west to east, and north to south) and differential stripping during times of subaerial erosion.

The period began with Wyoming emergent and vegetated with primitive vascular plants. Silurian strata were lost to erosion, and drainage systems developed on older bedrock. As far as can be told from the rock record, the maximum Early Devonian transgression onto the craton affected Wyoming only by turning the seaward ends of the valleys into estuaries. Sediments that accumulated in several of these are preserved as isolated lenses, as much as 75 feet thick, along the disconformable top of the Bighorn Dolomite in northern Wyoming.

Collectively known as the Beartooth Butte Formation, the lenses of conglomerate and carbonaceous dolomite are the only Lower Devonian rocks identified in Wyoming. The bizarre fossil assemblage obtained from them, including eurypterids, vascular plants, and fish, signifies their estuarine origin.

Wyoming was exposed to erosion during a major Middle Devonian regression that affected many parts of the world. When a Late Devonian sea encroached on the state, the initial depositional environments replicated the estuarine conditions of the Beartooth Butte Formation. The Upper Devonian channel deposits can be confused with their Lower Devonian counterparts in northern Wyoming, where both can be found along the disconformity at the base of the Devonian sequence.

The advance of Late Devonian sea water into the valleys draining the terrain of Bighorn Dolomite bedrock was the initial expression in Wyoming of a major rise in sea level. At the height of this transgression, marine conditions prevailed throughout the northern and western parts of the state. The resulting deposits consist of several hundred feet of sparsely fossiliferous carbonate rock, commonly dolomitized, with interbedded siltstone and sandstone. Montana nomenclature (Jefferson Limestone and Three Forks Formation) is applied to these Upper Devonian beds in northern Wyoming, whereas equivalent strata in the western part of the state are commonly called the Darby Formation. In the latter unit, beds of siltstone and sandstone become increasingly common eastward relative to dolomite intervals; the shore may not have been far beyond the present erosional limit of the formation.

Vacillation in water depth and supply of noncarbonate sediment during deposition of the Jefferson-Three Forks interval resulted in differences in bedding and lithology that led geologists in southwestern Montana to distinguish two members in each formation. Although carbonate rocks are dominant, mudstone is common in the upper part of the interval and an evaporitic facies a few tens of feet thick is present along the Idaho-Wyoming border.

The unconformity at the top of the sequence bevels it from northwest to southeast in such a way that successively older members cap the sequence southward from the state line to its southeastern limit. There, the remaining beds are inconspicuous and easily overlooked or misidentified.

Although the regional disconformity at the top of the Jefferson-Three Forks and Darby beds seems to signify the upper limit of the Devonian record in the state, this is not literally true. Late Devonian conodonts are present in a few tens of feet of dark gray shale and silty dolomite above the disconformity (Sandberg and Klapper, 1967). These unusual strata, constituting the basal member of the Madison Limestone, encompass the systemic boundary; Early Mississippian conodonts have been obtained from the upper beds.

To the southeast, a similar conodont succession places the Devonian-Mississippian boundary in a thin unit not far above Precambrian granite. In this area, the north end of the Laramie Mountains and vicinity, the conodonts are in siltstone and sandy dolomite separated from the crystalline basement by a variable thickness (6 to 186 feet) of resistant sandstone. In southeastern Wyoming, any such outcrop of unfossiliferous sandstone nonconformable on Precambrian granite is fair game for speculation as to geologic age. Nominations can start with the Cambrian, but evidence in this case favors Devonian.

The above evidence indicates that marine conditions had returned to Wyoming before the Devonian Period ended, but it does not imply that sea water covered the state at that point. Lithologic differences and lack of stratigraphic continuity between pertinent strata in northwestern and southeastern Wyoming suggest that the latest Devonian marine onlap did not completely cover central and southern Wyoming.

A review of the Devonian System in the Rocky Mountain region by Baars (1972) includes several thickness and lithofacies maps. Johnson and others (1988) offered a detailed interpretation of Early Devonian history of the western U.S., and Sandberg and others (1988) did the same for the Late Devonian. All three of these sources cite many references that deal specifically with Wyoming.

Mississippian Period

Far west of Wyoming, the plate margin changed from the passive behavior of its early Paleozoic history, and an allochthon of pre-Mississippian oceanic strata moved onto the continent margin. Although sediments derived from the resulting Antler orogenic belt did not reach the Wyoming shelf, the tectonic activity to the west may have influenced the advances and retreats of the sea recorded in the thick Mississippian carbonate sequence of Wyoming.

The Mississippian Period was characterized by carbonate deposition over a major part of North America. Wyoming's heritage from these warm, clear-water seas was a wedge of carbonate strata (**Figure 8**) thickening irregularly west and north from a zero edge in the southeast to more than 1,000 feet at the western border. Intercrystalline and vuggy porosity in some of these rocks makes them important as major aquifers and as oil and gas reservoirs in areas such as the Bighorn Basin.

Over most of the state, the carbonate strata are given formation rank as the Madison Limestone—a somewhat misleading term considering the extent of dolomitization. All but the uppermost of six formally designated members in central Wyoming are carbonate. They differ in ratio of dolomite to limestone, bedding type, texture, grain origin, and chert content. The Madison is treated as a group in western Wyoming, where two Montana names—Lodgepole Limestone and Mission Canyon Limestone—are applied to the lower and upper parts, respectively, of the thick section. At the other side of the state, the Black Hills term, Pahasapa Limestone, is employed for Madison-equivalent strata flanking the Black Hills, and correlative strata in the Hartville uplift to the south are called the Guernsey Formation.

As implied in the comments on Late Devonian history, the long interval of marine conditions represented by Madison strata began rather tentatively. The narrow seaway that extended into part of Wyoming in latest Devonian time was reestablished very early in the Mississippian Period after a brief absence. The limited areas drowned in these incursions received several tens of feet of conodont-bearing dark

Figure 8. Wind River Canyon (looking south) in north-central Wyoming. Cambrian rocks form slopes rising from the river; Bighorn Dolomite (Ordovician) and Madison Limestone (Mississippian) form cliffs. Silurian and nearly all Devonian strata were removed by pre-Madison erosion. The Wind River is bordered by a highway (left) and a railroad (right).

shale and silty dolomite now recognized as a basal member of the Madison sequence. A disconformity separates Devonian and Mississippian parts of the member where both are present. In some areas, only the upper tongue is found, and the member is missing entirely in parts of western and north-central Wyoming.

The shallow-bay environment terminated abruptly as a major eustatic rise produced a rapid transgression over the craton, which left only an area along Wyoming's southern border emergent. To the west, the basal black shale member of the Lodgepole Limestone grades upward into silty, variably cherty limestones of its middle member. At the western border of the state, water depths during deposition of these beds may have reached several hundred feet at times. Oxygen-deficient conditions below the photic zone are suggested by laminated rock with no algal remains and only rare shells. Correlative shelf strata in central Wyoming are now extensively dolomitized.

The thin beds, typically rich in skeletal debris, that typify the upper half of the Lodgepole Limestone represent a time when carbonate accumulation was catching up with sea-level rise. Repetition of small-scale, shoaling-upward cycles (mudstone-packstone-grainstone) reflect migration of tidal bars of oolitic and skeletal sand across the mud bottom. Dense populations of bryozoans and crinoids thrived in deeper water between the shoals, and grains in these less disturbed areas were typically micritized by endolithic algae. High-energy conditions were common in the shallower water to the east, as attested by crossbedding, oolite, and abundant skeletal debris. Such indicators are common in central Wyoming in the part of the Madison Limestone equivalent to the much thicker upper Lodgepole.

A second major sea-level rise was accompanied by progradation of the shelf until the shelf edge coincided with the present western border of Wyoming. Aggrading calcarenites and lime mud in this area formed the Mission Canyon Formation. The interbedding of these facies reflects rapid alternation of turbulent and less agitated environments as fluctuation in depth of wave action or shifts in tidal currents winnowed the mud sea floor. The reworked skeletal material was concentrated in shifting tidal bars, where smaller grains became nuclei for oolitic coatings.

Development of extensive shoals at the platform edge impeded water movement onto the shelf. Lagoonal conditions developed there, and the restricted circulation culminated more than once in precipitation of evaporites. When dissolution removed these beds from the sequence much later, collapse of superjacent rock produced layers of breccia. Two such zones, each several feet thick, are found in the Mission Canyon Limestone. Similar evidence of evaporite dissolution is present in the laterally

equivalent part of the Madison Limestone including the two upper members of the formation in central Wyoming—cherty dolomite overlain by red shale and stromatolitic carbonate.

The fossil content of Madison rocks is of interest in several respects. Some beds are virtual coquinas, whereas others are barren of fossils or exhibit only scattered crinoid columnals. The overall macrofauna includes solitary and colonial corals, fenestrate and nonfenestrate bryozoans, brachiopods of several orders, gastropods, trilobites, and plates and spines of various echinoderms. Conodonts and foraminifera are present in many beds, and thin sections of bioclastic rock commonly exhibit skeletal fragments attributable to green and red algae. Correlation of various parts of the Madison sequence with series and stages defined in the Mississippi Valley and Europe is based on conodonts and endothyroid foraminifera. Although more provincial, corals provide a zonation useful in correlating Madison strata with Mississippian units elsewhere in western North America.

Both rugose and tabulate corals are common in Madison strata but no reefs are present. These corals lived as solitary polyps and scattered colonies on loose sediment. Unlike many of their modern relatives, their growth habits did not involve lateral expansion by encrustation, and they did not form hard substrates above wave base. Also lacking in Wyoming Mississippian strata are Waulsortian mounds of the classic type described from outcrops of Mississippian and Lower Carboniferous outcrops elsewhere. Development of these enigmatic lenticular buildups of fossiliferous lime mud seems to have been favored by slope environments below greater water depths than those represented by most Madison strata.

Addition of strata to the Wyoming shelf was abruptly halted by a major regression that moved the shoreline to the western border of the state, exposing the entire platform to subaerial processes. Abundant meteoric water leached the surface, forming caverns, sinkholes and breccia (**Figure 9**), while subsurface evaporite layers were dissolved by ground water. West-flowing rivers draining the old highland along the southern border of the state built a delta southwest of Wyoming. Longshore currents brought arkosic sand north from that area and it was interbedded with carbonates that continued to accumulate in shallow water just offshore from the karst plain (DeJarnett, 1984).

Wyoming's well-developed karst topography was probably mantled by lateritic soil supporting a

Figure 9. Paleokarst on white Mississippian limestone (Guernsey Formation) overlain by red Pennsylvanian sandstone (Hartville Formation). Cliff overlooks the North Platte River near Guernsey in eastern Wyoming.

low-latitude plant community that provided habitat for insects and primitive amphibians. The picture seems reasonable, but there is no direct evidence other than red mudstone in some of the sinkholes; the rest was removed as the scene changed again to a seascape.

The final advance of the Mississippian sea affected only the western half of the state, where it deposited the first of three diverse members known today as the Amsden Formation. The foundation was thus laid for one of the most vexing controversies in Wyoming stratigraphy—the ages and lateral relationships of the various parts of that formation.

The basal member, the Darwin Sandstone, represents a dramatic change from the carbonate environments that produced the underlying Madison Limestone. The white, crossbedded sandstone is more than 150 feet thick in places. Its textural and compositional maturity implies that it is recycled material, possibly delivered by rivers draining lower Paleozoic sandstones far to the northeast. The unstable substrate in the advancing sea that reworked the sand was inhospitable for organisms, and the unfossiliferous aspect of the Darwin necessitates an age assignment based on circumstantial evidence. Although there is general agreement that the Darwin was deposited late in the Mississippian Period, there is no such consensus as to whether or not deposition was continuous from Mississippian into Pennsylvanian time.

The huge body of information compiled by Craig, Connor, and others (1979) on the Mississippian System in the U.S. puts the Wyoming record in continent-wide perspective. Maughan (1979) and Sando (1979) offered frank appraisals of their different interpretations of Amsden and related strata. A chronology of Devonian and Mississippian eustatic changes and epeirogenic events affecting the western U.S. as far east as Wyoming was compiled by Sandberg and others (1982) in a paper that includes five Mississippian paleogeographic maps. DeJarnett's (1984) detailed study of a thick Mississippian section in the thrust belt documented various biofacies and lithofacies that are widespread in rocks of the same age in western Wyoming.

Pennsylvanian Period

Had David Hume been a stratigrapher, he might have meditated that the existence of disconformities, as well as beauty, is in the mind of the observer. He might, that is, if he were a biostratigrapher arguing the "Amsden problem" with a physical stratigrapher. Although both camps cite faunal and physical evidence to support their contradictory views, the conclusion reached seems to depend on the weight given to certain fossils, as indicators of Mississippian age, versus lithostratigraphic criteria, as evidence for regional disconformities.

The current controversy centers on the relationship between the Amsden's basal member (Darwin Sandstone) and the two overlying members (Horseshoe Shale and Ranchester Limestone). One view holds that the Darwin is separated from the others by a regional disconformity and that Horseshoe strata are the initial deposits of a later transgression that initiated Pennsylvanian sedimentation in the area. The alternative view interprets the Horseshoe and Ranchester fauna (foraminifera, ostracodes, corals, brachiopods, and mollusks) to include Late Mississippian forms in the west and Early Pennsylvanian ones in central Wyoming. In this view, the Darwin-Horseshoe contact is conformable, and the three members are parts of a single transgressive episode that did not reach eastern Wyoming until Pennsylvanian time.

Part of the controversy concerns the relation of Amsden-like Mississippian strata in westernmost Wyoming to the Amsden of central Wyoming. If strata of the two areas were originally continuous, the transgressive theory is correct. The opposing school, however, maintains that the Mississippian wedge is overlain unconformably by Pennsylvanian strata. If so, similarities between units in that wedge and rocks of the Horseshoe and Ranchester members are coincidental and not grounds for postulating a time-transgressive relationship. The Amsden controversy is by no means the only one involving Wyoming Paleozoic rocks, but there is probably no better example of the problems confronting stratigraphers who deal with poorly exposed, sporadically fossiliferous, and heterogeneous formations.

The shelf conditions that characterized Wyoming during the Pennsylvanian contrasted sharply with localized areas of rapid subsidence to the west and

south (e.g., Sublett basin of Idaho, Oquirrh basin of Utah, central Colorado trough) and the rising mountains (e.g. ancestral Front Range uplift) in Colorado. The shelf was not, however, tectonically inactive. The extraordinary crustal instability to the west and south was mimicked in miniature by subtle warping of the platform as the period progressed. The positive areas that developed from time to time affected both sedimentation and preservation of the record. These aspects of the state's late Paleozoic history are discussed by Maughan (this volume) in the chapter on the ancestral Rocky Mountains.

The dominant role of terrigenous detrital sediment in Wyoming's Pennsylvanian strata, about 500 feet thick on the average, represents a major change from the Mississippian, when carbonate factories had little competition. In the Pennsylvanian, limestones formed from time to time but, with the exception of the Ranchester sea, clear-water conditions were typically brief. Their influence is most notable in the northeastern and eastern parts of the state, where the prominence of limestones in interbedded siliciclastic-carbonate units attests to the proximity of open seas in those directions.

Although opinions differ as to whether or not Wyoming was completely emergent at the beginning of Pennsylvanian time, all agree that shallow marine conditions were present early in the period. Mild crustal warping had produced a positive area along the Idaho border, and the northern end of the ancestral Front Range extended into south-central Wyoming. As a result, access of the Early Pennsylvanian sea to the Wyoming shelf seems to have been from the north, southwest, and southeast.

Today, the red mudstones of the Horseshoe Shale Member, commonly 100 feet thick, produce a distinctive zone of colorful soil separating ledge-forming Mississippian units below from the overlying Ranchester Limestone. The redbed depositional environments involved frequent flooding of coastal mudflats, but only rarely did an inundation persist long enough in central Wyoming to generate a thin limestone bed. Interbedded carbonate increases to the southwest, where the Horseshoe Shale grades into the Round Valley Limestone of Utah.

Expansion of the sea from the west into Wyoming resulted in the relatively clear-water conditions in which 100 feet or more of cherty carbonates with red mudstone partings were deposited (Ranchester Limestone Member). This interval of dominantly carbonate deposition was terminated by a major influx of siliciclastic sediments that comprise the bulk of the Tensleep Sandstone (**Figure 10**), one of the most important petroleum-producing formations in the state. The 200-to 300-foot thickness typical for the Tensleep includes numerous dolomite layers, some as much as 12 feet thick. Such units at the top of the formation can be confused with overlying Permian formations. Close-spaced carbonate layers at the base of the section pose a different problem, in that they are included in the Tensleep by some workers and in the Amsden by others.

As the formation name implies, the dolomite beds are a minor component of the Tensleep. The thick body of quartz sand they interrupt exhibits prominent crossbedding—some sets are more than 50 feet thick—as well as distinctive intervals of large-

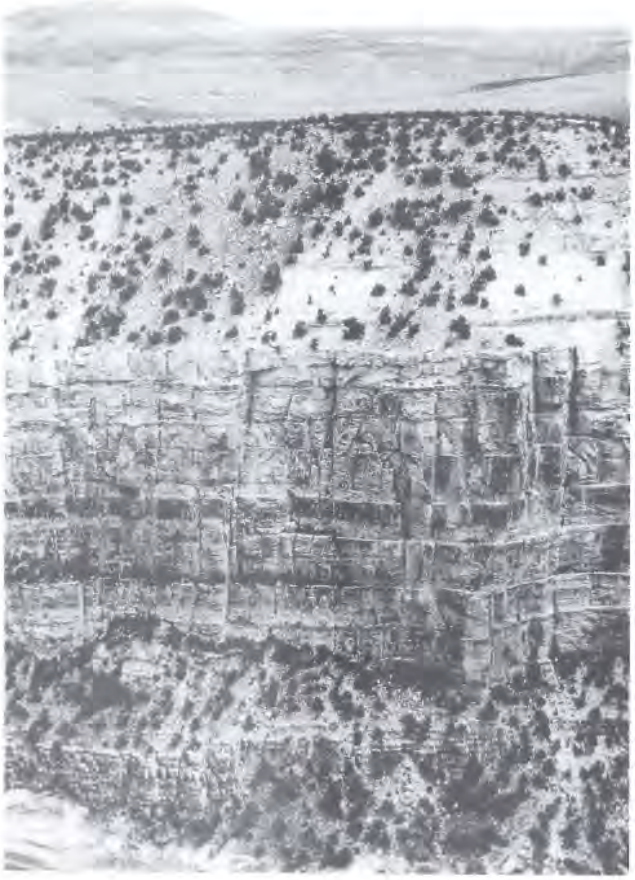

Figure 10. Cliff of Tensleep Sandstone (Pennsylvanian) at the north end of Wind River Canyon (east side). Tree-covered slope from cliff to canyon rim is formed by Park City Formation (Permian). (Highway at lower left corner.)

scale contorted bedding. A prolific source must have existed in Montana, northern Idaho, or the Canadian Shield to supply the great blanket of sand that spread over the Wyoming shelf, as well as adjacent areas where other formation names are applied (e.g., Quadrant in Montana, Wells in Idaho, and Weber in Utah).

Wind seems to have played a major role in the transport and deposition of the sand. Several eolian dune types, differentiated by distinctive bedding geometry and grain characteristics, have been identified in the formation. Other intervals lacking an eolian signature probably represent reworking of previous deposits by shallow seas that occasionally flooded the area. The more extensive incursions produced the intercalated carbonate units. Such evidence of fluctuating sea level is not surprising for a period of Earth history when glaciers were waxing and waning in the southern hemisphere.

Another factor that probably influenced distribution of marine and nonmarine facies within the Tensleep was variation in relief of the platform surface. Depositional topography in dune fields may have been significant, but slight differences in epeirogenic activity in different parts of the platform were probably more important. Positive areas would have been the sites of the most continuous eolian activity, while adjacent areas were more frequently submerged.

In eastern Wyoming, marine conditions were more continuous and clear-water environments more frequent than was true for the area of Tensleep deposition. The hundreds of feet of limestone and sandstone that accumulated in this area are now exposed in the Black Hills uplift, in the smaller Hartville uplift to the south, and along the flanks of the Laramie Mountains. By 1908, a local name had been applied to these rocks in each of the three areas. From north to south, the synonyms, Minnelusa, Hartville, and Casper mask the overall similarity in age and lithology of the rocks to which they apply.

Bryozoans, brachiopods, mollusks, and echinoderm plates are found in many beds of these formations, but fusulinids are of special interest because of their biostratigraphic importance. The succession of fusulinid species and genera present in each of the three formations establishes their mutual age equivalency. It also demonstrates that all four Pennsylvanian provincial series, as well as the lowest Permian one, are represented in the eastern Wyoming sequence.

During much of the Pennsylvanian Period, the northern part of the ancestral Front Range greatly influenced sedimentation in southeastern Wyoming. Gravel, sand, and clay derived from the exposed granite accumulated as an apron, hundreds of feet thick, of alluvial fans and braided-stream deposits flanking the highland. These arkosic fluviatile sediments comprise the Fountain Formation (**Figure 11**). The interplay of fluctuations in both sea level and supply of terrigenous sediment led to complex intertonguing of marine and nonmarine facies where the Casper Formation gives way to the Fountain. As the period progressed, this transition zone migrated toward the source area in response to the decreasing supply of terrigenous sediment. As the Pennsylvanian Period came to a close, strata continued to accumulate throughout much of eastern Wyoming while subaerial erosion was already erasing the latest part of the Pennsylvanian record elsewhere in the state.

The monumental study of the Pennsylvanian System in the U.S. produced by McKee, Crosby, and others (1975) includes two sections of text dealing with Wyoming and adjacent areas, and numerous lithofacies, isopach, and paleotectonic maps for the country as a whole. Another valuable synthesis for the Rocky Mountain region, by Mallory (1972), is illustrated with unusually colorful lithofacies maps. The report on the Tensleep Sandstone by Kerr and others (1986) illustrates the sedimentological complexities of that important formation.

Permian Period

In the Permian world, the part of the crust under discussion here was a tiny part of the great supercontinent Pangaea. Assembly of this greatest of all Phanerozoic landmasses had placed much of the margin of the North American craton far inland, but this was not true for the part of the margin bordering Wyoming. As had been true throughout its Paleozoic history, most of the state behaved tectonically as a

Figure 11. Nonconformity separating Proterozoic granite from Pennsylvanian fluviatile sandstone (Fountain Formation) at the Wyoming-Colorado border south of Laramie.

stable platform relative to the area now to the west, where passive-margin subsidence during the first half of the era was followed by more complicated tectonism.

As the period began, much of Wyoming was losing the last-formed part of its Pennsylvanian record. By contrast, Early Permian fusulinids in the upper beds of the Weber and Wells sandstones show that deposition continued along the state's western border, and similar evidence is found in the upper part of the Casper, Hartville, and Minnelusa formations of eastern Wyoming. There, the marine presence resulted in an interbedding of dolomite and sandstone interrupted, in the Minnelusa, by evaporite beds.

The Permian history of the Minnelusa is of special interest to the petroleum industry. The upper member, some 200 feet thick, consists of eolian sandstones alternating with marine carbonates and evaporites. The sandstone units have significant relief on their upper surfaces, and commercial quantities of oil have been trapped in the topographic highs. Relief on the top of the formation was created by an interlude of subaerial erosion that preceded deposition of overlying Permian redbeds. Lateral changes in thickness of lower sandstone units may reflect dune field topography modified by subsequent transgressions.

Farther south, a vestige of a coastal dune field that bordered the eastern sea is exposed at the Wyoming-Colorado border south of Laramie. The picturesque crossbedded sandstone, of special interest as the type locality for the term "festoon crosslamination" (Knight, 1929), overlies Pennsylvanian fluviatile strata of the Fountain Formation. The sandstone, however, is laterally equivalent to nearby strata of the upper Casper Formation that contain Early Permian fusulinids. Large-scale contorted bedding in the sandstone (**Figure 12**) is remarkably like that in several other formations (e.g., Tensleep) and is no better understood here than in the other occurrences.

The subaerial erosion that affected the central part of the state during the Pennsylvanian-Permian transition expanded to include the eastern area of earliest Permian deposition, thus producing the economically important disconformity at the top of the Minnelusa Formation. This surface, as well as the entire Wyoming platform, was then subjected to

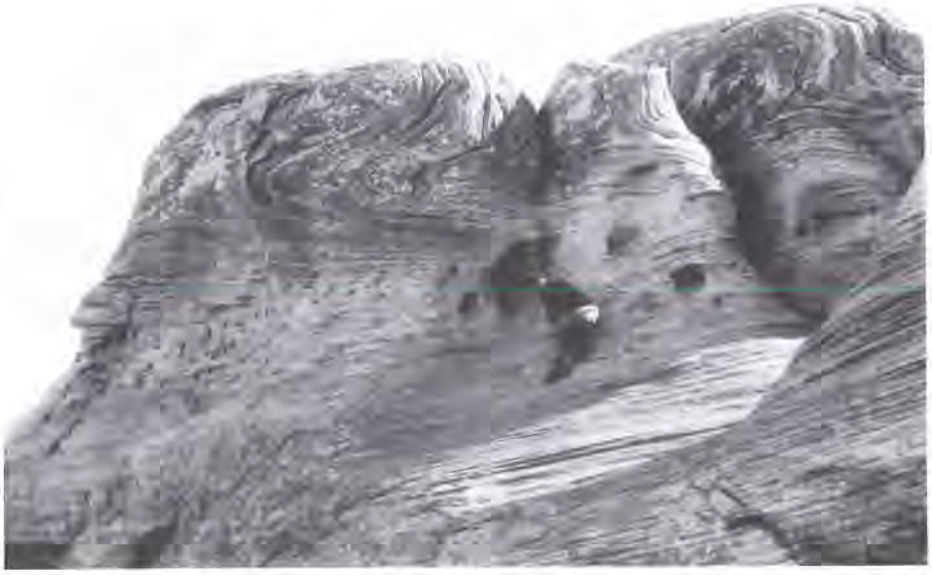

Figure 12. Contorted eolian sandstone (Permian part of Casper Formation) at the Wyoming-Colorado border south of Laramie.

aggradation until, by the end of the period, several hundred feet of Permian strata had been deposited over the main part of the shelf. This sequence accumulated as several contrasting depositional environments moved back and forth over the state and adjacent areas. The resulting complex of intertonguing rock units now exposed around Laramide uplifts in Wyoming, Utah, Idaho, and Montana has challenged stratigraphers of several generations. They, in turn, have created names for members, formations, and groups in such overlapping profusion as to render the word "nightmare" inadequate.

The basic picture involves deposition of redbeds (Goose Egg Formation) over the eastern half of the state while a peculiar sequence of phosphatic and cherty strata (Phosphoria Formation) accumulated along the western border. The intervening west-central area was characterized by carbonate deposition (Park City Formation), while sand spread into northwestern Wyoming from the north (Shedhorn Sandstone). The four formations represent end-member concepts more easily dealt with in theory than in practice. Nowhere in the state does one of them occur without including tongues of one or more of the others. At localities where tongues of two formations are equally prominent, the choice of one formation name for the section can seem very arbitrary. This has encouraged many geologists, particularly those in the petroleum industry, to disregard the term Park City Formation and to apply the term Phosphoria Formation as far east as the Goose Egg redbeds.

Carbonate members of the Park City Formation are important reservoirs in oil fields of the Wind River and Bighorn basins. Furthermore, the concentrations of phosphorite in the western facies have been commercially significant for several generations. Given the economic motivation, it is not surprising that the Phosphoria and Park City formations have been subjected to an unusual amount of study. It is safe to say that the resulting literature is more voluminous than that for any other Paleozoic formation in Wyoming.

The Phosphoria Formation of the overthrust belt is the eastern expression of unique depositional environments in a basin whose north-south axis was west of Wyoming. The long interval of sand deposition that had characterized the area during Pennsylvanian and earliest Permian time was terminated when an expansion of the sea halted erosion on the Wyoming platform. Basin flank and adjacent shelf were then blanketed with impure lime mud, which became the cherty and sandy dolomite comprising the basal member of the Park City Formation. Eastward of the carbonate limit, fine siliciclastic sediment covered the erosion surface. Thoroughly oxygenated during or soon after deposition, these layers became the first of the thick succession of Goose Egg redbeds.

The sedimentary history of the Phosphoria depositional basin is highlighted by two intervals when conditions favored accumulation of phosphatic sediments. The resulting stratigraphic units, the older

Meade Peak (below) and younger Retort Phosphatic Shale members, consist of black to brown shale and phosphorite. Beds of the latter vary in siliciclastic content and in texture. Some layers are oolitic, others are pelletal, and some consist mainly of fragmented valves of orbiculoid inarticulate brachiopods.

A completely satisfying explanation for the origin of the phosphatic members has yet to appear. Most interpretations invoke the upwelling of nutrient-rich waters from the depths of the basin onto the bordering ramp or shelf, and they typically envision high production of phytoplankton accompanied by slow sediment accumulation on an oxygen-deficient bottom. All workers agree that each of the two phosphatic members is part of a separate transgressive-regressive cycle, but opinions have differed as to whether or not deposition at the eastern limit of each member coincided with a highstand of the sea.

The two phosphatic members thin eastward to their distal edges in west-central Wyoming, where they are identifiable as thin beds in the Park City Formation. In basin sections where they achieve maximum thickness, the members come between and intertongue with equally enigmatic members composed of bedded chert and dark siliceous shale. Two concentrations of chert in different parts of the Phosphoria section have been formally designated as members. Their stratigraphic positions and dimensions, unlike those of typical lithologic units, may reflect localization of diagenetic rather than depositional environments. In any case, the chert members intertongue to the east with carbonate members of the Park City Formation (**Figure 10**), and both lithologies are interrupted by sandstone beds. These tongues of the Shedhorn Sandstone are commonplace in northwestern Wyoming, reflecting their Montana source.

The interval of sandy dolomite forming the base of the Phosphoria-Park City sequence is the lowest and least fossiliferous of the three carbonate members comprising the Park City Formation. While they were accumulating, the sea floor over much of the west half of Wyoming was formed of lime mud and skeletal debris. Percentages of these two components varied with time, as did the sites of thickest accumulation. The middle member is thickest in the west, where carbonate banks aggraded along the shelf margin. The thickest parts of the upper member are farther east on the shelf. Accumulating evidence indicates that lateral variations in thickness and carbonate facies of these members reflect the syndepositional influence of subtle structural highs and lows on the shelf.

The carbonate grains are typically skeletal fragments from bryozoans, brachiopods, and echinoderms. Ooids, pellets, and plates of phylloid algae are common in a few places. Packstone and wackestone fabrics predominate over grainstone, implying generally low-energy conditions in the carbonate-floored shelf seas. The type area for the term "fenestral fabric" (Tebbutt and others, 1965) is along the west flank of the Bighorn Mountains, where the distinctive rock is tens of feet thick in hogbacks formed by the upper Park City member. The same peritidal facies forms the petroleum reservoir in the highly productive Cottonwood Creek field not far to the south.

With the exception of a gypsum quarry operated by a Laramie cement plant, one searches in vain for Wyoming sites where the Goose Egg Formation produces something of economic interest. The redbeds play a critical role in some oil fields, where they seal underlying Minnelusa reservoirs or block lateral migration of petroleum at carbonate pinchouts. This function, however, has not served to motivate sedimentological study; little such work has been done on the Goose Egg Formation (**Figure 13**) relative to the effort lavished on the economically important correlative formations to the west.

Detailed subsurface correlations of the Goose Egg and Park City formations are facilitated by the vast eastward extent of several thin tongues of the latter formation. Each represents a brief time, presumably a highstand of the sea, when carbonate deposition interrupted the aggradation of fine siliciclastic sediments. Three carbonate tongues from the Park City have been named, as has each of the redbed intervals they separate. Add another pair at the top, and the Goose Egg Formation consists of eight members. The upper two are generally considered to be Triassic, but are included in the formation because the package forms a convenient unit for surface and subsurface mapping.

The lowest carbonate tongue (Minnekahta Limestone) is especially famous for its areal extent; it has been traced in the subsurface as far as the western parts of Nebraska and the Dakotas. The transgressions that produced the carbonate members did not expand the habitat for the brachiopod-bryozoan communities thriving in the western half of the state.

Only a few mollusks and fish probed the eastern environments, which no doubt became increasingly hostile in that direction. Some of the carbonate is stromatolitic, but much is nondescript dolomite that gives way laterally to evaporites. In fact, evaporite beds in the Goose Egg sequence typically correlate with, and are extensions of, carbonate members.

The great lateral extent of the thin carbonate-evaporite tongues implies that each originated in a standing body of water that had spread over a featureless surface essentially at sea level. The red clay-rich silt that forms most of the several hundred feet of Goose Egg strata apparently accumulated on such surfaces. Absence of paleosols and caliche suggests that any one surface was not exposed for long, although the ubiquitous iron oxide pigment demonstrates that oxygen was abundant in the diagenetic environment. The lack of ripplemarks and cut-and-fill structures argues against the fluviatile and tidal-flat origins often postulated for redbed sequences.

Perhaps these peculiar red siltstones are best understood as sediment transported by wind from an arid landscape to the east and deposited on a surface typically, but not invariably, covered by a shallow sheet of water (Renner, 1988). In this scenario, minor falls in sea level occasionally exposed broad areas of silt. At times of inundation, the silt-choked water was conducive to neither animal nor plant life. Carbonate deposition took place only when unusually high sea stands brought clear-water conditions.

To those who yearn for paleontological insight concerning the very last moment of the Paleozoic, it was a cruel trick of nature that recorded Wyoming's most complete record across the erathem boundary in the barren Goose Egg Formation, rather than in the fossiliferous sequence farther west. Not to say that deposition was literally continuous in eastern Wyoming, but no evidence, subsurface or surface, has been presented for a lengthy hiatus in aggradation of silt during the passage from Paleozoic to Mesozoic eras.

By contrast, paleontologists have long maintained that the faunal sequence in the Phosphoria and Park City formations is three bricks shy of a load, as the saying goes, relative to more complete Upper Permian sections in the Tethyan region. Six biostratigraphic zones, based on conodonts and brachiopods, have been documented in the Phosphoria-Park City sequence of Wyoming. The uppermost one is thought to be no younger than earliest Capitanian in

Figure 13. Slope-forming red siltstone and carbonate ledge in Goose Egg Formation (Permian) overlying Tensleep Sandstone (foreground); west flank of Sheep Mountain anticline, northeast Bighorn Basin.

the West Texas standard section. Furthermore, this zone has been identified only in west-central Wyoming. Farther west, the fact that uppermost Permian rocks bear representatives of older zones supports the lithostratigraphic evidence there for a significant gap in the record at the erathem boundary.

The absence of fusulinids from the Phosphoria-Park City rocks comes as an unpleasant surprise to those accustomed to using them for biostratigraphic work in this part of the Permian System. Their disappearance from this region is all the more mysterious considering their presence through much of Pennsylvanian and earliest Permian time. The best guess is that they were denied access to the Wyoming shelf from the west by low temperature waters of the upwelling system associated with the Phosphoria basin, and from the east by hypersaline conditions.

Unlike the fusulinids, several normal-marine groups continued to inhabit Wyoming while the Phosphoria-Park City sequence accumulated. Bryozoans, brachiopods, and crinoids are common constituents of all the carbonate members and can be found nearly to the top of the Park City Formation where it is overlain by Triassic mudstones. The highest beds of the upper member, however, show evidence of regression. At many localities, thin layers of laminated, unfossiliferous carbonate cap the member (**Figure 14**). Desiccation cracks are rare, but the upper surface commonly exhibits an alteration rind, silicified in places, suggestive of an unusual interval of exposure before sedimentation resumed with deposition of Triassic silt and clay.

Relief on this surface is typically on the order of inches rather than feet, and it is not overlain by a bed of Triassic conglomerate. The absence of a prominent disconformity contrasts sharply with the paleontological evidence of missing record and provides a final paradox for those who try to reconstruct the Paleozoic history of Wyoming.

Many valuable works dealing with Wyoming Permian rocks are referenced in important reviews by Peterson (1984) and Wardlaw and Collinson (1986). A regional synthesis by Rascoe and Baars (1972) provides perspective and is notable for illustrating subsurface relationships between the Permian of eastern Wyoming and adjacent states. Renner's (1988) study of the Permian-Triassic boundary beds is a fine example of integration of surface and subsurface evidence.

Figure 14. Thin carbonate beds of Park City Formation (Permian) overlain by drab, slope-forming mudstones of Dinwoody Formation (Lower Triassic), northwest end of Wind River Canyon.

Acknowledgments

Phillip Greer made an important contribution to this paper through literature research, preparation of figures and, together with Margaret Boyd, manuscript preparation. Careful reading of a preliminary draft by reviewers James E. Fox, James A. Peterson, and the editors resulted in a significantly improved final version.

References cited

Blackstone, D.L., Jr., 1963, Development of geologic structure in central Rocky Mountains, *in* Childs, O.E., and Beebe, B.W., editors, Backbone of the Americas: American Association of Petroleum Geologists Memoir 2, p. 160-179.

Chronic, J., McCallum, M.E., Ferris, C.S., Jr., and Eggler, D.H., 1969, Lower Paleozoic rocks in diatremes, southern Wyoming and northern Colorado: Geological Society of America Bulletin, v. 80, p. 149-156.

Chronic, L.M., 1988, The interrelation of fauna and lithology across a late Cambrian biomere boundary in Wyoming [M.S. thesis]: Laramie, University of Wyoming, 70 p.

Craig, L.C., Connor, C.W., and others, 1979, Paleotectonic investigations of the Misssissippian System in the United States: U.S. Geological Survey Professional Paper 1010, pt. I, 369 p.; pt. 2, 189 p.; pt. 3, 15 plates.

DeJarnett, J.G., 1984, Stratigraphy, sedimentation, corals, and paleogeographic significance of the Mississippian sequence at Mt. Darby, overthrust belt, Wyoming [M.S. thesis]: Laramie, University of Wyoming, 231 p.

Foster, N.H., 1972, Ordovician System, *in* Mallory, W.W., editor, Geologic atlas of the Rocky Mountain region: Denver, Colorado, Rocky Mountain Association of Geologists, p. 76-85.

Fouch, T.D., and Megathan, E.R., editors, 1980, Paleozoic paleogeography of the west-central United States: Rocky Mountain paleogeography symposium 1: Society of Economic Paleontologists and Mineralogists, 431 p.

Hausel, W.D., McCallum, M.E., and Roberts, J.T., 1985, The geology, diamond testing procedures, and economic potential of the Colorado-Wyoming kimberlite province -a review: Geological Survey of Wyoming Report of Investigations 31, 22 p.

Johnson, J.G., Sandberg, C.A., and Poole, F.G., 1988, Early and Middle Devonian paleogeography of western United States, *in* McMillan, N.J., Embry, A.F., and Glass, D.J., editors, Devonian of the world: Proceedings of the Second International Symposium of the Devonian System, Calgary, Canada: Canadian Society of Petroleum Geologists, v. 1, p. 161-182.

Kent, H.C., Couch, E.L., and Knepp, R.A., 1988, Central and southern Rockies region: correlation of stratigraphic units of North America (COSUNA) Project: American Association of Petroleum Geologists, Tulsa, Oklahoma.

Kerr, D.R., Wheeler, D.M., Rittersbacher, D.J., and Horne, J.C., 1986, Stratigraphy and sedimentology of the Tensleep Sandstone (Pennsylvanian and Permian), Bighorn Mountains, Wyoming: Wyoming Geological Association Earth Science Bulletin, v. 19, p. 61-77.

Knight, S.H., 1929, The Fountain and the Casper formations of the Laramie Basin: University of Wyoming Publications in Science, Geology, v. 1, 82 p.

Lochman-Balk, C., 1972, Cambrian System, *in* Mallory, W.W., editor, Geologic atlas of the Rocky Mountain region: Denver, Colorado, Rocky Mountain Association of Geologists, p. 60-75.

Love, J.D., and Christiansen, A.C., 1985, Geologic map of Wyoming: U.S. Geological Survey, scale 1:500,000.

Mallory, W.W., editor, 1972, Geologic atlas of the Rocky Mountain region: Denver, Colorado, Rocky Mountain Association of Geologists, 331 p.

Mallory, W.W., 1972, Regional synthesis of The Pennsylvanian System, *in* Mallory, W.W., editor, Geologic atlas of the Rocky Mountain region: Denver, Colorado, Rocky Mountain Association of Geologists, p. 111-142.

Martin, W.D., Fischer, H.J., Keogh, R.J., and Moore, K., 1980, The petrology of the limestones in the upper Gros Ventre and Gallatin Limestone formations (Middle and Upper Cambrian) northwestern Wind River Basin, Wyoming: Wyoming Geological Association 31st Annual Field Conference Guidebook, p. 37-51.

Maughan, E.K., 1979, Pennsylvanian (Upper Carboniferous) System of Wyoming, *in* The Mississippian and Pennsylvanian (Carboniferous) Systems in the United States: U.S. Geological Survey Professional Paper 1110, p. U16-U33.

McKee, E.D., Crosby, E.J., and others, 1975, Paleotectonic investigations of the Pennsylvanian System in the United States: U.S. Geological Survey Professional Paper 853, pt. 1, 349 p.; pt. 2, 192 p.; pt. 3, 60 plates.

Middleton, L.T., Steidtmann, J.R., and DeBour, D.A., 1980, Stratigraphy and depositional setting of some Middle and Upper Cambrian rocks, Wyoming: Wyoming Geological Association 31st Annual Field Conference Guidebook, p. 23-35.

Peterson, J.A., 1984, Permian stratigraphy, sedimentary facies, and petroleum geology, Wyoming and adjacent area: Wyoming Geological Association 35th Annual Field Conference Guidebook, p. 25-64.

_____ 1987, Pre-thrusting regional stratigraphy and paleotectonics, northern Rocky Mountains and adjacent Cordilleran shelf, U.S.: Wyoming Geological Association 38th Annual Field Conference Guidebook, p. 17-26.

Peterson, J.A. and Smith, D.L., 1986, Rocky Mountain paleogeography through geologic time, *in* Peterson, J.A., editor, Paleotectonics and sedimentation in the Rocky Mountain region, United States: American Association of Petroleum Geologists, Memoir 41, p. 3-19.

Rascoe, B.R., Jr., and Baars, D.L., 1972, Permian System, *in* Mallory, W.W., editor, Geologic atlas of the Rocky Mountain region: Denver, Colorado, Rocky Mountain Association of Geologists, p. 143-165.

Renner, J.M., 1988, Placement and paleogeographic significance of Permian-Triassic boundary, central and southeast Wyoming [M.S. thesis]: Laramie, University of Wyoming, 135 p.

Ross, R.J., Jr., 1976, Ordovician sedimentation in the western United States, *in* Bassett, M.G., editor, The Ordovician System: Proceedings of the Paleontological Association Symposium, Cardiff, Wales: University of Wales Press, p. 73-105.

Sandberg, C.A., and Klapper, G., 1967, Stratigraphy, age, and paleotectonic significance of the Cottonwood Canyon Member of the Madison Limestone in Wyoming and Montana: U.S. Geological Survey Bulletin 1251-B, 70 p.

Sandberg, C.A., Gutschick, R.C., Johnson, J.G., Poole, F.G., and Sando, W.J., 1982, Middle Devonian to Late Mississippian geologic history of the overthrust belt region, *in* Powers, R.B., editor, Geologic studies of the Cordilleran thrust belt, v. II: Denver, Colorado, Rocky Mountain Association of Geologists, p. 691-719.

Sandberg, C.A., Poole, F.G., and Johnson, J.G., 1988, Upper Devonian of western United States, *in* McMillan, N.J., Embry, A.F., and Glass, D.J., editors, Devonian of the world: Proceedings of the Second International Symposium on the Devonian System, Calgary, Alberta, Canada: Canadian Society of Petroleum Geologists, v. 1, p. 183-220.

Sando, W.J., 1979, Lower part of the Carboniferous, *in* The Mississippian and Pennsylvanian (Carboniferous) Systems in the United States: U.S. Geological Survey Professional Paper 1110, p. U2-U16.

Sando, W.J., and Sandberg, C.A., 1987, New interpretations of Paleozoic stratigraphy and history in the northern Laramie Range and vicinity, southeast Wyoming: U.S. Geological Survey Professional Paper 1450, 39 p.

Scotese, C.R., and McKerrow, W.S., 1990, Revised world maps and introduction, *in* McKerrow, W.S., and Scotese, C.R., editors, Palaeozoic palaeogeography and biogeography: Geological Society of London Memoir 12, p. 1-21.

Sloss, L.L., 1963, Sequences in the cratonic interior of North America: Geological Society of America Bulletin, v. 74, p. 93-114.

Stewart, J.H., Stevens, C.H., and Fritsche, A.E., editors, 1980, Paleozoic paleogeography of the western United States: Pacific coast Paleogeography Symposium 1, Los Angeles, California: Society of Economic Paleontologists and Mineralogists, 502 p.

Tebbutt, G.E., Conley, C.D., and Boyd, D.W., 1965, Lithogenesis of a distinctive carbonate rock fabric: University of Wyoming Contributions to Geology, v. 4, p. 1-13.

Wardlaw, B.R., and Collinson, J.W., 1986, Paleontology and deposition of the Phosphoria Formation: University of Wyoming Contributions to Geology, v. 24, p. 107-142.

Frontispiece. Camel Rock, a prominent landmark at the Colorado-Wyoming border south of Laramie, Wyoming. Most of the butte consists of Upper Pennsylvanian arkosic sandstones and conglomerates of the Fountain Formation, an apron of alluvial deposits fringing the ancestral Front Range uplift to the southwest. The "camel" lying on the pedestal is Lower Permian eolian sandstone of the Casper Formation. Photograph by D.W. Boyd.

The Ancestral Rocky Mountains in Wyoming

Edwin K. Maughan
U.S. Geological Survey
Denver Federal Center
Denver, Colorado 80225

Abstract

The Ancestral Rocky Mountains and contemporaneously formed lowlands in the Western Interior of the United States is a complex of northwest-trending uplifts of late Paleozoic age. These ancestral uplifts occupied approximately the same region of the Central Rocky Mountains as the late Cretaceous-early Tertiary Laramide uplifts. However, the more-or-less north-south trend of the Laramide ranges differs from the northwest-southeast trend of the Ancestral Rocky Mountains. The late Paleozoic uplifts formed along a belt in the western cratonic shelf where diastrophic compressional forces were transferred northwestward into the region from the Ouachita-Marathon orogenic belt of Oklahoma and Texas. These compressional forces were caused by the continental collision of the African and South American plate with the southern margin of the North American craton. Compressional forces directed into Colorado, Wyoming, and adjacent areas by the continental collision reactivated older structures of the craton. Recurrent structural movements throughout the region are expressed by diastrophism in a rectilinear orthogonal pattern.

The Ancestral Rocky Mountains diastrophism was characterized by orogeny in the Proterozoic terrane of Colorado, where elevated mountain blocks were eroded to produce large volumes of sediment. In contrast, epeirogeny in the tectonically more stable Archean terrane of Wyoming, resulted in lowland uplifts, which were eroded to produce only minor amounts of sediment. The Wyoming lineament crosses the Archean province from southwest to northeast and separates regions of greater epeirogeny in the southeast from less intense epeirogeny in the northwest.

Principal events of Ancestral Rocky Mountains diastrophism occurred at the onset of the Pennsylvanian Period, during late Atokan to early Des Moinesian time, and at the end of the Pennsylvanian. Some minor uplift, which occurred during the Mississippian Period in middle to late Meramecian time, preceded the Ancestral Rocky Mountains diastrophic events; and another minor uplift, which occurred during the Permian Period in Leonardian to Roadian time, succeeded the Pennsylvanian events.

Introduction

The Ancestral Rocky Mountains is a system of northwest-trending spurs on the northwest flank of the Transcontinental arch (**Figure 1**). The uplifts in Colorado and Wyoming southeast of the Wyoming lineament (Ransome, 1915, p. 294-295) formed a complex of en echelon ridges ranging from the principal orogenic highlands of the Ancestral Rocky Mountains—the Ancestral Uncompahgre uplift and the Ancestral Front Range—to low uplifts in eastern Wyoming—the Pathfinder uplift and a lowland in the vicinity of the Chadron arch and the Black Hills. Similar northwest-trending lowlands of lower amplitude

Maughan, E. K., 1993, The Ancestral Rocky Mountains in Wyoming, *in* Snoke, A.W., Steidtmann, J.R., and Roberts, S.M., editors, Geology of Wyoming: Geological Survey of Wyoming Memoir No. 5, p. 188-207.

than those in eastern Wyoming developed northwest of the Wyoming lineament. The principal northwest-oriented feature of this northwestern region was the Bannock highland in eastern Idaho and westernmost Wyoming. Farther east, in the region northwest of the lineament, other lowlands of probable northwest orientation are tenuously evident where they merge into the nearly east-west oriented Beartooth platform. Uplifts that formed north of the Wyoming lineament during the Pennsylvanian include: Gallatin ridge in northwestern Wyoming, an adjacent area in southwestern Montana, and several low-amplitude uplifts farther to the east that include an area of the present-day southern Bighorn Mountains (Dull Knife ridge); Darton ridge in the northern Bighorns (Todd, 1966); and the Miles City arch in southeastern Montana.

Late Paleozoic sedimentation and stratigraphy in Wyoming

Pennsylvanian strata in Wyoming and adjacent areas are bounded by regional unconformities that record the major tectonic events of the Ancestral Rocky Mountains diastrophism. The lithologies, thicknesses, and distribution of the Carboniferous and Permian sedimentary strata, especially those of the Pennsylvanian Amsden Formation, provide most of the clues to the interpretation of the late Paleozoic tectonic history. Erosional unconformities, lacunas in the rock record, and lithologic facies indicative of nearby terrigenous sources for the sediments identify epeirogenically uplifted areas in the region.

Mississippian strata

Mississippian strata in the Western Interior are composed dominantly of planar-bedded, shallow-water marine carbonate rocks of the Lodgepole Limestone and thick to massive bedded dolomite of the Mission Canyon Limestone (the Lower and Upper Mississippian Madison Group, respectively) (Smith, 1972, 1977; Craig, Connor, and others, 1979). These strata, deposited in a shallow, epeiric sea on the Wyoming shelf, thin regionally toward the Transcontinental arch from the Cordilleran miogeocline to the west and troughs northwest and north of the Wyoming shelf. Strata of the Upper Mississippian Big Snowy Group, which includes eolian dunes of the Darwin Sandstone and red mudstone beds of the equivalent Kibbey Formation, were deposited on a sabkha plain above the Madison. Strata in the Big Snowy Group above the Kibbey are mostly intracratonic lagoonal beds composed dominantly of mudstone and limestone. The Big Snowy Group, like the Madison Group, may have been deposited across most of the Wyoming shelf; but prior to Pennsylvanian deposition, the strata of this Upper Mississippian depositional sequence were eroded from most of the region except westernmost Wyoming. Remnants of the Darwin Sandstone occur beneath the Pennsylvanian strata at many places farther east from western to central Wyoming, but the Pennsylvanian overlaps older Madison strata in eastern Wyoming and Precambrian rocks in the southeastern part of the State.

Amsden sequence

The first depositional sequence in the Pennsylvanian Period, which followed the Mississippian-Pennsylvanian episode of differential uplift, is referred to as the Amsden sequence in this report. The Amsden sequence is an unconformity-bounded depositional subsequence that is coeval with the lower part of the Absaroka Sequence of Sloss (1963). The Amsden sequence includes: the Tyler Formation and Alaska Bench Limestone of the Amsden Group in Montana; the upper part of the Manning Canyon Formation and Round Valley Limestone in Utah and parts of southwestern Wyoming; the Amsden Formation (restricted to exclude the Darwin Sandstone Member) in northwestern Wyoming; the lower member of the Casper, Hartville, and Minnelusa formations in eastern Wyoming; and the lower member of the Fountain Formation adjacent to the Ancestral Front Range uplift in south-central Wyoming and Colorado (**Figure 2**). These Pennsylvanian sediments were deposited unconformably on rocks of Mississippian age in most of the region and on Precambrian rocks in southeastern Wyoming and adjacent parts of Colorado and Nebraska.

Sea level rose during early Pennsylvanian (Morrowan and early Atokan) time and sediments of the Amsden sequence covered the uneven, low-relief

topography of the Wyoming shelf, Transcontinental arch, and flanks of the Ancestral Rocky Mountains. The oldest deposits of the Amsden sequence indicate a sequential overlap of valley-filling fluvial, deltaic, and marine deposits. During this early depositional stage, the Wyoming shelf was a lowland, where subaerially exposed Mississippian carbonate rocks were weathered and dissolved to form karst, regolithic breccias, and an accumulation of lateritic terra rosa soils that were incorporated into the Horseshoe Member of the Amsden Formation. Alluviation in the valleys and accumulation of the lateritic soils was succeeded by marine deposition (Alaska Bench Limestone in Montana and Round Valley Limestone in northern Utah and adjacent areas in southwestern Wyoming) as the Pennsylvanian sea inundated these troughs. The shallow sea subsequently spread to inundate the lowland shelf in Wyoming and adjacent areas, depositing the Ranchester Member of the Amsden Formation.

The lateritic soils on the Wyoming shelf were eroded in the intertidal zone of the transgressing Early Pennsylvanian sea and redeposited with clay, silt, and

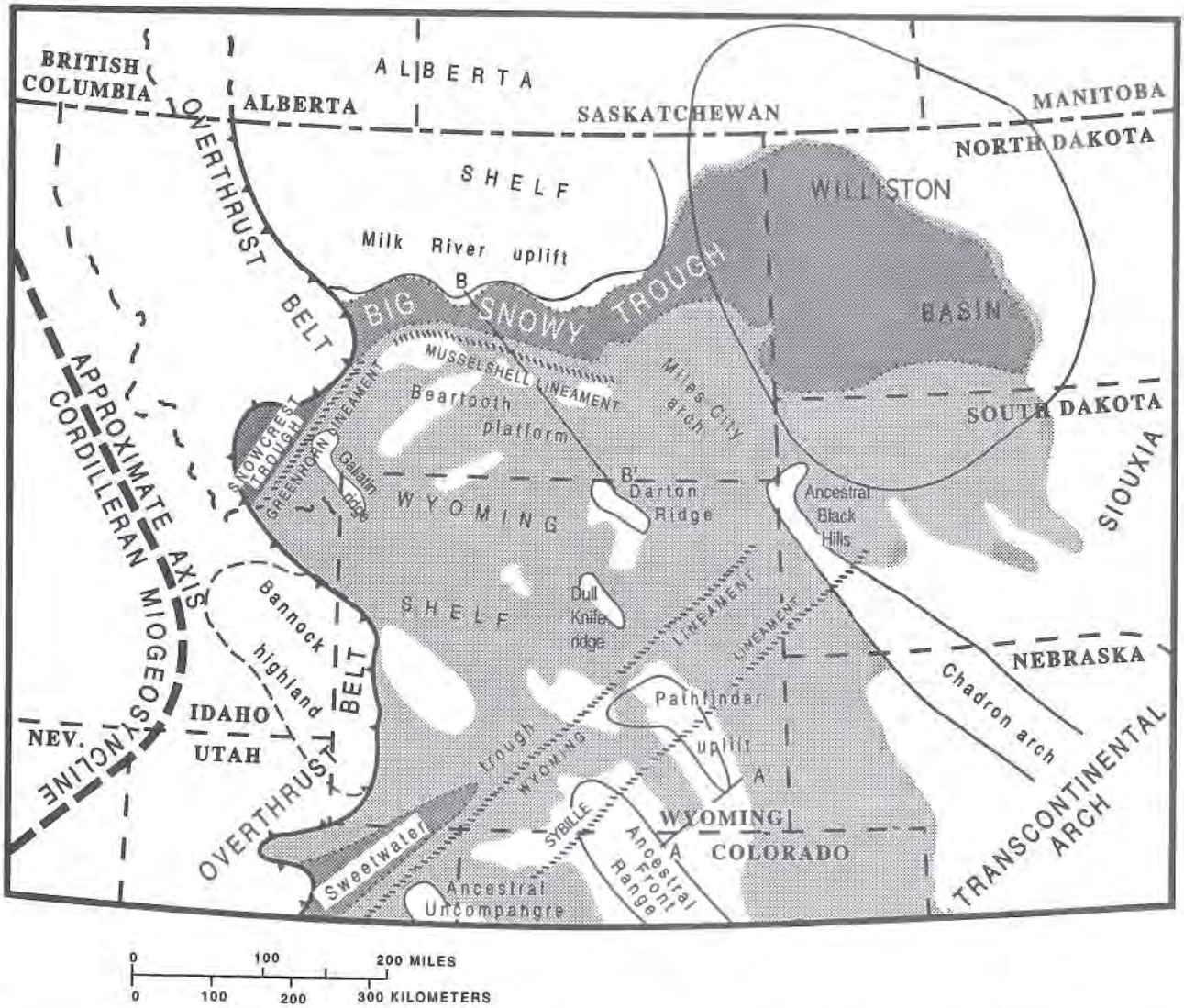

Figure 1. Map showing Ancestral Rocky Mountain structures. Shading indicates the distribution of Amsden Formation and equivalent strata (adapted from McKee and others, 1975), which reflects the Mississippian-Pennsylvanian and the Middle Pennsylvanian epeirogenic diastrophism: Dark shading=areal distribution of early stages of deposition of the Amsden sequence in structural sags; light shading=distribution of late stages of deposition of the Amsden sequence on lowlands; blank areas=Pennsylvanian uplifts where Amsden was not deposited or has been eroded. Amsden Formation is not shown west of the barbed line, which is the eastern limit of thrusts of the Sevier orogenic belt.

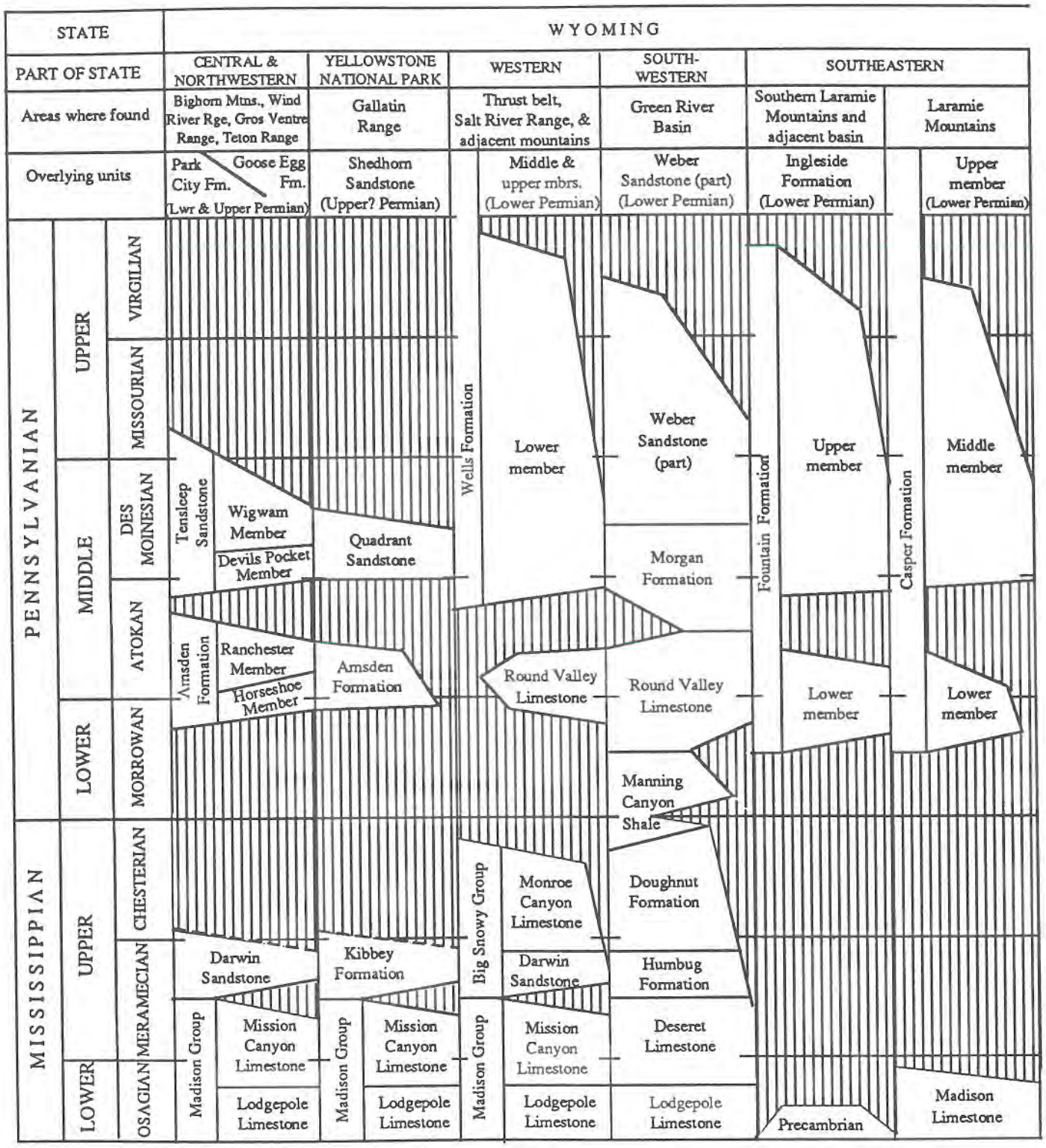

Figure 2. Summary of nomenclature and correlation of Upper Mississippian and Pennsylvanian rocks in Wyoming and parts of adjacent states as used in this report. [This figure does not conform, in all respects, to the stratigraphic chart of Love and others (this volume, map pocket).]

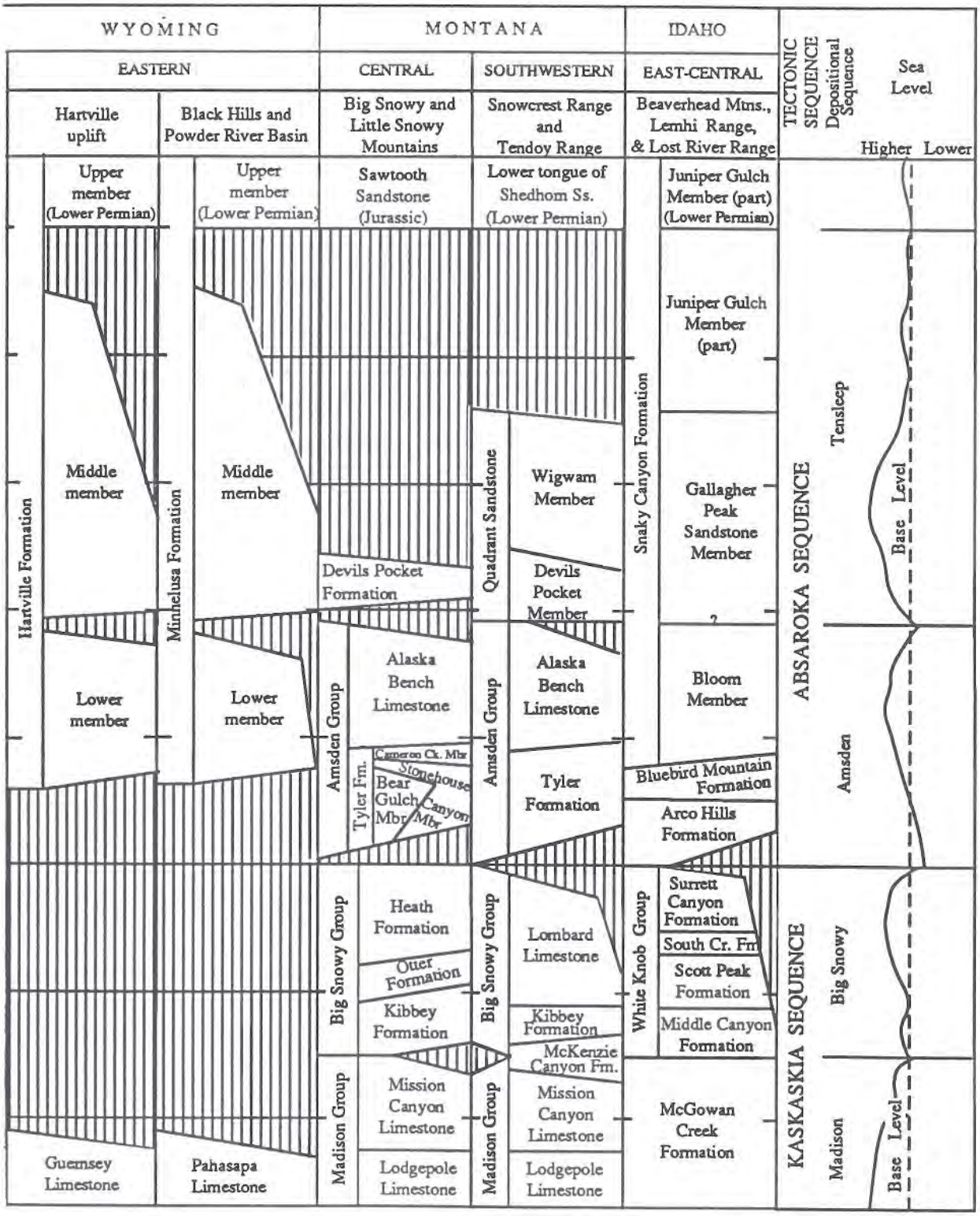

Figure 2. Continued

fine sand derived from the mountains and from Siouxia to form intertidal deposits of redbeds across most of Wyoming in the Horseshoe Member of the Amsden Formation and equivalent strata (**Figure 2**). Subsequent deepening of the epicontinental sea during early Middle Pennsylvanian (Atokan) time is indicated by the transition from mudstone in the Horseshoe Member to thin, interbedded limestone and red mudstone of the Ranchester Member of the Amsden Formation and its equivalents. Intercalated paleosols in coeval thin-bedded limestone in the lower member of the Hartville Formation in southeastern Wyoming is evidence for oscillations of sea level adjacent to the lowland near the crest of the Transcontinental arch.

Arkose and arkosic sand from the uplands of the Ancestral Rocky Mountains were deposited in the lower member of the Fountain Formation during Early to Middle Pennsylvanian time. The Fountain preserves fluvial fan-delta sediments deposited adjacent to the mountains on coastal plains and in intertidal mudflats in Colorado as the rising Early Pennsylvanian sea engulfed the lowlands adjacent to the mountains. The Middle Pennsylvanian diastrophism and its associated epeirogenic warping terminated Amsden deposition in Wyoming.

Absence of the Amsden sequence beneath the Tensleep sequence at many places on the Wyoming shelf indicates Early or Middle Pennsylvanian lowland uplifts of the Ancestral Rocky Mountains. The Bannock uplift, Beartooth platform, Miles City arch, Pathfinder uplift, and Ancestral Front Range uplift are documented by large areas where the Amsden and equivalent strata are missing. Numerous smaller areas of erosionally truncated or bevelled Amsden, including the Darton ridge, demonstrate that the Middle Pennsylvanian epeirogeny also produced a complex of smaller uplifted blocks throughout Wyoming.

Tensleep sequence

The second depositional sequence in the Pennsylvanian, which was initiated by the Middle Pennsylvanian Ancestral Rocky Mountains diastrophism, is referred to in this report as the Tensleep sequence. This unconformity-bounded depositional subsequence is coeval with a middle part of the Absaroka Sequence of Sloss (1963). The Tensleep sequence includes the Quadrant Sandstone of southwestern Montana; Tensleep Sandstone of northwestern Wyoming; equivalent middle members of the Casper, Hartville, and Minnelusa formations in eastern Wyoming, and the Wells Formation in central western Wyoming; the Morgan Formation and Weber Sandstone in southwestern Wyoming; and the upper member of the Fountain Formation in south-central Wyoming and areas adjacent to the Ancestral Front Range uplift in Colorado.

Middle Pennsylvanian uplift initiated a large supply of quartzose sand from an unidentified northern provenance. Well-sorted, fine- and medium-grained quartz sand is a major component of the Tensleep sequence. The inclusion of quartz sand differentiates this upper Pennsylvanian depositional sequence from the lower Pennsylvanian sequence, which contains no quartz sand except in the lowermost parts of the Amsden and in areas proximal to early Pennsylvanian uplands. Windblown, southerly transported quartz sand is the major component of the Quadrant and the Tensleep sandstones (Saperstone and Ethridge, 1984; Desmond and others, 1984), and tongues of eolian-transported sand occur in eastern Wyoming in equivalent parts of the Casper, Hartville, and Minnelusa formations (Tromp, 1984) and in the Wells Formation in western Wyoming.

Arkosic sand similar to the Lower Pennsylvanian arkose in these areas, which was derived more locally from Siouxia to the east and from rejuvenated mountainous terrains in the Ancestral Front Range and Uncompahgre uplifts, was incorporated into the upper member of the Fountain Formation and equivalent strata in Colorado. Tongues of arkose from these upland sources extend into the epeiric marine sediments of the middle member of the Casper Formation, the Hartville Formation in south-central and southeastern Wyoming, and the Morgan Formation in southwestern Wyoming and adjacent areas in northeastern Utah.

The Quadrant-Tensleep sand sea prograded across the Wyoming shelf from the north or northwest during Middle Pennsylvanian (Des Moinesian) and probably through most of Upper Pennsylvanian (Missourian and Virgilian) time. Shallow-water epeiric marine deposits of thin, interbedded sandy dolomite, sandy mudstone, and sandstone that comprise the Devils Pocket Formation in central Montana and the sandy, dolomitic Devils Pocket Member in the lower part of the Tensleep Sandstone in Wyoming were

succeeded by eolian dunes of the Wigwam Member of the Quadrant Formation in Montana and the Tensleep Sandstone in northwestern Wyoming. Tongues of these subaqueous and eolian facies extend into the Morgan and Weber formations, into the middle member of the Casper Formation in southern Wyoming, and into the middle members of the Hartville and Minnelusa formations in eastern Wyoming (Tromp, 1984; Desmond and others, 1984). Equivalent strata in western Wyoming are mostly sandy limestone and dolomite beds in the Wells Formation that were deposited in a chiefly marine environment. The dominantly eolian sandstone beds of this sequence intertongue with fan-delta and fluvial greywacke and arkosic sand deposits of the upper member of the Fountain Formation in coastal plain and nearshore areas adjacent to the Ancestral Front Range.

Deposition of the Tensleep sequence ended during Late Pennsylvanian to Early Permian uplift of the Wyoming arch (H.D. Thomas, personal communication, 1957), which trended south from the Milk River uplift in central Montana to the Ancestral Front Range in Colorado (Maughan, 1967). An east-west cross section of Pennsylvanian and Lower Permian strata in Wyoming (Love, 1954) shows the bevelling, thinning, and onlapping of these strata across this arch, and gives indication of the Pathfinder uplift and some of the more localized Pennsylvanian tectonic perturbations.

Permian sediments

Sand, eroded in Early Permian time from the Pennsylvanian beds exposed on the Milk River uplift and on the Wyoming arch, was deposited on the east and southeast flanks of these uplifts in eolian sandstone units of the upper member of the Minnelusa Formation, in equivalent age rocks in the upper members of the Hartville and the Casper formations, and in the Ingleside Formation. Coeval sand formed tongues of the Shedhorn Sandstone and the lower part of the Grandeur Member of the Park City Formation ("Nowood member" of McCue, 1953) on the west side of these uplifts. Arkose was deposited very locally adjacent to the Ancestral Front Range in Colorado and south-central Wyoming. The limited dispersal of this arkose provides an indication of the low relief of this late stage of uplift.

Highlands of the Ancestral Rocky Mountains in Wyoming

The Ancestral Uncompahgre and Front Range, the major features of the Ancestral Rocky Mountains, were mostly in Colorado; but the latter highland extended into south-central Wyoming to the site of the present-day Sierra Madre. The central Colorado trough, also a northwest-trending feature, separated these two ranges. The high relief of these mountain ranges is indicated by the large volume of coarse-grained and conglomeratic arkose deposited in adjacent sediments.

The uplifts that were formed in southeastern Wyoming by the Ancestral Rocky Mountains diastrophism were minor by comparison to those in Colorado. The Uncompahgre, Front Range, and Pathfinder uplifts, and the low uplift in the vicinity of the Chadron arch and the Black Hills comprise a system of northwest-trending spurs on the west flank of the Transcontinental arch. These uplifts terminate at the Sweetwater trough; however, similar low uplifts north of the trough continued the trends of the Ancestral Rocky Mountains in northwestern Wyoming onto the Beartooth platform in south-central Montana.

Ancestral Front Range uplift

Episodic uplift of the Ancestral Front Range is indicated by depositional sequences of conglomeratic beds of Early Mississippian, Early, Middle and Late Pennsylvanian, and Early and middle Permian age on the flank of the uplift. The sequences are separated by erosional unconformities. The older sequences are erosionally bevelled and are overlapped toward the axis of the Front Range by successively younger sequences. **Figure 3** is a generalized southwest to northeast cross section that illustrates this bevelling and overlapping from the eastern flank of the Medicine Bow Mountains to the eastern flank of the Laramie Mountains. On the western flank of the Medicine Bow Mountains, Upper Permian rocks of the upper part of the Goose Egg Formation (not shown on **Figure 3**)

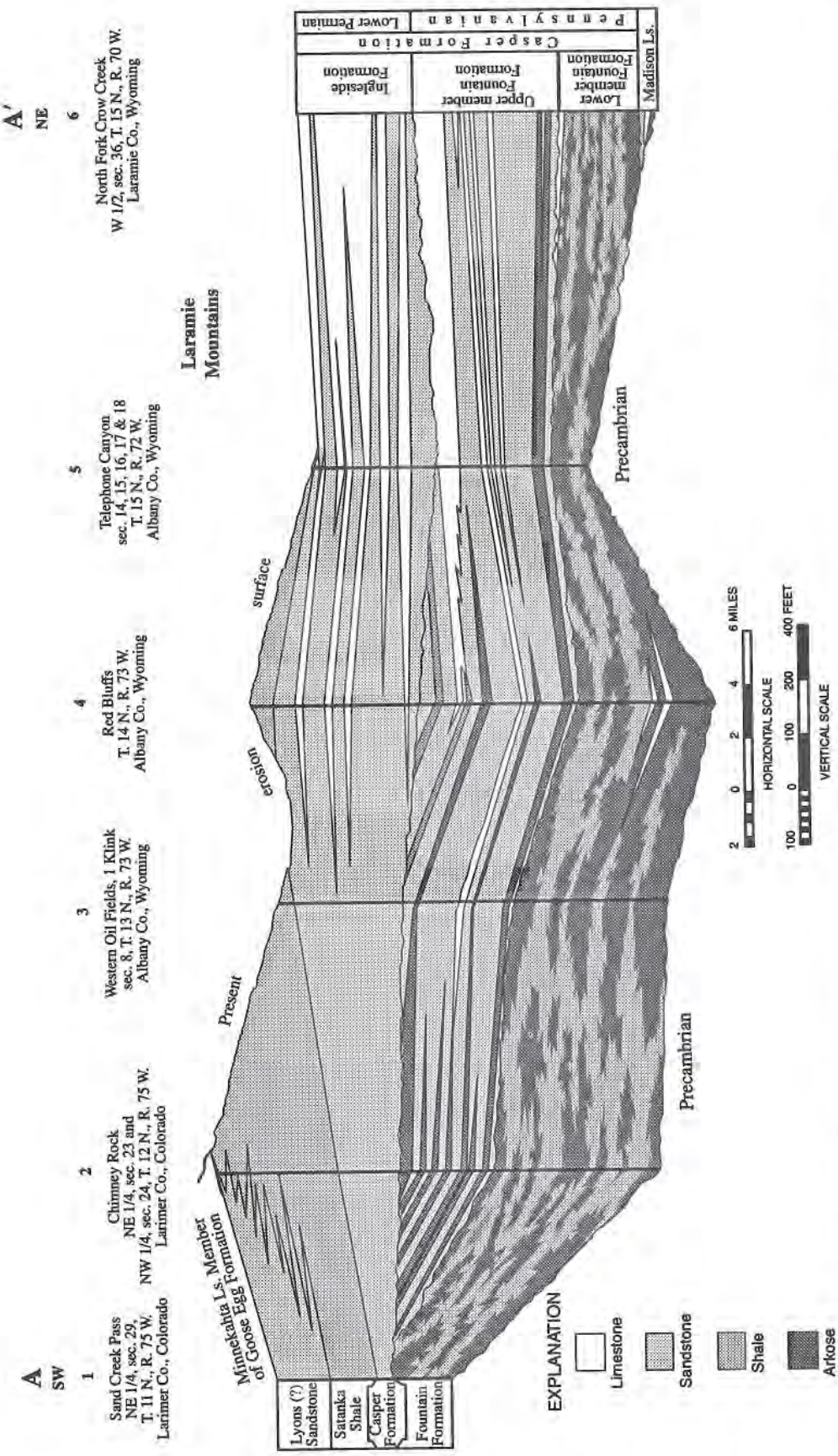

Figure 3. Cross section AA' of upper Paleozoic rocks showing depositional onlap and erosional truncation of Pennsylvanian sequences beneath an unconformable contact with Lower Permian strata. The cross section is approximately normal to the axis of the Ancestral Front Range and runs northeast from the eastern flank of the Medicine Bow Mountains in north-central Colorado through the Laramie Basin to the northeastern flank of the Laramie Mountains in southeastern Wyoming. Approximate location shown on Figure 1.

occur unconformably upon Precambrian rocks in northeastern North Park, Colorado. Still farther west, Upper Permian strata were not deposited or were erosionally bevelled in northwestern North Park, where Triassic beds lie unconformably above Precambrian rocks near the axis of the Ancestral Front Range. Conglomerate in the Pennsylvanian sequences is thick and coarse with clasts that range up to cobble size, but Permian conglomeratic beds are thin, areally limited, and composed of small clasts. In large part, the Permian conglomerate is redeposited from erosion of the conglomeratic Fountain Formation. The conglomeratic beds are generally unfossiliferous, but they intertongue with sparsely fossiliferous marine beds that provide paleontological ages. The overlap of the lower Permian sequence is indicated by fusulinids of Wolfcampian age (L.G. Henbest, written communication, 1965) in arkosic sandstone that lies unconformably on Precambrian crystalline rocks on the flank of Sheep Mountain near Centennial, and along the upper course of Wagonhound Creek in the Medicine Bow Mountains south of Arlington.

Pathfinder uplift

Uplift during the Pennsylvanian in the northern Laramie Mountains (Thomas and others, 1953) and westward in the Alcova and Pathfinder areas is identified as the Pathfinder uplift (Mallory, 1963). Pennsylvanian strata overlap Mississippian strata and lie unconformably on Precambrian rocks similar to the depositional onlap of Pennsylvanian strata on the flank of the Ancestral Front Range. Precambrian rocks are deeply weathered and karst is well developed beneath the Pennsylvanian rocks, indicating longer subaerial exposure prior to burial by the sediments on the uplift as compared to adjacent areas. Uplift during the Pennsylvanian is also indicated by the overlapping of Casper Formation strata corresponding to the Amsden sequence by strata corresponding to the younger Pennsylvanian Tensleep sequence. Upper Pennsylvanian strata are unconformable upon Mississipppian and Precambrian rocks in the Casper Mountain area (Thomas and others, 1953); but thin Amsden beds at Fremont Canyon (**Figure 4**) and thicker Amsden farther west indicate the onlap of this lower depositional sequence on the west flank of the Pathfinder uplift. Amsden exposed in the cliffs of Fremont Canyon includes only two thin units: red mudstone of the Horseshoe Member that fills karstic sink holes in the Madison Limestone, and a thin limestone bed of the Ranchester Member that lies unconformably upon the Madison and the karst-filled sink holes. Similar onlapping relationships are evident on the east flank of the Pathfinder uplift in the northern Laramie Mountains east of Casper Mountain. The local and regional relationship of these Amsden strata indicate that the Pennsylvanian sea submerged the Early Pennsylvanian uplifted terrane after the subaerial formation of terra rosa on the Mississippian carbonate rocks and subsequent erosional stripping of these redbeds. The limestone beds that usually occur in the upper part of the Amsden were either only thinly deposited, or a thicker limestone sequence was deposited and erosionally removed from the uplift during subsequent Middle Pennsylvanian rejuvenation.

Bannock uplift

The Bannock highland (Williams, 1962, p. 166), occupies an area where strata of the Amsden sequence are mostly absent. The area of this uplift is approximately outlined in **Figure 1**, and it may have extended farther northwest to the Wood River region in central Idaho. [Upper Mississippian strata that are equivalent to the Upper Mississippian Big Snowy Group of Montana have been miscorrelated and misidentified as Amsden on this Pennsylvanian lowland (Maughan, *in* Lageson and others, 1979; Maughan, in press). These Upper Mississippian strata were deposited earlier and are unconformably overlain by the redbeds and limestone of the Amsden sequence that occur at some places in western Wyoming adjacent to the Bannock uplift.] The Bannock "highland" was an area of low relief where Upper Mississippian rocks are unconformably overlain by the Middle and Upper Pennsylvanian Wells Formation (identified as Ranchester Member of the Amsden Formation by Sando and others, 1975), which corresponds to the Middle and Upper Pennsylvanian Tensleep sequence. The Wells Formation, like equivalent Middle and Upper Pennsylvanian strata elsewhere in Wyoming, is composed primarily of sandy carbonate rock and sandstone beds quite unlike the interbedded limestone and shale that is characteristic of the Amsden. Thin remnants of Amsden-like rocks of late Morrowan or Atokan age that locally occur within the Bannock uplift have commonly been included as part of the Wells Formation. Remnants of the Amsden in the region of the Bannock uplift are not extensive, although rocks of the Upper Mississippian Big Snowy

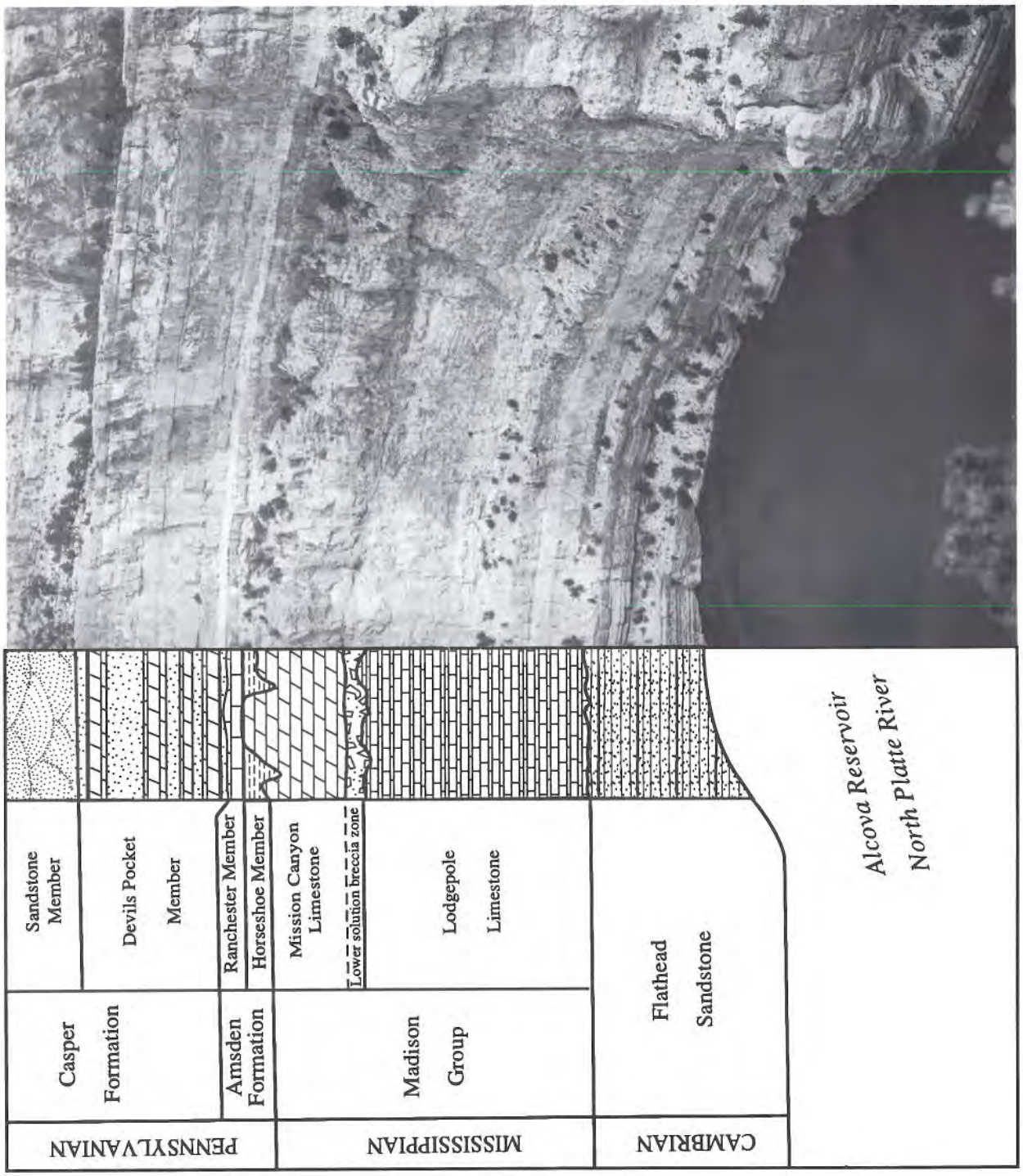

Figure 4. Photograph at Fremont Canyon on the flank of the Pathfinder uplift. Sink holes filled with red mudstone of the Horseshoe Member and a thin bed of limestone of the Ranchester Member separate the Lower Mississippian part of the Madison Limestone from the Middle or Upper Pennsylvanian beds of the Casper Formation.

Group are shown as Amsden on some geologic maps in the region, such as the maps of the Bedford and Afton quadrangles (Rubey, 1958, 1973).

The Bannock uplift may be a northwest extension of the ancestral Uncompahgre uplift. However, this uplift has been distorted and transported eastward from its original position by post-Paleozoic thrusting. Regional stratigraphic relationships indicate that it developed during the early Pennsylvanian in a way similar to the Pathfinder uplift. However, the Bannock uplift was not rejuvenated in Middle to Late Pennsylvanian time, and it remained an area of sediment accumulation. Minor, post-Pennsylvanian uplift is indicated where upper members of the Phosphoria and Park City formations were not deposited or were erosionally bevelled during Late Permian time.

Beartooth platform

The Beartooth platform (Beartooth shelf of Peterson, 1981, 1986; Maughan and Perry, 1986) is an area of Pennsylvanian uplift in south-central Montana adjacent to the Snowcrest trough on the west and the Big Snowy trough on the north (Maughan, 1984). The platform sloped south into northwestern Wyoming during Pennsylvanian deposition. The bevelled and onlapping strata across the platform is illustrated in **Figure 5**. Thick strata of the late Meramecian and Chesterian Big Snowy Group in the troughs in Montana are abruptly truncated and were eroded from the Beartooth platform adjacent to the Greenhorn and Musselshell lineaments. Farther south, remnants of the Darwin Sandstone, an equivalent of the upper Meramecian to Chesterian(?) Kibbey Formation, indicate that at least the lower part of the Big Snowy Group was deposited and locally preserved on the Beartooth platform and southward in central Wyoming. The Amsden Group, while it overlaps the truncated strata of the Big Snowy Group, also abruptly thins by depositional onlap across the Greenhorn and Musselshell lineaments; and it is absent at many places in the northern part of the platform. At a few places on the platform, the Alaska Bench Limestone (Ranchester equivalent) overlaps older Pennsylvanian strata and lies unconformably upon the Mission Canyon Limestone similar to the relationships observed at Fremont Canyon (**Figure 5**) and in other parts of the Pathfinder uplift. This onlapping relationship of the Amsden sequence indicates Late Mississippian-Early Pennsylvanian uplift of the Beartooth platform.

The Tensleep sequence is also thin adjacent to the Beartooth platform and the Amsden may have been bevelled or removed at some places on the platform, indicating Middle Pennsylvanian rejuvenation. Whether rejuvenation was due to Middle or Late Pennsylvanian epeirogeny is not clear. There is inadequate paleontological control of the Tensleep sequence to assess whether thinning of these strata was by depositional onlap or erosional bevelling. I suspect that the tectonic history was similar to other parts of the Wyoming region and that both depositional thinning and erosion account for this thinning. Most of the thinning in the vicinity of the Beartooth platform was contemporaneous with the Pennsylvanian to Permian development of the Milk River uplift and Wyoming arch.

Minor uplifts

Gallatin ridge, Dull Knife ridge, Darton ridge, and the Chadron arch-Black Hills uplift are smaller areas where Pennsylvanian uplift is evident in ways similar to the larger areas described above. At Gallatin ridge, the Amsden sequence is absent and Permian strata are also missing, indicating Early or Middle Pennsylvanian and Early Permian uplift of this feature. Dull Knife ridge is indicated in the southern Bighorn Mountains, where strata of the Amsden sequence are thin or absent and where Lower Permian strata overlap and pinch out on the Tensleep Sandstone. Darton ridge is defined by thinning of the Tensleep Sandstone in the northern Bighorn Mountains (Todd, 1966). The Chadron arch-Black Hills uplift is indicated by the absence of the Amsden sequence in the lower part of the Minnelusa Formation at places in the Black Hills and in subsurface sections to the south in South Dakota and Nebraska. Locally missing strata of the Amsden or the Tensleep sequences at many other places in the Western Interior suggest additional minor ridges and uplifts of the Ancestral Rocky Mountains diastrophism may be defined in the region by further stratigraphic studies.

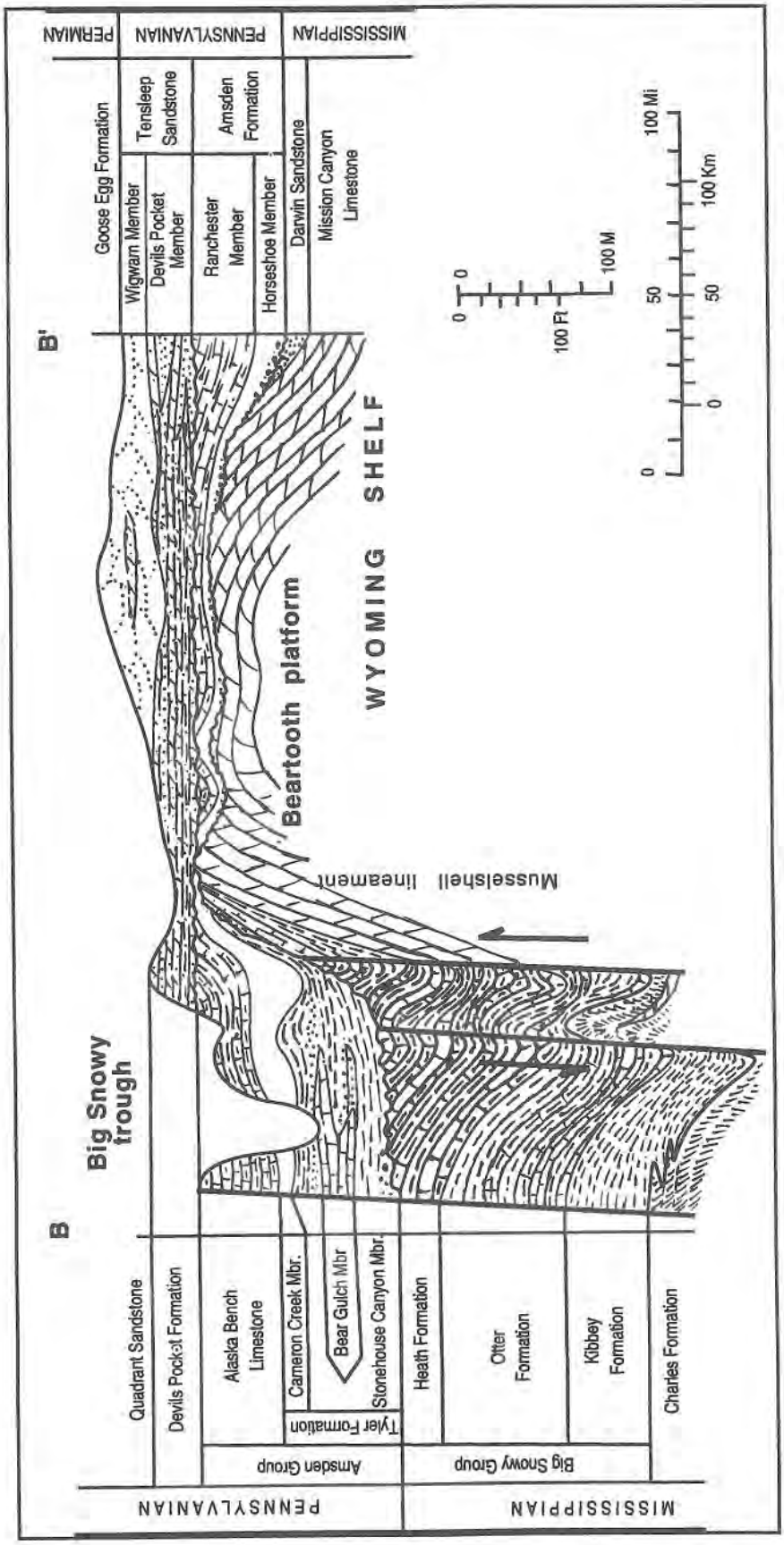

Figure 5. Cross section BB' of Upper Mississippian and Pennsylvanian strata showing relationships of Beartooth Platform and Big Snowy trough (see Figure 1) from the vicinity of Amsden Creek in the northern Bighorn Mountains to the northern flank of the Big Snowy Mountains (modified from Maughan and Roberts, 1967). Approximate location shown on Figure 1.

Late Paleozoic regional tectonic patterns

The Ancestral Rocky Mountains developed in response to stresses during the late Paleozoic from the suturing of the North American plate in the Ouachita-Marathon orogenic belt with the African and South American plates (**Figure 6**; Kluth, 1986). The North American continent was subject to moderate to intense diastrophism during the late Paleozoic that increased notably in intensity during the Mississippian, especially on the eastern margin of the continent; culminated during the Pennsylvanian on the southern margin; and diminished during the Permian on the southern margin and in the western Cordilleran region. Continental collision in the Appalachian orogenic belt preceded collision and orogeny along the southern margin that contributed to the Ancestral Rocky Mountains diastrophism of the Western Interior.

The rock record and structures in the region that was the western continental margin (Cordillera) also indicate there was moderate to appreciable instability and diastrophism in that part of North America during late Paleozoic time. Recent studies (Trexler and others, 1991) suggest timing of tectonic events in the Cordilleran region was approximately contemporaneous with Pennsylvanian and Permian events in Wyoming and adjacent areas of the Western Interior. Diastrophism in the Ancestral Rocky Mountains during the late Paleozoic shifted from east to west similar to the shift of orogeny from the Ouachita to the Marathon region along the southern continental margin. As noted by Kluth (1986), the similar times of deformation and consequent accumulation of sediments derived from the Ancestral Rocky Mountains were too close in time to those of the Ouachita-Marathon orogens to be coincidental.

Archean crust that underlies most of Wyoming (Tonnsen, 1986) seems to have limited the intensity of the late Paleozoic epeirogenic disturbances of the Wyoming shelf. The low amplitude of epeirogenic deformation in Wyoming, in contrast to the high-relief orogeny in Colorado, may be attributed to a greater stability of Archean crust as opposed to the younger

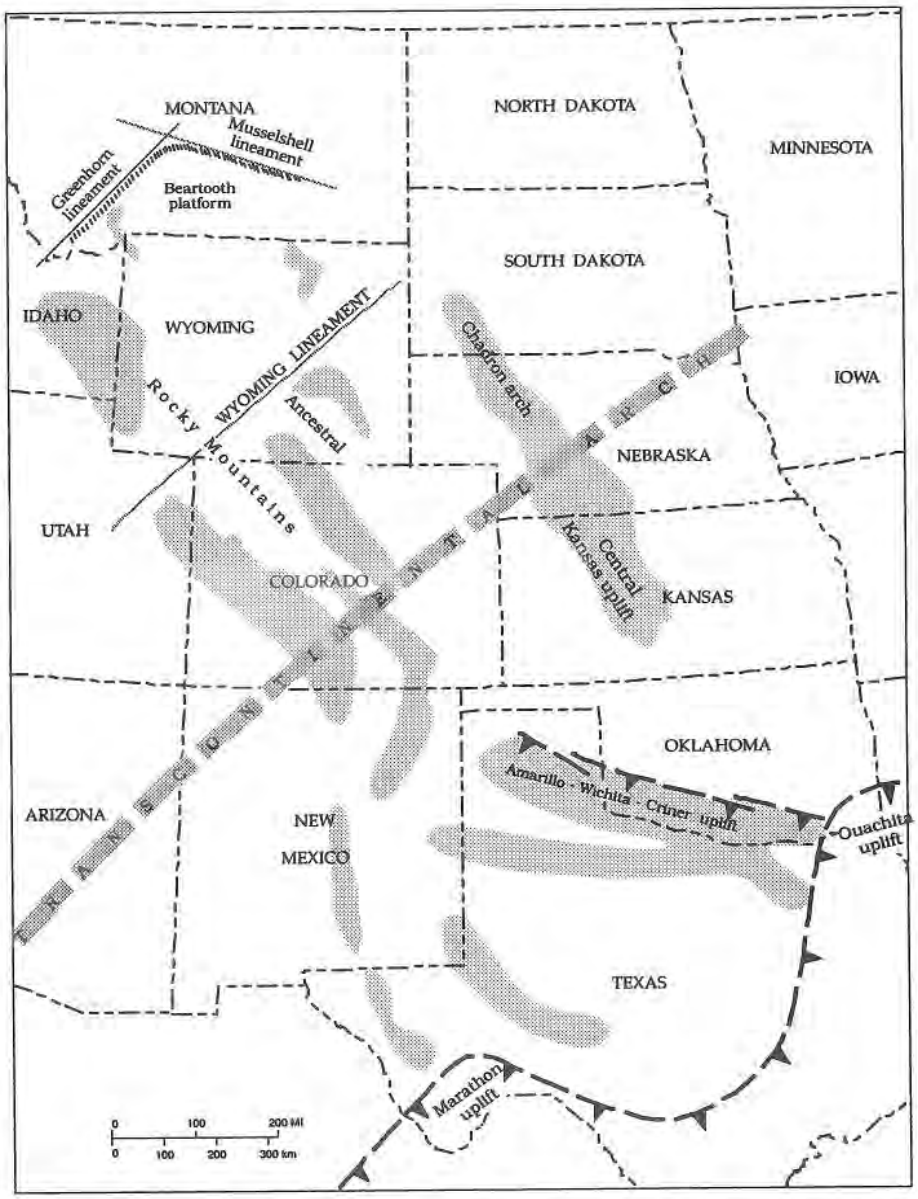

Figure 6. Map showing spatial relationships of major uplifts of the Ancestral Rocky Mountains in Wyoming and other Pennsylvanian uplifts apparently related to the Ouachita-Marathon continental collision zone (adapted from Kluth, 1986).

and apparently less stable Proterozoic crust, upon which the Ancestral Front Range in Colorado and southernmost Wyoming and Ancestral Uncompahgre uplift in Colorado and Utah were formed.

The Wyoming Archean province lies between the Sybille lineament in southeastern Wyoming and the Big Snowy trough in central Montana (**Figure 1**), but it is dissected by the Sweetwater trough along the "Wyoming lineament" of Ransome (Maughan and Perry, 1986). The Wyoming lineament and associated trough separate the Ancestral Rocky Mountains epeirogenic structures of the Wyoming shelf into a southeastern and a northwestern structural region. The southeastern structural region is approximately coincident with the southern Wyoming Precambrian paleotectonic block of Tonnsen (1986, figure 4, p. 24) and it is in the area of a postulated early Proterozoic subduction zone (Hills and Houston, 1979; Tonnsen, 1986, p. 25; Houston, this volume). The northwestern structural region of the Wyoming shelf is approximately coincident with Tonnsen's stable Archean paleotectonic block.

Two precursor tectonic events in the Western Interior, which occurred during Late Devonian (about 360 Ma) and early Late Mississippian time (about 330 Ma), foreshadowed the Ancestral Rocky Mountains diastrophism, which consisted of three principal tectonic events during the Pennsylvanian Period. The three events are evident from the erosional unconformities shown in **Figure 3**, and from the hiatuses indicated on the nomenclature chart, **Figure 2**. The first major epeirogenic event of the Ancestral Rocky Mountains diastrophism took place during latest Mississippian to earliest Pennsylvanian time (about 330 to 320 Ma). The second event took place during Middle Pennsylvanian (late Atokan, about 315 Ma). The third, a weaker event, took place during Late Pennsylvanian to Early Permian time (about 285 Ma). This latter event may have been preceded by at least one, and possibly two, Late Pennsylvanian events (Missourian and Virgilian), for which there are only hints in the mostly continental, eolian sediments of the region. Two successive tectonic events, one about late Early Permian (about 250 Ma) and the other during Late Permian (between about 240 and 230 Ma), weakly echo the major Ancestral Rocky Mountains diastrophism in the Western Interior. These tectonic events were recorded in the depositional sequences and erosional intervals of the late Devonian through Permian strata of the Western Interior North American cratonic shelf.

During the Mississippian, broad areas of epeiric warping of the craton in the Western Interior, especially in the eastern part of the region, formed in response to early phases of continental collision—primarily along the eastern continental margin. The Wyoming region was a slowly subsiding, tectonically stable shelf during most of the Mississippian Period. Subsidence was greater northwestward toward the axis of the Cordilleran miogeosyncline in Utah and Idaho and the intracratonic Snowcrest and Big Snowy troughs in western and central Montana. The thickness of the Mississippian rocks generally increases westward and northwestward in the region (Craig, Connor, and others, 1979). Subsidence during the Mississippian diminished southeastward and eastward toward the Transcontinental arch and the Siouxia extension of the Canadian shield, where Mississippian strata overlap, thin, and tongue into siliciclastic sediments adjacent to the lowlands formed by these paleotectonic features (Macke, in press).

Normal faults coincident with north-northwest-trending lineaments (Maughan, 1983; Maughan and Perry, 1986) bound the uplifts and define a complex set of horsts and grabens that comprise the Ancestral Rocky Mountains system in the Western Interior. This tectonic pattern indicates northeast-southwest extension in response to the northwest-directed compressional stress of the Ouachita-Marathon orogeny (Kluth, 1986). Most of the uplifts terminate along conjugate lineaments that trend east-northeast. The principle east-northeast-trending Wyoming lineament approximately marks the northwestern termini of the Uncompahgre, Front Range, and Pathfinder uplifts. Ransome's Wyoming lineament approximates the parallel east-northeast trend of the axis of the Sweetwater trough (Mallory, 1972, figure 4, p. 115), which was tectonically negative during much of the Paleozoic Era (Macke, in press).

Late Paleozoic low uplifts in northwestern Wyoming between the Sweetwater trough and the Beartooth platform continue the trends of the Ancestral Rocky Mountains in northwestern Wyoming and southwestern Montana (**Figure 1**). The Bannock uplift, a late Paleozoic feature that was subsequently tectonically telescoped and transported eastward in

the overthrust belt of western Wyoming, may be a northwest extension of the Ancestral Uncompahgre uplift or of another Ancestral Rocky Mountain uplift farther west in Utah (not considered in this study). The Gallatin ridge, in the vicinity of the southern Gallatin Range in the Yellowstone Park area, continued the trend of the Ancestral Front Range northwestward onto the western edge of the Beartooth platform. Dull Knife ridge, in the vicinity of the present southern Bighorn Mountains, extended the trend of the Pathfinder uplift to the northwest. The Miles City arch in southeasternmost Montana formed where the Chadron arch-ancestral Black Hills intersected the east-west-trending uplift of the Beartooth platform.

Late Mississippian and Early Pennsylvanian structural trends in south-central Montana were west-northwest. The orientation of the Big Snowy trough of this area is related to a probable ancient aulacogen in central Montana. However, most other Mississippian structural features in the Western Interior are oriented primarily northwest-southeast and secondarily are northeast-southwest. Broad, northwest-oriented Mississippian uplift in the vicinity of Laramie Mountains, Medicine Bow Mountains, and Sierra Madre, foreshadowed the Pathfinder and Ancestral Front Range uplifts of the Pennsylvanian Period. Mississippian deposits of sandstone and arkosic sandstone adjacent to elevated areas in southeastern Wyoming are overlain by carbonate rocks deposited during subsequent transgressive inundation of the epeiric sea.

During the first major tectonic event, which was coincident with Early Pennsylvanian continental collision and the first phase of the Ouachita orogeny in Oklahoma (Kluth, 1986), the Ancestral Rocky Mountains were orogenically elevated and Precambrian rocks were exposed and eroded in Colorado. The Wyoming shelf was elevated and Mississippian deposition was terminated as the sea withdrew from the Western Interior. The shelf in Wyoming was epeirogenically deformed by low-amplitude, northwest oriented folding and faulting. Elevated Mississippian rocks were deeply eroded in some areas. Other areas remained low, and a thick terra rosa paleosol was generated during prolonged subaerial weathering of the Mississippian carbonate rock before it was covered by the transgressing Pennsylvanian sea. Still other areas subsided and there was a minimum of weathering and little erosional truncation of the Mississippian strata prior to inundation by the Pennsylvanian sea (the Big Snowy trough in central Montana, Snowcrest trough in southwestern Montana, and Sweetgrass trough in south-central Wyoming and adjacent areas in Utah).

The more-or-less east-west trend of the Beartooth platform adjacent to the Big Snowy trough in south-central Montana (Maughan and Perry, 1986; Peterson, 1986) can be explained by differently directed epeirogenic stresses in that area or by deflection of strain into strike-slip movement along pre-existing west-northwest structures. Elsewhere in the Western Interior, the Pennsylvanian structures trend mostly northwest-southeast.

The second Ancestral Rocky Mountains diastrophic event occurred during Middle Pennsylvanian (probably late Atokan) time. This event was coincident with further continental collision and orogeny in Oklahoma that extended west of the Ouachita region to include the Amarillo-Wichita-Criner Hills trend (Kluth, 1986). The Ancestral Uncompahgre and Ancestral Front Range uplifts in Colorado were rejuvenated by tectonic stresses that projected northwestward from the diastrophism in Oklahoma. The Wyoming shelf adjacent to the Ancestral Rocky Mountains was differentially deformed by low-amplitude folds and faults. The Pathfinder, Bannock, and other previously elevated areas were rejuvenated; but for the most part they were only slightly emergent or remained shallowly submerged. Precambrian rocks exposed in the highly elevated mountains of Colorado were the source of thick arkosic sand and gravel deposited on the surrounding coastal plain. Amsden strata on the epeirogenically deformed shelf were locally exposed and erosionally bevelled in some areas and entirely eroded in other places.

The Western Interior was regionally, but differentially, elevated during Pennsylvanian to Permian diastrophism. Pennsylvanian to Permian regional uplift was preceded by Missourian and Virgilian sedimentation that may have included a Late Pennsylvanian diastrophic event not evident in the remnants of the dominantly terrigenous Upper Pennsylvanian clastic rocks of the Wyoming shelf. Diastrophism during the Late Pennsylvanian is evident farther west by unconformities recorded in the southern Rocky Mountain and Cordilleran regions that may be attributed to increased orogeny in the Marathon region as

diastrophism diminished in the Ouachita region during the Late Pennsylvanian (Kluth, 1986).

Pennsylvanian deposition was terminated in the Western Interior by Late Pennsylvanian (Virgilian) to Early Permian (early Wolfcampian) uplift of the region. Differential uplift is indicated by Lower Permian sediments that lie disconformably above eroded Pennsylvanian strata as young as Virgilian at places in the Laramie Mountains and in the Colorado Front Range, but lap unconformably onto older Pennsylvanian and Precambrian rocks at other places, such as in the Medicine Bow Mountains. The amplitude of the uplifts of this third stage of the Ancestral Rocky Mountains diastrophism were minor except that the Ancestral Front Range and Uncompahgre uplifts were rejuvenated and again were sources of arkosic sediments. The Ancestral Uncompahgre is indicated to have been elevated more than the Front Range by the greater accumulation in adjacent troughs of Lower Permian arkosic sediments derived from these areas. Elsewhere in the Western Interior, the Late Pennsylvanian-Early Permian diastrophism is primarily expressed by the development of the Wyoming arch, which connected elevated terrains in Colorado and Montana, and by the broad Milk River uplift in Montana. Pennsylvanian rocks subaerially exposed on these lowlands were the source of sand deposited during the Early Permian.

Middle to Late Permian diastrophism is scarcely detectable in the Permian strata. The Phosphoria and equivalent Goose Egg Formation are nearly conformable upon older Permian strata. There is subtle evidence in most places in the Western Interior for weathering or erosion or other indications of a hiatus at this contact. Minor epeirogeny is indicated by regional bevelling of the underlying units, and faulting is evident in a few places. Conglomerate in the Opeche Shale Member of the Goose Egg Formation on the west flank of the southern Bighorn Mountains (J.D. Love, personal communication, 1958) was derived from uplift of the Dull Knife ridge, and abrupt thickening of the Opeche from the Miles City arch into the Williston basin along the Cedar Creek structure are notable indications of faulting related to the Middle Permian diastrophism.

Late Permian to Early Triassic was a period of remarkable tectonic stability in the Western Interior. Upper Permian strata do not occur in the region and the Lower Triassic is paraconformable above the Upper Permian lacuna (Newell, 1967; Schock and others, 1981).

Conclusions

The evidence for the Ancestral Rocky Mountains epeirogeny is mostly contained within less than 1,000 ft (300 m) of rock strata throughout the Wyoming region except for the much greater thicknesses and a more complete stratigraphic range in the Sweetwater, Snowcrest, and Big Snowy troughs. The troughs and the major positive elements—the Ancestral Front Range, Ancestral Uncompahgre, Pathfinder, Bannock, and Beartooth uplifts—as well as the minor uplifts, show a similar history of development that was related to a series of tectonic disturbances accompanied by marine regressions and transgressions and associated erosion and deposition in the Western Interior. Diastrophism in the region was concurrent with orogeny during continental collision with the African and South American plates along the southern margin of North America. The depositional sequences, lithofacies, and erosional intervals discussed above can be observed at many places in the Wyoming region.

Acknowledgments

The interpretations of late Paleozoic tectonic events summarized in this report are the result of many years of investigation by me and the assimilation of data and understanding of many unnamed persons. I have drawn liberally from the U.S. Geological Survey paleotectonic maps of the Mississippian (Craig, Connor, and others, 1979), Pennsylvanian (McKee, Crosby, and others, 1975), and Permian (McKee, Oriel, and others, 1967a; 1967b). Some of this work is acknowledged in the cited references; but I

must express special gratitude to J.D. Love and D.L. Blackstone, Jr., as well as W.W. Mallory, H.D. Thomas, A.E. Roberts, W.J. Sando, J.A. Momper, G.J. Verville, and H.I. Saperstone, who contributed additional significant information to help formulate these interpretations. The manuscript was critically reviewed by James A. Peterson, William W. Mallory, and the editors of this volume, whose comments have been most helpful and are greatly appreciated.

References cited

Craig, L.C., Connor, C.W., and others, 1979, Paleotectonic Investigations of the Mississippian System in the United States: U.S. Geological Survey Professional Paper 1010, 559 p.

Desmond, R.J., Steidtmann, J.R., and Cardinal, D.F., 1984, Stratigraphy and depositional environments of the middle member of the Minnelusa Formation, central Powder River Basin, Wyoming, *in* Goolsby, J., and Morton, D., editors, The Permian and Pennsylvanian Geology of Wyoming: Wyoming Geological Association 35th Annual Field Conference Guidebook, Casper, Wyoming, p. 213-239.

Harland, W.B., Armstrong, R.L., Cox, A.V., Craig, L.E., Smith, A.G., and Smith, D.G., 1990, A geologic time scale 1989; Cambridge University Press, 263 p.

Hills, F.A., and Houston, R.S., 1979, Early Proterozoic tectonics of the central Rocky Mountains, North America: University of Wyoming Contributions to Geology, v. 17, p. 89-109.

Kluth, C. F., 1986, Plate tectonics of the Ancestral Rocky Mountains, *in* Peterson, J.A., editor, Paleotectonics and sedimentation in the Rocky Mountain region, United States: American Association of Petroleum Geologists Memoir 41, p. 353-369.

Lageson, D.R., Maughan, E.K., and Sando, W.J., 1979, Wyoming, *in* Yochelson, E.L., editor, The Mississippian and Pennsylvanian (Carboniferous) Systems in the United States: U.S. Geological Survey Professional Paper 1110, pt. II, p. U1-U38.

Love, J.D., 1954, Tentative diagrammatic correlation of Tensleep, Amsden, Casper, and Hartville formations in Wyoming: Wyoming Geological Association 9th Annual Field Conference Guidebook, plate in pocket.

Macke, D.L., in press, Cambrian through Mississippian rocks of the Powder River Basin, Wyoming, Montana, and adjacent areas, *in* Evolution of sedimentary basins—Powder River Basin: U.S. Geological Survey Bulletin 1917.

Mallory, W.W., 1963, Pathfinder uplift of Pennsylvanian age in southern Wyoming: U.S. Geological Survey Professional Paper 450-E, p. E57-E60.

_____ 1972, Regional synthesis of the Pennsylvanian System, *in* Mallory, W.W., editor, Geologic atlas of the Rocky Mountain region: Rocky Mountain Association of Geologists, Denver, p. 111-127.

Maughan, E.K., 1967, Eastern Wyoming, eastern Montana, and the Dakotas, *in* McKee, E.D., and Oriel, S.S. editors, Paleotectonic investigations of the Permian System in the United States: U.S. Geological Survey Professional Paper 515, p. 125-152.

_____ 1983, Tectonic setting of the Rocky Mountain region during the late Paleozoic and early Mesozoic, *in* Symposium on genesis of Rocky Mountain ore deposits—changes with time and tectonics: Denver Region Exploration Geologists Society Proceedings Volume, p. 31-50.

_____ 1984, Paleogeographic setting of the Pennsylvanian Tyler Formation and relation to underlying Mississippian rocks in Montana and North Dakota: American Association of Petroleum Geologists Bulletin, v. 68, p. 178-195.

_____ in press, The Mississippian Darwin Sandstone, the Pennsylvanian Amsden Formation, and associated strata in the Western Interior, U.S.A.: U.S. Geological Survey Bulletin.

Maughan, E.K., and Perry, W.J., Jr., 1986, Lineaments and their tectonic implications in the Rocky Mountains and adjacent plains region, *in* Peterson, J.A., editor, Paleotectonics and sedimentation in the Rocky Mountain region, United States: American Association of Petroleum Geologists Memoir 41, p. 41-53.

Maughan, E.K., and Roberts, A.E., 1967, Big Snowy and Amsden groups and the Mississippian-Pennsylvanian boundary in Montana: U.S. Geological Survey Professional Paper 554-B, 27p.

McCue, J.J., 1953, Facies changes within the Phosphoria Formation in the southeast portion of the Big Horn

Basin [M.A. thesis]: Laramie, University of Wyoming, 88 p.

McKee, E.D., Crosby, E.J., and others, 1975, Paleotectonic investigations of the Pennsylvanian System in the United States: U.S. Geological Survey Professional Paper 853, 541 p.

McKee, E.D., Oriel, S.S., and others, 1967a, Paleotectonic investigations of the Permian System in the United States: U.S. Geological Survey Professional Paper 515, 271 p.

_____ 1967b, Paleotectonic maps of the Permian System: U.S. Geological Survey Miscellaneous Geologic Investigations Map I-450, 164 p.

Newell N.D., 1967, Paraconformities, *in* Essays in paleontology and stratigraphy - R.C. Moore commemorative volume: Kansas State University Department of Geology Special Publication 2, p. 349-367.

Peterson, J.A., 1981, General stratigraphy and regional paleostructure of the western Montana overthrust belt: Montana Geological Society Field Conference and Symposium Guidebook, Southwest Montana, p. 5-35.

_____ 1986, General stratigraphy and regional paleotectonics of the western Montana overthrust belt, *in* Peterson, J.A., editor, Paleotectonics and sedimentation in the Rocky Mountain region, United States: American Association of Petroleum Geologists Memoir 41, p. 57-86.

Ransome, F.L., 1915, The Tertiary orogeny of the North American cordillera and its problems, *in* Rice, W.N., and others, editors, Problems of American geology: New Haven, Connecticut, Yale University Press, p. 287-376.

Rubey, W.W., 1958, Geology of the Bedford Quadrangle, Wyoming: U.S. Geological Survey Geologic Quadrangle Map GQ-109, scale 1:62,500.

_____ 1973, Geologic map of the Afton Quadrangle and part of the Big Piney Quadrangle, Lincoln and Sublette counties, Wyoming: U.S. Geological Survey Miscellaneous Geologic Investigations Map I-686, scale 1:62,500.

Sando, W.J., Gordon, M., Jr., and Dutro, J.T., Jr., 1975, Stratigraphy and geologic history of the Amsden Formation (Mississippian and Pennsylvanian) of Wyoming: U.S. Geological Survey Professional Paper 848-A, 83 p.

Saperstone, H.I., and Ethridge, F.G., 1984, Origin and paleotectonic setting of the Pennsylvanian Quadrant Sandstone, southwestern Montana, *in* Goolsby, J., and Morton, D., editors, The Permian and Pennsylvanian geology of Wyoming: Wyoming Geological Association 35th Annual Field Conference Guidebook, p. 309-331.

Schock W.W., Maughan, E.K., and Wardlaw, B.R., 1981, Permian - Triassic boundary in southwestern Montana and western Wyoming: Montana Geological Society Field Conference and Symposium Guidebook, Southwest Montana, p. 59-69.

Sloss, L.L., 1963, Sequences in the cratonic interior of North America: Geological Society of America Bulletin, v. 74, p. 93-114.

Smith, D.L., 1972, Depositional cycles of the Lodgepole Formation (Mississippian) in central Montana: Montana Geological Society 21st Annual Field Conference Guidebook, Billings, Montana, p. 29-35.

_____ 1977, Transition from deep- to shallow-water carbonates, Paine Member, Lodgepole Formation, central Montana, *in* Enos, P., and Cook, H.E., editors, Deep-water carbonate environments: Society of Economic Paleontologists and Mineralogists Special Publication 25, p. 187-201.

Thomas, H.D., Thompson, M.L., and Harrison, J.W., 1953, Stratigraphy of the Casper Formation, pt. I *of* Fusulinids of the Casper Formation of Wyoming: Wyoming Geological Survey Bulletin 46, p. 5-14.

Todd, T.W., 1966, Darton Ridge, Pennsylvanian feature of Wyoming shelf: American Association of Petroleum Geologists Bulletin, v. 50, p. 2519-2546.

Tonnsen, J.J., 1986, Influence of tectonic terranes adjacent to the Precambrian Wyoming province on Phanerozoic stratigraphy in the Rocky Mountain region: *in* Peterson, J.A., editor, Paleotectonics and sedimentation in the Rocky Mountain region, United States: American Association of Petroleum Geologists Memoir 41, p. 21-39.

Trexler, J.H., Jr., Snyder, W.S., Cashman, P.H., Gallegos, D.M., and Spinosa, C., 1991, Mississippian through Permian orogenesis in eastern Nevada: post-Antler, pre-Sonoma tectonics of the western Cordillera, *in* Cooper, J.D., and Stevens, C.H., editors, Paleozoic paleogeography of the western United States-II: Pacific Section, Society of Economic Paleontologists and Mineralogists, v. 1, p. 317-329.

Tromp, P.L., 1984, Leo depositional environments, southeastern Powder River Basin: Wyoming Geological Association Earth Science Bulletin, v. 17, p. 117-118.

Williams, J.S., 1962, Pennsylvanian System in central and northern Rocky Mountains, *in* Branson, C.C., editor, Pennsylvanian System in the United States—a symposium: American Association of Petroleum Geologists, Tulsa, Oklahoma, p. 159-187.

Part IV

Mesozoic history

Frontispiece. Lower Triassic Red Peak Formation exposed on the east wall of Red Canyon, south of Lander, Wyoming. Photograph by D.W. Boyd.

The early Mesozoic history of Wyoming

M. Dane Picard
Department of Geology and Geophysics
University of Utah
Salt Lake City, Utah 84112

Abstract

In the Late Triassic, Early Jurassic, and much of the Late Jurassic, the Wyoming shelf was emergent, a terrestrial plain covered by lakes and streams and sand seas. For most of the rest of the early Mesozoic, shallow seas covered the shelf. The Triassic rocks in Wyoming are the Dinwoody Formation (older) and the Chugwater Group (younger). From oldest to youngest, the Chugwater Group includes four formations: Red Peak (Lower Triassic), Alcova, Crow Mountain (Middle? Triassic), and Popo Agie (Upper Triassic). In southeast Wyoming, the Chugwater Formation is overlain by the Upper Triassic Jelm Formation. The Jurassic formations are: Nugget (Lower? Jurassic), Gypsum Spring (Middle Jurassic), Sundance (Middle Jurassic), and Morrison (Upper Jurassic).

The Early Triassic sea (Griesbachian Stage) transgressed quickly to the east, somewhat beyond the former basin of the Permian Phosphoria Formation, and covered the Wyoming shelf. Griesbachian strata of the Dinwoody Formation occur as far east as central Wyoming. In southeast Wyoming, the Freezeout Shale and the Little Medicine members of the Goose Egg Formation — Permian-Triassic redbeds, carbonates, and evaporites — grade to the west into yellowish calcareous siltstone in the lower Dinwoody Formation. Before the end of the Griesbachian, terrigenous silty sediments began to prograde west over the Wyoming shelf. During deposition of the Red Peak redbeds, a complex current system—dominant current directions to the northeast and northwest and a minor southwest current—existed in the shallow sea and tidal plain over the Wyoming shelf. The five Red Peak facies—silty claystone (older), lower platy, alternating, upper platy, and sandy—are characterized by their red color (except for the sandy facies), high silt and very fine sand content, abundant and diverse sedimentary structures (especially ripple mark varieties), gypsum content, and scarcity of fossils. The Alcova Limestone is a marine tongue extending eastward well out onto the shelf from the sandstone and limestone unit of the upper Thaynes Formation of southwest Wyoming and southeast Idaho. One of the world's great marker beds, the Alcova is up to 25 feet of micrite, biomicrite, pelmicrite, biolithite (algal beds in growth position), microsparite, and pseudosparite. The Crow Mountain Sandstone—the best Triassic reservoir rock and most important petroleum-producing interval—accumulated during a westward regression of the shelf sea. A tidal flat, beach, and marsh setting prevailed during deposition of the upper Crow Mountain. An unconformity separates the Crow Mountain and the overlying—probably Upper Triassic—unnamed redbed unit (central and western Wyoming) and the fluvial Jelm Formation (southeast Wyoming). The Jelm (or unnamed redbed unit) was laid down on a westward-prograding fluvial-deltaic plain in central Wyoming. Farther west, the interval was probably deposited in a shallow marine to paralic setting. The Popo Agie Formation, the youngest Triassic strata, was deposited in a vast river and lake system. Lake Popo Agie, one of the largest ancient lakes known, occupied a basin of at least 70,000 mi^2. During Popo Agie time, volcanoes rained ash over most of western Wyoming and on parts of Idaho, Utah, Colorado and, likely, on adjacent areas in the western United States.

Picard, M.D., 1993, The early Mesozoic history of Wyoming, *in* Snoke, A.W., Steidtmann, J.R., and Roberts, S.M., editors, Geology of Wyoming: Geological Survey of Wyoming Memoir No. 5, p. 210-248.

Dominantly eolian strata of Nugget Sandstone unconformably overlie the Popo Agie Formation. Locally, older beds have been tilted and folded and the unconformity is an angular one. In Wyoming and northern Utah, the Nugget contains beds that were laid down in several environments—eolian, small lakes within dune areas, inland sabkhas, and streams. The marine Gypsum Spring Formation—its lower evaporite and red fine-grained clastic unit—lies on a prominent unconformity above the Nugget Sandstone. The evaporites and associated beds accumulated on sabkhas in arid and semiarid climates. Before advance of the invading Sundance Formation seas, the stable Wyoming shelf was part of a regional low-lying erosion surface. The lower (Callovian) and upper (Oxfordian) Sundance divisions each include a major transgressional/regressional marine sequence. The advancing lower Sundance sea is represented by the Canyon Springs Sandstone and the lower part of the Stockade Beaver Shale, the prograding retreat by the upper Stockade Beaver Shale, the Hulett Sandstone, and the Lak Redbeds. During the Late Jurassic, the Wyoming shelf had a paleolatitude between about 35° and 39° N. The climate was warm and dry—winds blew from west to east over the Western Interior. Sundance seas were succeeded by terrestrial environments represented in the Morrison Formation by alluvial fans, braided and meandering streams, and lakes. Rainfall was sporadic. The climate was strongly seasonal with high rainfall interrupted by brief dry seasons.

Dedication

This work is dedicated to my mother, Velma Vestal Stubblefield Picard, dead at fifty-three in 1963 of complications from multiple sclerosis, but remembered every day with love and longing and pain. She came to Wyoming from southern Missouri near the Ozarks in the late 1920s and began teaching in a one-room schoolhouse that rested on Triassic sandstone just above the Alcova Limestone—the great Wyoming marker bed—and ripple-marked flagstone of the Red Peak Formation, on Bridger Creek in north-central Wyoming. She taught all the grade school children on Bridger Creek. I was a reluctant student in the schoolhouse, but from the time I began to crawl, a fervent one among the early Mesozoic rocks.

Introduction

Beds of the Lower Triassic Red Peak Formation—the redbed sequence of the Chugwater Group—are perhaps the most striking sedimentary strata in Wyoming. Wherever they occur in long bands—on the northeast flank of the Wind River Range, on the enclosing rim of the Bighorn Basin, in the thrust sheets of the fold-and-thrust belt, in Jackson Hole —they glow with the remembered warmth of the Triassic seas and tidal plains. It is almost impossible for a geologist or anyone else to come down the northeast flank of the Wind River Range on Wyoming Highway 28 (**Figure 1**), look northward toward Lander, and overcome the urge to stop in the Triassic to follow by eye the Red Peak band that sweeps northwest for almost 100 uninterrupted miles.

Travellers affected by rocks will remember forever this redbed land. Of all outcrops redbeds are probably the most spectacular rocks to tourists and geologists alike. The widespread, notable, red bands of this region are the Permian-Triassic Goose Egg Formation, the Triassic Red Peak and Jelm formations, and the Jurassic lower Nugget and Gypsum Spring strata. [see Love and others, Stratigraphic chart showing Phanerozoic nomenclature for the State of Wyoming, this volume].

Triassic rocks in Wyoming belong to the Dinwoody Formation (older) and the Chugwater Group (younger). From oldest to youngest, the Chugwater includes: Red Peak Formation (Lower Triassic), Alcova Limestone, Crow Mountain Sandstone (Middle? Triassic), (pronounced Pō-pō-sah) Formation (Upper Triassic). In southeast Wyoming, the Chugwater Formation is overlain by the Upper Triassic Jelm Formation. The Jurassic rocks are: Nugget Sandstone (Lower? Jurassic), Gypsum Spring Formation (Middle Jurassic), Sundance Formation

Figure 1. Part of the Triassic and Jurassic sequence exposed on the northeast flank of the Wind River Range. View from State Highway 28 to the northwest. Red Peak Formation (hogback cliffs in middleground), Alcova Limestone (A and arrow), Crow Mountain Sandstone, unnamed redbed unit, Popo Agie Formation, and Nugget Sandstone (N).

(Middle Jurassic), and Morrison Formation (Upper Jurassic). The fold-and-thrust belt rocks bear different names, to be identified at the appropriate places. **Table 1** includes a stratigraphic column and other information. Place names are shown on **Figure 2**.

In most of Wyoming, the Permian Phosphoria Formation and related rocks underlie the Dinwoody Formation (Lower Triassic). The Morrison Formation is overlain by Lower Cretaceous beds, generally the Cloverly Formation, but in the Yellowstone volcanic area, the Kootenai Formation, and in the Powder River Basin and Black Hills, the Lakota Formation of the Inyan Kara Group.

Table 1. Stratigraphic sequence, depositional environments, and sandstone types of early Mesozoic strata, Wyoming.

Age	Formation	Depositional environment[1]	Rock type[2]	Ss and siltstone type; QFL (ss, sltst)	Thickness (ft)
Jurassic	Morrison	A, L	F, Ss, Cgl, Carb, V, R	quartzarenite, sublitharenite	100-500
	Sundance				
	Windy Hill	M	Ss, F	quartzarenite, sublitharenite	5-57
	Redwater	M(td)	F, Ss, Carb		0-135
	Pine Butte	M	Ss, F		0-35
	Lak	E, M(s)	Ss, F, Ev, R	quartzarenite, sublitharenite	0-75
	Hulett	M (wt)	Ss, F	quartzarenite, sublitharenite	3-100
	Stockade Beaver	M(o)	F		0-95
	Canyon Springs	M(td, cs)	Ss, F, Carb	quartzarenite, sublitharenite	1-65
	Gypsum Spring	M(s)	F, Ev, Carb, R		0-250
	Nugget	E, L	Ss, F, Carb, Ev, R	82-14-4, 74-24-2	0-800
Triassic	Jelm	A, L, M(s)	Ss, F, Carb, R		25-650
	Popo Agie	L, A	F, Ss, Cgl, V, R		0-275
	Crow Mountain	M(td)	Ss, F, R	85-13-2, 79-16-5	0-175
	Alcova	M	Carb, Ev	77-18-5	0-25
	Red Peak	M(td)	F, Ss, Carb, Ev, R	73-24-3, 60-31-9	400-1,250
	Dinwoody	M	F, Ss, Carb		15-250

[1] Abbreviations: A = alluvial; E = eolian; L = lacustrine; M = marine; s = shallow; td = tide dominated; wt = wave and tide dominated; cs = clastic shoreline; o = offshore

[2] Abbreviations: Cgl = conglomerate; Ss = sandstone; F = siltstone and claystone; Carb = carbonate rocks; Ev = evaporites; R = redbeds or varicolored rocks; V = volcanic or volcaniclastic rocks

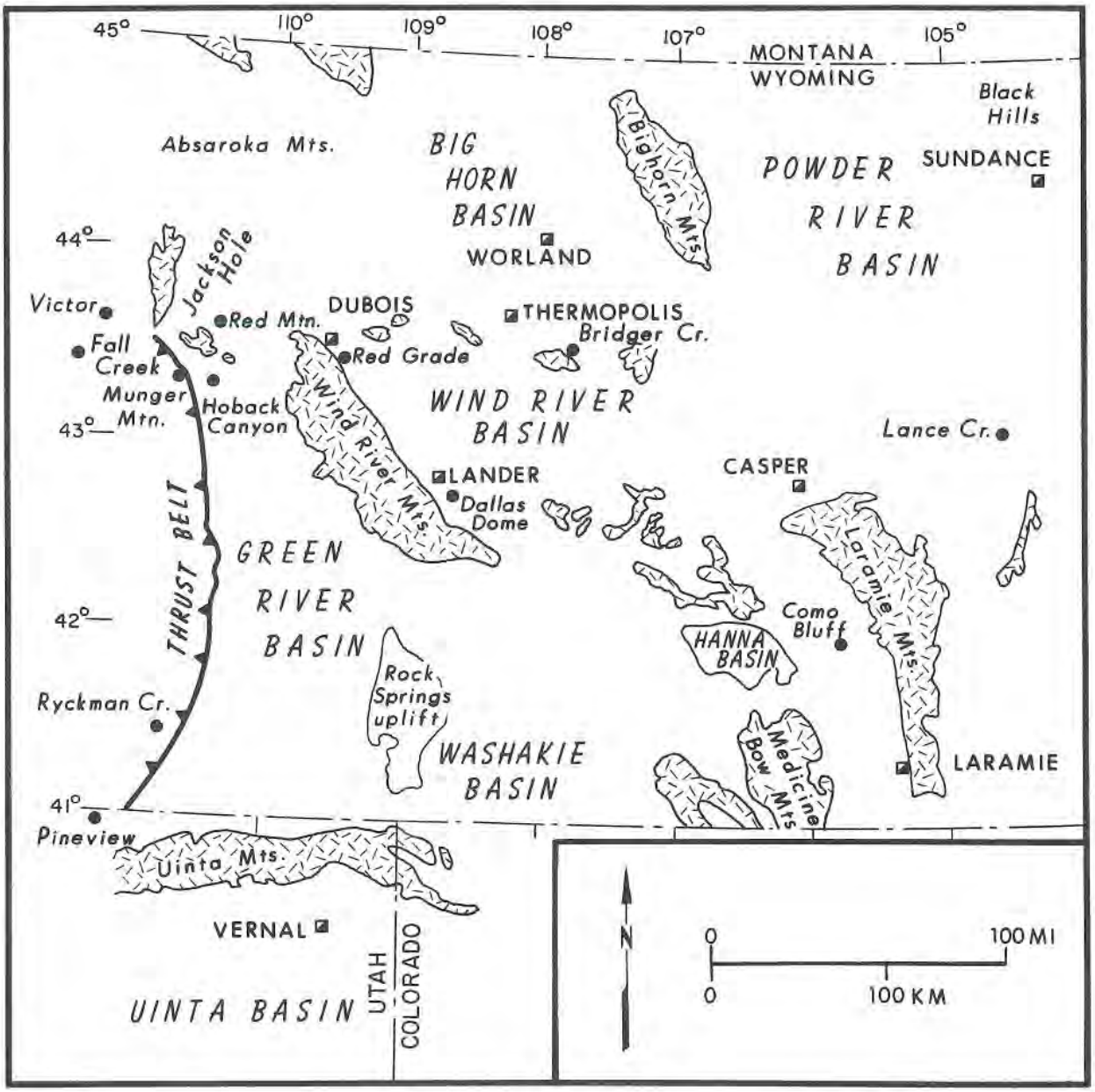

Figure 2. Index map of Wyoming, showing ranges, basins, and place names referred to in the text. Patterned areas indicate Precambrian rock outcrops. (Cr. = Creek, Mts. = Mountains, Mtn. = Mountain).

Evolution of Chugwater names

In 1904, Nelson Horatio Darton, one of those exceptional early 20th Century field geologists who mapped by horseback, defined the Chugwater Formation, named for Chugwater Creek in the Laramie Mountains. Darton's Chugwater included all of the redbeds in eastern Wyoming between the Pennsylvanian Tensleep Formation and the Jurassic Sundance Formation. Prior to his study, the sequence of redbeds was termed "Red beds" or "Laramie Plains Redbeds" (Knight, 1902). Also in 1904, Williston used the name "Popo Agie beds" for outcrops that yielded vertebrate remains along the Popo Agie River near

Lander in northwest Wyoming. Williston gave the thickness of the unit and the approximate distances from the top and bottom of the redbeds, but did not further define the Popo Agie.

From studies in the Bighorn Mountains, Darton (1906a) recognized that the basal part of his Chugwater Formation differed from the main body of redbeds and proposed the Embar Formation to include most of the light colored limestone and claystone between the redbeds and the Tensleep Sandstone. This interval is now considered to be the Permian Phosphoria and Triassic Dinwoody formations (Thomas, 1934; Thomas and Krueger, 1946). The Dinwoody extends somewhat stratigraphically above Darton's Embar (1906a) to include all limestone below the redbeds. Darton (1906b) also extended the Chugwater nomenclature into central Wyoming, where he noted the presence of a thin but widespread sheet of limestone near the top of his Chugwater Formation. This limestone, recognizable in Darton's (1906a) measured sections and in a cross section by Knight (1897), was named the Alcova Limestone Member by Lee (1927).

In 1939, in the published version of his dissertation on the southern margin of the Absaroka Mountains, J. David Love subdivided the Chugwater Formation into four members: Red Peak, Crow Mountain, Popo Agie, and Gypsum Spring. All were new names, except for the Popo Agie, which he formally defined for the first time. Love did not mention Alcova Limestone. Apparently it is not present in the outcrops he studied.

Branson and Branson (1941) made several suggestions concerning new names for the Chugwater sequence, based on field work in the Wind River Mountains. Their intent was to raise the Chugwater to group status and redefine all of its subdivisions as formations, to include the Dinwoody in the Chugwater, and to split-off the lower part of Love's Gypsum Spring Member and call it the "Wyopo formation". The Wyopo formation never gained acceptance and was soon abandoned in favor of the Nugget Sandstone, an extension of the Nugget from southwestern Wyoming (Imlay, 1945; Love and others, 1945a, b). The Gypsum Spring Formation, which the Bransons (1941) included in their Chugwater Group, is now known to be Middle Jurassic (Imlay, 1945). It is unconformable on underlying strata (Love, 1957). Similarly, the Dinwoody Formation was not accepted as part of the Chugwater (McKee and others, 1959). The elevation of Chugwater to a group (High and Picard, 1967) was about the only proposal of the Bransons' that gained acceptance, though with fewer formations than originally proposed.

Dinwoody Formation

By the latest Paleozoic, all of the continents were assembled to form the universal megacontinent Pangaea. Rifting with an outpouring of basalt about 200 Ma (early in the Jurassic period), signaled the breakup of the supercontinent. By the end of the Jurassic, breakup had been underway for 65 m.y.

Among the world's Foremost Five mass extinctions—Foremost Six if we add recent human havoc—the greatest of them all occurred at the end of the Paleozoic (250 Ma). The other principal extinctions are those in the Ordovician, Devonian, Triassic, and Cretaceous.

Of the four orders of amphibians alive at the end of the Permian, only one survived into the Triassic. Of about 50 genera of mammal-like reptiles present, only one (Dicynodon) came through to give rise in the Late Triassic to the first true mammals, a close call for us. A startling 54% of all marine families died out. As many as 90 to 96% of all species alive in the Upper Permian may have disappeared in this most ravishing of all mass extinctions, according to J.J. Sepkoski and D.M. Raup. However, Raup (1991) recently stressed that 96% is probably an upper limit. Whatever the actual percent, no other mass extinction has been so awesome as the one that closed the Paleozoic era.

Though hordes of different taxa disappeared by the end of the Permian, it is uncertain how abruptly they did so. My bias on mass extinctions is that they have been geologically brief.

Unfortunately, as in most of the rest of the world, the sequence of strata in Wyoming from the Upper

Permian into the Lower Triassic is not complete. Far from it. Some geologists have extravagantly estimated that 1 to 15 million years of geologic history is missing in the unconformity between the Triassic Dinwoody Formation and the Permian Phosphoria Formation (McKee and others, 1959). But in central and eastern Wyoming, the discordance between Permian and Triassic rocks is generally slight or not apparent; the rocks above and below the boundary are very similar; and fossils are rare or absent (Love, 1948; Kummel, 1954; Burk, 1956). Long ago, Love (1939, 1948) suggested that the discordance is physically apparent only in regional studies. Boyd and Maughan (1973) concluded that deposition in western Wyoming was continuous during the latest Permian and earliest Triassic and placed the era boundary at the base of the Dinwoody Formation.

It seems unlikely that a time gap of 10 to 15 million years exists between Permian and Triassic rocks anywhere in Wyoming. Rather, the gap may be closer to 2 to 3 million years, or less. Where the Permian-Triassic boundary falls within a redbed sequence in southeast Wyoming, erosional surfaces occur within the redbeds, but which surface, if any, marks the boundary is impossible to say.

The last widespread episode of marine deposition in the Cordilleran miogeocline that followed a depositional and structural pattern inherited from the late Paleozoic, and possibly from the late Precambrian (Carr and Paull, 1983), is recorded in Lower Triassic rocks (**Figure 3**). Early Triassic strata register the end of marine deposition along the passive continental margin of western North America. Speed (1978, 1979) suggested that the great range in depositional and tectonic patterns in the eastern Cordillera during the Early Triassic was related to the accretion of a Permian oceanic-arc terrane on the western margin of North America.

The Dinwoody Formation occupies about the same geographic area as the Phosphoria Formation—western Wyoming, southwest Montana, southeast Idaho, and northern Utah. The basin's center was in southeast Idaho, where the Dinwoody reaches a maximum thickness of 2,400 feet and includes strata both older and younger than those in the type locality in the Wind River Range near Dubois, Wyoming.

Siltstone, a sedimentary rock with few enthusiasts among the world's sedimentologists, is the principal rock in the Dinwoody Formation. It is light colored—gray or green or light brown and, in some places, orange. Dolomite is the dominant cement. The siltstone is sandy (very fine grains), clayey, micaceous, and streaked and interbedded with anhydrite in the subsurface and gypsum at the outcrop.

The masters of the Dinwoody seas in western Wyoming were gastropods and bivalves, but they were much less diverse than those living on the outer shelf in what is now southeasternmost Idaho. At the end of the Permian, there were few gastropods to be seen at all and "Paleozoic-like snails are simply more characteristic of the Triassic than they are of the Upper Permian," says Eldredge (1991). David Jablonski calls these Lazarus taxa. They seem to disappear, but show up again after their supposed demise. In the limey siltstone of western Wyoming, horizontal-paired trails and less common U-shaped burrows of the Cruziana shallow-marine association are well preserved (Carr and Paull, 1983).

In the subsurface, thin beds of dolomite, limestone, and anhydrite (gypsum at the surface) occur at the top of the Dinwoody Formation. On geophysical logs, the Dinwoody rocks show high resistivities compared with low resistivities of the overlying Red Peak Formation. In outcrops, the Dinwoody-Red Peak contact is marked by a color change from greenish gray below to red above, and in some places by a change from limestone or dolomite to claystone, clayey siltstone, or mudstone. The change from Dinwoody rocks to Red Peak rocks is generally abrupt, with fine-grained clastic rocks containing clay minerals (illite, chlorite, mixed-layer clays) characterizing the basal Red Peak (Picard, 1967). Sorting is also poorer in the Red Peak. In general, the Triassic Dinwoody-Red Peak contact is easier to distinguish on logs of boreholes and in outcrops than is the Phosphoria-Dinwoody contact.

The Early Triassic sea (Griesbachian Stage) transgressed rapidly to the east, somewhat beyond the former Phosphoria basin, and covered the Wyoming shelf. Griesbachian deposits of the Dinwoody Formation are apparent as far east as central Wyoming (Carr and Paull, 1983). In southeast Wyoming, the Freezeout Shale and Little Medicine members of the Goose Egg Formation—Permian-Triassic redbeds, carbonates, and evaporites—grade westward into yellowish calcareous siltstone in the lower part of the Dinwoody Formation (Maughan, 1964).

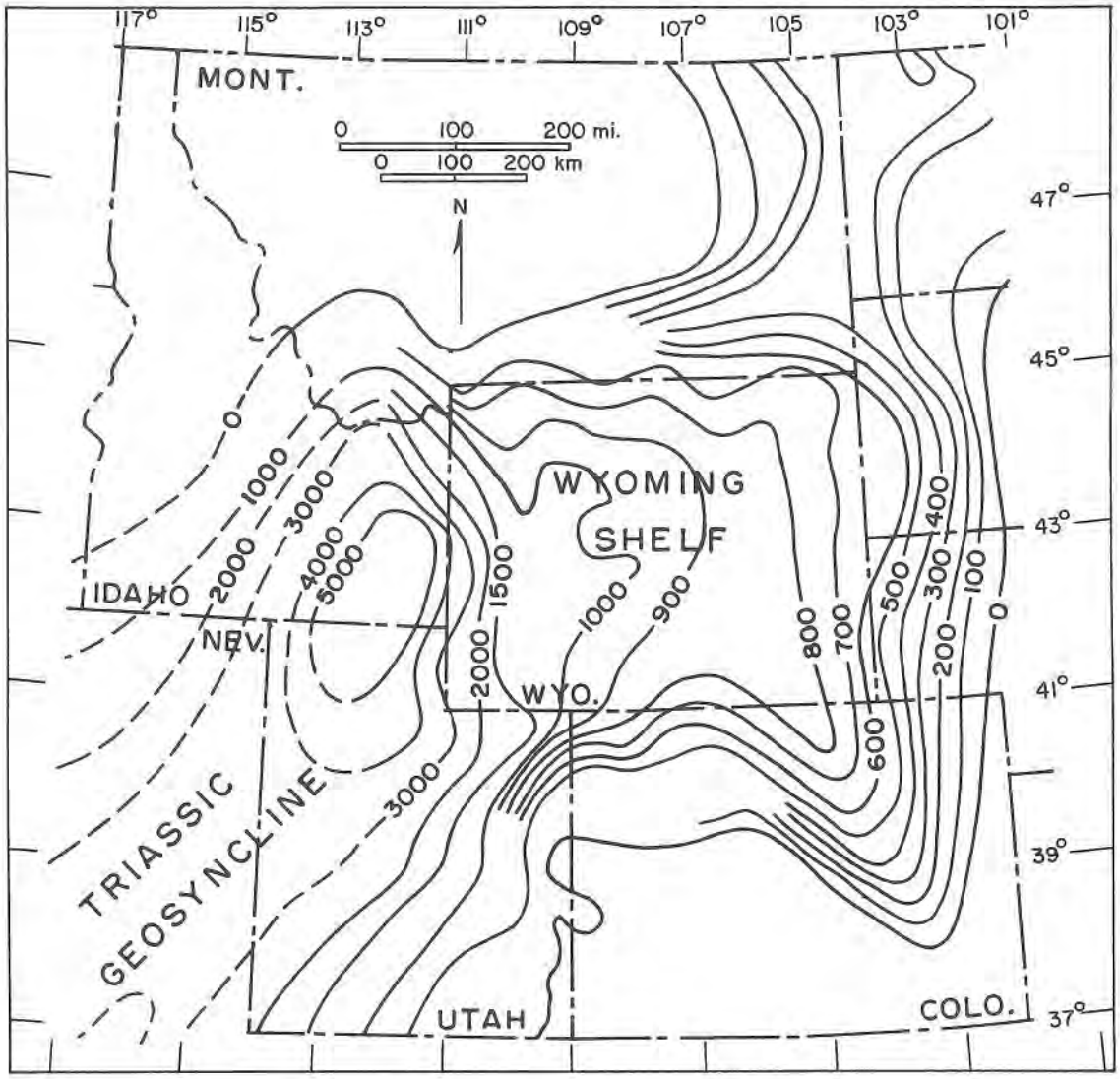

Figure 3. Regional paleogeographic map of the Western Interior during Early Triassic time (after McKee and others, 1959). Isopachs are thicknesses of Lower Triassic strata (in feet); in western Wyoming they include the Dinwoody and Red Peak formations. (Contour intervals vary.)

Across the Wyoming shelf the basin gradient was low. Thus, slight variations in sediment supply or a minor change in relative sea level affected broad areas (McKee and others, 1959; Collinson and Hasenmueller, 1978).

Before the end of the Griesbachian, terrigenous silty sediments began to prograde westward over the Wyoming shelf (Carr and Paull, 1983). This "progressive regression with minor fluctuations" continued throughout the Dienerian (McKee and others, 1959).

Red Peak Formation

The most notable feature of the Early Triassic Red Peak Formation is its red color. When the Chugwater Group is labelled a redbed sequence, it is the Red Peak Formation that has impressed the observer. The rocks are dominantly grayish red and pale reddish brown and in some places dark reddish brown, gray-

ish red, pale red, and moderate reddish brown (Goddard and others, 1948, color chart). Where the iron oxides have been reduced, common rock colors are light greenish gray, yellowish gray, greenish gray, and moderate yellowish brown. The red pigmentation occurred during diagenesis (Picard, 1964, 1965, and 1966); the sediment was not red, and terrigenous grains were not coated with hematite at deposition.

In my dissertation (Picard, 1964), I compared the magnetism of pairs of samples taken from the same or closely adjacent beds, in which the bedding of one sample is more disturbed than the bedding in the other sample—for example, planar and convolute bedding or slightly disturbed stratification and greatly disturbed stratification. There is little difference in magnetization in these sample pairs (an average of 18° in declination, 20° in inclination), indicating that the magnetization occurred after the bedding disturbance. This is strong evidence (if not proof) that the remanent magnetization was induced diagenetically. The magnetization resides primarily in hematite, the red pigment of these strata. The Red Peak is thus an important formation around the world in understanding the origin of red sedimentary rocks. When I found the relationship between the sample pairs during the summer of 1962, and saw the diagenetic relationships between red pigment, carbonate and silica cement, and quartz and feldspar grains, I thought that I might be about to attain my fifteen minutes in the sun. It was not to be.

After the Red Peak interval, there is no widespread similar sequence in the geologic record in Wyoming or in adjacent states. There are similar rocks, however, of approximately the same age in Utah (Moenkopi Formation in the Uinta Mountains; Ankareh, Thaynes, and Woodside formations in the western Uintas, Wasatch Mountains, and southeast Idaho), in northwest Colorado (Moenkopi Formation), and in western South Dakota (Spearfish Formation). The generally uniform red coloration, high silt and very-fine-sand content, abundant and diverse primary sedimentary structures (especially ripple marks), gypsum content, and rarity of fossils characterize these strata. Based on petrographic studies (modal analyses), the average, well-sorted, Red Peak siltstone contains these constituents: quartz and chert, 36%; feldspar, 22%; rock fragments, 5%; carbonate cement (calcite, dolomite), 28%; gypsum, 4%; and matrix, 5%. I include these data in remembrance of how hard they were won (Picard, 1966).

Long ago, the cyclic nature of the Red Peak was recognized (Picard, 1967). Plants growing in the thin soils formed on Red Peak siltstone and claystone below the cyclic, hogback-forming alternating, upper platy, and sandy facies support stock on range and pasture lands in the Bighorn and Wind River basins.

In Wyoming, the Red Peak Formation contains five recognizable facies that are, from base to top: silty claystone, lower platy, alternating, upper platy, and sandy (**Figures 4** and **5**; Picard, 1967, 1978). Like other informal stratigraphic names, these have not become wildly popular or widely used. But neither has any alternative terminology, and subdivision of the Red Peak, even informally, has led to the recognition of important relationships that might not have been seen otherwise. Especially notable is the general upward increase in abundance of coarser grains and the general upward increase in number and thickness of coarser beds. The thin upper platy facies (about 20

Figure 4. Alternating and upper platy facies of Red Peak Formation at Red Grade southeast of Dubois. Alcova Limestone caps outcrops of steep cliff.

Figure 5. Upper platy facies of Red Peak Formation, variegated sandy facies, Alcova Limestone (A), and Crow Mountain Sandstone near Red Grade.

to 75 feet thick) reflects a return to the depositional conditions of the lower platy facies.

Though many of the geologists who have studied the Red Peak Formation worked on it during periods when nonmarine—lake, stream, "desert" — depositional settings were favored for similar formations, they almost exclusively said the Red Peak redbeds originated in shallow marine environments. Branson (1915, 1927) proposed a marine origin for all of the Chugwater Group except for the Popo Agie. Reeside (1929) agreed with Branson (1927), saying a marine origin for the redbeds was likely. From his study of Phosphoria and Dinwoody tongues in the lower Chugwater Group of central and southeast Wyoming, Thomas (1934) postulated a specialized marine environment for the red shale tongues. Darton (1906a) thought the Chugwater of the Bighorn Mountains had accumulated in a widespread saline lake.

In geological studies, as in other research, it sometimes is tempting to begin anew. When I began studying the Red Peak Formation during 1961, I was skeptical of the paleomagnetic work that had been done (Collinson and Runcorn, 1960) because it was not tied closely to the stratigraphy. I also wondered about previous stratigraphic and petrologic research, especially interpretations of the depositional environments. After months of a largely unsuccessful nose-on-the-outcrop search for fossils and of tramping up and down over many stratigraphic sections, I turned to the sedimentary structures and bedding types to make an interpretation. I constructed histograms that show the percentage frequency of internal bedding structures in the facies (Picard, 1967). I studied about 155 beds in each rock unit. The histograms are sufficiently dissimilar to characterize the stratigraphic units over regional areas (perhaps 10,000 mi² or so).

From the character, abundance, and associations of bedding types and sedimentary structures, it is possible to distinguish the principal depositional environments. For each facies, these are: silty claystone = transitional paralic; lower platy = tidal flat; alternating = tidal flat and shelf; upper platy = tidal flat; variegated sandy = nearshore marine.

From the thin (1 to 2 feet thick) gypsum beds (especially in the lower platy and alternating facies), casts of salt cubes, mud cracks, raindrop impressions, and scarcity of fossils in the Red Peak Formation, it is possible to suggest that the climate was warm to hot and semiarid to arid during its deposition (Picard, 1966). Oxidizing conditions prevailed. The depositional basin was within 30° of the Early Triassic equator. In the dry climate, there was little vegetation and a low water table, which facilitated formation and preservation of ferric oxides in the redbeds. Van Houten (1961) suggested a similar climatic setting for the Red Peak and places many other redbed formations around the world in the same group.

The Red Peak facies persist laterally for tens of miles in outcrops (Picard, 1967). Bedding and sedimentary structures are also remarkably continuous in the field (see figure 18 in Picard, 1967). Long ago, Burk (1953), Love (1957), and Picard (1967) showed the striking persistence of Red Peak horizons as correlated on electric logs. Picard and Wellman (1965) traced a five-foot-thick, grayish red and reddish brown, claystone interval in the alternating facies for

more than 73 miles east-west in the southern Bighorn Basin. The north-south extent is likely more than 110 miles. Along the east-west line of section, the base of the claystone interval is from 98 to 138 feet below the base of the Alcova Limestone, the interval between the two units thickening westward at less than 2 feet per mile toward the deeper part of the basin.

Little variation in water depth occurred over the Wyoming shelf. A geologist standing on eastern Wyoming in the Early Triassic as the tide went out might have been tempted to walk to the west, persuaded by the flatness of the tidal plain and the tide's disappearance that it would not return.

During deposition of the Red Peak Formation, a complex current system existed in the shallow sea over the Wyoming shelf. Its waters moved in two major directions—to the northeast and northwest—with a minor southwest-directed current (Picard and High, 1968). Those three Red Peak current directions apparently record onshore, offshore, and longshore movement produced by wave drift, rip, and longshore currents, respectively. Choosing between two possible reconstructions that would satisfy the inferred current system, Picard and High (1968) suggested that the average shorelines trended northwest-southeast. A northwest-southeast-trending shoreline agrees closely with thickness trends of the Dinwoody and Red Peak formations in western Wyoming and with a detailed thickness map of the Red Peak (Picard, 1967).

If one judges the quality of life during Red Peak time by the fossils found in these Early Triassic redbeds, overcrowding was not a problem. Few are the instances of a sequence as thick and widespread displaying such excellent outcrops while revealing so few fossils.

There are small burrows, but they are not definitive as to maker or environment and have not been studied in any detail (**Figure 6**). Lull (1942) described small reptile footprints from strata about 35 ft below the Alcova Limestone in the upper platy facies in central Wyoming. Branson (1947) and Peabody (1948) gave additional information on Lull's material. Love (1948) reported a single pelecypod from the northern Wind River Basin. Picard (1967) found fish scales in the alternating facies in the southern Bighorn Basin. At three Red Peak localities representing different stratigraphic horizons, Boyd and Loope (1984) described distinctive sole marks that they interpreted as scratches made "by the toes of amphibious tetrapods." No tetrapod skeletal remains have been found.

These indications of Red Peak life are all that is known—small burrows, small reptile footprints, a lonely pelecypod, fewer fish scales than one would see near any fishing hole, and indications that a mysterious small group of amphibious tetrapods gained geological immortality by scratching in the mud in several places tens of miles apart. Speculation about these redbed depositional environments thus rests largely on the physical evidence in the rocks and not on the biologic evidence, since diagnostic fossils do not exist.

The redbeds intertongue in western Wyoming and eastern Idaho with limestone, dolomite, sandstone, and siltstone of the Thaynes Formation (Picard and others, 1969; Picard, 1975a). These rocks preserve

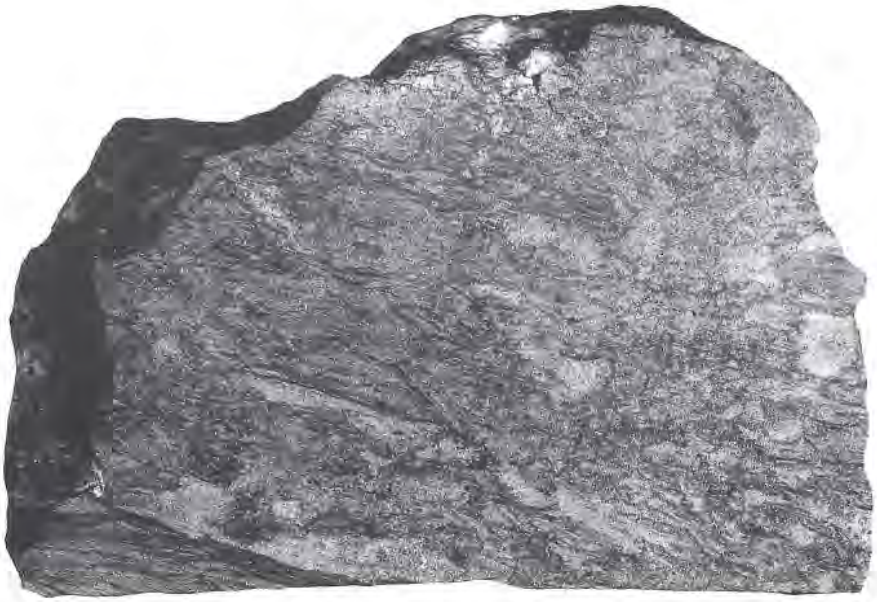

Figure 6. Disturbed stratification in massive siltstone of alternating facies, Red Peak Formation. Rock is burrowed. Width of specimen is 5 inches.

for us, even in the dolomitized intervals, pelecypods and crinoids, ammonoids, and, less abundantly, brachiopods, gastropods, cephalopods, bryozoans, foraminifers, and algae. At Hoback Canyon in western Wyoming, where the sequence is still dominantly red siltstone and sandstone, there are rare invertebrates—pelecypods especially—in the carbonate tongues and redbed intervals.

Paleocurrent data from the middle part of the Hoback Canyon section are similar to those from the redbed sequences farther east—major directions to the northeast, southwest, and northwest. Abundant gypsum and dolomite in the upper part of the sections at Red Mountain (**Figure** 7), Hoback Canyon, and Munger Mountain indicate deposition in a restricted marine environment. Similar environments probably prevailed also during deposition of the lower part of the Red Peak-Thaynes sequence at the same localities. To the west, the Thaynes is more calcareous, and only a few feet of dolomite occurs at Fall Creek in eastern Idaho. A series of carbonate banks on the shelf edge in eastern Idaho would have produced restricted conditions in the shallow water among and just behind the banks (**Figure 8**). Sediment accumulating in this area therefore would contain hypersaline pore solutions. The resulting penecontemporaneous dolomitization, associated with minor bedded gypsum, is reflected in the facies relations between western Wyoming (Red Mountain) and easternmost Idaho (Victor). On the east, the wide Wyoming shelf was largely unaffected by the shelf-margin banks. Water circulation was generally unrestricted (Picard and High, 1968).

As noted in western and west-central Wyoming, there is a conspicuous change in rock types at the Dinwoody-Red Peak (silty claystone facies) contact. Poorly sorted, fine-grained material lies above the carbonate, evaporite, and siltstone strata of the

Figure 7. Upper part of Red Peak Formation at Red Mountain northeast of Jackson, showing interval containing alternating facies of Red Peak, upper platy facies, variegated sandy facies, Alcova Limestone, and unnamed redbed unit.

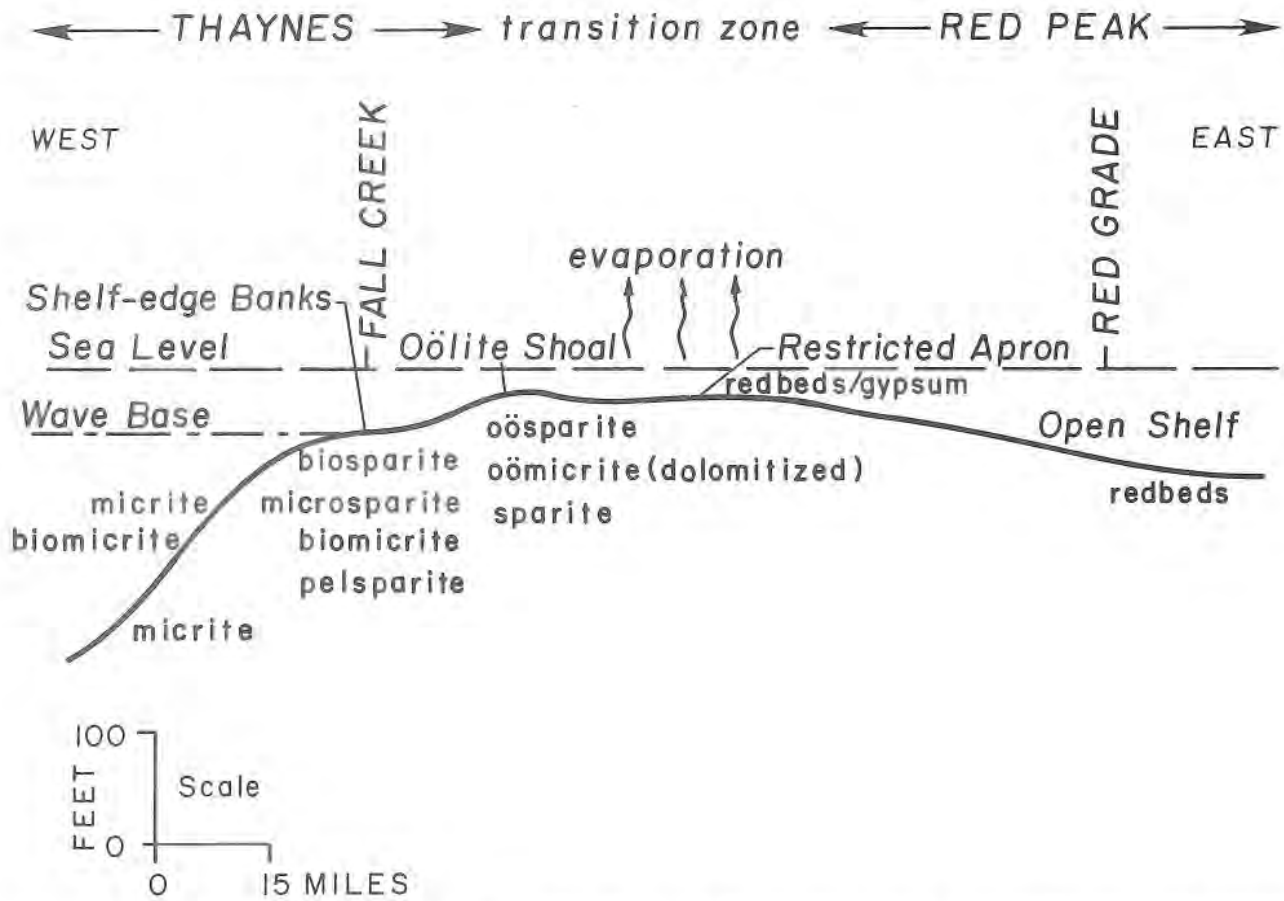

Figure 8. Paleogeography during deposition of Red Peak and Thaynes formations, western Wyoming and eastern Idaho.

Dinwoody. Though there is a general upward coarsening, deposition of similar fine-grained material continued nearly to the end of Red Peak deposition. In the Red Peak Formation, silt is the dominant clastic constituent of the rocks, followed by very-fine sand, and then clay-size particles.

I believe that large amounts of wind-blown silt may have fallen on the Wyoming shelf, beginning with Red Peak deposition. The last Dinwoody sea was retreating slowly and was very shallow or partly ponded when lowermost Red Peak grains began to accumulate. The Wyoming shelf then had a paleolatitude between about 15° and 25° N (Robinson, 1971, 1973). Silt rained down on the land adjoining the sea, on islands, and in the shallow sea from great dust storms carried by northeasterly trade winds. Waves and currents in the remnant sea sorted the grains and formed sedimentary structures and bedding.

The lowermost Red Peak unit, the silty claystone facies, is not well exposed. It forms valleys, or the upper part may form gentle slopes. Trenches and boreholes reveal that silty claystone is the dominant rock (about three-fourths of the facies), followed by siltstone (about 15%), claystone (5-10%), and very-fine-grained sandstone (2-4%). Cross stratification (dominantly micro cross stratification) and horizontal stratification are the major bedding types. Ripple stratification and wavy stratification are significant bedding types in the silty claystone facies. Most of the silt and clay grains settled from suspension, producing horizontal bedding. The other bedding types are the result of deposition in lower-flow regimes.

Limited data suggest that paleocurrent systems in the seas were similar during deposition of the upper part of Dinwoody and the silty claystone facies.

At Red Grade, the dominant paleocurrent directions are about 75° and 285° in the upper Dinwoody and 70° and 265° in the lower part of the lower platy facies immediately above the silty claystone facies.

The end of typical Red Peak deposition came with a flood from the east of very fine sand over well-sorted and poorly sorted silt of the upper platy facies. In the time that followed, sand and carbonate was deposited in a shallow sea and tidal flat across the Wyoming shelf. The youngest Red Peak strata, informally called the sandy facies, show great variation in color—grayish red, pale red, pale olive, pale green, dark yellowish orange—where the Alcova Limestone overlies the sandy facies, and are dominantly red at localities where the Alcova Limestone is absent. The variegated nature of the sandy facies is related to reduction of iron oxides by water expelled from the Alcova during diagenesis.

Alcova Limestone

On a clear day you can see the Alcova Limestone forever. It is the most widespread and easily recognized marker bed in the early Mesozoic strata of Wyoming, and certainly one of the most widespread marker beds in North America, covering at least 50,000 square miles. It is an incredibly thin formation to blanket such a large area—less than a foot thick in places. During Alcova deposition the Wyoming shelf was stable, one of the stillest places and times of the Mesozoic era.

The Alcova sea transgressed quickly over the Wyoming shelf to east-central Wyoming and, after leaving what is now up to about 25 feet of carbonate rock, regressed with dispatch westward toward the continental margin in westernmost Wyoming and adjacent Idaho. The top of the Alcova Limestone is a delight to map, and one's biggest concern is the rattlesnakes that inhabit the sandstone caves just below the Alcova and live in the Crow Mountain sandstone facies (**Figure 9**) just above it. They also love the Alcova setting.

Though the Alcova is the only carbonate tongue that extends out of the basinal carbonate rocks well into the Triassic redbed facies, it is difficult to know with what basinal rocks it is to be correlated. Distances between outcrops are great, in some places tens of miles. Wells are scarce in the critical parts of Wyoming and Idaho where they are necessary for confident correlation of the buried Alcova. In western Wyoming and eastern Idaho, structural complexity makes correlation difficult. The precise correlation of the Alcova Limestone with the southeast Idaho section is thus especially perplexing to geologists (see table 1 in Picard and others, 1969). It is assigned to the Early or Middle Triassic (Pipiringos 1953, 1957), Middle Triassic (Zangerl, 1963, *in* Burk, 1953), Middle or Late Triassic (Colbert, 1957; Carini, 1964), and Late Triassic (McKee and others, 1959; Zangerl, 1963; Bower, 1964).

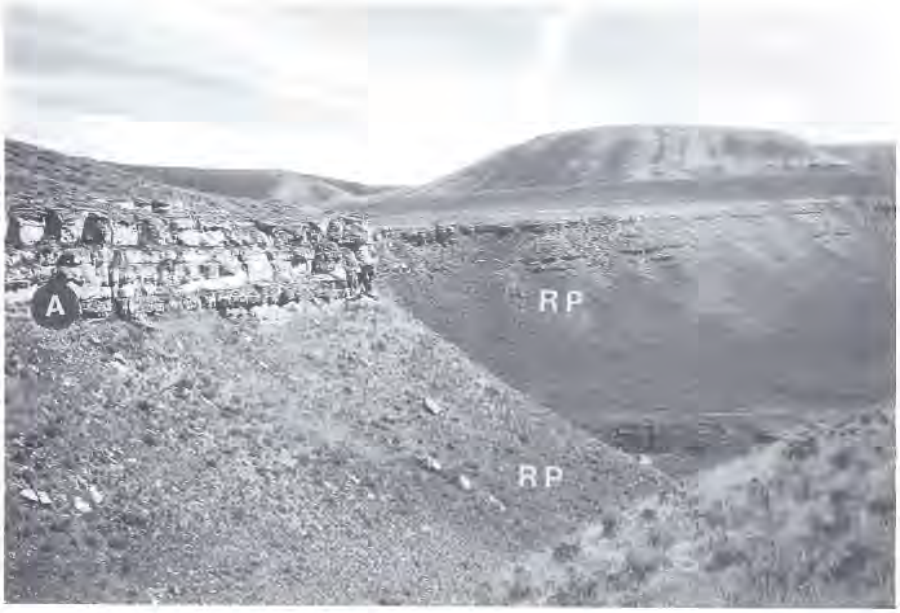

Figure 9. Cliff of variegated sandy facies of the Red Peak Formation (RP), Alcova Limestone (A), and Crow Mountain Sandstone (light colored sandstone above Alcova in foreground left).

In 1969, Picard and others suggested that the Alcova is a marine tongue extending eastward onto the Wyoming shelf from the sandstone and limestone unit of the upper Thaynes Formation (Kummel, 1954). The exact position of the Alcova equivalent in the "sandstone and limestone unit," which is about 150 feet thick at Hoback Canyon, could not be determined. In fact, there are several thin carbonate layers within about 90 feet of dolomite, gypsum, and fine-grained terrigenous redbeds at Red Mountain, which is about 53 miles west of the well-studied section at Red Grade, southeast of Dubois. At Red Grade there is only a single thin carbonate unit in the redbed facies, the Alcova Limestone.

In the Bighorn Basin, the Alcova Limestone occurs along the southern margin, but it is absent to the north by truncation or by local facies change to sandstone. The Alcova is locally missing in the northwest part of the Wind River Basin, because in this area there were islands in the Alcova sea. The interval is represented by sandstone, part of the Crow Mountain Sandstone.

The Alcova sea may have been full of life, but the remains are slight, restricted, and undistinctive. In frustration, J. David Love has said there is such an absence of diagnostic fossils in the Alcova that no one can tell if it formed in fresh or salt water (*in* McPhee, 1986). Love's impatience with the fauna comes from his long experience with the formation and from knowing the results of Carini's (1964) careful but unsuccessful search for diagnostic fossils.

The undistinguished Alcova biota includes molluscan, reptilean, and algal components. "The molluscan assemblage comprises two genera of pelecypods similar in external configuration and ornamentation to the fresh-water forms Naiadites and Sphaerium, and one genus of gastropod (non Natica) possibly allied to the basommatophorids," says Carini. Case (1936) described *Corosaurus alcovensis*, a semi-aquatic reptile, from the Alcova Limestone. Later, von Huene (1948) redefined the reptile, considering it to be an ancestral plesiosaur. Carini noted an undescribed thecodont reptile, a phytosaur or Coelophysis-like dinosaur.

The Alcova flora has given character to the rocks to a greater extent than the few molluscs and reptiles. Stromatolitic algae, inferred to be the work of blue-green (cyano bacteria) or green algae, is spectacularly developed locally, especially in the lower Alcova (Carini, 1964). Within the lowermost 2 to 4 feet, there is 1 to 3 feet of stromatolitic algal limestone at almost every outcrop. Algal mats "grade upward to closely packed and laterally-linked algal stromatolite mounds as much as 2 ft in radius" (Cavaroc and Flores, 1991). The algae is the most volumetrically significant organic constituent in the formation.

The large amount of calcite recrystallization and, to a lesser extent, dolomitization, have obscured and destroyed the majority of fossils. It has altered original textures, sedimentary structures, and bedding. What newly born Alcova limestone looked like is conjectural. If one uses Folk's classification (1959), Alcova rocks are micrite (dominant), biomicrite, pelmicrite, biolithite (algal beds in growth position), silty microsparite, and pseudosparite (Picard, 1969). Bisparite and biomicrosparite with gastropods, pelecypods, and ostracods (?) occur in small amounts. Several types of dolomite—dolomicrite, dolomicrosparite, dolosparite—that are usually silty, also occur in the Alcova. Carbonate pebble conglomerate attests to local erosional episodes. The pale rock colors—light olive gray, grayish pink, pale yellowish brown—are those of the Turner water colors of Venezia (Picard, 1978).

The Alcova Limestone is the deposit of a "desalted isolated lake-sea comparable to the extant Caspian Sea or Sea of Aral," said Carini (1964). When he wrote, few criteria existed for recognizing ancient lacustrine strata, and he cited little actual evidence of an inland sea or lake. In his view, the lack of saline-marine fossils meant that Alcova waters were fresh to brackish. Though I revere lacustrine rocks, and recognize them wherever I can, I interpret the Alcova depositional environments differently.

Limited stable isotope values from Alcova algal facies lend no support to Carini's lake hypothesis. $\delta^{13}C$ values of three samples are -1.0133 (the mean); the $\delta^{18}O$ values are -5.2203 (Cavaroc and Flores, 1991). Cavaroc and Flores seem to suggest that these results indicate brackish water conditions. An alternative interpretation would be that the Alcova $\delta^{13}C$ values are far from indicating fresh or brackish water, but are close to typical chalks. All three $\delta^{18}O$ values are typical of marine limestone. The Ca:Mg ratios are greater than 70. Nothing particularly unusual can be said of the few microprobe and stable isotope measurements other than that they are compatible with

the interpretation of a marine origin for the Alcova Limestone (Picard and others, 1969).

Pipiringos and O'Sullivan (1978) postulated an "inconspicuous but widespread" unconformity (their 'Tr-2') separating the Alcova Limestone and the Crow Mountain Sandstone. Its duration is unknown. They recognize it "at the base of the Crow Mountain Sandstone in north-central Wyoming and at the base of the Jelm Formation in [southeastern] Wyoming and north-central Colorado." Pebbles of Alcova Limestone occur in the basal few inches of the Crow Mountain Sandstone and the Jelm Formation (Love and others, 1945b; Love and others, 1947; Woodward, 1957; Tohill and Picard, 1966; Pipiringos, 1968). High and Picard (1969) looked for Alcova limestone pebbles in southeast Wyoming at the base of the Jelm in the Freezeout Mountains but did not see them. Several miles east, the Alcova is absent and Jelm stream beds lie on the Red Peak Formation (High and Picard, 1969). The probable contact is marked by a thin interval of algal plates.

Crow Mountain Sandstone

Recalling the Crow Mountain rocks from a great distance, I think immediately of field experiences. Bruce Tohill, my first graduate student, did his research on Crow Mountain strata in northwest Wyoming. We spent many long days measuring cross strata, the most abundant bedding structure in the formation, and divided the formation into a basal sandstone and an upper sandstone and siltstone facies (Tohill and Picard, 1966)—first at Thermopolis, where I had earlier spent many weeks with Lee High looking at the Crow Mountain while gathering information for my dissertation (Picard, 1964).

When I was a boy on Bridger Creek, I climbed all over the olive and olive-brown basal sandstone, there soon aware of the enormous Crow Mountain Sandstone rattlesnakes that dwarfed their cousins living in and on other Triassic terrain. My mother warned me often about the snakes, aware of their affinity for warm sandstone in summer and dark caves in winter.

South of the small town of Ten Sleep, in the early 1970s, I tried to convince my father, who was rightly skeptical of what we could see, that an ancient shallow ocean laid down the grains of the 120-feet-thick, reddish brown and yellowish red, basal sandstone. In that red desert valley, I was unconvincing and, for my father, no seas had ever pounded the dusk-drowned headlands.

Crow Mountain is the coarsest Triassic sandstone band in Wyoming. The grand hogbacks are held up by the sandy facies, the thin resistant Alcova Limestone, and the lower part of the basal Crow Mountain Sandstone.

The only common indications of ancient life in the Crow Mountain are trace fossils in the sandstone and siltstone. Trails that parallel bedding planes in cross-stratified sandstone are notable. Some specimens contain an internal structure of meniscate backfill. There are small vertical, inclined, and horizontal burrows. The burrowing organisms continued to churn sediments in some intervals, so that all of the original bedding was destroyed.

In northwestern Wyoming, currents in the Crow Mountain sea apparently moved onshore to the northeast and offshore to the southwest (Tohill and Picard, 1966). At many localities, a significant number of paleocurrent directions are discernable at approximate right angles to the predominant northeast or southwest directions. These probably reflect currents moving along shore to the northwest or southeast. The orientation of the average shoreline is interpreted to have been northwest-southeast, at least in what is now northwest Wyoming.

About half of the Crow Mountain paleocurrent measurements are from cross strata, and half from ripple marks. Cross stratification characterizes the basal sandstone unit of the Crow Mountain, which is red, reddish brown, yellowish red, and brown calcareous sandstone with well-sorted, subrounded, very fine grains (Tohill and Picard, 1966). Fine and medium grains occur, but in smaller amounts. Grains have been recycled, the majority of them several times. The medium- and large-scale trough (dominant) and planar cross stratification signifies deposition in upper parts of the lower-flow regime. Current action in the shallow sea was wave and tidal driven.

Wave-formed ripple marks, which indicate formation in the lower part of the lower-flow regime, characterize the upper sandstone and siltstone unit. Red and reddish brown and drab (non-red), calcareous, very-fine-grained sandstone interbedded with red and drab calcareous siltstone distinguish the sequence. The average well-sorted siltstone contains: quartz and chert (49%), feldspar (11%), rock fragments (3%), carbonate cement (33%), and clay-size matrix particles (4%). The upper unit includes less porous and permeable layers than lower Crow Mountain Sandstone. Depositional breaks are common; sediments were periodically exposed as indicated by the frequency of shrinkage cracks and claystone-pebble conglomerate.

We have suggested a tidal flat, beach, and marsh setting during upper sandstone and siltstone deposition (Tohill and Picard, 1966). Tohill and Picard (1966) also suggested that the Crow Mountain accumulated during a westward regression of the shelf sea. At the beginning of sandy facies deposition, regional uplift of the basin and source areas on the north, east, and south occured. The basal sandstone thickens toward the north and east, and the clastic strata are coarser grained on the north and east.

Although minor oil production comes from the Dinwoody Formation at T.E. Ranch and from the Red Peak Formation at Dallas Dome, the Crow Mountain Sandstone contains the most important producing Triassic intervals in Wyoming because of its favorable reservoir qualities. Based on about two dozen modal analyses, the average productive sandstone (subarkose) is composed of: quartz and chert (67%), feldspar (10%), rock fragments (2%), carbonate cement (13%), and matrix (8%). It is very fine to fine grained and well sorted. The grains are subrounded. Porosity in the producing fields varies from 14 to 24%. Limited measurements show permeabilities from 18 to 112 millidarcies (md). Pay thicknesses range from 2 to 66 ft, with an average of about 35 ft. The sand grains are from sedimentary sources (dominant), gneiss-schist terranes, and felsic plutonic rocks (Tohill and Picard, 1966). Volcanic and mafic igneous rocks contributed small amounts of sand. The principal reservoir intervals are in the basal sandstone unit. Because of its porosity and permeability, existing oil fields, and showings of oil in boreholes and outcrops, the basal Crow Mountain is a secondary target for new exploration.

Dinwoody and Red Peak rocks do not make good reservoirs for oil and gas, and most exploration geologists attached to major companies would not propose a wildcat well to test either sequence.

Crow Mountain production is dominantly in the Bighorn and Wind River basins, of which Grass Creek in the southern Bighorn Basin is by far the largest field. Nearly all of the fields produce from anticlines or faulted anticlines. None of the reservoirs is filled to the closing structural contour with oil or gas. The effective pay is much less than the subsurface closure at or near the productive intervals. At the North Tisdale field, facies changes in the Crow Mountain contribute greatly to the trap.

"Although both the Crow Mountain and the underlying Red Peak members of the Chugwater are oil stained in many parts of the basin, the source of this oil is not obvious," said Hunt and Forsman (1957, p. 108). Thirty-five years later it is still not obvious. Above the Dinwoody, the Triassic rocks are dominantly redbeds. Exploration geologists have held some or all of these partly or wholly faulty, premises: 1) oil does not occur in such redbed sequences, 2) oil does not originate in nonmarine sediments, and the Triassic sequence above the Dinwoody is nonmarine, and 3) Triassic oil must have migrated into the interval from marine Permian source beds (Picard, 1988).

Some of the Triassic oil clearly did originate in the Permian Phosphoria, as its chemical characteristics and proximity to the formation indicate. The oil in some Crow Mountain fields (N Tisdale, NW Sheldon, Grass Creek) is low gravity (25.7% °API) and high sulfur (2.46%; Picard, 1978). Such oil is similar to Phosphoria oils and to Pennsylvanian Tensleep Sandstone oils in Wyoming (**Table 2**). I tend to think that other Crow Mountain occurrences are less readily attributable to Permian sources. Because of local structural relationships, it is difficult to account for all of the oil-impregnated sandstone and siltstone by migration from Permian source beds. There are places in the Wind River and Bighorn basins, for example, where oil-impregnated intervals occur in the upper part of the Red Peak and lower part of the Crow Mountain in sections that are not sharply folded and are unfaulted. I cannot, however, point to likely source beds within these Triassic sequences, though the Alcova Limestone should be checked for source-bed characteristics.

Table 2. API gravity and sulfur characteristics of various oils in Wyoming.

Occurrences	Gravity (°API) (number of fields)	Sulfur (wt. %) (number of fields)
Tertiary in Green River Basin	38.9 (15)	0.07 (7)
Cretaceous in Green River Basin	40.1 (39)	0.17 (39)
Cretaceous in Wind River Basin	42.2 (15)	
Triassic Crow Mountain Sandstone, Wyoming	25.7 (10)	2.46 (3)
Permian Phosphoria Formation, Wyoming	23.5 (48)	2.65 (29)
Pennsylvanian Tensleep Sandstone, Wyoming	25.0 (41)	2.62 (41)

In the sixties, above the Crow Mountain in the Wind River Basin and in the southern Bighorn Basin, Tohill and Picard (1966) recognized a redbed unit—sandstone dominantly, but also siltstone, claystone, claystone-pebble conglomerate—to which they gave no formal name. An unconformity separates the unnamed redbed unit and the Crow Mountain. The Crow Mountain is Middle (?) Triassic, the overlying redbed interval probably Upper Triassic. Pipiringos and O'Sullivan (1978) have called the unconformity 'Tr-3', and said it "is one of the most widespread, cospicuous, and widely recognized unconformities" in the Triassic and Jurassic in the Western Interior United States. In northeast Utah, it lies between the Gartra Formation and the Moenkopi Formation (McCormick and Picard, 1969). Pipiringos and O'Sullivan (1978) placed the unconformity within the Crow Mountain Sandstone in the Wind River and Bighorn basins, but apparently they defined the Crow Mountain there differently than we did (Tohill and Picard, 1966). Pipiringos and O'Sullivan (1978) suggested that the Tr-3 lasted less than a million years.

Jelm Formation

During deposition of the Crow Mountain Sandstone, much of the Wyoming shelf was flooded by a shallow sea. Streams emptying into it in southeast Wyoming deposited the lower Jelm Formation. A general withdrawal followed, during which the fluvial and fluvial-lacustrine sediment of the Jelm and Popo Agie formations prograded over the shallow marine Crow Mountain Sandstone.

In 1917, Samuel H. (Doc) Knight — son of W.C. Knight who preceded him as Geology Department Chairman at the University of Wyoming—separated the Jelm Formation from the Chugwater Formation in southeast Wyoming because it is unconformable on the Chugwater (Red Peak Formation). In southeast Wyoming, the upper 250 feet of the redbed sequence includes a bed of bone- and plant-bearing conglomerate containing a Triassic (?) vertebrate fauna. Inasmuch as the Alcova does not extend that far east, exact placement of the Chugwater-Jelm contact is unknown relative to the Chugwater of central Wyoming. It lies at the approximate position of the Alcova, however, and the Jelm in the type area is thus approximately equivalent to the Crow Mountain and Popo Agie of central and western Wyoming described by previous workers. The relationships have not been demonstrated. We have much to learn.

Branson (1927) believed the Jelm and Popo Agie deposits to be representatives of local, short duration environments that probably were not contemporaneous. Hubbell (1954) used Jelm and Popo Agie interchangeably. Pipiringos (1968) considered the Jelm equivalent to the Crow Mountain of central Wyoming. High and Picard (1969) interpreted the Jelm Formation to be a facies equivalent of the upper Crow Mountain Sandstone in southeast Wyoming, and to unconformably overlie the Crow Mountain throughout central Wyoming.

The central Wyoming Jelm (or unnamed redbed unit) differs from more eastern sections in the rarity of conglomerate and the presence of clayey limestone and platy, ripple-marked, carbonate-cemented sandstone. Cross-stratified, channel-filling, red sandy siltstone and sandstone remain the dominant rocks. They were deposited on a generally westward-prograding fluvial deltaic plain (High and Picard, 1969; Picard, 1978).

From their study of the Chugwater Group along the southwest margin of the Powder River Basin, Cavaroc and Flores (1991) also interpreted the redbeds as representatives of fluvial-deltaic plain deposits. They noted thick (as much as 35 ft) lenticular sandstone, and "poorly sorted channel fills and tabular splays" (generally <10 ft thick). The cross strata in the channels indicate lower-flow regime conditions, but the planar lamination represents deposition in the upper-flow regime. Channel-filling sandstone grades upward into ripple-dominated beds. Some sandstone shows abundant burrows.

High and Picard (1969) showed the Jelm tongue grading into the basal part of the Ankareh Formation (**Figure 7**) in western Wyoming. The interval consists of dark reddish brown, platy, calcareous siltstone and very fine- to fine-grained sandstone with abundant small-scale cross stratification and ripple marks. Likely, now we would assign these beds in western Wyoming to the unnamed redbed unit, which Tohill and Picard (1966) used. These rocks closely resemble platy facies of the Red Peak Formation, which, on the basis of sedimentary structures and stratigraphic relationships, are interpreted to be tidal-flat deposits. Thus, in western Wyoming this sequence may be shallow marine to paralic.

Popo Agie Formation

The Popo Agie Formation was deposited in a vast river and lake system. During deposition, volcanoes rained ash over most of western Wyoming and on adjacent parts of what is now Idaho, Utah, and Colorado. In south-central, central, and western Wyoming, High and Picard (1965, 1967, 1969) recognized four easily distinguishable rock units: lower carbonate (oldest), purple, ocher, and upper carbonate (**Figures 10** and **11**). The upper three units also crop out in the Uinta Mountains area of Utah and Colorado, and extend westward to north-central Utah, maintaining thicknesses comparable to those in correlative outcrops on the western end of the Uintas.

Of all places to see the Popo Agie rocks, I find Red Grade (**Figure 10**) the most satisfying. Lee High and I spent several wonderful weeks there in the early 1960s looking at all the Popo Agie layers, and digging trenches to describe and sample hidden beds.

Lake Popo Agie was one of the largest (70,000+ mi^2) of the known ancient lakes. It would be the world's second largest modern lake, more than twice the size of Lake Superior—70,000 mi^2 compared with 31,654 mi^2—and probably less than half the size of the Caspian Sea, which is about 166,000 mi^2 (table 1 in Picard and High, 1985).

Figure 10. Unconformity separating lower Nugget Sandstone (Jurassic) from Popo Agie Formation (Late Triassic) at Red Grade in the Wind River Basin. The boys are standing near the base of the Popo Agie.

Figure 11. Purple, ocher, and upper carbonate units of Popo Agie Formation unconformably overlain by Nugget Sandstone southeast of Dubois on U.S. Highway 287.

Overlying strata truncate the Popo Agie Formation on the north and east. The lake thus may have been much larger than 70,000 mi². On the west and south, lake beds of the Popo Agie Formation grade into river beds.

The lower carbonate unit of the Popo Agie Formation is a carbonate pebble conglomerate deposited in a stream environment and associated local ponds and small lakes. The purple unit is a silty smectitic mudstone and claystone laid down on floodplains by low-gradient steams. Local beds of analcimolite (sedimentary rock with 50% or more of the zeolite mineral analcime) indicate that isolated lakes existed. Location of volcanoes there at the time is unknown. Ash, washed in by streams and carried to the basin by winds, settled on the vast alluvial plain and was altered to clay minerals (mostly smectite). The ocher unit is silty, analcimic, smectitic mudstone and analcimolite. It represents a widespread and persistent lake. The volcanic source areas continued to be active during deposition of the ocher unit. The same general conditions continued during deposition of the upper carbonate unit, which is mostly clayey dolomite and dolomitic mudstone. Evidently volcanism ended, however, while the lake was still active, and deposition of analcimic smectitic mud was replaced by illitic dolomite in the upper carbonate unit.

In northeast Utah and northwest Colorado, the Popo Agie Formation conformably overlies the stream-deposited Gartra Formation [Upper (?) Triassic], which McCormick and Picard (1969) discussed in detail. The lower carbonate unit of the Popo Agie is absent. An additional stream deposit—the sandstone and conglomerate unit—partially replaces the ocher unit in Colorado. Locally, the fluvial purple unit thickens at the expense of the lacustrine ocher unit, indicating nearness to shorelines. Similar relationships are evident in extreme eastern Idaho, indicating the western extent of the lake there. North of Nephi on Mount Nebo in north-central Utah, the Popo Agie Formation is still at least 300 feet thick. The western reaches of Lake Popo Agie appear to have spread at least tens of miles west of the Wasatch Mountains.

The proposed area of Lake Popo Agie grew as detailed studies of its formation continued. In 1963, High suggested that it probably occupied "an area of at least 3,500 mi²." By 1972, Picard and High estimated the area at 50,000 (+) mi². By 1993, this very large Late Triassic lake appeared to have covered an area that included large portions of Idaho, Wyoming, Colorado, and Utah, amounting to at least 70,000 mi². Probably it was much larger during its maximum extent. By comparison, England, Wales, Scotland, and Northern Ireland cover an area of about 94,000 mi².

The lack of bedding and sedimentary structures in the Popo Agie Formation is striking: it is similar in its few bedding types and primary structures to many shallow marine carbonate units. This contrasts sharply with the abundant and diverse bedding and sedimentary structures in the shallow marine, fine-grained, terrigenous clastics of the Red Peak Formation and the diverse structures in the lacustrine Eocene Green River Formation in the Uinta Basin (Picard and High, 1972). Disturbed bedding and intraformational conglomerate characterize the Popo

Agie. Horizontal stratification, cross stratification, homogeneous (no apparent bedding) stratification, and sedimentary dikes occur rarely in the formation. The Popo Agie is burrowed; the abundance of homogeneous bedding, disturbed bedding, and burrows indicates that much original bedding has been destroyed.

On the basis of its fauna, the Popo Agie Formation is assigned to the Late Triassic, when dinosaurs dominated land habitats and all of the present continents remained joined in the supercontinent Pangaea.

The Popo Agie vertebrate fauna consists of the phytosaurs Paleorhinus and Angistorhinus, the metoposaurid Eupelor, a pseudosuchian Dolichobrachium, the therapsids Brachybrachium and Eubrachiosaurus, a fresh-water lungfish Ceratodus, and the dinosaurs Poposaurus and Agialopus (Colbert, 1957; Gregory, 1957). High and others (1969) found the anterior end of a vertebra–probably from about the last third of a reptile tail—with phytosaur remains in the Uinta Mountains area north of Vernal, Utah. Wann Langston, Jr. (personal communication, 1969) suggested that it was from Trilophosaurus, which is best known from the Upper Triassic Dockum Group of Texas.

In the Late Triassic, phytosaurs were among the most numerous reptiles, similar in habits and appearance to modern crocodiles. They were, as well, the ecological predecessors of these forms, although not in themselves directly ancestral (Romer, 1945).

The fresh-water pelecypod, Unio, is the only reported invertebrate in the Popo Agie Formation (Berry, 1924; Keller, 1952). Coprolites occur. Fossil plants include a large Equisetum, cycadophytes, and many wood fragments (Berry, 1924).

Reconstruction of the paleogeography gives the broad outlines of Lake Popo Agie. A lake origin for much of the Popo Agie is inferred from paleontologic, mineralogic, geochemical, and regional stratigraphic considerations (High and Picard, 1965). The Popo Agie fauna is nonmarine. Although distinctions between river and lake environments usually are not definitive based on fossils, the presence in the Popo Agie of large predators such as phytosaurs and labyrinthodont amphibians indicates semi-permanent water bodies.

The abundant analcime and carbonate in the Popo Agie Formation also suggests a lake origin rather than a stream origin. Inasmuch as streams are commonly acidic, and calcite is unstable at pH values less than about 7.8, fresh-water limestone indicates a lake origin. Similarly, authigenic analcime requires conditions more basic and higher concentrations of alkalis than are usual in streams.

The mass extinction at the end of the Triassic ranks with the other cataclysms for species as one of the Foremost Five terminations (Eldredge, 1991). More than 20% of known families also became extinct. Terrestrial extinctions were notably severe. Losses among marine invertebrates were also heavy. Ammonoids, gastropods, corals, and bivalves suffered great familial extinctions, and conodonts vanished (Bice and others, 1992).

The cause of the Triassic-Jurassic boundary extinctions is uncertain. Recently, however, Bice and others (1992) apparently have found evidence of a meteorite impact—shock-metamorphosed quartz—in three closely spaced limey claystone beds from the uppermost Triassic ("Rhaetian") near Corfino, Northern Tuscany, Italy. They note that 5 to 10% of quartz grains "within these layers exhibit one or more sets of planar deformational features whose orientations cluster around the rational crystallographic planes ... most commonly observed in shocked quartz." It is conceivable, though unlikely from their description, that their "shocked quartz" may be displaying Böhm lamellae, a result of tectonism. Long ago, we found quartz with Böhm lamellae in the Upper Triassic unnamed redbed interval in northwest Wyoming (Tohill and Picard, 1966). Or did we see shocked quartz? I will certainly sample this interval again.

The shocked quartz crystals suggest that three closely spaced impacts occurred at the end of the Triassic, say Bice and colleagues, who propose multiple collisions in the latest Triassic, perhaps during a comet shower. The upper limey claystone coincides with the sudden end of the singular, uppermost Triassic, Rhaetavicula fauna. Lower Jurassic rocks overlie the claystone.

The dinosaurs, thus, may have risen about 204 Ma, following a cosmic collision whose effects devastated the dominant species, then left Earth with a similar bang when an 140-million-year-younger

cataclysmic impact ended the dinosaurs' long rein. Unfortunately for students of early Mesozoic history of Wyoming and Utah, there may be a 7- to 10-million-year time gap between the terrestrial Popo Agie and the overlying terrestrial Nugget Sandstone (Pipiringos and O'Sullivan, 1978). Evidence of the dinosuar's rise in Wyoming may have been carried into some Triassic-Jurassic (?) sea.

Nugget Sandstone

J. David Love, certainly one of the most experienced and gifted field geologists to study early Mesozoic strata since Nelson Horatio Darton nearly a century ago, wrote in 1957 that there is intricate intertonguing of the lower part of the Nugget Sandstone and the upper part of the Popo Agie Formation (then a member).

Earlier students of this boundary made similar interpretations. Hubbell (1954) postulated an interfingering of the Chugwater and Nugget formations along the north flank of the Great Divide and Hanna basins. In the Green River Basin, Anderman (1956) interpreted the Nugget Sandstone as a westward sandstone facies of the upper part of the Popo Agie Formation. Similarly, Burk (1956) reported that, "Just south of the Wind River Basin, stratigraphic correlations indicate that at least the lower part of the Nugget is a sandstone facies of the Triassic Popo Agie redbeds." Burk's study was confined to the subsurface and to mechanical logs, which do not show the character of the rocks in sufficient detail to determine that the Popo Agie-Nugget boundary is more complicated than a simple facies change from fine-grained Popo Agie strata into coarse clastic beds of the Nugget Sandstone.

The supposed facies or intertonguing relationships between the lower Nugget Sandstone and the upper Popo Agie Formation are cited as evidence that the Nugget Sandstone may be Triassic rather than Jurassic in age (Love, 1957). In 1963, while eating lunch under a sandstone overhang at the Nugget-Popo Agie boundary southeast of Dubois, High and Picard (1965) discovered evidence of an unconformity at the base of the Nugget Sandstone (**Figure 10**). Between bites of tuna fish, asparagus, and dill pickles, we noticed yellow pebbles and other pieces of Popo Agie rocks in conglomerate of the basal Nugget Sandstone. Later on, in support of a regional unconformity at the boundary, we noted: 1) the Popo Agie upper carbonate unit is absent at most localities on the southwest margin of the Wind River Basin; 2) the ocher unit varies in thickness; and 3) the purple unit thins abruptly between Dallas Dome and Red Canyon near Lander. Our serendipitous discovery of the unconformity in the Wind River Basin led to study of the boundary at many other localities. It occurs throughout Wyoming and is present in Utah and northwest Colorado (High and Picard, 1965, 1969; Pipiringos, 1968; Pipiringos and O'Sullivan, 1978). Locally, older beds have been tilted and folded and the unconformity is an angular one. This is especially notable in the southern Uinta Mountains area, where broad folds formed during pre-Nugget Sandstone warping (High and others, 1969).

In Wyoming and Utah, marked change is apparent in the rock types and mineral content between the analcimic rocks of the purple and ocher units of the Popo Agie and the sandstone and siltstone of the lower Nugget Formation. Illite is the characteristic clay mineral in the Nugget, smectite in the underlying Popo Agie. Analcime does not occur in the lower Nugget except in the ocher granules and pebbles of the basal conglomerate. Ocher, light green, and other variously colored granules and pebbles (up to 0.5 inches in diameter) in the conglomerate are the result of erosion of the Popo Agie, but were not transported far.

Crustaceans, molluscs (fresh-water bivalves), reptiles, fragmentary plant remains, scorpion tracks, and organic trails of unknown origin are present in the Nugget Sandstone and in the probably equivalent Navajo Sandstone south of the Uinta Mountains in Utah and northern Arizona (Picard, 1977a). However, fossils are rare in the Nugget, as is the case in ancient wind deposits throughout the world. The Nugget and Navajo formations are much studied, but no one has found them to contain marine fossils.

The Nugget Sandstone in Wyoming exhibits less evidence of ancient life than is the case on the south

flank of the Uinta Mountains, in the north-central Wasatch Mountains, and in equivalent strata farther south. In 1953, Wroble found a fossil trail in the upper part of the Nugget in central Wyoming, which A.A. Ekdale said resembles Gyrochorte (Picard, 1975b). Hallam (1970) interpreted Gyrochorte to be the collapsed tunnel of an amphipod burrowing just slightly below the sediment surface; Heinberg (1973) believed it to be the burrow of a worm-like organism moving obliquely through the sediment. Investigations of other trace fossils in the formation in Wyoming have so far been few.

Nugget Sandstone in the Wind River and Uinta mountains is divided into two informal rock units, an older thinly bedded facies and a younger cross-stratified facies (**Figure 12**). The thinly bedded facies is a variable sequence of clayey siltstone, siltstone, mudstone, silty claystone, sandstone, limestone, and dolomite (classification of fine-grained terrigenous rocks after Picard, 1971). In contrast, the cross-stratified facies is almost entirely sandstone or siltstone (Picard, 1977b). The thickness of the formation varies from less than 100 feet to about 1,000 feet. The thinly bedded facies ranges from about 25 to 125 feet thick in the subsurface. A similar rock unit, the Bell Springs Member that Pipiringos (1968) recognized, ranges from 0 to 240 feet thick in south-central Wyoming. The extent to which the Bell Springs Member corresponds to the thinly bedded facies remains as an open question.

At a time when few controversies stirred sedimentologists, Freeman and Visher (1975) started a spirited one when they suggested the Navajo Sandstone was laid down in a marine environment rather than a desert-eolian setting (**Table 3**). This debate never became a major geological confrontation, but it had its moments, and professors still use their article and the subsequent discussions as a provocative introduction for students to eolian and shallow marine environments.

Until Freeman and Visher (1975) published their paper—Freeman's dissertation—nearly everyone accepted the Navajo and Nugget sandstones as desert-eolian strata based on their large-scale, high-angle (>20°) cross stratification, lack of marine fossils, high quartz content, trace amounts of coarse mica, well-sorted and frosted quartz grains, (+)-skewed sands, strong bimodality of grains, unimodal paleocurrent patterns, eolian ripple marks (ripple indices >15), and so on (Picard, 1977b). If the magnificent, sweeping, Navajo cross strata in Zion National Park, for example, were not laid down by desert winds, what ancient sandstone in the world could be attributed to ancient winds? So wondered the eolian specialists. They were prepared to bet everything on the Zion Navajo. For a moment they were shaken by Freeman and Visher who seemed to have new evidence and wanted to label the strata "marine" (**Table 3**). It should also be said that Stanley, and others (1971) had earlier suggested that the Nugget Sandstone in western and central Wyoming originated in a shallow marine environment.

Figure 12. Nugget Sandstone at Lander dome. Thinly bedded facies of Nugget unconformably overlies fine-grained facies of Popo Agie Formation. Light colored cliffs are Nugget cross-stratified sandstone.

Within a few months, the results and interpretations Freeman and Visher presented were refuted or reinterpreted by others (Folk, 1977; Steidtmann, 1977; Ruzyla, 1977; Picard, 1977a). A few examples: the pelletal glauco-

Table. 3. Evidence for interpreting the Navajo sandstone as a marginal marine, tide-dominated shelf-floor sequence according to Freeman and Visher (1975).

1. The log-probability curve shapes of samples from the Navajo and modern tidal-current environments show that they were deposited by similar processes.
2. The Navajo Sandstone intertongues with the overlying marine Carmel Limestone.
3. Pelletal glauconite in the Nugget Sandstone of the Wind River Basin indicates a marine environment.
4. Sands from the North Sea tidal banks are moderately to very well sorted, as are those in the Navajo sandstone.
5. "Roundness lacks environmental significance in ancient-modern analog models and the evidence is that frosting on Navajo grains is a result of diagenetic solution and precipitation of quartz rather than mechanical action."
6. The large-scale, high-angle Navajo cross stratification is similar in size and morphology to sands in modern marine environments—sand waves and tidal-current ridges.
7. Small dinosaurs found in the Navajo Sandstone near Shonto, Arizona, may have been carried out to sea by rivers. The lack of marine fossils "does not preclude a marine origin" for these reasons: a tide-dominated environment is not "conducive to the support of marine benthonic forms"; biogenic structures are difficult to see in "homogeneous" sandstone; water conditions may have been abnormal (highly saline or alkaline); the high porosity and permeability of the sandstone are adverse for the preservation of hard parts of fossils.
8. Bioturbation such as that found in the Navajo is solely a subaqueous feature, suggesting a marine environment.

nite found in the Nugget Sandstone turns out to have been possibly three glauconite grains in a thin section (out of about 50 thin sections studied); bioturbation is, of course, not solely a subaqueous feature; and the marine Carmel Limestone unconformably overlies the Navajo Sandstone.

The reported occurrence of a single marine pelecypod, Trigonia, supposedly found in the Wasatch Mountains by Mathews (1931), was a mistake. This was probably not a fossil, says Wm. Lee Stokes, let alone a marine pelecypod, and its reported occurence six decades ago gives no marine aura to the Nugget Sandstone today.

Folk (1977) replotted the five Freeman and Visher samples, and said "it appears that four or five have size distributions matching desert ergs, and one (Buckhorn Wash) matches a dune flank." Folk also said that there was no match between the log-probability curve shapes of Navajo samples and sands from modern tidal-current environments. Walker and Middleton (1979) noted that the steep faces of tidal sand ridges and sand waves are commonly inclined about 5°, rather than the 20°or so Freeman and Visher needed to find cross strata in modern marine environments of similar size and morphology to eolian sandstone.

The Nugget Sandstone in Wyoming and northern Utah contains beds that were laid down in several environments—eolian, small lakes within dune areas, inland sabkhas, and streams (Picard, 1975b; High and Picard, 1975; Knapp, 1978). The climate was hot and dry. It was trodden by dinosaurs, crocodiles, scorpions, and many other animals. Burrowers were locally abundant in what is now northeast Utah and the Wind River Range and probably elsewhere in Wyoming. The Navajo Sandstone of central and southern Utah includes rocks that are similar to those of the Nugget Sandstone. Interpretations of Navajo environments are also similar.

Galton (1971) postulated that most of the Navajo Sandstone in northeast Arizona is Late Triassic rather than Early or Middle Jurassic, based on biostratigraphic evidence—the small, prosauropod dinosaur Ammosaurus and the crocodile Protosuchus. Earlier, after reviewing the paleontologic and stratigraphic evidence, Lewis and others (1961) suggested that the Kayenta Formation underlying the Navajo may be Late Triassic, but referred the Navajo to the Jurassic.

Many other workers, including myself, believe the Navajo is Early and (or) Middle Jurassic in age (Baker and others, 1936; Harshbarger and others, 1957; Welles, 1954, 1970; Picard, 1975b).

When a formation becomes a large producer of petroleum or any other valuable commodity, it becomes the object of frantic attention and study. The geological interpretations may be critical to successful exploration, leading some geologists to emotional outbursts more typical of a frenzied search for wealth and fame than the selfless pursuit of knowledge. Following the discoveries in northeast Utah at Pineview and in southwest Wyoming at Ryckman Creek, the Nugget became a hot formation. In the mid-1970s, some of the emotional responses growing out of pet theories about Nugget oil landed on me. My life became a soap opera—I got anonymous letters and strange telephone calls. At large luncheon meetings a few fellow geologists bristled when I so much as asked for mashed potatoes. All this only because I had suggested that part of the Nugget oil might have formed in lacustrine intervals of the lower Nugget and migrated into permeable parts of the upper Nugget (Picard, 1975b, 1976). I noted (1975b) that Nugget oils resemble Cretaceous and Tertiary oils. I discounted the Cretaceous possibility on the basis of regional relationships and on the grounds that the Nugget fields discovered to that time were largely controlled by structures (anticlines and faulted anticlines), but were well short of being full of oil or gas. None of the Nugget fields was full because only small amounts of oil originated in the minor lacustrine intervals in the formation, I said.

In 1976, I stressed the possibility of large-scale migration from Cretaceous sources into Nugget reservoirs along fault planes. This is essentially what happened where large Nugget fields occur in the fold-and-thrust belt. I did not completely retreat, however, from the idea that some oil might have originated within the lacustrine intervals and migrated to other parts of the formation. My earlier limited and partly incorrect interpretation was not immediately forgiven. The prodigal son does not always get the fatted calf.

The building blocks and facings of some of the most attractive public buildings and homes in Wyoming and Utah have come from Nugget quarries. Nugget beds are short on fossils, other than burrows, but the warm colors—orange-pink, pale orange, grayish orange, moderate reddish orange, and moderate red—hold their color moderately well in these semiarid to arid climates. The cements—silica, the first formed, then calcite and dolomite—maintain the sandstone grains, though there is weathering of feldspars in the sandstone.

Gypsum Spring Formation

Though they have become caprocks over Nugget petroleum reservoirs in Wyoming and Utah, though evaporites overlie carbonates that contain one-half of the world's petroleum reserves (Kirkland and Evans, 1981), Gypsum Spring rocks are little studied. It is a formation that droops and slumps and slides. The abundant gypsum beds (anhydrite at depth) in the lower part (**Figures 13** and **14**) lead to these instabilities and deformation within the formation. The anhydrite is interbedded with and underlies sealing claystone in Nugget fields.

Love (1939) named the Gypsum Spring Formation after Gypsum Spring on Red Creek, 18 miles southeast of Dubois, Wyoming. Since then the name has been misspelled (Gypsum Springs) about as frequently as it has been spelled correctly. An example from Gretel Ehrlich's piece "Spring" that first appeared in *Antaeus* (1986): "Now I'm sitting on a fin of Gypsum Springs rock looking west." Such a slip may cause a Jurassic geologist to wince, but is scarcely noticed by anyone else.

Apparently, the Gypsum Spring is a formation easily forgetten. Yet the contact between these earliest Middle Jurassic rocks (Bajocian) and underlying strata represents one of the most prominent unconformities in the Paleozoic and Mesozoic record of Montana, Wyoming, and Utah, said Downs (1949). Pipiringos and O'Sullivan, in their study (1978), assigned 2 to 3 million years to this unconformity (J-1), the contact between the Gypsum Spring Formation and the underlying Nugget Sandstone in Wyoming. They correlated the Temple Cap Sandstone of

Figure 13. Uppermost Nugget Sandstone (N), Gypsum Spring Formation (G), and lower part of Sundance Formation (light-colored strata at upper left), southeast of Dubois on U.S. Highway 287.

Figure 14. Gypsum Spring Formation at Lander dome, Wind River Basin. In the foreground, the photograph shows almost all of the formation.

southwest Utah and the Nesson Formation of the Williston Basin with the Gypsum Spring Formation—"they are here considered nearly exact correlatives" (p. A-20). Pipiringos and O'Sullivan believed the lower unconformity (J-O) between the Nugget Sandstone and the underlying Popo Agie Formation or, in the Wasatch Mountains, the Nugget Sandstone and the Ankareh Formation, lasted much longer (7 to 10 my), though they assigned a Jurassic (?) and Triassic (?) age to the Nugget Sandstone. To our dismay, they called the Popo Agie Formation in the Uinta Mountains the Chinle Formation, extending Chinle from southern Utah and northern Arizona across the deeply buried early Mesozoic rocks of the Uinta Basin. They ignored the earlier work of High and others (1969), who correlated, in detail, uppermost Triassic rocks of the Uinta Mountains with the Wyoming Popo Agie Formation. The duration of their J-0 cannot be well constrained between the slightly fossiliferous Popo Agie and Nugget formations in Wyoming and Utah.

From a maximum thickness of about 250 feet in the northwest corner of the Wind River Basin, the Gypsum Spring thins east and south and is absent in the southeast part of the basin, largely because of truncation below the Sundance Formation (Burk, 1956). To the west, the Gypsum Spring thickens, gains limestone beds, and grades into the lower part of the Twin Creek Limestone.

The lower part of the Gypsum Spring is the most widespread. The basal evaporite unit occurs at the wedge-edge in the Wind River Basin. Based on subsurface studies, Burk (1956) said that, "Throughout its extent in the Wind River Basin, the Gypsum Spring overlies the Nugget Sandstone."

To the north, in the Bighorn Basin, the unconformity beneath the Gypsum Spring cuts successively down through Popo Agie, Jelm, Crow Mountain, Alcova, and upper Red Peak beds (Picard, 1967). About 35 miles east of Sunlight Basin, in the northern Bighorn Basin, the Gypsum Spring lies on Red Peak beds about 350 feet below the top of the Red Peak Formation. Loss of Gypsum Spring rocks by erosion occurs progressively on the east side of the Bighorn Basin, with the basal anhydrite unit present in all wells of Mills's (1956) cross section. Mills placed the Gypsum Spring-Red Peak contact at the base of the anhydrite in the subsurface.

In central Wyoming, the Gypsum Spring Formation generally is a lower unit of gypsum or anhydrite and red claystone and siltstone; a middle unit of limestone, dolomite, red and green claystone, and minor gypsum; and an upper fine-grained clastic unit that locally contains gypsum (**Figure 14**) (Peterson, 1957a). Characteristic colors of the fine-grained "redbeds" are moderate orange-pink, moderate red, grayish red, and pale reddish brown. Various shades of green are also characteristic of the fine-grained beds in the upper unit.

The marine limestone of the middle member preserves pelecypods and ammonites together with crinoids, corals, and gastropods (Love and others, 1945a). As in other parts of the world, an ammonite is very hard to find, perhaps requiring a day or much more of searching by a specialist. The limestone and some of the intertidal fine-grained clastic strata contain abundant foraminifera and ostracods (Peterson, 1957a).

To the south, in northeast Utah, and on the west in southeast Idaho, the Twin Creek Limestone contains the Gypsum Spring Member at its base. This interval is partially equivalent to the Gypsum Spring Formation of the Wind River Basin.

On the pronounced unconformity (J-1) at the top of the widespread wind-deposited Nugget Sandstone sheets, the Gypsum Spring sea transgressed from the north into Wyoming and Utah. Thus began a period of marine evaporite deposition, probably on sabkhas, an Arabic word for salt flat. Deposition resumed, after a time gap of several million years, during another period of arid and semiarid climate. Evaporation was greater than rainfall plus inflow of surface and subsurface water into the basin.

Sundance Formation

The Sundance Kid, mythic bank and stagecoach robber and sidekick of Butch Cassidy, got his name from the same tiny, northeast Wyoming town that gives the Late Jurassic Sundance Formation its name. Darton named the Late Jurassic rocks in 1899.

Before the invading Sundance seas, the stable Wyoming shelf was part of a regional low-lying erosion surface now preserved as the 'J-2' surface or 'J-2' unconformity. There was little relief throughout the whole region.

The lowermost few inches of the Canyon Springs Member, the oldest member of the Sundance Formation, are characterized by weathered chert pebbles (Rautman, 1975). Pipiringos and O'Sullivan (1978) estimated that 80% of the chert is from the Gypsum Spring Formation. The Canyon Springs sandstone in north-central Colorado is the youngest unit deposited over the J-2 surface. The oldest deposition on the J-2 surface occurred in the Williston Basin of Montana, Canada, and the western Dakotas about 161 Ma. The initial transgression of the Sundance sea to cover an area about 310 miles east-west and 500 miles north-south, took approximately 5 my, which gives an average rate of transgression of about 60 to 100 miles per million years (Pipiringos and O'Sullivan, 1978).

During Sundance time, sea dominated the land. The formation shows striking bands in the Black Hills of northeast Wyoming and southwest South Dakota, where Darton first recognized their singularity (Darton 1899; Darton and O'Hara, 1909). The pleasing green and yellow Sundance outcrops, characterized by badlands of resistant sandstone and much thinner fine-grained intervals, are now easily recognized throughout much of central, south-central, and southeast Wyoming (**Figure 15**).

Geologists' propensity—even their need—to recognize a lower part and an upper part of a formation is readily accommodated by the Sundance

Figure 15. Sundance Formation at Lander dome. All of the outcrop in the foreground is assigned to the Sundance. View is toward the northwest.

Formation. Each part is a major transgressional/regressional marine sequence (Brenner, 1983). The lower Sundance, from base upward—Canyon Springs Sandstone, Stockade Beaver Shale, Hulett Sandstone, and Lak Redbeds—is Callovian in age (Rautman, 1975). The upper Sundance—Pine Butte Sandstone, Redwater Shale, and Windy Hill Sandstone—is Oxfordian in age (Uhlir and others, 1988).

The advance of the lower Sundance sea is apparently represented by the Canyon Springs Sandstone and the lower part of the Stockade Beaver Shale, the prograding retreat by the upper Stockade Beaver Shale, the Hulett Sandstone, and the Lak Redbeds (Rautman, 1978). Rautman interpreted the transgressive phase to have been characterized by large submarine sand waves (and/or tidal-current ridges), the regressive phase by non-marine deposits on the southeast in western Nebraska and South Dakota, passing northwestward into lagoons, a barrier-island complex, a submergent bar complex, and offshore silt and clay in central and northwest Wyoming (see Rautman, 1978, figure 14).

The Stockade Beaver Shale grades vertically into Hulett Sandstone. "The Hulett Sandstone is inferred to have been deposited in the various subenvironments of a barrier-island complex, including shoreface and beach, tidal channels, and back-barrier lagoon and tidal flats," said Rautman (1978, p. 2278). An ichnofauna of vertical, tubelike Monocraterion and Diplocraterion presumes very shallow water depths. Body fossils are rare. Wright (1973) reported only five bivalve genera from the Hulett.

Though an enigma, the Lak Redbeds are interpreted to be nonmarine, perhaps a wind-blown unit (Rautman, 1978). Like all of these early Mesozoic redbed facies, the Lak contains siltstone, sandy siltstone, claystone, and gypsum. It is unfossiliferous except for possible trace fossils. It lacks well-developed bedding and sedimentary structures. The wispy, mottled, swirled, sublenticular lamination resembes stratification and burrowed fabrics in the Red Peak Formation (**Figure 6**). According to Peterson (1957b), the Lak was not laid down in northern Wyoming.

Brenner and coworkers suggested that sandstone and coquina facies of the upper Sundance are the deposits of offshore sand bodies (Brenner and Davies, 1973, 1974; Brenner and others, 1985). Uhlir and others (1988) said Brenner and his colleagues may be right in their interpretation of the upper Sundance in some parts of Wyoming, but are wrong for the Bighorn Basin, where Uhlir and his colleagues believed the uppermost 50 to 165 feet represent a tidal inlet, back-barrier shoal and sandy tidal-flat that closes the marine Jurassic. As is true in many geological disputes, this one is courteous and unresolved, and seems to revolve around the question of which outcrops the protagonists have seen.

In the coquina facies, the shells are finely broken. Fragments typically are no larger than coarse sand. Rarely, whole disarticulated valves of *Camptonectes bellistriatus*, *Ostrea strigilecula*, and *Meleagrinella curta* (Imlay, 1956) rest in concave-down positions in the shell hash (Uhlir and others, 1988). The sandstone facies is fine, monocrystalline quartz sand "with 0 to 15% spheroidal glauconite and trace amounts of sand-sized dark colored chert" (Uhlir and others, 1988, p. 739).

During the Late Jurassic, the stable Wyoming shelf had a paleolatitude between about 35° and 39° N. North was the equivalent of our northwest during the Jurassic. The climate then was generally warm and dry, as suggested by the abundance of redbeds, evaporites, and shallow-water carbonate rocks (Brenner, 1983). Wind direction was west to east over the Western Interior. In the Oxfordian, the climate became more humid as moist westerly winds off the Pacific Ocean passed over newly uplifted elements on the west. The moist westerlies and moisture from the epicontinental sea combined to generate storms over the Western Interior sea (Brenner, 1983). These storms greatly influenced sediment dispersal patterns in the Sundance seas.

The transgressing and regressing shallow Sundance seas came in and went out over the Wyoming shelf, which was bounded on the west by the Utah-Idaho trough. On the east, the limiting feature was the Transcontinental arch, a high area through the late Mesozoic (Rautman, 1978). Farther west (**Figure 16**), an active Andean-type subduction zone, produced by the convergence of the Pacific and North American plates, raised positive areas along the western edge of the Sundance sea (Brenner, 1983).

The causes of fluctuating sea levels are diverse. Vail and others (1984) suggested that changes in ocean basin volumes may be the result of sea-floor spreading. Local and regional uplift also play a role in sea level fluctuation. In the Late Jurassic, the east-west Belt Island trend, which originated in central Montana, was an effective barrier to invading marine waters from the north (Brenner and Davies, 1974). As the western Cordillera rose during the Oxfordian, the sea was halted and reversed. Deposition exceeded subsidence, leading to a further regression.

The Sundance Formation is not a prolific petroleum producer in Wyoming, but there is notable production from the Canyon Springs Sandstone and the Lak-Hulett interval at Lance Creek and Poison Spider. A number of smaller oil pools are present in the Lower Sundance reservoirs.

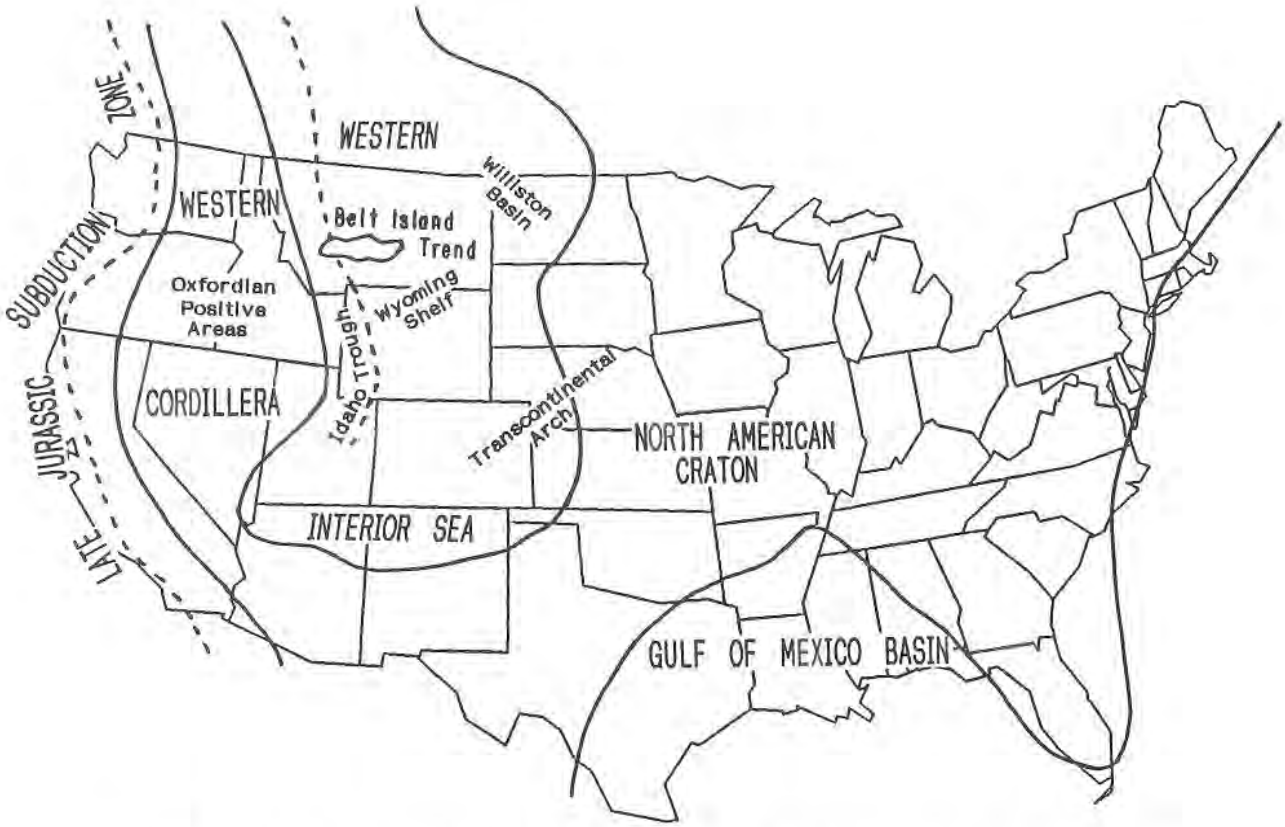

Figure 16. Regional tectonic features and setting during the Late Jurassic (after Brenner, 1983).

The Canyon Springs oil on the Lance Creek anticline is complexly trapped. It is not just in sheet sandstone arrayed across a Laramide anticline as was first thought. The oil distribution is controlled by the thickness of sand deposited within an ancient valley, by a stratigraphic pinchout along the edge of a hill on the field's south side, by the permeable sandstone distributed in the upper unit, and by normal faults (Curry and Hegna, 1970). Lance Creek contains an estimated 170 million barrels of oil in place in the Canyon Springs.

Morrison Formation

Wm. Lee Stokes, longtime student of the Upper Jurassic Morrison Formation in Utah and Colorado, believes it is the most studied formation in the world. Although such assertions are unprovable and are seldom objective—Stokes (1944) did his dissertation and much other research on the Morrison—the Morrison is renowned throughout the world of paleontologists and economic geologists for its dinosaur graveyards and uranium deposits.

Outcrops of the formation at Como Bluff, southeast Wyoming, made Brontosaurus "a household word in the 1880s"... and "for the first time Europe had to look to America for the lead in the paleontology of a major geological period" (Bakker, 1986). The famous brontosaur (now apatosaur) quarry is in the middle part of the sequence in gray floodplain claystone, siltstone, and mudstone. It is about 100 feet above the base of the Morrison. After an afternoon walk through the Como Bluff badlands, Robert T. Bakker, author of *The dinosaur heresies* and a consultant to Michael Crichton on his return-of-the-disturbed-dinosaurs novel *Jurassic Park*, said "Dinosaurs were everywhere."

I recall a Saturday saunter through less dinosaur-laden strata at Como Bluff in 1948 with S.H. Knight and other members of his class in physical and historical geology at the University of Wyoming. We did not lose our senses or our footing on copious femurs. But we were bowled over that day at the sight of the bones Doc Knight had staked out. The roar of imagined angry brontosaurs drowned out the radios of the few students who were listening to the University of Wyoming football game. We were terrified by the terrible reptile cries. For our benefit, Doc added Jurassic history, a reconstruction of the ancient plains, basins, and mountains, and magic on a chalkboard, Doc's art of illustrating the geologically little-known.

About 140 million years ago, "the waves of the Sundance sea beat their last cadence," said Bakker (1986). The Sundance seas were succeeded by terrestrial environments represented in the Morrison Formation by alluvial fans, braided and meandering streams, and lakes. Purple or green claystone and mudstone of the Morrison lie on fossiliferous limestone, sandstone, or siltstone of the Sundance. Sundance sandstone may be highly glauconitic; green Morrison rocks owe their color to clay minerals. At some outcrops, the glauconitic rocks were reworked and glauconite occurs "several inches up into Morrison strata" (Moberly, 1960). The uppermost Sundance was scoured and channeled. Mud cracks and raindrop inpressions on lower Morrison beds attest to the change to terrestrial conditions.

The Morrison lake basins were small compared with such large ancient basins as those occupied by Eocene Lake Uinta and Triassic Lake Popo Agie. The Morrison lakes were ephemeral. Rainfall was sporadic. The climate was strongly seasonal with high rainfall interrupted by brief dry seasons.

Subsurface studies of the Morrison Formation throughout Wyoming and northeast Utah show that it is an upward-fining sequence (see the cross sections in *Wyoming stratigraphy*, Wyoming Geological Association, 1956). Outcrops of the Morrison characteristically display a lower unit of stream-deposited sandstone, siltstone and conglomerate, and an upper unit of more variable rocks, typified by fine-grained strata—claystone, mudstone, and siltstone. There are lenses of channel sandstone and siltstone in the upper unit and braided sandstone sheets of greater lateral extent. There also are carbonate beds and very limey siltstone, which formed in the small lake basins on the vast Morrison alluvial plain.

The fine-grained terrigenous rocks are variegated—red, maroon, green, gray, and brown. From a distance, the striking and characteristic color is purple—pale purple, grayish purple, and very dusky purple. Throughout the Rocky Mountain area, Morrison outcrops are more extensive than those of any other single formation, cropping out in badlands (**Figure 17**) from New Mexico and Arizona on north into Canada. This vast low-lying area was about 1,400 miles long from north to south and about 800 miles wide from east to west. Moberly (1960) has said that the land must have been near sea level because hypsometric curves "show very little of the earth's surface more than a few hundred meters in elevation." One wonders if, when Eldridge (1896) named the formation from outcrops near the village of Morrison in Colorado, he had an inkling of the extent of the strata or how famous the beds would become.

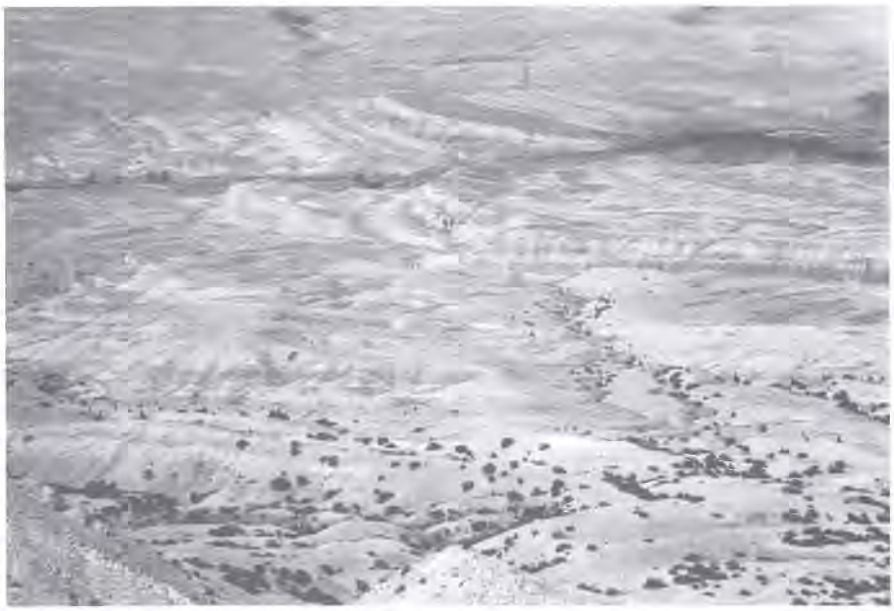

Figure 17. Badlands of Morrison Formation. View is northeast from Sheep Mountain, Bighorn Basin.

In Wyoming, Morrison rocks have not attracted great sedimentological attention. Dinosaur hunters do not always look closely at the beds in which the bones lie. The sedimentologist Ralph Moberly did, however, make a notable study of uppermost Jurassic and lowermost Creteacous strata in the northern Bighorn Basin. Like Stokes's research, Moberly's study (1960) was part of his dissertation at Princeton University.

The Morrison Formation produces a moderate amount of oil and gas throughout the Rocky Mountains. It is a formation much explored by independent operators. The small reservoirs are dominantly in lower Morrison sandstone, but younger sandstone intervals also produce petroleum. Facies changes are common in the lenticular sandstone units, leading to stratigraphic traps. From an exploration perspective, the problem is a lack of source strata in the formation. Contrary to an oil company's television advertisement of several years ago, dinosaurs did not yield gigantic amounts of hydrocarbons to the world's reserves.

The world's largest sedimentary uranium deposits lie in the Morrison Formation in the Grants uranium region in northwest New Mexico. A fine guide to all aspects of the formation and a basin analysis, edited by Turner-Peterson and others (1986), is available and valuable. The Grants uranium region has yielded 40% of the total United States production, holds about 53% of the reserves, and is estimated to contain in excess of 2.6 million tons U_3O_8 in undiscovered ore deposits, according to Kirk and Condon (1986) and others they cite. Most uranium production and reserves come from sandstone in the Westwater Canyon Member (Adams and Saucier, 1981). The Morrison Forma-tion, from oldest to youngest members in the San Juan Basin, includes Bluff Sandstone (eolian deposits), Salt Wash (stream deposits with minor eolian beds and rare lake beds), Recapture (stream and eolian deposits), Westwater Canyon (vertically stacked braided-stream deposits), and Brushy Basin (stream and lake deposits). The Dakota Sandstone (Lower Cretaceous) unconformably overlies the Morrison Formation.

Reading the article by Condon and Peterson (1986) on Middle and Upper Jurassic rocks of the basin and looking at their photographs brings memories of 1951, when I traced key Morrison layers through the Four Corners area, the common corner of Utah, Colorado, New Mexico, and Arizona. I was

searching for oil structures (closed anticlines); I found the best exposed nonmarine depositional sequences I had ever seen. None of the Morrison outcrop bands in northern Utah or Wyoming have been studied so assiduously. The exposures are not as good to the north and—probably the principal reason—the huge uranium reserves found in northwest New Mexico have not been found there. The potential for boomer riches concentrates a geological explorer's mind and inflames his company's interest.

Older uranium deposits—primary, prefault, tabular, or trend ores—occur within reduced fluvial Morrison sandstone (Westwater Canyon Member, Jackpile Sandstone). The uranium in the host rocks is consistently older than 130 Ma (Late Jurassic or Early Cretaceous), indicating that it formed soon after deposition of the host rock (Turner-Peterson and Santos, 1986). These primary ore deposits are termed "humate" because the uranium is intimately associated with pore-filling organic matter, presumably terrestrial in origin, that coats detrital grains and fills sandstone pore space. Redistribution of primary ore, which probably began less than 30 Ma, led to the formation of younger roll-front type deposits similar to those found in Tertiary rocks of Wyoming and Texas (Turner-Peterson and Santos, 1986). These are called redistributed, postfault, or stacked ore in the Grants uranium region.

Concluding remarks

The Triassic and Jurassic endured for 101 or 115 million years, or something in between, depending on which authorities one consults. The maximum thickness of early Mesozoic rocks, using the thickest sequence for each formation, reaches about 4,000 feet for Wyoming and northeast Utah. Using 8,000 feet of sediment as a maximum thickness before compaction and lithification, and about 100 million years for its deposition, the depositional rate would have been 0.00008 feet per year. The 12,500 years necessary to accumulate a foot of early Mesozoic sediment nearly exceeds human presence in North America.

As Ager (1981) has said so agreeably in *The nature of the stratigraphical record*, gaps in the record are more important than the record. The postulated duration of the principal unconformities (Pipiringos and O'Sullivan, 1979) in the Wyoming sequence totals about 18 million years, at least one-sixth of early Mesozoic time. The bulk of 80 to 100 million years may be represented by a large number of smaller unconformities. For the early Mesozoic, as for most stratigraphic sequences, a few beds contain the story of what has taken place during the abyss of geologic time.

Roughly equal amounts of sediment were laid down in continental settings—lake, stream, eolian—and in shallow marine or deltaic-plain settings—delta, beach, marsh, tidal flat, shallow shelf. The Nugget and Navajo sandstones show incomparable outcrops and details of one of the world's great ancient eolian sandstone sheets. No geologist traveling through the Western United States could have a better opportunity to see a record of dominantly eolian deposition. Similarly, though much more difficult to study, the Popo Agie lake beds offer one of the world's most interesting fine-grained formations. Some of the earliest interpretations of tidal flat deposits were made on the Red Peak and Crow Mountain formations. The variety of primary sedimentary structures and bedding types in the Red Peak Formation, and in correlative beds in Utah, is enormous. The fine detail of lamellae; the contrasts between reddish brown and dark red and light grayish green claystone, siltstone, and very-fine sandstone; and the vivid expression of small-scale sedimentary structures has attracted students to these outcrops for generations. Finally, we should not forget the importance of the Morrison Formation in the geology of the West. Dinosaurs and uranium deposits, the largest ancient beasts and the biggest bangs in our time—what a juxtaposition in channel conglomerate and sandstone!

Clastic rocks are overwhelmingly dominant in the early Mesozoic stratigraphic columns of the region. In order of decreasing abundance, they are: sandstone, siltstone, claystone, carbonates, evaporites, and claystone-pebble conglomerate. Siltstone is nearly as common as sandstone.

During the early Mesozoic, the Wyoming shelf was emergent or covered by a very shallow sea. The

continentality of the Triassic and Jurassic sequence sets it off from preceding and succeeding geologic periods. Major petroleum source beds occur in the Permian and Cretaceous in the Rocky Mountains; they are absent or very minor in the Triassic and Jurassic. Permian and Cretaceous seas were deeper, covered far more of the craton, and persisted longer; marine organisms were, of course, much more abundant. Whereas early Mesozoic sedimentary environments were dominantly oxidizing, Permian and Cretaceous environments were dominantly reducing.

Redbeds (including varicolored badlands strata) constitute about 55% of these early Mesozoic sedimentary stratigraphic sections. The Red Peak, Crow Mountain, and Gypsum Spring redbeds—approximately one-half of all the redbeds in the sequence—accumulated primarily in shallow marine environments. The Red Peak, in particular, has been well studied, partly because, as Ager (1981) noted, "Much is hidden in the mists of the Early Triassic, which is probably the least-known episode in the long history of Phanerozoic time."

The lateral persistence of facies has struck nearly all students of the early Mesozoic in the Rocky Mountain region. Many such instances are noted here. On a larger scale, Triassic rocks in the Rocky Mountains are very much like Triassic rocks in northwest Europe, South Africa, and so on. A Triassic specialist, no matter where one is, can find rocks he knows and loves.

Acknowledgments

I thank Donald W. Boyd, Robert L. Brenner, Patricia Faye Cowley, Earle F. McBride, Kitty Lou Milliken, Craig Sanders, Arthur Snoke, and James R. Steidtmann for helpful reviews of the manuscript. Boyd provided the Morrison Formation photograph. McBride lent his support in many ways besides his editorial suggestions. On a recent trip to Laramie, Boyd and Steidtmann generously gave further help. Word processing is the work of Jeanette Stubbe and Missy Grow. The Mineral Leasing Funds of the University of Utah, through several grants, gave partial funding for this study and for extensive work on the geologic history and petroleum potential of early Mesozoic rocks in Utah and Wyoming.

From 1963 through 1985, Lee R. High, Jr., and I coauthored the research memoir *Sedimentary structures of ephemeral streams*, 26 articles, and 16 abstracts, many of them on Triassic history, stratigraphy, and sedimentary petrology in Wyoming, Idaho, and Utah. The citations here to some of that work do not adequately reflect Lee's contributions to my understanding of Triassic rocks in the Rocky Mountain area.

When I read this article straight through for about the fortieth time, I couldn't help noticing the many rattlesnakes. I believe that I have been unusually conscious of them all my life out of my mother's fears while I grew up on the mountain. I remember those early years, and am still fascinated by rattlesnakes, startled by them sometimes, and pleased to yield as much sandstone as they want.

References cited

Adams, S.S., and Saucier, A.E., 1981, Geology and recognition criteria for uraniferous humate deposits, Grants uranium region, New Mexico: U.S. Department of Energy Report GJBX-2 (81), 226 p.

Ager, D.V., 1981, The nature of the stratigraphical record, 2nd edition: New York, MacMillan Publishers Ltd., 122 p.

Anderman, G.G., 1956, Subsurface stratigraphy of the pre-middle Niobrara formations in the Green River Basin, Wyoming, *in* Wyoming stratigraphy: Wyoming Geological Association, p. 49-68.

Baker, A.A., Dane, C.H., and Reeside, J.B., Jr., 1936, Correlation of the Jurassic formations of parts of Utah, Arizona, New Mexico and Colorado: U.S. Geological Survey Professional Paper 183, 66 p.

Bakker, R.T., 1986, The dinosaur heresies—new theories unlocking the mystery of the dinosaurs and their

extinction: New York, William Morrow and Company, Inc., 481 p.

Berry, E.W., 1924, Fossil plants and unios in the red beds of Wyoming: Journal of Geology, v. 32, p. 488-497.

Bice, D.M., Newton, C.R., McCauley, S., Reiners, P.W., and McRoberts, C.A., 1992, Shocked quartz at the Triassic-Jurassic boundary in Italy: Science, v. 255, p. 443-446.

Bower, R.R., 1964, Stratigraphy of Red Peak Formation, Alcova Limestone, and Crow Mountain Member of Popo Agie Formation (Triassic) of central Wyoming [Ph.D. dissertation]: Norman, University of Oklahoma, 174 p.

Boyd, D.W., and Loope, D.B., 1984, Probable vertebrate origin for certain sole marks in Triassic red beds of Wyoming: Journal of Paleontology, v. 58, p. 467-476.

Boyd, D.W., and Maughan, E.K., 1973, Permian-Triassic boundary in the Middle Rocky Mountains, *in* The Permian and Triassic Systems and their mutual boundary: Canadian Society of Petroleum Geologists, p. 294-317.

Branson, E.B., 1915, Origin of the red beds of western Wyoming: Geological Society of America Bulletin, v. 26, p. 217-230.

_____ 1927, Triassic-Jurassic "red beds" of the Rocky Mountain region: Journal of Geology, v. 35, p. 607-630.

_____ 1947, Triassic (Chugwater) footprints from Wyoming: Journal of Paleontology, v. 21, p. 588-590.

Branson, E.B., and Branson, C.C., 1941, Geology of Wind River Mountains, Wyoming: American Association of Petroleum Geologists Bulletin, v. 25, p. 120-151.

Brenner, R.L., 1983, Late Jurassic tectonic setting and paleogeography of Western Interior, North America, *in* Mesozoic paleogeography of the west-central United States: Rocky Mountain Section, Society of Economic Paleontologists and Mineralogists, Symposium 2, p. 119-132.

Brenner, R.L., and Davies, D.K., 1973, Storm-generated coquinoid sandstone—genesis of high energy marine sediments from the Upper Jurassic of Wyoming and Montana: Geological Society of America Bulletin, v. 84, p. 1685-1698.

_____ 1974, Oxfordian sedimentation in Western Interior United States: American Association of Petroleum Geologists Bulletin, v. 58, p. 407-428.

Brenner, R.L., Swift, D.S.P., and Gaynor, G.C, 1985, Reevaluation of coquinoid sandstone depositional model, Upper Jurassic of central Wyoming and south-central Montana: Sedimentology, v. 32, p. 363-372.

Burk, C.A., 1953, Electric log correlation of the Triassic rocks in southeastern Wyoming: Wyoming Geological Association Eighth Annual Field Conference Guidebook, p. 29-33.

_____ 1956, Subsurface stratigraphy of the pre-Niobrara formations in the Wind River Basin, central Wyoming, *in* Wyoming stratigraphy: Wyoming Geological Association, p. 23-33.

Carini, G.F., 1964, Regional petrographic and paleontologic analysis of the Triassic Alcova Limestone Member in central Wyoming [Ph.D. dissertation]: Columbia, University of Missouri, 165 p.

Carr, T.R., and Paull, R.K., 1983, Early Triassic stratigraphy and paleogeography of the Cordilleran miogeocline, *in* Mesozoic paleogeography of the west-central United States: Rocky Mountain Section, Society of Economic Paleontologists and Mineralogists, Symposium 2, p. 39-55.

Case, E.C., 1936, A nothosaur from the Triassic of Wyoming: Contributions of the Museum of Paleontology, University of Michigan, v. 5, p. 1-36.

Cavaroc, V.V., and Flores, R.M., 1991, Red beds of the Triassic Chugwater Group, southwestern Powder River Basin, Wyoming: U.S. Geological Survey Bulletin 1917, p. E1-E17.

Colbert, E.H., 1957, Triassic vertebrates of the Wind River Basin: Wyoming Geological Association 12th Annual Field Conference Guidebook, p. 89-93.

Collinson, D.W., and Runcorn, S.K. 1960, Polar wandering and continental drift: evidence from paleomagnetic observations in the United States: Geological Society of America Bulletin, v. 71, p. 915-958.

Collinson, J.W., and Hasenmueller, W.A., 1978, Early Triassic paleogeography and biostratigraphy of the Cordilleran miogeosyncline, *in* Mesozoic paleogeography of the western United States: Society of Economic Paleontologists and Mineralogists, Pacific Section, Pacific Coast Paleogeography Symposium, p. 175-186.

Condon, S.M., and Peterson, F., 1986, Stratigraphy of Middle and Upper Jurassic rocks of the San Juan Basin: historical perspective, current ideas, and remaining problems, *in* A basin analysis case study: the Morrison Formation, Grants uranium region, New Mexico: American Association of Petroleum Geologists, Tulsa, Oklahoma, p. 7-26.

Crichton, M., 1990, Jurassic Park: New York, Alfred A. Knopf, Inc., 401 p.

Curry, W.H., and Hegna, E.T., 1970, Stratigraphic oil accumulations in the Lower Sundance Canyon Springs sandstones of Wyoming: Wyoming Geological Association 22nd Annual Field Conference Guidebook, p. 51-74.

Darton, N.H., 1899, Jurassic formations of the Black Hills of South Dakota: Geological Society of America Bulletin: v. 10, p. 383-396.

_____ 1904, Comparison of the stratigraphy of the Black Hills, Bighorn Mountains, and Rocky Mountain Front Range: Geological Society of America Bulletin, v. 15, p. 379-448.

_____ 1906a, Geology of the Bighorn Mountains: U.S. Geological Survey Professional Paper 51, 129 p.

_____ 1906b, Geology of the Owl Creek Mountains: 59th Congress, First Session, Senate Document 219, 48 p.

Darton, N.H., and O'Hara, C.C., 1909, Description of the Belle Fourche Quadrangle, South Dakota: U.S. Geological Survey Atlas, Belle Fourche Folio, No. 164, p. 3.

Downs, G.R., 1949, Mesozoic rocks of the northern Powder River Basin, Wyoming: Wyoming Geological Association 4th Annual Field Conference Guidebook, p. 46-51.

Ehrlich, G., 1987, Spring: The best American essays, p. 58-69.

Eldredge, N., 1991, The Miner's canary: New York, Prentice Hall Press, 246 p.

Eldridge, G.H., 1896, Mesozoic geology, *in* Emmons, S.F., Cross, W., and Eldridge, G.H., editors, Geology of the Denver Basin in Colorado: U.S. Geological Survey Monograph 27, p. 51-150.

Folk, R.L, 1959, Practical petrographic classification of limestone: American Association of Petroleum Geologists Bulletin, v. 43, p. 1-38.

_____ 1977, Stratigraphic analysis of the Navajo Sandstone: a discussion: Journal of Sedimentary Petrology, v. 47,. p. 483-484.

Freeman, W.E., and Visher, G.S., 1975, Stratigraphic analysis of the Navajo Sandstone: Journal of Sedimentary Petrology, v. 45, p. 651-668.

Galton, P.M., 1971, The prosauropod dinosaur Ammosaurus, the crocodile Protosuchus, and their bearing on the age of the Navajo Sandstone in northeastern Arizona: Journal of Paleontology, v. 45, p. 781-795.

Goddard, E.N., and others, 1948, Rock color chart: Washington D.C., National Research Council, 6 p.

Gregory, J.T., 1957, Significance of the fossil vertebrates for correlation of Late Triassic continental deposits of North America, *in* El Mesozoico del Hemisferio Occidental y sus correlationes mundiales: 20th International Geological Congress, Mexico, 1956, Section 2, p. 7-25.

Hallam, A., 1970, Gyrochorte and other trace fossils in the Forrest Marble (Bathonian) of Dorset England: Geological Journal Special Issue 3, p. 189-200.

Harshbarger, J.W., Repenning, C.A., and Irwin, J.H., 1957, Stratigraphy of the Navajo country: U.S. Geological Survey Professional Paper 291, 74 p.

Heinberg, C., 1973, The internal structure of the trace fossils Gyrochorte and Curvolithus: Lethaia, v. 6, p. 227-238.

High, L.R., Jr., 1963, Sedimentology and mineralogy of the Popo Agie Member of the Chugwater (Triassic) Formation, western Wyoming [A.B. thesis]: Princeton, New Jersey, Princeton University, 75 p.

High, L.R., Jr., Hepp, D.M., Clark, T., and Picard, M.D., 1969, Stratigraphy of Popo Agie Formation (Late Triassic), Uinta Mountain area, Utah and Colorado: Intermountain Association of Geologists 16th Annual Field Conference Guidebook, p. 181-192.

High, L.R., Jr., and Picard, M.D., 1965, Sedimentary petrology and origin of analcime-rich Popo Agie Member, Chugwater (Triassic) Formation, west-central Wyoming: Journal of Sedimentary Petrology, v. 35, p. 49-70.

_____ 1967, Rock units and revised nomenclature, Chugwater Group (Triassic), western Wyoming: The Mountain Geologist, v. 4, p. 73-80.

_____ 1969, Stratigraphic relations within upper Chugwater Group (Triassic), Wyoming: American Association of Petroleum Geologists Bulletin, v. 53, p. 1091-1104.

_____ 1975, Sedimentary cycles in the Nugget Sandstone, northeastern Utah: Utah Geology, v. 2, p. 117-124.

Hubbell, R.G., 1954, Upper Triassic facies relations in northern Carbon County, Wyoming: American Association of Petroleum Geologists Bulletin, v. 40, p. 2743-2748.

Hunt, J.M., and Forsman, J.P., 1957, Relation of crude oil composition to stratigraphy in the Wind River Basin: Wyoming Geological Association 12th Annual Field Conference Guidebook, p. 105-112.

Imlay, R.W., 1945, Occurrence of Middle Jurassic rocks in Western Interior of United States: American Association of Petroleum Geologists Bulletin, v. 29, p. 1019-1027.

_____ 1956, Marine Jurassic exposed in Bighorn Basin, Pryor Mountains, and northern Bighorn Mountains, Wyoming and Montana: American Association of Petroleum Geologists Bulletin, v. 40, p. 562-599.

Keller, W. D., 1952, Analcime in the Popo Agie Member of the Chugwater Formation: Journal of Sedimentary Petrology, v. 22, p. 70-82.

Kirk, A.R., and Condon, S.M., 1986, Structural control of sedimentation patterns and the distribution of uranium deposits in the Westwater Canyon Member of the Morrison Formation, northwestern New Mexico—a subsurface study, *in* A basin analysis case study: the Morrison Formation, Grants uranium region, New Mexico: American Association of Petroleum Geologists, p. 105-143.

Kirkland, D.W., and Evans, R., 1981, Source-rock potential of evaporitic environment: American Association of Petroleum Geologists Bulletin, v. 65, p. 181-190.

Knapp, R.R., 1978, Depositional environments and diagenesis of the Nugget Sandstone, south-central Wyoming, northeast Utah, and northwest Colorado: Wyoming Geological Association 30th Annual Field Conference Guidebook, p. 131-138.

Knight, S.H., 1917, Age and origin of the red beds of southeastern Wyoming [abstract]: Geological Society of America Bulletin, v. 28, p. 168-169.

Knight, W.C., 1897, The petroleum of the Shoshone anticlinal, Part 1, The geology of the Popo Agie, Lander, and Shoshone fields: University of Wyoming Petroleum Series, Bulletin 2, p. 7-20.

_____ 1902, The Laramie Plains Red Beds and their age: Journal of Geology, v. 10, p. 413-422.

Kummel, B., 1954, Triassic stratigraphy of southeastern Idaho and adjacent areas: U.S. Geological Survey Professional Paper 254-11, p. 165-194.

Lee, W.T., 1927, Correlation of geologic formations between east-central Colorado, central Wyoming, and southern Montana: U.S. Geological Survey Professional Paper 149, 80 p.

Lewis, G.E., Irwin, J.H., and Wilson, R.F., 1961, Age of the Glen Canyon Group (Triassic and Jurassic) on the Colorado Plateau: Geological Society of America Bulletin, v. 72, p. 1437-1440.

Love, J.D., 1939, Geology along the southern margin of the Absaroka Range, Wyoming: Geological Society America Special Paper 20, 134 p.

_____ 1948, Mesozoic stratigraphy of the Wind River Basin, central Wyoming: Wyoming Geological Association 3rd Annual Field Conference Guidebook, p. 96-111.

_____ 1957, Stratigraphy and correlation of Triassic rocks in central Wyoming: Wyoming Geological Association 12th Annual Field Conference Guidebook, p. 39-45.

Love, J.D., Thompson, R.M., Johnson, C.O., Sharkey, H.H.R., Tourtelot, H.A., Zapp, A.D., and Nace, H.L., 1945a, Stratigraphic sections and thickness maps of Lower Cretaceous and non-marine Jurassic rocks in central Wyoming: U.S. Geological Survey Oil and Gas Investigations Preliminary Chart 13.

Love, J.D., Johnson, C.O., Nace, H.L., Sharkey, H.H.R., Thompson, R.M., Tourtelot, H.A., and Zapp, A.D., 1945b, Stratigraphic sections and thickness maps of Triassic rocks in central Wyoming: U.S. Geological Survey Oil and Gas Investigations Preliminary Chart 17.

Love, J.D., Tourtelot, H.A., Johnson, C.O., Thompson, R.M., Sharkey, H.H.R., and Zapp, A.D., 1947, Stratigraphic sections of Mesozoic rocks in central Wyoming: Wyoming Geological Survey Bulletin 38, 59 p.

Lull, R. S., 1942, Chugwater footprints from Wyoming: American Journal of Science, v. 240, p. 500-504.

Mathews, A.A.L., 1931, Mesozoic stratigraphy of the central Wasatch Mountains: Oberlin College Laboratory Bulletin, New Series No. 1, 50 p.

Maughan, E. K., 1964, The Goose Egg Formation in the Laramie Range and adjacent parts of southeastern Wyoming: U. S. Geological Survey Professional Paper 501-B, p. B53-B60.

McCormick, C.D., and Picard, M.D., 1969, Petrology of Gartra Formation (Triassic), Uinta Mountain area, Utah and Colorado: Journal of Sedimentary Petrology, v. 39, p. 1484-1508.

McKee, E.D., Oriel, S.S., Ketner, K.B., MacLachlan, M.E., Goldsmith, J.W., MacLachlan, J.C., and Mudge, M.R., 1959, Paleotectonic maps of the Triassic System: U.S.

Geological Survey Miscellaneous Geologic Investigations Map I-300, 9 plates, 33 p.

McPhee, J., 1986, Rising from the plains: New York, The Noonday Press, 214 p.

Mills, N.K., 1956, Subsurface stratigraphy of the pre-Niobrara formations in the Big Horn Basin, Wyoming, *in* Wyoming Stratigraphy: Wyoming Geological Association, p. 9-22.

Moberly, R., 1960, Morrision, Cloverly, and Sykes Mountain formations, northern Bighorn Basin, Wyoming and Montana: Geological Society of America Bulletin, v. 71, p. 1137-1176.

Peabody, F.E., 1948, Reptile and amphibian trackways from the lower Triassic Moenkopi Formation of Arizona and Utah: University of California Publications, Bulletin of the Department of Geological Sciences, 27, p. 295-468.

Peterson, J.A., 1957a, Gypsum Spring and Sundance formations, central Wyoming: Wyoming Geological Association 12th Annual Field Conference Guidebook, p. 47-54.

_____ 1957b, Marine Jurassic of northern Rocky Mountains and Williston Basin: American Association of Petroleum Geologists Bulletin, v. 41, p. 399-440.

Picard, M.D., 1964, Paleomagnetic correlation of units within Chugwater Formation (Triassic), west-central Wyoming: American Association of Petroleum Geologists Bulletin, v. 48, p. 269-291.

_____ 1965, Iron oxides and fine-grained rocks of Red Peak and Crow Mountain Sandstone members, Chugwater (Triassic) Formation, Wyoming: Journal of Sedimentary Petology, v. 35, p. 49-70.

_____ 1966, Petrography of Red Peak Member, Chugwater Formation (Triassic), west-central Wyoming: Journal of Sedimentary Petrology, v. 36, p. 904-926.

_____ 1967, Stratigraphy and depositional environments of the Red Peak Member of the Chugwater Formation (Triassic), west-central Wyoming: University of Wyoming Contributions to Geology, v. 6, p. 39-67.

_____ 1969, Oriented, linear-shrinkage cracks in Alcova Limestone Member (Triassic), southeastern Wyoming: University of Wyoming Contributions to Geology, v.8, p.1-7.

_____ 1971, Classification of fine-grained sedimentary rocks: Journal of Sedimentary Petrology, v. 41, p. 179-195.

_____ 1975a, Shelf edge carbonate-redbed transitions, Red Peak and Thaynes formations (Triassic), western Wyoming and adjacent Idaho, *in* Deep drilling frontiers in the Central Rocky Mountains: Rocky Mountain Association of Geologists—1975 Symposium, p. 99-107.

_____ 1975b, Facies, petrography, and petroleum potential of Nugget Sandstone (Jurassic), southwestern Wyoming and northeastern Utah, *in* Deep drilling frontiers in the Central Rocky Mountains: Rocky Mountain Association of Geologists—1975 Symposium, p. 109-127.

_____ 1976, Finds in Wyoming and Utah spark look at Nugget's petroleum potential: Oil and Gas Journal, v. 74, no. 30, p. 194-198.

_____ 1977a, Stratigraphic analysis of the Navajo Sandstone: A discussion: Journal of Sedimentary Petrology, v. 47, p. 475-483.

_____ 1977b, Petrology of the Jurassic Nugget Sandstone, northeast Utah and southwest Wyoming: Wyoming Geological Association 29th Annual Field Conference Guidebook, p. 239-258.

_____ 1978, Stratigraphy of Triassic rocks in west-central Wyoming: Wyoming Geological Association 30th Annual Field Conference Guidebook, p. 101-130.

_____ 1988, Origin of Triassic oil in Wyoming [abstract]: Society of Economic Pelontologists and Mineralogists Midyear Meeting, Columbus, Ohio, v. 5, p. 42.

Picard, M.D., Aadland, R., and High, L.R., Jr., 1969, Correlation and stratigraphy of Triassic Red Peak and Thaynes formations, western Wyoming and adjacent Idaho: American Association of Petroleum Geologists Bulletin, v. 53, p. 2274-2289.

Picard, M.D., and High, L.R., Jr., 1968, Shallow marine currents on the Early(?) Triassic Wyoming shelf: Journal of Sedimentary Petrology, v. 38, p. 411-423.

_____ 1972, Criteria for recognizing lacustrine rocks: Society of Economic Palentologists and Mineralogists Special Publication No. 16, p. 108-145.

_____ 1985, Geologic features of lakes, *in* Geology and Energy Resources, Uinta Basin of Utah: Utah Geological Association, Salt Lake City, Utah, p. 61-79.

Picard, M.D., and Wellman, S.S., 1965, Persistence of variegated claystone in Red Peak Member, Chugwater (Triassic) Formation, Big Horn Basin, Wyoming: University of Wyoming Contributions to Geology, v. 4, p. 69-73.

Pipiringos, G.N., 1953, Correlation of Marine Jurassic and related rocks in the Laramie Basin, Wyoming: Wyoming Geological Association 8th Annual Field Conference Guidebook, p. 34-39.

_____ 1957, Stratigraphy of the Sundance, Nugget and Jelm formations in the Laramie Basin, Wyoming: Wyoming Geological Survey Bulletin 47, 63 p.

_____ 1968, Correlation and nomenclature of some Triassic and Jurassic rocks in the south-central part of Wyoming: U.S. Geological Survey Professional Paper 594-D, 26 p.

Pipiringos, G.N., and O'Sullivan, R.B., 1978, Principal unconformities in Triassic and Jurassic rocks, Western Interior United States—a preliminary survey: U.S. Geological Survey Professional Paper 1035-A, 29 p.

Raup, D.M., 1991, Extinction: bad genes or bad luck: New York, W.W. Norton, 210 p.

Rautman, C.A., 1975, Sedimentology of the "Lower Sundance" Formation (Upper Jurassic), Wyoming Region: Wyoming Geological Association Earth Science Bulletin, v. 8, p. 1-16.

_____ 1978, Sedimentology of Late Jurassic barrier-island complex—Lower Sundance Formation of Black Hills: American Association of Petroleum Geologists Bulletin, v. 62, p. 2275-2289.

Reeside, J.B., Jr., 1929, Triassic-Jurassic "red beds" of the Rocky Mountain region: a discussion: Journal of Geology, v. 37, p. 47-63.

Robinson, P.L., 1971, A problem of faunal replacement on Permo-Triassic continents: Paleontology, v. 14, p. 131-153.

_____ 1973, Paleoclimatology and continental drift, *in* Implications of continental drift to the Earth sciences, New York, Academic Press, p. 451-476.

Romer, A.S., 1945, Vertebrate paleontology: Chicago, Illinois, University of Chicago Press, 687 p.

Ruzyla, K., 1977, Stratigraphic analysis of the Navajo Sandstone: a discussion: Journal of Sedimentary Petrology, v. 47, p. 489-491.

Speed, R.C., 1978, Paleogeographic and plate tectonic evolution of the early Mesozoic marine province of the western Great Basin, *in* Mesozoic paleogeography of the western United States: Society of Economic Paleontologists and Mineralogists, Pacific Section, Pacific Coast Paleogeography Symposium 2, p. 253-270.

_____ 1979, Collided Paleozoic microplate in the western United States: Journal of Geology, v. 87, p. 279-292.

Stanley, K.O., Jordan, W.M., and Dott, R.H., 1971, Early Jurassic paleogeography and sediment dispersal for the western United States: American Association of Petroleum Geologists Bulletin, v. 55, p. 10-19.

Steidtmann, J.R., 1977, Stratigraphic analysis of the Navajo Sandstone: a discussion: Journal of Sedimentary Petrology, v. 47, p. 484-489.

Stokes, W.L., 1944, Morrison Formation and related deposits in and adjacent to the Colorado Plateau: Geological Society of America Bulletin, v. 55, p. 951-992.

Thomas, H.D., 1934, Phosphoria and Dinwoody tongues in lower Chugwater of central and southeastern Wyoming: American Association of Petroleum Geologists Bulletin, v. 18, p. 1655-1697.

Thomas, H.D., and Krueger, M.L., 1946, Late Paleozoic and Mesozoic stratigraphy of Uinta Mountains: American Association of Petroleum Geologists Bulletin, v. 30, p. 1255-1293.

Tohill, B., and Picard, M.D., 1966, Stratigraphy and petrology of Crow Mountain Sandstone Member (Triassic), Chugwater Formation, northwestern Wyoming: American Association of Petroleum Geologists Bulletin, v. 50, p. 2547-2565.

Turner-Peterson, C.E., and Santos, E.S., 1986, Overview and summary, *in* A basin analysis case study: the Morrison Formation, Grants uranium region, New Mexico: Tulsa, Oklahoma, American Association of Petroleum Geologists, p. 1-6.

Turner-Peterson, C.E., Santos, E.S., and Fishman, N.S., editors, 1986, A basin analysis case study: the Morrison Formation, Grants uranium region, New Mexico: Tulsa, Oklahoma, American Association of Petroleum Geologists, 391 p.

Uhlir, D.M., Akers, A., and Vondra, C.F., 1988, Tidal inlet sequence, Sundance Formation (Upper Jurassic), north-central Wyoming: Sedimentology, v. 35, p. 739-752.

Vail, P.R., Hardenbol, J., and Todd, R.G., 1984, Jurassic unconformities, chronostratigraphy, and sea level changes from seismic stratigraphy and biostratigraphy, *in* Interregional unconformities and hydrocarbon accumulation: American Association of Petroleum Geologists Memoir no. 36, p. 129-144.

Van Houten, F.B., 1961, Climatic significance of red beds, *in* Descriptive palaeoclimatology: New York, Interscience Publishers, p. 89-139.

von Huene, F.R., 1948, *Simosaurus* and *Corosaurus*: American Journal of Science, v. 246, p. 41-43.

Walker, R.G., and Middleton, G.V., 1979, Eolian sands, *in* Facies models: Geoscience Canada, Reprint Series 1, p. 33-41.

Welles, S.P., 1954, New Jurassic dinosaur from the Kayenta Formation of Arizona: Geological Society of America Bulletin, v. 65, p. 591-598.

_____ 1970, *Diplophosaurus* (Reptilia: Saurischia), a new name for a dinosaur: Journal of Paleontology, v. 44, p. 989.

Williston, S.W., 1904, Notice of some new reptiles from Upper Jurassic of Wyoming: Journal of Geology, v. 12, p. 688.

Woodward, T.C., 1957, Geology of Deadman Butte area, Natrona County, Wyoming: American Association of Petroleum Geologists Bulletin, v. 41, p. 212-262.

Wright, R.P. 1973, Marine Jurassic of Wyoming and South Dakota—its paleoenvironments and paleobiogeography: Michigan University Museum of Paleontology Papers on Paleontology, no. 2, 49 p.

Wroble, J.L., 1953, Stratigraphy and sedimentation of the Popo Agie, Nugget, and Sundance formations in central Wyoming [M.A. thesis]: Laramie, University of Wyoming, 151 p.

Zangerl, R., 1963, Preliminary results of a restudy of *Corosaurus alcovensis* (Case), the only known New World nothosaur: University of Wyoming Contributions to Geology, v. 2, p. 117-123.

Frontispiece. Type section of the Haystack Mountains Formation of the Mesaverde Group along the North Platte River, 7 mi (11.2 km) north of Sinclair, Wyoming, on the Seminoe Road. Massive sandstone cliffs separated by shale slopes in the lower part of the section comprise the Haystack Mountains Formation. It is overlain by thinner-bedded sandstone and shale of the Allen Ridge Formation (center) and the Pine Ridge Sandstone (shadowed cliff in upper right), both of the Mesaverde Group. Photograph courtesy of O.J. Martinsen.

The Cretaceous foreland basin and its sedimentary record

James R. Steidtmann
Department of Geology and Geophysics
University of Wyoming
Laramie, Wyoming 82071

Abstract

Cretaceous sedimentary rocks in Wyoming record deposition in a foreland basin that formed, in part, as a flexural response to crustal loading by the fold-and-thrust belt of western North America and, in part, as a response to subduction of the Farallon plate. This process generated an asymmetric geometry with substantially greater subsidence and, consequently, much thicker sediments in the foredeep adjacent to the fold-and-thrust belt to the west. Although the basin retained its integrity as a regional downwarp throughout most of Cretaceous time, there is evidence that early in its history it was tectonically partitioned by uplifts and basins that controlled depositional patterns and which, in some cases, evolved into major features when Laramide basement deformation finally segmented the foreland in the Late Cretaceous.

The Cretaceous foreland basin was flooded by an epicontinental sea that began as a separate elongate northern arm and a short southern arm, which joined in Late Albian time, connecting the proto-Gulf of Mexico with the Cretaceous circumpolar sea. At the time of its maximum extent, the seaway reached more than 3,000 mi (4,800 km) from Arctic Canada to the Gulf of Mexico and 1,200 mi (1,920 km) from Utah and Idaho to Iowa and Minnesota. Relative sea level rose and fell frequently throughout Cretaceous time and, together with varying sediment supply, produced a distinct but complex record of transgressive-regressive cycles in the sedimentary record.

Lower Cretaceous sedimentary rocks in Wyoming range in thickness from 5,500 ft (1,677 m) in the west to less than 500 ft (152 m) over most of the rest of the state. The record of Neocomian events is missing in all but westernmost Wyoming, where alluvial-fan and lake deposits formed adjacent to the western highlands. In Early Aptian time, gravels from these fans spread eastward, leaving the first Cretaceous sedimentary record over much of the state. In Late Albian time, the first Cretaceous marine invasion spread across the state and began the record of marine transgressions and regressions that characterizes most deposition until mid-Maastrichtian time in Wyoming.

Upper Cretaceous sedimentary rocks range in thickness from 18,000 ft (5,490 m) in the western foredeep and 16,000 ft (4,880 m) in south-central Wyoming to less than 4,000 ft (1,220 m) in central-western Wyoming. During the Late Cretaceous transgressions and regressions, a north-south belt of complexly intercalated shallow marine, deltaic, barrier-island, and coastal-plain sediments formed across Wyoming, separating dominantly marine deposits to the east from dominantly nonmarine and marginal-marine deposits to the west.

Cretaceous strata in Wyoming are of great academic and economic significance. Nearly every Cretaceous marine sedimentary unit in Wyoming contains one or more laterally continuous bentonite beds, the product of contemporaneous volcanic activity to the west. Radiometric dating of these ash beds, to-

Steidtmann, James R., 1993, The Cretaceous foreland basin and its sedimentary record, *in* Snoke, A.W., Steidtmann, J.R., and Roberts, S.M., editors, Geology of Wyoming: Geological Survey of Wyoming Memoir No. 5, p. 250-271.

gether with detailed biozonation, provides the ideal combination of chronostratigraphic and biostratigraphic control for formulating and testing new stratigraphic principles. In addition, the complex intertonguing of marine shale and sandstone provides both source and reservoir rocks for hydrocarbons, and the thick coastal plain deposits provided the ideal setting for the formation of coal. As a consequence, Cretaceous rocks are among the most prolific oil, gas, and coal producers in the state.

Introduction

The black shale and tan sandstone, typical of Cretaceous rocks in Wyoming, stand in sharp contrast to the colorful Jurassic and Triassic rocks below. Yet, these Cretaceous rocks form spectacular outcrops that have attracted the critical attention of hundreds of geologists anxious to decipher the geologic history held within. In addition, these rocks have been penetrated by tens of thousands of drill holes in the search for oil and gas, providing even more information in the form of cores, cuttings, and wire-line logs. As a result, the body of stratigraphic, sedimentologic, paleontologic, and petrographic information on Cretaceous rocks in Wyoming is extensive and provides an invaluable data set for the study of marine and marginal-marine depositional systems. In particular, the combination of detailed biostratigraphic zonation and radiometrically dated bentonite beds provides a framework that is arguably the best available for stratigraphic studies in marine rocks.

The literature on Cretaceous rocks and the Cretaceous history of Wyoming is voluminous, and a complete discussion of it is beyond the scope of this synthesis. Readers searching for new information or a new interpretation will not find it here. Instead, I have tried to provide an overview of what has gone before, including discussions on the origin of the basin, the character of the seaway, the main depositional systems, and the basic stratigraphy. To some extent, the treatment is historical, so that the evolution of thought on the various topics can be followed. References cited, and the bibliographies therein, provide the reader with more information on each of these topics. The stratigraphic nomenclature chart by Love and others in the map pocket of this volume shows the major stratigraphic relationships and terminology for Cretaceous rocks in Wyoming. The reader should be aware, however, that because of the evolution of the Cretaceous time scale and differing interpretations by the various authors cited, there are some geochronologic and stratigraphic inconsistencies between the information summarized in this paper and that shown in this stratigraphic nomenclature chart. In these cases, the reader is encouraged to examine the original references. Stages of the Cretaceous for which there is a rock record in Wyoming, ammonite zones, and radiometric ages determined by Obradovich (in press) are shown in **Figure 1**.

Foreland basin tectonics

In spite of the tremendous amount of work done on Cretaceous rocks of the western United States since they were first described by geologists during the early surveys of the West, little was written on the origin of the basin itself prior to the early 1970s. Whereas the existence of the basin was not questioned, neither was the reason for its existence. This lack of attention was not, however, peculiar to the Western Interior Cretaceous basin, for it was not until the 1970s and 1980s that basin genesis and mechanisms for basin subsidence in general became the objectives of modern geological and geophysical studies.

Foreland basins are sedimentary basins that lie between the fronts of mountain chains and adjacent cratons (Allen and others, 1986). Basins having this tectonic setting have long been recognized. Kay (1951) recognized this basinal setting in the context of geosynclinal theory and coined the term exogeosyncline for a basin on the continental margin which fills with sediment shed toward the craton from a marginal orogenic belt. Subsidence was assumed to result from sedimentary loading within the basin. Dickinson (1974) formalized the term foreland basin within the context of plate tectonic theory and cited loading of the crust by tectonic

thickening in the adjacent fold-and-thrust belt as the driving mechanism for subsidence.

Flexure of the lithosphere as a cause of subsidence in the foreland basin of western Canada was suggested earlier by Price (1973), and followed even earlier work on warping of the lithosphere from loads imposed by Pleistocene ice sheets (e.g., Walcott, 1970). This model indicates that any large load, either supracrustal or intracrustal, will cause isostatic subsidence not only directly beneath, but also adjacent to the load because of the rigidity of the lithosphere. The subsidence is greatest immediately in front of the load, where a foredeep trough forms, and decreases with distance so that the basin is asymmetric. The width and depth of the depression depends on the geometry and magnitude of the load and the flexural rigidity of the lithosphere.

Subsequent modeling work by Beaumont (1981) in western Canada and Jordan (1981) in Wyoming confirmed that crustal loads due to tectonic thickening in the fold-and-thrust belt of western North America could indeed cause subsidence in the adjacent foreland basin as well as the basin asymmetry observed today. Jordan's (1981) work is particularly significant because it was well constrained by dates of thrusting events and by stratigraphic control in the basin. Her modeling assumed that the crust behaved elastically, and the results indicate that: (1) basin geometry was not only a function of tectonic loading, but also of the redistribution of this load as the source area was eroded and the basin filled; (2) thrust loading produced a foredeep immediately in front of the load; (3) thrust loading produced a forebulge on the craton side of the foredeep where the crust rose above its pre-loading level; and (4) the foredeep and forebulge migrated eastward in response to the eastward tectonic transport in the thrust belt as thrusting progressed.

It is probably safe to say there is general consensus that tectonic loading and the redistribution of this load by erosion and deposition played a major role in the subsidence and geometry of the Cretaceous foreland basin. However, the cause or causes of contemporaneous subsidence in the eastern part of the foreland basin far from the fold-and-thrust belt is not clear. The modeling by Jordan (1981) does not pertain to this part of the basin and another mechanism must be sought. Cross and Pilger (1978) recognized two spatially and temporally disjunct modes of subsidence in the Cretaceous foreland of the western United States. One was identified in isopachs of Upper Albian through Santonian strata and corresponded to the foredeep in front of the fold-and-thrust belt. The second was identified in Campanian through Maastrichtian strata and covered a broad area in southeastern Wyoming and adjacent parts of Colorado. Cross and Pilger (1978) postulated that sublithospheric loading and cooling related to shallow-slab subduction were sufficient to cause this second mode of subsidence. Modeling by Bird (1984) confirmed that the additional weight of the subducted plate would have depressed the region by at least the observed amount of subsidence unattributable to thrust loading. In contrast, the modeling by Mitrovica and others (1989) suggested that sublithospheric flow related to subduction would cause tilting of the continental interior sufficient to provide accommodation space for the Cretaceous sediments observed in the eastern part of the foreland basin.

Two modes of subsidence are also reflected in Kauffman's (1985) structural subdivision of the Western Interior Cretaceous basin, which includes both a foredeep that formed in response to thrust and sediment loading and a broad, axial basin separated from the foredeep by a discontinuous forebulge. In addition, Kauffman (1984) proposed a theory for a dynamic relationship between the development of the Western Interior Cretaceous basin and global events, which includes the following linkages: (1) high rates of seafloor spreading, contractional events in the fold-thrust belt, greatly increased volcanism, rapid basin subsidence, rapid sedimentation, and elevated global sea level; and (2) low rates of seafloor spreading, little contraction in the fold-and-thrust belt, greatly decreased volcanism, low rates of basin subsidence, slow sedimentation, and falling global sea level.

Although the western foreland basin maintained its integrity as a regional downwarp throughout most of Cretaceous time, there is a growing body of evidence, including that mentioned above, which indicates that intrabasinal highs and lows developed periodically throughout its history. Steidtmann and Middleton (1991) and Cerveny and Steidtmann (1993) present evidence that the site of the Laramide Wind River Range was positive as early as 100 Ma. Channel patterns in the Muddy Sandstone mapped by Dolson and others (1991) also indicate that the

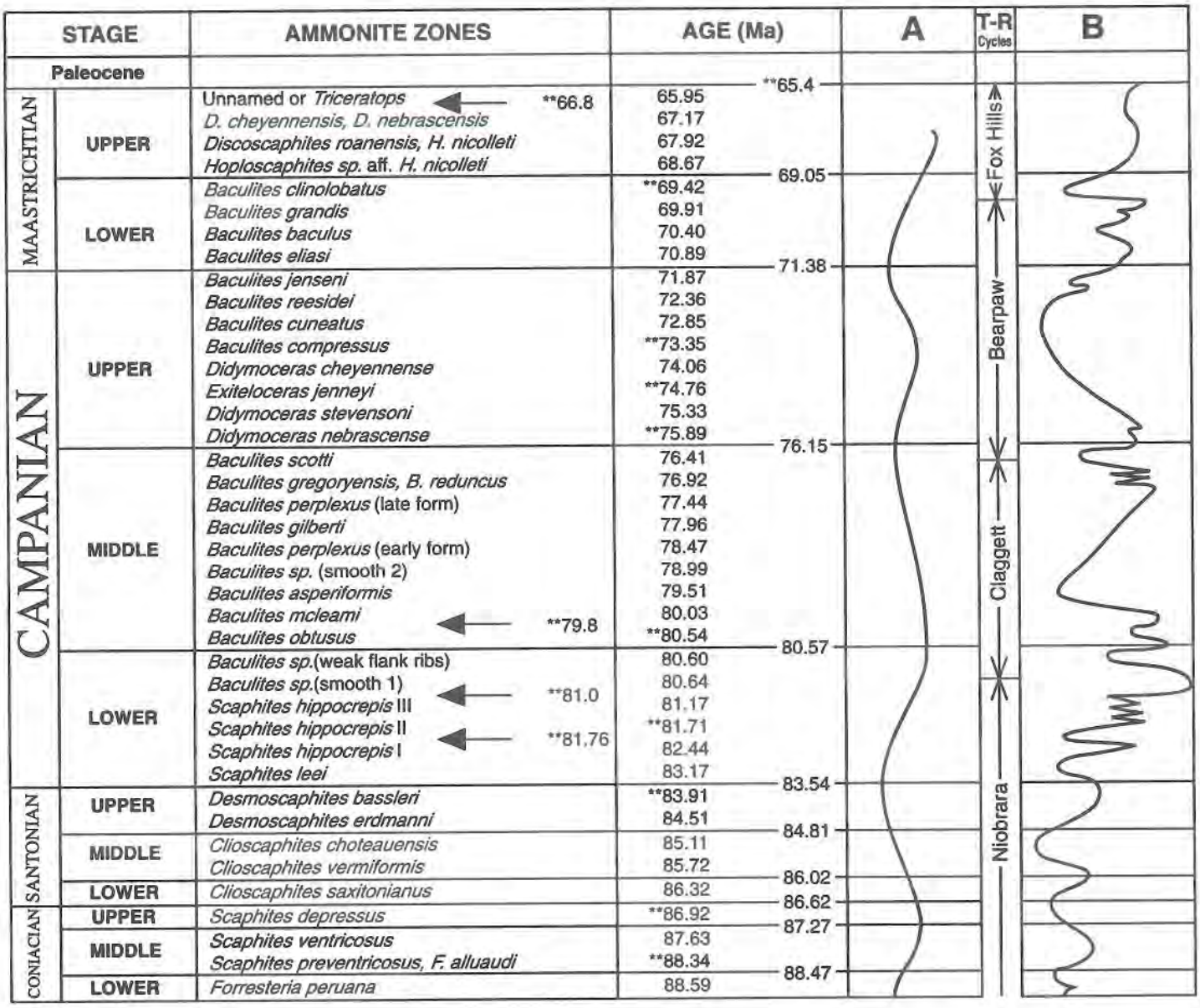

Figure 1. Biozonation, geochronology, and cyclicity of the United States Western Interior Cretaceous. (1) Traditional Early Cretaceous-Late Cretaceous boundary. (2) New Early Cretaceous-Late Cretaceous boundary proposed by Cobban and Kennedy (1989). ** Indicates new $^{40}Ar/^{39}Ar$ ages from Obradovich (in press). Remaining values interpolated between dated levels based on assignment of equal time durations to biozones (Kauffman and others, in press). *** Indicates new ages in parentheses (Obradovich, in press) are incompatible with new bounding dates and appear next to calculated value based on new bounding dates. After Kauffman and others (1992) and Kauffman (in preparation). Column A is sea-level curve from Weimer (1983). Transgressive and regressive cycles (T-R cycles) and sea-level curve in column B from Kauffman and Caldwell (in press). Terrestrial setting on the left and marine environment on the right.

TURONIAN	UPPER	*S. corvensis, P. germari*	88.84		Niobrara
		Scaphites nigricollensis	89.11		
		Scaphites whitfieldi	89.39		
		Scaphites ferronensis	89.66		
		Scaphites warreni	89.94		
		P. macombi, C. colleti	**90.21	90.35	
	MIDDLE	*Prionocyclus hyatti*	**90.51		
		Prionocyclus percarinatus	90.97		
		Collignoniceras woollgari regulare	91.42		
		Collignoniceras woollgari woollgari	91.88	92.11	
	LOWER	*Mammites nodosoides*	92.34		
		Vascoceras birchbyi	92.8 (***93.4)		
		Pseudaspidoceras flexuosum	**93.25		
		Watinoceras devonense	93.35	93.40	
CENOMANIAN	UPPER	*Nigericeras scotti*	93.46		Greenhorn
		Neocardioceras juddii	**93.56		
		Burroceras clydense	93.67		
		Euomphaloceras septemseriatum	93.78 (***93.49)		
		Vascoceras diartianum	**93.90		
		Dunveganoceras conditum	94.08		
		Dunveganoceras albertense	94.27		
		Dunveganoceras problematicum	94.45		
		C. canituarinum, D. pondi	**94.63	94.71	
	MIDDLE	*Plesiacanthoceras wyomingense*	94.78		
		Acanthoceras amphibolum	**94.93		
		Acanthoceras bellense	95.14		
		Acanthoceras muldoonense	95.36		
		Acanthoceras granerosense	95.57		
		Conlinoceras tarrantense	**95.78	95.98	
	LOWER	*Beattonoceras beattonense*	96.18		
		Irenicoceras bahani	96.58		
		Neogastroplites septimus	96.97	**97.17	
(1)		*Neogastroplites macleami*	97.36		
		Neogastroplites americanus	**97.75		
		Neogastroplites muelleri	98.14	98.33	
(2)	UPPER	*Neogastroplites comutus*	**98.52		Kiowa-Skull Cr.
		Neogastroplites haasi	**98.54		
		Unzoned (with *Eopachydiscus?*)	99.61		
		Inoceramus bellvuensis	100.68		
		Inoceramus comancheanus	101.75		
		Unzoned	102.82	103.36	
ALBIAN	MIDDLE	*Stelckiceras liardense*	103.89		
		Gastroplites sp.cf. cantianus	104.96		
		Gastroplites canadensis	106.03		
		Pseudopulchellia pattoni	**107.10		
		Unnamed	107.75	108.08	
	LOWER	*Arcthoplites macconnelli*	108.41		
		Arcthoplites irenense	109.06		
		Arcthoplites belli	109.71		
		Lemuroceras sp.*cf. L. indicum*	110.37		
		Cleoniceras sp.*cf. C. subbaylei*	111.02		
		Sonneratia sp.*cf. S. kitchini*	111.67	112.0	

Figure 1. *Continued.*

sites of many of the Laramide ranges were positive at 100 Ma. Similarly, DeCelles (1986) and Schwartz and DeCelles (1988) suggested that by the beginning of Cretaceous time the foreland basin in southwestern Montana was partitioned into uplifts, which occupied sites of eventual Laramide ranges. Reynolds (1976) presented stratigraphic evidence for recurrent structural growth on anticlines in south-central Wyoming throughout Late Cretaceous time.

In comparison, the biostratigraphic work by Merewether (1983) and Merewether and Cobban (1986), noting regions of Wyoming characterized by the omission or condensation of ammonite biozones, defined 90 Ma highs in areas now occupied by Laramide uplifts and several arches and swells, which formed between 100 and 90 Ma, but which did not subsequently become Laramide ranges. Numerous other studies (e.g., Weimer, 1980; Slack, 1981; Martinsen and Marrs, 1985) indicate that arching and basement faulting in the Rocky Mountain foreland controlled Cretaceous depositional patterns, but only in rare cases did these same highs evolve into Laramide ranges.

The significance of these intrabasinal structures is not clear. If uplifts similar to those described by DeCelles (1986), Schwartz and DeCelles (1988), and Steidtmann and Middleton (1991) indicate initial break-up of the foreland, then it began much earlier than the commonly assumed Late Cretaceous age of the first Laramide deformation. The arches or swells identified by unconformities (Reynolds, 1976; Merewether, 1983) or the concentration of offshore sandbodies (Tillman and Martinsen, 1984) may be related to the formation and eastward migration of forebulges in response to eastward tectonic transport in the thrust belt. This mechanism was proposed for the Sweetgrass arch in the Cretaceous foreland basin in Montana by Lorenz (1982), as a control of depositional patterns in the Appalachian foreland basin by Tankard (1986), and was mentioned as a depositional control in the Western Interior Cretaceous basin by Kauffman and Caldwell (in press). As an alternative, Cloetingh (1988) and Heller and others (in press) suggested that intraplate stresses related to plate-margin tectonics are of sufficient magnitude to have important consequences on basin stratigraphy, and this interesting concept warrants further investigation.

Whatever the cause of these varied intrabasinal structures evidenced throughout the Cretaceous, it is clear that by Maastrichtian time widespread breakup of the foreland basin was underway (Dickinson and others, 1988), and Laramide deformation, including uplift of basement-cored ranges and subsidence of intermontane basins, dominated the foreland of Wyoming.

The Western Interior Seaway

There is no good modern analogue for the great epicontinental seaway that flooded western North America during much of the Cretaceous, so there is little chance of deducing much about its character by uniformitarian comparisons. Instead, most of what we surmise about its extent, bathymetry, circulation patterns, and eustasy has been derived from numerous detailed studies and interpretations of the rock record and its fossil content. Many years of work on these subjects was presented by Kauffman (1984, 1985), a leader in Cretaceous stratigraphic and paleontologic research, and most recently by Kauffman and Caldwell (in press), and much of what follows comes from this work and a summary by Slingerland (1992).

The Western Interior Cretaceous Seaway owed its existence to two major factors: the presence of the subsiding foreland trough described above and a eustatic rise in sea level. This rise in sea level has been attributed to a period of spreading-ridge and mantle-plume development (Pitman, 1978; Kauffman, 1985; Larson, 1991), when increased spreading rates and the consequent production of hotter, higher-standing oceanic crust displaced sea level 1,000 ft (300 m) or more above the present stand and ocean waters flooded low-lying parts of the continents. In western North America, this rise in sea level flooded the evolving foreland basin. The Cretaceous Seaway started as separate northern and southern arms in early Neocomian time; with continued subsidence and sea-level rise, the northern and southern arms of the sea expanded into the foreland basin and connected the proto-Gulf of Mexico with the Cretaceous circumpolar sea in middle Late Albian time. The arms briefly disconnected, and

then reconnected in latest Albian-earliest Cenomanian time.

Although relative sea level rose and fell many times, the seaway remained a continuous marine passage across the continent for the next 38 m.y. At peak flooding (Early Turonian-Middle Santonian time), the seaway extended over 3,000 mi (4,800 km) from north to south and 1,200 mi (1,920 km) from west (Utah and Idaho) to east (Minnesota, Iowa, and South Dakota) and attained depths of up to 1,000 ft (300 m) (Kauffman, 1985).

Because of the relatively flat topography, particularly along its eastern shoreline, even small fluctuations in sea level produced widespread, essentially synchronous strand-line migrations. The position of the western shoreline also varied widely through time and was controlled by the complex interaction of changing relative sea level and the varying supply of sediments shed by the rising fold-and-thrust belt to the west. Gill and Cobban (1973) used the western extent of marine units, as defined by ammonite biostratigraphy, to determine the position of the western shoreline during the Late Cretaceous. This approach was expanded by Lillegraven and Ostresh (1990) when they established correspondences between the ammonite zones of Obradovich and Cobban (1975) and North American Land Mammal "Ages," thus more precisely locating the marine-nonmarine transition along the western edge of the interior seaway as it evolved during Late Cretaceous time.

There have been several attempts to interpret water circulation and stratification patterns for the interior seaway. Kauffman (1975) discussed this in some detail and pointed out that the factors influencing currents and water-mass distribution include: (1) northward movement of warm water from the south, (2) southward movement of cool, less saline water from the north, (3) the nature of the interface between these two water masses, (4) eustatic changes in sea level, (5) width and wind fetch across the basin, and (6) tidal exchange. Furthermore, Kauffman (1975) noted that, because the basin was filled from the north and south by waters with different physical and chemical characteristics, the water mass of the Western Interior Cretaceous Seaway was probably complexly stratified.

An excellent review of water circulation in the Cretaceous Seaway was given by Parrish and others (1984), who described both a theoretical modeling approach, using general principles of known physical processes with Cretaceous Seaway boundary conditions, and empirical models derived from information in the rock record. Numerical simulations by Ericksen and Slingerland (1990) indicate that circulation in the seaway was storm-dominated. Typical winter storms generated shore-parallel currents that initially flowed weakly northward but which flowed strongly southward later during the storm. Tidal ranges in the seaway were mesotidal to macrotidal along the southeastern margin but microtidal everywhere else. From the geological point of view, this kind of information is important for understanding the controls of sediment and organism distribution, and thus the evolution of the sedimentary and paleontologic record of the seaway. The models described have numerous discrepancies, but they also show a certain amount of commonality and therefore may be useful in interpreting the genesis of sedimentary units. Of particular interest is the pattern of bottom-current velocities computed for Campanian time (Parrish and others, 1984), which shows a uniform southerly flow across the western shelf and corresponds closely with measured paleocurrents from Campanian shelf-sand ridges (Tillman and Martinsen, 1984). On the other hand, maps prepared by Ericksen and Slingerland (1990) show a storm-generated northward flow followed by a strong southward flow as the storm passed across the seaway from west to east. Evidently, there is need for refinement of modeling techniques before the causal relations between ancient circulation patterns and the evolution of the Cretaceous marine sedimentary record will be fully understood.

The obvious, repetitive sandstone and shale strata of the Cretaceous sedimentary record lead one inescapably to the conclusion that the character of the seaway itself was cyclic, but discriminating among effects of the many controlling variables can be difficult at the local scale. Only when synchronous boundaries can be traced on an intercontinental scale can controls be identified as eustatic (long term) or climatic (short term). In those portions of the basin away from the influence of rapid clastic deposition and thrust-related deformation along the western margin, the effects of eustasy and oceanographic processes most likely dominated the sedimentary record. Along the clastic-dominated western margin of the basin, cyclicity in the sedimentary record was mainly controlled by a complex interplay of eustasy, climate, and sediment supply. A detailed

discussion of the effects of these variables on the cyclicity in the sedimentary record was given by Kauffman (1985). The orders of cyclicity discussed below refer to those in Haq and others (1988).

Several orders of cyclicity are recorded in the Cretaceous stratigraphy of the western foreland basin. Two Cretaceous first-order cycles (30 - 50 m.y. duration) are superposed on the overall flooding of the craton of the western United States from Jurassic to Paleocene time. The deposits of these cycles are not completely represented in the western foreland basin because second- and third-order regressions resulted in removal of part of the stratigraphic record. The most obvious cyclic controls on sedimentation in the western foreland basin are second-order (6-10 m.y. duration) and third-order (1-5 m.y. duration) fluctuations in relative sea level that are expressed as landward and seaward movements of the strand line on both the western and eastern margins of the basin, and as time-equivalent, large-scale cyclothems in the basin center. These second- and third-order cycles are tied to the major times of transgression and regression long recognized in the Cretaceous rocks of Wyoming. Sea-level curves for the Cretaceous have been published by Hancock (1975), Kauffman (1977, 1984, 1985), Hancock and Kauffman (1979), and Kauffman and Caldwell (in press). These authors relate major transgressive-regressive peaks in the Western Interior Cretaceous Seaway to those in Europe, and relate these events to eustatic sea-level change. Kauffman and Caldwell (in press) define nine transgressive-regressive (T-R) cycles of second-order scale for the entire Cretaceous, but the marine rock record containing T1 through R3 is not present in Wyoming. The formation names of the widely distributed shale units deposited during the transgressions were applied to the "seas" that expanded during the transgressions (McGookey and others, 1972) and, more recently, to the second-order cycles related to the transgressions. Thus, Kauffman and Caldwell's (in press) T-R 4 is informally referred to as the Kiowa-Skull Creek cycle, T-R 5 is the Greenhorn cycle, T-R 6 is the Niobrara cycle, T-R 7 is the Claggett cycle, T-R 8 is the Bearpaw cycle, and T-R 9 is the Fox Hills cycle (**Figure 1**). The Maastrichtian Fox Hills cycle is a relatively small transgressive reversal during the general fall in global sea level toward the end of the Cretaceous. It is best recorded in the rock record of South Dakota, but not obviously reflected in the Cretaceous sedimentary record in Wyoming.

Broad application of these transgressive-regressive cycles is complicated by the difficulties involved in separating local tectonic effects from eustatic controls for individual localities or regions. As a result, there is less than complete agreement on the significance of some of the T-R cycles. For example, the work by Lillegraven and Ostresh (1990), which portrays the positions of the western strandline of the foreland basin for each standard ammonite zone from earliest Campanian through Maastrichtian, suggests that there was a general regression during that time, and that the Claggett and Bearpaw T-R cycles are perturbations related to local and subregional tectonism, not to global eustatic sea-level changes. On the other hand, Hancock (1975) identified these peaks in Europe, thus supporting the interpretation of eustatic control. Sea-level curves for the Cretaceous of the western United States developed by Weimer (1983), together with Kauffman and Caldwell's (in press) transgressive-regressive cycles, are shown in **Figure 1**.

Fourth-order cycles described by Ryer (1983) are represented by smaller-scale progradational sequences on the western margin of the basin. Kauffman (1985) attributed these to short-term stillstand or fall in relative sea level. More recently, Ryer (1993) has suggested that these clastic wedges on the western margin of the basin are of three general types: those related to changes in relative sea level, those related to varying rates of sediment delivery, and hybrids of these two end members.

Kauffman (1985) related even smaller-scale cyclicity to changing climatic conditions. One- to ten-meter bedding cycles are common throughout the basin, and are expressed as shale-limestone bedding couplets in the basin center and as prograding sandstone sequences truncated by black shale beds near the basin margin. Radiometric dating of these couplets indicates that they generally fall into three groups relative to the amount of time they represent: 21 ka, 42 ka, and 100 ka. These groupings may correspond to Milankovitch cycles, which reflect orbital parameters of the Earth (Kauffman, 1985). Barron and others (1985) presented sedimentologic, geochemical, and biological data that indicate the shale-carbonate cycles of these magnitudes reflect wet and dry climatic episodes.

The sedimentary record

The Cretaceous foreland basin of the western United States was segmented into basement-cored uplifts and intermontane basins during the Laramide orogeny of Late Cretaceous and early Tertiary time. Erosion removed Cretaceous strata from most of the ranges so that reconstruction of the original depositional basin requires correlation of the strata preserved in the various Laramide basins. Because of the stratigraphic control provided by biozonation (**Figure 1**), radiometric dating of bentonite beds (**Figure 1**), and subsurface information from closely spaced wells, good correlation can be made throughout much of the Cretaceous stratigraphic section. McGookey and others (1972) have compiled the most complete summary of Cretaceous stratigraphy for the western foreland basin.

During the Early Cretaceous, sediments were derived from both sides of the basin, though the thickest strata were deposited along the western margin. During the Late Cretaceous, most sediment came from the west, and lithofacies were controlled by changes in environments from coastal plain to shoreline to marine shelf and the deeper water of the basin. This intertonguing of nonmarine strata on the west with marine strata in the center of the basin is depicted in the generalized cross section from Weimer (1960) in **Figure 2**, which shows the Cretaceous foreland basin from the tectonically active margin in western Wyoming to the central basin area in northeastern Wyoming. Times of major eastward progradation of clastic detritus from the west have been used to date deformation in the fold-and-thrust belt (Dorr and others 1977; Wiltschko and Dorr, 1983; and Royse, this volume). In contrast, Heller and Paola (1989) suggested that times of thrusting are indicated by areally restricted gravels near the thrust front.

Weimer (1983) focused on tectonic influences on sedimentation and related unconformities in the Cretaceous foreland basin fill. He recognized nine

Figure 2. Diagrammatic restored cross section of Upper Cretaceous rocks extending from southwest to northeast Wyoming. From Weimer (1960).

unconformities that could be placed in a regional context and used them to construct the restored section shown in **Figure 3**. The unconformities are of three types: those completely within nonmarine strata; those involving both marine and nonmarine strata; and those totally within marine strata. Where significant time is missing, the approximate ages cited for these unconformities are those of the top of the subjacent unit. These ages are: (1) Late Neocomian to Early Aptian, 125 Ma, (2) Late Aptian-Early Albian, 112 Ma, (3) Albian, 101 Ma, (4) Early Cenomanian, 95 Ma, (5) Late Turonian, 90 Ma, (6) Late Turonian- Early Coniacian, 88 Ma, (7) Early Campanian, 80 Ma, (8) Late Campanian-Early Maastrichtian, 73 Ma, and (9) Late Maastrichtian, 66 Ma. Many of these unconformities can be related to sea-level changes and to recognized transgressive-regressive cycles, but as previously discussed, there is almost always some uncertainty in determining whether a locally or regionally recognized unconformity is related to tectonism, sea-level change, or both.

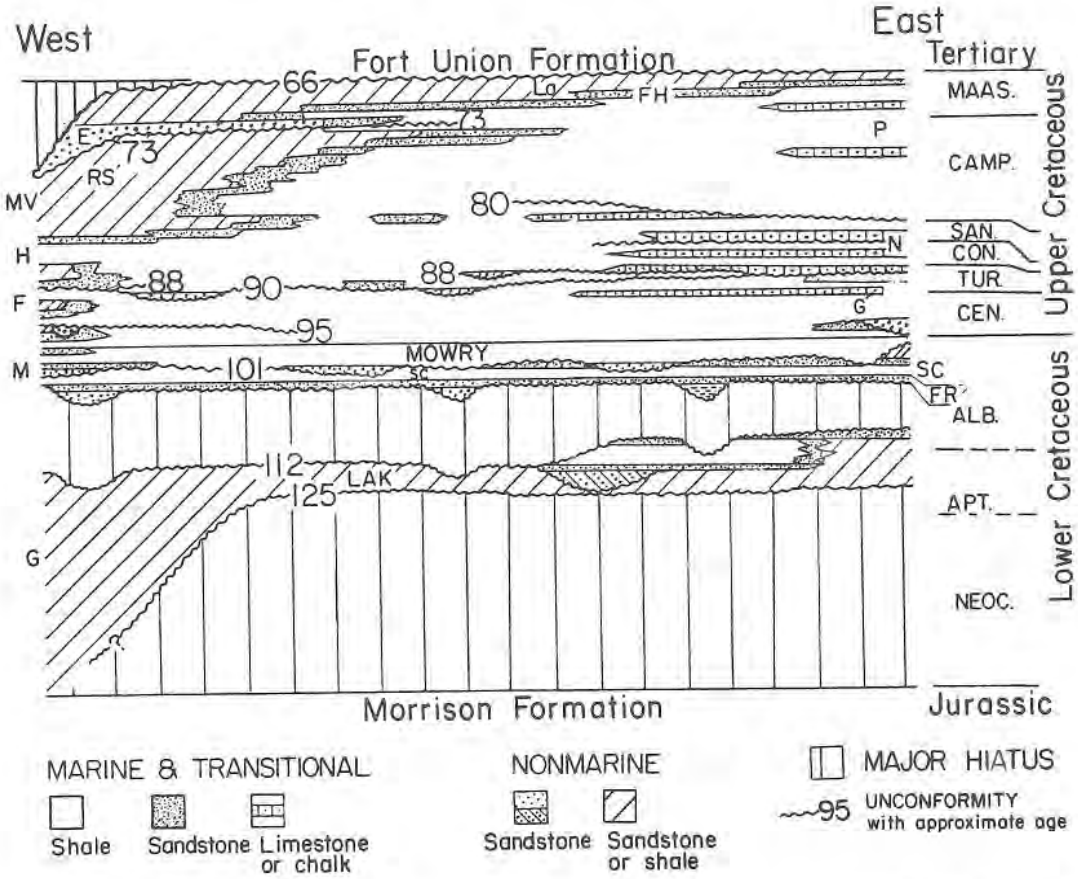

Figure 3. Diagrammatic restored cross section across the Cretaceous foreland basin from its western margin eastward to its geographic center. The stratigraphic positions of major intrabasin unconformities are shown by wavy lines which include approximate ages in millions of years. Strata are dominantly nonmarine in the western portion of the basin and dominantly marine in the geographic center of the basin. Unconformities are in three positions: those completely within nonmarine strata, those involving both marine and nonmarine strata, and those totally within marine strata. Wavy lines completely across the diagram represent times when the entire basin was subjected to subaerial or submarine erosion. Formations or groups to the west are: G = Gannett; M = Mowry; F = Frontier; H = Hilliard; MV = Mesaverde; RS = Rock Springs; E = Ericson; FH = Fox Hills; La = Lance. To the east, formations are: LAK = Lakota; FR = Fall River; SC = Skull Creek; G = Greenhorn; N = Niobrara; P = Pierre. The vertically ruled lines represent unconformities where a major hiatus is recognized. Ruling is omitted where gap is small. Modified from Weimer (1983) to reflect new ages from Obradovich (in press).

Lower Cretaceous

Neocomian through Early Albian sedimentary rocks in Wyoming range in thickness from 4,000 ft (1,220 m) in the west to less than 400 ft (122 m) over most of the state (**Figure 4a**). Haun and Barlow (1962) gave a general summary of Lower Cretaceous stratigraphic relationships for much of Wyoming. Most of Neocomian time is not represented by strata in the state. In the west, however, the lower part of the Gannett Group may be as old as Late Neocomian. Strata of this group represent alluvial-fan and ponded lake deposits that formed adjacent to the western highlands (Eyer, 1969; Furer, 1970). In Early Aptian time, gravels of the Cloverly Formation spread eastward, leaving the first Cretaceous sedimentary record over much of the state. Several studies, including those by Eicher (1969), MacKenzie and Ryan (1962), and McCubbin (1969), focused on the paleodrainage of these fluvial deposits. Heller and Paola (1989) interpret these gravels to indicate a broad, east- to northeast-directed stream system flowing from the fold-and-thrust belt out across the foreland basin. In contrast, DeCelles (1986) and Kvale and Beck (1985) argued that local variability of paleocurrents suggests local sources and indicates partitioning of the foreland basin.

Middle and Late Albian rocks in Wyoming range in thickness from 1,500 ft (457 m) in the west to less than 300 ft (91 m) in the east (**Figure 4b**). During this time, the first Cretaceous marine invasion (the transgressive phase of the Kiowa-Skull Creek T-R cycle) spread across Wyoming, and the dark shales of the Skull Creek Formation in northeastern Wyoming and Thermopolis Shale over most of the state, were deposited. However, this transgression was relatively short lived, and a regional lowstand surface of subaerial exposure and erosion formed during the major regression that followed. Valleys were incised into the exposed surface and soils formed on drainage divides. Subsequently, these valleys were filled with sediments which formed the Muddy Sandstone as the Greenhorn T-R cycle began and the Mowry sea flooded the foreland basin from the north. Dolson and others (1991) mapped the regional trends of these valleys throughout much of the Rocky Mountain area and showed that the drainage patterns outline paleotopographic highs, some of which continued as structurally positive areas during the Laramide orogeny.

The Muddy Sandstone is a thin, but widespread and complex stratigraphic unit consisting of a variety of nonmarine and marine strata that filled the valleys. Gustason and others (1988) and Martinsen (1992) have shown that, in the Powder River Basin, the Muddy Sandstone contains one or more lowstand surfaces of erosion and numerous transgressive surfaces of erosion, which provide both horizontal and lateral seals for hydrocarbon accumulations and give rise to stratigraphic compartments.

Because the Mowry sea was bounded on the south by the Transcontinental arch and not connected to the proto-Gulf of Mexico, it became stagnant as it deepened, thus promoting the formation of black shale and hydrocarbon source beds. The Aspen Shale of northwestern Wyoming and the Mowry Shale throughout the remainder of the state were deposited in this sea. The reader is cautioned here concerning the age of the Mowry. Merewether (1983) and Weimer (1983), as well as most other workers, indicate that it is entirely Late Albian, whereas Love and others (*Stratigraphic nomenclature chart of Wyoming*, map pocket) indicate that it is at least partly Early Cenomanian, based on a recent reassessment of ammonite zones and their ages by Cobban and Kennedy (1989).

The most complete study of the Mowry and contemporaneous rocks is that by Reeside and Cobban (1960), in which they looked at this widespread unit in both the western United States and Canada. In Wyoming, the Mowry consists of porcellanitic shale, porcellanite and bentonite, all products of a long period of volcanism. These rocks have yielded both brackish-water and marine invertebrates and are well known for concentrations of disarticulated fish remains.

Upper Cretaceous

Upper Cretaceous sedimentary rocks in Wyoming range in thickness from 18,000 ft (5,490 m) in the western foredeep and 16,000 ft (4,880 m) in the south-central part of the state to less than 4,000 ft (1,220 m) in central-western Wyoming (**Figure 4c**). During the transgressions and regressions that continued throughout Late Cretaceous time, a north-south belt of complexly intercalated marine, deltaic, barrier-island, and coastal-plain sediments formed across Wyoming and separated dominantly marine

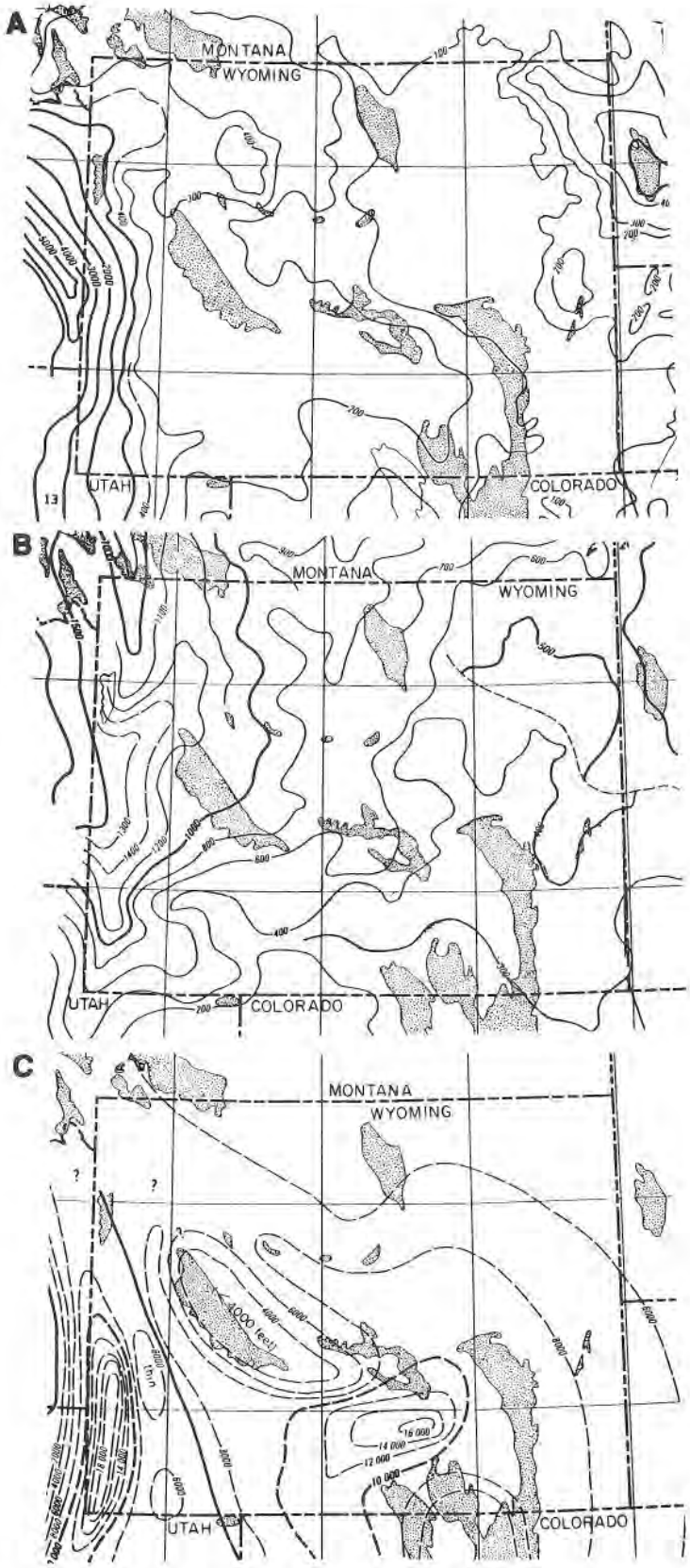

Figure 4. Thickness in feet of Cretaceous rocks in Wyoming and immediately adjacent areas: (a) lower part of Lower Cretaceous (Neocomian, Aptian, Early Albian); (b) upper part of Lower Cretaceous (Middle and Late Albian); (c) Upper Cretaceous. From McGookey and others (1972). Stippled pattern indicates Precambrian cores of Laramide uplifts.

deposits to the east from dominantly nonmarine and marginal-marine deposits to the west.

Eustatic sea level in the Mowry seaway continued to rise, finally overtopping the Transcontinental arch in Early Cenomanian time, reestablishing a through-flowing connection with the proto-Gulf of Mexico, and forming the Greenhorn Sea (Kauffman, 1984, 1985; Weimer, 1983). In Early Turonian, the Greenhorn seaway reached the highest eustatic sea level of the Cretaceous, and clastic sediments of the Frontier Formation spread eastward across the Aspen and Mowry shales along the western margin of this seaway. Merewether (1983) indicated that deposition of the Frontier began as early as latest Albian in the western part of the state and continued into the Coniacian, whereas Weimer (1983) indicated that all of the Frontier is above the Albian-Cenomanian boundary. In eastern Wyoming, sedimentary units equivalent in age to the Frontier include the Belle Fourche Shale, Greenhorn Formation, and Carlile Shale (Merewether and others, 1979).

The Frontier Formation is an extremely variable unit with regard to lithology, age, and thickness because of internal unconformities and facies changes related to transgressions and regressions along the western margin of the Greenhorn Seaway. As a consequence, a complex internal stratigraphic nomenclature, described in the references cited herein, has been developed from surface and subsurface information. Thickness of the Frontier ranges from less than 164 ft (50 m) near the Uinta Mountains to more than 2,000 ft (610 m) in the eastern part of the fold-and-thrust belt. In the southwestern part of the state, the Frontier contains beds of conglomerate (Schmitt, 1982), but over most of Wyoming it consists of sandstone, siltstone, shale, and coal. Deposition in almost every conceivable marginal- and shallow-marine environment has been documented in numerous detailed studies (e.g., Siemers, 1975; Ryer, 1977; Merewether and others, 1979; Schmitt, 1982; Merewether, 1983)

Internal stratigraphy of the Frontier includes evidence of transgressions and regressions caused by local tectonism as well as by the fluctuations of sea level recognized elsewhere (Merewether, 1983). Specifically, the areal distribution of some nearshore marine and nonmarine strata and the spatial and temporal magnitude of hiatuses indicate positive areas of tectonic origin at 90 to 91 Ma in western Wyoming, 89.8 Ma in southeastern and northwestern Wyoming, and 89.3 Ma in southeastern, central, and northwestern Wyoming (Merewether and Cobban, 1986). In addition, two regional unconformities within the Frontier (see *Stratigraphic nomenclature chart of Wyoming* by Love and others, map pocket) most likely indicate lowered relative sea level and subaerial exposure.

Marine conditions once again prevailed throughout most of Wyoming as the Niobrara T-R cycle began. The Niobrara transgression spread rapidly across the state during Late Turonian and Early Coniacian time, flooding the seaway with the second highest sea-level highstand of Cretaceous time. This seaway was unique among Cretaceous transgressions in that it maintained a prolonged interval of flooding with moderate third-order sea-level fluctuations. During this time, the widespread, thick shale units of the Hilliard and Baxter shales in the west and the Cody Shale in central Wyoming were deposited. In eastern Wyoming, the chalks and marls of the Niobrara Formation were deposited during this interval and probably record times of transgression and peak flooding of the Niobrara sea. Maximum thickness of sedimentary rocks formed during this time may be as great as 6,000 ft (1,830 m) in the western foredeep, whereas the thickness of equivalent units in the east is approximately 800 ft (248 m). These extensive, fine-grained marine deposits provide an excellent natural laboratory for micropaleontological studies and extensive work on the biostratigraphy and paleoceanography of these units has been carried out by Frerichs (1980, 1988), Hattin (1982), and Kent (1967).

Regression of the Niobrara sea is marked by the Early Campanian appearance of clastic rocks of the Mesaverde Group over much of the western and central part of the state while fine-grained sediments continued to accumulate in the east. The position of the boundary separating the rock records of the Niobrara and Claggett T-R cycles is not clear but it probably occurs at the base of the Rock Springs and Haystack Mountain formations in the lower part of the Mesaverde Group.

The Mesaverde Group is nearly 7,000 ft (2,135 m) thick along the Wyoming-Utah state line and thins eastward, finally pinching out into Cody and Steele shales in eastern Wyoming. The stratigraphic relationships generated by variations in basin subsid-

ence, sediment supply, eustasy, and facies migrations are extremely complex and have prompted a complicated and evolving stratigraphic terminology. Roehler (1990) gave an excellent discussion of Mesaverde stratigraphy for southwestern Wyoming, and his cross section is shown in **Figure 5**. In this area, a regional unconformity separates the lower part of the Mesaverde Group, consisting of the Blair and Rock Springs formations, and the lower part of the Ericson Sandstone from the upper Mesaverde, which includes the the upper part of the Ericson Sandstone and Almond Formation. The lower Mesaverde prograded eastward, terminating with the distal Allen Ridge Formation, which overlies the Haystack Mountains Formation in the south-central part of the state. The upper part of the Ericson Sandstone and the Pine Ridge Sandstone (and equivalent Teapot Sandstone to the north) were deposited on the erosional surface, which was tectonically enhanced and in places truncates as much as 1,700 ft (518 m) of the lower Mesaverde (Roehler, 1990). At the top of the Mesaverde Group, the Almond Formation intertongues eastward with the Lewis Shale.

As with the Frontier Formation, almost every conceivable fluvial, coastal-plain, marginal-marine, and near-shore environment is represented by rocks of the Mesaverde Group. Recently, marine trace fossils and sedimentary structures of tidal origin have been found in the Ericson Sandstone, previously thought to be fluvial in origin (O.J. Martinsen, personal communication). In addition, a shelf sand-ridge origin for some Mesaverde-equivalent sandstone units was suggested by Spearing (1976) and Tillman and Martinsen (1984), and a similar interpretation of sandstone units in the Haystack Mountains Formation was made by Martinsen and Tillman (1989). In contrast, Walker and Bergman (1993) interpreted some of these same sand bodies as lowstand shoreface deposits. These latest findings are representative of the many new interpretations based on the premise that there were large fluctuations in sea level and consequent erosion during the Cretaceous.

Although there are numerous bentonite and bentonitic beds through most of the Upper Cretaceous, one deserves particular mention. The Ardmore ben-

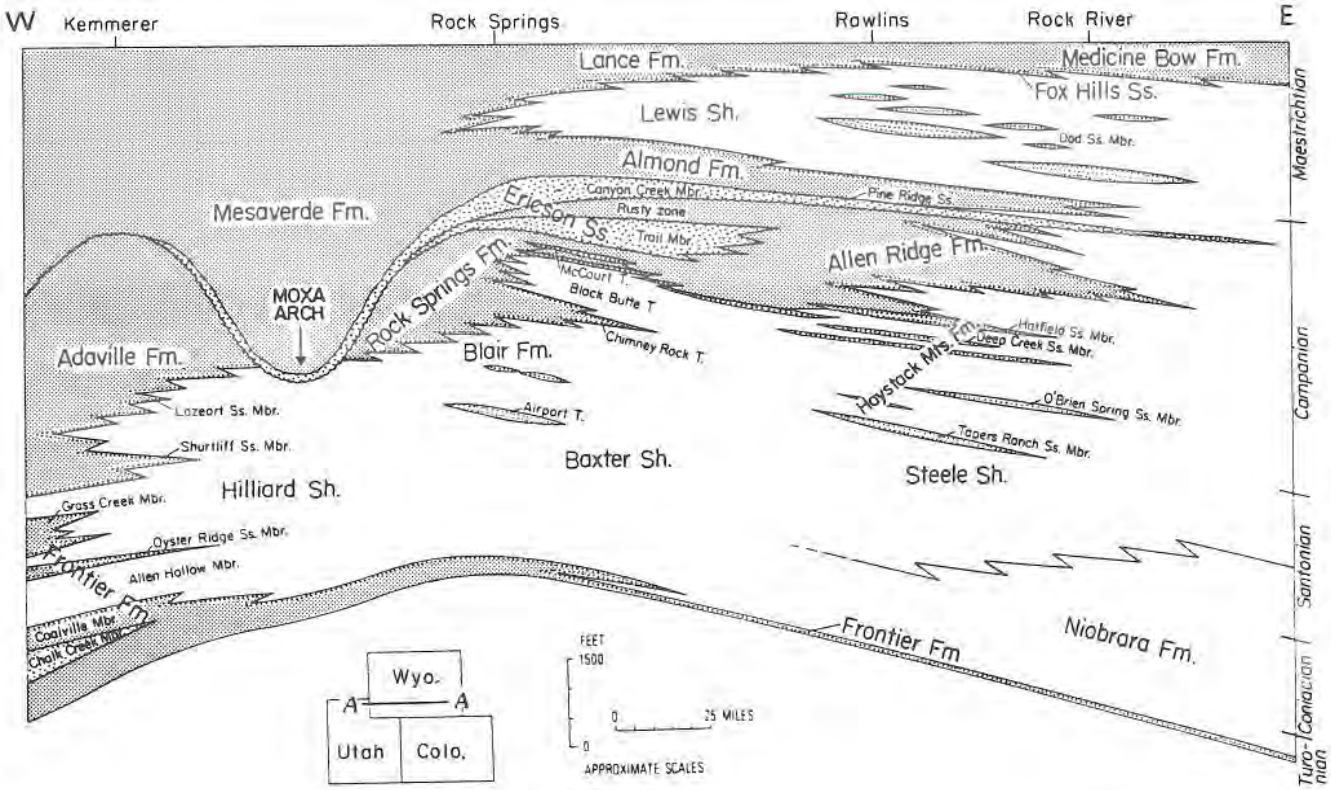

Figure 5. Cross section showing restored Upper Cretaceous rocks across northern Utah and southern Wyoming. Rocks of continental origin are shaded; alluvial-plain and marine-shoreline, shelf, slope, and basin sandstone and siltstone units are shown by dot pattern; marine shale and limestone are unpatterned. From Roehler (1990).

tonite, of Early Campanian age, is a bed or series of beds approximately 5 ft (1.5 m) thick that forms an excellent time-stratigraphic marker over much of the northern Rocky Mountain region. In Wyoming, it is interbedded with sedimentary rocks of the Mesaverde Group and Cody Shale, and reflects large-scale volcanism in west-central Montana at about 80 Ma.

Roehler (1990) stated that the transgressions and regressions indicated by Mesaverde stratigraphic relations in southwestern Wyoming do not correspond precisely with the T-R cycles of Kauffman (1977). One of the implications of this interpretation is that the the effects of tectonism have overprinted those of eustasy. Devlin and others (in press) have shown that stratal stacking patterns in the Mesaverde of southwest Wyoming are related to subsidence rates, which are, in turn, related to times of thrusting in the fold-and-thrust belt and/or uplift of basement-cored Laramide structures. Martinsen and others (1993) also point to the effects of tectonism on deposition of upper Mesaverde sediments in the southeastern part of the state. In general, however, beds of the lower part of the Mesaverde Group were deposited during the Niobrara regression and the Claggett transgression, whereas beds of the upper part of the Mesaverde Group were deposited at the beginning of the Bearpaw transgression. To the east, the Lewis shale was deposited during the transgressive and regressive phases of the Claggett T-R cycle, and later, during the transgressive phase of the Bearpaw T-R cycle, it covered the Mesaverde clastic rocks over most of the state. In this regard, it should be noted that the Lewis Shale in Wyoming is significantly younger than the Lewis Shale at its type locality in southern Colorado, and is correlative with the Bearpaw Shale of Montana (Weimer, 1960).

These stratigraphic relations were described by Gill and others (1970) for south-central Wyoming, where the Lewis Shale reaches a maximum thickness of as much as 2,600 ft (793 m). Northeast-southwest cross sections of the Lewis display a pattern of submarine topography that Asquith (1970) interpreted as shelf, slope, and basin marine environments, and Winn and others (1985) identified shelf, delta-front, and turbidite deposits in the Lewis. Perman (1990) also identified deltaic deposits in the Lewis and interpreted the Dad Sandstone Member as a shelf sand-ridge.

The Bearpaw regression represents the final retreat of the Cretaceous epicontinental seaway from the Rocky Mountain area and deposition during this time records the final transition from marine to nonmarine conditions. In Wyoming, this time is represented by the Fox Hills Sandstone, which intertongues with, and overlies, the Lewis Shale. Estimates of the thickness of the Fox Hills by Gill and others (1970) range from 200 ft (61 m) to 700 ft (214 m) in south-central Wyoming, but Fox (1971), using different criteria for the upper boundary, indicated that it may be as much as 1,000 ft (305 m) thicker than previously estimated. Except in south-central Wyoming, where sediments of the Fox Hills represent deltaic deposition (Weimer, 1961), the Fox Hills was deposited on a sandy shoreline as the seaway retreated toward the northeast.

As the edge of the seaway continued its retreat eastward across the state, nonmarine conditions prevailed throughout Wyoming and the sediments of the Lance Formation and equivalent units were deposited. In parts of southeastern Wyoming, equivalent sedimentary rocks are called the Medicine Bow Formation. In the far west, conglomerates of the Harebell Formation and part of the Evanston Formation were deposited. In central Wyoming, the Lance is up to 5,000 ft (1,670 m) thick (Keefer, 1965; Gillespie and Fox, 1991) and records the transition from coastal-plain and delta-plain environments to fluvial deposition as the sea receded (Gillespie and Fox, 1991; Flemings and Nelson, 1991).

In southeastern Wyoming, the Lance-equivalent Medicine Bow Formation is 6,300 ft (1,900 m) thick. Fox (1971) established the position of the marine to continental transition in the lower part of the Medicine Bow using the first occurrence of fresh-water fossils. As an aside, it should be mentioned that use of the term Medicine Bow Formation for Lance-equivalent strata in this area stems from a stratigraphic debate referred to as the "Laramie problem," which went on for several decades in the late 1800s and early 1900s. The term "Laramide orogeny" was derived from this debate, and a brief history of the roots of this nomenclature is discussed elsewhere in this volume (see overview chapter by Snoke).

Many workers (e.g., Keefer, 1965; MacLeod, 1981; Flemings and Nelson, 1991; Gillespie and Fox, 1991) cited thickness variations and unconformities

in the Lance as evidence for Laramide tectonic influence on deposition. Lillegraven and Ostresh (1988) showed the influence of early Laramide uplifts on drainage patterns during deposition of Lance sediments, and Dickinson and others (1988) used the presence of local depocenters and sediment sources as indicators of the onset of Laramide deformation during Maastrichtian time. In the far western part of the state, conglomerate units continued to be generated in and adjacent to the fold-and-thrust belt. Conglomerates in the Evanston and Harebell formations were shed by interior, ramp-supported uplifts during Maastrichtian time (Salat and Steidtmann, 1991; Schmitt and Steidtmann, 1990).

Economic considerations

The complex intertonguing of Cretaceous marine shale and sandstone and the resulting thick, widespread coastal plain deposits provide the geologic setting responsible for much of Wyoming's natural resources. The petroleum geology of Cretaceous rocks is described in greater detail elsewhere in this volume by DeBruin and Cretaceous coals are discussed in this volume by Moore and Shearer.

Hydrocarbon source beds are abundant in marine shale units such as the Thermopolis, Mowry, Niobrara, and Cody formations, and the sandstone units laterally associated with these shales provide high-quality reservoirs. Although over half of the oil and gas produced in Wyoming comes from structures, many of these traps have a stratigraphic component related to facies changes, diagenesis, or erosional truncation, which was critical to the formation of the reservoir. Some of the largest hydrocarbon reservoirs in Wyoming are in Cretaceous sandstones, such as the valley-fill deposits of the Muddy Sandstone, shelf-sand ridges of the Shannon and Sussex sandstones, shoreface sandstones of the Frontier Formation, and barrier-island deposits of the Almond Formation. However, the future of Wyoming's petroleum business may well rest in the enormous gas reserves in low-permeability or "tight" gas sands of the Mesaverde Group in the western part of the state.

Wyoming has the largest in-place coal resources of any state except Alaska, and many of Wyoming's coal fields include coal beds of Cretaceous age. The most widespread of these are in the deltaic and coastal plain deposits of the Mesaverde Group and equivalent units. Because of this depositional setting, many of the coal beds are relatively thin and laterally extensive, and because these beds were subsequently buried by marine sediments, they have a relatively high sulfur content compared to the Tertiary coal beds that accumulated in separate, rapidly subsiding Laramide basins.

Acknowledgments

I thank E.G. Kauffman and R.S. Martinsen for their informative discussions and help with reference material, and C.L. Angevine, J.E. Deibert, E.G. Kauffman, R.S. Martinsen, and T.A. Ryer for reviewing the manuscript.

References cited

Allen, P.A., Homewood, P., and Williams, G.D., 1986, Foreland basins: an introduction, *in* Allen, P.A., and Homewood, P., editors, Foreland basins: International Association of Sedimentologists Special Publication 8, p. 3-12.

Asquith, D.O., 1970, Despositional topography and major marine environments, Late Cretaceous, Wyoming: American Association of Petroleum Geologists Bulletin, v. 54, p. 1184-1224.

Barron, E.J., Arthur, M.A., and Kauffman, E.G., 1985, Cretaceous rhythmic bedding sequences—a plausible link between orbital variations and climate: Earth and Planetary Science Letters, v. 72, p. 327-340.

Beaumont, C., 1981, Foreland basins: Geophysical Journal of the Royal Astronomical Society, v. 65, p. 291-329.

Bird, P., 1984, Laramide crustal thickening event in the Rocky Mountain foreland and Great Plains: Tectonics, 3, p. 741-758.

Cerveny, P.F., and Steidtmann, J.R., 1993, Fission track thermochronology of the Wind River Range, Wyoming: evidence for timing and magnitude of Laramide exhumation: Tectonics, v. 12, p. 77-91.

Cloetingh, S., 1988, Intraplate stress: a new element in basin analysis, *in* Kleinspehn, K.L., and Paola, C., editors, New perspectives in basin analysis: New York, Springer-Verlag, p. 205-230.

Cobban, W.A., and Kennedy, W.J., 1989, The ammonite *Metengonoceras hyatt*, 1903, from the Mowry Shale (Cretaceous) of Montana and Wyoming: U.S. Geological Survey Bulletin 1787-L, 11 p.

Cross, T.A., and Pilger, R.H., Jr., 1978, Tectonic controls of Late Cretaceous sedimentation, Western Interior: Nature, v. 274, p. 653-657.

DeCelles, P.G., 1986, Sedimentation in a tectonically partitioned nonmarine foreland basin: the Lower Cretaceous Kootenai Formation, southwestern Montana: Geological Society of America Bulletin, v. 97, p. 911-931.

Devlin, W.J., Rudolph, K.W., Shaw, C.A., and Ehman, K.D., in press, The effect of tectonic and eustatic cycles on accommodation and sequence stratigraphic framework in the Upper Cretaceous foreland basin of southwestern Wyoming, *in* Posamentier, H.W., Summerhayes, C.P., Haq, B.U., and Allen, G.P., editors, Stratigraphy and facies association in a sequence stratigraphic framework: International Association of Sedimentologists Special Publication 18.

Dickinson, W.R., 1974, Plate tectonics and sedimentation, *in* Dickinson, W.R., editor, Tectonics and Sedimentation: Society of Economic Paleontologists and Minerologists Special Publication 22, p. 1-27.

Dickinson, W.R., Klute, M.A., Hayes, M.J., Janecke, S.U., Lundin, E.R., McKittrick, M.A., and Olivares, M.D., 1988, Paleogeographic and paleotectonic setting of Laramide sedimentary basins in the central Rocky Mountain region: Geological Society of America Bulletin, v. 100, p. 1023-1039.

Dolson, J., Muller, D., Evetts, M.J., and Stein, J.A., 1991, Regional paleotopographic trends and production, Muddy Sandstone (Lower Cretaceous), central and northern Rocky Mountains: American Association of Petroleum Geologists Bulletin, v. 75, p. 409-435.

Dorr, J.A., Spearing, D.R., and Steidtmann, J.R., 1977, Deformation and deposition between a foreland uplift and an impinging thrust belt: Hoback Basin, Wyoming: Geological Society of America Special Paper 177, 82 p.

Eicher, D.L., 1969, Cenomanian and Turonian planktonic foraminifera from the Western Interior of the United States: First International Conference on Plantonic Microfossils, Geneva, 1967, Proceedings v. 2, p. 163-174.

Ericksen, M.C., and Slingerland, R. , 1990, Numerical simulations of tidal and wind-driven circulation in the Cretaceous Interior Seaway of North America: Geological Society of American Bulletin, v. 102, p. 1499-1516.

Eyer, J.A., 1969, Gannett Group of western Wyoming and southeastern Idaho: American Association of Petroleum Geologists Bulletin, v. 53, p. 1368- 1390.

Flemings, P.B., and Nelson, S.N., 1991, Paleogeographic evolution of the latest Cretaceous and Paleocene Wind River Basin: The Mountain Geologist, v. 28, p. 36-52.

Fox, J.E., 1971, Invertebrate fossils and environments of the Fox Hills and Medicine Bow formations (Late Cretaceous) in south-central Wyoming [Ph.D. dissertation]: Laramie, University of Wyoming, 162 p.

Frerichs, W.E., 1980, Paleoceanographic control of planktonic foraminiferal distributions in the Late Cretaceous Niobrara Formation of the Western Interior, North America, *in* Sliter, W.V., editor, Studies in marine micropaleontology and paleoecology, a memorial volume to Orville L. Bandy: Cushman Foundation for Foraminiferal Research, Special Publication 19, p. 196-201.

_____ 1988, Distribution of the *Heterohelicidae* in Upper Cretaceous strata of the Western Interior: University of Wyoming Contributions to Geology, v. 26, p. 99-106.

Furer, L.C., 1970, Petrology and stratigraphy of nonmarine Upper Jurassic-Lower Cretaceous rocks of western Wyoming and southeastern Idaho: American Association of Petroleum Geologists Bulletin, v. 54, p. 2282-2302.

Gill, J.R., Merewether, E.A., and Cobban, W.A., 1970, Stratigraphy and nomenclature of some Upper Cretaceous and Lower Tertiary rocks in south-central Wyoming: U.S. Geological Survey Professional Paper 667, 53 p.

Gill, J.R., and Cobban, W.A., 1973, Stratigraphy and geologic history of the Montana Group and equivalent rocks, Montana, Wyoming, and North and South Dakota: U.S. Geological Survey Professional Paper 776, 37 p.

Gillespie, J.M, and Fox, J.E., 1991, Tectonically influenced sedimentation in the Lance Formation, eastern Wind River Basin, Wyoming: The Mountain Geologist, v. 28, p. 53-66.

Gustason, E.R., Ryer, T.A., and Odland, S.K., 1988, Stratigraphy and depositional environments of the Muddy Sandstone northwestern Black Hills, Wyoming: Wyoming Geological Association Earth Science Bulletin, v. 20, p. 49-60.

Hancock, J.M., 1975, The sequence of facies in the Upper Cretaceous of northern Europe compared with that in the Western Interior, *in* Caldwell, W.G.C., editor, The Cretaceous System in the Western Interior of North America: Geological Association of Canada Special Paper 13, p. 82-118.

Hancock, J.M., and Kauffman, E.G., 1979, The great transgressions of the Late Cretaceous: Journal of the Geological Society of London, v. 136, p. 175-186.

Haq, B.U., Hardenbol, J., and Vail, P.R., 1988, Mesozoic and Cenozoic chronosratigraphy and cycles of sea level change, *in* Wilgus, C.K., and others, editors, Sea level changes: an integrated approach: Society of Economic Paleontologists and Mineralogists Special Publication 42, p. 71-108.

Hattin, D.E., 1982, Stratigraphy and depositional environment of Smoky Hill Chalk Member, Niobrara Chalk (Upper Cretaceous) of the type area, western Kansas: Kansas Geological Survey Bulletin 225, 108 p.

Haun, J.D., and Barlow, J.A., Jr., 1962, Lower Cretaceous stratigraphy of Wyoming: Wyoming Geological Association 17th Annual Field Conference Guidebook, p. 15-22.

Heller, P.L., and Paola, C., 1989, The paradox of Lower Cretaceous gravels and the initiation of thrusting in the Sevier orogenic belt, United States Western Interior: Geological Society of America Bulletin, v. 101, p. 864-875.

Heller, P.L., Beekman, F., Angevine, C.L., and Cloetingh, S., in press, Cause of tectonic reactivation and subtle uplifts in the Rocky Mountain region and its effect on the stratigraphic record: Geology, v. 21.

Jordan, T.E., 1981, Thrust loads and foreland basin evolution, Cretaceous, western United States: American Association of Petroleum Geologists Bulletin, v. 65, p. 2506-2520.

Kauffman, E.G., 1975, Dispersal and biostratigraphic potential of Cretaceous benthonic bivalvia in the Western Interior, *in* Caldwell, W.G.E., editor, The Cretaceous System in the Western Interior of North America: Geological Association of Canada Special Paper 13, p. 163-194.

_____ 1977, Geologic and biological overview, Western Interior Cretaceous basin, *in* Kauffman, E.G., editor, Cretaceous facies, faunas, and paleoenvironments across the Western Interior basin: The Mountain Geologist, v. 14, p. 75-99.

_____ 1984, Paleobiogeography and evolutionary response dynamic in the Cretaceous Western Interior Seaway of North America, *in* Westermann, G.E.G., editor, Jurassic-Cretaceous biochronology and paleogeography of North America: Geological Association of Canada Special Paper 27, p. 273-306.

_____ 1985, Cretaceous evolution of the Western Interior basin of the United States, *in* Fine-grained deposits and biofacies of the Cretaceous Western Interior Seaway: evidence of cyclic sedimentary processes: Society of Economic Paleontologists and Mineralogists Field Trip Guidebook, no. 4, 10 p.

Kauffman, E.G., Obradovich, J., and Cobban, W.A., 1992, The evolution of Cretaceous biostratigraphy in the Western Interior basin of North America: Society of Economic Paleontologists and Mineralogists 1992 theme meeting, Mesozoic of the Western Interior, Abstracts with program, Fort Collins, Colorado.

Kauffman, E.G., and Caldwell, W.G.E., in press, The Western Interior basin in space and time, *in* Caldwell, W.G.E., and Kauffman, E.G., editors, Mesozoic evolution of the Western Interior Basin of North America: Geological Association of Canada Special Paper 39.

Kauffman, E.G., Sageman, B.B., Kirkland, J.I., Elder, W.P., Harries, P.J., and Villamil, T., in press, Molluscan, biostratigraphy of the Western Interior Cretaceous Basin, North America, *in* Caldwell, W.G.E., and Kauffman, E.G., editors, Mesozoic evolution of the Western Interior Basin of North America: Geological Association of Canada Special Paper 39.

Kay, M., 1951, North American geosynclines: Geological Society of America Memoir 48, 143 p.

Keefer, W.R., 1965, Stratigraphy and geologic history of the uppermost Cretaceous, Paleocene, and lower Eocene rocks in the Wind River Basin, Wyoming: Geological Survey Professional Paper 495-A, 76 p.

Kent, H.C., 1967, Microfossils from the Niobrara equivalent portion of the Mancos Shale (Cretaceous) in northwestern Colorado: Journal of Paleontology, v. 41, p. 1433-1456.

Kvale, E.P., and Beck, R.A., 1985, Thrust-controlled sedimentation patterns of the earliest Cretaceous nonmarine sequence of the Montana-Idaho-Wyoming Sevier foreland basin: Geological Society of America Abstracts with Programs, v. 17, no. 7, p. 636.

Larson, R.L., 1991, Geological consequences of superplumes: Geology, v. 19, p. 963-966.

Lillegraven, J.A., and Ostresh, L.M., 1988, Evolution of Wyoming's early Cenozoic topography and drainage patterns: National Geographic Research, v. 4, p. 303-327.

_____ 1990, Late Cretaceous (earliest Campanian/Maastrichtian) evolution of western shorelines of the North American Western Interior Seaway in relation to known mammalian faunas, *in* Bown T.M, and Rose, K.D., editors, Dawn of the Age of Mammals in the northern part of the Rocky Mountain Interior, North America: Geological Society of America Special Paper 243, p. 1-30.

Lorenz, J.C., 1982, Lithospheric flexure and the history of the Sweetgrass arch, northwestern Montana: Rocky Mountain Association of Geologists 1982 Symposium, p. 77-89.

MacKenzie, F.T., and Ryan, J.D., 1962, Cloverly-Lakota and Fall River paleocurrents in the Wyoming Rockies: Wyoming Geological Association 17th Annual Field Conference Guidebook, p. 44-61.

MacLeod, M.L., 1981, The Pacific Creek anticline: buckling above a basement thrust fault: University of Wyoming Contributions to Geology, v. 18, p. 143-160.

Martinsen, O.J., Martinsen, R.S., and Steidtmann, J.R., 1993, Mesaverde Group (Upper Cretaceous), southeastern Wyoming, USA: allostratigraphy versus sequence stratigraphy in a tectonically active area: American Association of Petroleum Geologists Bulletin, v. 77, p. 1351-1373.

Martinsen, R.S., 1982, Stratigraphic compartmentalization of reservoir sandstones: examples from the Muddy Sandstone, Powder River Basin, Wyoming and Montana: University of Wyoming Geology and Geophysics Department, report for the Gas Research Institute, #GRI 92/0484, 69 p.

Martinsen, R.S., and Marrs, R.W., 1985, Comparison of major lineament trends to sedimentary rock thicknesses and facies distribution, Powder River Basin, Wyoming: Fourth Thematic Conference, Remote Sensing for Exploration Geology, San Francisco, California, p. 1-11.

Martinsen, R.S., and Tillman, R.W., 1989, Haystack Mountains Formation: Wyoming Geological Association 40th Annual Field Conference Guidebook, p. 263-268.

McCubbin, D.G., 1969, Cretaceous strike-valley sandstone reservoirs, northwestern New Mexico: American Association of Petroleum Geologists Bulletin, v. 52, p. 2114-2140.

McGookey, D.P., Haun, J.D., Hale, L.A., Goodell, H.G., McCubbin, D.G., Weimer, R.J., and Wulf, G.R., 1972, Cretaceous System, *in* Mallory, W.W., editor, Geologic atlas of the Rocky Mountain region: Denver, Colorado, Rocky Mountain Association of Geologists, p. 190- 228.

Merewether, E.A., 1983, The Frontier Formation and mid-Cretaceous orogeny in the foreland of southwestern Wyoming: The Mountain Geologist, v. 20, p. 121-138.

Merewether, E.A., and Cobban, W.A., 1986, Biostratigraphic units and tectonism in the mid-Cretaceous foreland of Wyoming, Colorado and adjoining areas, *in* Peterson, J.A., editor, Paleotectonics and sedimentation in the Rocky Mountain region, United States, American Association of Petroleum Geologists Memoir 41, p. 443-468.

Merewether, E.A., Cobban, W.A., and Cavanaugh, E.T., 1979, Frontier Formation and equivalent rocks in eastern Wyoming: The Mountain Geologist, v. 16, p. 67-102.

Mitrovica, J.X., Beaumont, C., and Jarvis, G.T., 1989, Tilting of continental interiors by the dynamical effects of subduction: Tectonics, v. 8, p. 1079-1094.

Obradovich, J.D., in press, A Cretaceous time scale, *in* Caldwell, W.G.E., and Kauffman, E.G., editors, Mesozoic evolution of the Western Interior basin of North America: Geological Association of Canada Special Paper 39.

Obradovich, J.D., and Cobban, W.A., 1975, A time-scale for the Late Cretaceous of the Western Interior of North America, *in* Caldwell, W.G.E., editor, The Cretaceous System in the Western Interior of North America: Geological Association of Canada Special Paper 13, p. 31-54.

Parrish, J.T., Gaynor, G.C., and Swift, D.J.P., 1984, Circulation in the Cretaceous Western Interior Seaway of North America, review, *in* The Mesozoic of middle North America: Canadian Society of Petroleum Geologists Memoir 9, p. 221-231.

Perman, R.C., 1990, Depositional history of the Maastrichtian Lewis Shale in south-central Wyoming: deltaic and interdeltaic, marginal marine through deep-water marine environments: American Association of Petroleum Geologists Bulletin, v. 74, p. 1695-1717.

Pitman, W.C., III, 1978, Relationship between eustasy and stratigraphic sequences of passive margins: Geological Society of America Bulletin, v. 89, p. 1389-1403.

Price, R.A., 1973, Large-scale gravitational flow of supracrustal rocks, southern Canadian Rockies, *in* DeJong, K.A., and Scholton, R., editors, Gravity and tectonics: Wiley Interscience, New York, p. 491-502.

Reeside, J.B., Jr., and Cobban, W.A., 1960, Studies of the Mowry Shale (Cretaceous) and contemporary formations in the United States and Canada: U.S. Geological Survey Professional Paper 355, 126 p.

Reynolds, M.W., 1976, Influence of recurrent Laramide structural growth on sedimentation and petroleum accumulation, Lost Soldier area, Wyoming: American Association of Petroleum Geologists Bulletin, v. 60, p. 12-33.

Roehler, H.W., 1990, Stratigraphy of the Mesaverde Group in the central and eastern greater Green River Basin, Wyoming, Colorado, and Utah: U.S. Geological Survey Professional Paper 1508, 52 p.

Ryer, T.A, 1977, First Day, Coalville and Rockport areas, Utah: The Mountain Geologist, v. 14, p. 105-128.

_____ 1983, Transgressive-regressive cycles and the occurrence of coal in some Upper Cretaceous strata of Utah: Geology, v. 11, p. 207-210.

_____ 1993, Multiple origins of clastic wedges in the Western Interior foreland basin - A stratigrapher's approach: Montana Geological Society Newsletter, v. 37, no. 1, p. 2.

Salat, T.S., and Steidtmann, J.R., 1991, Provenance, dispersal, and tectonic significance of the Evanston Formation and Sublette Range Conglomerate, Idaho-Wyoming-Utah thrust belt: The Mountain Geologist, v. 28, p. 25-36.

Schmitt, J.G., 1982, Origin and sedimentary tectonics of Upper Cretaceous Frontier Formation conglomerates in the Wyoming-Idaho-Utah thrust belt [Ph.D. dissertation]: Laramie, University of Wyoming, 225 p.

Schmitt, J.G., and Steidtmann, J.R., 1990, Interior ramp-supported uplifts: implications for sediment provenance in foreland basins: Geological Society of America Bulletin, v. 102, p. 494-501.

Schwartz, R.K., and DeCelles, P.G., 1988, Cordilleran foreland basin evolution in response to interactive Cretaceous thrusting and foreland partitioning, southwestern Montana, *in* Schmidt, C.J., and Perry, W.J., editors, Interaction of the Rocky Mountain foreland and the Cordilleran thrust belt: Geological Society of America Memoir 171, p. 489-514.

Siemers, C.T., 1975, Paleoenvironmental analysis of the Upper Cretaceous Frontier Formation, northwestern Bighorn Basin, Wyoming: Wyoming Geological Association 27th Annual Field Conference Guidebook, p. 85-100.

Slack, P.B., 1981, Paleotectonics and hydrocarbon accumulation, Powder River Basin, Wyoming: American Association of Petroleum Geologists Bulletin, v. 65, p. 730-743.

Slingerland, R.L., 1992, The great Western Interior Seaway: Earth and Mineral Sciences, v. 61, no. 3, p. 56-61.

Spearing, D.R., 1976, Upper Cretaceous Shannon Sandstone: an offshore shallow marine sand body: Wyoming Geological Association 28th Annual Field Conference Guidebook, p. 65-72.

Steidtmann, J.R., and Middleton, L.T., 1991, Fault chronology and uplift history of the southern Wind River Range, Wyoming: implications for Laramide and post-Laramide deformation in the Rocky Mountain foreland: Geological Society of America Bulletin, v. 103, p. 472-485.

Tankard, A.J., 1986, Depositional response to foreland deformation in the Carboniferous of eastern Kentucky: American Association of Petroleum Geologists Bulletin, v. 70, p. 853-868.

Tillman, R.W., and Martinsen, R.S., 1984, The Shannon shelf-ridge sandstone complex, Salt Creek anticline area, Powder River Basin, Wyoming, *in* Tillman, R.W.,

and Siemers, C.T., editors, Siliciclastic shelf sedimentation: Society of Economic Paleontologists and Mineralogists Special Publication 34, p. 85-142.

Walcott, R.I., 1970, Isostatic response to loading of the crust in Canada: Canadian Journal of Earth Sciences, v. 7, p. 716-726.

Walker, R.G., and Bergman, K.M., 1993, Shannon Sandstone in Wyoming: a shelf-ridge complex reinterpreted as lowstand shoreface deposits: Journal of Sedimentary Petrology, v. 63, p. 839-851.

Weimer, R.J., 1960, Upper Cretaceous stratigraphy, Rocky Mountain area: American Association of Petroleum Geologists Bulletin, v. 44, p. 1-20.

_____ 1961, Uppermost Cretaceous rocks in central and southern Wyoming, and northwest Colorado: Wyoming Geological Association 16th Annual Field Conference Guidebook, p. 17-28.

_____ 1980, Recurrent movements on basement faults, a tectonic style for Colorado and adjacent areas, *in* Kent, H.C., and Porter, K.W., editors, Colorado geology: Denver, Colorado, Rocky Mountain Association of Geologists symposium, p. 23-35.

_____ 1983, Relation of unconformities, tectonics and sea level changes, Cretaceous of the Denver Basin and adjacent areas, *in* Reynolds, M.W., and Dolly, E.D., editors, Mesozoic paleogeography of west-central United States: Society of Economic Paleontologists and Mineralogists, Rocky Mountain Section, Rocky Mountain Paleogeography Symposium 2, p. 359-376.

Wiltschko, D.V., and Dorr, J.A., Jr., 1983, Timing of deformation in overthrust belt and foreland of Idaho, Wyoming and Utah: American Association of Petroleum Geologists Bulletin, v. 67, p. 1304- 1322.

Winn, R.D., Jr., Bishop, M.G., and Gardner, P.S., 1985, Lewis Shale, south-central Wyoming: shelf, delta front and turbidite sedimentation: Wyoming Geological Association 36th Annual Field Conference Guidebook, p. 113-130.

Frontispiece. The leading edge of the Prospect thrust system (i.e., Cliff Creek thrust) exposed at Battle Mountain, Hoback River Canyon area, Wyoming. At this locality, the Jurassic (?)-Triassic (?) Nugget Sandstone is thrust onto vertebrate fossil-bearing sandstone and claystone of the Paleocene Hoback Formation. Photograph by Jack Rathbone.

An overview of the geologic structure of the thrust belt in Wyoming, northern Utah, and eastern Idaho

Frank Royse, Jr.
6984 Urban Street
Arvada, Colorado 80004

Abstract

The Cordilleran thrust belt in Wyoming, northern Utah, and eastern Idaho is composed of five major thrust fault systems arranged in an eastward overlapping array. They are (from west to east with time intervals of major motion): Paris-Willard (Aptian? through Albian); Meade-Laketown (Cenomanian through Turonian); Crawford (Coniacian through Santonian); Absaroka (Santonian through Early Paleocene); and Darby (Paleocene through Early Eocene). The Darby system includes the Granite Creek, Prospect, Game Hill, Hogsback, and Jackson thrusts.

Each major thrust system contains more than one significant thrust fault, which may have more than one time of movement. Maximum displacement of the whole system including folds was about 103 miles (165 km), and total shortening was about 70%. Together, the thrust sheets form an east-tapering wedge bounded below by a regional décollement within basal Cambrian shale and carbonate that overlies autochthonous Cambrian sandstone and crystalline Archean basement. Basement is anomalously involved in thrusting in the central Wasatch Range. The Paris-Willard and Meade-Laketown thrust sheets include a thick Proterozoic clastic section not seen in thrust sheets farther east. The fault surfaces have a ramp-flat geometry that is controlled by stratification and lithologic changes, with Paleozoic carbonate and sandstone forming the main thrust sheet struts. The general convex eastward map configuration appears to reflect the prethrust thickness pattern of Jurassic, Triassic, and Paleozoic rocks. Post-Campanian phases of thrusting coincide with times of foreland basement deformation (such as the Wind River uplift) that interrupted the simple "foredeep" sedimentary basin pattern that existed earlier. The Uinta Mountains foreland uplift appears to be linked directly to the thrust sheets via the merger of the Hogsback thrust fault and the North Flank fault. Widespread normal faults of post-early Eocene to Holocene age form large half grabens and commonly merge with thrust faults, reactivating them as extensional faults. Fission-track data indicate significant Neogene uplift of the Wasatch fault hanging wall along the western thrust belt margin.

Introduction

The thrust belt of western Wyoming, northern Utah, and eastern Idaho is one of the first where major "thin-skinned" thrust sheets were recognized as a distinct tectonic style, and geologic endeavors there have played a major role in the development of understanding thrust belts worldwide (**Figure 1**).

Royse, Frank, Jr., 1993, An overview of the geologic structure of the thrust belt in Wyoming, northern Utah, and eastern Idaho, *in* Snoke, A.W., Steidtmann, J.R., and Roberts, S.M., editors, Geology of Wyoming: Geological Survey of Wyoming Memoir No. 5, p. 272-311.

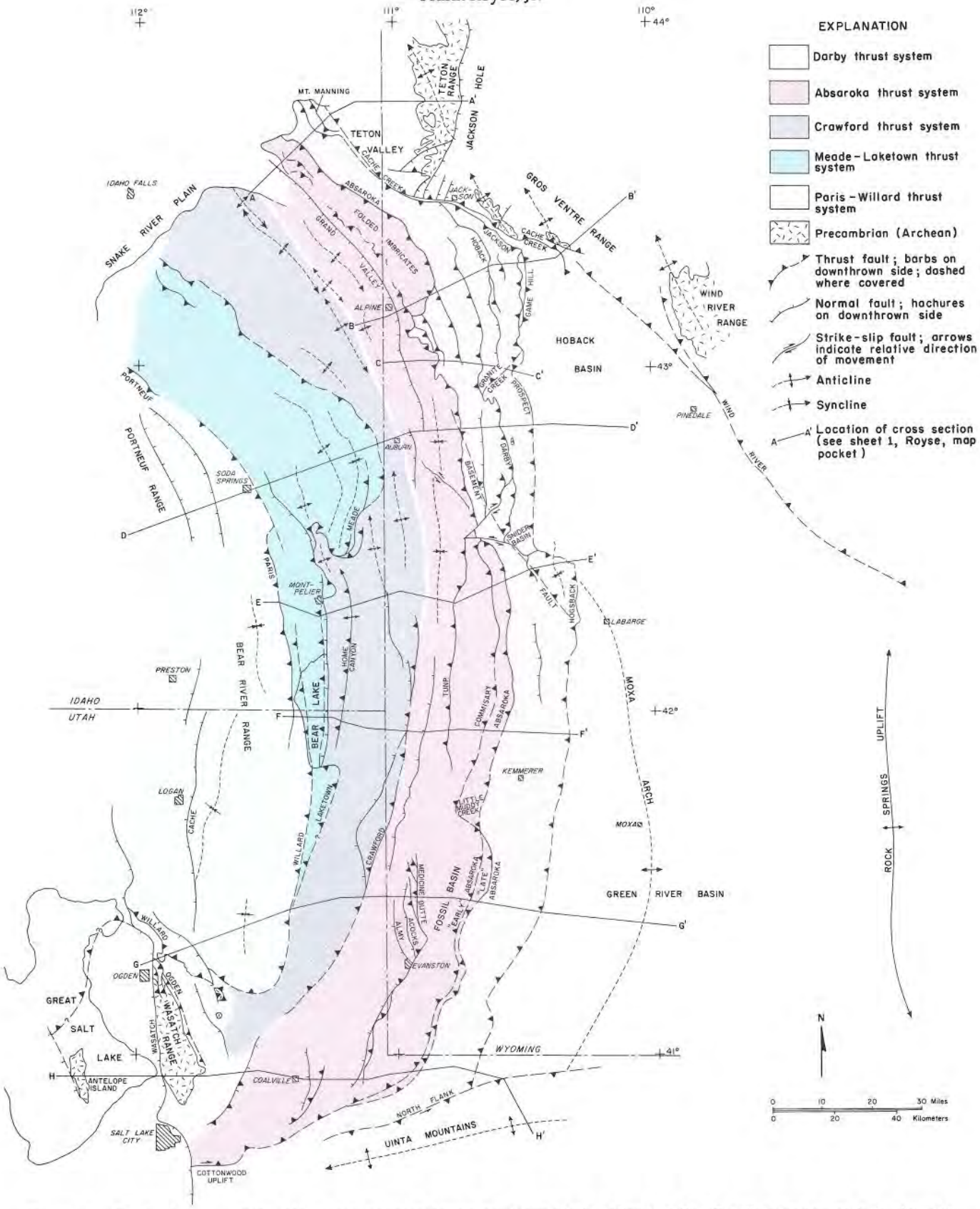

Figure 1. Tectonic map of the Wyoming-eastern Idaho-northern Utah salient of the Cordilleran thrust belt showing principal thrust faults and thrust fault systems, extensional faults, and major fold axes. Uncertainty of division between Crawford and Absaroka systems is indicated by white areas.

The area described is a part of the Cordilleran thrust belt of Cretaceous and early Tertiary age, which is about 100 miles (160 km) wide and extends more or less continuously from the Brooks Range in Alaska to Mexico, a distance of nearly 3,000 miles (4,800 km).

This paper presents a descriptive overview of the structure of the thrust belt in Wyoming and adjacent areas, and highlights certain features of special interest. The paper is intended to inform the geologist unfamiliar with the area as well as to offer ideas and interpretations for the consideration of those with local expertise. Toward this end, a tectonic index map (**Figure 1**), a series of eight regional structural cross sections (**Sheet 1**, Royse, map pocket) and a series of eight regional restored stratigraphic isopach maps (**Figure 2**) of the entire Phanerozoic section involved in thrusting are presented as key illustrations along with several supportive diagrams. The units included in each isopach map are bounded by regional stratigraphic markers, which, considering the large area, are as near to time lines as possible. A relatively flat surface topography is assumed, so that isopachs are considered to reflect basement structure at a small scale at the end of the different time periods. It is recommended that the reader of this paper use the published state geologic maps (1:500,000) for reference.

General summary

Thrusting in Wyoming and adjacent areas was episodic albeit quasi-continuous during at least a 70 million year time period from Early Cretaceous (Aptian?) until middle Eocene. A westward thickening wedge of mostly shallow-water marine sediments of Proterozoic through Jurassic age was thrust eastward on several major thrust fault systems. Synorogenic clastic debris was shed eastward from the rising thrust sheets into adjacent subsiding basins and then incorporated into younger thrust sheets and subsequently recycled into younger basins as deformation proceeded eastward onto the craton. These deposits include coarse conglomerate, thick coal-bearing fluvial and deltaic strata, and marine shale rich in organic carbon. Major marine regressions, widespread floods of conglomerates, and general increase in rates of deposition probably indicate times of major thrusting. Advances in paleontologic (mostly palynologic) dating techniques applied to these deposits have made possible a reasonable reconstruction of the tectonic history. Times of movement on specific major faults can be bracketed by dating angular unconformities and synorogenic clastic rocks, and by provenance and sedimentologic studies. Problems in dating thrust faults in this area are discussed in some detail by Oriel and Armstrong (1966) and in general by Jordan and others (1988).

The major thrust systems as defined in this report and the time intervals of major displacement are (from west to east): Paris-Willard (Aptian? through Albian); Meade-Laketown (Cenomanian through Turonian); Crawford (Coniacian through Santonian); Absaroka (Santonian through Early Paleocene); and Darby (Paleocene through Early Eocene) (**Figure 1**). Each of these thrust systems contains more than one significant thrust fault. Although major thrust displacement progressed in time toward the east, parts of each system were reactivated or imbricated by younger thrusts. Older thrust sheets became integral parts of younger ones and consequently underwent uplift and deformation subsequent to their major displacement. The eastward younging of major displacements and minor subsequent reactivations appear to be a consequence of the continuous maintenance of the eastward tapering wedge shape of the thrusted section, perhaps as hypothesized by Chapple (1978) and Davis and others (1983). Time intervals of motion on major thrusts probably overlapped. Maximum displacement of the whole system was about 103 miles (165 km), and total displacement on individual thrust faults is as much as 40 miles (64 km) according to this interpretation. Apparent along-strike displacement changes are not completely understood in some cases.

A wealth of geologic data indicate that the Archean crystalline basement was not involved in thrusting except in the central Wasatch Range, north of Salt Lake City, Utah, and that a regional décollement existed within basal Cambrian shale and carbonate near the top of the Archean basement for the Crawford, Absaroka, and Darby thrust systems. The Paris-Willard and Meade-Laketown thrust systems include a thick Proterozoic clastic section not seen in thrust sheets farther east. The Paris-Willard is the oldest and structurally highest major thrust sheet.

The thrust fault surfaces have a ramp-flat geometry similar to that described by Rich (1934) in the southern Appalachian Valley and Ridge province. The fault configuration is controlled by stratification

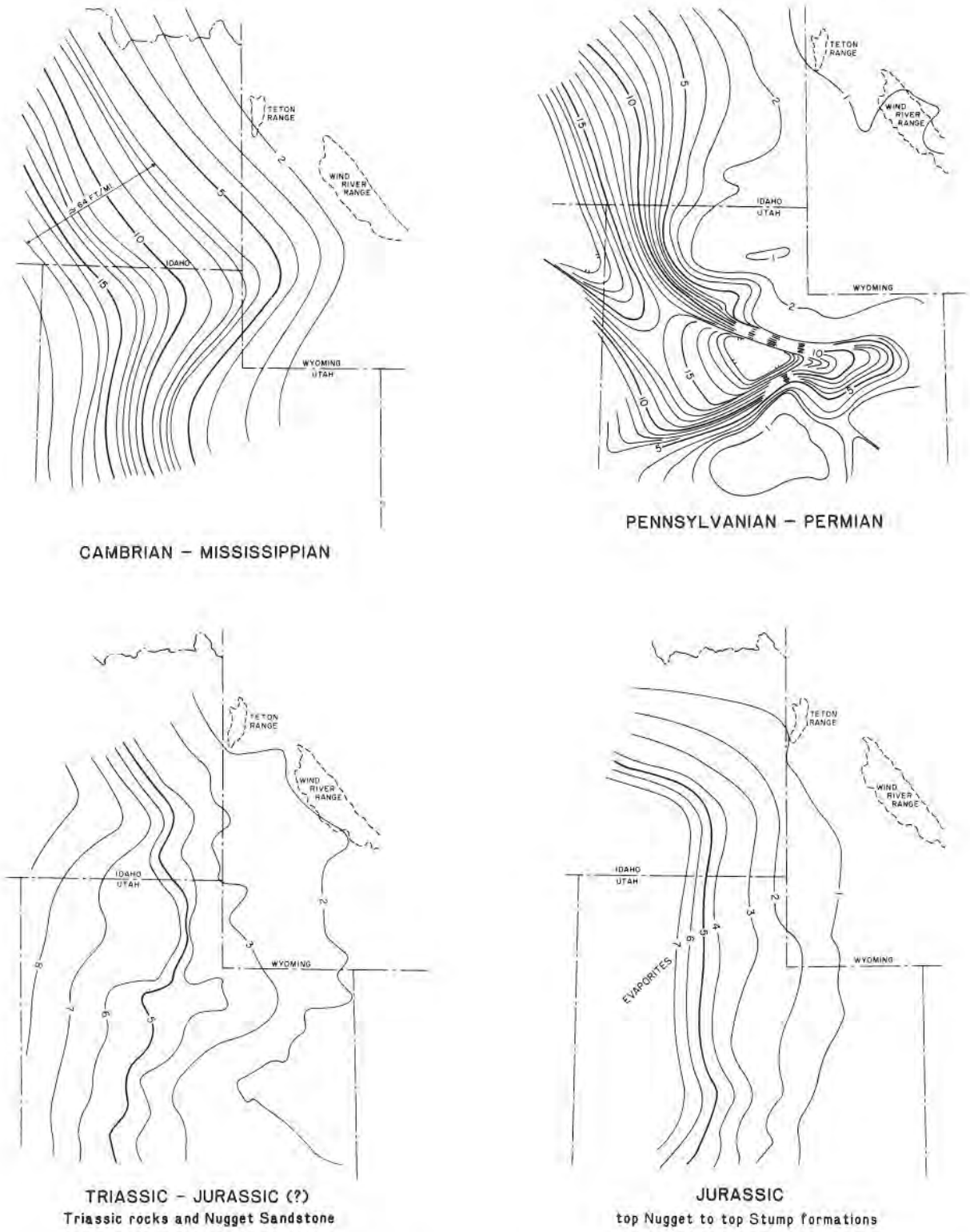

Figure 2. Eight isopach maps of Phanerozoic sediments restored to pre-deformed shape. Contour interval = 1,000 ft. Political boundaries and geographic features are current and remain fixed. Contours are restored to their position at time of top of interval. Faults shown provided major source terrains for the interval. Open teeth denote inactive and solid teeth denote active faults during the time interval shown. The Cretaceous and Tertiary isopach intervals do not specifically match the time intervals of motion of major thrust systems.

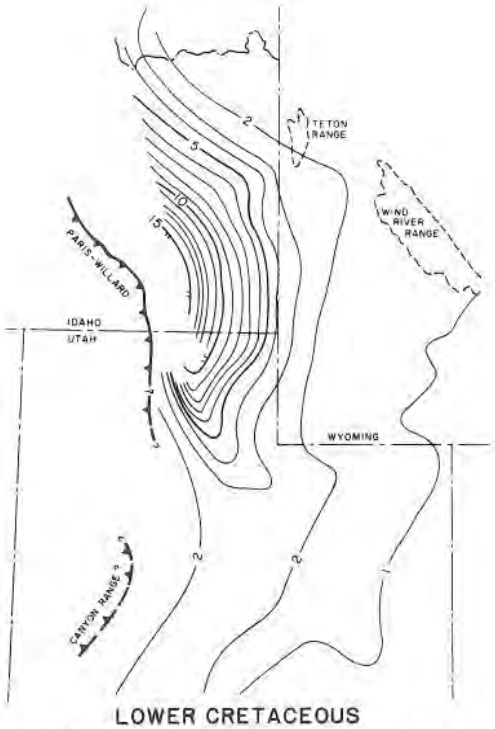

LOWER CRETACEOUS
top Stump to top Mowry – Aspen formations

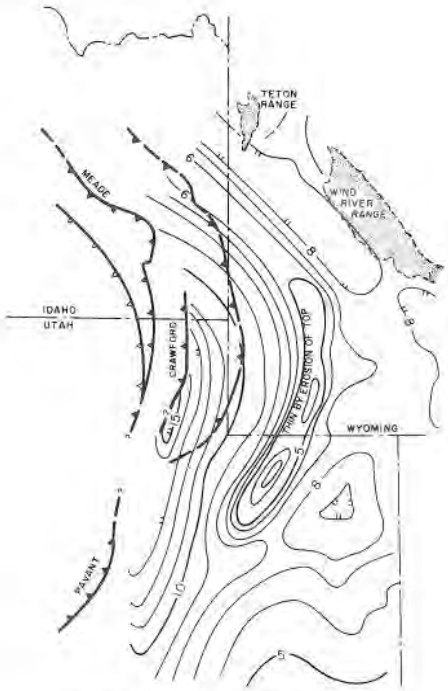

CENOMANIAN – CAMPANIAN
top Mowry – Aspen to top Adaville
("Mesaverde") formations

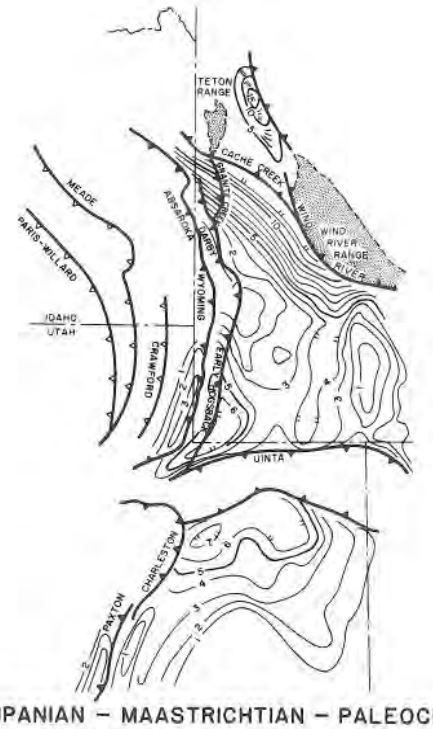

CAMPANIAN – MAASTRICHTIAN – PALEOCENE
Evanston – Fort Union – Hoback formations

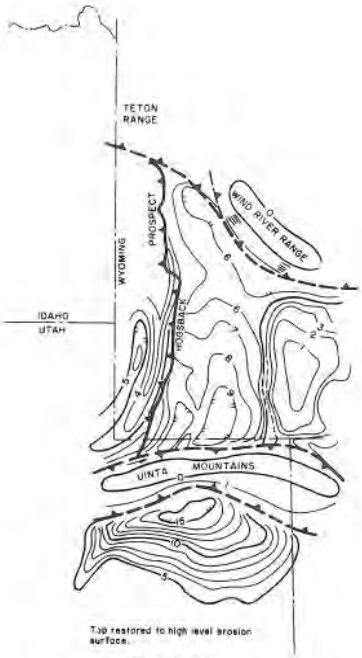

EOCENE
Wasatch – Green River formations

Figure 2. *(Continued)*

and by lithologic and thickness changes in the sediments. Structurally weak layers such as Cambrian shale, Triassic and Jurassic evaporite, and Cretaceous shale and coal gather faults, and contain extensive flats, whereas ramps tend to form in rocks that are relatively more competent such as Paleozoic carbonate and Jurassic sandstone. Seismic reflection data indicate that the angle between bedding and fault for major ramps in the Absaroka and Darby thrust systems is generally 25° to 35°. Transport of nearly flat-lying beds over these ramps created folds and promoted imbrication within the thrust plates. Ramps may be oriented at any angle to net slip direction; movement over lateral ramps resulted in complex plunging structures transverse to regional strike. Extensive flats are the sites of "piggyback" basins such as the Fossil Basin.

The thrust plates have been cut by numerous, mostly west-dipping normal (extensional) faults of post early Eocene to Holocene age, such as the Hoback and Grand Valley faults (**Figure 1**). These faults have imparted a significant amount of east-west horizontal extension—probably 6 miles (10 km) or so—to the entire thrust belt. Many of these normal faults are known to merge with or terminate against the older thrust faults, thus reactivating them as extensional faults. Beds on the down-thrown side of normal faults commonly are rotated so as to dip into the fault, creating folds that are products of extension, not compression.

History of investigations

Geologic investigations in the general area of the thrust belt began as early as 1870, with government sponsored surveys headed by F.V. Hayden and Clarence King. By 1916, most of the major tectonic features had been identified and named, in spite of rugged field conditions. Major contributors to this phase of mapping were A.C. Peale (1879), Orestes St. John (1879), A.C. Veatch (1907), A.R. Schultz (1914), and G.R. Mansfield (1927) and their many assistants. Veatch was especially perceptive, early to recognize and interpret the thrust-faulted terrain in spite of the fact that the area he mapped in southwest Wyoming has much Tertiary cover and very complex structure and stratigraphy. A more detailed surface mapping program by geologists of the U.S. Geological Survey followed, and continues sporadically to the present. This mapping program derived impetus first from the need to evaluate phosphate and coal deposits noted by early workers, and later from a need to evaluate oil and gas potential and recreational and wilderness aspects, since most of the land involved was owned by the government. Among the many outstanding geologists who contributed to this program were W.W. Rubey and S.S. Oriel, whose maps are still the standard. Landmark publications by Cressman (1964), Armstrong and Oriel (1965), Oriel and Armstrong (1966), and Rubey and Hubbert (1959) introduced what might be considered the modern era of Wyoming-eastern Idaho thrust belt geology.

The discovery of oil and gas in commercial quantities during the 1970s resulted in a literal explosion of expensive subsurface information mostly in the form of drill hole, reflection seismic, and paleontologic (mostly palynologic) data. Timely development of common depth point (CDP) digital portable seismic techniques was especially critical. Integration of these data with conventional surface maps provides a three-dimensional view that allows a resolution of structure not seen in other thrust belts. Use of palynology provides a time dimension when applied to synorogenic deposits.

Understandably, increase in data resulted in a marked increase in publications. Royse and others (1975) published one of the first papers to combine drill hole, seismic, aeromagnetic, palynologic, and surface work, along with a new appreciation of geometric constraints on structural form, to present a general quantitative picture of thrust belt structure. Blackstone (1977) applied his wide knowledge of Rocky Mountain tectonics to present an overview of this part of the Cordilleran fold-and-thrust belt. Jordan (1981) presented a thoughtful analysis of Cretaceous foreland basin evolution, which quantified the relationship between thrust sheet emplacement, subsidence, and deposition of synorogenic deposits. Dixon (1982) published a regional structural synthesis based mostly upon seismic data. Wiltschko and Dorr (1983) presented an indepth review of evidence used to date thrusting. Lamerson's (1982) paper on the Fossil Basin area is a good example of work that makes maximum use of valuable subsurface and palynologic data, much of which is not generally available. Many other valuable articles appear in thrust belt symposium guidebooks published by the Rocky Mountain Association of Geologists and the Wyoming Geological Association.

Generalized stratigraphy

In a regional sense, four main periods of sedimentation are generally recognized based on original tectonic setting. First, there was an early miogeoclinal stage made up of a westward thickening wedge of Proterozoic through mid-Devonian shallow-water marine beds that were deposited as a passive margin sequence along the rifted border of the craton. A second stage, from late Devonian through Jurassic time, consisted of marine sedimentation in successively eastward shifting basins associated with the mid-Paleozoic Antler and Permian-Pennsylvanian Ancestral Rocky Mountain orogenies and Jurassic magmatism and uplift in the west (Hintze, 1988). A third stage, during Cretaceous and early Tertiary, was characterized by thick eastward thinning synorogenic shallow-marine and continental sediments derived mostly from thrust sheets and deposited in basins that migrated eastward onto the foreland along with the eastward migration of thrust sheets. Later phases of this stage, in latest Cretaceous and early Tertiary, had mixed sources from foreland uplifts as well as thrust sheets. A fourth stage consisted of post-orogenic continental redbeds that were deposited during extensional deformation in mid-Eocene(?) to Holocene; they include significant thicknesses of lacustrine and volcanic ash beds and, in the north, basalt.

A series of restored isopachs (**Figure 2**), a generalized stratigraphic column (**Figure 3**), a diagram of synorogenic deposits (**Figure 4**), and cross sections of Lower Paleozoic and Precambrian rocks (**Figure 5**) illustrate certain important aspects of the stratigraphy. Other summaries can be found in Armstrong and Oriel (1965) and Peterson (1987). Hintze (1988) presented a valuable comprehensive summary of the Utah area. Complex correlations and terminology of Cretaceous and lower Tertiary rocks were well illustrated by Wiltschko and Dorr (1983). The total pre-Cretaceous (pre-thrusting) sedimentary section (excluding Proterozoic) that is involved in thrusting formed a west thickening wedge about 7,000 feet (2 km) thick on the east and 45,000 feet (14 km) thick on the west. The shape of the crystalline basement surface before thrusting was nearly planar, and its dip varied from about 3° on the east to as much as 6° on the west. Control exerted by stratigraphy upon structure will be mentioned in subsequent sections.

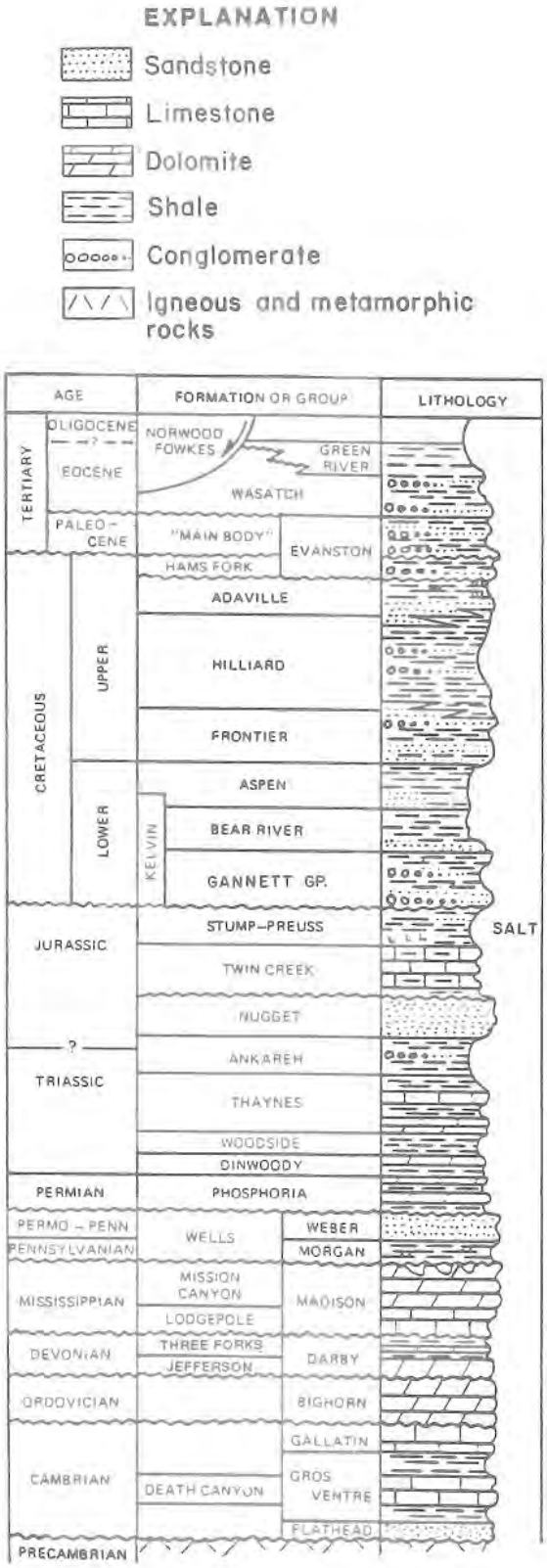

Figure 3. Generalized stratigraphic column of the Wyoming portion of the thrust belt (from Lamerson, 1982).

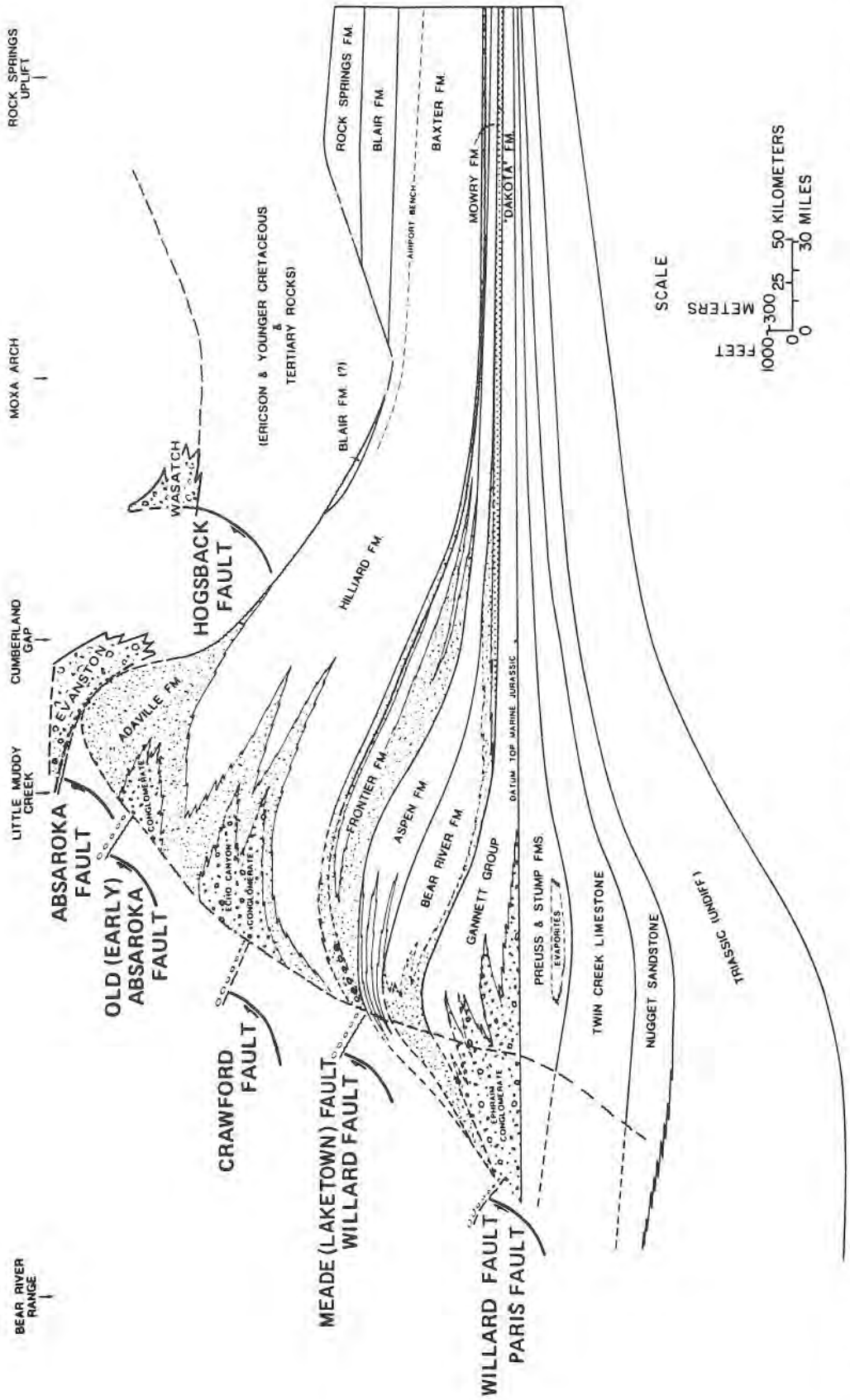

Figure 4. Stratigraphic diagram of restored Mesozoic rocks in western Wyoming and northern Utah, showing general relationship between thrust faulting and sedimentation. Line of section lies between cross sections G-G' and H-H' of Sheet 1. (Modified from Royse and others, 1975.)

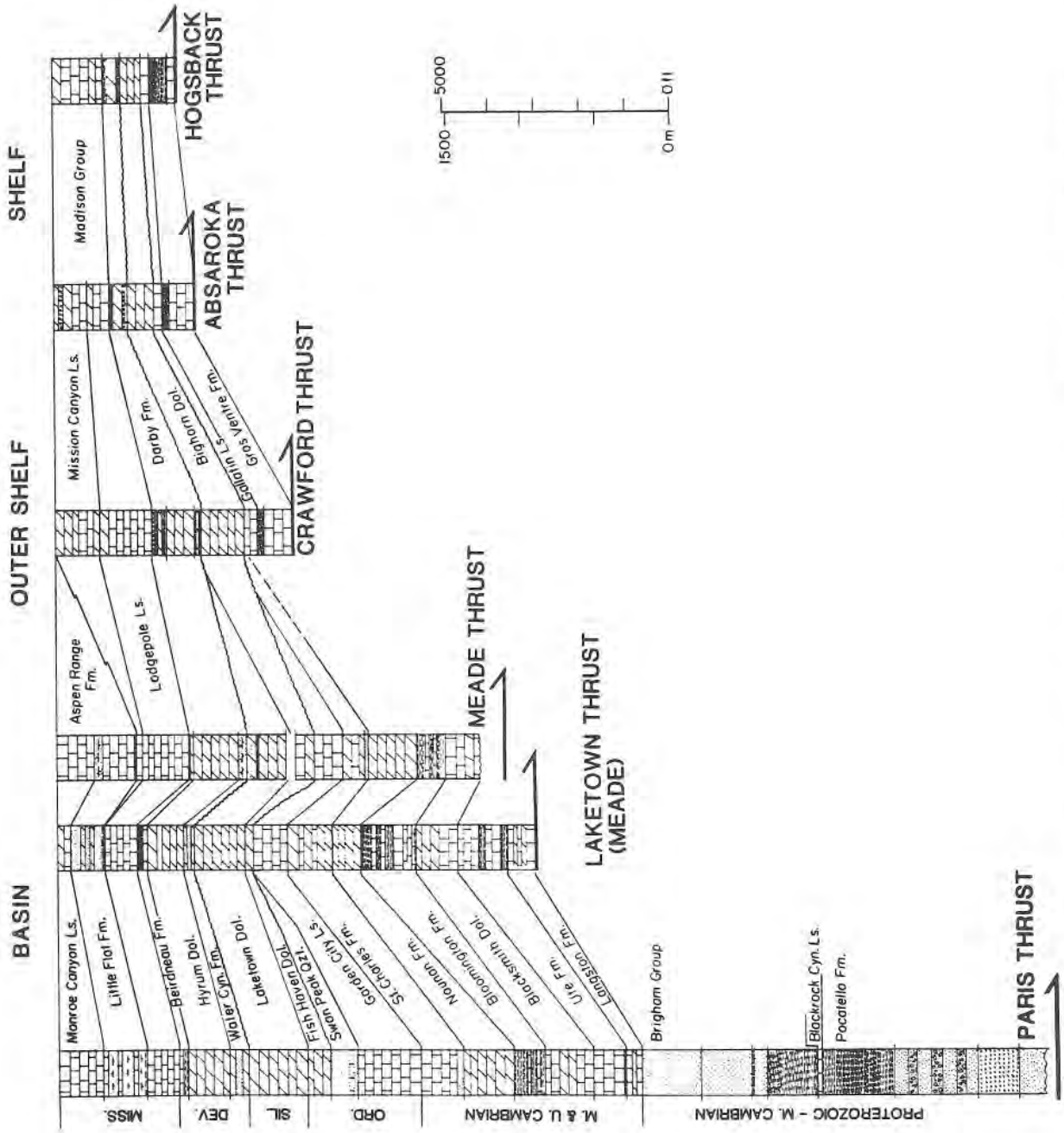

Figure 5A. Composite Paleozoic thrust sheet stratigraphy from surface and well data for the central part of the thrust belt (from Coogan and Royse, 1990). Information for the Meade thrust hanging wall is from the American Quasar #22-1 Jensen, sec. 22, T13N-R44E, and from the Ladd #3-24 Bennington, sec. 3, T12N-R44E, in Bear Lake County, Idaho.

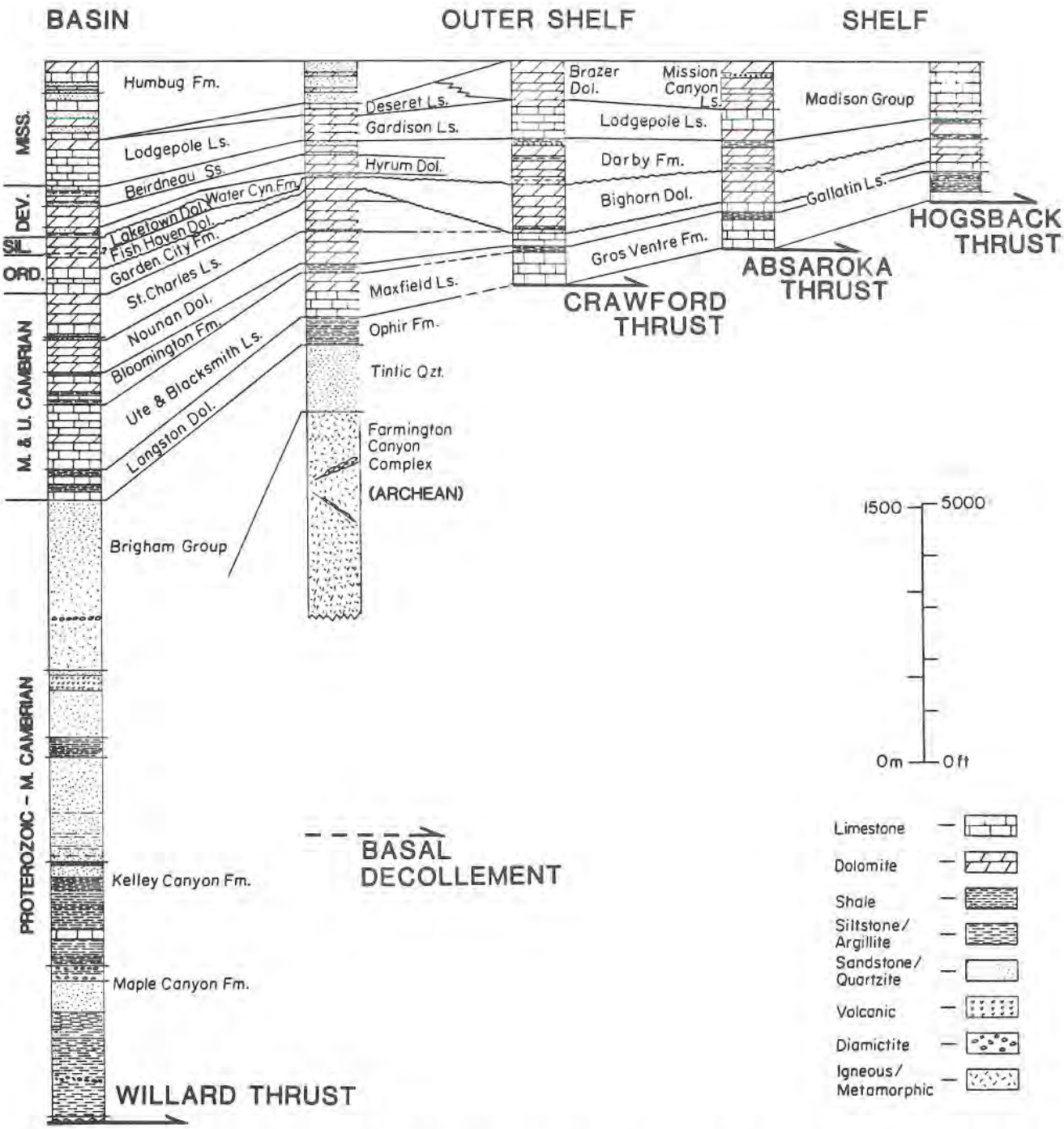

Figure 5B. Composite Paleozoic thrust sheet stratigraphy from surface and well data for the southern part of the thrust belt (from Coogan and Royse, 1990).

Precambrian rocks are represented by two major units: (1) a crystalline complex composed of gneiss, schist, amphibolite, and quartz monzonite of Archean age, and (2) a slightly metamorphosed, rift-phase clastic sequence of Middle (?) and Late Proterozoic age as thick as 20,000 feet (6 km). According to Bryant (1988), the Archean crystalline rocks (Farmington Canyon Complex) were metamorphosed under granulite(?) facies conditions about 2,600 Ma and remetamorphosed under amphibolite facies conditions about 1,790 Ma. These rocks crop out only within the western part of the thrust belt in the central Wasatch Range south and east of Ogden, Utah, where they are involved in thrusting with Lower Paleozoic rocks. They are characterized by many shallow-dipping, anastomosing mylonitic shear zones, which exhibit retrograde metamorphism under greenschist conditions according to Bryant (1988). Rocks of similar age and lithologies probably form the basement under most of the thrust belt and also comprise the core of nearby major foreland uplifts such as the Teton, Gros Ventre, and Wind River.

Proterozoic clastic rocks (quartzite, siltite, argillite) crop out along the western margin of the thrust belt in the Bear River and North Wasatch ranges, where they comprise the basal part of the Paris-Willard thrust sheet. They also crop out to the south in the Uinta Mountains and Cottonwood uplift east of Salt Lake City, Utah. The Uinta Mountains was the site of an east-striking Proterozoic aulacogen described by many authors (e.g., Wallace and Crittenden, 1969; Sears and others, 1982). The source of the clastic strata was the Archean craton (Peterson, 1987). The basement contact upon which these rocks were deposited is exposed within the thrust belt only on Antelope Island in the Great Salt Lake.

Paleozoic rocks within the thrust belt are mostly shallow-water marine limestone, dolomite, and fine-grained sandstone with minor shale, which were deposited along the miogeoclinal border of the craton. They are the dominant structural component of all the major thrust sheets, and their stratigraphy is useful in solving structural problems such as thrust sheet correlation and relative timing (**Figure 5**). Isopachs show that before thrusting, Paleozoic rocks thickened westward from about 2,000 feet (0.6 km) on the Wyoming shelf to about 35,000 feet (11 km) in central Idaho and western Utah. Pennsylvanian and Permian rocks exhibit especially abrupt thickness changes that are probably related to orogeny and faulting of that age, and which subsequently may have localized thrust faulting. Major source area of Paleozoic clastic rocks was the craton (Peterson, 1987).

Triassic and Jurassic rocks crop out extensively throughout the thrust belt except in the westernmost part (Paris-Willard thrust plate), where they have been eroded. They consist mostly of shaley, shallow-water marine carbonate that intertongues eastward with a clastic shaley redbed sequence. An eolian sandstone deposit (Nugget Sandstone) of Early Jurassic age represents a major marine regression. The position of the Triassic-Jurassic systems boundary is in dispute; it may be contained within a regionally correlatable regolith(?) in the upper Ankareh Formation. Isopachs show that, prior to thrusting, Triassic and Jurassic rocks together thickened westward from about 4,000 feet (1.2 km) in western Wyoming to about 15,000 feet (4.6 km) in central Idaho and western Utah. Of special note are thick halite and anhydrite deposits of Late Jurassic age, which play an important role in localizing faults. The glauconitic Stump Formation (Oxfordian) is the youngest pre-thrust marine unit; it provides a useful regional datum for stratigraphic and structural studies.

Cretaceous rocks are a paralic complex of shale, siltstone, and sandstone of mixed fluvial lacustrine, deltaic, and marine origin, which were deposited along the western margin of the intracontinental seaway during the time of thrusting. Coal and conglomerate are important constituents. Sequentially rising thrust plates were source areas on the west. The shoreline migrated eastward in response to the general eastward progression in age of thrusting (**Figure 4**), and fluctuated according to varying rates of thrusting, sediment input, and subsidence. Projection of westward rates of thickening toward the restored position of the the source area show that as much as 15,000 feet (4.6 km) of mostly nonmarine Lower Cretaceous clastic rocks were deposited in a basin (foredeep) adjacent to the Willard-Paris thrust sheet (**Figure 2**). Toward the east, those rocks intertongue with marine shale and rapidly thin to less than 2,000 feet (0.6 km). Pre-Maastrichtian Upper Cretaceous rocks have a similar facies pattern and thin eastward from a maximum of about 15,000 feet (4.6 km) to about 5,000 feet (1.5 km) on the foreland. Eastward thinning in this case is partly due to pre-Maastrichtian erosion of the top of the unit on the Moxa arch.

Angular unconformities separate pre-Maastrichtian rocks from overlying non-marine carbonaceous shale, siltstone, sandstone, and conglomerate of Maastrichtian-Paleocene age. Rocks deposited during this time are assigned to the Evanston Formation in the south and to the Hoback Formation in the north. They are extensively preserved as erosional remnants within the southern part of the thrust belt as far west as the Wasatch Range in northern Utah, where they overlie folded and faulted Paleozoic and Proterozoic rocks of the Paris-Willard thrust sheet. As much as 3,500 feet (1 km) of these rocks lie undeformed upon the Absaroka thrust plate in the central part of the Fossil Basin (Lamerson, 1982). In the northern thrust belt, rocks of the Paleocene Hoback Formation are preserved only as far west as the Clause Peak area near Hoback Canyon, where they lie both angularly upon and are overridden by the Prospect thrust sheet. East of the thrust belt, Maastrichtian(?) - Paleocene rocks thicken markedly eastward into the Hoback Basin toward the Wind River uplift, where thicknesses approach 12,000 feet (3.7 km) (**Figure 2**). Regional thickness and facies patterns for rocks of this age are quite different from the simple symmetrical pattern of older Cretaceous rocks and are as much the result of emplacement of foreland basement uplifts as of thin-skinned thrusting in the thrust belt. Sediment was derived both from sources within the thrust belt and from the Teton-Gros Ventre, Wind River, and Uinta uplifts. Source terrains can be identified by the lithology of the clasts.

Eocene rocks (Wasatch and Green River formations) are a continental, clastic, redbed, intermontane basin-filling sequence that contains significant lacustrine shale and carbonate and volcanic ash. Precise identifications of the Paleocene-Eocene-Oligocene boundaries are uncertain in many localities. Thrust faulting and uplift within the thrust belt proper ended in Early Eocene, and debris from highlands buried most of the southern part. The Uinta, Wind River, and Gros Ventre-Teton mountains were major highland source areas as well as highlands west of the Wasatch Range. Wasatch (Eocene?) redbeds lie on Archean crystalline rocks near the high reaches of the Wasatch Range north of Salt Lake City, Utah. Early Eocene lacustrine and coarse- to fine-grained redbed deposits overlap the eroded toe of the easternmost thrusts (Prospect-Hogsback). Late-stage thrusting produced source areas in ramp positions for isolated "piggyback" depositional basins, which formed over thrust plane flats such as the Fossil Basin (Hurst and Steidtmann, 1986; Coogan, 1989). The Eocene isopach (**Figure 2**) may include Oligocene beds; it is an attempt to show restored thickness prior to erosion and exhumation of basins in Miocene and younger time. The top of the Eocene shown in this illustration is largely in the air and is a projection of the highest regional high-level erosion surface exposed in the Wind River and Uinta mountains.

Post Eocene rocks are a locally derived, discontinuous clastic sequence including cobble conglomerate, siliceous tuffs, and large gravity-slide blocks of older rocks, which were deposited in grabens as they formed within the thrust belt. Thicknesses as great as 10,000 feet (3 km) of Pliocene-Pleistocene rocks crop out in Swan Valley near Alpine, Wyoming. Quaternary basalt occupies valleys in the northern area near the Snake River Plain.

Structural geology

A general view of thrust belt structure is shown by eight regional structural cross sections, which are spaced more or less evenly from north to south (**Sheet 1**, Royse, map pocket). Locations are shown on the index map (**Figure 1**) along with distribution of major tectonic features. The small scale precludes showing much detail, but it is sufficient to show most of the regionally important features. The structure at the surface is fairly well known and has been mostly mapped for some time, thanks to efforts of the U.S. Geological Survey and numerous graduate students. There are areas of uncertainty where exposures are poor and where dating and correlations of synorogenic deposits is poorly constrained (e.g., near the Uinta Mountains and in the northern extremities in eastern Idaho). However, in general, the surface structure is well exposed and accessible. An important aspect that gives this thrust belt the reputation as the best known in the world is the wealth of subsurface data acquired during the past 15 years by oil companies, much of which has filtered out to the general geologic public. The cross sections in this

report (**Sheet 1**, Royse, map pocket) incorporate much of this subsurface information. This is not to say that much interpretation has not been built into these sections, especially in the west. One never has enough data to produce a precisely correct structural section, as anyone who has tried to predict the outcome of a wildcat well will agree. Geometric (volumetric) constraints to section construction in brittle domains, which were well presented by Dahlstrom (1969, 1970), are the primary means of projecting structural forms past areas of control. These sections are believed to be accurate representations of the structural style, considering the large area involved. They are probably not balanced in the sense of being perfectly restorable to pre-deformation configuration; it would be fortuitous if they were. Attention was paid to basic guidelines of section construction such as rough matching of hanging-wall and footwall stratigraphic cutoffs, and transfers of displacement from fault to fold. But the effort and time required to draw precisely balanced sections is not warranted here when one considers the small-scale, the gaps in control, and the changing orientation of the sections to take advantage of well and outcrops (the direction of transport of thrust sheets is considered to be west to east with little deviation). In this case, a precisely balanced section would only mean that one has taken the time to draw it that way and, in the absence of close and detailed control, would be no better than many others that could be drawn using the same data.

These cross sections show that this part of the Cordilleran thrust belt is characterized by several large coherent thrust systems that do not involve the crystalline Archean basement except in the central Wasatch Range north of Salt Lake City, Utah. Structural continuity along strike is better here than in regions north of the Snake River Plain or to the south, in central and southwestern Utah. In those regions, much of the thrust belt structure has been obscured by a combination of Tertiary cover, magmatism, interaction with foreland basement structures, and pronounced overprint by extensional faulting. The major thrust systems can be grouped into two main categories: (1) those in the eastern part, which share a common décollement in lower Cambrian shale, namely the Darby, Absaroka, and Crawford systems; and (2) those in the west, which employ a major décollement in Proterozoic clastic rocks, namely the Meade-Laketown and Paris-Willard systems (Coogan 1987). Thrust faults dip west and each thrust sheet lies in shingled array above the next sheet to the east. Each sheet becomes an integral part of the one to the east, and movement of one affects all of the thrust sheets west of it. This is an important feature when evaluating possible source areas for synorogenic deposits.

Definition of major thrust fault systems, as used here, is largely a matter of scale, and is based on map continuity, fault linkages, common branch line ("liftoff") from a basal décollement, and similar times of major motion. Such a division of the thrust belt into thrust systems is informal, somewhat arbitrary, and not completely consistent as one might expect if the thrust belt is viewed in total as a dynamic linked system of faults that was more or less continuously active over a long time period. As Price (1988) stated, *our perceptions of the nature of thrust faults change with the scale at which we observe them.* At the scale presented here, these systems fall more or less naturally and practically into place, and they are convenient vehicles for discussion. The following sections are a short descriptive discussion of each major thrust fault system in east-to-west order.

Darby thrust system and the Moxa arch

The Darby is the easternmost and youngest (Maastrichtian?-early Eocene) thrust system. Major components are, from north to south, the Mt. Manning, Jackson, Darby, Prospect, Granite Creek, and Hogsback thrusts (**Figure 1**). Probably, more is known about the structure of this system than any other because it has been prospected extensively for oil and gas, and seismic data are generally of good quality; but much controversy remains, especially in regard to timing (e.g., Wiltschko and Dorr, 1983; Dixon, 1982; Kraig and others, 1988; Craddock and others, 1988).

In the interpretation presented here, thrust fault displacement on the Darby system in the northern area totaled as much as 18 miles (29 km) and was accomplished in two major episodes: (1) a Maastrichtian through Early Paleocene phase of 10 to 14 miles (16-23 km), which occurred on the Darby-Granite Creek thrusts, and (2) a mid-Paleocene-Early Eocene phase of 3 to 4 miles (5-6 km), which occurred on the Prospect thrust (**Sheet 1**, Royse, map pocket). (The Hogsback fault in the south is a composite of

Darby and Prospect faults, discussed later). An earliest time limit of Maastrichtian is indicated by outcrops in the Fossil Basin area, where beds of the lower Evanston Formation conform with the west-dipping ramp structure of the Hogsback thrust sheet (e.g., Lamerson, 1982, plate 5). The early Eocene upper time limit is established by the overlap of beds of this age over the trace of the Prospect-Hogsback thrust (Wiltschko and Dorr, 1983). Separation of deformation into two episodes is discussed later.

The Darby system extends in a nearly straight line north from the Uinta Mountains to the Gros Ventre-Teton uplift area, where it bends abruptly and continues northwest across Teton Valley to the Snake River Plain (**Figure 1**). Regional tectonic transport of the hanging wall was west to east so that the northwest aligned part is a manifestation of oblique left-lateral shear. Stratigraphic studies indicate that the Darby system thrust sheets were emplaced during the same time interval that the Gros Ventre-Teton uplift was emplaced on the northeast-dipping Cache Creek thrust. The Teton block overrides rocks of the Darby thrust system (Jackson thrust sheet) at Teton Pass. Structural restoration to pre-Maastrichtian (pre-Darby thrust system) time would move the original site of these features apart by several miles, so the northwest strike of this part of the Darby system must reflect its original shape, a strike more or less in alignment with the Gros Ventre-Teton uplift. The shape of the thrust belt here appears to be controlled by the thickness of the Phanerozoic section and a basement arch that existed between the Teton block and the toe of the Absaroka thrust sheet prior to movement of the Darby thrust system (**Figure 6**). The arch probably was created by the loading and flexural subsidence of the basement under the Gros Ventre-Teton uplift.

Several workers have proposed en masse counterclockwise rotation of thrust sheets (i.e., the older Paris, Meade, and Absaroka sheets) about a vertical axis during and after emplacement. They considered rotation to be caused by a buttressing effect during the uplift of the basement-cored Laramide Gros Ventre-Teton block. This is incorrect because such an interpretation requires large adjustments of rock volume due to bending and refolding of thrust sheets and pronounced along-strike changes in displacement of Darby system thrust sheets, which are not evident. Furthermore, the influence of the buttress would have had to been felt over 50 miles (80 km) to the west in order to bend the Absaroka and Meade thrust sheets. Paleomagnetic data (Eldridge and Van der Voo, 1988) show that counterclockwise rotation of thrusted rocks is confined to the leading edge of the Darby system near where it abuts the Gros Ventre-Teton uplift and is not present in the interior of the thrust belt. This is what would be expected if the zone of actual abutment is a left-lateral oblique-slip shear zone between the toes of the Cache Creek and Darby system faults. Pronounced horizontal slickensides and fault horses of Jurassic rocks within the shear zone near Teton Pass and the left-stepping en echelon arrangement of the Wind River-Gros Ventre-Teton uplifts support this interpretation. Presumably the Archean basement beneath the surface juncture of thrust belt and Teton Range is through-going and unaffected by thrusting.

Southward toward the Uinta Mountains, the Darby thrust system is composed essentially of a single thrust sheet, the Hogsback, which has numerous hanging-wall imbrications. The geometry of the Hogsback sheet is probably the simplest of all the major thrust sheets, having no major deflections (transverse ramps) or changes in stratigraphic position for more than 100 miles (160 km). Although it is mostly covered by lower Eocene redbeds and lacustrine deposits, the position and geometry are well known from drill hole and seismic data (e.g., Delphia and Bombolakis, 1988). Displacement on the Hogsback thrust east of the Fossil Basin area is about 12 miles (19 km), which is somewhat less than the 18 miles (29 km) maximum displacement estimated for the Darby thrust system in the north. In map view, the subcropping toe of the Hogsback thrust strikes nearly south and intersects the Uinta Mountains at a large angle without noticeable deflection or curvature. No buttressing effects are seen. The Uintas were emplaced on a south-dipping (±20°) thrust fault (North Flank thrust, **Sheet 1H**, Royse, map pocket) during and after emplacement of the Hogsback thrust sheet. Since there is no counterpart to the Hogsback thrust sheet in rocks of comparable age, which are completely exposed on the Uinta uplift, it must be concluded that the displacement of the Hogsback sheet either was transferred to the Uinta block, or a zone of low-angle, south-dipping right-lateral shear exists between them. The map pattern is similar to that in the north, with the Gros Ventre-Tetons being the Uinta Mountains counterpart, except there the Prospect thrust fault crops out and its trace swings abruptly northwestward to continue more or less par-

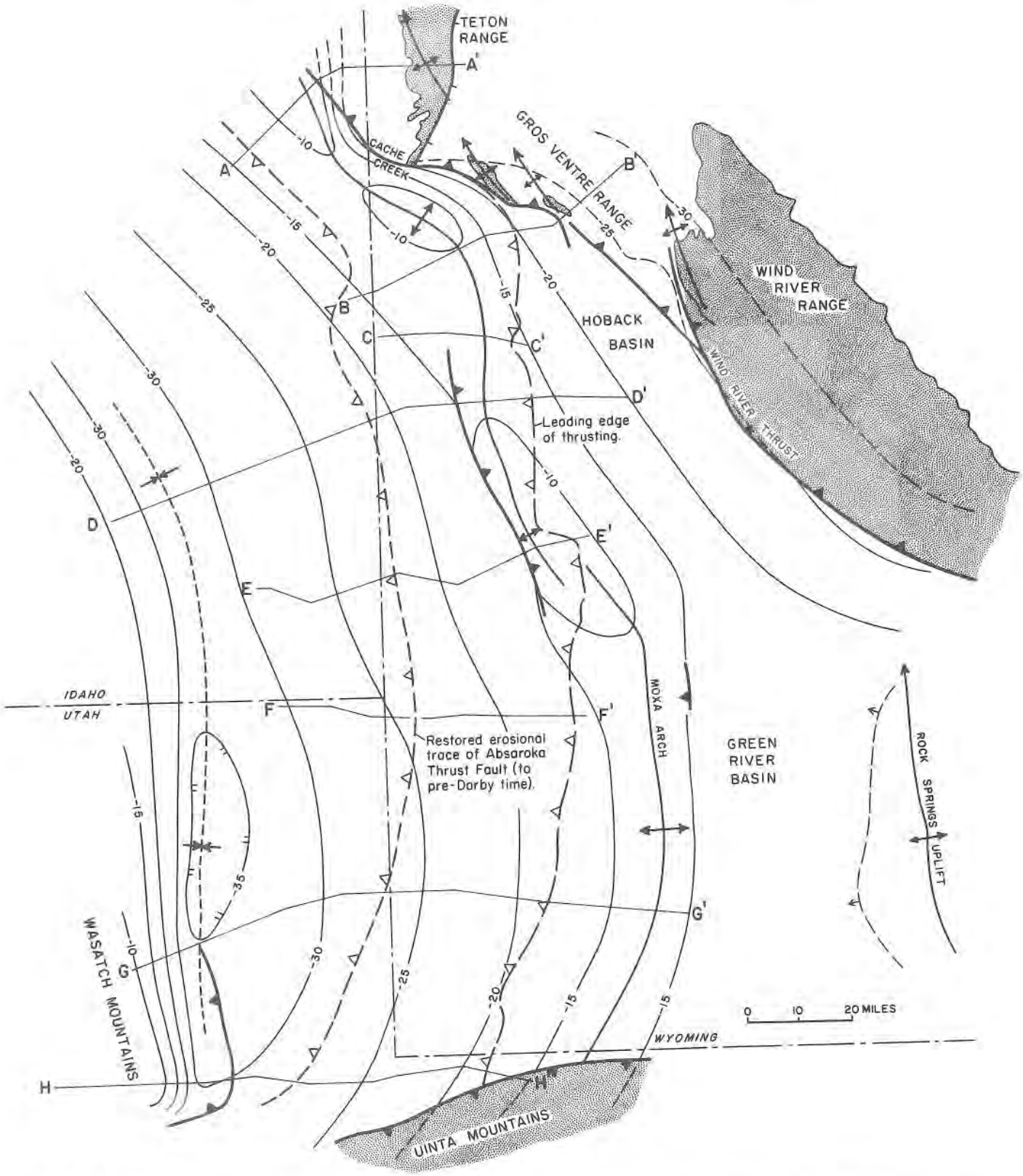

Figure 6. Structure map of top of Archean basement, showing present position of eastern edge of the thrust belt, and the position of the toe of the Absaroka thrust sheet prior to emplacement of the Darby system thrust sheets. Contour interval = 5,000 ft.

allel to the Gros Ventre-Tetons, whereas the Hogsback disappears under the Uinta block. Since the North Flank thrust dies out to the west with the west-plunging Uinta Mountain structure, it appears that the Uinta Mountains are part of the Hogsback thrust sheet and that eastward thrust displacement was transferred to the Uinta block during emplacement by merging of the Hogsback and North Flank thrusts. Bruhn and others (1986) and Bradley and Bruhn (1988) discussed this interpretation and its regional ramifications. It is possible that a similar linkage of basal décollements between thrust sheet and foreland structure exists at basement level between the thrust belt and the Gros Ventre-Teton block.

The area of intersection of the Darby, Prospect, and Hogsback thrust faults northwest of LaBarge, Wyoming, near Snider Basin (**Figure 7**) has been one of much controversy in spite of good surface exposures, many drill holes, and good quality seismic profiles. Many workers now agree that the Prospect fault joins the Darby southward across a lateral ramp in the Prospect fault plane to form the Hogsback thrust fault. The Hogsback is then a composite of the Darby and Prospect faults (Royse and others, 1975).

Below the thrusts in the area of intersection there is a pronounced west-verging, reverse-faulted, basement uplift with at least 8,000 feet (1.5 km) of structural relief (**Figure 6**). Cross-section E-E' (**Sheet 1**, Royse, map pocket) shows an interpretation of this structure based largely upon good quality seismic data tied to well control. The east-dipping basement fault is shown to link with the west-dipping Hogsback along a décollement in Triassic rocks to form a sort of triangle zone, although most of the displacement of the basement is by folding. The basement fault dies out about 40 miles (64 km) to the north and also 12 miles (19 km) to the south, where the basement assumes a nearly flat regional west dip (**Figure 6**). This pronounced basement-cored anticlinal uplift is superimposed upon an extensive basement flexure called the Moxa arch.

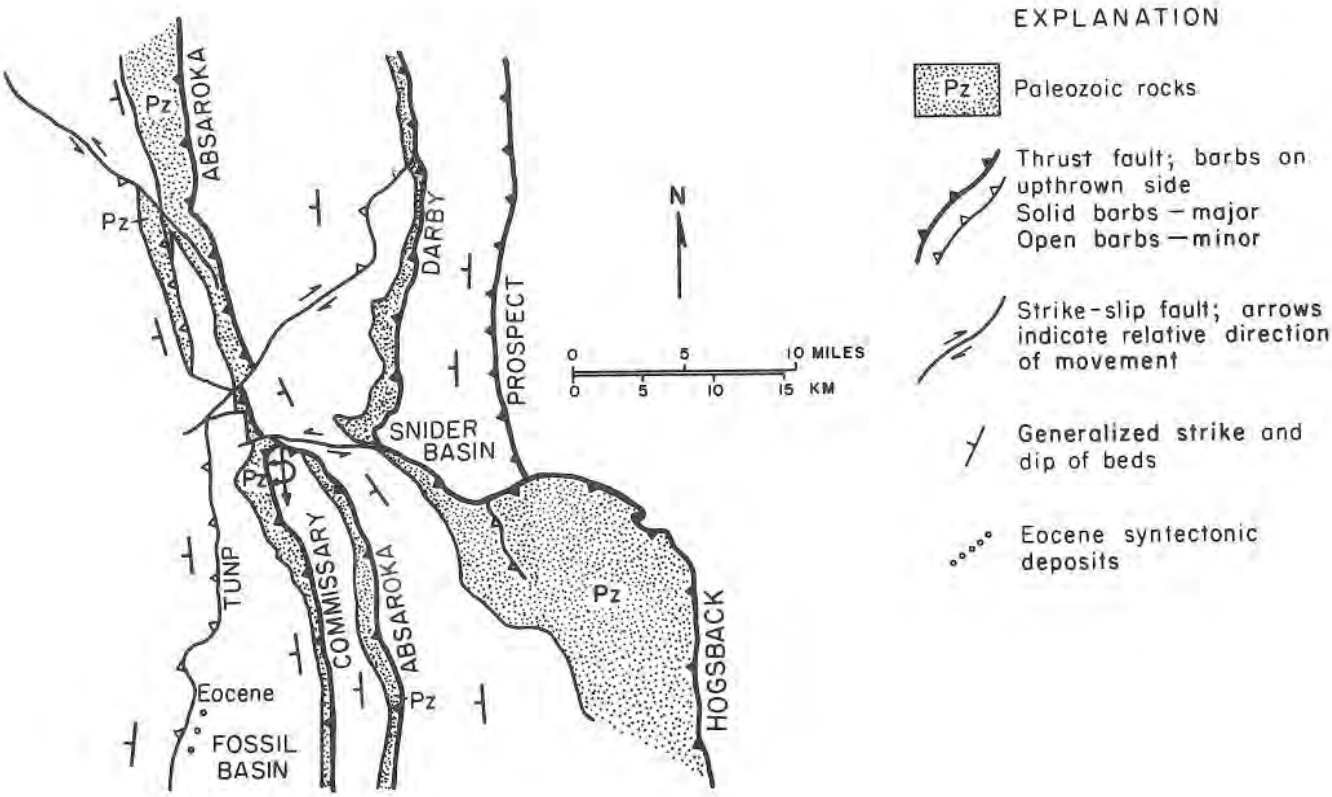

Figure 7. Generalized geologic map of the central part of the Wyoming thrust belt after Rubey (1973) and Rubey and others (1980), showing intersections in the Snider Basin area of the Commissary and Absaroka thrust faults, and of the Prospect and Darby faults to form the Hogsback fault. Note linkage of thrust faults by transverse faults.

The Moxa arch trends northward from its juncture with the Uinta Mountains to the LaBarge, Wyoming area, where the axis shifts westward beneath the Hogsback thrust sheet (**Figures 1** and **6**). From here, it continues northward under the Darby thrust plate. Evolution of the arch was different under the thrust belt north of LaBarge than it was to the south. In the south, in the Green River Basin, the axis of the arch is truncated by nearly flat-lying beds of Maastrichtian age (Erickson Formation = Lower Evanston Formation); Maastrichtian and younger beds are essentially unfolded (**Sheet 1G**, Royse, map pocket). Here, the west flank of the arch is a nearly planar panel, which dips west under the thrust belt at about 3°. Generally the east flank is only slightly steeper (but is locally steep and reverse faulted near Fontenelle, Wyoming). Northward along the axis of the arch north of Moxa, Wyoming, Paleocene beds (Fort Union Formation = upper Evanston Formation) truncate and overlap Maastrichtian rocks till they lie unconformably upon the lower Adaville coaly sequence (Santonian?) near LaBarge, Wyoming. From LaBarge northward, the configuration of the arch changes to abrupt west asymmetry, the axis shifts abruptly westward, and the east flank becomes the west flank of the Hoback Basin (**Figure 6**). The Hoback Basin has a long history of Maastrichtian through lower Eocene subsidence, probably in response to emplacement of the Wind River and Gros Ventre-Teton uplifts (Shuster and Steidtmann, 1988). The part of the arch that is under the thrust belt north of LaBarge evolved differently and through a longer time interval than the part that is to the south in the Green River Basin, and they could be considered separate features.

Seismic sections show that rocks of Cenomanian through Campanian age (Adaville and Hilliard Formations) thicken internally westward out of the Hoback Basin. They were deposited above west dipping basement before the arch developed. Initial development of the arch followed with uplift and erosion of several thousand feet of these rocks in the LaBarge area synchronous with initial uplift of the Wind River Range, before deposition of and overlap by Paleocene beds and before (or during) emplacement of the Darby-Granite Creek thrust sheets (Warner and Royse, 1987). The Darby-Granite Creek thrust sheets were then emplaced and overlapped by mid-Paleocene beds. (These faults are discussed in following paragraphs). Subsequently, the Prospect sheet was emplaced, merging southward with the Darby to form the Hogsback. The Prospect-Hogsback sheet overrode Paleocene beds a short distance and then was overlapped by Lower Eocene (Wasatch Formation) beds as the Hoback Basin area continued to subside under the load of the Wind River Range and rotate the east flank of the basement arch. Remnants of unconformable Paleocene deposits are preserved on and overridden by the Prospect-Hogsback thrust sheet. Minor antithetic east-dipping thrust faults cut the Paleocene in the Tip Top Field area (**Sheet 1E, Royse**, map pocket; Webel, 1977). Continued minor (?) contractional deformation is indicated by coaxial folding of the thrust sheets, the Precambrian basement surface, and the unconformably overlying Eocene beds (Wasatch Formation).

The above interpretation of the structure of the Moxa arch is similar to that proposed by Kraig (1987) and Kraig and others (1988), with some important differences, especially in the evolution of the arch with regard to the Prospect and Darby thrusts and the lack of involvement of Paleozoic beds in the Prospect sheet in the Snider Basin area shown here (**Sheet 1D**, Royse, map pocket). The Eocene age uplift of basement and folding of thrust sheets proposed by Royse (1985) is down-graded from a major to a minor role with major uplift being an earlier pre-Darby thrust phenomenon, as proposed by Kraig and others (1988), although dips in lower Eocene beds do indicate post Darby-Hogsback deformation.

From Snider Basin north to the Hoback Canyon area near the Gros Ventre uplift, the Darby thrust system is composed of three major thrust faults, the Darby, the Granite Creek, and the Prospect with its many hanging-wall imbricates (Shepard, Bear, etc.) A large antithetic (east-dipping) thrust, the Game Hill fault, crops out near Hoback Canyon (**Figure 1**); it is the easternmost thrust in this area. The subsurface configuration of these faults can be observed on cross-sections B, C, and D (**Sheet 1**, Royse, map pocket). Hunter (1988) presented a detailed interpretation of structure in the Hoback Canyon area.

The Granite Creek fault is of special interest because it is the only major thrust that doesn't crop out, and consequently was not known until recently (Royse, 1985). It is hidden by mid-Paleocene deposits and by the overriding Prospect (Cliff Creek of Hunter, 1988) and Game Hill thrust sheets. It was found unexpectedly during the drilling of the Chevron #1-34 well in 1984 (**Sheet 1B**, Royse, map pocket)

and its discovery caused a major revision of interpretations of structural geometry, thrust displacement, and thrust timing in this area. Well data show that structures in the Granite Creek thrust sheet are overlapped by mid-Paleocene rocks (Hoback Formation) which are cut by the Prospect and the antithetic (east-dipping) Game Hill thrusts. The Game Hill fault is overridden by the Prospect, which is overlapped by lower Eocene deposits (Lookout Mountain Conglomerate) (Wiltschko and Dorr, 1983), so the sequence and timing of thrusting is well established by both structure and stratigraphy as Granite Creek first, then Game Hill, then Prospect. In this locale, the Prospect thrust developed as a back-limb imbricate of the Granite Creek, and with the east-dipping Game Hill fault, forms a triangle zone. The Game Hill fault can be seen in seismic reflections to sole eastward into bedding in upper Cretaceous shale (coal ?); possibly it is linked to the Granite Creek thrust via a detachment in the bedding in the Upper Cretaceous. Such a link is indicated by the fact that the Game Hill thrust sheet plunges southward and terminates where the Granite Creek fault trace bends westward and links with the Darby thrust. Possible direct linkage to the north between Game Hill and Cache Creek thrusts is not indicated by the map pattern.

One should note that the major thrust displacement in the Hoback Canyon area occurred on the oldest thrust, the cryptic Granite Creek thrust, and not the Prospect as previously thought. Southward from cross-sections B-B′ to C-C′ (**Sheet 1**, Royse, map pocket) the subsurface trace of the hidden toe of the Granite Creek thrust swings westward and is overridden by the Prospect sheet. Displacement on the Prospect fault is fairly constant along strike, but the structural elevation of the Prospect sheet decreases abruptly southward, mostly because of the loss of the Granite Creek sheet. The south plunge of the Prospect sheet is evident on surface maps. Proceeding farther south to cross section D-D′ (**Sheet 1**, Royse, map pocket), the Granite Creek sheet is completely gone and the Prospect sheet has lost the Paleozoic section. The Prospect fault plane cuts up section southward from cross section C-C′ along strike and joins the Darby fault plane at a position above and east of the Darby Paleozoic ramp, so that south of cross-section D-D′, the Darby thrust sheet geometrically is a hanging-wall imbricate of the Prospect thrust sheet, and Paleozoic rocks are confined to the Darby portion of the hanging wall. An example of local stratigraphic control on the position of thrust faults is indicated by the fact that the Prospect fault follows bedding in a clay-rich, evaporitic shale sequence of Triassic age (Boyer, 1982) for over 6 miles (10 km) in the direction of transport before ramping eastward to the surface.

The structural relationship between the Darby and the Granite Creek faults may provide a means to date the Darby fault. Displacement on the Darby decreases northward from the Mt. McDougal (between cross sections D-D′ and C-C′) area to essentially zero in a fold near Munger Mountain, whereas displacement on the Granite Creek fault has the opposite pattern. This inverse relationship of displacements, plus the fact that the Granite Creek and Darby faults are linked through a common basal décollement in Cambrian, indicates displacement transfer and synchroneity of motion. The Granite Creek fault can be dated as pre-middle Paleocene, and so perhaps can major motion on the Darby.

The northwestward bend in the Darby thrust system (to parallel the Gros Ventre-Teton uplift) is a structurally complex feature. The northwestward continuity of the Prospect, Game Hill, and Granite Creek faults is uncertain. The antithetic (east-dipping) Game Hill fault appears to terminate northward in a north-plunging fold, similar to its southern termination. The Prospect thrust and associated minor imbricate thrusts curve and continue northwestward toward Jackson Hole and Teton Pass where it is called the Jackson thrust. The Granite Creek fault is not recognized at the surface, which is perplexing because it accommodated over 10 miles (16 km) of displacement in the Hoback Canyon area. It may extend northwestward in the subsurface below the Paleocene and Upper Cretaceous sediments that crop out between the thrust belt and Gros Ventre Range and link with the northeast dipping Cache Creek thrust fault forming a triangle zone, which involves the Archean basement.

Support for this interpretation comes from data from a well drilled south of Victor in southernmost Teton Valley, Idaho. The Anschutz-Victor #15-16 (sec. 16, T3N, R4E) penetrated west-southwest dipping Triassic and Paleozoic rocks of the Jackson thrust sheet below the valley alluvium and cut the Jackson thrust fault at 6,112 feet, where it passed from Cambrian into Upper Cretaceous Frontier Formation. (This is the same sequence that crops out 4 miles (6.4 km) to the southeast along strike on the west side

of Teton Pass.) At 7,950 feet, the well encountered a 1,200-ft-thick, mostly conglomerate section overlying a coaly sandstone and shale sequence containing post-Frontier (Campanian?) Cretaceous palynomorphs and bottomed at 13,514 feet. Clasts in the conglomerate were largely Precambrian quartzites similar to those found in the Pinion and Harebell formations of the Jackson Hole area. This sequence indicates that the Frontier is faulted over the conglomerate on a cryptic fault that may be the correlative of the Granite Creek thrust. Just how this information applies along strike to the northwest near the Snake River Plain, (**Sheet 1A**, Royse, map pocket), is uncertain. Drill hole and seismic data show conclusively that the Precambrian crystalline basement of the Teton uplift extends to the west at shallow depth under the whole of Teton Valley, a feature that restricts interpretations of the configuration of the western extent of the Teton block. A Phillips Petroleum well in Horseshoe Basin (west of Teton Valley in sec. 28, T5N, R44E) drilled a normal Lower Cretaceous through upper Paleozoic section that appears to belong to the foreland between the thrust belt and the Teton block (**Sheet 1A**, Royse, map pocket) without encountering a Granite Creek thrust counterpart.

Absaroka thrust system

The Absaroka thrust system has an arcuate map trace that extends without significant interruption from the Snake River Plain south to the Salt Lake City area, a distance of about 150 miles (240 km) (**Figure 1**). It is, perhaps, the most renowned of all the thrust systems in the region, thanks to spectacular topography and outcrops in the north and to the presence of associated oil and gas fields in the south, where it lies mostly buried under lower Tertiary deposits.

In the north, the system is composed of the Absaroka thrust and its many folded hanging-wall imbricate thrusts, such as the St. John, Elk, Needle, Baldy, etc. Woodward (1986) described nine major imbricate sheets in the Snake River Range that were emplaced sequentially from west to east with older (higher) sheets being folded by emplacement of younger sheets. In the Salt River Range, immediately south of the Snake River Range, Lageson (1984) interpreted a major culmination in the Absaroka thrust sheet (Stewart Peak culmination) to be a large-scale duplex structure bounded on the north and south by steep lateral ramps in large footwall imbricate thrusts, the Murphy and Firetrail thrusts (**Sheet 1C**, Royse, map pocket). Using Mackin's (1950) method of down-plunge (down-dip) viewing of geologic maps, one can obtain a somewhat distorted strike cross section of this culmination by viewing the State geologic map (1:500,000) with west at the top. This reveals how the faults link together along strike and what changes in stratigraphic position (lateral ramps) must occur in the subsurface to match those seen on the surface.

In the south, the Absaroka system is composed of the Tunp and Commissary thrusts and associated minor imbricates and the "early" Absaroka, and "late" Absaroka thrusts. This is a geometric grouping, as there are significant time differences in emplacement of these sheets. Lamerson (1982) presented a detailed interpretation of structure in the Fossil Basin and area to the southwest with the use of much valuable palynological, drill hole, and seismic data.

General concave westward curvature in the trace of the Absaroka thrust system is probably due to changes in stratigraphy and thickness of the sedimentary rocks involved in thrusting (especially the Lower Paleozoic and Lower Cretaceous) and to the presence of a basement arch between the thrust sheet and the Gros Ventre-Teton thrust uplift (**Figure 6**), and not to buttressing effects of foreland basement uplifts. Regional structural trends show that tectonic transport on thrust faults must have been essentially west to east. This implies that there are major lateral ramps in the thrust system with the southwest trend near the Uinta Mountains being one of oblique right-lateral shear, and the northern part near the Teton-Gros Ventre block being one of oblique left-lateral shear. In the south, seismic data clearly show that the westward curvature of the Absaroka thrust sheet as it nears the Uinta Mountains is accomplished without deformation of the footwall section, and that footwall and hanging-wall cutoffs of stratigraphic units swing west in conformance with the surface trace. A large lateral ramp exists in the Absaroka fault plane whereby the fault cuts upsection to the south from a basal Cambrian décollement to Cretaceous (see Lamerson, 1982, plate 12). Bruhn and others (1986), presented a discussion of the possible consequences of this geometry. The time of first major movement of the Absaroka thrust system is Santonian according to data from the Little Muddy Creek area, Wyoming

(Royse and others, 1975; Lamerson, 1982), and this predates uplift of the Uinta block, which is considered to be no older than late Campanian (Hansen, 1986; Bryant and Nichols, 1988). In similar fashion, the northwest swing in the northern Absaroka thrust system follows stratigraphic and isopach changes in pre-thrust rocks (**Figure 2**).

In the area west of Snider Basin, two major components of the Absaroka thrust system, the Commissary and Absaroka faults, join. The surface geology here is well exposed and mapped (Rubey, 1973; Rubey and others, 1980) (**Figure 7**). The map pattern appears to be an inverse image of the Darby-Prospect intersection just 10 miles (16 km) to the east. The Commissary and Absaroka faults join northward to form a single fault, which must be a composite of the two. Turning the map sideways with west at the top to view it down, regional dip provides a strike cross section perspective of the structure. The Absaroka fault joins the Commissary across a steep major lateral ramp in its hanging wall where the Absaroka fault plane cuts abruptly upsection from lower Paleozoic to Jurassic rocks to intersect the Commissary. South of the intersection, the Absaroka hanging-wall section and overlying Commissary fault plane are coaxially folded, whereas the west-dipping outcrops of the Commissary hanging-wall section continue northward without significant interruption. From this information, it appears that the Commissary sheet was emplaced first, and the single Absaroka fault north of the intersection is a composite of the "type" Absaroka (named from exposures to the south on Absaroka Ridge) and Commissary faults (just as the Hogsback is a Darby-Prospect composite, but in the opposite direction). This implies that the displacement on the single fault north of the intersection should be the sum of displacements on the Commissary and type Absaroka faults.

Southward along strike in the northern Fossil Basin the Commissary and Absaroka thrust planes join again in the Little Muddy Creek area (**Figure 1**; Vietti, 1974; Royse and Warner, 1987). The geometry is like a mirror image of the juncture west of Snider Basin just discussed, but is more complex. A down-dip projection of the geometry of the intersection is shown in **Figure 8**. The Little Muddy Creek outcrop area is a key locality in understanding the Absaroka thrust system because of unique exposures and the presence of dated synorogenic and overlapping deposits. There is a major west-northwest striking, northward facing lateral ramp in the Absaroka thrust fault plane west of here, which is indicated by the hanging-wall cutoffs shown on **Figure 8**, and by an abrupt westward deflection in the hanging-wall cutoff trace of Paleozoic beds on the Commissary and the type Absaroka thrusts in the subsurface to the west. The fault cuts up section along strike southward from Paleozoic to Triassic rocks, and forms an extensive flat in Triassic hanging-wall beds throughout the southern Fossil Basin (see Lamerson, 1982 for a more comprehensive view of this geometry).

There is little doubt that the Absaroka and the Darby-Hogsback thrust fault systems stem from a regional décollement within Cambrian shale and carbonate near the top of the Archean basement surface. Basal Cambrian sandstone is attached to the basement and not involved in the thrusting. This feature was recognized some time ago by workers (e.g., Rubey and Hubbert, 1959) who noted that although Cambrian shale and carbonate were exposed extensively along strike of major thrusts, the basal sand that crops out in nearby foreland uplifts never appeared. Seismic data verifies this décollement feature and, in some places, shows the precise "liftoff" position (branching point) of thrusts from the throughgoing near-basement reflection. However, the Archean basement (Farmington Canyon Complex) cored anticlinal uplift, which comprises the central Wasatch Range north of Salt Lake City, Utah, is allochthonous and part of the thrust system (cross section H-H'). Evidence of this comes from structural cross sections supported by seismic data and palynological dating of overlapping deposits that show the time of basement uplift is at least as old as Absaroka thrusting, and the regional décollement in Cambrian rock must pass under the uplift (Royse and others, 1975). Apatite fission-track dating of Archean rocks (Naeser and others, 1983) indicate uplift to be no older than 94.4 ± 10.5 Ma and mostly younger. The anticlinal geometry of the uplift indicates it was a product of movement on a décollement that must ramp westward into the basement at a distance west of the basement hanging-wall cutoff at least equal to the displacement of the Absaroka and Hogsback thrust sheets. If one assumes the basement hanging-wall cutoff is just east of easternmost basement surface exposures, as cross sections indicate, then the footwall cutoff would be about 42 miles (67 km) to the west, which would place it just west of Antelope Island in the Great Salt Lake (**Figure 1**). This appears to be a logical position from the standpoint of re-

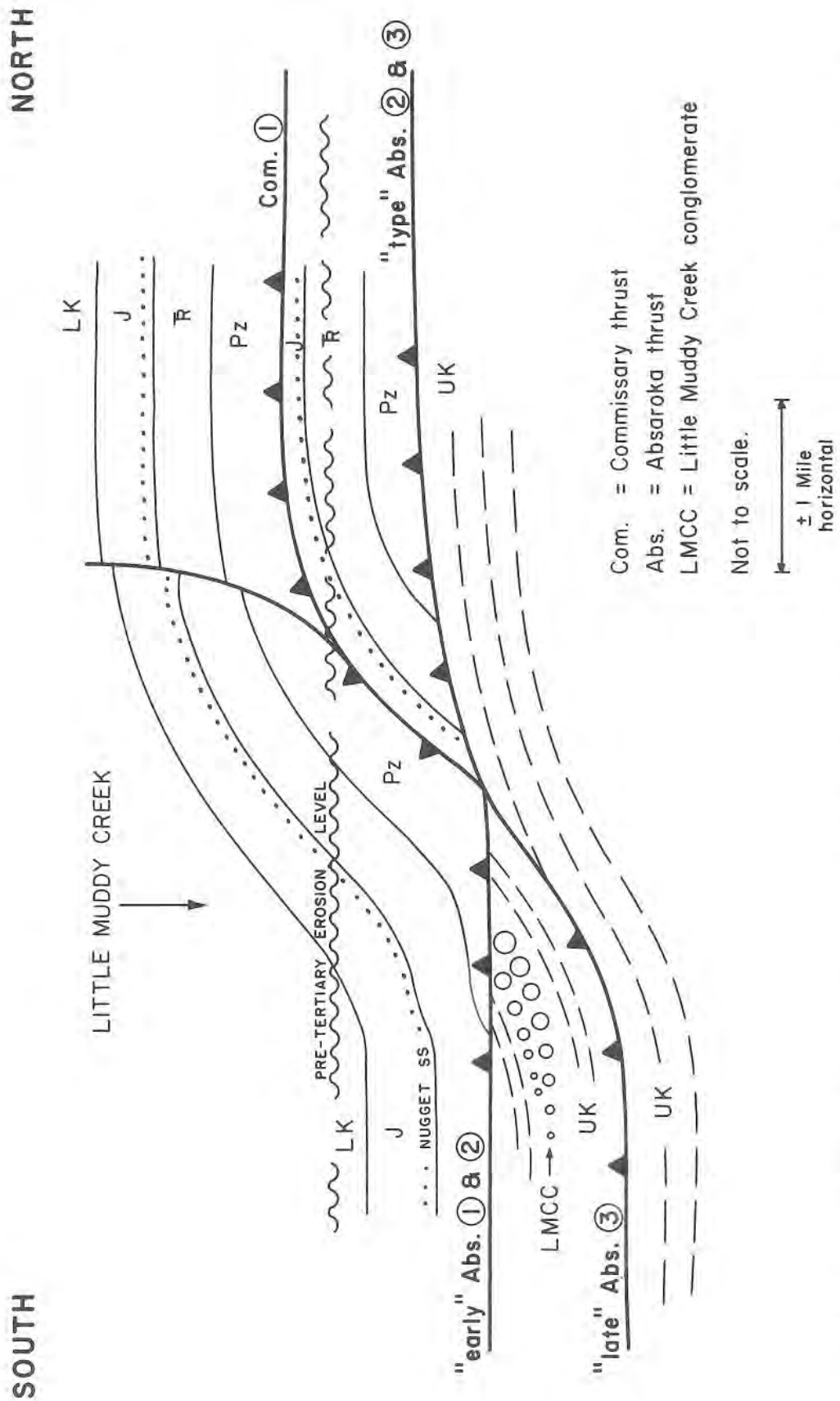

Figure 8. Diagrammatic south to north cross section (with projection of rocks from out of the plane of section) in the Little Muddy Creek area (see Figure 1), showing stratigraphic position and linking of major faults. Circled numbers indicate sequence of fault movements: 1 and 2 = pre-early Campanian major displacements and 3 = pre-mid Paleocene lesser displacement. Displacement direction of the hanging wall is toward the observer. See text for explanation.

gional geology, since Antelope Island (part of the Absaroka hanging wall) is the westernmost exposure of Archean basement within the thrust belt. The steep southward and northward plunges of the basement uplift must be expressions of west-striking lateral fault plane ramps within the basement farther west. Whether or not these ramps are reactivated Proterozoic or Paleozoic faults is conjectural.

Coogan (1991) presented an argument for an earlier time for basement uplift. He suggests that Crawford, not Absaroka, thrusting is responsible for initial uplift. If so, the addition of as much as ±20 miles (32 km) of Crawford displacement to the aforementioned Hogsback and Absaroka displacements would place the basement ramp about 62 miles (99 km) west of the hanging-wall cutoff, or about the position of the Lakeside Mountains on the west shore of the Great Salt Lake. Further discussion of this problem is included in the section on the Crawford thrust.

The amount of displacement on the total Absaroka thrust system is best established in the northern Fossil Basin, where seismic and drill hole data and outcrops yield the most complete and reliable information. Cross sections E-E' and F-F' (**Sheet 1**, Royse, map pocket) show the type Absaroka fault to have about 20 miles (32 km) and the Commissary fault to have about 7 miles (11 km) of displacement of Mississippian beds. The type Absaroka (named from its exposure on Absaroka Ridge in the northern Fossil Basin) is a composite of the "early" Absaroka and "late" Absaroka faults (**Figure 8**). The Tunp fault, a major hanging-wall imbricate, has about 1 mile (1.6 km) of displacement. Thus the total displacement of the Absaroka thrust system in the northern Fossil Basin is approximately 28 miles (45 km). Estimates of displacement in other areas are not as certain. [Displacement appears to decrease southward toward the Uinta Mountains, but this is probably due to the westward swing in stratigraphic cutoffs, and the inclusion of a major basement-cored fold (Wasatch Range) as part of the hanging wall.] Although there are many fault plane bifurcations, the total displacement probably does not change significantly along strike; if it does, the mechanism of displacement transfer is not apparent.

The Little Muddy Creek area and northern Fossil Basin contain outcrop and well data that allow the most precise dating of fault movement in the Absaroka thrust system. The first stratigraphic sign of fault movement was the deposition of a very coarse proximal alluvial fan deposit of late Santonian to early Campanian age (Jacobson and Nichols, 1983). This conglomerate was informally named the Little Muddy Creek conglomerate (Royse and others, 1975), and was derived from Jurassic, Triassic and Paleozoic rocks of the Commissary thrust sheet. Movement along the aforementioned northwest-striking lateral ramp in Paleozoic beds probably localized the uplift that produced the conglomerate (**Figure 8**). Younger Campanian-Maastrichtian conglomerate beds lie with marked angular discordance upon the Commissary and Absaroka thrust sheets, indicating major displacement before that time. Finally, "late" Absaroka fault motion deformed the Little Muddy Creek conglomerate, cut and deformed Campanian-Maastrichtian beds, and was overlapped by mid-Paleocene conglomeratic deposits. North of Little Muddy Creek, the "late" Absaroka fault merges with the "type" Absaroka fault, whereas to the south the "late" Absaroka is a frontal imbricate of the "early" Absaroka fault. Further discussion of dating sedimentary beds in this area can be found in Lamerson (1982).

A summary of times and magnitudes of fault displacement (**Figure 8**) is as follows: (1) the Commissary sheet (which extended south into northern Utah) was displaced about 7 miles (11 km) in pre-early Campanian to post early Santonian time; (2) the "early" Absaroka sheet (which includes the "type" Absaroka and Commissary sheet) was displaced about 14 miles (22 km) during the latter part of the same time period; and (3) the "late" Absaroka thrust sheet, which incorporates all of the earlier mentioned sheets, was displaced about 6 miles (10 km) before mid-Paleocene (offset of Maastrichtian beds appears to be less than 6 miles). The age of boulder beds that lie unconformably upon the west flank of the Lazeart syncline in NW T22N, R116W northwest of Kemmerer, Wyoming are critical to this interpretation. They were mapped as the Ham's Fork Member of the Evanston Formation (Campanian-Maastrichtian) by Rubey and others (1975) but have subsequently yielded a mid-Paleocene fauna (Lamerson, 1982). In the western Fossil Basin, in the ramp region of the Absaroka thrust system, minor movement (±1 mile, .6 km) occurred on the Tunp thrust (**Sheet 1F**, Royse, map pocket) during deposition of the Wasatch Formation in early Eocene (Hurst and Steidtmann, 1986).

The traces of the Absaroka thrust system faults merge and bifurcate along strike as shown in **Figure 1**. The youngest significant movement on the Absaroka fault system occurred during the same time period as did movement on the Darby-Granite Creek faults; i.e., pre mid-Paleocene and post-Campanian-Maastrichtian. Also, in the Fossil Basin, structures and angular unconformities associated with the Absaroka fault have been rotated where they overlie the Hogsback thrust ramp by post-Paleocene movement on the Hogsback thrust. Angular unconformities and pulses of conglomerate indicate discrete faulting episodes, but these episodes cannot yet be fully discriminated by paleontology. Fault movements probably overlapped both in time and space, in a locally episodic, but regionally quasi-continuous way, as suggested by Oriel and Armstrong (1966).

Crawford thrust system

The Crawford is perhaps the most enigmatic of the major thrust systems. In the type area in the Crawford Mountains, the Cambrian is thrust over Upper Cretaceous Frontier Formation. Royse and others (1975) interpreted the Crawford thrust to be a frontal imbricate of the Willard thrust, and also to have been active during the same period as the Meade thrust. The Meade and Crawford were believed to be linked physically in the subsurface to the west by a common décollement in hanging-wall Proterozoic sediments, and temporally by what appeared on the surface to be a classic zone of displacement transfer where displacement on the Crawford fault decreased northward to be replaced by increased displacement on the Meade (**Figure 1**). This interpretation was generally accepted until recently, when Coogan (1991) used both stratigraphic and structural analysis to show that the Meade and Crawford are not directly linked either physically or temporally (**Figure 9**). Using lower Paleozoic stratigraphy and limited seismic data, he showed that the Crawford fault was not a frontal imbricate of the Willard but that it branched from the same basal Cambrian shale décollement as the Absaroka and Darby thrust systems, and that major folds in the Crawford thrust sheet (e.g., Sublette anticline) deform the Meade thrust fault plane. Valenti (1987) presented a detailed study of the Crawford thrust in the subsurface by using much proprietary seismic and well control; his analysis supports Coogan's interpretation.

An interesting feature of Crawford thrusting is the involvement of Jurassic evaporite beds as major frontal footwall décollement horizons, which accommodate significant displacements of Cretaceous beds east of the toe of the Crawford thrust fault (**Sheet 1E, F, and G**, Royse, map pocket). The east flank of the Jurassic evaporite basin (**Figure 2**) was in position to localize Crawford thrusting. Two main stratigraphic positions of frontal décollement are the anhydritic beds in the basal Twin Creek Limestone (Gypsum Spring Formation), which are just above the competent Nugget Sandstone, and the halite and anhydrite deposits, which occur in the basal Preuss Formation above the Twin Creek Limestone. Structural detachment at these stratigraphic positions shows clearly on surface maps (e.g., Rubey and others, 1980; Cressman, 1964; Coogan, 1991) and cross sections. Drill hole and seismic data from the southern Fossil Basin and Coalville, Utah area define an extensive detachment in the Preuss salt section, which links westward to the Crawford fault and is folded by Absaroka thrusting. An important aspect of this detachment and others like it is that they have been active during several periods, first to accommodate compression in Upper Cretaceous and lower Tertiary, and later, in post-Eocene time, to provide for east-west extension. This behavior can be traced along strike over a huge region from southeastern Idaho to southwestern Utah, including the Wasatch Plateau, essentially the entire east flank of the Jurassic evaporite basin.

Displacement on the Crawford fault decreases northward from an apparent maximum of about 20 miles (32 km) in the vicinity of the Crawford Mountains (**Sheet 1G**, Royse, map pocket). The northward displacement decrease is clearly indicated by surface exposures, and it becomes zero (tip point) in Lower Cretaceous beds along the eastern flank of the Sublette anticline. Displacement may have been transferred westward to the Sheep Creek and Home Canyon thrusts and associated folds and imbricates via the basal Cambrian décollement (**Sheet 1E and F**, Royse, map pocket). The means by which Crawford fault displacement was extended along strike northeast of the Meade thrust outcrop area toward the Snake River Plain is not known; it may be expressed as the many large-scale folds seen in outcrops of Triassic through Lower Cretaceous beds which accommodate significant horizontal shortening east of the Meade thrust and northwest of Alpine, Wyoming.

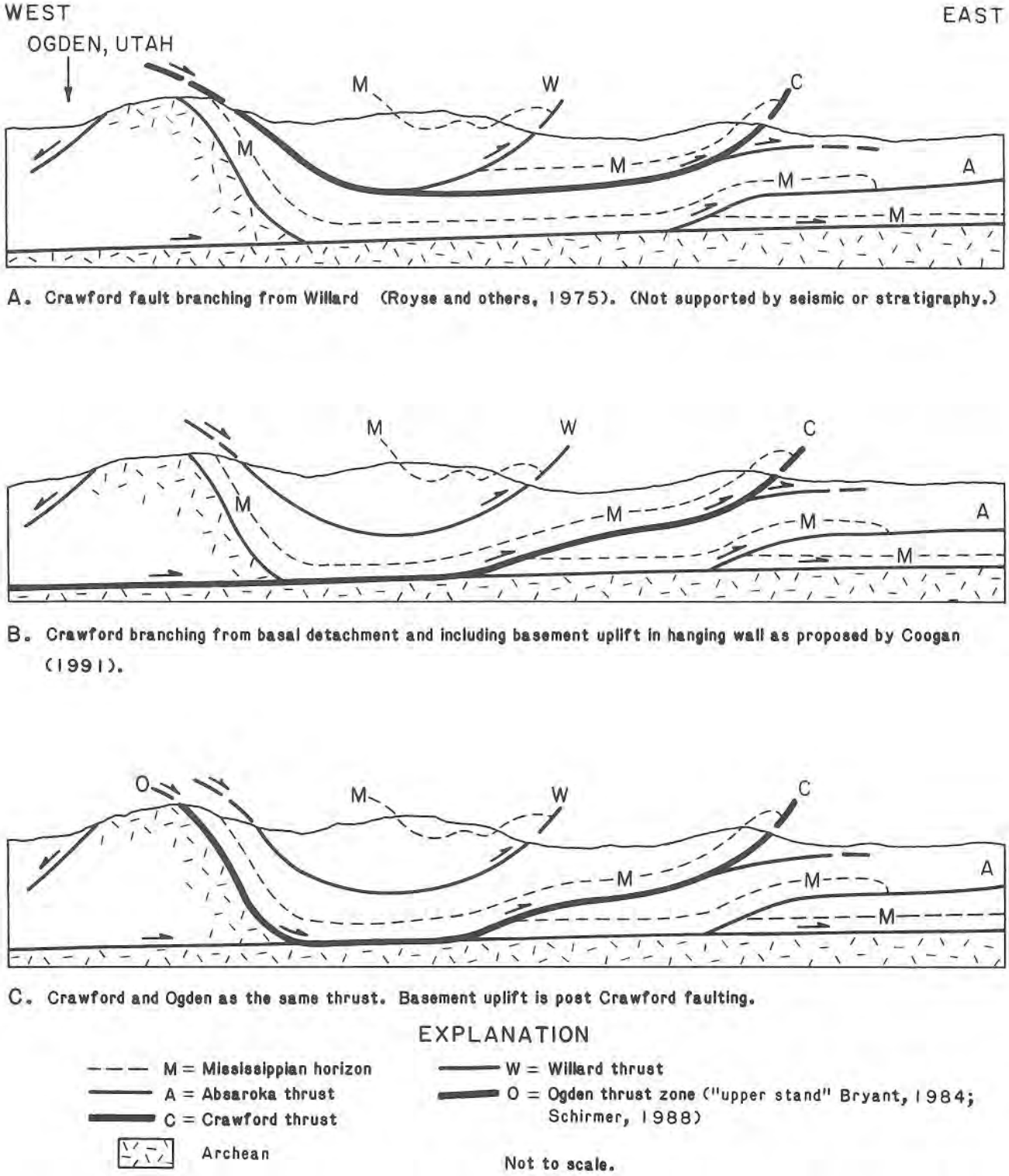

Figure 9. Diagrammatic cross sections showing three different interpretations of the Crawford thrust geometry in the area of cross section G-G' (see Figure 1).

The zone between the Crawford and Meade thrust sheets contains several thrust faults and folds in Triassic and Jurassic beds that crop out east of Bear Lake valley. Together these structures represent a significant amount of horizontal displacement. Notable among these are the Home Canyon and Sheep Creek (blind) thrusts and the Home Canyon and Sheep Creek anticlines. J.C. Coogan (personal communication, 1990), using sparse seismic data, interpreted the Sheep Creek thrust to branch from the same regional basal Cambrian shale décollement that is employed by the Crawford, Absaroka, and Darby faults, and the Home Canyon thrust to be a frontal imbricate of the Meade (Laketown). For the purpose of this report, they are grouped with the Crawford as being of the same thrust system. Eastward projections of the Sheep Creek and Home Canyon fault planes follow bedding in anhydritic beds of the basal Twin Creek Limestone (Jurassic) and separate tight disharmonic folds above from less deformed Nugget Sandstone below. This décollement is folded to conform with large folds in Nugget Sandstone, such as the Sheep Creek anticline, and its history of motion is probably very complex. The Home Canyon, Sheep Creek, and Crawford faults may form a more or less contemporaneous thrust system with displacement transfer between them via the regional Cambrian shale décollement. Just how the large displacement of the Home Canyon thrust sheet shown in cross section E-E' (**Sheet 1**, Royse, map pocket) is accommodated along strike is unknown.

The southward continuation of the Crawford fault is perplexing. South of the Crawford Mountains outcrop area, the trace of the fault is buried beneath lower Tertiary and Maastrichtian beds, and it does not reappear in a recognizable form in the continuous outcrops that flank the Cottonwood uplift and central Wasatch Range uplift. Valenti (1987) traced the Crawford fault at least as far south as T5N with well control and seismic. Remembering that well control and seismic data analyzed by Coogan (1991) showed that the Crawford fault branches from the regional basal Cambrian décollement near the top of crystalline basement, there appears to be two possibilities. First, the Crawford fault may be the same as the upper strand of the Ogden thrust zone, which occupies a lower Cambrian shale décollement position in outcrops on the north plunge of the central Wasatch Range east of Ogden, Utah (Bryant, 1984; Schirmer, 1988) (**Sheet 1G**, Royse, map pocket). In other words, the Crawford fault plane passes over the basement uplift by riding in basal Cambrian shale and is eroded from the crest (**Figure 9C**). In this case, basement uplift would be essentially post-Crawford thrusting and coincident with Absaroka thrusting.

A second possibility is that the Crawford fault plane merges with the regional Cambrian décollement and passes under the Archean basement uplift. If this is true, initial basement uplift was a product of Crawford thrusting. In this case, fault displacement may decrease rapidly southward along strike, possibly by displacement transfer from faulting to folding to form the huge basement uplift (central Wasatch Range) as a sort of tip anticline (Boyer and Elliot, 1982) but just where the tip line of the Crawford fits on the map is not apparent.

Figure 9 is a schematic illustration of possible Crawford thrust interpretations. Available data do not indicate absolutely which interpretation is correct, if any. The age of the basement-cored uplift is pertinent in choosing. Palynological dating of shales lying conformably upon synorogenic conglomerates, which lie with marked structural discordance upon the east flank of the basement uplift, are as old as Campanian-Maastrichtian. Some workers have correlated these conglomerates with the Echo Canyon Conglomerate of late Coniacian-Santonian age (Jacobson and Nichols, 1983) and the Echo Canyon Conglomerate is generally considered to be a product of uplift due to Crawford thrusting (**Figure 4**). However, the lithology of the type Echo Canyon Conglomerate is very dissimilar to the synorogenic conglomerates that lie unconformably upon the basement uplift. Proterozoic quartzite clasts (as large as 2 feet (.6 m) in diameter) are characteristic of the unconformable conglomerates, whereas that lithology is essentially not present in the type Echo Canyon Conglomerate, which lies conformably nearby upon marine sandstone and shale of the Henefer Formation east of the uplift. The outcrop localities are too close and the Proterozoic quartzite clasts are too resistant for the difference to be explained by a simple facies change. Therefore, correlation of the type Echo Canyon Conglomerate with those lying angularly upon the basement uplift does not appear to be justified [in spite of different opinions of DeCelles (1988) and Bryant and Nichols (1988)]. Even though the uplift can only be dated from stratigraphy as Campanian-Maastrichtian or older, it seems that basement uplift resulted from Absaroka thrusting based on the correlation proposed here of the unconformable conglomerates with

the Campanian-Maastrichtian lower Evanston Formation, both of which contain much Proterozoic quartzite clasts, and the fact that they are structurally conformable with overlying shale of Campanian-Maastrichtian age. The lower Evanston is known from widespread angular and overlapping relations to have been deposited during the waning phase of Absaroka thrusting. No Archean basement clasts have been reported from either the Echo Canyon or the unconformable conglomerate. If the basement block which comprises the Wasatch Range is part of the Crawford hanging-wall (**Figure 9B**) then Proterozoic quartzite clasts should appear earlier and in abundance in the Echo Canyon Conglomerate, but they do not. Therefore, this interpretation favors correlation of the Crawford thrust with the upper strand of the Ogden thrust of Bryant (1984) (**Figure 9C**). Apatite fission-track data (Naeser and others, 1983) is inconclusive regarding time of basement uplift, with disparate ages in adjacent samples. A complex uplift (thermal) history is indicated, with Archean basement ages ranging from 5 Ma to 94 Ma. The oldest date could represent uplift caused by either Crawford or early Absaroka thrusting.

A problem common to both interpretations is that the southern extension of either the tipline or surface trace of the Crawford fault below Tertiary cover must still be accounted for. Commonly, the surface trace is shown to either end arbitrarily with a question mark somewhere below cover southeast of Lost Creek Reservoir or to swing westward and join the Willard fault southeast of Huntsville, Utah. Coogan (1991) demonstrated that joining the Willard (**Figure 9A**) could not be the case because a restoration to pre-thrusting time would require the Lower Paleozoic of the Crawford hanging wall to have been derived from areas west of the Willard footwall exposures seen in Ogden Canyon, contrary to stratigraphic analysis (**Figure 5**). Also, there does not appear to be enough room between the outcropping northeast flank of the basement uplift and the Proterozoic exposures on the Willard thrust sheet southeast of Huntsville to accommodate a separate Crawford hanging-wall Paleozoic section. A partial solution to this problem may be that displacement on the main Crawford thrust dies out rapidly south of the Crawford Mountains by being transferred to the frontal décollement(s) in Jurassic evaporite, locally called the Medicine Butte thrust. However, although this décollement(s) accommodates significant displacement of post-Jurassic rocks, the problem of southward disappearing displacement of Triassic and Paleozoic rocks remains. It may be that the Crawford fault is in bedding in the Jurassic evaporitic sequence that is exposed in Emigration Canyon east of Salt Lake City.

Meade-Laketown thrust system

The Meade-Laketown thrust sheet is characterized by the involvement of a thick, distinct, western-facies miogeoclinal Paleozoic sequence, including Silurian dolomite, which is not seen to the east in the Crawford, Absaroka, and Darby thrust sheets. This sequence is exposed to the west in the Bear River Range, where it occurs in normal succession above a thick Proterozoic clastic section as part of the Paris-Willard thrust sheets (**Figure 5**). Using well control, scattered seismic data, and Paleozoic stratigraphy of hanging-wall sediments, Coogan (1991) showed that the Meade thrust may be traced southward from its type locality east of Georgetown, Idaho, into the subsurface in Bear Lake Valley and under Bear Lake to connect with the Laketown thrust of Valenti (1982) (**Figure 1**). The Laketown thrust is exposed for a limited distance just south of Bear Lake, where its steep dip and east strike indicate a lateral ramp and fold or tear in the thrust sheet, with Devonian carbonate in the hanging wall to the south faulted against Jurassic Nugget Sandstone. The hanging-wall stratigraphic cutoff geometry of the Laketown sheet (where exposed) is quite different from that of the Meade in its type area. The entire hanging-wall section, from at least Silurian to Triassic, is abruptly cut off at Laketown, whereas the Meade fault in the type area rides in Mississippian for a long distance, thus requiring a lateral ramp or en echelon interchange between the localities. The southward continuation of the Laketown thrust is covered by lower Tertiary fluvial beds, but its position is constrained by the Marathon Otter Creek well (sec. 21, T12N, R6E), which penetrated it. A postulated connection to the Willard thrust just north of Woodruff Creek is buried by lower Tertiary beds. There is little doubt that the Meade-Laketown thrust sheet proper contains typical western-facies Paleozoic rocks; however, it is uncertain whether Proterozoic clastic rocks in the subsurface to the west are directly involved. Cross section D-D′ (**Sheet 1**, Royse, map pocket) shows Proterozoic rocks in the hanging wall of the Meade thrust below the Paris thrust fault, but it could be drawn without Proterozoic and still honor the available data.

The exposure of the Meade thrust sheet in the type area north of Montpelier, Idaho, is unusual in that both hanging-wall and footwall sections are more or less continuously exposed for a distance over 15 miles (24 km) measured across strike normal to the direction of transport. Maps by Cressman (1964) show that both hanging-wall and footwall cutoffs of like Triassic and Jurassic units are exposed, thereby enabling a close estimate of fault displacement that does not rely upon seismic data, well control, or geometric projection. At this locality, total shortening of Triassic units above the Meade thrust, including folding, is as much as 25 miles (40 km). The control of stratigraphy upon the shape of the Meade fault is well displayed in outcrop. The parallel attitude of the fault plane with respect to bedding, as shown in cross section D-D′ (**Sheet 1**, Royse, map pocket) is a generalized northward projection of outcrop relations. The fault is shown to occupy salt-bearing Upper Jurassic beds in the footwall and Lower Mississippian shaly carbonate beds in the hanging wall for about 20 miles (32 km). The influence of Jurassic salt in localizing thrusting is obvious, and the northward change in strike of the Meade thrust sheet from north to northwest may indicate control by the shape of the Jurassic salt basin. The extensive hanging-wall cutoff of Lower Mississippian beds requires a matching footwall cutoff in the subsurface to the west under the Bear River Range.

Time of emplacement of the Meade-Laketown thrust sheet(s) is not closely constrained by crosscutting or overlapping relationships. The oldest overlapping rocks are lower Tertiary for the Laketown, and Miocene(?) for the Meade. The youngest rocks cut by the Meade are Lower Cretaceous in age (Wayan Formation). Folding of the Meade fault plane by Crawford thrusting indicates a pre-Crawford (pre-late Coniacian-Santonian) age. These items considered, it seems likely that the emplacement of the Meade-Laketown thrust sheet was the cause of the uplift and erosion that produced conglomerate beds in the Frontier Formation of Turonian age (**Figure 4**). Outcrops of this conglomerate occur to the south in the East Canyon Creek and Coalville, Utah area, where they lie above the well-dated Oyster Ridge Sandstone and Allen Valley Shale members; the conglomerate also occurs to the north in the Big Hole Mountains in Tie Canyon (SW 1/4 T3N, R44E) where it lies disconformably on the Lower Cretaceous Aspen Formation.

The Meade thrust sheet in the type area must have extended a considerable distance to the south and east of its present outcrop trace prior to uplift and erosion by Crawford thrusting. Cobble-size quartzite clasts from Meade footwall outcrops of Ephraim Conglomerate (Lower Cretaceous) preserved in the Red Mountain syncline are fractured, with offsets that involve matrix, suggesting deep burial by the Meade sheet (Gray and Platt, 1988). Also, analysis of illite crystallinity by Mitra and Yonkee (1985) indicates that temperatures in the footwall Twin Creek Limestone (Jurassic) exceeded 130°C. This could only be a result of burial by practically the full original thickness of the Meade sheet (±5 km, not including Lower Cretaceous), if a reasonable temperature gradient range of 25° to 30°C/km is used.

Paris-Willard thrust system

The Paris-Willard is the westernmost, oldest, and structurally highest of all the major thrust systems. Actual outcrops of the faults are meager and widely spaced, but the stratigraphy of the thrust sheet is distinctive enough to enable general tracing of the faults through covered areas with confidence. The Paris-Willard thrust sheet comprises the entire Bear River and Portneuf ranges. These ranges contain a Middle Cambrian and Proterozoic quartzite and argillite sequence as thick as 19,500 feet (6 km) (Hintze, 1988), which is not seen in outcrops to the east, and a lower Paleozoic, mostly carbonate passive margin, shallow water sequence over 14,000 feet (4.5 km) thick, which includes units not present in much thinner correlative rocks to the east (**Figure 5**).

At the type locality in Paris Canyon west of Montpelier, Idaho, the Paris thrust places Proterozoic quartzite over an overturned section of upper Paleozoic rocks. Northward, the thrust trace is buried by upper Tertiary rocks, and map relations indicate a rapid decrease in stratigraphic separation north of Soda Springs. Displacement is probably transferred westward to the Putnam thrust (**Figure 1**), a little-known fault with similar stratigraphic separation that crops out along the east flank of the Portneuf Range about 20 miles (32 km) northeast of Pocatello (Platt and Royse, 1989). Southward from the type area, the Paris thrust loses stratigraphic separation and probably terminates west of Bear Lake, as progressively older rocks appear in the footwall. Displacement is

presumed to be transferred to the Willard thrust, which extends from a tip point in Bear Lake Valley southward beneath Bear Lake according to seismic profiles. Thus, the Willard, Paris, and Putnam thrust fault traces form a left-stepping en echelon array along the east margin of the Bear River and Portneuf ranges. The en echelon geometry and change in structural trend from north to northwest suggests that a component of left-lateral shear operated as thrust sheets were emplaced.

The type area of the Willard thrust near Ogden, Utah, is a spectacular exposure of its hindward part at a position where the fault plane ramps eastward from a Cambrian shale décollement through lower Paleozoic strata carrying Proterozoic quartzite and argillite as old as 1.66 Ga (Crittenden and Sorensen, 1980) in the hanging wall. Another unusual feature in Ogden Canyon is the pronounced east dip of the fault plane, which was mostly imposed long after thrusting in Neogene time, as indicated by overlap of east-dipping Tertiary beds in Huntsville Valley, and by fission-track data reported by Naeser and others (1983). Much has been published about this well-exposed and well-mapped area (e.g., Bryant, 1984; Bruhn and Beck, 1981; Crittenden, 1972; Sorensen and Crittenden, 1972, 1979; Schirmer, 1988; Yonkee and others, 1989;). Although the eastward extent of the Willard fault is masked by Tertiary cover and normal faulting, its trace south of Huntsville, Utah, and north to an outcropping toe position on the east flank of the Bear River Range in the Woodruff Creek drainage is constrained by outcrops in the Causey Creek Dam area (Mullens, 1969) of distinctive hanging-wall Proterozoic and lower Paleozoic strata, which compose the thrust sheet. On Woodruff Creek, there is an overturned panel of Triassic and Jurassic rocks below Proterozoic quartzite. From here, the Willard fault trace extends northward under Maastrichtian and Lower Tertiary cover to link in left-stepping en echelon fashion with the Paris thrust previously mentioned. Cross section G-G′ (**Sheet 1**, Royse, map pocket) shows the Willard thrust sheet to have been folded by basement uplift related to both younger thrusting and to post-Eocene (post thrusting) extension.

The amount of displacement of the Willard-Paris thrust sheet is uncertain. Fortunately, post-thrusting uplift and erosion has exposed enough of hanging-wall and footwall stratigraphic cutoffs to allow an estimation. If, as maps indicate, the hanging-wall cutoff of lower Paleozoic beds (which appears to occur in the covered area south of the Woodruff Creek outcrop) can be matched with footwall cutoffs exposed to the west, north of Ogden, then the displacement on the Willard fault is about 40 miles (62 km). One should realize that this figure includes displacement attributed to the Laketown-Meade thrust system, since the Laketown thrust must join the Willard under cover north of Woodruff Creek. Assuming that displacement on the Laketown at its branch point with the Willard is the same as the 25-mile (40 km) slip on the Meade in its type area, then initial pre-Meade displacement of Willard sheet alone would be 15 miles (24 km). Maps also show that south of Woodruff Creek the Willard fault plane cuts upsection toward the south in the hanging wall, and that near Ogden it cuts upsection toward the south in the footwall. This indicates that a north-facing lateral ramp exists in the fault plane, mimicking the shape of the Absaroka and maybe the Crawford thrusts. Such along-strike changes in stratigraphic position of the fault plane may produce errors when matching hanging-wall and footwall cutoffs for the purpose of determining displacement, depending upon where one selects matching points. For example, an intensely deformed outcrop of Cambrian Maxfield Dolomite below Proterozoic about 2 miles (3.2 km) east of Huntsville (Crittenden, 1979) is 6 miles (9.7 km) east of footwall cutoffs of younger Paleozoic rocks in Ogden Canyon; this raises questions about the positions of footwall stratigraphic cutoffs below the Willard sheet.

The sedimentary record indicates an Early Cretaceous, probably Aptian-Albian, age for time of major displacement of the Willard-Paris thrust sheet. Emplacement of the sheet is generally considered to have begun with or shortly before deposition of the Ephraim Conglomerate (Armstrong and Cressman, 1963) and to have continued through a phase of rapid subsidence, which resulted in deposition of clastic foredeep deposits of Lower Cretaceous age possibly 15,000 feet (4.6 km) thick (**Figure 2**). Subsidence is presumed to have been a result of flexural downwarp of the basement due to loading by the Willard-Paris thrust sheet (Jordan, 1981). The age of the Ephraim Conglomerate was thought to be as old as latest Jurassic by the U.S. Geological Survey; however, Heller and others (1986) favor an Aptian age based on scanty fossil data and subsidence history. More recently, Heller and Paola (1989) contended that distinctive clast lithology and widespread distribution of lower

Ephraim and correlative conglomerates eastward throughout the Rocky Mountain foreland is evidence that deposition occurred prior to subsidence and that the conglomerates were derived in part from sources far to the west of the Willard-Paris thrust sheet, thereby reinforcing their argument that thrusting is not significantly older than Aptian. It is difficult to reconcile their interpretation that the conglomerate doesn't indicate thrusting with Armstrong and Cressman's (1963) discussion of the Ephraim Conglomerate in the Red Mountain area. Armstrong and Cressman reported unique lithologies, clasts as large as two feet in diameter, and very rapid westward thickening, all indicating that the Willard-Paris thrust sheet (Bear River Range) was a nearby source. However, precise definition of the Ephraim Conglomerate at Red Mountain is uncertain, and the basal chert-pebble-bearing part may be significantly older (Jurassic?) than the rest of the unit.

The possibility that thrusting began earlier than Aptian in the west is indicated by subsidence and deposition of over 7,000 feet (2,135 m) of marine clastic sediments and evaporites in Middle to Late Jurassic time in western Utah and south-central Idaho. Jordan (1985) discussed the possibility that this Jurassic basin is a foredeep filled with clastic rocks derived mostly from thrusted highlands to the west. (Older clastic rocks were derived wholly from the craton to the east.) However, the Jurassic uplift was coincident with magmatism, which suggests a thermal origin (Heller and Paola, 1989) rather than a thrust uplift. Allmendinger and others (1984) reported minor thrusting in northwest Utah of Jurassic age. In any case, no thrust sheets comparable in magnitude to the Willard-Paris sheet have yet been recognized to the west.

Extensional deformation

East-west horizontal extension of late Eocene(?) through Holocene age is pervasive in the thrust belt. Extension was a result of movement on mostly west dipping normal faults, which merged with and occupied older thrust fault planes so that a part of the major thrust planes accommodated composite movement, early contractional deformation, and later extension (Royse, 1983; Royse and others, 1975).

Surface maps, seismic data, and well data together show conclusively that the position and shape of normal faults was controlled by that of the thrust faults, which were controlled by stratigraphy, especially Jurassic evaporites. The basement below the regional Cambrian décollement east of the Wasatch fault was not affected. Ramps in the thrust fault planes localized the surface traces of normal faults, and along-strike terminations of normal faults coincide with strike terminations of thrust fault ramps in the subsurface. For example, the Grand Valley fault joins and follows a major ramp in the Absaroka thrust (**Sheet 1B**, Royse, map pocket), and the Hoback fault position coincides with a ramp in the Prospect thrust system (Royse and others, 1975). Near Evanston, Wyoming, the Acocks and Almy normal faults merge with a ramp in the Medicine Butte thrust, which follows bedding in Jurassic evaporites. East of the Fossil Basin a network of minor normal faults parallels the ramp in the Hogsback thrust, and, like the Hogsback thrust, these normal faults do not extend onto the Uinta Mountain block. Other examples are shown on the cross sections (**Sheet 1**, Royse, map pocket).

Characteristic normal fault structure at the surface is a half graben bounded on the east by a fault. Many of these half graben are expressed topographically as broad linear valleys, such as Grand, Thomas Fork, Bear Lake, and Cache valleys. Rocks on the downthrown side, including graben fill, are rotated and dip eastward into the fault, forming noncompressional folds (e.g., Hoback fault motion produced the Willow Creek anticline). Rotation of downthrown beds is a result of motion on a fault whose attitude changes from a steep surface dip to a gentler dip in the subsurface where the fault joins and assumes the path of a thrust fault. Whether the fault planes are actually curved (listric) or not is a matter of interpretation; seismic data and lack of volume-compensating antithetic faults indicate some of them are. Most downthrown beds are rotated eastward because the thrust fault ramps that localize the normal faults dip westward. Important exceptions occur where graben-fill beds are rotated westward into normal faults that follow thrust-faulted east-dipping panels of incompetent units such as the evaporitic beds of the Jurassic Preuss Formation in the East Canyon Reservoir area, Utah (**Sheet 1H**, Royse, map pocket).

Seismic profiles commonly show that graben-fill beds fan outward toward the fault, a feature which indicates deposition during faulting. More precise ages and correlations of these beds would allow better estimations of ages and rates of faulting than we have now. It is not certain whether these graben-fill deposits are as old as Eocene (Armstrong and Oriel, 1965). The Miocene through Pleistocene ages reported for most of the graben fill indicate major extensions occurred during that interval. Offsets of Holocene sediments along the Wasatch fault (Smith and Bruhn, 1984) show that extension is probably occurring today.

The total net east-west horizontal extension within the thrust belt east of the Wasatch fault appears to be on the order of 5 to 6 miles (8-10 km). The amount of net slip on a single fault may be quite large; the Grand Valley fault has about 16,000 feet (5 km) of net slip near Alpine, Wyoming and the Bear Lake valley fault has about 15,000 feet (4.6 km) of slip north of Bear Lake, Idaho.

Possible thrust fault control on the Wasatch fault (zone) in this area is not obvious. It may merge in the subsurface with the basal thrust décollement within the basement. Northward from the Ogden area, stratigraphic separation and slip on the Wasatch fault appear to decrease. Displacement may be relayed eastward to the Cache Valley fault. If so, linkage through such a regional décollement is indicated, perhaps for the entire normal fault trend north to the Snake River Plain. Southward, the Wasatch fault trend is interrupted by a promontory north of Salt Lake City (Traverse Mountains), which coincides with the steep south plunge of the Archean basement thrust uplift and the abrupt southward appearance of thick Proterozoic deposits in the Cottonwood uplift outcrop area (**Sheet 1H**, Royse, map pocket). There is a fundamental, but poorly understood, east-west striking structural discontinuity at this latitude, which has influenced structural development from Proterozoic through periods of thrusting and extension until the present (Bryant and Nichols, 1988; Bruhn and others, 1986).

The interpretation of the Wasatch fault shown on cross section G-G′ and H-H′ (**Sheet 1**, Royse, map pocket) indicates modification of the footwall by post-10 Ma uplift. Footwall uplift of this age is indicated by fission-track studies (Naeser and others, 1983). Fission-track dates of hanging-wall Proterozoic rocks at Little Mountain, about 12 miles (19 km) west of Ogden, Utah, are reported to be in the range of 67 to 75 Ma (Absaroka thrust time), indicating that Tertiary uplift is essentially confined to the Wasatch fault footwall. Tertiary uplift may be due to an isostatic response of the crust to extensional faulting and unloading of the hanging-wall rocks in a manner similar to that described by Wernicke and Axen (1988) for the Virgin and Beaver Dam mountains in southwestern Utah.

Unlike the Uinta Mountains, the Teton-Gros Ventre block adjacent to the thrust belt has been extended by normal faulting similar to that seen in the thrust belt proper, a process that produced the spectacular topography seen there, such as the Teton Range and Jackson Hole. Movement on several mostly north-south striking east-dipping normal faults has rent this Archean basement-cored foreland thrust sheet into a series of west-tilted blocks, the largest of which is the Teton Range. Others are West and East Gros Ventre Buttes near Jackson, Wyoming. Tilting of downthrown beds suggests a listric fault shape, and the apparent termination of the faults southward against the surface trace of the Cache Creek thrust indicates that faulting is confined to the Cache Creek thrust sheet. Possible domino-like planar rotation of fault planes (Wernicke and Burchfiel, 1982) to produce the tilted blocks rather than curved fault planes has not been ruled out. The largest fault, the Teton fault, dips eastward about 35° and has accommodated as much as 23,000 feet (7 km) of displacement, much of which is less than 9 Ma old (Behrendt and others, 1968). The other faults appear to mimic the Teton fault. Of interest is the fact that the southern termination of the Teton fault is nearly opposite the northern termination of the Hoback fault, each being confined to thrust sheets but with opposite senses of dip and displacement (**Figure 1**).

Discussion

Restored section

In thrust belt settings, the component of horizontal translation is so large when compared to the vertical that many geologic analyses cannot be made without employing some sort of structural restoration. The foregoing discussions of the various thrust faults have underscored the difficulty in accounting for along-strike displacement balance, the map balance which must exist. The series of isopachs in **Figure 2** are an attempt to show restored thicknesses of certain regionally correlatable stratigraphic packages but only on a very small scale; restoration was made by moving isopach data points westward by an amount equal to their total horizontal displacement according to structural cross sections, and then contouring them. Control is sparse to nonexistent in some western areas, but the simple form of the isopachs on a small scale allows a reasonable projection of data and restoration of eroded material.

A structural restoration to a time near the end of the Jurassic and before emplacement of the Willard-Paris thrust sheet is illustrated in cross section along latitude 41°15′N on **Sheet 2**, Royse (map pocket) close to the line of cross section G-G′ (**Figure 1**). The top of marine Jurassic rocks (Stump Formation) is a reliable datum throughout most of the thrust belt, and it provides a convenient reference line for displaying the original cross-sectional shape of stratigraphic units deposited before, during, and after thrusting. Restoration was made by constructing thickness profiles according to the restored stratigraphic isopachs (**Figure 2**) and by plotting thrust fault trajectories on them in their prefault positions. Thrust fault sheets were placed in a prethrust position by moving each fault sequentially westward, beginning with the Hogsback and ending with the Willard, by an amount equal to their displacement according to structural cross sections, while maintaining footwall stratigraphic cutoff geometry. Longitude marks are in present-day positions. The restored section is plotted in both natural scale and in a 1:4 vertically exaggerated scale. It is important to realize that at this latitude, the Laketown fault has merged with the Willard, so that the fault shown is a composite of the two. Total horizontal displacement of Mississippian rocks is about 103 miles (163 km); a zone originally about 143 miles (229 km) wide has been compressed into approximately 40 miles (64 km), or about 70% total shortening. This is somewhat larger than the 65 miles (104 km) and 50% shortening reported by Royse and others (1975). The discrepancy is due to the addition at this latitude of the Laketown (Meade) displacement to the Willard displacement—a feature not recognized in the 1975 paper.

There are too many generalizations and assumptions in this restoration for it to be considered a conclusive interpretation; however, certain speculative features are worth mentioning. The shape of the restored prethrusting wedge is largely dependent upon two items: (1) the position of the thick (+20,000 feet, 6 km) Proterozoic section, and (2) the shape of the upper Paleozoic isopach. In this interpretation, the Proterozoic section is portrayed as appearing suddenly at a fault boundary (rifted margin?), and the upper Paleozoic is shown as a rapidly westward expanding section by spacing contours evenly between the control points used to make the isopach. Prior to thrusting, the surface was near sea level and the west dip of the top of Archean basement below the sedimentary wedge was about 3° on the east and 6° on the west. A different portrayal of the Proterozoic section (for instance as an evenly east tapering wedge) or portrayal of the upper Paleozoic thickening as occurring across late Paleozoic fault(s) could modify this shape. Proterozoic faulting is shown to localize the position of the Willard thrust basement ramp—this is a common speculation. The sudden thickening of upper Paleozoic rocks creates an inflection in an otherwise planar basement surface and may have influenced the shape of the Willard thrust and localized younger thrust fault involvement of the crystalline basement.

The original position of the Archean basement block, which now forms the core of the anticlinal central Wasatch Range uplift, is shown to be just west of Antelope Island, following the interpretation that uplift began in Santonian(?) with Absaroka thrusting and that displacement of the block would be equal to that of the Absaroka and Hogsback thrust sheets combined (±43 miles, 69 km). If Crawford displacement is added, the basement block would have originated as much as an additional 20 miles (32 km) farther west, a position not supported by this analysis. The thickness of the Archean basement block is conjectural, but cross sections indicate that it must be ±40,000 feet (12 km). If true, this would mean that the

basal décollement had shifted down well into the basement from its original position on top of the basement block. A possible cause of this downward shift in the position of the basal detachment could be maintenance of a critical wedge shape in the overthrust block.

Another item of interest is that the restored spacing of points where major thrusts branch from the top basement décollement increases eastward toward the foreland—36 miles (57 km) between Willard-Laketown and Crawford branch points, 40 miles (63 km) between Crawford and Absaroka, and 48 miles (77 km) between Absaroka and Hogsback. Increased spacing eastward may result from decreasing eastward taper of the thrust block caused by the progressive introduction of weak ductile décollement horizons in the eastward migrating, deforming wedge such as Jurassic evaporites and Cretaceous coal.

Wedge hypothesis

Although it is tempting to quantitatively apply the critical wedge hypothesis (Chapple, 1978; Davis and others, 1983; Dahlen and others, 1984) to the evolution of this thrust belt using restorations such as **Sheet 2**, Royse (map pocket) along with intermediate steps, such a study is beyond the scope of this paper. The overall regional consistency in stratigraphic features that affect the mechanical properties of the wedge, such as thickness and lithology, coupled with the availability of critical data, make this area a likely one for such a study. Obviously, the thrust sheets were wedge shaped, and they slid coherently on basal décollements (the shape of the initial thrust sheet, the Willard is the most uncertain). Woodward's (1987) concerns about the applicability of the hypothesis to the Wyoming thrust belt may be alleviated by proper integration of all available data. The repeated floods of coarse conglomerates derived from the west indicate episodic uplift in the interior of the wedge over major fault plane ramps. It appears that after initial failure, the wedge may have remained "supercritical" during thrusting by incorporating new weak basal décollements at the toe. Minor interior adjustments such as the Tunp thrust accompanied final phases of thrusting in Lower Eocene time.

The localization of the Archean basement uplift to the area of the present central Wasatch Range and eastern Great Salt Lake may have been predetermined by pronounced thickness changes of the upper Paleozoic section. Coincidence between the area of basement involvement and the marked thinning of isopachs in the upper Paleozoic rocks (**Figure 2**) suggest that the basement became involved in thrusting as a means of maintaining a critical shape (thickness) to the overall regional thrust wedge.

Thrusting and sedimentation

It has become almost axiomatic that foreland basins develop by flexure of the continental lithosphere induced by thrust sheet loads (Price, 1973). Many have used this concept to quantitatively analyze sedimentation associated with thrusting (e.g., Beaumont, 1981; Quinlan and Beaumont, 1984; Royden and Karner, 1984; Stockmal and others, 1986). Jordan (1981) successfully applied this model to the Idaho-Wyoming thrust belt to explain the eastward shift in pre-Santonian Cretaceous subsidence and sedimentation there, and Heller and others (1986) used it to conclude that onset of thrusting was probably no older than Aptian.

A commonly accepted corollary to this hypothesis is that thrusting means subsidence. This does not appear to be always the case in Wyoming. The emplacement of the Absaroka and Darby system of thrust sheets did not produce subsidence of the lithosphere according to a reconstruction of the thermal and depositional history (Warner and Royse, 1987). In the Fossil Basin, the sedimentary section above the crystalline basement was at least as thick before emplacement of the Absaroka thrust sheet as after. In essence, the Absaroka thrust sheet replaced the Jurassic-Cretaceous section, which was eroded as thrusting proceeded. In the LaBarge, Wyoming area, the basement surface was actually buried deeper before emplacement of the Darby-Hogsback thrust sheet than after (Warner and Royse, 1987). Apparently, no extra load was placed upon the lithosphere as a result of thrusting because the thrust sheets were eroded as they were emplaced, and the eroded material was transported eastward and deposited in subsiding basins on the foreland such as the Green River-Hoback and Washakie basins. The cause of foreland basin subsidence is probably more complex than simple flexural subsidence due to top loading of the lithosphere by major thrust-bounded uplifts and may be related to events within the crust and mantle (e.g., see

Dickinson and Snyder, 1978; Cross, 1986). In some areas such as the southern Wyoming thrust belt, the Uinta Basin, and the Green River Basin subsidence was not symmetrical with uplifts and it continued after basin-margin faulting had ceased. Also, lack of an Early Cretaceous foredeep in central Utah is curious. Interestingly, the thrusts considered responsible for the Aptian through Santonian foredeep basins (the Willard-Paris and Meade-Laketown) are the ones dated by the date of the basin (subsidence) presumed to be caused by them—a circular argument against which, in the light of provenance studies, there is no apparent reasonable alternative; but one wonders what is cause and what is effect? Jordan and others (1988) presented a comprehensive discussion of basin subsidence due to thrust faulting.

Some areas in the interior of the thrust belt, such as the Fossil Basin and Bear Lake plateau, received significant thicknesses of sediment (±4000 feet, 1.2 km), which has remained essentially undeformed except at the very margins (**Sheet 1G** and **H**, Royse, map pocket; Lamerson, 1982; Hurst and Steidtmann, 1986; Coogan, 1989). These have been called piggyback basins, probably because they evolved while being transported on the basal Cambrian thrust décollement as part of younger thrust sheets. The basins are not discretely subsiding units like the Early Cretaceous foredeep or the Hoback Basin, but they are local areas that lie within a much larger subsiding region and were partly isolated topographically by local structural movements. Delineation of the Fossil Basin as a structurally discrete sedimentary basin was by minor thrust uplift of early Eocene age (Tunp and Medicine Butte thrusts) in the ramp region of the Absaroka thrust to form the western border and by uplift of the Hogsback thrust sheet over the Hogsback ramp in early Paleocene(?) through early Eocene to form the eastern border. The Hogsback ramp originated some 14 miles (22 km) east of its present position and migrated westward relative to the hanging wall, shedding nonresistent Cretaceous deposits by erosion as Hogsback thrusting proceeded. The topographic ridges that comprise the eastern margin of the Fossil Basin formed when resistant lower Mesozoic beds were exposed by uplift and erosion of the Hogsback hanging wall, and when lower Mesozoic and Paleozoic beds of the Absaroka hanging wall were carried up the Hogsback ramp. Southward, the eastern margin loses definition as the Eocene rocks overlap the ridges and thicken toward the Uinta Mountains and the trend of Hogsback and Absaroka thrust ramps diverge. It seems from the foregoing discussion that sedimentation is not related to thrusting in a simple way.

Conclusions and suggestions for future study

The Wyoming-eastern Idaho-northern Utah segment of the Cordilleran thrust belt is one of the better known worldwide because of the wealth of geologic information available. The thin-skinned structural style has been well documented by integrating data from widespread surface exposures, numerous well bores, extensive good-quality reflection seismic coverage, and gravity and aeromagnetic surveys. Much paleontologic data has been collected which, along with sparse radiometric analyses, document the Cretaceous and early Tertiary age and the time range of emplacement of major thrust sheets.

The stratigraphic control on thrust fault geometry is striking. The pronounced continuity, coherency, large breadth, and shape of major thrust sheets are due to the simple, wide-ranging, homogeneous, layer-cake stratigraphy and thickness pattern of prethrust Proterozoic through Jurassic rocks. These rocks formed a west-thickening wedge that was optimally oriented with respect to the east-directed compressional stress to produce extensive, coherent, wedge-shaped thrust sheets. Paleozoic carbonate and sandstone and Jurassic sandstone units formed the struts within major thrust sheets. Major décollement horizons were localized in widespread homogeneous stratigraphic units, whose ductilities contrasted strongly with that of more brittle underlying units. Notable among these are Jurassic halite and anhydrite beds and basal Cambrian shale and carbonate beds. Cretaceous coal and shale provided added major décollement horizons as thrusting proceeded eastward and involved foredeep deposits derived from the erosion of earlier thrust sheets. The whole thrust belt system rides upon the basal Cambrian décollement; however, the oldest thrusts—the Willard-Paris and the Meade-Laketown—involve a thick Proterozoic clastic section not seen in thrust

sheets farther east. The general eastward progression in time of thrusting is a natural consequence of the maintenance of an eastward tapering "critical" wedge shape. The anomalous involvement in thrusting of crystalline basement rock in the central Wasatch Range may be due to the existence there of a late Paleozoic positive feature and relatively thin prethrust sedimentary section. The occurrence of several distinct, widespread Cretaceous and lower Tertiary conglomerate units signifies episodic uplift due to thrust faulting and, lacking dated, crosscutting or overlapping units, provides a means for general dating and discriminating specific thrust fault episodes. Post-Campanian phases of thrust faulting coincided with foreland deformation (e.g., Green River Basin, Wind River Range, etc.), which interrupted the classic foredeep sedimentary basin pattern that existed earlier. The cause of this later widespread phase of basin subsidence appears not to be due simply to top loading of the lithosphere by thrust sheets but to stresses within the crust and mantle. The general utilization of thrust fault surfaces by younger normal (extensional) faults was a result of the extensional strain direction being normal to the strike of the thrust faults.

Even though this thrust belt has been studied extensively and is relatively well known, much remains to be done. Most research has concentrated on large-scale regional features; there are numerous smaller scale problems and tasks to be addressed, such as determining mechanisms and means of along-strike displacement balance of specific faults (e.g., the Granite Creek and Crawford faults), and detailed descriptions and analyses of specific fault surfaces. This appears to be a good area to analyze the kinematic and rheologic attributes of a thrust fault without having to resort to abstract models. The geometry of subsurface structure in the westernmost part, the roots of the thrust faults, is uncertain and deserves more study. A project that investigates the applicability of the critical wedge hypothesis (Davis and others, 1983) to this area may provide a better understanding as well as new quantitative data. Fission-track data, although expensive, could refine tectonic (uplift) and thermal history and possibly indicate where erroneous interpretations have been made. It seems that the more one knows about the geology of a region, the more there is left to be known.

Acknowledgments

The author's first field experience with thrust belt geology was as a graduate student at the University of Wyoming under the guidance of D.L. Blackstone, Jr. Most thrust belt knowledge was attained while employed by Chevron U.S.A., Incorporated and through association with members of Chevron's Rocky Mountain Exploration staff, especially M.A. "Boone" Warner, Don Reese, Paul Lamerson, Clint Dahlstrom, Peter Verrall, and Bill Brown. Many thanks are due to Jim Coogan, who reviewed the cross sections and provided much new map data and insightful interpretation of the complex geology of the Meade and Crawford thrust systems. Adolph Yonkee shared his knowledge of the structural evolution of the central Wasatch Range. Reviewers R.W. Allmendinger, R.L. Bruhn, and editor A.W. Snoke suggested many alterations and corrections which significantly improved the manuscript. Drafting of illustrations was provided by The Geological Survey of Wyoming under the direction of Sheila M. Roberts.

References cited

Allmendinger, R.W., Miller, D.M., and Jordan, T.E., 1984, Known and inferred Mesozoic deformation in the hinterland of the Sevier belt, northwest Utah: Utah Geological Association Publication 14, p. 21-34.

Armstrong, F.C., and Cressman, E.R., 1963, The Bannock thrust zone, southeastern Idaho: U.S. Geological Survey Professional Paper 374-J, p. J1-J22.

Armstrong, F.C., and Oriel, S.S., 1965, Tectonic development of Idaho-Wyoming thrust belt: American Association of Petroleum Geologists Bulletin, v. 49, p. 1847-1866.

Beaumont, C., 1981, Foreland basins: Geophysical Journal of the Royal Astronomical Society, v. 65, p. 291-329.

Behrendt, J.S., Tibbetts, B.L., Bonini, W.E., and Lavin, P.M., 1968, A geophysical study in Grand Teton National Park and vicinity, Teton County, Wyoming: U.S. Geological Survey Professional Paper 516-E, 23 p.

Blackstone, D.L., Jr., 1977, The overthrust belt salient of the Cordilleran fold belt, western Wyoming-southeastern Idaho-northeastern Utah, *in* Heisey, E.L., Lawson, D.E., Norwood, E.R., Wach, P.H., and Hale, L.A., editors, Rocky Mountain thrust belt geology and resources: Wyoming Geological Association 29th Annual Field Conference Guidebook (with Montana Geological Society and Utah Geological Society), p. 367-384.

Boyer, D.L., 1982, Severe drilling hazards associated with the Thaynes-Woodside transition zone in the Wyoming Thrust Belt, *in* Powers, R.B., editor, Geologic studies of the Cordilleran thrust belt: Rocky Mountain Association of Geologists, p. 641-648.

Boyer, S.E., and Elliot, D., 1982, Thrust systems: American Association of Petroleum Geologists Bulletin, v. 66, p. 1196-1230.

Bradley, M.D., and Bruhn, R.L., 1988, Structural interactions between the Uinta arch and the overthrust belt, north-central Utah: implications of strain trajectories and displacement modeling, *in* Schmidt, C.J., and Perry, W.J., Jr., editors, Interaction of the Rocky Mountain foreland and the Cordilleran thrust belt: Geological Society of America Memoir 171, p. 431-446.

Bruhn, R.L., and Beck, S.L., 1981, Mechanics of thrust faulting in crystalline basement, Sevier orogenic belt, Utah: Geology, v. 9, p. 200-204.

Bruhn, R.L., Picard, M.D., and Isby, J.S., 1986, Tectonics and sedimentology of Uinta arch, western Uinta Mountains, and Uinta Basin, *in* Peterson, J.A., editor, Paleotectonics and sedimentation in the Rocky Mountain region, United States: American Association of Petroleum Geologists Memoir 32, p. 333-352.

Bryant, B., 1984, Reconnaissance geologic map of the Precambrian Farmington Canyon Complex and surrounding rocks in the Wasatch Mountains between Ogden and Bountiful, Utah: U.S. Geological Survey Map I-1447, scale 1:50,000.

_____ 1988, Geology of the Farmington Canyon Complex, Wasatch Mountains, Utah: U.S. Geological Survey Professional Paper 1476, 54 p.

Bryant, B., and Nichols, D.J., 1988, Late Mesozoic and early Tertiary reactivation of an ancient crustal boundary along the Uinta trend and its interaction with the Sevier orogenic belt, *in* Schmidt, C.J., and Perry, W. J., Jr., editors, Interaction of the Rocky Mountain foreland and the Cordilleran thrust belt: Geological Society of America Memoir 171, p. 411-430.

Chapple, W.M., 1978, Mechanics of thin skinned fold-and-thrust belts: Geological Society of America Bulletin, v. 89, p. 1189-1198.

Coogan, J.C., 1987, Thrust systematics and displacement transfer in the Wyoming-Idaho-Utah thrust belt: Geological Society of American Abstracts with Programs, v. 19, no. 7, p. 622.

_____ 1989, Distinguishing reactivated thrust slip vs. footwall uplift sedimentation patterns in hanging wall basins, Fossil Basin and Bear Lake Plateau, WY-ID-UT thrust belt: Geological Society of America Abstracts with Programs, v. 21., no. 6., p. 366.

_____ 1992, Thrust systems and displacement transfer in the Wyoming-Idaho-Utah thrust belt [Ph.D. dissertation]: Laramie, University of Wyoming, 240 p.

Coogan, J.C., and Royse, F. Jr., 1990, Overview of recent developments in thrust belt interpretation, *in* Roberts, S.M., editor, Geologic field tours of western Wyoming and parts of adjacent Idaho, Montana, and Utah: Geological Survey of Wyoming Public Information Circular 29, p. 89-126.

Craddock, J.P., Kopania, A.A., and Wiltschko, D. V., 1988, Interaction between the northern Idaho-Wyoming thrust belt and bounding basement blocks, central western Wyoming, *in* Schmidt, C.J., and Perry, W.J., Jr., editors, Interaction of the Rocky Mountain foreland and the Cordilleran thrust belt: Geological Society of America Memoir 171, p. 333-352.

Cressman, E.R., 1964, Geology of the Georgetown-Snowdrift Mountain area, southeastern Idaho: U.S. Geological Survey Bulletin 1153, 115 p.

Crittenden, M.D., Jr., 1972, Willard thrust and the Cache autochthon, Utah: Geological Society of America Bulletin, v. 83, p. 2871-2880.

_____ 1979, Geologic map of the Huntsville Quadrangle, Weber and Cache Counties, Utah: U.S. Geological Survey Geologic Quadrangle Map GQ-1503, scale 1:24,000.

Crittenden, M.D., Jr., and Sorensen, M.L., 1980, The Facer Formation, a new Early Proterozoic unit in northern Utah: U.S. Geological Survey Bulletin 1482-F, p. F1-F28.

Cross, T.A., 1986, Tectonic controls of foreland basin subsidence and Laramide style deformation, western

United States: International Association of Sedimentologists Special Publication no. 8, p. 15-39.

Dahlen, F.A., Suppe, J., and Davis, D., 1984, Mechanics of fold-and-thrust belts and accretionary wedges - Cohesive Coulomb Theory: Journal of Geophysical Research, v. 89, p. 10,087-10,101.

Dahlstrom, C.D.A., 1969, Balanced cross sections: Canadian Journal of Earth Sciences, v. 6, p. 743-757.

_____ 1970, Structural geology in the eastern margin of the Canadian Rocky Mountains: Bulletin of Canadian Petroleum Geology, v. 18, p. 332-406.

Davis, D., Suppe, J., and Dahlen, F.A., 1983, Mechanics of fold-and-thrust belts and accretionary wedges: Journal of Geophysical Research, v. 88, p. 1153-1172.

DeCelles, P.G., 1988, Lithologic provenance modeling applied to the Late Cretaceous synorogenic Echo Canyon Conglomerate, Utah: a case for multiple source areas: Geology, v. 16, p. 1039-1043.

Delphia, J.G., and Bombolakis, E.G., 1988, Sequential development of a frontal ramp, imbricates, and a major fold in the Kemmerer region of the Wyoming thrust belt: Geological Society of America Special Paper 222, p. 207-222.

Dickinson, W.R., and Snyder, W.S., 1978, Plate tectonics of the Laramide orogeny: Geological Society of America Memoir 151, p. 355-366.

Dixon, J.S., 1982, Regional structural synthesis, Wyoming salient of western overthrust belt: American Association of Petroleum Geologists Bulletin, v. 66, p. 1560-1580.

Eldridge, S., and Van der Voo, R., 1988, Paleomagnetic study of thrust sheet rotations in the Helena and Wyoming salients of the northern Rocky Mountains, *in* Schmidt, C.J., and Perry, W.J., Jr., editors, Interaction of the Rocky Mountain foreland and the Cordilleran thrust belt: Geological Society of America Memoir 171, p. 319-332.

Gray, M.B., and Platt, L.B., 1988, Regional implications of pebble deformation in the Gannett Group conglomerates, Idaho-Wyoming: Geological Society of America Abstracts with Programs, p. 417.

Hansen, W.R., 1986, History of faulting in the eastern Uinta Mountains, Colorado and Utah: Rocky Mountain Association of Geologists 1986 Symposium Guidebook, p. 5-17.

Heller, P.L., Bowdler, S.S., Chambers, H.P., Coogan, J.C., Hagen, E.S., Shuster, M.W., and Winslow, N.S., 1986, Timing of initiation of the Sevier orogeny, Idaho-Wyoming and Utah thrust belts: Geology, v. 14, p. 388-391.

Heller, P.L., and Paola, C., 1989, The paradox of Lower Cretaceous gravels and the initiation of thrusting in the Sevier orogenic belt, United States western interior: Geological Society of America Bulletin, v. 101, p. 864-875.

Hintze, L.F., 1988, Geologic history of Utah: Provo, Utah, Brigham Young University Geology Studies Special Publication 7, Provo, Utah, 202 p.

Hunter, R.B., 1988, Timing and structural interaction between the thrust belt and foreland, Hoback basin, Wyoming, *in* Schmidt, C.J., and Perry, W.J., Jr., editors, Interaction of the Rocky Mountain foreland and the Cordilleran thrust belt: Geological Society of America Memoir 171, p. 367-396.

Hurst, D.J., and Steidtmann, J.R., 1986, Stratigraphy and tectonic significance of the Tunp conglomerate in the Fossil Basin, southwest Wyoming: The Mountain Geologist, v. 23, p. 6-13.

Jacobson, S.R., and Nichols, D.J., 1983, Palynological dating of syntectonic units in the Utah-Wyoming thrust belt: the Evanston Formation, Echo Canyon Conglomerate, and Little Muddy Creek Conglomerate, *in* Powers, R.D., editor, Geologic studies of the Cordilleran thrust belt, 1982: Rocky Mountain Association of Geologists, p. 735-750.

Jordan, T.E., 1981, Thrust loads and foreland basin evolution, Cretaceous, western United States: American Association of Petroleum Geologists Bulletin, v. 65, p. 2506-2520.

_____ 1985, Tectonic setting and petrography of Jurassic foreland basin sandstones, Idaho-Wyoming-Utah: Utah Geological Association Publication 14, p. 201-213.

Jordan, T.E., Flemings, P.B., and Beer, J.A., 1988, Dating thrust-fault activity by use of foreland-basin strata, *in* Kleinspehn, K.L., and Paola, C., editors, Frontiers in sedimentary geology: new perspectives in basin analysis: New York, Springer-Verlag, p. 307-330.

Kraig, D.H., 1987, Interaction of basement uplift and thin-skinned thrusting, Moxa arch and the western overthrust belt, Wyoming: a hypothesis: Geological Society of America Bulletin, v. 99, p. 654-612.

Kraig, D.H., Wiltschko, D.V., and Spang, J.H., 1988, The interaction of the Moxa arch (LaBarge platform) with the Cordilleran thrust belt, south of Snider Basin, southwestern Wyoming, *in* Schmidt, C.J., and Perry, W.J., Jr., editors, Interaction of the Rocky Mountain foreland and the Cordilleran thrust belt: Geological Society of America Memoir 171, p. 395-410.

Lageson, D.R., 1984, Structural geology of Stewart Peak culmination, Idaho-Wyoming thrust belt: American Association of Petroleum Geologists Bulletin, v. 68, p. 401-416.

Lamerson, P.R., 1982, The Fossil Basin and its relationship to the Absaroka thrust system, Wyoming and Utah, *in* Powers, R.B., editor, Geologic studies of the Cordilleran thrust belt, 1982: Rocky Mountain Association of Geologists, p. 279-340.

Mackin, J.H., 1950, The down-structure method of viewing geologic maps: Journal of Geology, v. 58, p. 55-72.

Mansfield, G.R., 1927, Geography, geology and mineral resources of part of southeastern Idaho: U.S. Geological Survey Professional Paper 152, 453 p.

Mitra, G., and Yonkee, W.A., 1985, Relationship of spaced cleavage to folds and thrusts in the Idaho-Utah-Wyoming thrust belt: Journal of Structural Geology, v. 7, p. 361-373.

Mullens, T.E., 1969, Geologic map of the Causey Dam Quadrangle, Weber County, Utah: U.S. Geological Survey Geologic Quadrangle Map GQ-790, scale 1:24,000.

Naeser, C.W., Bryant, B., Crittenden, M.D., Jr., and Sorensen, M.L., 1983, Fission-track ages of apatite in the Wasatch Mountains, Utah: an uplift study: Geological Society of America Memoir 157, p. 29-36.

Oriel, S.S., and Armstrong, F.C., 1966, Times of thrusting in Idaho-Wyoming thrust belt: reply: American Association of Petroleum Geologists Bulletin, v. 50, p. 2614-2621.

Peale, A.C., 1879, Report on the geology of the Green River district: U.S. Geological and Geographic Survey of the Territories, Eleventh Annual Report, p. 509-646.

Peterson, J.A., 1987, Pre-thrusting regional stratigraphy and paleotectonics, northern Rocky Mountains and adjacent Cordilleran shelf, U.S.: Wyoming Geological Association 38th Annual Field Conference Guidebook, p. 17-26.

Platt, L.B., and Royse, F., Jr., 1989, The Idaho-Wyoming thrust belt: 28th International Geological Congress field trip guidebook T135, Washington, D.C., American Geophysical Union, 34 p.

Price, R.A., 1973, Large-scale gravitational flow of supracrustal rocks, southern Canadian Rockies, *in* DeJong, K.A., and Scholton, R., editors, Gravity and tectonics: New York, Wiley Interscience, p. 491-502.

_____ 1988, The mechanical paradox of large overthrusts: Geological Society of America Bulletin, v. 100, p. 1898-1908.

Quinlan, G.M., and Beaumont, C., 1984, Appalachian thrusting, lithospheric flexure, and the Paleozoic stratigraphy of the eastern interior of North America: Canadian Journal of Earth Science, v. 21, p. 973-996.

Rich, J.L., 1934, Mechanics of low-angle overthrust faulting as illustrated by Cumberland thrust block, Virginia, Kentucky and Tennessee: American Association of Petroleum Geologists Bulletin, v. 18, p. 1584-1596.

Royden, L., and Karner, G.D., 1984, Flexure of lithosphere beneath Appennine and Carpathian foredeep basins: evidence for an insufficient topographic load: American Association of Petroleum Geologists Bulletin, v. 68, p. 704-712.

Royse, F., Jr., 1983, Extensional faults and folds in the foreland thrust belt, Utah, Wyoming, Idaho: Geological Society of America Abstracts with Programs, v. 15, no. 5, p. 295.

_____ 1985, Geometry and timing of the Darby-Prospect-Hogsback thrust fault system, Wyoming: Geological Society of America Abstracts with Programs, v. 17, no. 4, p. 263.

Royse, F., Jr., and Warner, M.A., 1987, Little Muddy Creek area, Lincoln County, Wyoming, *in* Beus, S., editor, Centennial Field Guide: Rocky Mountain Section: Boulder, Colorado, Geological Society of America, Centennial Field Guide volume 2, p. 213-216.

Royse, F., Jr., Warner, M.A., and Reese, D.L., 1975, Thrust belt structural geometry and related stratigraphic problems, Wyoming-Idaho-northern Utah, *in* Bolyard, D.W., editor, Deep drilling frontiers of the central Rocky Mountains: Rocky Mountain Association of Geologists Symposium, p. 41-54.

Rubey, W.W., 1973, Geologic map of the Afton Quadrangle and part of the Big Piney Quadrangle, Lincoln and Sublette counties, Wyoming: U.S. Geological Survey Miscellaneous Geologic Investigations Map I-686, scale 1:48,000.

Rubey, W.W., and Hubbert, M.K., 1959, Role of fluid pressure in mechanics of overthrust faulting, part II. Overthrust belt in geosynclinal area of western Wyoming in light of fluid-pressure hypothesis: Geological Society of America Bulletin, v. 70, p. 115-206.

Rubey, W.W., Oriel, S.S., and Tracey, J.I., Jr., 1975, Geology of the Sage and Kemmerer 15-minute quadrangles, Lincoln County Wyoming: U.S. Geological Survey Professional Paper 855, 18 p.

_____ 1980, Geological map and structure sections of the Cokeville 30-minute quadrangle, Lincoln and Sublette counties, Wyoming: U.S. Geological Survey Miscellaneous Investigations Map I-1129, scale 1:62,500.

Schultz, A.R., 1914, Geology and geography of a portion of Lincoln County, Wyoming: U.S. Geological Survey Bulletin 543, 139 p.

Sears, J.W., Graff, P.J., and Holden, G.S., 1982, Tectonic evolution of Lower Proterozoic rocks, Uinta Mountains, Utah and Colorado: Geological Society of America Bulletin, v. 93, p. 990-997.

Schirmer, T.W., 1988, Structural analysis using thrust-fault hanging-wall sequence diagrams: Ogden duplex, Wasatch Range, Utah: American Association of Petroleum Geologists Bulletin, v. 72, p. 573-585.

Shuster, M.W., and Steidtmann, J.R., 1988, Tectonic and sedimentary evolution of the northern Green River Basin, western Wyoming, *in* Schmidt, C.J., and Perry, W.J., Jr., editors, Interaction of the Rocky Mountain foreland and the Cordilleran thrust belt; Geological Society of America Memoir 171, p. 515-529.

Smith, R.B., and Bruhn, R.L., 1984, Intraplate extensional tectonics of the eastern Basin-Range: inferences on structural style from seismic reflection data, regional tectonics, and thermal-mechanical models of brittle-ductile deformation: Journal of Geophysical Research, v. 89, p. 5733-5762.

Sorensen, M.L., and Crittenden, M.D., Jr., 1972, Preliminary geologic map of part of the Wasatch Range near Ogden, Utah: U.S. Geological Survey Miscellaneous Field Studies Map MF-428, scale 1:24,000.

_____ 1979, Geologic map of the Huntsville Quadrangle, Weber and Cache counties, Utah: U.S. Geological Survey Geologic Quadrangle Map GQ-1503, scale 1:24,000.

Stockmal, G.S., Beaumont, C., and Boutilier, R, 1986, Geodynamic models of convergent margin tectonics: the transition from rifted margin to overthrust belt and the consequences for foreland basin development: American Association of Petroleum Geologists Bulletin, v. 70, p. 43-62.

St. John, O.H., 1879, Geological Report of the Teton Division: U.S. Geological Survey of the Territories 11th Annual Report, p. 321-508.

Valenti, G.L., 1982, Structure of the Laketown Quadrangle and petroleum exploration in the Bear Lake area, Rich County, Utah, *in* Powers, R.B., editor, Geologic studies of the Cordilleran thrust belt: Rocky Mountain Association of Geologists, p. 859-868.

_____ 1987, Review of the hydrocarbon potential of the Crawford thrust plate, Wyoming-Idaho-Utah thrust belt: Wyoming Geological Association 38th Annual Field Conference Guidebook, p. 257-266.

Veatch, A.C., 1907, Geology of a portion of southwestern Wyoming: U.S. Geological Survey Professional Paper 56, 178 p.

Vietti, J.S., 1974, Structural geology of the Ryckman Creek anticline area, Lincoln and Uinta counties, Wyoming [M.S. thesis]: Laramie, University of Wyoming, 102 p.

Wallace, C.A., and Crittenden, M.D., Jr., 1969, The stratigraphy, depositional environment, and correlation of the Precambrian Uinta Mountain Group, western Uinta Mountains, Utah: Intermountain Association of Petroleum Geologists 16th Annual Field Conference Guidebook, p. 127-141.

Warner, M.A., and Royse, F., Jr., 1987, Thrust faulting and hydrocarbon generation: discussion: American Association of Petroleum Geologists Bulletin, v. 71, p. 882-889.

Webel, S., 1977, Some new perspectives on the old Nugget oil fields of the LaBarge platform: Wyoming Geological Association 29th Annual Field Conference Guidebook, p. 665-671.

Wernicke, B., and Burchfiel, B.C., 1982, Modes of extensional tectonics: Journal of Structural Geology, v. 4, p. 105-115.

Wernicke, B., and Axen, G.J., 1988, On the role of isostasy in the evolution of normal fault systems: Geology, v. 6, p. 848-851.

Wiltschko, D.V., and Dorr, J.A., Jr., 1983, Timing of deformation in overthrust belt and foreland of Idaho, Wyoming and Utah: American Association of Petroleum Geologists Bulletin, v. 67, p. 1304-1322.

Woodward, N.B., 1986, Thrust fault geometry of the Snake River Range, Idaho and Wyoming: Geological Society of America Bulletin, v. 97, p. 178-193.

_____ 1987, Geological applicability of critical-wedge thrust-belt models: Geological Society of America Bulletin, v. 99, p. 827-832.

Yonkee, W.A., 1992, Basement-cover relations, Sevier orogenic belt, northern Utah: Geological Society of America Bulletin v. 104, p. 280-302.

Yonkee, W.A., Parry, W.T., Bruhn, R.L., and Cashman, P.H., 1989, Thermal models of thrust faulting: constraints from fluid-inclusion observations, Willard thrust sheet, Idaho-Utah-Wyoming thrust-belt: Geological Society of America Bulletin, v. 101, p. 304-315.

Frontispiece. North view of west flank of the Bighorn Mountains (T. 55N., R.91W.), between Shell Canyon on the south and Five Springs on the north. White bed exposed in the monocline is the Mississipian Madision Limestone. Photograph graciously provided by Bob Lynn, Denver.

Structural style of Laramide basement-cored uplifts and associated folds

William G. Brown
Department of Geology
Baylor University
Waco, Texas 76798

Abstract

Laramide deformation of the Wyoming foreland was controlled by the direction and rate of convergence between the North American and Farallon plates along the western margin of North America during the period of 80 to 40 Ma. The N40° to 50°E direction of convergence resulted in formation of primary reverse-faulted structures oriented northwest-southeast.

The sequence of deformation of the foreland progressed as a tectonic front beginning at the western margin of the foreland in the vicinity of the Moxa arch in Campanian time. This tectonic front moved eastward through time, deforming the Wind River uplift primarily in Maastrichtian. The Owl Creek Mountains were uplifted during Paleocene and early Eocene. To the north and east, the Bighorn and Beartooth ranges were uplifted in early Eocene, with final movements occurring after the middle Eocene.

No single model applies to all structures throughout the Wyoming foreland. Evidence presented here leads to the conclusion that the orientation of structural features within the inferred northeast-oriented Laramide horizontal stress field dictated the type of structure that developed. Primary Laramide structures trend in a northwest orientation, with subordinate trends of northeast, east, and north superimposed across the northwest grain. This intersection of primary and subordinate trends results in a block-like pattern of faulted folds. The northwest-trending features display basic characteristics of major contractile (crustal shortening) structures such as thrusts, thrust-folds, basement wedges, or fold-thrusts. These primary fault systems created large magnitudes of crustal shortening in a northeast-southwest direction.

Interpretations of northwest-trending uplifts as nonshortening (noncontractile) features formed through differential vertical uplift are structurally out of balance (length of the basement/sediment contact is too short compared to length of the overlying sedimentary layers). Correct application of nonshortening (differential vertical uplift) models to the foreland is dependent upon finding direct evidence of vertical motion (slickensides), and/or structures which allow bed-lengthening or bed-thinning, as predicted by theoretical and experimental work by Hafner and Sanford.

Although the dominant direction of motion along foreland faults is reverse dip-slip, locally there are areas where the dominant motion is vertical. This condition exists where: (1) a northwest-trending anticline is segmented by a high-angle transverse fault, and (2) at the corner formed by the intersection of northwest-striking thrusts and east-striking high-angle faults. A vertical component is therefore achieved as a component of oblique-slip motion along the transverse fault.

Magnitude of Laramide crustal shortening is reasonably consistent across the Wyoming foreland when measured parallel to the southwest and northeast direction of regional tectonic transport. Values of total crustal shortening approach 30 miles and represent approximately 15% strain across the foreland. Magnitudes of lateral offsets are surprisingly small when compared to the total shortening. A general lack of

Brown, W.G., 1993, Structural style of Laramide basement-cored uplifts and associated folds, *in* Snoke, A.W., Steidtmann, J.R., and Roberts, S.M., editors, Geology of Wyoming: Geological Survey of Wyoming Memoir No. 5, p. 312-371.

significant en echelon *fold trends argues against a wrench-fault system as the dominant mechanism of foreland deformation. Instead, the total magnitude of lateral offset appears to have been distributed across the foreland on individual faults (with dominantly east and northeast orientations) in a style called compartmental deformation. The presence of northeast- and southwest-verging, low-angle reverse faults is compatible with theoretical predictions for horizontal compression. This is another indication that the foreland basement yielded along a conjugate set of reverse faults, and thus it can be inferred that the northeast-southwest compressive stress was generated by the northeast-southwest direction of convergence between the North America and Farallon plates during the Laramide orogeny.*

Introduction

The Rocky Mountain foreland is located immediately east of the Cordilleran thrust belt and provides a distinct contrast in structural style to the thin-skinned thrusting in the Cordillera; yet both styles are intimately related, in both time and space, to the late Mesozoic-early Cenozoic plate interaction along the west coast of North America (see Snoke, this volume). The Wyoming foreland (**Figure 1**) is an important part of the larger Rocky Mountain foreland, and lies immediately east of the Wyoming salient of the thrust belt. The well-exposed outcrops throughout the Wyoming foreland have provided opportunities for geologists to study the basement-involved deformation typical of foreland regions. Many theories and models of basement-involved deformation have been developed in Wyoming and applied throughout the Rocky Mountain region and also to other foreland areas. Some of these theories and models describe: (a) deformation mechanisms of basement rocks (Bucher, 1920; Wilson, 1934; Wise, 1964), (b) segmentation of large mountain uplifts (Demorest, 1941; Bell, 1956; Hoppin and Jennings, 1971), (c) mechanical stratigraphy and deformation mechanisms of sedimentary rocks (Fanshawe, 1971; Stearns, 1978; Petersen, 1983), and (d) structural models of drape folds and upthrust structures (Prucha and others, 1965; Stearns, 1971), wedge-uplift (Chamberlain, 1925; Erslev, 1986; Robbins and Erslev, 1986) and fold-thrusts (Berg, 1962b; Gries, 1983a; Brown, 1983). Other structural concepts such as structural balance conceived in other areas, have been tested in and applied to the Wyoming foreland.

The structural style of the Wyoming foreland has been interpreted in many different ways over the past century. In general, these differences are related to each author's concept of the orientation of the stresses involved in the deformation. There are two basic concepts of foreland deformation: (a) differential vertical uplift (nonshortening) accomplished primarily through vertically directed stresses, and (b) crustal shortening accomplished primarily through horizontal compressive stresses. Various structural models have been proposed for individual foreland structures, based upon which concept is accepted; often different models have been applied to interpret the same structure. The magnitude of total crustal shortening across the Wyoming foreland also has certain implications for interpretation of possible strike-slip motions within the foreland.

This chapter presents an historical review of the development of geologic thought with respect to the mode of deformation of the foreland. The historical review is followed by a discussion of structural observations on the character of Precambrian basement and the sedimentary rocks involved in the foreland structures. Various structural models proposed for individual foreland structures are discussed, along with evidence to support or deny the models. The magnitude of total crustal shortening across the Wyoming foreland is discussed as it relates to regional structural balance within the foreland and whether or not large magnitude strike-slip has occurred.

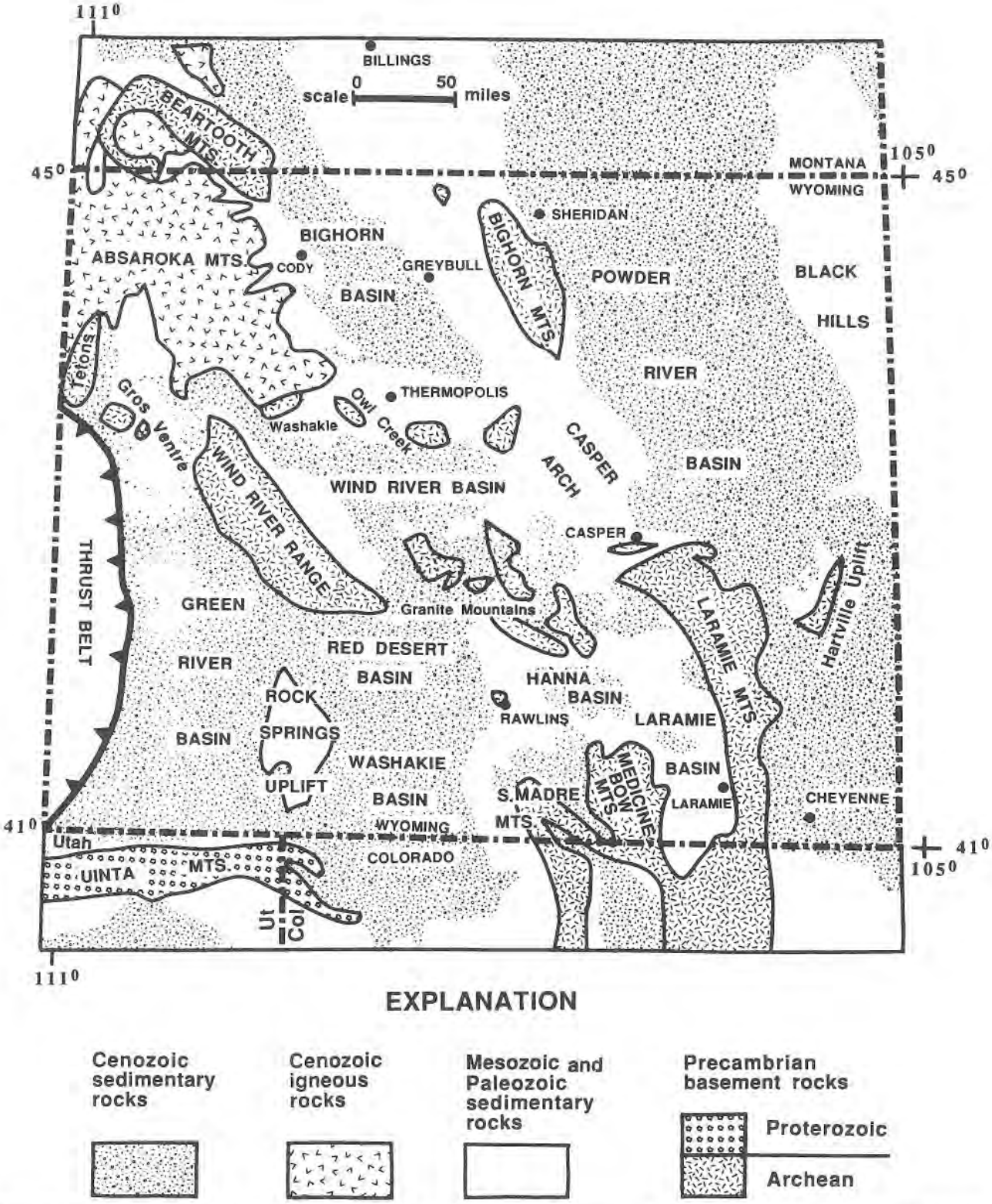

Figure 1. Index map of the Wyoming foreland showing distribution of Precambrian-cored ranges and intervening basins. The Wyoming foreland is comprised of those ranges and basins east of the thrust belt, and west of the Black Hills (modified from Stearns, 1978; reprinted by permission of Geological Society of America).

Historical review

For purposes of this discussion, the development of geologic thought concerning the structural style of the Wyoming foreland has been divided into four major (unequal) periods: (a) early geologic studies (1867 to 1919); (b) development of earliest structural concepts (1920 to 1940); (c) development of modern structural models (1941 to 1970); and (d) debate over various structural models (1971 to Present). Evolution of geologic thought during these periods generally followed the acquisition of more and better subsurface data. The following discussion has been modified from Brown (1987).

Early geologic studies (1867 to 1919)

Earliest geologic studies in the region were carried out in conjunction with the initial military and topographic surveys as the frontier moved westward. Most of these early studies were primarily concerned with the stratigraphic succession and initial surface mapping. For example, in 1868, the F.V. Hayden Survey mapped in the Medicine Bow Mountains west of Laramie and in the Yellowstone-Teton-Jackson Hole region. O.C. Marsh led the Yale Scientific Expedition in exploring the Bighorn Basin in 1870 (William F. "Buffalo Bill" Cody was employed as guide). Clarence King (later to become director of the U. S. Geological Survey) reached Fort Bridger in southwestern Wyoming in 1871 during his survey eastward along the 40th Parallel.

In 1894, a geological reconnaissance in northern Wyoming was published as U.S. Geological Survey Bulletin 119 (Eldridge, 1894) in which the author gave very general description of the major uplifts in the region, and also assumed a horizontal compressional origin of those uplifts. N.H. Darton worked in the Bighorn and Owl Creek Mountains, and Laramie Basin during the late 1890s. The former studies were published as U.S. Geological Survey Professional Paper 51, entitled "Geology of the Bighorn Mountains" and Folios 141 and 142 (Darton, 1906a, b, c).

Many of the present-day giant oil fields such as Elk Basin, Grass Creek, Hamilton Dome, Little Buffalo Basin, and Oregon Basin, along with several smaller fields, were first drilled and discovered during this period of investigation. D.F. Hewitt and Charles T. Lupton studied the anticlines in the southern part of the Bighorn Basin, and the results were published as U.S. Geological Survey Bulletin 656 (Hewitt and Lupton, 1917). In this work, the authors interpreted the major anticlines as being asymmetric, but generally did not show the dip of the faults that control the folds. What few faults were indicated on their cross sections were shown as high-angle faults.

Development of earliest foreland structural concepts (1920 to 1940)

During the early part of this period, three prominent structural geologists made important contributions to the basic understanding of the foreland structural style. W.H. Bucher (1920) was the author of a study on mechanical interpretation of rock joints, which served as the forerunner of later studies attempting to determine the mechanisms of basement deformation within the foreland. W.T. Thom (1923) described the relationship of foreland structural features to possible deep-seated faults in the central Montana portion of the Rocky Mountain foreland. R.T. Chamberlain (1925) postulated his "wedge theory" of diastrophism, and related it to mountain-building in the foreland. The wedge uplift was bounded on both sides by oppositely verging reverse faults.

C.W. Wilson, Jr. studied the Five Springs area on the west flank of the Bighorn Mountains, east of Lovell, Wyoming. He interpreted the Five Springs thrust as dipping approximately 10° to 20° east, and related its development to Chamberlain's wedge theory (Wilson, 1934). Wilson also conducted detailed studies of the Precambrian basement rocks in the same area. His observations have been used by later workers to explain basement deformation of some Laramide structures (Berg, 1962b). G. Duncan Johnson's work on Rattlesnake Mountain anticline west of Cody was published in the *Journal of Geology* in 1934. His was perhaps the first interpretation of what was later to be called the "drape fold" model, wherein the sedimentary section was interpreted to have passively draped over the edge of a basement block, uplifted along a high-angle fault.

J.D. Love, one of this volume's honorees, began his career with the U.S. Geological Survey during this period. One of Love's early publications (1934) was on the geology of the western Owl Creek Mountains, a foreland uplift partially buried beneath Tertiary sedimentary and volcaniclastic rocks. Love's interpretation of the structures present in the area were controlled only by surface outcrops. Inferred faults were interpreted to be low-angle reverse faults; those that were observable on the surface were indicated to dip as low as 10°.

Observation of low-angle reverse faults, which crop out in the sedimentary section along the steep flanks of several foreland uplifts, combined with the prevailing wedge theory of uplift, led early workers to interpret these features to have been uplifted by tangential stresses. The influence of previous workers can be seen in the published cross sections of Beckwith (1938) and Fanshawe (1939). In these two reports, the southwest margin of the Laramie Basin and the Owl Creek Mountains were interpreted as being uplifted along low-angle (30° or less) reverse faults.

D.L. Blackstone, Jr. (1940), this volume's second honoree, interpreted the monoclines of the Pryor Mountains (northern Wyoming-southern Montana) to have been created by movement on curved (concave upward) low-angle reverse faults. As this period of geologic investigation came to a close, the concept of foreland uplifts bounded by low-angle reverse faults that were developed as a consequence of regional horizontal compression, was firmly entrenched in the literature.

Development of modern structural models (1941 to 1970)

The low-angle reverse fault concept continued to prevail in the early years of this period. Classic areas such as Elk Mountain (Beckwith, 1941) and the Bighorn Mountains (Demorest, 1941) were interpreted in this manner. Nelson and Church (1943) described the geometry of foreland reverse faults as having the concave-upward shape of "sled runners." Chamberlain (1945) continued his studies of deformed basement rocks and adopted the concept of localization of large Laramide uplifts by Precambrian basement structures.

Beginning in the post-World War II years, Blackstone presented interpretations of several local foreland structures (1947, 1948, 1949, 1951, 1956, 1963, 1970). He also summarized previously interpreted dip-angles of foreland faults, and argued for horizontal tangential stresses as the cause of Laramide foreland deformation (1963, figure 13, p. 173).

Beginning in the early 1950s, structural models were being developed that are presently in use. Hafner (1951) presented the results of theoretical mathematical models of structural development created by both horizontal and vertical stresses. In the same decade, results of Sanford's (1959) theoretical and experimental sandbox models of vertical uplift were published. Bell (1956) postulated the transverse segmentation of Laramide fold systems which he interpreted as having been created by horizontal stresses.

The decade of the 1960s saw publication of perhaps the greatest variety of structural works up to that time. The vertical uplift concept discussed by Hafner (1951) and Sanford (1959) was first employed in actual interpretations by Osterwald (1961). The structural terms *drape fold* and *upthrusts* were formalized by Prucha and others (1965). Berg (1962b) proposed what he called the *thrust uplift* and *fold-thrust* models of basement-involved foreland uplifts. Berg's study was apparently the first published interpretation predicated largely on subsurface well control and seismic reflection data. Although Berg did not specifically invoke horizontal compression in his interpretation, his argument that folding accompanied thrusting along foreland mountain flanks led other workers to conclude that only horizontal compression could account for such large-scale deformation.

The role played by Precambrian basement rocks in the development of Laramide structures continued to be studied. Workers such as Foose and others (1961), Hoppin (1961), Wise (1964), Hoppin and Palmquist (1965), Hoppin and others (1965), Palmquist (1967), and Jennings (1967) published major studies on the role of and mode of deformation of basement rocks in the Beartooth, Bighorn, and Owl Creek Mountains. From these studies came ideas about basement deformation by brittle fracture and the possible reactivation of Precambrian zones of weakness by Laramide stresses.

J.D. Love has made many contributions to the understanding of the structural geology of the Wyoming foreland. His work on the nature of the south flank of the Granite Mountains-Sweetwater arch (Love, 1970) is still the most definitive of the area. In this publication, Love documents the low-angle nature of the Emigrant Trail thrust (Berg, 1962b) and the South Granite Mountains thrust. Love has also written numerous articles on the geology of the Teton and Yellowstone areas, one of the most recent being a discussion of the Targhee uplift of northwestern Wyoming and southwestern Montana (1982) which was broken into local mountain ranges during the Tertiary period of extension.

Sales (1968) created experimental models by using barite mud deformed by pure shear, which reproduced the map patterns of many Wyoming foreland structures. Cross sections through the hardened models displayed structural geometries often encountered in the subsurface in the Wyoming foreland. Stone (1969) introduced the concept of wrench-faulting to explain the deformation in the Wyoming foreland.

Debate of various structural models (1971 to present)

As a result of the Arab oil embargo, the price of oil began to escalate in the mid-1970s, resulting in a major increase in the number of exploratory wells drilled along the margins of foreland uplifts. Accompanying this increased drilling, major advances in the quality of reflection seismic data provided numerous examples of mountain overhangs of large areal extent, as predicted by Berg (1962b).

Differential vertical uplift, requiring little or no crustal shortening, was a prominent concept in foreland structural studies, and it was widely accepted as the "ruling" model during the early years of this period. Stearns (1971) presented his interpretation of Rattlesnake Mountain anticline near Cody, Wyoming, as an example of a major drape fold created by differential vertical uplift. For most of the decade, work by Stearns dominated the literature on the structural style of the Wyoming foreland (Stearns, 1975, 1978; Stearns and Weinberg, 1975; Cook and Stearns, 1975; Weinberg and Stearns,1978; Stearns and others, 1978; Stearns and Stearns, 1978; Couples and Stearns, 1978). A significant aspect of these works was deformation experiments in which small slabs of real rocks were deformed into so-called drape folds under confining pressures simulating depth of burial during the Laramide orogeny.

The differences of opinions between the proponents of differential vertical uplift (little or no crustal shortening) and proponents of horizontal shortening were brought into sharp focus by several events in the late 1970s and early 1980s. First was the publication of Geological Society of America Memoir 151 (Matthews, 1978), entitled "Laramide folding associated with basement block faulting in the western United States," which was a collection of papers espousing the concept of differential vertical uplift. Second was the convening of a symposium on Rocky Mountain foreland basement tectonics (1981) as a joint meeting of the Wyoming Geological Association, Geological Survey of Wyoming, and University of Wyoming Department of Geology and Geophysics, and publication of a volume entitled "Rocky Mountain foreland basement tectonics" (Boyd and Lillegraven, 1981). The vast majority of interpretations presented at this meeting displayed low-angle reverse faults as the mode of deformation in the Laramide orogeny. The third event was the convening of a Geological Society of America Penrose Conference on Wyoming foreland tectonics at Red Lodge, Montana, in 1982. Discussion and disagreement of the significance of various outcrops visited during the conference was carried on in a spirited manner. The fourth and final event was the Rocky Mountain Association of Geologists' symposium and publication on foreland basins and uplifts held in 1983. Numerous examples of low-angle reverse faulting throughout the foreland documented by outcrops, well control, and seismic data were published in the meeting's guidebook (Lowell, 1983).

Just as the previous decade of work on Laramide deformation was dominated by interpretations of vertical uplift (non-shortening), the decade of the 1980s was dominated by interpretations invoking horizontal compression, and displaying large magnitudes of crustal shortening.

Gries (1981, 1983a) documented the penetration of several basement overhangs along Laramide mountain fronts, as disclosed by boreholes drilled since Berg's original article (1962b). Brown (1983) corroborated Berg's (1962b) fold-thrust sequential model with outcrop examples of low-angle reverse

faults. Petersen (1983) documented numerous occurrences of bedding-plane detachment-thrusts in the sedimentary section of foreland structures, and demonstrated their relationship to a compressive origin. Scheevel (1983) published mathematical models of stress trajectories for horizontal compression that suggested basement-rooted foreland thrust faults should dip approximately 30° to 35°, and propagate *downward* from the initial break in the upper crust. The early 1980s also saw publication of a number of compressional interpretations as alternates to Stearns' (1971) drape-fold (differential vertical uplift) interpretation of Rattlesnake anticline (Cook, 1983, 1988; Schmidt and Garihan, 1983; Brown, 1984a; Erslev, 1985, 1986, 1990).

Even as evidence favoring horizontal crustal shortening was accumulating, differences of opinions surfaced concerning the consistency of orientation of the stress field during the Laramide orogeny. Gries (1983b) interpreted a reorientation of the horizontal compressive stress field from northeast-southwest, to a north-south orientation during the latter part of the Laramide orogeny, basing her ideas on a change in plate motions and the presence of several east-west-trending mountain ranges. However, Brown (1988) argued that the direction of plate convergence rather than simple plate motion controlled the direction of regional compression, and that the Laramide compressive stresses remained in an orientation of approximately N40°E.

During this same period, modern seismic lines were published which demonstrated large basement overhangs of several major Laramide uplifts which seemingly could only be caused by horizontal compression (Gries, 1983b; Lowell, 1983; Skeen and Ray, 1983; Sprague, 1983). The Consortium On Continental Reflection Profiling (COCORP) shot long record-time seismic reflection lines across the Wind River Range and the Laramie Mountains in an attempt to obtain deep crustal data. These data were interpreted showing shallow-dipping boundary faults for both uplifts (Smithson and others, 1978; Johnson and Smithson, 1985).

The decade of the 1980s also saw a marked increase in application of the concept of *structural balancing* (Dahlstrom, 1969b) to the foreland. Brown (1982, 1984a), Cook (1983, 1988), Erslev (1985, 1986), Hennings and Spang (1985), and Spang and others (1985), have all presented methods for balancing the magnitude of deformation of the Precambrian basement with that of the overlying sedimentary section.

Presently, studies appear to be strongly oriented towards investigating the role of Precambrian basement rocks in the development of Laramide structures, and in the determination of deformation mechanisms active in the basement rocks. Studies presented at the 1990 Rocky Mountain Section Meeting of the Geological Society of America (e.g., Evans and others, 1990; Giegengack and others, 1990; Harlan and others, 1990; McConnell and Wilson, 1990; Miller and Lageson, 1990; Mitra, 1990) were concerned with the interaction of the basement and sedimentary section in numerous Laramide anticlines throughout the foreland. Several of these will be discussed in the following section on the basement complex.

Recent studies have continued to unravel the structural complexities of the Five Springs area (Narr and Suppe, 1990; Tucker and Willis, 1990). Also present-day workers are still striving to understand the significance of the wedge-appearance of many foreland uplifts (Erslev, 1986).

Structural observations

This discussion of the Wyoming foreland (**Figure 1**) structural style begins with observations on characteristics of the Precambrian basement *forcing block*, which has directly or indirectly influenced the location and style of structures in the overlying sedimentary section. These characteristics include the type of basement rocks, the structural fabric of these rocks, inclination and orientation of basement-rooted Laramide faults, and the geometry of the basement/sediment contact. Following that, I address the response of the sedimentary section to the upward movement of the basement forcing block. Finally, I describe the geometry of the folds in the sedimentary section and the significance of bedding-plane detachment thrusts which result from volumetric crowding occurring in the cores of folds.

Basement complex

The Wyoming foreland is characterized by large mountain uplifts that expose Precambrian basement rocks in their eroded cores (**Figure 1**). There has been much discussion concerning the definition of *basement* in the Wyoming foreland. To some, the term means any rocks below the Cambrian Flathead Sandstone, that are older than the Uinta or Belt Supergroups; but to others, it means only those rocks that are ". . . statistically homogeneous and isotropic, which behave in a brittle manner to depths of at least 50,000 feet (15,000m), and below which layered rocks do not occur" (Stearns, 1971, p. 125).

Some foreland workers have concluded that most Laramide structures have no relationship to Precambrian anisotropies (summarized by Houston, 1971). Still others place major importance on the role Precambrian basement structure has played in localization of Laramide faults (Hoppin and others, 1965; Houston and others, 1968; Brown, 1988).

Rock composition

The variety of rock types described throughout the foreland clearly indicates that the basement of the Wyoming province (Engel, 1963) is not a single homogeneous igneous body, but rather a heterogeneous complex (Brown, 1987, Table 5). Large areas of the foreland are underlain by well-foliated quartzo-feldspathic gneiss (Lageson, written communication, 1991). Basement rocks exposed throughout the foreland include granitic rocks (quartz diorite to monzogranite), anorthosite, and metasedimentary/metavolcanic rocks. For further discussion of Precambrian basement rocks, please refer to Frost and Frost (this volume) and Houston (this volume).

The most significant apparent coincidence between the locations of Laramide faults and major changes in basement rock types are along the Tensleep fault (Hoppin, 1961; Hoppin and others, 1965) and the Cheyenne belt (Houston and others, 1968; Duebendorfer and Houston 1987). The ancestral Tensleep fault separates different Precambrian crustal rocks (Palmquist, 1978), as does the Cheyenne belt (Duebendorfer and Houston, 1987).

Structural fabric

Basement outcrops in the Wyoming foreland commonly display complex Precambrian structures, including: (a) foliation, (b) small-scale folds, (c) shear zones, and (d) igneous dikes. The strike of Precambrian structural fabric displays a variety of geographic orientations, with the the most prominent directions being: (1) northeast-southwest, (2) east-west, and (3) north-south, in order of importance. At this time, there is no known consistent relationship between structural trends in the basement and the major *northwest-trending* Laramide uplifts in Wyoming (Mitra and Frost, 1981; Houston, 1971). In southwest Montana, however, Schmidt and Garihan (1979, 1983, 1986) and Schmidt and others (1988) have shown several instances of northwest-striking Laramide faults that are controlled by faults of Proterozoic ancestry.

The effect of small-scale fabric elements such as ***foliation***, on Laramide structures, appears to be minor with respect to the large area of the foreland. However, Miller and Lageson (1990) demonstrated that in areas where the angle between Precambrian metamorphic foliation and the overlying Cambrian sedimentary section is small, the Precambrian basement rocks deformed by *oblique flexural-slip* on foliation surfaces. Laramide features such as Casper Mountain and Corral Creek faults (Brown,1975) and the Boysen normal fault (Brown, 1987) display strong parallelism to adjacent east- and northeast-striking Precambrian foliation.

Precambrian ***fold axes*** trend north-south in the Beartooth uplift (Foose and others, 1961), Tongue River area (Jennings, 1967), the Horn area (Palmquist, 1978), and other areas of the Bighorn Mountains (Osterwald, 1959). In all of these areas, Laramide faulting parallels the trend of adjacent Precambrian folds. Some Precambrian fold axes trend northeastward in the central and southern Wind River Mountains (Perry, 1967, *in* Houston, 1971; Worl, 1963), but Laramide faults in these areas strike northwest. Miller and Lageson (1990) have shown that Archean folds interfered with flexural slip on basement foliation surfaces, resulting in macrogranular breakup of the basement rocks in the cores of some Laramide folds.

Precambrian ***shear zones*** generally strike east or northeast and have been recognized using gravity and magnetic data (Kulik and Bankey, 1990). East-striking shear zones parallel the Laramide age Tensleep (Hoppin, 1961) and Florence Pass faults (Hodgson, 1965) and the Piney Creek "tear" fault

(Hoppin and others, 1965). Northeast-striking shear zones parallel the Tongue River lineament (Jennings, 1967) and the Cheyenne belt (Nash Fork-Mullen Creek shear zone of Houston and others, 1968).

Precambrian ***igneous dikes*** have a dominant northeast strike within the foreland. Laramide faults, such as Corral Creek (Brown, 1975) and Tongue River (Jennings, 1967), are parallel to northeast-striking dikes, while the Deep Creek fault is adjacent to a north-northeast-striking Precambrian dolerite dike (Nicols, 1965). The northeast-striking faults in the Five Springs area (Hoppin, 1970) and the Shirley Mountains (**Figure 2**) are also immediately adjacent to Precambrian dikes (Brown, 1987).

Apparent control of Laramide features by some Precambrian structural fabrics suggests that the basement is not isotropic. Laramide structures parallel or coincide with Precambrian zones of weakness where such zones were favorably oriented to the inferred orientation of the Laramide stress field. Reactivation of these ancient structures appears to have played a significant role in the development of foreland structural patterns (Brown, 1987).

Orientation of basement-rooted Laramide faults

There appears to be a consistent geometric relationship between strike orientation of Laramide basement-rooted faults and the angle of dip of these faults (Brown, 1987). Location and orientation of major *high-angle* reverse faults in the foreland are shown in **Figure 3**. Faults that strike north, or north-northeast generally dip from 45° to 60°. Faults that strike east or east-northeast generally dip between 60° and 80°. These high-angle reverse faults also have a component of lateral slip (Brown, 1987, 1988; Molzer and Erslev, 1991). Therefore all of the above faults are best classified as *oblique-slip* faults (Lageson, 1987; Furner, 1989; Paylor, 1990). Faults that strike northeast are parallel to the inferred orientation of the Laramide stress field, are nearly vertical and may represent the extensional fractures observed in some uniaxial rock compression tests.

I consider the major Laramide reverse faults to strike northwestward (**Figure 4**), have large areas of overhang, and dip at low angles (20° to 45°) either northeast or southwest (**Figure 5**). The strike direction and bidirectional dip of these observed faults is compatible with the conjugate reverse fault patterns predicted in Hafner's (1951) solution for horizontal compressive stresses (**Figure 6**). This suggests that these northwest-striking faults are *primary conjugate shears*, which developed from horizontal compressive stresses. Basement homogeneity assumed for the theoretical models (Hafner, 1951; Sanford, 1959) might therefore be applicable in a regional sense to the foreland basement. Reactivation of the east- and

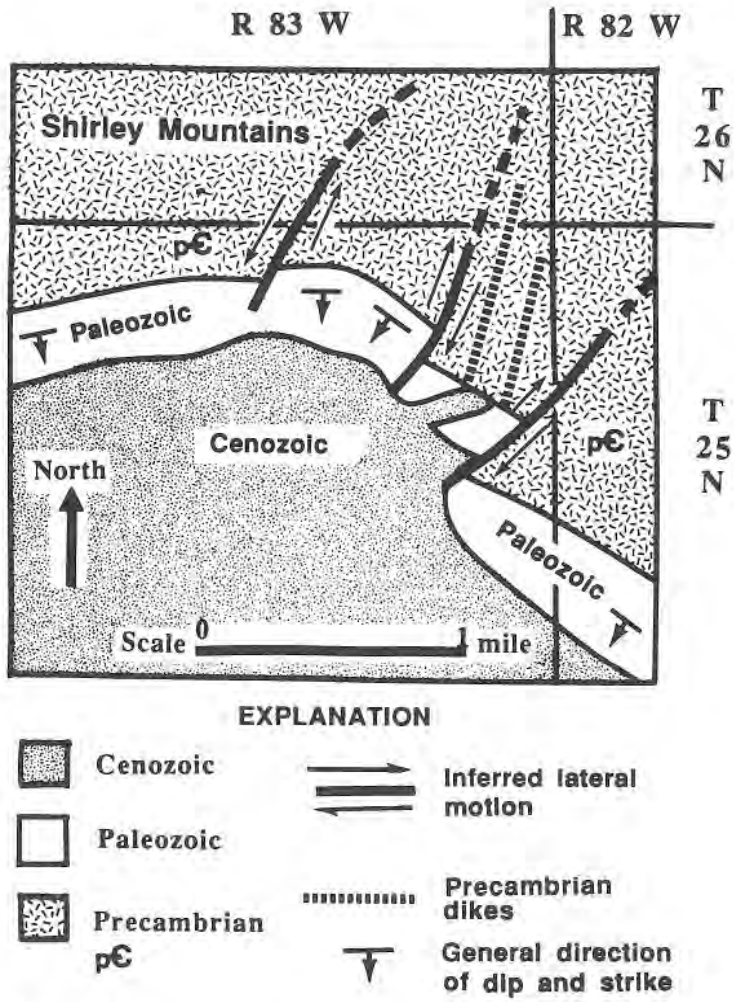

Figure 2. Many Laramide structures appear to be controlled, in location and/or trend, by Precambrian igneous dikes. Geologic map (modified from Love and Christiansen, 1985) of the western end of Shirley Mountains, shows where northeast-striking faults offset basement-Paleozoic contact in a left- and right-lateral sense. Laramide faults strike parallel and along side of the Precambrian dikes.

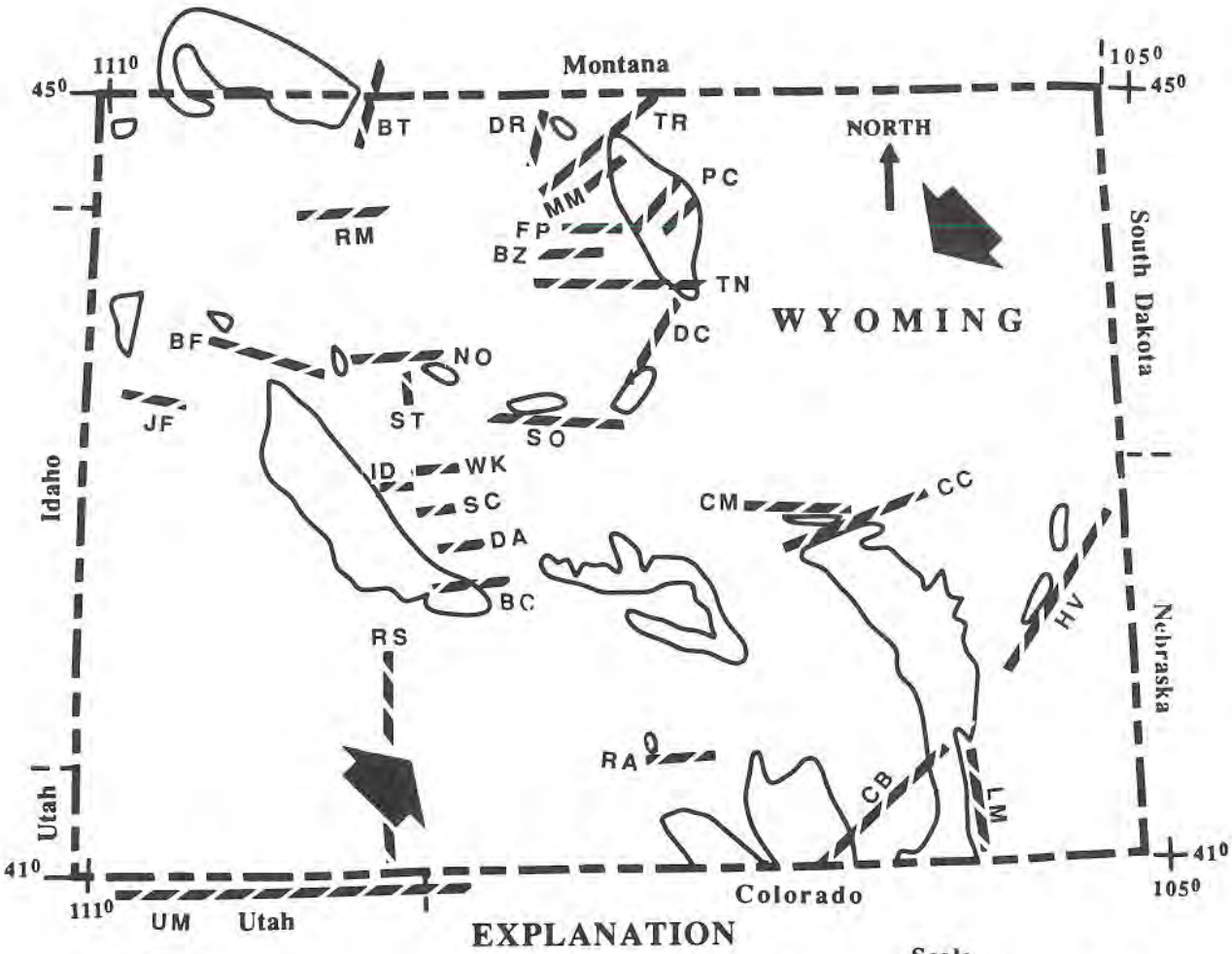

Alphabetical listing of major high-angle (>45⁰) reverse faults:

BC-Beaver Creek
BF-Buffalo Fork, south
BT-Beartooth, east
BZ-Bonanza-Zeisman
CB-Cheyenne Belt
CC-Cache Creek
CM-Casper Mountain
DA-Dallas Dome, south
DC-Deep Creek
DR-Deer Creek
FP-Florence Pass
JF-Jakeys Fork
HV-Hartville uplift
ID-Igneous dike
LM-Laramie Mountains
MM-Medicine Mountain
NO-North Owl Creek
PC-Piney Creek (no. & so.)
RA-Rawlins, south
RM-Rattlesnake (south)
RS-Rock Springs
SC-Sage Creek (north)
SO-South Owl Crk. (deep)
ST-Stagner fault
TN-Tensleep fault
TR-Tongue River
UM-Uinta Mountains
WK-Winkleman (north)

Figure 3. Major high-angle (dip >45°) reverse faults in the Wyoming foreland. Letters refer to individual structural features. Arrows indicate inferred direction of Laramide regional horizontal compression.

Alphabetical listing of major low-angle (<45°) reverse faults:

AR-Arlington
BT-Beartooth
CA-Casper arch
CC-Cache Creek
EA-E/A thrust
EB-Elk Basin
ET-Emmigrant Trail
DC-Dry Creek
FS-Five Springs
GM-Granite Mountains
HO-The Horn
LM-Laramie Mountains
MC-Mud Creek
OB-Oregon Basin
PM-Phlox Mountain
PC-Piney Creek
RW-Rawlins uplift
SM-Sheep Mountain
SO-South Owl Creek
TP-Tripod thrust
UM-Uinta Mts. (shallow)
WR-Wind River thrust

Figure 4. Major low-angle (dip <45°) reverse faults in the Wyoming foreland. Most of these faults have the primary Laramide orientation of northwest-southeast. Two major exceptions are the east-west trending South Owl Creek thrust (SO) and the Uinta Mountain thrust (UM). Arrows indicate inferred direction of Laramide regional horizontal compression.

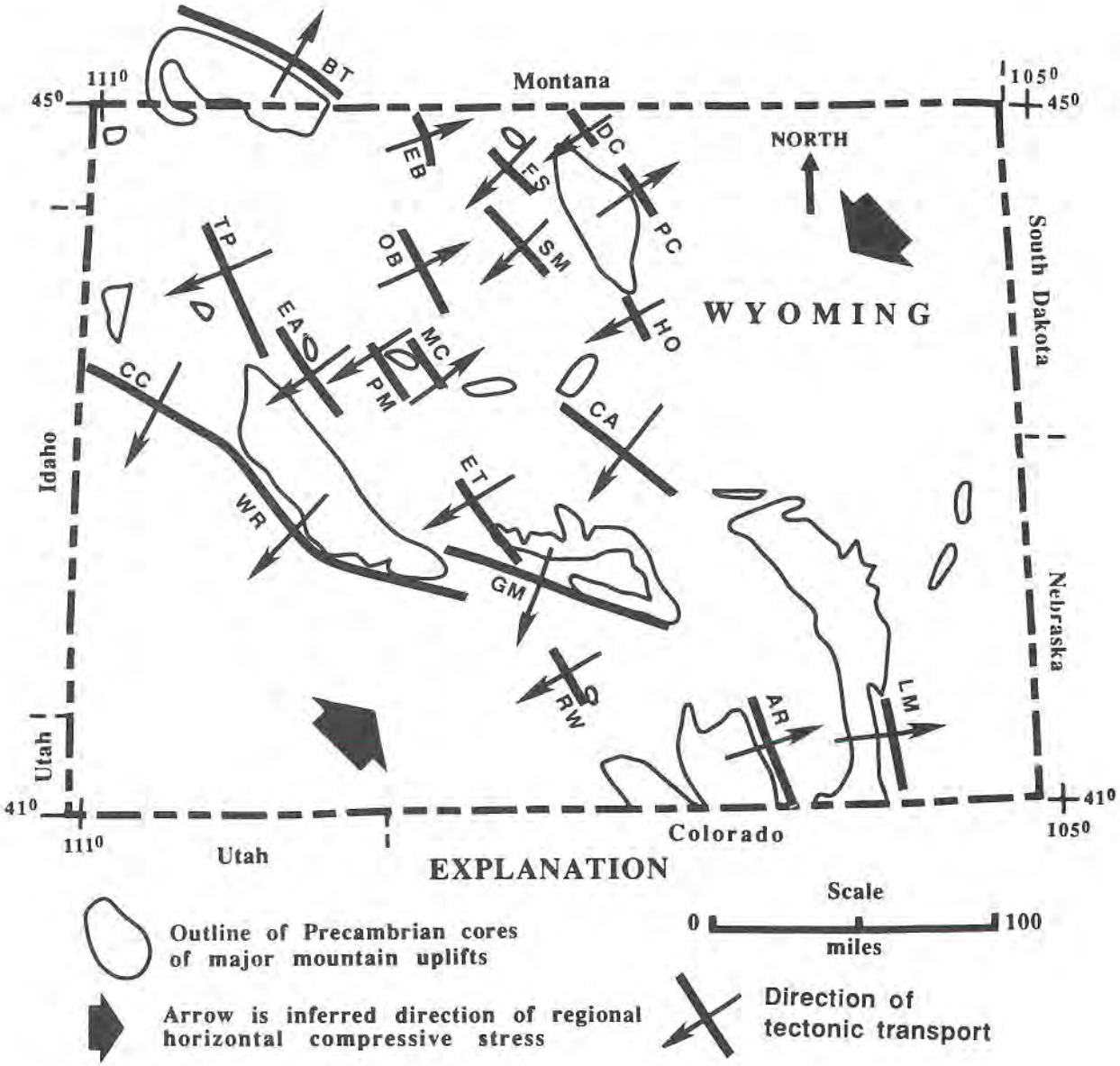

Alphabetical listing of SW- and NE-verging low-angle reverse faults:

Southwest-verging

CA-Casper arch
EA-E/A thrust
ET-Emmigrant Trail
CC-Cache Creek
DC-Dry Creek
FS-Five Springs
GM-Granite Mountains
HO-The Horn
PM-Phlox Mountain
RW-Rawlins
SM-Sheep Mountain
TP-Tripod
WR-Wind River

Northeast-verging

AR-Arlington
BT-Beartooth
EB-Elk Basin
LM-Laramie Mountains
MC-Mud Creek
OB-Oregon Basin
PC-Piney Creek

Figure 5. Index map showing directions of vergence of low-angle reverse faults in the Wyoming foreland. The northeast and southwest directions of tectonic transport may be interpreted as representing a conjugate set of basement reverse faults, which are the primary response to a N40° to 45°E regional horizontal compressive stress (large arrows). These faults also have the largest areas of mountain overhangs in the foreland.

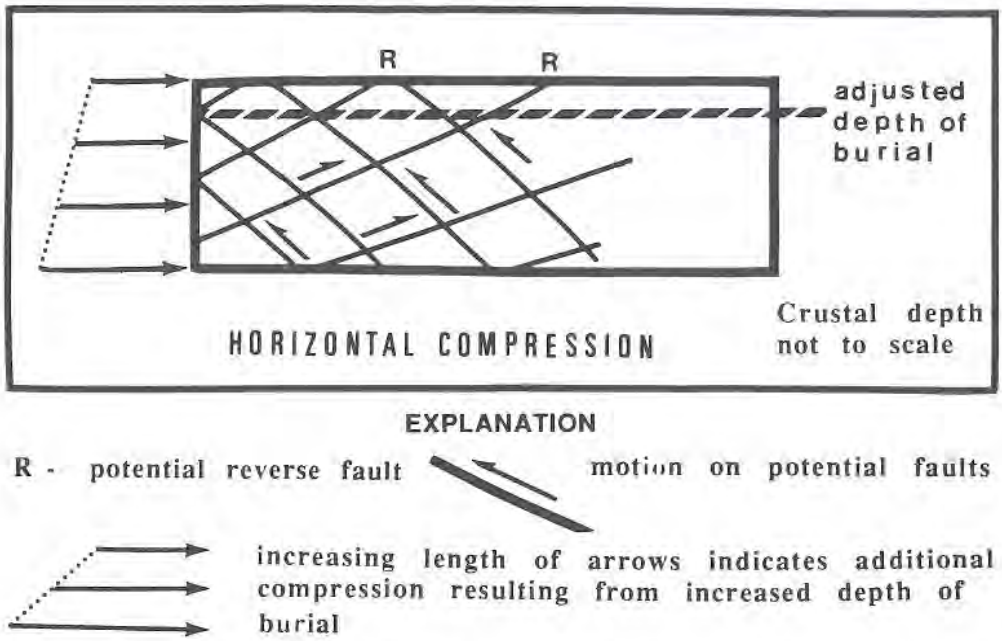

Figure 6. Orientation of potential fault planes determined from theoretical mathematical stress analyses (data from Hafner, 1951) for horizontal compression (modified from Brown, 1988; reprinted by permission of Geological Society of America). Dashed line represents level of basement surface adjusted for depth of burial at onset of Laramide orogeny (Stearns, 1975).

northeast-striking Precambrian zones of weakness have broken the primary northwest trends of Laramide structures into a heterogeneous pattern of blocks.

Folding of basement rocks

The basement/sedimentary rock contact appears to have been folded into anticlines and synclines, based upon map patterns and outcrop observations. The term *folded basement* means different things to different geologists. To some, it simply refers to anticlinal or synclinal curvature expressed at the basement/sediment interface. To others, it implies flexural slip or some ductile folding mechanism. Mechanisms which can result in basement curvature include: (1) rigid rotation, (2) cataclasis, (3) macrofracturing, (4) flexural slip, and (5) fault-propagation and fault-bend folding. Curvature created by mechanisms 1, 4, and 5 above imply that shortening of the upper basement surface has been accomplished, regardless of the method. However, curvature accomplished by cataclasis or macrofracturing may be independent of crustal shortening.

Brown (1984b; 1987, table 6; 1988) documented the presence of anticlinal and synclinal curvature of the basement/sediment contact in structures throughout the foreland. Anticlinal curvature is present on the hanging wall of several reverse faults, including: (1) Canyon Mouth anticline, Beartooth Mountains (**Figure 7**), (2) Hunt Mountain, western flank of the Bighorn Mountains (**Figure 8**), and (3) Bald Mountain, north flank of the Hanna Basin. Synclinal curvature, or basinward dip of the basement/sediment contact is present: (1) on the footwall of the Beartooth fault, north side of Clarks Fork Canyon (**Figure 9**), (2) on Porcupine Creek anticline, west flank of the Bighorn Mountains (**Figure 10**), and (3) in the Five Springs area, west flank of the Bighorn Mountains. In the latter two examples, the basement surface on the hanging wall of these faults is planar, and dips gently away from the faults. The resulting geometric form is that of an anticline that is faulted at or near the crest. In areas such as Rattlesnake Mountain anticline (west of Cody), where the basement/sediment contact is planar and gently dipping on the upthrown block, synclinal curvature may still be present on the buried downthrown side of the fault (Brown, 1984b; Blackstone,1986).

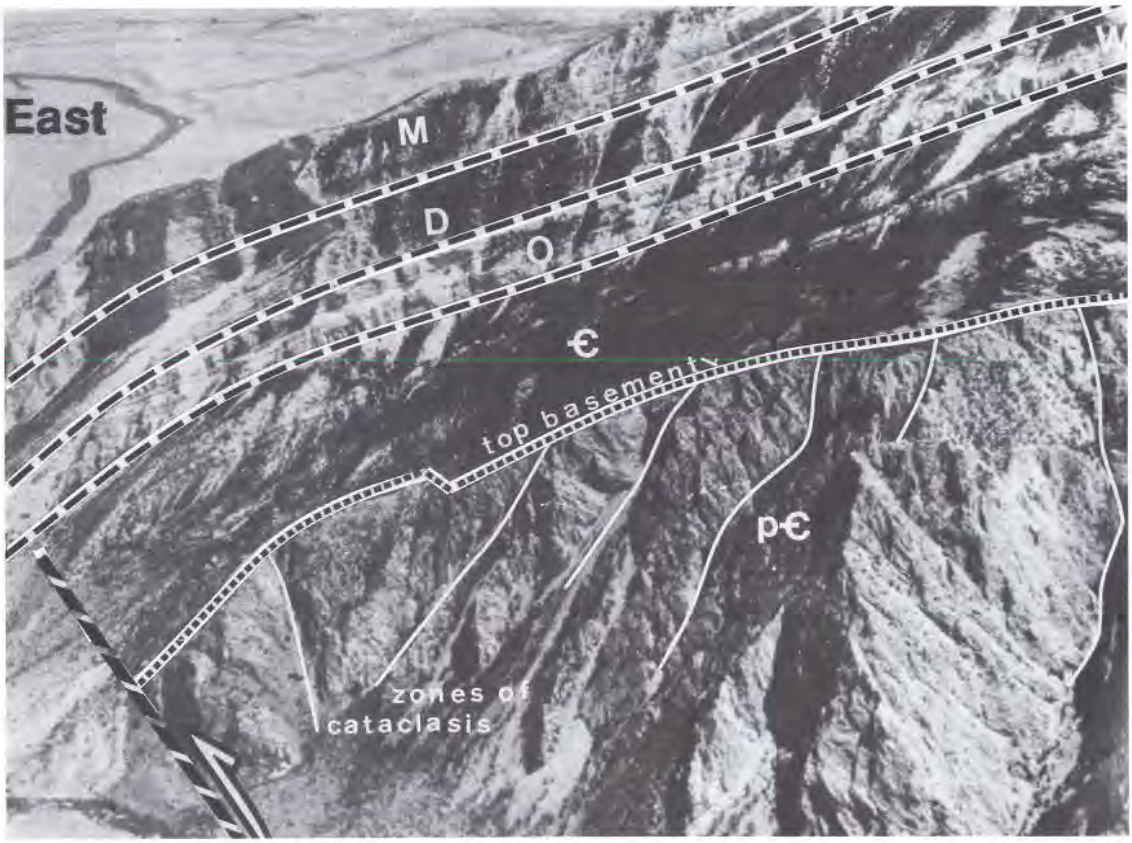

- Inferred position of Beartooth fault
- Stratigraphic contacts
- M - Mississippian
- D - Devonian
- O - Ordovician
- € - Cambrian
- Top of Precambrian basement
- p€ - Precambrian

Figure 7. Photograph of curved Precambrian basement surface of the Canyon Mouth anticline, exposed on the south canyon wall of Clarks Fork River (T56N, R103W). Zones of cataclasis (white lines in gullies) may have resulted from folding forced by the geometry of the fault plane, (from Brown, 1988; reprinted by permission of Geological Society of America).

Workers with strong backgrounds in rock mechanics (Stearns, 1971; Couples and Stearns, 1978; Weinberg, 1978; Matthews and Work, 1978) object to the concept that foreland basement can be folded because of its "brittle and homogeneous" nature (mechanical basement of Stearns, 1971). Interpretations of foreland structures employing a mechanical basement generally show the basement/sediment contact to be planar on both the upthrown and downthrown blocks. Any inclination of these planar surfaces is also considered to result from rigid rotation along curved faults (Narr and Suppe, 1990; Stearns, 1971).

Stearns (1971) and Hudson (1955) discussed the presence of a curved basement surface on a small fold near Manitou Springs, Colorado, as the product of cataclasis. Miller and Lageson (1990) also noted macrogranulation (cataclastic flow) of basement

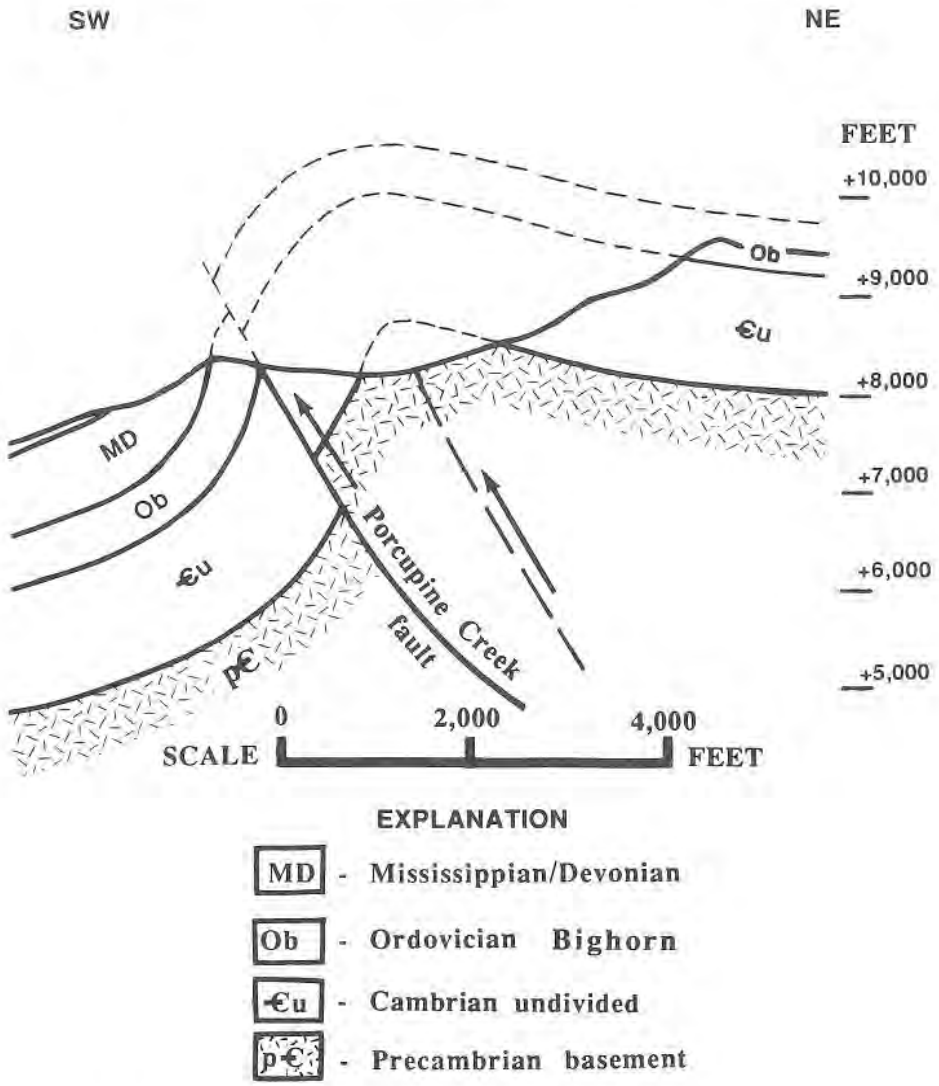

Figure 8. Cross section of Precambrian basement core of Porcupine Creek anticline, exposed in the Hunt Mountain area (T55N, R91W) of the Bighorn Mountains. Porcupine Creek anticline displays approximately 4,500 feet of structural relief on the basement surface accomplished by a combination of structural dip and offset across Porcupine Creek fault. Basement is reverse faulted near the crest of the structure, typical of many foreland folds. Anticlinal form remains after restoration of fault offset of basement/sediment contact, suggesting basement/sediment contact was folded before faulting occurred.

rocks in Laramide folds in southwestern Montana, where Archean foliation surfaces are at high angles to the basement/sediment contact. Macrofracturing is also often suggested as a method of creating curvature on the basement surface without producing crustal shortening (Prucha and others, 1965). However, Stearns (1971) argued that macrofracturing present in the basement at Rattlesnake Mountain anticline did not result in a curved basement surface. DuBois and Evans (1990) and Mitra (1990) documented macrofracturing of the basement rocks in the cores of local structures in the Wind River Range, but did not interpret significant folding of the basement surface.

Flexural-slip folding of the basement, utilizing Archean foliation surfaces, has been documented by Miller and Lageson (1990) in the Bridger Mountains anticline and the Canyon Mountain anticline in southwestern Montana. Wilson (1934), Berg (1962b),

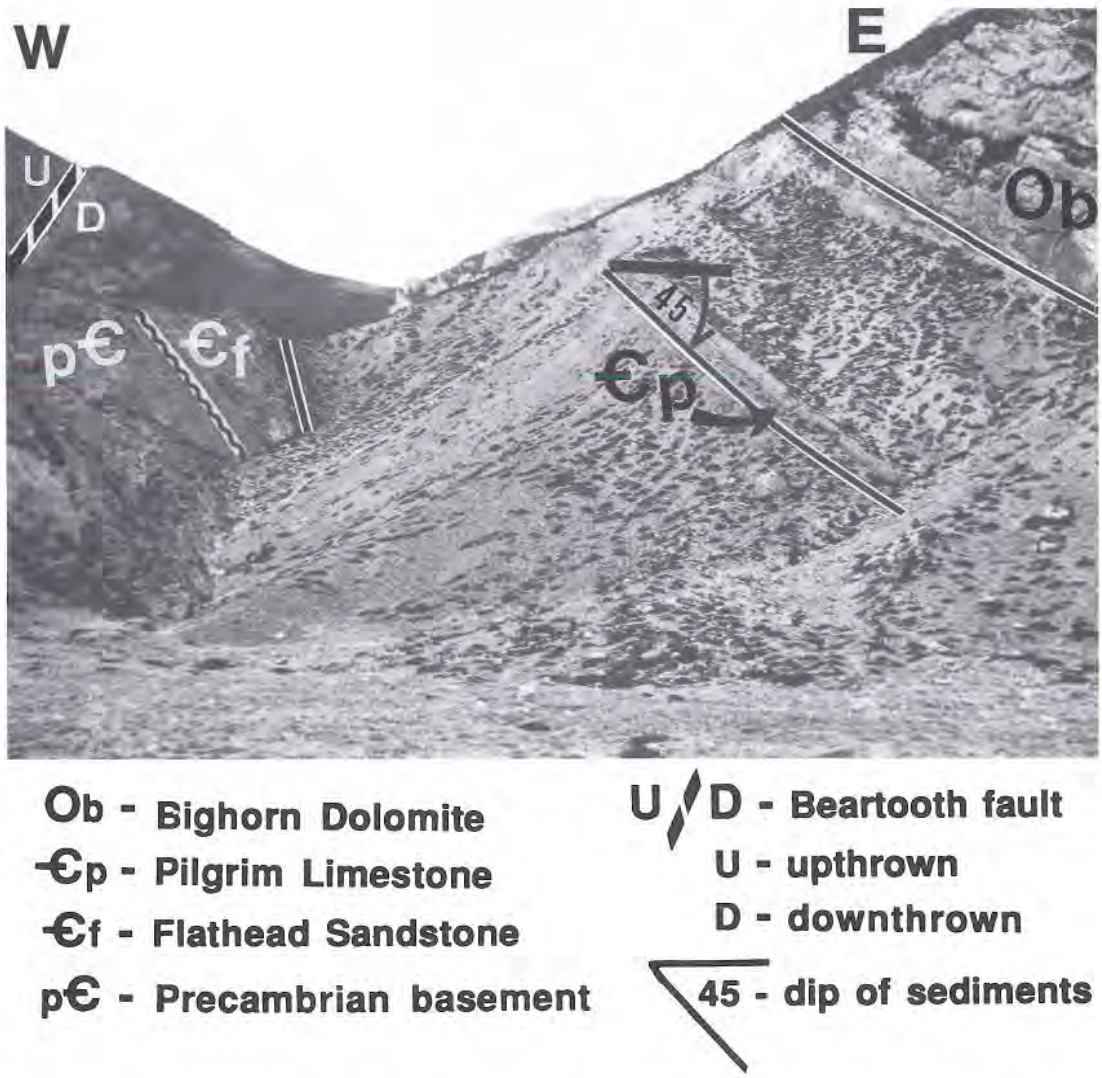

Figure 9. Photograph of Precambrian basement surface exposed on the north wall of Clarks Fork River canyon which dips 45° east towards the Bighorn Basin. Basement/Flathead contact dips parallel to the overlying sedimentary section. Exposure is on the footwall (east side) of the Beartooth fault.

Hoppin (1970), and Brown (1987) discussed the presence of *relict sheeting joints* oriented parallel to the basement/sediment contact in the Five Springs area, of the western Bighorn Mountains. These joints are aligned in an arcuate concave upward pattern, parallel to the basement/sediment contact. Slickensides on these joint surfaces are evidence that slippage has taken place along these surfaces during uplift and folding of the mountain flank, mimicking a form of flexural-slip folding. Triaxial compression tests often display primary extensional fractures parallel to the plane containing σ_1 and σ_2. Horizontal compression during the Laramide orogeny could have created horizontal extension fractures (vertical σ_3), as well as conjugate reverse faults, in basement rocks. Such horizontal fractures would have provided surfaces that were properly oriented to accommodate flexing of basement rocks.

For several years, I have applied the concept of upward and/or lateral *fault-to-fold interchanges* to foreland structures as a means of maintaining structural balance (Brown, 1982, 1984b). A more quantitative approach using the fault-propagation fold model (Suppe, 1985) has recently begun to be applied to the Wyoming foreland (Narr and Suppe, 1990). The concept of fault-bend folding (Suppe, 1985) has also been applied to basement-rooted Laramide faults in the

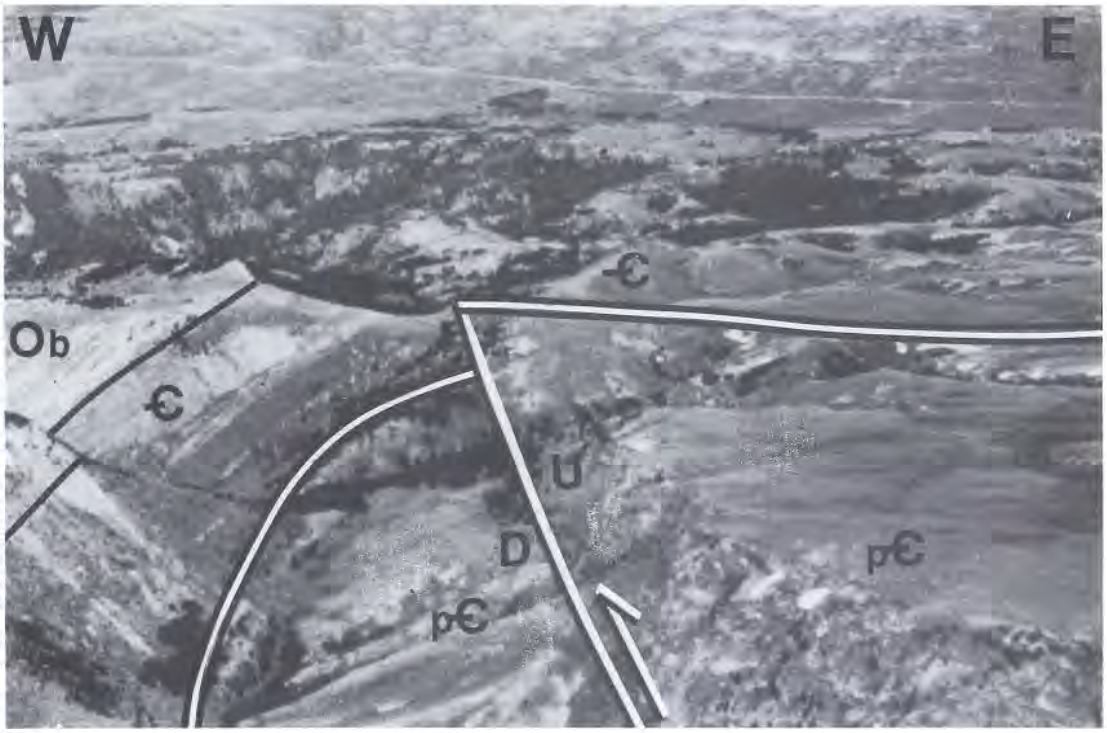

Ob - Bighorn Dolomite
Ꞓ - Cambrian
pꞒ - Precambrian basement
D\U - Porcupine Creek fault

Figure 10. Photograph of Porcupine Creek anticline, west flank of Bighorn Mountains (T55N, R91W). Basement/sediment contact on the hanging wall is planar, with 5° east dip, but the same contact on the footwall flattens downward away from fault, parallel to the overlying sedimentary section.

Wyoming foreland (Brown; 1988; Erslev, 1986; Spang and Evans, 1988). The occurrence of fault-propagation/fault-bend fold geometries may explain the curvature of the basement surface and highly fractured basement rocks seen in the cores of some Laramide uplifts throughout the foreland (**Figure 11**). No other aspect of Laramide deformation needs more study than does the concept of *folded* basement.

Structural characteristics of the sedimentary section

The large-scale forms of Laramide structures are controlled by the upward movement of a Precambrian basement forcing-block (Stearns, 1981). The response of the sedimentary section to this forcing is determined by deformational mechanisms peculiar to each lithology, which in turn are controlled by depth of burial and pore pressure. Fold geometry indicates that flexural slip was the dominant folding mechanism in the sedimentary section. This mechanism produced disharmonic folds and detachment thrusts, which were the product of volumetric crowding in the cores of the larger folds.

Mechanical stratigraphy

The stratigraphic section in the foreland is divisible into sequences, which are chiefly a single lithology and deform according to the deformational mechanism characteristic of that lithology. Sequences of different lithologies form packages in which deformational mechanisms are determined by the dominant lithology.

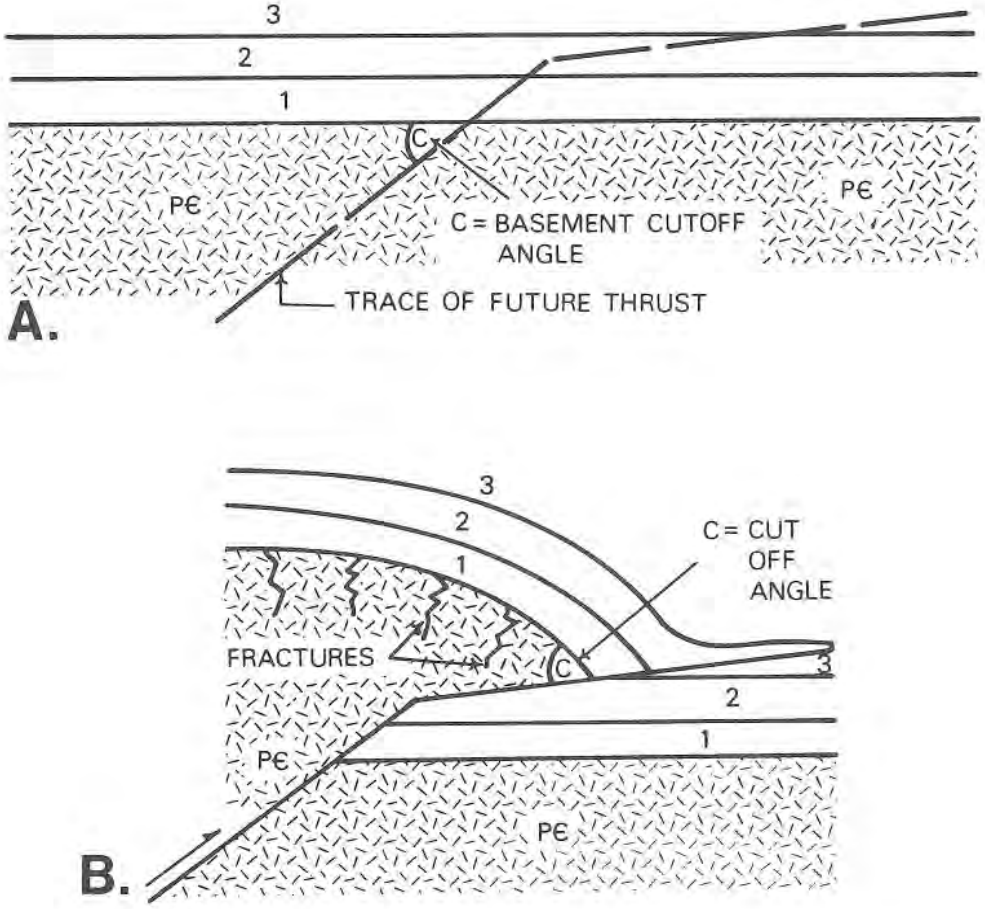

Figure 11. Application of ramp-anticline, or fault-bend fold model to basement-involved reverse fault. A. Ramp is developed as fault breaks through the basement/sediment contact with a cut-off angle "C". B. Fault flattens in the sedimentary section and basement/sediment contact is forced to fold as cut-off angle "C" rotates on flattening fault plane (b), resulting in an anticlinal basement surface. Fractures shown are diagrammatic of brittle (cataclastic) deformation of basement rock as it conforms to fault plane geometry.

The concept of *mechanical stratigraphy* was first introduced into the foreland literature by Stearns (1978), who described three general categories of responses of the sedimentary section to forced folding, based upon the nature of the dominant member in the sedimentary section and the nature of the unit that separates the dominant member from the forcing block. These are: (1) nonwelded, nonthinning, (2) welded, nonthinning, and (3) welded, ductile (or thinning) (Stearns, 1978).

Examples of the ***nonwelded, non-thinning*** condition are present over much of the Wyoming foreland where the Ordovician-to-Mississippian carbonates, Pennsylvanian sandstone, and the Permian carbonates (where present) act as the dominant structural member. The Cambrian shales and shaley limestones act as the ductile unit and facilitate detachment thrusting between the dominant member and the basement forcing block and allows the dominant structural member to deform with minimal faulting (Stearns, 1978). The ***welded, nonthinning*** condition is present in south-central Wyoming, where the Cambrian is represented by a thick sandstone facies. The absence of Cambrian shales and limestones inhibit detachment thrusting between the basement and the dominant structural member, but facilitates upward propogation of faulting with less overall displacement (Stearns, 1978). The ***welded, ductile*** condition was originally described in northwest Colorado, where the Triassic Chinle-to-Wingate clastic section lies directly on the Precambrian basement (Stearns,

1978). Stearns viewed the thinning of the clastic sequence by cataclastic flow as "... very macroscopically ductile behavior" (1978, p. 29). The cataclastic flow results in extreme thinning in the Triassic sandstones (Stearns, 1978). A similar stratigraphic situation exists in southern and southeastern Wyoming, where Pennsylvanian sandstones lie on the Precambrian basement.

Fold geometry

Equally important in the deformation of the sedimentary section is the presence of numerous bedding-plane detachments. Fanshawe (1971) summarized the role that stratigraphy played in localizing preferred zones of bedding-plane slip and detachment thrusting in the Bighorn Basin. Bedding-plane detachments occur in a number of units in the stratigraphic section of the Wyoming foreland (**Figure 12**). Petersen (1983) and Brown (1983, 1987, 1988) documented many examples of detachment thrusting in the Wyoming foreland.

Petersen illustrated how various detachments result from both anticlinal and synclinal volumetric crowding (**Figure 13**). Upward movement of the basement forcing block along reverse faults results in highly asymmetric parallel-folded anticlines (and synclines). The folds commonly overlie an anticlinal shape in the basement, which is faulted at or near the crest. The strongly asymmetric anticline causes the syncline to be more tightly folded upward along its axial surface.

Parallel-folded anticlines (**Figure 14**) typically tighten down their axial surfaces, resulting in increasingly steep dips and repetition of section by thrust faults. Parallel-folded synclines tighten upward along their axial surfaces, creating volume problems in the upper part of the syncline. These volume problems are resolved through interbed slip, with movement from the synclinal hinge toward the anticlinal hinge. Bedding-plane slip is then transferred into detachment thrusts

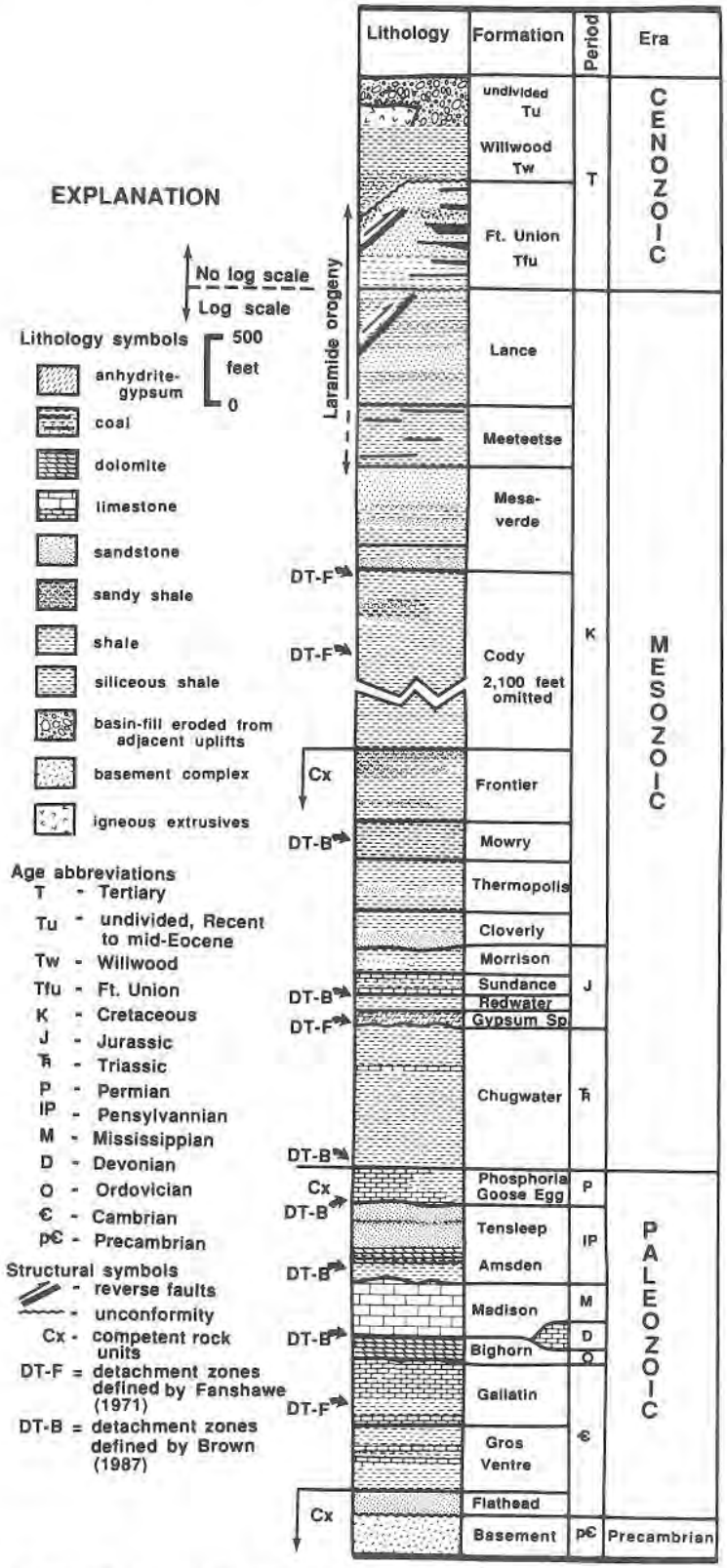

Figure 12. Stratigraphic column of Bighorn Basin rocks (modified from Fanshawe, 1971), which is also somewhat representative of much of the Wyoming foreland.

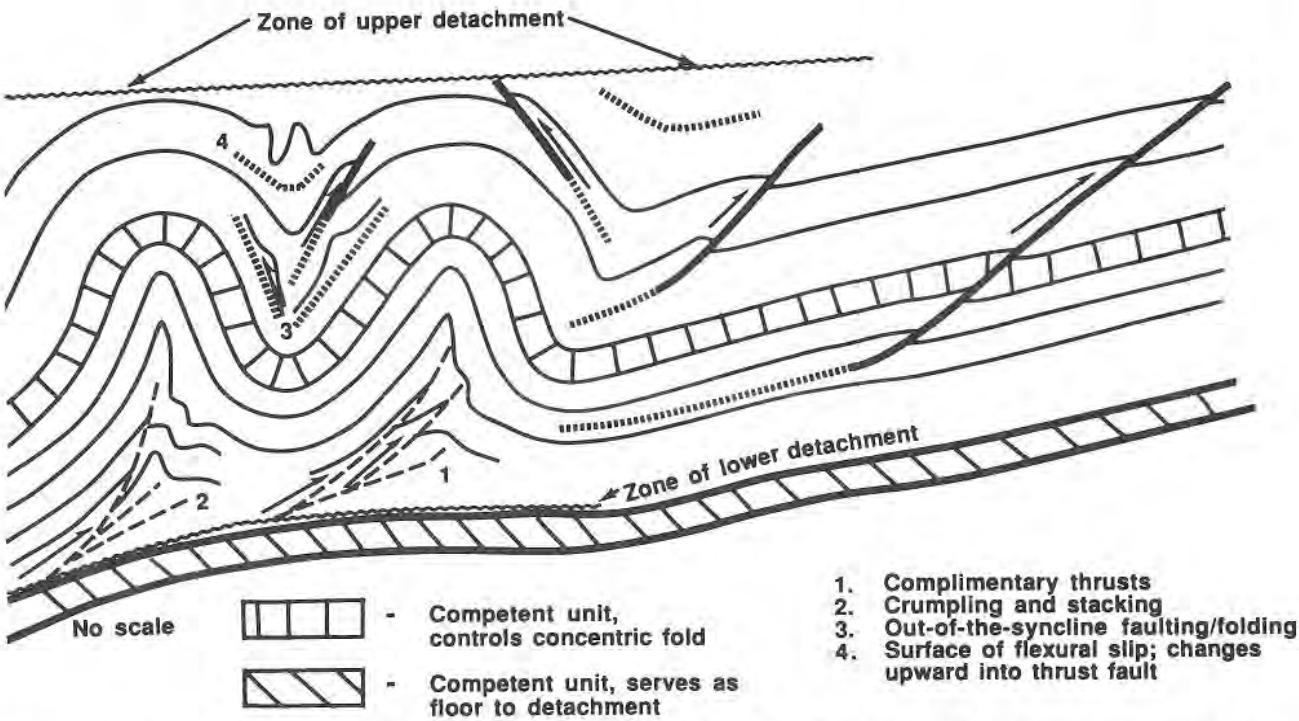

Figure 13. Diagram of concentric (parallel) fold behavior (modified from Petersen, 1983). Multiple detachments are the result of volumetric constrictions downward in anticlines and upward in synclines. Folds in the foreland sedimentary section have been documented to behave in this manner over several orders of magnitude.

near the position of the anticlinal axial line. The thrusting dies out upward through a fault-to-fold interchange (Brown, 1984b) as a fault-propagation fold (Suppe, 1985).

Solution of these volume problems results in development of an *upper detachment* (Dahlstrom, 1969a), as shown in **Figure 15**, or out-of-the-syncline *crowd structures* (Brown, 1982). Structures resulting from out-of-the-syncline crowding are called: (1) back-limb folds, (2) cross-crestal folds, and (3) rabbit-ear folds (**Figure 16**). The presence of numerous detachment-prone horizons in the sedimentary section results in the development of subsidiary folds and multiple detachments (**Figure 17**; Brown, 1988).

Foreland structural models

Structural models applied to the origin of major Laramide uplifts and folds of the Wyoming foreland commonly reflect the choice between the two basic concepts of horizontal compression (crustal shortening) and differential vertical uplift (nonshortening). It is my opinion that no single model applies to all foreland uplifts, since the dip of foreland faults appears to vary with changes in strike, as noted previously. I will present several models (**Figure 18**) that have been proposed for foreland structures, and note the specific structural characteristics these models require. Next, I will compare the models against the structural observations described in the previous section, to determine which models are supported by the data.

The models

In the past, adoption of a model has generally led to the mutual exclusion of all other models. This has resulted in the publication of widely divergent interpretations of the same Laramide structure [e.g., Osterwald (1961) versus Berg (1962a); Prucha and others (1965) versus Blackstone (1983); Stearns (1971) versus Brown (1984a)].

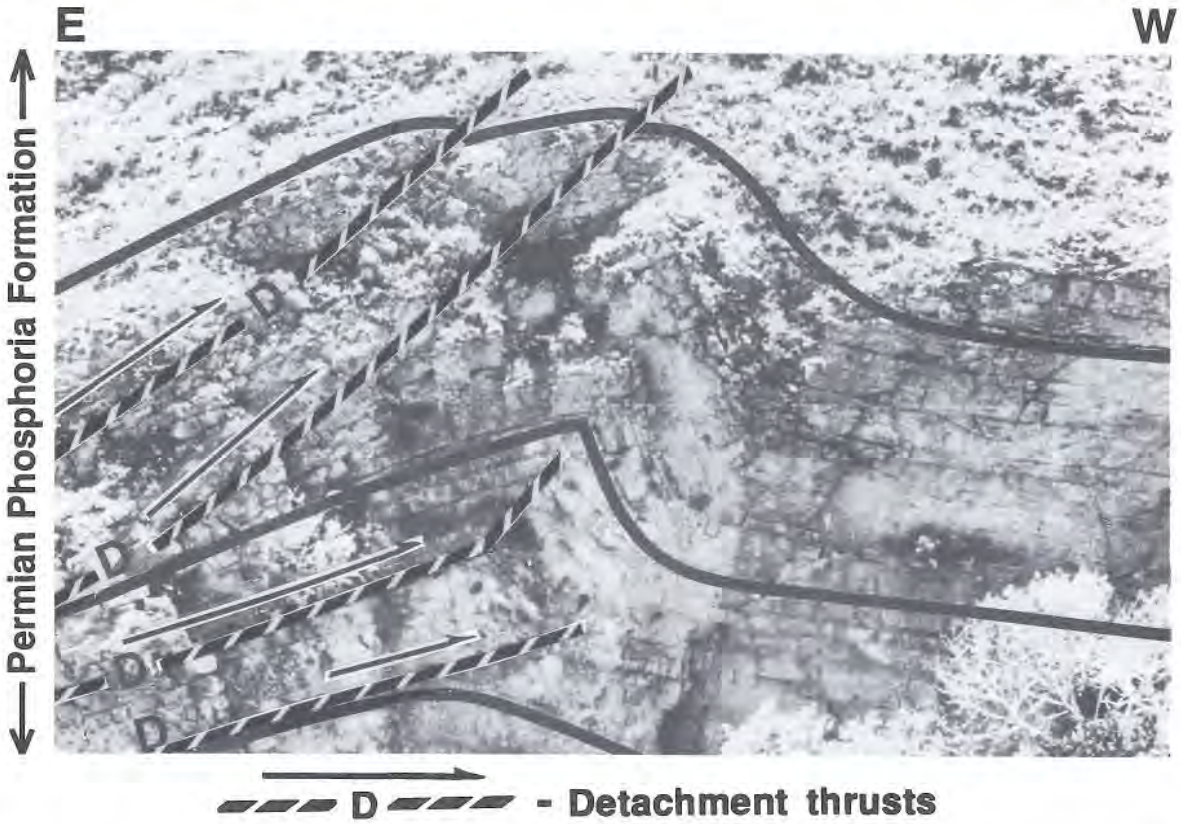

Figure 14. Photograph of tightly folded and faulted core of West Mud Creek anticline (east end of Embar anticline; T8N, R2E, WRM) exposed in Permian Phosphoria Formation. Overlying fold in Triassic Chugwater Formation (not shown) tightens downward to this level as a parallel fold. Small thrusts at crest of anticline are traceable downward into bedding-plane detachments. Notice how fold resumes a more broadly-folded form beneath the zone of detachments.

Crustal shortening models

Crustal shortening is defined as the decrease in distance between two reference points before and after deformation, as determined by subtracting present-day map distance between the points from the length of the same stratigraphic horizon between those points. Crustal shortening must be measured in the direction of regional tectonic transport (N40° to 50°E in the Wyoming foreland). Total crustal shortening may be obtained by measuring the cumulative shortening of individual structures along a single line which is parallel to the direction of tectonic transport. Total crustal shortening along any cross section oriented approximately N45°E, equals the heave of all reverse faults crossing the line of section, plus the shortening from all folding, minus any measurable extension. For a more detailed discussion of methods of determining values of crustal shortening with limited subsurface data, refer to Brown (1987, section 9.3, p. 255).

There is no consensus of opinion as to what classification should be used when discussing major Laramide structures that are considered to have formed under horizontal compressive stresses (Berg, 1962b; Stone,1983; Erslev, 1986). Erslev (personal communication, 1990) suggested a dual-level classification, with one level describing the structure as it is seen today, and the second level inferring a kinematic sequence. I agree that there should be a consistency in the use of terms, and urge future workers to adopt such a consensus.

As noted previously, many early foreland workers such as Wilson (1934), Beckwith (1938), and Fanshawe (1939) interpreted foreland uplifts to be bounded by extremely low-angle thrust faults. In all cases, the bounding fault was depicted as a single fault plane, which placed older rocks over right-side-up younger rocks. Berg (1962b) referred to this as the ***thrust uplift*** model (**Figure 18a**). It was not until

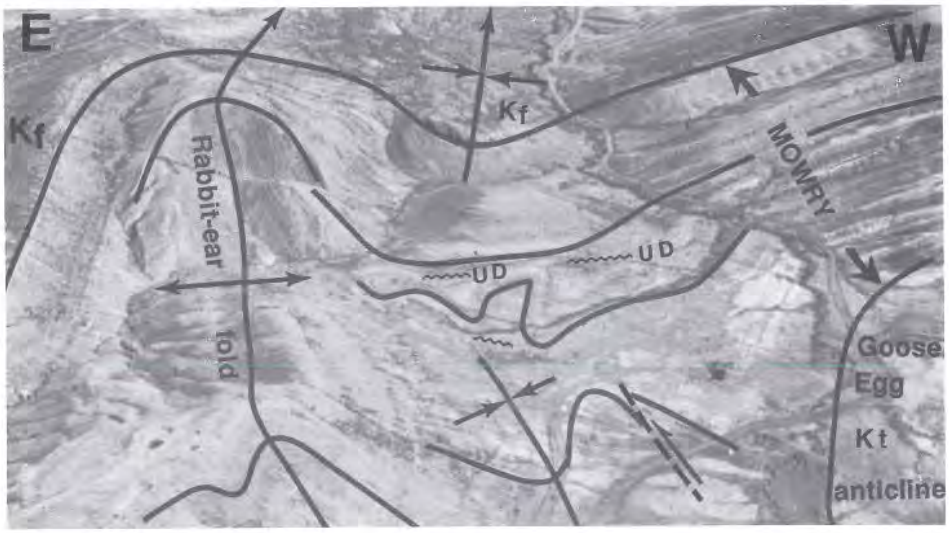

A.

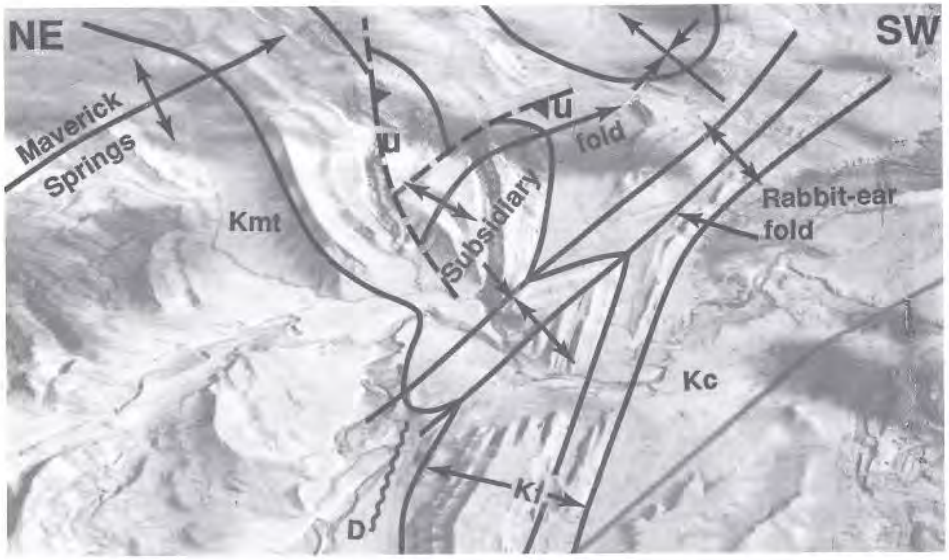

B.

Kc - Cody Fm.

Kf - Frontier Fm.

Kmr - Mowry Fm.

Kt - Thermopolis Fm.

UD - upper detachment

D - detachment

u thrust fault

anticline

syncline

Figure 15. A. Subsidiary rabbit-ear fold and adjacent syncline, developed in the Cretaceous Mowry Shale on the northeast flank of Goose Egg anticline, east flank of Bighorn Basin (T55N, R95W). Parallel-folded syncline has tightened up the axial surface until reaching a zone of detachment. Sinuous beds are just below the "upper detachment" UD. B. Subsidiary folds and detachment thrusts on the southwest flank of Maverick Springs anticline (T5N, R1W, WRM). These structures result from out-of-the-syncline movements originating from the deep syncline on the southwest flank of the fold, and the synclinal plunge-depression between Maverick Springs and Little Dome.

Berg's (1962b) work on the EA and Emigrant Trail thrusts was published, that many uplift-bounding faults were shown to be a zone of two major thrusts, which encase a slice of overturned sedimentary rocks. Berg called this the ***fold-thrust*** model **(Figure 18b)**, emphasizing his interpretation that folding at higher structural levels occurred at the same time as faulting in the deeper structural levels. All of the structures for which Berg demonstrated the dual fault system were northwest-trending Laramide uplifts.

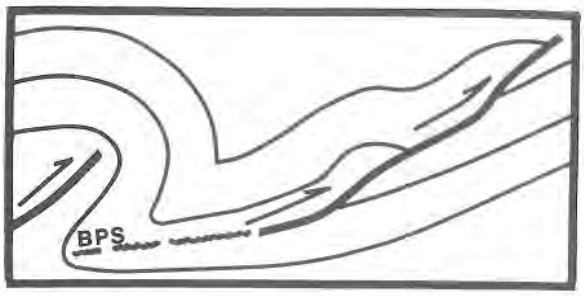

A. Back-limb fold

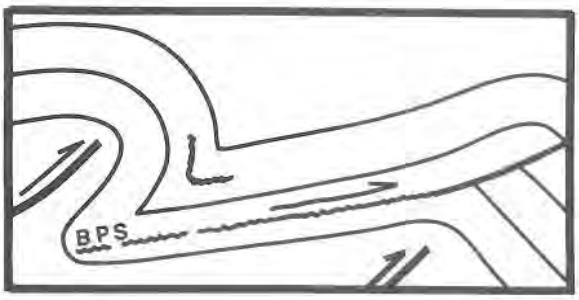

B. Cross-crestal fold

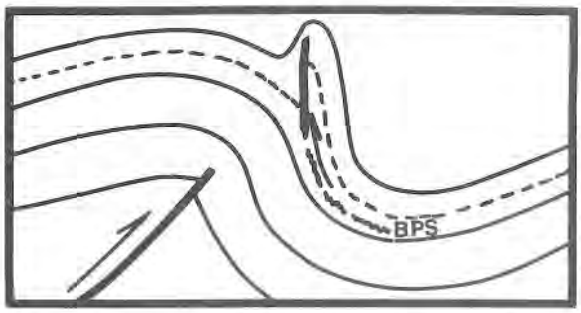

C. Rabbit-ear fold

BPS - bedding-plane slip ~~~~~ detachment

Figure 16. Synclinal parallel folding of sedimentary layers results in volumetric problems that are resolved by bedding-plane slip (BPS) that is directed away from synclinal axes. The BPS translates upward into reverse faults that in turn lose displacement upward into fault-propagation folds of three styles: A. back-limb, B. cross-crestal, and C. rabbit-ear folds (from Brown, 1988; reprinted by permission of Geological Society of America).

The distinction between Berg's thrust uplifts and fold-thrust uplifts **(Figure 18a, b)** is not clear-cut. It is generally based upon whether the uplift is bounded by a single thrust or a dual-fault zone (Brown, 1983) with overturned sediments (and basement) between the two faults. The problem arises as to whether these two styles are truly separable on some basis that will allow prediction of which style will be present in a given area. Brown (1987) suggested that such a basis of separation might be the difference in strike orientation of the fault zone. Fold-thrusts are northwest-trending uplifts, which developed perpendicular to inferred Laramide stresses (N40°E, Brown, 1987), whereas thrust uplifts should strike more north-south. There does appear to be a clear difference between the northwest-trending structures and the north, east, or northeast-trending features. The latter three more commonly have a single fault plane, while the northwest-trending structures appear to have a dual fault system.

Stone (1983) suggested that the term fold-thrust should be transposed into the term *thrust-fold* to more clearly depict the sequence of formation. However, Berg (1962b) had already recognized this relationship, and chose to call it fold-thrust because we typically observe the folded sedimentary section at various erosional levels more often than we see the fault at the basement level. I (Brown, 1984a) described the sequence envisioned for reverse-faulted foreland structures as a fault dipping approximately 30° at depth, steepening upward at the basement surface, with displacement decreasing to zero upward in the fold. While the term thrust-fold may more clearly describe the sequence of deformation, this author has chosen to continue use of the term fold-thrust because of the precedence established by Berg's term.

Robbins and Erslev (1986) and Erslev (1990) published interpretations of the Beartooth Mountains and Bighorn Basin using the terminology ***basement wedges and backthrusts*** **(Figure 19)**. Homan (1988) and Abercrombie (1989) presented interpretations of other Laramide structures using similar models. This

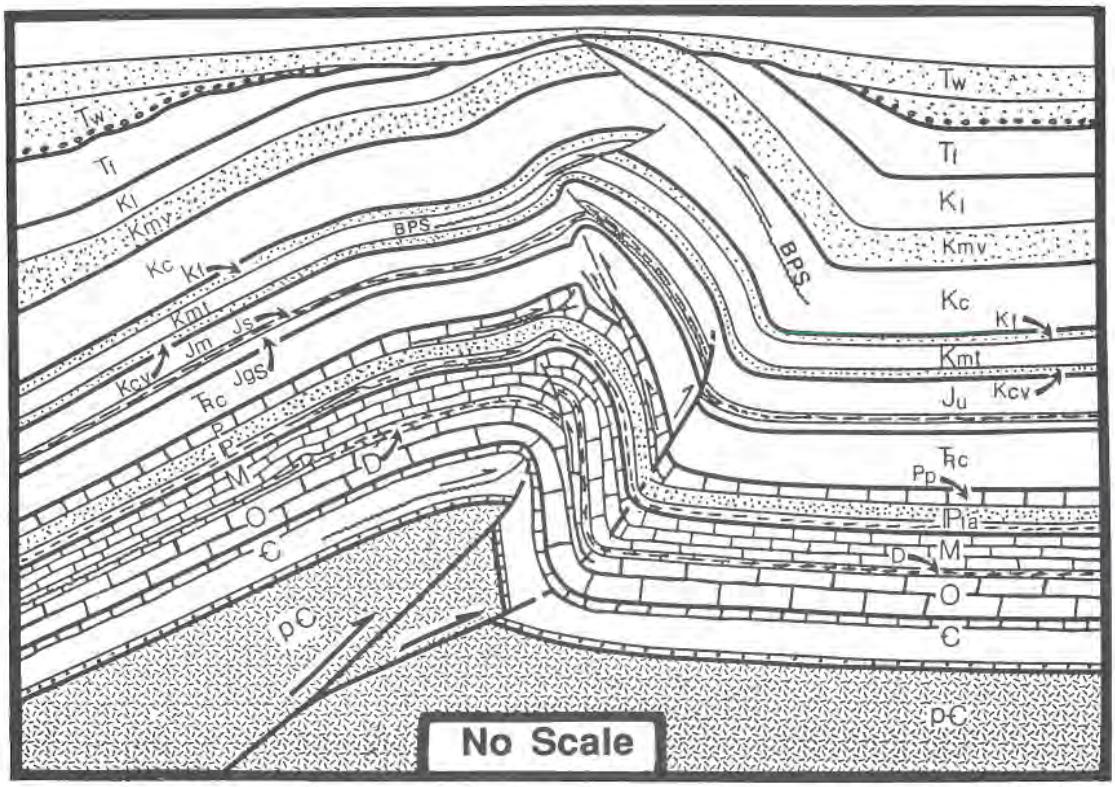

Tw	- Willwood (Eocene)	Kcv	- Cloverly	M	- Mississippian (Madison)
Tf	- Ft. Union (Paleocene)	Jm	- Morrison	D	- Devonian
Kl	- Lance-Meeteetse	Js	- Sundance	O	- Ordovician (Bighorn)
Kmv	- Mesaverde	Jgs	- Gypsum Spring	Є	- Cambrian
Kc	- Cody	TRc	- Triassic Chugwater	pЄ	- Precambrian
Kf	- Frontier	Pp	- Phosphoria	BPS	- bedding-plane slip
Kmt	- Mowry-Thermopolis	IPta	- Tensleep-Amsden		

Figure 17. Model of composite foreland basin-flank anticline derived from observations of numerous structures within the Wyoming foreland. The basement acts as the forcing-block, causing the sedimentary section to conform to the block in overall size and shape. Stratigraphic variations control the deformation mechanisms in the sedimentary section, one of which is the development of multiple zones of detachment that are activated by bedding-plane slip (BPS) as a consequence of volumetric adjustments in adjacent synclines. Multiple detachments allow the concentric-like fold to propagate to depth, with changes in asymmetry associated with the major zones of detachment (from Brown, 1988; reprinted by permission of Geological Society of America).

style provides a method of transfer of structural shortening from the basement forcing block upward into folds having an opposite sense of vergence to that of the underlying basement fault.

Nonshortening models

Although some very early foreland interpretations (Johnson, 1934) invoked vertical uplift, most such interpretations were made after the works of Hafner (1951) and Sanford (1959) were published. Hafner (**Figure 20a**) and Sanford (**Figure 20b**) presented some of the first mathematical and experimental models of the vertical uplift process. In these works, both had similar results in that the uplifted block was separated from the downthrown block by faults that generally steepened with depth, giving it a concave downward shape. This geometry is referred to as an ***upthrust*** (Link, 1930). Additionally, the Hafner (1951) and Sanford (1959) studies indicated

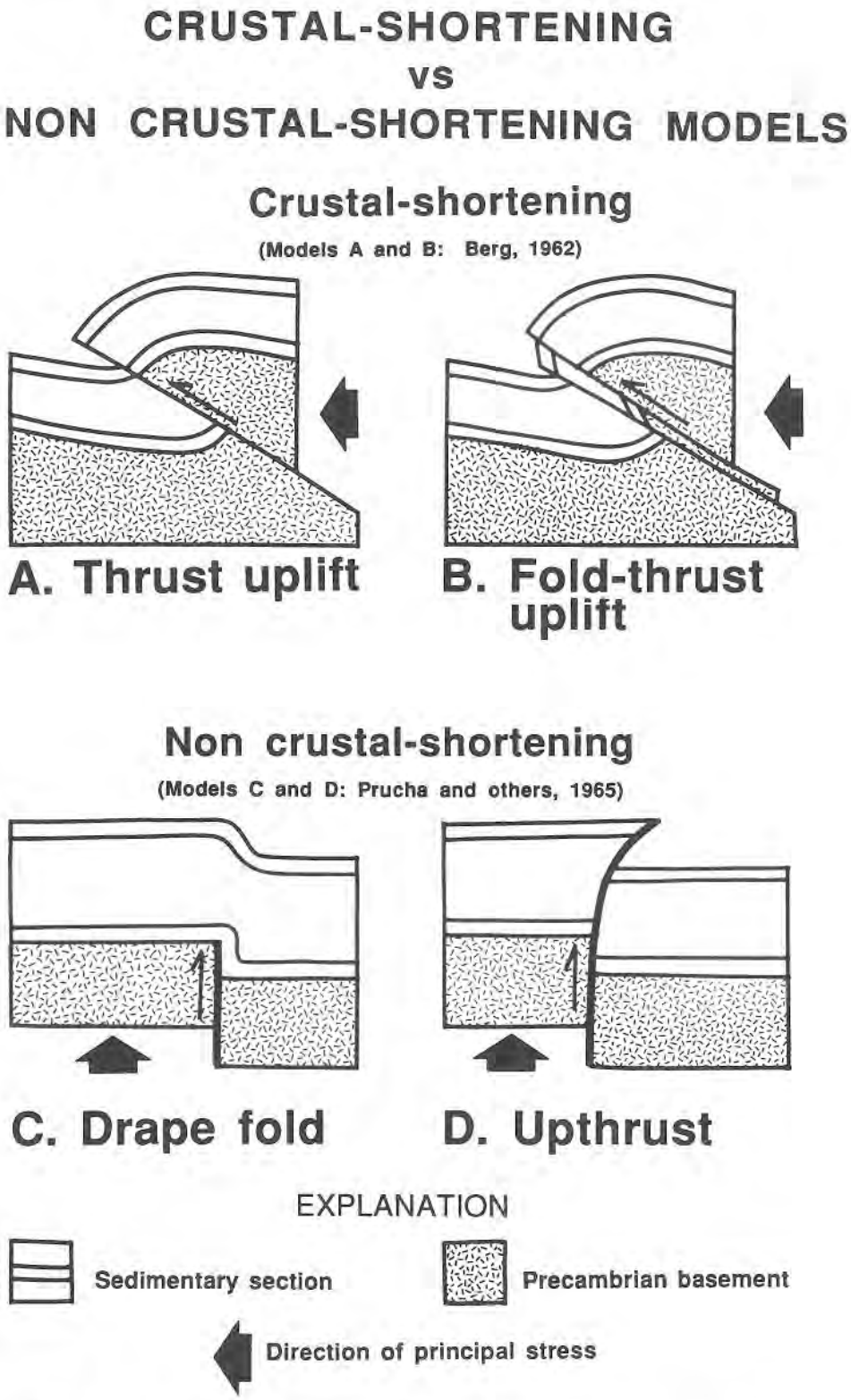

Figure 18. Four models of foreland deformation: crustal shortening models A. thrust uplift, B. fold-thrust uplift, and non crustal shortening models C. drape fold and D. upthrust (from Brown, 1988; reprinted by permission of Geological Society of America). Models a and b are after Berg (1962b); models c and d are after Prucha and others (1965).

that normal faults were present on the uplifted blocks. The curved shape of the upthrust faults resulted in vertical translation along the steep portion, and structural shortening by duplication along the low-angle thrust portion. Extension by normal faults on the upthrown block effectively balanced this discrepancy at different structural levels, by yielding a net zero for shortening and/or extension for the entire model.

Prucha and others (1965) described the ***drape fold*** (**Figure 18c**) as an intermediate stage in the process of uplift along *upthrust* faults. The name implies draping of the sedimentary section over the edge of the rising basement block, much as a table cloth drapes over the edge of a table. Neither the upthrust (**Figure 18d**) nor the drape fold depicted by Prucha and others (1965) displayed any of the extensional normal faults indicated in the Hafner (1951) and Sanford (1959) models. However, Prucha and others stated (p. 983) "The mechanism by which this [extension] is accomplished is . . . not known, although thinning of beds in the flexure probably is common." When applying the upthrust and drape fold models, many geologists have ignored these compensating normal faults required by the mathematical and experimental models, as well as the remarks by Prucha and others (1965) concerning bed-thinning.

Stearns (1971) popularized the drape fold in his interpretation of Rattlesnake Mountain anticline, west of Cody. He pointed out that neither normal faulting present at the surface, nor thinning of the Paleozoic section could account for the continuity of the normal thickness of Mississippian rocks over the edge of the drape fold. He therefore proposed that a

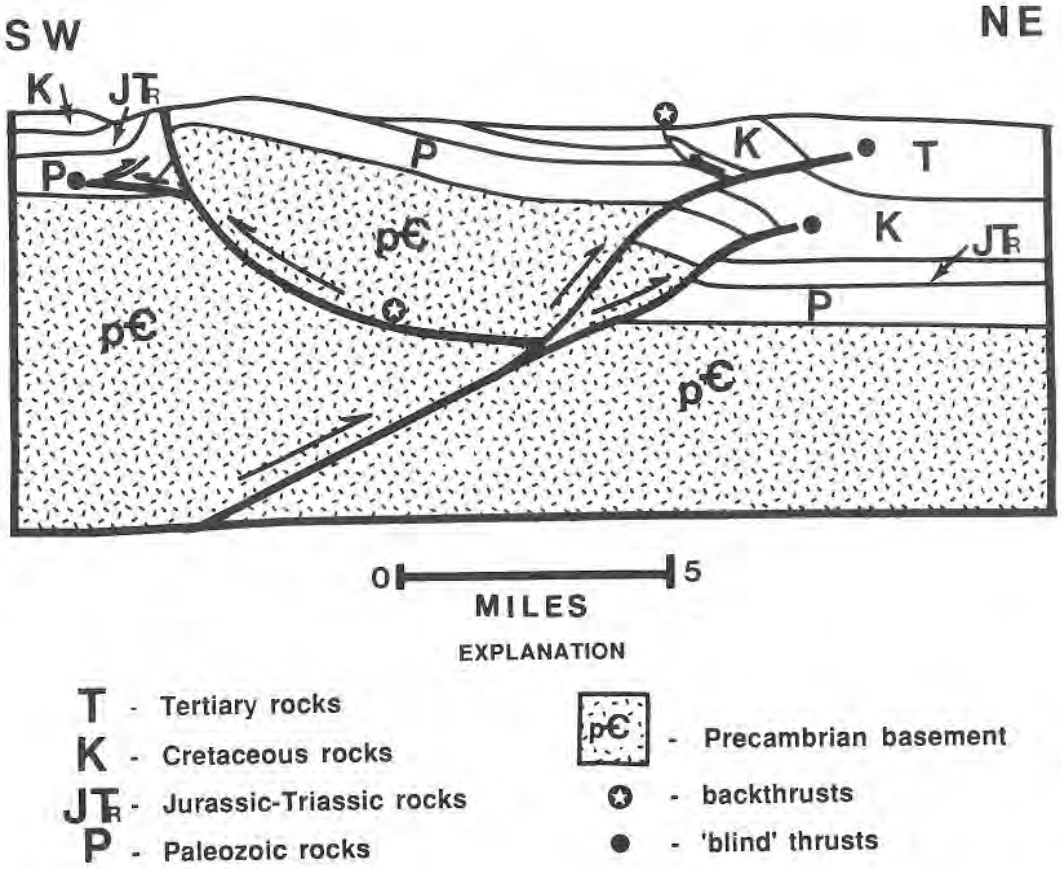

Figure 19. A style of basement wedges and backthrusts (modified from Erslev, 1990) can be structurally balanced and restored, and explains many relationships in the Wyoming foreland. Erslev (1986, 1990) has also shown that this style explains some of the changes in fault vergence along mountain fronts, such as the Beartooth Mountains. Typically, displacement on the main basement fault becomes zero upward (fault goes "blind") and basement-involved backthrusts form accompanied by thin-skinned detachment thrusting in the sedimentary section.

detachment fault could have allowed movement of the necessary volume of Paleozoic rock into the steep limb of the fold to account for the apparent imbalance in the bed lengths of the Precambrian basement surface and overlying Paleozoic layers.

Figure 21 illustrates three possible mechanisms to accommodate the bed-length problem of a drape fold. Lengthening of the sedimentary layers on the upthrown block by ductile thinning (**Figure 21a**) or normal fault extension (**Figure 21b**) should be observable on a drape fold that is not too deeply eroded. On the other hand, development of a detachment slide and void (**Figure 21c**) resulting from movement of large volumes of rock into the steep limb might be difficult to evaluate. However, in the case of Rattlesnake anticline, there are outcrops of Upper Cretaceous rocks present west of the fold for a distance of ten miles, and there is no apparent gap that would correspond to the volume of rocks needed to balance the drape-fold interpretation. A seismic line shot westward from the steep flank of Rattlesnake anticline (Brittenham and Tadewald, 1985) also indicates there is no gap from which sedimentary rocks have been removed (Blackstone, 1986). **Figure 21d, e** illustrates additional problems in the application of the detachment-void model of compensation for drape folds. In situations where two drape folds face one another with opposed asymmetries, or where multiple drape folds face the same direction, there is no place from which to obtain the volume of rock needed to maintain structural balance.

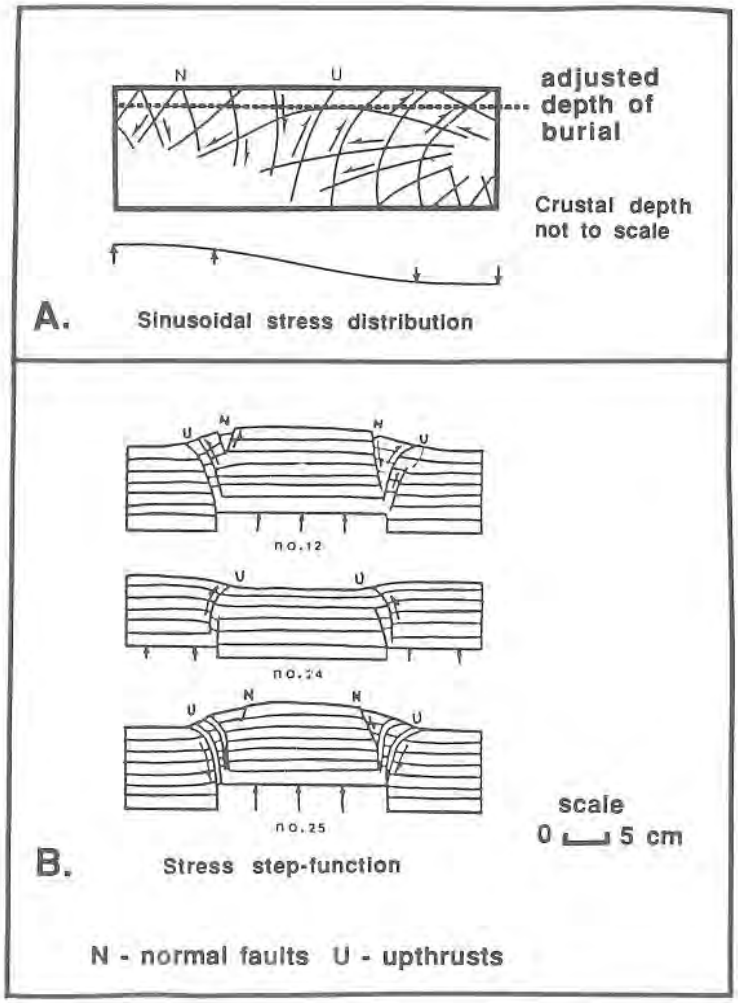

Figure 20. A. Orientation of potential fault planes determined from theoretical mathematical stress analysis (modified from Hafner, 1951) for differential vertical uplift. B. Development of upthrust fault geometry in sandbox experiments via vertically driven piston (Sanford, 1959). Numbers 12, 24, and 25 refer to different runs of experiment with different materials.

Although many nonshortening interpretations are suspect because of a lack of structural balance, the fact remains that theoretical and experimental data (Hafner, 1951; Sanford, 1959; **Figure 20**) require the application of the upthrust and drape fold models if the deforming force is differential vertical uplift. Therefore, we must recognize those specific places where the vertical component of uplift dominates over horizontal shortening. It should be obvious therefore that if non-shortening models cannot be balanced, and the necessary bed-length compensation is not observable, then the wrong model is being employed, but such is not always the case.

Structural evidence for the various models from the Wyoming foreland

Evidence directly supporting the nonshortening models of drape folding and upthrust faulting is sparse in the the Wyoming foreland, especially on the primary northwest-trending uplifts and folds. However, these non-shortening models should be applied where vertical translation dominates over horizontal shortening. This condition appears to take place at corners created by the intersection of northwest-trending anti-

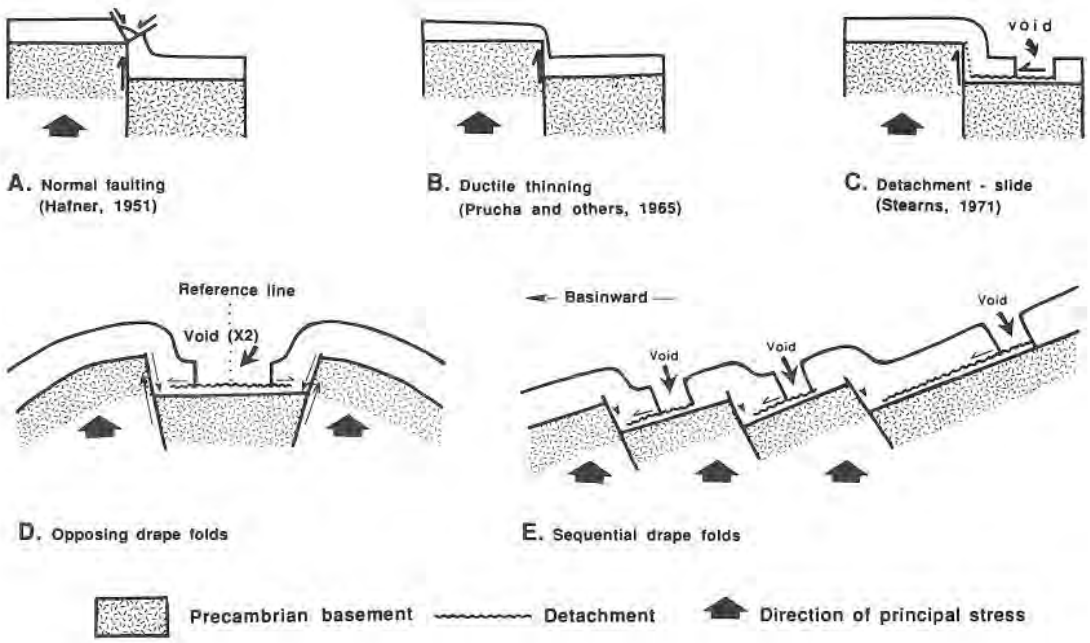

Figure 21. Bed-length accommodations needed to maintain structural balance of drape folds: A. ductile thinning of beds, B. extension by normal faulting, and C. development of a bedding-plane detachment to allow the sedimentary section to slide into the fold with normal stratigraphic thickness. Model c will result in the creation of an area devoid of the same volume of rock that slides into the drape fold, (from Brown, 1988; reprinted by permission of Geological Society of America). Model a is after Hafner (1951); model b is after Prucha and others (1965); model c is after Stearns (1971).

clines and east- or northeast-striking faults. Much detailed work needs to be done in these locations in order to obtain data to confirm this model.

Since 1962, when Berg first documented the existence of large overhangs along foreland mountain fronts in Wyoming, over two dozen additional wells have been drilled through numerous other mountain overhangs. Additionally, the quality of exploration seismic data has increased many fold, thus allowing at least a cursory inspection of almost all mountain fronts in the foreland. The accumulation of the new well and seismic data supports, more strongly than ever, the concept that the major northwest-trending Laramide mountain uplifts and associated subsidiary folds have accommodated significant crustal shortening along a northeast-southwest direction, parallel to the inferred direction of the Laramide horizontal compressional stress field.

The general lack of observed ductile stretching and/or extension by normal faulting on the steep limbs of northwest-striking Laramide anticlines suggests that a horizontal shortening model should be applied to these folds. However, structures that offer the best possibility for application of the nonshortening models trend east and northeast. It is more than simple coincidence that these are also the same trends as many of the inherited Precambrian zones of weakness.

Evidence for the crustal shortening model

Gries (1983a) documented the presence of major thrusting of basement rocks along many more of the northwest-striking uplifts in Wyoming since Berg (1962b) first postulated the fold-thrust model. **Table 1** lists selected wells that penetrate Precambrian basement overhangs throughout the Wyoming foreland. **Figure 22** shows the areal distribution of these same selected wells. It can be seen that most of the wells that penetrated basement were drilled on northwest-trending structures. Exceptions to this are: (1) the north end of the Laramie Mountains (well number 4, **Table 1, Figure 22**), along the northeast-striking Corral Creek fault, and (2) the north flank of the Uinta Mountains (well number 3, **Table 1, Figure 22**), in northeastern Utah, and (3) the south flank of the Owl Creek Mountains (well number 12, **Table 1, Figure 22**).

In addition to the Emigrant Trail (well number 1, **Table 1, Figure 22,**) and EA (well number 2, **Table 1, Figure 22**) thrusts, Berg (1962b) predicted that the Wind River Range also had an overhang of major magnitude and that Precambrian basement was thrust over sedimentary rocks along a dual fault system. In 1973, Husky Oil Company drilled to a depth of 12,944 feet (well number 5, **Table 1, Figure 22**; Ray and others, 1983). The well penetrated 6,247 feet of Precambrian basement on the hanging wall of the Wind River thrust and then penetrated upside down Devonian through Pennsylvanian beds to near total depth. Information circulating at the time indicated that the well had reached total depth in Pennsylvanian conglomerates. However, it is my interpretation that the well penetrated the lower fault of the dual system, which placed Pennsylvanian Tensleep Sandstone over Upper Cretaceous or Tertiary conglomerates. Subsequent drilling by other companies (well number 6, **Table 1, Figure 22**) has established the presence of Tertiary and Cretaceous rocks beneath the overturned Paleozoic rocks. Industry and COCORP seismic data (**Figure 23**) establish a minimum horizontal transport (heave) of 13 miles on the 25° to 30° dipping Wind River thrust.

Gries (1983b), Sprague (1983), and Skeen and Ray (1983) have all shown the northwest-striking Casper arch thrust to have approximately 8 to 12 miles of southwest directed displacement over the eastern margin of the Wind River Basin. Well and seismic data also indicate that the Casper arch thrust dips northeastward at angles varying from 20° to 40° (**Figure 24**), which gives the thrust a "step/flat" appearance (Brown, 1987; Skeen and Ray, 1983). The Moncrief 16-1 Tepee Flats (well number 8, **Table 1 Figure 22**) drilled 8,865 feet of Precambrian basement before drilling into overturned Triassic Chugwater Formation in the dual fault zone, and then eventually into Cretaceous rocks (well number 8, **Figure 24**). The Casper arch thrust strikes northwestward to the northeast corner of the Wind River Basin. In the vicinity of T39N, R89W, the Casper arch thrust either intersects the South Owl Creek fault, or changes to a west-northwest strike and becomes the South Owl Creek fault. The 8 to 10 miles of reverse dip-slip mapped on the Casper arch thrust suggests that the South Owl Creek fault should have a similar amount of reverse left-oblique slip. The Casper arch thrust also continues southeastward along the west flank of Casper arch. The lower fault of the dual fault zone was penetrated at Pine dome (number 15, **Table 1, Figure 22**; Cercone, 1989) at a depth of 19,000 feet.

In 1984, Gulf Oil Corporation drilled the 1-9-2D Granite Ridge well (well number 13, **Table 1, Figure 22**) on the Piney Creek block (**Figure 25**) to a depth of 15,710 feet. The location proves a minimum displacement of 3.3 miles (Brown, 1988) on the Piney Creek thrust, which dips westward at an angle of 25° to 35° (Furner, 1989).

The northwest-striking Beartooth thrust, southwest of Red Lodge, Montana has been interpreted by Bonini and Kinard (1983) to be a low-angle, southwest-dipping reverse fault. In 1988, Amoco Production Company drilled the Beartooth Unit A No. 1 (well number 18, **Table 1, Figure 22**), to a total depth of 14,000 feet, cutting the Beartooth thrust at a depth of 10,070 feet. The location of the well documents the Beartooth thrust as dipping approximately 30° to the southwest. Displacement of the basement has been estimated between 7.5 miles (Blackstone, 1986) to 10 miles (Brown, 1987).

Other Wyoming foreland uplifts have been drilled and/or explored seismically to the extent that faults and significant amounts of crustal shortening can be attributed to them. The west flank of the Bighorn Basin has been drilled in the Oregon Basin field by Hunt Oil Co. The #1 Lock Katrine (well number 18, **Table 1, Figure 22**) was drilled to a depth of 23,860 feet. Although this well did not actually penetrate Precambrian, Blackstone (1986) interpreted the Oregon Basin fault to dip approximately 40° to the west, having a heave component of almost 5 miles. Johnson and Smithson (1985) interpreted the COCORP seismic data across the Laramie Mountains as showing a low-angle reverse fault bounding the the east side of the uplift. Drilling in the Laramie Mountains has been concentrated at the north end, along the northeast-striking Corral Creek fault (Gries, 1983a), where seismic and well data (well number 4, **Table 1, Figure 22**) indicate a southward dip between 45° and 60°.

Evidence for the nonshortening model

When primary northwest-trending Laramide folds were transected by east- and northeast-striking transverse faults (**Figure 26a**), the dominant sense of motion was vertical at the anticlinal crest. Longitudinal sections (**Figure 26b, c**) would thus be expected to

Table 1. Selected wells that drilled through Precambrian basement along mountain fronts in the Wyoming foreland.

Well no.	Well name	Well location	Thrust penetrated-associated uplift
1.	Carter #1 Unit	sec. 32, T30N, R93W	Emigrant Trail thrust-Sweetwater arch
2.	Shell #1 Gov't	sec. 09, T42N, R105W	EA thrust-Washakie Range
3.	Shell #21X-9	sec. 09, T2N, R14E	Uinta thrust-northern Uinta Mountains
4.	True Oil-Rainbow #41-6 Shaffer	sec. 06, T32N, R75W	Corral Creek thrust-Laramie Mountains
5.	Husky #8-2 Fed.	sec. 02, T29N, R106W	Wind River thrust-Wind River Range
6.	American Quasar #1 Skinner Fed.	sec. 32, T28N, R101W	Wind River thrust-Wind River Range
7.	Supron Energy #1F-28-30-93	sec. 28, T30N, R93W	Emmigrant Trail thrust-Sweetwater arch
8.	Moncrief #16-1	sec. 16, T37N, R86W	Casper Arch thrust-Casper arch
9.	Champlin Oil #1 Rock Mtn. State	sec. 36, T19N, R79W	Arlington thrust-Medicine Bow Mountains
10.	Champlin Oil #21-11	sec. 11, T17N, R78W	Arlington thrust-Medicine Bow Mountains
11.	American Quasar #9-24 Tribal	sec. 09, T6N, R2W	Maverick Springs thrust-Mav. Spr. anticline
12.	Moncrief #12-2	sec. 12, T39N, R93W	So. Owl Creek thrust-Owl Creek Mountains
13.	Gulf #1-9-2D	sec. 09, T53N, R84W	Piney Creek thrust-Bighorn Mountains
14.	Arco #1-4	sec. 04, T50N, R83W	Clear Creek thrust-Bighorn Mountains
15.	Moncrief #35-1	sec. 35, T35N, R84W	Casper Arch thrust-Casper arch
16.	Hunt Energy #1 Loch Katrine	sec. 02, T51N, R100W	Oregon Basin thrust-Oregon Basin anticline
17.	Texaco #1 Sheets	sec. 21, T54N, R102W	Line Creek thrust (?)-Beartooth Mountains
18.	Amoco #1 Unit	sec. 09, T8S, R20E	Beartooth thrust-NE Beartooth Mountains
19.	Phillips Pet. Federal #1-9	sec. 15, T9S, R20E	Beartooth thrust-E. Beartooth Mountains
20.	Phillips Pet. #1 Federal-A	sec. 20, T43N, R106W	EA thrust (?)-Washakie Range

the show bed-lengthening required by the drape fold model. Unfortunately, few of these features have been studied in enough detail to provide unequivocal data either to support or contradict this interpretation.

One area where the required bed-lengthening may be present is Zeisman Dome on the east flank of the Bighorn Basin (T49N, R89W). Stricker (1984) has shown that northwest plunge is expressed by a steeply north dipping panel of Upper Triassic and Lower Jurassic rocks (**Figure 27**). Stone (1987) interpreted this panel to represent a buried basement wrench fault. Brown (1988) interpreted this same fault as a compartmental fault, with the steep north dip representing drape over the basement fault. Stricker mapped a west-striking normal fault exposed in the Pennsylvanian Tensleep Formation at

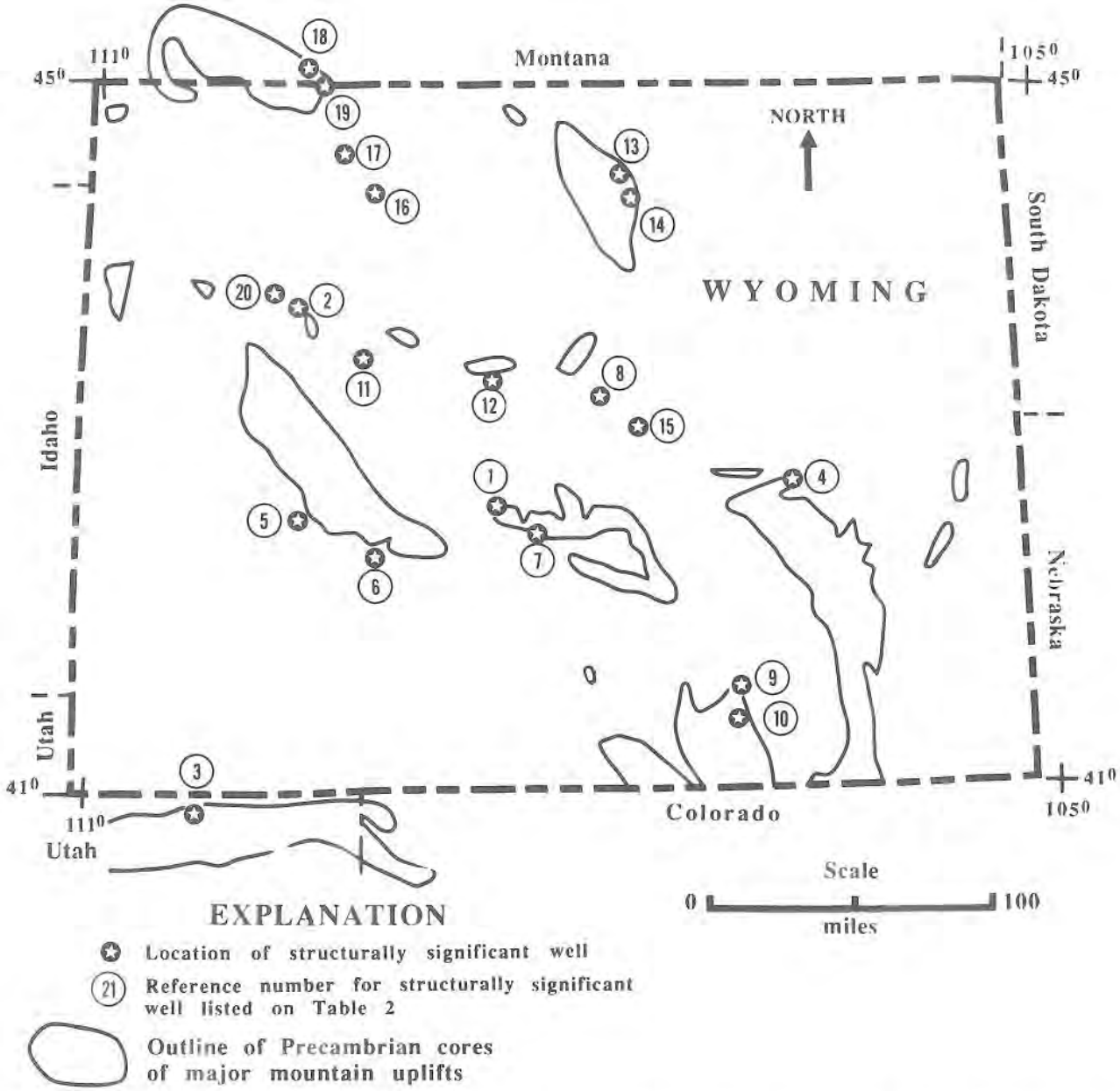

Figure 22. Map showing location of selected exploratory wells that have penetrated varying thicknesses of Precambrian basement rocks along mountain-flank overhangs in the Wyoming foreland, and have encountered sedimentary rocks beneath. A listing of these wells and the thrust faults they penetrated is given in Table 1. Wells 1 and 2 were used by Berg (1962b) in formulating his fold-thrust model. Well number 5 was the first well to penetrate the basement overhang of the Wind River uplift. Wells 3, 4 and 12 are the only wells that penetrated Precambrian and were not on northwest-trending uplifts.

the crest of the fold, on the north plunge-end (Figure 27). Such faulting is in the proper position to represent one of the extensional structures required for drape folding to occur over a buried high-angle fault.

Another area that may offer confirmation of this style is along the north flank of the Owl Creek Mountains, south and west of Embar anticline (T8N, Rs1E-1W). Brown (1988) presented preliminary data that suggests as much 30% thinning in some Paleozoic and Mesozoic units across the east-west striking

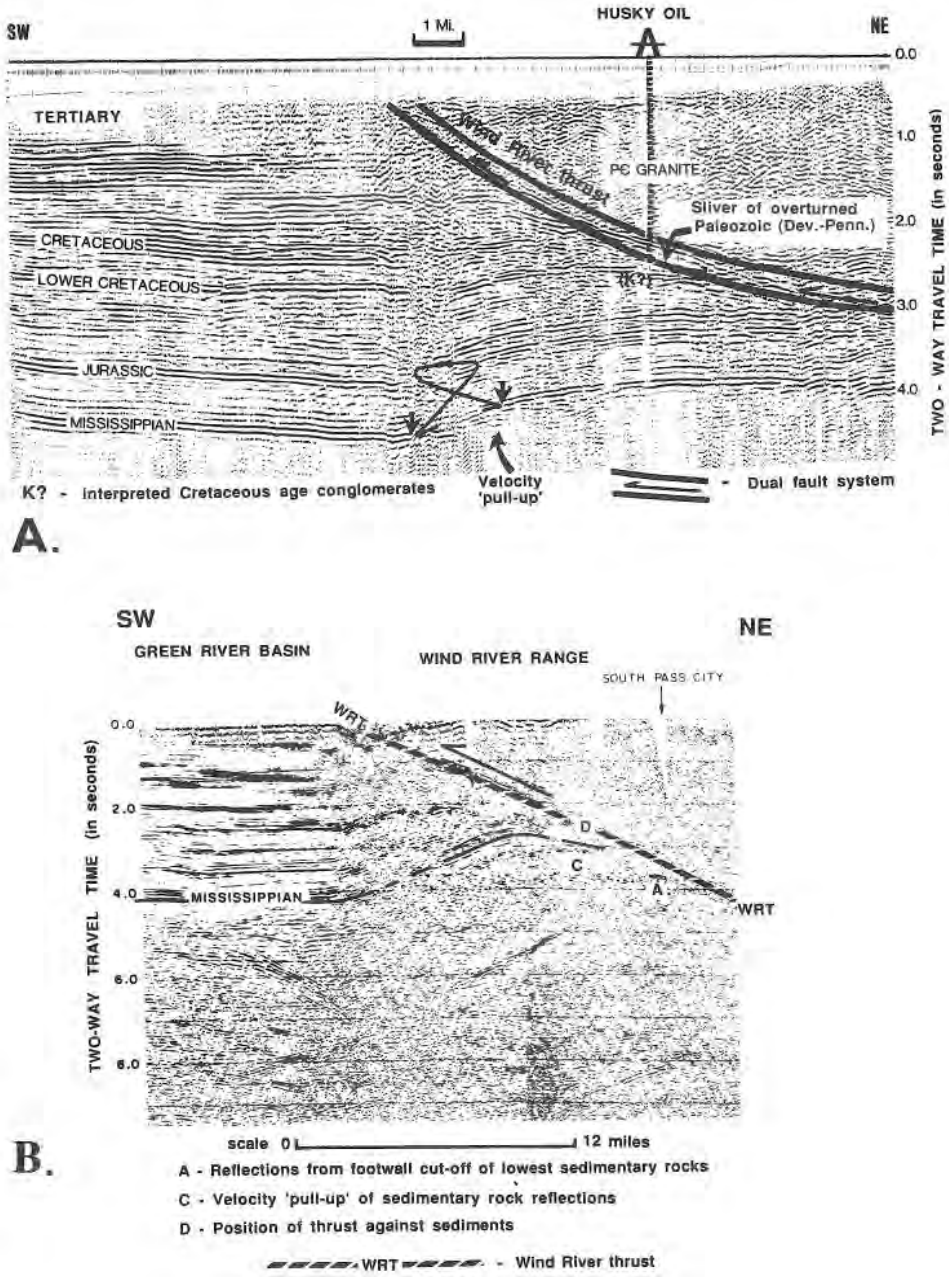

Figure 23. Reflection seismic line across the southwestern margin of the Wind River uplift. A. Husky Oil Co. (well number 5, Table 1, Figure 22) penetrated 6,247 feet of Precambrian basement and then encountered upside-down sedimentary section below the fault, ranging from Devonian to Pennsylvanian. Note the seismic velocity "pull-up", which results from higher seismic velocities through the basement (modified from Lowell, 1983). B. The COCORP (Consortium for Continental Reflection Profiling) seismic line demonstrates approximately 13 to 14 miles of Precambrian basement overhang (crustal shortening) developed along the low-angle Wind River thrust (modified from Smithson and others, 1978).

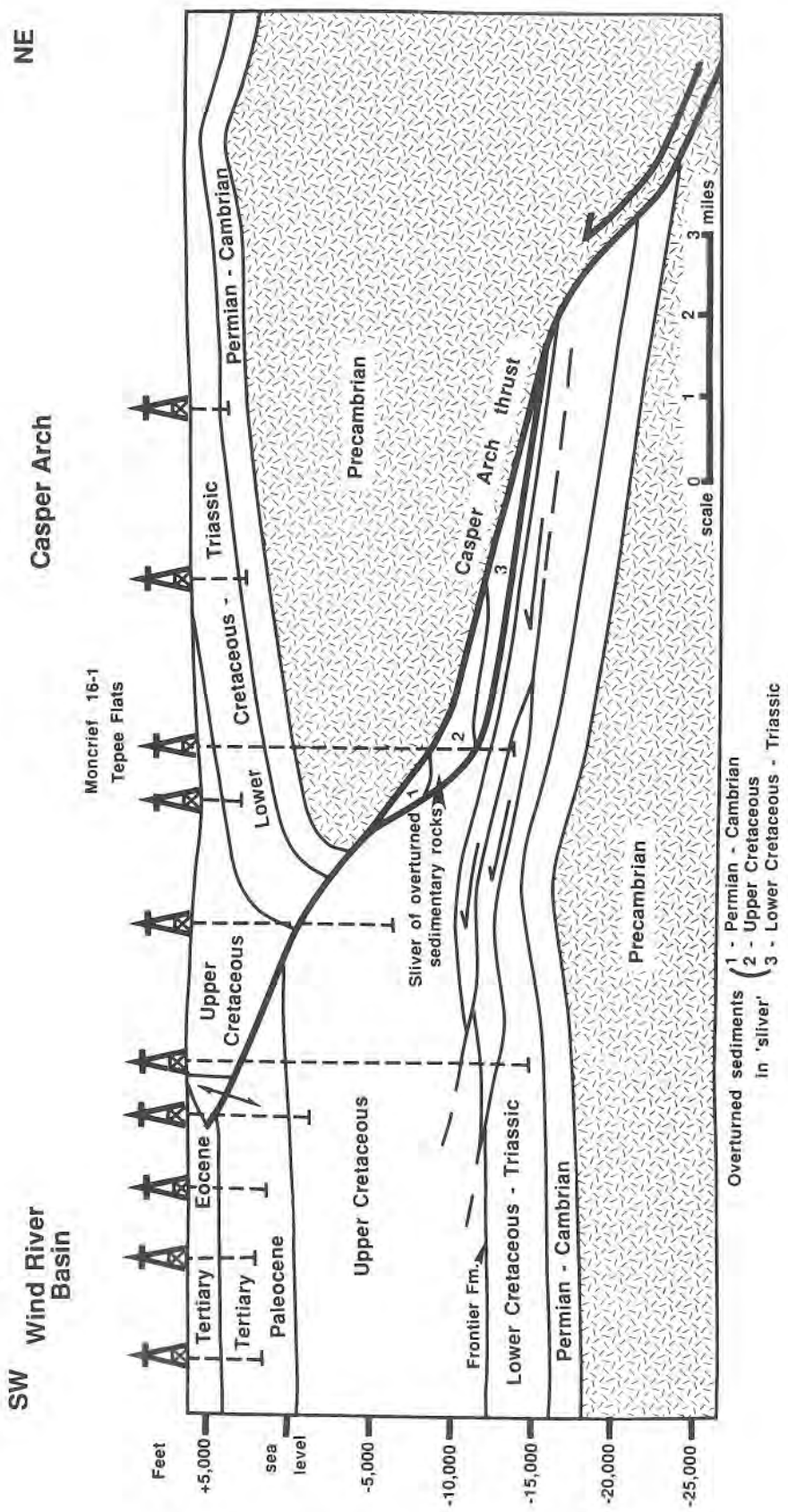

Figure 24. True-scale structural cross section of the Casper arch thrust (modified from Busby, 1982, *in* Skeen and Ray, 1983), based on well and seismic data. Geometry suggests a "step and flat" arrangement of the fault plane in the basement, typical of faults of the thin-skinned thrust belt.

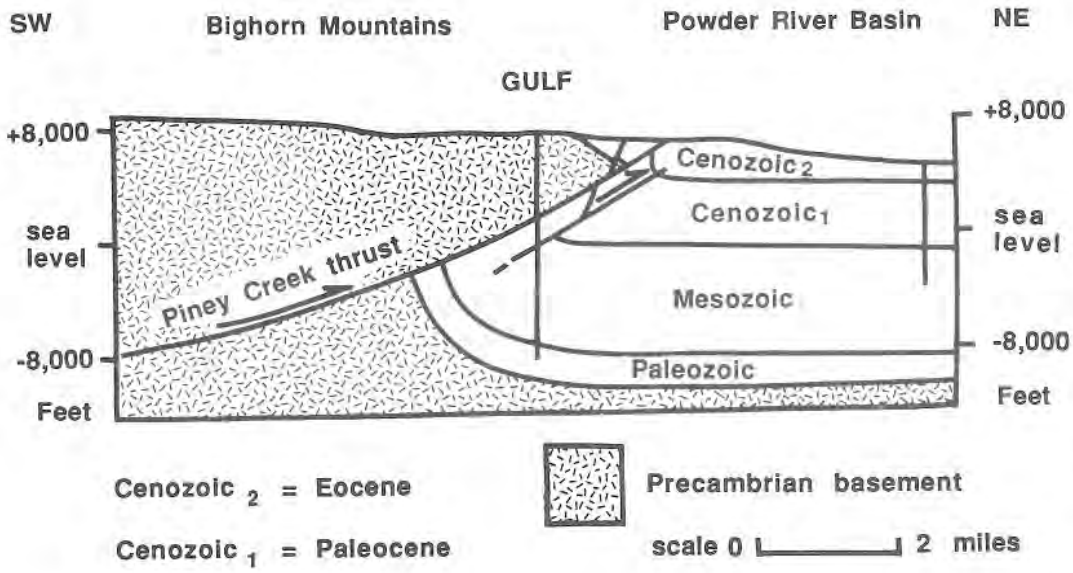

Figure 25. The east flank of the Bighorn Mountains has been pushed eastward approximately 3.3 miles along the Piney Creek thrust fault, which dips 25° to 35° west. The structure was penetrated to a depth of 15,710 feet by the Gulf Oil 1-9-2D Granite Ridge well (well number 13, Table 1, Figure 22; modified from Furner, 1989).

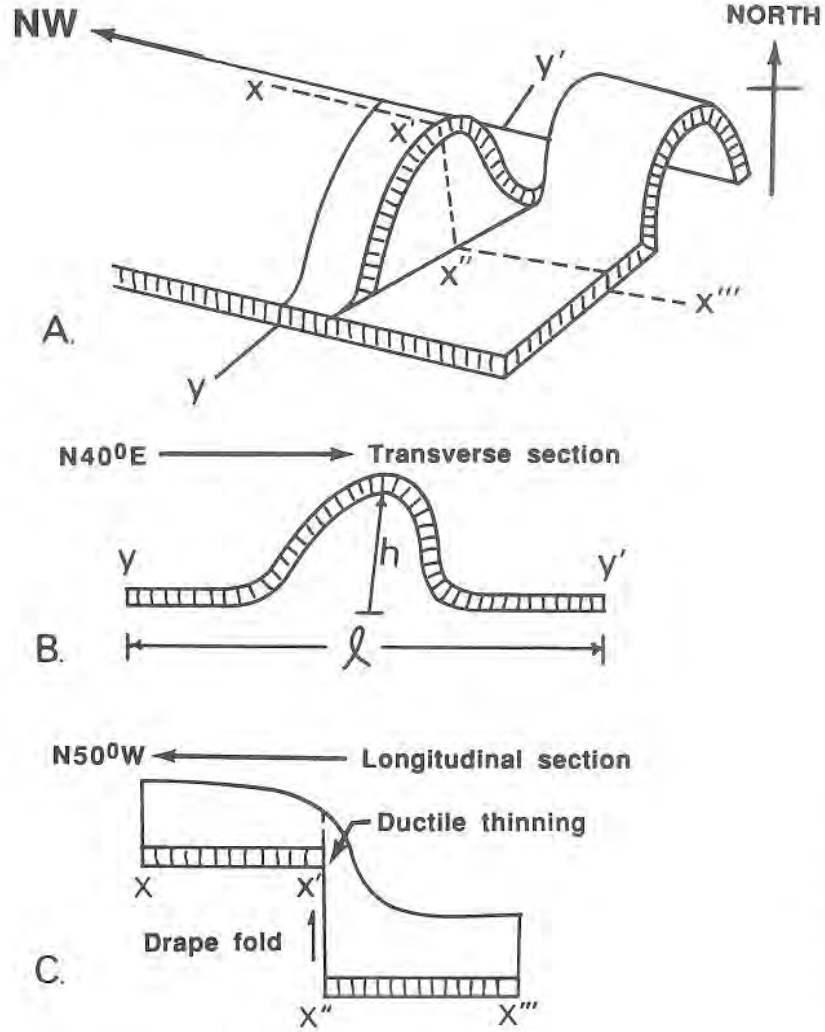

Figure 26. A. Northwest-trending Laramide folds are often cut by a transverse compartmental fault. B. This results in predominantly vertical motion along the fault at the anticlinal crest. C. A longitudinal section of the fold across the compartmental fault should show evidence of bed-lengthening and thus be interpreted as an east-trending drape fold.

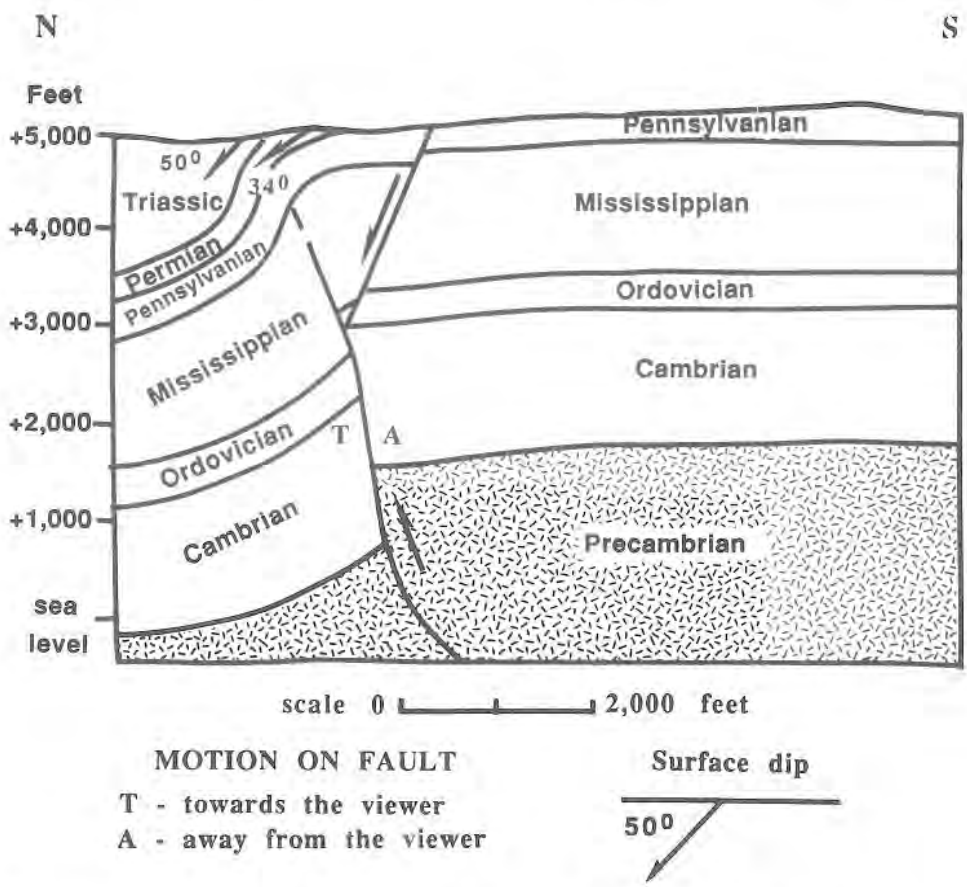

Figure 27. True scale north-south section showing steeply north dipping panel of rock, which terminates the northwest plunge of Zeisman dome (modified from Stricker, 1984). Presence of a normal fault on the hanging wall of the high-angle fault suggests bed lengthening to accommodate draping of sedimentary rocks across the buried Bonanza-Zeisman compartmental fault.

North Owl Creek fault. Application of a northeast-southwest oriented Laramide stress on this portion of the North Owl Creek fault implies that some magnitude of left oblique-slip should have occurred along the fault.

The nonshortening model of *upthrust faulting* has been applied by Prucha and others (1965) to the northwest-trending Bald Mountain anticline on the north flank of Hanna Basin (T25N, R81W). Their interpretation will be contrasted to the horizontal shortening model in a later section.

Precambrian basement exposed in the canyon of Wind River (T6N, R5E, WRM; T40N, R94W) displays a series of normal faults, of which the Boysen fault is the most significant. Boysen fault strikes east-west and dips 65° south. It has approximately 1,500 feet of down-to-the-south throw. South of the crest, the normal faults dip north, culminating in a keystone graben (Wise, 1963) at the crest of the range. I (Brown, 1988) interpreted this transect across the uplift using an upthrust model; the Boysen fault and keystone graben could provide the extension required in the application of the nonshortening model. The upthrust geometry (**Figure 28**) is also similar to that observed in deformation experiments by Logan and others (1978) and to *flower structures* created by wrench (or strike-slip) movement (Harding, 1990). Other workers Fanshawe, 1939; Gries, 1983b; (Blackstone, 1990) have inferred the South Owl Creek fault to dip gently northward for several miles. Seismic data in the vicinity of Wind River Canyon is of insufficient quality to prove this. Other seismic data (Gries, 1983b) which have been interpreted as gentle north dip, are actually related to the Casper arch thrust farther to the east (Brown, 1987).

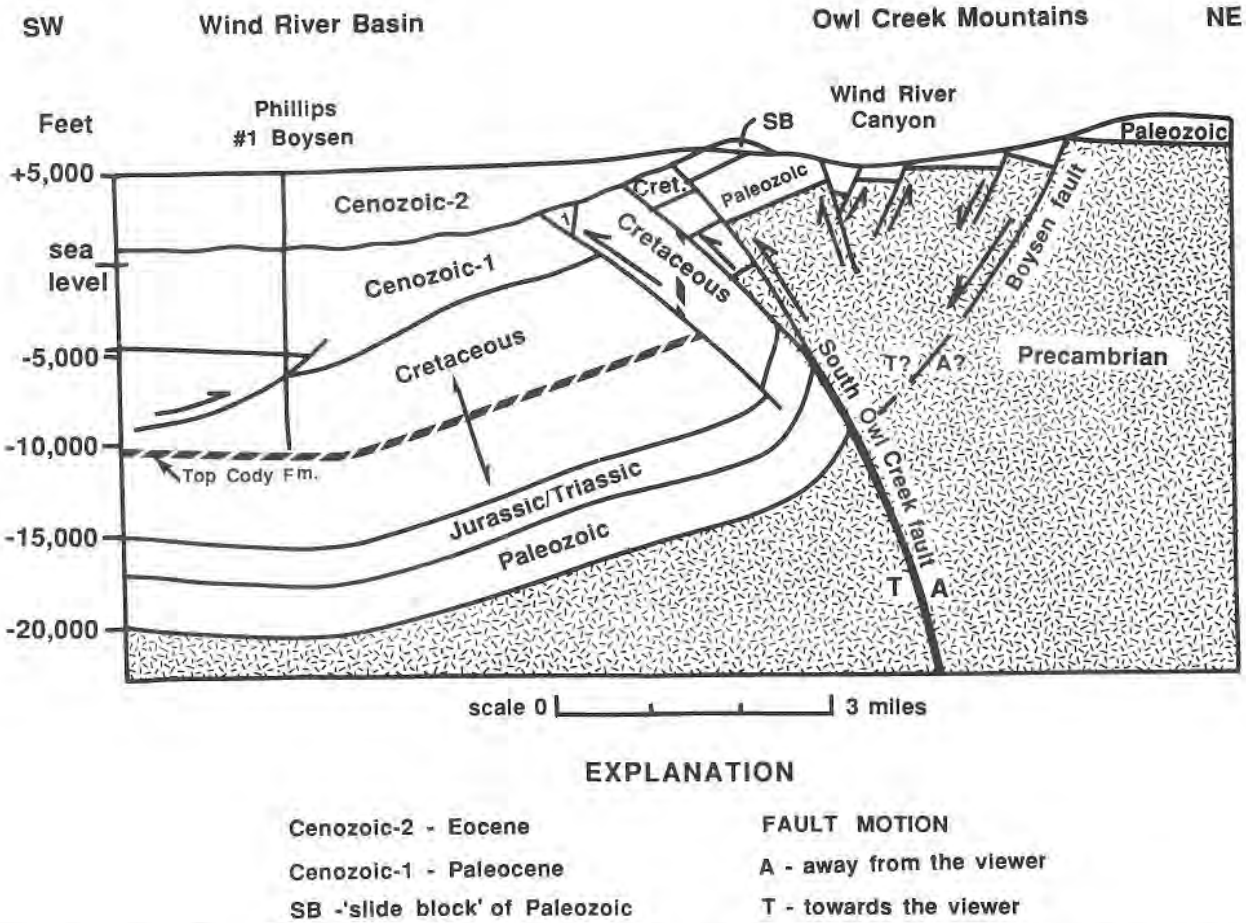

Figure 28. South flank of the Owl Creek uplift has been faulted over the Wind River Basin along the east-west striking South Owl Creek fault (SOCF; SO on Figures 3, 4). Extension on the hanging wall of the SOCF by the Boysen normal fault, along with development of a keystone graben, allows interpretation of the SOCF as an upthrust fault having reverse left oblique-slip. Comparison of this interpretation with experimental models (Logan and others, 1978) offers a reason for the development of a mountain overhang on east-west trending faults.

Comparison of horizontal crustal shortening and nonshortening models using the concept of structural balance

Structural balancing has been applied to thin-skinned thrust belt interpretations for some time (Dahlstrom, 1969b). Acceptance of the technique of structural balancing has been much slower by foreland workers than by thrust belt workers. Structural balance must be maintained across the deformed foreland unless there is a regional change in shortening; therefore measurements along parallel, northeast-trending lines across the foreland should show essentially the same magnitude of crustal shortening. Any discrepancy between such values may be the result of a change in the regional shortening, or an error in the interpretation along one or more cross sections.

Comparison of multiple interpretations of individual foreland structures that have been published are shown in **Table 2**. Stone's (1984) comparison of interpretations of Rattlesnake Mountain anticline (**Figure 29**; number 4, **Table 2**) shows not only the contrast between the horizontal shortening and nonshortening interpretations, but also shows the variety in horizontal shortening interpretations. Brown (1988) demonstrated that the Precambrian/Cambrian contact is approximately 5,000 feet short in contrast to the overlying Mississippian surface when the drape fold interpretation is compared to a reverse fault interpretation. Both Erslev (1986) and Matthews (1986)

Table 2. Comparisons of crustal shortening and non crustal-shortening models.

Area *	Nonshortening Model (Original reference)	Crustal Shortening Model (Original reference)	Reference to Comparison of Models
1.	Osterwald (1961)	Berg (1962a)	Brown (1988)
2.	Palmquist (1978)	Blackstone (1981)	Brown (1988)
3.	Matthews & Work (1978)	Brown (1983)	Brown (1987)
4a.	Stearns (1971)	Brown (1984a)	Brown (1988)
4b.		(See Figure 29)	Stone (1984)
	(a) Johnson (1934) (b) Pierce & Nelson (1968) (c) Stearns (1971)	(d) Cook (1983) (e) Schmidt & Garihan (1983) (f) Brown (1984a)	

* Key:
1. Soda Lakes area, Front Range, Colorado
2. Piney Creek area, Bighorn Mountains, Wyoming
3. Belleview Dome, Front Range Colorado

4a. Rattlesnake Mtn. anticline, Cody, Wyoming
4b. Rattlesnake Mtn. anticline, Cody, Wyoming

pointed out that Brown's interpretation (**Figure 29f**) is structurally balanced down to the top of the basement, but a volumetric problem exists within the footwall basement, if Brown's cross section is restored using the single fault depicted. Those interpretations showing a second fault in the basement on the footwall of the Rattlesnake fault (Erslev, 1986) are probably more accurate.

Another area in Wyoming where both models have been applied is the Bald Mountain anticline, north flank of Hanna Basin. Prucha and others (1965, p. 978) constructed a section across this fold showing a high-angle, upthrust-style interpretation (**Figure 30a**). Blackstone (1983, p. 4) interpreted the area using a horizontal shortening model (**Figure 30b**). The noticeable differences seen in such comparisons, are: (1) the dip-angle of the controlling fault, and (2) geometry of the basement/sediment contact. These two differences relate to the magnitude of crustal shortening, and lack of structural balance. The lack of extensional features present at Bald Mountain, plus the steep dip-angle of the upthrust fault result in the nonshortening model being structurally out of balance.

The topic of structural balancing was discussed at the 1982 Geological Society of America Penrose Conference on Wyoming Foreland Structures, held at Red Lodge, Montana. Generally, the concept of structural balance was accepted by those advocating a crustal shortening model, and dismissed by those advocating a nonshortening model of deformation. Beginning in 1983, several papers were published describing techniques of structural balancing as applied to basement-involved foreland folds. Cook (1983) presented a short discussion on structural balancing as it applied to Rattlesnake anticline, and then documented his technique in 1988. Spang and others (1985) presented their techniques of structural balancing with examples from the Wind River Basin. Erslev (1985, 1986) presented techniques of structural balancing, using Rattlesnake Mountain anticline and folds in the Beartooth uplift as examples.

Erslev (1986), and Robbins and Erslev (1986), invoked a style of interpretation referred to as *basement wedges and backthrusting* (**Figure 19**). In such a model, displacement on the master fault decreases to zero (goes blind) by transferring displacement to one or more oppositely verging backthrusts, allowing structural balance to be maintained even though the main fault dies out. Abercrombie (1989) invoked a similar model to explain the apparent changes in vergence of basement thrusts along the Sheep Mountain line of folding in the southwestern Wind River Basin. Homan (1988) also used basement wedges to explain the apparent eastward loss of displacement of the Bradley Peak thrust, as well as to explain a change in vergence on other faults on the southwest flank of the Sweetwater arch.

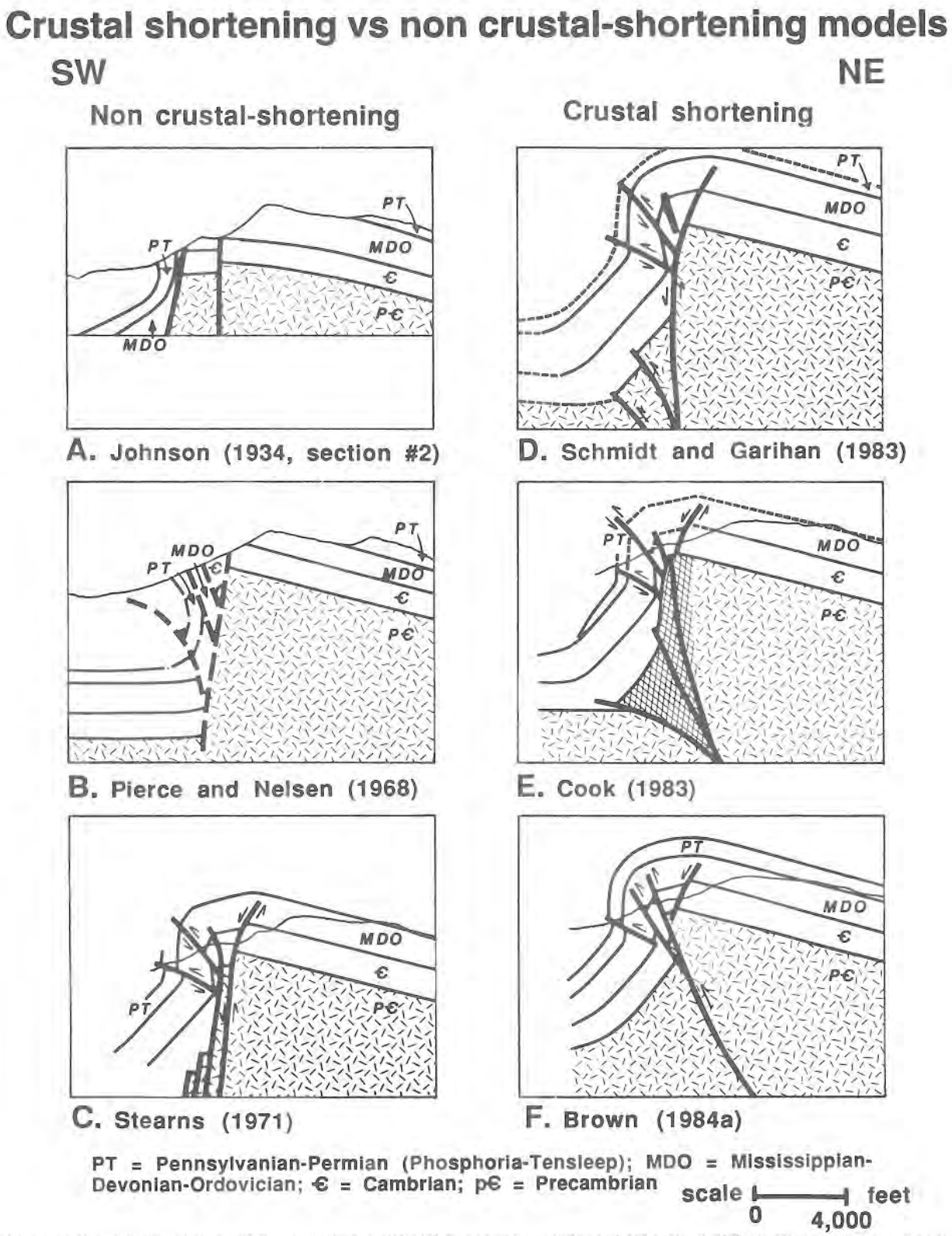

Figure 29. Comparison of interpretations of Rattlesnake Mountain anticline west of Cody, Wyoming contrasts crustal shortening and nonshortening models. Interpretations A. (Johnson, 1934), B. (Pierce and Nelsen, 1968) and C. (Stearns, 1971) are not in structural balance because length of sedimentary section is much longer than the top of the basement. The crustal shortening models D. (Schmidt and Garihan, 1983), E. (Cook, 1983), and F. (Brown, 1984a) are more nearly structurally balanced. The deep fault in E. allows the footwall block to rotate upward without causing a volume problem beneath it. (Modified from Stone, 1984.)

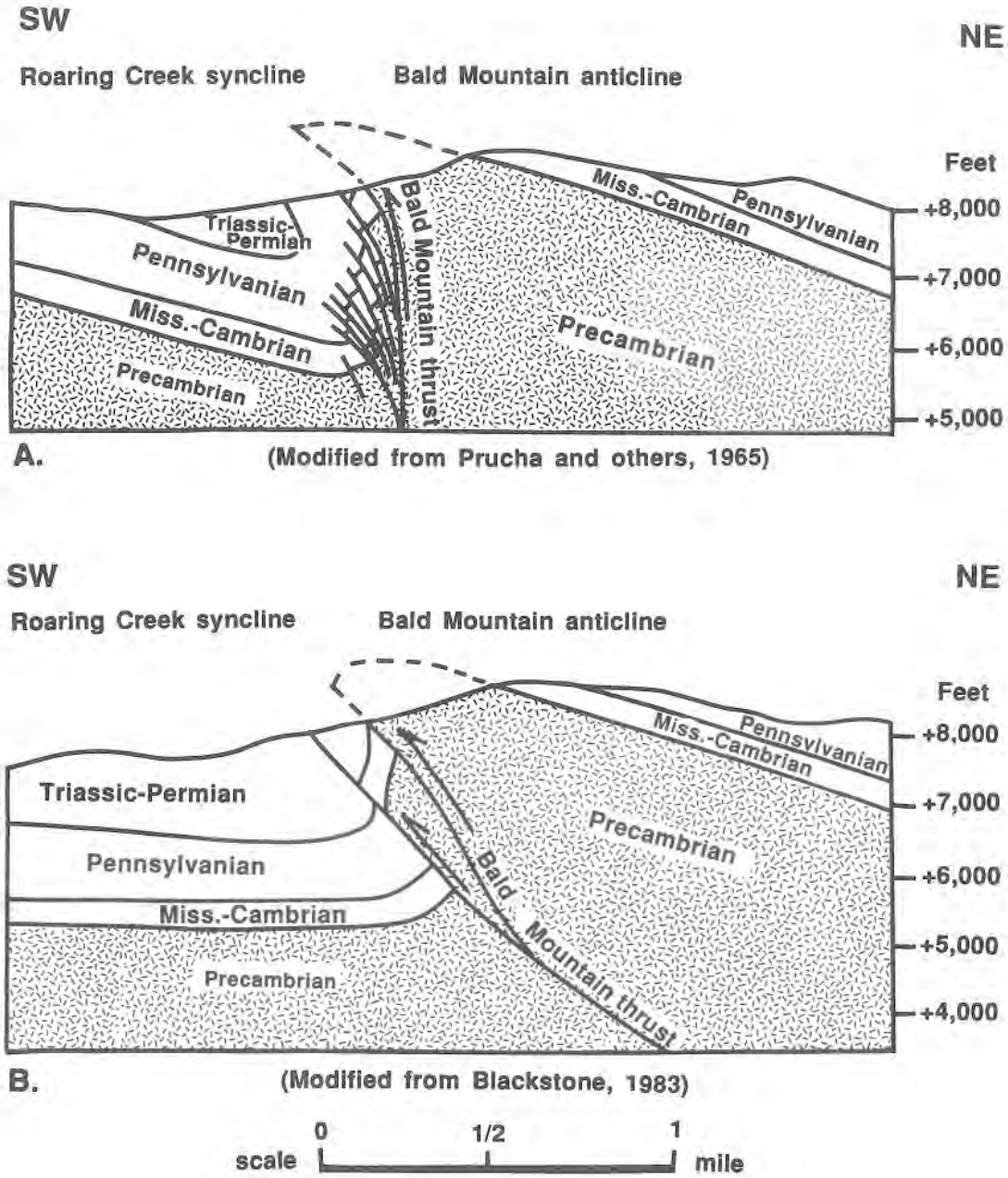

Figure 30. A. The nonshortening interpretation of Bald Mountain anticline (modified from Prucha and others, 1965) shows an upthrust system with multiple splay faults which are not present at the surface, even though the fault is exposed up-plunge. B. The crustal shortening interpretation (modified from Blackstone, 1983) displays a style encountered frequently across the foreland. A moderately dipping reverse dual fault system has vertical to overturned rocks between the two fault planes.

Crustal shortening and lateral movements

Consistency of crustal shortening values for the Wyoming foreland

Crustal shortening was pervasive throughout, and consistent across the Wyoming foreland during the Laramide orogeny. Brown (1987, table 11) determined crustal shortening values for over 30 individual structures within the Wyoming foreland. These values range up to approximately 13 miles for the Wind River thrust, whereas many individual folds display crustal shortening of one mile or less. Structures in the Wyoming foreland do not continue along trend for hundreds of miles, therefore when one structure plunges out, some other structure should demonstrate an increase in shortening to balance that loss. Such trade off of crustal shortening may be referred to as an accommodation zone or a displacement transfer zone (Dahlstrom, 1969b).

A cross section by Petersen (1983) displays approximately 17 miles of shortening across the foreland, but more recent drilling indicates that value to be too small. Brown (1988) calculated the total shortening across the Wyoming foreland along three northeast-striking cross sections (**Figure 31**), each covering over 200 miles in length. The values for total

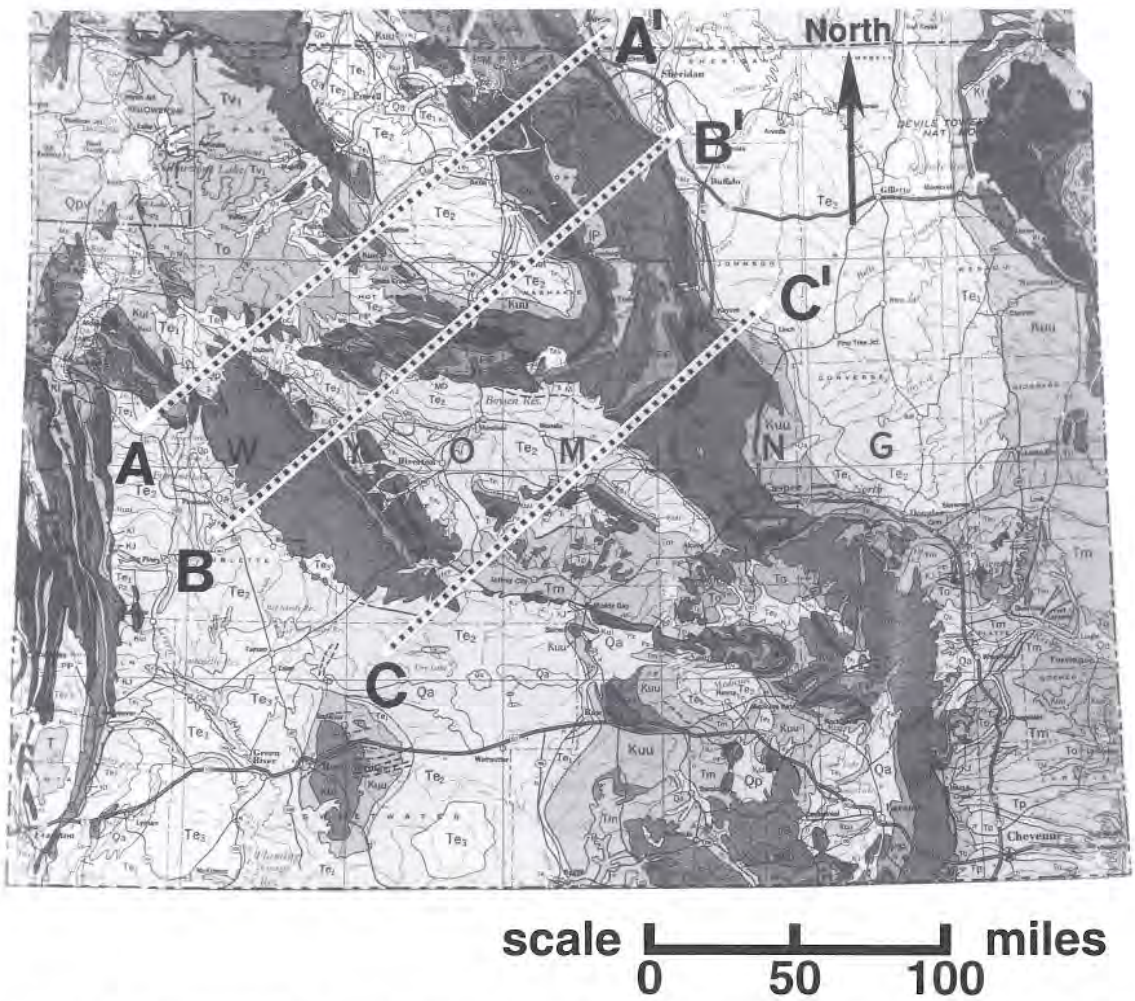

Figure 31. Geologic map of Wyoming (modified from Renfro and Feray, 1966) shows the lines of section for three northeast-southwest trending true-scale cross sections that have been used in determining the total crustal shortening across the Wyoming foreland. Values determined from these three sections range from 26.9 to 28 miles, or approximately 13% strain. A-A', C'C'- cross sections are discussed in text. Cross section B-B' is shown in Figure 32.

shortening on these three sections range from 26.9 miles (11.5% strain) to 29 miles (13% strain). Kanter and others (1981) calculated a value of at least 5% shortening for 15 regional cross sections across the Rocky Mountain foreland; however, their percentages were somewhat variable due to including large undeformed areas (e.g., Powder River Basin) in their calculations. Their line E-E' (Figure 5, 1981) is coincident with Brown's section B-B' (**Figure 32**) which demonstrates 28 miles of cumulative shortening across the central portion of the Wyoming foreland. Consistent crustal shortening values of this magnitude (approximately 28-29 miles and 13+ % strain) suggest that the Wyoming foreland has been deformed in a regionally uniform and unidirectional stress field.

Nature and extent of lateral movements

That a potential for large-scale lateral movements existed during the Laramide orogeny is indicated by the values of total crustal shortening presented above. However, those same values place an upper limit to the maximum amount of strike-slip or lateral offset in the Wyoming foreland. Faults that strike perpendicular to the axis of maximum crustal shortening should be low-angle, reverse dip-slip thrusts (**a-b** on **Figure 33**). Any fault not so oriented should have some component of lateral offset, and thus be an oblique-slip fault.

Faults that strike more north-south (between NNW and NNE; **c-d** and **e-f** on **Figure 33**) should logically show a component of right-slip, whereas those oriented more east-west (between ENE and ESE; **g-h** and **j-k** on **Figure 33**) should display a component of left-slip. As pointed out previously, the dominant orientations of apparent Laramide-reactivated Precambrian zones of weakness are northeast, east, and north, in that order. Therefore, a predominance of *left oblique-slip* should have occurred on a high percentage of these reactivated basement faults.

In the absence of linear geologic features that will produce piercing points (Sylvester, 1986) when offset by a fault, documentation of lateral offsets is principally deductive. For instance, along the northwest strike of the Beartooth front (southwest of Red Lodge, Montana), the northeast-striking Willow Creek fault has apparently offset the basement and Paleozoic rocks approximately 0.5 miles in a right-lateral sense. The presence of slickensides that plunge approximately 28° southwest within the fault zone offers substantiation for an interpretation of lateral slip on the Willow Creek fault and low-angle dip of the main Beartooth thrust.

Another area for which a strong case can be made for lateral offset is the northern boundary fault of the Piney Creek block (T53N, R84W) which strikes ENE, on the east flank of the Bighorn Mountains (**Figures 25, 34; Table 2**). Blackstone (1981) proposed that the Piney Creek block had been pushed east-ward along a low-angle reverse fault (Piney Creek thrust) and that the north-bounding fault of the Piney Creek block represented a left-lateral tear fault. Borehole penetration of this uplifted block has now established approximately 3.3 miles of horizontal motion on the Piney Creek thrust (**Figure 25**) and therefore the Piney Creek tear fault has 3.3 miles of left oblique-slip (Brown, 1988; Furner, 1989).

The potential for large lateral displacements and the reasonably sound determination of smaller magnitude lateral displacements, makes it surprising that there are so few areas that show the classic *en echelon* fold arrangement, expected in strike-slip regimes (Wilcox and others, 1973). Stone (1969) has been a leading proponent of strike-slip motion on many foreland faults. He has interpreted the Bonanza-Zeisman area on the east flank of the Bighorn Basin as a *wrench fault/thrust-fold* structure (Stone, 1987; italics added). However, none of the anticlines that terminate along a postulated northeast-striking basement fault (**Figure 35**) have developed any significant *left-stepping en echelon* arrangements (Brown, 1987), which would be expected of a true left-wrench system. An alternative to the wrench fault interpretation will be presented in a later section.

There are a few areas within the foreland that do show the classic acute angle between a fold and a possible wrench or strike-slip fault. One such area is the Sheep Creek anticline (T28N, R92W) on the south flank of the Sweetwater arch (**Figure 36**). The angle between this fold and the Sheep Creek thrust (South Granite Mountain fault) suggests a left-lateral component as well as reverse motion (Berg, 1962b).

Another area displaying fault and fold arrangements suggestive of lateral motion is along the north flank of the Owl Creek Mountains (T8N, Rs1E-1W).

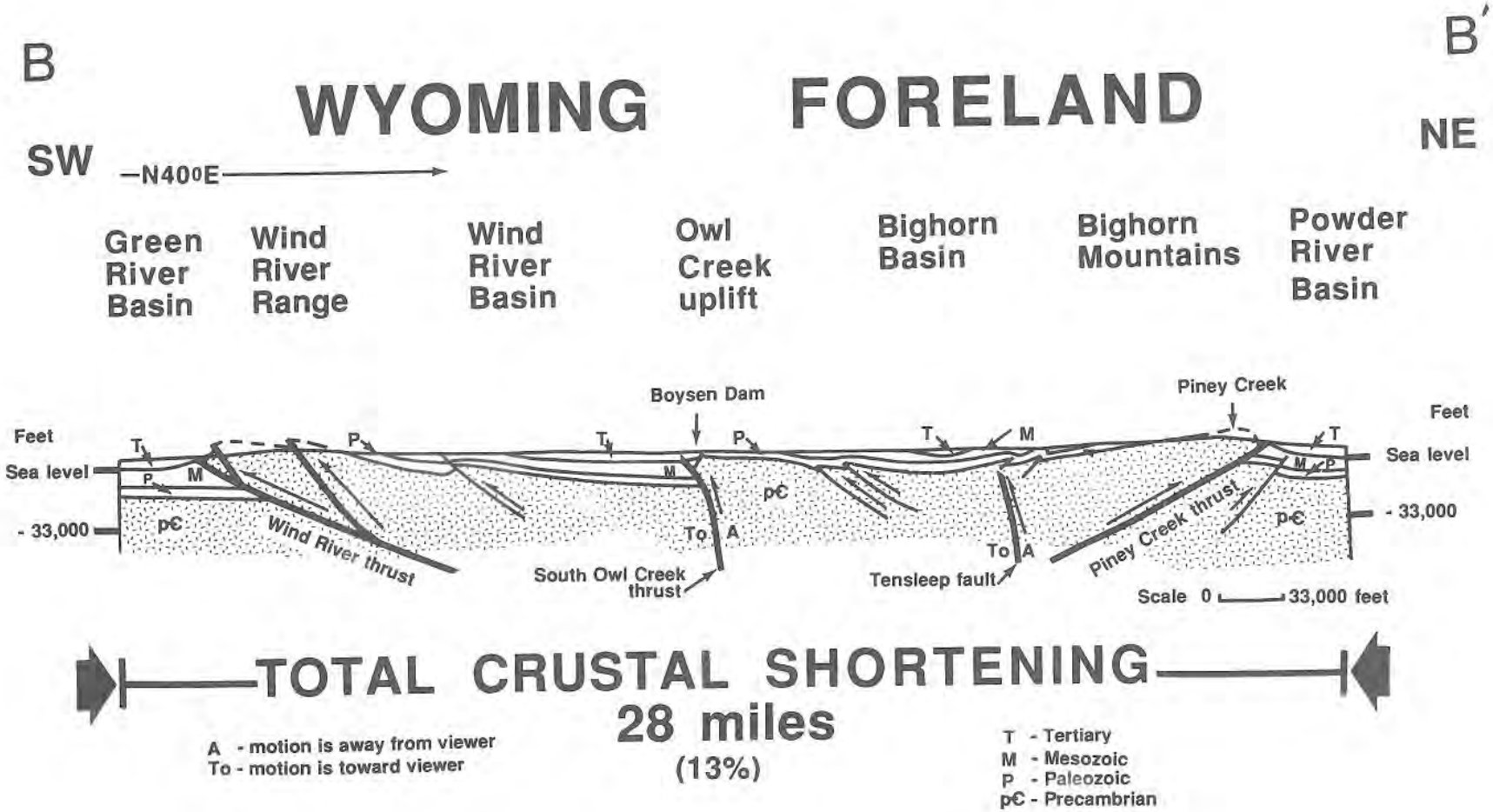

Figure 32. Southwest to northeast cross section BB' (location on Figure 31) demonstrates the conjugate nature of the basement-involved reverse faults typical of primary Laramide structures. Total crustal shortening across the foreland equals approximately 28 miles along this line of section (from Brown, 1988; reprinted by permission of Geological Society of America).

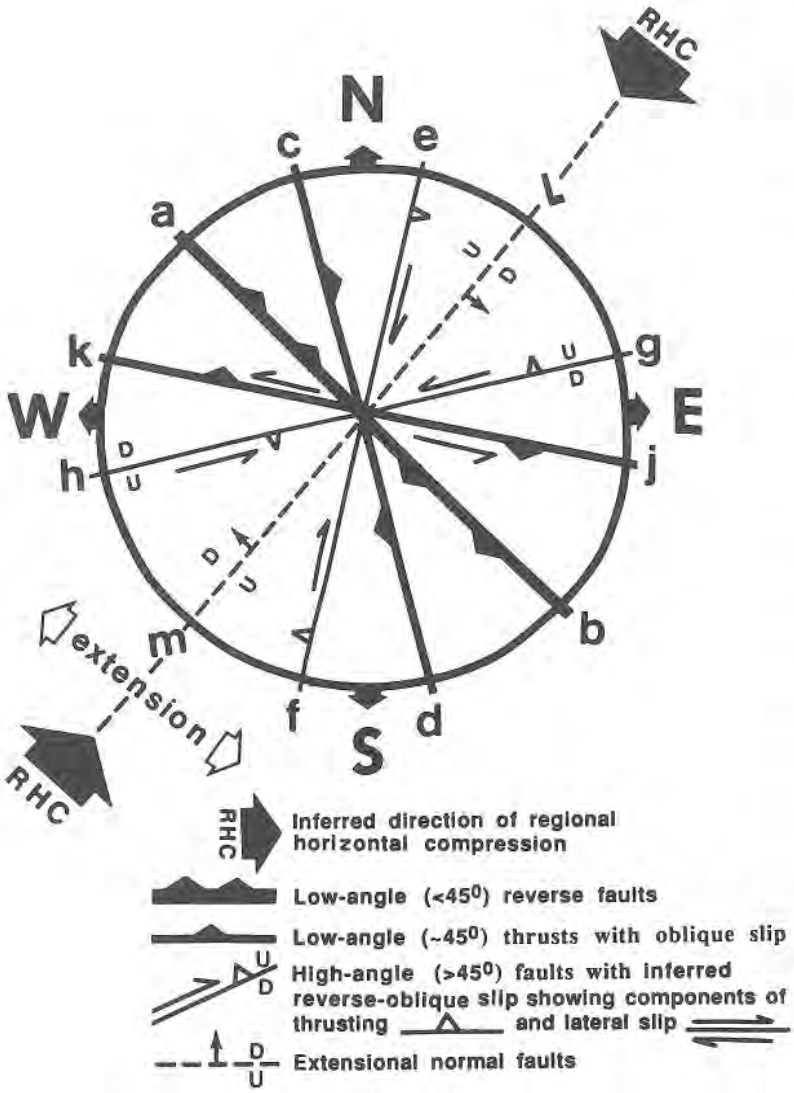

Figure 33. The two-dimensional strain ellipse for a northeast-southwest oriented regional horizontal compressional system (RHC) shows the orientation and sense of slip expected on a variety of fault orientations within the stress system. Primary conjugate thrusts (a-b) will develop at right angles to the RHC and have the greatest reverse dip slip motion. Fault sets c-d and j-k intersect the RHC at the an angle of 45° or greater, and will primarily have thrust motion with a component of either left or right oblique-slip. Fault sets e-f and g-h intersect the RHC at the an angle of 45° or less, and will have either left or right oblique-slip, with the strike-slip component being the greatest. Fracture L-m is parallel to RHC and could show normal oblique-slip motion.

The east-west strike of this high-angle fault within the inferred Laramide stress system implies a left-slip component on this up-to-the-south fault. The trend of Anchor anticline (**Figure 37**) also suggests that left-slip has occurred along the North Owl Creek fault. Until recently, this was as definitive as one could get in proving lateral motion along this fault. However, Paylor (1990) reported that this fault is very high angle (80°), north-side down, and changes from south dip on the east end to north dip on the west end. He presented slickenside data from the fault zone that proves left-oblique slip has taken place along this fault. Paylor estimated the lateral motion to be almost 6 miles. Brown (1988) estimated a minimum value of lateral motion to be 2.5 miles, equal to the shortening measured across the adjacent uplift. The North Owl Creek fault zone has been eroded deeply enough to expose Precambrian basement on the upthrown side, juxtaposed to upper Paleozoic and Triassic rocks on the downthrown side. This level of erosion may have removed evidence needed to determine if the overall geometry is that of an upthrust fault.

Results of rock deformation experiments (Logan and others, 1978) give some indication of the geometry of faults with reverse oblique-slip motion. The model (**Figure 38a**) is set up to represent the "corner" created by the intersection of a primary thrust-faulted fold and an oblique-slip fault that is transverse to the fold trend. The cross sections (**Figure 38b**) of multiple repetitions (**Runs I, II, III**) of the experiment yield a sequential series displaying progressive deformation with increased lateral and vertical offset. **Run I** displays the development of a drape fold with several splays of the fault present in the subsurface. This tells us that a drape fold can be created by oblique-slip on a fault without the fault reaching the surface. **Run II** documents that the first place where the fault splays reach the surface is at the lower hinge of the drape fold. With increasing displacement (**Run III**), additional splays develop progressively up the steep flank of the hanging-wall drape fold. These splays give the fault the appearance of a "flower structure" (Harding, 1990) typical of strike-slip faults. Additional displacement would be

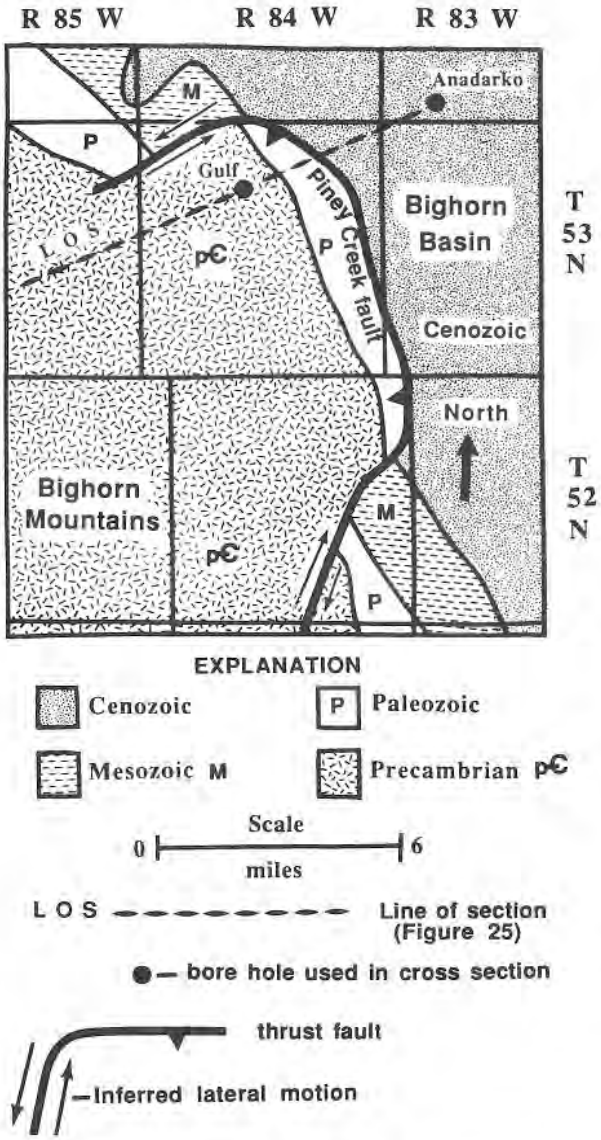

Figure 34. Geologic map modified from Love and Christiansen (1985) shows the Piney Creek block on the east flank of the Bighorn Mountains. The Piney Creek thrust terminates to the southeast and northwest into northeast striking tear faults. The Gulf well drilled in section 9 of T53N, R84W penetrated the Piney Creek thrust at a depth of 5,790 feet, thus establishing the dip on the fault plane to be between 25° and 35° west, proving a minimum horizontal displacement on the north Piney Creek tear fault of 3.3 miles.

needed for the fault to develop into a near-vertical surface feature located directly over the edge of the forcing block.

The near-vertical portion, along which reverse oblique-slip has occurred, is equivalent to the North Owl Creek fault described above. The drape fold displays the required bed-lengthening, which is accomplished by thinning of the model's multiple layers. **Run III** of the model shows the upward flattening typical of upthrust faults which is developed as a consequence of vertical stresses created when the forcing block moves up the 65°-dipping ramp.

This model has been applied to explain the south termination of Rattlesnake Mountain anticline (T52N, R102W; Brown, 1987). Brown's (1984a) reverse fault interpretation of Rattlesnake (**Figure 29**) has a crustal shortening value of 2,250 feet. The south plunge of the structure is intersected by a west-striking panel of steep south dip, forming the *corner problem* of Stearns (1978). In applying the oblique-slip upthrust model (Logan and others, 1978) to this corner, we find that a north-dipping reverse fault is exposed near the lower hinge of the south-facing drape fold. The separation of the Triassic/Jurassic contact along this fault is indicated to be between 5,000 feet (A/B, **Figure 39**) and 8,000 feet (A/C, **Figure 39**) in a left-lateral sense. This magnitude of lateral separation easily accommodates the 2,250 feet of lateral slip that would accompany the reverse dip-slip motion on the Rattlesnake reverse fault (Brown, 1984a). A north-south profile (**Figure 40**) across the steep south plunge illustrates the interpretation of the reverse left oblique-slip upthrust.

No doubt there are also structures where the upthrust fault is not yet exposed by erosion. These structures may not have had sufficient motion on the main reverse fault ramp to have caused the upthrust fault to propagate very high into the sedimentary section. Much detailed study of corner structures needs to be done across the foreland to fully document this style. Particular attention should be given to quantify the amount of motion required to cause the upthrust fault to propagate to the ground surface.

Compartmental deformation

There are numerous east- and northeast-striking faults that transect anticlines of different orders of magnitude but do not link into northwest-striking reverse faults (**Figure 26**). Brown (1975, 1988) has called these *compartmental faults*. Typically these faults have the following characteristics: (1) they are short in length, relative to the uplift on which they occur, (2) they separate changes in direction of fold

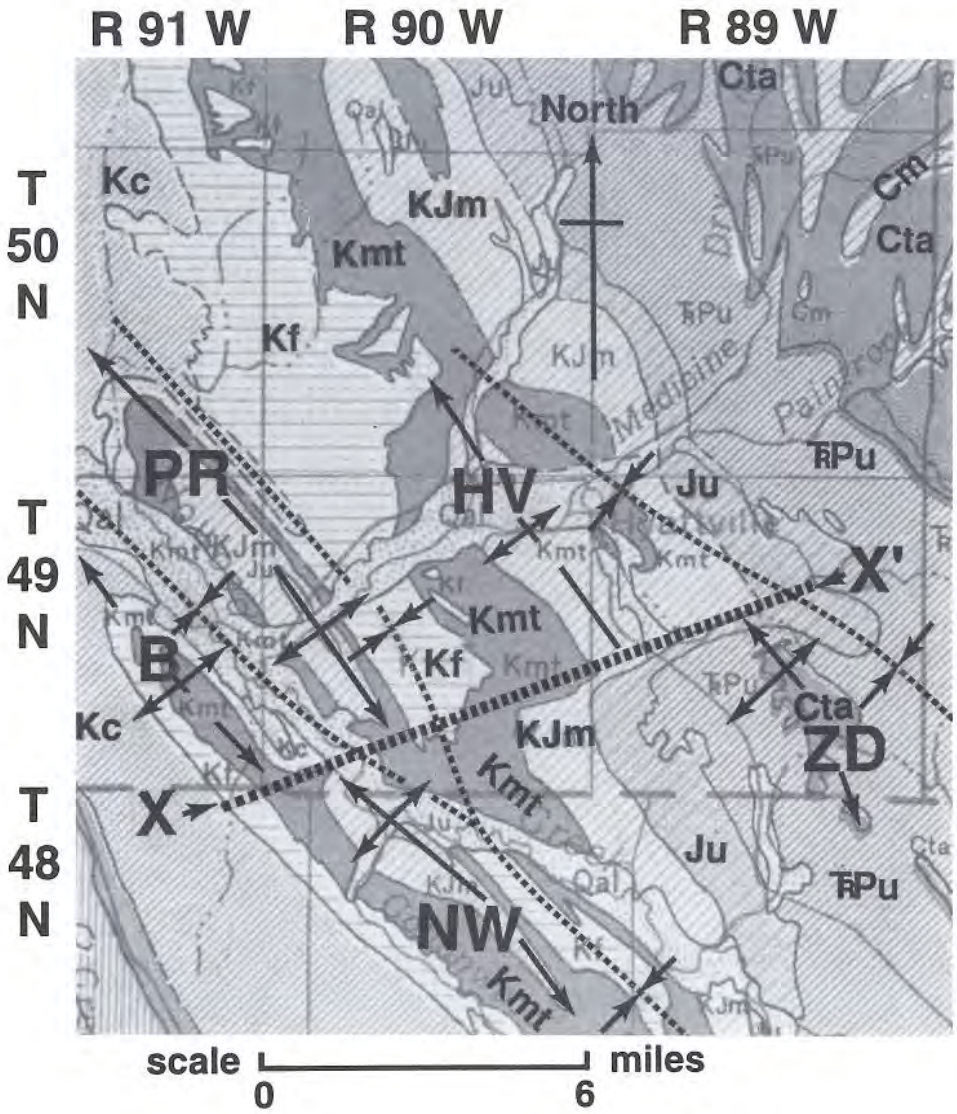

B - Bonanza
HV - Hyattville
NW - Nowood
PR - Paint Rock
ZD - Zeisman

anticline
syncline

Kc - Cody
Kf - Frontier
Kmt - Mowry, Thermopolis
KJm - Cloverly, Morrison
Ju - Sundance, Gypsum Spring
TRPu - Triassic, Permian
Cta - Tensleep, Amsden
Cm - Madison

X ····· X' - buried compartmental fault

Figure 35. Geologic map modified from Love and others (1955) showing the terminations of several northwest-trending anticlines along a line oriented east-northeast. This line of termination is interpreted as a buried compartmental fault that owes its existence to reactivation of a Precambrian zone of weakness by the Laramide stress system. North of this line, there are three anticlines: (B) Bonanza, (PR) Paintrock, and (HV) Hyattville; whereas south of the line there are only two anticlines: (NW) Nowood and (ZD) Zeisman dome. Although there is an imbalance in the number of structures, the total shortening across the area on both sides of the compartment fault is the same.

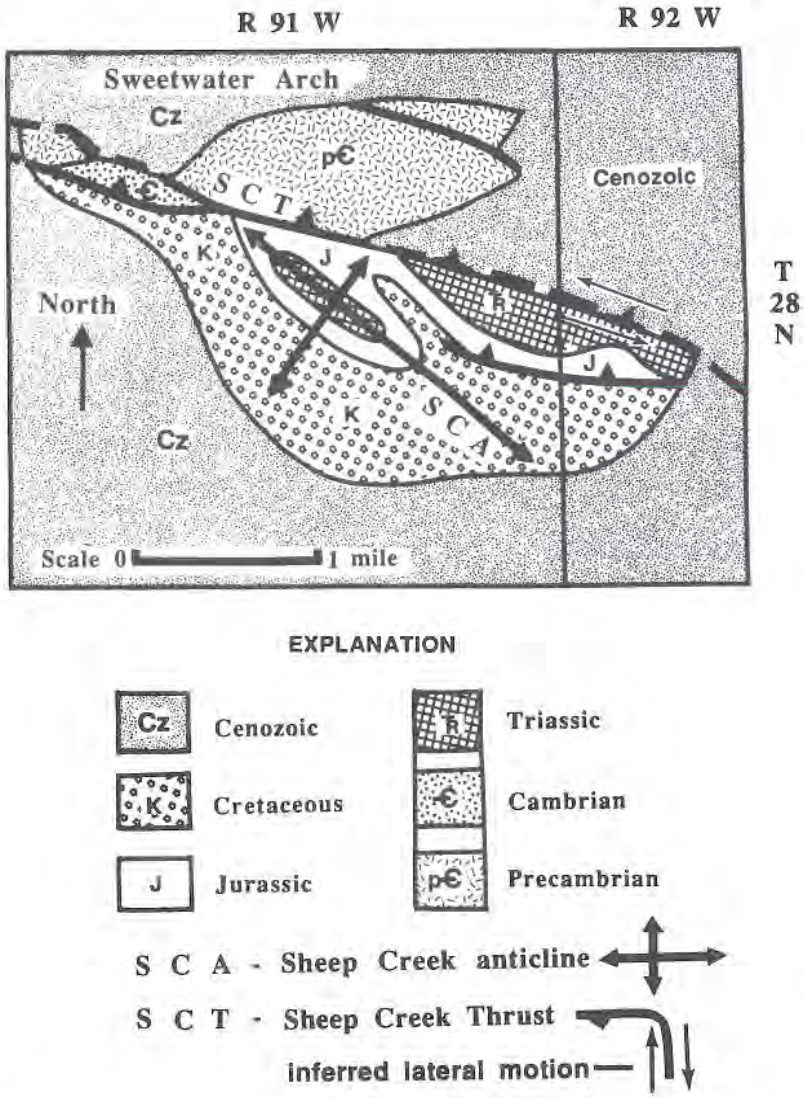

Figure 36. The Sheep Creek anticline (SCA) in T28N, R91W displays an acute angle with respect to the Sheep Creek thrust (SCT), suggesting a sense of left-slip on the fault. Reverse dip-slip on the SCT, demonstrable by well data indicates that the fault must have a reverse-oblique sense of motion. Map is modified from Love and Christiansen (1985).

asymmetry on each side of the fault, (3) they terminate fold trends on one or both sides of the fault, and (4) they allow structural balance to be maintained, often with shortening by one large structure being balanced by several smaller structures on the other side of the fault. The relatively short length of these faults places a limit on the magnitude of lateral motion that can occur along them. Since these faults are almost always associated with an anticlinal uplift, the sense of motion on these faults at the crest of the anticline is one of vertical translation (**Figure 26**). As discussed previously, this is the anticipated location for the development of small drape folds.

Many inferred compartmental faults are exposed at the surface today (e.g., Casper Mountain, Corral Creek, and Tensleep faults), but others are apparently still buried and can only be inferred from the arrangement of surface structures (Iron Creek-Oil Mountain, Barrett, 1989; Bonanza-Zeisman, Hudson, 1989), with subsurface data often insufficient to fully document them. An example of a buried compartmental fault (Hudson, 1989) is indicated in the Bonanza anticline-Zeisman dome area (T49N, Rs89-91W) on the east flank of the Bighorn Basin (**Figure 35**).

As mentioned earlier, Stone (1987) interpreted the Bonanza-Zeisman area as a wrench fault/thrust fold complex. Both Stone (1987) and Brown (1987) interpreted the alignment of fold-terminations to be along a Precambrian zone of weakness, which was reactivated during the Laramide orogeny as a northeast-striking, high-angle fault. The block diagram (**Figure 41a**) illustrates the concept that the zone of compartmentalization represents reactivation of individual segments of the Precambrian zone (**Figure 41b**) by the northeast vergence on the basement thrusts controlling each Laramide structure. This is in contrast to Stone's interpretation that this feature represents a continuous, through-going wrench fault.

If the overall tectonic model for foreland deformation were primarily a wrench-fault system, the structural style should be predominantly strike-slip faults and *en echelon* folds. Instead, the style appears to be predominantly basement-cored thrust structures that are segmented into block-like patterns by short compartmental faults, having minimum amounts of lateral motion.

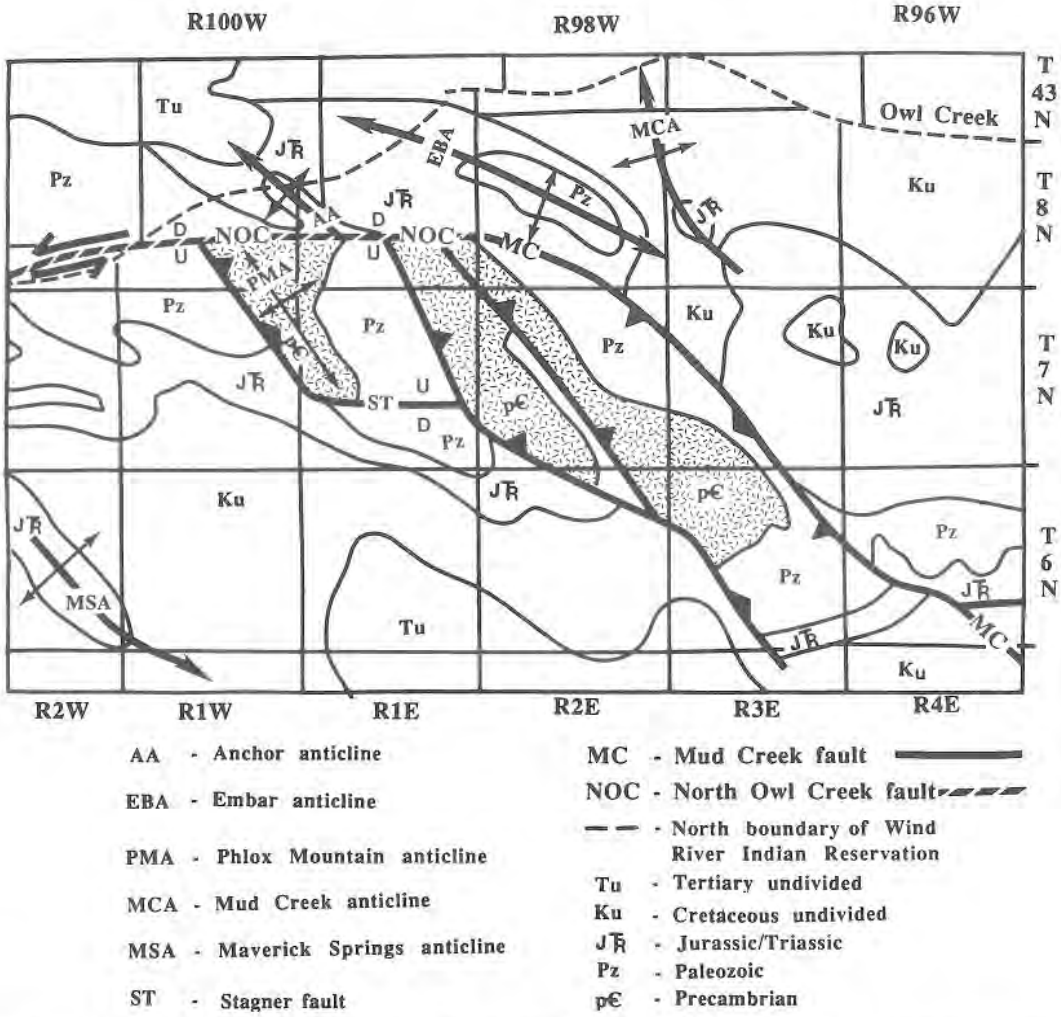

Figure 37. Geologic map of the Owl Creek uplift (modified from Love and Christiansen, 1985) displays a change in strike of the fault that bounds the north flank of this portion of the uplift. The Mud Creek fault (MC), strikes northwest and dips 20° south. In T8N, R1E, the fault changes direction to an east-west strike and becomes the high-angle North Owl Creek (NOC) fault. Crustal shortening across this uplift locally exceeds 2.5 miles. The northwest plunging Anchor anticline (AA) makes an acute angle with the NOC that suggests left-slip along the NOC. Slickensides on the east-west striking NOC (Paylor, 1990) confirms a lateral component of motion, which is also in agreement with the northeast directed sense of reverse dip slip on the MC fault. Magnitude of left-slip on the NOC could be as much as 2.5 miles, the shortening on the MC system. (Modified from Brown, 1988; reprinted by permission of Geological Society of America).

Sequence of foreland development

The Laramide orogeny was controlled by the direction and rate of convergence between the North American and Farallon plates along the western margin of North America, during the period of 80 to 40 Ma. The N40° to 50°E direction of plate convergence (Coney, 1978) resulted in the formation of primary reverse-faulted structures oriented northwest-southeast.

The initial deformation of the previously stable craton apparently began with crustal downwarp, at least in the area of the Owl Creek Mountains. Initially, downwarping was the dominant direction of crustal movement, but by the end of the Laramide, the component of uplift finally became dominant (Keefer, 1965, 1970). This crustal downwarp formed Laramide basins, and may have been accompanied

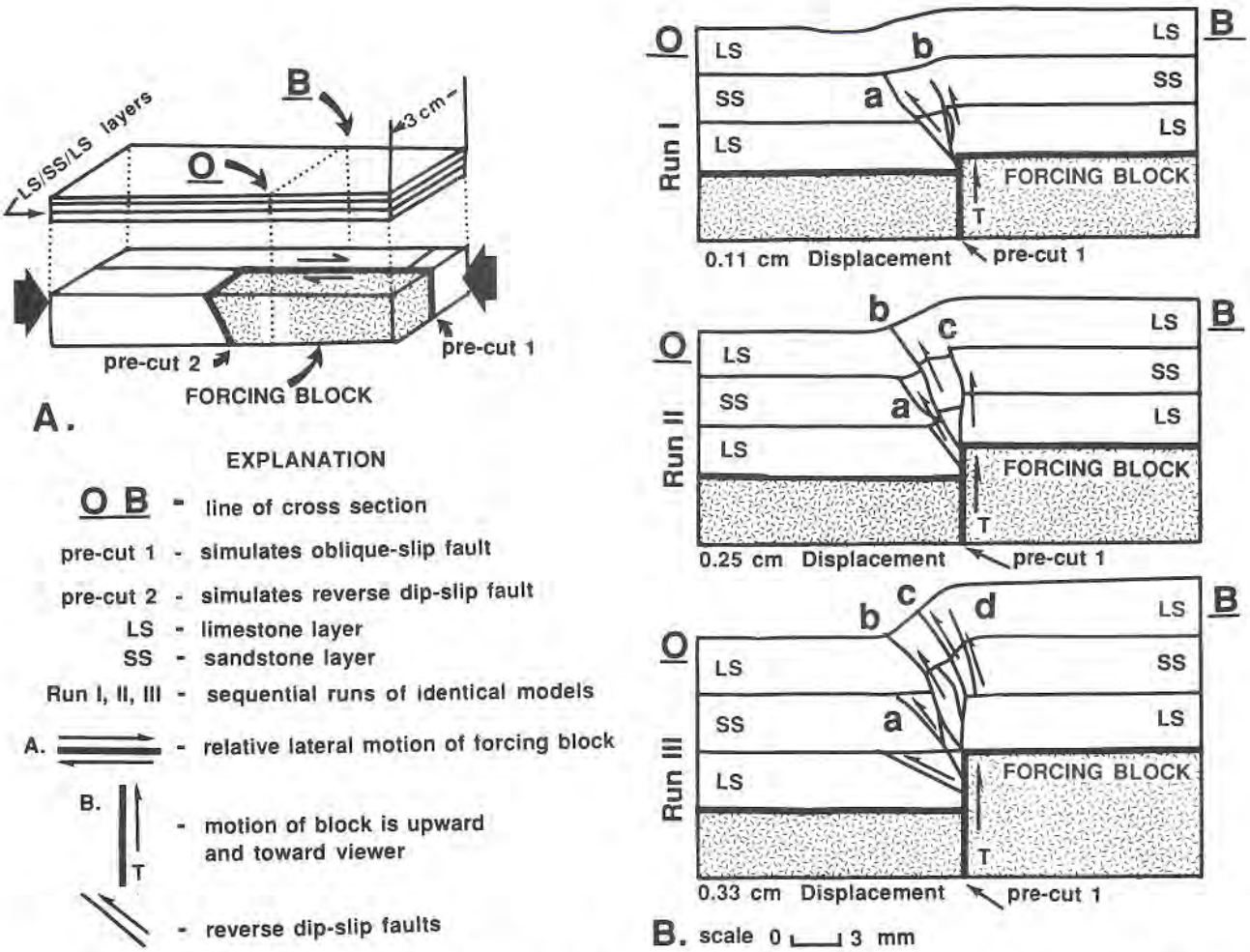

Figure 38. Results of rock deformation experiments on the "corner problem" by Logan and others (1978) lend credence to the interpretation that movement on compartmental-type faults will be reverse oblique-slip. A. The models are prepared so that they have a fault (pre-cut 1) that is transverse to the reverse fault ramp (pre-cut 2). This geometry allows the forcing block to move up the ramp, with right oblique-slip along the transverse fault. B. Results of repeated experiments with increasing displacement (Runs I, II, and III) illustrate the progressive development of an upthrust fault having reverse right oblique-slip, which first reaches the surface at the lower hinge of the early formed drape fold. Continued displacement results in the progressive movement of the upthrust up the flank of the drape fold. (Modified from Brown, 1988; reprinted by permission of Geological Society of America.)

by additional local compressional forces in the upper crust (**Figure 42a**) as a result of flattening the natural curvature of the Earth's surface (Dallmus, 1958). These compressive stresses forced shallow-rooted flakes of basement rock (**Figure 42b**) upward into the overlying sedimentary section (**Figure 42c**), along a conjugate set of low-angle reverse faults (**Figure 5**; Brown, 1988). The resulting structures are the typical Laramide anticlinal folds displayed as flank structures around the margins of the basins.

Primary Laramide structural features trend in a general northwest orientation, with subordinate trends of northeast, east, and north, superimposed across the northwest grain. The superposition of these four structural orientations results in a block-like pattern of faults and folds. Basin-flank anticlines trend parallel or subparallel to the mountain uplifts. Many individual anticlines display a blunt plunge end, controlled by steep, northeast- or east-striking compartmental faults (Brown, 1988).

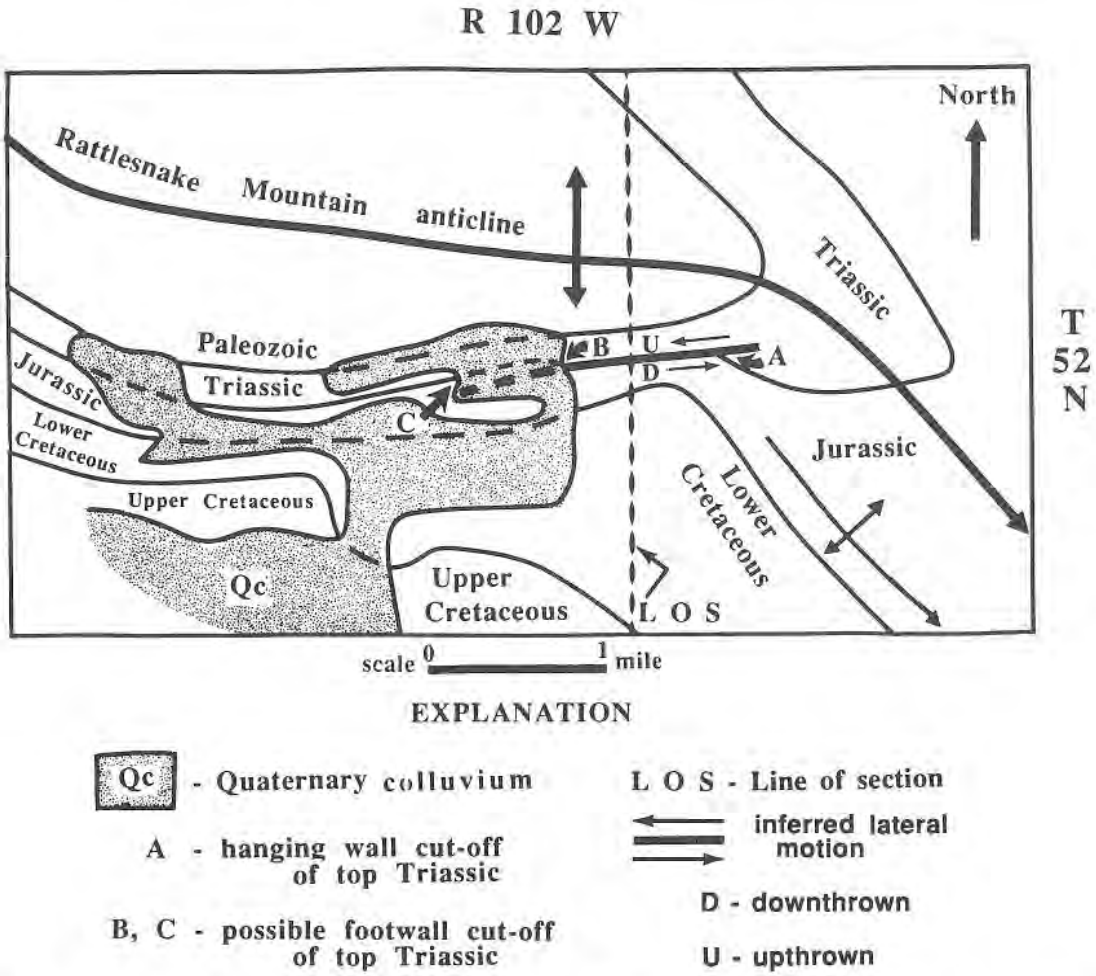

Figure 39. Interpretation of possible lateral movement along the south plunge of Rattlesnake Mountain anticline (map modified from Pierce and Nelsen, 1968). The south plunge is accomplished by a combination of steep dip and fault displacement. The South Rattlesnake Mountain compartmental fault strikes east-west and offsets the top of the Triassic with a sense of reverse left-separation. The footwall cut off of the top of the Triassic is at point A on the map. The location of the hanging wall cut off of the the same contact is obscured under the Quaternary colluvium, but must occur between points B and C. If the hanging wall cut off is at B, separation on the fault is 5,000 feet in a left lateral sense; however, if the cut off is at C, then the separation is 8,000 in a left lateral sense. The 5,000 feet to 8,000 feet of *left separation* on the South Rattlesnake Mountain compartmental fault is sufficient to accommodate the *left slip* which must be present to accommodate the 2,250 feet of *reverse dip slip* on the northwest trending Rattlesnake Mountain fault (Brown, 1988; Figure 22f). The position of the cross section shown in Figure 40 is along the line of section (LOS).

The sequence of deformation of the foreland has been shown to have progressed from west to east across the foreland (Gries, 1983b) along a *tectonic front* (Brown, 1988). This front began at the western margin of the foreland in the vicinity of the Moxa arch, in Campanian time, and formed the Wind River uplift, primarily in Maastrichtian time. This timing is indicated by the angular unconformity at the base of the Paleocene rocks on the northeast dip-slope of the Wind River Mountains. The Owl Creek Mountains were uplifted primarily during the Paleocene and early Eocene. Farther to the north, the Bighorn Mountains and the Beartooth Mountains were uplifted in early Eocene with final movements occurring post-middle Eocene.

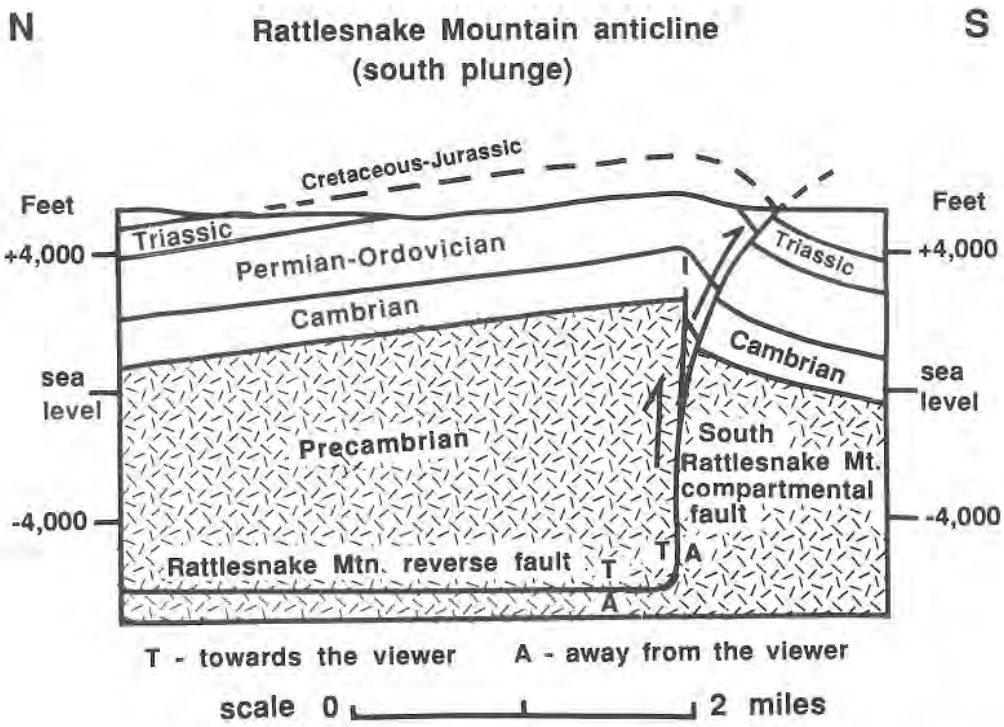

Figure 40. A north-south cross section across Rattlesnake Mountain anticline is interpreted using the results of experimental models (Logan and others, 1978). This section displays a critical factor relating to the geometry of fault planes at a "corner"—the low-angle reverse fault must turn up at the edge to become the high-angle oblique-slip fault; therefore the amount of dip slip on the Rattlesnake Mountain reverse fault must be equal to the lateral slip on the oblique slip South Rattlesnake Mountain compartmental fault.

Summary of foreland style

The evidence presented in this paper leads to the conclusion that the orientation of structural trends within the Laramide stress field was the controlling factor as to whether a crustal shortening or nonshortening structure developed. There is no single structural model which applies throughout the Wyoming foreland. Features displaying the basic characteristics of major contractile structures (thrusts, thrust-folds, basement wedges, or fold-thrusts) developed along a general northwest strike, as a primary response to the Laramide compressive stresses. It is not known whether fold-thrust uplifts (bounded by the dual-fault zone) are different from thrust uplifts (bounded by a single reverse fault) simply because of slight changes in strike orientation (from northwest, to north-northwest; **Figure 33**), or for some other reason. It is clear though, that the basement was deformed differently in these two cases, and in the overall structural picture both fault systems result in large magnitudes of crustal shortening in a northeast-southwest direction.

When northwest-striking faults have been interpreted as having formed through differential vertical uplift, such interpretations are structurally out of balance (length of the basement/sediment contact is too short when compared to the length of the overlying sedimentary layers). Correct application of nonshortening (differential vertical uplift) models to the foreland is dependent upon finding direct evidence of vertical motion (slickensides), and/or structures that allow bed-lengthening or bed-thinning, as predicted by theoretical and experimental work of Hafner (1951) and Sanford (1959).

Although the dominant direction of motion along foreland faults is reverse dip-slip, locally there are areas where the dominant motion is vertical. This

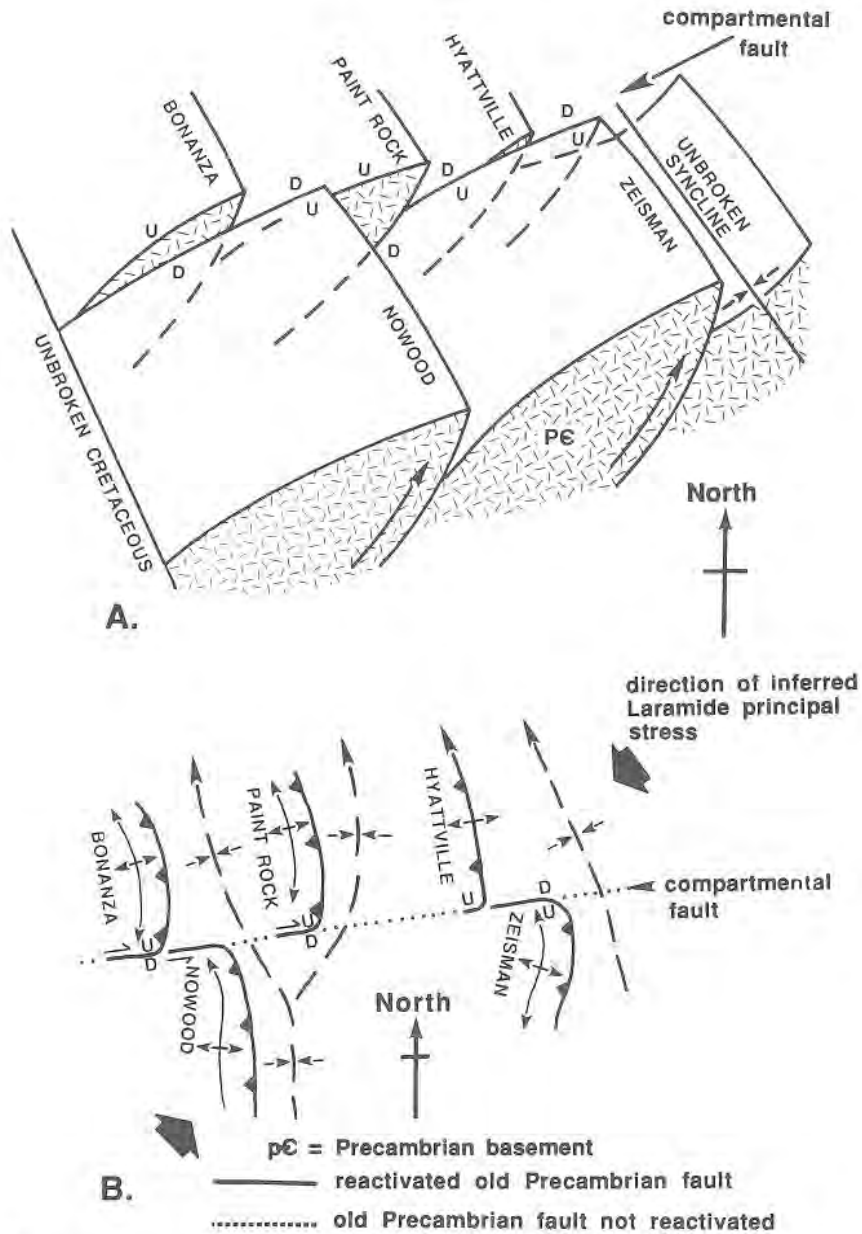

Figure 41. A. Block diagram and B. map of the buried Bonanza-Zeisman compartmental fault shows the apparent mismatch of surface anticlines created by movement along the east-northeast striking Laramide-reactivated Precambrian zone of weakness. Structural balance is maintained on both sides of the compartmental fault by varying magnitudes of displacement on the individual faults.

condition exists where a northwest-trending anticline is segmented by a high-angle transverse fault, and at the corner formed by the intersection of northwest-striking thrusts and east-striking high-angle faults. A vertical component is therefore achieved as a component of motion along the transverse oblique-slip fault.

The magnitude of crustal shortening across the Wyoming foreland during the Laramide orogeny is reasonably consistent when measured parallel to the northeast-southwest direction of tectonic transport. Values of total crustal shortening approach 30 miles and represent approximately 13 to 15 % strain across

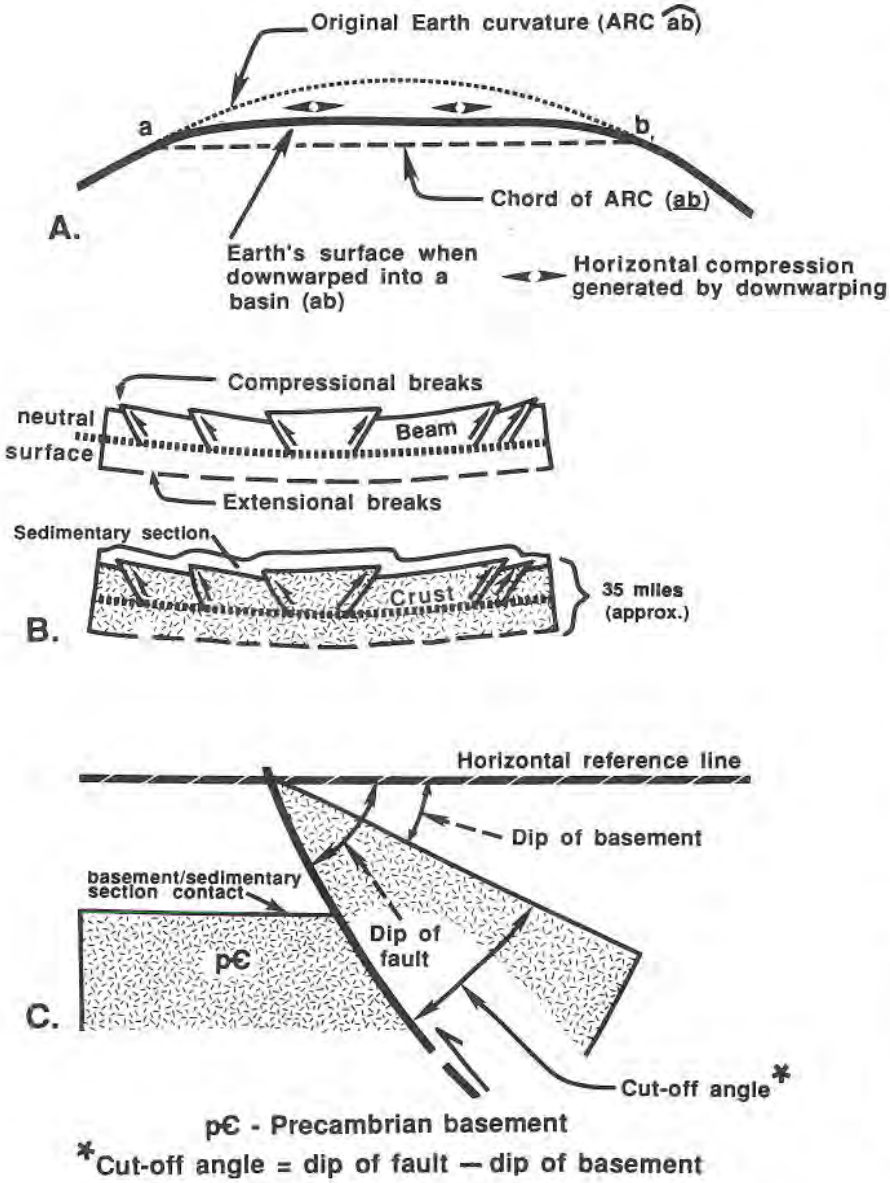

Figure 42. A. Local compressional forces were generated in the upper crust by the downwarping of basins in opposition to the curvature of the Earth as predicted by Dallmus (1958). B. (upper) A bent beam deforms by creating compressional breaks above and extensional breaks below the neutral surface. B. (lower) Basement-cored subsidiary anticlines on the flanks of Laramide basins appear to have been developed along similar compressive breaks caused by horizontal compressive stresses localized in the upper crust as the basin formed. These stresses cause the Precambrian basement to "flake off" by being detached in the shallow parts of the crust. These flakes then become forcing blocks, causing the overlying sediments to fold and conform to the size and shape of the basement block. Examples of this style along the Derby-Dallas fold trend are seen on the COCORP seismic line across the Wind River Range. C. The fault cut-off angle is determined by taking the difference between the dip angle of the upper portion of the basement fault and the angle of rotation of the basement-sediment contact. This cut off angle represents the dip of the fault that controls the basement flake at the moment the fault broke the top of the horizontal basement.

the entire foreland. Documented kinematic indicators of lateral motion (Lageson, 1987; Furner, 1989; Paylor, 1990; Molzer and Erslev, 1991) are surprisingly few in the foreland. Magnitudes of lateral slip are small, when considered against the overall potential of much larger offsets indicated by total shortening values. The general lack of development of significant trends of *en echelon* folds argues against invoking a dominantly wrenching mechanism. Instead, it appears that potential lateral movements are distributed across the foreland on properly oriented faults in a style of compartmental deformation. The presence of both northeast- and southwest-verging, low-angle reverse faults is another indication that the foreland basement yielded along a set of conjugate reverse faults, generated by stresses resulting from northeasterly-directed plate convergence during the Laramide orogeny.

Acknowledgments

I wish to acknowledge the influence which the two honorees of this volume, Don Blackstone and Dave Love, have had on my understanding of the structural geology of Wyoming. I also wish to express my appreciation to the organizers and editors of this volume for giving me the opportunity to participate in honoring these two men. The historical review presented in this chapter is not intended to be an all inclusive listing of workers who have published on the Wyoming foreland. Instead, it is meant to document major cornerstones and turning points in the interpretation of the foreland structural style. To anyone who feels their work has been slighted or ignored, I humbly apologize. I wish to express my appreciation to David Lageson, Arthur Snoke, and Sheila Roberts for reviewing this paper; their comments have greatly improved the text and clarified several points of discussion. I also gratefully acknowledge my previous 23-year association with Chevron USA, Inc., and the benefits derived from that association through the exchange of ideas and concepts with numerous Chevron geologists and geophysicists. The concepts presented in this chapter are an outgrowth of this past association and present dialog with students who have worked in Wyoming under my direction. However, sole responsibility for the interpretations made here is mine.

References cited

Abercrombie, S., 1989, Structural analysis of the Sheep Mountain-Beaver Creek thrust area, Fremont County, Wyoming [M.S. thesis]: Waco, Texas, Baylor University, 71 p.

Barrett, E.L., 1989, Structural analysis of the Poison Spider-Oil Mountain-Iron Creek trend, Natrona County, Wyoming [B.S. thesis]: Waco, Texas, Baylor University, 99 p.

Beckwith, R.H., 1938, Structure of the southwest margin of the Laramie Basin, Wyoming: Geological Society of America Bulletin, v. 49, p. 1515-1544.

_____ 1941, Structure of the Elk Mountain district, Carbon County, Wyoming: Geological Society of American Bulletin, v. 49, p. 1445-1486.

Bell, W.G., 1956, Tectonic setting of Happy Springs and nearby structures in the Sweetwater uplift area, central Wyoming, *in* Geological Record, Rocky Mountain section: American Association of Petroleum Geologists, p. 81-86.

Berg, R.R., 1962a, Subsurface interpretation of Golden fault at Soda Lakes, Jefferson County, Colorado: American Association of Petroleum Geologists Bulletin, v. 46, p. 704-707.

_____ 1962b, Mountain flank thrusting in Rocky Mountain foreland, Wyoming and Colorado: American Association of Petroleum Geologists Bulletin, v. 46, p. 2019-2032.

Blackstone, D.L., Jr., 1940, Structure of the Pryor Mountains, Montana: Journal of Geology, v. 48, p. 590-618.

_____ 1947, Structural relationships of the Pryor Mountains: Wyoming Geological Association Bighorn Basin Field Conference Guidebook: p. 182-188.

_____ 1948, Structural relationships of northeast margin of the Laramie Mountains [abstract]: Geological Society of America Bulletin, v. 59, p. 1397-1398.

_____ 1949, Structural pattern of the Powder River Basin, Wyoming: Wyoming Geological Association 4th Annual Field Conference Guidebook, p. 35-36.

_____ 1951, An essay on development of structural geology in Wyoming: Wyoming Geological Association 6th Annual Field Conference Guidebook, p. 15-18.

_____ 1956, Introduction to the tectonics of the Rocky Mountains, *in* Geological record, Rocky Mountain section: American Association of Petroleum Geologists, p. 3-19.

_____ 1963, Development of geologic structure in central Rocky Mountains, *in* Backbone of the Americas, a symposium: American Association of Petroleum Geologists Memoir 2, p. 160-179.

_____ 1970, Structural geology of the Rex Lake Quadrangle, Laramie Basin, Wyoming: Geological Survey of Wyoming Preliminary Report 11, 17 p.

_____ 1981, Compression as an agent in deformation of the east-central flank of the Bighorn Mountains, Sheridan and Johnson counties, Wyoming: University of Wyoming Contributions to Geology, v. 19, p.105-122.

_____ 1983, Laramide compressional tectonics, southeastern Wyoming: University of Wyoming Contributions to Geology, v. 22, p. 1-38.

_____ 1986, Structural geology—northwest margin, Bighorn Basin, Park County, Wyoming and Carbon County, Montana: Montana Geological Society and Yellowstone Bighorn Research Association Joint Field Conference and Symposium, p. 125-135.

_____ 1990, Rocky Mountain foreland structure exemplified by the Owl Creek Mountains, Bridger Range and Casper arch, central Wyoming: Wyoming Geological Association 41st Annual Field Conference Guidebook, p. 151-166.

Bonini, W.E., and Kinard, R.E., 1983, Gravity anomalies along the Beartooth front, Montana: Wyoming Geological Association 34th Annual Field Conference Guidebook, p. 89-95.

Boyd, D.W., and Lillegraven, J.A., editors, 1981, Rocky Mountain foreland basement tectonics, University of Wyoming Contributions to Geology v. 19, no. 2, 181 p.

Brittenham, M.D., and Tadewald, B.H., 1985, Detachment and basement-involved structures beneath the Absaroka Range volcanics, *in* Gries, R.R., and Dyer, R.C., editors, Seismic exploration of the Rocky Mountain region: Rocky Mountain Association of Geologists and Denver Geophysical Society, p. 31-43.

Brown, W.G., 1975, Casper Mountain area, Wyoming—a model of Laramide deformation [abstract]: American Association of Petroleum Geologists Bulletin, v. 59, p. 906.

_____ 1982, New tricks for old dogs, a short course in structural geology: Southwest Section American Association of Petroleum Geologists, 79 p.

_____ 1983, Sequential development of the fold-thrust model of foreland deformation, *in* Lowell, J.D., editor, Rocky Mountain foreland basins and uplifts: Rocky Mountain Association of Geologists, p. 57-64.

_____ 1984a, Rattlesnake Mountain anticline—a reverse fault interpretation: The Mountain Geologist, v. 21, p. 32-35.

_____ 1984b, Basement involved tectonics—foreland areas: American Association of Petroleum Geologists Continuing Education Course Note Series #26, 92 p.

_____ 1987, Structural style of the Laramide orogeny, Wyoming foreland [Ph.D. dissertation]: Fairbanks, University of Alaska, v. 1 (text), 342 p., v. 2 (figures), 193 p.

_____ 1988, Deformational style of Laramide uplifts in the Wyoming foreland, *in* Schmidt, C.J., and Perry, W.L. Jr., editors, Interaction of the Rocky Mountain foreland and the Cordilleran thrust belt: Geological Society of America Memoir 171, p. 1-25.

Bucher, W.H., 1920, The mechanical interpretation of joints: Journal of Geology, v. 28, p. 707-730.

Chamberlain, R.T., 1925, The wedge theory of diastrophism: Journal of Geology, v. 33, p. 755-792.

_____ 1945, Basement control in Rocky Mountain deformation: American Journal of Science, v. 243-A, p. 98-116.

Cercone, D.P., 1989, Structural geology of Pine Mountain and Boone dome, west flank of the Casper arch, Natrona County, Wyoming [M.S. thesis]: Waco, Texas, Baylor University, 100 p.

Coney, P.J., 1978, Mesozoic-Cenozoic Cordilleran plate tectonics, *in* Smith, R.B., and Eaton, G.P. editors, Cenozoic tectonics and regional geophysics of the western Cordillera: Geological Society of America Memoir 152, p. 33-50.

Cook, D.G., 1983, The northern Franklin Mountains, Northwest Territories, Canada,—a scale model of the Wyoming province, *in* Lowell, J.D., editor, Rocky Mountain foreland basins and uplifts: Rocky Mountain Association of Geologists, p. 314-338.

_____ 1988, Balancing basement-cored folds of the Rocky Mountain foreland and the Cordilleran thrust belt, *in* Schmidt, C.J., and Perry, W.L. Jr., editors, Interaction of the Rocky Mountain foreland and the Cordilleran thrust belt: Geological Society of America Memoir 171, p. 53-64.

Cook, R.A., and Stearns, D.W., 1975, Mechanisms of sandstone deformation: a study of the drape folded Weber Sandstone in Dinosaur National Monument, Colorado and Utah, *in* Bolyard, D.W., editor, Deep drilling frontiers of the central Rocky Mountains: Rocky Mountain Association of Geologists, p. 21-32.

Couples, G., and Stearns, D.W., 1978, Analytical solutions applied to structures of the Rocky Mountain

foreland on local and regional scales, *in* Matthews, V., III, editor, Laramide folding associated with basement block faulting in the western United States: Geological Society of America Memoir 151, p. 313-335.

Dahlstrom, C.D.A., 1969a, The upper detachment in concentric folding: Canadian Petroleum Geology Bulletin, v. 17, p. 326-346.

_____ 1969b, Balanced cross sections: Canadian Journal of Earth Sciences, v. 6, p. 743-757.

Dallmus, K.F., 1958, Mechanics of basin evolution and its relation to the habitat of oil in the basin, *in* Weeks, W.G., editor, Habitat of oil: American Association of Petroleum Geologists, p. 883-931.

Darton, N.H., 1906a, Description of the Bald Mountain and Dayton, Wyoming quadrangles: U.S. Geological Survey Folio 141, 15 p.

_____ 1906b, Geology of the Bighorn Mountains, U.S. Geological Survey Professional Paper 51, 129 p.

_____ 1906c, Description of the Cloud Peak and Ft. McKinney, Wyoming quadrangles: U.S. Geological Survey Folio 142, 16 p.

Demorest, M.H., 1941, Critical structural features of the Bighorn Mountains, Wyoming: Geological Society of America Bulletin, v. 62, p. 161-176.

Dubois, M.A., and Evans, J.P., 1990, Internal deformation of the Wind River thrust sheet along Laramide and Precambrian zones: detailed structural analyses and scales of brittle deformation, NE Wind River Range, Wyoming: Geological Society of America Abstracts with Programs, v. 22, no. 6, p. 8.

Duebendorfer, E.M., and Houston, R.S., 1987, Proterozoic accretionary tectonics at the southern margin of the Archean Wyoming craton: Geological Society of America Bulletin, v. 98, p. 554-568.

Eldridge, G.H., 1894, A geological reconnaissance in northern Wyoming: U.S. Geological Survey Bulletin 119, p. 13-69.

Engel, A.E.J., 1963, Geologic evolution of North America: Science, v. 140, p. 143-152.

Erslev, E.A., 1985, Balanced cross sections of small fold-thrust structures; Comment: The Mountain Geologist, v. 22, p. 91-93.

_____ 1986, Basement balancing of Rocky Mountain foreland uplifts: Geology, v. 14, p. 259-262.

_____ 1990, Heterogeneous Laramide deformation in the Rattlesnake Mountain anticline, Cody, Wyoming, *in* Field Trip Guidebook: Trip No. 7, part 1: Rocky Mountain Section, Geological Society of America, p. 141-147.

Evans, J.P., Batatian, D., Derr, D., Dubois, M., Harlan, S., Malizzi, L., McDowell, R., Nelson, G., Parke, M., Schmidt, C., and Weberg, E., 1990, Mechanisms and kinematics of a Precambrian-cored fold and fault structure: Jakey's Fork, Wyoming: Geological Society of America Abstracts with Programs, v. 22, no. 6, p. 10.

Fanshawe, J.R., 1939, Structural geology of the Wind River Canyon area, Wyoming: American Association of Petroleum Geologists Bulletin, v. 23, p. 1439-1492.

_____ 1971, Structural evolution of the Bighorn Basin: Wyoming Geological Association 23rd Annual Field Conference Guidebook, p. 35-37

Foose, R.M., Wise, D.U., and Garbarini, G.S., 1961, Structural geology of the Beartooth Mountain block, Montana and Wyoming: Geological Society of America Bulletin, v. 72, p. 1147-1172.

Furner, R.B., 1989, Structural analysis of the Walker Mountain-northern Piney Creek area, Bighorn Mountains, Wyoming [M.S. thesis]: Waco, Texas, Baylor University, 146 p.

Giegengack, R.,O., G.I., Lutz, T., and Soloyanis, S., 1990, Geometry of basement-rock deformation adjacent to overthrust margins of the Bighorn and Beartooth Mountains, Wyoming-Montana: Geological Society of America Abstracts with Programs, v. 22, no. 6, p. 12.

Gries, R., 1981, Oil and gas prospecting beneath the Precambrian of foreland thrust plates in the Rocky Mountains: The Mountain Geologist, v. 18, p.1-18.

_____ 1983a, Oil and gas prospecting beneath Precambrian of foreland thrust plates in the Rocky Mountains: American Association of Petroleum Geologists Bulletin, v. 67, p. 1-26.

_____ 1983b, North-south compression of Rocky Mountain foreland structures, *in* Lowell, J.D., editor, Rocky Mountain foreland basins and uplifts: Rocky Mountain Association of Geologists, p. 9-32.

Hafner, W., 1951, Stress distribution and faulting: Geological Society of America Bulletin, v. 62, p. 373-398.

Harding, T.P., 1990, Identification of wrench faults using subsurface structural data: criteria and pitfalls:

American Association of Petroleum Geologists Bulletin, v. 74, p. 1590-1609.

Harlan, S., Batatian, D., Evans, J., Derr, D., Malizzi, L., McDowell, R., Nelson, G., Parke, M., Schmidt, C., and Weberg, E., 1990, Mechanical behavior of footwall basement rocks, Scarface thrust, central Madison Range, Montana: Geological Society of America Abstracts with Programs, v. 22, no. 6, p. 13.

Hennings, P.H., and Spang, J.S., 1985, Crystalline basement geometry from three dimensionally balanced cross-sections: Dry Fork Ridge, northeastern Bighorn Mountains, Wyoming: Geological Society of America Abstracts with Programs v. 17, no. 7, p. 607.

Hewitt, D.F., and Lupton, C.T., 1917, Anticlines in the southern part of the Bighorn Basin, Wyoming: U.S. Geological Survey Bulletin 656, 192 p.

Hodgson, R.A., 1965, Genetic and geometric relations between structures in basement and overlying sedimentary rocks with examples from Colorado Plateau and Wyoming: American Association of Petroleum Geologists Bulletin, v. 49, p. 935-939.

Homan, K.S., 1988, Structural analysis of the south flank of the Sweetwater uplift, Carbon County, Wyoming [M.S. thesis]: Waco, Texas, Baylor University, 160 p.

Hoppin, R.A., 1961, Precambrian rocks and their relationship to Laramide structure along the east flank of the Bighorn Mountains near Buffalo, Wyoming: Geological Society of America Bulletin, v. 72, p. 351-367.

_____ 1970, Structural development of Five Springs Creek area, Bighorn Mountains, Wyoming: Geological Society of America Bulletin, v. 81, p. 2403-2416.

Hoppin, R.A., and Jennings, T.V., 1971, Cenozoic tectonic elements, Bighorn Mountain region, Wyoming-Montana: Wyoming Geological Association 23rd Annual Field Conference Guidebook, p. 39-47.

Hoppin, R.A., and Palmquist, J.C., 1965, Basement influence on later deformation—the problem, techniques of investigation, and examples from Bighorn Mountains, Wyoming: American Association of Petroleum Geologists Bulletin, v. 49, p. 993-1003.

Hoppin, R.A., Palmquist, J.C., and Williams, L.O., 1965, Control by Precambrian basement structure on the location of the Tensleep-Beaver Creek faults, Bighorn Mountains, Wyoming: Journal of Geology, v. 73, p. 189-195.

Houston, R.S., 1971, Regional tectonics of the Precambrian rocks of the Wyoming province and its relationship to Laramide structure: Wyoming Geological Association 23rd Annual Field Conference Guidebook, p. 19-28.

Houston, R.S., and others, 1968, A regional study of rocks of Precambrian age in that part of the Medicine Bow Mountains lying in southeastern Wyoming, with a chapter on the relationships between Precambrian and Laramide structures: Geological Survey of Wyoming Memoir 1, 167 p.

Hudson, F.S., 1955, Folding of unmetamorphosed strata superjacent to massive basement rocks: American Association of Petroleum Geologists Bulletin, v. 29, p. 2038-2052.

Hudson, S.D., 1989, Structural analysis of Paintrock anticline, Bighorn Basin, Wyoming [B.S. thesis]: Waco, Texas, Baylor University, 42 p.

Jennings, T.V., 1967, Structural analysis of the northern Bighorn Mountains, Wyoming [Ph.D. dissertation]: Iowa City, University of Iowa, 224 p.

Johnson, G.D., 1934, Geology of the mountain uplift transected by the Shoshone Canyon, Wyoming: Journal of Geology, v. 42, p. 809-835.

Johnson, R.A., and Smithson, S.B., 1985, Thrust faulting in the Laramie Mountains, Wyoming, from reanalysis of COCORP data: Geology, v. 13, p. 534-537

Kanter, L.R., Dyer, R., and Dohmen, T.E., 1981, Laramide crustal shortening in the northern Wyoming province: University of Wyoming Contributions to Geology, v. 19, p. 135-142.

Keefer, W.R., 1965, Stratigraphy and geologic history of the uppermost Cretaceous, Paleocene, and lower Eocene rocks in the Wind River Basin, Wyoming: U.S. Geological Survey Professional Paper 495-A, p. A1-A77.

Kulik, D.M., and Bankey, V.L., 1990, Basement terrains in Wyoming as interpreted from aeromagnetic and gravity data: Geological Society of America Abstracts with Programs, v. 22, no. 6, p. 18.

Lageson, D.R., 1987, Laramide uplift of the Gros Ventre Range and implications for the origin of the Teton fault: Wyoming Geological Association 38th Annual Field Conference Guidebook, p. 79-89.

Link, T.A., 1930, Experiments relating to salt-dome structures: American Association of Petroleum Geologists Bulletin, v. 14, p. 483-508.

Logan, J.M., Friedman, M., and Stearns, M.T., 1978, Experimental folding of rocks under confining pressure, Part VI, Further studies of faulted drape folds, *in* Matthews, V., III, editor, Laramide folding associated with basement block faulting in the western United States: Geological Society of America Memoir 151, p. 79-99.

Love, J.D., 1934, The geology of the western end of the Owl Creek Mountains, Wyoming: Geological Survey of Wyoming Bulletin 24, 33 p.

_____ 1970, Cenozoic geology of the Granite Mountains area, central Wyoming: U.S. Geological Survey Professional Paper 495-C, p. C1-C154.

_____ 1982, A possible gap in the western thrust belt in Idaho and Wyoming; *in* Powers, R.B., editor, Geologic studies of the Cordilleran thrust belt, 1982: Rocky Mountain Association of Geologists, v. 1, p. 247-260.

Love, J.D., and Christiansen, A.C., 1985, Geologic map of Wyoming: U. S. Geological Survey, scale 1:500,000.

Love, J.D., Weitz, J.L., and Hose, R.K., 1955, Geologic map of Wyoming: U. S. Geological Survey, scale 1:500,000.

Lowell, J.D., editor, 1983, Rocky Mountain foreland basins and uplifts: Rocky Mountain Association of Geologists, 392 p.

Matthews, V., III, 1986, A case for brittle deformation of the basement during the Laramide revolution in the Rocky Mountain foreland province: The Mountain Geologist, v. 23, p. 1-5.

Matthews, V., III, and Work, D.F., 1978, Laramide folding associated with basement block faulting along the northeastern flank of the Front Range, Colorado, *in* Matthews, V., III, editor, Laramide folding associated with basement block faulting in the western United States: Geological Society of America, Memoir 151, p. 101-124.

McConnell, D.A., and Wilson, T.G., 1990, Linkage between deformation of basement rocks and sedimentary rocks in foreland folds: Geological Society of America Abstracts with Programs, v. 22, no. 6, p. 38.

Miller, E.W., and Lageson, D.R., 1990, Laramide basement deformation in the northern Gallatin Range and southern Bridger Range, southwest Montana: Geological Society of America Abstracts with Programs, v. 22, no. 6, p. 39.

Mitra, G., 1990, Deformation processes in brittle deformation zones in granitic basement rocks: a case study from the Torey Creek area, Wind River Mountains: Geological Society of America Abstracts with Programs, v. 22, no. 6, p. 39.

Mitra, G. and Frost, B.R., 1981, Mechanisms of the deformation within Laramide and Precambrian deformation zones in basement rocks of the Wind River Mountains: University of Wyoming Contributions to Geology, v. 19, p. 161-173.

Molzer, P.C., and Erslev, E.A., 1991, Oblique thrusting in east-west Laramide foreland uplifts; Geological Society of America Abstracts with Programs, v. 23, no. 4, p. 50.

Narr, W., and Suppe, J., 1990, Deformational behavior of basement in low-temperature, basement-involved, compressive structures: Geological Society of America Abstracts with Programs, v. 22, no. 6, p. 40.

Nelson, V.E., and Church, V., 1943, Critical structures of the Gros Ventre and northern Hoback Ranges, Wyoming: Journal of Geology, v. 51, p. 143-166.

Nicols, C.E., 1965, Geology of a segment of Deep Creek fault zones, southern Bighorn Mountains, Wyoming [Ph.D. dissertation]: Iowa City, University of Iowa, 216 p.

Osterwald, F.W., 1959, Structure and petrology of the northern Bighorn Mountains, Wyoming: Geological Survey of Wyoming Bulletin 48, 47 p.

_____ 1961, Critical review of some tectonic problems in Cordilleran foreland: American Association of Petroleum Geologists Bulletin, v. 45, p. 219-237.

Palmquist, J.C., 1967, Structural analysis of the Horn area, Bighorn Mountains, Wyoming: Geological Society of America Bulletin, v. 78, p. 282-298.

_____ 1978, Laramide structures and basement block faulting: two examples from the Bighorn Mountains, Wyoming, *in* Matthews, V., III, editor, Laramide folding associated with basement block faulting in the western United States: Geological Society of America Memoir 151, p. 125-138.

Paylor, E.D., II, 1990, A strike-slip fault system in the Wyoming foreland: Geological Society of America Abstracts with Programs, v. 22, no. 6, p. 42.

Petersen, F.A., 1983, Foreland detachment structures, *in* Lowell, J.D., editor, Rocky Mountain foreland basins and uplifts: Rocky Mountain Association of Geologists, p. 65-77.

Pierce, W.G., and Nelson, W.H., 1968, Geologic Map of the Pat O'Hara Mountain Quadrangle, Park County, Wyoming: U.S. Geological Survey Geologic Quadrangle Map GQ-755, scale 1:62,500.

Prucha, J.J., Graham, J.A., and Nickelsen, R.P., 1965, Basement-controlled deformation in Wyoming province of Rocky Mountain foreland: American Association of Petroleum Geologists Bulletin, v. 49, p. 966-992.

Ray, R.R., Gries, R., and Babcock, J.W., 1983, Acoustic velocities, synthetic seismograms, and lithologies of thrusted Precambrian rocks, Rocky Mountain foreland, *in* Lowell, J.D., editor, Rocky Mountain foreland basins and uplifts: Rocky Mountain Association of Geologists, p. 125-135.

Renfro, H.B., and Feray, D.E., compilers, 1966, United States geological highway map no. 5, Northern Rocky Mountain region (Idaho, Montana, Wyoming): American Association of Petroleum Geologists, scale 1:1,875,000.

Robbins, E.A., and Erslev, E.A., 1986, Basement wedges, back-thrusting, and thin-skinned deformation in the northwest Beartooth Mountains near Livingston, Montana: Montana Geological Society and Yellowstone Bighorn Research Association Joint Field Conference and Symposium, p. 111-123.

Sales, J.K., 1968, Cordilleran foreland deformation: American Association of Petroleum Geologists Bulletin, v. 52, p. 2000-2015.

Sanford, A.R., 1959, Analytical and experimental study of simple geologic structures: Geological Society of American Bulletin, v. 79, p. 19-51.

Scheevel, J.R., 1983, Horizontal compression and a mechanical interpretation of Rocky Mountain foreland deformation: Wyoming Geological Association 34th Annual Field Conference Guidebook, p. 53-62.

Schmidt, C.J., and Garihan, J.M., 1979, A summary of Laramide basement faulting in the Ruby, Tobacco Root, and Madison ranges and its possible relationship to Precambrian continental rifting: Geological Society of America Abstracts with Programs, v. 11, no. 6., p. 301.

Schmidt, C.J., O'Neill, J.M., and Brandon, W.C., 1988, Influence of Rocky Mountain foreland uplifts on the development of the frontal fold and thrust belt, southwestern Montana, *in* Schmidt, C.J., and Perry, W.L., Jr., editors, Interaction of the Rocky Mountain foreland and the Cordilleran thrust belt: Geological Society of America Memoir 171, p. 171-201.

Skeen, R.C., and Ray, R.R., 1983, Seismic models and interpretation of the Casper arch thrust: application to Rocky Mountain foreland structure, *in* Lowell, J.D., editor, Rocky Mountain foreland basins and uplifts: Rocky Mountain Association of Geologists, p. 99-124.

Smithson, S.B., Brewer, J., Kaufman, S., Oliver, J., and Hurich, C., 1978, Question of the Wind River thrust, Wyoming resolved by COCORP deep reflection data and by gravity: Wyoming Geological Association 30th Annual Field Conference Guidebook, p. 227-234.

Spang, J.S., and Evans, J.P., 1988, Geometrical and mechanical constraints on basement-involved thrusts in the Rocky Mountain foreland province, *in* Schmidt, C.J., and Perry, W.L., Jr., editors, Interaction of the Rocky Mountain foreland and the Cordilleran thrust belt: Geological Society of America Memoir 171, p. 41-51.

Spang, J.S., Evans, J.P., and Berg, R.R., 1985, Balanced cross sections of small fold-thrust structures: The Mountain Geologist, v. 22, p. 41-46.

Sprague, E.L, 1983, Geology of the Tepee Flats-Buffington fields, Natrona County, Wyoming, *in* Lowell, J.D., editor, Rocky Mountain foreland basins and uplifts: Rocky Mountain Association of Geologists, p. 339-343.

Stearns, D.W., 1971, Mechanisms of drape folding in the Wyoming province: Wyoming Geological Association 23rd Annual Field Conference Guidebook, p. 125-143.

_____ 1975, Laramide basement deformation in the Bighorn Basin—the controlling factor for structure in the layered rocks: Wyoming Geological Association 27th Annual Field Conference Guidebook, p. 149-158.

_____ 1978, Fault and forced folding in the Rocky Mountains foreland, *in* Matthews, V., III, editor, Laramide folding associated with basement block faulting in the western United States: Geological Society of America Memoir 151, p. 1-37.

Stearns, D.W., Couples, G., and Stearns, M.T., 1978, Deformation of non-layered material that affect structures in layered rocks: Wyoming Geological Association 30th Annual Field Conference Guidebook, p. 213-225.

Stearns, D.W., and Stearns, M.T., 1978, Geometric analysis of multiple drape folds along the northwest Bighorn Mountains front, Wyoming, *in* Matthews, V., III, editor, Laramide folding associated with basement block faulting in the western United States: Geological Society of America Memoir 151, p. 139-156.

Stearns, D.W., and Weinberg, D.M., 1975, A comparison of experimentally created and naturally formed drape folds: Wyoming Geological Association 27th Annual Field Conference Guidebook, p. 159-166.

Stone, D.S., 1969, Wrench faulting and the Rocky Mountain tectonics: The Mountain Geologist, v. 6, p. 67-79.

_____ 1983, The Greybull Sandstone pool (Lower Cretaceous) on the Elk Basin thrust-fold complex, Wyoming and Montana, *in* Lowell, J.D., editor, Rocky Mountain foreland basins and uplifts: Rocky Mountain Association of Geologists, p. 345-356.

_____ 1984, The Rattlesnake Mountain, Wyoming debate: a review and critique of the models: The Mountain Geologist, v. 21, p. 37-46.

_____ 1987, A wrench fault/thrust-fold clay model study and comparison with the Bonanza-Zeisman area of the eastern Bighorn Basin: The Mountain Geologist, v. 24, p. 87-94.

Stricker, J.L., 1984, A structural and stratigraphic interpretation from the surface geology of Zeisman Dome, Bighorn Basin, Wyoming [B.S. thesis]: Waco, Texas, Baylor University, 66 p.

Suppe, J., 1985, Principles of structural geology: Englewood Cliffs, New Jersey, Prentice-Hall, 537 p.

Sylvester, A.G., 1986, Working with faults: shortcourse notes for AAPG structural geology school: American Association of Petroleum Geologists, Park City, Utah, 120 p.

Thom, W.T., 1923, Relationship of deep-seated faults to the surface structural features of central Montana: American Association of Petroleum Geologists Bulletin, v. 7, p. 1-13.

Tucker, D.R., and Willis, J.J., 1990, Fold-thrust structures of the northern Bighorn Mountains and Bighorn Basin: Geological Society of America Abstracts with Programs, v. 22, no. 6, p. 48.

Weinberg, D.M., 1978, Some two-dimensional kinematic analyses of the drape-fold concept, *in* Matthews, V., III, editor, Laramide folding associated with basement block faulting in the western United States: Geological Society of America Memoir 151, p. 551-578.

Weinberg, D.M., and Stearns, D.W., 1978, Kinematic analysis of drape folds in the Rocky Mountains foreland: some geological implications: Wyoming Geological Association 30th Annual Field Conference Guidebook, p. 199-212.

Wilcox, R.E., Harding, T.P., and Seely, D.R., 1973, Basic wrench tectonics: American Association of Petroleum Geologists Bulletin, v. 57, p. 74-96.

Wilson, C.W., Jr., 1934, A study of the jointing in the Five Springs Creek area, east of Kane, Wyoming: Journal of Geology, v. 42, p. 498-522.

Wise, D.U., 1964, Microjointing in basement, middle Rocky Mountains of Montana and Wyoming: Geological Society of America Bulletin, v. 75, p. 287-306.

_____ 1963, Keystone faulting and gravity sliding driven by basement uplift of Owl Creek Mountains, Wyoming: American Association of Petroleum Geologists Bulletin, v. 47, p. 586-598.

Worl, R.G., 1963, Superimposed deformations in Precambrian rocks near South Pass, Wyoming [Ph.D. dissertation]: Laramie, University of Wyoming, 53 p.

Part V

Cenozoic history

Frontispiece. Aerial view of Devils Tower (5,112 ft) exposed in the Wyoming portion of the Black Hills uplift, Crook County, Wyoming. Photograph by the Wyoming State Highway Department.

Laramide evolution of the Black Hills uplift

Alvis L. Lisenbee
Department of Geology and Geological Engineering
South Dakota School of Mines and Technology
Rapid City, South Dakota 57701

Ed DeWitt
United States Geological Survey
Denver Federal Center
Denver, Colorado 80225

Abstract

Fundamental questions regarding Laramide development of the Black Hills uplift concern timing, structural styles and their relationship to stresses, the origin of such stresses, and the character and origin of syntectonic alkalic magmatism. Timing and patterns of sedimentation indicate that the shoreline of the Cretaceous Western Interior Seaway retreated eastward or southeastward across the future Black Hills in late Maastrichtian (69 Ma). Sedimentation patterns in the eastern Powder River Basin indicate eastward flow of streams across the future site of the Black Hills uplift in early Paleocene (Tullock time, 66.5 to 65 Ma) and westward flow from an eastern sediment source for the syntectonic Lebo (approximately 65 to 63 Ma) and Tongue River (approximately 63 to 59 Ma) members of the Fort Union Formation in middle and late Paleocene. A second tectonic pulse may have occurred in earliest Eocene time (approximately 56 Ma) during deposition of the Wasatch Formation. The uplift was reduced to a local sediment source by the time of initiation of deposition of the post-tectonic, late Eocene (37 Ma) Oligocene White River Group. Erosion rates during the interval from initiation of uplift to 54 Ma averaged 4 to 5 inches per 1,000 years, whereas during the period from 54 to 37 Ma the minimum rate was 2.5 inches per 1,000 years.

North- and northwest-trending monoclines, chiefly west facing, bound the uplift on the west and are common at smaller scales across it. Such features are inferred to lie above thrust faults formed during regional horizontal compression oriented approximately east-northeast to west-southwest. Minor components of wrench tectonics are suggested by en echelon folds at the north and south ends of the eastern block and along monoclines on the western block.

Emplacement of stocks, dikes, sills, and laccoliths accompanied initial tectonism (62 Ma) across the northern Black Hills uplift, but was most active at 50 to 58 Ma. These plutons of alkalic and alkali-calcic rocks are undersaturated to oversaturated with respect to silica and are interpreted to have evolved from two magma sources, one yielding olivine gabbro and one yielding alkali gabbro. Fractional crystallization during ascent through the crust led to both phonolitic and quartz syenitic differentiation products from the alkali gabbro and alkali-calcic hornblende-bearing granodiorite from the olivine gabbro. Partial crustal melting and assimilation by the olivine gabbro magma produced

Lisenbee, A.L., and DeWitt E., 1993, Laramide evolution of the Black Hills uplift, *in* Snoke, A.W., Steidtmann, J.R., and Roberts, S.M., editors, Geology of Wyoming: Geological Survey of Wyoming Memoir No. 5, p. 374-412.

alkali-calcic granite. Initial melting may have occurred above a subducted lithospheric slab and partial crustal melting in zones of dilation in the regional wrench system present at the north end of the Laramide foreland province.

Plate-tectonic solutions to the origin of this easternmost Laramide uplift in North America suggest some combination of interaction of the subducted Farallon plate and northward movement of the Colorado Plateau microplate. Regional shortening of the Wyoming Rocky Mountains, chiefly across northwest-striking range-margin thrusts, require strike-slip components along west-striking Laramide features in Montana and extending to the Black Hills uplift. Such movement acts to decouple the Rocky Mountains from the undeformed Canadian foreland to the north.

Introduction

The newest 1:500,000-scale geologic map of the State of Wyoming, compiled by Love and Christiansen (1985), is an artful display that outlines in colors and shapes the basins and uplifts present across this geologically exciting state. In the northeast, browns and tans on the map indicate the north-northwest-trending Powder River Basin and its syntectonic fill of Paleocene and Eocene clastic strata. Adjacent to this large basin on the east, and occupying the extreme northeast corner of the state, greens and blues on the map indicate older strata, dominantly of Mesozoic age, exposed on one of the uplifts created by the great mountain-building event known as the Laramide orogeny. This structure extends northward into Montana and southeastward into South Dakota, but is named for the structurally more elevated regions to the east in the Black Hills. The uplift and the Tertiary igneous rocks that cut it (shown in red hues on the state geologic map) are the subjects of this paper.

Because the topographic feature of the Black Hills is surrounded by the northern Great Plains, it appears deceptively unrelated to other mountainous uplifts of the Wyoming Rocky Mountains. Newton and Jenny (1880) recognized the domal nature of the Black Hills (**Figure 1**), but the first synthesis of the geometry of the entire uplift was by Darton (1904). Such a synthesis was possible only because of the extensive detailed field work that he and his colleagues had completed in South Dakota and Wyoming, much of which was not published until later (Darton, 1904, 1919; Darton and O'Harra, 1905a, 1905b, 1907, 1909; Darton and Paige, 1925; Darton and Smith, 1904). The structure-contour map Darton prepared (**Figure 2**) first demonstrated that the uplift covers an area more than twice the size of the topographic feature of the Black Hills. The map also showed, in the many areas of linear, closely spaced contour lines, that the major monoclinal boundary features are similar to those of other uplifts in Wyoming and that the Black Hills uplift is similar in size and trend to those uplifts as well.

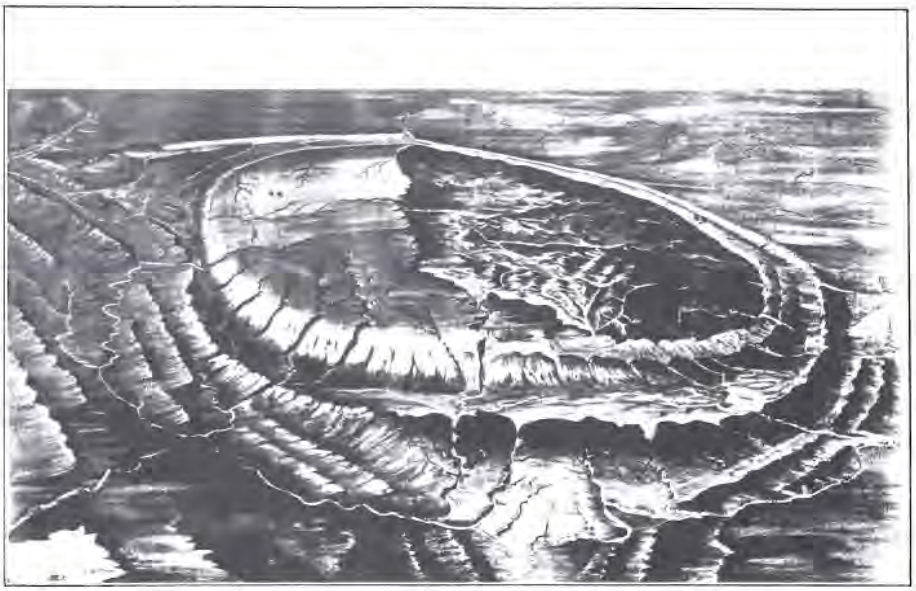

Figure 1. "Birds-eye view" of the Black Hills as depicted by Newton and Jenney (1880). The Precambrian core and outward-dipping rings of Phanerozoic strata of the eastern block of the uplift are viewed from the south.

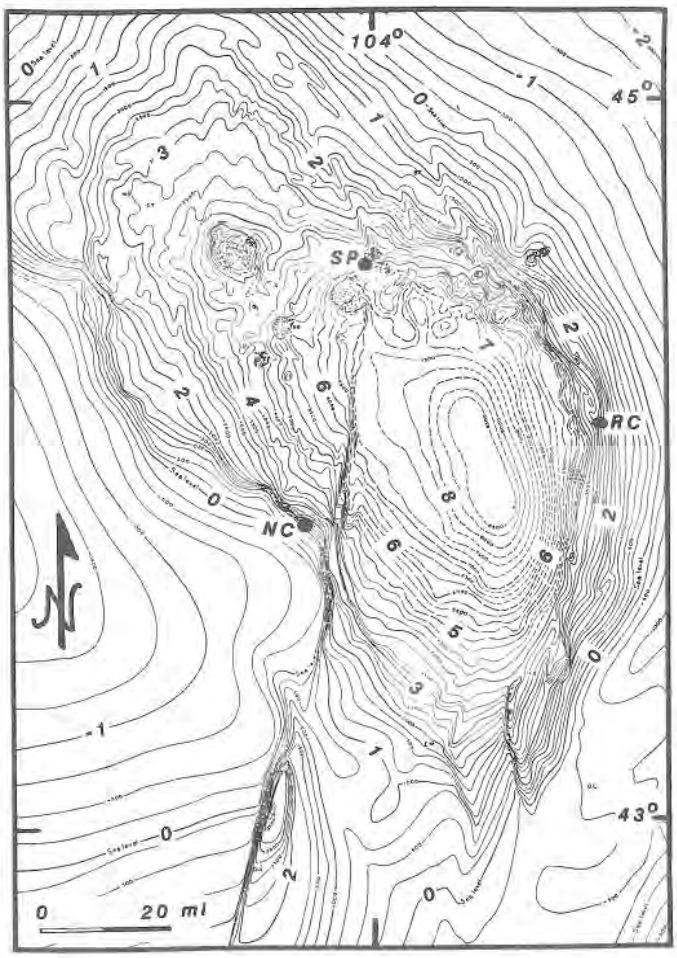

Figure 2. Structure contour map of the Black Hills uplift drawn on the Lower Permian Minnekahta Limestone (adapted from Darton, 1904). The size, trend, and many details of the Black Hills uplift are defined. The area shown in the diagram of Newton and Jenney (Figure 1) represents only the structurally higher eastern half of this large feature. Contour interval is 250 ft and the numbers represent elevations in thousands of feet relative to sea level. NC = Newcastle, Wyoming; SP = Spearfish, and RC = Rapid City, South Dakota. Dashed contours are projected above land surface.

The numerous works of Nelson Horatio Darton are benchmark contributions to the study of the Black Hills. Because his findings of a century ago were presented in the form of geologic maps, they constitute the backbone of most later studies. These maps remain the most reliable source of information for the local geology of some areas, but in others they have been superseded by more detailed maps by members of the U.S. Geological Survey, state geological surveys, or the academic community.

At the time of the work of N.H. Darton, Wyoming was, as it remains, a large and sparsely populated state. J.D. Love recounted a charming story to one of us in 1981 concerning his first meeting with Darton, which occurred during graduate student days in New York and illustrates the interconnection of those who have lived and worked in this state. Upon hearing the family name of Love, Mr. Darton asked if he was from Wyoming and by any chance from a ranch on the Wind River. As the story developed, Darton revealed that during the beginning of one spring's field work in the Wind River Basin, his buggy and all his field equipment had been swept away crossing a river. By great fortune a rancher was passing and lassoed him, saving his life, although the field maps and equipment were lost. That rancher was Mr. John Love, the father of J.D. Love. The subsequent understanding of American geology contributed by N.H. Darton owes much to John Love's generous effort, which allowed the remarkable geologist another half century of productivity.

The purpose of this volume, as noted by the editors, is two-fold. In the first instance, the articles are to provide a synthesis of some aspect of the geology of Wyoming, in this case the Black Hills uplift. Additionally, these syntheses are to present at least some insight as to the development of understanding of fundamental geologic questions involved. During the past hundred years, several fundamental geologic questions have been posed regarding the geological evolution of the Black Hills. What is the age of Laramide deformation here? What types of structural features are present on the uplift or in adjoining basins and what do they tell of the origin of the uplift? What stresses acted to form this easternmost mountain range of the Cordillera at a point so distant from a plate boundary? Is the syntectonic, alkalic magmatic activity related to tectonic processes specifically associated with the uplift or to deep-seated events associated with the larger aspects of crustal activity at the northeastern edge of the Laramide orogenic belt?

We will attempt in this paper to outline the stratigraphic, structural, and igneous development of the Black Hills region during the latest Cretaceous and early Tertiary, to comment on the tectonic setting in the context of the larger Laramide orogeny, and to

present models of possible uplift origins. Geologic understanding of the Black Hills is the product of years of labor by numerous scientists, each of whom added to the cumulative knowledge. The following summary, based on our personal experiences and the works of those scientists referenced here, undoubtedly overlooks many who have enjoyed triumphs in unraveling the geologic story of the Black Hills and to them we extend such apologies as may be appropriate.

Geologic setting

The Black Hills uplift is the structurally highest segment of a 600-mi-long positive feature that includes the Miles City arch to the northwest and the Chadron and Cambridge arches to the southeast (**Figure 3**). The Miles City arch connects on the northwest with the Porcupine dome, the easternmost feature on a structural high that continues 155 mi west (Dobbin and Erdmann, 1955).

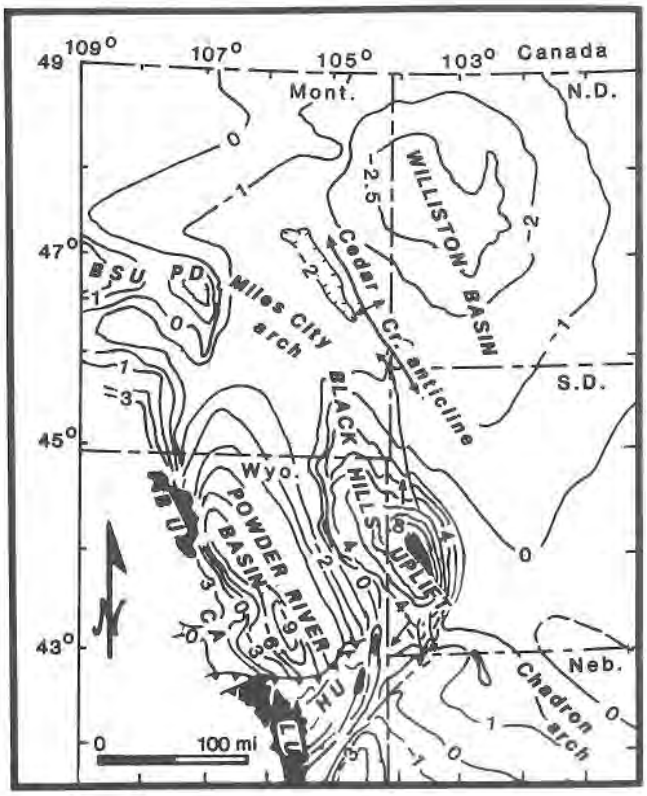

Figure 3. Generalized tectonic map of the northern Great Plains area. Structure contours, in 1000s of feet, drawn on top of the Lower Cretaceous Fall River Formation and equivalent formations. BSU = Big Snowy uplift, BU = Bighorn uplift, CA = Casper arch, HU = Hartville uplift, LU = Laramie uplift, PD = Porcupine dome (from Lisenbee, 1985).

As noted previously, the Black Hills uplift is bordered on the west by the Powder River Basin, of Laramide age. On the north and east is the Williston Basin, which had a long-lived Phanerozoic history, including a Laramide phase. The northeast-trending Hartville uplift, which borders a part of the Powder River Basin on the south, connects to the southwest margin of the Black Hills uplift across a broad structural saddle.

Early Tertiary erosion produced the north-trending elliptical outcrop pattern of the Black Hills uplift (**Figure 4**). The innermost exposures, as defined by Redden and French (1989), are dominantly multiply deformed Precambrian (1.8 to 2.1 Ga) metagraywacke, metabasalt, and schist, intruded by a 1.7 Ga granite, although Archean (2.5 Ga) granite crops out in two small areas. A strong north-northwest-striking structural fabric of folds and cleavage, produced especially during the last stage of folding (Redden and French, 1989), resulted in a strongly anisotropic basement. The uplift is situated at the eastern margin of the Wyoming Archean province (**Figure 5**). This boundary between a dominantly granitic basement to the west and a dominantly foliated metamorphic one (the Trans-Hudson province) to the east extends northward and southwestward from the uplift beneath Phanerozoic cover. The contrast in crustal character at the boundary between these two major Precambrian tectonic provinces may have served in some, as yet undefined, fashion to localize Laramide deformation.

Surrounding the Precambrian core are outward-dipping Paleozoic marine shelf and Mesozoic continental and shallow marine strata (Lisenbee, 1985; Redden and Lisenbee, 1990). Removal of these Phanerozoic strata and some underlying crystalline rocks from the core area provided a source of some of the Laramide age sediments, which were deposited in the Powder River and Williston basins. The resulting strata provide a continuous record across the Creta-

ceous-Tertiary boundary, a record that extends from the waning phase of the Cretaceous Western Interior Seaway (Lillegraven and Ostresh, 1990) through the formation of the adjacent Laramide basins.

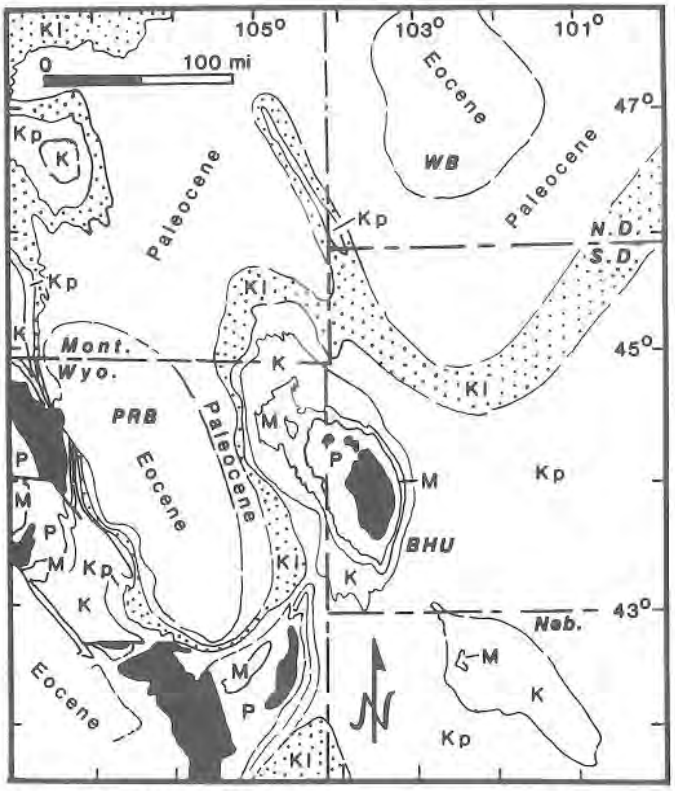

Figure 4. Interpreted subcrop pattern beneath Oligocene strata of the northern Great Plains and adjacent Rocky Mountains for the time interval shortly following deposition of the White River Group. Black areas are Precambrian; P = Paleozoic strata; M = Triassic and Jurassic strata; K = pre-Pierre Shale Cretaceous strata; Kp = Pierre Shale and Fox Hills Sandstone; Kl = Lance and Hell Creek Formations; WB = Williston Basin; PRB = Powder River Basin; BHU = Black Hills uplift.

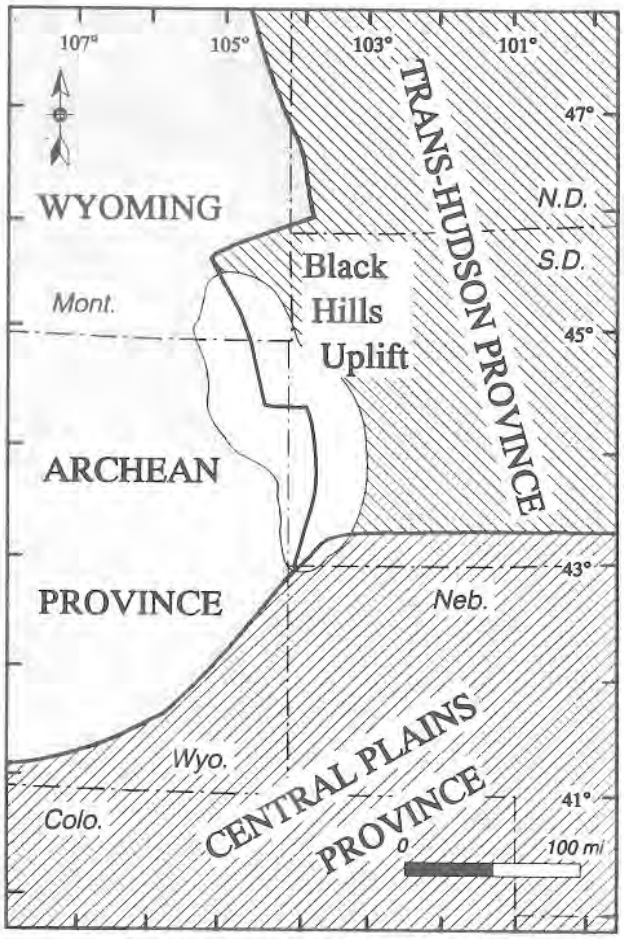

Figure 5. Generalized map of Precambrian terranes, northern Great Plains region. The Black Hills uplift (stippled) lies along a part of the boundary of the Wyoming Archean and the Proterozoic Trans-Hudson provinces.

Age of the Laramide Black Hills uplift — sedimentologic evidence

Preorogenic sedimentation

The age of a tectonic event is typically bracketed by the oldest strata that are not deformed and the youngest strata that are. Such a method is not definitive, for it gives only maximum and minimum ages and not the specific timing of tectonism. Chuck Chapin (oral communication, 1981) made the general observation that "...the history of the uplift is read in the book of the basin." He recognized the importance of syntectonic deposits in defining the timing of erosional stripping of source terranes, which may retain little direct evidence of the timing of their tectonic elevation. In the case of the Black Hills uplift, Paleocene strata were deformed by the uplift and Oligocene strata were not, which suggests a late Paleocene or Eocene age of orogeny. The Paleocene and Eocene strata in the adjoining basins, however, permit the detailed "reading" of the Laramide history of the Black Hills uplift and show that a source area for part

of the Paleocene deposits in the Powder River Basin was an uplift to the east. Paleocene deposits on the eastern side of the Powder River Basin were either deformed by a second tectonic pulse or tectonism was synchronous with deposition.

As the Cretaceous neared an end, the seas of the foreland basin (the Cretaceous Western Interior Seaway) east of the Wyoming thrust belt and the developing Laramide foreland were regressing across the area of the future Black Hills uplift. Sediments deposited during the regression formed a shallowing-upward sequence (**Figure 6**) from the offshore marine Pierre Shale to the nearshore marine Fox Hills Sandstone to the fluvio-deltaic Lance Formation (Hell Creek Formation in Montana and North Dakota) (Buswell, 1982; Cherven and Jacob, 1985). Although the shoreline had trended north throughout much of the Late Cretaceous, its orientation during deposition of the Fox Hills Sandstone has had two interpretations, one east trending, the other northeast trending.

McGookey and others (1972) and Buswell (1982) interpreted the strand line as east-trending across the area of the future uplift. Cherven and Jacob (1985) interpreted this strand line in the Black Hills area to lie along the southern margin of the great Sheridan delta that built eastward across eastern Montana (**Figure 7**). The east-trending shoreline of this Late Cretaceous delta is defined by Gill and Cobban (1973) as the northern limit of strata containing the ammonite *Baculites clinolobatus* and shown to trend directly across the site of the future Black Hills uplift. W.A. Cobban and J.D. Obradovich (written communication, 1990) place the age of *B. clinolobatus* as approximately 70 Ma.

Lillegraven and Ostresh (1990) presented a further refinement of the location of the retreating Cretaceous shoreline. They showed a northeast-trending shore at the time of *B. clinolobatus*, but placed the Black Hills region southeast of the strand line of the delta located in eastern Montana and North Dakota. Lillegraven and Ostresh (1990) showed that approximately one million years later, at the time of the zone fossil *Discoscaphites roanensis* (69 Ma; Obradovich and Cobban, written communication, 1990) a north-trending shoreline was located along a line approximately 50 mi east of the future site of Rapid City. Neither the paleogeographic reconstructions of McGookey and others (1972), Cherven and Jacob (1985), nor Lillegraven and Ostresh (1990) indicated a positive feature in the Black Hills area in the latest Cretaceous (69 to 70 Ma), but the area was at or near sea level at this time.

Following regression of the Cretaceous shoreline, the Lance and equivalent Hell Creek formations were deposited during the last three million years of the Cretaceous Period. Based on a study of thickness, composition, and paleocurrent indicators (crossbeds at 48 localities), Connor (1988) defined a fluvial origin for the Lance/Hell Creek sediments in which streams flowed eastward from the east side of the Powder River Basin, indicating that the Black Hills uplift was not yet in existence.

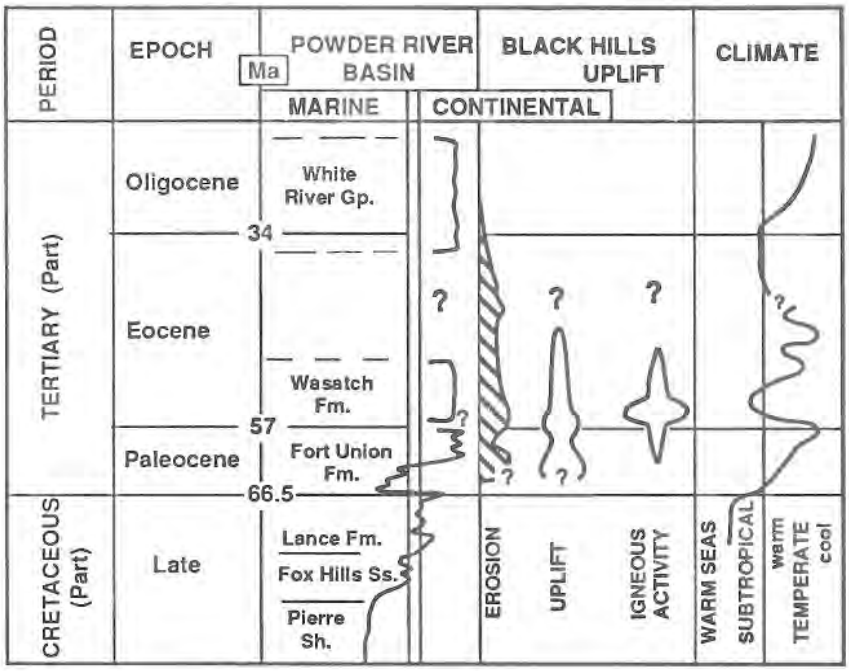

Figure 6. Diagram showing the late Mesozoic and Tertiary sedimentary environments in the Williston and Powder River basins; timing of uplift, erosion, and igneous activity of the Black Hills uplift; and climatic fluctuations. Marine conditions shown for the early and middle Paleocene are for the Williston Basin north and northeast of the Black Hills uplift. Absolute ages are from Lillegraven (this volume).

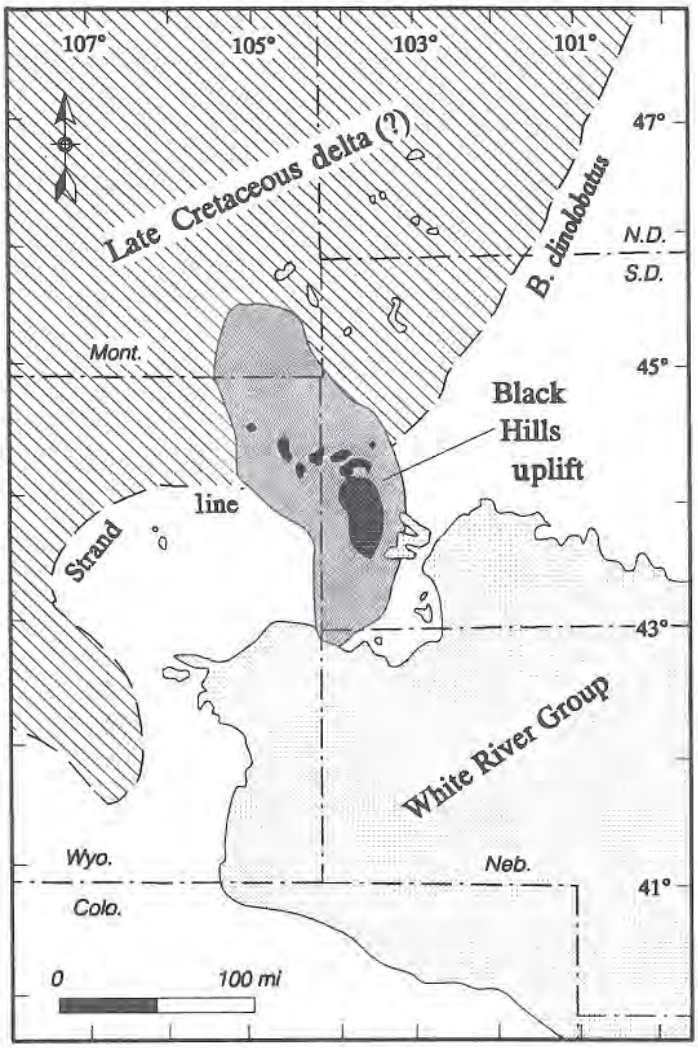

Figure 7. Area of the Black Hills uplift and relation to Late Cretaceous (69 Ma) pre-tectonic (McGookey and others, 1972) and Eocene and Oligocene post-tectonic sedimentary units. Black areas in the uplift area represent alkalic rocks emplaced at 50 to 62 Ma.

Synorogenic sedimentation

The first "reading" of a Tertiary age for syntectonic sediments from the Black Hills uplift was by Love (1960). Knowledge regarding early Tertiary sedimentation in the Powder River and Williston basins has increased markedly in the past 10 to 15 years. Although undertaken primarily to seek an understanding of the origin and placement of coal and uranium deposits found there, recent studies provide an improved and growing, although still controversial, picture of the evolution of the basins and, indirectly, of the development of the source terranes. In the Powder River Basin, these rocks include the Paleocene Fort Union Formation (composed in ascending order of the Tullock, Lebo, and Tongue River members) and the Eocene Wasatch Formation; in the Williston Basin they are, in ascending order, the Paleocene Ludlow, Slope, and Bullion Creek formations and Paleocene-Eocene Golden Valley Formation (Winczewski, 1982). Paleocene depositional sequences in the two basins are continuous across the Miles City arch. The age of initiation of the Black Hills uplift is found in the changing paleogeographic patterns of these Paleocene and Eocene rocks. As will be described below, initial indicators in the Powder River Basin have been assigned to both the lowest member, the Tullock, and the middle member, the Lebo.

Subsurface analyses of sandstone percentage (Lewis and Hotchkiss, 1981; Flores and Ethridge 1985) and isopach and maximum sandstone thickness (Ayers, 1986) in the Powder River Basin have been interpreted by these authors to indicate a sediment source to the east and northeast for the oldest member of the Fort Union Formation (the Tullock). Tongues containing sand as 60% or greater of total sediment extend westward from the outcrops of the Tullock (**Figure 8A**) in the eastern Powder River Basin near Gillette. Along the Montana-Wyoming state line a west-trending tongue extends across the entire basin (Lewis and Hotchkiss, 1981). In outcrops of the west-trending tongue along the east side of the basin, Flores and Ethridge (1985) noted bimodal north-south paleocurrent directions, based on cross-bed measurements at one location, and interpreted the combination of features to imply the presence of a source terrain on the Black Hills uplift in earliest Paleocene (Tullock) time. Lillegraven (this volume) interprets deposition of the Tullock to have occurred between 66.5 Ma and approximately 64 Ma. In this scenario, tectonic elevation of the Black Hills uplift would have begun at about 65.5 Ma.

Isopach and maximum sand thickness maps prepared by Ayers (1986) revealed that the overall thickness of the Tullock Member increased to the southwest and that maximum sand thicknesses occurred in narrow, elongate bands of northeast trend. Ayers (1986) interpreted these features of thickness and trend to indicate a maximum depocenter in the area

of the southwestern part of the Powder River Basin, fed by streams carrying sand from the rising Black Hills uplift to the northeast.

In marked contrast to the interpretation of west-flowing streams from the area of the Black Hills uplift in Tullock time, Seeland (1988) and Seeland and others (1988) stated that crossbedding azimuths at 39 localities for the Tullock on the east side of the Powder River Basin indicated an east trend in Montana and an east-northeast trend in Wyoming (**Figure 8B**). Such an east-northeast trend is parallel to the elongate sand bodies defined by Ayers (1986) in the Powder River Basin, and Seeland (1988) and Seeland and others (1988) interpreted this parallelism to demonstrate that streams flowed east-northeast. In this more likely scenario, the sand lobes described by Lewis and Hotchkiss (1981) and the northeast-trending bodies of Ayers (1986) were actually built eastward across the future sites of the Powder River Basin and Black Hills uplift by streams flowing across a coastal plain to the Cannonball Sea in western North and South Dakota.

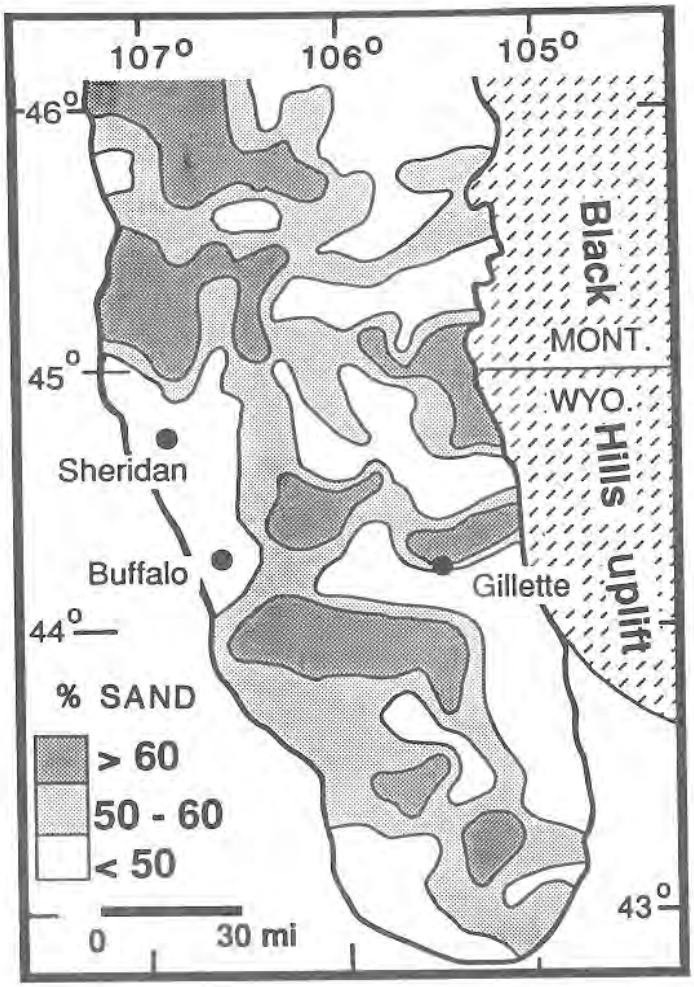

Figure 8A. Sandstone-percentage map adapted from Lewis and Hotchkiss (1981) for the Tullock Member of the Lower Fort Union Formation.

The lithofacies pattern present in the Lebo Member is similar to that in the underlying Tullock according to Lewis and Hotchkiss (1981), although the percentage of sand in the Gillette area is less and the axis of deposition is shifted northward to the Wyoming state line. In general, the percentage of sand decreases westward from the Black Hills uplift (Flores and Ethridge, 1985; Lewis and Hotchkiss, 1981), implying the presence of a source area to the east. Seeland (1988) noted that crossbed trends in rare channel sandstone bodies in the Lebo are similar to those in the overlying Tongue River Member (**Figure 8B**), i.e., north-northwest along the eastern side of the basin. According to Seeland, these crossbed trends, combined with the thickening of the Lebo along the structural axis of the basin (Curry, 1971; Ayers, 1986), are the first evidence of an eastern source for Fort Union Formation sediments and indicate that the initial phase of uplift in the Black Hills had begun. Lillegraven (this volume) interprets the time of deposition of the Lebo to be approximately 63 to 65 Ma; an average age for the initiation of the Black Hills uplift, based on this interpretation, would be approximately 64 Ma.

For the uppermost member of the Fort Union (the Tongue River), sand-percent maps prepared by Kaiser and Ayers (1983) and Ayers (1986) also showed strongly developed, west-trending sand bodies, best developed westward from the Gillette area, and an overall increase in percentage of sand toward the Black Hills uplift. Paleocurrent indicators (crossbeds) determined by Seeland (1988) indicate a north-northwest transport direction (**Figure 8B**) for streams in the eastern Powder River Basin. Although the direction of sediment transport indicated by the crossbeds is approximately perpendicular to the sand bodies of Kaiser and Ayers (1983), both lines of evidence suggest that at least the central and southern Black Hills uplift acted as a source of sediments during deposition of the Tongue River Member. Paleocurrent indicators (crossbeds) suggest that a major stream flowed eastward in Lebo (Flores and Ethridge, 1985) and Tongue River (Flores and Ethridge, 1985; Seeland and others, 1988) time across

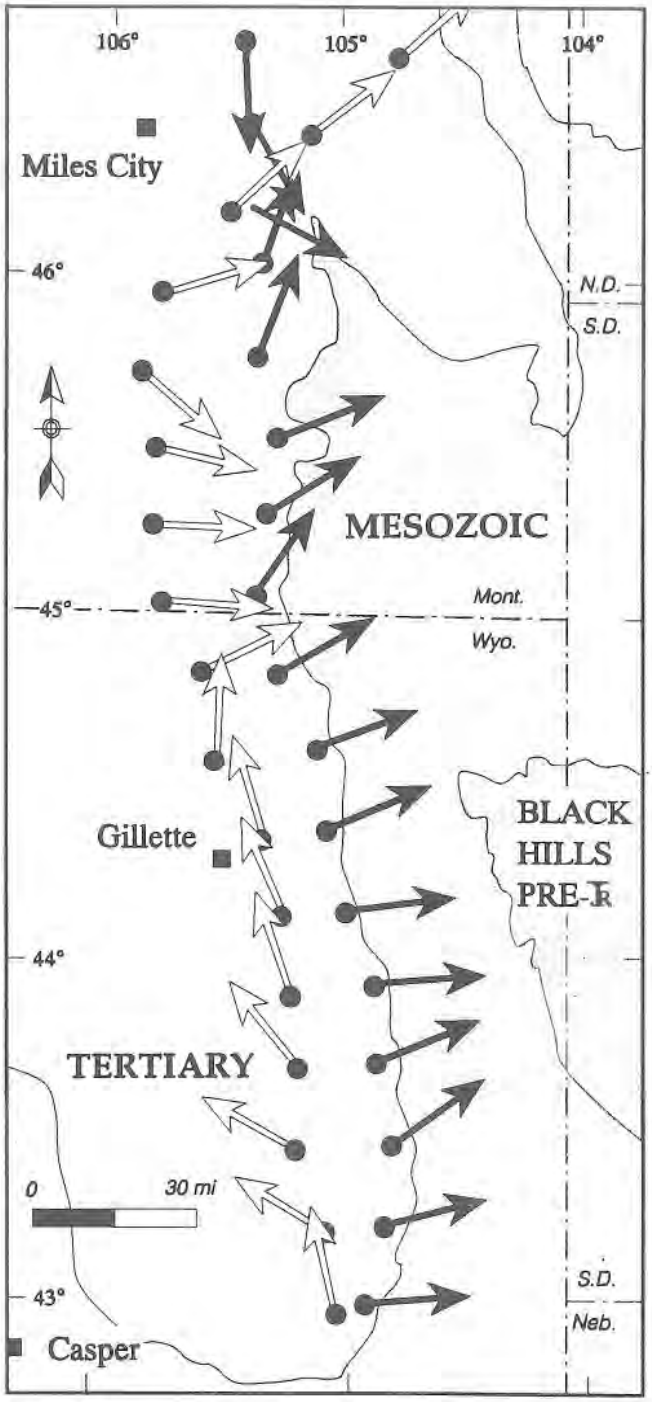

Figure 8B. Generalized geologic map (Seeland, 1991, unpublished figures) showing paleocurrent directions (sliding average cross bedding) for the lower Paleocene Tullock (black arrows) and upper Paleocene Tongue River (white arrows) members of the Fort Union Formation. Eastward paleocurrent trends in the Tullock suggest flow of streams toward the future site of the Black Hills uplift at this time. In contrast, Tongue River paleocurrent directions in Wyoming are northwest suggesting flow away from a rising source terrain on the Black Hills uplift.

the northern, structurally lower, extension of the Black Hills uplift in Montana.

Interpretations of the environments in which these sand bodies developed are generally of two types. In one (Kaiser and Ayers, 1983), sand lobes in the Tongue River represent westward bifurcating deltaic bodies supplied by sediment from the Black Hills uplift. The thick coal deposits of the Powder River Basin formed in swamps across this delta plain (**Figure 9**). In contrast, Flores and Ethridge (1985) suggested a fluvial origin for the Tullock and Tongue River Members in which coal deposits formed in backswamp environments between streams; they postulated a fluvio-deltaic and lacustrine environment for the Lebo Member.

North of the Black Hills uplift, lower Paleocene sedimentary units in southwestern North Dakota are interpreted to have formed as streams carried sediments onto deltas prograding eastward (**Figure 9**) into the Cannonball Sea (Winczewski, 1982; Winczewski and Groenewold, 1982; Cherven and Jacob, 1985; Flores and Ethridge, 1985). This sea is the successor to the Cretaceous Western Interior Seaway and, according to Cherven and Jacob (1985), retreated slowly eastward during deposition of much of the Paleocene strata. The resulting regressive sequence, which includes part of the Cannonball Formation and the Slope, Bullion Creek, Sentinel Butte, and Golden Valley formations, contains abundant coal deposits interpreted to have formed in backswamp environments adjacent to channels within the delta system (Winczewski, 1982).

Tectonic activity within this region continued throughout the middle and late Paleocene. In the area of the 120-mi-long Cedar Creek anticline, sedimentary patterns of streams preserved in lower Paleocene strata (**Figure 3**) change from east-flowing to southeast-flowing during deposition of the middle Paleocene Bullion Creek Formation (Cherven and Jacob, 1985). This change is interpreted by Winczewski (1982) and Winczewski and Groenewald (1982) to have resulted from uplift of the Cedar Creek anticline, blockage of direct west-to-east drainage, and sediment transport around the north end of the anticline into the southeast-trending axial area of the Williston Basin. In a similar fashion, sedimentary patterns in the late Paleocene Sentinel Butte Formation reflect development of north-northwest-trending anticlines in Billings

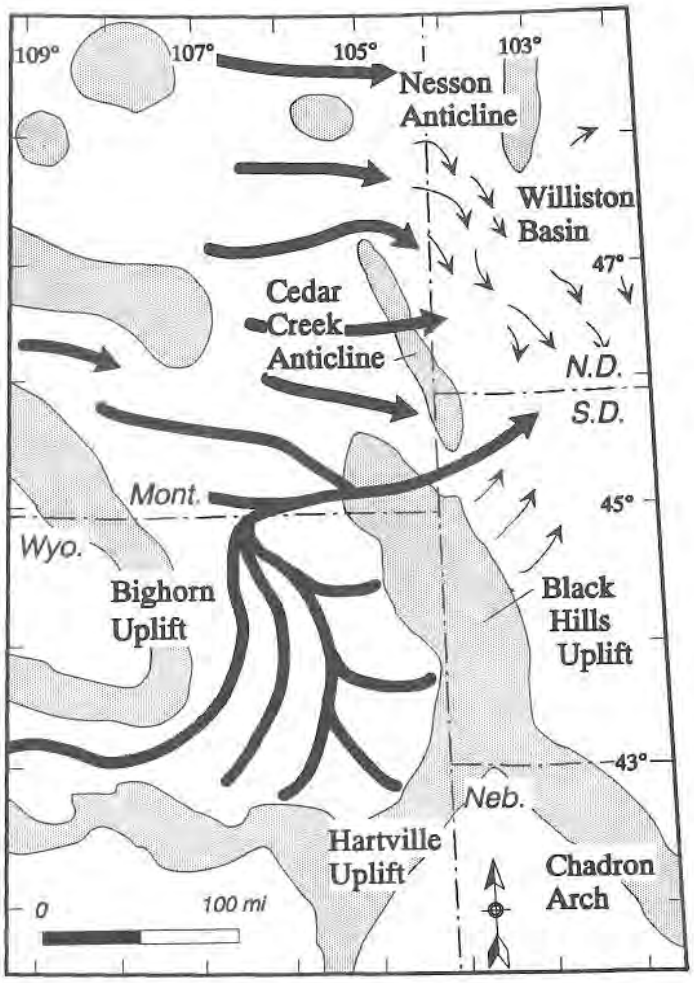

Figure 9. Generalized paleogeographic map of the Powder River and Williston basins and associated uplifts in late Paleocene time illustrating stream flow toward the Cannonball Sea in North Dakota and northwestern South Dakota. Stream transport directions in Wyoming and Montana adapted from Seeland (1976, 1988, and written communication, 1991) and those in North Dakota from Winczewski (1982) and Winczewski and Groenewold (1982). Stippled pattern indicates positive tectonic elements active during late Paleocene time.

County, North Dakota, northeast of the Cedar Creek anticline (Winczewski, 1982).

Although direct input of sediment to the Cannonball Sea from the Black Hills uplift likely existed in the early Paleocene, strata which record such evidence are absent on the east margin of the uplift. During or immediately following the latest Paleocene the southern part of the Williston Basin was uplifted (Winczewski, 1982), resulting in Eocene erosion that removed any evidence of the Paleocene depositional record along the east and northeast margins of the uplift.

The presence of a Paleocene seaway not more than 100 mi from the rising landmass of the Black Hills uplift is a revealing aspect of the nature of the structural and topographic development of the region. Laramide tectonic activity ultimately caused a 9,000 ft differential uplift of the Black Hills relative to adjacent basins. During the tectonic activity, the surface of these basins was near or even below sea level. Paleocene units deposited at that time were subsequently elevated 2,500 to 4,000 ft as a result of broad regional uplift of basins and surrounding uplifts in Montana, Wyoming and North and South Dakota, either due to Laramide activity in the early Eocene or to post-Laramide epeirogeny.

Unfortunately, the oldest Eocene strata are not exposed on or directly against the Black Hills uplift and, therefore, do not afford as detailed a reading in regard to later Laramide tectonic pulses. Eocene deposits of the Powder River and Williston basins lack a connecting link across the Miles City arch. Seeland (1976, 1985, 1988) used crossbeds as paleocurrent indicators to show that the Wasatch Formation in the Powder River Basin formed in a fluvial system with input from three sides. The model shows a major trunk stream that flowed from the north margin of the basin and which was not interpreted by Seeland (1976) to cross the northern end of the Black Hills uplift as had been the case in late Paleocene. This northern portion of the Black Hills uplift, therefore, may have risen during the early Eocene and diverted the flow of the major trunk stream westward.

Two aspects of the Wasatch Formation suggest that a second pulse of tectonism affected the Black Hills uplift during deposition of this unit. The first was presented at the Geological Society of America annual meeting in 1984, in which Bion Kent defined an angular unconformity and weathered surface at the base of Eocene strata in the Gillette area (not mentioned in his abstract for the meeting). Kent (1984) suggested that the sedimentary wedge above this unconformity resulted from uplift to the east and that other periods of quiescence and rapid sedimentation were intermixed. The second aspect of tectonic activity is the recognition by Seeland (1988) that sandstones of the Wasatch Formation, which he defined as of latest Paleocene and Eocene age, are coarser grained than those of the underlying Tongue River Member in the eastern Powder River Basin. He

considered this increase in grain size to result from strong uplift at the basin margins, although the granitic Precambrian core of the uplifted Laramie or Hartville uplifts to the south may have also supplied such arkose.

In summary, the Tertiary sedimentary record of the Powder River and Williston basins suggests a two-phase development for the Black Hills uplift. Initial uplift, as recorded in the eroded detritus, appears to have begun during deposition of the Lebo Member (63 to 65 Ma) of the Fort Union Formation, although a somewhat older initiation during deposition of the Tullock Member (65 to 66.5 Ma) has also been suggested. A similar age is indicated for the Laramide phase of subsidence in the Powder River and Williston basins. Uplift began in the middle Paleocene at the Cedar Creek anticline north of the Black Hills, and in late Paleocene at folds northeast of the Cedar Creek structure. A second tectonic pulse in the Black Hills uplift in latest Paleocene/early Eocene is suggested by the angular unconformity at the base of the Wasatch Formation on the east side of the Powder River Basin and the coarser sediments within this unit as compared to the underlying Tongue River Member of the Fort Union Formation.

Postorogenic sedimentation

The entire northern Great Plains region was beveled (Denson and Gill, 1965) by late Eocene time (37 Ma). At the northern end of the continuous Tertiary cover of the Great Plains and east of the Black Hills is the White River Badlands. Exposures of Chadronian age mauve and tan siltstone and sandstone and minor white tuff of the highly fossiliferous White River Group (Clark and others, 1967) rest unconformably on the yellow and red Interior Paleosol, developed on the Pierre Shale.

In regional context, the basal beds of the White River Group lie with angular unconformity on the older strata. Across a distance of 275 mi to the north of the Badlands, scattered remnants of the Eocene paleosol rest on successively higher units (Pettijohn, 1966) so that in the central Williston Basin it rests on Eocene strata. To the west, the erosion surface cuts into successively lower units. In a distance of 60 mi, the surface cuts across the entire Phanerozoic section and, in the core of the Black Hills uplift southwest of Rapid City, the paleosol is developed on Early Proterozoic basement. The age of the basal Oligocene strata on the uplift appears to vary from place to place. Both uppermost Eocene Chadronian strata (P.R. Bjork, oral communication, 1990) at about 36 to 37 Ma (Swisher and Prothero, 1990) and upper Oligocene Whitneyan (McDonald, 1982) at 29 to 30 Ma (Swisher and Prothero, 1990) locally overlie the east-dipping Paleozoic rocks.

Oligocene sedimentary material in the Chadron and overlying Brule formations in the Badlands is composed of a combination of far-travelled volcanic ash, locally derived material, and debris from the Black Hills uplift (Clark, 1975). Stream channels extended from both the northern and southern portions of the topographic Black Hills (**Figure 10**), carrying distinctive minerals from the Tertiary igneous and

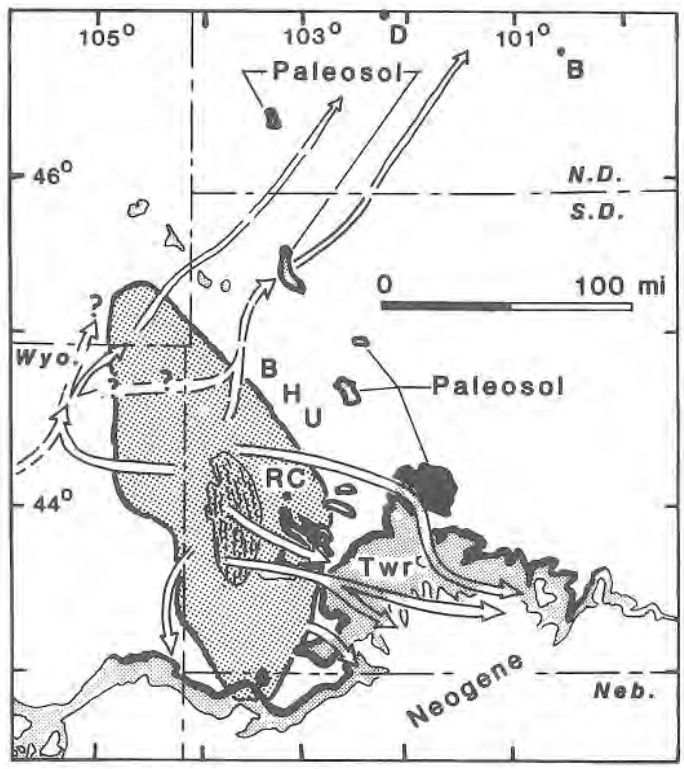

Figure 10. Oligocene paleogeography of the northern Great Plains region. Heavy line surrounding area with stippled pattern represents the approximate boundary of the Black Hills uplift and the area of short curving lines within the uplift represents exposed Precambrian core. Black areas are Eocene Interior Paleosol (Pettijohn, 1966), stippled pattern represents areas of Eocene-Oligocene White River Group as shown by Trimble (1980). The arrows show direction of transport of Oligocene drainages as reconstructed by Clark (1975) and Seeland (1985). B = Bismark, D = Dickinson, RC = Rapid City.

Precambrian igneous and metamorphic terranes (Clark and others, 1967). Small exposures of Oligocene strata are present in the central Powder River Basin at Pumpkin Buttes. McKenna and Love (1972) interpreted these isolated outcrops as the only remaining evidence of a continuous unit extending from outcrops on the Bighorn uplift to those on the Black Hills uplift. The erosion surface was developed on Eocene strata in the central basin and older rocks toward the basin margins. The source of most, if not all, of the material remaining at Pumpkin Buttes appears to have been uplifts to the west (McKenna and Love, 1972). Clark (1975), however, indicated a probable radial drainage pattern from the Black Hills uplift, with streams carrying material to now eroded areas to the west. In a similar fashion, northward drainage from the Black Hills uplift to the Williston Basin is postulated, and Seeland (1985) suggested that a major stream crossed the northern portion of the uplift flowing from the Powder River Basin to the Williston Basin.

Paleoclimate

The climate during Laramide activity, the climate under which erosion from the uplift and deposition in the adjoining coal basins occurred (**Figure 6**), was reviewed succinctly for the Williston Basin by Winczewski (1982) as follows:

> *The climate of the Late Cretaceous was subtropical; the climate cooled to warm temperate during the Paleocene (Sloan, 1970). The Paleocene Rocky Mountain flora was similar in part to the modern East Asian Flora. Leopold and MacGinitie (1972) concluded that the Paleocene flora changed to a modern one, having affinity to Central America floras, during Eocene time. They concluded that the climate throughout the Paleocene was relatively stable in the Rocky Mountain area, based on the persistence of certain plant and pollen types. They believed that the low relief of the Laramide highlands, in contrast to that of the modern Rockies, contributed to the floral stability.*
>
> *The climate became unstable in latest Paleocene to earliest Eocene time. Based on fossils in the lower Golden Valley Formation, Hickey (1972) concluded that the climate cooled somewhat. In early Eocene, the climate returned temporarily to subtropical, similar to that of the Late Cretaceous. Leopold and MacGinitie (1972) concluded that thereafter the Rocky Mountain area became more temperate (drier winters) with both humid and dry cycles. The trend was toward drier and cooler climates.*

The distinctive alternating color bands of the Oligocene sequence in the White River Badlands were interpreted by Retallack (1983) to be fossil soil horizons. He used the soil type and associated fossil remains to define both climatic conditions and vegetation types; they indicate a change from subtropical woodlands in the early Oligocene to warm to cool temperate grasslands in the late Oligocene.

Structural characteristics of the Black Hills uplift

What is the structural character of the uplift from which the syntectonic sediments were shed? What are the structural styles of the uplift and what might they tell, if anything, of its origin? The Black Hills uplift appears to be a large, doubly plunging anticline or elongated dome as seen on the *Geologic map of the United States* (King and Beikman, 1974), the more detailed (1:250,000) map of DeWitt and others (1986, 1989), or the tectonic map of Lisenbee (1988; **Figure 11** in this paper). The axis of the large fold forms an open S with north-trending segments at the ends connected by a northwest-trending center section. The fold extends at least 185 mi north-northwest from the South Dakota-Nebraska border, where it joins the Chadron arch, to an indistinct merging with the Miles City arch in southeastern Montana (**Figure 3**). Structure contour maps (Darton, 1902; Lisenbee, 1988) (**Figures 2** and **11** in this paper), which show more clearly the shape of the uplift, both refine and modify this concept of a large fold. A more detailed descrip-

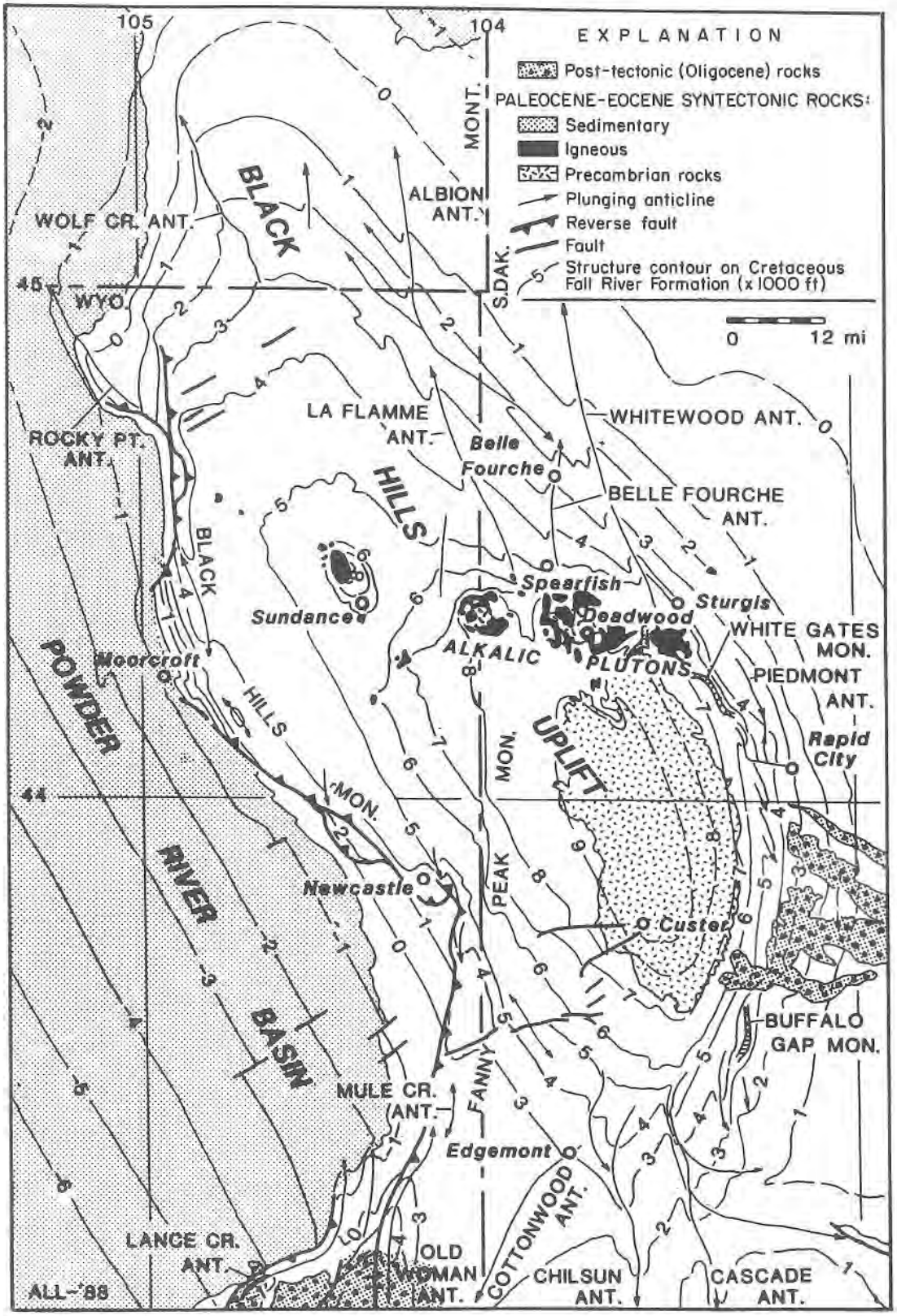

Figure 11. Tectonic map of the Black Hills uplift and eastern Powder River Basin (revised from Lisenbee, 1988). Railroad pattern for the Buffalo Gap and Whitegates structures used to distinguish the only east-facing monoclines of the Black Hills uplift. ANT. = anticline; MON. = monocline. (Reprinted with permission of the Wyoming Geological Association.)

tion of individual structures superimposed upon the larger fold is given in Lisenbee (1978), and the following discussion draws heavily on that work.

West-vergent monoclines are present across the uplift and the two largest monoclines separate the Black Hills uplift from the Powder River Basin on the west. The eastern flank of the uplift, in strong contrast, is a broad arch with small, superimposed monoclinal folds, both with and opposed to regional dip. These structures, as well as the overall outline of the uplift, trend north and north-northwest. If the monoclinal folds are associated with basement thrusting, as is probable, they result from regional compression in which the maximum compressive stress was oriented approximately west-northwest. Several tectonic models involving such basement thrusting are outlined in a later section of this paper. En echelon folds at the northern and southern ends of the uplift are consistent with a model of limited wrench tectonics (left slip on the north, right slip on the south), in which the uplift moved east-northeast relative to the adjoining areas. Minor strike-slip may also have occurred on the north- and northwest-trending monoclines along the margin between the uplift and the Powder River Basin.

Figure 12. View north of the Minnelusa Formation flatirons exposed in the Fanny Peak monocline northeast of Newcastle, Wyoming (from Lisenbee, 1988). This west-vergent fold separates the eastern and western blocks of the Black Hills uplift. (Reprinted with permission of the Wyoming Geological Association.)

Although in its entirety the uplift clearly trends northwest (**Figure 3**), Noble (1952a) recognized two blocks, a western block that plunged northward and an eastern block that plunged southward, separated approximately along the Wyoming-South Dakota boundary by the west-facing Fanny Peak monocline (**Figure 12**). This detail is worthy of note for the trend of Laramide uplifts is believed to have varied with time (Chapin and Cather, 1981, 1983) and Gries (1983a and b) suggested that the north trends formed in latest Cretaceous and the northwest trends during the Paleocene. As a unit, the two blocks in the Black Hills present an overall north-northwest trend compatible with the suggested Paleocene age and this age is independently established from the syntectonic sedimentation record. Differential uplift of the eastern block relative to the western block, as much as 1,100 ft across the Fanny Peak monocline, resulted in deeper erosion on the east, exposing the Precambrian core. The Fanny Peak monocline almost certainly lies along a preexisting zone of basement weakness, for in addition to the Laramide tectonism, Weimer and others (1982) use sedimentation patterns along this same feature to document movement during Early Cretaceous deposition.

A similarity of style for folds on the uplift as well as at the west margin of the uplift (the Fanny Peak and Black Hills monoclines), suggests a similarity of origin. With only three exceptions along the east flank of the uplift [Whitegates (**Figure 13**) and Buffalo Gap monoclines and a faulted structure near the

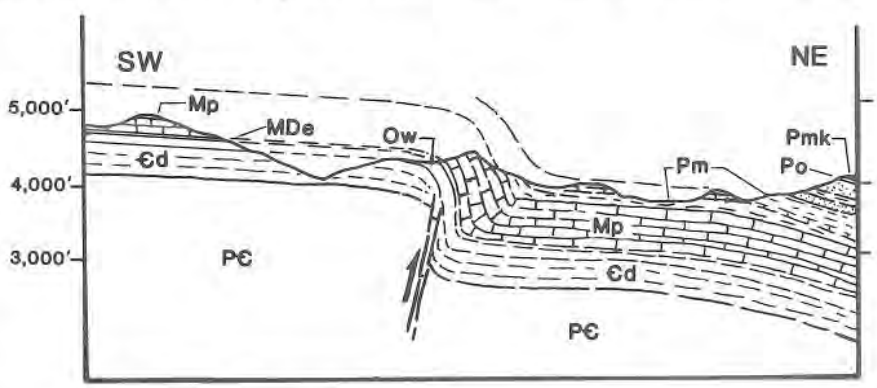

Figure 13. Cross sectional view of Whitegates monocline, located 2 mi west of Piedmont, South Dakota. Folded strata are interpreted here to drape over a reverse fault in the Precambrian basement. Pmk = Minnekahta Limestone; Po = Opeche Shale; ℙm = Minnelusa Formation; Mp = Pahasapa Limestone; MDe = Englewood Limestone; Ow = Winnipeg Formation; Ꞓd = Deadwood Formation; PꞒ = Precambrian basement.

Stratobowl southwest of Rapid City (not shown on **Figure 11**)], all of the folds are west-vergent (**Figure 11**) and, with the exception of the Cottonwood anticline, strongly asymmetric.

At the largest scale, the two flanks of the uplift are deformed in contrasting styles (**Figure 11**). On the west, the Black Hills (**Figure 14**) and Fanny Peak (**Figure 15**) monoclines, which separate the uplift from the Powder River Basin, are as much as 110 mi long and have a maximum structural relief of 5,500 ft. Based on similarities with Laramide structures elsewhere in Wyoming and on the gravity data of Black and Roller (1961) for the Black Hills monocline, the monoclines are interpreted to lie above or in the hanging wall of blind reverse/thrust faults, which may reach to the base of the Cretaceous strata (**Figure 11**), at least in those areas of near vertical dips in outcrop. Planar strata of low dip are present on both the uplift and in the Powder River Basin. The east side of the uplift, however, comprises a broad half arch, across which Phanerozoic strata descend eastward into the southern end of the Williston Basin.

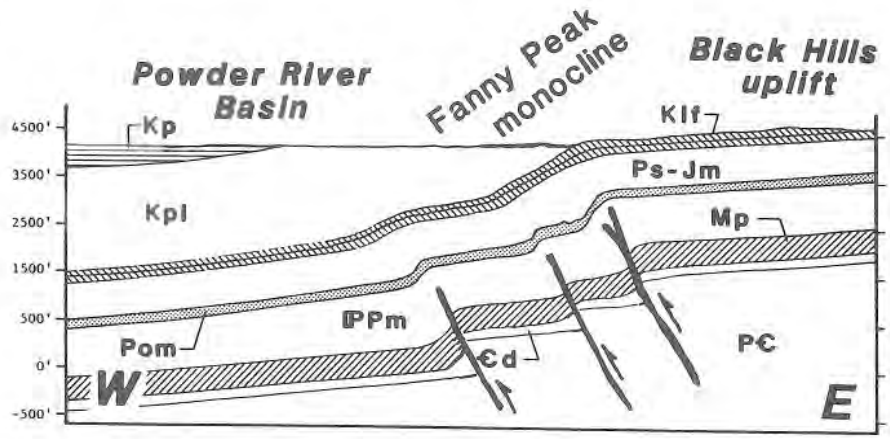

Figure 15. Cross sectional view of the boundary between the Powder River Basin and Black Hills uplift separated by the Fanny Peak monocline. The section (Lisenbee, 1978), based on surface geology and gravity data by Black and Roller (1961), is located a few miles south of the latitude of Newcastle, Wyoming. Kp = upper part of the Pierre Shale; Kpl = lower part of the Pierre Shale; Klf = Lakota and Fall River Formations; Ps-Jm = Spearfish, Sundance, and Morrison Formations; Pom = Opeche Shale and Minnekahta Limestone; PIPm=Minnelusa Formation; Mp = Pahasapa Limestone; Ꞓd = Deadwood Formation; PꞒ = Precambrian rocks, undifferentiated.

Numerous monoclines of smaller scale, both with and opposed to regional dip, are superimposed upon the Black Hills uplift. These smaller scale folds may extend for 10 miles or more, have structural relief of 500 to 1,200 feet, and dips of as much as 90° in the rotated limb. West of the axis of the uplift, where strata dip to the west, west vergence results in monoclinal folds. East of the axis, most folds have the same west vergence, but form asymmetric anticline-syncline couples. Both groups were inferred by Lisenbee (1978) to form by the mechanism of folding of Phanerozoic strata above a fault in the Precambrian basement and both represent monoclines from a mechanical point of view.

Figure 14. View eastward from Powder River Basin across the Black Hills monocline near Oshoto, Wyoming (from Lisenbee, 1988). Missouri Buttes (left skyline) and Devils Tower (right skyline) are stocks emplaced within Mesozoic strata on the western block of the Black Hills uplift. This monocline, having approximately 4,000 ft of structural relief, is notable for the lack of topographic expression in the Cretaceous clastic strata. (Reprinted with permission of the Wyoming Geological Association.)

In map view, the axes of such folds have consistent C-shaped patterns (either singly or as a series of connected scallops). The block diagram of **Figure 16** is a view of the interpreted basement configuration beneath the Cascade anticline. In this model, the scallops result from dog-leg bends in the strikes of the underlying faults. Curvilinear patterns are also found in folds associated with thrust faults, such as those described by Dahlstrom (1970) and Royse and others (1975) for fold-thrust belts of Canada and western Wyoming, respectively, and may imply that the faults

present here beneath monoclines are of more gentle dip than shown in **Figure 16**.

Smaller-scale structures are also aligned along the Fanny Peak and Black Hills monoclines. Lisenbee (1978) described the structures as terraces, ramps (a term used with different meaning in thrust tectonics), and anticlines resulting from vertical movement on several subparallel basement fractures. Shurr and others (1988) reinterpreted the structures (**Figure 17**) as suggesting that small components of right slip on the Fanny Peak monocline and left slip on the Black Hills monocline accompanied the dominantly vertical movement and formed in-line lenses, restraining and releasing bends, and oblique folds and faults such as are present along major wrench zones. The strike-slip component on the Fanny Peak and Black Hills structure, however, would be small.

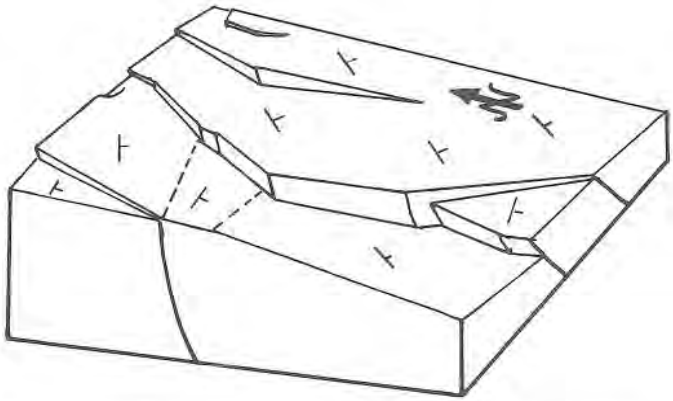

Figure 16. Three-dimensional diagram illustrating possible Precambrian basement configuration beneath the Cascade anticline near Hot Springs, South Dakota. The strata folded over this basement template form asymmetric anticline-syncline couples and display a C-shape in map view. Dotted lines are flexures. Dip and strike symbols show the average attitudes of strata within blocks. The north-south dimension for the area shown is approximately 18 mi. (Adapted from Lisenbee, 1978.)

In an unusual feature, the Fanny Peak and Black Hills monoclines cross near Newcastle, Wyoming (**Figures 17** and **18**). If major components of either strike-slip or thrusting were present on basement faults such as those illustrated in **Figure 18**, strata in the area of intersection would experience strong compression as the uplifted blocks impinged. Although surface exposures of the basal Cretaceous sandstones in the basinward-plunging syncline that marks this intersection are strongly fractured, they are not deformed to the degree expected from substantial strike-slip movement on either monocline.

Another pattern suggestive of wrench movement is found in folds at the north and south ends of the eastern block. As shown in **Figure 3**, anticlines and synclines on the south appear to be part of a larger group of en echelon folds, many of which are present on the crest of the Hartville uplift. Such a grouping is suggestive of a wrench-fault pattern produced

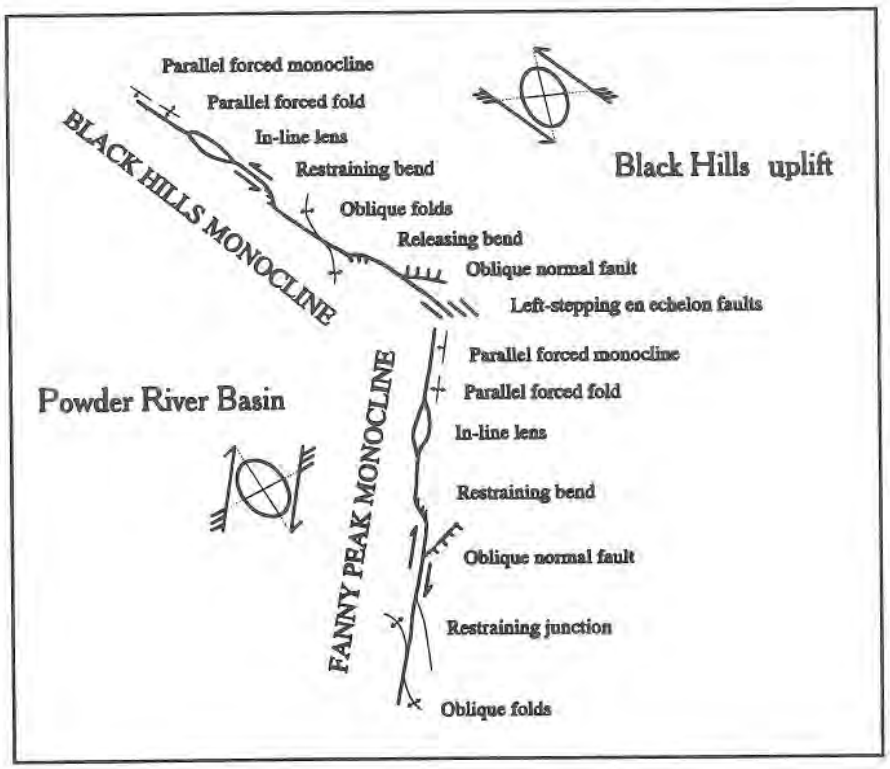

Figure 17. Tectonic summary of elements along the Black Hills and Fanny Peak monoclines interpreted by Shurr and others (1988) as indicative of a component of left slip on the former and right slip on the latter. The north-south dimensions of the areas shown are approximately 60 mi.

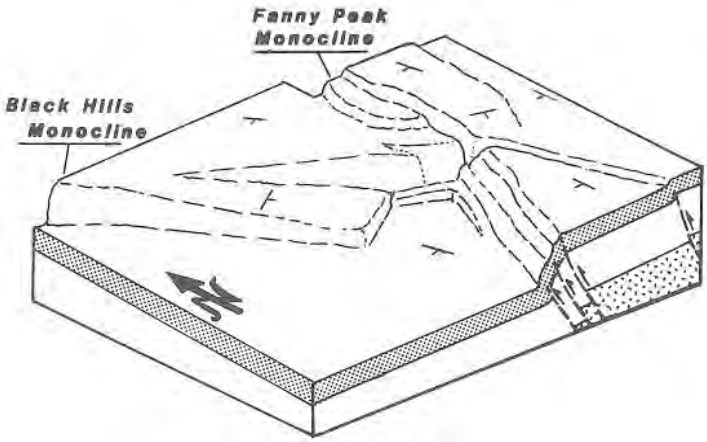

Figure 18. Three dimensional diagram illustrating configuration of strata deformed by faulting and folding above faulted basement blocks along the Black Hills and Fanny Peak monoclines in the Newcastle, Wyoming, area. The various blocks are interpreted based on surface geology and a gravity survey of the Fanny Peak structure by Black and Roller (1961). Dip and strike symbols show the average attitudes of strata within blocks. The west edge of the area shown is approximately 9 mi long. (Adapted from Lisenbee, 1978.)

by right slip. The mirror image pattern at the north end of the block is suggestive of possible left slip, which would result in shortening due to buckling in the central portion of the Black Hills uplift, the area of recognized maximum structural relief.

Laramide igneous activity

A magmatic event, whose results are most dramatically exemplified by the monolith of Devils Tower (**Figure 19**), also affected part of the Black Hills during Laramide time. Igneous activity during the period 50 to 62 Ma (DeWitt and others, 1986) began shortly after initial tectonism (**Figure 6**). Some intrusive bodies [such as those along the Fanny Peak monocline (Shapiro, 1971) and Whitewood anticline (Sottek, 1959)] appear to abut Laramide structures (**Figure 20**) without being deformed; whereas others [such as the laccolithic complex at Theodore Roosevelt (Heidt, 1977)] are strongly shattered, possibly by continuing Laramide stresses or later emplacement of other intrusions. Although there may have been a second magmatic pulse at about 39 Ma, based on a limited number of age determinations from the Bear Lodge Mountains near Sundance (Staatz, 1983), we believe that these ages are probably spurious and that the majority of the igneous activity occurred between 50 and 58 Ma.

Placement of plutonism within the larger framework of Laramide development is of fundamental importance. What is the petrologic character of these rocks and was the parent magma derived from the crust, the mantle, or both? Was the molten rock part of a regional event or only local? How does the magma generation fit within plate tectonic concepts?

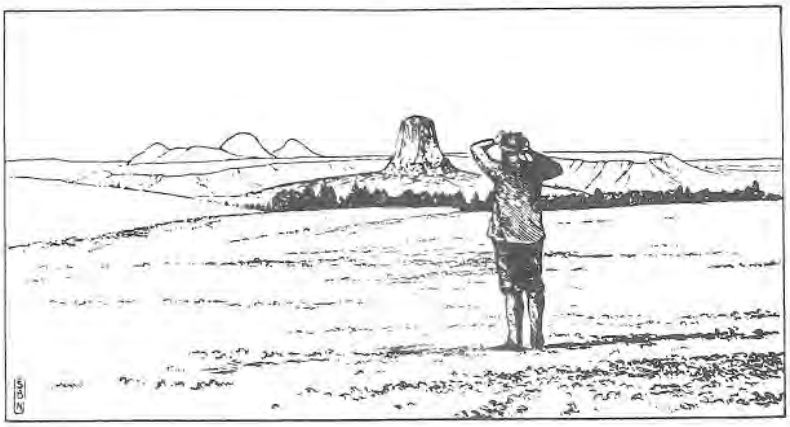

Figure 19. Figure 95 in Jaggar's (1901) study of laccoliths in the Black Hills. The stock of Devils Tower was known as Mato Tepee (Bear Lodge) and was incorrectly interpreted by Jaggar to be a laccolithic remnant fed from plutons in the distant Missouri Buttes.

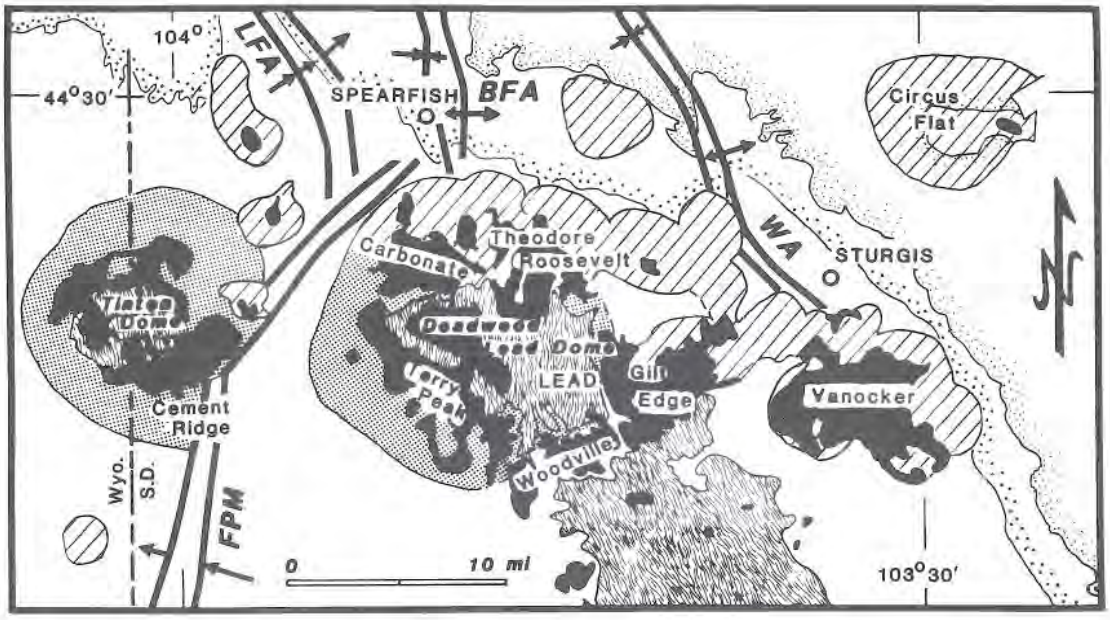

Figure 20. Generalized geologic map of the eastern intrusive centers in the Black Hills. The heavily stippled pattern indicates the igneous-related basement domes (Tinton, Deadwood-Lead). The diagonal lines show areas of individual laccoliths or laccolithic clusters (Vanocker, Theodore Roosevelt, Terry Peak, Gilt Edge, Circus Flats). Anastomosing pattern indicates Precambrian basement. FPM = Fanny Peak monocline; WA = Whitewood anticline and adjacent syncline; LFA = La Flamme anticline and adjacent syncline; BFA = Belle Fourche anticline and adjacent syncline.

As outlined by Jaggar (1901), igneous activity on the Black Hills uplift was first reported by F.V. Hayden to the Philadelphia Academy of Science in 1869, at which time Hayden described the prominent bulk of Bear Butte (**Figure 21**) as a ...*protrusion of basalt* (it is actually rhyolite). In the succeeding twelve decades, dozens of studies of these rocks have been undertaken. Investigations include those of their contained mineral deposits including gold, silver, lead, copper, rare-earth elements, molybdenum, and thorium (Irving and Emmons, 1904; Connolly and O'Harra, 1929; Connolly, 1927; Shapiro and Gries, 1970; DeWitt and others, 1986; Paterson and others, 1989; Staatz, 1983); of their forms and mechanisms of emplacement, especially as dikes and laccoliths (Jaggar, 1901; Darton and Paige, 1925; Noble, 1952b;

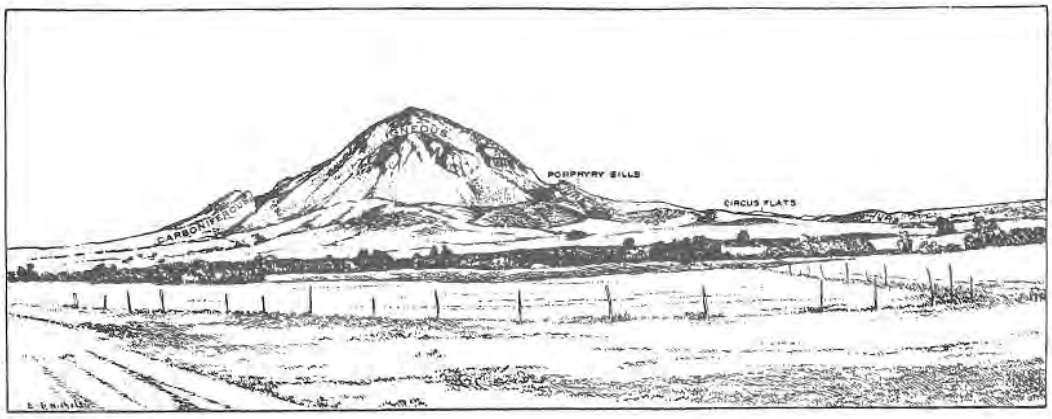

Figure 21. Plate XXXI from Jaggar (1901) showing the stock at Bear Butte from the northwest.

Beck, 1976; Lisenbee and Martin, 1988); and more recently of their chemical character and origin (Olson, 1976; Beintema and Montgomery, 1986; Karner, 1985; Halvorson, 1980; DeWitt and others, 1986; Shearer, 1990).

These plutons represent a diverse group of predominantly alkalic, iron-rich, metaluminous to slightly peraluminous igneous rocks, which intrude the Archean and Proterozoic basement and its cover of Paleozoic and Mesozoic sedimentary rocks along a linear, west-northwest-trending belt in the northern Black Hills (**Figure 11**). Numerous laccoliths and sills, lesser numbers of stocks, and many dikes contain rocks ranging in chemical composition from ijolite and essexite, through syenite and nepheline syenite, to quartz monzonite and granite (De la Roche and others, 1980). Because of the confusion surrounding the great number of rock names applied to igneous rocks in the past [see reviews in DeWitt and others (1986), and Shearer (1990)], we (**Figure 22**) will use the nomenclature for plutonic rocks described by De la Roche and others (1980). Many of the Eocene-Paleocene igneous rocks in the northern Black Hills are fine grained and porphyritic and, therefore, in this discussion we place volcanic rock names in parentheses where appropriate. Chemical data are from a variety of sources and were derived by a variety of techniques. Some rocks are fresh and unaltered, others are not. Some analyses sum very close to 100 weight %, others do not or have been normalized to 100 weight %. A detailed treatment is beyond the scope of this review paper, and the available data will be combined on diagrams designed to reveal their patterns of alteration.

Both alkalic and alkali-calcic igneous rocks are present and they display a broad-scale geographic separation. Alkalic rocks, dominated by syenite (trachyte), nepheline syenite (phonolite), and quartz syenite, are most common in the western half of the belt, from west of Lead to the westernmost exposures at Missouri Buttes. Within this alkalic group, plutons of mafic alkalic rocks are most numerous at Tinton, near the center of the belt, and near Galena, toward the eastern end of the belt. Carbonatite is restricted to the core of the Bear Lodge Mountains, near the western end, and within the Mineral Hill complex at Tinton. Alkali-calcic igneous rocks dominated by granite (rhyolite) are most numerous in the eastern half of the belt, from Lead to the easternmost exposures at Bear Butte, but are present as far west as the southern Bear Lodge Mountains. The entire suite of rocks is predominantly average to very iron rich and metaluminous; however, alkali-calcic granite (rhyolite) is locally very magnesium rich and strongly peraluminous. Details of the chemistry and petrology of the igneous rocks will be discussed from west to east, along the length of the belt following a general outline of the petrographic character of the major igneous rock types.

Petrography

Syenite and quartz syenite (trachyte and quartz trachyte) most commonly consist of a fine-grained groundmass of sanidine, orthoclase, undifferentiated

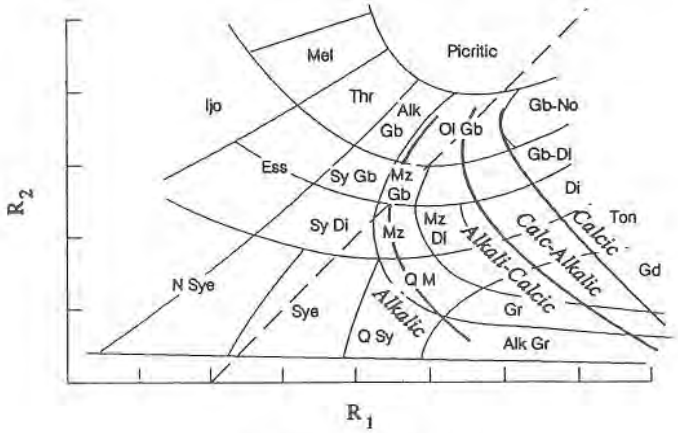

EXPLANATION

Alk Gb=alkali gabbro	Mz Gb=monzogabbro
Alk Gr=alkali granite	Mz=monzonite
Di=diorite	N Sye=nepheline syenite
Ess=essexite	Ol Gb=olivine gabbro
Gb-Di=gabbro-diorite	Q M=quartz monzonite
Gb-No=gabbro-norite	Q Sy=quartz syenite
Gr=granite	Sy Di=syenodiorite
Gd=granodiorite	Sy Gb=syenogabbro
Ijo=ijolite	Sye=syenite
Mel=meltigite	Thr=theralite
Mz Di=monzodiorite	Ton=tonalite

Figure 22. Major-element (R1-R2) chemical classification of De la Roche and others (1980). Dashed, diagonal line separates nepheline-normative rocks in upper left from quartz-normative rocks in lower right. R1 = 4,000 Si - 11,000 (Na + K) -2,000 (Fe + Ti); R2 = 6,000 Ca + 2,000 Mg + 1,000 Al.

alkali feldspar, albite, aegirine-augite, and minor quartz. Phenocrysts, which make up 5 to 20% of the rock, are albite and low-calcium plagioclase, sanidine, anorthoclase, aegirine-augite, and minor hastingsite, sphene, and biotite. Nepheline syenite (phonolite) has a fine-grained groundmass of sanidine, albite, anorthoclase, aegirine-augite, nepheline, and analcime. Five to 25 % of the rock is phenocrysts of sanidine, orthoclase, anorthoclase, aegirine-augite, sphene, sodalite, and plagioclase. Granite (all bodies are rhyolite) has a fine-grained groundmass of orthoclase and undifferentiated alkali feldspar, low-calcium plagioclase, quartz, and minor biotite. Phenocrysts, which make up 3 to 15% of the rock, are oligoclase, biotite, and minor orthoclase. Syenodiorite and syenogabbro (trachyandesite and trachybasalt) have a fine-grained groundmass of plagioclase, orthoclase, and biotite, and phenocrysts of anorthoclase, hastingsite and ferrohastingsite, augite, and oligoclase.

Bear Lodge Mountains, Wyoming

Syenite and lesser amounts of nepheline syenite, syenodiorite, and quartz syenite are the main rock types in the core of the Bear Lodge Mountains (**Figure 23A**). The unaltered and non-metasomatized syenite, nepheline syenite, syenodiorite, and quartz syenite are predominantly iron rich to very iron rich (**Figure 23B**) and are metaluminous to mildly peraluminous (**Figure 23C**). Extensive carbonatitic alteration in the core of the Bear Lodge Mountains (Wilkinson, 1982; Jenner, 1984a and b) drives the bulk composition of much of the syenite into the essexite field (open squares, **Figure 23A**). The alteration also intensifies the iron-rich to very iron-rich nature of the rocks and results in SiO_2 concentrations of less than 50 weight % (**Figure 23B**). The resulting calcium-rich rocks are strongly metaluminous (**Figure 23C**). Potassium metasomatism associated with the carbonatitic alteration (Jenner, 1984a and b) drives the composition of much of the syenite and quartz syenite into the peraluminous field (open triangles, **Figure 23C**).

Outside the core of the Bear Lodge Mountains, relatively unaltered equivalents of the igneous rocks associated with carbonatite and potassium-metasomatized rocks are exposed. In these areas, nepheline syenite, syenite, and lesser amounts of syenodiorite and syenogabbro are noted (**Figure 23A**). In one intrusive body on the north side of the Bear Lodge Mountains, nepheline-normative syenogabbro apparently grades into quartz-normative syenite (filled triangles, **Figure 23A**). This gradation suggests fractional crystallization at low confining pressures and crossing of the thermal divide between nepheline-normative and quartz-normative compositions. Specifically, mafic nepheline-normative magmas in the Bear Lodge Mountains may have given rise to two more felsic products: (1) typical syenite to nepheline syenite; and (2) syenite to quartz syenite, and possibly alkali granite (alkali rhyolite). Most igneous rocks outside the core of the Bear Lodge Mountains are average to very iron rich (**Figure 23B**) and are metaluminous (**Figure 23C**).

Of note for rocks in both the core of the range and in the outlying parts of the Bear Lodge Mountains is the presence of minor amounts of alkali-calcic rhyolite (**Figures 23A**), most common in the laccolith of Sundance Mountain, south of Sundance (**Figure 11**). The rhyolite of Sundance Mountain is average to very magnesium rich (**Figure 23B**) and strongly peraluminous (**Figure 23C**), and chemically it resembles other rhyolite bodies near and east of Lead, South Dakota.

All other areas, Wyoming

Nepheline syenite (phonolite and trachyphonolite) at Devils Tower and Missouri Buttes (**Figure 24A**) is chemically similar to nepheline syenite in the Bear Lodge Mountains, but it shows no spatial association with more mafic rocks (Halvorson, 1980). A rather large compositional variation (R1 values from -1,000 to +400) with very little variation of R2 of the nepheline-normative rocks suggests a syenitic parent material. Nepheline syenite from the Black Buttes and from Barlow Canyon, northeast of Devils Tower, have slightly higher R2 values, but this difference may not be significant. Most of these nepheline syenites are iron rich to very iron rich (**Figure 24B**) and metaluminous to mildly peraluminous (**Figure 24C**).

The ring dike complex at Mineral Hill, west of Tinton (Welch, 1974) (**Figure 20**) contains the most mafic rocks in the belt. Although chemical analyses are not available for all the mafic rocks, ijolite and essexite (nephelinite and tephrite) are noteworthy (**Figure 24A**). These mafic rocks are also very iron rich (**Figure 24B**) and plot off the bottom of the alumina saturation diagram (**Figure 24C**).

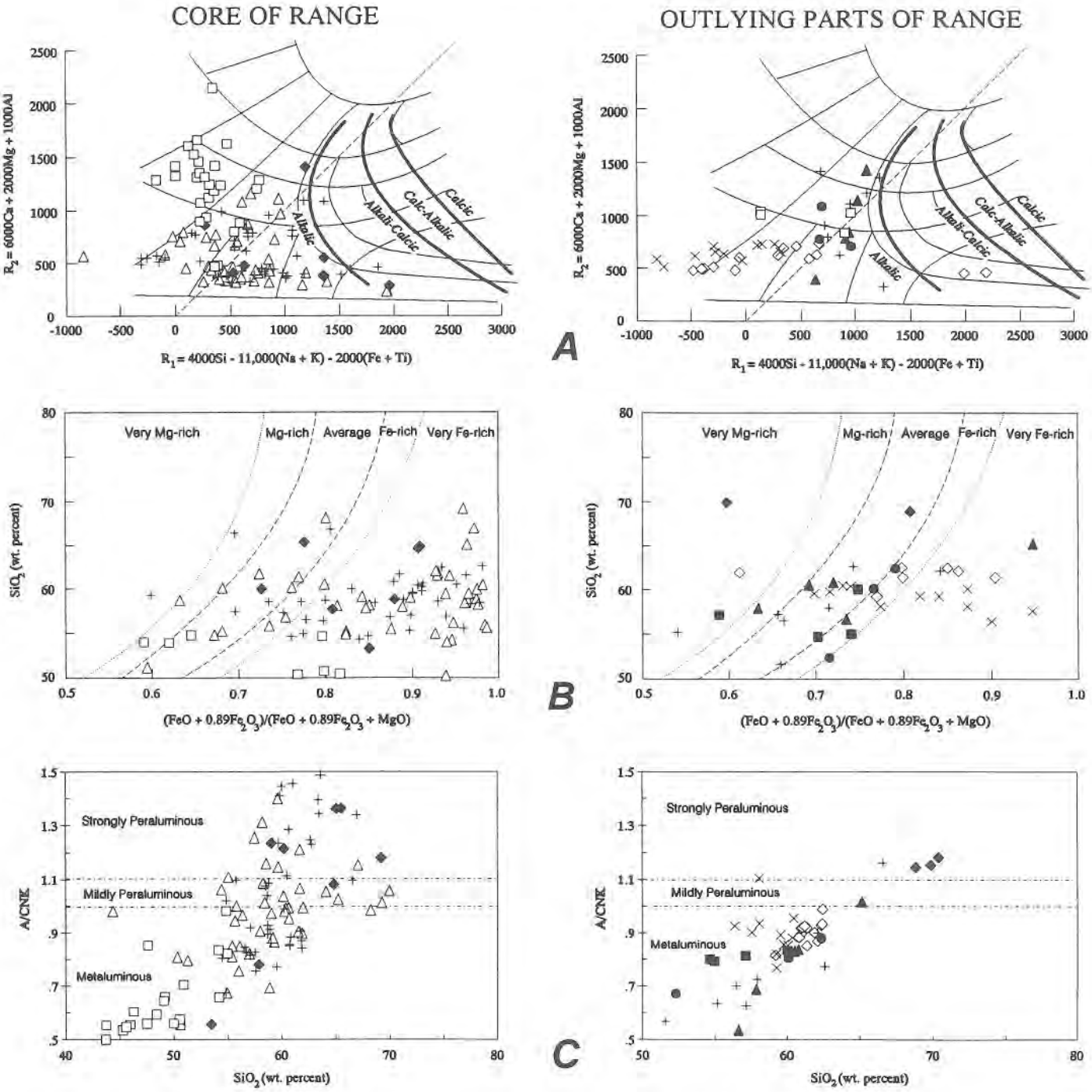

EXPLANATION

- △ Core of range, surface samples
- □ Core of range, drill-hole samples
- ◆ Northwest part of core, surface samples
- + Southeast part of core, surface samples
- ▲ Hershey Creek
- ◇ Jim Wayne Canyon
- + Ladogar Flats
- ■ North Lytle Creek
- × Ragged Top, Reuter Campground
- ◆ Sundance Mountain
- ● South of Lytle Creek

Figure 23. Tertiary intrusive rocks, Bear Lodge Mountains, northwestern Black Hills. A. Major-element (R1-R2) chemical classification (De la Roche and others, 1980). B. Iron variation diagrams (fields of very Mg-rich to very Fe-rich rocks from DeWitt, and others, 1986). Some open squares plot well below the diagram, to as low as 45% SiO_2, and into very iron-rich field. C. Alumina saturation diagrams. A/CNK = molar Al_2O_3/(molar CaO + Na_2O + K_2O). Data from Darton (1905), Jenner (1984), O'Toole (1981), Staatz (1983), White (1980), and Wilkinson (1982).

Samples from a sill and dike complex at Tinton (Ray, 1979) plot in both the alkalic and alkali-calcic fields (**Figure 24A**) and represent compositions approximating syenite and monzodiorite to quartz monzonite, respectively. All rocks are average to iron rich (**Figure 24B**) and range from metaluminous to strongly peraluminous (**Figure 24C**). Whether or not two distinct intrusive suites are represented by the rocks at Tinton is unknown at present.

Phonolitic rocks, South Dakota

Nepheline syenite (phonolite and trachyphonolite) is widespread in the eastern half of the belt in South Dakota, but is most abundant westward from Lead (Irving, 1899; Kirchner 1971). Overall, the slope of a line defined by all values of R1 and R2 for nepheline syenite in South Dakota (**Figure 25A**) is slightly steeper than a similar line defined by such values for nepheline syenite in Wyoming (**Figures 23A**, outlying parts of range, and **Figure 24A**) and may suggest

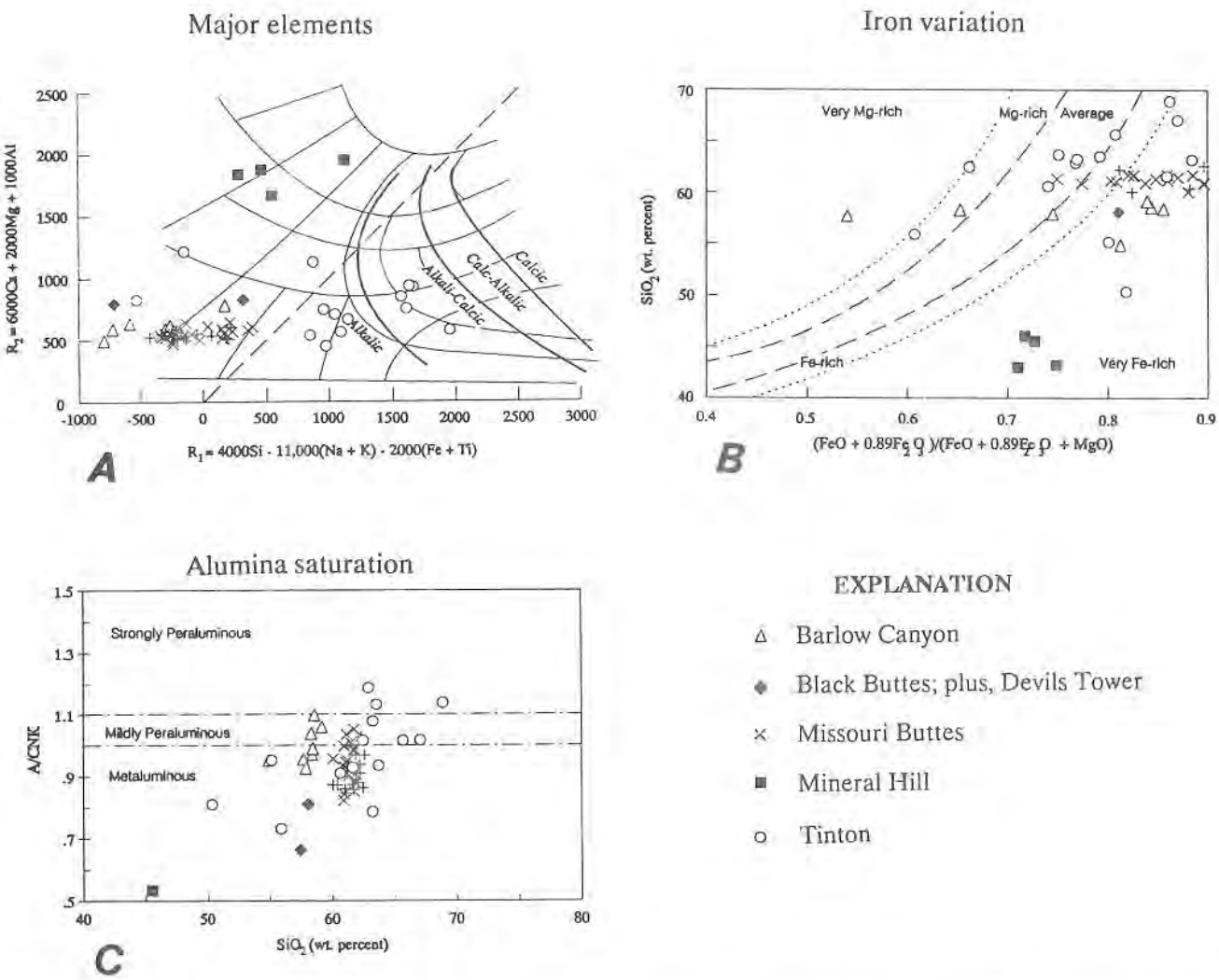

Figure 24. Tertiary intrusive rocks in Wyoming, exclusive of the Bear Lodge Mountains, western to west-central Black Hills. A. Major-element (R1-R2) chemical classification. Field boundaries and rock type names as in Figure 22. B. Iron variation diagram. Fields as in Figure 23B. C. Alumina saturation diagram. Most filled squares plot off the bottom of the diagram. Fields and abbreviations as in Figure 23C. Data from Darton and O'Harra (1907), Fashbaugh (1979), Halvorson (1980), and Ray (1979).

derivation of the phonolitic magmas in the eastern half of the belt from a slightly more mafic parent than those in the western half of the belt. Mafic nepheline syenite (open diamonds, **Figure 25A**) and mafic syenite (closed diamonds, **Figure 25A**) from along Bear Butte Creek and west of Lead, respectively, suggest derivation from magmas at least as mafic as syenodiorite, and probably syenogabbro. All nepheline-normative rocks are average to very iron rich (**Figure 25B**) and follow a fractional crystallization trend of increasingly iron-rich compositions with increase in R1. The nepheline syenites range from metaluminous to mildly peraluminous (**Figure 25C**).

Nonphonolitic rocks, South Dakota

The transition from alkalic rocks near and west of Lead to alkali-calcic rocks near and east of Lead is displayed by nonphonolitic rocks in the eastern half of the belt (**Figure 26A**). The Cutting stock, west of Lead, contains both alkalic syenite and quartz syenite (trachyte and quartz trachyte) and alkali-calcic granite and alkali granite (rhyolite and alkali rhyolite) as shown by the solid diamonds in **Figure 26A**. These rocks are very iron rich (**Figure 26B**) and metaluminous (**Figure 26C**) in the Cutting stock. Similarly, both alkalic quartz syenite (quartz tra-

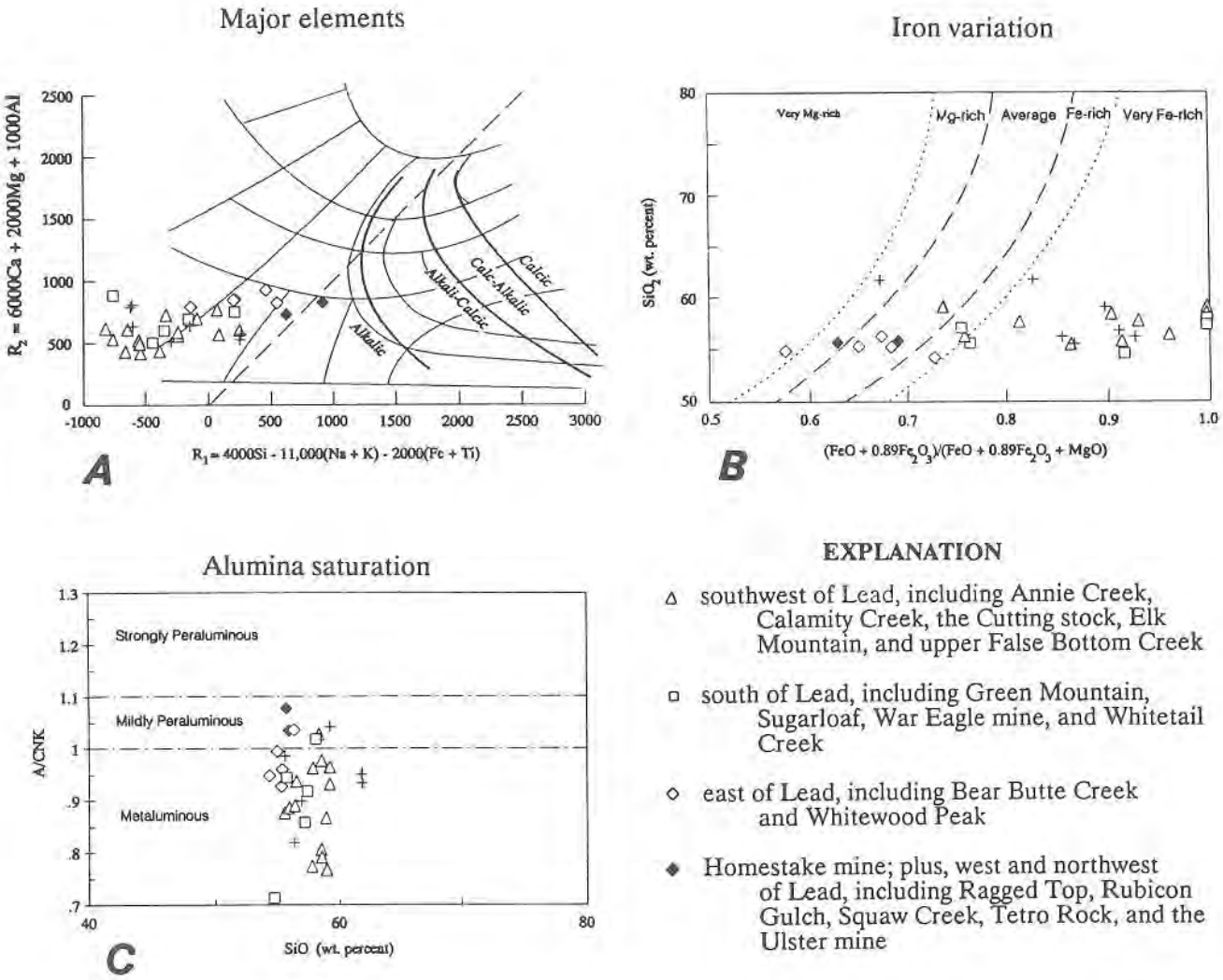

Figure 25. Phonolitic Tertiary intrusive rocks in South Dakota, central to eastern Black Hills. A. Major-element classification. Field boundaries and rock type names as in Figure 22. B. Iron variation diagram. Fields as in Figure 23B. C. Alumina saturation diagram. Fields and abbreviations as in Figure 23C. Data from Boyd (1975), Grunwald (1970), Irving (1899), Irving and Emmons (1904), Kirchner (1971), Larsen (1977), and Parkhill (1976).

chyte) and alkali-calcic granite (rhyolite) are exposed at Whitewood Peak, 1 mi east of Lead (open boxes and solid boxes, **Figure 26A**). Interestingly, these rocks at Whitewood Peak are very magnesium rich; many samples plot off the left side of the iron variation diagram (**Figure 26B**). The strongly peraluminous nature of the alkali-calcic granite (rhyolite) (**Figure 26C**) does not appear to be related to the magnesium enrichment, as alkalic granite is also strongly peraluminous to mildly peraluminous. Alkali-calcic rhyolite in the Homestake mine (Noble, 1948) ranges from normal rhyolite (solid circle, **Figure 26A**) to high-K rhyolite (open circle, **Figure 26A**); both varieties are predominantly very magnesium rich (**Figure 26B**) and their magnesium-rich nature is independent of alumina saturation (**Figure 26C**). East of the longitude of Whitewood Peak in the Galena and Bear Butte areas, most rocks are alkali-calcic granite (rhyolite).

Two compositional groups having different alkalinities are also recognized near Galena (Grunwald, 1970), where alkalic syenodiorite (trachyandesite) to quartz syenite (quartz trachyte) crops out in sill and dike complexes (open diamonds and crosses, **Figure 26A**), and alkali-calcic granite (rhyolite) is

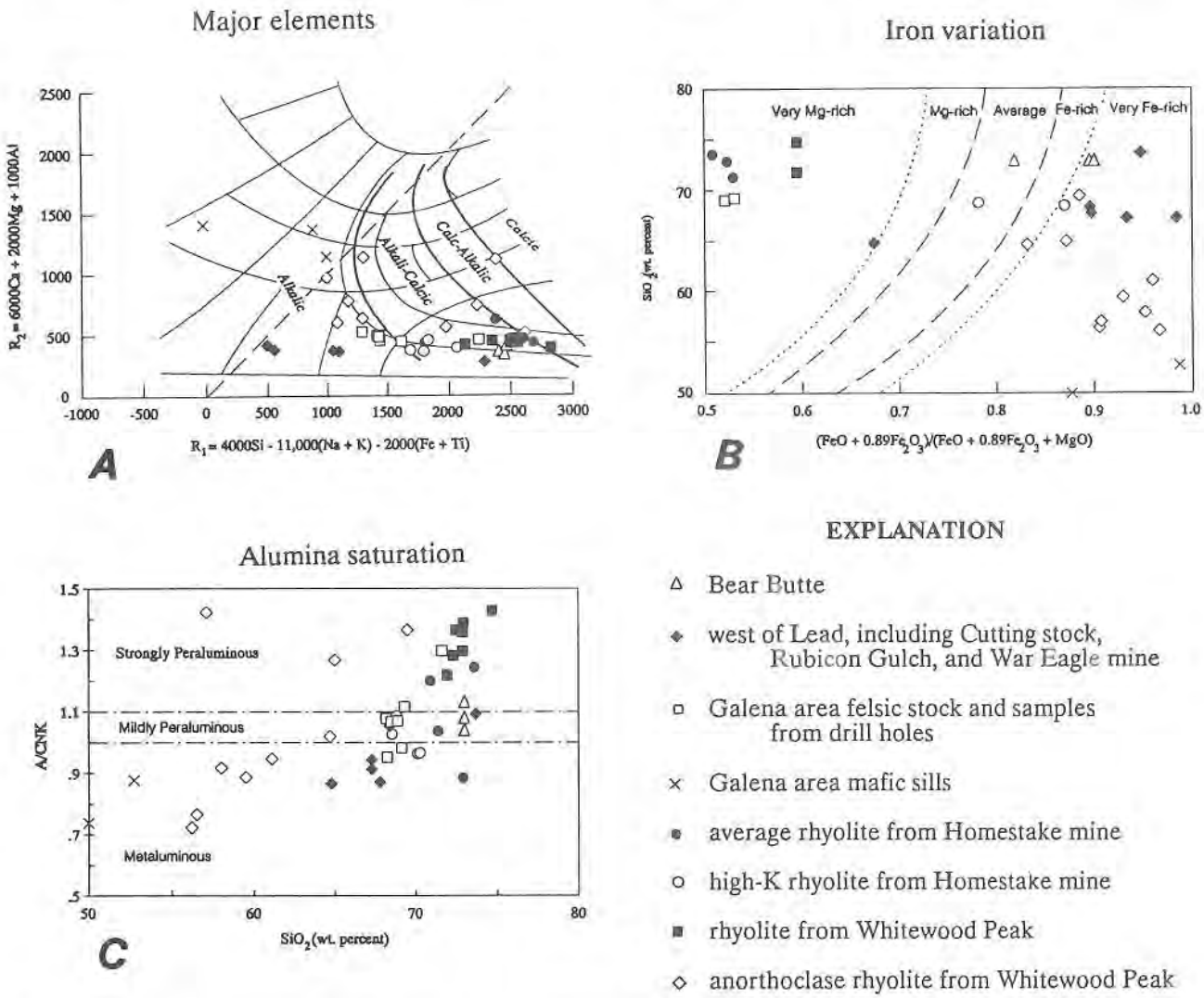

Figure 26. Nonphonolitic Tertiary intrusive rocks in South Dakota, central to eastern Black Hills. A. Major-element classification. Field boundaries and rock type names as in Figure 22. B. Iron variation diagram. Fields as in Figure 23B. Many open and closed boxes plot off the diagram to the left, as do many open and closed circles. C. Alumina saturation diagram. Fields and abbreviations as in Figure 23C. Data from Boyd (1975), DeWitt (1973), Grunwald (1970), Irving (1899), Irving and Emmons (1904), Larsen (1977), Noble (1948), and Parkhill (1976).

present within small stocks (open diamonds, **Figure 26A**). The trachyandesite and quartz trachyte are very iron rich (**Figure 26B**) and metaluminous where not altered (**Figure 26C**). The rhyolite is iron rich and mildly peraluminous where fresh, but strongly peraluminous where hydrothermally altered (**Figure 26C**). Alkali-calcic granite (rhyolite) similar in composition to the laccolith at Sundance Mountain on the far western end of the belt in Wyoming is exposed at Bear Butte at the far eastern end of the belt in South Dakota (DeWitt, 1973). The rhyolite is average to very iron rich (**Figure 26B**) and mildly peraluminous (**Figure 26C**).

Minor-element and isotope geochemistry

Published trace-element data for the Paleocene-Eocene igneous rocks of the Black Hills are limited, but indicate that nepheline normative and syenitic rocks are enriched in many distinctive elements. Phonolites commonly are enriched in strontium (Sr > 2,000 ppm), barium (Ba > 2,000 ppm), niobium (Nb > 50 ppm), zirconium (Zr > 400 ppm), and light rare-earth elements as shown by Olson (1976), Larsen (1977), Parkhill (1976), and Shearer (1990). Trachytes are enriched in barium (Ba > 2,000 ppm), rubidium (Rb > 300 ppm), thorium (Th > 70 ppm), zirconium (Zr > 400 ppm), hafnium (Hf > 10 ppm), strontium (Sr > 1,500 ppm), and niobium (Nb > 40 ppm) and light rare-earth elements as shown by Larsen (1977), Parkhill (1976), Boyd (1975), and Shearer (1990). Quartz-normative rocks, especially rhyolite, do not exhibit these high concentrations of rubidium, zirconium, strontium, and thorium, but are surprisingly barium rich (Ba > 1,000 to 1,700 ppm) as shown by Boyd (1975) and Larsen (1977) and are enriched in the light rare-earth elements (Shearer, 1990).

Olson (1976) reported low values of initial $^{87}Sr/^{86}Sr$ (0.7048 to 0.7054) and Rb/Sr (0.044 to 0.188) for phonolite in the northern Black Hills and interpreted the ratios to indicate a noncontaminated mantle source in the late stage of differentiation from a parent alkali basalt. Shearer (1990) supported this concept of derivation from an "enriched" mantle for the trachyte-phonolite suite based on the preferential enrichment of incompatible elements in phonolite and trachyte [rare earth elements (REE), Ba, Zr], the agreement of Sr and Pb isotopic data (Bientama and Montgomery, 1986), and the association of carbonatite, rocks with carbonatitic affinities, and trachyte. We extend the cogenetic nature of the phonolite-trachyte suite to include the fractional crystallization of syenogabbro to syenodiorite, syenite (trachyte), nepheline syenite (phonolite), and quartz syenite (quartz trachyte) as discussed above, thereby eliminating one of the four evolutionary trends suggested by Shearer (1990). Interestingly, the mafic rocks at Mineral Hill (**Figure 24A**) fall well off this fractional crystallization path, and may represent yet another variant. Based on a comparison with the experimentally derived system for the analcime-liquid stability field, Halvorsen (1980) interpreted that the feldspathoid-bearing alkali trachyte and analcime phonolite at Devils Tower and Missouri Buttes was derived at depths of 18 to 43 km and temperatures of 600 to 640°C and was propelled to the surface by the pressure of contained H_2O and CO_2. This maximum depth is approximately equal to the crustal thickness in northeastern Wyoming and may represent either the source depth or a transitory stopping point of the magma during ascent.

For rhyolite in the Deadwood-Lead area, Beintema and Montgomery (1986) interpreted initial $^{87}Sr/^{86}Sr$ ratios (0.7063 to 0.7101) and a wide range of Pb and Sr isotopic values to indicate crustal contamination of phonolitic magma. However, contamination of a phonolitic magma with variable amounts of average deep continental crust (calc-alkalic granodiorite) will yield a quartz monzonitic mixture, not a rhyolite. Quartz monzonite (quartz latite) is unknown in the Black Hills (**Figures 22, 23A, 24A, 25A, 26A**), except for very minor outcrops in the Tinton area. Also because we do not know which rhyolite bodies (i.e., alkalic versus alkali-calcic) in the Deadwood-Lead area were analyzed by Bientema and Montgomery (1986), we cannot tell whether the low $^{87}Sr/^{86}Sr$ values of 0.7063 are associated with alkalic rocks (syenite and quartz syenite) or alkali-calcic rocks. A more likely model for creation of the alkali-calcic rhyolite suite is by variable degrees of partial melting of lower crust (Shearer, 1990). Rocks of intermediate composition in the Vanocker laccolithic complex, modeled on the basis of Nd and Sm values by Farmer and DePaulo (1984), suggest mixing of a depleted mantle source and Precambrian crust.

We consolidate the four magmatic trends suggested by Shearer (1990) to two magmatic trends (**Figure 27**). Reservoir 1 is envisioned to be enriched mantle, which partially melts to form a parent alkali

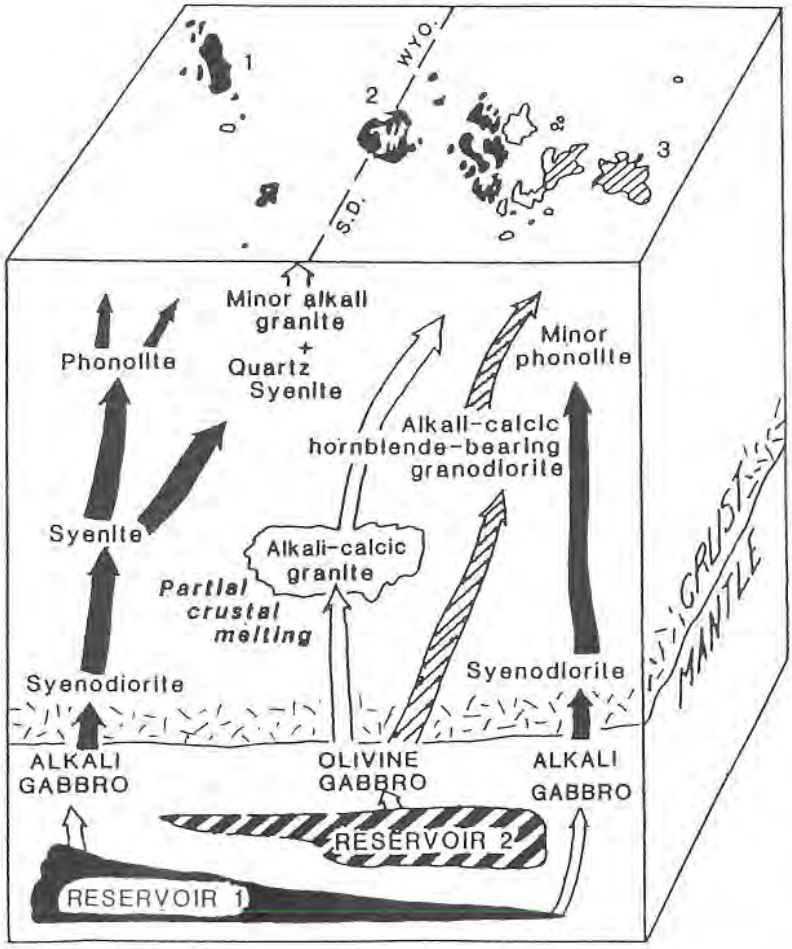

Figure 27. Block diagram modified from Shearer (1990), illustrating the distribution of Tertiary igneous centers and related rock types across the central Black Hills uplift and the two possible magma sources relative to the crust and mantle. Centers shown in a diagonal pattern are dominated by silica-saturated rocks; those in white are dominated by silica-oversaturated rhyolite and potassium rhyolite; those in black are dominated by alkalic silica-undersaturated rocks. 1 = Bear Lodge igneous complex and dome; 2 = Tinton igneous complex and dome; 3 = Vanocker laccolithic cluster.

gabbro. Fractional crystallization of this gabbro gives rise to the alkalic suite of syenogabbro, syenodiorite, syenite, and nepheline syenite, as well as the minor amount of quartz syenite and alkali-calcic alkali granite formed by low-pressure fractional crystallization and crossing of the thermal divide between nepheline normative and quartz normative magmas. This reservoir is present beneath all the northern Black Hills igneous province, as indicated by alkalic rocks as far east as Galena.

Reservoir 2 is envisioned as non-enriched mantle, which partially melts to form olivine gabbro. Some of this gabbro intrudes the base of the crust, partially melts it, and forms the bulk of the alkali-calcic rhyolite that is common east of Lead. Some of Reservoir 2 must be present in the far western part of the belt to account for the alkali-calcic rhyolite at Sundance Mountain, south of the Bear Lodge Mountains. The olivine gabbro also fractionally crystallizes within the crust to give rise to the hornblende-bearing granodiorite in the Vanocker laccolithic complex. Carbonatite formation and associated potassic metasomatism are viewed as cogenetic hydrothermal activity associated with fractional crystallization of Reservoir 1. Reservoir 2 may not be necessary if the alkali gabbro of Reservoir 1 were to partially melt small amounts of the crust throughout the belt, thereby giving rise to the alkali-calcic rhyolite and the hornblende-bearing granodiorite of the Vanocker laccolithic complex. Models of the development of the Eocene-Paleocene igneous suite are obviously in their initial stages.

Because erosion levels across the Black Hills uplift span Precambrian basement to Cretaceous, a view of the igneous bodies over a vertical range of almost 4,000 feet is presented. Throughout this vertical range, margins of the bodies are generally parallel to bedding or schistosity. Stocks, dikes, and ring dikes are common within the Precambrian basement; where abundant plutons form composite bodies they swell the basement into the large Bear Lodge, Tinton, and Deadwood-Lead domes (**Figure 20**). Such forceful emplacement was first documented by Noble (1952b) for rhyolite dikes in the Homestake mine and a similar origin extrapolated to the domes. These rhyolite dikes and the sills they feed are seen in the incomparable exposures of the Homestake Mine open cut in Lead. Numerous similar examples, such as that shown by Jaggar (1901) from the Bald Mountain area southwest of Lead (**Figure 28**), are exposed in the Deadwood-Lead region.

Sills and laccoliths are most abundant in the subhorizontal, lower Paleozoic section, although stocks

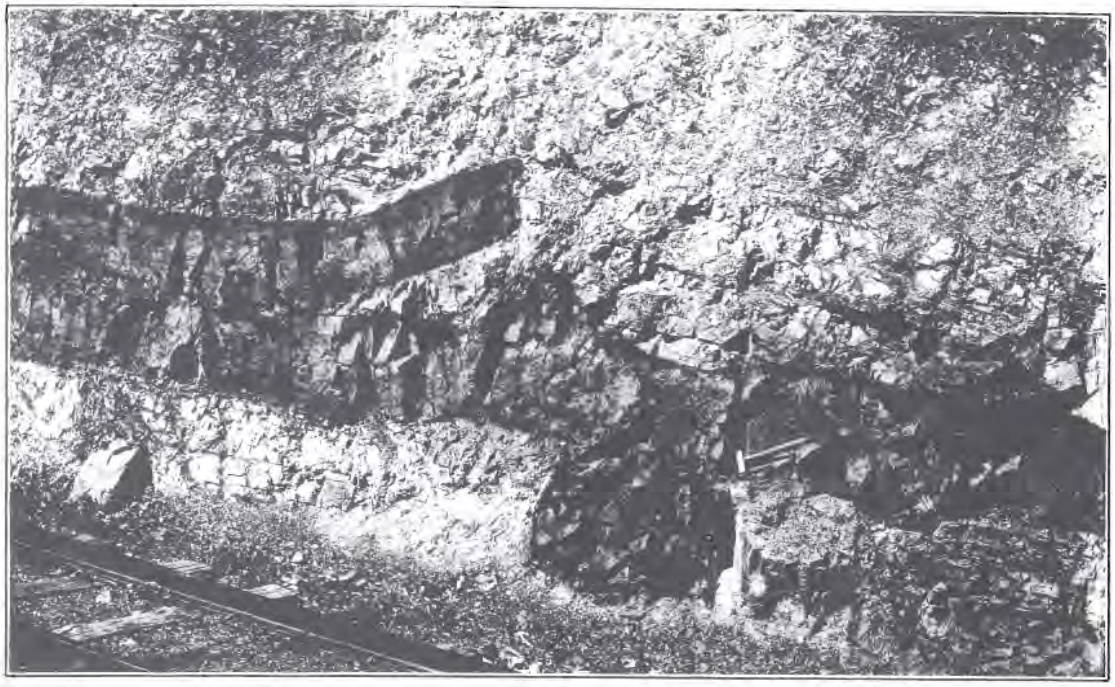

Figure 28. Plate XXXIV from Jaggar (1901), showing a dike-to-sill transition (dark colored rocks) in Cambrian Deadwood Formation in roadcuts of the Fremont Railroad (long defunct) on Bald Mountain, approximately 4 mi southwest of Lead, South Dakota.

and diatremes reach into the Cretaceous. The generalized geologic map of **Figure 20** outlines the location of several such features, including the Tinton and Deadwood-Lead domes and the Theodore Roosevelt and Vanocker laccolithic clusters. Single laccoliths have diameters of roughly 1 mile, whereas laccolithic clusters are up to 6 miles in diameter (**Figure 20**).

The first detailed study of these bodies was by Jaggar (1901), who mapped and described them as laccoliths and in whose publication is a section by Ernest Howe on experiments simulating laccolithic emplacement. Howe placed numerous layers of sand, plaster, and dust of coal and marble onto a 3-foot square table and from an underlying hydraulic piston injected them with a red-colored, liquid, plaster of Paris *...with about the consistency of cream.* Although this experiment was not balanced for time, scale, rheology, etc., it was the first to attempt to match field observations about laccoliths with laboratory models. Howe was able to duplicate enough of the attributes of the field examples to predict that the size and shape of such laccoliths vary depending upon the viscosity of the magma and the rigidity and thickness of the overlying strata and to establish several generalizations concerning such relationships.

An additional aspect of these igneous complexes is the fact that carbonatitic rocks are present and that diatremes and breccia pipes indicative of high volatile content are widespread. Carbonatites are present in the Bear Lodge Mountains, largely within breccia pipes (Staatz, 1983; Jenner, 1989), and in the Tinton dome (Welch, 1974). Diatremes, such as those at Devils Tower, Missouri Buttes, and the Tomahawk area south of Lead, reach maximum diameters of 1 mile, are cored by tuffs, and contain abundant xenoliths from both higher and lower in the stratigraphic section (Lisenbee and Roggenthen, 1990). At Tomahawk, which is exposed at the level of the Precambrian basement, clasts of fossiliferous Upper Cretaceous Mowry Shale (Runner, 1957) indicate that at 54 Ma, the time of rhyolitic activity here (Redden and others, 1983), the core of the Black Hills was covered with at least 3,300 ft of Phanerozoic strata, a fact useful in reconstructing the erosional history of the rising uplift.

A fundamental question in regard to this igneous activity is whether plutonism and volcanism are related to tectonic processes specifically associated with the uplift or with a larger-scale event. The answer appears to be some of both.

Laramide magmatism is uncommon in the Wyoming Rocky Mountains (excluding the calc-alkalic event in the Yellowstone region), but plutonic rocks similar to those of the Black Hills are present to the west in Montana (Little Belt, Big Snowy, and Judith Mountains, for example) along the continuation of the structural high that includes the Black Hills uplift. Similar rocks are also exposed to the north of this zone in the Bearpaw Mountains and Little Rocky Mountains. Apparently, magmatism in the Black Hills is temporally and spatially part of a larger scheme.

Within the uplift itself the west-northwest trend of the belt of plutons is similar to the trend of several wrench faults (Nye-Bowler, Cat Creek) in Montana (Dobbin and Erdmann, 1955). Also, the plutons lie along a zone that offsets major magnetic and gravity contours, which Roggenthen and Lisenbee (1986) interpreted to represent an offset in the boundary between the Wyoming Archean province and the Early Proterozoic Trans-Hudson province (**Figure 5**). This deep basement structure is envisioned as a zone of weakness that facilitated the rise of buoyant magma to the upper crust, where it followed the north-northwest-striking fabric of the Precambrian rocks.

Paleogene stripping and Neogene exhumation of the uplift

The sedimentary cover has been removed twice from the Black Hills uplift. The first episode accompanied the Laramide orogeny and provided the source of syntectonic sediment shed into the Powder River and Williston basins described above. The uplift was then covered by post-tectonic White River Group clastic rocks, which were themselves generally stripped away in the Pliocene(?).

Removal of Mesozoic strata must have begun with the initial phase of uplift at approximately 64 Ma or 65.5 Ma. Two techniques reveal information about the rate at which these strata were stripped away. The first considers the arrival time in the basin of various types and ages of rocks stripped from the adjoining uplifts. Phyllite grains in sandstone of the upper part of the Tongue River Member of the Fort Union Formation near the Recluse oil field south of the Montana-Wyoming border in the Powder River Basin, lead Merin and Lindholm (1986) to conclude that Precambrian rocks were breached on some surrounding uplift by late Paleocene time, approximately 58 Ma. Because low-grade metamorphic rocks are more common in the northern and central Black Hills than in other uplifts, Merin and Lindholm concluded that this uplift was the most likely source of the phyllite. Seeland (1988) also suggested a late Paleocene age (58 Ma?) for unroofing of the Precambrian core of the Black Hills, based on the presence of scarce, coarse-grained arkosic sandstones in the Tongue River Member east of Wright, Wyoming, in an area where Pierce and Johnson (1988) reported metamorphic rock fragments in the Tongue River. If these fragments are indeed from the Black Hills, and not from other uplifts marginal to the southern end of the Powder River Basin, approximately 7,000 ft of Phanerozoic rock would have to have been removed in 6 to 7.5 million years. This is a high rate of erosion, averaging 11 to 14 inches per 1,000 years. Seeland and others (1988), however, noted that the arkosic sands were more likely derived from the Laramie Mountains at the southern margin of the Powder River Basin. Therefore, the timing of exposure of the Precambrian core of the Black Hills is still unresolved.

The interpretation that all Phanerozoic strata were removed from the Black Hills uplift by the end of the Paleocene (58 Ma) is at odds with the presence of fossiliferous Upper Cretaceous Mowry Shale (Runner, 1957) in the 54-Ma (Redden and others, 1983) Tomahawk diatreme south of Deadwood (Lisenbee and Roggenthen, 1990). These shale fragments imply that strata of Cretaceous age remained on the uplift and that only about 4,000 to 5,000 ft of post-Mowry sandstone and shale had been removed at 54 Ma. Limiting values for the erosion rate vary with the interpretation of the time of initial uplift. If uplift began during deposition of the Tullock Member (approximately 65.5 Ma) of the Fort Union Formation in the Powder River Basin (Lewis and Hotchkiss, 1981), then the erosion rate was 5 to 6 inches per 1,000 years; if uplift began at approximately 64 Ma during Lebo Member deposition (Seeland, 1988), the rate would be 4 to 5 inches per 1,000 years. The approximately 3,300 ft of Mesozoic and Paleozoic sandstone, shale, and limestone remaining on the uplift at 54 Ma were removed in the 17 Ma period before deposition of the post-tectonic White River Group beginning at 37 Ma.

This implies a minimum stripping rate of 2.5 inches per 1,000 years.

The depositional thickness of White River Group strata across the uplift is unknown, but exhumation of the Black Hills from beneath this dominantly Oligocene cover probably occurred in the Plio-Pleistocene during a period of epeirogenic uplift (Lisenbee, 1988). Direct evidence of this timing is unclear on the uplift, but is supported by nearby regional studies. Love (1960) described Pliocene excavation of the filled Laramide basins in Wyoming and the superposition of rivers across mountains and basins during this time. From studies of the Tertiary strata east of the Black Hills, Harkson and Macdonald (1969) concluded that western South Dakota had been uplifted as much as 1,200 ft in the last 4.5 Ma. From stratigraphic relationships along the Chadron arch of Nebraska, Swinehart and others (1985) defined a period of regional uplift at about 5 Ma that caused downcutting of canyons 1,000 ft below the Miocene Ogallala Group present on adjoining tablelands. Trimble (1980) stated that post-Ogallala epeirogenic uplift affected all of the Great Plains region with a differential rise of as much as 7,000 ft on the west and 1,000 ft on the east. Uplift relative to base level produced increased gradients on all streams flowing within the area and concommitantly increased their erosional capacity. Prior to this period of erosion, Devils Tower may have stood only 150 ft above the surrounding plain. The spheroidal weathering and horizontal fracturing of the upper part of the Tower is above the restored level of the sandstone of the Fall River Formation (Halvorsen, 1980). Erosion from this level to the present Belle Fourche River at the foot of the tower would be a total of 1,125 ft, indicating an average of 2.7 inches per 1,000 years during the past 5 Ma.

Summary of geologic evolution

Before a final discussion of possible causes of formation of the Black Hills uplift, we will summarize the geologic characteristics described in the preceding sections; for it is from these characteristics that any explanation of origin must be drawn.

As read in the sedimentary record, the "book of the basin," no uplift was present near the end of the Cretaceous (68 to 70 Ma). Marine conditions of the great Western Interior Cretaceous Seaway, the foredeep basin of the Wyoming fold-and-thrust belt, and the growing foreland uplifts to the west, came to a close as the shoreline retreated southeastward across the area of the future Black Hills uplift.

Paleocene and Eocene strata within the adjoining Powder River Basin show an input of sediments from the Black Hills area that is interpreted to indicate an initial phase of uplift either in the early Paleocene (Lewis and Hotchkiss, 1981; Flores and Etheridge, 1985) at approximately 65.5 Ma or, more likely, in late early Paleocene (Seeland, 1988; Seeland and others 1988) at approximately 64 Ma. The continued supply of detritus was enhanced by a second phase of tectonic activity in latest Paleocene and Eocene (Kent, 1984; Seeland, 1988). The presence of the nearby Cannonball Sea in early Paleocene time indicates that the uplift was rising above a region of low elevation.

By late Eocene Chadronian time (37 Ma), continental deposits of the White River Group blanketed the quiescent uplift and deposition continued into the Oligocene. Paleo-valleys containing these deposits show that the topographic form of the present Black Hills was essentially carved before deposition of these strata. The surface elevation in the Black Hills at the end of the period of uplift, as well as that of the Oligocene plains surrounding the foothills, is not known.

The growing uplift presented the general character of a large, doubly plunging, northwest-trending anticline, but there is a contrast in styles on the two flanks. Monoclines on the west disrupt the gentle homoclinal dip of strata and, presumably, the basement across the basin-to-uplift margin. On the east, the basement appears folded across a 15-mi-wide transition zone between the Laramide foreland and the tectonically quiescent Interior Lowlands province. The location of the uplift coincides with part of the east margin of the Wyoming Archean province at its boundary with the Trans-Hudson province. This boundary may coincide with the Fanny Peak monocline or it may be transitional in the subsurface beneath the uplift.

The 50 to 62 Ma, west-northwest-trending belt of syntectonic and late tectonic, alkalic-calcic to alkalic stocks, dikes, laccoliths, and diatremes that represent the easternmost Laramide magmatic activity are similar to contemporaneous rocks in Montana and Wyoming, which are associated with other Laramide basement uplifts. On the Black Hills uplift, these igneous rocks appear to lie above a major zone of offset in the transition between Archean and Early Proterozoic basement and to have been fed from parental reservoirs in both the mantle and lower crust.

Possible models of formation of the Black Hills uplift

Tectonic interpretation at the regional scale must explain both the formation of a specific uplift and its place within the larger framework of Laramide evolution. The factors to consider are numerous, but four of paramount significance are: timing, structural style, orientation of the uplift, and causative forces. In the case of the Black Hills uplift, these factors involve a Paleocene-Eocene uplift of northwest trend, in which the basement is interpreted to have reacted to regional stresses by both large-scale faulting and folding. The forces involved must have been transmitted through the lithosphere, either horizontally from distant plate margins or vertically.

Five potential methods of elevating the crust to form the Black Hills uplift are shown diagrammatically in **Figure 29**. A brief outline of each model will be given followed by an overview of their relative compatibility with the known geology. Model A follows the suggestion of Berg (1981) that the uplift rose due to a push by a rising batholith. Minor igneous intrusions of the correct age are present across the northern part of the uplift.

Model B suggests that during regional horizontal compression the relatively more ductile metamorphic rocks of the early Proterozoic Trans-Hudson province acted as a shock absorber against the blunt margin of a thick, granitic, Wyoming Archean province.

Models C, D, and E suggest uplift resulting from deep-seated thrust or reverse faulting in which crustal slabs undergo translation, uplift, and rotation in the hanging wall. In case C, the dip of the west-dipping thrust fault flattens into a detachment in the upper crust. In the region of dip change, the hanging wall is rotated in a fault-propagation-type fold. In such a model, all west-vergent monoclines would result from antithetic back thrusts above the major thrust, although only the sharp monocline (a combination of Fanny Peak and Black Hills monoclines) on the western flank of the uplift is shown in this case. Because strata in both the hanging wall and the footwall have similar dips across the western monocline, the model necessitates that this back thrust have a uniform dip.

Model D also shows a deep-seated thrust, but of a listric or sled-runner type. Lateral translation is accommodated by a combination of imbrication that forms several faults in the upper crust and folding of the latest Proterozoic basement rocks. As in Model C, the west-vergent monoclines result from antithetic back thrusts. An additional advantage of this form of thrust is that the curving fault produces a rotation of the hanging-wall block. Such a rotation would help to explain the gentle west dip on the west flank of the uplift and in the Powder River Basin. DeWitt and others (1986) proposed that the large-scale, west-vergent anticline-syncline couples at the north and south ends of the Black Hills overlie a master, east-dipping thrust fault (Model E), which produced the monoclines on the west side of the Black Hills uplift. In such a model, the arching of the eastern flank of the uplift overlies closely spaced, high-angle reverse faults in the underlying Precambrian basement.

An additional model, not shown in **Figure 29**, involves crustal-scale folding due to shortening. Brittle deformation of the upper crust (faulting and drape folding) would modify the crest of the resulting large anticline. Such folding would be possible if accompanied by ductile flow and shortening within the lower crust or mantle.

None of these models presents a unique solution and each has varying probabilities if reconciled with known geology. In model A, the vertical push and arching would produce extension across the crest of the uplift and should result in structures indicative of such a stress regime. Extensional features have not been identified in the Black Hills, nor does this mechanism explain the near ubiquitous west-facing

nature of the lengthy monoclines that are present. In addition, most other foreland uplifts of similar age, trend, and style lack associated igneous activity.

Although the uplift is approximately along the boundary suggested in model B, there is no evidence of penetrative deformation of the Precambrian basement during the Laramide. The contrast in basement rheology, however, may have helped to localize stresses at this ancient tectonic break and may be significant in explaining the contrasting deformation styles on opposing flanks of the uplift.

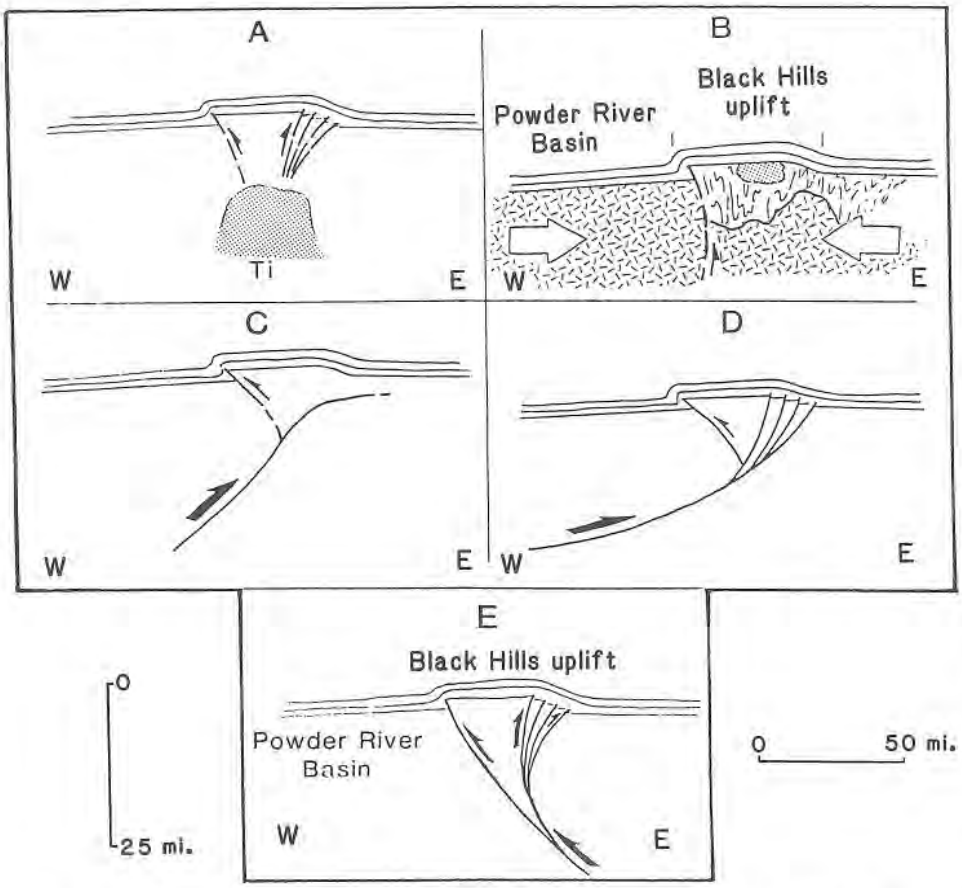

Figure 29. Alternative models for uplift mechanisms of the Black Hills uplift.

A. Uplift due to batholithic push from below. The alkalic intrusions of the northern Black Hills are the only possible surface manifestation.

B. "Accordian" uplift due to horizontal compression that squeezed Proterozoic basement against rigid buttress of the Wyoming Archean province.

C. Uplift due to deep-seated, west-dipping thrust. The eastern flank of metamorphic rocks are rotated in a fault-bend-type fold. The west flank is bounded by a monocline, formed by folding of strata over a back-thrust in the Precambrian basement.

D. Uplift due to a deep-seated, west-dipping thrust. Folding along the eastern margin overlies imbricate stack in the basement. The west flank is bounded by a monocline, as in Model C.

E. Uplift due to a deep-seated, east-dipping thrust or reverse fault. Folding along the eastern margin of the uplift overlies steeply dipping faults with reverse sense of movement at higher levels. The Fanny Peak and Black Hills monoclines along the west margin of the uplift represents the surface manifestation of the major reverse fault.

The thrust models C, D, and E are speculative; no major thrust faults are proven for this uplift, although they are common in others (Bighorn, Beartooth) of similar age and trend, but greater structural relief. Thrust models are consistent with the concept of Laramide compression suggested by numerous authors (Gries, 1983a, 1983b; Chapin and Cather, 1981, 1983; Dickinson and Snyder, 1978), among whom D.L. Blackstone, Jr. (1947, 1980, 1981, 1990) has long been a leading proponent.

Within the framework of timing and space, the Black Hills uplift represents the easternmost major crustal response within the Laramide orogen. The trend of the uplift suggests that maximum compressive stresses acting here during the early Paleocene were oriented east-northeast to west-southwest, compatible with the regional Laramide trend postulated by Gries (1983a and b) and Chapin and Cather (1981, 1983) for this time. Al-

though numerous origins for these forces have been postulated, the final verdict is not at hand. Suggested origins include: (1) a regional-scale left-lateral wrench system, in which the Colorado Plateau moves eastward relative to the Canadian foreland (Sales, 1968); (2) clockwise rotation of the Colorado Plateau northward as a microplate (Hamilton, 1981); (3) northward movement of the Colorado Plateau during a second phase of Laramide activity (Chapin and Cather, 1981, 1983); (4) basal shear between the North American plate and a flat-dipping, subducted Farallon plate (Dickinson and Snyder, 1978); and (5) stresses resulting from the interaction of the opening of the North Atlantic Ocean and the subducting Farallon plate (Gries, 1983b; Chapin and Cather, 1981, 1983).

Because not all Laramide uplifts are synchronous, movement of the Colorado Plateau as a microplate is unlikely, in itself, to explain Laramide deformation. However, some combination of these ideas, involving movement of the Colorado Plateau microplate within a larger plate-tectonic framework, is necessary.

Regional horizontal compression is necessary to produce the crustal shortening indicated by major thrust faults at the margins of many of the Laramide foreland uplifts. The termination of such shortening in central Montana, south of the Canadian foreland, requires a left-lateral wrench component of movement at the northern limit of the Laramide foreland. Wrench zones of this type are linear, en echelon fault systems such as the Nye-Bowler and Cat Creek (Dobbin and Erdmann, 1955).

Of the several models mentioned above, only that of Dickinson and Snyder (1978) includes an explanation of the source of the magma. In their scenario, diapirs of magma derived from a nearly flat-lying subducted slab rise passively through the overlying crust. In the specific case of the north margin of Laramide foreland deformation, we believe that the movement paths may have favored local areas of extension within a wrench system. Also, areas of reduced lithostatic pressure within such crustal-scale fractures may have independently facilitated partial melting of lower crust and upper mantle.

Sources of magma within both the crust and mantle for the plutons in the Black Hills uplift, as postulated in this paper, do not distinguish between the mechanisms of flat subduction and deep fracturing, and do not require a subducted plate, only a source of heat. Alternatives to melting of a subducted plate were proposed by Dudás (1991) and O'Brien and others (1991) for igneous rocks in the Crazy Mountains and the Highwood Mountains, respectively. These areas in Montana lie along the westward continuation of the structurally elevated zone containing the Black Hills uplift. Dudás (1991) noted possible advection of a thermal anomaly by mantle upwelling and O'Brien and others (1991) proposed a combination of fluid derived sequentially from the descending slab, the overlying asthenospheric mantle, and the mantle keel of the Wyoming Archean province. Distinction of flat subduction as opposed to intraplate tectonic movements for generation of appropriate stresses and of the magma is in a preliminary stage and awaits much further clarification.

Acknowledgments

Critical reviews by D. Seeland, R. Tysdal, J. Lillegraven, F. Karner, A.W. Snoke, and S.M. Roberts added to both the content and the clarity of the final manuscript; and we are indebted to them for their assistance.

References cited

Ayers, W.B., Jr., 1986, Lacustrine and fluvial-deltaic depositional systems, Fort Union Formation (Paleocene), Powder River Basin, Wyoming and Montana: American Association of Petroleum Geologists, v. 70, p. 1651-1673.

Beck, J.A., Jr., 1976, Geology of the Lexington Hill-Pillar Peak area, Lawrence County, South Dakota [M.S. thesis]: Rapid City, South Dakota School of Mines and Technology, 102 p.

Beintema, C., and Montgomery, C.W., 1986, Petrogenesis of Tertiary volcanics of the Black Hills inferred from isotopic data: Geological Society of America Abstracts with Programs, v. 18, p. 341.

Berg, R.R., 1962, Mountain flank thrusting in Rocky Mountain foreland, Wyoming and Colorado: American Association of Petroleum Geologists Bulletin, v. 46, p. 2019-2032.

_____ 1981, Review of thrusting in the Wyoming foreland: University of Wyoming Contributions to Geology, v. 19, p. 93-104.

Black, R.A., and Roller, J.C., 1961, Relationship between gravity and structures of part of the western flank of the Black Hills, South Dakota and Wyoming: U.S. Geological Survey Professional Paper 424-C, p. 260-262.

Blackstone, D.L., Jr., 1947, Montana and Wyoming examples of overthrusting in relation to petroleum accumulation [abstract]: Oil and Gas Journal, v. 45, no. 47, p. 116.

_____ 1980, Foreland deformation: compression as a cause: University of Wyoming Contributions to Geology, v. 18, p. 83-101.

_____ 1981, Compression as an agent in deformation of the east-central flank of the Bighorn Mountains, Sheridan and Johnson Counties, Wyoming: University of Wyoming Contributions to Geology, v. 19, p. 105-122.

_____ 1990, Rocky Mountain foreland structure exemplified by the Owl Creek Mountains, Bridger Range and Casper arch, central Wyoming, *in* Specht, R.W., editor, Wyoming sedimentation and tectonics: Wyoming Geological Association 41st Annual Field Conference Guidebook, p. 151-166.

Boyd, T.M., 1975, Bedrock geology of the Whitewood Peak area, Lawrence County, South Dakota [M.S. thesis]: Toledo, Ohio, University of Toledo, 89 p.

Brown, W.G., 1984, Basement involved tectonics foreland areas: American Association of Petroleum Geologists Continuing Education Course Note Series #26, 92 p.

Buswell, M., 1982, Subsurface geology of the Oshoto uranium deposit, Crook County, Wyoming [M.S. Thesis]: Rapid City, South Dakota School of Mines and Technology, 84 p.

Chapin, C.E., and Cather, S.M., 1981, Eocene tectonics and sedimentation in the Colorado Plateau—Rocky Mountain area, *in* Dickinson, W.R., and Payne, W.D., editors, Relations of tectonics to ore deposits in the southern Cordillera: Arizona Geological Society Digest, v. XIV, p. 173-198.

_____ 1983, Eocene tectonics and sedimentation in the Colorado Plateau—Rocky Mountain area, *in* Lowell, J.D., editor, Rocky Mountain foreland basins and uplifts: Denver, Colorado, Rocky Mountain Association of Geologists, p. 33-56.

Cherven, V.B., and Jacob, A.R., 1985, Evolution of Paleogene depositional systems, Williston Basin, in response to global sea level changes, *in* Flores, R.M., and Kaplan, S.S., editors, Cenozoic paleogeography of the west-central United States, Rocky Mountain Paleogeography Symposium 3: Society of Economic Paleontologists and Mineralogists, Rocky Mountain Section, p. 127-170.

Clark, J., 1975, Controls of sedimentation and provenance of sediments in the Oligocene of the Central Rocky Mountains, *in* Curtis, B.F., editor, Cenozoic history of the southern Rocky Mountains: Geological Society of America Memoir 144, p. 95-117.

Clark, J., Beerbower, J.R., and Kietzke, K.K., 1967, Oligocene sedimentation, stratigraphy, paleogeography, and paleoclimatology in the Big Badlands of South Dakota: Fieldiana—Geology Memoir, v. 5, 1158 p.

Connolly, J.P., 1927, The Tertiary mineralization of the northern Black Hills: South Dakota School of Mines and Technology Bulletin 15, 130 p.

Connolly, J.P., and O'Harra, C.C., 1929, The mineral wealth of the Black Hills: South Dakota School of Mines Bulletin 16, 418 p.

Connor, C.W., 1988, The Lance Formation, Powder River Basin and beyond: Geological Society of America Abstracts with Programs, v. 20, p. 80.

Curry, W.H., III, 1971, Laramide structural history of the Powder River Basin, Wyoming, *in* Renfro, A.R., Madison, L.V., Jarre, G.A., and Bradley, W.A., editors, Symposium on Wyoming tectonics and their economic significance: Wyoming Geological Association 28th Annual Field Conference Guidebook, p. 49-60.

Dahlstrom, C.D.A., 1970, Structural geology of the eastern margin of the Canadian Rocky Mountains: Bulletin of Canadian Petroleum Geology, v. 18, p. 332-406.

Darton, N.H., 1901, Preliminary description of the geology and water resources of the southern half of the Black Hills and adjoining regions in South Dakota and Wyoming: U.S. Geological Survey Twenty-first Annual Report, Part 4, p. 489-599.

_____ 1902, Oelrichs (quadrangle), South Dakota: U.S. Geological Survey Geologic Atlas of the United States, Folio 85, 6 p.

_____ 1904 Newcastle (quadrangle), Wyoming-South Dakota: U.S. Geological Survey Geologic Atlas of the United States, Folio 107, 9 p.

_____ 1919, Newell (quadrangle), South Dakota: U.S. Geological Survey Geologic Atlas of the United States, Folio 209, 7 p.

Darton, N.H., and O'Hara, C.C., 1905a, Sundance (quadrangle), Wyoming-South Dakota: U.S. Geological Survey Geologic Atlas of the United States, Folio 127, 12 p.

_____ 1905b, Aladdin (quadrangle), Wyoming-South Dakota-Montana: U.S. Geological Survey Geologic Atlas of the United States, Folio 128, 8 p.

_____ 1907, Devils Tower (quadrangle), Wyoming: U.S. Geological Survey Geologic Atlas of the United States, Folio 150, 10 p.

_____ 1909, Belle Fourche (quadrangle), South Dakota: U.S. Geological Survey Geologic Atlas of the United States, Folio 164, 9 p.

Darton, N.H., and Paige, S., 1925, Central Black Hills (quad-rangle), South Dakota: U.S. Geological Survey Geologic Atlas of the United States, Folio 219, 34 p.

Darton, N.H., and Smith, W.S.T., 1904, Edgemont (quadrangle), South Dakota: U.S. Geological Survey Geologic Atlas of the United States, Folio 108, 10 p.

De la Roche, E., Leterrier, J., Grandclaude, P., and Marchal, M., 1980, A classification of volcanic and plutonic rocks using R1-R2 diagram and major-element analyses—its relationships with current nomenclature: Chemical Geology, v. 29, p. 183-210.

Denson, N.M., and Gill, J.R., 1965, Uranium-bearing lignite and carbonaceous shale in the southwestern part of the Williston Basin—a regional study: U.S. Geological Survey Professional Paper 473, 75 p.

DeWitt, E., 1973, The geology of the Bear Butte area, Fort Meade Quadrangle, South Dakota [B.S. thesis]: Rapid City, South Dakota School of Mines and Technology, 45 p.

DeWitt, E., Redden, J.A., Wilson, A.B., and Buscher, D., 1986, Mineral resource potential and geology of the Black Hills National Forest, South Dakota and Wyoming: U.S. Geological Survey Bulletin 1580, 135 p.

_____ 1989, Geologic map of the Black Hills area, South Dakota and Wyoming: U.S. Geological Survey Miscellaneous Investigations Map I-1910, scale 1:250,000.

Dickinson, W.R., and Snyder, W.S., 1978, Plate tectonics of the Laramide orogeny, *in* Matthews, V., III, editor, Laramide folding associated with basement block faulting: Geological Society of America Memoir 151, p. 355-366.

Dobbin, C.E., and Erdmann, C.E., 1955, Structure contour map of the Montana plains: U.S. Geological Survey Oil and Gas Investigations Map OM 178-B, scale 1:1,000,000.

Dudás, F.Ö., 1991, Geochemistry of igneous rocks from the Crazy Mountains, Montana, and tectonic models for the Montana alkalic province: Journal of Geophysical Research, v. 96, p. 13,261-13,277.

Ethridge, F.R., and Jackson, T.J., 1980, Regional depositional framework of the uranium- and coal-bearing Wasatch (Eocene) and Fort Union (Paleocene) Formations, Powder River Basin, Wyoming, *in* Guidebook to the coal geology of the Powder River coal basin, Wyoming: Field Trip No. 5: Energy Minerals Division, American Association of Petroleum Geologists, p. 2-27.

Fashbaugh, E.F., 1979, Geology of igneous extrusive and intrusive rocks in the Sundance area, Crook County, Wyoming [M.S. thesis]: Grand Forks, University of North Dakota, 97 p.

Farmer, G.L., and DePaolo, D.J., 1984, Origin of Mesozoic and Tertiary granite in the western United States and implications for pre-Mesozoic crustal structure: 2. Nd and Sr isotopic studies of unmineralized and Cu- and Mo-mineralized granite in the Precambrian craton: Journal of Geophysical Research, v. 89, p. 10,141-10,160.

Flores, R.M., and Ethridge, F.G., 1985, Evolution of intermontane fluvial systems of Tertiary Powder River Basin, Montana and Wyoming, *in* Flores, R.M., and Kaplan, S.S., editors, Cenozoic paleogeography of the west-central United States, Rocky Mountain Paleogeography Symposium 3: Society of Economic Paleontologists, and Mineralogists, Rocky Mountain Section, p. 107-126.

Gill, J.R., and Cobban, W.A., 1973, Stratigraphy and geologic history of the Montana Group and equivalent rocks, Montana, Wyoming and North and South Dakota: U.S. Geological Survey Professional Paper 776, p. 1-37.

Gries, R., 1983a, North-south compression of Rocky Mountain foreland structures, *in* Lowell, J.D., editor, Rocky Mountain foreland basins and uplifts: Rocky Mountain Association of Geologists, p. 9-32.

_____ 1983b, Oil and gas prospecting beneath Precambrian of foreland thrust plates in Rocky Mountains: American Association of Petroleum Geologists Bulletin, v. 67, p. 1-28.

Grunwald, R.R., 1970, Geology and mineral deposits of the Galena mining district, Black Hills, South Dakota [Ph.D. dissertation]: Rapid City, South Dakota School of Mines and Technology, 321 p.

Halvorson, D.L., 1980, Geology and petrology of the Devils Tower, Missouri Buttes, and Barlow Canyon area, Crook County, Wyoming [Ph.D. dissertation]: Grand Forks, University of North Dakota, 218 p.

Hamilton, W., 1981, Plate-tectonic mechanism of Laramide deformation: University of Wyoming Contributions to Geology, v. 19, p. 87-92.

Harkson, J.C., and Macdonald, J.R., 1969, Guidebook to the major Cenozoic deposits of southwestern South Dakota: South Dakota Geological Survey Guidebook 2, 103 p.

Heidt, J.H., 1977, Geology of the Mount Theodore Roosevelt-Maitland area, Lawrence County, South Dakota [M. S. thesis]: Rapid City, South Dakota School of Mines and Technology, 141 p.

Hickey, L.J., 1972, Stratigraphic summary of the Golden Valley Formation (Paleocene-Eocene) of western North Dakota, *in* Depositional environments of the lignite-bearing strata in western North Dakota: North Dakota Geological Survey Miscellaneous Series No. 50, p. 105-122.

Irving, J.D., 1899, A contribution to the geology of the northern Black Hills: New York Academy of Sciences Annals, v. 12, no. 9, p. 187-340.

Irving, J.D., and Emmons, S.F., 1904, Mining geology, Part 2, *in* Irving, J.D., Emmons, S.F., and Jaggar, T.A., Jr., Economic resources of the northern Black Hills: U.S. Geological Survey Professional Paper 26, p. 43-222.

Jaggar, T.A., Jr., 1901, The laccoliths of the Black Hills, with a chapter on Experiments illustrating intrusion and erosion, by Ernest Howe: U.S. Geological Survey Twenty-first Annual Report, Part 3, p. 163-303.

Jenner, G.A., Jr., 1984a, Eocene igneous activity and related metasomatic and hydrothermal events, Bear Lodge Mountains, Crook County, Wyoming, *in* Karner, F.R., editor, Devils Tower—Black Hills alkalic igneous rocks and general geology: 28th International Geological Congress Field Trip Guidebook T131, p. 50-66.

_____ 1984b, Tertiary alkalic igneous activity, potassic fenitization, carbonatitic magmatism, and hydrothermal activity in the central and southeastern Bear Lodge Mountains, Crook County, Wyoming [M.S. thesis]: Grand Forks, University of North Dakota, 232 p.

_____ 1989, I-type and S-type carbonatites? Evidence from the Bear Lodge Mountains, Crook County, Wyoming, *in* Karner, F.R., editor, Devils Tower—Black Hills alkalic igneous rocks and general geology: 28th International Geological Congress Field Trip Guidebook T131, p. 75-82.

Kaiser, W.R., and Ayers, W.B., Jr., 1983, Estimation of uncertainty in coal resources, *in* Tewalt, S.J., and others, editors, Electric Power Research Institute Research Project Report No. 1367-1, 137 p.

Karner, F.R., 1985, Geologic relationships in the western centers of the northern Black Hills Cenozoic igneous province, *in* Rich, F.J., editor, Geology of the Black Hills, South Dakota and Wyoming: American Geological Institute, p. 126-134.

Kent, B., 1984, Evolution of thick coal deposits in the Powder River Basin, northeastern Wyoming: Geological Society of America Abstracts with Programs, v. 85, p. 558.

King, P.B., and Beikman, H.M., 1974, Geologic map of the United States (exclusive of Alaska and Hawaii): U.S. Geological Survey, scale 1:2,500,000.

Kirchner, J.G., 1971, The petrography and petrology of the phonolite porphyry intrusions of the northern Black Hills, South Dakota [Ph.D. dissertation]: Des Moines, University of Iowa, 197 p.

Larsen, R.K., 1977, Geology, alteration, and mineralization of the northern Cutting Stock, Lawrence County, South Dakota [M.S. thesis]: Rapid City, South Dakota School of Mines and Technology, 147 p.

Leopold, E.B., and MacGinitie, H.D., 1972, Development and affinities of Tertiary floras in the Rocky Mountains, *in* Floristics and paleofloristics of Asia and eastern North America: New York, Elsevier, p. 147-200.

Lewis, B.D., and Hotchkiss, W.R., 1981, Thickness, percent sand, and configuration of shallow hydrologic units in the Powder River Basin, Montana and Wyoming: U.S.

Geological Survey Miscellaneous Investigations Map I-1317.

Lillegraven, J.A., and Ostresh, L.M., 1990, Late Cretaceous (earliest Campanian/Maastrichtian) evolution of western shorelines of the North America Western Interior Seaway in relation to known mammalian faunas, *in* Bown, T.M., and Rose, K.D., editors, Dawn of the age of mammals in the northern part of the Rocky Mountain interior, North America: Geological Society of America Special Paper 243, p. 1-30.

Lisenbee, A.L., 1978, Laramide structure of the Black Hills uplift, South Dakota-Wyoming-Montana, *in* Matthews, V., III, editor, Laramide folding associated with basement block faulting: Geological Society of America Memoir 151, p. 165-196.

_____ 1985, Tectonic map of the Black Hills uplift, Montana, Wyoming, and South Dakota: Geological Survey of Wyoming Map Series 13, scale 1:250,000.

_____ 1988, Tectonic history of the Black Hills uplift, *in* Diedrich, R.P., Dyka, M.A.K., and Miller, W.R., editors, Eastern Powder River Basin—Black Hills: Wyoming Geological Association 39th Annual Field Conference Guidebook, p. 45-52.

Lisenbee, A.L., and Martin, J.E., 1988, Igneous-related structure of the southeastern Bear Lodge dome, Crook County, Wyoming, *in* Diedrich, R.P., Dyka, M.A.K., and Miller, W.R., editors, Eastern Powder River Basin—Black Hills: Wyoming Geological Association 39th Annual Field Conference Guidebook, p. 67-76.

Lisenbee, A.L., and Roggenthen, W.M., 1990, Diatremes and breccia pipes of the northern Black Hills, South Dakota—Wyoming, *in* Paterson, C.J., and Lisenbee, A.L., editors, Metallogeny of gold in the Black Hills: Society of Economic Geologists Guidebook Series Volume 7, p. 175-181.

Love, J.D., 1960, Cenozoic sedimentation and crustal movement in Wyoming: American Journal of Science, Bradley Volume, v. 258-A, p. 204-214.

Love, J.D., and Christiansen, A.C., 1985, Geologic map of Wyoming: U.S. Geological Survey, scale 1:500,000.

Merin, I.S., and Lindholm, R.C., 1986, Evidence that the crystalline cores of uplifts adjacent to the Powder River Basin were breached during Paleocene time: The Mountain Geologist, v. 23, p. 128-131.

McDonald, J.R., 1982, Preliminary report on a late Oligocene fissure fill in the Pahasapa Limestone near Rockerville, South Dakota: Proceedings of the South Dakota Academy of Science, v. 61, p. 172-173.

McGookey, D.P., Haun, J.D., Hale, L.A., Goodell, H.G., McCubbin, D.G., Weimer, R.J., and Wulf, G.R., 1972, Cretaceous System, *in* Mallory, W.W, Mudge, M.R., Swanson, V.E., Stone, D.S., and Lumb, W.E., editors, Geologic atlas of the Rocky Mountain region: Rocky Mountain Association of Geologists, p. 190-228.

McKenna, M.C., and Love, J.D., 1972, High-level strata containing early Miocene mammals on the Bighorn Mountains, Wyoming: American Museum Novitates, no. 2490, 31 p.

Newton, H., and Jenny, W.P., 1880, Report of the geology and resources of the Black Hills of Dakota: U.S. Geographic and Geological Survey, Rocky Mountain Region (Powell), 566 p.

Noble, J.A., 1948, High-potash dikes in the Homestake mine, Lead, South Dakota: Geological Society of America Bulletin, v. 59, p. 927-940.

_____ 1952a, Structural features of the Black Hills and adjacent areas developed since Precambrian time, *in* Sonnenberg, F.P., editor, Black Hills-Williston Basin: Billings Geological Society 3rd Annual Field Conference Guidebook, p. 31-37.

_____ 1952b, Evaluation of criteria for the forcible intrusion of magma: Journal of Geology, v. 60, p. 34-57.

O'Brien, H.E., Irving, A.J., and McCallum, I.S., 1991, Eocene potassic magmatism in the Highwood Mountains, Montana: petrology, geochemistry, and tectonic implications: Journal of Geophysical Research, v. 96, p. 13,237-13,260.

Olson, K.R., 1976, The isotopic composition of strontium and the origin of igneous intrusive rocks in the northern Black Hills province of western South Dakota [M.S. thesis]: Rapid City, South Dakota School of Mines and Technology, 52 p.

O'Toole, F.S., 1981, Petrology of the Cenozoic phonolites and related rocks of the Houston Creek area, Bear Lodge Mountains, Wyoming [M.S. thesis]: Grand Forks, University of North Dakota, 112 p.

Parkhill, T.A., 1976, Geology of the Tertiary igneous rocks in the Richmond Hill intrusive complex, northern Black Hills, South Dakota [M.S. thesis]: Rapid City, South Dakota School of Mines and Technology, 45 p.

Paterson, C.J., Uzunlar, N., Groff, J., and Longstaffe, F.J., 1989, A view through an epithermal-mesothermal precious metal system in the northern Black Hills, South Dakota: a magmatic origin for the ore-forming fluids, *in* Keays, R.R., Ramsay, W.R.H., and Skinner,

B.J., editors, The geology of gold deposits: the perspective in 1988: p. 564-570.

Pettijohn, W.G., 1966, Eocene paleosol in the northern Great Plains, in Geological Survey Research 1966: U.S. Geological Survey Professional Paper 550-C, p. C61-C65.

Pierce, F.W., and Johnson, E.A., 1988, Preliminary facies analysis of the sequence of rocks below the upper Wyodak coal bed, Paleocene Fort Union Formation, southeastern Powder River Basin, Wyoming (abstract): U.S. Geological Survey Circular 1025, p. 47.

Ray, J.T., 1979, Petrology of the Cenozoic igneous rocks of the Tinton district, Black Hills, South Dakota-Wyoming (Lawrence County) [M.S. thesis]: Grand Forks, University of North Dakota, 115 p.

Redden, J.A., Obradovich, J.D., Naeser, C.W., Zartman, R.W., and Norton, J.J., 1983, Early Tertiary age of pitchstone in the northern Black Hills, South Dakota: Science, v. 220, p. 1153-1154.

Redden, J.A., and French, G.M., 1989, Geologic setting and potential exploration guides for gold deposits, Black Hills, South Dakota, *in* Shawe, D., editor, United States gold terranes—Part I: U.S. Geological Survey Bulletin 1857, p. B45-B74.

Redden, J.A., and Lisenbee, A.L., 1990, Geologic setting, Black Hills, South Dakota, *in* Paterson, C.J., and Lisenbee, A.L., editors, Metallogeny of gold in the Black Hills: Society of Economic Geologists Guidebook Series Volume 7, p. 1-9.

Retallack, G.J., 1983, A paleopedological approach to the interpretation of terrestrial sedimentary rocks: The mid-Tertiary fossil soils of Badlands National Park, South Dakota: Geological Society of America Bulletin, v. 94, p. 823-840.

Rich, J.L., 1934, Mechanics of low-angle overthrust faulting as illustrated by Cumberland thrust block, Virginia, Kentucky, and Tennessee: American Association of Petroleum Geologists Bulletin, v. 18, p. 1584-1596.

Roggenthen, W.M., and Lisenbee, A.L., 1986, Laramide development of the Black Hills uplift: Geological Society of America Abstracts with Programs, v. 87, p. 77.

Royse, F., Jr., Warner, M.A., and Reese, D.C., 1975, Thrust belt structural geometry and related stratigraphic problems, Wyoming-Idaho-northern Utah, *in* Bolyard, D.W., editor, Symposium on deep drilling frontiers in the Central Rocky Mountains: Rocky Mountain Association of Geologists, p. 41-54.

Runner, J.J., 1957, Origin of the Upper Cretaceous shale inclusions in volcanic agglomerate cutting Precambrian and Paleozoic rocks in the Black Hills, South Dakota: Geological Society of America Bulletin, v. 68, p. 1790.

Sales, J.K., 1968, Regional tectonic setting and mechanics of origin of the Black Hills uplift, *in* Wulf, G.R., editor, Black Hills area, South Dakota, Montana, Wyoming: Wyoming Geological Association 20th Annual Field Conference Guidebook, p. 10-27.

Seeland, D.A., 1976, Relationships between early Tertiary sedimentation patterns and uranium mineralization in the Powder River Basin, *in* Curry, W.H., III, and Runge, J.S., editors, Geology and energy resources of Powder River Basin: Wyoming Geological Association 28th Annual Field Conference Guidebook, p. 221-230.

_____ 1985, Oligocene paleogeography of the northern Great Plains and adjacent mountains, *in* Flores, R.M., and Kaplan, S.S, editors, Cenozoic paleogeography of the west-central United States, Rocky Mountain Symposium 3: Society of Economic Paleontologists and Mineralogists, Rocky Mountain Section, p. 187-206.

_____ 1988, Laramide paleogeographic evolution of the eastern Powder River Basin, Wyoming and Montana, *in* Diedrich, R.P., Dyka, M.A.K., and Miller, W.R., editors, Eastern Powder River basin—Black Hills: Wyoming Geological Association 39th Annual Field Conference Guidebook, p. 17-20.

Seeland, D.A., Flores, R.M., Johnson, E.A., and Pierce, F.W., 1988, Some paleogeographic inferences from paleocurrents of the Tongue River Member, Fort Union Formation, Powder River, Bull Mountains and southwestern Williston Basins, Montana and Wyoming, *in* Tafoya, R.E., editor, Geological Society of America Field Trip Guidebook, Centennial Meeting - Denver, Colorado: Professional Contributions - Colorado School of Mines, no. 12, p. 191-225.

Shapiro, L.H., 1971, Structural geology of the Black Hills region (South Dakota and Wyoming) and implications for the origin of the uplifts of the middle Rocky Mountain province [Ph.D. dissertation]: Minneapolis, University of Minnesota, 343 p.

Shapiro, L.H., and Gries, J.P., 1970, Ore deposits in rocks of Paleozoic and Tertiary age, northern Black Hills, South Dakota: U.S. Geological Survey Open File Report 70-300, 235 p.

Shearer, C.K., 1990, Geochemistry of Laramide igneous intrusions, northern Black Hills, with implications for

petrogenetic relationships and magma sources, *in* Paterson, C.J., and Lisenbee, A.L., editors, Metallogeny of gold in the Black Hills: Society of Economic Geologists Guidebook Series Volume 7, p. 35-42.

Shurr, G.W., Watkins, I.W., and Lisenbee, A.L., 1988, Possible strike-slip components on monoclines at the Powder River Basin-Black Hills uplift margin, *in* Diedrich, R.P., Dyka, M.A.K., and Miller, W.R., editors, Eastern Powder River Basin—Black Hills: Wyoming Geological Association 39th Annual Field Conference Guidebook, p. 53-66.

Sloan, R.E., 1970, Cretaceous and Paleocene terrestrial communities of western North America: North American Paleontological Convention, Chicago, 1969, Proceedings E., p. 427-453.

Sottek, T.C., 1959, Geology of the Deadman Mountain and Whitewood anticline area, Meade-Lawrence Counties, South Dakota [M.S. thesis]: Rapid City, South Dakota School of Mines and Technology, 41 p.

Staatz, M.H., 1983, Geology and description of thorium and rare-earth deposits in the southern Bear Lodge Mountains, northeastern Wyoming: U.S. Geological Survey Professional Paper 1049-D, 52 p.

Swinehart, J.B., Souders, V.L., Degraw, H.M., and Diffendahl, R.F., 1985, Cenozoic paleogeography of western Nebraska, *in* Flores, R.M., and Kaplan, S.S., editors, Cenozoic paleogeography of the west-central United States, Rocky Mountain Symposium 3: Society of Economic Paleontologists and Mineralogists, Rocky Mountain Section, p. 209-299.

Swisher, C.C., III, and Prothero, D.R., 1990, Single-crystal $^{40}Ar/^{39}Ar$ dating of the Eocene-Oligocene transition in North America: Science, v. 249, p. 760-762.

Trimble, D.E., 1980, Cenozoic tectonic history of the Great Plains contrasted with that of the southern Rocky Mountains: a synthesis: The Mountain Geologist, v. 17, p. 59-69.

Warren, G.K., 1875, Preliminary report of exploration in the Nebraska and Dakota in 1855, 1856, 1857: U.S. Army, Engineer Department, 125 p.

Weimer, R.J., Emme, J.J., Farmer, C.L., Anna, L.O., Davis, T.L., and Kidney, R.L., 1982, Tectonic influence on sedimentation, Early Cretaceous, east flank Powder River Basin, Wyoming and South Dakota: Colorado School of Mines Quarterly, v. 77, no. 4, 61 p.

Welch, C.M., 1974, A preliminary report on the geology of the Mineral Hill area, Crook County, Wyoming [M.S. thesis]: Rapid City, South Dakota School of Mines and Technology, 83 p.

White, S.F., 1980, Petrology of the Cenozoic igneous rocks of the Lytle Creek area, Bear Lodge Mountains, Wyoming [M.S. thesis]: Grand Forks, University of North Dakota, 69 p.

Wilkinson, M., 1982, Petrology and alteration in the core of the Bear Lodge Tertiary intrusive complex, Bear Lodge Mountains, Crook County, Wyoming [M.S. thesis]: Grand Forks, University of North Dakota, 127 p.

Winczewski, L.M., 1982, Paleocene coal-bearing sediments of the Williston basin, North Dakota: An interaction between fluvial systems and intracratonic basin [Ph.D. dissertation]: Grand Forks, University of North Dakota, 94 p.

Winczewski, L.M., and Groenewold, G.H., 1982, A tectonic-fluvial model for Paleocene coal-bearing sediments, Williston Basin, south-North Dakota, *in* Gurgel, K.D., editor, Utah Geological and Mineralogical Survey Bulletin 118, p. 76-88.

Frontispiece. View to west at northeastern extreme of Hanna Basin, south-central Wyoming. Steeply dipping Upper Cretaceous Almond Formation (coaly deltaic sandstone) and overlying Lewis Shale (shallow marine) dominate the view. Person at skyline stands on veneer of orthoquartzite conglomerates in lower reaches of Upper Paleocene Hanna Formation, set with marked angular unconformity upon the Cretaceous strata.

Correlation of Paleogene strata across Wyoming — a users' guide

Jason A. Lillegraven
Departments of Geology/Geophysics and Zoology/Physiology
University of Wyoming
Laramie, Wyoming, 82071

Abstract

In reference to Paleogene (i.e., Paleocene through Oligocene) time, the geologic record of Wyoming is better understood than any other comparably sized tract of Earth's dry land. The following graphical devices are presented as means of summarizing the status of knowledge of Wyoming's Paleogene history:

1. A map of Wyoming, showing statewide distribution of remnants of two temporal components (pre-Chadronian versus post-Duchesnean) of Paleogene sedimentary rocks;

2. A series of 30 locally representative Paleogene stratigraphic sections, including almost all named non-Absarokan formations and members (set on a radiometrically calibrated time scale, but emphasizing primacy of correlation using North American Land Mammal "Ages"), coordinated with listings of primary research literature for each surrounding area; and

3. Statewide, interbasinal comparative diagrams showing consistency of presence or absence of sedimentary records for each estimated million-year interval of the Paleogene.

Wyoming's Paleogene record is dominated by Paleocene through earlier Eocene strata; early parts (Paleocene into late Wasatchian) represent influence of subsidence associated with the Laramide orogeny, and later parts (late Wasatchian through Uintan) reflect increased influence of local volcanism. Sudden, massive influx of distantly derived volcaniclastic debris began in the late Eocene (Chadronian) and continued with sporadic interruptions until late in the Tertiary; Wyoming probably experienced generally aggradational conditions throughout that entire interval. Important, geographically widespread episodes of erosion occurred statewide during the following intervals of the Paleogene:

1. Early Paleocene (largely restricted to tectonically unstable basin margins);

2. Late Wasatchian (also of localized importance, as Laramide subsidence abated);

3. Late Eocene (Duchesnean; profoundly important, affecting much of western North America); and

4. Late Oligocene (probably medial Arikareean; affecting Wyoming generally, and perhaps nearby parts of western Montana).

Introduction

Hundreds of man-years of field and laboratory effort and millions of dollars have been invested into research on the Cenozoic geologic history of Wyoming. Because of the nature of the State's preserved record, most of the investment has been applied to Paleocene through Oligocene (Paleogene) components of the story.

Lillegraven, J.A., 1993, Correlation of Paleogene strata across Wyoming—a users' guide, *in* Snoke, A.W., Steidtmann, J.R., and Roberts, S. M., editors, Geology of Wyoming: Geological Survey of Wyoming Memoir No. 5, p. 414-477.

Love and others (1963) published a pioneering paleogeographic summary of Wyoming's geologic history, involving the latest Cretaceous and all of Cenozoic time. In 1988, in cooperation with my colleague Lawrence M. Ostresh, Jr., I provided an updated synthesis of latest Cretaceous through earliest Oligocene tectonic/depositional evolution of Wyoming. The review was structured around a full-color series of nine statewide paleogeographic reconstructions that emphasized influence of the Laramide orogeny and post-Laramide basin fill on patterns of ancient drainage. Each reconstruction was supplemented by descriptive text that summarized the sequence of tectonic events shaping Wyoming's Paleogene landscape. Almost simultaneously, Dickinson and others (1988) presented a less detailed but much broader review, describing Laramide evolution of most major U.S. basins of the Rocky Mountain region.

The present work should be considered, in part, as a supplement to the paper by Lillegraven and Ostresh (1988), here focusing upon detailed chronology of Wyoming's Paleogene stratigraphy, along with a more thorough and updated listing of pertinent literature. Additionally, the present study extends in time to the earliest Miocene. Materials summarized herein, however, formed the informational base for the earlier paper.

Purposes

I had the following goals in mind while constructing the present work:

1. Development of a map that shows statewide distribution of two genetically different temporal components (defined below) of Paleogene sedimentary rocks;
2. Presentation of a statewide series of 30 representative Paleogene stratigraphic sections, including almost all named formations and members;
3. Detailed evaluation of the temporal limits of each stratigraphic unit within each section, set on a radiometrically calibrated time scale but emphasizing primacy of correlation to North American Land Mammal "Ages";
4. Designation of essential primary research literature on Paleogene history for the vicinity of each representative stratigraphic section; and
5. Graphical display showing the consistency of statewide interbasinal occurrences of Paleogene strata. I have not, however, provided thorough stratigraphic coverage of the Absaroka volcanic field (see Sundell, this volume).

Paleogene nature of Wyoming's present landscape

The modern landscape of Wyoming is a topographically complex assemblage of mountain ranges and intermontane basins (**Figure 1**) that has obvious northwest-southeast and east-west structural grains (see Blackstone, 1990; Woodward, 1988). Nearly all physiographic features identified in the upper part of **Figure 1** were defined most importantly during Paleogene time, principally in association with basement-involved Laramide-style structures (see Brown, 1988; Hamilton, 1988; and Steidtmann, this volume). Only the defining features of areas 1 (in part), 2, 4, and 5 (in part) were constructed later and, even there, the Neogene geologic events were superimposed upon an older, Laramide structural framework. Area 15 experienced Cretaceous through early Eocene thin-skinned thrusting, and areas 7 and 21 resulted principally from outpourings of middle Eocene volcanic rocks that partly buried older Laramide structures. Northwestern parts of area 14 were also influenced by Paleogene volcanism, but at a much less important scale. Despite these few qualifications, the present-day topography of Wyoming profoundly reflects inheritance from an essentially early Eocene, structurally defined landscape.

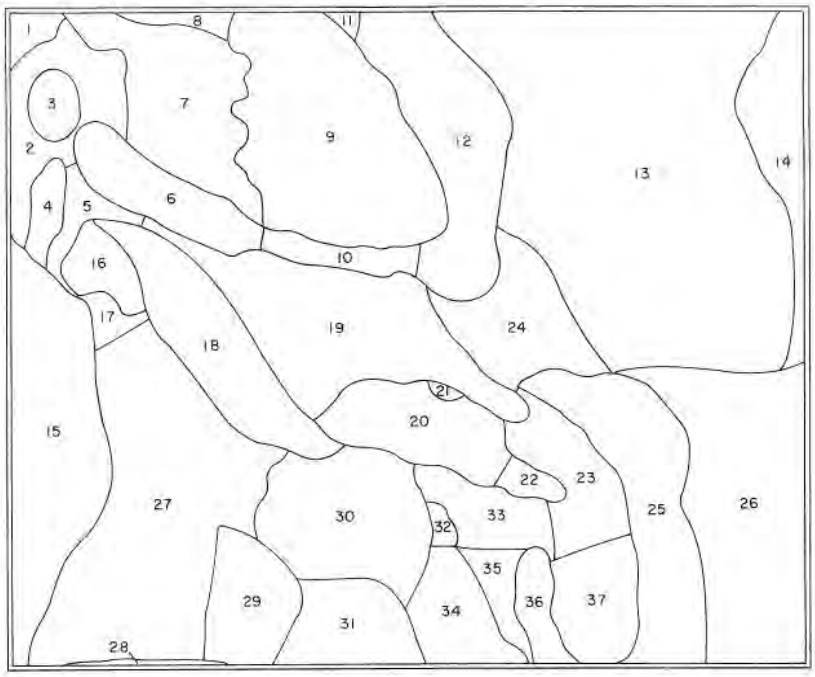

A

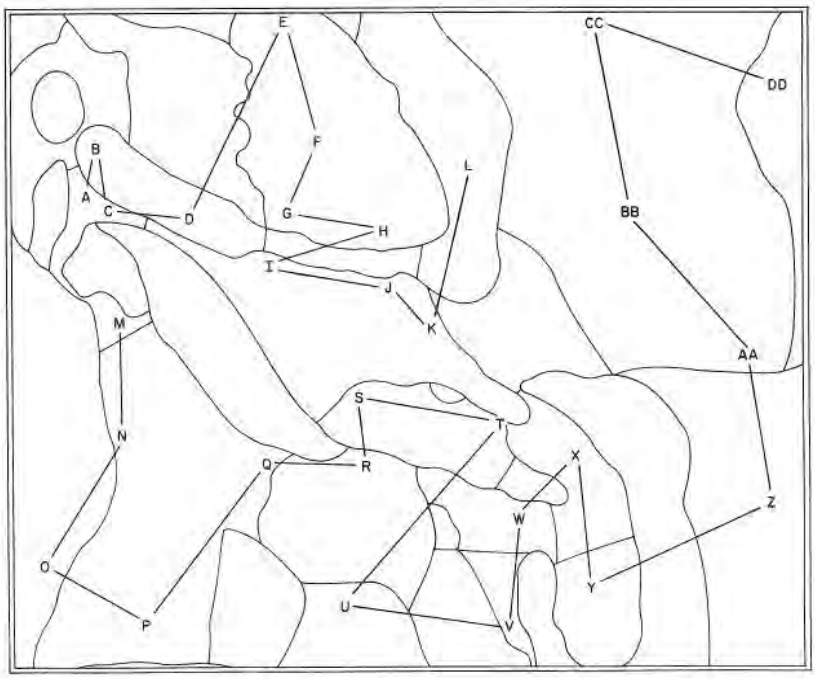

B

Figure 1. A. Reference map of dominant physiographic features of Wyoming. Names are as appear in: *Webster's New Geographical Dictionary*, (1984) and U.S. Geological Survey *Geographic Names Information System, State of Wyoming* (1981). B. Reference map locating general geographic areas appropriate to stratigraphic sections presented in Figures 4A-DD (also see Figure 2).

1. complex mountainous terrain characteristic of southwestern Montana
2. combination of eastern edge of Snake River Plain, Teton Basin (Pierre's Hole), and Yellowstone National Park
3. Basin Creek uplift
4. Teton Range
5. Jackson Hole
6. Washakie Range (largely buried by Absaroka volcanic sequences)
7. Absaroka Range
8. Beartooth Mountains
9. Bighorn Basin
10. Owl Creek Mountains
11. Pryor Mountains
12. Bighorn Mountains
13. Powder River Basin
14. Black Hills
15. Wyoming-Idaho overthrust belt
16. Gros Ventre Range
17. Hoback Basin
18. Wind River Range
19. Wind River Basin
20. Granite Mountains (Sweetwater arch or uplift)
21. Rattlesnake Hills volcanic field
22. Shirley and Freezout Mountains
23. Shirley Basin and Bates Hole
24. Casper arch
25. Laramie Mountains
26. Hartville uplift, Goshen Hole, and Denver-Julesburg Basin
27. Green River Basin proper and Bridger Basin
28. Uinta Mountains
29. Rock Springs uplift
30. Great Divide (Red Desert) Basin and Bison Basin
31. Wamsutter arch and Washakie Basin
32. Rawlins uplift
33. Hanna Basin and Carbon Basin
34. Sierra Madre
35. Saratoga Basin
36. Medicine Bow Mountains (including Snowy Range)
37. Laramie Basin

Distribution of Wyoming's remaining Paleogene strata

Figure 2 shows the breadth of distribution of remaining Paleogene sedimentary rocks across Wyoming. Paleogene remnants are present in outcrop or in subsurface across most of the state, with important exceptions being the mountainous crests of Laramide anticlinal features, basin-margin settings, northern parts of the Overthrust Belt, and most of the greater vicinity of Yellowstone National Park. Utter absence of Paleogene strata within major parts of basins themselves is limited to the eastern third of the Powder River Basin, to eastern parts of the Laramie Basin, and to western reaches of the Hanna Basin.

I subdivided the pattern of remnant Paleogene strata as seen in **Figure 2** into older (pre-Chadronian; see **Figure 3**) and younger (post-Duchesnean) components. By so doing, the fundamental genetic difference is emphasized between distributions of:

1. The older component (related to major basin filling during the Laramide orogeny and, immediately following, less thick, post-orogenic basin fill contributed by relatively local volcanic centers); and
2. The younger component (related to basin filling dominated by massive input of more distantly derived volcaniclastic sediments). As discussed in the final parts of this paper, an interval of profound, statewide erosion separated the younger from the older depositional events.

Although geographic distribution of pre-Chadronian components certainly dominates the area covered by **Figure 2**, post-Duchesnean sediments almost certainly represent greatly eroded remnants of a blanket that virtually covered the state, even until quite late in Tertiary time. The younger components today are being stripped away rapidly by erosion, thereby exhuming older Paleogene structural features that dominate Wyoming's modern landscape.

Paleogene time scale

Conventions used

The principal chronological framework against which the present work is set is North American Land Mammal "Ages" (NALMAs); the system was initiated by Wood and others (1941). Because of chronic uncertainties associated with correlating North American terrestrial strata with European sections (from which all epochal names for the Tertiary stem), Wood and others developed a provincial set of terms, defined on the basis of mammalian fossil assemblages, that was intended to apply:

1. To nonmarine strata across the entire North American continent; and
2. To all of Tertiary time. The system initiated by Wood and others (1941) has been refined greatly since then, with the most recent general summary existing as the volume edited by Woodburne (1987a). A broader treatment, which attempted to link North American chronology with other land-based vertebrate faunas across Earth, was provided by Savage and Russell (1983).

The sequence of NALMAs pertinent to Paleogene time (i.e., Puercan through early Arikareean) is presented in **Figure 3** (column B). Evernden and others (1964) pioneered constraint of limits of the various NALMAs by radiometric dates. Especially important, more recent general attempts to refine radiometric limits of Paleogene NALMAs include the following: *Paleogene as a whole* (Aubry and others, 1988; Woodburne, 1987b); *Puercan-Clarkforkian* (Archibald and others, 1987); *Wasatchian-Duchesnean* (Flynn, 1986; Krishtalka and others, 1987); *Chadronian-Whitneyan* (Emry and others, 1987; Swisher and Prothero, 1990); and *Arikareean* (Tedford and others, 1987). I used the compromise scheme of NALMA boundaries relative to radiometric time as shown in **Figure 3** (column C).

The boundary estimates used in **Figure 3** (column C) surely will require significant alteration as more refined geochronometric data becomes available. Also, readers should be aware that, during the process of developing **Figure 4** (**A** through **DD**), I put principal emphasis for temporal control of forma-

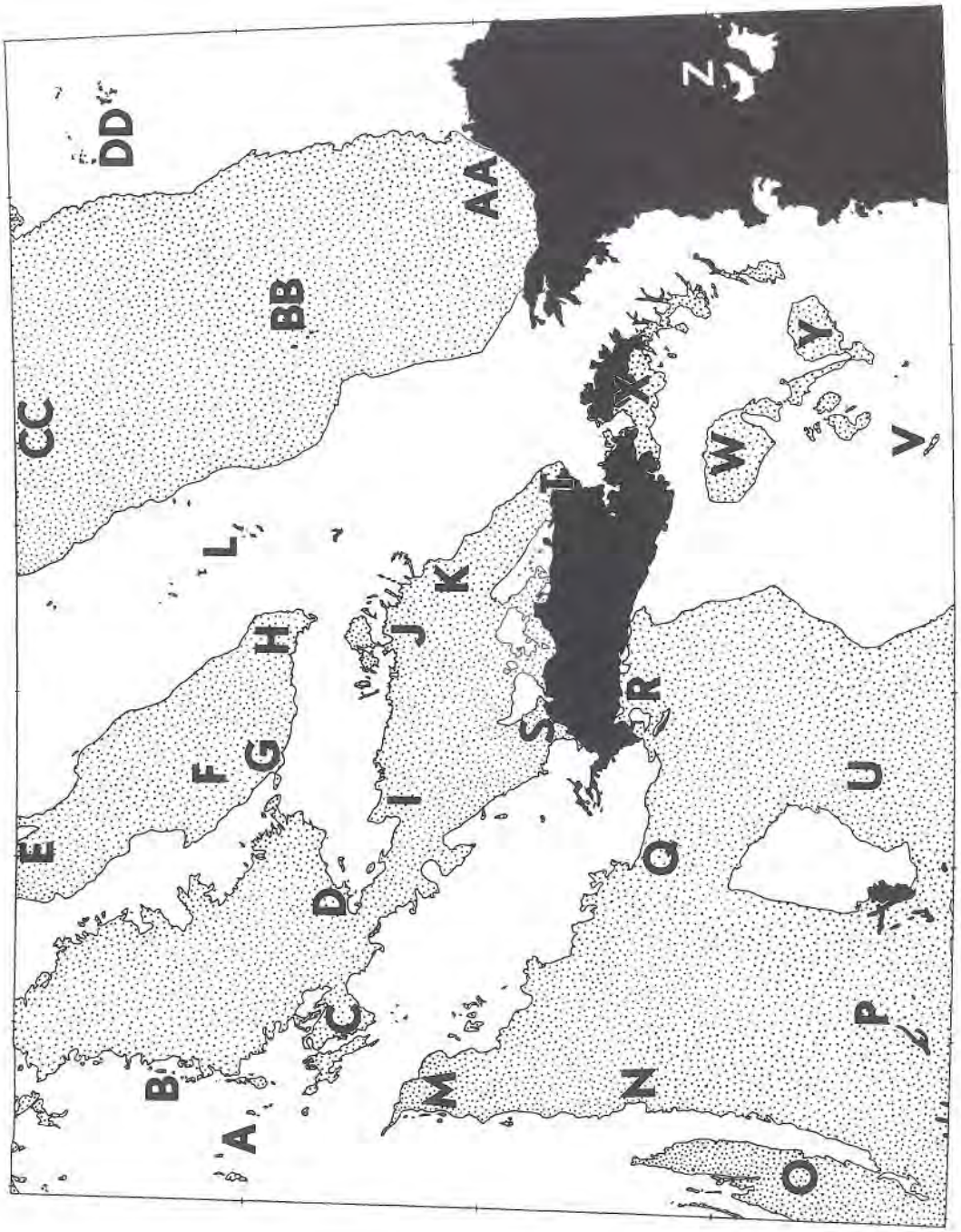

Figure 2. Stippled pattern indicates presence of Paleocene and Eocene strata (exclusive of the White River Formation and its presumed temporal equivalents). Black patterning indicates presence of the late Eocene-Oligocene White River Formation (or its presumed correlatives), commonly associated with overlying, variously-named pre-Miocene strata. Many approximations of the black pattern were required along eastern flanks of Laramie Mountains and southern border of Granite Mountains because the White River Formation commonly is covered by Neogene strata. Erosional windows of Goshen Hole are shown, but most other interruptions within the black pattern (e.g., Hartville uplift, granite knobs in Granite Mountains) are not. Many additional small patches of "White River Formation" would be necessitated on flanks of the Bighorn Mountains through recently published maps by Denson and others (1990), Hinrichs and others (1991), and Ver Ploeg (in press); stratigraphic identification of none, however, has been confirmed paleontologically or radiometrically. Base map is Love and Christiansen (1985). Right page. A through DD designations (as seen in lower part of Figure 1) are general geographic areas appropriate to stratigraphic sections presented in Figures 4A-DD.

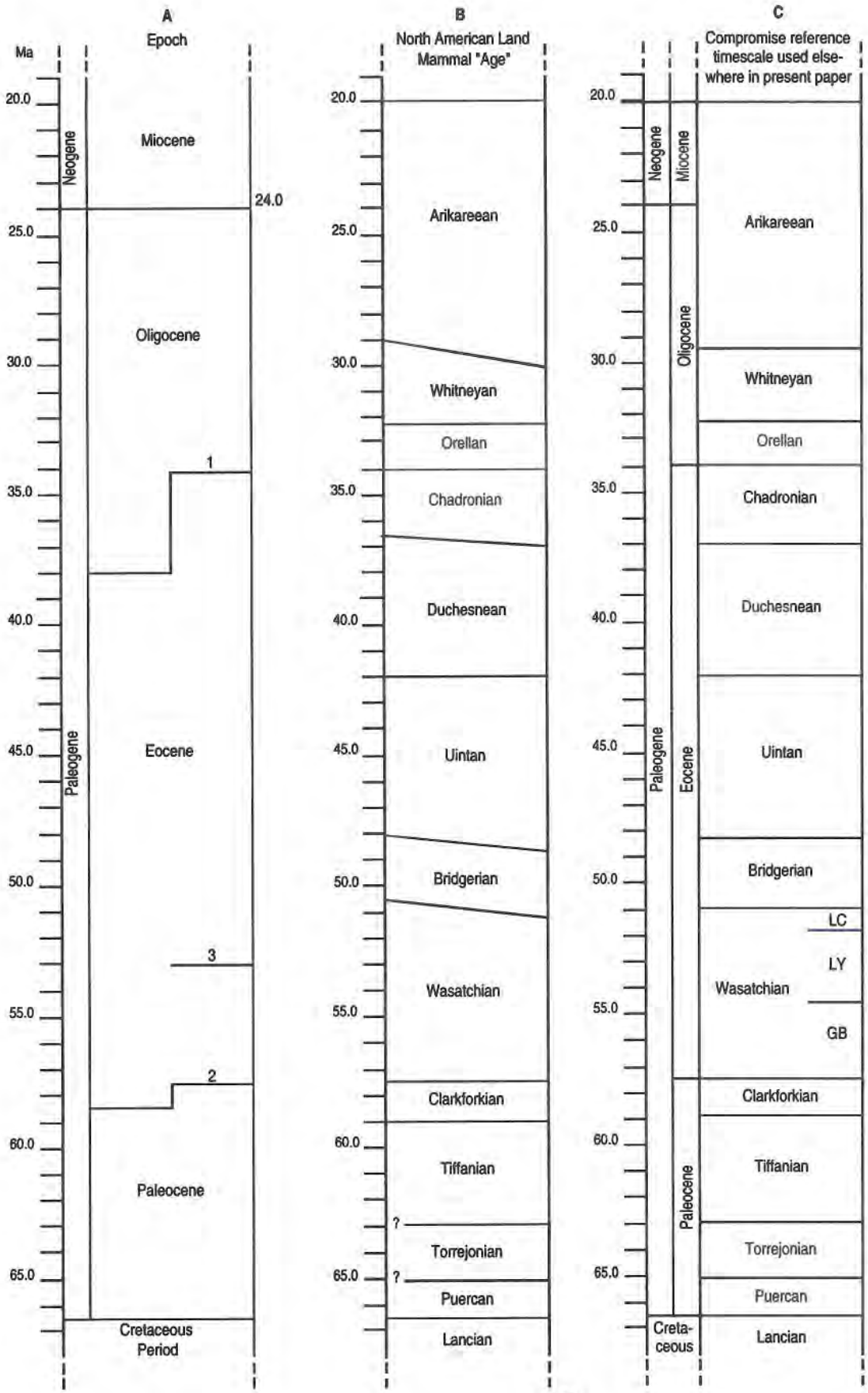

Figure 3. Paleogene time scale.
Column A. Boundaries of European-based epochs as summarized in Woodburne (1987a; 1987b, Figure 10.1). "1" indicates reordered Eocene-Oligocene boundary (accepted herein) as proposed by Swisher and Prothero (1990); "2" indicates reordered Paleocene-Eocene boundary (accepted herein) as proposed by Gingerich (1989a); and "3" indicates position of Paleocene-Eocene boundary as tentatively suggested by Odin and Odin (1990).
Column B. Estimated boundaries of North American Land Mammal "Ages" as calibrated against radiometric time scale in Woodburne (1987a,b); bracketed part indicates reordered Duchesnean through Arikareean boundaries (accepted herein) as proposed by Swisher and Prothero (1990). Diagonaled boundary-lines suggest ranges of uncertainty of boundaries relative to radiometric time scale.
Column C. Compromise reference time scale used for Figures 4A through DD in present paper. Abbreviations ("subages" of the Wasatchian; scaled against radiometric time following Woodburne, 1987b, Figure 10.1): LC = Lostcabinian; LY = Lysitean; and GB = Graybullian (including Sandcouleean sensu Woodburne, 1987b, Figure 10.1 and "zone Wa0" of Gingerich, 1989a).

tional tops and bottoms upon interpretations of mammalian faunas, with available radiometric dates being of secondary consideration. As suggested by Flynn and others (1984), experimental error for most published Paleogene radiometric dates are of greater magnitude than the error in relative dating (set against ranges of NALMAs) expected for correlation using fossil mammals.

Quite a different problem involves appropriate assignment of European epochal boundaries (marine-based, except for the Paleocene) within nonmarine stratigraphic sequences present in the North American western interior. Placements of Paleocene-Eocene, Eocene-Oligocene, and Oligocene-Miocene boundaries have shifted dramatically within the past two decades relative both to the global radiometric time scale and the limits of NALMAs. As pertinent and recent examples of such instability, the left half of column A in **Figure 3** represents placement of epochal boundaries within the radiometric time scale as used by Woodburne (1987b); relationships of those choices of boundaries to beginnings and endings of NALMAs are seen by comparison with column B.

The right half of column A in **Figure 3**, however, shows recent suggestions for significant change. Swisher and Prothero (1990) suggested that, relative to European chronology, the Chadronian is better considered as latest Eocene, rather than early Oligocene as has been the traditional use. Similarly, Gingerich (1989a) returned to an older concept that puts the Paleocene-Eocene boundary at the Clarkforkian-Wasatchian transition, rather than within Clarkforkian time. Finally, should it prove that Odin and Odin's (1990) suggested younger placement (to about 53 Ma) of the Paleocene-Eocene boundary is correct, much of Wasatchian history would have occurred during Paleocene time. For purposes of the present paper, I have accepted (**Figure 3**, column C) the alterations suggested by Swisher and Prothero (1990) and Gingerich (1989a).

Practical advantages in use of a provincial chronology

As discussed immediately above, application of European-based epochal names to terrestrial Paleogene stratigraphic sequences in the North American western interior has been a highly unreliable process. As examples of resulting terminological instability, the type Bridger Formation, which almost universally has been visualized by the geological community as "middle Eocene" in age, on the present time scale must be considered as partly early Eocene. Similarly, at least lower reaches of the White River Group (or Formation as it usually is termed in Wyoming), previously universally referred to the Oligocene, now should be considered as of late Eocene age. Because of such ever-changing use of European-based geochronologic terminology, communication within the North American research community for purposes of recognition of synchronous Paleogene geological/biological events ("correlation") has suffered from much lower levels of precision than is actually possible. What would be meant today, for example, by unqualified designation in Wyoming of so vague a term as "early Eocene"?

The great majority of Paleogene deposits in Wyoming, and across most of the Rocky Mountains in general, have been dated on the basis of assemblages of fossil mammals. Even paleobotanical chronologies for Paleogene sequences of the Rocky Mountains (e.g., Brown, 1962; Leopold and MacGinitie, 1972; MacGinitie, 1974; Wing, 1984; Wolfe, 1987) usually have been linked directly to vertebrate history. The system of NALMAs has been applied widely to Wyoming's Paleogene stratigraphic sequences by vertebrate paleontologists, with consequent important refinements in interbasinal correlation. NALMAs have proven themselves to be remarkably stable entities, providing tools for detailed correlation across a wide variety of depositional settings.

Nevertheless, despite such practical advantages and such a record of success within the paleontological community, it is an unfortunate fact that many otherwise highly capable geologists who have published important research on the Paleogene history of Wyoming have not reaped benefits from the added increments of precision at their avail all along through integration of paleontological knowledge and use of a better defined system of reference to specific intervals of Paleogene time. As an indication of the compartmentalization of the science of geology, and even of stratigraphy itself, the NACSN (1983) included no discussion of the (1941) concept of North American Land Mammal "Ages." Hopefully, the present paper will help encourage the general community of geologists practicing in Paleogene sequences of the Rocky Mountains to take better advantage of the vertebrate fossils for purposes of detailed correlation.

A statewide series of 30 generalized stratigraphic sections

Conventions used

Figure 4 (A through DD) presents a series of thirty generalized stratigraphic columns for the Paleogene that represent all parts of the state (see lower part of **Figure 1** and **Figure 2**). The sections include virtually all presently recognized Paleogene formations and their members, with the exception of many volcanogenic units found within the Absaroka Range (see Sundell, this volume).

In large part because of the much narrower focus applied here (strictly the Paleogene), I have employed a number of procedural conventions that differ from those used on correlation charts developed by Love and Christiansen (1980) and Love and others (this volume). Although practical application of the sections within the present paper itself is limited in scope, I hope the various columns will provide a sound temporal framework for the recording and integration of a wide variety of geological information by future researchers.

As discussed above, I designated the temporal limits of individual stratigraphic units principally in terms of North American Land Mammal "Ages," with available radiometric dates, in most cases, having been given second-level consideration. One added advantage of using limits constrained by NALMAs (or their "subages") is that the relative magnitudes of hiatuses within a stratigraphic column can be visualized more realistically. Compare, for example, the improved precision available when it is possible to state that a particular rock unit was deposited during the "late Wasatchian", as contrasted to such a generalized term as "early Eocene."

I selected the locations for sections under guiding criteria of: (1) provision of greatest completeness; and (2) presentation of stratigraphic relationships that are most typical for the surrounding area. In some areas (e.g., Laramie Basin, **Figure 4Y**), there exists, at no single place, the complete stratigraphic column as drawn. Where sections are markedly composite, however, subareas of formational occurrence are specified in the figure captions. Reported thicknesses (in feet) are presented for most Paleogene stratigraphic subunits of the columns, generally as measured in outcrop. Usually, the reported thickness is a maximum for the local area. In situations in which local thicknesses are highly variable, the site of reported measurement (again, usually a maximum value) is specified within the caption.

Associated with each column is a brief listing of the most important literature pertinent to Paleogene geologic history of the immediate area. In most cases, I attempted to restrict the listing to relatively recent publications. Only a few unpublished, graduate theses and dissertations are referenced, and all are from The University of Wyoming; these were cited only for situations in which important information is included that is not otherwise available.

Queries are used liberally throughout the various columns to suggest degrees of uncertainty in temporal limits of tops or bottoms of individual stratigraphic units. Absence of a query suggests high confidence in temporal resolution. A single query is intended to suggest minor uncertainty for the correlation. A double query is intended to imply major uncertainty in timing of the event. In development of **Figures 5** through **7**, however, counts were made from positions of stratigraphic tops and bottoms as they stand in **Figure 4** (A through DD), regardless of status of uncertainty in correlation.

Standard formational and member names are capitalized in the columns, with informal designations (as used within existing literature) enclosed by quotation marks. Informal names lacking quotation marks are my own designations, unique to the present paper. Alternatively used formational names are enclosed within parentheses.

Paleogene geologic evolution of Wyoming

As mentioned in the introduction, the present work should be considered, in part, as a documentary supplement to the paper by Lillegraven and Ostresh (1988). Readers are therefore referred to that reference for a statewide paleogeographic reconstruction (and associated descriptive text) for each of the following intervals:

9. *early Chadronian* (latest Eocene of present paper)
8. *early Uintan* (later medial Eocene)
7. *late Wasatchian and Bridgerian* (earlier medial Eocene)
6. *early Wasatchian* (early Eocene)
5. *Clarkforkian* (latest Paleocene of present paper)
4. *Tiffanian* (late Paleocene)
3. *Torrejonian* (early Paleocene)
2. *Puercan* (earliest Paleocene)
1. *Lancian* (latest Cretaceous; see Lillegraven and McKenna, 1986; Lillegraven and Ostresh, 1990)

Dramatic changes in sizes and shapes of hydrographic basins occurred across Wyoming during Paleogene time. These were related to sequentially changing interactions of basin filling associated with Laramide tectonism, mid-Eocene local volcanism, and latest Eocene through Oligocene volcanism at distant sites. Major areal features of hydrographic basinal evolution through the Paleogene were evaluated quantitatively by Lillegraven and Ostresh (1988, Table 2).

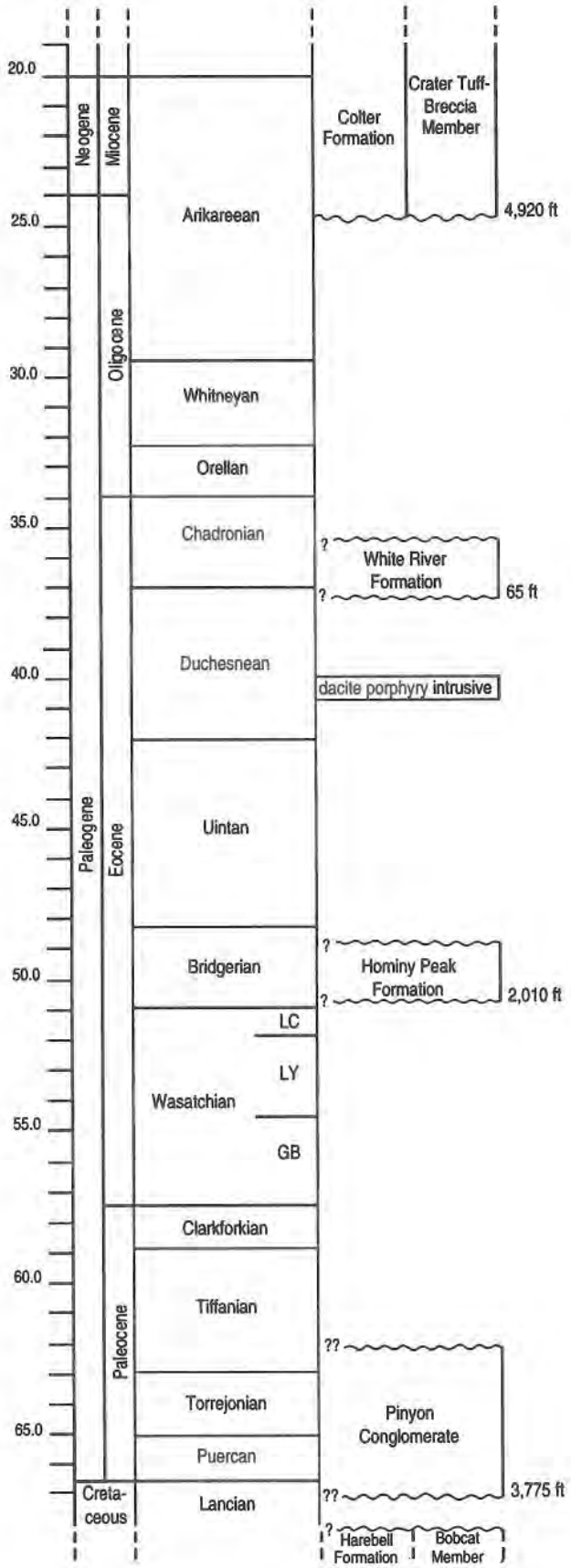

Figure 4A. Generalized Paleogene stratigraphy in vicinity of Section A (Figures 1 and 2) — **Jackson Hole, northern and western flanks of Teton Range**, northwestern Wyoming. *Locations and/or local thicknesses*: Colter Formation (total formation) at Pilgrim Creek; White River Formation at East Fork Pilgrim Creek; Hominy Peak Formation on northwest flank of Teton Range; Pinyon Conglomerate at Pinyon Peak (at type section, capped by 200 to 400 ft of undated "lower Tertiary volcanic rocks"). "Dacite porphyry intrusive" found at Birch Hills.

Key literature to Paleogene history in vicinity of Section A
Albertus, 1985
Barnosky, 1984, 1986
Blackstone and De Bruin, 1987
Lindsey, 1972
Love, 1973
J. D. Love and others, 1976, 1978
McKenna and Love, 1970
Schmitt and Steidtmann, 1990
Steidtmann and Schmitt, 1988
Sutton and Black, 1975

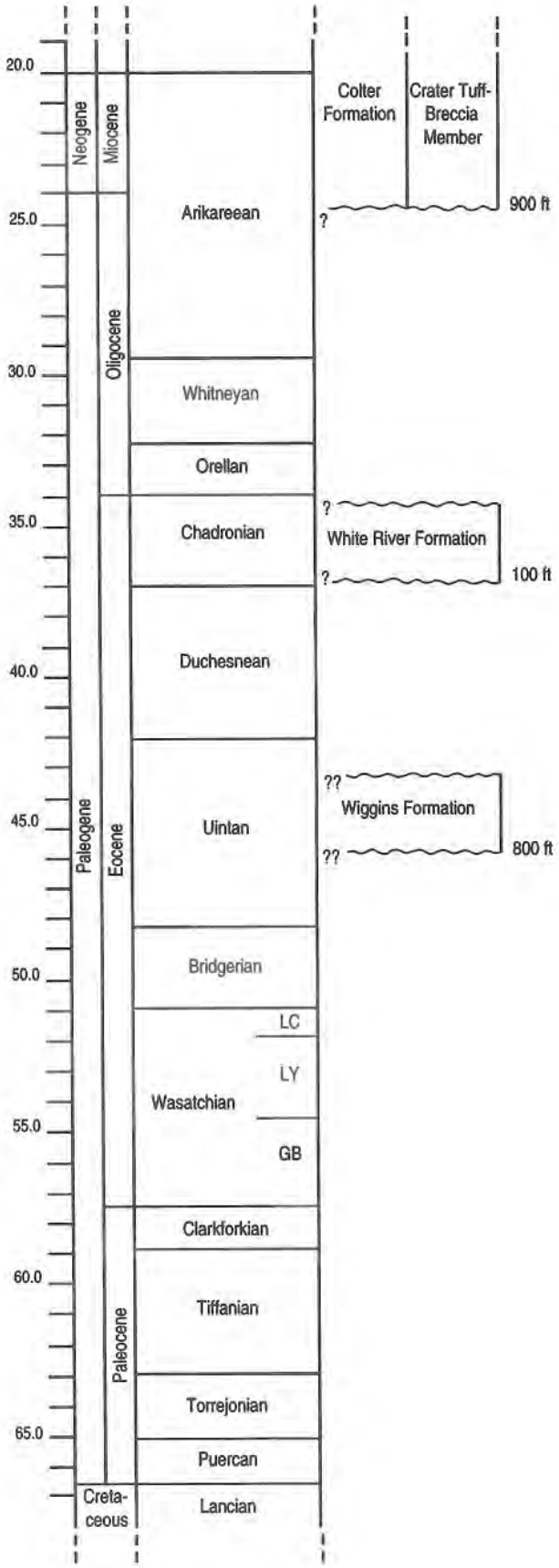

Figure 4B. Generalized Paleogene stratigraphy in vicinity of Section B (Figures 1 and 2) — **Emerald Lake (summit of west end of Washakie Range)**, northwestern Wyoming.

Key literature to Paleogene history in vicinity of Section B
Barnosky, 1986
Love and Keefer, 1975
J. D. Love and others, 1976
Smedes and Prostka, 1972

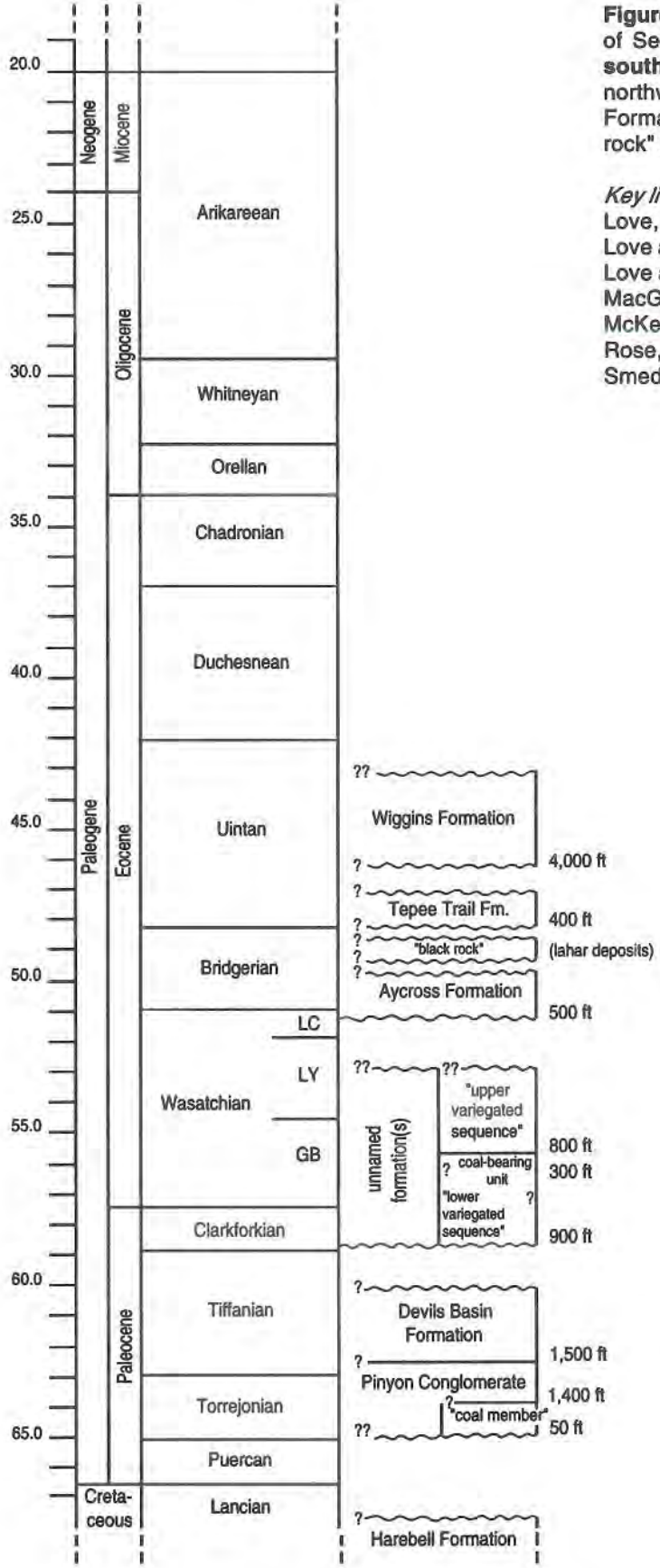

Figure 4C. Generalized Paleogene stratigraphy in vicinity of Section C (Figures 1 and 2) — **Togwotee Pass to southern headwaters of Gros Ventre River drainage,** northwestern Wyoming. "?Tepee Trail Fm." is "Aycross Formation" of Love and others (1978). Thickness of "black rock" lahar deposits unspecified.

Key literature to Paleogene history in vicinity of Section C
Love, 1947, 1973, 1989
Love and Christiansen, 1985
Love and others, 1978
MacGinitie, 1974
McKenna, 1980a
Rose, 1981
Smedes and Prostka, 1972

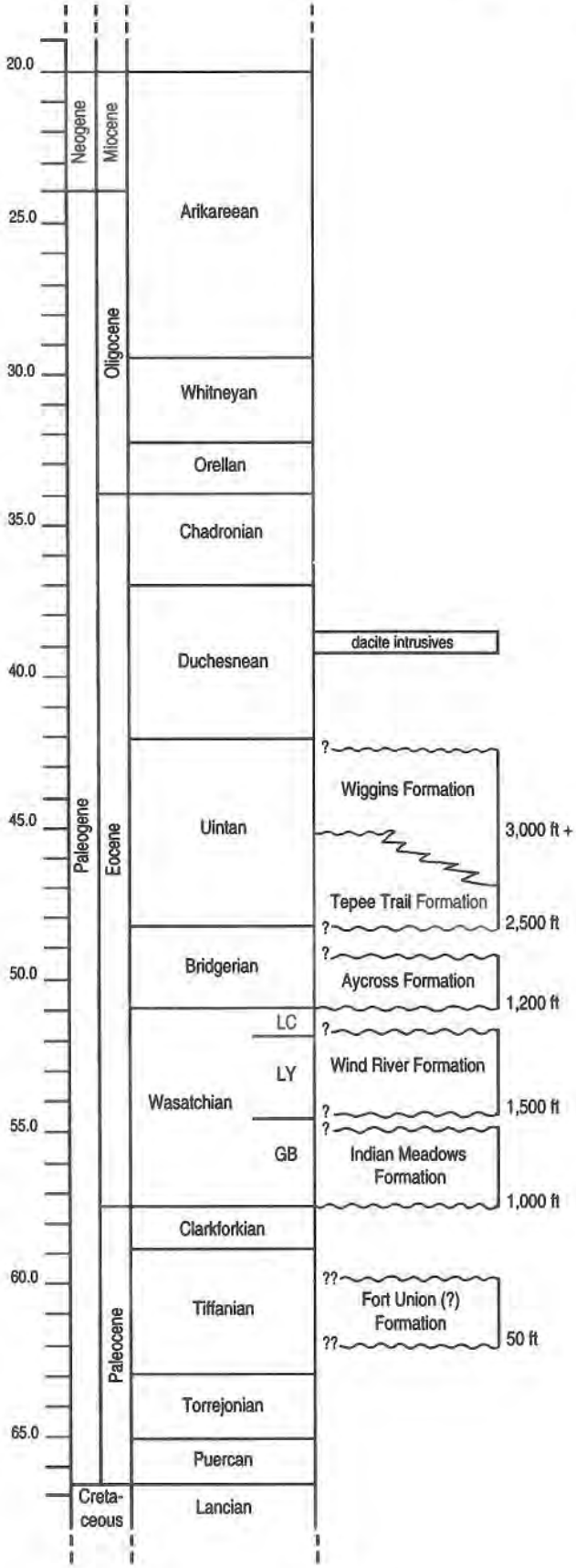

Figure 4D. Generalized Paleogene stratigraphy in vicinity of Section D (Figures 1 and 2) — **southeastern Absaroka Range, Washakie Range, northwesternmost Wind River Basin**, northwestern Wyoming. "Dacite intrusives" found at Washakie Needles and Dome Mountain.

Key literature to Paleogene history in vicinity of Section D

Bown, 1982
Eaton, 1982
Flynn, 1986
Keefer, 1957, 1965, 1970
Love, 1939
L. L. Love and others, 1976
MacGinitie, 1974
MacFadden, 1980
McKenna, 1990
Rohrer and Obradovich, 1969
Smedes and Prostka, 1972
Sundell, 1982
Sundell and Eaton, 1982
Sundell and others, 1984
Winterfeld, 1986
Winterfeld and Conard, 1983

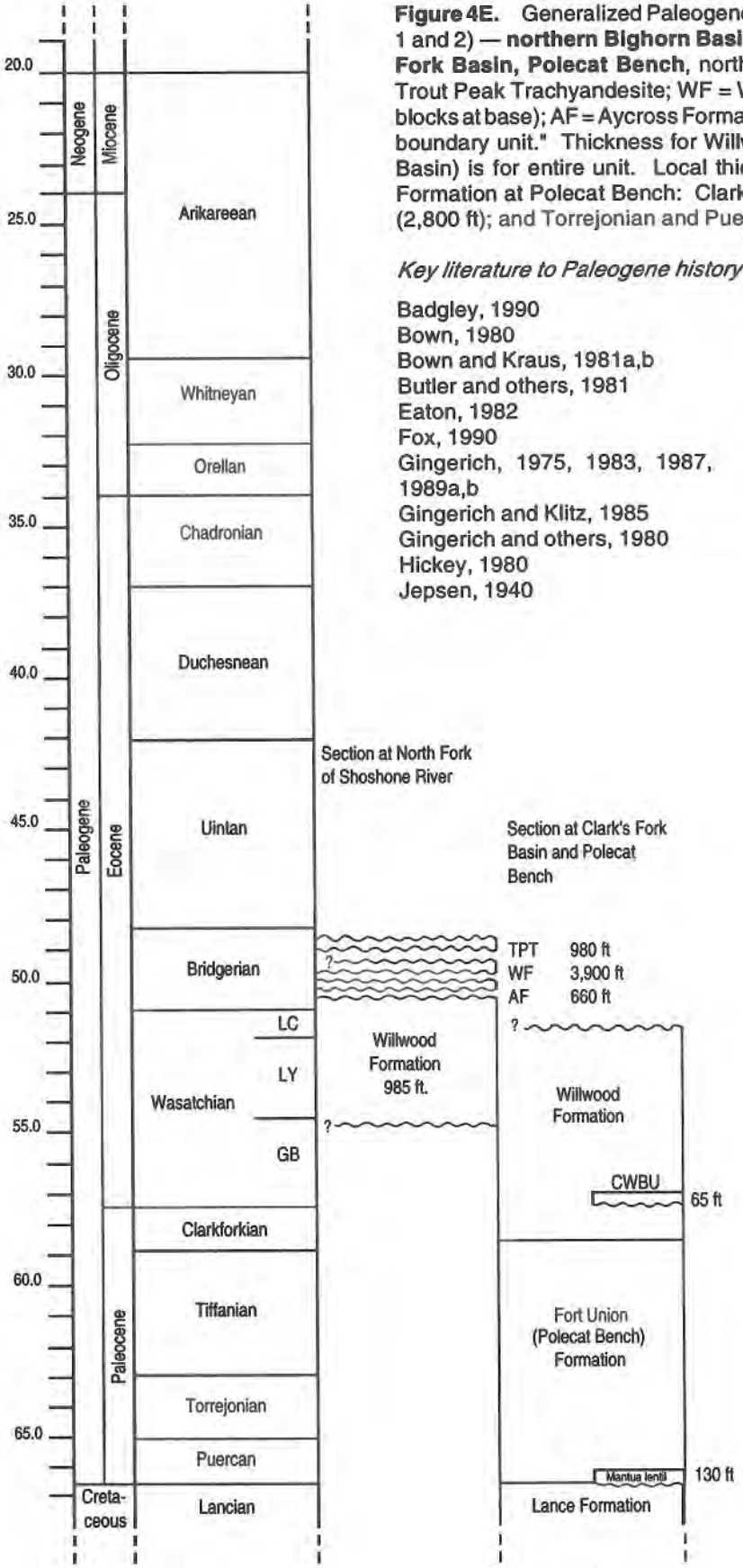

Figure 4E. Generalized Paleogene stratigraphy in vicinity of Section E (Figures 1 and 2) — **northern Bighorn Basin, North Fork of Shoshone River, Clark's Fork Basin, Polecat Bench**, northwestern Wyoming. Abbreviations: TPT = Trout Peak Trachyandesite; WF = Wapiti Formation (with Heart Mountain fault blocks at base); AF = Aycross Formation; and CWBU = "Clarkforkian-Wasatchian boundary unit." Thickness for Willwood Formation (measured in Clark's Fork Basin) is for entire unit. Local thicknesses of Fort Union (= Polecat Bench) Formation at Polecat Bench: Clarkforkian section (1,900 ft); Tiffanian section (2,800 ft); and Torrejonian and Puercan sections combined (330 ft).

Key literature to Paleogene history in vicinity of Section E

Badgley, 1990
Bown, 1980
Bown and Kraus, 1981a,b
Butler and others, 1981
Eaton, 1982
Fox, 1990
Gingerich, 1975, 1983, 1987, 1989a,b
Gingerich and Klitz, 1985
Gingerich and others, 1980
Hickey, 1980
Jepsen, 1940
Kraus, 1980, 1987
Krause and Maas, 1990
Love, 1988b
Nelson and Pierce, 1968
Parker, 1986
Parker and Jones, 1986
Rose, 1981
Torres, 1985
Wing, 1984
Winkler, 1983
Yuretich and others, 1984

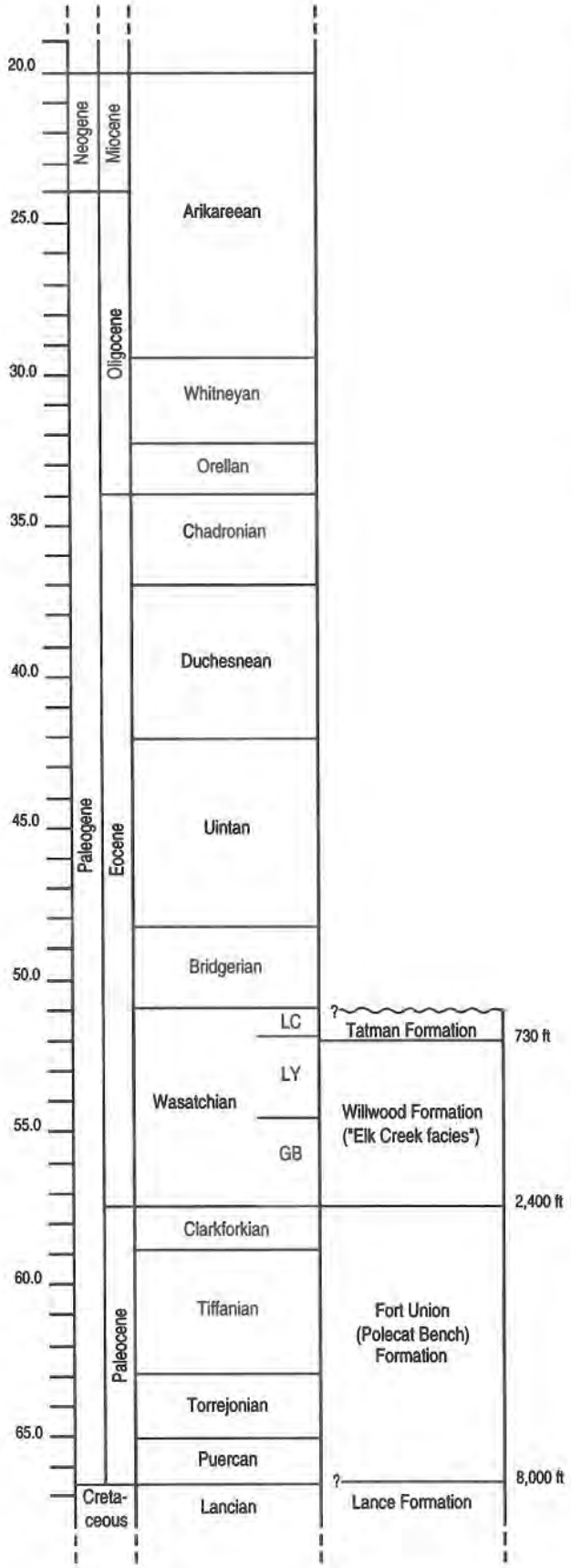

Figure 4F. Generalized Paleogene stratigraphy in vicinity of Section F (Figures 1 and 2) — **central Bighorn Basin, Tatman Mountain**, northwestern Wyoming. Fort Union (= Polecat Bench) Formation in this area is wholly subsurface.

Key literature to Paleogene history in vicinity of Section F
Badgley, 1990
Bown, 1980
Bown and Beard, 1990
Bown and Kraus, 1987
Bown and Rose, 1987
Bown and others, in press
Gingerich, 1989a
Love, 1988b
Neasham and Vondra, 1972
Parker, 1986
Parker and Jones, 1986
Rohrer and Smith, 1969
Schankler, 1980
Stone, 1985a,b
Van Houten, 1944

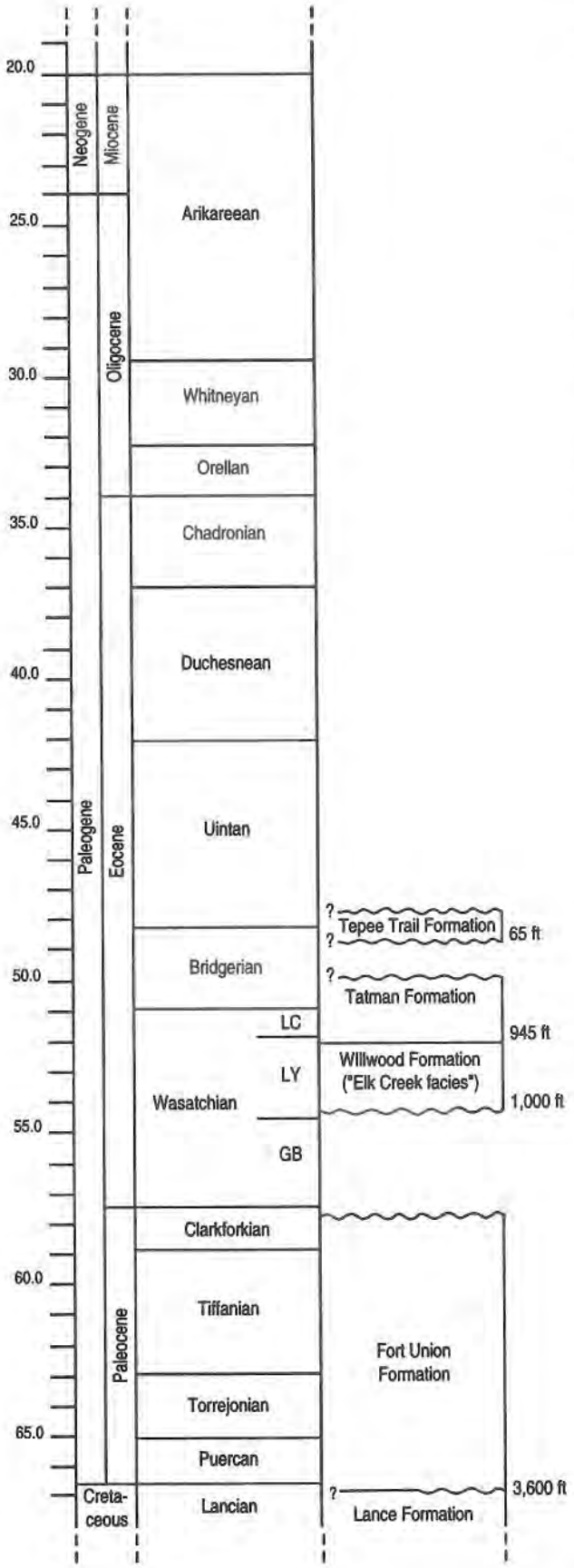

Figure 4G. Generalized Paleogene stratigraphy in vicinity of Section G (Figures 1 and 2) — **southwestern Bighorn Basin, Squaw Teats, Blue Mesa, Golden Eagle Dome,** northwestern Wyoming. Tepee Trail Formation in this area occurs as a detachment fault klippe, derived from eastern Absaroka Range. Base of Willwood Formation becomes significantly older eastward.

Key literature to Paleogene history in vicinity of Section G
Blackstone, 1986
Bown, 1982
Bown and others, in press
Kraus, 1985
Leite, in prep.
Love, 1988b
Neasham and Vondra, 1972
Parker, 1986
Parker and Jones, 1986
Rohrer, 1966
Rohrer and Smith, 1969
Van Houten, 1944

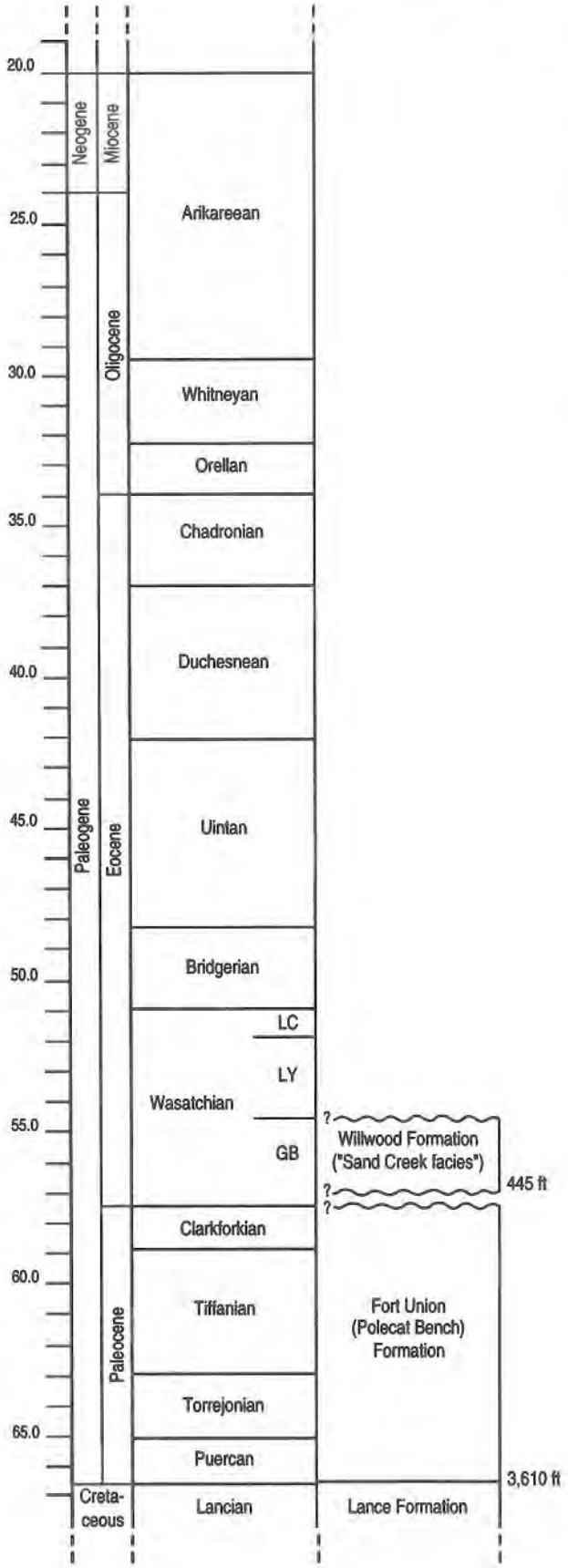

Figure 4H. Generalized Paleogene stratigraphy in vicinity of Section H (Figures 1 and 2) — **southeastern Bighorn Basin (east of Bighorn River)**, northwestern Wyoming.

Key literature to Paleogene history in vicinity of Section H
Blackstone, 1986
Bown, 1979, 1980
Bown and Rose, 1987
Bown and others, in press
Hartman, 1986
Horn, 1963
Keefer and Love, 1963
Love, 1988b
Parker, 1986
Parker and Jones, 1986

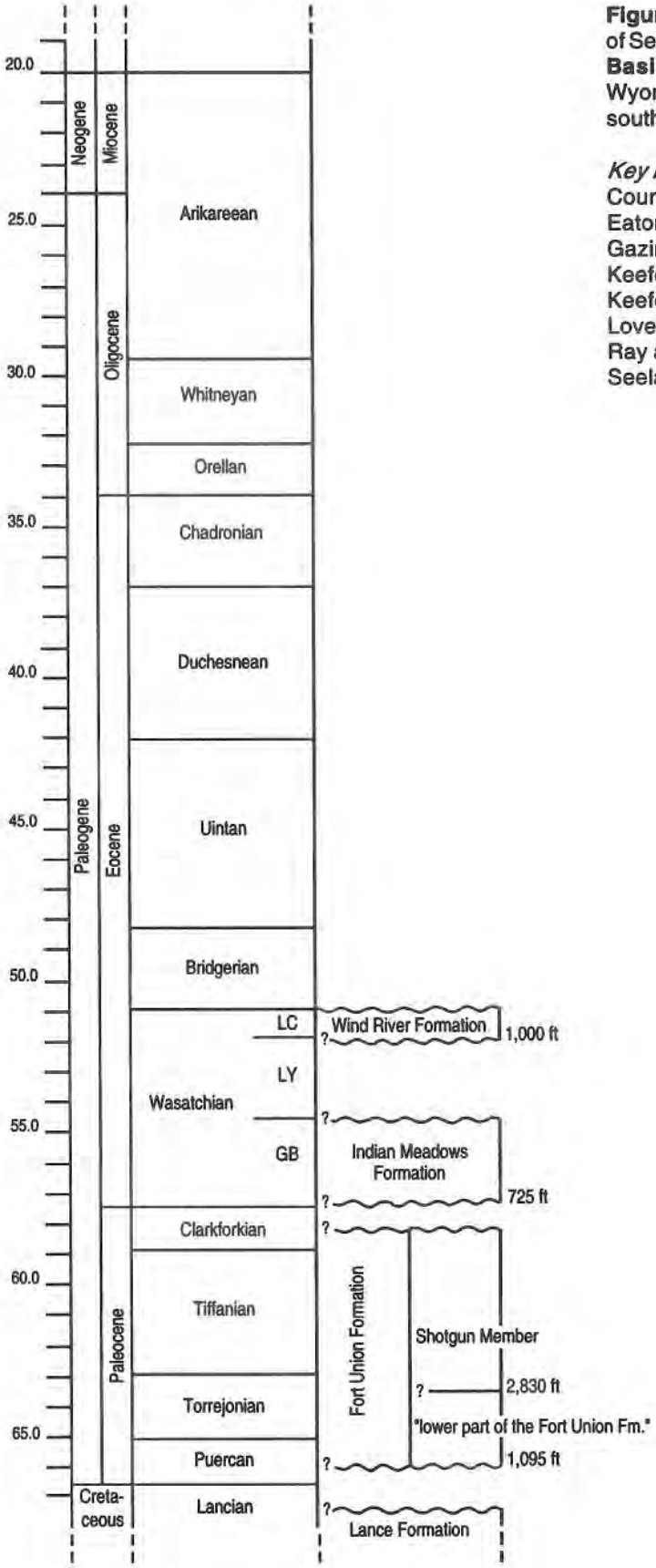

Figure 4I. Generalized Paleogene stratigraphy in vicinity of Section I (Figures 1 and 2) — **northwestern Wind River Basin (Shotgun Butte, Twin Buttes)**, north-central Wyoming. Wind River Formation measured from outcrops south of Shotgun Butte.

Key literature to Paleogene history in vicinity of Section I
Courdin and Hubert, 1969
Eaton and others, 1989
Gazin, 1971
Keefer, 1961, 1965, 1970
Keefer and Troyer, 1964
Love, 1988a
Ray and Keefer, 1985
Seeland, 1978a,b

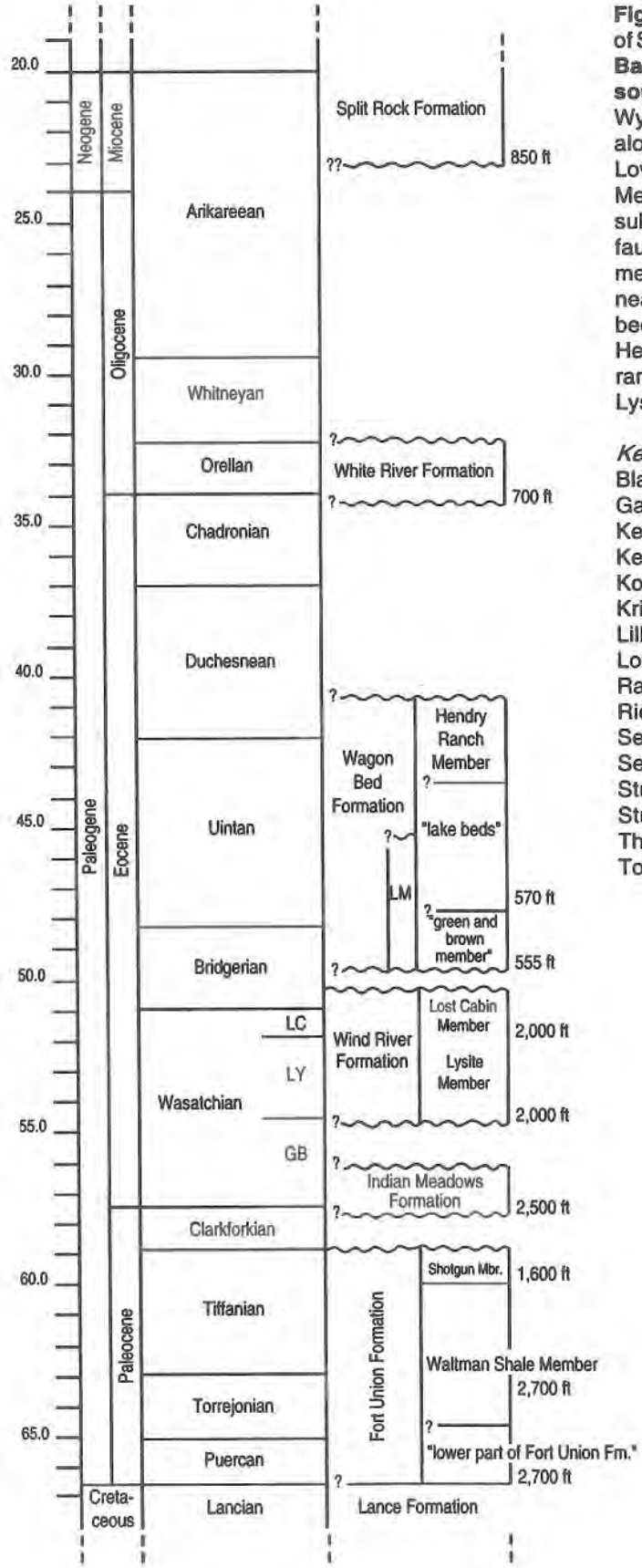

Figure 4J. Generalized Paleogene stratigraphy in vicinity of Section J (Figures 1 and 2) — **northeastern Wind River Basin (Badwater Creek, Cedar Ridge, Lysite Mountain, southern extreme of Bighorn Mountains)**, north-central Wyoming. Split Rock and White River formations measured along north side of Cedar Ridge normal fault system. Lower part of Fort Union Formation and Waltman Shale Member of Fort Union Formation occur in this area only in subsurface; outcrop of Shotgun Member exists locally in fault contact against lower units. Lost Cabin and Lysite members of Wind River Formation exist in fault contact near Lysite and along Cedar Ridge. Thickness for "lake beds" of Wagon Bed Formation is measured to top of Hendry Ranch Member. *Abbreviation:* LM = presumed range of Wagon Bed Formation (520 ft) as recognized at Lysite Mountain on summit of Owl Creek Mountains.

Key literature to Paleogene history in vicinity of Section J

Black, 1969
Gazin, 1956d
Keefer, 1961, 1965, 1970
Keefer and Love, 1963
Korth, 1980, 1982
Krishtalka and others, 1975
Lillegraven and others, 1981
Love, 1978, 1988a
Ray and Keefer, 1985
Riedel, 1969
Seeland, 1978a,b
Setoguchi, 1978
Stucky, 1984a-c
Stucky and others, 1989, 1990
Thaden, 1980a-c
Tourtelot, 1953, 1957

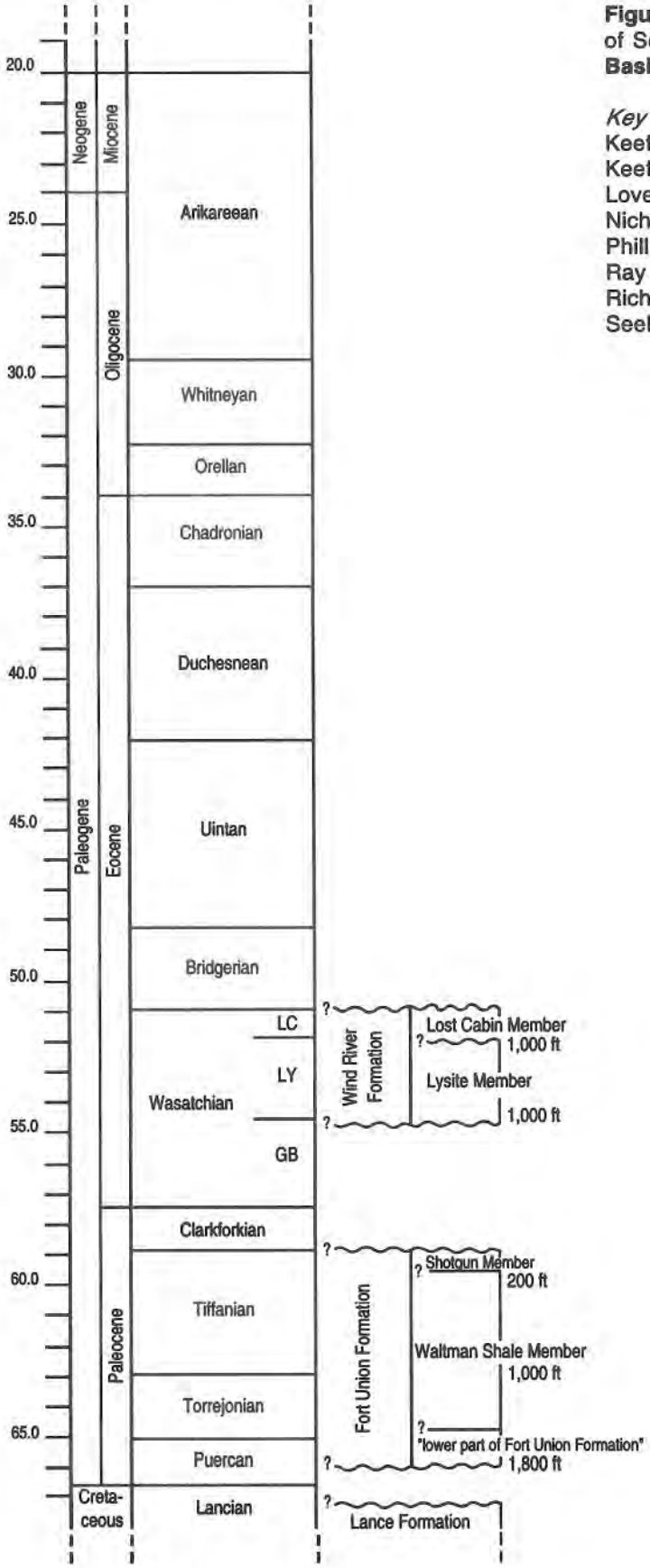

Figure 4K. Generalized Paleogene stratigraphy in vicinity of Section K (Figures 1 and 2) — **eastern Wind River Basin (Waltman, Hells Half Acre)**, north-central Wyoming.

Key literature to Paleogene history in vicinity of Section K
Keefer, 1961, 1965, 1970
Keefer and Love, 1963
Love, 1988a
Nichols and Ott, 1978
Phillips, 1983
Ray and Keefer, 1985
Rich, 1962
Seeland, 1978a,b

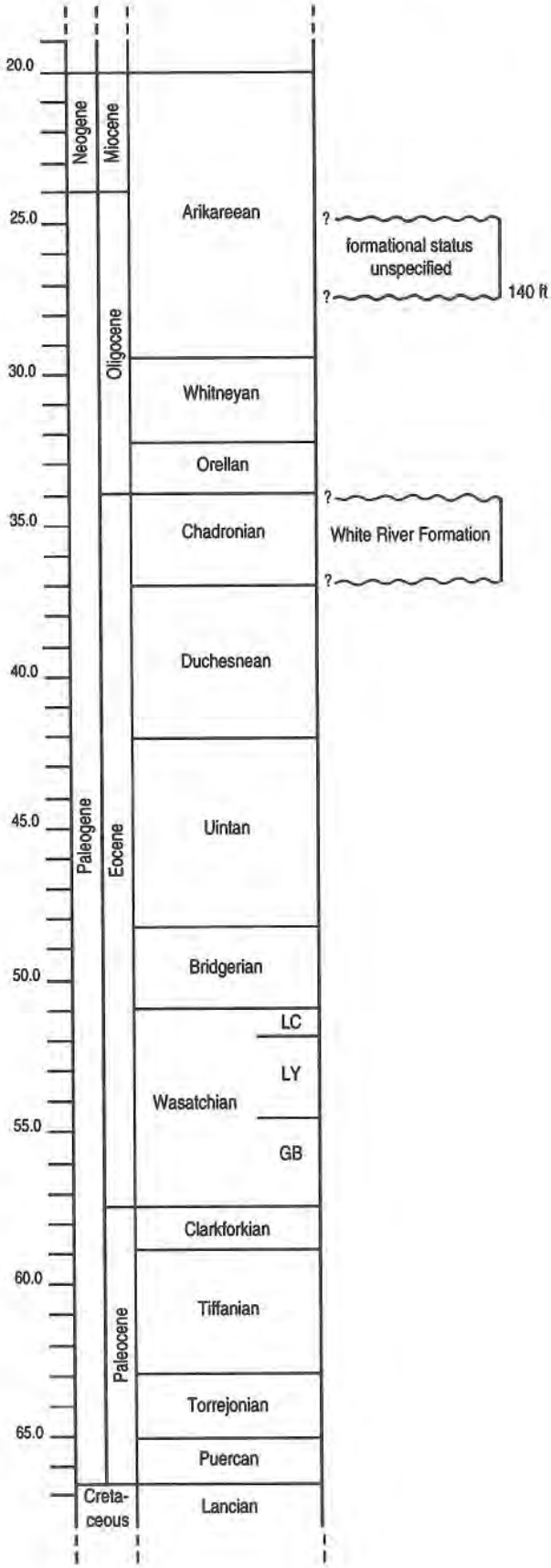

Figure 4L. Generalized Paleogene stratigraphy in vicinity of Section L (Figures 1 and 2) — **high-level deposits on Bighorn Mountains (exclusive of southern extreme)**, north-central Wyoming. Early Arikareean section measured at Darton's Bluff. White River Formation variously represented locally at Camp Creek (15 ft +), north of Clear Creek, headwaters of Gronmund Creek, and North Fork Crazy Woman Creek (300 ft).

Key literature to Paleogene history in vicinity of Section L
Darton, 1906
Hose, 1955
Kochel and Ritter, 1982
Love, 1978
McKenna, 1980b
McKenna and Love, 1972
Mapel, 1959
Osterwald, 1959

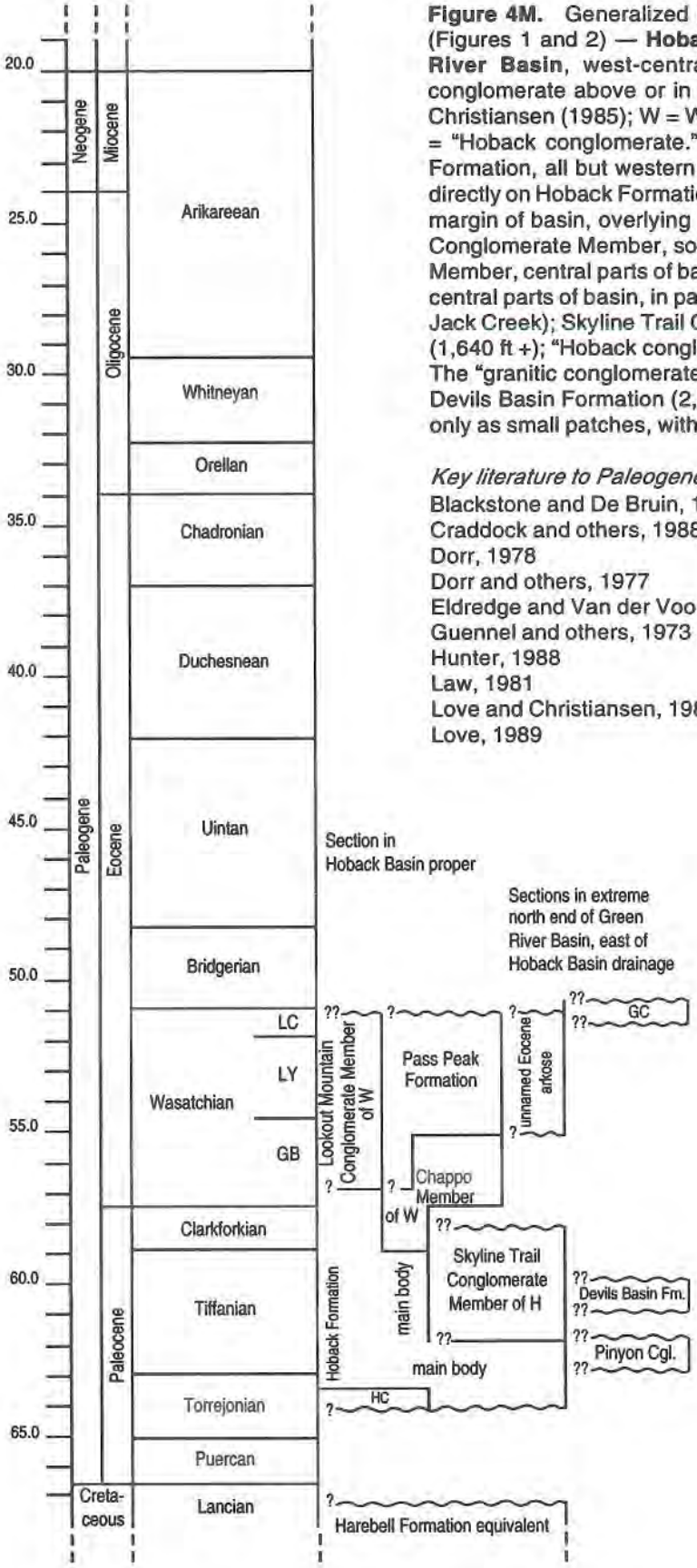

Figure 4M. Generalized Paleogene stratigraphy in vicinity of Section M (Figures 1 and 2) — **Hoback Basin and adjacent northernmost Green River Basin**, west-central Wyoming. *Abbreviations*: GC = "granitic conglomerate above or in upper part of Wasatch Formation" of Love and Christiansen (1985); W = Wasatch Formation.; H = Hoback Formation.; HC = "Hoback conglomerate." *Locations and local thicknesses*: Pass Peak Formation, all but western and eastern margins of basin, occasionally set directly on Hoback Formation (1,510 ft); "unnamed Eocene arkose," eastern margin of basin, overlying Hoback Formation (8,000 ft); Lookout Mountain Conglomerate Member, southwestern margin of basin (2,200 ft +); Chappo Member, central parts of basin (1,970 ft); "main body" of Hoback Formation, central parts of basin, in part enclosing Chappo Member (15,000 ft, north of Jack Creek); Skyline Trail Conglomerate Member, northern margin of basin (1,640 ft +); "Hoback conglomerate," northwestern margin of basin (100 ft). The "granitic conglomerate above or in upper part of Wasatch Formation," Devils Basin Formation (2,000 ft.), and Pinyon Conglomerate occur locally only as small patches, with most thicknesses uncertain.

Key literature to Paleogene history in vicinity of Section M

Blackstone and De Bruin, 1987
Craddock and others, 1988
Dorr, 1978
Dorr and others, 1977
Eldredge and Van der Voo, 1988
Guennel and others, 1973
Hunter, 1988
Law, 1981
Love and Christiansen, 1985
Love, 1989
Rose, 1981
Schmitt and Steidtmann, 1990
Shaughnessy and Butcher, 1974
Shuster and Steidtmann, 1988
Steidtmann and Middleton, 1991
Steidtmann and others, 1989
Steidtmann and Schmitt, 1988
Sullivan, 1980
Wiltschko and Dorr, 1983

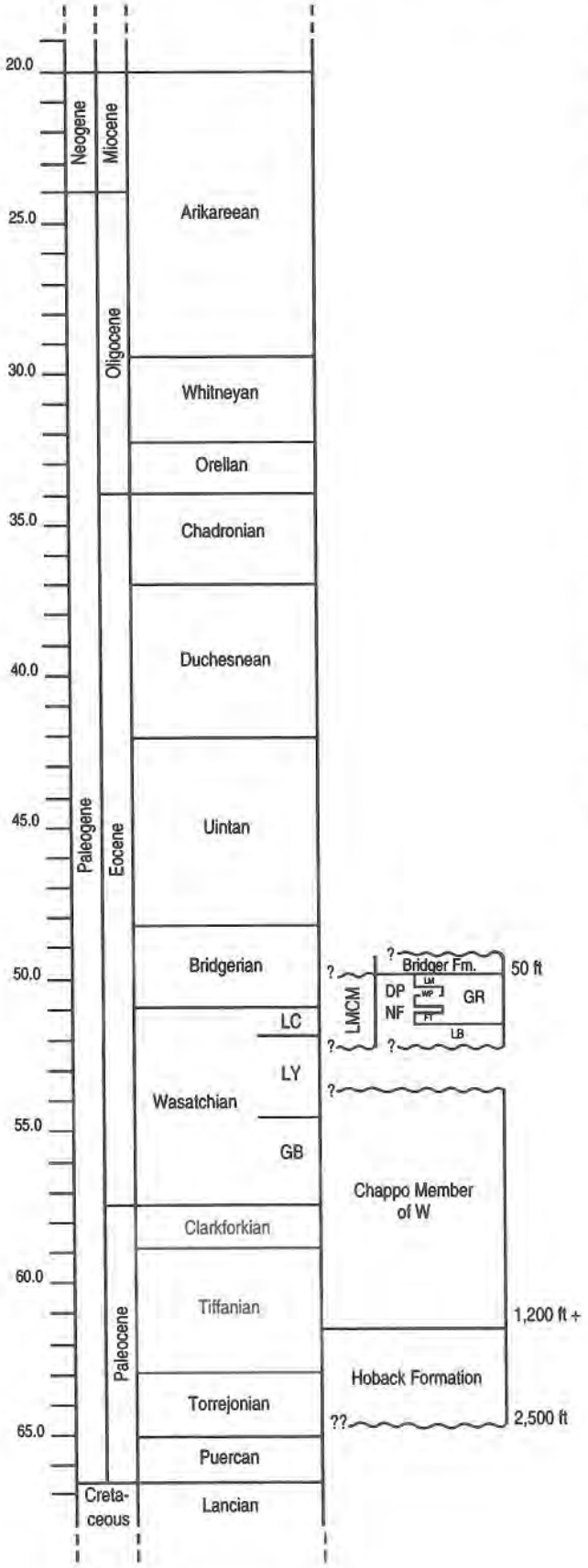

Figure 4N. Generalized Paleogene stratigraphy in vicinity of Section N (Figures 1 and 2) — **northwestern Green River Basin (La Barge)**, southwestern Wyoming. Hoback Formation occurs locally only in subsurface. *Abbreviations and local thicknesses*: GR = Green River Formation; LM = Laney Member of Green River Formation (250 ft); WP = Wilkins Peak Member of Green River Formation (295 ft); and FT = Fontenelle Tongue of Green River Formation (Tipton Tongue of more easterly Green River Basin) (150 ft); W = Wasatch Formation — DP = Desertion Point Tongue (200 ft); NF = New Fork Tongue (300 ft); LB = La Barge Member (1,500 ft); and LMCM = Lookout Mountain Conglomerate Member (3,000 ft +).

Key literature to Paleogene history in vicinity of Section N

Blackstone, 1979
Blackstone and De Bruin, 1987
Bradley, 1964
Dorr and Gingerich, 1980
Gazin, 1956c, 1962
Kraig and others, 1987
Lamerson, 1982
Markochick and others, 1982
Oriel, 1961, 1962, 1969
Rose, 1981
Ryder, 1988
Shuster and Steidtmann, 1988
Sullivan, 1980
Surdam and Stanley, 1979
West, 1970
West and Dawson, 1973
Wiltschko and Dorr, 1983

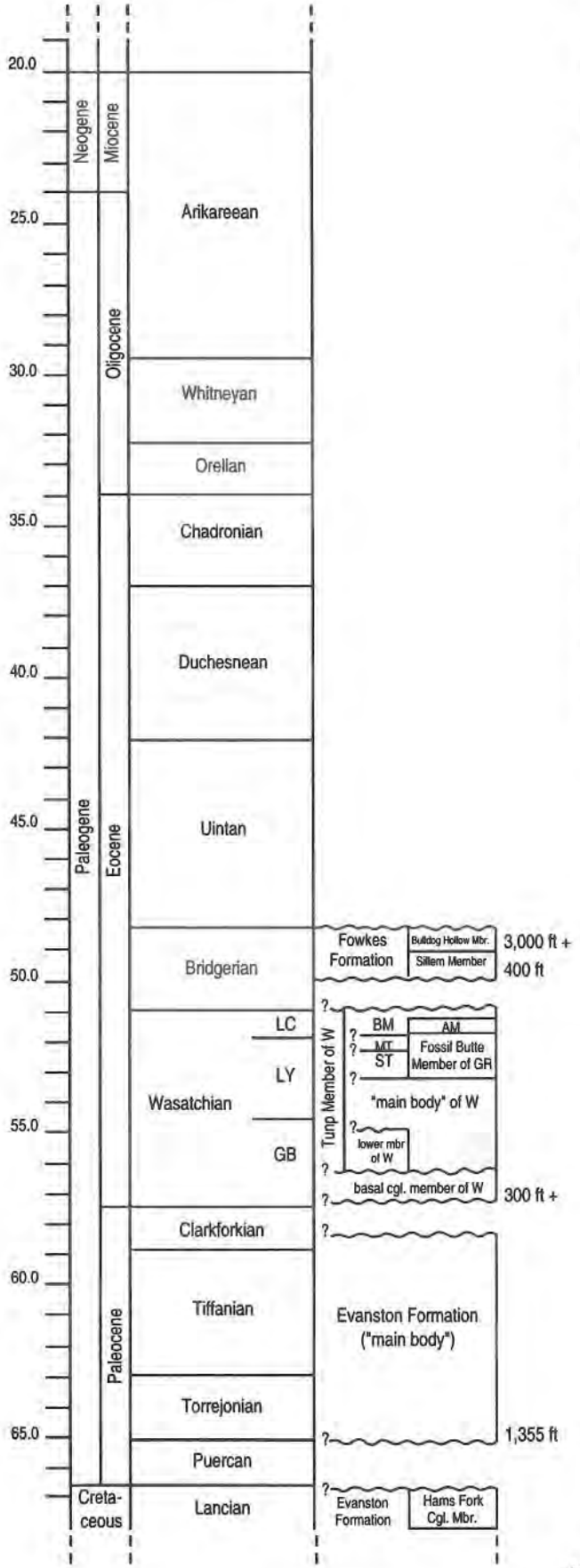

Figure 4O. Generalized Paleogene stratigraphy in vicinity of Section O (Figures 1 and 2) — **Fossil Basin**, southwestern Wyoming. Fowkes Formation measured north of Evanston. *Abbreviations and/or local thicknesses*: GR = Green River Formation — AM = Angelo Member (200 ft); and Fossil Butte Member (210 ft at Fossil Butte); W = Wasatch Formation — BM = Bullpen Member (320 ft); MT = "mudstone tongue" (60 ft); ST = "sandstone tongue" (50 ft); Tunp Member (500 ft); "main body" (1,700 ft at south end of basin); and "lower member" (300 ft).

Key literature to Paleogene history in vicinity of Section O
Blackstone and DeBruin, 1987
Bradley, 1964
Bryant and Nichols, 1988
Gazin, 1952, 1956a, 1962, 1969
Grande, 1984
Hansen, 1985
Hurst and Steidtmann, 1986
Jacobson and Nichols, 1982
Kraig and others, 1987
Lamerson, 1982
McGrew and Casilliano, 1975
Nelson, 1973, 1979
Oriel and Tracey, 1970
Roehler and others, 1977
Rubey and others, 1975
Steidtmann and Schmitt, 1988
Wiltschko and Dorr, 1983

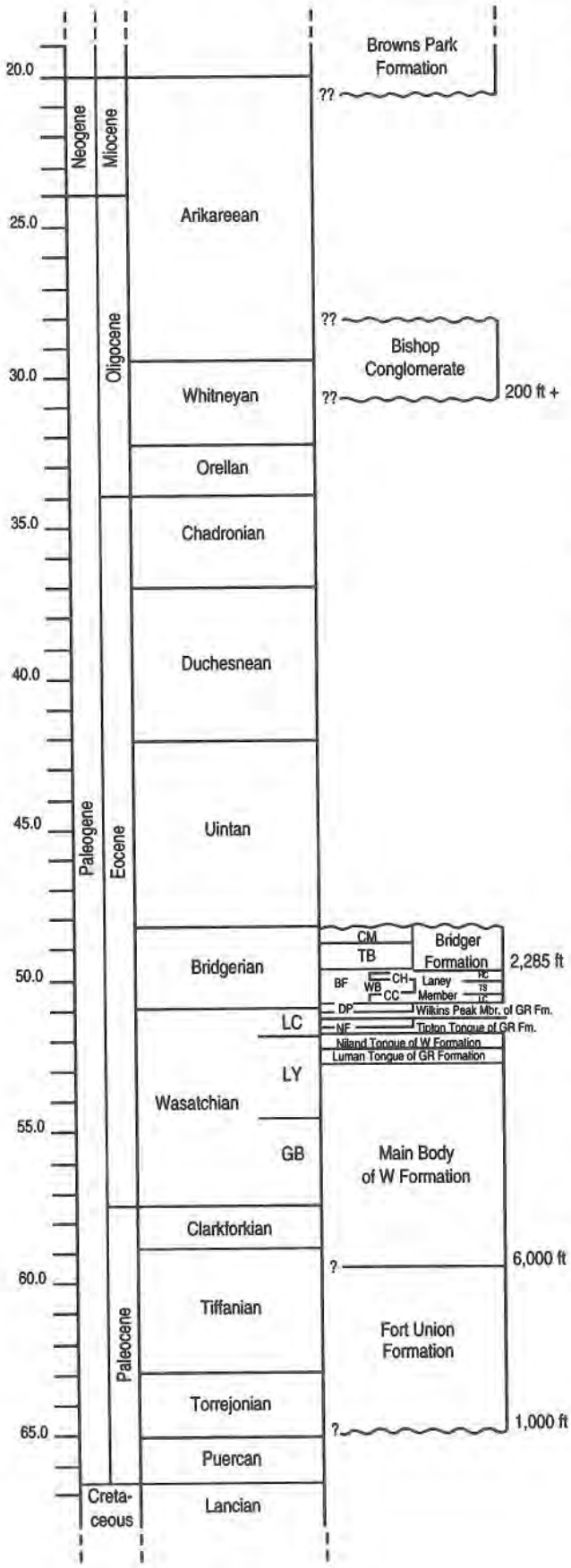

Figure 4P. Generalized Paleogene stratigraphy in vicinity of Section P (Figures 1 and 2) — **Bridger Basin, northern Uinta Mountains, southwestern Rock Springs uplift,** southwestern Wyoming. *Locations of thickness measurements:* Bishop Conglomerate (Aspen Mountain in southwestern Rock Springs uplift); Bridger Formation (north of Lonetree); Main Body of Wasatch Formation (southwest of Rock Springs uplift); and Fort Union Formation (southwest flank of Rock Springs uplift). *Abbreviations:* Bridger Formation — CM = Cedar Mountain Member (= Bridger "E" of Matthew, 1909); TB = Twin Buttes Member (= Bridger "C" plus "D" of Matthew, 1909); BF = Blacks Fork Member (= Bridger "A" plus "B" of Matthew, 1909); and WB = Whiskey Butte Bed; GR = Green River Formation (with all following terms relating to its Laney Member.) — CH = Cow Hollow Bed; CC = Craven Creek Bed; HC = Hartt Cabin Bed; TS = Tower Sandstone Lentil (term generally abandoned); and LC = La Clede Bed; W = Wasatch Formation — DP = Desertion Point Tongue; and NF = New Fork Tongue. Local designation of Tipton Tongue of Green River Formation is Fontenelle Tongue of western Green River Basin.

Key literature to Paleogene history in vicinity of Section P

Bradley, 1936, 1964
Buchheim and Surdam, 1977
Eugster and Hardie, 1975
Eugster and Surdam, 1973
Gazin, 1976
Grande, 1984
Hanley, 1976, 1977
Hansen, 1965, 1984, 1985
Kirschbaum, 1987
Kirschbaum and Nelson, 1988
McGrew and Sullivan, 1970
Markochick and others, 1982
Matthew, 1909
Mauger, 1977
Ritzma, 1971
Roehler, 1973a,b, 1977, 1983
Roehler and others, 1977
Ryder, 1988
Sklenar and Andersen, 1985
Smoot, 1983
Stockton and Hawkins, 1985
Sullivan, 1980, 1985
Surdam and Stanley, 1979, 1980
Surdam and Wolfbauer, 1975
West, 1976
West and Hutchison, 1981

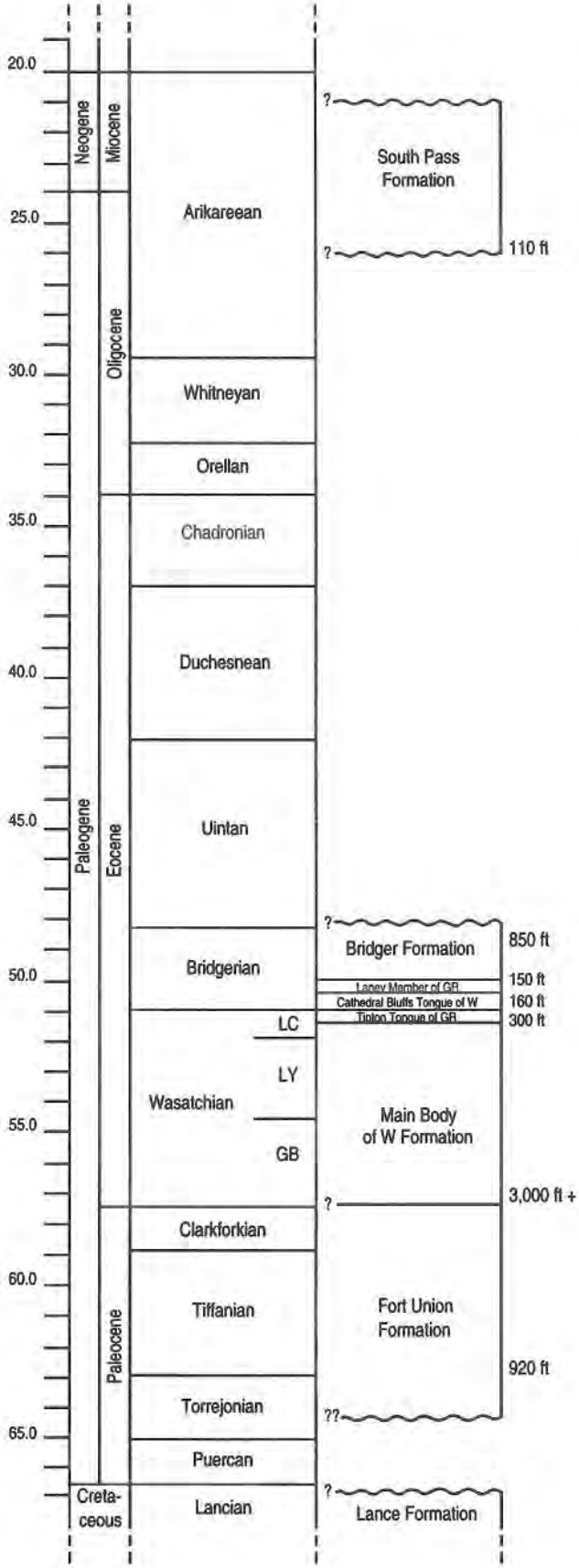

Figure 4Q. Generalized Paleogene stratigraphy in vicinity of Section Q (Figures 1 and 2) — **northeastern Green River Basin, southern Wind River Range**, south-central Wyoming. *Locations of thickness measurements:* South Pass Formation (north of Continental fault); Bridger Formation (west of Oregon Buttes); Laney Member (Oregon Buttes); Cathedral Bluffs Tongue (east of Oregon Buttes); Tipton Tongue (Oregon Buttes); Main Body of Wasatch Formation (near Oregon Buttes); and Fort Union Formation (outcrop along north flank of Rock Springs uplift, becoming dramatically thicker in subsurface along southwestern flank of Wind River Range). *Abbreviations:* GR = Green River Formation and W = Wasatch Formation.

Key literature to Paleogene history in vicinity of Section Q

Antweiler and others, 1980
Bottjer, 1984
Bradley, 1964
Groll, 1986
Groll and Steidtmann, 1987
Jackson, 1984
Law, 1981
McGrew and others, 1959
McKenna and others, 1962
Roehler, 1977, 1983
Ryder, 1988
Shuster and Steidtmann, 1988
Stanley and Surdam, 1978
Steidtmann and others, 1983, 1986, 1989
Steidtmann and Middleton, 1986, 1991
Sullivan, 1980
Surdam and Stanley, 1980
West, 1973
Zeller and Stevens, 1969

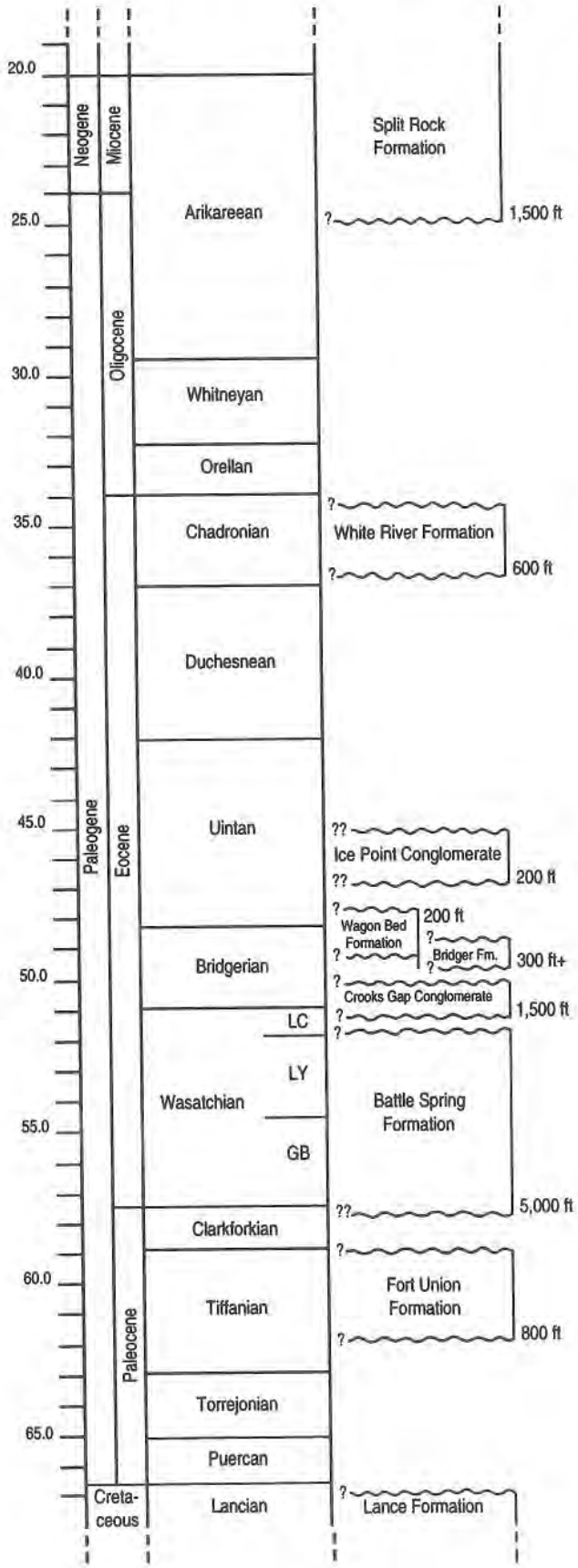

Figure 4R. Generalized Paleogene stratigraphy in vicinity of Section R (Figures 1 and 2) — **northern Great Divide Basin, Bison Basin, southern Granite Mountains**, south-central Wyoming. *Locations of thickness measurements*: Split Rock Formation (north of Crooks Mountain); White River Formation (southwestern flanks of Granite Mountains); Ice Point Conglomerate (at type section on southwestern flank of Granite Mountains); Wagon Bed Formation (north of Flattop fault); Bridger Formation (south of Flattop fault); Crooks Gap Conglomerate (Crooks Mountain); Battle Spring Formation (estimated subsurface maximum in northern Great Divide Basin); and Fort Union Formation (Bison Basin).

Key literature to Paleogene history in vicinity of Section R
Bell, 1955
Denson and Pipiringos, 1974
Gazin, 1956b
Keefer and Love, 1963
Love, 1970
Munthe, 1979
Pipiringos, 1961
Pipiringos and Denson, 1970

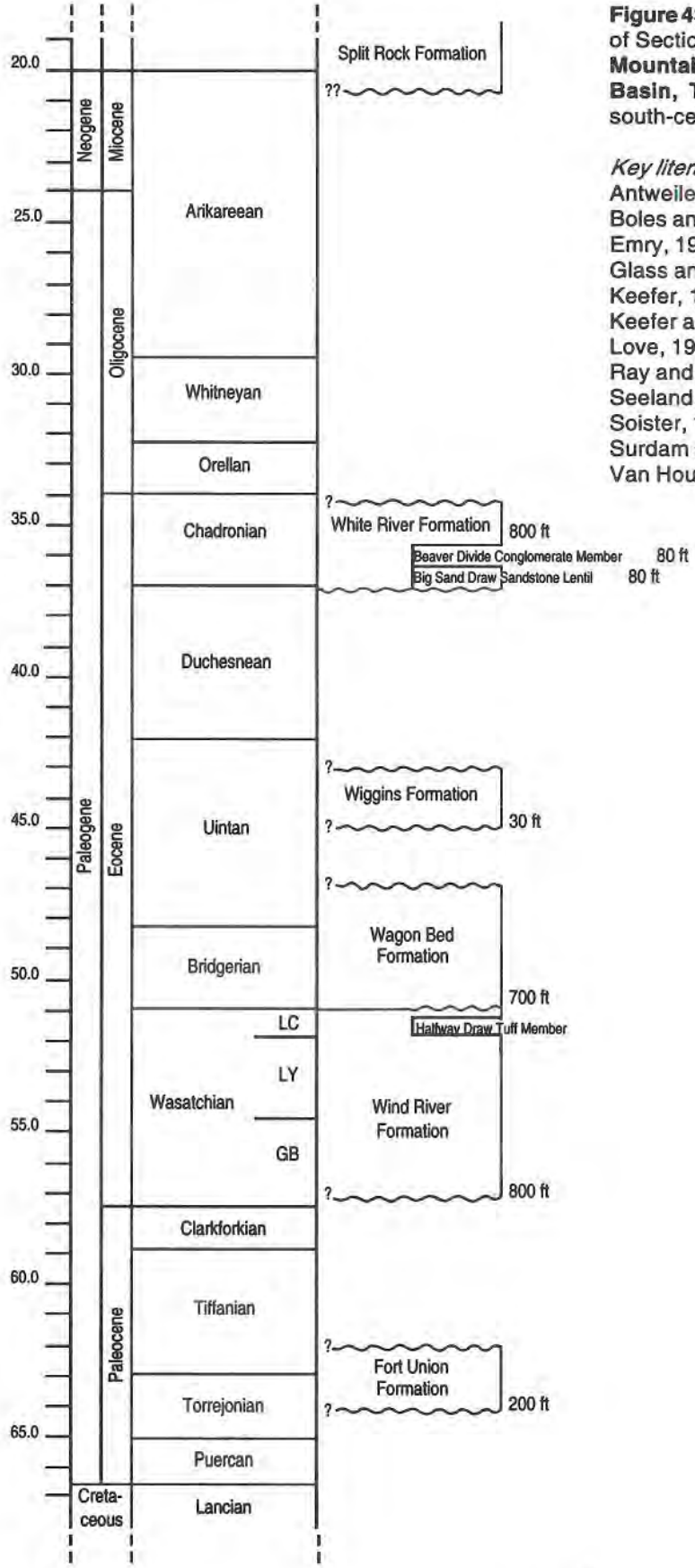

Figure 4S. Generalized Paleogene stratigraphy in vicinity of Section S (Figures 1 and 2) — **northwestern Granite Mountains (Beaver Rim), southwestern Wind River Basin, Twin Creek (southeastern Wind River Range),** south-central Wyoming.

Key literature to Paleogene history in vicinity of Section S
Antweiler and others, 1980
Boles and Surdam, 1971,1979
Emry, 1975
Glass and Roberts, 1978
Keefer, 1965, 1970
Keefer and Love, 1963
Love, 1970, 1988a
Ray and Keefer, 1985
Seeland, 1978a,b
Soister, 1968
Surdam and Stanley, 1980
Van Houten, 1955, 1964

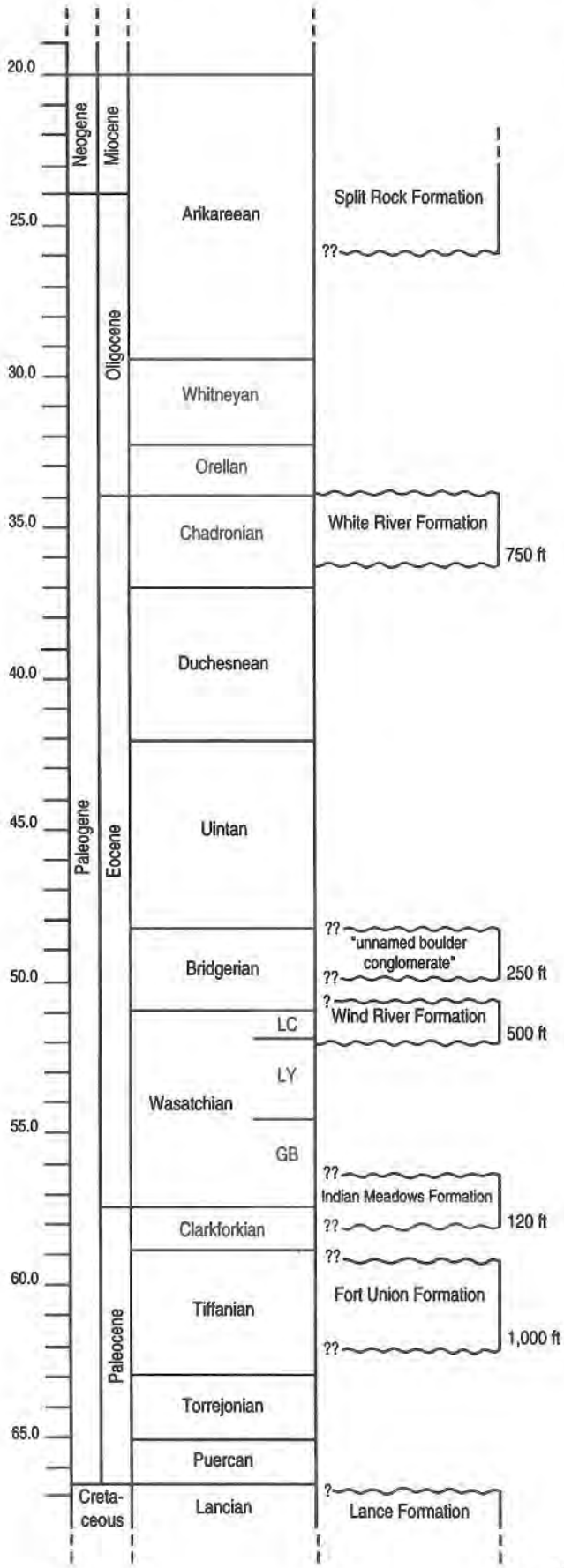

Figure 4T. Generalized Paleogene stratigraphy in vicinity of Section T (Figures 1 and 2) — **northeastern Granite Mountains (Flagstaff Rim, Ledge Creek), southeastern Wind River Basin**, south-central Wyoming. *Locations of thickness measurements*: "unnamed boulder conglomerate" (Clarkson Hill and Flat Top); Wind River Formation (outcrop in southeastern salient of Wind River Basin, becoming much thicker in subsurface); Indian Meadows Formation (east side of Clarkson Hill); and Fort Union Formation (margins of southeastern salient of Wind River Basin).

Key literature to Paleogene history in vicinity of Section T

Emry, 1973
Glass and Roberts, 1978
Keefer, 1965, 1970
Lillegraven and others, 1981
Love, 1970, 1988a
Pekarek, 1978
Prothero, 1985
Prothero and others, 1982, 1983
Ray and Keefer, 1985
Rich, 1962
Seeland, 1978a,b
Sheriff and Shive, 1980
Skinner and Gooris, 1966
Swisher and Prothero, 1990

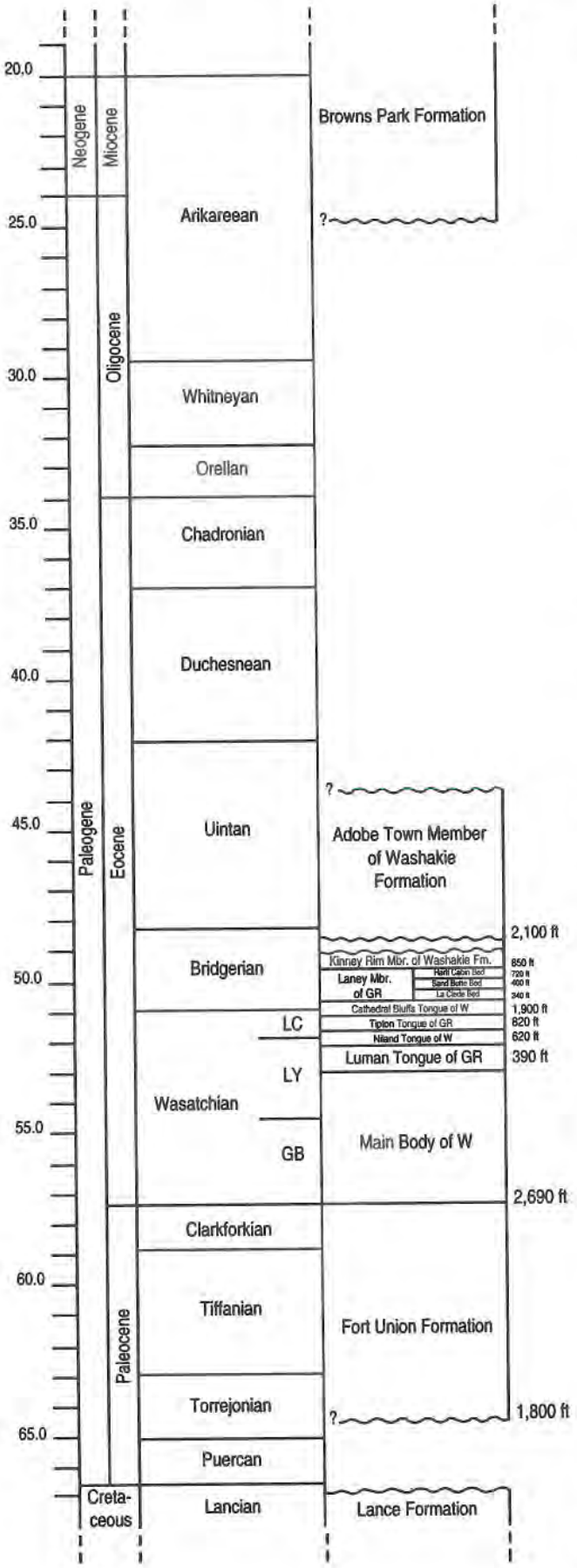

Figure 4U. Generalized Paleogene stratigraphy in vicinity of Section U (Figures 1 and 2) — **eastern Rock Springs uplift, Wamsutter arch, Washakie Basin, western Sierra Madre**, south-central and southeastern Wyoming. Browns Park Formation occurs locally only along south rim of Washakie Basin. Hettinger and others (1991) and Honey and Hettinger (1989) report on "unnamed Cretaceous and Tetiary sandstone unit" (up to 1,100 ft. thick) along eastern flank of Washakie Basin. *Locations of thickness measurements*: Adobe Town Member (Adobe Town Rim); Kinney Rim Member (southwestern Washakie Basin); Laney Member (including Hartt Cabin, Sand Butte, and La Clede beds; central Washakie Basin); Cathedral Bluffs Tongue, Tipton Tongue, Niland Tongue, Luman Tongue, and Main Body (south of Bitter Creek Station); and Fort Union Formation (vicinity of Black Butte Coal Company Mine). *Abbreviations*: GR = Green River Formation and W = Wasatch Formation.

Key literature to Paleogene history in vicinity of Section U

Breithaupt, 1982
Colson, 1969
Flynn, 1986
Grande, 1984
Hanley, 1976, 1977
Hettinger and others, 1991
Honey and Hettinger, 1989
Izett, 1975
Izett and others, 1970
Korengay and Surdam, 1980
McKenna, 1960
Mauger, 1977
Morris, 1954
Rigby, 1980
Roehler, 1973a,b, 1977, 1979a,b, 1983
Rose, 1981
Ryder, 1988
Savage and Russell, 1983
Sklenar and Andersen, 1985
Stanley and Surdam, 1978
Sullivan, 1980
Surdam and Stanley, 1979, 1980
Surdam and Wolfbauer, 1975
Turnbull, 1978, 1991
Turnbull and Martill, 1988
Winterfeld, 1982

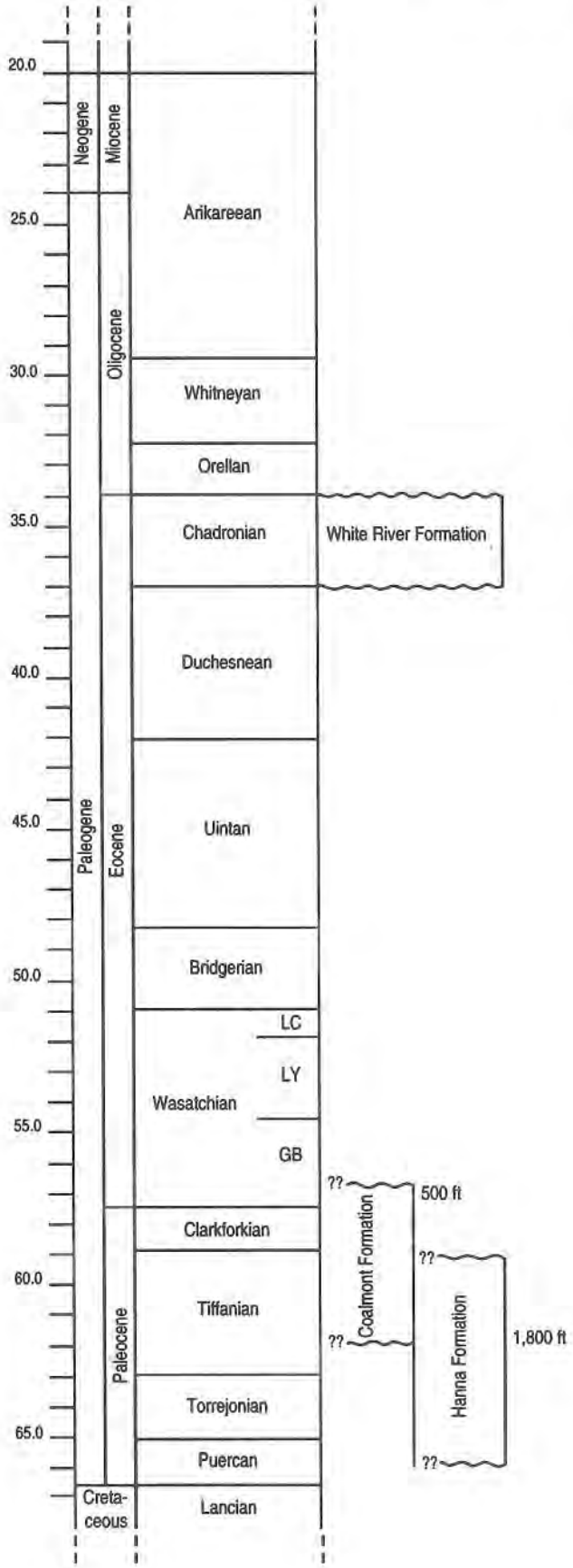

Figure 4V. Generalized Paleogene stratigraphy in vicinity of Section V (Figures 1 and 2) — **Saratoga Basin, northwestern and southwestern Medicine Bow Mountains**, south-central and southeastern Wyoming. White River Formation is present immediately across state boundary with Colorado on southwestern flanks of Medicine Bow Mountains (thickness undesignated). Coalmont Formation occurs locally in southwestern Saratoga Basin. Hanna Formation exists locally as coarse facies on northwestern flanks of Medicine Bow Mountains. According to Malcolm C. McKenna (written communication, 1991), the base of the rock unit mapped by Montagne (1957) as "Browns Park Formation" in Big Creek Park (southeastern Sierra Madre), Wyoming may represent late Arikareean time.

Key literature to Paleogene history in vicinity of Section V

Evanoff, 1990
Blackstone, 1975
Gries, 1964
Houston and others, 1968
Love and Christiansen, 1985
Love and others, 1987
McCallum, 1968
McGrew, 1953
Montagne, 1957, 1991

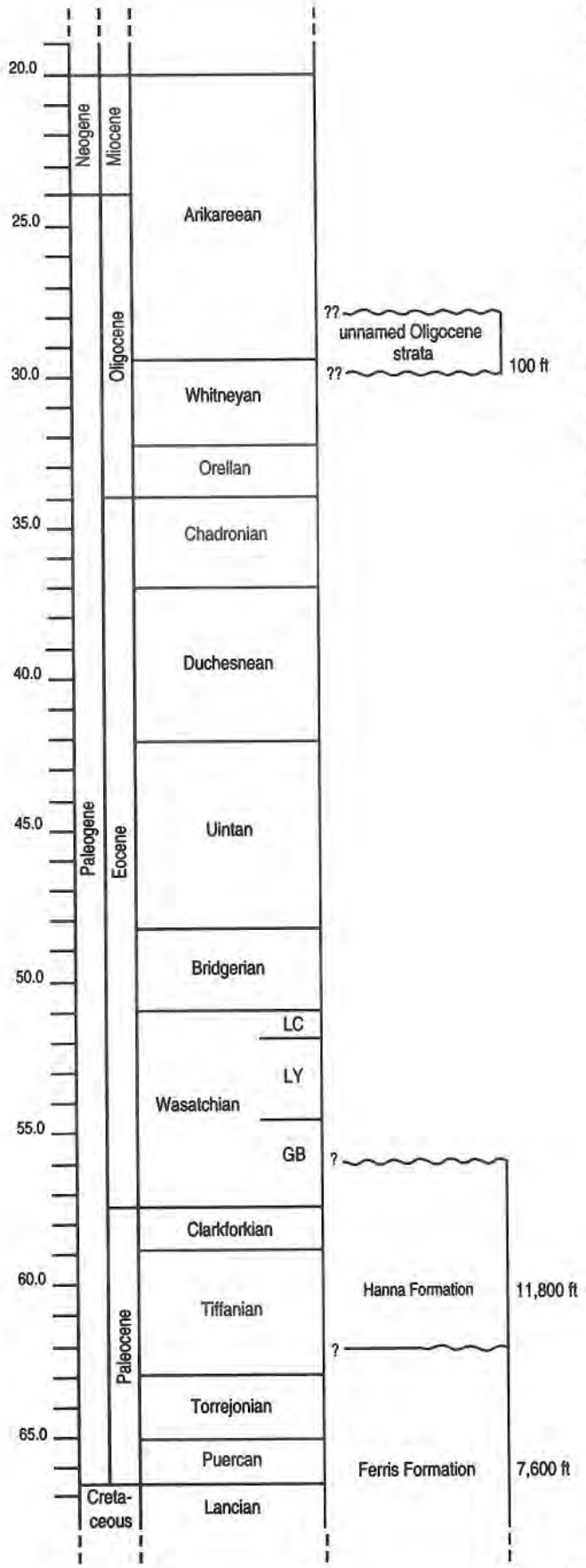

Figure 4W. Generalized Paleogene stratigraphy in vicinity of Section W (Figures 1 and 2) — **Hanna Basin, Carbon Basin**, south-central and southeastern Wyoming. "Unnamed Oligocene strata" (sensu LeFebre, 1988) are present on northern margin of Hanna Basin, set on Ferris and Medicine Bow formations. Contacts between Hanna and Ferris formations, while probably conformable in midreaches of Hanna Basin, occur with angular unconformities in Carbon Basin and eastern Hanna Basin. Hanna Formation measured in "The Breaks" (northeastern corner of Hanna Basin) by the author. Basal Hanna Formation is Torrejonian in age in Carbon Basin.

Key literature to Paleogene history in vicinity of Section W

Blackstone, 1975, 1983
Blanchard and Comstock, 1980
Bowen, 1918
Cardinal and Parsons, 1982
Dobbin and others, 1929
Gill and others, 1970
Glass, 1975
Glass and Roberts, 1980a,b, 1984
Hansen, 1986
Kaplan and Skeen, 1985
Kirschner, 1984
Knight, 1951
LeFebre, 1988
Ryan, 1977
Teerman and others, 1985

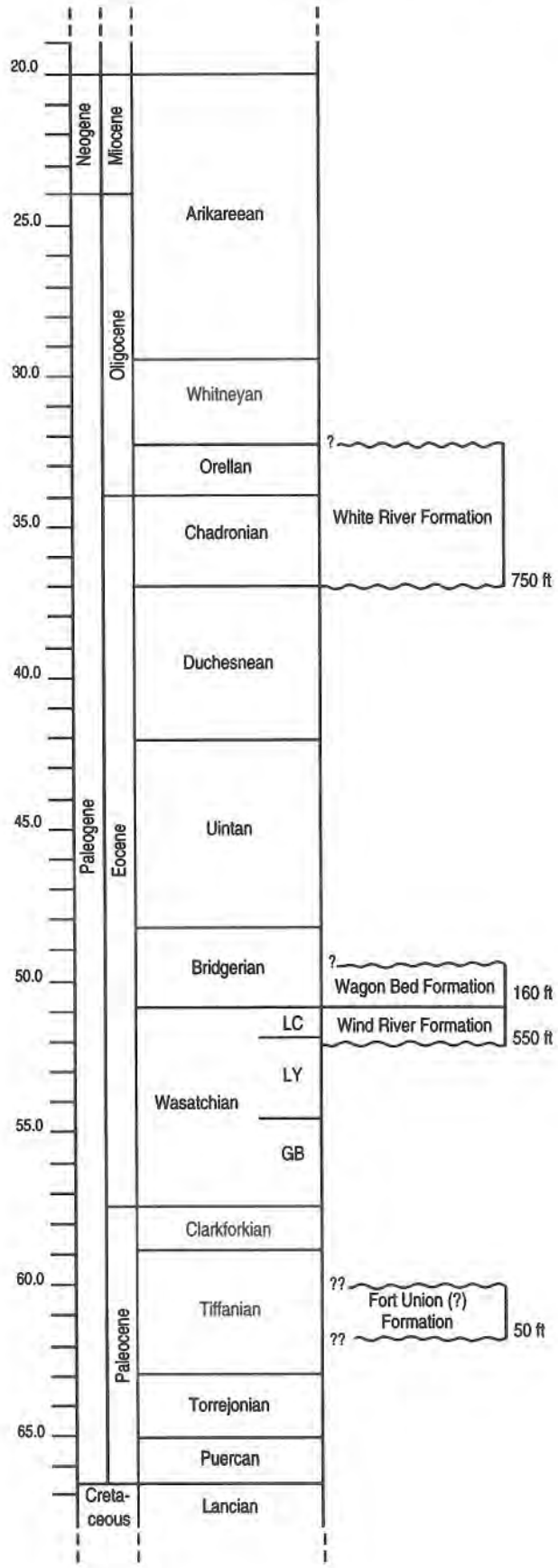

Figure 4X. Generalized Paleogene stratigraphy in vicinity of Section X (Figures 1 and 2) — **Shirley Basin, Bates Hole, northwestern Laramie Mountains**, south-central and southeastern Wyoming. The "Arikaree Formation" of Harshman (1972) probably is post-Arikareean in age (see Roehler, 1958).

Key literature to Paleogene history in vicinity of Section X
Denson and Harshman, 1969
Evanoff, 1990
Harshman, 1968, 1972
Roehler, 1958
Seeland, 1985

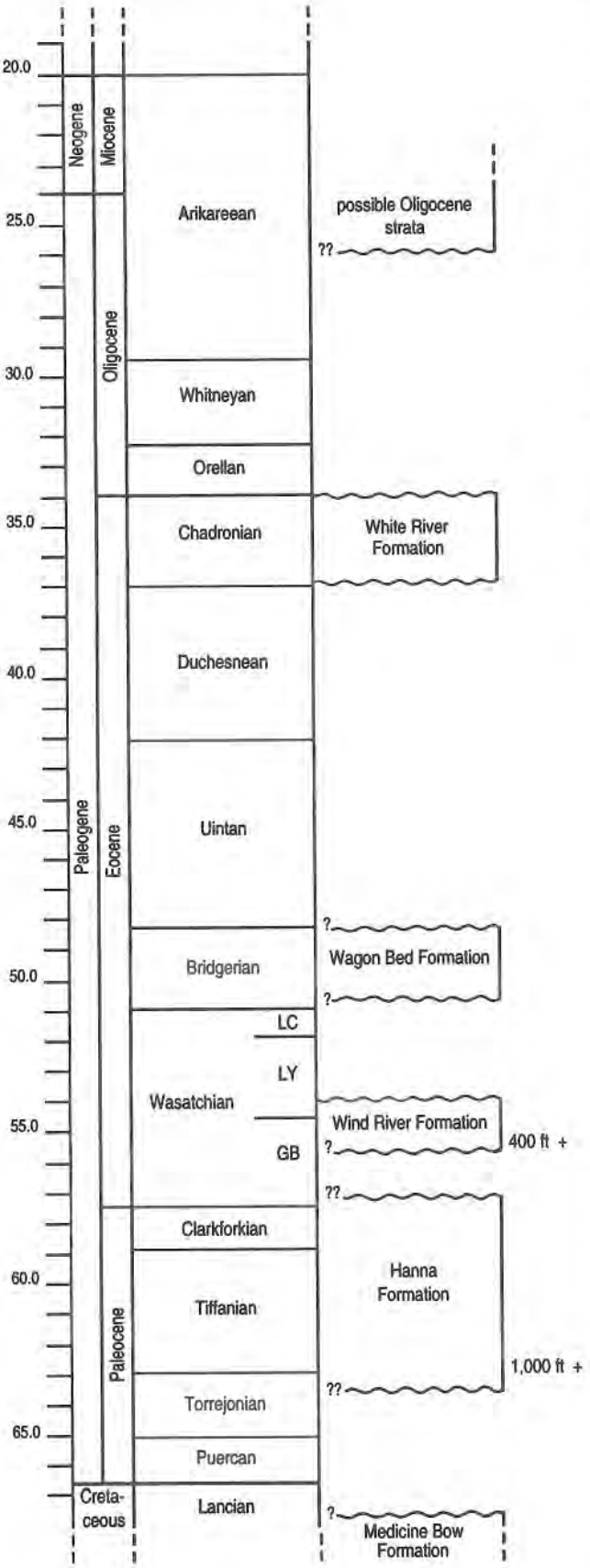

Figure 4Y. Generalized Paleogene stratigraphy in vicinity of Section Y (Figures 1 and 2) — **northeastern and southeastern Medicine Bow Mountains, Laramie Basin (Cooper Lake Basin)**, southeastern and east-central Wyoming. *Locations of sections*: "possible Oligocene strata" (southeastern flanks of Medicine Bow Mountains; thickness unreported); White River Formation (southern extreme of Centennial Valley; 300 ft); Wagon Bed Formation (northeastern corner of Laramie Basin; thickness unreported); Wind River Formation (Cooper Lake Basin); and Hanna and Medicine Bow formations (northeastern flank of Medicine Bow Mountains). Hanna Formation includes Foote Creek (upper parts) and Dutton Creek formations of Hyden and others (1965).

Key literature to Paleogene history in vicinity of Section Y
Beckwith, 1942
Blackstone, 1975, 1983, 1987
Davidson, 1987
Hyden and others, 1965
Knight, 1953
Love and Christiansen, 1980, 1985
McCallum, 1968
McGrew, 1953
Prichinello, 1971

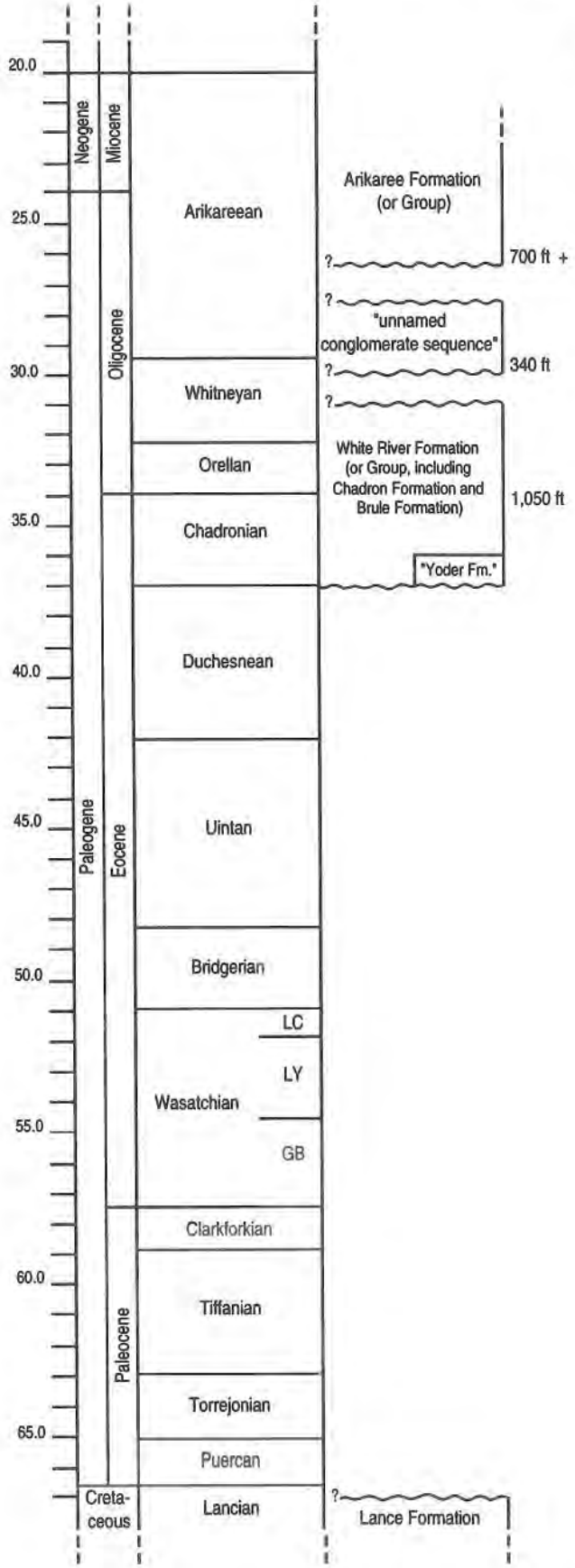

Figure 4Z. Generalized Paleogene stratigraphy in vicinity of Section Z (Figures 1 and 2) — **eastern Laramie Mountains, northern Denver-Julesburg Basin, Goshen Hole**, southeastern and east-central Wyoming. The "unnamed conglomerate sequence" (see McGrew, 1963) uniquely occurs near Fort Laramie.

Key literature to Paleogene history in vicinity of Section Z

Albrandt and Groen, 1987
Curtis, 1988
Denson and Botinelly, 1949
Emry and others, 1987
Hunt, 1985, 1990
Johnson and Smithson, 1985
McGrew, 1963
Moore, 1960
Prothero and others, 1983
Schlaikjer, 1935
Stanley, 1976
Swinehart and others, 1985

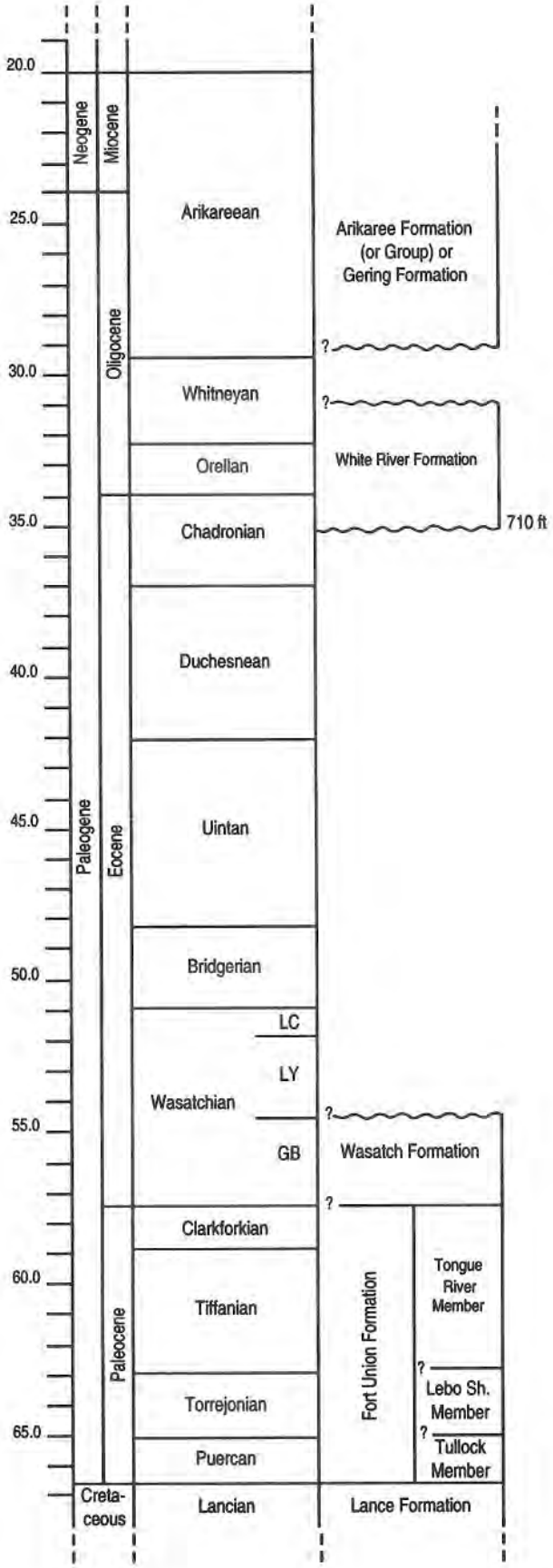

Figure 4AA. Generalized Paleogene stratigraphy in vicinity of Section AA (Figures 1 and 2) — **northeastern Laramie Mountains, Hartville uplift, Pine Ridge, southeastern Powder River Basin**, southeastern and east-central Wyoming. Thickness measurement for White River Formation is from Dilts Ranch, where only Chadronian and Orellan parts of section are preserved. Total local thickness for Fort Union Formation is 1,500 ft.

Key literature to Paleogene history in vicinity of Section AA
Ayers, 1986
Ayers and Kaiser, 1984
Curry, 1971
Denson and Botinelly, 1949
Evanoff, 1990
Flores and Ethridge, 1985
Kron, 1978
Leffingwell, 1970
Love, 1988c
Marrs and Raines, 1984
Prothero, 1985
Prothero and others, 1982, 1983
Seeland, 1976
Swisher and Prothero, 1990

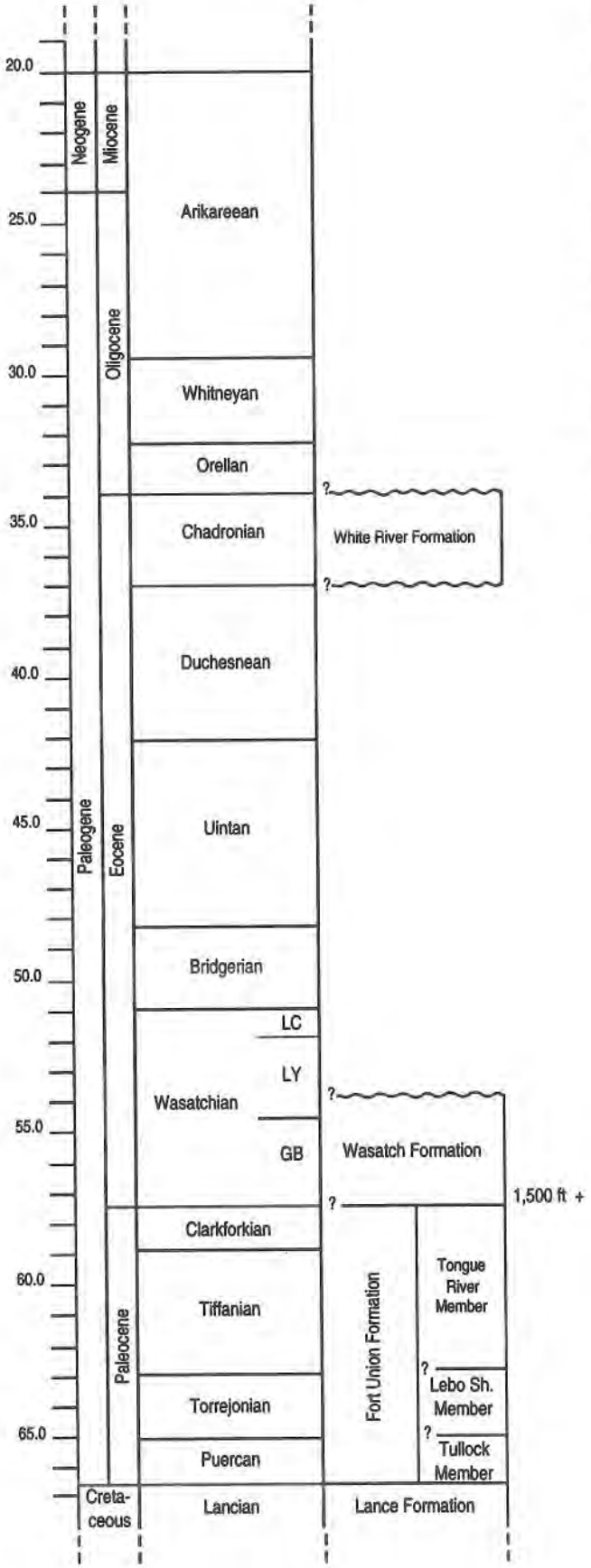

Figure 4BB. Generalized Paleogene stratigraphy in vicinity of Section BB (Figures 1 and 2) — **central Powder River Basin, Pumpkin Buttes**, southeastern and east-central Wyoming. Local thickness of White River Formation (caprock at Pumpkin Buttes) is in dispute: 250 ft (Love, 1952) versus 50 ft (Sharp and others, 1964). Total local thickness for Fort Union Formation is 2,800 ft. According to Malcolm C. McKenna (written communication, 1991), the White River Formation at Pumpkin Buttes may be Orellan in age (not Chadronian), as based upon undescribed mammalian fossils in collections at The American Museum of Natural History.

Key literature to Paleogene history in vicinity of Section BB

Curry, 1971
Delson, 1971
Flores and Ethridge, 1985
Love, 1952, 1988c
McKenna and Love, 1972
Marrs and Raines, 1984
Seeland, 1976
Sharp and others, 1964

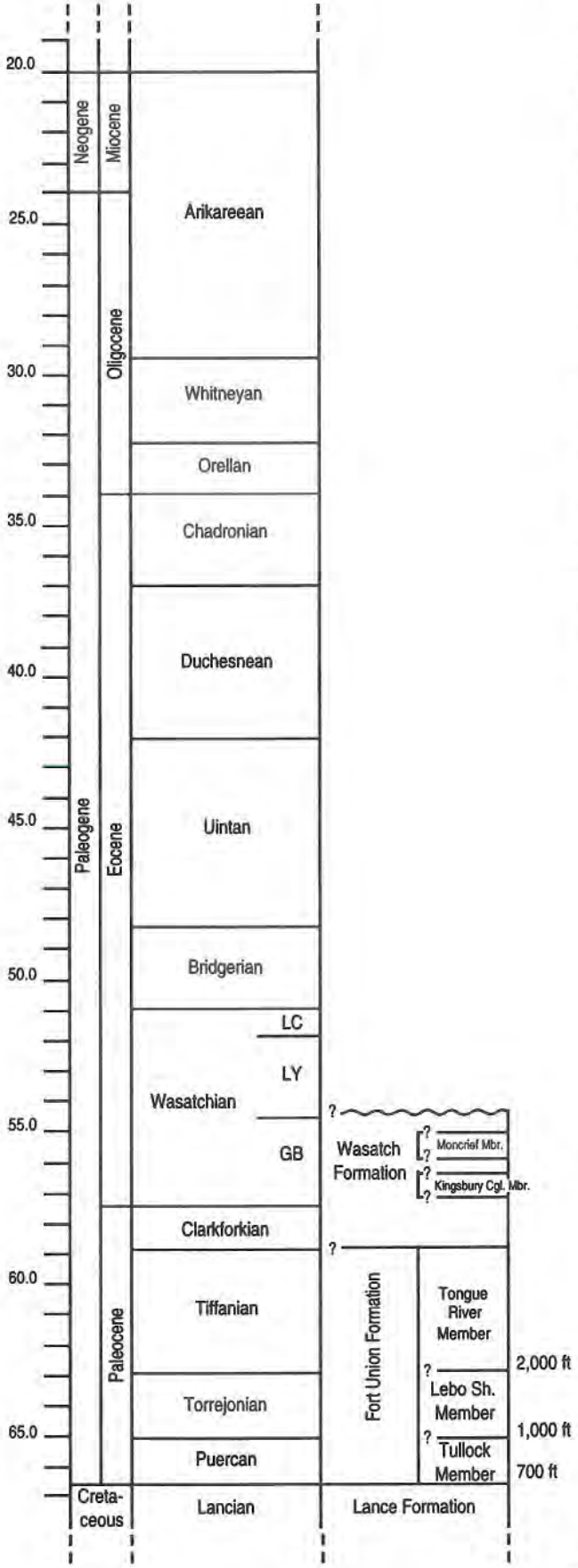

Figure 4CC. Generalized Paleogene stratigraphy in vicinity of Section CC (Figures 1 and 2) — **northern Powder River Basin**, northeastern Wyoming. Moncrief Member (1,400 ft) and Kingsbury Conglomerate Member (800 ft) are restricted to easternmost flanks of Bighorn Mountains and adjacent edges of Powder River Basin. Total local basinal thickness of Wasatch Formation is 2,000 ft.

Key literature to Paleogene history in vicinity of Section CC

Ayers, 1986
Ayers and Kaiser, 1984
Bressler and Elston, 1981
Brown, 1948
Curry, 1971
Flores and Ethridge, 1985
Flores and Hanley, 1984
Hose, 1955
Law and others, 1979
Love, 1988c
Mapel, 1959
Marrs and Raines, 1984
Merin and Lindholm, 1986
Obernyer, 1979
Pocknall, 1987a,b
Seeland, 1976
Tschudy, 1976

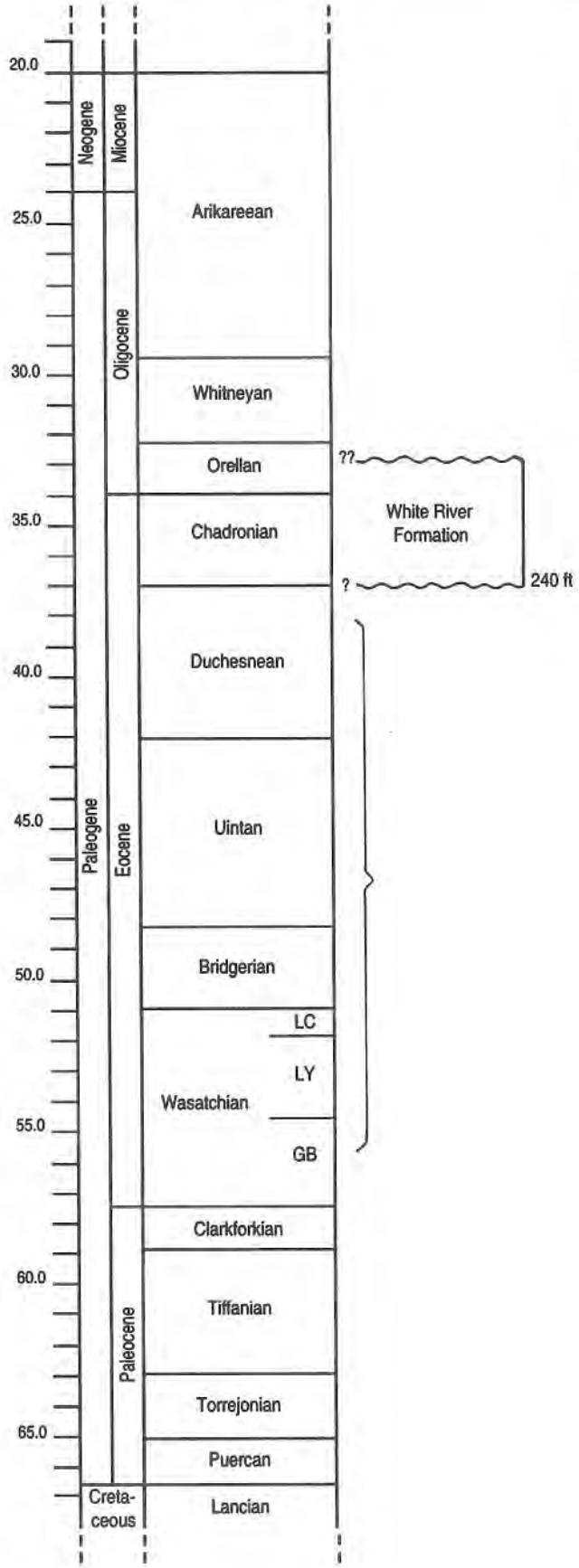

Figure 4DD. Generalized Paleogene stratigraphy in vicinity of Section DD (Figures 1 and 2) — **uplands of northwestern Black Hills**, northeastern Wyoming. Thickness measurement for White River Formation is characteristic for sections at Missouri Buttes and Bear Lodge Mountains. Bracket indicates range of Paleogene radiometric dates reported from several intrusives in Wyoming parts of northwestern Black Hills (as summarized by Lisenbee, 1985).

Key literature to Paleogene history in vicinity of Section DD
Chadwick, 1985
Flanagan, 1990
Lisenbee, 1978, 1985, this volume
McKenna and Love, 1972
Robinson and others, 1964

General features of Wyoming's Paleogene stratigraphic record

Consistency of interbasinal stratigraphic representation through Paleogene time

Although the following discussion cannot be couched in any formal statistical sense, comparative inspection of sections A through DD (**Figure 4A** through **DD**) provides an excellent sense for the consistency of interbasinal completeness, or lack thereof, of Wyoming's Paleogene stratigraphic record. In constructing **Figure 5**, I made the assumption that all formational tops and bottoms are correct as they appear on columns presented in **Figures 4A** through **4DD**. As can be seen by the relative ubiquity of queries (single and double) on those sections, however, my assumption of the correctness in correlation cannot be defended at any fine level of detail. Nevertheless, the resulting distribution of presence (dark-stippled pattern) or absence (light-stippled pattern) of Paleogene strata shows a temporal consistency that I believe realistically reflects local geologic history. Because I was interested specifically in the nature of hiatuses that developed during Paleogene time, the light-stippled pattern in **Figure 5** was used only within sections capped by Arikareean or older strata. **Figures 6** and **7** are derivatives of **Figure 5**.

Figure 6 shows the absolute dominance of Paleocene through earlier Eocene strata in preserved parts of Wyoming's Paleogene record. Earlier parts of this excellent record (Paleocene through much of the Wasatchian) represents basin filling related to subsidence and uplift during the Laramide orogeny. Except for long-lived tectonic persistence in the vicinity of the Uinta Mountains (and probably the Rock Springs uplift), effects of the Laramide orogeny as seen in Wyoming were reduced greatly during late Wasatchian time. Beginning in the late Wasatchian, major volcanic centers came into being in northwestern Wyoming, southwestern Montana, and east-central Idaho; all of these contributed importantly, both through fluvial and airfall processes, to continuation of sedimentary aggradation across Wyoming's basins and mountain flanks. Volcanic input, combined with detrital influx by way of localized erosion within enormous hydrographic basins that involved large areas of adjacent states (see Lillegraven and Ostresh, 1988), was especially important across Wyoming during Bridgerian and Uintan time. Most of Wyoming's Laramide uplands remained largely exposed during that interval, also contributing locally derived clastic debris to surrounding basins.

An end result of the combined influences cited immediately above was that sedimentary accumulation across Wyoming's basins, which resulted initially from Laramide subsidence (i.e., Paleocene into late Wasatchian), continued virtually unabated during post-orogenic time, at least through the Uintan. As discussed below, however, much of the post-Bridgerian through pre-Chadronian record subsequently was lost as a result of profound erosion during Duchesnean time.

Figure 6 depicts effects of sudden influx across Wyoming during Chadronian time of massive volumes of ashfall, derived from distant volcanic sources. Contributing volcanic centers to the west (and perhaps south) of Wyoming certainly were multiple, but involved most notably, from a volumetric point of view, Nevada and adjacent parts of the Great Basin (see Armstrong and Ward, in press). Although remnant distribution of Chadronian and Oligocene sedimentary rocks in Wyoming is limited (**Figures 2** and **6**), Chadronian through early Arikareean volcaniclastic strata are widespread across southwestern Montana, western South Dakota and Nebraska, and northeastern Colorado; prodigious output of debris from western volcanoes thus is clearly shown to have continued throughout this interval.

As suggested in **Figure 8**, aggradation of distantly derived volcaniclastic sediments probably continued across the landscape of Wyoming well beyond the end of the Chadronian, through most of Oligocene time, and even into the late Neogene (see Flanagan and Montagne, this volume). The basins of Wyoming gradually became filled, with sediments lapping high onto the flanks of Laramide ranges by late Neogene time. Prior to the latest Paleogene, however, most of Wyoming's mountains remained topographically higher than the surrounding aggradational plains. Steidtmann and others (1989)

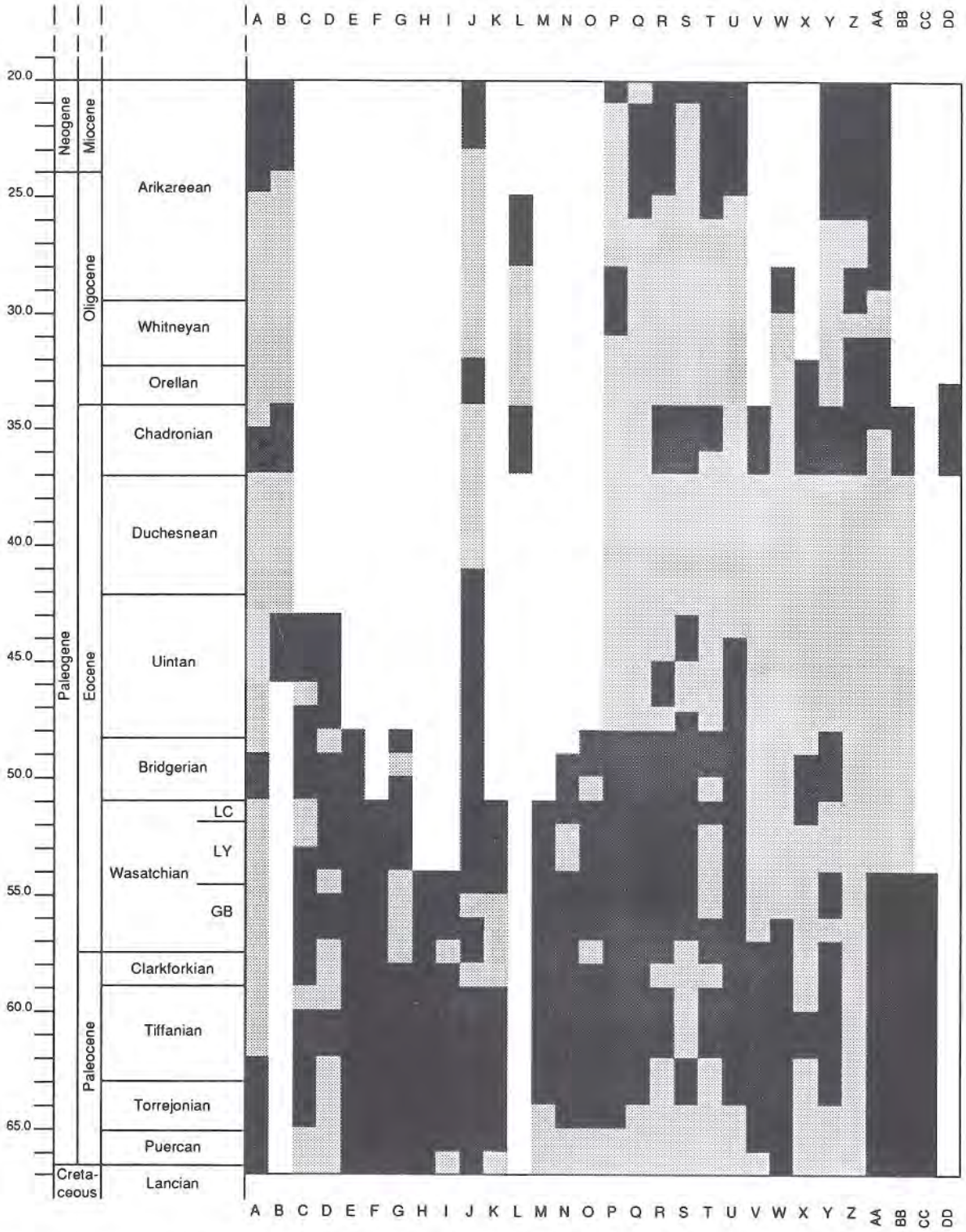

Figure 5. Summary chart comparing distributions of geologic ranges of sedimentary occurrences (dark-stippled pattern) and temporal hiatuses (light-stippled pattern) seen within Figure 4 (A through DD), as rounded to estimated million-year intervals. Light-stippled pattern is applied only within sections capped by rocks of Arikareean age, or older. Because the bases of Figure 4 (B, L, and DD) are set upon much older rocks (and probably never did have an older Paleogene component), the light-stippled pattern is not used in those columns below the oldest represented sedimentary rocks. Figures 6 and 7 are derived from (horizontal) counts, for each approximately million year interval, of presence of an actual rock record (Figure 6) or a hiatus (Figure 7).

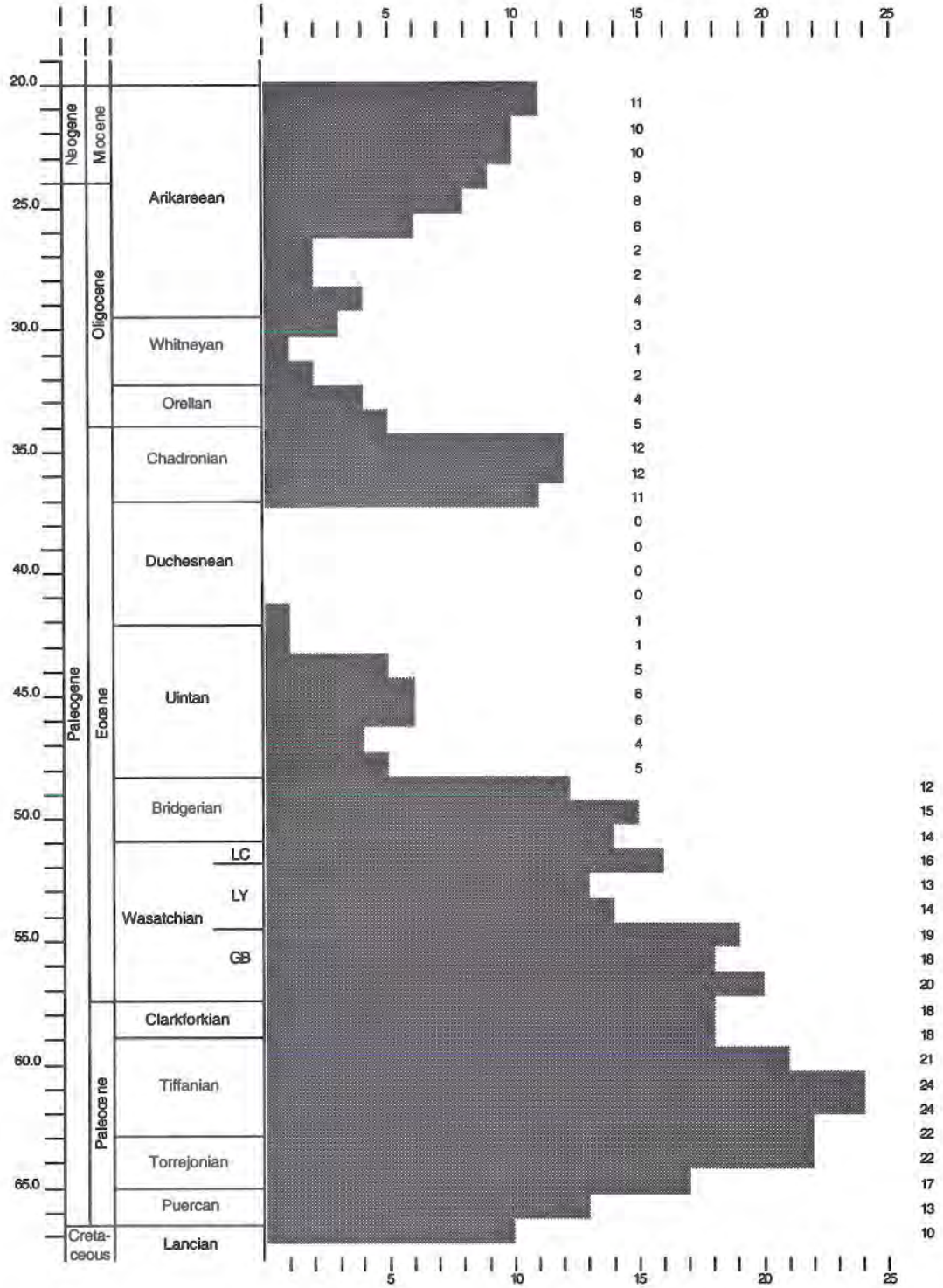

Figure 6. Histogram derived from occurrences of sedimentary records in Figure 4 (A through DD) (dark-stippled patterns), as summarized in Figure 5. Consistency of occurrences across the state shows that the Paleogene record of Wyoming is dominated by sedimentary rocks of Torrejonian through Bridgerian age, initially representing basinal fills associated with the Laramide Orogeny, then followed without interruption (beginning in late Wasatchian) by major volcaniclastic input from the local Absaroka/Gallatin/Challis volcanic centers (refer to Fig. 8). A secondary sedimentary cover is represented by massive influx of more distantly-derived, Chadronian volcaniclastics. In all probability, aggradational depositional regimes continued statewide throughout Uintan and Orellan-early Arikareean times, with subsequent losses resulting from at least two discrete intervals of widespread erosion (see Fig. 7).

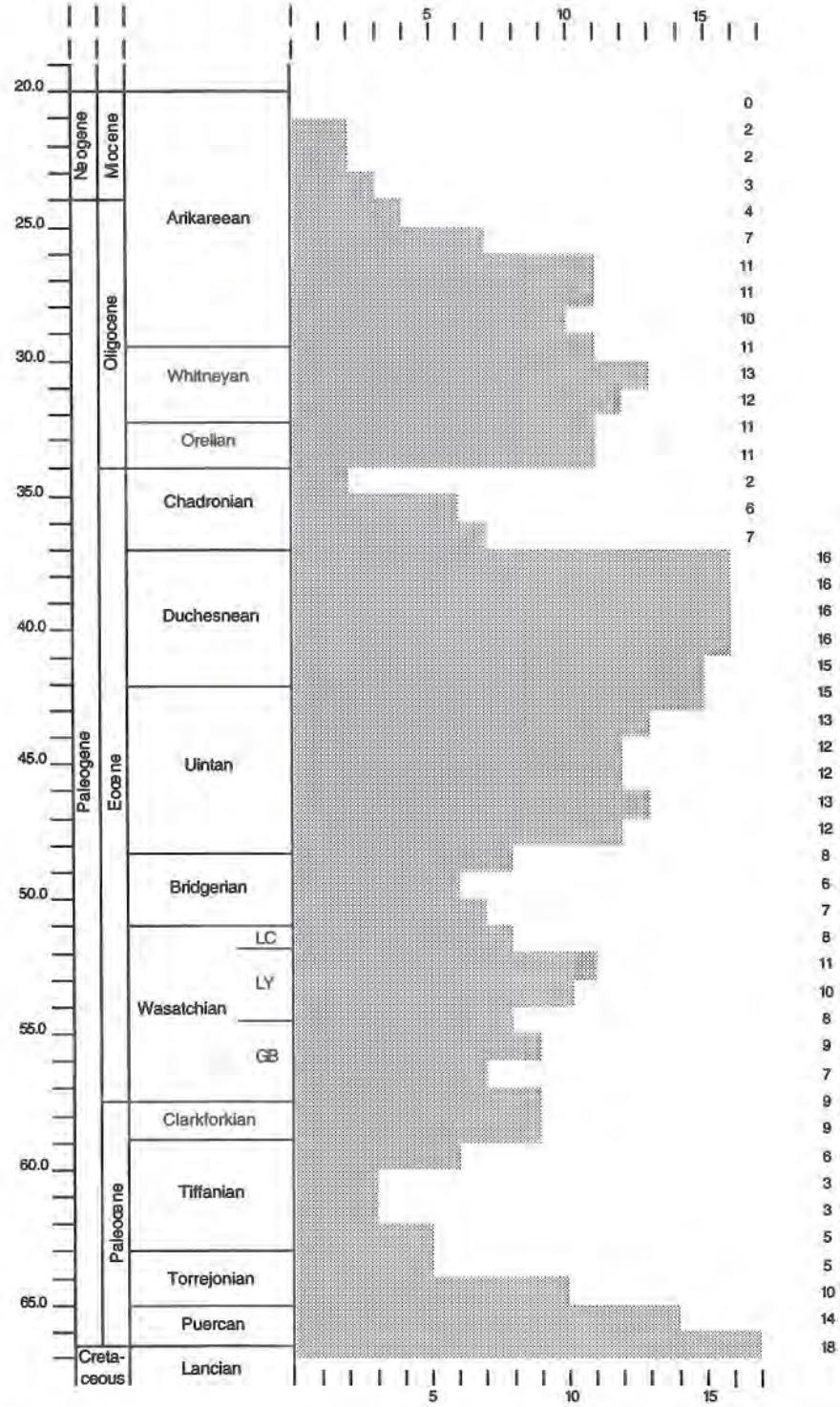

Figure 7. Histogram derived from occurrences of temporal hiatuses within sedimentary records of Figure 4 (A through DD) (light-stippled pattern), as summarized in Figure 5. The widespread hiatus indicated for the Puercan (and perhaps part of Torrejonian) probably was restricted largely to basinal margins, associated with early uplift histories of large, adjacent Laramide structures (refer to Fig. 8). The late Eocene hiatus is much more profound, having occurred statewide; the all-encompassing late Eocene gap in Wyoming's sedimentary record probably represents a Duchesnean interval of intense erosion that was influential across much of western North America. A final Paleogene interval of nearly statewide erosion appears to have occurred during some part of the earlier half of Arikareean time.

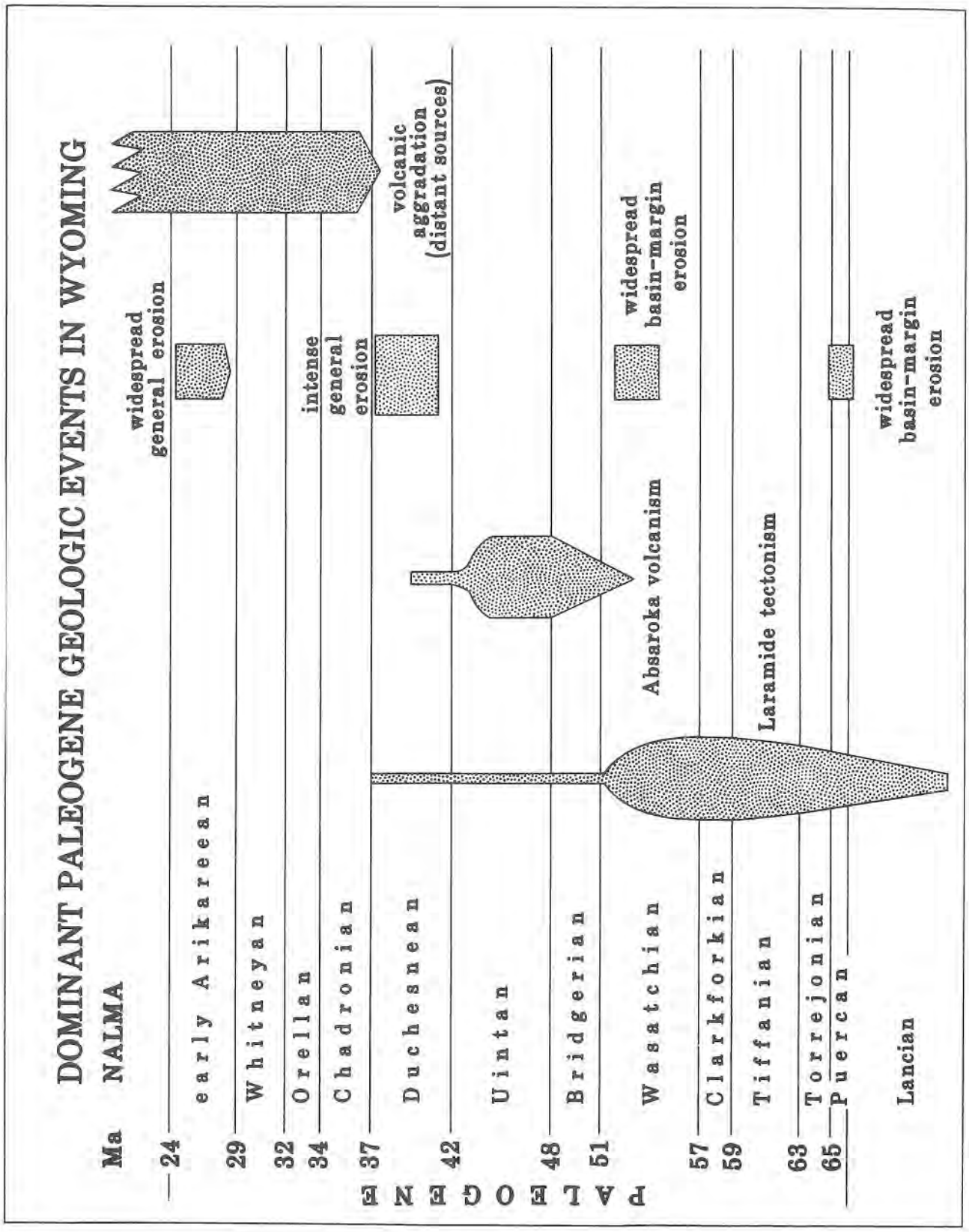

Figure 8. Qualitative balloons suggesting relative timings and magnitudes of major geological events that profoundly influenced the landscape of Wyoming during latest Cretaceous and Paleogene time. Aggradation of volcanic sediments derived from distant sources continued across Wyoming into the late Miocene. Modified and redrafted from Lillegraven and Ostresh (1988).

suggested that the core of the Wind River Range exhibited differential uplift relative to surrounding basins during the Oligocene, with elevation beginning well after the end of the Laramide orogeny.

Statewide consistency of missing section through Paleogene time

The statewide consistency of Paleogene hiatuses (as defined in **Figure 5**) is summarized in **Figure 7**. Because many of the stratigraphic columns presented in **Figures 4 (A through DD)** represent tectonically unstable, basin-margin paleoenvironmental settings, it is not surprising that so many brief diastems exist through the total record. Commonly across the state, for example, earliest Paleocene strata (Puercan and part of the Torrejonian) are missing. In all probability, however, deposition was essentially uninterrupted in central parts of most of Wyoming's basins from latest Cretaceous through early Paleocene time.

Figures 5 and **7** indicate important but geographically scattered centers of erosion during late Wasatchian. These probably were restricted to localized areas in which Laramide subsidence had abated (or even ceased), but in which influx of locally derived volcanic debris had not yet become a major feature.

Much more clearly demonstrable is the consistency of a late Eocene, pre-Chadronian interval of erosion. As suggested in **Figure 6**, strata of late Duchesnean age are unknown in Wyoming. Evanoff (1990) and many other previous workers recognized that Chadronian strata across Wyoming typically were deposited upon topographically complex, deeply incised, erosional surfaces. As can be inferred from **Figure 5**, basinal rocks of the White River Formation in Wyoming typically were deposited on erosional surfaces cut into strata of Uintan, Bridgerian, or Wasatchian age. Only on high-level surfaces of the Washakie Range, Bighorn Mountains, southern Medicine Bow Mountains, and Black Hills, and in northern parts of the Denver-Julesburg Basin was the White River Formation deposited exclusively upon pre-Cenozoic rocks.

It seems highly probable, therefore, that an interval of profound erosion dominated Wyoming during pre-Chadronian, late phases of Eocene time. Specifically, I suggest that it occurred during some part of the Duchesnean. As summarized by Lillegraven and Ostresh (1988) and Epis and Chapin (1975), such an interval of intense erosion affected not only Wyoming statewide, but also the Rocky Mountains in general and, perhaps, most of western North America. The late Eocene erosional interval in Wyoming and adjacent areas was terminated by massive influx of distantly derived volcaniclastic sediments in Chadronian time; such input and subsequent aggradational depositional settings continued, with sporadic interruptions, into the late Tertiary.

I infer from **Figures 5** and **7** the existence of a final, pre-Neogene erosional interval that affected much of Wyoming's landscape. Sediments of Arikareean age in Wyoming generally are set with marked erosional unconformity upon older rocks, typically Chadronian or older. As pointed out above, adjacent parts of states surrounding Wyoming exhibit important volcaniclastic-dominated sections of Orellan, Whitneyan, and early Arikareean age, thus showing almost certainly that sedimentary influx continued across the state during that interval. Accumulation of volcaniclastic sediments probably continued to blanket Wyoming from Orellan through at least early Arikareean time, most sediments of which were eroded away before early phases of the Neogene.

The correlation chart for mid-Tertiary basins of western Montana developed by Fields and others (1985) shows several examples of missing section for the late Oligocene and earliest Miocene, suggesting influence of Arikareean erosion beyond the northern border of Wyoming. Also, Love (1970) clearly suggested that a major interval of erosion, affecting much of southern and southeastern Wyoming, occurred prior to deposition of the local Miocene sequences. Although available evidence from Wyoming provides little opportunity for precision in dating, I suggest that this last interval of widespread erosion occurred late in Paleogene time, probably during the medial Arikareean.

A broad-brush look at Wyoming's Paleogene geological evolution

Figure 8 provides a generalized, graphic summary of the sequence of most important geologic events that influenced evolution of Wyoming's Paleogene landscape. Additional detail can be gained from the paleogeographic reconstructions and text presented by Lillegraven and Ostresh (1988), from the figures and text of the present paper, and from the large sampling of pertinent literature cited in conjunction with **Figure 4 (A through DD)**, above.

Clearly, there still exist highly significant gaps in our knowledge of Wyoming's Paleogene history; many exciting revelations and surprises await additional inquiry. Nevertheless, in reference to Paleogene time, the geologic history of Wyoming is better understood than any other comparably sized tract of Earth's dry land. Profound influences upon attainment of that level of scientific knowledge have derived from career-long efforts in the field, laboratory, and classroom by D.L. Blackstone, Jr. and J. David Love.

Acknowledgments

I extend sincere thanks to the professional staff of The University of Wyoming's Geology Library, especially to Christine L. Van Burgh, Keith E. Clarey, and Linda R. Zellmer. U.W. geology students Sheryl A. Hansen, Cheryl C. Jaworowski, and Michael B. Leite contributed information for sections of the paper dealing with the Powder River, Wind River, and Bighorn basins, respectively. The following institutions provided various kinds of support to the project: National Science Foundation (grant DEB-8105454 and EAR-8205211); National Geographic Society's Committee for Research and Exploration (grant 4280-90); Alexander von Humboldt Stiftung; Kuehn Committee, U.W. College of Arts and Sciences; and U.W. Office of Research and Graduate Studies. Drs. D.L. Blackstone, Jr., Malcolm C. McKenna, and Donald E. Savage provided technical criticism of the manuscript. My wife, Linda E. Lillegraven, also helped in its preparation in innumerable ways. I thank Arthur W. Snoke, James R. Steidtmann, and Sheila Roberts for the opportunity to participate in this tribute. Finally, and most importantly, I thank Drs. D.L. Blackstone, Jr. and J. David Love for the professional inspiration and personal friendship that both have given me over the past 15 years.

References cited

Ahlbrandt, T.S., and Groen, W., 1987, The Goshen Hole uplift: a brief review of its geologic history and exploration potential: The Mountain Geologist, v. 24, p. 34-44.

Albertus, R.G., 1985, Eastern Jackson Hole, *in* Gries, R.R., and Dyer, R.C., editors, Seismic exploration of the Rocky Mountain region: Rocky Mountain Association of Geologists and Denver Geophysical Society, p. 67-72.

Antweiler, J.C., Love, J.D., Mosier, E.L., and Campbell, W.L., 1980, Oligocene gold-bearing conglomerate, southeast margin of Wind River Mountains, Wyoming: Wyoming Geological Association 31st Annual Field Conference Guidebook, p. 223-237.

Archibald, J.D., Clemens, W.A., Gingerich, P.D., Krause, D.W., Lindsay, E.H., and Rose, K.D., 1987, First North American land mammal ages of the Cenozoic Era, *in* Woodburne, M.O., editor, Cenozoic mammals of North America: geochronology and biostratigraphy: Berkeley, University of California Press, p. 24-76.

Armstrong, R.L., and Ward, P., in press, Late Triassic to earliest Eocene magmatism in the North American Cordillera: implications for the Western Interior Basin, *in* Caldwell, W.G.E., and Kauffman, E.G., editors, The Western Interior Basin: Geological Association of Canada Special Paper 39.

Aubry, M.-P., Berggren, W.A., Kent, D.V., and others, 1988, Paleogene geochronology: an integrated approach: Paleoceanography, v. 3, p. 707-742.

Ayers, W.B., Jr., 1986, Lacustrine and fluvial-deltaic depositional systems, Fort Union Formation (Paleocene), Powder River Basin, Wyoming and Montana: American Association of Petroleum Geologists Bulletin, v. 70, p. 1651-1673.

Ayers, W.B., Jr., and Kaiser, W.R., 1984, Lacustrine-interdeltaic coal in the Fort Union Formation (Paleocene), Powder River Basin, Wyoming and Montana, *in* Rahmani, R.A., and Flores, R.M., editors, Sedimentology of coal and coal-bearing sequences: Oxford, Blackwell Scientific Publications, International Association of Sedimentologists Special Publication 7, p. 61-84.

Badgley, C., 1990, A statistical assessment of last appearances in the Eocene record of mammals, *in* Bown, T.M., and Rose, K.D., editors, Dawn of the Age of Mammals in the northern part of the Rocky Mountain Interior, North America: Geological Society of America Special Paper 243, p. 153-167.

Barnosky, A.D., 1984, The Colter Formation: evidence for Miocene volcanism in Jackson Hole, Teton County, Wyoming: Wyoming Geological Association Earth Science Bulletin, v. 17, p. 49-97.

_____ 1986, Arikareean, Hemingfordian, and Barstovian mammals from the Miocene Colter Formation, Jackson Hole, Teton County, Wyoming: Carnegie Museum of Natural History Bulletin 26, p. 1-69.

Beckwith, R.H., 1942, Structure of the upper Laramie River valley, Colorado-Wyoming: Geological Society of America Bulletin, v. 53, p. 1491-1532.

Bell, W.G., 1955, The geology of the southeastern flank of the Wind River Mountains Fremont County, Wyoming [Ph.D. dissertation]: Laramie, University of Wyoming, 204 p.

Black, C.C., 1969, Fossil vertebrates from the late Eocene and Oligocene, Badwater Creek area, Wyoming, and some regional correlations: Wyoming Geological Association 21st Annual Field Conference Guidebook, p. 43-47.

Blackstone, D.L., Jr., 1975, Late Cretaceous and Cenozoic history of the Laramie Basin region, southeast Wyoming, *in* Curtis, B.F., editor, Cenozoic history of the southern Rocky Mountains: Geological Society of America Memoir 144, p. 249-279.

_____ 1979, Geometry of the Prospect-Darby and La Barge faults at their junction with the La Barge platform, Lincoln and Sublette counties, Wyoming: Geological Survey of Wyoming Report of Investigations 18, 34 p.

_____ 1983, Laramide compressional tectonics, southeastern Wyoming: University of Wyoming Contributions to Geology, v. 22, p. 1-38.

_____ 1986, Foreland compressional tectonics: southern Bighorn Basin and adjacent areas, Wyoming: Geological Survey of Wyoming Report of Investigations 34, 32 p.

_____ 1987, Northern Medicine Bow Mountains, Wyoming: revision of structural geology, northeast flank: University of Wyoming Contributions to Geology, v. 25, p. 1-9.

_____ 1990 (revised), Precambrian basement map of Wyoming: outcrop and structural configuration: Geological Survey of Wyoming Map Series 27, scale 1:1,000,000.

Blackstone, D.L., Jr., and De Bruin, R.H., 1987, Tectonic map of the Overthrust Belt, western Wyoming, northwestern Utah, and southeastern Idaho, showing oil and gas fields and exploratory wells in the Overthrust Belt and adjacent Green River Basin: Geological Survey of Wyoming Map Series 23, scale 1:316,800.

Blanchard, L.F., and Comstock, M.C., 1980, Geologic map and coal sections of the Pats Bottom Quadrangle, Carbon County, Wyoming: U.S. Geological Survey Open File Report 80-052, 2 sheets (with map), scale 1:24,000.

Boles, J.R., and Surdam, R.C., 1971, Authigenesis of the Wagon Bed Formation, central Wyoming: University of Wyoming Contributions to Geology, v. 10, p. 141-144.

_____ 1979, Diagenesis of volcanogenic sediments in a Tertiary saline lake: Wagon Bed Formation, Wyoming: American Journal of Science, v. 279, p. 832-853.

Bottjer, R.J., 1984, Depositional environments and tectonic significance of the South Pass Formation, southern Wind River Range, Wyoming [M.S. thesis]: Laramie, University of Wyoming, 229 p.

Bowen, C.F., 1918, Stratigraphy of the Hanna Basin, Wyoming: U.S. Geological Survey Professional Paper 108, p. 227-235.

Bown, T.M., 1979, Geology and mammalian paleontology of the Sand Creek facies, lower Willwood Formation (lower Eocene), Washakie County, Wyoming: Geological Survey of Wyoming Memoir 2, 151 p.

_____ 1980, Summary of latest Cretaceous and Cenozoic sedimentary, tectonic, and erosional events, Bighorn Basin, Wyoming, *in* Gingerich, P.D., editor, Early Cenozoic paleontology and stratigraphy of the Bighorn Basin, Wyoming: University of Michigan Papers on Paleontology 24, p. 25-32.

_____ 1982, Geology, paleontology, and correlation of Eocene volcaniclastic rocks, southeast Absaroka Range, Hot Springs County, Wyoming: U.S. Geological Survey Professional Paper 1201-A, 75 p.

Bown, T.M., and Beard, K.C., 1990, Systematic lateral variation in the distribution of fossil mammals in alluvial paleosols, lower Eocene Willwood Formation, Wyoming, *in* Bown, T.M., and Rose, K.D., editors, Dawn of the Age of Mammals in the northern part of the Rocky Mountain interior, North America: Geological Society of America Special Paper 243, p. 135-151.

Bown, T.M., and Kraus, M.J., 1981a, Lower Eocene alluvial paleosols (Willwood Formation, northwest Wyoming, U.S.A.) and their significance for paleoecology, paleoclimatology, and basin analysis: Palaeo-geography, Palaeoclimatology, Palaeoecology, v. 34, p. 1-30.

_____ 1981b, Vertebrate fossil-bearing paleosol units (Willwood Formation, lower Eocene, northwest Wyoming, U.S.A.): implications for taphonomy, biostratigraphy, and assemblage analysis: Palaeogeography, Palaeoclimatology, Palaeoecology, v. 34, p. 31-56.

_____ 1987, Integration of channel and floodplain suites, I. Developmental sequence and lateral relations of alluvial paleosols: Journal of Sedimentary Petrology, v. 57, p. 587-601.

Bown, T.M., and Rose, K.D., 1987, Patterns of dental evolution in early Eocene anaptomorphine primates (Omomyidae) from the Bighorn Basin, Wyoming: Paleontological Society Memoir 23, 162 p.

Bown, T.M., Rose, K.D., Simons, E.L., and Wing, S.L., in press, Distribution and stratigraphic correlation of upper Paleocene and lower Eocene fossil mammal and plant localities of the Fort Union, Willwood, and Tatman formations, southern Bighorn Basin, Wyoming: U.S. Geological Survey Professional Paper.

Bradley, W.H., 1936, Geomorphology of the north flank of the Uinta Mountains: U.S. Geological Survey Professional Paper 185-I, p. 163-204.

_____ 1964, Geology of Green River Formation and associated Eocene rocks in southwestern Wyoming and adjacent parts of Colorado and Utah: U.S. Geological Survey Professional Paper 496-A, 86 p.

Breithaupt, B.H., 1982, Paleontology and paleoecology of the Lance Formation (Maastrichtian), east flank of Rock Springs uplift, Sweetwater County, Wyoming: University of Wyoming Contributions to Geology, v. 21, p. 123-151.

Bressler, S.L., and Elston, D.P., 1981, Preliminary magnetostratigraphic correlations in upper Fort Union Formation (Paleocene) and lower Wasatch Formation (Eocene), northern Powder River Basin, Wyoming and Montana: U.S. Geological Survey Open File Report 81-876, 22 p.

Brown, R.W., 1948, Age of the Kingsbury Conglomerate is Eocene: Geological Society of America Bulletin, v. 59, p. 1165-1172.

_____ 1962, Paleocene flora of the Rocky Mountains and Great Plains: U.S. Geological Survey Professional Paper 375, 119 p.

Brown, W.G., 1988, Deformational style of Laramide uplifts in the Wyoming foreland, *in* Schmidt, C.J., and Perry, W.J., Jr., editors, Interaction of the Rocky Mountain foreland and the Cordilleran thrust belt: Geological Society of America Memoir 171, p. 1-26.

Bryant, B., and Nichols, D.J., 1988, Late Mesozoic and early Tertiary reactivation of an ancient crustal boundary along the Uinta trend and its interaction with the Sevier orogenic belt, *in* Schmidt, C.J., and Perry, W.J., Jr., editors, Interaction of the Rocky Mountain foreland and the Cordilleran thrust belt: Geological Society of America Memoir 171, p. 411-430.

Buchheim, H.P., and Surdam, R.C., 1977, Fossil catfish and the depositional environment of the Green River Formation, Wyoming: Geology, v. 5, p. 196-198.

Butler, R.F., Gingerich, P.D., and Lindsay, E.H., 1981, Magnetic polarity stratigraphy and biostratigraphy of Paleocene and lower Eocene continental deposits, Clark's Fork Basin, Wyoming: Journal of Geology, v. 89, p. 299-316.

Cardinal, D.F., and Parsons, G.T., 1982, Catalog of Hanna Basin stratigraphy: Wyoming Geological Association Earth Science Bulletin, v. 15, p. 45-126.

Chadwick, R.A., 1985, Overview of Cenozoic volcanism in the west-central United States, *in* Flores, R.M., and Kaplan, S.S., editors, Cenozoic paleogeography of the west-central United States: Society of Economic Paleontologists and Mineralogists, Rocky Mountain Section, Rocky Mountain Paleogeography Symposium 3, p. 359-382.

Colson, C.T., 1969, Stratigraphy and production of the Tertiary formations in the Sand Wash and Washakie basins: Wyoming Geological Association 21st Annual Field Conference Guidebook, p. 121-128.

Courdin, J.L., and Hubert, J.F., 1969, Sedimentology and mineralogical differentiation of sandstones in the Fort Union Formation (Paleocene), Wind River Basin, Wyoming: Wyoming Geological Association 21st Annual Field Conference Guidebook, p. 29-37.

Craddock, J.P., Kopania, A.A., and Wiltschko, D.V., 1988, Interaction between the northern Idaho-Wyoming thrust belt and bounding basement blocks, central western Wyoming, *in* Schmidt, C.J., and Perry, W.J., Jr., editors, Interaction of the Rocky Mountain foreland and the Cordilleran thrust belt: Geological Society of America Memoir 171, p. 333-351.

Curry, W.H., III, 1971, Laramide structural history of the Powder River Basin, Wyoming: Geological Association of Wyoming 23rd Annual Field Conference Guidebook, p. 49-60.

Curtis, B.F., 1988, Basins of the Rocky Mountain region: sedimentary rocks of the Denver Basin, *in* Sloss, L.L., editor, Sedimentary cover — North American Craton: U.S.: Geological Society of America, The Geology of North America, v. D-2, p. 182-196.

Darton, N.H., 1906, Geology of the Bighorn Mountains: U.S. Geological Survey Professional Paper 51, 129 p.

Davidson, J.R., 1987, Geology and mammalian paleontology of the Wind River Formation, Laramie Basin, southeastern Wyoming: University of Wyoming Contributions to Geology, v. 25, p. 103-132.

Delson, E., 1971, Fossil mammals of the early Wasatchian Powder River local fauna, Eocene of northeast Wyoming: American Museum of Natural History Bulletin, v. 146, p. 305-364.

Denson, N.M., and Botinelly, T., 1949, Geology of the Hartville uplift, eastern Wyoming: U.S. Geological Survey Oil and Gas Investigations Preliminary Map OM 102, 2 sheets, scale unspecified.

Denson, N.M., and Harshman, E.N., 1969, Map showing areal distribution of Tertiary rocks, Bates Hole-Shirley Basin area, south-central Wyoming: U.S. Geological Survey Miscellaneous Geologic Investigations Map I-570, scale 1:125,000.

Denson, N.M., and Pipiringos, G.N., 1974, Geologic map and sections showing areal distribution of Tertiary rocks near the southeastern terminus of the Wind River Range, Fremont and Sweetwater counties, Wyoming: U.S. Geological Survey Miscellaneous Investigations Series Map I-835 (2 sheets), scale 1:48,000.

Dickinson, W.R., Klute, M.A., Hayes, M.J., and others, 1988, Paleogeographic and paleotectonic setting of Laramide sedimentary basins in the central Rocky Mountain region: Geological Society of America Bulletin, v. 100, p. 1023-1039.

Dobbin, C.E., Bowen, C.F., and Hoots, H.W., 1929, Geology and coal and oil resources of the Hanna and Carbon basins, Carbon County, Wyoming: U.S. Geological Survey Bulletin 804, 88 p.

Dorr, J.A., Jr., 1978, Revised and amended fossil vertebrate faunal lists, early Tertiary, Hoback Basin, Wyoming: University of Wyoming Contributions to Geology, v. 16, p. 79-84.

Dorr, J.A., Jr., and Gingerich, P.D., 1980, Early Cenozoic mammalian paleontology, geologic structure, and tectonic history in the Overthrust Belt near La Barge, western Wyoming: University of Wyoming Contributions to Geology, v. 18, p. 101-115.

Dorr, J.A., Jr., Spearing, D.R., and Steidtmann, J.R., 1977, Deformation and deposition between a foreland uplift and an impinging thrust belt: Hoback Basin, Wyoming: Geological Society of America Special Paper 177, 82 p.

Eaton, J.G., 1982, Paleontology and correlation of Eocene volcanic rocks in the Carter Mountain area, Park County, southeastern Absaroka Range, Wyoming: University of Wyoming Contributions to Geology, v. 21, p. 153-194.

Eaton, J.G., Kirkland, J.I., and Doi, K., 1989, Evidence of reworked Cretaceous fossils and their bearing on the existence of Tertiary dinosaurs: Palaios, v. 4, p. 281-286.

Eldredge, S., and Van der Voo, R., 1988, Paleomagnetic study of thrust sheet rotations in the Helena and Wyoming salients of the northern Rocky Mountains, *in* Schmidt, C.J., and Perry, W.J., Jr., editors, Interaction of the Rocky Mountain foreland and the Cordilleran thrust belt: Geological Society of America Memoir 171, p. 319-332.

Emry, R.J., 1973, Stratigraphy and preliminary biostratigraphy of the Flagstaff Rim area, Natrona County, Wyoming: Smithsonian Contributions to Paleobiology 18, 43 p.

_____ 1975, Revised Tertiary stratigraphy and paleontology of the western Beaver Rim divide, Fremont

County, Wyoming: Smithsonian Contributions to Paleobiology 25, 20 p.

Emry, R.J., Bjork, P.R., and Russell, L.S., 1987, The Chadronian, Orellan, and Whitneyan North American land mammal ages, *in* Woodburne, M.O., editor, Cenozoic mammals of North America: geochronology and biostratigraphy: Berkeley, University of California Press, p. 118-152.

Epis, R.C., and Chapin, C.E., 1975, Geomorphic and tectonic implications of the post- Laramide, late Eocene erosion surface in the southern Rocky Mountains, *in* Curtis, B.F., editor, Cenozoic history of the southern Rocky Mountains: Geological Society of America Memoir 144, p. 45-74.

Eugster, H.P., and Hardie, L.A., 1975, Sedimentation in an ancient playa-lake complex: the Wilkins Peak Member of the Green River Formation of Wyoming: Geological Society of America Bulletin, v. 86, p. 319-334.

Eugster, H.P., and Surdam, R.C., 1973, Depositional environment of the Green River Formation of Wyoming: a preliminary report: Geological Society of America Bulletin, v. 84, p. 1115- 1120.

Evanoff, E., 1990, Early Oligocene paleovalleys in southern and central Wyoming: evidence of high local relief on the late Eocene unconformity: Geology, v. 18, p. 443-446.

Evernden, J.F., Savage, D.E., Curtis, G.H., and James, G.T., 1964, Potassium-argon dates and the Cenozoic mammalian chronology of North America: American Journal of Science, v. 262, p. 145-198.

Fields, R.W., Rasmussen, D.L., Tabrum, A.R., and Nichols, Ralph, 1985, Cenozoic rocks of the intermontane basins of western Montana and eastern Idaho: a summary, *in* Flores, R.M., and Kaplan, S.S., editors, Cenozoic paleogeography of the west-central United States: Society of Economic Paleontologists and Mineralogists, Rocky Mountain Section, Rocky Mountain Paleogeography Symposium 3, p. 9-36.

Flanagan, K.M., 1990, Late Cenozoic geology of the Pathfinder region, central Wyoming, with tectonic implications for adjacent areas [Ph.D. thesis]: Laramie, University of Wyoming, 186 p.

Flores, R.M., and Ethridge, F.G., 1985, Evolution of intermontane fluvial systems of Tertiary Powder River Basin, Montana and Wyoming, *in* Flores, R.M., and Kaplan, S.S., editors, Cenozoic paleogeography of the west-central United States: Society of Economic Paleontologists and Mineralogists, Rocky Mountain Section, Rocky Mountain Paleogeography Symposium 3, p. 107- 126.

Flores, R.M., and Hanley, J.H., 1984, Anastomosed and associated coal-bearing fluvial deposits: upper Tongue River Member, Paleocene Fort Union Formation, northern Powder River Basin, Wyoming, U.S.A., *in* Rahmani, R.A., and Flores, R.M., editors, Sedimentology of coal and coal-bearing sequences: Oxford, Blackwell Scientific Publications, International Association of Sedimentologists Special Publication 7, p. 85-103.

Flynn, J.J., 1986, Correlation and geochronology of middle Eocene strata from the western United States: Palaeogeography, Palaeoclimatology, Palaeoecology, v. 55, p. 335-406.

Flynn, J.J., MacFadden, B.J., and McKenna, M.C., 1984, Land-mammal ages, faunal heterochrony, and temporal resolution in Cenozoic terrestrial sequences: Journal of Geology, v. 92, p. 687-705.

Fox, R.C., 1990, *Pronothodectes gaoi* n. sp. from the late Paleocene of Alberta, Canada, and the early evolution of the Plesiadapidae (Mammalia, Primates): Journal of Paleontology, v. 64, p. 637-647.

Gazin, C.L., 1952, The lower Eocene Knight Formation of western Wyoming and its mammalian faunas: Smithsonian Miscellaneous Collections, v. 117, no. 18, 82 p.

_____ 1956a, The occurrence of Paleocene mammalian remains in the Fossil Basin of southwestern Wyoming: Journal of Paleontology, v. 30, p. 707-711.

_____ 1956b, Paleocene mammalian faunas of the Bison Basin in south-central Wyoming: Smithsonian Miscellaneous Collections, v. 131, no. 6, 57 p.

_____ 1956c, The upper Paleocene Mammalia from the Almy Formation in western Wyoming: Smithsonian Miscellaneous Collections, v. 131, no. 7, 18 p.

_____ 1956d, The geology and vertebrate paleontology of upper Eocene strata in the northeastern part of the Wind River Basin, Wyoming, part 2. The mammalian fauna of the Badwater area: Smithsonian Miscellaneous Collections, v. 131, no. 8, 35 p.

_____ 1962, A further study of the lower Eocene mammalian faunas of southwestern Wyoming: Smithsonian Miscellaneous Collections, v. 144, no. 1, 98 p.

_____ 1969, A new occurrence of Paleocene mammals in the Evanston Formation, southwestern Wyoming: Smithsonian Contributions to Paleobiology 2, 17 p.

_____ 1971, Paleocene primates from the Shotgun Member of the Fort Union Formation in the Wind River Basin, Wyoming: Biological Society of Washington Proceedings, v. 84, p. 13- 37.

_____ 1976, Mammalian faunal zones of the Bridger middle Eocene: Smithsonian Contributions to Paleobiology 26, 25 p.

Gill, J.R., Merewether, E.A., and Cobban, W.A., 1970, Stratigraphy and nomenclature of some Upper Cretaceous and lower Tertiary rocks in south-central Wyoming: U.S. Geological Survey Professional Paper 667, 53 p.

Gingerich, P.D., 1975, New North American Plesiadapidae (Mammalia, Primates) and a biostratigraphic zonation of the middle and upper Paleocene: University of Michigan Museum of Paleontology Contributions, v. 24, p. 135-148.

_____ 1983, Paleocene-Eocene faunal zones and a preliminary analysis of Laramide structural deformation in the Clark's Fork Basin, Wyoming: Wyoming Geological Association 34th Annual Field Conference Guidebook, p. 185-195.

_____ 1987, Early Eocene bats (Mammalia, Chiroptera) and other vertebrates in freshwater limestones of the Willwood Formation, Clark's Fork Basin, Wyoming: University of Michigan Museum of Paleontology Contributions, v. 27, p. 275-320.

_____ 1989a, New earliest Wasatchian mammalian fauna from the Eocene of northwestern Wyoming: composition and diversity in a rarely sampled high-floodplain assemblage: University of Michigan Papers on Paleontology 28, 97 p.

_____ 1989b, Paleocene and early Eocene of the Bighorn and Clark's Fork basins, Wyoming, *in* Flynn, J.J., editor, Mesozoic/Cenozoic vertebrate paleontology: classic localities, contemporary approaches: American Geophysical Union, Washington, D.C., International Geological Congress Field Trip Guidebook T322, p. 47-57.

Gingerich, P.D., and Klitz, K., 1985, Paleocene and early Eocene fossil localities in the Fort Union and Willwood formations, Clark's Fork Basin, Wyoming: University of Michigan Museum of Paleontology [map, series unspecified, scale unspecified].

Gingerich, P.D., Rose, K.D., and Krause, D.W., 1980, Early Cenozoic mammalian faunas of the Clark's Fork Basin-Polecat Bench area, northwestern Wyoming, *in* Gingerich, P.D., editor, Early Cenozoic paleontology and stratigraphy of the Bighorn Basin, Wyoming: University of Michigan Papers on Paleontology 24, p. 51-68.

Glass, G.B., 1975, Analyses and measured sections of 54 Wyoming coal samples (collected in 1974): Geological Survey of Wyoming Report of Investigations 11, 219 p.

Glass, G.B., and Roberts, J.T., 1978, Update on the Wind River Coal Basin: Wyoming Geological Association 30th Annual Field Conference Guidebook, p. 363-377.

_____ 1980a, Update on the Hanna Coal Field, Wyoming: Wyoming Geological Association 31st Annual Field Conference Guidebook, p. 239-262.

_____ 1980b, Coals and coal-bearing rocks of the Hanna Coal Field, Wyoming: Geological Survey of Wyoming Report of Investigations 22, 43 p.

_____ 1984, Analyses and measured sections of 25 coal samples from the Hanna Coal Field of southcentral Wyoming (collected between 1975 and 1979): Geological Survey of Wyoming Report of Investigations 27, 104 p.

Grande, L., 1984, Paleontology of the Green River Formation, with a review of the fish fauna: Geological Survey of Wyoming Bulletin 63, 333 p.

Gries, J.C., 1964, The structure and Cenozoic stratigraphy of the Pass Creek Basin area, Carbon County, Wyoming [M.S. thesis]: Laramie, University of Wyoming, 69 p.

Groll, P.E., 1986, Sedimentation and tectonics of the upper Bridger Formation, southern Wind River Range, Wyoming [M.S. thesis]: Laramie, University of Wyoming, 138 p.

Groll, P.E., and Steidtmann, J.R., 1987, Fluvial response to Eocene tectonism, the Bridger Formation, southern Wind River Range, Wyoming, *in* Ethridge, F.C., and Flores, R.M., editors, Recent developments in fluvial sedimentology: Society of Economic Paleontologists and Mineralogists Special Volume 39, p. 263-268.

Guennel, G.K., Spearing, D.R., and Dorr, J.A., Jr., 1973, Palynology of the Hoback Basin: Wyoming Geological Association 25th Annual Field Conference Guidebook, p. 173-185.

Hamilton, W.B., 1988, Laramide crustal shortening, *in* Schmidt, C.J., and Perry, W.J., Jr., editors, Interaction of the Rocky Mountain foreland and the Cordilleran thrust belt: Geological Society of America Memoir 171, p. 27-39.

Hanley, J.H., 1976, Paleosynecology of nonmarine Mollusca from the Green River and Wasatch formations (Eocene), southwestern Wyoming and northwestern Colorado, *in* Scott, R.W., and West, R.R., editors, Structure and classification of paleocommunities: New York, Dowden, Hutchinson, and Ross, Inc., p. 235-261.

_____ 1977, Lithostratigraphic relations, nonmarine Mollusca, and depositional environments of a portion of the Green River and Wasatch formations south of the Rock Springs uplift, Sweetwater County, Wyoming, with appendices of measured stratigraphic sections: U.S. Geological Survey Open File Report 77-588, 223 p.

Hansen, D.E., 1986, Laramide tectonics and deposition of the Ferris and Hanna formations, south-central Wyoming, *in* Peterson, J.A., editor, Paleotectonics and sedimentation in the Rocky Mountain region, United States: American Association of Petroleum Geologists Memoir 41, p. 481-495.

Hansen, W.R., 1965, Geology of the Flaming Gorge area, Utah-Colorado-Wyoming: U.S. Geological Survey Professional Paper 490, 196 p.

_____ 1984, Post-Laramide tectonic history of the eastern Uinta Mountains, Utah, Colorado, and Wyoming: The Mountain Geologist, v. 21, p. 5-29.

_____ 1985, Drainage development of the Green River Basin in southwestern Wyoming and its bearing on fish biogeography, neotectonics, and paleoclimates: The Mountain Geologist, v. 22, p. 192-204.

Harshman, E.N., 1968, Geologic map of the Shirley Basin area, Albany, Carbon, Converse, and Natrona counties, Wyoming: U.S. Geological Survey Miscellaneous Geologic Investigations Map I-539, scale 1:48,000.

_____ 1972, Geology and uranium deposits, Shirley Basin area, Wyoming: U.S. Geological Survey Professional Paper 745, 82 p.

Hartman, J.E., 1986, Paleontology and biostratigraphy of lower part of Polecat Bench Formation, southern Bighorn Basin, Wyoming: University of Wyoming Contributions to Geology, v. 24, p. 11-63.

Hettinger, R.D., Honey, J.G., and Nichols, D.J., 1991, Chart showing correlations of Upper Cretaceous Fox Hills Sandstone and Lance Formation, and lower Tertiary Fort Union, Wasatch, and Green River Formations, from the eastern flank of the Washakie Basin to the southeastern part of the Great Divide Basin, Wyoming: U.S. Geological Survey Miscellaneous Investigations Series I-2151.

Hickey, L.J., 1980, Paleocene stratigraphy and flora of the Clark's Fork Basin, *in* Gingerich, P.D., editor, Early Cenozoic paleontology and stratigraphy of the Bighorn Basin, Wyoming: University of Michigan Papers on Paleontology 24, p. 33-49.

Honey, J.G., and Hettinger, R.D., 1989, Cross section showing correlations of Upper Cretaceous Fox Hills Sandstone and Lance Formation, and lower Tertiary Fort Union and Wasatch formations, southeastern Washakie Basin, Wyoming, and eastern Sand Wash Basin, Colorado: U.S. Geological Survey Miscellaneous Investigations Series I-1964.

Horn, G.H., 1963, Geology of the east Thermopolis area, Hot Springs and Washakie counties, Wyoming: U.S. Geological Survey Oil and Gas Investigations Map OM-213, scale 1:48,000.

Hose, R.K., 1955, Geology of the Crazy Woman Creek area, Johnson County, Wyoming: U.S. Geological Survey Bulletin 1027-B, p. 33-118.

Houston, R.S., and others, 1968, A regional study of rocks of Precambrian age in that part of the Medicine Bow Mountains lying in southeastern Wyoming — with a chapter on the relationship between Precambrian and Laramide structure: Geological Survey of Wyoming Memoir 1, 167 p.

Hunt, R.M., Jr., 1985, Faunal succession, lithofacies, and depositional environments in Arikaree rocks (lower Miocene) of the Hartville Table, Nebraska and Wyoming, *in* Martin, J.E., editor, Fossiliferous Cenozoic deposits of western South Dakota and northwestern Nebraska: Dakoterra, v. 2, part 2, p. 155-204.

_____ 1990, Taphonomy and sedimentology of Arikaree (lower Miocene) fluvial, eolian, and lacustrine paleoenvironments, Nebraska and Wyoming; a paleobiota entomed in fine-grained volcaniclastic rocks, *in* Lockley, M.G., and Rice, A., editors, Volcanism and fossil biotas: Geological Society of America Special Paper 244, p. 69-111.

Hunter, R.B., 1988, Timing and structural interaction between the thrust belt and foreland, Hoback Basin,

Wyoming, *in* Schmidt, C.J., and Perry, W.J., Jr., editors, Interaction of the Rocky Mountain foreland and the Cordilleran thrust belt: Geological Society of America Memoir 171, p. 367-393.

Hurst, D.J., and Steidtmann, J.R., 1986, Stratigraphy and tectonic significance of the Tunp Conglomerate in the Fossil Basin, southwest Wyoming: The Mountain Geologist, v. 23, p. 6-13.

Hyden, H.J., McAndrews, H., and Tschudy, R.H., 1965, The Foote Creek and Dutton Creek formations, two new formations in the north part of the Laramie Basin, Wyoming: U.S. Geological Survey Bulletin 1194-K, 12 p.

Izett, G.A., 1975, Late Cenozoic sedimentation and deformation in northern Colorado and adjoining areas, *in* Curtis, B.F., editor, Cenozoic history of the Southern Rocky Mountains: Geological Society of America Memoir 144, p. 179-209.

Izett, G.A., Denson, N.M., and Obradovich, J.D., 1970, K-Ar age of the lower part of the Browns Park Formation, northwestern Colorado: U.S. Geological Survey Professional Paper 700-C, p. 150-152.

Jackson, K.E., 1984, Geology of the Circle Bar Lake Quadrangle, Fremont and Sweetwater counties, Wyoming [M.S. thesis]: Laramie, University of Wyoming, 73 p.

Jacobson, S.R., and Nichols, D.J., 1982, Palynological dating of syntectonic units in the Utah- Wyoming thrust belt: the Evanston Formation, Echo Canyon Conglomerate, and Little Muddy Creek Conglomerate, *in* Powers, R.B., editor, Geologic studies of the Cordilleran thrust belt: Rocky Mountain Association of Geologists, v. II, p. 735-750.

Jepsen, G.L., 1940, Paleocene faunas of the Polecat Bench Formation, Park County, Wyoming, Part I: American Philosophical Society Proceedings, v. 83, p. 217-340.

Johnson, R.A., and Smithson, S.B., 1985, Thrust faulting in the Laramie Mountains, Wyoming, from reanalysis of COCORP data: Geology, v. 13, p. 534-537.

Kaplan, S.S., and Skeen, R.C., 1985, North-south regional seismic profile of the Hanna Basin, Wyoming, *in* Gries, R.R., and Dyer, R.C., editors, Seismic exploration of the Rocky Mountain region: Rocky Mountain Association of Geologists and Denver Geophysical Society, p. 219-224.

Keefer, W.R., 1957, Geology of the Du Noir area, Fremont County, Wyoming: U.S. Geological Survey Professional Paper 294-E, p. 155-221.

_____ 1961, Waltman Shale and Shotgun members of Fort Union Formation (Paleocene) in Wind River Basin, Wyoming: American Association of Petroleum Geologists Bulletin, v. 45, p. 1310-1323.

_____ 1965, Stratigraphy and geologic history of the uppermost Cretaceous, Paleocene, and lower Eocene rocks in the Wind River Basin, Wyoming: U.S. Geological Survey Professional Paper 495-A, 77 p.

_____ 1970, Structural geology of the Wind River Basin, Wyoming: U.S. Geological Survey Professional Paper 495-D, 35 p.

Keefer, W.R., and Love, J.D., 1963, Laramide vertical movements in central Wyoming: University of Wyoming Contributions to Geology, v. 2, p. 47-54.

Keefer, W.R., and Troyer, M.L., 1964, Geology of the Shotgun Butte area, Fremont County, Wyoming: U.S. Geological Survey Bulletin 1157, 123 p.

Kirschbaum, M.A., 1987, Stratigraphic and sedimentologic framework of Paleocene rocks, southwest flank of the Rock Springs uplift, Sweetwater County, Wyoming: U.S. Geological Survey Miscellaneous Field Studies Map MF-1973, 2 sheets (no map).

Kirschbaum, M.A., and Nelson, S.N., 1988, Geologic history and palynologic dating of Paleocene deposits, western Rock Springs uplift, Sweetwater County, Wyoming: University of Wyoming Contributions to Geology, v. 26, p. 21-28.

Kirschner, W.A., 1984, Nonmarine molluscan paleontology and paleoecology of early Tertiary strata, Hanna Basin, Wyoming [M.S. thesis]: Laramie, University of Wyoming, 157 p.

Knight, S.H., 1951, The Late Cretaceous-Tertiary history of the northern portion of the Hanna Basin—Carbon County, Wyoming: Wyoming Geological Association 6th Annual Field Conference Guidebook, p. 45-53.

_____ 1953, Summary of the Cenozoic history of the Medicine Bow Mountains, Wyoming: 8th Annual Field Conference Wyoming Geological Association Guidebook, p. 65-76.

Kochel, R.C., and Ritter, D.F., 1982, Depositional environments of high-level sand and gravel deposits, western Bighorn Mountains, Wyoming: University of Wyoming Contributions to Geology, v. 20, p. 111-122.

Kornegay, G.L., and Surdam, R., 1980, The Laney Member of the Green River Formation, Sand Wash Basin, Colorado, and its relationship to Wyoming: Wyoming

Geological Association 31st Annual Field Conference Guidebook, p. 191-204.

Korth, W.W., 1980, *Paradjidaumo* (Eomyidae, Rodentia) from the Brule Formation, Nebraska: Journal of Paleontology, v. 54, p. 933-941.

_____ 1982, Revision of the Wind River faunas, early Eocene of central Wyoming. Part 2: Geologic setting: Carnegie Museum of Natural History Annals, v. 51, p. 57-78.

Kraig, D.H., Wiltschko, D.V., and Spang, J.H., 1987, Interaction of basement uplift and thin-skinned thrusting, Moxa arch and the western Overthrust Belt, Wyoming: a hypothesis: Geological Society of America Bulletin, v. 99, p. 654-662.

Kraus, M.J., 1980, Genesis of a fluvial sheet sandstone, Willwood Formation, northwest Wyoming, *in* Gingerich, P.D., editor, Early Cenozoic paleontology and stratigraphy of the Bighorn Basin, Wyoming: University of Michigan Papers on Paleontology 24, p. 87-94.

_____ 1985, Early Tertiary quartzite conglomerates of the Bighorn Basin and their significance for paleogeographic reconstruction of northwest Wyoming, *in* Flores, R.M., and Kaplan, S.S., editors, Cenozoic paleogeography of the west-central United States: Society of Economic Paleontologists and Mineralogists, Rocky Mountain Section, Rocky Mountain Paleogeography Symposium 3, p. 71-91.

_____ 1987, Integration of channel and floodplain suites, II. Vertical relations of alluvial paleosols: Journal of Sedimentary Petrology, v. 57, p. 602-612.

Krause, D.W., and Maas, M.C., 1990, The biogeographic origins of late Paleocene-early Eocene mammalian immigrants to the western interior of North America, *in* Bown, T.M., and Rose, K.D., editors, Dawn of the Age of Mammals in the northern part of the Rocky Mountain interior, North America: Geological Society of America Special Paper 243, p. 71-105.

Krishtalka, L., Black, C.C., and Riedel, D.W., 1975, Paleontology and geology of the Badwater Creek area, central Wyoming. Part 10: A late Paleocene mammal fauna from the Shotgun Member of the Fort Union Formation: Carnegie Museum of Natural History Annals, v. 45, p. 179-212.

Krishtalka, L., Stucky, R.K., West, R.M., and others, 1987, Eocene (Wasatchian through Duchesnean) biochronology of North America, *in* Woodburne, M.O., editor, Cenozoic mammals of North America: geochronology and biostratigraphy: Berkeley, University of California Press, p. 77-117.

Kron, D.G., 1978, Oligocene vertebrate paleontology of the Dilts Ranch area, Converse County, Wyoming [M.S. thesis]: Laramie, University of Wyoming, 185 p.

Lamerson, P.R., 1982, The Fossil Basin and its relationship to the Absaroka thrust system, Wyoming and Utah, *in* Powers, R.B., editor, Geologic studies of the Cordilleran thrust belt: Rocky Mountain Association of Geologists, v. 1, p. 279-340.

Law, B.E., 1981, Section C-C' subsurface correlations of some Upper Cretaceous and Tertiary rocks, northern Green River Basin, Wyoming: U.S. Geological Survey Open File Report 81-663, 1 sheet.

Law, B.E., Barnum, B.E., and Wollenzien, T.P., 1979, Coal bed correlations in the Tongue River Member of the Fort Union Formation, Monarch, Wyoming, and Decker, Montana, areas: U.S. Geological Survey Miscellaneous Investigation Series Map I-1128, 1 sheet (fence diagram).

LeFebre, G.B., 1988, Tectonic evolution of Hanna Basin, Wyoming: Laramide block rotation in the Rocky Mountain foreland [Ph.D. dissertation]: Laramie, University of Wyoming, 240 p.

Leffingwell, H.A., 1970, Palynology of the Lance (Late Cretaceous) and Fort Union (Paleocene) formations of the type Lance area, Wyoming, *in* Kosanke, R.M., and Cross, A.T., editors, Symposium on palynology of the Late Cretaceous and early Tertiary: Geological Society of America Special Paper 127, p. 1-64.

Leite, M.B., in prep., Paleontology of the Fort Union Formation in the southwestern Bighorn Basin, Wyoming [Ph.D. dissertation]: Laramie, University of Wyoming.

Leopold, E.B., and MacGinitie, H.D., 1972, Development and affinities of Tertiary floras in the Rocky Mountains, *in* Graham, A., editor, Floristics and paleofloristics of Asia and eastern North America: Amsterdam, Elsevier Publishing Company, p. 147-200.

Lillegraven, J.A., and McKenna, M.C., 1986, Fossil mammals from the "Mesaverde" Formation (Late Cretaceous, Judithian) of the Bighorn and Wind River basins, Wyoming, with definitions of Late Cretaceous North American Land-Mammal "Ages": American Museum of Natural History Novitates 2840, 68 p.

Lillegraven, J.A., McKenna, M.C., and Krishtalka, L., 1981, Evolutionary relationships of middle Eocene and younger species of *Centetodon* (Mammalia, Insectivora, Geolabididae) with a description of the dentition of *Ankylodon* (Adapisoricidae): University of Wyoming Publication 45, 115 p.

Lillegraven, J.A., and Ostresh, L.M., Jr., 1988, Evolution of Wyoming's early Cenozoic topography and drainage patterns: National Geographic Research, v. 4, p. 303-327.

_____ 1990, Late Cretaceous (earliest Campanian/ Maastrichtian) evolution of western shorelines of the North American western interior seaway in relation to known mammalian faunas, *in* Bown, T.M., and Rose, K.D., editors, Dawn of the Age of Mammals in the northern part of the Rocky Mountain interior, North America: Geological Society of America Special Paper 243, p. 1-30.

Lindsey, D.A., 1972, Sedimentary petrology and paleocurrents of the Harebell Formation, Pinyon Conglomerate, and associated coarse clastic deposits, northwestern Wyoming: U.S. Geological Survey Professional Paper 734-B, 68 p.

Lisenbee, A.L., 1978, Laramide structure of the Black Hills uplift, South Dakota-Wyoming-Montana, *in* Matthews, V., III, editor, Laramide folding associated with basement block faulting in the western United States: Geological Society of America Memoir 151, p. 165-196.

_____ 1985, Tectonic map of the Black Hills uplift, Montana, Wyoming, and South Dakota: Geological Survey of Wyoming Map Series 13, scale 1:250,000.

Love, J.D., 1939, Geology along the southern margin of the Absaroka Range, Wyoming: Geological Society of America Special Paper 20, 134 p.

_____ 1947, Tertiary stratigraphy of the Jackson Hole area, northwestern Wyoming: U.S. Geological Survey Oil and Gas Investigations Preliminary Chart OC-27 (1 sheet).

_____ 1952, Preliminary report on uranium deposits in the Pumpkin Buttes area, Powder River Basin, Wyoming: U.S. Geological Survey Circular 176, 37 p.

_____ 1970, Cenozoic geology of the Granite Mountains area, central Wyoming: U.S. Geological Survey Professional Paper 495-C, 154 p.

_____ 1973, Harebell Formation (Upper Cretaceous) and Pinyon Conglomerate (uppermost Cretaceous and Paleocene), northwestern Wyoming: U.S. Geological Survey Professional Paper 734-A, 54 p.

_____ 1978, Cenozoic thrust and normal faulting, and tectonic history of the Badwater area northeastern margin of Wind River Basin, Wyoming: Wyoming Geological Association 30th Annual Field Conference Guidebook, p. 235-238.

_____ 1988a Basins of the Rocky Mountain region: Geology of the Wind River Basin, central Wyoming, *in* Sloss, L.L., editor, Sedimentary cover — North American craton: U.S.: Geological Society of America, The geology of North America, v. D-2, p. 196- 200.

_____ 1988b, Basins of the Rocky Mountain region: Geology of the Bighorn Basin, northern Wyoming and southern Montana, *in* Sloss, L.L., editor, Sedimentary cover — North American craton: U.S.: Geological Society of America, The geology of North America, v. D-2, p. 201-204.

_____ 1988c, Basins of the Rocky Mountain region: geology of the Powder River Basin, northeastern Wyoming and southeastern Montana, *in* Sloss, L.L., editor, Sedimentary cover - - North American craton: U.S.: Geological Society of America, The geology of North America, v. D-2, p. 204-208.

_____ 1989, Names and descriptions of new and reclassified formations in northwestern Wyoming: U.S. Geological Survey Professional paper 932-C, 45 p.

Love, J.D., and Christiansen, A.C., 1980, Preliminary correlation of stratigraphic units used on 1° x 2° geologic quadrangle maps of Wyoming: Wyoming Geological Association 31st Annual Field Conference Guidebook, p. 279-282.

_____ 1985, Geologic map of Wyoming: U.S. Geological Survey, scale 1:500,000.

Love, J.D., Christiansen, A.C., and Ver Ploeg, A.J., 1992, Stratigraphic nomenclature chart for Wyoming: Geological Survey of Wyoming Open File Report 92-2, 1 sheet.

Love, J.D., and Keefer, W.R., 1975, Geology of sedimentary rocks in southern Yellowstone National Park, Wyoming: U.S. Geological Survey Professional Paper 729-D, 60 p.

Love, J.D., Leopold, E.B., and Love, D.W., 1978, Eocene rocks, fossils, and geologic history, Teton Range, northwestern Wyoming: U.S. Geological Survey Professional Paper 932-B, 40 p.

Love, J.D., McGrew, P.O., and Thomas, H.D., 1963, Relationship of latest Cretaceous and Tertiary deposition and deformation to oil and gas in Wyoming, *in* Childs, O.E., editor, Backbone of the Americas — Tectonic history from pole to pole: a symposium: American Association of Petroleum Geologists Memoir 2, p. 196-208.

Love, J.D., McKenna, M.C., and Dawson, M.R., 1976, Eocene, Oligocene, and Miocene rocks and vertebrate fossils at the Emerald Lake locality, 3 miles south of Yellowstone National Park, Wyoming: U.S. Geological Survey Professional Paper 932-A, 28 p.

Love, L.L., Kudo, A.M., and Love, D.W., 1976, Dacites of Bunsen Peak, the Birch Hills, and the Washakie Needles, northwestern Wyoming, and their relationship to the Absaroka volcanic field, Wyoming and Montana: Geological Society of America Bulletin, v. 87, p. 1455-1462.

MacFadden, B.J., 1980, Eocene perissodactyls from the type section of the Tepee Trail Formation of northwestern Wyoming: University of Wyoming Contributions to Geology, v. 18, p. 135-143.

MacGinitie, H.D., 1974, An early middle Eocene flora from the Yellowstone-Absaroka volcanic province, northwestern Wind River Basin, Wyoming: University of California Publications in Geological Sciences, v. 108, 103 p.

McCallum, M.E., 1968, Cenozoic history of the east-central Medicine Bow Mountains, Wyoming: The Mountain Geologist, v. 5, p. 69-81.

McGrew, L.W., 1963, Geology of the Fort Laramie area, Platte and Goshen counties, Wyoming: U.S. Geological Survey Bulletin 1141-F, 39 p.

McGrew, P.O., 1953, Tertiary deposits of southeastern Wyoming: Wyoming Geological Association 8th Annual Field Conference Guidebook, p. 61-64.

McGrew, P.O., Berman, J.E., Hecht, M.K., and others, 1959, The geology and paleontology of the Elk Mountain and Tabernacle Butte area, Wyoming: American Museum of Natural History Bulletin, v. 117, p. 117-176.

McGrew, P.O., and Casilliano [sic], M., 1975, The geological history of Fossil Butte National Monument and Fossil Basin: U.S. National Park Service Occasional Paper 3, 37 p.

McGrew, P.O., and Sullivan, R., 1970, The stratigraphy and paleontology of Bridger A: University of Wyoming Contributions to Geology, v. 9, p. 66-85.

McKenna, M.C., 1960, Fossil Mammalia from the early Wasatchian Four Mile Fauna, Eocene of northwest Colorado: University of California Publications in Geological Sciences, v. 37, 130 p.

_____ 1980a, Late Cretaceous and early Tertiary vertebrate paleontological reconnaissance, Togwotee Pass area, northwestern Wyoming, *in* Jacobs, L.L., editor, Aspects of vertebrate history: Flagstaff, Museum of Northern Arizona Press, p. 321-343.

_____ 1980b, Remaining evidence of Oligocene sedimentary rocks previously present across the Bighorn Basin, Wyoming, *in* Gingerich, P.D., editor, Early Cenozoic paleontology and stratigraphy of the Bighorn Basin, Wyoming: University of Michigan Papers on Paleontology 24, p. 143-146.

_____ 1990, Plagiomenids (Mammalia: ?Dermoptera) from the Oligocene of Oregon, Montana, and South Dakota, and middle Eocene of nortwestern Wyoming, *in* Bown, T.M., and Rose, K.D., editors, Dawn of the Age of Mammals in the northern part of the Rocky Mountain Interior, North America: Geological Society of America Special Paper 243, p. 211-234.

McKenna, M.C., and Love, J.D., 1970, Local stratigraphic and tectonic significance of *Leptoceratops*, a Cretaceous dinosaur in the Pinyon Conglomerate, northwestern Wyoming: U.S. Geological Survey Professional Paper 700-D, p. 55-61.

_____ 1972, High-level strata containing early Miocene mammals on the Bighorn Mountains, Wyoming: American Museum Novitates 2490, 31 p.

McKenna, M.C., Robinson, P., and Taylor, D.W., 1962, Notes on Eocene Mammalia and Mollusca from Tabernacle Butte, Wyoming: American Museum Novitates 2102, 33 p.

Mapel, W.J., 1959, Geology and coal resources of the Buffalo-Lake De Smet area, Johnson and Sheridan counties, Wyoming: U.S. Geological Survey Bulletin 1078, 148 p.

Markochick, D.J., Law, B.E., and Spencer, C.W., 1982, Section E-E'. Preliminary subsurface correlations of some Cretaceous and Tertiary rocks from Moxa arch to Rock Springs uplift, Green River Basin, Wyoming: U.S. Geological Survey Open File Report 82-455, 2 sheets.

Marrs, R.W., and Raines, G.L., 1984, Tectonic framework of Powder River Basin, Wyoming and Montana, interpreted from Landsat imagery: American Association of Petroleum Geologists Bulletin, v. 68, p. 1718-1731.

Matthew, W.D., 1909, The Carnivora and Insectivora of the Bridger Basin, middle Eocene: American Museum of Natural History Memoir 9, p. 291-567.

Mauger, R.L., 1977, K-Ar ages of biotites from tuffs in Eocene rocks of the Green River, Washakie, and Uinta basins, Utah, Wyoming, and Colorado: University of Wyoming Contributions to Geology, v. 15, p. 17-41.

Merin, I.S., and Lindholm, R.C., 1986, Evidence that the crystalline cores of uplifts adjacent to the Powder River Basin were breached during Paleocene time: The Mountain Geologist, v. 23, p. 128-131.

Montagne, J. de la, 1957, Cenozoic structural and geomorphic history of northern North Park and Saratoga Valley, Colorado and Wyoming, *in* Guidebook to the geology of North and Middle Parks Basin, Colorado,: Rocky Mountain Association of Geologists, p. 36-41.

_____ 1991, Cenozoic history of the Saratoga Valley area, Wyoming and Colorado: University of Wyoming Contributions to Geology, v. 29, p. 13-70.

Moore, F.E., 1960, Summary of Cenozoic history, southern Laramie Range, Wyoming and Colorado, *in* Weimer, R.J., and Haun, J.D., editors, Guide to the geology of Colorado: Rocky Mountain Association of Geologists, p. 217-222.

Morris, W.J., 1954, An Eocene fauna from the Cathedral Bluffs Tongue of the Washakie Basin, Wyoming: Journal of Paleontology, v. 28, p. 195-203.

Munthe, J., 1979, Summary of Miocene vertebrate fossils of the Granite Mountains Basin, central Wyoming: University of Wyoming Contributions to Geology, v. 18, p. 33-46.

NACSN (North American Commission on Stratigraphic Nomenclature), 1983, North American stratigraphic code: American Association of Petroleum Geologists Bulletin, v. 67, p. 841- 875.

Neasham, J.W., and Vondra, C.F., 1972, Stratigraphy and petrology of the lower Eocene Willwood Formation, Bighorn Basin, Wyoming: Geological Society of America Bulletin, v. 83, p. 2167-2180.

Nelson, M.E., 1973, Age and stratigraphic relations of the Fowkes Formation, Eocene, of southwestern Wyoming and northeastern Utah: University of Wyoming Contributions to Geology, v. 12, p. 27-31.

_____ 1979, K-Ar age for the Fowkes Formation (middle Eocene) of southwestern Wyoming: University of Wyoming Contributions to Geology, v. 17, p. 51-52.

Nelson, W.H., and Pierce, W.G., 1968, Wapiti Formation and Trout Peak Trachyandesite, northwestern Wyoming: U.S. Geological Survey Bulletin 1254-H, 11 p.

Nichols, D.J., and Ott, H.L., 1978, Biostratigraphy and evolution of the *Momipites- Caryapollenites* lineage in the early Tertiary in the Wind River Basin, Wyoming: Palynology, v. 2, p. 93-112.

Obernyer, S.L., 1979, Basin-margin depositional environments of the Fort Union and Wasatch formations in the Buffalo-Lake De Smet area, Johnson County, Wyoming: U.S. Geological Survey Open File Report 79-712, 116 p.

Odin, G.-S., and Odin, C., 1990, Echelle numerique des temps geologiques: Geochronique, no. 35, p. 12-21.

Oriel, S.S., 1961, Tongues of the Wasatch and Green River formations, Fort Hill area, Wyoming: U.S. Geological Survey Professional Paper 424-B, p. 151-152.

_____ 1962, Main body of Wasatch Formation near La Barge, Wyoming: American Association of Petroleum Geologists Bulletin, v. 46, p. 2161-2173.

_____ 1969, Geology of the Fort Hill Quadrangle, Lincoln County, Wyoming: U.S. Geological Survey Professional Paper 594-M, 40 p.

Oriel, S.S., and Tracey, J.I., Jr., 1970, Uppermost Cretaceous and Tertiary stratigraphy of Fossil Basin, southwestern Wyoming: U.S. Geological Survey Professional Paper 635, 53 p.

Osterwald, F.W., 1959, Structure and petrology of the northern Bighorn Mountains, Wyoming: Geological Survey of Wyoming Bulletin 48, 47 p.

Parker, S.E., 1986, Tectonostratigraphic relationships of the Upper Cretaceous and lower Tertiary strata of the Bighorn Basin, Wyoming [M.S. thesis]: Laramie, University of Wyoming, 125 p.

Parker, S.E., and Jones, R.W., 1986, Isopachous map of the Tertiary overburden above the latest Cretaceous Lance Formation, Bighorn Basin, Wyoming: Geological Survey of Wyoming Open File Report 86-8, scale 1:250,000.

Pekarek, A.H., 1978, Stratigraphy and structural geology of the Rattlesnake Hills, Wyoming: Wyoming Geological Association 30th Annual Field Conference Guidebook, p. 239-253.

Phillips, S.T., 1983, Tectonic influence on sedimentation, Waltman Member, Fort Union Formation, Wind River

Basin, Wyoming, *in* Lowell, J.D., and Gries, R., editors, Rocky Mountain foreland basins and uplifts: Rocky Mountain Association of Petroleum Geologists, p. 149-160.

Pipiringos, G.N., 1961, Uranium-bearing coal in the central part of the Great Divide Basin: U.S. Geological Survey Bulletin 1099-A, 104 p.

Pipiringos, G.N., and Denson, N.M., 1970, The Battle Spring Formation in south-central Wyoming: Wyoming Geological Association 22nd Annual Field Conference Guidebook, p. 161-168.

Pocknall, D.T., 1987a, Paleoenvironments and age of the Wasatch Formation (Eocene), Powder River Basin, Wyoming: Palaios, v. 2, p. 368-376.

_____ 1987b, Palynomorph biozones for the Fort Union and Wasatch formations (upper Paleocene-lower Eocene), Powder River Basin, Wyoming and Montana, U.S.A.: Palynology, v. 11, p. 23-35.

Prichinello, K.A., 1971, Earliest Eocene mammalian fossils from the Laramie Basin of southeast Wyoming: University of Wyoming Contributions to Geology, v. 10, p. 73-87.

Prothero, D.R., 1985, Chadronian (early Oligocene) magnetostratigraphy of eastern Wyoming: implications for the age of the Eocene-Oligocene boundary: Journal of Geology, v. 93, p. 555-565.

Prothero, D.R., Denham, C.R., and Farmer, H.G., 1982, Oligocene calibration of the magnetic polarity time scale: Geology, v. 10, p. 650-653.

_____ 1983, Magnetostratigraphy of the White River Group and its implications for Oligocene geochronology: Palaeogeography, Palaeoclimatology, Palaeoecology, v. 42, p. 151-166.

Ray, R.R., and Keefer, W.R., 1985, Wind River Basin, central Wyoming, *in* Gries, R.R., and Dyer, R.C., editors, Seismic exploration of the Rocky Mountain region: Rocky Mountain Association of Geologists and Denver Geophysical Society, p. 201-212.

Rich, E.I., 1962, Reconnaissance geology of Hiland-Clarkson Hill area, Natrona County, Wyoming: U.S. Geological Survey Bulletin 1107-G, p. 447-540.

Riedel, D.W., 1969, Geology of the Tepee Trail Formation, Badwater area Fremont and Natrona counties, Wyoming: Wyoming Geological Association 21st Annual Field Conference Guidebook, p. 39-41.

Rigby, J.K., Jr., 1980, Swain Quarry of the Fort Union Formation, middle Paleocene (Torrejonian), Carbon County, Wyoming: geologic setting and mammalian fauna: Evolutionary Monographs 3, 179 p.

Ritzma, H.R., 1971, Faulting on the north flank of the Uinta Mountains, Utah and Colorado: Wyoming Geological Association 23rd Annual Field Conference Guidebook, p. 145-150.

Robinson, C.S., Mapel, W.J., and Bergendahl, M.H., 1964, Stratigraphy and structure of the northern and western flanks of the Black Hills uplift, Wyoming, Montana, and South Dakota: U.S. Geological Survey Professional Paper 404, 134 p.

Roehler, H.W., 1958, Geology of Bates Hole, Wyoming [M.A. thesis]: Laramie, University of Wyoming, 58 p.

_____ 1973a, Stratigraphy of the Washakie Formation in the Washakie Basin, Wyoming: U.S. Geological Survey Bulletin 1369, 40 p.

_____ 1973b, Stratigraphic divisions and geologic history of the Laney Member of the Green River Formation in the Washakie Basin in southwestern Wyoming: U.S. Geological Survey Bulletin 1372-E, 28 p.

_____ 1977, Geologic map of the Rock Springs uplift and adjacent areas, Sweetwater County, Wyoming: U.S. Geological Survey Open File Report 77-242, scale 1:125,000, 2 sheets.

_____ 1979a, Geological and energy resources of the Sand Butte Rim NW Quadrangle, Sweetwater County, Wyoming: U.S. Geological Survey Professional Paper 1065-A, 54 p.

_____ 1979b, Geology of the Cooper Ridge NE Quadrangle, Sweetwater County, Wyoming: U.S. Geological Survey Professional Paper 1065-B, 45 p.

_____ 1983, Stratigraphy of Upper Cretaceous and lower Tertiary outcrops in the Rock Springs uplift, Wyoming: U.S. Geological Survey Miscellaneous Investigations Series Map I-1500, 1 sheet (no map).

Roehler, H.W., Swanson, V.E., and Sanchez, J.D., 1977, Summary report of the geology, mineral resources, engineering geology and environmental geochemistry of the Sweetwater-Kemmerer area, Wyoming. Part A: Geology and mineral resources: U.S. Geological Survey Open File Report 77-360, 80 p.

Rohrer, W.L., 1966, Geology of the Adam Weiss Peak Quadrangle, Hot Springs and Park counties, Wyoming: U.S. Geological Survey Bulletin 1241-A, 39 p.

Rohrer, W.L., and Obradovich, J.D., 1969, Age and stratigraphic relations of the Tepee Trail and Wiggins formations, northwestern Wyoming: U.S. Geological Survey Professional Paper 650-B, p. 57-62.

Rohrer, W.L., and Smith, J.W., 1969, Tatman Formation: Wyoming Geological Association 21st Annual Field Conference Guidebook, p. 49-54.

Rose, K.D., 1981, The Clarkforkian land-mammal age and mammalian faunal composition across the Paleocene-Eocene boundary: University of Michigan Papers on Paleontology 26, 197 p.

Rubey, W.W., Oriel, S.S., and Tracey, J.I., Jr., 1975, Geology of the Sage and Kemmerer 15-minute quadrangles, Lincoln County, Wyoming: U.S. Geological Survey Professional Paper 855, 18 p.

Ryan, J.D., 1977, Late Cretaceous and early Tertiary provenance and sediment dispersal, Hanna and Carbon basins, Carbon County, Wyoming: Geological Survey of Wyoming Preliminary Report 16, 17 p.

Ryder, R.T., 1988, Basins of the Rocky Mountain region: Greater Green River Basin, *in* Sloss, L.L., editor, Sedimentary cover — North American craton: U.S.: Geological Society of America, The geology of North America, v. D-2, p. 154-165.

Savage, D.E., and Russell, D.E., 1983, Mammalian paleofaunas of the world: London, Addison-Wesley Publishing Company, xvii + 432 p.

Schankler, D.M., 1980, Faunal zonation of the Willwood Formation in the central Bighorn Basin, Wyoming, *in* Gingerich, P.D., editor, Early Cenozoic paleontology and stratigraphy of the Bighorn Basin, Wyoming: University of Michigan Papers on Paleontology 24, p. 99-114.

Schlaikjer, E.M., 1935, Contributions to the stratigraphy and palaeontology of the Goshen Hole area, Wyoming. III: A new basal Oligocene formation: Bulletin of the Museum of Comparative Zoology at Harvard College, v. 76, p. 69-93.

Schmitt, J.G., and Steidtmann, J.R., 1990, Interior ramp-supported uplifts: implications for sediment provenance in foreland basins: Geological Society of America Bulletin, v. 102, p. 494-501.

Seeland, D.A., 1976, Relationships between early Tertiary sedimentation patterns and uranium mineralization in the Powder River Basin, Wyoming: Wyoming Geological Association 28th Annual Field Conference Guidebook, p. 53-64.

_____ 1978a, Sedimentology and stratigraphy of the lower Eocene Wind River Formation, central Wyoming: Wyoming Geological Association 30th Annual Field Conference Guidebook, p. 181-198.

_____ 1978b, Eocene fluvial drainage patterns and their implications for uranium and hydrocarbon exploration in the Wind River Basin, Wyoming: U.S. Geological Survey Bulletin 1446, 21 p.

_____ 1985, Oligocene paleogeography of the northern Great Plains and adjacent mountains, *in* Flores, R.M., and Kaplan, S.S., editors, Cenozoic paleogeography of the west-central United States: Society of Economic Paleontologists and Mineralogists, Rocky Mountain Section, Rocky Mountain Paleogeography Symposium 3, p. 187-205.

Setoguchi, T., 1978, Paleontology and geology of the Badwater Creek area, central Wyoming. Part 16: The Cedar Ridge local fauna (late Oligocene): Carnegie Museum of Natural History Bulletin 9, 61 p.

Sharp, W.N., McKay, E.J., McKeown, F.A., and White, A.M., 1964, Geology and uranium deposits of the Pumpkin Buttes area of the Powder River Basin, Wyoming: U.S. Geological Survey Bulletin 1107-H, p. 541-638.

Shaughnessy, J., and Butcher, R.H., 1974, Geology of Wagon Wheel nuclear stimulation project, Pinedale Field, Wyoming: American Association of Petroleum Geologists Bulletin, v. 58, p. 2250-2259.

Sheriff, S.D., and Shive, P.N., 1980, The Rattlesnake Hills of central Wyoming revisited: further paleomagnetic results: Geophysical Research Letters, v. 7, p. 589-592.

Shuster, M.W., and Steidtmann, J.R., 1988, Tectonic and sedimentary evolution of the northern Green River basin, western Wyoming, *in* Schmidt, C.J., and Perry, W.J., Jr., editors, Interaction of the Rocky Mountain foreland and Cordilleran thrust belt: Geological Society of America Memoir 171, p. 515-529.

Skinner, S.M., and Gooris, R.J., 1966, A note on *Toxotherium* (Mammalia, Rhinocerotoidea) from Natrona County, Wyoming: American Museum Novitates 2261, 12 p.

Sklenar, S.E., and Andersen, D.W., 1985, Origin and early evolution of an Eocene lake system within the Washakie Basin of southwestern Wyoming, *in* Flores, R.M., and Kaplan, S.S., editors, Cenozoic paleogeography of the west-central United States: Society of Economic Paleontologists and Mineralogists, Rocky Mountain Section, Rocky Mountain Paleogeography Symposium 3, p. 231-245.

Smedes, H.W., and Prostka, H.J., 1972, Stratigraphic framework of the Absaroka Volcanic Supergroup in the Yellowstone National Park region: U.S. Geological Survey Professional Paper 729-C, 33 p.

Smoot, J.P., 1983, Depositional subenvironments in an arid closed basin; the Wilkins Peak Member of the Green River Formation (Eocene), Wyoming, U.S.A.: Sedimentology, v. 30, p. 801-827.

Soister, P.E., 1968, Stratigraphy of the Wind River Formation in south-central Wind River Basin, Wyoming: U.S. Geological Survey Professional Paper 594-A, 50 p.

Stanley, K.O., 1976, Sandstone petrofacies in the Cenozoic high plains sequence, eastern Wyoming and Nebraska: Geological Society of America Bulletin, v. 87, p. 297-309.

Stanley, K.O., and Surdam, R.C., 1978, Sedimentation on the front of Eocene Gilbert-type deltas, Washakie Basin, Wyoming: Journal of Sedimentary Petrology, v. 48, p. 557-573.

Steidtmann, J.R., McGee, L.C., and Middleton, L.T., 1983, Laramide sedimentation, folding, and faulting in the southern Wind River Range, Wyoming, *in* Lowell, J.D., and Gries, R., editors, Rocky Mountain foreland basins and uplifts: Rocky Mountain Association of Petroleum Geologists, p. 161-167.

Steidtmann, J.R., and Middleton, L.T., 1986, Eocene-Pliocene stratigraphy along the southern margin of the Wind River Range, Wyoming: revisions and implications from field and fission-track studies: The Mountain Geologist, v. 23, p. 19-25.

_____ 1991, Fault chronology and uplift history of the southern Wind River Range, Wyoming: implications for Laramide and post-Laramide deformation in the Rocky Mountain foreland: Geological Society of America Bulletin, v. 103, p. 472-485.

Steidtmann, J.R., Middleton, L.T., and Shuster, M.W., 1989, Post-Laramide (Oligocene) uplift in the Wind River Range, Wyoming: Geology, v. 17, p. 38-41.

Steidtmann, J.R., Middleton, L.T., Bottjer, and others, 1986, Geometry, distribution, and provenance of tectogenic conglomerates along the southern margin of the Wind River Range, Wyoming, *in* Peterson, J.A., editor, Paleotectonics and sedimentation in the Rocky Mountain region, United States: American Association of Petroleum Geologists Memoir 41, p. 321-332.

Steidtmann, J.R., and Schmitt, J.G., 1988, Provenance and dispersal of tectogenic sediments in thin-skinned, thrusted terrains, *in* Kleinspehn, K.L., and Paola, C., editors, New perspectives in basin analysis: Berlin, Springer-Verlag, p. 353-366.

Stockton, S.L., and Hawkins, C.M., 1985, Southern Green River Basin/Moxa arch, *in* Gries, R.R., and Dyer, R.C., editors, Seismic exploration of the Rocky Mountain region: Rocky Mountain Association of Geologists and Denver Geophysical Society, p. 73-78.

Stone, D.S., 1985a, Geologic interpretation of seismic profiles, Bighorn Basin, Wyoming, Part I: east flank, *in* Gries, R.R., and Dyer, R.C., editors, Seismic exploration of the Rocky Mountain region: Rocky Mountain Association of Geologists and Denver Geophysical Society, p. 165-174.

_____ 1985b, Geologic interpretation of seismic profiles, Bighorn Basin, Wyoming, Part II: west flank, *in* Gries, R.R., and Dyer, R.C., editors, Seismic exploration of the Rocky Mountain region: Rocky Mountain Association of Geologists and Denver Geophysical Society, p. 175-186.

Stucky, R.K., 1984a, Revision of the Wind River faunas, early Eocene of central Wyoming. Part 5: Geology and biostratigraphy of the upper part of the Wind River Formation, northeastern Wind River Basin: Carnegie Museum of Natural History Annals, v. 53, p. 231-294.

_____ 1984b, Revision of the Wind River faunas, early Eocene of central Wyoming. Part 6: Stratigraphic sections and locality descriptions, upper part of the Wind River Formation: Carnegie Museum of Natural History Annals, v. 53, p. 295-325.

_____ 1984c, The Wasatchian-Bridgerian land mammal age boundary (early to middle Eocene) in western North America: Carnegie Museum of Natural History Annals, v. 53, p. 347-382.

Stucky, R.K., Krishtalka, L., and Dawson, M.R., 1989, Paleontology, geology and remote sensing of Paleogene rocks in the northeastern Wind River Basin, Wyoming, USA, *in* Flynn, J.J., editor, Mesozoic/Cenozoic vertebrate paleontology: classic localities, contemporary approaches: International Geological Congress, Field Trip Guidebook T322, American Geophysical Union, Washington, D.C., p. 34-44.

Stucky, R.K., Krishtalka, L., and Redline, A.D., 1990, Geology, vertebrate fauna, and paleoecology of the Buck Spring Quarries (early Eocene, Wind River Formation), Wyoming, *in* Bown, T.M., and Rose, K.D., editors, Dawn of the Age of Mammals in the northern part of the Rocky Mountain interior, North America: Geological Society of America Special Paper 243, p. 169-186.

Sullivan, R., 1980, A stratigraphic evaluation of the Eocene rocks of southwestern Wyoming: Geological Survey of Wyoming Report of Investigations 20, 50 p.

_____ 1985, Origin of lacustrine rocks of Wilkins Peak Member, Wyoming: American Association of Petroleum Geologists Bulletin, v. 69, p. 913-922.

Sundell, K.A., 1982, Geology of the headwater area of the North Fork of Owl Creek, Hot Springs County, Wyoming: Geological Survey of Wyoming Report of Investigations 15, 51 p.

Sundell, K.A., and Eaton, J.G., 1982, Stratigraphic relations within the southeastern Absaroka volcanic sequence, northwestern Wyoming: Wyoming Geological Association 33rd Annual Field Conference Guidebook, p. 65-71.

Sundell, K.A., Shive, P.N., and Eaton, J.G., 1984, Measured sections, magnetic polarity and biostratigraphy of the Eocene Wiggins, Tepee Trail and Aycross formations within the southeastern Absaroka Range, Wyoming: Wyoming Geological Association Earth Science Bulletin, v. 17, 48 p.

Surdam, R.C., and Stanley, K.O., 1979, Lacustrine sedimentation during the culminating phase of Eocene Lake Gosiute, Wyoming (Green River Formation): Geological Society of America Bulletin, v. 90, p. 93-110.

_____ 1980, Effects of changes in drainage-basin boundaries on sedimentation in Eocene Lakes Gosiute and Uinta of Wyoming, Utah, and Colorado: Geology, v. 8, p. 135-139.

Surdam, R.C., and Wolfbauer, C.A., 1975, Green River Formation, Wyoming: a playa-lake complex: Geological Society of America Bulletin, v. 86, p. 335-345.

Sutton, J.F., and Black, C.C., 1975, Paleontology of the earliest Oligocene deposits in Jackson Hole, Wyoming. Part 1: Rodents exclusive of the family Eomyidae: Carnegie Museum of Natural History Annals, v. 45, p. 299-315.

Swinehart, J.B., Souders, V.L., DeGraw, H.M., and Diffendal, R.F., Jr., 1985, Cenozoic paleogeography of western Nebraska, *in* Flores, R.M., and Kaplan, S.S., editors, Cenozoic paleogeography of the west-central United States: Society of Economic Paleontologists and Mineralogists, Rocky Mountain Section, Rocky Mountain Paleogeography Symposium 3, p. 209- 229.

Swisher, C.C., III, and Prothero, D.R., 1990, Single-crystal $^{40}Ar/^{39}Ar$ dating of the Eocene- Oligocene transition in North America: Science, v. 249, p. 760-762.

Tedford, R.H., Galusha, T., Skinner, M.F., and others, 1987, Faunal succession and biochronology of the Arikareean through Hemphillian interval (late Oligocene through earliest Pliocene epochs) in North America, *in* Woodburne, M.O., editor, Cenozoic mammals of North America: geochronology and biostratigraphy: Berkeley, University of California Press, p. 153-210.

Teerman, S.C., Crelling, J.C., and Glass, G.B., 1985, Petrology of Hanna and Ferris Formation coals from the Hanna Coal Field, Wyoming: Geological Survey of Wyoming Report of Investigations 32, 23 p.

Thaden, R.E., 1980a, Geologic map of the De Pass Quadrangle, Fremont and Hot Springs counties, Wyoming: U.S. Geological Survey Geologic Quadrangle Map GQ-1526, scale 1:24,000.

_____ 1980b, Geologic map of the Guffy Peak Quadrangle showing chromolithofacies in the Wind River Formation, Fremont and Hot Springs counties, Wyoming: U.S. Geological Survey Geologic Quadrangle Map GQ-1527, scale 1:24,000.

Thaden, R.E., 1980c, Geologic map of the Picard Ranch Quadrangle, showing chromolithofacies and coal beds in the Wind River Formation, Fremont County, Wyoming: U.S. Geological Survey Geologic Quadrangle Map GQ-1539, scale 1:24,000.

Torres, V., 1985, Stratigraphy of the Eocene Willwood, Aycross, and Wapiti formations along the North Fork of the Shoshone River, north-central Wyoming: University of Wyoming Contributions to Geology, v. 23, p. 83-97.

Tschudy, R.H., 1976, Pollen changes near the Fort Union-Wasatch boundary, Powder River Basin: Wyoming Geological Association 28th Annual Field Conference Guidebook, p. 73- 81.

Tourtelot, H.A., 1953, Geology of the Badwater area, central Wyoming: U.S. Geological Survey Oil and Gas Investigations Map OM-124, 2 sheets, scale unspecified.

_____ 1957, The geology and vertebrate paleontology of upper Eocene strata in the northeastern part of the Wind River Basin, Wyoming. Part 1: Geology: Smithsonian Miscellaneous Collections, v. 134, no. 4, 27 p.

Turnbull, W.D., 1978, The mammalian faunas of the Washakie Formation, Eocene age, of southern Wyoming. Part I: Introduction: the geology, history, and setting: Field Museum of Natural History Fieldiana (Geology), v. 33, p. 569-601.

_____ 1991, *Protoptychus hatcheri* Scott, 1895. The mammalian faunas of the Washakie Formation, Eocene age, of southern Wyoming. Part II: The Adobetown Member, middle division (=Washakie B), Twka/2 (in part): Fieldiana, Geology, New Series, no. 21, 33 p.

Turnbull, W.D., and Martill, D.M., 1988, Taphonomy and preservation of a monospecific titanothere assemblage from the Washakie Formation (late Eocene), southern Wyoming: an ecological accident in the fossil record: Palaeogeography, Palaeoclimatology, Palaeoecology, v. 63, p. 91-108.

Van Houten, F.B., 1944, Stratigraphy of the Willwood and Tatman formations in northwestern Wyoming: Geological Society of America Bulletin, v. 55, p. 165-210.

_____ 1955, Volcanic-rich middle and upper Eocene sedimentary rocks northwest of Rattlesnake Hills, central Wyoming: U.S. Geological Survey Professional Paper 274-A, 14 p.

_____ 1964, Tertiary geology of the Beaver Rim area, Fremont and Natrona counties, Wyoming: U.S. Geological Survey Bulletin 1164, 99 p.

West, R.M., 1970, Sequence of mammalian faunas of Eocene age in the northern Green River Basin, Wyoming: Journal of Paleontology, v. 44, p. 142-147.

_____ 1973, Geology and mammalian paleontology of the New Fork-Big Sandy area, Sublette County, Wyoming: Field Museum of Natural History Fieldiana (Geology), v. 29, 193 p.

_____ 1976, Paleontology and geology of the Bridger Formation, southern Green River Basin, southwestern Wyoming. Part 1: History of field work and geological setting: Milwaukee Public Museum Contributions in Biology and Geology 7, 12 p.

West, R.M., and Dawson, M.R., 1973, Fossil mammals from the upper part of the Cathedral Bluffs Tongue of the Wasatch Formation (early Bridgerian), northern Green River Basin, Wyoming: University of Wyoming Contributions to Geology, v. 12, p. 33-41.

West, R.M., and Hutchison, J.H., 1981, Geology and paleontology of the Bridger Formation, southern Green River Basin, southwestern Wyoming. Part 6: The fauna and correlation of Bridger E: Milwaukee Public Museum Contributions in Biology and Geology 46, 8 p.

Wiltschko, D.V., and Dorr, J.A., Jr., 1983, Timing of deformation in overthrust belt and foreland of Idaho, Wyoming, and Utah: American Association of Petroleum Geologists Bulletin, v. 67, p. 1304-1322.

Wing, S.L., 1984, A new basis for recognizing the Paleocene/Eocene boundary in Western Interior North America: Science, v. 226, p. 439-441.

Winkler, D.A., 1983, Paleoecology of an early Eocene mammalian fauna from paleosols in the Clarks Fork Basin, northwestern Wyoming (U.S.A.): Palaeo-geography, Palaeoclimatology, Palaeoecology, v. 43, p. 261-298.

Winterfeld, G.F., 1982, Mammalian paleontology of the Fort Union Formation (Paleocene), eastern Rock Springs uplift, Sweetwater County, Wyoming: University of Wyoming Contributions to Geology, v. 21, p. 73-111.

_____ 1986, Laramide tectonism, deposition, and early Cenozoic stratigraphy of the northwestern Wind River Basin and Washakie Range, Wyoming [Ph.D. dissertation]: Laramie, University of Wyoming, 248 p.

Winterfeld, G.F., and Conard, J.B., 1983, Laramide tectonics and deposition, Washakie Range and northwestern Wind River Basin, Wyoming, *in* Lowell, J.D., and Gries, R., editors, Rocky Mountain foreland basins and uplifts: Rocky Mountain Association of Petroleum Geologists, p. 137-148.

Wolfe, J.A., 1987, An overview of the origins of the modern vegetation and flora of the northern Rocky Mountains: Missouri Botanical Gardens Annals, v. 74, p. 785-803.

Wood, H.E., 2nd., Chaney, R.W., Clark, J., and others, 1941, Nomenclature and correlation of the North American continental Tertiary: Geological Society of America Bulletin, v. 52, 48 p.

Woodburne, M.O., editor, 1987a, Cenozoic mammals of North America: geochronology and biostratigraphy: Berkeley, University of California Press, xv + 336 p.

_____ 1987b, A prospectus of the North American mammal ages, *in* Woodburne, M.O., editor, Cenozoic mammals of North America: geochronology and biostratigraphy: Berkeley, University of California Press, p. 285-290.

Woodward, L.A., 1988, Tectonic map of the Rocky Mountain region of the United States, *in* Sloss, L.L., editor, Sedimentary cover — North American craton: U.S.: Geological Society of America, The geology of North America, v. D-2, Plate 2, scale 1:2,500,000.

Yuretich, R.F., Hickey, L.J., Gregson, B.J., and Hsia, Y.-L., 1984, Lacustrine deposits in the Paleocene Fort Union

Formation, northern Bighorn Basin, Montana: Journal of Sedimentary Petrology, v. 54, p. 836-852.

Zeller, H.D., and Stevens, E.V., 1969, Geology of the Oregon Buttes area, Sweetwater, Sublette, and Fremont counties, southwestern Wyoming: U.S. Geological Survey Bulletin 1256, 60 p.

ISBN 1-884589-00-6

GEOLOGY OF WYOMING

Editors

Arthur W. Snoke
James R. Steidtmann
Sheila M. Roberts

Memoir No. 5
The Geological Survey of Wyoming
Gary B. Glass, State Geologist

Geology of Wyoming

Dedicated to

Donald L. Blackstone, Jr.

and

J. David Love

Volume 2

Editors

Arthur W. Snoke

James R. Steidtmann

Sheila M. Roberts

Geological Survey of Wyoming Memoir No. 5

Gary B. Glass, State Geologist

Laramie, Wyoming

1993

WYOMING STATE GEOLOGICAL SURVEY
Lance Cook, *State Geologist*

GEOLOGICAL SURVEY BOARD

Ex Officio

Jim Geringer, *Governor*
Randi S. Martinsen, *University of Wyoming*
Don J. Likwartz, *Oil and Gas Supervisor*
Lance Cook, *State Geologist*

Appointed

Ronald A. Baugh, *Casper*
Nancy M. Doelger, *Casper*
Charles M. Love, *Rock Springs*
Stephen L. Payne, *Casper*
John E. Trummel, *Gillette*

STAFF

Computer Services Unit
Susan McClendon - *Manager*

Geologic Sections
James C. Case, *Staff Geologist - Geologic Hazards*
Rodney H. De Bruin, *Staff Geologist - Oil and Gas*
Ray E. Harris, *Staff Geologist - Industrial Minerals and Uranium*
W. Dan Hausel, *Senior Economic Geologist - Metals and Precious Stones*
Alan J. Ver Ploeg, *Senior Staff Geologist - Geologic Mapping*
Robert M. Lyman, *Staff Geologist - Coal*

Publications Section
Richard W. Jones - *Editor*
Jaime R. Bogaard - *Editorial Assistant*
Lisa J. Alexander - *Sales Manager*
Fred H. Porter - *Cartographer*
Phyllis A. Ranz - *Cartographer*
Joseph M. Huss - *GIS Specialist*

Supportive Services Unit
Susanne G. Bruhnke - *Office Manager*
Joan E. Binder - *Administrative Assistant*

People with disabilities who require an alternative form of communication in order to use this publication should contact the Editor, Wyoming State Geological Survey at (307) 766-2286. TDD Relay operator 1(800) 877-9975.

This and other publications available from: Wyoming State Geological Survey
P.O. Box 3008
Laramie, Wyoming 82071-3008
(307) 766-2286

First edition, second printing of 1,000 copies by Pioneer Printing and Stationery Company, Cheyenne, Wyoming.

Geology of Wyoming: edited by Arthur W. Snoke, James R. Steidtmann, and Sheila M. Roberts
ISBN 1-884589-00-6 (volume 1)
ISBN 1-884589-01-4 (volume 2)
ISBN 1-884589-02-2 (2 volume set)

A cooperative project of the Wyoming State Geological Survey and the Department of Geology and Geophysics, University of Wyoming.

Table of Contents

page

Volume 1

Preface and acknowledgments ..... *Arthur W. Snoke, James R. Steidtmann, and Sheila M. Roberts* v

Dedication to Donald L. Blackstone, Jr. ..... *Robert S. Houston* vii

Dedication to J. David Love ..... *William R. Keefer* xi

"Geologists' Camp". ..... *Phyllis Ranz* xiv

Part I: Overview

Geologic history of Wyoming within the tectonic framework of the North American Cordillera ..... *Arthur W. Snoke* 2

Part II: Precambrian history

The Archean history of the Wyoming province ..... *Carol D. Frost and B. Ronald Frost* 58

Late Archean and Early Proterozoic geology of southeastern Wyoming ..... *Robert S. Houston* 78

The Laramie Anorthosite Complex and the Sherman batholith: geology, evolution, and theories of origin ..... *B. Ronald Frost, Carol D. Frost, Donald H. Lindsley, James S. Scoates, and Jeremy N. Mitchell* 118

Part III: Paleozoic history

Paleozoic history of Wyoming ..... *Donald W. Boyd* 164

The Ancestral Rocky Mountains in Wyoming ..... *Edwin K. Maughan* 188

Part IV: Mesozoic history

The early Mesozoic history of Wyoming ..... *M. Dane Picard* 210

The Cretaceous foreland basin and its sedimentary record ..... *James R. Steidtmann* 250

An overview of the geologic structure of the thrust belt in Wyoming, northern Utah, and eastern Idaho ..... *Frank Royse, Jr.* 272

Structural style of Laramide basement-cored uplifts and associated folds ..... *William G. Brown* 312

Part V: Cenozoic history

Laramide evolution of the Black Hills uplift ..... *Alvis L. Lisenbee and Ed DeWitt* 374

Correlation of Paleogene strata across Wyoming—a users' guide ..... *Jason A. Lillegraven* 414

Volume 2

Part V: Cenozoic history *(continued)*

A geologic overview of the Absaroka volcanic province ..... *Kent A. Sundell* 480

Petrographic and geochemical characteristics of mid-Tertiary igneous rocks in the Rattlesnake Hills, central Wyoming, with a comparison to the Bear Lodge intrusive suite of northeastern Wyoming ..... *Anthony R. Hoch and Carol D. Frost* 508

page

The Heart Mountain detachment, northwestern Wyoming: 100 years of controversy ..... *Thomas A. Hauge* 530

Neogene stratigraphy and tectonics of Wyoming ..... *Kathryn M. Flanagan and John Montagne* 572

Geomorphic history of Wyoming and high-level erosion surfaces ..... *Brainerd Mears, Jr.* 608

The Teton fault, Wyoming: seismotectonics, Quaternary history, and earthquake hazards ..... *Robert B. Smith, John O.D. Byrd, and David D. Susong* 628

Seismic surveys and Quaternary history of Jackson Lake, Wyoming ..... *Robert B. Smith , Kenneth L. Pierce, and Richard J. Wold* 668

Topographic signature, space-time evolution, and physical properties of the Yellowstone-Snake River Plain volcanic system: the Yellowstone hotspot ..... *Robert B. Smith and Lawrence W. Braile* 694

Part VI: Topical aspects

The influence of Laramide foreland structures on modern ground-water circulation in Wyoming artesian basins ..... *Peter W. Huntoon* 756

Geologic applications of remote sensing and GIS: A Wyoming landscape perspective ..... *Ronald W. Marrs and Dennis N. Grasso* 790

Metal and gemstone deposits of Wyoming ..... *W. Dan Hausel* 816

Overview of oil and gas geology of Wyoming ..... *Rodney H. De Bruin* 836

Processes and possible analogues in the formation of Wyoming's coal deposits ..... *T.A. Moore and J.C. Shearer* 874

Geologic classification and origin of radioactive mineralization in Wyoming ..... *Ray E. Harris and Jon K. King* 898

Industrial minerals and construction materials of Wyoming ..... *Ray E. Harris* 918

Map pocket (CD-ROM in Vol. 2, second printing)

Geologic map of Precambrian rocks of the Wyoming province (Sheet 1, Robert S. Houston)

Eight regional structural cross sections in the Wyoming-Utah-Idaho thrust belt (Sheet 1, Frank Royse, Jr.)

Restored structural cross section along latitude 41° 15' Wyoming-Utah thrust belt (Sheet 2, Frank Royse, Jr.)

Generalized geologic map of the Heart Mountain detachment, northwestern Wyoming (Sheet 1, Thomas A. Hauge)

Map of the Quaternary trace of the Teton fault (Sheet 1, R.B. Smith, J.O.D. Byrd, and D.D. Susong)

Bathymetric map of Jackson Lake, Wyoming (Sheet 1, R.B. Smith, K.L. Pierce, and R.J. Wold)

Seismic reflection profiles of Jackson Lake (Sheet 2, R.B. Smith, K.L. Pierce, and R.J. Wold)

Stratigraphic chart showing Phanerozoic nomenclature for the State of Wyoming (J.D. Love, Ann Coe Christiansen, Alan J. Ver Ploeg)

Revised Precambrian basement map of Wyoming: outcrop and structural configuration (D.L. Blackstone, Jr.)

Wyoming geologic highway map (1:1,000,000)

Part V

Cenozoic history
(continued)

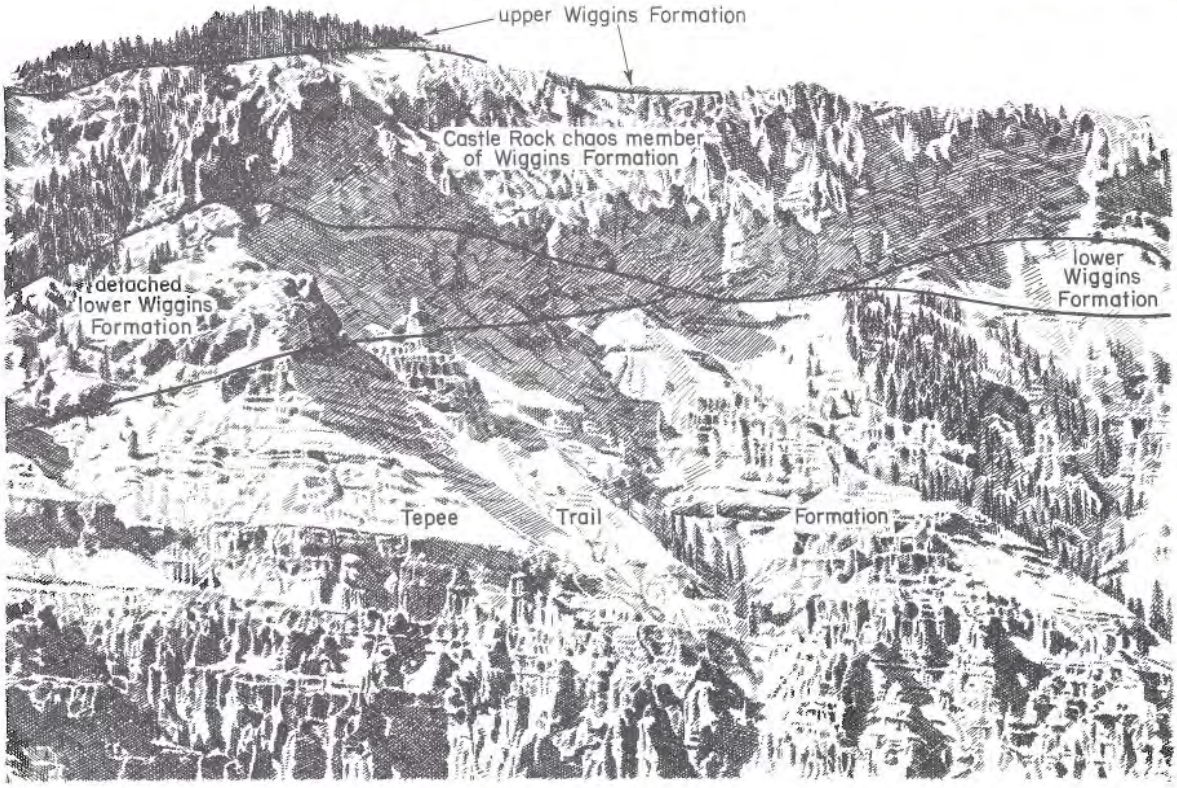

Frontispiece. Head of South Fork of Cottonwood Creek (N 1/2 section 7, T. 44 N., R. 101 W.). View to south of the Castle Rocks Chaos Member of the Wiggins Formation (landslide/debris flow) overlying the Teepee Trail Formation (fluvial epiclastic rocks) with a detached white sliver of lower Wiggins Formation in between. Sketch by Phyllis A. Ranz.

A geologic overview of the Absaroka volcanic province

Kent A. Sundell
Ram Oil Company/Absaroka Exploration Company
Casper, Wyoming 82602

Abstract

The Absaroka volcanic province is composed of Eocene andesitic volcanic rocks, covering 9,000 mi² (23,310 km²) of northwestern Wyoming and southwestern Montana. Volcanism occurred between 53 and 38 Ma, when 10,000-ft-high (3,050 m) andesitic stratovolcanoes formed and were rapidly eroded and redistributed into a >6,000-ft-thick (1,830 m) blanket of reworked, epiclastic volcanic rocks. The present erosion cycle carves a spectacular, rugged, mountainous topography into the thick volcanic pile that overlies a Paleozoic, Mesozoic, and Tertiary sedimentary and tectonic basin. Regional stratigraphic, structural, and geophysical investigations suggest that the Absaroka basin has significant potential for oil and gas accumulations and locally contains precious and base minerals. Stratigraphic relationships are very complex due to extensive reworking of the primary volcanic rocks and large-scale mass movements. Three of the largest subaerial landslide deposits known on Earth are within the Absaroka volcanic province. Thick stratigraphic sequences containing interbedded radiometrically dated rocks, vertebrate fossils, and plant fossils, and the availability of paleomagnetic data make the Absaroka volcanic province exceptional for worldwide correlation of middle Eocene rocks. The rugged and remote nature of the Absaroka volcanic province has hindered research and exploration. Vast areas are relatively unexplored, and the potential for significant geologic discoveries is great.

General description

The Absaroka Range, a rugged 155-mi-long (250 km), northwest-trending mountain range in northwestern Wyoming and southwestern Montana, forms the central core of the Absaroka volcanic province (AVP) (**Figure 1**). The AVP is composed chiefly of Eocene volcaniclastic rocks, including volcanic sandstone, siltstone, claystone, conglomerate, and breccia. The amounts of intercalated primary volcanic rocks, including hypabyssal igneous rocks, lava flows, flow breccias, pyroclastic breccias, and tuffs increase near eruptive centers. The inferred depositional setting was a belt of large andesitic stratovolcanoes flanked by coalescing alluvial aprons. Volcanic sediments rapidly filled a shallow foreland basin, mantled the adjacent Paleozoic- and Precambrian-cored mountain uplifts, and were dispersed throughout nearby basins by fluvial and eolian processes. The present AVP is an erosional remnant of an accumulation of volcanic material that extended across northwestern Wyoming. It is the largest Eocene volcanic field in the Northern Rocky Mountains, covering about 9,000 mi² (23,310 km²), and the rocks within the range have collectively been named the Absaroka Volcanic Supergroup (Smedes and Prostka, 1972).

Sundell, K. A., 1993, A geologic overview of the Absaroka volcanic province, *in* Snoke, A.W., Steidtmann, J.R., and Roberts, S.M., editors, Geology of Wyoming: Geological Survey of Wyoming Memoir No. 5, p. 480-506.

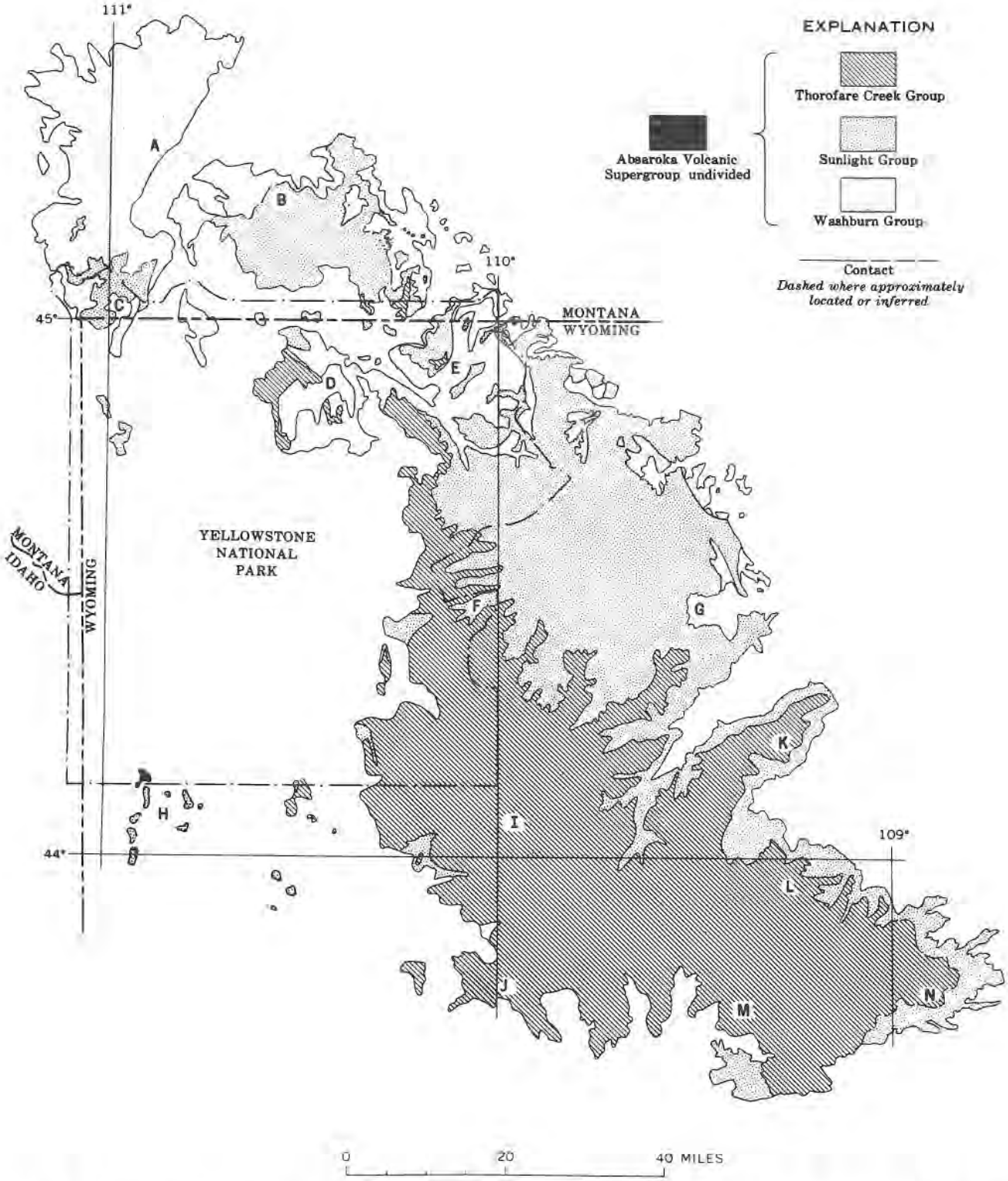

Figure 1. Generalized geologic map of the Absaroka volcanic field. Intrusive rocks are not shown (after Smedes and Prostka, 1972). Letters A through N refer to locations of stratigraphic sections in Figures 5A and 5B.

The AVP covers most of the largest roadless area in the conterminous United States, including portions of four wilderness areas, four national forests, and the eastern half of Yellowstone National Park.

Regional setting

The Absaroka Range is bordered on the east by the Bighorn Basin, on the northeast by the Beartooth Mountains, on the northwest by the Gallatin Range, on the west by the Yellowstone Plateau, on the southwest by Jackson Hole and the Mt. Leidy Highlands, and on the south by the northwestern Wind River Basin and Owl Creek Mountains (**Figure 2**). Absaroka volcanic rocks were deposited upon an early Eocene paleotopography with local relief of several thousand feet, similar to the present topography in the western Owl Creek Mountains immediately adjacent to the southeastern margin of the AVP. This paleotopography is being exhumed by erosion along all margins of the AVP (Love, 1939; Sundell, 1985). The volcanic field is highly dissected by erosion that began in the late Eocene (Sundell, 1985), and the original paleorelief (>10,000 ft) (>3,050 m) associated with large Eocene stratovolcanoes is no longer evident (Fritz, 1982; Sundell, 1985). Eocene igneous rocks intruded and unconformably overlie folded, faulted, and truncated early Tertiary, Mesozoic, Paleozoic, and Precambrian rocks (Love and Christiansen, 1985). The AVP is unconformably overlain by late Pliocene and Quaternary volcanic rocks of the Yellowstone volcanic plateau along most of its western margin in Yellowstone National Park (Blackstone, 1966; Christiansen and Blank, 1972).

Before the onset of Absaroka volcanism during the early Eocene (about 53 Ma), uplifts related to the Late Cretaceous to early Tertiary Laramide orogeny formed the primary tectonic elements in northwestern Wyoming. These included the Beartooth, Gallatin, Washakie, Owl Creek, and Cody uplifts, which outlined and separated the Absaroka basin from the adjacent Bighorn, Wind River, and Fish Creek basins to the east, south, and west, respectively (Sundell, 1990) (**Figure 2**). The Absaroka basin was a relatively broad, shallow Laramide basin covering more than 7,000 mi^2 (18,130 km^2) and containing at least several thousand feet of prevolcanic, synorogenic lower Eocene sediments. The Absaroka basin filled rapidly during the middle Eocene, contemporaneous with Absaroka volcanism. In contrast, the adjacent Laramide basins were filled with more than 10,000 ft (3,050 m) of synorogenic Paleocene and lower Eocene sediments prior to initiation of Absaroka volcanism.

Eocene volcanism was common in the northwestern United States during subduction of the East Pacific plate beneath North America (Lipman and others, 1972). One of the largest accumulations of Eocene volcanic rocks, the AVP remains rather enigmatic in regards to its distance from the subduction zone (>1,000 mi/1,610 km) and its position near the southeast terminus of a broad northwest-trending magmatic arc that extends from southwestern Canada across Washington and Idaho, and into Montana (Snyder and others, 1976). The unique coupling of Absaroka volcanism with the latest stage of the Laramide orogeny provided a fundamental regional control of depositional, tectonic, and volcanic processes during the middle Eocene (Sundell, 1990).

Volcanologic and petrologic aspects

Absaroka volcanism began in southern Montana during the early Eocene (about 53 Ma) (Chadwick, 1969, 1970, 1981) and continued throughout the middle Eocene over the entire volcanic field. Probably the last eruption was in the southeastern Absaroka Range during the late Eocene (about 38 Ma) (L.L. Love and others, 1976; Sundell, 1985). The rocks are dominantly calc-alkaline andesites, with locally important basalts, trachyandesites, dacites, and rhyolites. The vast majority of AVP rocks are epiclastic deposits, including volcanic sandstones, siltstones, claystones, conglomerates, and breccias, derived by reworking of primary volcanic rocks. The major volcanic eruptive centers are commonly spaced 15 to 25 mi (24 to 40 km) apart and contain abundant intrusions, breccias, pyroclastic rocks, tuffs, and lava

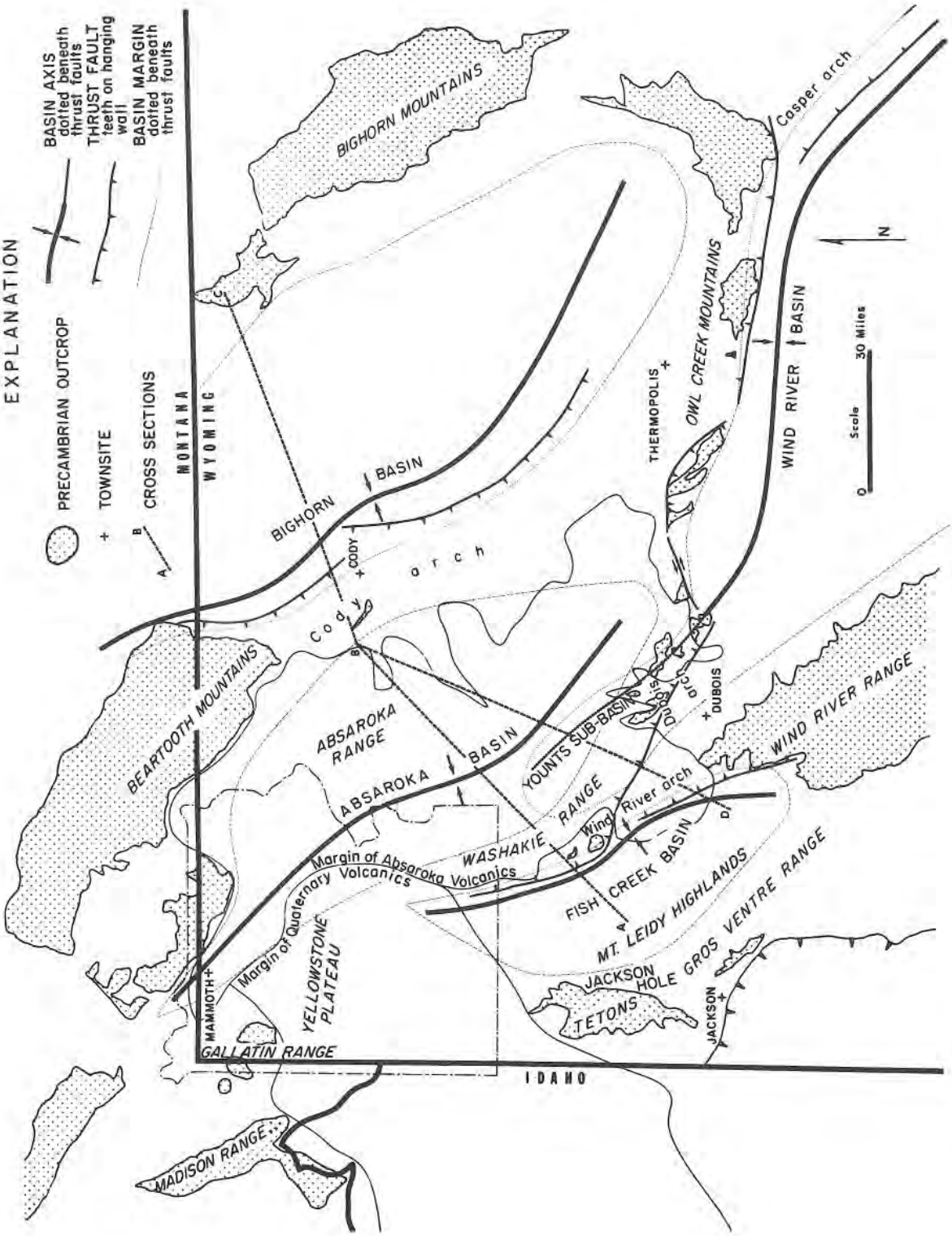

Figure 2. Generalized tectonic map of northwestern Wyoming. Heavy dashed straight lines refer to cross sections A-B-C and D-B shown on Figure 6.

flows interspersed with minor epiclastic rocks. The areas between volcanic centers are filled chiefly with epiclastic rocks and reworked airfall tuffs derived from adjacent volcanic centers.

Two subparallel belts of Absaroka volcanic eruptive centers may have been localized by zones of Precambrian structural weakness that were reactivated during the Laramide orogeny (Chadwick, 1969, 1970; Garihan and others, 1983). Zones of dilation, providing excellent sites for magma generation and ascent through the crust, may have developed in the Absaroka Range along the southeast portion of northwest-striking sinistral faults observed in the foreland province of southwest Montana (i.e., Gardiner/Spanish Peak fault system) (Sundell, 1990). These northwest-striking zones of crustal weakness and dilatancy propagated southeastward into Wyoming and probably influenced the timing of eruption and localization of deposition of Absaroka volcanic rocks.

Excellent examples of deposits preserved from virtually every type of volcanic eruption can be found within the Absaroka volcanic sequence. The locally spectacular cross-sectional exposures on steep mountain slopes and cliff faces provide a perfect opportunity to identify depositional analogs to modern eruption processes. The Blue Point marker (Sundell and Eaton, 1982) is a thick (>250 ft/76 m), widespread (>2,000 mi^2/5,180 km^2) sequence of primary and reworked Plinian airfall deposits (**Figure 3**). The Trout Peak Trachyandesite (Nelson and Pierce, 1968) and extensive lava flows within the Wapiti Formation show episodes of Hawaiian-style vent facies and dike-fed lava flows and the formation of large, 300-ft-deep (92 m) lava lakes. A myriad of vent-facies flow breccias and pyroclastic breccias have been described throughout the Absaroka Range and may represent variations of Vesuvian, Strombolian, and Pelean eruptions (Parsons, 1939b, 1974; Wilson, 1963, 1964; Rubel, 1971; LaPointe,

Figure 3. North flank of Carter Mountain showing epiclastic fluvial conglomerates of Wiggins Formation (top left) overlying pyroclastic reworked tuffs of the Blue Point marker (white). A single widespread continuous flow (lava lake) of the Trout Peak Trachyandesite is separated from multiple valley-filling flows in the Wapiti Formation (bottom right) by an unnamed sequence of fine-grained epiclastic rocks and lake sediments (trees). Photo by Jeff Eaton.

1977). The Slough Creek Tuff is a welded ash-flow tuff in the northern portion of the AVP (Hickenlooper and Gutmann, 1982). The Castle Rocks chaos, which deposited more than 70 mi^3 (293 km^3) of material over a 350 mi^2 (900 km^2) area (Sundell, 1985), formed by the complete collapse of a giant stratovolcano in the southeastern Absaroka Range that was one hundred times larger than the Mt. St. Helens sector collapse (**Figure 4**). Unfortunately, the details of most of these spectacular eruptive episodes and individual eruptions remain unstudied. Many others are yet to be discovered and described.

Calc-alkaline mafic to felsic andesites predominate in the Absaroka volcanic sequence, but rhyolites, dacites, basalts, and a variety of potassium-rich rocks are locally important (Hague and others, 1899; Parsons, 1939a, 1969; Wilson, 1964; Chadwick, 1970; Smedes and Prostka, 1972; Ketner and Fisher, 1978). In general, the Sunlight Group contains more mafic rock types than either the underlying Washburn or overlying Thorofare Creek groups. Potassium-rich rocks, including trachyandesites, trachybasalts, syenites, trachytes, monzonites, quartz latites, absarokite, shoshonite, and banakite, occur along the eastern belt of eruptive centers in the northern Absaroka Range (Hague and others, 1899; Parsons, 1939a; Chadwick, 1970; Smedes and Prostka, 1972; Gest and McBirney, 1979). The potassium-rich mafic rocks may be of a hybrid origin, not derived from primary potassic mafic magmas (Nicholls and Carmichael, 1969; Prostka, 1973; Meen and Eggler, 1987, 1989). Rhyodacitic and quartz latite ash flows are locally present in the northern Absaroka Range (Smedes and Prostka, 1972; Hickenlooper and Gutmann, 1982), and rhyolitic rocks are common constituents of the Wiggins Formation in the southeastern Absaroka Range (Wilson, 1964; Sundell, 1982). Basaltic rocks are most common in the Sunlight Group (Wilson, 1964; Chadwick, 1970; Smedes and Prostka, 1972; Sundell, 1982), but also occur locally in older rocks

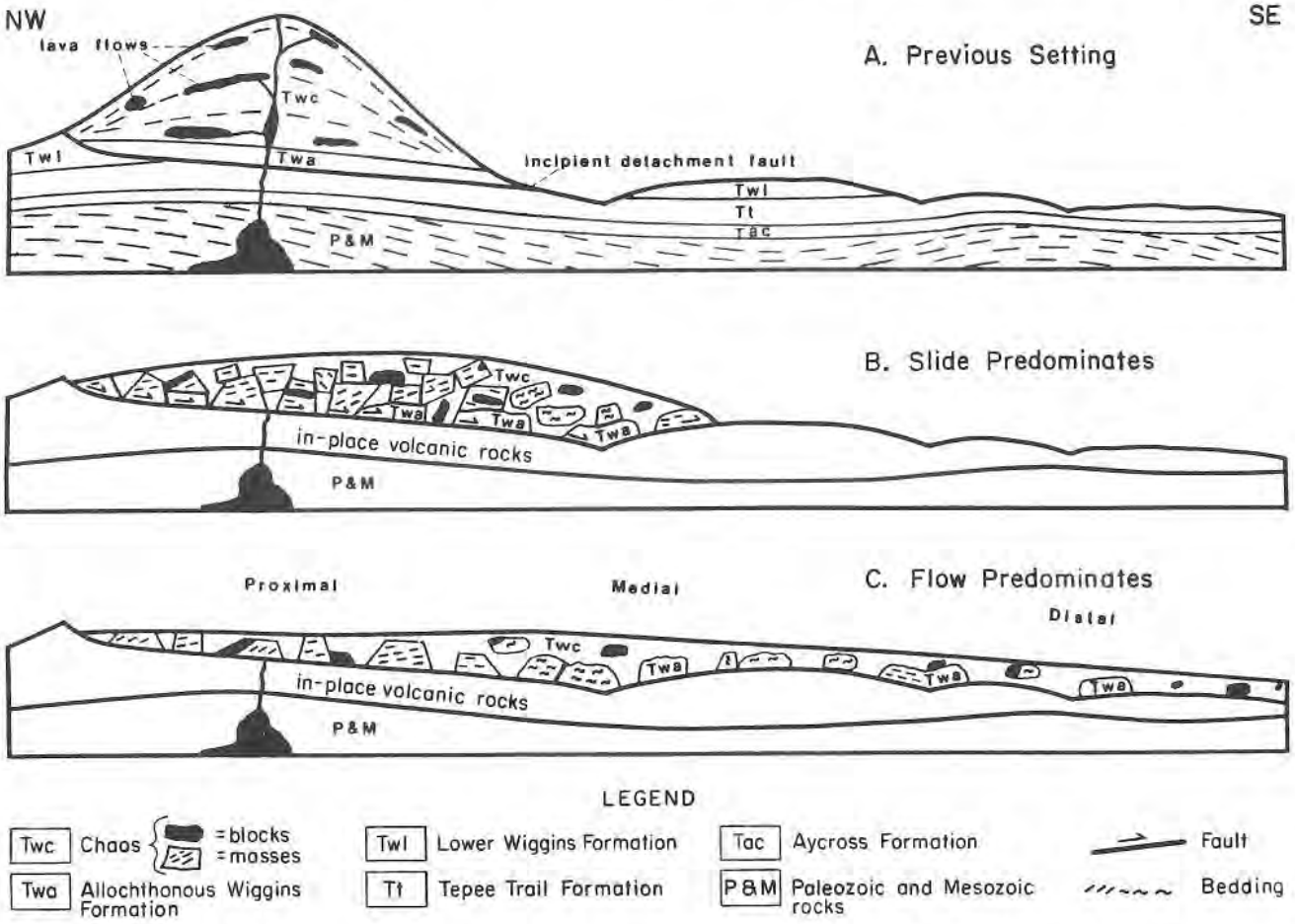

Figure 4. Schematic diagram showing the development of the Castle Rocks chaos (after Sundell, 1985).

(Elk Creek Basalt of Smedes and Prostka, 1972) and cap the Wiggins Formation in the youngest rocks of the volcanic sequence (Love, 1939; Blackstone, 1966). Unfortunately, the available petrologic data represent a small fraction of the igneous rocks present in the Absaroka Range, and analyses have concentrated on a few near-vent mineralized areas and limited areas of easy access. Geochemical data are virtually absent from intrusive and hypabyssal rocks in the central and southern parts of the Absaroka Range, and thick sequences (>1,000 ft/300 m) of lava flows remain unstudied in the South Fork of the Shoshone and Greybull river areas.

Stratigraphic relationships

The Eocene volcanic rocks of the Absaroka Range were derived from multiple eruptions emanating from localized extrusive centers throughout the volcanic field. The primary volcanic material was rapidly and continuously reworked and mixed by fluvial, mass wasting, and eolian processes. The resultant deposits form a very complex heterogeneous assemblage of primary vent-facies rocks and reworked alluvial-facies rocks derived from many source areas at different times. Many nomenclature problems have developed in trying to group these rocks into mappable lithostratigraphic units (Sundell and Eaton, 1982).

The Absaroka Volcanic Supergroup (Smedes and Prostka, 1972) encompasses all volcanic rocks within the AVP and associated outliers deposited during the Eocene. The stratigraphic relationships between mapped formations within the Absaroka Volcanic Supergroup were summarized by Smedes and Prostka in 1972; an updated correlation diagram is shown in **Figures 5A** and **5B**. One notable change to Smedes and Prostka's (1972) work is recognition of the Blue Point marker (Wilson, 1964; Sundell and Eaton, 1982) as a widespread distinctive sequence of airfall and reworked tuffs throughout the southern half of the AVP. The Blue Point marker (**Figure 5**) has a distinctive lithologic character, age, and reverse polarity that aids in correlation of strata throughout the Absaroka Range (Sundell and Eaton, 1982; Shive and Sundell, 1986). Correlation of the Blue Point marker and paleomagnetic data suggest that the Aycross Formation is laterally and temporally equivalent to the Wapiti Formation and should be included within the Sunlight Group. The lower portions of the Aycross Formation may correlate to rocks within the Washburn Group, but at present the Aycross has not been effectively subdivided due to stratigraphic and structural complexities. The name "Pitchfork formation" (Hay, 1956) has been abandoned (Sundell and Eaton, 1982; Bown, 1982a; Decker, 1990). Tracing of the Blue Point marker and detailed stratigraphic and paleontologic studies (Sundell, 1982, 1985; Eaton, 1982, 1985; Sundell and Eaton, 1982) show the Tepee Trail Formation in the southeastern Absaroka Range to be laterally equivalent to the Wiggins Formation on Carter Mountain. The Wiggins Formation is time transgressive, becoming younger from northwest to southeast, with the youngest sedimentary rocks of the AVP occurring within the upper Wiggins in the southeasternmost Absaroka Range (**Figure 5B**).

Several other major stratigraphic problems are indicated by **Figures 5A** and **5B**. The lower part of the Wiggins Formation (sections F and G of **Figure 5A**) along the divide between the upper Yellowstone River and the South Fork of the Shoshone River drainages is portrayed on the *Geologic map of Wyoming* (Love and Christiansen, 1985) as laterally equivalent to both the Langford and Two Ocean formations. Smedes and Prostka (1972) believed the Wiggins Formation unconformably overlies the Langford and Two Ocean formations. Extensive detailed mapping, paleomagnetic data, and tracing of marker beds within the Wiggins Formation of the central Absaroka Range is needed to determine its actual relationship to the Langford and Two Ocean formations.

In sections D and E of **Figure 5A** the lower portions of the Sepulcher, Lamar River, and Cathedral Cliffs formations are all laterally equivalent. Detailed stratigraphic analysis of these formations is warranted to help resolve the current argument of which volcanic rocks are involved in the Heart Mountain allochthon and to provide critical data on translation and rotation of large volcanic blocks and masses. Bridgerian age (early middle Eocene) epiclastic rocks lie beneath Paleozoic carbonates of

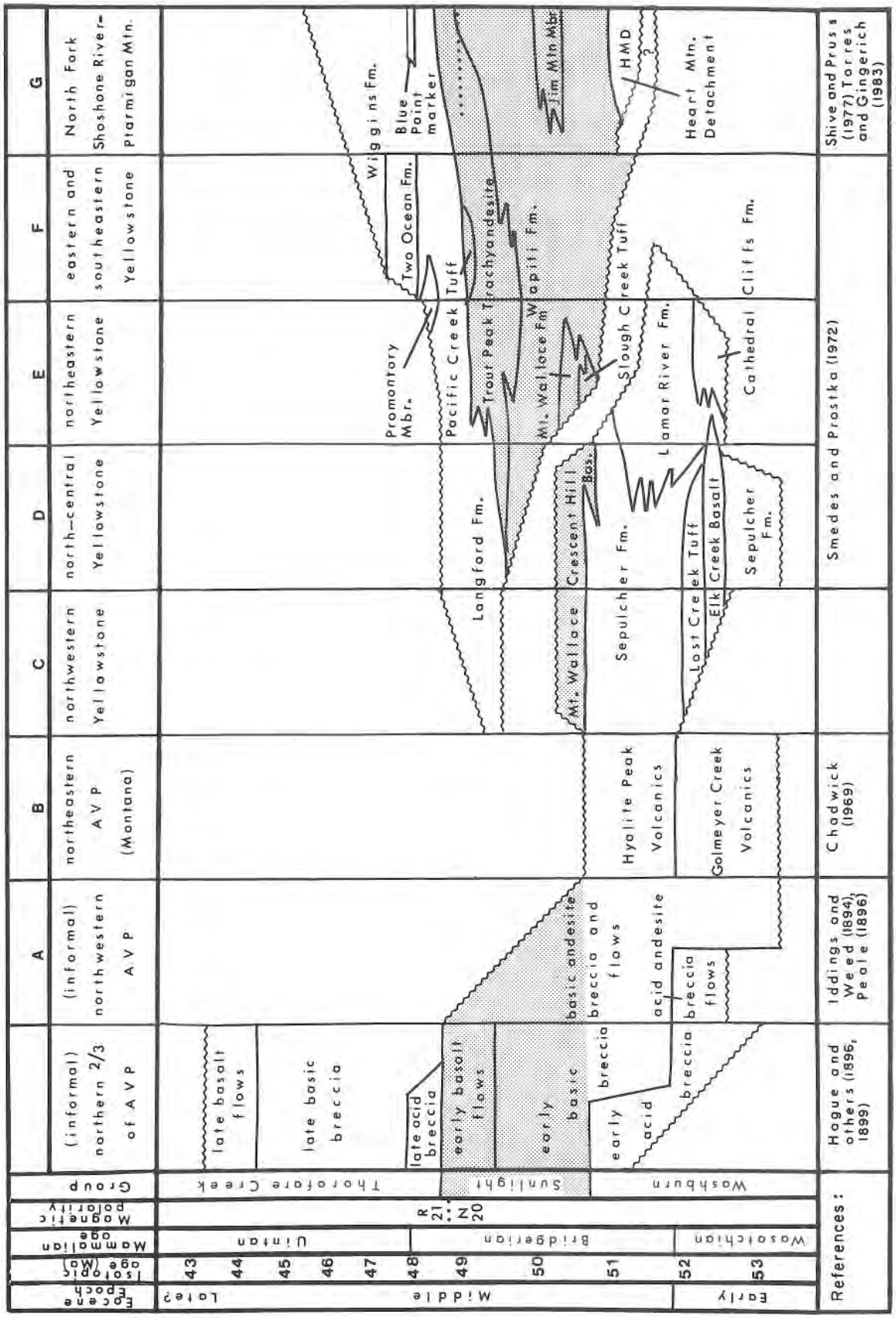

Figure 5A. Regional stratigraphic correlation diagram of the Absaroka Volcanic Supergroup sequence from the northwest to the central Absaroka Range. See Figure 1 for the location of sections A through G (AVP is the Absaroka volcanic plateau).

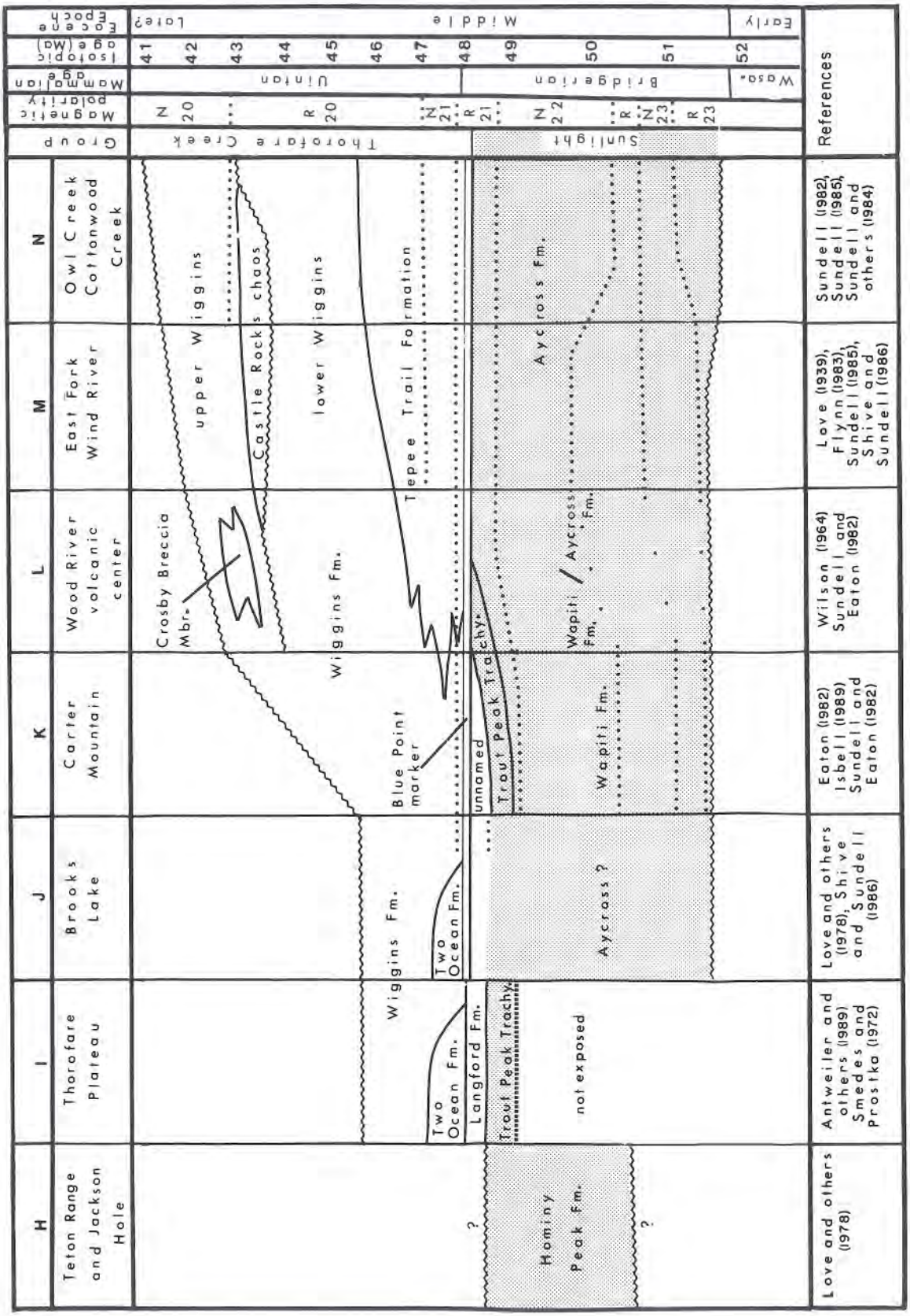

Figure 5B. Regional stratigraphic correlation diagram of the Absaroka volcanic sequence from central to southeast Absaroka Range. In magnetic polarity column, N=normal and R=reversed. See Figure 1 for the location of sections H through N.

the Heart Mountain allochthon along the North Fork of the Shoshone River (**Figure 5A**, section G). Torres and Gingerich (1983) referred to the epiclastic rocks as the Aycross Formation, but with additional detailed mapping, petrology, and stratigraphic correlations these rocks may eventually be referred to the Lamar River, Sepulcher, Cathedral Cliffs (Pierce, 1963b), or a fluvial facies of the Wapiti Formation. A detailed understanding of the in-place volcaniclastic rocks beneath, laterally adjacent to, and overlying the Heart Mountain allochthon is essential to deciphering the displacement history and the role of volcanic rocks in the allochthon. Additionally, the Hominy Peak Formation (Love and others, 1978) (**Figure 5B**, section H) is included within the Sunlight Group of the Absaroka Volcanic Supergroup, although the upper and lower age limits of the formation are not certain.

Laterally extensive marker beds are scarce within the Absaroka Volcanic Supergroup. The best marker beds are widespread airfall tuffs (Blue Point marker of Sundell and Eaton, 1982), lava flows (Trout Peak Trachyandesite of Nelson and Pierce, 1968), ash flows (Hickenlooper and Gutmann, 1982), and gigantic (>100 mi^2/259 km^2) mass-movement deposits such as the Castle Rocks chaos (Sundell, 1985). The Slough Creek Tuff, Pacific Creek Tuff, Lost Creek Tuff, Crescent Hill Basalt, Elk Creek Basalt (Brown, 1961; Smedes and Prostka, 1972; Hickenlooper and Gutmann, 1982), and Crosby Breccia (Wilson, 1964) are the only formal names applied to a single volcanic event or a genetically related sequence of events.

Local stratigraphy has generally been established in the northernmost Absaroka Range and Gallatin Range of Montana (Chadwick, 1969), the north-central Absaroka Range (Hague and others, 1899; Brown, 1961; Smedes and Prostka, 1972; Fritz, 1980b, 1982), the southeastern Absaroka Range (Love, 1939; Sundell, 1982; Sundell and others, 1984), and the southwestern Absaroka Range (Love and Keefer, 1975; Love, J. D., and others, 1976; Antweiler and others, 1989). However, due to the lack of regional marker beds, correlations between these areas are not well established. The stratigraphy within the volcanic field is greatly complicated by multiple source areas, reworking, synorogenic deposition, and post-depositional deformation including regional tectonism, volcanism, large-scale detachments, and gravity mass-movement events (Sundell, 1990).

The regional stratigraphic relationships indicate a general shift in the locus of eruption and deposition towards the southeast through time (Smedes and Prostka, 1972). However, the detailed eruption history is certainly much more complex (Sundell, 1982, 1990). Virtually all of the formations in the Absaroka Volcanic Supergroup contain many volcanogenic units, including a great variety of rock types derived from multiple source areas. The detailed stratigraphic work of matching vents to primary volcanic deposits and correlating to reworked deposits is largely lacking. Descriptions of composite units and their possible source affinities are most typical of stratigraphic studies (Love, 1939; Smedes and Prostka, 1972). Several studies (Sundell, 1982, 1985; Flynn, 1983; Sundell and others, 1984) have demonstrated the usefulness of multiple correlation techniques within the primary volcanic and reworked volcaniclastic rocks, including isochronous lithologic markers, paleontology, magnetostratigraphy, and radiometric dating (**Figures 5A** and **5B**). Detailed tracing and correlation between the vent and alluvial facies of most volcanic centers is possible using magnetostratigraphy in conjunction with the other correlation techniques.

Structural geology

The Absaroka Range is unique within the Wyoming foreland province, formed primarily by deposition and partial erosion of a thick volcanic sequence. Its origin therefore, sharply contrasts with the structural uplift of adjacent folded and faulted mountain ranges such as the Beartooth, Owl Creek, and Wind River ranges. The Laramide orogeny (Late Cretaceous-Eocene) deformed early Tertiary, Mesozoic, Paleozoic, and Precambrian rocks prior to initiation of Absaroka volcanism. Contractile deformation during the Laramide orogeny reactivated and/or produced northwest-striking zones of weakness and dilatancy that localized eruption and deposition of the Absaroka Volcanic Supergroup. In addition, the orogeny formed the Absaroka basin, a structural and depositional basin that presently contains the bulk of

the volcanic-derived sediments within the AVP (Sundell, 1990).

The Absaroka basin formed concurrent with the development of surrounding basement-cored uplifts and adjacent Paleogene sediment-filled Tertiary basins, including the Owl Creek uplift to the southeast, the eastern Washakie uplift to the south, the western Washakie uplift to the southwest, the southern Gallatin-Madison uplift to the northwest (in northwestern Yellowstone National Park), the Beartooth uplift to the north and northeast, and the Cody arch to the east (**Figures 2** and **6**) (Sundell, 1990). These major foreland uplifts separate the Absaroka basin from the surrounding Paleogene sediment-filled basins, including the Bighorn, Wind River, and Fish Creek basins. The majority of bounding uplifts indicate episodic Laramide movements during the Late Cretaceous (Maastrichtian) through middle Eocene (Love, 1939, 1978; Keefer, 1957, 1965; Thomas, 1965; Fanshawe, 1971; Seeland, 1978; Winterfeld and Conard, 1983; Schmidt and Garihan, 1983; Gingerich, 1983; Sundell, 1986a, 1986b, 1985, 1990; Winterfeld, 1990).

The Absaroka basin is shallow (generally <12,000 ft/3,658 m of sedimentary rocks) relative to adjacent Laramide basins (>20,000 ft/6,100 m). However, as shown on **Figure 6**, local deep depositional sites may be inferred based on gravity data (Love, 1985; Antweiler and others, 1989; Sundell, 1990) and surface hydrocarbon seeps (Clifton and others, 1990; Lorenson and others, 1991). This has not been confirmed because of restrictions on drilling and seismic acquisition in most of the central AVP.

Deformation of the Absaroka volcanic rocks has occurred by four primary processes: the Laramide orogeny, intrusive igneous activity, gravitational mass movements, and post-volcanic compaction and extension.

Many of the folds and faults in the lower volcanic units were formed by the last episodes of the Laramide orogeny (Sundell, 1990). However, strata in the upper Thorofare Creek Group commonly lie horizontal above northwest-striking folded and faulted volcanic rocks and similarly deformed nonvolcanic rocks (Rouse, 1937, 1947; Nelson and others, 1980; Sundell, 1982, 1985, 1990). Deformation attributed to the Laramide orogeny apparently ceased in the late middle Eocene (about 45 Ma), whereas local volcanic activity continued into the late Eocene (Sundell, 1986a, 1990).

Numerous structural features in the Absaroka volcanic rocks resulted directly from igneous activity. The intrusion of magma as dikes, sills, stocks, and other shallow intrusives caused folding, faulting, and doming of the surrounding rocks (Hague and others, 1899; Rouse, 1937, 1940; Love, 1939; Wilson, 1964; Sundell, 1985) during Absaroka magmatism (53 to 38 Ma). In addition, volcanic activity may have triggered and/or helped transport some of the ubiquitous mass-movement deposits within the AVP (Bucher, 1933; Pierce, 1973; Decker, 1990).

A unique geologic feature of the Absaroka Range is the occurrence of multiple episodes of large-scale mass movements during accumulation of the volcanic pile (Pierce, 1973, 1986; Wilson, 1975a; Bown, 1982a, 1982b; Sundell, 1982, 1985, 1990; Sales, 1983; Decker, 1990; Hauge, this volume). Large plates, blocks, and megablocks of volcanic and nonvolcanic strata periodically detached in the central volcanic region and moved downslope by a combination of slide and flow processes towards the adjacent Bighorn and Wind River basins. These detached masses form extensive folded, faulted, brecciated, and chaotic structural features within the volcanic sequence. Gravity detachments occur throughout the volcanic sequence and involve many different rock units. This ubiquitous process of tectonic sediment dispersal within the AVP was caused by rapid deposition in the central volcanic region, abundance of poorly consolidated and water-saturated sediments within the Absaroka basin, erosion along the margins of the AVP, ongoing late Laramide tectonism, and periodic volcanic activity (Sundell, 1990).

Three of the largest subaerial landslides recognized on Earth occurred along the eastern margin of the Absaroka basin during the middle Eocene (51-43 Ma). The Heart Mountain allochthon, recognized and studied for many years (see Pierce, 1973, 1987; Hauge, 1982, 1985, and this volume for a general review of voluminous literature and recent references), displaced scattered Paleozoic fragments and some volcanic material (Pierce, 1941, 1982, 1987; Prostka, 1978; Hauge, 1985, 1990; Pierce and Nelson, 1986) over a 1,300 mi^2 (3,400 km^2) area of the eastern margin of the Absaroka basin during early middle Eocene time. The Enos Creek-Owl Creek detachment

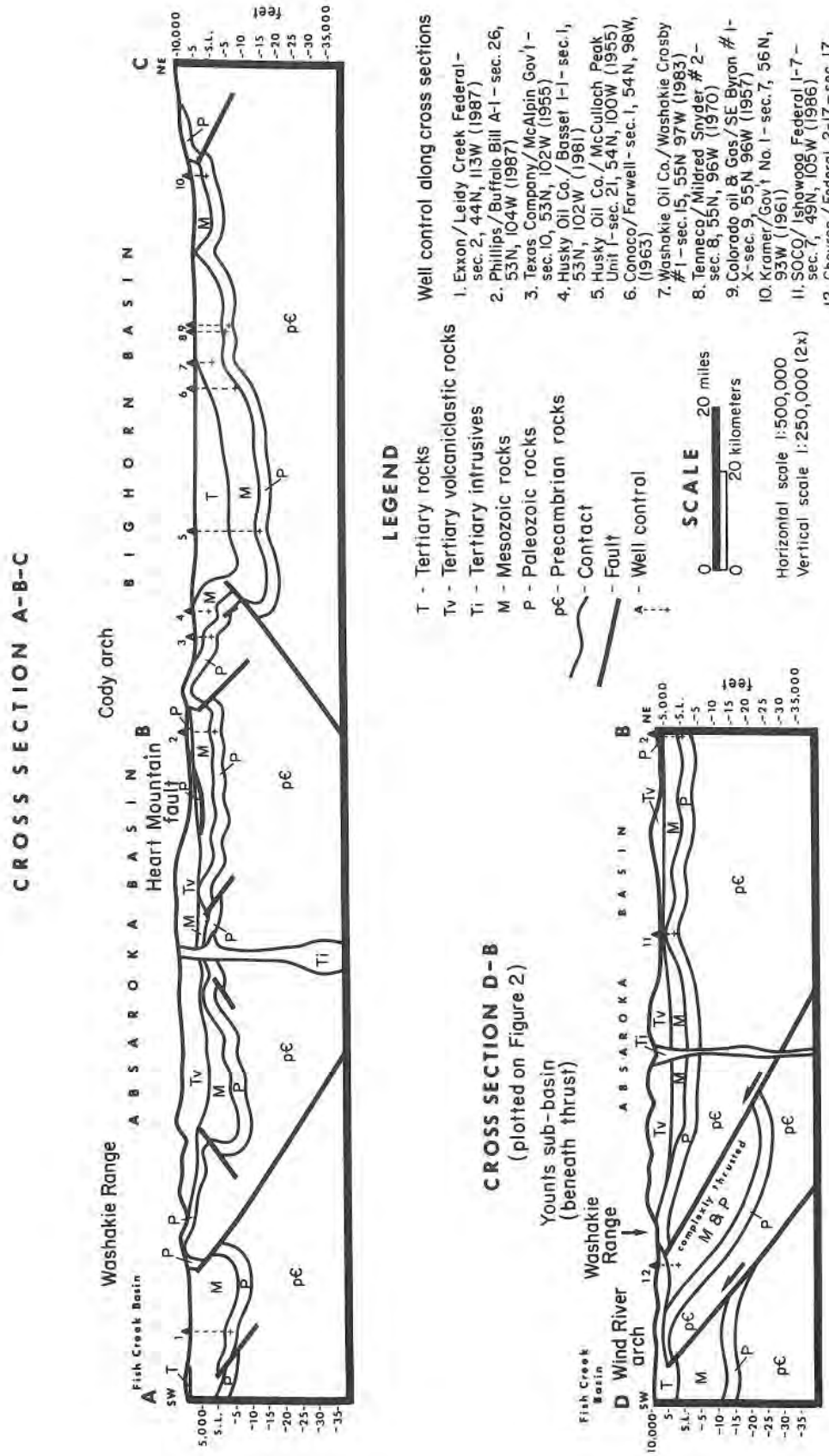

Figure 6. Geologic cross sections of the Absaroka basin and adjacent areas in northwest Wyoming. The location of sections A-B-C and D-B are shown on Figure 2. The Absaroka basin structure is inferred from regional geophysical data.

fault (Bown, 1982a, 1982b; Sundell, 1985) emplaced volcaniclastic rocks over a 350 mi² (900 km²) area during the early middle Eocene in the southeastern Absaroka Range. The Castle Rocks chaos (**Figure 4**) (Sundell, 1982, 1985) is 70 mi³ (293 km³) of primary volcanic and volcaniclastic material of predominantly the Wiggins Formation emplaced over a 350 mi² (900 km²) area during the Middle Eocene in the southeastern Absaroka Range.

Several smaller detachment faults, including the South Fork and Reef Creek faults (Pierce, 1941, 1963a, 1973, 1986; Blackstone, 1985; Clarey, 1990), have been described in the northern Absaroka Range. Four other megamictites and teramictites (Sundell and Fisher, 1985), containing rock fragments greater than 32.8 ft (10 m) and 328 ft (100 m) in diameter, respectively, have been described within middle Eocene Absaroka volcanic rocks. They have been variously interpreted as primary volcanic deposits (Hay, 1954), gravitational detachment faults (Eaton, 1982; Barnes, 1985; Malone, 1992a, 1992b), and domains of in-situ liquefaction (Decker, 1990) (see teramictite in **Figure 7**). These distinct episodes of large-scale disruption represent a time of regional geologic instability within the Absaroka basin, rather than a single event (Sales, 1983; Sundell, 1985).

Minor postvolcanic normal faults and compaction folds have been described in the uppermost layers of the AVP (Ketner and Fisher, 1968; Sundell 1982, 1990). The timing of postvolcanic deformation is very poorly constrained (late Eocene to Quaternary), but is likely related to compaction of volcanic materials and extensional faulting following the cessation of Laramide shortening.

Future structural studies in the Absaroka Range might attempt to separate features produced by the Laramide orogeny, direct action of volcanic activity, large-scale mass movements, and post-volcanic deformation as well as to search for relationships between the features. Interpretations of the regional tectonic framework of the AVP, and northwestern Wyoming in general, is rapidly changing as a result of extensive oil and gas exploration along the margins of the AVP (Sundell, 1983, 1990). Understanding the relationships between Laramide deformation in the volcanic rocks and in underlying oil-bearing Mesozoic and Paleozoic rocks will be critical for future hydrocarbon exploration. The classic mechanical enigma of the Heart Mountain allochthon (fault) must be re-evaluated in light of the possible inclusion of extensive amounts of volcanic material (Malone, 1992a, 1992b; Hauge, this volume) and the similarities with other gigantic detachment features within the AVP (Sundell, 1990). Mapping the extent of poorly known detachments and understanding the mechanism of emplacement of each of these events are of critical importance. Solutions to these problems will probably only come with extensive detailed mapping of the allochthons, in conjunction with detailed stratigraphic studies of in-situ strata behind the

Figure 7. Southeast-facing cliff at the confluence of Cabin Creek and the South Fork of the Shoshone River. Well-bedded fluvial epiclastic rocks (at base of cliff) of the Wapiti Formation are overlain by a 300-ft-thick teramictite, interpreted as resulting from either landsliding (this author) or in-situ liquifaction (Decker 1990, plate VII). Note the 60 ft thick white and dark banded clast (left center). Upper cliffs are epiclastic fluvial rocks overlain by 300 ft thick flows (lava lakes) of the Wapiti Formation and Trout Peak Trachyandesite (top). Bright white rocks are dikes and sills crosscutting the volcaniclastic rocks of the Wapiti Formation.

breakaway faults, and the use of all available stratigraphic correlation techniques (paleomagnetic data, paleontology, etc.) to confirm precise translations of large volcanic blocks and plates.

Geophysical investigations

Reflection seismic data from along the eastern and southern margins of the AVP in regions outside of designated wilderness areas have been extensively collected by private oil and gas exploration companies (**Figure 8**). Only two seismic lines have been published (Brittenham and Tadewald, 1985). An estimated 500 miles (805 km) or more of data have been acquired in areas covered by Absaroka volcanic rocks during the past 15 years and additional studies continue. Approximately 85% of the AVP is in Yellowstone National Park or adjacent wilderness areas, where the use of seismic reflection data acquisition techniques is prohibited.

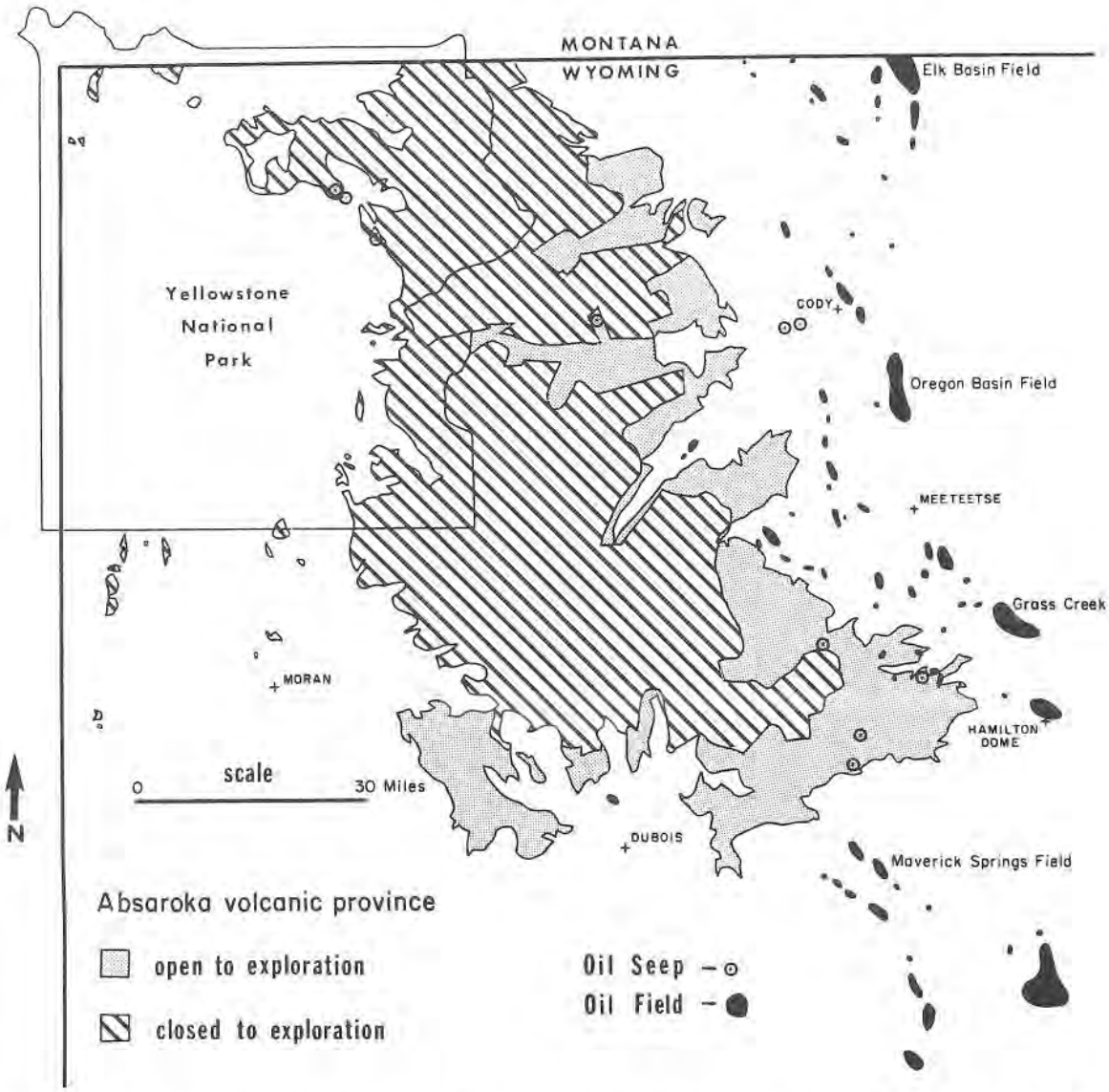

Figure 8. Land use restriction map of the Absaroka volcanic plateau of northwestern Wyoming showing the location of adjacent producing oil and gas fields and oil seeps.

The quality of data acquisition methods and processing has improved greatly over the past 15 years and the industry is developing the ability to "see through" the volcanic cover to potential underlying Mesozoic and Paleozoic oil reservoirs. Difficult access, rugged topography, complex geology, poor velocity control, sparse well control, and statics problems still have a significant adverse affect on data quality. Portable, deep shothole acquisition techniques usually give the best results, but "Polter" and "Vibroseis" methods are locally effective in areas of easier access and low relief. Seismic refraction/reflection data from earthquakes within the seismically active Yellowstone area have also provided information on the present tectonic system and subvolcanic crustal structure along the western margin of the AVP (Smith and Braile, 1982; Lehman and others, 1982).

Regional gravity surveys (Blank and Gettings, 1974; Smith and Braile, 1982; Lehman and others, 1982; Lyons and O'Hara, 1982; Antweiler and others, 1989; Sundell, 1990) indicate the presence of a generally shallow, northwest-trending Absaroka basin beneath the central portion of the AVP. Several deeper sub-basins are inferred in northeastern Yellowstone (Smith and Braile, 1982) and in the southwestern portion of the AVP (Antweiler and others, 1989). On the basis of regional structural relationships and nearby seismic reflection data, Sundell (1990) interpreted the large gravity low in the southwestern AVP to be related primarily to thrusting of the Washakie Range over the Younts sub-basin of the Wind River Basin. Detailed gravity surveys (Rubel and Romberg, 1971) are scarce and generally are proprietary data of mineral resource companies.

Regional aeromagnetic maps of the AVP show pronounced effects of topography and regionally high magnetic values due to the high proportion of magnetic minerals within the Absaroka Volcanic Supergroup (U.S. Geologic Survey, 1973; Long, 1985; Antweiler and others, 1989). Structural interpretations are extremely difficult due to the overprinting of topographic and near-surface anomalies. However, near-surface intrusives are easily identifiable by the magnetic surveys (Long, 1985; Antweiler and others, 1989).

Magnetostratigraphy has proven to be an extraordinarily useful tool in time-stratigraphic correlation within the epiclastic volcanic rocks (Shive and Pruss, 1977; French and Van Der Voo, 1978; Shive and others, 1980; Sundell and Eaton, 1982; Flynn, 1983; Lee and Shive, 1983; Sundell and others, 1984; Shive and Sundell, 1986; Isbell, 1989) and could be used to correlate alluvial and vent facies strata through the complex lateral lithologic changes. Local, regional, and worldwide correlations and refinements of the magnetostratigraphic, radiometric, and biostratigraphic time scales may be made for the middle Eocene from layered sequences within the AVP (Flynn, 1983; Sundell and others, 1984). Paleomagnetic techniques were also used in the AVP to calculate the geomagnetic pole for North America for the Eocene (Pruss, 1975; Shive and Pruss, 1977). Isbell (1989) used paleomagnetic data to help elucidate the sedimentation and tectonic history during Laramide deformation of the basal volcanic sequence. Determining the amount of rotation and minimum translation of large detached plates in the Heart Mountain allochthon and other detachment structures within the AVP is another possible use of paleomagnetic data. Mimura and others (1982) used paleomagnetic data to prove rotation of large blocks within debris avalanches and rockslides associated with volcanoes in Japan. Paleomagnetic techniques are also used in determining cooling histories (Nyblade and others, 1987) and could be useful in stratigraphic and structural studies within the AVP.

Geochronometric studies of rocks in the AVP have provided a chronologic framework for the province (53 to 38 Ma) (Chadwick, 1969, 1970, 1981; Rohrer and Obradovich, 1969; Smedes and Prostka, 1972; L. L. Love and others, 1976; Sundell and others, 1984). Biotite, hornblende, and feldspar K-Ar dates are most common but some fission-track dating of apatite and sphene has also been done (L.L. Love and others, 1976). Given the size of the AVP, the geochronometric data base is small, and most exposed intrusive rocks have not been dated. Radiometric dating has also been used in a few detailed petrogenetic studies of the AVP (Meen, 1983; Meen and Eggler, 1987, 1989).

Several electrical geophysical techniques have been used locally in mineralized areas such as the Kirwin and Sunlight Basin mining districts (Hausel, 1982a, 1982b). The development and use of wilderness-compatible geophysical surveys, such as magnetotellurics, may be essential in helping verify the regional tectonic framework of the AVP.

Geomorphology

The Absaroka Range is characterized by rugged mountainous terrain (**Figure 9**) ranging in elevation from 6,000 to 13,140 ft (1,830 m to 4,006 m) (Francs Peak). This maturely dissected volcanic plateau contains abundant V-shaped valleys, sharp ridges, narrow floodplains, cliffs, waterfalls, talus, and high relief (Hague and others, 1899; Love, 1939; Wilson, 1964; Ketner and others, 1966; Rohrer, 1966; Breckenridge, 1974, 1975; Nelson and others, 1980; Sundell, 1982). A well-developed high-level erosion surface is present in the Thorofare, Buffalo Fork, and upper South Fork of the Shoshone River areas in the southwestern Absaroka Range. The terrain in this area is characterized by relatively flat, rolling mountain tops between 10,000 ft and 11,000 ft (3,050 m and 3,350 m) in elevation separated by deep U-shaped glacial valleys. It is typical "biscuit board" topography (Wilson, 1964; Ketner and others, 1966; Ketner and Fisher, 1968). The age of this surface is not well constrained; it may have formed during the late Eocene at the close of the Absaroka volcanic depositional cycle (Sundell, 1985) or during subsequent depositional and erosional cycles, as suggested by other workers (McKenna and Love, 1972).

Extensive glaciation occurred throughout the Absaroka Range during the Pleistocene and continues locally (K.L. Pierce, 1979; Richmond, 1964). Glaciers, ice-cored rock glaciers, and rock glaciers are presently active in the Absaroka Range (**Figure 9**) (Potter, 1974). Cirques, U-shaped valleys, hanging valleys, and outwash terraces are the most notable evidence of past glacial activity throughout the Absaroka Range (Keefer, 1957; Breckenridge, 1975; Pierce, K.L., 1979; Nelson and others, 1980). However, tarns, erratics, moraines, striated bedrock, and other glacial features are also locally preserved. Glacial features are not as well preserved in the AVP as in nearby Precambrian-cored uplifts (e.g., Wind River Range) because the volcaniclastic rocks are easily eroded and extensively reworked by subsequent fluvial and mass-movement processes (Keefer, 1957; Breckenridge, 1975; Sundell, 1982).

Conspicuous terraces are developed along all major and most minor stream drainages throughout the AVP. The easily erodible nature of the volcanic rocks in the AVP allows for rapid development of terraces. No comprehensive study of the terraces within the AVP has ever been attempted, although local information has been gathered from all major drainage basins, including the Bighorn River (Rouse, 1934; Mackin, 1937; Moss and Bonini, 1961; Moss, 1974; Breckenridge, 1974, 1975; Sundell, 1980; Palmquist, 1983; Ritter and Kauffman, 1983), the Wind River (Blackwelder, 1915; Keefer, 1957; Morris, 1959), the Snake River (Love and Reed, 1968), and the Yellowstone River (Richmond, 1964; K.L. Pierce, 1979).

Figure 9. View to the south from Dike Mountain across Sunlight Creek. Ice-cored rock glaciers, cirques, arêtes, and other aspects of typical glacial topography occur in upper Galena Creek within the Sunlight mining district. All exposed rock is Wapiti Formation.

An important feature of the Absaroka Range is the occurrence of ubiquitous mass-wasting phenomena. Rockslides, rockfall, slump, earthflow, mudflow, soil creep, and virtually all combinations of, and transitions between, these processes are common. Large mass movements are generally more common in the southeastern Absaroka Range where there

are extensive reworked alluvial rocks and primary airfall deposits altered to bentonitic clays (Pierce, 1968; Breckenridge, 1975; Sundell and Eaton, 1982; Sundell, 1982). As evidenced by the abundance of coarse-grained, poorly sorted, fragmental rocks (megamictites and teramictites of Sundell and Fisher, 1985), mass-wasting processes have been important throughout the depositional and erosional history of the AVP.

Paleontology

The epiclastic volcanic conglomerates, sandstones, siltstones, and claystones are excellent environments for the deposition and preservation of fossils. The fossil trees of Yellowstone National Park have been known and studied for more than a century (Holmes, 1879; Hauge and others, 1899; Dorf, 1964, 1980; Wheeler, 1978; Fritz, 1980a; Yuretich, 1984). Fossil floras have been found throughout the AVP (Darton, 1906; Berry, 1930; Love, 1939; Dorf, 1964; Rohrer and Obradovich, 1969; Leopold and MacGinitie, 1972; MacGinitie, 1974; Love and others, 1978; Sundell, 1982). Leaves, pollen, and thin carbonaceous beds are generally more common in the basal volcanic strata (Sunlight Group), deposited in gentle fluvial, overbank, paludal, and lacustrine environments. Fossil wood, logs, stumps, and locally complete forest assemblages can be found in virtually all epiclastic deposits, but are most common in sequences of stacked cobble- to boulder-size laharic breccias, formed by mudflows from the flanks of large stratovolcanoes (**Figure 10**) (Fritz, 1980b, 1982; Sundell, 1982; Yuretich, 1984).

Known vertebrate mammal localities were rare prior to the 1980s (Jepson, 1939; Love, 1939), but recent research (Eaton 1980, 1982, 1985; McKenna 1980; MacFadden, 1980; Bown 1982a; Sundell, 1982; Sundell and Eaton, 1982; Torres and Gingerich, 1983; Flynn, 1983; Sundell and others, 1984) has proven them to be more common than previously believed,

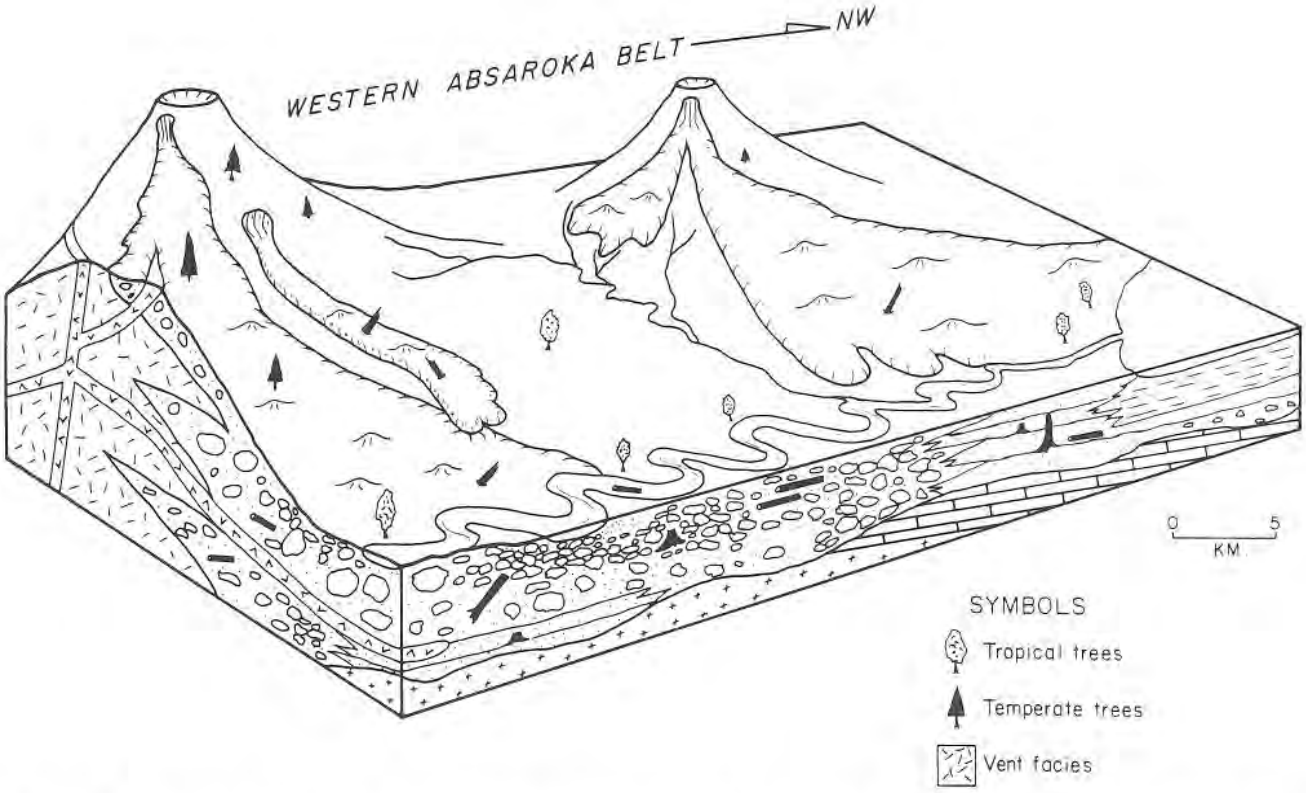

Figure 10. Block diagram showing depositional environments of "fossil forests" in Lamar River Formation (after Fritz, 1980a,b). Mixing of tropical and temperate flora in volcanic and fluvial deposits reflects high topographic relief.

and to be useful for correlation within the AVP. Time-stratigraphic correlations throughout the southeastern Absaroka Range have been greatly improved by recognition of the Bridgerian-Uintan transition (North American Land Mammal Ages) and the use of paleomagnetic data and radiometric dating (Sundell and Eaton, 1982; Flynn, 1983; Sundell and others, 1984; Isbell, 1989). These correlations may be carried into the northern Absaroka Range and possibly other Rocky Mountain Tertiary basins by future investigations.

The unique combination of thick volcanogenic sedimentary deposits containing isotopically datable rocks, vertebrate fossils, plant fossils, and distinct paleomagnetic reversals may make the AVP one of the best localities in the world to compare and refine radiometric, biostratigraphic, and paleomagnetic time scales for the middle Eocene (52-43.6 Ma). Compositional and morphological differences in similar-age faunas and floras provide strong evidence for inferring high paleorelief (>10,000 ft/3,050 m) between the stratovolcanoes and adjacent lowlands (Fritz, 1982; Yuretich, 1984; Eaton, 1985). Enormous areas within the central and northern AVP remain to be examined, and the potential for remarkable paleontological discoveries remains great.

Economic geology

Oil and gas, coal, precious and base metals, and several industrial minerals are present within or beneath the AVP. The AVP unconformably overlies proven oil and gas producing strata from Cody to Anchor, Wyoming (>50 mi/>130 km) along the entire western margin of the Bighorn Basin and portions of the northwestern Wind River Basin (**Figure 8**). Moderate to high potential for oil and gas accumulations probably exists on more than two-thirds of the total area covered by the AVP (>7,000 mi^2/>18,130 km^2). At least 36 hydrocarbon seeps occur within the volcanic rocks (Love and Good, 1970; Love, 1985; Sundell and Love, 1986; Clifton and others, 1990; Lorenson and others, 1991) and several oil fields have been discovered beneath the edge of the volcanic rocks (Tonnsen, 1982). Domal structures in Mesozoic and Paleozoic rocks beneath the volcanic rocks, typical of Bighorn Basin oil fields (Stone, 1967), are the primary exploration targets. Timing of depositional and tectonic events also suggests a great potential for stratigraphic traps at the angular unconformity between the volcanic strata and all principal oil producing horizons along the margins of the Bighorn, Absaroka, Wind River, and Fish Creek basins (Sundell, 1983, 1990). Given the oil production history of the adjacent Bighorn and Wind River basins (Cardinal and others, 1989), several billion barrels of recoverable oil may lie undiscovered beneath the AVP. The virtually unexplored subvolcanic portions of the Cody arch, Wind River arch, and Dubois arch (**Figure 2**) are presently the areas of highest potential for future oil and gas discoveries (Sundell, 1990).

Coal occurs within Cretaceous rocks underlying the Absaroka volcanic rocks, but the economic potential of production by conventional methods is greatly diminished by the volcanic overburden.

Metallic minerals, including gold, silver, copper, molybdenum, lead, zinc, and less significant amounts of other metals, are found near intrusive centers throughout the Absaroka Range (Parsons, 1937; Osterwald and others, 1966; Wilson, 1971, 1975b, 1980, 1986; Fisher, 1972, 1981, 1983; Fisher and others, 1977; Nelson and others, 1980; Elliot, 1980; Fisher and Antweiler, 1980; Hausel, 1982a, 1982b; Nelson and Williams, 1984; Elliot and Stotelmeyer, 1984; Wedow and Bannister, 1984). Only minor production has been reported (Osterwald and others, 1966), but significant potential for large Cu-Mo porphyry deposits and smaller precious metal deposits does exist (Wilson, 1971, 1980; Fisher, 1981, 1983; Hausel, 1982a, 1982b).

Bentonites from Cretaceous rocks beneath the volcanic strata and from within the Eocene volcanic rocks (Dunrud, 1962; Sundell, 1982) and zeolites within the volcanic rocks (Sundell, 1985) are the principal nonmetallic minerals of potential importance. No production of nonmetallic minerals has been reported from the volcanic terrane. Additional studies are needed to adequately determine if the reported bentonites and zeolites in the volcanic rocks are of economic quality and quantity.

Much of the AVP lies within restricted areas of Yellowstone National Park and adjacent wilderness areas. Most reported occurrences of nonmetallic minerals and coal do not lie within restricted areas. The major localities for metallic minerals were excluded from the protected regions, although some potential areas are located within the wilderness (Hausel, 1982a, 1982b). Approximately 850 mi^2 (2,200 km^2) of high-potential oil and gas acreage are presently available for exploration and production. The success of mineral exploration and development on nonrestricted areas will help determine the potential of restricted areas in the Absaroka Range. Economic mineral resources will be discovered within protected areas only if technology makes exploration and development compatible with wilderness values, or if extreme emergencies dictate development of the resource. The harsh climate and difficult access within the volcanic terrain also hinder exploitation of mineral resources.

Acknowledgments

Foremost, I would like to thank Dave Love and Don Blackstone for being extraordinary teachers and mentors. Their friendly willingness to share knowledge, continual encouragement, and professional manner has positively shaped my mind and spirit. I thank all the authors and geologists mentioned herein who often braved great physical and mental hardships to increase our scientific knowledge and understanding of this unique rugged part of the world. I would like to thank Jeff Eaton, Paul Decker, and Art Snoke for effectively reviewing and improving the manuscript. Finally, I thank Meg and the kids for their patience and support during my mental and physical absence from family life.

References cited

Antweiler, J. C., Love, J. D., Prostka, H., Kulik, D. M., Anderson, L. A., Williams, F. E., Jinks, J. E., and Light, T. D., 1989, Mineral resources of the Teton Wilderness study area, Teton County, Wyoming: U.S. Geological Survey Bulletin 1781, 105 p.

Barnes, B. K., 1985, Stratigraphy of Eocene volcaniclastic rocks, Dick Creek Lakes quadrangle, Wyoming [M.S. thesis]: Ames, Iowa State University, 221 p.

Berry, E. W., 1930, A flora of the Green River age in the Wind River Basin of Wyoming: U.S. Geological Survey Professional Paper 165-B, p. 488-497.

Blackstone, D. L., Jr., 1966, Pliocene vulcanism, southern Absaroka Mountains, Wyoming: University of Wyoming Contributions to Geology, v. 5, p. 21-30.

_____ 1985, South Fork detachment fault, Park County, Wyoming: Geometry—extent—source: University of Wyoming Contributions to Geology, v. 23, p. 47-62.

Blackwelder, E., 1915, Post-Cretaceous history of the mountains of central western Wyoming: Journal of Geology, v. 23, p. 97-117, 193-217, 307-340.

Blank, H. R., Jr., and Gettings, M. E., 1974, Complete Bouguer gravity map: Yellowstone-Island Park region: U.S. Geological Survey Open File Map 74-22, scale 1:125,000.

Bown, T. M., 1982a, Geology, paleontology and correlation of Eocene volcaniclastic rocks, southeast Absaroka Range, Hot Springs County, Wyoming: U.S. Geological Survey Professional Paper 1201A, 75 p.

_____ 1982b, Catastrophic large-scale late Cenozoic detachment faulting of Eocene volcanic rocks, southeast Absaroka Range, northwest Wyoming: Wyoming Geological Association 33rd Annual Field Conference Guidebook, p. 185-201.

Breckenridge, R. M., 1974, Quaternary and environmental geology of the upper Wood River area, Absaroka Range, Wyoming [Ph.D. dissertation]: Laramie, University of Wyoming, 139 p.

_____ 1975, Quaternary geology of the Wood River area, Wyoming: Wyoming Geological Association 27th Annual Field Conference Guidebook, p. 45-54.

Brittenham, M. D. and Tadewald, B. H., 1985, Detachment and basement-involved structures beneath Absaroka Range volcanics *in* Seismic Exploration of the Rocky Mountain region: Denver, Colorado, Rocky Mountain

Association of Geologists and Denver Geophysical Society, p. 31-43.

Brown, C. W., 1961, Cenozoic stratigraphy and structural geology, northeast Yellowstone National Park, Wyoming and Montana: Geological Society of America Bulletin, v. 72, p. 1173-1194.

Bucher, W. H., 1933, Volcanic explosions and overthrusts: American Geophysical Union 14th Annual Meeting Transcript, p. 238-242.

Cardinal, D. F., Miller, T., Stewart, W. W., and Trotter, J. F., 1989, Wyoming oil and gas fields symposium: Bighorn and Wind River basins: Wyoming Geological Association, p. 4.

Chadwick, R. A., 1969, The northern Gallatin Range, Montana: northwestern part of the Absaroka-Gallatin volcanic field: University of Wyoming Contributions to Geology, v. 8, p. 150-166.

_____ 1970, Belts of eruptive centers in the Absaroka-Gallatin volcanic field: Geological Society of America Bulletin, v. 81, p. 267-273.

_____ 1981, Chronology and structural setting of volcanism in southwestern and central Montana: Montana Geological Society 1981 Field Conference Guidebook, p. 301-310.

Christiansen, R. L., and Blank, H. R., Jr., 1972, Volcanic stratigraphy of the Quaternary rhyolite plateau in Yellowstone National Park: U.S. Geological Survey Professional Paper 729-B, 18 p.

Clarey, T. L., 1990, Thin-skinned shortening geometries of the South Fork fault: Bighorn Basin, Park County, Wyoming: The Mountain Geologist, v. 27, p. 19-26.

Clifton, C. G., Walters, C. C., and Simoneit, B. R. T., 1990, Hydrothermal petroleums from Yellowstone National Park: Applied Geochemistry, v. 5, p. 169-191.

Darton, N. H., 1906, Geology of the Owl Creek Mountains: 59th Congress, 1st session, Senate Document 219, 48 p.

Decker, P. L., 1990, Style and mechanics of liquefaction-related deformation lower Absaroka Volcanic Supergroup (Eocene), Wyoming: Geological Society of America Special Paper 240, 71 p.

Dorf, E., 1964, The petrified forests of Yellowstone National Park: Scientific American, v. 210, p. 106-114.

_____ 1980, Petrified forests of Yellowstone: Washington, D.C., U.S. Government Printing Office, 31 p.

Dunrud, C. R., 1962, Volcanic rocks of the Jack Creek area, southeastern Absaroka Range, Park County, Wyoming [M.S. thesis]: Laramie, University of Wyoming, 92 p.

Eaton, J. G., 1980, A preliminary report on paleontological exploration of southeastern Absaroka Range, Wyoming, *in* Early Cenozoic paleontology and stratigraphy of the Bighorn Basin, Wyoming: University of Michigan Museum Papers on Paleontology 24, p. 139-142.

_____ 1982, Paleontology and correlation of Eocene volcanic rocks in the Carter Mountain area, Park County, southeastern Absaroka Range, Wyoming: University of Wyoming Contributions to Geology, v. 21, p. 153-194.

_____ 1985, Paleontology and correlation of the Eocene Tepee Trail and Wiggins formations in the area of the North Fork of Owl Creek, southeastern Absaroka Range, Hot Springs County, Wyoming: Journal of the Society of Vertebrate Paleontologists, v. 5, p. 345-370.

Elliot, J. E., 1980, Mineralization of the Sunlight mining region, *in* North Absaroka Wilderness and vicinity, Park County, Wyoming: U.S. Geological Survey Bulletin 1447, p. 57-58.

Elliot, J. E., and Stotelmeyer, R. B., 1984, North Absaroka study area, Montana, *in*, Marsh, S. P., Kropschot, S. J., and Dickinson, R. G., editors, Wilderness mineral potential: assessment of wilderness mineral resource potential in U.S. Forest Service lands studied 1964-1984: U.S. Geological Survey Professional Paper 1300, p. 731-733.

Fanshawe, J. R., 1971, Structural evolution of the Bighorn Basin: Wyoming Geological Association 23rd Annual Field Conference Guidebook, p. 35-37.

Fisher, F. S., 1972, Tertiary mineralization and hydrothermal alteration in the Stinkingwater mining region, Park County, Wyoming: U.S. Geological Survey Bulletin 1332-C, 33 p.

_____ 1981, Controls and characteristics of metallic mineral deposits in the southern Absaroka Mountains, Wyoming: Montana Geological Society Symposium Guidebook, p. 343-348.

_____ 1983, Porphyry copper deposits associated with the Needle Creek igneous center, southern Absaroka Mountains, Wyoming, *in*, Babcock, J. W., editor, The genesis of Rocky Mountain ore deposits; changes with time and tectonics: Denver, Colorado, Proceedings of the Denver Region Exploration Geologist Society 1983 Symposium, p. 87-93.

Fisher, F. S., and Antweiler, J. C., 1980, Preliminary geological and geochemical results from the Robinson Creek, Birthday and Cloud's Home Peak mineralized areas in the Washakie Wilderness, Wyoming: U.S. Geological Survey Open File Report 80-781, 12 p.

Fisher, F. S., Antweiler, J. C., and Welsch, E. P., 1977, Preliminary geological and geochemical results from the Silver Creek and Yellow Ridge mineralized areas in the Washakie Wilderness, Wyoming: U.S. Geological Survey Open File Report 77-225, 11 p.

Flynn, J. J., 1983, Correlation and geochronology of middle Eocene strata from the western United States [Ph.D. dissertation]: New York, Columbia University, 345 p.

French, A. N., and Van Der Voo, R., 1978, Absaroka Mountains, Yellowstone National Park, a summary report of paleomagnetic study of lower Eocene volcanics: Yellowstone National Park Library, 10 p.

Fritz, W. J., 1980a, Reinterpretation of the depositional environments of the Yellowstone "fossil forests": Geology, v. 8, p. 309-313.

_____ 1980b, Stratigraphic framework of the Lamar River Formation in Yellowstone National Park: Northwest Geology, v. 9, p. 1-18.

_____ 1982, Geology of the Lamar River Formation, northeastern Yellowstone National Park: Wyoming Geological Association 33rd Annual Field Conference Guidebook, p. 73-101.

Garihan, J. M., Schmidt, C. J., Young, S. W., and Williams, M. A., 1983, Geology and recurrent movement history of the Bismark-Spanish Peaks-Gardiner fault system, southwest Montana, *in* Lowell, J. D., editor, Rocky Mountain foreland basins and uplifts: Denver, Colorado, Rocky Mountain Association of Geologists, p. 295-314.

Gingerich, P. D., 1983, Paleocene-Eocene faunal zones and a preliminary analysis of Laramide structural deformation in the Clark's Fork Basin, Wyoming: Wyoming Geological Association 34th Annual Field Conference Guidebook, p. 185-195.

Gest, D. E., and McBirney, A. R., 1979, Genetic relations of shoshonitic and absarokitic magmas, Absaroka Mountains, Wyoming: Journal of Volcanological and Geothermal Research, v. 6, p. 85-104.

Hague, A., Iddings, J. P., Weed, W. H., Walcott, C. D., Girty, G. H., Stanton, T. W., and Knowlton, F. H., 1899, Descriptive geology, petrography, and paleontology, of Geology of the Yellowstone National Park, Part II : U.S. Geological Survey Monograph 32, 893 p. and folio atlas of 27 sheets.

Hague, A., Weed, W. H., and Iddings, J. P., 1896, Description of the Yellowstone National Park quadrangle [Wyoming]: U.S. Geological Survey Geological Atlas, Folio 30.

Hauge, T. A., 1982, The Heart Mountain detachment fault, northwest Wyoming: involvement of Absaroka volcanic rock: Wyoming Geological Association 33rd Annual Field Conference Guidebook, p. 175-179.

_____ 1985, Gravity-spreading origin of the Heart Mountain allochthon, northwestern Wyoming: Geological Society of America Bulletin, v. 96, p. 1440-1456.

_____ 1990, Kinematic model of a continuous Heart Mountain allochthon: Geological Society of America Bulletin, v. 102, p. 1174-1188.

Hausel, W. D., 1982a, Ore deposits of Wyoming: Wyoming Geological Survey Preliminary Report 19, 39 p.

_____ 1982b, General geologic setting and mineralization of the porphyry copper deposits, Absaroka volcanic plateau, Wyoming: Wyoming Geological Association 33rd Annual Field Conference Guidebook, p. 297-313.

Hay, R. L., 1954, Structural relationships of tuff-breccia in the Absaroka Range, Wyoming: Geological Society of America Bulletin, v. 65, p. 605-620.

_____ 1956, Pitchfork Formation, detrital facies of early basic breccia, Absaroka Range, Wyoming: American Association of Petroleum Geologists Bulletin, v. 40, p. 1863-1898.

Hickenlooper, J. W., Jr., and Gutmann, J. T., 1982, Geology of the Slough Creek Tuff, northern Absaroka volcanic field, Park County, Montana: Wyoming Geological Association 33rd Annual Field Conference Guidebook, p. 55-63.

Holmes, W. H., 1879, Fossil forests of the volcanic Tertiary formations of Yellowstone National Park: U.S. Geological and Geographic Survey of the Territories Bulletin, v. 2, p. 125-132.

Iddings, J. P., and Weed, W. H., 1894, Description of the Livingston quadrangle [Montana]: U.S. Geological Survey Geological Atlas, Folio 1.

Isbell, W. B., 1989, Paleomagnetic study of volcanic and volcaniclastic rocks from the Absaroka Mountains, northwestern Wyoming [M.S. thesis]: Laramie, University of Wyoming, 108 p.

Jepsen, G. L., 1939, Dating Absaroka volcanic rocks by vertebrate fossils: Geological Society of America Bulletin, v. 50, p. 1914.

Keefer, W. R., 1957, Geology of the Du Noir area, Fremont County, Wyoming: U.S. Geological Survey Professional Paper 294-E, p. 155-221.

_____ 1965, Geologic history of the Wind River Basin, central Wyoming: American Association of Petroleum Geologists Bulletin, v. 49, p. 1878-1892.

Ketner, K. B., and Fisher, F. S., 1968, Later Tertiary syncline in the southern Absaroka Mountains, Wyoming, *in* Geological Survey Research: U.S. Geological Survey Professional Paper 600-B, p. 144-147.

_____ 1978, Lithic and chemical composition of samples from the Wiggins and Tepee Trail formations, southern Absaroka Range, Wyoming: U.S. Geological Survey Open File Report, 2 p.

Ketner, K. B., Keefer, W. R., Fisher. F. S., Smith, D. L., and Raabe, R. G., 1966, Mineral resources of the Stratified Primitive Area, Wyoming: U.S. Geological Survey Bulletin 1230-E, p. 1-56.

Kudo, A. M., and Broxton, D. E., 1985, High-potassium intrusive rocks of the Crandall ring-dike complex, Absaroka Mountains, Wyoming: Geological Society of America Bulletin, v. 96, p. 522-528.

LaPointe, D. D., 1977, Geology of a portion of the Eocene Sylvan Pass volcanic center, Absaroka Range, Wyoming [M.S. thesis]: Missoula, University of Montana, 60 p.

Lee, T., and Shive, P. N., 1983, Paleomagnetic study of the volcanic and volcaniclastic rocks from the Absaroka Mountains, northwest Wyoming: Bulletin for the Institute of Earth Sciences Academia Sinica, v. 3, p. 155-172.

Lehman, J. A., Smith, R. B., Schilly, M. M., and Braile, L. W., 1982, Upper crustal structure of the Yellowstone caldera from delay time analyses and gravity correlations: Journal of Geophysical Research, v. 87, p. 2713-2730.

Leopold, E. B., and MacGinitie, H. D., 1972, Development and affinities of Tertiary floras in the Rocky Mountains, *in* Graham, A., editor, Floristics and paleofloristics of Asia and eastern North America: Amsterdam, Holland, Elsevier Publishing Company, p. 147-200.

Lipman, P. W.,Prostka, H.J., and Christiansen, R.L., 1972, Cenozoic volcanism and plate tectonic evolution of the western United States, I. Early and middle Cenozoic: Royal Society of London Philosophical Transactions, ser. A., v. 271, p. 217-248.

Long, C. L., 1985, Geophysical survey map of the Washakie Wilderness and adjacent roadless areas, Park County, Wyoming: U.S. Geological Survey Miscellaneous Field Studies Map MF-1597, scale 1:125,000.

Lorenson, T. D., Kvenvolden, K. A., Simoneit, B. R. T., and Leif, R. N., 1991, Composition of gas seeps in northwestern Wyoming: U.S. Geological Survey, Open-File Report 91-121, 26 p.

Love, J. D., 1939, Geology along the southern margin of the Absaroka Range, Wyoming: Geological Society of America Special Paper 20, 134 p.

_____ 1978, Cenozoic thrust and normal faulting and tectonic history of the Badwater area, northeastern margin of the Wind River Basin, Wyoming: Wyoming Geological Association 30th Annual Field Conference Guidebook, p. 235-238.

_____ 1985, Oil and gas potential of the Washakie (south Absaroka) Wilderness and adjacent study areas, Wyoming: Wyoming Geological Survey Report of Investigations 33, 10 p.

Love, J. D., and Christiansen, A. C., 1985, Geologic map of Wyoming: U.S. Geological Survey, scale 1:500,000.

Love, J. D., and Good, J. M., 1970, Hydrocarbons in thermal areas, northwestern Wyoming: U.S. Geological Survey Professional Paper 644-B, 23 p.

Love, J. D., and Keefer, W. R., 1975, Geology of sedimentary rocks in southern Yellowstone National Park, Wyoming: U.S. Geological Survey Professional Paper 729-D, 69 p.

Love, J. D., Leopold, E. B., and Love, D. W., 1978, Eocene rocks, fossils, and geologic history, Teton Range, northwestern Wyoming: U.S. Geological Survey Professional Paper 932-B, 40 p.

Love, J. D., McKenna, M. C., and Dawson, M. R., 1976, Eocene, Oligocene and Miocene rocks and vertebrate fossils at the Emerald Lake locality, 3 miles south of Yellowstone National Park, Wyoming: U.S. Geological Survey Professional Paper 932-A, 28 p.

Love, J. D., and Reed, J. C., Jr., 1968, Creation of the Teton landscape, the geologic story of Grand Teton National Park and vicinity: Grand Teton Natural History Association, 120 p.

Love, L. L., Kudo, A. M., and Love, D. W., 1976, Dacites of Bunsen Peak, the Birch Hills and Washakie Needles, northwest Wyoming, and their relationship to the Ab-

saroka volcanic field, Wyoming-Montana: Geological Society of America Bulletin, v. 87, p. 1455-1462.

Lyons, P. L., and O'Hara, W. O., 1982, Gravity anomaly map of the United States: Society of Exploration Geophysicists.

MacFadden, B. J., 1980, Eocene perissodactyls from the type section of the Tepee Trail Formation of northwestern Wyoming: University of Wyoming Contributions to Geology, v. 18, p. 135-143.

MacGinitie, H. D., 1974, An early middle Eocene flora from the Yellowstone-Absaroka volcanic province, northwestern Wind River Basin, Wyoming: California Universities Publications in Geological Science, v. 108, 103 p.

Mackin, J. H., 1937, Erosional history of the Bighorn Basin, Wyoming: Geological Society of America Bulletin, v. 48, p. 813-893.

Malone, D. H., 1992a, Evidence for large-scale detachment faulting within the lower Wapiti Formation, Absaroka Volcanic Supergroup (Eocene), Wyoming: Geological Society of America Abstracts with Programs, v. 24, no. 5, p. 24.

_____ 1992b, Evidence for Wapiti Formation volcanic blocks involvement in Heart Mountain faulting, implications for the continuous allochthon and tectonic denudation models: American Association of Petroleum Geologists Bulletin, v. 76, no. 8, p. 1263.

McKenna, M. C., 1980, Late Cretaceous and early Tertiary vertebrate paleontological reconnaissance, Togwotee Pass area, northwestern Wyoming, *in* Jacobs, L. L., editor, Aspects of vertebrate history: essays in honor of Edwin Harris Colbert: Museum of Northern Arizona Press, p. 331-343.

McKenna, M. C., and Love, J. D., 1972, High-level strata containing early Miocene mammals on the Bighorn Mountains, Wyoming: American Museum of Natural History Novitaties, no. 2490, 31 p.

Meen, J. K., 1983, Isotopic composition of some Laramide volcanics, Absaroka Mountains, Montana: Yearbook of the Carnegie Institution of Washington, v. 82, p. 481-486.

Meen, J. K., and Eggler, D. H., 1987, Petrology and geochemistry of the Cretaceous Independence volcanic suite, Absaroka Mountains, Montana: Geological Society of America Bulletin, v. 98, p. 238-247.

_____ 1989, Chemical and isotopic compositions of Absaroka granitoids, southwestern Montana, evidence for deep-seated Archean amphibolite basement in the Beartooth region: Contributions to Mineralogy and Petrology, v. 102, p. 462-477.

Mimura, K., Kawachi, S., Fujimoto, U., Taneichi, M., Hyuga, T., Ichikawa, S., and Koizumi, M., 1982, Debris avalanche hills and their natural remnant magnetization-Nirasaki debris avalanche, central Japan: Journal of the Volcanological Society of Japan, v. 88, p. 653-663.

Morris, D. A., 1959, Groundwater resources of the Riverton irrigation project area, Wyoming: U.S. Geological Survey Water Supply Paper, no. 1375, 205 p.

Moss, J. H., 1974, The relation of river terrace formation to glaciation in the Shoshone River basin, western Wyoming, *in* Coates, D. R., editor, Glacial geomorphology: State University of New York, Binghamton, Publications in Geomorphology, p. 293-314.

Moss, J. H., and Bonini, W., 1961, Seismic evidence supporting a new interpretation of the Cody terrace near Cody, Wyoming: Geological Society of America Bulletin, v. 72, p. 547-556.

Nelson, W. H., and Pierce, W. G., 1968, Wapiti Formation and Trout Peak Trachyandesite, northwestern Wyoming: U.S. Geological Survey Bulletin 1254-H, 11 p.

Nelson, W. H., Prostka, H. J., and Williams, F. E., 1980, Geology and mineral resources of the North Absaroka Wilderness and vicinity, Park County, Wyoming: U.S. Geological Survey Bulletin 1447, 101 p.

Nelson, W. H., and Williams, F. E., 1984, North Absaroka Wilderness, Wyoming, *in*, Marsh, S. P., Kropschot, S. J., and Dickinson, R. G., editors, Wilderness mineral potential: assessment of wilderness mineral resource potential in U.S. Forest Service lands studied 1964-1984: U.S. Geological Survey Professional Paper 1300, p. 1151-1152.

Nicholls, J., and Carmichael, I. S. E., 1969, A commentary on the absarokite-shoshonite-banakite series of Wyoming, U.S.A.: Schweizerische Mineralogische und Petrographische Mitteilungen, v. 49, p. 47-64.

Nyblade, A. P., Shive, P. N., and Furlong, K. P., 1987, Rapid secular variation recorded in thick Eocene flows from the Absaroka Mountains of northwest Wyoming: Earth and Planetary Science Letters, v. 81, p. 419-424.

Osterwald, F. W., Osterwald, D. B., Long, J. S., and Wilson, W. H., 1966, Mineral resources of Wyoming: Geological Survey of Wyoming Bulletin 50, 287 p.

Palmquist, R., 1983, Terrace chronologies in the Bighorn Basin, Wyoming: Wyoming Geological Association 34th Annual Field Conference Guidebook, p. 217-231.

Parsons, W. H., 1937, The ore deposits of the Sunlight mining region, Park County, Wyoming: Economic Geology, v. 32, p. 844-846.

_____ 1939a, Volcanic centers of the Sunlight area, Park County, Wyoming: Journal of Geology, v. 47, p. 1-26.

_____ 1939b Criteria for the recognition of volcanic breccias—review: Geological Society of America Memoir 115, p. 263-304.

_____ 1969, Types of intrusives in the Absaroka volcanic province: Geological Society of America Special Paper 121, p. 619-620.

_____ 1974, Volcanic rocks of the Absaroka-Yellowstone region *in* Voight, B., and Voight, M. A., editors, Rock mechanics: the American northwest: Pennsylvania State University, p. 94-101.

Peale, A. C., 1896, Description of the Three Forks quadrangle [Montana]: U.S. Geological Survey Geological Atlas, Folio 24, 7 p., 4 maps.

Pierce, K. L., 1979, History and dynamics of glaciation in the northern Yellowstone National Park area: U.S. Geological Society Professional paper 729-F, 90 p.

Pierce, W. G., 1941, Heart Mountain and South Fork thrusts, Park County, Wyoming: American Association of Petroleum Geologists Bulletin, v. 25, p. 2021-2045.

_____ 1963a, Reef Creek detachment fault, northwestern Wyoming: Geological Society of America Bulletin, v. 74, p. 1225-1236.

_____ 1963b, Cathedral Cliffs Formation, the early acid breccia unit of northwestern Wyoming: Geological Society of America Bulletin, v. 74, p. 9-21.

_____ 1968, The Carter Mountain landslide area, northwest Wyoming in Geological Survey Research 1968: U.S. Geological Survey Professional Paper 600-D, p. 235-241.

_____ 1973, Principal features of the Heart Mountain fault and the mechanism problem, *in* DeJong, K. A., and Scholten, R., editors, Gravity and tectonics: New York, New York, John Wiley and Sons, p. 457-471.

_____ 1982, Relation of volcanic rocks to the Heart Mountain Fault: Wyoming Geological Association 33rd Annual Field Conference Guidebook, p. 181-183.

_____ 1986, The South Fork detachment fault, Park County, Wyoming: discussion and reply: University of Wyoming Contributions to Geology, v. 24, p. 77-90.

_____ 1987, The case for tectonic denudation by the Heart Mountain fault — a response: Geological Society of America Bulletin, v. 99, p. 552-568.

Pierce, W. G., and Nelson, W. H., 1986, Some features indicating tectonic denudation by the Heart Mountain fault: Montana Geological Society and Yellowstone-Bighorn Research Association Joint Field Conference Guidebook, p. 155-164.

Potter, N., Jr., 1974, Snow avalanches and rock glaciers, Sunlight mining region, northern Absaroka Mountains, Wyoming, *in* Voight, B., and Voight, M. A., editors, Rock mechanics: the American northwest: Pennsylvania State University, p. 51-55.

Prostka, H. J., 1973, Hybrid origin of the absarokite-shoshonite-banakite series, Absaroka volcanic field, Wyoming: Geological Society of America Bulletin, v. 84, p. 697-701.

_____ 1978, Heart Mountain fault and Absaroka volcanism, Wyoming and Montana, U.S.A., *in* Voight, B., editor, Slides and avalanches: Developments in Geotechnical Engineering, volume 1, no. 14A, Amsterdam, Holland, Elsevier, p. 423-437.

Pruss, E. F., 1975, Paleomagnetic study of basalt flows from the Absaroka Mountains, Wyoming: Wyoming Geological Association 27th Annual Field Conference Guidebook, p. 257-266.

Richmond, G. M., 1964, Glacial geology of the West Yellowstone Basin and adjacent parts of Yellowstone National Park: U.S. Geological Survey Professional Paper 435-T, p. 223-236.

Ritter, D. F., and Kauffman, M. E., 1983, Terrace development in the Shoshone River Valley near Powell, Wyoming and speculations concerning the sub-Powell terrace: Wyoming Geological Association 34th Annual Field Conference Guidebook, p. 197-203.

Rohrer, W. L., 1966, Geology of the Adam Weiss Peak Quadrangle, Hot Springs and Park Counties, Wyoming: U.S. Geological Survey Bulletin 1241-A, 39 p, map scale 1:24,000.

Rohrer, W. L., and Obradovich, J. D., 1969, Age and stratigraphic relations of the Tepee Trail and Wiggins formations, northwestern Wyoming in Geological Survey Research 1969: U.S. Geological Survey Professional Paper 650-B, p. 57-62.

Rouse, J. T., 1934, The physiography and glacial geology of the Valley region, Park County, Wyoming: Journal of Geology, v. 42, p. 738-752.

_____ 1937, Genesis and structural relationships of the Absaroka volcanic rocks, Wyoming: Geological Society of America Bulletin, v. 48, p. 1257-1295.

_____ 1940, Structural and volcanic problems in the southern Absaroka Mountains, Wyoming: Geological Society of America Bulletin, v. 51, p.1413-1427.

_____ 1947, The Absaroka volcanic field: Wyoming Geological Association 2nd Annual Field Conference Guidebook, p. 165-172.

Rubel, D. H., 1971, Independence volcano: a major Eocene eruptive center, northern Absaroka volcanic province: Geological Society of America Bulletin, v. 82, p. 2473-2494.

Rubel, D. H., and Romberg, F. E., 1971, Gravity interpretation of the Silver Tip structure, northern Absaroka volcanic field, Montana: Geologic Society of America Bulletin, v. 82, p. 2611-2615.

Sales, J. K., 1983, Heart Mountain— blocks in a giant volcanic rock glacier: Wyoming Geological Association 34th Annual Field Conference Guidebook, p. 117-165.

Schmidt, C. J., and Garihan, J. M., 1983, Laramide tectonic development of the Rocky Mountain foreland of southwestern Montana, *in* Lowell, J. D., editor, Rocky Mountain foreland basins and uplifts: Rocky Mountain Association of Geologists, Denver, Colorado, p. 271-294.

Seeland, D., 1978, Sedimentology and stratigraphy of the lower Eocene Wind River Formation, central Wyoming: Wyoming Geological Association 30th Annual Field Conference Guidebook, p. 181-198.

Shive, P. N., and Pruss, E. F., 1977, A paleomagnetic study of basalt flows from the Absaroka Mountains, Wyoming: Journal of Geophysical Research, v. 82, p. 3039-3048.

Shive, P. N., Sundell, K. A., and Rutledge, J., 1980, Magnetic polarity stratigraphy of Eocene volcaniclastic rocks from the Absaroka Mountains of Wyoming: EOS, v. 61, p. 945.

Shive, P. N., and Sundell, K. A., 1986, Magnetostratigraphic correlation of Eocene rocks from the Absaroka Mountains, Wyoming: American Association of Petroleum Geologists Bulletin, v. 70, p. 1056.

Smedes, H. W., and Prostka, H. J., 1972, Stratigraphic framework of the Absaroka Volcanic Supergroup in the Yellowstone National Park region: U. S. Geological Survey Professional Paper 729-C, 33 p.

Smith, R. B., and Braile, L. W., 1982, Crustal structure and evolution of an explosive silicic volcanic system at Yellowstone National Park: Wyoming Geological Association 33rd Annual Field Conference Guidebook, p. 233-250.

Snyder, W. S., Dickinson, W. R., and Silberman, M. L., 1976, Tectonic implications of space-time patterns of Cenozoic magmatism in the western United States: Earth and Planetary Science Letters, v. 32, p. 91-106.

Stone, D. S., 1967, Theory of Paleozoic oil and gas accumulation in Bighorn Basin, Wyoming: American Association of Petroleum Geologists Bulletin, v. 51, p. 2056-2114.

Sundell, K. A., 1980, Geology of the North Fork of Owl Creek area, Hot Springs County, Wyoming [M.S. thesis]: Laramie, University of Wyoming, 158 p.

_____ 1982, Geology of the headwater area of the North Fork of Owl Creek, Hot Springs County, Wyoming: Geological Survey of Wyoming Report of Investigation 15, 51 p.

_____ 1983, Volcanic stratigraphy, timing and petroleum exploration in the southeastern Absaroka Range, Bighorn Basin, Wyoming: American Association of Petroleum Geologists Bulletin, v. 67, p. 1357-1358.

_____ 1985, The Castle Rocks chaos: a gigantic Eocene landslide-debris flow in the southeastern Absaroka Range, Wyoming [Ph.D. dissertation]: Santa Barbara University of California 332 p.

_____ 1986a, Introduction to the Absaroka volcanics and roadlogs: Wyoming Geological Association Earth Science Bulletin, v. 19, p. 84-115.

_____ 1986b, Petroleum exploration in the Absaroka basin of northwestern Wyoming: American Association of Petroleum Geologists Bulletin, v. 70, p. 1058.

_____ 1990, Sedimentation and tectonics of the Absaroka basin of northwestern Wyoming: Wyoming Geological Association 41st Annual Field Conference Guidebook, p. 105-122.

Sundell, K. A., and Eaton, J. G., 1982, Stratigraphic relations within the southeastern Absaroka volcanic sequence, northwestern Wyoming: Wyoming Geological Association 33rd Annual Field Conference Guidebook, p. 65-71.

Sundell, K. A., and Fisher, R. V., 1985, Very coarse-grained fragmental rocks: a proposed size classification: Geology, v. 13, p. 692-695.

Sundell, K. A., and Love, J. D., 1986, Oil and gas seeps within the Absaroka volcanics of northwestern Wyoming: American Association of Petroleum Geologists Bulletin, v. 70, p. 1058-1059.

Sundell, K. A., Shive, P. N., and Eaton, J. G., 1984, Measured sections, magnetic polarity and biostratigraphy of the Wiggins, Tepee Trail and Aycross Formations within the southeastern Absaroka Range, Wyoming: Wyoming Geological Association Earth Science Bulletin, v. 17, p, 1-48.

Thomas, L. E., 1965, Sedimentation and structural development of the Bighorn Basin: American Association of Petroleum Geologists Bulletin, v. 49, p. 1867-1877.

Tonnsen, J. J., 1982, Petroleum geology of the northern part of Yellowstone National Park: Wyoming Geological Association 33rd Annual Field Conference Guidebook, p. 289-295.

Torres, V., and Gingerich, P. D., 1983, Summary of Eocene stratigraphy at the base of Jim Mountain, North Fork of the Shoshone River, northwestern Wyoming: Wyoming Geological Association 34th Annual Field Conference Guidebook, p. 205-208.

U.S. Geological Survey, 1973, Aeromagnetic map of Yellowstone National Park and vicinity, Wyoming, Montana, and Idaho: U.S. Geological Survey Open File Report 73-304, scale 1:125,000.

Wedow, H. Jr., and Bannister, D. P., 1984, Absaroka Primitive Area and vicinity, Montana, *in*, Marsh, S. P., Kropschot, S. J., and Dickinson, R. G., editors, Wilderness mineral potential: assessment of wilderness mineral resource potential in U.S. Forest Service lands studied 1964-1984: U.S. Geological Survey Professional Paper 1300, p. 659-660.

Wheeler, E., 1978, Fossil dicotyledonous woods from Yellowstone National Park, part II: Journal of the Arnold Arboretum, v. 59, p. 1-26.

Wilson, W. H., 1963, Correlation of volcanic rock units in the southern Absaroka Mountains, northwest Wyoming: University of Wyoming Contributions to Geology, v. 2, p. 13-20.

_____ 1964, Geologic reconnaissance of the southern Absaroka Mountains, northwest Wyoming: Part I - the Wood River-Greybull River area: University of Wyoming Contributions to Geology, v. 3, p. 60-77.

_____ 1971, Volcanic geology and mineralization, Absaroka Mountains, northwest Wyoming: Wyoming Geological Association 23rd Annual Field Conference Guidebook, p. 151-155.

_____ 1975a, Detachment faulting in volcanic rocks, Wood River area, Park County, Wyoming: Wyoming Geological Association 27th Annual Field Conference Guidebook, p. 167-171.

_____ 1975b, The copper-bearing Meadow Creek granodiorite, upper Wood River area, Park County, Wyoming: Wyoming Geological Association 27th Annual Field Conference Guidebook, p. 235-241.

_____ 1980, The Kirwin mineralized area, Park County, Wyoming: Geological Survey of Wyoming Preliminary Report 2, 20 p.

_____ 1986, Volcanic geology and mineralization in the upper Wood River-Kirwin area, Absaroka Mountains, Park County, Wyoming, *in* Roberts, S., editor, Metallic and nonmetallic minerals of Wyoming and adjacent areas: Geological Survey of Wyoming Public Information Circular 25, p. 92-93.

Winterfeld, G. F., 1990, Summary of Laramide depositional and tectonic events East Fork area, northwestern Wind River Basin and adjacent Washakie Range, Wyoming: Wyoming Geological Association 41st Annual Field Conference Guidebook, p. 167-168.

Winterfeld, G. F., and Conard, J. B., 1983, Laramide tectonics and deposition, Washakie Range and northwestern Wind River Basin, Wyoming, *in* Lowell, J.D., editor, Rocky Mountain foreland basins and uplifts: Denver, Colorado, Rocky Mountain Association of Geologists, p. 137-148.

Yuretich, R. F., 1984, Yellowstone fossil forests: new evidence for burial in place: Geology, v. 12, p. 159-162.

Frontispiece. Discordant columnar jointing exposed in a 250 ft (75 m) high phonolite plug (SE 1/4, NW 1/4, sec. 14, T32N, R88W).

Petrographic and geochemical characteristics of mid-Tertiary igneous rocks in the Rattlesnake Hills, central Wyoming, with a comparison to the Bear Lodge intrusive suite of northeastern Wyoming

Anthony R. Hoch and Carol D. Frost
Department of Geology and Geophysics
University of Wyoming
Laramie, Wyoming 82071

Abstract

Approximately 50 mid-Tertiary plugs, dikes, and sills are exposed along a northwest-trending anticline in the Rattlesnake Hills. Magma emplacement post-dated Laramide folding, but predated the last displacement along the east-striking North Granite Mountains fault zone, which truncates the Rattlesnake anticline. The Tertiary intrusive rocks are divided into three distinct groups: central alkalic group, eastern felsic group, and western felsic group. The central alkalic group is located near the axis of the Rattlesnake anticline and consists of phonolite, trachyte, and latite intrusions. The eastern felsic group lies on the northeast limb of the Rattlesnake anticline and is comprised of less alkali-rich quartz latites and rhyolites. The western felsic group lies in the southwest part of the complex, near the North Granite Mountain fault zone, and is mineralogically and chemically similar to the eastern felsic group, but texturally different.

Although sodium-rich trachytes, phonolites, and latites are scarce rock types, they are comparable to intrusions in the Bear Lodge Mountains of northeastern Wyoming. Intrusive rocks of the Bear Lodge Mountains are similar in age and structural setting and display similar mineral assemblages and geochemical characteristics. The major difference between the Bear Lodge Mountains and Rattlesnake Hills intrusive complexes is the comparative paucity of intrusions of subalkaline quartz latite and rhyolite in the former.

The origin of the Rattlesnake Hills intrusive complex and other similar alkaline complexes is poorly understood. Laramide structural features apparently enabled the alkaline and subalkaline magmas to ascend to shallow crustal levels. Magma mixing played an important role in the generation of the western felsic group and central alkalic group rocks, but was less important in the eastern felsic group. The most mafic magmas were not derived from a depleted mantle; they may reflect the composition of subcontinental mantle that has been isolated and chemically modified during the last 3.5 billion years. Archean country rocks have made only a modest contribution to Rattlesnake Hills alkaline intrusive complex magmas.

Hoch, A.R., and Frost, C.D., 1993, Petrographic and geochemical characteristics of mid-Tertiary igneous rocks in the Rattlesnake Hills, central Wyoming, with a comparison to the Bear Lodge intrusive suite of northeastern Wyoming, *in* Snoke, A.W., Steidtmann, J.R., and Roberts, S.M., editors, Geology of Wyoming: Geological Survey of Wyoming Memoir No. 5, p. 508-528.

Introduction

Alkaline rocks, although a volumetrically minor constituent of the Earth's total igneous rocks, have nevertheless attracted the interest of petrologists because of their exotic phenocryst assemblages and enigmatic petrogenesis. In Wyoming, alkaline rocks are found in the Rattlesnake Hills, Leucite Hills, Absaroka Range, and western Black Hills area, including Devils Tower and the Bear Lodge Mountains. Alkaline rocks from the Leucite Hills are potassic, whereas alkaline rocks of the Rattlesnake Hills and the Black Hills region are dominated by sodium-rich trachytes and phonolites. In this paper we discuss the characteristics of the latter, as they are exposed in the Rattlesnake Hills.

Location and geologic setting

The Rattlesnake Hills alkaline intrusive complex (RHAC) is located in the southern part of the northwest-trending Rattlesnake Hills about 15 mi (25 km) southeast of the geographical center of Wyoming in western Natrona County (**Figure 1**). It is bordered on the north by the Wind River Basin, on the south by the Granite Mountains, and on the west by the Beaver Rim.

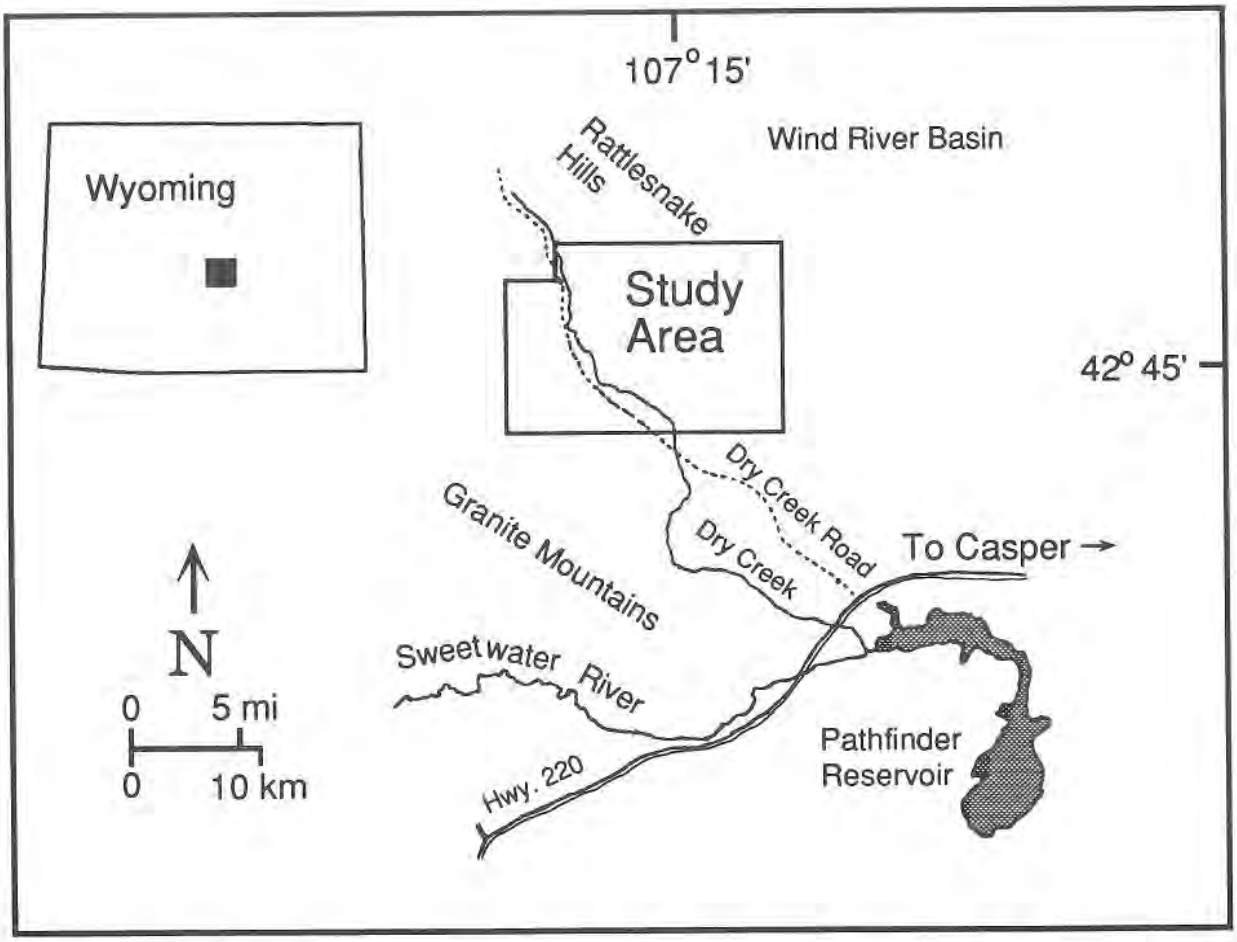

Figure 1. Regional map of central Wyoming showing the location of the Rattlesnake Hills (modified from Stupak, 1984).

Eocene trachytic, phonolitic, latitic, and rhyolitic magmas were emplaced into Archean granite gneiss, amphibolite, and overlying Phanerozoic sediments at a very high (subvolcanic) crustal level (Carey, 1959). Plugs and dikes occur in three distinct clusters or groups (**Figure 2**): central alkalic group (CAG), western felsic group (WFG), and eastern felsic group (EFG). The trachytes and phonolites of the CAG are centrally located in the predominately amphibolite core of the northwest-trending, Rattlesnake anticline of Laramide age. Large, coarsely porphyritic bodies of quartz latite and rhyolite of the EFG intruded the northeast limb of the anticline. Finer grained bodies of quartz latite and rhyolite of the WFG are exposed in granitic country rock southwest of the central alkaline intrusions and south of the North Granite Mountains (NGM) fault. The east-striking NGM fault truncated the Rattlesnake anticline during the earliest Eocene with a relative displacement of as much as 5,000 ft (1,500 m) across the fault zone (Love, 1970). Structural, textural, and geochemical evidence suggest that the NGM fault was a late Laramide reactivation of a subvertical Proterozoic zone of weakness that extends from the northern Laramie Mountains to the southern Wind River Range (Love, 1970; Bayley and others, 1973; Peterman and Hildreth, 1978). Middle Eocene through early Oligocene volcanic and intrusive activity in the Rattlesnake Hills postdates the uplift of the Granite Mountains. This was followed by a reversal of slip along the NGM fault and the downward displacement of the Granite Mountains structural block in the late Tertiary (Rachou, 1951; Love, 1970).

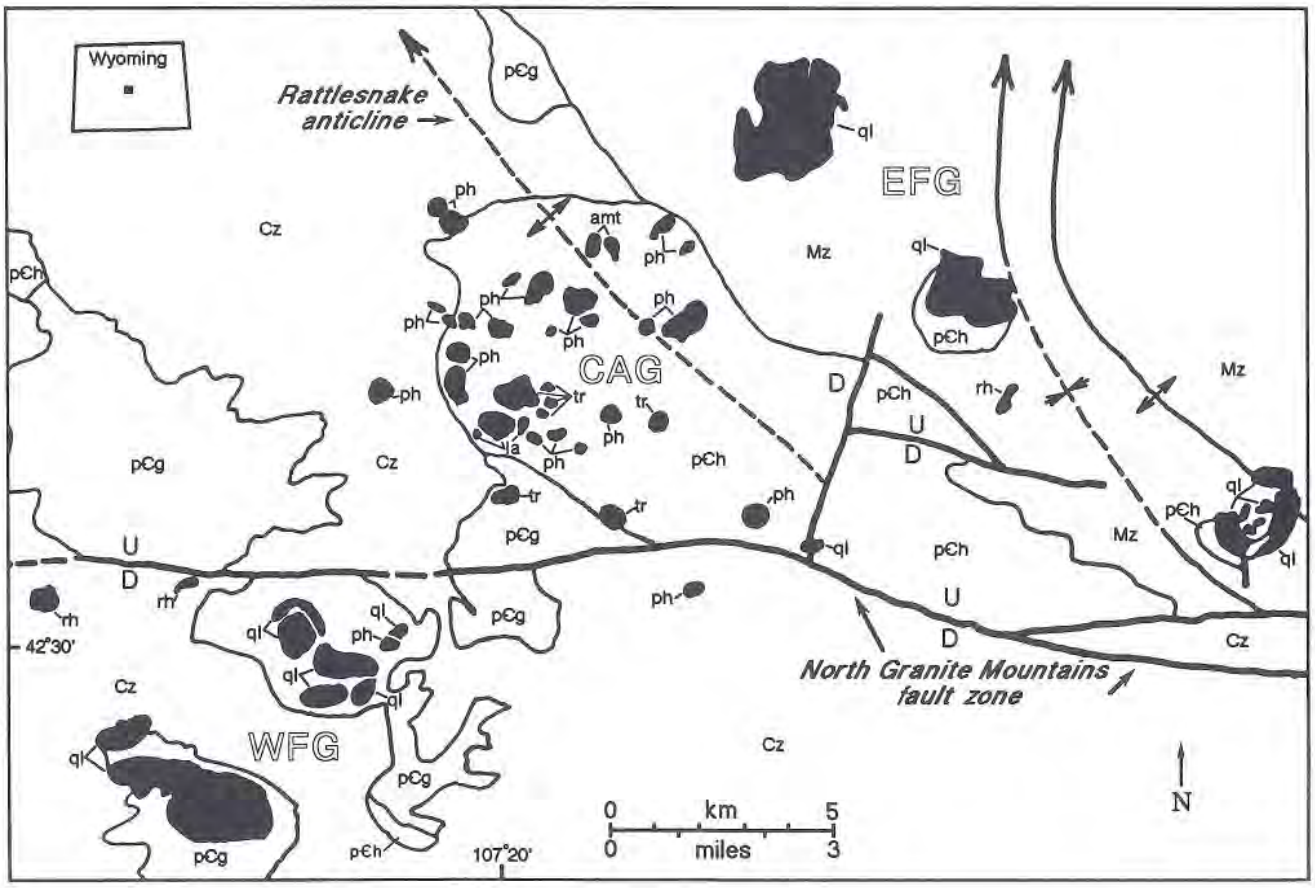

Figure 2. Schematic map showing local geology and distribution of igneous intrusive bodies (black). The Rattlesnake Hills alkalic complex is comprised of three groups: western felsic group (WFG), central alkalic group (CAG), eastern felsic group (EFG). Abbreviations are as follows: ph = phonolite, tr = trachyte, amt = alkali mela-trachyte, la = latite, ql = quartz latite, rh = rhyolite, Cz = Cenozoic surficial deposits, Mz = Mesozoic rocks, pCh and pCg = Archean hornblende schist and granitic gneiss. For structural and stratigraphic details see Pekarek (1974) from which this figure is modified.

Previous investigations

The Rattlesnake Hills were first noted in the territorial surveys of Hayden (1869) and King (1876). However, the first description of the igneous rocks is found in Cross (1897), which includes a chemical analysis of a "dacite" from Garfield Peak. Knight and Slossen (1901) and Hares (1916) recognized that the volcanic necks of the Rattlesnake Hills comprise "porphyritic andesite" or "porphyritic trachyte." Blackstone (1951) suggested that the post-eruptive, large-scale normal faulting in the region was a result of emplacement of magma from depth to the surface, which necessitated crustal readjustment. The Tertiary stratigraphic sequence of the area, which consists of intercalated tuff, breccia, sandstone, and claystone, was studied by Rachou (1951). He concluded that volcanism initially occurred over a 10 million year period beginning in the mid-Eocene. A second pulse of volcanism occurred during the early Oligocene. From a study of volcanogenic sediments on the Beaver Rim, 9.3 mi (15 km) west of the Rattlesnake Hills, Van Houten (1955) concluded that latitic lavas were erupted prior to the phonolitic and trachytic lavas. Houston (1964) mentioned the Rattlesnake Hills alkaline center in a report on Tertiary stratigraphic correlation and contrasted the undersaturated phonolites and trachytes with the contemporaneous andesitic volcanic debris of the Yellowstone and Absaroka volcanic provinces. Love (1970) published a comprehensive report on the Cenozoic geology of the Granite Mountains area, which included chemical analyses of RHAC rocks and postulated a complex displacement history for the North and South Granite Mountains fault systems.

The first detailed study of the Rattlesnake Hills volcanic plugs and dikes was undertaken by Carey (1959). Carey mapped 38 plugs, flows, and dikes in the complex; described the small-scale deformation associated with magma emplacement; and defined nine rock types based on petrography. He concluded that the alkaline phonolites and trachytes were produced as a result of the "desilicication of quartz latite magmas" by assimilation of amphibolite country rock. The quartz latite magma was inferred to have been the product of crystal fractionation from an unknown basaltic parent magma.

The second major study of the RHAC (Pekarek, 1974; Pekarek and others, 1974) attempted to synthesize the local igneous geology into the regional structural framework proposed by Love (1970). Petrographic and geochemical descriptions were presented along with K-Ar radiometric ages of feldspars from a quartz latite and a phonolite. Both units yielded ages of about 44 Ma, suggesting that, at least in some instances, emplacement of alkalic and subalkalic magmas was contemporaneous. Pekarek (1974) recognized the significance of the pre-eruptive uplift of the Granite Mountains and proposed decompression melting of the lower crust or upper mantle to produce distinct phonolitic and quartz latitic magmas; trachytes were considered to be mixing products of the two primary magmas.

The whole-rock chemical database was increased significantly by Stupak (1984) who acquired major- and trace-element analyses on 115 samples from the RHAC. Rare-earth element data and several analyses for volatile content were obtained on 12 samples. Geochemical modelling indicated that fractional crystallization and crystal retention could account for variations within each rock type, but relationships between rock types were not addressed by Stupak. Petrogenetic inferences were based on petrographic observations in conjunction with bulk rock geochemistry. Quartz latitic and rhyolitic magmas were inferred to have been a product of crustal melting resulting from calc-alkaline, arc-type volcanism. In contrast, trachytes and phonolites were thought to have been produced by partial melting of the upper mantle in response to postsubduction release of compression (Stupak, 1984).

This study of the RHAC combines previous data and observations with new petrographic and geochemical information, and provides a comparison with similar suites of rocks in Wyoming.

Petrography of the mid-Tertiary igneous rocks

Petrographic nomenclature for all rock samples is taken from Pekarek (1974) and is based on the Streckeisen (1967) classification scheme. Xenolith classification is based on texture and mineral content. Petrographic units are defined as spatially separate plugs, dikes, or flows. For further clarification, petrographic units are grouped based on relative location and presence or absence of modal quartz. The CAG comprises 21 phonolite, six trachyte, and two latite intrusions. The WFG includes six quartz latite units, two rhyolite units, and one small phonolite intrusion. The EFG includes three large quartz latite complexes and one smaller rhyolitic unit. A summary of mineral assemblages of individual rock types is given in **Figure 3**; representative modal analyses are given in **Table 1**.

Rock units of the central alkalic group (CAG)

Phonolite

The phonolites of the CAG are nepheline normative and contain modal feldspathoid (nosean, hauyne, or nepheline), alkali feldspar (sanidine), and clinopyroxene (salite > Cr-diopside > augite > aegirine). Amphibole may or may not be present. Sphene, apatite, magnetite, and phlogopite are present in trace amounts. Stupak (1984) divided the CAG phonolites into two groups: group A, a geographically central group, and group B, which lies near the perimeter of the CAG. Group A is characterized by a mafic phenocryst assemblage that includes

	Rock type	olivine	clinopyroxene	hornblende	phlogopite	alkali feldspar	plagioclase	sphene	apatite	magnetite	sodalite	nepheline	quartz	garnet	cpx-mica cumulate
CAG	alkali mela-trachyte	Tp	Ae	As	As				Ae	Ca					C
CAG	trachyte	Tp	Ae	Aa	Ta	As	As	Ae	Ae	Ca	Ce				C
CAG	phonolite	Ta	Ae	Cs	Ta	Ae		Ae	Ae	Ta	Ae	Ta		Ta	C
CAG	latite	Tp	Ae	Aa	Ta	Ae	As	Ae	Ae	Ca					C
WFG	quartz latite		Ta	As	Ta	Ta	As	Ae	Ae	Ta					
WFG	rhyolite		Ta	As			As	Ae	Ae	Ta	Te		Ca		
EFG	quartz latite		Ta	Ae			Ae	Ae	Ae	Ta					
EFG	rhyolite			Ae			Ae	Ae	Ae	Ta			Ta		

A = Always present
C = Common
T = Trace

e = euhedral
s = subhedral
a = anhedral
p = pseudomorph

Figure 3. Summary of mineral assemblages and textures for intrusive lithologies (cpx = clinopyroxene).

Table 1. Representative model phenocryst (> 0.05 mm) abundances. (1000 points counted for each sample; tr = trace abundance).

Sample	1[1] RH11	2 RH13	3 RH32	4 RH18	5 RH25	6 RH7	7 RH2	8 RH36	9 RH4	10 RH38
alkali feldspar		1.4	2.0	1.1	1.8	8.8				
plagioclase		17.0	6.3			39.2	38.0	23.9	31.5	27.3
feldspathoid			0.1	3.0	25.3					tr
clinopyroxene	15.7	11.9	4.5	11.3	2.3	4.0	0.3		0.6	
hornblende	3.5	0.6	2.1	4.0	tr	3.8	7.7	6.4	3.7	3.8
phlogopite	0.2			tr		0.4			tr	
olivine	tr			tr						
magnetite	2.0	1.2	0.1	0.2	tr	1.2			0.2	0.1
apatite	0.9	0.4	0.1	1.0		0.6	0.1	0.2	tr	tr
sphene		0.4	0.5	1.0		0.8	1.0	0.3		tr
quartz							0.5	tr		2.2
nepheline				tr						
Total phenocrysts	22.3	32.9	15.7	21.6	29.4	58.8	47.6	30.8	36.0	33.4

[1]Sample descriptions:

1. alkali mela-trachyte
2. trachyte (no feldspathoid)
3. trachyte (feldspathoid present)
4. phonolite (Group A)
5. phonolite (Group B)
6. latite
7. quartz latite
8. rhyolite
9. quartz latite
10. rhyolite

abundant euhedral pyroxene, zoned from diopside to ferrosalite; anhedral amphibole; and rare olivine(Fo_{87}). The olivine crystalsare surrounded by salite + phlogopite + magnetite reaction rims (**Figure 4**). Variable zoning in pyroxene is evident in thin section under plane-polarized light; clear zones are Mg-rich diopside and salite, whereas green areas are more Fe-rich (ferrosalite) (**Figure 5**). Felsic phenocrysts in Group A include tabular sanidine phenocrysts and smaller feldspathoid phenocrysts, which are mostly altered to zeolite (Pekarek, 1974). Group B contains larger and more abundant feldspathoid phenocrysts; smaller, more potassic sanidine crystals; and less abundant, sodium-rich ferrosalite phenoc-

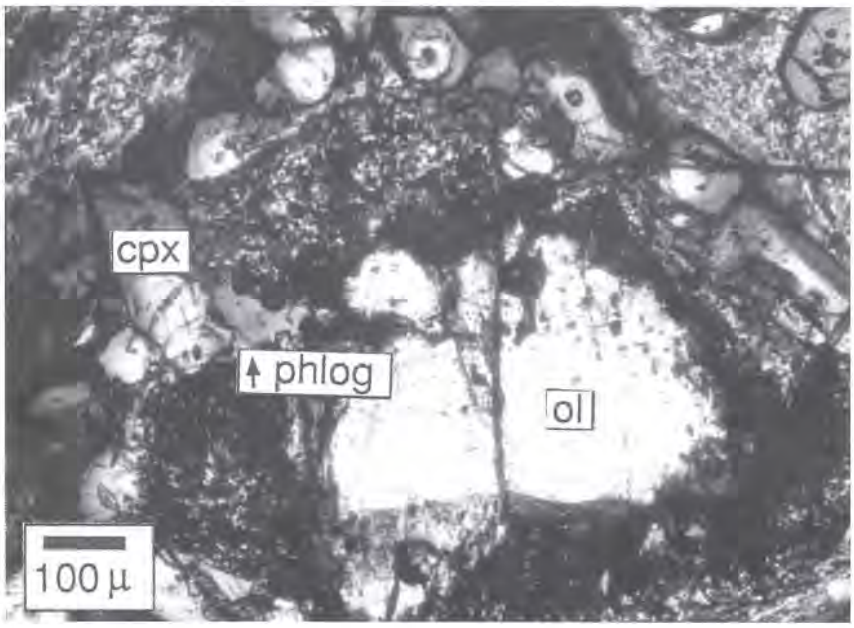

Figure 4. Photomicrograph of a resorbed olivine (ol) grain in phonolite. Minerals in reaction zone include phlogopite (phlog), salite (cpx), apatite, and magnetite (plane-polarized light).

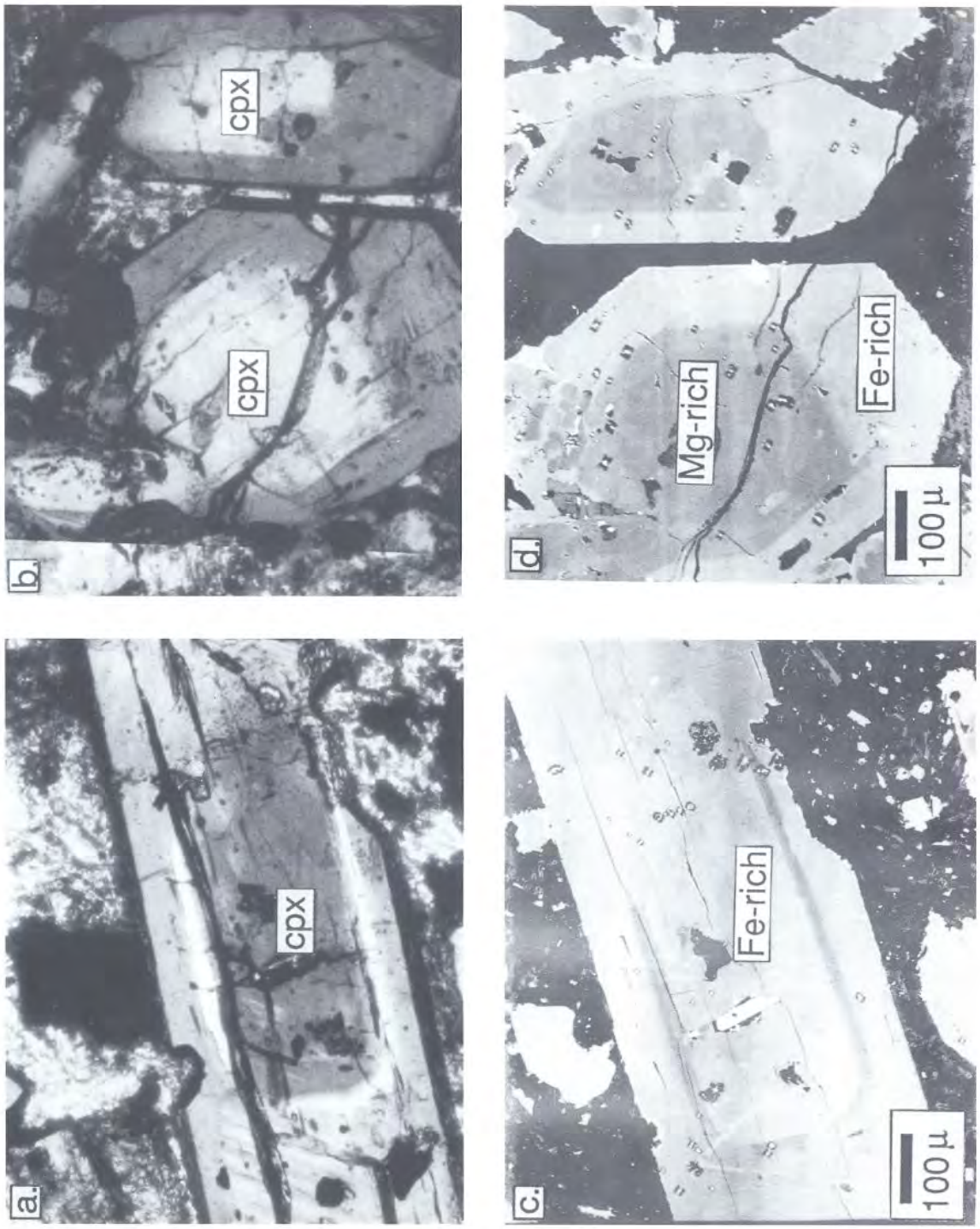

Figure 5. Photomicrographs of zoned salite (cpx) in phonolite: plane-polarized light images: (a) grain has a dark green (dark gray) ferrosalite core, partially surrounded by a clear zone of Mg-rich salite, and mantled by light green (light gray) ferrosalite; (b) normal zoned salite grains have clear Mg-rich cores and green (gray) Fe-rich rims. (c) and (d) are backscattered electron images of (a) and (b) showing compositional differences as a function of average atomic weight: lighter average atomic weight appears darker, whereas heavier average atomic weight appears lighter.

rysts. Scarce phenocrysts of melanite, a Ti-rich variety of andradite garnet, are also present in two of the outer intrusions of group A.

Euhedral sphene, apatite, and magnetite crystals are present in all phonolites. Trace amounts of anhedral nepheline also occur in both groups of phonolites. Groundmass constituents of all phonolites include alkali feldspar, aegirine and/or augite, feldspathoid, and magnetite. No crustal xenoliths were observed in the phonolites, but many samples contain clinopyroxene or clinopyroxene-mica cognate inclusions up to 5 mm in diameter.

Trachyte

The trachytes of the CAG may be either quartz normative or nepheline normative. They are characterized petrographically by the occurrence of both alkali feldspar and plagioclase phenocrysts in a trachytic groundmass. Subhedral plagioclase (oligoclase) phenocrysts are larger and much more abundant than subhedral alkali feldspar (anorthoclase) phenocrysts. Feldspathoid phenocrysts are absent. Clinopyroxene (salite-ferrosalite) is the most abundant mafic mineral, occurring both as euhedral phenocrysts and in clinopyroxene-mica cognate inclusions. Clinopyroxene commonly exhibits reverse zoning, which is apparent in thin section (**Figure 6**). Anhedral hornblende phenocrysts are partially or completely replaced with salite + magnetite + sanidine + sphene (**Figure 7**). Phlogopite is present in trace amounts as phenocrysts and occurs in cognate inclusions with clinopyroxene. Sphene, apatite, zircon, and magnetite occur as accessory minerals. The trachytic groundmass consists chiefly of sanidine laths with lesser amounts of augite, magnetite, sphene, and apatite.

Alkali mela-trachyte

Alkali mela-trachyte is the most mafic rock type in the RHAC and is found in only one locality in the CAG. Feldspar and feldspathoid phenocrysts are absent. Clino-pyroxene is the most abundant phenocryst and exhibits normal, reverse, and complex zoning patterns with compositions ranging from Cr-diopside to ferrosalite. Hornblende, the next most abundant phenocryst, is commonly rimmed by clinopyroxene + magnetite. Sodium-rich phlogopite phenocrysts occur in trace amounts. Other phenocrysts include magnetite and smoky apatite. Pseudomorphs of calcite after olivine are also present and are rimmed by clinopyroxene, phlogopite, and magnetite. Sphene, a ubiquitous phase in trachyte and phonolite, is notably absent. The groundmass mineral assemblage of alkali mela-trachyte is similar to that of trachyte.

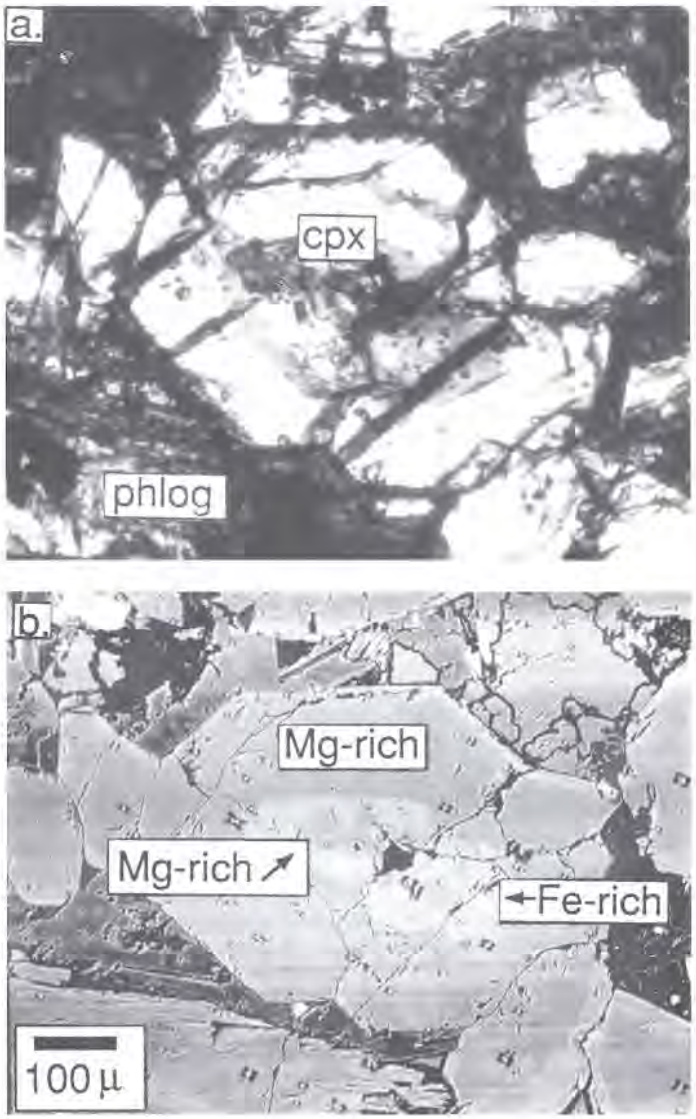

Figure 6. Complexly zoned salite (cpx) in trachyte: (a) The small clear zone in the green (gray) core is an Mg-rich nucleus surrounded by Fe-rich ferrosalite, which is surrounded by clear Mg-rich salite. Also present in this cognate inclusion is phlogopite (phlog) and magnetite (plane polarized light). (b) Backscattered electron image of the same grains, showing variable shades as a function of chemical composition: lighter average atomic weight appears darker, whereas heavier average atomic weight appears lighter.

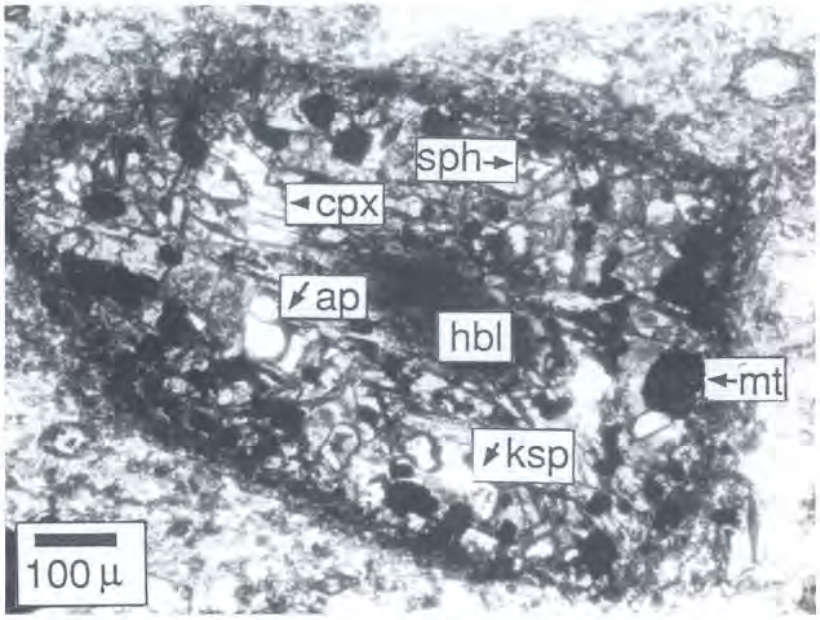

Figure 7. Resorbed hornblende core (hbl) in hornblende replacement pseudomorph. Replacement minerals include salite (cpx), magnetite (mt), apatite (ap), sanidine (ksp), and sphene (sph) (plane polarized light).

Latite

Latite, the largest exposed unit in the CAG, has petrographic similarities to both CAG trachytes and to quartz latites of the EFG and WFG. It is grouped with the CAG because it is surrounded by phonolite and trachyte intrusions typical of the CAG. Latite contains >50% phenocrysts, which range in size from groundmass (0.05 mm) to 1 cm. Plagioclase (oligoclase-andesine) is the largest and most abundant phase, followed by alkali feldspar (anorthoclase), clinopyroxene, and hornblende, which has the same reaction texture as in trachytes (**Figure 6**). Accessory minerals include phlogopite, sphene, apatite, and magnetite. A small percentage of plagioclase phenocrysts have resorbed cores or zones of resorption. Smaller plagioclase crystals are commonly enclosed by larger alkali feldspar phenocrysts (**Figure 8**). Clinopyroxene-mica cognate inclusions are common and may be as large as 10 cm in diameter. Hornblende cognate inclusions with interstitial plagioclase are also present. Individual hornblende grains may also contain salite, phlogopite, and apatite. The groundmass mineral assemblage is identical to those of the trachytes, with the addition of trace amounts of zircon.

Clinopyroxene-mica cognate inclusions

Clinopyroxene-mica cognate inclusions or malignite (Dudás and Eggler, 1989) occur in most units of the CAG. These were thought by Pekarek (1974) to be reaction products of unstable hornblende, but more recently Dudás and Eggler (1989) speculated that they are cumulate products of crystal settling in mid-crustal to shallow magma chambers. Backscattered electron imaging reveals complex compositional zoning in clinopyroxene (**Figure 5**), a possible indication of repeated cycles of crystal retention and settling during magma evolution. The mica is an unusual sodium-rich phlogopite (wt.% Na_2O = K_2O). Clinopyroxene compositions range from Cr-

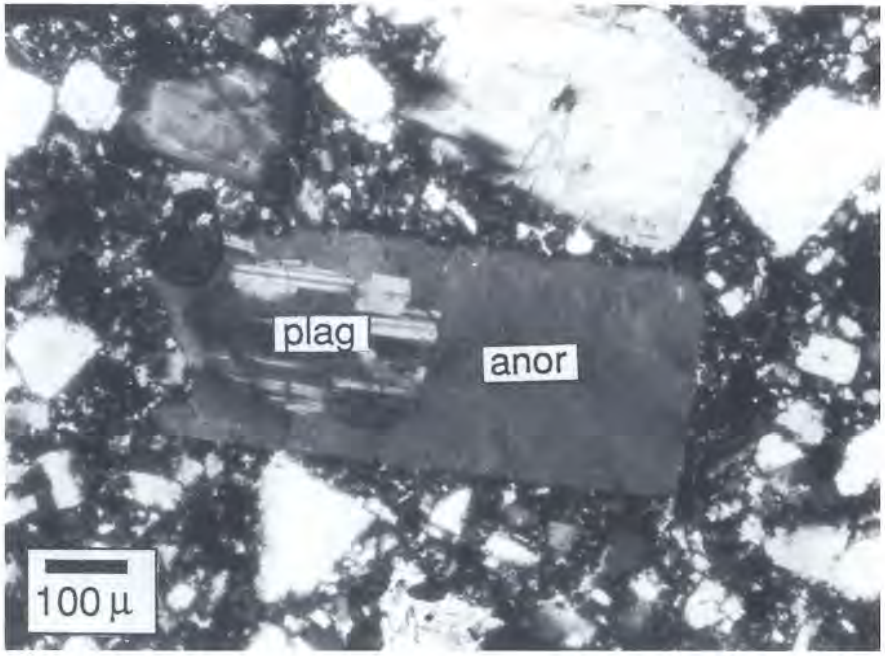

Figure 8. Subhedral plagioclase grain (pl) surrounded by euhedral anorthoclase (anor) in a latite sample from the CAG (plane-polarized light).

rich diopside to ferrosalite. Nepheline, apatite, and magnetite also occur in trace abundances in some cumulates. These cognate inclusions, which range in size from a few mm to several cm, are distinctive from smaller (<1mm) clinopyroxene-mica clusters that formed as a reaction product of olivine + magmatic fluids.

Rock units of the eastern felsic group (EFG)

Quartz latite

EFG quartz latites are very coarsely porphyritic with euhedral, homogeneous oligoclase phenocrysts up to 1.5 cm long. Large, euhedral hornblende phenocrysts are also abundant, and may contain inclusions of apatite, zircon, or sphene. Trace amounts of magnetite, sphene, apatite, and biotite also occur as phenocrysts. Quartz is restricted to the groundmass, which is glassy. The groundmass also contains sanidine, hornblende, magnetite, apatite, phlogopite, zircon, and sphene. EFG quartz latites are very homogeneous, and no cognate inclusions or xenoliths have been observed.

Rhyolite

Rhyolite occurs in the EFG in much smaller volume than the quartz latite. The presence of quartz phenocrysts and a higher silica content distinguish rhyolite from quartz latite. Subhedral plagioclase (oligoclase) is the most abundant phenocryst phase. Hornblende is the next most abundant phase, as in quartz latite. Apatite, magnetite, and sphene are also present in trace amounts. Groundmass texture and mineral assemblage are similar to those of EFG quartz latites.

Rock units of the western felsic group (WFG)

Quartz latite

The quartz latite units of the WFG are porphyritic with mineral assemblages and phenocryst abundances similar to those of the EFG. However, the phenocrysts are about one half the size of those in EFG quartz latites (**Figure 9**). Plagioclase compositions are slightly more variable than those in the EFG, ranging from oligoclase to andesine. Many of the plagioclase phenocrysts exhibit zones of resorption or resorbed cores, which contain trace amounts of potassium feldspar (**Figure 10**). Euhedral hornblende phenocrysts are abundant, along with trace amounts of magnetite, sphene, apatite, phlogopite, and clinopyroxene. The groundmass is holocrystalline and includes quartz, sanidine, magnetite, hornblende, apatite, and sphene.

Rhyolite

Rhyolite units of the WFG are much less voluminous than nearby quartz latite units. Large resorbed quartz and feldspar phenocrysts similar to those in WFG quartz latite are common. Hornblende is also present. Apatite, magnetite, and sphene phenocrysts occur in trace amounts. In one sample, a euhedral feldspathoid xenocryst was observed in close proximity to a resorbed quartz phenocryst (**Figure 11**). Texturally, the groundmass is more glassy than WFG quartz latites, but the mineral assemblages are similar.

Figure 9. Quartz latite hand samples from the WFG (left) and the EFG (right) illustrate textural differences between the two groups of subalkaline rocks. These rocks have very similar mineral assemblages and chemical compositions.

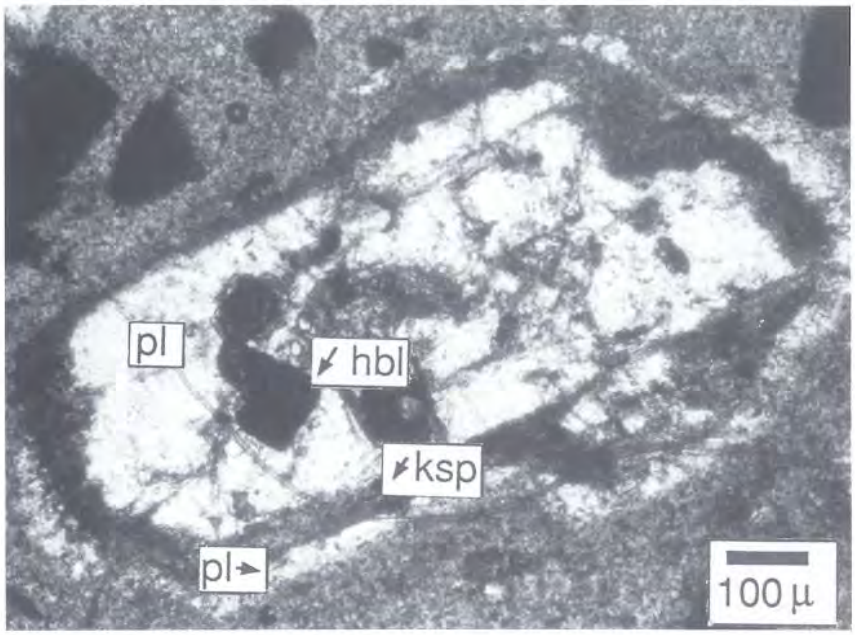

Figure 10. Plagioclase phenocryst (pl) with sanidine-rich (ksp) zone of resorption from the western felsic group. This texture is common in both the rhyolite and quartz latite in the western felsic group. The hornblende (hbl) inclusion in plagioclase is common in all plagioclase-bearing rocks of the Rattlesnake Hills intrusive complex (plane-polarized light).

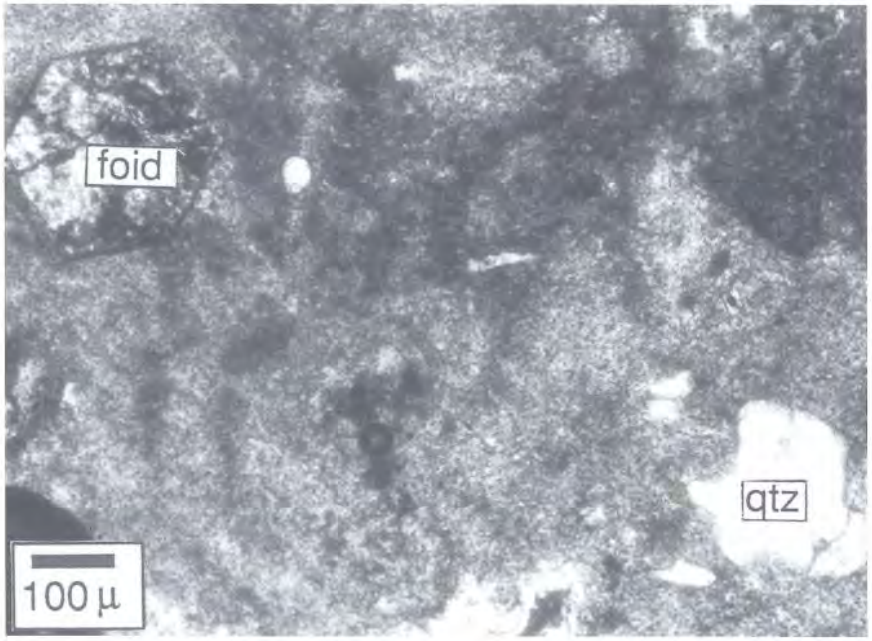

Figure 11. Euhedral feldspathoid (foid) and anhedral quartz (qtz) coexisting in a rhyolite sample from the western felsic group.

Whole-rock chemical data

Major-element compositions

Major-element analyses were performed on 40 samples, including 18 phonolites, seven trachytes (including one alkali mela-trachyte), one latite, nine quartz latites, two rhyolites, and a clinopyroxene-mica cognate inclusion. Representative analyses are presented in **Table 2**.

CAG phonolites have highly variable major-element contents at nearly constant silica concentrations, whereas CAG trachytes vary in silica con-

Table 2. Representative whole-rock chemical compositions (b.d. = below detection limit; x-ray fluorescence analyses by XRAL Laboratory).

Sample	1[1] RH11	2 RH13	3 RH32	4 RH18	5 RH25	6 RH2	7 RH36	8 RH35	9 RH38
Major elements in weight % oxide									
SiO_2	51.80	56.00	58.20	53.70	55.00	64.80	69.80	65.60	71.60
TiO_2	1.03	0.80	0.54	0.66	0.20	0.36	0.29	0.38	0.21
Al_2O_3	14.90	17.70	18.40	17.80	20.80	15.30	14.30	16.70	14.40
Fe_2O_3	7.92	5.23	3.88	5.00	2.28	3.27	2.44	1.89	1.84
MnO	0.19	0.18	0.16	0.18	0.11	0.11	0.07	0.04	0.05
MgO	3.78	1.64	1.04	1.58	0.64	1.05	0.68	0.43	0.37
CaO	6.40	4.36	4.07	3.83	1.93	3.30	2.60	2.34	1.60
Na_2O	3.60	5.94	5.99	7.98	8.20	5.67	5.11	4.68	5.46
K_2O	5.08	4.81	4.80	5.23	4.94	3.77	3.05	4.23	3.48
P_2O_5	0.44	0.21	0.13	0.18	0.03	0.21	0.16	0.17	0.11
H_2O/LOI	3.62	2.16	2.16	1.62	5.85	1.77	1.16	2.23	1.00
Trace elements in ppm									
Ba	930	890	840	980	140	820	860	830	1200
Co	19	20	21	25	10	36	20	22	22
Cr	64	15	11	62	26	16	13	19	21
Cu	40	b.d.	b.d.	38	b.d.	b.d.	b.d.	b.d.	b.d.
Mo	b.d.	b.d.	b.d.	b.d.	b.d.	b.d.	b.d.	b.d.	b.d.
Nb	34	38	33	54	57	15	22	32	13
Ni	34	b.d.	b.d.	17	b.d.	b.d.	b.d.	b.d.	b.d.
Pb	25	27	32	35	97	b.d.	16	15	33
Rb	23	103	120	117	193	85	73	114	106
Sr	1180	2090	1950	2820	2220	1510	1580	1530	1330
Th	b.d.	12	17	28	48	b.d.	14	15	13
U	b.d.	b.d.	b.d.	b.d.	22	b.d.	b.d.	b.d.	b.d.
Y	b.d.	32	33	39	31	18	35	b.d.	17
Zn	76	86	89	100	130	120	66	55	54
Zr	200	260	290	300	610	190	180	170	130
Total wt.%	99.06	99.43	99.76	98.28	100.40	99.92	99.98	99.00	100.40

[1]Sample descriptions:

1. CAG alkali mela-trachyte
2. CAG trachyte (feldspathoid)
3. CAG trachyte (feldspathoid present)
4. CAG phonolite (Group A)
5. CAG phonolite (Group B)
6. EFG quartz latite
7. EFG rhyolite
8. WFG quartz latite
9. WFG rhyolite

tent and follow linear compositional trends (**Figure 12**). The composition of latite is generally intermediate between trachyte and quartz latite. The clinopyroxene-mica cognate inclusion bears no chemical similarity to any other rock type. Quartz latite and rhyolite compositions from the EFG and WFG are similar and are more silica enriched than any rocks of the CAG. All rocks of the RHAC have relatively low concentrations of MgO and Fe_2O_3 and high concentrations of alkalis.

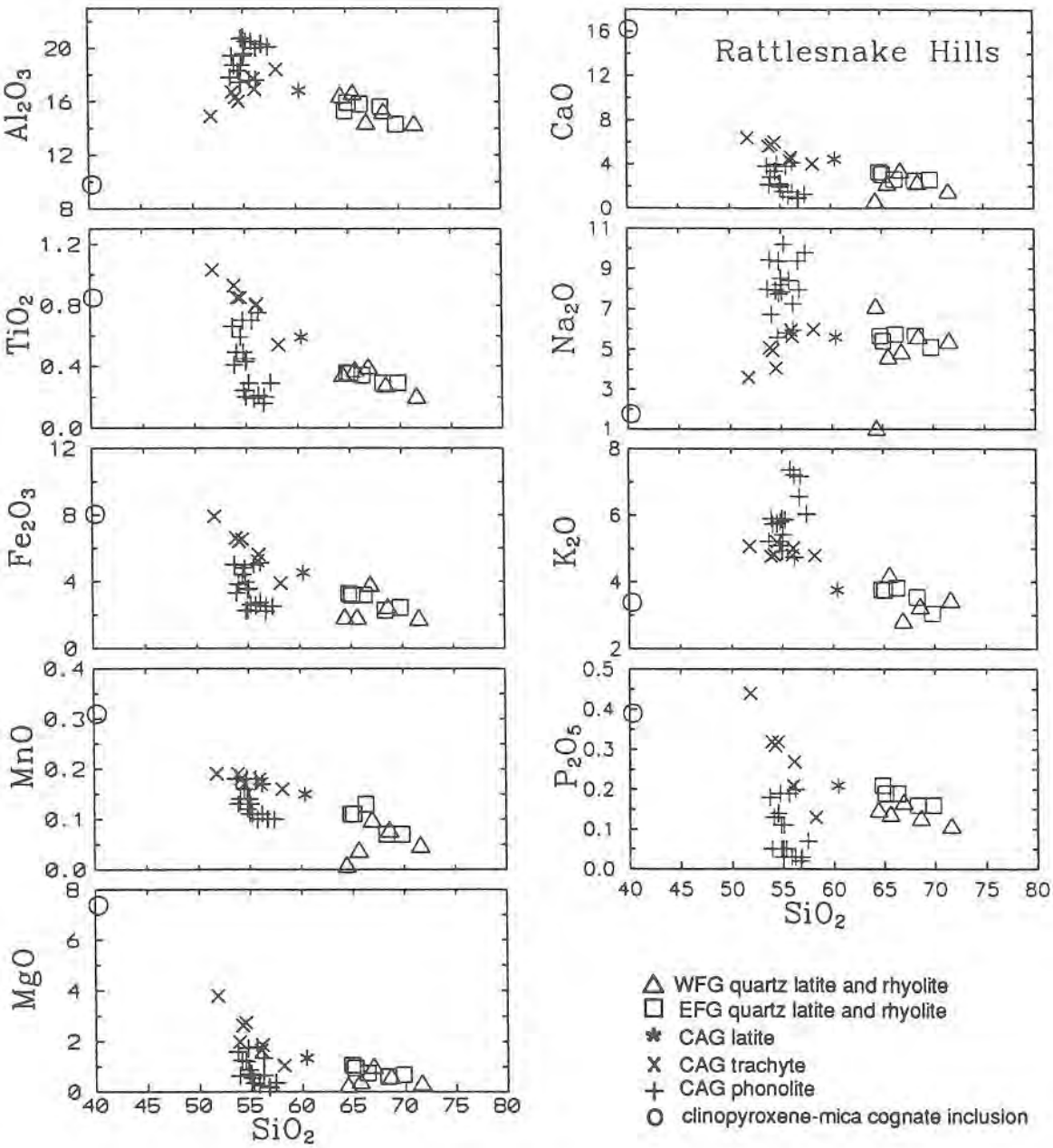

Figure 12. Harker variation diagrams for major-element compositions of the Rattlesnake Hills intrusive rocks, including an analysis of a clinopyroxene-mica cognate inclusion from a trachyte sample. Note the low variability of silica in phonolite. The latite composition is intermediate between trachyte and quartz latite compositions, both of which form individual linear trends (units are in weight % oxide).

Trace-element compositions

Rocks of the RHAC were also analyzed for 14 trace-element concentrations; representative analyses are listed in **Table 2**. All RHAC rock types are extremely enriched in Sr, and all rocks except for some phonolites are enriched in Ba (**Figure 13**). All rock types have appreciable contents (>50 ppm) of "incompatible" elements such as Zn, Zr, and Rb. Concentrations of Cu, Mo, Ni, and U are below detection limits in almost all analyzed samples. All rock types are strongly enriched in light rare-earth elements (LREE) (Stupak, 1984).

Preliminary isotopic data

Sr and Nd isotopic analyses were performed for four samples of the RHAC—phonolite, trachyte, alkali mela-trachyte, and clinopyroxene-mica cumulate—and also for samples of amphibolite and granitic gneiss country rock (**Table 3**). Initial $^{87}Sr/^{86}Sr$ ratios range from 0.70398 to 0.70446 for the RHAC samples. These values are very different from those of the country rocks at the time of RHAC emplacement, which are $^{87}Sr/^{86}Sr$ = 0.71192 and 0.91943 for the amphibolite and granitic gneiss, respectively. Initial ϵ_{Nd} values for the RHAC range from -3.96 to -6.85, which contrast with country rock values of -18.64 and -28.49.

The Sr and Nd isotopic values of the four RHAC rock types are not within analytical error of one another, despite petrographic similarities and spatial proximity.

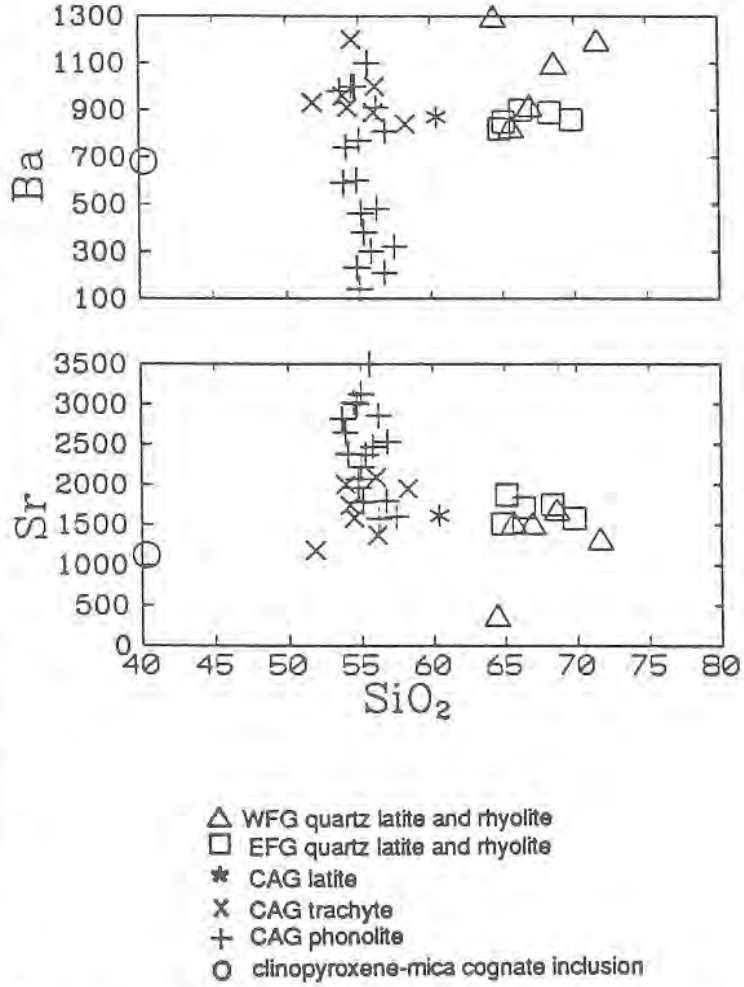

Figure 13. Harker variation diagrams showing highly enriched concentrations of Ba and Sr in Rattlesnake Hills igneous rocks (SiO_2 is in weight % oxide; Sr and Ba are in parts per million).

Comparison to Tertiary intrusive rocks in the the Bear Lodge Mountains area

A wide variety of petrographically and geochemically distinct rocks occur in Tertiary intrusions associated with Laramide uplift structures in Montana and Wyoming (Larsen, 1940; Eggler and others, 1988). Among these, the intrusive complex that bears the most striking resemblance to the Rattlesnake Hills complex is in the Bear Lodge Mountains, Wyoming. The Bear Lodge Mountains (BLM) are located in the northeast corner of Wyoming approximately 200 mi (300 km) northeast of the Rattlesnake Hills and 12 mi (20 km) west of the Black Hills. Intrusions lie along a northwest-trending axis, which is roughly parallel to Laramide folding axes associated with the Black Hills uplift. The aerial extent of the intrusions is approximately 45 mi^2 (110 km^2) (Staatz, 1983), compared to the RHAC which, covers approximately 125 mi^2 (300 km^2).

Table 3. Preliminary Sm, Nd, Rb and Sr concentrations and Nd and Sr isotopic data. [Initial values (ϵ^{t}_{Nd} and I^{t}_{Sr}) were calculated for an age of 44 Ma; errors in the last two decimal places are in parentheses.]

Sample	Sm ppm	Nd ppm	$^{147}Sm/^{144}Nd$	$^{143}Nd/^{144}Nd$	ϵ_{Nd}	ϵ^{t}_{Nd}	Rb ppm	Sr ppm	$^{87}Rb/^{86}Sr$	$^{87}Sr/^{86}Sr$	I^{t}_{Sr}
CAG phonolite											
RH18	12.7	67.6	0.113602	0.512287 (18)	-6.85	-6.38	134.2	2486.6	0.247823	.704172 (17)	0.704096
CAG trachyte											
RH13	10.8	55.1	0.118522	0.512268 (17)	-7.22	-6.78	201.1	788.1	0.309001	.704649 (11)	0.704456
CAG alkali mela-trachyte											
RH11	5.5	22.7	0.146511	0.512336 (13)	-5.89	-5.61	123.3	1195.4	0.292809	.704881 (24)	0.704298
CAG clinopyroxene-mica cognate inclusion (from RH15 trachyte)											
RH15x	5.6	24.1	0.140513	0.512470 (15)	-3.28	-2.96	118.7	368.6	0.313463	.704178 (11)	0.704298
EFG quartz latite											
RH2	10.5	54.1	0.117364	0.512435 (16)	-3.96	-3.51	134.2	521.5	0.247823	0.704604 (18)	0.704449
Archean country rock											
p-€gg	1.3	4.9	0.160402	0.511659 (29)	-19.08	-18.64	202.9	43.8	13.68898	0.927995 (16)	0.919439
p-€hs2	2.9	15.3	0.114583	0.511154 (18)	-28.95	-28.49	44.4	284.1	0.452278	0.712205 (20)	0.711922

K-Ar radiometric ages of four phonolite samples in the BLM range from 38.3 Ma to 50.5 Ma (Staatz, 1983), bracketing K-Ar ages from the Rattlesnake Hills.

Tertiary igneous rock types in the BLM include: phonolite, trachyte, latite, lamprophyre, nepheline syenite, and carbonatite. Large intrusions along the northwest-trending core of the complex are surrounded by lower Paleozoic strata, which were folded along the margins of the intrusive igneous rocks. The centrally located Bear Lodge dome is the largest intrusion [5.5 mi x 2.5 mi (9km x 4km)], consisting of rocks which are gradational between phonolite and trachyte (Staatz, 1983). Included in the Bear Lodge dome are exposures of Archean granite country rock, into which alkalic magmas were emplaced. A large [0.35 mi^2 (1km^2)] latite body lies 1.2 miles (2 km) northwest of the Bear Lodge dome. Smaller intrusive domes, plugs, dikes, and sills are on the same scale as those in the RHAC [<.35 mi^2 (1 km^2)]. Approximately 30 smaller phonolite and trachyte bodies occur peripherally to the perimeter of the larger intrusions. Two lamprophyre plugs and one sill occur on the western edge of the complex in Mesozoic sedimentary strata. Syenite and nepheline syenite (plutonic equivalents of trachyte and phonolite) occur within larger trachyte and phonolite bodies. Scarce stringers of carbonatite have also been noted in the Bear Lodge dome (Staatz, 1983).

Petrographically, trachytes and phonolites of the BLM are similar to those of the RHAC with a few exceptions: melanite garnet and nepheline phenocrysts occur more commonly in BLM rocks. Other phenocryst occurrences are similar, as is the notable paucity of olivine. Lamprophyre intrusions of the BLM are analogous to alkali mela-trachyte of the RHAC. Both are porphyritic igneous rocks whose phenocrysts consist entirely of mafic minerals (Ca-rich clinopyroxene, phlogopite, and hornblende). Latites in the BLM complex are chemically similar to latites in the RHAC and have similar mineral assemblages with smaller phenocrysts. Carbonatite veins in BLM alkaline intrusions are present, although not obvious; they were found during bulldozer excavation (Staatz, 1983). The occurrence of carbonatites in the RHAC has not been yet observed. However, replacement of phenocrysts by magmatic carbonate (Stupak, 1984) and presence of calcite along

microfractures in phonolite are evidence of the possible presence of carbonatites at depth associated with the RHAC.

A major petrographic difference between the RHAC and the BLM complex is a lack of subalkaline lithologies in the BLM. Quartz latite and rhyolite make up two large groups within the RHAC, whereas only one subalkaline intrusion is present in the BLM complex. Alkaline phonolite and trachyte are by far the dominant lithologies in the BLM, whereas there is a more even distribution between alkaline and subalkaline rocks in the RHAC.

Major-element compositions of the two complexes are compared in **Figure 14**. The BLM rocks are not as rich in silica as those of the RHAC. This reflects the absence of quartz latite and rhyolite in the BLM. The majority of major-element compositions of BLM rocks fall within RHAC compositional fields, due to the similarity between the alkaline rocks of the two complexes.

Chronological, petrographic, and geochemical similarities between the alkaline intrusions of the BLM and RHAC are striking; however, more work is needed in both localities before any petrogenetic relationships may be established.

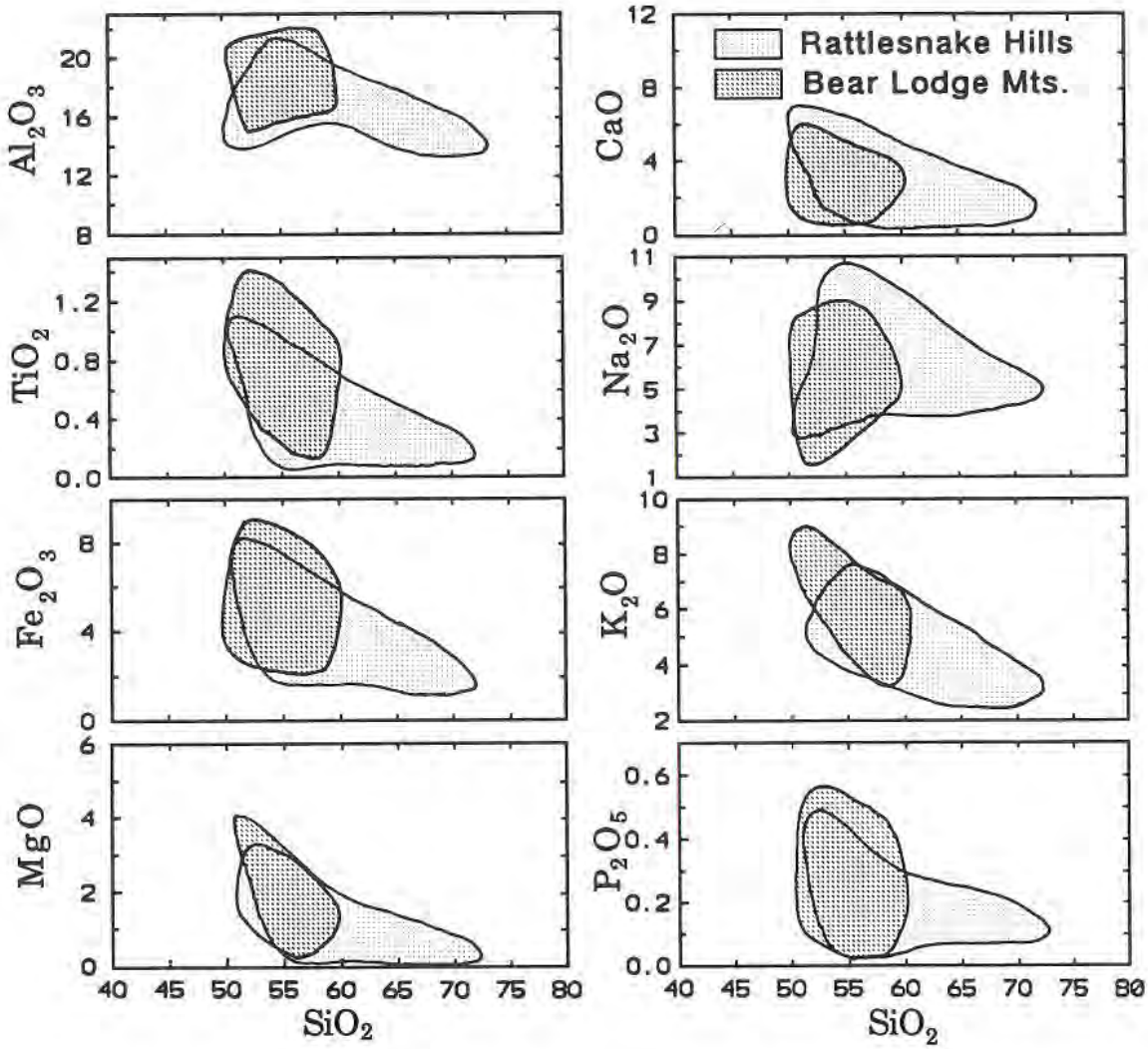

Figure 14. Comparison of major-element compositions of Tertiary intrusive rocks of the Rattlesnake Hills and the Bear Lodge Mountains (BLM). Rock compositions of the BLM coincide with phonolite and trachyte of the Rattlesnake Hills. Quartz latites and rhyolites are absent from the BLM. [BLM data are from Staatz (1983) and Jenner (1989)].

Preliminary speculations on petrogenesis of the igneous intrusions of the Rattlesnake Hills

Relationship of magmatism to structural features

Alkaline magmatism is associated chronologically and spatially with Laramide orogenic activity in the RHAC and BLM. Tertiary folding and faulting is presumably responsible for reactivating Precambrian zones of crustal weakness, along which magmas could ascend. It is not known whether alkaline magmas were produced only in the Rattlesnake Hills and Black Hills areas or whether they were generated more widely, but did not ascend to shallow crustal levels in all locations.

Magmatic differentiation

The petrologic relationships between different rock types within the RHAC are complicated. The presence of large unzoned phenocrysts in the EFG suggests that mixing of magmas was unimportant in this geographic area of the complex. In contrast, the rocks of the WFG include petrographic evidence of resorption of feldspars, and some rhyolites contain euhedral sodalite coexisting with anhedral quartz. It appears that mixing of a felsic parental magma with a silica-poor, sodalite-bearing magma produced the WFG rocks. The CAG rocks contain multiple populations of clinopyroxene phenocrysts; including unzoned green salite or ferrosalite, normally zoned clinopyroxene with Cr-diopside cores and green salite or ferrosalite rims, and grains with green salite cores with clear bands of Mg-rich salite. Multiple magma-mixing events involving clinopyroxene-phyric magmas are required to produce the different clinopyroxene populations in the CAG rocks.

The complex mixing relations indicated by the petrography of the RHAC are also reflected in the major- and minor-element Harker variation diagrams. No simple curve or straight line relationships encompass all RHAC rock types, as would be expected if simple fractionation or two-component mixing was responsible for the geochemical variation of the suite. In addition, the Sr and Nd isotopic compositions for four RHAC rock types are outside of analytical error of one another, ruling out a relationship of crystal fractionation alone. The isotopic data form a cluster rather than defining a single binary mixing or assimilation/fractional-crystallization trend, again confirming that the relationships between RHAC rock types are complex.

Evidence of parental magma(s) characteristics: significance of clinopyroxene-mica cognate inclusions

The clinopyroxene-mica cognate inclusions or cumulates are common in all CAG rock types. The Cr-diopside-rich clinopyroxene grains exhibit complex compositional zoning, indicating possible repeated cycles of crystal retention and settling in magmas that were more primitive than those exposed in the RHAC (Hoch, 1991). Bulk chemical composition and isotopic composition also suggest that they have been less affected by mixing with evolved magmas or other types of crustal interaction than have other RHAC rock types (Hoch, 1991). More than any of the lithologies presently exposed, the clinopyroxene-mica cumulates preserve information about one or more mafic parental magmas involved in the generation of the RHAC.

If the geochemical and isotopic characteristics of the clinopyroxene-mica cumulates are representative of a mafic parental magma or magmas, then this mafic end member cannot be from a Rb and LREE depleted mantle source like that found beneath mid-ocean ridges. Lithospheric material with high concentrations of incompatible elements may be formed by the ascent and solidification of small melt fractions generated in the upper mantle. The decay of ^{87}Rb and ^{147}Sm in this metasomatized mantle lithosphere can produce large isotopic contrasts to the convecting upper mantle. This contrast appears to be greatest beneath Archean cratons, where the chemical anomaly is longest lived (McKenzie, 1989). The isotopic data for the clinopyroxene-mica cumulate and other rocks of the RHAC are consistent with the involvement of a geochemically and isotopically modified mantle source (Hoch, 1991). Another well-documented occurrence of chemically modified, mantle-derived, hypabyssal rocks in Wyoming is in

the Leucite Hills of southwestern Wyoming (Vollmer and others, 1984).

Origin of evolved felsic magmas

Petrographic, geochemical, and isotopic evidence all suggest that silica-poor magmas mixed with felsic magmas to produce many of the rock types of the RHAC. Archean country rocks are possible sources of these felsic magmas. Although the country rocks presently exposed in the Rattlesnake Hills are not necessarily the same as those at depth, granitic gneisses and amphibolite are the dominant Archean rock types exposed in the basement-cored uplifts throughout the Wyoming province (Frost and Frost, this volume). Binary bulk assimilation mixing models, in which magmas with the isotopic composition of the clinopyroxene-mica cumulate are mixed with the amphibolite, suggest that less than 20% country rock is required to produce magmas with the isotopic composition of the phonolite, quartz latite, or trachyte (**Figure 15**). Although such elementary modelling is undoubtedly a gross simplification of the actual magmatic processes (see Hoch, 1991 for a more complete evaluation), it underlines the important point that Archean country rock played a minor role in the generation of the RHAC.

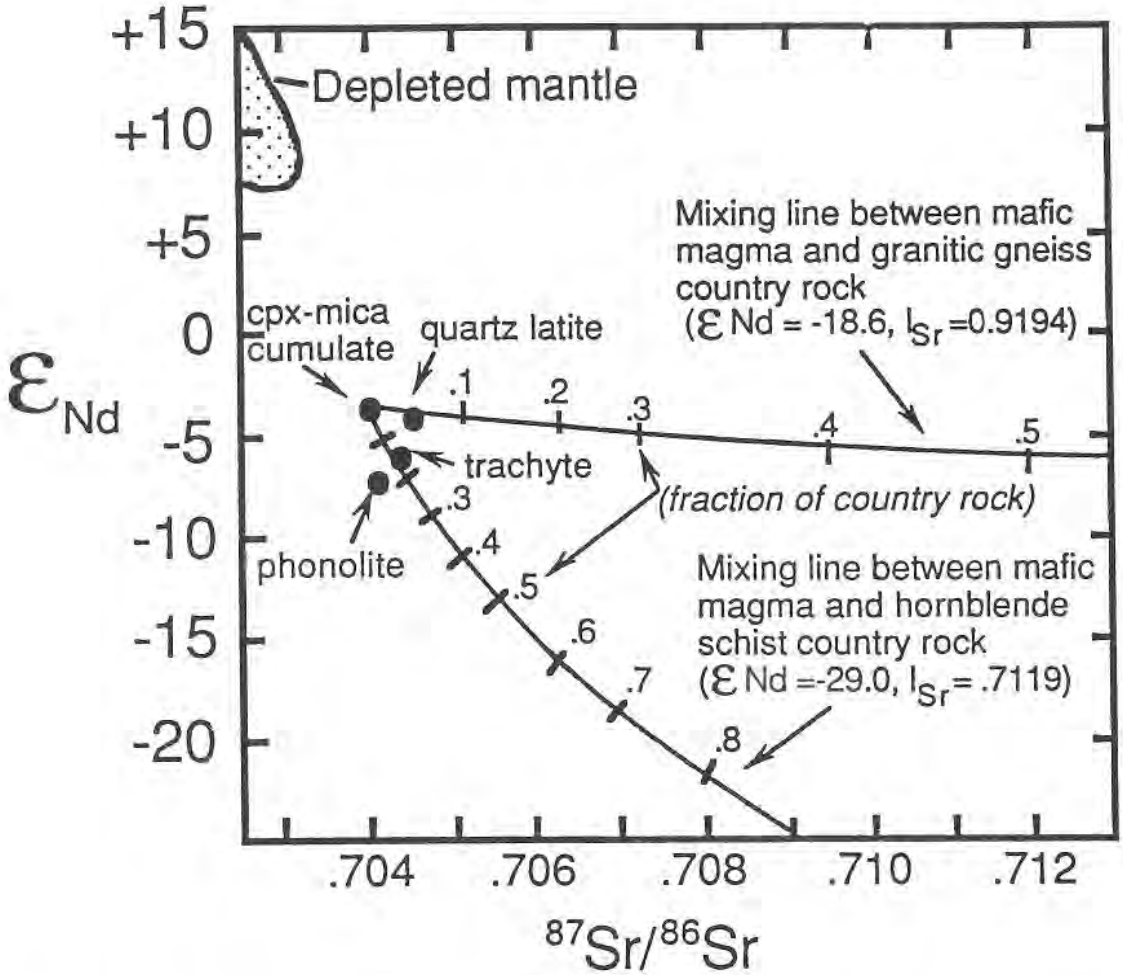

Figure 15. Simple binary mixing model for Sr and Nd isotopes. Isotopic ratios of clinopyroxene (cpx)-mica cumulate represent those of a possible RHAC parental magma. Isotopic values of Archean country rock plot off the diagram. Mixing of relatively minor amounts of country rock with parental magma could produce daughter magmas with isotopic ratios similar to those of Rattlesnake Hills rocks. [Depleted mantle data are from Frost and Snoke (1989)].

Summary

The mid-Tertiary igneous rocks of the Rattlesnake Hills are intruded near the intersection of two major Laramide structures as three distinct groups. The central alkalic group (CAG) is comprised of phonolites, trachytes, and latites, which are exposed near the axis of the Rattlesnake anticline. The eastern felsic group (EFG) is east of the CAG on the northeast limb of the anticline and consists of texturally homogeneous, coarsely porphyritic quartz latite and rhyolite. The western felsic group (WFG) is also comprised of quartz latites and rhyolites, and is situated near the North Granite Mountains fault zone, southwest of the CAG. Although the WFG rocks are chemically similar to those of the EFG, they are finer grained and texturally heterogeneous.

Many comparisons can be made between the Rattlesnake Hills intrusive rocks and the Tertiary intrusions of the southern Bear Lodge Mountains of northeastern Wyoming. Similarities include age, structural setting, and petrographic and geochemical characteristics of the alkaline rocks.

The origin of continental alkaline rock complexes such as those exposed in the Rattlesnake Hills and the Bear Lodge Mountains is unclear, but certainly bears some relationship to local structure and regional tectonics. In the Rattlesnake Hills, some constraints can be placed on the late-stage evolution of the intrusive rocks: magma mixing played an important role in the generation of the CAG and WFG rocks, but not in the EFG. Based on isotopic and geochemical characteristics, the most mafic magmas in the Rattlesnake Hills were probably not derived from a depleted mantle, but from a subcontinental mantle that had been isolated and chemically modified since Archean time. Archean country rocks in the Rattlesnake Hills appear to have made, at most, a modest contribution to the Tertiary magmas.

Acknowledgments

Many thanks go to James Myers, Susan Swapp, Art Snoke, and James Scoates for their editorial assistance. We are also extremely grateful to Chuck Sylvester and Tim Fenster of the Circle Bar Ranch, Con Murphy of the Murphy Ranch, and Norman Park of the Dumbell Ranch for their hospitality and for granting us access to the study area. This study was supported in part by National Science Foundation grants EAR-8707296 and EAR-8917354.

References cited

Bayley, R.W., Proctor, P.D., and Condie, K.C., 1973, Geology of the South Pass area, Fremont County, Wyoming: U.S. Geological Survey Professional Paper 793, 39 p.

Blackstone, D.L., Jr., 1951, An essay on the development of structural geology in Wyoming: Wyoming Geological Association 6th Annual Field Conference Guidebook, p. 16-28.

Carey, B.D., 1959, Geology of the Rattlesnake Hills Tertiary volcanic field, Natrona County, Wyoming [Ph.D. dissertation]: Laramie, University of Wyoming, 274 p.

Cross, C.W., 1897, Analyses of rocks, with a chapter on analytical methods, laboratory of the United States Geological Survey, 1880-1896: U.S. Geological Survey Bulletin 148, 306 p.

Dudás, F.Ö., and Eggler, D.H., 1989, Crazy Mountains, Montana: *in* Henshaw, P.M., editor, Volcanism and plutonism of western North America: American Geophysical Union Field Trip Guide, v. 2, p. T346:7-T346:14.

Eggler, D.H., Meen, J.K., Welt, F., Dudás, F.Ö., Furlong, K.P., McCallum, M.E., Carlson, R.W, 1988, Tectonomagmatism in the Wyoming province: Colorado School of Mines Quarterly, v. 83, no. 2, p. 25-40.

Frost, C.D., and Snoke, A.W., 1989, Tobago, West Indies, a fragment of a Mesozoic island arc: petrochemical

evidence: Journal of the Geological Society, London, v. 146, p. 953-964.

Hares, C.J., 1916, Anticlines in central Wyoming: U.S. Geological Survey Bulletin 641, p. 233-279.

Hayden, F.V., 1869, Geological report of the exploration of the Yellowstone and Missouri rivers under the direction of Captain W.F. Raynolds: 1858-1860.

Hoch, A.R., 1991, Petrological and geochemical evolution of the Rattlesnake Hills alkaline-intrusive complex, Natrona County, Wyoming [M.S. thesis]: Laramie, University of Wyoming, 150 p.

Houston, R.S., 1964, The petrographic calendar, *in* Parker, R.B., editor, Non-paleontological methods of correlation of rocks of Tertiary age in Wyoming: University of Wyoming Contributions to Geology, v. 3, no. 1, p. 15-26.

Jenner, G., 1989, Eocene igneous activity and related metasomatic and hydrothermal events, Bear Lodge Mountains, Crook County, Wyoming: *in* Karner, F.R., editor, Devil's Tower-Black Hills alkalic igneous rocks and general geology: 28th International Geological Congress Field Trip Guide T131, American Geophysical Union, p. 50-66.

King, C., 1876, Annual report upon the geological exploration of the Fortieth Parallel from the Sierra Nevada to the eastern slope of the Rocky Mountains: Washington, D.C., 6 p.

Knight, W.C., and Slossen, E.E., 1901, The Dutton, Rattlesnake, Arago, Oil Mountain and Powder River oil fields: University of Wyoming School of Mines Petroleum Series, Bulletin 4, 57 p.

Larsen, E.S., 1940, Petrographic province of central Montana: Geological Society of America Bulletin, v. 51, p. 887-948.

Love, J.D., 1970, Cenozoic geology of the Granite Mountains area, central Wyoming: U.S. Geological Survey Professional Paper 495-C, 154 p.

McKenzie, D., 1989, Some remarks on the movement of small melt fractions in the mantle: Earth and Planetary Science Letters, v. 95, p. 53-72.

Pekarek, A.H., 1974, Structural geology and volcanic petrology of the Rattlesnake Hills, Wyoming [Ph.D. dissertation]: Laramie, University of Wyoming, 113 p.

Pekarek, A.H., Marvin, R.F., and Mehnert, H.H., 1974, K-Ar ages of the volcanics in the Rattlesnake Hills, central Wyoming: Geology, v. 2, p. 283-285.

Peterman, Z.E., and Hildreth, R.A., 1978, Reconnaissance geology of the Precambrian of the Granite Mountains, Wyoming: U.S. Geological Survey Professional Paper 1055, 23 p.

Rachou, J.F., 1951, Tertiary stratigraphy of the Rattlesnake Hills, central Wyoming [M.S. thesis]: Laramie, University of Wyoming, 70 p.

Staatz, M.H., 1983, Geology and description of thorium and rare-earth deposits in the southern Bear Lodge Mountains, northeastern Wyoming: U.S. Geological Survey Professional Paper 1049-D, 52 p.

Streckeisen, A.L., 1967, Classification and nomenclature of igneous rocks: Neues Jahrbuch für Mineralogie Abhandlungen, v. 107, p. 144-240.

Stupak, W.A., 1984, The petrography and petrochemistry of the Eocene volcanics, Rattlesnake Hills, central Wyoming [M.S. thesis]: Fredericton, University of New Brunswick, 318 p.

Van Houten, F.B., 1955, Volcanic rich middle and upper Eocene sedimentary rocks northwest of Rattlesnake Hills, central Wyoming: U.S. Geological Survey Professional Paper 274-A, 14 p.

Vollmer, R., Ogden, P., Schilling, J.G., Kingsley, R.H., and Waggoner, D.G., 1984, Nd and Sr isotopes in ultrapotassic rocks from the Leucite Hills, Wyoming: Contributions to Mineralogy and Petrology, v. 87, p. 359-368.

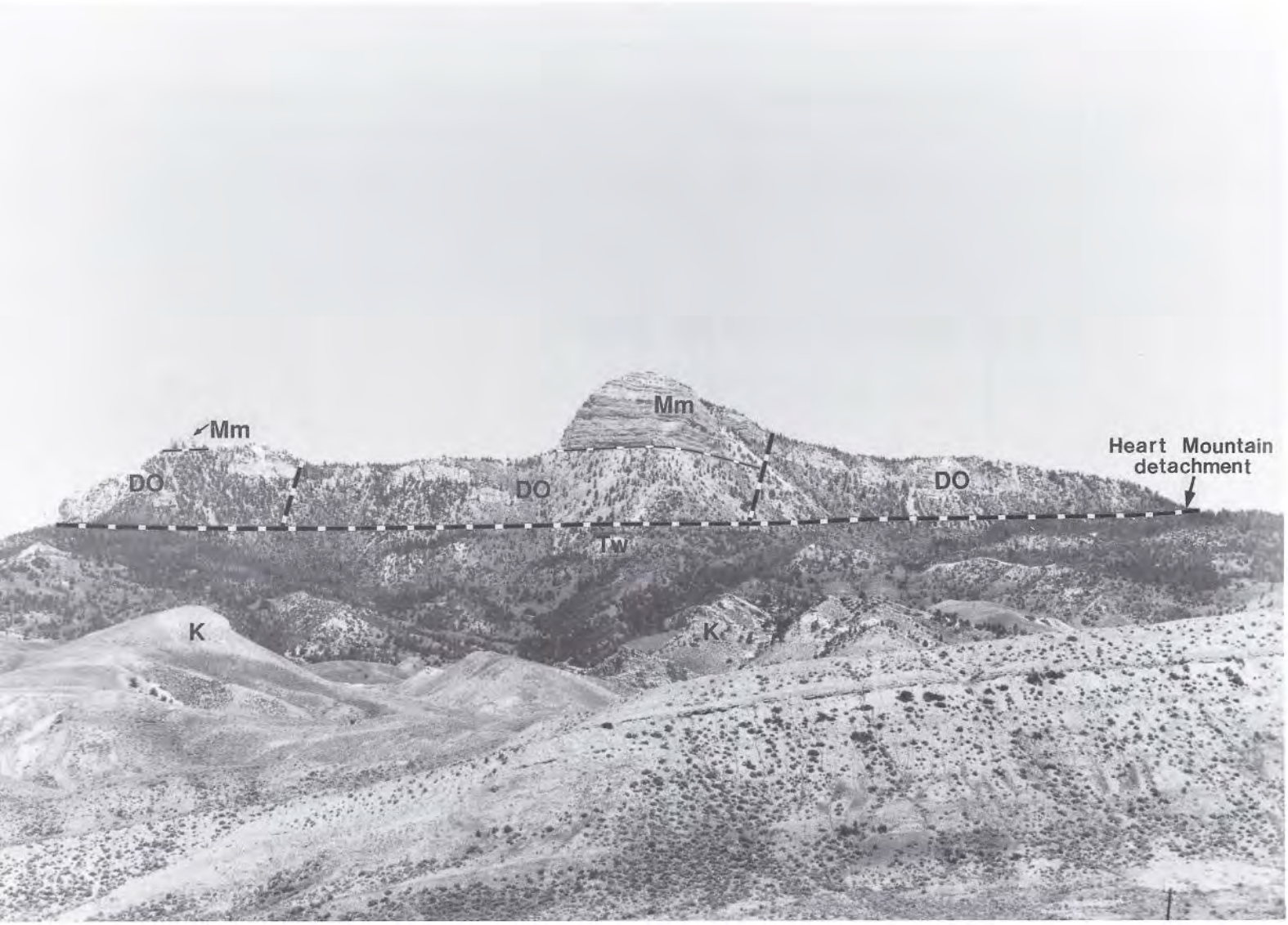

Frontispiece. View to the north of Heart Mountain, viewed from Wyoming State Highway 120 north of Cody. DO = Devonian Three Forks and Jefferson formations and Ordovician Bighorn Dolomite; Mm = Mississippian Madison Limestone; K = Cretaceous rocks; Tw = Eocene Willwood Formation. Maximum thickness of klippe is about 700 ft (215 m); length of klippe is about 1 mi (1.6 km).

The Heart Mountain detachment, northwestern Wyoming: 100 years of controversy

Thomas A. Hauge
Exxon Production Research Company
P.O. Box 2189
Houston, Texas 77252

"It is never possible to introduce only observable quantities in a theory. It is the theory which decides what can be observed." Albert Einstein (Heisenberg, 1983, p. 10)

Abstract

Despite more than 100 years of study, the Heart Mountain detachment remains among the world's most puzzling geologic structures. Its major features — an areally extensive (1,300 mi²/3,400 km²), demonstrably rootless detachment, with average dip of less than 2°; an internally extended upper plate; a breakaway defining the proximal boundary of the detachment area; younger-over-older (Tertiary and Paleozoic over Paleozoic) relationships across the detachment in its proximal portion, giving way to older-over-younger (Paleozoic over Tertiary) in the distal ("toe") portion; and tectonic transport distances of as much as 30 mi (50 km) or more— were, at the times of their discoveries (1880s to 1950s), without known analog. From the 1930s to the 1980s, relationships were attributed to emplacement at catastrophic rates of numerous detached blocks, many 1,000 ft (300 m) or more thick and one or more mi² in areal extent. The mechanisms of detachment and long-distance transport of the envisioned detached blocks were enigmatic, and in the 1960s and 1970s the Heart Mountain detachment became a focus of discussion of the mechanics of thrust faulting (and low-angle faulting in general). In the early 1980s the upper plate of the Heart Mountain detachment was reinterpreted as a continuous extensional allochthon, emplaced noncatastrophically, that included large volumes of volcanic rock previously thought to postdate faulting. The problem of the mechanics of emplacement of the upper plate may be resolved by the continuous allochthon model. However, disagreement continues as to whether the traditional detached-block model or the more recent continuous allochthon model is better supported by field relationships.

Introduction

One thousand feet (300 m) of Paleozoic strata form the steep upper slopes of Heart Mountain (**Frontispiece**), yet the surrounding lowlands of the western Bighorn Basin consist of Eocene basin-fill strata. Since the first recognition of this relationship more than 100 years ago, features associated with what became known as the Heart Mountain detachment were among the most widely known, enigmatic, and controversial structural features of North American geology. The initial controversy (1916 to 1950) focused on the apparent contradiction between "thrust" (older-over-younger) relationships across

Hauge, T.A., 1993, The Heart Mountain detachment, northwestern Wyoming: 100 years of controversy, *in* Snoke, A.W., Steidtmann, J.R., and Roberts, S.M., editors, Geology of Wyoming: Geological Survey of Wyoming Memoir No. 5, p. 530-571.

the detachment and a suite of features, such as regional setting, timing problems, and internal extension rather than contraction of the "thrust sheet," that seemed incompatible with the thrust interpretation. This controversy was resolved when the idea of a once-continuous thrust sheet was replaced by that of an upper plate that consisted of numerous mountain-size detached blocks. The detached-block model was a conceptual orphan, in that all other known allochthons were then thought to be contractional and the closest known "extensional" analogs were long-runout landslides, which deposited chaotic rubble rather than coherent detached blocks.

The second major controversy (1935 to 1982) focused on the mechanics of emplacement of mountain-size, coherent, detached blocks on the Heart Mountain detachment. This controversy appeared to be of broad importance, bearing on the mechanics of low-angle faulting in general. The detachment and rapid transport of extending detached blocks, without benefit of a "push from behind," suggested the action of undiscovered processes that reduce friction along low-angle faults. Numerous workers were attracted to this mechanical enigma, but no consensus arose regarding its resolution.

A third controversy (1935 to present; mostly post-1973) existed among field workers in the Absaroka Range regarding the volume of volcanic rocks involved in Heart Mountain faulting. For many years this third controversy seemed insignificant in the context of the mechanics problem. However, since 1982 it became of paramount importance in the development of a radically different concept of Heart Mountain faulting, which led to the fourth (and presently dominant) controversy: did the upper plate consist of numerous detached blocks, as long envisioned, or was it a continuous *extensional* allochthon (**Figure 1**)? The latter model requires involvement of large volumes of volcanic rocks in faulting. This most recent controversy bears strongly on the issue of mechanics: the continuous allochthon model allows non-catastrophic emplacement of the allochthon and may be addressed with Coulomb-wedge concepts like those applied to thrust-sheet emplacement.

This review of the Heart Mountain detachment problem begins with a description of field relationships, followed by a history of the development of concepts of Heart Mountain faulting, an overview of the present state of controversy, and a suggestion as to how the most recent controversy may be resolved.

General Features

Scale, tectonic setting, and age

The Heart Mountain detachment is a rootless low-angle normal fault that accommodated transport of upper-plate rocks for distances of up to 30 mi (50 km) or more (**Sheet 1**, Hauge, map pocket). Transport was largely southeastward, from the northeast flank of the northern Absaroka Range, a Laramide basement uplift and volcanic center, into the western margin of the Laramide Bighorn Basin. The detachment and overlying allochthonous rocks are well preserved in the Absaroka Range, with excellent exposure along the steep-sided glacial valleys of the Clarks Fork of the Yellowstone River, the Shoshone River, and their tributaries. In contrast, in the Bighorn Basin Neogene erosion has left only a few remnants of the detachment and allochthonous rocks. The detachment is preserved over an area of at least 1,300 mi^2 (3,400 km^2), although it probably covered a somewhat larger area of the Bighorn Basin before erosion.

Based on its relationship to Eocene sedimentary and volcanic rocks, the Heart Mountain allochthon is interpreted to have been emplaced during the late stages of the Laramide orogeny. Allochthonous Paleozoic rocks at Heart Mountain and McCulloch Peak overlie nonmarine lower Eocene (Wasatchian) Willwood strata, indicating that emplacement of the allochthon postdated most of the Laramide fill of the Bighorn Basin. Thus, most of the offset across the basement-involved fault zone that defines the boundary between the Bighorn Basin and adjacent uplifts to the west had taken place by the time of Heart Mountain faulting. Wise (1983) has shown that the north-trending portion of this fault zone postdated northwest-trending structures along the Beartooth range front, and he inferred that the north-

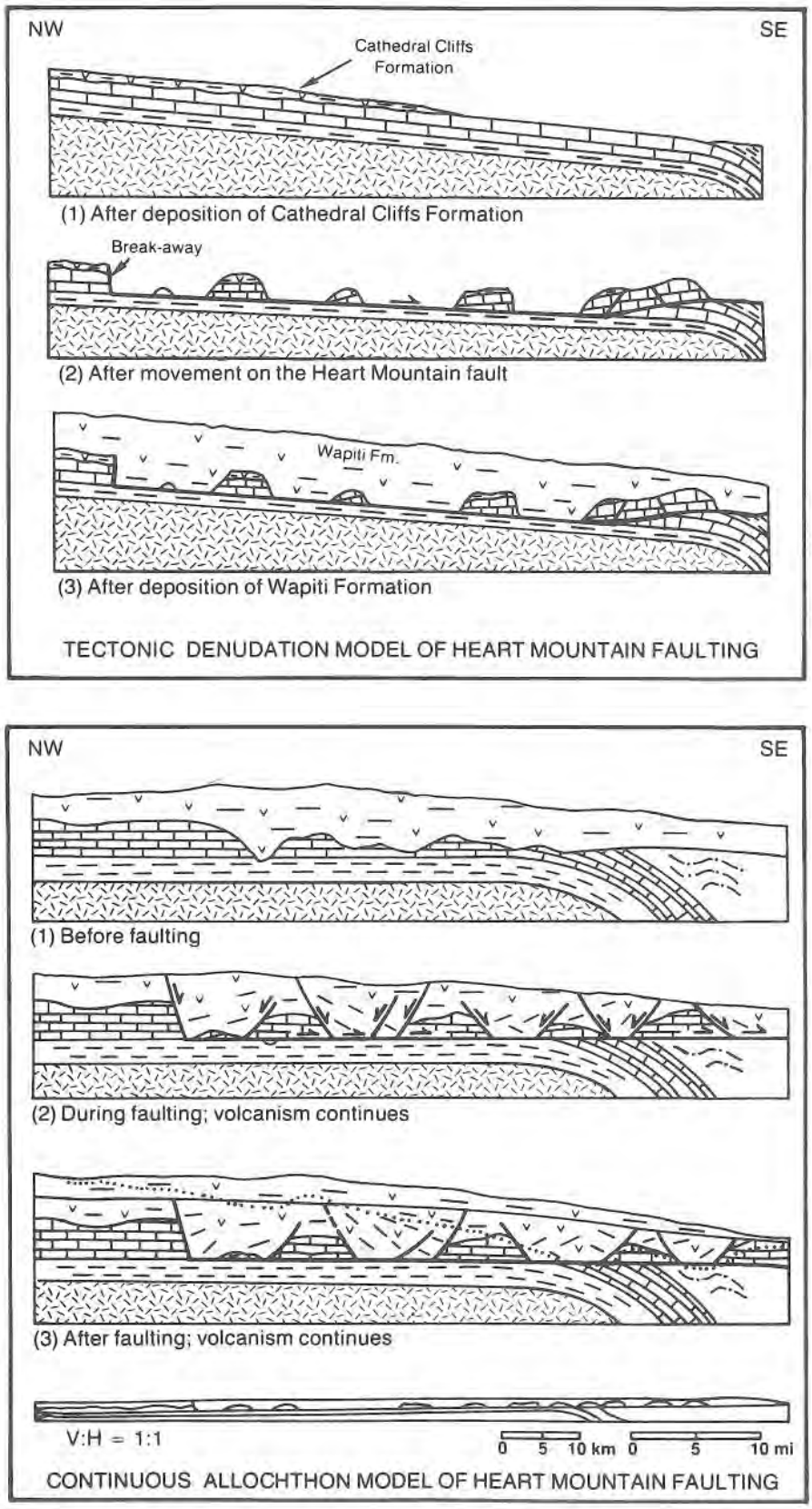

Figure 1. Two models of Heart Mountain faulting.:
a. The tectonic denudation model, modified from Pierce (1960). (1) Before faulting occurred, volcanic rocks (Cathedral Cliffs Formation) locally overlay Paleozoic strata. (2) When the detachment formed, Paleozoic strata and overlying volcanic rocks detached along a basal Ordovician bedding plane and were emplaced at catastrophic rates as numerous detached blocks along the bedding-plane detachment, up a transgressive ramp, and across the Eocene land surface. (3) Immediately after faulting, catastrophic volcanism (Wapiti Formation) blanketed the disrupted terrane.
b. The continuous allochthon model, modified from Hauge (1985). (1) Before faulting occurred, volcanic rocks 0.6 mi (1 km) or more thick overlay deeply eroded Paleozoic strata and younger strata to the southeast. (2) When the detachment formed, Paleozoic strata above the detachment and overlying volcanic rocks underwent lateral translation and extension as a continuous allochthon, and structurally high (largely volcanic) rocks were downfaulted, tilted, and translated. Displacement was noncatastrophic [0.4 in (1 cm) per year?] and coeval with volcanism (feeders out of plane of the section). (3) After faulting ceased, volcanism continued. Dotted line is present erosion surface.
Patterns: random dash = Precambrian basement; dash = Cambrian shale; brick = Ordovician to Mississippian sedimentary rocks, largely carbonate; dot-dash = late Paleozoic and younger sedimentary rocks; dash-v = Eocene volcanic rocks.

west-trending boundary between the Absaroka Range and the Beartooth Mountains was also probably an earlier Laramide structure. Thus, development of the presently observed basement framework of Laramide structures in the detachment area was essentially complete when Heart Mountain faulting occurred, and little subsequent tectonic deformation has affected the region.

Further constraints on the age of Heart Mountain faulting are provided by relationships west of Buffalo Bill Reservoir, where allochthonous Paleozoic rocks overlie middle Eocene strata (Bridgerian Aycross Formation), indicating emplacement of the allochthonous rocks in this area as middle Eocene or younger (Torres and Gingerich, 1983). A middle Eocene upper age limit for Heart Mountain faulting is also indicated by the Bridgerian age of volcanic rocks overlying the allochthonous Paleozoic rocks at this locality (Torres and Gingerich, 1983). These Bridgerian rocks are assigned to the Wapiti Formation and Trout Peak Trachyandesite (Pierce and Nelson, 1968). The Wapiti Formation and Trout Peak Trachyandesite have been interpreted as postdating Heart Mountain faulting (Pierce, 1987a), which would indicate that faulting was wholly Bridgerian (pre-Wapiti) in age. Alternatively, rocks assigned to the Wapiti Formation have been interpreted as allochthonous (Hauge, 1985), and the Trout Peak Trachyandesite, which locally comprises the hanging wall of the breakaway fault and the Black Mountain fault (**Sheet 1**, Hauge, map pocket), has been interpreted as involved in the final phases of Heart Mountain faulting (Hauge, 1990). This alternative interpretation suggests that Heart Mountain faulting was complete slightly later in the Bridgerian (after Trout Peak Trachyandesite time). By either interpretation, Heart Mountain faulting may have been wholly Bridgerian (47.5 to 49.5 Ma; Torres and Gingerich, 1983), though earlier minor movements (Pierce and Nelson, 1973) are not precluded by the data.

Composition and general character of the allochthon

Heart Mountain faulting involved rocks ranging in age from Ordovician to middle Eocene (**Figure 2**). The most conspicuously allochthonous rocks are the Paleozoic cratonic strata, which underlie the steep upper slopes of Heart Mountain and form bold cliffs up to 1,300 ft (400 m) high along the Clarks Fork valley. These rocks are Ordovician dolomite and dolomitic limestone; Devonian dolomite, limestone, siltstone, and shale; and Mississippian limestone, which are locally tilted and offset across upper-plate normal faults. Exposures of these strata are up to a mile or more (several kilometers) wide and are separated by areas a mile or more wide that are underlain by volcanic rocks (**Sheet 1**, Hauge, map pocket). The distances separating the masses of allochthonous Paleozoic rocks exposed along the Clarks Fork valley are an indication of the amount of extension that characterizes the allochthon. Less obviously allochthonous, but perhaps comprising a greater volume of the allochthon, are the largely andesitic Eocene volcanic breccias, tuffs, volcanic sediments, and lava flows that lie between and upon the masses of allochthonous Paleozoic rocks. These volcanic rocks commonly lack the apparent tabular stratification and lateral continuity of the Paleozoic cratonic strata, and stratification in the volcanic breccias, which comprise most of these volcanic rocks, is typically difficult to discern. As a result, distinction between primary fabric elements in the volcanic rocks and those that indicate deformation during Heart Mountain faulting is difficult in many areas, and for many years no volcanic rocks were recognized as allochthonous. Recent workers differ widely on how large a volume of volcanic rocks they interpret as involved in faulting (**Figures 1** and **2**; **Sheet 1**, Hauge, map pocket). In addition, non-volcanic Eocene (?) fluvial conglomerate comprises a minor component of the allochthon. Another possible minor component of the preserved allochthon is allochthonous Willwood Formation which overlies in situ Willwood along the Clarks Fork River in the Bighorn Basin (**Sheet 1**, Hauge, map pocket). These masses of allochthonous Willwood have been interpreted as slide blocks derived from the Beartooth Mountains (Wise, 1957), but it is possible that they are klippen of the Heart Mountain allochthon.

Components of the detachment

Breakaway fault

The Heart Mountain fault can be subdivided into three components (**Figure 1**; **Sheet 1**, Hauge, map pocket). The first is the breakaway fault, which forms the western boundary of the detachment area. It is spectacularly exposed across 2,100 ft (650 m) of relief near the northeast entrance to Yellowstone National Park 1.25 mi (2 km) west of Silver Gate, Mon-

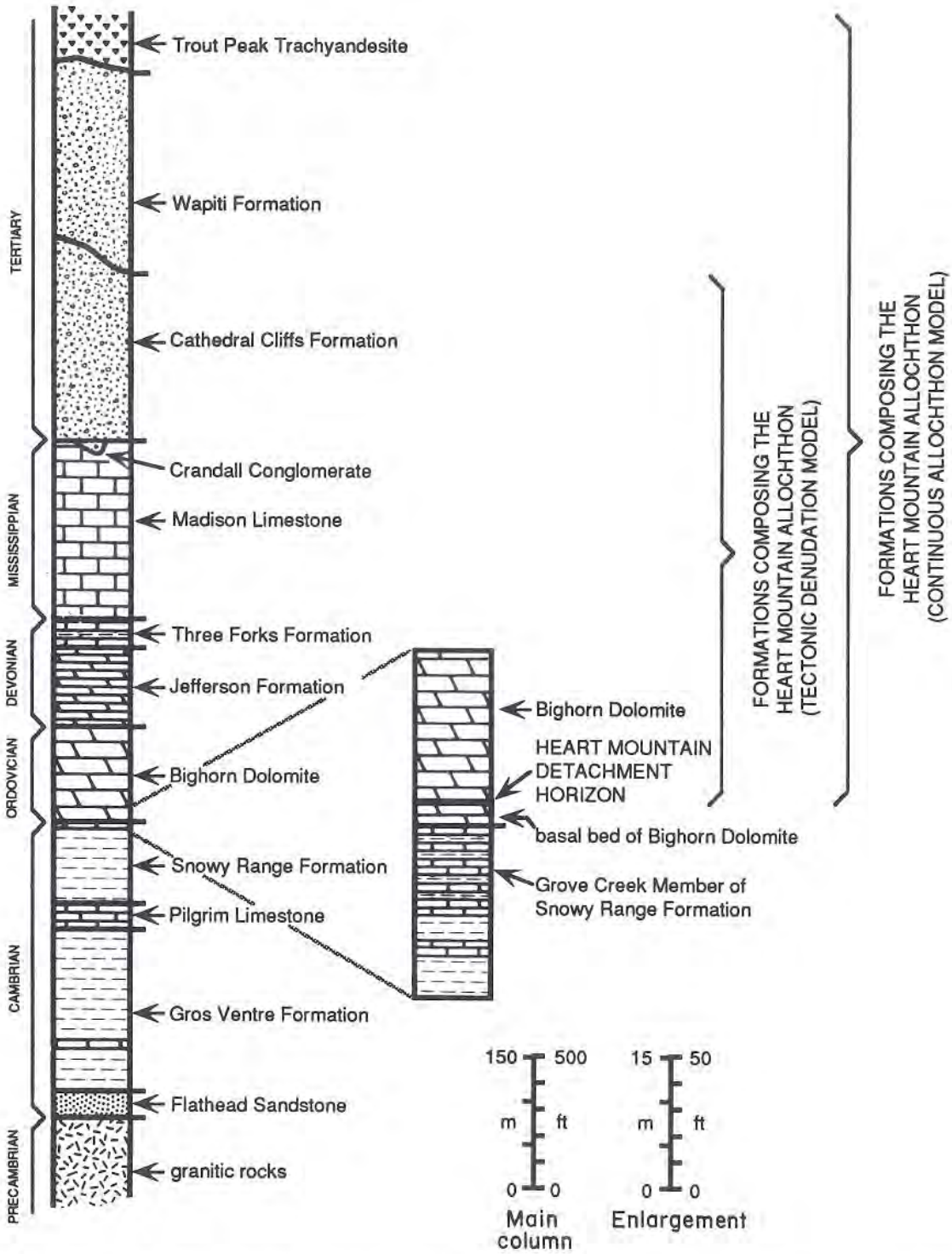

Figure 2. Generalized stratigraphic section showing the formations associated with the Heart Mountain detachment, modified from Pierce (1973). Use of the terms Wapiti Formation, Cathedral Cliffs Formation, and Lamar River Formation in the detachment area has proven problematic (see text). Crandall Conglomerate, of Eocene (?) age (Pierce and Nelson, 1973), overlies units as old as the Snowy Range Formation.

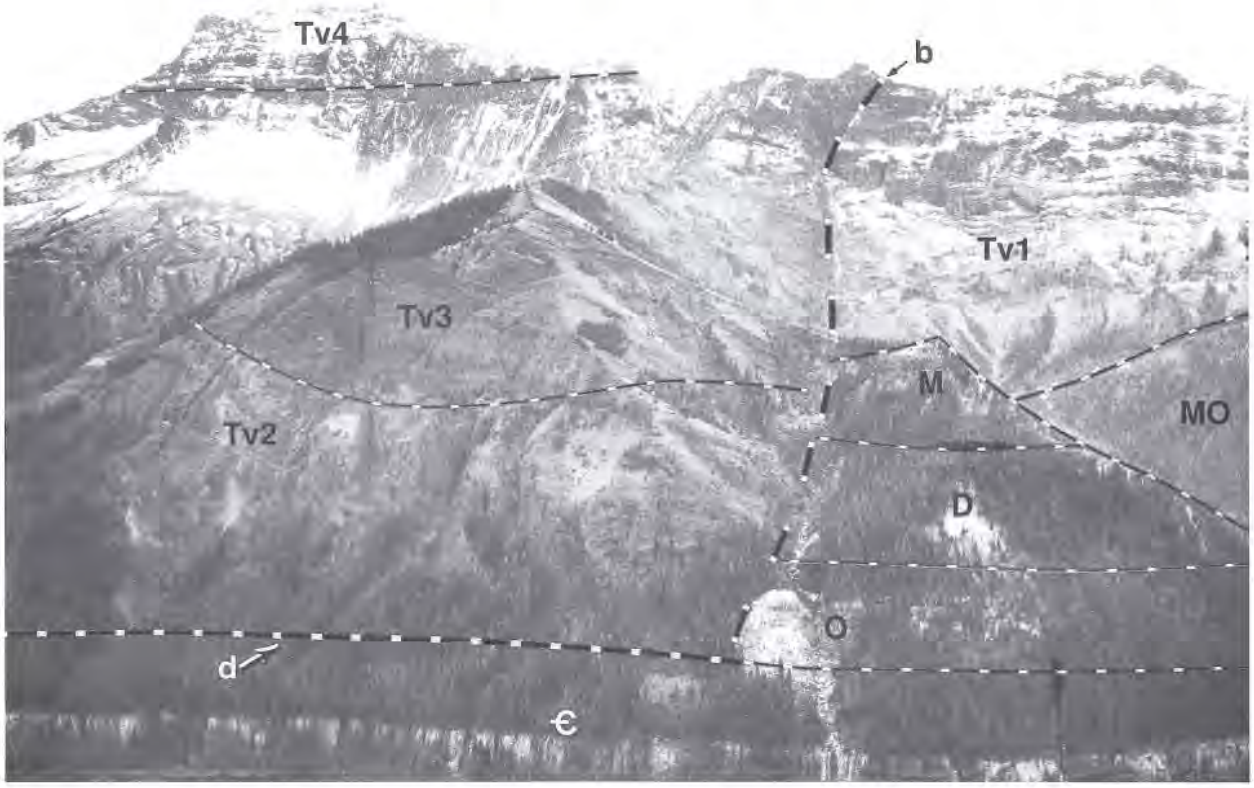

Figure 3. View to south of breakaway of the Heart Mountain detachment. Viewpoint is about 1 mi (1.6 km) north of and 2,000 ft (600 m) higher than the northeast entrance to Yellowstone National Park. The breakaway (b) dips steeply (about 70°) eastward and truncates downward at the detachment (d). Rocks visible in the footwall of the detachment (€) are Pilgrim Limestone (cliff near base of photo), about 80 ft (25 m) thick, and overlying shale and limestone of the Snowy Range Formation, about 240 ft (75 m) thick. About 6 ft (2 m) of Ordovician Bighorn Dolomite, not shown, immediately underlies the detachment. The footwall of the breakaway consists of about 300 ft (90 m) of Bighorn Dolomite (O), 300 ft (90 m) of Devonian Three Forks and Jefferson formations (D), 240 ft (75 m) of Mississippian Madison Limestone (M), and about 1,300 ft (400 m) of Eocene volcanic rocks, partly snow-covered, of the Lamar River and Cathedral Cliffs formations (Tv1). The hanging wall consists of a basal 600 ft (180 m) of Eocene volcanic rocks (Tv2) variably assigned to the Lamar River Formation (Prostka and others, 1975), Lamar River and Cathedral Cliffs formations (Pierce and others, 1973), and the Wapiti Formation (Pierce, 1980), overlain by about 1500 ft (450 m) of Eocene volcanic rocks (Tv3) assigned to the Wapiti Formation by these workers. The topographically highest volcanic rocks (Tv4), with apparent subhorizontal bedding, are Wapiti Formation and Trout Peak Trachyandesite (Pierce and others, 1973; Prostka and others, 1975); these strata overlap the breakaway out of view to the southeast (figure 6 of Pierce, 1980) and therefore postdate Heart Mountain faulting. Note apparent southwestward dips of Tv2, evident above "Tv2" annotation. Disagreement exists as to whether the upper-plate rocks were tectonically emplaced (Hauge, 1990) or were deposited on the detachment and breakaway (Pierce, 1987a) (see text).

tana (**Figure 3**). There, it dips 70° east and cuts steeply down through Eocene volcanic rocks and Mississippian, Devonian, and Ordovician sedimentary rocks in its footwall, ending near the base of the Ordovician at the detachment. The hanging wall consists of Eocene volcanic rocks. Pierce (1960a) coined the term "break-away" for this feature, and the term has subsequently come into general use (with the hyphen omitted) for analogous features associated with rooted low-angle normal faults (e.g., Wernicke, 1985).

In other areas, due to limited vertical exposure and difficult access, the trace and cross-sectional geometry of the breakaway are less well known. Pierce (1980) mapped its trace as 23 mi (37 km) long, from 6 mi (10 km) north of the Montana-Wyoming border, where it is removed by erosion, to 17 mi (27 km) south of that border, where Pierce (1980) interpreted it to be overlapped and concealed by volcanic rocks, although other interpretations differ (cf., Pierce and others, 1973; Pierce, 1978; Nelson and others, 1980). In Wyoming, one exposure documents a ramp-flat

breakaway geometry within volcanic rocks (figure 6 of Pierce, 1980), and at this locality volcanic rocks dip steeply toward the breakaway, compatible with a kinematic model of tilting of hanging-wall strata toward a listric normal fault. The breakaway may connect with the Black Mountain fault (**Sheet 1**, Hauge, map pocket), as first suggested by Voight (1974a).

Pierce (1960a, 1980) interpreted the breakaway as having been tectonically denuded and interpreted the volcanic rocks overlying it as Wapiti Formation that was deposited on the denuded surface of the breakaway. He described the breakaway fault as a *"half-fault," for only one side* [the footwall side] *is a fault surface; the other side* [the hanging-wall side] *is a surface of deposition* (Pierce, 1980, p. 276). In contrast, the hanging-wall volcanic rocks have been interpreted as in part (Prostka and others, 1975) or wholly (Hauge, 1982, 1985, 1990) allochthonous. This difference in interpretation bears directly on how the relationship between the breakaway and Black Mountain faults is interpreted. Pierce (1980, p. 279) interpreted them as different faults, in part because the Black Mountain fault offsets volcanic rocks that Pierce (1980) interpreted as younger than Heart Mountain faulting. Mapping of the Black Mountain fault in the Shoshone River valley (Pierce and Nelson, 1968) suggests that it may offset the Heart Mountain detachment and therefore is younger than the breakaway. The interpretation that the two faults are segments of the same fault is acceptable if the Wapiti Formation overlying the breakaway is allochthonous and the interpreted offset of the detachment by the Black Mountain fault is incorrect.

Bedding-parallel component

The second component is the portion of the basal detachment that parallels bedding in the homoclinal Paleozoic section of the northeastern Absaroka Range. This is the "bedding thrust" of Pierce (1957) and the "bedding plane fault" of Pierce (1973). The bedding-parallel component of the detachment lies along a bedding plane located about 6 ft (2 m) above the base of the Ordovician section. This stratigraphic position is remarkable from the perspective of rock mechanics, as discussed by Pierce (1973), because the detachment lies along a bedding plane within "strong" dolomite rather than within the thick, "weak" Cambrian shales that underlie it by only a few meters. In this sense it is comparable to *'strong décollement' foreland thrusts* described by Burchfiel and others (1982). The detachment does not cut below this stratigraphic horizon, and upper-plate units are no older than Ordovician and younger, indicating that the detachment is rootless. [Hauge (1983, p. 121) reported a small exposure of 50 ft (15 m) of Cambrian Snowy Range Formation above the detachment north of the mouth of Pilot Creek. This indicates that the detachment ramps down into the Cambrian section in at least one area where it is concealed, but such a relationship is exceptional.] The bedding-parallel component of the detachment is bounded to the west by the breakaway, to the northeast by erosion, to the southeast by a footwall ramp, and, perhaps, to the southwest, by the Black Mountain fault (**Sheet 1**, Hauge, map pocket) The southwestern boundary is not known with confidence, due to thick volcanic cover. The pre-erosional northeastern boundary may have coincided with the Clarks Fork fault (Voight, 1974b). The bedding-parallel component of the detachment presently dips an average of 3 to 5° to the south-southwest (Pierce, 1985), although an overall 2° southeastward dip, parallel to the dominant transport direction, has been inferred for the time of its activity (Pierce, 1973).

The bedding-parallel component of the detachment is well exposed along the Clarks Fork valley, in Sunlight Basin, and in the drainage of Dead Indian Creek. The autochthon in this area exhibits little deformation either related to or subsequent to faulting, in contrast to the allochthon, which was strongly extended during Heart Mountain faulting. Allochthonous Paleozoic rocks include 1300-ft (400-m)-thick untilted sections with little section missing along the detachment (**Figure 4**); sections tilted up to 30° or more with strata truncating downward at the detachment (**Figure 5**); and local exposures where Ordovician and Devonian strata are omitted along the detachment, without significant angular discordance. Multiple detachment levels at the breakaway or within the allochthon may explain the local omissions of section at the base of the allochthon.

Volcanic rocks lie between and upon the masses of allochthonous Paleozoic strata (**Figures 4** and **6**), but disagreements exist as to the involvement of these rocks in faulting. Some workers argue that in most areas the contact between volcanic rocks and the detachment is a "half fault" (Pierce, 1980), the volcanic rocks having been deposited upon the detachment after it had been tectonically denuded (Pierce, 1987a). Others infer the contact is in many

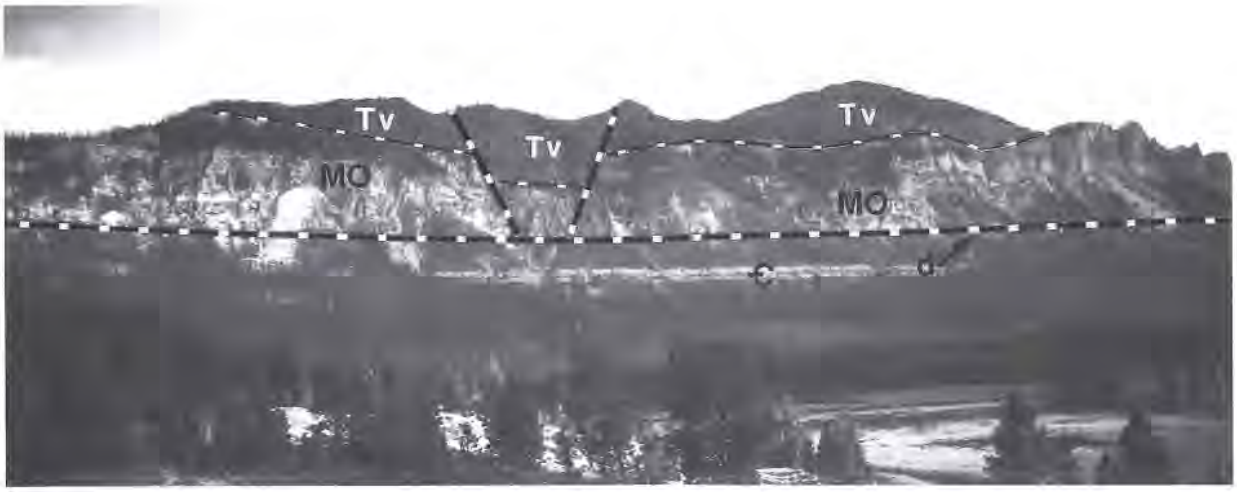

Figure 4. Photograph of Cathedral Cliffs, looking south from Wyoming State Highway 296. The allochthonous Paleozoic rocks (MO), largely untilted despite several kilometers of transport, are overlain by Eocene volcanic rocks (Tv) along a contact that is locally a well exposed upper-plate fault (figure 46 of Hauge, 1983). Numerous subvertical igneous dikes intrude the allochthon (not apparent at this distance) and die out downward at or above the detachment. The detachment (d) parallels strata in the footwall (Є); prominent cliff in the footwall is the Pilgrim Limestone, about 300 ft (90 m) below the detachment. Width of view is about 2 mi (3.2 km).

areas (Prostka, 1978) or everywhere (Hauge, 1982, 1985, 1990) tectonic. This is the essence of the present controversy between the tectonic denudation and continuous allochthon models of Heart Mountain faulting.

Detachment ramp

The third component of the detachment is a footwall ramp that, in general terms, cuts up-section to the southeast, from the bedding-parallel component of the detachment near the base of the Ordovician up to the middle Eocene (**Sheet 1**, Hauge, map pocket). Whereas the footwall of the bedding-parallel component of the detachment is a structurally simple homocline, the footwall of the detachment ramp is the structurally complex transition from the Absaroka Range to the Bighorn Basin, and the configuration of the detachment ramp reflects this footwall structure. The detachment ramp climbs abruptly in elevation eastward from ~6,600 ft (2,000 m) at the eastern margin of the bedding-parallel component to elevations of ~8,000 ft (2,400 m) to ~9,600 ft (2,900 m) atop Dead Indian Hill, Pat O'Hara Mountain, and Rattlesnake Mountain (the "Cody arch" of Sundell, 1990), as it climbs stratigraphically through the footwall Paleozoic section. From there it drops in elevation to ~7,400 ft (2,200 m) at Heart Mountain and ~6,400 ft (1,900 m) at McCulloch Peak, as it continues its stratigraphic climb through the Mesozoic and Eocene section of the Bighorn Basin (Pierce, 1985). Pierce (1957, 1960a, 1985) subdivided the detachment ramp into (1) a "shear thrust" (1957) or "transgressive fault" (1960a), where it climbs abruptly in elevation to the top of Dead Indian Hill, and (2) an "erosion thrust" (1957; after Hewett, 1920) or "fault on former land surface" (1960a) from Dead Indian Hill eastward. The 1-to-3-mi (3-to-5-km)-wide "transgressive fault" dips about 10° westward; the "fault on former land surface," up to 30 mi (48 km) wide, dips an average of 1° (and locally up to 4°) eastward.

The terms "transgressive fault" and "fault on former land surface" are avoided in the present discussion because, although it is probable that the toe of the Heart Mountain allochthon overrode the Eocene land surface, it is also likely that in much of the area of the "fault on former land surface" the detachment was within Eocene or older strata rather than on the land surface. No direct evidence of the allochthon having overridden its own debris has been described to constrain the location of a "former land surface". As a result, the descriptive term "detachment ramp" is used here in preference to the earlier more interpretative terms "transgressive fault" and "fault on former land surface," for which specific areas are connoted (Pierce, 1960a). The term "detachment ramp" is descriptively accurate with respect to both the "fault on former land surface"

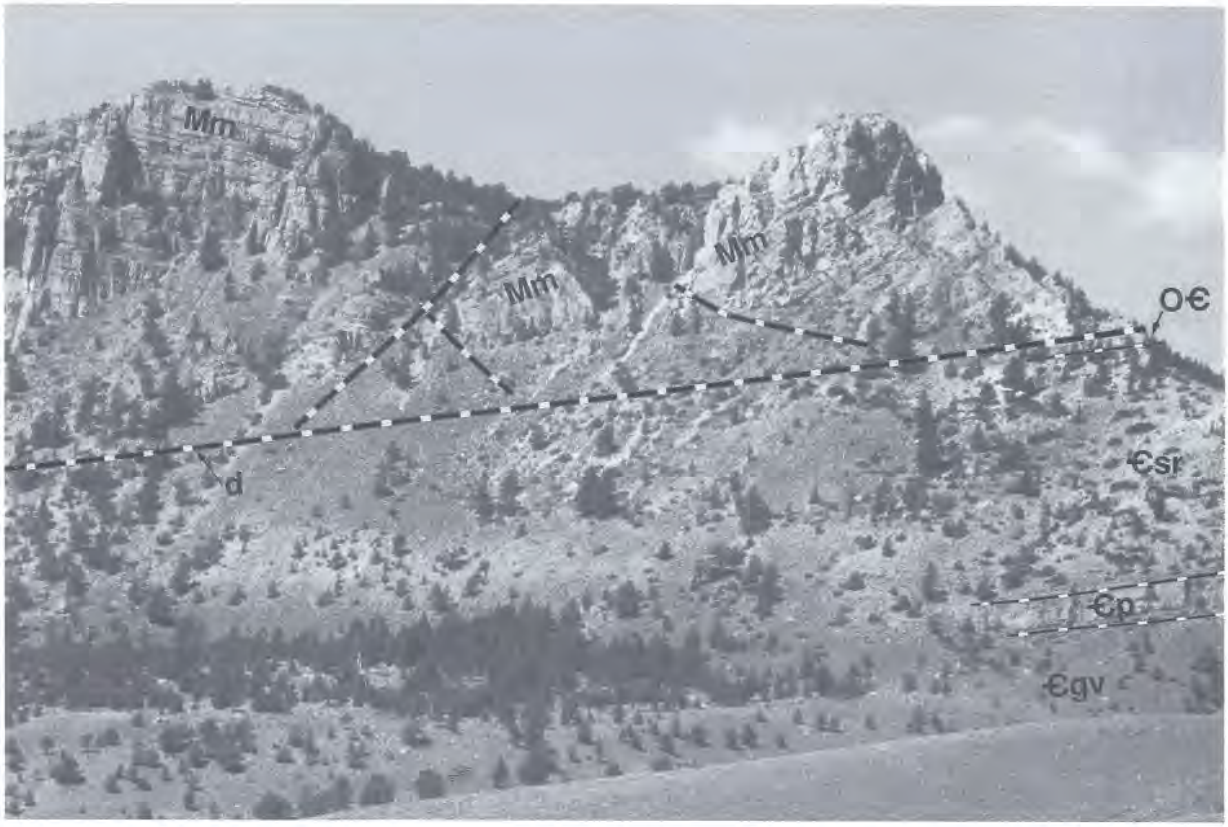

Figure 5. View to the west of the north end of Steamboat, from Wyoming State Highway 296 near Dead Indian Creek. Allochthonous Paleozoic strata, mostly Madison Limestone (Mm) are tilted to dips as steep as 30° across upper-plate faults. The detachment (d) parallels footwall strata, which dip about 7° south (to the left) and consist of: a 30 ft (10 m) cliff underlain by the basal 6 ft (2 m) of Bighorn Dolomite and uppermost limestone of the Snowy Range Formation (O€); the recessive shales of the Snowy Range Formation (€sr); the cliff-forming Pilgrim Limestone (€p); and shale and limestone of the Gros Ventre Formation (€gv). Transport across the detachment at this locality is inferred to be in excess of 6 miles (10 km).

and the "transgressive fault," because the detachment cuts up-section southeastward throughout its preserved extent. In the Bighorn Basin, footwall strata at McCulloch Peak, the most distal klippen, are younger than those at Heart Mountain [Wasatchian Wa_6 and Wasatchian Wa_{3-5} biostratigraphic zones, respectively (Gingerich, 1983)]. In the Shoshone River drainage, rocks as young as Bridgerian Aycross Formation underlie the allochthon.

The interpretation of the detachment having been below rather than upon the land surface in much of its distal area carries implications for the composition of the allochthon in this area. If the detachment was within Eocene and older strata rather than on the land surface throughout its preserved area, rocks of the entire post-Mississippian to pre-Eocene stratigraphic column of the Bighorn Basin may have been incorporated into the allochthon in the Bighorn Basin, depending upon where the detachment reached the land surface. However, erosion below the horizon of the detachment in most of this area has removed any direct evidence of such allochthonous rocks, if they existed. On the other hand, if the allochthon overrode the land surface where it presently overlies Mesozoic and Eocene strata, few of these Mesozoic and Eocene rocks need have been incorporated into the upper plate. The latter model has implications for the depositional history of the Willwood and Aycross formations, because it requires that both Willwood and Aycross formations, ranging in age from Wasatchian Wa_{3-5} to Bridgerian, were exposed at the time of Heart Mountain faulting. A third possibility

Figure 6. View to northeast of part of the east side of Painter Gulch. Volcanic strata (Tv) are tilted toward the listric fault and downfaulted to the detachment horizon (d), with complete mismatch of preserved section across the listric fault zone. Volcanic rocks are variably ascribed to the Wapiti Formation (Pierce and Nelson, 1971; Pierce, 1978), Lamar River Formation (Prostka, 1978), and Cathedral Cliffs Formation (Pierce, 1987a). Detachment is not exposed.

is that the toe of the detachment did not reach the land surface, but instead terminated as a contractional blind thrust. Any of a number of variations of these hypotheses is consistent with the few klippen that are preserved in the area of the detachment ramp.

Dip of the detachment

The present dip of the detachment is about 2° southwestward in the bedding-parallel component and variable, including westward dips of up to 10°, in the ramp component. The dip of the detachment at the time of faulting, however, is uncertain. Pierce (1973, 1985) suggested that the dip of the detachment, including the bedding-parallel and ramp components, was to the southeast at the time of faulting. He argued that the overall dip was less than 2°, based on the distance between, and inferred paleoelevations of, the breakaway and the most distal remnants of the allochthon. Pierce noted that the "transgressive phase" of the detachment presently dips about 10° northwest, opposite the direction of transport in this area, but that its dip may have been less during Heart Mountain faulting.

Deformation of the lower plate

Lower-plate rocks appear to have undergone only minor deformation during Heart Mountain faulting. Minor deformation in the footwall of the breakaway is visible in the exposure shown in **Figure 3**, where minor faults offset autochthonous volcanic strata by a few to perhaps ten or more meters. These offsets are small in comparison to the total mismatch of section across the breakaway, which at this locality is exposed across 2,100 ft (650 m) of topographic relief. Elsewhere the breakaway is not as well exposed, and no footwall deformation in these areas has been reported.

Along the bedding-plane portion of the detachment, the footwall is remarkable in most areas for its apparent lack of deformation, except for regional uplift and inferred tilting to gentle (typically less than 10°) south to southwestward dips. Only a few examples of footwall deformation have been cited: a few andesite dikes (Hauge, 1983, p. 100, 121, 142) and a minor fold (Hauge, 1983, p. 149) that predate cessation of faulting; apparently syntectonic local minor shattering and minor faults with offsets of about an inch (a few cm) within about an inch of the detachment (Hauge, 1983, p. 134, 138); and two faults, one south of Silver Gate, Montana (Elliott, 1979) and the other north of the mouth of Sunlight Creek (Pierce, 1965b), that offset the detachment about 50 to 100 ft (15 to 30 m) and postdate Heart Mountain faulting. In most areas no deformation of the footwall is evident. A prominent exception is folding and minor thrusting of the footwall that is associated with the Crandall Conglomerate (Pierce and Nelson, 1973; Hauge, 1990), and predates the cessation of Heart Mountain faulting. The Crandall Conglomerate and associated features are briefly described in a subsequent section.

Along the detachment ramp, exposures of the detachment are poor and little footwall deformation has been reported in the literature. In this area, footwall deformation is attributed to folding associated with Laramide basement-involved thrusting (Wise, 1983). Minor shearing of pebbles in Willwood strata of the footwall at Heart Mountain was reported by Stevens (1938), but Pierce (1941) described this as a local feature. In light of tectonic transport of as much as 30 mi (50 km) across it, the footwall of the Heart Mountain detachment is remarkably little deformed.

Deformation of the upper plate

Magnitude of extension

In contrast to the rocks of the lower plate, which are in most places virtually undeformed, the rocks of the upper plate range from little deformed to highly deformed, having undergone varying degrees of extension by faulting, stratal tilting, and igneous intrusion, accompanied by shearing and brecciation of the base of the allochthon. These features are well preserved and well exposed above the bedding-parallel component of the detachment at several locations in the Clarks Fork valley. Before faulting, the strata above the detachment horizon in this area consisted of an essentially unfaulted homocline of Ordovician, Devonian, and Mississippian strata up to 1,300 ft (400 m) thick. The homocline had been dissected by a few stream channels that cut as deeply as the Cambrian and were filled with non-volcanic Eocene (?) or older conglomerate and was overlain by Eocene volcanic rocks (**Figure 1**). [Pierce and Nelson (1973) inferred that these stream channels developed due to an early minor phase of Heart Mountain faulting, rather than having predated Heart Mountain faulting.] The extreme extension experienced by the upper plate during Heart Mountain faulting is most apparent from the large separation of masses of allochthonous Paleozoic strata in this area (**Sheet 1**, Hauge, map pocket). Presently, less than half of the exposed trace of the detachment is overlain by Paleozoic strata; the rest is overlain by Eocene volcanic rocks. Regardless of whether the volcanic rocks are viewed as largely younger than faulting or syntectonic and involved in faulting, the present distribution of Paleozoic rocks represents upper-plate extension of 100% to 200% or more (based on **Figure 4** of Pierce and Nelson, 1986). If volcanism was ongoing with extension, as suggested by Hauge (1985, 1990), the amount of extension of syntectonic strata would presumably decrease for progressively younger Eocene units within the allochthon.

Faults and tilted strata

Extension of the allochthon was accommodated by normal and normal-oblique faulting (Hauge, 1985), stratal tilting, and, in the view of the continuous allochthon model, extensive downfaulting of pretectonic and syntectonic volcanic rocks. The upper-plate faults that accommodate the extension are apparent within allochthonous Paleozoic rocks (**Figure 5**), within allochthonous Eocene volcanic rocks (**Figure 6**), and at contacts between allochthonous Paleozoic and Eocene rocks (**Figure 7**). Tilted strata typically comprise the hanging walls of upper-plate normal faults and dip toward the faults, as is locally apparent in Paleozoic strata (**Figure 5**) and in Eocene volcanic rocks where stratification is evident (**Figure 6**). Gently dipping strata are more typical of the footwalls of upper-plate normal faults which, in the better exposed lower parts of the allochthon, typically consist of Paleozoic strata; these rocks were translated along the detachment without appreciable tilting. Locally, gently tilted Mississippian (Pierce

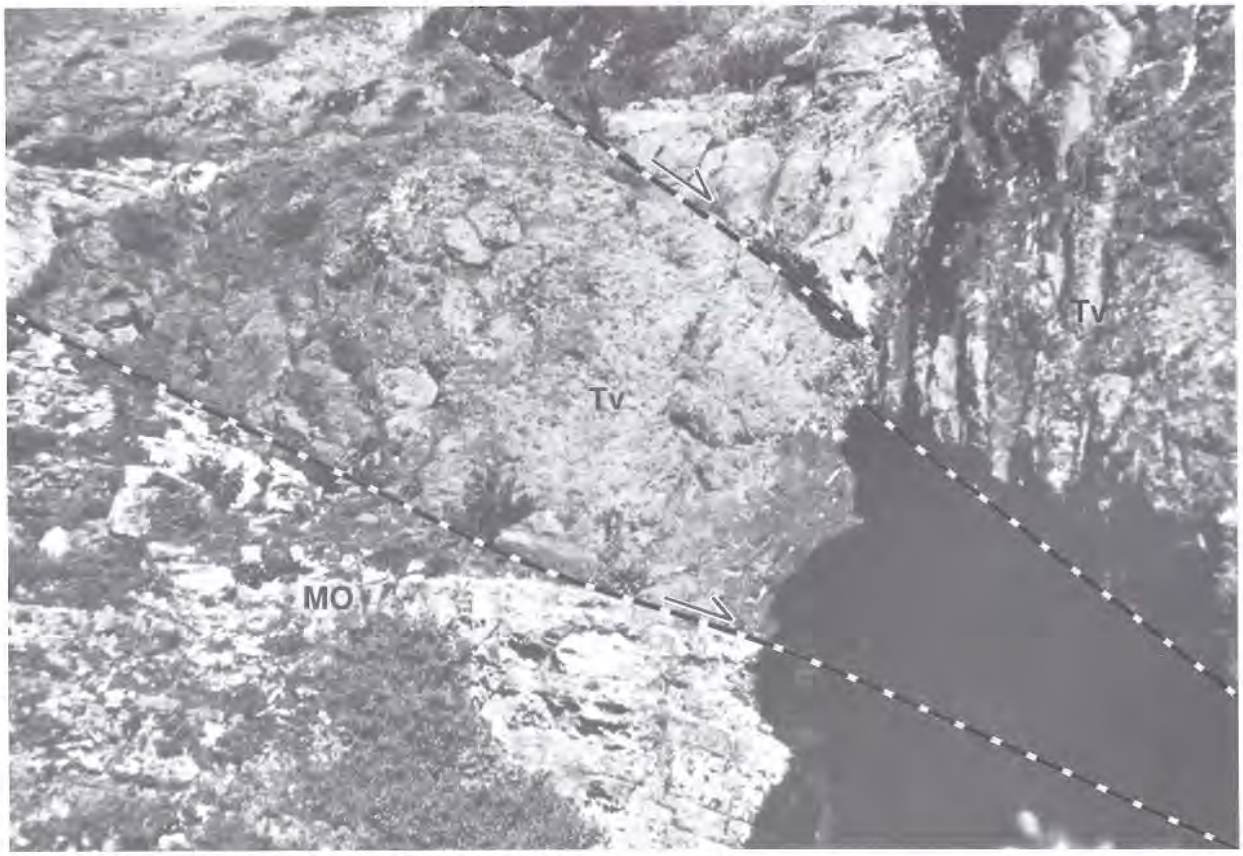

Figure 7. Two upper-plate faults (dashed lines), one at the contact between allochthonous Paleozoic carbonate rocks (MO) and Tertiary volcanic rocks (Tv) and the other within the allochthonous volcanic rocks. Field of view is ~60 ft (~20m) wide. Locality is the east side of Republic Creek; view is to the east. (From Hauge, 1983.)

and Nelson, 1971; Pierce and Nelson, 1968) or Eocene (Figure 34 of Hauge, 1983) strata directly overlie the detachment; these strata presumably originated above secondary bedding-parallel detachments within the allochthon or along the breakaway and were downfaulted to the basal detachment, having been temporarily tilted as they rode down ramps between detachment levels (Prostka, 1978; Pierce, 1980).

Commonly, however, stratification is difficult to discern in volcanic rocks above the detachment. This is particularly typical of massive volcanic breccias, for which bedding may be discerned from distant views but is commonly obscure in close examination (**Figures 3** and **8**). For example, the dominantly southeastward dips of volcanic strata described by Prostka (1978) in the areas of Pilot Peak, Jim Smith Peak, and Squaw Peak are discernible, though not obvious, from distant views, given favorable sun angle. However, in many areas the attitudes of these strata can be measured in only a few places on the outcrop. This lack of readily apparent stratification of Eocene strata has greatly hindered understanding of the extent of involvement of volcanic rocks in Heart Mountain faulting and the amount of internal extension of these rocks.

Basal shattering, brecciation, and shearing

At its base, the allochthon is characterized by shattering, brecciation, and shearing of Paleozoic (Pierce, 1979) and Tertiary volcanic (Hauge, 1982, 1985) rocks. Basal Paleozoic rocks may be deformed as much as 50 ft (15 m) or more above the detachment (Pierce, 1979) or may appear essentially undeformed immediately above the detachment. The deformed base of volcanic rocks shows a similar range of thickness (e.g., figures 4 and 5 of Hauge, 1985). Fault breccia composed of Paleozoic carbonate rock locally overlies the detachment, beneath volcanic rocks as well as beneath allochthonous Paleozoic rocks (Pierce, 1957, 1979). The absence of volcanic clasts

Figure 8. View to west of Republic Mountain, from U.S. Highway 212 east of Cooke City, Montana. The allochthon consists of Ordovician, Devonian, and Mississippian sedimentary rocks (MO) overlain by Eocene volcanic rocks (Tv). Note southward dip of volcanic strata, which are Lamar River and Cathedral Cliffs formations of Pierce and others (1973) and Wapiti Formation of Pierce (1978). Detachment (d) parallels fotwall strata (Є). Prominent cliff in the footwall is Pilgrim Limestone. Total relief shown is about 2,500 ft (750 m).

within all-carbonate fault breccia was viewed as support for the interpretation that volcanic rocks comprise only a small volume of the allochthon (Pierce and Nelson, 1970; Nelson and others, 1972). Pierce (1987a) argued that where all-carbonate fault breccia underlies the volcanic rocks, the volcanic rocks must be in depositional contact with the breccia. However, I (Hauge, 1985) observed deformation at the base of volcanic rocks that overlie such breccia and interpreted them as allochthonous. In addition to the all-carbonate fault breccia, fault breccia of mixed volcanic-carbonate composition and all-volcanic fault breccia have also been described (Nelson and others, 1972; Hauge, 1985).

Clastic dikes

Fault breccia along the detachment is locally intruded into overlying Paleozoic and Tertiary rocks as clastic dikes, as first described by Pierce (1968) and discussed in detail by Pierce (1979). Clastic dikes within Paleozoic rocks typically are composed entirely of carbonate breccia, although at White Mountain clastic dikes containing volcanic clasts intrude allochthonous Paleozoic rocks (Nelson and others, 1972). Clastic dikes within Tertiary volcanic rocks are composed of all-carbonate breccia, carbonate breccia with volcanic clasts (Pierce, 1979), and volcanic microbreccia (Hauge, 1985, p. 1445). The Tertiary volcanic rocks intruded by clastic dikes include rocks interpreted by Pierce (1973, 1979, 1987b) as deposited on the inferred surface of tectonic denudation. In the context of the tectonic denudation model of Heart Mountain faulting, emplacement of the clastic dikes is explained as follows (Pierce, 1979, p. 23):

> *Once the surface of tectonic denudation had been created by catastrophic movement on the Heart Mountain fault, water-saturated carbonate fault breccia, from 0 to 4 m or more thick, was irregularly distributed over the fault surface. As volcanic rock was poured out onto this land surface, some of the* [carbonate fault breccia] *was mixed with the volcanic rocks, some was caught up as irregular pods and lenses in the lower part of the Wapiti Formation, and some remained as irregular tabular bodies at the base of the volcanic rocks....As deposition of the volcanic rocks continued,....Lithostatic pressure on the unconsolidated fault breccia at the base of the upper plate increased with the thickening volcanic*

cover until the cohesive strength of the overlying rock was exceeded, and the [carbonate fault breccia] *was injected upward as dikes...regardless of whether the overlying rocks were upper-plate rocks or* [post-faulting] *volcanic rocks.*

In the context of the continuous allochthon model, I (Hauge, 1982, 1985, 1990) interpreted all the Tertiary and Paleozoic rocks intruded by clastic dikes as allochthonous, and I interpreted the dikes as having been intruded during extension and translation of the allochthon.

Igneous dikes

A small but significant amount of extension of the allochthon is accommodated by igneous dikes related to Absaroka volcanism. Many hundreds are mapped within the upper plate (e.g., plate 1 of Nelson and others, 1980; Pierce, 1978); fewer than ten dikes have been observed in the footwall (Hauge, 1983). Many upper-plate dikes form radial patterns around intrusive centers, and thus postdate most movement on the detachment, but many are faulted, indicating significant extension after dike injection (e.g., figure 40 of Hauge, 1983). At White Mountain, on the north side of Sunlight Creek, some dikes are folded and metamorphosed with the rocks they intrude (Nelson and others, 1972). The upper-plate dikes, typically 10 ft (3 m) thick, probably represent no more than a few percent overall extension of the allochthon, but in several areas (Hauge, 1983, p. 150, 157) swarms of dikes represent local extension of up to 50%.

Thermal metamorphism

Thermal metamorphism is a minor aspect of upper-plate deformation. Contact metamorphism is common along walls of dikes within the upper plate and is particularly conspicuous where carbonate rocks are bleached white along the margins of the dark gray dikes. At White Mountain, thermally metamorphosed and folded allochthonous Paleozoic rocks are exposed in an area of about 0.1 mi^2 (0.25 km^2) (Nelson and others 1972). These adjoin a monzonitic stock, exposed over a 0.2 mi^2 (0.5 km^2) area, away from which metamorphism decreases. The footwall underlying these metasediments is unmetamorphosed, indicating that the stock predates the faulting (Nelson and others, 1972).

Associated Features

Other detachments

Two other detachments have been interpreted in the Heart Mountain fault region — the South Fork fault (Pierce, 1957) and the Reef Creek fault (Pierce, 1963b). Discussion of these interpreted detachments is beyond the scope of the present paper. The reader is referred to Pierce (1963b) for a discussion of the similarities and differences between the South Fork, Reef Creek, and Heart Mountain faults, and to Bucher (1947), Brittenham and Tadewald (1985), Blackstone (1985), and Clarey (1990) for other interpretations of the South Fork fault. Large-scale landslides involving Absaroka volcanic rocks in the southern Absaroka Range have been described by Wilson (1975), Bown (1982a, 1982b), and Sundell (1982, 1985, 1990).

Crandall Conglomerate

The Crandall Conglomerate (Pierce, 1957) is a stream-channel deposit of Eocene (?) age (Pierce and Nelson, 1973) found in both the lower and upper plates of the Heart Mountain detachment. Its age with respect to Heart Mountain faulting is uncertain. It has been interpreted as coeval with faulting (Pierce, 1941), predating faulting (Pierce, 1950, 1968), and predating faulting in some areas and postdating it in others (Pierce, 1957). The significance of the unit to the history of Heart Mountain faulting arises from the interpretation that Heart Mountain faulting occurred in two episodes that were separated in time by deposition of the conglomerate (**Figure 9a**) (Pierce, 1958, 1987a; Pierce and Nelson, 1973). I (Hauge, 1985, 1990) interpreted the conglomerate as older than, and unrelated to, Heart Mountain faulting (**Figure 9b**).

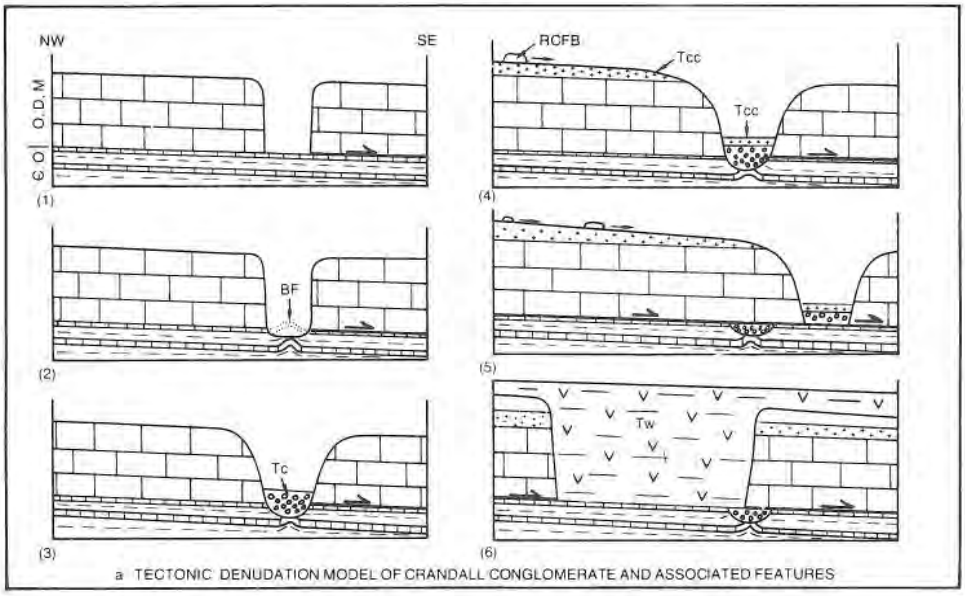

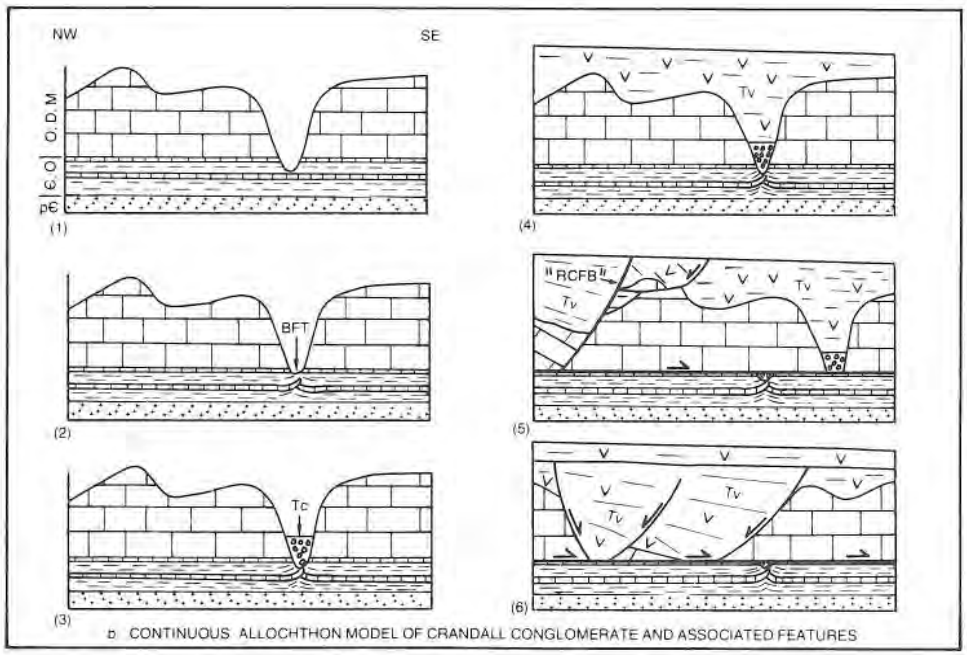

Figure 9. Two models of the origin of the Crandall Conglomerate, both shown with vertical exaggeration and varying vertical scale.

a. Tectonic denudation origin after Pierce (1987a) and Pierce and Nelson (1973). (1) An early, minor movement along part of the Heart Mountain detachment produced steep-walled canyons, into which Cambrian shale and limestone flowed laterally (2) to form the Blacktail fold (BF). (3) Next, the Crandall Conglomerate (Tc) was deposited within the canyons, followed by (4) local deposition of early volcanic rocks (Cathedral Cliffs Formation = Tcc) and emplacement of Reef Creek fault blocks (RCFB). (5) Finally, the main phase of Heart Mountain faulting displaced upper-plate blocks, including some Crandall Conglomerate, and (6) post-faulting volcanics (Wapiti Formation = Tw) blanketed the disrupted terrain.

b. Pre-detachment origin after Hauge (1983). (1) Stream channels, which formed by normal erosional processes, controlled the location of the Blacktail fold/thrust (BFT) (2), which formed as a minor detached splay of southeast-directed basement-involved Laramide thrusts bounding the south side of the Beartooth uplift. (3) Deposition of the Crandall Conglomerate was followed by (4) Absaroka volcanism and (5, 6) movement of the Heart Mountain allochthon, which locally placed Paleozoic rocks above Eocene rocks ("RCFB"). (6) Absaroka volcanism continued after faulting had ended.

Historical development of "overthrust" and "tectonic denudation" models

Recognition of the Heart Mountain "overthrust"

G.H. Eldridge, who visited the Bighorn Basin as part of a U.S. Geological Survey reconnaissance of northwest Wyoming, presented the first published description of Heart Mountain, *the structure of which was but indefinitely determined* (Eldridge, 1894, p. 30). [Johnson (1934) credited T.B. Comstock with the first (1873) geological reconnaissance of Heart Mountain area, but no citation of Comstock's work is given.] Eldridge observed the peak "capped with the quartzites and limestones of the Carboniferous" (p. 30) and surrounded at elevations 500 to 600 ft (150 to 180 m) lower by strata of Jurassic, Cretaceous, and Tertiary ages. Eldridge's (1894, p. 31) somewhat tentative interpretation was as follows.

> *The relations between the Cretaceous and Tertiary Formations and those entering into the structure of the peak itself are extremely obscure. The most plausible interpretation of the regional geology, however, seems to be that of an upward thrust, perhaps developed from extreme compression, by which the older beds, the Carboniferous and Jurassic, were carried through the surrounding formations of younger age, developing as it were between the two series of formations a practically circular fault, the strata in the immediate vicinity of which are in considerable confusion.*

The meaning of Eldridge's "upward thrust" and "circular fault" is unclear, but he appears to envision a cylindrical fault, with vertical axis, within which Madison and older rocks were uplifted as a plug to the level of the Tertiary (Hewett, 1920, p. 552). C.A. Fisher (1906, p. 37) reached a similar conclusion, although in his view the uplifted strata included the Madison limestone but not the Jurassic.

> *The underground structural relations of Heart Mountain are somewhat obscure, but the uplift is probably due to a circular fault, which raised the Madison Limestone several thousand feet above its original position.*

Neither Eldridge nor Fisher appears to have inferred what a few years later would be the obvious interpretation to the orthodox geologist, that a thrust fault must underlie the Paleozoic strata of Heart Mountain.

Such an interpretation may not have been obvious to these earliest workers because at the time of their studies of Heart Mountain the concept of thrust faults was still in its infancy, particularly in the Cordillera of the western United States. Thrusts had been described in Europe early in the Nineteenth Century (e.g., Murchison, 1849) and in the Appalachians of North America in the middle of the Nineteenth Century (Rogers and Rogers, 1843; Logan, 1860), but according to Hubbert and Rubey (1959), the concept of large overthrusts was not well established until the late Nineteenth Century (Peach and Horne, 1884). In western North America, thrusts were first described by McConnell (1887) in the Canadian Rockies, by Willis (1902) in Montana, by Richards and Mansfield (1912) in Idaho, and by Veatch (1907) and Schultz (1914) in Wyoming.

By the time C.L. Dake studied the Heart Mountain area in 1916, the existence of the Cordilleran foreland fold-and-thrust belt was documented and the time was right for the discovery of the "Hart Mountain thrust" (**Figure 10**; Dake, 1916). Dake's (1916) interpretation of Paleozoic rocks at Heart Mountain, in the Shoshone River drainage, and on Pat O'Hara Mountain as erosional remnants of a large thrust sheet was confident: "the supposition hardly admits of doubt that Hart Mountain constitutes a portion of the large fault block so widely exposed to the west" (p. 50). Dake further inferred eastward transport of the thrust sheet and a period of erosion between thrusting and volcanism:

> *If the movement was from west eastward, as will be shown later, the fault plane must pass* [as] *far west* [as the Trout Creek area], *hidden below the lava, but cut through by erosion before the lava was poured out. If this is the case, the amount of displacement must not have been less than 22 miles* [35 km] (p. 50).

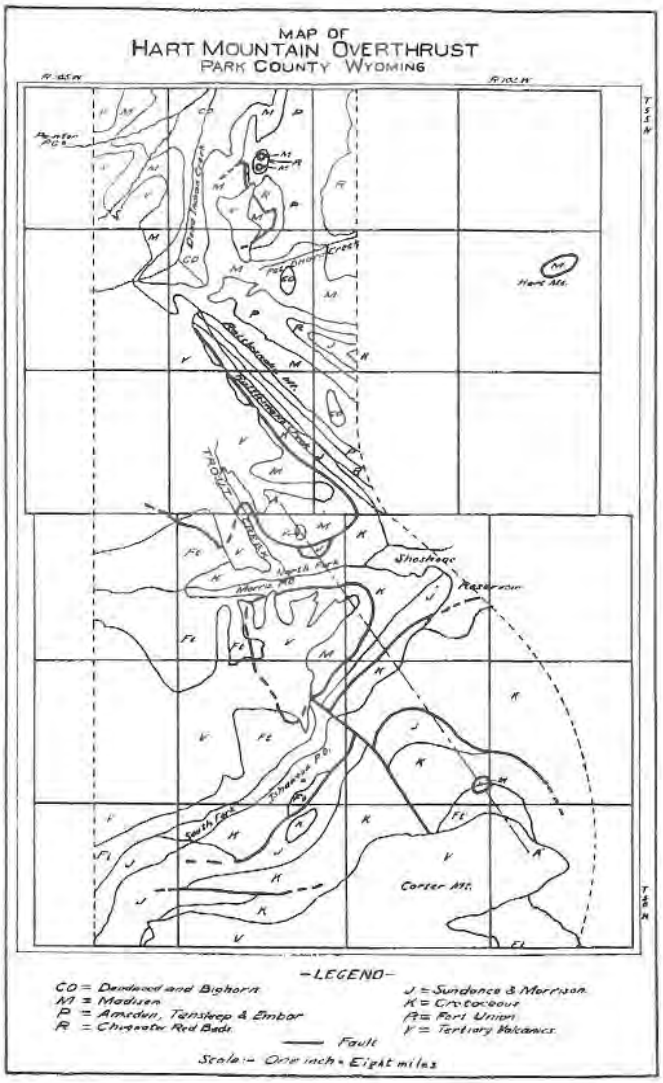

Figure 10. Dake's (1916) geologic map of the "Hart Mountain overthrust."

Dake also noted the internal structure of the allochthonous rocks:

> *The great limestone block above the fault plane is little folded. But while it presents the general aspect of a nearly flat-lying horizon, locally the dips are high, as a result of numerous small normal faults which appear to have been the result of the settling of the great block after thrusting ceased* (p. 53).

Thus Dake recognized two relationships that, among others, would ultimately lead future workers to abandon the thrust interpretation. The presence of normal faults rather than contractional structures within the allochthonous carbonate rocks would later be cited by Bucher (1935) as indicative of an allochthon of extended detached blocks rather than a continuous contractional thrust sheet. Similarly, the apparent pre-volcanic erosional unconformity would later be interpreted as the result of extension of the allochthon rather than erosion of a continuous thrust sheet. Bucher (1933, 1947) envisioned the unconformity as the result of emplacement of numerous detached blocks of Paleozoic rocks rather than a continuous thrust sheet, and I (Hauge, 1982, 1985) viewed the unconformity as highly disrupted due to extension of a continuous allochthon of Paleozoic and volcanic rocks. Nonetheless, between 1916 and 1941, most workers accepted the concept of a once-continuous overthrust sheet of Paleozoic strata which, after emplacement, suffered deep erosion and subsequent burial by volcanic rocks (Hewett, 1920; Johnson, 1934; Lawrence and Sheets, 1934; Sheets 1935; Rouse, 1937; Stevens, 1938; and Pierce, 1941).

The known areal extent of the Heart Mountain "overthrust" increased during this time. Hewett (1920) interpreted Mississippian rocks at the crest of McCulloch Peak as klippen of the "Heart Mountain overthrust," increasing the minimum transport distance to 28 mi (45 km) (p. 554). Pierce (1941) mapped klippen of the allochthon in the area of Rattlesnake Mountain, Pat O'Hara Mountain, and Sunlight Basin and suggested that the allochthon was probably present "a considerable distance farther northwest" (Pierce, 1941, p. 2023).

"Overthrust sheet" or "detached blocks"?

Although most workers from the time of Dake (1916) through the 1940s subscribed to the concept of the Heart Mountain overthrust, W.H. Bucher, in a series of publications from 1933 to 1947, argued for an entirely different concept, one that was to evolve into the model of Heart Mountain faulting that was generally accepted from the 1950s until the early 1980s. In its earliest form Bucher's model of Heart Mountain faulting was expressed tentatively (Bucher, 1933, p. 239):

The writer thinks it possible that the limestone-plates which constitute the thrust-masses of this region were thrust eastward and scattered much as they exist today by the horizontal component of the force of a large volcanic explosion.

In a later description of the model, Bucher (1947, p. 194 and 196) adopted a more confident tone:

the allochthonous masses of Paleozoic limestones in the Heart Mountain region do not represent erosion remnants of a once-continuous "thrust sheet", but are independent fragments that came into existence by a process radically different from that of normal orogeny and at a rate very much greater than that of normal orogenic processes. The writer suggests that the same temporary uptilting that caused the outer sedimentary mantle to crack along tangential and radial fractures and locally to sag into folds and thrust planes produced local overthrusts higher up, where erosion had laid bare the surface of the Madison limestone. From these, wedge-shaped slices of limestone, some several square miles in area, broke loose, sheared off the base of the Bighorn limestone and across the higher beds, landed on the temporarily steepening slope, and slid downward under the action of gravity, probably aided by frequent earthquake shocks that preceded the outbreak of volcanic activity. It is possible that volcanic explosions, associated with the earliest acid phase of eruptions, had an active part in the dislodging of individual units.

Bucher's arguments against the overthrust concept of Heart Mountain faulting display elements of geologic reasoning at its best, diluted occasionally by dogmatism:

The "Heart Mountain overthrust" differs from all other known overthrusts in several remarkable ways....The Heart Mountain thrust mass consists, at present, of a few patches of Paleozoic limestone, not more than a quarter of a mile thick, scattered over a roughly triangular area of some 400 square miles....The once-continuous thrust sheet...has been inferred to have moved...28 [to] *48 miles. Such horizontal displacement would be not at all remarkable in regions where a belt of parallel folding and thrusting is proof of strong unidirectional horizontal movement, such as accompanies the great thrusts of southeastern Idaho or the Northern Rocky Mountains from the Lewis Range northward. It is wholly startling, however, in a region that is conspicuous for the lack of such folded belts and in which, quite to the contrary, each uplift possesses its own local thrust pattern.* (1947, p. 189-190)

this rather fantastic hypothetical thrust sheet must not only have come into existence, but about seven-eighths of it must have been destroyed by erosion within a fraction of the time represented by one vertebrate fossil zone of the Eocene....(1947, p. 193)

Minor thrust faulting and imbrication should be a conspicuous feature of the internal structure of the preserved portions [of a contractional thrust sheet]. *None could be found. Instead, "normal" faulting and corresponding jointing dominate their structure.* (1940, p. 167)

All the limestone masses, except that of Logan Mountain, are wedge-shaped, with the thrust sole cutting across the beds in such a way that on one side the Ordovician Bighorn limestone, on the opposite side the Mississippian Madison limestone forms the base of the thrust block....In other parts of the world, thrust sheets of this character result from the shearing off along bedding planes, and over much of the thrust sheet the formations involved in it lie parallel to the thrust plane....The only [conclusion] *is that there were no flat parts in the thrust sheet, that the beds dipped everywhere. In that case the fault plane must have cut so neatly across the folded beds as to never cut below the base of the Bighorn, slicing off a layer less than a quarter mile thick over an area of 400 square miles. Such a transecting thrust plane seems mechanically incomprehensible.* (1947, p. 194)

Wherever the writer has seen the base of a limestone thrust sheet, he has always found it criss-crossed by a network of calcite veins....The writer has seen no sign of calcite filling anywhere [in the base of the Heart Mountain allochthon]. *This can have but one meaning: The thrust blocks travelled to their final resting place so fast that ground water had no time to*

produce its normal effects — certainly faster by several orders of magnitude than typical thrust sheets. (1947, p. 194).

Unlike the interpretations of proponents of a continuous Heart Mountain overthrust sheet, Bucher's arguments were made in a context without close supportive analogs. Bucher (1933) suggested as a possible analog the Ries Basin in Germany, where volcanic explosions were interpreted to have displaced sedimentary strata radially outward from the extrusive center. He noted that laboratory experiments employing explosives had produced similar geometries. However, Bucher (1933, p. 241) qualified these analogies by observing that:

> *the energy required to produce...effects* [similar to those of the experiments] *on the scale of the Ries Basin and, more so, on the scale of the Heart Mountain thrust-sheets, is truly stupendous. It would require activity on a scale far greater than that of explosions of historic time.*

Later, Bucher (1935, 1940, 1947) suggested as possible analogs the Bearpaw Mountains of Montana and other areas that show *structural patterns, including local overthrusts, that may be expected when intrusive activity produces local uparchings* (1947, p. 196). However, none of these analogs combines the scale of detachment area, transport distance, and displacement rate required by Bucher's view of Heart Mountain faulting.

The first indication in the literature that other workers had accepted Bucher's interpretations is in an abstract by Pierce (1950). Although Pierce refers to the "Heart Mountain thrust sheet" and to "remnants of the thrust block" in this abstract, suggesting that at this time he maintained his interpretation of a continuous allochthon, he no longer viewed it as a typical thrust: *Strata down to the base of the Bighorn dolomite were then sheared from the underlying Gallatin and were moved, probably with the aid of gravity, southeastward down the south limb of the Beartooth mountain uplift.*

Seven years later Pierce (1957) clearly had accepted Bucher's detached-block model of the Heart Mountain allochthon, and he championed that concept, with minor modification, for more than thirty years.

Development of the tectonic denudation model

In Pierce's 1957 paper, most of the components of the tectonic denudation model (Pierce, 1987a) were in place. By 1957, Pierce had mapped the detachment along the Clarks Fork valley as far northwest as Pilot Peak, increasing its known northwest-southeast dimension from 37 mi (60 km) to nearly 60 mi (100 km). In the Clarks Fork area, Pierce mapped the detachment as following the base of the Ordovician, which rendered highly unlikely the existence of a thrust-like "root" beneath the Absaroka volcanic rocks. Pierce (1957) recognized a "bedding thrust," which paralleled the base of the Ordovician along the Clarks Fork margin of the Absarokas; a "shear thrust" where the detachment cut up section toward the Bighorn Basin; and the "erosion thrust" where the upper plate overrode Eocene strata. Hewett (1920) first proposed an erosion thrust across Wasatch (now Willwood Formation) strata, although no supporting data were presented: *the surface upon which the overthrust moved...is probably a surface of erosion* (p. 554), and Pierce (1957) adopted the concept with little discussion. In the area of the "bedding thrust", Pierce interpreted Paleozoic strata as allochthonous on the detachment and early basic breccia as in depositional contact with the "bedding thrust." The geologic history Pierce (1957, p. 617) envisioned is as follows:

> *it is thought that the thrust sheet was broken into numerous blocks, and those on the front or southeast part of the advancing sheet moved farther than the northwest part, thereby causing the blocks to become separated, with large gaps between them. In these gaps or openings between the thrust blocks, the thrust plane at the top of the Grove Creek formation was laid bare, thus producing a feature which de Sitter (1954, p. 325) called "tectonic denudation".... Before erosion could appreciably modify the thrust plane, the "early basic breccias" blanketed the area.*

The remaining fundamental components of the tectonic denudation model were added in the next few years. Pierce's (1958) abstract contains the first recognition since Hares (1933) of the involvement of volcanic rocks in Heart Mountain faulting. [However, Pierce did not recognize volcanic rocks as allochthonous in the area studied by Hares until 1987 (Pierce, 1987a).] Pierce (1960a) reported discovery of

the "break-away fault" and adopted the now-traditional phrases "Heart Mountain detachment fault," "bedding fault," "transgressive fault," and "fault on former land surface." He observed "early acid volcanics" in the footwall of the breakaway fault, further evidence of involvement of volcanic rocks in Heart Mountain faulting. Pierce (1960b, 1963b), following Bucher, added *the shaking motion of many earthquakes* (1963b, p. 1225) to *the force of gravity* (1957, p. 615) as an essential component of the mechanism of detachment and emplacement of the detached masses, completing the basic framework of the tectonic denudation model. Much of Pierce's mapping is published as a series of 1:62,500 U.S. Geological Survey geologic maps (Pierce, 1965a, 1965b, 1966b; Pierce and Nelson, 1968, 1969, 1971; Pierce and others, 1973, 1982; see also Pierce, 1978; Elliott, 1979; Nelson and others, 1980; and Prostka and others, 1975). These are the most detailed and comprehensive maps of the detachment area available (**Sheet 1**, Hauge, map pocket).

Later work by Pierce introduced or elaborated upon other features of the detachment area that he interpreted as supportive of the tectonic denudation model. These include: clastic dikes intruded upward from the detachment (Pierce, 1968, 1979, 1987b), the Crandall Conglomerate (Pierce and Nelson, 1973), and the break-away fault (Pierce, 1980, 1987b). Arguments in support of the tectonic denudation model are summarized in Pierce (1987a).

Pierce, like Bucher, was hard-pressed to cite close analogs to support his interpretation of the Heart Mountain detachment. Low-angle normal faults had been mapped by Longwell (1945) in southern Nevada, but general acceptance of the common occurrence of extensional detachment faults did not follow until much later (e.g., Crittenden and others, 1980). Pierce (1957) cited de Sitter's (1954) interpretation of the Bearpaw Mountains as the only other known example of tectonic denudation, and he made the following observations about rootless low-angle faults (Pierce, 1957, p. 625):

> *The Heart Mountain and South Fork thrusts are by no means the only thrusts without roots. Particularly in the Jura Mountains of Switzerland and France, but in other places also, there are more widely known examples of the décollement or detachment type of structure. In many of these, erosion has removed most of the geologic record from what seems to be the "source area" for the thrusts. However, it may be possible to fill in a very significant part of the geologic record of the Heart Mountain and South Fork thrusts, because soon after the thrusting took place, the entire area was buried under a great mass of volcanic rock, Here the geologic record remained, protected as though it were cast in a mold, from middle Eocene to the present, and it is only now being exposed as the processes of erosion remove the cover of volcanic rock.*

In the context of the present interpretation of the Jura as rooted thrusts with continuous contractional allochthons, this analog seems inappropriate. Pierce did not subsequently invoke it, nor have better analogs to the tectonic denudation interpretation of Heart Mountain faulting been recognized.

Heart Mountain faulting and Absaroka volcanism

Although the involvement of volcanic rocks in Heart Mountain faulting was first suggested in the 1930s (Hares, 1933), the involvement of even minor amounts of volcanic rocks in faulting was not generally accepted until the late 1950s (Pierce, 1958). This was after development of the tectonic denudation model, which was first presented in Pierce (1957). Since 1958, greater and greater volumes of volcanic rocks have been recognized as allochthonous by a number of workers, notably Pierce (1960a, 1960b, 1963b, 1987a) and Prostka (1978), and these workers modified the original tectonic denudation model of Pierce (1957) to accommodate allochthonous volcanic rocks. I (Hauge, 1982, 1985) believed, unlike previous workers, that all volcanic rocks immediately overlying the detachment are allochthonous, which led me to develop the alternate interpretation of a continuous extensional allochthon.

Interpretation that Absaroka volcanic rocks postdate Heart Mountain faulting

The first statement regarding the relative ages of volcanic rocks and Heart Mountain faulting was by Dake (1916, p. 54): *Following the faulting long erosion had trenched the region deeply and in places completely cut away the fault block, before the Basic Breccia was laid down.*

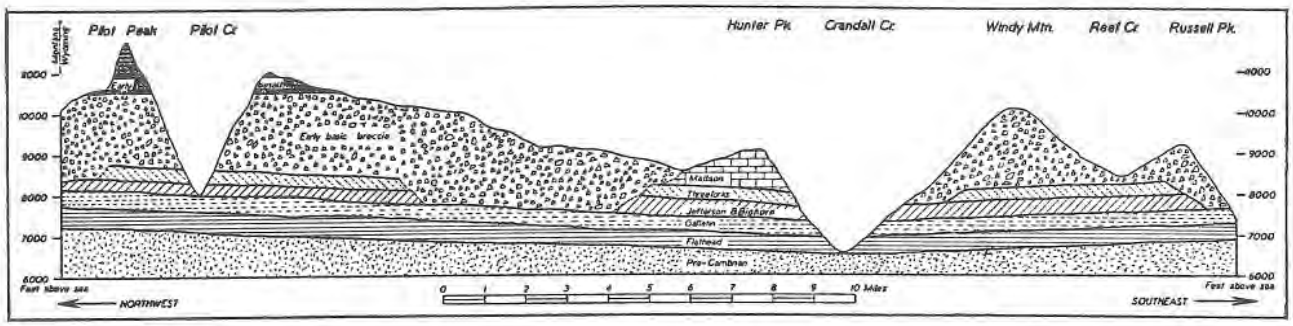

Figure 11. Rouse's (1937) cross section of the southeast side of the Clarks Fork valley, northern Absaroka Range.

This interpreted unconformity (**Figure 11**) was described by Rouse (1937, p. 1261) as follows:

> *In many instances, where present streams have cut down through the covering of volcanic rocks and into the underlying Paleozoic rocks, the old land surface can be seen in cross-section in continuous exposures, showing a relief of between 1000 and 1500 feet. The most spectacular example is on the southern side of the Clarks Fork River where the breccias and lavas can be seen resting unconformably on Paleozoic rocks. From Cooke City the same unconformity can be seen on the north slope of Republic Mountain. Numerous other examples of this spectacular unconformity might be cited in the Sunlight Basin, Wyoming, and many other areas.*

In the areas cited here the subvolcanic unconformity was also mapped in reconnaissance by Hague (1899); and other workers, most of whom worked in the Shoshone River Valley, reached the same conclusion. Hewett (1920) confirmed Dake's interpreted period of deep erosion between thrusting and "early basic breccia" volcanism. However, in the Owl Creek - Wood River area of the southern Absaroka Range, Hewett observed no major unconformity between Wasatch basin-fill strata and Absaroka volcanic rocks (correlated with the older "early acid breccia"). Hewett concluded (and Rouse later agreed) that *the overthrust took place after the deposition of the "early acid breccias" and before the outbursts of "early basic breccias"* (p. 537), but there was no explicit statement that volcanic rocks were involved in thrusting. A number of other workers, including Johnson (1934), Lawrence and Sheets (1934), Sheets (1935), Rouse (1937), Stevens (1938), and Pierce (1941) inferred a geologic history of emplacement of a continuous thrust sheet of Paleozoic rocks followed by deep erosion and subsequent "early basic breccia" volcanism. Although faults were observed offsetting both the Paleozoic rocks of the allochthon and overlying volcanic rocks by Lawrence and Sheets (1934), these faults were thought by these workers to offset the thrust surface and therefore postdate Heart Mountain faulting.

During this period, only one worker argued for involvement of volcanic rocks in Heart Mountain overthrusting. In an abstract, C.J. Hares (1933) recognized an apparent difficulty for the concept of the Heart Mountain overthrust: *what overburden held less than one thousand feet of limestone together while being moved thirty miles or more is a very pertinent question.* Hares also noted that *secondary faults displace both the agglomerate and the limestone* [**Figure 12**]; *they were apparently contemporaneous with the main overthrust.* Hares concluded that *the unconformity was thrust with the Paleozoic limestone,* that the *Tertiary agglomerate* predated thrusting, and that *the agglomerate was the overburden which held the thrusted masses of limestone together.* Judging from a lack of subsequent reference to his ideas, they seem not to have gained even minor acceptance. It was not until the work of Pierce (1957) that this unconformity was recognized as a result of profound extension of the Paleozoic section above the Heart Mountain detachment.

The last suggestion that no volcanic rocks were involved in Heart Mountain faulting was in Pierce (1957). Pierce (1957, p. 609) accepted the arguments of previous workers that the deposition of early basic breccia postdated faulting, and he added several new lines of evidence, among which was the following:

> *If in some way the early basic breccia was faulted into its present position on the Grove*

Figure 12. Oblique aerial view to east of tilted fault blocks at Logan Mountain on the east side of Trout Creek, illustrating domino-style extension of the allochthon. This locality is visible from U.S. Highway 14-16-20 west of Cody, Wyoming, about 1 mi (1.6 km) west of Trout Creek.

> *Creek formation during the emplacement of the Heart Mountain thrust masses, then with the volcanic breccia and limestone masses moving together as a thrust sheet, one would expect to find a few fragments of volcanic rock along the fault beneath some of the limestone thrust masses particularly either in the area of the bedding thrust or the erosion thrust, but none have been found.*

This line of evidence was cited by Pierce (1987a) as proof that the continuous allochthon model of Hauge (1985) is unsupported by field relationships.

Pierce (1957) acknowledged the presence of early acid breccia in the detachment area but did not make explicit an interpretation of whether these rocks were involved in Heart Mountain faulting. In stating that *none* [of the rock formations in the thrust blocks] is *younger than the Madison limestone* (p. 591) he implied that the early acid breccia postdates faulting. In apparent contradiction to this statement, the first event he mentions after Heart Mountain faulting is the deposition of early *basic* breccia, suggesting that the older early acid breccia predates faulting. Pierce's apparent uncertainty in this regard was eliminated in his next publication.

Interpretation that Absaroka volcanic rocks were involved in Heart Mountain faulting

Clear involvement of Absaroka volcanic rocks in Heart Mountain faulting was documented in Pierce (1958, 1960b) at Cathedral Cliffs and in Pierce (1960a) at the breakaway fault. Pierce (1963a, p. 15) defined the Cathedral Cliffs Formation to replace the informal term "early acid breccia" of Hague (1899) and defined it as the Absaroka volcanic rocks that predated Heart Mountain faulting: *Both the Reef Creek and the Heart Mountain fault masses were emplaced after deposition of the Cathedral Cliffs Formation and before deposition of the early basic breccia* [Wapiti Formation of Nelson and Pierce, 1968].

Pierce (1963b) interpreted all allochthonous volcanic rocks in the detachment area as Cathedral Cliffs Formation and all of the younger "early basic breccia" as younger than faulting (figure 2 of Pierce, 1963b). This interpretation was reiterated when the early basic breccia was redefined as the Wapiti Formation (Nelson and Pierce, 1968, p. H9):

> *In a number of places the Wapiti Formation surrounds and buries blocks of Paleozoic rock, mostly carbonate, some of them hundreds of feet thick and thousands of feet across. These blocks were dispersed on the early Eocene land surface by the Heart Mountain detachment fault before deposition of the Wapiti Formation.*

Similarly, Nelson and others' (1972) interpretation of relationships at White Mountain in Sunlight Basin subdivided volcanic and associated intrusive rocks into allochthonous Cathedral Cliffs Formation and post-tectonic Wapiti Formation. In their description of the stratigraphic framework of the Absaroka Volcanic Supergroup, Smedes and Prostka (1972, p. C24-25) corroborated the interpretation of Wapiti Formation as younger than Heart Mountain faulting:

East of [Yellowstone National Park], *the pre-Wapiti formations have been extensively disrupted by sliding along the Heart Mountain detachment fault. There, the tectonically denuded fault plane and allochthonous blocks of Paleozoic strata and pre-Wapiti volcanic rocks* [Cathedral Cliffs Formation] *were buried by the Wapiti Formation immediately after the sliding occurred.*

Thus, the general concept that Heart Mountain faulting was a catastrophic event defining the temporal boundary between distinct volcanic formations, the older Cathedral Cliffs and younger Wapiti formations, apparently was generally accepted in the early 1970s. However, disagreement with this concept arose in the literature almost immediately. The first indication was in the U.S. Geological Survey geologic map of the Pilot Peak Quadrangle (Pierce and others, 1973), in which the name Lamar River Formation was introduced into the detachment area. The Lamar River Formation was defined west of the detachment area (Smedes and Prostka, 1972) and was described as in part younger than and in part older than Heart Mountain faulting (Pierce and others, 1973). The coauthors of Pierce and others (1973) agreed that rocks they mapped as Cathedral Cliffs Formation were allochthonous and those mapped as Wapiti Formation were in situ, but they disagreed as to whether large volumes of volcanic rocks which they mapped as Lamar River Formation (or as undifferentiated Lamar River and Cathedral Cliffs formations) were allochthonous (H.L. Prostka) or in situ (W.G. Pierce and W.H. Nelson). The area of disagreement included most of the exposures of volcanic rocks on the detachment in this quadrangle. In the late 1970s, three schools of thought were evident in the literature regarding the mapping of volcanic rocks overlying the detachment: Pierce (1978) mapped the contact between volcanic rocks and the detachment in most places as Wapiti deposited on the detachment; Nelson and others (1980) mapped the contact as in most places depositional, but mapped some of these rocks as Lamar River and Cathedral Cliffs formations; and Prostka (1978) interpreted much of the northwestern part of the detachment as being overlain tectonically by Lamar River and Cathedral Cliffs formations. Prostka (1978, p. 430) recognized steep dips of fine-grained volcaniclastic rocks in these areas and interpreted them as evidence of tectonic tilting. The areas of disparate mapping of these authors are shown on **Sheet 1**, Hauge, map pocket. Unlike previous workers, I (Hauge, 1982, 1985, 1990) interpreted the contact between volcanic rocks and the detachment as everywhere tectonic, leading me to abandon the tectonic denudation model.

Mechanism problem of the tectonic denudation model

The tectonic denudation model of Heart Mountain faulting evolved at a time when the mechanics of thrust faults was an unresolved paradox. [For historical perspectives on the mechanical paradox of thrust faulting, see, for example, Hubbert and Rubey (1959), Voight, (1976), and Price (1988).] The tectonic denudation model of Heart Mountain faulting seemed to present even greater mechanical difficulties, because it envisioned mountain-size detached blocks transported across slopes of less than 2°, for distances of up to 30 mi (50 km), at rapid rates, without the aid of a "push from the rear." Pierce (1960b, 1963b, 1973, 1987a) has long argued that earthquake oscillations, in conjunction with the body force of gravity, best explain the emplacement of the detached blocks. However, the lack of general acceptance of this or any other of the proposed mechanisms of Heart Mountain faulting is indicated by the periodic publication, between 1959 and 1981, of new hypothetical mechanisms to explain Heart Mountain faulting.

Gravity as the moving force

The first mechanism proposed to explain the emplacement of the Heart Mountain "thrust sheet" as numerous detached blocks was presented only one paragraph after the concept of the allochthon as numerous detached blocks was first suggested (Bucher, 1933, p. 239):

The writer thinks it possible that the limestone-plates which constitute the thrust-masses

of this region were thrust eastward and scattered much as they exist today by the horizontal component of the force of a large volcanic explosion.

Throughout the Beartooth Mountains in the north, intrusive igneous rocks have tended to spread laterally within the thick Cambrian shales. It is thought that something like this occurred in a broad uplift which occupied the center of the volcanic area west of the thrust-sheets. The volcanic gases, perhaps largely pent-up steam, exploded in such a way as to shear off large sheets of limestone from the highly mica-ceous Cambrian shales and to drive them east-ward (or, perhaps better, southeastward), down the pediment slope onto the plain. Following the later extrusion of vast quantities of agglomerates and lavas, the central zone of volcanic activity was depressed in the form of a broad gentle syn-cline, carrying the underlying structural uplift out of sight.

The volcanic uplift/explosion model soon gave way to the idea of "gravity as the moving force," suggested in an abstract by Bucher (1935) for the South Fork fault, and, by comparison, for the Heart Mountain fault as well. Bucher (1933, 1935) implied that no "push from the rear" was involved in emplacing the detached blocks he envisioned, thereby setting the mechanics of the Heart Mountain allochthon distinctly apart from thrust mechanics.

Pierce (1950) accepted Bucher's (1947) concept of a rootless allochthon emplaced by gravity, abandoning the idea of a rooted thrust expressed in Pierce (1941):

After anticlinal uplift of the Beartooth Mountains, strata at the top of the uplift above the resistant Madison Limestone were removed by erosion and conglomerate was deposited. Strata down to the base of the Bighorn dolomite were then sheared from the underlying Gallatin and were moved, probably with the aid of gravity, southeastward down the south limb of the Beartooth Mountain uplift. (Pierce, 1950, p. 1493).

Here, Pierce differed from Bucher in envisioning the Beartooth uplift rather than the Absaroka Range as the source area of the allochthon and in referring to a "thrust sheet" (p. 1493) rather than numerous detached blocks, but he seems to have dismissed the possibility that a "push from the rear" facilitated emplacement of the allochthon.

That gravity alone was an inadequate mechanism to emplace the detached blocks was probably apparent from the beginning, but further discussion of this issue did not appear until Bucher returned to it more than ten years later.

Earthquake oscillations

Bucher (1947) augmented his idea of "gravity as the moving force" of allochthon emplacement by suggesting that the detached blocks moved down steepened slopes with the aid of earthquakes, calling upon movement across a *temporarily steepening slope, ...under the action of gravity, probably aided by frequent earthquake shocks that preceded the outbreak of volcanic activity* (Bucher, 1947, p. 196). Following Bucher, Pierce (1957) recognized that gravity alone seemed inadequate to emplace Heart Mountain detached blocks but did not subscribe explicitly to Bucher's "earthquake shocks" concept. Instead, Pierce (1957) suggested two possible mechanisms of formation of the detachment, specifically *volcanic activity or events associated with the 'early acid breccia'* and *intrusion of a sill or laccolith* (p. 615). Pierce (1957, p. 615-616) suggested a range of possible mechanisms for continuing movement of the allochthon after initial detachment:

Once this detachment or shearing-off had started, the force of gravity may in considerable part account for the continuing movement of the thrust mass....As the Heart Mountain thrust mass moved southeast, perhaps as a series of intermittent movements wherein the strata below the thrust were the actively moving block or platform, the strata above the fault plane could have been free to move by a combination of the forces of gravity and inertia, such as has been suggested by Stevens (1936). Or the initial movement of the thrust sheet may have been extremely violent and sudden; possibly a sudden movement of the entire mass might better account for the separation and scattering of the blocks toward the southeast.

By the early 1960s, Pierce had formulated the concept of Heart Mountain fault mechanics that he would advocate for the next thirty years. Pierce (1960b, 1963b) incorporated Bucher's (1947) model of

earthquakes as facilitating the gravity-driven emplacement of the Heart Mountain allochthon, described here as detached fault blocks rather than a thrust sheet:

> *The Reef Creek and Heart Mountain detachment faults are in part the result of gravity movement, but gravity alone is inadequate for the low slope involved. Along the western border of the Bighorn Basin vertical displacement of 20,000 feet, mostly during Tertiary time, undoubtedly was accompanied by many earthquakes. Extrusion of the volcanic rocks, closely associated in time with the fault movements, can be presumed to have been preceded and accompanied by repeated tremors. It is suggested that the shaking motion of innumerable earthquakes, combined with the constant force of gravity, caused the detached fault blocks to move great horizontal distances on a slope of a few degrees.* (Pierce, 1960b, p. 1944).

Pierce and Nelson (1970) elaborated on this mechanism:

> *If under certain conditions an upward acceleration approaching 1 G were imparted to the rocks above the fault plane, then the stress normal to the fault as a result of gravity would approach zero. With repetitions of upward acceleration, the rocks above the fault would then be nearly unrestrained by friction and periodically would be free to move laterally on a very low slope* (p. 121).

However, Voight (1972, p. 698) pointed out several difficulties with the earthquake oscillation concept:

1) *extreme assumptions required for large-motion durations and/or displacement per oscillation;*
2) *a "time-problem" which arises with reasonable assumption of duration and frequency;*
3) *slight deformation engendered by slide blocks;*
4) *lack of deformation below the décollement.*

In addition to envisioning earthquakes as having facilitated movement along the detachment, Pierce (1963b, p. 1234-1235) suggested that earthquake energy may have created the detachment:

> *some additional factor, as yet undetermined, may have been required to produce the initial rupture along the* [detachment]. *Strong seismic waves traveling horizontally along adjacent thick units of different lithology, such as dolomite and shale which have significantly different wave velocities, may have been a factor.*

This suggestion received support from the concept of acoustic fluidization of Melosh (1981, 1983), who used it to explain the localization of the detachment along bedding within dolomite rather than within subjacent shale. Melosh (1981, p. 1046) envisioned an "acoustically activated" Heart Mountain detachment, along which movement was maintained by acoustic rather than earthquake energy:

> *The initial movement...was along a bedding-plane fault in the Bighorn Dolomite, 2 to 3 meters above its contact with the Grove Creek Formation and the underlying shale units of the Snowy Range Formation. The peculiar fact that the fault plane lies in the apparently strongest unit rather than the weaker underlying shale is readily explained by an acoustic lubrication mechanism. Some form of lubrication is required to allow the upper block to slide down the 2° regional slope. This can be provided by a strong acoustic wave partially trapped on the interface between the dolomite and shale. The largest vertical stress fluctuations induced by this wave are in the dolomite, approximately 1/4 wavelength away from the contact. Field evidence indicates a wave of ca. 40 m wavelength (50 Hz). Once sliding begins, the acoustic wave is maintained by transformation of potential energy to acoustic energy.*

However, as pointed out by Stearns and others (1974), a detachment at this horizon is also present where these strata are folded across a basement-involved fault exposed at Rattlesnake Mountain, suggesting empirically that this bedding surface is not inherently "strong." Stearns and others (1974) also cite experimental data indicating that sliding of dolomite on dolomite is characterized by relatively low friction and might be favored over sliding along a dolomite-limestone contact. This is in contrast to Kehle (1970), whose suggestion that the Heart Mountain detachment lies along a low-viscosity zone seems contradicted by its occurrence within dolomite. Thus, the detachment, like the " 'strong decollement' foreland thrusts" of Burchfiel and

others (1982), may be localized along a stratigraphic horizon that is only apparently strong, so that the "enigma" of the detachment lying along a "strong" bedding plane may be more apparent than real, and no acoustic activation, or other unusual mechanism, is needed to localize it there.

Abnormal fluid pressure: early applications to Heart Mountain faulting, 1959-1966

The first suggestion that friction along the base of the Heart Mountain allochthon may have been reduced by abnormal fluid pressure was in Hubbert and Rubey's (1959) introduction of that idea as applied to thrust faults, although they did not develop the idea explicitly in terms of Heart Mountain faulting. Pierce (1963b, p. 1234) argued against the possibility:

> *Pressure of interstitial fluids (Hubbert and Rubey, 1959) as a means of reducing the force required for movement does not seem applicable...; the faults were at shallow depth, and high fluid pressure is not expected, but if there was an abnormal pressure, it would be lost as soon as the fault mass began to break up.*

Davis (1965) raised the same point in a discussion of Hubbert and Rubey (1959), arguing that several low-angle faults, among them the Heart Mountain detachment, were not amenable to reduction of basal friction by abnormal fluid pressure. Rubey and Hubbert's (1965) reply admitted the difficulties of applying their model to the Heart Mountain detachment but, in a passage (p. 469-470) that followed the suggestion of Hares (1933) and foreshadowed the conclusions of Hauge (1982, 1985), they suggested that certain field relationships might be reinterpreted:

> *Pierce's interpretation (1957; 1963*[b]*) of the Heart Mountain and associated South Fork and Reef Creek faults of Wyoming is convincing to us in almost all details. He himself remarks (1957, p. 617), however, that his "picture of fault blocks, separated in some as yet undetermined manner, with the fault plane exposed only briefly in areas between the fault blocks, seems fantastic if not impossible."* [Pierce (1966a) objected to Rubey and Hubbert's selective quotation: "This gives an incorrect impression as to the intent of the statement...The original sentence ...continued as follows: '...but there are several lines of evidence that point to it; if this concept is discarded, several unusual features must be explained, of which the following are particularly significant,' " after which Pierce lists the four points quoted below.] *One may wonder, then, whether any of the field evidence clearly disproves the possibility that movement on the Heart Mountain thrust, which began before the accumulation of early basic breccia..., may also have continued during it* [emphasis added]. *If so, the intrusive emplacement of some of the volcanic breccia..., the large blocks of Paleozoic limestone caught up within it..., and the evidence of lateral movement of a mile or more by "underground mudflows" within the breccia... could support a broadened interpretation that some part of the fault movement was the result of relatively local movements within the volcanic breccia, and that another part was the result of large-scale movements of an extensive thrust sheet composed of limestone blocks plus breccia.*

Pierce (1966a) cited four lines of evidence that, in his view, contradicted Rubey and Hubbert's suggested reinterpretation of field relationships:

> *In the bedding-plane phase of the fault, the early basic breccia rests with depositional contact on a surface of tectonic denudation formed by the fault; the widespread areal pattern of isolated blocks of the upper plate that were not isolated by erosion requires that a tectonically denuded space be created first; and no early basic breccia debris is present in the Heart Mountain fault gouge (p. 595)...The numerous occurrences of Madison Limestone which rest...on the Heart Mountain fault plane...*[are] *most difficult if not impossible to explain as long as the upper plate is unbroken* (p. 566).

This argument went unchallenged for nearly 20 years, until I (Hauge, 1982, 1985) suggested that they could be explained within the context of a continuous allochthon model much like that suggested by Rubey and Hubbert. Meanwhile, however, a number of variations on the Hubbert and Rubey "beer can" fluid-pressure model were developed by other workers to explain the mechanics of Heart Mountain faulting in the context of the tectonic denudation model.

Abnormal fluid pressure: later variations, 1969-1982

Despite Pierce's dismissal of the possibility that abnormal fluid pressure facilitated emplacement of Heart Mountain detached blocks, numerous authors evoked fluid pressures, of a variety of imaginative origins, to explain the "fantastic if not impossible" emplacement history envisioned by the tectonic denudation model. Goguel (1969) suggested that dehydration of minerals such as gypsum and frictional heating along the detachment may have increased fluid pressure and facilitated sliding. Hsü (1969) evoked an "air-cushion" model analogous to that proposed for the Blackhawk landslide by Shreve (1968). Hughes proposed a "hovercraft" model, with flotation of upper-plate blocks supported by injection of volcanic gases, a model with which Pierce and Nelson disagreed, leading to an extended discussion in the literature (Hughes 1970a, 1970b, 1970c, 1973; Pierce and Nelson, 1970; Nelson and others, 1972, 1973). Pierce (1973), in a review dedicated largely to the mechanism problem, discounted all variants of fluid-pressure models, maintaining that "a combination of gravity and earthquake oscillations is the only mechanism that has been suggested (Bucher, 1947, p. 196; Pierce, 1963b, p. 1234) which is compatible with the observed features of the Heart Mountain fault" (p. 468).

Nonetheless, new variations on the fluid pressure theme continued to be suggested to explain the mechanics of Heart Mountain faulting. Voight, who accepted Pierce's interpretations of the field relationships, developed a particularly vivid vision of the detachment history. Voight (1972), whose problems with the earthquake oscillation mechanism were quoted above, proposed a "fluid wedge" model in which abnormal fluid pressures due to magmatic activity were envisioned not only as reducing friction along the detachment horizon, but also as imparting a lateral component of acceleration to induce detachment and provide initial motion of the allochthon (Voight, 1972, 1973a, 1973b, 1973c, 1974a, 1974b, 1974c). Movement of allochthonous blocks on the land surface was envisioned as having been facilitated by elevated fluid pressures that were *generated by the frontal portions of the glide blocks* (1972, p. 698). Voight inferred maximum block velocities to be "ca. 10^2 knots" (1972, p. 234) and envisioned that *the whole event, in the bedding plane and transgressive fault areas, occurred in merely a geological instant — vs. on the order of an hour* (1974b, p. 116). In support of this model, Voight argued that clastic dikes within the base of the allochthon and lack of deformation beneath the allochthon "demand" a fluid "flotation" mechanism (1973a, p. 233) (an argument to which Pierce, 1979, took issue), and suggested the Turnagain Heights, Anchorage, Alaska landslide as an analog.

Still more suggestions arose to explain the mechanics of Heart Mountain faulting. Prostka (1978, p. 435) argued that:

> *The fluid-wedge hypothesis of Voight (1972), or some variation of it, seems to me to best fit the geological facts as they are presently known... Because extremely rapid injection of large volumes of fluid is required, volcanic gas — mainly steam — seems to me to be the only reasonable possibility...This model is obviously similar to the mechanism originally suggested by Bucher (1933).*

Finally, Straw and Schmidt (1981a, 1981b) proposed yet another variation, a "phreatomagmatic/hydraulic" mechanism, which envisioned high fluid pressures due in part to magmatic activity, dislodging of the allochthon by earthquake activity, and synextensional pressure reduction causing overpressured, superheated water to flash into steam, expand, and thereby provide continuous buoyancy to aid downslope movement. The "acoustic fluidization" concept of Melosh (1981, 1983) was also applied to Heart Mountain faulting, as described previously.

These numerous mechanical models, in my view, reflect the astonishment facing these geologists as they attempted to explain Heart Mountain faulting in the context of the tectonic denudation model: they seem to have been, in effect, in a similar state as were Rubey and Hubbert (1965, p. 469) in terms of thrust faults in general: *We — like others — still react toward thrust faults with something of the incredulity of the farmer on seeing his first giraffe.*

The combination of features that comprise the "giraffe" of Heart Mountain detached blocks is the combination of long distances of transport, rapid rates of transport, low slope of detachment, large size of detached blocks, and lack of profound internal deformation of detached blocks and footwall. This combination of features seems to require nearly total elimination of friction along the detachment horizon, leading most workers to invoke a form of abnormal

fluid pressure ("beer can," "hovercraft," "air-cushion," "phreatomagmatic/hydraulic," "pnuematic-hydraulic plastic wedge," and "acoustic fluidization" versions). However, although *several mechanisms have been proposed...as yet, no thoroughly convincing case has been made for any of them* (Prostka, 1978, p. 433).

In the view of the continuous allochthon model, discussed next, the apparent mechanical impossibility of the tectonic denudation model arises from its mistaken view of the nature of the upper plate. When the upper plate is viewed as a continuous allochthon rather than as numerous detached blocks, catastrophic emplacement velocities are no longer indicated, and the mechanics of gravity spreading (Davis and others, 1983), which requires no elevated fluid pressures, may resolve the enigma of the mechanics of Heart Mountain faulting.

Development of the continuous allochthon model

The concept of the Heart Mountain allochthon as numerous detached blocks rather than a continuous allochthon stood all but unchallenged for more than twenty years after its general acceptance (Pierce, 1957). A challenge arose in the early 1980s, when study of the volcanic rocks overlying the detachment led to development of the continuous allochthon model of Hauge (1982, 1983, 1985, 1990).

Observational basis and origin of the continuous allochthon model

My field study of the Heart Mountain detachment, the bulk of which was conducted in 1977, 1978, and 1980, was initially conceived by my thesis advisor Gregory A. Davis and myself as a search for the undiscovered critical field observations that would resolve the mechanical paradox of the tectonic denudation model. Initially, field study focused on the detachment horizon, both on the margins of the detachment area where it is unfaulted and within the detachment area where allochthonous Paleozoic rocks overlie the detachment. Because excellent U.S. Geological Survey geologic maps by Pierce, Nelson, and Prostka were available, acquisition of detailed structural data (both geometric and kinematic) was the technique chosen to augment the existing data. Not until 1980 did my field study turn to the volcanic rocks overlying the detachment. Early in that field season features of apparent tectonic origin were discovered within and along the base of volcanic rocks that had previously been mapped as in situ Wapiti Formation. Efforts were redirected to include study of all the masses of "Wapiti" mapped as in depositional contact with the detachment, and in every area evidence of tectonic emplacement of the volcanic rocks was discovered. The observations are summarized in Table 1 of Hauge (1985).

The suggestion, based on field observation, that all rocks immediately overlying the detachment are allochthonous led to a series of reinterpretations of the geologic history of Heart Mountain faulting that eventually took form as the continuous allochthon model. The first inference was that if all volcanic rocks immediately above the detachment are allochthonous, then a continuous allochthon rather than numerous detached blocks might be indicated. In contrast to the continuous contractional thrust sheet of Dake and other workers, the newly envisioned continuous allochthon was extensional and composed largely of Absaroka volcanic rocks (Wapiti and Cathedral Cliffs formations, with minor late-stage involvement of younger units). The second inference was that if the allochthon was continuous, tectonic denudation did not occur. This in turn implied that the catastrophic rates of faulting and immediately subsequent volcanism, which were required by the tectonically denudation model, were no longer indicated. Instead, slip rates in accord with those presently observed along low-angle faults are permitted if the allochthon was continuous. The mechanical difficulties of the tectonic denudation model were also thought to be eliminated, both because of reduced slip rates and because gravity spreading rather than gravity sliding would be the appropriate mechanical concept (see Mechanics section, below). Thus, the continuous allochthon model, if correct, renders moot the unresolved mechanical enigma of the tectonic denudation model.

My conclusions (Hauge, 1982, 1983, 1985) were based for the most part on study of the detachment horizon and the rocks exposed within a few tens of meters above it. These studies indicated that normal faults are present within volcanic rocks previously mapped as Wapiti and at contacts between these and other allochthonous rocks. However, not all

"Wapiti" volcanic rocks in the detachment area are involved in faulting. For example, the "Wapiti" overlapping the breakaway, shown in **Figure 3** of Pierce (1987a), clearly postdates faulting, but I interpret the Wapiti in the hanging wall of the breakaway as allochthonous. My field study documented the existence of numerous faults offsetting "Wapiti" volcanic rocks along the detachment, but only locally (e.g., areas of **Figures 6** and **11**) did I trace these faults more than a few meters above the detachment. Additional work is needed to map these faults at higher structural levels. The many normal faults mapped by Nelson and others (1980) as offsetting Wapiti Formation in the detachment area, such as the Black Mountain fault (**Sheet 1**, Hauge, map pocket), can be interpreted as detached on the Heart Mountain fault, and therefore, as supportive of my interpretations. [Pierce and Nelson (1968, 1969) mapped the Black Mountain fault as juxtaposing Wapiti Formation and Willwood For-mation, suggesting that it offsets, and is younger than, the Heart Mountain detachment. However, the contact is mapped as approximately located, allowing the possibility that the Black Mountain fault is detached.] If the Black Mountain fault soles into the Heart Mountain detachment, then extension and translation of the Heart Mountain allochthon must have continued after Wapiti time. This is implied by the offset of the Trout Peak Trachyandesite, which overlies the Wapiti Formation, across the Black Mountain fault (Nelson and others, 1980). [Trout Peak Trachyandesite is also present in the hanging wall of the breakaway (**Sheet 1**, Hauge, map pocket), but it is absent from the breakaway footwall. This permits the interpretation that it onlaps the breakaway, compatible with the tectonic denudation model. In contrast, both footwall and hanging-wall equivalents are preserved across the Black Mountain fault, demanding tectonic offset of Trout Peak Trachyandesite across it.]

Like Dake (1916), when he "discovered" the Heart Mountain "thrust," I (Hauge, 1982, 1985) worked within a conceptual context favorable to my interpretation of a continuous Heart Mountain allochthon. Detachments with continuous extensional allochthons in the southern Basin and Range province were becoming well known in the late 1970s (e.g., Crittenden and others 1980), although, unlike the Heart Mountain detachment, these detachments are rooted and are not typically localized along footwall bedding. In addition, the mechanics of the continuous allochthon I envisioned was apparently tractable via the recently developed Coulomb-wedge mechanics of thrust allochthons (Elliott 1976; Dahlen 1984). In the late 1970s the time was ripe for the "discovery" of the continuous Heart Mountain allochthon. A few years earlier, such an interpretation would have been, like Bucher's (1933) first detached-block model was at the time of its proposal, totally without supporting analogs.

Further implications of the continuous allochthon model

An aspect of the interpretation of the detachment region brought into question by these studies is the use of the formal stratigraphic names "Wapiti Formation" and "Cathedral Cliffs Formation" for volcanic rocks in the detachment region. (See Hauge, 1985, 1990; and Pierce, 1987a, for a discussion of this issue.) The Cathedral Cliffs Formation was defined by Pierce (1963a) as everywhere predating Heart Mountain faulting, whereas, the Wapiti Formation was defined by Nelson and Pierce (1968) as everywhere postdating Heart Mountain faulting. Field observations indicated to me (Hauge, 1982, 1985) that much Wapiti is allochthonous on the detachment; yet allochthonous Wapiti is a contradiction in terms. Because of this problem inherent in the definitions of the formations, I (Hauge, 1985, 1990) chose to abandon use of these two formation names. Remapping of these units was beyond the scope of my study, so I chose simply to refer to the volcanic rocks previously mapped as Cathedral Cliffs and Wapiti formations as undifferentiated Absaroka volcanic rocks. The suggestion that these two terms be abandoned seemed to be supported by the numerous differences in mapping of these volcanic rocks by previous workers who used the names Wapiti and Cathedral Cliffs. Figure 2 of Hauge (1985) shows the extensive areas where the maps of Pierce (1978), Nelson and others (1980), and Prostka (1978), who were the major workers in these rocks in the 1970s, differ in interpretation of Wapiti versus Cathedral Cliffs formations.

Another aspect of the interpretation of the detachment region brought into question by these studies is the nature of the allochthon in the area of the detachment ramp. Specifically, the involvement of large volumes of volcanic rocks in the Heart Mountain allochthon may lend support to the idea that the area of land surface overridden by the allochthon was more limited than is suggested in the tectonic denudation model. The presence of volcanic rocks in

the area of the breakaway and the bedding-parallel component of the detachment at the time of faulting suggests the likelihood that their distal equivalents were present in the adjacent Bighorn Basin as well. This argument holds for the tectonic denudation model, which acknowledges pre-faulting thicknesses of volcanic rocks to be at least 1,500 ft (450 m) at the breakaway fault, and more strongly for the continuous allochthon model, which allows volcanic thicknesses of up to several kilometers during faulting. However, Willwood Formation strata, which underlie the allochthon in the Bighorn Basin, contain little volcanic detritus (Van Houten, 1944). In the context of the tectonic denudation model, the presence of only traces of distal volcanic rock on the "fault on former land surface," despite abundant nearby volcanism, may seem fortuitous. In contrast, the continuous allochthon model allows the presence of significant volumes of distal volcanic rocks in the western Bighorn Basin before initiation of faulting, if the detachment was within rather than upon Willwood and older strata. Under these conditions, the distal volcanic facies of the Bighorn Basin would have been incorporated into the allochthon rather than overridden by it, and any toe area, which could have been narrow due to continuous erosion during emplacement of the allochthon, would have been to the east of McCulloch Peak.

The evidence presently available does not prove or disprove either the "fault on former land surface" interpretation of Pierce (1960) or the alternative "subsurface ramp" model proposed here. The former model is favored by the lack of allochthonous rocks younger than Mississippian identified in the Bighorn Basin. The latter model explains this in terms of aspects of the erosional model of the Bighorn Basin described by Mackin (1937): in the context of the continuous allochthon model, a large part of the eroded basin fill of the northwestern Bighorn Basin, which by Oligocene was thick enough to engulf Rattlesnake Mountain, was allochthonous on the Heart Mountain detachment rather than of direct sedimentary origin. During Neogene regional uplift and erosion, the less resistant rocks, such as allochthonous Willwood sediments and alluvial-facies Absaroka volcanic rocks, would have been preferentially removed, leaving behind the more resistant allochthonous rocks, such as the carbonate rocks of Heart Mountain and McCulloch Peaks. Volcanic rocks observed at McCulloch Peak (Rouse, 1937) are direct evidence that volcanic rocks were deposited or emplaced as far east as the easternmost known remnants of the allochthon. Fission-track data of Giegengack and others (1986, 1988) further support the idea of a once-extensive cover of volcanic rocks in the western Bighorn Basin. The "subsurface ramp" model described here is also compatible with the bedding-transgressive nature of the detachment between Heart Mountain and McCulloch Peak, as well as with the presence of allochthonous Willwood in the western Bighorn Basin near the mouth of the Clarks Fork river (**Sheet 1**, Hauge, map pocket — although these Willwood klippen need not be allochthonous on the Heart Mountain detachment (Wise, 1957).

An alternate view of the continuous allochthon

In an imaginative paper, Sales (1983, p. 117) embraced the concept of a continuous Heart Mountain allochthon:

> *By conventional interpretation,* [the Heart Mountain allochthon] *is some type of free-slide of blocks that predated their burial under Absaroka volcanics...By contrast, this paper suggests that they were moved as gigantic blocks of "ground moraine" in an equally gigantic Absaroka rock "glacier."*

Whereas I envisioned a slow rate of emplacement (Hauge, 1983), Sales (1983, p. 117) envisioned catastrophic emplacement of a continuous allochthon:

> *Arguments can be made for: a) a steady-state collapse linked to the rate of extrusion* [like that of Hauge, 1983a], *b) incrementally catastrophic collapse with earthquakes shaking down the pile every few tens to few hundred years, c) a single catastrophy* [sic] *in which an over-sized pile high on the dip slope was effectively liquified* [sic] *by seismic vibration, then began to override its swampy toe which floated the mass, and resulted in geologically instantaneous complete collapse. The latter is favored because it enhances the role of fluid overpressure.*

Sales, in part echoing Voight (1972), listed several objections to the tectonic denudation concept of Heart Mountain faulting, among which are the following:

I have never been impressed with the potential of earthquakes for triggering and maintaining motion on the Heart Mountain "detachment" under the free-sliding concept as suggested by Pierce (1975). That mechanism, sometimes characterized as the "shale-shaker" mechanism, would act much like frost-heaving, with each vertical acceleration moving the mass a minute distance downslope, with excessive repetitions required to do significant work on that 2 degree slope. Also, vertical accelerations that strong would have shaken the blocks down to rubble and would have left extensive talus aprons around the blocks. In other words, Heart Mountain blocks could not have hung together on a "shale-shaker". (p. 139)

Some blocks are vertical-sided and seem to have no talus at their feet. There are many 1500 foot cliffs, but none that I know of without talus aprons at their bases. Even if the blocks were exposed for only two minutes prior to burial and after movement stopped, there should be talus aprons at their bases. (p. 127)

the lowermost bed of dolomite [top of the footwall where the detachment follows Ordovician bedding] *is nearly undisturbed in contrast to the fragmented condition of many of the blocks above. Yet, apparently near-vertical-walled blocks up to 2,000 feet thick and several square miles in extent supposedly moved over it, with extreme differential loading if it were a free slide. I feel that it would be physically impossible for* [the Cambrian] *shale...to support blocks of that mass without their sinking into it and ripping up that delicate persistent bed* [of Ordovician dolomite] *between the detachment surface and the underlying shale under these conditions. This would be unlikely in a static situation, and doubly so in a dynamic one.* (p. 125)

Sales (1983) described his concept of Heart Mountain faulting in detail in this long (48 pages, 40 figures) paper, but in its most succinct form it reduces to the following:

I submit that six potential factors, each of which would have been unable to create the structure by itself, uniquely combined to create the Heart Mountain "detachment." These are:

1. *The presence of a long dip-slope above basin level.*
2. *The down-dip termination of that slope in a basin-facing monocline.*
3. *The development of a very large volcanic pile centered high on that dip-slope.*
4. *Fluidization of the entire pile by normal tectonic earthquakes*
5. *The presence of swamp terrain around the base of the volcanic pile.*
6. *Possible "floating of the toe" by artesian overpressure within the volcanic pile.* (p. 136-137)

the unique blending of the five or six [individual factors] *proved...to be...exceedingly catastrophic.* (p. 141)

One of the most logical reasons for a catastrophic collapse of the pile would be what I think of as the "concrete vibrator" mechanism. One cannot watch these in action on heavy construction without being impressed. Concrete is poured with minimum water for maximum ultimate strength, and it hangs up in one end of the form and on the reinforcing bars. The minute the vibrator is turned on, the concrete liquefies and instantly flows to a smooth horizontal surface in the bottom of the form. This is a much more potent mechanism than vibrating a free-standing block down a very gentle slope [the earthquake oscillation mechanism of the tectonic denudation model] *with the same "seismic" energy.* (p. 143)

Sales favored catastrophic emplacement of the continuous allochthon largely because he thought the mechanics of allochthon emplacement was more plausible in these terms. In contrast, I viewed Coulomb-wedge theory as an adequate explanation of the mechanics of gradual emplacement of the allochthon. Pierce and Nelson (1986), in countering my continuous allochthon model, argued that the volume of allochthonous volcanic rocks required by the continuous allochthon model indicates an unreasonably thick volcanic pile before emplacement of the allochthon. I viewed this argument as inappropriate, because the continuous allochthon model envisioned gradual growth of the allochthon by addition of volcanic rocks as it was emplaced coeval with volcanism (Hauge, 1990). Pierce and Nelson's assertion may be better directed against Sales' concept of emplacement of a continuous allochthon by catastrophic collapse of a volcanic edifice.

Mechanics of the continuous allochthon model

In comparison to the mechanics of emplacement of detached blocks, the mechanics of emplacement of a continuous Heart Mountain allochthon may be relatively tractable, due to its similarities to the mechanics of continuous contractional allochthons (thrust sheets). Gravitational spreading (Elliott, 1976) of the Heart Mountain allochthon, suggested by Hauge (1982, 1985), requires neither catastrophic emplacement rates nor simultaneous movement of the entire allochthon. Dahlen (1984), in a theoretical analysis of the mechanics of thrust sheets, demonstrated that for an extremely low coefficient of basal friction, an extensional allochthon such as that envisioned by the continuous allochthon model can develop. Price (1988) argued that a variety of mechanisms may reduce friction along thrust faults, and a similar range probably applies to the Heart Mountain allochthon (Hauge, 1985). Abnormal fluid pressure is one means by which friction along the detachment beneath a continuous allochthon might be reduced, whereas such pressures are unlikely either to develop or be maintained beneath rapidly moving detached blocks (Davis, 1965). Local development of low friction at the base of the Heart Mountain allochthon, by fluid pressure, seismicity, or other mechanisms, might have allowed a sequence of small displacements of portions of the allochthon, analogous to the movement of thrust sheets. In this view, the allochthon reached its present configuration by many such movements over many years.

Present controversy: continuous allochthon or tectonic denudation?

The present understanding of the Heart Mountain detachment is, like its past history, marked by controversy. Deep differences exist between advocates of the tectonic denudation and continuous allochthon models. In response to my (Hauge, 1985) development of the continuous allochthon model, Pierce (1987a) presented a comprehensive argument for the tectonic denudation model and against the continuous allochthon model. I (Hauge, 1990) further developed the continuous allochthon model and defended it against the arguments of Pierce (1987a). Nelson (1991) and Pierce and others (1991) focused discussion on lineations beneath volcanic rocks along the detachment, which they interpreted as depositional lineations and I (Hauge, 1985, 1991) interpreted as tectonic striae. A brief summary of the different interpretations of Pierce (1987a) and Hauge (1985, 1990) follows.

Recent arguments regarding the viability of the tectonic denudation model

In defense of the tectonic denudation model, Pierce (1987a) argued that the Wapiti Formation, which is mapped in many areas by Pierce (1987a) as in depositional contact with the detachment, must postdate faulting for several reasons. First, the breakaway fault is buried by rocks of the Wapiti Formation. Second, allochthonous carbonate rocks are underlain by detachment breccia that contains no volcanic material, yet such volcanic material should exist if the laterally adjacent volcanic rocks are allochthonous. Similarly (third), carbonate breccia containing no volcanic material underlies volcanic rocks along the detachment. If the volcanic rocks were allochthonous, this breccia should contain volcanic material, whereas if the volcanic rocks were deposited on a tectonic blanket of fault breccia on the tectonically denuded surface, the observed relationships are explained. Fourth, the Wapiti Formation is in depositional contact with upper-plate Paleozoic rocks. Fifth, volcanic fault breccia is absent where volcanic rocks overlie the detachment, and such breccia should exist if the volcanic rocks are allochthonous. Sixth, striae beneath volcanic rocks, which I interpreted as evidence of tectonic emplacement of the volcanic rocks (Hauge, 1985), are depositional rather than tectonic.

In the context of the continuous allochthon model, these arguments may be answered, respectively, as follows (Hauge 1985, 1990). First, only the volcanic rocks that overlap the breakaway fault are demonstrably younger than faulting, whereas those

in the hanging wall of the breakaway are allochthonous. Second, if slip along the detachment is largely accommodated along the microbreccia at the base of the volcanic fault breccia rather than by flow of the breccia, no mixing of carbonate and volcanic detachment breccia is required. This response also applies to the third argument. Fourth, depositional contacts between volcanic and carbonate rocks are predicted by both models. However, I interpreted many such contacts as tectonic that Pierce interpreted as depositional. Fifth, volcanic fault breccia is present in many areas where volcanic rocks overlie the detachment, as are other indications of tectonic deformation (table 1 of Hauge, 1985). Sixth, the striated, slickensided surface locally present at the base of volcanic rocks along the detachment is interpreted as tectonic not only because of its similarity to slickensides and striae typical of faults in general, but also because of the suite of other structures of tectonic origin associated with the striae and slickensides (e.g., figures 5, 6 of Hauge, 1985). The other features interpreted as tectonic include faulted, tilted, and truncated volcanic strata, and sheared, shattered, and brecciated basal volcanic rocks.

As further evidence of tectonic denudation, Pierce (1987a) argued that small masses of Mississippian and Devonian rocks overlying the detachment and engulfed by volcanic rocks are explained only if they were derived from the upper parts of larger detached blocks and were subsequently buried by volcanic rocks. I (Hauge, 1990) viewed these small masses as downfaulted along upper-plate faults within the continuous allochthon. Pierce (1987a) argued that relationships surrounding the Crandall Conglomerate require tectonic denudation; these arguments, and my rebuttal (Hauge, 1990), were reviewed in a previous section. Finally Pierce (1987a) cited relationships associated with clastic dikes as requiring tectonic denudation; these arguments, as well as my response (Hauge, 1990), were reviewed in a previous section.

Recent arguments regarding the viability of the continuous allochthon model

Pierce (1987a) contended, for several reasons, that the continuous allochthon model is inherently flawed. One argument was that faults to transport Wapiti Formation onto and along the detachment do not exist. I (Hauge, 1985, 1990) cited several areas where such faults exist, although mapping of these faults in less accessible areas of the allochthon has not been undertaken. A specific locality of disagreement in this regard is the contact between the carbonate cliffs and volcanic rocks at the west end of Cathedral Cliffs, which is easily accessible and exposed within a few meters of the detachment but is poorly exposed at higher levels. Pierce (1987a) also argued that "the volume of Wapiti filling the spaces between the allochthonous blocks in proportion to the volume of those blocks is much too great for the Wapiti to have been allochthonous" (p. 552). The continuous allochthon model of Hauge (1985, 1990) envisions extension of the allochthon coeval with volcanism (extrusion of Wapiti Formation), thus eliminating the perceived volume problem. In addition, Pierce (1987a) argued that most igneous dikes, many of which are within volcanic rocks mapped by Pierce as Wapiti (younger than faulting), were intruded after movement on the detachment and therefore could not accommodate extension of the allochthon. In contrast, I inferred that the volume occupied by these dikes, which have no lower-plate equivalents, was created by the last phase of extension of a continuous allochthon, documenting the involvement of Wapiti Formation strata in late-stage extension (Hauge, 1990). Finally, Pierce argued that upper-plate faults with strike-slip striae, such as I observed north of Pilot Creek (Hauge, 1985), are incompatible with the continuous allochthon model, although reasons for the alleged incompatibility are not stated. However, this argument is contradicted by the existence of strike-slip faults in other extensional allochthons, such as in the Whipple Mountains, southeastern California.

In summary, disagreements between the advocates of the tectonic denudation and continuous allochthon models are fundamental and wide ranging. They include differences in the nature of specific exposed field relationships, such as whether contacts are depositional or tectonic, and whether volcanic rocks are allochthonous or in situ. They include disagreement about the use of the terms Wapiti and Cathedral Cliffs formations as assigned to volcanic units in the detachment area. They also include disagreements as to whether the opposing models are geometrically and mechanically plausible. The differences between the interpretations are well defined, so that future workers will have a clear choice between the tectonic denudation model, the continuous allochthon model, and possibly other models that have yet to be formulated.

Discussion

The evolution of concepts of Heart Mountain faulting provides an object lesson regarding pitfalls in the process of scientific inquiry. One pitfall is the dependency of most scientists on the conceptual climate within which they work, or the scientific paradigm (Kuhn, 1970) dominant at the time of their endeavors. Another is the difficulty in recognizing that what we may take for granted as established truths may, in retrospect, appear to have been little more than poorly substantiated assumptions.

An example of the dependency of interpretations on the contemporary conceptual climate is the evolution of understanding of the basic nature of the Heart Mountain allochthon. The earliest workers (Eldridge, Fisher), who viewed Heart Mountain at a time when no low-angle faults were known from anywhere in the western United States, were unable to infer with confidence that older over younger relationships were most likely related to low-angle faulting. It was not until the time of Dake, whose work (1916) postdated the documentation of thrust faults in western Wyoming (1907, 1914), that the "obvious" (albeit incorrect) interpretation of the Heart Mountain "thrust" could be confidently made. Given that the conceptual climate regarding low-angle faults changed little until more than 60 years after Dake's interpretation, it is remarkable that Walter Bucher saw beyond its constraints and understood that the Heart Mountain allochthon was in many ways unlike thrust allochthons and was fundamentally extensional, not contractional. When I made the most recent, still controversial, reinterpretation of the Heart Mountain allochthon in the early 1980s, the conceptual climate was amenable to my reinterpretation because the concept of continuous extensional allochthons above low-angle normal faults was under active development in theories of metamorphic core complexes. Thus, in the history of understanding of Heart Mountain faulting, Walter Bucher deserves distinct honor for seeing clearly beyond the confines of his contemporary conceptual climate.

An example of the difficulty in recognizing that presumably "established truths" are instead poorly substantiated assumptions is the nature of the contact at the base of the early basic breccia (Wapiti Formation) in the area of the Heart Mountain fault. The pre-early basic breccia "unconformity," first mapped by Hague (1899), was confirmed in the Clarks Fork area by Rouse (1937) before the detachment was recognized in that area. Pierce (1957) deserves credit for the breakthrough discovery of the Heart Mountain detachment in the Clarks Fork area and his recognition that the "unconformity" beneath the early basic breccia was of tectonic rather than erosional origin. In the context of the tectonic denudation model, Pierce's (1957) publication marks the end of a misunderstanding that had been accepted with little question for nearly 60 years. Pierce (1957, p. 602-609) considered the possibility that the early basic breccia was allochthonous, but he dismissed it as unsupported by field relationships. From the perspective of the continuous allochthon model, which requires that the basal early basic breccia was allochthonous, Pierce (1957) was, like his predecessors, misled by the established idea of a sub-early basic breccia unconformity (either partly tectonic or wholly erosional in origin) and the lack of a concept of a continuous extensional allochthon within which allochthonous early basic breccia is understandable. However, from the alternative perspective of the tectonic denudation model, my continuous allochthon model of Heart Mountain faulting is a misapplication of an idea that may be appropriate only to rooted detachment systems such as metamorphic core complexes.

Conclusions

The history of understanding of Heart Mountain faulting is a history of controversies. Was the allochthon a contractional thrust sheet or extensional detached blocks? What triggered the formation of the detachment, and what mechanism allowed movement of the allochthon along it? To what degree were Absaroka volcanic rocks involved in faulting? Was the extensional allochthon comprised of numerous detached blocks or a continuous allochthon? To the degree that they have been re-

solved, each controversy was settled by careful field study. Similarly, additional mapping of the stratigraphy and structure of volcanic rocks in the detachment area is required in the next phase of investigation, to resolve the present outstanding question: are volcanic rocks overlying the detachment and breakaway everywhere allochthonous, or do localities exist where a depositional contact between volcanic rocks and the detachment can be proven? The former would support the continuous allochthon model; the latter the tectonic denudation model. The "South of Silver Gate" locality was presented by Pierce (1987b) as the showcase example of a depositional contact between volcanic rocks and the detachment, but Prostka (1978) and I (Hauge, 1985; 1990) interpreted the contact there as tectonic (**Figure 13**). Future workers might direct their attention to this locality as a first test of the two models.

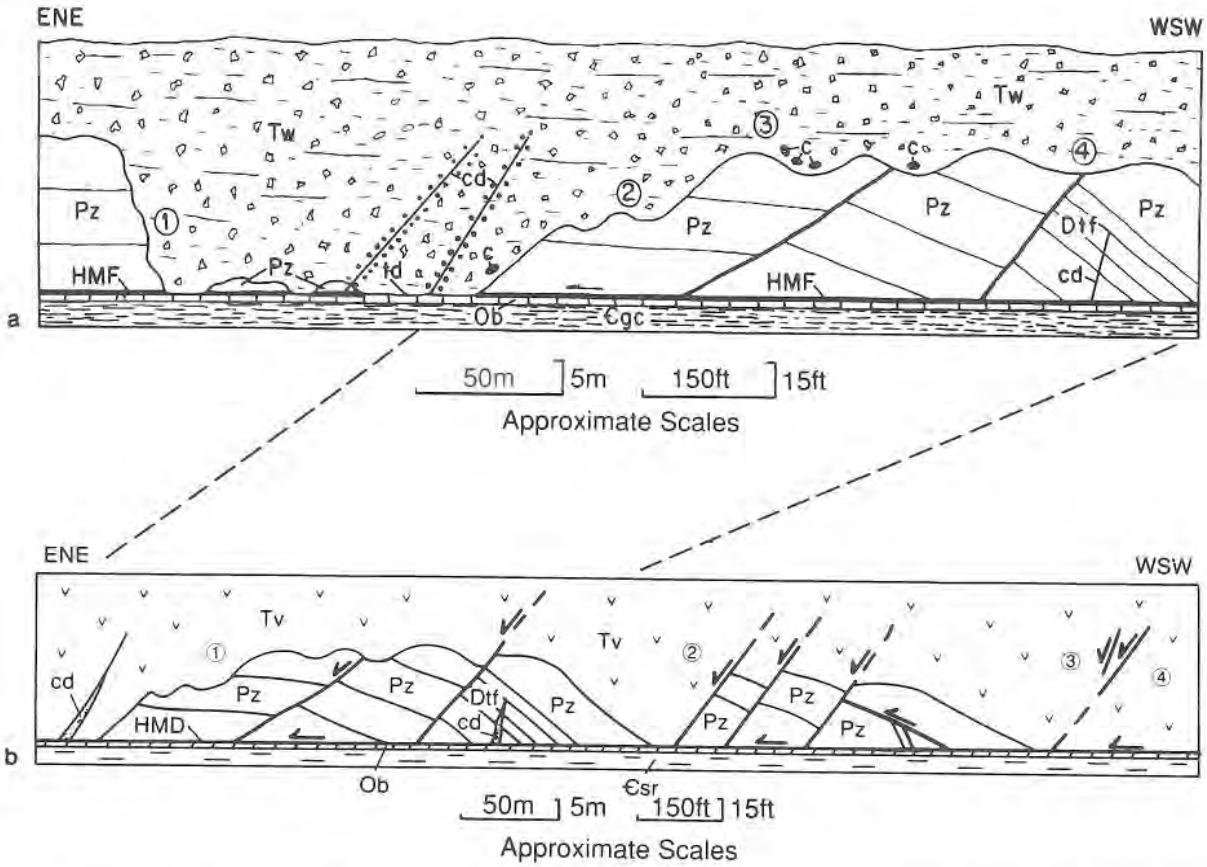

Figure 13. Two interpretations of relationships along the Heart Mountain detachment south of Silver Gate, Montana.
a. Interpretation of Pierce (1987a, p. 561): generalized cross section...showing relations between upper-plate blocks (Pz) of the Heart Mountain fault, volcanic rocks of the Wapiti Formation (Tw) containing scattered clasts of Paleozoic and Precambrian rocks (c), and dikes of carbonate fault breccia (cd). Faults in Paleozoic rocks do not extend into the Wapiti Formation. (Dtf) Three Forks Formation; (Ob) basal bed of Bighorn Dolomite; (Cgc) Grove Creek Limestone member of the Snowy Range Formation; (td) surface of tectonic denudation; dots along dikes indicate flow banding adjacent to dike and intermixing of carbonate fault breccia with volcanic rock; arrow indicates relative direction upper plate moved; numbers indicate locality referred to in text [of Pierce, 1987a]. From Pierce and Nelson, 1986.
b. Interpretation of Hauge (1990, p. 1181): generalized cross section depicting a steep exposure 1 km south of Silver Gate, Montana...; modified and expanded from Figure 9 of Pierce, 1987a. Allochthonous Tertiary volcanic rocks (Tv) and Paleozoic rocks (Pz, mostly Madison Limestone; Dtf, Three Forks Formation) are intruded by clastic dikes (cd) of fault breccia and are offset across faults that truncate into the Heart Mountain detachment (HMD). Footwall rocks are ~ 2 m of Bighorn Dolomite (Ob) underlain by Snowy Range Formation limestone and shale (Csr). Circled numbers indicate localities discussed in the text [of Hauge, 1990].

Acknowledgments

This paper has benefited greatly from reviews by D.L. Blackstone, Jr., S. Roberts, C. Rossen, A.W. Snoke, K.A. Sundell, and D.U. Wise. My work on the Heart Mountain detachment was aided greatly by the guidance and encouragement of G.A. Davis and by an introduction to the field relationships by W.G. Pierce.

References cited

Blackstone, D.L., Jr., 1985, South Fork detachment fault, Park County, Wyoming: geometry — extent — source: University of Wyoming Contributions to Geology, v. 23, p. 47-62.

Bown, T.M., 1982a, Geology, paleontology, and correlation of Eocene volcaniclastic rocks, southeast Absaroka Range, Hot Springs County, Wyoming: U.S. Geological Survey Professional Paper 1201A, 75 p.

_____ 1982b, Catastrophic large-scale late Cenozoic detachment faulting of Eocene volcanic rocks, southeast Absaroka Range, northwest Wyoming: Wyoming Geological Association 33rd Annual Field Conference Guidebook, p. 185-201.

Brittenham, M.D., and Tadewald, B.H., 1985, Detachment and basement involved structures beneath the Absaroka Range volcanics, *in* Gries, R.R., and Dyer, R.C., editors, Seismic exploration of the Rocky Mountain region: Rocky Mountain Association of Geologists and Denver Geophysical Society, p. 31-43.

Bucher, W.H., 1933, Volcanic explosions and overthrusts: Transactions of the American Geophysical Union, v. 14, p. 238-242.

_____ 1935, Remarkable local folding, possibly due to gravity, bearing on the Heart Mountain thrust fault problem [abstract]: Proceedings of the Geological Society of America for 1934, p. 69.

_____ 1940, The geology of the Cody region: Transactions of the New York Academy of Sciences, series 2, v. 2, no. 7, p. 165-168.

_____ 1947, Heart Mountain problem, *in* University of Wyoming—Wyoming Geological Association—Yellowstone Bighorn Research Association Field Conference in the Bighorn Basin Guidebook, p. 189-197.

Burchfiel, B.C., Wernicke, B., Willemin, J.H., Axen, G.J., and Cameron, C.S., 1982, A new type of décollement thrusting: Nature, v. 300, p. 513-515.

Clarey, T.L., 1990, Thin-skinned shortening geometries of the South Fork fault, Bighorn Basin, Park County, Wyoming: Wyoming Geological Association 41st Annual Field Conference Guidebook, p. 89-98.

Crittenden, M.D. Jr., Coney, P.J., and Davis, G.H., editors, 1980, Cordilleran metamorphic core complexes: Geological Society of America Memoir 153, 490 p.

Dahlen, F.A., 1984, Noncohesive critical Coulomb wedges: an exact solution: Journal of Geophysical Research, v. 89, p. 10,125-10,133.

Dahlen, F.A., Suppe, J., and Davis, D., 1983, Mechanics of fold-and-thrust belts and accretionary wedges: cohesive Coulomb theory: Journal of Geophysical Research, v. 89, p. 10,087-10,101.

Dake, C.L., 1916, The Heart Mountain overthrust and associated structures in Park County, Wyoming: Journal of Geology, v. 26, p. 45-55.

Davis, G.A., 1965, Role of fluid pressure in mechanics of overthrust faulting: discussion: Geological Society of America Bulletin, v. 76, p. 463-468.

Davis, D., Suppe, J., and Dahlen, F.A., 1983, Mechanics of fold-and-thrust belts and accretionary wedges: Journal of Geophysical Research, v. 88, p. 1153-1172.

de Sitter, L.U., 1954, Gravitational gliding tectonics, an essay in comparative structural geology: American Journal of Science, v. 252, p. 321-344.

Eldridge, G.H., 1894, A geological reconnaissance in northwest Wyoming: U.S. Geological Survey Bulletin 119, p. 30-31.

Elliott, D., 1976, The motion of thrust sheets: Journal of Geophysical Research, v. 81, p. 949-963.

Elliott, J.E., 1979, Geologic map of the southwestern part of the Cooke City Quadrangle, Montana and Wyoming: U.S. Geological Survey Miscellaneous Investigations Series, Map I-1084, scale 1:24,000.

Fisher, C.A., 1906, Geology and water resources of the Bighorn Basin, Wyoming: U.S. Geological Survey Professional Paper 53, 37 p.

Giegengack, R., Omar, G.I., and Lutz, T.M., 1986, A reconnaissance fission track uplift chronology for the northwest margin of the Bighorn Basin, *in* Garrison, P.B., editor, Geology of the Beartooth uplift and adjacent basins, Montana: Montana Geological Society and Yellowstone Bighorn Research Association Joint Field Conference Guidebook, p. 179-184.

Giegengack, R., Omar, G.I., Lutz, T.M., and Johnson, K.R., 1988, Tectono-thermal history of the Bighorn Basin and adjacent highlands, Montana-Wyoming: Geological Society of America Abstracts with Programs, v. 20, no. 6, p. 416.

Gingerich, P.D., 1983, Paleocene-Eocene faunal zones and a preliminary analysis of Laramide structural deformation in the Clarks Fork Basin, Wyoming: Wyoming Geological Association 34th Annual Field Conference Guidebook, p. 185-195.

Goguel, J., 1969, Le role de l'eau et de la chaleur dans les phenomines tectoniques (The role of the water and heat in tectonic phenomena): Revue de Geographie Physique et de Geologie Dynamique, v. 11, no. 2, p. 153-163.

Hague, A., 1899, Description of the Absaroka Quadrangle (Crandall and Ishawooa quadrangles): U.S. Geological Survey Geological Atlas, Folio 52, 6 p.

Hares, C.J., 1933, Relative age of the Heart Mountain overthrust and the Yellowstone Park volcanic series [abstract]: Proceedings of the Geological Society of America for 1932, p. 84.

Hauge, T.A., 1982, The Heart Mountain detachment fault, northwest Wyoming: involvement of Absaroka volcanic rock: Wyoming Geological Association 33rd Annual Field Conference Guidebook, p. 175-179.

_____ 1983, Geometry and kinematics of the Heart Mountain detachment fault, northwestern Wyoming and Montana [Ph.D. dissertation]: Los Angeles, California, University of Southern California, 265 p.

_____ 1985, Gravity-spreading origin of the Heart Mountain allochthon, northwestern Wyoming: Geological Society of America Bulletin, v. 96, p. 1440-1456.

_____ 1990, Continuous allochthon model of Heart Mountain faulting: Geological Society of America Bulletin, v. 102, p. 1174-1188.

_____ 1991, Continuous allochthon model of Heart Mountain faulting: reply: Geological Society of America Bulletin, v. 103, p. 719-722.

Heisenberg, W., 1983, Encounters with Einstein and other essays on people, places, and particles: Princeton, New Jersey, Princeton University Press, 141 p.

Hewett, D.F., 1920, The Heart Mountain overthrust, Wyoming: Journal of Geology, v. 28, p. 536-557.

Hsu, K.J., 1969, Role of cohesive strength in the mechanics of overthrust faulting and of landsliding: Geological Society of America Bulletin, v. 80, p. 927-952.

Hubbert, M.K., and Rubey, W.W., 1959, Role of fluid pressure in mechanics of overthrust faulting. I. Mechanics of fluid-filled porous solids and its application to overthrust faulting: Geological Society of America Bulletin, v. 70, p. 115-166.

Hughes, C.J., 1970a, Role of cohesive strength in the mechanics of overthrust faulting and of landsliding: discussion: geological Society of America Bulletin, v. 81, p. 607-608.

_____ 1970b, The Heart Mountain detachment fault—a volcanic phenomenon?: Journal of Geology, v. 78, p. 107-116.

_____ 1970c, The Heart Mountain detachment fault—a volcanic phenomenon? a reply: Journal of Geology, v. 78, p. 629-630.

_____ 1973, Igneous activity, metamorphism, and Heart Mountain faulting at White Mountain, northwestern Wyoming: discussion: Geological Society of America Bulletin, v. 84, p. 3109-3110.

Johnson, G.D., 1934, Geology of the mountain uplift transected by the Shoshone Canyon, Wyoming: Journal of Geology, v. 42, p. 809-838.

Kehle, R.O., 1970, Analysis of gravity sliding and orogenic translation: Geological Society of America Bulletin, v. 81, p. 1641-1664.

Kuhn, T. S., 1970, The structure of scientific revolutions: Chicago, Illinois, University of Chicago Press, 172 p.

Lawrence, R.A. and Sheets, M.M., 1934, Geology of Logan Mountain, Wyoming, and its bearing upon the Heart Mountain overthrust [abstract]: Proceedings of the Geological Society of America for 1933, p. 93-94.

Logan, W.E., 1860, Remarks on the fauna of the Quebec Group of rocks and the Primordial zone of Canada: Canadian Naturalist, v. 5, 472-477.

Longwell, C.R., 1945, Low-angle normal faults in the Basin and Range province: American Geophysical Union Transactions, v. 26, p. 107-118.

McConnell, R.G., 1887, Report on the geological structure of a portion of the Rocky Mountains, accompanied by a section measured near the 51st Parallel: Geological Survey of Canada Annual Report, 1886, v. 2, Report D, p. 5-41.

Mackin, J.H., 1937, Erosional history of the Bighorn Basin; Geological Society of America Bulletin, v. 48, p. 813-894.

Melosh, H.J., 1981, Acoustically activated décollement: mechanics of the Heart Mountain fault [abstract]: EOS., v. 62, no. 45, p. 1046.

_____ 1983, Acoustic fluidization: American Scientist, v. 71, p. 158-165.

Murchison, R.I., 1849, On the geologic structure of the Alps, Apennines, and Carpathians, more especially to prove a transition from Secondary to Tertiary rocks, and the development of Eocene deposits in southern Europe: Geological Society of London Quarterly Journal, v. 5, p. 157-312.

Nelson, W.H., 1991, Kinematic model of a continuous Heart Mountain allochthon: discussion: Geological Society of America Bulletin, v. 103, p. 718-719.

Nelson, W.H., and Pierce, W.G., 1968, Wapiti Formation and Trout Peak trachyandesite, northwestern Wyoming: U. S. Geological Survey Bulletin, 1254-H, p. Hl-Hll.

Nelson, W.H., Pierce, W.G., Parsons, W.H., and Brophy, G.P., 1972, Igneous activity, metamorphism, and Heart Mountain faulting at White Mountain, northwestern Wyoming: Geological Society of America Bulletin, v. 83, p. 2607-2620.

Nelson, W.H., Pierce, W.G., and Brophy, G.P., 1973, Igneous activity, metamorphism, and Heart Mountain faulting at White Mountain, northwestern Wyoming: reply: Geological Society of America Bulletin, v. 84, p. 3111-3112.

Nelson, W.H., Prostka, H.J., and Williams, F.E., 1980, Geology and mineral resources of the North Absaroka Wilderness and vicinity, Park County, Wyoming, with sections on mineralization of the Cooke City mining district by James E. Elliott and aeromagnetic survey by Donald L. Peterson: U. S. Geological Survey Bulletin 1447, 101 p.

Peach, B.N., and Horne, J., 1884, Report on the geology of north-west Sutherland: Nature, v. 31, p. 31-35.

Pierce, W.G., 1938, Intrusive breccia along east margin of Absaroka Range, Wyoming [abstract]: Geological Society of America Bulletin, v. 49, p. 1896-1897.

_____ 1941, Heart Mountain and South Fork thrusts, Park County, Wyoming: American Association of Petroleum Geologists Bulletin, v. 25, p. 2021-2045.

_____ 1950, Source and movement of the Heart Mountain thrust blocks, Park County, Wyoming [abstract]: Geological Society of America Bulletin, v. 61, p. 1493.

_____ 1957, Heart Mountain and South Fork detachment thrusts of Wyoming: American Association of Petroleum Geologists Bulletin, v. 41, p. 591-626.

_____ 1958, Detachment thrusts, with special reference to the Heart Mountain thrust, Wyoming [abstract]: Washington Academy of Science Journal, v. 48, no. 4, p. 142.

_____ 1960a, The "break-away" point of the Heart Mountain detachment fault in northwestern Wyoming: *in* Geological Survey Research 1960: U.S. Geological Survey Professional Paper 400-B, p. B236-B237.

_____ 1960b, Reef Creek detachment fault in northwestern Wyoming [abstract]: Geological Society of America Bulletin, v. 71, p. 1944.

_____ 1963a, Cathedral Cliffs Formation, the early acid breccia unit of northwestern Wyoming: Geological Society of America Bulletin, v. 74, p. 9-22.

_____ 1963b, Reef Creek detachment fault, northwestern Wyoming: Geological Society of America Bulletin, v. 74, p. 1225-1236.

_____ 1965a, Geologic map of the Clark Quadrangle, Park County, Wyoming: U.S. Geological Survey Geologic Quadrangle Map GQ-477, scale 1:62,500.

_____ 1965b, Geologic map of the Deep Lake Quadrangle, Park County, Wyoming: U.S. Geological Survey Geologic Quadrangle Map GQ-478, scale 1:62,500.

_____ 1966a, Role of fluid pressure in mechanics of overthrust faulting: discussion: Geological Society of America Bulletin, v. 77, p. 565-568.

_____ 1966b, Geologic map of the Cody Quadrangle, Park County Wyoming: U.S. Geological Survey Geological Quadrangle Map GQ-542, scale 1:62,500.

_____ 1968, Tectonic denudation as exemplified by the Heart Mountain fault, Wyoming, *in* Orogenic belts: 23rd International Geological Congress Proceedings, Prague, Czechoslovakia, 1968, Section 3, p. 191-197.

_____ 1973, Principal features of the Heart Mountain fault, and the mechanism problem, *in* DeJong, K.A., and Scholten, R., editors, Gravity and tectonics: New York, John Wiley and Sons, p. 457-471.

_____ 1978, Geologic map of the Cody 1° x 2° Quadrangle, northwestern Wyoming: U.S. Geological Survey Miscellaneous Field Studies Map MF-963, scale 1:62,500.

_____ 1979, Clastic dikes of Heart Mountain fault breccia, northwestern Wyoming, and their significance: U.S. Geological Survey Professional Paper 1133, p. 1-25.

_____ 1980, The Heart Mountain break-away fault, northwestern Wyoming: Geological Society of America Bulletin, v. 91, p. 272-281.

_____ 1985, Map showing present configuration of Heart Mountain fault and related features, Wyoming and Montana: Geological Survey of Wyoming Map Series MS-15, scale 1:125,000.

_____ 1987a, The case for tectonic denudation by the Heart Mountain fault—A response: Geological Society of America Bulletin, v. 99, p. 552-568.

_____ 1987b, Heart Mountain detachment fault and clastic dikes of fault breccia, and Heart Mountain break-away fault, Wyoming and Montana, *in* Beus, S.S., editor, Geological Society of America Centennial Field Guide, Rocky Mountain Section, p. 147-154.

Pierce, W.G., and Nelson, W.H., 1968, Geologic map of the Pat O'Hara Mountain Quadrangle, Park County, Wyoming: U.S. Geological Survey Geological Quadrangle Map GQ-755, scale 1:62,500.

_____ 1969, Geologic map of the Wapiti Quadrangle, Park County, Wyoming: U.S. Geological Survey Geological Quadrangle Map GQ-778, scale 1:62,500.

_____ 1970, The Heart Mountain detachment fault—a volcanic phenomenon? a discussion: Journal of Geology, v. 78, p. 116-122.

_____ 1971, Geologic map of the Beartooth Butte Quadrangle, Park County, Wyoming: U.S. Geological Survey Geological Quadrangle Map GQ-935, scale 1:62,500.

_____ 1973, Crandall Conglomerate, an unusual stream deposit, and its relation to Heart Mountain faulting: Geological Society of America Bulletin, v. 84, p. 2631-2644.

_____ 1986, Some features indicating tectonic denudation by the Heart Mountain fault, *in* Garrison, P.B., editor, Geology of the Beartooth uplift and adjacent basins, Montana: Montana Geological Society and Yellowstone Bighorn Research Association Joint Field Conference Guidebook, p. 155-164.

Pierce, W.G., Nelson, W.H., and Prostka, H.J., 1973, Geologic map of the Pilot Peak Quadrangle, Park County, Wyoming, and Park County, Montana: U.S. Geological Survey Miscellaneous Geologic Investigations Map I-816, 1:62,500.

_____ 1982, Geologic map of the Dead Indian Peak Quadrangle, Park County, Wyoming: U.S. Geological Survey Geological Quadrangle Map GQ-1564, scale 1:62,500.

Pierce, W.G., Nelson, W.H., Tokarski, A.K., and Piekarska, E., 1991, Heart Mountain, Wyoming, detachment lineations — are they in microbreccia or in volcanic tuff?: Geological Society of America Bulletin, v. 103, p. 1133-1145.

Price, R.A., 1988, The mechanical paradox of large overthrusts: Geological Society of America Bulletin, v. 100, p. 1898-1908.

Prostka, H.J., 1978, Heart Mountain fault and Absaroka volcanism, Wyoming and Montana, U.S.A., *in* Voight, B., editor, Rockslides and Avalanches I. Natural phenomena: New York, Elsevier Scientific Publishing Company, p. 423-437.

Prostka, H.J., Ruppel, E.T., and Christiansen, R.L., 1975, Geologic map of the Abiathar Peak Quadrangle, Yellowstone National Park, Wyoming and Montana: U.S. Geological Survey Geologic Quadrangle Map GQ-1244, scale 1:62,500.

Richards, R.W., and Mansfield, G.R., 1912, The Bannock overthrust, a major fault in southeastern Idaho and northeastern Utah: Journal of Geology, v. 20, p. 681-709.

Rouse, J.T., 1937, Genesis and structural relationships of the Absaroka volcanic rocks, Wyoming: Geological Society of America Bulletin, v. 48, p. 1257-1296.

Rogers, W.B., and Rogers, H.D., 1843, On the physical structure of the Appalachian chain, as exemplifying the laws which have regulated the elevation of great mountain chains, generally: Association of American Geologists and Naturalists Reports, p. 474-531, Plates 16, 18-21. *Reprinted in* Rogers, W.B., 1884, A reprint of

annual reports and other papers on the geology of the Virginias: New York, Appleton, p. 601-642, Plates 3-5.25.

Rubey, W.W., and Hubbert, M.K., 1965, Role of fluid pressure in mechanics of overthrust faulting: reply: Geological Society of America Bulletin, v. 76, p. 469-474.

Sales J.K., 1983, Heart Mountain — blocks in a giant volcanic rock glacier: Wyoming Geological Association 34th Annual Field Conference Guidebook, p. 117-165.

Schultz, A.R., 1914, Geology and geography of a portion of Lincoln County, Wyoming: U.S. Geological Survey Bulletin 543, 141 p.

Sheets, M.M., 1935, Structural detail near the western border of the thrust sheets north of Shoshone River, Wyoming: American Journal of Science, v. 29, p. 144-150.

Shreve, R.L., 1968, The Blackhawk landslide: Geological Society of America Special Paper 108, 47 p.

Smedes, H.W., and Prostka, H.J., 1972, Stratigraphic framework of the Absaroka Volcanic Supergroup in the Yellowstone National Park region: U.S. Geological Survey Professional Paper 729-C, 33 p.

Stearns, D.W., Logan, J.M. and Friedman, M., 1974, Structure of Rattlesnake Mountain and related rock mechanics investigations, *in* Voight, B., editor, Rock mechanics, the American Northwest: 3rd Congress International Society of Rock Mechanics Expedition Guidebook: Special Publication, Experiment Station, College of Earth and Mineral Sciences, The Pennsylvania State University, p. 18-25.

Stevens, E.H., 1936, Inertia as a possible factor in the mechanics of low-angle thrust faulting: Journal of Geology, v. 44, p. 729-736.

_____ 1938, Geology of the Sheep Mountain remnant of the Heart Mountain thrust sheet, Park County, Wyoming: Geological Society of America Bulletin, v. 49, p. 1233-1266.

Straw, W.T., and Schmidt, C.J., 1981a, Heart Mountain detachment fault: a phreatomagmatic-hydraulic hypothesis: Geological Society of America Abstracts with Programs, v. 13, no. 4, p. 227.

_____ 1981b, Heart Mountain detachment fault: a phreatomagmatic-hydraulic hypothesis: Geological Society of America Abstracts with Programs, v. 13, no. 7, p. 562.

Sundell, K.A., 1982, Geology of the headwater area of the North Fork of Owl Creek, Hot Springs County, Wyoming: Wyoming Geological Survey Report of Investigations 15, 51 p.

_____ 1985, The Castle Rocks chaos: a gigantic Eocene landslide—debris flow in the southeast Absaroka Range, Wyoming [Ph.D. dissertation]: Santa Barbara, University of California, 286 p.

_____ 1990, Sedimentation and tectonics of the Absaroka basin of northwestern Wyoming: Wyoming Geological Association 41st Annual Field Conference Guidebook, p. 105-122.

Torres, V., and Gingerich, P.D., 1983, Summary of Eocene stratigraphy at the base of Jim Mountain, North Fork of the Shoshone River, northwestern Wyoming: Wyoming Geological Association 34th Annual Field Conference Guidebook, p. 205-208.

Van Houten, F.B., 1944, Stratigraphy of the Willwood and Tatman formations in northwestern Wyoming: Geological Society of America Bulletin, v. 55, p. 165-210.

Veatch, A.C., 1907, Geography and geology of a portion of southwestern Wyoming: U.S. Geological Survey Professional Paper 56, 178 p.

Voight, B., 1972, Fluid-wedge hypothesis and the Heart Mountain and Reef Creek décollements northwestern Wyoming, U.S.A.: Geological Society of America Abstracts with Programs, v. 4, no. 7, p. 698.

_____ 1973a, Clastic fluidization phenomena and the role of fluid pressure in mechanics of natural rock deformation: Geological Society of America Abstracts with Programs, v. 5, no. 2, p. 233.

_____ 1973b, Role of fluid pressure in mechanics of South Fork, Reef Creek, and Heart Mountain rockslides: Geological Society of America Abstracts with Programs v. 5, no. 2, p. 233-234.

_____ 1973c, The mechanics of retrogressive block-gliding, with emphasis on the evolution of the Turnagain Heights landslide, Anchorage, Alaska, *in* DeJong, K.A., and Scholten, R., editors, Gravity and tectonics: New York, John Wiley and Sons, p. 97-121.

_____ 1974a, Architecture and mechanics of the Heart Mountain and South Fork rockslides, *in* Voight, B. and Voight, M.A., editors, Rock mechanics: the American Northwest: 3rd Congress International Society of Rock Mechanics Expedition Guidebook: Special Publication, Experiment Station, College of Earth and Mineral Sciences, The Pennsylvania State University, p. 26-36.

_____ 1974b, Roadlog: Wapiti-Heart Mountain area—canyon, *in* Voight, B. and Voight, M.A., editors, Rock Mechanics: The American Northwest: 3rd Congress International Society of Rock Mechanics Expedition Guidebook: Special Publication, Experiment Station, College of Earth and Mineral Sciences, The Pennsylvania State University, p. 112-124.

_____ 1974c, Thin-skinned graben, plastic wedges, and deformable-plate tectonics, *in* Illies, J. H., and Fuchs, K., editors, Approaches to taphrogenesis: (Inter-Union Commission on Geodynamics Scientific Report No. 8), Stuttgart, E. Schweizerbart'sche Verlagsbuchhandlung, 1974, p. 395-419.

_____ 1976, Editor's comments on papers 39 and 40, *in* Voight, B., editor, Mechanics of thrust faults and décollement: Stroudsburg, Pennsylvania, Dowden, Hutchinson and Ross, Benchmark Papers in Geology, v.32, p. 357-360.

Wernicke, B.P., 1985, Uniform-sense normal simple shear of the continental lithosphere: Canadian Journal of Earth Sciences, v. 22, p. 108-125.

Willis, B., 1902, Stratigraphy and structure, Lewis and Livingston ranges, Montana: Geological Society of America Bulletin, v. 13, p. 305-352.

Wilson, W.H., 1975, Detachment faulting in volcanic rocks, Wood River area, Park County, Wyoming: Wyoming Geological Association 27th Annual Field Conference Guidebook, p. 167-171.

Wise, D.U., 1957, Tectonics and tectonic heredity in the southern Beartooth Mountains, Wyoming [Ph.D. dissertation]: Princeton, New Jersey, Princeton University, 187 p.

_____ 1983, Overprinting of Laramide structural grains in the Clarks Fork Canyon area and eastern Beartooth Mountains of Wyoming: Wyoming Geological Association 34th Annual Field Conference Guidebook, p. 77-87.

Frontispiece. Air oblique view northeast showing course of North Platte River across Seminoe Mountains at Black Canyon. Indicated are Seminoe Reservoir (A), Kortes Dam (B), Precambrian rocks of Seminoe Mountains (C), surface beveling crest of Seminoe Mountains at elevation of 7,350 feet, 1,200 feet above Kortes Reservoir level (D), South Granite Mountains fault system (between points E-E), downfaulted Pliocene and Miocene rocks (F), Paleozoic rocks (G), and Precambrian rocks of downfaulted core of Granite Mountains (H). Photo by P. T. Jenkins and L.P. House. Collection of J.D. Love.

Neogene stratigraphy and tectonics of Wyoming

Kathryn M. Flanagan
Department of Geology
Southern Illinois University
Carbondale, Illinois 62901

John Montagne
Department of Earth Sciences
Montana State University
Bozeman, Montana 59717

Abstract

The Neogene history of Wyoming included widespread deposition, normal faulting, regional uplift, climatic changes, development of modern drainage systems, and basin excavation. During the late Paleogene and Neogene, basins that had initially developed during the Laramide orogeny were filled with abundant volcaniclastic detritus of remote origin as well as locally derived detrital sediments. Late Tertiary fluvial and terrace deposits indicate a minimum fill of approximately 500 to 1,500 ft (150-460 m), whereas many basins may have contained over 3,000 ft (915 m) of Neogene rocks. Erosion of the basins occurred during the Pliocene and Pleistocene after the establishment of large, through-flowing rivers.

Paleoenvironmental and geologic interpretations of Neogene deposits in Wyoming and Nebraska indicate the initiation of regional uplift during the middle Miocene (Hemingfordian). During the middle Neogene, extensional deformation, perhaps related to the Basin and Range province, is manifested by normal faulting in parts of Wyoming. Normal faulting chiefly occurred between 13 and 9 Ma, but some faults (e.g., Teton fault) indicate Holocene displacement.

Introduction

Neogene sedimentary rocks are located in isolated patches across Wyoming (**Figure 1**). They occur as valley fills, in small isolated tracts of strata high on mountain ranges, and in the downthrown blocks of normal faults. The Neogene deposits of northern and southwestern Wyoming are scarce but are preserved in small erosional remnants on the Bighorn Mountains and atop Aspen Mountain on the Rock Springs uplift (Love and Christiansen, 1985). In central and southern Wyoming, Neogene sedimentary rocks are preserved on the downdropped sides of normal faults. In eastern Wyoming, late Cenozoic rocks form a blanket that covers the top of the Bear Lodge Mountains in the northeast corner of the State,

Flanagan, K. M., and Montagne, J., 1993, Neogene stratigraphy and tectonics of Wyoming , *in* Snoke, A.W., Steidtmann, J.R., and Roberts, S.M., editors, Geology of Wyoming: Geological Survey of Wyoming Memoir No. 5, p. 572-607.

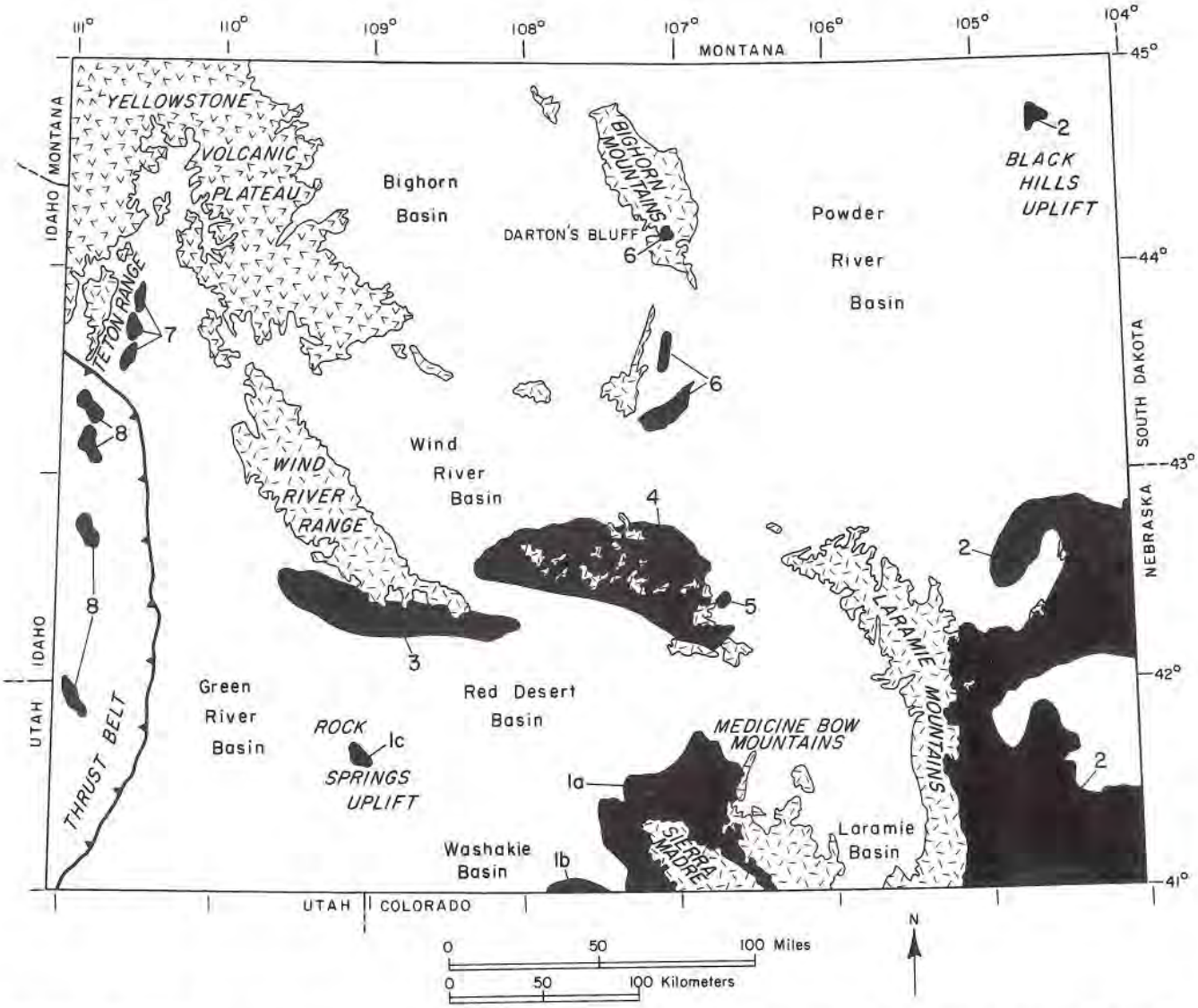

Figure 1. Geologic sketch map of Wyoming showing the general distribution of Neogene rocks in black. Numbers indicate locations of deposits discussed in the paper. 1, Browns Park Formation of Saratoga Valley (1a), Cherokee Ridge (1b), and Aspen Mountain (1c); 2, Arikaree and Ogallala formations of eastern Wyoming and the Ogallala Formation of the Bear Lodge Mountains; 3, Split Rock Formation, Circle Bar beds, and Leckie beds of the southern Wind River Range; 4, Split Rock, Moonstone, and Kortes formations of the Granite Mountains and Pathfinder areas; 5, Split Rock Formation of Bates Hole; 6, Split Rock Formation of Cedar Ridge and Darton's Bluff in the Bighorn Mountains; 7, Colter, Teewinot, Shooting Iron, and Camp Davis formations of northwest Wyoming; and 8, Salt Lake Formation of the thrust belt (compiled from Love and Christiansen, 1985). Very generalized areas of Precambrian (random line pattern) and Cenozoic igneous (v-pattern) rocks are also shown.

the top of the Laramie Mountains along ancient valley fills, and an area east of the Laramie Mountains that spreads into Nebraska. These patches of late Cenozoic sedimentary rocks have been correlated throughout the State on the basis of lithology, paleontological data, and geomorphic expression (e.g., Love, 1970; Denson, 1965a).

Neogene rocks have been mapped (Love, 1956a, 1961, 1970, 1978; Denson, 1965a, 1965b; Steidtmann and others, 1986; Montagne, 1955; Robinson and others, 1964; Staatz, 1983, and references therein) and discussed (McKenna and Love, 1972; Montagne, 1991) but due to lack of exposure, the late Cenozoic geologic history is still poorly understood. Scarcity of late Cenozoic rocks in Wyoming is the result of either Quaternary erosion or just nondeposition.

Geologic work on these deposits began with the first surveys of the West under the direction of

Hayden (1872). Subsequent mapping of the mountain fronts continued into the early twentieth century (Darton, 1906; Mansfield, 1927; Lovering, 1929), followed by mapping of the Neogene deposits in the basins. Many of the sedimentary deposits discussed in this paper were mapped but not described in detail. Several particularly interesting aspects of Wyoming's late Cenozoic geologic and tectonic history include: (1) the extent and depth to which Wyoming's basins were filled and subsequently excavated (Darton, 1906; Blackwelder, 1915; Mackin, 1937; Knight, 1953; Love, 1970; McKenna and Love, 1972); (2) the timing of normal faulting (Love, 1970, 1978; Steidtmann and Middleton, 1986); and (3) the timing and effects of regional uplift (Love, 1970; McKenna and Love, 1972; Bown, 1980; Swinehart and others, 1985).

The total extent to which Wyoming's basins were filled remains an unanswered question. Approximately 3,000 ft (1,000 m) of Oligocene to Pliocene rocks are preserved in parts of Wyoming (Emry, 1973; Love, 1952, 1970; Steidtmann and others, 1986). However, an important question is: How extensive was the original distribution of the Neogene deposits across Wyoming?

Widespread normal faulting occurred during the Neogene in Wyoming (**Figure 2**). The normal faults discussed are: North and South Granite Mountains

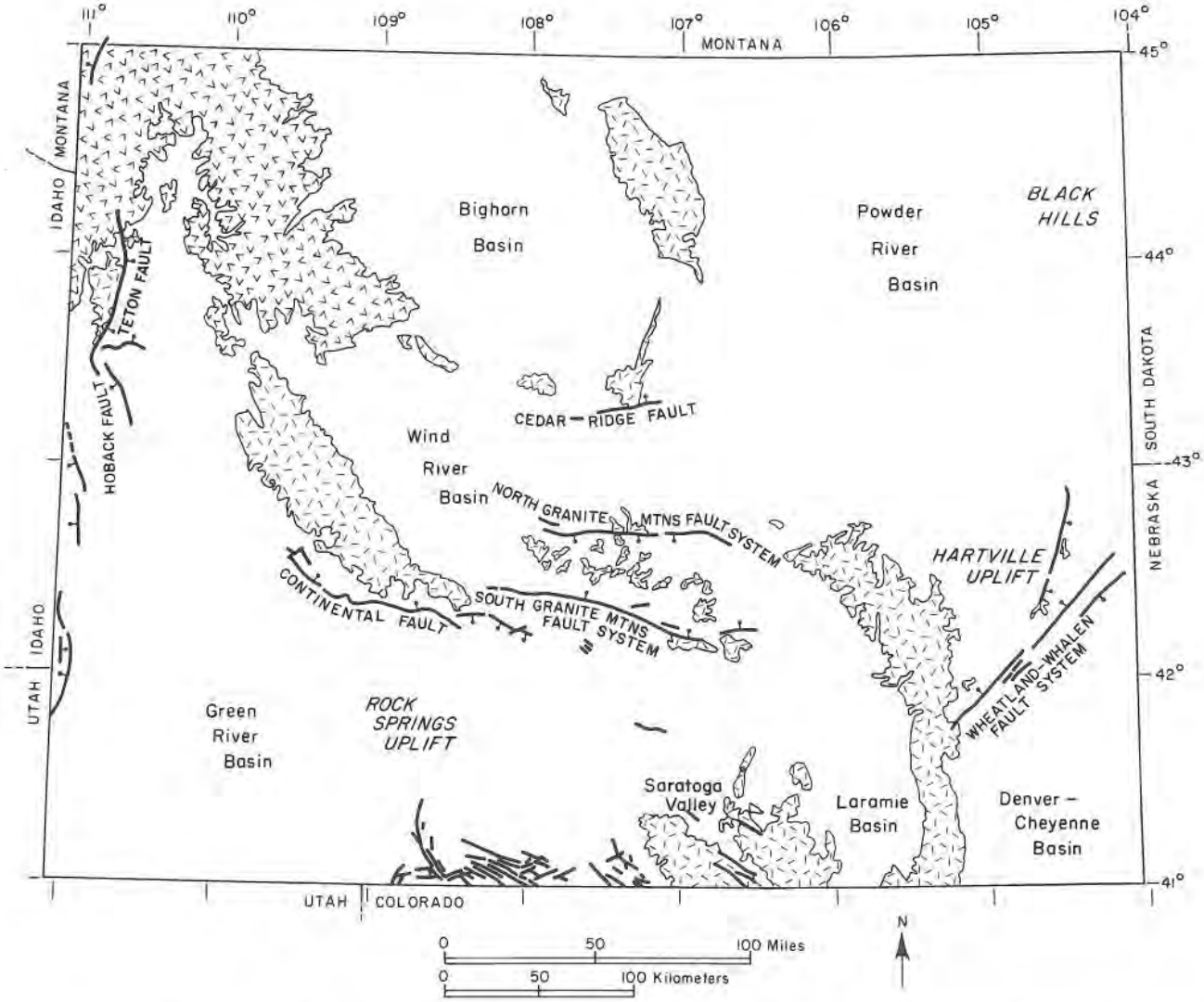

Figure 2. Location of Neogene normal faults in Wyoming (compiled from Witkind, 1975; Love and Christiansen, 1985; Steidtmann and others, 1986; and Montagne, 1991).

fault systems, Wheatland-Whalen fault system, Continental fault, Saratoga Valley faults, Cedar Ridge fault, Hoback fault, and Teton fault. Normal faulting formed mountain ranges (Tetons), downdropped large parts of ranges uplifted during the Laramide orogeny [Granite Mountains (Sweetwater uplift)], or cut the toes of large Laramide thrust faults (Wind River Range).

During the Laramide orogeny (late Cretaceous through early Eocene), Wyoming's basins formed and filled at or near sea level (Love, 1970; Blackstone, 1975; Bown, 1980; Angevine and Flanagan, 1987). Sometime during the Cenozoic, Wyoming rose to its present average elevation of approximately 5,000 ft (1,500 m) above sea level. The nature and timing of this uplift remains in question (Love, 1970; Angevine and Flanagan, 1987; Eaton, 1986). The uplift may have occurred: (1) as small changes over a long duration; (2) as large-scale events throughout the Cenozoic; or (3) as uplift over a relatively short period of time. Mechanisms responsible for the uplift in Wyoming also remain in question.

The time of initiation of uplift has been interpreted as late Oligocene (Swinehart and others, 1985; Steidtmann and others, 1989), mid-Miocene (Denson and Chisholm, 1971; Bown, 1980; Barnosky and Labar, 1989), or Pliocene (Love, 1960; Love, 1970; Blackstone, 1975), mostly based on local changes in sedimentation. Initiation of basin excavation may be related to or caused by regional uplift (Love, 1960). Stratigraphic evidence for late Cenozoic uplift is manifested by the Ogallala Group sediments preserved in Nebraska in large paleovalleys.

A review of the stratigraphy and sedimentology of the Neogene sedimentary rocks in Wyoming will set the background for the tectonic interpretation of these deposits. The rocks are grouped by geographic area rather than age because the precise ages of some strata are unknown. The dating of Cenozoic continental sedimentary rocks is commonly done on the basis of vertebrate fossil material. The North American sequences are divided into North American Land Mammal Ages (NALMA) (Wood and others, 1941), which are used in this paper (**Figure 3**). It is important to bear in mind when reviewing the literature that much of the stratigraphic work in Wyoming was done prior to 1976, when the late Miocene of the present time scale (e.g., Palmer, 1983) was included in the Pliocene (Cita, 1975; Berggren and others, 1985).

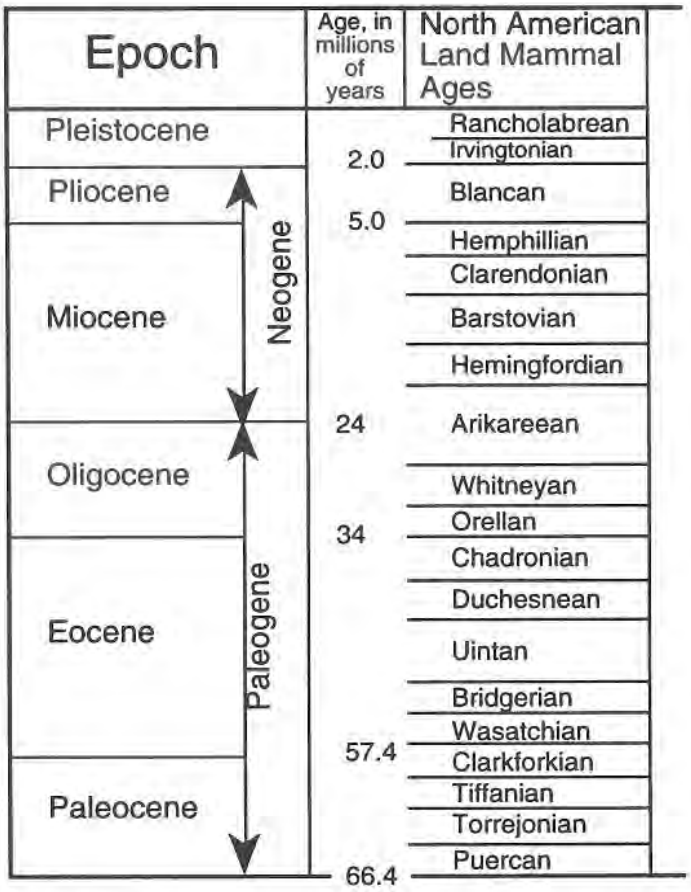

Figure 3. The Cenozoic North American Land Mammal Ages with suggested time boundaries after Palmer (1983), Woodburne (1987), and Swisher and Prothero (1990).

Key stratigraphic units

Southern Wyoming

A thick sequence of Arikareean, Hemingfordian, Barstovian, and younger sedimentary rocks, named the Browns Park Formation, is preserved in Saratoga Valley (Montagne, 1955, 1991). The valley is located in south-central Wyoming, along the Colorado/Wyoming border between the Sierra Madre

and Medicine Bow Mountains (**Figure** 4). Cenozoic rocks in this area are present on the flanks of the adjacent mountain ranges, in the mountains along drainage divides at present-day elevations in excess of 9,200 ft (2,800 m), and on the floor of Saratoga Valley.

Browns Park Formation

The Browns Park Formation was named by Powell (1876) for the upper Tertiary rocks of Browns Park, Colorado and Utah, a valley east of the Uinta Mountains. The formation was recognized in Wyoming south of the Washakie Basin (Sears, 1924) and consequently traced along the northern and western margins of the Park Range (Colorado) and Sierra Madre (Wyoming) (Buehner, 1936; Ritzma, 1949). The Neogene rocks of Saratoga Valley were correlated with the Browns Park Formation of Utah by Buehner (1936) and described in detail by Montagne (1955, 1991). Montagne also applied the name Browns Park Formation to the sedimentary strata of Big Creek, Cunningham, and Holroyd parks within the Sierra Madre (Montagne, 1953, 1955, 1991).

The Browns Park Formation in Wyoming consists of a basal conglomerate overlain by calcareous to siliceous siltstone and sandstone varying in color from green, gray, and tan to white. The middle units of the Browns Park Formation in Saratoga Valley consist of conglomerate and sandstone, limestone, thin beds of chalcedony, and volcanic ash. Although much of the formation is tuffaceous, the Browns Park Formation of Big Creek Park in the Sierra Madre is richer in pumicite and tuffaceous material than its counterpart in Saratoga Valley (Montagne, 1953, 1955).

The lower part of the Browns Park Formation is considered Arikareean and Hemingfordian in age from fossil mammals found in Saratoga Valley and Big Creek Park. A small fauna of fragmentary material from this area is in the paleontological collections at the University of Wyoming. The fauna contains *Gentilocamelus* sp. , *Merychyus arenarum, Hypolagus* (?) sp., and geomyid teeth (McGrew, 1951; Montagne, 1955). Radiometric ages from the Browns Park Formation in Saratoga Valley range from about 23 Ma to 14.5 Ma (Montagne, 1991). Radiometric

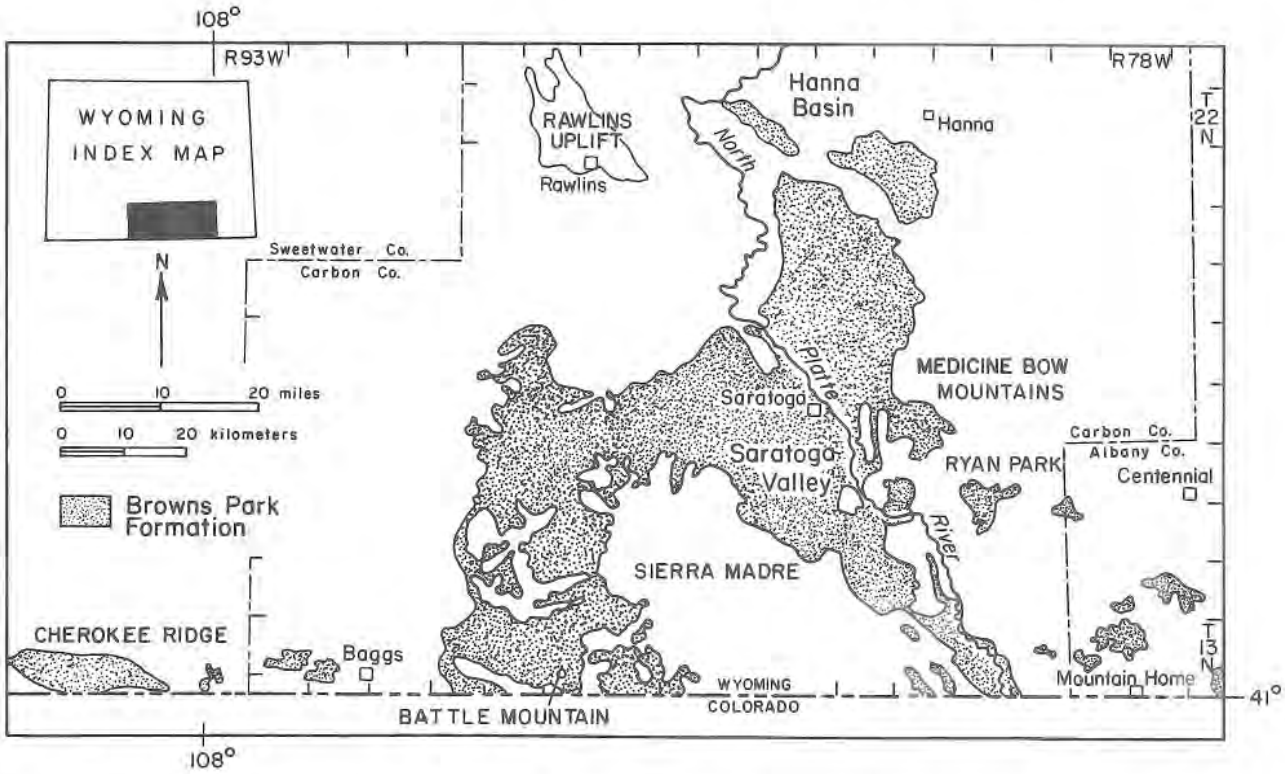

Figure 4. The location of Browns Park Formation in southern Wyoming including deposits in the Medicine Bow Mountains (compiled from Love and Christiansen, 1985; Luft, 1985; Montagne, 1955; 1991).

ages for rocks of the Browns Park Formation in the type area are 26 Ma near the base of the formation to 9 Ma at the top (Izett, 1975). Fossil mammalian faunas from four localities in northwestern Colorado (Moffat County) are late Arikareean, early to late Hemingfordian, and late Barstovian to early Clarendonian in age (Honey and Izett, 1988).

The upper part of the Browns Park Formation is best exposed in central Saratoga Valley, on the flanks of the Sierra Madre and Medicine Bow Mountains, and in Cunningham Park, a half-graben within the Sierra Madre (Montagne, 1955; Love and Christiansen, 1985). The sedimentary strata of the upper Browns Park Formation are composed of white, green, or tan calcareous siltstone and fissile shale, nodular limestone, chalcedonic sandstone, ash, and conglomerate. Sedimentary structures include crossbedding, graded bedding, and root casts. Fossils of the upper Browns Park Formation include ostracods, fossilized wood, algal material, and Barstovian-aged mammalian fauna. Dominantly grazers, the mammals include *Merychippus* and *Nannipus* (equids), *Merycodus* (antilocaprid), *Ustatochoerus* (oreodont), *Oreolagus* (rabbit), *Eucastor* (beaver), a camel, and a rhinoceros (Montagne, 1955).

Montagne (1955) divided the upper Browns Park Formation into three intertonguing fluvial facies: (1) channel; (2) back-fill; and (3) flank. The channel facies includes sandstone and conglomerate beds. The conglomerates are composed of rounded volcanic clasts from the volcanic fields of northern Colorado and Precambrian clasts from local sources. The back-fill facies is finer grained and includes tuffaceous siltstone, claystone, shale, marl, and algal limestone commonly cemented with calcium carbonate. The flank facies consists of angular clasts of mostly Precambrian material and reworked siltstone and sandstone fragments cemented with calcium carbonate. The flank facies coarsens toward the western mountain slopes, where the exposed beds rest unconformably on the early Cenozoic Coalmont Formation or Precambrian crystalline rocks. The upper part of the Browns Park Formation is conformable with the lower Browns Park near Pick Ranch, along the North Platte River (Montagne, 1955).

The Browns Park Formation was deposited in subsiding depressions by streams flowing from adjacent mountain ranges. Warping and minor faulting were syndepositional but *major* faulting in the Saratoga Valley followed deposition of the Browns Park Formation. Tuffaceous input may have been from the west and south and from reworking of pyroclastic material erupted in the Rabbit Ears Range of Colorado. During Browns Park deposition, a river system transported material from the Rabbit Ears volcanic field and the Never Summer Range into south-central Wyoming. The river system and adjacent overbank deposits filled a series of sagging depressions. Ponding took place in the northern part of the area resulting in a large lake. Sluggish streams in the backwater environments of the trunk river flourished with algae, while herbivores grazed on the floodplain. The flank facies represents colluvial deposits shed from the adjacent highlands of the partially buried Sierra Madre and Medicine Bow Mountains (Montagne, 1955). Before erosion, the Browns Park Formation was more than 2,800 ft (850 m) thick. Post-Barstovian erosion resulted in superposition of the present-day North Platte River through Northgate Canyon along the west flank of the Medicine Bow Mountains.

Aspen Mountain and Cherokee Ridge

Aspen Mountain and Cherokee Ridge are located in south-central Wyoming. Aspen Mountain is part of the Rock Springs uplift in the Green River Basin (**Figure 1**), whereas Cherokee Ridge is located on the south margin of the Washakie Basin (**Figures 1** and **4**). The deposits are discussed together because they have limited extent and are inferred to be Miocene in age based on stratigraphic position. However, these rocks have not yielded any datable material. The lithology consists of gray to orange, fine-grained sandstone and siltstone. Along Cherokee Ridge, the Browns Park Formation is preserved within a suite of normal-fault blocks (Luft, 1985). A sandstone unit mapped as a facies of the Oligocene Bishop Conglomerate atop Aspen Mountain may be equivalent to the Browns Park Formation and is mapped as Miocene on several geologic maps (Kirschbaum,1986; Love and Christiansen, 1985).

Eastern and northeastern Wyoming

Deposits of Neogene age are widespread in eastern Wyoming; they extend from the slopes of the Laramie Mountains into Nebraska, encompassing a part of the High Plains sequence (**Figure 5**). Neogene strata also cap Pine Bluffs and the Bear Lodge Mountains of northeastern Wyoming. There is much confusion concerning the formation names used in

eastern Wyoming. The question involves the "Arikaree Formation" and "Ogallala Formation" and the formations that are traced from the "Arikaree Group" and "Ogallala Group" of Nebraska into Wyoming.

Darton and others (1910) first identified Miocene rocks in Wyoming east of the Laramie Mountains as the Arikaree Formation.

> *The table-lands east of the eastern foothills of the Laramie Mountains are capped by a sheet of sand and gravel that is in places cemented into a loose sandstone or conglomerate, which probably represents the Arikaree formation. It has been cut away by Horse, Lodgepole and Crow creeks for 8 or 9 miles from the foot of the mountains and also in an irregular zone near the foothills across the divide north of Crow Creek.* (Darton and others, 1910, p. 11)

Conglomeratic beds containing Sherman granite and anorthosite clasts that cap this sequence were included originally in the Arikaree Formation but were subsequently placed in the younger Ogallala Formation.

Further work led stratigraphers in Nebraska to subdivide the Arikaree and Ogallala into formations and elevate Arikaree and Ogallala to group status. Geologists from the University of Wyoming followed suit and subdivided the Miocene rocks into several formations (Harrison, Monroe Creek, and Ash Hollow) (see Minick, 1951; P.O. McGrew, 1953; Moore, 1959; Cassiliano, 1980). Problems arose in publications from the 1950s onward. Some geologists preferred to use Nebraska nomenclature for beds traced from western Nebraska into eastern Wyoming. Other geologists, mostly from the U.S. Geological Survey, tended to use the older names Arikaree and Ogallala formations, but they were also aware that stratigraphers had attempted to bring in the Nebraska nomenclature. Denson and Bergendahl (1961) described the Neogene deposits of eastern Wyoming as Arikaree and Ogallala formations but stated: *In this report only the names of the chief rock units are used, without reference to the subordinate units recognized by the foregoing authors* (i.e., Lugn,

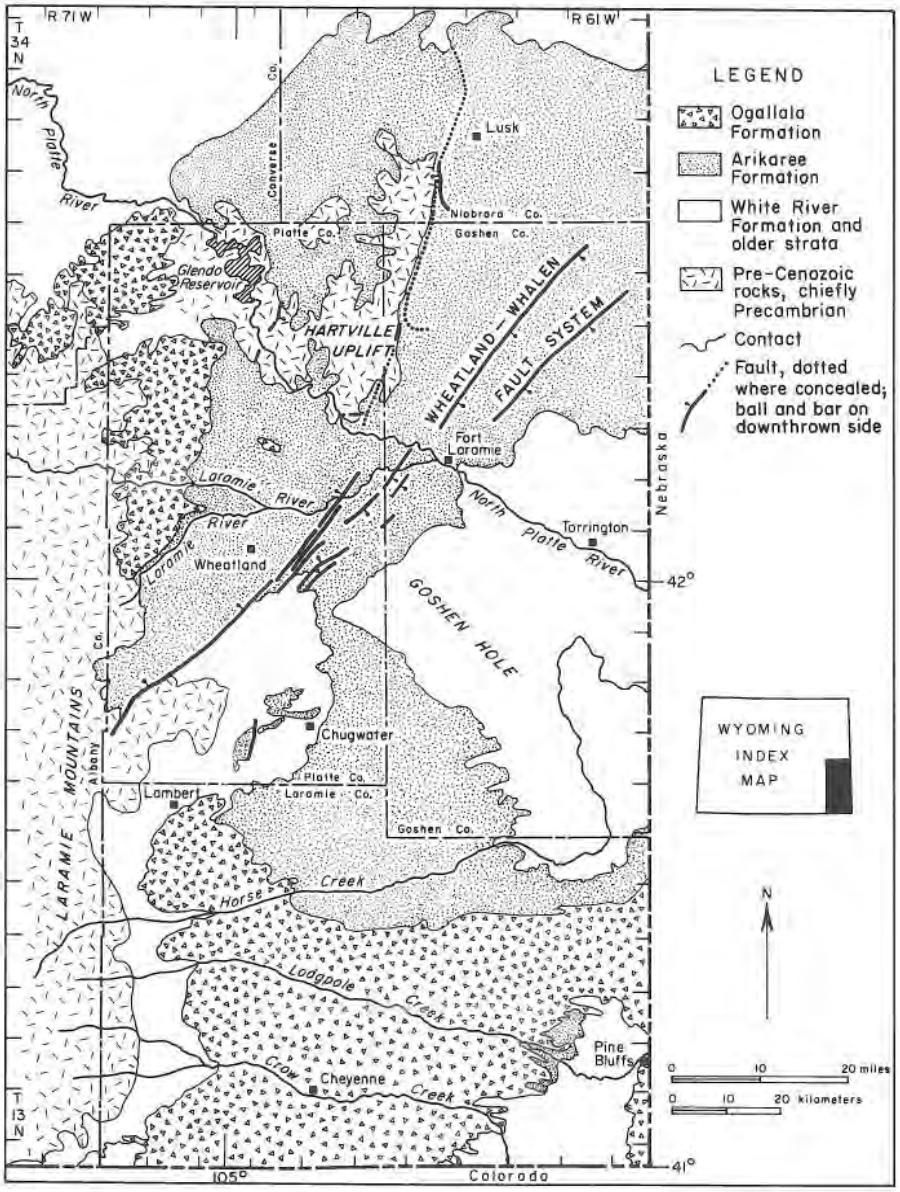

Figure 5. Map of the Arikaree and Ogallala formations of eastern Wyoming, as discussed in the text (compiled from Cassiliano, 1980; Hunt, 1990; Love and Christiansen, 1985; L.W. McGrew, 1963; Minick, 1951; Moore, 1959). Note that the blank areas include White River Formation as well as older subjacent rocks.

1939; P.O. McGrew, 1953; Galbreath, 1953). Ahlbrandt and Groen (1987) discussed the geology of Goshen Hole using the terms Arikaree and Ogallala *groups*.

Breyer (1975) traced the Ash Hollow Formation of Nebraska into Wyoming, further restricting the term "Ogallala Formation." Minick (1951) and Cassiliano (1980) continued to use Ash Hollow Formation for beds described as Ogallala Formation, and Cassiliano (1980) discussed some "unnamed Miocene rocks" within the area of Trail Creek/Horse Creek. Moore (1959) described the Neogene deposits as Arikaree and Ogallala formations, stating that, *no further subdivision is possible at present.* The *Geologic map of Wyoming* uses Arikaree and Ogallala formations for rock units east of the Laramie Mountains and "upper and lower Miocene" for rock units west of the Laramie Mountains (Love and Christiansen, 1985). Overuse of the names "Arikaree" and "Ogallala" has added to the confusion of stratigraphic terms in Wyoming, Nebraska, Kansas, and Texas, suggesting this gross classification of lithologies is no longer useful in light of modern geologic problems. However, by convention in this review, Arikaree and Ogallala formations will be discussed for rocks east of the Laramie Mountains.

Arikaree Formation

Darton and others (1910) discussed the Tertiary deposits of the Laramie and Sherman quadrangles in eastern Wyoming and described the Arikaree Formation as a fine-grained sandstone unit embedded with volcanic ashes of Miocene age. An overlying conglomerate was included in their description of the Arikaree Formation. L.W. McGrew (1963) who made a detailed study of the Arikaree Formation in the Fort Laramie area separated the uppermost conglomerates from the Arikaree Formation but did not apply a formal name. These conglomerates were discussed in a section entitled: "Deposits of post-early Miocene and pre-Pliocene age" and have subsequently been placed in the Ogallala Formation (e.g., Love and Christiansen, 1985). The Arikaree Formation of eastern Wyoming consists of siltstone, fine-grained sandstone, limestone, and volcanic ash. The rocks are mainly friable, gray, tuffaceous sandstone containing limy, tuffaceous, sandstone concretions. It is estimated to be 700 ft (200 m) thick in the Fort Laramie area and 262 ft (80 m) thick in southeastern Wyoming (L.W. McGrew, 1963; Cassiliano, 1980). The Arikaree Formation of southeastern Wyoming consists of gray sandstone cemented with calcium carbonate and some limestone lenses towards the top of the unit. There is some secondary replacement by silica throughout the strata (Cassiliano, 1980).

The Arikaree Formation of the Fort Laramie area can be divided into three units (L.W. McGrew, 1963). The first unit consists of the lower 200 to 300 ft (60-100 m) of friable, orange-gray, fine- to medium-grained, massive sandstone with a matrix rich in clay, and thin ash beds. Limy sandstone concretions form pipes and nodules, or sandstone is cemented to form ledges. Siliceous root casts increase in abundance towards the top of the unit. The second unit is composed of gray, fine- to medium-grained tuffaceous sandstone and freshwater limestone beds. This unit is approximately 200 ft (60 m) thick and differs from the underlying strata in that the rocks are lighter in color, less massive, richer in carbonate, and contain an increased abundance of root casts. There are a few coarse-grained sandstone and conglomerate deposits. Some of the limestone beds contain chert nodules. The third and uppermost unit is 200 ft (60 m) thick and consists of an orange-gray, fine- to medium-grained, massive sandstone, with minor claystone and ash beds. Again, pipey-shaped calcareous sandstone concretions are present and root casts are very abundant. The sandstone beds are rich in carbonate and in some places form resistant ledges.

The Arikaree Formation east of the Hartville uplift consists of mostly massive, tuffaceous silty, sandstone. Less extensive deposits are beds of tuffaceous siltstone, tabular limestone, carbonate mudstone, diatomite, and calcareous tuff (Hunt, 1990). Sedimentary structures in the Arikaree Formation include roots, burrows, laminated bedding, and horizontal, low-angle, and trough cross stratification (Hunt, 1990). The limestone lenses contain diatoms, gastropods, and ostracods (Hunt, 1990).

The Arikaree Formation of the Fort Laramie and Hartville areas is Arikareean in age (R. M. Hunt, personal communication, 1992). Fossils collected from this area include insectivores, rodents, lagomorphs, oreodonts, equids, antilocaprids, rhinocerotids, and an amphicyonid. The depositional environment was alluvial plains, in places blanketed by volcaniclastic loess produced by eolian processes, and punctuated by ephemeral, braided, fluvial systems (Hunt, 1990). Freshwater limestone indicates ponding occurred locally. After deposition

of the Arikaree Formation, a period of normal faulting took place in the Fort Laramie area along the Wheatland-Whalen fault system (McGrew, 1963).

The "middle Miocene formation" of southeastern Wyoming, as discussed by Cassiliano (1980), consists of an informal unit between the Arikaree Formation (or Marsland and Harrison formations) and the Ogallala Formation (or Ash Hollow). Fossil mammal material collected from the Horse Creek Quarry (R. M. Hunt, written communication, 1992) indicates the base of the "middle Miocene formation" is late Arikareean, whereas the top of the unit is late Hemingfordian to early Barstovian. The lithologies are sandstone, siltstone, claystone, shale, and volcanic ash with a measured thickness of 152 to 340 ft (46-104 m). Conglomerates containing limestone clasts are common at the top of the "formation". The depositional environment was broadly eolian; however, lacustrine sediments dominate at the base of the unit and fluvial sediments are common towards the top (Cassiliano, 1980). The "middle Miocene formation" is tentatively placed in the Arikaree Formation in this paper.

Ogallala Formation

The Ogallala Formation blankets the eastern flank of the Laramie Mountains to Pine Bluffs on the Wyoming/Nebraska border, and extends from the Colorado/Wyoming border north to Lambert, Wyoming (**Figure 5**). The Ogallala Formation then continues in patches along the northeastern edge of the Laramie Mountains and forms the resistant cap of the Bear Lodge Mountains in northeastern Wyoming.

The lithology of the Ogallala Formation is dominantly coarse-grained deposits ranging from gravel-sized conglomerate to boulder conglomerate. It is mainly coarse-grained near the mountain fronts and fines to siltstone, sandstone, ash, and limestone beds to the east (Minick, 1951; Moore, 1959; Stanley, 1976; Cassiliano; 1980; Staatz, 1983). The conglomeratic clasts are composed of Precambrian crystalline material from the Laramie Mountains, Bear Lodge Mountains, and Hartville uplift, and volcanic material from north-central Colorado.

Cassiliano (1980) carried the nomenclature of the Ogallala Group (of Nebraska) and its formations into the Horse Creek/ Trail Creek area north of Cheyenne. The Ash Hollow Formation of Cassiliano (1980) consists of tan, brown, and brown-gray, fine- to medium-grained sands and silty sands. Thin beds of clay (mostly altered ash) and tuff cemented with calcium carbonate are present. Conglomerates are composed of limestone clasts near the base of the formation. More commonly, Precambrian crystalline rocks with a sandstone or siltstone matrix are prevalent in southeastern Wyoming.

Sedimentary structures include graded bedding, crossbedding, laminar bedding, mudcracks, rip-up clasts, bioturbation, and root casts. Calichified paleosol horizons are also present. Fossils are found scattered throughout the formation. Trail Creek Quarry and Escarpment Quarry contain cranial and postcranial material of fish, reptiles, birds, and mammals. The mammalian fossils indicate that the Ogallala (or Ash Hollow) Formation at Trail Creek is Barstovian to Clarendonian in age, but a *Mammut* tooth suggests the uppermost part of the formation may be younger (Voorhies, 1965; Cassiliano, 1980). At Pine Bluffs, the Ogallala (or Ash Hollow) Formation is late Clarendonian to early Hemphillian in age (based on fossil seed zonation by Minick, 1951). Zircon fission-track ages on ash clasts from a conglomerate indicate the Ogallala Formation in the Bear Lodge Mountains is younger than 12 Ma (Flanagan, 1990). The age of the Ogallala Formation in eastern Wyoming is probably time transgressive from west to east, from mid- to late Miocene.

The thickness of the Ogallala Formation in Wyoming varies from 262 to 450 ft (80 to 137 m) in southeastern Wyoming to 300 ft (100 m) near the Laramie Mountains, to 90 ft (30 m) at Pine Bluffs, to about 50 ft (15 m) in the Bear Lodge Mountains (Minick, 1951; Moore, 1959; Cassiliano, 1980; Staatz, 1983).

Some of the volcanic material in the Ogallala Formation is from distant sources, perhaps the Basin and Range province, whereas local sources for the metamorphic and igneous material are the Laramie Mountains, Black Hills, Front Range, and Hartville uplift. The source of rhyolite clasts in the conglomerates near Cheyenne is northern Colorado (Stanley, 1976). Lithology of the clasts is similar to the Specimen Mountain volcanic rocks of north-central Colorado. Paleocurrent directions for transport of the volcanic clasts suggest a northeastward flow (from a southwest source) into the Cheyenne area across a filled Laramie Basin (Stanley, 1976).

The depositional environment of the Ogallala Formation east of the Laramie Mountains was a

semiarid alluvial plain with interspersed river systems and ponds. The sandstone and siltstone units of the alluvial plain were deposited by both eolian and fluvial processes, but deposition resulted more from fluvial processes than eolian. Limestones with freshwater algae were deposited in quiet-water, shallow ponds. Conglomerates, containing clasts of crystalline rocks from the Laramie Mountains and volcanic rocks from Specimen Mountain in northern Colorado (Stanley, 1976; Cassiliano, 1980), were deposited by large rivers that flowed northeast from Colorado across southeastern Wyoming into Nebraska (Stanley, 1976; Skinner and others, 1977). Rocks in Nebraska of similar age to the Ogallala Formation of Wyoming are dominantly coarse-grained conglomerates that filled large valleys cut during Ogallala time (Skinner and others, 1977; Diffendal, 1982; Diffendal and others, 1985; Swinehart and others, 1985). These fills include reworked blocks and boulders of Arikaree and Ogallala sandstones and Ogallala air-fall ash (Diffendal, 1983).

The Ogallala Formation of the Black Hills is composed of siltstone, an intraformational conglomerate of rounded sandstone clasts, and several massive, poorly sorted, pebble-to-boulder conglomerate beds. Most of the siltstone and the rounded-sandstone conglomerate beds are found approximately 6 mi (10 km) north and west of a massive conglomerate unit (Staatz, 1983; Flanagan, 1990). Siltstones of the lower unit are orange-tan in color and contain reworked ash with some limestone lenses. Caliche is present in the siltstones, and no fossils have been found.

Conglomeratic units make up the upper part of the Miocene strata in the Bear Lodge Mountains. Some well-exposed conglomerate beds have been described by Staatz (1983) from a landslide scarp in Cole Canyon. The conglomerates that cap the Bear Lodge Mountains contain pebble- to boulder-sized, angular clasts of igneous rocks identical to those atop Warren Peak, the highest topographic point in the Bear Lodge Mountains. The massive conglomeratic units are interbedded with finer grained siltstones. There are erosive contacts between beds and an overall coarsening upward of the formation. Imbrication is poorly developed but, when present, shows a southwest to northeast paleoflow direction. Boulder-sized clasts of ash were reworked into the conglomeratic units. The deposit is a fluvial/alluvial fan system that extended from Warren Peak eastward towards the Black Hills. The fluvial system consisted of braided rivers, minor overbank deposits, and debris flows.

The Bear Lodge Mountains area hosted dominantly fine-grained sedimentation in the Oligocene and early Miocene. The age of the lower Ogallala Formation of the Bear Lodge Mountains is not well documented. Lithologically, it is similar to late Oligocene- early Miocene beds elsewhere in Wyoming but this may be due to depositional environment rather than continuity of strata. The beds were deposited as a fine-grained alluvial fill prior to mid-Miocene conglomeratic deposition.

Large braided river deposits and debris flows now rest at an elevation of 7,000 ft (2,000 m), which is 2,000 to 3,000 ft (600-900 m) above the surrounding basin floor. The age of this deposit (upper part of the Ogallala Formation) is younger than 12 Ma (fission-track dating of zircons reported by Flanagan, 1990) and falls within the Clarendonian NALMA as determined by grass-seed zonation of Elias (1942) for *Biorbia fossilia* (Staatz, 1983). The Ogallala Formation (or Ash Hollow Formation), found elsewhere in eastern Wyoming, is also partly of Clarendonian age.

Central and north-central Wyoming

One of the thickest and most complete sections of Neogene strata in the State is preserved in central Wyoming. The deposits of central Wyoming occur in the southern Wind River Range, Granite Mountains, and Pathfinder areas.

The southern Wind River Range lies subparallel to the Sweetwater arch (Hares, 1916) along the trace of the Wind River thrust fault and Continental normal fault (**Figure 6**). Neogene rocks in this area will be referred to as the Split Rock Formation following Love (1970), although they have also been referred to as the Arikaree Formation (Denson, 1965a). The Burnt Gulch Formation and two other rock units that have been informally named the Circle Bar beds and Leckie beds will also be discussed.

The Granite Mountains area is presently a large asymmetrical graben in central Wyoming bordered to the north and south by the North Granite Mountains and South Granite Mountains fault systems, respectively (**Figure 7**). The northern margin of the Granite Mountains area along the Beaver Rim marks the southern extent of the Wind River Basin and

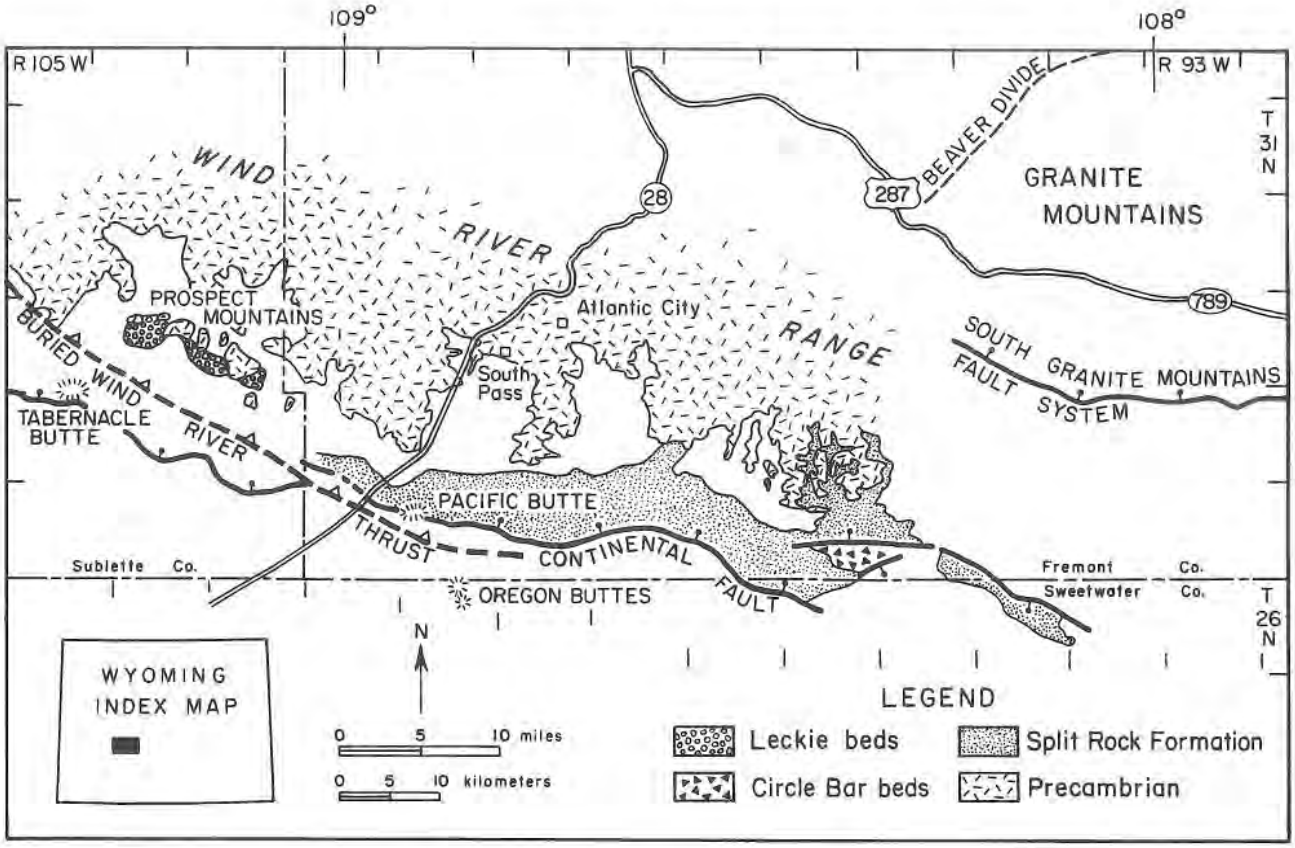

Figure 6. Map of the southern Wind River Range and the Neogene rocks of the Split Rock Formation, Circle Bar beds, and Leckie beds (modified from Love and Christiansen, 1985; Steidtmann and others, 1986). Split Rock Formation in the Granite Mountains is not delineated (see Love, 1970).

includes the Rattlesnake Hills. From east to west, the Seminoe, Ferris, Green, and Crooks mountains form the southern border of the Granite Mountains area. The Granite Mountains area is a Laramide uplift that was subsequently downfaulted along normal faults of the North and South Granite Mountains fault systems (Love, 1970). Within this large graben lies one of the best preserved Neogene sedimentary sequences in Wyoming—the Split Rock Formation (early to middle Miocene), Moonstone Formation (late Miocene), and Kortes formation (latest Miocene-Pliocene) (**Figure 8**).

The Pathfinder region encompasses the southeast corner of the Granite Mountains syncline (Love, 1970) or Sweetwater arch (Hares, 1916). It is located north of the Seminoe Mountains, along the shores of the North Platte River and Pathfinder Reservoir (see **Figures 8** and **9**). The area extends east to the Shirley Mountains and west to Windy Gap. The Pedro Mountains lie within the Pathfinder region, as do several other granitic knobs and ridges. The segment of the South Granite Mountains fault in the Pathfinder region was named the Kortes fault by Blackstone (1965). Two formations of Miocene and younger sedimentary rocks dominate the Pathfinder region, lapping onto the Precambrian granitic and metamorphic rocks. They are the Moonstone and Kortes formations, composed of fine-grained and coarse-grained strata, respectively.

The **Split Rock Formation** of the southern Wind River Range blankets an elongate area between South Pass City and Oregon Buttes (**Figure 6**). The formation consists of approximately 750 ft (230 m) of strata ranging from a basal conglomerate to gray, tuffaceous, fine-grained sandstone and siltstone cemented with calcium carbonate (Jackson, 1984; Steidtmann and others, 1986). The age of this formation was determined by fission-track studies to be latest Oligocene to early Miocene, and it is considered to be Miocene from sparse fossil evidence (Steidtmann and Middleton, 1986).

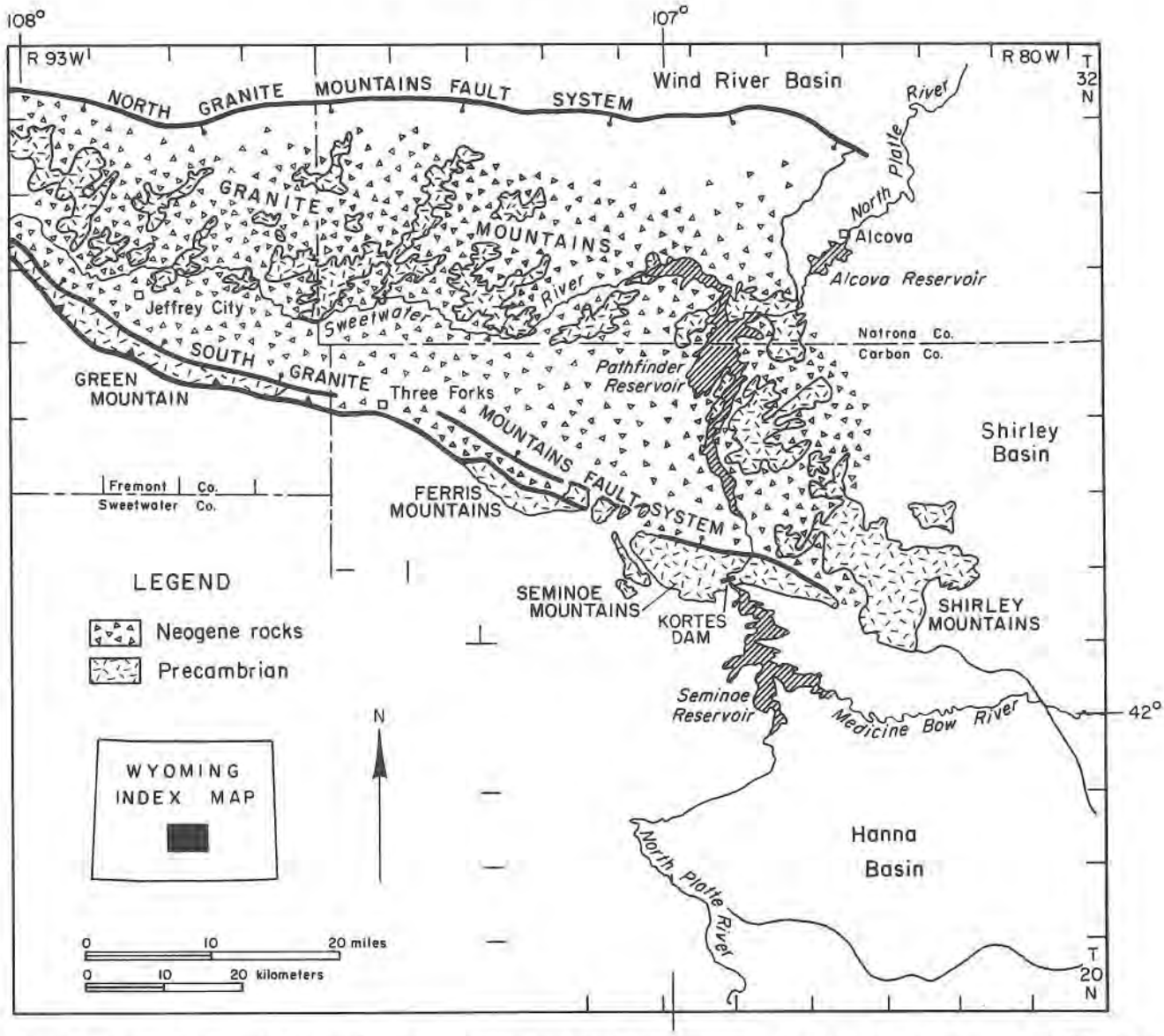

Figure 7. Map of the Granite Mountains or Sweetwater arch and the present-day North Platte, Sweetwater, and Medicine Bow rivers (complied from Love, 1970; Flanagan, 1990). Details are not delineated in the surrounding areas.

Circle Bar beds and Leckie beds are located along the southern margin of the Wind River Range (**Figure 6**). The Circle Bar beds are an informally named unit described by Jackson (1984) and later discussed by Steidtmann and others (1986) and Steidtmann and Middleton (1986). These deposits are composed of sandstone, volcanic ash, and conglomerate. The lower part of Circle Bar beds consists of tuffaceous sandstone coarsening upward to conglomeratic deposits. The lower gray sandstone unit contains silicic root casts and scattered pebbles of Precambrian crystalline rocks. Conglomerates overlie and are interbedded with the lower sandstone unit. The conglomerates consist of pebble- to boulder-sized clasts of metagraywacke, mafic metamorphic rocks, and reworked Split Rock sandstone (Jackson, 1984). Imbricated clasts provide paleocurrent directions of transport toward the north-northeast. The Circle Bar beds are 200 to 400 ft (60 - 120 m) thick and rest with angular unconformity on the Bridger and Split Rock formations. A fission-track age of 13 Ma was obtained from a tuffaceous unit within the beds (Steidtmann and Middleton, 1986). The beds were deposited as alluvial fans that were shed and reworked from the footwall block of the Continental fault.

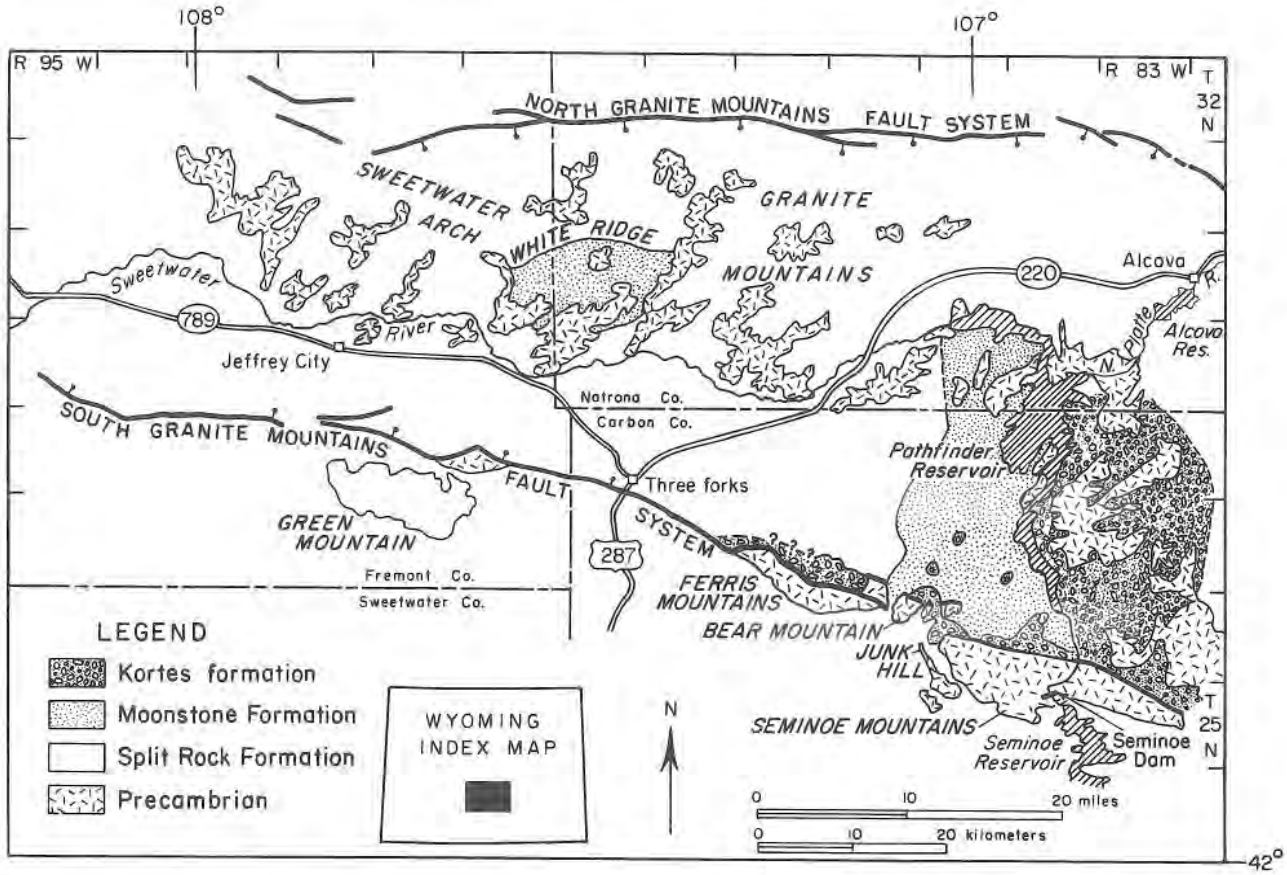

Figure 8. Generalized geologic map of the Granite Mountains including the Pathfinder region (from Love, 1970; Flanagan, 1990). Note that blank areas labelled "Split Rock Formation" also include older units.

Little is known about the Leckie beds except that they are an informally named coarse clastic deposit interpreted as a series of alluvial fans derived from the core of the Wind River Range and may be as young as late Miocene-Pliocene age (see Figure 2, Steidtmann and others, 1986). Conglomerates of the Leckie beds are composed of weathered granitoid boulders and bear some similarity to those described in the Burnt Gulch Formation.

The **Burnt Gulch Formation** is a late Pliocene to Pleistocene deposit located in canyons on the northeast flank of the Wind River Range and is composed of boulder conglomerates containing weathered Precambrian granitoid and meta-igneous clasts in an arkosic matrix (Martin and others, 1992). The overall upward gradation from large to small clasts and the presence of some relatively finer grained, nonconglomeratic units suggests alluvial fan deposition of dominantly debris-flow sedimentation (Martin and others, 1992).

The fine-grained sandstone deposits of the Granite Mountains area (**Figure 8**) were formally named Split Rock Formation by Love (1961). However, Denson (1965a) argued that these deposits should be called Arikaree Formation, carrying the nomenclature of eastern Wyoming into central Wyoming. Love (1970) further described the rocks of the Granite Mountains in detail using the name "Split Rock Formation." Both names have have been subsequently used for strata in this area (Sato and Denson, 1967; Reynolds, 1968 a, b; Denson and Harshman, 1969; Crist and Lowry, 1972; Denson and Pipiringos; 1974; King and Beikman, 1978; Peterman and Hildreth, 1978; Munthe, 1979). The nomenclature of Love (1961, 1970) is accepted in this paper for central Wyoming.

The Split Rock Formation throughout central Wyoming is dominantly fine-grained fluvial and eolian sandstone, volcanic ash, and limestone. Arkosic pebble-conglomerate beds characterize early Split Rock deposition and are interbedded throughout the

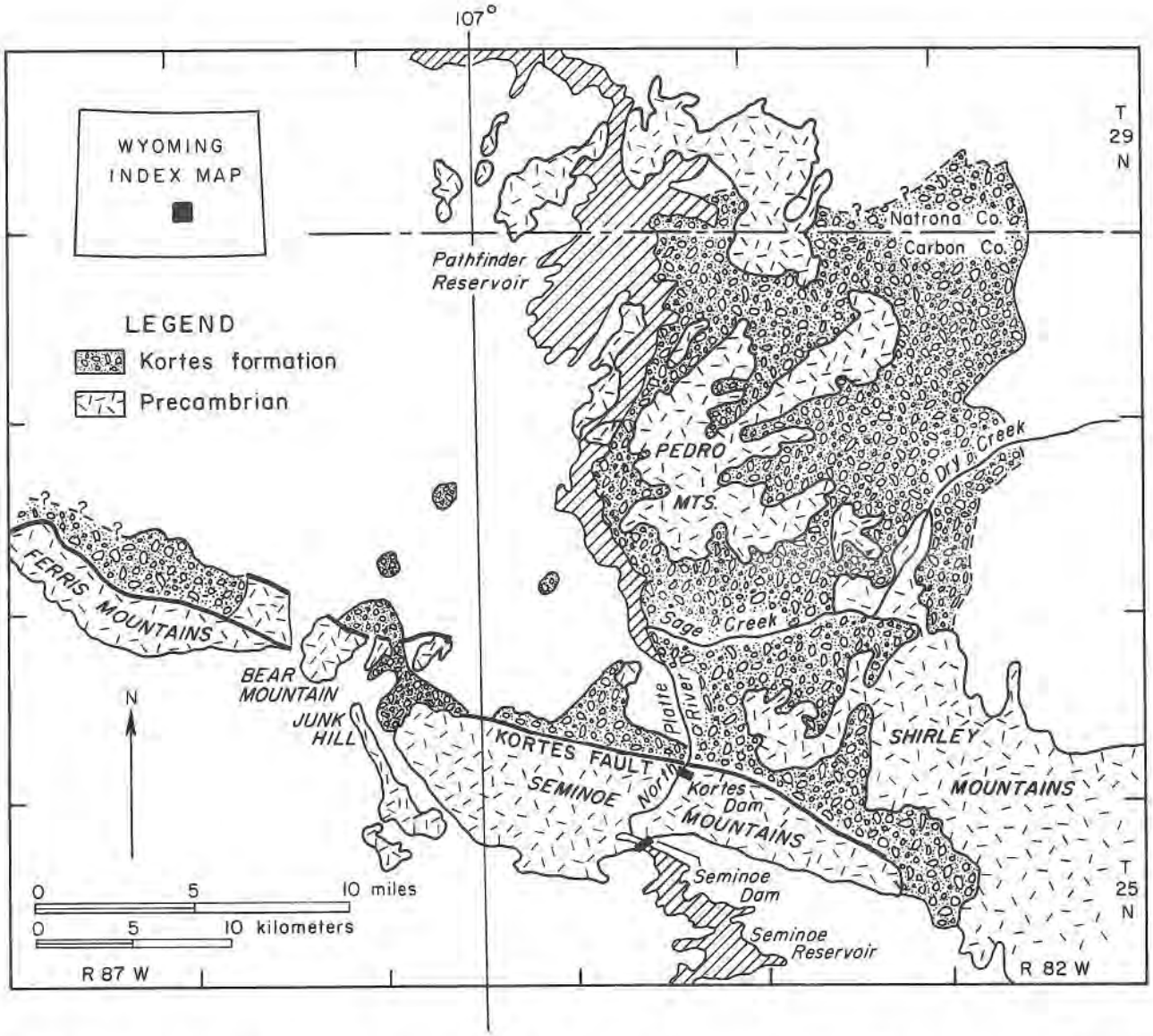

Figure 9. Map of the Pathfinder region, central Wyoming, showing the extent of the Kortes formation (Moonstone Formation is not shown [from Flanagan, 1990]).

fine-grained strata (Love, 1970; Munthe, 1979). Sedimentary structures include high-angle cross stratification, burrows, "pipey concretions," and root casts (Love 1970).

The depositional environment during Split Rock sedimentation was that of a semiarid open plain interspersed with freshwater ponds and dominated by eolian processes (Love, 1970; Munthe, 1979). The ecosystem supported a diverse fauna of reptiles and mammals.

The age of the Split Rock Formation in central Wyoming is early to middle Miocene [Arikareean(?)-Hemingfordian]. The sedimentary rocks have been dated by fossils, and a radiometric age of 17 Ma was obtained from tuff beds (Munthe, 1979). The fauna of the Split Rock Formation is composed of 67 taxa including insectivores, rodents, lagomorphs, oreodonts, equids, antilocaprids, chalicotheres, camels, and carnivores (Munthe, 1979).

The **Moonstone Formation** in the Granite Mountains is located in a depression within the center of a graben surrounded by granitic knobs (**Figure 8**). The sedimentary rocks are composed of tan to white shale, siltstone, sandstone, limestone, and conglomerates. There is some pumicite, bedded chalcedony,

zeolites, and salt within the type section at White Ridge, as well as radioactive shales and moss agates (Love, 1970; Mariner, 1971). Most of the Moonstone Formation at the type section is fine grained except for the lower part, which is an arkosic conglomerate.

The depositional environment of the type area of the Moonstone Formation was an alkaline saline lake surrounded by hill slopes and a vegetated alluvial plain (Mariner, 1971). A pollen assemblage of xeric vegetation (*Artemesia*) and (dominantly) conifers was collected from a shale at White Ridge (Love, 1970; Leopold and Denton, 1987). The pollen assemblage and sedimentary deposits suggest a closed basin in a semiarid environment in which eolian processes dominated.

The Moonstone Formation, formally named by Love (1961), crops out extensively in the southeast corner of the Granite Mountains syncline, west of the North Platte River (**Figure 8**). The Moonstone Formation in this area is composed of fine- to very fine-grained sandstone, medium-grained sandstone, reworked volcanic ash, siltstone, and limestone.

The Moonstone Formation in the Pathfinder region is mostly located on the west side of the North Platte River and can be traced west-northwest for approximately 25 miles. It is discontinuous with the type area (White Ridge), but is correlated on lithology. Maximum thickness of the Moonstone Formation in the Pathfinder region has not been determined. It is approximately 900 ft (300 m) thick and possibly more, since the lower contact with the Split Rock Formation is covered where the most complete sections are exposed.

Three facies of the Moonstone Formation exist in the Pathfinder region: (1) massive or finely laminated, orange-tan sandstone, ash, and siltstone; (2) thin-bedded orange-tan sandstone, white limestone, and volcanic ash; and (3) thick-bedded orange-tan sandstone, siltstone, and ash. The three facies represent a shallow freshwater lake, the shoreline of the lake, and the surrounding vegetated plain, respectively (Flanagan, 1990). Sedimentary structures within the Moonstone Formation include ripples with flattened crests, high-angle cross stratification, parting lineations, wavy bedding, load structures, soft-sediment deformation, burrows, root traces, and algal structures. The majority of sedimentary structures are in the sandstones of the thin-bedded facies (Flanagan, 1990).

Rocks of the massive or finely laminated facies were deposited in a quiet-water lake. Lack of any sedimentary features except fine laminations in this facies suggests the rocks underwent little deformation. The laminations do not show a change in grain size, but there is a lithologic change marked by an increase in either sand or ash content. Laminations of different lithology indicate a change in source, possibly caused by a change in wind direction.

The thin-bedded facies represents a lakeshore surrounded by a large mud flat. A highly bioturbated, gray ash unit is a diagnostic marker bed within the large mudflat deposit. Features indicative of the shore environment include thin beds, rapid lithologic changes, intraformational conglomerates, ripples with flattened crests, load structures, and soft-sediment deformation. The extensive mudflat and strandline sedimentary features indicate the lake was shallow with a broad, fluctuating shoreline.

The thick-bedded facies of sandstone, ash, and siltstone represents a vegetated plain environment adjacent to the shallow lake. The vegetated plain was composed primarily of fine-grained sand and silt. Vegetation is indicated by the abundant monopodial roots. Limestone lenses within the siltstones and sandstones of the vegetated plain were probably deposited in small ponds. Caliche indicates periods of nondeposition and episodic sedimentation. Thin beds of medium-grained sandstone were deposited by ephemeral streams during flash flooding.

The thick-bedded facies contains a small, late Barstovian-early Clarendonian fossil fauna of mostly ungulates and rabbits. The fossil material is generally isolated, disarticulated, postcranial skeletal material found associated with calichified horizons. A fission-track date of 11 Ma was obtained from a reworked ash bed in the middle of the Moonstone Formation (Flanagan, 1990). This age is within the radiometric age range for the late Barstovian of California (Tedford and others, 1987)

The shallow lake of the Moonstone Formation in the Pathfinder region formed in an open depression surrounded by gentle rolling hills. Ostracods and limestone deposits indicate the lake in the Pathfinder region was a different lake system from that of the type Moonstone Formation at White Ridge (Love, 1970). At White Ridge, an alkaline saline lake formed, resulting in deposition of evaporite deposits

including trona (Love, 1970; Mariner, 1971). The limestone beds and lack of evaporite minerals in the Pathfinder region suggest a shallow, freshwater lake. The Granite Mountains area subsided and had internal drainage until the late Barstovian. The Moonstone Formation was deformed by normal faulting along the Kortes fault during the Clarendonian (Flanagan, 1990).

The **Kortes formation**, named for Kortes Dam, is a newly recognized informally named unit that lies stratigraphically above the Moonstone Formation but in many places is topographically lower than the Moonstone Formation because of faulting. The Kortes is the major surface unit on the east side of the North Platte River, although outcrops are present on the west side of the river (**Figure 9**). It is composed of massive conglomerates (both matrix- and clast-supported), some limestone, and minor amounts of siltstone (Flanagan, 1990). The dominant strata throughout the Kortes formation are green conglomeratic beds consisting of clast-supported and matrix-supported arkosic conglomerate. The clasts are subangular to angular, metamorphic and granitic rocks ranging in size from pebbles to boulders, and are identical to the igneous and metamorphic rocks exposed in the Seminoe Mountains. The matrix is a fine-grained, tuffaceous sandstone cemented with calcite. Imbrication of the clasts indicates that the direction of flow was from south to north. Thin deposits of matrix-supported conglomerates interbedded with arkosic conglomerates and epidote-rich, green conglomerate beds are most prevalent on the east side of the river. Limestone beds are sandwiched between conglomeratic units near the mountain front east of the North Platte River. The limestones vary in thickness from 1 to 3 ft (0.3-1 m) and contain matrix- supported clasts of granite varying in size from pebbles to cobbles that are subangular to angular. The thicker limestone beds contain algal structures.

The middle part of the Kortes formation is composed of arkosic conglomerates, siltstones, and a massive clast-supported conglomeratic unit. The top of the middle part is capped by a massive, poorly sorted granule-to-boulder conglomerate [i.e., .1 in to 1.6 ft (3 mm-0.5 m)], which contains subrounded to angular clasts of granite and Paleozoic rocks (limestones and sandstones). The matrix is an ashy, fine-grained sandstone similar to that in the Moonstone Formation. Thin lenses of limestone are found in the conglomerate and pebbles of granite from the conglomerate are mixed within the limestones. Sedimentary structures in the middle part of the unit include low-angle cross stratification.

The upper Kortes formation consists of 300 ft (90 m) of clast-supported conglomerate, matrix-supported conglomerate, limestone, and tufa, typically including thick beds of matrix-supported pebble conglomerate, interbedded with clast-supported cobble to boulder conglomerate. The clasts of the conglomerates consist of subangular to angular granites and vein quartz varying in size from pebbles to boulders. Thin caliche beds, 1.5 to 3 ft (0.5-1 m) thick, indurated horizons, and root traces are found throughout the matrix-supported conglomerates. This upper part was deposited as a result of sporadic hyperconcentrated sediment flows or mud flows in a semiarid environment, and the mud flows indicate infrequent, high-intensity flood events (Flanagan, 1990).

The thickness of the Kortes formation is approximately 1,300 ft (400 m) and it laps horizontally onto and over the Precambrian knobs of the Seminoe, Granite, and Pedro mountains. The formation rests on the uppermost part of the Moonstone Formation and in some places lenses of clast-supported pebble conglomerate are in erosional contact with the uppermost beds of the Moonstone Formation.

The Kortes formation is younger than the Moonstone Formation and older than the Pleistocene conglomerates that cap and bevel the deposits. Mammal fossils assigned to the Clarendonian Land Mammal Age have been found in rocks now mapped as the Kortes formation, but they are sparse (Love, 1970). Therefore, the Kortes formation is probably latest Miocene to Pliocene in age.

The Kortes formation was deposited as alluvial fans shed off the Seminoe Mountains, Pedro Mountains, and various granite knobs as the eastern one—third of the Granite Mountains graben dropped approximately 2,000 ft (600 m) along the South Granite Mountains fault system and up to 1,000 ft (300 m) along the North Granite Mountains fault system (Love, 1970). Displacement on the Kortes fault segment of the South Granite Mountains fault system in the Pathfinder region is up to 1,300 ft (400 m) (Blackstone, 1965). The conglomerates are deposits of sheetwash and braided stream systems that flowed from south to north off the surrounding mountains. Ponds developed along the Kortes fault as down-

ward movement continued and were filled with conglomeratic debris from renewed river systems.

Two river systems entered the Pathfinder region after deposition of the Kortes sediments. Gravels of these river systems rest on and crosscut all facies of the Moonstone Formation and alluvial fans of the Kortes. A gravel and conglomerate deposit that bevels the Kortes formation west of the North Platte River is characterized by the predominance of angular to subangular clasts of banded iron formation (derived from the Seminoe Mountains), gneiss, granite, and schist. This conglomerate and gravel deposit caps the Moonstone and Kortes formations west of the North Platte River along the Seminoe Mountains and is very thick in the western part of the Pathfinder region.

Miocene deposits of Bates Hole

Bates Hole is located north of the Shirley Basin, south-southwest of Casper (**Figure 10**). Various pre-Cenozoic through late Tertiary age rocks are exposed, including Miocene sandstones and some younger gravels. Miocene rocks cap the older deposits along the western and eastern margins of Bates Hole. They are listed on the *Geologic map of Wyoming* (Love and Christiansen, 1985) as "lower Miocene rocks" and have been termed Arikaree Formation in some U. S. Geological Survey publications (e.g., Harshman, 1972). By restricting usage of the name Arikaree Formation to eastern Wyoming, these rocks will instead be called Split Rock Formation in this paper, following the terminology of Love (1970). The Miocene rocks of Bates Hole can be traced into the Granite Mountains and Beaver Rim areas on the western edge of Bates Hole and are of similar lithology. The Split Rock Formation at Bates Hole is dominantly a light gray, arkosic, calcareous sandstone, tuffaceous sandstone, minor conglomerate beds, and limestone (Harshman, 1972). The thickness of the Split Rock Formation in Bates Hole is 175 feet (53 m). It rests conformably on the White River Formation (Harshman, 1972).

Some Miocene fossils found in the Bates Hole area are in the collections at the University of Wyoming Geological Museum, but the assignment of a Miocene age to the Split Rock Formation of Bates Hole was on stratigraphic position alone. The rocks are of lacustrine, fluvial, and eolian origin and they contain a tuffaceous component (Harshman, 1972). Clasts of the conglomerates are from Precambrian rocks of the Granite Mountains. Sheetwash was the dominant process in the deposition of arkosic sandstones, suggesting semiarid conditions (Hooke, 1967; Harshman, 1972).

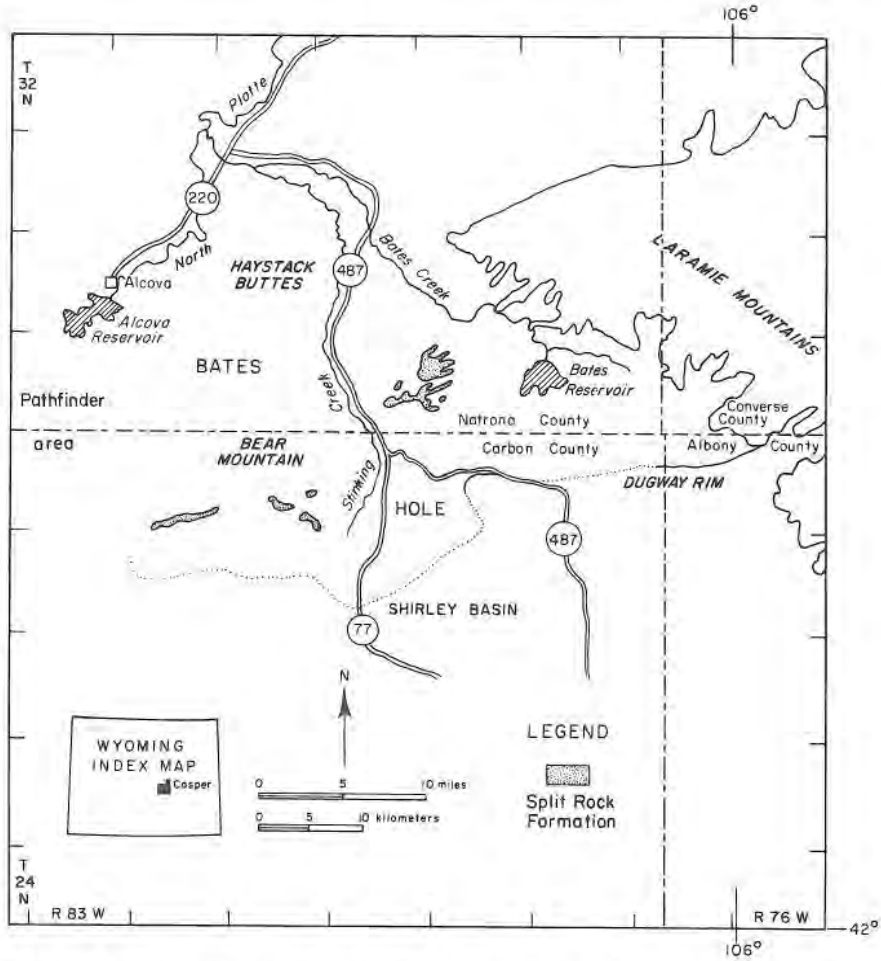

Figure 10. Neogene rocks of Bates Hole, east-central Wyoming (compiled from Harshman, 1972; Love and Christiansen, 1985). Details are not delineated in the surrounding areas.

Northern Wyoming

The Split Rock Formation at Cedar Ridge is located along Badwater Creek on the downthrown (northern) side of Cedar Ridge normal fault in the northeastern Wind River Basin, and is also found at higher elevations in the southern Bighorn Mountains north of Cedar Ridge. The Split Rock Formation is a poorly exposed deposit of fine-grained, tuffaceous sandstone and is termed Split Rock Formation because of the lithologic similarity to the Split Rock Formation along the southern margin of the Wind River Basin (Love, 1978). The sandstone is white, tan, or pale green and includes a few stringers of arkosic conglomerate containing clasts of Precambrian rocks. The Split Rock Formation overlies the late Eocene White River Formation in the southern Bighorn Mountains.

The Split Rock Formation at Darton's Bluff (**Figure 1**) consists of fine-grained sandstone and siltstone overlying a poorly sorted, cobble-to-boulder basal conglomerate, interpreted as an alluvial fan deposit. The fine-grained rocks are overlain by a sand and gravel deposit of braided stream origin (Kochel and Ritter, 1982). The age of the Split Rock deposits at Darton's Bluff is Arikareean based on a small fauna of fossil mammals (McKenna and Love, 1972; Love, 1978).

Northwestern and western Wyoming

The Neogene deposits of northwestern Wyoming are located primarily in the Jackson Hole area and northward into Grand Teton National Park (**Figure 11**). These deposits are less extensive than those in central and southern Wyoming, but they make up one of the most complete Neogene sections in the State. Another Neogene deposit, the Salt Lake Formation, crops out in the thrust belt of western Wyoming.

Colter Formation

The Colter Formation is preserved as isolated remnants located within Teton County, mostly in Jackson Hole (**Figure 11**). The best exposures are along Pilgrim Creek, east of Jackson Lake; and near Two Ocean Lake, Cunningham Hill, Shadow Mountain, and Ditch Creek (Barnosky, 1986). The Colter Formation was named by Love (1956a) and further studied in detail, including the fossil faunas by A.D. Barnosky (1984, 1986). It is dominantly a volcanic and volcaniclastic deposit consisting of waterlain pyroclastic rock, conglomerate, sandstone, siltstone, and claystone. The color varies from light gray and white for the finer grained tuff and sandstone and to red, brown, and green for coarser grained conglomerate and sandstone. There are two members of the Colter Formation, the Crater Member composed of tuff and tuff breccias of andesite, trachyte, and latite, and the overlying Pilgrim Creek Member, composed mostly of tuff, tuff-breccia, claystone, sandstone, and conglomerate. The Pilgrim Creek Member is rhyolitic and makes up the upper two-thirds of the Colter Formation. The upper (Pilgrim Creek) member differs from the lower (Crater) member in color and the occurrence of clasts of rounded quartzite cobbles in conglomerates that more commonly contain subrounded to angular clasts of volcanic material (Love, 1956a; Barnosky, 1986). The Pilgrim Creek Member is a complex deposit consisting of up to 70 beds of volcaniclastic lahar, surge, and ash deposits. The beds were laid down near vents and on the flanks of volcanoes located in the northern Jackson Hole area (Barnosky and Labar, 1989). The Colter Formation is 7,000 ft (2,000 m) thick near Pilgrim Creek.

Mammalian faunas of Arikareean, Hemingfordian, and Barstovian age in the Colter Formation include insectivores, rodents, lagomorphs, equids, oreodonts, antilocaprids, and camelids. The Colter faunas show a greater affinity to the faunas of the Great Plains than those to the west, although there is evidence that ecological differences in the Jackson area influenced both the Arikareean and Barstovian faunas. Ecological isolation of the Rocky Mountains from the west and Great Plains became evident by the late Barstovian (Barnosky, 1986).

The Colter Formation marks the first outpouring of Miocene volcanic rocks in the Jackson Hole area. The change in chemical composition from a relatively lower SiO_2 content in the Crater Member (<72%) to a higher SiO_2 content (72%) in the overlying Pilgrim Creek Member appears relatively synchronous with widespread extension and bimodal volcanism in the northern Basin and Range province (Barnosky, 1984; Barnosky and Labar, 1989; Zoback and others, 1981). This change took place during the Barstovian in northwestern Wyoming, as determined from paleontological evidence.

Teewinot Formation

The name Teewinot Formation was applied by Love (1956a) to a thick deposit of conglomerate,

sandstone, siltstone, claystone, tuff, and white limestone. The formation, named for Mt. Teewinot in the Teton Range, occurs as isolated outcrops in Jackson Hole (**Figure 11**) but may extend west into Idaho along Grand Valley.

The rocks are composed of a basal conglomerate facies fining upward into a middle facies of white limestone and pumicite, and an upper facies of claystone and pumicite (Love, 1956a). Interbedded with the basal conglomerate are sandstone, limestone, tuff, pumicite, and claystone beds. The clasts of the conglomerate include Paleozoic limestones and sandstones from the west flank of the Gros Ventre Mountains and scarce Precambrian and Mesozoic clasts. The middle facies is dominantly limestone and pumicite. The upper facies consists of claystone, limestone, pumicite, and thin conglomerate beds. Some claystone beds are laminated and interbedded with carbonaceous "paper" shales.

Algal structures, crossbedding, and laminated bedding occur, especially in the middle limestone facies, and imbrication occurs in the upper facies. A small fossil fauna and flora collected from the Jackson Hole area contains coquinas of molluscs and ostracods, a diatomite in the upper part of the formation, a fauna of terrestrial gastropods from a tuffaceous sandstone bed, a Clarendonian to Hemphillian mammal fauna, and a flora of xeric plants and conifers (Love, 1956a; A.D. Barnosky, 1984; Barnosky, 1986).

In Jackson Hole, the late Miocene Teewinot Formation is predominantly composed of fine-grained lacustrine rocks deposited in a subsiding basin formed prior to movement on the Warm Springs and Teton faults (Love, 1956a). Although uplift of the Teton Range did not occur during deposition of the Teewinot Formation, the Gros Ventre Range was exposed and provided a local source for the pebbles and cobbles of the basal Teewinot conglomerate (Love, 1956a; Barnosky and Labar, 1989). After deposition, the Teewinot Formation was deformed by uplift of the Teton Range. Outcrops of the Teewinot Formation dip up to 35° on flanks of anticlines and synclines in the area. Generally, rocks dip 10 to 30° to the west and *folding may be*

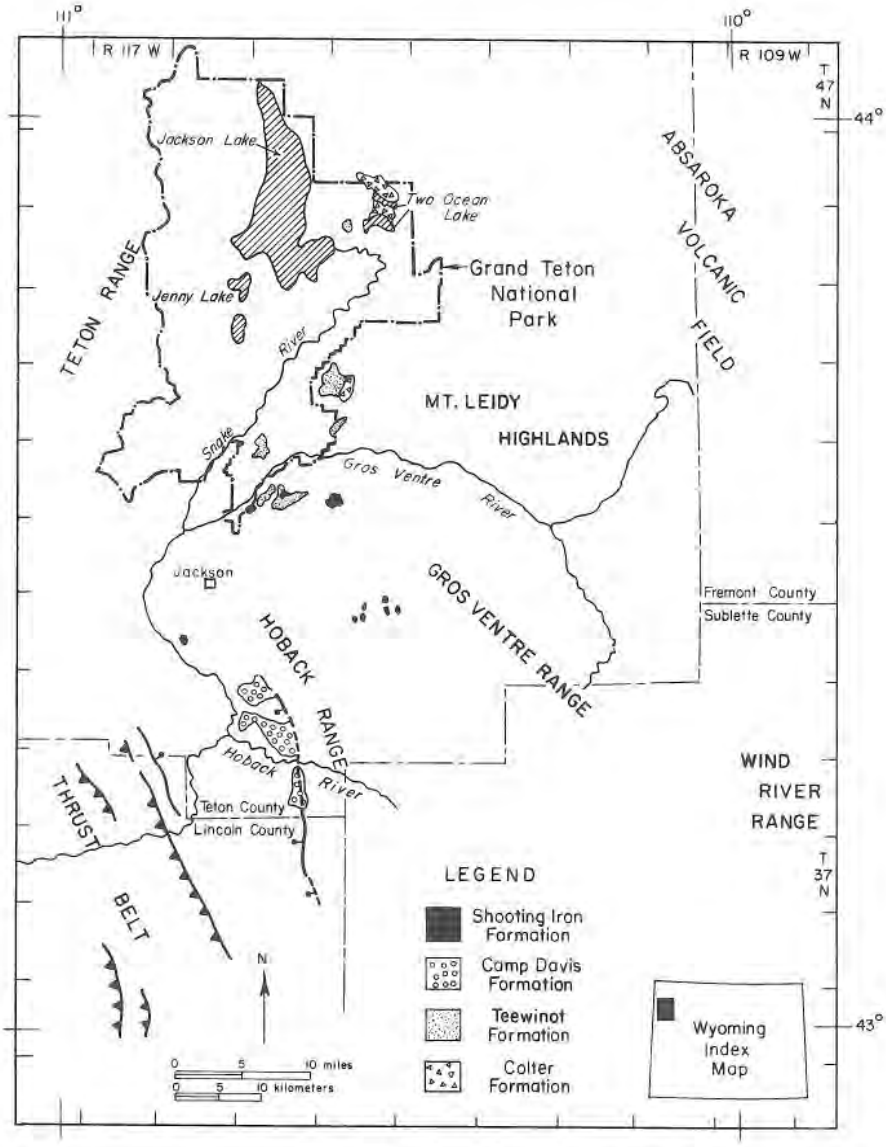

Figure 11. Neogene rocks of northwest Wyoming including Jackson Hole, part of Grand Teton National Park, and the Gros Ventre and Hoback ranges (compiled from Barnosky, 1986; Love, 1956a, 1990; Love and Christiansen, 1985; Olson and Schmitt, 1987).

more intense in areas of local faulting (Love, 1956a, p. 1910).

Camp Davis Formation

The Camp Davis Formation is located in northwestern Wyoming adjacent to the Hoback fault on the west flank of the Hoback Range, south of Jackson (**Figure 11**). It was first described by Eardley (1942) and more detailed studies were completed by Love (1956b, 1956c), Wanless and others (1955), Dorr (1956), Davis and Wilkinson (1983), and Olson and Schmitt (1987).

The Camp Davis Formation is divided into a lower conglomeratic member, a middle limestone and tuffaceous member, and an upper conglomeratic member. The lower member consists of a light gray to tan, cobble-to-pebble conglomerate and sandstone (Olson and Schmitt, 1987). The clast-supported conglomerate of the lower member is well cemented and resistant, forming prevalent pinnacles along U.S. Highway 187/189. Imbrication is scarce in the lower member as is planar and trough crossbedding; horizontal stratification is dominant (Olson and Schmitt, 1987). The sandstones are less resistant and show minor ripple and trough crossbedding and massive to horizontal stratification.

The middle member is much finer grained and is divided into three subfacies including: (1) rust-mottled carbonate mudstone, (2) oolitic sandstone and pisolitic conglomerate, and (3) carbonate siltstone and fine sandstone with pumice and volcanic ash. The carbonate mud of the first subfacies includes terrigenous clastic material, minor amounts of sand or granule-size grains, volcanic glass, algae, and gastropod and ostracod shell molds. The second subfacies consists of coarse-clastic deposits with calcareous grains, terrigenous quartz, and lithic material. The third subfacies of carbonate siltstone and fine-grained sandstone is slightly mottled by roots and contains some glass shards (Davis and Wilkinson, 1983).

The upper member is a granule-to-boulder, clast-supported diamictite with a sand and mud matrix. There is moderately developed horizontal stratification and locally well-developed clast imbrication with intervals of trough cross-stratified gravels, scour-fill sandstone, and horizontal to massive sandstone (Olson and Schmitt, 1987). A minor component of the upper member is a matrix-supported conglomerate cemented with a mud-rich matrix. The clasts are poorly sorted and mostly pebbles and cobbles. Sedimentary structures include cross stratification, graded bedding, scour-fill, and ripple laminae in the finer-grained material (Olson and Schmitt, 1987).

Clasts of the conglomerates in the Camp Davis Formation are predominantly Mesozoic and Paleozoic sedimentary units derived from the Gros Ventre and Hoback ranges. The lower member, however, also contains clasts of Precambrian quartzite and dacite from the Jackson area interpreted to be reworked material from the Harebell and Pinyon conglomerates (Late Cretaceous-Paleocene) of Jackson Hole. The upper member is largely composed of Mesozoic and Paleozoic clasts with an upward increase of Precambrian granite, granite gneiss, and mafic gneiss clasts (Olson and Schmitt, 1987).

The age of this deposit is uncertain; it has been assigned a late Miocene age based on a *Pliohippus* tooth from the middle member, but it may range in age from late Miocene to early Pliocene (Olson and Schmitt, 1987; Dorr and others, 1977). Thickness of the total unit is 5,000 ft (1,500 m) preserved on the downthrown side of the Hoback normal fault.

The depositional environment of the Camp Davis Formation was fluvial and lacustrine. There are two interpretations for the origin of the lower member. Davis and Wilkinson (1983, p. 46) suggested the lower member was deposited as *a syndeformational sedimentary sequence deposited in a tectonic basin immediately adjacent to and downthrown from its source area.* Olson and Schmitt (1987), however, favored a braided river system for the lower member and an alluvial fan sequence for the upper member, noting both the difference in clast composition and transport direction between the conglomerates of the upper and lower members. Lithology and sedimentary structures from the lower member indicate a braided river system that paralleled the axis of the Hoback fault and Camp Davis trough, similar to the present-day Snake River. The upper member is interpreted as an alluvial fan system based on the nature of the conglomerates (matrix-supported and diamictites) and the predominance of locally derived Mesozoic and Paleozoic clasts. The middle member represents a freshwater carbonate lake. In general, the Camp Davis Formation consists of fluvial/lacus-

trine sediments that were deposited prior to and during movement on the Hoback normal fault.

Shooting Iron Formation

The name Shooting Iron Formation was applied by Love (1990) to dominantly fine-grained sedimentary rocks located as isolated remnants throughout the Jackson Hole area, along the flanks of the Gros Ventre Range, and at approximately 10,000 ft (3,000 m) elevation in the Gros Ventre Range (**Figure 11**).

The Shooting Iron Formation is green, yellow, gray, and red claystone, siltstone, sandstone, and conglomerate with minor pumicite beds. Clasts of the conglomerates are composed of locally derived quartzite, limestone, volcanic rocks, granite, and sandstone (Love, 1990). The formation is most often capped by glacial deposits (till and gravel) or colluvium. Some sections of the Shooting Iron Formation are richer in conglomeratic beds than others. The clast size ranges from gravel to approximately 4-inch cobbles, with gravel-sized material to small cobble clasts being most common. The conglomerates are poorly cemented with a sandy matrix. Some claystones are slightly calcareous.

Many sections contain freshwater invertebrate fossils (pelecypods, ostracods, and gastropods) as well as fish and frog bones. A late Blancan (Pliocene) rodent assemblage has been described by Barnosky (1985). The depositional environment of the Shooting Iron Formation was lacustrine, lake margin, and fluvial.

Salt Lake Formation

The name Salt Lake Formation (**Figure 12**) was applied by Mansfield (1927) to conglomeratic beds overlying the early Tertiary deposits of the thrust belt of western Idaho and Utah. Patches of Salt Lake Formation have been mapped in the Wyoming thrust belt by Oriel and Platt (1980). Some of the Salt Lake Formation mapped in Star Valley near Afton west of the Teton Range is considered to be either Teewinot Formation (Love and Christiansen, 1985) or Salt Lake Formation (Oriel and Platt, 1980). In Wyoming, the Salt Lake Formation is a poorly defined term for

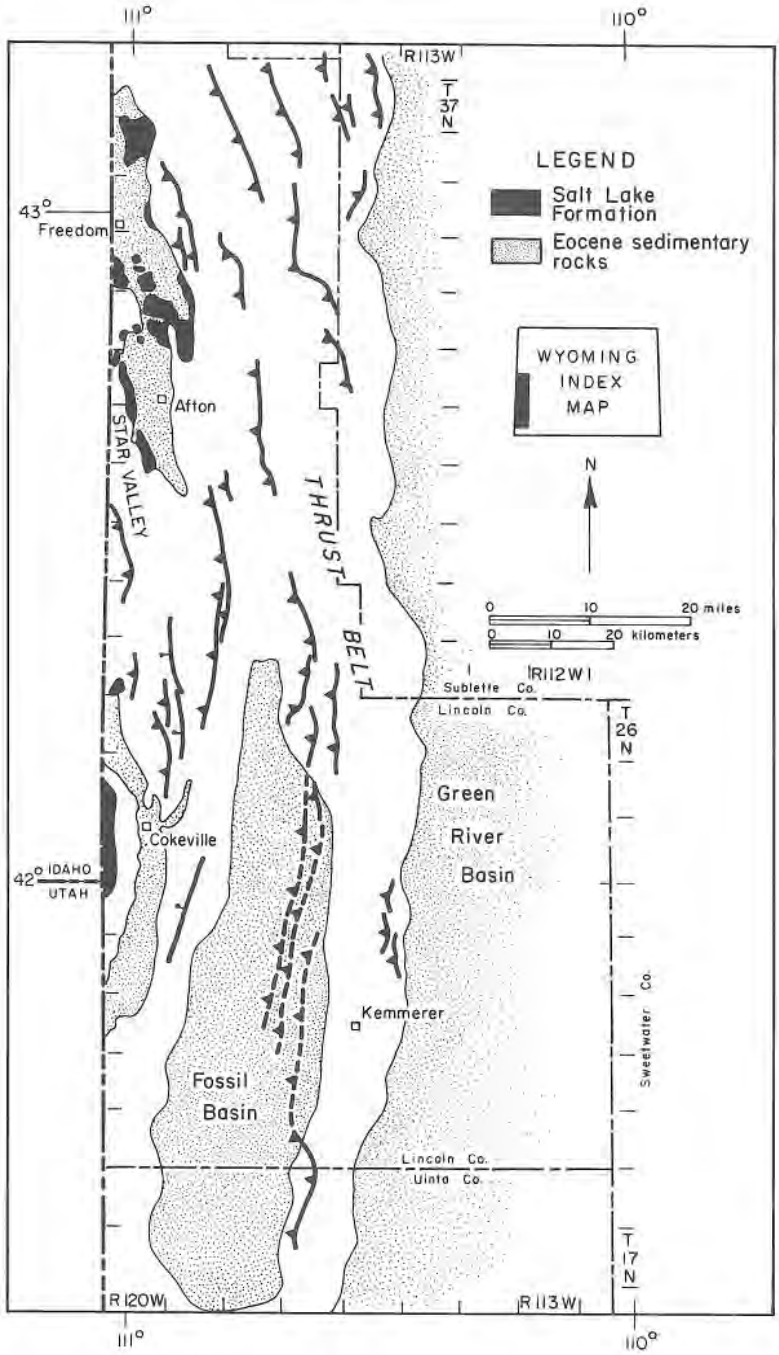

Figure 12. Neogene rocks of western Wyoming in the thrust belt showing the extent of the Salt Lake Formation (compiled from Mansfield, 1927; Love and Christiansen, 1985; Blackstone and DeBruin, 1987).

most post-Laramide, volcanic-rich sedimentary rocks in the thrust belt. The deposits of Salt Lake Formation consist of gray to pink, fine-grained, tuffaceous sandstone, siltstone, ash, pumicite, and conglomerate. The rocks are rich in calcium carbonate (Mansfield, 1927; Oriel and Platt, 1980).

The age of this deposit may range from Oligocene to Pliocene, but it is commonly considered late Miocene to Pliocene based on stratigraphic position. The thickness of the Salt Lake Formation is 1,000 to 1,200 ft (300-400 m).

Changing Neogene depositional environments

Early Miocene

There is notable similarity in depositional styles of Neogene sedimentary rocks in Wyoming (**Table 1**). A basal conglomerate characterizes most beds considered as earliest Miocene in the Granite Mountains area, Saratoga Valley, Bighorn Mountains, southern Wind River Range, northern Medicine Bow Mountains, Bates Hole, and eastern Wyoming. Such conglomeratic deposition was the continuation of widespread late Oligocene, coarse-grained sedimentation throughout central and southern Wyoming (Harshman, 1972; Hansen, 1986; Steidtmann and others, 1986). In the early Miocene there was a marked depositional change from late Oligocene style conglomerate to fine-grained sand. Above the basal conglomerate, the rocks fine upward into dominantly fine-grained sandstones. The early to middle Miocene deposits of the Browns Park and Split Rock formations are generally fine-grained volcaniclastic sandstone, limestone, volcanic ash, and minor conglomerate beds deposited in depressions, as some subsidence took place prior to normal fault movement. The Arikaree Formation in eastern Wyoming and western Nebraska is composed of tuffaceous silty sandstone and air-fall volcaniclastic loess (Hunt, 1990).

The fine grain size, absence of coarse granitic detritus from exposed Precambrian basement, and the eolian/lacustrine character of these sedimentary rocks suggest low topography throughout Wyoming and support the hypothesis that many of Wyoming's mountain ranges were essentially covered or were supplying very little locally derived debris in the early to middle Miocene (Blackwelder, 1915; Knight, 1953). Many of the Miocene fine-grained clastic rocks have since undergone deformation by normal faulting, but early to middle Miocene tectonic quiescence dominated all of Wyoming except in the Jackson area, where renewed volcanism resulted in coarse volcaniclastic deposits of the Colter Formation.

The overall climatic regime of Wyoming during the Neogene tended towards increased aridity accompanied by intense, episodic precipitation (Flanagan, 1990). Faunal evidence supports increasing dryness throughout the Miocene continuing into the Pliocene. Evidence of some ecological isolation in northwest Wyoming is provided by the Arikareean faunas of the Colter Formation (Barnosky, 1986). The Arikareean faunas of Darton's Bluff, Jackson Hole, eastern Wyoming, and possibly the Granite Mountains consisted mostly of browsers, suggesting that brushy vegetation was dominant.

Middle to late Miocene

By the mid-Miocene, the climate was arid to semiarid, as evidenced by eolian cross stratification, caliche soil horizons, interdunal pond deposits, and a pollen record dominated by semiarid vegetation. Fine-grained silt and sand deposition continued in the basins during the middle Miocene (Hemingfordian), including continued input of volcaniclastic material (Hunt, 1990). Approximately 2,000 ft (600 m) of Split Rock Formation filled a sagging depression along the valley of the modern Sweetwater River, and strata similar in lithology accumulated along Cedar Ridge in the Badwater area. Deposits of Browns Park Formation in southern Wyoming are dominantly fine grained, punctuated by fluvial and colluvial conglomeratic beds. Pollen from the Split Rock Formation of the Granite Mountains indicates an impoverished flora of deciduous and coniferous trees with an overall modern aspect. Elements of semiarid vegetation (*Artemesia*) appear in the pollen record (Leopold and MacGinitie, 1972; Leopold and Denton, 1987). Eolian and fluvial processes deposited several hundred feet of sandstone and siltstone

Table 1. A summary of sedimentation patterns, depositional environments, and tectonism during the Neogene in Wyoming.

	Land Mamal Ages	Northwestern and western Wyoming	Central Wyoming	Southern Wyoming	Eastern Wyoming	Tectonic interpretation
Pliocene	Blancan	fine-grained sedimentation	canyon cutting	canyon cutting	canyon cutting	widespread erosion after development of large river systems
5 my	Hemphillian	large river system develops, alluvial fans from Hoback fault	development of large river systems		development of large river systems	
	Clarendonian	uplift of Teton Range (?) fresh water lakes and fine-grained sedimentation	coarse-grained sedimentation, South Granite Mts. fault system active	beds cut by normal faulting (post-Browns Park Fm.)	ponds, fine grained sedimentation on interfluves beds of Arikaree Fm. cut by faults	episode of normal faulting
Miocene	Barstovian	normal faulting in the Jackson area	shallow fresh and alkaline-saline lakes Granite Mts. area	fine-grained sedimentation continues with some coarse-grained material	coarse-grained sedimentation in Bear lodge Mts.	
	Hemingfordian		coarse-grained sedimentation, Continental fault system	lake development	development of river systems with epiclastic bedload flowing off Laramie Mts. to east	initiation of regional uplift
	Arikareean	volcaniclastic sedimentation in the Jackson area	fine-grained eolian sedimentation and ponding basal conglomerate	small fluvial systems and fine-grained sedimentation basal conglomeate fine- to coarse-grained sandstone	fine-grained eolian sedimentation of volcaniclastic loess	basin filling and aggradation; quiescence in central, southern, and eastern Wyoming; volcanism in Jackson area
24 my						

in eastern, central, and southern Wyoming during the Hemingfordian, whereas lacustrine deposition took place in the northern Saratoga Valley. In northern Wyoming, the Miocene rocks of Cedar Ridge, southern Bighorn Mountains, and Bear Lodge Mountains suggest that fluvial and eolian processes were important. Volcanism continued in the Jackson area during the Hemingfordian. The initial cutting of large valleys in western Nebraska began in the Hemingfordian and continued throughout the Neogene, involving up to six cycles of scour and fill. Debris shed off the Laramie Mountains and Front

Range contributed much of the sedimentary infill during the cycles (Skinner and others, 1977; Swinehart and others, 1985). In summary, in the central regions of Wyoming fine-grained eolian deposition took place, to the west volcanic deposition occurred, and to the east conglomeratic deposition was renewed.

Fine-grained deposition slowed and was replaced by conglomeratic deposition in parts of eastern Wyoming during the Barstovian, and the erosion of large valleys by river systems continued in western Nebraska. Normal faulting began in the Jackson Hole area and along the Continental fault of the southern Wind River Range. Ecological isolation of the Rocky Mountains is evident by Barstovian time (Barnosky, 1986; Leopold and Denton, 1987; Flanagan, 1990). Barstovian faunas of the Jackson area contain species common to communities west (Great Basin, California) and east (Nebraska) of the Jackson area, but the overall composition of the fossil assemblage is unique. The latest Barstovian fauna of the Pathfinder region is mostly composed of grazers including equids, camelids, antilocaprids, rodents, rabbits, and ochotonids. Faunas of eastern Wyoming bear some similarity to those of central Wyoming but primarily resemble the faunas of the Great Plains and only slightly resemble the Jackson faunas. The Barstovian faunas of the Saratoga Valley contain oreodonts (small herbivores), rodents, camelids, antilocaprids, and equids. The middle Miocene faunas were dominated by grazing herbivores as the spread of grasses took place throughout North America, but the overall taxonomic diversity of faunas is not as great relative to those of the Great Basin and Great Plains. This may be a factor of either preservation or environment; the latter interpretation is supported by an impoverished flora at that time and semiarid conditions.

Late Barstovian to Clarendonian flora from the Granite Mountains, Saratoga Valley, and Jackson area contain pollen of modern aspect, primarily conifers (pines, spruce, and fir) and semiarid vegetation such as grasses, saltbush, and sagebrush (Leopold and MacGinitie, 1972; Leopold and Denton, 1987; Montagne, 1991). The flora indicate vegetated slopes surrounding semiarid valleys filled with shallow lakes (C.W. Barnosky, 1984). Algal limestones and evaporite beds in the Granite Mountains, Jackson area, and eastern Wyoming were deposited in shallow, freshwater to alkaline saline lacustrine systems, again suggesting a semiarid climate (Love, 1956a, 1970; Mariner, 1971; Flanagan, 1990).

Although the climatic trend toward aridity continued into the Clarendonian, conglomeratic deposition once again became widespread as an episode of normal faulting progressed eastward to encompass central, southern, and eastern Wyoming (Flanagan, 1990). Displacement along the normal faults resulted in the development of alluvial fans in some areas (Granite Mountains, southern Wind River Range, Camp Davis basin) but not others (Saratoga Valley, Sierra Madre, Cedar Ridge, and Jackson Hole). Eolian cross stratification, evaporite deposits, and caliche horizons are found in the late Miocene fine-grained sandstone and siltstone beds and all lithologies are cemented with calcium carbonate. The conglomerate beds have sheet- and ribbon-like geometries. The rivers carried locally derived sediments and flowed from the newly uplifted mountains into the basins. Mudflows in the Pathfinder region resulted from episodic sedimentation initiated by periodic, intense precipitation characteristic of semiarid to arid areas (Hooke, 1967; O'Brien and Julien, 1985; Schumm and others, 1987).

Clarendonian fossils are sparse in central Wyoming (Kortes formation), although camel, rhino, equid, and rabbit fragments have been reported (Love, 1970). The late Barstovian to early Clarendonian faunas of eastern Wyoming were primarily grazing herbivores similar to those of the Great Plains. Clarendonian fossils are also found in the lacustrine Teewinot Formation of Jackson Hole. From the Arikareean to early Clarendonian, reptile fossils indicate winters were warmer than today (Hutchison, 1982). There were probably very few prolonged periods of freezing temperatures, but the progressive disappearance of deciduous trees in the late Barstovian to Clarendonian floras of Wyoming and an increase in alpine vegetation suggests cooling was taking place (Cassiliano, 1980; Hutchison, 1982; Flanagan, 1990).

Latest Miocene - Pliocene

The nature of river systems changed during the latest Miocene through Pliocene (Hemphillian and Blancan). The clasts in the conglomerates became more rounded and more were derived from distant rather than local areas. The conglomeratic deposits

contain less matrix and are restricted to long narrow forms suggesting confined channels. These conglomeratic deposits are found throughout the State as isolated remnants on much of the highest topography in the basins. The upper Ogallala Formation in southeast Wyoming was formed by braided river systems carrying debris from the Laramie Mountains eastward into Nebraska. Although the North Platte River had established its initial northward flow into the Saratoga Valley by Hemingfordian time, rejuvenation occurred in late Barstovian time as the river system cut North Gate Canyon and the outlet near Ft. Steele, Wyoming. Downcutting in Lodore Canyon (Uinta Mountains) was caused by capture and rejuvenation of the Green River (Hansen, 1986). The Fenton Pass Formation, located in the Bighorn Basin atop Tatman Mountain, was deposited by a late Cenozoic river system (Rohrer and Leopold, 1963). Latest Miocene to early Pleistocene high terrace deposits are also present in the Green River Basin, Hanna Basin, Powder River Basin, Laramie Basin, and Granite Mountains syncline (Love, 1970; Hansen, 1986; Flanagan, 1990; Mears and others, 1991).

High terraces of large river systems are present in Kansas, Nebraska, Colorado, and Wyoming (Pearl, 1971; Stanley and Wayne, 1972; Larson and others, 1975; Diffendal and others, 1982; Diffendal and others, 1985; Aber, 1985; Eversoll, 1985). The terraces are the first evidence for modern drainage systems. Geomorphic processes of headward erosion by vigorous streams, and stream capture and piracy are recorded in the high terraces of the rivers (Pearl, 1971; Stanley and Wayne, 1972; Larson and others, 1975; Diffendal, 1982; Diffendal and Corner, 1983; Aber, 1985; Eversoll, 1985).

In summary, depositional styles of Miocene strata indicate that subsidence took place prior to movement on the normal faults. Between the Hemingfordian and Barstovian, internally drained areas surrounded by low topography were filled with eolian and lacustrine deposits. Normal faulting in Wyoming during the Miocene occurred in post-Barstovian time (around 10 Ma) except along the Continental fault, where movement took place at 13 Ma and in the Jackson area along the Warm Springs fault (Love and others, 1973). After movement on the normal faults, alluvial fan sedimentation took place in some areas but not in others. During the latest Miocene and Pliocene, development of large through-flowing river systems occurred, eroding older sediments from Wyoming's basins. This initiated the degradational regime in Wyoming that continues to the present.

Tectonic interpretations from the Neogene sedimentary record

Basin fill and excavation

The depth and timing of Wyoming's basin fill remains a controversial subject. The essential question is whether Wyoming's foreland basins were filled with volumetrically more Cenozoic sedimentary material between late Eocene and Pleistocene and then substantially excavated or whether the material in the basins today is the maximum sediment fill deposited in the basins throughout the Cenozoic. Darton (1906), while studying high-level surfaces in the Bighorn Mountains, first suggested that the basins had once been filled with volumetrically more material than remains today. He concluded that the surfaces were formed by erosion. Miocene sediments found on these surfaces were *probably the remnants of much more extensive sheets* (Darton, 1906, p. 110). Blackwelder (1915) and Mackin (1937) reinforced this interpretation based primarily on geomorphic evidence. Knight (1953) envisioned the paleotopography of Wyoming during the Miocene as a broad monotonous plain with only the high peaks of the mountain ranges rising above a thick sedimentary deposit. Subsequent work has both supported and challenged basin filling to the high-level surfaces (Love, 1960; Love and others, 1963; Love, 1970; McKenna and Love, 1972; Kochel and Ritter, 1982). Surfaces of low relief at approximately 10,000 ft (3,000 m) elevation (high-level surfaces) are present in all the major mountain ranges in Wyoming (Steidtmann and others, 1989; also see Mears, this volume).

The amount of basin fill is difficult to determine because there are only scattered remnants of Oligocene to Pliocene sedimentary rocks in the basins. Wyoming's basins are dominantly floored with rocks of middle Eocene age in the south and early Eocene

age in the north. The Laramie Basin of southeast Wyoming, the highest basin, is an exception and is partially floored by rocks of Late Cretaceous age. Lower Eocene sediments are preserved in Cooper Lake Basin, a small structural sub-basin of the Laramie Basin (Blackstone, 1975; Davidson, 1987). Evidence for filling of Wyoming's basins with an additional 3,000 ft (1,000 m) of sediment on top of the present basin floors is constrained by: (1) the presence of fine-grained Neogene sedimentary rocks at high elevations in the mountain ranges and basins of Wyoming; (2) the amount of overburden needed for maturation of source rocks for hydrocarbon and coal deposits; (3) geothermal fission-track work of Naeser (1984); (4) the petrography of the Miocene sedimentary rocks preserved throughout Wyoming; and (5) superposition of rivers across mountain ranges. The superposition of river systems suggest that the rivers were flowing across basins filled with sedimentary material to elevations of approximately 9,000 ft (2700 m).

Late Eocene to Miocene sedimentary rocks are present in canyon fills and atop mountain ranges and mesas (McKenna and Love, 1972; Love and Christiansen, 1985; Montagne, 1991). Oligocene to Miocene conglomerates and siltstones are present high in mountain ranges between approximately 7,000 and 9,000 ft (2,300 and 3,000 m). Siltstones and conglomerates from local sources, and alluvial fan deposits on Darton's Bluff occur as canyon fill and isolated exposures on the high-level surface in the Bighorn Mountains (Darton, 1906; McKenna and Love, 1972; Kochel and Ritter, 1982). Oligocene conglomerates and siltstones are preserved in paleovalleys in the Medicine Bow and Laramie ranges, where local high topography existed (Evanoff, 1990). Fine-grained Miocene sandstones are present atop the Laramie Mountains, Seminoe Mountains, and Sierra Madre (Knight, 1953; Montagne, 1953; Love, 1970; Love and Christiansen, 1985). The presence of fine-grained rocks high in the mountains indicates that parts of the mountain ranges were covered by a sedimentary blanket in the early to middle Neogene.

Measurement of the minimum amount of fill is also constrained by the elevation of late Miocene through Pleistocene fluvial deposits preserved on mesas in Wyoming's basins. The late Cenozoic Fenton Pass Formation caps Tatman Mountain in the Bighorn Basin, about 1,500 ft (500 m) above the basin floor (Rohrer and Leopold, 1963). Upper Eocene or lower Oligocene conglomerates cap Pumpkin Buttes in the Powder River Basin, about 1,000 ft (300 m) above the basin floor (Love, 1952). Work is now in progress to date other high-level fluvial deposits in the southern basins of Wyoming.

Fission-track thermochronology from the Green River Basin rules out the possibility of a thermal perturbation event causing the maturation of hydrocarbons (Naeser, 1984). A down-hole thermal history of Wagon Wheel Hole #1 indicates there was little change in thermal regime affecting the 110° isotherm throughout the middle to late Tertiary. Fission-tracks in apatites were annealed until about 4 Ma, when the rocks cooled through the 110° isotherm and tracks began to form. This suggests a lowering of the 110° isotherm in the Green River Basin near 4 Ma, and it is attributed to a major erosion event (Naesar, 1984).

The superposed rivers include: (1) the North Platte River across the Medicine Bow Mountains (through North Gate Canyon), Seminoe Mountains (through Black Canyon), and Granite Mountains (through Fremont Canyon); (2) the Wind River across the Owl Creek Mountains (through Wind River Canyon); (3) the Laramie River across the Laramie Mountains; (4) the Sweetwater River across the Granite Mountains; (5) the Green River across the Uinta Mountains; and (6) the Bighorn River across the Bighorn Mountains (Love, 1970; McKenna and Love, 1972; Love and Christiansen, 1985).

The large braided river systems that dominated deposition in the upper part of the Ogallala Formation (Bear Lodge Mountains), middle part of the Kortes formation, and lower part of the Camp Davis Formation were still aggrading, as evidenced by the preservation of conglomerates deposited by the river systems. The Neogene aggradational regime in Wyoming continued until latest Miocene-early Pliocene. Large-scale excavation of the basins began when through-flowing rivers with the capacity to carry large sediment loads developed. There is evidence for large, through-flowing rivers in the late Miocene, during deposition of the Kortes formation in central Wyoming. Evidence for through-flowing rivers is also seen in Saratoga Valley, the Bighorn Basin, the Camp Davis basin, and the Uinta Mountains/Green River Basin (Montagne, 1955; Rohrer and Leopold, 1963; Stanley, 1976; Hansen, 1986;

Olson and Schmitt, 1987). Perennial rivers were fed by the water released from large snowpacks. Increased snowfall aided in the development of mountain glaciers that are first recorded in Wyoming at approximately 3 Ma (Love and others, 1973). The combination of cold climate and large, through-flowing river systems during the Plio-Pleistocene resulted in continued basin excavation. Cut terraces along the North Platte River attest to the erosion both in central Wyoming and Saratoga Valley. The 4 Ma lowering of the 110° isotherm further supports an erosion event in the Pliocene of the Green River Basin (Naeser, 1984).

Initiation of modern drainages and development of large river systems took place during the late Miocene in the adjacent states of Colorado, Nebraska, and Idaho. Initiation of the modern Colorado River system occurred around 10 Ma (Larson and others, 1975). Two thousand feet (600 m) of downcutting has taken place over the last 8 million years on the Roaring Fork River in northern Colorado (Larson and others, 1975). The Ogallala-topped tablelands of Nebraska are 1,000 ft (300 m) above the North Platte River in central Scotts Bluff County (Swinehart and others, 1985). The modern North Platte River valley in Nebraska is slightly younger than 10 Ma (Swinehart and others, 1985). Development of modern drainages in the basins of southwestern Montana and eastern Idaho was also a late Miocene event (Fields and others, 1985).

During the last one million years, the Tongue River has cut down 1,000 ft (300 m) in the Powder River Basin (Mears and others, 1991). The North Platte River in Black Canyon has cut a total of 800 feet (250 m) in two episodes of downcutting in the Hanna Basin since Plio-Pleistocene time. Up to 1,500 ft (450 m) of erosion has occurred in the Bighorn Basin since late Tertiary.

Neogene normal faulting

The episode of normal faulting that began in Wyoming around 13 million years ago suggests mid-Miocene regional uplift. Steidtmann and Middleton (1986) dated movement on the Continental fault adjacent to the southern Wind River Range using fission-track techniques. They concluded that movement occurred around 13 Ma and resulted in the deposition of the Circle Bar beds shed off the upthrown fault block (Jackson, 1984; Steidtmann and Middleton, 1986). Normal faults which dropped Saratoga Valley down between the Medicine Bow Mountains and Sierra Madre are post-Barstovian to Holocene in age; the Barstovian upper Browns Park Formation was warped by the faulting in the Saratoga Valley (Montagne, 1991) and Cherokee Ridge area (Luft, 1985). Movement on the Cedar Ridge normal fault in the Badwater region has not been dated, but is also thought to be after Miocene deposition because of the presence of both flat-lying and structurally deformed Split Rock Formation adjacent to the fault (Love, 1978). The Wheatland-Whalen fault system of eastern Wyoming cuts Arikaree Formation of early Miocene age (Hunt, 1990). Movement on these faults is considered to be post early middle Miocene and no younger than latest Miocene (L.W. McGrew, 1963). The Granite Mountains of central Wyoming are within an asymmetrical graben formed by movement on the South Granite Mountains and North Granite Mountains fault systems. Movement on the faults began around 11 Ma and have continued into Quaternary time (Geomatrix Consultants, 1988; Flanagan, 1990). Sedimentary rocks of the Miocene Split Rock and Moonstone formations rest adjacent to and are deformed by the normal faults (Love, 1970; Flanagan, 1990). Normal faulting in the northwest corner of Wyoming was initiated in the post-Barstovian (Love, 1956a; A.D. Barnosky, 1984, 1986; Barnosky and Labar, 1989).

Between 18 and 16 Ma, Yellowstone Valley and the Jackson Hole area record subsidence and volcanism, interpreted to signal the onset of Neogene extension (Barnosky and Labar, 1989). Subsidence first began during the Hemingfordian, approximately 18 to 16 Ma, in central and south-central Wyoming (Granite Mountains and Saratoga Valley). At this time, initiation of major cut-and-fill sequences began in Nebraska from rivers originating along the Continental Divide. Accelerated regional uplift in Wyoming and possibly the entire Rocky Mountain region took place in the middle Miocene (Hemingfordian). By 10 Ma, Wyoming was at or near its present elevation.

There is no reason to decouple the Neogene tectonic history of Wyoming from the rest of the west (Basin and Range, Rio Grande Rift, Snake River Plain) even though the degree and style of tectonism experienced by these areas differed. The advent of

extensional tectonics in northwest Wyoming around 17 Ma, the mid-Miocene change in sedimentation in Nebraska, normal faulting at 13 Ma in the Wind River Range, and younger faulting to the east and north suggests tectonism related to the Basin and Range, Rio Grande Rift, and Snake River Plain. Timing of the tectonism in the Basin and Range corresponds well to middle Miocene volcanism and uplift, normal faulting, and resulting graben and half-graben structures in Wyoming (Stewart, 1978; Zoback and others, 1981; Anderson and others, 1983). The expression of these events is unique to Wyoming although the underlying causes may be linked. The uniqueness of Wyoming's tectonism is perhaps due principally to Wyoming's Archean crust and the lower thermal regime that underlies the mountain ranges of Wyoming (Decker and others, 1988).

Regional uplift

Regional uplift took place in a series of pulses. The first occurred during the Laramide, as evidenced by regression of the Western Interior seaway and Cannonball Sea. The second pulse occurred in the late Oligocene to early Miocene and is marked by a change in flow direction of some Rocky Mountain river systems, and by localized conglomeratic sedimentation in Wyoming and widespread conglomeratic sedimentation in Nebraska (Swinehart and others, 1985; Steidtmann and others, 1989). The third and major pulse of uplift began in the mid-Miocene (about 17 Ma) and continued through the Pleistocene. This large pulse of uplift is roughly contemporaneous with the initiation of bimodal volcanism in the Basin and Range province and in northwestern Wyoming (Stewart, 1978; Barnosky and Labar, 1989). Interpretation of climate and vegetation suggest that regional uplift elevated Wyoming to almost its present elevation by the Clarendonian, as ecological isolation continued. The area west of the Rocky Mountains, including Idaho, did not undergo a decline in the Miocene-type forests nor develop local grassland and steppe environments until late Pliocene to Pleistocene (Leopold and Denton, 1987), suggesting that warmer conditions continued to the west as cooler conditions developed in the Rockies.

The main body of evidence for initiation of regional uplift in Wyoming is not seen in the interior of the uplift, where little deformation of older rocks took place, but along the edge of the uplifted area, as recorded in the Miocene sedimentary history of Nebraska. Oligocene and early Miocene sedimentation in Nebraska was dominated by fine-grained sandstones and siltstones interbedded with conglomerates (Swinehart and others, 1985; Hunt, 1990). An episode of major channel cutting and related conglomeratic sedimentation took place around 28 Ma (Swinehart and others, 1985). After this channelling event, aggradation of fine-grained material resumed again in Nebraska. In the mid-Miocene (Hemingfordian-Barstovian), deposition of the Hemingford and Ogallala groups began as a series of channel scour-and-fill events with the erosion of large paleovalleys (Skinner and others, 1977). From mid-Miocene to Pleistocene there was a sequence of three to six cut-and-fill events (Skinner and others, 1977; Diffendal, 1982; Swinehart and others, 1985). Flow direction of rivers that cut the valleys was from west to east, off the Laramie Mountains and Front Range into Nebraska. Anorthosite and granite from the Laramie Mountains can be found as far as eastern Nebraska (Stanley and Wayne, 1972; Diffendal, 1982). Volcanic rocks from Specimen Mountain in north-central Colorado were carried by rivers across the site of the present Medicine Bow and Laramie mountains and deposited as clasts in the conglomerates of the Ogallala Formation near Cheyenne and to the east in Nebraska (Blackstone, 1975; Stanley, 1976; Swinehart and others, 1985).

The gradients of the North Platte's major valleys and their tributaries during deposition of the Ogallala Group in western Nebraska were similar to those of the North Platte valley and tributaries today (Diffendal, 1982; Goodwin and Diffendal, 1987). A period of nondeposition occurred in western Nebraska between 5 and 4 Ma (Swinehart and others, 1985; Diffendal, personal communication, 1989), correlating in time with a major erosion event in Wyoming (Naeser, 1984). Regional tilting, continued movement on normal faults, superposition of rivers across mountain ranges, and erosion in the basins confined many of Wyoming's major rivers to northward draining courses. Structural warping in Nebraska (Diffendal and Corner, 1983) and Kansas (Aber, 1985) may have caused the North Platte and Cheyenne rivers to flow east again.

Suggestions for future research

This paper is a broad review of what is known about Wyoming's Neogene geologic history. Many deposits remain to be studied in detail and placed into a regional context in order to address larger tectonic questions. This review has noted several problems with the nomenclature of the Neogene deposits. Basic mapping projects would help clarify some problems:

1. A comprehensive study of the rocks of the Arikaree and Ogallala formations in eastern Wyoming and the establishment of a useful nomenclature;

2. A comprehensive study of the Salt Lake Formation in the thrust belt of Wyoming, Utah, and Idaho, including radiometric ages and lithologic analyses of the deposits mapped as Salt Lake Formation in the various basins;

3. A study of the thickness of Miocene rocks in the Bighorn Mountains to determine if the rocks formed a thin veneer blanketing the mountains or if they are a thick deposit that once was part of the basin-filling sequence;

4. A detailed study of the Browns Park Formation in south-central Wyoming, including Aspen Mountain and Cherokee Ridge, to clarify their relationship to the deposits in Saratoga Valley and northern Colorado;

5. Determination of the extent of the Kortes formation throughout central Wyoming;

6. Mapping of the late Cenozoic high-level boulder conglomerate and lag deposits throughout Wyoming;

7. Better dating of the normal faults that displaced the Neogene deposits, especially along Cherokee Ridge, Wheatland-Whalen fault system, North Granite Mountains fault system, Cedar Ridge, and in the thrust belt;

8. A study of the dynamics of conglomeratic deposition in eastern Wyoming and the western Black Hills (Ogallala Formation);

9. A study of the relationships between regional tectonism in the western U.S. Cordillera during the Neogene and tectonic activity in Wyoming.

Acknowledgments

We thank two outstanding geologists and gentlemen, J. D. Love and D.L. Blackstone, Jr., for their continued support, advice, criticism, and the sharing of their knowledge with students of Wyoming geology. We wish to thank Bob Hunt, Art Snoke, Bob Diffendal, Don Blackstone, and Dave Love for reviewing this manuscript and for their insightful suggestions. Helpful discussions with Tony Barnosky, Dede Bohn, Tom Dunn, Emmett Evanoff, Karin Fischer, Tim Gubbels, Jay Lillegraven, Brainerd Mears, Jim Steidtmann, Mike Voorhies, and Jay Zimmerman are gratefully appreciated. We especially want to thank the Kortes and Richner families for their unwavering hospitality and friendship. This research was supported in part by the University of Wyoming Department of Geology and Geophysics, the Charles Hill Fellowship, a Geological Society of America Research Award, and the Sigma Xi Scientific Society.

References cited

Aber, J. S., 1985, Quartzite-bearing gravels and drainage development in eastern Kansas: TER-QUA Symposium Series 1, p. 105-110.

Ahlbrandt, T. S., and Groen, W., 1987, The Goshen Hole uplift: A brief review of its geologic history and exploration potential: The Mountain Geologist, v. 24, p. 33-43.

Anderson, R. E., Zoback, M. L., and Thompson, G. A., 1983, Implications of selected subsurface data on the structural form and evolution of some basins in the northern Basin and Range province, Nevada and Utah: Geological Society of America Bulletin, v. 94, p. 1055-1072.

Angevine, C. L., and Flanagan, K. M., 1987, Buoyant subsurface loading of the lithosphere in the Great Plains foreland basin: Nature, v. 327, p. 137-139.

Barnosky, A. D., 1984, The Colter Formation: Evidence for Miocene volcanism in Jackson Hole, Teton County, Wyoming: Wyoming Geological Association Earth Science Bulletin, v. 16, p. 50-101.

_____ 1985, Late Blancan (Pliocene) microtine rodents from Jackson Hole, Wyoming: biostratigraphy and biogeography: Journal of Vertebrate Paleontology, v. 5, p. 255-271.

_____ 1986, Arikareean, Hemingfordian, and Barstovian mammals from the Miocene Colter Formation, Jackson Hole, Teton County, Wyoming: Bulletin of Carnegie Museum of Natural History, no. 26, 69 p.

Barnosky, A. D., and Labar, W. J., 1989, Mid-Miocene (Barstovian) environmental and tectonic setting near Yellowstone Park, Wyoming and Montana: Geological Society of America Bulletin, v. 101, p. 1448-1456.

Barnosky, C. W., 1984, Late Miocene vegetational and climate variability inferred in a pollen record in northwestern Wyoming: Science, v. 223, p. 49-51.

Berggren,W.A., Kent, D.V., Flynn, J.J., and Van Couvering, J.A., 1985, Cenozoic geochronology: Geological Society of America Bulletin, v. 96, p. 1407-1418.

Blackstone, D. L., Jr., 1965, Gravity thrusting in the Bradley Peak and Seminoe Dam quadrangles, Carbon County, Wyoming, and the relationship to the Seminoe iron deposits: Geological Survey of Wyoming Preliminary Report 6, 13 p.

_____ 1975, Late Cretaceous and Cenozoic history of the Laramie Basin region, southeast Wyoming, *in* Curtis, B. F., editor, Cenozoic history of the Southern Rocky Mountains: Geological Society of America Memoir 144, p. 249-279.

Blackstone, D. L., Jr., and DeBruin, R. H., 1987, Tectonic map of the Overthrust Belt, western Wyoming, northwestern Utah, and southeastern Idaho: Geological Survey of Wyoming Map Series 23, scale 1:316,800.

Blackwelder, E., 1915, Post-Cretaceous history of the mountains of central western Wyoming: Journal of Geology, v. 23, p. 97-117, 193-217, and 307-340.

Bown, T. M., 1980, Summary of latest Cretaceous and Cenozoic sedimentary, tectonic, and erosional events, Bighorn Basin, Wyoming: University of Michigan Papers on Paleontology, no. 24, p. 25-32.

Breyer, J., 1975, The classification of Ogallala sediments in western Nebraska, *in* Studies on Cenozoic paleontology and stratigraphy: University of Michigan Papers on Paleontology, v. 3, no. 12, p. 1-8.

Buehner, J. H., 1936, Geology of an area north of the Sierra Madre, Carbon County, Wyoming [M.S. thesis]: Laramie, University of Wyoming, 37 p.

Cassiliano, M., 1980, Stratigraphy and vertebrate paleontology of the Horse Creek-Trail Creek area, Laramie County, Wyoming: University of Wyoming Contributions to Geology, v. 19, p. 25-68.

Cita, M.B., 1975, The Miocene/Pliocene boundary: history and definition, *in* Saito, T. and Burckle, L.H., editors, Late Neogene epoch boundaries: Micropaleontology Press, American Museum of Natural History, New York, p. 1-30.

Crist, M.A., and Lowry, M. E., 1972, Ground-water resources of Natrona County, Wyoming: U.S. Geological Survey Water-Supply Paper 1897, 92 p.

Darton, N. H., 1906, Geology of the Bighorn Mountains: U. S. Geological Survey Professional Paper 51, 129 p.

Darton, N. H., Blackwelder, E., and Siebenthal, C.E., 1910, Description of the Laramie and Sherman quadrangles [Wyoming]: U.S. Geological Survey Geological Atlas, Folio 173, 17 p.

Davis, R. L., and Wilkinson, B. H., 1983, Sedimentology and petrology of freshwater lacustrine-carbonate: mid-Tertiary Camp Davis Formation, northwestern Wyoming: University of Wyoming Contributions to Geology, v. 22, p. 45-55.

Davidson, J. R., 1987, Geology and mammalian paleontology of the Wind River Formation, Laramie Basin, southeastern Wyoming [M.S. thesis]: Laramie, University of Wyoming, 110 p.

Decker, E. R., Heasler, H. P., Buelow, K. L., Baker, K. H., and Hallin, J. S., 1988, Significance of past and recent heat-flow and radioactivity studies in the Southern Rocky Mountains region: Geological Society of America Bulletin, v. 100, p. 1851-1885.

Denson, N. M., 1965a, Miocene and Pliocene of central Wyoming, *in* Cohee, G. V., and West, W. S., editors, Changes in stratigraphic nomenclature by the U. S. Geological Survey, 1964: U.S. Geological Survey Bulletin 1224-A, p. A70-A74.

_____ 1965b, Relation of Tertiary drainage changes to uplift and collapse of a mountain arch, *in* Schultz, C. B., and Smith, H. T. U., editors, INQUA VII Congress, Northern and Middle Rocky Mountains, p. 22-28.

Denson, N. M., and Bergendahl, M. H., 1961, Middle and upper Tertiary rocks of southeastern Wyoming and adjoining areas: U.S. Geological Survey Professional Paper 424-C, p. 168-172.

Denson, N. M., and Chisholm, W. A., 1971, Summary of mineralogic and lithologic characteristics of Tertiary sedimentary rocks in the Middle Rocky Mountains and the Northern Great Plains: U.S. Geological Survey Professional Paper 750-C, p. C117-C126

Denson, N. M. and Harshman, E. N., 1969, Map showing areal distribution of Tertiary rocks, Bates Hole-Shirley Basin area, south-central Wyoming: U.S. Geological Survey Miscellaneous Geological Investigations Map I-570, scale 1:125,000.

Denson, N. M., and Pipiringos, G. N., 1974, Geologic map and sections showing areal distribution of Tertiary rocks near the southeastern terminus of the Wind River Range, Fremont and Sweetwater counties, Wyoming: U.S. Geological Survey Miscellaneous Investigations Map I-835, scale 1:48,000.

Dickinson, W. R., 1981, Plate tectonic evolution of the Southern Cordillera, *in* Dickinson, W. R., and Payne, W. D., editors, Relations of tectonics to ore deposits in the Southern Cordillera: Arizona Geological Society Digest, v. 14, p. 113-135.

Diffendal, R. F., Jr., 1982, Regional implications of the geology of the Ogallala Group (upper Tertiary) of southwestern Morrill County, Nebraska and adjacent areas: Geological Society of America Bulletin, v. 93, p. 964-976.

_____ 1983, Megaclasts in alluvial fills from the Ogallala Group (Miocene), Banner, Kimball, and Morrill counties, Nebraska: University of Wyoming Contributions to Geology, v. 22, p. 109-115.

Diffendal, R. F., Jr., and Corner, R. G., 1983, Asymmetrical distribution of Quaternary alluvial fills, Pumpkin Creek drainage basin, western Nebraska: Geological Society of America Bulletin, v. 94, p. 720-729.

Diffendal, R. F., Jr., Pabian, R. K., and Thomasson, J. R., 1982, Geologic history of Ash Hollow Park, Nebraska: Conservation and Survey, Institute of Agriculture and Natural Resources, The University of Nebraska-Lincoln, Educational Circular 5, 33 p.

Diffendal, R. F., Jr., Swinehart, J. B., and Gottula, J. J., 1985, Characteristics, age relationships, and regional importance of some Cenozoic paleovalleys, southern Nebraska panhandle: TER-QUA Symposium Series 1, p. 21-32.

Dorr, J. A., Jr., 1956, Post-Cretaceous geologic history of the Hoback Basin area, central western Wyoming: Wyoming Geological Association 11th Annual Field Conference Guidebook, p. 99-108.

Dorr, J. A., Jr., Spearing, D. R., and Steidtmann, J. R., 1977, Deformation and deposition between a foreland uplift and an impinging thrust belt, Hoback Basin, Wyoming: Geological Society of America Special Paper 177, 82 p.

Eardley, A. J., 1942, Tertiary trough near Camp Davis, Wyoming (abstract): Geological Society of America Bulletin, v. 53, p. 1800.

Eaton, G. P., 1986, A tectonic redefinition of the Southern Rocky Mountains: Tectonophysics, v. 132, p. 163-193.

Elias, M. K., 1942, Tertiary prairie grasses and other herbs from the High Plains: Geological Society of America Special Paper 41, 176 p.

Emry, R. J., 1973, Stratigraphy and preliminary biostratigraphy of the Flagstaff Rim area, Natrona County, Wyoming: Smithsonian Contributions to Paleobiology, no. 18, 43 p.

Evanoff, E., 1990, Early Oligocene paleovalleys in southern and central Wyoming: Evidence of high local relief on the late Eocene unconformity: Geology, v. 18, p. 443-446.

Eversoll, D. A., 1985, Preliminary report on a late Cenozoic channel deposit in southwestern Dundy County, Nebraska, containing very large cobbles and boulders: TER-QUA Symposium Series 1, p. 119-124.

Fields, R. W., Rasmussen, D. L., Tabrum, A. R., and Nichols, R., 1985, Cenozoic rocks of the intermontane basins of western Montana and eastern Idaho: a summary, *in* Flores, R. M., and Kaplan, S. S., editors, Cenozoic paleogeography of the west-central United States: Society of Economic Paleontologists and Mineralogists, Rocky Mountain Section, Symposium, v. 3, p. 9-36.

Flanagan, K. M., 1990, Late Cenozoic geology of the Pathfinder region, central Wyoming, with tectonic implications for adjacent areas [Ph.D. dissertation]: Laramie, University of Wyoming, 186 p.

Galbreath, E.C., 1953, A contribution to the Tertiary geology and paleontology of northeastern Colorado: The University of Kansas Paleontological Contributions, Vertebrata, Art. 4, p. 1-120.

Geomatrix Consultants, Inc., 1988, Seismotectonic evaluation of the Wyoming Basin geomorphic province for Seminoe, Kortes, Pathfinder, Alcova, and Gray Reef dams: Final Report prepared for U. S. Bureau of Reclamation, Contract no. 6-CS-81-07310, 167 p.

Goodwin, R. G., and Diffendal, R. F., Jr., 1987, Paleohydrology of some Ogallala (Neogene) streams in the southern panhandle of Nebraska, *in* Flores, R. M., and Ethridge, F., editors, Recent developments in fluvial sedimentology: Society of Economic Paleontologists and Mineralogists, p. 149-157.

Hansen, W. R., 1986, Neogene tectonics and geomorphology of the eastern Uinta Mountains in Utah, Colorado, and Wyoming: U.S. Geological Survey Professional Paper 1356, 78 p.

Hares, C. J., 1916, Anticlines in central Wyoming: U.S. Geological Survey Bulletin 641-I, p. 233-279.

Harshman, E. N., 1972, Geology and uranium deposits, Shirley Basin area, Wyoming: U.S. Geological Survey Professional Paper 745, 82 p.

Hayden, F. V., 1872, Preliminary report on the U.S. Geological Survey of Wyoming and portions of contiguous territories: Government Printing Office, Washington, D.C., p. 25-35.

Honey, J.G., and Izett, G.A., 1988, Paleontology, taphonomy, and stratigraphy of the Browns Park Formation (Oligocene and Miocene) near Maybell, Moffat County, Colorado: U.S. Geological Survey Professional Paper 1358, 52 p.

Hooke, R. L., 1967, Processes on arid-region alluvial fans: Journal of Geology, v. 75, p. 438-460.

Hunt, R.M., Jr., 1990, Taphonomy and sedimentology of Arikaree (lower Miocene) fluvial, eolian, and lacustrine paleoenvironments, Nebraska and Wyoming: a paleobiota entombed in fine-grained volcaniclastic rocks, *in* Lockley, M.G., and Rice, A., editors, Volcanism and fossil biotas: Geological Society of America Special Paper 244, p. 69-111.

Hutchison, J. H., 1982, Turtle, crocodilian, and champsosaur diversity changes in the Cenozoic of the north-central region of western United States: Palaeogeography, Palaeoclimatology, Palaeoecology, v. 37, p. 149-164.

Izett, G.A., 1975, Late Cenozoic sedimentation and deformation in northern Colorado and adjoining areas: Geological Society of America Memoir 144, p. 179-209.

Jackson, K. E., 1984, Geology of the Circle Bar Lake Quadrangle, Fremont and Sweetwater counties, Wyoming [M.S. thesis]: Laramie, University of Wyoming, 77 p.

King, P. B., and Beikman, H. M., 1978, The Cenozoic rocks; a discussion to accompany the geologic map of the United States: U.S. Geological Survey Professional Paper 904, 82 p.

Kirschbaum, M. A., 1986, Geologic map of the Kappes Canyon Quadrangle, Sweetwater County, Wyoming: U.S. Geological Survey Geologic Quadrangle Map GQ-1607, scale 1:24,000.

Knight, S. H., 1953, Summary of the Cenozoic history of the Medicine Bow Mountains, Wyoming: Wyoming Geological Association 8th Annual Field Conference Guidebook, p. 65-76.

Kochel, R. C., and Ritter, D. F., 1982, Depositional environments of high-level sand and gravel deposits, western Bighorn Mountains, Wyoming: University of Wyoming Contributions to Geology, v. 20, p. 111-122.

Larson, E. E., Ozima, M., and Bradley, W. C., 1975, Late Cenozoic basic volcanism in northwestern Colorado and its implications concerning tectonism and the origin of the Colorado River system: Geological Society of America Memoir 144, p. 155-177.

Leopold, E. B., and MacGinitie, H.D., 1972, Development and affinities of Tertiary floras in the Rocky Mountains, *in* Graham, A., editor, Floristics and paleofloristics of Asia and eastern North America: Amsterdam, Elsevier Publishing Co., p. 147-200.

Leopold, E. B., and Denton, M. F., 1987, Comparative age of grassland and steppe east and west of the Northern Rocky Mountains: Annals of the Missouri Botanical Garden, v. 74, p. 841-867.

Love, J. D., 1952, Preliminary report on the uranium deposits in the Pumpkin Buttes area, Powder River Basin, Wyoming: U. S. Geological Survey Circular 176, 37 p.

_____ 1956a, New formation names, Jackson Hole, Wyoming: American Association of Petroleum Geologists Bulletin, v. 40, p. 1899-1914.

_____ 1956b, Cretaceous and Tertiary stratigraphy of the Jackson Hole area, northwestern Wyoming: Wyoming Geological Association 11th Annual Field Conference Guidebook, p. 76-94.

_____ 1956c, Summary of geological history of Teton County, Wyoming, during Late Cretaceous, Tertiary and Quaternary times: Wyoming Geological Associa-

tion 11th Annual Field Conference Guidebook, p. 76-94.

_____ 1960, Cenozoic sedimenation and crustal movement in Wyoming: American Journal of Science, Bradley Volume, vol. 258-A, p. 204-214.

_____ 1961, Split Rock Formation (Miocene) and Moonstone Formation (Pliocene) in central Wyoming: U.S. Geological Survey Bulletin 1121-I, 39 p.

_____ 1970, Cenozoic geology of the Granite Mountains area, central Wyoming: U.S. Geological Survey Professional Paper 495-C, 154 p.

_____ 1978, Cenozoic thrust faulting and tectonic history of the Badwater area, northeastern margin of Wind River Basin, Wyoming: Wyoming Geological Association 13th Annual Field Conference Guidebook, p. 235-238.

_____ 1990, Names and descriptions of new and reclassified formations in northwestern Wyoming: U.S. Geological Survey Professional Paper 932-C, 45 p.

Love, J. D., and Christiansen, A. C., 1985, Geologic map of Wyoming: U.S. Geological Survey, scale 1:500,000.

Love, J. D., McGrew, P.O., and Thomas, H. D., 1963, Relationship of latest Cretaceous and Tertiary deposition and deformation to oil and gas occurrences in Wyoming, *in* Childs, O.E. and Beebe, B.W., editors, Backbone of the Americas: American Association of Petroleum Geologists Memoir 2, p. 196-208.

Love, J. D., Reed, J. C., Christiansen, R. L., and Stacey, J. R., 1973, Geologic block diagram and tectonic history of the Teton region: U.S. Geological Survey Miscellaneous Map Series I-730.

Lovering, T. S., 1929, The Rawlins, Shirley, and Seminoe iron-ore deposits, Carbon County, Wyoming: U.S. Geological Survey Bulletin 811, p. 203-235.

Luft, S. J., 1985, Generalized geologic map showing distribution and basal configuration of the Browns Park Formation and Bishop Conglomerate in northwestern Colorado, northeastern Utah, and southern Wyoming: U.S. Geological Survey Miscellaneous Field Studies Map MF-1821, scale 1:250,000.

Lugn, A. L., 1939, Classification of the Tertiary System in Nebraska: Geological Society of America Bulletin, v. 50, p. 1245-1276.

Mackin, J.H., 1937, Erosional history of the Bighorn Basin, Wyoming: Geological Society of America Bulletin, v. 48, p. 813-893.

Mansfield, G.R., 1927, Geography, geology, and mineral resources of part of southeastern Idaho: U.S. Geological Survey Professional Paper 152, 453 p.

Mariner, R. H., 1971, Experimental evaluation of authigenic mineral reactions in the Pliocene Moonstone Formation [Ph.D. dissertation]: Laramie, University of Wyoming, 133 p.

Martin, W. D., McWilliams, R. G., and Kochan, M., 1992, Occurrence and significance of the Burnt Gulch Formation: a Pliocene-Pleistocene fanglomerate, Wind River Basin, Wyoming: The Mountain Geologist, v. 29, p. 29-40.

McGrew, L. W., 1963, Geology of the Fort Laramie area, Platte and Goshen counties, Wyoming: U.S. Geological Survey Bulletin 1141-F, 39 p.

McGrew, P. O., 1951, Tertiary stratigraphy and paleontology of south-central Wyoming: Wyoming Geological Association 6th Annual Field Conference Guidebook, p. 54-57.

_____ 1953, Tertiary deposits of southeastern Wyoming: Wyoming Geological Association 8th Annual Field Conference Guidebook, p. 61-64.

McKenna, M. C., and Love, J. D., 1972, High-level strata containing early Miocene mammals on the Bighorn Mountains, Wyoming: American Museum Novitates, no. 2490, 31 p.

Mears, B., Jr., and Agard, S. S., and Sutherland, W. M., with a contribution on clinker by Coates, D. A., 1991, The Powder River Basin, *in* Morrison, R.B., editor, Quaternary non-glacial geology; Conterminous: Boulder, Colorado, Geological Society of America, The Geology of North America, v. K-2, p. 446-448.

Minick, J. N., 1951, Tertiary stratigraphy of southeastern Wyoming and northeastern Colorado [M.S. thesis]: Laramie, University of Wyoming, 53 p.

Montagne, de la, J. 1953, Late Tertiary normal faults along the east flank of the Park Range, Wyoming and Colorado: Wyoming Geological Association 8th Annual Field Conference Guidebook, p. 103-105.

_____ 1955, Cenozoic history of the Saratoga Valley area, Wyoming and Colorado [Ph. D. dissertation]: Laramie, University of Wyoming, 140 p.

Montagne, J., 1991, Cenozoic history of the Saratoga Valley area, Wyoming and Colorado: University of Wyoming Contributions to Geology, p. 13-70.

Moore, F. E., 1959, The geomorphic evolution of the east flank of the Laramie Range, Colorado and Wyoming

[Ph. D. dissertation]: Laramie, University of Wyoming, 123 p.

Munthe, J., 1979, Summary of Miocene vertebrate fossils of the Granite Mountains basin, central Wyoming: University of Wyoming Contributions to Geology, v. 18, p. 33-46.

Naeser, N. D., 1984, Fission-track ages from the Wagon Wheel No. 1 well, northern Green River Basin, Wyoming: evidence for recent cooling: *in* Law, B. E., editor, Geological characteristics of low-permeability Upper Cretaceous and lower Tertiary rocks in the Pinedale anticline area, Sublette County, Wyoming: U.S. Geological Survey Open File Report 84-0753, p. 66-77.

O'Brien, J. S., and Julien, P. Y., 1985, Physical properties and mechanics of hyperconcentrated sediment flows, *in* Bowles, D. S., editor, Delineation of landslides: Utah Water Research Laboratory, Utah State University, Logan, Utah, p. 260-279.

Olson, T. J., and Schmitt, J. G., 1987, Sedimentary evolution of the Miocene - Pliocene Camp Davis basin, northwestern Wyoming: Wyoming Geological Association 38th Annual Field Conference Guidebook, p. 225-243.

Oriel, S. S., and Platt, L. B., 1980, Geologic map of the Preston 1° x 2° Quadrangle, southeastern Idaho and western Wyoming: U.S. Geological Survey Miscellaneous Investigations Series Map I-1127, scale 1:250,000.

Palmer, A.R., 1983, Decade of North American Geology 1983 geologic time scale: Geology, v. 11, p. 503-504.

Pearl, R. H., 1971, Pliocene drainage of east-central Colorado and northwestern Kansas: The Mountain Geologist, v. 8, p. 25-30.

Peterman, Z. E., and Hildreth, R. A., 1978, Reconnaissance geology and geochronology of the Precambrian of the Granite Mountains, Wyoming: U.S. Geological Survey Professional Paper 1055, 22 p.

Powell, J. W., 1876, Report on the geology of the eastern portion of the Uinta Mountains and a region of country adjacent thereto: U.S. Geological and Geographical Survey of the Territories, v. 7, p. 1-218.

Reynolds, M. W., 1968a, Geologic map of the Muddy Gap Quadrangle, Carbon County, Wyoming: U.S. Geological Survey Quadrangle Map GQ-771, scale 1:24,000.

_____ 1968b, Geologic map of the Whiskey Peak Quadrangle, Carbon, Fremont, and Sweetwater counties, Wyoming: U.S. Geological Survey Geological Quadrangle Map GQ-772, scale 1:24,000.

Ritzma, H.R., 1949, Geology along the southwest flank of the Sierra Madre, Carbon County, Wyoming [M.S. thesis]: Laramie, University of Wyoming, 77 p.

Robinson, C. S., Mapel, W. J., and Bergendahl, M. H., 1964, Stratigraphy and structure of the northern and western flanks of the Black Hills uplift, Wyoming, Montana, and South Dakota: U.S. Geological Survey Professional Paper 404, 134 p.

Rohrer, W. L., and Leopold, E. B., 1963, Fenton Pass Formation (Pleistocene?), Bighorn Basin, Wyoming: U.S. Geological Survey Professional Paper 475-C, article 71, p. C45-C48.

Sato, Y., and Denson, N. M., 1967, Volcanism and tectonism as reflected by the distribution of nonopaque heavy minerals in some Tertiary rocks of Wyoming and adjacent states, *in* Geological survey research 1967: U.S. Geological Survey Professional Paper 575-C, p. C42-C54.

Schumm, S. A., Mosley, M. P., and Weaver, W. E., 1987, Experimental fluvial geomorphology: New York, John Wiley and Sons, 413 p.

Sears, J.D., 1924, Relations of the Browns Park Formation and the Bishop Conglomerate and their role in the origin of Green and Yampa Rivers: Geological Society of America Bulletin, v. 35, p. 259-304.

Skinner, M. F., Skinner, S. M., and Gooris, R. J., 1977, Stratigraphy and biostratigraphy of late Cenozoic deposits in central Sioux County, western Nebraska: Bulletin of American Museum of Natural History, v. 158, p. 263-371.

Staatz, M. H., 1983, Geology and description of thorium and rare-earth deposits in the southern Bear Lodge Mountains, northeastern Wyoming: U.S. Geological Survey Professional Paper 1049-D, 52 p.

Stanley, K. O., 1976, Sandstone petrofacies in the Cenozoic High Plains sequence, eastern Wyoming and Nebraska: Geological Society of America Bulletin, v. 87, p. 297-309.

Stanley, K. O., and Wayne, W. J., 1972, Epeirogenic and climatic controls of early Pleistocene fluvial sediment dispersal in Nebraska: Geological Society of America Bulletin, v. 83, p. 3675-3690.

Steidtmann, J. R., and Middleton, L. T., 1986, Eocene-Pliocene stratigraphy along the southern margin of the Wind River Range, Wyoming: revisions and im-

plications from field and fission-track studies: The Mountain Geologist, v. 23, p. 19-25.

Steidtmann, J. R., Middleton, L. T., Bottjer, R. J., Jackson, K. E., McGee, L. C., Southwell, E. H., and Lieblang, S., 1986, Geometry, distribution, and provenance of tectogenic conglomerates along the southern margin of the Wind River Range, Wyoming, *in* Peterson, J. A., editor, Paleotectonics and sedimentation in the Rocky Mountain Region, U.S.: American Association of Petroleum Geologists Memoir 41, p. 321-332.

Steidtmann, J. R., Middleton, L. T., and Shuster, M. W., 1989, Post-Laramide (Oligocene) uplift in the Wind River Range, Wyoming: Geology, v. 17, p. 38-41.

Stewart, J. H., 1978, Basin-range structure in western North America: a review: Geological Society of America Memoir 152, p. 1-31.

Swinehart, J. B., Souders, V. L., DeGraw, H. M., and Diffendal, R. F., Jr., 1985, Cenozoic paleogeography of western Nebraska, *in* Flores, R. M., and Kaplan, S. S., editors, Cenozoic paleogeography of the west-central United States: Society of Economic Paleontologists and Mineralogists, Rocky Mountain Section, Symposium, v. 3, p. 209-229.

Swisher, C.C., III, and Prothero, D.R., 1990, Single-crystal $^{40}Ar/^{39}Ar$ dating of th Eocene-Oligocene transition in North America: Science, v.249, p. 760-762.

Tedford, R. H., Skinner, M. F., Fields, R. W., Rensberger, J. M., Whistler, D. P., Galusha, T., Taylor, B. E., Macdonald, J. R., and Webb, S. D., 1987, Faunal succession and biochronology of the Arikareean through Hemphillian interval (late Oligocene through earliest Pliocene epochs) in North America, *in* Woodburn, M. O., editor, Cenozoic mammals of North America: Geochronology and biostratigraphy: Berkley, California, University of California Press, p. 153-210.

Van Houten, F. B., 1964, Tertiary geology of the Beaver Rim area, Fremont and Natrona counties, Wyoming: U.S. Geological Survey Bulletin 1164, p. 1-99.

Voorhies, M. R., 1965, The Carnivora of the Trail Creek fauna: University of Wyoming Contributions to Geology, v. 4, p. 21-25.

Wanless, H. R., Belknap, R. L., and Foster, H., 1955, Paleozoic and Mesozoic rocks of Gros Ventre, Teton, Hoback, and Snake River ranges, Wyoming: Geological Society of America Memoir 63, 90 p.

Witkind, I.J., 1975, Preliminary map showing known and suspected active faults in Wyoming: U.S. Geological Survey Open File Report 75-279, 36 p.

Wood, H. E., Chaney, R. W., Clark, J., Colbert, E. H., Jepsen, G. L., Reeside, J. B., Jr., and Stock, C., 1941, Nomenclature and correlation of the North American continental Tertiary: Geological Society of America Bulletin, v. 52, p. 1-48.

Woodburne, M.O., 1987, Cenozoic mammals of North America, geochronology and biostratigraphy: Berkeley, University of California Press, 336 p.

Zoback, M. L., Anderson, R. E., and Thompson, G. A., 1981, Cainozoic evolution of the state of stress and style of tectonism of the Basin and Range province of the western United States: Philosophical Transactions of the Royal Society of London, A 300, p. 407-434.

Frontispiece. Oblique aerial photograph of the northwestern flank of the Wind River Mountains, immediately southwest of Green River Lakes. Prominent flat-topped peak in the right-foreground is Gypsum Mountain (el. 11,515 ft; 3,510 m), located on the Big Sheep Mountain, Wyo. 1:24,000 USGS topographic quadrangle. The high-level erosion surface truncates well-bedded Phanerozoic strata that dip steeply off Archean rocks that form the core of the range. Canyon of the Green River lies in shadow in the middle distance (from left-center to upper-right corner). Photo taken in September, 1986, after the first autumn snowfall by David R. Lageson, Montana State University.

Geomorphic history of Wyoming and high-level erosion surfaces

Brainerd Mears, Jr.
Department of Geology and Geophysics
University of Wyoming
Laramie, Wyoming 82071

Abstract

The geomorphic evolution of the Precambrian-cored mountains of Wyoming and their truncated uplands remain lively research topics. A late Eocene age for the prominent subsummit surface is the doctrine for most geologists in Colorado. However, dissenters in Wyoming consider the surface late Miocene, based on field evidence for the following history.

At the climax of the Laramide orogeny, during the latest Paleocene and earliest Eocene, the relief of the mountains exceeded that of the present, but the basin floors were closer to sea level. Following the end of major deformation in the early mid-Eocene, the crests of the mountains were lowered by erosion and the mountain valleys and broad intermontane basins were filled. The basin deposits were partially excavated during a widespread late Eocene interval of regional erosion that preceded the onset of renewed basin filling in the latest Eocene. During the ensuing aggradation, clastic debris derived from the mountains was overwhelmed by ash from distant volcanic eruptions. The rising level of Oligocene and then Miocene deposits eventually lapped across the lower segments of the crystalline-cored uplands that finally had been eroded down to broad subsummit surfaces surmounted by residual hills and peaks. At some time during this aggradational episode, broad regional uplift began to raise the mountains to their present-day elevations. The exhumation of the present broad basin floors and adjacent mountain valleys began in mid-Miocene time, following the end of massive volcanic ash falls and accompanying the acceleration of regional uplift. This uplift may have contributed to the onset of late Cenozoic alpine glaciation in the mountains of Wyoming.

Various geomorphic processes have been proposed for the origin of the high-level erosion surfaces. The ruling theory was originally peneplanation, which involves prolonged erosion of a region to near sea level, followed by uplift to present-day elevations. Thereafter, pedimentation has been the generally favored process, wherein surfaces are developed along the bases of retreating mountain fronts at levels controlled by local master streams. Altiplanation, the reduction of mountain tops by intense frost-action above timberline, is another possible process. In places, some surfaces may represent the exhumed top of the Precambrian basement rock, from which the formerly overlying Paleozoic strata have been stripped by erosion. The most recent proposal involves primary denudation, wherein (prior to accelerated uplift) the rise of a Precambrian-cored block is so slow that its eroding planation surface remains approximately level with the top of the fill accumulating in an adjacent subsiding basin. In general, geologists dealing with the origin of high-level erosion surfaces have commonly propounded one particular hypothesis. However, such surfaces are complex and probably are the products of several different processes.

Mears, B., Jr., 1993, Geomorphic history of Wyoming and high-level erosion surfaces, *in* Snoke, A.W., Steidtmann, J.R., and Roberts, S.M., editors, Geology of Wyoming: Geological Survey of Wyoming Memoir No. 5, p. 608-626.

Introduction

Wyoming is an Indian word[1] which means "land between the mountains" (S.H. Knight, oral communication) or "at the big plains" (Larson, 1978). Either translation aptly depicts the landscape. Forested mountains with crests rising above timberline are the most impressive scenic element, but mountains (**Figure 1**) only occupy about 29% of the State's 97,914 square-mile area (if we include the Wyoming part of the Black Hills and the Absaroka and Yellowstone volcanic plateaus). The rest of the State, almost 71%, is in shrub grasslands, which include the Great Plains east of the Rocky Mountain front and the mountain-rimmed plains of the various intermontane basins (**Figure 1**). The plains, however, are underlain by deep structural basins (Love, 1960) filled with sedimentary rocks that reach a maximum depth of 30,000 feet below sea level in the Green River Basin (Blackstone, 1990, and **map pocket**). This area is only 16 miles southwest of Gannett Peak, Wyoming's highest pinnacle, where Precambrian basement rocks are 13,804 feet above sea level. From a geomorphic perspective, the mountains and basins of Wyoming record a long Cenozoic history of tectonic, volcanic, depositional, and erosional events.

Geomorphic history

That "the present is the key to the past" was a necessary concept for the founding fathers of modern geology. However, the converse—that "the past is the key to the present" (R.A. Bryson, oral communication) — better suits an introduction to the geomorphology of Wyoming. Thus, the following synopsis of the State's geologic-geomorphic evolution during the past 70 million years provides a framework for the ensuing discussion of the much debated high-level erosion surfaces planating the major Laramide ranges in Wyoming and adjacent states.

The evolution of the present Wyoming landscape begins with the Laramide orogeny. Thus, I treat the Precambrian rocks now exposed in the mountain cores as "basement complex" that was planated during a major episode of erosion[2] prior to the advance of the Cambrian sea. Paleozoic and Mesozoic strata, which accumulated in marine and terrestrial environments on the continental foreland, are treated as geomorphic features: the flatirons, strike valleys, and hogbacks along present-day mountain flanks. [An interpretation of the two and one-half billion-year geomorphic history of southeastern Wyoming from Archean to present, which is illustrated with a wealth of his outstanding block diagrams, is available in the posthumous publication of S.H. Knight (1990) on the Medicine Bow Mountains.]

Laramide evolution of the mountains and basins

For the stratigraphic, structural, and temporal aspects of the following geomorphic interpretations, I am much indebted to discussions with, and the extensive publications of, D.L. Blackstone, Jr., (e.g., 1975), S.H. Knight (e.g., 1953), J.D. Love (e.g., 1960), and J.A. Lillegraven (e.g., 1988, with L.J. Ostresh, Jr.).

The rise of the Wyoming Rockies and subsidence of broad intervening basins began in late Cretaceous time. Along the western margin of the State, elongate ridges and valleys developed in miogeoclinal rocks, now exposed in the fold-and-thrust belt (Royse, this volume). Here Paleozoic, Mesozoic, and early Cenozoic rocks were complexly folded and

[1] Some other Indian names were proposed in the U.S. Congress when the area of the future (1890) 44th state was separated from the Dakota Territory (Larson, 1978). Absaroka was rejected as giving a priority in the roll call of states; Cheyenne because it sounded like the French word for a female dog. Wyoming, a Delaware Indian word for a part of Pennsylvania (where James M. Ashley, a proponent of the name, was born), was considered beautiful, harmonious, and "easy to spell".

[2] The Lipalian interval of Walcott (1910), a long-obsolete term that was in vogue when D.L. Blackstone, Jr., and J.D. Love (to whom this volume is dedicated) were graduate students.

jammed eastward in great imbricate, fault-bounded plates that were detached from, and moved over, the Precambrian basement, that is, Sevier-style of deformation. Throughout some 95% of the State's area,

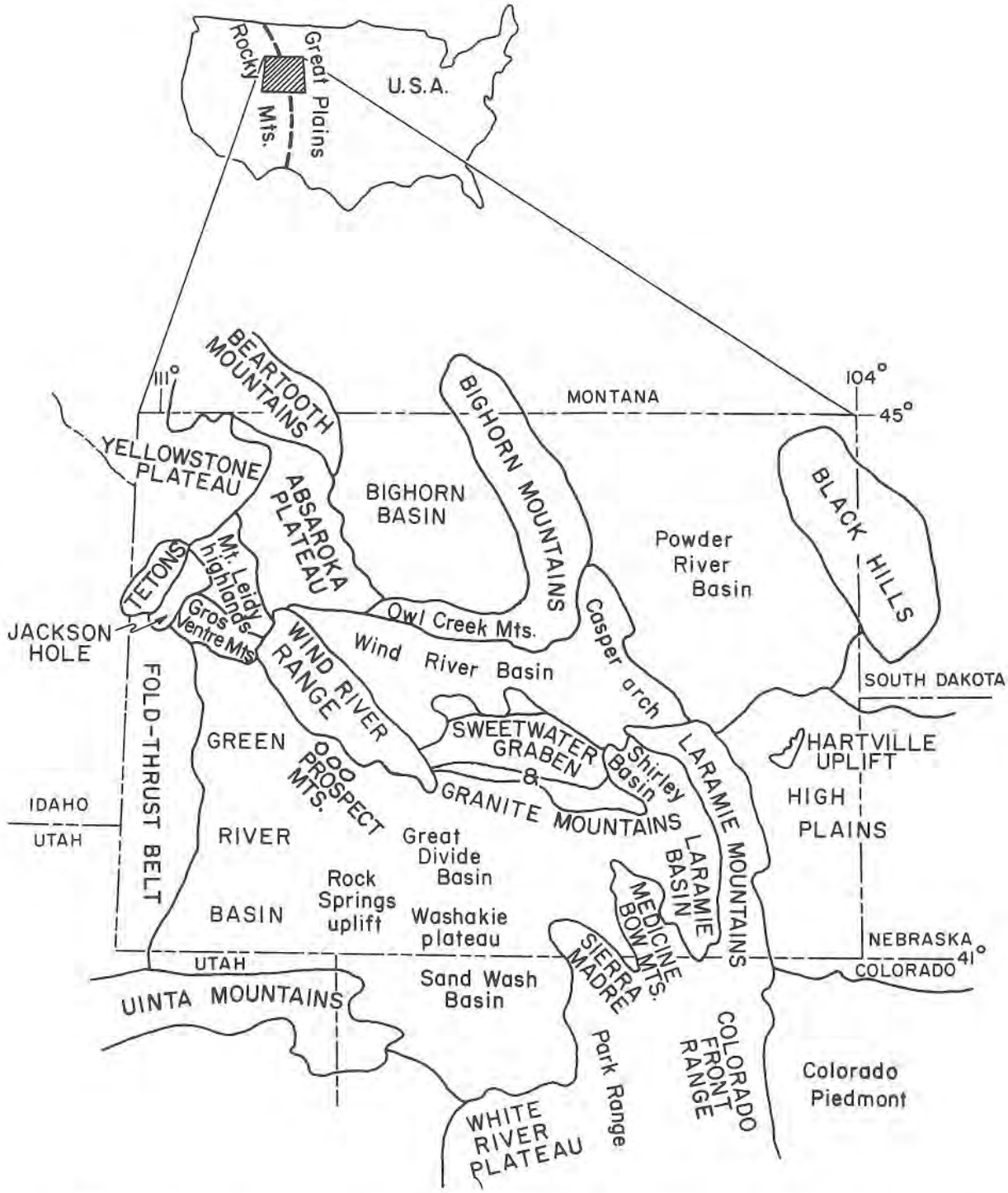

Figure 1. Regional geomorphic features of Wyoming and adjacent areas. (Names entirely in capital letters are those mentioned in the text.)

Precambrian-cored uplifts of Laramide style (Brown, this volume) developed in the foreland. The initial Laramide uplifts in latest Cretaceous to earliest Cenozoic time are interpreted as broad, flat-topped anticlines elevated along incipient reverse faults (**Figure 2**). Relicts of this stage of geomorphic development may be represented by the present-day Black Hills and White River Plateau (**Figure 1**), which still have plateau-like covers of Paleozoic rocks. As the major Laramide ranges continued to rise in latest Paleocene and earliest Eocene time, erosion stripped the sedimentary strata from the Precambrian mountain cores, an event marked by a change in dominance from sedimentary to crystalline clasts in the deposits that were accumulating in adjacent basins (**Figure 3**). In the major ranges of Wyoming, where the exposed cores are complexly deformed crystalline rocks, their origin as broad flat-topped anticlines is less obvious than in the Uinta Mountains (**Figure 1**) where, as noted by Powell (1876), the broad upland surface is underlain by near-horizontal layers of Proterozoic quartzite.

Post-Laramide events

Laramide mountain building ended during the early Eocene, except in the Uinta Mountains and White River plateau. Major lakes developed, such as Lake Gosiute in the Green River Basin and Lake Tatman in the Bighorn Basin. By mid-Eocene to earliest late Eocene time, the mountain tops were being reduced by erosion and the intermontane basins were being aggraded (**Figure 4**). The lacustrine deposits were buried by clastic deposits derived from the eroding mountains and increasingly supplemented by volcaniclastic debris from eruptive centers in the Absaroka and more distant volcanic areas. Most of the late Eocene was a time of regional erosion. Streams excavated the relatively nonresistant basin-fill sediments to create a landscape rather like that of the present day (**Figure 5**); however, the region as a whole was at lower elevations. Whether this erosional episode resulted from a marked decrease of Absaroka volcanism (whose products had previously overloaded the streams), a broad regional (epeirogenic) uplift, or both has not been established. In any case, during most of the Eocene, the region as a whole was near sea level and the climate was subtropical, based on fossil flamingos, crocodiles, fig palms, and magnolias in the Green River Basin (McGrew, 1980).

During latest Eocene, Oligocene, and much of Miocene time (**Figure 6**), the Wyoming basins were progressively filled with airborne pyroclastic debris from enormous eruptions in the Basin and Range province and Colorado Rocky Mountains. The ash was picked up and redeposited by streams, along with channel gravels derived from Precambrian outcrops in local mountains. By the end of the mid-Miocene, when the basins were largely filled, prolonged erosion had reduced the once-rugged Laramide mountains to isolated peaks and hills on broadly planated Precambrian bedrock surfaces. In places, the major streams flowed across mountain axes that had been buried by coalescing basin fills.

The epeirogenic rise of the Wyoming region is documented by normal faulting commencing in the mid-Miocene. The faults, interpreted as listric (**Figure 6**), offset the erosion surfaces on the crystalline uplands and trapped Oligocene and Miocene deposits, which are still preserved along downthrown blocks in the Sierra Madre and Medicine Bow Mountains. The most extensive downfaulted Miocene deposits are in the Sweetwater graben (**Figure 1**), the collapsed core of a major Laramide uplift. Elsewhere, post-orogenic normal faults formed prominent scarps in the fold-and-thrust belt and created the imposing east face of the Tetons, Wyoming's youngest mountain range.

The last major episode in the geomorphic evolution of Wyoming (**Figure 7**) began in late Miocene time. The onset of regional erosion followed the end of catastrophic Cordilleran volcanism that had filled the basins with volcaniclastic deposits. During the ensuing 10,000 years of regional uplift, as much as 1,000 feet of basin excavation is indicated by relicts of Oligocene and Miocene deposits and by the exhumed mountain fronts and transverse canyons of superposed rivers.

Throughout post-Laramide time, the climate became drier and cooler. Vertebrate fossils (and limited paleobotanical data) indicate the development of open, unforested, intermontane and piedmont plains: Oligocene savannas; Miocene steppes; and eventually Pleistocene periglacial steppes (underlain by permafrost), when the Yellowstone region was covered by ice and mountain glaciers on the major ranges extended onto the adjacent plains. Overall geological evidence for the geomorphic and climatic history of the Wyoming region fits the hypothesis of

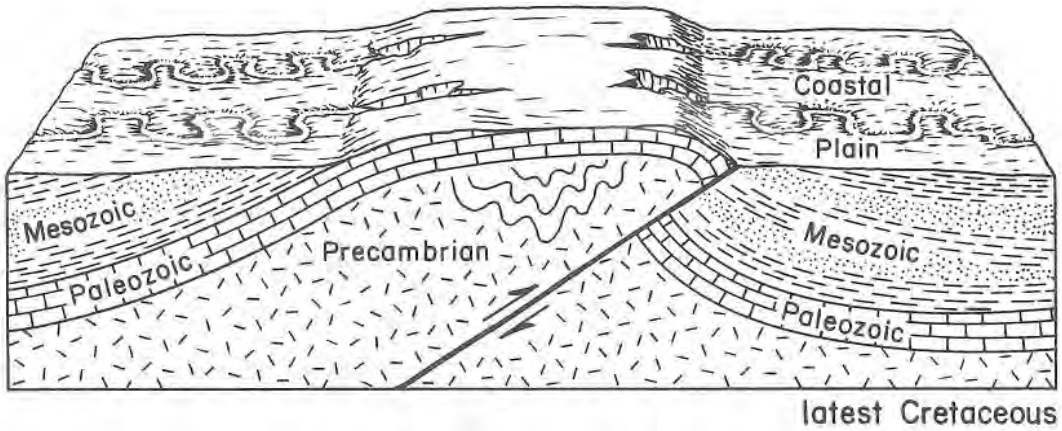

Figure 2. Initial Laramide origin of mountains and subsiding basins.

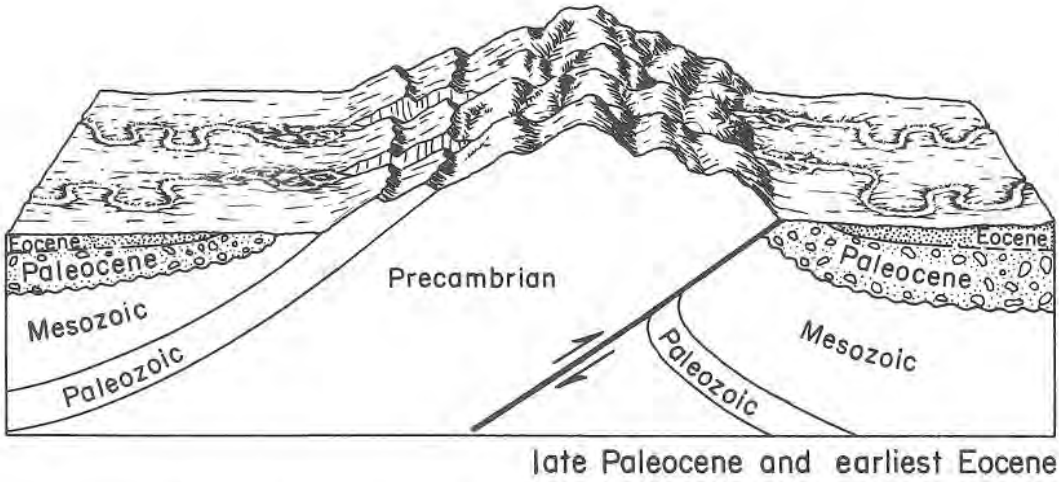

Figure 3. Maximum local relief during climax of Laramide orogeny.

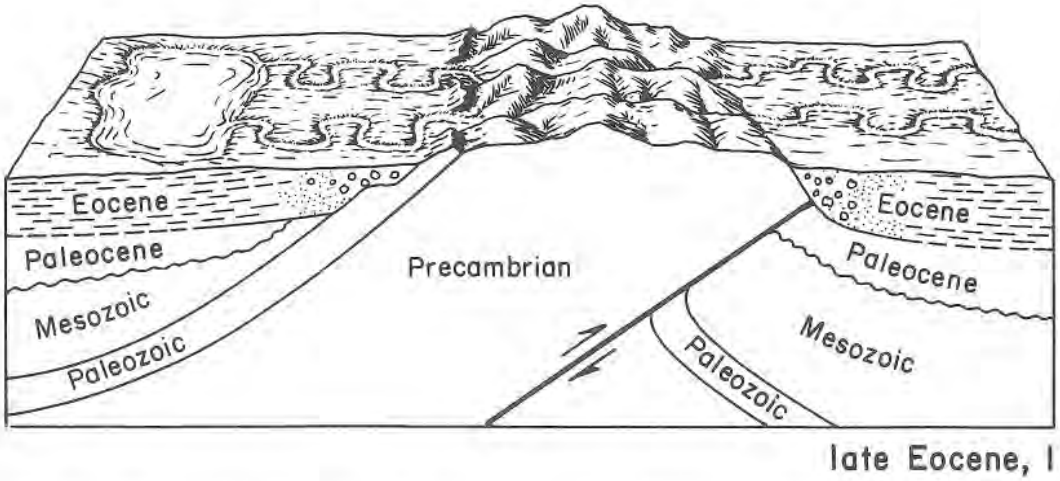

Figure 4. Post-orogenic stability, with erosion of mountain uplands and deposition in the basins.

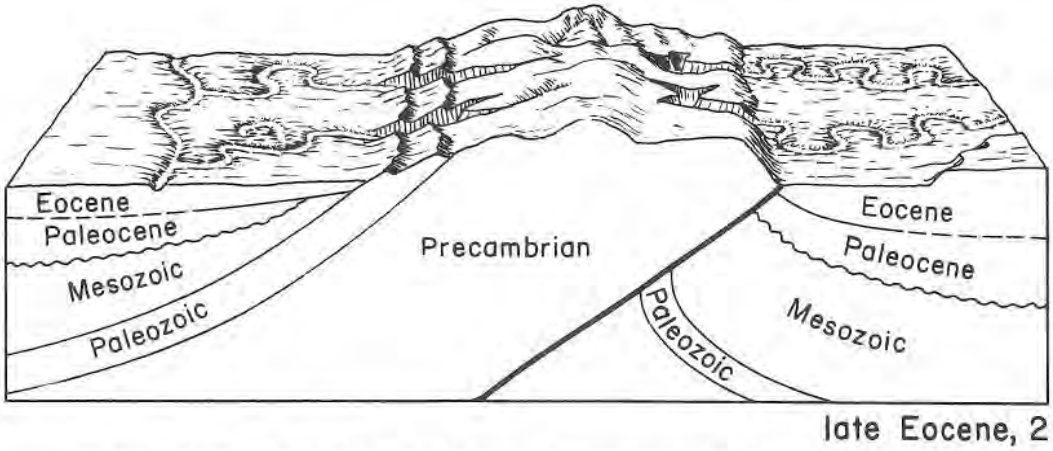

Figure 5. Excavation of basin-fill sediments accompanying regional erosion.

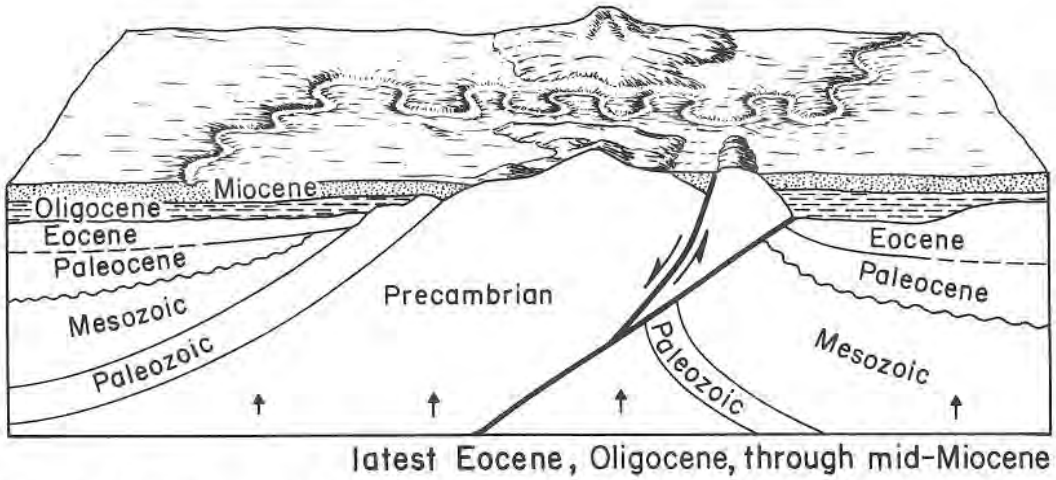

Figure 6. Progressive filling of basins with ash from remote eruptions; onset of regional uplift and normal faulting; streams crossing buried parts of subdued erosion surfaces.

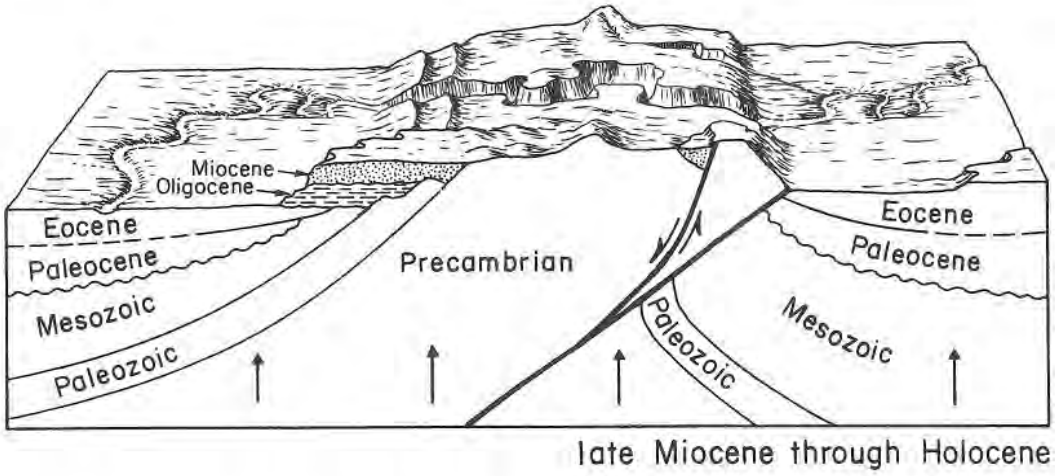

Figure 7. Excavation of basins-fill sediments and superposition of streams accompanying uplift; isolation of high-level surfaces.

Ruddiman and Kutzbach (1989). These authors attribute late Cenozoic cooling in the Northern Hemisphere to the concurrent regional uplift of central Asia (in and around the great Plateau of Tibet) and western North America, whose heartland is Wyoming.

High-level erosion surfaces

The plateau-like uplands on Colorado and Wyoming mountains have been studied and their nature debated since first reported by Marvine (1874). Today, well over a century later, there is still no complete agreement as to the number of different surfaces, their age, or how they formed.

The number

It has been argued (but not by geologists working in the Wyoming and Colorado Rockies) that there are no high-level erosion surfaces. This interpretation is from the folded Appalachian province (**Figure 8**), where Hack (1960) proposed that the peneplains of earlier geomorphologists are misconceptions from "eyeballing" across a succession of seemingly accordant ridge tops. The same argument could apply to the ridges in the northern part of the Wyoming fold-and-thrust belt, except that those crests do reach about the same level as the extensive upland surface on the nearby Wind River Range. High-level erosion surfaces are a reality on the basement-cored mountains of Colorado and Wyoming, but the number of such surfaces has been debated. In the Colorado Front Range, the proposed numbers (**Figures 9A-C**) range from 1, as first described by Marvine (1874), to 11, as reported by Van Tuyl and Lovering (1935). However, Wahlstrom (1947) recognized only one surface that had been offset by faulting and in places eroded to different levels. The enthusiasm for peneplains was not restricted to geomorphologists, such as Van Tuyl. Lovering was a "hard rock" geologist. Wahlstrom was also a petrologist with wide experience in Rocky Mountain geology. The profuse literature on the surfaces in the Colorado Front Range is nicely distilled by Bradley (1987).

In Wyoming, no more than two high-level erosion surfaces have been proposed (**Figure 9D**), and these surfaces are at higher levels on higher mountains. The "undue multiplication of entities" by Van Tuyl and Lovering has also been avoided by rejecting abandoned upland valleys and shoulders along present-day canyons as partial peneplains. Only one high-level erosion surface is evident on the mountains of southeastern Wyoming: the Sherman surface on the Laramie Mountains, the Libby Flats surface on the Medicine Bow Mountains, and an unnamed surface on the Sierra Madre (Price, 1973). Although Blackwelder (1909) suggested that the

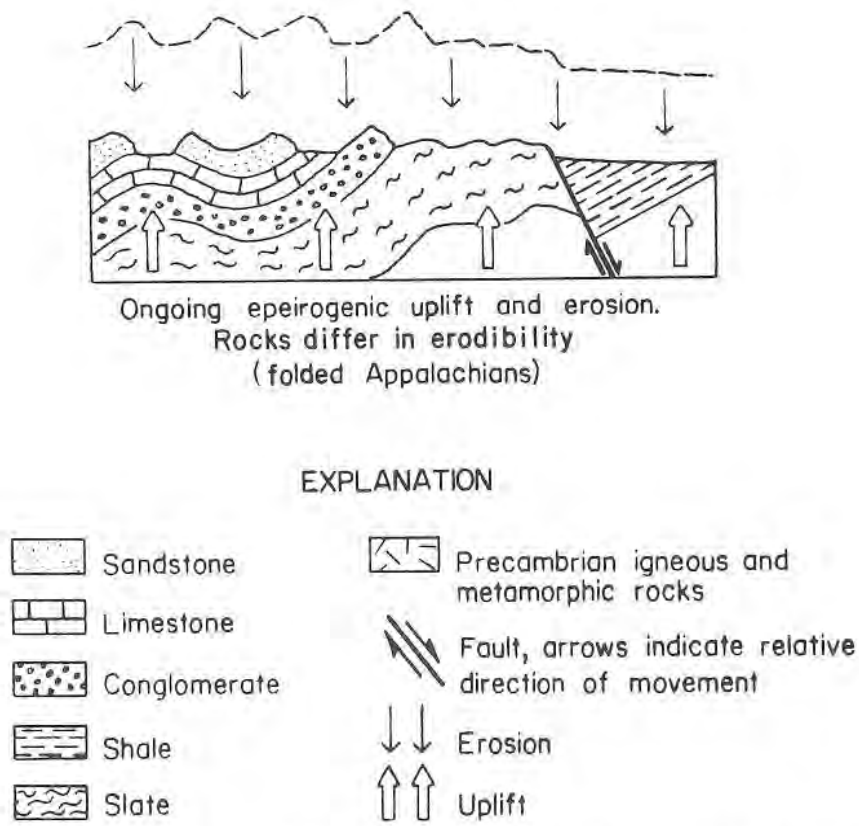

Figure 8. Illustration of J.T. Hack's (1960) concept that accordant ridge crests and lower surfaces are products of ongoing degradation of differing rock types, not dissected remains of former erosion surfaces.

Laramie Mountains had relicts of another peneplain above the Sherman surface, there is no evidence of relict flats on the higher tors and hills.

On the Precambrian core of the Wind River Range, Westgate and Branson (1913) recognized one surface, which they called an uplifted peneplain, surmounted by higher peaks. However, Blackwelder (1915) noted two different levels of high surfaces on the Wind River mountains. In addition to the dissected surface reported by Westgate and Branson at 12,000- to 11,000-foot levels, Blackwelder recognized

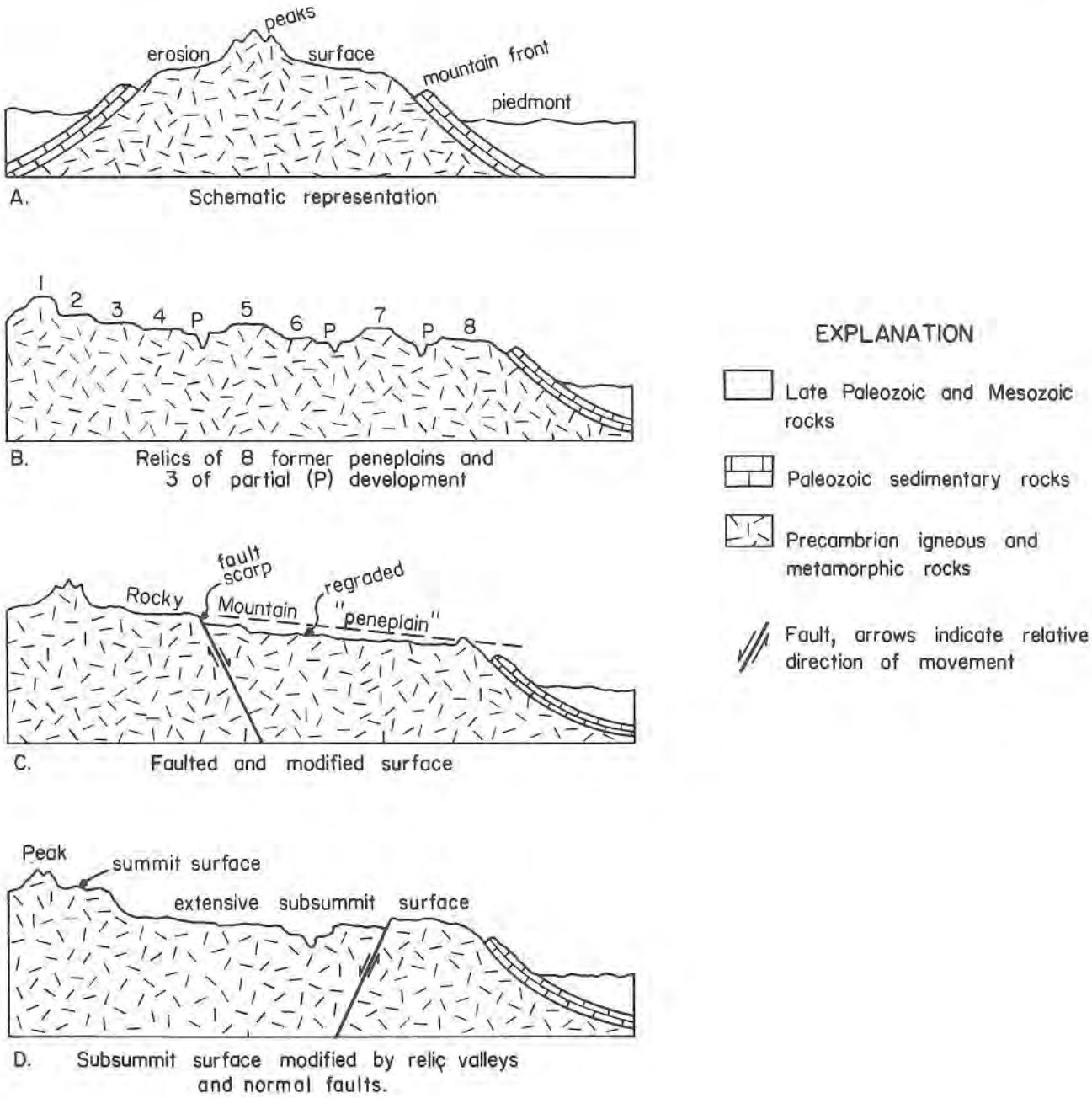

Figure 9. The evolution of geologists' interpretations of the number of high-level surfaces in the Colorado Front Range: A. one high-level surface as originally recognized by Marvine (1874); B. multiple surfaces as proposed by Van Tuyl and Lovering (1935); C. single surface, displaced and eroded (derived from Wahlstrom, 1947); D. best current estimate, two surfaces.

another prominent surface at 10,500 to 10,000 feet along the west side of the range, west of the high peaks. He suggested that the lower surface might be younger than the higher one. In the Beartooth Mountains, Bevan (1925) reported two surfaces: the higher at 12,400- to 12,000-foot elevations, mainly in Montana, is represented by the "flattish" tops on ridges and peaks; the lower, mainly in Wyoming, is a more continuous surface at about 9,500 feet. In the Bighorn Mountains, Mackin (1947) noted that the higher summit surface is broadly rounded and bounded by steeper slopes cut by cirques, and that the lower and more extensive subsummit surface gradually increases in elevation from 8,000 feet at the brink of the steep mountain front to 11,000 feet.

Proposed ages

Eliot Blackwelder fathered two schools of thought on the ages of high-level erosion surfaces. He initially proposed (1909) that the Libby Flats surface on the Medicine Bow Mountains is Eocene, by projecting it across the excavated Laramie Basin to the tops of the tors and hills on the Sherman surface. He dated the Sherman surface as Pliocene, because it graded evenly onto the surface of the "Gangplank", an isolated relict of uppermost "Pliocene"[3] deposits in the Great Plains. In his classic paper on the post-Cretaceous history of the Wind River Range, Blackwelder (1915) concluded that all of the major high-level surfaces are Pliocene. He saw that Eocene deposits in the Wind River Basin have a coarse conglomeratic facies, reflecting valley fill adjacent to mountainous relief (e.g., **Figure 4**).

Late Eocene

Knight (1953) strongly advocated a late Eocene age for the Libby Flats surface on the Medicine Bow Mountains. His interpretation (**Figure 10A**) is based on unfossiliferous volcaniclastic and conglomeratic deposits of Tertiary age found in a shallow valley on Libby Flats and along the downthrown side of a normal fault near the mountain front (e.g., **Figures 6** and **7**). The deposits are probably Oligocene but may be as young as Miocene. For the crystalline-cored Laramide ranges of Colorado, Epis and Chapin (1975) and Scott (1975) presented a well-reasoned case for a single major upland surface that had developed by late Eocene time. Their argument is based on radiometrically dated Oligocene and Miocene rocks (such dates are not yet available in Wyoming) that are underlain by alluvial gravels in "shallow" valleys of the erosion surface. Thus the early Tertiary age for the subsummit erosion surfaces has respectable advocates in both Wyoming and Colorado, but there are dissenters.

Wahlstrom (1947) concluded that, in the Front Range of Colorado, Oligocene and Miocene lavas and pyroclastic deposits had buried a rugged topography. In Wyoming there is abundant evidence for a rugged late Eocene landscape (**Figures 4** and **5**). Love (1960), in his summary article on Cenozoic sedimentation and crustal movements in Wyoming, reported bouldery Eocene facies adjacent to all the Laramide mountains and a late Eocene topography of marked relief. Blackstone (1975) presented detailed stratigraphic and structural evidence for considerable early Tertiary relief in his report on the mountains and basins of southeastern Wyoming. The most convincing geomorphic evidence is provided by the steep mountain fronts, canyons, and outlying hills now being exhumed from Oligocene and Miocene deposits (**Figures 6** and **7**). The critical sites are mainly in the mountains and uplifts of southeastern Wyoming because Oligocene and Miocene deposits are scarce in the rest of the state.

The westernmost diagnostic site is the southeast end of the Wind River Range, where Antweiler and others (1980) reported a paleovalley at least 1,900 feet deep that extends 4 miles into the Precambrian and is largely filled with Oligocene deposits. Along the southwest margin of the Wind River Range, Precambrian-cored hills (the Prospect Mountains, **Figure 1**) are encircled by Oligocene basin fill. The easternmost site is in the High Plains, where Paleozoic rocks along the axis of the Hartville uplift are being exhumed from their Tertiary cover (Mears, 1991). The most comprehensive study of pre-Oligocene topography is by Evanoff (1990) in the Laramie Mountains, where he described 14 paleovalleys that extend as much as 16 miles into the Precambrian core. The valley floors are as much as 2,700 feet below the existing upland and are underlain by relict Oli-

[3] Today that designation could be late Miocene because of the recent change of the Pliocene/Miocene time boundary from 12 Ma to 5 Ma (Berggren and others, 1985).

gocene fills. He concluded that the relief of the range during Oligocene deposition was considerably greater than the present and that the subdued upland surface was developed during Miocene time.

Late Miocene

Several lines of evidence indicate a generally subdued late Miocene landscape (**Figure 6**) extending across the sediment-filled basins and the broadly truncated basement rocks, locally forming isolated hills and peaks in the mountain cores. A small but significant relict late Miocene landscape is preserved along the southeast flank of the Laramie Mountains. Here, the surface across uppermost deposits of the Miocene Ogallala Formation of the "Gangplank" (see **Figure 10B**) merges evenly with the truncated surface of the Sherman granite (Moore, 1960). The evidence for a subdued mid-Miocene topography across all of southeastern Wyoming was presented by Blackstone (1975). He plotted the widespread sites of distinctive rhyolitic pebbles and cobbles uniquely derived from Oligocene to early Miocene eruptive centers to the southwest in Colorado. These fragments had been transported across planated mountains and deposited in the southern part of the High Plains of Wyoming and northern Colorado.

In terms of the numerical Cenozoic time scale and associated geologic events (see Lillegraven, this volume), the 40 million-year interval from the end of the Laramide orogeny to the mid-Miocene is a reasonable amount of time for planation of the crystalline-cored major mountains. The alternative interpretation of a late Eocene age for planation, previously discussed, would require truncation of the rugged Laramide mountains in some 14 million years.

Concerning origins

The history of thinking about high-level erosion surfaces, shows that our interpretations are strongly influenced by the prevailing frame of reference, often a "school doctrine", and that seemingly similar forms, such as the high-level surfaces, may have differing origins.

Peneplains

In the heyday of the "erosion cycle" — the conceptual scheme of William Morris Davis that dominated most (but not all) geomorphic studies in the late 19th and first half of the 20th centuries — the prevailing explanation for high-level erosion surfaces was the "peneplain." It was the end product of an erosion cycle wherein mountains were uplifted and then progressively eroded during tectonic stability to produce a subdued plain near sea level (**Figure 11**). During this long process, the landscape gradually evolved through stages, namely: "youth", when valleys were deepening; "maturity", the time of greatest relief and steepest slopes; and finally "old age", as slopes became subdued and the region was slowly worn down to near sea level (which was considered to be the ultimate base level of stream erosion). Thereafter, renewed uplift could make peneplains high-level surfaces. The erosion cycle was based on the accepted geologic concepts of the late 19th and early 20th centuries: the gradualism of Lyell, Powell's "ultimate level of subaerial erosion," and Darwin's organic evolution. Davis and his enthusiastic followers applied the scheme to various structural types: plains

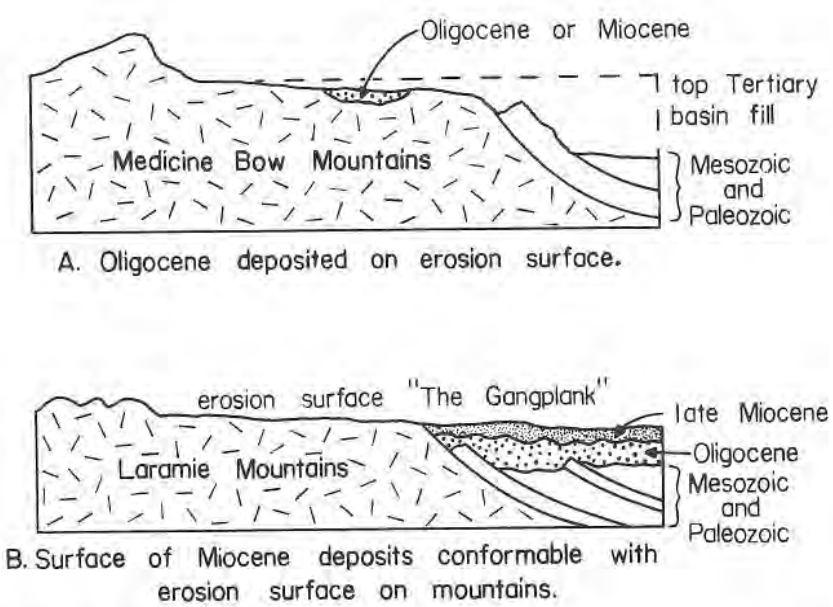

Figure 10. Two different interpretations for the age of high-level surfaces: A. late Eocene (after Knight, 1953); B. late Miocene (after Moore, 1960).

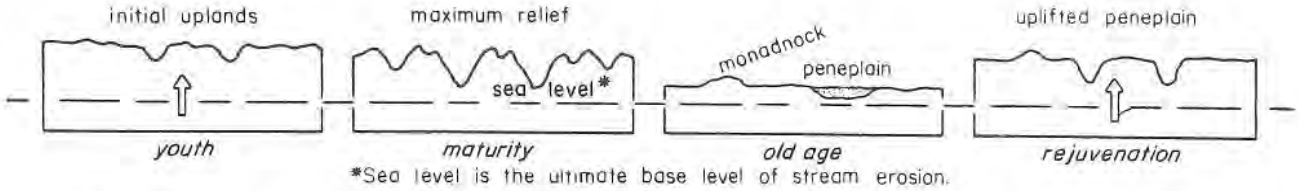

Figure 11. The geomorphic cycle of Davis (1909): erosion to near sea level, followed by renewed uplift.

and plateaus, domes, folded and block mountains, complex crystalline-cored mountains and volcanoes; and to variations related to processes of streams, glaciers, waves, and wind (e.g., see A.K. Lobeck's well-illustrated 1939 textbook).

Enthusiasm for the Davis scheme has waned markedly since the 1940s because of doubts about his theory of slope evolution and the objection that there are no present-day peneplains at or near sea level. American geomorphic investigations now deal largely with the quantitative aspects of fluvial processes. This worthy project, largely avoided by Davis and his school, was pioneered by G.K. Gilbert, Davis's contemporary, who is generally considered the foremost of American geologists (see *The scientific ideas of G.K. Gilbert*, 1980, E.L. Yochelson, editor). In retrospect, the Davisian cyclic concept was a worthy attempt to set up a broad conceptual scheme of the sort that Conant (1951) considered the mark of a mature science — which geologists did acquire for the Earth's crustal processes during the plate-tectonic revolution. Today, peneplains are not in vogue with avant-garde geomorphologists. But, could the planated, crystalline-cored, Laramide uplands be comparable products of prolonged post-orogenic erosion, prior to epeirogenic uplift, provided such surfaces were divorced from some Davisian concepts of slope evolution and of regional reduction to near sea level?

Pediments

A currently favored explanation for the planated Rocky Mountain uplands is pedimentation, a process controlled by local base levels, which may be well above sea level (**Figure 12**). Pediments (called pediplains where extensive) are gently sloping to flat bedrock surfaces, thinly veneered by alluvial deposits that extend outward from the base of mountain fronts. Such surfaces were first recognized (and their origin discussed) by Gilbert (1877) in his classic report on the geology of the Henry Mountains of Utah; however, McGee (1897) first applied the term pediment (from the similarity to the low-pitched gables of Greek temples). There has been much debate as to whether pediments are products of lateral planation by streams emerging from mountain fronts (e.g., Blackwelder, 1931), weathering and retreat of mountain fronts involving rill wash and transportation of debris across the pediment surface (e.g., McGee, 1897; Lawson, 1915), or a combination of such processes (e.g., Bryan, 1922; Sharp, 1940). For a concise review of the much-discussed pediment problem, see Hadley (1967).

Johnson (1931) proposed that the high-level surfaces in the Rocky Mountains are pediments that formed near their present elevations. Although today late Cenozoic epeirogenic uplift of the surfaces is well established, his suggestion did eliminate the necessity for regional degradation to near sea level, inherent in the Davisian peneplain concept. Johnson's views (not unexpectedly) influenced his former graduate students, as is evident in A.D. Howard's short article (1941), "Rocky Mountain peneplanes or pediments", and the classic papers of J. Hoover Mackin (1937, 1947), based primarily on his work in the Bighorn Basin and adjacent Bighorn Mountains, which is relevant to all Wyoming mountains and basins. Mackin argued, convincingly, that the subsummit uplands are former pediments. He pointed out that the surfaces rise gradually from the

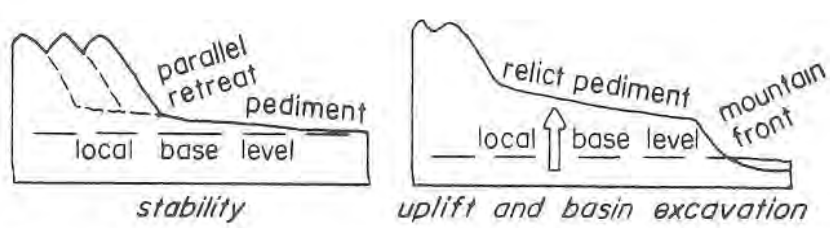

Figure 12. Pedimentation and uplift of pediment to produce high-level surface (after Howard, 1941).

brink of the mountain fronts to the central mountain axes, a form indicative of pediments. A regional Davisian peneplain would have required secondary upwarping of each mountain to produce such surfaces.

Mackin's most significant contribution to the problem of the origin of high-level surfaces had important implications for interpretations of the Cenozoic tectonic history of Wyoming. Establishing that the subsummit uplands were pediments greatly reduced the amount of epeirogenic uplift required to raise the planated surfaces to their present elevations. Davisian peneplains, resulting from prolonged erosion that reduced the landscape to near sea level, would have required 6,000 feet or more of vertical uplift to bring them to the present levels of the subsummit surfaces. Pediments, in contrast, are controlled by the local base levels of erosion, which in Wyoming would have been thousands of feet above sea level along stream courses that were 1,500 to 2,000 miles inland from the coast. Thus, Mackin (1947) concluded that, at most, 2,000 feet of late Tertiary uplift had occurred. That figure seems reasonable based on the comparable depth of basin excavation during the ongoing, post-mid-Miocene episode of regional erosion. Mackin (1937, 1947) presented a convincing case for pedimentation as the process forming the now uplifted subsummit mountain surfaces. However, he attributed the summit surfaces at 13,000- to 11,000-foot levels to a different process.

Altiplanation

In the rigorous environments above timberline, many flat and terrace-like surfaces are attributed to altiplanation (**Figure 13**), a term proposed by Eakin (1916) from work in Alaska. The processes include frost shattering of bedrock and associated nivation that produces cirque-like hollows resulting from freeze-thaw, solifluction, and related mass movements, as well as meltwater runoff. The significance of "high-country" periglacial processes in the Sierra Nevada and Rocky Mountains was recognized by Matthes (1930) and R.J. Russell (1933), who pointed out that the extent of the affected surfaces had received scant attention by geologists who had mainly studied the more spectacular glacial cirques and U-shaped troughs.

As far back as 1896, Dawson noted that, except for some higher peaks, most mountain crests in the Canadian Coast Range were at 8,000-foot-levels, a phenomenon he attributed to the intense frost action and erosion above timberline. This process, called altiplanation, is illustrated in **Figure 13**. South of the Canadian border, an accordance of summits in the Cascade Mountains was also observed by geologists who, imbued with the Davisian concept, interpreted the isolated mountain tops as relicts of a much-dissected peneplain (e.g., I.C. Russell, 1900; Willis, 1903; Smith, 1903). Shortly thereafter, Daly (1912) recognized a lower concordance of gently sloping alpine meadows (such as the Swiss use for summer pasture) at 6,000-foot levels near timberline in the Cascades. Daly attributed these surfaces to strong periglacial action when timberlines were much lower during Pleistocene glacial times. Thompson (1962) strongly supported the altiplanation concepts of Dawson and Daly in his paper "Cascade alp slopes and gipfelfluren as clima-geomorphic indicators". *Gipfelfluren* is a term proposed by Penck (1919) for a former "summit plain" deduced from an approximate accordance of isolated peaks. As evidence for the periglacial origin of the gently sloping alpine surfaces at lower elevations, Thompson noted that they conform with the progressively lower timberlines from northern California to Alaska.

In Wyoming, the extensive subsummit surfaces are clearly not primary products of Pleistocene periglacial processes, because they were present in mid-Miocene time. However, the summit surfaces (**Figure 14**) may well result from ongoing Quaternary altiplanation, as suggested by Mackin (1947). The evidence of intense frost action above timberline includes: stone nets and stripes, shattered blocks of rugged bedrock (felsenmeer), nivation hollows, solifluction terraces and lobes, massive talus, and protalus in glacial cirques (e.g., R.J. Russell, 1933; Richmond, 1949; Mears, 1953; Price, 1973; Breckenridge, 1974).

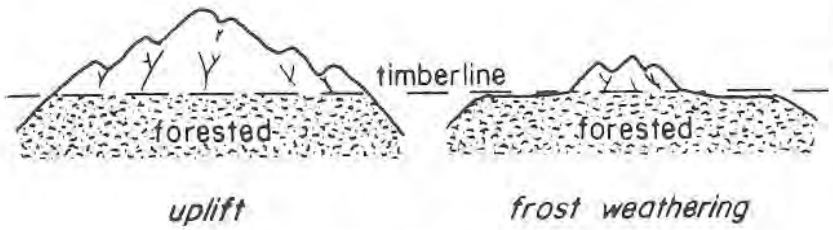

Figure 13. Altiplanation (after Mackin, 1937).

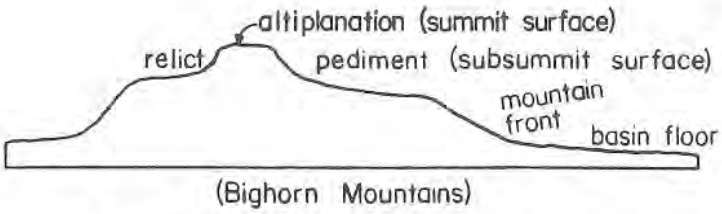

Figure 14. Two origins of high-level surfaces in the same mountain range (after Mackin, 1947).

Stripped Precambrian surfaces

In places, the plateau-like uplands (and/or mountain flanks) are relict planated Precambrian surfaces across which the basal Paleozoic strata had been deposited (**Figure 15**). Hughes (1933) was the first to report such a surface on the Beartooth Mountains in northern Wyoming, where a remnant of Cambrian sandstone, in Beartooth Butte, is preserved on the crystalline-cored upland. Simons and Armbrustmacher (1976) agreed with Hughes' interpretation and, based on five projected profiles, they suggested that isolated remnants of the stripped Precambrian surface were present on the higher ridge tops and peaks of the Beartooth Mountains in Montana. Mackin (1947) recognized a small relict stripped Precambrian surface on the Bighorn Mountains, but dismissed it as irrelevant to the origin of the extensive subsummit surface (which he considered a late Tertiary pediment) or to the summit levels (which he attributed to altiplanation).

The stripped surfaces, where present, are significant as relict broad-backed, Precambrian-cored anticlines that preceded the climax of the Laramide orogeny and ensuing development of extensive high-level subsummit surfaces. These surfaces are complex and not entirely stripped Precambrian surfaces (offset in places by high-angle faults) as evidenced in the Medicine Bow Mountains, whose structure and Precambrian history have been mapped and studied in great detail by Houston and others (1968). Here, the east face of the Snowy Range (**Figure 10A**), which rises 1,000 feet above the extensive Libby Flats erosion surface, is clearly not related to Laramide or post-Laramide high-angle faulting. The face is purely an erosional scarp resulting from the contrast between the extremely hard, near-vertical quartzite beds forming the Snowy Range and less resistant Precambrian crystalline rocks across which the subsummit surface developed.

Differential weathering

Interpretations of the surface on the Laramie Mountains had followed the prevailing schools of thought from the peneplain of Blackwelder (1909) to the pediment of Moore (1960). Whatever its primary origin, this surface has special features attributed to differences in weathering of the coarse-crystalline Sherman granite. The extensive subdued upland, the Sherman surface, is characteristically underlain by grus, a thick weathering mantle of loose quartz, feldspar, and rock particles (**Figure 16**). In places, however, notably less-weathered granite forms clusters of tors, steep-sided hills whose surfaces are characterized by thick sheet-like slabs with horizontal joints attributed to "unloading," a process involving a slight expansion of the surficial bedrock during regional denudation.

The cause for the difference in weathering in areas of deep grus and of tors is not evident from studies of hand specimens and thin sections. However, an explanation was proposed by Eggler and others (1969) when they studied polished sections of granite from both the tors and Sherman

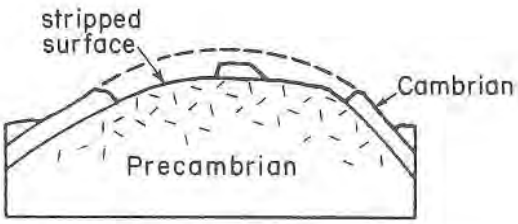

Figure 15. Stripped Precambrian surfaces, Beartooth Mountains (after Hughes, 1933).

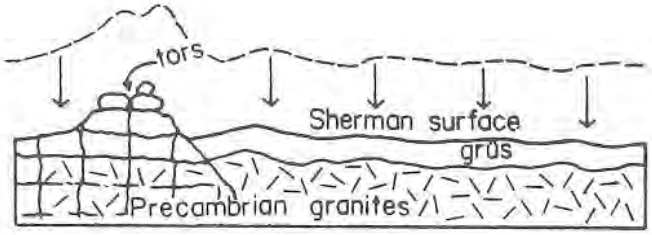

Figure 16. Differential weathering of Sherman granite in the Laramie Mountains (after Eggler and others, 1969).

surface under oil at high magnifications (1,000 x) and also obtained x-ray diffraction patterns. They concluded that the difference in weathering of the Sherman granite was primarily a product of biotite disruption. In the Precambrian granite bodies emplaced at higher temperatures, oxidation products along intergranular biotite cleavage surfaces produced a looser structure than in bodies emplaced at lower temperatures. During exposure to surficial processes in Cenozoic time, the looser biotite cleavage surfaces expanded as much as 40 percent in volume to create the grus of the Sherman surface. In contrast, in areas of tors this process was much less effective. Eggler and others (1969) also proposed that the general form of the topography was established in the early Tertiary and that it has remained little changed during progressive weathering and removal of material to the present time [a dynamic equilibrium of the sort proposed by Hack (1960)].

The above studies in the Laramie Mountains were all restricted to the dominantly granitic southern area. As Blackstone (1975) pointed out, the same upland extends well northward across the anorthositic bodies mapped by Newhouse and Hagner (1957). Thus, Blackstone suggested that the term "Sherman surface" should also include the areas of anorthosite, a rock consisting almost exclusively of plagioclase feldspar (andesine to labradorite) and devoid of biotite.

Primary denudation

The most recent hypothesis for the high-level erosion surfaces involves a process here called primary denudation. This concept stems from a study by Steidtmann and others (1989) of the Tertiary deposits on and adjacent to the southwest flank of the Wind River Range. They proposed that during the Laramide orogeny, spanning latest Cretaceous through most of the early Eocene, the accumulation of thick fills deposited in the deeply subsiding adjacent Green River Basin kept pace with the slow denudation of the very gradually rising Precambrian-cored tectonic block (**Figure 17**). Thus, the surface of primary denudation, across the crystalline bedrock, remained essentially concordant with the top of the aggrading basin fill. Thereafter, in the late early Eocene, the erosion surface was uplifted to its present relative position by reverse faulting in the hanging wall of the Wind River thrust fault. By mid-Eocene time, the erosion surface had been largely overlapped by deposits that were greatly supplemented by volcaniclastic deposits transported southward from concurrent eruptions in the Absaroka region. Steidtmann and others (1989) attributed the climactic rise creating the high peaks of the Wind River Range to Oligocene uplift characterized by reverse faulting within the crystalline-cored mountain mass. The event is recorded in coarse conglomerates derived from the mountain core.

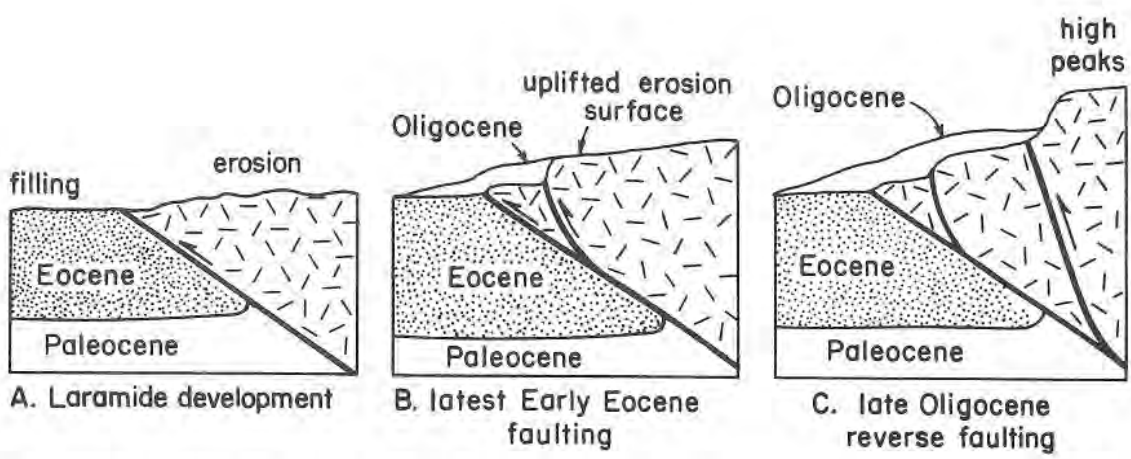

Figure 17. Development of high-level erosion surface in the Wind River Range (after Steidtmann and others, 1989). A. Surface of primary denudation, B. uplifted erosion surface, and C. later differential uplift of high peaks.

This model introduces several new concepts for the evolution of the Wind River Range. Except for the deposition of thick fill in a deeply subsiding adjacent basin, a Laramide erosion surface of primary denudation is reminiscent of the "primärrumpf" of Walther Penck (1924). As a possible alternative to Davis' assumption of geologically rapid initial uplift followed by prolonged stability and degradation that ultimately produced a peneplain, Penck proposed that if uplift were slow, an extensive erosion surface would develop at a relatively low level. That an Eocene erosion surface had been uplifted to form the surface across the Wyoming uplands and some of the higher peaks had been previously suggested (e.g., Baker, 1946; Granger and others, 1971; Pearson and others, 1971). The new proposals of Steidtmann and others (1989) include: (1) the absence of mountainous relief throughout most of Laramide time because of ongoing erosion during a prolonged phase of gradual Laramide deformation; and (2) the rise of the high mountain peaks during accelerated reverse faulting in late Oligocene time. These hypotheses need verification.

Based on his field work in the Wind River Range, B.R. Frost doubts that the flattish summits on high peaks are the remains of a once-continuous erosion surface (personal communication, 1992). He points out that the alignment of the successive peaks does not correspond to the dominantly north- and northeast-striking fault systems in the Precambrian core of the range [mapped in some detail by Worl and others (1986)]. However, Steidtmann and others (1989) attributed the late Oligocene rise of the peaks to reactivation along shear zones considered Precambrian in age by Mitra and Frost (1981) in a small study area in the northeast part of the range. In their very detailed study of Precambrian rocks in the Medicine Bow Mountains of southeastern Wyoming, Houston and others (1968) mapped a major east-striking shear zone. However, that zone is truncated by the extensive subsummit level and is not responsible for the 1,000-foot-high, precipitous east face of quartzite that forms Snowy Range ridge above the erosion surface. Moreover, D.L. Blackstone, Jr. (personal communication, 1992) remains to be convinced of any major reverse faulting in post-Laramide time, based on his extensive knowledge of Wyoming structures (buttressed by his many serial cross sections). Whatever the final verdict, the innovative proposals of Steidtmann and others (1989) indicate the ongoing interest in the number, age, and origins of the controversial high-level erosion surfaces.

Conclusions concerning high-level erosional surfaces

Rather than end with a seemingly open-minded summary, I conclude with personal opinions. Following the latest Cretaceous through early Eocene rise of high mountains and deep subsidence of broad intervening basins during Laramide deformation of the continental foreland, a rugged Wyoming landscape was progressively buried by deposits, greatly supplemented by pyroclastic debris from remote sources, during the Oligocene and much of the Miocene. Progressive reduction of the initially rugged mountains eventually produced a mid-Miocene surface of low relief, extending across planated crystalline uplands and deep, sediment-filled basins. After the onset of broad regional (epeirogenic) uplift, which was characterized by normal faulting beginning in the mid-Miocene, progressive regional erosion has excavated the broad intermontane basins.

Genesis of the high-level erosion surfaces involves several processes. Moreover, the various interpretations of the surfaces have commonly reflected the generally accepted schemes of particular times (comparable to the thinking of most American geologists before and after the plate-tectonic revolution).

The Precambrian-cored mountains have one major subsummit surface level and a much less extensive summit surface level. If the subsummit level formed in early Tertiary time, it would have been at appreciably lower levels prior to epeirogenic uplift and could have resembled a Davisian peneplain. The evidence of significant late Eocene topography, currently being exhumed from Oligocene and Miocene basin fills, better fits a late Tertiary origin for the subsummit surface. In addition, in the late Tertiary, arid or semi-arid conditions conducive to pedimentation prevailed. In contrast, the summit surfaces developed during Quaternary time in the periglacial environments prevailing above Rocky Mountain timberlines.

Acknowledgments

I thank D.L. Blackstone, Jr., and William C. Bradley for many helpful suggestions on an initial manuscript, and Emmett Evanoff and Jason Lillegraven for comments that improved a later version. The polished drafting of the final block diagrams was done by Phyllis A. Ranz.

References cited

Antweiler, J.C., Love, J.D., Mosier, E.L., and Campbell, W.L., 1980 Oligocene gold-bearing conglomerate, southeast margin of Wind River Mountains, Wyoming: Wyoming Geological Association 31st Annual Field Conference Guidebook, p. 223-237.

Baker, C.L., 1946, Geology of the northwestern Wind River Mountains, Wyoming: Geological Society of America Bulletin, v. 57, p. 565-596.

Berggren, W.A., Kent, D.V., Flynn, J.J., et. al., 1985, Cenozoic geochronology: Geological Society of America Bulletin, v. 96, p. 1407-1418.

Bevan, A., 1925, Rocky Mountain peneplains northeast of Yellowstone Park: Journal of Geology, v. 33, p. 563-587.

Blackstone, D.L., Jr., 1975, Late Cretaceous and Cenozoic history of Laramie Basin region, southeast Wyoming, *in* Curtis, B.F., editor, Cenozoic history of the southern Rocky Mountains: Geological Society of America Memoir 144, p. 249-279.

_____ 1990, Precambrian basement map of Wyoming: outcrop and structural configuration: Geological Survey of Wyoming Map Series 27, scale 1:1,000,000.

Blackwelder, E., 1909, Cenozoic history of the Laramie region, Wyoming: Journal of Geology, v. 17, p. 429-444.

_____ 1915, Post-Cretaceous history of the mountains of central western Wyoming: Journal of Geology, v. 23, p. 97-117, 193-217, 307-340.

_____ 1931, Desert plains: Journal of Geology, v. 39, p. 137-140.

Bradley, W.C., 1987, Erosion surfaces of the Colorado Front Range: a review, *in* Graf, W.L. editor, Geomorphic systems of North America: Geological Society of America Centennial Special volume 2, p. 215-220.

Breckenridge, R.M., 1974, Quaternary and environmental geology of the upper Wood River area, Absaroka Range, Wyoming [Ph.D. thesis]: Laramie, University of Wyoming, 138 p.

Bryan, K., 1922, Erosion and sedimentation in the Papago County, Arizona: U.S. Geological Survey Bulletin 730-B, p. 19-90.

Conant, J.B., 1951, Science and common sense: New Haven, Yale University Press, 344 p.

Daly, R.A., 1912, The geology of the North American Cordillera: Canada Department of Mines, Geological Survey Memoir 38, part 2, p. 631-641.

Davis, W.M., 1909, The geographical cycle, *in* Geographical essays: Dover Press reprint (1954), p. 249-278.

Dawson, G.M., 1896, Report on the area of the Kamloops map sheet, British Columbia: Canadian Geological Survey, New Series VII, Report B for 1894.

Eakin, H.M., 1916, The Yukon-Koyukuk region: U.S. Geological Survey Bulletin 631, p. 67-82.

Eggler, D.H., Larson, E.E., and Bradley, W.C., 1969, Granites, grusses, and the Sherman erosion surface, southern Laramie Range, Colorado-Wyoming: American Journal of Science, v. 267, p. 510-522.

Epis, R.C., and Chapin, C.E., 1975, Geomorphic and tectonic implications of the post-Laramide, late Eocene erosion surface in the southern Rocky Mountains, *in* Curtis, B.F., editor, Cenozoic history of the Southern Rocky Mountains: Geological Society of America Memoir 144, p. 45-74.

Evanoff, E., 1990, Early Oligocene paleovalleys in southern and central Wyoming: evidence of high local relief on the late Eocene unconformity: Geology, v. 18, p. 443-446.

Gilbert, G.K., 1877, Geology of the Henry Mountains (Utah): U.S. Geographical and Geological Survey of The Rocky Mountain Region, U.S. Government Printing Office, Washington, D.C., 160 p.

Granger, H.C., McKay, E.J., Mattick, R.E., Patten, L.L., McIlroy, P., 1971, Mineral resources of the Glacier primitive area, Wyoming: U.S. Geological Survey Bulletin 1319-F, 113 p.

Hack, J.T., 1960, Interpretation of erosional topography in humid temperate regions: American Journal of Science (Bradley Volume), v. 258-A, p. 80-96.

Hadley, R.F., 1967, Pediments and pediment-forming processes: Journal of Geological Education, v. 15, p. 83-89.

Houston, R.S., and others, 1968, A regional study of rocks of Precambrian age in that part of the Medicine Bow Mountains lying in southeastern Wyoming — with a chapter on the relationship between Precambrian and Laramide structure: Wyoming Geological Survey Memoir No. 1, 167 p.

Howard, A.D., 1941, Rocky Mountain peneplanes or pediments: Journal of Geomorphology, v. 4, p. 138-141.

Hughes, R.V., 1933, Peneplanation of the Beartooth Mountains: Pan-American Geologist, v. 59, p. 321-327.

Johnson, D.W., 1931, Planes of lateral corrosion: Science, v. 73, no. 1885, p. 174-177.

Knight, S.H., 1953, Summary of the history of the Medicine Bow Mountains, Wyoming: Wyoming Geological Association 8th Annual Field Conference Guidebook, p. 65-76.

_____ 1990, Illustrated geologic history of the Medicine Bow Mountains and adjacent areas, Wyoming: Geological Survey of Wyoming Memoir 4, 48 p.

Larson, T.A., 1978, History of Wyoming, 2nd editon, revised: Lincoln and London, University of Nebraska Press, 663 p.

Lawson, A.C, 1915, The epigene profiles of the desert: California University Publications in Geology, v. 9, p. 23-48.

Lobeck, A.K., 1939, Geomorphology: New York, McGraw-Hill Book Company, Inc., 731 p.

Lillegraven, J.A., and Ostresh, L.J., Jr., 1988, Evolution of Wyoming's early Cenozoic topography and drainage patterns: National Geographic Research, v. 4, no. 3, p. 303-327.

Love, J.D., 1960, Cenozoic sedimentation and crustal movement in Wyoming: American Journal of Science (Bradley Volume), v. 258A, p. 204-213.

Mackin, J.H., 1937, Erosional history of the Bighorn Basin, Wyoming: Geological Society of America Bulletin, v. 48, p. 813-894.

_____ 1947, Altitude and local relief of the Bighorn area during the Cenozoic: Wyoming Geological Association 2nd Annual Field Conference Guidebook, p. 103-120.

Marvine, A.R., 1874, Report for the year 1873, *in* 7th Annual Report of the U.S. Geological and Geographical Survey of the Territories (Hayden Survey): Washington, D.C., p. 83-192.

Matthes, F.E., 1930, Geological history of the Yosemite Valley: U.S. Geological Survey Professional Paper 160, 137 p.

McGee, W.J., 1897, Sheetflood erosion: Geological Society of America Bulletin, v. 8, p. 87-112.

McGrew, P.O., 1980, An Eocene flamingo nesting area, Sweetwater County, Wyoming: National Geographic Society Research Reports, v. 12, p. 473-478.

Mears, B., Jr., 1953, Quaternary features of the Medicine Bow Mountains, Wyoming: Wyoming Geological Association Eighth Annual Field Conference Guidebook, p. 81-84.

_____ 1991, The High Plains of Wyoming, *in* Morrison, R.B., editor, Quaternary nonglacial geology of the conterminous United States: Geological Society of America Centennial Special volume K-2, p. 450-452.

Mitra, G., and Frost, B.R., 1981, Mechanisms of deformation within Laramide and Precambrian deformation zones in basement rocks of the Wind River Mountains: University of Wyoming, Contributions to Geology, v. 19, p. 161-173.

Moore, F.E., 1960, Summary of Cenozoic history, southern Laramie Range, Wyoming and Colorado, *in* Guide to the geology of Colorado: Geological Society of America-Rocky Mountain Association of Geologists, Colorado Scientific Society publication, p. 217-222.

Newhouse, W.H., and Hagner, A.F., 1957, Geologic map of anorthosite areas, southern part of Laramie Range, Wyoming: U.S. Geological Survey Minerals Investigation Map MF-119, scale 1:63,360.

Pearson, R.C, Killsgaard, T.H., Patten, L.L., 1971, Mineral resources of the Popo Agie Primitive Area; Fremont and Sublette counties, Wyoming: U.S. Geological Survey Bulletin 1353-B, p. B1-B55.

Penck, A., 1919, Die Gipfelflur der Alpen: Berlin, Sitzber, Preuss. Akad. Wiss. v. 17, 256 p.

Penck, W., 1924, Die Morpologische Analyse: J. Engelhorn's Nachfolger, Stuttgart, 283 p. (translation by H. Czech and K.C. Boswell, 1953, as *Morphological analysis of landforms*, St. Martins Press, New York, 429 p.)

Powell, J.W., 1876, Geology of the eastern portion of the Uinta Mountains, U.S. Geological and Geographical Survey of the Territories: Washington, D.C., 218 p.

Price, C., 1973, Glacial and drainage history of the upper Cow Creek drainage, Sierra Madre Range [*sic*], Wyoming [M.A. thesis]: Laramie, University of Wyoming, 82 p.

Richmond, G.M., 1949, Stone nets, stone stripes, and soil stripes in the Wind River Mountains, Wyoming: Journal of Geology, v. 57, p. 143-153.

Ruddiman, W.F., and Kutzbach, J.E., 1989, Forcing of late Cenozoic Northern Hemisphere climate by plateau uplift in southern Asia and the American West: Journal of Geophysical Research, v. 94, p. 18,409-18,427.

Russell, I.C., 1900, A preliminary paper on the geology of the Cascade Mountains in northern Washington: U.S. Geological Survey 20th Annual Report, part 2, p. 193-204.

Russell, R.J., 1933, Alpine land forms of western United States: Geological Society of America Bulletin, v. 44, p. 927-950.

Scott, G.R., 1975, Cenozoic surfaces and deposits in the Southern Rocky Mountains, *in* Curtis, B.F., editor, Cenozoic history of the Southern Rocky Mountains: Geological Society of America Memoir 144, p. 227-248.

Sharp, R.P., 1940, Geomorphology of the Ruby-East Humboldt Range, Nevada: Geological Society of America Bulletin, v. 51, p. 337-371.

Simons, F.S., and Armbrustmacher, T.J., 1976, High-level plateaus of the southeastern Beartooth Mountains, Montana and Wyoming—remnants of an exhumed sub-Cambrian marine plain: U.S. Geological Survey Journal of Research, v. 4, no. 4, p. 387-396.

Smith, G.O., 1903, Geology and physiography of central Washington: U.S. Geological Survey Professional Paper 19, p. 3-40.

Steidtmann, J.R., Middleton, L.T., and Shuster, M.W., 1989, Post-Laramide (Oligocene) uplift in the Wind River Range, Wyoming: Geology, v. 17, p. 38-41.

Thompson, W.F., 1962, Cascade alp slopes and gippelfluren as clima-geomorphic phenomena: Erdkunde, band XVI, heft 2, p. 81-94.

Van Tuyl, F.M., and Lovering, T.S., 1935, Physiographic development of the Front Range: Geological Society of America Bulletin, v. 46, p. 1291-1350.

Wahlstrom, E.E., 1947, Cenozoic history of the Front Range, Colorado: Geological Society of America Bulletin, v. 58, p. 551-572.

Walcott, C.D., 1910, Abrupt appearance of the Cambrian fauna on the North American continent: Smithsonian Miscellaneous Collections, v. 57, p. 1-16.

Westgate, L.G., and Branson, E.B., 1913, the later Cenozoic history of the Wind River Mountains, Wyoming: Journal of Geology, v. 11, p. 142-159.

Willis, B., 1903, Physiography and deformation of the Wenatchee-Chelan district, Cascade Range: U.S. Geological Survey Professional Paper 19, p. 41-101.

Worl, R.G., Koesterer, M.E., and Hulsebosch, T.P., 1986, Geologic map of the Bridger Wilderness on the Green-Sweetwater Roadless Area, Sublette and Fremont Counties, Wyoming: U.S. Geological Survey Miscellaneous Field Investigations Map MF-1636-B, scale 1:250,000.

Yochelson, E.L., editor, 1980, The scientific ideas of G.K., Gilbert, an assessment on the occasion of the Centennial of the U.S. Geological Survey (1879-1979): Geological Society of America Special Paper 183, 148 p.

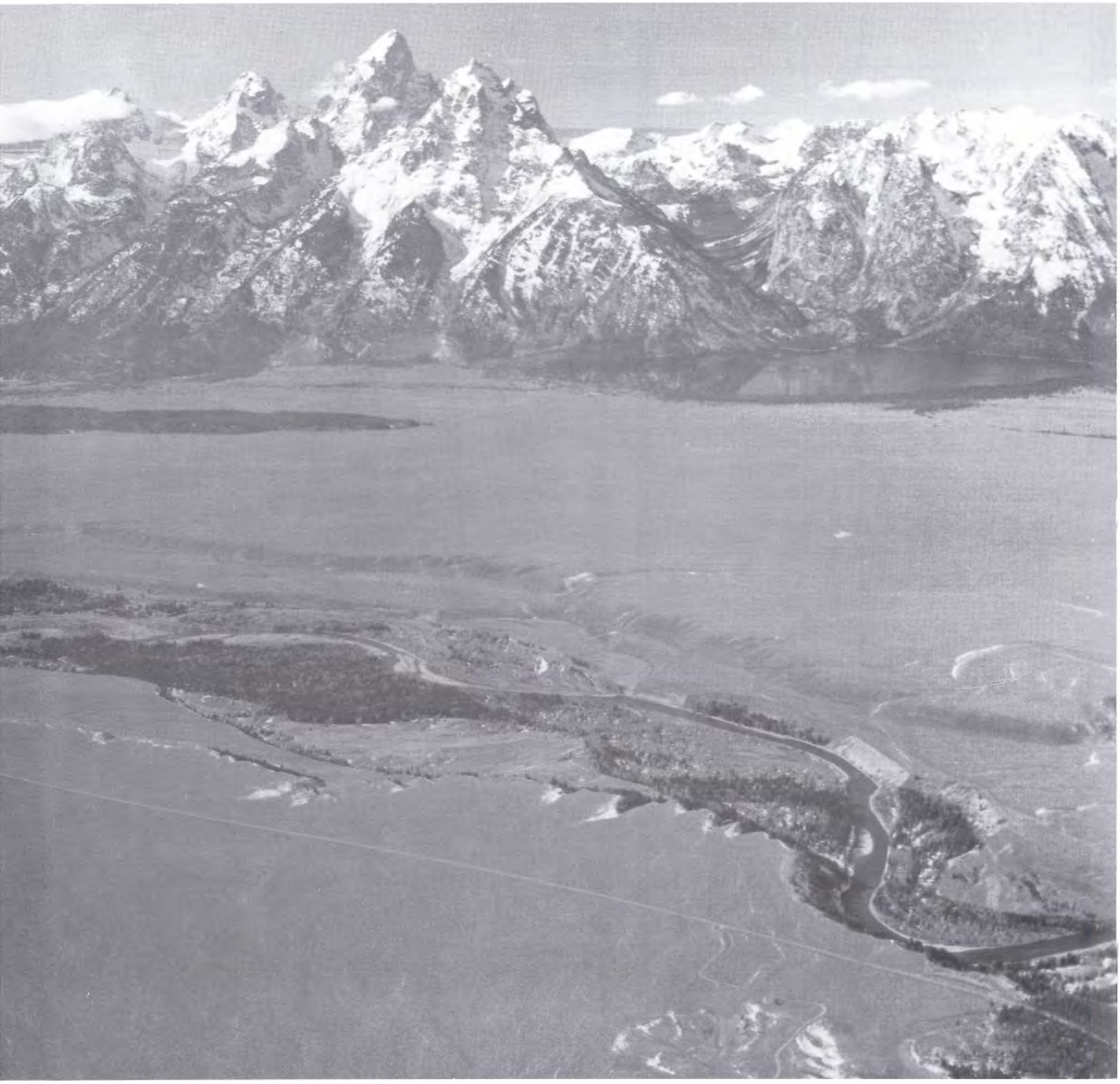

Frontispiece. Aerial view of the Teton Range (looking southwest) showing the spectacular topographic relief (~2,100 m) of the range due pimarily to 6-9 km of stratigraphic offset along the east-facing Teton normal fault. The Quaternary expression of the Teton fault is at the base of the range and generally extends along the top of the wooded slopes between Garnet Canyon on the left and Jenny Lake on the right. The Snake River at Deadman's Bar is shown in the lower left foreground. The valley of Jackson Hole (foreground) occupies the down-dropped, hanging-wall sediment basin now filled by lake beds, alluvium, and glacial deposits. Photograph courtesy of David R. Lageson, Montana State University.

The Teton fault, Wyoming: seismotectonics, Quaternary history, and earthquake hazards

Robert B. Smith and John O.D. Byrd
Department of Geology and Geophysics
University of Utah
Salt Lake City, Utah 84112

David D. Susong
Water Resources Division
U.S. Geological Survey
Salt Lake City, Utah 84104

Abstract

The more than 2 km of topographic relief of the spectacular Teton Range, Wyoming, is attributed to uplift along the Teton fault. Movement on this major, range-bounding normal fault is thought to have begun as early as 5 to 13 million years ago and the fault has been active during Quaternary time, producing well-preserved fault scarps up to 50 m high and over 55 km long. These young scarps offset Pinedale-age (~14 ka) glacial deposits and younger fluvial and alluvial deposits. The total stratigraphic offset of the Teton fault is estimated to be 6 to 9 km. The youthful nature and magnitude of Quaternary faulting demonstrate its capability for producing large, scarp-forming earthquakes despite evidence that the Teton fault has been seismically quiescent in historic time. We believe that a 4.1 m vertical displacement in near-surface alluvium and glacial deposits, observed in a trench exposure on the southern segment of the Teton fault, represents the most recent displacement(s) on the fault and is the product of two large Holocene earthquakes. The oldest of these events occurred 7,175 ± 190 years ago (radiocarbon date) and resulted in 2.8 m of slip, whereas a younger and yet undated event produced a 1.3 m slip. Stratigraphic displacements of Quaternary volcanic rocks and results from the trench suggest Holocene slip rates of 0.45 to 1.6 mm/yr for the Teton fault. These rates are consistent with a range of recurrence intervals for large, scarp-forming earthquakes of 1,600 to 6,000 years. An area of unusual topographic subsidence, up to 26 m, was located 0.5 to 2 km east of the central part of the Teton fault and is similar to a pattern of down-to-west tilt of the valley floor against the Teton fault in southern Jackson Hole. This anomalous pattern of subsidence may reflect, in part, hanging-wall deformation associated with large prehistoric earthquakes.

To assess the contemporary deformation of the Teton fault, a 22 km-long profile of 50 precisely surveyed benchmarks was established across the Teton fault in 1988 and surveyed in 1988 and 1989 in a cooperative project with the University of California, Santa Barbara. During that period, the valley of

Smith, R.B., Byrd, J.O.D., and Susong, D.D., 1993, The Teton fault, Wyoming: seismotectonics, Quaternary history, and earthquake hazards, *in* Snoke, A.W., Steidtmann, J.R., and Roberts, S.M., editors, Geology of Wyoming: Geological Survey of Wyoming Memoir No. 5, p. 628-667.

Jackson Hole (hanging wall) rose up to 8 mm relative to the Teton Range (footwall), opposite to the pre-seismic deformation expected for a normal fault. This unexpected deformation may have resulted from non-tectonic mechanisms, such as near-surface inflation due to alluvial expansion from groundwater introduced during the refilling of Jackson Lake, or tectonic processes such as aseismic reverse creep.

We consider that the Teton fault has the potential for large scarp-forming earthquakes of $M_s = 7.2 \pm 0.3$. Earthquakes of this size could damage or destroy lifelines, produce strong ground motion, and trigger landslides and snow and rock avalanches. Moderate magnitude (M_s=5.5 to 6.3), nonsurface-rupturing earthquakes are also important because of their more frequent occurrence, but they would affect smaller areas than less frequent, larger earthquakes.

Introduction

The Teton fault is an important element of the 1,300 km-long Intermountain seismic belt (referred to hereafter as ISB), an intraplate zone of seismicity (**Figure 1**) that extends northward from southern Utah, through eastern Idaho and western Montana, and encompasses western Wyoming and the Teton fault (Smith and Sbar, 1974; Smith and Arabasz, 1991). The pre-Quaternary expression of the Teton fault extends north-south for up to 70 km on the east side of the Teton Range, and it has a total stratigraphic separation estimated to be from 6 to 9 km (Love and Reed, 1971). A striking aspect of this major fault is a string of well-preserved fault scarps in Quaternary glacial deposits that extend 55 km along the base of the range (**Frontispiece**). The Teton fault is considered by us as the single most important factor contributing to the ~2,150 m (~7053 feet) of topographic relief and therefore to the spectacular scenery of the Teton Range—the essence of Grand Teton National Park.

The seismotectonic significance of the Teton fault is evident when it is compared to similar range-front normal faults associated with three large scarp-forming earthquakes in the Basin and Range province in historic time: (1) the Dixie Valley fault, associated with the M_s = 6.8, 1954, Dixie Valley, Nevada, earthquake (Slemmons, 1957; Doser, 1988); (2) the Hebgen Lake and Red Canyon faults, associated with the M_s = 7.5, 1959, Hebgen Lake, Montana, earthquake (Myers and Hamilton, 1964; Doser, 1985); and (3) the Lost River fault, Idaho, site of the M_s = 7.3, 1983, Borah Peak, Idaho, earthquake (Doser and Smith, 1985; Richins and others 1987; Crone and others, 1987). These well-studied events nucleated at mid-crustal depths of 15 ± 5 km and were the result of rupture on 45° to 60° dipping, planar normal faults (see **Figure 1** for locations of the Hebgen Lake and Borah Peak earthquakes). Hanging-wall subsidence associated with these large earthquakes was as large as 6 m and surface ruptures extended up to 34 km in length. The similarities among these three earthquakes have led to a conceptual working model for normal-faulting earthquakes (Smith and others, 1985; King and others, 1988; Smith and Arabasz, 1991) that enables us to hypothesize the magnitude and extent of surface rupture and ground deformation that may accompany large scarp-forming earthquakes, such as those expected on the Teton fault.

We report here the results of a four-year study focused on the seismotectonics, Quaternary history, and earthquake hazards of the Teton fault. Preliminary results of this work were given by Susong and others (1987), Byrd and others (1988), and Smith and others (1990a, b, c). Our research was supported by the University of Wyoming-National Park Service Research Center, U.S. Geological Survey, and Geological Survey of Wyoming.

Regional tectonic setting

The structural evolution of the Teton Range and the Teton fault (**Figure 2**) has been influenced by four major orogenic tectonic-volcanic events: (1) Precambrian deformation, metamorphism, and plutonism

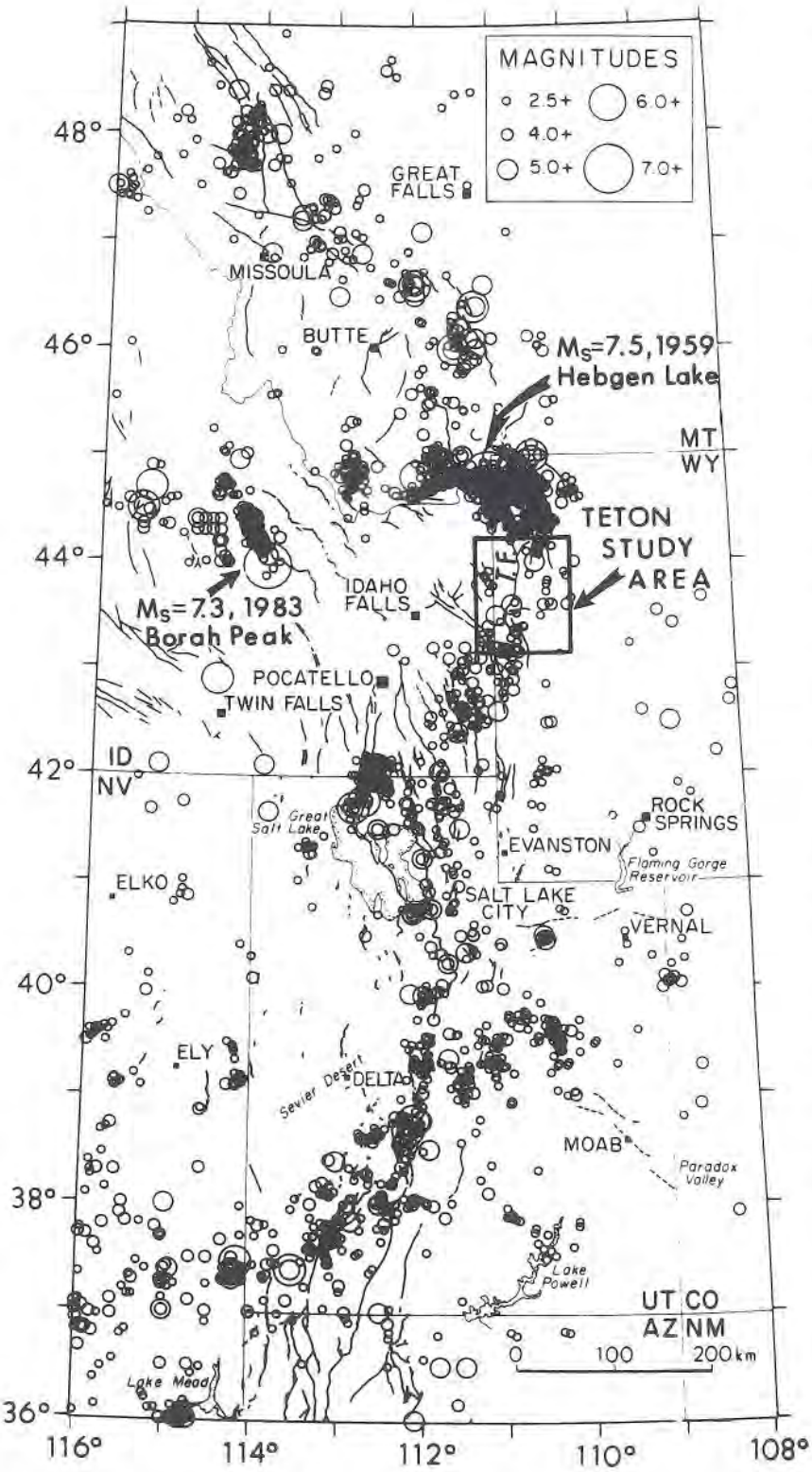

Figure 1. Seismicity of the Intermountain seismic belt for 1850 through 1985 (from Smith and Arabasz, 1991). Teton fault study area outlined by box.

forming the core of the range; (2) Mesozoic to early Tertiary crustal shortening, including thrust faulting and folding of the Wyoming-Idaho thrust belt and the Laramide foreland provinces; (3) late Tertiary to Quaternary, Basin and Range epeirogeny accompanied by east-west crustal extension and normal faulting; and (4) late Tertiary-Quaternary silicic volcanism and crustal uplift and subsidence associated with the Yellowstone-Snake River Plain volcanic system. These diverse tectonic regimes have no doubt had a profound effect on the Teton region, but we believe the late Tertiary crustal extension attributed to Basin and Range tectonism has had the dominant influence on the topographic development of the Teton Range and on the structural evolution of the Teton normal fault (**Figure 3** and **Sheet 1**, Smith, Byrd, and Susong, map pocket).

On a more regional scale, the seismic quiescence of the eastern Snake River Plain, a late Tertiary, bimodal rhyolite-basalt province, with its pronounced seismically active "shoulders" (**Figures 4** and **5**), led several workers (Smith and others, 1985, 1990b; Smith and Braile, this volume; Anders and others, 1989; Pierce and Morgan, 1990) to postulate the effect of the Yellowstone hotspot on the seismotectonics of the central Intermountain region. Smith and others (1985, 1990b), Smith and Braile (this volume), and Anders and others (1989) suggest that a lithospheric thermal disturbance associated with the Yellowstone hotspot extends outward from the center of the Snake River Plain, influencing the regional stress field and resulting in an aseismic central region and a roughly parabolic-shaped pattern of earth-

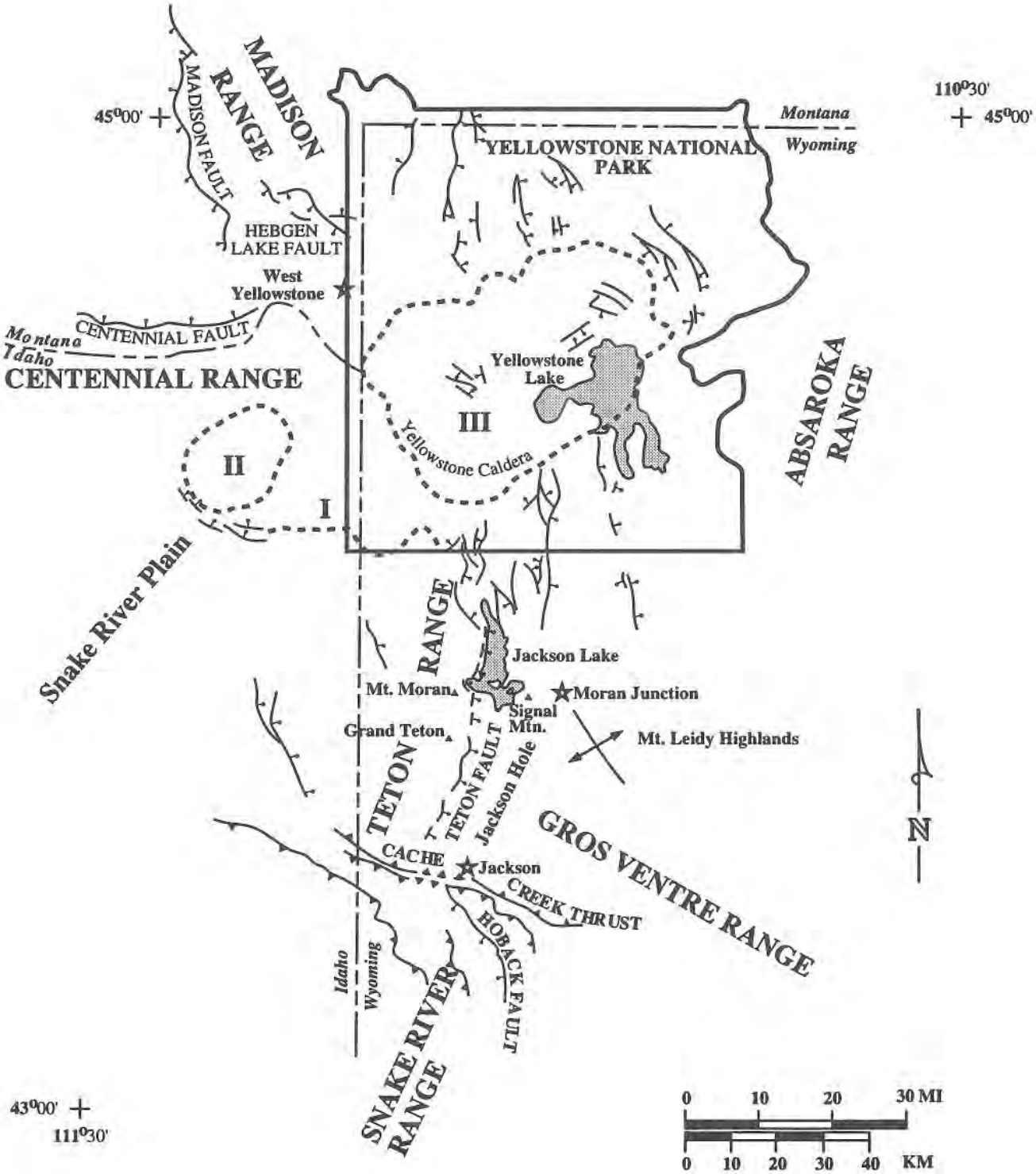

Figure 2. Tectonic index map of the Teton Range and Yellowstone Plateau of Wyoming, Idaho, and Montana. Ages of Yellowstone calderas (outlined with dashes): I = 2.0 Ma, II = 1.2 Ma, and III = 0.6 Ma. (Standard symbols for normal faults, thrust faults, and anticline.)

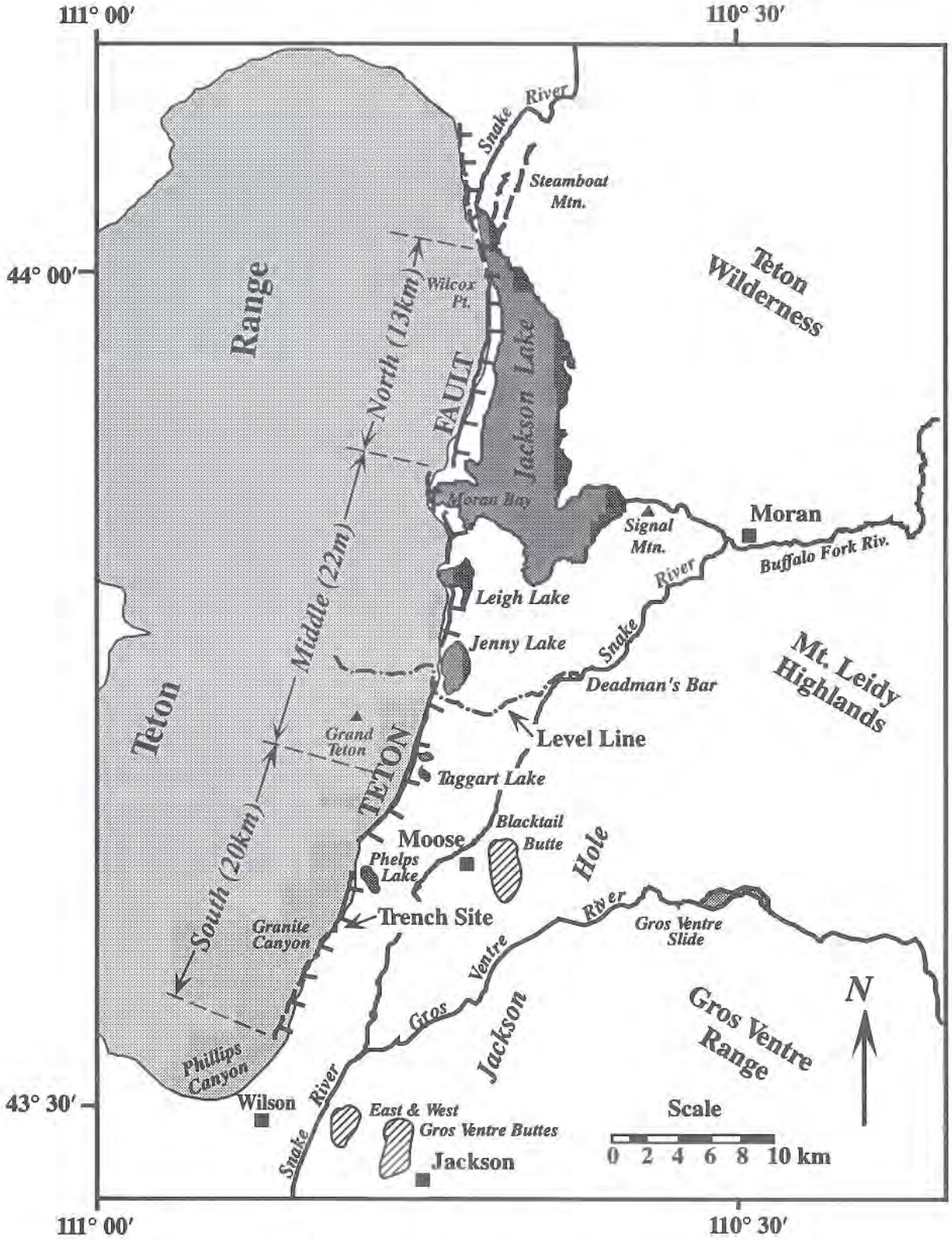

Figure 3. Map of the Teton Range-Jackson Hole region showing the Quaternary expression of the Teton fault and proposed segment boundaries. The map also shows key geographic features cited in the text. Light grey pattern is area of Precambrian outcrop. Cross-hachured areas are outcrops of Palozoic rocks in Jackson Hole.

quakes surrounding the volcanic province. The Teton region is located within the eastern branch of the parabolic-shaped area of seismicity located east of the Snake River Plain (**Figure 4**). It is also east of a belt of late Cenozoic normal faulting that appears to have been relatively inactive throughout Holocene time (Scott and others, 1985; Smith and others, 1985).

Evidence for Late Cretaceous initiation of deformation along the Teton Range was provided by a study of apatite fission-track age-determinations taken from samples acquired along the eastern range front (Roberts and Burbank, 1988, 1993). They determined dates of 85 to 25.8 Ma with decreasing sample elevation and inferred uplift of 1 to 1.5 km of the Teton Range in the Late Cretaceous. Roberts and Burbank (1988, 1993) further speculated that the post-30 Ma uplift of the Teton Range was represented by approximately 2 km of offset of the 2 Ma Huckleberry Ridge Tuff.

Notably, earlier studies of the Teton region by Blackwelder (1915) and Horberg and others (1955) pointed out that the Teton fault may be a fault-line scarp, an hypothesis that it is consistent with the Late Cretaceous uplift suggested by Roberts and Burbank (1988, 1993). Furthermore, Lageson (1992) suggested that the Teton fault may reflect reactivation on the northeast-dipping Cache Creek thrust (**Figure 2**) that flanked a Laramide basement high. If these hypotheses are correct, then the Teton Range has had a complex history of pre-Tertiary uplift and Tertiary erosion, followed by Plio-Pleistocene range uplift and valley subsidence along the Teton fault.

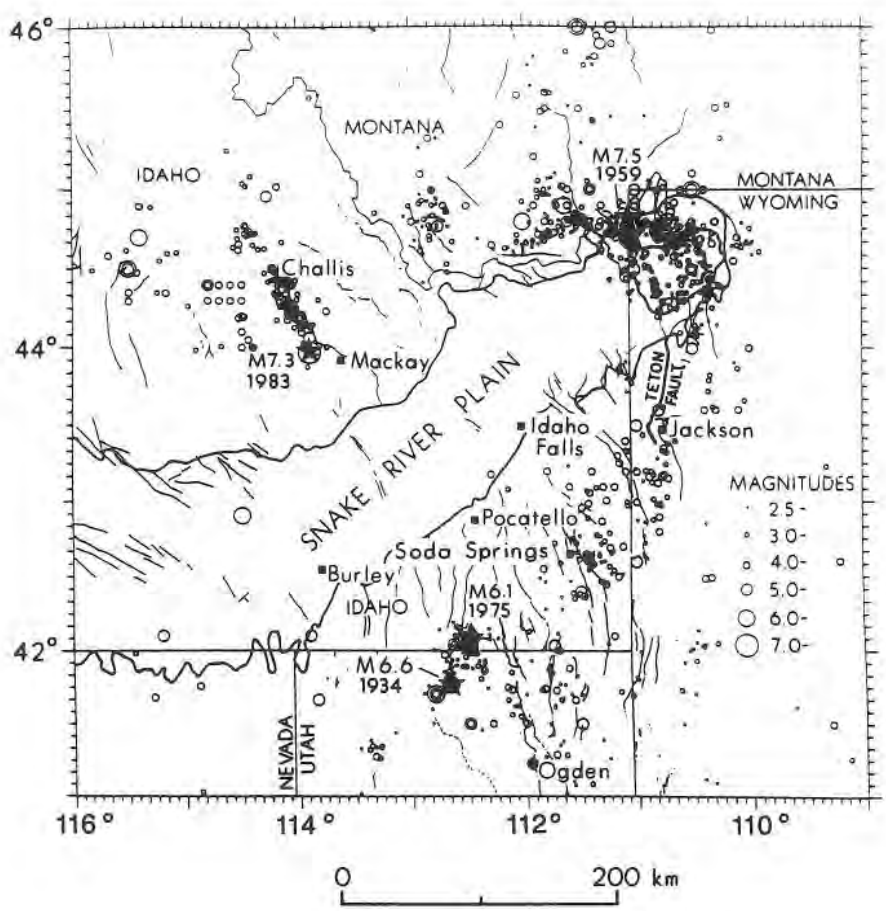

Figure 4. Regional seismicity of Yellowstone-Snake River Plain-Teton region for the period ~1900 to 1985. Map modified from Smith and others (1990a) and Smith and Arabasz (1991).

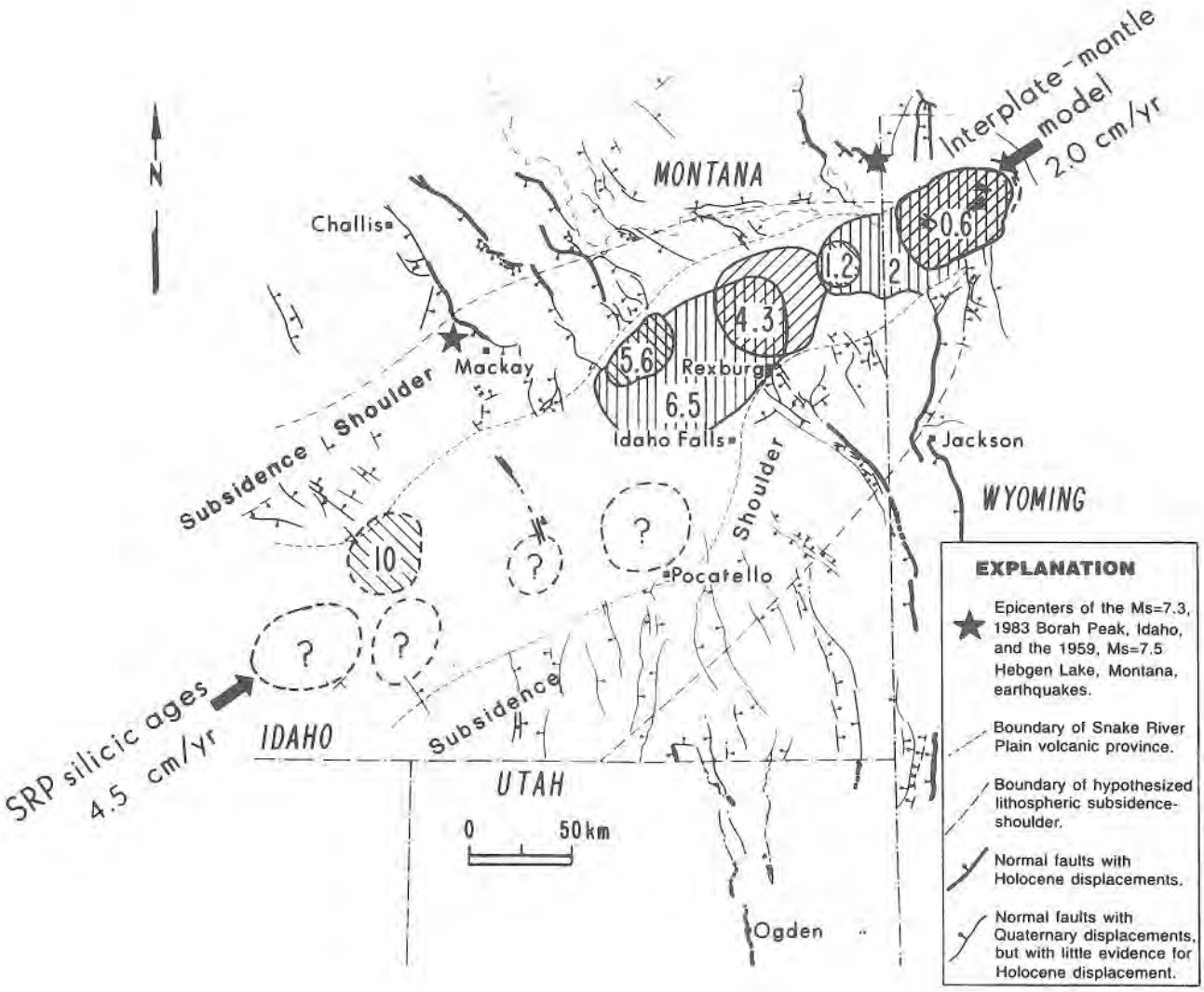

Figure 5. Distribution of calderas (with ages in millions of years), late Cenozoic normal faults, and deformation zones associated with the Snake River Plain-Yellowstone volcanic system. The arrow at Yellowstone is the direction of motion of the North American plate relative to the Yellowstone hotspot with an absolute velocity of ~2 cm/yr, and the arrow at the southwest end of the Snake River Plain (SRP) is the direction of progressively younger silicic volcanism of 4 cm/yr (after Smith and Braile, this volume). Map modified from Smith and others (1990a) and Smith and Braile (this volume).

General geology

The geological setting of the Teton region is well known and is not described here except to point out the general features that relate to our study. The reader is referred to discussions of the geology and tectonics of the Teton Range and the Jackson Hole area by Love (1956), Love and Reed (1971), Love and others (1972), and Love (1977).

The Teton Range consists primarily of a core of Precambrian igneous and metamorphic rocks including quartz monzonite, gneiss, and diabase (Reed, 1973; Reed and Zartman, 1973). These crystalline basement rocks are overlain by westward-tilted Paleozoic strata and Quaternary silicic volcanic rocks that form the western dip slope of the Teton Range

(Love and Reed, 1971; Love and others, 1992). **Figure 6** shows our interpreted west-east geologic cross section of the Teton Range and Jackson Hole with the corresponding aerial view of the Teton Range looking north. On the east side of the Teton Range, a 70 km-long valley, Jackson Hole, occupies the hanging wall of the Teton fault and appears to be underlain by an asymmetric, west-dipping Tertiary-Quaternary basin. The Quaternary strata are fluvial, glacial, and volcaniclastic deposits and are underlain by Tertiary lacustrine, fluvial, and volcaniclastic units. A relatively continuous section of Paleozoic and Mesozoic sedimentary rocks is thought to underlie Jackson Hole based on the results of geophysical surveys (Behrendt and others, 1968; Tibbetts and others, 1969) and on exploratory wells in the Gros Ventre Range and the Mount Leidy Highlands (**Figure 6b**). The Paleozoic strata are well exposed on the west flank of the Teton Range and serve as a geometric marker of the uplifted and westward tilted hanging wall of the Teton fault.

Although several bedrock buttes, consisting of westward- to vertically-dipping Paleozoic and Tertiary sedimentary and volcanic rocks are exposed in the central and southern parts of Jackson Hole (Love, 1956; Love and Albee, 1972; Love and Love, 1978; Love, unpublished maps), the structural configuration and thicknesses of formations underlying the basin are poorly known. The estimated total stratigraphic offset of the Teton fault (6 km, **Figure 6b**) could be in error by as much as ± 50% or more, especially if our assumptions of a planar-dipping fault and formation geometry and thicknesses are incorrect.

The floor of Jackson Hole is marked by widely distributed Pleistocene glacial deposits that provide evidence for at least two periods of Pleistocene glaciation. These were the Bull Lake (100 to 150 ka) and Pinedale (14 to 30 ka) stages that filled Jackson Hole with up to 790 m of ice (Porter and others, 1983; Pierce, 1979; Pierce and Good, 1990; Smith and others, this volume). The younger Pinedale age glaciers flowed south and southwest from the Yellowstone ice cap, depositing the terminal moraines that form the southern margin of Jackson Lake. Smaller Pinedale valley glaciers carved the steep canyons in the Teton Range and produced terminal moraine complexes at the canyon mouths that have been offset by the Teton fault (for example, see the first discussions of these features in Fryxell, 1938a,b). The lateral extent and configuration of the fault scarps that offset these and younger deposits define the Quaternary trace of the fault and were the focus of our first-year mapping project.

The Snake River and the streams emanating from the Teton Range form a rather unusual drainage pattern across the floor of Jackson Hole (**Figure 3** and **Sheet 1**, Smith, Byrd, and Susong, map pocket). The Snake River is the main drainage of Jackson Hole and exits Jackson Lake at its southeast margin, north of Signal Mountain. It follows a course along the eastern side of Jackson Hole until the channel works its way to the west side of the valley at the southern end of the valley. A surprising aspect of the fluvial drainage is the generally southward flow of several streams exiting the canyons of the central and southern parts of the Teton Range. Rather than draining eastward into the Snake River, these streams appear to have been diverted southward from Leigh Lake and south of Phelps Lake along the western side of Jackson Hole (**Sheet 1**, Smith, Byrd, and Susong, map pocket). The geomorphic features responsible for the diversion of these streams may be due to damming by glacial and fluvial features. However, we suggest that the diversion appears to be in part related to hanging-wall subsidence associated with prehistoric earthquakes and thus agree with Love and Montagne (1956) who suggested that prehistoric earthquakes on the Teton fault played a significant role in developing this unusual drainage pattern at the south end of the Teton fault.

In contrast to the youthful Teton Range, the Gros Ventre Range, east of Jackson Hole (**Figures 2** and **3**), evolved as part of the Wyoming foreland province during the Laramide orogeny (Nelson and Church, 1943). The Gros Ventre Range consists of a core of Precambrian igneous rocks that underlies a generally continuous Paleozoic, Mesozoic, and Tertiary sedimentary section. The rocks are exposed in a series of north-northwest-trending folds that developed in response to uplift along the Cache Creek thrust and a series of high-angle reverse faults within the range (e.g., Nelson and Church, 1943; Simons and others, 1981; Lageson, 1987).

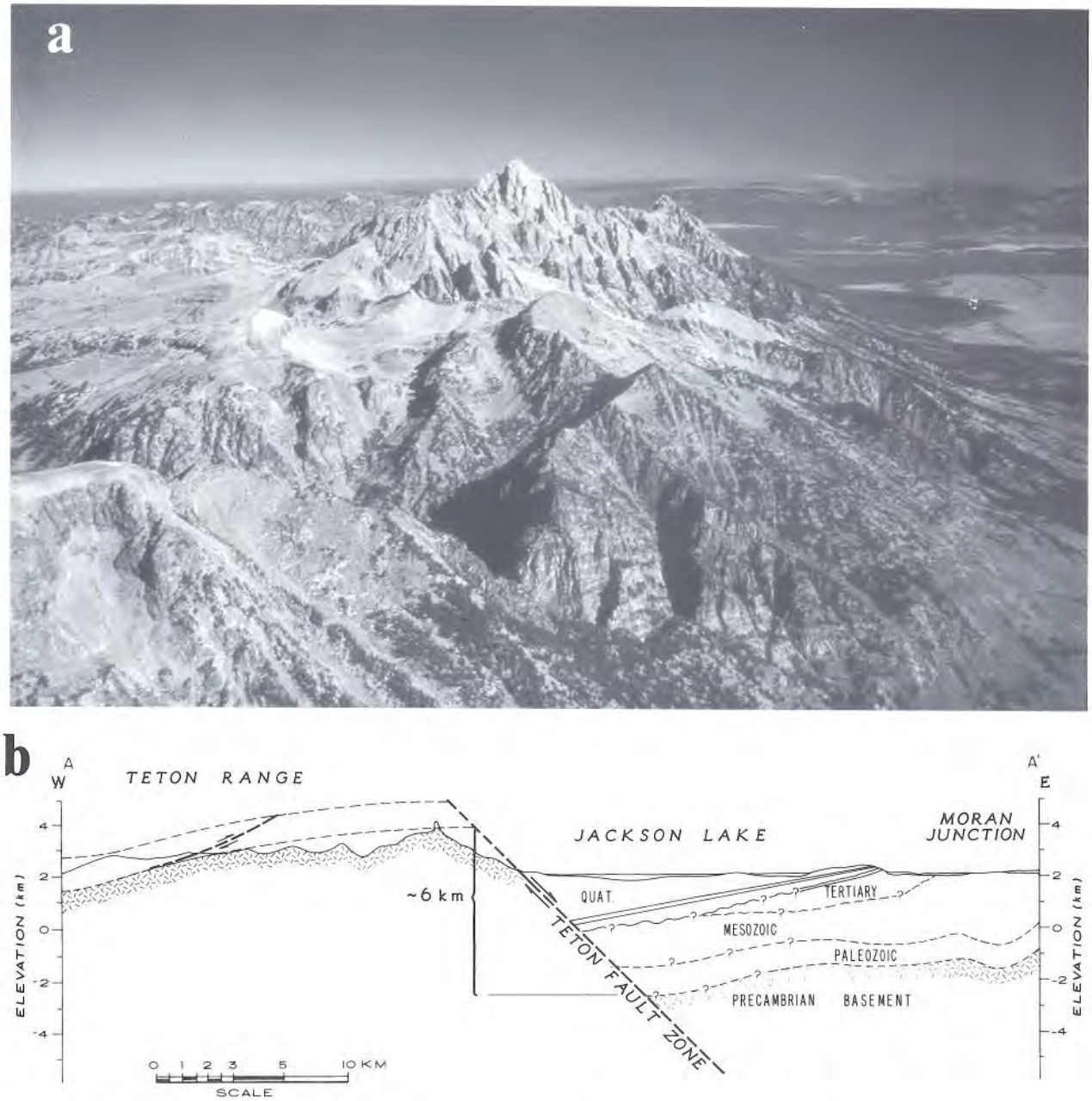

Figure 6. (a) Aerial view of the Teton Range and the Grand Teton looking north. (This picture corresponds to the cross-section in Figure 6b.) The hanging-wall valley of Jackson Hole (upper right) is bounded on the west by the uplifted Teton Range. Note the west-dipping Paleozoic strata to left of the Grand Teton (photograph by Robert B. Smith). (b) Schematic geologic cross section of the Teton Range and Jackson Hole showing a total stratigraphic offset of ~ 6 km of the Teton fault. The total displacement was estimated from offsets of the Cambrian Flathead Sandstone exposed on top of Mt. Moran to its projected depth in Jackson Hole. The subsurface configuration of Mesozoic and Paleozoic sediments beneath Jackson Hole is based on a projection of limited outcrop data and well data taken from Love and others (1992), Behrendt and others (1968), and Tibbetts and others (1969).

Seismicity of the Teton region

The Teton Range lies within the central part of the ISB (**Figures 1** and **4**). This zone of intraplate seismicity is characterized by a diffuse zone of epicenters, up to 200 km wide, that generally do not correlate with the surface traces of Quaternary faults (Smith and Arabasz, 1991). The ISB represents the general boundary between the Basin and Range province on the west and the Colorado Plateau-Middle Rocky Mountains on the east. Focal mechanisms and patterns of Quaternary faulting in the ISB commonly reflect normal to oblique-slip faulting and focal depths are shallow, seldom exceeding 15 km (Smith and Sbar, 1974; Smith and Arabasz, 1991). Studies of focal mechanisms and seismic moment[1] rates of historical earthquakes suggest that contemporary deformation of the Teton region is characterized by general east-west crustal extension accommodated on normal- to oblique-slip faults, but at relatively low horizontal deformation rates of 0.01 mm/yr or less (Eddington and others, 1987; Doser and Smith, 1983; Wood, 1988). These rates are much lower than those determined for other areas in the ISB (Eddington and others, 1987) and are also much lower than the long-term slip estimated for the Teton fault during Quaternary time.

The central ISB has experienced some of the largest earthquakes in the conterminous United States (**Figures 1** and **4**). These include the $M_S = 7.5$, 1959, Hebgen Lake, Montana, earthquake. This is the largest historic earthquake in the Rocky Mountains and it was located only 90 km northwest of the Teton Range. Most recently, the $M_S = 7.3$, 1983, Borah Peak, Idaho, earthquake occurred 200 km west of the Teton Range on the northwest side of the Snake River Plain. In addition, earthquakes as large as $M_L = 6.1$ and extensive earthquake swarms characterize the Yellowstone Plateau. Earthquakes of the Yellowstone volcanic system begin just 10 km north of the Teton Range (Smith and Arabasz, 1991).

Historical seismicity

Earthquakes have been commonly reported by inhabitants of Jackson Hole since the late 1800s (Blackwelder, 1926). Until about the 1950s, earthquake locations in the western U.S. were based upon the personal felt reports of ground-shaking based on the Modified Mercalli intensity scale and are considered accurate to ± 50 km (Smith and others, 1976). Earthquakes in the Teton region from the 1950s to the early 1960s were recorded by a few seismographs scattered throughout the western U.S., which, along with the intensity reports, provided only a marginal increase in epicenter accuracy. Following the installation of networks of seismographs throughout the western U.S. beginning in 1962, epicenter accuracy increased to about ± 10 km for the Teton region (Smith and Arabasz, 1991). When the more densely spaced, temporary and permanent seismograph networks were installed in the Teton-Yellowstone area beginning the early 1970s, the epicenter accuracy increased to ± 1 to 2 km (Doser and Smith, 1983; Smith and Arabasz, 1991). This is the accuracy of the current U.S. Bureau of Reclamation network coverage of the Teton region (Wood, 1988), making these data sufficiently accurate for seismotectonic assessments.

The historical seismicity of the Teton region is characterized by a relatively large number of earthquakes reported by the small and isolated population of Jackson Hole from the early 1900s to the early 1930s. Several earthquakes up to intensity VI that caused minor damage throughout this period were reported in the Gros Ventre Canyon (Blackwelder, 1926; Fryxell, 1933; Gale, 1940; Coffman and Von Hake, 1973). However, after about 1933, the incidence of felt earthquakes in the Teton area perceptibly decreased in Jackson Hole and no significant ground shaking was reported until 1959, when the $M_S = 7.5$, Hebgen Lake, Montana, earthquake produced significant shaking throughout the valley. Love (1973) documented several earthquakes that were felt in the area in 1968, 1970, and 1972; however, no felt events were reported in the Jackson Hole area from 1972 to 1979 (see U.S. Geological Survey's annual publications *United States Earthquakes, 1985*, Stover and Brewer, 1991). From 1979 to the present, small to moderate shocks, some as large as $M_L = 4.6$, were reported in the southern Jackson Hole area, although the most recent U.S. Geological Survey earthquake compilation is only current through 1985. These felt events were recorded on regional networks, and the locations of their epicenters are poorly known, precluding their assignment to specific faults.

[1]Seismic moment is a term that quantitatively describes the size of an earthquake by its length, width, and coefficient of shear rigidity.

Regional earthquake monitoring

Earthquake monitoring, focused on the Teton Range and Jackson Hole, was initiated by the University of Utah in 1973 (Smith and others, 1977) and was conducted intermittently during summer field seasons through 1981 (Doser and Smith, 1983). These surveys used portable seismographs and located earthquakes as small as approximately $M_L \sim 1.0$; however, calibrated magnitudes were not determined for these events. The U.S. Bureau of Reclamation established a permanent seismograph network surrounding Jackson Lake, the Palisades reservoir, Idaho, and west side of the Teton Range in the summer of 1986 (Wood, 1988). The U.S. Bureau of Reclamation network includes 22, short-period, vertical-component seismographs centrally recorded in Denver, Colorado (Wood, 1988).

Epicenter data from the University of Utah temporary networks, combined with data from the U.S. Bureau of Reclamation permanent network for 1986 to 1988, illustrate the distribution of earthquakes in the Teton region in recent years (**Figure 7**). The epicenters define a diffuse pattern of small earthquakes that extends at least 80 km northeastward from the Wyoming and Snake River Ranges to an area west of the Hoback Junction and northeastward into the Gros Ventre Range-Mt. Leidy area. An area of sparse earthquakes is also noted on the west flank of the Teton Range. Note the general lack of small-magnitude earthquakes on the Teton fault and in Jackson Hole, extending north from the vicinity of Moose for at least 50 km (**Figure 7**). The epicenters shown in the northern part of **Figure 7** are at the southern end of a band of persistent north-trending seismic activity that extends 30+ km northward beneath the southern part of the Yellowstone caldera (**Figure 4**). These epicenters may reflect earthquakes on a buried extension fault or zone of weakness related to the Teton fault now covered by Quaternary volcanic rocks in Yellowstone National Park (Smith, 1988; Smith and others 1990b).

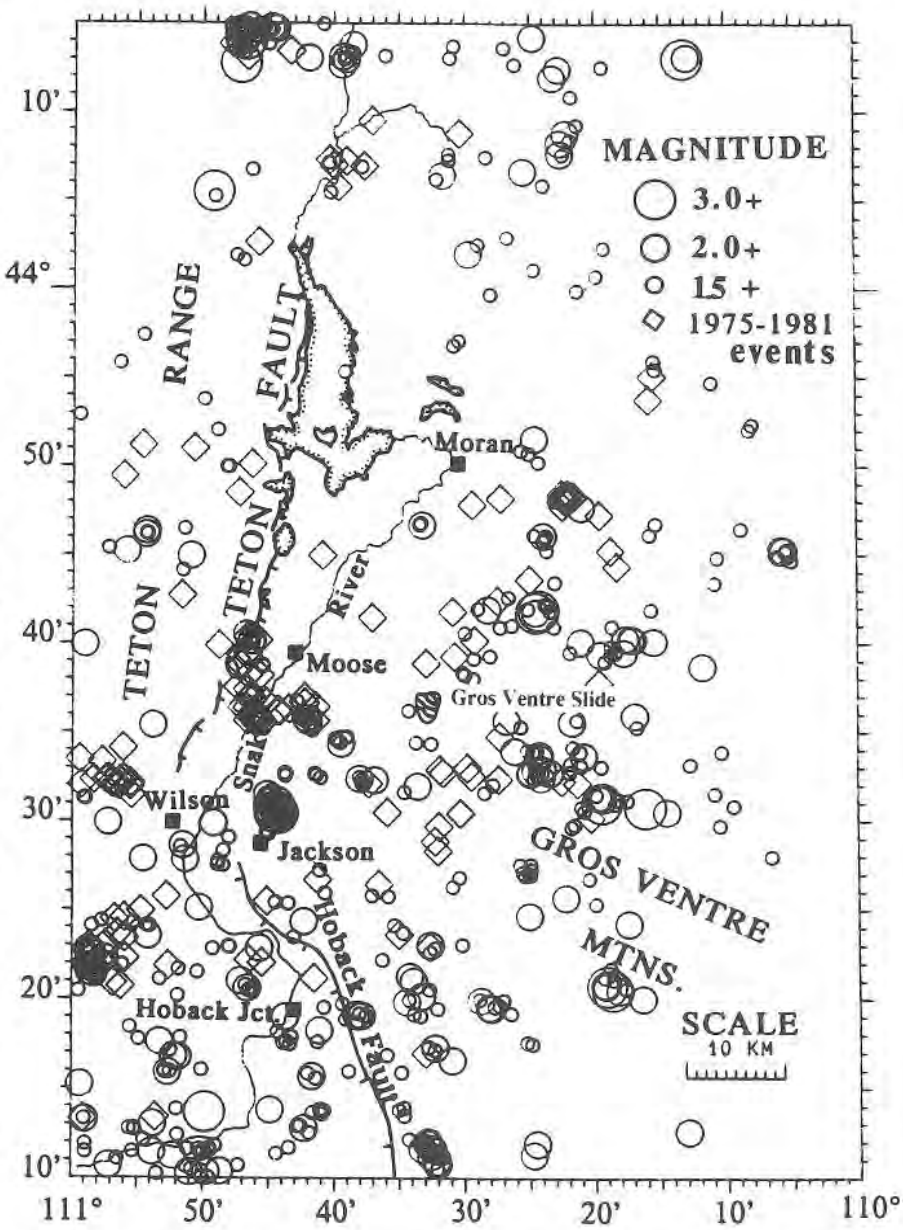

Figure 7. Earthquake epicenter map of the Teton region from 1973 to 1981 and 1983 to 1988. [1973 to 1981 data from the University of Utah (Smith and others, 1976; Doser and Smith, 1985; University of Utah unpublished data); and 1986 to 1988 data from the U.S. Bureau of Reclamation (Wood, 1988).]

Doser and Smith (1983) noted a correlation of epicenters in the Gros Ventre Range-Mt. Leidy area with a 5.5 to 7 km-deep, Laramide thrust zone identified from seismic reflection profiles. Although Doser and Smith (1983) could not definitely show that the earthquakes were associated with thrust faults, their close spatial correlation suggests that the background seismicity of the Gros Ventre region may result, in part, from displacements associated with pre-existing zones of weakness.

A notable north-trending belt of earthquakes near the southern end of the Teton fault and the two distinct clusters of epicenters between Jackson and Moose (Figure 7) are the likely sources of several felt earthquakes reported in Jackson in the late 1980s. The foci of these tremors are generally less than 5 km (Wood, 1988) and the projection of a 45°-60° eastward-dipping Teton fault into this area places the fault plane at depths of 10 to 15 km. The shallow foci of these earthquakes are therefore not on the eastward projection of the Teton fault and may be related to movement on related, yet unknown, structures in the hanging wall.

The pattern of historic earthquakes of the central ISB shows that the Teton fault has been notably aseismic for magnitudes $M_L \geq 2$ (**Figure 8**) for the period 1959 to 1989. The very low regional strain rate (Eddington and others, 1987) and the general seismic quiescence of the Teton area compared to the rest of the ISB led Smith (1988) to suggest a possible "gap" in the historic seismicity of this region at the $M_L > 3$ level. If his interpretation is valid, the Teton fault may be "locked" and the area of seismic quiescence may be expected to reactivate with moderate to large earthquakes in the future. However, possible alternate interpretations for the aseismic nature of the Teton fault include: (1) the Teton fault is no longer active and therefore is not storing significant strain energy required for earthquake nucleation. However, based on the Holocene history of faulting and the long-term geologic record, we have no reason to believe that the Teton fault is not active; (2) the main belt of regional seismicity may have migrated eastward onto unknown structures in the Gros Ventre Range, thereby relieving stress accumulation on the fault; and (3) the period of historic seismological observations may not be sufficiently long to accurately assess the temporal pattern of the long-term seismicity .

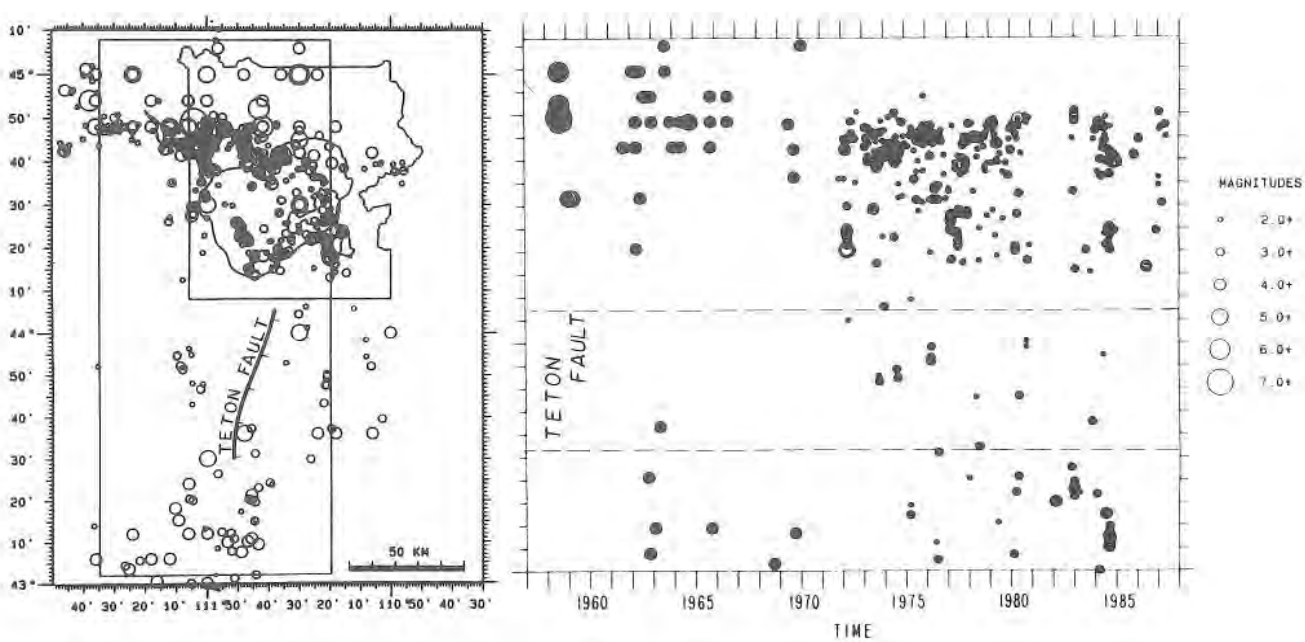

Figure 8. Space-time distribution of seismicity for the Teton region from 1959 to 1989 showing: (a) regional epicenter map, and (b) temporal distribution of corresponding earthquakes.

The Teton fault zone

The Quaternary expression of the Teton fault was first described on a general scale by Fryxell (1938a,b) and Horberg (1938), and the location of the fault was incorporated into the geologic maps of the Teton Range and the surrounding area by Love and Reed (1971) and Love and others (1972, 1992). **Figure 9** shows pictures of well-developed Quaternary fault scarps along the central part of the Teton fault. A detailed study of Quaternary faulting at specific locations along the Teton fault was made by Gilbert and others (1983) for an earthquake safety assessment of the Jackson Lake dam and included a map of the Quaternary trace of the Teton fault that was detailed at several specific locations.

Movement on the Teton fault may have begun as early as 13 Ma (Barnosky, 1984), although Love (1977) estimated movement on the fault began at 5 Ma based on the lack of coarse clastic detritus in the Miocene Teewinot Formation. Barnosky's interpretation was made on the basis of a 15° angular unconformity between the Miocene Colter Formation and the overlying Teewinot Formation exposed on the northeast side of Jackson Hole. Nonetheless, the Teton fault appears to have been generally influenced by the Basin and Range extensional tectonism that began earlier, ~17 to 20 Ma, in Utah and Nevada.

A number of interpretations of the magnitude of stratigraphic separation and geometry of the Teton fault have been proposed. Love and Reed (1971) and Love and others (1972) estimated a total stratigraphic separation ranging from 6 to 9 km (also see **Figure 6**). They implied that the Teton fault dips 70° to 80° east and is more than 90 km long, extending well beyond the southern end of the main topographic expression of the Teton Range. Tibbetts and others (1969) estimated that the Teton fault dips 30° east on the basis of seismic refraction measurements and gravity data. Lageson (1992) argued that the Teton fault terminates or ramps downward on a footwall ramp of the Cache Creek thrust. The geometry of Lageson's model implies that if the Teton fault is a planar, 45° to 60° dipping structure, it may occupy a north-striking ramp of the Cache Creek thrust or alternately, it may sole out into a listric geometry along the thrust. Unfortunately, none of these studies provide unequivocal information on the subsurface geometry of the fault.

Quaternary fault mapping

Expanding upon the work of previous investigators (e.g., Gilbert and others, 1983), we (D.D.S. and J.O.D.B.) have mapped the Quaternary scarps of the Teton fault at a scale of 1:9,000, extending from Phillips Canyon on the south to Steamboat Mountain on the north (**Figure 3**). Preliminary versions of the fault map were presented by Susong and others (1987) and Smith and others (1990a,b) and form the basis for the large-scale map of the Teton fault shown in **Sheet 1** (Smith, Byrd, and Susong, map pocket). The Quaternary expression of the Teton fault was delineated based upon identification of fault scarps that offset Pinedale glacial deposits, younger fluvial and alluvial deposits, and related neotectonic features. The detailed distribution and characteristics of glacial, alluvial, fluvial, and colluvial deposits adjacent to the fault were not mapped, except in special study areas discussed in the next section.

Quaternary fault scarps, from 3 m to 50 m high, are exposed for 41 km along the 55 km length of the Teton fault. The discontinuity in fault scarps, accounting for the 14 km deficit, is from the lack of identifiable exposures of faulting in areas of steep topography, lakes, and landslides. The Quaternary scarps define a prevalent N10°E strike along most of the fault and a down-to-the-east, normal sense of displacement (**Figure 3** and **Sheet 1**, Smith, Byrd, and Susong, map pocket). A distinct right-stepping, en echelon pattern characterizes the distribution of scarps in the central and southern sections of the Teton fault, whereas a linear pattern parallel to the topography of the range-front characterizes the northern part of the fault.

Bathymetric maps of Jackson Lake (Hayden, 1969) were examined for possible lake-bottom scarps but none were clearly observed. Some slope breaks were identified in the bathymetry data in Jenny and Leigh lakes that may represent fault scarps. Divers from the U.S. Bureau of Reclamation (J. Gilbert, personal communication, 1987) identified submerged trees beneath the west side of Jenny Lake, originally suggested as evidence for a recent large displacement on the Teton fault, but now thought to be a submerged landslide. They also identified a small topographic scarp near the west shore of the lake that

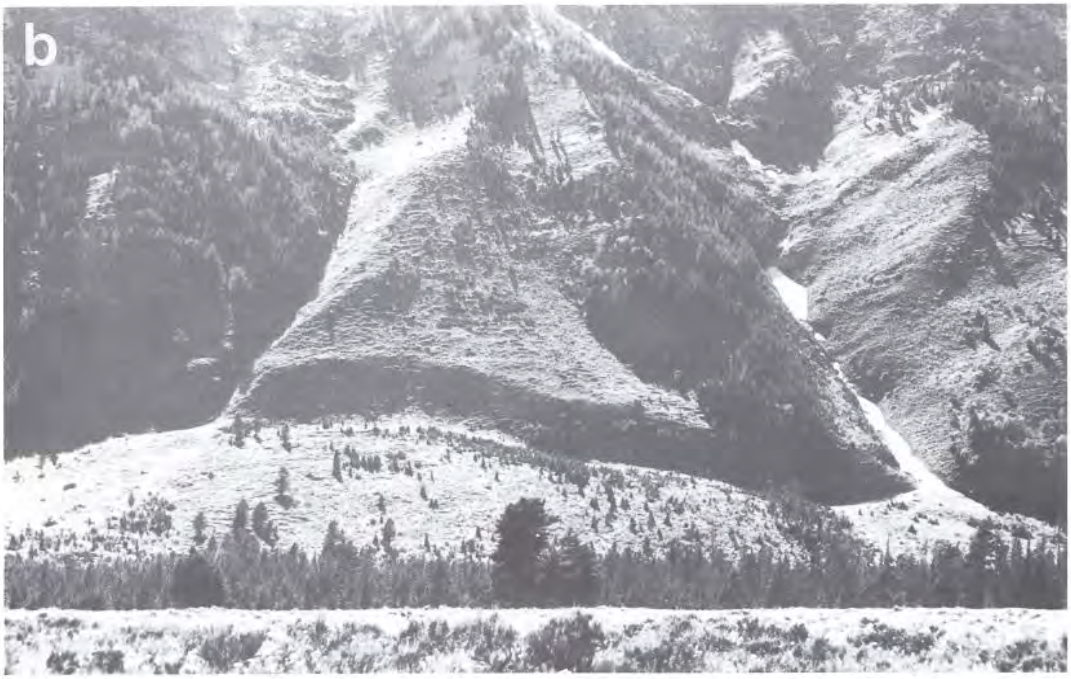

Figure 9. Pictures of post-glacial fault scarps of the Teton fault: (a) aerial view of the scarp west of String Lake between Jenny Lake (left) and Leigh Lake (right side) looking toward the Grand Teton (scarp is near the center of the photo), and (b) closeup view of the String Lake post-glacial fault scarp taken from the Cathedral Group scenic turnout. The String Lake scarp has a height of 34 to 50 m, which corresponds to a surface offset of 22 to 27 m. (Photo 9a by Robert B. Smith, 9b by Don Cushman of the National Park Service.)

corroborates our identification of the fault in that area.

In the central part of the Teton fault, near Taggart Lake, the fault bends approximately 24° clockwise (**Figure 3** and **Sheet 1**, Smith, Byrd, and Susong, map pocket). In this area, offset moraine crests suggest a left-lateral oblique separation of 8 to 26 m. The inferred strike-slip component may account for up to 50% of the slip on the fault in this area. This apparent horizontal displacement may be due to the interaction between the northeast strike of the fault and a predominant east-west sense of dip slip (Ostenaa, 1988). However, it should be noted that the evidence for lateral offset is equivocal given the complex geometry of intersecting nested glacial moraines that obscure the correlation of these features across the fault. We also note the lack of evidence for similar horizontal displacements on the southernmost and northern parts of the fault, where similar glacial features are offset vertically.

Previous workers (Behrendt and others, 1968; Tibbetts and others, 1969; Gilbert and others, 1983) concluded that a splay of the Teton fault extended beneath the west side of Jackson Lake. However, seismic reflection profiles along the west side of Jackson Lake and across Moran Bay (Smith, Pierce, and Wold, this volume) revealed no evidence of significant displacement of Quaternary sediments. This suggests that the scarps we have mapped along the range front west of the lake shore represent the most recent rupture(s) in this area. An alternative explanation may be that the recent faults are not preserved in the incompetent lake-bottom sediments, precluding their identification in the seismic profiles.

Near Steamboat Mountain, north of Jackson Lake, the Teton fault splays into a series of north-northeast-striking faults (**Sheet 1**, Smith, Byrd, and Susong, map pocket). These smaller and discontinuous faults offset Pinedale glacial deposits and the 2.0 Ma Huckleberry Ridge Tuff with both a down-to-the-west and a down-to-the-east sense of offset (**Sheet 1**, Smith, Byrd, and Susong, map pocket). This pattern of fault bifurcation, along with the decreasing magnitude of stratigraphic displacement across the northern end of the Teton fault, suggests that overall displacement is distributed northward onto multiple, right-stepping faults. A possible manifestation of this can be seen in the northeast-stepping pattern of Quaternary normal faults that extend into the southern Yellowstone Plateau (**Figure 2**; Locke and others, 1992).

On the basis of our mapping, the well-preserved, large Quaternary fault scarps at the south end of the Teton fault extend to the vicinity of Phillips Canyon and terminate north of the east-west-striking, Laramide Cache Creek and Jackson thrusts at the south end of the Teton Range (**Figures 2, 3** and **Sheet 1**, Smith, Byrd, and Susong, map pocket). The Teton fault has been postulated to extend south of the town of Wilson by J.D. Love (personal communication, 1988) and Love and others (1992). However, we could not find unequivocal evidence for large Quaternary faults in this area on the basis of reconnaissance mapping. Thus, if the Quaternary expression of the fault extends south of Phillips Canyon, the recent scarps have either been eroded, or the Quaternary displacement on the Teton fault is obscured by river and stream terraces and is not as prominent here as it is observed to the north.

Detailed study areas

We constructed detailed topographic and geologic maps and fault scarp profiles at several locations along the Teton fault using an electronic distance measuring device (EDM) to measure the amount of Quaternary fault offset, scarp morphology, and scarp height. The EDM resolves the height and distance of individual points with a precision of 1 or 2 cm. Locations of these detailed study areas are shown on **Sheet 1** (Smith, Byrd, and Susong, map pocket).

Stewart Draw and Avalanche Canyon

Excellent Quaternary exposures of the Teton fault with an apparent left-lateral component of slip are present at the bottom of Stewart Draw and at the mouth of Avalanche Canyon south of Taggart Lake. At Stewart Draw (**Figure 10**), the Teton fault displaces a moraine crest with up to 26 m of left-lateral and 32 m of vertical slip. An antithetic fault scarp with a 2 m offset marks the east side of a back-tilted graben that extends some hundreds of meters north and south from this location (located off the map in **Figure 10**).

A similar fault geometry was observed at the Avalanche Canyon site (**Figure 11**) where the fault

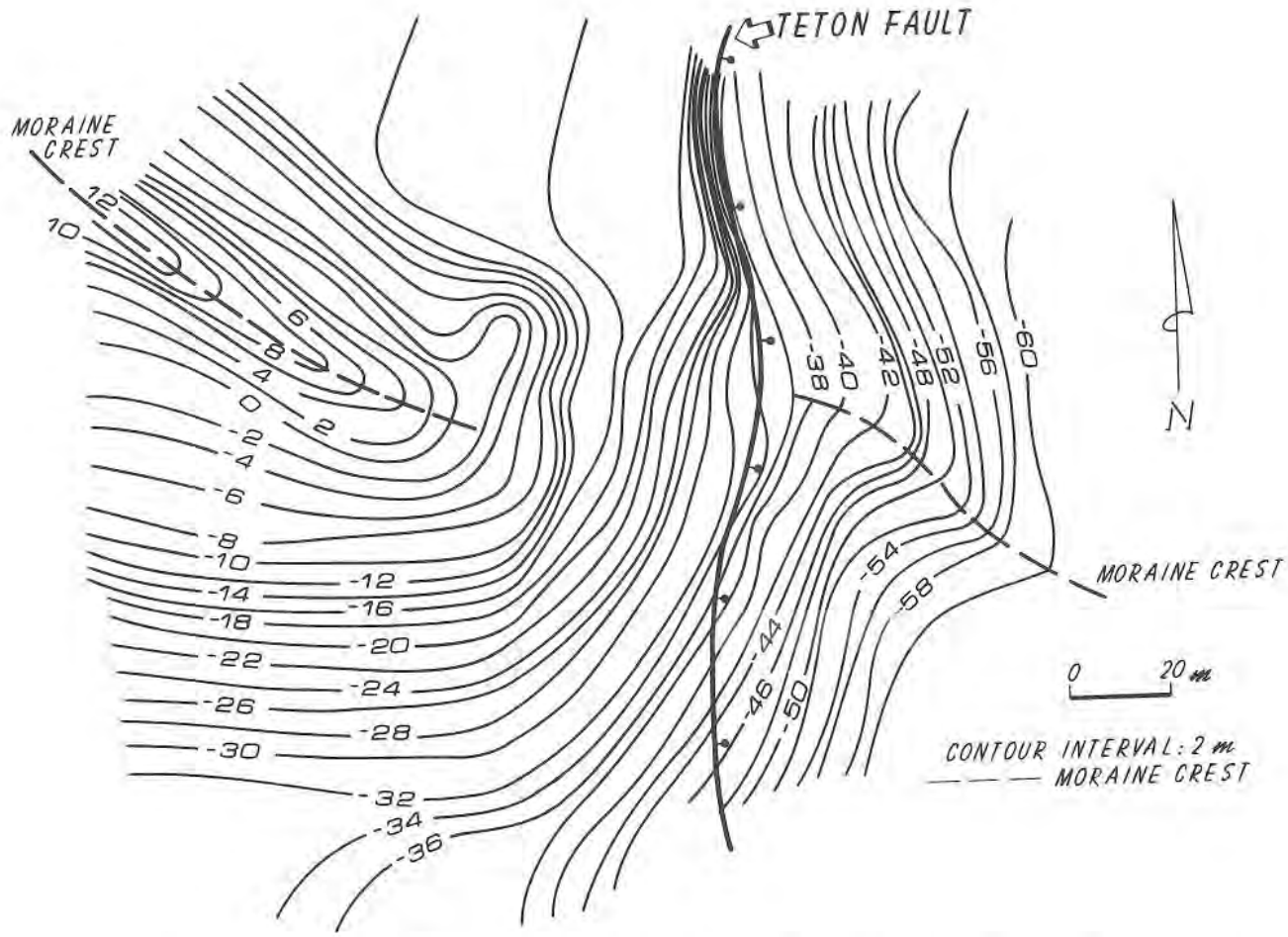

Figure 10. Topographic map of the Teton fault scarp on the south side of Stewart Draw. Location of study site is shown on Sheet 1 (Smith, Byrd, and Susong, map pocket). The Teton fault is shown as a heavy line with downthrown (with ball and bar) block to the east. Left-lateral displacement of 26 m is based on extrapolation of the moraine crest on the upthrown block into the fault trace. Data acquired in 1987 using an EDM.

offsets a moraine crest 8 m vertically and 9 m left-laterally. The two components of displacement suggest a total of 42 m of left-lateral oblique displacement at Stewart Draw, and 12 m at Avalanche Canyon.

We note, however, that the apparent left-lateral displacements exposed in glacial moraines at these locations can be amplified by the geometry of the fault scarps relative to the slopes of the moraine. For example, a component of left-lateral oblique displacement of an east-west trending moraine will produce apparently larger displacements on the north side of the moraine crest and smaller displacements on the south side. For this reason, the scarps appear to be relatively small, 0 to 2 m, on the north (right) side of the Avalanche Canyon lateral moraine. On the south (left) side, scarp heights are as large as 10+ m. As a result, care was exercised in estimating the total Quaternary tectonic offset in these areas of coalescing glacial and topographic features.

Jenny Lake

The Quaternary trace of the Teton fault changes from N10°E, 1 km south of Jenny Lake, to N50°E where it cuts the Pinedale-aged lateral moraine (**Figure 12**). The moraine crest is offset approximately 16 m vertically across the fault. The fault trace turns back to a N10°E strike about 1/2 km north, where it intersects the west shore of Jenny Lake (**Sheet 1**, Smith, Byrd, and Susong, map pocket). This relatively abrupt change in fault strike corresponds to a 350 m eastward step in the fault trace that also coin-

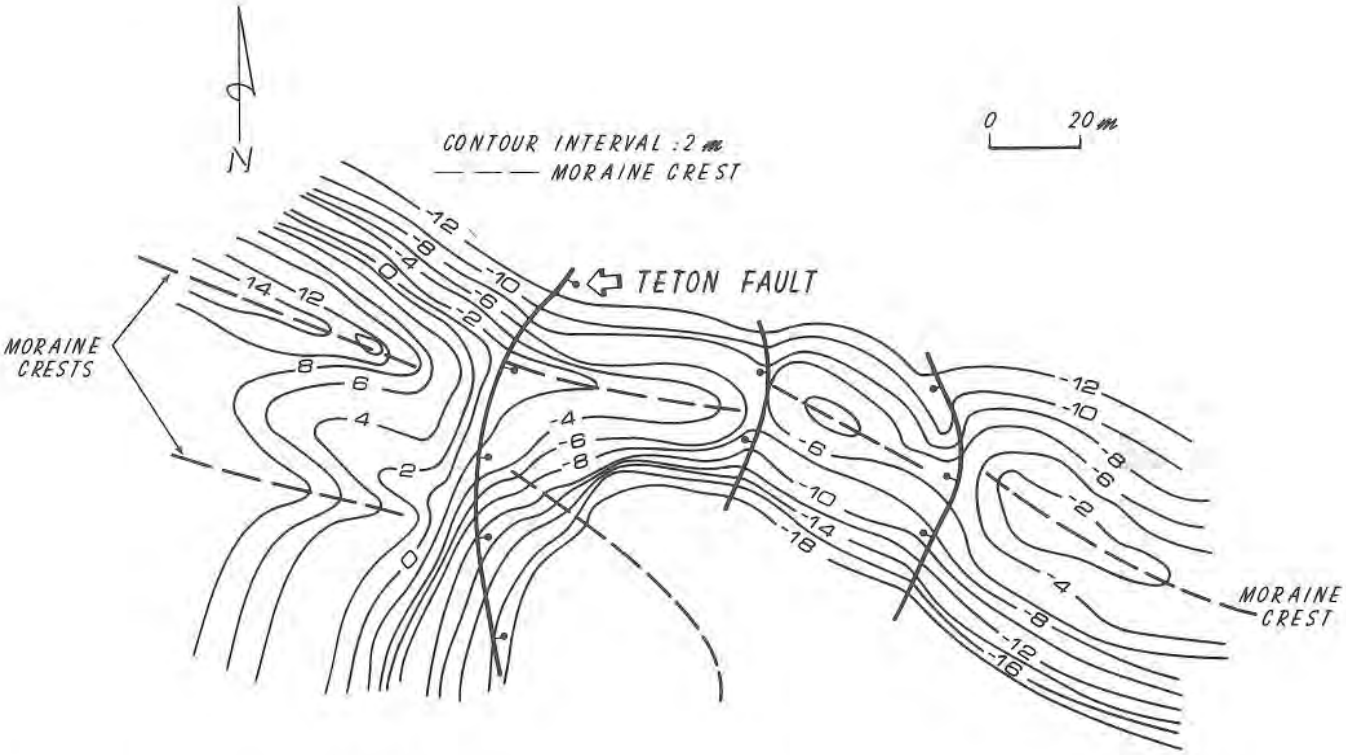

Figure 11. Topographic map of the Teton fault scarp on the south side of the mouth of Avalanche Canyon. Location of study site is shown on Sheet 1 (Smith, Byrd, and Susong, map pocket). Teton fault and antithetic fault are shown in heavy line with ball and bar on downthrown block. Interpreted left-lateral displacement of 9 m is based on extrapolation of the trace of the moraine crests on the upthrown block into the fault trace. Data acquired in 1987 using an EDM.

cides with a marked increase in the thickness of surficial glacial deposits. Extrapolation of a predominantly east-west-trending normal-slip vector onto the fault implies a left-lateral sense-of-slip for the N 50° E striking portion of the fault. Unfortunately, the complex anastomosing pattern of nested moraines precludes an unequivocal identification of horizontal displacement in the south Jenny Lake moraine.

Lateral variations of scarp height and offset

Seventeen elevation profiles of Quaternary scarps along the Teton fault were surveyed with an EDM to determine scarp heights and surface offsets. Geologists of the U.S. Bureau of Reclamation (Gilbert, and others, 1983) measured eight additional scarp profiles using a Jacobs staff and inclinometer. These data are summarized in **Table 1** with profile locations shown on **Sheet 1** (Smith, Byrd, and Susong, map pocket).

Scarp profile locations were selected to evaluate sites representative of Quaternary faulting. Fault scarps modified by slumping or gullies were not profiled. Surface deposits along the profiles consisted of glacial till, alluvium, and colluvium with sand- to boulder-sized clasts. Measured scarp-slope angles range from 14° to 40° with the steeper slopes at or near the angle of repose for the bouldery deposits.

In our analysis of the fault scarp profiles, we employed the definitions of scarp height and surface offset by Bucknam and Anderson (1979). Scarp height is defined as the vertical height of the scarp measured from the toe to the top of the scarp. Surface offset is generally defined as the vertical offset across the fault between the tectonically undeformed footwall and hanging-wall slopes (**Figure 13**), but we modified the definition to be the measured offset determined by projecting the hanging-wall slope to the top of the scarp. In the absence of trench data, the

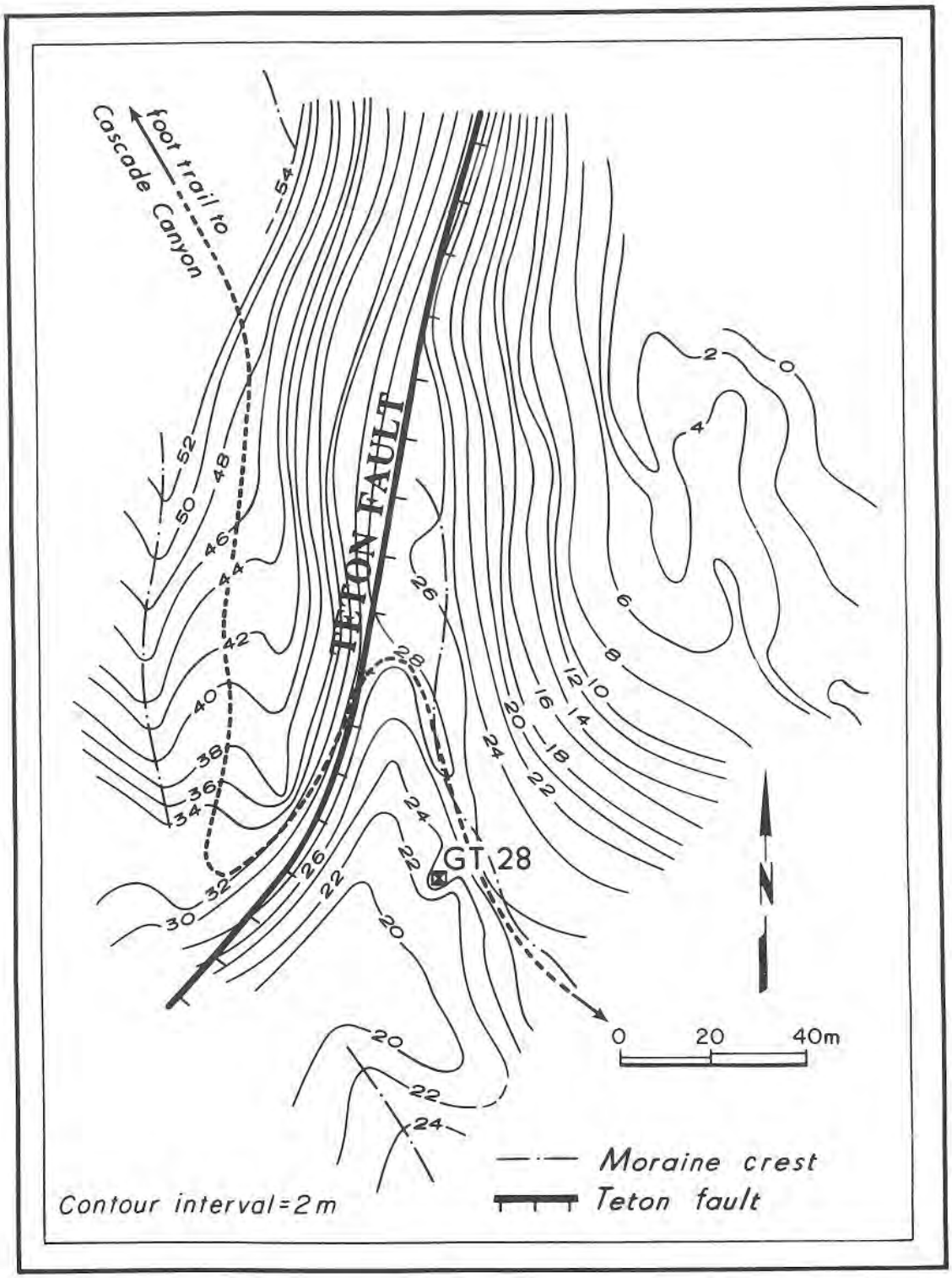

Figure 12. Topographic map of the Teton fault at the south Jenny Lake moraine. Location of study site is shown on Sheet 1 (Smith, Byrd, and Susong,map pocket). Teton fault is shown in heavy line with hachures, downthrown block is to the east. Data acquired in 1989 using an EDM. GT28 corresponds to a leveling benchmark in Figure 19.

surface offset is considered the best measure of the fault slip since it does not include the apparent displacement due to rotation of the footwall or hanging-wall surface into the fault. Calculation of surface offset assumes that the footwall and hanging-wall slopes were continuous prior to faulting, or that the slope angles were known prior to the most recent ground-rupturing event. If surficial deposits are moved from the footwall to the hanging wall and no erosion takes place in the hanging wall adjacent to the original fault scarp, then the scarp degradation effectively decreases the amount of tectonic displacement that can be measured in the field. As a result, our estimates of tectonic displacement from surface offset data are considered to define the minimum.

Measured Quaternary scarp heights along the Teton fault (**Figure 14**) range from 3.6 m to 50 m and surface offsets range from 3 m to 28 m (**Table 1**). Based on these data, the average surface offset appears to increase from 10 to 13 m (18.6 m maximum) in the southern section of the fault to about 20 m (28.4 m maximum) in the middle section (**Figure 14**). Insufficient data preclude estimation of average surface offsets for the northern part of the fault.

The south-to-north variations in Quaternary surface offset along the Teton fault generally coincide with lateral variations in average topographic relief along the crest of the Teton Range (**Figure 14**) and suggest a causal relationship between the areas of

Table 1. Morphologic properties of Quaternary scarps of the Teton fault. Scarp topography determined by EDM for our study and by hand level for the results of Gilbert and others (1983). Profile number corresponds to profile locations on Sheet 1.

Profile name	No.	Scarp height (m)[1]	Surface offset (m)[2]	Surface offset (m)[3]	Scarp slope angle (°)[1]
		Southern segment			
Granite Canyon	trench	3.6	3.0		14 - 21
Granite Canyon	11	12.7 - 14.0	10.9- 12.6		15 - 35
Granite Canyon	12	10.4 - 11.0	9.8 - 10.1	11.3	25 - 36
Teton Village	13	12.2 - 48.5	10.8 - 18.6	7.3- 7.9	28 - 35
Teton Village	14	26 - 36	13.6 - 15.5		28 - 35
Average			**13**		
		Middle segment			
Lupine Meadows	1	19 - 25	13.0 - 19.3	>10.7	32 - 38
Lupine Meadows	2	25.0	18.4 - 25.4		30 - 38
Burned Wagon Gulch	3	9.2 - 12.4	7.6 - 9.3		26 - 29
Avalanche Canyon	—	5.2 - 7.9		5.2- 7.0	26 - 27
Bradley Lake	4	15.0	9.2 - 14.0		25 - 34
Bradley Lake	5	11.3 -14	10.7 - 11.2		16 - 34
Taggart Lake	6	22.0	17.5 -19.4		25 - 38
Taggart Lake	7	17.3 - 22	11.0 - 13.0	11.6	19 - 30
Taggart Lake	8	12 - 29	12.5 - 14.8	12.2	24 - 33
Beaver Creek	9	17.0 - 22	8.7 - 12.9		30
String Lake	10	34.4 - 50.0	22.0 - 26.6	19.2	27 - 40
Trapper Lake	15	30.2 - 47.8	23.4 -28.4	23.8[1]	26 - 32
Moran Bay	17	14.0 - 14.5	10.3 - 11.9		31 - 33
Average			**15**		
		Northern segment			
Colter Canyon	16	20.8	11.0 - 18.2		22 - 29
Wilcox Point	Estim.	4.5 - 12.0			

[1]Range of values reflects data from this study and that of Gilbert and others (1983).
[2]Surface offsets were calculated by projecting the hanging-wall slope to the top of the scarp.
[3]Data from Gilbert and others (1983).

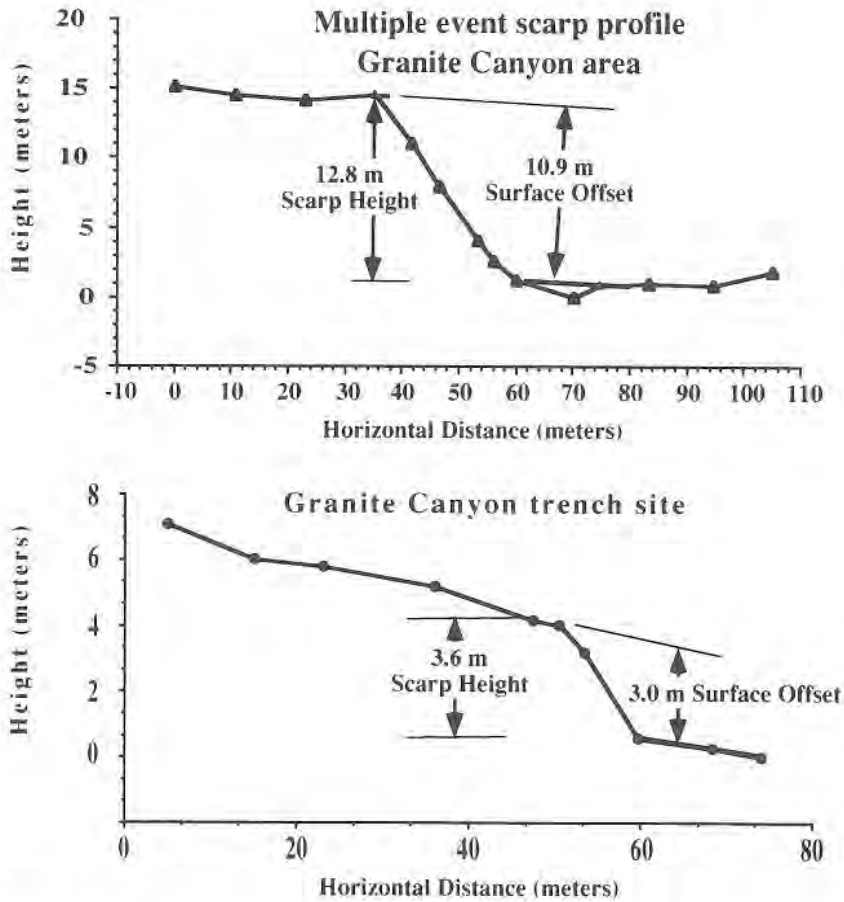

Figure 13. Topographic profiles of Quaternary fault scarps at the mouth of Granite Canyon: (a) multiple-event scarp approximately 120 m north of the trench site; and (b) scarp profile at the trench site.

highest topography and the areas of greatest Quaternary fault displacement. Fryxell (1938a) first noted that the area of highest topographic relief along the central part of the Teton Range does not coincide directly with the north-south-trending drainage boundary of the range. It is displaced approximately 3 to 4 km east of the drainage divide where it is marked by the highest peaks, e.g., Grand Teton, South and Middle Tetons, Mt. Moran, etc. (**Sheet 1,** Smith, Byrd, and Susong, map pocket). This systematic, eastward uplift of the highest topography of the Teton Range is consistent with concomitant uplift and westward tilt of the range at rates that exceed those of erosion.

Fault segmentation

Correlation of surface ruptures associated with a single earthquake and individual segments of normal faults forms the basis for the "characteristic earthquake model" proposed by Schwartz and Coppersmith (1984). Therefore, identification of individual fault segments can provide a general guideline for evaluating the seismogenic capacity of a fault zone. Schwartz and Coppersmith (1984) and Machette and others (1991) have suggested a number of criteria for identification of fault segmentation, such as extent of similar aged faulting, changes in fault trend, changes in range topography, lateral variations in fault strike and footwall structures, and

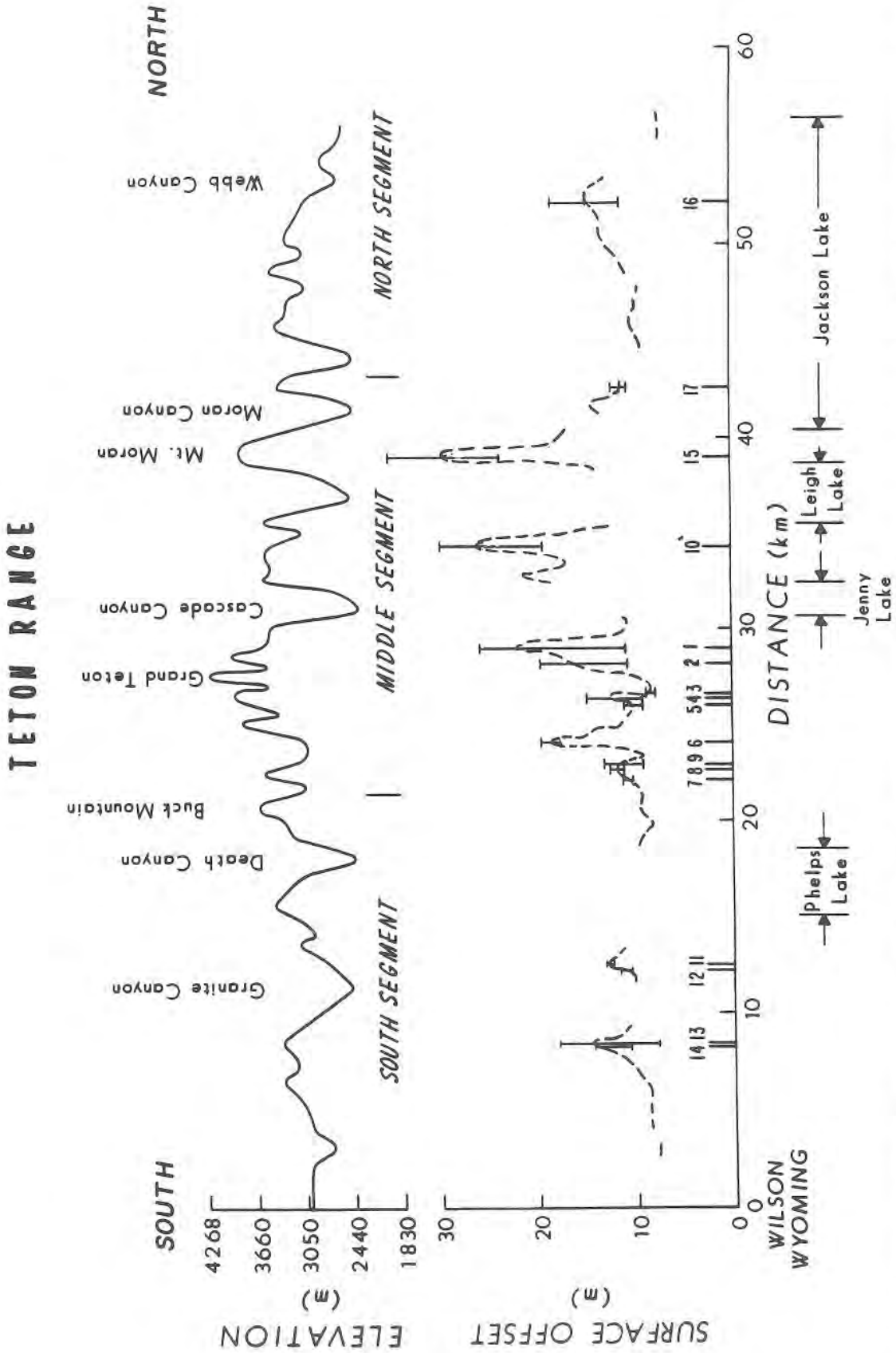

Figure 14. Lateral variation of Quaternary surface offsets of the Teton fault and averaged maximum elevation on the adjacent Teton Range. Vertical lines = locations of detailed scarp profiles. Numbers correspond to scarp profile locations shown on Sheet 1 (Smith, Byrd, and Susong, map pocket) and detailed information is given in Table 1. Fault offsets dashed where inferred.

variations in hanging-wall geometry interpreted from gravity anomalies. Using the above criteria, we suggest that the Quaternary expression of the Teton fault is made up of two and possibly three fault segments (**Figure 3**).

The southern segment begins 5 km south of Teton Village and extends north for approximately 20 km to the vicinity of Taggart Lake (**Figure 3** and **Sheet 1**, Smith, Byrd, and Susong, map pocket). The general strike of the southern segment is N20°E and the surface offsets averages 13 m. The highest topography in this area of the Teton Range is about 3,000 m. The identification of a separate middle segment is somewhat problematical. However, variations of surface offset, fault strike, footwall topography, and gravity anomalies in the hanging-wall block suggest that a separate segment extends about 22 km from Taggart Lake north to Moran Bay (**Figure 3** and **Sheet 1**, Smith, Byrd, and Susong, map pocket). This segment has the largest surface offsets and its boundary with the southern segment is marked by a change in strike from N24°E to almost north-south, north of Taggart Lake. The middle section of the Teton fault also corresponds to the area of highest topography of the Teton Range that ranges from 3,810 m to 4,200 m and averages ~ 3,500 m compared to < ~3,000 m to the north and south. We also note that the best evidence for a component of left-lateral displacement at Avalanche Canyon and Stewart Draw is in this area, but we cannot definitely attribute this observation to a kinematic property of the faulting.

The boundary between the southern and middle segments is further suggested by the location of the southern end of a large negative Bouguer gravity anomaly (**Figure 15**) located at the boundary between two alluvial-filled sedimentary basins beneath Jack-

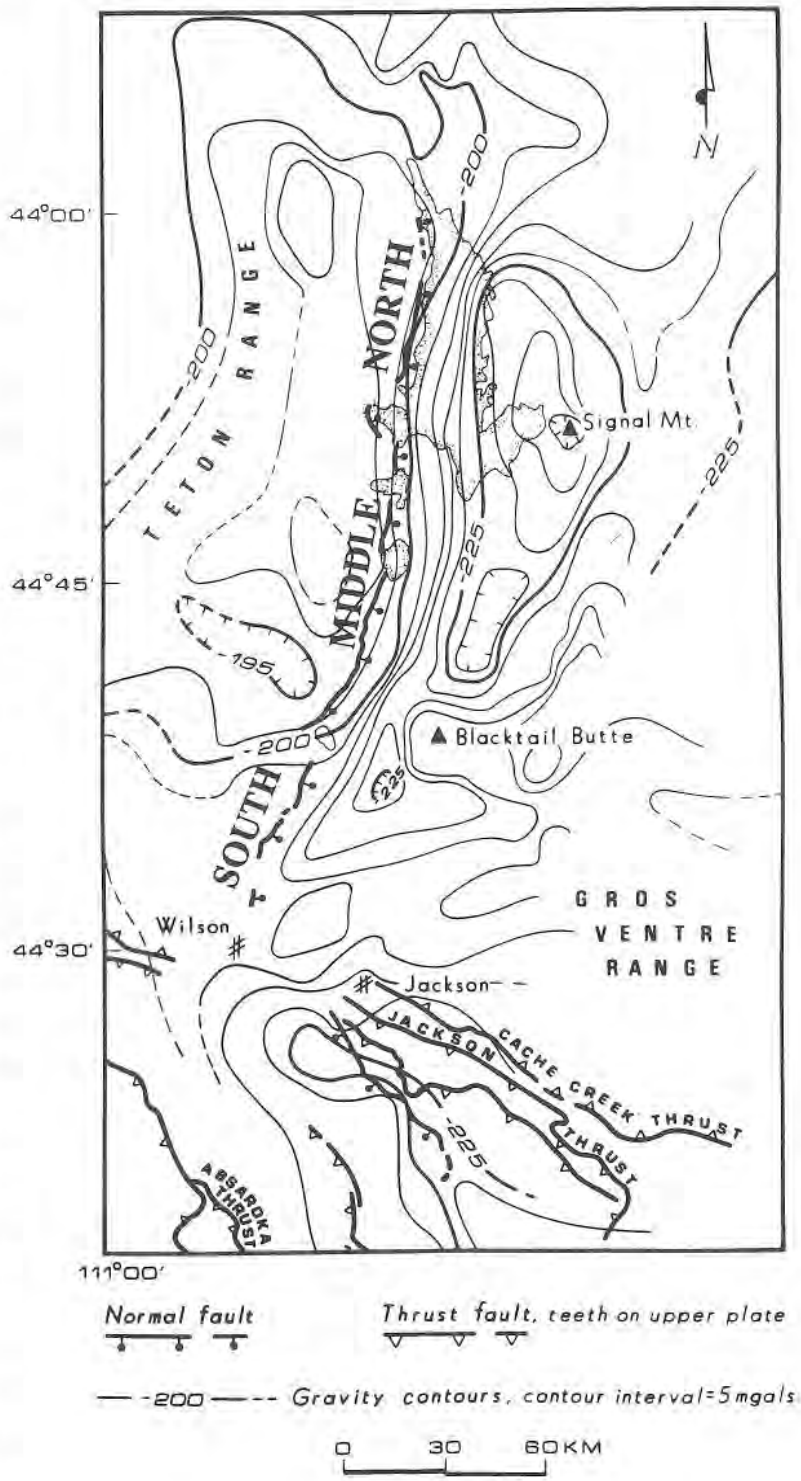

Figure 15. Complete Bouguer gravity map of the Jackson Hole region showing the Teton fault and proposed fault segments (gravity map modified from Behrendt and others, 1968).

son Hole (Behrendt and others, 1968). We ascribe the east-west gravity gradient to shallowing of high-density footwall basement rocks beneath the valley coincident with the eastward projection of the segment boundary.

On the basis of interpreted slip directions of the Teton fault, Ostenaa (1988) concluded that the change in fault strike and the presence of the gravity high in this area do not necessarily indicate the existence of a segment boundary. In his interpretation, the southern and middle segments represent a single, 42 km-long segment. This is a reasonable interpretation, especially if one considers that the 1.3- and 2.8-m most recent surface displacements (Byrd, 1991), such as those exposed in the Granite Canyon trench (discussed in a later section), generally correspond to surface ruptures that extend 30 km or more and are expected to be associated with magnitude 7+ earthquakes (Mason and Smith, 1990; de Polo and others, 1991).

The boundary between the northern and middle segments of the Teton fault (**Figure 3**) is located on the north side of Moran Bay where the middle segment terminates against Precambrian footwall rocks (also see **Sheet 1**, Smith, Byrd, and Susong, map pocket). The northern segment then steps 1.5 km eastward and extends 13 km northward from the north side of Moran Bay along the west side of Jackson Lake to Wilcox Point (**Figure 3** and **Sheet 1**, Smith, Byrd, and Susong, map pocket). North of Wilcox Point, the fault extends beneath the northernmost end of Jackson Lake and the Snake River delta, reemerging east of the lake as the series of N10°E striking faults in the Steamboat Mountain area. Other branches of the fault may extend north-northwest along the Snake River and the northern base of the Teton Range to the boundary of Yellowstone National Park. Evidence of surface displacements along these splays has not been identified by reconnaissance mapping of this area by the U.S. Bureau of Reclamation (Dean Ostenaa, personal communication, 1990).

The implication of the contrasting segmentation models, i.e., two versus three fault segments, is particularly important for assessing the expected size of future earthquakes on the Teton fault. As a result, we include both two- and three-segment models in subsequent discussions of future earthquakes.

Dating Quaternary displacements on the Teton fault

Preliminary results from trenching

Stratigraphic interpretation of trench exposures of active faults can provide definitive data on the age and magnitude of surface displacements and hence on the recurrence intervals of prehistoric earthquakes. To acquire this information, a small trench was excavated across a 3.6 m fault scarp at the mouth of Granite Canyon near the southern end of the Teton fault (see **Figure 3** and **Sheet 1**, Smith, Byrd, and Susong, map pocket, for location). Details of the trench are not given here because this aspect is the focus of an on-going study. However, we summarize the initial findings from the trenching given by Byrd and Smith (1990a,b, 1991) and Byrd (1991).

The Granite Canyon trench exposed fluvial and debris flow deposits overlying Pinedale glacial till that were offset 4.1 m down-to-the-east on an 85°E dipping fault plane (Byrd and Smith, 1990b, 1991; Byrd, 1991). The estimated offset is based on correlation of fining-upward fluvial deposits capped by a 2 to 6 cm-thick floodplain deposit exposed in the hanging-wall and footwall blocks. Westward back tilt of ~ 3° was observed in the hanging-wall block, whereas units in the footwall block exhibited an average 2° east depositional slope. Subtracting the 5° of back tilt in the hanging-wall units yields a net tectonic displacement of 4 m.

Two charcoal samples collected from the base of the colluvial wedge overlying the floodplain deposit and from the base of the floodplain deposit yielded radiocarbon ages of 7,150 ± 120 years and 7,240 ± 190 years, respectively (Byrd and Smith, 1990a). We believe that these samples represent the same burn event due to the overlap of the standard deviations of calculated ages, the inferred rapid deposition of the floodplain deposit, and the 150-year to 250-year recurrence of major forest fires (Peter Hayden, personal communication, 1991) in this region. The average of the two samples is 7,175 ± 100 radiocarbon years and conversion of radiocarbon years to calendar years (Stuiver and Reimer, 1986) gives a calendar

age of 7,980 ± 210 years (we refer to radiocarbon ages to be consistent with previous citations of the age of Pinedale glaciation by other workers). This averaged age represents the maximum calendar age for a single faulting event exposed in the trench.

We note from the recent analyses of Byrd and Smith (1990a,b) and Byrd (1991) that it is quite probable that the 4.1 m displacement is the product of two prehistoric slip events. If a younger event contributed to the displacement, the total tectonic displacement could be divided into a 2.8 m offset associated with the oldest, (7,175 year) event and 1.3 m offset accompanying a younger slip. Additional radiocarbon dating is being done to assess the ages of faulting for this Holocene, multiple-event scenario.

Dendochronological dating of the Teton fault

Attempts to determine the age of the most recent faulting on the Teton fault using dendochronologic techniques were made by Gordon Jacoby of Lamont Doherty Geological Observatory, Columbia University in 1987, who concluded that the oldest trees he sampled along or on the Quaternary scarps in the middle and southern parts of the Teton fault were about the same age (approximately 130 years old). We suspect that large forest fires between 1840 and 1890 (Loope and Gruell, 1973) destroyed most older trees along the Teton Range front, thereby precluding the use of dendochronology to estimate the age of faulting before that time.

Slip rates and earthquake recurrence intervals for the Teton fault

Comparison of long-term rates of displacement with point samples of single or multiple prehistoric earthquakes can often be misleading. Large errors in the magnitude of displacement and time intervals, short-term fluctuations from an "average rate", and a lack of multiple prehistoric events can contribute to misinterpretations of short-term versus long-term deformation rates. As a result, comparisons of long-term (13 to 9 Ma), Quaternary (2 Ma), and post-glacial (14 ka) displacement rates should be made with caution, especially with regard to evaluating the contemporary earthquake capability of the fault.

Estimates of post-glacial displacement rates are based on a single slip-event scenario at the Granite Creek trench and an extrapolation of the surface offset to the multiple-event, 12.8 m-high fault scarps (**Figure 13**) exposed in Pinedale glacial deposits 120 m to the north. As a result, these are estimates of post-glacial surface offset rates and should be considered as conservative. A 3 m surface offset is associated with the 3.6 m scarp at the Granite Canyon site (**Figure 13**). Subtracting this surface offset from the 10.9 m offset on the larger scarps, and assuming a 14,000 year age for the cessation of Pinedale glaciation (Porter and others, 1983), results in an average 1.6 mm/yr surface-offset rate and an estimated recurrence interval of 1,650 years (**Figure 16**). This estimate assumes the 7,175 ± 100-year event is the youngest on this portion of the fault and the displacement and surface offset is the same at the trench site as on the adjacent larger scarps. However, for the Holocene two-event scenario, the younger but undated slip event will decrease the 14,000 to 7,175 yr surface offset rate (Byrd and Smith, 1990b). A lower slip rate is implied if one assumes an average of 30,000 years for the end of Pinedale glaciation (Pierce and others, 1976). In this scenario, a lower slip rate of 0.45 mm/yr is implied with a recurrence interval of approximation 6,000 years for four equivalent M_S=7+ postulated events (**Figure 16**).

Estimates of Quaternary displacement rates for the Teton fault were also made on the basis of a projection of the 2.0 Ma old Huckleberry Ridge Tuff into the postulated location of the fault (Gilbert and others, 1983; Smith, Pierce, and Wold, this volume). Gilbert and others (1983) compared the elevations of the westward-dipping exposures of the Huckleberry Ridge Tuff exposed on Signal Mountain, 12 km east of the Teton fault (**Figure 4**), to the highest elevation of the tuff on the west side of the Teton Range and proposed a 2.8 km offset. Smith, Pierce, and Wold (this volume) and Gilbert and others (1983) projected the location of the Huckleberry Ridge Tuff from exposures east and north of Jackson Lake to suggest an estimated offset of 2.5 ± 0.4 km. The average Quaternary displacement rates corresponding to these projected offsets are estimated in the range of 1.0 to 1.4 mm/yr (**Figure 16**). However, the magnitude of

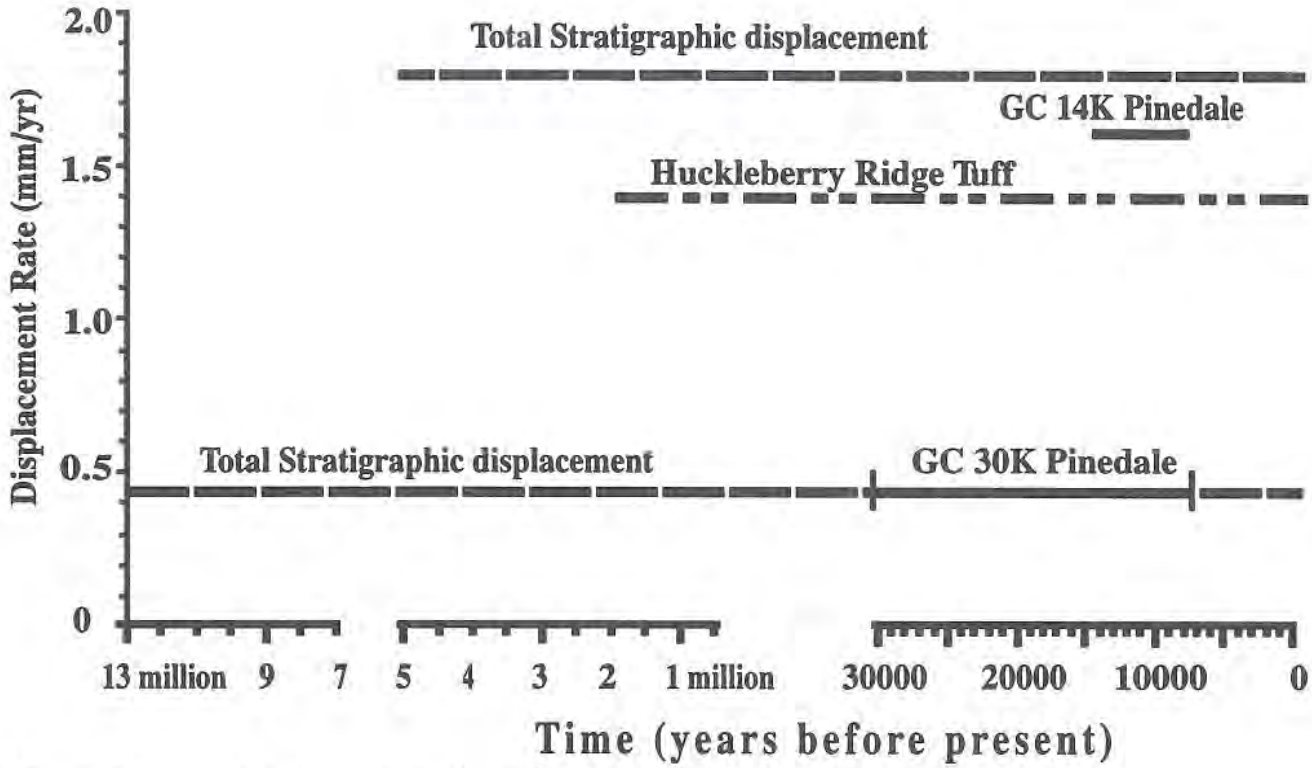

Figure 16. Estimated displacement rates for the Teton fault. The two different total stratigraphic displacement rates reflect maximum and minimum estimates based on 5 Ma (Love, 1977) to 13 Ma (Barnosky, 1984) and 6 km to 9 km stratigraphic separation across the Teton fault. Huckleberry Ridge Tuff rates are from Gilbert and others (1983) and Smith and others (this volume). GC 14K Pinedale (14 ka) and GC 30K Pinedale (30 ka) are youngest and oldest ages of glacial deposits and a single faulting event resulting in 4.0 m surface offset at Granite Canyon trench site.

westward tilting of Signal Mountain caused by possible movement on a small normal fault east of Signal Mountain (Gilbert and others, 1983) is not known or included in these estimates; therefore, the offsets and resulting displacement rates are considered maximum values.

Initial estimates of recurrence intervals for large $7.0 < M_s < 7.5$ earthquakes on the Teton fault were made by Gilbert and others (1983), who suggested a range from 700 to 2,000 years with an average interval of 1,400 years. These estimates were based on comparisons of measured surface offsets on the Teton fault with observations from historic earthquakes in the Intermountain region. Doser and Smith (1983) estimated a recurrence interval of 800 to 1,800 years for an $M_s = 7.5$ event on the Teton fault using the summation of seismic moments of historical earthquakes. These estimates span the 1,650-year return rate suggested from our trenching study.

If one extrapolates the 0.45-mm/yr and 1.6-mm/yr slip rates from 7,175 ± 100 years to the present, then the southern segment of the Teton fault has accumulated a "slip deficit" from 3.2 m to 14 m, respectively. The lower estimate of a 0.45-mm/yr slip rate implies that the Teton fault may be accumulating stress at a "normal rate" because the 3.2-m slip deficit is comparable to the surface displacements accompanying M_s =7.2+ normal-faulting earthquakes (Bonilla and others, 1984; Mason and Smith, 1990; de Polo and others, 1991). The higher 1.6-mm/yr slip rate suggests that the southern part of the fault has already stored sufficient energy for an $M_s \sim 7.2+$ earthquake. An earthquake of this magnitude, however, would rupture most if not all the Quaternary trace of the Teton fault. Note that there is no other information on Holocene slip rates for the middle and northern segments of the fault, thus precluding a definitive determination of the Holocene slip rates and recurrence intervals for the entire Teton fault.

Ground deformation associated with the Teton fault

Subsidence and asymmetric tilt of the hanging-wall block is a significant component of the co-seismic ground deformation associated with large, scarp-forming normal-faulting earthquakes (**Figure 17**). These phenomena have been observed with three historic earthquakes: (1) M_s=6.8 Dixie Valley, Nevada (Slemmons, 1957; Snay and others, 1985); (2) M_s=7.3, Borah Peak, Idaho (Stein and Barrientos, 1985); and (3) M_s=7.5, Hebgen Lake, Montana (Myers and Hamilton, 1964; Savage and Hastie, 1966). These large normal-faulting earthquakes demonstrated relatively small (generally less than 15%) footwall uplift compared to substantial hanging-wall subsidence and asymmetric tilt of adjacent valleys (**Figure 17**).

Co-seismic ground deformation associated with normal faulting has also been modeled theoretically by King and others (1988). In their boundary-element model, a 45°-dipping normal fault was simulated in a 16 km-thick elastic half-space with an underlying fluid layer (**Figure 18**) and 1 m dip-slip displacement along the entire fault corresponding to an M_s = 7.1 earthquake. The results of King and others (1988) modeling show that the theoretical ratio of hanging-wall subsidence to footwall uplift is about 4:1, which is similar to that observed with large historic normal-faulting earthquakes (**Figure 17**). If this ratio is typical for large normal faults, then we can assume that deformations accompanying prehistoric earthquakes along the Teton fault have had a greater component of hanging-wall valley subsidence than footwall uplift.

In southern Jackson Hole, an area of anomalous down-to-the west tilt and subsidence of the ground

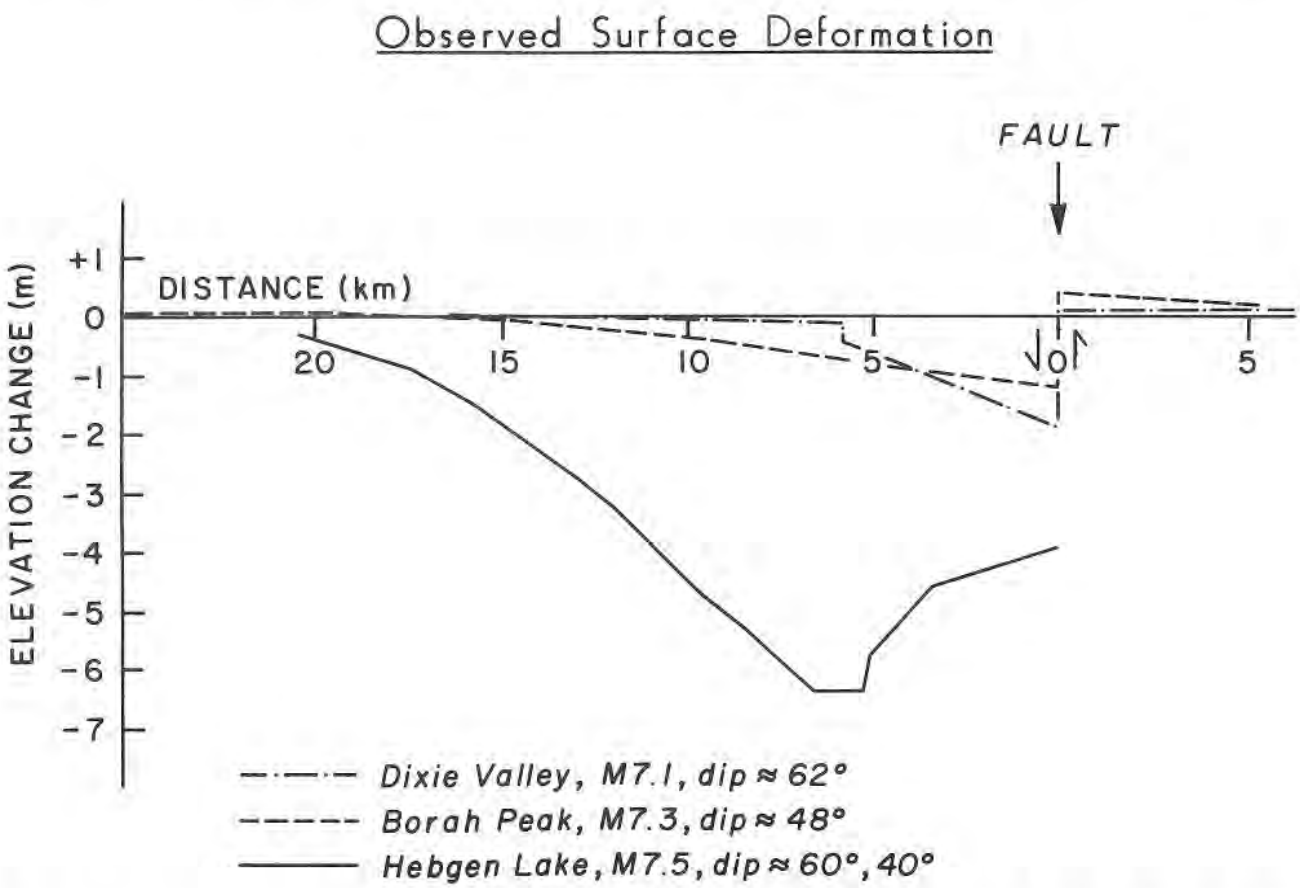

Figure 17. Co-seismic, vertical ground deformation accompanying three large, scarp-forming Basin and Range province earthquakes: (1) M_s = 6.8, 1954, Dixie Valley, Nevada (Slemmons, 1957; Snay and others, 1985); (2) M_s = 7.5, 1959, Hebgen Lake, Montana (Savage and Hastie, 1966); and (3) M_s = 7.3, 1983, Borah Peak, Idaho (Stein and Barrientos, 1985).

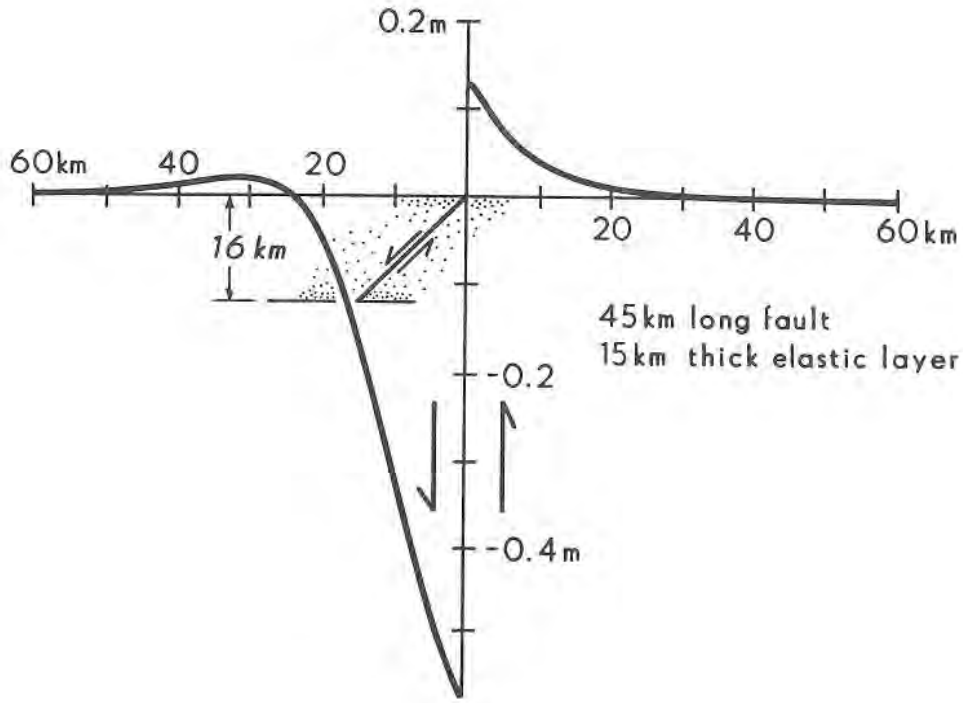

Figure 18. Theoretical ground deformation produced by a large, normal-faulting earthquake from boundary element modeling of the free surface, assuming a co-seismic displacement of 1 m on a 45°-dipping normal fault (from King and others, 1988).

surface (**Figure 19**) was reported by Love and Montagne (1956) and is similar to that shown in **Figures 17** and **18**. Using an altimeter to measure elevations, they documented this unusual topography extending from the Teton fault a few kilometers eastward across the valley floor (**Figure 19**). Their topographic profiles were constructed beginning on the north from Lupine Meadows, extending south to the vicinity of the town of Wilson (general location shown on **Figure 3**). While altimetry is not as precise as geodetic leveling, it is usually accurate to a few meters over tens of kilometers of profile length and is considered sufficiently accurate to resolve large-scale variations in height. It should be noted that Love and Montagne (1956) postulated prehistoric earthquakes accounted for this anomalous pattern of ground deformation. Their observations were made several years before the general style of hanging-wall subsidence associated with normal faulting was known as an important kinematic property of large, scarp-forming earthquakes in the Basin and Range province.

Streams emanating from the Teton Range would normally be expected to flow directly eastward to the Snake River (**Sheet 1**, Smith, Byrd, and Susong, map pocket). However, the topographic depression documented by Love and Montagne (1956) apparently influences streams flowing from the range south of Phelps Lake to turn south, parallel to the Snake River. Range-front capture of streams south of Leigh Lake to the vicinity of Taggart Lake provides evidence for topographic depression along the Teton fault in this area. This area of subsidence was revealed by a detailed topographic profile, constructed from a 1st-order level line across the valley of Jackson Hole (see **Figure 19** and discussion in the next section), which reveals up to 26 m of subsidence (Byrd and others, 1988). We suspect this topographic depression may also reflect, in part, tectonic deformation (hanging-wall subsidence) associated with prehistoric scarp-forming earthquakes on the fault. Other interpretations include an apparent westward tilt of the valley resulting from a westward flow along preexisting stream drainages emanating from the terminal moraines near Jackson Lake or aggradation of sediments deposited by the Snake and Gros Ventre Rivers. However, we agree with Love and Montagne (1956) that the juxtaposition of the westward-tilted valley block against the Teton fault is in part associated with large prehistoric earthquakes on the Teton fault.

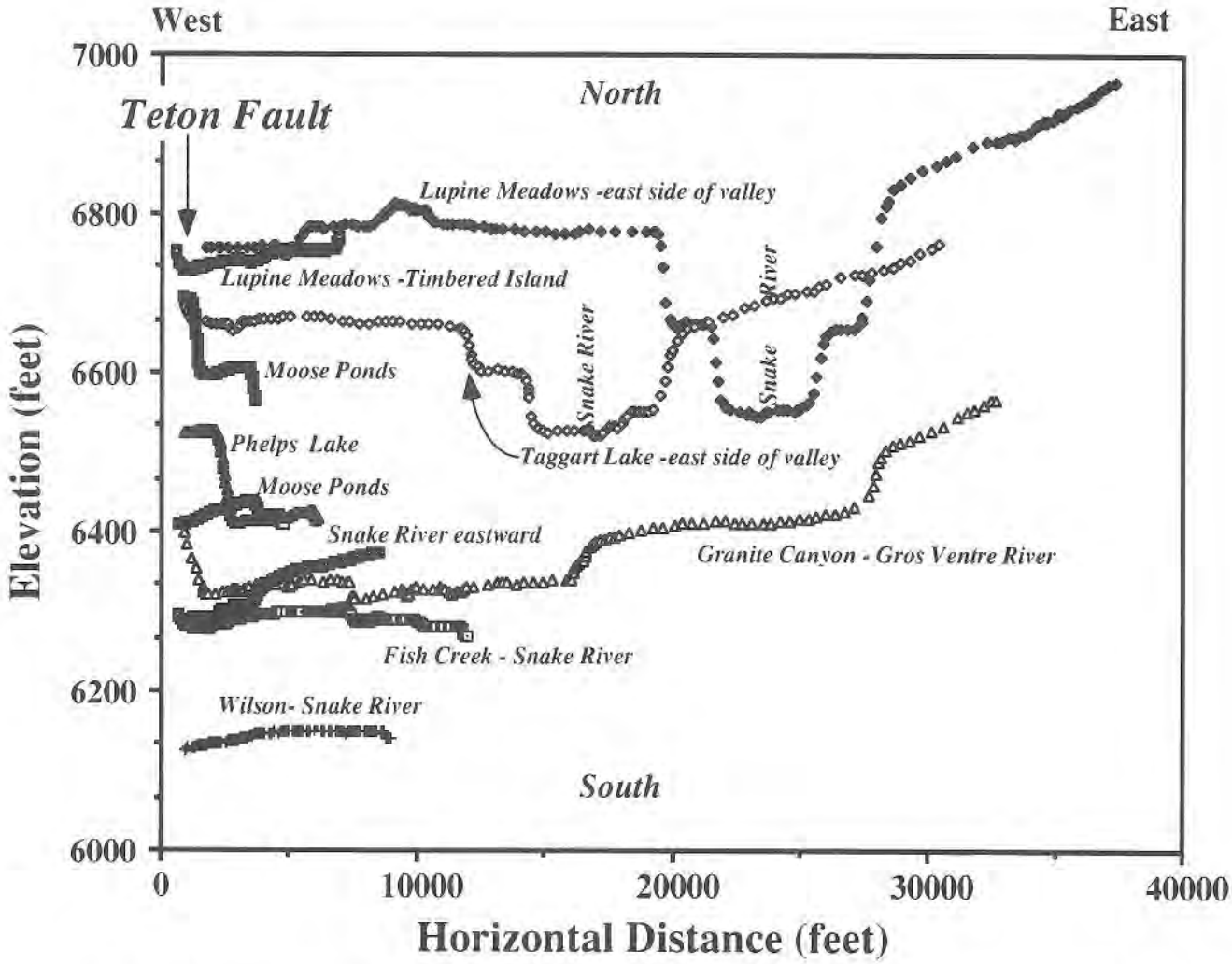

Figure 19. Topographic profiles across the floor of Jackson Hole, east of the Teton fault. Elevation data were digitized from altimeter profiles acquired by Love and Montagne (1956). Individual symbols indicate digitization points, not spacing of original altimeter readings. Heights are in feet above sea level. See Sheet 1 (Smith, Byrd, and Susong, map pocket) for geographic locations.

Contemporary deformation of the Teton fault

In a cooperative project between Professor Arthur G. Sylvester of the University of California, Santa Barbara, and the University of Utah, an east-west line of permanent benchmarks across the Teton fault was established in 1988 (Byrd and others, 1988). These marks were precisely surveyed in 1988, 1989 (Sylvester and others, 1991), and 1991. The level line was established to assess possible contemporary deformation and to provide a long-term reference frame for neotectonic studies of the Teton fault (**Figure 20** and **Sheet 1**, Smith, Byrd, and Susong, map pocket). Only the 1988-1989 leveling data are discussed here as the analyses of the 1991 data are in progress.

The Teton leveling profile is 22.1 km long and consists of 50 permanent benchmarks at approximately 500 m intervals (**Figure 20** and **Sheet 1**, Smith, Byrd, and Susong, map pocket). The west end of the level line begins well within the footwall block of the Teton fault, near the center of the Teton Range in Cascade Canyon (**Sheet 1**, Smith, Byrd, and

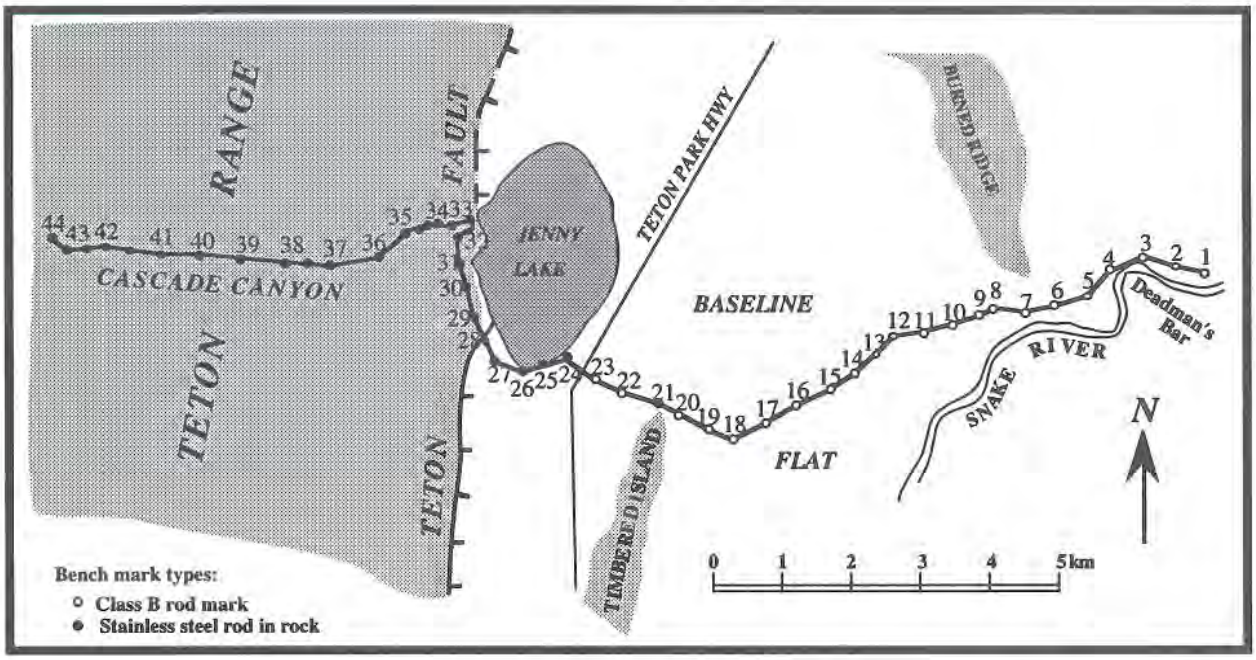

Figure 20. Map of Teton fault 1st-order level line from Cascade Canyon to Deadman's Bar (after Sylvester and others, 1991; Byrd and others, 1988). Benchmarks GT-1, 12, 24, 35 and 37 were observed using GPS (Global Positioning Satellite) receivers and will be reoccupied for future measurements of deformation.

Susong, map pocket). It extends eastward and crosses the Teton fault west of Jenny Lake and continues around the north end of Timbered Island to well within the hanging wall at Deadman's Bar on the Snake River (**Figure 21**). Details of the benchmark standards and surveying procedures are given in Sylvester and others (1990, 1991) and Byrd and others (1988). The combined observed closure of all the segments from the 1988 survey was 12.4 mm, and 12.2 mm for the 1989 survey (Sylvester and others, 1991). If the closure error is spread equally among the benchmarks for both surveys, then the probable error associated with a single benchmark is ± 0.28 mm in 1988, and ± 0.25 mm in 1989, and are equivalent to "tectonic 1st-order" surveying standards.

Results from the initial reobservation of the level line in 1989 (Sylvester and others, 1991) showed that in the one-year period, 1988 to 1989, the hanging-wall valley block rose from 4 to 8 mm relative to the westernmost benchmark within the Teton Range (**Figure 21**). The greatest height change occurred across a ~1,500 m wide zone that straddles the surface trace of the Teton fault west of Jenny Lake. These measurements indicate an unexpected reverse sense of relative motion, with the hanging wall moving up. A normal fault with the geometry of the Teton fault is expected to respond to inter-seismic tectonic loading by relative hanging-wall subsidence as in the case of co-seismic deformation observed on normal faults during large earthquakes (see **Figure 17**). Nonetheless, it is noteworthy that regardless of the sense of deformation, the displacement rate of 8 mm/yr is from 4 to 18 times greater than those determined from the geologic and paleoseismic data (**Figure 16**).

Some plausible interpretations for this unusual aseismic behavior of the Teton fault include: (1) seismic energy release on unknown faults to the east or west, such as may be associated with the background seismicity of the Gros Ventre Range, may have locked the Teton fault in horizontal compression; (2) inter-event seismic energy may be accumulating [see Sylvester and others (1991) for a complete discussion]; and (3) measurements may reflect nontectonic behavior such as ground-water flow or surveying or analysis errors. Sylvester and others (1991) preferred the conclusion that the measured displacement occurred as aseismic creep, i.e., not accompanied by earthquakes. However, the rapid change in elevation across a 1 km width argues that creep took place at relatively shallow depths, probably less than 5 km.

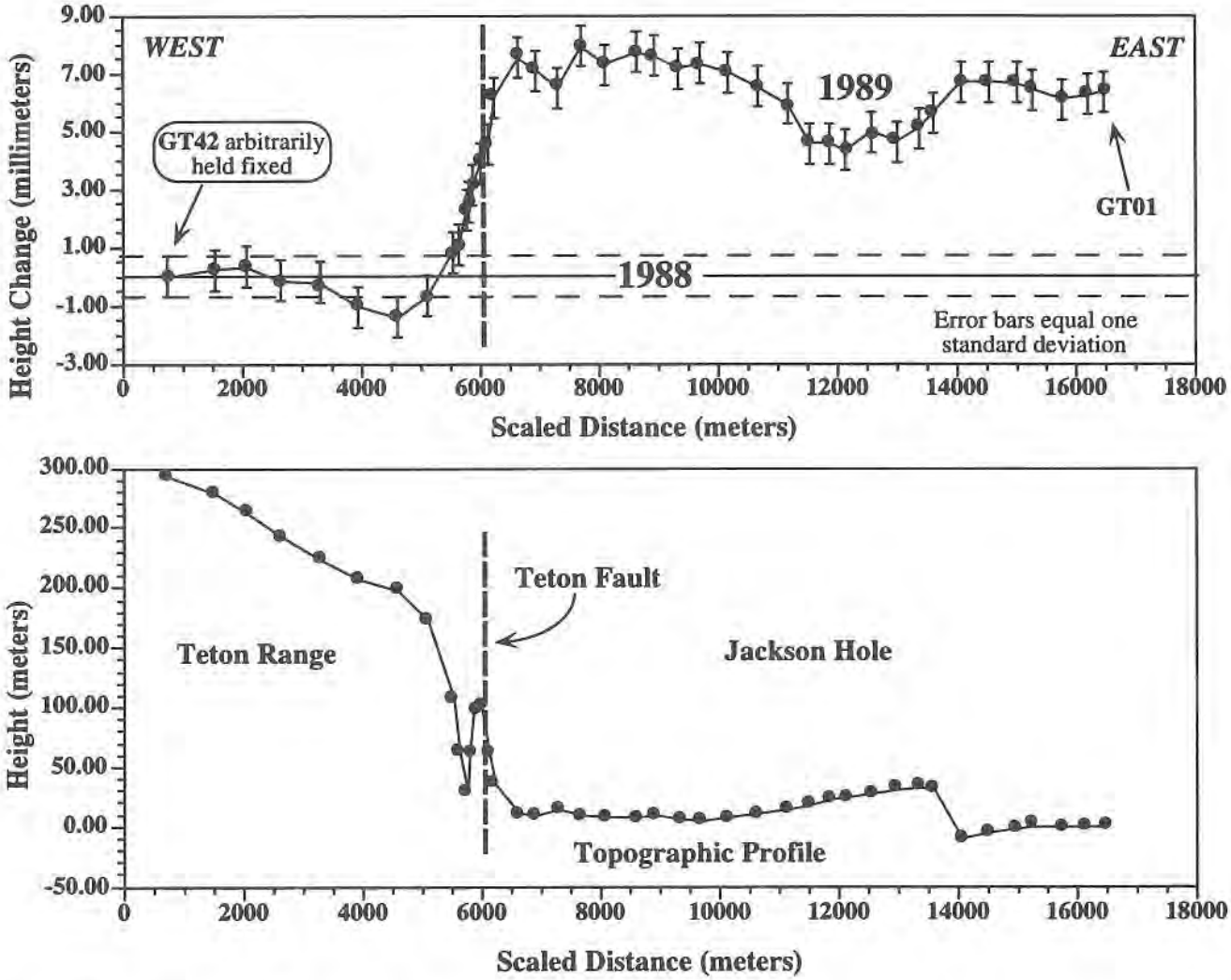

Figure 21. (a) Results from 1988 and 1989 precise leveling surveys showing height difference of benchmarks from Cascade Canyon (GT 42) to Deadmans Bar GT01 (from Sylvester and others, 1991). Elevations are in millimeters with respect to station GT42 on the western end of leveling line that was arbitrarily fixed as a zero-deformation base station. (b) Corresponding topographic profile along the Teton level line.

Preliminary analyses of the 1991 leveling results suggest that heights of benchmarks in the hanging-wall block indicate a reversal from a hanging-wall uplift to hanging-wall subsidence, with a maximum height difference of 4 mm between the 1989 and 1991 surveys. While the 1989-1991 period was also characterized by seismic quiescence along the Teton fault, these preliminary results suggest that the anomalous uplift of the hanging wall may have changed to a more characteristic deformation associated with pre-seismic loading of a normal fault (footwall uplift and hanging-wall subsidence). These observations represent the first documented occurrence of aseismic vertical creep across a normal fault in the United States.

Earthquake hazards of the Teton region

In the Teton region, contemporary seismicity and faulting are considered a natural consequence accompanying active mountain-building processes. Based on the evidence of Quaternary faulting and the

historic record of large earthquakes in the ISB, future large earthquakes of M_s=6.3 to 7.5 are expected to occur every few hundred to few thousands of years (Gilbert and others, 1983; Doser and Smith, 1983; Piety and others, 1986; Smith and Arabasz, 1991). While the repeat times of large earthquakes in the ISB are large compared to the expected lifetimes of man-made structures and of man himself, the occurrence of a large earthquake in the Teton region will have a major impact on roads, structures, and human safety. Based on the results of our research and observations from historic normal-faulting earthquakes in the western U.S., we describe here possible scenarios for the Teton region in the event of a large, scarp-forming earthquake.

We emphasize that the minimum-magnitude threshold for scarp-forming earthquakes in the Basin and Range province (Arabasz and others, 1992) is $M_s = 6.3 \pm 0.3$. Furthermore, although moderate magnitude earthquakes of $5.5 < M_s < 6.3$, which occur without surface rupture, are not as large as scarp-forming events, they generally have shorter recurrence intervals (on the order of hundreds of years). Such earthquakes also pose a hazard to the Teton region because of their more frequent occurrence. Our study did not assess the attendant hazards accompanying this class of intermediate magnitude earthquakes because of insufficient data for the Teton area.

We also note that if the Teton fault has a listric geometry, as implied by one of Lageson's (1992) models, then our application of a planar, normal-faulting model derived from the large scarp-forming earthquakes of the Basin and Range province would be inappropriate. However, Jackson (1987) and Doser and Smith (1989) found no evidence of scarp-forming, normal-faulting earthquakes with dips less than 30°, implying that a listric fault model is not appropriate for normal-faulting earthquake nucleation.

Ground deformation and fault rupture

Extrapolation of data from numerical models of large normal-faulting earthquakes (**Figure 18**), coupled along with observations of the magnitude of surface rupture and displacement accompanying historic normal-faulting earthquakes around the world (Bonilla and others, 1984; de Polo and others, 1991; Mason and Smith, 1990), provide scaling laws that we used to estimate the expected magnitudes for earthquakes on the Teton fault. Applying the hypothetical working model of Smith and others (1985) and Smith and Arabasz (1991) to the Teton fault, one could expect nucleation of large-magnitude earthquakes to occur east of the surface trace of the fault on a 45°- to 60°-dipping plane and at a depth of 15 ± 5 km. Furthermore, if unilateral rupture characterizes the nucleation of the Teton fault, such as the $M_s = 7.3$, 1983, Borah Peak, Idaho, earthquake (Richins and others, 1987) and as suggested for the $M_s = 7.5$, 1959, Hebgen Lake earthquake (Bruhn and others, 1987), then potential nucleation would occur at the ends of individual segments and would propagate upward to the surface and toward the opposite end of the segment. Note that for the Teton fault, the expected nucleation (starting) point would be at the bottom of the fault, displaced 10 to 20 km to the east of the Teton Range, probably at the end of a segment boundary.

The Quaternary expression of the Teton fault is interpreted by us to consist of two or three independent fault segments 13 km to 42 km long. Extrapolation of the individual segment lengths to the magnitudes of causative normal-faulting earthquakes (after Mason and Smith, 1990) suggests a minimum $M_s = 6.6 \pm 0.3$ associated with the northern segment and a $M_s = 6.8 \pm 0.3$ earthquake associated with the south or middle segment. If the 4.1-m displacement at Granite Creek is composed of two separate slip events of 2.8 m and 1.3 m, as suggested by Byrd and Smith (1990b) and Byrd (1991), then the corresponding magnitudes of the causative earthquake would be $M_s = 7.2 \pm 0.3$ and 6.9 ± 0.3, respectively. In either case, these are large earthquakes with the potential for significant ground deformation and damage that would rupture most, if not all, the southern and middle segments.

The expected magnitudes and displacements of earthquakes along the Teton fault (**Table 2**) assume rupture of a single segment or of multiple segments. Note that the $M_s = 7.3$, 1983, Borah Peak, Idaho, earthquake ruptured one 20-km-long segment entirely and propagated about 14 km into an adjacent segment. Thus, if the southern and middle segments of the Teton fault represent a single 42-km-long segment, then a rupture of this length would correspond to an $M_s = 7.1 \pm 0.3$ earthquake using the relationships of Mason and Smith (1990).

Table 2. Expected magnitudes (M_s) and displacements for large earthquakes on the Teton fault. Estimates from scaling laws for normal-faulting earthquakes by Bonilla and others (1984) de Polo and others (1991), and Mason and Smith (1990).

Segment name	Rupture length (km)	Magnitude (M_s)	Surface displacement (m)
South	20	6.8 ± 0.3	1.0
Middle	22	6.8 ± 0.3	1.0
North	13	6.6 ± 0.3	0.5
South/middle segments combined	42	7.1 ± 0.3	2.8
Rupture of the entire length of Quaternary faulting	55	7.2 ± 0.3	4.0

Associated with these fault displacements, the valley floor of Jackson Hole could tilt westward against the fault and subside in a manner similar to that observed in other large normal-faulting earthquakes (see **Figures 17** and **18**). This effect could lead to rechanneling of rivers and streams and possible flood inundation of low-lying areas, depending upon the location of the subsidence and local hydrologic conditions. However, we cannot state unequivocally what would happen in the Teton area in the event of a large earthquake, because we do not know the actual fault attitude and geometry, stress condition, etc. Therefore, we must rely upon models of normal-fault nucleation based upon the observations of the large, historic normal-faulting earthquakes (**Figure 17**).

Ground shaking

Strong ground motions (peak ground accelerations) of the Earth's surface accompanying a major earthquake produce most of the seismically related damage to man-made structures. Strong ground-shaking occurs not only along the fault, but at distances up to several 10s of km from the surface rupture. Strong shaking damages structures and roads, produces loss of soil strength resulting in liquefaction and failure of the ground surface, and can induce rock and snow slides. Ground shaking may also be amplified at a particular site by a number of factors such as the thickness and competency of unconsolidated rocks, ground-water conditions, focusing of seismic energy due to local geologic conditions, or poor construction/design of structures. To date, there has been little research done on determining engineering properties of soils and site-specific conditions in the Teton region, therefore, a site-specific evaluation of strong ground motion and expected damage accompanying a large earthquake in this region is not possible.

Secondary effects

Secondary effects accompanying a large earthquake on the Teton fault are expected to include rock and snow avalanches, landslides, liquefaction, rechanneling of streams and rivers, and generation of seiches within lakes. The potential impact of these effects in the Teton region depends, in various ways, on the time of year, amount of precipitation, exposure to the fault, etc. For example, high runoff during wet springs may saturate soils and thus amplify the potential for landslides and liquefaction. Similarly, a heavy snow pack in the surrounding mountains would increase the threat of seismically induced snow avalanches.

Earthquake-induced landslides

The influence of earthquakes on potential landslides is particularly important to the Teton region. Investigations by Bailey (1972) and Case and others (1991) revealed the presence of large areas susceptible to landslides in the Teton, Snake River, and Gros Ventre Ranges. The earthquake-related landslide hazard of the Teton region is emphasized by Smith and others (1976), who examined the possibility that the June 23, 1925, Lower Gros Ventre slide (location shown in **Figure 7**) may have been triggered by earthquakes.

The Lower Gros Ventre slide occurred at the western end of Gros Ventre Canyon and catastrophically released 38 x 106 m^3 of bedrock that slid down the north-facing side of the Gros Ventre Canyon and dammed the Gros Ventre River (Voight, 1974). Failure of the rock-slide dam caused the disastrous Kelly flood two years later. Smith and others (1976) compiled the personal accounts of several residents living in the Gros Ventre Canyon and in the town of Moran prior to the 1925 Lower Gros Ventre slide. Their study revealed evidence for earthquake swarms and persistent background seismicity several years before this catastrophic slide. It appears that earthquakes in the Jackson Hole area were more common for several years preceding the 1925 Gros Ventre slide than for several years following the slide

(Smith and others, 1976). In their accounts, residents noted a significant increase of small earthquakes in the spring of 1925, including an earthquake of magnitude 3 to 4 in the northern Jackson Hole-Kelly area 20 hours before the slide (personal communication, Slim Lawrence to R. B. Smith). Although the evidence is equivocal, this earthquake and the persistent earthquake swarms, in the presence of highly susceptible landslide terrain, may have induced ground creep followed by the massive slide several hours later.

As pointed out in the section on seismicity of the Teton region (see **Figure 7**), the Gros Ventre Range is a seismically active area, and earthquake-induced landslides may be more common here than in other areas in the Teton region. Of course not all landslides in the region have necessarily been seismically induced, but if even a small percentage were related to earthquakes, they pose an important long-term hazard.

Other earthquake hazards characteristic of the Teton region include large rock slides and debris flows in steep canyons that could be triggered by even moderate-magnitude earthquakes. Earlier accounts of earthquakes in the region (Fryxell, 1933) told of large rock falls and avalanches occurring after small earthquakes. It is likely that a major earthquake along the Teton fault would trigger significant snow avalanches during winter months along the steep range fronts and within the steep-sided canyons of the Teton Range.

Rock falls and landslides following a moderate to large earthquake could disrupt crucial transportation routes and power lines in and out of Jackson Hole. In addition, excess water could be expelled by natural springs, which could disrupt stream and river flows. For example, in the first few weeks following the 1983 Borah Peak earthquake, up to 0.5 km^3 of ground water (Wood, 1985) was released from areas adjacent to and along the ground rupture. Similar phenomena may accompany a large earthquake along the Teton fault.

Seismically-induced waves, or seiches, in lakes along the Teton Range (such as Jackson Lake) could result from earthquakes on the northern Teton fault. Seiches accompanying the M_s = 7.5 1959 Hebgen Lake earthquake localized flooding of the shorelines of Hebgen Lake, Montana (Myers and Hamilton, 1964). It should be noted that the presence of large islands on the east shore of Jackson Lake would likely reduce, but not preclude, seiche damage to areas on the east side of the lake. However, the juxtaposition of smaller lakes adjacent to the Teton fault (**Figure 3** and **Sheet 1**, Smith, Byrd, and Susong, map pocket) increases the likelihood of damage resulting from tilting and small-scale seiches.

Conclusions

Our study reveals that the well-preserved Quaternary scarps of the Teton fault extend for 55 km at the base of the Teton Range. Since its inception 5 to 13 Ma, the Teton fault has accumulated an estimated 6 to 9 km of stratigraphic separation, including up to 28 m of surface offset in just the past 14 ka, and several meters of Holocene displacement. Thus, we believe that the Teton fault is an active structure and has been the dominant factor contributing to the 2,150 m of topographic relief of the Teton Range in at least the last 2 Ma.

On the basis of lateral offsets of Quaternary scarps, scarp height variation, and variations in trends of faulting, two to three fault segments from 13 to 42 km long have been defined for the Teton fault. Each of these segments is considered capable of rupturing during large scarp-forming earthquakes of $M_s = 6.3 \pm 0.3$ or larger. Rupture of the entire 55 km length of the Teton fault may correspond to an earthquake as large as $M_s = 7.2 \pm 0.3$.

The 3.6-m fault scarp at the mouth of Granite Canyon contrasts in offset with larger scarps, up to 13 m in height, 120 m north of the trench location. The larger scarps are the products of several scarp-forming, prehistoric earthquakes that offset 14 to 30 ka Pinedale glacial deposits. Rates of surface offset (corresponding to conservative estimates of slip rates) projected from the trench data and the adjacent scarps, suggest average slip rates of 0.45 to 1.6 mm/yr for this segment of the fault, with recurrence intervals for scarp-forming earthquakes from 1,600 to 6,000 years.

Initial interpretations of a trench at Granite Creek on the southern segment of the Teton fault revealed 4.1 m of vertical displacement in alluvial and glacial deposits. Byrd (1991) recently suggested that the slip was composed of two separate events identified by radiocarbon dating that supports a two-event, Holocene, displacement record with a 7,175 ± 100-yr slip event associated with 2.8 m of displacement and a younger event, associated with 1.3 m of displacement. Scaling of the Holocene fault displacements from historic normal faulting earthquakes to these paleo-slip events (Mason and Smith, 1990) suggests a scenario of two corresponding scarp-forming earthquakes of $M_s = 7.0 \pm 0.3$ and 6.9 ± 0.3, respectively, with estimated rupture lengths of approximately 32 km and 25 km.

In a study of the contemporary deformation of the Teton fault, Sylvester and others (1991) found that the hanging-wall block rose 8 mm ± 0.7 mm relative to the footwall block (the Teton Range) during a period of seismic quiescence between 1988 to 1989. This finding was unexpected, because an active normal fault ought to behave with hanging-wall subsidence and footwall uplift during elastic strain accumulation. The unusual deformation measured on the Teton fault has been tentatively interpreted as aseismic creep, but we cannot rule out a non-tectonic origin. Preliminary analyses of the 1991 leveling results, however, suggest that heights of benchmarks in the hanging-wall block decreased ~ 4 mm relative to those in the footwall and may be diagnostic of strain associated with loading of a normal fault. If the deformation observed across the Teton fault indeed represents the occurrence of vertical creep, then it is the first observation of this phenomenon across an active normal fault in the United States.

A possible implication for the aseismic creep on the Teton fault is that it is currently undergoing stress buildup prior to a large earthquake. This interpretation is consistent with the concept that the seismic quiescence on the Teton fault is a seismic gap that may end with a large event. Occurrence of a large-magnitude earthquake ($M_s \geq 6.3$) on the Teton fault would most likely result in significant ground deformation and disruption of roads and structures. However, smaller magnitude ($5.5 \geq M_s \geq 6.3$) but more frequent earthquakes also pose a notable hazard to the Teton-Jackson Hole area.

Acknowledgments

A project of the scope presented here represents the contributions of many colleagues, students, research managers, and friends. It also represents our long-term interest in seismotectonics and regional geophysics of the Yellowstone-Teton-Hebgen Lake region. This paper presents the principal findings of a three-year (1987-1989) research project entitled: "Earthquake hazards of the Grand Teton National Park: emphasizing the Teton fault" that was funded by the University of Wyoming-National Park Service Research Center, grant #532724. We are grateful to Mark Boyce and Ken Diem of the University of Wyoming-National Park Service Research Center who have always been interested in our projects and have encouraged this work. Funds for the 1989 and 1991 releveling surveys across the Teton fault were provided by the U.S. Geological Survey, National Earthquake Hazards Reduction Program grants #14-08-00001-G1349 and #14-08-0001-G1970. The Geological Survey of Wyoming also supported our 1991 dating and field efforts.

We gratefully acknowledge the excellent cooperation of the Grand Teton National Park staff including the superintendent, Jack Stark, and other staff members: Marshall Gingery, Peter Hayden, Roger Haney, and Patrick Smith. The Granite Creek trenching component of the Teton fault study was approved through a finding of no significant impact for the National Park Service subject environmental assessment "Trenching Teton fault" by the Acting Regional Director, Jack Neckels, dated August 17, 1989. We thank Marshall Gingery for his endeavors in obtaining approval to conduct this aspect of our study.

Arthur G. Sylvester and students from the University of California, Santa Barbara, and the University of Utah made the leveling measurements. Ronald Bruhn of the University of Utah frequently discussed with us the regional tectonic context of the Teton fault and provided insight into the mechanics of normal faulting. Gordon Jacoby of Lamont

Doherty Geological Observatory, Columbia University, kindly provided the tree-ring dating of the Teton fault at no cost to the project. The University of Utah provided support for computing. Art Sylvester and Jim Case provided critical and very helpful reviews of the manuscript.

William Hardman, Dan Trentman, Susan Olig, Adolph Yonkee, and Colin Zelt from the University of Utah, and Chris Hitchcock, Barbara Belding, and Ken Perez of University of California, Santa Barbara, assisted with the EDM profiling and trenching studies. A team of geologists with expertise in fault trenching and geology of the Teton region also assisted us and participated in a critical review of the final trenching results including: Ron Bruhn, Dean Ostenaa, William Lund, J. David Love, Jim McCalpin, and Ken Pierce. Chris Wood of the U.S. Bureau of Reclamation kindly provided earthquake data from the Jackson Lake seismic network. We also thank Jack Shea of the Teton Science School for providing housing and logistical support during our field work in 1989, 1990, and 1991.

We are especially indebted to J. David Love for his many years of encouragement, for his ideas on the geology of the region, and for graciously sharing his unpublished data with us. In addition, we thank Dean Ostenaa and Jerry Gilbert for contributing their knowledge of the Teton fault and for their help with the trenching project. We have also benefited from the discussions with Ken Pierce regarding his ideas of the Quaternary history of the region and his suggestion of the Granite Creek trench site.

References cited

Anders, M.H., Geissman, J.W., Piety, L.A., and Sullivan, J.T., 1989, Parabolic distribution of circum-eastern Snake River Plain seismicity and latest Quaternary faulting—migratory pattern and association with the Yellowstone hotspot: Journal of Geophysical Research, v. 94, p. 1589-1621.

Arabasz, W.J., Pechmann, J.C., and Brown, E.D., 1992, Observational seismology and the evaluation of earthquake hazards and risk in the Wasatch front area, Utah, *in* Hays, W.W., and Gori, P.L., editors, Assessment of regional earthquake hazards and risk along the Wasatch front, Utah, v. 1: U.S. Geological Survey Professional Paper 1500-A-J, p. D1-D39.

Bailey, R.G., 1972, Landslide hazards related to land use planning in Teton National Forest, northwest Wyoming: U.S. Department of Agriculture, Forest Service, 131 p.

Barnosky, A.D., 1984, The Colter Formation: evidence for Miocene volcanism in Jackson Hole, Teton County, Wyoming: Wyoming Geological Association Earth Science Bulletin, v. 17, p. 49-95.

Behrendt, J.S., Tibbetts, B.L, Bonini, W.E., and Lavin, P.M., 1968, A geophysical study in Grand Teton National Park and vicinity, Teton County, Wyoming: U.S. Geological Survey Professional Paper 516-E, 23 p.

Blackwelder, E., 1915, Post-Cretaceous history of the mountains of central Wyoming, part II: Journal of Geology, v. 51, p. 143-166.

_____ 1926, Earthquakes in Jackson Hole, Wyoming: Seismological Society of America Bulletin, v. 16, p. 196.

Bonilla, M.G., Mark, R.K., and Lienkaemper, J.J., 1984, Statistical relations among earthquake magnitude, surface rupture length, and surface fault displacement: Seismological Society of America Bulletin, v. 74, p. 2379-2411.

Bruhn, R.L., Gibler, P.R., and Parry, W.T., 1987, Rupture characteristics of normal faults: example from the Wasatch fault zone, Utah, *in* Coward, M.P., Dewey, J.F., and Hancock, P.L., editors, Continental extensional tectonics: Geological Society of London Special Publication 28, p. 337-353.

Bucknam, R.C., and Anderson, R.E., 1979, Estimation of fault-scarp ages from scarp height-slope angle relationship: Geology, v. 7, p. 11-14.

Byrd, J.O.D., 1991, Paleoseismicity of the southern section of the Teton fault, Wyoming: Geological Society of America Abstracts with Programs, v. 23, no. 5, p. A481.

Byrd, J.O.D., Geissman, J.W., and Smith, R.B., 1988, Seismotectonics of the Teton fault and possible relationship to the Yellowstone hotspot: Eos, Transactions, American Geophysical Union, v. 44, p. 1419.

Byrd, J.O.D., and Smith, R.B., 1990a, Dating recent faulting and estimates of slip rates for the southern segment of

the Teton fault, Wyoming: Geological Society of America Abstracts with Programs, v. 22, no. 6, p. 33.

_____ 1990b, Paleoseismicity and earthquake capability of the Teton fault, Wyoming: Eos, Transactions, American Geophysical Union, v. 71, p. 1452.

_____ 1991, Paleoseismicity, near-surface fault geometry, and segmentation of the Teton fault: Eos, Transactions, American Geophysical Union, v. 72, p. 316.

Case, J.C., Gilmer, D.R., Larsen, L.L., Cannia, J.C., and Coombs, L.A., 1991, Landslide map of the Driggs 1° x 2° Quadrangle: Geological Survey of Wyoming Open File Report 91-2E, scale: 1:250,000.

Coffman, T.L., and Von Hake, C.A,. 1973, Earthquake history of the United States: U.S. Department of Commerce, National Oceanic and Atmospheric Administration Publication 41-1, 208 p.

Crone, A.J., Machette, M.N., Bonilla, M.G., Lienkaemper, J.J., Pierce, K.L., Scott, W.E., and Bucknam, R.C., 1987, Surface faulting accompanying the Borah Peak earthquake and segmentation of the Lost River fault, central Idaho: Seismological Society of America Bulletin, v. 77, p. 739-770.

de Polo, C.M., Clark, D.G., Slemmons, D.B., and Ramelli, A.R., 1991, Historical surface faulting in the Basin and Range province, western North America: implications for fault segmentation: Journal of Structural Geology, v. 13, p. 123-136.

Doser, D.I., 1985, Source parameters and faulting processes of the 1959 Hebgen Lake, Montana, earthquake sequence: Journal of Geophysical Research, v. 90, p. 4537-4555.

_____ 1988, Source mechanisms of earthquakes in the Nevada seismic zone (1915-1943): Journal of Geophysical Research, v. 93, p. 15,001-15,016.

Doser, D.I., and Smith, R.B., 1983, Seismicity of the Teton-southern Yellowstone region, Wyoming: Seismological Society of America Bulletin, v. 73, p. 1369-1394.

_____ 1985, Source parameters of the October 28, 1983 Borah Peak, Idaho, earthquake from body-wave analysis: Seismological Society of America Bulletin, v. 75, p. 1041-1051.

_____ 1989, An assessment of source parameters of earthquakes in the Cordillera of the western United States: Seismological Society of America Bulletin, v. 79, p. 1383-1409.

Eddington, P.J., Smith, R.B., and Renggli, C., 1987, Kinematics of Basin-Range intraplate extension, *in* Coward, M.P., Dewey, J.F., and Hancock, P.L., editors, Continental extensional tectonics: Geological Society of London Special Publication 28, p. 371-392.

Fryxell, F.M., 1933, Earthquake shocks in Jackson Hole, Wyoming: Seismological Society of America Bulletin, v. 23, p. 167-168.

_____ 1938a, The Tetons, interpretations of a mountain landscape: Berkeley, University of California Press, 77 p.

_____ 1938b, Postglacial faulting in the Teton Range, Wyoming [abstract]: Geological Society of America Bulletin, v. 49, p. 1881.

Gale, B.T., 1940, Communication, further earthquake shocks in Jackson Hole, Wyoming: Seismological Society of America Bulletin, v. 30, p. 85.

Gilbert, J.D., Ostenaa, D., and Wood, C., 1983, Seismotectonic study Jackson Lake dam and reservoir: U.S. Bureau of Reclamation Seismotectonic Report 83-8, Minidoka Project, Idaho-Wyoming, 123 p.

Hayden, P.S., 1969, Jackson Lake limnological investigations: National Park Service Progress Report, 1968-1969, Aquatic Research Biologist, Division of Natural Science Studies, Washington, D.C., 37 p.

Horberg, L., 1938, The structural geology and physiography of the Teton Pass area, Wyoming: Augustana Library Publications, 16, p. 1-86.

Horberg, L., Edmund, R.W., and Fryxell, F.M., 1955, Geomorphic and structural relations of Tertiary volcanics in the northern Teton Range and Jackson Hole, Wyoming: Journal of Geology, v. 63, p. 501-511.

Jackson, J.A., 1987, Active normal faulting and crustal extension, *in* Coward, M.P., Dewey, J.F., and Hancock, P.L., editors, Continental extensional tectonics: Geological Society of London Special Publication 28, p. 3-17.

King, G.C.P., Stein, R.S., and Rundle, J.B., 1988, The growth of geological structures by repeated earthquakes 1, conceptual framework: Journal of Geophysical Research, v. 93, p. 307-318.

Lageson, D.R., 1987, Laramide uplift of the Gros Ventre Range and implications for the origin of the Teton fault, Wyoming: Wyoming Geological Association 38th Annual Field Conference Guidebook, p. 78-89.

_____ 1992, Possible Laramide influence on the Teton normal fault, western Wyoming, *in* Link, P.K., Kuntz, M.A., and Platt, L.B., editors, Regional geology of eastern Idaho and western Wyoming: Geological Society of America Memoir 179, p. 183-196.

Locke, W.M., Meyer, G.A., and Pings, J.C., 1992, Morphology of a postglacial fault scarp across the Yellowstone (Wyoming) caldera margin and its implications: Seismological Society of America, v. 82, p. 511-516.

Loope, L.L., and Gruell, G.E., 1973, The ecological role of fire in the Jackson Hole area, northwestern Wyoming: Quaternary Research, v. 3, p. 425-443.

Love, J.D., 1956, General history of Teton County during Late Cretaceous, Tertiary, and Quaternary: Wyoming Geological Association 11th Annual Field Conference Guidebook, p. 140-150.

_____ 1973, Map showing differences in the stability of the ground, Jackson Quadrangle, Teton County, Wyoming: U.S. Geological Survey Miscellaneous Geologic Investigations Map I-769-F, scale 1:24,000.

_____ 1977, Summary of Upper Cretaceous and Cenozoic stratigraphy and of tectonic and glacial events in Jackson Hole, northwestern Wyoming: Wyoming Geological Association 29th Annual Field Conference Guidebook, p. 585-593.

Love, J.D., and Montagne, J., 1956, Pleistocene and recent tilting of Jackson Hole, Teton County, Wyoming: Wyoming Geological Association 11th Annual Field Conference Guidebook, p. 169-178.

Love, J.D., and Reed, J.C., Jr., 1971, Creation of the Teton landscape, the geological story of Grand Teton National Park: Grand Teton Natural History Association, Moose, Wyoming, 120 p.

Love, J.D., and Albee, H.F., 1972, Geologic map of the Jackson Quadrangle, Teton County, Wyoming: U.S. Geological Survey Miscellaneous Geologic Investigations Map I-769-A, scale 1:24,000.

Love, J.D., and Love, C.M., 1978, Geologic map of the Cache Creek Quadrangle, Teton County, Wyoming: U.S. Geological Survey Open File Report 78-480, scale 1:24,000.

Love, J.D., Reed, J.C., Jr., Christiansen, R.L., and Stacy, J.R., 1972, Geologic block diagram and tectonic history of the Teton region, Wyoming-Idaho: U.S. Geological Survey Miscellaneous Geologic Investigations Map I-730.

Love, J.D., Reed, J.C., Jr., and Christiansen, A.C., 1992, Geologic map of the Grand Teton National Park area: U.S. Geological Survey Miscellaneous Investigations Series Map I-2031, scale 1:62,500.

Machette, M.N., Personius, S.F., Nelson, A.R., Schwartz, D.P., and Lund, W.R., 1991, The Wasatch fault zone, Utah—segmentation and history of earthquakes: Journal of Structural Geology, v. 13, p. 137-149.

Mason, D.B., and Smith, R.B., 1990, Paleoseismicity of the Intermountain seismic belt from magnitude scaling of Quaternary fault lengths and displacements: Eos, Transactions, American Geophysical Union, v. 71, p. 1559.

Myers, W.B., and Hamilton, W., 1964, Deformation accompanying the Hebgen Lake earthquake, August 17, 1959, *in* The Hebgen Lake, Montana, earthquake of August 17, 1959: U.S. Geological Survey Professional Paper 435, p. 37-98.

Nelson, V.E., and Church, V., 1943, Critical structures of the Gros Ventre and northern Hoback Ranges, Wyoming: Journal of Geology, v. 23, p. 193-217.

Ostenaa, D.A., 1988, Late Quaternary behavior of the Teton fault, Wyoming: Geological Society of America Abstracts with Programs, v. 20, no. 7, p. A14.

Pierce, K.L., 1979, History and dynamics of glaciation in the northern Yellowstone National Park area: U.S. Geological Survey Professional Paper 729-F, 90 p.

Pierce, K.L., and Good, J., 1990, Quaternary geology of Jackson Hole, Wyoming, *in* Roberts S., editor, Geologic Field Tours of western Wyoming and parts of adjacent Idaho, Montana, and Utah: Geological Survey of Wyoming Public Information Circular 29, p. 79-88.

Pierce, K.L., Obradovich, J.D., and Friedman, I., 1976, Obsidian hydration dating and correlation of Bull Lake and Pinedale glaciations near West Yellowstone, Montana: Geological Society of America Bulletin, v. 87, p. 703-710.

Pierce, K., and Morgan, L.A., 1990, The track of the Yellowstone hot spot: volcanism, faulting, and uplift: U.S. Geological Survey Open File Report 90-415, 46 p.

Piety, L.A., Wood, C.K., Gilbert, J.D., Sullivan, J.T., and Anders, M.H., 1986, Seismotectonic study for Palisades dam and reservoir, Palisades Project: U.S. Bureau of Reclamation, Engineering and Research Center Seismotectonic Division, Denver, Colorado, and Pacific Northwest Region Geology Branch, Boise, Idaho, Seismotectonic Report no. 86-3, p. 198.

Porter, S.C., Pierce, K.L., and Hamilton, T.D., 1983, Late Wisconsin mountain glaciation in the Western United States, *in* Wright, H.E., Jr. , editor, Late Quaternary environments of the United States, v. 1, The Late Pleistocene: University of Minnesota Press, p. 71-111.

Reed, J.C., 1973, Geologic map of the Precambrian rocks of the Teton Range, Wyoming: U.S. Geological Survey Open File Report 73-230, scale 1:62,500.

Reed, J.C., and Zartman, A.E., 1973, Geochronology of Precambrian rocks of the Teton Range: Geological Society of America Bulletin, v. 84, p. 561-582.

Richins, W.D., Pechmann, J.C., Smith, R.B., Langer, C.J., Goter, S.K., Zollweg, J.E., and King, J.J., 1987, The 1983 Borah Peak, Idaho, earthquake and its aftershocks: Seismological Society of America Bulletin, v. 77, p. 694-723.

Roberts, S.M., and Burbank, D.W., 1988, Late Cretaceous to Recent differential uplift in the Teton Range, N.W. Wyoming, by apatite fission-track dating: Geological Society of America Abstracts with Programs, v. 20, no. 6, p. 465.

_____ 1993, Uplift and thermal history of the Teton Range defined by apatite fission-track dating: northwest Wyoming: Earth and Planetary Science Letters (in press).

Savage, J.C., and Hastie, L.M., 1966, Surface deformation associated with dip-slip faulting: Journal of Geophysical Research, v. 71, p. 4897-4904.

Schwartz, D.P., and Coppersmith, K.J., 1984, Fault behavior and characteristic earthquakes: examples from the Wasatch and San Andreas fault zones: Journal of Geophysical Research, v. 89, p. 5681-5698.

Scott, W.E., Pierce, K.L., and Hait, M.H., Jr., 1985, Quaternary tectonic setting of the 1983 Borah Peak earthquake, central Idaho: Seismological Society of America Bulletin, v. 75, p. 1053-1066.

Simons, F.S., Love, J.D., Keefer, W.R., Harwood, D.S., and Bienwieske, C.L., 1981, Mineral resources of the Gros Ventre Wilderness study area, Teton and Sublette counties, Wyoming: U.S. Geological Survey Open File Report 81-510, 94 p.

Slemmons, D.B., 1957, Geological effects of the Dixie Valley-Fairview Peak, Nevada, earthquakes of December 16, 1954: Seismological Society of America Bulletin, v. 47, p. 353-375.

Smith, R.B., 1988, Seismicity and earthquake hazards of the Borah Peak-Hebgen Lake-Yellowstone-Teton region—implications for earthquakes in extensional and active volcanic regimes: Geological Society of America Abstracts with Program, v. 20, no. 7, p. A12.

Smith, R.B., and Sbar, M.L., 1974, Contemporary tectonics and seismicity of the western United States with emphasis on the Intermountain seismic belt: Geological Society of America Bulletin, v. 85, p. 1205-1218.

Smith, R.B., and Arabasz, W.J., 1991, Seismicity of the Intermountain Seismic Belt, *in* Slemmons, D.B., Engdahl, E.R., Zoback, M.L., and Blackwell, D.D., editors, Neotectonics of North America: Geological Society of America, Decade Map Volume 1, p. 185-228.

Smith, R.B., Pelton, J.R., and Love, J.D., 1976, Seismicity and the possibility of earthquake related landslides in the Teton-Gros Ventre-Jackson Hole area: University of Wyoming Contributions to Geology, v. 14, p. 57-64.

Smith, R.B., Shuey, R.T., Pelton, J.R., and Bailey, J.P., 1977, Yellowstone hot spot, crustal properties from new earthquake and magnetic data: Journal Geophysical Research, v. 82, p. 3665-3676.

Smith, R.B., Richins, W.D., and Doser, D.I., 1985, The Borah Peak earthquake: seismicity, faulting kinematics, and tectonic mechanism, *in* Workshop XXVII, the Borah Peak earthquake: U.S. Geological Survey Open File Report 85-290, p. 236-263.

Smith, R.B., Byrd, J.O.D., Susong, D.D., Sylvester, A.G., Bruhn, R.L., and Geissman, J.W., 1990a, Three year progress report, an evaluation of earthquake hazards of the Grand Teton National Park emphasizing the Teton fault: Unpublished report to the University of Wyoming-National Park Service Research Center by the Department of Geology and Geophysics, University of Utah, Salt Lake City, 149 p.

Smith, R.B., Byrd, J.O.D., and Susong, D.D., 1990b, Neotectonics and structural evolution of the Teton fault, *in* Roberts, S., editor, Geologic field tours of western Wyoming and parts of adjacent Idaho, Montana, and Utah: Geological Survey of Wyoming Public Information Circular 29, p. 126-138.

Smith, R.B., Byrd, J.O.D., Sylvester, A.G., and Susong, D.D., 1990c, Neotectonics and earthquake hazards of the Teton fault: Geological Society of America Abstracts with Program, v. 22, no. 6, p. 45.

Snay, R.A., Cline, M.W., and Timmerman, E.L., 1985, Dislocation models for the 1954 earthquake sequence in Nevada, *in* Workshop XXVII, the Borah Peak earthquake: U.S. Geological Survey Open File Report 85-290, p. 531-555.

Stein, R.S., and Barrientos, S.E., 1985, Planar high-angle faulting in the Basin and Range: geodetic analysis of the 1983 Borah Peak, Idaho, earthquake: Journal of Geophysical Research, v. 90, p. 11,355-11,366.

Stover, C.W., and Brewer, L.R., 1991, United States earthquakes, 1985: U.S. Geological Survey Bulletin 1954, 170 p.

Stuiver, M., and Reimer, P.J., 1986, A computer program for radiocarbon age calibration: Radiocarbon, v. 28, p. 1,022-1,030.

Susong, D.D., Smith, R.B., and Bruhn, R.L., 1987, Quaternary faulting and segmentation of the Teton fault zone, Grand Teton National Park, Wyoming: Eos, Transactions, American Geophysical Union, v. 68, p. 1452.

Sylvester, A.G., Byrd, J.O.D., and Smith, R.B., 1990, Aseismic(?) reverse creep across the Teton fault, Wyoming, with implications for interseismic strain: Geological Society of America Abstracts with Programs, v. 22, no. 3, p. 88.

_____ 1991, Geodetic evidence for aseismic reverse creep across the Teton normal fault: Geophysical Research Letters, v. 18, p. 1083-1086.

Tibbetts, B.L., Behrendt, J.C., and Love, J.D., 1969, Seismic-refraction measurements in Jackson Hole, Wyoming: Geological Society of America Bulletin, v. 80, p. 1109-1122.

Voight, B., 1974, The Lower Gros Ventre (Kelly) slide, *in* Rock mechanics, the American Northwest, Expedition Guide, International Society of Rock Mechanics 3rd Congress: Pennsylvania State University, University Park, Pennsylvania, p. 164-166.

Wood, C., 1988, Seismicity of the Teton region, Wyoming and Idaho: perspective from a newly installed telemetered network: Geological Society of America Abstracts with Programs, v. 20, no. 7, p. A14.

Wood, S., 1985, The Borah Peak, Idaho earthquake of October 28, 1983—hydrologic effects: Earthquake Spectra, v. 2, p. 127-150.

Frontispiece. Aerial view of the south end of Jackson Lake, Wyoming, looking southwest toward Mt. Moran (in background). Foreground shows Elk Island, with Moran Bay in right background. Jackson Lake occupies an ancestral basin developed by west-dipping hanging-wall deformation accompanying the Quaternary evolution of the Teton fault, followed by scouring by glaciers that entered the basin from the north and east. The lake basin sediments are dominantly alluvium, lacustrine sediments, and glacial debris. Photograph courtesy of David R. Lageson, Montana State University.

Seismic surveys and Quaternary history of Jackson Lake, Wyoming

Robert B. Smith
Department of Geology and Geophysics
University of Utah
Salt Lake City, Utah 84112

Kenneth L. Pierce
U.S. Geological Survey
Denver, Colorado 80225

Richard J. Wold
Terra Sense Inc.
Sunnyvale, California 94086

Abstract

This report describes the structure and Quaternary sedimentation history of Jackson Lake, Wyoming, as evaluated by seismic reflection and refraction surveys. Interpretations of these data were correlated with the glacial geology and Quaternary history of the Teton-Jackson Hole area and the Quaternary volcanic history of the nearby Yellowstone Plateau to assess the evolution of this high intermontane lake. High-resolution seismic reflection profiles (7.5 kHz source) were used to construct a bathymetic map of Jackson Lake that revealed two topographic troughs: (1) a western trough along the main north-south axis of the lake up to 437 ft (133 m) deep, and (2) a separate, shallower, eastern trough up to 142 ft (43 m) deep. The deeper penetrating, air-gun reflection data (1-in^3 source) revealed a sub-lake basin composed of unconsolidated to semiconsolidated Quaternary sediments that underlies the western topographic trough. It consists of up to 375 ft (115 m) of undisturbed to moderately deformed sediments. In contrast, the air-gun data from the eastern part of Jackson Lake exhibit gently dipping Quaternary sediments in a separate basin to depths of 165 ft (50 m) with deeper, alternately east- and west-dipping layers separated by angular unconformities. The sedimentary pattern in the eastern basin is thought to represent subaqueous progradation of Quaternary sediments deposited from ice flowing into the trough from different directions.

The thickness of postglacial Holocene sediments on the west side of the western lake basin exceeds 70 ft (21 m) adjacent to the Teton fault but decreases to 40 ft (12 m) on the eastern edge of this basin. This variation of sediment thickness is consistent with both: (1) greater sediment rain-out in the western part of the lake, and (2) asymmetric astratal westward tilt

Smith, R.B., Pierce, K.L., and Wold, R.J., 1993, Seismic surveys and Quaternary history of Jackson Lake, Wyoming, *in* Snoke, A.W., Steidtmann, J.R., and Roberts, S.M., editors, Geology of Wyoming: Geological Survey of Wyoming Memoir No. 5, p. 668-693.

associated with hanging-wall subsidence of Jackson Lake produced by faulting accompanying large prehistoric earthquakes along the Teton fault.

Basement penetrating, wide-angle seismic refraction/wide-angle reflection data (40-in^3 source) revealed a 42° west-dipping reflection, 5,000 to 10,000 ft (1.5 - 3.0 km) beneath the southern part of Jackson Lake. This westward tilted horizon is located beneath the projection of the west-dipping, 2-Ma Huckleberry Ridge Tuff, whose dip, in surface exposures, increases from 9° to 28° westward towards the Teton fault. The underlying westward dipping reflection may thus be the top of older volcanic, Mesozoic, or Paleozoic units. The westward increasing dips of the tuff and that of the deeper reflection indicate asymmetric tilt of hanging-wall layers into the Teton fault and are consistent with a listric geometry for the fault at depth. Notably, there was little evidence from our seismic data for the proposed trace of the Teton fault or any other significant faulting in the Quaternary sediments mapped in our surveys.

Overall, the reflection data revealed that Jackson Lake was formed when late Pleistocene glaciation scoured out weakly consolidated Quaternary sediments from a basin produced by tectonic subsidence associated with deformation along the Teton fault. The basin was dammed by moraines and outwash buildup at the southern end. Our interpretation of the seismic data is that the eastern trough of Jackson Lake was scoured out by the west-flowing Pacific Creek glacial lobe (75 to 25 ka), and later the western trough was scoured out by the south-flowing Snake River glacial lobe (40 to 15 ka). Following glacial recession, diatomaceous sediment rained out of the lake water to form the sub-bottom layer that accumulated in quiet sites where sediments were not swept away by lake currents.

Introduction

Jackson Lake occupies a north-south trending natural basin at the north end of Jackson Hole, Wyoming. It is bounded on the west by the Precambrian-cored Teton Range and on the east by low-lying hills of the Teton Wilderness and an area of northern Jackson Hole drained by the Snake River (**Figures 1** and **2**). Jackson Lake attained a maximum depth of about 400 ft (122 m) before 1910. Construction of the Jackson Lake dam, completed in 1916, increased the maximum depth to about 437 ft (135 m). The Snake River, which drains a large part of the Yellowstone volcanic plateau to the north, is the main tributary of the lake. It enters Jackson Lake at its north end and exits on the southeast side, flowing eastward around Signal Mountain (**Figure 2**).

A combination of widespread Quaternary glaciation of the Jackson Hole region and long-term displacement on the Teton fault during its 5 to 9 million year history have been the primary factors in the evolution of Jackson Lake. Late Cenozoic normal faulting controlled the general location of Jackson Lake by producing a down-faulted hanging-wall depression against the Teton fault (**Figure 2**). However, the greatest effect on the topography around and beneath Jackson Lake results from the last (Pinedale) glaciation.

The latest glaciation consisted of three phases (**Table 1**). During the first phase (Burned Ridge interval) westward flow of ice down the valleys of Pacific Creek and Buffalo Fork (see **Figure 3**) scoured several troughs. One of these troughs trends westward down Pacific Creek, westward around the north side of Signal Mountain, and under the Jackson Lake dam to beneath Jackson Lake between Signal Mountain and Donoho Point (**Figure 3a**). During the second (Hedrick Pond) and third (Jackson Lake) phases (**Figure 3b**), southward flow of ice from the Yellowstone plateau scoured the western trough along the main north-south axis of the lake and deposited moraines and outwash that enclose the southern side of Jackson Lake.

The primary objectives of our geophysical surveys were to acquire detailed seismic reflection and refraction data with ancillary information from piston coring of shallow sediments for paleomagnetic analyses and determining the composition of the recent sediments. Subsequently, we combined this geophysical data with the results of glacial geologic studies of the Jackson Hole region to determine the Quaternary geologic history of Jackson Lake.

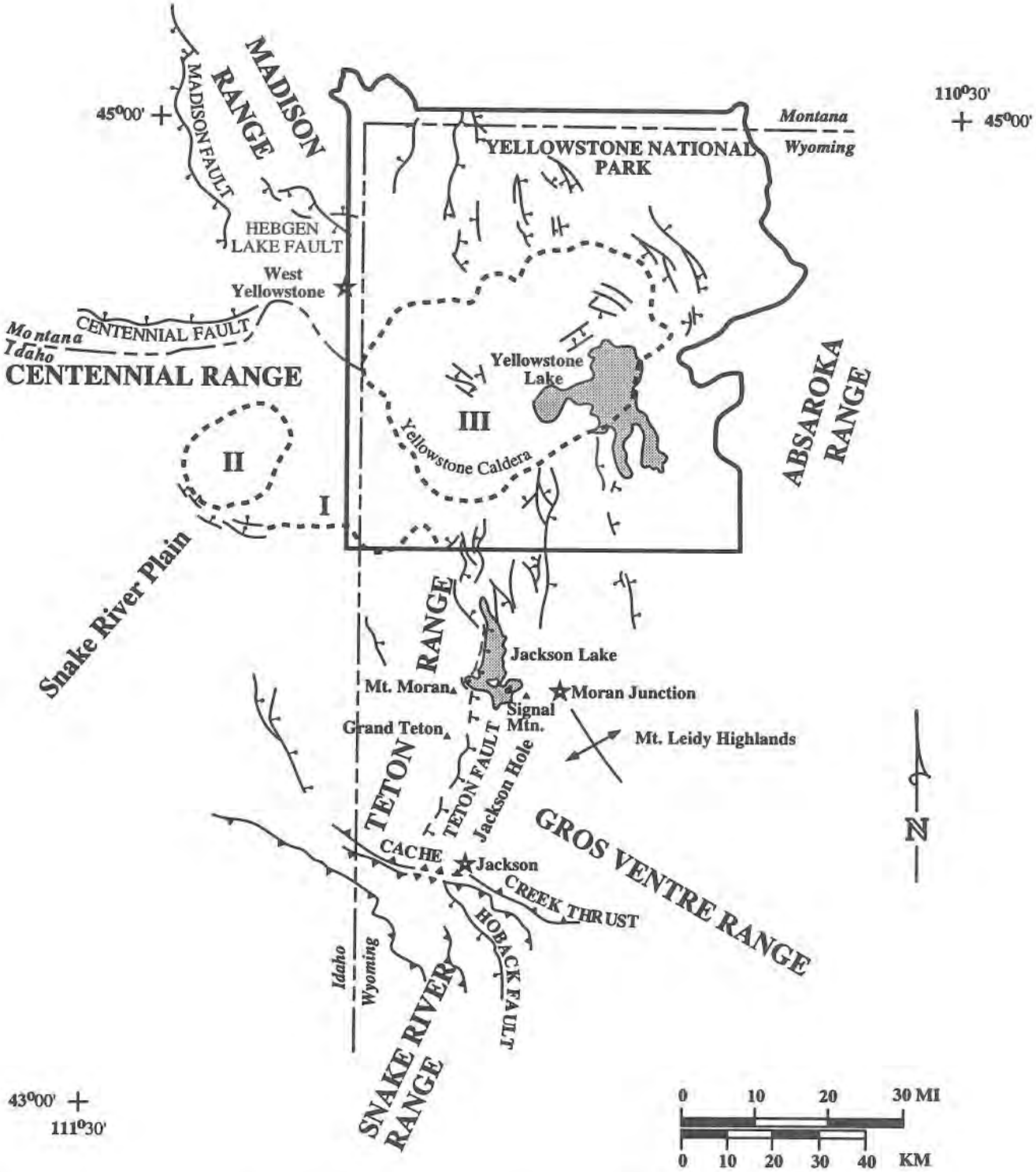

Figure 1. Regional tectonic map of the area surrounding Jackson Lake, Wyoming, showing the relationships between Jackson Lake, the Teton Range, Jackson Hole, the Teton fault, and the Yellowstone plateau and volcanic system. Outlines and ages of Yellowstone Quaternary calderas are noted: I = 2.0 Ma, II = 1.2 Ma and III = 0.6 Ma. Standard symbols for normal faults, thrust faults, and anticline.

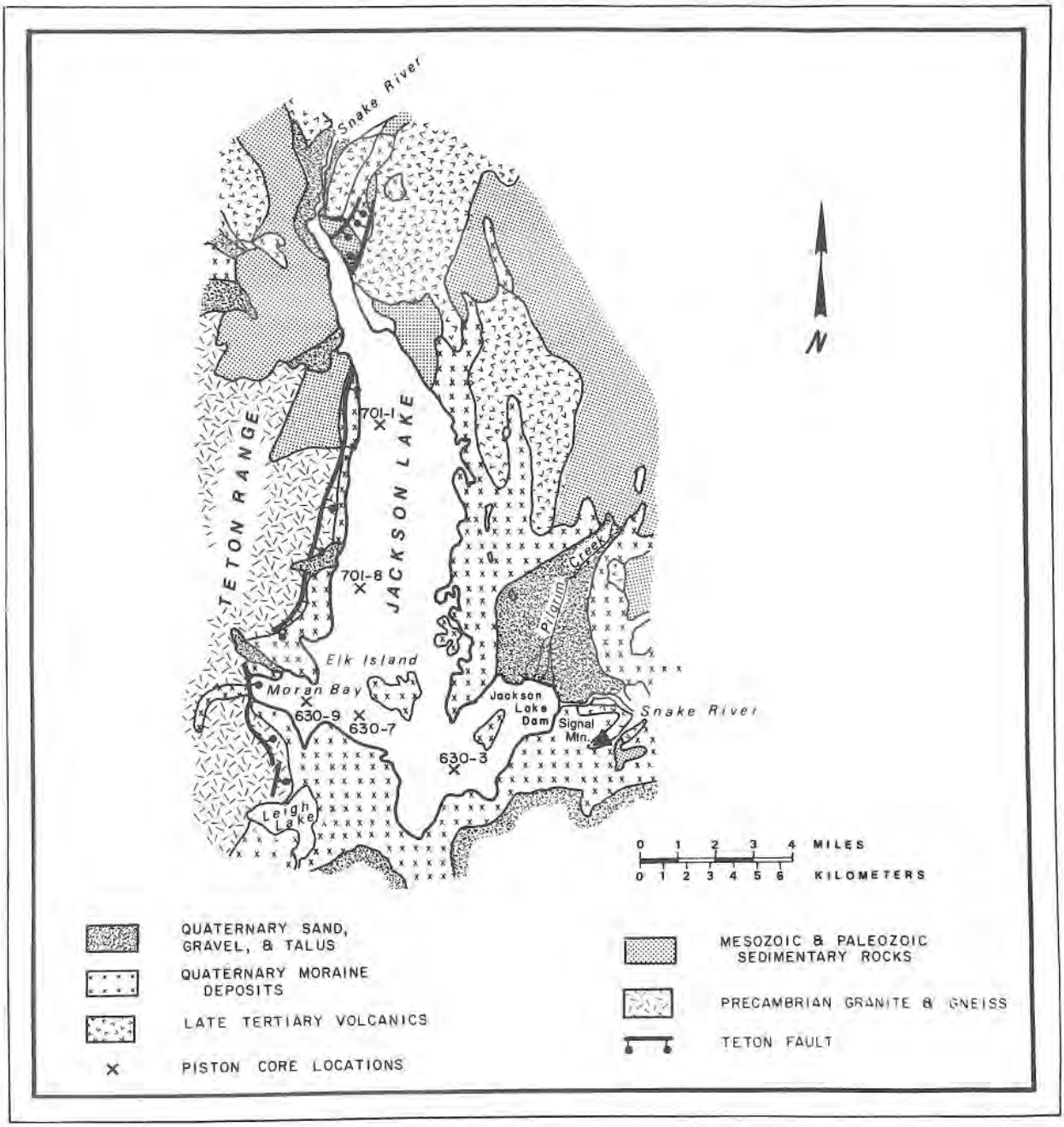

Figure 2. Generalized geology of Jackson Lake, Wyoming, area. Data compiled from Love and Reed (1971) and Reed (1973). Location of Teton fault from Smith and others (1990) and Smith, Byrd, and Susong (this volume).

Geology of the Jackson Lake area

Jackson Lake has been influenced by its proximity to the Teton Range and the range-bounding Teton fault, located immediately west of the lake (**Figures 1** and **2**). The Teton Range consists primarily of an intensely deformed and metamorphosed Precambrian gneiss and quartz monzonite core (Reed, 1973). These crystalline basement rocks are overlain by generally west- to northwest-tilted Paleozoic and Mesozoic sedimentary and late Cenozoic silicic volcanic rocks that are exposed on the west side of the Teton

Table 1. Three glacial lobes that terminated in the northern Jackson Hole region and their relative size during the three phases of the last glaciation (Pinedale). Phases are listed from youngest to oldest.

Glacial phases	(West) Snake River	Lobe Pacific Creek	(East) Buffalo Fork
Jackson Lake	XX	XX	O
Hedrick Pond	X	XXX	O
Burned Ridge	O	X	XXX

Explanation of symbols:
O = lobe not confluent with others at terminus,
X = lobe confluent but subordinate at terminus,
XX = lobe confluent and of similar size at terminus,
XXX = lobe confluent and dominates at glacial terminus.

Range (Love and Reed, 1971; Love and others, 1992). Jackson Hole and Jackson Lake occupy the hanging wall of the northern segment of the Teton fault and the regional structure suggests that Paleozoic, Mesozoic, Tertiary, and Quaternary strata extend westward beneath Jackson Lake (Behrendt and others, 1968; Tibbetts and others, 1969). Latest Tertiary ash-flow tuffs are exposed north of Jackson Lake and extend discontinuously east of Jackson Lake southward to and beyond Signal Mountain (**Figure 2**). Quaternary deposits around Jackson Lake consist mostly of glacial till and outwash with some alluvial, lacustrine, and landslide deposits. The principal units mapped by our seismic surveys were Quaternary sediments.

Information on the upper-crustal structure of northern Jackson Hole was provided by seismic refraction surveys around the western and southern margins of Jackson Lake (Behrendt and others, 1968; Tibbetts and others, 1969; Schilly and others, 1982). Interpretations of these data suggest an average P-wave velocity of 20,000 ft/s (6.1 km/s) for the crystalline basement rocks beneath Jackson Lake that were interpreted to be highly consolidated Paleozoic carbonate rocks or Precambrian granitic rocks. Paleozoic and Mesozoic strata, up to 2.5 mi (4 km) thick, are exposed on the east side of Jackson Hole (Love and Reed, 1971) and are projected to overlie Precambrian basement and also to underlie Jackson Lake.

Seismotectonics

The close proximity of Jackson Lake to the Teton fault (**Figure 2**) suggests that processes associated with large prehistoric earthquakes on this fault have influenced the structural evolution of Jackson Lake. For example, subsidence and westward tilt of the hanging-wall block of the Teton fault is consistent with westward-dipping late Tertiary volcanic units exposed in northern Jackson Hole (**Figure 2**). These include the 2 Ma Huckleberry Ridge Tuff, exposed on Signal Mountain 0.5 to 2.8 mi (1 to 5 km) east of Jackson Lake, which dips about 11° west, and an underlying 6 to 4.2 Ma tuff, also exposed on Signal Mountain, which dips approximately 22° west (Gilbert and others, 1983). The 10 to 9 Ma Teewinot Formation, exposed near Signal Mountain, dips west at 20° to 25° (Gilbert and others, 1983). The similarity of westward dips for these 10 to 4.2 Ma units implies that displacement on the Teton fault continued after 6 to 4.2 Ma (Smith and others, 1990; Pierce and Morgan, 1990; Smith, Byrd, and Susong, this volume).

Comparisons of ground deformation associated with large historic earthquakes of the Basin and Range province by Smith and Arabasz (1991) and Smith, Byrd, and Susong (this volume) suggest subsidence and asymmetric tilt of the hanging wall accompanied large, normal-faulting earthquakes. This pattern of deformation is also postulated to have accompanied large scarp-forming prehistoric earthquakes on the Teton fault, with the Jackson Lake basin occupying the subsided, hanging-wall block.

Total offset on the Teton fault is estimated to be ~18,000 to 30,000 ft (6-9 km) (Love and Reed, 1971). Quaternary scarps up to ~33 ft (~10 m) high in alluvial material and glacial moraines occur within 0.3 to 0.6 mi (0.5 to 1 km) of the west edge of Jackson Lake and reflect repeated movement along the fault from about 14 ka (Smith and others, 1990; Smith, Byrd, and Susong, this volume). Postglacial slip of up to 79 ft (24 m) has been measured southwest of Jackson Lake and at least 7,000 ft (2,100 m) of offset along the Teton fault has occurred since deposition of the Huckleberry Ridge Tuff on the northern end of the range (Gilbert and others, 1983; Smith and others, 1990; Smith, Byrd, and Susong, this volume). Estimates of Quaternary slip rates on the Teton fault by Smith, Byrd, and Susong (this volume), based upon trenching and stratigraphic offsets, range from 0.02 to 0.07 in/yr (0.4 to 1.8 mm/yr) and suggest that the fault has been an active element in the development of the Jackson Lake basin.

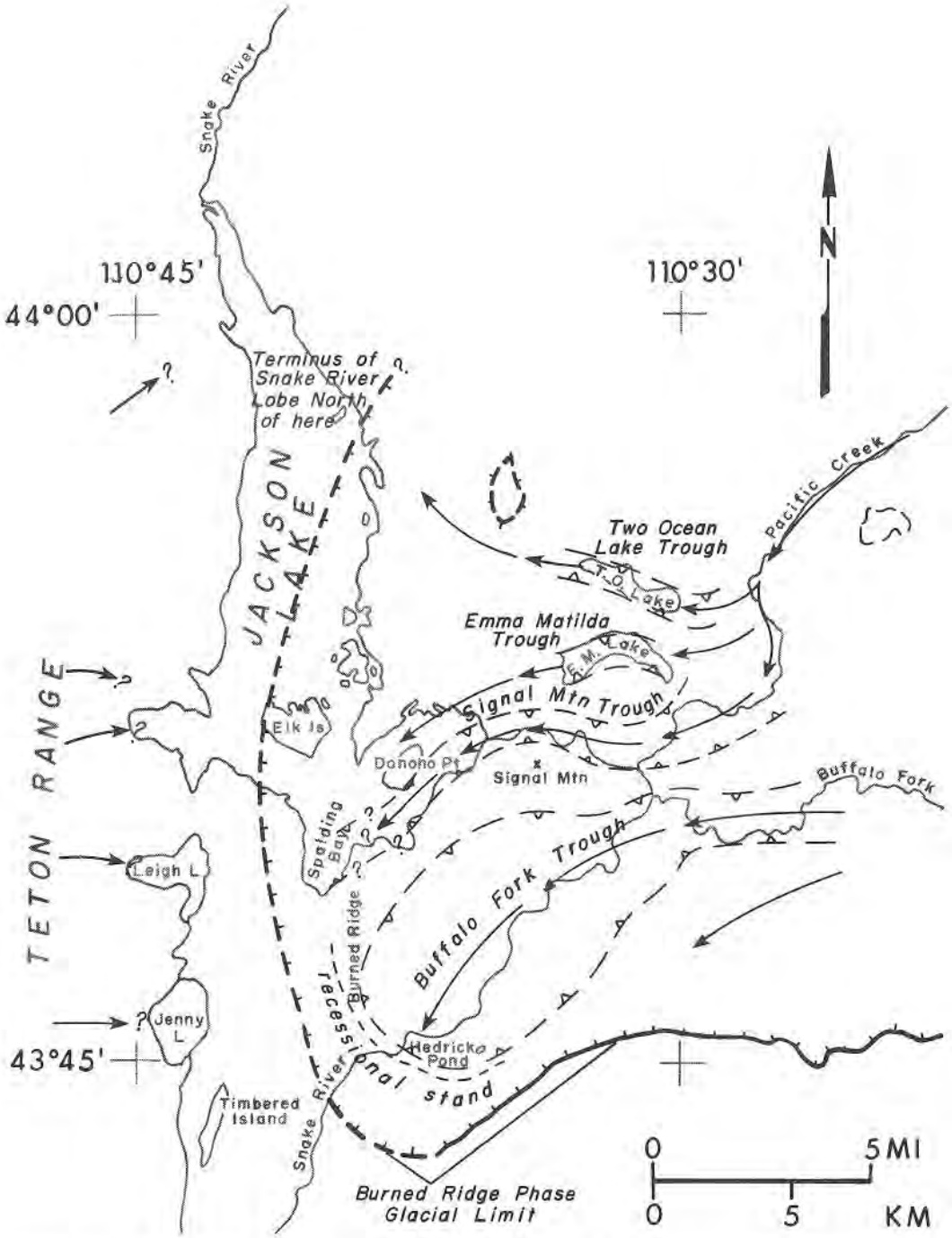

Figure 3a. Contrasting ice flow directions during the Burned Ridge phase of the last (Pinedale) glaciation. Glacial flow directions indicated by arrows. Glacial termini are shown by hachured lines except along the Teton Range where they are not known. Borders of troughs shown by long dashed line with small triangles on trough side. The Burned Ridge ice phase was associated with westward flow of the Buffalo Fork and Pacific Creek ice lobes, resulting in several glacial-scour troughs including the eastern trough of Jackson Lake

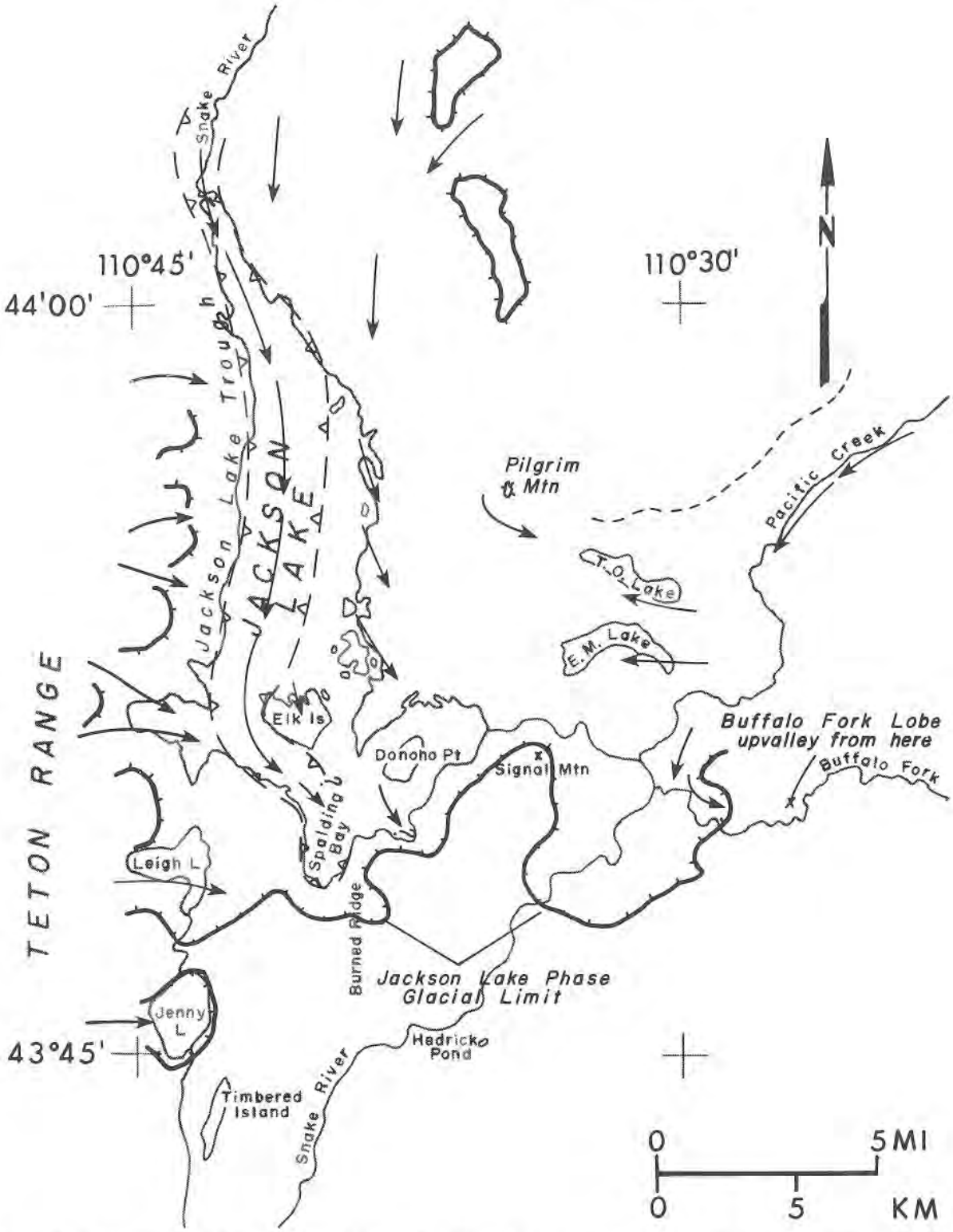

Figure 3b. Contrasting ice flow directions during the Jackson Lake phase of the last (Pinedale) glaciation. Glacial flow directions indicated by arrows. Glacial termini and ice margins are shown by hachured lines with open triangles on the ice contact side of the line. The Jackson Lake ice phase was associated with southward flow of the Snake River ice lobe that scoured the deep western trough down the main axis of Jackson Lake. Ice margins on valley walls shown by hachured line. North of Jenny Lake, the Snake River lobe was joined by valley glaciers (arrows) from the Teton Range.

Geologic mapping by Love and others (1972) and the seismic refraction studies of Behrendt and others (1968) indicated that the Teton fault extends along the western side of Jackson Lake and crosses the east side of Moran Bay. Behrendt and others (1968) and Tibbetts and others (1969) also interpreted a subsidiary north-trending fault extending through the center of the lake. However, as discussed below, we found no evidence from our reflection data for these proposed faults or any other significant faulting beneath the lake. This finding confirmed the conclusions of Smith and others (1990) and Smith, Byrd, and Susong (this volume), who reported that the main Quaternary scarp of the Teton fault is confined to on-shore areas, 0.1 to 1.2 mi (0.2 to 2 km) west of Jackson Lake.

Glaciation

Pleistocene glacial processes that scoured sedimentary troughs and deposited the extensive moraines and outwash in the Jackson Lake area are key elements necessary for understanding the seismic data and interpretations presented here. The glacial record of the Jackson Hole region was first discussed by Fryxell (1929, 1938) and later elaborated upon by Montagne (1956). Pierce (1979) described the glacial history and dynamics of the northern Yellowstone ice cap and Pierce and Good (1990) summarized their glacial geology studies conducted in Jackson Hole from 1985 to 1990.

Prior to the last glaciation (Pinedale), there were perhaps ten or more glacial intervals, during which glaciers may have reached the floor of Jackson Hole and contributed sediments to the Quaternary fill of northern Jackson Hole. The fill is estimated to be about 8,000 ft (2,460 m) thick above the 2 Ma Huckleberry Ridge Tuff just east of the Teton fault. Of these many possible pre-Pinedale glaciations, only deposits and effects of the next-to-last (Munger) glaciation are clearly identified in northern Jackson Hole. The Munger glaciation is tentatively correlated with the Bull Lake glaciation, whose age in the West Yellowstone, Montana, area is about 140 ka (Pierce and others, 1976). The Munger glaciation was much more extensive than the Pinedale glaciation; it extended about 30 miles (50 km) south of the Pinedale glacial terminus and filled Jackson Hole with more than 3,000 ft (1 km) of ice (Love and Reed, 1971; Pierce and Good, 1990).

During the Pinedale glaciation, three glacial lobes (**Figure 3a** and **3b**; **Table 1**) fed into northern Jackson Hole from the southern margin of the Yellowstone-Absaroka ice sheet (Pierce and Good, 1990). These lobes are, from east to west, Buffalo Fork, Pacific Creek, and Snake River (**Table 1**; **Figure 3a**). Three temporal phases are also distinguished, among which the relative size of these lobes changed, with the biggest lobe changing through time from sources to the east to sources north of Jackson Lake (**Table 1**). However, the ages of these phases are poorly constrained. Pinedale glaciers of the Jackson Lake phase receded from the area by 15 to 11 ka and the Jackson Lake and Hedrick Pond phases probably occurred between 40 and 15 ka. The Burned Ridge phase is at least 25 ka and may be as old as 75 ka (Pierce and Good, 1990).

During the first (Burned Ridge) phase, ice from the combined Buffalo Fork and Pacific Creek lobes flowed westward into the Jackson Lake basin nearly to the Teton Range (**Figure 3a**). At this time, the Snake River lobe did not join the other two lobes but terminated somewhere north of Jackson Lake. The ice front of this advance reached more than 6 mi (10 km) south of Jackson Lake (Fryxell, 1929; Love and Reed, 1971; Pierce and Good, 1990). This flow covered Signal Mountain and scoured deep basins north and south of Signal Mountain. The scour trough on the north side of Signal Mountain extends down the Pacific Creek valley and into the Snake River valley beneath the Jackson Lake damsite to at least the deep trough between Signal Mountain and Donoho Point (**Figure 3a**). Beneath the dike north of the concrete section of Jackson Lake dam, drilling shows that this scour basin is more than 600 ft (185 m) deep and is filled largely with unconsolidated lake sediments (Gilbert and others, 1983).

During the second (Hedrick Pond) and third (Jackson Lake) phases, ice from the Snake River (Richmond, 1973) and Pacific Creek (Richmond and Pierce, 1971) lobes joined and flowed southward into northern Jackson Hole (**Figure 3b**). At this time, the Buffalo Fork glacial lobe did not join the other two lobes but terminated several miles up Buffalo Fork. The southern margin of Jackson Lake is dammed by moraines and outwash deposited mostly during the Jackson Lake phase and built up to heights of ~100 to 300 ft (30 to 90 m) above Jackson Lake (Fryxell, 1929; Love and Reed, 1971). The deep trough beneath the long north-south axis of Jackson Lake and the

drumlinoid topography on islands east of Jackson Lake were formed at this time (Pierce, 1987). This ice flowed southward to moraines about halfway up the north side of Signal Mountain. Such flow was nearly perpendicular to the westward flow during Burned Ridge time (**Figure 3a**). At this time (Jackson Lake phase), ice from the northern part of the Teton Range joined the south-flowing Snake River lobe. A glacial lobe flowing eastward from Moran Canyon through Moran Bay joined the Snake River lobe and deflected it southeastward around the southwest side of Elk Island.

Geophysical data acquisition and processing

The geophysical data for our Jackson Lake study were acquired in June and July 1974 as part of a comprehensive investigation of several lakes in the Intermountain region. A transportable 26-ft (8-m) research vessel was rigged with an air-gun seismic reflection and refraction system, a 500 cfm air compressor, a digital magnetometer, a 16-ft (5-m)-long piston corer and a high-resolution seismic-profiling device. Studies with this and similar equipment have been made of Yellowstone Lake, Wyoming (Otis and others, 1977; Nelson, 1974); Bear Lake, Utah, (Skeen, 1975); and the Great Salt Lake, Utah (Mikulich and Smith, 1974). These surveys and an earlier seismic investigation of Lake Tahoe, California-Nevada by Henyey and others (1972) demonstrated the effectiveness of marine techniques to acquire seismic information on the Quaternary geologic record in continental lacustrine environments of the western U.S.

The primary seismic reflection system used in the Jackson Lake surveys consisted of a 1-in^3 (16.4-cm^3) air gun, pressurized to 2,000 psi and fired at 4-second intervals. The data were received on a 40-element, single-channel hydrophone streamer and recorded on an FM analog recorder, providing 78 mi (125 km) of profile coverage (**Figure 4**). The 1-in^3 source had a maximum depth of penetration of about 1,100 ft (350 m) and provided a vertical resolution of ± 10 ft (3 m).

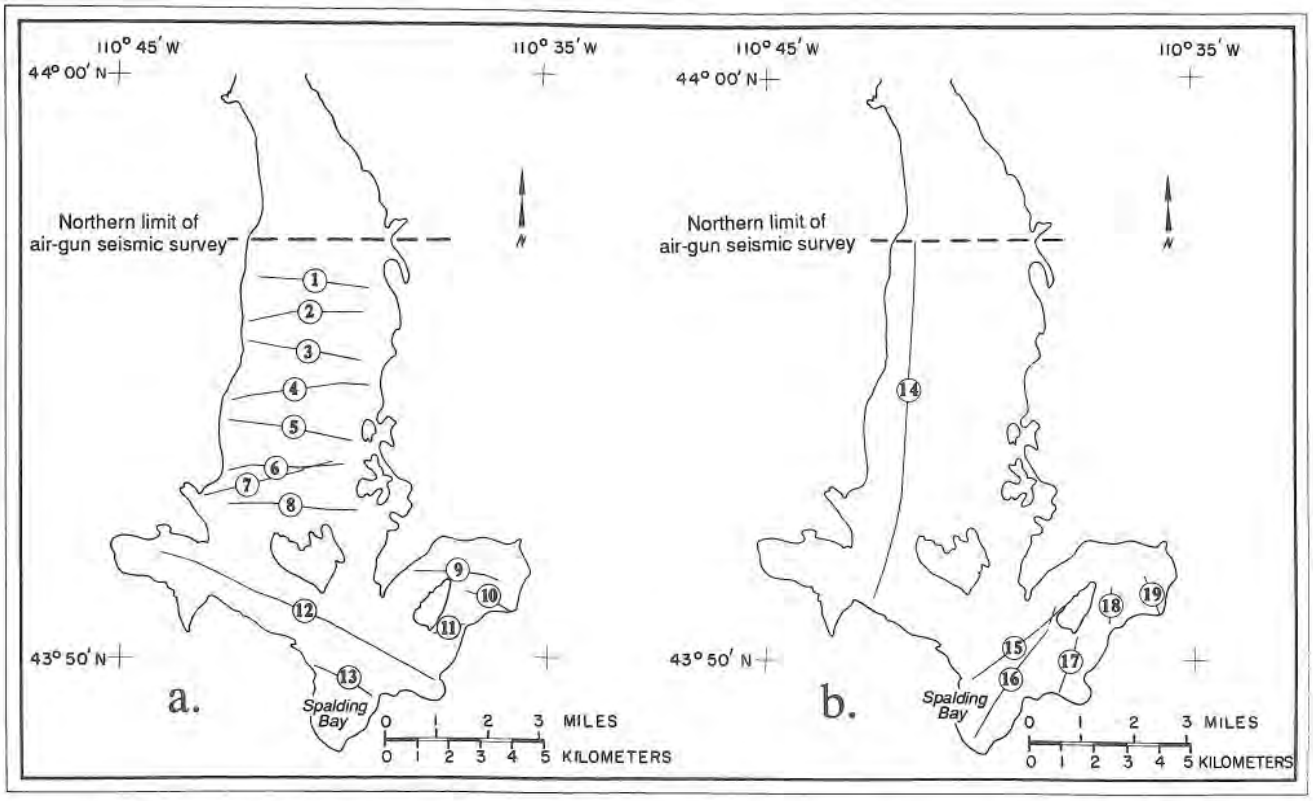

Figure 4. Index map of air-gun seismic reflection profiles of Jackson Lake. 4a numbers correspond to profiles shown on Sheet 2A and 4b numbers correspond to profiles shown on Sheet 2B.

The analog reflection data were digitized on a PDP-10 computer at the University of Utah. Homomorphic log-spectral averaging (Otis and Smith, 1976) was applied to these data to eliminate the bubble-pulse and other reverberations. Unfortunately, because none of the seismic data exist now in a digital form, we cannot reprocess them with state-of-the-art processing algorithms. The reflection data also were not migrated because of the lack of multichannel information, and also because of the lack of software for seismic processing in the late 1970s, while the data were available in a digital form.

The seismic data presented here are from both processed and unprocessed analog record sections reproduced from 9-inch, high-precision CRT displays in a continuous-tone format. Photographs were then taken of the CRT images and enlarged to obtain permanent plots of the reflection profiles. Interpretations were made on both processed and field-recorded analog record sections. We note the distortion of the reflection data ranges from 10 to 20:1 because of vertical to horizontal exaggeration.

Supplementing the seismic data, several 6.5- to 13-ft (2- to 4-m) piston cores were acquired for paleomagnetic analyses, to estimate the postglacial sedimentation rates, and to determine the composition of the sub-bottom lake sediments of Jackson Lake (Shuey and others, 1977). A radar-range microwave Mini-Ranger provided navigation for the surveys (transponder locations are shown on **Figure 5**). Locations from this system are considered accurate to about ± 3 ft (± 1 m).

Most seismic interpretations for this paper were made from the CRT-photographed seismic profiles. However, because the photographic images of the seismic record sections were not adequate for reproduction, hand-drawn picks were made to produce interpreted seismic cross sections. As an example of this process, we show two reflection profiles that

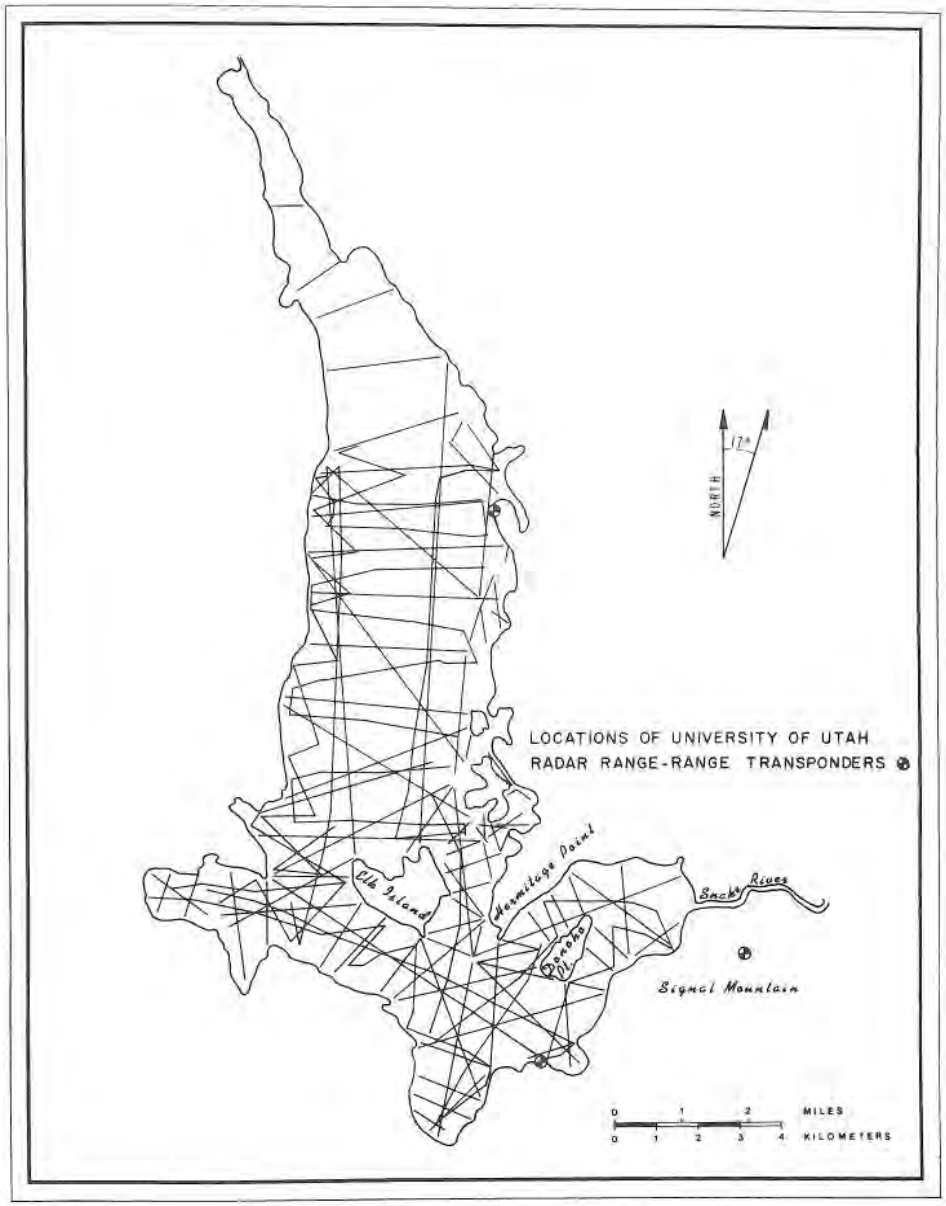

Figure 5. Locations of high-resolution seismic reflection profiles used to construct the bathymetric map of Jackson Lake. Bathymetry from 7.5 kHz high-frequency seismic reflection system with radar-range transponders for navigation. Additional data taken in areas inaccessible by our research vessel were from fathometer readings and dead-reckoning navigation by Hayden (1969).

were drawn from the accompanying photographic images in **Figures 6** and **7** (profiles 6 and 12).

Profile 6 (**Figure 6**) extends east-west across the main Jackson Lake basin and shows our interpretation of the continuous reflectors outlining unit A, which are underlain by discontinuous and unconformable reflectors, underlain by more coherent layers C and D. Profile 12, which crosses the south end of Jackson Lake (**Figure 7**), illustrates the lack of discontinuity in reflections that are expected at the projected location of the Teton fault across the east end

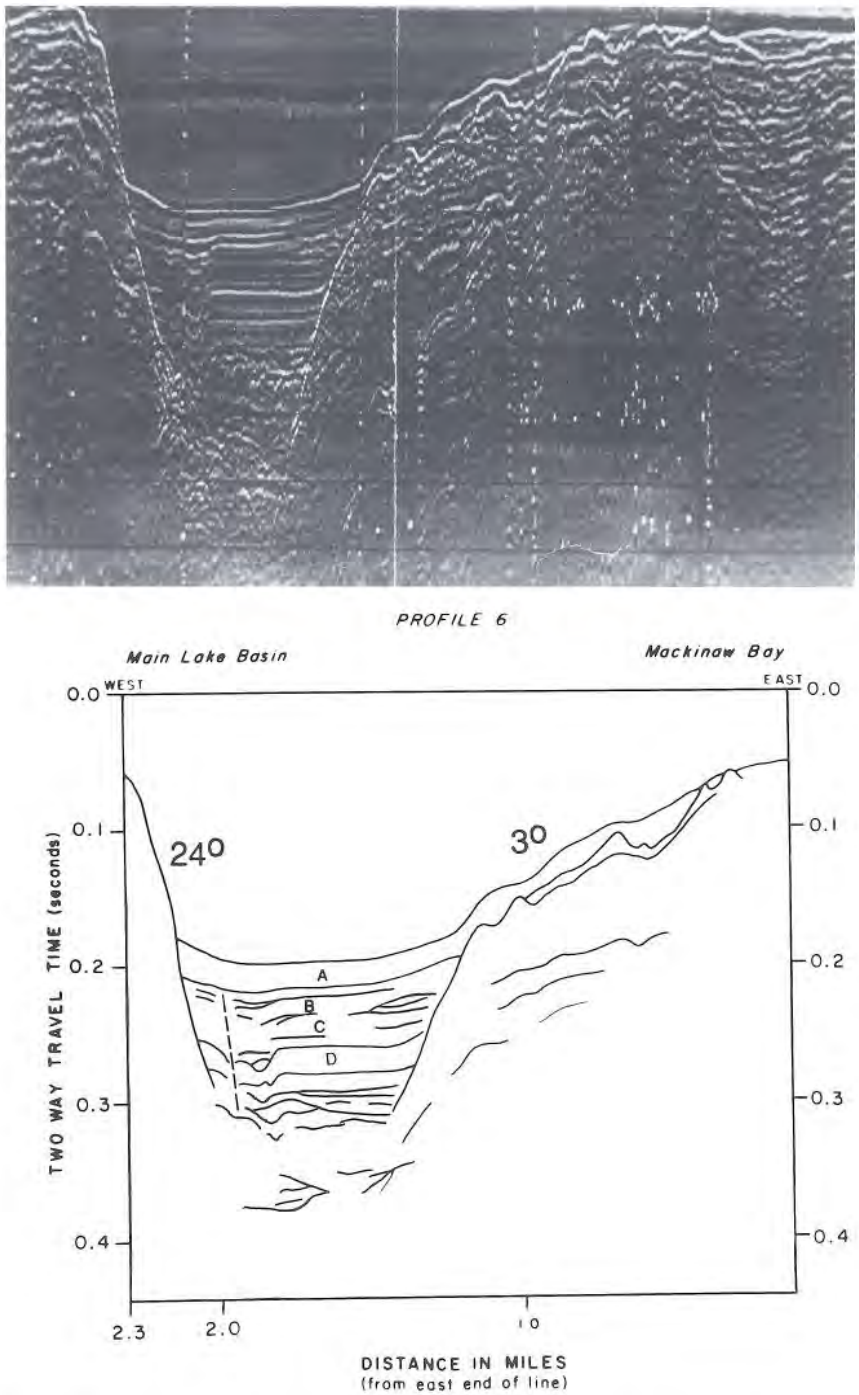

Figure 6. Seismic reflection profile no. 6 (east-west) and corresponding interpreted cross section across the main lake basin of Jackson Lake (also shown on Sheet 2A). Slopes of the water-bottom basin margins are shown in degrees.

of Moran Bay. **Figure 7** also demonstrates the excellent definition of reflector units A, B, and C in the Signal Mountain-Spalding Bay trough.

Due to the distortion caused by the exaggeration of the reflection profiles, we have noted the true dip of the water bottom on several of the figures to provide a better perspective of the lake-bottom geometry. For example, on profiles 6 and 12 (**Figures 6** and 7), the lake-bottom slopes range from 3° to 24°, representing typical values for both sides of the western lake basin. The maximum dips of the deeper geologic reflectors are correspondingly less, but they were not calculated due to the lack of migrated seismic data.

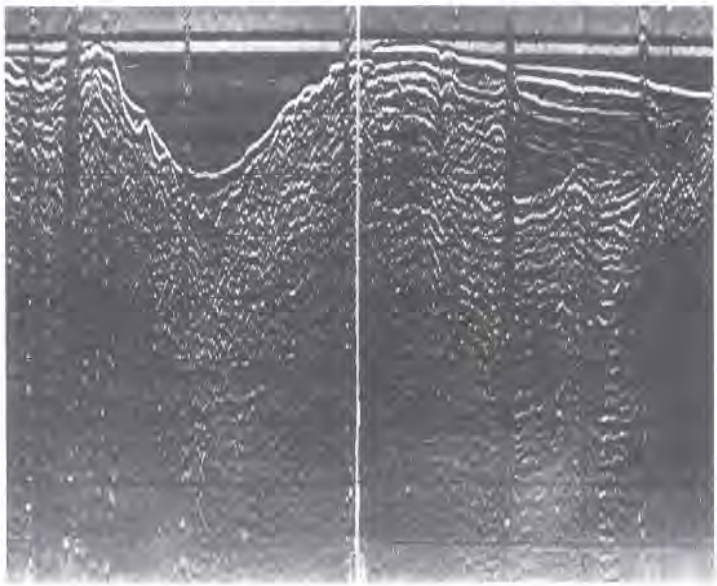

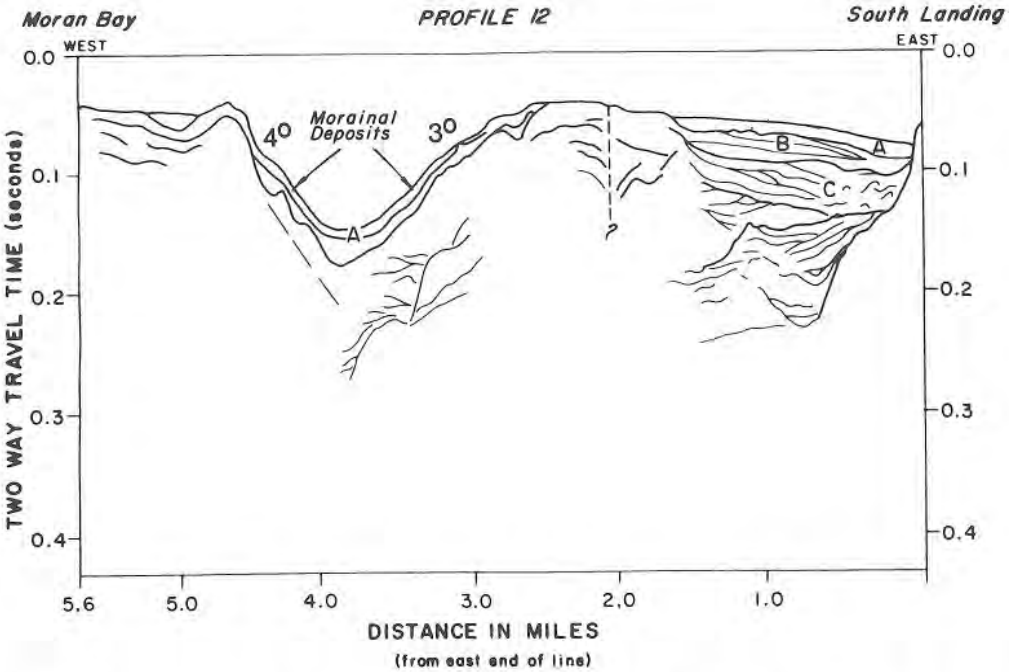

Figure 7. Seismic reflection profile no. 12 (east-west) from Moran Bay to the Signal Mountain-Spalding Bay trough with corresponding interpreted cross section (also shown on Sheet 2B). Slopes of the water-bottom basin margins are shown in degrees.

Bathymetry of Jackson Lake

An important objective of our project was to produce a detailed bathymetric map of Jackson Lake (**Sheet 1**, Smith and others, map pocket). This was accomplished by acquiring high-resolution reflection profiles of the shallow lake-bottom sediments using the 7.5 kHz-source seismic reflection system. The high-resolution data provided about 3 ft (~1 m) of vertical resolution to maximum depths of about 125 ft (~40 m) and were recorded along 207 mi (333 km) of profiles (**Figure 5**).

The depth of the water bottom was determined using the velocity of about 4,750 ft/s (1.4 km/s), determined from the refraction profiles of Oxley (1975), to convert lake bed reflections to depth. The water bottom was penetrated by five piston cores to depths of about 12-ft (4-m) and was generally composed of up to 90% fluid, grading from water into silt-sized diatom particles (Shuey and others, 1977). Thus our use of the water bottom was not at an idealized water-mud boundary, but incorporated a gradational water-to-saturated mud interface. The lake bottom is estimated to be within 1 to 3 ft (0.3 to 1 m) of the bottom of the 100% water column. Note that we were unable to acquire seismic data with our research vessel in shallow water, such as the north end of Jackson Lake on the Snake River delta and around several of the islands. In these areas we supplemented our data with fathometer depth-sounding data acquired by Hayden (1969).

From the Jackson Lake bathymetry map (**Sheet 1**, Smith and others, map pocket), two topographic troughs are apparent. The deeper western basin extends north-south and attains a maximum depth of 437 ft (133 m). A smaller eastern trough trends southwest around the north side of Signal Mountain and reaches a maximum depth of 142 ft (43 m). These troughs are separated by a shallow ridge that extends southwest from Hermitage Point. The main lake trough is bounded by generally linear margins, the western side of which has been thought to be a fault scarp. However, as noted above, the dips of these basin margins do not exceed 28° and most are less than 20°. Because the trough is two-sided (symmetrical) and much too high to represent a postglacial fault scarp, we interpret both sides of the trough to have resulted from north-to-south glacial scouring of unconsolidated Quaternary sediments deposited in a basin formed immediately east of the Teton fault.

Sediment record of Jackson Lake

The air-gun seismic reflection profiles were the primary source of data for our interpretations of the structure and sedimentation of Jackson Lake. These data consisted of 78 mi (125 km) of air-gun reflection profiles, supplemented by 207 mi (333 km) of high-resolution (7.5 kHz) reflection profiles (**Figures 4** and **5**). Nineteen of the air-gun profiles have been reproduced on **Sheet 2A** (east-west profiles) and **2B** (north-south profiles) (Smith and others, map pocket). [Also see **Figures 6** and **7** for enlarged figures of reflection profiles 6 and 12]. Examination of **Sheet 2A** and **2B** reveals that the general subsurface structure of Jackson Lake corresponds to two sedimentary basins located beneath the two bathymetric troughs, described below as the western and eastern basins.

Western basin

The shallowest distinguishable reflector marks the bottom of a unit identified as A. Unit A generally lacks strong reflectors, is widespread beneath the lake bottom, and is interpreted to represent postglacial, mostly Holocene, lake sediments. In the center of the main lake basin, unit A has a generally uniform thickness of about 55 ft (17 m) (**Figure 8**). According to analyses of 3- to 12-ft (1- to 4-m) piston cores from Jackson Lake (Shuey and others, 1977), the uppermost part of this layer consists of up to 90% water with up to 50% silt-sized diatom frustules and several percent of sand-sized detritus composed of quartz, feldspar, mica and other minerals, and up to 10% clay.

Unit A is thickest on the west side of the main lake (the west side of the bathymetric basin), reaching a maximum thickness of 70 ft (23 m) (**Figure 8**). There is little evidence (see profile 6) for westward tilt of unit A. The thickening of this layer west of the axis of the main bathymetric basin may result from turbid Snake River inflow observed to extend southward along the west side of the lake. In the eastern trough, unit A thins to about 50 ft (15 m) (**Figure 8**).

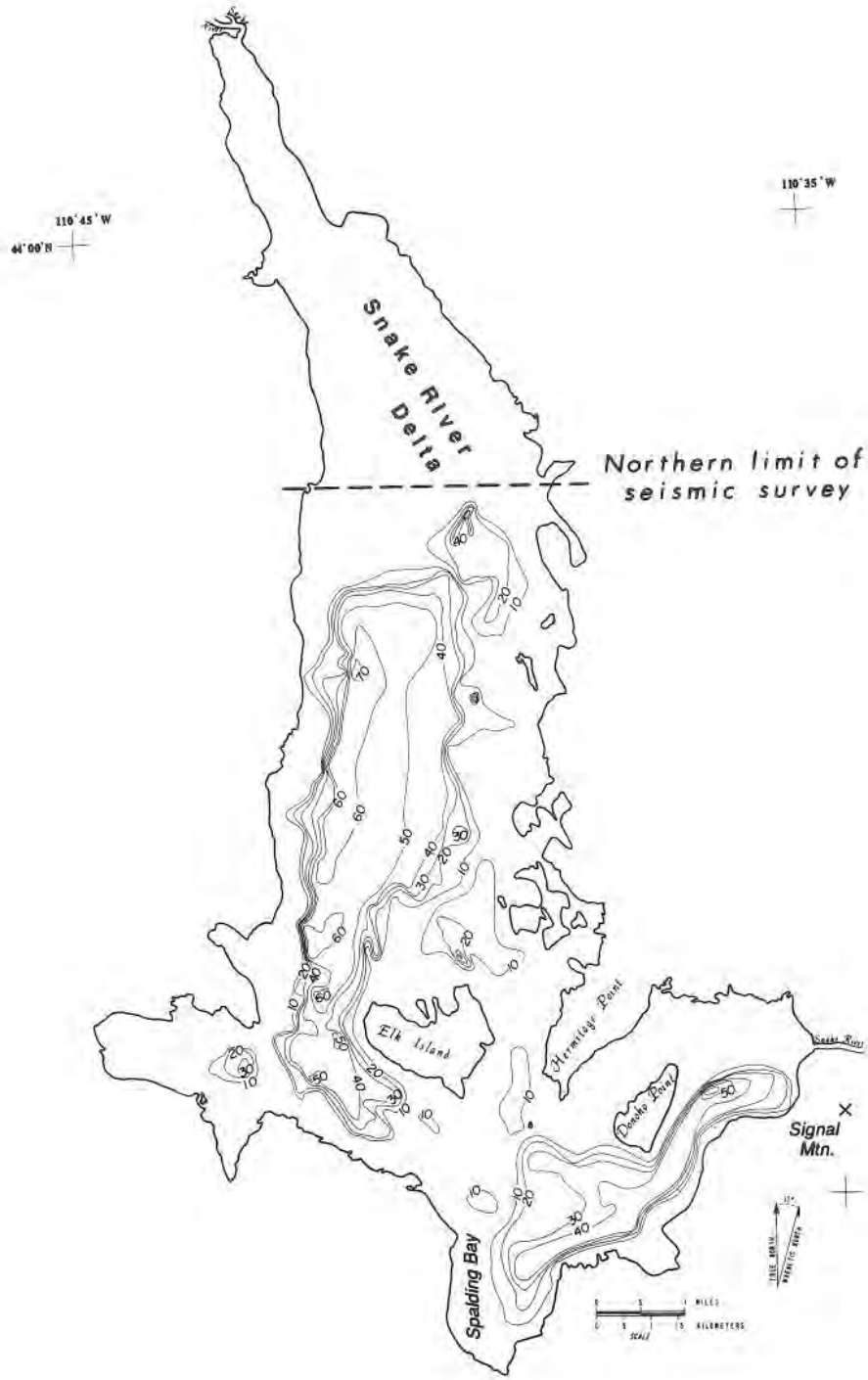

Figure 8. Isopach map of postglacial sediments in Jackson Lake, Wyoming. Contour interval = 10 ft (3.3 m). Velocity model: sediment velocity = 5,280 ft/s (1.6 km/s). This postglacial layer is interpreted to be between the lake bottom and the bottom of layer A. Thicknesses of less than 10 ft were not considered resolvable.

The seismic reflection data of Jackson Lake were carefully examined for evidence of faulting or other notable structural deformation in the postglacial sediments, primarily in layer A. However, we did not recognize any significant displacements in this layer, including across the east side of Moran Bay, where the Teton fault has been postulated by other workers (see Behrendt and others, 1968; and Love and others, 1972).

As seen in profiles 1 through 8, unit A averages 55 ft (16 m) thick, and piston cores of the upper 6.5 to 13.1 ft (2 to 4 m) from this unit show that it is composed dominantly of diatoms (Shuey and others, 1977). Dissolved silica, necessary to form the diatomaceous sediment, probably came from thermal springs in the Yellowstone volcanic plateau drained by the Snake River. This composition suggests that unit A was accumulated by a rain of diatoms growing in waters of a relatively clean lake. The environment of deposition has probably remained essentially unchanged since the drainage basin was deglaciated in the latest Pleistocene time.

For the main lake basin, units B and C (for example on profile 3, **Sheet 2A**) are noted as packets of discontinuous reflectors and are bounded by unconformities. These units are also evident on profile 6 (**Figure 6**). At the north end of the main lake basin, the seismic data reveal a more erratic nature of reflections in units B and C (between units A and D) that are marked by short discontinuous reflections and diffractions (profiles 3, 4, and 5, **Sheet 2A**). Units B and C apparently represent more disturbed sediments characterized by discontinuous reflections and unconformities. As shown in profile 14 (**Sheet 2B**), the slopes of units B and C decrease from north to south. This slope variation is consistent with their derivation from sources at the north end of the lake, perhaps by slumping from the Snake River delta and southward transport of this watery sediment mass by gravity into and along the deep western trough.

While there are deeper discontinuous reflections, unit D is the deepest coherent reflection package that was visible in our data. On reflection profiles 3, 4, 5, 6, and 7 (**Sheet 2A**), layer D can be recognized as a set of weak discontinuous reflections at 0.25 to 0.30 s (two-way travel time). The homogeneous nature of this unit suggests that it was deposited during a period of continuous deposition, although the possibility of multiple reflection paths cannot be ruled out. Beneath layer D, a zone of discontinuous reflectors makes up the deepest sediments seen in the reflection data of Jackson Lake at depths of 660 to 980 ft (200 to 300 m). However, these reflectors lack the lateral continuity to identify them as separated sediment packages (**Sheet 2**), although their internal character is similar to that of units B and C.

In the center of the main-lake basin, profiles 3 through 7 (**Sheet 2A**) show that the sediment packages A, C, and D have dips generally less than 5°. At the north end of Jackson Lake, a gentle eastward dip on these units can be seen on profile 1 (**Sheet 2A**), opposite to that expected for a westward tectonic backtilt. On profile 8 (**Sheet 2A**), at the south end of the main basin, the reflectors beneath the coherent sediment layers dip westward on the east side of the basin. We interpret that the western basin (**Figure 9**) contains at least 375 ft (115 m) of sediments (see profile 14, **Sheet 2B**; and profiles 1 through 8, **Sheet 2A**). South of Elk Island (profile 12, **Sheet 2A**), either the base of the sediment-filled trough rises to the base of unit A or the set of recessional glacial moraines south of Elk Island have restricted adequate seismic imaging of underlying reflectors.

The sediment supply to Jackson Lake during late glacial time was probably greatest into the Snake River delta at the north end of Jackson Lake. Also, layer A is thinnest or absent near the Snake River delta, where deposition of terrigenous clastics continued into the late Holocene. As will be discussed later, the deepest part of the inferred scour basin is north of the currently deepest part of the lake, also suggesting a northern source of sediment (profiles 1 through 8, **Sheet 2A**). However, unit A is also commonly absent in the shallow parts of the lake basin, possibly scoured away by modern lake currents as fast as it accumulates.

Secular changes of remnant magnetization from four piston cores extracted from Jackson Lake (locations on **Figure 2**) were analyzed by Shuey and others (1977) to estimate paleoinclination for the past ~ 1,800 years. They concluded that the sharp swings in inclination correlate among the four cores (as shown by the dashed lines in **Figure 10**). The time scale was determined by comparison with the archeomagnetic data of the western U.S. described by Shuey and others (1977). From these paleomagnetic data, the predicted paleomagnetic inclination curves indicate a maxima at 1175 A. D. and a minima at 800 A. D. and lead to estimates of the sedimentation rates for the youngest sediments in Jackson Lake (**Table 2**).

The sedimentation rates determined for the uppermost sub-lake bottom sediments of Jackson Lake (**Table 2**) ranged from 0.04 to 0.08 in/yr (0.11 to 0.21 cm/yr) for the period 800 to 1175 A.D. and from 0.04 to 0.06 in/yr (0.09 to 0.15 cm/yr) for the period 1175 to 1974 A.D. Averaging these rates gives a range of 0.04 to 0.07 in/yr (0.09 to 0.17 cm/yr) for about a 800 to 1,900 year interval with an average of 0.06 in/yr or 5 ft/1,000 yr (0.14 cm/yr or 1.4 m/1,000 yr).

The minimum age of unit A, calculated using the layer thickness and the average sedimentation rate, is about 10,000 years and is notably less than the 14,500-year age of the near-total deglaciation of Yellowstone Lake (Porter and others, 1983). However, the sedimentation rate used for this calculation is based on only the upper one-tenth of the thickness of unit A, and the expected compaction of this unit with

depth would result in a closer match between the age of deglaciation based on sedimentation and that based on carbon-dating.

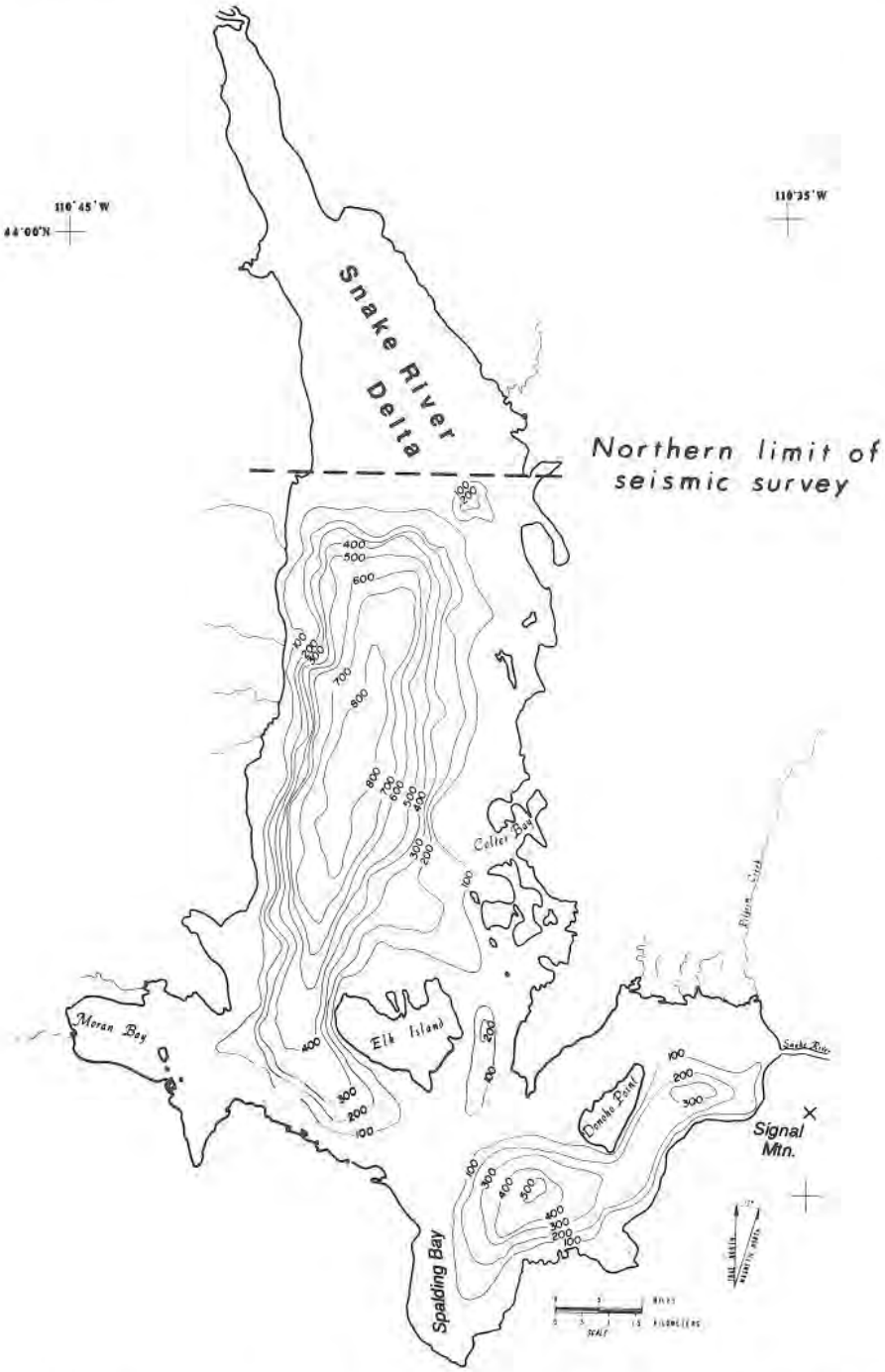

Figure 9. Depth to base of poorly consolidated Quaternary sediments in Jackson Lake, Wyoming. Contour interval=100 ft (30.5 m). Datum is the surface of Jackson Lake in 1974. Velocity model: water velocity = 4,785 ft/s (1.45 km/s), sediment velocity = 5,280 ft/s (1.6 km/s). Isopachs of sediment thicknesses can be determined by subtracting the bathymetrically determined depths on Sheet 1 (Smith and others, map pocket) from data in this figure.

Sediment units B and C are generally much thicker than layer A, and their ages are not known. However, they are considered to date from the time when sediment delivery by the Snake River was quite high. A large increase in deposition rate, perhaps fifty times greater than that characterizing the Holocene, determined here from the paleomagnetic analyses, is required for an interval of a few thousand years. This is not unreasonable because: (1) deposition rates in water bodies near glaciers are typically very high (decimeters/yr), and (2) the 40:1 ratio of the sediment source area to deposition area would result in a strong sediment-focusing effect. The western trough of Jackson Lake has an area of about 9.6 mi^2 (25 km^2), whereas the glaciers draining into the basin had an area of about 380 mi^2 (1,000 km^2). Thus the high rate of late-glacial accumulation in not unreasonable.

The deeper coherent units, B and C, are identified at their tops and bottoms by unconformities (see for example, profiles 3, 5, and 6, **Sheet 2A**). Plausible interpretations for the unconformities are: (1) partial erosion of the sedimentary fill deposited by a glacial advance, followed by deposition of more sediment; (2) periodic lowering of lake levels by at least several hundred feet with ensuing subaerial erosion, followed by raising of lake level and renewed lake deposition; and (3) slumps of water-rich unconsolidated sediment from the steep front of the Snake

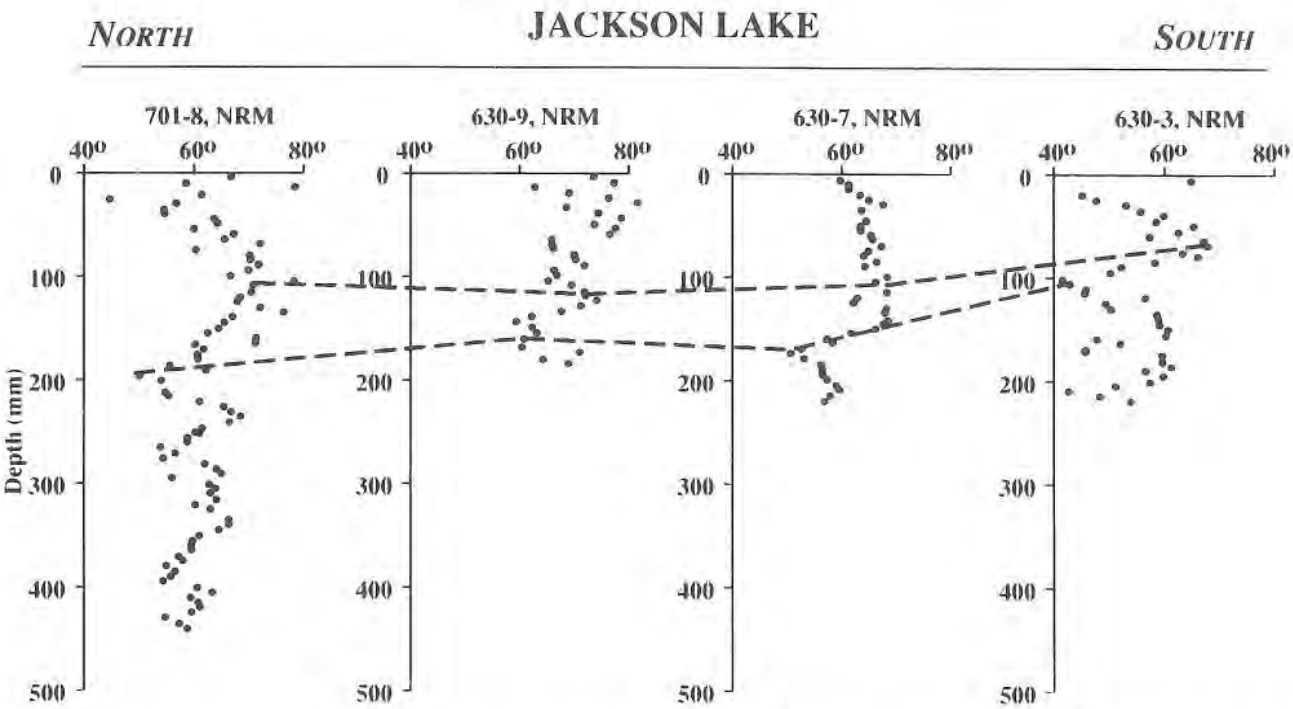

Figure 10. Correlation of paleomagnetic inclinations from piston cores (dashed lines), Jackson Lake, Wyoming (modified from Shuey and others, 1977). See Figure 2 for piston core locations. The data are NRM (natural remnant magnetization) and were demagnetized in fields of 50, 100, or 150 oersteds.

River delta and gravity transport of this sediment mass to the floor of the deep trough, producing contorted sediment packets with relatively flat tops.

The first explanation is considered unlikely because any significant overriding by glacial ice would probably scour out all the soft sediment and because glacial overriding is not likely to leave a similar section everywhere along the trough. A more plausible variation of the first explanation might include glacial standstills or minor readvances of about 0.6 mi (1 km) during overall retreat of ice northward.

The second explanation is considered unlikely because the lowest level of the lake is currently controlled by a bedrock threshold at the Jackson Lake dam site at an elevation of 6,700 ft (2,045 m). The discontinuities in the reflection profiles are all greater than 100 ft (300 m) deeper than this threshold, and displacements more than 100 ft (300 m) on the Teton fault would thus be required for base-level changes of this magnitude.

The third explanation seems plausible. Slumping of sediment from the Snake River delta at the north end of the lake and the development of southward-flowing mass movements down the trough may be responsible for units B and C, separated by planar unconformities. Slumped and rotated beds may also produce inclined layers truncated by subhorizontal unconformities. Such slumps are likely to have occurred during large scarp-forming earthquakes on the Teton fault. Large earthquakes on the Teton fault are estimated to have occurred at intervals averaging 1,600 to 6,000 years (Smith and others, 1990; Smith, Byrd, and Susong, this volume), and there have probably been several large, scarp-forming earthquakes since deglaciation about 14 ka. If such slumps oc-

Table 2. Sedimentation rates [in/yr (cm/yr)] calculated from paleomagnetic data of piston cores from Jackson Lake, Wyoming (after Shuey and others, 1977). Piston core locations shown in Figure 2.

Core no.	800-1175 A.D.	1175-1974 A.D.	Averaged by core
701-8	0.08 (0.21)	0.06 (0.15)	0.07 (0.17)
630-9	0.05 (0.13)	0.06 (0.15)	0.06 (0.15)
630-7	0.07 (0.17)	0.06 (0.14)	0.06 (0.15)
630-3	0.04 (0.11)	0.04 (0.10)	0.04 (0.10)
Averaged by age	0.06±0.02	0.05±0.01	0.06 ±0.01

curred, they most likely formed in late-glacial time and not in Holocene time, because unit A reaches its full thickness in the main trough, suggesting units B and C are pre-Holocene in age.

Eastern basin

Similar sedimentary layers, identified in the western, main-lake, basin are also present beneath the eastern bathymetric trough that consists of two sub-basins: Spalding Bay and Signal Mountain. They are described separately because the Spalding Bay trough has a more complex genesis, having been occupied and scoured(?) first by the southwest-flowing Pacific Creek lobe in Burned Ridge time and then by the south-flowing Snake River lobe in Jackson Lake time. The seismic data for this area (see profile 12, **Sheet 2A**; profiles 18 and 19, **Sheet 2B**) correspond to a total sediment thickness of about 600 ft (180 m). Other profiles—10 and 11 (**Sheet 2A**) and 17 (**Sheet 2B**)—reveal sedimentary fill of only about half this thickness. However, the bases of the scour troughs may not be apparent on these profiles and thus may be much deeper.

A continuity of main reflectors between the western (main) and eastern sedimentary troughs was not visible from our seismic reflection data. This area, however, corresponds to the location where westward-flowing ice from the Pacific Creek and Buffalo Fork lobes would have coalesced with the south-flowing ice of the main lake basin southwest of Hermitage Point. This configuration may have produced a ridge of more consolidated lateral morainal sediments that could not be penetrated by our seismic reflection system.

Spalding Bay sub-basin

Beneath Spalding Bay, sedimentary units B and C generally have eastward dips of a few degrees (less than 5°) and some have basal angular unconformities (**Figure 7**; profile 12, **Sheet 2A**). Profiles 15 and 16 (**Sheet 2B**) are located in the same area as profile 12 but show essentially horizontal bedding in units B and C, indicating that the apparent dips shown in profile 12 are essentially the maximum dips. These gentle east dips suggest deposition from a source to the west and are thought to indicate subaqueous density flows of sediment emerging into a lake from the base of the Snake River lobe when it terminated south of Elk Island. Two ages relative to the glacial sequence might be postulated: (1) units B and C on profile 12 accumulated during recession of ice from the Jackson Lake position, when a glacier front was between Elk Island and Hedrick Pond area; or (2) unit C accumulated during the Hedrick Pond glacial advance and unit B accumulated during recession from the Jackson Lake phase. The second option seems less likely because the advance to the Hedrick Pond position seems likely to have eroded unit C.

Signal Mountain sub-basin

Several hundred feet of sediment fill are present beneath the trough adjacent to Signal Mountain. Dips of beds in units B and C in this area are not systematic, as in the western main lake trough. For layer B, the following apparent dips are indicated: west (profiles 10 and 11, **Sheet 2A**), north (profile 18, **Sheet 2B**), and south (profile 19, **Sheet 2B**). For unit C, apparent dips are south (profile 18), and north (profile 19). Perhaps these diverse directions represent subaqueous filling by density flows pouring around both ends of Donoho Point and into the trough from the northwest and northeast.

Structure of the Jackson Lake basin

The upper crustal, basement structure of northern Jackson Hole has been evaluated by seismic refraction profiling around the east and south ends of Jackson Lake. Two-dimensional interpretations of refraction data were made by Behrendt and others (1968) and Tibbetts and others (1969), who interpreted Mesozoic and Paleozoic consolidated sediments to be as deep as 13,120 ft (4,000 m). These layers are interpreted to underlie Jackson Lake.

Information on the Jackson Lake sub-basin units was also interpreted from seismic refraction and wide-angle reflection data acquired in our surveys. These data were initially interpreted by Oxley (1975) but have been reinterpreted by us using new ray-tracing codes. The seismic refraction data were recorded with a fixed, radio-telemetered, single-channel sonobuoy from a moving 40-in^3 (650-cm^3) air gun on the research vessel. Seven refraction profiles

were recorded in the main basin and across the south end of the lake (**Figures 11** and **12**). We discuss the generalized one-dimensional velocity determinations first (**Figure 11**), then summarize the two-dimensional structure of the southern end of Jackson Lake (**Figure 12**) using wide-angle reflection data.

To determine the general Jackson Lake basin structure, P-wave arrivals from the refraction profiles (**Figure 11**) were used to determine one-dimensional P-wave velocity models for Jackson Lake (**Figure 12**). We note that the refraction profiles were not well reversed because of the low-energy source and the resultant lack of reciprocity. The one-dimensional P-wave models were then combined into a three-dimensional diagram to display a generalized velocity model for Jackson Lake (**Figure 12**), which extends to depths of about 975 to 1,100 ft (300-400 m).

Figure 12 shows that the first layer is representative of the water column. The water layer is in turn underlain by a second layer of unconsolidated sediments characterized by an averaged velocity of 6,890 ft/s (2.1 km/s). This layer generally coincides with sediment layer A interpreted from the reflection data, and it is interpreted as upper Quaternary. This layer is thickest [~ 650 ft (200 m)] at the north end of the main lake basin, suggesting filling of a glacial scour basin by the Snake River delta and slumps from that delta. The second sediment layer underlies the entire lake and appears thickest [~ 1,000 ft (300 m)] in the center of the main lake basin. Its velocity of 8,530 ft/s (2.6 km/s) reflects increasing consolidation with depth and age compared to the lower velocity overlying layers. This layer is inter-

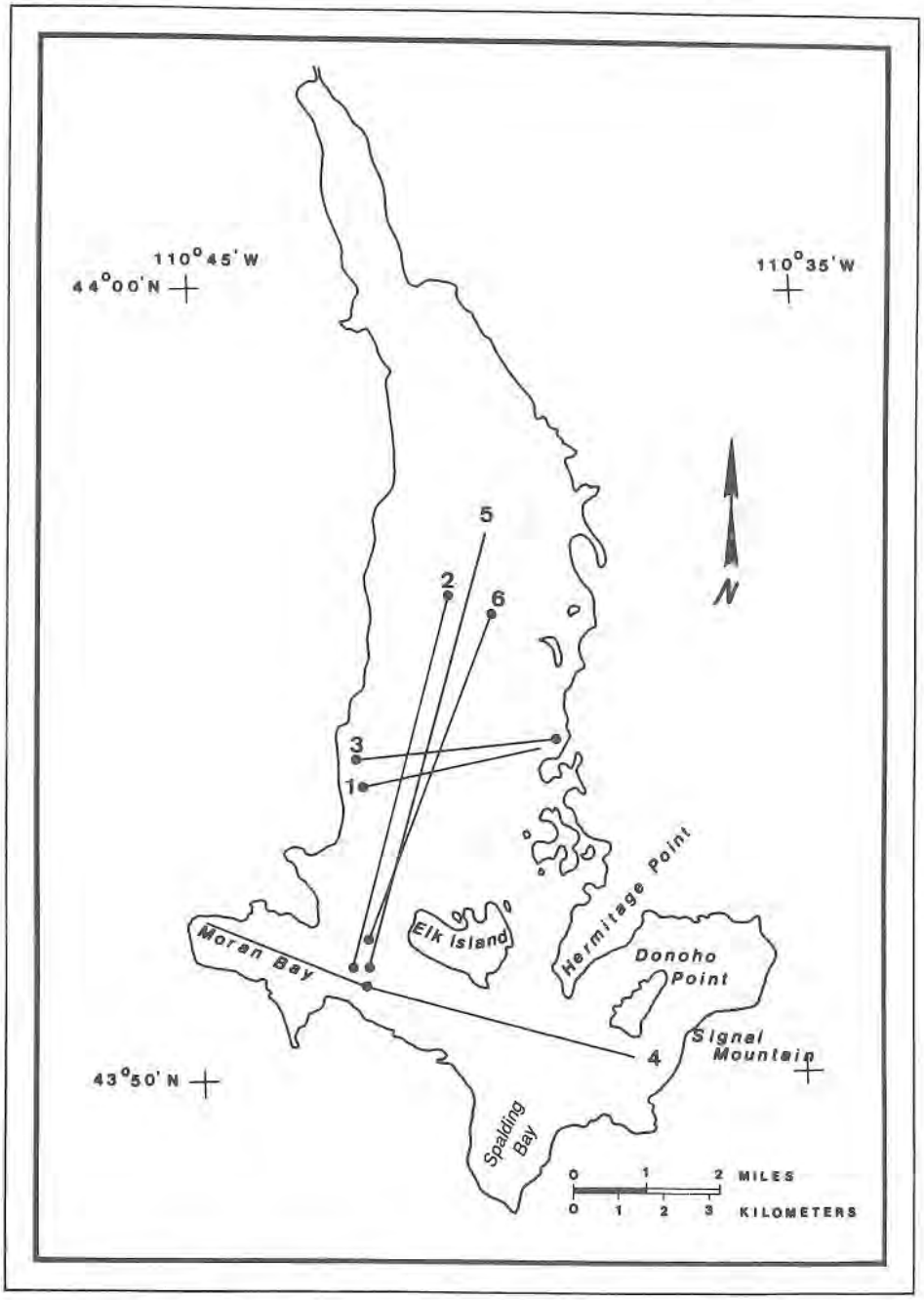

Figure 11. Locations of refraction profiles used to construct the generalized velocity structure of Jackson Lake basin. Fixed sonobuoys were located at the ends of the profiles (shown as solid dots). Note that there are two off-end seismic profiles across the southern end of Jackson Lake recorded from a single sonobuoy southwest of Elk Island.

layers. This layer is interpreted to be composed of lower Quaternary sediments, into which the late Pleistocene (Pinedale) glacial scour trough was excavated.

The third sediment layer has velocities of 11,480 ft/s (3.5 km/s) to 14,760 ft/s (4.5 km/s) and is interpreted to be composed of consolidated Tertiary and Mesozoic deposits (**Figure 12**). The deepest units discernible from the refraction data likely represent Mesozoic or Paleozoic rocks, interpreted by Behrendt and others (1968) from nearby refraction measurements south of Jackson Lake, with velocities of 8,040 ft/s (2.45 km/s) to 12,800 ft/s (3.9 km/s). Deeper Paleozoic and Precambrian rocks, identified by Behrendt and others (1968), Tibbetts and others (1969), and Schilly and others (1982), have considerably higher velocities of 20,000 ft/s (6.1 km/s) and occur at greater depths (~ 10,000 ft/3 km) than penetrated by our seismic profiles.

Figure 13 shows a detailed refraction/wide-angle reflection profile (corresponding to the location of profile 4, **Figure 11**) re-

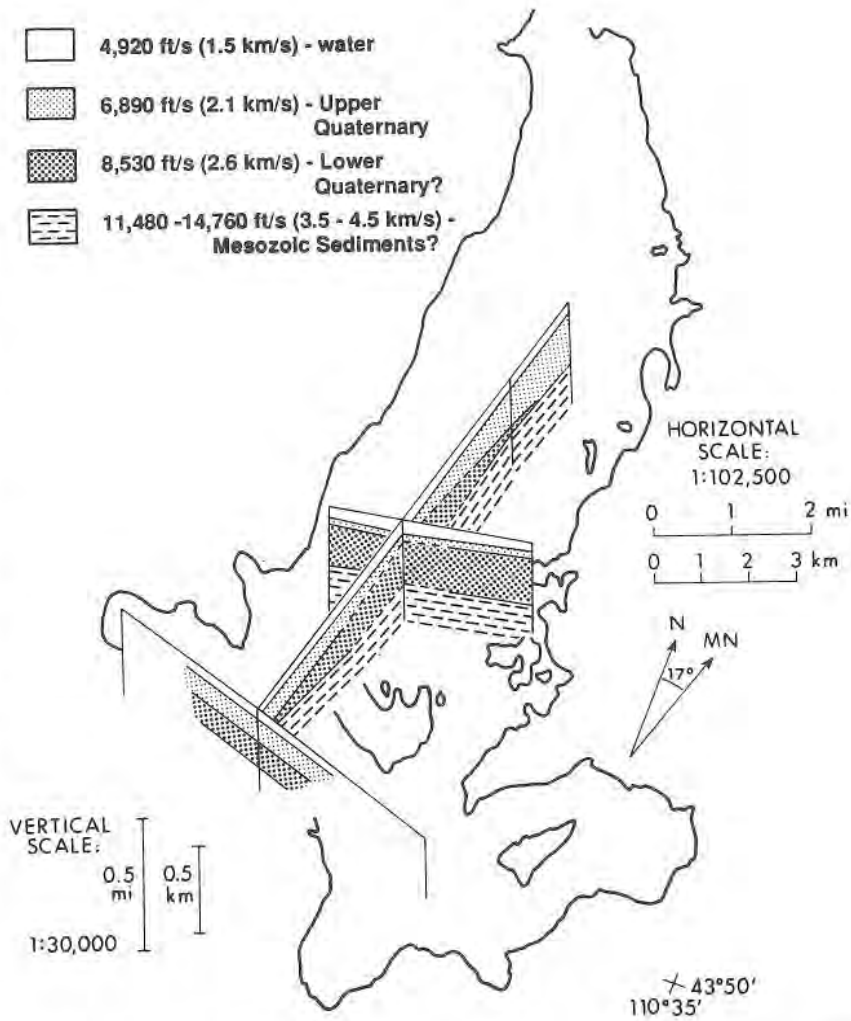

Figure 12. Diagram of the P-wave velocity structure of upper ~ 1,500 ft (0.5 km) of the Jackson Lake basin. Velocities and depths were determined by ray-tracing for one-dimensional models of unreversed refraction lines shown in Figure 11.

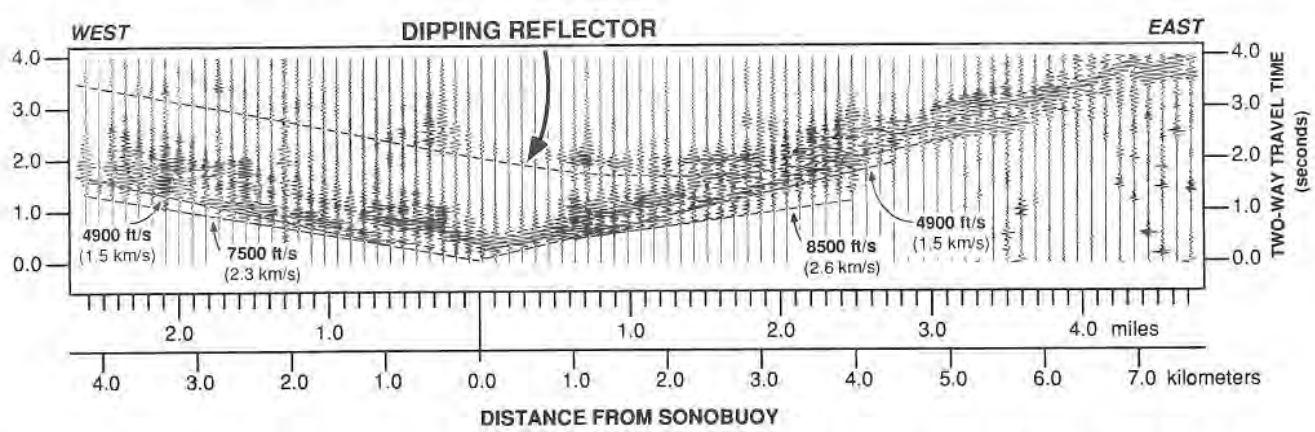

Figure 13. Seismic refraction and wide-angle reflection profile across the south end of Jackson Lake from south of Elk Island to Signal Mountain. Location corresponds to line 4 on Figure 11. A radio-telemetered, single-channel sonobuoy (recorder) was placed southwest of Elk Island and the source was towed east and west to the ends of the profiles.

corded from a fixed air-gun source (southwest of Elk Island) eastward toward Signal Mountain and westward across Moran Bay. The notable arrivals on this profile (**Figure 13**) include a direct wave associated with the water-bottom saturated sediments at a P-wave velocity of 4,757 ft/s (1.45 km/s). A second arrival represents a refractor from a layer that is interpreted to represent shallow lake sediments with a velocity of 6,560 ft/s (2.3 km/s) and an average thickness of 430 ft (130 m).

A secondary arrival on this record section is seen between 2 and 3 seconds two-way time as a hyperbolic travel-time branch and is interpreted to be a wide-angle reflection from a sub-basin or basement layer. Using an averaged velocity of about 9,850 ft/s (3 km/s), estimated from the moveout of this arrival, the top of this reflecting layer (**Figure 13**) is calculated to be about 2.7 mi (4.3 km) below Elk Island and the dip is 42° west.

To examine the relationship of this west dipping reflection, we have constructed a generalized east-west cross section across the southern end of Jackson Lake (**Figure 14**) on the basis of the seismic data shown in **Figure 13** and the projection of on-shore mapped exposures of the 2 Ma Huckleberry Ridge Tuff by Gilbert and others (1983). The projection of the Teton fault, at a postulated eastward dip of 60° (estimated by Smith, Byrd, and Susong, this volume), is also shown.

The dip of the Huckleberry Ridge Tuff in northern Jackson Hole increases westward toward the Teton fault (**Figure 14**). The change in dip with distance from the Teton fault shown in **Figure 14** is taken from dips of the Huckleberry Ridge Tuff mapped by Gilbert and others (1983, figure D-3) around the east and north sides of Jackson Lake. It should be noted, however, that a component of the tilt of these units may be due to local tilting on a small, north-striking down-to-the-east normal fault east of Signal Mountain. The projected position of the Huckleberry Ridge Tuff at a depth of 6,000 ft (1.8 km) beneath Elk Island (dashed line, **Figure 14**) is shallower than the 42° dipping reflector beneath Elk Island (heavy line, **Figure 14**), but these lines intersect between Elk Island and Hermitage Point. If the prominent reflector is Huckleberry Ridge Tuff, it dips much steeper than projected from surface outcrops. It also could be an older layer, such as the 6 to 4.2 Ma tuff exposed on Signal Mountain or the inter-

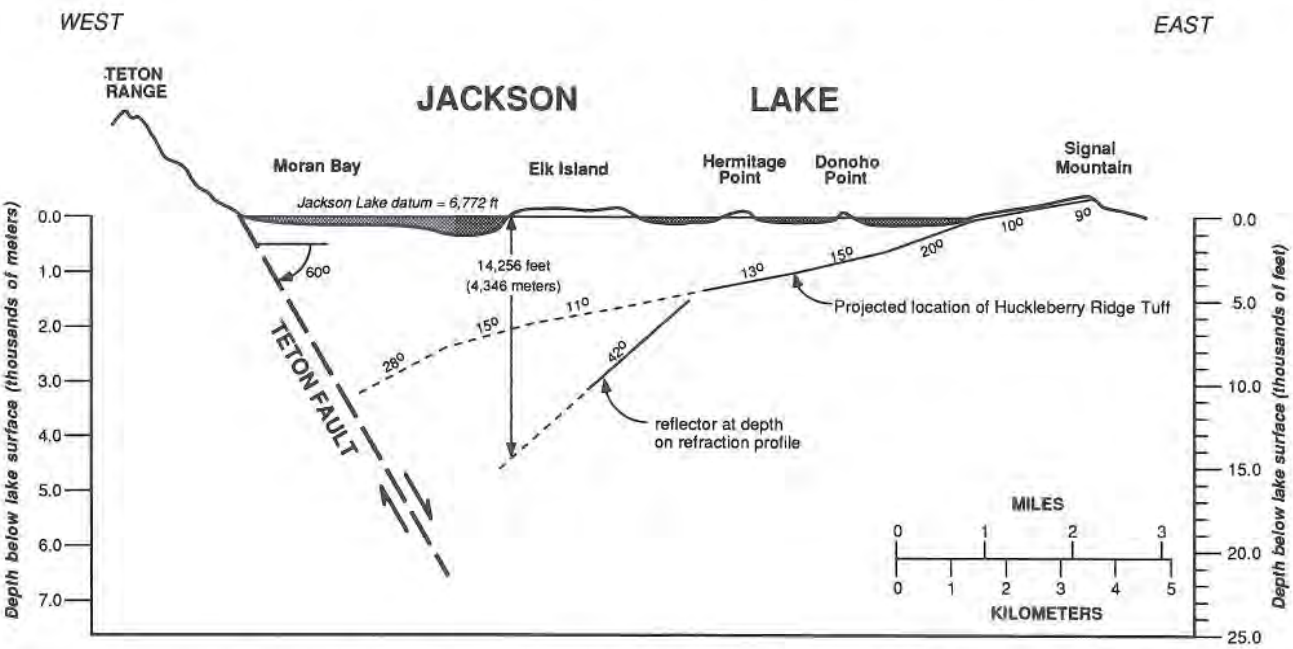

Figure 14. Interpreted geologic east-west cross section of the southern Jackson Lake basin. The profile represents the bathymetry and upper-crustal structure along a generalized east-west line from Moran Bay to Signal Mountain. The cross section shows the projection of the westward-dipping Huckleberry Ridge Tuff (from Gilbert and others, 1983) exposures north of Jackson Lake (dashed lines) and on and near Signal Mountain (solid lines). The projected location of the Teton fault is from Smith, Byrd, and Susong (this volume). Lake depths are exaggerated.

face between much older Mesozoic and Paleozoic consolidated units or Precambrian rocks. Nonetheless, the steeper westward dip of the reflector is consistent with hanging-wall subsidence of the sediments produced by large scarp-forming earthquakes on the Teton fault (see Smith, Byrd, and Susong, this volume, for a detailed example). Note that the westward increase of dip of both the Huckleberry Ridge Tuff and the deep reflector are consistent with a listric geometry for the Teton fault at depth. However, the data are insufficient to confidently determine the fault geometry.

Conclusions

The structure and Quaternary history of Jackson Lake were delineated by seismic reflection and refraction data, paleomagnetic data, and piston cores and integrated with the glacial history of the region. The high-resolution (7.5kHz) seismic reflection data used to determine the bathymetry of Jackson Lake showed a main western trough up to 437 ft (133 m) deep and a separate but shallower trough up to 142 ft deep (43 m) on the east side of the lake. Distinguishable sediment packets were recognized by coherent reflections bounded by notable unconformities, which are interpreted to represent different episodes of glacial and postglacial sedimentation in the lake. The floor of Jackson Lake is underlain by Quaternary deposits marked by angular unconformities and locally interbedded undisturbed and disturbed layers. Sediments recovered from four 6.5- to 12-ft (2 to 4 m) long piston cores in the upper 3 or 4 m of unit A were composed dominantly of silt-sized (4 to 60 mm) diatom frustules mixed with a few percent solid detritus of quartz, feldspar, and mica (Shuey and others, 1977).

Sediments in the upper part of the western (main) basin of Jackson Lake consist of an undisturbed near-surface layer up to 70 ft (23 m) thick interpreted to have been deposited in postglacial time, which includes all of Holocene time (last 10,000 years or more) and a few thousand years of latest Pleistocene time. Deeper units form packets between subhorizontal boundaries, but contain contorted and steeply inclined beds interpreted as slumps of unconsolidated sediment from the Snake River delta. In contrast, the reflection data in the Signal Mountain-Spalding Bay basin show tilted sediment layers with alternately east- and west-dipping units interpreted to indicate primary dips inclined away from glacial sources of sediment to both the northwest and northeast.

Sedimentation rates of Holocene sediments of Jackson Lake, estimated from paleomagnetic determinations of paleoinclinations of piston cores, averaged 0.06 to 0.08 in/yr (0.1 to 0.2 cm/yr) for the past 1,800 years (Shuey and others, 1977). The sedimentation rate for the upper part of this unit (0.15 cm/yr) yields an age of 10 ka for unit A, which is a minimum age because it does not account for sediment compaction with time and depth.

Our interpretations of the seismic data from Jackson Lake correlate well with the glacial history of northern Jackson Hole. Along the southern margin of the greater Yellowstone ice-mass in late Pleistocene time, three glacial lobes pushed into northern Jackson Hole and produced the main features of the Jackson Lake basin by scouring and deposition of sediments, first in a glacial trough on the east side of the lake and then in a larger one to the west. During the first phase (Burned Ridge) of the last glaciation (Pinedale), westward flow of the Pacific Creek glacial lobe (75 ka to 25 ka) scoured the Signal Mountain trough to depths of 600 ft (185 m). During the second and third phases (Hedrick Pond and Jackson Lake) of the last glaciation (40 to 15 ka), southward flow of the Snake River lobe scoured out the deep western trough to a depth of about 800 ft (245 m). This trough was subsequently about half filled with late glacial and postglacial sediment.

We did not identify any significant evidence in the reflection data of faulting within the Quaternary sediments of Jackson Lake or along the projection of the Teton fault zone across the east side of Moran Bay. This finding is substantiated by detailed mapping (Smith, Byrd and Susong, this volume), which has documented that the Quaternary trace of the Teton fault is located onshore at the west side of Moran Bay and farther north to the Snake River

delta. The thickening of the postglacial Holocene sediments along the west side of the western lake basin and adjacent to the Teton fault is consistent with either: (1) up to 100 ft (30 m) of hanging-wall subsidence in the last ~10,000 years, or (2) sediment accumulation in that area due to a plume of sediment discharged from the Snake River. It is possible that both mechanisms contributed.

The general characteristics of Jackson Lake basin sedimentation were controlled by late Pleistocene glaciation. However, the seismic profiles do not have sufficient resolution to reveal the gentle tilting of trough-filling sediments toward the Teton fault because of the very small magnitude of the postglacial tilts. These are estimated to be less than 1° based on the simple geometry of < 20 m downthrow from a hinge up to 9.4 mi (15 km) away from the fault. We note that this predicted postglacial tilt is much smaller than the expected primary sedimentary dips of up to several degrees, whereas the older Quaternary(?) sediments, into which these basins were excavated, exhibit dips into the Teton fault that tend to increase with depth and which may be tectonic. This interpretation is consistent with large, scarp-forming, prehistoric earthquakes, $6.5 \leq M_S \leq 7.5$, thought to have dropped the hanging-wall block of the Teton fault several kilometers during the 9 to 6 Ma structural evolution of Jackson Lake (Smith, Byrd, and Susong, this volume).

In northern Jackson Hole, glacial scour during the last glaciation locally removed as much as 800 feet (250 m) of the weakly consolidated sediments, first by excavation of the east-west Signal Mountain trough and then the north-south western basin. We thus interpret that the general evolution of the sedimentary basin in which Jackson Lake is located is the result of localized, hanging-wall subsidence produced by earthquake slip on the Teton fault during the past 5 to 9 m.y. However, the principal evolution of the Jackson Lake sedimentary basin was by glacial scouring of this sediment-filled structural basin and buildup of moraine and outwash embankments on the southern margin of the lake. Following glaciation, Jackson Lake received deposits of relatively undisturbed, silica-rich diatomaceous muds.

Acknowledgments

The geophysical surveys of Jackson Lake were supported primarily by the National Science Foundation, grant numbers GA-12870 and GA-30768 to the University of Utah, and by a National Science Foundation grant to the University of Wisconsin-Milwaukee. The University of Utah Computer Science Department provided computer time and data-processing facilities.

We expressly thank the personnel of Grand Teton National Park for their permission and help in conducting the field work. We are grateful to Ken Diem, former director of the University of Wyoming-National Park Service Research Center (UW-NPS), for his encouragement and support in the late stages of this project, and to Mark Boyce and Glen Plumb, also of the UW-NPS Research Center, for their encouragement. Tiny Wiley, of the Grand Teton Lodge Company, donated dock space for our research vessel that is greatly appreciated.

Natalie Kelsey assisted with the calculations, drafting, editing, and reviews of the manuscript. Robert Otis, Jack Pelton, David Oxley, Van Henson, and Ron Jaworski assisted with the seismic data acquisition and data processing. Discussions of the glacial history and maps of glacial features outlined in this paper were based primarily upon field studies from 1985 to 1991 by Ken Pierce and John Good. Tom Henyey and Paul Carrara provided insightful and critical reviews of this paper.

We especially appreciate the encouragement of and discussions with J. David Love, U.S. Geological Survey, who provided important insights into the geological history of the region and asked thoughtful questions.

References cited

Behrendt, J.C., Tibbetts, B.L., Bonini, W.E., and Lavin, P.M., 1968, A geophysical study in Grand Teton National Park and vicinity, Teton County, Wyoming: U.S. Geological Survey Professional Paper 516-E, 23 p.

Fryxell, F.M., 1929, Glacial features of Jackson Hole, Wyoming [Ph.D. dissertation]: Chicago, Illinois, University of Chicago, 128 p.

_____ 1938, The Tetons, interpretations of a mountain landscape: Berkeley, University of California Press, 77 p.

Gilbert, J.D., Ostenna, D., and, Wood, C., 1983, Seismotectonic study, Jackson Lake dam and reservoir, Minidoka project, Idaho-Wyoming: U.S. Bureau of Reclamation Seismotectonic Report 83-8, 123 p.

Hayden, P.S., 1969, Jackson Lake limnological investigations: National Park Service Progress Report, 1968-1969, Division of Natural Science Studies, Washington, D.C., 37 p.

Henyey, N.J., Chelminski, P., Court, J.E., Gorsline, D.S., and Goldman, C.H., 1972, Quaternary history of Lake Tahoe, California-Nevada: Geological Society of America Bulletin, v. 83, p. 1435-1448.

Love, J.D., and Reed, J.C., Jr., 1971, Creation of the Teton landscape, Teton National Park: Grand Teton Natural History Association, Moose, Wyoming, 120 p.

Love, J.D., Reed, J.C., Jr., Christiansen, R.L., and Stacey, J.R., 1972, Geologic block diagrams and tectonic history of the Teton region, Wyoming-Idaho: U.S. Geological Survey Miscellaneous Geological Investigations Map I-730, scale 1:62,500.

Love, J.D., Reed, J.C., Jr., and Christiansen, R.L., 1992, Geologic map of Grand Teton National Park: U.S. Geological Survey Miscellaneous Investigations Series Map I-2031, scale 1:62,500.

Montagne, J., 1956, Review of glacial studies in Jackson Hole: Wyoming Geological Association Eleventh Annual Field Conference Guidebook, p. 29-32.

Mikulich, M.J., and Smith, R.B., 1974, Seismic reflection and aeromagnetic surveys of the Great Salt Lake, Utah: Geological Society of America Bulletin, v. 85, p. 991-1002.

Nelson, H.R., 1974, A reflection seismic study of the Quaternary sediments of Yellowstone Lake [B.S. thesis]: Salt Lake City, University of Utah, 23 p.

Otis, R.M., and Smith, R.B., 1976, Homomorphic deconvolution by log spectral averaging: Geophysics, v. 42, p. 1146-1157.

Otis, R.M., Smith, R.B., and Wold, R.J., 1977, Geophysical surveys of Yellowstone Lake, Wyoming: Journal of Geophysical Research, v. 82, p. 3705-3718.

Oxley, D.R., 1975, Magnetic and refraction surveys on Jackson Lake, Wyoming [M.S. thesis]: Milwaukee, University of Wisconsin-Milwaukee, 74 p.

Pierce, K.L., 1979, History and dynamics of glaciation in the northern Yellowstone National Park area: U.S. Geological Survey Professional Paper 729-F, 90 p.

_____ 1987, Geologic setting of eight archeological sites investigated in 1986, Jackson Lake, Wyoming, *in* Conner, M., Site testing at Jackson Lake: Midwest Archeological Center, National Park Service, Lincoln, Nebraska, p. 100-123.

Pierce, K.L., and Good, J., 1990, Quaternary geology of Jackson Hole, Wyoming, *in* Roberts, Sheila, editor, Geologic field tours of western Wyoming and parts of adjacent Idaho, Montana, and Utah: Geological Survey of Wyoming Public Information Circular 29, p. 79-88.

Pierce, K.L., and Morgan, L.A., 1990, The track of the Yellowstone hotspot: volcanism, faulting, and uplift: U.S. Geological Survey Open File Report 90-415, 46 p.

Pierce, K.L., Obradovich J.D., and Friedman, I., 1976, Obsidian hydration dating and correlation of Bull Lake and Pinedale glaciations near West Yellowstone, Montana: Geological Society of America Bulletin, v. 87, p. 703-710.

Porter, S.C., Pierce, K.L., and Hamilton, T.D., 1983, Late Wisconsin mountain glaciation in the western United States, *in* Wright, H.E., Jr., editor, Late Quaternary environments of the United States, v. 1, The Late Pleistocene: Minneapolis, University of Minnesota Press, p. 71-111.

Reed, J.C., Jr., 1973, Geologic map of the Precambrian rocks of the Teton Range, Wyoming: U.S. Geological Survey Open File Report 73-2, scale 1:62,500.

Richmond, G.M., 1973, Surficial geologic map of the Huckleberry Mountain Quadrangle, Yellowstone National Park and adjoining area, Wyoming: U.S. Geological Survey Miscellaneous Geological Investigations Map I-639, scale 1:62,500.

Richmond, G.M., and Pierce, K.L., 1971, Surficial geologic map of the Mount Hancock Quadrangle, Yellowstone National Park and adjoining area, Wyoming: U.S. Geological Survey Miscellaneous Geological Investigations Map I-636, scale 1:62,500.

Schilly, M.M., Smith, R.B., Ansorge, J., Lehman, J.H., and Braile, L.W., 1982, The Yellowstone-eastern Snake River Plain seismic profiling experiment: upper-crustal structure: Journal of Geophysical Research, v. 84, p. 2692-2704.

Shuey, R.T., Ugland, R.O., and Schmidt, C.R., 1977, Magnetic properties and secular variation in cores from Yellowstone and Jackson lakes, Wyoming: Journal of Geophysical Research, v. 82, p. 3739-3746.

Skeen, R.C., 1975, A reflection seismic study of the subsurface structure and sediments of Bear Lake, Utah-Idaho [B.S. thesis]: Salt Lake City, University of Utah, 24 p.

Smith, R.B., and Arabasz, W.J., 1991, Seismicity of the Intermountain seismic belt, *in* Slemmons, D.B., Engdahl, E.R., Zoback, M.L., and Blackwell, D.D., editors, Neotectonics of North America: Geological Society of America, SMV V-1, Decade Map Volume 1, p. 185-228.

Smith, R.B., Byrd, J.O.D., Susong, D.D., Sylvester, A.G., Bruhn, R.L., and Geissman, J.W., 1990, Three year progress report, an evaluation of earthquake hazards of the Grand Teton National Park emphasizing the Teton fault: Unpublished report to the University of Wyoming-National Park Service Research Center by the Department of Geology and Geophysics, University of Utah, Salt Lake City, 149 p.

Tibbetts, B.L., Behrendt, J.C., and Love, J.D., 1969, Seismic-refraction measurements in Jackson Hole, Wyoming: Geological Society of America Bulletin, v. 80, p. 1109-1122.

Frontispiece. Photograph of Steamboat Geyser, Norris Junction, Yellowstone National Park, in full eruption on July, 6, 1984 (photograph by Robert B. Smith).

Topographic signature, space-time evolution, and physical properties of the Yellowstone-Snake River Plain volcanic system: the Yellowstone hotspot

Robert B. Smith
Department of Geology and Geophysics
University of Utah
Salt Lake City, Utah 84112-1183

Lawrence W. Braile
Department of Earth and Atmospheric Sciences
1397 Civil Engineering Building
Purdue University
West Lafayette, Indiana 47907-1397

Abstract

The track of the Yellowstone hotspot— an 800 km linear age progression of silicic volcanic centers that runs through the Snake River Plain to the Yellowstone caldera— provides direct evidence for mantle plume-plate interaction as the mechanism responsible for the Yellowstone-Snake River Plain (YSRP) 16 million-year volcanic system. Caldera-forming rhyolitic volcanism, active crustal deformation, extremely high heat flow (30 times the continental average), and intensive earthquake activity are manifestations of the hotspot currently active at Yellowstone National Park. Anomalously low P-wave velocities in the upper crust of the Yellowstone caldera are interpreted as solidified but still hot granitic rocks, partial melts, hydrothermal fluids, and sediments. Unprecedented deformation of the Yellowstone caldera of as much as 1 m of uplift from 1923 to 1984, followed by subsidence of as much as ~12 cm from 1985 to 1991, clearly reflects a giant caldera at unrest.

The regional signature of the Yellowstone hotspot is highlighted by an anomalous, 600 m high, approximately 600 km wide, topographic bulge centered on the caldera. We suggest that this feature reflects long-wavelength tumescence of the hotspot. Yellowstone is also the center of a +10 m to +12 m geoid anomaly—the largest in North America—which extends about 500 km laterally from the caldera, similar in width to the geoid anomalies of oceanic hotspots and swells. The 16 million year trace of the Yellowstone hotspot, the seismically quiescent Snake River Plain, is surrounded by "bow-wave" or parabolic-shaped regions of earthquakes and high topography. The systematic topographic decay southwest along the Snake River Plain, totaling 1,300 m, fits a

Smith, R.B., and Braile, L.W., 1993, Topographic signature, space-time evolution, and physical properties of the Yellowstone-Snake River Plain volcanic system: the Yellowstone hotspot, *in* Snoke, A.W., Steidtmann, J.R., and Roberts, S.M., editors, Geology of Wyoming: Geological Survey of Wyoming Memoir No. 5, p. 694-754.

model of lithospheric cooling and subsidence that is consistent with the passage of the North American plate across a mantle heat source. The rate of silicic-volcanic age progression of the YSRP (4.5 cm/yr) includes a component of southwest motion of the North American plate, modeled at ~2.5 cm/yr, and a component of concomitant crustal extension estimated to be 1 to 2 cm/yr. The YSRP also exhibits anomalous crustal structure, which we believe is inherited from magmatic and thermal processes associated with the Yellowstone hotspot. This includes a thin, (2 - 5 km thick) surface layer composed of basalt and rhyolites and an unusually high-velocity (6.5 km/s), mid-crustal mafic layer that we suggest reflects extinct "Yellowstone" magma systems, which have replaced much of the normal granitic upper crust. Direct evidence for a mantle connection for the YSRP system is from anomalously low P-wave velocities which extend from the crust to depths of approximately 200 km. These properties and the kinematics of the YSRP are consistent with an analytic model for plume-plate interaction that produces a "bow-wave" or parabolic pattern of upper mantle flow southwest from the hotspot, similar to the systematic patterns of regional topography and seismicity. Our unified model for the origin of the YSRP is consistent with the geologic evidence: basaltic magmas ascend from a mantle plume to interact with a silicic-rich continental crust, producing partial melts of rhyolitic composition and the characteristic caldera-forming volcanism of Yellowstone. Cooling and contraction of the lithosphere follows the passage of the plate over the hotspot, with continuing episodic eruptions of mantle-derived basalts along the SRP.

Introduction

Our knowledge of mantle hotspots has been derived largely from observations of active volcanoes located primarily in oceanic settings. The Yellowstone-Snake River Plain (YSRP) volcanic system of Idaho, Wyoming, and Montana , including the Yellowstone silicic volcanic field and the related bimodal basaltic-rhyolitic volcanic field of the eastern Snake River Plain (SRP), affords an opportunity to investigate the dynamics and properties of one of the Earth's largest silicic-dominated volcanic systems. We will develop a unifying model for the origin of the YSRP that reflects mantle plume-plate interaction consistent with observed geologic and geophysical data. We will also show how the Yellowstone hotspot has affected more than 20% of the western United States during its 16 million year evolution (**Figure 1**).

The currently active element of the YSRP is a large caldera complex located at Yellowstone National Park, Wyoming. However, unlike most of the Earth's volcanic and tectonic features generally found at or near plate boundaries, Yellowstone National Park (here loosely called Yellowstone) is located ~2,000 km from the western margin of the North American plate. Yellowstone is also located at the boundary of two major tectonic provinces, the Basin and Range and the Rocky Mountains. Here, the immense scale of its Pleistocene volcanism, extremely high heat flow (~30 times the continental average), intense seismicity, widespread hydrothermal activity, and unprecedented crustal deformation makes Yellowstone a natural laboratory for investigating volcanic and related tectonic processes (**Frontispiece**).

The 1983, M_s = 7.3, Borah Peak, Idaho, earthquake has recently focused attention on the influence of the Yellowstone hotspot on the seismotectonics of the YSRP (Smith and others, 1985). To examine this relationship we plotted the regional topography, locations of silicic volcanic centers (**Figure 2**), earthquakes, and late Cenozoic normal faults in a region we believe has been affected by the hotspot (**Figures 3** and **4**). The most important features of **Figures 3** and **4** are: (1) a northeast progression of decreasingly younger silicic volcanic centers along the YSRP, (2) "bow-wave" or parabolic-shaped areas of high topography and seismicity surrounding the aseismic SRP, and (3) systematic patterns of similar-aged normal faulting subparallel to the SRP which follow the general patterns of topography and seismicity. In this paper, we will relate these features to a model for plume-plate interaction and show how the geophysical and geodetic data of the YSRP are consistent with a mantle hotspot source.

What is a hotspot?

We associate the term "hotspot" with a geologic feature of long-lived active volcanism and high heat flux originating from the asthenosphere and resulting in regional topographic uplift and undulations of the geoid. These features have been interpreted for various oceanic swells and linear tracks of oceanic volcanism as evidence of upwelling mantle plumes. Our use of the term hotspot also reflects the generalized definition of Crough (1978) of a region of midplate or anomalous ridge crest volcanism that is either persistent or accompanied by a broad topographic swell. These definitions encompass such oceanic features as the Hawaiian chain, Cape Verde Rise, the Azores, and the Galapagos spreading center, all of which share properties with the YSRP.

As discussed by Thompson and Gibson (1991), we expect that the hotspot location (defined by surface manifestations of deep-seated processes) is within the plane of the axis of an underlying mantle plume. We thus define the Yellowstone hotspot as a large area of voluminous silicic volcanism that has evidence for mantle heat and a basaltic magmatic source. Further discussions of hotspots and plumes are contained in recent reviews by Richards and others (1989), Sleep (1990), and Duncan and Richards (1991).

The Yellowstone-Snake River Plain volcanic system

The heart of Yellowstone National Park's majestic mountain scenery is a large, Pleistocene, silicic volcanic field that is distinguished by three large calderas with a total eruptive volume of ~8,500 km³ (Christiansen and Blank, 1972; Christiansen, 1984, 1993). This area is best known for its spectacular display of geysers, fumeroles, and hot springs (**Frontispiece**). However, the accumulated effect of Yellowstone's volcanism is a ~2,500 m high, relatively flat and undulating mountainous terrain, termed the Yellowstone Plateau, which is surrounded by high peaks of the Rocky Mountains, some exceeding 4,000 m elevation.

To the southwest, the Snake River Plain occupies an 800 km long and 80 km wide topographic depression that descends to elevations of ~1,200 m in southwestern Idaho (**Figure 3**).

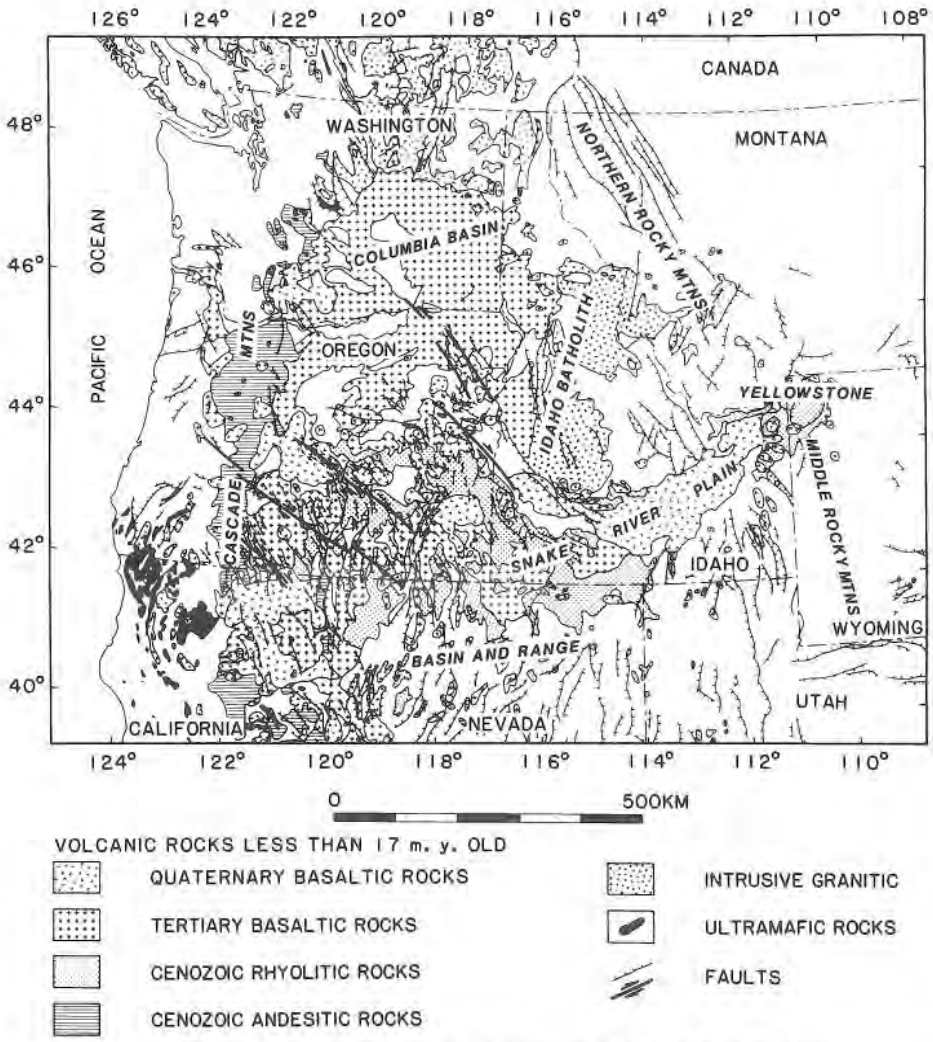

Figure 1. Generalized tectonic map of the northwestern United States showing the Yellowstone and Snake River Plain region.

Figure 2. Photograph of Big Southern Butte, an example of a siliceous volcanic cone (in the far distance), and Middle Butte, a basaltic cone (in the distance) on the Snake River Plain near Arco, Idaho (photograph by Lawrence W. Braile).

The Snake River Plain, covered primarily by late Cenozoic basalt flows, is underlain by silicic volcanic rocks (**Figure 2**) similar in composition to those found in Yellowstone. The volcanic rocks age progressively to the southwest, from 0.6 Ma at Yellowstone to as old as 16 Ma in southwestern Idaho and northern Nevada (Armstrong and others, 1975). The systematic increase in the age of the silicic volcanic centers and the decrease in topography along the SRP are the best and most important surface manifestations of the Yellowstone hotspot. We will show corroborating evidence from geophysical and geodetic data for this hypothesized mantle source.

Early naturalists in Yellowstone

We point out the role of Yellowstone, not only as one of the world's greatest scenic wonders, but as the birthplace of the U. S. National Park system. Ferdinand V. Hayden (1872, 1873) was the first scientist to describe Yellowstone during his exploration of "Coulter's Hell", as it was known by fur trappers in the early 19th century for its rumored expanse of geysers and hot springs in a largely unexplored region of the Rocky Mountains. Hayden's perspective and championing of Yellowstone's geologic wonders and spectacular mountain scenery lead to the enactment of legislation in 1872 establishing the first national park in the world, Yellowstone National Park, and helped establish the beginnings of the global environmental ethic.

Impressed with Yellowstone's magnificent high mountain scenery and evidence of youthful volcanism, Hayden summarized an insightful interpretation of its origin that is still valid today:

> *From the summit of Mt. Washburn, a bird's-eye view of the entire basin may be obtained with the mountains surrounding it on every side without any apparent break in the rim. This basin has been called by some travelers the vast crater of an ancient volcano. It is probable that during the Pliocene period the entire country drained by the sources of the Yellowstone and the Columbia was the scene of as great volcanic activity as that of any portion of the globe. It might be called one vast crater, made up of thousands of smaller volcanic vents and fissures out of which the fluid interior of the earth, fragments of rocks, and volcanic dust were poured in unlimited quantities.*
>
> Hayden (1872)

Hayden's experiences and insight into the significance of the scientific opportunities at Yellowstone were amplified by the views of Lt. Gustavus C. Doane, the military leader of a 1870 expedition into Yellowstone and cited from his personal journal entry on September 24, 1870. Doane's statement emphasizes the importance of Yellowstone as a multidisciplinary natural laboratory:

> *As a country for sight seers, it is without parallel. As a field for scientific research it prom-*

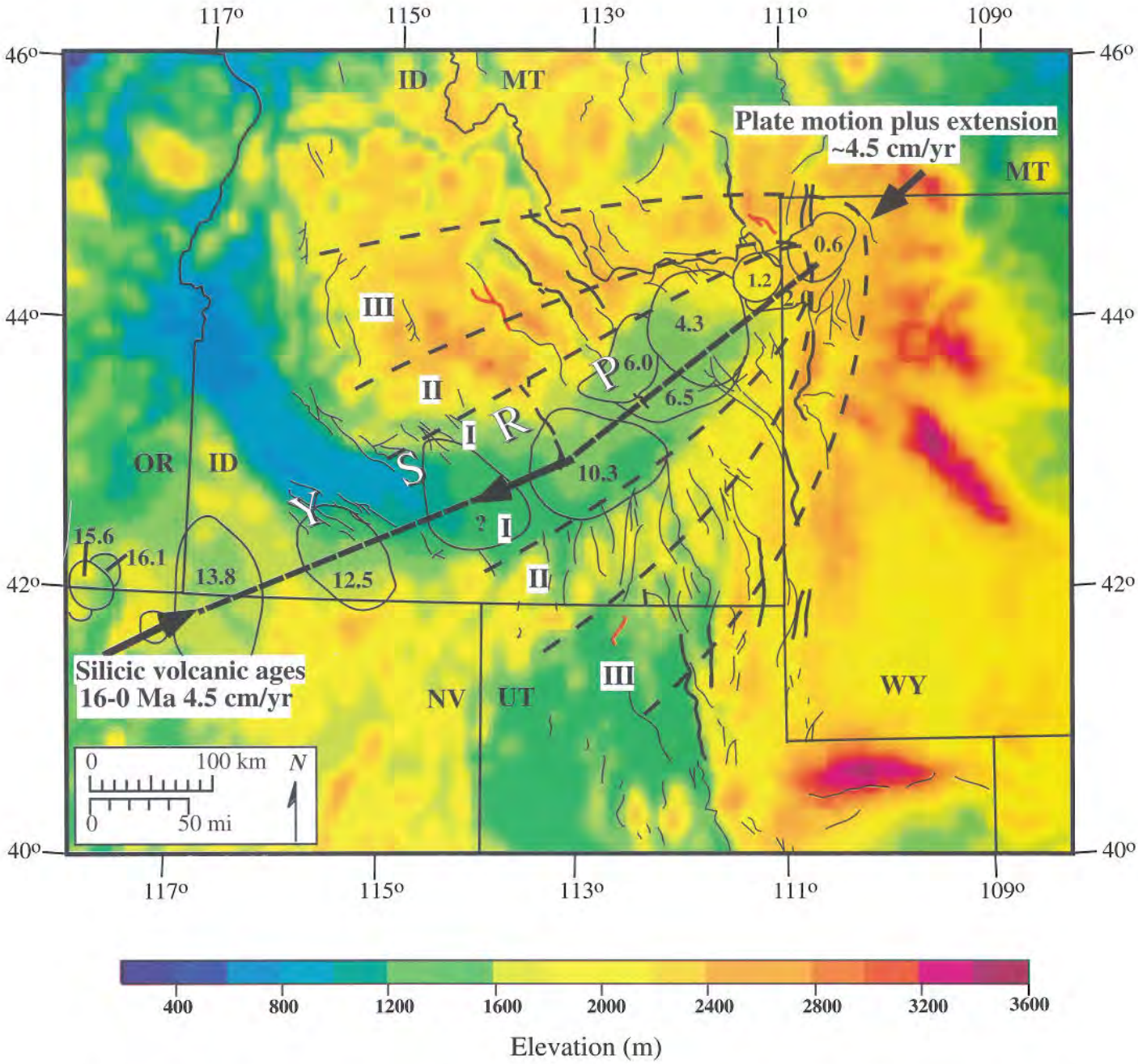

Figure 3. Topography, late Cenozoic faulting, and volcanic features of the Yellowstone-Snake River Plain. The digitized topography was contoured by color with the warmest colors (reds, purples) corresponding to the highest topography (exceeding 3,500 m), grading to lowest elevations, (~1,200 m) shown by the cooler colors of green, blue and, magenta. The locations of silicic volcanic centers are from the maps of Christiansen (1984, 1993) for Yellowstone and Island Park; and for the Snake River Plain, from Mel Kuntz (U. S. Geological Survey, 1985, personal communication), Morgan and others (1984), and Pierce and Morgan (1990, 1992). The dashed line corresponds to the estimated center line of the YSRP. The plate motion and silicic volcanism progression vectors are from this paper (see Table 1). Selected late Cenozoic normal faults from compilation of Smith and Arabasz (1991). Light lines = late Cenozoic to late Quaternary, bold lines = faults ≤ 14,000 ^{14}C years, and red lines = faults with historic rupture. This figure is modified and updated from earlier versions by Smith and others (1985, 1990) and Smith (1989, 1990).

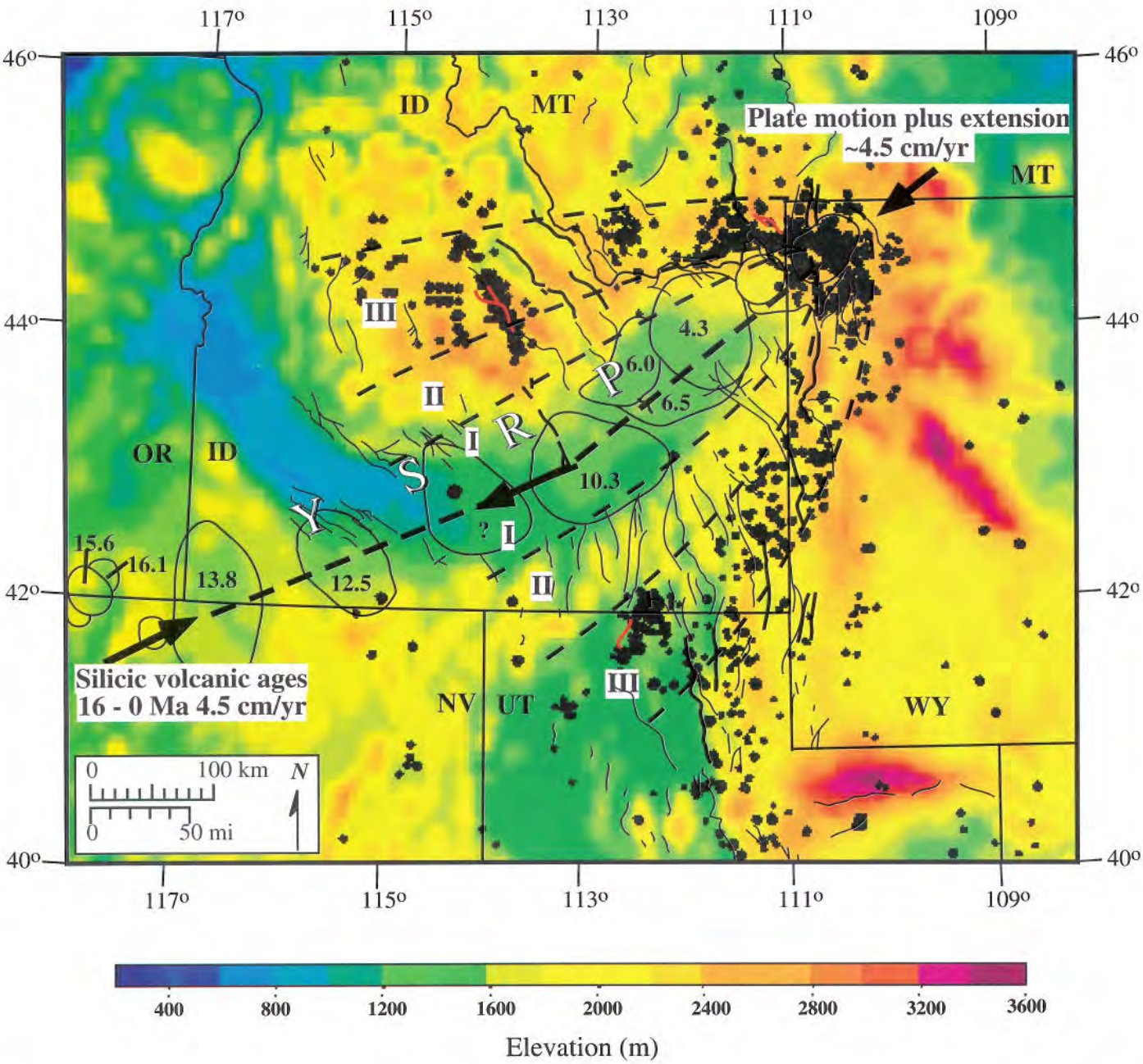

Figure 4. Topographic and seismicity signature of the Yellowstone hotspot, showing the "bow-wave" or parabolic-shaped seismotectonic domains (defined in text) I, II and III. Earthquake epicenters are shown as black filled circles and are scaled in size to magnitude; $2.5 \leq M \leq 7.5$, for the period, ~1900 to 1985. The earthquake data are from earthquake compilations of the Intermountain region by the University of Utah (Eddington and others, 1987; Smith and Arabasz, 1991) and Engdahl and Rinehart (1988).

ises great results, in the branches of Geology, Mineralogy, Botany, Zoology, and Ornithology. It is probably the greatest laboratory that nature furnishes on the surface of the globe.

Doane (1870)[1]

We show throughout this paper that the YSRP system is indeed a natural laboratory and provides an unusual window into the workings of the Earth's interior revealing information on such important processes as mantle derived volcanism, magmatic transport and heatflow, and surficial manifestation of plume-plate interactions. We will address these topics by first summarizing the late Cenozoic volcanic history of the YSRP, then describing the distinctive physical properties of this system such as seismic velocity structure, heat flow, gravity and geoid fields, topographic features, and finally, concluding with a discussion of a mantle plume-plate model which accounts for many of the observations.

We include a discussion of the geophysical and geological evidence regarding the space-time evolution and physical properties of the YSRP volcanic system as it pertains to an origin associated with a mantle hotspot. We conclude with a discussion emphasizing the corroboration of diverse geophysical findings of the YSRP with the results of volcanological, geomorphic, and petrological studies and comment on the unusually good agreement between these data and a unified model for plume-plate interaction as the mechanism responsible for the Yellowstone hotspot.

Track of the Yellowstone hotspot—the Snake River Plain

The volcanic history of the Snake River Plain is not as well known as that of Yellowstone, primarily because most of the late Cenozoic silicic volcanic rocks and related calderas are buried beneath younger basalts (**Figure 2**). Nonetheless, the first definitive evidence for a systematic time-progressive volcanic origin of this region was recognized by Armstrong and others (1975), who mapped and dated silicic volcanic rocks by the K-Ar method along the Snake River Plain. Morgan and others (1984) employed paleomagnetic methods and identified several large calderas in the northern part of the SRP with dimensions similar to those of Yellowstone (**Figure 3**). Leeman (1982) summarized the Snake River Plain volcanic system based on petrology and trace-element analysis of volcanic rocks.

Discussions of the YSRP must also include its possible relationship to the Miocene Columbia Plateau basalt field of western Oregon and Washington, which has been attributed by several authors to a mantle plume. For example, Thompson (1977) and Draper (1991) suggested that the short-lived magmatism of the Columbia Plateau volcanic field was fed by upper mantle dikes from a "Yellowstone" plume located in southwestern Idaho, 16 to 17 Ma. While there is no directional age progression of the Columbia Plateau basalts, the immense scale of this volcanic field suggests that a mantle source cannot be ruled out; however, there is little geophysical data for the Columbia Plateau or its transition to the Snake River Plain. We therefore will not attempt to address the possible relationships between these provinces, but we offer, in a later section, reasons why we believe that the YSRP is not directly related to this flood basalt province.

Age progression of silicic volcanic centers

The best evidence for systematic motion of the North American plate across a mantle magmatic source is the progressive increase in age of silicic volcanic rocks southwest along the YSRP (**Figure 5**). The youngest silicic volcanic centers, in the Yellowstone volcanic field, are less than 2.0 Ma. These are followed by a sequence of silicic centers at about 6 Ma, southwest of Yellowstone. A third group, about 10 Ma, is centered near Pocatello, Idaho. The oldest mapped silicic rocks of the SRP, about 16 Ma, are distributed across a 150 km wide zone in southwestern Idaho and northern Nevada, the suspected origin point of the YSRP (**Figure 3**). See **Table 1** for a compilation of data relating to plate motions of the YSRP. **Appendices I** and **II** contain the data used in the linear regression models shown in **Figure 5**.

[1] Cited in Bonney and Bonney (1970, p. 387).

A 3.5 cm/yr systematic northwestward decrease in age of silicic volcanic rocks of the YSRP was first described by Armstrong and others (1975). However, these authors did not speculate on a mechanism. Since Armstrong's pioneering work on the Snake River Plain, his results have been cited by various authors as evidence for the track of the North American plate across a mantle plume. Smith (1990) and Smith and others (1990) used Armstrong's data and calculated a 4 cm/yr rate for the silicic volcanic age progression, which is similar to the rate of 4.5 cm/yr given by Rodgers and others (1990).

We have also calculated the silicic volcanic age-progression rate by fitting a linear regression of silicic volcanic ages and locations along the YSRP (**Figure 5**). Our analysis shows an average rate of silicic volcanic age progression of 4.5 cm/yr for the past 20 million years, similar to that of several other studies cited here. However, we think that the data distinguish two regimes: (1) a rate of 3.3 cm/yr for the 0 to 8 Ma period, and (2) a rate of 6.1 cm/yr. for the 16 to 8 Ma period. Variations in the rates of age progression may be due in part to varying episodes of superimposed Basin and Range extension, to the combined scatter of the reported dates by various authors, and to spatial variations in the reported locations and widths of the silicic centers. Nonetheless, the 0 to 16 Ma averages for all reported age rates fall within 4±1 cm/yr.

Plate tectonic models

The first recognition of plate motion at Yellowstone was by Morgan (1972), who calculated a southwest-trending vector for the North American plate of 1 to 2 cm/yr from a hypothesized plume beneath Yellowstone with a track along

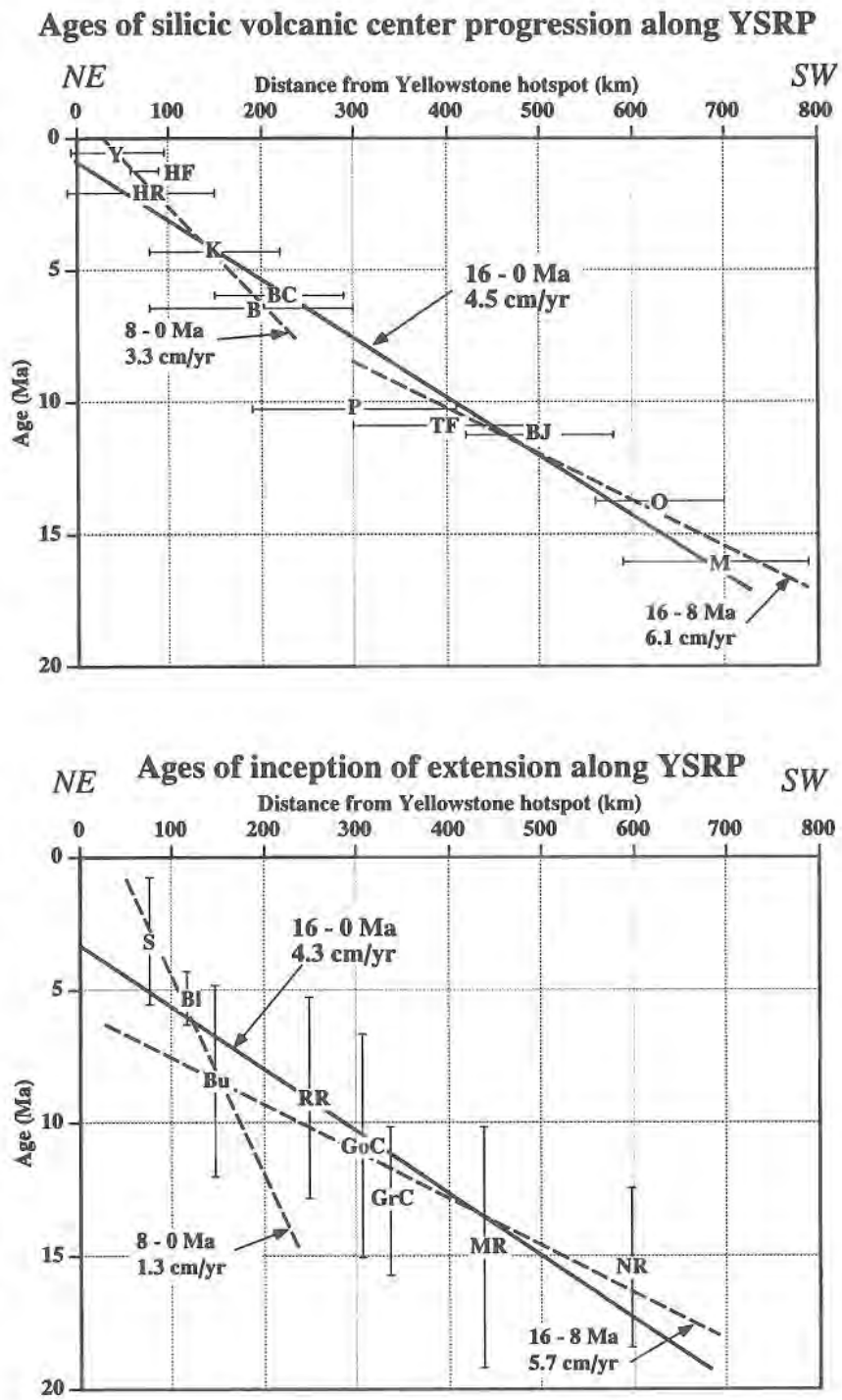

Figure 5. (Top) calculated rates of silicic volcanic age progression. (Bottom) rates of inception of crustal extension (data from Rodgers and others, 1990) for the YSRP. See Appendix I and II for references and lists of data used to construct the regression models. Solid lines are fits to all of the data. Brackets give an indication of errors due to the size of calderas (top) and the uncertainties in ages (bottom). Bold dashed lines are fits to data in two periods: 0-8 Ma and 10-16 Ma.

the Snake River Plain.[2] A plate motion vector at Yellowstone of 2.5 cm/yr and at an azimuth of 245° was calculated by Smith and Sbar (1974) for the relative motion between the North American plate at Yellowstone with respect to the Juan de Fuca and Pacific plates. They also calculated a rate of 4.5 cm/yr and a 245° azimuth for plate motion at Yellowstone, constrained by a 6 cm/yr rate of interplate motion between the North American and Pacific plates along the San Andreas fault. Using an average displacement rate of 2.4 cm/yr along the San Andreas fault (Wallace, 1990) and the same data as Smith and Sbar (1974), we calculated a plate motion rate at Yellowstone of 3.4 cm/yr. These rates compare well with values determined from a global multi-plate inversion of 2 to 3.1 cm/yr evaluated at Yellowstone (**Table 1**). The differences in the various plate motion vectors come from errors in the calculated Euler poles produced by variations in such data as oceanic paleomagnetic anomalies, slip vectors from earthquakes, and the various assumptions of net-rotation and net-torque models.

The most recent models of plate motion at Yellowstone are from DeMets and others (1990), who determined rates of North American plate motion using variations of the multi-plate model, NUVEL-1, and incorporated fixed hotspot models of Gripp and Gordon (1989, 1990). Their calculations yielded plate velocities at Yellowstone of 0.9 cm/yr to 2.5 cm/yr. We have used a rate of ~ 2 cm/yr that is averaged for the absolute plate motion at Yellowstone by excluding the extreme values of multiplate NUVEL-1 models (**Table 1**).

Rate of inception of extension

The rates of plate motion implied by the silicic volcanic age progression (Armstrong and others, 1975) include the accompanying extension of the SRP and the surrounding Basin and Range crust. Richard L. Armstrong first suggested to one of us (RBS) that he believed the apparent progression of the inception of normal faulting adjacent to the Snake River Plain reflected regional extension related to the age progression of silicic volcanism. Scott and others (1985) and Pierce and Morgan (1990) noted similar progressions of the inception of normal faulting along the SRP, whereas Rodgers and others (1990) used the ages of inception of sedimentation in basins on the south side of the SRP as evidence for inception of regional extension (**Figure 5**).

We have also examined the rates of inception of crustal extension by modeling the ages of inception of sedimentation given by Rodgers and others (1990). We excluded the Teton fault because new evidence suggests that this feature may have evolved as early as the Miocene (Byrd and Smith, 1991). From our calculations (**Figure 5**), we suggest that the ages of inception of extension reflect the same two regimes as noted in the silicic volcanic age progressions. In the first phase, from 16 to 8 Ma, the rate of inception of extension of 5.7 cm/yr compares with the rate of 6.1 cm/yr from the age progression of silicic volcanic centers (**Figure 5**). Whereas for the younger regime of 8 to 0 Ma, the rate of extension inception of 1.3 cm/yr is smaller than the silicic age rate of 3.3 cm/yr. Our 16 to 0 Ma rate was 4.3 cm/yr which is remarkably similar to the silicic volcanic age progression rate of 4.5 cm/yr.

How the Pacific and North American plate motions have affected the SRP evolution during its 16 million-year history is discussed by Pollitz (1988). He made calculations of rates based upon the silicic volcanic ages and moreover noted two regimes: (1) 20 to 10 Ma with a rate of 3.1 cm/yr at an azimuth of 267°, and (2) 9 to 0 Ma, marked by a change in azimuth to 234° with a rate of 2.9 cm/yr (**Table 1**). Our model (**Figure 5**) also reveals the change at 8 to 10 Ma that we believe marks a distinct decrease in the relative rates of either plate motion or extension rate. Pollitz (1988) attributed the change in plate direction at ~ 9 Ma to either a plate reorientation or to a change in the magnitude of forces acting on the northwest margin of the Pacific plate. The 10 to 8 Ma change is also near the time of inferred clockwise rotation (estimated to be about 45°) of the least principal stress direction from ENE-WSW to WNW-ESE in the northern Basin and Range province at approximately 10 Ma (Zoback and others, 1981). Thus, the change in rate and the inception of extension at 8 to 10 Ma on the YSRP may be associated with late Cenozoic intraplate adjustment within the western U. S.

An important factor not incorporated into previous estimates of Yellowstone plate motion is the effect of concomitant crustal extension associated with the evolution of the Basin and Range province. We estimated the long-term extension rate of the SRP by

[2] Note that these azimuths are for the direction of plate motion and are opposite to the directions implied by the progression of silicic ages.

Table 1. Table of calculated and observed rates of plate motion for the North American plate relative to the Yellowstone hotspot.

No.	Feature	Type of measurement	Rate cm/yr	Azm. (°)
North American plate motion modeled at Yellowstone				
1.	Yellowstone hotspot	Multiplate model	1 to 2	SW
2.	Yellowstone hotspot	North American-Pacific interplate model	4.5	246°
			2.4	246°
3.	Yellowstone hotspot	Multiplate model	2.4	214°
4.	Yellowstone hotspot	North American-Pacific plate model	~ 2	225
5.	Trend of the YSRP	Intraplate model	2.8 3.0	234° 245°
6.	Yellowstone hotspot	NUVEL1-HS3 multiplate model with hotspots (Gripp and Gordon, 1989)	0.9	258°
7.	Yellowstone hotspot	NUVEL1-HS2 multiplate model with hotspots (Gripp and Gordon, 1990)	2.3	238°
8.	Yellowstone hotspot	NUVEL1-NNR (no net rotation) multiplate model with hotspots (Argus and Gordon, 1991)	1.9	238°
9.	Yellowstone hotspot	N. America-Pacific interplate model	2.5	240°
Age progression of silicic volcanic rock along YSRP volcanic system				
10.	YSRP	Age determinations of dated silicic volcanic rocks	3.5	SW
11.	YSRP	Map projection of dated silicic volcanic rocks	4.0	065°
12.	YSRP	Map projection of dated silicic volcanic rocks	4.5	056°
13.	YSRP	Map projection of dated silicic volcanic rocks	2.9 7.0	054° 070°-075°
14.	YSRP	Map projection of dated silicic volcanic rocks	2.9 7.0	054° 073°
Inception of normal faulting and extension adjacent to YSRP				
15.	Northern Basin and Range	Intraplate motion across the Basin and Range at lat. 41° N.	1.7	E-W
16.	Southeast of SRP	Inception of normal faulting	1.0	——
17.	Southeast of SRP	Inception of normal faulting	3.7	056°
18.	Southeast of SRP	Inception of normal faulting	1	——
19.	North of SRP	Inception of late Quaternary normal faulting	1	——
20.	Basin-Range	Inception of normal faulting	1	——
21.	South side of SRP	Late Quaternary faults	~1-2	SW

Table 1. *Continued.*

Comments	Reference
Generalized interplate motions	Morgan, 1972
Constrained by San Andreas motion at 6 cm/yr	Smith and Sbar, 1974
Constrained by San Andreas motion of 3.4 cm/yr	Wallace, 1990
Improved multiplate inversion model	Minster and Jordan, 1978
Multiplate model 50 - 0 Ma	Engebretson and others, 1985
9 - 0 Ma 20 - 10 Ma	Pollitz, 1988
Multiplate inversion using hotspot framework	Calculated by C. DeMets for this paper.
Multiplate inversion using hotspot framework	Calculated by C. DeMets for this paper.
Multiplate inversion using hotspot framework	Calculated by C. DeMets for this paper.
Relative motion with respect to Juan de Fuca plate	This paper
Dating silicic and basaltic volcanic rocks of the YSRP	Armstrong and others, 1975
Re-evaluation of silicic volcanic ages of Armstrong and others	Smith and others, 1990
Re-evaluation of silicic age rate and related extension	Rodgers and others, 1991
Re-evaluation of silicic age rates 10 - 0 Ma 16 - 10 Ma	Pierce and Morgan, 1992
Re-evaluation of silicic age rates 10 - 0 Ma 17 - 10 Ma	This paper
Paleomagnetic rotations in the northern Basin and Range	Magill and Cox, 1981
Estimated extension rate from dike intrusion and inception of faulting	Anders and others, 1989
Evaluation of extension inception in basins adjacent to the southern SRP	Rodgers and others, 1990
Inception of late Cenozoic normal faulting adjacent to southern boundary of SRP	Pierce and Morgan, 1992
Estimated extension rate from Quaternary faulting, NW side of SRP	Knuepher and others, 1990
Estimated extension rate from dike intrusion and inception of faulting	Zoback and others, 1981
Estimated from distribution of normal faults along and adjacent to the YSRP	This paper

subtracting the age-progression rate determined from the ages of silicic volcanic rocks (which we assume reflects the combined effects of extension and plate motion) from the modeled plate motion rates. As shown in **Figure 5**, this suggests, for the period 9 to 0 Ma, an extension rate of ~2 cm/yr. Distinguishing extension from plate motion is critical to analytical models of plate-plume interaction (discussed in later sections) as well as for differentiating magmatic-related deformation from crustal extension as inferred from geologic data.

Topographic expression of the YSRP

Perhaps the most striking surface feature of the YSRP is the systematic decrease in average elevation along the Snake River Plain from ~2,500 m at the Yellowstone Plateau, to an average elevation of ~ 1,200 m in southwestern Idaho about 800 km to the southwest (**Figure 3**). The SRP depression is about 80 km wide and generally corresponds to the extent of basaltic volcanism. However, we point out a ~15° change in direction at about 250 km from Yellowstone (**Figure 3**), which appears to be related to the large-scale plate reorientation at 8 to 10 Ma discussed in the previous section.

Arcuate topographic highs extend southwest from Yellowstone in two branches to form a "bow-wave" or parabolic-shaped pattern of high topography surrounding the

depression (**Figure 3**). The systematic topographic features of the SRP were first recognized by Myers and Hamilton (1964), who pointed out the arcuate pattern of surrounding earthquakes and suggested they were the result of general topographic collapse. Suppe and others (1975) hypothesized that the topographic doming of the Yellowstone Plateau was due to a mantle plume. The topographic rims surrounding the SRP were also discussed by Smith and others (1985) and Smith (1989) in their assessments of the seismotectonics of the YSRP and by Anders and others (1989, 1992) who ascribed the systematic parabolic-shaped topography of the YSRP to the Yellowstone hotspot. Pierce and Morgan (1990, 1992) also associated the topography with a crescent-shaped uplift, warping around Yellowstone, which they attributed to a mantle hotspot.

Lithospheric deformation associated with large-scale mantle processes generally has an observable response in river drainage systems. To examine this possibility, we plotted the rivers and streams of the YSRP and surrounding region (**Figure 6**). The resulting pattern reveals the high topographic divides surrounding the SRP, which separate the Snake River and Salmon River drainages to the northwest and the Great Basin and ancestral Snake River drainages to the southeast. The highest topography is associated with the topographic divides at 1,500 to 2,000 m in elevation (also shown in **Figure 3**) . The bordering topographic shoulders extend southwestward from Yellowstone for 400 km, wrapping around the SRP in the characteristic parabolic pattern. The width between the drainage divides increases to ~200 km, 300 km southwest of Yellowstone.

We also included on **Figure 6** the locations of the larger, $M_s > 5.7$, earthquakes of the region, which demonstrate an important observation, namely that the background seismicity is generally located in the

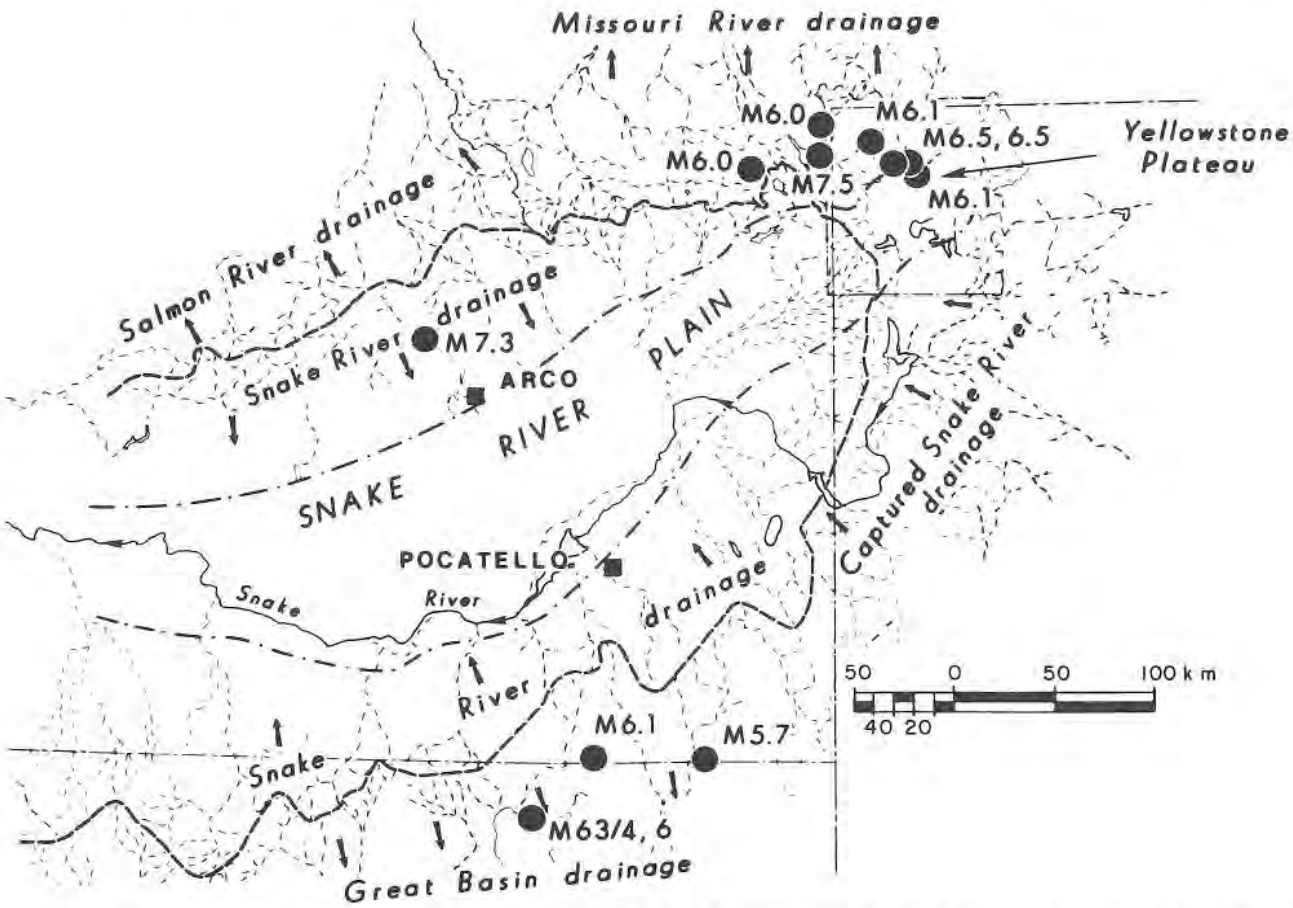

Figure 6. Drainage patterns of the upper Snake River basin and surrounding regions of the YSRP. Light dashed lines correspond to rivers and streams, bold dashed lines are the main drainage divides. Epicenters of the larger ($M_s \geq 5.7$) historic earthquakes from Table 3 are shown.

areas of the SRP drainage divides (except for the 1983 Borah Peak nucleation point, which is 25 km southeast, but its surface rupture extends northwest beyond the drainage divide). This correlation suggests a common mechanism for the elevated topography and seismicity (Smith and others, 1985).

The residual topography of the Yellowstone Plateau and the Snake River Plain (**Figure 7**) also reveals anomalous properties. For Yellowstone, the topographic residual was determined by radially averaging digital elevation data out to distances of 400 km. We selected the Yellowstone data in two azimuthal windows: (1) to the northeast and (2) to the southwest. This reveals a distinct ~600 km wide topographic anomaly of up to 600 m in height that we suggest reflects the region now affected by the Yellowstone hotspot (**Figure 7**). We also note that the area of the high topography is more than ten times larger than the ~2,500 km² Yellowstone caldera and encompasses the nearby Hebgen Lake fault zone to the west, the Teton Range to the south, and the Absaroka and Beartooth ranges to the east—the general definition of the Yellowstone Plateau.

Subsidence of the SRP is revealed by a 300 km long, residual topographic profile (**Figure 7**). The SRP topographic residual anomaly, produced by removing a long-wavelength linear trend from the digital topographic profile across the SRP, exhibits a pronounced 200 - 300 m depression surrounded by topographically high shoulders with relief in excess of 400 m. The surrounding uplift shoulder and central subsidence anomaly have a dimension of ~650 km, about the same width as the regional topographic uplift anomaly of the Yellowstone Plateau.

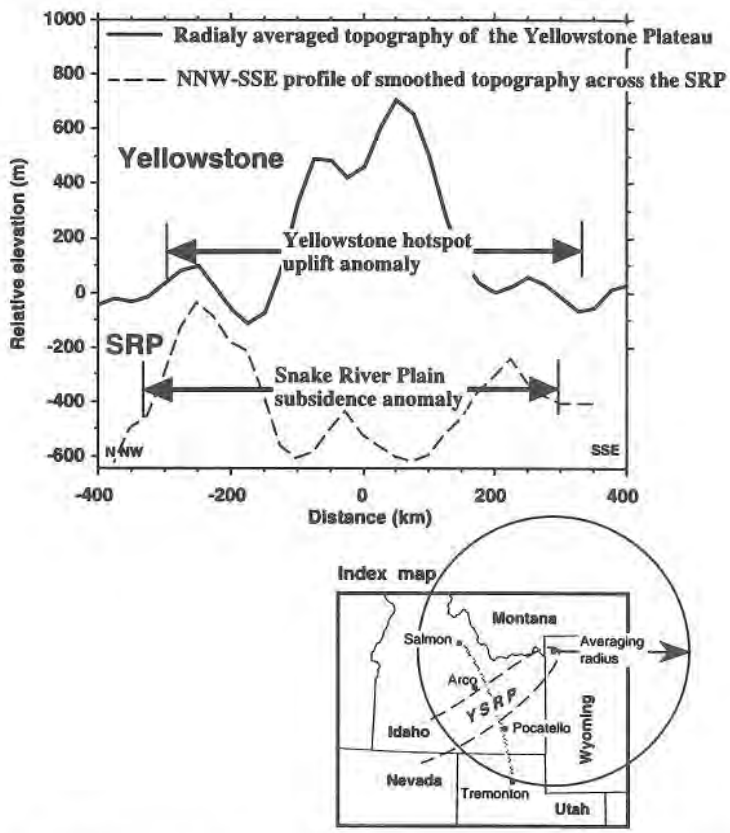

Figure 7. Topographic anomalies of the Yellowstone Plateau and the Snake River Plain affected by the Yellowstone hotspot. The Yellowstone topographic anomaly was determined by radially averaging (smoothing) the digitized topography in Figure 3 out to distances of 400 km. The Snake River Plain residual topography was computed by removing a linear regional trend and was plotted along a general north-northwest-trending profile from Salmon, Idaho (north of the SRP), across the SRP (zero distance), to Tremonton, Utah (south of the SRP).

Comparison of YSRP topography with oceanic mantle hotspots

The long-wavelength topographic response of the Yellowstone hotspot (**Figure 7**) can be compared with those of oceanic hotspots such as the Cape Verde, Galapagos, Azores, and Hawaiian islands (Crough, 1983). Topographic highs associated with these features range from 1 to 2 km above the abyssal plain and their widths range from 700 km to 1,500 km (**Table 2**). We caution that there may not be a direct one-to-one comparison between the topography of Yellowstone and the oceanic features because of differing thicknesses and compositions of oceanic versus continental crust, age of crust, and thermal regimes. Nonetheless, the 600 km wide topographic anomaly of Yellowstone (**Figure 7**) (and the ~1000 km wide geoid anomaly to be discussed in a later section) is similar to those associated with oceanic swells and hotspots and provides corroborative evidence for a mantle hotspot origin of Yellowstone.

We note the striking similarity between the anomalous Yellowstone topography (**Figure 7**) and the excess lithospheric topography modeled by Hill and others (1992) for a rising mantle plume interacting with a stationary continental lithosphere,

i.e., without shearing the top of the plume near the base of the overriding plate. They suggested up to 500 m of excess topographic uplift across 1,000 km wide zones and describe the YSRP as a "plume tail province." This width compares with that of Yellowstone; however, we assume that there is a significant component of shearing of mantle material accompanying the plume-plate interaction of the North American plate, plus a component of concomitant plate extension. We discuss our plume-plate model for Yellowstone in a later section.

Patterns of late Cenozoic faulting

The style of late Cenozoic normal faulting of the YSRP and its related deformational patterns (**Figure 3**) is discussed using a compilation of late Tertiary to Holocene normal faults taken from Smith and Arabasz (1991). The systematic pattern of late Cenozoic faulting paralleling the YSRP has been noted by Smith and others (1985), Scott and others (1985), and Pierce and Morgan (1990, 1992) as evidence related to the track of the Yellowstone hotspot. Here we differentiate areas of faulting of similar age and seismicity, which we designate as Zones II and III (**Figures 3** and **4**). Zone I corresponds to the generally undeformed and seismically quiescent SRP volcanic field. The areas of similar-aged faulting are differentiated on the basis of recency of slip, not on direction of fault motion, and are generally oblique to orthogonal to individual faults trends. Zones encompassing faults of common age are generally parallel to the boundaries of the SRP (**Figures 3** and **4**).

Zone II extends outward ~80 km from the boundaries of the SRP and is characterized by faults whose most recent displacements are generally older than post-glacial, i.e., generally greater than ~14,000 ^{14}C years (marked by thin lines in **Figures 3** and **4**). Zone II was suggested by Smith and others (1985) as possibly related to a thermal shoulder of the Yellowstone hotspot. Zone III encompasses the active earthquake zones surrounding the SRP and appears to have been much more active throughout Holocene and historic time than Zone II. Faults that have ruptured in historic time are generally within Zone III and are indicated by bold red lines on **Figures 3** and **4**. Although Pierce and Morgan (1990, 1992) subdivided the region of faulting into six divisions based upon age, height of adjacent triangular facets, etc., we could not distinguish the finer divisions of fault activation that they proposed.

Regional seismicity

In this section, we summarize the seismicity of the YSRP and surrounding region (**Figures 4, 6** and **8**). We also point out important observations from the Intermountain Seismic Belt (ISB) that are relevant to the patterns of earthquakes associated with the Yellowstone hotspot. Our seismicity data

Table 2. Topographic and geoid characteristics of the Yellowstone-Snake River Plain volcanic system.

Long Wave Length Topography	Width (km)	Height/ Subsidence (km)
Yellowstone Plateau		
Radially averaged topography (Figure 6)	600 km	~650 m
Snake River Plain		
Width of volcanic province, Zone I, 300 km southwest of Yellowstone (Figure 3)	~ 80 km	- 200 m[1]
Width of Zones I and II, 300 km south west of Yellowstone (Figure 3)	250 km	-
Maximum width; Zones I, II and III 500 km southwest of Yellowstone (Figure 3)	600 km	-
Oceanic Swells [2]		
Hawaiian	1100 km	2 km
Cape Verde Rise	1500 km	2 km
Azores	1500 km	2 km
Galapagos	900 km	1 km
Yellowstone Hotspot Geoid Anomaly		
GEOID90 model[3] (Figure 7)	~1,000 km	+10 to +12 m anomaly

[1]At 300 km distance from Yellowstone. The Snake River Plain has subsided an additional 200 m with respect to the averaged topography of the Yellowstone Plateau.

[2]From Crough (1983).

[3]From Milbert (1991).

are taken from regional seismograph network compilations summarized by Smith and Arabasz (1991). They noted that the networks in the Intermountain region consist generally of widely spaced seismic stations, averaging 30 to 50 km separation. This spacing precludes accurate focal depth determinations, except in the case of Yellowstone, where focused monitoring, using a dense array of seismographs with about 15 km spacing, provides sufficiently accurate focal depths to correlate with structure.

The coherence of the dual-branched pattern of seismicity surrounding the YSRP (Zone III in **Figures 3, 4** and **8**) has become apparent with evolving compilations of seismicity of the Intermountain region, starting with Smith and Sbar (1974). The regional continuity of the ISB led Smith and Arabasz (1991) to distinguish three parts referred to as the southern, central, and northern ISB (**Figure 8**). The central region, which we believe has been affected by the Yellowstone hotspot, extends from latitude 42° 15' to 45° 25' N and, in part, follows the Basin and Range-Middle Rocky Mountains transition. However, this zone is complicated by a west-trending branch defining an arc that "wraps around" the eastern Snake River Plain (Smith and others, 1985; Anders and others, 1989).

Thirty moderate to large earthquakes ($5.5 < M_s < 7.5$) since 1900 (**Table 3**) characterize the historical seismicity of the YSRP. This area is also distinguished by the occurrence of the two largest, scarp-forming earthquakes in the Intermountain region in historical time: (1) the M_s = 7.5, 1959 Hebgen Lake, Montana, and (2) the M_s = 7.3, 1983 Borah Peak, Idaho, earthquakes (also see **Figure 6**). In contrast, the SRP is seismically quiescent at the magni-

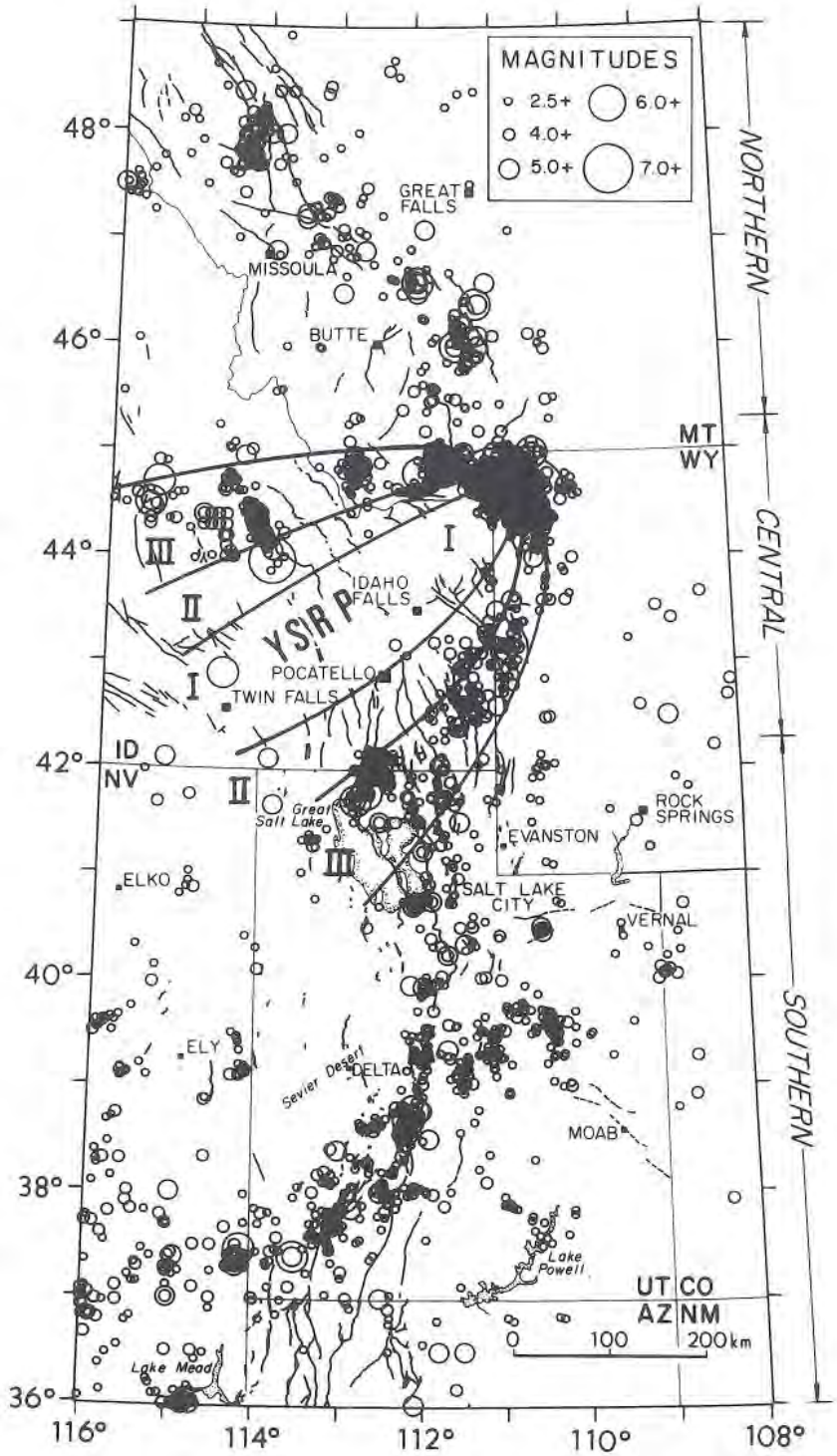

Figure 8. Earthquake epicenters of the Intermountain region, 1900-1985, outlining the Intermountain seismic belt (ISB) and the YSRP volcanic system (epicenters taken from Smith and Arabasz, 1991). The fault data were taken from published information on late Tertiary to Holocene normal faults in the Intermountain region, summarized by Smith and Arabasz (1991). Quaternary faults in Yellowstone taken from maps by Christiansen (1984, 1993). Roman numerals correspond to the seismotectonic domains of Figures 3 and 4.

tude 2+ level (Smith and Arabasz, 1991; S. M. Jackson and others, unpublished data).

Beginning at the southern margin of the YSRP (**Figures 6** and **8**), earthquakes near the Utah-Idaho border occur near a change in direction between the southern and central parts of the ISB (Smith and Arabasz, 1991). North of the Utah border there is a marked discordance between the northeast-trending seismicity belt and northwest-trending zones of late Cenozoic normal faulting that we believe reflects the influence of the Yellowstone hotspot. Seismicity studies by Piety and others (1986) of the region between southeastern Idaho and western Wyoming showed little correlation between earthquakes and Quaternary faults. Seismicity of the Idaho-Wyoming border area, encompassing the Teton region, reveals a scattered northeast trend, approximately paralleling the SRP, that continues into the southern Yellowstone Plateau but with a notable gap in historical seismicity along the Teton fault (**Figure 8**).

Seismicity continues north across about a 100 km wide, north-trending zone, intersecting the caldera in the vicinity of Yellowstone Lake. Within Yellowstone, widespread earthquake swarms characterize the caldera with a distinct change in regional trend from north-south at the southern Yellowstone Pla-

Table 3. Thirty earthquakes in the Yellowstone-Snake River Plain region of magnitude 5.5 and greater, 1900 through 1985 (area defined from Lat. 41°N to 46°N, Long. 110°W. to 116°W). Earthquakes accompanied by surface faulting have their origin time and location in bold print. Table summarized from Smith and Arabasz (1991).

No.	Date (GMT)		Time[1] (GMT) hr mn	Lat. (°N)	Long. (°W)	Magnitude[2] M_{conv}	M_w	Region
1.	1905	Nov 11	21:26	42.9	114.5	(5.5 ±)	—	South central Idaho (Shoshone)
2.	1909	Oct 06	02:50	41.8	112.7	(6 ±)	—	NW Utah (Hansel Valley)
3.	1914	May 13	17:15	41.2	112.0	(5.5 ±)	—	Ogden, Utah
4.	1925	Jun 28	01:21	46.00	111.50	6.75	6.6	Clarkston Valley, Mont.
5.	1930	Jun 12	09:15	42.6	111.0	5.8	—	Grover, Wyo.
6.	**1934**	**Mar 12**	**15:05**	**41.77**	**112.67**	**6.6**	**6.6**	**Hansel Valley, Utah**
7.	1934	Mar 12	18:20	41.57	112.75	6	5.9	Hansel Valley, Utah, aftershock
8.	1934	Apr 07	02:16	41.5	111.5 ?	5.5	—	Hansel Valley, Utah, aftershock?
9.	1934	Apr 14	21:26	41.73	112.60	5.6	—	Hansel Valley, Utah, aftershock
10.	1934	May 06	08:09	41.96	112.82	5.5	—	Hansel Valley, Utah, aftershock
11.	1944	Jul 12	19:30	44.41	115.06	6.1	—	Central Idaho (Seafoam)
12.	1945	Feb 14	03:01	44.61	115.09	6.0	—	Central Idaho (Clayton ?)
13.	1947	Nov 23	09:46	44.92	111.53	6.25	6.1	Virginia City, Mont.
14.	1959	Aug 18	06:37	44.88	111.11	6.3	6.3	Hebgen Lake, Mont., double event
15.	**1959**	**Aug 18**	**06:37**	**44.84**	**111.03**	**7.5**	**7.3**	**Hebgen Lake, Mont., double event**
16.	1959	Aug 18	07:56	45.00	110.70	6.5	—	Hebgen Lake, Mont., aftershock
17.	1959	Aug 18	08:41	45.08	111.80	6	—	Hebgen Lake, Mont., aftershock
18.	1959	Aug 18	11:03	44.94	111.80	5.5 +	—	Hebgen Lake, Mont., aftershock
19.	1959	Aug 18	15:26	44.85	110.70	6.3	6.3	Hebgen Lake, Mont., aftershock
20.	1959	Aug 19	04:04	44.76	111.62	6	6.0	Hebgen Lake, Mont., aftershock
21.	1962	Aug 30	13:35	41.92	111.63	5.7	5.6	Cache Valley (Logan), Utah
22.	1964	Oct 21	07:38	44.86	111.60	5.8	5.6	Hebgen Lake, Mont., aftershock
23.	1975	Mar 28	02:31	42.06	112.53	6.0	6.2	Pocatello Valley (Idaho-Utah border)
24.	1975	Jun 30	18:54	44.69	110.62	6.1	—	Yellowstone Park, Wyo.
25.	1976	Dec 08	14:40	44.76	110.80	5.5	—	Yellowstone Park, Wyo., aftershock
26.	**1983**	**Oct 28**	**14:06**	**43.97**	**113.92**	**7.3**	**6.9**	**Borah Peak, Idaho**
27.	1983	Oct 28	19:51	44.05	113.92	5.8	5.4	Borah Peak, Idaho, aftershock
28.	1983	Oct 29	23:29	44.24	114.06	5.8	5.5	Borah Peak, Idaho, aftershock
29.	1983	Oct 29	23:39	44.24	114.11	5.5	—	Borah Peak, Idaho, aftershock
30.	1984	Aug 22	09:46	44.37	114.06	5.8	5.6	Borah Peak, Idaho, aftershock

[1]The local time (Mountain Standard Time) for the earthquakes in this table is found by subtracting seven hours from Greenwich Mean Time. In some cases (War Time, Daylight Savings Time), the difference is six hours. Non-instrumental and instrumental earthquake locations are listed with one- and two-decimal-point accuracy, respectively.

[2]Abbreviations for earthquake magnitude: M_{conv} = conventional magnitude, M_L (local magnitude), M_S (surface-wave magnitude), and ^{m}b (body-wave magnitude); M_w = moment magnitude.

teau to northwest on the northwest margin of the caldera.

West of the Yellowstone caldera, a pronounced east-west band of earthquakes passes through the Hebgen Lake, Montana region, including the epicenter of the $M_s = 7.5$, 1959 Hebgen Lake earthquake that occurred about 30 km west of the caldera. This earthquake produced a 26 km long, west- to northwest-striking rupture with a maximum vertical displacement variously cited as 5.5 to 6.7 m (see Smith and Arabasz, 1991). Earthquakes in this area are part of the divergent belt of seismicity that extends more than 400 km along the north side of the SRP in a west-southwest direction into central Idaho. Smith and Sbar (1974) characterized this as an independent seismic zone and Stickney and Bartholomew (1987) called it the "Centennial tectonic belt". However, Smith and others (1985) included the area within a "V-shaped" pattern of seismicity surrounding the YSRP and suggested that this zone of seismicity was related to the Yellowstone hotspot.

Along the northwest side of the SRP, **Figures 4** and **8** reveal a northwest alignment of epicenters that corresponds to the mainshock and aftershocks of the $M_s = 7.3$, 1983 Borah Peak, Idaho, earthquake. This large scarp-forming earthquake (**Table 3**) was accompanied by a 34 km long fault with up to 2.7 m of coseismic vertical slip. It occurred 60 km northwest of the Snake River Plain in an area characterized by late Quaternary Basin and Range faulting (Scott and others, 1985) and widespread hot springs, but low background seismicity.

We note the relative seismic quiescence of the SRP and the abrupt increase in earthquake activity about 50 km to 100 km from its margins (see **Figures 4** and **8**). The low seismicity of the SRP with pronounced seismically active "shoulders" is enigmatic, and led Smith and others (1985), Anders and others (1989), and Anders and Sleep (1992) to suggest thermal and magmatic mechanisms associated with the Yellowstone hotspot. Parsons and Thompson (1991) postulated that magmatic overpressuring in the SRP reduced the normal stresses on incipient fractures, thereby precluding earthquakes. However, their mechanism does not account for the lack of seismicity in the adjacent aseismic area, Zone II, which extends up to 100 km beyond the boundary of the SRP volcanic field and which shows little evidence of volcanic features or high heat flow. Nonetheless, if the surrounding belt of seismicity, Zone III, is a signature of the regional stress field associated with the Yellowstone hotspot, then its effects on stress extends 100 to 200 km beyond the boundary of the SRP volcanic field.

Geoid anomaly

Just as the Earth's topographic field responds to crustal sources, the long-wavelength gravity field generally reflects deeper, lithospheric sources. The isostatic properties of the YSRP can be seen by examining the geoid model, GEOID90, from Milbert (1991) for North America (**Figure 9**). The geoid is considered to represent the degree of isostatic compensation and is an equipotential surface reflecting an amalgam of topographic relief and density variation. Most of the local geoid features are due to topographic variation. Density variations form a secondary, but important source of the geoid anomaly.

The most significant geoid anomaly of the entire North American continent is a very broad (about 1,000 km wide +10 to +12 m) circular geoid high centered at Yellowstone (**Figure 9**). We suggest that the major component of the Yellowstone geoid anomaly is the approximately 600 m high excess topography (**Figure 6**) of the Yellowstone Plateau, with a superimposed long-wavelength geoid signal produced by a large upper-mantle low-density body associated with the mantle hotspot. The radius of this anomaly (marked by the outer dashed line in **Figure 9**) is similar to the radii of geoid anomalies associated with oceanic swells and rises which range from ~800 to 1,500 km and average 10 to 15 m in amplitude (Crough, 1983).

The 1,000 km wide Yellowstone geoid anomaly, however, is not a direct indicator of the hotspot dimensions. The gravitational signal has been upward-continued to the Earth's surface from 100 to 200 km depths, thus indicating a smaller dimension at the source. We suggest that the geoid anomaly reflects the effects of buoyancy and lateral flow of the upper mantle, spreading out from a plate-plume interaction at Yellowstone with source dimensions of ~150 km. This model will be discussed in detail in a later section. The affect of the overriding plate across a rising heat source is also indicated in the lateral deflections of the +8 m to+12 m contours, streaming to the southwest adjacent to the SRP. This pattern is similar to the parabolic-shaped patterns of topography and seismicity surrounding the YSRP (**Figures 3** and **4**).

Plate tectonic framework of the YSRP

The significance of the YSRP within the plate framework of North America can be examined by plotting the location of the Yellowstone hotspot and several of the major tectonic features of the western U. S. at systematically older ages of 0, 5, 10, and 15 Ma (**Figure 10**), corresponding to the 16 million year evolution of the YSRP. These figures were produced by assuming a rigid-body framework for tectonic sub-provinces of western North America (for example, the Sierra Nevada, Great Valley, Cascade

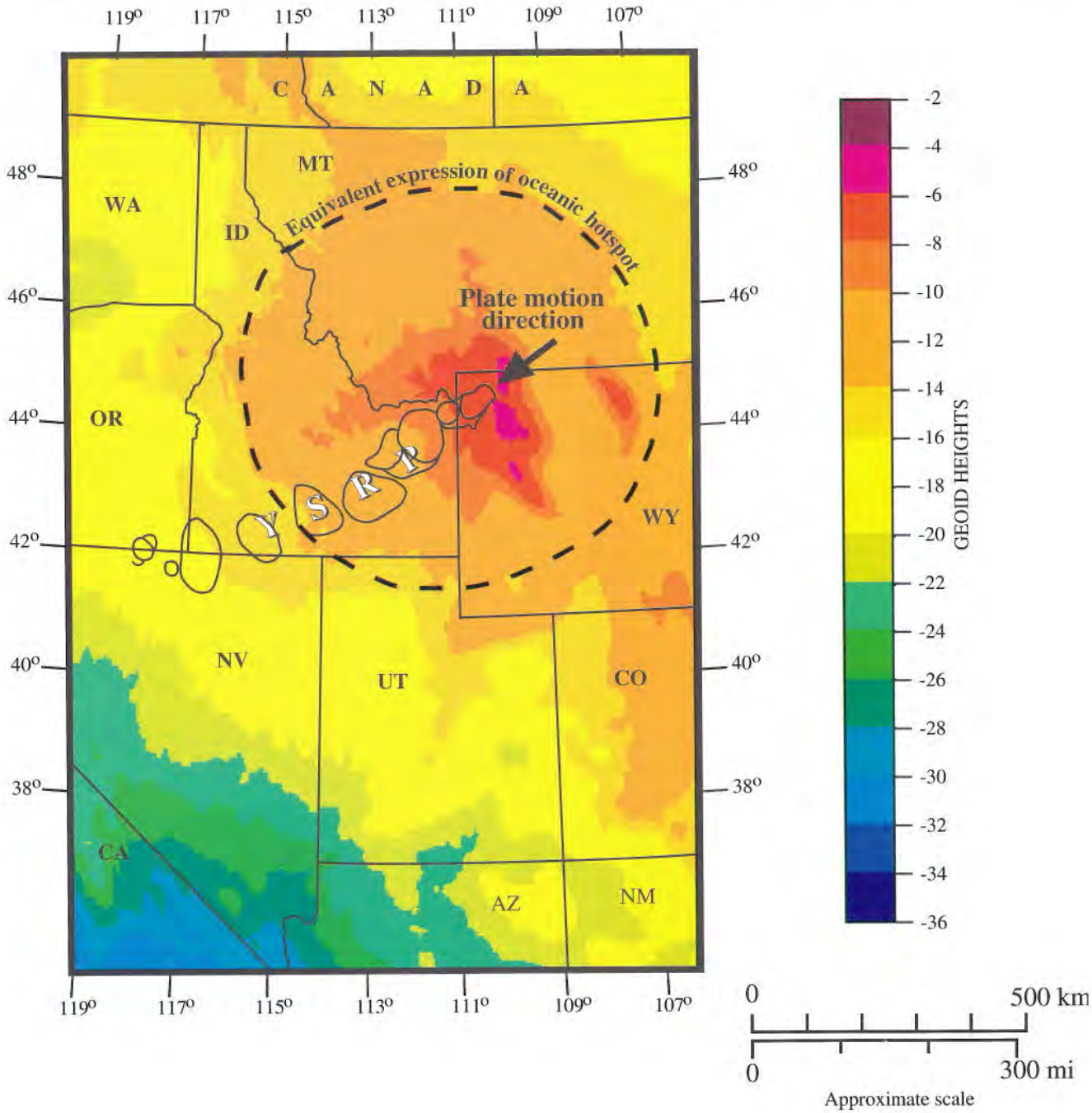

Figure 9. Map of geoid heights for the western United States from the GEOID90 model of Milbert (1991). Geoid heights are contoured at 2 m intervals. YSRP calderas are shown for reference. Dashed line marks the outline of geoid height anomaly of approximately 10 m, which is similar to geoid anomalies for oceanic hotspots and is considered a combined topographic-density signature of the Yellowstone hotspot.

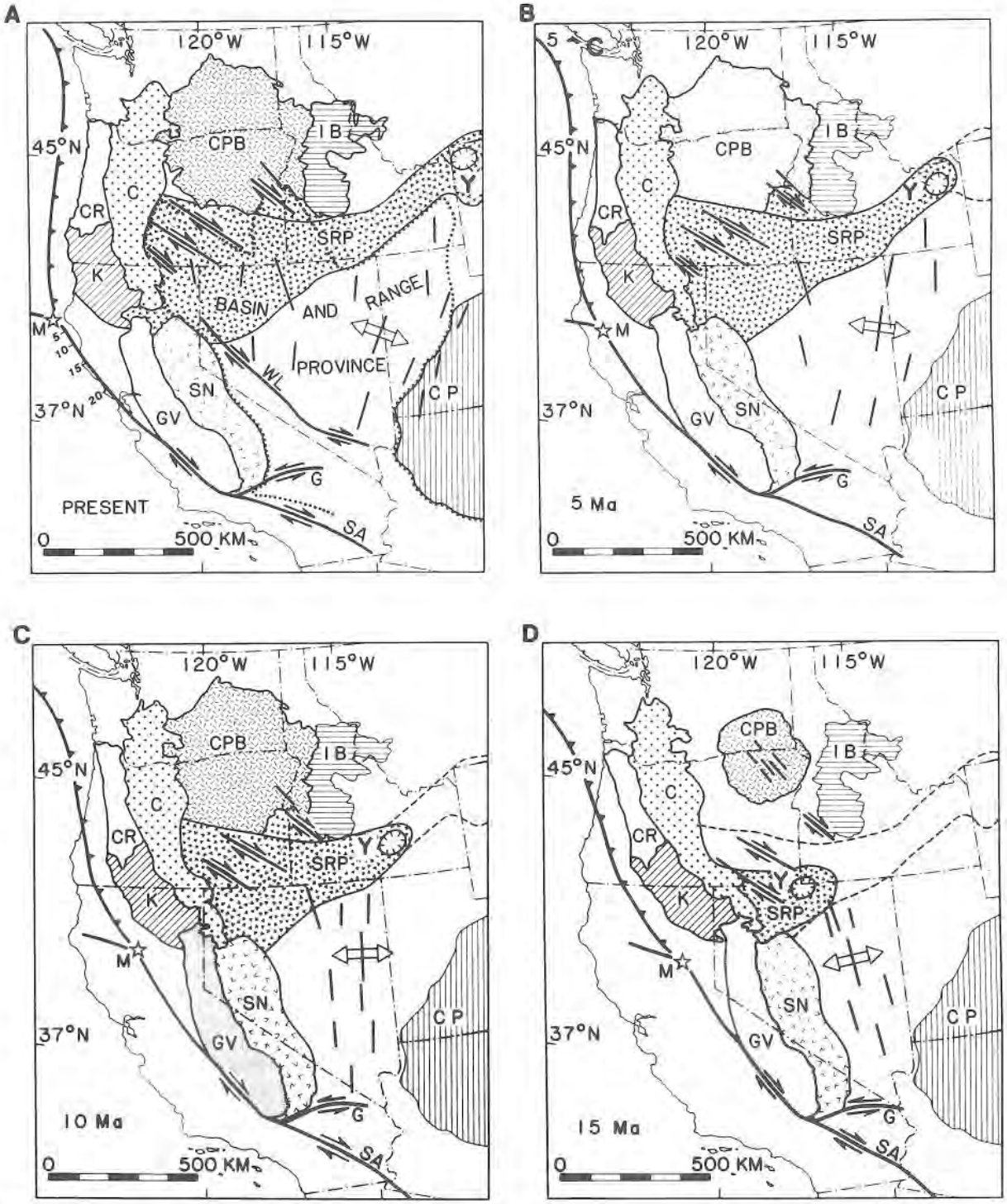

Figure 10. Maps showing plate reconstructions and the related tectonic framework of the western United States. Reconstructions were made at 5 Ma, 10 Ma, and 15 Ma taking into account the relative motion of the North American plate of ~2.5 cm/yr southwest and a regional east-west extension rate of the Basin and Range province of ~1.7 cm/yr (from Magill and Cox, 1981). The bimodal rhyolitic-basaltic volcanic rocks of the YSRP are shown as the same pattern as those of the High Lava Plains of southern Oregon. SRP = Snake River Plain, Y = Yellowstone hotspot, M = Mendocino triple junction, CP = Colorado Plateau, SA = San Andreas fault, GV = Great Valley, G = Garlock fault, SN = Sierra Nevada, K = Klamath Mountains, C = Cascade Range, CR = Coast Ranges, CPB = Columbia Plateau basalt field, IB = Idaho batholith.

Range, etc.) with a superimposed east-west extension rate of ~1.7 cm/yr and for the northern Basin and Range given by Magill and Cox (1981). We then projected the North American plate motion backwards in time at ~2.5 cm/yr in a southwest direction, with respect to the location of the Yellowstone hotspot, subtracting the component of east-west regional extension accompanying Basin and Range evolution.

The primary features of the intraplate reconstructions are as follows (**Figure 10**):

0 Ma—The Yellowstone hotspot is at its present location and the Basin and Range province is fully extended (100 % of its original width).

5 Ma—The Yellowstone hotspot volcanic center was located approximately 75 km southwest of its current position, at Island Park, and the Basin and Range was extended approximately 70% of its original width.

10 Ma—The Yellowstone hotspot was located near the center of the eastern Snake River Plain near Pocatello, Idaho. The northern Basin and Range was about half of its present width, and the western North American plate boundary was approximately 200 km east of its current position.

15 Ma—This time is near the age of the oldest silicic volcanic rocks of the Snake River Plain, at about 16 Ma, and at a position about 700 km southwest of Yellowstone in southwestern Idaho and northern Nevada. This location is also where most authors place the inception of YSRP volcanism based upon the oldest YSRP silicic volcanic rocks. This was also near the time of initiation of widespread extension in the Basin and Range province at 17 to 20 Ma (Zoback and others, 1981).

We have also examined the hypothesis that the Yellowstone hotspot originated earlier by continuing the intraplate reconstructions to 20 and 23 Ma. At 20 Ma, the reconstruction would place the Yellowstone hotspot in northern California, where there is little evidence for volcanic rocks of this age. The Yellowstone hotspot may have passed beneath the Sierra Nevada crust, approximately 20 km thicker than Basin and Range crust (Coney and Harms, 1984), without producing surface volcanism. Presumably much more heat would be required to penetrate the thick and cool Sierra Nevada crust, and possibly this thicker crust was not heated sufficiently to bring magmatic material to the surface.

Speculating further, at about 23 Ma our model places the Yellowstone hotspot near the subducting margin of the west coast of North America and near the Mendocino triple junction (within the error of ± 100 km of our calculations). A location for the Yellowstone hotspot at approximately 50 Ma at the western plate margin was suggested by Engebretson and others (1985), who constructed models of relative motions between the North American and Pacific plates for the past 180 million years. Their estimate did not consider the extension of the Basin and Range province that in 16 million years could have increased its width by 100% and thus could also be in error by 100 km or more (Engebretson and others, 1985). Nonetheless, both of these models indicate the possibility of a hotspot location at or near the plate boundary in middle Tertiary time.

Despite the uncertainties in these reconstructions, they offer insight into the general space-time behavior of the YSRP volcanic system for at least the last 16 million years and support the origin of the YSRP as an interaction between the North American plate (moving southwest) and a fixed mantle magmatic source.

The Yellowstone hotspot today

As described in the previous section, the present location of the YSRP hotspot is thought to be beneath Yellowstone. In this section we discuss the volcanic history and physical properties of the crust and mantle of Yellowstone assessed primarily by geophysical and geodetic surveys. The resulting models reveal an active volcanic system controlled by vigorous magmatic and heat sources originating in the upper mantle, which are manifested in the upper-crust by marked thermal, earthquake, gravity, and crustal deformation signals.

Volcanic history of Yellowstone

The most comprehensive treatment of Yellowstone's volcanic history is from Christiansen and Blank (1972), Christiansen (1984), and maps and data from Christiansen's (1993) forthcoming U. S. Geological Survey Professional Paper. Keefer (1971) summarized Yellowstone's complete geologic history since Precambrian time, including an overview of its volcanic history. A detailed review of Yellowstone's volcanic history is given by Christiansen (1984), and a recent account of the isotopic content of Yellowstone volcanic rocks is given by Hildreth and others (1991). Christiansen (1982) also discussed the volcanic history of the Henry's Fork transitional area between Yellowstone and the Snake River Plain. We also recommend summaries of the geology and geophysics of the Yellowstone volcanic system by Smith and Christiansen (1980) and a National Research Council report on the objectives for deep scientific drilling in Yellowstone National Park (Yellowstone National Park Task Group to the Continental Drilling Committee, 1987) for further reading.

The earliest scientific account of Yellowstone's volcanism and earthquakes was given by Hayden (1872, 1873), based upon his late 19th century, pioneering field expeditions into Yellowstone. Hayden recognized that the Yellowstone region was the center of a giant volcanic system and remarked on the occurrence of numerous small- to moderate-magnitude earthquakes:

> *While we were encamped on the northeast side of the lake* [Yellowstone Lake] *on the night of the 20th of July* [1871], *we experienced several severe shocks of an earthquake, and these were felt by two other parties, fifteen to twenty-five miles distant, on different sides of the lake. We were informed by mountain-men that these earthquake shocks are not uncommon, and at some seasons of the year very severe, and this fact is given by the Indians as the reason why they never visit that portion of the country. I have no doubt that if this part of the country should ever be settled and careful observations made, it will be found that earthquake shocks are of very common occurrence.* Hayden (1872)

So persistent were the tremors on Yellowstone Lake that Hayden named this camp "Earthquake Camp," an aptly named site, for we will show later in this section that Yellowstone Lake has persisted as one of the most notable areas of earthquake swarms in the entire Yellowstone region.

Geologic studies by various U. S. Geological Survey and university scientists continued through the early 20th century to the present. Interest in the seismotectonics of the region was heightened by the occurrence of the 1959, $M_S = 7.5$, Hebgen Lake, Montana, earthquake, the largest earthquake in the Intermountain region in historic time. Following this earthquake, investigations by Hamilton (1959) distinguished the Yellowstone caldera from the nearby Island Park caldera and further resolved the differences in volcanism between Yellowstone and the Snake River Plain. However, it has been the detailed volcanological studies of Yellowstone by geologists of the U. S. Geological Survey that led to an elucidation of the cyclic nature and the immense scale of Pleistocene volcanism (e.g., see Christiansen and Blank, 1972; Christiansen, 1984, 1993; Hildreth and others, 1991).

The history of the Yellowstone volcanic system is dominated by three catastrophic, caldera-forming eruptions (**Figure 11**), which produced more than ~4,800 km³ of ash flows at 2.0 Ma, 1.2 Ma, and 0.6 Ma (Christiansen, 1984, 1993). The first cycle of Yellowstone's silicic volcanism, Huckleberry Ridge Tuff, occurred at 2.0 Ma (denoted as I in **Figure 11**) and produced a large caldera that is now mostly covered by younger volcanic flows and is thought to have had an eruptive volume of 2,500 km³. The second-cycle, Henry's Fork caldera (denoted as II in **Figure 11**) was restricted to the Island Park area, southwest of the Yellowstone Plateau, and produced 280 km³ of ash-flow tuff. Following the 0.6 Ma caldera-forming eruption of 1,000 km³ (denoted as III), drainage of a large magma chamber released roof support, causing it to collapse and produce the 45 km wide by 75 km long "Yellowstone caldera." In the last 150,000 years, there have been 40 or more silicic volcanic eruptions on the Yellowstone Plateau and several basaltic eruptions on the margin of the plateau, with the most recent magmatic activity at 70 Ka (Christiansen, 1993). The cumulative effects of post-caldera eruptions have produced the gently rolling and forested topography of the Yellowstone Plateau.

Following caldera collapse at 0.6 Ma, magmatic resurgence formed two structural domes: (1) the

Sour Creek dome, in the northeast caldera, began its uplift following the main eruption at 0.6 Ma; and (2) the Mallard Lake dome (**Figure 12**), in the southern caldera, was initiated at 0.15 Ma (Christiansen, 1984). Both of these domes are thought to have been produced by uplift above magmatic sources and are considered to be active (Christiansen, 1984, 1993). Following the explosive eruption of 0.6 Ma, the roof of the magma chamber was downdropped several hundred meters, producing the subsided floor of the Yellowstone caldera that was later covered by post-caldera flows and sediments (Christiansen, 1993). Glacial moraines and alluvial fans are offset across northwest-striking normal faults along the crests of both domes, and the circular caldera rim-boundary fault has accommodated caldera-wide subsidence and extension.

On a regional scale, the Quaternary tectonic story of the Yellowstone Plateau is dominated by normal faulting and crustal extension associated with general Basin and Range epeirogeny. The main Quaternary faults of the Yellowstone Plateau are the Gallatin, Madison, and Teton fault zones of late Tertiary age that strike north-south at the northern and southern margins of the plateau (**Figure 13**). Buried extensions of these faults may exist in areas covered by the Quaternary silicic volcanic rocks.

The youngest mapped faults of the Yellowstone caldera (**Figure 13**) are Holocene in age and have several meters of offset (Meyer and Locke, 1986). These faults extend along the west side of the South Arm of Yellowstone Lake in an area of pronounced seismicity, to be discussed later. These faults are part of a regional right-stepping fault zone that extends south of the Yellowstone Plateau in an *en echelon* series of north-south striking faults to the Teton fault. On the northwest side of the Yellowstone Plateau, the seismically active Hebgen Lake fault zone extends about 30 km east-southeast toward the caldera boundary, but its relationship to the rim boundary fault is not known. The relationship of the north-south striking Gallatin fault, that extends south of Mammoth and terminates at the northwest caldera, is poorly defined because of limited access and extensive cover.

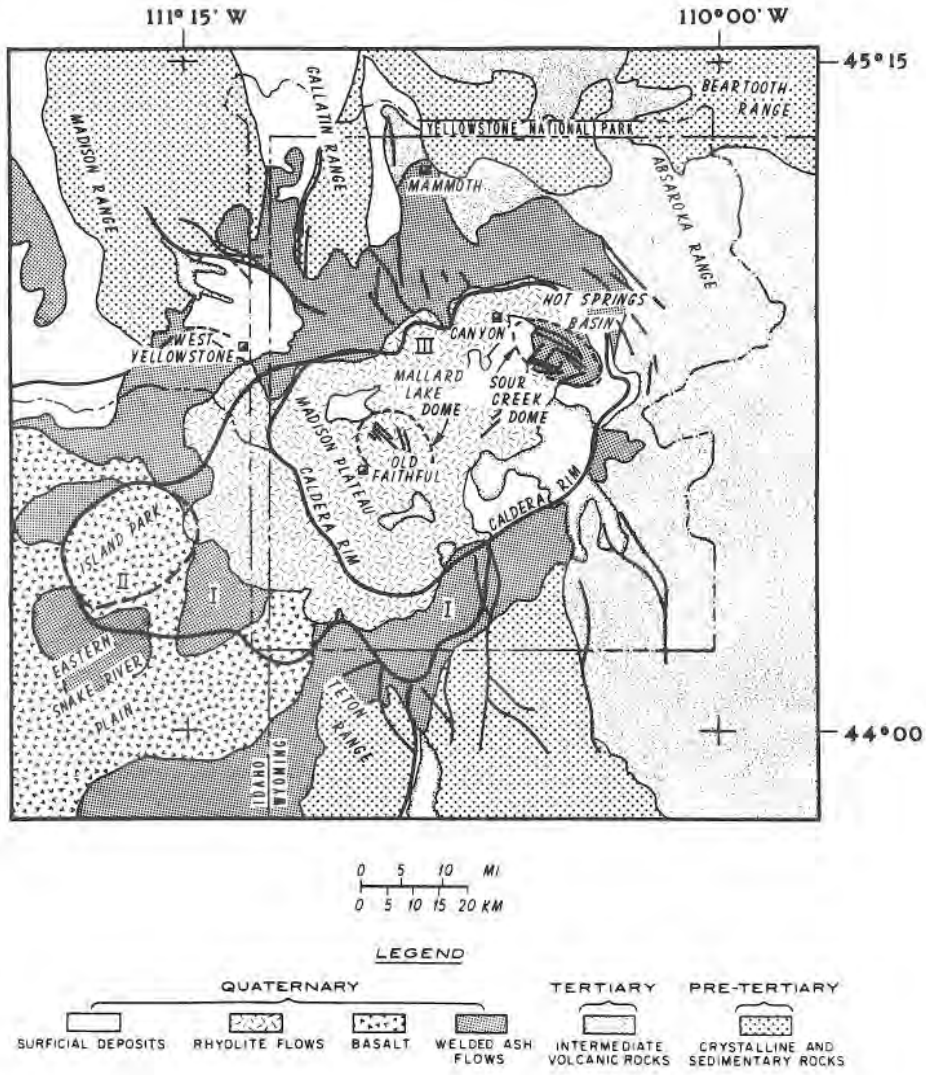

Figure 11. Geologic map of the Yellowstone Plateau showing the locations of Yellowstone calderas, Quaternary volcanic flows, and late Cenozoic normal faults (modified from Christiansen, 1984). Yellowstone calderas are shown by age: I = 2.0 Ma, II = 1.2 Ma, and III = 0.6 Ma.

Figure 12. Photograph of the Mallard Lake resurgent dome, southeastern Yellowstone caldera, looking northeastward across the Yellowstone Plateau and showing the approximate 400 m topographic dome and the northwest-striking central graben. The dome is highlighted by a fresh snow cover. Aerial photo taken in February, 1989, by Rick Hutchinson, National Park Service.

On **Figure 13** we have also plotted the locations of volcanic vents that fed the post-collapse caldera flows. The vents form two distinct groups: (1) a northwest alignment in the southwest Yellowstone caldera, and (2) a similar north to northwest alignment in the northwest caldera that projects into a series of west- to northwest-striking Quaternary faults near Norris Junction. On the basis of contemporary seismicity, we believe that the vents southeast of Norris Junction are related to an active fault system that may continue southeast beneath the central caldera.

Global significance of Yellowstone's explosive volcanism

To portray the importance of Yellowstone's volcanism, we have plotted the eruptive volumes of several well-known volcanic eruptions of global significance along with those of Yellowstone (**Figure 14**). The smallest eruption in this comparison was in 1980 at Mt. St. Helens, Washington. While this dacitic volcano produced substantial destruction and ash that was deposited in areas of several surrounding states, its eruptive volume is thought to be only about 0.7 km^3. The 1991 eruption of Mt. Pinatubo, The Philippines, killed more than 600 persons and expelled 10 km^3 of ash. Another major volcanic eruption of North America was the 6.8 Ka Mazama volcano, which ejected 75 km^3 of ash and was responsible for producing the high mountain lake at Crater Lake National Park, Oregon. Another large historic eruption was that of Krakatoa, southwest Pacific, which expelled more than 18 km^3 tephra in 1883. The even larger Tambora, Indonesia, eruption of 1815 produced 150 km^3 tephra.

However, none of these eruptions comes even close to the smallest of Yellowstone's Pleistocene, caldera-forming, explosive eruptions. In **Figure 14**, Yellowstone's climactic eruptions (**Figure 11**) expelled ash flows with volumes of: (1) 2,500 km^3 as 2.0 Ma Huckleberry Ridge Tuff , (2) 280 km^3 as the 1.2 Ma Mesa Falls Tuff, and (3) 1,000 km^3 as the 0.6 Ma Lava Creek Tuff (Christiansen, 1984, 1993). Continuous small-scale rhyolitic and basaltic eruptions between the climactic events contributed an additional 3,500 km^3 of volcanic material for a total of about 8,000 km^3. These volumes make Yellowstone one the world's largest, if not the largest, known center of active silicic volcanism. We suggest that the Pleistocene volcanism of Yellowstone likely compares in volume with the eruptions from the older late Tertiary calderas of the Snake River Plain volcanic system shown in **Figure 3**.

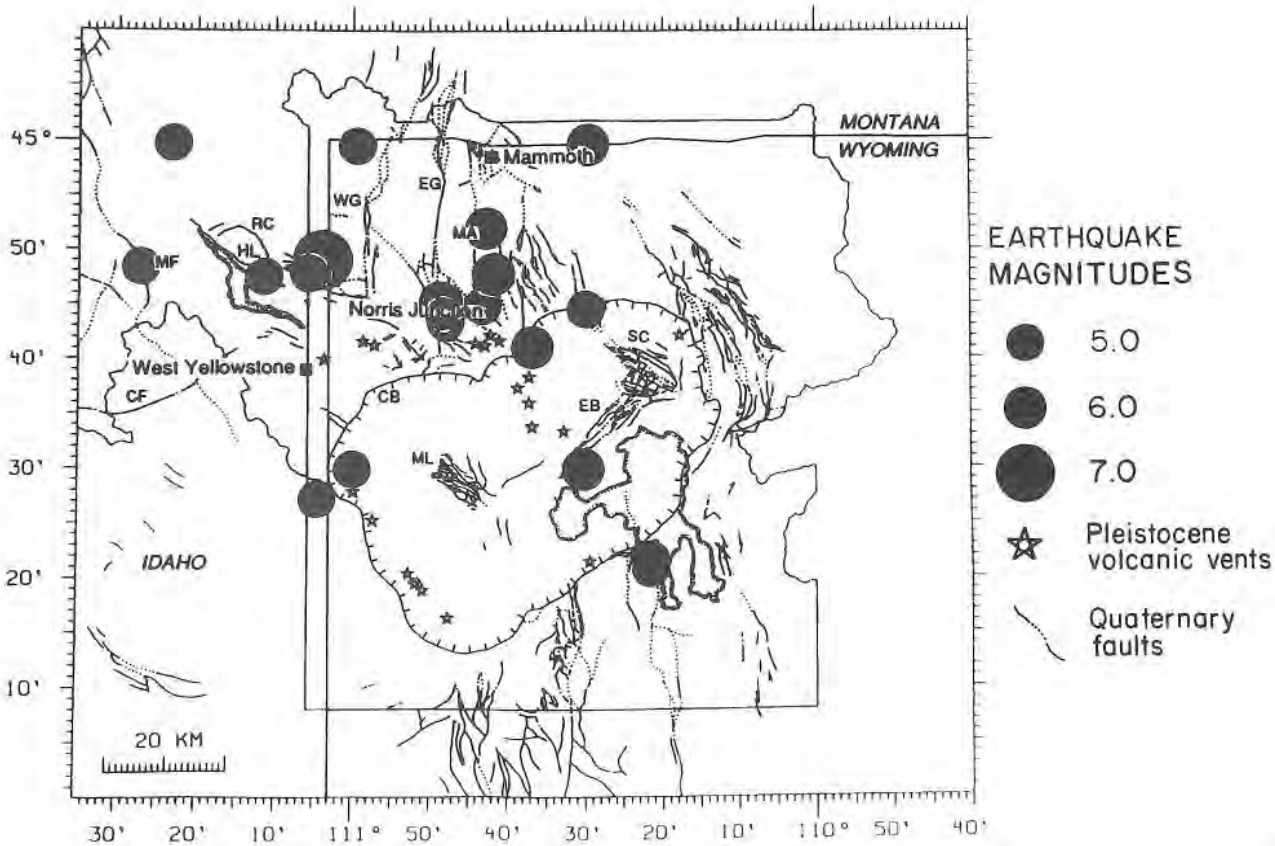

Figure 13. Map of Quaternary faults, Pleistocene volcanic vents, and larger, historic earthquakes (M > 5.5) of the Yellowstone Plateau. Volcanic vents are from U. S. Geological Survey 15-minute geologic quadrangle maps. Faults were digitized from the maps of Christiansen (1993). Fault zones are: RC = Red Canyon, HL = Hebgen Lake, WG = West Gallatin, EG = East Gallatin, CB = caldera boundary, EB = Elephant Back, and MA = Mammoth corridor. ML = Mallard Lake dome and SC = Sour Creek dome.

To further portray the scale of Yellowstone's silicic volcanism, we plotted the areas covered by ash deposits from four large eruptions in the western U. S. (**Figure 15**). These include: (1) the 0.74 Ma Bishop tuff with 500 km^3 of ash from the Long Valley caldera, California (Sarna-Wojcicki and Davis, 1993); (2) the 0.6 Ma Lava Creek Tuff of Yellowstone (Sarna-Wojcicki and Davis, 1993); (3) the 2 Ma Huckleberry Ridge Tuff of Yellowstone (Christiansen, 1984); and (4) the 1980 Mt. St. Helens volcano, Washington (Dzurisin and Newhall, 1988). The significance of these eruptions is evident by the immense areas of ash coverage, from thicknesses of a few

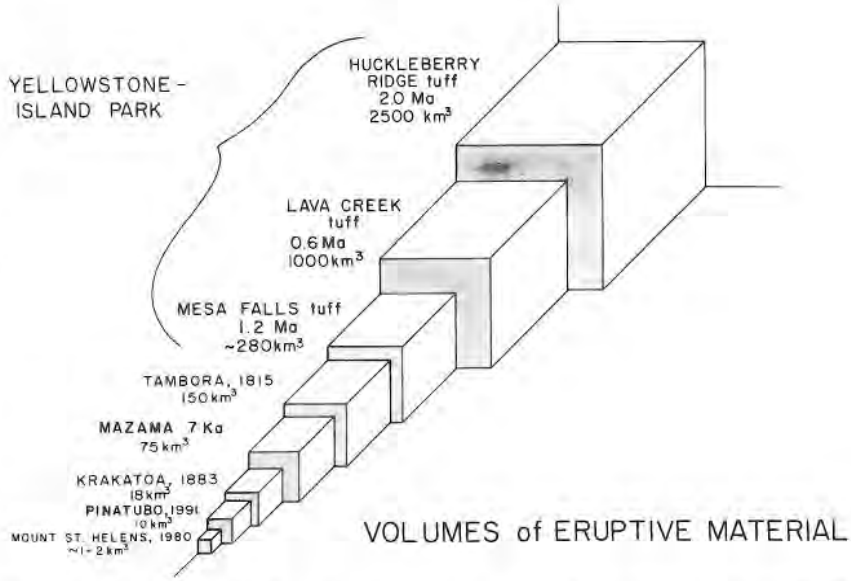

Figure 14. Volumes of Yellowstone's explosive volcanic eruptions compared with other well-known volcanic eruptions of the world. Data in part taken from Dzurisin and Newhall (1988) and Decker and Decker (1989).

millimeters to several meters, that blanketed much of western North America. For example, the Bishop tuff covered most of the southwestern U. S. and northern Mexico. Ash from Yellowstone's Huckleberry Ridge and Lava Creek tuffs, however, covered the entire western U. S., much of the Midwest, parts of the eastern Pacific, and northern Mexico. Compared to the ash fall coverage of Mt. St. Helens, which had such a dramatic affect on the landscape and the population of western Washington and Oregon, the scale of Yellowstone's prehistoric caldera-forming eruptions is immense. And while the Mt. Pinatubo and Mt. St. Helens eruptions had disastrous effects, they are very small compared to Yellowstone's past and potential for future catastrophic, caldera-forming eruptions.

Geophysical properties of Yellowstone

In this section we focus on the geophysical and geodetic properties of Yellowstone and show how heat flow, seismic velocity structure, seismicity, and crustal deformation are consistent with crustal heat flow from magmatic sources beneath the Yellowstone caldera. Previous geophysical summaries by Smith and others (1974, 1977), Eaton and others (1975), and Smith and Braile (1984) provide an interesting perspective on these issues that have changed with the acquisition of much new data since their publication.

Heat flow

There is a single physical property that sets Yellowstone apart from virtually all other continental regions, namely its extremely high heat flow of

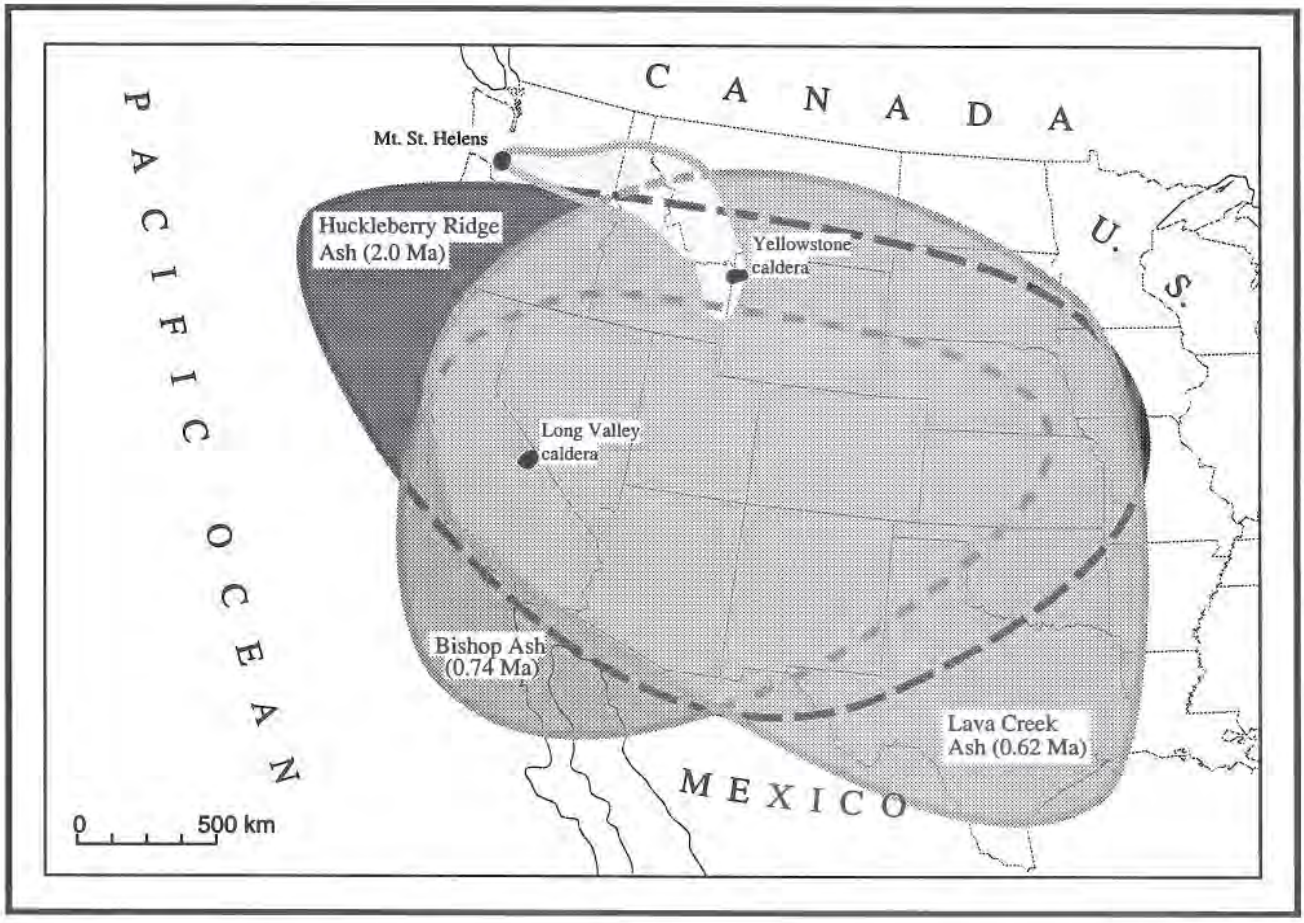

Figure 15. Map showing areas covered by airborne ash flows, tuffs, and pumices of four large Cenozoic volcanic eruptions of the western U. S.; the 0.6 Ma Yellowstone eruption, the 2.0 Ma Yellowstone eruption, the 0.7 Ma Long Valley caldera eruption, and the 1980 Mt. St. Helens eruption. Data from Sarna-Wojcicki and Davis (1993) and Sarna-Wojcicki and others (1982) for Mt. St. Helens.

~2,000 mWm^{-2}, which is about 30 times the continental average (**Figure 16**). Not only is heat an essential property of the youthful volcanism and hydrothermal activity of Yellowstone, we believe it drives such important mechanisms as thermal buoyancy, which affects the topography and the distribution of earthquakes of the YSRP system.

The coherence of a distinct thermal province associated with the YSRP became apparent with evolving compilations of heat-flow measurements (Blackwell, 1978; Lachenbruch and Sass, 1978; Blackwell and others, 1991). The regional heat flow of the Snake River Plain ranges from 40 to 100 mWm^{-2} (Brott and others, 1981; Blackwell and others, 1991). In contrast, the heat flux north and east of Yellowstone in the Beartooth and Absaroka mountains is 50 to 80 mWm^{-2} (Heasler and Hinckley, 1985). Thus there is a clear distinction between the high heat flow of Yellowstone (2,000 mW/m^2) and those of the Basin and Range province (75 to 90 mWm^{-2}), transitional values of ~100 mWm^{-2} within the Snake River Plain, and much lower values of 50 - 80 mWm^{-2} north and east of the YSRP.

Only a few borehole measurements of temperature have been made in the Yellowstone Plateau and those revealed temperatures exceeding 240°C and higher at depths less than 300 m (White and others, 1975; David Blackwell, personal communication, 1989). These measurements document a shallow, high-temperature regime but also reveal that conductive heat-flow measurements of Yellowstone are contaminated by pervasive ground-water circulation, primarily associated with the widespread hydrothermal systems.

The convective heat-flow component of Yellowstone, however, can be estimated using chloride content of hot water drained through hot springs and geysers and collected in streams and rivers. Fournier (1989) and Fournier and Pitt (1985) estimated a total convective flux for the entire Yellowstone Plateau of 4x10^{16} cal/yr (using geochemical methods), which corresponds to a heat-flow value of about 2,000 mWm^{-2}. Unfortunately, the chemical method of heat-flow measurements cannot differentiate between individual heat sources, such as localized magma bodies, because the measurements were from rivers that collect chloride from large drainage basins of the Yellowstone Plateau.

The only conductive heat-flow measurements in the Yellowstone caldera were made by Morgan and others (1977) in Yellowstone Lake using marine-type thermal probes in shallow sub-bottom sediments (**Figure 16**). Their mapped values ranged from 125 to 300 mWm^{-2} in the southern arms of Yellowstone Lake and rapidly increased northward across the caldera boundary, with an average value of 1,600 mWm^{-2} for the main lake basin. This dramatic change in thermal flux is compelling evidence for a

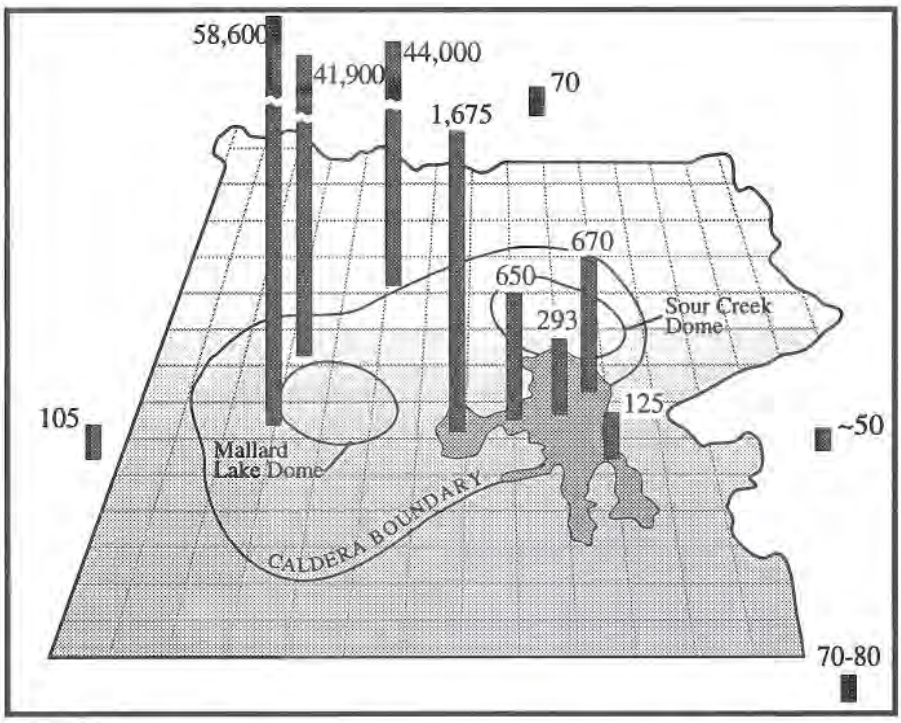

Figure 16. Heat-flow distribution of the Yellowstone Plateau (in units of mWm^{-2}). Heat-flow values in Yellowstone Lake were determined by thermal probe measurements and are considered the most reliable indicators of the conductive heat flux of the Yellowstone caldera (Morgan and others, 1977). Heat-flow values for the western caldera were estimated from geochemical determinations by Fournier (1989) and mainly reflect the convective component of heat flow. Heat-flow values of the surrounding region are from Blackwell (1989) and Heasler and Hinckley (1985).

shallow heat source beneath the northern and western parts of Yellowstone Lake. Fournier (1989) showed that the 2,000 mWm^{-2} heat flux is consistent with the release of heat by crystallization and cooling of about 0.1 km^3 of rhyolitic magma per year from 900°C to 500°C. We believe that this estimate is a reasonable value of magmatic recharge rate for Yellowstone and is therefore good evidence that magmas, Partial melts, and extensive hydrothermal systems are present beneath the caldera.

The significance of Yellowstone's heat flow on a global scale can also be seen by comparing its 2,000 mWm^{-2} flux with the background heat flow of the North American continent of 40 to 60 mWm^{-2} (**Table 4**). The thermal energy release of Yellowstone is of the same order as such large volcanic features as the entire Cascade Range, the Columbia Plateau, and the ignimbrite fields of the Basin and Range province. Moreover, it is 2 to 3 times greater than that of the Valles, New Mexico, and Long Valley, California, calderas. Blackwell (1978) estimated that fully 5% of the total thermal energy of the entire U. S. Cordillera is released at Yellowstone, which occupies less than 0.1 % of its area.

Regional gravity field of the YSRP

The YSRP Bouguer gravity field mimics the regional patterns of topography (compare with **Figure 3**), i.e., gravity lows correspond to topographic highs, and vice versa, and consequently we have not included it in this paper. On large-scale compliations, the gravity signature of the YSRP is a pronounced arcuate positive gravity anomaly that systematically decreases northeastward along the SRP from values of -110 mGal in southwestern Idaho, to -190 mGal at the transitional Island Park area, then rapidly decreases to a regional -200 mGal value and a pronounced -60 mGal closed low at Yellowstone.

Interpretations of the SRP crustal structure were made from a 300 km-long northwest-southeast gravity profile (**Figure 17**) across the SRP in conjunction with seismic velocity determinations from the 1978 YSRP seismic refraction experiment (Sparlin and others, 1982). The SRP model revealed an 80 mGal positive gravity anomaly centered over the volcanic province that suggests significant density and compositional variations compared to the surrounding thermally undisturbed region. The combined SRP

Table 4. Comparison of continental heat production with that of Yellowstone. Data taken in part from Blackwell (1978), Dzurisin and Newhall (1988), and the Yellowstone National Park Task Group to the Continental Drilling Committee (1987).

Feature	Area (km^2)	Time span (Ma)	Total energy (cal/s)	Total heat flow (mWm^{-2})
General volcanism				
Cascade Range	17,500	20	4.1×10^9	20
Andes	--	10	--	6 - 10
Columbia Plateau	250,000	3	3×10^9	55
Basin-Range ignimbrites	180,000	20	2.6×10^8	6
San Juan caldera, Colorado	25,000	3	2.7×10^8	46
Magmatic intrusion–conduction				
Andes				~16
Yellowstone caldera	2,500	15	3×10^8	~400
Hydrothermal convection				
Western United States	2,300,000	----	$> 2.4 \times 10^8$	0.4
Yellowstone caldera	2,500		1.2×10^9	1,400 - 2,000
Stored heat energy				
U. S. Cordillera	2,000,000	40-80	~4×10^{10} watts	~80
Other U. S. calderas				
Long Valley, California	450	0.7 m. y.	0.7×10^8	630
Valles, New Mexico	150	1.1 m. y.	0.2×10^8	500

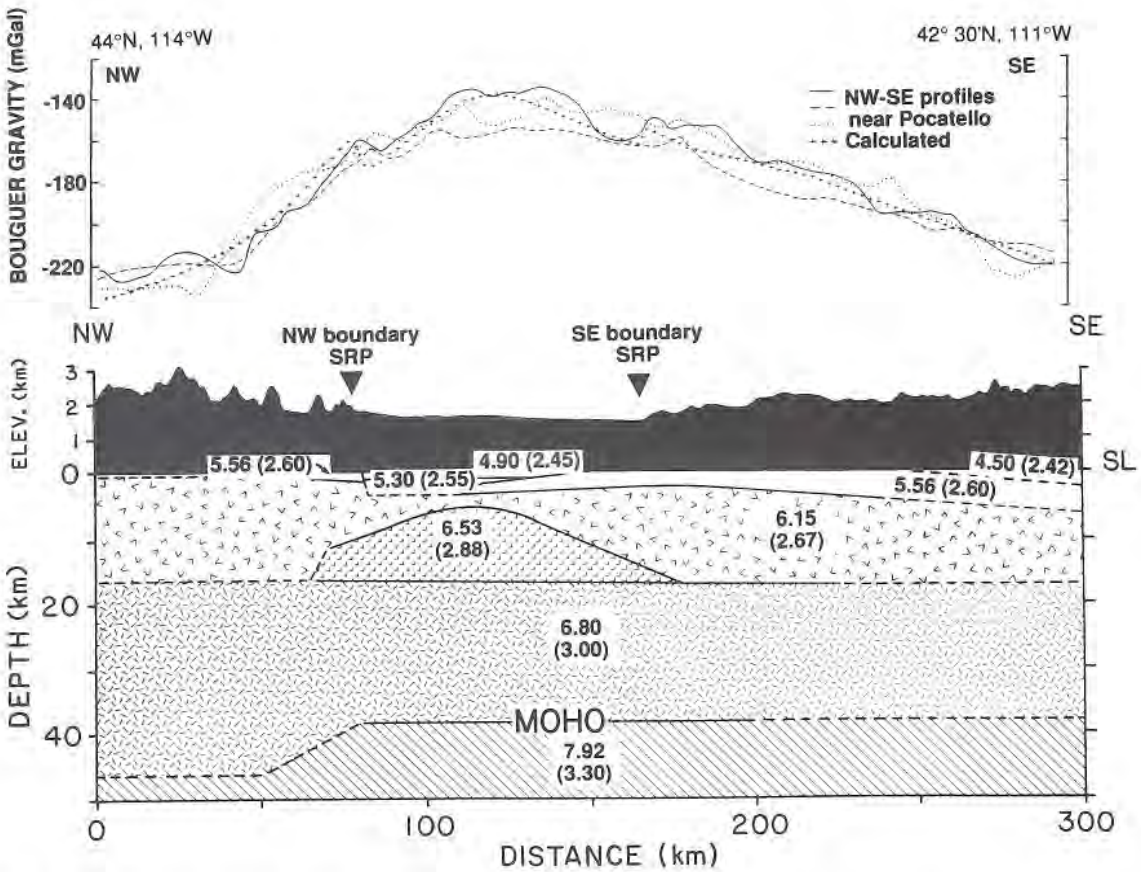

Figure 17. Bouguer gravity and crustal P-wave velocity and density model across the Snake River Plain determined by two-dimensional modeling of a reversed seismic refraction profile between Arco and Pocatello, Idaho (from Sparlin and others, 1982). See Figure 6 for locations of towns. Numbers are P-wave velocities in km/s and numbers in parentheses are densities in gm-cm^{-3}.

seismic velocity and density model of Sparlin and others (1982) is characterized by:

1. a thin (~1 km-thick) surface basalt layer underlain by a 2 to 3 km thick silicic volcanic layer with relatively low densities of 2.45 and 2.55 gm-cm^{-3}, respectively;
2. a thin to non-existent 6.15 km/s layer, which is a continuation of the typical granitic upper crust of the surrounding thermally undisturbed region;
3. an anomalous ~10 km-thick, high-velocity (6.5 km/s) and high density (2.88 gm-cm^{-3}) body that underlies the entire SRP at mid-crustal depths of 8 to 18 km;
4. a uniform lower crust with a density and velocity similar to the lower crust of the surrounding Basin and Range province; and
5. a crust-mantle boundary at depths of 40 to 45 km.

In contrast, the Bouguer gravity field of Yellowstone (**Figure 18**) is characterized by a large negative anomaly that was first identified by Hill and Pakiser (1966) as a separate feature from the SRP. **Figure 18** shows that Yellowstone's gravity field is dominated by a - 60 mGal residual low centered over the caldera, but notably extends northward, about 25 km beyond the caldera, encompassing the northeastern Yellowstone Plateau. An additional localized -20 mGal low is centered in the northeastern Yellowstone Plateau, located on the north side of the Sour Creek dome and near the largest hydrothermal system in Yellowstone, Hot Springs Basin.

The negative gravity anomaly of Yellowstone thus contrasts with the pronounced positive gravity anomaly of the SRP and suggests notable differences in crustal composition. Eaton and others (1975) modeled the regional gravity low of Yellowstone and

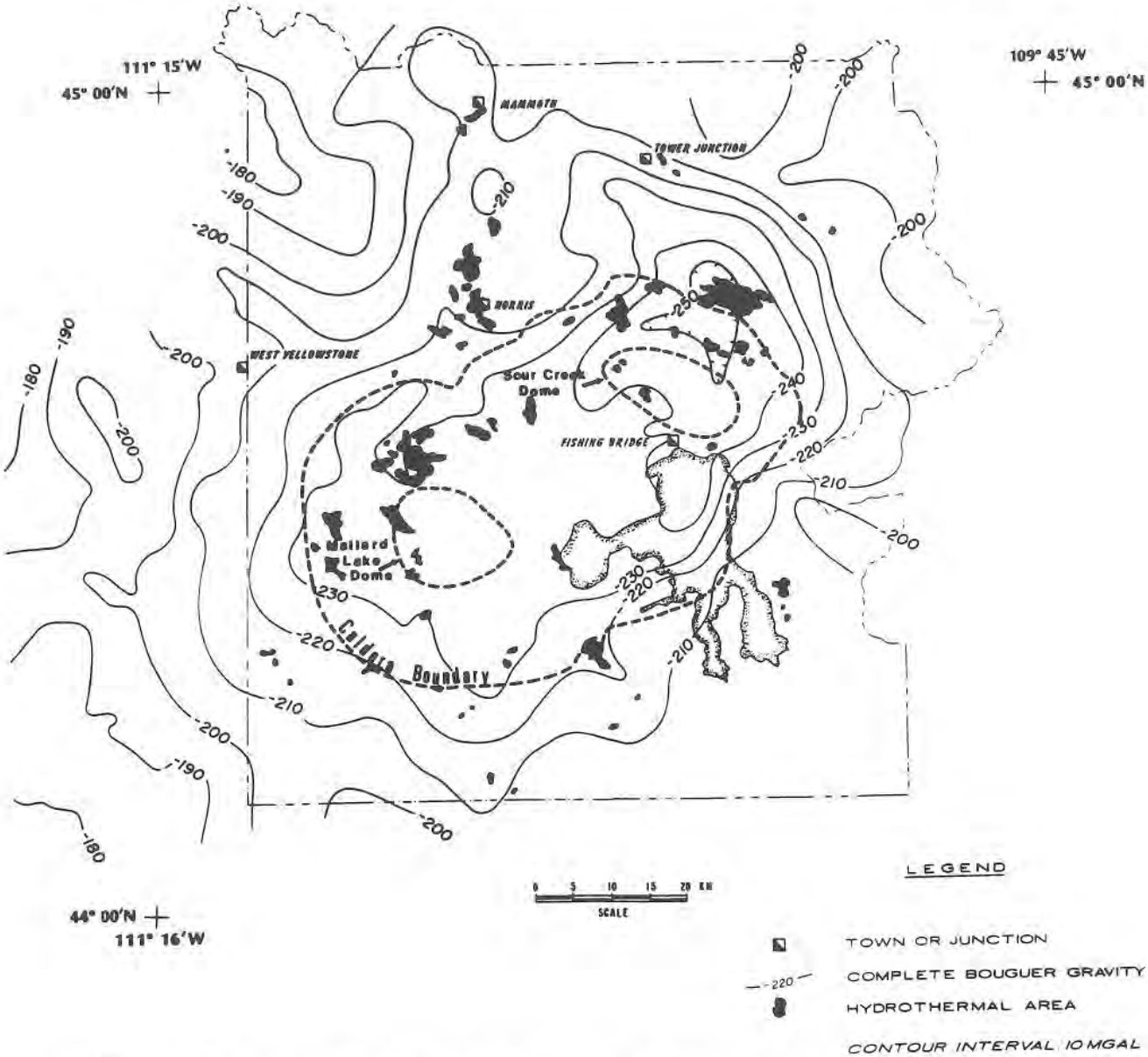

Figure 18. Complete Bouguer gravity anomaly map of the Yellowstone Plateau (modified from Lehman and others, 1982).

interpreted that the surficial rhyolites were underlain by hydrothermally altered basement rocks with molten to partially melted rhyolites and basalts. However, their models were not as well constrained as those by Lehman and others (1982), who incorporated the three-dimensional P-wave velocity distribution of the upper crust with a three-dimensional density model that reveals (**Figure 19**): (1) a 2.4-2.5 gm-cm^{-3} layer, 1-2 km thick, corresponding to caldera sediment fill and rhyolite flows; (2) a 2.6-2.7 gm-cm^{-3} upper-crustal layer beneath most of the caldera, which corresponds to a 10% P-wave velocity decrease and is interpreted to be a hot but generally solid, granitic body of batholithic proportions; and (3) an unusually low density body of 2.40 gm-cm^{-3} at depths of 1 to ~10 km beneath the northeast caldera. The low-density body of the northeast caldera corresponds to an additional ~15% velocity decrease and is consistent with models ranging from thick sediment fill to hydrothermally altered near-surface material underlain by a body dominated by hydrothermal fluids or silicic partial melts of up to 15% (Lehman and others, 1982).

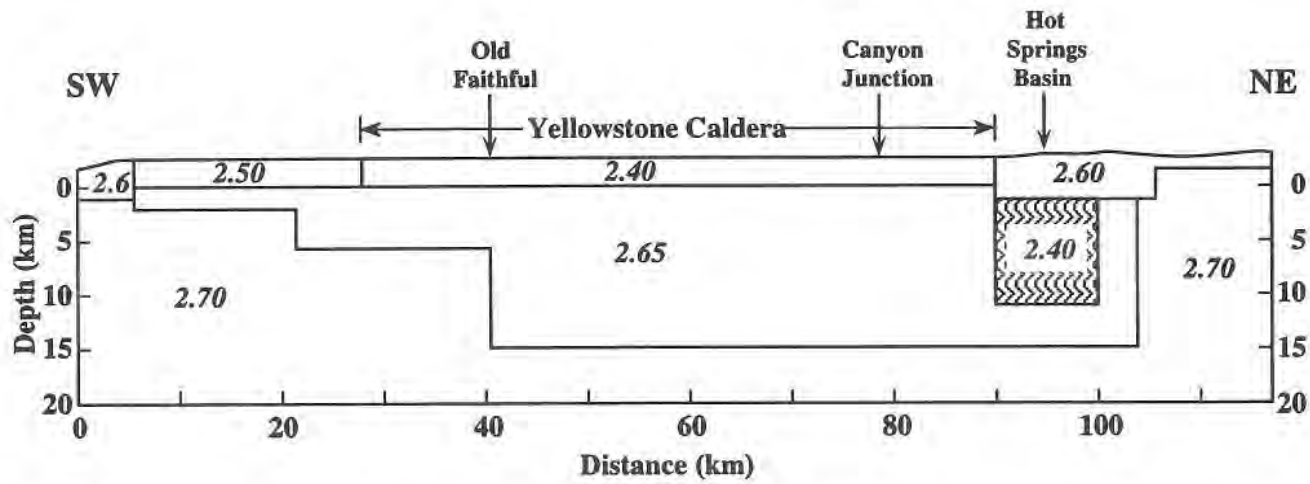

Figure 19. Density model of the upper crust of the Yellowstone Plateau. The gravity model was determined by analyzing the two-dimensional velocity and density data of Lehman and others (1982) using three-dimensional time-term analyses of seismic refraction data acquired in the 1978 seismic experiment. Numbers are densities in gm-cm^{-3}.

Curie depths of the Yellowstone caldera

The unusually high heat flow and lateral variations in velocity structure of Yellowstone suggest significant variations in thermal sources. To examine this property and to estimate the locations of excess heat in the crust, we investigated the temperature field by determining the depths of the Curie isotherm, the temperature at which rocks lose their magnetization, here assumed to be about 575°C. Smith and others (1974) first determined a one-dimensional Curie depth model of the Yellowstone Plateau by spectral analyses of the magnetic field and inferred the depth to the bottom of magnetic crust as 10± 3 km. This value corresponds to a thermal gradient of 45°C/km and a conductive heat flow of about 113 mWm^{-2}. This Curie depth was corroborated by Bhattarcharya and Leu (1975) who determined a two-dimensional Curie isotherm map of Yellowstone that averaged 5 to 6 km beneath the central caldera, a circular zone 6 to 8 km deep outside the caldera, and 10 km deep and greater northwest of the caldera. These values correspond to a conductive thermal flux of 170 mWm^{-2} for the central caldera and an average heatflow of 152 mWm^{-2} for the remaining parts of caldera.

We employed an extension of the Curie depth method by Barnoff (1977) to investigate the three-dimensional distribution of heat sources at Yellowstone (**Figure 20**). This involved a comparison of the observed Bouguer gravity field, $\vec{G}$, with that of the pseudogravity field deduced from the transformation of the Earth's magnetic field due to the magnetized crust. The magnetic ($\vec{M}$) and Bouguer gravity ($\vec{G}$) fields of Yellowstone were digitized at 2.1 km intervals from the Bouguer gravity map of Yellowstone (**Figure 18**) by Blank and Gettings (1974) and from an unpublished magnetic map of Yellowstone (U. S. Geological Survey aeromagnetic map of Yellowstone, 1973). We then converted the magnetic field to an equivalent-stratum gravity field called the pseudogravity field and subtracted it from the observed gravity field (**Figure 20A**). This gives a residual gravity field that is a reflection of mass at temperatures exceeding the Curie isotherm (~575°C), i.e., "hot" rocks. The residual pseudogravity anomalies in **Figure 20B** reflect the distribution of rocks that exceed the Curie temperature and reveal three features: (1) the caldera is characterized by small residual anomalies of + 5 to +15 mGal surrounded by a distinctive circular pattern of positive anomalies of +20 mGal along the southwest caldera rim; (2) a separate and large + 30 mGal anomaly over the northeast caldera; and (3) a transitional gravity gradient from the caldera at its north and south margins.

We have not modeled these data, but the southwestern caldera anomaly has a half-width of 6 to 8 km, implying shallow heat sources in the upper crust. These anomalies coincidentally correspond to the area of the youngest (150 Ka to 70 Ka) post-collapse caldera flows of Yellowstone (Christiansen, 1984, 1993) and could represent ring dikes or cupolas of shallow low-density material. The northeastern anomaly is more circular, suggesting a spherical or a

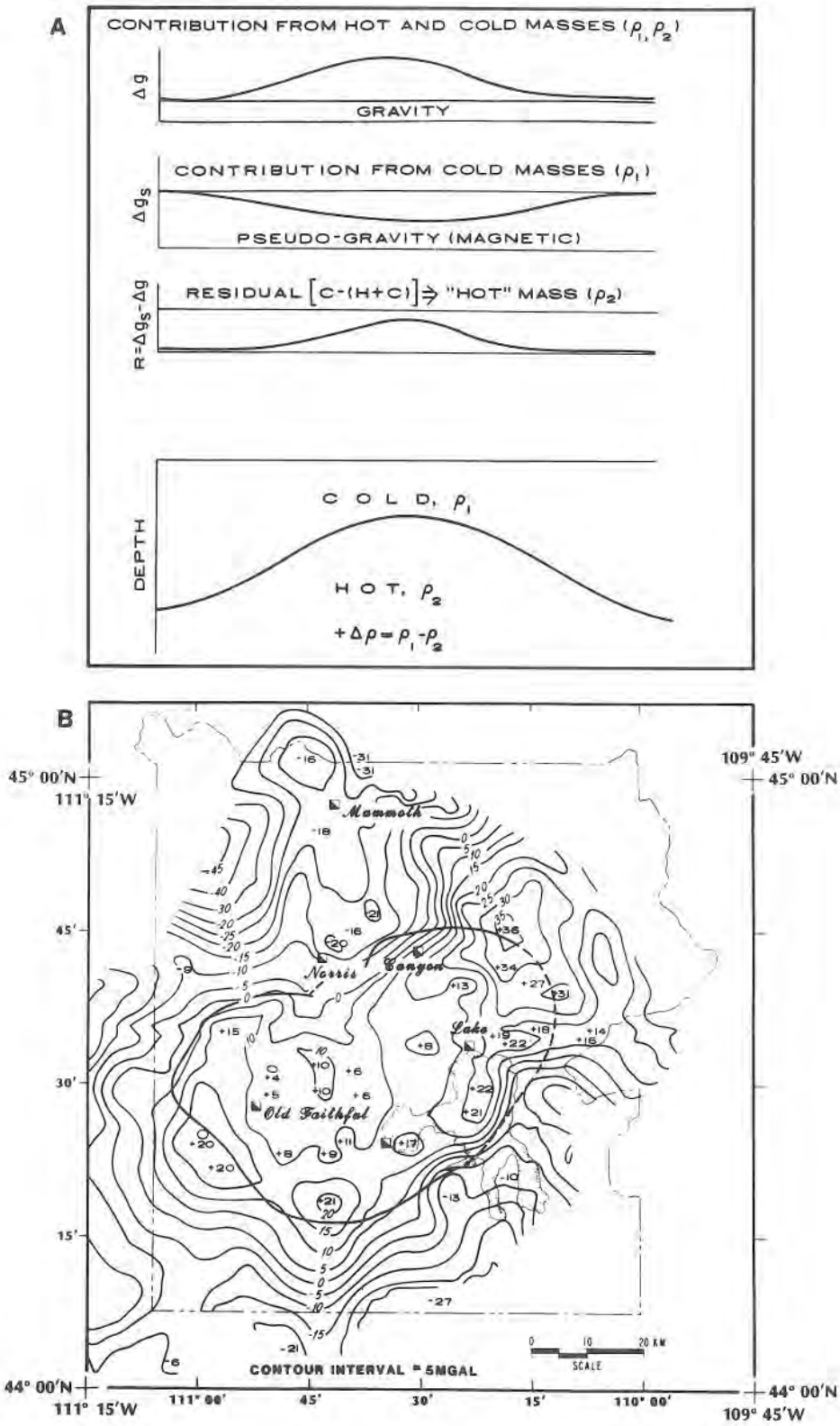

Figure 20. Curie depth-gravity response of high-temperature crustal rocks at Yellowstone using the pseudogravity field method. A, Cartoon of method; and B, Curie-depth residual gravity field (pseudogravity minus observed gravity) of the Yellowstone Plateau. Positive residual anomalies correspond to crustal rocks at temperatures in excess of the Curie isotherm of ~ 575°C.

vertical-cylindrical shaped source. The half-width is about 6 km for a spherical source and suggests the presence of a shallow upper-crustal source. While we cannot determine the temperature distribution associated with these inferred bodies, we suggest that their association with the young Yellowstone Plateau rhyolite flows on the southwest rim and other anomalous geophysical properties, to be discussed in the next sections, reflect remnant magma/partial melt-zones or hydrothermal fluid-filled bodies.

Crustal structure

The YSRP has been the focus of two major seismic refraction experiments in 1978 and 1980 (Braile and others, 1982; Smith and others, 1982). The 1978 project targeted the large-scale tectonic and volcanic features of the YSRP. The 1980 project focused on the upper crust of the volcanically covered SRP and evaluated anomalous features revealed in the 1978 project.

The first observations of the Yellowstone velocity structure were summarized by Schilly and others (1982). They recognized large P-wave delays (up to 1.5 sec) compared to zero traveltime delays in a uniform upper-crustal velocity model of 5.95 km/s (**Figure 21**). Lehman and others (1982), using a three-dimensional time-term analysis of these data, deduced a two-dimensional upper-crustal low-velocity body of 4.0 - 4.8 km/s compared to a thermally undisturbed, 6.05 km/s, Precambrian upper crust outside the caldera.

The upper-crustal, three-dimensional P-wave structure of Yellowstone was investigated by Brokaw (1985) using the combined 1978 and 1980 refraction seismic experiments. This structure is shown by a northeast-southwest profile from Island Park to Yellowstone that extends to depths of 10 km (**Figure 22**) and reveals: (1) a general caldera-wide upper crustal velocity of 5.4 km/s, which is 0.6 km/s slower than the surrounding thermally undisturbed crust of the Rocky Mountains; (2) a low-velocity zone of 4.8 km/s in a restricted area in the northeast caldera; and (3) a transitional zone between the Yellowstone caldera and Island Park with P-wave velocities of 5.4 to 5.6 km/s, intermediate between those of the caldera and the Snake River Plain to the southwest. The intermediate-depth crustal structure was not as well determined by the refraction data, but is based primarily upon wide-angle reflections recorded in the 1980 experiment. A thin remnant of the 6.15 km/s layer, observed to be 15 km thick, was modeled by Chiang and Braile (1984) for the Yellowstone to Snake River Plain transition.

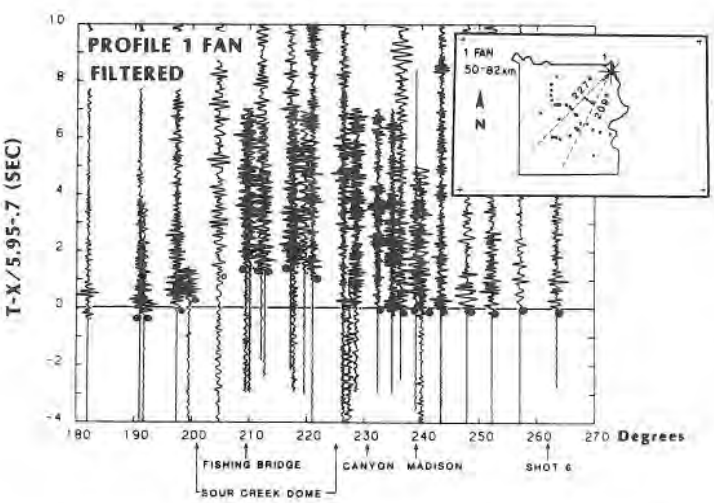

Figure 21. Pg-traveltime arrivals across the northern Yellowstone Plateau plotted versus azimuth, showing the traveltime delays of up to 1.8 sec. The delays were interpreted to be the result of a major upper-crustal low-velocity zone by Schilly and others (1982). Data were reduced to a flat datum using a reducing velocity of 5.95 km/s.

The three-dimensional P-wave structure of the upper crustal structure of Yellowstone has also been studied by tomographic inversion of traveltimes from local earthquakes recorded by the Yellowstone seismograph network. Benz and Smith (1984) first inverted the traveltimes of P waves from local earthquakes recorded in Yellowstone to epicentral distances of up to 100 km with an average station spacing of approximately 15 km recorded on 25 stations. Their study revealed two areas of anomalously low velocities, with up to a 10% velocity reduction compared to a homogeneous model for areas surrounding the YSRP. They occur at depths between 3 and 15 km and are located in the northeast caldera and in the southwest caldera. Nagy and Smith (1988) inverted the P-wave structure of Yellowstone using the expanded Yellowstone seismograph network and traveltime arrivals from ~500

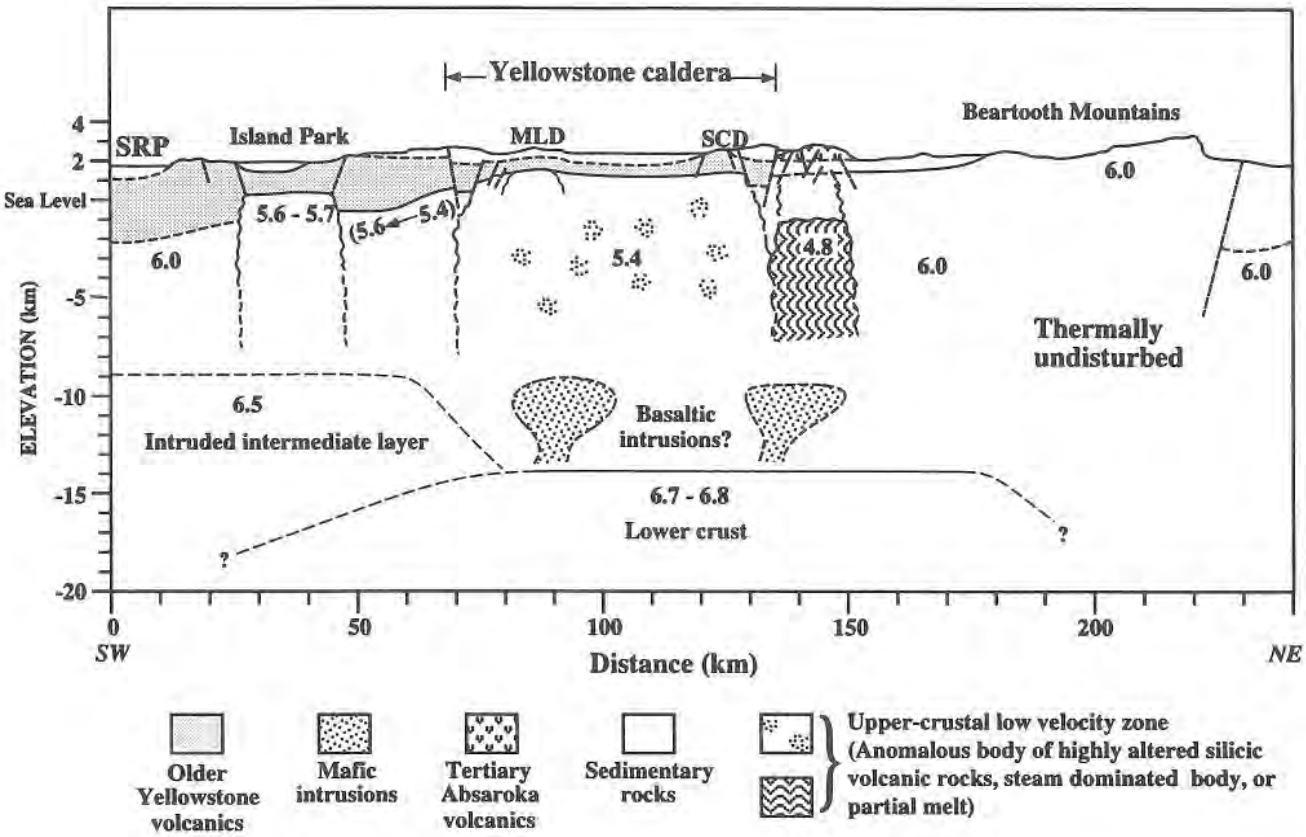

Figure 22. Cross section (northwest-southeast) of the upper-crustal P-wave velocity structure of the Yellowstone Plateau; numbers are km/s (from Brokaw, 1985). Interpretation based upon two-dimensional ray trace modeling of data from the 1978 and 1980 YSRP seismic experiments. MLD = Mallard Lake dome and SCD = Sour Creek dome.

local earthquakes. They determined a 15% decrease in velocity at depths of 3 to 15 km in the northeastern caldera and general caldera-wide 3-5% velocity reduction in upper crust. These results compare to Kissling's (1988) study of Yellowstone's velocity structure at depths from 3 and 12 km with up to a 6% velocity reduction for the caldera.

Seismicity

The historical seismicity of Yellowstone is characterized by a large, scarp-forming earthquake, the 1959, Hebgen Lake, Montana, $M_S = 7.5$ event located on the northwest margin of the caldera; its extensive aftershock sequence; and widespread earthquake swarms within the Yellowstone caldera. Here we describe the spatial and depth distribution of the earthquakes of the Yellowstone Plateau, outlining what is known about the association of seismicity with tectonic and volcanic features (**Figure 23**).

Intense swarms of shallow earthquakes and occasional moderate-sized events as large as the 1975, $M_L = 6.1$, Norris Junction earthquake characterize the well defined 1973-1990 seismicity of the Yellowstone region (**Figure 23**). The general pattern of background seismicity in the northwestern caldera is oriented northwest, similar to the orientation of nodal planes of focal mechanisms for the 1975 Norris Junction event and its aftershock sequence (Pitt and others, 1979). These features also parallel the northwest-trending, post-caldera volcanic vents (**Figure 13**) and suggest that the same stress field is responsible for both the tectonic and magmatic features.

However, seismicity notably varies across the caldera. Within the caldera, inner-ring fracture-zone earthquakes have not exceeded magnitude $M_L = 4.5$, and epicenters are generally scattered, except for

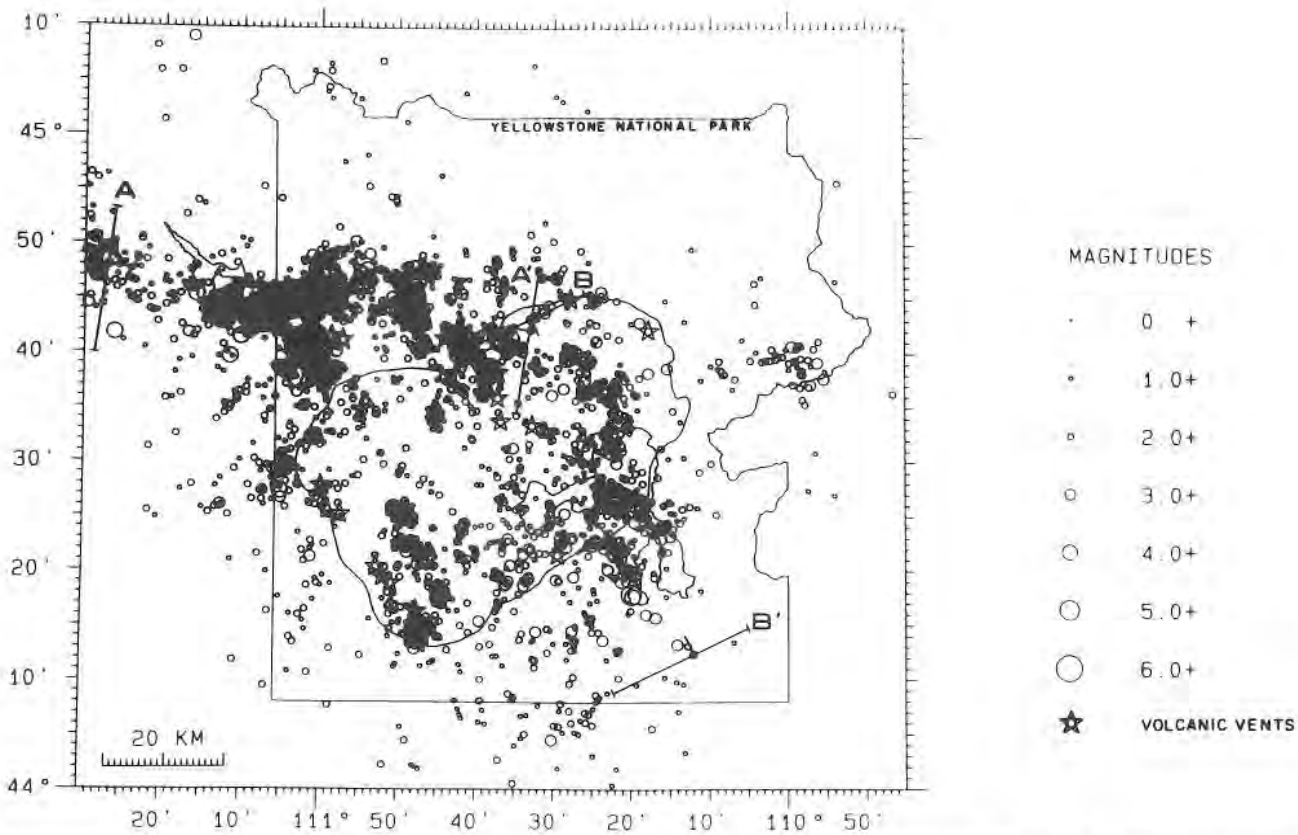

Figure 23. Seismicity map of the Yellowstone Plateau. Earthquakes of magnitude M_L=1.5 or greater are from compilations by the U. S. Geological Survey for 1973-1981 (Pitt, 1989) and by the University of Utah for the period 1984-1990. A-A' and B-B' define the end points of the cross section shown in Figure 25.

alignments spatially associated with volcanic vents. In several examples, there is a good correlation of seismicity with the onset of new hydrothermal activity (Pitt and Hutchinson, 1982) suggesting seismic slip on the boundaries of small upper-crustal blocks, which may reflect a combination of deformation caused by local magma/hydrothermal fluid transport and by the regional tectonic stress field.

The temporal distribution of earthquakes in Yellowstone (**Figure 24**) demonstrates the importance of the long-lasting earthquake swarms. Hayden (1872) first commented on the occurrence of extensive earthquakes (swarms) during his exploration of Yellowstone in 1871, described in an earlier section. Trimble and Smith (1975) and Pitt (1989) noted the occurrence of earthquake swarms with magnitudes as large as M_L = 4.5. Pitt and Hutchinson (1982) documented a major swarm with focal depths less than 5 km deep in 1978, between Yellowstone Lake and Canyon Junction, which lasted for several months and coincided with major changes in hydrothermal features.

The 1985 northwestern caldera swarm was the largest and most persistent in the historic record (**Figure 24**). Nagy and Smith (1988) documented a 6-month period of intense earthquake activity that peaked in frequency of occurrence with earthquakes of magnitude as large as M_L ~ 4.5 in November and December, 1985. Focal depths for these events ranged from 3 to 10 km, and the epicenters extended along a 15 km long northwest-trending zone next to the caldera boundary. Focal mechanisms for this swarm were dominated by strike-slip solutions with a common left-lateral slip nodal plane striking to the northwest and aligned with the trend of the swarm epicenters. Notably, the trend of this swarm projected northwest, orthogonal to the caldera boundary, suggesting a radial fracture extending from the caldera, perhaps either a propagating fracture extending from the Hebgen Lake fault toward the caldera or a magma-filled fracture extending radially outward from the caldera.

On the southeastern side of the caldera, epicenters associated with background seismicity are

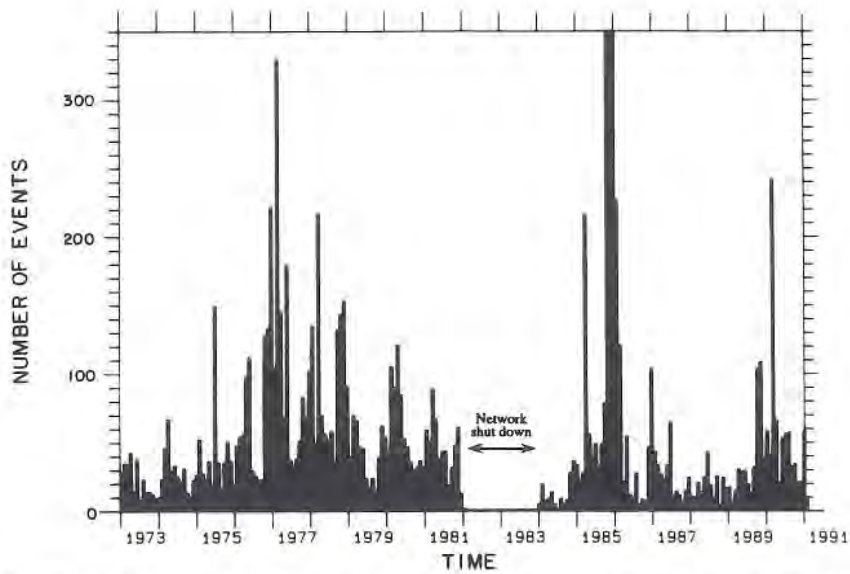

Figure 24. Temporal variation of recorded earthquakes in Yellowstone. Numbers of earthquakes are plotted in one-month intervals between 1973 and 1990. Note the sporadic and intense earthquake swarms. Source of data is the same as in Figure 23.

aligned with north-south-trending zones, including epicenters near a normal fault along the west side of the Yellowstone Lake that exhibits several meters of Holocene slip (Meyer and Locke, 1986). The alignment of epicenters in the southern Yellowstone Plateau may reflect a buried extension of the Teton fault (**Figures 13** and **23**).

Focal depth variations and temperatures of the Yellowstone caldera

Lateral variations in focal depths of earthquakes of the Yellowstone caldera are thought to reflect variations in depth to the brittle-ductile transition (**Figure 25**). Maximum focal depths outside the caldera are generally less than 15 to 20 km, but decrease to less than 5 km beneath the caldera. This distinctive shallowing suggests a thin seismogenic brittle layer above a major heat source. Within the caldera, the crust appears to be in a quasi-plastic state at depths exceeding 5 km and at temperatures greater than 350° to 450°C, incapable of supporting shear stresses (Sibson, 1982; Smith and Bruhn, 1984).

If we assume that the 80th percentile of focal depths of the Yellowstone caldera reflects the depth to the 350°C isotherm, as hypothesized by Smith and Bruhn (1984) for extensional regimes, we can estimate the temperature gradient. The maximum focal depths occur at about 10 km immediately outside and west of the caldera and correspond to a thermal gradient of 35°C/km. Inside the caldera, the average 80th-percentile depth at ~5 km corresponds to a gradient of 70°C/km (**Figure 25**) and a corresponding conductive heat flow value is ~200 mWm^{-2}. These data suggest that the conductive heat flow of the caldera is ~200 mWm^{-2}, which is ~ 10 times smaller than the total heat flux of the caldera (~2,000 mWm^{-2}) and thus requires a convective heat transfer of ~ 1,800 mWm^{-2}.

The ratio of conductive to convective heat flux provides a measure of the relative magnitude of thermal convective heat transport as specified by the Nusselt number, which is defined as the ratio of the convective to conductive heat flow. For Yellowstone, a Nusselt number of 10 compares with Nusselt numbers, calculated by the same method by Hill (1992) for the 0.7 Ma Long Valley caldera, California, of 6 to 8.

Crustal deformation

While subsidence of the Snake River Plain over its 16 million year history reflects the long-term deformation pattern of that region, the Yellowstone Plateau has been the site of unprecedented crustal deformation in historic time. Pelton and Smith (1982) first documented the historical uplift of the Yellowstone caldera of up to 76 cm based upon repeated 1st-order precision leveling in 1975-76-77 at benchmarks originally surveyed in 1923 (**Figure 26**). From the mid-1970s to 1984, leveling surveys revealed an additional 25 cm of uplift. However, by 1985, the deformation reversed to subsidence which exceeded about 12 cm by 1990 (Dzurisin and Yamashita, 1987; Meertens and others, 1992).

Vasco and others (1990) modeled the uplift data (**Figure 27**) by dividing the crust into a number of discrete blocks, each of which may undergo a fractional dilatational volume change, (Δvolume/volume). Their three-dimensional model extended from the surface to 9 km depth. For the uplift data, a maximum volume change of 0.22 km^3, in the 3 km to 6 km depth range was determined in the southern

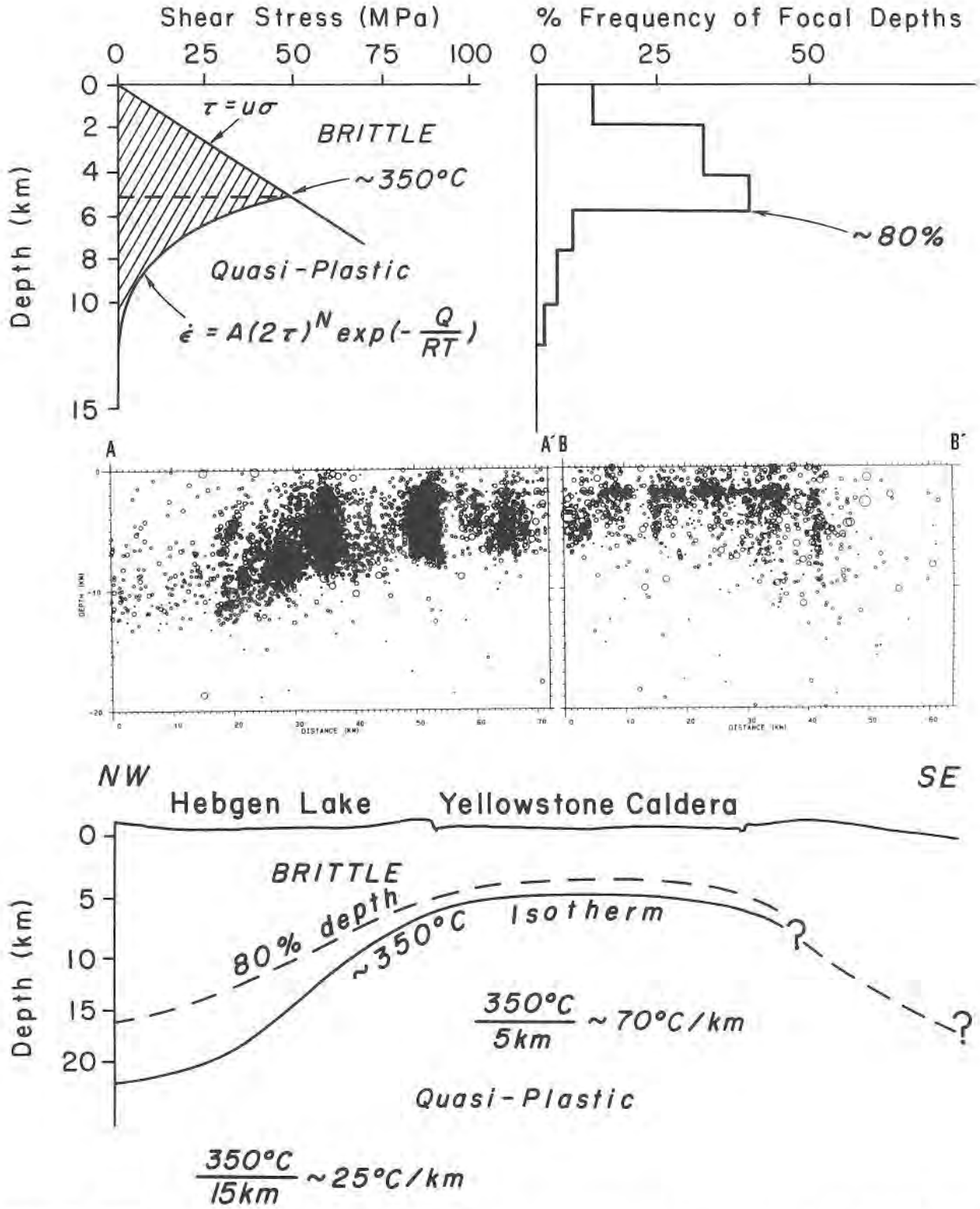

Figure 25. Cross sections of rheology properties, earthquake foci and idealized rheological model for the Yellowstone Plateau. Focal depths correspond to profiles A-A′ and B-B′ in Figure 23, but extended to all shocks of $M_L > 0$. The brittle-ductile transition was calculated from rheological parameters with a quartz rheology, a regional strain rate of $\sim 10^{-16} s^{-1}$, and for a high conductive heat flow, exceeding 100 mWm^{-2}.

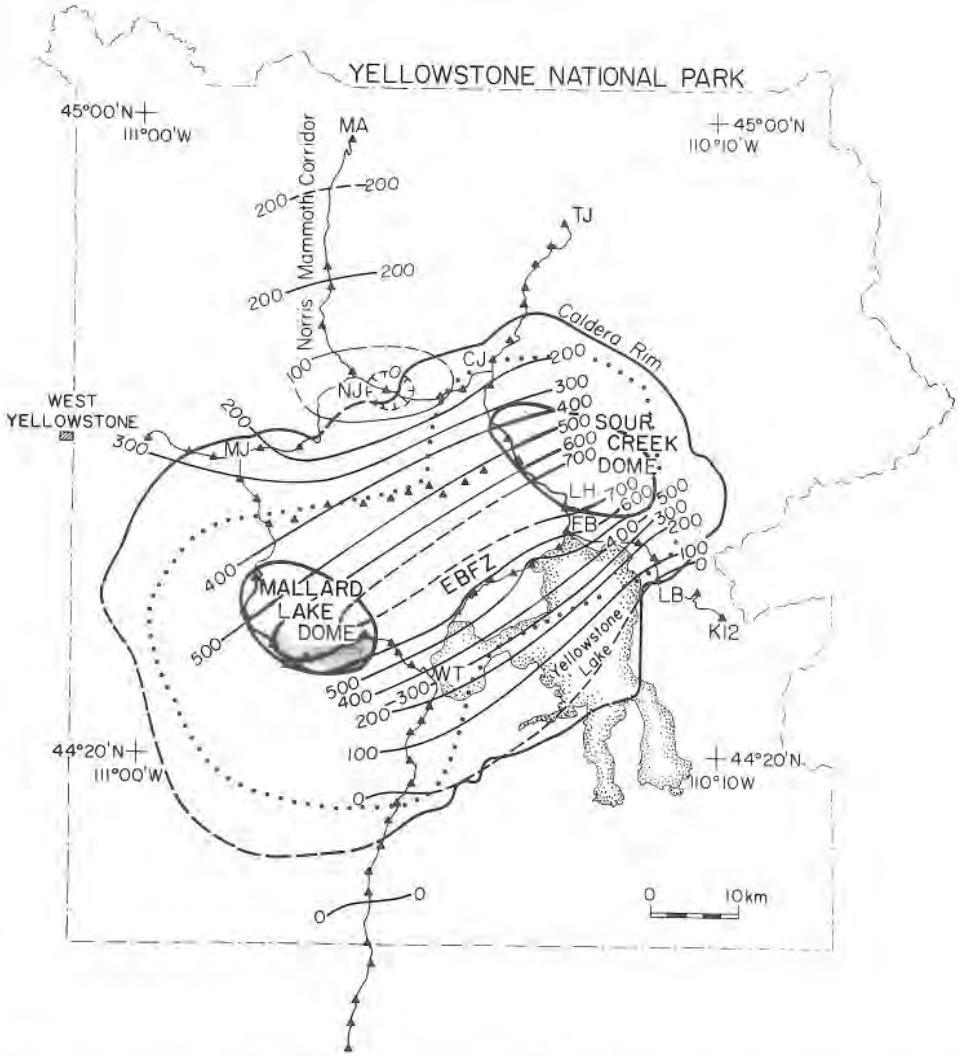

Figure 26. Map of 1923 to 1977 surface uplift of the Yellowstone caldera (modified from Pelton and Smith, 1982). Contours are in millimeters relative to a reference base station, K12, on the east side of the caldera that was assumed least affected by volcanic or tectonic activity of Yellowstone. Dotted line shows inner edge of caldera-rim fracture zone. EBFZ-Elephant Back fault zone, MA-Mammoth Hot Springs, TJ-Tower Junction; WT-West Thumb; MJ-Madison Junction; NJ-Norris Junction; CJ-Canyon Junction; FB-Fishing Bridge; and LB-Lake Butte.

caldera and a second source of 0.18 km³ volume increase was located in the northeast caldera (**Figure 27**). The total volume change for the 1923 to 1977 data totaled approximately 0.73 km³, which corresponds to an inflation rate of 0.01 km³/yr to 0.03 km³/yr. Vasco and others (1990) attributed the volume change to migration of magmas and/or hydrothermal fluids into the upper crust.

Causative mechanisms for the caldera-wide uplift, summarized by Pelton and Smith (1982), included magmatic, tectonic, and glacial-isostatic sources, but these authors suggested that the most likely source of the 1923 to 1977 uplift was transport of magma. Dzurisin and others (1990) concluded that basaltic intrusions into the middle or upper crust or pressurization of a deep hydrothermal system (by magmatic gas or brine released by crystallization of a rhyolitic melt) were also plausible sources for the uplift.

Following the 50-year episode of historical uplift, deformation abruptly changed to subsidence of up to 6 cm between 1984 and 1985 (Dzurisin and others, 1990), and subsidence has continued to 1991. Meertens and others (1992) reported subsidence of

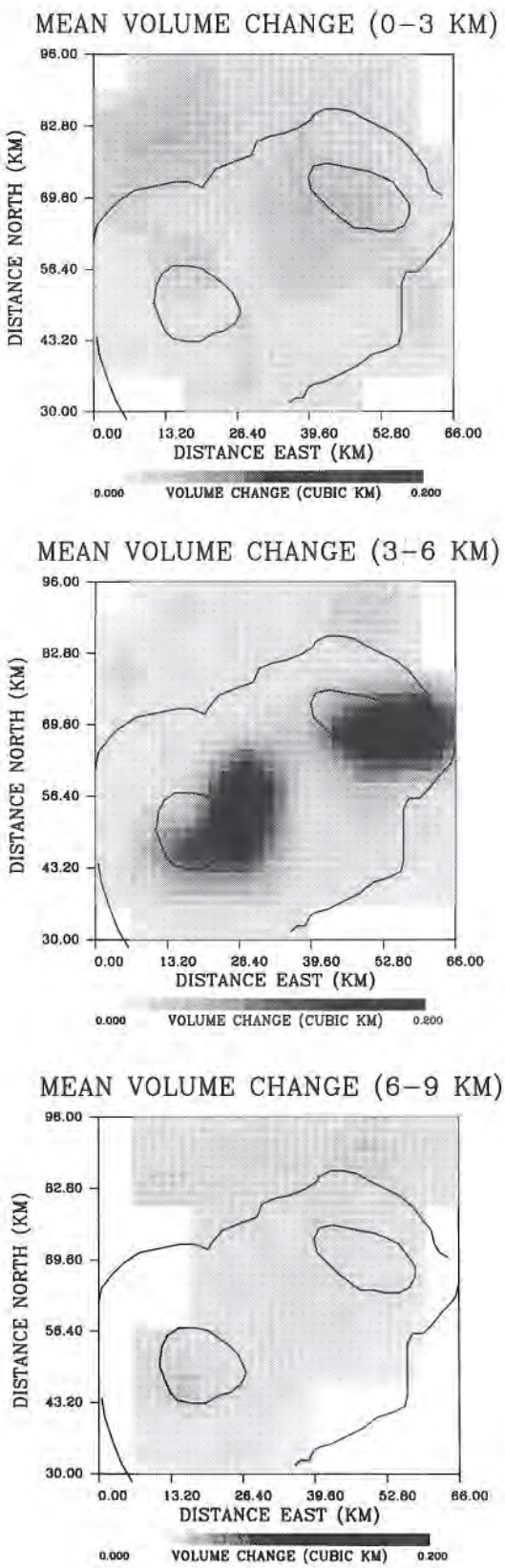

Figure 27. Locations and volumes of sources modeled for the 1923 to 1977 uplift of the Yellowstone caldera at 0-3 km, 3-6 km and 6-9 km depth ranges. Gray-scale contoured to volumetric increases in km^3 (from Vasco and others, 1990).

up to 7 cm for the period 1987 to 1991 over the entire caldera using GPS (Global Positioning Satellites) surveys corresponding to the same general area that experienced uplift from 1923 to 1977 (**Figure 28**). The spatial correlation between the area of uplift and the area of subsidence suggests related mechanisms. The uplift phase of the Yellowstone caldera is postulated to have resulted from intrusion of magma and/or hydrothermal fluid into the 3 to 6 km-deep upper crust. These fluids may have, in turn, produced excess hydrothermal fluids in a shallow overlying layer, which then degassed and/or experienced a reduced rate of input, producing the observed subsidence.

Evidence of a widespread magmatic connection between the Yellowstone caldera and the Hebgen Lake fault was recently suggested by Savage and others (1993), who modeled the strain field of the Hebgen Lake trilateration network for the period 1973 to 1987. They calculated a uniaxial extension of approximately 0.27 μstrain/yr at an azimuth of 015°. Although these data can be explained by dislocation on a southward dipping normal fault at Hebgen Lake, their data imply significant deformation north of the surface projection of the Hebgen Lake fault. Savage and others (1993) suggested an alternate mechanism related to magmatism, namely inflation of a vertical dike and accompanying rift that extends west-northwest about 100 km from the Yellowstone caldera to the Hebgen Lake fault zone. This is a provocative interpretation, as it provides a tie between tectonic and magmatic mechanisms across a large area of the Yellowstone Plateau.

Nonetheless, we believe that the migration of magma and/or hydrothermal fluids into the middle and upper crust of the Yellowstone caldera is the most plausible explanation for the modern crustal deformation. This mechanism must have been important over much of the 2-million-year volcanic history of Yellowstone, and magma intrusion must have been the principal mechanism in the development of

the resurgent domes. The modeled volume changes of Yellowstone's historic crustal deformation are commensurate with intrusion of hydrothermal fluids and rhyolitic/basaltic melts into the upper crust as a likely mechanism.

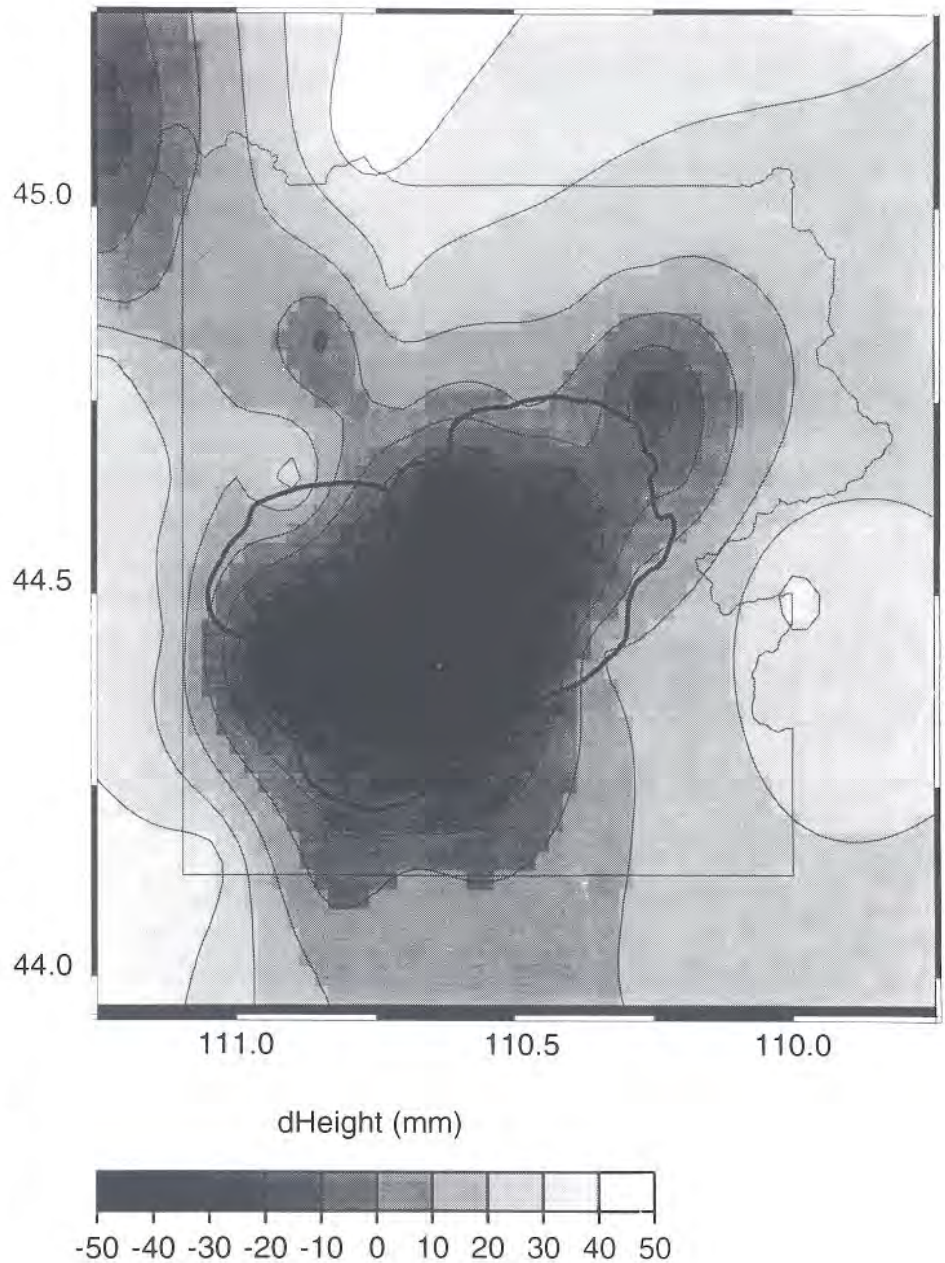

Figure 28. Map of 1987 to 1991 Yellowstone caldera subsidence from Global Positioning Satellite (GPS) measurements (from Meertens and others, 1992). Height changes, dHeight, are gray-scale contoured in mm. Base level taken by averaging measurements of GPS stations outside the caldera that are assumed to be least influenced by the Yellowstone hotspot. Caldera boundary is shown by heavy black line.

Mantle origin of the YSRP

An enormous amount of heat and a continuous supply of magma are required for the 16-million-year history of YSRP silicic volcanism as well as the 2,000 mWm^{-2} heatflow of Yellowstone. We believe this requires a mantle source and suggest that mantle plume-plate interaction (the Yellowstone hotspot) is responsible for the time-spatial characteristics of the YSRP. In this section, we build upon the picture of a seismically and thermally active Yellowstone caldera as the active element of the YSRP and examine the evidence for mantle coupling by a plume-plate model. We also comment on alternate mechanisms that may account for some of the observations.

Lithospheric structure of the YSRP

Perhaps the most compelling evidence for a plume-plate model for the YSRP is the progression in silicic volcanism ages discussed in an earlier section of this paper. The P-wave crustal structure of the YSRP also reveals a similar systematic variation in thicknesses, velocities, and compositions of intermediate- and upper-crustal layers that corresponds to the variation in ages of the silicic volcanic rocks. In **Figure 29**, the upper crustal structure of the YSRP is plotted along with the averaged surface elevation. The granitic upper crust of the North American continent, which is normally 10 to 15 km thick with a P-wave velocity of 5.9 - 6.1 km/s (Braile and others, 1989), is absent or thin along the entire YSRP. We believe it has been largely replaced by silicic volcanic rocks and mafic intrusions related to the Yellowstone hotspot. At the Yellowstone caldera, a heterogeneous upper crust extends to depths of about 10 km.

Along the SRP, a southwest decrease in topography also reflects a systematic change in crustal structure. The near-surface basaltic layer thins from 2 km in southwestern Idaho to zero at Island Park and is apparently absent at Yellowstone. Correspondingly, the deeper, 2 km-thick, silicic volcanic layer extends from southwestern Idaho 800 km northeastward to Yellowstone beneath the younger basalt wedge. The high-velocity (6.5 km/s) intermediate crustal layer is interpreted as a solidified mafic remnant of the crustal magma sources. Neither the Moho nor the seismic velocity structure of the lower crust of the SRP is as well determined as the velocity structure of the upper crust, but these features appear relatively homogeneous and resemble the lower crust of the surrounding thermally undisturbed regions.

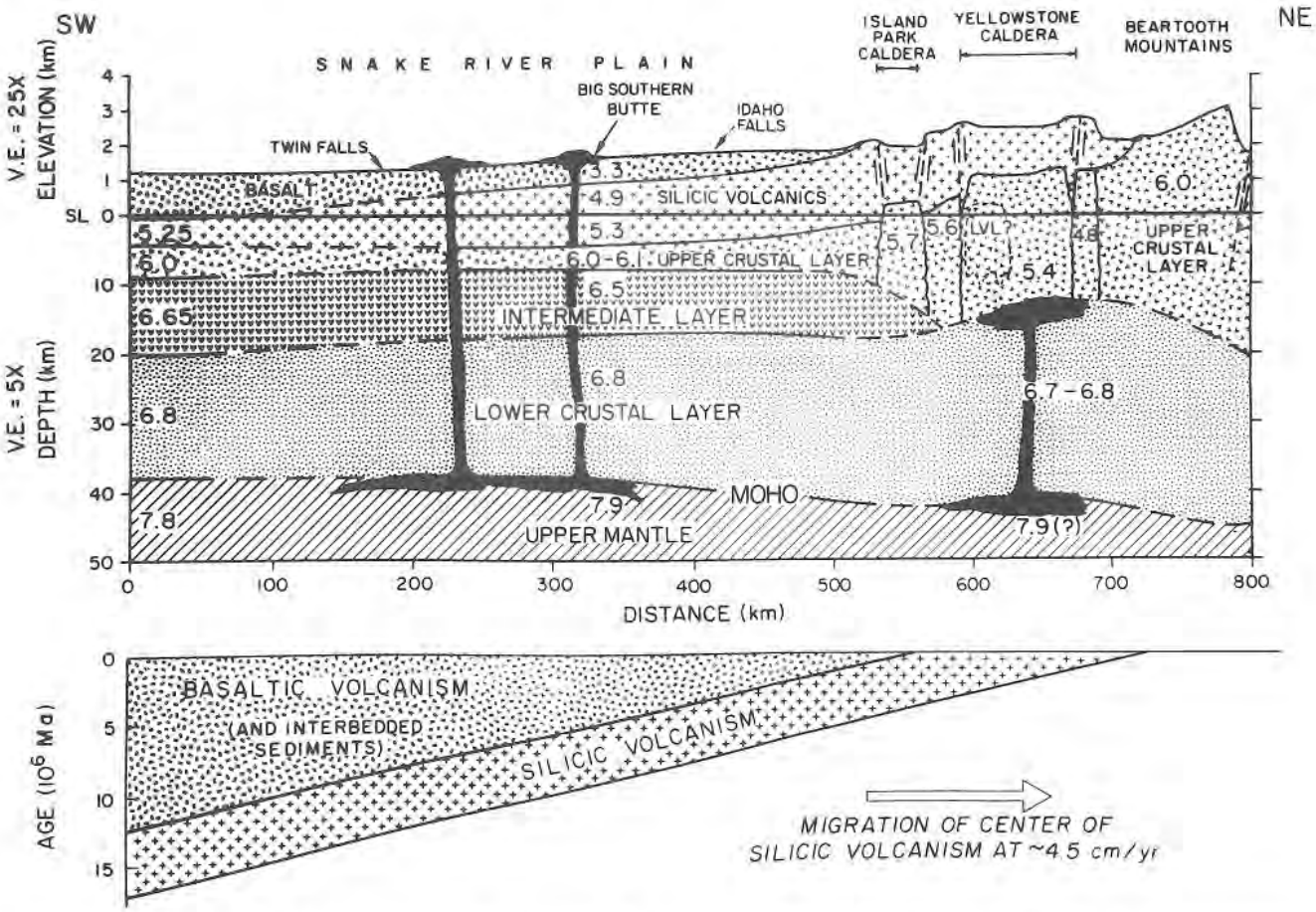

Figure 29. Generalized crustal structure and topography along the path of the Yellowstone hotspot from southwestern Idaho and northern Nevada to the Yellowstone Plateau. Figure compiled from the data and models of Hill and Pakiser (1966), Braile and others (1982), Smith and others (1982), Elbring (1984), and Brokaw (1985). P-wave velocities (numbers within patterned areas) are in km/s. Basaltic rocks thin and silicic volcanic rocks thicken with decrease in the ages of the silicic centers shown in Figure 3. Idealized locations of mantle-derived basaltic intrusions noted by black pattern. V.E.=vertical exaggeration.

Mantle velocity structure

The most definitive information on upper mantle structure comes from observations of seismic traveltimes from earthquakes, using tomographic inversion. These studies used P-wave seismic traveltimes from earthquakes recorded at teleseismic distances (greater than 5,000 km) to provide information on deeper structure of the lithosphere and suggest an anomalously low-velocity crust and upper mantle structure of the entire YSRP.

The first detailed teleseismic P-wave study of the upper mantle of Yellowstone, by Iyer and others (1981), revealed caldera-wide delays as large as 1.5 sec. They modeled the traveltime anomalies as the result of velocity decreases of up to 10% in the upper crust, 5% in the lower crust, and 6% in the upper mantle, with velocity anomalies evidenced as deep as 165 km. Evoy (1978) used the same teleseismic traveltime data simultaneously with the long-wavelength Bouguer gravity field for a combined velocity-density distribution model to depths of about 100 km. His model identified density anomalies of ± 0.1 gm-cm^{-3} for the heterogeneous upper crust and - 0.05 to - 0.10 gm-cm^{-3} reduction for the lower crust and upper mantle.

The most recent study of the upper mantle structure is from teleseismic P-wave data acquired by regional seismic networks in the YSRP (Dueker and Humphreys, 1989). These authors modeled teleseismic P-wave delays along three 300 km-long profiles across the YSRP from depths of 40 km to 200 km, which are characterized by low velocities, with up to a 3% reduction compared with the surrounding thermally undisturbed Rocky Mountains (**Figure 30**). Dueker and Humphrey's (1993) model also includes a zone of P-wave reduction (up to a 3%) in the crust beneath Yellowstone that is underlain by a pervasive upper-mantle low-velocity body with up to a 3% reduction at depths of 40 km to 100 km. Low-velocity mantle extends southwest beneath the SRP to depths of 200 km, indicating a deepening and broadening mantle anomaly, whereas the crustal anomaly decreases in its magnitude and extent (**Figure 30**). Anomalously low crust and upper mantle P-wave velocities along the entire YSRP are consistent with models that suggest of partial melting and excess fluids in the lithosphere.

Geochemical evidence

He^3/He^4 ratios determined from samples acquired in the Yellowstone's hydrothermal systems by Craig and others (1978) and Kennedy and others (1985) are also consistent with a mantle source. This conclusion was corroborated by anomalous isotopic ratios of Nd and radiogenic isotopes of Pb and Sr in the YSRP, which are also consistent with an undepleted mantle source (Doe and others, 1982; Leeman, 1982). Additional evidence for mantle coupling comes from an assessment of Nd, Sr, Pb, and O isotopic compositions of basalts and post-caldera rhyolite flows of the Yellowstone Plateau (Hildreth and others, 1991). Their data reveal variations in the isotopic compositions of these elements that were interpreted to reflect sources from subcaldera upper-crustal regions and sources independent of the caldera magma system. These authors universally argue that the isotopic composition of Yellowstone rhyolites requires deep-crustal sources that have been pervasively altered by mantle-derived basalts.

Stress-field directions

Earthquake focal mechanisms, fault slip directions, and orientations of volcanic dikes and vents are the main sources of information on stress directions for the YSRP. Because the dominant mode of contemporary deformation in the ISB is extension, the direction of maximum extensional strain, corresponding to the T-axes of focal mechanisms, is assumed to be in the same direction as σ_{hmin} (**Figure 31**). However, Peyton (1991) made a detailed study of the stress field of Yellowstone by inversion of focal mechanisms and showed that vectors orthogonal to mapped faults, dikes, and rifts are not necessarily in the direction of σ_{hmin}. We have thus only included reliable stress direction indicators that have been evaluated in published studies. The stress field data in **Figure 31** are from Eddington and others (1987) and from a summary by Zoback and Zoback (1989).

Beginning with the south side of the YSRP (**Figure 31**), the directions of σ_{hmin} are generally southeast- to east-trending throughout southeastern Idaho and western Wyoming, an area of moderate seismicity. Northward into the Yellowstone region, the directions of σ_{hmin} from inversion of focal mechanisms are northeast (Peyton, 1991). Northwest of the Snake River Plain, σ_{hmin} orientations are also northeast.

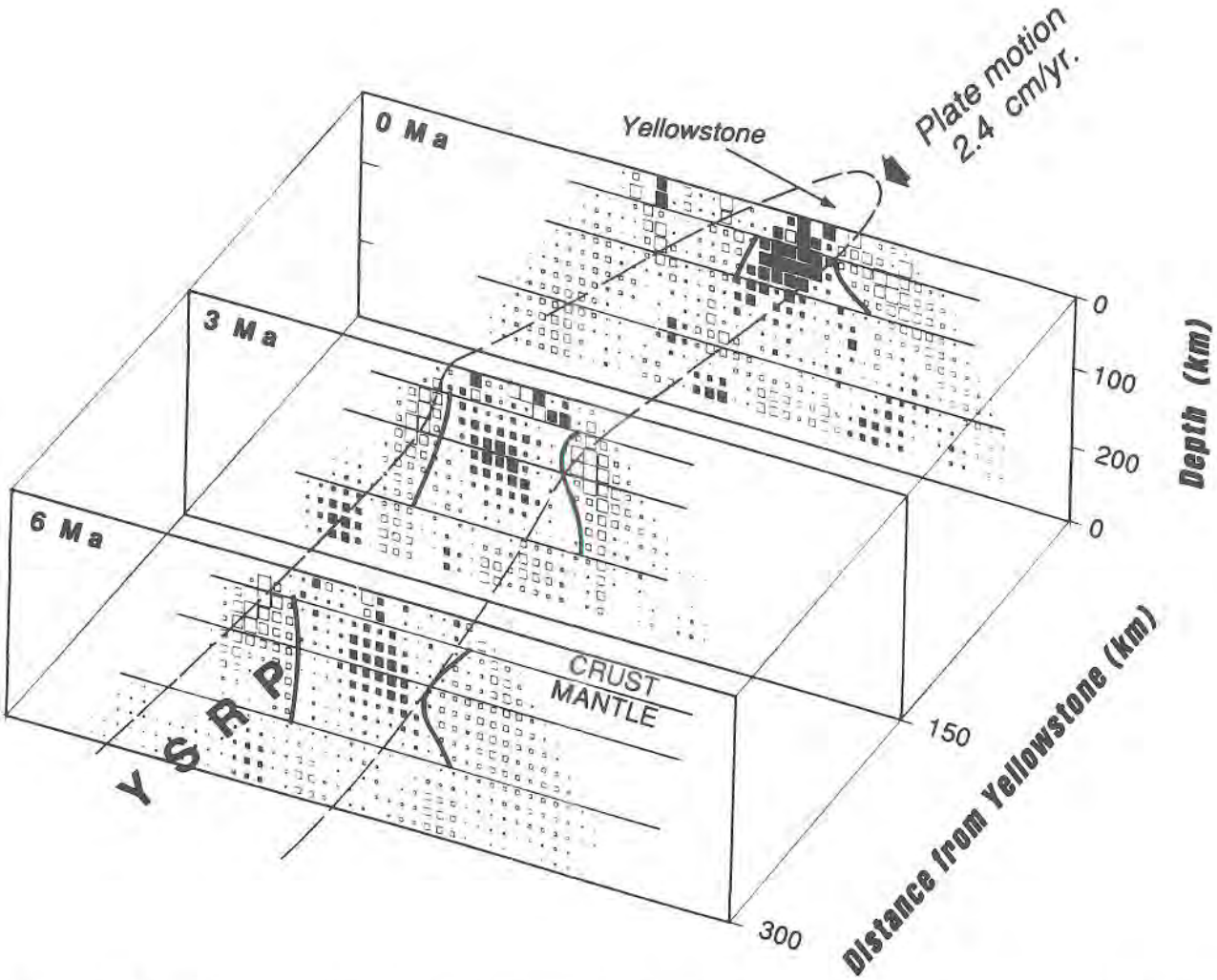

Figure 30. P-wave velocity profiles of the crust and upper mantle of the YSRP from the surface to depths of approximately 300 km determined from inversion of traveltime delays of teleseismic earthquakes (from Dueker and Humphreys, 1989, 1993). The velocity-depth profiles correspond to 0, 150, and 300 km distances from the Yellowstone Plateau. Velocity differences are scaled from a laterally homogeneous model and are shown by square symbols that are scaled in size to the percent velocity perturbation. The largest symbols are ±3%, dark = slow velocities and open = fast velocities.

On the basis of focal-mechanism studies west of Yellowstone National Park, Smith and others (1977) and Stickney and Bartholomew (1987) identified a localized stress regime with a north-trending σ_{hmin}. This region is distinguishable from the northern ISB in the vicinity of the Montana-Idaho border where σ_{hmin} trends northeast, the same as south of Yellowstone (**Figure 31**). We suggest that this restricted regime of north-south σ_{hmin} is a perturbation of the stress field perhaps associated with lithospheric bulging. It may also be associated with an east-west zone of magmatic related-rifting, which is hypothesized by Savage and others (1993) to extend 100 km westward from the northern Yellowstone caldera to Hebgen Lake.

An important feature of the regional YSRP stress field is the 45° rotation of σ_{hmin}, from northeast on the northwest side of the eastern SRP, to east-west southeast of the SRP (**Figure 31**). The older Basin and Range normal faults northwest of the SRP and vents and fissures located on the SRP are consistent with northeast-trending σ_{hmin}. This suggests that structures within the SRP were influenced by the same stress field as that of Yellowstone. However, a change in direction of σ_{hmin} to east-west is evident

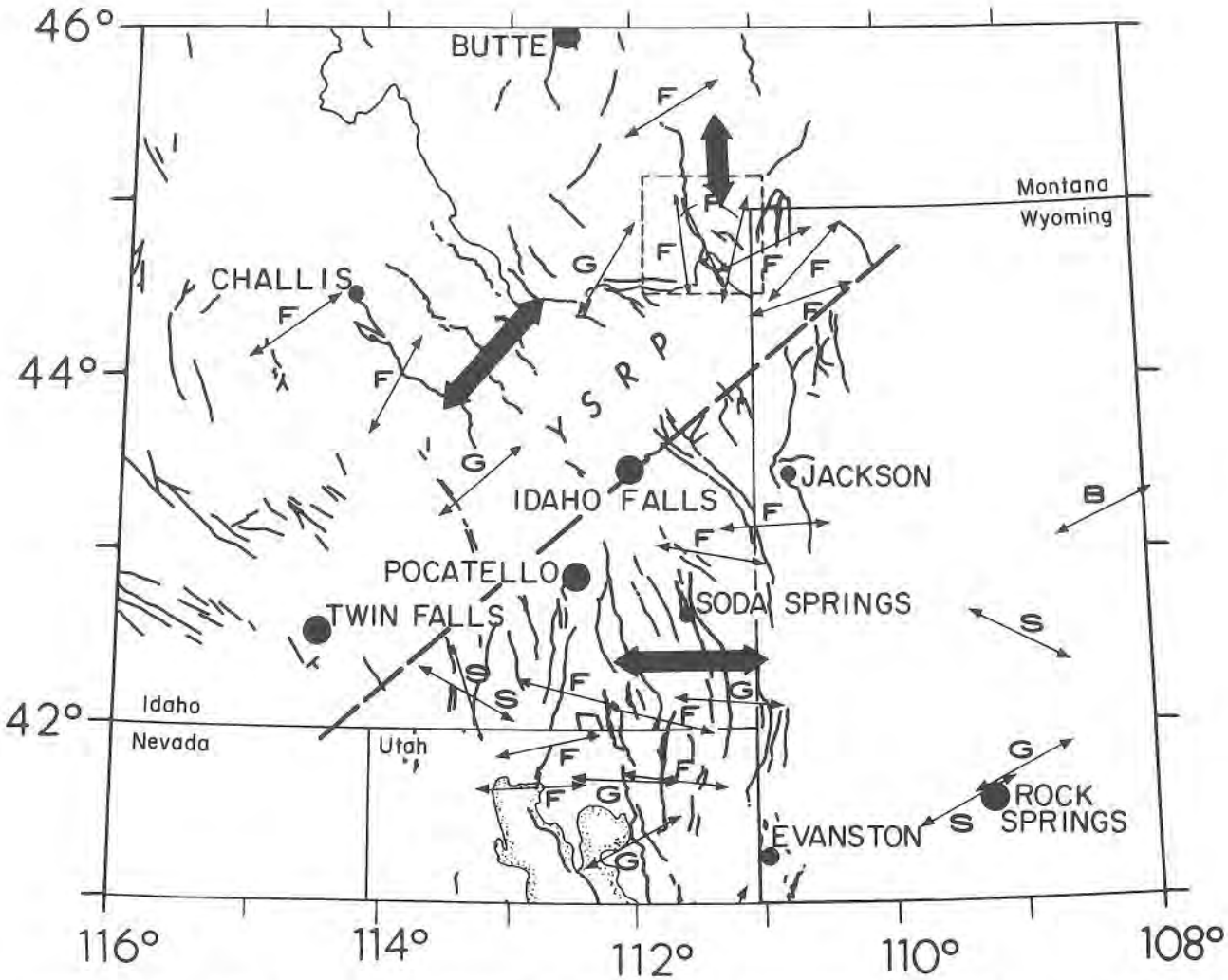

Figure 31. Map showing the orientations of crustal extension of the YSRP, assumed to be in the direction of minimum horizontal compressive stress, σ_{hmin} (modified from Smith and Arabasz, 1991). Data are from compilations by Eddington and others (1987) and Zoback and Zoback (1989), and include selected Cenozoic faults shown in Figure 3. Stress indicators: F = focal mechanism; G = geologic; and S = in situ stress.

from the alignment of normal faults on the southeast side of the caldera and the *en echelon* zone of apparently right-stepping, north-trending normal faults extending to the Teton fault. Along the southeastern edge of the SRP, the stress field appears to change trend to east-west (**Figure 31**) and continues into southeastern Idaho, where the seismicity belt becomes discordant with northwest-striking Quaternary faults near this stress-field boundary.

Topographic decay of the YSRP

Spatial variations in topography and the elevations of crustal boundaries attributed to thermal mechanisms are shown in **Figure 32**. The systematic topographic decay along the SRP was first noted by Brott and others (1978, 1981), who fitted curves corresponding to the averaged topography in response to the passage of a crustal heat source. They postulated that the overriding plate produced cooling and thermal contraction of the surface and the corresponding 1.5 to 2 km topographic subsidence of the eastern Snake River Plain.

We have also fitted the averaged surface elevations along the YSRP (**Figure 32**), the boundary between the basaltic and rhyolite layers, and the boundary between the rhyolite and the 6.0 km/s basement layer. The surface topographic decay fits an expression, $z = 3.07 - 0.52\sqrt{t}$, (where t is the age of the silicic volcanism in millions of years). This

expression is the common scaling law for fitting topography behind oceanic hotspots and mid-ocean ridges (Sclater and Francheteau, 1970; Parsons and Sclater, 1977). Moreover, the boundaries between the rhyolite and the granitic crustal layers also fit a decay curve of $z = 1.22 - 1.53\sqrt{t}$. This curve reflects a faster decay than the surface topography and may be the result of additional crustal intrusion by basalts as well as isostatic adjustment for the additional load of the high-density mid-crustal layer, sediments, and basaltic eruptions in the SRP.

Mantle plume-plate interaction of the Yellowstone hotspot

Smith and Sbar (1974) first suggested that the influence of convective upper-mantle flow on the

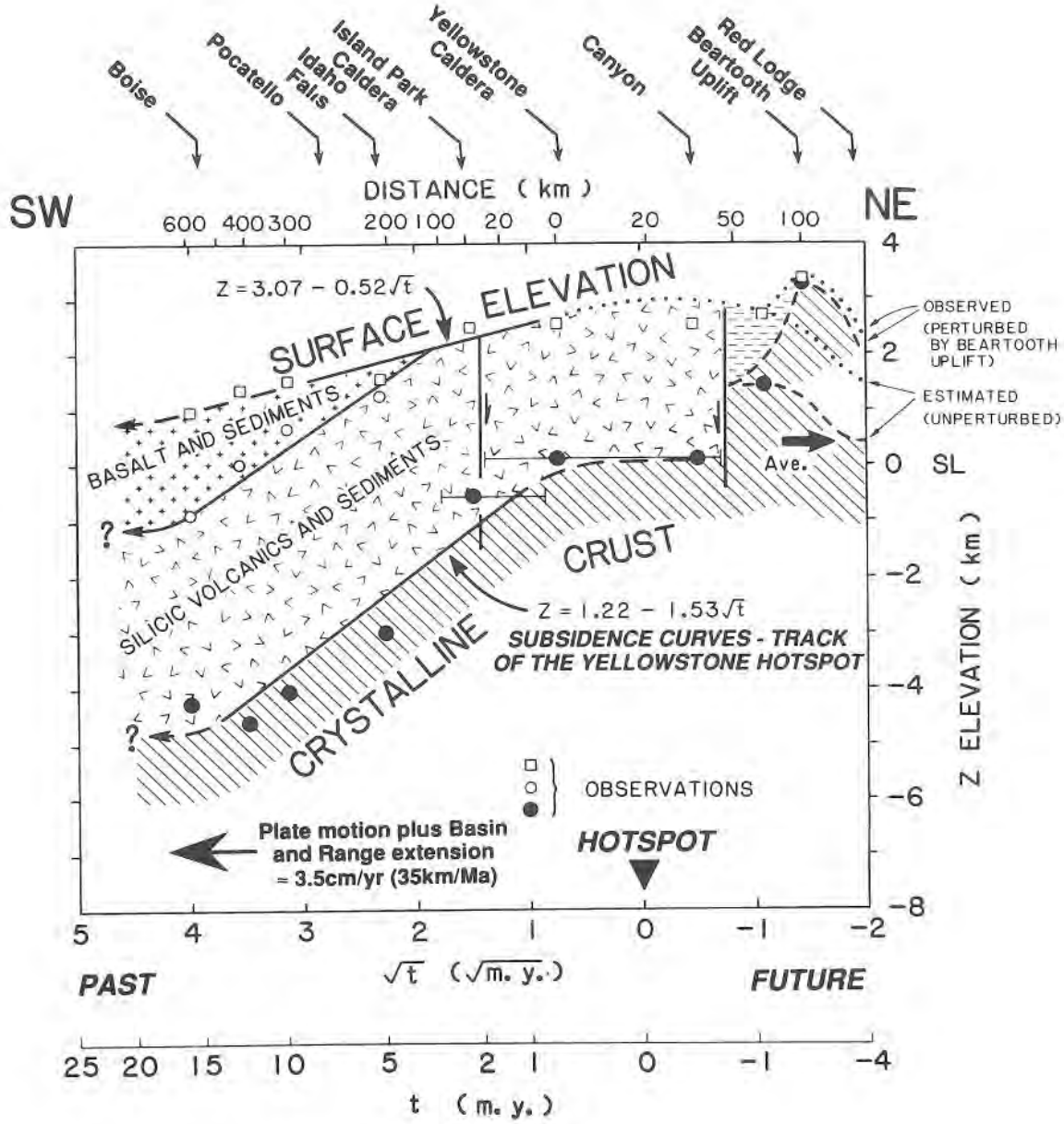

Figure 32. Plot of surface topography and elevations of the boundaries between the silicic and basaltic rocks and the crystalline granitic crust along the YSRP, showing the systematic elevation decay proportional to the $\sqrt{t}$. t is the age of the silicic volcanic rocks in millions of years from Armstrong and others (1975).

overlying North American plate may contribute to differential intraplate velocities across the Yellowstone region and hence to the tectonic processes manifest at the surface. More recently, Westaway (1989) described an analytic model for interaction of return flow associated with an hypothesized Yellowstone plume with the overlying North American plate to explain the dual-branched pattern of seismicity and similar patterns of faulting surrounding the Snake River Plain. Pierce and Morgan (1990, 1992) also described idealized models of plume ascension and lateral spreading at the base of the lithosphere to account for the parabolic patterns of seismicity of the YSRP.

To analytically evaluate the surface manifestation of a mantle plume-plate interaction at Yellowstone, we collaborated with Neil Ribe, Yale University, who developed a three-dimensional fluid-flow modeling code incorporating the interaction of an upwelling mantle plume with a southwestward moving lithospheric plate (Ribe and Christensen, 1992a,b). **Figure 33** shows the preliminary plume-plate model for the Yellowstone hotspot, described as a rectangular box filled with a fluid whose viscosity varies as a function of depth, temperature, and strain rate. We assumed conditions and properties deduced for the YSRP including a cooler, 80 km thick lithosphere, determined from surface-wave analyses for the northern Basin and Range province (Priestly and others, 1980) and represented by higher viscosity material near the top of the model. The motion of the lithosphere was simulated by imposing a horizontal velocity of 3.5 cm/yr (including a 2.5 cm/yr North American plate velocity and a 1 cm/yr concomitant extension rate) on a low-viscosity layer.

A thermal profile is specified as an upstream boundary condition and all sides of the model except for the top are open to permit flow through the boundaries. The imposed surface velocity drives large-scale shear flow in the box that contains a buoyant thermal plume, which was produced by imposing a Gaussian-shaped temperature anomaly on the bottom of the model (**Figure 33**). The rising plume spreads out against the base of the overlying lithosphere and at the same time is swept downstream by the shear flow. For this model, the buoyancy flux was perturbed until the "stagnation line"(Sleep, 1990) matched the outer margin of Zone III, i.e., the outer margin of the seismicity of the YSRP. This yielded a buoyancy flux of 0.38 Mg/sec (**Figure 33**). A vertical cross section (AA') of the resulting temperature field (**Figure 33**) shows the upper mantle plume at a depth of 80 km.

While **Figure 33** represents a preliminary model, it provides some important insights into the expected patterns of observable quantities such as topography, seismicity, and stresses. Material supplied by the plume flows in from the right and is separated by a sharp front of roughly parabolic shape, corresponding to the stagnation streamline. Note how the stagnation line has the same shape as the stream-line features observed along the YSRP, including the dual-branched parabolic-shaped seismicity and topography (**Figures 3** and **4**).

While we have not performed a quantitative analysis of this model, the correspondence of the distinctive patterns of seismicity and topographic highs surrounding the SRP with downwelling mantle flow may reflect surface loads buoyed up above the outer wake of the plume as it impinges on the stable mantle. This model fits a narrow (approximately 150 km-wide) hot core at Yellowstone that cools to the southwest behind the hotspot, producing the systematic topographic decrease along the SRP attributed to thermal decay (**Figure 32**).

We realize our model for the Yellowstone hotspot does not explicitly require a mantle plume, but a model for plume-plate interaction matches the general properties of the observed topography and seismicity that distinguish the YSRP. Further work is required to incorporate such features as concomitant crustal extension and explain how the plume would initially develop. These considerations are beyond the scope of this paper.

A unified model for the space-time evolution of the YSRP

We complete our discussion by remarking on the excellent correlation between the space-time evolution of Yellowstone's silicic volcanism, its signature in the topographic field, and its regional geophysical properties. We believe that the observations and data discussed throughout this paper are consistent with a unified working hypothesis for a hotspot origin of Yellowstone's volcanic system.

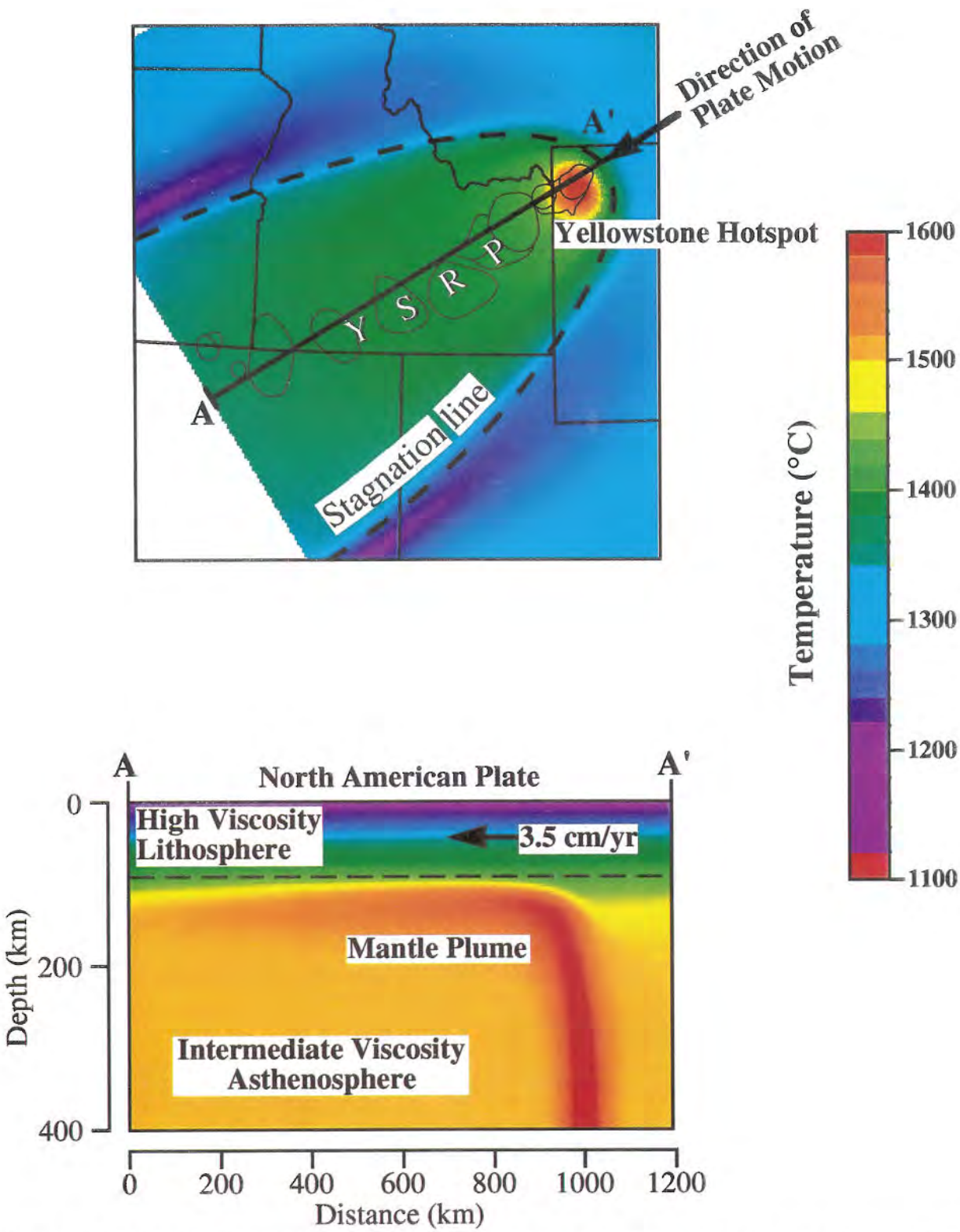

Figure 33. Model of Yellowstone hotspot origin from a mantle plume-plate interaction. The model is characterized by its temperature field contoured in °C. Top: planform view showing the "bow-wave" shaped flow lines taken from a horizontal cross section at the 100 km depth. The dark line corresponds to the approximated stagnation line of Sleep (1990), which separates up-flowing from down-flowing mantle and also corresponds to the outer edge of anomalous YSRP seismicity. Bottom: vertical cross section of the interaction of the plume with the overriding lithospheric plate. Mantle plume-plate model courtesy of Neil Ribe of Yale University.

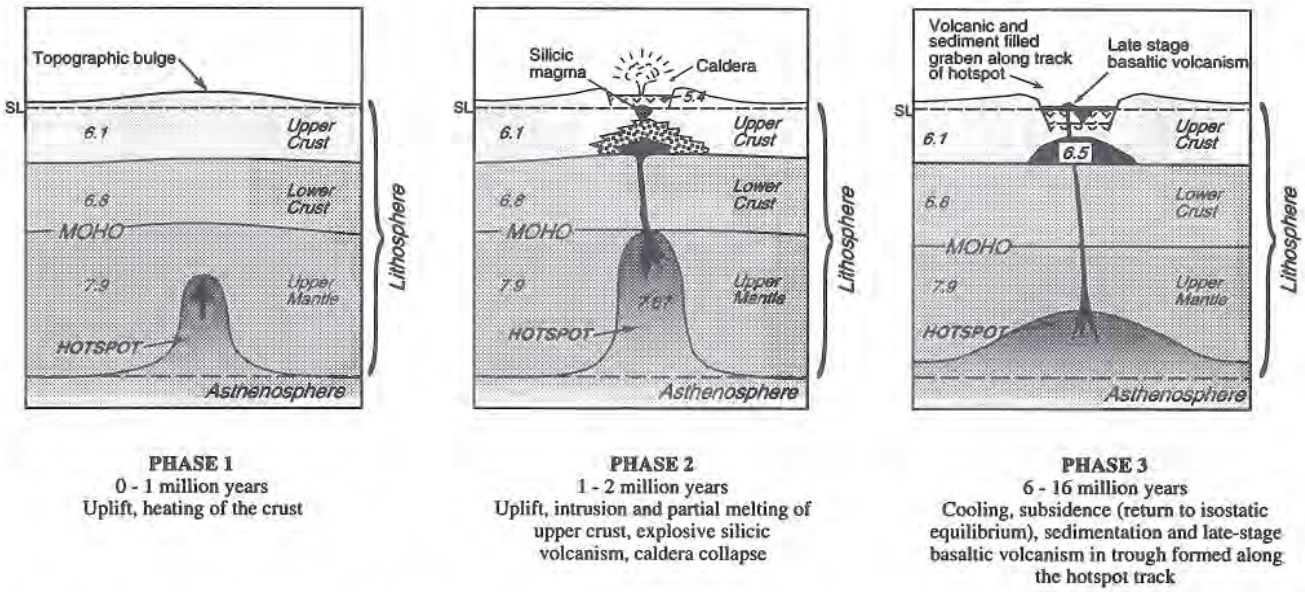

PHASE 1
0 - 1 million years
Uplift, heating of the crust

PHASE 2
1 - 2 million years
Uplift, intrusion and partial melting of upper crust, explosive silicic volcanism, caldera collapse

PHASE 3
6 - 16 million years
Cooling, subsidence (return to isostatic equilibrium), sedimentation and late-stage basaltic volcanism in trough formed along the hotspot track

Figure 34. Models of lithospheric evolution along the track of the Yellowstone hotspot, showing the generalized P-wave velocity structure and topography: (Phase 1) the pre-caldera phase—regional topographic tumescence associated with initial hotspot interaction with the lithosphere, (Phase 2) the "Yellowstone" phase—explosive, silicic volcanism and caldera formation with accompanying caldera collapse, and (Phase 3) the "Snake River Plain" phase—cooling and thermal contraction of the lithosphere with episodic eruptions of mantle-derived basalts.

Together, **Figures 34** and **35** summarize our model for the 16-million-year space-time evolution of the YSRP and its origin as related to the interaction between a plume and the southwestward moving North American plate. The systematic variations in lithospheric structure of the YSRP are seen by plotting three time-slice cross-sections at: 0, 1 to 2, and 6 to 16 Ma (**Figure 34**). Physical properties such as topography, heat flow, and gravity are shown as a function of distance and age of silicic volcanism along the YSRP, plus our conceptual model for the hotspot (**Figure 35**). A hypothetical working model for the lithospheric evolution of the YSRP, which corroborates the scenario of basaltic and rhyolitic magma generation proposed by Leeman (1982) for the SRP and for Yellowstone by Christiansen (1984; 1993), includes these observations (**Figures 33** and **34**). Our model is consistent with those of Hildreth (1981), Glazner and Ussler (1989), and Johnson (1991), who describe how silicic magmas originate from mid-crustal melts accompanying the buoyant ascent of plume generated basalts.

Pre-caldera phase

In the first, or pre-caldera phase, parental basaltic magmas originate in an upper mantle "keel" (defined by Leeman, 1982) that is thought to provide a coupling between the hotspot and crust. The keel corresponds to the trailing portion of our plume model. The combined effects of heating and partial melting reduce P-wave velocities to ~7.8 km/s, compared to 8.0 - 8.1 km/s upper mantle velocities determined beneath the stable craton (Braile and others, 1989). At this stage, ascent of basaltic magmas into the upper mantle begins to produce long-wavelength lithospheric tumescence.

Eventually, a heat flux of ~2,000 mWm^{-2} is available in the crust to produce melting. This corresponds to accelerated tumescence of the lithosphere. Mafic magma bodies likely stagnate below the crust because of density variations (**Figures 22, 33,** and **34**), then ascend through or into the lower crust (Hildreth and others, 1991) in response to buoyancy and extensional pressure release at the base of the upper crust. These bodies act as localized heat sources, which in turn produce partial melting by pressure release, yielding the characteristic rhyolitic magmas of the YSRP.

Yellowstone phase

Beginning the "Yellowstone" phase, the rise of rhyolitic magmas forms batholith-scale bodies in the upper crust (**Figure 21**), perhaps as a single batholith with two near-surface cupolas manifest by the two resurgent domes in Yellowstone (Christiansen,

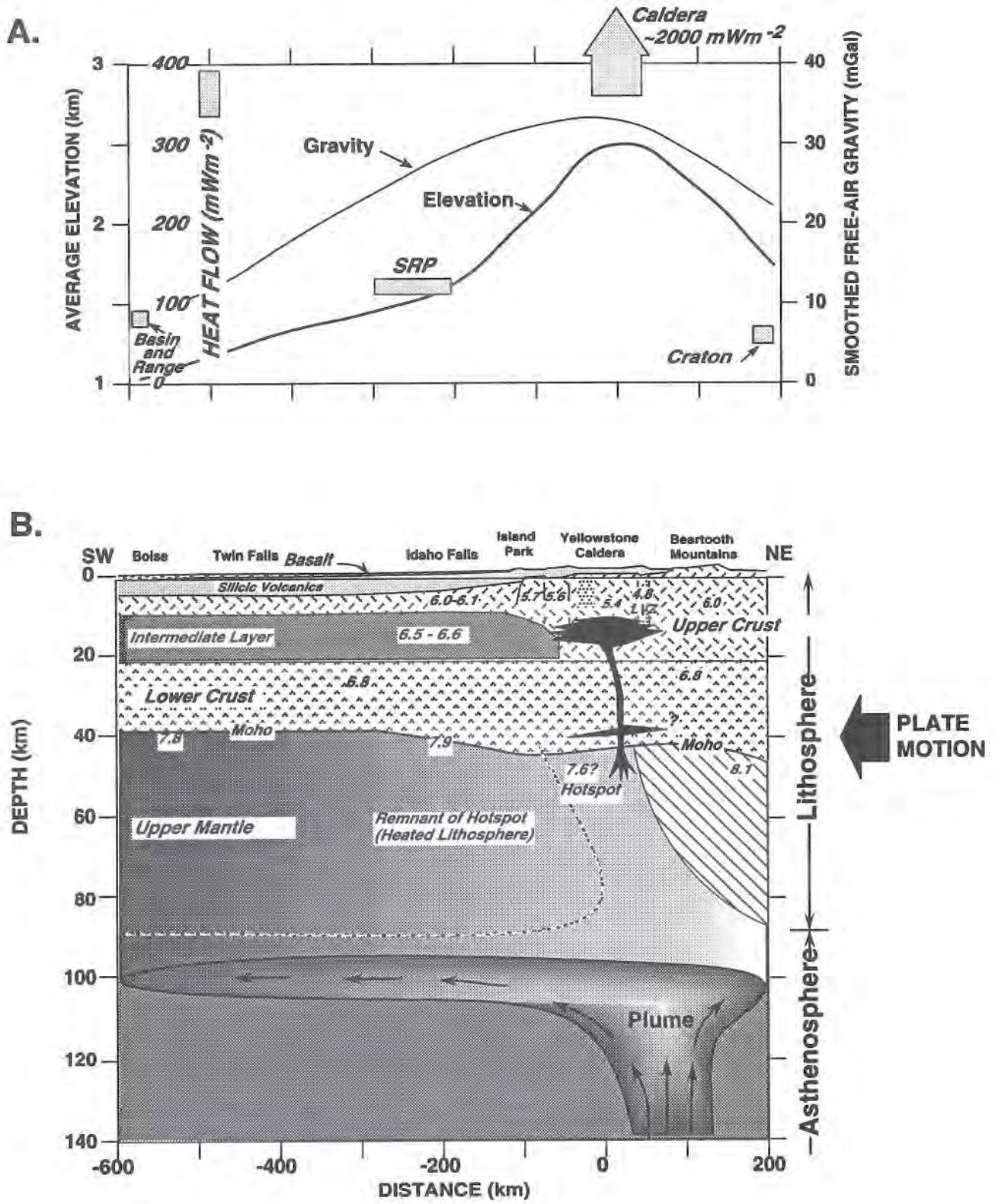

Figure 35. Lithospheric structure, physical properties, and model of hypothesized mantle plume associated with the YSRP volcanic system: (A) profiles of topography, silicic ages, heat flow, and smoother free-air corrected gravity; and (B) seismic velocity (numbers in patterned areas are km/s) and inferred structure of the crust and upper mantle, showing the hypothesized plume-plate interaction responsible for the Yellowstone hotspot. Solid black is inferred basaltic intrusion (see Figure 22).

1984). The upper-crustal batholith in turn produces ring-fracture zones, a process that is accentuated by the superimposed northeast Basin and Range regional extension. Seismicity is accelerated at shallow depths, where heat flow is still sufficiently low to permit brittle failure. As rhyolitic magmas ascend, thermal expansion and magma transport produce crustal uplift on a caldera-wide scale. The batholithic basement is evidenced by the low P-wave velocities (4.8 to 5.6 km/s) and concomitant low-density zones that are interpreted as rhyolitic and basaltic magmas, solidified but hot granitic rocks, partial melts, and hydrothermal fluids. These are in contrast to 6.0 km/s for the thermally undisturbed and colder basement of the surrounding Rocky Mountains. The low-velocity bodies extend to depths of about 10 km and are primarily responsible for the negative gravity anomaly of the Yellowstone Plateau and generally reflect the location of Yellowstone's batholith. Localized crustal deformation, like that measured historically in Yellowstone, reflects ephemeral episodes of uplift and subsidence associated with the migration of magma and hydrothermal fluids in the upper crust. Earthquakes occur along crustal zones of weakness (**Figure 23**), such as pre-existing fault zones or alignments of volcanic vents with high temperatures, limiting the depth of brittle failure within the caldera to less than ~5 km (**Figure 25**).

During the climactic stage of the "Yellowstone" phase of silicic volcanism, violent caldera-scale eruptions are produced when shallow magma chambers intersect pre-existing faults or other zone of weakness. Explosive volcanism is likely exacerbated by ruptures accompanying large earthquakes that reduce the confining pressure and produce rapid gas exsolution at a rate greater than can be physically accommodated. This results in violent pyroclastic, caldera-forming eruptions with concomitant loss of roof support and caldera roof collapse.

As the siliceous magmas cool, mafic magmas are erupted at the margins of the caldera, which continue to subside. Residual magma bodies and subsidence of the caldera continue to feed the resurgent domes. Magmatic and hydrothermal fluids beneath or near Yellowstone's domes fit our models of quasi-plastic flow and source volumes responsible for Yellowstone's modern crustal deformation (**Figures 25** and **27**), as well as the localized gravity and seismic-velocity anomalies. Ultimately, cooling and fracturing of the Yellowstone batholith allows the parental basalts to flood the surface.

Snake River Plain phase

The last phase of YSRP volcanism is hypothesized as the "Snake River Plain" stage (**Figures 17** and **34**). In this stage, thermal contraction, surface loading from episodic basaltic magmatism, and subsurface loading associated with the high-density mid-crustal body produce the notable topographic decay of the eastern SRP. Heat flow is reduced to background values of ~100 mWm^{-2}. The velocity structure of the upper crust in this late stage reflects the characteristic bimodal volcanism manifested by a near-surface basalt layer (4.9 km/s) underlain by a rhyolite layer (5.3 km/s) (**Figure 29**). The anomalous, high-velocity (6.5 km/sec), high-density intermediate crustal layer is interpreted as a mafic remnant of the crustal differentiation process and is primarily responsible for the positive gravity anomaly of the SRP.

We note that upper-mantle teleseismic P-wave and density models do not resolve physical properties to depths greater than ~250 km. Thus our model (**Figure 25**) does not necessarily specify the depth of origin of the Yellowstone hotspot, it simply accounts for a mantle source of magmatism and heat.

Alternate hypotheses for the origin of Yellowstone

Several hypotheses have been variously suggested for the origin of the YSRP, varying from mantle plume models to lithospheric fracturing. Eaton and others (1975) attributed the mechanism for the YSRP to mantle-derived magmas, which ascended along a northeast-striking, pre-existing zone of weakness identified by subtle trends in regional magnetic anomalies. Morgan (1972) and Smith and Sbar (1974) proposed plume models to account for the progressive volcanism of the YSRP. Smith (1977) proposed a regional model of a dual-branched—northeast (the YSRP) and northwest (into the High Lava Plains of Oregon)—rift emanating from a mantle bulge, continental triple junction, in north-central Nevada. The rifting model also resembles the concept of "unzipping" along a lithospheric fracture (see Furlong, 1979), with buoyant ascent of mantle magmas to account for the systematic variations of

silicic volcanism for the YSRP. However, the models of Smith (1977) and Draper (1991) require northwest progression of silicic volcanic centers into the southern Oregon volcanic province, but this silicic zone of volcanism does not have a well-defined age progression of silicic centers nor the volume of volcanic rocks that would be expected.

Christiansen and McKee (1978) suggested that the silicic volcanic age progression of the YSRP originated along a transform fault boundary with right-lateral offset. However, there is little evidence for strike-slip offset along the boundary of the SRP. Furthermore, the direction of regional northwest Basin and Range extension, i.e., σ_{hmin}, has persisted since about 17 Ma and is inconsistent with the proposed strike-slip offset. Christiansen and McKee (1978), while agreeing with the idea of a melting anomaly at Yellowstone, argued against a deep mantle plume and suggested that concentrations of radioactive minerals in the upper mantle could produce the required heat to drive the YSRP. Our plume-plate model cannot differentiate a shallow or deep (core-mantle boundary) plume. On the other hand, the idea of concentrations of radioactrive minerals in the mantle is speculative and untested.

Several authors have attributed the origin of the Miocene Columbia River flood basalts to the initial development of the Yellowstone plume in southeastern Oregon. For example, Thompson (1977) suggested shallow-rooted mantle diapiric upwelling for the origin of the YSRP, beginning as early as Oligocene, which he suggested was also the source of the basaltic volcanism of the Columbia Plateau. White and McKenzie (1989) characterize flood basalts, such as in the Columbia Plateau, as a passive response to rifting or extension above the head of a mantle plume that spreads out beneath the lithosphere. This model requires a dimension larger than 200 km, indeed as large as 1,000 km, and we believe there is little evidence now for such a large-scale feature. Thompson and Gibson (1991) recently suggested that the Miocene volcanism of the Columbia Plateau was the result of a lithospheric "thinspot" that may have originated when the Yellowstone "plume" was located beneath southwestern Oregon and western Idaho at ~ 17-15 Ma. However, these authors could not link the narrow and linear volcanic pattern of the YSRP to the hypothesized thinspot. Draper (1991) suggested that the Miocene basalts of southeastern Oregon originated from a shallow plume source initiated at 18 Ma. He failed to note that the Columbia Plateau magmatism declined at the time when silicic volcanism of the Oregon lava plains began to propagate.

Duncan (1982), Thompson and Gibson (1991), and Pierce and Morgan (1990, 1992) link the origin of the voluminous Columbia river basalts with the initiation of the Yellowstone plume about 16 Ma. However, plate reconstructions are inconsistent with the hotspot track implied by these models. For this reason, Thompson and Gibson (1991) suggested that a pre-existing lithospheric "thinspot" at the location of the Columbia Basin may have allowed the rising Yellowstone plume head to spread laterally as it reached the base of the lithosphere and produce the Columbia River basalt eruptions away from the axis of the plume.

Despite the unknown, deep source of the Yellowstone hotspot, the uncertainty about the nature of the initial interaction of the hotspot with the North American plate before 16 Ma, and the unclear relationship between the Yellowstone hotspot and the Columbia River basalts, we believe that the mantle plume-plate model described in this paper and schematically illustrated in **Figures 34** and **35** currently represents the best working model for the late Cenozoic evolution of the YSRP tectono-magmatic system. Although there is much to learn about the exact mechanisms of plume interactions with the continental lithosphere, the model explains the main characteristics of the YSRP system including: (1) a source of intense heat, mantle-derived basalts, and siliceous partial melts; (2) the systematic age progressions of silicic volcanism, topographic bulging and subsidence of the Yellowstone caldera along with topographic decay of the SRP; (3) plate reconstructions for which we can infer the former positions of the Yellowstone hotspot; (4) systematic variations in crustal velocity structure along the YSRP; and (5) the parabolic pattern of seismicity and topography observed in the YSRP region.

Concluding remarks

We conclude by discussing the stress field and the possibility of magmatic sources at Yellowstone and speculating on the future of volcanism and earthquakes in this region.

Extensional stress field at Yellowstone

We have discussed the evidence that the historic uplift of the Yellowstone caldera has a magmatic or hydrothermal origin. These observations suggest an important question about the long-term processes of Yellowstone; namely, what is the regional pattern of crustal deformation excluding the influence of the hotspot? To examine one possible scenario, Meertens and others (1989) constructed three-dimensional, finite-element models of the Yellowstone-Hebgen Lake region assuming an elastic layer over a fluid half-space with the Yellowstone caldera as a soft inclusion that was loaded by tectonic and volcanic mechanisms. Their modeling suggested that the occurrence of the 1959, M_S = 7.5 Hebgen Lake earthquake may have stressed the Yellowstone caldera, causing uplift within a region dominated by crustal extension. This mechanism is consistent with the modeling of the 1987 to 1991 caldera subsidence (Meertens and others, 1992), which requires both a component of caldera subsidence at 1 to 2 cm/yr and the superposition of regional northeast extension.

Additional evidence for long-term crustal extension is given by Peyton's (1991) study of the stress field by inversion of focal mechanisms. Her study revealed a dominant north-northeast direction of σ_{hmin}, which is also consistent with the strain directions implied by trilateration networks in the same region (see Dzurisin and others, 1990; Savage and others, 1993) and by the orthogonal direction to the alignment of volcanic vents associated with the post-caldera rhyolite flows (see **Figure 13**).

These observations suggest the Yellowstone Plateau has been dominated by northeast crustal extension that has been active since at least the time of the volcanic vent emplacements 0.6 Ma. On the basis of evidence for long-term regional extension from these geologic and geophysical indicators, we thus believe that the northeast-trending extensional stress field has persisted for at least the last 10 million years and that the Yellowstone Plateau has been largely influenced by Basin and Range extension that continues today.

However, the stress field of Yellowstone must be episodically interrupted by tectonic events (large earthquakes) and magmatic events (eruptive and non-eruptive emplacements of magmas and hydrothermal fluids), which produce caldera-wide uplift, such as that observed historically. Nonetheless, we believe that these short-term perturbations are followed by relaxation and continued extension with resulting caldera subsidence.

Present-day magmatic fluids at Yellowstone

For Yellowstone, one of the key issues implied by the Quaternary silicic volcanic record (Christiansen, 1984; 1993) is the extent and location of magma sources. Geophysical and geodetic surveys by their nature, provide inferential information on physical properties and hence on locations of magmatic systems. However, these models do not uniquely define the locations of the hypothesized magmatic systems, but rather provide constraints on plausible models. We suggest that the ~ 2,000 mWm^{-2} thermal flux is the key parameter that characterizes the evolution of Yellowstone's volcanic system, because heat flow of this magnitude must originate from the upper mantle, implying a long-lived magmatic process.

Direct evidence for shallow magmatic/hydrothermal fluids at Yellowstone is the unprecedented 1923-1984 period of uplift totaling about 1 m followed by subsidence of about 25 cm from 1985 to 1991. The synchroneity of caldera-wide uplift and the rapid change to subsidence across the entire caldera is the best evidence for a shallow, connected source zone. Vasco and others (1990) suggested that low-viscosity fluids such as hydrothermal brines or gases associated with deeper magmatic sources may be transported through an upper-crustal conduit system along the entire 75 km long Yellowstone caldera or connected between the two cupolas underlying the resurgent domes. This idea is consistent with modeling of the crustal deformation data,

which places the source of 1923 to 1977 uplift in the 3 to 6 km depth range near the resurgent domes, whereas the 1987 to 1991 subsidence was modeled in the 3 to 6 km depth zone along the entire caldera. A magma or partial melt may have invaded the deeper zone producing crustal uplift, then generating hydrothermal fluids and gases.

In an earlier section, we showed the distribution of excess mass that exceeded the Curie temperature. The Curie depth anomaly on the southwest side of the caldera appears to reflect bodies with upper crustal sources, implying hot material in the upper crust at 6 to 8 km depths. This area also corresponds to the youngest (150 Ka to 70 Ka) post-collapse caldera flows of Yellowstone (Christiansen, 1984) and the circular nature of this anomaly around the caldera rim suggests that it could represent ring dikes or bodies that follow the inner-caldera rim fracture zone. Together with the upper crustal low-velocity body in the northeast caldera, these observations suggest the presence of magmatic and hydrothermal or highly altered rock bodies in the northeast caldera, near the Sour Creek dome, around the southwest caldera rim, and near the Mallard Lake dome. The continuous nature of the 1974 to 1991 subsidence of the entire central caldera also argues for a connection between the northern and southern caldera, perhaps zones of hydrothermal fluid flow.

Future of volcanism at Yellowstone

We close by speculating on the future of tectonic and magmatic activity of the Yellowstone Plateau. Smith and Christiansen (1980) and Christiansen (1984) pointed out that there is little evidence that Yellowstone's volcanism has ceased and, therefore, that volcanic eruptions are quite likely in the future. The record of unprecedented modern crustal deformation of the Yellowstone caldera and its Quaternary record of rather continuous silicic volcanism, interrupted by the caldera-forming explosions, reflects an intense and long-lived heat source that drives the Yellowstone system. While the anomalous crustal properties do not indicate what form the volcanism might take, Smith and Christiansen (1980) suggest it could range from small phreatic and hydrothermal explosions throughout the caldera, to eruptions of small rhyolite and basalt flows at the margins of the caldera, to medium-sized eruptions of rhyolitic lava within the caldera, and finally, to catastrophic explosive eruptions of ash. While we do not know where we are in the present cycle, Christiansen (1993) suggests that we may be in the end of the third cycle or in the beginning of a new fourth cycle.

Note that the total volume of source material modeled for the 1923 to 1976 caldera uplift episode is on the order of about 1 km^3, which is about the same volume as that expelled in the historic 1980, Mt. St. Helens explosive eruption. Thus the storage chamber(s) for the historic uplift of the Yellowstone caldera reflects a sufficiently large source to produce a sizable volcanic or phreatic eruption. However, we point out that the historic crustal deformation and inferred source models do not necessarily imply imminent volcanic eruptions at Yellowstone. Nonetheless, the Quaternary volcanic record, the extremely high heat flow, extensive hydrothermal activity, active crustal deformation, and the historic record of large earthquakes warrant systematic and continued monitoring of the Yellowstone region.

We feel that any renewal of volcanism at Yellowstone would be preceded by increased earthquake activity, increased rates of crustal deformation, and increased gas emissions—all phenomena that can be monitored with modern surveillance equipment. Surveillance for long- and short-term volcanic and earthquake precursors and related hazards should include systematic geodetic measurements (GPS, leveling, and gravity), earthquake monitoring, and monitoring of gases and hydrothermal fluids.

We also suggest that large earthquakes, $M_S \leq 7.5$, could occur on the periphery of the Yellowstone Plateau with intense earthquake swarms and $M_S \leq 6.5$ earthquakes around the periphery of the caldera and shallow earthquakes within the caldera. The modern record of seismicity and hydrothermal activity suggests that Yellowstone's geysers, hot springs, and fumeroles will continue to evolve, but may also be extinguished by related volcano-tectonic processes and strong ground shaking accompanying earthquakes. There is no reason to believe that uplift and subsidence of the caldera on the scale measured in historic time will not continue. Over longer periods—tens of millions of years—we suggest that lithospheric tumescence, magmatism, and seismicity associated with the Yellowstone hotspot will progress to the northeast, affecting southern Montana.

We close by quoting T. A. Jaggar (1922), the founder of the Hawaiian Volcano Observatory, who visited Yellowstone in 1920 by horseback and whose keen observations noted the dynamic processes so well manifested in Yellowstone:

> *Anyone who has spent summers with pack-train in a place like Yellowstone comes to know the land to be leaping....The mountains are falling all the time and by millions of tons. Something underground is shoving them up....How much is the ground tilting?* Jaggar (1922)

How prophetic are Jaggar's words. We now recognize Yellowstone as one of the world's largest and most active calderas and one that we believe owes its existence to the interaction between a mantle plume and the overriding North American plate. Indeed, Yellowstone deserves recognition as the "The Yellowstone National Hotspot."

Acknowledgments

This paper presents the findings of multiple investigations made by the University of Utah in Yellowstone and studies by Purdue University in the Snake River Plain with related work from other researchers. We are particularly grateful for cooperative ties made with scientists of the U. S. Geological Survey; in particular, for the fruitful collaborations with R. L. Christiansen, who generously assisted in integrating our geophysical and geodetic data with his volcanological findings.

Funds for the crustal deformation surveys were provided by the National Science Foundation, research grants EAR 86-8618341 and EAR 89-04473 to the University of Utah. The U. S. Geological Survey, Volcano Hazards and Geothermal Research program, grant 1434-92-A-0975 supports the recording and maintenance of the Yellowstone Seismograph Network at the University of Utah Seismograph Stations. Partial support for this research was also furnished by NSF grants, EAR 77-23357 and EAR 84-01330, and by U. S. Geological Survey grant #14-08-0001-G674 to Purdue University.

We gratefully acknowledge the permission and excellent cooperation of the National Park Service and the personnel of Yellowstone National Park and their long-term support and assistance. We especially thank Superintendent Robert Barbee and members of his staff: John Varley, Rick Hutchinson, Wayne Hamilton, and John Lounsbury. Many other Yellowstone National Park rangers, naturalists, and staff members have also assisted us, and we thank them all.

Several students and staff from the University of Utah have worked on projects in Yellowstone and surrounding areas since 1971 and contributed to this paper. Natalie Kelsey materially assisted with the preparation of the paper, especially for drafting of the figures using computer graphics, for editing, and for general assistance. Sue Nava assisted with the preparation of the earthquake data. Anthony Lowry assisted with the color plotting. Walter Nagy was particularly helpful with preparation and interpretation of the earthquake data and the development of the color graphics. We are indebted to many other University of Utah graduate students who have worked on Yellowstone and related projects including: Al Trimble, Terry Daw, Jeff Evoy, Bob Otis, Jim Bailey, Mike Schilly, Jay Lehman, Harley Benz, Diane Doser, Mark Brokaw, Steve Clawson, Walter Nagy, Lynn Peyton, Bill Hardman, and John Byrd. Dan Trentman assisted with computer matters such as data bases, earthquake interpretation, and general computations. Erwin McPherson, Walt Arabasz, Linda Hall, and Sue Nava contributed to technical support and management of Yellowstone Seismograph Network through their affiliation with the University of Utah Seismograph Stations. We also thank graduate students Greg Elbring, Mark Baker, Keith Peregrine, Carl Daudt, and Mark Sparlin from Purdue University for their assistance on the Snake River Plain seismic experiments. Donald Browne pointed out the original references pertaining to the quote of Lt. Gustavus C. Doane.

Neil Ribe contributed the computer models of plume-plate interactions. Chuck Meertens was involved with the Global Positioning Satellite measurements and modeling of crustal deformation. Dave Blackwell cooperated in the heat flow measurements of Yellowstone Lake, and with thermal interpretations of the Snake River Plain, and made a pre-

print of unpublished work available. Dan Dzurisin provided information on crustal deformation from published and unpublished leveling data. In addition, we thank Robert Fournier, Mitch Pitt, Ken Pierce, and Dave Love of the U. S. Geological Survey for contributing their knowledge and data on Yellowstone. Mark Anders and Ken Pierce kindly provided preprints of unpublished work. Charles DeMets computed plate motions for various NUVEL-1 models. Gene Humphreys and Ken Dueker provided unpublished data on the lithospheric velocity structure of the YSRP. David Fountain, Tom Hanks, David Blackwell, and Robert Fournier provided critical and constructive reviews of the manuscript, which are much appreciated.

Appendices

I. Ages of silicic volcanic fields of the Yellowstone-Snake River Plain region, with distances from Yellowstone.

Data from Armstrong and others (1975), Morgan and others (1984), Rodgers and others (1990), Pierce and Morgan (1990, 1992), and Mel Kuntz (U. S. Geological Survey, personal communication, 1985).

Volcanic field	Caldera	Volcanic unit	Age (Ma)	Distance (km)	Error (km)	Symbol
Yellowstone, Wyo.	Yellowstone	Lava Creek Tuff	0.6	45	50	Y
Yellowstone, Wyo.	Henry's Fork	Mesa Falls Tuff	1.3	75	15	HF
Yellowstone, Wyo.	Huckleberry Ridge	Huckleberry Ridge Tuff	2.1	70	80	HR
Heise, Ida.	Kilgore	Kilgore Tuff	4.3	150	70	K
Heise, Ida.	Blue Creek	Walcott Tuff	6.0	220	70	BC
Heise, Ida.	Blacktail Creek	Blacktail Ck. Tuff	6.5	190	110	B
Picabo, Ida.	Blackfoot	Arbon Valley Tuff	10.3	300	110	P
Twin Falls, Ida.	Not specifically identified	multiple tuffs	10.9 (average)	400	100	TF
Bruneau-Jarbidge, Ida.	Not specifically identified	Cougar Point tuff	11.3	500	80	BJ
Owyhee, Ida.-Nev.	Juniper Mtn	multiple tuffs	13.8	630	70	O
McDermitt, Nev.	multiple	multiple tuffs	16.1	690	100	M

II. Inception of extension along Yellowstone-Snake River Plain system, with distances from Yellowstone

Data taken from Rodgers and others (1990, GSA Repository Item # 90-28, Supplementary data), excluding data from the Teton fault. Average age and error estimate (this paper).

Location of extensional basin	Inception age (Ma)	Cessation age (Ma)	Average (Ma)	Error (Ma)	Distance (km)	Symbol
Swan Valley, Ida.	2	4.4	3.2	2.4	80	S
Blackfoot Mtn, Ida.	4.9	5.9	5.4	1	120	Bl
Buckskin Mtn, Ida.	6.7	10.3	8.5	3.6	150	Bu
Raft River., Ida.	7.2	11	9.1	3.8	250	RR
Goose Ck., Ida-Utah.	8.8	13	10.9	4.2	310	GoC
Grouse Ck., Ida-Utah	11.6	14.4	13	2.8	340	GrC
Mary's River., Nev.	12.5	17	14.75	4.5	440	MR
Northern Nev.	14	17	15.5	3	600	NR

References cited

Anders, M.H., and Sleep, N.H., 1992, Lithospheric strengthening by magmatic intrusion: thermal and mechanical affects of the Yellowstone hotspot: Journal of Geophysical Research, v. 97, p. 15,379-15,394.

Anders, M.H., Geissman, J.W., Piety, L., and Sullivan, T., 1989, Parabolic distribution of circum-eastern Snake River Plain seismicity and latest Quaternary faulting: migratory pattern and association with the Yellowstone hotspot: Journal of Geophysical Research, v. 94, p. 1589-1621.

Anderson, D.L., Tanimoto, T., and Zhang, Y., 1992, Plate tectonics and hotspots: the third dimension: Science, v. 256, p. 1645-1651.

Argus, D.F., and Gordon, R.G., 1991, No-net-rotation model of current plate velocities incorporating plate motion model NUVEL-1: Geophysical Research Letters, v. 18, p. 2039-2042.

Armstrong, R.L., Leeman, W.P., and Malde, H.E., 1975, K-Ar dating, Quaternary and Neogene volcanic rocks of the Snake River Plain, Idaho: American Journal of Science, v. 275, p. 225-251.

Barnoff, V., 1977, A new method for interpretation of aeromagnetic maps: Pseudogravimetric anomalies: Geophysics, v. 22, p. 827-829.

Benz, H.M., and Smith R.B., 1984, Simultaneous inversion for lateral velocity variations and hypocenters in the Yellowstone region using earthquake and refraction data: Journal of Geophysical Research, v. 89, p. 1208-1220.

Bhattacharyya, B.K., and Leu, L., 1975, Analysis of magnetic anomalies over Yellowstone National Park: mapping of curie-point isothermal surface for geothermal reconnaissance: Journal of Geophysical Research, v. 80, p. 4461-4465.

Blackwell, D.D., 1978, Heat flow and energy loss in the western United States, *in* Smith R.B., and Eaton, G.P., editors, Cenozoic tectonics and regional geophysics of the western Cordillera: Geological Society of America Memoir 152, p. 175-208.

_____ 1989, Regional implications of the heat flow of the Snake River Plain, northwestern United States: Tectonophysics, v. 164, p. 323-343.

Blackwell, D.D., Steele, J.L., and Carter, L.S., 1991, Heat-flow patterns of the North American continent; a discussion of the Geothermal map of North America, *in* Slemmons, D.B., Engdahl, E.R., Zoback, M.D., and Blackwell, D.D., editors, Neotectonics of North America: Geological Society of America, Decade Map Volume 1, p. 423-436.

Blank, H.R., Jr., and Gettings, M.E., 1974, Complete Bouguer gravity map: Yellowstone-Island Park region: U.S. Geological Survey Open File Map 74-22, scale 1:125,000.

Bonney, O., and Bonney, L., 1970, Battle drums and geysers: Chicago, Illinois, Sage Books, Swallow Press, 622 p. Original citation from Gustavus Doane from: Lt. Gustavus C. Doane, The Yellowstone Expedition of 1870, Senate Executive Committee Document, 51, Serial 1440, 41st Congress, 3rd Session, Washington, D.C.

Braile, L.W., Smith, R.B., Ansorge, J., Baker, M.R., Sparlin, M.A., Prodehl, C., Schilly, M.M., Healy, J.H., Mueller, S.T., and Olsen, K.H., 1982, The Yellowstone-Snake River Plain seismic profiling experiment: crustal structure of the eastern Snake River Plain: Journal of Geophysical Research, v. 87, p. 2597-2609.

Braile, L.W., Hinze, W.J., von Frese, R.R.B., and Keller, G.R., 1989, Seismic properties of the crust and uppermost mantle of the continuous United States and adjacent Canada, *in* Pakiser, L.C., and Mooney, W.C., editors, Geophysical framework of the continental United States: Geological Society of America Memoir 172, p. 655-680.

Brokaw, M.A., 1985, Upper crustal interpretation of Yellowstone determined from ray-trace modeling of seismic refraction data [M.S. thesis]: Salt Lake City, University of Utah, 179 p.

Brott, C.A., Blackwell, D.D., and Mitchell, J.C., 1978, Tectonic implications of the heat flow of the western Snake River Plain, Idaho: Geological Society of America Bulletin, v. 89, p. 1697-1707.

Brott, C.A., Blackwell, D.D., and Ziagos, J.P., 1981, Thermal and tectonic implications of heat flow in the eastern Snake River Plain, Idaho: Journal of Geophysical Research, v. 86, p. 11,709-11,734.

Byrd, J.O.D., and Smith, R.B., 1991, Paleoseismicity, near-surface fault geometry, and segmentation of Teton fault: Eos, Transactions of the American Geophysical Union, v. 72, p. 316.

Chiang, C.S., and Braile, L.W., 1984, An example of two-dimensional synthetic seismogram modeling: Bulletin of the Seismological Society of America, v. 74, p. 509-519.

Christiansen, R.L., 1982, Late Cenozoic volcanism of the Island Park area, eastern Idaho, *in* Bonnichsen, B., and Breckenridge, R.M., editors, Cenozoic geology of Idaho: Idaho Bureau of Mines and Geology Bulletin, v. 26, p. 345-368.

_____ 1984, Yellowstone magmatic evolution: its bearing on understanding large-volume explosive volcanism, *in* Explosive volcanism, its inception, evolution and hazards: Washington, D.C., National Academy of Science, p. 84-95.

_____ 1993, The Quaternary and Pliocene Yellowstone volcanic field of Wyoming, Idaho, and Montana: U.S. Geological Survey Professional Paper 729-G, in press.

Christiansen, R.L., and Blank, H.R., Jr., 1972, Volcanic stratigraphy of the Quaternary rhyolite plateau in Yellowstone National Park: U.S. Geological Survey Professional Paper 729-B, 18 p.

Christiansen, R.L., and McKee, E., H., 1978, Late Cenozoic volcanic and tectonic evolution of the Great Basin and Columbia intermountain regions, *in* Smith, R.B., and Eaton, G.P., editors, Cenozoic tectonics and regional geophysics of the western Cordillera: Geological Society of America Memoir 152, p. 283-311.

Coney, P.J., and Harms, T.A., 1984, Cordilleran metamorphic core complexes: Cenozoic extensional relics of Mesozoic compression: Geology, v. 12, p. 550-554.

Craig, H., Lupton, J.E., Welhan, J.A., and Poreda, R., 1978, Helium isotope ratios in Yellowstone and Lassen Park volcanic gases: Geophysical Research Letters, v. 5, p. 897-900.

Crough, T.S., 1978, Thermal origin of mid-plate hot-spot swells: Geophysical Journal of the Royal Astronomical Society, v. 55, p. 451-469.

_____ 1983, Rifts and swells: Geophysical constraints and causality: Tectonophysics, v. 94, p. 23-38.

Decker, R., and Decker, B., 1989, Volcanoes: New York, W.H. Freeman and Co., 285 p.

DeMets, C., Gordon, R.G., Argus, D.F., and Stein, S., 1990, Current plate motions: Geophysical Journal International, v. 101, p. 425-478.

Doe, B.R., Leeman, W.P., Christiansen, R.L., and Hedge, C.E., 1982, Lead and strontium isotopes and related trace elements as genetic tracers in the Upper Cenozoic rhyolite-basalt association of the Yellowstone Plateau volcanic field, U.S.A.: Journal of Geophysical Research, v. 87, p. 4785-4806.

Draper, D.S., 1991, Late Cenozoic bimodal magmatism in the northern Basin and Range province of southeastern Oregon: Journal of Volcanology and Geothermal Research, v. 47, p. 299-328.

Dueker, K., and Humphreys, E., 1989, Upper mantle velocity structure beneath the eastern Basin and Range: evidence for small-scale convection: Eos, Transactions of the American Geophysical Union, v. 70, p. 122.

_____ 1993, Upper mantle velocity structure along the Yellowstone volcanic field: Journal of Geophysical Research (in press).

Duncan, R.A., 1982, A captured island chain in the Coast Range of Oregon and Washington: Journal of Geophysical Research, v. 87, p. 10,827-10,837.

Duncan, R.A., and Richards, M.A., 1991, Hotspots, mantle plumes, flood basalts, and true polar wander: Reviews of Geophysics, v. 29, p. 31-50.

Dzurisin, D., and Newhall, C., 1988, Historic unrest at large calderas of the world: U.S. Geological Survey Bulletin 1855, vols. 1 and 2, 1108 p.

Dzurisin, D., and Yamashita, K.M., 1987, Vertical surface displacements at Yellowstone caldera, Wyoming, 1976-1986: Journal of Geophysical Research, v. 92, p. 13,753-13,766.

Dzurisin, D., Savage, J.C., and Fournier, R.O., 1990, Recent crustal subsidence at Yellowstone caldera, Wyoming: Bulletin of Volcanology, v. 52, p. 247-270.

Eaton, G.P., Christiansen, R.L., Iyer, H.M., Pitt, A.M., Mabey, D.R., Blank, H.R., Jr., Zietz, I., and Gettings, M.E., 1975, Magma beneath Yellowstone National Park: Science, v. 188, p. 787-796.

Eddington, P.K., Smith, R.B., and Renggli, C., 1987, Kinematics of Basin-Range intraplate tectonics, *in* Coward, M.P., Dewey, J.F., and Hancock, P.L., editors, Continental extensional tectonics: Geological Society of London Special Publication 28, p. 371-392.

Elbring, G., 1984, A method for inversion of two-dimensional seismic refraction data with applications to the Snake River Plain region of Idaho [Ph.D. dissertation]: Lafayette, Indiana, Purdue University, 123 p.

Engdahl, E.R., and Rinehart, W.A., 1988, Seismicity map of North America, Continent-scale Map-004, Decade of North American Geology: Geological Society of America, scale 1:5,000,000.

Engebretson, D.C., Cox, A., and Gordon, R.G., 1985, Relative motions between oceanic and continental plates

in the Pacific basin: Geological Society of America Special Paper 206, 59 p.

Evoy, J.A., 1978, Precision gravity re-observations and simultaneous inversion of gravity and seismic data from subsurface structure of Yellowstone [M.S. thesis]: Salt Lake City, University of Utah, 212 p.

Fournier, R.O., 1989, Geochemistry and dynamics of the Yellowstone National Park hydrothermal system: Annual Review of Earth and Planetary Sciences, v. 17, p. 13-53.

Fournier, R.O., and Pitt, A.M., 1985, The Yellowstone magmatic-hydrothermal system, *in* Stone, C., editor, International symposium on geothermal energy (transactions): Geothermal Resources Council 1985, p. 319-327.

Furlong, K.P., 1979, An analytic stress model applied to the Snake River Plain (northern Basin and Range province, U.S.A.): Tectonophysics, v. 58, p. T11-T15.

Glazner, A.F., and Ussler, W., 1989, Crustal extension, crustal density, and the evolution of Cenozoic magmatism in the Basin and Range of the western United States: Journal of Geophysical Research, v. 94, p. 7952-7960.

Gripp, A.E., and Gordon, R.G., 1989, Current plate motion relative to hotspots: Eos, Transactions of the American Geophysical Union, v. 70, p. 1351.

_____ 1990, Current plate velocities related to hotspots incorporating the NUVEL-1 global plate motion model: Geophysical Research Letters, v. 17, p. 1109-1112.

Hamilton, W., 1959, Yellowstone Park area, Wyoming: a possible modern lopolith: Geological Society of America Bulletin, v. 70, p. 225-228.

Hayden, F.V., 1872, Preliminary report of the United States Geological Survey of Montana and portions of adjacent Territories, *in* Hayden, F.V. editor, U.S. Geological and Geographical Survey of the Territories Fifth Annual Report [for 1871] 13-204, 538 p.

_____ 1873, Report of the United States Geological Survey of the Territories, *in* Hayden, F.V., editor, U.S. Geological and Geographical Survey of the Territories Sixth Annual Report [for 1872] 13-85, 844 p.

Heasler, H.P., and Hinckley, B.S., 1985, Geothermal resources of the Bighorn Basin, Wyoming: Geological Survey of Wyoming Report of Investigations No. 29, 20 p.

Hildreth, W., 1981, Gradients in silicic magma chambers: implications for lithospheric magmatism: Journal of Geophysical Research, v. 86, p. 10,153-10,192.

Hildreth, W., Halliday, A.Z., and Christiansen, R.L., 1991, Isotopic and chemical evidence concerning the genesis and contamination of basaltic and rhyolitic magma beneath the Yellowstone Plateau volcanic field: Journal of Petrology, v. 52, p. 63-138.

Hill, D.P., 1992, Temperatures at the base of the seismogenic crust beneath Long Valley caldera, California, and the Phlegrean fields caldera, Italy, *in* Gasparini, P., editor, Proceedings in Volcanology: Volcanic Seismology, v. 3, p. 432-460.

Hill, D.P., and Pakiser, L.C., 1966, Crustal structure between the Nevada Test Site and Boise, Idaho, from seismic-refraction measurements, *in* Steinhart, J.S., and Smith, T.J., editors., The earth beneath the continents: American Geophysical Union Monographs, v. 10, p. 391-419.

Hill, R.I., Campbell, I.H., Davies, G.F., and Griffiths, R.W., 1992, Mantle plumes and continental tectonics: Science, v. 256, p. 185-193.

Iyer, H.M., Evans, J.R., Zandt, G., Stewart, R.M., Jr., Coakley, J., and Roloff, J., 1981, A deep magma body under the Yellowstone caldera: delineated using teleseismic P-wave residuals and tectonic interpretation: Geological Society of America Bulletin, v. 92, p. 1471-1646.

Jaggar, T.A., 1922, A plea for geophysical and geochemical observatories: Journal of the Washington Academy of Science, v. 12 (15), p. 343-353.

Johnson, C.M., 1991, Large-scale crust formation and lithosphere modification beneath middle to late-Cenozoic calderas and volcanic fields, western North America: Journal of Geophysical Research, v. 96, p. 13,485-13,507.

Keefer, W.R., 1971, The geologic story of Yellowstone National Park: U.S. Geological Survey Bulletin 1347, 92 p.

Kennedy, B.M., Lynch, M.A., Reynolds, J.H., and Smith, S.P., 1985, Intensive sampling of noble gases in fluids at Yellowstone: I. Early overview of the data; regional patterns: Geochimica et Cosmochimica Acta, v. 49, p. 1251-1261.

King, P.B., compiler, 1969, Tectonic map of North America: U.S. Geological Survey, scale 1:5,000,000.

Kissling, E., 1988, Geotomography with local earthquake data: Reviews of Geophysics, v. 26, p. 659-698.

Knuepher, P.K., Baltzer, E.M., and Turko, J.M., 1990, Late Quaternary earthquake recurrence and seismic hazard of the Lemhi fault, Idaho: Geological Society of America Abstracts with Programs, v. 22, no. 6, p. 17.

Lachenbruch, A.H., and Sass, J.H., 1978, Models of an extending lithosphere and heat flow in the Basin and Range province, *in* Smith, R.B., and Eaton, G.P., editors, Cenozoic tectonics and regional geophysics of the western Cordillera: Geological Society of America Memoir 152, p. 209-250.

Lawrence, R.D., 1976, Strike-slip faulting terminates the Basin and Range province in Oregon: Geological Society of America Bulletin, v. 87, p. 846-850.

Leeman, W.P., 1982, Development of the Snake River Plain-Yellowstone Plateau province, Idaho and Wyoming: an overview and petrologic model, *in* Bonnichsen, B., and Breckenridge, R.M., editors, Cenozoic geology of Idaho: Idaho Bureau of Mines and Geology Bulletin, v. 26, p. 155-178.

Lehman, J.A., Smith, R.B., Schilly, M.M., and Braile, L.W., 1982, Upper crustal structure of the Yellowstone caldera from delay time analyses and gravity correlations: Journal of Geophysical Research, v. 87, p. 2713-2730.

Magill, J., and Cox, A., 1981, Post-Oligocene tectonic rotation of the Oregon western Cascade Range and the Klamath Mountains: Geology, v. 9, p. 27-131.

Meertens, C.M., Levine, J., and Busby, R., 1989, Tilt observations using borehole tiltmeters: 2. Analysis of data from Yellowstone National Park: Journal of Geophysical Research, v. 94, p. 587-601.

Meertens, C.M., Smith, R.B., and Vasco, D.M., 1992, Crustal deformation of the Yellowstone caldera from first GPS measurements: 1987-1989: Geophysical Research Letters, v. 18, p. 1763-1766.

Meyer, G.A., and Locke, W.W., 1986, Origin and deformation of Holocene shoreline terraces, Yellowstone Lake, Wyoming: Geology, v. 14, p. 699-702.

Milbert, D.G., 1991, GEOID90: a high-resolution geoid for the United States: Eos, Transactions of the American Geophysical Union, v. 72, p. 49.

Minster, J.B., and Jordan, T.H., 1978, Present day plate motions: Journal of Geophysical Research, v. 36, p. 5331-5354.

Morgan, L.A., Doherty, D.J., and Leeman, W.P., 1984, Ignimbrites of the eastern Snake River Plain: evidence for major caldera-forming eruptions: Journal of Geophysical Research, v. 89, p. 8665-8678.

Morgan, P., Blackwell, D.D., Spafford, R.E., and Smith, R.B., 1977, Heat flow measurements in Yellowstone Lake and the thermal structure of the Yellowstone caldera: Journal of Geophysical Research, v. 82, p. 3719-3732.

Morgan, W.J., 1972, Deep mantle convection plumes and plate motions: American Association of Petroleum Geologists Bulletin, v. 56, p. 203-213.

Myers, W.B., and Hamilton, W., 1964, Deformation accompanying the Hebgen Lake earthquake of August 17, 1959: U.S. Geological Survey Professional Paper 435, p. 55-98.

Nagy, W.C., and Smith, R.B., 1988, Seismotectonic implications of the 1985-86 Yellowstone earthquake swarm from velocity and stress inversion: Seismological Research Letters, v. 59, p. 20.

Parsons, B., and Sclater, J.G., 1977, An analysis of the variation of ocean floor bathymetry and heat flow with age: Journal of Geophysical Research, v. 82, p. 803-827.

Parsons, T., and Thompson, G.A., 1991, The role of magma overpressuring in suppressing earthquakes and topography: worldwide examples: Science, v. 253, p. 1399-1402.

Pelton, J.R., and Smith, R.B., 1982, Contemporary vertical surface displacements in Yellowstone National Park: Journal of Geophysical Research, v. 87, p. 2745-2761.

Peyton, S.L., 1991, Contemporary tectonics of the Yellowstone-Hebgen Lake region from earthquake focal mechanisms and stress-field inversion [M. S. thesis]: Salt Lake City, University of Utah, 96 p.

Pierce, K.L., and Morgan, L.A., 1990, The track of the Yellowstone hot spot: volcanism, faulting, and uplift: U.S. Geological Survey Open File Report 90-415, 49 p.

_____ 1992, The track of the Yellowstone hotspot: volcanism, faulting and uplift, *in* Link, P.K., Kuntz, M.A., and Platt, L.B., editors, Regional geology of eastern Idaho and western Wyoming: Geological Society of America Memoir 179, p. 1-53.

Piety, L.A., Wood, C.K., Gilbert, J.D., Sullivan, J.T., and Anders, M.H., 1986, Seismotectonic study for Palisades Dam and Reservoir, Palisades Project: U.S. Bureau of Reclamation, Engineering and Research Center Seismotectonic Division, Denver, Colorado, and Pacific Northwest Region Geology Branch, Boise, Idaho, Seismotectonic Report 86-3, 198 p.

Pitt, A.M., 1989, Map showing earthquake epicenters (1964-81) in Yellowstone National Park and vicinity, Wyoming, Idaho, and Montana: U.S. Geological Sur-

vey Miscellaneous Field Studies Map MF-2022, scale 1:250,000.

Pitt, A.M., and Hutchinson, R.A., 1982, Hydrothermal changes related to earthquake activity at Mud Volcano, Yellowstone National Park, Wyoming: Journal of Geophysical Research, v. 87, p. 2762-2766.

Pitt, A.M., Weaver, C.S., and Spence, W., 1979, The Yellowstone Park earthquake of June 30, 1975: Bulletin of the Seismological Society of America, v. 69, p. 187-205.

Pollitz, F.F., 1988, Episodic North American and Pacific plate motions: Tectonics, v. 7, p. 711-726.

Priestly, K., Orcutt, J.A., and Brune, J.N., 1980, Higher-mode surface waves and structure of the Great Basin of Nevada and western Utah: Journal of Geophysical Research, v. 85, p. 7166-7174.

Ribe, N.M., and Christensen, U.R., 1992a, A 3D dynamical modeling of plume-lithsophere interaction: Eos, Transactions of the American Geophysical Union, v. 14, p. 303.

_____ 1992b, A 3D dynamical model of the Hawaiian plume: Eos, Transactions of the American Geophysical Union, v. 43, p. 578.

Richards, M.A., Duncan, R.A., and Courtillot, V.E., 1989, Flood basalts and hotspot tracks: plume heads and tails: Science, v. 246, p. 103-107.

Rodgers, D.W., Hackett, W.R., and Ore, H.T., 1990, Extension of the Yellowstone plateau, eastern Snake River Plain, and Owyhee plateau: Geology, v. 18, p. 1138-1141.

Sarna-Wojcicki, A.M., and Davis, J.O., 1993, Quaternary tephrochronology, Decade of North American Geology volume on Tephrochronology (in press).

Sarna-Wojcicki, A.M., Shipley, S., Waitt, R.B., Jr., Dzurisin, D., and Wood, S.H., 1982, Areal distribution, thickness, mass, volume, and grain size of air-fall ash from the six major eruptions of 1980, *in* The 1980 eruptions of Mount St. Helens, Washington: U.S. Geological Survey Professional Paper 1250.

Savage, J.C., Lisowski, M., Prescott, W.H., and Pitt, A.M., 1993, Deformation from 1973 to 1987 in the epicentral area of the 1959 Hebgen Lake, Montana, earthquake (M_s = 7.5): Journal of Geophysical Research, v. 98, p. 2145-2153.

Schilly, M.M., Smith, R.B., Ansorge, J., Lehman, J.A., and Braile, L.W., 1982, The Yellowstone-eastern Snake River Plain seismic profiling experiment: upper-crustal structure: Journal of Geophysical Research, v. 87, p. 2692-2704.

Sclater, J.G., and Francheteau, J., 1970, The implications of terrestrial heat flow observations on current tectonic and geochemical models of the crust and upper mantle of the Earth: Geophysical Journal of the Royal Astronomical Society, v. 20, p. 509-542.

Scott, W.E., Pierce, K.L., and Hait, M.H., Jr., 1985, Quaternary tectonic setting of the 1983 Borah Peak earthquake, central Idaho: Bulletin of the Seismological Society of America, v. 75, p. 1053-1066.

Sibson, R.H., 1982, Fault zone models, heat flow, and the depth distribution of earthquakes in the continental crust of the United States: Bulletin of the Seismological Society of America, v. 72, p. 151-164.

Sleep, N.H., 1990, Hotspots and mantle plumes: Some phenomenology: Journal of Geophysical Research, v. 95, p. 6715-6730.

_____ 1992, Hotspot volcanism and mantle plumes: Annual Review of Earth and Planetary Sciences, v. 20, p. 19-43.

Smith, R.B., 1977, Intraplate tectonics of the western North American plate: Tectonophysics, v. 37, p. 323-336.

_____ 1989, Kinematics and dynamics of the Yellowstone hotspot: Eos, Transactions of the American Geophysical Union, v. 10, p. 1356.

_____ 1990, Evolution and kinematics of the Yellowstone hotspot: Geological Society of America Abstracts with Programs, v. 22, no. 6, p. 45.

Smith, R.B., and Arabasz, W.J., 1991, Seismicity of the Intermountain seismic belt, *in* Slemmons, D.B., Engdahl, E.R., Zoback, M.D., and Blackwell, D.D., editors, Neotectonics of North America: Geological Society of America, Decade Map Volume 1, p. 185-228.

Smith, R.B., and Braile, L.W., 1984, Crustal structure and evolution of an explosive silicic volcanic system at Yellowstone National Park, *in* Explosive volcanism, its inception, evolution, and hazards: Washington, D.C., National Academy of Science, p. 96-109.

Smith, R.B., and Bruhn, R.L., 1984, Intraplate extensional tectonics of the western U.S. Cordillera: inferences on structural style from seismic reflection data, regional tectonics and thermal-mechanical models of brittle-ductile deformation: Journal of Geophysical Research, v. 89, p. 5733-5762.

Smith, R.B., and Christiansen, R.L., 1980, Yellowstone Park as a window on the Earth's interior: Scientific American, v. 242, p. 104-117.

Smith, R.B., and Sbar, M.L., 1974, Contemporary tectonics and seismicity of the western United States, with emphasis on the Intermountain seismic belt: Geological Society of America Bulletin, v. 85, p. 1205-1218.

Smith, R.B., Shuey, R.T., Freidline, R.O., Otis, R.M., and Alley, L.B., 1974, Yellowstone hot spot: new magmatic and seismic evidence: Geology, v. 2, p. 451-455.

Smith, R.B., Shuey, R.T., Pelton, J.R., and Bailey, J.T., 1977, Yellowstone hot spot: contemporary tectonics and crustal properties from new earthquake and aeromagnetic data: Journal of Geophysical Research, v. 82, p. 3665-3676.

Smith, R.B., Braile, L.W., Schilly, M.M., Ansorge, J., Prodehl, C., Baker, M., Healey, J.H., Mueller, S., and Greensfelder, R., 1982, The Yellowstone-eastern Snake River Plain seismic profiling experiment: crustal structure of Yellowstone: Journal of Geophysical Research, v. 87, p. 2583-2596.

Smith, R.B., Richins, W.D., and Doser, D.I., 1985, The Borah Peak earthquake: seismicity, faulting kinematics and tectonic mechanism, *in* Workshop XXVIII on the Borah Peak Earthquake: U.S. Geological Survey Open File Report 85-290, p. 236-263.

Smith, R.B., Byrd, J.O.D., and Susong, D.D., 1990, Neotectonics and structural evolution of the Teton fault, *in* Roberts, S., editor, Geologic field tours of western Wyoming and parts of adjacent Idaho, Montana, and Utah: Geological Survey of Wyoming Public Information Circular No. 29, p. 126-138.

Sparlin, M.A., Braile, L.W., and Smith, R.B., 1982, Crustal structure of the eastern Snake River Plain determined from ray-trace modeling of seismic refraction data: Journal of Geophysical Research, v. 87, p. 2619-2633.

Stewart, J.H., and Carlson, J.E., 1978, Generalized maps showing distribution, lithology, and age of Cenozoic igneous rocks in the western United States, *in* Smith, R.B., and Eaton, G.P., editors, Cenozoic tectonics and regional geophysics of the western Cordillera: Geologic Society of America Memoir 152, p. 263-264.

Stickney, M.C., and Bartholomew, M.J., 1987, Seismicity and late Quaternary faulting of the northern Basin and Range province, Montana and Idaho: Bulletin of the Seismological Society of America, v. 77, p. 1602-1625.

Suppe, J., Powell, J.C., and Berry, R., 1975, Regional topography, seismicity, Quaternary volcanism and the present-day tectonics of the western United States: American Journal of Science, v. 275-A, p. 397-436.

Thompson, R.N., 1977, Columbia/Snake River—Yellowstone magmatism in the context of western U.S.A. Cenozoic geodynamics: Tectonophysics, v. 39, p. 621-636.

Thompson, R.N., and Gibson, S.A., 1991, Subcontinental mantle plumes, hotspots and pre-existing thinspots: Journal of the Geological Society of London, v. 148, p. 973-977.

Trimble, A.B., and Smith, R.B., 1975, Seismicity and contemporary tectonics of the Hebgen Lake-Yellowstone Park region: Journal of Geophysical Research, v. 80, p. 733-741.

United States Geological Survey, 1973, Aeromagnetic map of Yellowstone National Park and vicinity, Wyoming, Montana, and Idaho: U.S. Geological Survey Open-File Report 73-304, scale 1:125,000.

Vasco, D.W., Smith, R.B., and Taylor, C., 1990, Inversion of Yellowstone vertical displacements and gravity changes, 1923 to 1975-1977 to 1986: Journal of Geophysical Research, v. 95, p. 19,839-19,856.

Wallace, R.E., 1990, General features in the San Andreas fault system, California: U.S. Geological Survey Professional Paper 1515, p. 3-21.

Westaway, R., 1989, Deformation of the NE Basin and Range province: the response of the lithosphere to the Yellowstone plume?: Geophysical Journal International, v. 99, p. 33-62.

White, D.E., Fournier, R.O., Muffler, L.J.P., and Truesdell, A.H., 1975, Physical results of research drilling in thermal areas of Yellowstone National Park: U.S. Geological Survey Professional Paper 892, 70 p.

White, R., and McKenzie, D., 1989, Magmatism at rift zones: the generation of volcanic continental margins and flood basalts: Journal of Geophysical Research, v. 94, p. 7685-7730.

Yellowstone National Park Task Group to the Continental Drilling Committee, 1987, The objectives for deep scientific drilling in Yellowstone National Park: Board of Earth Sciences, Commission on Physical Sciences, Mathematics, and Resources, National Research Council, National Academy Press, 69 p.

Zoback, M.L., and Zoback, M.D., 1989, Tectonic stress field of the continental United States, *in* Pakiser, L.C., and Mooney, W.D., editors, Geophysical framework of the continental United States: Geological Society of America Memoir 172, p. 523-539.

Zoback, M.L., Anderson, R.E., and Thompson, G.A., 1981, Cenozoic evolution of the state of stress and style of tectonism of the Basin and Range province of the western United States: Philosophical Transactions of the Royal Society of London, v. A300, p. 407-434.

Part VI

Topical aspects

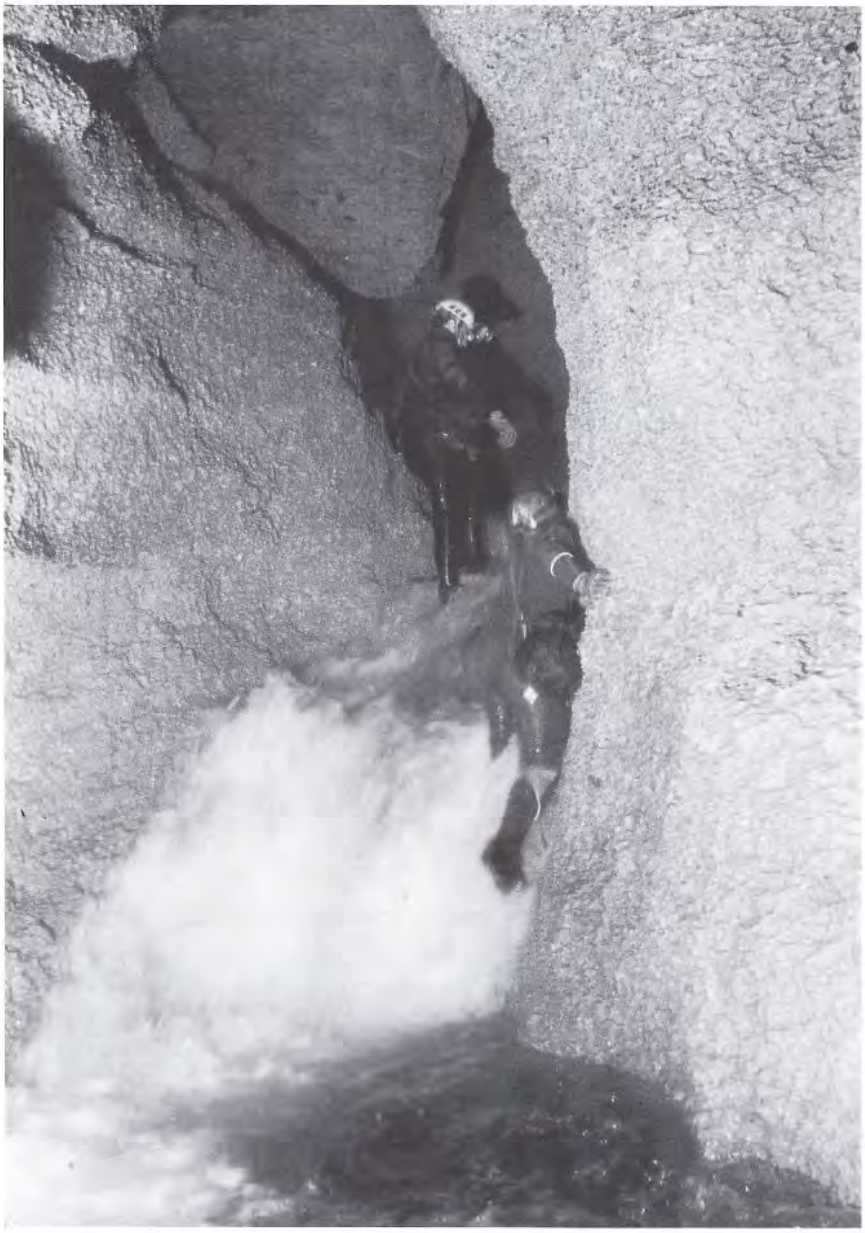

Frontispiece. Stream passage in Great X cave dissolved Bighorn Dolomite on the homoclinal west flank of the Bighorn Mountains, northeast of Hyattville, Wyoming. These modern passages are localized on partings along bedding and joints. Local steepening within the potentiometric surface caused by the topographic positions of recharge and discharge points on the homocline dictate which specific bedding partings and joints dissolved. (Photograph by Norm Pace.)

The influence of Laramide foreland structures on modern ground-water circulation in Wyoming artesian basins

Peter W. Huntoon
Department of Geology and Geophysics
University of Wyoming
Laramie, Wyoming 82071

Abstract

Ground-water circulation in the Paleozoic rocks in Wyoming artesian basins is strongly influenced by highly anisotropic permeabilities imparted on the rocks during Laramide deformation. Laramide structural elements both enhance and diminish permeabilities. Laramide range-bounding thrust faults and large-displacement faults that occur in the cores of anticlines sever the hydraulic continuity within aquifers in directions perpendicular to the trend of the anticlines. On the other hand, extensional fractures, both parallel and oblique to trend, greatly enhanced permeabilities in the crestal parts of Laramide anticlines. Crestal fracture permeabilities are highly anisotropic, with fractures oriented oblique and parallel to trend vying for dominance as to which will locally define the maximum principal permeability tensor within the fold. Other classes of Laramide fractures strongly contribute to whole-rock permeabilities, particularly within anticlines. Bedding-plane stylolites with separations opened during Laramide folding contribute to lateral permeabilities. Small-scale thrust, reverse, and normal faults, which crosscut confining strata within folds, provide the most important vertical pathways for fluid migration in foreland basins.

Ground-water circulation in the Wyoming foreland artesian basins is primarily parallel to bedding. Circulation patterns take advantage of the highly transmissive fracture zones, in many cases solution enhanced, along the crests of anticlines. The tendency for circulation to converge on the permeable anticlinal crests and orient parallel to trend is reinforced by the presence of the large-displacement faults that occur in the cores of anticlines and preclude circulation perpendicular to trend.

The potential for ground-water recharge to Wyoming foreland basins is regulated by the basin-margin architecture imposed by Laramide tectonism. Range-bounding thrust faults along almost half the basin margins fully sever the lateral continuity of aquifers between mountain recharge areas and the basin interiors. In contrast, Laramide anticlines that trend across unsevered basin margins hydraulically link the mountain recharge areas with the deep basins. The fracture-enhanced permeabilities along the crests of such anticlines serve as important recharge conduits.

Vertical circulation within the Wyoming artesian basins is very limited owing to the presence of areally extensive, thick confining strata. The vertical circulation pathways that do exist usually are fractures and faults within Laramide anticlines. These vertical conduits can link two or more aquifers or they can link several aquifers to the land surface. The latter explains the discharge of waters that originate from several aquifers in the underlying Paleozoic section through springs such as the Thermopolis Hot Springs in the Bighorn Basin.

Huntoon, P.W., 1993, The influence of Laramide foreland structures on modern ground-water circulation in Wyoming artesian basins, *in* Snoke, A.W., Steidtmann, J.R., and Roberts, S.M., editors, Geology of Wyoming: Geological Survey of Wyoming Memoir No. 5, p. 756-789.

Introduction

The objective of this article is to summarize how ground-water recharge into and regional circulation through Paleozoic rocks in Wyoming foreland basins are strongly influenced by the presence of thrust faults and reverse-fault-cored anticlines developed during Laramide contraction.

Laramide deformation not only shaped the perimeters of the foreland basins, but caused internal deformation within them as well. This deformation and accompanying erosion established the hydraulic boundaries for areally extensive ground-water circulation systems in the basins. In addition, the deformation produced highly localized zones of large but anisotropic permeabilities that strongly influence circulation patterns and rates within the basin interiors.

The primary focus of this discussion is the tectonic enhancement or diminution of permeabilities in Laramide structures—structures which are shortening features that owe their development to horizontal compression. A tenet underlying this work is that when it comes to permeability enhancement, any fracture is generally better than none, recognizing, of course, that subsequent diagenesis can close fracture openings or seal fracture surfaces.

A rather consistent view emerging from this work is that fracture permeabilities are maximized in zones of extension and minimized in zones of shortening. Despite the fact that Laramide foreland structures formed in a regionally compressional tectonic environment, highly localized zones within them have undergone extension. The implication for ground-water exploration is that large, tectonically imprinted permeabilities are possible where such extension occurred. Extension-fracture permeability generally overwhelms most other classes of permeability and therefore strongly influences regional circulation.

The Madison problem

A serious misconception colors, even plagues, exploration and development hydrogeology in Wyoming. It is the popular and often professional expectation that the Madison aquifer, comprising the Madison Limestone and underlying Paleozoic carbonate rocks, will yield unlimited quantities of water to wells drilled into it. This myth has developed to the point that it now imbues the Madison section with the characteristics of a vast underground reservoir that extends beneath all of Wyoming's basins. The myth has been nurtured by a few spectacularly productive water wells that were completed in saturated, active karst systems in the Madison aquifer within the homoclinal flanks of some Wyoming mountain ranges. The naive extrapolation of these high-yield properties deep into the basins is legitimized by reports of exceptional yields of fluids from the Madison Limestone or underlying carbonates from some petroleum wells drilled into anticlines within the interiors of the basins. With these facts serving as anchors, other evidence seems to be everywhere. For example, the Madison commonly contains dynamic cave systems in alpine and subalpine exposures. Many of the caves swallow entire streams and rivers, the best example of this being The Sinks, along the Popo Agie River south of Lander. In addition, large springs discharge from the Madison Limestone or underlying carbonates along the lower flanks of most Wyoming mountain ranges. The uplifted outcrops of the Madison Limestone are riddled with caves that seem to prove ubiquitous sponge-like cavern permeability, no matter that these holes actually represent shallow surface weathering of ancient paleokarst infillings within the unit.

The truth is that the bulk of occurrences of strata comprising the Madison aquifer in the state, especially the large structurally undeformed sections within the basins, have the permeabilities of tombstones. Large-yield sections are actually quite anomalous and represent a combination of very special geologic conditions to have rendered them permeable. Specifically, the largest permeabilities are associated with modern karsts developed on the flanks of the ranges, or with fractured cores of anticlines within the basin interiors.

Another myth has emerged among some professionals regarding the character of the permeability found in the Madison Limestone. This vision holds that the paleokarst in the upper part of the Madison Limestone is characterized by large permeabilities resulting from interconnected, open caves dating from late Mississippian time when that karst developed. The fact is that the paleokarst, although it adds incrementally to permeability, is generally unimportant because it is largely infilled, collapsed, and cemented. Large, localized Madison permeabilities are attributed primarily to either distinct geologically young karst superimposed on all the carbonates comprising the Madison aquifer or to fracture permeability associated with Laramide and younger orogenesis. Consequently, Wyoming geohydrologists work in an environment where ground-water exploration is as complex as the search for oil. One does not successfully produce ground water from Wyoming's Paleozoic Madison section simply by drilling a hole anywhere into it.

Classic basin circulation

Ground-water circulation in a basin is from areas of greatest to least hydraulic head. Hydraulic head is defined as:

$$h = z + P/\rho g$$

where:

h = hydraulic head,
z = elevation of point of interest in an aquifer,
P = pressure at point of interest in an aquifer,
ρ = density of fluid,
g = acceleration due to gravity.

The lowest hydraulic head in hydraulically interconnected rocks is the lowest elevation of a surface stream in the basin. The greatest heads occupy the recharge areas on the basin perimeters.

Figure 1 illustrates the heads and circulation pattern in an idealized foreland basin. Notice lateral flows dominate. Also notice that heads increase with depth under any given location in the basin. The increase in head with depth is a direct consequence of the successively higher elevations of the outcrops of progressively older units in the recharge areas. The key assumption inherent in this model is that there is hydraulic interconnection throughout the basin. If permeability seals exist either as a result of impermeable facies, structural severing of permeable strata, or diagenetic destruction of permeability, circulation is necessarily diminished or precluded. Highly overpressured or underpressured fluid or gas zones can then develop that are independent of or very poorly linked to the regional ground-water circulation system.

Aquifer architecture within the Wyoming foreland

The large part of Wyoming east of the thrust belt (**Figure 2**) lies within the foreland tectonic province, a region characterized by elongate mountain uplifts that separate deep sedimentary basins. The structural relief on the Precambrian-Paleozoic contact is as great as 6 miles, measured between the tops of the mountains and the depths of the basins. The altitudes of this contact now range from -3.5 to +2.5 miles (e.g., Blackstone, 1990). The Paleozoic strata, which once blanketed the region in flat sheets at or below sea level, are equally deformed.

Paleozoic strata comprise the base of a pre-Laramide sedimentary section that in places exceeds 20,000 feet thick, but which has been largely eroded from the mountain uplifts. Several units in this sequence are regionally important aquifers, most notably the Mississippian Madison Limestone and underlying permeable carbonate rocks, which together constitute the Madison aquifer. The Paleozoic section in the Bighorn Basin shown on **Figure 3** is a good example.

The strata comprising the great artesian aquifers of Wyoming, including the Madison aquifer, traditionally have been viewed as highly permeable, areally continuous units interbedded between confining layers. These layered rocks were envisioned as

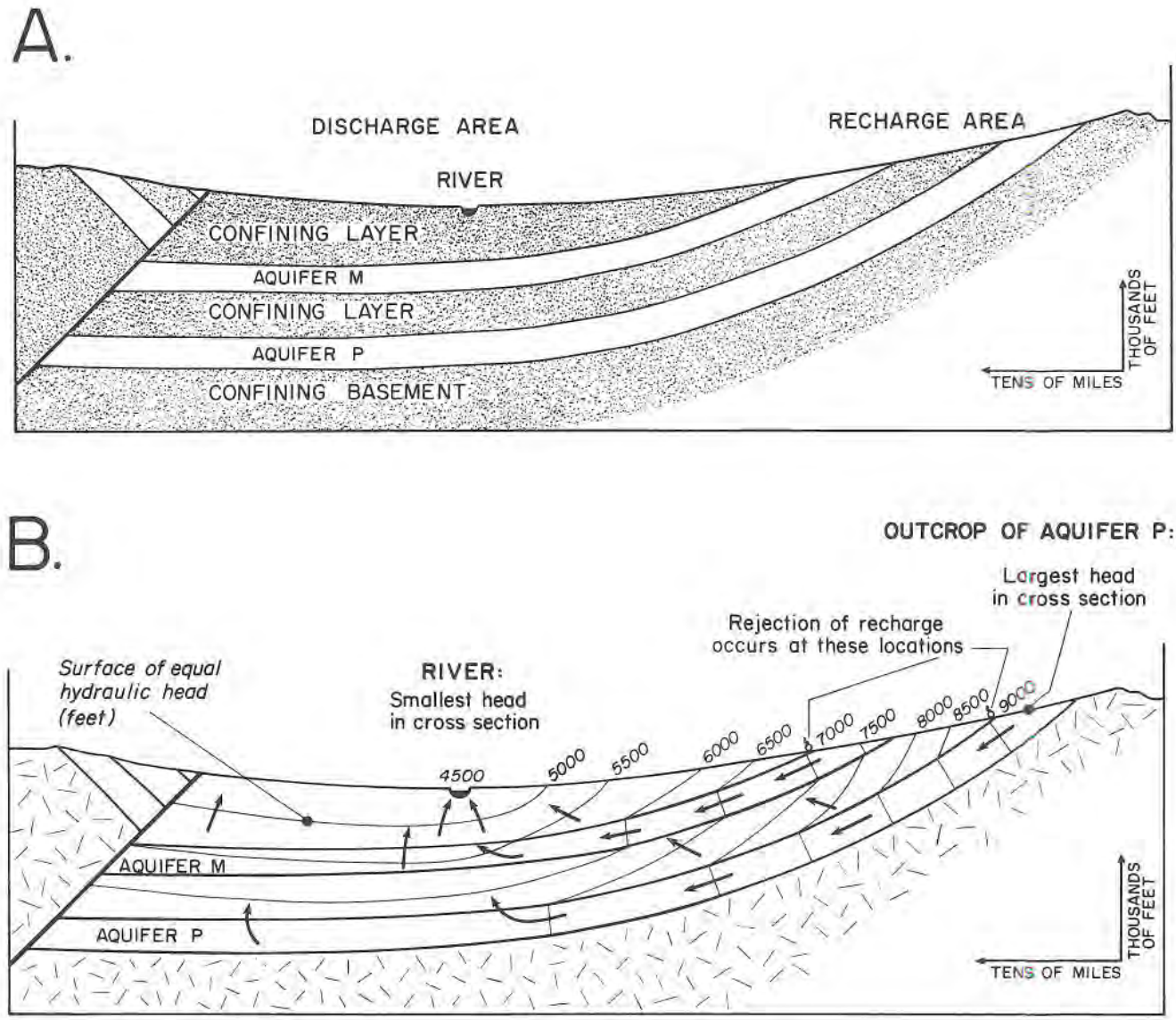

Figure 1. Idealized (A) hydrostratigraphic architecture and (B) head configuration within a profile through a typical Wyoming foreland artesian basin. Notice that the hydraulic heads increase with depth under any point in the basin, thereby producing upward gradients through the section.

folded into broad synclines and anticlines to create Wyoming's basins and mountain ranges. The upturned eroded edges of the aquifers along the perimeters of the basins were imagined to allow for plentiful recharge.

These precepts have been shattered. First, the permeabilities of the Paleozoic rocks comprising the regional aquifers in Wyoming basins generally have been found to be very small to negligible. Large productions tend to be limited to localized zones of large fracture permeability and to zones of modern karstification that are usually restricted to the mountain flanks. Second, the expectation of areal continuity of the aquifers has been successfully challenged.

The prosaic view concerning the areal continuity of aquifers in foreland basins has radically changed, mainly through improved structural models for Wyoming basins developed by oil explorationists. Wyoming's foreland mountain ranges are now known to be uplifts that have ridden up Laramide

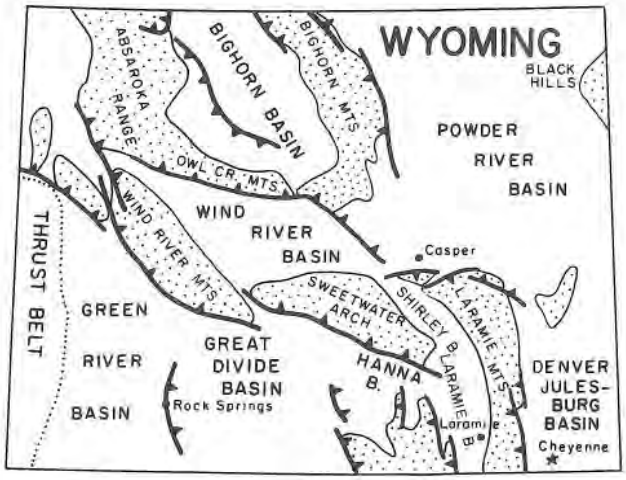

Figure 2. Simplified map showing the locations of foreland uplifts (stippled) and basins in Wyoming. Notice that approximately half of the basin margins are bounded by thrust faults, which sever the hydraulic continuity of the Paleozoic and Mesozoic strata between the recharge areas in the uplifts and the artesian aquifers in the basins.

thrust faults. As shown on **Figure 4**, the configuration that results is an uplift bounded by (1) a fault-severed margin on one flank and (2) a homoclinal dip slope on the other. The basin perimeters in the region are almost equally divided into one or the other of these types. Gone is the model of stratigraphic, and thus hydraulic, continuity between the mountain recharge areas and basin interiors along the fault-severed margins.

The general form of a fault-severed margin is one of large-displacement thrusts that parallel the mountain front (Gries, 1983). Good examples of Wyoming basin margins of this type are the eastern and northern flanks of the Laramie Mountains, the southwestern flank of the Wind River Range, and the eastern flank of the Bighorn Mountains (**Figure 2**). The dip-slip displacements along these range-bounding thrusts is measured in miles, 3 to 6 being rather typical. Obviously, fault severing largely precludes ground-water circulation into the basins. As **Figure 5** illustrates, units comprising the aquifers, such as the Madison section, are fully or partially severed within the thrust-related anticlines, precluding or impeding ground-water circulation perpendicular to trend.

The lateral compression that created the range-bounding thrusts also shortened the sedimentary deposits within the basins. Horizontal telescoping characteristically took place across numerous asymmetric anticlines with thrust or reverse faults in their cores. The faults in the cores exhibit dip-slip displacements that commonly range upward from a thousand feet to a mile or more.

The currently favored model for Wyoming foreland deformation is that the structures represent Laramide shortening caused by horizontal compression. This thesis gained currency with publication of drillhole-controlled cross sections such as those by Berg (1962, 1976) (**Figure 6**) and seismic profiles such as the COCORP line across the Wind River Range (Smithson and others, 1979). The classic papers by Blackstone (1980, 1981) firmly advanced compression as the agent responsible for shaping the Laramide structural basins of Wyoming. Brown's (1987 and this volume) treatise traced the evolution of foreland structural models and comprehensively documented the accumulated outcrop, drillhole, and seismic data used to support a shortening origin.

Emergence of the compressional model brought with it a substantially improved vision of foreland structural geometries, which was in turn employed with great advantage to identify previously unrecognized traps for oil and gas in the deeply buried footwall block below thrust faults (Gries, 1983). These geometric insights radicalized exploration geohydrology by forcing a reassessment of permeability distributions within the province, both as they occur in individual structures and as they impact the lateral continuity of permeable strata (Huntoon, 1985b).

The kinematics of deformation are as important to the geohydrologist as are the resulting geometries. The essence of the kinematic issue is that, in general, extension favors permeability enhancement, whereas contraction diminishes permeability.

Is the foreland environment a geohydrologic writeoff with its omnipotent compressive stress regime? To answer this question, it is necessary to assess the opportunities for localized permeability enhancement within typical foreland structures, as well as to document the magnitude of compression-induced damage elsewhere.

The composite cross sections, reproduced here as **Figures 7** and **8**, respectively, capture the principal classes of mesoscopic structures that, in part, accom-

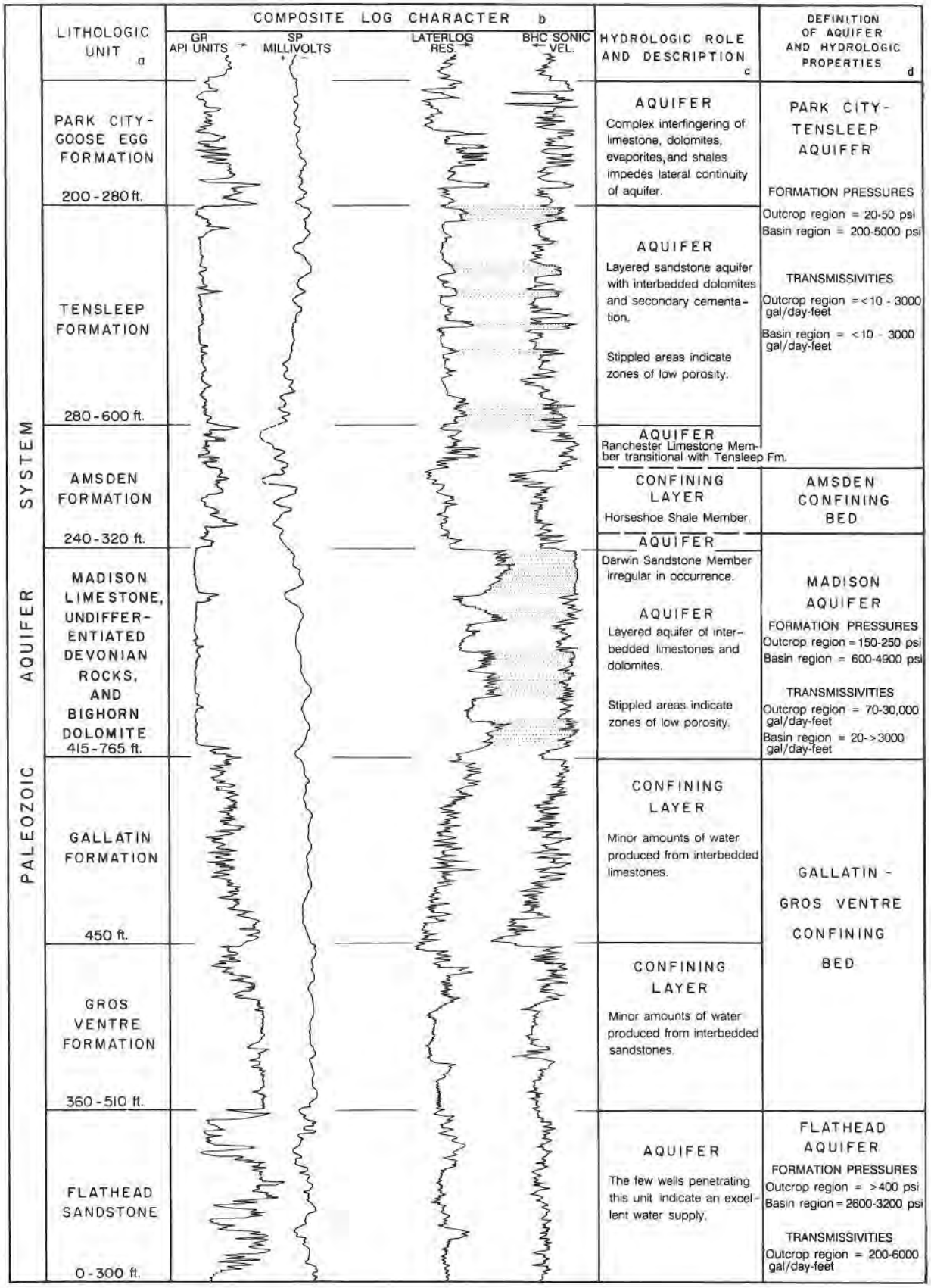
LITHOLOGIC UNIT a
COMPOSITE LOG CHARACTER b
GR API UNITS
SP MILLIVOLTS
LATERLOG RES.
BHC SONIC VEL.
HYDROLOGIC ROLE AND DESCRIPTION c
DEFINITION OF AQUIFER AND HYDROLOGIC PROPERTIES d
PALEOZOIC
AQUIFER
SYSTEM
PARK CITY-GOOSE EGG FORMATION
200-280 ft.
AQUIFER
Complex interfingering of limestone, dolomites, evaporites, and shales impedes lateral continuity of aquifer.
PARK CITY-TENSLEEP AQUIFER
FORMATION PRESSURES
Outcrop region = 20-50 psi
Basin region = 200-5000 psi
TRANSMISSIVITIES
Outcrop region = <10 - 3000 gal/day-feet
Basin region = <10 - 3000 gal/day-feet
TENSLEEP FORMATION
280-600 ft.
AQUIFER
Layered sandstone aquifer with interbedded dolomites and secondary cementation.
Stippled areas indicate zones of low porosity.
AQUIFER
Ranchester Limestone Member transitional with Tensleep Fm.
AMSDEN FORMATION
240-320 ft.
CONFINING LAYER
Horseshoe Shale Member.
AMSDEN CONFINING BED
AQUIFER
Darwin Sandstone Member irregular in occurrence.
MADISON LIMESTONE, UNDIFFERENTIATED DEVONIAN ROCKS, AND BIGHORN DOLOMITE
415-765 ft.
AQUIFER
Layered aquifer of interbedded limestones and dolomites.
Stippled areas indicate zones of low porosity.
MADISON AQUIFER
FORMATION PRESSURES
Outcrop region = 150-250 psi
Basin region = 600-4900 psi
TRANSMISSIVITIES
Outcrop region = 70-30,000 gal/day-feet
Basin region = 20->3000 gal/day-feet
GALLATIN FORMATION
450 ft.
CONFINING LAYER
Minor amounts of water produced from interbedded limestones.
GALLATIN - GROS VENTRE CONFINING BED
GROS VENTRE FORMATION
360-510 ft.
CONFINING LAYER
Minor amounts of water produced from interbedded sandstones.
FLATHEAD SANDSTONE
0-300 ft.
AQUIFER
The few wells penetrating this unit indicate an excellent water supply.
FLATHEAD AQUIFER
FORMATION PRESSURES
Outcrop region = >400 psi
Basin region = 2600-3200 psi
TRANSMISSIVITIES
Outcrop region = 200-6000 gal/day-feet

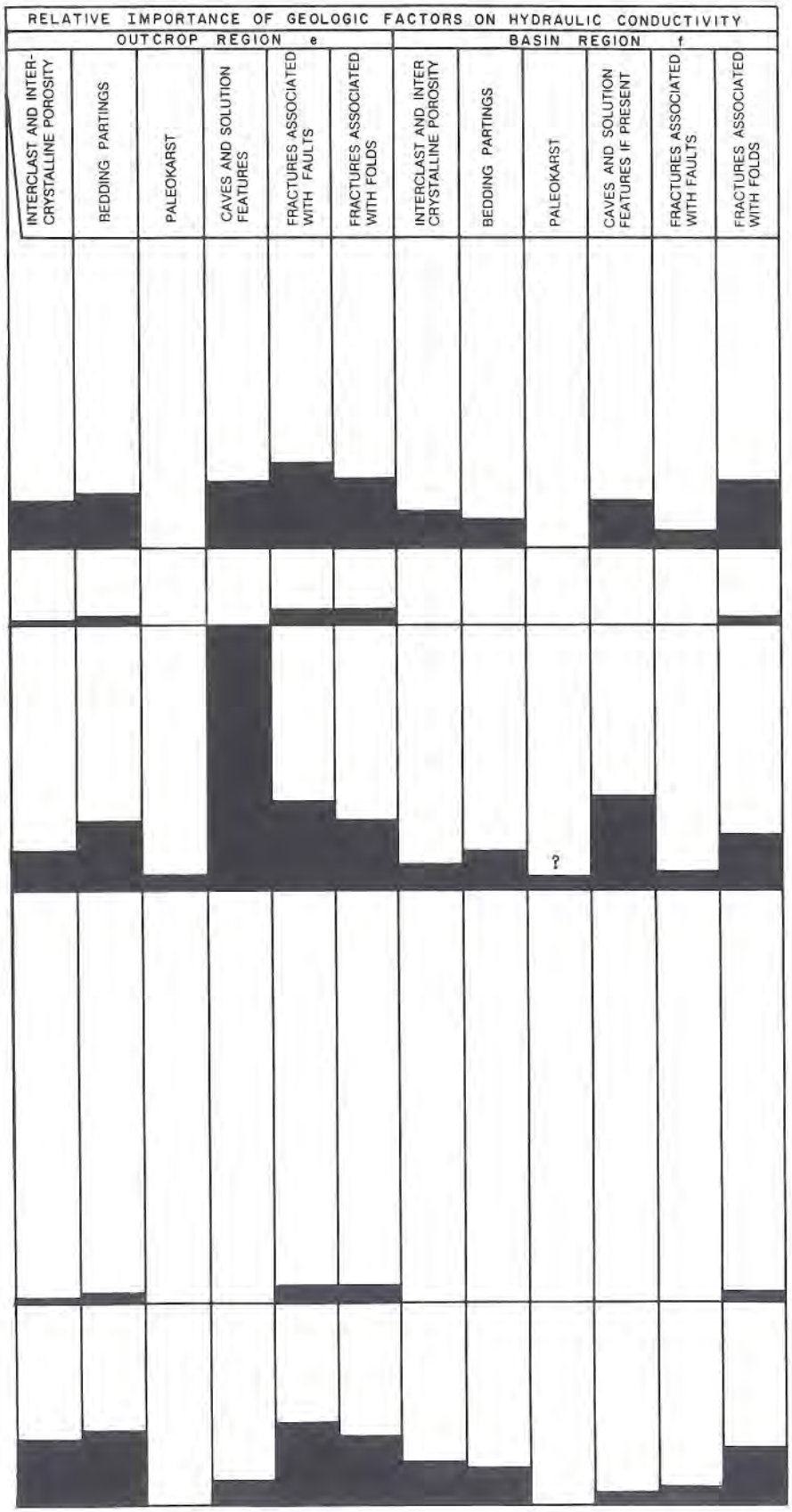

Figure 3. Hydrostratigraphy of Paleozoic rocks in the southern Bighorn Basin, Wyoming. Heights of bars indicate the relative importance of geologic factors on hydraulic conductivity. (Adapted from Jarvis, 1986, figure 9.)

Footnotes:

[a] Thicknesses from Jarvis (1986, figure 3).

[b] Composite log from Parraffine Oil 1 State (SW NE, sec. 9, T42N, R88W) and Husky Oil Worland 1 (NW SE, sec. 12, T49N, R91W) wells.

[c] Summarized from Swenson and Bach (1951), Mankiewicz and Steidtmann (1979), Cooley (1984), well logs, pressure tests, and water chemistry data.

[d] Sources of data: outcrop region -- Burnham and Kelly (1979), Kelly (1980) and Cooley (1984); and basin region -- Wyoming Geological Association (1957), Heasler and Hinckley (1982), and drill stem test data.

[e] Based on field observations.

[f] Based on observations reported in Emmett and others (1971), Morgan and others (1977), Heasler and Hinckley (1982), Andrews and Higgins (1984), and borehole televiewer logs of well in SE NE SE, sec. 6, T57N, R87W.

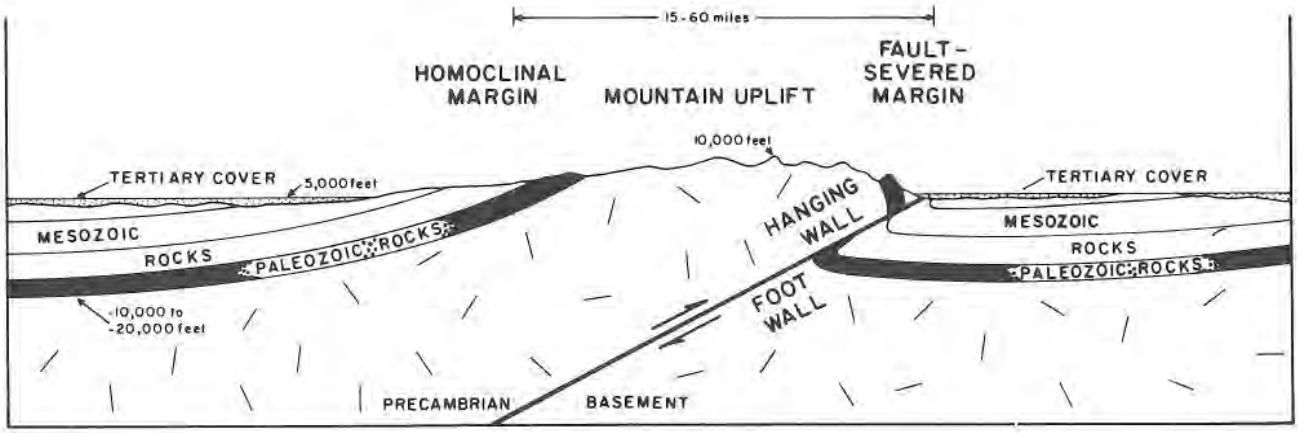

Figure 4. Schematic cross section through a Wyoming foreland uplift showing the style of deformation that produced approximately equal percentages of fault-severed and homoclinal basin margins. Notice that the thrust fault subcrop is basinward from the flank of the range, where it is buried by Tertiary rocks. (From Huntoon, 1985a.)

modate and accompany folding in the thick sedimentary sections involved in foreland fault-cored folds. Notice the overwhelming dominance of shortening (compressive) faults at the mesoscopic scale.

The impact of compressional tectonism on permeability was not always negative. Consider that many of the small-scale faults in fault-cored Laramide folds crosscut confining strata, which improves vertical permeabilites. Also consider that parts of the folds have actually undergone extension during folding, which improves permeabilities along trend. Small-scale faults that crosscut strata have the potential for providing vertical circulation pathways through regional confining strata. More important are extensional fractures along anticlinal crests, which provide highly transmissive lateral circulation pathways parallel to trend.

The Bighorn Basin (**Figure 9**) contains excellent, well-documented examples of permeability architectures, found throughout the Wyoming foreland province. Consequently, Bighorn Basin examples will be the focus of much of the following discussion.

Permeability anisotropy

Cross joints and through-going joints oriented parallel to the crest compete for permeability dominance within the Bighorn Basin anticlines. The cross joints dominate in Garland and parts of Little Sand Draw anticlines cited by Hurley (1990), so in those fields the maximum principal permeability tensor is locally oriented perpendicular to trends of the fold axes and parallel to bedding. In contrast, at Sheep Mountain, dissolutional widening along the through-going joints has resulted in a maximum principal permeability tensor oriented parallel to trend and parallel to bedding.

It is my opinion that maximum principal permeability tensors within the carbonate sections eventually became oriented parallel to trend in anticlines that contained dynamic ground-water circulation systems, regardless of the orientations of the maximum principal permeability tensor immediately following Laramide tectonism. Laramide extensional fracturing, both parallel and perpendicular to trend, increased permeabilities along the anticlinal crests significantly above permeabilities in adjacent undeformed rocks. This localized permeability enhancement caused circulation to converge on and concentrate along the anticlinal crests. The presence of faults in the anticlinal cores, which severed the hydraulic continuity of the aquifers perpendicular to trend, ensured that the flow roughly paralleled the crests. Dissolution accompanying circulation then preferentially widened the fractures oriented parallel to the crest. This process produces a permeability regime in which the maximum principal permeability tensor in the crest is parallel to the trend of the anticline.

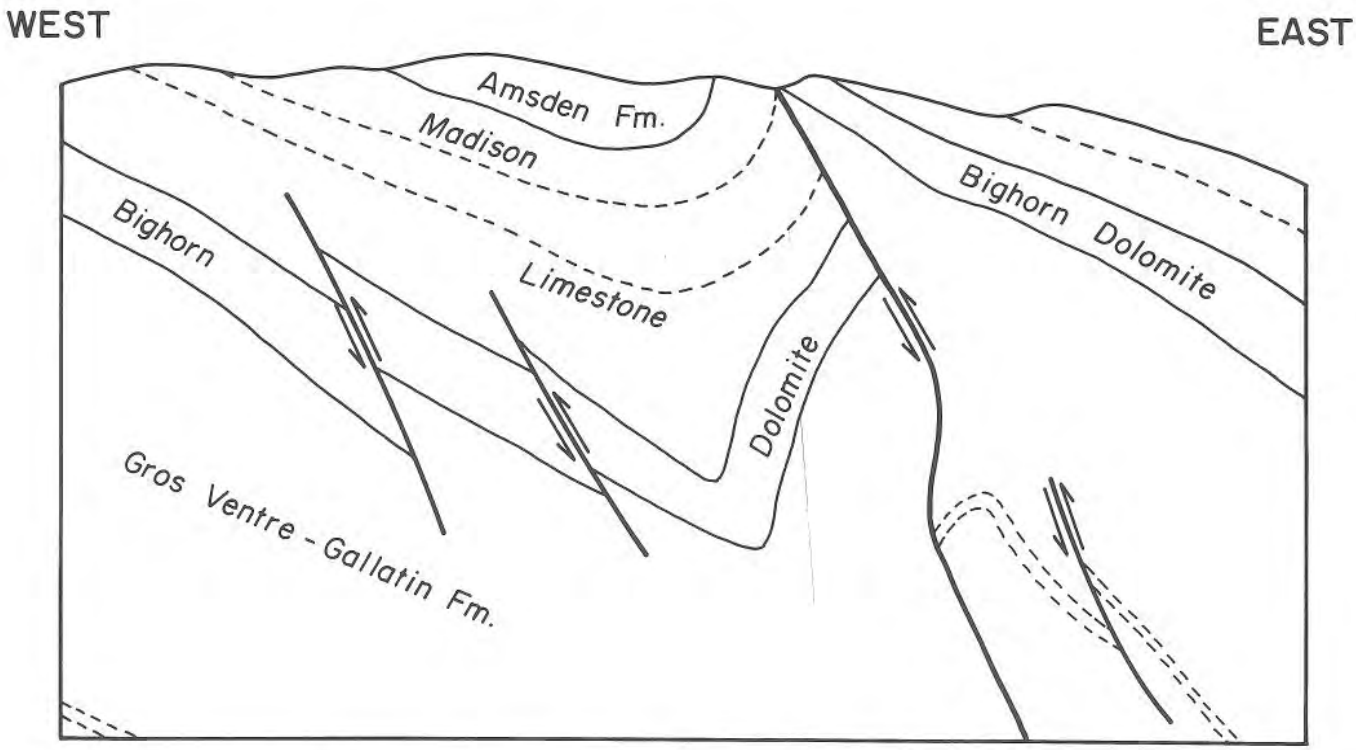

Figure 5. Profile across the Wolf Creek thrust-cored anticline along the east flank of the Bighorn Mountains west of Wolf, Wyoming, in which the Paleozoic carbonate section is partially severed. There is approximately a half mile of dip-slip displacement along this thrust fault, in contrast to 3 to 6 miles along a typical range-bounding thrust fault in the Wyoming foreland province. View is toward the north.

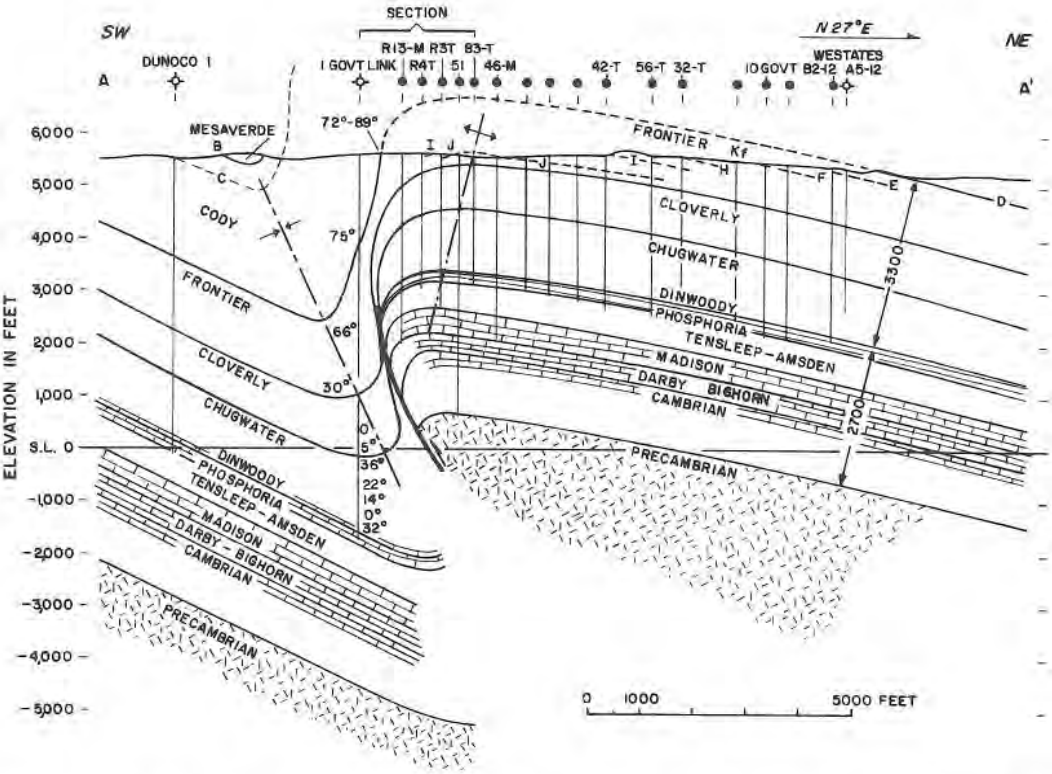

Figure 6. Drillhole-controlled cross section by Berg (1976) through Hamilton Dome, Bighorn Basin, Wyoming, illustrating that (1) this type of Laramide anticline developed above a reverse fault in the basement, (2) Precambrian rocks in the hanging wall overlie potential producing strata in the footwall, and (3) faults sever the Paleozoic carbonates perpendicular to the trend of the anticline. Dips in #1 Govt Link well are from dipmeter measurements. (Redrafted and reprinted by permission.)

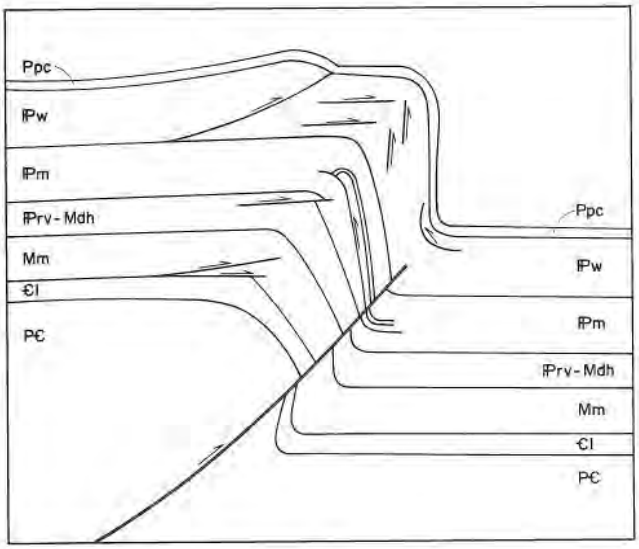

Figure 7. Composite cross section by Bernaski (1985, figure 23) through a Laramide fault-cored fold in the southeastern Uinta Mountains, southwestern Colorado and northeastern Utah, showing styles of mesoscopic faulting within the Paleozoic section that accommodated some of the shortening across the structures.

EXPLANATION

IPpc	Permian Park City Formation
IPw	Pennsylvanian Weber Formation
IPm	Pennsylvanian Morgan Formation
IPrv-Mdh	Pennsylvanian Round Valley Limestone and Mississippian Doughnut and Humbug formations
Mm	Mississippian Madison Limestone
€l	Cambrian Ladore Formation
P€	Precambrian rocks

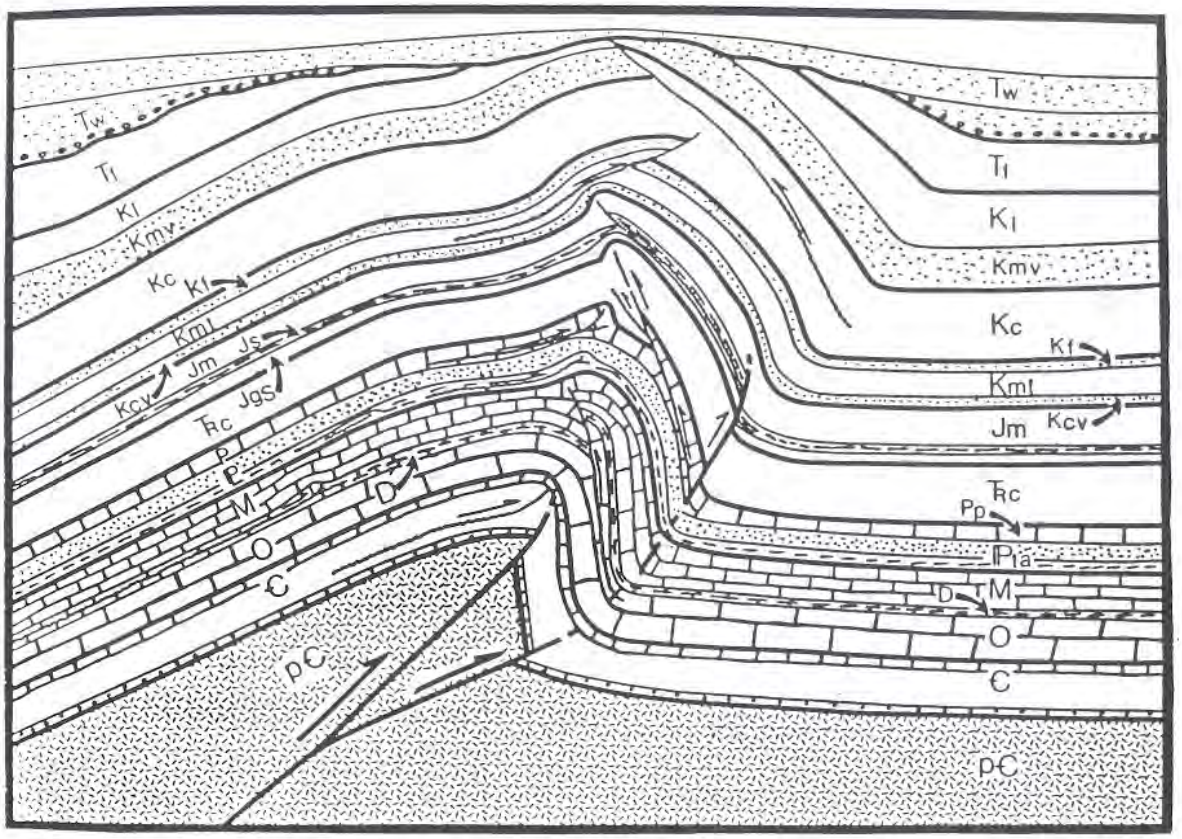

Figure 8. Composite cross section by Brown (1987, figure 47) through a typical Laramide fault-cored anticline in the Wyoming foreland province, showing mesoscopic faults including out-of-the-syncline thrusts that accommodated some of the shortening across the structures. (Reprinted by permission.)

EXPLANATION

Tw	Tertiary White River Formation	Jgs	Jurassic Gypsum Spring Formation
Tf	Tertiary Fort Union Formation	Ꞧc	Triassic Chugwater Formation
Kl	Cretaceous Lance Formation	Pp	Permian Phosphoria Formation
Kmv	Cretaceous Mesaverde Formation	Pta	Pennsylvanian Tensleep and Mississipian-Pennsylvaniuan Amsden formations
Kc	Cretaceous Cody Shale	M	Mississippian Madison Limestone
Kf	Cretaceous Frontier Formation	D	Devonian rocks
Kmt	Cretaceous Mowry and Thermopolis formations	O	Ordovician rocks
Kcv	Cretaceous Cloverly Formation	Є	Cambrian rocks
Jm	Jurassic Morrison Formation	PЄ	Precambrian rocks
Js	Jurassic Sundance Formation		

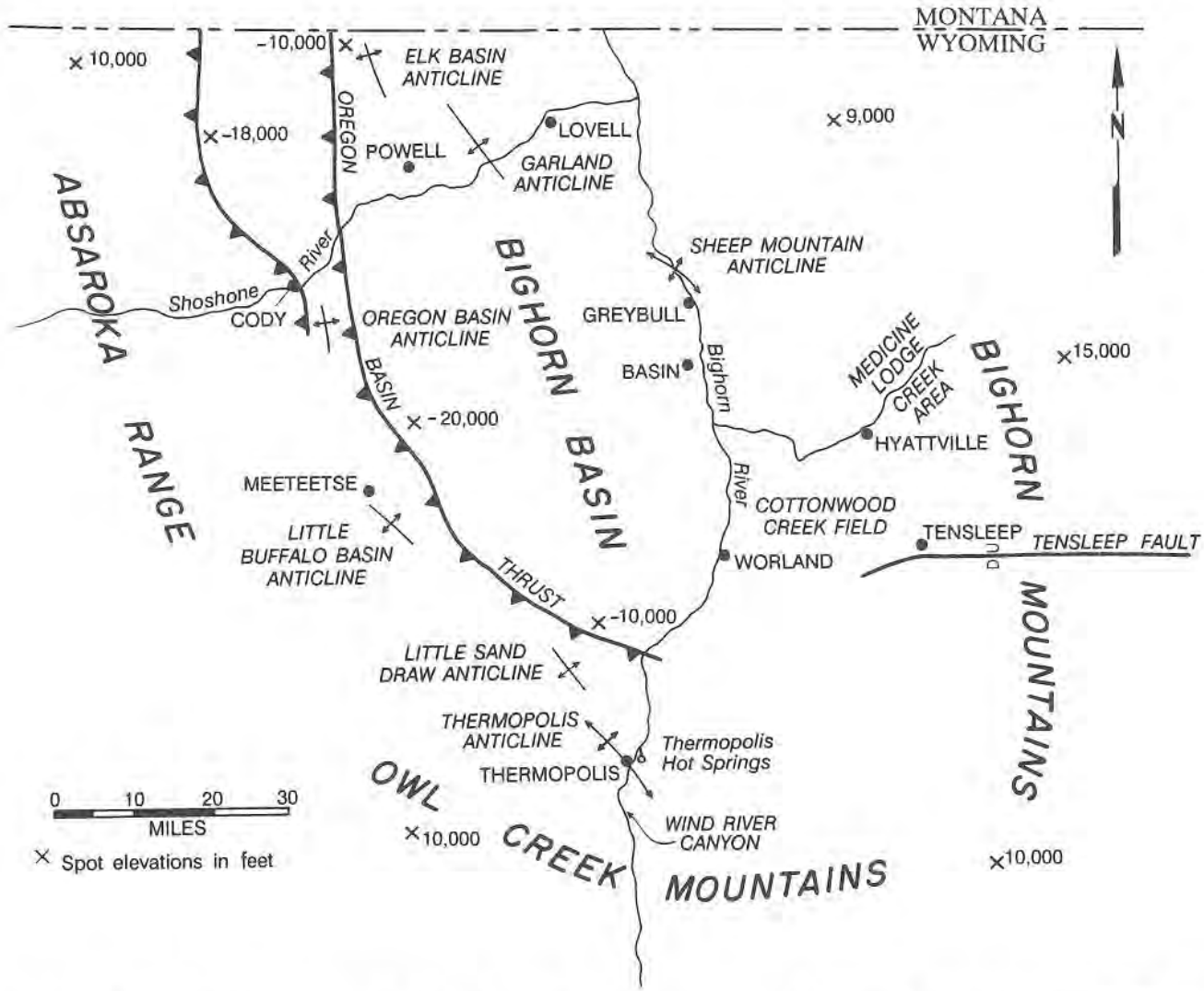

Figure 9. Locations of selected structures in the Bighorn Basin, Wyoming, cited in the text. Spot elevations are for the top of the Precambrian basement (from Blackstone, 1990).

Conversely, the persistence over geologic time of maximum permeability tensors that are oriented perpendicular to trend in carbonate sections implies saturation with static fluids. Consequently, it is conceivable that directional permeabilities could become zoned within an anticline where the maximum principal permeability tensors were originally oriented perpendicular to trend. For example, if a static oil reservoir developed above a dynamic groundwater system, the static oil would preserve the original anisotropy. However, the maximum principal permeability tensor in the underlying ground-water system would eventually reorient to a direction parallel to trend as dissolution proceeded in that zone.

Enhancement of vertical permeability in fractured anticlines

To this point, attention has focused on the role of fractures, particularly vertical extension joints, in increasing lateral permeabilities along the crests of foreland anticlines. Fracturing is also important in creating vertical hydraulic connections between aquifers within the crestal parts of the anticlines, manifested as vertical integration of oil pools in many Bighorn Basin fields and in a few cases by localization of springs in the cores of the anticlines, which derive water from several underlying Paleozoic units. Both vertical extensional joints and variously dipping faults are involved. Many small-scale

thrust faults associated with shortening within foreland anticlines are potential conduits, particularly those shown on **Figures 7** and **8**, which crosscut formations and thus fracture through confining strata. Some transmit fluid even though they formed under compressional stress regimes and are not as open as the fractures formed under extension. The point is that a small-scale fault through a confining bed is potentially more permeable than no fault, regardless of kinematic origin. This is borne out in the field by alteration along some of these shortening faults, commonly in the form of chemically reduced zones extending away from the fracture surfaces, which demonstrate past fluid circulation.

The role that subsidiary faults and vertical fractures play in hydraulically linking multizoned oil pools within the Paleozoic section along the crests of many Bighorn Basin anticlines was comprehensively documented by Stone (1967). The primary evidence used by Stone to demonstrate such communication is (1) the similar chemical composition of the crude oils and (2) similar quality of the associated formation waters within each anticline, regardless of producing horizon. Cooley (1986), Jarvis (1986), and Spencer (1986) used similarities in ground-water quality and common hydraulic heads within stacked aquifers as evidence for vertical circulation between Paleozoic zones within various Bighorn Basin anticlines. Hinckley and others (1982) found virtually isothermal conditions in temperature profiles within the Paleozoic section in the Thermopolis anticline, revealing vertical circulation inclusive of at least the Madison and Park City (Phosphoria) formations in that structure.

Incomplete summary data in Jarvis (1986) and Spencer (1986) from the aquifers in the Paleozoic section in the Bighorn Basin anticlines indicate a tendency for the degree of vertical hydraulic interconnection to increase proportionately to the offset on the basement fault that produced the anticline. This tentative conclusion appears plausible because fractures within the fold serve as the primary vertical hydraulic conduits, and the degree of fracturing within the fold increases with displacement on the fault.

The finding by McCaleb and Willingham (1967) that extensional fracturing is enhanced in the more brittle carbonate Phosphoria facies as contrasted to the shale facies within the Cottonwood Creek field implies that, given two similar structures, greater opportunities for vertical interconnection should be expected in the structure containing brittle facies. Consistent with this line of reasoning is Stone's (1967) observation that the thick, ductile, lower Mesozoic section serves as a regional confining layer, even where sharply folded, thus largely isolating ground-water circulation in the Paleozoic rocks from those above.

Oblique fracturing in anticlines

Subsurface faulting, much of it rather small scale, that is oblique to the trends of anticlines within foreland basins is known to disrupt fluid circulation along the crests of some anticlines. The result is localized compartmentalization within producing oil fields. A good example is the Tensleep reservoir in the Oregon Basin fold in the Bighorn Basin, in which Morgan and others (1977) found that obliquely striking faults divide the reservoir into several hydraulically disconnected production zones.

Fractures in petroleum reservoirs

The importance of extensional fractures on permeability enhancement in the crestal parts of Bighorn Basin anticlines has been recognized by the petroleum industry (Harris and others, 1960; Stone, 1967). However, various workers have found that not all classes of fractures contribute to permeability. For example, Morgan and others (1977) reported that small-scale vertical fractures in well-indurated parts of the Tensleep Sandstone in the Oregon Basin anticline have little impact on whole-rock permeability, and in fact, permeabilities are decreased in directions normal to the fracture surface. Similarly, Emmett and others (1971) found that small, vertical, closed fractures in the Tensleep Sandstone in the Little Buffalo Basin anticline do not contribute significantly to permeability, and permeabilities perpendicular to the fracture surfaces are decreased between 10 and 30%. The fractures examined in cores from the Tensleep Sandstone in Little Buffalo Basin field exhibited impediments to flow including: lining with shale and filling with anhydrite, fine-grained sand or silt, and asphalt residue. This type of fracture appears to be analogous to the sealed small-scale vertical fractures and microfractures observed in outcrops of the Madison Limestone in Sheep Mountain anticline (to be described below).

Emmett and others (1971) also encountered open extensional fractures in cores recovered from the Tensleep Sandstone at Little Buffalo Basin anticline, which contrast sharply in character to the small-scale closed fractures:

> *Core from north-end Well 62 was almost continuously fractured, and upon completion it produced 100 percent water even though analysis of the matrix rock indicates it should produce oil. Historically, producing wells in the north and west area of the field, where there is a preponderance of open vertical fractures, at first produced clean oil but soon began producing water.*

Obviously the extreme permeabilities of such fractures, in contrast to the small permeability of the matrix, allowed ground water from below to quickly invade the oil-saturated zone and bypass the oil-saturated matrix. These same fractures were shown by Emmett and others (1971) to have lateral continuity based on rapid gas breakthroughs between a natural-gas injection well and producing wells located along the strike of the fractures. The practical issue faced in developing the Little Buffalo Basin field was that permeabilities resulting from extensional fracturing in the Tensleep Sandstone caused premature watering out of production wells. Only 4.5% of the oil in place was recovered by primary production.

McCaleb and Willingham (1967) used gas- and water-injection test results to document the importance of permeability enhancement along extensional fractures within the Phosphoria Formation dolomites in the Bighorn Basin Cottonwood Creek field. Such findings were generalized by Stone (1967) as follows:

> *Prominence of fractures in the Paleozoic carbonate and calcareous sandstone is shown by core information from all productive formations. Fractures, usually "bleeding oil," are described from cores of producing zones in every Bighorn Basin Paleozoic field; below the oil-water interface, "dead oil" or "asphalt" stains in the fractures commonly are described.*

An excellent paper by Hurley (1990) draws appropriate and needed attention to the contribution to permeability made by fractures oriented orthogonally and obliquely to the fold axis in producing anticlines in the Bighorn Basin. His observations are based on fracture orientations in outcrops at Sheep Mountain anticline (**Figure 10**) and on fracture and permeability data from subsurface cores, a fracture logging tool, and interference tests in Paleozoic reservoir rocks in the Garland and Little Sand Draw anticlines. Although he found that fracture densities are greatest along trend, fracture aperture measurements and interference testing in the Garland and Little Sand Draw anticlines reveal that the orthogonally and obliquely striking extensional fractures have greater permeabilities. He concludes: *Fractures with the greatest effect on short-term fluid flow trend roughly perpendicular to fold axes.* He states further: *Permeability anisotropy would probably be aligned roughly parallel and perpendicular to the fold axis.* Open extensional fractures with orientations perpendicular or oblique to the trends of the two anticlines were attributed to extension within the crest resulting from the doubly plunging geometries of the folds.

Permeability in synclinal hinges

Deformation in the steeply dipping limb and adjacent synclinal hinge of foreland fault-cored anticlines was not conducive to the development of open fractures. Consequently, ground-water and oil production from these parts of the fold are diminished. The Paleozoic rocks in the steep limb tend to be highly deformed, characterized by dips that increase with depth and bedding that is attenuated in thickness (Berg, 1976). Emmett and others (1971) found that the Tensleep Sandstone is thinned by only approximately 10% on the flank of Little Buffalo Basin anticline, yet hydrocarbon production from the thinned strata is roughly 1% of that in the non-attenuated strata. The rocks in such synclines are highly compressed, and exhibit tight, small-scale folding and out-of-the-syncline thrust faulting where the sense of motion is that of transporting rocks away from the syncline (see **Figure 8**). The Laramide compressional stresses within the synclines adjacent to typical foreland fault-cored anticlines tended to destroy interstitial porosity and to tightly compress the opposing sides across fractures, both of which diminished permeabilities.

Figure 10. Exposures of Paleozoic rocks in Sheep Mountain anticline, Bighorn Basin, Wyoming. Cliffs facing the 760-foot-deep Sheep Canyon are the Madison Limestone. View is toward the southwest.

Permeabilities in homoclinal basin margins

Homoclinal margins (**Figure 4**), characterized by stratigraphic and thus hydraulic continuity between the mountain uplifts and basin interiors, appear made to order for conducting large volumes of water into the major aquifers in the basins. Examples of this type of margin are found along the flanks of the Black Hills, west flank of the Laramie Mountains, and parts of the west flank of the Bighorn Mountians (**Figure 2**). In reality, recharge through the homoclinal margins is surprisingly meager. The problem is that transmissivities decrease basinward (Bredehoeft, 1964; Head and Merkel, 1977). The result is that regardless of rock type, most of the water that infiltrates outcrops in the recharge areas discharges from springs located at the toes of the dip slopes (Huntoon, 1985b). The water is thus rejected from the aquifers before it can become trapped beneath overlying confining beds and enter the artesian systems within the basins (Mancini, 1976). The potentiometric surface flattens appreciably basinward from the points of rejection. In some cases the basinward gradients are a tenth of their slope within the homocline (Lundy, 1978).

Rejection of recharge makes sense in the context of the diametrically opposed diagenetic environments between the outcrops and basin parts of the system. Since these regions became differentiated in Laramide time, permeabilities in the recharge areas have been increasing through dissolution. Wholesale modern karstification of the carbonate sections in the homoclines is common. A good example is the cave networks that drain and are spatially restricted to the Paleozoic carbonate section within the west flank of the Bighorn Mountains (Huntoon, 1985c). Dissolutional enlargement of pores also takes place within the clastic units such as in the Tensleep or Casper aquifers, where soluble cements are removed. Such dissolution is facilitated by the good-

quality waters that circulate through these upland parts of the system.

In contrast, the basin parts of the system are characterized by a diagenetic environment undergoing recrystallization, cementation, and compaction, all operating to destroy permeability. The rates of solutional enhancement of permeabilities within the basins are substantially less than those in the recharge areas. Todd (1963) documented decreases in permeability in the Tensleep aquifer in the Bighorn Basin resulting from precipitation of coarse dolomite in pore spaces in post-Laramide time. Similarly, Mankiewicz and Steidtmann (1979) found that Tensleep permeability is being lost through calcite pore filling and anhydrite and silica fracture filling. McCaleb and Wayhan (1969) observed that Laramide fractures in the lower parts of the Madison Limestone in Elk Basin field are filled, in order of abundance, by anhydrite, quartz, and dolomite. They also observed that fractures in the upper part of the Madison section in closer proximity to the paleokarst zone are filled with clays derived from both insoluble limestone residues and the overlying Amsden Formation.

One consequence of the differences in diagenetic regimes between the uplifted and basinal parts of homoclines is that permeability contrasts have been accentuated with time between the two regions. The deterioration of permeability basinward has important ramifications because the small permeabilities in the basin region govern basinward circulation rates, and thus recharge. Even with hydraulic continuity within the homocline, recharge rates are small owing to the reduced permeabilities basinward.

In contrast, the parts of the homoclines up dip from the basin perimeter are now sites of very active ground-water circulation. The waters involved have among the finest qualities found in the foreland province and are actively dissolving their host aquifers. Permeability enhancement in the homoclines is not uniformly large, although net increases can be expected almost everywhere over background perme-abilities found in the same rocks in the basin interiors. Permeability enhancement has been, in part, proportional to the total volume of ground water that has circulated through the rocks since Laramide uplift. Consequently, those parts of the homocline favored with the highest circulation rates tended to develop the largest dissolution permeabilities.

The steepest hydraulic gradients and greatest permeabilities in homoclines occur in carbonate rocks in close proximity to and under deeply incised canyons, which trend downdip across the homoclines and which have breached the overlying confining strata (Huntoon, 1985c). Caves in the Bighorn-Madison section have developed in greater number and larger size under the canyons than in the intercanyon parts of the broad homocline on the west flank of the Bighorn Mountains. However, cavern development under the canyons abruptly diminishes beyond the points in the floors of the canyons where the Bighorn-Madison section dips into the subsurface beneath the Amsden confining strata. The caves do not continue into the basin because water is rejected through springs along the floors of the canyons at these points.This results in a sharp basinward decrease in gradient that inhibited cavern dissolution in the geologic past.

Ground-water exploration efforts tend to focus on the homoclinal basin perimeters because production rates and water qualities are good. The liability of these sites is twofold: (1) circulation rates are large, and thus the systems are particularly sensitive to degradation by upslope pollution sources and detrimental land-use practices; and (2) these sites are usually connected hydraulically to fully appropriated surface streams.

An example of system sensitivity was revealed by dye tracings in the Medicine Lodge Creek area on the west flank of the Bighorn Mountains (**Figure 9**). Here, water lost to sinkholes in upland areas travels at surface-water velocities through open caves in the Bighorn-Madison section to springs at the toes of the homocline (Vietti, 1977; Huntoon, 1985c). Travel times through these karst systems are a matter of several hours to days over distances of 5 miles or more.

At Natural Bridge, on the north flank of the Laramie Mountains, Anderson and Kelly (1987) documented that direct hydraulic connection can exist between a water well drilled into a fracture zone in a basinward-plunging anticline and a nearby stream. Their example involved a 900-foot-deep well drilled into the Casper-Madison carbonate section along the crest of a sharply folded anticline. The well is located approximately 1/2 mile downdip from exposures of the Casper Formation along the crest of the fold in the bed of La Prele Creek. Pumpage from the well caused depletions in stream flow within

hours of the onset of production. After 21 days, at a pumpage rate of 2,600 gallons/minute, depletions from the stream had gradually progressed to 1,400 gallons/minute. The streamflow recovered when pumping stopped.

Madison permeability in Sheep Mountain anticline

The magnificently exposed outcrops of the Madison Limestone in the core of Sheep Mountain anticline, through which large volumes of fluids have circulated, serve as a vehicle for differentiating among the classes of permeability found in a foreland fold. The contribution to total Madison permeability attributable to intercrystalline porosity is very small. Consequently, a detailed petrographic treatment is not warranted, and the discussion can focus on the nonstratigraphic elements.

Sheep Mountain anticline (**Figure 10**) is located along the Bighorn River in the northern Bighorn Basin (**Figure 9**). The anticline is a northwest-trending, doubly plunging, 15-mile-long, asymmetric, east-verging structure with over 4,000 feet of structural relief (Harris and others, 1960). Some dips on the east limb approach vertical. Hennier and Spang (1983) consider the fold to have developed largely through flexural slip in a compressive stress regime. Bed lengths and thicknesses are fairly uniform over the fold, although the thickness of at least the upper part of the Madison Limestone is attenuated on the east limb by 15 to 20% or so in outcrops in Sheep Canyon.

The 760-foot-deep Sheep Canyon, carved by the Bighorn River, combines with the Burlington Northern railroad cut along the northwest canyon wall to provide virtually unsurpassed exposures of key permeability elements within the Madison Limestone. In order to place fracture enhancement of permeability, especially that due to extensional fracturing, into perspective, it is important to identify all classes of permeability present in the unit. Consider first the Madison paleokarst zones of nontectonic origin.

Madison paleokarst

At least two prominent, laterally extensive paleokarst zones developed one above the other in the upper third of the Madison Limestone during late Mississippian time (Sando, 1974). A similar paleokarst in the Madison- equivalent Redwall Limestone in the Grand Canyon of Arizona is infilled with Chesterian sediments (McKee and Gutschick, 1969; Billingsley and Beus, 1985), thus providing timing for the karstification.

The paleokarst zones in both Wyoming and the Grand Canyon presently contribute very little to whole-rock permeabilities within the Madison Limestone because of the poor hydraulic interconnectedness within the paleokarst zones. The karstic permeabilities were largely destroyed through cementation or infilling with younger sediments, and, to a lesser degree, by collapse and compaction. The paleokarst certainly increases Madison permeabilities, but its total contribution ranks as minor in comparison to that of certain classes of overprinted tectonic fractures.

The Madison paleokarst zones developed as a result of one or more episodes of uplift that raised the Madison surface above sea level. Ground-water circulation through the Madison Limestone under unconfined conditions pervasively dissolved two prominent paleokarst horizons that crop out at Sheep Mountain. The upper involves a section approximately 50 feet thick and the lower a section from 100 to 250 feet thick. Dissolution within each appears to have spread from a labyrinth of horizontal intersecting caves that were localized in permeable strata along joints and bedding. As shown on **Figure 11**, a dissolution front at the base of the lower paleokarst zone extends variable distances downward into the massive limestones at Sheep Mountain anticline, thus explaining the variable thickness of the lower paleokarst section. An analog for the environment that produced the Madison paleokarst is the modern karst in the flat-lying limestones that crop out over the Yucatan Peninsula in Mexico.

The most highly dissolved zones in the Madison paleokarst horizons at Sheep Mountain are readily identified as laterally extensive, pervasively brecciated limestones that commonly erode into benches

near their bases and massive cliffs above. Cavities and small amphitheaters have eroded into the incompletely cemented, less resistant basal breccias. The breccia clasts at Sheep Mountain are typically fist size, but larger clasts measuring up to several feet across are present. The clasts are from collapse of roof rock and disaggregation of the dissolved strata. The infilling cement is generally a microcrystalline limestone, possibly an indurated lime mud. The bedding overlying the paleokarst zones at Sheep Mountain is only slightly deformed by differential sag into the karst below, yet stratigraphic thinning within the dissolution zone must have been quite significant.

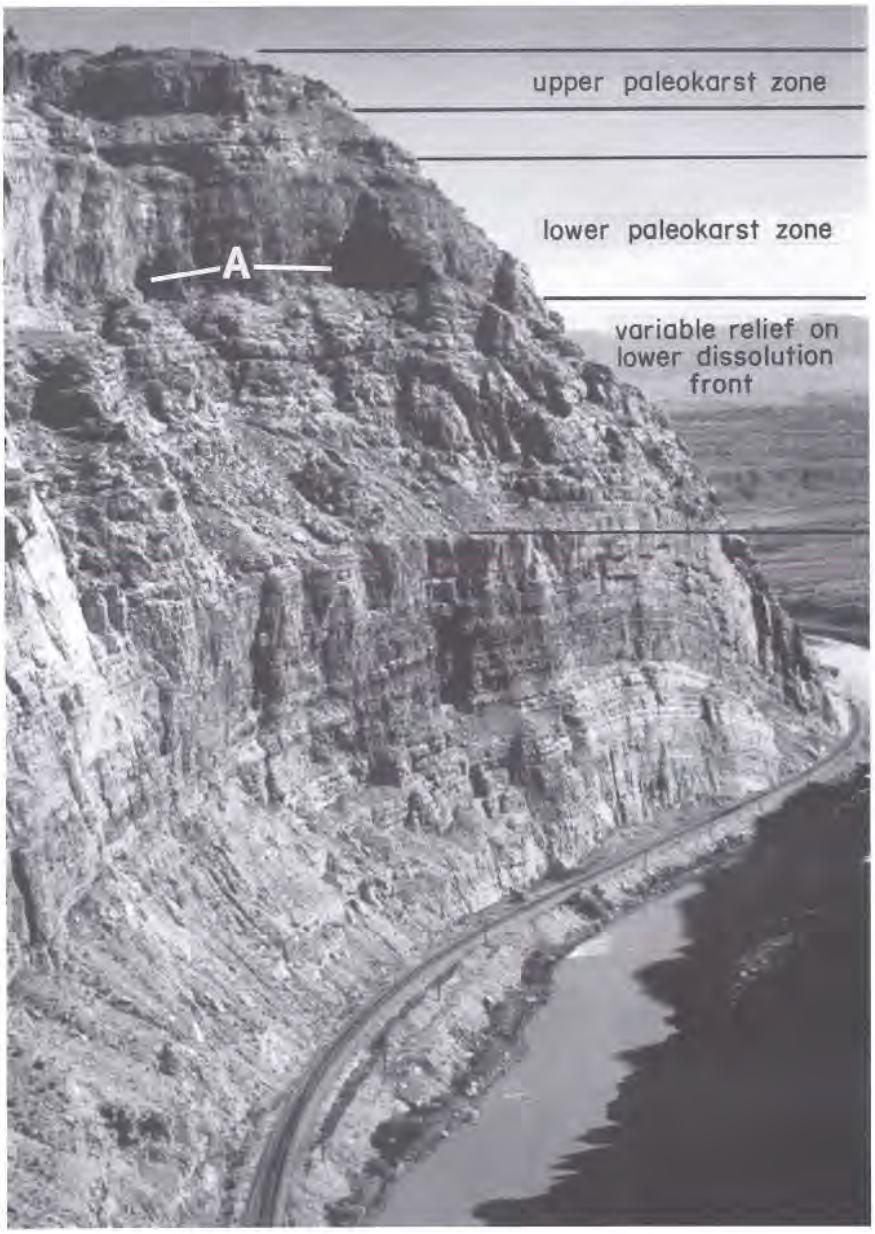

Figure 11. Madison Limestone cliff on 760-foot-high northwest wall of Sheep Canyon, Wyoming, with the two most prominent paleokarst zones identified. Reentrants labeled A are eroded from massively bedded dissolution paleokarst breccias. View is toward the northeast.

Limestone beds overlying the Madison paleokarst in outcrops along the Medicine Lodge creeks, 35 miles to the southeast (**Figure 9**), exhibit a greater degree of collapse and disaggregation. Collapse and stoping features extend upward from the paleocavities, infilled sinkholes connect the cavities to the Mississippian-Pennsylvanian erosion surface, and the roof rocks over the paleokarst zones are differentially tilted, subsided, and faulted on a small scale. In both the Sheep Mountain and Medicine Lodge areas, the original caves were destroyed through collapse and brecciation of host rock and filled with insoluble residues, externally derived sediments, or water-borne cements. In contrast, some outcrops containing the Redwall paleokarst in the Grand Canyon exhibit preserved remnants of the original caves, which are invariably filled with externally derived sediments, cemented breccias, or collapsed roof rock.

The Madison paleokarst breccias are recemented. Color variations between the clasts and cements are sufficiently muted to defy differentiation from a distance. What are in fact thick zones of cemented breccias appear to be massive, irregularly bedded, cliff-forming limestones. Modern cavities eroded into the zones are localized in poorly cemented breccia pockets within the total mass. Stylolites with random orientations occur

within the paleokarst, but the opposing faces are typically tightly fitted together.

The presence of dissolution fronts extending downward into the massive limestones underlying the lower paleokarst zone is revealed by breccia-filled, solution-widened, vertical joints. Minor tilting occurs in some columns of undissolved limestone between the widened joints.

Wayhan and McCaleb (1969) and McCaleb and Wayhan (1969) documented in great detail the presence, extent, and petrology of the Madison paleokarst and its negative impact on permeabilities in the prolific Elk Basin field. Using subsurface information, these workers found that, in general, permeabilities were destroyed within the solution breccias in the paleokarst zones. Loss of permeability was attributed primarily to cementation of carbonate clasts by insoluble residues, and externally introduced clays and fine-grained quartz detritus. The result is laterally extensive solution-breccia horizons that form confining layers within the reservoir and massive, vertically brecciated zones that compartmentalize the upper producing intervals in the field.

A lack of spring and seep discharge from the paleokarst zones throughout the region demonstrates that the paleokarst does not contribute significantly to whole-rock permeability within the Madison Limestone. This finding is supported on the outcrop by a lack of interconnection between vugs and cavities within the paleokarst. In an apparent contradiction, springs discharge from the level of the Madison paleokarst to the Bighorn River at Sheep Mountain anticline, mostly along the east side of the canyon from the west limb of the fold. The total discharge from the springs above river level is reported to be slightly greater than 1 ft^3/sec (Doremus, 1986). Although the springs discharge from the paleokarst horizon, they appear to be localized on vertical extensional fractures. Therefore, I do not attribute localization of the springs to paleokarst permeability; rather it is more closely tied to fracture permeability created by considerably younger extension within the fold. Dissolution widening along other through-going vertical joints elsewhere in the fold reveals that the permeability found in the paleokarst zones at Sheep Mountain anticline is primarily fracture permeability imprinted on the paleokarst zones during Laramide folding.

Fracture permeability

The following types of fractures can be discriminated in the Madison outcrops in Sheep Mountain anticline: partings along bedding, stylolites developed along bedding, through-going vertical joints, small-scale vertical joint sets, vertical stylolites, small-scale, low-angle, conjugate thrust faults, high-angle-to-bedding minor normal faults, and localized microfracturing of diverse orientations. Two of these contribute significantly to permeability: the through-going vertical joints and selected stylolites that were opened during the folding of the anticline.

The following chronology for the origin of the various classes of fractures found in Sheep Mountain anticline appears to be plausible. Bedding planes and many small-scale vertical joints date from deposition and diagenesis in Mississippian time. Considerable microfracturing accompanied paleokarst development in Late Mississippian time. The stylolites that developed along bedding planes resulted from pressure solution in a stress regime where the maximum principal stresses were vertical. They could date from any period when the Madison section was deeply buried, from late Paleozoic to late Cretaceous time. Through-going vertical joints, vertical stylolites, small-scale thrust and normal faults, some small-scale jointing and microfracturing, and partings along bedding planes including open stylolites resulted from folding of the anticline, and are thus dated as Laramide features. Notice that the two classes of fractures identified here as contributing most to permeability—through-going joints and sprung stylolites—are of Laramide origin. Dissolutional enlargement along the permeable Laramide fractures dates from Laramide and post-Laramide time and is still taking place where these rocks are in contact with chemically undersaturated waters.

The judgement as to whether a class of fractures contributes significantly to permeability was made in the field using objective criteria. Foremost was the recurrent presence of interconnected dissolution cavities developed along the fractures in a given class. Next in importance was the occurrence of consistent separations along the fracture surfaces within a class. The presence of alteration halos and crystal growths on fracture surfaces demonstrate past circulation of ground water. Alteration halos exposed in Sheep Mountain consist of bleached (re-

duced) zones, which commonly penetrate from 1/2 to 2 inches into the rock from the surfaces of the fractures.

Through-going vertical joints

Through-going vertical joints refer to joints that are oriented parallel or subparallel to the trend of the fold and penetrate entirely or most of the way through the massive sections of the Madison Limestone (**Figure 12**). The vertical dimensions of such joints are measured in many tens to hundreds of feet. Spacings are highly variable, ranging from several feet to 100 to 150 feet or more. They are restricted to the crestal parts of folds; however, joint density is less in the immediate vicinity of the crestal axes than in the inflected beds lying to either side. Joints in this class are extension fractures, along which open separations developed. Solution widening and horizontal solution tubes localized on through-going joints demonstrate that ground waters have circulated along strike. The solution tubes are concentrated at the tops of the joints, producing a keyhole-shaped cross section. The tubes are generally less than 1.5 feet in diameter. The density of solution tubes decreases with depth in the section regardless of the position of the parent joint in the fold. Many joints in this class extend into or through the paleokarst zones. Most of the permeability in the Madison section at Sheep Mountain is attributed to these joints and the dissolution enlargement that has occurred along them.

Stylolites

Although the presence of stylolites demonstrates significant ground-water circulation, the opposing surfaces across most stylolites found in the Madison Limestone in Sheep Mountain anticline are tightly fitted together, with dissolution residuals filling the gaps. They also generally lack alteration halos, revealing that they were not permeable when reducing fluids were circulating through the other fracture sets. There are, however, a number of stylolites on

Figure 12. Exposures of through-going vertical extensional joints in the Madison Limestone within the crest of Sheep Mountain anticline, Wyoming. Dissolution widening such as at A produces keyhole cross sections along these permeable joints. View is toward the southeast across Sheep Canyon.

the limbs of the fold in the upper part of the Madison section that, for want of a better term, appear to be consistently "sprung." The stylolites were clearly sprung during shearing parallel to bedding caused by flexural slip within the fold. As shown on **Figure 13**, the younger bed moved perceptibly toward the axis of the anticline, whereas the older bed moved toward the syncline. This shearing left small openings along the surfaces in the stylolite that are oriented parallel to strike and dip toward the anticlinal axis. In contrast, surfaces in the stylolite that are oriented parallel to strike, but which dip toward the synclinal axis, are tightly locked. The sprung stylolites contribute most to permeability along the flanks of the fold, where flexural slip was greatest, not along the axis.

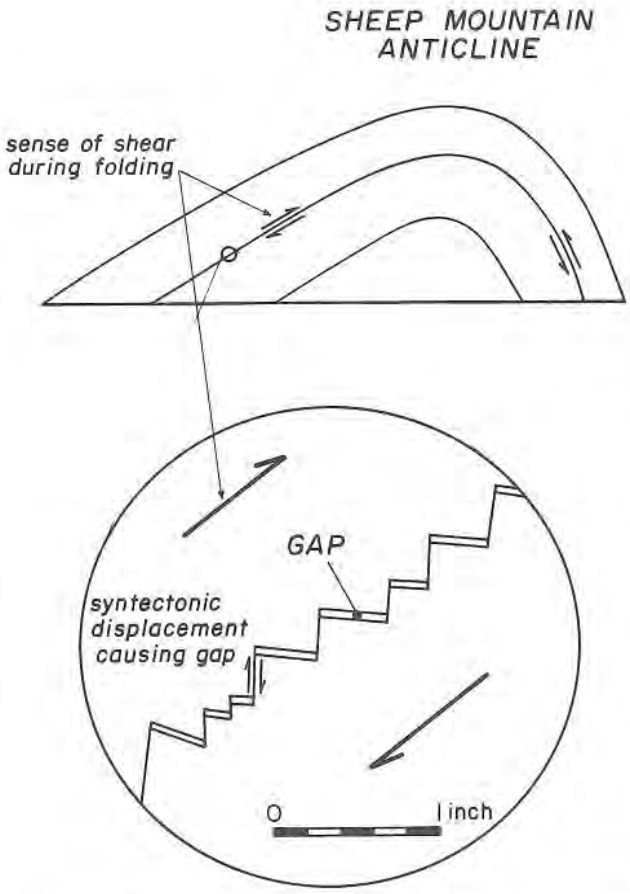

Figure 13. Mechanism for the development of permeable gaps along "sprung" stylolites resulting from small displacements across stylolites developed along bedding planes in the upper thin-bedded parts of the Madison Limestone at Sheep Mountain anticline, Wyoming. Shearing across the bedding planes was caused by flexural slip as the limbs of the fold deformed.

The stylolites along bedding in the Madison Limestone in Sheep Mountain anticline have a relief of less than 1 inch. The surfaces are rough, characterized by a series of pointed peaks or wave forms rather than rectilinear columns with flat tops. Such non-locked geometries allowed for minor flexural slip as shearing stresses developed parallel to bedding. More firmly locked stylolitized surfaces comprised of rectilinear columns, which are also present, are not sheared and sprung.

The most densely spaced bedding-plane stylolites occur in the upper, thin-bedded part of the Madison above the uppermost paleokarst zone. Vertical spacings between these stylolites range from 1 to 14 inches in typical thin-bedded outcrops. Stylolites in the lower, massive bedded, cliffed sections are rare to nonexistent. The permeable sprung stylolites occur mostly in the upper thin-bedded exposures.

Minor faults

In general, the minor faults—both normal and thrust—do not contribute appreciably to permeability because the compressive stresses that operated across them, coupled with their smooth surfaces, precluded the development of laterally extensive, interconnected gaps. Low-angle conjugate thrust faults occur on both the gentle and steep limbs of Sheep Mountain anticline and parallel the strike of the fold. The extent of these faults is generally a few tens to a few hundred feet in the dip direction. The best developed faults in a conjugate set are those that dip toward the syncline. The sense of displacement along these faults is upper plate toward the anticline, consistent with flexural slip within the fold. The fracture surfaces are generally smooth and terminate in the slip directions in splays along bedding, in ductile folds at termini, or in breccias at termini. Separations are generally absent, and alteration is minor to nonexistent, hence these minor faults do not contribute appreciably to whole-rock permeability.

Conjugate sets of small-scale normal faults that strike parallel to the fold are largely restricted to the steeply dipping east limb in Sheep Mountain anticline. Collectively, they account for some of the thinning of the limestones observed on the steeply dipping east limb. These faults are oriented at high angles to bedding, but they have rotated to subhorizontal attitudes, owing to the steep dips where they are found. Their minor displacements

account for the numerous steps found on the surfaces of beds on the flanks of the fold. The vertical extent of these faults is several tens of feet, and maximum offsets are measured in a few feet. Those observed did not appear to contribute appreciably to permeability.

Microfracturing

Microfracturing is especially well developed in the higher outcrops within the Madison section, and it increases in density with proximity to the paleokarst features. Therefore, much microfracturing appears to be related to paleokarst development, probably resulting from partial collapse of the host strata into the paleokarst zones. Other microfractures appear to be related to folding of the anticline. Both are characterized by very close spacings, multiple orientations, and healing. Some outcrops appear to be shattered by microfractures, which occur every inch or two in all directions. In others, the microfractures are best discerned as etching along their traces on the outcrops. In either case, the fractures are closed and usually filled with veins of calcite or other cementing agents; they appear to be unimportant to whole-rock permeability. Owing to cementation, microfractures can be readily observed in cores taken from wells drilled into the unit.

Permeability ranking

The relative contribution to Madison whole-rock permeability by the various structures exposed in Sheep Mountain anticline appears to be as follows. Most important are the solution-widened through-going vertical extensional joints in the crestal part of the fold. Next are the sprung stylolites along bedding, which occur on the flanks of the fold in the upper thin-bedded part of the unit. A poor third appears to be the limited permeability within the paleokarst zones. The collective contribution of all other classes of fractures appears to be small. Because both the solution widened through-going vertical joints and sprung stylolites owe their origin to anticlinal folding of the Madison Limestone, it is clear that, at this location, Laramide fracture permeability subsequently enhanced by dissolutional widening dominates the permeability regime.

The through-going vertical extensional joints concentrated along the crestal parts of the anticlines and the flexural slip sprung stylolites along bedding on the flanks provide some degree of permeability in the Madison Limestone under most areas of the anticline. Ideally, members within these two classes of fractures that are oriented approximately orthogonal to each other intersect sufficiently to allow a degree of hydraulic interconnection throughout the Madison Limestone within the anticline. Notice that the resulting whole-rock permeability is strongly anisotropic. At Sheep Mountain anticline, the combination of solution-widened, through-going joints parallel to trend and sprung stylolites operate to produce a maximum principal permeability tensor that is oriented parallel to both trend and bedding.

Circulation in foreland folds—the Thermopolis anticline

Ground-water circulation within Wyoming basins is strongly influenced by the presence of foreland anticlines. The impacts are manifested as alterations in regional circulation patterns and rates of circulation resulting from the combination of (1) fault severing of aquifers by the faults coring the anticlines, and (2) large fracture permeabilities along the crests of the anticlines. The net result is a highly anisotropic permeability regime, which leads to a lack of flow across the trends of the structures and to concentration of circulation along the crests parallel to trend. The best documented example of this involves circulation of ground water through the Paleozoic rocks within the Thermopolis anticline in the southern Bighorn Basin. The discussion that follows summarizes the detailed work of Jarvis (1986) and Spencer (1986).

The Thermopolis anticline (location on **Figure 9**) trends north-northwest for approximately 25 miles within the southern part of the Bighorn Basin (Paylor and others, 1989). The structure has approximately 3,000 feet of structural closure. Its trend is parallel to the north flank of the Owl Creek Mountains, which bounds the basin 10 miles to the south. The Thermopolis anticline is a member of a group of

north-northwest-trending anticlines in the southern part of the Bighorn Basin that developed over reverse or thrust faults that propagated upward from the basement into the Phanerozoic section (**Figure 14**). These anticlines are highly asymmetri-cal in cross section, with most verging toward the southwest. The basement faults appear to be back thrusts in the hanging-wall plate above the southwest dipping Oregon Basin thrust fault (Blackstone, 1986).

The Bighorn River has breached the Thermopolis anticline to the level of the Chugwater Group. Hot ground water discharges from sharply flexed Chugwater strata near the hinge of the fold. The Thermopolis Hot Springs, which discharge about 6 ft^3/sec at a temperature of 133°F, comprise the largest natural outlet for ground water in the Paleozoic section within the interior of the 8,000 mi^2 Bighorn Basin. The ultimate source for the water is recharge through outcrops of Paleozoic rocks in the Owl Creek Mountains to the south and in the southernmost part of the Bighorn Mountains to the east. Two important hydrologic questions emerge. First, what permeability regime accounts for the volume of water discharged through the Thermopolis Hot Springs; and second, how is the water heated to the observed temperatures?

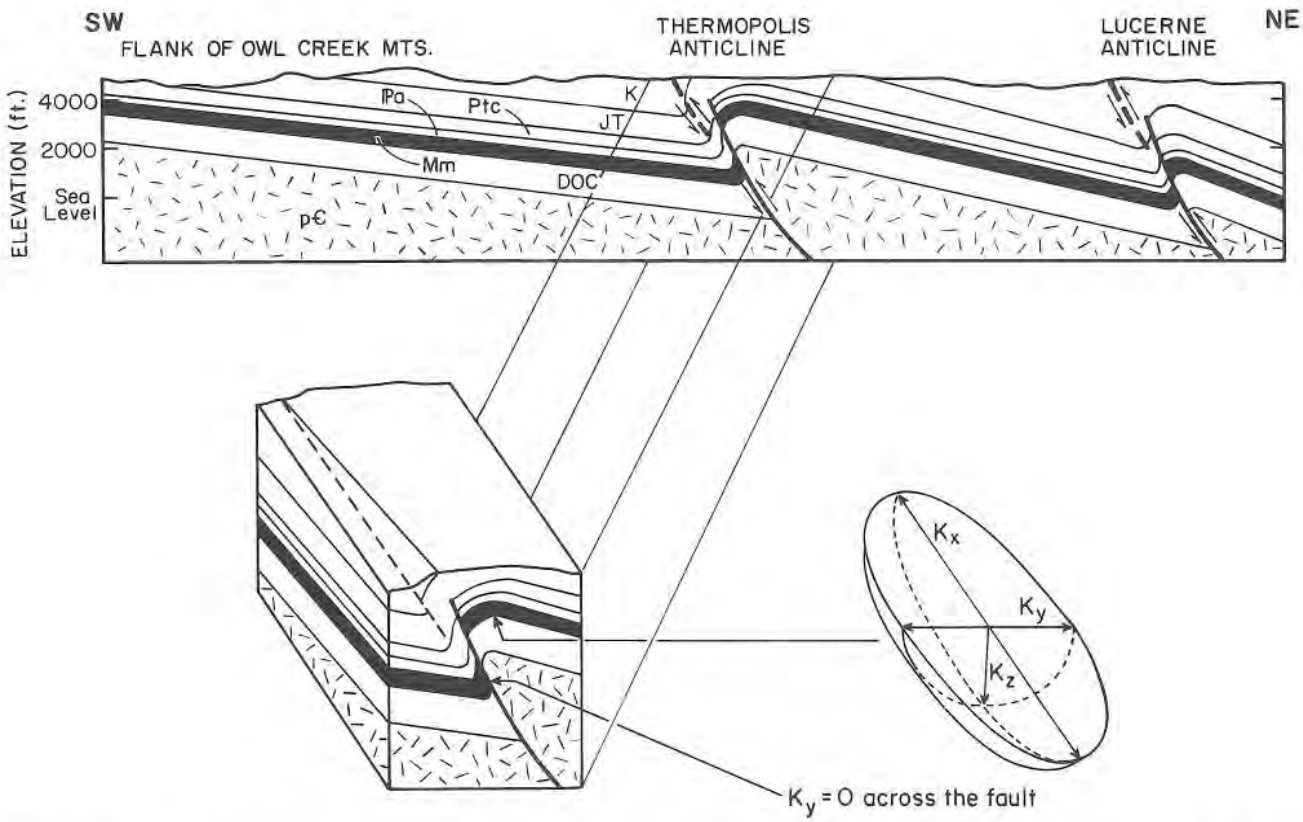

Figure 14. Structural cross section through the Thermopolis anticline (above), and a block diagram (below) showing the permeability tensors within the Madison aquifer in the crest of the anticline. Notice that the permeability tensor parallel to trend is greatest, reflecting large permeabilities associated with dissolution-widening of extensional fractures along trend within the crest of the fold. The fault in the core of the anticline is a barrier to fluid circulation perpendicular to trend. (Adapted from Jarvis, 1986, figure 16.)

EXPLANATION

K	undivided Cretaceous rocks
JT	Triassic Chugwater Group and Jurassic rocks undivided
IPPtc	Pennsylvanian-Permian Tensleep and Park City (Phosphoria) formations
IPa	Mississippian-Pennsylvanian Amsden Formation
Mm	Mississippian Madison Limestone
DO€	Devonian, Ordovician and Cambrian rocks
p€	Precambrian rocks

The comprehensive circulation model developed by Spencer (1986) and Jarvis (1986) for the Thermopolis hydrothermal system is summarized on **Figure 15**. Recharge to the Paleozoic section takes place in outcrops along the Owl Creek Mountains and southernmost part of the Bighorn Mountains. The water moves northward into the Bighorn Basin, where it reaches great depths and is geothermally heated. The water cannot circulate across the large-displacement fault in the core of the Thermopolis anticline. Consequently, it circulates through the footwall block parallel to the fault plane until it bypasses the fault barrier near the termini of the fold. The geothermally heated water then enters the highly transmissive crestal part of the fold, where the water circulates up plunge but down gradient to the springs. The elevations of the springs along the Bighorn River represent the lowest hydraulic heads in the system. The highest heads are the driving heads in the recharge areas imparted on the system by the elevations of the saturated upstream parts of the Paleozoic aquifers in the Owl Creek Mountains. Details supporting this model follow.

Figure 15 clearly illustrates elongated depressions in the Tensleep- Phosphoria head surface that coincide with the trends of the anticlines. The potentiometric low along the Thermopolis anticline is natural, as is the one directly to the south. The lowest hydraulic heads in the latter are the elevations of another group of thermal springs along the Bighorn River. The potentiometric configuration shown provides the gradients that deliver water to the springs.

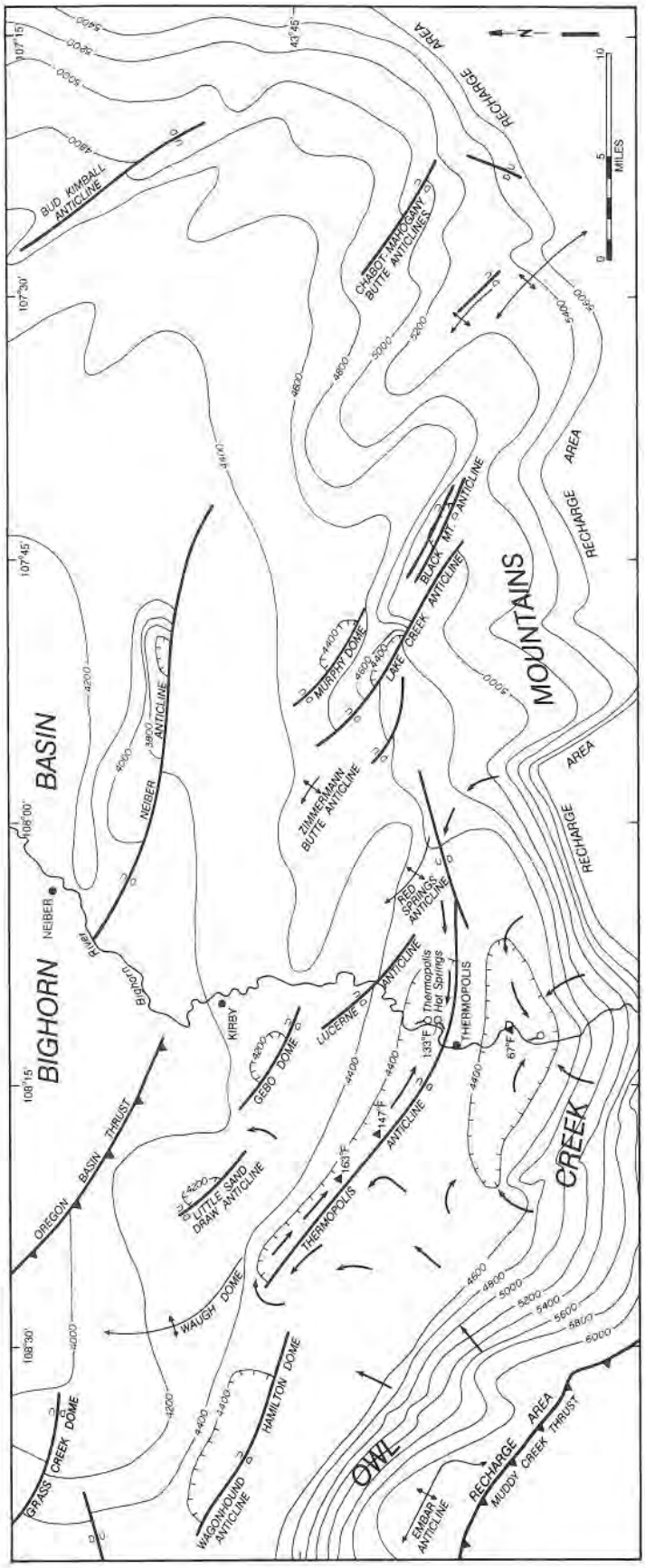

Figure 15. Potentiometric surface for the Park City-Tensleep aquifer, southern Bighorn Basin, Wyoming. Contours show elevations of equal hydraulic head within the aquifer. Heavy arrows are ground-water flow vectors in the vicinity of the Thermopolis anticline that illustrate the Jarvis-Spencer model for ground-water circulation from the Owl Creek recharge areas to Thermopolis Hot Springs. Ground-water temperatures along Thermopolis anticline, which cool toward the springs, are shown. (Adapted from Jarvis, 1986; and Spencer, 1986.)

The other potentiometric depressions on **Figure 15**, such as at Hamilton Dome, Little Sand Draw, Gebo, Neiber, Murphy, Lake Creek, and Black Mountain anticlines, have developed in response to production of petroleum fluids from the Tensleep-Phosphoria aquifer at those locations. The elongation of these depressions reflects both the distribution of production along strike and the highly anisotropic permeabilities within the crests of the anticlines. The shapes of the head declines demonstrate that the crests of the anticlines are highly permeable and that the large-displacement segments of the faults in the cores of the anticline are impermeable perpendicular to the trend of the folds. The available head data indicate that the production- induced potentiometric depressions have not propagated across the large-displacement parts of the faults in the cores of the anticlines, revealing that the faulting has severed the hydraulic continuity within the Paleozoic aquifers perpendicular to strike. This same anisotropic permeability regime is applied to the Thermopolis anticline.

There is a paucity of quantitative data on transmissivities in the Park City (Phosphoria)-Tensleep aquifer along the Thermopolis anticline; however, there is evidence that the transmissivities are extremely large. Collier (1920) and Heasler and Hinckley (1982) reported highly variable penetration rates and lost circulation problems in the Park City (Phosphoria)-Tensleep in wells drilled along the crest of the structure. In addition, head recoveries were virtually instantaneous in slug and pump tests in three wells analyzed by Heasler and Hinckley (1982).

The stratigraphic source for the waters discharging through the Thermopolis Hot Springs is inclusive of at least the Park City (Phosphoria) through Madison formations, based on homogeneous water qualities (Jarvis, 1986) and isothermal temperatures (Heasler and Hinckley, 1982) found in that stratigraphic interval near Thermopolis. The implication is that extensional fracturing along the crest of the fold allows for good vertical hydraulic connection between the various Paleozoic units.

Geothermal work by Hinckley and others (1982) and Heasler (1984) provide both water temperature data and a data-based thermal model for circulation along the Thermopolis anticline west of the hot springs. As shown on **Figure 15**, water temperatures are greatest in the northwest plunging part of the fold and decrease gradually toward the springs. Heasler (1984) concluded that the direction of ground-water flow in this part of the fold was southeastward along the crest of the structure, up-plunge toward the springs. The source for the geothermally heated waters were the depths in excess of 7,000 feet below the land surface to the northwest of the fold. The observed decrease in temperature of the ground water as it neares the hot springs was explained by Heasler (1984) as conductive heat loss as the water moves up plunge, but down gradient, along the anticline into regions of progressively thinner cover. This flow and thermal regime is mirrored in the anticline to the east of the springs; however, the maximum depths within the aquifers there are shallower.

Recharge to basins

Range-bounding thrust faults and reverse and thrust faults that occur in the cores of anticlines in the foreland basins commonly sever the hydraulic continuity of aquifers perpendicular to the trend of the anticline (**Figure 4**) and serve as barriers to flow. **Figure 2** shows that there is hydraulic severing of aquifers by faulting along approximately half of the basin perimeters in Wyoming. As a result, the opportunities for recharge between the uplifts and basins are proportionately diminished. The Paleozoic rocks in the footwall are deeply buried in the majority of cases. Accordingly, two completely separate circulation systems develop along the range-bounding faults, one restricted to the hanging wall on the flank of the range, and the other to the same rocks in the footwall within the basin. Three criteria are used to demonstrate the independence of the systems (Huntoon, 1985a): (1) head differences occur across the fault; (2) water qualities are dramatically different such that, in the extreme, fresh waters occupy the hanging-wall block; and brines and petroleum occur in the footwall block; and (3) geothermally heated waters occur in the deeply buried footwall block.

The northern and eastern flanks of the Laramie Mountains are bounded by thrust faults located as shown on **Figure 16**. These commonly have well in excess of 2 miles of dip slip (Jenkins and Rea, 1978; Richter and Huntoon, 1982; Johnson and others, 1982). **Figure 17** is an idealized composite cross section through the flank of the range based on the style of deformation documented by Wiersma (1989). Notice that (1) the Paleozoic aquifers in the hanging wall and footwall are isolated from each other, and (2) the structure has been dissected by erosion to various levels at different locations.

The A and F, and B and G profiles represent the two most common situations found along the fault-severed perimeters of Wyoming basins. These settings are characterized by the preservation of grand hogbacks of Paleozoic rocks on the hanging wall, which dip toward the basin. Many of the structurally isolated hanging-wall blocks have been falsely identified as recharge areas for the Paleozoic aquifers in the adjacent basins. The fact is that the Paleozoic hogbacks in the hanging-wall blocks have self-contained ground-water circulation systems. These generally drain along strike to gaining reaches of streams that cross the blocks, to springs located in topographic low spots along the Paleozoic outcrops, or to Tertiary aquifers that bury the leading edges of the hanging-wall blocks. Consequently, the hydraulic gradients within the hanging-wall blocks are dominantly parallel to the strike of the rocks, not down dip into the basin. Mancini (1976) documented the expected gains in stream flows from such Paleozoic outcrops along the northern Laramie Mountains.

The land surface in profile E on **Figure 17** is beveled across the deformed Paleozoic rocks in the fault-bounded overturned limb of the fold. The sheared and attenuated strata within the fault-bounded sliver are also hydraulically isolated from the aquifers in the basin. Circulation through these slivers is very similar to that in the hanging-wall blocks, being dominantly parallel to strike toward topographic lows rather than down dip.

Recharge through anticlines

The lateral permeabilities associated with extensional fracturing along the crests of anticlines are of paramount importance in facilitating ground-water recharge to foreland basins. Recharge rates are maximized in locations where anticlines trend from the recharge area to the basin interior. Zones of high-quality water penetrate deeply into the basins along the trends of such structures. Jarvis (1986) and Spencer (1986) documented that this was occurring within the aquifers in the Paleozoic section in the Bighorn Basin and used the following criteria to isolate examples: (1) hydraulic gradients flatten along the trends of anticlines, indicating the presence of large transmissivities; (2) fresh water penetrates deeply into the basin along anticlines; and (3) water temperatures in the anticlines are commonly cooler than those in the adjacent rocks. The result is a basinward-plunging antiform in the regional potentiometric surface that coincides spatially with the anticline. An example of this is the potentiometric bulge associated with the basinward-plunging structures southwest of the Chabot-Mahogany trend shown on on **Figure 17**.

A particularly good example, documented by Jarvis (1986), is that of recharge along the Tensleep fault-fold complex, which trends westward from the Bighorn Mountains toward the town of Worland. Potentiometric contours for the Park City (Phosphoria)-Tensleep aquifer bulge westward and flatten along the axis of the structure, producing a basinward-dipping antiform in the potentiometric surface that is characteristic of such a recharge zone. Some heads in the zone are 200 to 300 feet greater than those found in the adjacent undeformed strata (Jarvis, 1986, plate VI). Jarvis also found that total dissolved solids in the Park City (Phosphoria)-Tensleep aquifer in the hanging wall were one-half to one-quarter of those found in the footwall. Likewise, Heasler and Hinkley (1985) documented a 2°C difference in temperatures between the cooler hanging-wall (anticline) waters and those in the footwall.

Diminished recharge

The prospects for large-volume, deep-basin recharge are dim in the Wyoming foreland when viewed in light of the geologic constraints imposed by fault-severed basin margins and basinward deterioration of permeabilities in the remaining homoclinal margins. For example, net deep-basin recharge to the Paleozoic section under the 8,000 mi^2 Bighorn Basin cannot be measured in units of more than a few tens of ft^3/sec based on total

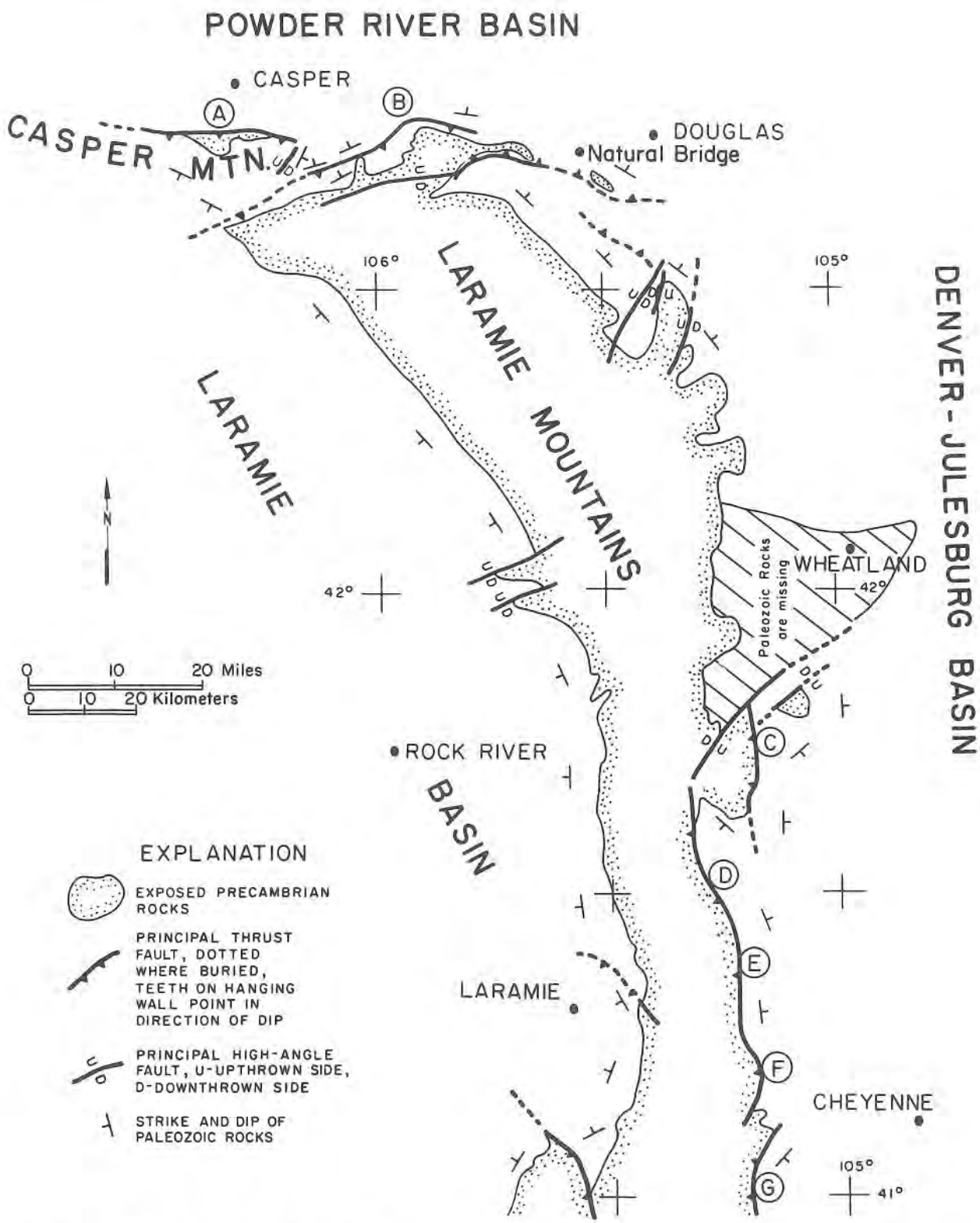

Figure 16. Generalized tectonic map for the Laramie Mountains, southeastern Wyoming, showing the range-bounding thrust faults that sever the Paleozoic aquifers. The lettered locations correspond to the lettered profiles shown on Figure 17.

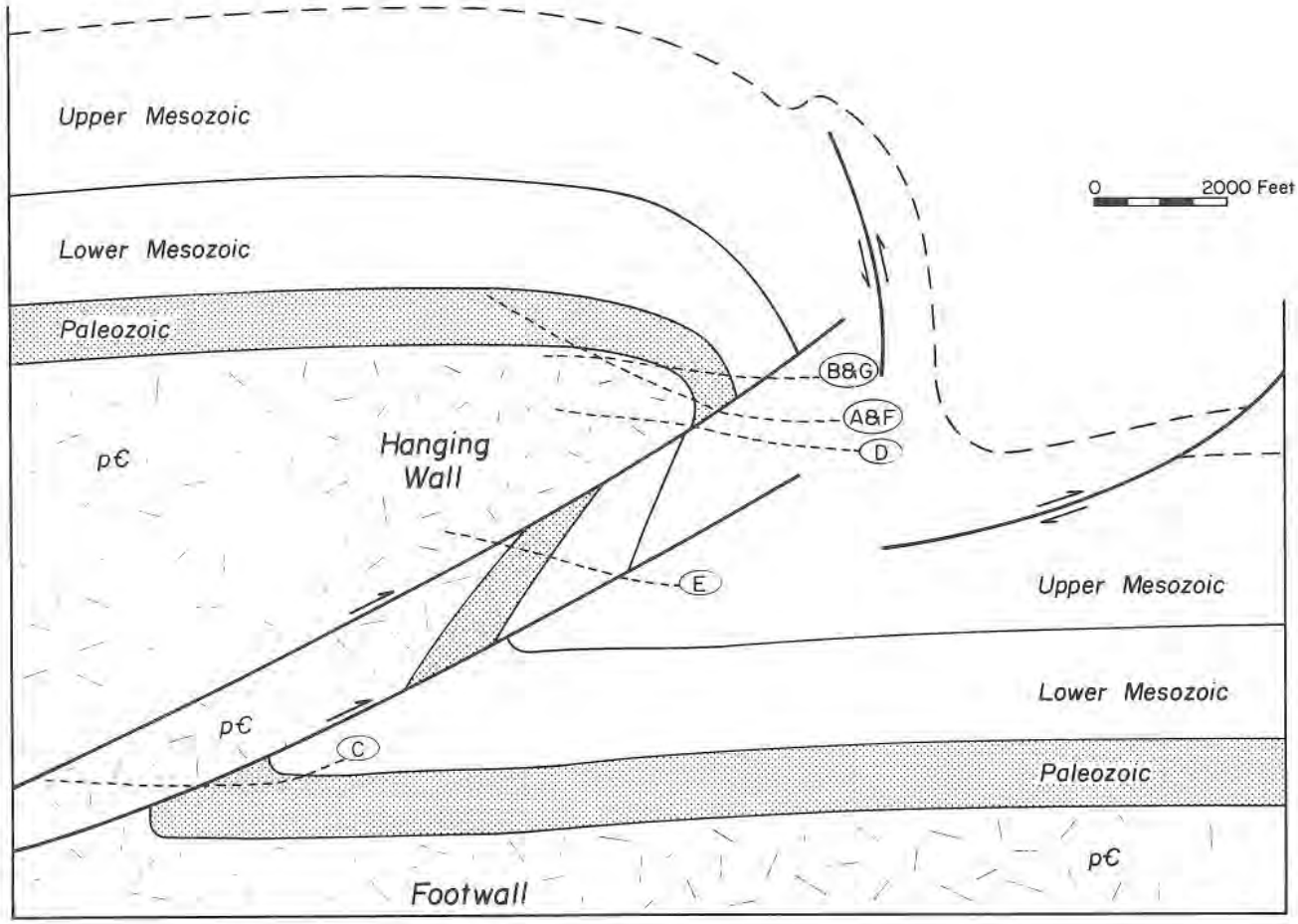

Figure 17. Composite cross section through the range-bounding Laramide thrusts along the eastern and northern flanks of the Laramie Mountains based on styles of deformation documented by Wiersma (1989). The dashed lines show the land surface profiles at the lettered locations on Figure 16.

predevelopment spring discharges from those rocks within the interior of the basin. The contribution to this total through most homoclinal margins is modest; the contribution through the fault-severed margins, negligible. Potentiometric data such as on **Figure 15** reveal that the bulk of the recharge is taking place through homoclinal margins containing basinward-plunging anticlines. These anticlines hydraulically link the uplifted recharge areas with the basin interiors. Extensional fractures trending basinward within the crests of these anticlines provide the largest capacity conduits for deep-basin recharge.

Discussion

Regionally extensive foreland artesian aquifers such as the Madison aquifer in Wyoming do not offer developers unbridled opportunities for high-quality, large-yield water supplies. The permeabilities of the Paleozoic rocks are highly variable, with a tendency for most to be small to negligible. A complicating variable is water qualities that are weighted toward the unpotable. The fickleness of these aquifers is predicated by uneven permeability distribution. Consequently, ground-water exploration in the foreland artesian basins has become increasingly dependent on targeting highly transmissive zones identified on the basis of favorable structural and geochemical factors.

Among the highest priority tasks for the explorationist is to carefully identify and map geologic structures in the domain of interest and develop insights into the kinematics responsible for the emplacement of those structures. Kinematic analysis will reveal the parts of the structures that have experienced permeability enhancement as a result of the deformation—preferably extensional fracturing—and drilling targets will emerge. Locations favored with a post-Laramide geochemical regime characterized by circulation of large volumes of fresh water will benefit additionally from dissolution enhancement of permeabilities.

In general, it is counterproductive in the foreland setting to drill Paleozoic aquifers in the footwall blocks along fault-severed basin margins because low permeabilities and brines will be encountered. Drilling the crests of anticlines within basins holds the potential for yielding appreciable volumes of water, but that water is most likely to be warm and of marginal quality. Drilling anticlines that plunge into the basins across unsevered homoclinal margins enhances the probability that large volumes of high-quality water will be present. Risks inherent in homoclinal sites include: (1) system sensitivity that attends rapid-response, highly transmissive zones; (2) vulnerability to pollution; (3) problems in intersecting highly localized, large-capacity targets such as saturated caves in otherwise tight rock; and (4) interference with fully appropriated streams. Updip locations on homoclinal margins have increased risk of ephemeral saturation of strata.

One characteristic of the permeability regime imposed on the foreland basins by Laramide tectonism is its extreme anisotropy. On a regional scale, the maximum principal permeability tensors are aligned roughly parallel to the trends of the Laramide structures (**Figure 14**). On a local basis, within doubly plunging anticlines, work such as that by Hurley (1990) reveals that the maximum permeability tensor can be oblique or perpendicular to trend if the extensional fractures oriented oblique or perpendicular to trend are more transmissive than those parallel to trend.

Fluid production from highly anisotropic aquifers results in head declines that radiate from the production center, but which elongate parallel to the maximum permeability tensor. In the case of an anticline where the maximum tensor is oriented perpendicular to trend, the head decline will tend to propagate rapidly toward the flanks of the anticline rather than along it until the limits of the extensional fractures are reached. The head decline will necessarily have to expand laterally along strike, ultimately coalescing with declines propagating from other wells. The result will be an elongated decline that parallels trend and has an appearance similar to the decline expected had the maximum permeability tensor been oriented parallel to trend to begin with.

It is immaterial whether the maximum or intermediate permeability tensor is oriented parallel to the crests of Laramide anticlines when considering regional circulation through aquifers in the foreland basins. Circulation will always converge on and concentrate along the crests of the anticlines in either case because both the maximum and intermediate tensors are significantly greater than background permeabilities. If dissolution attends circulation, permeability enhancement will preferentially take place in the fractures oriented parallel to the hydraulic gradient along trend. Anticlines that contain or have contained active ground-water systems ultimately develop maximum permeability tensors that parallel trend. This occurs at the Thermopolis and Sheep Mountain anticlines. In contrast, the original tensor characteristics of the Laramide fracture-enhanced permeability regime in the nonactive parts of the system can be preserved over long periods of geologic time if the fluids in the anticlines are stagnant or if the zones contain static hydrocarbons above dynamic water systems.

It is clearly inappropriate to mathematically characterize or model the ground-water aquifers and petroleum reservoirs in the Laramide foreland basins using transport equations that assume isotropic permeabilities. Even equations predicated on highly heterogeneous permeabilities are inadequate. The pioneering 2-dimensional planimetric model utilizing anisotropic transmissivities developed by Spencer (1986) to forecast the impacts of fluid withdrawals from the Paleozoic section on spring discharges at the Thermopolis Hot Springs is a step in the right direction.

Acknowledgments

The Wyoming State Board of Charities and Reform and University of Wyoming Water Research Center supported this research. Preparation of the manuscript was in part sponsored by the Gas Research Institute, contract 5089-260-1894. W. Todd Jarvis (J.M. Montgomery Consulting Engineers) and Neil F. Hurley (Marathon Oil Company) provided thorough technical reviews, which greatly improved this manuscript.

D.L. Blackstone, Jr.

It is fitting that this paper appear in a volume in part dedicated to D.L. Blackstone, Jr. Blackstone championed ground water as a discipline within geology and as a topic important to the welfare of Wyoming. He taught ground-water geology at the University of Wyoming from 1950 until 1973. His prescience, coming before massive environmental programs, was instrumental in establishing a full-time ground-water professorship in the Department of Geology in 1974.

Blackstone actively participated with me on the Master of Science thesis committees for the following students whose detailed work and insights comprise the foundation upon which this paper builds: Barbara Vietti (1977), Don Lundy (1978), Keith Thompson (1979), Mark Stock (1981), O. Glenn Heyman (1983), John Copeland (1984), Gregory Bernaski (1985), Todd Jarvis (1986), Sue Spencer (1986), Dale Doremus (1986), John Mills (1989), and Ursula Wiersma (1989). Some of these researchers worked exclusively on foreland structure, others on ground-water geology, but most integrated the two. The quality and scope of their efforts comprise a testament to yet another facet of Blackstone's career—a career that continues in active thesis advising in ground-water geology to this day despite his formal retirement in 1974.

References cited

Anderson and Kelly, 1987, Hydrogeologic evaluation of the Natural Bridge well, Converse County, Wyoming: Consultants report by Anderson and Kelly, a division of James M. Montgomery, Consulting Engineers, for ARIX Corporation and the Wyoming Water Development Commission, 60 p.

Andrews, S., and Higgins, L.S., 1984, Influence of depositional facies on hydrocarbon production in the Tensleep Sandstone, Bighorn Basin, Wyoming, a working hypothesis: Wyoming Geological Association 35th Annual Field Conference Guidebook, p. 183-197.

Berg, R.R., 1962, Mountain flank thrusting in Rocky Mountain foreland, Wyoming and Colorado: American Association of Petroleum Geologists Bulletin, v. 46, p. 2019-2032.

_____ 1976, Deformation of Mesozoic shales at Hamilton Dome, Bighorn Basin, Wyoming: American Association of Petroleum Geologists Bulletin, v. 60, p. 1425-1433.

Bernaski, G.E., 1985, Compressional Laramide deformation in the southwestern Uinta Mountains, northwestern Colorado, and northwestern Utah [M.S. thesis]: Laramie, University of Wyoming, 154 p.

Billingsley, G.H., and Beus, S.S., 1985, The Surprise Canyon Formation, an Upper Mississippian and Lower Pennsylvanian(?) rock unit in the Grand Canyon, Arizona: U.S. Geological Survey Professional Paper 1173, p. 137-147.

Blackstone, D.L., Jr., 1980, Foreland deformation, compression as a cause: University of Wyoming Contributions to Geology v. 18, p. 83-100.

_____ 1981, Compression as an agent in deformation of the east-central flank of the Bighorn Mountains, Sheridan and Johnson counties, Wyoming: University of Wyoming Contributions to Geology, v. 19, p. 105-122.

_____ 1986, Structural geology of the northwest margin, Bighorn Basin, Park County, Wyoming, and Carbon County, Montana: Montana Geological Society Field Conference Guidebook, p. 125-135.

_____ 1990, Precambrian basement map of Wyoming: outcrop and structural configuration: Geological Survey of Wyoming Map Series 27, scale 1:1,000,000.

Bredehoeft, J.D., 1964, Variation of permeability in the Tensleep Sandstone in the Bighorn Basin, Wyoming, as interpreted from core analyses and geophysical logs: U.S. Geological Survey Professional Paper 501–D, p. D166-D170.

Bredehoeft, J.D., and Bennett, R.B., 1971, Potentiometric surface of the Tensleep Sandstone in the Bighorn Basin, west-central Wyoming: U.S. Geological Survey Open File Report 72-461.

Brown, W.G., 1987, Structural style of the Laramide orogeny, Wyoming foreland [Ph.D. dissertation]: Fairbanks, University of Alaska, v. 1, 342 p., v. 2, 193 p.

Burnham, W.L., and Kelly, J.E., 1979, Potential for development of ground-water supplies for hatchery use, Renner Ranch area, Phase 1 report: Consultants report by Anderson and Kelly, Consultants in Engineering and Geology, for the Wyoming Game and Fish Department, 23 p.

Collier, A.J., 1920, Oil in the Warm Springs and Hamilton dome near Thermopolis, Wyoming: U.S. Geological Survey Bulletin 711, p. 61-73.

Cooley, M.E., 1984, Artesian pressures and water quality in Paleozoic aquifers in the Tensleep area of the Bighorn Basin, north-central Wyoming: U.S. Geological Survey Water Supply Paper 2289, 53 p.

Copeland, J.R., 1984, Laramide structural deformation at the interface between the Laramie Mountains and the Denver-Julesburg Basin, southeastern Wyoming [M.S. thesis]: Laramie, University of Wyoming, 49 p.

Doremus, D.M., 1986, Groundwater circulation and water quality associated with the Madison aquifer in the northeastern Bighorn Basin, Wyoming [M.S. thesis]: Laramie, University of Wyoming, 81 p.

Emmett, W.R., Beaver, K.W., and McCaleb, J.A., 1971, Little Buffalo Basin Tensleep heterogeneity, its influence on drilling and secondary recovery: Journal of Petroleum Technology, v. 23, p. 161-169.

Gries, R., 1983, Oil and gas prospecting beneath Precambrian of foreland thrust plates in Rocky Mountains: American Association of Petroleum Geologists Bulletin, v. 67, p. 1-28.

Harris, J.F., Taylor, G.L., and Walper, J.L., 1960, Relation of deformational fractures in sedimentary rocks to regional and local structure: American Association of Petroleum Geologists Bulletin, v. 44, p. 1853-1873.

Head, W.J., and Merkel, R.H., 1977, Hydrologic characteristics of the Madison Limestone, the Minnelusa Formation, and equivalent rocks as determined by well logging formation evaluation, Wyoming, Montana, South Dakota, and North Dakota: U.S. Geological Survey Journal of Research, v. 5, p. 473-485.

Heasler, H.P., 1984, An analysis of the geothermal potential near Western Area Power Administration's facility in Thermopolis, Wyoming: Report by the University of Wyoming Water Research Center for the U.S. Department of Energy, Western Area Power Administration, 28 p.

Heasler, H.P., and Hinckley, B.S., 1982, Preliminary investigation for proposed geothermal development, Thermopolis, Wyoming: Consultants report by Anderson and Kelly, Consultants in Engineering and Geology, for the Town of Thermopolis, 61 p.

Heasler, H.P., and Hinckley, B.S., 1985, Geothermal resources of the Bighorn Basin, Wyoming: Geological Survey of Wyoming Report of Investigations 29, 28 p.

Hennier, J., and Spang, J.H., 1983, Mechanisms for deformation of sedimentary strata at Sheep Mountain anticline, Bighorn Basin, Wyoming: Wyoming Geological Association 34th Annual Field Conference Guidebook, p. 96-111.

Heyman, O.G., 1983, Regional compression as the cause for Laramide deformation of the northwestern Uncompahgre Plateau, western Colorado and eastern Utah [M.S. thesis]: Laramie, University of Wyoming, 128 p.

Hinckley, B.S., Heasler, H.P., and King, J.K., 1982, The Thermopolis hydrothermal system with an analysis of Hot Springs State Park: Geological Survey of Wyoming Preliminary Report 20, 42 p.

Huntoon, P.W., 1985a, Fault-severed aquifers along the perimeters of Wyoming artesian basins: Groundwater, v. 23, p. 176-181.

_____ 1985b, Rejection of recharge water from the Madison aquifer along the eastern perimeter of the Bighorn artesian basin, Wyoming: Groundwater, v. 23, p. 345-353.

_____ 1985c, Gradient-controlled caves, Trapper-Medicine Lodge area, Bighorn Basin, Wyoming: Groundwater, v. 23, p. 443-448.

Hurley, N.F., 1990, Characterization of natural fractures in Bighorn Basin anticlines, *in* Ewing, R.E., Kline, L.I., and Copeland, D., editors, Proceedings of the Fifth Wyoming Enhanced Oil Recovery Symposium: En-

hanced Oil Recovery Institute, University of Wyoming, Laramie, p. 99-111.

Jarvis, W.T., 1986, Regional hydrogeology of the Paleozoic aquifer system, southeastern Bighorn Basin, Wyoming, with an impact analysis on Hot Springs State Park [M.S. thesis]: Laramie, University of Wyoming, 224 p.

Jenkins, C.E., and Rea, B.D., 1978, Cross sections, Casper Mountain-Muddy Mountain area, Natrona County, Wyoming, *in* Knittel, P., editor, A field guide to the Casper Mountain area: Wyoming Field Science Foundation, Casper, Wyoming, 80 p.

Johnson, R.A., and others, 1982, Interpretation of foreland structure in the Laramie Mountains from reprocessed COCORP deep crustal reflection data: Society of Exploration Geophysicists 52nd Annual International Meeting and Exposition technology progress abstracts and biographies, p. 86-87.

Kelly, J.E., 1980, Recommendations for development of ground-water supplies for hatchery use, Renner Ranch area, Phase 2 report: Consultants report by Anderson and Kelly, Consultants in Engineering and Geology, for the Wyoming Game and Fish Department, 20 p.

Lundy, D.A., 1978, Hydrology and geochemistry of the Casper aquifer in the vicinity of Laramie, Albany County, Wyoming [M.S. thesis]: Laramie, University of Wyoming, 76 p.

Mancini, A.J., 1976, Investigation of recharge to groundwater reservoirs of northeastern Wyoming: Wyoming State Engineer's Office, Cheyenne, 111 p.

Mankiewicz, D., and Steidtmann, J.R., 1979, Depositional environments and diagenesis of the Tensleep Sandstone, eastern Bighorn Basin, Wyoming: Society of Economic Paleontologists and Mineralogists Special Publication no. 26, p. 319-336.

McCaleb, J.A., and Wayhan, D.A., 1969, Geologic reservoir analysis, Mississippian Madison Formation, Elk Basin Field, Wyoming-Montana: American Association Petroleum Geologists Bulletin, v. 53, p. 2094-2113.

McCaleb, J.A., and Willingham, R.W., 1967, Influence of geologic heterogeneities on secondary recovery from Permian Phosphoria reservoir, Cottonwood Creek field, Wyoming: American Association of Petroleum Geologists Bulletin, v. 51, p. 2122-2132.

McKee, E.D., and Gutschick, R.C., 1969, History of the Redwall Limestone of northern Arizona: Geological Society of America Memoir 114, 726 p.

Mills, J.P., 1989, Foreland structure and karstic groundwater circulation in the eastern Gros Ventre Range, Wyoming [M.S. thesis]: Laramie, University of Wyoming, 101 p.

Morgan, J.T., Cordiner, F.S., and Livingston, A.R., 1977, Tensleep reservoir study, Oregon Basin field, Wyoming-reservoir characteristics: Journal of Petroleum Technology, v. 29, p. 886-896.

Paylor, E.D., Muncy, H.L., Lang, H.R., Conel, J.E., and Adams, S.L., 1989, Testing some models of foreland deformation at the Thermopolis anticline, southern Bighorn Basin, Wyoming: The Mountain Geologist, v. 26, p. 1-22.

Richter, H.R., and Huntoon, P.W., 1982, Ground-water development potential for the Paleozoic aquifer along the flanks of the Laramie Mountains and Hartville uplift, southeastern Wyoming: Consultants report by Western Water Consultants, Incorporated, for the Wyoming Water Development Program, 88 p.

Sando, W.J., 1974, Ancient solution phenomena in the Madison Limestone (Mississippian) of north-central Wyoming: U.S. Geological Survey Journal of Research, v. 2, p. 133-141.

Smithson, S.B., Brewer, J., Kaufman, S., Oliver, J., and Hurich, C., 1979, Wind River uplift, Wyoming, from COCORP deep reflection data and from gravity data: Journal of Geophysical Research, v. 84, p. 5955-5972.

Spencer, S.A., 1986, Groundwater movement in the Paleozoic rocks and impact of petroleum production on water levels in the southwestern Bighorn Basin, Wyoming [M.S. thesis]: Laramie, University of Wyoming, 118 p.

Stock, M.D., 1981, The geohydrology of the shallow aquifers in the vicinity of the Old Woman anticline, Niobrara County, Wyoming [M.S. thesis]: Laramie, University of Wyoming, 87 p.

Stone, D.S., 1967, Theory of Paleozoic oil and gas accumulation in Bighorn Basin, Wyoming: American Association of Petroleum Geologists Bulletin, v. 51, p. 2056-2114.

Swenson, F.A., and Bach, W.K., 1951, Ground-water resources of the Paintrock Irrigation Project, Wyoming, with a section on the quality of the water by H.A. Swenson: U.S. Geological Survey Circular 96, 45 p.

Thompson, K.S., 1979, Prediction of water level declines in the Casper aquifer in the vicinity of Laramie, Wyoming [M.S. thesis]: Laramie, University of Wyoming, 74 p.

Todd, T.W., 1963, Post depositional history of Tensleep Sandstone (Pennsylvanian), Bighorn Basin, Wyoming: American Association of Petroleum Geologists Bulletin, v. 47, p. 599-616.

Vietti, B.T., 1977, The geohydrology of the Black Butte and Canyon Creek areas, Bighorn Mountains, Wyoming [M.S. thesis]: Laramie, University of Wyoming, 49 p.

Wayhan, D.A., and McCaleb, J.A., 1969, Elk Basin Madison heterogeneity, its influence on performance: Journal of Petroleum Technology, v. 21, p. 153-159.

Wiersma, U.M., 1989, Structural obstruction of recharge to the Paleozoic aquifer in the Denver-Julesburg Basin along the Laramie Mountains, Wyoming [M.S. thesis]: Laramie, University of Wyoming, 56 p.

Wyoming Geological Association, 1957 (updated 1989), Wyoming oil and gas fields symposium, 579 p.

Frontispiece. Photograph of the south face of the Oregon Buttes, an outcrop of interbedded, brightly colored Tertiary sedimentary rocks. The high ridge on the skyline (shadowed) forms the western limb of the Continental Divide and the western boundary of the Great Divide Basin in south-central Wyoming. The Oregon Buttes (2,594 m) was a familiar skyline landmark for early westward travelers on the Oregon Trail. (Photograph by D. N. Grasso, 1989.)

Geologic applications of remote sensing and GIS: A Wyoming landscape perspective

Ronald W. Marrs and Dennis N. Grasso
Department of Geology and Geophysics
University of Wyoming
Laramie, Wyoming 82071

Abstract

Improvements in remote-sensing instruments over the past two decades have greatly enhanced capabilities for detailed mapping, lithologic identification, and remote mineralogical and chemical assessments. User-friendly software and affordable computers now permit full-capability processing of images and integration of pertinent ancillary landscape information. The regional perspective furnished by modern satellite imagery also offers geologists an unprecedented view of region-wide geologic relationships.

The advantages afforded by these new tools have been particularly evident in Wyoming, where excellent exposures and a broad variety of geologic problems are ideal for testing improvements in the application of remote-sensing techniques. In Wyoming, remote-sensing has been used for structural and stratigraphic interpretation, resource exploration, and geomorphic analysis. Examples are presented to illustrate the capabilities and potential of the present generation of remote-sensing systems.

The integration of satellite imagery with field data, aerial photography, and map information has significantly improved region-wide geologic interpretation and modeling in Wyoming. Eolian landforms have been investigated by correlating interpretations of high-altitude aerial photography and Landsat imagery with wind-velocity soundings, topography, sediment characteristics, and radiocarbon dates. This technique helped to identify and map areas of exceptionally high wind-energy potential across southern Wyoming. From the combined information, patterns of climatic change were interpreted.

A subsequent project, employing a geographic information system (GIS) approach, in which Landsat multispectral satellite data is digitally merged with topographic landscape information, was used to identify and interpret lacustrine features in Wyoming's Great Divide Basin. A multi-dimensional analysis of these combined data revealed the maximum extent of a large late Quaternary lake that once occupied some 2,000 square kilometers of this topographically closed hydrologic basin. Some of the more important procedures of this investigation are presented to illustrate the application of the remote-sensing/GIS approach to paleolandscape reconstructions. They also show how multispectral remote sensing can be a more effective tool when used in conjunction with appropriate forms of ancillary landscape information.

Marrs, R.W., and Grasso, D.N., 1993, Geologic applications of remote sensing and GIS: A Wyoming landscape perspective, *in* Snoke, A.W., Steidtmann, J.R., and Roberts, S.M., editors, Geology of Wyoming: Geological Survey of Wyoming Memoir No. 5, p. 790-814.

Introduction

The launch of the first Landsat (ERTS) satellite in July 1972 began a new era in mapping the Earth's surface. The Landsat imaging system provided the first regular global coverage with both the detail and broad overview necessary for regional resource analysis. Landsat's Multispectral Scanner (MSS) recorded energy reflected from surface materials in four separate spectral bands and proved effective for mapping at scales of 1:250,000 and smaller. Later Landsat imaging systems contributed still greater spatial and spectral capabilities.

The well-exposed and diverse geology of Wyoming was immediately recognized as an excellent test area for these new remote-sensing tools. The work of Tomes and others (1973), Blackstone (1972, 1973), Hoppin and others (1973), Earle (1977), Marrs and Raines, (1984), Gubbels (1987), Paylor and others (1989), and Blundell and Marrs (1991) showed that Landsat imagery could be effectively used for geologic mapping and structural analysis, whereas Houston (1973), Kaminsky (1977), and Raines and Marrs (1983) pioneered efforts to use Landsat multispectral image data to identify and map contrasting surface lithologies. Detailed analyses of spectral responses recorded by Landsat also proved useful in locating exposed zones of mineral alteration and surface anomalies of the type sometimes associated with subsurface petroleum reservoirs (Kolm, 1975; Short and Marrs, 1975; Froman, 1976; Marrs and Kaminsky, 1977; Levinson, 1979; Richers and others, 1982; Lang and others, 1984a; Marrs and Paylor, 1987). Satellite images have been effectively used in regional geomorphic analyses in Wyoming (Breckenridge, 1973; Kolm, 1977; Gaylord, 1982; Grasso, 1990). Without the broad-scale coverage and multispectral detail of Landsat, such regional evaluations may not have been possible.

Satellite image analysis has become an important part of many regional geologic studies. Various experimental aircraft and satellite systems, such as the Thermal Infrared Multispectral Scanner (TIMS), Airborne Imaging Spectrometer (AIS), Skylab Earth Resources Experiments Package (EREP), Heat Capacity Mapping Mission (HCMM), Seasat, and the Shuttle radar systems (SIR-A and SIR-B), have shown promise in a broad range of geologic applications. Subsequently, some of the best features of these experimental systems have been incorporated into operational remote-sensing systems, such as the Landsat Thematic Mapper (TM) and Systeme Probatoire d'Observation de la Terre (SPOT).

Each successive improvement in instrumentation has further augmented the utility of remote sensing as a geologic tool. For example, one can now purchase imagery acquired from orbital altitudes with enough detail to resolve objects 5 to 12 meters across. At the same time, the spectral range of orbiting sensors has been expanded from the visible and near-infrared wavelengths (400 to 1,100 nm) into the mid-infrared (1,100 to 5,000 nm) and thermal infrared (8,000 to 14,000 nm) regions of the electromagnetic spectrum. Repetitive coverage and stereographic images are also available.

Discussions of equipment parameters, data formats, processing routines, and the various geologic applications of remote sensing appear in several good textbooks and other summary publications (Sabins, 1986; Siegal and Gillespie, 1980; Jensen, 1986; Kahle, 1980a; Elachi, 1982; McCauley, 1982). Such discussions are certainly beyond the scope of this paper, but they demonstrate the utility of remote sensing as a geologic tool.

The challenge now is to provide professional geologists with an adequate background in remote sensing and ready access to the necessary processing capabilities via desktop computers with the appropriate peripheral devices (**Figure 1**). Menu-driven image processing software for microcomputers is user friendly and able to handle both image and map data in either raster or vector formats. Better techniques are being developed for data compression and correlation, which now allow the full range of image-processing functions.

Recent efforts have also been directed toward improved training. Short courses and training modules have been developed to provide geoscientists with the necessary background to select and combine computerized data. For example, using a geographic information system (GIS), image data can be integrated with other forms of landscape information (**Figure 2**). Many new remote-sensing techniques have been devised and tested by application to real geologic problems in Wyoming.

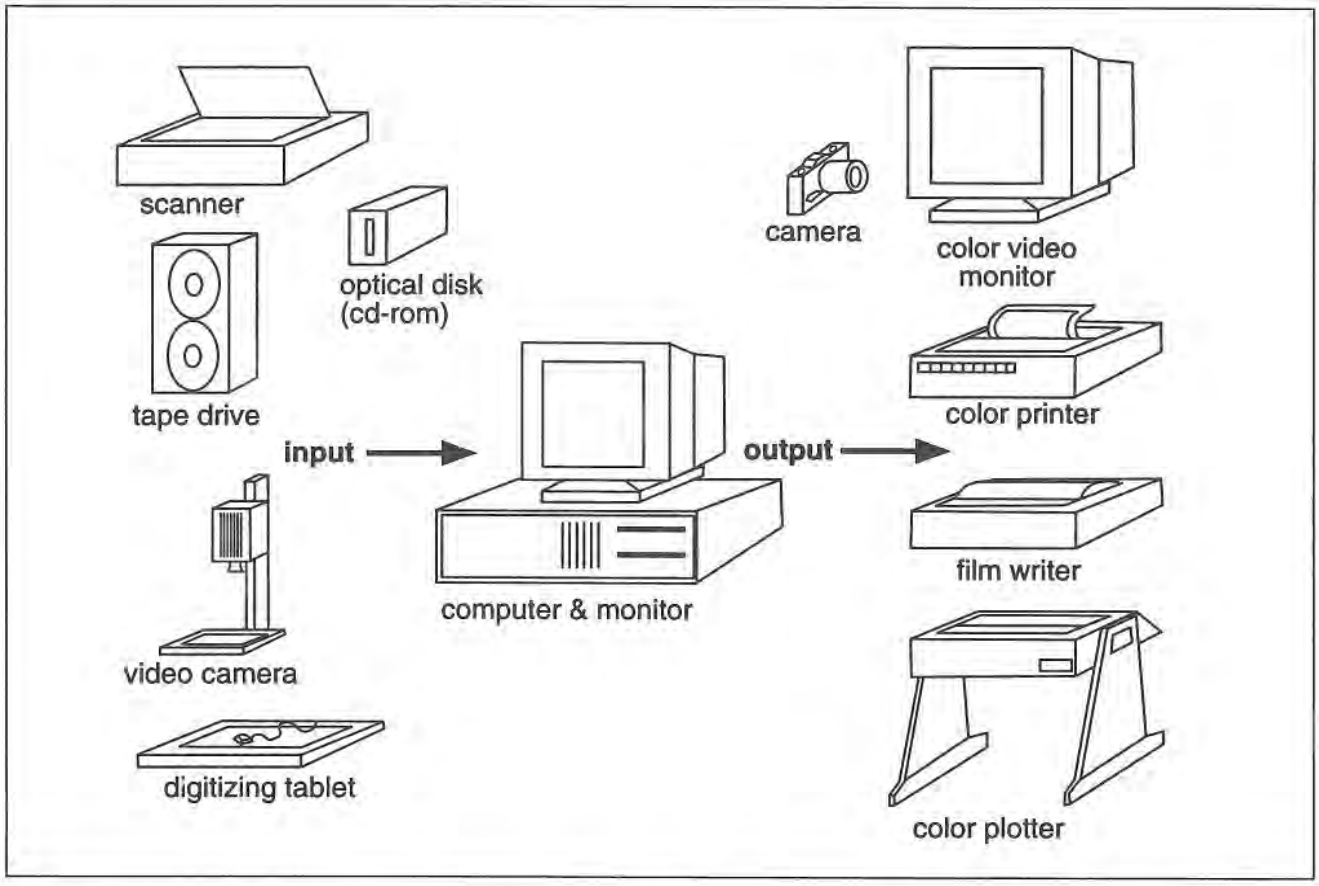

Figure 1. Diagram of a typical desktop computer with peripheral equipment appropriate for image processing. Input to the system can be from optical disk, digital magnetic tape, image and map scanner, video camera, digitizing tablet or computer keyboard. Hardcopy output devices may include pen plotter, film writer, printer, or camera set up to photograph the video monitor. Various peripheral devices may or may not be necessary depending upon the intended application.

Operational remote-sensing systems (Landsat, SPOT, NAPP, NHAP)

The following synopsis of the current generation of remote-sensing systems is not intended as a comprehensive survey of all remote-sensing tools. Instead, it gives a general overview of the current capabilities and limitations of remote-sensing systems applicable to geologic problems in Wyoming.

Landsat

Since its launch in 1972, Landsat has provided a nearly continuous supply of multispectral imagery. Early satellites (ERTS/Landsat 1, 2, and 3) carried a Return-Beam Vidicon (RBV) system and a 4-channel Multispectral Scanner (MSS). The MSS system was soon recognized as a superior instrument for most Earth resources applications and it became the primary instrument on each of the first three Landsat satellites. On Landsat 3, a thermal-infrared band was added and the 3-band RBV system was replaced by a twin-camera, high-resolution vidicon system to provide detailed imagery in black-and-white that would better complement the MSS imaging system. In later Landsat systems (Landsat 4 and 5), the RBV system was supplanted by an improved, 7-band multispectral scanner, called the Thematic Mapper (TM), that provides both higher spatial resolution and broader spectral coverage than the MSS instrument (**Table 1**).

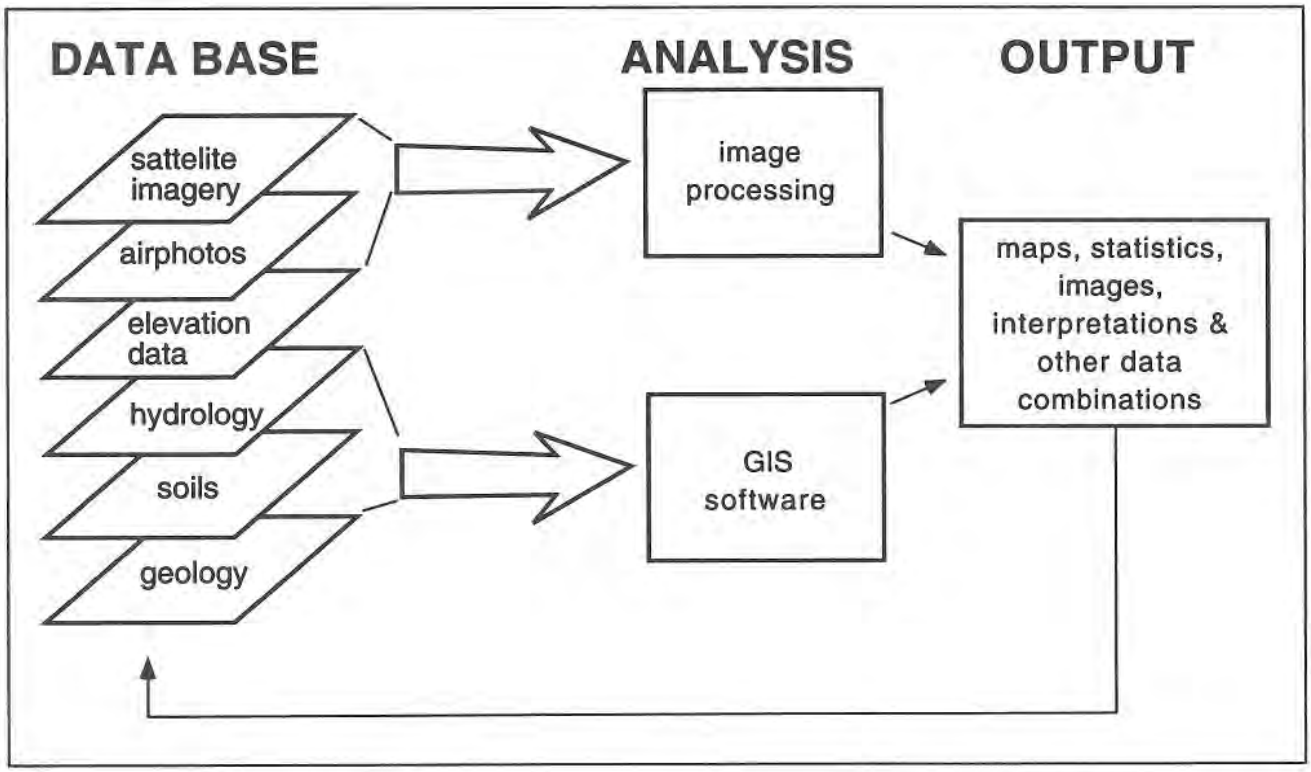

Figure 2. Flow diagram showing how data from a multi-layer data base may be used for landscape analysis or resource evaluations by coupling image processing with geographic information system software.

Table 1. Sensor characteristics of Landsat and SPOT satellites.

	LANDSAT			SPOT	
SENSOR	MSS	RBV-III	TM	PAN	MSS
NUMBER OF BANDS	4	3	7	1	3
SPECTRAL RANGE: (in nanometers)					
Visible	500 - 700	500 - 750	450 - 700	10 - 730	500 - 680
Near infrared	700 - 1100	(none)	700 - 2350	(none)	790 - 890
Thermal infrared	(none)	(none)	10500 - 12500	(none)	(none)
GROUND COVERAGE (in kilometers)					
Along track	185	99	185	60	60
Across track	185	99	170	60	60
RESOLUTION (in meters)					
Width x Length	79 x 57	40 x 40	28.5 x 28.5	20 x 20	10 x 10
*Thermal band			*120 x 120		
DETECTORS/BAND	6	na	16	6000	3000
NUMBER OF PIXELS (in millions)					
In single band	7.6	6.1	39	36	9
In all bands	30.4	6.1	273	36	27

These improvements allowed the Thematic Mapper to quickly replace Landsat MSS as the instrument of choice for most geoscience applications. However, the 4-band Landsat MSS system has been retained for program continuity.

In its present mode, Landsat's orbit path tracks north to south across the sunlit side of the globe approximately 14 times each day. On each pass, the scanners view and record imagery along a swath 185 km wide. As the Earth rotates beneath the satellite, the coverage paths shift westward so that the entire Earth (except for a small area near each pole) is covered every 16 days. Therefore, satellite images from the MSS and TM instruments are available for nearly all cloud-free portions of the Earth's surface on a 16-day return cycle.

Landsat MSS and TM imagery is available from:

Earth Observation Satellite Company
4300 Forbes Boulevard
Lanham, Maryland 20706
Phone: (800) 367-2801

SPOT

In February, 1986, France launched a multispectral remote-sensing system, known as SPOT (Systeme Probatoire d'Observation de la Terre), which provides both single-band, black-and-white (panchromatic) imagery at 10-meter resolution and 3-band color (multispectral) imagery at 20-meter resolution (**Table 1**). Like Landsat, SPOT provides global coverage, but its sensors do not always view the Earth vertically. Instead, SPOT's sensors can be tilted to obtain "off-track" views of the Earth. Hence, SPOT is able to view the same site every five days or view the same site from adjacent tracks for stereographic imaging.

SPOT imagery is available from:

SPOT Image Corporation
1897 Preston White Drive
Reston, Virginia 22091-4368
Phone: (703) 620-2200

A comparison of the overall characteristics of SPOT and Landsat (**Table 1**) reveals that the Landsat TM system provides both a broader view of the Earth (185-km swath) and superior spectral coverage (visible to thermal). Hence, Landsat is better suited for discriminating between various lithologic units and mapping alteration patterns or other geologic features expressed on the imagery as subtle differences in spectral reflectance. On the other hand, SPOT provides superior resolution (10 m and 20 m) and stereographic coverage often necessary for geomorphic and structural analyses where topographic detail is of particular importance.

Aerial photography

The U. S. Geological Survey National Aerial Photography Program (NAPP) is an important source of remotely acquired data for geologic interpretation in the United States. During the 1980s, the National High-Altitude Aircraft Program (NHAP), the predecessor to the present program, furnished both black-and-white, high-altitude photographic coverage at 1:80,000 scale, and color-infrared coverage at 1:58,000 scale centered on 7.5-minute topographic quadrangle areas. These photographs were used by the U.S. Geological Survey to produce 1:24,000-scale orthophoto quadrangle maps for many areas.

The current NAPP program obtains color-infrared photography at 1:40,000 scale. Frames are acquired that center on each quarter of a 7.5-minute topographic quadrangle map. They can therefore be rectified and enlarged to produce 1:24,000-scale image maps (orthophoto quads) of the Earth's surface. The intent of the NAPP program is to provide complete photographic coverage of the United States with regular updates. Index maps for NAPP photographic coverage and ordering information for either photographs or orthophoto quad maps may be obtained from agencies that distribute the aerial photographs.

NAPP and NHAP aerial photographs are available from:

U. S. Department of Agriculture
ASCS, Aerial Photography Field Office
P.O. Box 30010
Salt Lake City, Utah 84103-0010
Phone: (801) 524-5856

or

Customer Services NAPP
USGS EROS Data Center
Sioux Falls, South Dakota 57198
Phone: (605) 594-6151

Geologic investigations in Wyoming

Satellite imagery has been used in many different ways to augment the study of Wyoming geology. Most applications use the broad regional perspective of the imagery to view region-wide landscape relationships. The satellite image is often interpreted in much the same way as a color or black-and-white aerial photograph. While such applications may be effective, they fail to make use of the multispectral attribute and digital format of these image data, which provide extended capabilities for a more in-depth analysis.

In recent years, multispectral satellite imagery has played a key role in structural, stratigraphic, mineralogic, and geomorphic investigations throughout Wyoming. These studies hinge on the ability of multispectral images and high-resolution (aircraft or satellite) spectrometry to distinguish surface mineralogic differences.

The works of Stucky and Krishtalka (1991) and Lang and others (1987, 1990) demonstrate that Landsat multispectral data are particularly useful for characterizing mineralogic variations in exposed stratigraphic sequences. Lang and others (1990) showed that laboratory reflectance or emittance spectra, derived from representative rock samples, can be employed to construct "type" spectra characterizing distinct sedimentary rock units. Each type spectrum exhibits absorption bands characteristic of specific mineral species. Gypsum, for instance, is represented by the presence of reflectance minima (absorption bands) at 1,000, 1,200, 1,450, 1,480, 1,530, 1,750, 1,940, 2,220 and 2,260 nm wavelengths. Because most geologic units contain more than one mineral, they can be characterized by a unique mix of type spectra. The combinations are sometimes ambiguous, but certain geologic units are sufficiently unique in their multispectral character to serve as markers for regional mapping and stratigraphic correlation. For example, Schmidt (1991) examined sequences of sedimentary rocks near Como Bluff and Medicine Bow, Wyoming, and found that the Triassic Chugwater Formation and the Cretaceous Mowry Formation are particularly distinctive and may serve as marker units.

The capabilities of Landsat multispectral data have also proven useful for mineral and petroleum exploration. A number of investigators have employed this approach in Wyoming with considerable success (Levinson, 1979; Marks, 1985; Lang and others, 1984a; Froman, 1976; Marrs and Kaminsky, 1977; Marrs, 1984). In each of these studies, variations in spectral reflectance were used to detect surface anomalies associated with petroleum and/or mineral deposits. In cases where surface alterations are associated with uranium, vanadium, or sulfide ores, for example, the most detectable constituent is often ferric iron (Levinson, 1979; Lang and others, 1984a), which may be detected as red soils. Thus, digital processing of appropriate spectral bands, which enhances variations in soil color, can aid mineral detection.

Multispectral remote sensing is often useful in petroleum exploration. Since hydrocarbon reservoirs are seldom, if ever, completely sealed, the lighter hydrocarbons will slowly seep from a "leaky" reservoir and chemically alter overlying rock and soil (Donovan and others, 1974; Richers and others, 1982). The escaping hydrocarbons may also indirectly affect vegetation and ground-water flow patterns. Thus, multispectral remote sensing can be used to identify these surface features and aid detection of subsurface reserves.

Using this approach, Marrs and Paylor (1987) investigated a surface anomaly at the Table Rock oil field in the Green River Basin, Wyoming. They identified a spectral anomaly directly above the Table Rock oil reservoir (in this case, an abundance of smectite and mixed-layered clay minerals) that was represented by a reflectance minimum in the 2,200 nm wavelength region. In addition, they found an excess of iron near the central part of the anomalous zone. This concentration was associated with a slight increase in red and yellow reflectance, visible on enhanced Landsat images, and formed a halo or donut-shaped soil anomaly above the Table Rock reservoir. Others have also attempted to relate surface spectral anomalies to petroleum accumulations in Wyoming in the hope that remote sensing might provide a direct exploration tool by helping to locate spectral, geochemical, soil, or vegetation anomalies (Froman, 1976; Marrs and Kaminski, 1977; Lang and others, 1984a). The most comprehensive of these efforts was the work conducted at Patrick Draw, Wyoming, and other selected locations by the Geosat Team, a consortium of petroleum companies and other agencies (Lang and others, 1984a).

Geomorphic applications of multispectral remote sensing in Wyoming have proven quite successful. Two applications are described in detail in the following sections. These applications are particularly significant in that they illustrate the general utility of digital, multispectral satellite imagery and the effectiveness of combining these data with other types of computerized landscape information. Distinct combinations of these data have enabled investigators to identify and map subtle geologic and geomorphic features in Wyoming that have never before been fully recognized.

Interpretation of eolian landforms and wind power potential

An early application of Landsat multispectral imagery employed the regional perspective to map eolian landforms and interpret airflow patterns across south-central Wyoming. This work spanned several years and involved a number of workers interested in evaluating present wind patterns, long-term climatic change, and wind-power potential from eolian landforms (Kolm, 1973, 1977, 1982; Dawson and Marwitz, 1982; Martner and Marwitz, 1982; Marrs and Kolm, 1982; Marrs and Gaylord, 1982; Gaylord, 1982, 1987, 1991; Marrs and others, 1987). These investigations were given impetus by a short-lived enthusiasm for alternate energy sources that emerged as a result of the 1973-74 energy crisis (Grove, 1974). The development of wind power was considered especially attractive in areas where wind-generated power could be used to augment hydroelectric power during winter months, so that more winter runoff could be retained in reservoirs for later use as irrigation water.

Kolm (1973) used Landsat imagery to map dune fields of south-central Wyoming, an area well known for its strong winter winds. Because of the regional overview provided by Landsat, he was better able to appreciate the relationship between numerous eolian landforms and the topographic features that control airflow across Wyoming. Consequently, he used his interpretations of Landsat imagery to define the "Wyoming wind corridor". He later expanded his interpretation by mapping major dune complexes, wind-scour streaks, blowout playas, and playa-related features (Kolm, 1977). He interpreted trends and concentrations of eolian features and was able to map the general pattern of surface airflow. Ultimately, he identified areas of topographic confluence having persistent high winds (areas of exceptional windpower potential) (**Figure 3**). Dawson and Marwitz (1982) supplemented this work by using airborne wind sensors to measure three-dimensional wind vectors. From these measurements they correlated between measured wind velocities, local wind patterns, and terrain features that control near-surface air movement.

Recognizing the relationship between airflow patterns and eolian features, Marrs and Kolm (1982) used Landsat imagery and air photos to interpret large-scale landform characteristics such as dune and draa orientation, size, form, and spacing. They also used repetitive coverage to determine rates of dune migration. Sand samples were collected for size analyses so that quantitative estimates of wind velocity and overall wind power could be estimated. Their work demonstrates that eolian landforms can be accurately mapped from Landsat satellite imagery and that these landforms can be used to interpret important environmental parameters such as wind direction, persistence, and maximum and mean velocities which can, in turn, be used to develop estimates of wind-power potential for an area.

Recently, Gaylord (1987) and Gaylord and Dawson (1987) combined satellite image and air photo interpretations with field data, airborne wind-velocity soundings, and topographic information to evaluate wind and terrain interactions in the Ferris dune field and at Windy Gap in central Wyoming. They found that dune forms in the Windy Gap area are influenced by accelerated airflow through the mountain pass (**Figure 4**). The dunes within the gap are extremely elongate and lack leeward slip faces typical of most dunes. On the upwind side of the gap, the dunes are transformed into sand streaks that merge downwind with phytogenic dunes, which have been stabilized by heavier growths of vegetation. Sediment samples reveal that dune sands at Windy Gap show a general downwind decrease in grain size; the coarser sand being left behind as a lag deposit as winds carry the finer sand up slope through the gap.

To evaluate airflow patterns through Windy Gap, a series of wind velocity and temperature soundings were used to construct potential temperature and isovelocity profiles (**Figure 5**). These profiles show that a weak velocity jet forms beneath a stable, constricting air layer that usually develops

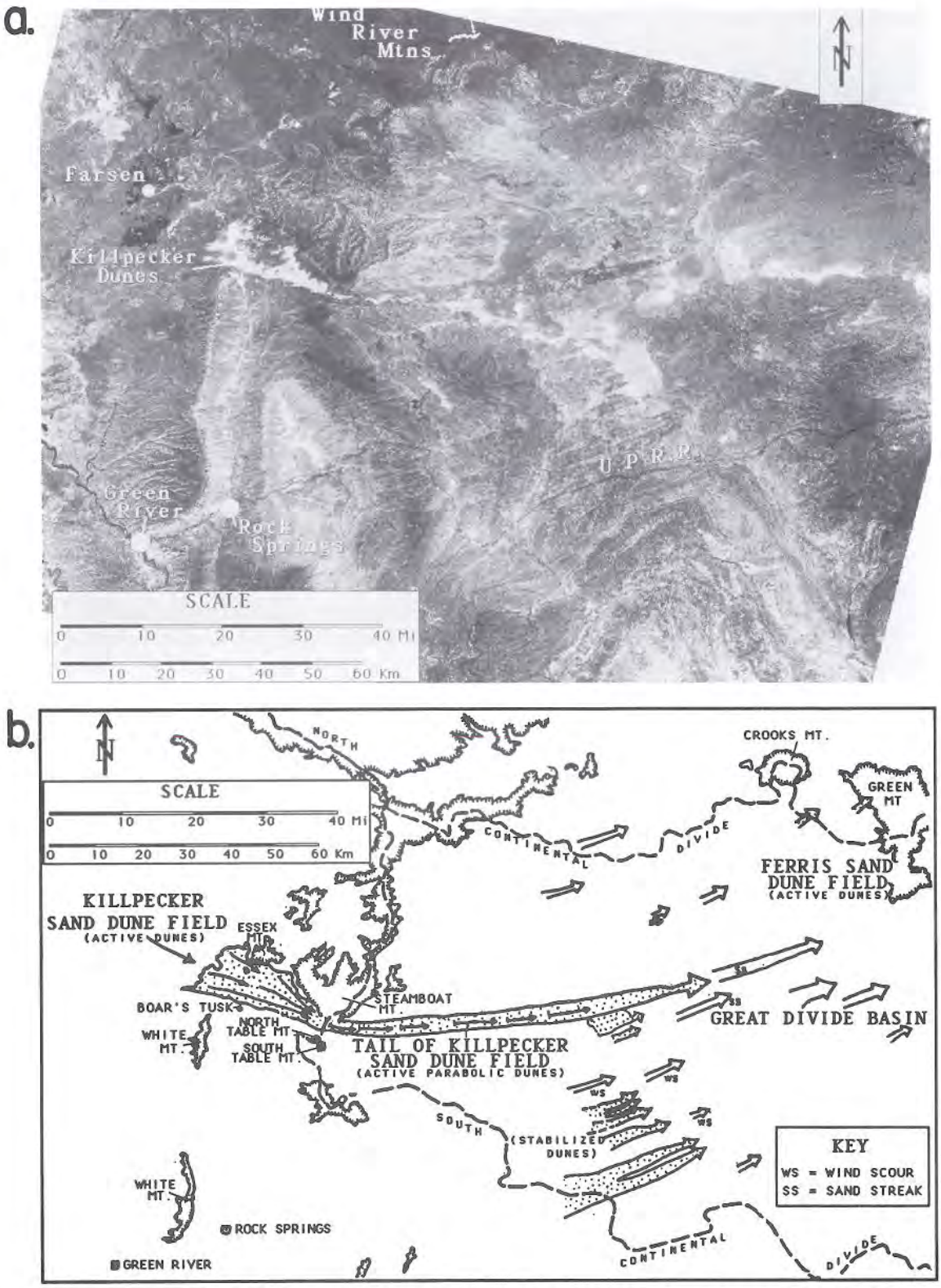

Figure 3. (a) Landsat MSS image (June 17, 1978; I.D. #3010517234; red band) of the Killpecker Dunes and surrounding area of south-central Wyoming and (b) interpretation of eolian landforms and high-wind areas in the region (from Kolm, 1977). Note that streamlines may be interpreted directly from the orientation of eolian landforms. The strongly aligned features indicate that persistent strong winds in this area are nearly unidirectional. Areas where streamlines converge may be interpreted as regions of particularly high wind-energy potential.

a.

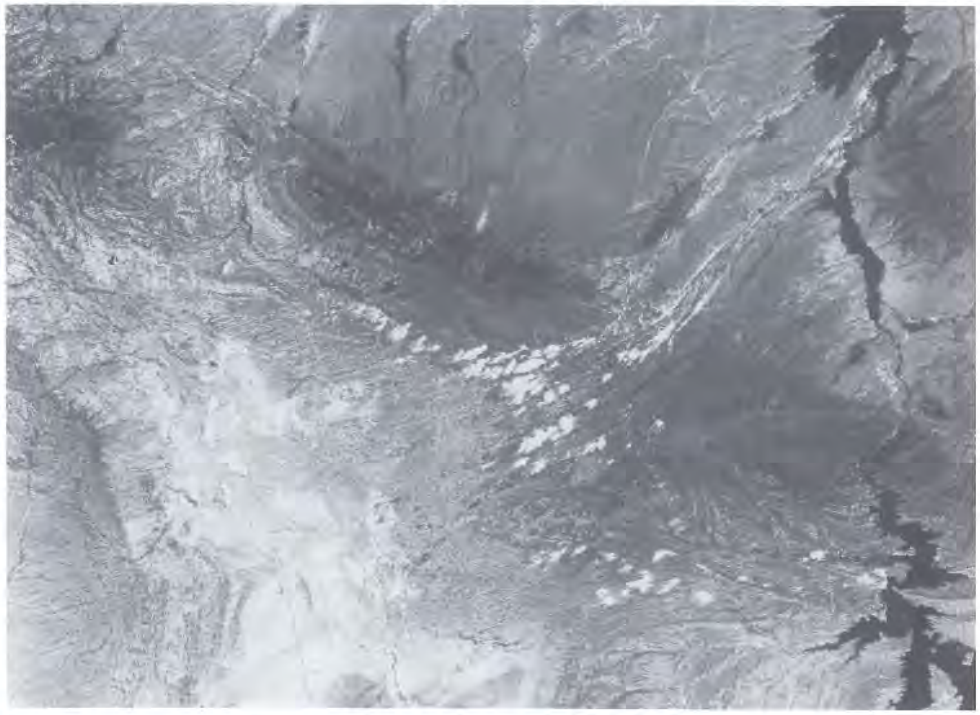

b.

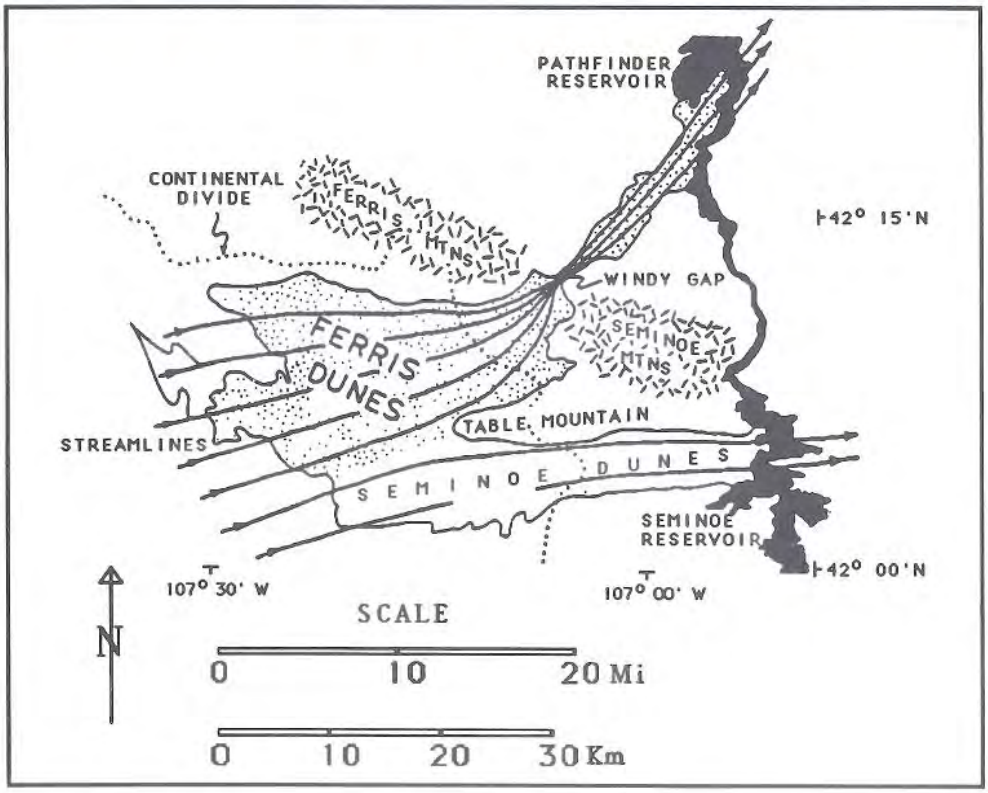

Figure 4. (a) Landsat Thematic Mapper image (July 7, 1984; red band) of the Windy Gap area near Seminoe and Pathfinder reservoirs in central Wyoming. The dunes visible on this image show a pattern that responds to the bifurcation of near-surface airflow and the effects of the acceleration of flow through Windy Gap. (b) Eolian sand deposits mapped from the satellite imagery and airflow streamlines interpreted from dune patterns. The streamlines indicate direction of dominant airflow across the area. Note the confluence of airflow through Windy Gap and the change in direction of flow as it passes on either side of Table Mountain (from Gaylord and Dawson, 1987).

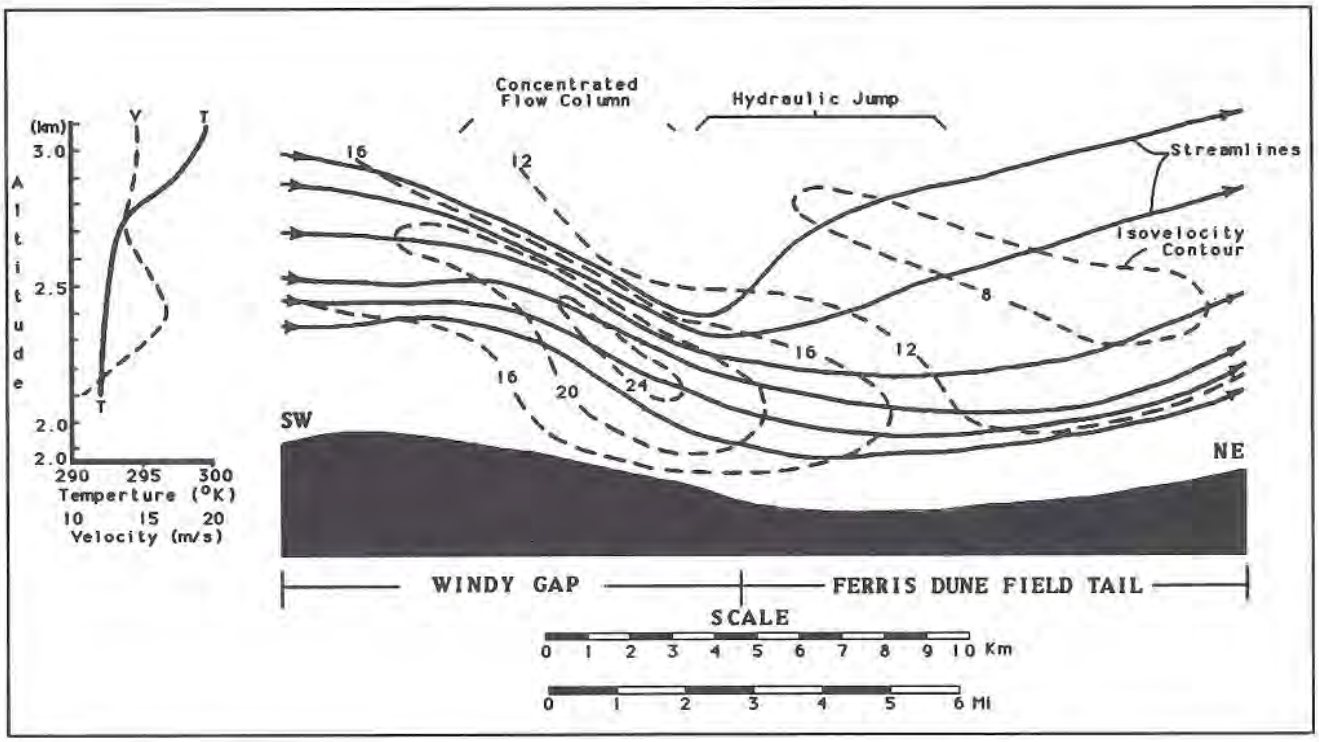

Figure 5. Vertical profile through Windy Gap showing the configuration of airflow streamlines and their relationship to wind velocities (V) and potential temperature (theta) (from Gaylord and Dawson, 1987).

some 750 meters above the ground. Thus, the vertical and horizontal confluence through the narrow mountain gap generates a distinct acceleration (funneling) of airflow. As air descends the downwind side of Windy Gap, the concentrated flow column develops a standing wave pattern analogous to a hydraulic jump. The turbulent flow has very high kinetic energy that enhances erosion, as evidenced by an elongate deflation hollow about 100 meters deep. The surface of the hollow is covered with a thin, discontinuous sheet of debris that was left behind as eolian sediments were swept downwind and deposited in a less turbulent environment.

The regional perspective provided by Landsat imagery and high-altitude aerial photography was critical to this study in that it enabled recognition of large-scale spatial relationships between topographic features and airflow processes. In addition, the image detail was suitable for the recognition and interpretation of individual sand dunes and deflation hollows.

Defining a late Quaternary paleolake basin

In the high desert of south-central Wyoming, Grasso (1990) applied a geographic information system approach to examine the geomorphology of a late Quaternary paleolake, Lake Wamsutter, that may have once occupied some 2,000 square kilometers of the Great Divide Basin (**Figure 6**). The study employed a multi-dimensional analysis of Landsat TM and MSS satellite data and ancillary landscape information (i.e., digital elevation and slope models, digitized aerial photographs and maps, and field data) to identify lacustrine sediments, wave-cut terraces, and fan-delta complexes that formed in direct response to Lake Wamsutter. The spatial distributions of lacustrine landforms and unique Quaternary sediment types were subsequently combined into a region-wide model showing the late Quaternary geologic history of the basin and the paleogeographic extent of the lake.

Figure 6. Digital elevation model of the Great Divide Basin, an internally drained hydrologic basin entirely encircled by the Continental Divide. Five-meter topographic contour levels are displayed in 240 shades of gray. Low elevations (basins) are displayed in dark gray, while high elevations (mountains) are displayed light gray. The approximate maximum extent of Lake Wamsutter is shown at the 2,040-45 meter level in white. Remnant wave-cut terraces and deltas at Lost Creek (LCD), Stewart Creek (SCD), and the Stratton Draw site (SDS) reveal that the lake was approximately 67 meters (220 feet) deep in the vicinity of Battle Spring Flat (BSF; elevation 1,973 m). At this level, Lake Wamsutter would have engulfed two smaller basins: Red Desert Basin (RDB) to the west and an east-trending basin now occupied by Lost Creek Basin (LCB), Battle Spring Flat, and Chain Lakes Flat (CLF). The dotted line west of Separation Flats (SF) marks the former site of basin closure. Here the incised channel of Separation Creek cuts near-vertical rocks of the west flank of the Rawlins uplift (A). The deepest parts of the lake basin (less than 2,010 meters) are displayed in black. Some were sites of closed-basin lakes that formed during a middle Holocene lake event (modified from Grasso, 1990).

Ultimately, this investigation demonstrated that the currently arid environment of the Great Divide Basin may have been dominated by cooler and wetter climatic conditions similar to those that characterized the Great Basin physiographic province of the western United States during the late Pleistocene. This relationship suggests that south-central Wyoming may have been a distant, northeastern extension of the Great Basin; an area where some 100 late Pleistocene perennial lakes formerly occupied topographically closed basins (Benson, and others, 1990; Benson and Thompson, 1987; Smith and Street-Perrott, 1983; Feth, 1964).

The following sections of this paper give a summary of some of the more important remote-sensing/GIS procedures Grasso (1990) used to identify remnant lacustrine features of Lake Wamsutter. They

exemplify how a combination of Landsat multispectral satellite data and ancillary terrain information can be used to interpret and map past and present geologic landscapes.

The remote-sensing/GIS approach

Geomorphologists have commonly relied on aerial photography to locate and map the former extent of Quaternary paleolakes (Reeves, 1968). Today, regional satellite coverage, advancements in computer technologies, and software capable of integrating digital and analog landscape information offer an improved approach. For example, surface sediment composition can be identified using a number of well-established image enhancement and analysis procedures, including band ratioing, density slicing, principal-components analysis, and a host of other multispectral analysis procedures (Drury, 1987; Jensen, 1986; Lang and others, 1984a, 1984b; Kahle, 1980a). The digital (raster) format of these modern satellite data also provides a ready means for combining other forms of digital terrain information (e.g., digital elevation and slope models) through the use of mathematical and/or statistical manipulation techniques.

Throughout the 1980s, various methods were proposed to merge spectral (surface composition) and spatial (topographic) information. Particular combinations of data enabled investigators to successfully examine such features as the Holocene extent of the Great Salt Lake (Merola and others, 1989), geologic structures (Chorowicz and others, 1989), arid geomorphic surfaces (Shih and Schowengerdt, 1983), soil and land cover classes (Moore, 1984; Franklin, 1987), vegetation communities (Frank, 1988), and a number of land use patterns (Stow and Estes, 1981).

The discrimination of sediments and identification of landforms associated with a large lake system, such as Lake Wamsutter (**Figure 6**), was possible through a basin-wide analysis of surface sediment composition and landform morphology. For example, remnant wave-cut shorelines of silica-rich sand and gravel border the basin's perimeter at elevations corresponding to lake level stillstands, whereas clay-rich lacustrine sediments, characteristic of quiet, deep-water areas of the lake, occupy flat, low-lying areas of the basin center. A region-wide geomorphic investigation of lacustrine features in the Great Divide Basin was therefore possible by combining the Landsat multispectral analysis of surface sediment composition with a digital elevation model (DEM) analysis of basin morphology.

The physical basis of this approach is that geologic surface materials can be recognized and mapped using multispectral remote sensing (Drury, 1987; Lang and others, 1984a, 1984b; Richason, 1983; Rowan and others, 1983; Viljoen and Viljoen, 1983; Goetz and Rowan, 1981; Moik, 1980; Siegal and Gillespie, 1980; Condit, 1970), and that corresponding landforms can be identified based on their unique morphology (Jenson and Domingue, 1988; Townshend, 1981; Way, 1978). The merger of multispectral Landsat data and multispatial digital elevation and slope information therefore provided a means for distinguishing unique lacustrine sediment types for a given elevation, elevation range, or slope class related to one or more of the former depositional environments of Lake Wamsutter. Using this approach, remnant landforms of this lake system were identified and mapped based on both their lithologic composition and morphologic character. Ultimately, this spectral and spatial information was used to reconstruct the paleogeographic extent of Lake Wamsutter, and to model the late Quaternary geologic history of the basin.

Paleogeographic reconstruction of Lake Wamsutter

In the Great Divide Basin, a predictable correspondence was identified between the maximum high-water stillstand of Lake Wamsutter and remnant lacustrine sediments and littoral zone landforms (Grasso, 1990). At the 2,035-45 meter level, paleolake sediments and landforms (e.g., remnant shorelines, deltas, and lake-marginal sand dunes) mark the maximum stillstand (deepwater) level of the lake (**Figure 6**). In addition, many of these paleolake features were uniquely identified by an unsupervised classification algorithm, which numerically classified spectral and spatial data for the basin into discrete geologic feature types. This information was subsequently combined to produce a composite image map of the basin showing the spatial relationship between paleolake features and former lake levels of Lake Wamsutter.

Figure 7 shows the results of the multi-dimensional analysis procedure applied to Landsat spectral bands MSS-4, MSS-5, and MSS-7 and co-registered digital elevation and slope models. The image displays the maximum extent of Lake Wamsutter as identified by remote sensing and field investigations (shown in shades of green at digital elevation levels 2,035-40 m and 2,040-45 m), and by the multi-dimensional numerical classification approach (shown in medium blue). The extent of post-lacustrine fluvial and eolian sediments, which have invaded the basin and now cover large portions of the former lake bed, is also shown.

It is particularly noteworthy that the maximum predicted level of the lake is closely paralleled by the maximum extent of clay-rich lacustrine sediments in the basin (i.e., the paleolake feature class), since the former was based on the location of remnant paleolake landforms (e.g., shorelines, deltas, and lakemarginal sand dunes) and the latter was derived numerically. The visible discordance that exists between the predicted and numerically-identified lake levels was shown by field examinations and supplemental image analysis to be the result of both basin morphology and post-lacustrine sediment deposition. The most important of these are: (1) the steeper slope of the lake's former nearshore zone caused the classifier to disassociate this zone from the more gently sloping offshore area, (2) the dissimilarity between coarse, silica-rich littoral zone sediments and clay-rich lake deposits of the basin's center caused the classifier to separate the littoral-zone from the paleolake feature class, and (3) the recent influx of Holocene-age fluvial, colluvial, and eolian sediments that invaded the lake basin and now bury large portions of the former nearshore zone were identified by the classifier to be unlike lacustrine sediments in the basin since the composition of these younger deposits are spectrally different than the deposits of the exposed lake bed.

Although the more recent Holocene sediments caused misclassifications, they provide chronological evidence for a late Pleistocene existence of Lake Wamsutter. Along the north margin of the east subbasin, in the vicinity of the Stewart Creek delta site (SCD; **Figure 7**), colluvium buries a middle to late Holocene paleosol containing prehistoric Indian hearths to a depth of one meter. Similarly, the east margin and central parts of the Red Desert Basin (RDB) are concealed beneath Holocene-age eolian sheet sands and sand dunes, the most obvious being the elongate "tail" of the Killpecker dune field. These dunes, estimated to be 10,000 years old (Gaylord, 1982), bury Quaternary alluvium (Qa) derived from red clastic units of the Tertiary Cathedral Bluffs Tongue (Twc), which in turn buries lacustrine sediments of Lake Wamsutter. The underlying lake deposits therefore pre-date both fluvial and eolian sediments since the invasion of either of these sediments into the lake would have resulted in sediment mixing and dispersal by lacustrine processes rather than the conspicuous stratigraphic sequence of Quaternary sediments seen in the basin today. Thus, this sedimentary sequence indicates a minimum late Pleistocene age for Lake Wamsutter.

Combining aerial photographs and Landsat images

A limitation of Landsat remote sensing is its relatively poor resolution of small-scale landforms. Thus, small shoreline remnants and deltas at the margins of Lake Wamsutter could not be readily identified and mapped from satellite data alone. To solve this problem, Landsat image bands were digitally combined with high-altitude aerial photographs. The result was a hybrid data set containing both spectral and high-resolution spatial information.

The procedure employs a mathematical transformation that orthogonally transforms red, green, and blue (RGB) image display components into more easily perceived hue, intensity, and saturation (HIS) elements of human color perception (Buchanan and Pendergrass, 1980). The intensity component, which contains surface reflectance (albedo) information corresponding to surface roughness (or texture), renders topography of the site at the resolution of the sensor (Gillespie, 1980). Conversely, hue and saturation contain spectral (color) information related to the electromagnetic range of the three Landsat input bands, for example MSS-7 as red, MSS-5 as green, and MSS-4 as blue. Hue therefore defines the combined average color of surface reflected light within the spectral range of the sensors (500 to 1100 nm), while saturation depicts the purity (or richness) of the color.

If these HIS elements are reverse transformed back to their red, green, and blue counterparts, the resulting RGB image will contain the same information as the original bands used in the forward (RGB to

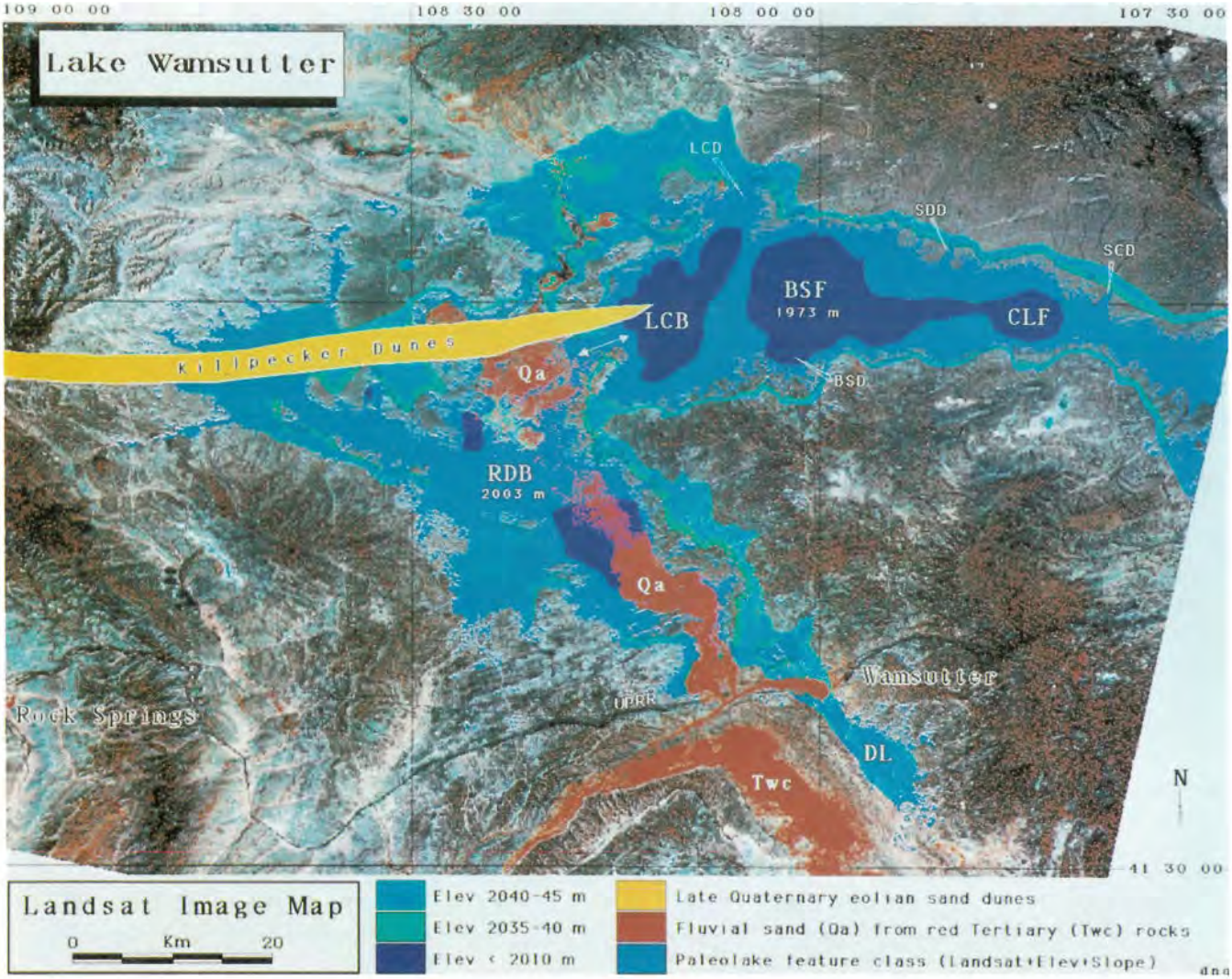

Figure 7. Landsat image map of the Great Divide Basin showing the paleogeographic extent of Lake Wamsutter and the distribution of post-lacustrine alluvium (Qa) derived from red sandstones of the Cathedral Bluffs Tongue of the Wasatch Formation (Twc), and eolian sands forming the prominent "tail" of the Killpecker dune field. The image was prepared using a standard, geometrically corrected, MSS false-color image base and six coregistered overlays: three digital elevation levels (2,040-45, 2,035-40, and (< 2,010 meters); and three geologic-feature classes identified from numerical analyses of spectral and spatial data. The paleolake class (medium blue) was derived based on its unique lacustrine sediment composition and morphometric (i.e., elevation and slope) characteristics. The chronostratigraphic relationship between Quaternary fluvial (Qa) and eolian sediments, which invaded the basin following the demise of Lake Wamsutter, and underlying lacustrine deposits indicate a minimum late Pleistocene age for the lake. Other noteworthy geologic features are: (1) remnant deltas at the mouths of Lost Creek (LCD), Stratton Draw (SDD), and Stewart Creek (SCD), (2) a remnant shoreline to the west of Dry Lake (DL), (3) dispersion patterns of red fluvial sands derived from Twc outcrops north and south of the Red Desert Basin, and (4) the nearly flat basin surface (2,040-45 m) that is graded to the maximum level of Lake Wamsutter; the latter most noticeable to the north of Lost Creek Basin. The double-sided arrow shows the location of a former spillway (wind gap) that connected west and east subbasins of Lake Wamsutter during its maximum stillstand (modified from Grasso, 1990).

HIS) transformation. However, if the intensity element is enhanced to improve topographic discrimination, or simply replaced with another image containing more detail, the effective resolution of the RGB image components is improved to the resolution of the replacement intensity image.

Figure 8 shows that the 80 x 80-meter pixel resolution of a standard, geometrically-corrected Landsat MSS image can be effectively increased to the 10x10-meter pixel resolution of a digitized aerial photograph by replacing the intensity component from the RGB-to-HIS transformed Landsat image with a co-registered, high-resolution aerial photograph and performing the reverse (HIS to RGB) transformation. The resulting hybrid image (**Figure 8b**) not only retains the primary spectral information (i.e, hue and saturation) supplied by Landsat, but also gains the high-resolution spatial information (i.e., intensity) furnished by the aerial photograph. The color transformation therefore yields an eight-fold improvement in spatial resolution over the Landsat image, and produces a data set with spatial and spectral characteristics similar to that furnished by the more advanced SPOT satellite system.

This approach was recently used by Carper and others (1990) to merge SPOT 30-meter multispectral and 10-meter panchromatic image data. The result was a three-fold improvement in the resolution of SPOT multispectral imagery. The reverse HIS color transformation has also been shown by Harris and others (1990) to be an effective method for merging spectrally and spatially dissimilar data sets, such as multispectral satellite image bands with radar, magnetometer, and geologic map information.

Since the color-transformed hybrid image is in digital (raster) format it can also be spectrally enhanced to improve geologic discrimination or combined with other forms of digital map information to improve spatial analysis and mapping. **Figure 8b** explicitly shows, for example, that a well-preserved, remnant delta extends from the mouth of Stratton Draw (SDD, **Figure 7**) out onto the dry lake bed of Lake Wamsutter, while this lake-marginal landform is barely discernible on a standard Landsat image of the site (**Figure 8a**). The improved textural (topographic) resolution of the image also shows the boundary between the smoother lake bed (A) and more dissected terrain to the north (B), and the irregular terrain of shoreline sand dunes (C) that reside downwind (east) of the delta. Moreover, the superimposed elevation contours, derived from a 1:24,000-scale U.S. Geological Survey topographic map, greatly improve mapping and morphometric interpretation of these lake-marginal landforms.

Multispectral sediment discrimination

Multispectral discrimination of sediment composition is best achieved by comparing known reflectance and/or thermal emittance properties of pure and mixed geologic materials with the derived spectral values of the material of interest. This method, known as spectral signature analysis, is based on the fact that Earth materials have unique visible, infrared, and thermal-infrared properties (Jensen, 1986; Kahle, 1980b; Hunt, 1977, 1979; Hunt and Ashley, 1979). The geologic application of this multispectral remote-sensing technique is particularly well documented for differentiating semiarid surface sediment, soil, and vegetation cover types at Patrick Draw, Wyoming, southwest of the Great Divide Basin (Lang and others, 1984a), near Coyanosa, Texas (Lang and others, 1984b), and by spectral stratigraphic studies in the Wind River and Big Horn basins of Wyoming (Lang and others, 1990). The work of Lang and others (1984a) in the Patrick Draw area and that by Kahle (1980b) were especially valuable to the Lake Wamsutter study in that they: (1) furnished field spectra of unique surface-sediment types in south-central Wyoming, (2) illustrated the use of Landsat TM band ratios, and (3) exemplified the effectiveness of using Landsat short-wave-infrared (TM-5 and TM-7) and thermal-infrared (TM-6) bands for geologic remote sensing.

In the Separation Flats area, east of the proposed boundary of Lake Wamsutter (**Figure 6**), Landsat TM infrared data were used to distinguish between lacustrine and fluvial sediments associated with a natural spillway of the lake. Using preliminary field investigations and Landsat spectral analyses for the area, Grasso (1990) showed that three Landsat infrared bands (TM-4, TM-6, and TM-7) could be used to effectively differentiate geologic sediments and landforms associated with Lake Wamsutter. These bands noticeably improved landform interpretation and ultimately helped to unravel the geologic history of the lake basin to the west.

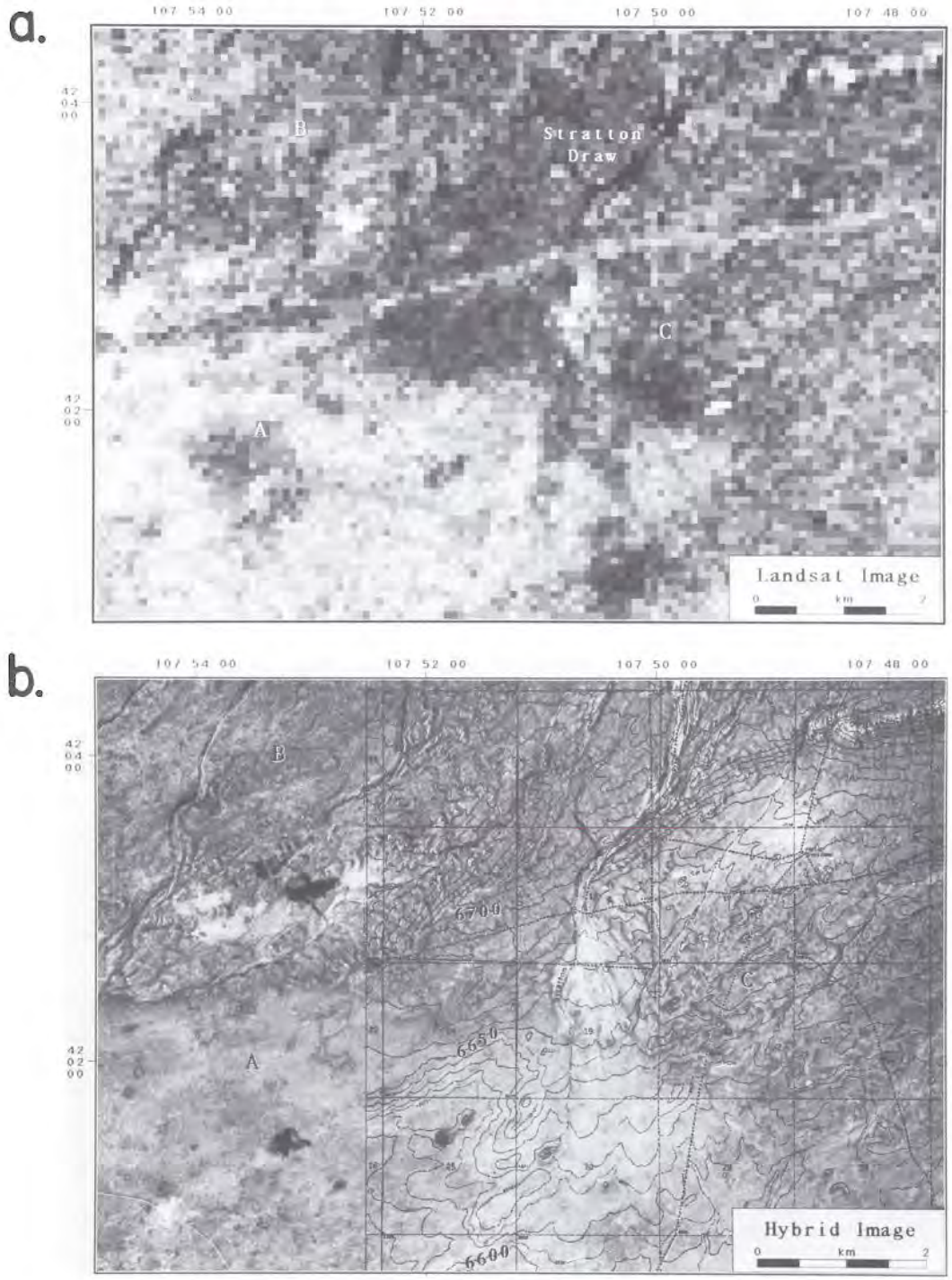

Figure 8. Landsat MSS-5 image (a) and HIS color-transformed hybrid image (b) of the Stratton Draw site (SDS, Figure 6). A comparison of these images illustrates the improved resolution produced by the forward and reverse HIS color transformation procedure. The blocky appearance of the geometrically corrected Landsat image is due to the 800 percent enlargement needed to match (coregister) it to the 10-meter pixel resolution of the digitized high-altitude aerial photograph. The 1:24,000-scale topographic contour map (overlain in black) was used to improve geologic interpretation and mapping of the delta and associated paleolake features. The improved resolution of the hybrid image clearly delineates the boundary between the smooth paleolake bed of Lake Wamsutter (A) and the dissected terrain (B) to the north, and shows the irregular topography of lake-marginal sand dunes (C) east (downwind) of the delta. (Modified from Grasso, 1990.)

Figure 9 shows the results of geologic remote sensing and field investigations in the Separation Flats area. This falsecolor infrared image map of the proposed spillway at the eastern margin of Lake Wamsutter was prepared using spectrally and spatially calibrated Landsat bands TM-4 (near infrared), TM-7 (short-wave infrared), and TM-6 (thermal infrared). The image effectively differentiates spectrally dissimilar surface-sediment types and associated landforms and illustrates the application of these nonvisible bands for geologic investigations. The discriminating power of the three bands (**Table 2**) was particularly important in identifying and mapping a former outlet channel and alluvial plain associated with Lake Wamsutter. The paleochannel (brown trend) extends from the lake basin to the southwest and cuts near-vertical rocks along the west flank of the Rawlins uplift. Sediments comprising a large alluvial plain (yellow areas) spread radially across Separation Flats from the narrow, v-shaped mouth of the channel. The morphology of this alluvial sediment plume suggests that it was deposited as a result of rapid outwash from the Lake Wamsutter basin to the west.

A numerical analysis of spectral reflectance and thermal-emittance properties (**Figure 10**) reveals that the paleochannel contains clay-rich, fluvio-lacustrine sediments (low TM-7 values); is warmer than the surrounding alluvial plain (higher TM-6 values); and supports a heavier growth of sagebrush (slightly higher TM-4 values) due to subsurface ground-water flow. This analysis and the results of field investigations show that the paleochannel is a prior spillway (outlet) channel of the lake.

Stratigraphic investigations of sediments in the Separation Flats area showed that clay-rich lacustrine sediments from the paleolake basin were deposited within the paleochannel by an eastward-flowing stream as the lake drained into Separation Flats (**Figure 9**). The surrounding fan-shaped alluvial plain also contains sands, silts, and clays (i.e., fluvio-lacustrine sediments) that were deposited by an eastward-flowing distributary network of braided streams. Sediment composition, stratigraphy, and dispersion patterns all suggest that Lake Wamsutter overtopped its eastern divide along the west flank of

Table 2. Physical basis for the discrimination potential of Landsat TM bands used to prepare the false-color infrared image map of the Separation Flats site (see Figure 9).

TM-4 (Red)	Enhances the distribution of green healthy vegetation due to high near-infrared reflectance properties of chlorophyll. Areas of dense sagebrush and grass along ephemeral streams and around playa lakes are displayed in bright red. Bright (high albedo) surfaces, such as active sand dunes or playa lake flats, have high TM-4 values due to mirror-like (specular) reflectance characteristics of their surfaces, a condition that results in high spectral values for all Landsat TM reflectance bands.
TM-7 (Green)	Enhances subtle differences in sediment and rock composition. Band TM-7 (2,080 to 2,350 nm) is most useful for differentiating silica-rich from clay-rich geologic materials due to a distinctive clay absorption feature within the spectral range of the band. Clays and clay- rich sediments, such as comprise lacustrine sediments and playa mud flats, absorb incident solar radiation and appear darker (low pixel values) than silica-rich deposits, such as sand dunes and alluvial channel or fan deposits.
TM-6 (Blue)	Enhances temperature/emittance differences of the Earth's surface. Cool surfaces are dark (low pixel values), while warm surfaces are bright (high pixel values). Southeast-facing, sunlit slopes heat up more quickly during the morning hours of Landsat's overpass and are therefore considerably warmer than surrounding (shaded) areas. Lakes, streams, and moist sediment surfaces are also warmer in the morning hours due to the higher thermal capacity of water as compared with dry soil.

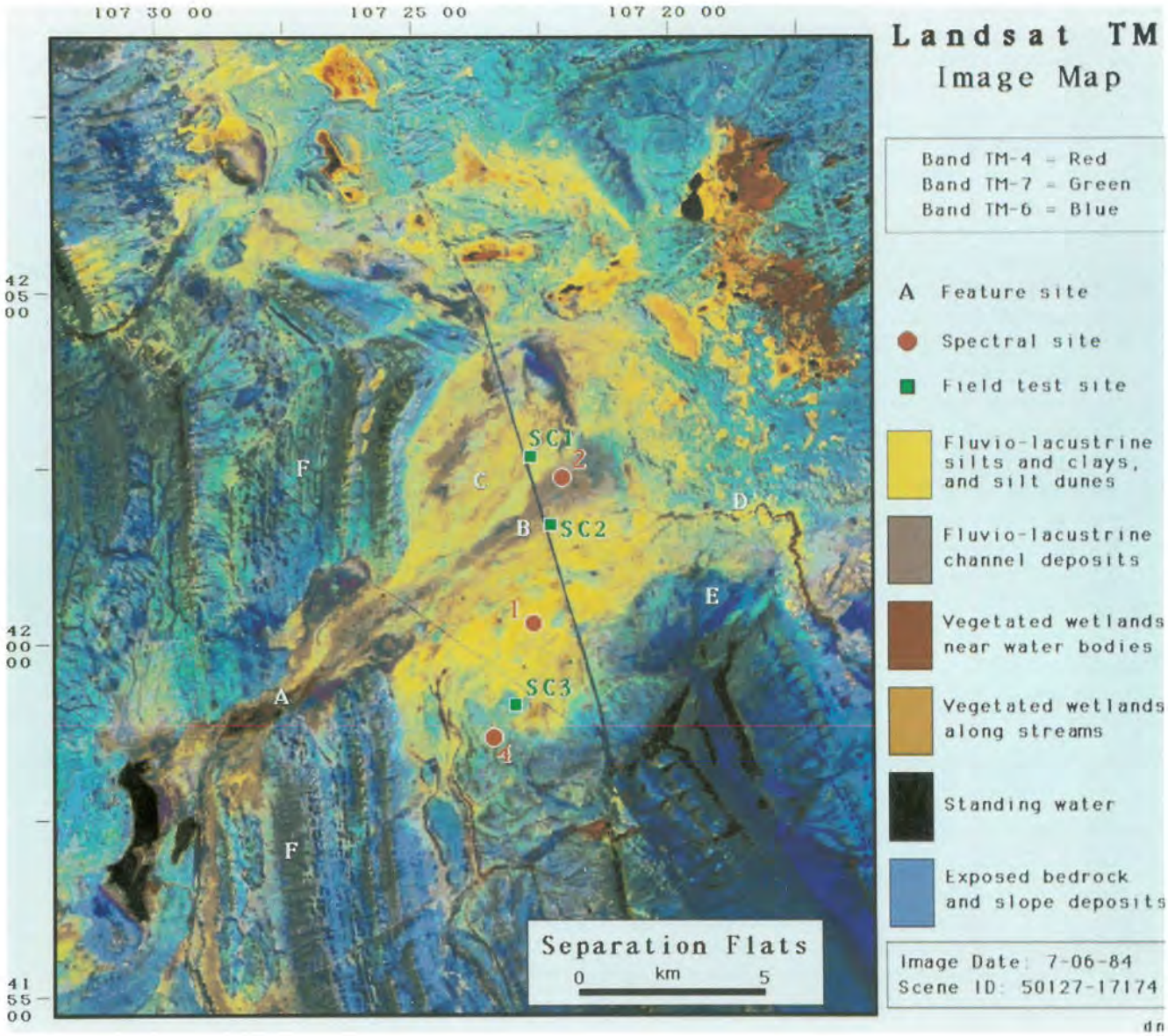

Figure 9. Landsat TM false-color infrared image map of Separation Flats showing the radial dispersion pattern of a Quaternary fluvio-lacustrine alluvial plain (yellow) deposited at the mouth of a prominent natural spillway (brown) of Lake Wamsutter. Fine-grained sands, silts, and interbedded clays that compose this alluvial sediment plume are thought to have been deposited during a rapid draining of the lake. Its sedimentary stratigraphy and composition indicate that these materials were deposited by an east-flowing distributary network of braided streams that spread radially from the narrow, 750-meter-wide mouth (A) of a channel cut through near-vertical rocks along the west flank of the Rawlins uplift (F). The dry paleochannel (A to B) at the center of the alluvial plain (C) contains an abundance of clay similar to that of the Lake Wamsutter basin to the west. The modern meandering channel of Separation Creek (D) is barely visible south of the paleochannel. Modern playa lakes are sites of dense vegetation cover (deep red). South of Separation Flats, hogbacks forming Browns Canyon Rim (slate gray to blue in lower right corner of scene) have shed debris northward into the flats. At the northern end of Browns Canyon Rim, a large 2-km-long alluvial fan (E) and coalescing fans (bajada) to the southwest (spectral site 4) have encroached on, and buried, Quaternary fluvio-lacustrine sediments comprising the alluvial plain along the south side of Separation Flats. The prominent north-trending road is Highway 287 (Muddy Gap Road). Pixel size is 28.5 x 28.5 meters. (Modified from Grasso, 1990.)

the Rawlins uplift (A; **Figure 6**) and drained into Separation Flats and the North Platte River to the east. The lack of well-defined, recessional shorelines in the Lake Wamsutter basin similarly indicates that the lake may have quickly drained from its maximum stillstand level as a result of rapid spillway erosion. This scenario is supported by the fact that no evidence (e.g., shorelines) for the existence of Lake Wamsutter was found in the Separation Flats area.

Today, the small channel of Separation Creek intermittently flows from the basin following a course southeast of and parallel to the larger paleochannel. It is likely that some of the modern drainage flows in the subsurface along the course of the paleochannel, since as **Figures 9** and **10** show, a distinctly warmer trend of higher thermal emittance was identified by the thermal-infrared band (TM-6) along this channel (spectral site 2) as compared to the surrounding alluvial plain (spectral site 1).

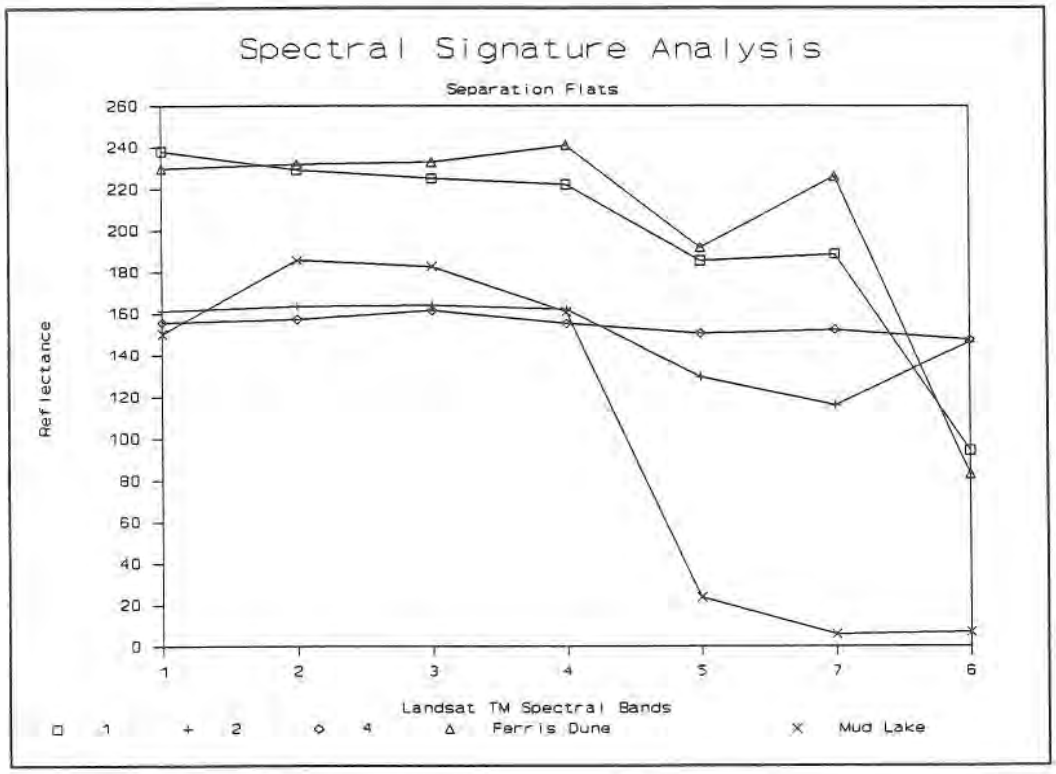

Figure 10. Landsat TM spectra of surface sediment types in and around Separation Flats (see Figure 9 for locations). Spectral properties of the exposed sediment of a modern sand dune (Ferris Dune) and playa mud flat (Mud Lake) are shown for comparison. Note that spectral similarities exist in the visible (TM-1, TM-2 and TM-3) and near-infrared (TM-4) bands, but that the middle-infrared (TM-5 and TM-7) and thermal-infrared (TM-6) bands show greater separation due to intrinsic mineralogical differences. Band TM-7 (2,080-2,350 nm) detects changes in clay content due to a prominent clay-absorption feature in its spectral range. Clay-rich deposits of Mud Lake therefore have the lowest TM-7 value, while silica-rich (clay-poor) eolian sands (Ferris Dune) have the highest TM-7 value. The prominent paleochannel (spectral site 2) crossing Separation Flats has a greater abundance of clay than either alluvial plain (spectral site 1) or fan (spectral site 4) deposits. The thermal band TM-6 (10,400-12,500 nm) also reveals important geologic features. The alluvial plain (spectral site 1) and Ferris Dune which both have bright (high albedo) surfaces are cool (low thermal emittance) since most incoming solar radiation is reflected away. Mud Lake, having a red-brown, clay-rich surface and the lowest thermal emittance value, is relatively cold due to rapid capillary rise of near-surface ground water; its evaporation actively cooling the playa surface. The spectral range of TM bands (X-axis) are: TM-1 (450-520 nm), TM-2 (520-600 nm), TM-3 (630-690 nm), TM-4 (760-900 nm), TM-5 (1550-1750 nm), TM7 (2,080-2,350 nm), and TM-6 (10,400-12,500 nm). (Modified from Grasso, 1990.)

Summary and conclusions

In the past ten years the capabilities for geologic remote sensing have improved dramatically. The spatial resolution of satellite sensor systems has steadily increased, while their spectral range and resolution have been enhanced to permit more accurate discrimination of the mineralogical and chemical composition of surface materials. At the same time, the regional overview provided by these systems is still one of their most important attributes. Several systems, including Skylab S-190B, Shuttle LFC, and SPOT, also offer stereographic coverage for more detailed analyses of landscape morphology.

The regional view provided by satellites and the extension of our vision into spectral regions beyond the visible have been beneficial to many geologic applications. The digital, raster-based format of multispectral satellite data aides interpretation by allowing numerical analyses and enhancements of spectral contrasts in geologic surface materials. These digital processing techniques also improve image interpretation and can be effectively used to generate automated numerical classifications of diverse landscape attributes. Moreover, multispectral satellite data, and the thematic information these generate, are an important component of a geographic data base because they are already in formats compatible with other types of numerical landscape information and the image coverage is regularly updated.

In Wyoming, remote sensing has already contributed significantly to our understanding of geomorphic, structural, stratigraphic, and mineralogic relationships. Various interpretation and multispectral analysis techniques have been used as tools to effectively identify and map these geologic characteristics. The integration of Landsat and high-altitude aerial photographic interpretations with wind-velocity profiles, isotopic age determinations, and sedimentological measurements was shown, for example, to contribute a comprehensive overview of region-wide airflow patterns and their relationships to eolian landforms across south-central Wyoming. In a second example, Landsat multispectral data and ancillary digital elevation and slope information were used to quantify variations in surface-sediment composition corresponding to remnant landforms of a late Quaternary paleolake (Lake Wamsutter) that once occupied the now arid region of the Great Divide Basin. A numerical classification of these merged multispectral and multispatial data showed that lacustrine sediments and remnant paleolake landforms (e.g., shorelines and deltas) delineate the paleogeographic extent of this ancient lake system. This investigation was further augmented by detailed large-scale aerial photographic interpretations, topographic mapping, and field analyses of sediment and landform types. Ultimately, a remote-sensing/GIS approach was used to interpret this multi-dimensional data set and to reconstruct the paleogeography of the ancient lake basin.

In the future, new remote-sensing tools and GIS techniques will be developed to rapidly integrate satellite spectral data and landscape information derived from thematic (e.g., geologic, geographic, and topographic) maps with linear and positional data, such as seismic lines and well logs. The potential for extending the utility of these new tools by amalgamation of data sets has already been demonstrated. Using these new merging techniques, the analyst of the future will be able to effectively assimilate a greater diversity of information to more accurately interpret, classify, and map geologic landscape characteristics.

References cited

Benson, L.V., Currey, D.R., Dorn, R.I., Lajoie, K.R., Oviatt, C.G., Robinson, S.W., Smith, G.I., and Stine, S., 1990, Chronology of expansion and contraction of four Great Basin lake systems during the past 35,000 years: Palaeogeography, Palaeoclimatology, Palaeoecology, v. 78, p. 241-286.

Benson, L.V., and Thompson, R.S., 1987, The physical record of lakes in the Great Basin, *in* Ruddiman, W.F., and Wright, H.E., Jr., editors, North America and adjacent oceans during the last deglaciation: The Geology of North America, v. K-3, Boulder, Colorado, Geological Society of America, p. 241-260.

Blackstone, D.L., Jr., 1972, Tectonic analysis of southwestern Wyoming from ERTS-1 imagery: NASA Technical Report #72-10377, submitted for NASA/UW contract NAS5-21799, 8 p.

_____ 1973, Geology of photo-linear elements, Great Divide Basin, Wyoming: NASA Technical Report #73-10958/WR, submitted for NASA/UW contract NAS5-21799, 14 p.

Blundell, J.S., and Marrs, R.W., 1991, Precambrian control of Laramide faulting, Sheep Ridge anticline, western Owl Creek Mountains, Wyoming: Mountain Geologist, v. 28, p. 83-90.

Breckenridge, R.M., 1973, Glaciation of northwestern Wyoming interpreted from ERTS-1 imagery: Symposium on significant results obtained from ERTS-1, NASA Report SP-327, NTIS, Washington, D.C., p. 363-370.

Buchanan, M.D., and Pendergrass, R., 1980, Digital Image Processing: Can intensity, hue, and saturation replace red, green, and blue?: Electro-Optical Systems Design (EOSD), March, 1980.

Carper, W.J., Lillesand, T.M., and Kiefer, R.W., 1990, The use of intensity-hue-saturation transformations for merging SPOT panchromatic and multispectral image data: Photogrammetric Engineering and Remote Sensing, v. 56, p. 459-467.

Chorowicz, J., Kim, J., Manoussis, S., and Rudant, J.P, 1989, A new technique for recognition of geological and geomorphological patterns in digital terrain models: Remote Sensing of Environment, v. 29, p. 229-239.

Condit, H.R., 1970, The spectral reflectance of American soils: Photogrammetric Engineering and Remote Sensing, v. 36, p. 955-966.

Currey, D.R., 1990, Quaternary palaeolakes in the evolution of semidesert basins, with special emphasis on Lake Bonneville and the Great Basin, U.S.A.: Palaeogeography, Palaeoclimatology, Palaeoecology, v. 76, p. 189-214.

Dawson, P.J., and Marwitz, J.D., 1982, Wave structures and turbulent features of the winter airflow in southern Wyoming: Geological Society of America Special Paper 192, p. 55-64.

Donovan, T.J., Friedman, I., and Gleason, J.D., 1974, Recognition of petroleum-bearing traps by unusual isotopic compositions of carbonate-cemented surface rocks: Geological Society of America Bulletin, v. 85, p. 351-354.

Drury, S.A., 1987, Image interpretation in geology: London, Allen and Unwin, 243 p.

Earle, J., 1977, A study of the tectonics of Wyoming and adjacent areas using photo-linear elements mapped from Landsat-1 and Skylab imagery [M.S. thesis]: Laramie, University of Wyoming, 90 p.

Elachi, C., 1982, Shuttle imaging radar experiment: Science, v. 218, p. 996-1003.

Feth, J.H., 1964, Review and annotated bibliography of ancient lake deposits (Precambrian to Pleistocene) in the western United States: U.S. Geological Survey Bulletin, no. 1080, 119 p.

Frank, T.D., 1988, Mapping dominant vegetation communities in the Colorado Rocky Mountain Front Range with LANDSAT thematic mapper and digital terrain data: Photogrammetric Engineering and Remote Sensing, v. 54, p. 1727-1734.

Franklin, S.E., 1987, Terrain analysis from digital patterns in geomorphometry and LANDSAT MSS spectral response: Photogrammetric Engineering and Remote Sensing. v. 53, p. 59-65.

Froman, N.L., 1976, Petroleum exploration using Landsat imagery [M.S. thesis]: Laramie, University of Wyoming, 96 p.

Gaylord, D.R., 1982, Geologic history of the Ferris dune field, south-central Wyoming: Geological Society of America Special Paper 192, p. 65-82.

_____ 1987, Airflow-terrain and hydrologic controls on eolian sedimentation and Holocene paleoclimatic fluctuations in Wyoming: University of Wyoming Contributions to Geology, v. 25, p. 157-165.

_____ 1991, Holocene paleoclimatic fluctuations revealed from dune and interdune strata in Wyoming: Journal of Arid Environments, in press.

Gaylord, D.R., and Dawson, P.J., 1987, Airflow-terrain interactions through a mountain gap, with an example of eolian activity beneath an atmospheric hydraulic jump: Geology, v. 15, p. 789-792.

Gillespie, A.R., 1980, Digital techniques of image enhancement, *in* Siegal, B.S., and Gillespie, A.R., editors, Remote sensing in geology: New York, John Wiley and Sons, p. 139-226.

Goetz, A.F.H., and Rowan, L.C., 1981, Geologic remote sensing: Science, v. 211, p. 781-791.

Grasso, D., 1990, Recognition and paleogeography of Quaternary Lake Wamsutter (A proposed lake in Wyoming's Great Divide Basin) combining LANDSAT remote sensing and digital elevation modeling [Ph.D. dissertation]: Laramie, University of Wyoming, 184 p.

Grove, N., 1974, Oil - the dwindling treasure: National Geographic Magazine, v. 145, p. 792-825.

Gubbels, T.L., 1987, Structural and geomorphic evolution of the north flank of the eastern Owl Creek Mountains, Wyoming [M.S. thesis]: Laramie, University of Wyoming, 181 p.

Harris, J.R., Murray, R., and Hirose, T., 1990, IHS transformation for the integration of radar imagery with other remotely sensed data: Photogrammetric Engineering and Remote Sensing. v. 56, p. 1631-1641.

Hoppin, R.A, Manley, R.D., Tappmeyer, D.M., and Voldseth, N.E., 1973, Geologic interpretation of ERTS-1 imagery, Bighorn Mountains: University of Wyoming Contributions to Geology, v. 12, p. 33-42.

Houston, R.S., 1973, Geologic mapping using space images: University of Wyoming Contributions to Geology, v. 12, p. 77-98.

Hunt, G.R., 1977, Spectral signatures of particulate minerals in the visible and near infrared: Geophysics, v. 42, p. 501- 513.

_____ 1979, Near infrared (1300-2400 nm) spectra of alteration minerals - potential for use in remote sensing: Geophysics, v. 44, p. 1974-1986.

Hunt, G.R., and Ashley, R.P., 1979, Spectra of altered rocks in the visible and near infrared: Economic Geology, v. 74, p. 1613- 1629.

Jensen, J.R., 1986, Introductory digital image processing: a remote sensing perspective: Englewood Cliffs, New Jersey, Prentice-Hall, 379 p.

Jenson, S.K., and Domingue, J.O., 1988, Extracting topographic structure from digital elevation data for geographic information system analysis: Photogrammetric Engineering and Remote Sensing, v. 54, p. 1593-1600.

Kahle, A.B., 1980a, Middle infrared MSS aircraft scanner data: analysis for geologic applications: Applied Optics, v. 19, p. 2279-2290.

_____ 1980b, Surface thermal properties, *in* Siegal, B.S., and Gillespie, A.R., editors, Remote sensing in geology: New York, John Wiley and Sons, p. 257-273.

Kaminsky, B., 1977, Correlation of Landsat multi-spectral data to rock reflectance measurements [M.S. thesis]: Laramie, University of Wyoming, 55 p.

Kolm, K.E., 1973, ERTS MSS imagery applied to mapping and economic evaluation of sand dunes in Wyoming: University of Wyoming Contributions to Geology, v. 12, p. 69-76.

_____ 1975, Selenium in soils of the lower Wasatch Formation, Campbell County, Wyoming: NASA Special Report, submitted under NASA/UW contract NAS9-13298, 98 p.

_____ 1977, Predicting the surface wind characteristics of southern Wyoming from remote sensing and eolian geomorphology [M.S. thesis]: Laramie, University of Wyoming, 141 p.

_____ 1982, Predicting wind velocities from sand dune and draa spacings determined by Fourier analysis: Geological Society America Special Paper 192, p. 19-24.

Lang, H.R., Alderman, W.H., and Sabins, F.F., Jr., 1984a, Patrick Draw, Wyoming, petroleum test case report, section 11, *in* Abrams, M.J., Conel, J.E., and Lang, H.R., editors, The joint NASA/Geosat test case project: American Association of Petroleum Geologists Special Publication, Part 2, Volume II, p. 11-1 - 11-112.

Lang, H.R., Nicolais, S.M., and Hopkins, H.R., 1984b, Coyanosa, Texas, petroleum test site report, section 13, *in* Abrams, M.J., Conel, J.E., and Lang, H.R., editors, The joint NASA/Geosat test case project: American Association of Petroleum Geologists Special Pub-lication, Part 2, Volume II, p. 13-1 - 13-81.

Lang, H.R., Adams, S.L., Conel, J.E., McGuffie, B.A., and Paylor, E.D., 1987, Multispectral remote sensing as a stratigraphic and structural tool, Wind River and Bighorn Basin area, Wyoming: American Association of Petroleum Geologists Bulletin, v. 71, p. 389-402.

Lang, H.R., Bartholomew, J., Grove, C.I., and Paylor, E.D., 1990, Spectral reflectance characterization (0.4 to 2.5 and 8.0 to 12.0um) of Phanerozoic strata, Wind River Basin and southern Bighorn Basin areas, Wyoming: Journal of Sedimentary Petrology, v. 60, p. 504-524.

Levinson, R.A., 1979, Remote sensing applied to uranium exploration in Wyoming [M.S. thesis]: Laramie, University of Wyoming, 244 p.

Marks, J., 1985, Multispectral remote sensing techniques applied to exploration for kimberlite diatremes, Laramie Range, Wyoming-Colorado [M.S. thesis]: Laramie, University of Wyoming, 164 p.

Marrs, R.W., 1984, Examination of visible and near-infrared reflectance for spectral detection of kimberlite: Transactions of the Society of Mining Engineers of the AIME, v. 278, p. 1871-1876.

Marrs, R.W., and Gaylord, D.R., 1982, Techniques for interpretation of windflow characteristics from eolian landforms: Geological Society America Special Paper 192, p. 3-18.

Marrs, R.W. and Kaminsky, B., 1977, Detection of petroleum-related soil anomalies from LANDSAT: Wyoming Geological Association 29th Annual Field Conference Guidebook, p. 71-79.

Marrs, R.W., and Kolm, K.E., editors, 1982, Interpretation of windflow characteristics from eolian landforms: Geological Society America Special Paper 192, 109 p.

Marrs, R.W., Kolm, K.E., and Gaylord, D.R., 1987, Dunes of the Wyoming wind corridor, southern Wyoming: Geological Society of America Centennial Field Guide - Rocky Mountain Section, p. 209-212.

Marrs, R.W., and Paylor, E.D., 1987, Investigation of a surface spectral anomaly at Table Rock gas field, Wyoming: Geophysics, v. 52, p. 841-857.

Marrs, R.W., and Raines, G.L., 1984, Tectonic framework of the Powder River Basin, Wyoming and Montana, interpreted from LANDSAT imagery: American Association of Petroleum Geologists Bulletin, v. 68, p. 1718-1731.

Martner, B.E., and Marwitz, J.D., 1982, Wind characteristics in southern Wyoming: Journal of Applied Meteor-ology, v. 21, p. 1815-1827.

McCauley, J.F., 1982, Subsurface valleys and geoarcheology of the eastern Sahara revealed by Shuttle radar: Science, v. 218, p. 1004-1019.

Merola, J.A., Currey, D.R., and Ridd, M.K., 1989, Thematic mapper laser profile resolution of Holocene lake limit, Great Salt Lake Desert, Utah: Remote Sensing of Environment, v. 28, p. 233-244.

Moik, J.G., 1980, Digital processing of remotely sensed images: NASA Special Publication SP-431, 330 p.

Moore, J., 1984, Soil classification in Indiana from a regression modified ratio of LANDSAT data: Terre Haute, Indiana State University Professional Paper No. 16, p. 50-59.

Paylor, E.D., Muncy, H.L., Lang, H.R., Conel, J.E., and Adams, S.L., 1989, Testing some models of foreland deformation at the Thermopolis anticline, southern Bighorn Basin, Wyoming: Mountain Geologist, v. 26, p. 1-22.

Raines, G.L., and Marrs, R.W., 1983, Lithofacies map, cross-section, and favorable areas for uranium deposits, Powder River Basin, Wyoming and Montana: U.S. Geological Survey Miscellaneous Investigations Map I-1501, Scale 1:500,000.

Reeves, C.C., Jr., 1968, Introduction to paleolimnology: Developments in Sedimentology 11, New York, Elsevier Publishing Company, 228 p.

Richason, B.F., Jr., editor, 1983, Introduction to remote sensing of the environment: Dubuque, Iowa, Kendal/Hunt Publishing Company, 582 p.

Richers, D.M., Reed, R.J., Horstman, K.C., Michels, G.D., Baker, R.N., Lundell, L., and Marrs, R.W., 1982, Landsat and soil-gas geochemical study of Patrick Draw oil field, Sweetwater County, Wyoming: American Association of Petroleum Geologists Bulletin, v. 66, p. 903-922.

Rowan, L.C., Wetlaufer, P.H., Goetz, A.F.H., Billingsley, F.C., and Stewart. J.H., 1983, Discrimination of rock types and detection of hydrothermally altered areas in southcentral Nevada by use of computer enhanced ERTS images *in* Watson, K., and Regan, R.D., editors, Remote sensing: Geophysics Reprint Series, no. 3, p. 23-57.

Sabins, F.F., 1986, Remote sensing: principles and interpretation: New York, W.H. Freeman and Company, 446 p.

Schmidt, K.J., 1991, Spectral stratigraphy applied to analysis of Cretaceous units at Como and Flat Top anticlines, southeast Wyoming [M.S. thesis]: Laramie, University of Wyoming, 104 p.

Shih, E.H.H., and Schowengerdt, R.A., 1983, Classification of arid geomorphic surfaces using LANDSAT spectral and textural features: Photogrammetric Engineering and Remote Sensing, v. 49, no. 3, p. 337-347.

Short, N.M., and Marrs, R.W., 1975, Anatomy of an anomaly, *in* The first NASA earth resources survey symposium: NASA Report TM X-58168 (also JSC-09930), p. 641-663.

Siegal, B.S., and Gillespie, A.R., 1980, Remote sensing in geology: New York, John Wiley and Sons, 702 p.

Smith, G.I., and Street-Perrott, F.A., 1983, Pluvial lakes in the western United States, *in* Wright, H.E., Jr., and Porter, S.C., editors, Late Quaternary of the United States, Volume 1, The Pleistocene: Minneapolis, University of Minnesota Press, p. 190-212.

Stow, D.A., and Estes, J.E., 1981, LANDSAT and digital terrain data for county-level resource management: Photogrammetric Engineering and Remote Sensing, v. 47, p. 215-222.

Stucky, R.K., and Krishtalka, L., 1991, Application of geologic remote sensing to vertebrae biostratigraphy: general results from the Wind River Basin: Mountain Geologist, v. 28, p. 75-82.

Tomes, B.J., Marrs, R.W., Parker, R.B., and Houston, R.S., 1973, Comparison of ERTS, Skylab 190A and 190B sensors, and aircraft photos for lineation mapping: University of Wyoming Contributions to Geology, v. 12, p. 61-69.

Townshend, J.R.G., editor, 1981, Terrain analysis and remote sensing: London, Allen and Unwin, 232 p.

Viljoen, R.P., and Viljoen, M.J., 1983, ERTS-1 imagery: an appraisal of applications in geology and mineral exploration, *in* Watson, K., and Regan, R.D., editors, Remote sensing: Geophysics Reprint Series, no. 3, p. 23-57.

Way, D.S., 1978, Terrain analysis: Stroudsburg, Pennsylvania, Dowden, Hutchinson and Ross, Inc., 438 p.

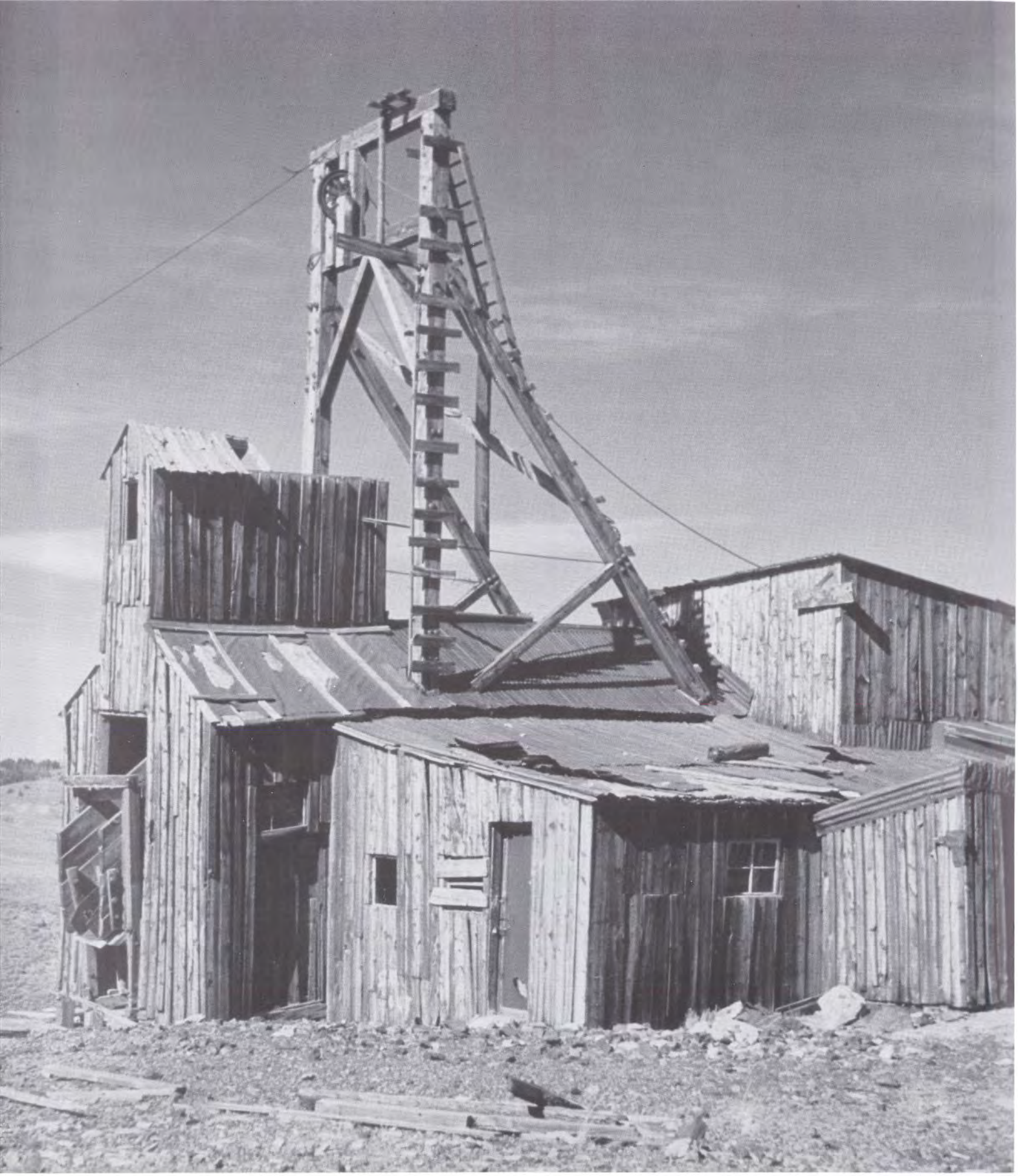

Frontispiece. The Duncan headframe and shaft house located in the South Pass-Atlantic City mining district (photograph by W.D. Hausel, 1978).

Metal and gemstone deposits of Wyoming

W. Dan Hausel
Geological Survey of Wyoming
Laramie, Wyoming 82071

Abstract

Magmatic mineral deposits in Wyoming include some important precious and strategic metal and gemstone resources including diamond, platinum-group elements, gold, titanium, vanadium, and chromium. Magmatic hydrothermal deposits include large resources of copper, silver, gold, rare-earth elements, thorium, and associated lead and zinc. Metamorphogenic mineral resources include well-developed auriferous shear zones and quartz veins. Stratabound and stratiform mineral deposits of sedimentary affiliation include banded iron formation, curpiferous quartzite, and copper-silver-zinc redbeds. Placer and paleoplacer deposits host a variety of heavy minerals of potential significance.

Introduction

The lack of geochemical information on many metal and gemstone deposits in the Cowboy State requires heavy reliance on host-rock geology and geological setting for metallogenic provenance. The available data indicate mineral deposits in Wyoming can be grouped into a variety of ore types. Classification of these deposits leads to groups with temporal and/or spatial associations indicating the presence of mineral provinces and districts.

Because of time and space constraints, I have restricted this discussion to some of the more interesting gemstones and metal occurrences and deposits. An overview on many deposits not included in this paper can be found in Osterwald and others (1960).

More detailed information on precious-metal deposits is available in Hausel (1989).

Magmatic deposits

Magmatic deposits in Wyoming include platinum, palladium, chromite, magnetite, and ilmenite in layered mafic complexes; chrome in serpentinites and in ultramafic schists; titaniferous magnetite in anorthosite; and diamonds in kimberlite. Disseminated and cumulate mineralization provide direct textural evidence of crystallization from the host magma. This intimate association links mineralization to the host igneous rock implying the mineralization and host rock have a common heritage.

Other than nickeliferous schists and diamondiferous lamproite, most types of magmatic deposits have been recognized in Wyoming in one form or another. And since a major lamproite field occurs in southwestern Wyoming and high-magnesian schists with peridotitic komatiite composition occur in more than one mountain range in the state, it is possible these latter deposits may someday be found.

Hausel, W.D.,1993, Metal and gemstone deposits of Wyoming, *in* Snoke, A.W., Steidtmann, J.R., and Roberts, S.M., editors, Geology of Wyoming: Geological Survey of Wyoming Memoir No. 5, p. 816-835.

Platinum group mineralization

Worldwide, platinum-group elements (PGE) show a strong affinity for large, intracontinental, layered mafic complexes of tholeiitic affinity. This affinity is demonstrated in southeastern Wyoming, where PGE mineralization is intimately associated with two ~1.8 Ga (age from Houston and others, 1968) Precambrian layered mafic intrusives (Lake Owen and Mullen Creek) in the Medicine Bow Mountains (**Figure 1**). These layered complexes in the Medicine Bow Mountains intrude Proterozoic schist and gneiss of the Green Mountain terrane. This terrane is interpreted as part of a Precambrian island arc that was accreted to the Wyoming craton about 1,770 Ma. The terrane was intruded by the Mullen Creek mafic complex at about the time of accretion (Loucks and others, 1988).

In mineralized layered complexes elsewhere in the world, the PGE have been described to occur in sulfides in stratiform layers spatially associated with cyclic cumulus pyroxenite, dunite, anorthosite, and troctolite. Platinum-bearing sulfides include cooperite, sperrylite, braggite, and laurite (Edwards and Atkinson, 1986).

Typically, PGE metals are found in cyclic cumulate layers of undisturbed layered complexes. In the Lake Owen intrusive, anomalous platinum is syngenetic and found in gabbroic norite (Loucks, 1991). In the Mullen Creek mafic complex, however, significant platinum mineralization is epigenetic and found in hydrothermally altered igneous rock. The effects of deformation on the Lake Owen and Mullen Creek complexes differ greatly.

The nearby Centennial Ridge district shows similar evidence for epigenesis, in that minor platinum and palladium occur with gold in shear zones in discontinuous mafic intrusives. Elsewhere, platinum nuggets have been recovered from placers of the Douglas Creek district downstream from the Mullen Creek mafic complex.

Mullen Creek mafic complex

The northeastern edge of the 60 mi^2 Mullen Creek mafic complex is intensely sheared and truncated by the Mullen Creek-Nash Fork shear zone, which contributed greatly to the deformation of the complex. Platinum and palladium occur in shear zones in hydrothermally altered metadiorite, metagabbro, metapyroxenite, and metaperidotite (McCallum and others, 1975). McCallum and others (1975) recognized two hydrothermal alteration assemblages overprinted by supergene assemblages at the New Rambler mine. Hydrothermal propylitic mineral assemblages include chlorite, epidote, clinozoisite, albite, magnetite, and pyrite. Phyllic alteration assemblages consist of sericite, quartz, and pyrite.

Sporadic mining activity between 1900 and 1918 in the mineralized shears at the New Rambler mine produced at least 6,100 tons of copper ore with credits in gold, silver, platinum, and palladium (McCallum and Orback, 1968). The U.S. Bureau of Mines (1942) reported mine production at 1.75 million pounds of copper, 170 ounces of gold, 7,350 ounces of silver, 170 ounces of platinum, and 451 ounces of palladium. Actual production of platinoids was higher than reported by the U.S. Bureau of Mines because 4,000 tons of high-grade copper ore mined at the turn of the century was sent to the smelter before platinum and palladium were discovered in the ore (McCallum and Orback, 1968). Taking this into account, Silver Lake Resources (1985) estimated platinum and palladium production at 910 ounces of platinum and 16,870 ounces of palladium.

The New Rambler shaft was sunk in a 75-foot-thick oxidized cap of malachite and azurite, with subordinate cuprite, tenorite, chalcotrychite, and chalcopyrite. Native copper, atacamite, chalcanthite, tetrahedrite, and bornite are sparsely distributed with rare orpiment, realgar, and lorandite. From 75 to 100 feet deep, the oxidized cap grades into a supergene enriched blanket of platiniferous covellite and chalcocite. The supergene assemblages grade into primary mineralized rock at 100 feet deep. Primary ore includes quartz-pyrite-chalcopyrite veins with minor sperrylite (McCallum and Orback, 1968).

Loucks and others (1988) recognized more than 21 cyclic units in the Mullen Creek complex. It is not known if syngenetic platinum is associated with these units, but the association of platinum and palladium with shear zones in the layered complex suggests remobilization of the metals from the complex.

Lake Owen mafic complex

In contrast to the Mullen Creek complex, the Lake Owen complex is virtually unaffected by defor-

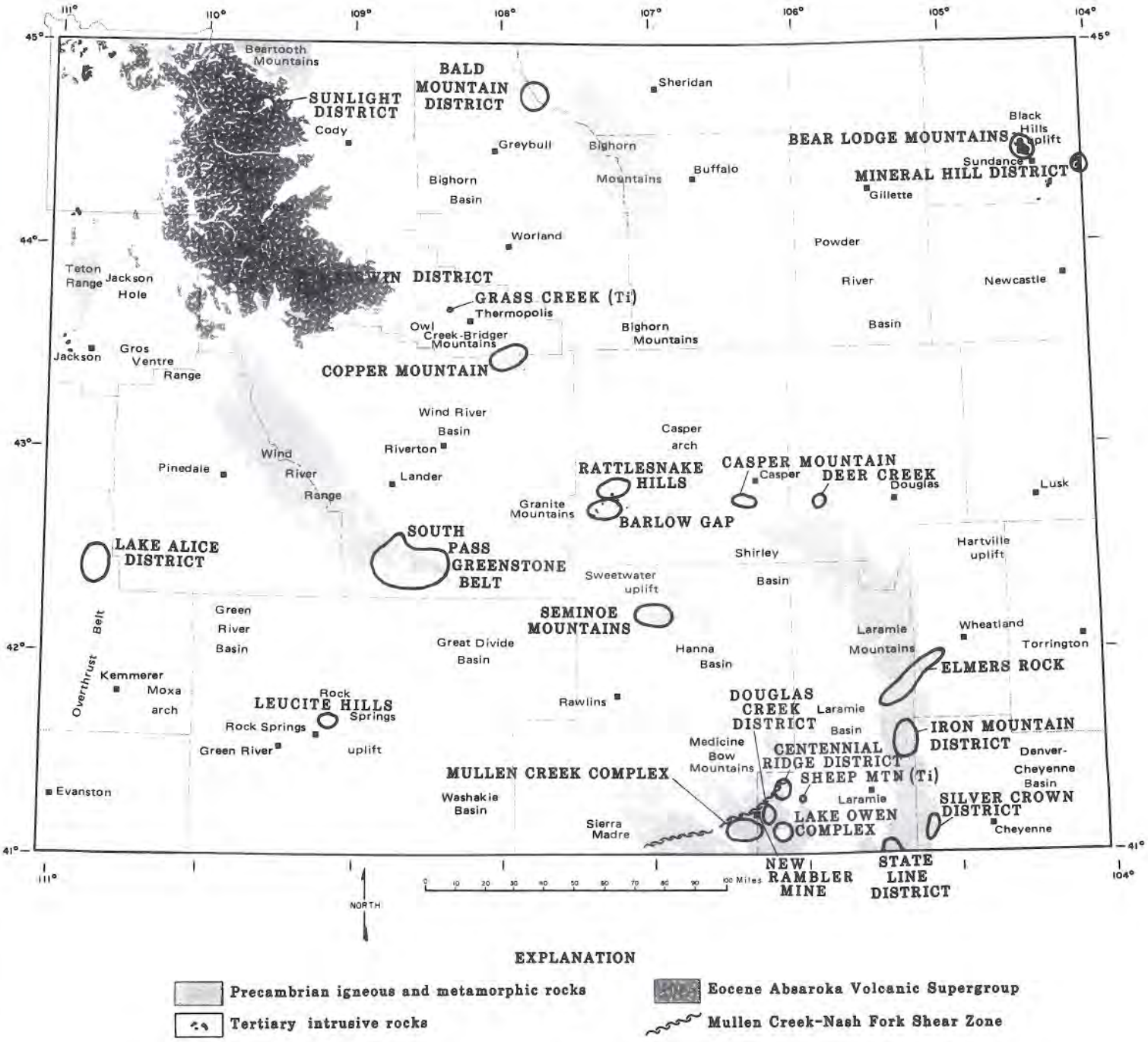

Figure 1. Location map of metal and gemstone deposits of Wyoming. Deposits are described in the text.

mation and metamorphism. It forms a 20 to 25 mi^2 funnel-shaped intrusion tilted 75° on its side to expose a cross section of at least 16 cyclic units. Vanadiferous titanomagnetite cumulates are persistent in gabbronorite near the tops of some cyclic units (Loucks, 1991).

Cumulus sulfides occur in at least 12 stratigraphic horizons in the complex, with some zones containing elevated gold and platinum ± palladium. Four of the horizons have laterally persistent precious-metal anomalies of a few hundred to a few thousand ppb and contain Au-Ag alloys, Pt-arsenides, Pt-Pd tellurides and sulfides associated with disseminated chalcopyrite, pentlandite, pyrrhotite, pyrite, gersdorffite, bornite, millerite, and PGE-bearing carrollite. The mineralized zones are generally lensy and spotty and include zones up to 15 feet thick with strike lengths of more than 1 mile (Loucks, 1991).

Centennial Ridge district

North of the Lake Owen complex in the Centennial Ridge district, late 19th Century mine developers cut mafic metaigneous rock in search of gold associated with platinum-group metals. The mineralization is spotty and found in shears and veins. The richest ores were found in sulfide-rich zones in mafic mylonites, in graphitic fault gouge, and in strongly chloritized zones (McCallum, 1968).

It is apparent some Wyoming platinum is magmatic as well as hydrothermal. Platinum in the Lake Owen complex is clearly magmatic and associated with cumulus layers. In the New Rambler district in the Mullen Creek complex, the platinum is in hydrothermally altered mafic cataclastics. Possibly, the New Rambler ore was leached from discrete mafic rock units by hydrothermal solutions or remobilized from the deformed layered complex (McCallum and Orback, 1968). Platinum in the Centennial Ridge district is restricted to narrow zones of altered, mafic, metaigneous schist and gneiss and appears to have been remobilized from the mafic country rock (McCallum, 1968).

Titaniferous magnetite

Titaniferous magnetite is found within a 350 mi^2 anorthosite batholith of the Laramie Mountains, and in stratiform layers of the Lake Owen mafic complex of the Medicine Bow Mountains (refer to the "Platinum group mineralization" section above for information on Lake Owen). In addition to titanium, these deposits also contain significant iron and anomalous vanadium and chromium.

Titaniferous magnetite in the Laramie Mountains forms one of the largest deposits of this type in North America. The titaniferous magnetite is distributed in more than 30 separate deposits of disseminated and massive magnetite-ilmenite (Dow, 1961). Many of these occupy the crest of an antiform in the Laramie anorthosite complex (Hagner, 1968).

The deposits consist of lenses of ilmenite, magnetite, and magnetite-ilmenite intergrowths containing minor to accessory olivine, apatite, spinel, mica, and sulfides (pyrrhotite and pyrite). The magnetite and ilmenite occur as discrete grains and as intergrowths and overgrowths. The intergrowths consist of fine interpenetrating networks of ilmenite lamellae along octahedral partings in magnetite. In some samples, the titaniferous magnetite partially replaces feldspar and pyroxene indicating the metals are paragenetically late (Hagner, 1968). Early workers interpreted these deposits as magmatic segregations or injections (Diemer, 1941). Later work by Hagner (1968) considered the titaniferous magnetite to have formed by replacement of the anorthosite along a zone of en echelon fractures. More recently, the titaniferous magnetite has been considered as either a crystal cumulate or the result of magma unmixing (Frost and Simons, 1991).

Dow (1961) described two types of ore: (1) massive ore and (2) disseminated ore. Chemical analyses of the massive ore show 16 to 23% TiO_2. The ore is enriched in vanadium (<1.0% V_2O_5) and locally enriched in chromium (0.03% to 2.45% Cr_2O_3) (Diemer, 1941; Hagner, 1968). In addition to massive deposits, disseminated titanomagnetite forms relatively large, low-grade deposits in the complex (Dow, 1961; Frost and Simons, 1991).

Available resource estimates based on drilling and magnetic surveys indicate reserves of massive titaniferous magnetite ore in the Laramie anorthosite complex at 30 million tons, averaging 45% Fe, 20% TiO_2; and 0.64% V_2O_5 with little or no sulfur, and disseminated ore at 148 million tons, averaging 20% Fe, 9.7% TiO_2, 0.17% V_2O_5, and 0.17% S (Dow, 1961). The amount of disseminated ore in the Strong Creek

area is reported to be at least 100 million tons (Frost and Simons, 1991).

In the 1950s, 1,091,452 tons of titaniferous magnetite were mined from the anorthosite complex. The ore was used in a heavy-mineral concrete in submerged petroleum pipelines in the Gulf Coast.

Chromite

The principal chromite deposits of the world are magmatic and are associated with >2.0 Ga layered complexes (Edwards and Atkinson, 1986). With the exception of the Lake Owen layered complex, most of the known Wyoming chromium deposits are associated with serpentinites and ultramafic schists in greenstone belts and related supracrustal successions. Typically, these deposits occur as weakly anomalous zones to low-grade mineralized zones in the high-MgO rocks. Although no nickel anomalies have been identified in Wyoming, some high MgO and Cr_2O_3 serpentinites have whole-rock compositions similar to nickeliferous peridotitic komatiites in Western Australia.

Anomalous chromium is reported in the Casper Mountain, Elmers Rock, South Pass, and Deer Creek Canyon Archean supracrustal belts. In these terranes, chromite occurs as disseminations, pods, layers, and/or veinlets in serpentinite, talc-tremolite schist, and tremolite-talc-chlorite schist. The chromium is found in chromite (spinel), and in kammererite and wolchonskoite (chromian chlorites). However, the silicates (chlorites) are of no economic value. Chrome-rich spinels are also reported in the Lake Owen layered complex (Loucks, 1991).

The known Wyoming chromite deposits are too low grade or too small to be considered economic (Hausel, 1987a). However, some chromite schist mined from the Deer Creek deposit in 1908 and during the First World War yielded economic grades of 35 to 45% Cr_2O_3 (Spencer, 1916; Beckwith, 1955). The chromite schist on Casper Mountain averages only 2% Cr_2O_3, but includes bands of high grade chromitite that vary from 5 to 25% Cr_2O_3. Drilling by the U.S. Bureau of Mines on Casper Mountain identified relatively large low-grade resources (Julihn and Moon, 1945). These chromitites are stratified and associated with serpentinized cumulate peridotite and magnetite-talc-chlorite schist.

A significant amount of the world's nickel deposits occur in peridotitic komatiites with >38% MgO (volatile free). These komatiites are aluminum undepleted with CaO/Al_2O_3 ratios of about 1, Al_2O_3/TiO_2 ratios of nearly 20, and flat chondrite-normalized heavy rare-earth element (HREE) patterns. They are depleted in light rare earth elements (LREE) and TiO_2 (Marston and others, 1981).

Rocks with compositions similar to the Western Australia nickeliferous rocks occur in some Wyoming greenstone belts. In the South Pass greenstone belt, serpentinites and talc-tremolite-chlorite-serpentine schists of the lowermost unit of the greenstone belt vary from 22.3% to 43.5% MgO (volatile free), 1,700 ppm to 34,600 ppm Cr, and 289 ppm to 2,570 ppm Ni. The CaO/Al_2O_3 ratios average about 0.6, and the Al_2O_3/TiO_2 ratios average about 22. These rocks yield some weak Cr_2O_3 anomalies, but nickel systematically in creases with increasing MgO and is not anomalous in any of the samples collected to date (Hausel, 1991). The available REE analyses of these rocks are incomplete. Two ultramafic samples, partially analyzed for REE chemistry, possess flat HREE patterns similar to the Australian rocks, but the LREE data are lacking.

Serpentinites from the Seminoe Mountains have compositions consistent with peridotitic komatiite (Klein, 1981). Chemically, they have 25.7 to 36.7% MgO, 1,900 ppm to 6,200 ppm Cr, 810 ppm to 1,600 ppm Ni. CaO/Al_2O_3 ratios average 0.41; Al_2O_3/TiO_2 ratios average 27. Tremolite schists with spinifex texture have 7.01 to 28.4% MgO, 150 to 6,000 ppm Cr, and 60 to 1,400 ppm Ni. CaO/Al_2O_3 ratios average 0.86 and Al_2O_3/TiO_2 ratios average 23.

In the Elmers rock greenstone belt, similar ultramafic schists have 11.2 to 28.4% MgO and 713 to 4,900 ppm Cr. CaO/Al_2O_3 ratios average 1.25; Al_2O_3/TiO_2 ratios average 21 (Smaglik, 1987). Five samples were analyzed for REE content and only one sample showed a REE pattern consistent with the Western Australia nickeliferous komatiites. The remaining samples showed LREE enrichment inconsistent with the Western Australia rocks.

Diamondiferous kimberlite

Worldwide, commercial diamond deposits are confined to kimberlites in stable cratons, lamproites

along craton margins, and placer deposits presumably derived from these and related mantle rocks. Kimberlite and lamproite intrusives have unique nodules, mineral assemblages, and geochemistry indicative of mantle origin. Pressure-temperature estimates based on the chemistry of mineral associations of some ultramafic xenoliths and diamond xenocrysts place the source terrane of the kimberlite intrusives at minimum depths of 120 miles. Phanerozoic mobile belts tend to lack penecontemporaneous diamondiferous kimberlite.

Diamondiferous and barren kimberlite, placer diamonds, and lamproite all occur in Wyoming, and the distribution of kimberlitic heavy (satellite) minerals in stream sediments suggest dozens of kimberlites or related intrusives remain undiscovered. Although the known Wyoming kimberlites intrude the Proterozoic basement along the margin of the Wyoming craton, the distribution of kimberlitic satellite minerals suggest that the Colorado-Wyoming kimberlite province may extend into the Archean craton.

Geochemically, kimberlite is a potassic ultrabasic igneous rock. Whole-rock analyses of kimberlite from the Colorado-Wyoming region show SiO_2 contents of 24.8 to 34.2%; K_2O contents of 0.16 to 1.4%; and MgO contents in the range of 12.6 to 31.2% (Smith and others, 1979). The intrusives are Early Devonian dikes, blows, and diatremes that range from inches wide to the largest known pipe in the region (Sloan 1), with dimensions of 1,800 by 500 feet (McCallum and others, 1977). Kimberlite eruption in Wyoming was enhanced by deep north-northwest fractures developed during the Early Devonian. These intrusives exhibit a variety of textures including porphyries and breccias (McCallum and Mabarak, 1976). Many of the kimberlites, particularly the diamondiferous intrusives, host abundant mantle and lower crustal xenoliths.

During the early 1980s, several kimberlite intrusives in the Colorado-Wyoming province were evaluated for diamond content (**Figure 2**). The evaluations showed a high percentage of the State Line intrusives were diamondiferous but subeconomic. In the Wyoming portion of the State Line district, kimberlites yielded low diamond grades of only 0.5 to 1.0 carat/100 tonnes with gem and near gem to industrial ratios of nearly 1:1. The largest diamond recovered was a 0.86-carat gem. In Colorado, kimberlites yielded grades as high as 20 carats/100 tonnes at the Sloan 1 and 2 pipes (Gold, 1984) and as high as 135 carats/100 tonnes at the George Creek dikes (McCallum and Waldman, 1991). The largest Colorado diamond was a 2.6-carat industrial (Frank Yaussi, personal communication, 1989). In total, more than 100,000 diamonds have been recovered from the State Line district (McCallum and Waldman, 1991).

The potential for the discovery of additional kimberlite intrusives is high. To date, only modern drainages have been sampled, and these have yielded over a hundred kimberlitic heavy mineral anomalies. Additionally, several magnetic and conductivity anomalies in the State Line district have not been tested.

Figure 2. Aerial view of diamond-evaluation project at the Sloan 5 (Evelyn) kimberlite pipe in the Colorado-Wyoming State Line district. The intrusive lies within an open park. A prominent linear fracture along the edge of the pipe is visible in the right-bottom corner of the photo. Mining equipment provides scale.

The lamproites of the Leucite Hills lie within the confines of the Wyoming province. These lamproites are relatively young (~1.0 Ma) and form volcanic cones, flows, and necks (Ogden, 1979). They are ultrapotassic, basic to ultrabasic, volcanic and volcaniclastic rocks, and include both olivine-bearing and leucite lamproites. Geochemically, these rocks have SiO_2 contents in the range of 43.0 to 56.5%; K_2O from 3.3 to 12.7%; and MgO from 5.2 to 11.2%. A few hundred pounds of both olivine-bearing and leucite lamproite have been tested for diamonds by the Geological Survey of Wyoming with negative results. Although no diamonds have been found, sampling has been minimal.

Magmatic hydrothermal deposits

Hydrothermal alteration accompanies many magmatic metalliferous deposits. Temperature gradients associated with the deposits result in zoned alteration and mineralization. The classic magmatic hydrothermal deposits are the porphyry copper deposits and their associated vein systems. Spatially associated with some porphyries with high average Au/Ag ratios are large-tonnage, disseminated gold deposits. Porphyries, veins, and disseminated gold mineralization have all been recognized in Wyoming. Volcanogenic massive sulfides, another type of magmatic hydrothermal deposit, have also been recognized in Wyoming.

Porphyry deposits and disseminated gold

Several large copper-silver porphyries (with high Ag/Au ratios) occur in the Absaroka Mountains of northwestern Wyoming (Fisher, 1981; Hausel, 1982). This region includes one of Wyoming's great copper districts, but limited accessibility has precluded development and extensive exploration of these deposits. Total copper, molybdenum, lead, zinc, silver, titanium, and gold resources are unknown, but the available drilling records indicate ore tonnages exceed a hundred million tons.

The Absaroka Mountains form a deeply dissected Tertiary volcanic plateau of calc-alkaline flows and flow breccias. Some eruptive centers possess classical hydrothermal alteration mineral assemblages and zonation typically seen in many porphyry copper deposits in the southwestern United States. Several mineralized porphyries have been recognized, but only the Kirwin and Sunlight districts are accessible.

In the Kirwin district in the southern Absaroka Mountains, at least three intrusive centers have been recognized (Wilson, 1964), but only the Bald Mountain porphyry has been extensively drilled. This porphyry is surrounded by deuterically altered andesite containing secondary calcite, chlorite, and clay. The andesite gives way to hydrothermally propylitized (quartz-epidote-montmorillonite-calcite-chalcopyrite with chalcopyrite-calcite-quartz veinlets) andesite within 1,500 feet of the intrusive center. Near the intrusive center, phyllically altered assemblages are overprinted by argillic assemblages (quartz-sercite-pyrite-biotite-kaolinite-chlorite-illite/montmorillonite). This phyllic-argillic altered zone encloses a poorly defined potassic zone represented by secondary orthoclase, quartz, and veinlet sulfides (Wilson, 1964; Nowell, 1971).

Zoned mineralization is characteristic of these deposits. Copper-molybdenum-trace gold mineralization surrounds the stocks and gives way to zinc-lead-silver mineralization laterally. Drill-hole data show a pyrite-chalcopyrite-molybdenite stockwork at Kirwin with a secondary enriched blanket of chalcocite, digenite, and covellite over a portion of the stockworks (Wilson, 1964). Veins in the altered area are chalcopyrite-pyrite-molybdenite-quartz veins (Wilson, 1960). Wilson (1964) reported vein and mine dump samples to assay a trace to 8.58 ppm Au and a trace to 3,835 ppm Ag (123.3 opt). The ore body was drilled by AMAX Exploration, which outlined geologic reserves totalling 196 million tons averaging 0.505% Cu and 0.022% MoS_2 (Rostad, 1983). Estimated contained metals in the porphyry include 1.23 billion lbs of Cu, 121,000 oz of Au, 5.6 million oz of Ag with significant Pb, Zn, Mo, and anomalous Ti (Pay Dirt, 1985) worth more than $1.5 billion (1989 prices).

In the Silver Crown district of the southern Laramie Mountains, copper is disseminated in Proterozoic quartz monzonite and foliated granodiorite

(**Figure 1**). This porphyry (Copper King) possesses a hydrothermal alteration halo of propylitic and potassic alteration assemblages. Near the old shaft, a zone of intense silicification is expressed by intersecting quartz veins and veinlets. Extending outward from the shaft is a narrow potassically altered zone containing secondary biotite and K-feldspar. This halo is in turn enclosed by a propylitized zone that includes secondary epidote, chlorite, sulfides, and quartz. The ore body is oxidized to depths of 30 to 150 feet. Below 150 feet, sulfides dominate. The ore body is 300 feet wide by 600 to 700 feet long and is continuous to depths greater than 1,000 feet. Drilling by the U.S. Bureau of Mines established a 35-million-ton ore body with average grades of 0.21% Cu and 0.755 ppm Au. A higher grade zone (4.5 million tons averaging 1.51 ppm Au) was later outlined by company drilling (Hausel, 1989).

A possibly similar deposit of Proterozoic age was recently examined by the author in the southern Sierra Madre. This property was developed as the Kurtz-Chatterton copper mine somewhere near the turn of the last century. The mine is surrounded by a well-developed mineralized zone with a 3,500-foot strike length and a minimum width of 600 feet. The mineralized zone is confined to the Sierra Madre granite and contains secondary (?) K-feldspar, biotite, muscovite, and propylitic mineral assemblages in sheared granite. Historic reports indicate the mined ore contained 10 to 20% Cu with some gold and silver (Hausel, 1989, p. 156). Hand specimens contain chalcopyrite, cuprite, malachite, and minor chrysocolla.

The Bear Lodge Mountains in the northwestern Black Hills of Wyoming (**Figure 1**), are a large multiple intrusive complex of alkalic igneous rock ranging in age from 38.0 to 50.0 Ma (Staatz, 1983; Lisenbee, 1985). Staatz (1983) described the complex as a porphyry-type intrusive containing one of the largest, low-grade, disseminated and vein-type REE and thorium deposits in the United States. Disseminated gold mineralization is also associated with feldspathic breccia in the complex (Jenner, 1984). One mineralized zone discovered in an elongate intrusive breccia (2,000 by 120 ft) was recently drilled yielding gold values of 0.343 to 1.72 ppm (Anonymous, 1988). Current geologic resource estimates for the intrusive breccia are 8.2 million tons averaging 0.686 ppm gold (Anonymous, 1991).

Twelve to 15 miles southeast of the Bear Lodge Mountains, another Tertiary alkalic intrusive at Mineral Hill shows similar mineralization. Anomalous gold is reported in feldspathic breccia, quartz veins, and jasperoid (Welch, 1976). Welch (1976) reported breccias with 6 ppm Au and 115 ppm Ag and jasperoids with 5 ppm Au and 7 ppm Ag. Recently, the author collected quartz vein samples at Mineral Hill that assayed 130 ppm Au and 330 ppm Ag. The possibility for similar mineralization at Black Buttes, 6 miles to the southwest, is indicated by the presence of epithermal replacement galena, wulfenite, fluorite, and hemimorphite in altered Pahasapa Limestone along a contact with Tertiary alkalic igneous rock (Hausel, 1989).

Some potential for epithermal disseminated gold exists in the Rattlesnake Hills of central Wyoming in the vicinity of UT Creek, where American Copper and Nickel Company identified several gold anomalies between 1983 and 1987. This area is underlain by Archean supracrustal rocks intruded by Tertiary alkalic rocks and includes some jasperoids (Hank Hudspeth, personal communication, 1988). Aspen (Quaking Asp) Mountain, along the Rock Springs uplift south of Rock Springs, is another anomalous area with highly silicified sandstones and siltstones covering several square miles. Alunite, kaolinite, localized jasperoid(?), and minor travertine have been identified. Some weak gold anomalies were recently detected in the silicified zone (Hausel and others, 1992).

Volcanogenic massive sulfides

South of the Mullen Creek-Nash Fork shear zone in the Sierra Madre, volcanogenic zinc-copper-silver massive sulfides occur in epidote-actinolite-magnetite exhalites in differentiated calc-alkaline metarhyolites and meta-andesites of the Green Mountain Formation. These are stratabound deposits of pyrite, chalcopyrite, and sphalerite, with secondary tenorite, and marmatite spatially associated with vol-caniclastics containing clasts up to several inches in length. Locally, samples of colloform pyrite mantled by chalcopyrite in a magnetite matrix are found near some vent breccias.

Wallrock alteration associated with the massive sulfide mineralization consists of localized sericite-

pyrite with broad zones of sausseritization (epidote ± chlorite ± garnet ± calcite ± actinolite) (Conoco Minerals Company, 1982). The geological setting and physical characteristics of these deposits suggests formation by sulfide precipitation in mounds near vents on a Proterozoic sea floor.

Veins

Quartz veins are common in both volcanic and metamorphic terranes. In Tertiary volcanic rocks, veins are clearly associated with hydrothermal activity and commonly show classical ore zonation. Some Proterozoic veins in southeastern Wyoming show similar characteristics. In the Archean craton, the association is often not clear, and many veins are undoubtedly related to metamorphic secretion during regional metamorphism and deformation rather than magmatic hydrothermal processes.

Quartz veins associated with the porphyry stocks of the Absaroka Mountains are zoned. In the Sunlight district, copper-rich veins with trace gold occur near the porphyry center and grade into lead-silver and barren veins away from the stock. Some Proterozoic veins are also zoned. Spencer (1904) described precious metal zonation in the Bridger vein of the Sierra Madre, where gold decreased and silver increased with depth.

Several factors related to host-rock chemistry and structure may cause ore shoots in hydrothermal veins. For example, Schoen (1953) noted a close association of host-rock lithology and the type of metals found in the Albion mine. Copper dominated the ore assemblage in metalimestone, and lead and silver dominated in quartzite. In the Mineral Hill district, the strongly mineralized, near-horizontal, pyritiferous veins of the Treadwell mine are reported to form ore shoots at intersections with a series of vertical fractures.

Metamorphogenic deposits

During regional metamorphism, fluids released at elevated temperatures and pressures may leach metals from the surrounding rocks and transport them to dilational zones, forming shear-zone and vein deposits. Contact metamorphic deposits may result by the intrusion of igneous rock into country rock, leading to recrystallization and replacement at elevated temperatures. These types of deposits are closely related to metamorphic processes.

Shear-zone gold

During the initial stages of deformation (D_1) of Wyoming's Archean supracrustal belts, regional shortening produced isoclinal folding (F_1), regional foliation (S_1), and shear zones parallel to S_1 and to the F_1 fold hinges. Regional metamorphism during D_1 liberated fluids from the supracrustal pile, which tended to focus in the shear structures. Precipitation of silica synchronous with this early stage of deformation produced quartz veins that were stretched, boudinaged, and sheared parallel to S_1. Wallrock alteration associated with gold mineralization is chlorite-carbonate-quartz dominated with minor sericite, microcline, and tourmaline. Most zones are stained by hematite.

At South Pass, gold is closely associated with shear-zone structures in a variety of rock types. Bow (1986) showed that there was a close association of gold to carbonated tremolite/actinolite schists with basaltic to peridotitic komatiite compositions, and Spry and McGowan (1989) showed there was also an association with the metagreywacke suite. Additionally, several other rock types in the district host auriferous shears suggesting more than one source rock contributed gold. The variety of source rocks supports the interpretation that the gold originated by metamorphic secretion from the supracrustal pile during a 2.8 Ga regional metamorphic event.

The shears and veins contain trace gold with sporadic ore shoots enriched in gold (Hausel, 1987). Where recognized, fold closures, shear-fault, and shear-shear intersections appear to localize some ore shoots. The Hidden Hand shaft in the Lewiston district was sunk at the intersection of coalescing shears in metagreywacke. The chloritized-hematized shear intersection is many feet wide with a gold tenor of a trace to 3,100 opt (ounces per ton) (Pfaff, 1978). At the Bullion mine on Strawberry Creek, a shoot was mined at the intersection of an Archean shear and a Laramide(?) tear fault. The localization of this latter shoot suggests gold may have been mobilized syn-

chronous or subsequent to Laramide deformation. My impression is the intersection produced a zone of high permeability that was supergene enriched. Thus this shoot may be surficial and not extend below the ground water level.

Tight to open fold closures control shoots at several mines including the Carissa, Alpine, Diana, Duncan, and Miners Delight. The Duncan shaft was sunk on a steeply plunging drag fold in hornblendic amphibolite. Compared to the adjacent shear splay, the fold closure is more than 10 times enriched in gold. A 2-foot channel sample from the fold nose assayed 33 ppm Au compared to a 37-foot composite chip sample taken in the shear splay that averaged 2.5 ppm Au.

In general, the shears occur as relatively narrow, foliation-parallel zones with brittle and ductile deformation. They are traceable for hundreds of feet to more than 11,000 feet along strike (Hausel, 1991) and are continuous to minimum depths of at least 900 feet based on drilling (deQuadros, 1989).

Later mineralizing episodes occurred after the development of the auriferous shear zones. This is clearly seen at South Pass, where a swarm of copper-gold-silver quartz veins cut the earlier auriferous shears. These veins occur in greater frequency near the margins of the greenstone belt and have also been identified in the adjacent granodiorite plutons, implying a possible relationship to the cratonization event that produced the major 2.6 Ga batholiths along the margin of the greenstone belt.

Veins

Veins related to metamorphic processes are characteristically not zoned. The Mary Ellen vein (Archean) in the South Pass-Atlantic City district along the northwestern flank of the South Pass greenstone belt (**Figure 1**) is a crosscutting vein hosted by metatonalite porphyry. This milky quartz vein is dominated by gold with uncommon pyrite. Gold values are found to increase where the vein pinches, and no mineralogical zonation has been noted. Veins along the Sweetwater River in the Lewiston district to the southeast parallel foliation and contain argentiferous arsenopyrite and minor gold. Again, no mineralogical zonation has been noted.

In the Seminoe Mountains greenstone belt, gold-chalcopyrite-pyrite-quartz veins occur in a 1/4-mile-diameter chlorite-calcite-sulfide alteration haloe in metagabbro and metabasalt (Klein, 1981). The quartz veins develop shoots at vein intersections and in fold closures.

Skarns

The intrusion of rock by magma and its associated hydrothermal fluids often leads to replacement and recrystallization. When such hot mineralizing fluids contact carbonates, the resulting replacements (skarns) can be profound. These contact metamorphic deposits, until very recently, have been essentially unknown in Wyoming.

Some localized replacement lead-zinc-silver mineralization has been described in the Black Buttes area of the Black Hills. Recent mapping in the Cooper Hill district of the Medicine Bow mountains led to the discovery of several skarns in metalimestone of Proterozoic age associated with gabbroic and basaltic intrusives (Hausel and others, 1992). These include (1) garnet (hydrogrossular)-epidote-actinolite-chlorite-idocrase(?)-calcite-limonite-(±) magnetite hornfels, (2) epidote-pyrite-calcite-quartz hornfels, (3) magnetite hornfels, (4) calcite-epidote-actinolite-pyrite-magnetite marble, (5) actinolite-calcite-quartz-chlorite-(±) chalcopyrite hornfels, (6) tremolite-calcite-quartz marble, and (7) uvarovite-magnetite-calcite hornfels.

Stratiform and stratabound deposits of sedimentary affiliation

Stratiform and stratabound deposits of sedimentary affiliation include some of the largest known metalliferous deposits in Wyoming. The source of the metals of these deposits is not always clear. Typically, the stratiform deposits contain mineralization that is concordant to stratification, the stratabound deposits are confined stratigraphically, and mineralization can be either concordant or disconcordant to stratification.

Cupriferous quartzite

The Ferris-Haggerty mine in the Sierra Madre was Wyoming's premier copper mine. The Ferris-Haggerty ore body is a stratabound massive sulfide, hosted by a contact breccia in quartzite formed between a hanging-wall schist and the footwall quartzite of the Magnolia Formation (Proterozoic). The massive sulfide is as much as 20 feet thick and grades into laminated disseminated sulfides in the nonbrecciated quartzite. The ore deposit was reported to average 6 to 8% Cu with some high-grade shoots containing 30 to 40% Cu with some Ag and 3.43 to 12.7 ppm Au (Beeler, 1905).

The mine operated from 1902 until 1908. Operations terminated following a series of disasters. The mill at Riverside was partially destroyed by fire in 1906, followed by the destruction of the Riverside smelter by fire in 1907 and a 35% drop in the price of copper in 1908. The ore body was not exhausted and large blocks of 'low-grade' ore (averaging about 5% Cu) remain unmined (Ralph Platt, personal communication, 1988). In addition to the Ferris-Haggarty deposit, similar quartzite-hosted deposits are described at several other locations in the Sierra Madre (Hausel, 1986).

Copper-silver-zinc redbeds

Copper-silver-zinc redbed mineralization is widespread in the thrust belt of western Wyoming (Hausel and Harris, 1983). Many of these deposits and occurrences lie along the contact of the Nugget Sandstone (Triassic-Jurassic) and the overlying Gypsum Spring Member (Jurassic) of the Twin Creek Limestone (Boberg, 1986) Some deposits show evidence of both structural and stratigraphic control. The redbeds are bleached, indicating the mineralizing fluids were reducing.

The best exposure of this type is at the Griggs mine in the Lake Alice district (**Figure 1**), where several adits were driven into mineralized sandstone. Fluid-inclusion studies indicate the mineralizing fluids were deposited at less than 100°C (Loose and Boberg, 1987). The source of these fluids may have been interformational fluids generated during deformation of the thrust belt (Boberg, 1986), or they may have originated from metalliferous hydrocarbons (Love and Antweiler, 1973). The ore fluids migrated into anticlinal traps along permeable fault and breccia zones (Loose and Boberg, 1987; Loose, 1988) and produced a mineralized zone 300 feet thick (Love and Antweiler, 1973).

Ore shipped from the district between 1914 and 1920 and ore recovered from the mine in 1942 averaged 3.5% Cu and 254 ppm Ag (Allen, 1942). Samples collected by Love and Antweiler (1973) contained 180 ppm to 6.7% Cu, a trace to 0.5% Pb, 26 ppm to 3.2% Zn, and a trace to 1,200 ppm Ag.

Banded iron formation

Significant resources of Archean banded iron formation (BIF) occur in the Copper Mountain, South Pass, and Seminoe Mountains supracrustal belts, and additional BIF is found in the Barlow Gap, Rattlesnake Hills, Sellers Mountain, and Elmers Rock belts. In the Hartville uplift of southeastern Wyoming, giant resources of hematite schist occur in a eugeoclinal belt of Archean (?) age.

Banded iron formation in the South Pass greenstone belt occurs in a metasedimentary-metaigneous unit containing quartzite, metapelite, and amphibolite. The BIF typically shows well-developed banding expressed by alternating magnetite-rich and meta-chert-rich layers with subordinate amphibole (principally hornblende and grunerite), chlorite, and local sulfides (pyrite and chalcopyrite). The rock averages 33.0% iron (Bayley, 1963). Ninety million tons of taconite were mined at the Atlantic City mine between 1962 to 1983. Bayley (1968) reported indicated resources in the range of 300 million tons suggesting a substantial resource remains in place (Hausel, 1991).

Sulfides are uncommon in the BIF, but locally may form up to 5% of the rock. The sulfides (pyrite with subordinate chalcopyrite) are principally stratiform with some crosscutting veinlets. The BIF has been structurally thickened by internal folding and plication and by repetition by slippage along faults.

Gold distribution has been incompletely examined in the BIF. Available records indicate one mine was developed in a crosscutting quartz vein adjacent to BIF at the Atlantic City iron mine. The ore averaged 2.06 ppm Au (Bayley, 1963). Elsewhere, samples of BIF have assayed as high as 1.1 ppm Au with some quartz stingers containing 0.4 ppm Au (Hausel, 1991).

Banded iron formation in the Copper Mountain district crops out as four, relatively continuous, narrow beds along an 8-mile strike. These rocks contain both quartz and magnetite but also have abundant grunerite (Hausel and others, 1985). Near the center of the district, a shaft was sunk (McGraw mine) in copper-stained magnetite-rich iron formation. No production history is available for the mine, but it is suspected the shaft was sunk to test a nearby cupriferous strike vein.

Banded iron formation in the Seminoe Mountains greenstone belt forms a large resource in the Bradley Peak thrust sheet (Blackstone, 1965). The iron formation is intercalated in metasediments, follows schistosity in metabasalt and metagabbro, and occurs as interflow sediments between basaltic komatiite flows. Locally, the BIF is structurally thickened to produce a giant iron ore resource. Harrer (1966) indicated the north slope of Bradley Peak contains a resource of 100 million tons. The iron deposits continue beyond the north slope, suggesting the total resource to be much greater. Chemical analyses of the Seminoe BIF give iron contents of 28.7% to 68.7% Fe (Harrer, 1966). Localized gold and silver anomalies have been detected (Hausel, 1989).

Banded iron formation in the Rattlesnake Hills supracrustal belt of the Granite Mountains (**Figure 1**) is found in a meta-volcanic-metasedimentary sequence intruded by Tertiary alkalics. Gold anomalies have been identified in a variety of rock types in this area (John T. Ray, personal communication, 1991) including iron formation (Bob Kellie, personal communication) and metachert (Hausel, 1989).

Iron deposits in the Hartville uplift were commercially mined until 1981. About 45 million tons of ore were mined from the Sunrise deposit, where the ore occurs as hematite schist in the Silver Springs Schist (Snyder and others, 1989). Gold anomalies have also been detected in some hematite schists in the Hartville uplift (Woodfill, 1987).

Placer deposits

One of the greatest untapped resources in the state is extensive paleoplacers and placers that cover thousands of square miles of surface area. Paleoplacers have been recognized in rocks of Precambrian, Cambrian, Jurassic, Cretaceous, and Tertiary age. Precambrian conglomerates of Archean and Proterozoic age in the state exhibit possible equivalents to the Blind River, Canada, and Witwatersrand, South Africa uranium and gold deposits. Cambrian conglomerates exhibit possible equivalents to the Deadwood, South Dakota, gold deposits, and the vast auriferous Cretaceous and Tertiary conglomerates may someday yield commercial gold deposits. But incredibly, much of these remain essentially unexplored.

Modern placers have yielded some gold and other valuable heavy minerals in the historic past. These placers range from relatively restricted occurrences to widespread deposits.

Gold paleoplacers

Paleoplacers are widespread in the state. To date, production from paleoplacers and their associated reworked placers has been minimal, although the shear volume of paleoplacer material implies that these deposits should become important sources of gold and other heavy minerals in the future.

Paleoplacers of Late Archean, Early Proterozoic, Cambrian, Jurassic, Late Cretaceous, and Tertiary age have been identified. The Late Archean and Early Proterozoic paleoplacers in southeastern Wyoming are part of a thick wedge of miogeoclinal metasedimentary rocks that unconformably overlie Archean basement rocks. Following the discovery of radioactive metaconglomerates in the Medicine Bow Mountains, comparisons were made to the Blind River conglomerates of Canada and Witwatersrand deposits of South Africa (Houston and Karlstrom, 1979). A few conglomerate samples were tested for gold, producing several anomalies including one sample from the Sierra Madre that yielded 10 ppm Au (Houston and others, 1979).

Cambrian paleoplacers have been described at several locations in the state. At South Pass, Flathead Sandstone conglomerates were explored for gold, although the paleocurrent directions (into the greenstone belt) indicate limited gold content. In the Bald

Mountain district of the Bighorn Mountains, low-grade gold and monazite paleoplacers form relatively large resources. At several other localities in the state, the Flathead Sandstone has yielded anomalous monazite, gold, or other heavy minerals. One similar unexplored conglomerate is the Fountain Formation(?) conglomerate of Pennsylvanian age. In southeastern Wyoming near the State Line district, native copper and copper carbonate were discovered in this conglomerate prior to 1906. The conglomerate remains unexplored for other heavy minerals.

Tertiary paleoplacers are abundant in the state. These consist of fanglomerates and fluvial conglomerates that locally include giant boulders eroded from the nearby uplifts. The more highly mineralized conglomerates lie adjacent to greenstone belts. For example, the South Pass greenstone belt is flanked by two giant paleoplacers known as the Twin Creek (Antweiler and others, 1980) and Oregon Buttes paleoplacers (Love and others, 1978; Hausel and Love, 1991), and large areas of the greenstone belt are also overlain by additional paleoplacers. One of these was recently explored by magnetic surveys and trenching that revealed a complex braided paleo-channel with gold values (Fred Groth, personal communication, 1989).

Titaniferous black sandstone

Titaniferous black sandstone (Late Cretaceous) is relatively widespread. These paleobeach sands occur primarily in the Mesaverde Formation. The black sandstones are enriched in heavy-mineral suites that include anatase, sphene, rutile, ilmenite, titanomag-netite, magnetite, monazite, zircon, and gold. Minerals of potential economic value include the titanium-bearing assemblage of sphene, rutile, anatase, ilmenite, and titanomagnetite; zircon for zirconium and hafnium; monazite for rare earth metals; a niobium-bearing opaque; and gold (Houston and Murphy, 1962, 1970).

The deposits differ greatly in grade and size. The Grass Creek deposit in the Bighorn Basin is the largest high-grade deposit in Wyoming (Houston and Murphy, 1962) and includes significant resources of titanium (averages 16% TiO_2) and zircon (3 million tons averaging 4.8% $ZrSiO_4$) (William Graves, personal communication, 1990). Some younger deposits (i.e., Sheep Mountain in southeastern Wyoming and deposits in northeastern Wyoming) contain a similar suite of heavy minerals and are also anomalous in gold (Madsen, 1978). Values as high as 1.3 ppm Au have been reported by Houston and Murphy (1970) and 1.7 ppm by William Graves (personal communication, 1990).

Modern placers

Gold tenors of modern placers in the state range from a trace to more than an 1.0 oz/yd^3. Generally, the commercial placers average about 0.01 oz/yd^3, although exceptional placers have averaged 0.1 oz/yd^3.

Some extensive placers extend from their river beds into the adjacent terraces, covering hundreds of square miles. These widespread placers typically contain fine gold flakes and "colors" difficult to recover by mechanical concentration. The placers of the Wind River were mined in 1910, but recovery was difficult even though gravels encountered by two dredges averaged 0.014 oz/yd^3 and 0.038 oz/yd^3 (Hausel, 1989). This placer was found along much of the Wind River and was reported to be 12 to 14 feet thick with widths as great as 3 to 4 miles (Schrader, 1913).

Nuggets recovered from Wyoming placers include walnut-size nuggets from Mineral Hill, Douglas Creek, and the South Pass greenstone belt. The largest nugget found in Wyoming may have been a fist-size specimen of mixed rock with 24 ounces of gold reported to have been found on Rock Creek in the South Pass area prior to 1905. Another interesting specimen found in the same area consisted of country rock with an estimated 630 ounces of gold. Several other nuggets ranging in weight up to 5 ounces have been described (Hausel, 1991). Most nuggets in the state are rounded typical of detrital transport, although Day and others (1988) reported slivers and hairs of gold from gravels in the Lewiston district. In addition to placer gold, other heavy minerals of potential value have been identified in Wyoming placers (**Table 1**).

A recent study of sand and gravel deposits for gold occurrences resulted in the identification of gold "colors" at many of the locations sampled (Hausel and others, 1992). This widespread occurrence of gold could lead to the recovery of by-product gold from some sand and gravel operations.

Table 1. Dominant heavy minerals reported in some modern placers in Wyoming.

Gold placer or district	Heavy minerals
Lewiston district, South Pass	Gold, scheelite, cassiterite
South Pass-Atlantic City district	Gold, scheelite, cassiterite, chromite
Crows Nest, South Pass	Gold, scheelite
Mineral Hill district, Black Hills	Gold, cassiterite, tantalite
Douglas Creek, Medicine Bow Mountains	Gold, platinum, palladium
Cortez Creek, Medicine Bow Mountains	Gold, diamond
Clarks Camp, Wind River Mountains	Gold, monazite
Bald Mountain, Bighorn Mountains	Gold, monazite
Nugget Creek, Sierra Madre	Silver, gold
Muddy Creek, Shirley Basin	Monazite

Gemstones

Gemstones are found in a variety of geologic settings and may be the result of crystal growth and/or replacement during regional metamorphism producing jade, sapphire, or ruby; magma cooling producing peridote or aquamarine phenocrysts or megacrysts; partial melting at great depths where diamond xenocrysts may be captured and brought to the earth's surface; or simply low-temperature silica replacement of fossils and wood at the earth's surface. In the past, the State has been noted for its abundant and high-quality jade and varieties of chalcedony, although a variety of gemstones and semi-precious and lapidary stones have been found in Wyoming.

Nephrite jade

Wyoming jade (nephrite) is a monomineralic rock composed of calcium- and magnesium-rich amphibole. Nephrite has been found at a number of localities in central Wyoming including the Prospect Mountains of the southern Wind River Range, the Granite Mountains, the Seminoe Mountains, the northern Laramie Mountains, and it has also been found in fanglomerates derived from these areas. The jade recovered in the past has included material ranging from the poorest quality black jade to some of the highest quality apple green jade ever found in the world.

In the Granite Mountains, nephrite is associated with amphibolite inclusions in quartzo-feldspathic gneiss. The Granite Mountains have been the primary source area of jade in the state (Sutherland, 1990). Other areas include the Laramie Mountains, where nephrite has been identified in orthoamphibolite dikes containing quartz veins. In the Seminoe Mountains, nephrite is reported with amphibolite inclusions and dikes (Sherer, 1969).

Field, chemical, and petrographic data suggest nephrite was formed by metasomatic alteration of amphibolite. Sherer (1969) suggested the following reaction in the presence of water: hornblende → prismatic actinolite → fibrous actinolite (nephrite) → chlorite + talc → serpentine.

Diamonds

Based on a small sampling of 78 diamonds recovered from the Colorado-Wyoming district, McCallum and others (1979) reported the majority of the diamonds were aggregates, octahedra, and transitional octahedra-dodecahedra crystals (**Figure 3**). Subordinate morphologies include macles, irregulars, flattened dodecahedra, and dodecahedra. Octahedra and macles were the principal growth forms. Dodecahedral forms evolved from octahedra.

Diamonds recovered from Wyoming kimberlites include both gem and industrial quality diamonds. Data provided by Cominco American Incorporated show that a few of the gemstones are brown to tinted but most are white or better with GIA (Gemological Institute of America) color grades of H-I or better. Some gems have exceptional white colors and GIA color grades as high as D-E-F (grading system ranges from D to X with diamonds of grades D to I being most desirable; see Hurlbut and Switzer, 1979, p.130-132). The clarity of the gems varies from VVS (very very slightly included) to I (imperfect), thus some gems are lightly included, although near inclusion-free diamonds also occur.

Other gemstones

Rubies from the Granite Mountains of central Wyoming commonly range in size from 0.1 to 0.5 inch and occur in soft, light green, aphanitic nodular masses enclosed by a darker green to grey mica schist. Diffraction patterns of the nodules encasing the rubies show a homogeneous mass of sericite. Gem-quality rubies have been recovered from at least two localities in the Granite Mountains, and float schist with high-quality rubies have been found on Green Mountain. Also in the Granite Mountains, pale blue to colorless sapphires occur in rounded nodules in biotite-chlorite schist. The schist forms an enclave in granite (Sutherland, 1990).

Aquamarine beryl-bearing pegmatites occur locally in the Copper Mountain district of the Owl Creek Mountains. Additionally, a pegmatite from the Anderson Ridge area of South Pass contains rare aquamarine. One translucent, light blue, prismatic, hexagonal aquamarine from the Anderson Ridge area at South Pass probably weighed more than a thousand carats (Sutherland, 1990).

a

b

Figure 3. (a) Wyoming's largest gemstone diamond (0.86 carat) octahedra fragment and (b) well-developed dodecahedra gemstone (millimeter scale).

Pyrope garnet and chromian diopside are found in ant hills in the Green River Basin. These minerals produce attractive faceted stones. The source of the stones is unknown.

Beautiful high-quality amethyst and smoky quartz has been recovered from open-space fractures in granite south of the Battle Lake area in the Sierra Madre (Ralph E. Platt, personal communication, 1989). Amethyst and drusy lavender chalcedony was also recently found at the Artic mine in the Mineral Hill district (Sutherland, 1990).

Some other attractive gemstones found in Wyoming include labradorite in the Buttes area of the Laramie anorthosite complex, which produces a 'fire' similar to opal. Small amounts of poor-quality opal and some gem-quality amber are found in the Absaroka Mountains. Peridote crystals up to 1 to 2 cm in diameter are found in some of the olivine lamproites in the Leucite Hills. Information on these and other gemstones can be found in Sutherland (1990).

Acknowledgments

W.W. Boberg and Robert S. Houston reviewed this manuscript and provided helpful suggestions and comments. I very much appreciate their comments and suggestions and I am indebted to both Bill and Bob for helping me clarify some of my ideas. Sheila Roberts' editorial review greatly improved the organization of the paper. Thanks again Sheila for your help.

References cited

Allen, F.S., 1942, Letter to the Board of Directors of the Polaris Mining Company: Geological Survey of Wyoming mineral files (unpublished), 3 p.

Anonymous, 1988, International Curator Resources Ltd. annual report: Denver Colorado, 4 p.

_____ 1991, Exploration roundup: Engineering and Mining Journal, April, 1991, p. 8.

Antweiler, J.C., Love, J.D., Mosier, E.L., and Campbell, W.C., 1980, Oligocene gold-bearing conglomerate southeast margin of Wind River Mountains, Wyoming: Wyoming Geological Association 32nd Annual Field Conference Guidebook, p. 223-237.

Bayley, R.W., 1963, Preliminary report on Precambrian iron deposits near Atlantic City, Wyoming: U.S. Geological Survey Bulletin 1142-C, 23 p.

_____ 1968, Ore deposits of the Atlantic City district, Fremont County, Wyoming *in* Ridge, J.D., editor, Ore deposits of the United States, 1933-1967: AIME, New York, p. 589-604.

Beckwith, R.H., 1955, Chromite in Wyoming: Geological Survey of Wyoming Mineral Report MR55-8 (unpublished), 3 p.

Beeler, H.C., 1905, Mining in the Grand Encampment copper district, Carbon and Albany counties, Wyoming: Office of the State Geologist, Cheyenne, Wyoming, 31 p.

Blackstone, D.L., Jr., 1965, Gravity thrusting in the Bradley Peak-Seminoe Dam quadrangles, Carbon County, Wyoming and relationships to the Seminoe iron deposits: Geological Survey of Wyoming Preliminary Report 6, 13 p.

Boberg, W.W., 1986, Lake Alice copper district, Lincoln County, Wyoming, *in* Roberts, S.M., editor, Metallic and nonmetallic deposits of Wyoming and adjacent areas, 1983 conference proceedings: Geological Survey of Wyoming Public Information Circular 25, p. 54-55.

Bow, C.S., 1986, Structural and lithologic controls on greywacke-hosted gold mineralization within the Sweetwater district, Wyoming USA, *in* Ayres, L.D., Thurston, P.C., Card, K.D., and Weber, W., editors, Turbidite-hosted gold deposits: Geological Association of Canada Special Paper 32, p.107-113.

Bowdin, H., 1918, Report on Williams-Luman copper mine at DePass, Wyoming: Geological Survey of Wyoming Mineral Report MR18-1 (unpublished), 7 p.

Conoco Minerals Company, 1982, Project summary report on the Fletcher and Huston Parks massive sulfides: Geological Survey of Wyoming files (unpublished), 110 p.

deQuadros, A.M., 1989, Report on the diamond drill program (July-August 1989) at the Carissa mine property, South Pass City, Fremont County, Wyo-ming: Consolidated McKinney Resources Ltd., Vancouver, B.C., 76 p.

Diemer, R.A., 1941, Titaniferous magnetite deposits of the Laramie Range, Wyoming: Geological Survey of Wyoming Bulletin 31, 23 p.

Dow, V.T., 1961, Magnetite and ilmenite resources, Iron Mountain area, Albany County, Wyoming: U.S. Bureau of Mines Information Circular 8037, 35 p.

Edwards, R., and Atkinson, K., 1986, Ore deposit geology: London, Chapman and Hall, 466 p.

Fisher, F.S., 1981, Controls and characteristics of metallic mineral deposits in the southern Absaroka Mountains, Wyoming: Montana Geological Society 1981 Field Conference Guidebook, p. 343-348.

Frost, B.R., and Simons, J.P., 1991, Fe-Ti oxide deposits of the Laramie anorthosite complex: their geology and proposed economic utilization: Wyoming Geological Association 42nd Field Conference Guidebook, p. 41-48.

Gold, D.P., 1984, A diamond exploration philosophy for the 1980s: Pennsylvania State University Earth and Mineral Sciences, v. 53, no. 4, p. 37-42.

Hagner, A.F., 1968, The titaniferous magnetite deposit at Iron Mountain, Wyoming, *in* Ridge, J.D., editor, Ore deposits of the United States, 1933-1967: AIME, New York, p. 666-680.

Harrer, C.M., 1966, Wyoming iron-ore deposits: U.S. Bureau of Mines Information Circular 8315, 112 p.

Hausel, W.D., 1982, General geologic setting and mineralization of the porphyry copper deposits, Absaroka Volcanic Plateau, Wyoming: Wyoming Geological Association 33rd Annual Field Conference Guidebook, p. 297- 313.

_____ 1986, Mineral deposits of the Encampment mining district, Sierra Madre, Wyoming-Colorado: Geological Survey of Wyoming Report of Investigations 37, 31 p.

_____ 1987, Structural control of Archean gold mineralization within the South Pass greenstone terrain, Wyoming (USA), *in* Hurst, R.W., Davis, T.E., and Augustithis, S.S., editors, The practical application of trace elements and isotopes to environmental biogeochemistry and mineral resources evaluation: Theophrastus Publications, Athens, Greece, p. 199-216.

_____ 1989, The geology of Wyoming's precious metal lode and placer deposits: Geological Survey of Wyoming Bulletin 68, 248 p.

_____ 1991, Economic geology of the South Pass granite-greenstone belt, southern Wind River Range, Wyoming: Geological Survey of Wyoming Report of Investigations 44, 129 p.

Hausel, W.D., Graff, P.J., and Albert, K.G., 1985, Economic geology of the Copper Mountain supracrustal belt, Owl Creek Mountains, Fremont County, Wyoming: Geological Survey of Wyoming Report of Investigations 28, 33 p.

Hausel, W.D., and Harris, R.E., 1983, Metallogeny of some Wyoming deposits: Colorado Mining Association 1983 Mining Yearbook, p. 46-63.

Hausel, W.D., and Love, J.D., 1991, Field guide to the geology and mineralization of the South Pass region, Wind River Range, Wyoming: Wyoming Geological Association 42nd Field Conference Guidebook, p. 181-200.

Hausel, W.D., Marlatt, G., Neilsen, E., and Gregory, R.W., 1992, Preliminary study of precious metals and stones along the Union Pacific right-of-way of southern Wyoming: Geological Survey of Wyoming Mineral Report 92-1, 63 p.

Houston, R.S., and Karlstrom, K.E., 1979, Uranium-bearing quartz pebble conglomerates-exploration model and United States resource potential: U.S. Department of Energy Open File Report GJBX-1(80), 510 p.

Houston, R.S., Karlstrom, K.E., and Graff, P.J., 1979, Progress report on the study of radioactive quartz-pebble conglomerate of the Medicine Bow Mountains and Sierra Madre, southeastern Wyoming: U.S. Geological Survey Open File Report 79-1131, 41 p.

Houston, R.S., and Murphy, J.R., 1962, Titaniferous black sandstone deposits of Wyoming: Geological Survey of Wyoming Bulletin 49, 120 p.

_____ 1970, Fossil beach placers in sandstones of Late Cretaceous age in Wyoming and other Rocky Mountain states: Wyoming Geological Association 22nd Annual Field Conference Guidebook, p. 241-249.

Hurlbut, C.S., and Switzer, G.S., 1979, Gemology: New York, John Wiley & Sons, 243 p.

Jenner, G.A., 1984, Tertiary alkalic igneous activity, potassic fenitization, carbonatitic magmatism, and hydrothermal activity in the central and southeastern Bear Lodge Mountains, Crook County, Wyoming [M.S. thesis]: Grand Forks, University of North Dakota, 232 p.

Julian, C.E., and Moon, L.B., 1945, Summary of the Bureau of Mines exploration projects on deposits of raw material resources for steel production: U.S. Bureau of Mines Report of Investigations 3801, 55 p.

Klein, T.L., 1981, The geology and geochemistry of the sulfide deposits of the Seminoe district, Carbon County, Wyoming [Ph.D. dissertation]: Golden, Colorado School of Mines, 232 p.

Lisenbee, A.L., 1985, Tectonic map of the Black Hills uplift, Montana, Wyoming, and South Dakota: Geological Survey of Wyoming Map Series 13, scale 1:250,000.

Loose, S.A., 1988, Sedimentary facies, ore mineralogy, and paragenesis of the Lake Alice Cu-Ag-Pb-Zn district in the Wyoming Overthrust Belt [M.S. thesis]: Laramie, University of Wyoming, 177 p.

Loose, S.A., and Boberg, W.W., 1987, Sedimentary facies control on mineralization at the Lake Alice district in the Wyoming overthrust belt: Wyoming Geological Association 38th Annual Conference Guidebook, p. 309-327.

Loucks, R.R., 1991, Platinum-gold and vanadiferous magnetite mineralization in the Early Proterozoic Lake Owen layered mafic intrusion, Medicine Bow Mountains, Wyoming: Wyoming Geological Association 42nd Field Conference Guidebook, p. 37-38.

Loucks, R.R., Premo, W.R., and Snyder, G.L., 1988, Petrology, structure, and age of the Mullen Creek layered mafic complex and age of arc accretion, Medicine Bow Mountains, Wyoming: Geological Society of America Abstracts with Programs, v. 20, p. A73.

Love, J.D., and Antweiler, J.C., 1973, Copper, silver, and zinc in the Nugget Sandstone, western Wyoming: Wyoming Geological Association 25th Annual Field Conference Guidebook, p. 139-147.

Love, J.D., Antweiler, J.C., and Mosier, E.L., 1978, A new look at the origin and volume of the Dickie Springs-Oregon Gulch placer gold at the south end of the Wind River Mountains: Wyoming Geological Association 30th Annual Field Conference Guidebook, p. 379-391.

Madsen, M., 1978, A statistical analysis of heavy mineral variations in upper Cretaceous black sandstone deposits of the Rocky Mountain states [M.S. thesis]: Laramie, University of Wyoming, 138 p.

Marston, R.J., Groves, D.I., Hudson, D.R., and Ross, J.R., 1981, Nickel sulfide deposits in Western Australia: a review: Economic Geology, v. 76, p. 1330-1363.

McCallum, M.E., 1968, The Centennial Ridge gold-platinum district, Albany County, Wyoming: Geological Survey of Wyoming Preliminary Report 7, 12 p.

McCallum, M.E., Eggler, D.H., Coopersmith, H.G., Smith, C.B., and Mabarak, C.D., 1977, Field guide to the Colorado-Wyoming State Line District: Colorado State University Department of Earth Resources, Second International Kimberlite Conference, 23 p.

McCallum, M.E., Loucks, R.R., Carlson, R.R., Cooley, E.F., and Doerge, T.A., 1975, Platinum metals associated with hydrothermal copper ores of the New Rambler mine, Medicine Bow Mountains, Wyoming: Economic Geology, v. 71, p. 1429-1450.

McCallum, M.E., and Mabarak, C.D., 1976, Diamond in State Line kimberlite diatremes, Albany County, Wyoming, Larimer County, Colorado: Geological Survey of Wyoming Report of Investigations 12, 36 p.

McCallum, M.E., Mabarak, C.D., and Coopersmith, H.G., 1979, Diamonds from kimberlites in the Colorado-Wyoming State Line District, *in* Boyd, F.R., and Meyer, H.O.A., editors, Kimberlites, diatremes, and diamonds: their geology, petrology, and geochemistry: American Geophysical Union, Washington D.C., p. 42-58.

McCallum, M.E., and Orback, C.J., 1968, The New Rambler copper-gold-platinum district, Albany and Carbon Counties, Wyoming: Geological Survey of Wyoming Preliminary Report 8, 12 p.

McCallum, M.E., and Waldman, M.A., 1991, The diamond resources of the Colorado-Wyoming State Line district: kimberlite indicator mineral chemistry as a guide to economic potential: Wyoming Geological Association 42nd Field Conference Guidebook, p. 77-90.

Nowell, W.B., 1971, The petrology and alteration of the Kirwin mineralized area, Park County, Wyoming [M.S. thesis]: Missoula, University of Montana, 72 p.

Ogden, P.R., 1979, The geology, major element chemistry, and petrogenesis of the Leucite Hills volcanic rocks, Wyoming [Ph.D. dissertation]: Laramie, University of Wyoming, 137 p.

Osterwald, F.W., Osterwald, D.B., Long, J.S., Jr., and Wilson, W.H., 1960, Mineral resources of Wyoming: Geological Survey of Wyoming Bulletin 50, 287 p.

Pay Dirt, 1985, Do you want a mine or a beautiful summer retreat? See AMAX: Rocky Mountain Pay Dirt, October, 1985, p. 32A.

Pfaff, B.C., 1978, Atlantic City nuggets: Baroil, Wyoming, 155 p.

Rostad, O.H., 1983, Data summary, AMAX's Kirwin project — Park County, Wyoming: AMAX Exploration report, Geological Survey of Wyoming mineral files (unpublished), 4 p.

Schrader, F.C., 1913, Gold placers on Wind and Bighorn rivers, Wyoming: U.S. Geological Survey Bulletin 580, p. 127-142.

Sherer, R.L., 1969, Nephrite deposits of the Granite, the Seminoe, and the Laramie mountains, Wyoming [Ph.D. dissertation]: Laramie, University of Wyoming, 194 p.

Silver Lake Resources, Inc., 1985, Annual report for 1985: Geological Survey of Wyoming Mineral files, 27 p.

Smaglik, S.M., 1987, Petrogenesis and tectonic implication for Archean mafic and ultramafic magmas in the Elmer's Rock greenstone belt, Laramie Range, Wyoming [M.S. thesis]: Golden, Colorado School of Mines, 126 p.

Smith, C.B., McCallum, M.E., Coopersmith, H.G., and Eggler, D.H., 1979, Petrochemistry and structure of kimberlites in the Front Range and Laramie Range, Colorado-Wyoming, *in* Boyd, F.R., and Meyer, H.O.A., editors, Kimberlites, diatremes, and diamonds: their geology, petrology, and geochemistry: American Geophysical Union, Washington, D.C., p. 179-189.

Snyder, G.L., Hausel, W.D., Klein, T.L., Houston, R.S., and Graff, P.J., 1989, Precambrian rocks and mineralization, southern Wyoming province: 28th International Geological Congress Field Trip Guidebook T332: American Geophysical Union, Washington D.C., 48 p.

Spencer, A.C., 1916, The Atlantic gold district and the north Laramie Mountains: U.S. Geological Survey Bulletin 626, 85 p.

Spry, P.G., and McGowan, K.I., 1989, Origin of Archean lode gold mineralization at Atlantic City-South Pass, Wyoming: fluid inclusion and stable isotope study: 28th International Geological Congress Abstracts, American Geophysical Union, Washington D.C., p. 3-163.

Staatz, M.H., 1983, Geology and descriptions of thorium and rare earth deposits in the southern Bear Lodge Mountains, northeastern Wyoming: U.S. Geological Survey Professional Paper 1049-D, 52 p.

Sutherland, W.M., 1990, Gemstones, lapidary materials, and geologic collectibles in Wyoming: Geological Survey of Wyoming Open File Report 90-9, 53 p.

U.S. Bureau of Mines, 1942, Rambler mine, Albany County, Wyoming: U.S. Bureau of Mines War Minerals Report 17, 7 p.

Welch, C.M., 1974, A preliminary report on the geology of the Mineral Hill area, Crook County, Wyoming [M.S. thesis]: Rapid City, South Dakota School of Mines and Technology, 83 p.

Wilson, W.H., 1960, Petrology of the Wood River area, southern Absaroka Mountains, Park County, Wyoming [Ph.D. dissertation]: Salt Lake City, University of Utah, 121 p.

_____ 1964, The Kirwin mineralized area, Park County, Wyoming: Geological Survey of Wyoming Preliminary Report 2, 20 p.

Woodfill, R.D., 1987, Hartville uplift, southeastern Wyoming: Geological Survey of Wyoming mineral files (unpublished), 20 p.

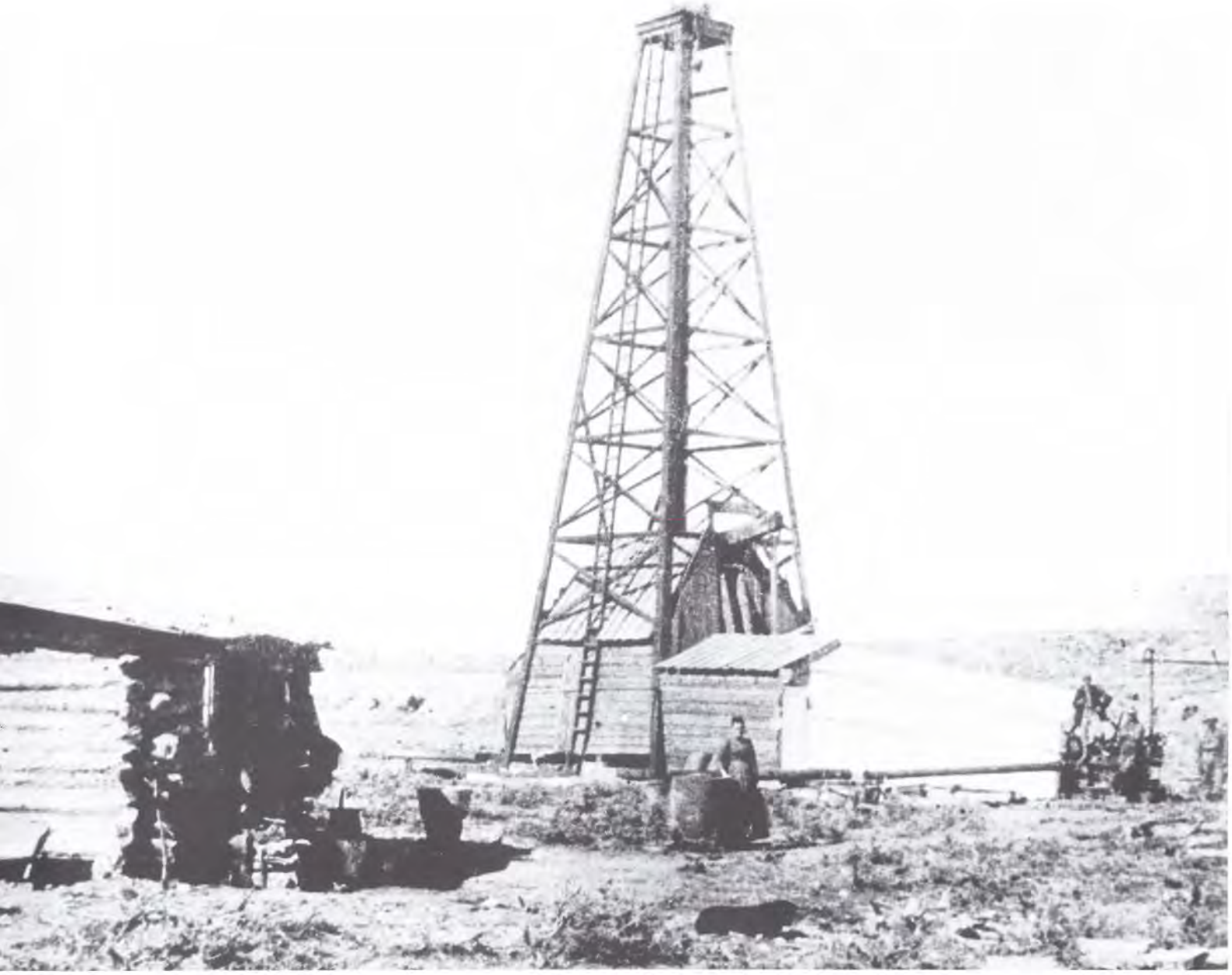

Frontispiece. P.M. Shannon drilled the first producing well in Natrona County in 1889 near an oil seep. The well, shown above, was drilled less than a mile north of what would later be known as Salt Creek field. Five to 10 barrels of oil per day were produced from this well at a depth of 700 feet in the Shannon Sandstone. Oil was discovered in 1906 just 3 miles southwest of this well at a well drilled on the Salt Creek anticline. In 1908, the Dutch No. 1 well discovered oil in the Wall Creek Sandstone Member of the Frontier Formation. This and subsequent discoveries in deeper reservoirs established Salt Creek field as one of the most significant fields in the Rocky Mountain region. Salt Creek field has produced over 640 million barrels of oil and over 700 billion cubic feet of gas from 12 different reservoirs. Photograph courtesy of University of Wyoming, American Heritage Center.

Overview of oil and gas geology of Wyoming

Rodney H. De Bruin
Geological Survey of Wyoming
Laramie, Wyoming 82071

Abstract

The first commercial oil well in Wyoming was completed in 1884 near an oil seep. Over 1,500 oil and gas fields have since been discovered in Wyoming, and these fields have produced over 6 billion barrels of oil and nearly 17 trillion cubic feet of natural gas. Since 1884, a number of advances, such as the application of the anticlinal theory of oil and gas accumulation, the recognition of trap types other than the anticlinal occurrence, and the recognition that depositonal environments of sedimentary rocks play an important role in the heterogeneity of reservoirs, have helped to develop the State's oil and gas resources. The development of seismic techniques and down-hole geophysical logs helped geologists recognize stratigraphic traps and buried structural traps (without surface expression) and led to the discovery of many oil and gas fields.

In Wyoming, oil and gas are produced from sedimentary rocks ranging in age from Tertiary to Cambrian. Formations that contain most of the largest hydrocarbon reservoirs are: the Mississippian Madison Limestone, Pennsylvanian Tensleep Sandstone, Permian/Pennsylvanian Minnelusa Formation, Permian Phosphoria Formation, Jurassic/Triassic Nugget Sandstone, Lower Cretaceous "Dakota" Sandstone and Muddy Sandstone, and the Upper Cretaceous Frontier Formation, Almond Formation, and Shannon Sandstone. Sandstone reservoirs were deposited in a variety of environments that include coastal, fluvial, deltaic, nearshore, shelf, and deepwater. Most carbonate reservoirs were deposited in a peritidal or shallow shelf environment. Over 90% of Wyoming's oil has been produced from the Powder River, Bighorn, and Wind River basins and over 75% of the gas has been produced from the Greater Green River Basin and overthrust belt.

Over half of Wyoming's oil and gas has been produced from reservoirs in anticlines. A component of the oil and gas produced from these structures was trapped stratigraphically. Stratigraphic traps have produced nearly half of Wyoming's hydrocarbons. Stratigraphic traps include: asphalt seals (scarce), impermeable shale, porosity variations including depositional and diagenetic influences, and erosional truncation. Hydrodynamic flow is partly responsible for off-structure production in several fields.

Primary source rocks that have provided hydrocarbons for reservoirs in Wyoming range in age from Tertiary to Pennsylvanian. Notable source rocks are the Pennsylvanian black shales of the Minnelusa Formation; the Retort and Meade Peak shale members of the Permian Phosphoria Formation; and Cretaceous shales of the Thermopolis Shale, Mowry Shale, Frontier Formation, Cody Shale, Aspen Shale, Skull Creek Shale, Niobrara Formation, and Carlile Shale. Lacustrine shales of Tertiary formations contribute to natural gas reserves located principally in deep basin centers. Cretaceous and Tertiary coals have generated significant hydrocarbons, but as yet have accounted for little production.

De Bruin R.H., 1993, Overview of oil and gas geology of Wyoming, *in* Snoke, A.W., Steidtmann, J.R., and Roberts, S.M., editors, Geology of Wyoming: Geological Survey of Wyoming Memoir No. 5, p. 836-873.

Introduction

This paper presents an account of some exploration theories and technological advances that have been applied in Wyoming (and other areas) and have contributed to the discovery of many oil and gas fields in the State. Major plays in the Powder River, Bighorn, Wind River, and Greater Green River basins, overthrust belt, and southeastern Wyoming basins are catalogued with respect to reservoir ages, depositional environments, and trap types. A "play" encompasses an area within which hydrocarbon accumulations are expected to be geologically similar in terms of: reservoir age, porosity and permeability, trap type, source rock, diagenetic alteration, hydrocarbon type, and depositional environment. The present productive limit and the most productive fields of the individual plays are shown. A section on source rocks summarizes some current theories on which rocks generated and discharged hydrocarbons to the main reservoirs in the State.

Historical perspective

The first written account of an oil discovery, in the area which would later become the State of Wyoming, was in Washington Irving's book *Adventures of Captain Bonneville* (1849). Irving described Captain Bonneville's 1833 discovery of a "great tar spring" on the Popo Agie River, approximately 8 miles southeast of present-day Lander. The "tar" from that spring was used by hunters and trappers for medicinal purposes (Knight, 1897) and later was used by the military and early travelers as lubrication for their wagon wheels (Roundtree, 1984).

E.L. Drake's discovery of oil in western Pennsylvania in 1859 was the beginning of the modern oil industry in the United States (Levorsen, 1967), as it demonstrated drilling as an effective production method to obtain oil in large volumes. Following Drake's discovery, early drillers began to search for the best places to drill oil wells. Wells were most often drilled near oil seeps.

In 1884, 25 years after Drake's discovery, Mike Murphy completed the first well drilled for commercial oil production in Wyoming and opened the Dallas oil field. This well was drilled to a depth of 300 feet adjacent to the "great tar spring" that was discovered by Captain Bonneville. Dallas field is still producing oil more than 109 years later and has produced a total of 11 million barrels, chiefly from the Tensleep Sandstone and Phosphoria Formation. Another oil seep, at Jackass Spring, probably influenced Mark Shannon to file mining claims on Federal land around that spring. In 1889, Shannon drilled the discovery well for Shannon field on the north plunge of Salt Creek anticline, approximately 40 miles north of Casper. The well produced from a Cretaceous age sandstone (now named for him) and established commercial production in the area just north of what later became Salt Creek field. The Shannon field is insignificant in hydrocarbon volume when compared to Salt Creek field, which has produced 631 million barrels of oil and 712 billion cubic feet of gas.

I.C. White's field work on gas occurrences in Pennsylvania led to publication of the anticlinal theory of gas accumulation in 1885. The theory simply states that gas collects in anticlines because of its volatile nature and because fracturing necessary to form a large reservoir takes place most readily in anticlines, where tension in response to bending is greatest (White, 1885).

The success that White achieved with his theory led to its widespread application in oil exploration in Wyoming and in other parts of the country. Early wildcatters in Wyoming drilled wells on anticlines along the margins of the Powder River, Bighorn, Wind River, and Greater Green River basins. Between 1906 and 1928, 13 giant fields were discovered in the State following this exploration philosophy. These 13 giant fields have produced nearly half of Wyoming's cumulative oil through 1991 and nearly 13% of Wyoming's cumulative gas through 1991 (**Table 1**). Many other fields were discovered in surface mapped anticlines in this period as well, but the amount of discovered oil and gas was minor when compared to those 13 giant fields.

The seismic method of exploration was developed in the Gulf Coast during the 1920s and its application caused another significant advance in Wyo-

Table 1. Giant fields discovered in Wyoming between 1906 and 1928.

Field	Discovery date	Cumulative oil production through 1991 (millions of barrels)	Cumulative gas production through 1991 (billons of cubic feet)
Garland	1906	170	138
Salt Creek	1908	639	713
Oregon Basin	1912	410	192
Grass Creek	1914	191	8
Little Buffalo Basin	1914	124	121
Elk Basin	1915	440	343
Lost Soldier	1916	219	112
Winkleman	1917	89	2
Hamilton Dome	1918	237	—
Byron	1918	123	13
Lance Creek	1918	107	143
Wertz	1920	106	109
Frannie	1928	114	—
Total		**2,969**	**1,894**

ming oil exploration. Quealy Dome, which was discovered in 1934 by the California Company, was the first field in the Rocky Mountain region that was found through the use of seismic exploration methods. At first, seismic techniques were used to find anticlines that could not be identified through surface mapping techniques. Later, as the seismic techniques were refined and resolution of discrete beds and reservoirs was achieved, stratigraphic traps were identified.

In 1936, the first electric log in Wyoming was run by Schlumberger. After this it became common practice to run down-hole surveys of wells drilled in the State. Other geophysical logs such as acoustic, formation density, gamma ray, neutron, and dipmeter were developed and became important tools used by geologists to interpret subsurface structure, stratigraphy, fluid content, and reservoir properties including porosity. Subsurface geological work has played a significant role in the discovery of many oil and gas fields in Wyoming.

The term "trap" was introduced by McCullough (1934) and was applied to reservoirs that trapped oil by asphalt seals, impermeable rocks, porosity variations, truncation, overlap, and folding and faulting. Although most of the oil and gas found in Wyoming before 1956 was discovered because of its relationship to structures, it is recognized that a part of the oil and gas was trapped by variations in lithology. Pedry (1975) discussed the role that hydrodynamic flow may have played in trapping oil in several large fields in the Bighorn Basin. Curry (1984) discussed the possibility that the Tensleep Sandstone reservoir at Bonanza field in the Bighorn Basin is a buried paleohill that forms a stratigraphic trap, even though the hydrocarbons occur on a structure.

Cottonwood Creek, in the Bighorn Basin, is a large stratigraphic trap that was discovered through subsurface geological work. This field had produced 55 million barrels of oil through 1991. It produces from the Permian Phosphoria Formation. The field was discovered in 1953 and is the first major discovery of a purely stratigraphic trap in Wyoming (Herrod, 1980).

Before 1960, exploration for oil from the Minnelusa Formation in the Powder River Basin concentrated on structural accumulations. Raven Creek field was discovered in 1960. Additional development drilling at Raven Creek showed that a stratigraphic trap was present. This discovery resulted in renewed interest in the Minnelusa (Trotter, 1963). The Minnelusa became the most active play in the United States in the last 30 years in terms of wildcat wells drilled. More than 260 fields have been discovered in the Minnelusa (DeBruin and Boyd, 1990) and this play is still one of the most active in the State. Over 21 million barrels of oil were produced during 1991 in Wyoming from reservoirs in the Minnelusa Formation (Wyoming Oil and Gas Conservation Commission, 1992). Most of this oil was produced from traps related to eolian dunes overlain by Opeche Shale.

The first significant development of reservoirs in the Muddy/Newcastle Sandstone in Wyoming was at Moorcroft field (discovered in 1887) and Osage field (discovered in 1919). The Fiddler Creek and Clareton field areas in the Powder River Basin of eastern Wyoming were developed in the 1950s. After the Bell Creek field was discovered in the southeastern Montana portion of the Powder River Basin in 1967, the play extended throughout northeastern Wyoming and resulted in the discovery of major hydrocarbon accumulations at Recluse, Gas Draw, Kitty, Hilight, and Amos Draw fields (Berg and

others, 1985). Muddy Sandstone reservoirs at these fields had produced over 450 billion cubic feet of gas and 145 million barrels of oil through 1991 (Wyoming Oil and Gas Conservation Commission, 1992). Muddy and Newcastle sands that now form the reservoirs were deposited in fluvial, and marine environments adjacent to less permeable muddy sediments that form stratigraphic traps.

Following the discovery of Pineview field in Utah in 1975, major accumulations of oil and gas were discovered in the overthrust belt of Wyoming. Reservoirs occur in several different formations, and are in folds related to thrust faults, where Paleozoic and Mesozoic rocks are thrust over, or are in juxtaposition with, younger Cretaceous source beds. Because of the structural complexity, high-quality seismic data, resulting from advances in technology and data processing, were necessary to find the best places to drill. Discoveries at Whitney Canyon-Carter Creek, Painter Reservoir, Painter Reservoir East, Ryckman Creek, Clear Creek, and Yellow Creek fields nearly doubled Wyoming's measured reserves of natural gas. The reserves estimated by The Energy Information Administration (1980, 1983) increased from 5.3 trillion cubic feet in 1976 to 10.1 trillion cubic feet in 1982.

Horizontal drilling now under way in the Upper Cretaceous Niobrara Formation and drilling into Upper Cretaceous and Tertiary coal beds may be the next wave of exploration that will increase Wyoming's oil and gas reserves. Geologic conditions are such that horizontal drilling targets may also develop in the Cretaceous Mowry Shale and Frontier Formation. Horizontal drilling will almost certainly be used in tight gas sands and coal seams as well. Overpressured low-permeability Cretaceous and Tertiary sandstone reservoirs in the Greater Green River Basin contain an estimated 5,063 trillion cubic feet of in-place gas (Law and others, 1989). Large volumes of this gas may be recovered if gas prices increase enough and if production technology advances.

In Wyoming, oil and gas are produced from reservoirs of Tertiary, Cretaceous, Jurassic, Triassic, Permian, Pennsylvanian, Mississippian, Devonian, Ordovician, and Cambrian age. Commercial oil and gas production comes from every major basin and the overthrust belt of western Wyoming. Over 75% of Wyoming's oil production presently comes from reservoirs in the Powder River, Bighorn, and Wind River basins, whereas nearly 85% of Wyoming's gas production comes from reservoirs in the Greater Green River Basin and overthrust belt (Wyoming Oil and Gas Conservation Commission, 1992).

Most production from the overthrust belt and from the major basins in the State (**Figure 1**) can be divided into several major plays. These plays are based on depositional environments, reservoir ages, and trap types. Some of these identified plays are catalogued in the text that follows, arranged in ascending stratigraphic order by basin.

Powder River Basin

Basin margin structural play

Nearly one billion barrels of oil and one trillion cubic feet of gas have been produced from multiple reservoirs on large anticlines located on the western and southern margins of the Powder River Basin (**Figure 2**). Many of these anticlines have normal faults on their crests and reverse faults depth. Principal reservoirs in these structures are in the Pennsylvanian Tensleep Sandstone and Permian-Pennsylvanian Minnelusa Formation, the Lower Cretaceous Fall River Formation (informally "Dakota Sandstone") and Muddy Sandstone, and the Upper Cretaceous Frontier Formation (see Stratigraphic nomenclature chart of Wyoming, Love and others, **map pocket**). These fields were discovered in the early exploration of the Powder River Basin.

Major fields in this play include Salt Creek, Lance Creek, Big Muddy, and Teapot. These four fields have produced over 800 million barrels of oil and nearly 0.9 trillion cubic feet of associated gas. Salt Creek is the most productive field in Wyoming, with over 630 million barrels of oil and over 0.7 trillion cubic feet of associated gas produced (Wyoming Oil and Gas Conservation Commission, 1992). The first and second Wall Creek sands in the Frontier Formation account for over 500 million barrels of oil at Salt Creek field.

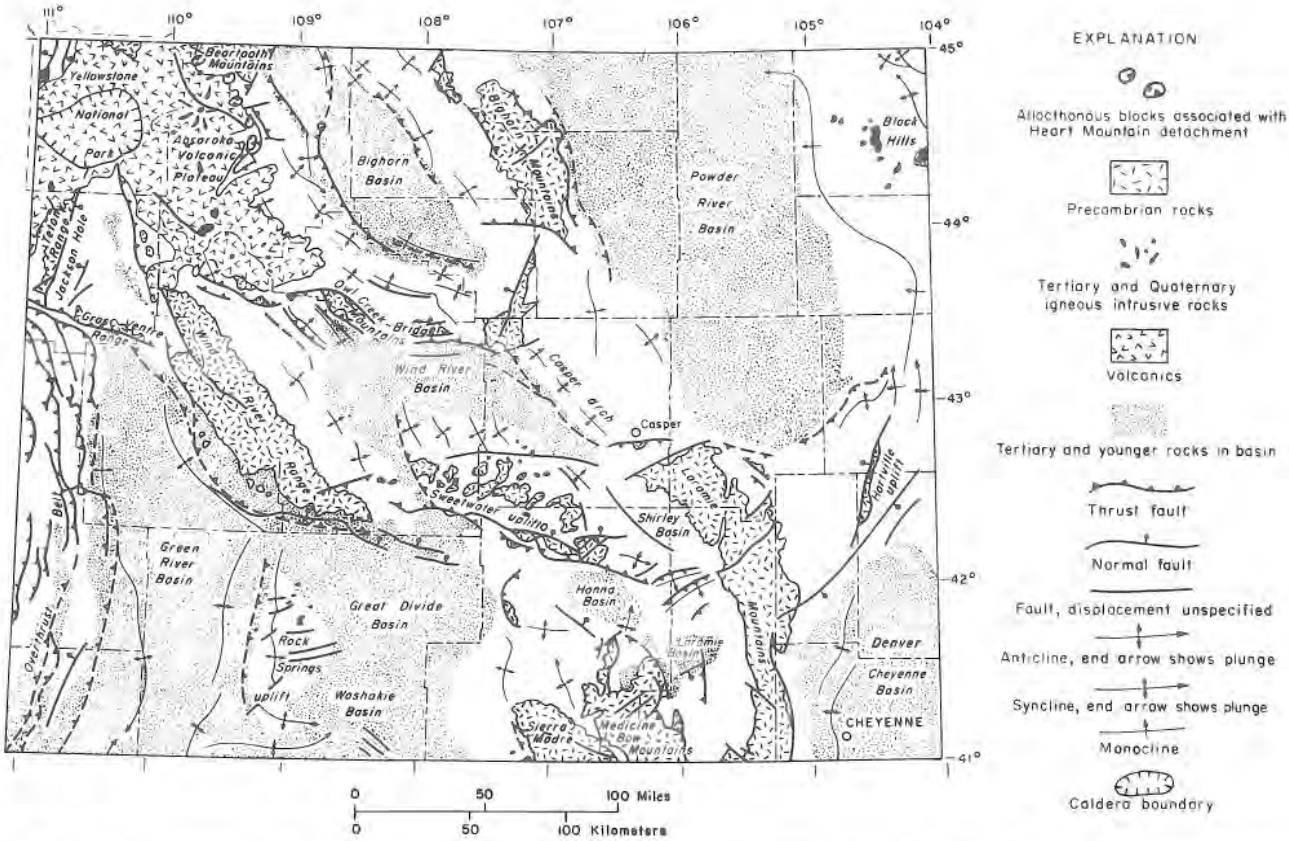

Figure 1. Index map of Wyoming that shows the location of the major hydrocarbon-producing basins and the overthrust belt. Modified from Blackstone (1987).

Permian upper Minnelusa Formation play

This play is located in the northeastern part of the Powder River Basin, Wyoming, and occurs in sandstone reservoirs of Permian age in the upper part of the Minnelusa Formation (**Figure 3**). The reservoirs are mainly eolian dune sandstones within a cyclic sequence of carbonates and sandstones of marine and nonmarine origin (Van West, 1972; Fryberger, 1984; George, 1984).

Oil in the Minnelusa is trapped in: paleotopographic highs overlain and sealed by Opeche Shale at the top of the formation; preserved dune forms with dolomite draped over the top (partly due to compaction); permeability pinchouts of depositional and diagenetic origin; and structural closures due to folding (Van West, 1972; Fryberger, 1984).

This play is still one of the most active in the State; over 260 fields with upper Minnelusa reservoirs have been discovered. Raven Creek field is the largest in terms of cumulative production, with over 44 million barrels produced through 1989. Timber Creek, Dillinger Ranch, Stewart, Halverson, and Duvall Ranch fields have each produced over 12 million barrels of oil (Wyoming Oil and Gas Conservation Commission, 1992). These six fields have produced over 116 million barrels of oil through 1991. In 1991, upper Minnelusa reservoirs produced over 21 million barrels of oil, which currently makes the Minnelusa the most prolific oil-producing formation in the State (Wyoming Oil and Gas Conservation Commission, 1992).

Lower Cretaceous Fall River Formation play

The Fall River Formation ("Dakota Sandstone") play is located in the east-central and southern areas of the Powder River Basin. On the northeastern flank of the Powder River Basin (**Figure 4**) sands were deposited in environments related to the regression of the Cretaceous sea. Most reservoirs are interpreted as point-bar sandstones sealed updip by fine-grained channel deposits (Berg, 1968; Mettler, 1968) and as

barrier bar sandstones (Miller, 1963). Chisholm (1970) interpreted the reservoir at Coyote Creek field as a tidal channel deposit.

Recent discoveries of oil and gas in the Fall River Formation of the southern Powder River Basin at Nutcracker, Buck Draw, and Buck Draw North fields (**Figure 4**) support the interpretation of Rasmussen and others (1985) that Lower Cretaceous sands in this part of the basin were deposited in environments related to deltas. Most oil and gas producing sandstone reservoirs discovered in the southern Powder River Basin are interpreted as distributary channel deposits (Hawkins and Formhals, 1985). Hoyle and others (1981) describe the "Dakota" rocks at Glenrock South field as meandering stream channel deposits reworked by marine processes.

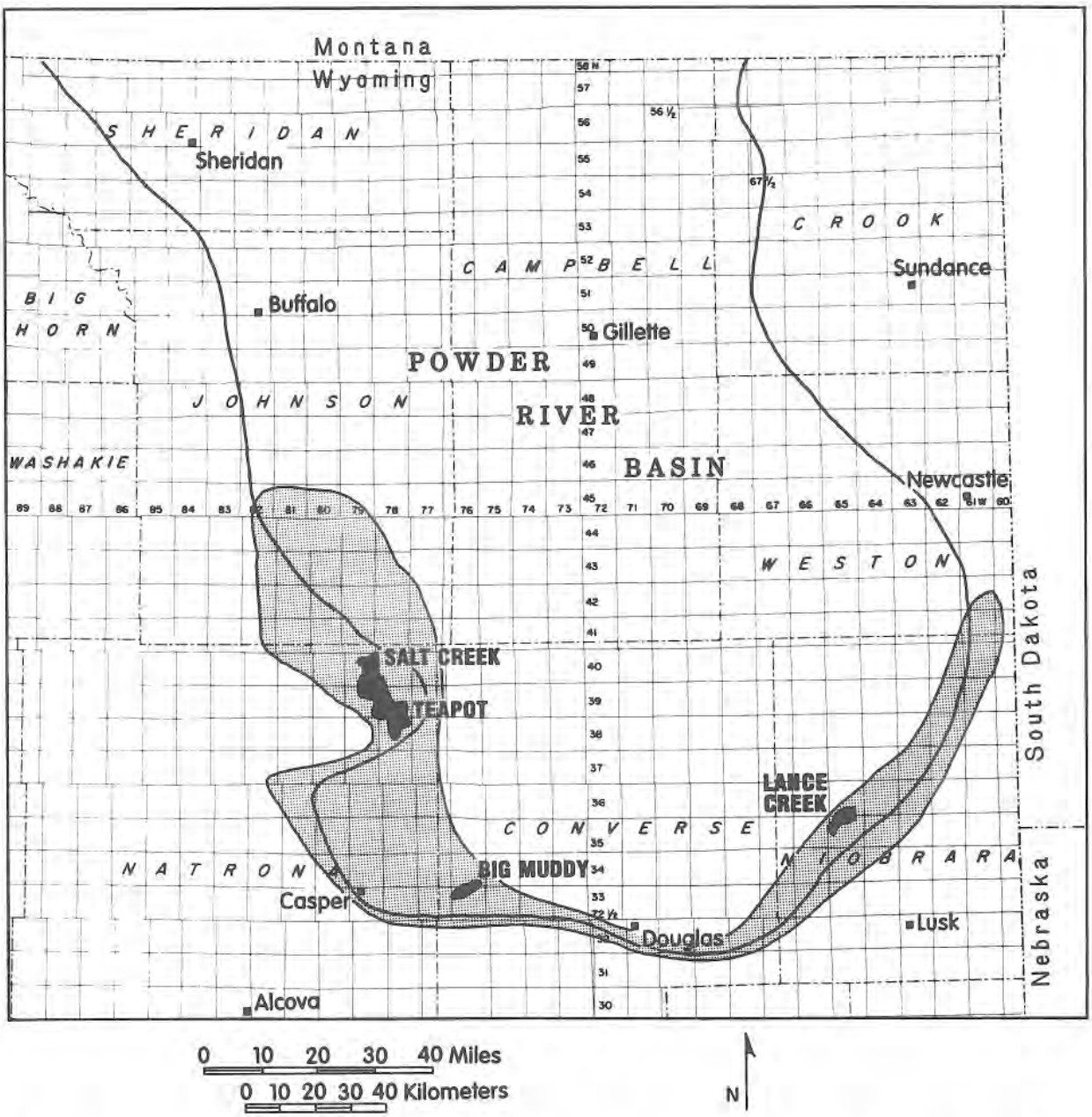

Figure 2. Present productive limit of the basin margin structual play (shaded) in the Wyoming portion of the Powder River Basin. Major fields in the play are shown in black.

Lower Cretaceous Muddy Sandstone and Newcastle Sandstone play

This play is developed in a suite of stratigraphic traps related to the depositional environments of the reservoirs (Dolton and others, 1990). The reservoirs along the eastern edge of the basin are interpreted as alluvial and estuarine deposits filling channels incised into the underlying marine Skull Creek Shale (Stone, 1972). This productive trend is predominantly northeast to southwest and major fields include Fiddler Creek, Fiddler Creek East, Osage, Clareton, Skull Creek and Mush Creek (**Figure 5**). Production from these six fields through 1991 was

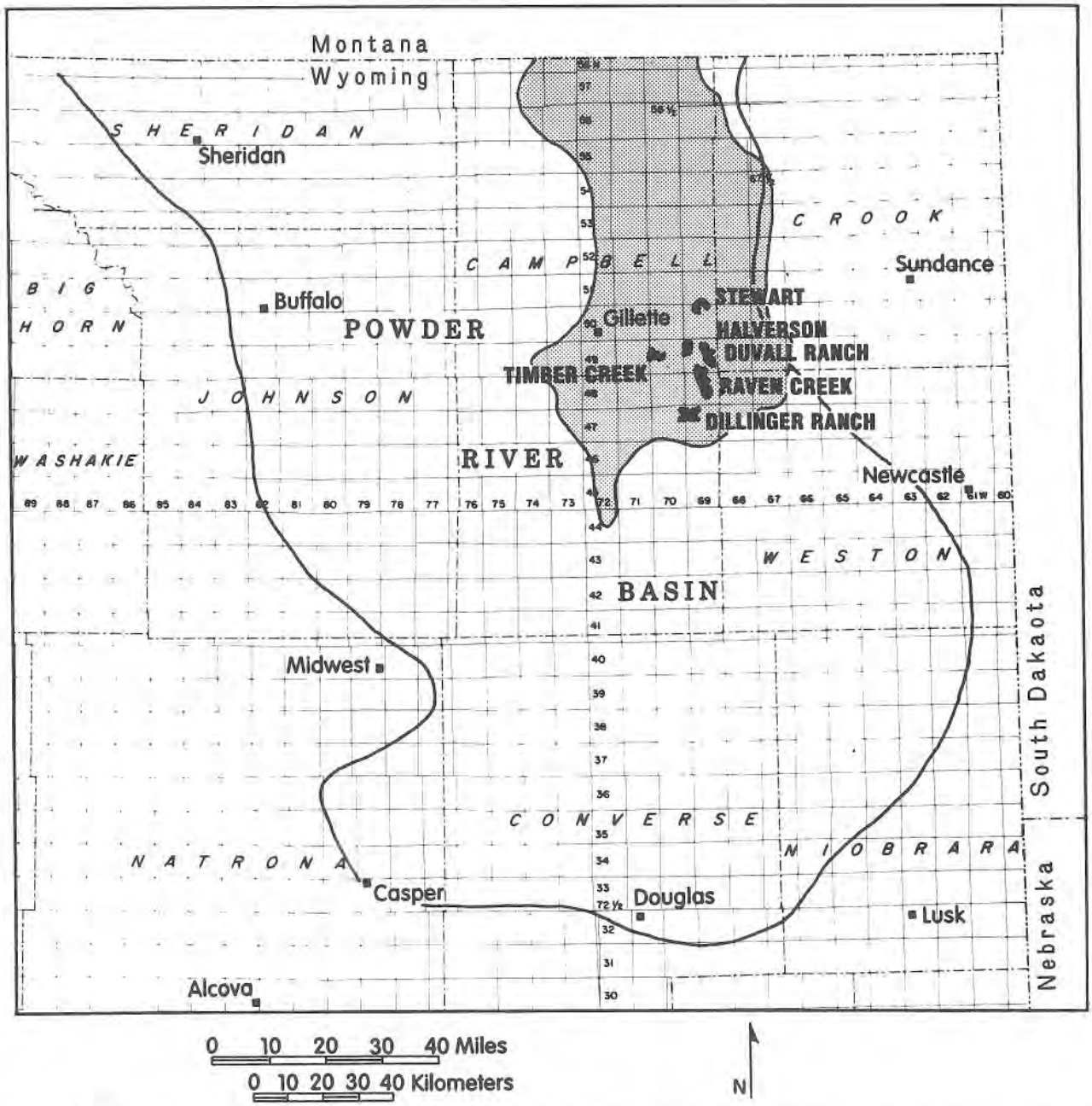

Figure 3. Present productive limit of the Permian upper Minnelusa Formation play (shaded) in the Wyoming portion of the Powder River Basin. Major fields in the play are shown in black.

over 74 million barrels of oil and 5 billion cubic feet of gas (Wyoming Oil and Gas Conservation Commission, 1992).

In parts of the basin, reservoirs are nearshore marine sandstones (Von Drehle, 1985; Stone, 1972) and channel and valley-fill sandstones (Dolson and others, 1991). Important fields such as Kitty (Larberg, 1980), Gas Draw (Stone, 1972), Hilight (Prescott, 1970), and Recluse (Berg, 1976) (**Figure 5**) produce from stacked reservoirs, which include nearshore marine, fluvial, and valley-fill sandstones. The Muddy Sandstone produces from fluvial and barrier-bar sandstones at Glenrock South field (Hoyle

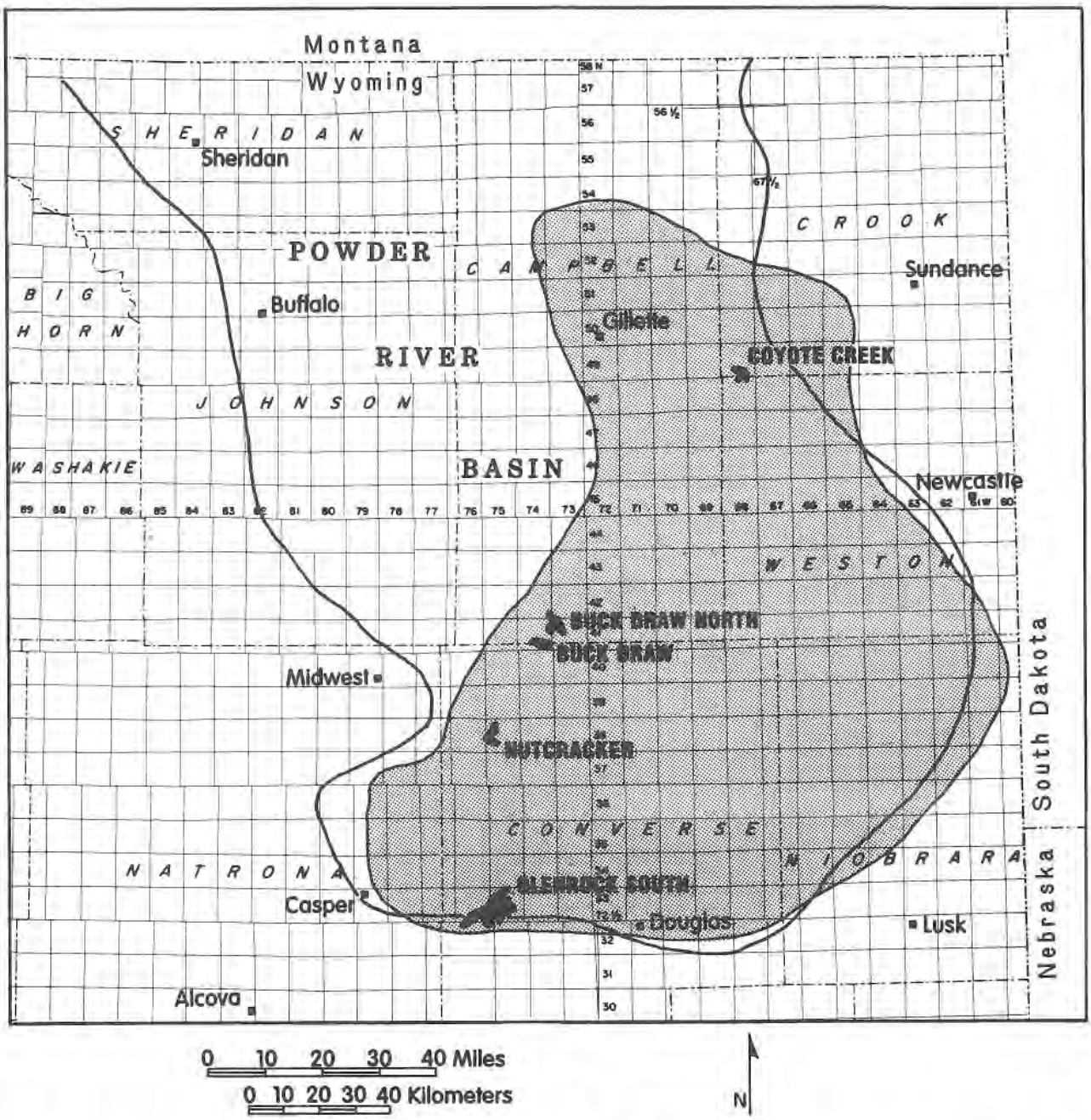

Figure 4. Present productive limit of the Lower Cretaceous Fall Fiver Formation play (shaded) in the Wyoming portion of the Powder River Basin. Major fields in the play are shown in black.

and others, 1981) and from a marine barrier bar complex at Amos Draw field (Von Drehle, 1985) (**Figure 5**).

Upper Cretaceous Frontier Formation and Turner Sandy Member play

This play is developed in sandstone reservoirs of the lower Turner Sandy Member of the Carlile Shale in the southeastern portion of the basin and in Frontier Formation sandstone reservoirs to the west in the south-central part of the basin (**Figure 6**) (see Stratigraphic nomenclature chart of Wyoming, Love and others, **map pocket**). While the Frontier Sandstone reservoirs at Salt Creek in the basin margin structural play are interpreted as deltaic and nearshore marine (Maynard and others, 1981), the reservoirs in this play are mainly shelf deposits in the west (Haun, 1958; Rice and Keighin, 1988) and offshore sand-

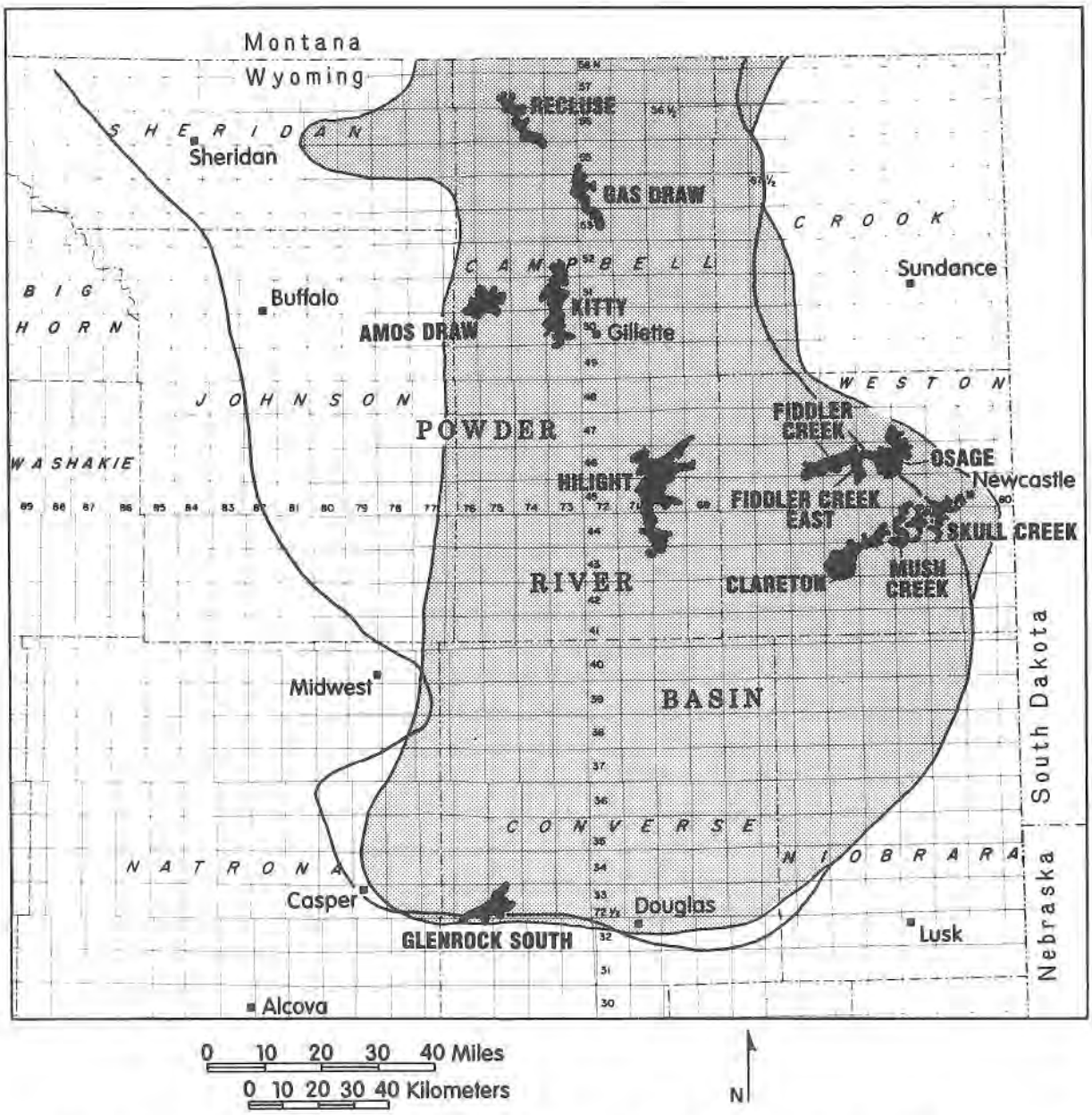

Figure 5. Present productive limit of the Lower Cretaceous Muddy Sandstone and Newcastle Sandstone play (shaded) in the Wyoming portion of the Powder River Basin. Major fields in the play are shown in black.

stones farther to the east (Merewether and others, 1979). The sandstones mostly trend northwest-southeast but they sometimes coalesce to form unpredictable configurations (Winn and others, 1983). Major fields in this play include Powell, Spearhead Ranch, and Finn-Shirley.

Upper Cretaceous Shannon Sandstone and Sussex Sandstone play

The Shannon and Sussex sandstones are members of the Steele (or Cody) Shale. Reservoirs are stratigraphically trapped sandstones deposited on

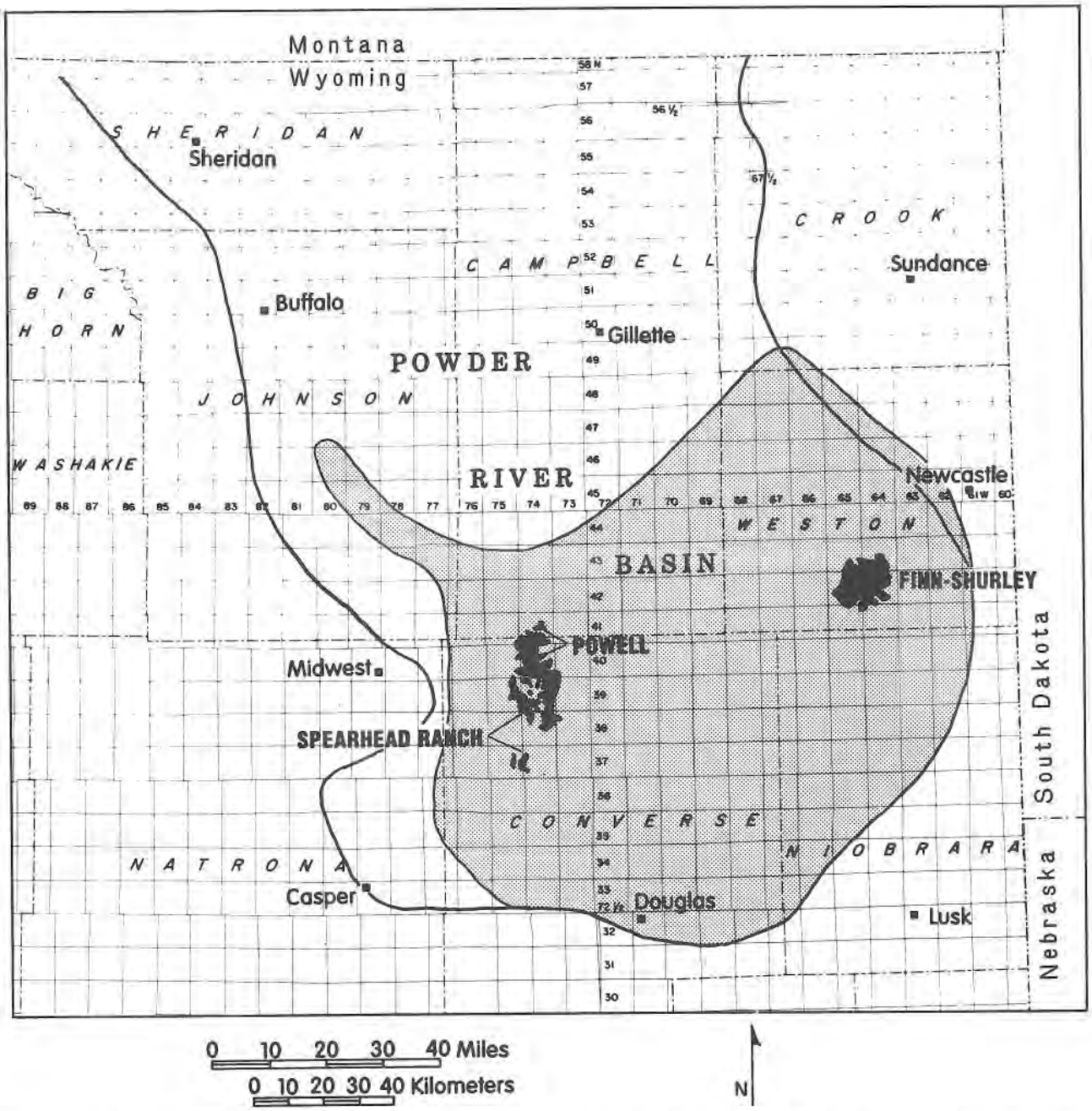

Figure 6. Present productive limit of the Upper Cretaceous Frontier Formation and lower Turner Sandy Member play (shaded) in the Wyoming portion of the Powder River Basin. Major fields in the play are shown in black.

the middle to outer shelf (Asquith, 1974; Davis, 1976; Spearing, 1976; Berg, 1975; Tillman and Martinsen, 1984, 1987). An interpretation by Hansley and Whitney (1990) suggests that Shannon sand ridges were originally deposited as a shoreline facies, then were reworked during a transgression and redeposited on the shelf. Shale encases the sandstones and forms the seal. The known extent of the play is in the western half of the Powder River Basin (**Figure 7**). Production from younger Sussex sandstones is east of fields productive from the Shannon Sandstone (Crews and others, 1976) and the Sussex sandstones do not extend as far north as the Shannon sandstones. The sandstone bodies in both the Shannon

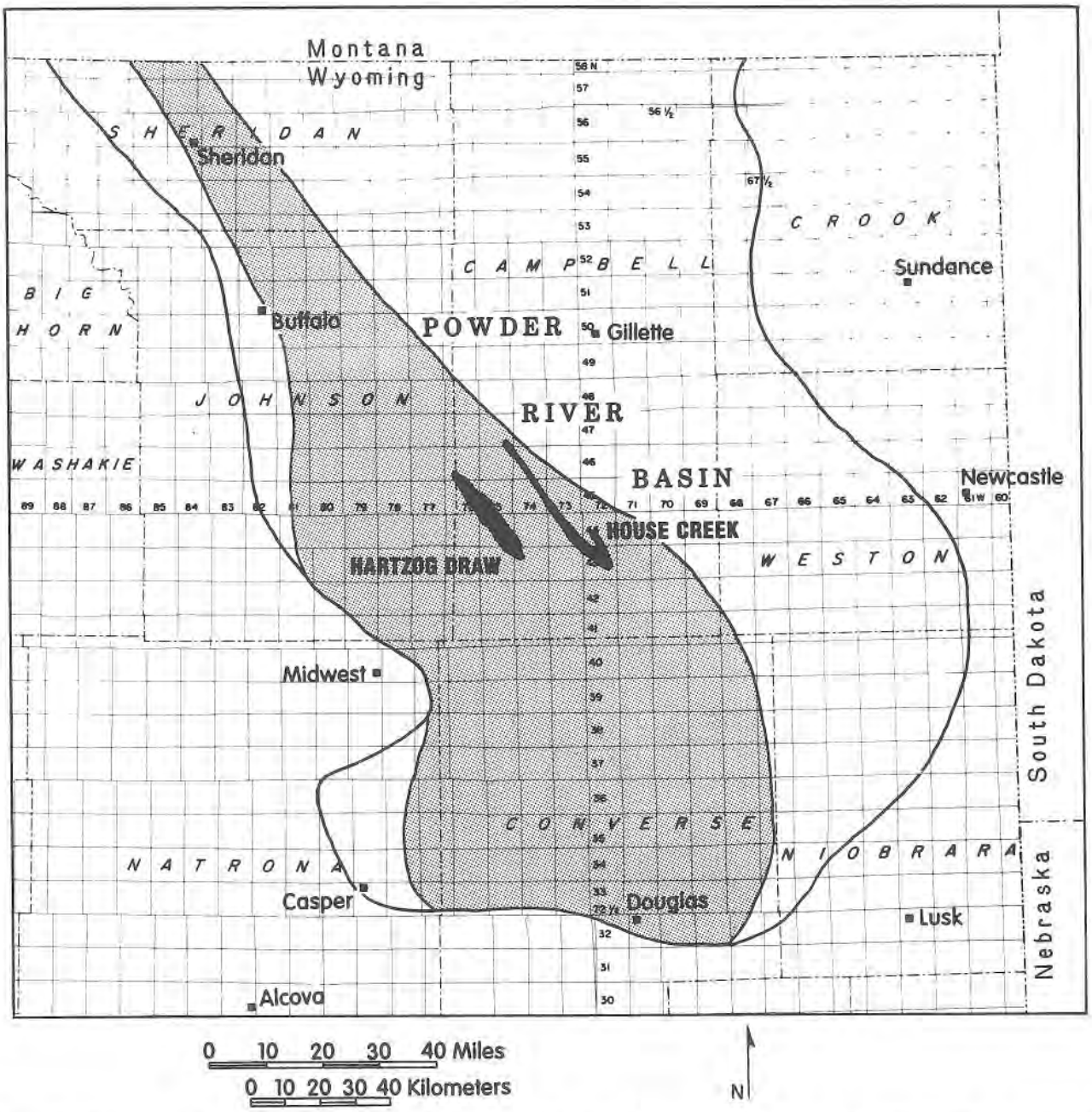

Figure 7. Present productive limit of the Upper Cretaceous Shannon Sandstone and Sussex Sandstone play (shaded) in the Wyoming portion of the Powder River Basin. Major fields in the play are shown in black.

non Sandstone and Sussex Sandstone trend northwest-southeast. The best developed porosity is usually in the thickest part of the Shannon and Sussex reservoirs. Significant fields in this play include Hartzog Draw, which has produced over 80 million barrels of oil and nearly 30 billion cubic feet of gas from the Shannon since its discovery in 1976, and House Creek, which has produced over 21 million barrels of oil and over 20 billion cubic feet of gas from the Sussex since its discovery in 1968 (Wyoming Oil and Gas Conservation Commission, 1992).

Upper Cretaceous Parkman, Teapot, and Teckla sandstones play

The Parkman and Teapot sandstones are members of the Upper Cretaceous Mesaverde Formation. The Teckla Sandstone is a member of the Upper Cretaceous Lewis Shale (see Stratigraphic nomenclature chart of Wyoming, Love and others, **map pocket**). Most of the oil and gas is trapped stratigraphically in marine sandstones with the seal provided by the updip pinchout of the sand into siltstones and shales

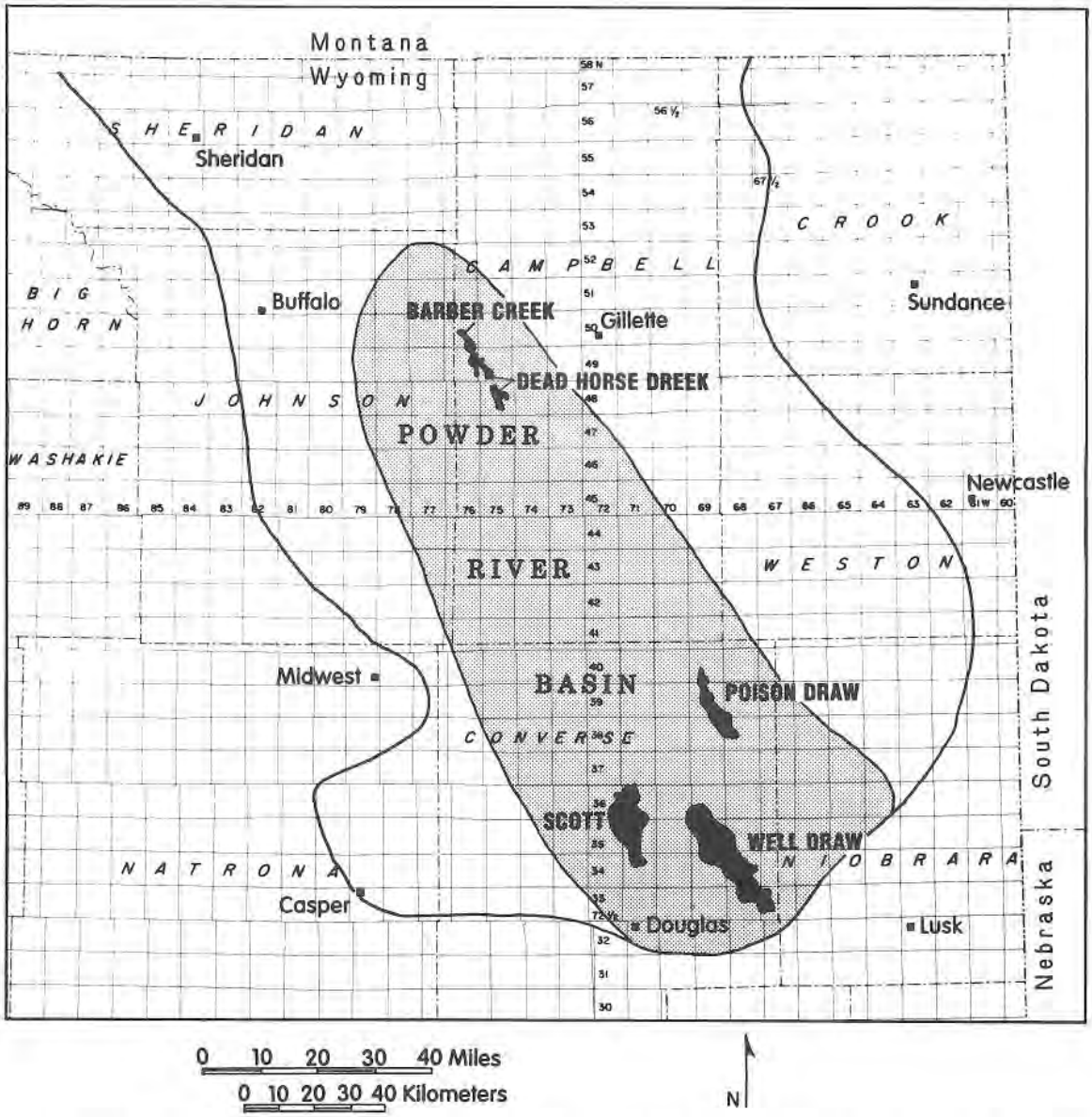

Figure 8. Present productive limit of the Upper Cretacceous Parkman Sandstone, Teapot Sandstone, and Teckla Sandstone play (shaded) in the Wyoming portion of the Powder River Basin. Major fields in the play are shown in black.

(Runge and others, 1973; Isbell and others, 1976). The currently known productive trend for sandstones in all three of these units is generally northwest-southeast; the productive area is in the central and south-central part of the basin (**Figure 8**). To the west of this play, the Parkman and Teapot were deposited on southeast prograding deltas (Curry, 1973, 1976); the Teckla was deposited on a third, more localized, prograding delta (Dolton and others, 1990). The major fields in this play include: Dead Horse Creek, Barber Creek, Well Draw, Scott, and Poison Draw. These five fields have produced over 65 million barrels of oil and 117 million cubic feet of gas through 1991 (Wyoming Oil and Gas Conservation Commission, 1992).

Bighorn Basin

Basin margin structural play

Nearly all of the oil and gas produced in the Bighorn Basin has come from sandstone and carbonate reservoirs associated with large anticlines around the margins of the basin. Most of these structures are related to reverse faults. Eight fields in this play have each produced a minimum of 100 million barrels of oil (Elk Basin, Oregon Basin, Hamilton Dome, Frannie, Grass Creek, Little Buffalo Basin, Byron, and Garland) (**Figure 9**). These eight fields have produced a total of 1.81 billion barrels of oil and 0.8 trillion cubic feet of natural gas (Wyoming Oil and Gas Conservation Commission, 1992). Seven of these fields were discovered between 1906 and 1918. Elk Basin, which extends into Montana, is the largest field in terms of past production. The Wyoming part of the field has produced over 440 million barrels of oil and over 343 billion cubic feet of gas (Wyoming Oil and Gas Conservation Commission, 1992).

Oil and gas have been produced at fields in this play from reservoirs that range in age from Cambrian through Cretaceous. Five fields first produced oil and gas from Frontier Formation sandstones, which are shallow and the first reservoirs encountered. Completions in Paleozoic reservoirs came later as drilling technology improved and the market developed for the heavy, commonly sour crude oil from these reservoirs. Most production in this play is associated with sandstone reservoirs of the Pennsylvanian Tensleep Sandstone and carbon-

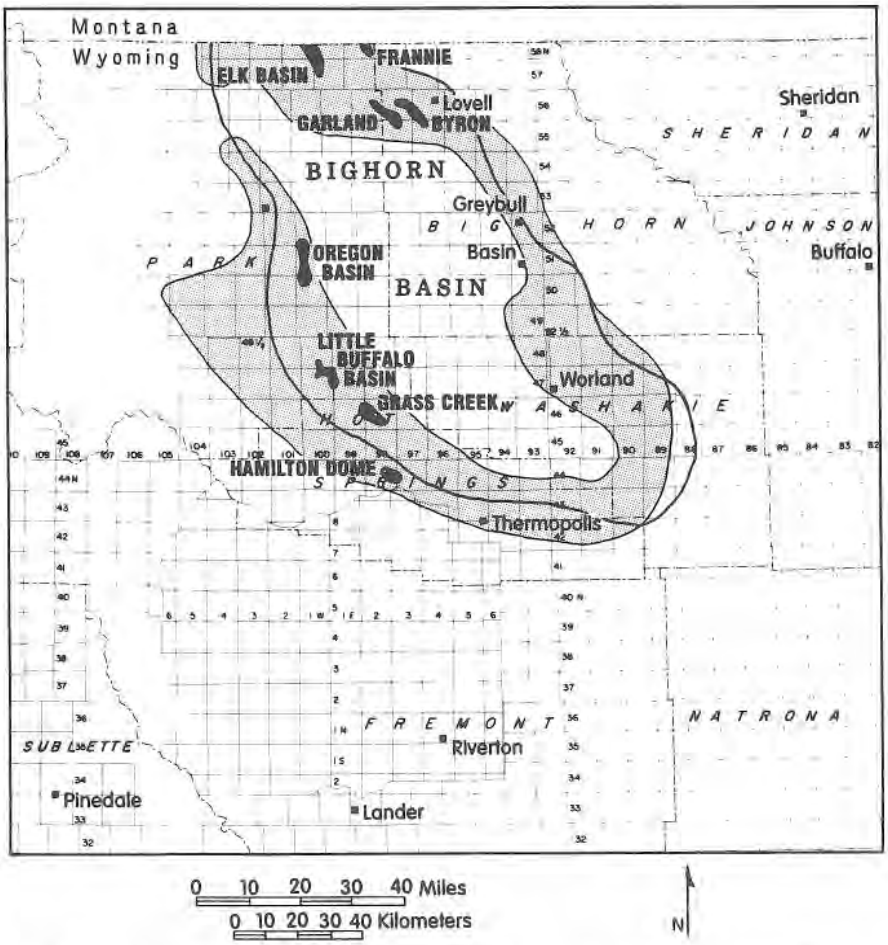

Figure 9. Present productive limit of the basin margin structural play (shaded) in the Wyoming portion of the Bighorn Basin. Major fields are shown in black.

ate reservoirs of the Permian Phosphoria Formation. It is common practice for field operators to commingle production from reservoirs in these two adjacent formations. Carbonate reservoirs in the Mississippian Madison Limestone and sandstone reservoirs in the Upper Cretaceous Frontier Formation are also important oil and gas producers. Other reservoirs which have produced oil and gas, but which are only important locally, are in the Lower Cretaceous Muddy Sandstone and Cloverly Formation, the Triassic Crow Mountain Sandstone, the Pennsylvanian-Mississippian Amsden Formation, and the Ordovician Bighorn Dolomite. These reservoirs produce on structures where faults provided an oil migration pathway into them.

Basin margin off-structure play

Most production from Tensleep Sandstone reservoirs in the Bighorn Basin is related to fields in the basin margin structural play; however, some of these fields produce oil from traps that have a stratigraphic component. The Tensleep Sandstone in the Bighorn Basin is often divided on the basis of facies into an upper and lower unit (Mankiewicz and Steidtmann, 1979; Andrews and Higgins, 1984). The lower unit was deposited in a nearshore marine environment and the upper unit contains eolian facies. Most of the hydrocarbon production is associated with the eolian facies.

Pedry (1975) suggested downdip hydrodynamic flow, in combination with updip stratigraphic thinning of a reservoir sand, is the trapping mechanism for off-structure Tensleep production at Murphy Dome, Lake Creek, Water Creek, Oregon Basin South, Frannie, Sage Creek, Deaver, and Homestead fields (**Figure 10**). Lawson and Smith (1966) also attributed off-structure production from the Tensleep to updip sand pinchout or permeability loss, unconformity traps, tar seals, channeling, and preserved paleohills. Curry (1984) suggested that oil in the Tensleep at Bonanza field (**Figure 10**) was trapped stratigraphically.

Permian Phosphoria Formation stratigraphic play

Cottonwood Creek field was the first major discovery in Wyoming drilled on the basis of a carbonate stratigraphic play (Pedry, 1975). The field has produced over 54 million barrels of oil and over 41 million cubic feet of gas since its discovery in 1953. Although there is a complex intertonguing relationship between the Phosphoria and Goose Egg formations in the area of this play, I chose to label this play

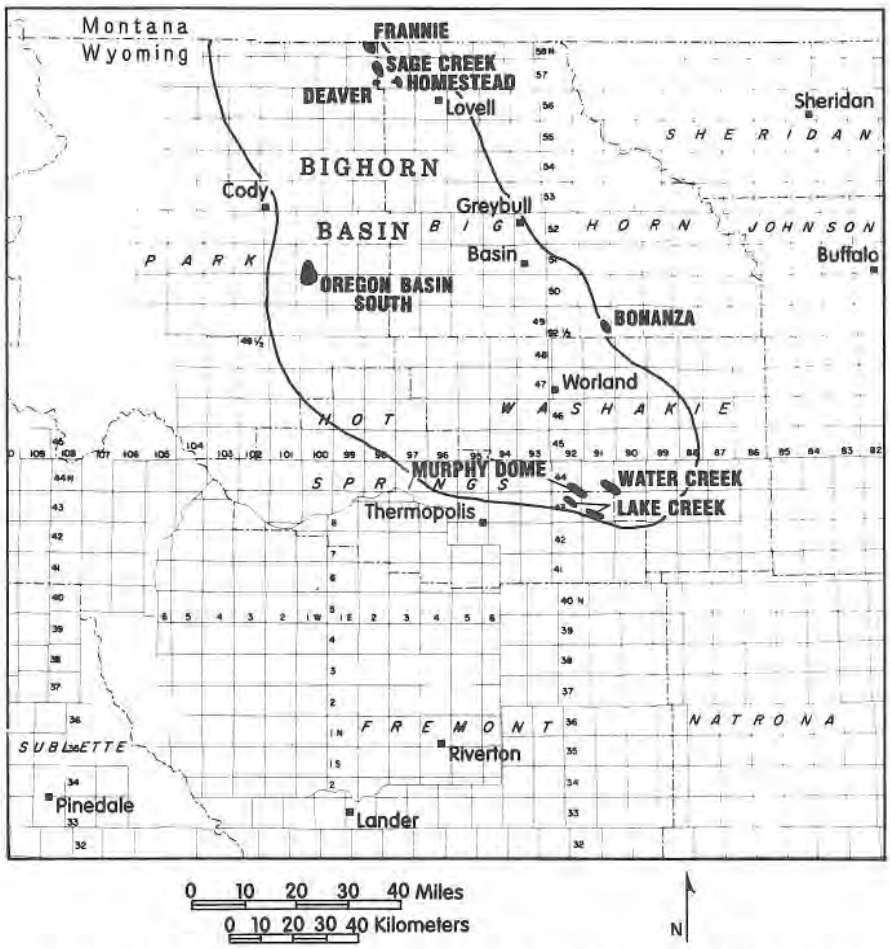

Figure 10. Fields in the Wyoming portion of the Bighorn Basin that produce oil and gas from Tensleep Sandstone reservoirs that have a stratigraphic component to the trapping mechanism.

the Permian Phosphoria Formation stratigraphic play. The productive reservoir is described as a facies-controlled higher porosity pod within peritidal carbonates of the Ervay Member (Herrod, 1980). Production comes from intertidal carbonates in the eastern and central parts of the field and from subtidal carbonates in the western part of the field. Herrod (1980) described the updip seal as supratidal dolomitic mudstones and evaporites and the (downdip) seal to the south as intertidal fenestral-fabric carbonates plugged with anhydrite. Porosity is enhanced by fractures (McCaleb and Willingham, 1967) and is due to fenestral fabric, in what Boyd (1975) described as the fenestral facies of the Ervay Member in the Phosphoria rock complex. Other important fields developed in this play, some of which include combination structural trapping mechanisms, are Worland, Nowater Creek, Rattlesnake, Frisby South, South Fork, Marshall, and Slick Creek (**Figure 11**). These fields have cumulative production through 1991 of more than 85 million barrels of oil and nearly 500 cubic feet of gas (Wyoming Oil and Gas Conservation Commission, 1992).

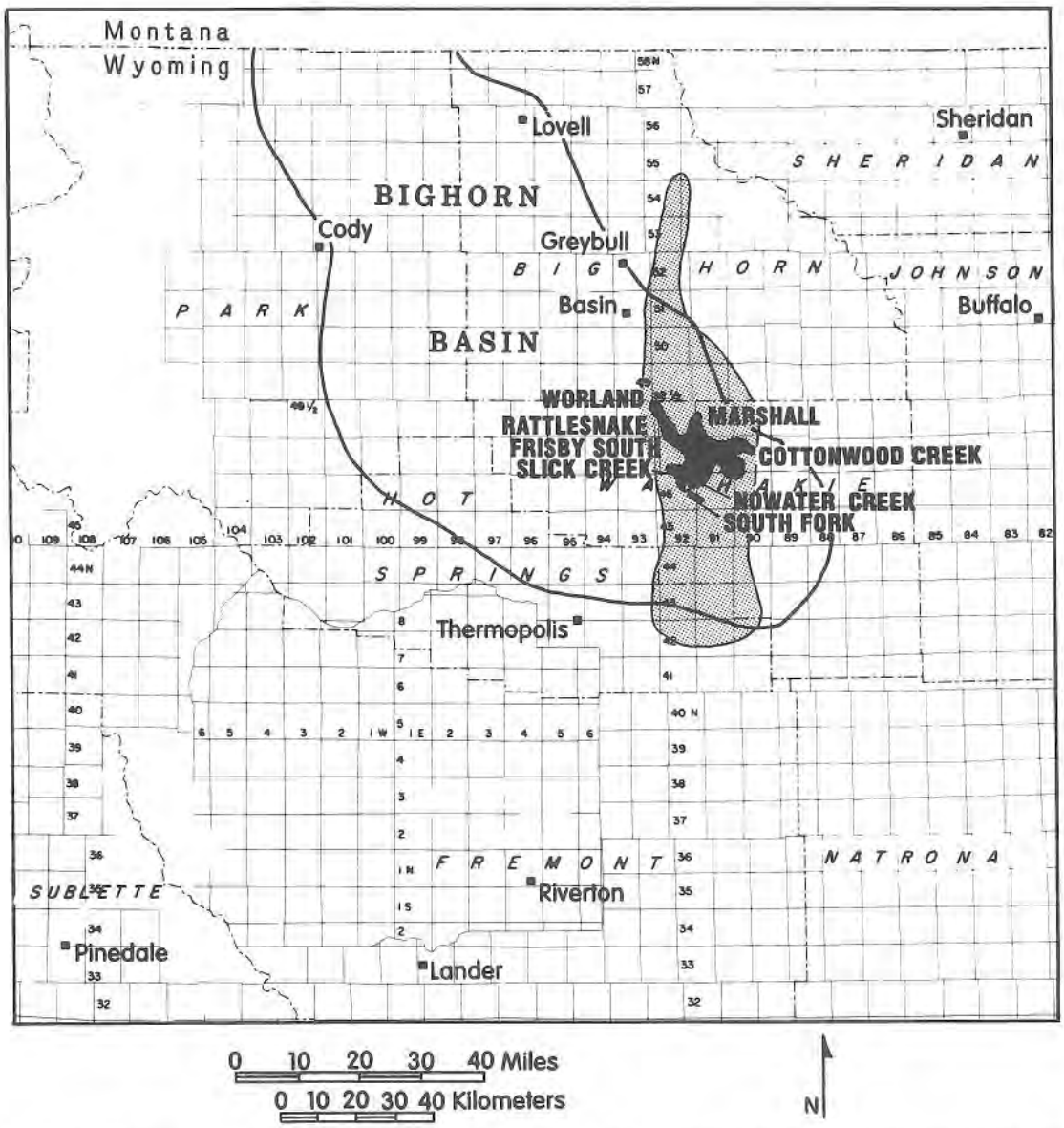

Figure 11. Present productive limit of the Permian Phosphoria Formation stratigraphic play (shaded) in the Wyoming portion of the Bighorn Basin. Major fields are shown in black.

Wind River Basin

Structural play

This play has structural and reservoir similarity to the basin margin structural play in the Bighorn Basin. Oil and gas are trapped in reservoirs ranging in age from Mississippian to Tertiary that occur along the western, northern, and eastern edges of the basin, primarily in anticlines with reverse faulting on the steeply dipping flank. Fields along the western margin that have each produced 10 million barrels or more of oil are Steamboat Butte, Pilot Butte, Winkleman, Maverick Springs, Lander, Circle Ridge, and Dallas (**Figure 12**). Dallas, the first field discovered in Wyoming, is still producing oil. Important fields along the eastern and northern margins of the basin are Casper Creek South, Poison Spider West, and Madden (**Figure 12**). These three fields produced over 26 million barrels of oil and 372 billion cubic feet of gas through 1991 (Wyoming Oil and Gas Conservation Commission, 1992). Northward-trending structures in the southwestern portion of the basin host the Beaver Creek, Riverton Dome, Riverton Dome East, and Big Sand Draw fields (**Figure 12**). These four fields produced over 116 million barrels of oil and nearly one trillion cubic feet of gas through 1991 (Wyoming Oil and Gas Conservation Commission, 1992).

Most of the oil production in this play is from reservoirs in the Permian Phosphoria Formation and the Pennsylvanian Tensleep Sandstone. Reservoirs which are locally productive occur in the Tertiary Fort Union Formation; the Cretaceous Lance, Mesaverde, Cody Shale, Muddy Sandstone, and Cloverly formations; the Jurassic Morrison and Sundance formations; the Jurassic-Triassic Nugget Sandstone; the Triassic Chugwater Formation; and the Mississippian Madison Limestone. Along the basin margins, most fields in this play produce relatively low-gravity crude oil which grades into higher gravity crude oil, condensate, and natural gas in the deeper productive areas of the basin at Beaver Creek, Riverton Dome, and Big Sand Draw fields. At Madden field, a structural closure in the north-central area of the basin, natural gas is produced from shallow reservoirs in the Tertiary Fort Union Formation and from reservoirs below a depth of 13,000 feet in the Upper

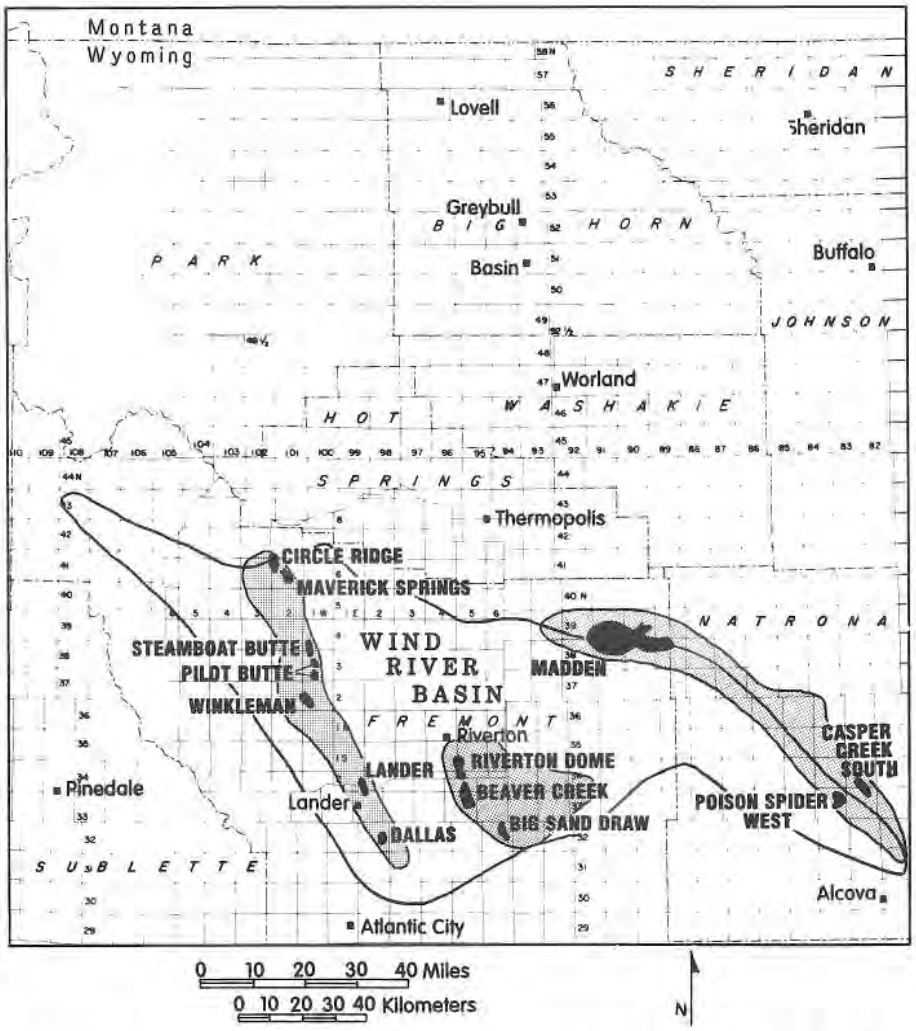

Figure 12. Present productive limits of the structural play (shaded) in the Wind River Basin. Major fields in the play are shown in black.

Cretaceous Lance and Mesaverde formations and Cody Shale. Two ultradeep wells at Madden field have been completed below 23,000 feet in the Mississippian Madison Limestone. These two wells established the deepest commercial production in the Rocky Mountain region; however, production cannot begin until a gas plant is constructed to remove high concentrations of hydrogen sulfide from the gas.

Lower Cretaceous Muddy Sandstone play

This play is developed in sandstone reservoirs of the lower Muddy Sandstone in the southeastern part of the basin. These reservoirs are interpreted as fluvial (Curry, 1985) or estuarine sandstones (Mitchell, 1978; Dresser, 1974) deposited in the "Grieve" paleovalley cut into the underlying Thermopolis Shale. The most important fields, in terms of cumulative production, are Grieve, North Grieve, and Sun Ranch (**Figure 13**). Production at all three fields consists of high-gravity oil and natural gas. Grieve field, discovered in 1954, has produced over 30 million barrels of oil and over 105 billion cubic feet of gas (Wyoming Oil and Gas Conservation Commission, 1992). The stratigraphic trap at Grieve is an updip pinchout of sandstone which is up to 50 feet thick (Mitchell, 1978). Sun Ranch Field, discovered in 1987, has not been fully developed.

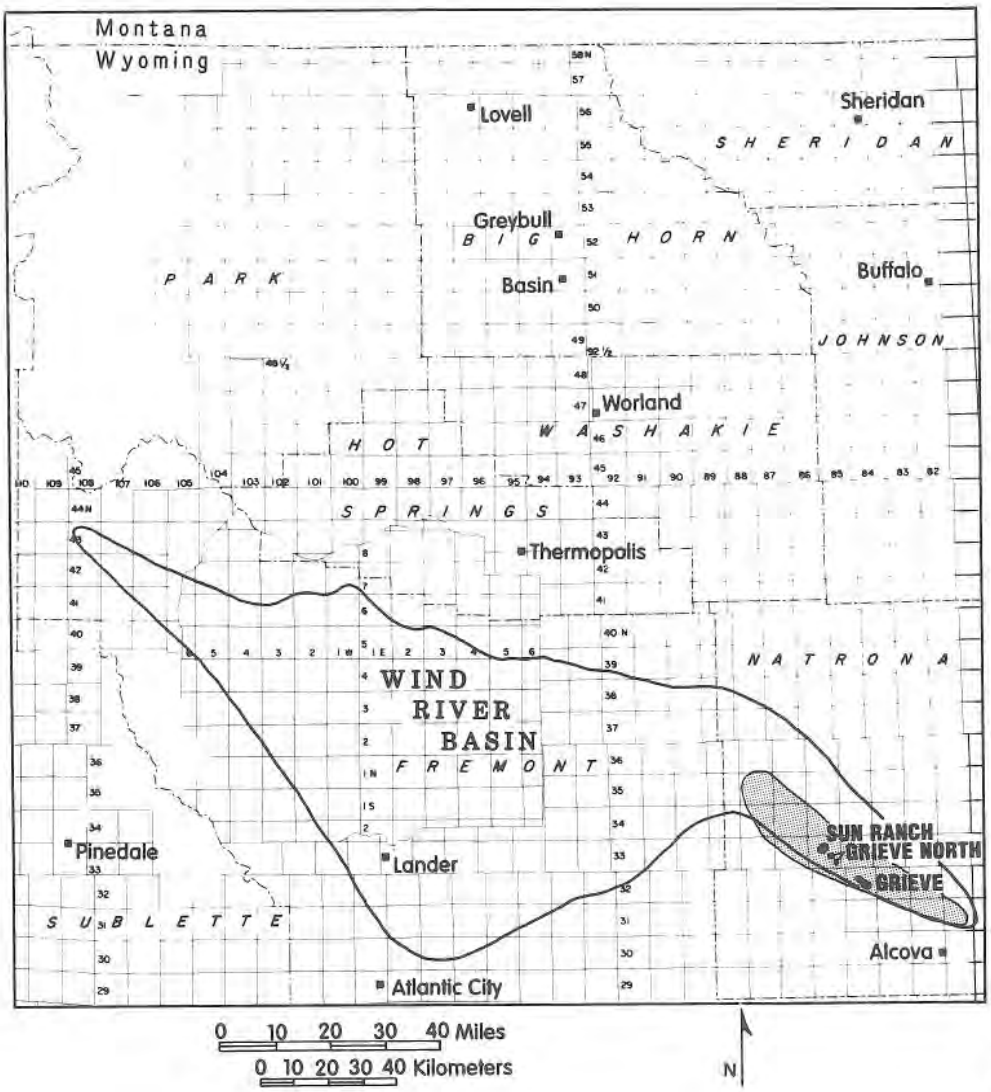

Figure 13. Present productive limit of the Lower Cretaceous Muddy Sandstone play (shaded) in the Wind River Basin. Major fields are shown in black.

Tertiary Fort Union Formation play

Gas production with some condensate occurs in multiple fluvial sandstone reservoirs (Keefer, 1965; Arro, 1969; Boyd, 1969; Barrett and Hubley, 1969) in the Paleocene Fort Union Formation at several fields in the central and northern Wind River Basin. The most productive fields in this play are Pavillion, Frenchie Draw, Fuller Reservoir, Muddy Ridge, Waltman, Cooper Reservoir, and Madden (**Figure 14**). These fields have produced over 300 billion cubic feet of gas from the Fort Union through 1991 (Wyoming Oil and Gas Conservation Commission, 1992). The traps are combination structural and stratigraphic.

Structural closure may be the most identifiable trapping mechanism; however, variations in lithology commonly define the productive limits of the reservoirs. Reservoirs are generally lenticular with limited extent. One of the characteristics of this play is the occurrence of multiple pay zones. New production tools, which were used at the Fuller Reservoir field, allow completions in multiple reservoirs and may help to improve the economics of this play.

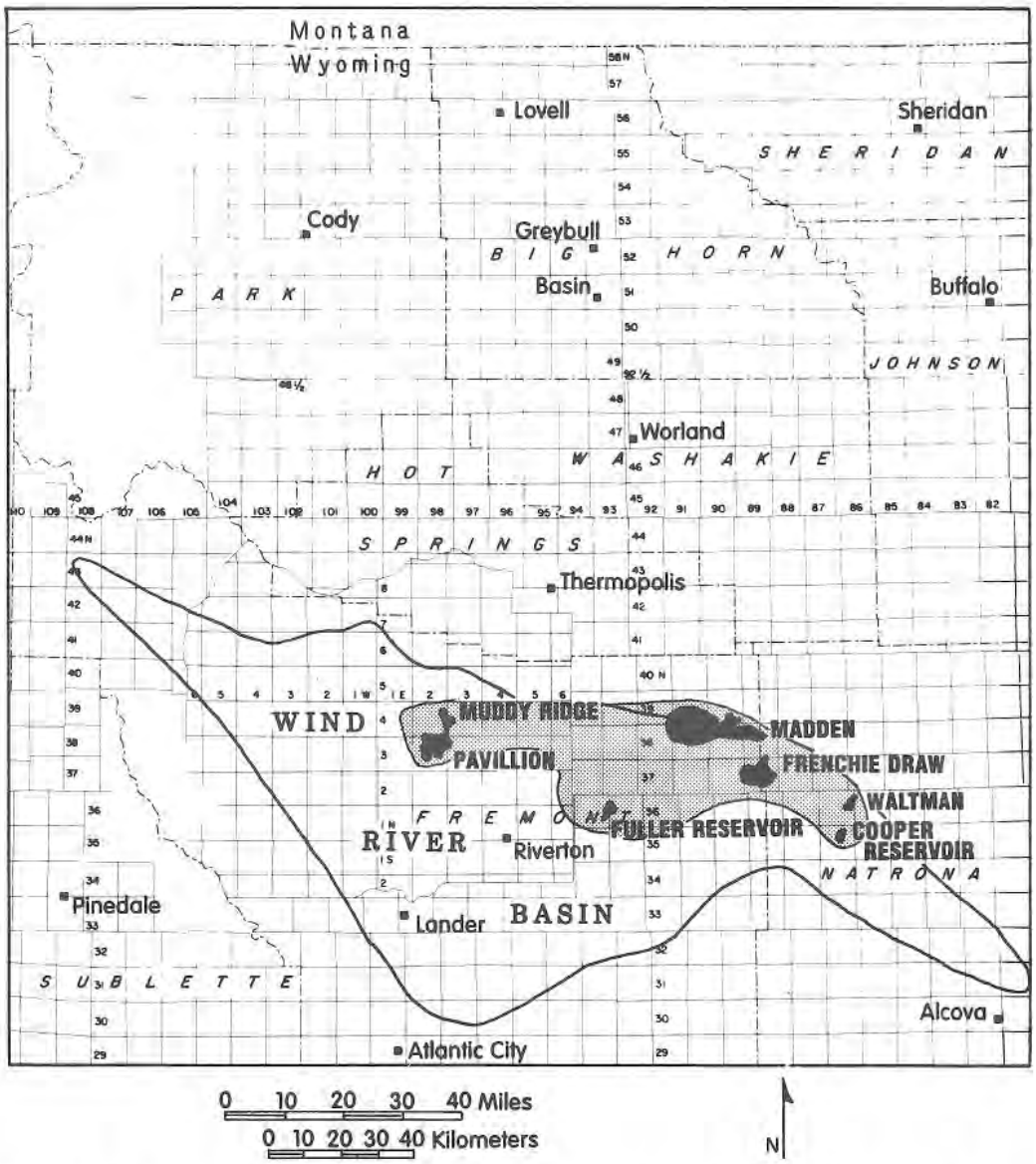

Figure 14. Present productive limit of the Tertiary Fort Union Formation play (shaded) in the Wind River Basin. Major fields are shown in black.

Overthrust belt

The discovery of Pineview field in northeastern Utah in 1975 set off a wave of exploration that rapidly spread into southwestern Wyoming. Within five years, reserves of oil and gas discovered at Ryckman Creek, Yellow Creek, Clear Creek, Painter Reservoir, Whitney Canyon-Carter Creek, Painter Reservoir East, and Anschutz Ranch East fields (**Figure 15**) more than doubled Wyoming's reserves. These fields have produced nearly 100 million barrels of oil and condensate and over 1.7 trillion cubic feet of natural gas in just over 10 years. Whitney Canyon-Carter Creek field alone had produced one trillion cubic feet of gas in less than 10 years of production by 1992. The geology of the overthrust belt is extremely complex (Blackstone and De Bruin, 1987); improvements in reflection seismic techniques and in deep drilling technology were needed to make these discoveries possible.

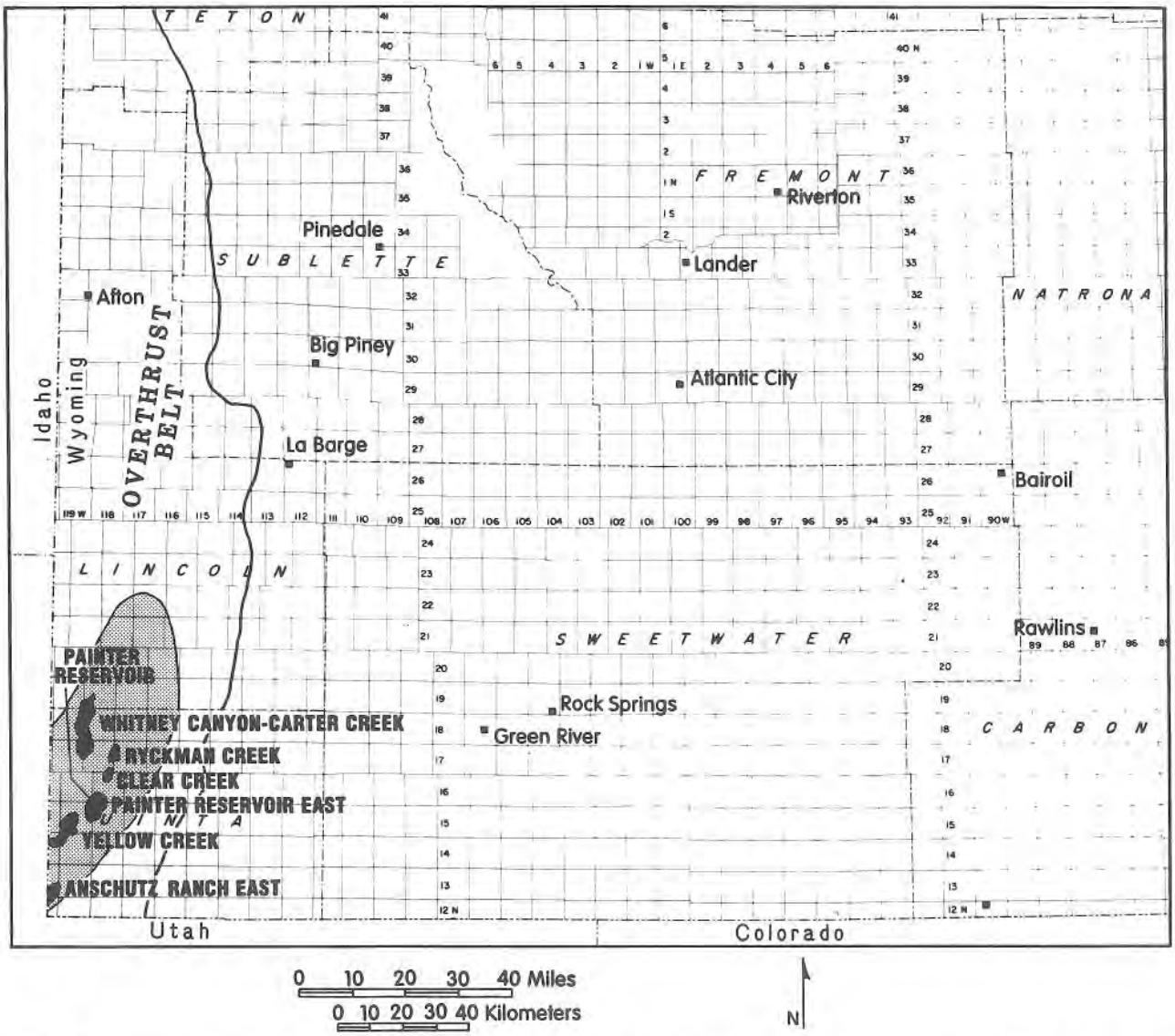

Figure 15. Present productive limit of the Absoraka structural play (shaded) in the Wyoming portion of the overthrust belt. Major fields are shown in black.

The major discoveries in the overthrust belt occur on anticlines in the hanging wall of the Absaroka thrust fault, where productive reservoirs have been thrust over and are in juxtaposition with Cretaceous source rocks (Frank and others, 1982,; Hoffman and Balcells-Baldwin, 1982; Couples and others, 1987; Lelek, 1982; Kelley and Hine, 1977; Ver Ploeg and De Bruin, 1982; Royse, this volume). Most oil and condensate production and a large part of the gas production in this play are from reservoirs in the Jurassic-Triassic Nugget Sandstone of eolian origin (Picard, 1977; Doelger, 1987). Reservoirs in the Jurassic Twin Creek Limestone and Triassic Thaynes Limestone produce small amounts of hydrocarbons. Reservoirs in Paleozoic rocks generally produce hydrogen sulfide-rich gas. The most important Paleozoic reservoir, in terms of cumulative gas production, is the Madison Limestone at Whitney Canyon-Carter Creek field. The Madison produced over 900 billion cubic feet through 1991 (Wyoming Oil and Gas Conservation Commission, 1992). Other Paleozoic reservoirs are the Permian Phosphoria Formation, Pennsylvanian Weber Sandstone, and Ordovician Bighorn Dolomite.

Greater Green River Basin

The Greater Green River Basin is a gas prone area with production from reservoirs ranging from Mississippian to Tertiary in age. Important reservoirs are the Tertiary "Almy" (Fort Union) Formation; the Upper Cretaceous Lewis Shale, Mesaverde Formation or Group, and Frontier Formation; the Lower Cretaceous Bear River Formation and "Dakota" Sandstone (Cloverly Formation); the Jurassic-Triassic Nugget Sandstone; the Pennsylvanian Weber Sandstone; and the Mississippian Madison Limestone (see *Stratigraphic nomenclature chart of Wyoming*, Love and others, map pocket).

Moxa arch structural play (Paleozoic reservoirs)

Gas production from Paleozoic reservoirs is associated with structural closures on the Moxa arch. The most productive reservoir at the present time is in the Mississippian Madison Limestone, with cumulative production of nearly one trillion cubic feet of gas in just over five years of production (from 15 wells). Production is from the Lake Ridge, Fogarty Creek, and Graphite units (**Figure 16**) on the northern end of the Moxa arch at La Barge anticline. The gas has a composition of 66% carbon dioxide, 22% methane, 7% nitrogen, 4.5% hydrogen sulfide, and 0.5% helium. The carbon dioxide is used in several tertiary or enhanced oil recovery operations within Wyoming (principally in the northeastern Green River Basin) and at the Rangely field in Colorado. Carbon dioxide production far exceeds demand, and the excess production is currently vented to the atmosphere. The gas processing plant also recovers about 300,000 tons of sulfur and nearly one billion cubic feet of helium a year. This volume of helium ranks the plant as the largest helium producer in the United States. Other Paleozoic gas production in this play is from the Pennsylvanian Morgan Formation on the southern end of the Moxa arch at the Church Buttes and Butcher Knife Springs fields (**Figure 16**).

Basin margin structural play

Several fields produce oil and gas from anticlinal traps along the northeastern margin of the Greater Green River Basin. This basin segment is the Great Divide Basin. Most of the production in this play has been from the Lost Soldier and Wertz fields (**Figure 17**). These two fields have produced over 325 million barrels of oil through 1991 (Wyoming Oil and Gas Conservation Commission, 1992). The most important reservoirs are the Pennsylvanian Tensleep Sandstone and Mississippian Madison Limestone; however, reservoirs in the Upper Cretaceous Frontier Formation, Lower Cretaceous Muddy Sandstone and Cloverly Formation, Jurassic Morrison and Sundance formations, Jurassic-Triassic Nugget Sandstone, Mississippian Darwin Sandstone, and Cambrian Flathead Sandstone are also productive. Both fields are currently being flooded with carbon dioxide produced from the Madison Limestone on the northern end of the Moxa arch (as previously discussed). This ter-

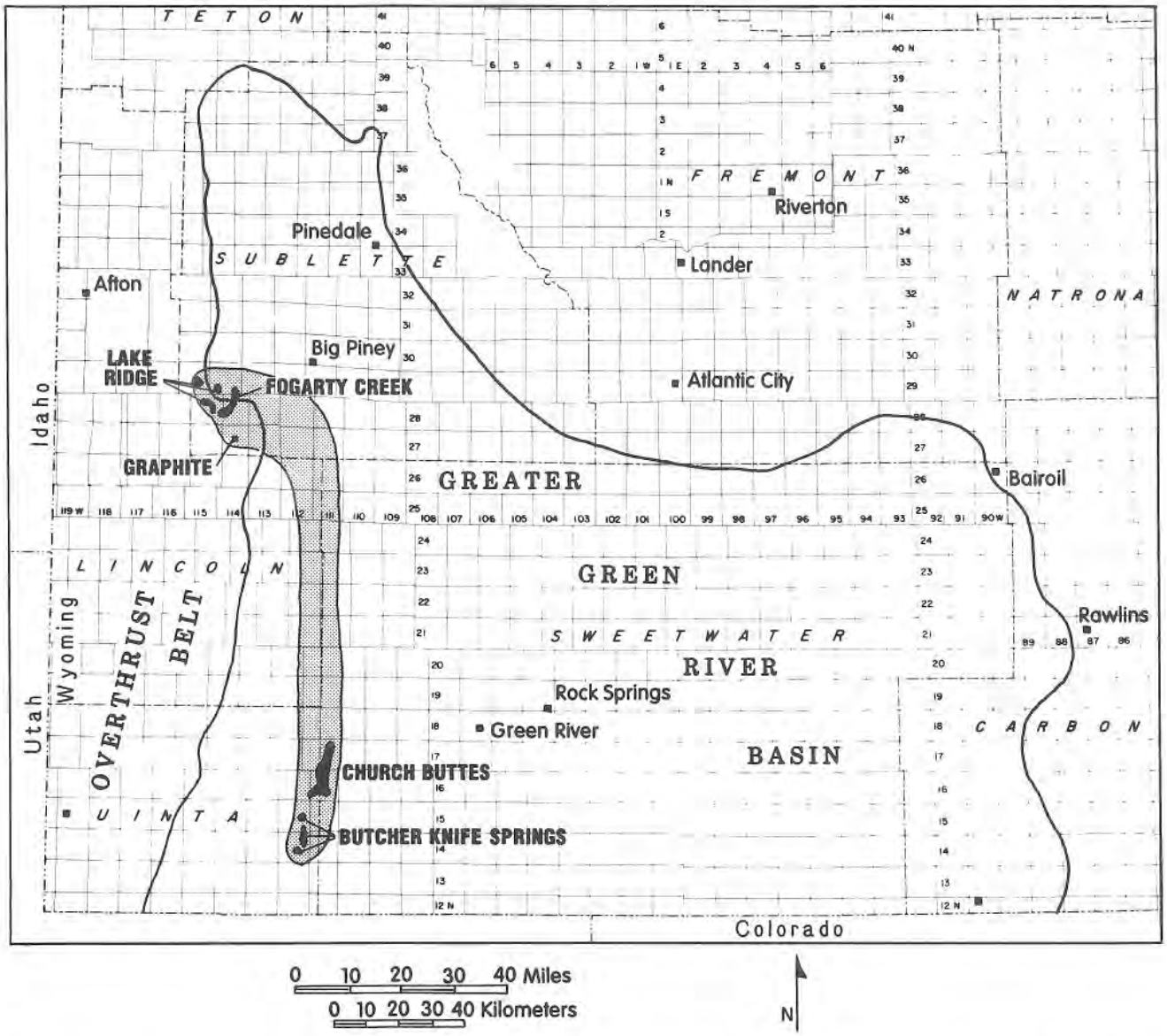

Figure 16. Present productive limit of Paleozoic reservoirs of the Moxa arch structural play (shaded) in the Wyoming portion of the Greater Green River Basin. Major fields are shown in black.

tiary project is expected to recover an additional 38 million barrels of oil from the Tensleep Sandstone, Darwin Sandstone, and Madison Limestone.

Other structural plays

Structural traps occur at Baxter Basin North, Middle, and South fields in faulted anticlines on the Rock Springs uplift (**Figure 18**). Over 230 billion cubic feet of gas has been produced from sandstone reservoirs that are mainly in the Upper Cretaceous Frontier Formation and Lower Cretaceous "Dakota" (Cloverly) Formation. At Baxter Basin North, important reservoirs include the Jurassic Morrison Formation and Jurassic-Triassic Nugget Sandstone.

Brady Field (**Figure 18**) is developed on a seismically defined structure that has no surface expression (Brock and Nicolaysen, 1975). Reservoirs are the Upper Cretaceous Frontier Formation, Lower Cretaceous "Dakota" (Cloverly) Formation, Jurassic Sundance Formation, Jurassic-Triassic Nugget Sandstone, Permian Phosphoria Formation, and Pennsyl-

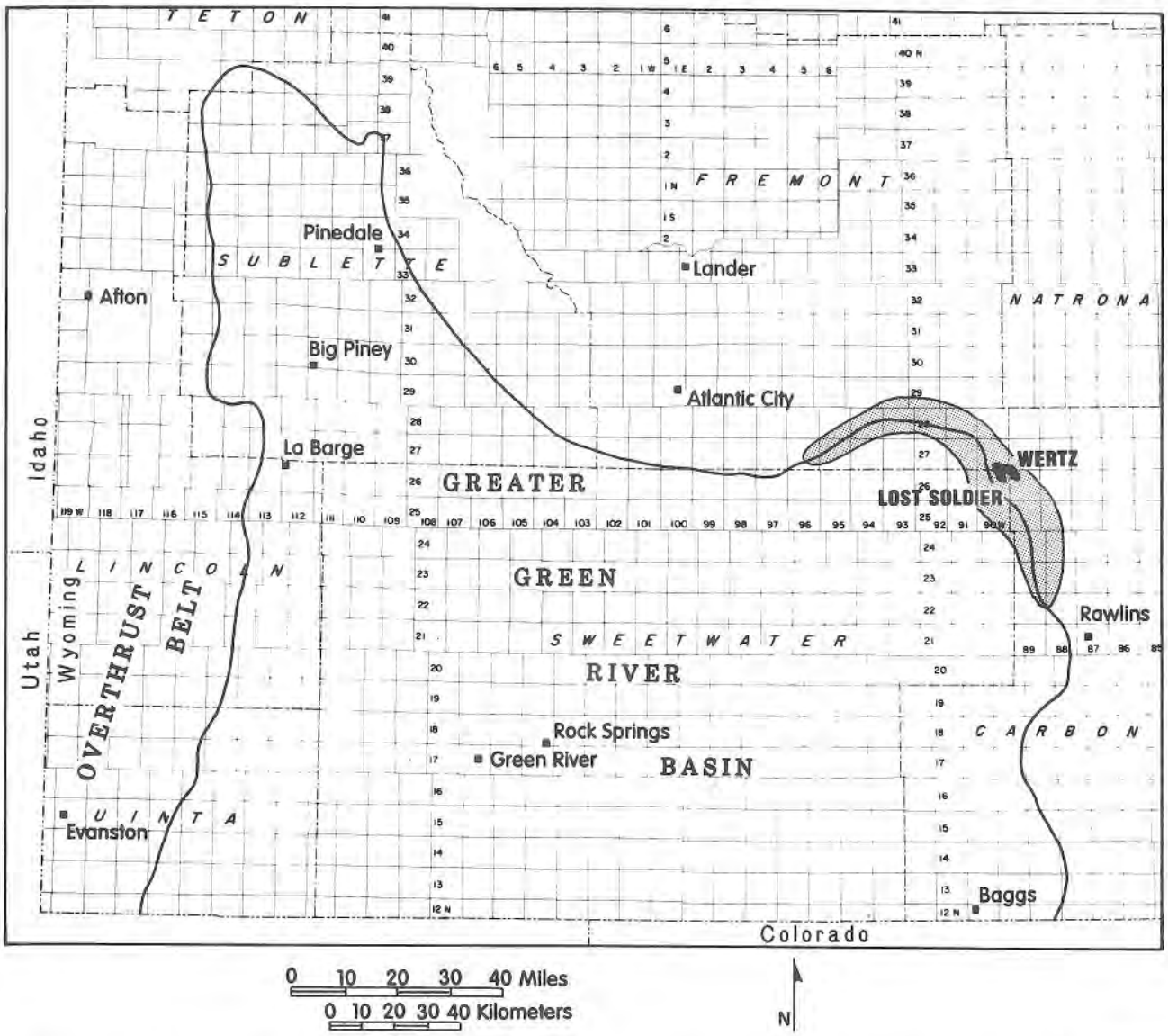

Figure 17. Present productive limit of the basin margin structural play (shaded) in the Wyoming portion of the Greater Green River Basin. Major fields are shown in black.

vanian Weber Sandstone. Drilling depths range from 10,000 ft to 15,000 ft. Brady has produced over 60 million barrels of oil and condensate and 357 billion cubic feet of gas since its discovery in 1973 (Wyoming Oil and Gas Conservation Commission, 1992).

Cherokee ridge is an east-west structure that separates the Washakie Basin in Wyoming from the Sand Wash Basin in Colorado (McDonald, 1975). Fields in Wyoming are Baggs South, Hiawatha, and West Side Canal (**Figure 18**). These three fields have produced over 250 billion cubic feet of gas and small amounts of oil. The traps in these fields are complexly faulted structural traps with stratigraphic variations. Production is from the Tertiary Wasatch and Fort Union formations, Upper Cretaceous Lance and Almond formations, and Lewis Shale.

Lower Cretaceous "Dakota sandstone" play

Reservoirs in this play in the area of the Moxa arch are sandstones informally reported by oil and gas operators as the "Dakota", which are older than the Mowry Shale and younger than the Cloverly

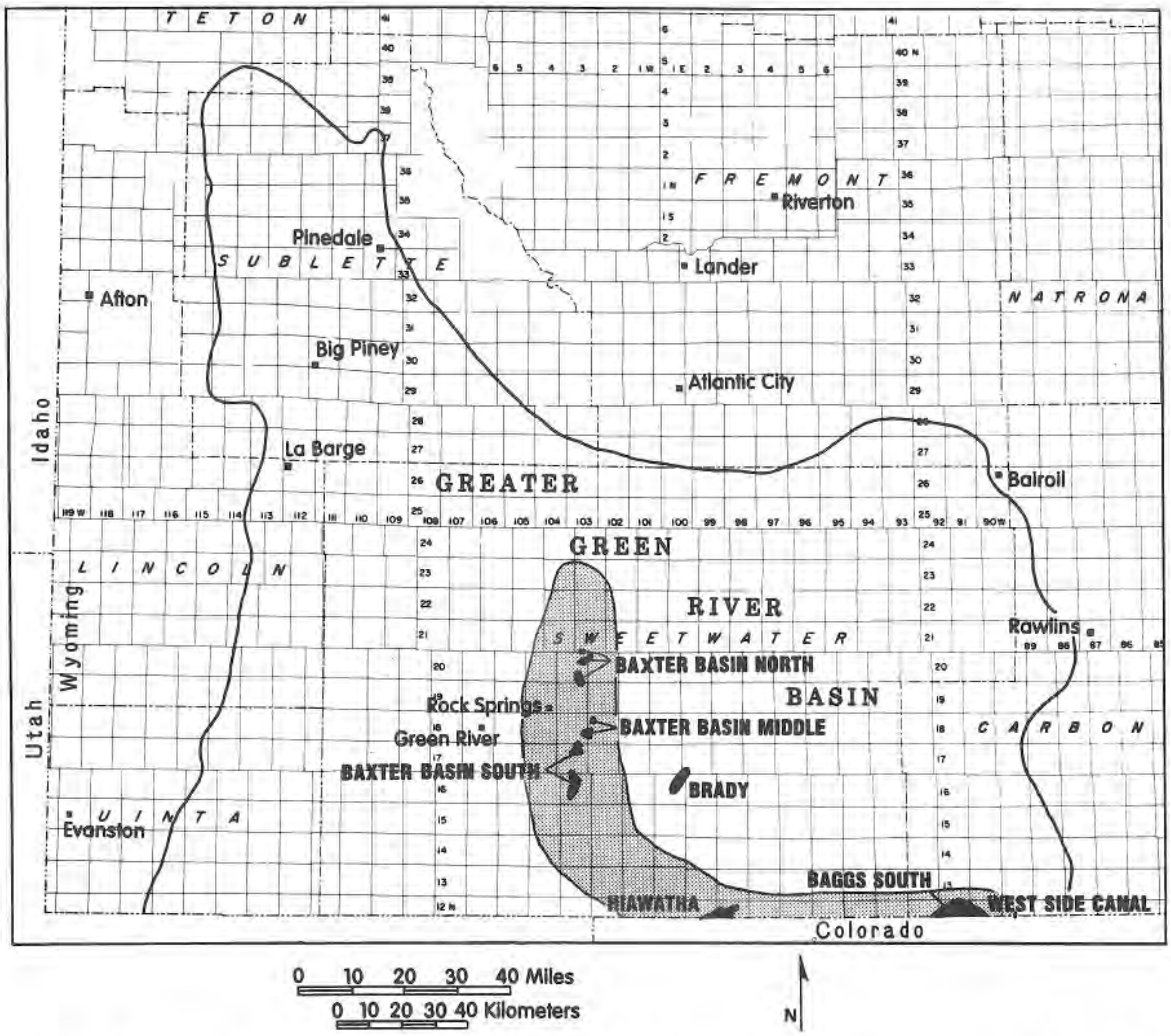

Figure 18. Present productive limit of other structural plays (shaded) in the Wyoming portion of the Greater Green River Basin. Major fields are shown in black.

Formation (Ryer, and others, 1987). The "Dakota" is in part equivalent to the Bear River Formation of the overthrust belt (Wallem and others, 1981) and is productive on the northern end of the Moxa arch (from the Birch Creek, Bird Canyon, and Green River Bend fields) (**Figure 19**). "Dakota" reservoirs are primarily marine shoreline sandstones on the northern part of the Moxa arch and mainly fluvial sandstones on the southern part of the Moxa arch (Webb, 1975; Ryer and others, 1987). Upper "Dakota" reservoirs have a general northeastward trend (Ryer, and others, 1987) and are productive at Swan, Lincoln Road, and Blue Forest fields; lower "Dakota" reservoirs trend north-northwest, were deposited in a fluvial environment, and are productive at Luckey Ditch, Henry, Taylor Ranch, and Church Buttes fields. Fields on the central portion of the Moxa arch, such as Bruff and Whiskey Buttes, have reservoirs that are both marine and non-marine. Traps in this play are primarily stratigraphic, but subtle structure often enhances production.

Upper Cretaceous Frontier Formation play

Reservoirs in this play are developed in two Frontier deltaic sequences known (by industry terminology) as first and second Frontier sandstones. De Chadenedes (1975) interpreted the productive

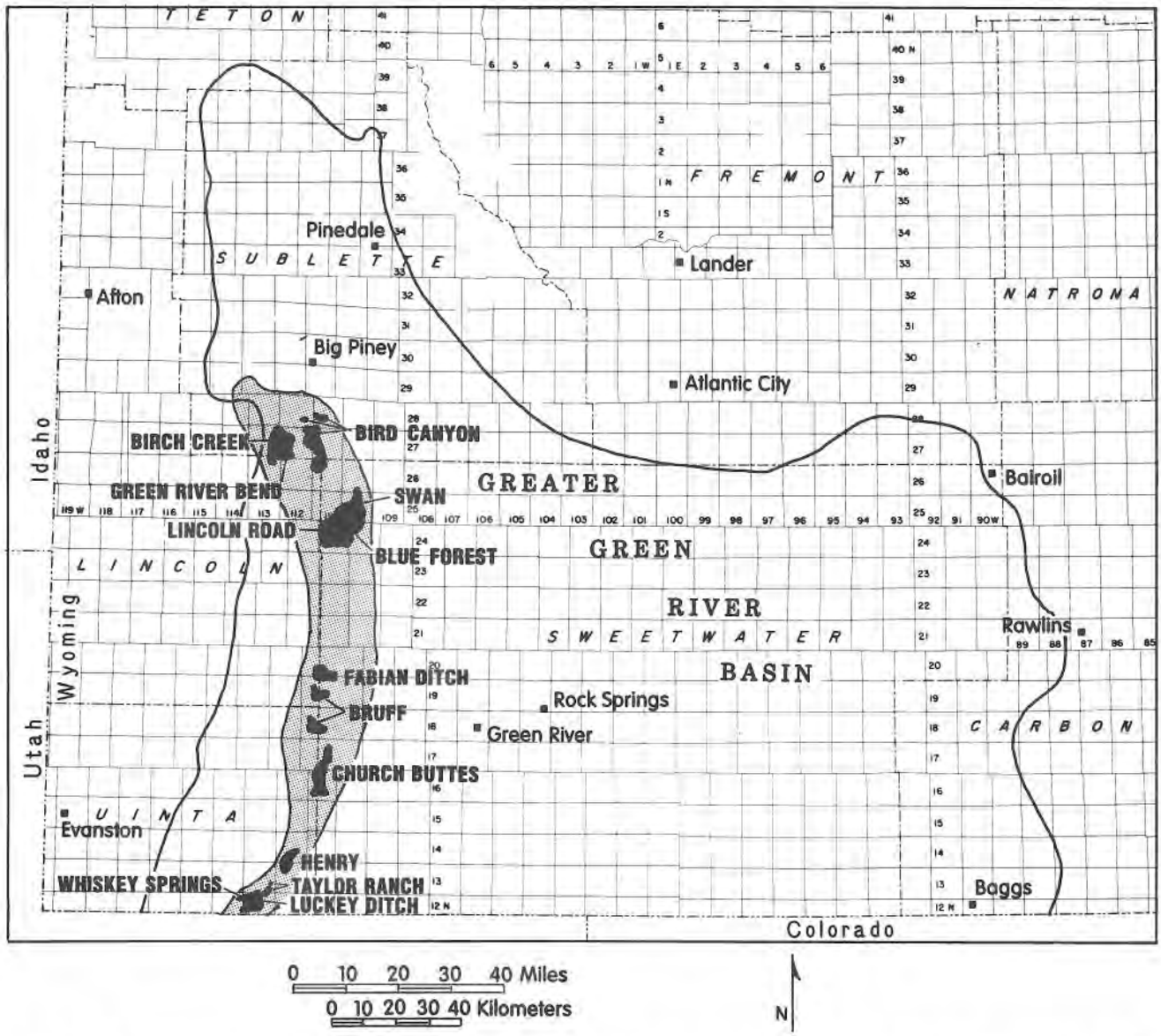

Figure 19. Present productive limit of the Lower Cretaceous "Dakota sandstone" play (shaded) in the Wyoming portion of the Greater Green River Basin. Major fields are shown in black.

sandstones of the first Frontier as two northwest-trending offshore marine bars, which are draped across and limited to the northern Moxa arch. The second Frontier sandstone is more extensive and produces from reservoirs related to deltaic facies [point bars, channel fills, channel mouth bars, and marginal marine sandstones (De Chadenedes, 1975)]. Several areas of deltaic rocks are mappable at the northern end of the Moxa arch near the present-day Uinta-Lincoln County line, and on the southern Moxa arch. Schultz and Lafollette (1989) interpret the second Frontier as a fluvial-deltaic sequence of sandstones, siltstones, shales, and conglomerates. Gas production comes from stratigraphic traps associated with the first Frontier sandstone at the northern end of the Moxa arch and from stratigraphic traps in the second Frontier sandstone at fields along the central Moxa arch. The southern Moxa arch is generally non-productive from the Frontier Formation. The most productive fields in this play include Fontenelle, Birch Creek, La Barge, Tip Top, Hogsback, Swan, Blue Forest, Lincoln Road, Fabian Ditch, Bruff, Whiskey Butte, and Church Buttes (**Figure 20**).

Upper Cretaceous stratigraphic play

Sandstones in formations of the Mesaverde Group and the overlying Lewis Shale are productive from stratigraphic traps in the eastern segments of the Greater Green River Basin known as the Washakie and Great Divide basins, respectively. Drilling depths for reservoirs in this play are currently less that 12,000 feet. The Mesaverde Group and Lewis Shale were deposited during a major cycle of marine regression and transgression in response to shifting deltas with associated marginal marine and marine sedimentation (Asquith, 1975). Cumulative production from the major fields in this play, including Patrick Draw, Desert Springs, Table Rock, Echo Springs, Canyon Creek, Standard Draw, Hay Reservoir, Wamsutter, and Wild Rose (**Figure 21**), exceeds 60 million barrels of oil and 1.6 trillion cubic feet of gas (Wyoming Oil and Gas Conservation Commission, 1992). The Almond Formation of the Mesaverde Group has produced a total of 50 million barrels of oil and nearly a trillion feet of gas at Patrick

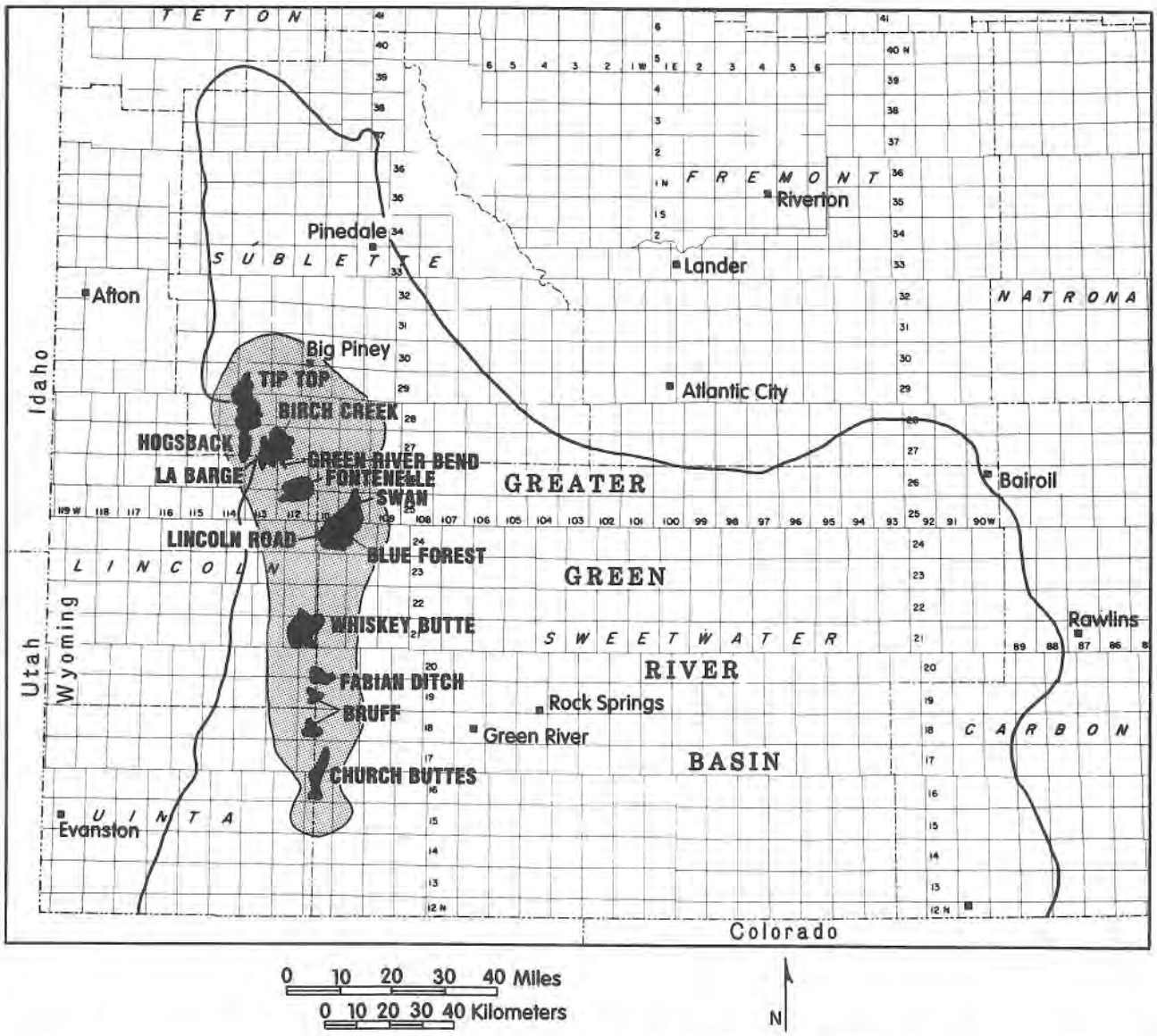

Figure 20. Present productive limit of the Upper Cretaceous Frontier Formation play (shaded) in the Wyoming portion of the Greater Green River Basin. Major fields are shown in black.

Draw, Desert Springs, Table Rock, and Wamsutter fields from reservoirs interpreted as barrier bars (Weimer, 1965). Reservoirs in the Ericson Sandstone of the Mesaverde Group are productive at Canyon Creek field and are interpreted as fluvial (Asquith, 1975). Most Lewis production is at Wamsutter and Hay Reservoir fields. The sands at these fields may have been deposited in deep water by high-density turbidity currents (Winn and others, 1985). However, Perman (1990) interpreted the reservoirs at these two fields as sandy shelf and nearshore sandstones; she placed turbidite deposits farther south. These two fields produced over 155 billion cubic feet of gas through 1991 (Wyoming Oil and Gas Conservation Commission, 1992).

Upper Cretaceous Mesaverde Formation play

This structural-stratigraphic play is developed in marine sandstone reservoirs (McDonald, 1973) on the Big Piney - La Barge structural platform. Major production is from the Big Piney, La Barge, Mickelson Creek, and Saddle Ridge fields (**Figure 22**) with minor production from several other

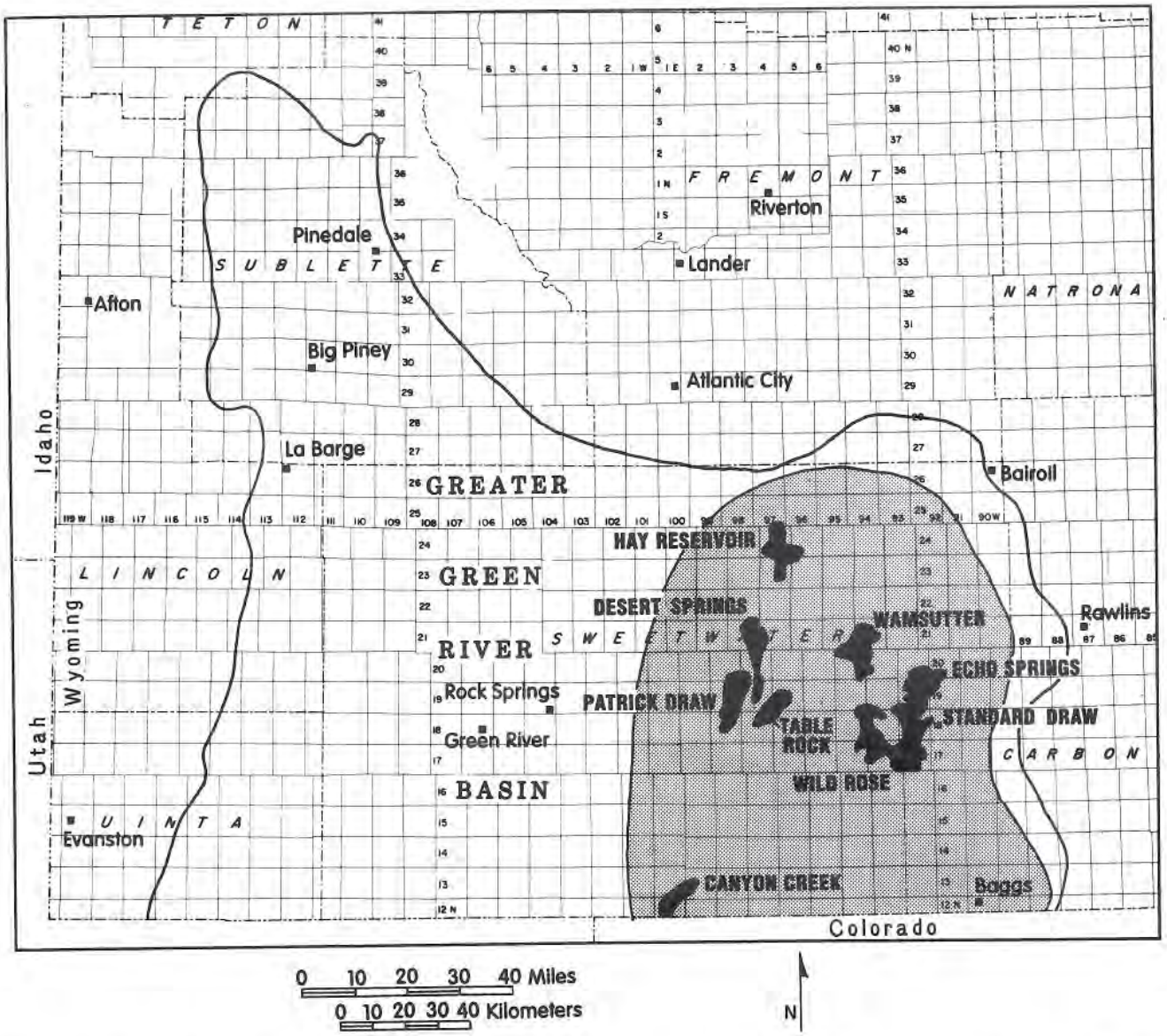

Figure 21. Present productive limit of the Upper Cretaceous stratigraphic play (shaded) in the Wyoming portion of the Greater Green River Basin. Major fields are shown in black.

fields. Trapping mechanisms include anticlinal closure and the Paleocene-Cretaceous angular unconformity, where Mesaverde sandstones underlie nonporous Tertiary rocks.

Tertiary "Almy" play

Reservoirs in this structural-stratigraphic play also produce oil and gas from fields located on the Big Piney - La Barge structural platform. Major fields in this play include: Big Piney, La Barge, Ruben, McDonald Draw, and Chimney Butte (**Figure 23**). Although productive sandstones in this play are Paleocene in age, they are commonly known as "Almy". The type section of the Almy, originally named by Veatch (1907), is Eocene. Stratigraphically, the reservoirs should probably be described as Hoback Formation (Oriel, 1969) or Fort Union Formation (Dunnewald, 1969). Several types of traps have been described for the "Almy" sandstones. These include: eastward deflection of sand deposition onto a paleostructural uplift resulting in traps from sandstone pinchout on monclinal dip; coincidence of sandstone pinchouts across anticlinal noses; and structural closure. Dunnewald (1969) and

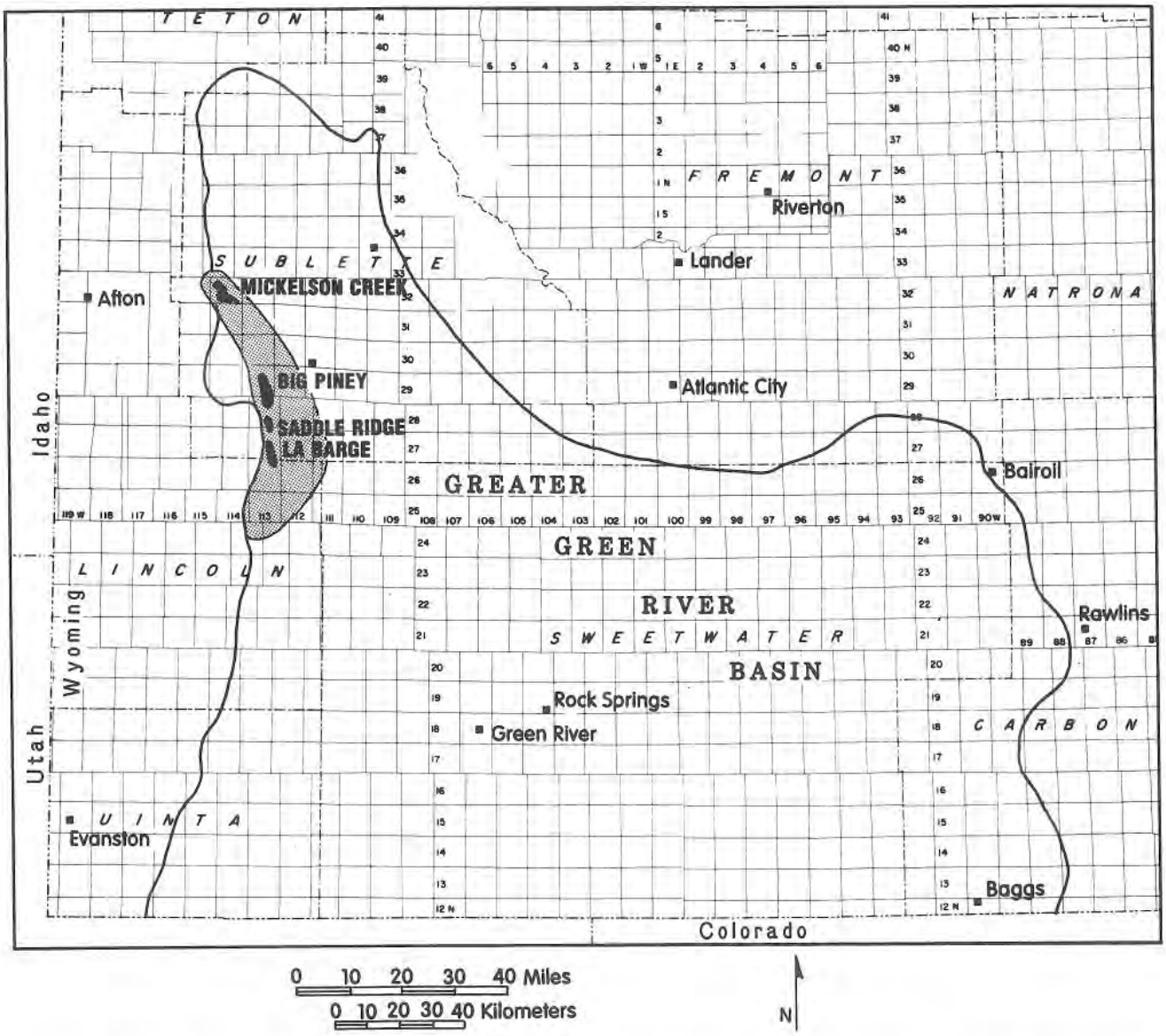

Figure 22. Present productive limit of the Upper Cretaceous Mesaverde Formation play (shaded) in the Wyoming portion of the Greater Green River Basin. Major fields are shown in black.

McDonald (1973) suggested that the reservoirs are mostly point bar and stream channel deposits, whereas Krueger (1968) suggested the reservoirs were deposited as sand bars, delta deposits, and sand- filled estuaries on the west side of the Paleocene/Eocene Lake Gosiute. Dunnewald (1969) explained the lacustrine shale and limestone in the "Almy" as oxbow-type lake deposits.

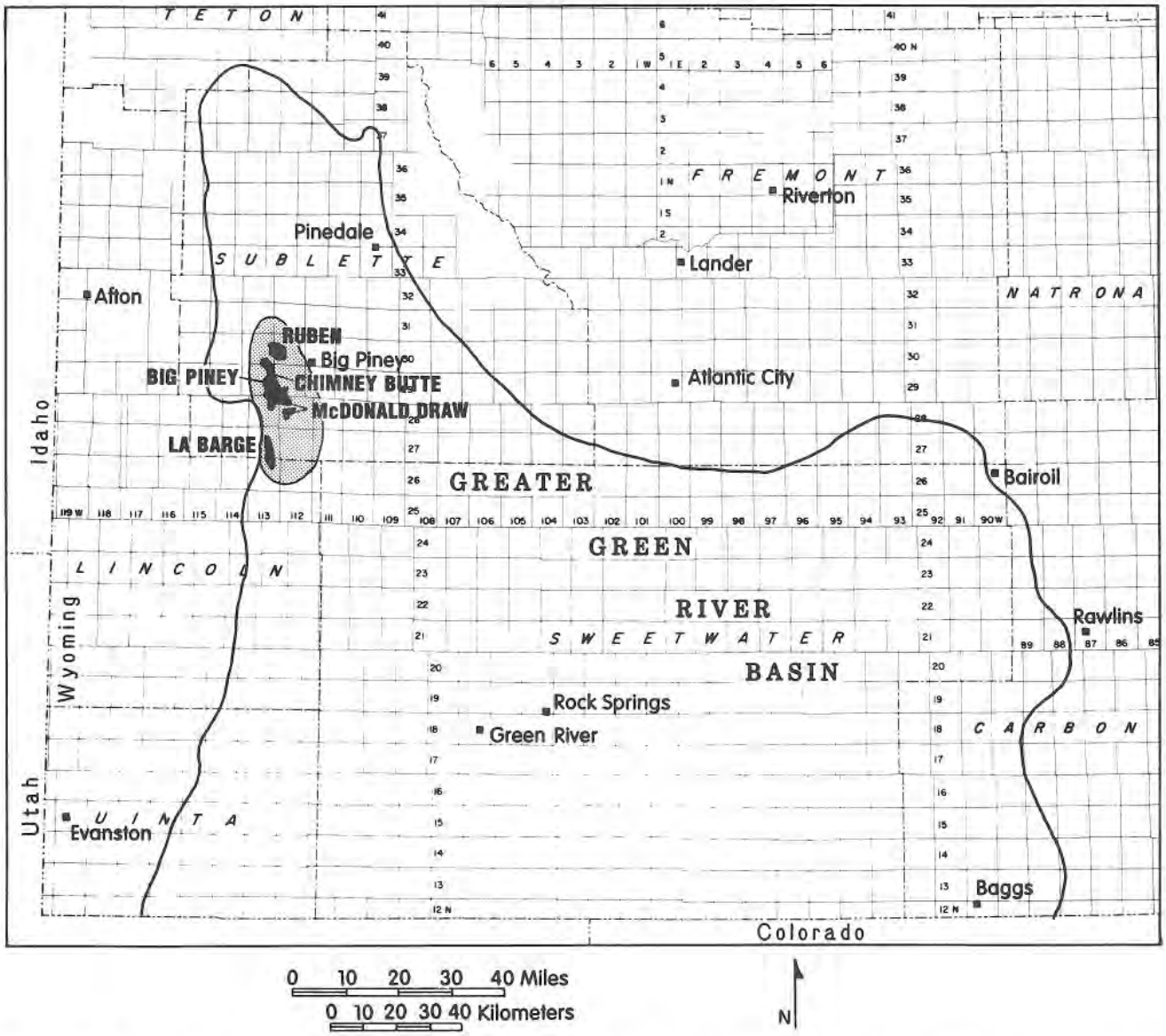

Figure 23. Present productive limit of the Tertiary "Almy" play (shaded) in the Wyoming portion of the Greater Green River Basin. Major fields are shown in black.

Southeastern Wyoming

Basin margins structural play

Six anticlinal fields, located along the southeastern margin of the Hanna Basin (Big Medicine Bow field), along the western and northwestern margin of the Laramie Basin (Quealy, Cooper Cove, and Rock River fields), and along the western margin of the Denver-Cheyenne Basin (Borie and Horse Creek

fields) (**Figure 24**), have produced nearly 70 million barrels of oil and 19 billion cubic feet of gas. The largest field in terms of cumulative production is Rock River, which has produced nearly 39 million barrels of oil and over nine billion cubic feet of gas. The traps in this play are primarily structural closures and the main productive reservoirs are within the Lower Cretaceous Muddy Sandstone. Significant production is also from reservoirs in the Lower Cretaceous "Dakota" (Cloverly) Sandstone, Jurassic Sundance Formation, and Permian-Pennsylvanian Casper Formation.

Upper Cretaceous Niobrara Formation play

This play has recently been developed in fractured Niobrara reservoirs. The extent and significance of the play is not yet known. Over fifteen horizontal wells have been completed in the Niobrara Formation since 1989 in and around the previously defined Silo field in the Denver-Cheyenne Basin.

Before horizontal drilling technology, an estimated four million barrels of oil and three billion

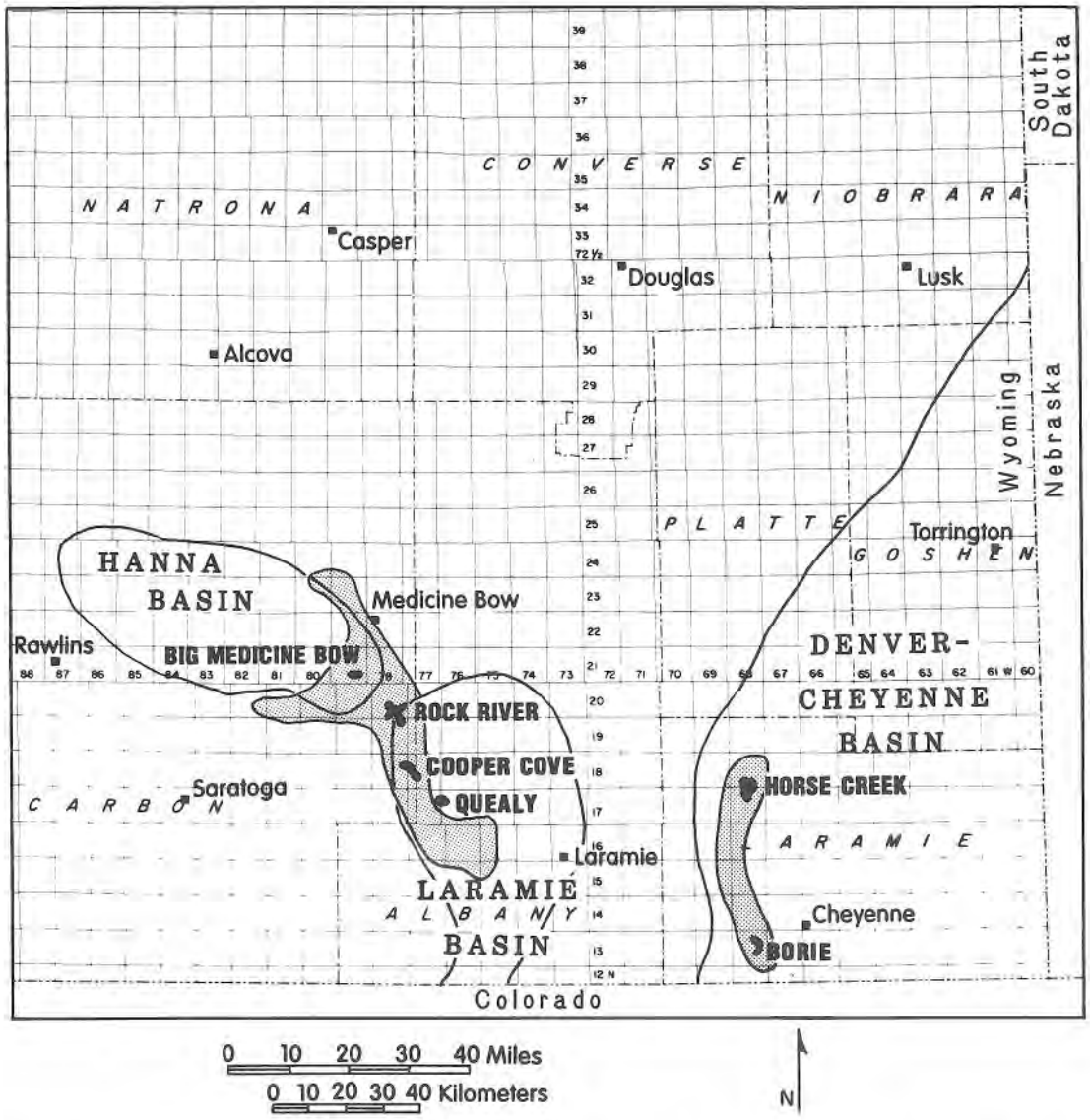

Figure 24. Present productive limits of the basin margins structural play (shaded) in the Hanna, Laramie, and Denver-Cheyenne basins of southeast Wyoming. Major fields are shown in black.

cubic feet of gas (De Bruin, 1990) had been produced from vertically drilled Niobrara Formation wells in several fields in the eastern half of the State (**Figure 25**).

The Niobrara Formation is subdivided into two members in the southeastern part of the State: the lower Fort Hays Limestone Member and the upper Smoky Hill Member. The Smoky Hill Member is generally comprised of limestones (chalks) and calcareous shales. Chalks of the Smoky Hill Member were deposited in deep water and are laterally extensive, with only slight facies variation. Most Niobrara production in Wyoming is from the fractured chalks and calcareous shales of the Smoky Hill Member. Post-depositional deformation accounts for the Niobrara Formation fracturing; there is very little interstitial porosity in the brittle chalks and calcareous shales (Pollastro and Scholle, 1984).

Experience gained by horizontal drilling in the Niobrara in Wyoming and other producing areas may cause more widespread application of the technology. The Mowry Shale, Frontier Formation, tight gas sands, and coal beds have geological characteristics favorable for horizontal drilling applications.

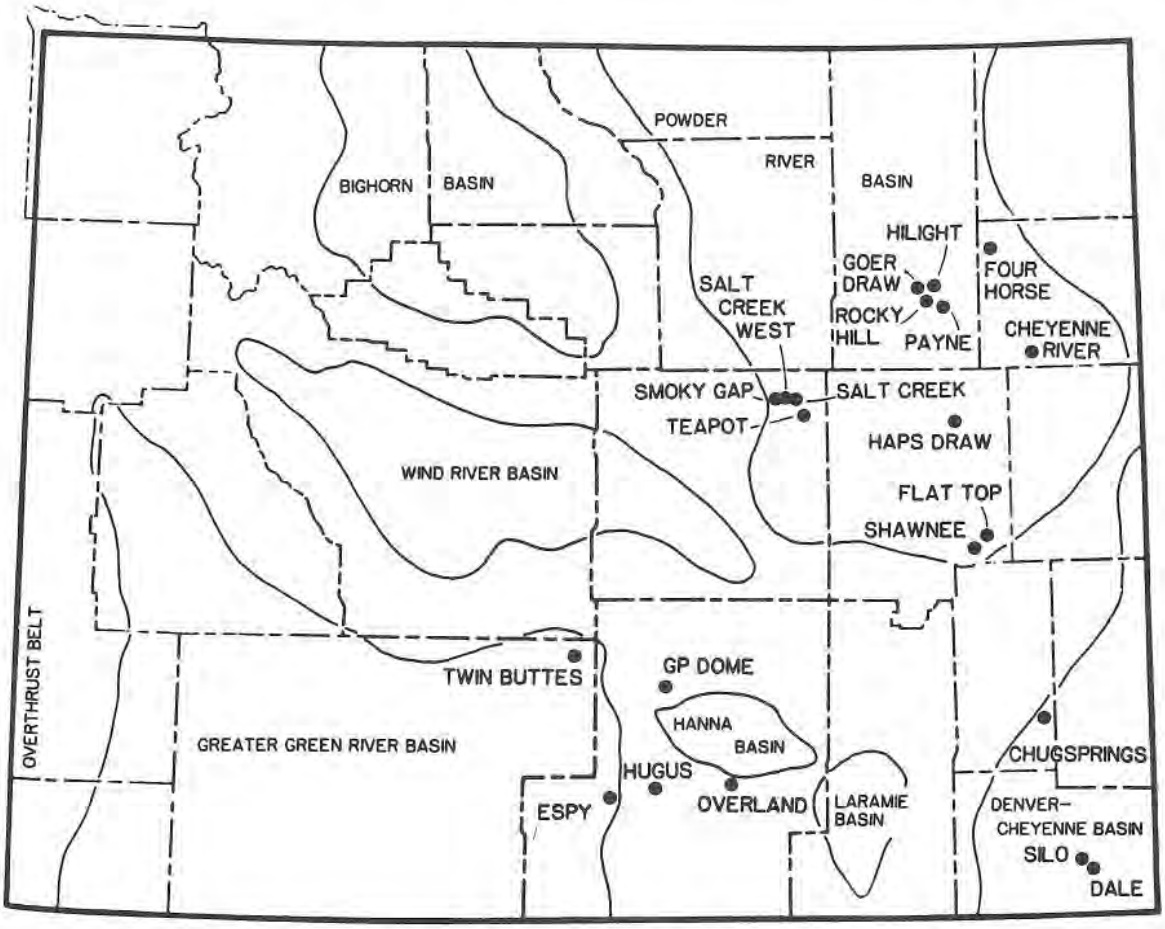

Figure 25. Oil and gas fields in Wyoming with production from the Niobrara Formation.

Statewide coalbed methane

Methane is a major component of the volatile matter released during the coalification process. In Wyoming, methane in coal beds and related reservoir rocks may be a product of either low-temperature coalification, dominated by biogenic processes, or of higher temperature coalification, dominated by thermogenic processes (Jones and De Bruin, 1990).

Exploration for coalbed methane has occurred in the Powder River Basin (Fort Union Formation), the Green River Basin (Mesaverde and Rock Springs formations) and the Hanna Basin (Ferris and Hanna formations) (Jones and De Bruin, 1990) (**Figure 26**).

This play includes production from sandstone reservoirs at several fields in the northern part of the Powder River Basin. Sandstones in the Tongue River Member of the Paleocene Fort Union Formation are apparently charged with methane sourced by the adjacent coal beds (Randall, 1989). Most production (over two billion cubic feet) in this play has been from the Oedekoven and Chan fields. One field in the Powder River Basin, Moose Draw, produced gas from sandstone reservoirs in the Eocene Wasatch Formation.

There is an estimated 7.25 to 145.0 trillion cubic feet of coalbed methane in Wyoming (Jones and De Bruin, 1990), based on the amount of coal in the State and on estimates of the average amount of methane in the coal.

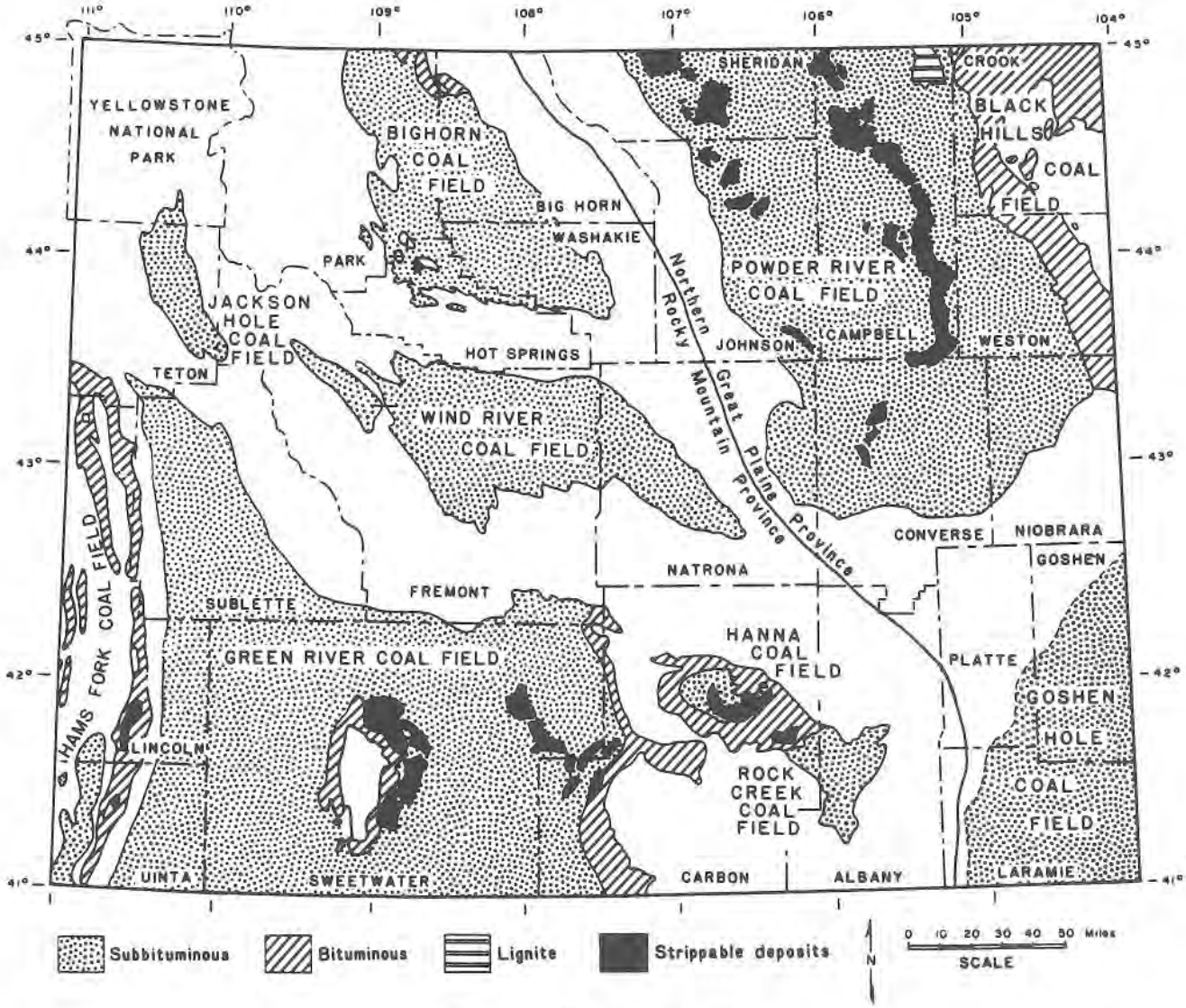

Figure 26. Wyoming coal fields.

Source rocks

Source rocks are organic-rich sediments that have been subjected to sufficient temperatures and pressures through geologic time to have generated and discharged hydrocarbons. Source rocks that have provided hydrocarbons for reservoirs in Wyoming range in age from at least Pennsylvanian to Tertiary, and may also include older formations (e.g., the Madison Limestone and Bighorn Dolomite).

The Permian Phosphoria Formation includes two organic-rich shales in western Wyoming, southeastern Idaho, and northern Utah—the Retort and Meade Peak phosphatic shale members. Most of the Meade Peak contains greater than 0.5% organic carbon, which is considered adequate for source rock. The average organic carbon content of the Retort is about 4.9%, based on 82 samples from 22 localitites (Maughan, 1984). The Phosphoria Formation is thought by some workers to be the source of much of the oil in Paleozoic reservoirs in the Bighorn and Wind River basins. Sheldon (1967) and Claypool and others (1978) proposed that oil migrated from western Wyoming and may have been trapped as far east as the eastern Powder River Basin in the Permian-Pennsylvanian age Minnelusa Formation. Stone (1967) presented evidence that oil in Paleozoic reservoirs of the Bighorn Basin was sourced by the Phosphoria Formation, and Keefer (1969) presented similar evidence for the Wind River Basin. An opposing view presented by Clayton and Ryder (1984) suggested that oil from reservoirs in the Permian-Pennsylvanian Minnelusa Formation in the Powder River Basin is geochemically different from oil associated with reservoirs in the Phosphoria Formation in the Bighorn Basin. They concluded that oil in Minnelusa reservoirs probably was sourced by Pennsylvanian black shales in the Minnelusa of the Powder River Basin.

Hagen and Surdam (1984) evaluated the source rock potential of the Lower Cretaceous Thermopolis and Mowry shales and the Upper Cretaceous Frontier Formation and Cody Shale in the Bighorn Basin. They concluded that good-quality source rocks exist throughout a 2,000- to 4,000-ft-thick section and that the source rocks are oil and gas prone.

The Lower Cretaceous Mowry and Skull Creek shales and their equivalent formations (Aspen and Thermopolis shales) are the primary sources for hydrocarbons in reservoirs in the Jurassic Nugget Sandstone in southwestern Wyoming, the Lower Cretaceous Muddy Sandstone of the Powder River Basin, and possibly other Cretaceous reservoirs in the State such as the Dakota and Frontier (Burtner and Warner, 1984). The Mowry Shale has expelled as much as 11.9 billion barrels of oil in the Powder River Basin (Momper and Williams, 1984).

The Upper Cretaceous Niobrara Formation and the Carlile Shale are sources for oil in Upper Cretaceous reservoirs in the Powder River Basin (Momper and Williams, 1984). The Lower Cretaceous Fuson Shale and the Upper Cretaceous Frontier Formation include shales that may have expelled some oil in the Powder River Basin (Momper and Williams, 1984). Generally, Cretaceous marine shales in the State that have undergone sufficient thermal maturation are potential hydrocarbon source rocks.

Cretaceous and Tertiary coals were probably the source for a portion of the natural gas produced from Tertiary and Upper Cretaceous reservoirs in the State. Deeply buried Cretaceous coals in the Bighorn, Wind River, and Greater Green River basins have most likely generated significant amounts of thermogenic methane (Jones and De Bruin, 1990). Some deeply buried Tertiary coals in these basins also may have generated thermogenic methane. Less thermally mature coals in the Tertiary Wasatch and Fort Union formations in the Powder River Basin generated biogenic methane. Coal beds can serve as both the source and reservoir for natural gas.

Summary

Over six billion barrels of oil and nearly 16 trillion cubic feet of gas have been produced over the past 107 years from a variety of hydrocarbon traps in Wyoming. Most oil and gas production in Wyoming can be classified according to geologic play based on trapping mechanism, reservoir age and facies, source rock, and hydrocarbon type within the Bighorn, Powder River, Wind River, and greater Green River

basins, the overthrust belt, and several basins in southeastern Wyoming.

The most prolific source rocks occur in the Minnelusa Formation, Phosphoria Formation, Mowry and Thermopolis shales, and Cretaceous and Tertiary coals.

Horizontal drilling and multiple completion production tools will open up new exploration objectives in the State. There is also good potential for gas discoveries in the deep portions of Wyoming basins, where drilling has been sparse.

References cited

Andrews, S., and Higgins, L.S., 1984, Influence of depositional facies on hydrocarbon production in the Tensleep Sandstone, Bighorn Basin, Wyoming: a working hypothesis: Wyoming Geological Association 35th Annual Field Conference Guidebook, p. 183-197.

Arro, E. 1969, Waltman field: Wyoming Geological Association 21st Annual Field Conference Guidebook, p. 105-110.

Asquith, D.O., 1974, Sedimentary models, cycles, and deltas, Upper Cretaceous, Wyoming: American Association of Petroleum Geologists Bulletin, v. 58, p. 2274-2283.

_____ 1975, Petroleum potential of deeper Lewis and Mesaverde sandstones in the Red Desert, Washakie, and Sand Wash basins, Wyoming and Colorado, *in* Bolyard, D.W., editor, Symposium on deep drilling frontiers in the central Rocky Mountains: Denver, Colorado, Rocky Mountain Association of Geologists, p. 159-162.

Barrett, W.J., and Hubley, M.D., 1969, The Madden gas field, Fremont County, Wyoming: Wyoming Geological Association 21st Annual Field Conference Guidebook, p. 115-120.

Berg, R.R., 1968, Point-bar origin of Fall River Sandstone reservoirs, northeastern Wyoming: American Association of Petroleum Geologists Bulletin, v. 52, p. 2116-2122.

_____ 1975, Depositional environment of Upper Cretaceous Sussex Sandstone, House Creek field, Wyoming: American Association of Petroleum Geologists Bulletin, v. 59, p. 2099-2110.

_____ 1976, Trapping mechanisms for oil in Lower Cretaceous Muddy Sandstone at Recluse field, Wyoming: Wyoming Geological Association 28th Annual Field Conference Guidebook, p. 261-272.

Berg, R.R., Larberg, G.M.B., and Recker, L.D., 1985, Hydrodynamic flow in the Lower Cretaceous Muddy Formation, northeast Powder River Basin, Wyoming and Montana: Wyoming Geological Association 36th Annual Field Conference Guidebook, p. 149-156.

Blackstone, D.L., Jr., and De Bruin, R.H., 1987, Tectonic map of the Overthrust Belt, western Wyoming, northwestern Utah, and southeastern Idaho, showing oil and gas fields and exploratory wells in the Overthrust Belt and adjacent Green River Basin: Geological Survey of Wyoming Map Series 23, scale 1:316,800.

Boyd, D.W., 1975, Fenestral fabric in Permian carbonates of the Bighorn Basin: Wyoming Geological Association 27th Annual Field Conference Guidebook, p. 101-106.

Boyd, J.B., 1969, Cooper Reservoir field: Wyoming Geological Association 21st Annual Field Conference Guidebook, p. 111-114.

Brock, W.G., and Nicolaysen, J., 1975, Geology of the Brady Unit, Sweetwater County, Wyoming, *in* Bolyard, D.W., editor, Symposium on deep drilling frontiers in the central Rocky Mountains: Denver, Colorado, Rocky Mountain Association of Geologists, p. 225-237.

Burtner, R.L., and Warner, M.A., 1984, Hydrocarbon generation in Lower Cretaceous Mowry and Skull Creek shales of the northern Rocky Mountain area, *in* Woodward, J., Meissner, F.F., and Clayton, J.L., editors, Hydrocarbon source rocks of the greater Rocky Mountain region: Denver, Colorado, Rocky Mountain Association of Geologists, p. 449-467.

Chisolm, W.A., 1970, Depositional history and petrography of two Fall River Formation sandstone reservoirs in the eastern Powder River Basin and their relationship to oil entrapment: Wyoming Geological Association 22nd Annual Field Conference Guidebook, p. 169-185.

Claypool, G.E., Love, A.H., and Maughan, E.K., 1978, Organic geochemistry, incipient metamorphism, and oil generation in black shale members of Phosphoria Formation, Western Interior United States: American Association of Petroleum Geologists, v. 62, p. 98-120.

Clayton, J.L., and Ryder, R.T., 1984, Organic geochemistry of black shales and oils in the Minnelusa Formation (Permian and Pennsylvanian), Powder River Basin, Wyoming, *in* Woodward, J., Meissner, F.F., and Clayton, J.L., editors, Hydrocarbon source rocks of the greater Rocky Mountain region: Denver, Colorado, Rocky Mountain Association of Geologists, p..231-253.

Couples, G.D., Weir, G.M., and Jamison, W.R., 1987, Structural development and hydrocarbon entrapment at Whitney Canyon and Yellow Creek fields, Wyoming overthrust belt: Wyoming Geological Association 38th Annual Field Conference Guidebook, p. 275-285.

Crews, G.C., Barlow, J.A., and Haun, J.D., 1976, Upper Cretaceous Gammon, Shannon, and Sussex sandstones, central Powder River Basin, Wyoming: Wyoming Geological Association 28th Annual Field Conference Guidebook, p. 9-20.

Curry, W.H., III, 1973, Parkman delta in central Wyoming: Wyoming Geological Association Earth Science Bulletin, v. 6, p. 5-18.

_____ 1976, Late Cretaceous Teapot delta of southern Powder River Basin, Wyoming: Wyoming Geological Association 28th Annual Field Conference Guidebook, p. 21-28.

_____ 1984, Paleotopography at the top of the Tensleep Sandstone, Bighorn Basin, Wyoming: Wyoming Geological Association 35th Annual Field Conference Guidebook, p. 199-211.

_____ 1985, Grieve paleovalley of the Muddy Sandstone in the eastern Wind River Basin, Wyoming: Wyoming Geological Association 36th Annual Field Conference Guidebook, p. 75-79.

Davis, M.J.T., 1976, An environmental interpretation of the Upper Cretaceous Shannon Sandstone, Heldt Draw field, Wyoming: Wyoming Geological Association 28th Annual Field Conference Guidebook, p. 125-138.

De Bruin, R.H., 1990, Horizontal drilling in the Upper Cretaceous Niobrara Formation: Geological Survey of Wyoming Geo-notes, no. 27, p. 41-43.

De Bruin, R.H., and Boyd, C.S., 1990, Oil and gas fields map of the Powder River Basin, Wyoming: Geological Survey of Wyoming Map Series 31, scale 1:316,800.

De Chadenedes, J.F., 1975, Frontier deltas of the western Green River Basin, Wyoming, *in* Bolyard, D.W., editor, Symposium on deep drilling frontiers in the central Rocky Mountains: Denver, Colorado, Rocky Mountain Association of Geologists, p. 149-157.

Doelger, N.M., 1987, The stratigraphy of the Nugget Sandstone: Wyoming Geological Association 38th Annual Field Conference Guidebook, p. 163-178.

Dolson, J., Muller, D., Evetts, M.J., and Stein, J.A., 1991, Regional paleotopographic trends and production, Muddy Sandstone (Lower Cretaceous), central and northern Rocky Mountains: American Association of Petroleum Geologists Bulletin, v. 75, p. 409-435.

Dolton, G.L., Fox, J.E., and Clayton, J.L., 1990, Petroleum geology of the Powder River Basin, Wyoming and Montana: U.S. Geological Survey Open File Report 88-450P, 68 p.

Dresser, H.W., 1974, Muddy Sandstone—Wind River Basin: Wyoming Geological Association Earth Science Bulletin, v. 7, p. 4-70.

Dunnewald, J.B., 1969, Big Piney-La Barge Tertiary oil and gas field: Wyoming Geological Association 21st Annual Field Conference Guidebook, p. 139-144.

Energy Information Administration, 1980, U.S. crude oil and natural gas reserves, 1977 annual report: Washington, D.C., Energy Information Administration, 82 p.

_____ 1983, U.S. crude oil, natural gas, and natural gas liquids reserves, 1982 annual report: Washington, D.C., Energy Information Administration, 99 p.

Frank, J.R., Cluff, S., and Bauman, J.M., 1982, Painter Reservoir, East Painter Reservoir, and Clear Creek fields, Uinta County, Wyoming, *in* Powers, R.B., editor, Geologic studies of the Cordilleran thrust belt: Denver, Colorado, Rocky Mountain Association of Geologists, v. 2, p. 601-612.

Fryberger, S.G., 1984, The Permian upper Minnelusa Formation, Wyoming: Ancient example of an offshore-prograding eolian sand sea with geomorphic facies, and system boundary traps for petroleum: Wyoming Geological Association 35th Annual Field Conference Guidebook, p. 241-271.

George, G.R., 1984, Cyclic sedimentation and depositional environments of the upper Minnelusa Formation, central Campbell County, Wyoming: Wyoming Geological Association 35th Annual Field Conference Guidebook, p. 75-95.

Hagan, E.S., and Surdam, R.C., 1984, Maturation history and thermal evolution of Cretaceous source rocks of the Bighorn Basin, Wyoming and Montana, *in* Woodward, J., Meissner, F.F., and Clayton, J.L., editors, Hydrocarbon source rocks of the greater Rocky Mountain Region: Denver, Colorado, Rocky Mountain Association of Geologists, p. 281-294.

Hansley, P.L., and Whitney, C.G., 1990, Petrology, diagenesis, and sedimentology of oil reservoirs in Upper Cretaceous Shannon Sandstone beds, Powder River Basin, Wyoming: U.S. Geological Survey Bulletin 1917, chapter C, p. C1-C33.

Haun, J.D., 1958, Early Upper Cretaceous stratigraphy, Powder River Basin, Wyoming: Wyoming Geological Association 13th Annual Field Conference Guidebook, p. 84-89.

Hawkins, C.M., and Formhals, S., 1985, Geology and engineering aspects of Buck Draw field, Campbell and Converse counties, Wyoming: Wyoming Geological Association 36th Annual Field Conference Guidebook, p. 33-43.

Herrod, W.H., 1980, Relationship of Cottonwood Creek field, Washakie County, Wyoming to carbonate facies of Permian Goose Egg Formation, eastern Bighorn Basin: Wyoming Geological Association 31st Annual Field Conference Guidebook, p. 67-89.

Hoffman, M.E., and Balcells-Baldwin, R.N., 1982, Gas giant of the Wyoming Thrust Belt: Whitney Canyon-Carter Creek field, *in* Powers, R.B., editor, Geologic studies of the Cordilleran thrust belt: Denver, Colorado, Rocky Mountain Association of Geologists, v. 2, p. 613-618.

Hoyle, B.L., Kraus, G.P., and Swanson, J., 1981, Glenrock South: Wyoming Geological Association Symposium, Oil and Gas Fields Powder River Basin, p. 164-165.

Irving, W., 1849, The adventures of Captain Bonneville, U.S.A., in the Rocky Mountains and the far west: New York, New York, G.P. Putnam, 428 p.

Isbell, E.B., Spencer, C.W., and Seitz, T., 1976, Petroleum geology of the Well Draw Field, Converse County, Wyoming: Wyoming Geological Association 28th Annual Field Conference Guidebook, p. 165-174.

Jones, R.W., and De Bruin, R.H., 1990, Coalbed methane in Wyoming: Geological Survey of Wyoming Public Information Circular 30, 15 p.

Keefer, W.R., 1965, Stratigraphy and geology history of the uppermost Cretaceous, Paleocene, and lower Eocene rocks in the Wind River Basin, Wyoming: U.S. Geological Survey Professional Paper 495-A, p. A1-A77.

_____ 1969, Geology of petroleum in Wind River Basin, central Wyoming: American Association of Petroleum Geologists Bulletin, v. 53, p. 1839-1865.

Kelly, J.M., and Hine, F.O., 1977, Ryckman Creek field, Uinta County: Wyoming Geological Association 29th Annual Field Conference Guidebook, p. 619-628.

Knight, W.C., 1897, The petroleum of the Shoshone anticlinal: Wyoming University School of Mines Petroleum Series Bulletin 2, part 1, p. 1-20.

Krueger, M.L., 1968, Occurrence of natural gas in Green River Basin, Wyoming: American Association of Petroleum Geologists Memoir 9, p. 780-797.

Larberg, G.M.B., 1980, Depositional environments and sand body morphologies of the Muddy sandstones at Kitty field, Powder River Basin, Wyoming: Wyoming Geological Association 31st Annual Field Conference Guidebook, p. 117-135.

Law, B.E., Spencer, C.W., Charpentier, R.R., Corvelli, R.A., Mast, R.F., Dolton, G.L., and Wandrey, C.J., 1989, Estimates of gas resources in overpressured low-permeability Cretaceous and Tertiary sandstone reservoirs, Greater Green River Basin, Wyoming, Colorado, and Utah: Wyoming Geological Association 40th Annual Field Conference Guidebook, p. 39-61.

Lawson, D.E., and Smith, J.R., 1966, Pennsylvanian and Permian influence on Tensleep oil accumulation, Bighorn Basin, Wyoming: American Association of Petroleum Geologists Bulletin, v. 50, p. 2197-2200.

Lelek, J.L., 1982, Anschutz Ranch East field, northeast Utah and southwest Wyoming, *in* Powers, R.B., editor, Geologic studies of the Cordilleran thrust belt: Denver, Colorado, Rocky Mountain Association of Geologists, v. 2, p. 619-631.

Levorsen, A.I., 1967, Geology of petroleum: San Francisco, California, W.H. Freeman and Company, 724 p.

Mankiewicz, D., and Steidtmann, J.R., 1979, Depositional environments and diagenesis of Tensleep Sandstone: eastern Bighorn Basin, Wyoming: Society of Economic Paleontologists and Mineralogists Special Publication 26, p. 319-336.

Maughan, E.K., 1984, Geological setting and some geochemistry of petroleum source rocks in the Permian Phosphoria Formation, *in* Woodward, J., Meissner, F.F., and Clayton, J.L., editors, Hydrocarbon source rocks of the greater Rocky Mountain Region: Denver, Colorado, Rocky Mountain Association of Geologists, p. 281-294.

Maynard, J.E., Rickles, S.E., Sackreiter, D.K., and Ver Steeg, D.J., 1981, Salt Creek: Wyoming Geological Association Symposium, Oil and Gas Fields Powder River Basin, p. 358-361.

Mitchell, G., 1978, Grieve oil field: A Lower Cretaceous estuarine deposit: Wyoming Geological Association 30th Annual Field Conference Guidebook, p. 147-165.

McCaleb, J.A., and Willingham, R.W., 1967, Cottonwood Creek field, Wyoming: American Association of Petroleum Geologists Bulletin, v. 51, p. 2122-2132.

McCullough, E.H., 1934, Structural influence on the accumulation of petroleum in California, *in* Problems of petroleum geology: Tulsa, Oklahoma, American Association of Petroleum Geologists, p. 735-760.

McDonald, R.E., 1973, Big Piney-La Barge producing complex, Sublette and Lincoln counties, Wyoming: Wyoming Geological Association 25th Annual Field Conference Guidebook, p. 57-77.

_____ 1975, Structure, correlation, and depositional environments of the Tertiary Sand Wash and Washakie basins, Colorado and Wyoming, *in* Bolyard, D.W., editor, Symposium on deep drilling frontiers in the central Rocky Mountains: Denver, Colorado, Rocky Mountain Association of Geologists, p. 100-103.

Merewether, E.A., Cobban, W.A., and Cavanaugh, E.T., 1979, Frontier Formation and equivalent rocks in eastern Wyoming: The Mountain Geologist, v. 16, p. 67-102.

Mettler, D.E., 1968, West Moorcroft and Wood Dakota fields, Crook County, Wyoming: Wyoming Geological Association 20th Annual Field Conference Guidebook, p. 89-94.

Miller, D.N., Jr., 1963, Subsurface aspects of the Fall River Sandstone, northern Black Hills: Wyoming Geological Association and Billings Geological Society 1st Joint Field Conference Guidebook, p. 117-122.

Momper, J.A., and Williams, J.A., 1984, Geochemical exploration in the Powder River Basin, *in* Demaison, G., and Morris, R.J., editors, Petroleum geochemistry and basin evaluation: American Association of Petroleum Geologists Memoir 35, p. 181-191.

Oriel, S.S., 1969, Geology of the Fort Hill Quadrangle, Lincoln County, Wyoming: U.S. Geological Survey Professional Paper 594-M, 40 p.

Pedry, J.J., 1975, Tensleep Sandstone stratigraphic-hydrodynamic traps, northeast Bighorn Basin, Wyoming: Wyoming Geological Association 27th Annual Field Conference Guidebook, p. 117-127.

Perman, R.C., 1990, Depositional history of the Maastrichtian Lewis Shale in south-central Wyoming: deltaic and interdeltaic, marginal marine through deep-water marine environments: American Association of Petroleum Geologists Bulletin, v. 74, p. 1695-1717.

Picard, M.D., 1977, Petrology of the Jurassic Nugget Sandstone, northeast Utah and southwest Wyoming: Wyoming Geological Association 29th Annual Field Conference Guidebook, p. 239-258.

Pollastro, R.M., and Sholle, P.A., 1984, Hydrocarbons exploration, development from low-permeability chalks—Upper Cretaceous Niobrara Formation, Rocky Mountains area: Oil and Gas Journal, v. 82, no. 16, p. 140-145.

Prescott, M.W., 1970, Hilight field, Campbell County, Wyoming: Wyoming Geological Association 22nd Annual Field Conference Guidebook, p. 89-106.

Randall, A.G., 1989, Shallow Tertiary gas production, Powder River Basin, Wyoming: Wyoming Geological Association 40th Annual Field Conference Guidebook, p. 83-96.

Rasmussen, D.L., Jump, C.J., and Wallace, K.A., 1985, Deltaic systems in the Early Cretaceous Fall River Formation, southern Powder River Basin, Wyoming: Wyoming Geological Association 36th Annual Field Conference Guidebook, p. 91-111.

Rice, D.D., and Keighin, C.W., 1988, Relation of major sea level fall, regional unconformity, and hydrocarbon accumulations, Upper Cretaceous Turner Sandy Member of Carlile Shale, Black Hills uplift, *in* Carter, L.M.H., editor, USGS research on energy resources—1988, Program and abstracts: U.S. Geological Survey Circular 1025, p. 51-52.

Roundtree, R., 1984, Western Oil Reporter's Rocky Mountain oil history: Denver, Colorado, Hart Publications Inc., 210 p.

Runge, J.S., Wicer, W.L., and Eckelberg, D.J., 1973, A subsurface type section on the Teckla Sand Member of the Lewis Shale formation: Wyoming Geological Association Earth Science Bulletin, v. 6, p. 3-18.

Ryer, T.A., McClurg, J.J., and Muller, M.M., 1987, Dakota-Bear River paleoenvironments, depositional history and shoreline trends-implications for foreland basin paleotectonics, southwestern Green River Basin and southern Wyoming overthrust belt: Wyoming Geological Association 38th Annual Field Conference Guidebook, p. 179-206.

Sheldon, R.P., 1967, Long-distance migration of oil in Wyoming: The Mountain Geologist, v. 4, p. 53-65.

Shultz, M.S., and Lafollette, R.F., 1989, Effect of drilling and completion methods on Frontier gas production, northern Moxa arch, southwest Wyoming: Wyoming Geological Association 40th Annual Field Conference Guidebook, p. 247-254.

Spearing, D.R., 1976, Upper Cretaceous Shannon Sandstone: an offshore shallow-marine sand body: Wyoming Geological Association 28th Annual Field Conference Guidebook, p. 65-72.

Stone, D.S., 1967, Theory of Paleozoic oil and gas accumulation, Bighorn Basin, Wyoming: American Association of Petroleum Geologists Bulletin, v. 51, p. 2056-2114.

Stone, W.D., 1972, Stratigraphy and exploration of the Lower Cretaceous Muddy Formation, northern Powder River Basin, Wyoming and Montana: The Mountain Geologist, v. 9, p. 355-378.

Tillman, R.W., and Martinsen, R.S., 1984, The Shannon shelf-ridge sandstone complex, Salt Creek anticline area, Powder River Basin, Wyoming, *in* Tillman, R.W., and Siemers, C.T., editors, Siliciclastic shelf sediments: Society of Economic Paleontologists and Mineralogists Special Publication 34, p. 85-142.

_____ 1987, Sedimentologic model and production characteristics of Hartzog Draw field, Wyoming, a Shannon shelf-ridge sandstone, *in* Tillman, R.W., and Weber, K.J., editors, Reservoir sedimentology: Society of Economic Paleontologists and Mineralogists Special Publication 40, p. 15-112.

Trotter, J.F., 1963, The Minnelusa play of the northern Powder River Basin, Wyoming and adjacent areas: Wyoming Geological Association and Billings Geological Society 1st Joint Field Conference Guidebook, p. 117-122.

Van West, F.P., 1972, Trapping mechanisms of Minnelusa oil accumulations, northeastern Powder River Basin, Wyoming: The Mountain Geologist, v. 9, p. 3-20.

Veach, A.C., 1907, Geography and geology of a portion of southwestern Wyoming with special reference to oil and coal: U.S. Geological Survey Professional Paper 56, 178 p.

Ver Ploeg, A.J., and De Bruin, R.H., 1982, The search for oil and gas in the Idaho-Wyoming-Utah salient overthrust belt: Geological Survey of Wyoming Report of Investigations 21, 108 p.

Von Drehle, W.F., 1985, Amos Draw field, Campbell County, Wyoming: Wyoming Geological Association 36th Annual Field Conference Guidebook, p. 11-31.

Wallem, D.B., Steidtmann, J.R., and Surdam, R.C., 1981, Depositional environments and diagenesis of the Bear River Formation, western Wyoming: Wyoming Geological Association 32nd Annual Field Conference Guidebook, p. 23-29.

Webb, J.E., 1975, Sedimentology and clay cementation, Dakota Formation, Bridger Lake Field, Utah, *in* Bolyard, D.W., editor, Symposium on deep drilling frontiers in the central Rocky Mountains: Denver, Colorado, Rocky Mountain Association of Geologists, p. 217-224.

Weimer, R.J., 1965, Stratigraphy and petroleum occurrences, Almond and Lewis formations (Upper Cretaceous), Wamsutter arch, Wyoming: Wyoming Geological Association 19th Annual Field Conference Guidebook, p. 65-80.

White, I.C., 1885, The geology of natural gas: Science, v. 5, p. 521-522.

Winn, R.D., Stoneciher, S.A., and Bishop, M.G., 1983, Depositional environments and diagenesis of offshore sand ridges, Frontier Formation, Spearhead Ranch field, Wyoming: The Mountain Geologist, v. 20, p. 41-58.

Winn, R.D., Jr., Bishop, M.G., and Gardner, P.S., 1985, Lewis Shale, south-central Wyoming: shelf, delta front, and turbidite sedimentation: Wyoming Geological Association 36th Annual Field Conference Guidebook, p. 113-130.

Wyoming Oil and Gas Conservation Commission, 1992, Oil and gas statistics 1991: Casper, Wyoming, Wyoming Oil and Gas Conservation Commission, 226 p.

Frontispiece. Leaf impressions from Taxodiaceae vegetation (mostly *Metasequoia occidentalis* and *Glyptostrobus europaeus*) of the Late Paleocene Fort Union Formation. Species of the Taxodiaceae are thought to have been major contributors to the peats of Wyoming Tertiary mires. Specimen dimensions are 30 x 63 cm (from the Denver Museum of Natural History; collected by Clarence Johnsrud; photographed by Rick Wicker).

Processes and possible analogues in the formation of Wyoming's coal deposits

Timothy A. Moore
Geological Survey of Wyoming
Laramie, WY 82071

Jane C. Shearer
Geological Survey of Wyoming
Laramie, WY 82071
and
Department of Botany
University of Wyoming
Laramie, WY 82071

Abstract

Coal deposits in Wyoming formed within a variety of depositional settings. Modern environments provide analogues for some of these deposits, whereas others cannot be directly related to modern depositional settings. For example, the Cretaceous Pintail coal bed (Almond Formation, Green River coal field) developed in association with marginal-marine barrier-bar sediments, although a low abundance of inorganic constituents in the coal suggests that the peat was not affected by clastic sedimentation. Subsequent burial by sulfate-bearing marine sediments resulted in a relatively high concentration of sulfur in the coal bed. Palynological analysis of the Pintail coal bed indicates that it formed dominantly from angiosperms, ferns, and mosses. Large, intact plant material observed in the coal bed, however, are solely derived from gymnosperms. A modern analogue for the Pintail coal bed may be the Okefenokee Swamp in the southeastern United States. In this mire, peat is accumulating adjacent to a relict barrier-bar.

In contrast to the Pintail coal bed, the Tertiary Anderson coal bed (Fort Union Formation, Powder River coal field) formed in a freshwater, fluvial-dominated environment far removed from marine sedimentation. Although the Anderson coal bed formed in close proximity to sites of clastic fluvial and overbank sedimentation, it has a low concentration of sulfur and inorganic constituents. The surface of the Anderson palaeo-mire may have been raised in the manner of modern mires, which have been documented in the Indo-Malesian region. In particular, the Palangkaraya mire in Kalimantan, Indonesia, has compositional and floral similarities to observed organic constituents in the Anderson coal bed. Plant succession can be noted in both deposits, although the Anderson coal bed was dominated by gymnosperms and the Palangkaraya mire is dominated by angiosperms. In addition, oxidized plant remains at the tops of both deposits may be the result of a lowered water table. A lowered water table may signify the death of the

Moore, T.A., and Shearer, J.C., 1993, Processes and possible analogues in the formation of Wyoming's coal deposits, *in* Snoke, A.W., Steidtmann, J.R., and Roberts, S.M., editors, Geology of Wyoming: Geological Survey of Wyoming Memoir No. 5, p. 874-896.

Palangkaraya mire and may also have been responsible for termination of the Anderson palaeo-mire.

Although analogues exist for the Pintail and Anderson coal beds, finding modern equivalents for other coal beds in Wyoming that are very thick (>80 ft/ 25 m) is difficult. Part of the problem is that known maximum peat thickesses (56 ft/17 m) are not comparable when the thick coal beds are decompacted using even a modest (3:1) compaction ratio. However, when these thick coals are examined in detail, most are found to contain multiple inorganic and/or degradational 'partings', which represent terminations of peat accumulation. The coal between these partings can be equated to individual mires and are relatively comparable to peat thicknesses, even when uncompacted.

Introduction

The State of Wyoming contains vast coal deposits, many of which remain largely unexplored and unexploited. In fact, with the exception of Alaska, Wyoming has the largest in-place coal resources of any state (1.44 trillion tons). Wyoming coal beds range in age from Early Cretaceous to Eocene and their degree of metamorphism (*i.e.*, rank) ranges from sub-bituminous to high-volatile A bituminous. Much of Wyoming coal is readily marketable because it has low ash and sulfur contents. Coal deposits in Wyoming are found within ten major coal fields, as shown in **Figure 1**. A list of the coal-bearing formations and the general attributes of coal beds in each coal field are given in **Table 1**.

All Wyoming coal fields contain Cretaceous-age coal beds (Glass and Jones, 1991). The most widespread Cretaceous coal deposits are in the Mesaverde Group (Powder River, Green River, Bighorn, Wind River, Jackson Hole and Rock Creek coal fields) and its western equivalent, the Adaville Formation (Hams Fork coal field). Paleocene coals crop out in all coal fields except the Black Hills and Goshen Hole fields and occur mainly in the Fort Union, Ferris, and Hanna formations. The greatest number of Paleocene coal beds occur in the Hanna coal field (Glass and Jones, 1991), but the thickest coal beds (up to 200 ft/61 m) are found in the Powder River coal field. The major-

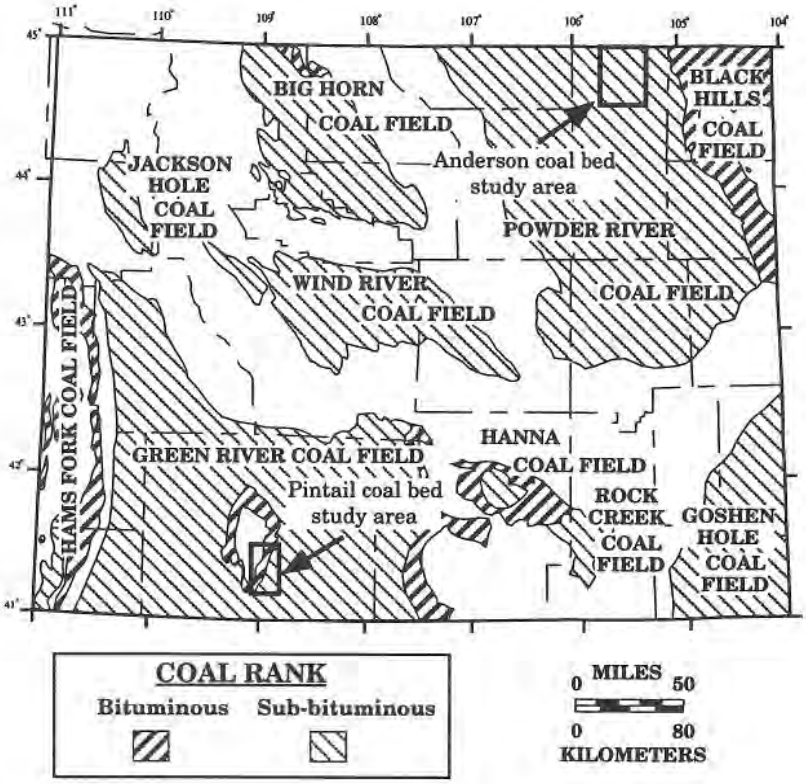

Figure 1. The location of major coal fields of Wyoming and predominant ranks of the near-surface coals. The positions of the Anderson and Pintail coal bed study areas are shown in Figures 2 and 3. Areas in white on the map are non-coal-bearing regions. (County lines are dashed.)

ity of Eocene coal beds are also in the Powder River coal field, and the Wasatch Formation is the most widespread Eocene coal-bearing formation. The thickest coal bed in Wyoming occurs in the Wasatch Formation in the Powder River coal field; this is the Lake de Smet coal bed, which reaches a maximum thickness of 250 ft (75.8 m) (Obernyer, 1980). Thick Wasatch Formation coals also occur in the Green River and Hanna coal fields; Eocene-age coals are not found in the Hams Fork, Black Hills, Rock Creek, or Goshen Hole coal fields.

Cretaceous and Tertiary coal beds in Wyoming differ as a result of the contrasting tectonic and sedimentary regimes in which they formed (Glass, 1977b). Cretaceous peat deposits were most often located in deltaic, coastal plain, or other nearshore settings along the Cretaceous epeiric seaway. As a result, Cretaceous coal beds are generally laterally extensive but are relatively thin (less than 9 ft/3 m) and often relatively high in sulfur (frequently > 1%). In contrast, Tertiary coal beds accumulated as peats in smaller more localized sedimentary basins formed during the Laramide orogeny (Glass, 1977b). Tertiary mires were associated with fluvial or fluvio-lacustrine depositional systems and their proximity to these systems, coupled with migration of the fluvial systems, restricted the lateral extent of the mires. Tertiary coal beds tend to be more areally restricted but are often thicker (greater than 200 ft/61 m) than Cretaceous coal beds. Because they were not exposed to marine water, the total sulfur in Tertiary coal beds tends to be low (< 1%). The percentage of inorganic constituents in both Cretaceous and Tertiary coal beds is related to the specific sedimentary environment in which peat accumulated and ranges from less than 5% to more than 50% of the coal.

The contrasts between Cretaceous and Tertiary coals demonstrate how coal bed formation can be influenced by the original depositional environment. Therefore, this paper will concentrate on two specific coal beds, the Cretaceous Pintail coal bed (Green River coal field) and the Paleocene Anderson coal bed (Powder River coal field) (**Figure 1**). The differences between these coal deposits will be examined and modern analogues suggested from which the settings of these Wyoming palaeo-mires may be interpreted. Finally, a brief discussion on the problem of coal bed thickness is included, as this conundrum is still not completely explained by modern analogues.

Comparison of two Wyoming coal settings

Lithologic relationships

The Anderson and Pintail coal beds occur in very different sedimentary settings, as shown in **Figures 2** and **3**. Major differences between these settings can be seen in the fossils and the contrasting morphologies and internal sedimentary structures of sandstone units. In addition, the fine-grained sediments in the two areas differ. A final contrast is provided by the relationships of coal beds to clastic sediments in the two settings.

Marine fossils are abundant in Cretaceous strata associated with the Pintail coal bed. In particular, oyster beds and *Ophiomorpha* traces are most common. In contrast, the Paleocene sediments associated with the Anderson coal bed contain numerous freshwater bivalves and gastropods (Flores and Hanley, 1984).

The different sedimentary structures in sandstone units of the two areas also distinguish the marine Cretaceous from the terrestrial Paleocene sediments. The Cretaceous sandstones are more variable in morphology and internal structure compared to those of the Paleocene. Sandstones associated with the Pintail coal bed are either thick (160 ft or 48 m), laterally continuous sandstone bodies with gradational upper and lower surfaces, or thinner (90 ft or 27 m) laterally discontinuous sandstone bodies with erosional bases. The laterally continuous sandstones are typically burrowed and generally exhibit massive bedding in their lower parts and crossbedding in their upper parts. In contrast, the discontinuous sandstone units are crossbedded throughout and not burrowed. These two types of sandstone units have been interpreted by Roehler (1988) as barrier-bar shoreface (thick, continuous sandstones) and tidal channel (discontinuous sandstones).

Table 1. General characteristics of Wyoming coals[1]

COAL FIELD Formation	AGE	TYPICAL BED ABUNDANCE[2]	TYPICAL BED THICKNESS[3]	APPARENT RANK	TYPICAL RANGE OR AVERAGE ASH (%)
POWDER RIVER					
Mesaverde	Upper Cretaceous	rare	thin	subC	9
Lance	Upper Cretaceous	common	thin	subC	9
Fort Union	Paleocene	common	intermediate to thick	sub	3–12
Wasatch	Eocene	common	mostly intermediate, sometimes thick	sub	4–22
GREEN RIVER					
Mesaverde Group	Upper Cretaceous	abundant	thin to intermediate	hvCb	2–28
Lance	Upper Cretaceous	common	intermediate	subB	4–6
Fort Union	Paleocene	common	intermediate	hvCb	8–14
Wasatch	Eocene	common	thin to thick	sub	7–8
HANNA					
Almond	Upper Cretaceous	common	thin to intermediate	subA to hvCb	8
Medicine Bow	Upper Cretaceous	common to abundant	thin to intermediate	subA to hvCb	4
Ferris	Paleocene	abundant	thin to intermediate	subA to hvCb	4–21
Hanna	Paleoc. to Eoc.	abundant	thin to intermediate	subA to hvCb.	4–21
HAMS FORK					
Bear River	Upper Cretaceous	rare	thin	bit (?)	ND
Frontier	Upper Cretaceous	common	thin, rarely intermediate	hvCb to hvAb	3–15
Adaville	Upper Cretaceous	abundant	thin to intermediate	sub	3–9
Blind Bull	Upper Cretaceous	ND	thin, occasionally intermediate	hvBb	2–10
Evanston	Paleocene	rare	intermediate	sub	7–16
BIGHORN					
Mesaverde	Upper Cretaceous	ND	thin, rarely intermediate	subA to hvCb	2–9
Meeteetse	Upper Cretaceous	ND	thin, rarely intermediate	subA to hvCb	6–17
Fort Union	Paleocene	ND	intermediate	subA to hvCb	5–9
WIND RIVER					
Mesaverde	Upper Cretaceous	abundant	thin to intermediate, occasionally thick	subC to hvCb	3–12
Meeteetse	Upper Cretaceous	ND	thin to intermediate	subA	8
Fort Union	Paleocene	common	thin	sub (?)	5–15
JACKSON HOLE					
Bacon Ridge Ss	Upper Cretaceous	ND	thin to intermediate	sub	13.2
Sohare sequence	Upper Cretaceous	abundant	thin to intermediate	sub	ND
Mesaverde	Upper Cretaceous	ND	thin	sub	ND
Pinyon Cg	U. Cret. to Paleocene	rare	thin to intermediate	sub	ND
Devils Basin	Paleocene	common	thin	sub	ND
Wind River	Eocene	rare	thin to thick	sub	ND
BLACK HILLS					
Lakota Sandstone	Early Cretaceous	rare	thin to intermediate	hvCb	17
ROCK CREEK					
Mesaverde	Late Cretaceous	common	mostly thin, rarely intermediate	sub	ND
Medicine Bow	Late Cretaceous	rare	mostly thin, some intermediate	sub	ND
Hanna	Paleocene	abundant	thin	sub	ND
GOSHEN HOLE					
Lance	Late Cretaceous	rare	thin	sub	ND

[1] Data sourced from Glass and others (1975), Glass (1976, 1977a, 1978, 1981), Glass and Roberts (1978; 1979), Jones (1982), Warlow and others (1986) and Glass and Jones (1991)
[2] "rare" is 3 or fewer seams, "common" is 4 to 10 beds, "abundant" is more than 10 beds
[3] "thin" is ≤ 6 ft (1.8 m), "intermediate" is 6 to 30 ft (1.8 to 9 m), "thick" is ≥ 30 ft (9 m)
[4] Total in-place coal resources (Wood and Bour, 1988).
"ND" = Not documented in available literature.
Rank abbreviations = sub (subbituminous); subA - C (subbituminous A to C); hvAb (high-volatile A bituminous); hvBb (high-volatile B bituminous); hvCb (high volatile C bituminous)

Table 1. Continued

TYPICAL RANGE OR AVERAGE SULFUR (%)	IN-PLACE RESOURCES[4] (billion short tons)
	1,030.6
0.7	
0.7	
0.1–1.1	
0.3–3.3	
	213.1
0.3–2.8	
0.4–1.1	
0.7–2.7	
0.7–1.5	
	23.3
0.7	
0.7	
0.2–0.7	
0.2–2.3	
	49.6
ND	
0.4–2.7	
0.2–1.8	
0.3–1.0	
0.2–4.5	
	23.5
0.4–0.8	
0.3–0.7	
0.3–0.6	
	81.0
0.3–1.3	
0.4	
0.2–2.1	
	6.3
0.8	
ND	
ND	
ND	
ND	
ND	
	7.9
4.9	
	3.4
ND	
ND	
ND	
	0.2
ND	
TOTAL IN GROUND RESOURCES	1,438.9

Paleocene Fort Union Formation sandstones associated with the Anderson coal bed are lenticular bodies with erosional bases and gradational tops. They contain lateral accretion surfaces and are composed of fining-upward successions of conglomerate and coarse-grained sandstone that grade vertically into fine-grained sandstone and siltstone (Flores, 1983). These sandstone units are trough crossbedded near their bases and bedding changes upward to tabular crossbeds and ripple laminations. Laterally, the lenticular sandstones interfinger with highly root-penetrated siltstone and claystone or with tabular coarsening-upward (from siltstone to sandstone) intervals that are parallel laminated. Flores (1980, 1981) and Pocknall and Flores (1987) interpret these types of lenticular sandstone units in the Powder River Basin as fluvial channel deposits. Tabular coarsening-upward sandstones lateral to the channel sandstones are interpreted as overbank and crevasse-splay deposits associated with the channels.

The fine-grained sediments of the Anderson coal bed also differ from those of the Pintail coal bed. Thin (<6 ft/1.8 m) discontinous limestones occur interbedded with clastically derived sediments in association with the Anderson coal bed. In contrast, fine-grained sediments associated with the Pintail coal bed are composed exclusively of detrital clastic material. Additionally, the fine-grained sediments in the Anderson study area are often extensively root penetrated (indicating deposition in relatively shallow water), whereas in the Pintail coal study area, fine-grained sediments are generally finely laminated and do not display rooting (suggesting deposition in slightly deeper water where plants could not root).

In addition to the contrasting types of detrital sediment associated with the Pintail and Anderson coal-bearing sequences, there is also an important difference in the relationship between the coal and clastic sediments in the two areas. The Pintail coal bed, and also the Finch coal bed (which underlies the Pintail coal bed) are split by (or interbedded with) carbonaceous siltstone interpreted to represent salt marshes adjacent to the freshwater mires (coal) (Roehler, 1988). In contrast, the Anderson coal bed is split by channel sandstones and associated fine-grained claystone and siltstone deposited as overbank and splay sediments.

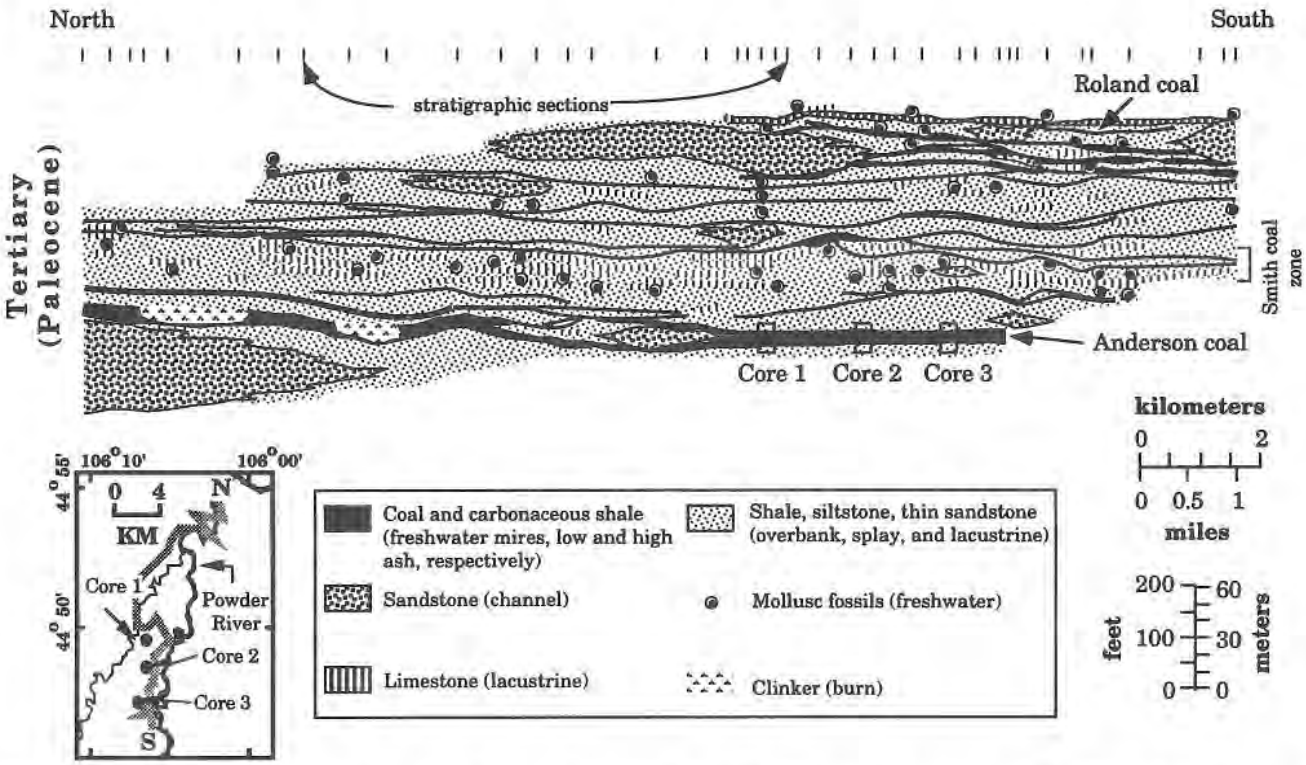

Figure 2. Stratigraphic cross section through the Anderson coal bed study area. Note the position of cores 1, 2, and 3, which are shown in greater detail in Figure 4. Inset shows location of cross section (modified from Flores, 1981; Moore and others, 1990).

Coal composition

The Anderson and Pintail coal beds can be differentiated on the basis of both inorganic and organic composition (**Table 2**) as well as sedimentary setting. The main difference in their inorganic content is in their total sulfur values. The Pintail coal bed contains more than 8% sulfur on average, as compared to less than 1% in the Anderson coal bed. The total inorganic contents of the two coals are similar, ranging from 5 to 6% in the Pintail coal bed and 7 to 8% in the Anderson coal bed.

The organic composition of the two coals differs in the proportions of preserved plant tissue and oxidized tissue, although it should be noted that the limited analyses performed on the Pintail coal bed preclude detailed interpretations. The Pintail coal bed contains generally higher concentrations of plant cell-wall material compared to the Anderson coal bed, which has significantly higher concentrations of finer grained organic material (humic gels and fragments of cell walls and cell infillings) (Roehler, 1988). Large pieces of plant material in the Pintail coal bed are composed of gymnosperm wood (Roehler, 1988). In addition, the Pintail coal has more plant material that has been oxidized (either through fire or microbial alteration) than the Anderson coal bed. Detailed petrographic analysis of the Anderson coal bed (Moore and others, 1990), summarized in **Figure 4**, shows a vertical change in coal composition. Two intervals, including the upper 3.3 ft (1 m) of the coal bed, contain an abundance of oxidized plant remains (**Figure 5**, mean = 11.7%), as opposed to the remainder of the coal, which contains an average of less than 4% oxidized plant material. The oxidized plant remains in these intervals do not occur as discrete lenses in the coal (*i.e.*, fusain) but rather as disseminated fragments throughout.

Palynological analyses of the Pintail (Roehler, 1988) and the Anderson (Pocknall, 1986; Pocknall and Flores, 1987; Moore and others, 1990) coal beds indicate that they formed from totally different floral communities (**Table 3**). The Pintail coal bed is dominated by pollen from angiosperms (44%) and spores from ferns and mosses (36%), with only a minor component of gymnosperms (16%). In contrast, the Anderson coal bed is dominated by pollen of gymnosperms (65%) with subordinate concentrations of

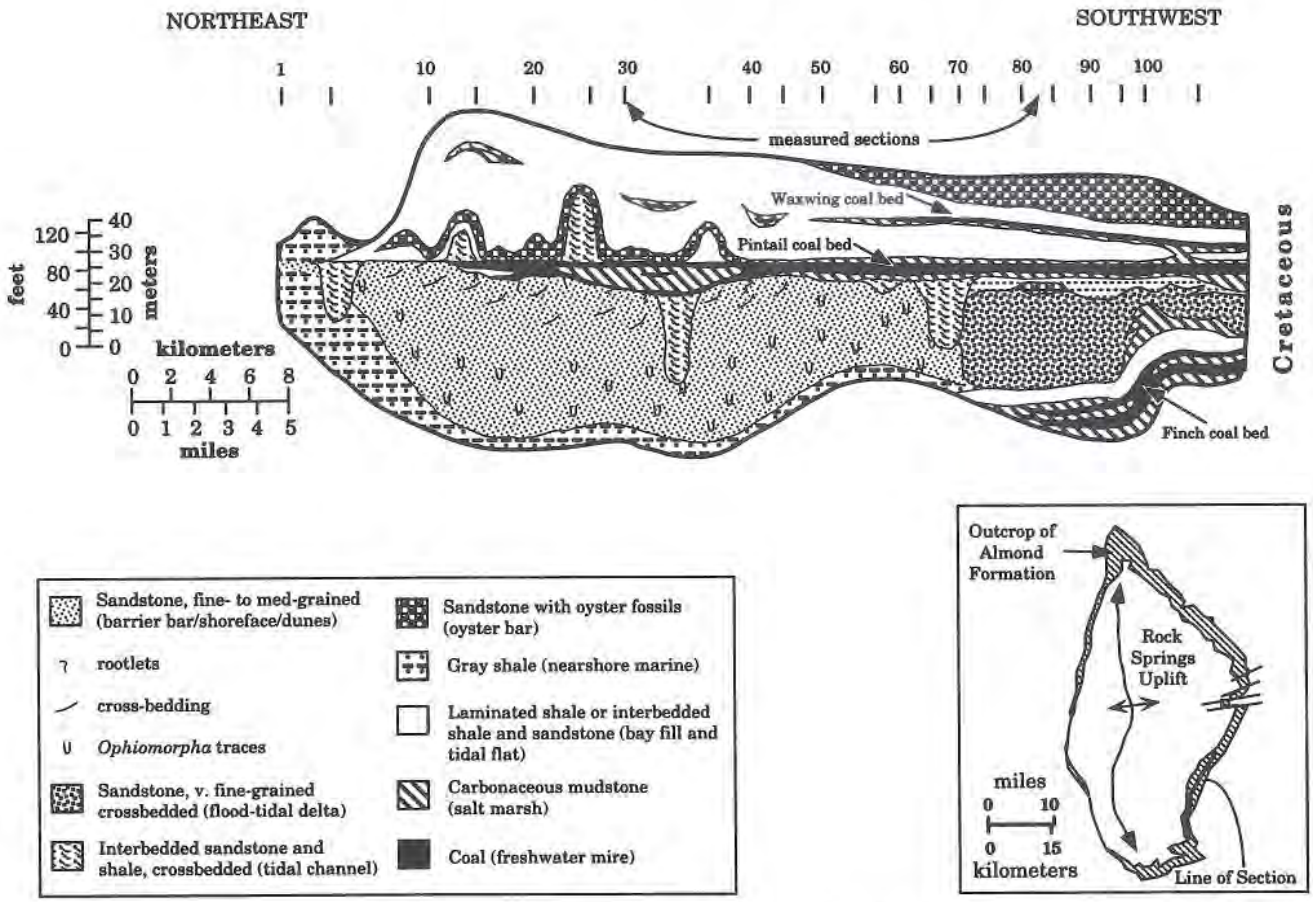

Figure 3. Stratigraphic cross section through the Pintail coal bed and associated sediments. Inset shows the location of the cross section (modified from Roehler, 1988).

Table 2. Average organic composition (in percent) of the Pintail and Anderson coal beds. Numbers in bold are means, and values in parentheses represent ranges (Pintail coal bed) or standard deviations (Anderson coal bed). Data compiled from Roehler (1988) and Moore and others (1990).

Organic component	*Cretaceous* (Almond Formation) Pintail coal bed[1]		*Tertiary* (Fort Union Formation) Anderson coal bed[2]	
Unoxidized (vitrinite)				
cell wall material (telocollinite & telinite)	**77**	(71-83)	**47**	(10.0)
cell fillings (corpocollinite)	**3**	(1-5)	**6**	(2.5)
humic gels and fragments of cell walls (desmocollinite)	**1.5**	(1-2)	**35**	(10.3)
Oxidized (inertinite)				
slightly oxidized cell wall material (semifusinite)	**9**	(8-10)	**1**	(1.5)
highly oxidized cell wall material (fusinite)	**1**	(-)	**1**	(1.0)
unidentifiable oxidized fragments (inertodetrinite)	**6**	(3-9)	**2**	(2.1)
fungal remains (sclerotinite)	-		**Trace**	
Resins, waxes, spores-pollen, Bitumen & Cuticle (liptinite)	**3.5**	(2-3)	**10**	(1.2)

[1]2 samples from one outcrop
[2]25 samples from three cores

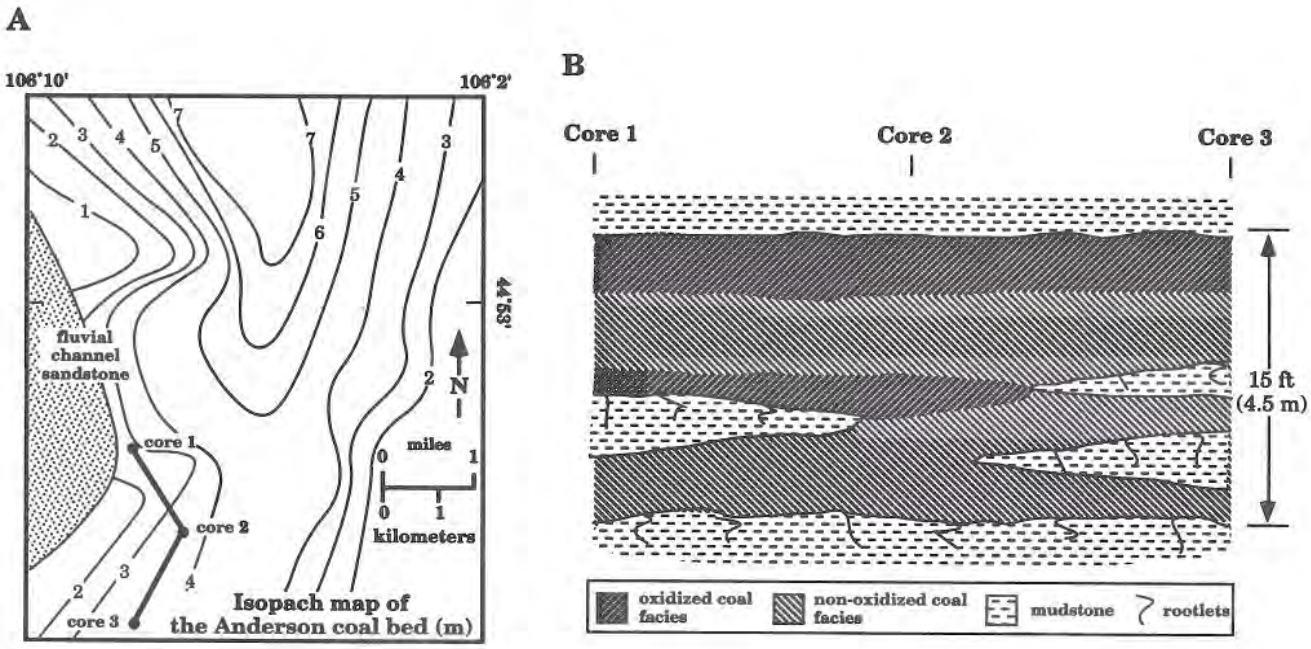

Figure 4. (A) Thickness map of the Anderson coal bed in a portion of northeastern Wyoming (modified from Pocknall and Flores, 1987; Moore and others, 1990). (B) Cross section of the Anderson coal bed showing the distribution of oxidized and non-oxidized organic facies (modified from Moore and others, 1990). See location map in Figure 2 for location of cores.

angiosperms (34%) and only trace amounts of spores (1%).

Detailed pollen analysis of the Anderson coal bed suggests a vertical succession of plant types (Moore and others, 1990). Throughout the accumulation of the Anderson palaeo-mire, the flora was dominated by *Glyptostrobus*, a bald-cypress-like plant. However, the initial mire vegetation was characterized by a riparian vegetation of *Platanus* (sycamore) and *Ulmus* (elm). As peat thicknesses increased, the mire flora changed to one typified by *Nyssa* (sour gum), *Carya* (hickory, pecan), Betulaceae (birch) and *Pinus/Picea* (pine and spruce).

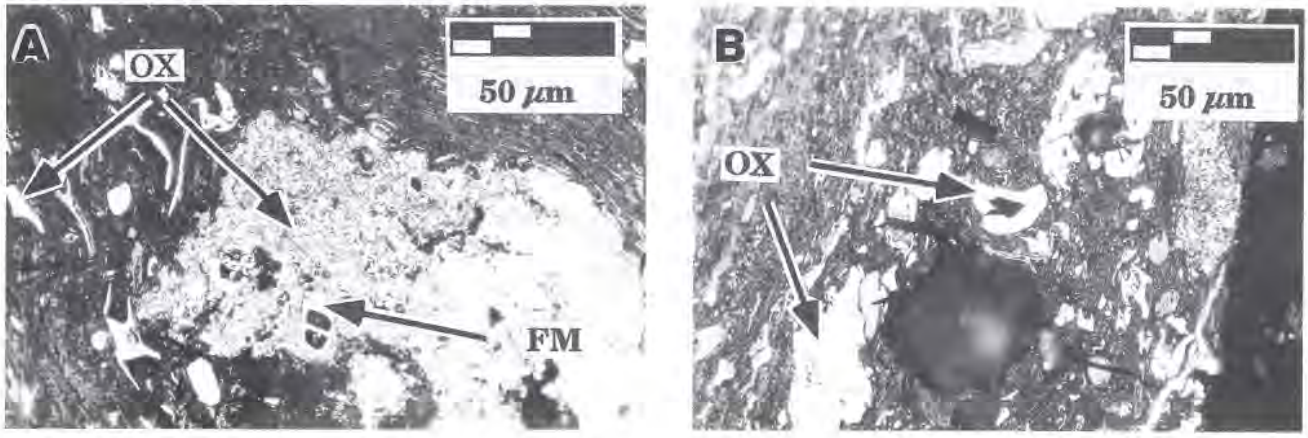

Figure 5. Photomicrographs of oxidized plant remains in the Anderson coal bed. Fragments of oxidized material (OX) are commonly associated with fungal remains (FM).

Table 3. Average palynomorph composition (in percent) of the Pintail (Cretaceous) and Anderson (Tertiary) coal beds. Numbers in bold are means, and standard deviations are shown in parentheses. Data is compiled from Pocknall (1986) and Roehler (1988).

Palynomorphs	Cretaceous (Almond Formation) Pintail coal bed[1]	Tertiary (Fort Union Formation) Anderson coal bed[2]
Pollen		
Gymnosperms	**16** (1.5)	**65** (11.7)
Angiosperms	**44** (4.9)	**34** (11.5)
Spores		
Pteridophytes & Bryophytes	**36** (3.8)	**1** (1.0)

[1]3 samples from three localities.
[2]21 samples from three cores.

Modern analogues

Understanding any sedimentologic setting depends on testing assumptions with modern analogues. Unfortunately, in comparison to other fields of sedimentary geology, there have been only limited studies on modern peat environments. However, in the case of the Pintail and Anderson coal beds, modern analogues have been proposed. Roehler (1988) cited the Okefenokee Swamp in the southeastern United States as an analogue to the Pintail coal bed. Flores (1981), Pocknall and Flores (1987), and Moore and others (1990) have suggested that the Anderson coal bed formed in a similar manner to modern mires in the Indo-Malesian region. Unfortunately, there rarely exists an exact match between modern and ancient systems. Sometimes this results from the lack of a true analogue, but more often it is because data collected are not wholly comparable. In the case of the Pintail and Anderson coal beds, criteria for an extensive point-by-point comparison with a modern analogue is not possible because of apparent data incompatibility. However, certain features of both the depositional setting and/or composition of the Pintail and Anderson coal beds suggest they may be correlative in many aspects to the modern settings of the Okefenokee and Palangkaraya mires, respectively.

Okefenokee swamp—Pintail coal bed

The Okefenokee Swamp lies 50 miles (90 km) west of the current Atlantic coastal shoreline (Figure 6). The swamp-marsh complex covers an area of approximately 1,020 square miles (1,700 square km) and peat ranges in thickness from 3.3 to 15 ft (1 to 4.6 m) (Cohen and others, 1984). Although open

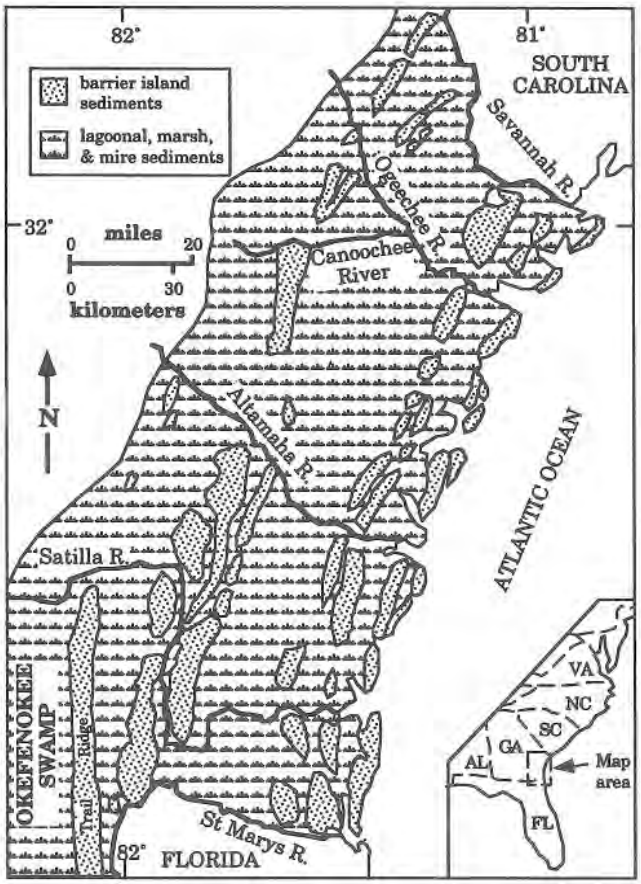

Figure 6. Distribution of Pleistocene relict barrier-bar sands on the eastern seaboard of the United States (modified from Cohen and others, 1984).

Figure 7. Photographs of Okefenokee Swamp. (A) Open water prairie with aquatic vegetation in the foreground and forest mire in the background. (B) Tree-dominated area of the Okefenokee.

areas of standing water and aquatic vegetation (known as prairies) are common, slightly elevated shrub and tree swamps are the dominant mire type (**Figure 7**). The swamp-marsh complex is bounded on the east by a sand high known as Trail Ridge. A number of theories exist for the origin of Trail Ridge, including development as a terrace, spit, or as a result of weathering. However, the theory that is generally accepted is from Hoyt and Hails (1969) and Pirkle (1984), who state that Trail Ridge, along with other sand ridges which parallel the coastal plain (**Figure 6**), are relict barrier-bar sequences deposited during the Pleistocene. The sand ridges are terraced, in the sense that seaward (eastward), each ridge occurs at a slightly topographically lower level than sand ridges to the west. The sand that comprises Trail Ridge is quartz dominated, well sorted and fine grained. The muds between the sand ridges are estuarine and lagoonal in origin and thus are bioturbated and sometimes rooted.

The peat of Okefenokee Swamp originated in disconnected, open, freshwater marshes long after the shoreline had prograded eastward (Cohen, 1973a). Using ^{14}C, the oldest peat in Okefenokee Swamp has been dated at 6,500 years BP (Cohen and others, 1984). The peat is low in inorganic material (ash <4%) and sulfur (<0.4%). The composition of the peat is determined by the original vegetation (Cohen, 1973b). Dominant peat types in Okefenokee Swamp are derived from *Nymphaea* (water lily) (55%) and *Taxodium* (bald-cypress) (35%). Peat from *Nymphaea* vegetation is fine grained, reddish brown, and fibrous to granular. Peat from the *Taxodium*-dominated forest is dark brown, coarse, and granular to woody. The remainder of the peat types (*Woodwardia*, *Panicum*, *Decodon*, and *Carex*-dominated) are termed "transitional" and represent less than 10% of all peat in the Okefenokee swamp-marsh complex (**Figure 8**). The composition of the peat from Okefenokee Swamp can be described as a ratio of intact plant parts versus fine-grained matrix (Cohen, 1973a). In the *Nymphaea* peats, there tends to be less well-preserved plant material and more abundant fine-grained matrix (ratio = 0.79). The transitional and *Taxodium* peats have roughly equal amounts of plant parts to matrix. *Taxodium* peats also contain more than 3% oxidized plant material derived from fire.

The most convincing feature of the Pintail coal bed relating it to Okefenokee Swamp is the association with barrier-bar sands. Cohen (1984) proposed that the Okefenokee Swamp may be a useful analogue to some coal beds associated with barrier-bar sediments. The model for Pintail palaeo-mire development in **Figure 9** integrates the ideas of Cohen (1984) and Roehler (1988). In the interpretation of

Roehler (1988), peat accumulation is in near proximity to offshore sedimentation. However, the low inorganic matter present within the coal indicates that it must have been sheltered from clastic sedimentation. Indeed, active accumulation of barrier-bar sands implies a high-energy environment (Barwis and Hayes, 1979), a setting practically incompatible with the development of low-ash peat. Therefore, the Pintail palaeo-mire may have formed after the barrier sands and lagoonal/estuarine environments were abandoned during shoreline progradation. Other barrier-bar sequences that may represent this shoreline progradation occur in the Almond Formation, and these underlie and overlie the Pintail coal bed and associated sediments (Flores, 1978; McCubbin, 1981; Roehler, 1988). The cause of the progradation is unknown, but may have been the result of any one of a number of factors, including drop in sea level or tectonism.

Other than general depositional setting, features of the Pintail coal bed are hard to correlate with those of the Okefenokee. For example, the composition of the Pintail coal tends to have a greater abundance of preserved plant material than the Okefenokee Swamp. In part this may be related to differences in plant type such as the presence of highly degraded *Nymphaea* peat in the Okefenokee Swamp, which has no correlative in the Pintail coal bed. Interestingly, both deposits contain a large fraction of recognizable tissue derived from conifers (gymnosperms), but this may be related to the decay-resistant nature of gymnosperms over that of other plant types.

Another difference between peat in Okefenokee Swamp and the Pintail coal bed is the low sulfur content of the peat as compared to the coal. Commonly, sulfur is introduced into buried peat from overlying marine sediments, rather than during peat accumulation. In the case of the Pintail coal bed, sulfur was probably introduced to the peat just after burial by the marine bay-fill sediments that overlie the coal.

Palangkaraya mire—Anderson coal bed

Areas of mire development in the Indo-Malesian region are extensive. In contrast to the Okefenokee Swamp, most of the mires in this region are characterized by surfaces that are raised up to 20 ft (6 m) above the level of surrounding streams. These raised surfaces are created by the large volumes of organic matter. The raised surface is maintained by continu-

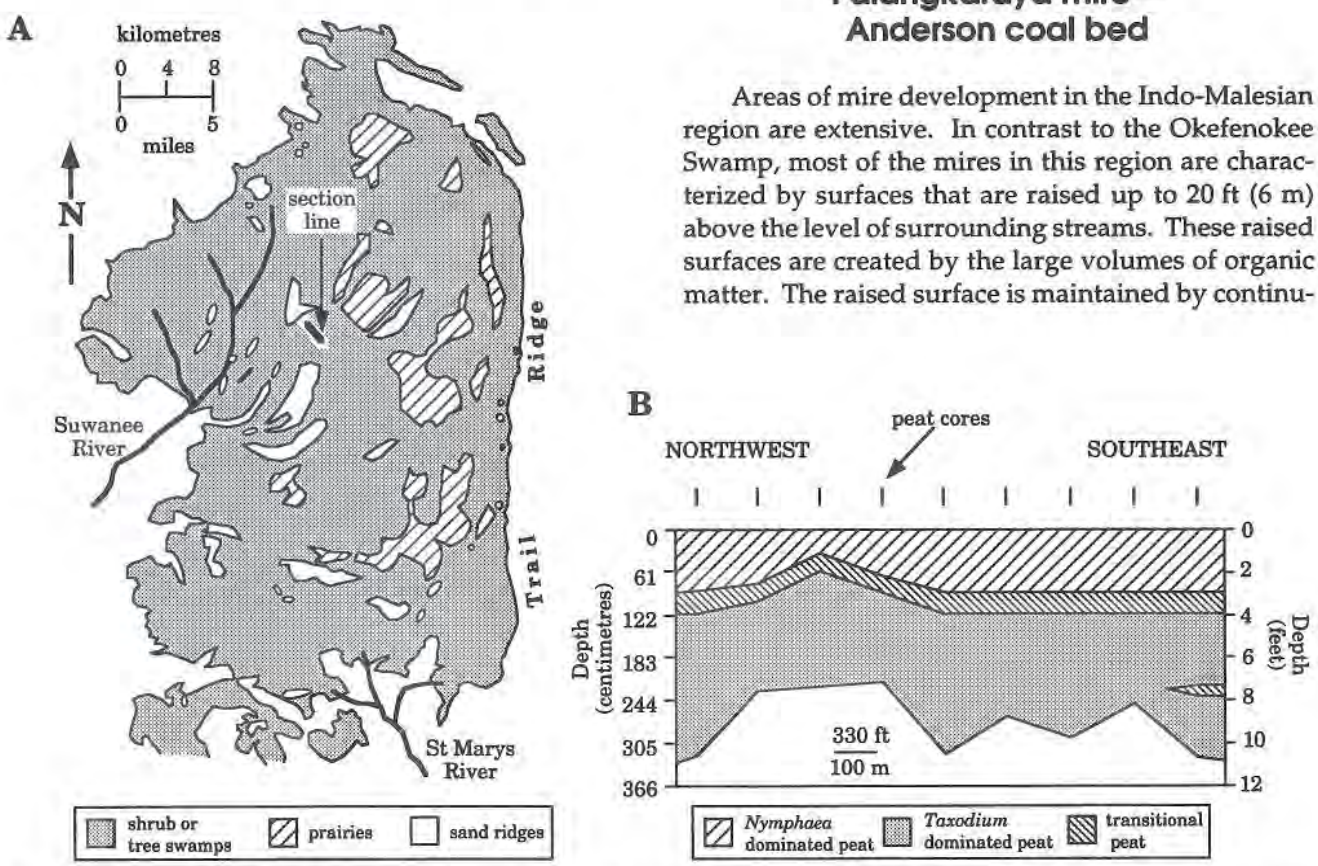

Figure 8. (A) Distribution of prairies and forests in Okefenokee Swamp. (B) Cross section through a portion of the mire showing peat types (modified from Cohen and others, 1984).

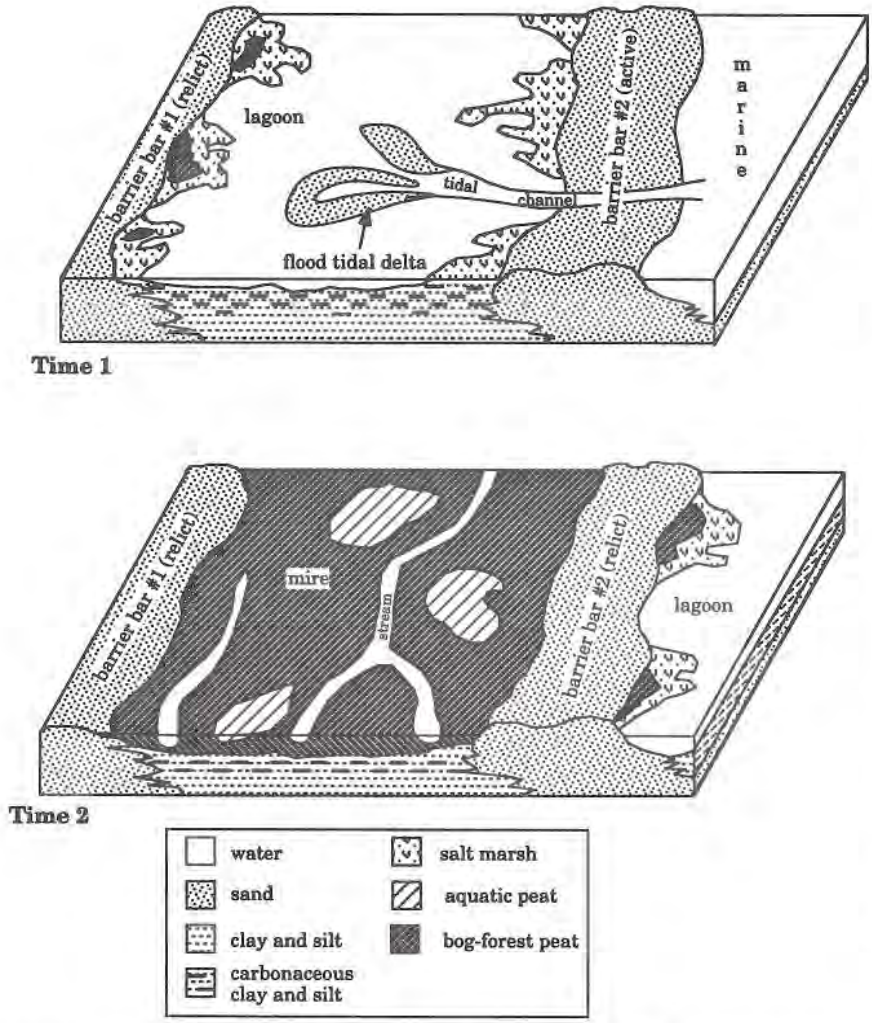

Figure 9. Interpretative model of depositional setting during the formation of the Pintail coal bed (modified from Roehler, 1988).

ous rain throughout the year, which aids in sustaining a perched water table essential to raised peat accumulation. Some mire surfaces have a pronounced relief of 17 to 20 ft (5 to 6 m), such as mires in the Baram River area of Sarawak, Malaysia (Anderson, 1964; Esterle and others, 1989; Esterle, 1990) and the Teluk Keramat deposit in Kalimantan Barat (Moore and Hilbert, 1992). Not all mires have such conspicuous relief; for example, the Jambi deposit in Sumatra (Cameron and others, 1990; Esterle, 1990) does not have an appreciably raised surface. Other deposits, such as some in the Kutai Basin, Kalimantan Timur (Moore, 1991), may have had a raised relief, but the surfaces have been deflated by fire and subsequently flooded and buried by clastic sediments (Staub and Cohen, 1979).

The Palangkaraya in Kalimantan Tengah, Borneo, Indonesia (**Figure 10**) is a raised mire dissected by a number of fluvial systems. Some of these fluvial systems are sourced from upland deposits such as the Rungan and Kahayan Rivers, which are sediment laden as evidenced from abundant point bar sequences (**Figure 11A**). Other streams, sourced within the mire, such as the Kemipang and Sebangau Rivers, carry essentially no sediment and are known as blackwater streams because of their high concentrations of dark colored tannic and humic acids.

The peat in the Palangkaraya mire can reach up to 19.8 ft (6 m) thick (**Figure 12**). Initiation of peat accumulation was approximately 10,000 years BP (Neuzil and Cecil, 1992), which is much older than the 6,000-7,000 years BP observed in other Indo-Malesian mires (Cameron and others, 1990; Esterle, 1990; Moore and Hilbert, 1992; Neuzil and Cecil, 1992). Not much is known of the substrate except that it is usually a dark gray mudstone, which is root penetrated from the overlying peat. Sometimes a leached white sand occurs below the peat (Prof. G. Sieferman, ORSTOM, Yogyakarta, personal communication, 1989). Lateral to the mire, levees have formed and are heavily vegetated (**Figure 11A**).

There are five peat types in the Palangkarya mire: (1) sapric—black, granular to amorphous (the least abundant type); (2) sapric/hemic—dark brown-black, granular to fibrous; (3) fine-grained hemic—brown, woody to fibrous; (4) coarse-grained hemic—brown and woody; and (5) clayey—contains high (>20%) concentrations of inorganic material.

The sapric and sapric/hemic peat types tend to occur at the top of the deposit and are the most degraded peat types. The surface of the mire is

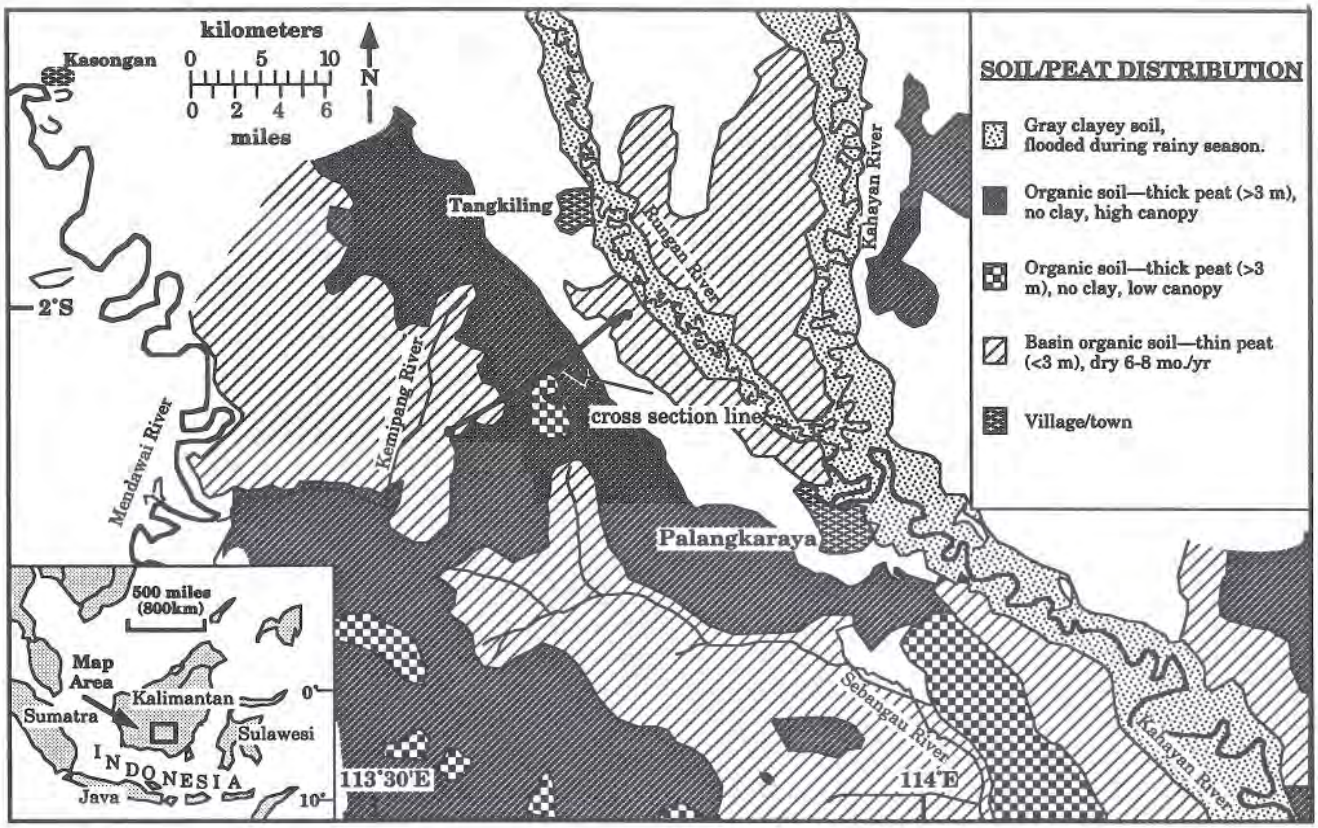

Figure 10. Soil distribution map in a modern peat-forming area in Kalimantan Tengah, Indonesia (modified from G. Sieferman, OSTROM, unpublished map, 1989). Cross section is shown in detail in Figure 12.

highly degraded because it remains aerobic, and allows higher levels of microbial decay than anaerobic (water-logged) peat. Unlike other domed mires, which have a perched water table near the surface (within 8 in/20 cm), the water table in the Palangkaraya deposit is often ~3 ft (1 m) below the surface. The cause of the low water table is not known but may be the result of a lack of continuous rain throughout the year (Prof. G. Siefermann, ORSTOM, Yogyakarta, personal communication, 1989). Preliminary microscopic analysis of the upper ~3 ft (1 m) of the peat also shows a high (10-15%)

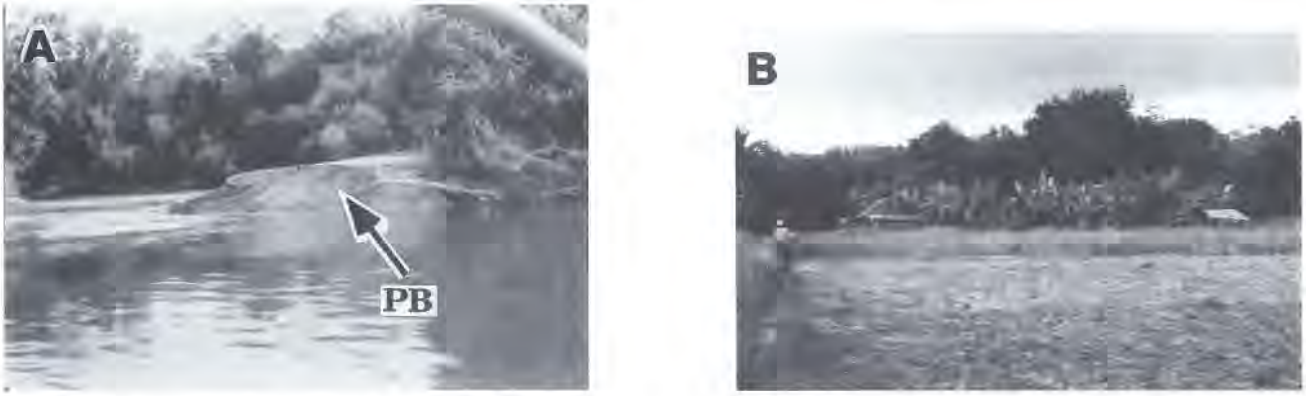

Figure 11. Photographs of peat-forming areas in the Palangkaraya mire. (A) Point-bar (PB) and levee (trees in the background) deposits on the east side of the Palangkaraya mire. (B) Rice farming on thin areas of peat in Kalimantan. Trees in background mark the beginning of thick (> 7 ft/2 m) peat.

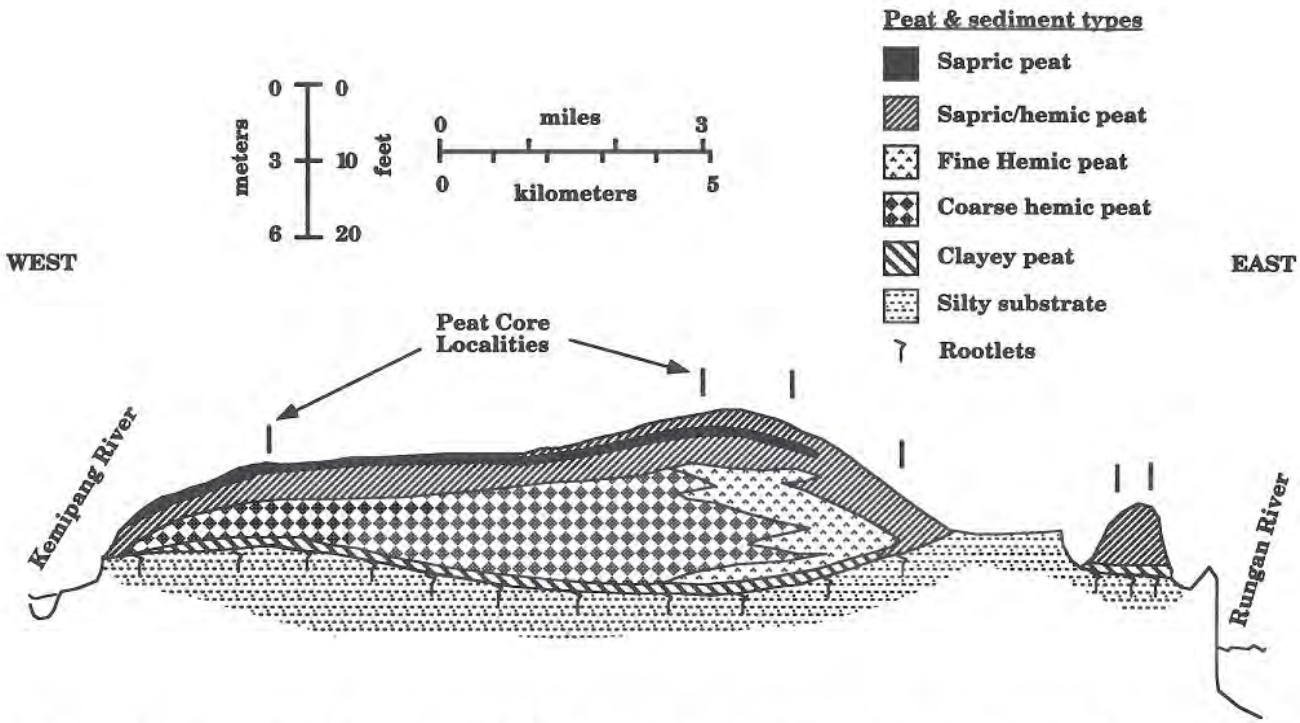

Figure 12. Cross section of the Palangkaraya mire showing distribution of peat types (modified from T.A. Moore and C.B. Cecil, unpublished data, 1990).

concentration of oxidized plant remains (**Figure 13**). The high amount of degradation may signal the death of the Palangkarya mire. A continued low water table will result in further degradation and oxidation (Prokopovich, 1985) , thus lowering the raised peat surface (Edil and others, 1986) and allowing clastic sediment to bury the mire.

The vegetation in the mires of the Palangkaraya area has been studied by Morley (1981). His pollen analysis indicates that the initial mire community was dominated by reeds, mosses, and palms. However, with development of a thick (>3 ft/1 m) peat substrate, the vegetation changed to one dominated by arborescent angiosperms such as *Shorea*,

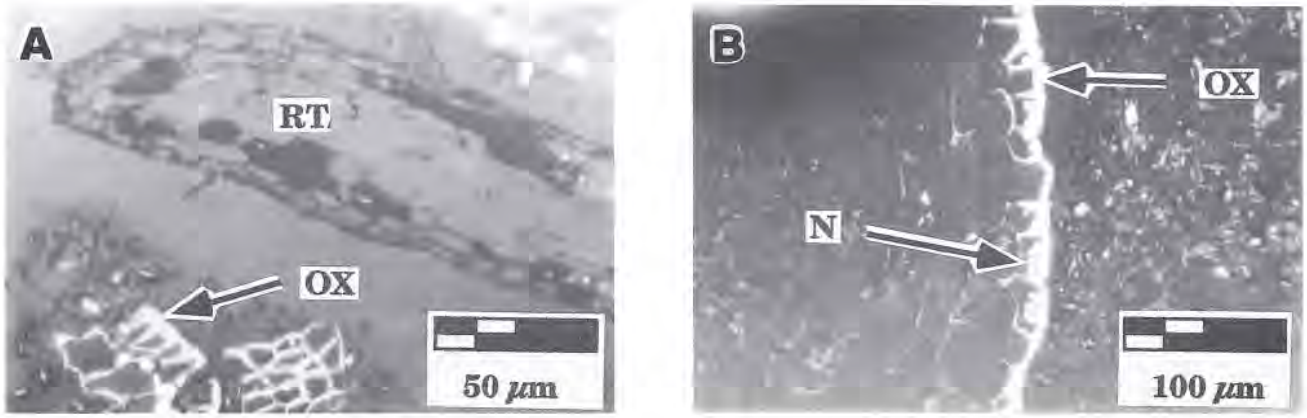

Figure 13. Photomicrographs of oxidized plant material from the top of the Palangkaraya peat. (A) RT is an unoxidized root with only primary tissue as compared to oxidized cell-wall material (OX). (B) Oxidized epidermal layer of a primary root (OX) with intercellular nodules, which indicate aerobic fungal alteration.

Combretocarpus and *Campnosperma*, and the gymnosperm *Dacrydium*.

Several lines of evidence make the Anderson coal bed comparable to the Palangkaraya peat deposit in Kalimantan Tengah, Indonesia. First, the interpreted depositional setting of the Anderson coal bed is similar to that of the Palangkaraya mire. The Palangkaraya peat has formed within a fluvial depositional setting well removed from marine sedimentation. Interpretation of the Anderson coal bed depositional setting also places it within a freshwater fluvial sedimentary regime 100 miles (160 km) from sites of marine sedimentation (Flores, 1983). Specific clastic sediments associated with both deposits are derived from fluvial point-bar channel sands and overbank/levee silts and sands. **Figure 14** is a reconstruction of the depositional setting and ultimate termination of the Anderson palaeo-mire based on the observations made in this paper and by Pocknall and Flores (1987) and Moore and others (1990). It should be noted, however, that alternative peat-forming models have been proposed for other Powder River Basin coal beds, for example the models of Ayers and Kaiser (1984) and McClurg (1988).

In addition to the similarity in sedimentary setting, the Anderson coal bed is compositionally similar to the Palangkarya mire. In both the coal and peat, there are significant concentrations of oxidized plant remains near the top of the deposit. As in the Palangkaraya mire, the oxidized plant material in the upper Anderson coal bed may indicate a lowered water table, which resulted in increased microbial oxidation and deflated the mire surface to a point where burial by clastic sediments could occur.

The vegetation of the Palangkaraya and Anderson deposits are not directly comparable because of their disparate ages and geographic locations. However, succession in plant types [as deduced from palynological analyses by

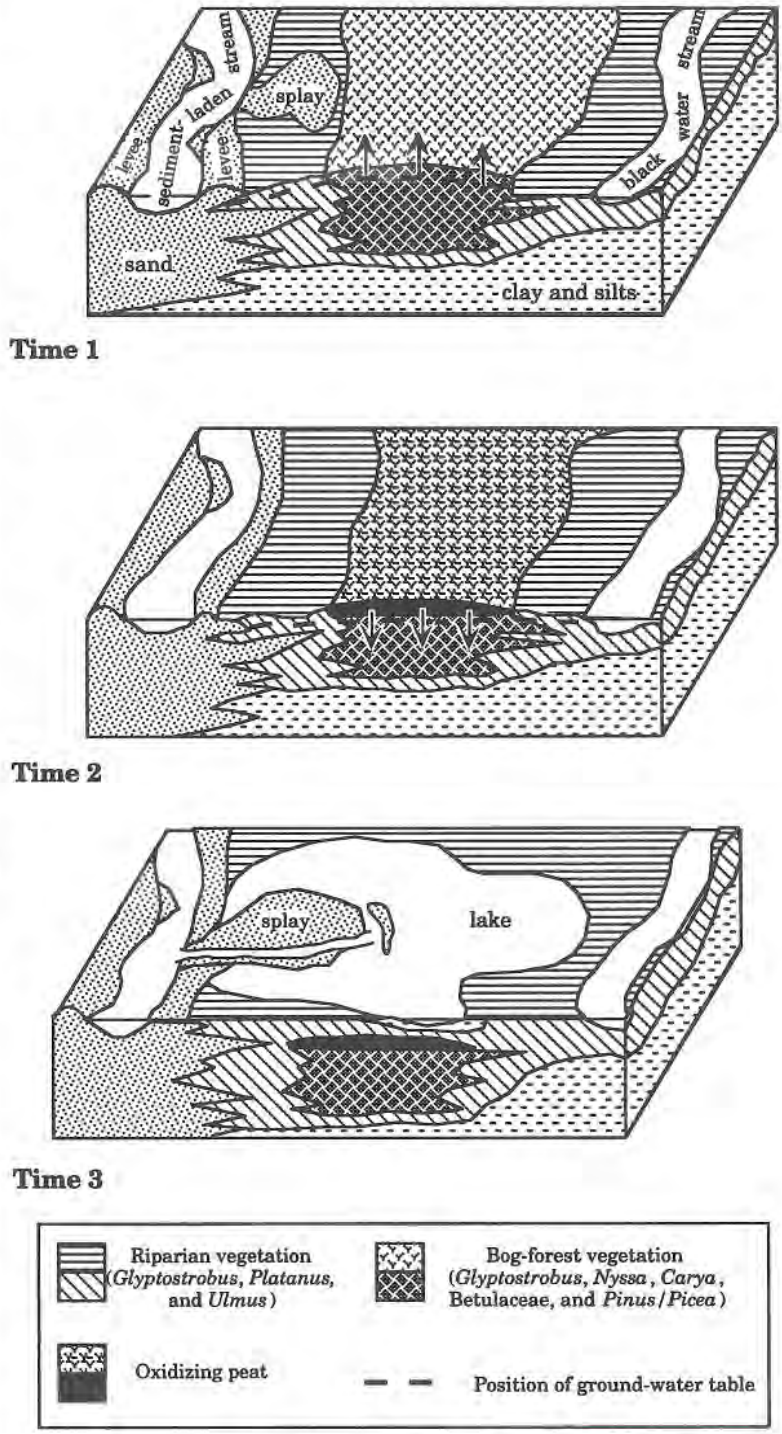

Figure 14. Interpretative model of depositional setting during formation of the Anderson coal bed. Time 1: Peat accumulation in a domed mire with a perched (from abundant rainfall) water table. Arrows indicate that the mire surface is actively accreting upwards. Time 2: Hydrology of the mire is changed (possibly from a decrease in rainfall) and drop in water table causes upper layer of peat to oxidize and 'deflate'. Arrows indicate that the surface is being lowered in relation to surrounding stream levels. Time 3: With the surface of the peat mire lowered, ponds or lakes form, which are subsequently filled with sediment that terminates peat accumulation.

Morley (1981), Moore and others (1990)] from initial mire communities to well-developed mires is seen in both the Anderson coal and the Palangkaraya peat. Change (*i.e.*, succession) in the vegetation within the modern (and ancient) mires is probably related to the development of a thicker, more nutrient-poor peat substrate, in which only certain types of vegetation are able to flourish (Morley, 1981).

The conundrum of thickness

Defining criteria for recognition of modern analogues is not always easy. As has been shown in both the Pintail/Okefenokee and Anderson/Palangkaraya comparisons, some criteria fit while others do not. It is for this reason that geologists must have recourse to their imagination and the scientific method. Coal-bed thickness is one discrepancy that affects not only the Okefenokee Swamp and Palangkaraya mires as modern analogues for coal formation, but all other presently known peat environments. Estimates of compaction ratios from peat to coal range from 3:1 (3 ft of peat is needed to make 1 ft of coal) to over 20:1 (Ryer and Langer, 1980). Even a conservative estimate of 3:1 would require peat thicknesses of 300 ft (90 m) or more to explain some of Wyoming's thick coal deposits. Such thicknesses have never been observed in modern mires. Therefore, addressing the conundrum of peat and coal bed thicknesses, which are apparently not comparable, is paramount when evaluating the validity of modern peat analogues and applying them to ancient coal equivalents.

When evaluating the suitability of modern peat models in regard to thickness of resultant coal beds, two aspects must be considered. The first is determination of the actual amount of compaction peat undergoes to produce coal, which involves estimates of compaction of organic constituents themselves in relation to the loss of the surrounding pore space. The second aspect relates to mire development—does a single coal bed represent accumulation of peat in a single mire or a sucession of mires separated by hiatuses in peat deposition?

Compaction

As stated earlier, compaction ratios for peat to coal vary widely. Common misconceptions are that compaction is relatively uniform throughout a single peat deposit (or coal bed) and that the majority of the compression of peat occurs after burial of the deposit. Some experimental peat compression studies show that different peat types have different compressibilities. Berry and Poskit (1972) found that peat composed mostly of fine fibrils of well-preserved plant material are extremely compressible, whereas peat types composed of fine-grained amorphous material have a plastic structural resistance to compression similar to clays. It is also known that wood (secondary xylem) preserved in peat does not compress appreciably even into the subbituminous stage of coalification. Therefore the variation in peat compressibility is related at least in part to peat type. A mire containing more than one peat type, as is seen in both the Okefenokee Swamp and Palangkarya mire, will undergo differential compaction in areas where the different peat types occur. Applied to coal beds, differential compaction means that a highly degraded coal type (durain or cannel coal) or a very woody coal, (vitrain rich) will have been compressed much less than finely banded coal (clarain).

Another aspect of compaction which needs to be considered is determination of what exactly is being compressed and when this compression is occurring. Comparisons of the size of peat constituents with that of similar organic particles found in coals (lignite to bituminous in rank), have shown that the particles have not been compressed appreciably after the peat stage (Esterle and others, 1992; Moore and Ferm, 1992; Moore and Hilbert, 1992; Demchuk and Moore, 1993). Instead of a decrease in organic particle size, compression of the peat is primarily a loss of pore space between the organic particles. Fenton (1980) and Johnson and others (1990) found that compression of organic components in peat occurs in the upper 8 to 11 in (20 - 30 cm) of the mire. In this zone, compression of plant material by as much as 5:1 is a result of a loss of organic material within plant structures from microbial decay. Below this zone, compression of plant material halts and the weight of the overlying accumulating peat mass causes a loss in pore space and a gain in bulk density.

Trying to apply compaction ratios to coal beds involves extremely complex formulations because compaction will vary vertically and laterally as a result of changing peat types. If realistic estimates of compaction are to be made, detailed examination of vertical peat profiles and coal beds must be performed and volumetric evaluation of various peat (or coal) types within a single bed must be delineated. In addition, further work on mires is needed to estimate the degree of autocompaction that has occurred at different levels in the peat.

Stacked peat bodies

Even though compaction ratios are difficult to calculate it seems as though proposed ratios are so large that comparison of peat to coal bed thickness change is incompatible. The maximum thickness of peat observed anywhere in the world is 56 ft (17 m), in Borneo (Anderson, 1964; Esterle and others, 1989). In contrast, coal bed thicknesses in Wyoming reach 200 ft (61 m) and greater. Even with a compaction ratio of 3:1, there is an order of magnitude difference between the thickness of Bornean peat and Wyoming coal. However, when coal beds are examined in detail it becomes apparent that, in thick seams, inorganic sediments (partings) as well as highly degraded and/or oxidized intervals are present. Intervals of coal between these partings are referred to as benches or plys. Staub (1991) postulated that a single bench of coal may be compared to a single peat body, rather than comparing the whole seam to a single mire. Thus, each parting or degraded interval may represent the termination of an individual mire, and stacked coal benches separated by partings may represent several generations of individual mire deposits.

A conceptual problem in stacking of mires is that one envisions a peat 'hill' developing to provide enough material for a thick coal seam when compacted. However, significant peat compaction must be occurring before and after deposition of partings as it is clear that stacks of peat several hundreds of feet (tens of meters) thick cannot occur. Staub (1991) documented sequential compaction of peat during burial of a Carboniferous palaeo-mire (coal bed). Compaction allowed for subsequent influx of sediment, which covered the peat surface. Relatively thin inorganic partings deposited on a peat would place a load pressure on the surface and result in further compression of the underlying peat material (Fielding, 1984; Flood and Brady, 1985; Edil and others, 1986; Moore, 1991). In this way, the peat of each mire would be significantly compacted before initiation of the next mire. In some cases, as in the Palangkaraya deposit, a lowering of the water table may have the same effect as an inorganic parting. It is well documented that oxidation of the peat when the water table is lowered results in a 'deflation' of the peat surface (Prokopovich, 1985; Edil and others, 1986). There is evidence for both oxidative deflation and compression as a result of sediment incursion in the case of the Anderson palaeo-mire (see **Figure 4**).

In reporting coal-bed geometry, total seam thickness is usually reported, but partings less than 1 ft (0.3 m) thick are typically ignored. Thus, an erroneous impression may be imparted that thick coal beds exhibit no evidence of stacked mire development. Close examination of the thick Powder River Basin coal beds reveals that most are dissected into significantly smaller benches by partings. For example, the Big George coal bed in the the Powder River Basin has a reported thickness of 201 ft (61 m), but the coal is split by at least six inorganic partings, whose thicknesses range from 1 to 3 in (3 to 7 cm) (Chao and others, 1984). The thickness of the coal benches between the inorganic partings range from 3 to 21 ft (1 to 7 m). When decompacted using a 5:1 ratio, a postulated peat thickness for those benches would range from 16.5 to 105 ft (5 to 32 m), which is of the same magnitude as observed modern peat thicknesses.

In another example, the Wyodak-Anderson coal bed in the eastern Powder River Basin has a reported thickness of 175 ft (53 m), but contains partings 1.5 to 6 ft (0.5 to 2 m) thick (Warwick and Stanton, 1988). These partings divide the coal bed into benches ranging from 20 to 56 ft (6 to 17 m) thick and when decompacted (5:1) they would range from 100 to 280 ft (30 to 85 m) thick. In this case, the thickest bench cannot be easily explained in terms of modern observed peat thicknesses. However, recognition of intervals that may have signaled a hiatus in peat accumulation can be difficult. For example, identification of cessation of peat accumulation as a result of oxidative deflation (as is thought to be occurring in the Palangkaraya mire) requires detailed sampling and analysis. Although the Wyodak-Anderson coal

bed was studied petrographically, the intervals sampled were relatively thick [generally 1.5 to 9 ft (0.5 to 3 m)]. This coarseness of sampling may have precluded detection of intervals that were high in oxidized plant remains. In the study of the Anderson coal bed, incremental increases in oxidized plant material could only be detected by using relatively fine sampling units.

The presence of inorganic partings (mire terminations) may also be difficult to recognize because the bulk of the inorganic material may have been removed or because the parting was not deposited throughout the peat. Inorganic material (partings) may be removed through intense leaching, which would be expected in an acidic mire environment (Triplehorn and others, 1991) or by flocculation at mire margins (Staub and Cohen, 1979). Thus, degradation and mire death may occur without development or preservation of a parting. Flocculation of sediment at the margins may have occurred in the thick (53 ft or 16 m) Anderson-Dietz #1 coal bed in the northwestern part of the Powder River Basin (Moore, 1991). Eastward, the coal bed is split into two benches by as much as 149 ft (45 m) of detrital inorganic sediment. The thicknesses of the coal benches are approximately 26 ft (8 m) (the upper Anderson coal bed) and 20 ft (6 m)(the lower Dietz #1 coal bed). The thicknesses of the two benches taken together are comparable to the total thickness of coal where the two seams merge into one coal bed with no parting. Detailed chemical and petrographic analysis of the coal from where the benches are merged shows an interval (about 2 ft or 0.6 m thick) that is high in degraded plant material but low in inorganic content. This interval is thought to be laterally equivalent to the inorganic sediments. Cessation of peat accumulation (and possibly even losses of plant material in the peat deposit) probably occurred during this time, although it is not marked by an inorganic parting.

If both oxidized layers and inorganic partings are used to indicate benches in the Anderson coal bed (**Figure 4**), then the thickest bench is less then 8.3 ft (2.5 m). Using a moderate compaction ratio of 5:1, this would yield a 41.5 ft thick (12.6 m) peat, which is well within documented peat thicknesses described in Sarawak, Malaysia (Anderson, 1964; Esterle and others, 1989). The Pintail coal bed, which has no more than 5.3 ft (1.6 m) of unsplit coal would have originated from a peat less than 26.5 ft (8.0 m) thick.

From the data cited for the Wyodak-Anderson, Anderson-Dietz #1, and Big George coal beds, it appears that thick coal deposits, which are generally referred to as single entities, are actually composed of a number of benches separated by partings (either true inorganic partings or degradative 'partings'). These benches probably represent complete and separate mire systems, each of which underwent appreciable compaction when loaded by inorganic sediment or autocompaction during oxidation. When coal is viewed as one bench equals one mire (Staub, 1991), observed peat thicknesses of modern mires are much more comparable. One apparent problem is that most modern peat studies have not identified stacked mires separated by partings. This may be the result of peat sampling methods. Typically, the coring apparatus used for peat sampling does not penetrate more than 4 to 11 in. (10 to 30 cm) into the inorganic substrate below a mire, thus precluding documentation of stacked peat deposits.

Conclusions

Wyoming coal deposits formed in a variety of depositional settings ranging from coastal plain to freshwater, fluvial-dominated environments. The Cretaceous Pintail coal bed peat accumulated in association with barrier-bar and lagoonal/estuarine sediments. It is not clear when the Pintail palaeopeat accumulation occurred relative to deposition of the surrounding clastic sediments. However, it is likely that the peat was deposited after active sedimentation had ceased in the area, as evidenced by the low inorganic content of the Pintail coal bed. Burial by sulfate-bearing marine sediments could account for the high sulfur content in the coal bed. Floral composition, as determined by palynological analysis, indicates that the Pintail palaeo-mire was comprised dominantly of angiosperms, ferns, and

mosses with only a minor component of gymnosperms. Limited botanical data, however, shows that the Pintail coal bed contains plant material of gymnosperm secondary xylem. A modern analogue for the Cretaceous Pintail coal bed may be Okefenokee Swamp in the southeastern United States. Although floral and compositional differences do exist, the depositional settings are comparable.

In contrast to the coastal plain setting of the Pintail coal bed, the Tertiary Anderson coal bed formed well removed from marine sedimentation in a freshwater, fluvial-dominated environment. Although the Anderson coal bed formed proximal to fluvial channels and associated overbank and splay environments, the coal bed is consistently low in inorganic constituents. The majority of the palaeo-mire may have been shielded from surrounding clastic sedimentation by doming in a manner similar to modern raised mires of the Indo-Malesian region. The surfaces of these mires are topographically higher than surrounding streams as a result of biomass accumulation over a raised water table. The raised surfaces of these mires help to prevent the influx of sediment from surrounding channels. The organic and floral composition of the Anderson coal bed is comparable to that of the Palangkaraya mire in Kalimantan, Indonesia. Plant succession is seen in both deposits, although a fundamental difference is that the Anderson coal bed was apparently dominated by gymnosperm vegetation with subordinate amounts of angiosperms, whereas the Palangkaraya mire is dominated by arborescent angiosperms. Changing plant communities reflected in both the Anderson coal bed and the Palangkaraya peat are probably an ecological adaptation of the vegetation to a thickening of the peat substrate and consequent decrease in nutrient supply. Oxidized plant remains also occur in high concentrations near the tops of both the Anderson coal bed and Palangkaraya peat. The oxidized remains in the Palangkaraya mire are probably the result of a drop in water table, which allowed microbial alteration of the peat. This oxidized zone may signal the death and subsequent 'deflation' of the Palangkaraya mire and may also be analogous to the termination of peat accumulation in the Anderson palaeo-mire.

Finally, when comparing coal bed thicknesses with those of modern mires, studies must be made on a bench-by-bench basis rather than on the scale of whole coal beds. Each bench of coal equates to an individual peat deposit and thus thick seams, such as those in Wyoming, are probably derived from stacked peat bodies. The intervals that separate benches (*i.e.*, individual mires) may be very evident where inorganic sediment accumulation has occurred. However, some of these intervals may be degradational 'partings' represented in the coal only by highly degraded and sometimes oxidized plant remains. In these cases, recognition of coal benches becomes problematic, and detailed petrographic and chemical analyses are needed.

Acknowledgments

The concepts and ideas presented in this paper are largely a product of numerous discussions with our colleagues. We would especially like to thank C.B. Cecil, J.S. Esterle, J.C. Ferm, R.M. Flores, J. Newman, R.W. Stanton, J.R. Staub, and P.D. Warwick, all of whom have contributed much to the authors' understanding of coal (peat) development. Specific data for the Palangkaraya mire in Indonesia were obtained as part of a National Research Council Post-Doctoral Fellowship at the U.S. Geological Survey granted to the senior author. The peat project in Indonesia was part of a broader study of modern analogues of coal formation being conducted by the U.S. Geological Survey and the Directorate of Mineral Resources of Indonesia. Thanks to Professor G. Sieferman for his kind assistance in the field and numerous discussions on processes controlling the formation of mires in Indonesia. Many thanks to C. Blaine Cecil for his enthusiasm for peat research and for providing the opportunity to study the mires in Indonesia. The authors also wish to acknowledge the great care Stephen B. Roberts, R. Farley Fleming, and Gary B. Glass took in reviewing this paper.

References cited

Anderson, J. A. R., 1964, The structure and development of the peat swamps of Sarawak and Brunei: Journal of Tropical Geography, v. 18, p. 7-16.

Ayers, W. B., and Kaiser, W. R., 1984, Lacustrine-interdeltaic coal in the Fort Union Formation (Paleocene), Powder River Basin, Wyoming and Montana, *in* Rahmani, R.A., and Flores, R. M., editors, Sedimentology of coal and coal-bearing sequences: International Association of Sedimentologists Special Publication 7, p. 61-84.

Barwis, J. H., and Hayes, M. O., 1979, Regional patterns of modern barrier island and tidal inlet deposits as applied to paleoenvironmental studies, *in* Ferm, J. C., and Horne, J. C., editors, Carboniferous depositional environments in the Appalachian region: Columbia, South Carolina, Carolina Coal Group, Department of Geology, University of South Carolina, p. 472-498.

Berry, P. L., and Poskitt, T. J., 1972, The consolidation of peat: Géotechnique, v. 22, p. 27-52.

Cameron, C. C., Esterle, J. S., and Palmer, C. A., 1990, The geology, botany and chemistry of selected peat-forming environments from temperate and tropical latitudes, *in* Lyons, P. C., and Alpern, B., editors, Peat and coal: origin, facies and depositional models: International Journal of Coal Geology, v. 12, p. 105-156.

Chao, E. C. T., Minkin, J. A., Back, J. M., and Pierce, F. W., 1984, Petrographic characteristics and depositional environment of the Paleocene 61-m-thick subbituminous Big George coal bed, Powder River Basin, Wyoming: 1984 Symposium on the Geology of Rocky Mountain Coal, Bismarck, North Dakota, North Dakota Geological Society, p. 41-60.

Cohen, A. D., 1973a, Petrology of some Holocene peat sediments from the Okefenokee swamp-marsh complex of southern Georgia: Geological Society of America Bulletin, v. 84, p. 3867-3878.

_____ 1973b, Possible influences of subpeat topography and sediment type upon the development of the Okefenokee swamp-marsh complex of Georgia: Southeastern Geology, v. 15, p. 141-151.

_____ 1984, The Okefenokee Swamp: a low-sulphur end-member of a shoreline-related depositional model for coastal plain coals, *in* Rahmani, R.A., and Flores, R. M., editors, Sedimentology of coal and coal-bearing sequences: International Association of Sedimentologists Special Publication 7, p. 231-240.

Cohen, A. D., Andrejko, M. J., Spackman, W., and Corvinus, D., 1984, Peat deposits of the Okefenokee Swamp, *in* Cohen, A. D., Casagrande, D. J., Andrejko, M. J., and Best, G. R., editors, The Okefenokee Swamp: its natural history, geology and geochemistry: Los Alamos, New Mexico, Wetland Surveys, p. 493-553.

Demchuk, T. D., and Moore, T. A., 1993, Palynofloral and organic characteristics of a Miocene bog-forest, Kalimantan, Indonesia: Organic Geochemistry, v. 20, p. 119-134.

Edil, T. B., Bosscher, P. J., and DeWitt, C. B., 1986, Compression and gravity drainage as means of dewatering peat, *in* Fuchsman, C. H., editor, Peat and water: Amsterdam, Elsevier, p. 21-36.

Esterle, J. S., 1990, Trends in petrographic and chemical characteristics of tropical domed peats in Indonesia and Malaysia as analogues for coal formation [Ph.D. dissertation]: Lexington, University of Kentucky, 270 p.

Esterle, J. S., Ferm, J. C., and Yiu-Liong, T., 1989, A test for the analogy of tropical domed peat deposits to "dulling up" sequences in coal beds—preliminary results: Organic Geochemistry, v. 14, p. 333-342.

Esterle, J. S., Moore, T. A., and Shearer, J. C., 1992, Comparison of macroscopic and microscopic size analyses of organic components in both coal and peat: 26th Newcastle Symposium: Advances in the study of the Sydney Basin, Newcastle, NSW, Australia, April 3-5, 1992, p. 143-149.

Fenton, J. H. C., 1980, The rate of peat accumulation in Antarctic moss banks: Journal of Ecology, v. 68, p. 211-228.

Fielding, C. R., 1984, 'S' or 'Z' shaped coal seam splits in the coal measures of County Durham: Proceedings of the Yorkshire Geological Society, v. 45, p. 85-89.

Flood, P. G., and Brady, S. A., 1985, Origin of large-scale crossbeds in the Late Permian coal measures of the Sydney and Bowen basins, eastern Australia: International Journal of Coal Geology, v. 5, p. 231-245.

Flores, R. M., 1978, Barrier and back-barrier environments of deposition of the Upper Cretaceous Almond Formation, Rock Springs uplift, Wyoming: The Mountain Geologist, v. 15, p. 57-65.

_____ 1980, Fluvial coal settings of the Tongue River Member of the Fort Union Formation in the Powder

River-Clear Creek area, Wyoming, *in* Glass, G. B., editor, Guidebook to the coal geology of the Powder River Basin, Wyoming: Geological Survey of Wyoming Public Information Circular 14, p. 71-95.

_____ 1981, Coal deposition in fluvial paleoenvironment of the Paleocene Tongue River Member of the Fort Union Formation, Powder River Area, Wyoming and Montana, *in* Ethridge, F. G., and Flores, R. M., editors, Recent and ancient nonmarine depositional environments: models for exploration: Society of Economic Paleontologists and Mineralogists Special Publication 31, p. 169-190.

_____ 1983, Basin facies analysis of coal-rich Tertiary fluvial deposits, northern Powder River Basin, Montana and Wyoming, *in* Collinson, J. D., and Lewin, J., editors, Modern and ancient fluvial systems: International Association of Sedimentologists Special Publication 6, p. 501-515.

Flores, R. M., and Hanley, J. H., 1984, Anastomosed and associated coal-bearing fluvial deposits: Tongue River Member, Paleocene Fort Union Formation, northern Powder River Basin, Wyoming, *in* Rahmani, R. A., and Flores, R. M., editors, Sedimentology of coal and coal-bearing sequences: International Association of Sedimentologists Special Publication 7, p. 85-103.

Glass, G. B., 1976, Analyses and measured sections of 54 Wyoming coal samples: Geological Survey of Wyoming Report of Investigations 11, 219 p.

_____ 1977a, Update on the Hams Fork coal region: Wyoming Geological Association 29th Annual Field Conference Guidebook, p. 689-706.

_____ 1977b, Wyoming coal deposits, *in* Murray, D.K., editor, Geology of Rocky Mountain coal: Colorado Geological Survey Resource Series 1, p. 73-84.

_____ 1978, Wyoming coal fields: Geological Survey of Wyoming Public Information Circular 9, 91 p.

_____ 1981, Coal deposits of Wyoming: Wyoming Geological Association 32nd Annual Field Conference Guidebook, p. 181-236.

Glass, G. B., and Jones, R. W., 1991, Coal fields and coal beds of Wyoming: Wyoming Geological Association 42nd Annual Field Conference Guidebook, p. 133-167.

Glass, G. B., and Roberts, J. T., 1978, Update on the Wind River coal basin: Wyoming Geological Association 30th Annual Field Conference Guidebook, p. 363-377.

_____ 1979, Remaining strippable coal resources and strippable reserve base of the Hanna coal field in southcentral Wyoming: Geological Survey of Wyoming Report of Investigations 17, 166 p.

Glass, G. B., Westervelt, K., and Oviatt, C. G., 1975, Coal mining in the Bighorn coal basin of Wyoming: Wyoming Geological Association 27th Annual Field Conference Guidebook, p. 221-228.

Hoyt, J. H., and Hails, T. P., 1969, Pleistocene shorelines in a relatively stable area, southeastern Georgia, U.S.A.: Giornale de Geologia, v. 35, p. 105-117.

Johnson, L. C., Damman, A. W. H., and Malmer, N., 1990, *Sphagnum* macrostructure as an indicator of decay and compaction in peat cores from an ombrotrophic south Swedish peat bog: Journal of Ecology, v. 78, p. 633-647.

Jones, R. W., 1982, The Jackson Hole coal field: Wyoming Geological Association 33rd Annual Field Conference Guidebook, p. 315-321.

McClurg, J. E., 1988, Peat-forming wetlands and the thick Powder River Basin coals: Wyoming Geological Association 39th Annual Field Conference Guidebook, p. 229-236.

McCubbin, D. G., 1981, Barrier-island and strand-plain facies, *in* Scholle, P. A., and Spearing, D., editors, Sandstone depositional environments: American Association of Petroleum Geologists Memoir 31, p. 247-279.

Moore, T. A., 1991, The effects of clastic sedimentation on organic facies development within a Tertiary subbituminous coal bed, Powder River Basin, Montana, U.S.A.: International Journal of Coal Geology, v. 18, p. 187-209.

Moore, T. A., and Ferm, J. C., 1992, Composition and grain-size of an Eocene coal bed in southeastern Kalimantan, Indonesia: International Journal of Coal Geology, v. 21, p. 1-30.

Moore, T. A., and Hilbert, R. E., 1992, Petrographic and anatomical characteristics of plant material from two peat deposits of Holocene and Miocene age, Kalimantan, Indonesia: Review of Palaeobotany and Palynology, v. 72, p. 199-227.

Moore, T. A., Stanton, R. W., Pocknall, D. T., and Flores, R. M., 1990, Maceral and palynomorph facies from two Tertiary peat-forming environments in the Powder River Basin, U.S.A.: International Journal of Coal Geology, v. 15, p. 293-316.

Morley, R. J., 1981, Development and vegetation dynamics of a lowland ombrogenous peat swamp in

Kalimantan Tengah, Indonesia: Journal of Biogeography, v. 8, p. 383-404.

Neuzil, S. G., and Cecil, C. B., 1992, Evidence in peat of Late Quaternary climate and sea level change, western Indonesia: Geological Society of America Abstracts with Programs, v. 24, no. 7, p. A50.

Obernyer, S. L., 1980, The Lake De Smet coal seam, *in* Glass, G. B., editor, Guidebook to the coal geology of the Powder River Basin, Wyoming: Geological Survey of Wyomin, Public Information Circular 14, p. 31-70.

Pirkle, F. L., 1984, Environment of deposition of Trail Ridge sediments as determined from factor analysis, *in* Cohen, A. D., Casagrande, D. J., Andrejko, M. J., and Best, G. R., editors, The Okefenokee Swamp: its natural history, geology and geochemistry: Los Alamos, N.M., Wetland Surveys, p. 629-650.

Pocknall, D. T., 1986, Palynological data from the Fort Union and Wasatch formations, Powder River Basin, Wyoming and Montana. U.S. Geological Survey Open File Report 86-117, 58 p.

Pocknall, D. T., and Flores, R. M., 1987, Coal palynology and sedimentology in the Tongue River Member, Fort Union Formation, Powder River Basin, Wyoming: Palaios, v. 2, p. 133-145.

Prokopovich, N. P., 1985, Subsidence of peat in California and Florida: Bulletin of the Association of Engineering Geologists, v. 22, p. 395-420.

Roehler, R. W., 1988, The Pintail coal bed and barrier bar G —a model for coal of barrier bar-lagoon origin, Upper Cretaceous Almond Formation, Rock Springs Coal Field, Wyoming: U.S. Geological Survey Professional Paper 1398, 60 p.

Ryer, T. A., and Langer, A. W., 1980, Thickness change involved in the peat-to-coal transformation for a bituminous coal of Cretaceous age in central Utah: Journal of Sedimentary Petrology, v. 50, p. 987-992.

Staub, J. R., 1991, Comparisons of central Appalachian Carboniferous coal beds by benches and a raised Holocene peat deposit: International Journal of Coal Geology, v. 18, p. 45-69.

Staub, J. R., and Cohen, A. D., 1979, Snuggedy Swamp of South Carolina: a back-barrier estuarine coal-forming environment: Journal of Sedimentary Petrology, v. 49, p. 133-149.

Triplehorn, D. M., Stanton, R. W., Ruppert, L. F., and Crowley, S. S., 1991, Volcanic ash dispersed in the Wyodak-Anderson coal bed, Powder River Basin, Wyoming: Organic Geochemistry, v. 17, p. 567-575.

Warlow, R. C., Bragg, L. J., Windolph, J. F., Hickling, N. L., Oman, J. K., Kerr, P. T., and Baker, J. W., 1986, Chemical analysis and evaluation of 40 samples from Upper Cretaceous coal beds from the Wind River Basin, Wyoming. U.S. Geological Survey Open File Report 86-187, 42 p.

Warwick, P. D., and Stanton, R. W., 1988, Petrographic characteristics of the Wyodak-Anderson coal bed (Paleocene), Powder River Basin, Wyoming, U.S.A.: Organic Geochemistry, v. 12, p. 389-399.

Wood, G. H., Jr., and Bour, W. V., III, 1988, Coal map of North America: U.S. Geological Survey Special Geologic Map, scale 1:5,000,000.

Frontispiece. "Discovery roll" the first discovery of uranium in Tertiary sandstone in Wyoming was made at Pumpkin Buttes, Powder River Basin on October 15, 1951, by J.D. Love. The photograph shows black manganese and uraninite-bearing sandstone (dark) containing yellow oxidized uranium streaks (light). The cross-bedded sandstone is within the Eocene Wasatch Formation. Photograph by J.D. Love, October 15, 1951.

Geological classification and origin of radioactive mineralization in Wyoming

Ray E. Harris and Jon K. King[1]
Geological Survey of Wyoming
Laramie, WY, 82071

Abstract

Wyoming is a uranium province. In Wyoming, uranium and thorium occur together in igneous rocks due to their similar behavior during igneous processes. In sedimentary rocks, the solubility of uranium varies with oxidation state, resulting in the formation of uranium roll-front deposits, for which Wyoming is famous. The source of the uranium in the roll-front deposits is a topic of conjecture. Other important types of uranium occurrences are found in Wyoming in sedimentary rocks and at unconformities. Thorium is also an important radioactive element in Wyoming, because one of the largest potential thorium resources in the United States is in igneous rocks in the Black Hills.

Introduction

Wyoming is a uranium province (Houston, 1979). Almost every stratigraphic unit and every county in the state contains uranium mineralization (**Figure 1** and **Table 1**), and Wyoming has been a major producer and reserve holder of uranium in the United States (**Table 2**). Thorium and radium mineralization in the State have also attracted interest, because one of the largest potential thorium resources in the United States is in Wyoming, and radium ore was mined in Wyoming in the years just after World War I. Present demand for radium is easily met by its creation in nuclear reactors (Kirk, 1981). The largest and most important uranium deposits in Wyoming occur in roll-front deposits in Eocene and Paleocene sedimentary rocks in the Gas Hills, Shirley Basin, Crooks Gap, southern Powder River Basin, and Pumpkin Buttes uranium districts (**Figure 1**). Other types of uranium deposits in the State have been mined to various extents.

Uranium was mined in Wyoming by several methods. The first mines were small open pits, trenches or small underground workings. Later, beginning in the mid-1960s, larger open-pit mines (**Figure 2**) and underground mines were developed. Later developments included: (1) the extraction of uranium from a large pile of ore by spraying the pile with a uranium-dissolving solution and recovering the uranium from the solution after it passed throught the pile (heap leaching), and (2) the extraction of uranium from underground by injecting a leaching solution into the host rock and through the ore body, and pumping the uranium-containing solution to the surface, where the uranium was recovered from the solution (in-situ production).

Uranium is extracted from ore by milling and leaching; the shipped product is yellowcake, which is ammonium diuranate, sodium diuranate, or ura-

[1] Current address: Utah Geological Survey, Salt Lake City, UT 84109

Harris, R.E., and King, J.K., 1993, Geological classification and origin of radioactive mineralization in Wyoming, *in* Snoke, A.W., Steidtmann, J.R., and Roberts, S.M., editors, Geology of Wyoming: Geological Survey of Wyoming Memoir No. 5, p. 898-916.

nium peroxide. By 1979, most operations were producing yellowcake that contained at least 95% uranium oxide (U_3O_8) (List and Coleman, 1979). Yellowcake produced by mills in the 1950s and 1960s contained 60% to 75% U_3O_8 (Merritt, 1971, table 7-1).

Uranium, thorium, and radium have diverse applications. Most uranium is used as fuel in nuclear power plants for the generation of electricity (Kirk, 1980). This fuel is enriched uranium, made from yellowcake. Minor uses of uranium include the manufacture of detonators made of super-enriched uranium for nuclear (fusion) weapons, whereas depleted uranium (a by-product of the enrichment process) is used for armor-piercing projectiles, reactor shielding, chemical catalysts, and counterweights (Kirk, 1980). Thorium is used in refractory materials, incandescent lamp mantles, aerospace alloys, electronic components, and chemical catalysts (Hedrick, 1985). Radium is used in medical and other miscellaneous applications like well-logging tools, luminous dials, and smoke detectors (Landa, 1987; also Kirk, 1981).

The remainder of this review chapter includes summaries of the: (1) geochemistry of uranium, thorium, and radium; (2) geologic classifications of selected radioactive occurrences in Wyoming; and (3) uranium source and age of Wyoming redox deposits. For the best and most recent summary of the history of uranium exploration, discoveries, and production in Wyoming the reader is referred to Chenoweth (1991).

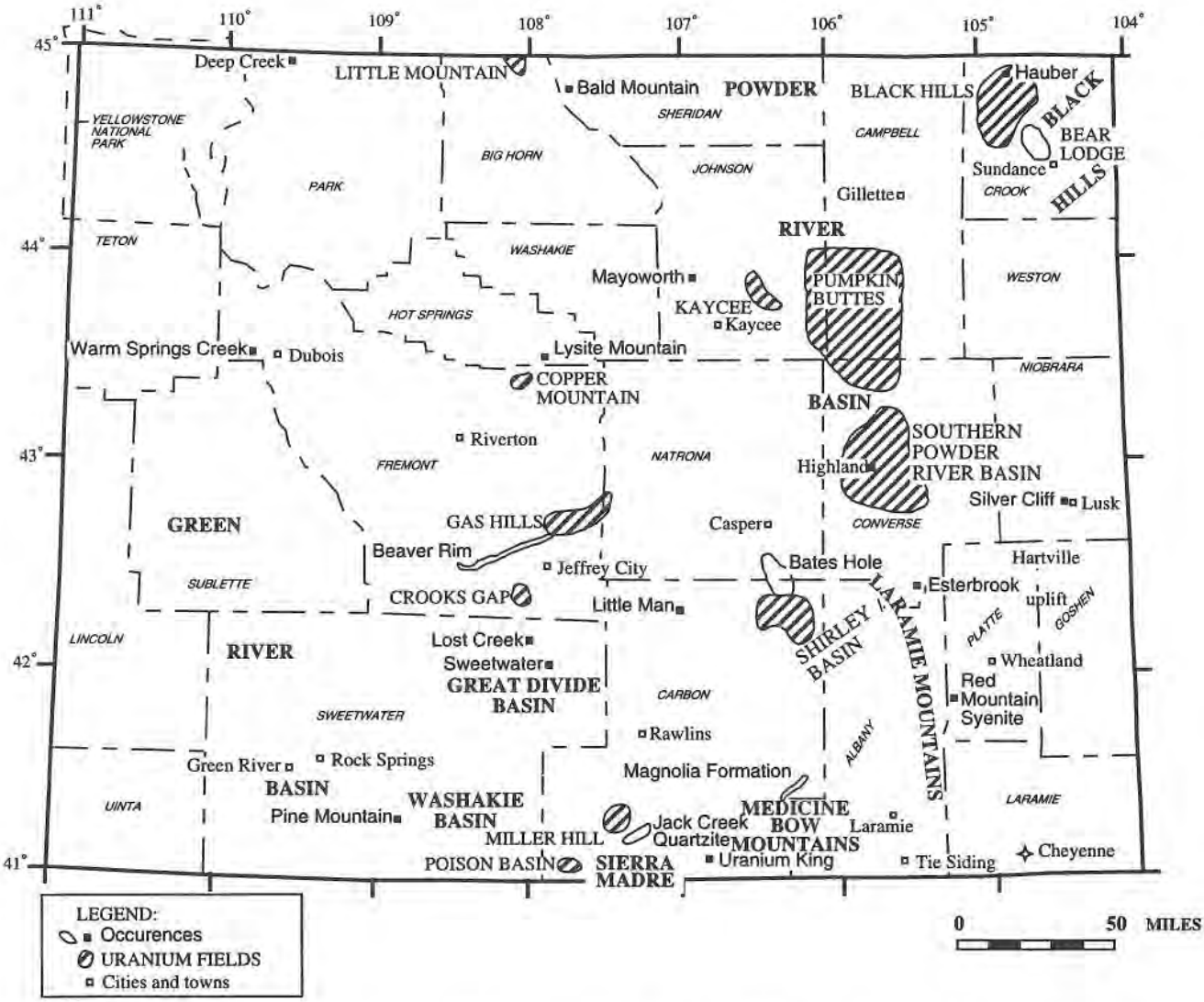

Figure 1. Generalized map of selected radioactive localities in Wyoming. County names are shown in all capital letters in italic type.

Table 1. Geologic units in Wyoming that host known uranium occurrences; units with significant past uranium production are noted in bold.

Age	Geologic Unit	Location
Pliocene	Bug Formation	central Wyoming
Miocene	"Miocene rocks, undifferentiated"	statewide
	North Park Formation	central southern Wyoming
	Browns Park Formation	central southern Wyoming
	Ogallala Formation	southeastern Wyoming
	Arikaree Formation	southeastern Wyoming
Miocene/Oligocene	"Miocene and Oligocene rocks, undifferentiated"	northeastern Wyoming
Oligocene	White River Formation	statewide
	Brule Formation	southeastern Wyoming
	Chadron Formation	southeastern Wyoming
Eocene	Bridger Formation	southwestern Wyoming
	Wagon Bed Formation	southwestern & central Wyoming
	Wasatch Formation	statewide
	Green River Formation	southwestern Wyoming
	Willwood Formation	Big Horn Basin
	Wind River Formation	southeastern Wyoming
	Eocene igneous rocks	northeastern Wyoming
	Battle Spring Formation	central southern Wyoming
Paleocene	**Fort Union Formation**	statewide
Paleocene and Cretaceous	Evanston & Hoback formations	southwestern Wyoming
Cretaceous	Medicine Bow Formation	south central Wyoming
	Lance Formation	southern & northeastern Wyoming
	Fox Hills Sandstone	southern & eastern Wyoming
	Lewis Shale	central southern Wyoming
	Pierre Shale	eastern Wyoming
	Mesaverde Formation (Group)	statewide
	Ericson Sandstone	Rock Springs uplift
	Rock Springs Formation	Rock Springs uplift
	Cody Shale	central & central southern Wyoming
	Frontier Formation	southern & northeastern Wyoming
	Newcastle Sandstone	northeastern Wyoming
	Cloverly Formation	statewide
	Inyan Kara Group	northeastern Wyoming
	Fall River Formation	northeastern Wyoming
	Lakota Formation	northeastern Wyoming
Jurassic	Morrison Formation	statewide
	Sundance Formation	central & northeastern Wyoming
	"Canyon Springs Member, Sundance Formation"	northeastern Wyoming
Triassic	Chugwater Formation	Bighorn Basin & central Wyoming
Permian	Phosphoria Formation	western Wyoming
Pennsylvanian and Permian	Casper Formation	southeastern Wyoming
Pennsylvanian	Tensleep Sandstone	northern & central Wyoming
	Minnelusa Formation	eastern Wyoming
	Fountain Formation	southeastern Wyoming
Pennsylvanian and Mississippian	Amsden Formation	northern & central Wyoming
Mississippian	Madison Limestone	statewide
	Pahasapa Limestone	Black Hills uplift
Devonian	Jefferson Formation	northwestern Wyoming
Ordovician	Bighorn Dolomite	Bighorn Mountains
Cambrian	Gros Ventre Formation	central Wyoming
	Deadwood Formation	eastern Wyoming
	Flathead Sandstone	statewide
Precambrian	undifferentiated	statewide

Table 2. Cumulative uranium production and reserves of Wyoming and other states, in millions of pounds of U_3O_8 (Energy Information Administration, 1990).

	Wyoming	Colorado	New Mexico	Texas	Utah	Other
Cumulative production	187	71	322	42	58	179[3]
Economic reserves [1]	217	—	54	35	—	31[4]
Reasonably assured resources [2]	66	—	174	4	—	32[5]

[1] Economic at the time of calculation
[2] Economic at $30 per pound U_3O_8
[3] Includes Arizona, Colorado, Florida, Louisiana, Nebraska, New Mexico, South Dakota, Texas, Utah, and Washington
[4] Includes Arizona, Colorado, Nebraska, and Utah
[5] Includes Arizona, California, Colorado, Idaho, Montana, Nebraska, Nevada, North Dakota, Oregon, South Dakota, Utah, and Washington

Geochemistry of uranium, thorium, and radium

The geochemistry of uranium (U), thorium (Th), and radium (Ra) plays an important role in their concentration. The average amount of uranium and thorium in the Earth's crust is about 2 ppm and 8 to 10 ppm, respectively (Boyle, 1982; Taylor and McLennan, 1985). The long-term existence of radium, a gaseous radioactive-decay daughter-product of uranium, is almost totally dependent on the presence of uranium, and rocks normally contain only about one millionth of a ppm radium (Dyck, 1978). Therefore, abundant radium is only found in nature with uranium ores. The chemical behavior of radium is basically like that of barium, under most conditions (Boyle, 1982), and unlike the behaviors of uranium and thorium.

The chemical behaviors of uranium and thorium are almost the same under high-pressure, high temperature (>350°C) conditions, with concentration in differentiated and alkaline igneous rocks and in veins and pegmatites in metamorphic rocks (Kimberley, 1978; Boyle, 1982; Keppler and Wyllie, 1990). Behavior of thorium and uranium in the temperature range between 100° and 350° C is incompletely understood (Boyle, 1982; Romberger, 1984). Uranium, thorium, and radium are commonly found together in igneous and metamorphic rocks.

Figure 2. Air photo of active open-pit uranium mines in the Gas Hills, *circa* 1967, showing typical uranium mines in the days of active exploration and development. Pits in the foreground were operated by Federal American Partners. Those in the middle distance (farthest pits) were operated by Western Nuclear, Inc. Spoil piles of overburden extend to the left of the pits. These mines have been reclaimed. (Photo from C.L. Van Alstine, Office of the U. S. Atomic Energy Commission, Casper, Wyoming, donated to the Geological Survey of Wyoming by W.L. Chenoweth. Exact date of photo and name of photographer unknown.)

At temperatures below about 100° C, temperatures usually encountered in sedimentary rocks and the zone of weathering, the geochemical behavior of uranium differs markedly from that of thorium and radium. At these temperatures uranium has two valences, tetravalent (reduced) and hexavalent (oxidized). Uranium is readily soluble in water when oxidized and is insoluble in water when reduced. In contrast, thorium and radium have only one valence; thorium is insoluble in water and radium is soluble in water, regardless of the amount of oxygen (Langmuir, 1978; Langmuir and Herman, 1980; Boyle, 1982). These differences in solubility mean that uranium can migrate when it is oxidized, leaving thorium behind, and later be deposited when it encounters a reducing environment. The effective solubility of radium versus uranium is not well understood, but radium is strongly adsorbed by manganese and iron oxides (Boyle, 1982; Burnett and others, 1990), and therefore, the transport of Ra in an oxidizing environment may vary depending on the Mg and Fe oxides. Consequently, radioactive mineralization in sedimentary rocks, other than placers, usually has high U/Th ratios and quite variable U/Ra ratios.

The differences in the geochemical behavior of uranium, thorium, and radium at low temperatures are significant in exploration. The solubility of oxidized uranium, and the relative lack of mobility of radium and insolubility of thorium under the same conditions, leads to radioactive disequilibrium. The equilibrium U/Ra ratio is about 2.86 million (Boyle, 1982). Oxidized uranium occurences have a low U/Ra ratio. Conversely, reduced uranium occurrences have a high U/Ra ratio. A thorough discussion of this subject is beyond the scope of this chapter, and the reader is referred to Lillie (1986) for more information.

Geological classification of selected radioactive element occurrences in Wyoming

Many schemes have been devised to classify radioactive element occurrences. The scheme adopted for this article is based on suspected origin (**Table 3**) and was modified from Mickle and Mathews (1978). Examples from Wyoming have been selected on the basis of economic and geologic importance. Because the characteristics of these classes commonly overlap and the differences between classes are gradational, many occurrences in Wyoming are unclassified. Other occurrences are not yet classified due to insufficient data.

Occurrences in sedimentary rocks

A wide variety of radioactive occurrences are present in sedimentary rocks in Wyoming. Most of these occurrences and the majority of the uranium ore mined in the State were formed by the oxidation-reduction (redox) process. Other types of occurrences in sedimentary rocks are placers, chemical-codepositional, carbonate-hosted, desert evaporite, and coal-hosted occurrences.

Redox occurrences

Redox deposits and mineralization were formed by low-temperature geochemical processes, and include roll-front, tabular, and near-surface occurrences. A brief summary of these complex geochemical processes follows. Meteoric water in carbonate or phosphate complexes usually contains sufficient dissolved oxygen to oxidize and transport uranium. When oxygen is used up in the oxidation of organic carbon and/or pyrite, uranium will be precipitated as the insoluble reduced tetravalent ion. If sulfides such as pyrite are oxidized, sulfuric acid will also form. This sulfuric acid can be neutralized if calcite is present. These chemical reactions can be facilitated by bacterial action. Continued influx of oxygenated water causes a "roll-front" to migrate down the ground-water flow gradient and tabular deposits can be formed. Erosion and changes in the water table lead to movement of near-surface mineralization as pre-existing roll-front and tabular occurrences are oxidized by meteoric water and transported to new locations (for reviews see Harshman and Adams, 1981; Galloway and others, 1979; Rackley, 1976; Gruner, 1956; and the references in the geochemistry section).

In Wyoming, redox roll-front and tabular occurrences are found in a variety of sedimentary environments (refer to **Table 1**), including: (1) fluvial sandstones and conglomerates in the White River, Wind

Table 3. Classification of Wyoming uranium, thorium, and radium occurrences (classes modified from Mickle and Mathews, 1978).

Classification	Wyoming examples
	Occurrences in sedimentary rocks
Redox	
roll-front [1]	Tertiary basins (Fort Union and Wasatch formations)
tabular [1]	Northern Black Hills (Inyan Kara Group)
near-surface [1]	Gas Hills and Pumpkin Buttes (Eocene rocks)
Placer	
beach placer [2]	widespread (Mesaverde Formation)
fluvial placer [2]	Bald Mountain (Flathead Sandstone)
quartz-pebble conglomerate [2]	Medicine Bow Mtns. (Magnolia Formation)
Chemical codepositional	
marine black shale	eastern Wyoming (Minnelusa Formation)
marine phosphorite [2]	western Wyoming (Phosphoria Formation)
lacustrine phosphorite	Green River Basin (Green River Formation)
Carbonate-hosted	
acid neutralization [1]	Little Mountain (Madison Limestone)
surficial coating	Miller Hill (Browns Park Formation)
reduction-related	Mayoworth (Sundance Formation)
Desert evaporite	Lost Creek (various)
Coal-hosted	Great Divide Basin (Wasatch Formation)
	Occurrences in igneous rocks
Orthomagmatic	Laramie Mtns. (Precambrian granites)
Pegmatitic	Tie Siding (Sherman granite)
Magmatic hydrothermal [2]	Bear Lodge Mtns. (Tertiary veins)
Autometasomatic [2]	Bear Lodge Mtns. (Tertiary carbonatites)
	Occurrences in metamorphic rocks
Anatectic	Uranium King (Precambrian gneiss)
Redox	Little Man (Archean metamorphic rocks)
Vein	Esterbrook (Archean metamorphic rocks)
	Unconformity-related occurrences [2]
	Copper Mountain (various)
Unclassified occurrences [3]	
	numerous (e.g., Ramsbottom)

[1] Types of occurrences with important past production in Wyoming
[2] Types of occurrences with the potential for production in Wyoming
[3] Unknown due to insufficient or contradictory available information

River, Wasatch, Battle Spring, Fort Union, Cloverly, Morrison, and Lakota formations; (2) alluvial deposits in the Battle Spring Formation; (3) eolian sandstones in the Browns Park Formation and Tensleep Sandstone; (4) deltaic sandstones in the Lance and Fall River formations, and Teapot Member of the Mesaverde Formation; and (5) beach and barrier-bar sandstones in the Fox Hills and Fall River formations.

The first discovery of uranium in Tertiary sandstones, which led to the discovery of the major deposits in the Wyoming basins (**Figure 1**) was a near-surface roll-front type of redox deposit. This discovery (see **Frontispiece**) was made by J.D. Love on October 15, 1951.

Roll-front uranium deposits occur in sandstones and conglomerates and are bound above and below by less permeable shales. They follow a sinuous linear trend in plan view and are usually C-shaped in cross-section (**Figures 3** and **4**). This cross-sectional configuration was first called a "roll" by Colorado and Utah miners in the early 1940s. In Wyoming, the rolls are at the boundary between unaltered (reduced) sandstone, typically containing organic carbon and pyrite, and altered (oxidized) sandstone, typically containing iron oxides. The roll is convex into unaltered ground and concave from altered ground. Sometimes, as in the southern Powder River Basin, this boundary is distinctly visible as a gray (unaltered) to red (altered) color change in the rock. In other locations, such as the Shirley Basin, the alter-

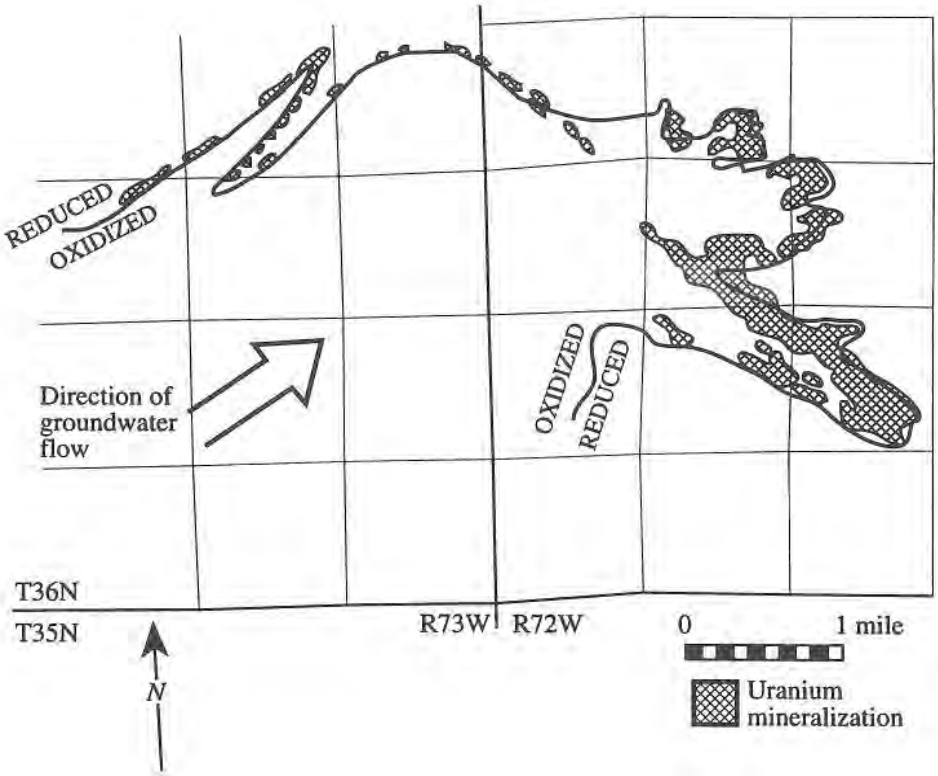

Figure 3. Uranium mineralization and redox boundary in plan view, Highland mine area, southern Powder River Basin uranium district, Wyoming (modified from Dahl and Hagmaier, 1976).

ation is more subtle, with color changes from gray in the unaltered zone to yellowish gray in altered rock (**Figures 4** and **5**).

In an idealized roll-front uranium deposit, uranium concentrations decrease abruptly into oxidized rock away from the concave boundary, and concentrations gradually decrease away from the convex boundary in reduced rock. However, uranium is not a necessary ingredient in the formation of a roll front, and uranium is irregularly distributed and may not be present everywhere along a roll front. The pattern of uranium mineralization in plan view illustrates this phenomena (**Figure 3**). In addition to uranium, other elements that can be concentrated in or associated with a roll front include: vanadium, selenium, molybdenum, copper, silver, lead, and zinc (Harris, 1982). Near-economic grades of selenium (Hough, 1956), silver (Shockey, 1974), and molybdenum (Harris, 1982) have been found along roll fronts.

Uranium ore along roll fronts is commonly found where coarse-grained sandstones grade into finer grained or clay-bearing equivalents, which are commonly subparallel to pinch-outs of sandstone-filled channels. The finer grained sandstones appear to contain more organic debris than the coarse-grained sandstone, and the decreased permeability apparently slowed ground-water flow. Because roll-front migration is directly related to ground-water flow, these zones of lower permeability are commonly the loci of roll fronts (Harris, 1982; Gaylord, 1981).

Tabular redox uranium occurrences are found in many areas of Wyoming; the most prominent deposits are in the Cretaceous Inyan Kara Group in the Black Hills. The uranium mines in New Mexico and many other parts of the Colorado Plateau are also tabular deposits. The name describes their irregular tabular form, within which reduced conditions and uranium mineralization are present. The tabular bodies are roughly parallel to bedding, unlike the roll-front mineralization, which crosses bedding. In Wyoming, tabular bodies are associated with redox boundaries but can be surrounded by non-mineralized, usually altered (oxidized), sandstone and conglomerate or are bounded by impermeable rocks on one or more sides.

The formation of tabular redox uranium occurrences in Wyoming is incompletely understood. This mineralization could have formed by processes like the uraniferous humate and/or two-solution interface models proposed for tabular mineralization on the Colorado Plateau (Adams and Saucier, 1981; Thamm and others, 1981). Alternatively, migrating redox boundaries played a role in the formation of Wyoming tabular occurrences (Chenoweth, 1988) or actually formed these occurrences (Harshman and Adams, 1981; Renfro, 1969).

In Wyoming, some tabular bodies in Tertiary rocks are the limbs and detached limbs of roll fronts

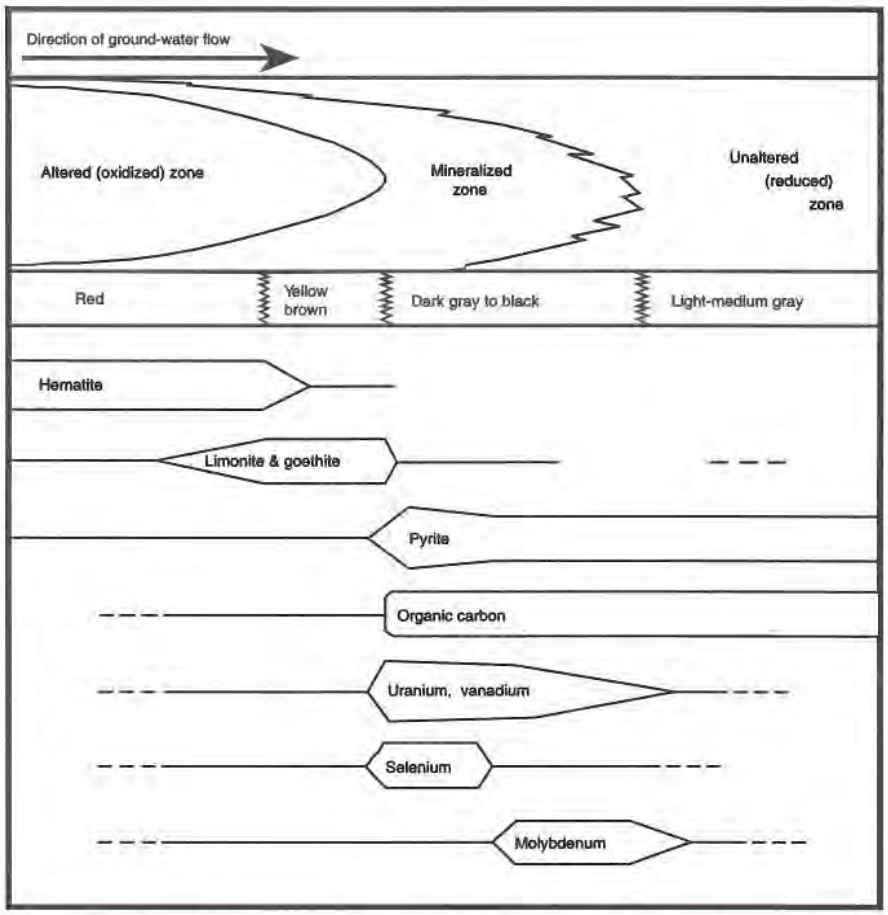

Figure 4. Generalized cross section of roll-front showing alteration, color, and mineralogical changes (modified from Gaylord, 1981).

left in less permeable rocks at fluvial channel margins. In other Wyoming occurrences, less permeable and often organic-rich zones within a channel will remain mineralized even though surrounded by oxidized rocks. Tabular bodies can also be preserved in oxidized rock due to high concentrations of reducing materials, such as coal, primary organic matter, pyrite, and possibly migrated hydrocarbons. Changes in the direction of ground-water flow can theoretically produce tabular uranium mineralization (Harris, 1988).

Near-surface redox occurrences come in a variety of forms and are very widespread in the State; but all are probably due to near-surface oxidation of pre-existing reduced roll-front and tabular mineralization. Examples include: (1) oxidized uranium mineralization above the present-day water table (low U/Ra ratios) as in the concretionary uranium occurences in the Pumpkin Buttes area; (2) reduced uranium mineralization at the water table (high U/Ra ratios), mined in the Gas Hills in the 1950s and 1960s; and (3) pods containing both oxidized and reduced uranium mineralization, like the manganese oxide concretions that were mined in the 1950s and 1960s in the Pumpkin Buttes uranium district (**Figure 1**). Oxidized mineralization above the water table is due to incomplete solution of uranium, often due to limited precipitation in semi-arid and arid climates. Reduced mineralization at the water table is the result of redeposition of uranium in reducing ground water after leaching from above. Mineralized pods are commonly concretions that formed in the subsurface; these pods retain uranium under oxidizing conditions because they are less permeable and/or because uranium is adsorbed onto various minerals.

Placer occurrences

Thorium and minor uranium are found as mechanical accumulations in beach and fluvial placers in Wyoming. Wyoming beach placers are ancient (Mesozoic), whereas Wyoming fluvial placers are both Quaternary and ancient (Tertiary and Cambrian). Quartz-pebble conglomerates in the northern Medicine Bow Mountains and Sierra Madre are a special type of Archean-Early Proterozoic fluvial placer. Wyoming placers have not yielded any thorium or uranium ores, but potential exists for by-product production with gold, zircon, rare-earth-bearing minerals, and magnetite-ilmenite (King, 1991).

The typical Wyoming fossil beach placer is an elongate body oriented parallel to the paleoshoreline. These black sandstones average 15 % heavy minerals and contain thin (1/4-inch) individual layers composed of up to 90 % heavy minerals. The occurrences are resistant to weathering and are exposed on ridges. The host rocks for most of the

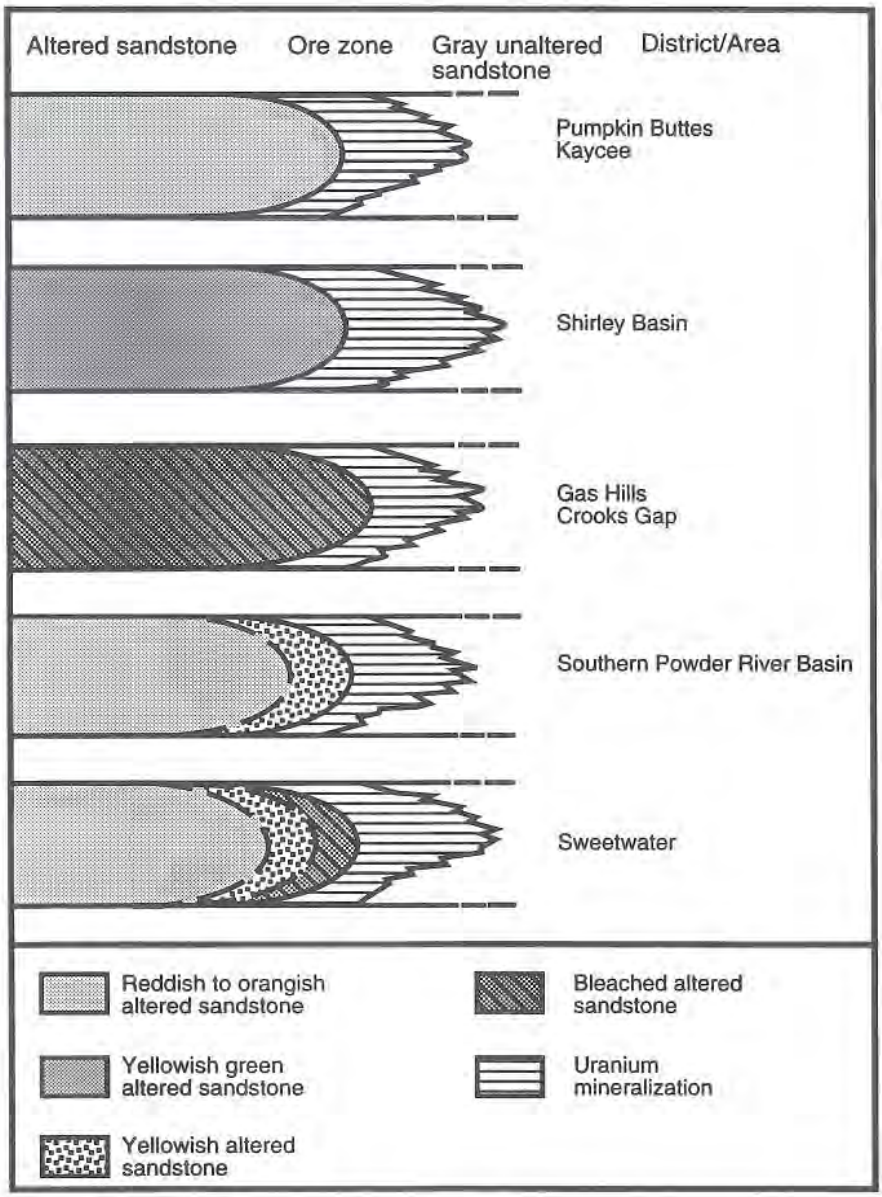

Figure 5. Generalized cross sections across roll fronts showing the most common color changes present in the various uranium districts and areas (modified from Harshman and Adams, 1981, figure 9).

occurrences are regressive beach sandstones of late Cretaceous age (Houston and Murphy, 1962, 1970, 1977; Houston and Love, 1956).

Examples of radioactive fluvial placers in Wyoming include: (1) Quaternary (Holocene and Pleistocene ?) placers in and along Warm Spring Creek near Dubois; (2) Cambrian placers in the Flathead Sandstone in northern and central Wyoming; and (3) Tertiary placers in the Wind River and/or White River formations in Bates Hole and the adjacent Shirley Basin (**Figure 1**). The Cambrian placers in the Bald Mountain area, on the Sheridan—Big Horn County line, are the most promising prospect (**Figure 1**) (King, 1991).

The Precambrian, radioactive, quartz-pebble conglomerates are fluvial paleoplacers with several unique characteristics. Such conglomerates are mined for uranium at Elliot Lake, Ontario, and for gold and uranium in the Witwatersrand, South Africa. They are unique because of the anastomosing nature of the fluvial channels and the presence of detrital pyrite, reduced uranium and thorium minerals, large clasts of what is probably vein quartz. In addition, they were only formed during the Archean and Early Proterozoic, when the Earth's atmosphere apparently contained less free oxygen than at present (Roscoe, 1973; Houston and Karlstrom, 1980).

Archean and Proterozoic metasedimentary rocks in the northern Sierra Madre and Medicine Bow Mountains have been examined for mineralized quartz-pebble conglomerates. The most radioactive, pyritic, gold- and rare-earth-bearing conglomerates were found in the thorium-rich, Jack Creek Quartzite in the Upper Archean Phantom Lake Metamorphic Suite in the northwestern Sierra Madre, and the uranium-rich, Magnolia Formation in the Lower Proterozoic Deep Lake Group in the northeastern Medicine Bow Mountains (**Figure 1**) (Karlstrom and others, 1981; Borgman and others, 1981).

Chemical codepositional occurrences

These types of mineralization are thought to have formed at the time of deposition of the host rock. The subclasses are based on the type of host

rock and include marine black shale, marine phosphorite, and lacustrine phosphorite.

In eastern Wyoming, oil wells have penetrated several radioactive marine black shales at depths of 2,000 to 7,000 feet in the Permian-Pennsylvanian Minnelusa Formation. These shales are not well exposed in Wyoming (Love, 1953; Dunagan and Kadish, 1977; Harris and Hausel, 1984). Other radioactive marine black shales are reported in the Phosphoria Formation (Permian) in western Wyoming; but most of these so-called black shales are actually phosphorites. Uranium in the black shale occurrences was probably precipitated with or adsorbed onto organic-rich, fine-grained sediments in an anoxic marine environment. The very low-grade uranium mineralization in these black shales is uneconomic, although these black shales are so extensive that large amounts of uranium are present.

In Wyoming, many uraniferous marine phosphates are reported in the Permian Phosphoria Formation. These phosphorites thicken and become more uraniferous to the west (Swanson and others, 1953; Sheldon, 1963). The uranium is interpreted to have coprecipitated with phosphate minerals upon the basin-to-shelf transition as upwelling basin seawater was warmed (De Voto and Stevens, 1979, v. 1, chp. 1). Uranium substituted for calcium in the lattice of calcium phosphate minerals (Altschuler and others, 1958). Wyoming uraniferous phosphorites contain enough uranium to warrant studies of by-product uranium extraction at existing phosphate processing plants, similar to what is being done with Florida phosphate (De Voto and Stevens, 1979, v. 2). Potential surface-mineable uraniferous phosphate resources in Wyoming are estimated at 77 million tons of 33.3 % P_2O_5 ore, containing on average of 82 ppm U (Bauer and Dunning, 1979, table 3-9).

Uraniferous phosphatic lake beds occur in Eocene sedimentary rocks in four areas of Wyoming: (1) Lysite Mountain in eastern Hot Springs County, (2) the Beaver Rim in Fremont County, (3) the central Green River Basin in Sweetwater County, and (4) Pine Mountain in the Washakie Basin in southern Sweetwater County (**Figure 1**) (Love, 1964). These phosphorites appear to have formed by evaporitic concentration in a restricted lacustrine environment, rather than by warming of saturated cold water (Mott and Drever, 1983). These lacustrine phosphorites are, at present, of geologic rather than economic interest.

Carbonate-hosted occurrences

Uranium mineralization occurs in carbonate host rocks at several localities in Wyoming. Three types of carbonate-hosted uranium mineralization are recognized: (1) oxidized mineralization in brecciated zones and cavern fill in paleokarst in the Upper Mississippian Madison Limestone that was probably due to carbonate neutralization of acidic, uranium-bearing ground water; (2) surficial and fracture coatings of oxidized uranium minerals of uncertain origin on Tertiary limestones, particularly in the Browns Park Formation of southern Wyoming ; and (3) occurrences related to reduction in fetid, oolitic marine limestones of the Jurassic Sundance Formation in Johnson County, similar to that mined from the Todilto Limestone of New Mexico. Uranium was mined from the Madison Limestone in the Little Mountain District of northernmost Big Horn County and from limestones in the Sundance Formation near Mayoworth, Johnson County (**Figure 1**).

Desert evaporite occurrences

Uranium has been found in caliche-like occurrences in the Lost Creek area of northern Sweetwater County, Wyoming (**Figure 1**) (Sheridan and others, 1961). This is the largest area of schroeckingerite [$NaCa_3(UO_2)(CO_3)_3(SO_4)F \bullet 10H_2O$] mineralization in the world. This mineralization was (and is) precipitated near and on the surface of Quaternary materials, and Eocene Wasatch, Green River, and Battle Spring formations due to evaporation of oxygenated uranium-rich, fluorine-bearing groundwater. Most mineralized samples from the area contain less than 0.05 % uranium (Sheridan and others, 1961), so the mineralization is not economic. During rainy periods, some of the schroeckingerite is dissolved and returns to the ground-water system. Then during dry periods, redeposition occurs, commonly at different locations. Therefore, the precise location of mineralization can change from season to season and after heavy rainfalls.

Coal-hosted occurrences

Coal can cause the precipitation of uranium from water through reduction (Vine, 1962; Drever and others, 1977). This precipitation can be syndepositional (actually chemical codepositional) or

postdepositional (actually redox) [see Vine (1962) for conflicting evidence on timing]. Significant amounts of uranium occur in lignite in the Eocene Wasatch Formation in the Great Divide Basin, northeastern Sweetwater County, Wyoming (**Figure 1**). The potential strippable resource in this area is 100,000,000 short tons of coal containing at least 0.003 % uranium. This mineralization is not economic given the low rank of the coal and low uranium contents of ash from burning (Masursky, 1962).

Occurrences in igneous rocks

The classification of igneous radioactive mineralization is based on origin, which is usually subject to some guesswork on the part of scientists (**Table 3**) (also Mathews, 1978). The four classes found in Wyoming—orthomagmatic, igneous pegmatite, magmatic-hydrothermal, and autometasomatic—were formed at relatively high temperatures and pressures by what are certainly igneous processes (references in geochemistry section). Each of these classes grade into each other.

Orthomagmatic occurrences

Orthomagmatic occurrences are formed when magmas crystallize; radioactive minerals are usually evenly distributed throughout the rock. The even distribution and attendant low grade usually preclude economic development. Uranium- and thorium-rich host rocks are commonly highly differentiated, and are enriched in fluorine, potassium, and sodium. In Wyoming, orthomagmatic radioactive occurrences have been found in Precambrian granitic rocks, like the Middle Proterozoic Red Mountain syenite and Sherman granitic rocks in the Laramie Mountains (**Figure 1**). The Archean granites in the Laramie and Granite Mountains also have indications of uranium enrichment, but deep weathering precludes determining the exact origin of the uranium enrichment .

Igneous pegmatite occurrences

Uranium and thorium are concentrated in pegmatites, which form during the late stages of magma crystallization. These are more attractive exploration targets than orthomagmatic occurrences, and have been mined elsewhere in the world. In Wyoming, radioactive igneous pegmatites have been found at several locations, in particular in the Sherman granite in the Tie Siding area of southernmost Albany County (**Figure 1**).

Magmatic-hydrothermal occurrences

In magmatic-hydrothermal occurrences, radioactive minerals are commonly found in veins and veinlets that contain primary quartz (usually smoky) with minor fluorite and calcite. These veins commonly contain more abundant radioactive elements than pegmatites, and are found in the same types of host rocks as orthomagmatic occurrences. Little difference exists between magmatic-hydrothermal and autometasomatic occurrences The usually accepted difference between radioactive magmatic-hydrothermal and autometasomatic occurrences is that the former are veins and the latter are disseminated (porphyry system). Yet, they are basically different results of the same process—fracturing and alteration by and deposition from hydrothermal fluids during the last stages of magma crystallization.

Autometasomatic occurrences

Autometasomatic radioactive occurrences form during the final crystallization of intrusive rocks due to reactions between already crystallized minerals and late-stage hydrothermal fluids. Plutons containing autometasomatic radioactive occurrences are typically alkaline to peralkaline and occur as shallow intrusives of relatively small size (1 to 12 square miles of exposure). Associated autometasomatic gangue minerals include calcite and fluorite (Mathews, 1978).

Wyoming contains one of the largest potential thorium resources in the United States in the southern Bear Lodge Mountains, Crook County, Wyoming (**Figure 1**) (Staatz, 1983). The prospect has characteristics of both the magmatic-hydrothermal and autometasomatic classes. It also contains abundant rare earth elements and some uranium mineralization, and is within and probably genetically related to a Tertiary carbonatite complex (Staatz, 1983).

Occurrences in metamorphic rocks

It is seldom possible to definitively state the origin of radioactive occurrences in metamorphic rocks, and the classification scheme is based more on physical and chemical characteristics. Types of occurrences in Wyoming include: anatectic, vein and re-

dox mineralization, and many unclassified occurrences. An important example of an unclassified occurrence is the Ramsbottom property in Archean, metamorphosed, allanite-bearing, calc-silicate rocks in the southern Bighorn Mountains (**Figure 1**) (King, 1991).

Anatectic occurrences

Radioactive pegmatites in metamorphic terrains are anatectic occurrences, and are thought to have been formed by partial melting of a pre-existing rock during incipient anatexis. Most have the characteristics of igneous pegmatites; the definitive difference is usually the type of host rock. In Wyoming, uranium production was reported from the Uranium King pegmatite in a Proterozoic gneiss terrane in southern Carbon County (**Figure 1**).

Redox occurrences

Radioactive redox occurrences in metamorphic rocks are similar to vein occurrences. The important differences are the lack of fractures zones, chloritization, hematization, and thorium in redox occurrences. In redox occurrences, host rocks are usually carbonaceous or graphitic, and sometimes calcareous, with minor calcite and/or quartz gangue. The Little Man occurrence in Precambrian metasedimentary rocks in Carbon County is an example of this type of mineralization (**Figure 1**). These redox occurrences are quite similar to radioactive unconformity-related occurrences.

Vein occurrences

Radioactive veins in metamorphic rocks are usually associated with fracture zones, without the presence of an unconformity (unconformity-related) or an igneous pluton (magmatic-hydrothermal). Chloritic, graphitic (or carbonaceous), and calcareous units are the most favorable host rocks. These veins contain reduced uranium minerals, generally with chlorite, hematite, pyrite, carbonate, and/or quartz, with or without complex metal sulfides and arsenides. Chloritic and hematitic alteration are common. Multiple generations of alteration and uranium mineralization have been documented. The producing Beaverlodge veins in northern Canada are a good example of this type of mineralization (Dahlkamp and Adams, 1981). Veins in Archean metamorphic rocks in the Esterbrook area of the northern Laramie Mountains, Albany and Converse counties, are examples of this type of mineralization in Wyoming (**Figure 1**). The source of uranium and thorium and the nature of the mineralizing solutions that produced these veins is speculative. This vein class grades into several others (unconformity-related, magmatic-hydrothermal, redox metamorphic).

Occurrences related to unconformities

Most of the largest producing uranium deposits in the world are found in Archean and Lower Proterozoic metasedimentary, metaigneous, and igneous rocks that are or were beneath unconformities overlain by Lower to Middle Proterozoic rocks. The deposits are in fractured rocks that are usually graphitic, carbonaceous, pyritic, and/or chloritic. Uranium mineralization is reduced, with very high uranium/thorium ratios indicative of transport in oxidizing solutions at submetamorphic temperatures. Gangue minerals are chlorite with or without hematite, quartz, and carbonate. Chloritic alteration is common with or without hematitic alteration. Mineralization is simple (uranium only) or contains complex metal sulfides and arsenides. Multiple generations of alteration and mineralization are common. The rocks above the unconformity are less metamorphosed or unmetamorphosed, oxidized, red, clastic or volcanoclastic sedimentary rocks. The largest such deposits are in northern Canada and northern Australia (Dahlkamp and Adams, 1981; Harris, 1986).

In Wyoming, unconformity-related uranium occurrences are found at unconformities of different ages. Many uranium occurrences are located at the unconformity between Tertiary units that directly overlie Precambrian rocks. The Copper Mountain uranium district in northeastern Fremont County is a prime example (**Figure 1**). Uranium mineralization is present in Cambrian sandstones and the unconformably underlying Precambrian rocks in the Hartville uplift in Goshen and Niobrara counties, Wyoming, for example the Silver Cliff mine (**Figure 1**). This uranium mineralization may have been emplaced during any of several erosional events since the Cambrian. Uranium mineralization is also reported in Cambrian rocks that unconformably overlie Archean rocks in Park County, Wyoming, though the origin of the mineralization is not certain. A few uranium anomalies, for example at Deep Creek in Park County (**Figure 1**), are reportedly asso-

ciated with unconformities between Proterozoic and Archean rocks in Wyoming, roughly the age of the unconformities associated with the Canadian and Australian deposits (Harris, 1986). Unconformities between Proterozoic and Archean rocks are found in Wyoming in the Medicine Bow Mountains, Sierra Madre, and Hartville uplift of southeastern Wyoming.

Uranium source and age of Wyoming redox deposits

Uranium source

The source of the uranium found in redox sedimentary-hosted mineralization in Wyoming is controversial. Four basic theories on the source of the uranium and other trace elements in these occurrences have been suggested: (1) leached uranium from overlying ash-fall tuffs; (2) leached uranium from igneous and metamorphic rocks in the highlands surrounding the basins; (3) leached uranium from the host sandstones themselves; and (4) hydrothermal uranium from a magma source at depth. Combinations of these theories have been proposed as well (Boberg, 1981). Currently, the most popular theories are the tuff leach (#1) and the highland leach (#2).

The tuff leach theory is supported by several kinds of data. The close spatial relationship between redox uranium occurrences in Wyoming and the uraniferous White River Formation (Oligocene) and other uraniferous, Tertiary, tuffaceous units has long been observed (Love, 1952). The tuff leach theory is also supported by extensive geochemical studies on uranium removal from tuff as reviewed in Zielinski (1983, 1984; also Trentham and Orajaka, 1986). Further, it was the tuff leach theory that led to the discovery of most of the large uranium deposits in the State (Love, 1952). A study by Zielinski (1983) on tuffs in the White River Formation in the Powder River Basin, Wyoming, showed that uranium leached from the tuffs was in amounts much greater than that needed to account for the uranium in the redox occurrences and deposits in the Powder River Basin. The tuff leach theory is indirectly supported over the highland leach theory by two types of evidence: (1) productive uranium deposits in Cretaceous rocks of the Black Hills of Wyoming and Tertiary rocks in south Texas have only tuffs as a possible uranium source; and (2) 60 to 80 % uranium loss in Archean granites in the Owl Creek Mountains apparently happened during the Laramide, and consequently, this source was not available during the deposition of uranium in the Copper Mountain district (e.g., see Stuckless and others, 1986).

On the other hand, many redox occurrences in Wyoming are found adjacent to crystalline rocks, especially the uraniferous granites of the northern Laramie and Granite mountains. Oxidized uranium leached from these crystalline terrains could have been transported to the sites of the present mineralization. This theory was implied by Gruner (1956) and might include the erosion of pre-existing Precambrian uranium deposits (Guilinger, 1963; also Rackley, 1976). Geochemical evidence for the highland leaching theory is available from uranium-loss studies of Precambrian granites in Wyoming. From surface and drill-hole samples, Stuckless and Nkomo (1978), Stuckless and others (1986), and Stuckless (1987) have shown that the Archean granites in the Granite Mountains lost 70 to 90% of their original uranium content in the Tertiary (about 10 to 40 Ma), more than about 100 times the amount needed to account for the uranium in the surrounding districts. Nkomo and others (1979) have shown both uranium loss and gain in Archean granites in the northern Laramie Mountains. The gains were about 75 to 250% of the original uranium contents, and occurred in the last 150,000 years (a documented period of near-surface mobilization); losses of about 50 to 75% of the original uranium content occurred prior to the gains (Nkomo and others, 1979), and might be Tertiary. The limited redox mineralization next to the Archean granites in the Wind River Range has been attributed to little uranium loss from the granites in the Tertiary and low original uranium contents (Stuckless and others, 1985). The near absence of redox mineralization near the uraniferous Middle Proterozoic Sherman granite in the southern Laramie Mountains might be due to less uranium loss than Archean granites and/or disequilibrium in the Sherman granite that indicates most uranium mobility was in the last 100,000 years (Zielinski and others, 1981).

The theory that the source of the uranium was the host sandstones and conglomerates (#3) has some adherents (Melin, 1964; Rackley and others, 1968; Renfro, 1969). Because the host sedimentary rocks in Wyoming are commonly arkoses that were eroded from nearby Precambrian granitic terrains, this remains a compelling theory. Convincing evidence in support of this theory would be that altered sandstones contain less uranium than unaltered sandstones. In partial support, Renfro (1969) reported that unaltered sandstones near Cretaceous-hosted tabular redox deposits of the Black Hills contain more uranium (14 ppm) than altered sandstones (5 ppm). However, these sandstones are neither arkosic nor tuffaceous, and other geochemical data do not suggest the host-rocks as a uranium source. Harshman (1972) and Davis (1969) reported that uranium in Tertiary rocks in the Shirley Basin and southern Powder River Basin districts was slightly more abundant in the altered zone (6 to 15 ppm; 6 ppm, respectively) than in the unaltered zone (4 to 8 ppm; 2 ppm, respectively). Comparisons using other elements (especially Se, V, As, and Mo), which behave similarly in roll-front chemical reactions, can also be made. Vanadium and selenium differences have been detected, but no conclusive relationships have been identified (Harshman, 1972; Harris, 1982). Specific studies designed to overcome the problems of low concentrations and minor differences between altered and unaltered rocks have yet to be attempted.

Because hydrothermal minerals and alteration are not found at redox uranium occurrences, especially those in Wyoming, most geologists have discounted a hydrothermal source (#4). Gabelman (1970), and Gabelman and Krusiewski (1963) proposed a modified hydrothermal origin for the redox deposits.

Age of uranium redox deposits

The reported ages of redox mineralization in Wyoming document several episodes of mobilization and deposition. Measurements obtained from U-Pb isotope studies on uranium ores in Tertiary rocks in the Gas Hills and Crooks Gap uranium districts in the 1950s and 1960s indicated that the date of mineralization was Pleistocene to Recent (Coleman, 1957; Zeller, 1957). Similar ages were reported from uranium deposits in Cretaceous rocks in the Wyoming portion of the Black Hills (Rosholt, 1961; Robinson and Rosholt, 1961). Because these dates were all on near-surface redox mineralization, they actually constrain only the last period of uranium movement, like the uranium mobility studies discussed for the highland leach theory. Other reported ages of uranium mineralization in Wyoming extend from this period back to about 20 Ma and probably indicate a mixture of younger and older uranium mobilization. Reliable determinations of older U-Pb ages from roll-front redox ores in the Shirley Basin, Gas Hills, and Crooks Gap uranium districts showed maximum ages of 28 to 43 Ma and minimum ages of 18 to 35 Ma for the formation of these ores (Ludwig, 1978, 1979; Zielinski, 1980). Supporting data for older ages are the 33 and 20 Ma ages of uraniferous silica in the White River Formation at Lance Creek (Zielinski, 1983) and in the Shirley Basin (Zielinski, 1980), respectively. These late Eocene to earliest Miocene dates support the earlier conceptual models of Childers (1974) and Rackley (1976), which suggested uranium was mobilized and deposited into redox, Tertiary-hosted roll-front and Cretaceous-hosted tabular mineralization from late Eocene into Oligocene time, when the host sediments and rocks were nearer the surface and oxygenated water from the surface could have entered these permeable units. Subtropical climatic conditions, most favorable for the mobilization of uranium, terminated near the end of the Oligocene (Childers, 1974; Rackley, 1976; also Bailey, 1980).

Given occurrence characteristics, the separate intervals of Quaternary and Tertiary U-Pb dates might also have been periods of uranium concentration from all types of preexisting deposits.

Acknowledgments

The authors wish to acknowledge technical reviews of this paper by distinguished uranium geologists William L. Chenoweth and E. N. Harshman. Any technical miscues remaining in this chapter are purely the responsibility of the authors. The writers are indebted to Richard W. Jones, Geological Survey

of Wyoming, and Sheila M. Roberts, University of Calgary, for detailed editorial comments. Helpful comments on the manuscript and the organization of this paper were provided by Arthur W. Snoke.

References cited

Adams, S.S., and Saucier, A.E., 1981, Geology and recognition criteria for uraniferous humate deposits, Grants uranium region, New Mexico: U.S. Department of Energy Open File Report GJBX-2(81), 225 p.

Altschuler, Z.S., Clark, R.J., Jr., and Young, E.J., 1958, Geochemistry of uranium in apatite and phosphorite: U.S. Geological Survey Professional Paper 314-D, 46 p.

Bailey, R.V., 1980, Comments on the Shirley Basin uranium deposits and on the age of all Wyoming uranium deposits in Eocene host rocks: Third annual uranium seminar, American Institute of Mining and Metallurgical Engineers, p. 41-59.

Bauer, C.W., and Dunning, C.P., 1979, Uraniferous phosphate resources of the western phosphate field, *in* De Voto, R.H., and Stevens, D.N., editors, Uraniferous phosphate resources and technology, and economics of uranium recovery from phosphate resources, United States and free world: U.S. Department of Energy Open File Report GJBX-110(79), v. 1, p. 123-248.

Boberg, W.W., 1981, Some speculations on the development of central Wyoming as a uranium province: Wyoming Geological Association 32nd Annual Field Conference Guidebook, p. 161-180.

Borgman, L.E., Sever, C. K., Quimby, W. F., Andrew, M. E., Houston, R. S., and Karlstrom, K. E., 1981, Uranium assessment for the Precambrian pebble conglomerates in southeastern Wyoming: U.S. Department of Energy Open File Report GJBX-139(81), v. 3, 153 p.

Boyle, R.W., 1982, Geochemical prospecting for thorium and uranium deposits: Elsevier Scientific Publishing Company, New York, Chapters 1 and 2, p. 1-121.

Burnett, W.C., Cowart, J.B., and Deetae, S., 1990, Radium in the Suwanee River and estuary: Biogeochemistry, v. 10, p. 237-255.

Chenoweth, W.L., 1988, Geology and production history of the uranium deposits in the northern Black Hills, Wyoming-South Dakota: Wyoming Geological Association 39th Annual Field Conference Guidebook, p. 263-270.

_____ 1991, A summary of uranium production in Wyoming: Wyoming Geological Association 42nd Annual Field Conference Guidebook, p. 169-179.

Childers, M.O., 1974, Uranium occurrences in Upper Cretaceous and Tertiary strata of Wyoming and northern Colorado: The Mountain Geologist, v. 2, p. 131-146.

Coleman, R.G., 1957, Mineralogical investigations, general investigations, mineralogy, and geochemistry of uranium deposits in the Gas Hills district, Wyoming: U.S. Geological Survey Trace Element Investigations Report TEI-690, p. 508-512.

Dahl, A.R., and Hagmaier, J.L., 1976, Genesis and characteristics of the southern Powder River Basin uranium deposits, Wyoming: Wyoming Geological Association 28th Annual Field Conference Guidebook, p. 243-252.

Dahlkamp, F.J., and Adams, S.S., 1981, Geology and recognition criteria for vein-like uranium deposits of the Lower to Middle Proterozoic unconformity and strata-related types: U.S. Department of Energy Open File Report GJBX-5(81), 253 p.

Davis, J.F., 1969, Uranium deposits in the Powder River Basin: University of Wyoming Contributions to Geology, v. 8, p. 131-142.

De Voto, R.H., and Stevens, D.N., editors, 1979, Uraniferous phosphate resources and technology, and economics of uranium recovery from phosphate resources, United States and free world: U.S. Department of Energy Open File Report GJBX-110(79), v. 1, 742 p., v. 2, 672 p.

Drever, J.I., Murphy, J.W., and Surdam, R.C., 1977, The distribution of As, Be, Cd, Cu, Hg, Mo, Pb, and U associated with the Wyodak coal seam, Powder River Basin, Wyoming: University of Wyoming Contributions to Geology, v. 15, p. 93-101.

Dunagan, J.F., Jr., and Kadish, K.A., 1977, Preliminary study of uranium in Pennsylvanian and Lower Permian strata in the Powder River Basin, Wyoming, Montana, and the northern Great Plains: U.S. Department of Energy Open File Report GJBX-81(77), 39 p.

Dyck, W., 1978, The mobility and concentration of uranium and its decay products in temperate surficial environments, *in* Kimberley, M.M., editor, Uranium deposits, their mineralogy and origin: Mineralogical Association of Canada Short Course Notes, University of Toronto Press, v. 3, p. 57-100.

Energy Information Administration, 1990, Uranium industry annual, 1989: U.S. Department of Energy, Energy Information Administration Report DOE/EIA-478(89), 121 p.

Gabelman, J.W., 1970, Metallotectonic control of uranium distribution, *in* Uranium exploration geology: International Atomic Energy Agency, Vienna, Austria, p. 187-204.

Gabelman, J.W., and Krusiewski, S.V., 1963, The application of hydrothermal zoning to Wyoming uranium deposits: Eighth annual uranium and mineral symposium, American Institute of Mining and Metallurgical Engineers, Wyoming section, p. 11-41.

Galloway, W.E., Kreitler, C.W., and McGowen, J.H., 1979, Depositional and groundwater flow systems in the exploration for uranium: Texas Bureau of Economic Geology, University of Texas, Austin, 267 p.

Gaylord, D.R., 1981, Stratigraphic and sedimentary controls on uranium mineralization in sandstones—with an example from the Highland mine, Converse County, Wyoming [M.S. thesis]: Laramie, University of Wyoming, 131 p.

Gruner, J.W., 1956, Concentration of uranium in sediments by multiple migration-accretion: Economic Geology, v. 51, p. 495-520.

Guilinger, R.R., 1963, Source of uranium in the Gas Hills area, Wyoming: Economic Geology, v. 50, p. 285-286.

Harris, R.E., 1982, Alteration and mineralization associated with sandstone uranium occurrences, Wyoming and New Mexico, [M.S. thesis]: Laramie, University of Wyoming, 102 p.

_____ 1986, The genesis of uranium deposits in Athabasca, Canada and northern Australia—Wyoming exploration significance, *in* Roberts, Sheila, editor, Metallic and nonmetallic deposits of Wyoming and adjacent areas, 1983 conference proceedings: Geological Survey of Wyoming Public Information Circular 25, p. 66-83.

_____ 1988, Tectonic control of sandstone uranium deposits, southern Powder River Basin, Wyoming and the Laguna-Paguate District, New Mexico, *in* Kisvarsanyi, G., and Grant, S.K., editors, North American Conference on tectonic control of ore deposits and the vertical and horizontal extent of ore systems: University of Missouri-Rolla, p. 166-173.

Harris, R.E., and Hausel, W.D., 1984, Mineral resources of Permian and Pennsylvanian rocks in Wyoming: Wyoming Geological Association 35th Annual Field Conference Guidebook, p. 369-381.

Harshman, E.N., 1972, Geology and uranium deposits, Shirley Basin area, Wyoming: U.S. Geological Survey Professional Paper 745, 73 p.

Harshman, E.N., and Adams, S.S., 1981, Geology and recognition criteria for roll-type uranium deposits in continental sandstones: U.S. Department of Energy Open File Report GJBX-1(81), 185 p.

Hedrick, J.B., 1985, Thorium, *in* Mineral facts and problems, 1985 edition: U.S. Bureau of Mines Bulletin 675, p. 835-846.

Hough, H.W., 1956, Shawano's new upgrader working: Uranium Magazine, v. 3, no. 11, p. 4-5, 30.

Houston, R.S., 1979, Introduction to second uranium issue and some suggestions for prospecting: University of Wyoming Contributions to Geology, v. 17, p. 85-88.

Houston, R.S., and Karlstrom, K.E., 1980, Uranium-bearing quartz-pebble conglomerates—exploration model and United States resource potential: U.S. Department of Energy Open-File Report GJBX-1(80), 510 p.

Houston, R.S., and Love, J.D., 1956, Titaniferous sandstone in marine rocks of Late Jurassic age, northwestern Wyoming: Wyoming Geological Association 11th Annual Field Conference Guidebook, p. 73-74.

Houston, R.S., and Murphy, J.F., 1962, Titaniferous black sandstone deposits of Wyoming: Geological Survey of Wyoming Bulletin 49, 120 p.

_____ 1970, Fossil beach placers in sandstones of Late Cretaceous age in Wyoming and other Rocky Mountain states: Wyoming Geological Association 22nd Annual Field Conference Guidebook, p. 241-249.

_____ 1977, Depositional environment of Upper Cretaceous black sandstones of the Western Interior: U.S. Geological Survey Professional Paper 994-A, 29 p.

Karlstrom, K.E., and others, 1981, A summary of the geology and uranium potential of Precambrian conglomerates in southeastern Wyoming: U.S. Department of Energy Open File Report GJBX-139(81), v. 1, 541 p.

Keppler, H., and Wyllie, P.J., 1990, Role of fluids in transport and fractionation of uranium and thorium in magmatic processes: Nature, v. 348, p. 531-533.

Kimberley, M.M. 1978, High temperature uranium geochemistry, *in* Kimberley, M.M., editor, Uranium deposits, their mineralogy and origin: Mineralogical Association of Canada Short Course Notes, University of Toronto Press, v. 3, p. 101-104.

King, J.K., 1991, Rare-earth elements and yttrium in Wyoming: Geological Survey of Wyoming Mineral Report MR91-3 (unpublished), 125 p.

Kirk, W.S., 1980, Depleted uranium, *in* Mineral facts and problems: U.S. Bureau of Mines Bulletin 671, p. 997-1003.

_____ 1981, Radium, *in* Mineral commodity summaries: U.S. Bureau of Mines, p. 122-123.

Landa, E.R., 1987, Buried treasure to buried waste—the rise and fall of the radium industry: Colorado School of Mines Quarterly, v. 82, no. 2, 87 p.

Langmuir, D., 1978, Uranium solution-mineral equilibria at low temperatures with applications to sedimentary ore deposits: U.S. Department of Energy Open File Report GJBX-54(78), 86 p.

Langmuir, D., and Herman, J.S., 1980, The mobility of thorium in natural waters at low temperatures: Geochimica et Cosmochimica Acta, v. 44, p. 1753-1766.

Lillie, D.W., 1986, Our radiant world: Iowa State University Press, Ames, Iowa, 226 p.

List, J. E., and Coleman, R. B., 1979, Current U.S. methods of yellowcake precipitation: Engineering and Mining Journal, v. 180, no. 12, p. 78-82.

Love, J.D., 1952, Preliminary report on uranium deposits in the Pumpkin Buttes area, Powder River Basin, Wyoming: U.S. Geological Survey Circular 176, 37 p.

_____ 1953, Uranium content of Middle Pennsylvanian black shales penetrated in wells in southeastern Wyoming: U.S. Geological Survey Trace Elements Memorandum Report TEM-122, 14 p.

_____ 1964, Uraniferous phosphatic lake beds of Eocene age in intermontane basins of Wyoming and Utah: U.S. Geological Survey Professional Paper 474-E, 66 p.

Ludwig, K.R., 1978, Uranium-daughter migration and U/Pb isotope apparent ages of uranium ores, Shirley Basin, Wyoming: Economic Geology, v. 56, p. 423-430.

_____ 1979, Age of uranium mineralization in the Gas Hills and Crooks Gap districts, Wyoming, as indicated by U/Pb isotope apparent ages: Economic Geology, v. 74, p. 1654-1668.

Masursky, H., 1962, Uranium-bearing coal in the eastern part of the Red Desert area, Wyoming: U.S. Geological Survey Bulletin 1099-B, 152 p.

Mathews, G.W., 1978, Uranium occurrences in and related to plutonic igneous rocks, *in* Mickle, D.G., and Mathews, G.W., Geologic characteristics of environments favorable for uranium deposits: U.S. Department of Energy Open File Report GJBX-67(78), p. 121-180.

Melin, R.E., 1964, Description and origin of uranium deposits in Shirley Basin, Wyoming: Economic Geology, v. 59, p. 835-849.

Merritt, R.C., 1971, The extractive metallurgy of uranium: Colorado School of Mines Research Institute, Golden, 576 p.

Mickle, D.G., and Mathews, G.W., 1978, Geologic characteristics of environments favorable for uranium deposits: U.S. Department of Energy Open File Report GJBX-67(78), 250 p.

Mott, L.V., and Drever, J.I., 1983, Origin of uraniferous phosphatic beds in Wilkins Peak Member of Green River Formation, Wyoming: American Association of Petroleum Geologists Bulletin, v. 67, p. 70-82.

Nkomo, I.T., Rosholt, J.N., and Dooley, J.R., Jr., 1979, U-Th-Pb systematics of Precambrian rocks in the Laramie Mountains, Wyoming: Wyoming Geological Association Earth Science Bulletin, v. 12, no. 4, p. 1-13.

Rackley, R.I., 1976, Origin of western-states type uranium mineralization, *in* Wolf, K.H., editor, Handbook of strata-bound and stratiform ore deposits: Elsevier, Amsterdam, v. 7, p. 89-156.

Rackley, R.I., Shockey, P.N., and Dahill, M.P., 1968, Concepts and methods of uranium exploration: Wyoming Geological Association 29th Annual Field Conference Guidebook, p. 115-124.

Renfro, A.R., 1969, Uranium deposits in the Lower Cretaceous of the Black Hills: University of Wyoming Contributions to Geology, v. 8, p. 87-92.

Robinson, C.S., and Rosholt, J.N., Jr., 1961, Uranium migration and geochemistry of uranium deposits in sandstone above, at, and below the water table, part II—Relationship of uranium migration dates, geology and chemistry of uranium deposits: Economic Geology, v. 56, p. 1404-1420.

Romberger, S.B. 1984, Transport and deposition of uranium in hydrothermal systems at temperatures up to 300°C—geological implications, *in* De Vivo, B., Ippolito, F., Capaldi, O., and Simpson, P.R., editors, Uranium geochemistry, mineralogy, geology, exploration and resources: The Institution of Mining and Metallurgy, London, England, p. 12-17.

Roscoe, S.M., 1973, The Huronian Supergroup, a paleo-Aphebian succession showing evidence of atmospheric evolution, *in* Young, G.M. , editor, Huronian stratigraphy and sedimentation: Geological Association of Canada Special Paper 12, p. 31-47.

Rosholt, J.N., Jr., 1961, Late Pleistocene and recent accumulation of uranium in ground-water saturated sandstone deposits: Economic Geology, v. 56, p. 423-430.

Sheldon, R.P., 1963, Physical stratigraphy and mineral resources of Permian rocks in western Wyoming: U.S. Geological Survey Professional Paper 313-B, p. B49-B271.

Sheridan, D.E., Maxwell, C.H., and Collier, J.T., 1961, Geology of the Lost Creek schroeckingerite deposits, Sweetwater County, Wyoming: U.S. Geological Survey Bulletin 1087-J, p. 391-479.

Shockey, P.N., 1974, Copper-silver solution fronts at Paoli, Oklahoma: Economic Geology, v. 69, p. 266-268.

Staatz, M.H., 1983, Geology and description of thorium and rare-earth deposits in the southern Bear Lodge Mountains, northeastern Wyoming: U.S. Geological Survey Professional Paper 1049-D, 52 p.

Stuckless, J.S., 1987, A review of applications of U-Th-Pb isotope systematics to investigation of uranium source rocks: Uranium, v. 3, p. 235-244.

Stuckless, J.S., Hedge, C.E., Worl, R.G., Simmons, K.R., Nkomo, I.T., and Wenner, D.B., 1985, Isotopic studies of late Archean plutonic rocks of the Wind River Range, Wyoming: Geological Society of America Bulletin, v. 96, p. 850-860.

Stuckless, J.S., and Nkomo, I.T., 1978, Uranium-lead isotope systematics in uraniferous alkali-rich granites from the Granite Mountains, Wyoming - implications for uranium source rocks: Economic Geology, v. 73, p. 427-441.

Stuckless, J.S., Nkomo, I.T., and Butt, K.A., 1986, Uranium-thorium-lead systematics of an Archean granite from Owl Creek Mountains, Wyoming: U.S. Geological Survey Professional Paper 1388-C, p. 23-48.

Swanson, R.W., McKelvey, V.E., and Sheldon, R.P., 1953, Progress report on investigations of western phosphate deposits: U.S. Geological Survey Trace Elements Investigations Report TEI-246, 29 p.

Taylor, S.R., and McLennan, S.M., 1985, The continental crust—it's composition and evolution: Blackwell, Oxford, England, 312 p.

Thamm, J.K., Kovschuk, A.A., Jr., and Adams, S.S., 1981, Geology and recognition criteria for sandstone uranium deposits of the Salt Wash type, Colorado Plateau province, Final report: U.S. Department of Energy Open File Report GJBX-6(81), 135 p.

Trentham, R.C., and Orajaka, I.P., 1986, Leaching of uranium from felsic volcanic rocks: experimental studies: Uranium, v. 3, p. 55-67.

Vine, J.D., 1962, Geology of uranium in coaly carbonaceous rocks: U.S. Geological Survey Professional Paper 346-D, p. 113-170.

Zeller, H.D., 1957, The Gas Hills uranium district and some probable controls for ore deposition: Wyoming Geological Association 12th Annual Field Conference Guidebook, p. 156-160.

Zielinski, R.A., 1980, Uranium in secondary silica—a possible exploration guide: Economic Geology, v. 75, p. 592-602.

_____ 1983, Tuffaceous sediments as source rocks for uranium—a case study of the White River Formation, Wyoming: Journal of Geochemical Exploration, v. 18, p. 285-306.

_____ 1984, Volcanic rocks as sources of uranium, *in* Uranium deposits in volcanic rocks: International Atomic Energy Agency, Vienna, Austria, p. 83-95.

Zielinski, R.A., Peterman, Z.E. Stuckless, J.S., Rosholt, and J.N., Nkomo, I.T., 1981, The chemical and isotopic record of rock-water interaction in the Sherman granite, Wyoming and Colorado: Contributions to Mineralogy and Petrology, v. 78, p. 209-219.

Frontispiece. Industrial minerals geologists, developers, and landowners examine marble deposits (the light-colored outcrops in the foreground and on the hills in the center background) at Little Wildcat Canyon, Goshen County, Wyoming.

Industrial minerals and construction materials of Wyoming

Ray E. Harris
Geological Survey of Wyoming
Laramie, Wyoming 82071

Abstract

Industrial minerals and construction materials have been used by people since the Stone Age. Wyoming's first inhabitants used mineral pigment for decoration, salt for preserving meat, and stone for tools. Now, Wyoming produces industrial minerals used in space-age technology. Wyoming boasts the world's largest producing trona deposit, the nation's largest production of bentonite, and important production of limestone, gypsum, recovered sulfur, decorative stone and aggregate, and railroad ballast. Zeolites and silica sand are examples of industrial minerals in Wyoming with development potential.

Introduction

Industrial minerals and construction materials have always been instrumental to civilization. From the first stone used as a tool, rock products have been essential. In Wyoming, the first inhabitants of the region quarried chert and obsidian for tools, talc and clay for implements, iron ore (mineral pigment) for decoration, and salt for a preservative. Early settlers used salt and made bricks from clay, glass from silica sand, plaster from limestone and gypsum, and other products from Earth materials. Today, Wyoming produces industrial minerals for export, including trona, bentonite, sodium sulfate, gypsum, decorative stone and aggregate, recovered sulfur, and many others.

As defined by the U. S. Bureau of Mines, industrial minerals are *rocks and minerals not produced as sources of metals but excluding mineral fuels* (Thrush, 1968, p. 577). This definition leaves room for minerals not generally considered industrial, such as gemstones. The industrial minerals considered here are those covered by the above definition, but excluding gemstones. Industrial minerals are generally produced in relatively large volumes and at relatively low prices. Construction materials are industrial minerals used specifically for construction of buildings, dams, highways, and other projects. Some of these minerals are also used for non-construction projects. Gypsum is a construction material when used in cement or drywall, but is not a construction material when used to produce chemicals. Construction materials generally have the lowest cost of all industrial minerals. Construction materials are grouped with the other industrial minerals in this chapter. **Table 1** lists industrial minerals found in Wyoming that may be used in construction.

It is the price structure that determines the suitability of industrial minerals, though quality does affect the usefulness of an industrial mineral. Industrial minerals and construction materials grade all the way from sand and gravel, priced in cents per ton, to oxides of rare earths and related minerals, priced in hundreds of dollars per ounce. Transportation costs have always been a major factor in the development of industrial minerals. For this reason,

Harris, R.E., 1993, Industrial minerals and construction materials of Wyoming, *in* Snoke, A.W., Steidtmann, J.R., and Roberts, S.M., editors, Geology of Wyoming: Geological Survey of Wyoming Memoir No. 5, p. 918-937.

it has always been desirable to locate industrial mineral sources as close as possible to the point of use.

This chapter summarizes the occurrence, use, and development potential of some industrial minerals and construction materials that occur in Wyoming. **Figure 1** shows selected occurrences of industrial minerals and construction materials summarized in the text. Some industrial minerals found in Wyoming have only limited extent or little or no possibility for development. For these minerals, and their current references, see **Table 2**.

Table 1. Construction materials found in Wyoming.

Aggregate
Construction aggregate [sand, gravel (river rock), and crushed stone]
Decorative aggregate
Lightweight aggregate (includes pumice and pumicite, expanded shale, vermiculite and others)
Roofing granules
Cement and cement raw materials
Limestone
Gypsum
Shale, marl, and other additives
Iron oxide and other mineral additives used in relatively small amounts
Stone
Dimension stone
Facing and other cut and natural slab stone
Decorative stone
Insulating material (includes vermiculite and other materials)

Industrial minerals and construction materials

Aggregate

Aggregates are crushed stone, gravel, or sand, which are usually sized, and are used to provide mass and weight to concrete, fill, paving material, or similar materials or used separately as in landscape rock or gravel road surfacing. Construction aggregate is the rock used in construction to provide weight or volume. It can be used separately, as in fill for dikes and levees, or it can be mixed with a binder such as asphalt or cement. The material is usually graded as to strength and sized. The largest construction aggregate consists of boulder-sized pieces and is called rip-rap. Fine sand is used in some applications. Ballast is a specialty construction aggregate used in railroad construction. Decorative aggregates are used for the same purposes, but are also selected for their color or other visual qualities.

Gravel deposits are usually found in Quaternary alluvium, as river gravels or in terrace deposits. Some older material, for example the Eocene Kingsbury Conglomerate near Sheridan, can also be used. Glacial deposits sometimes serve as sources of gravel, but they often have a wide variation in clast size, so that a large volume of material must be processed to get the material required. Gravel deposits may be screened to provide the required size or they may be crushed and screened. Uncrushed gravel is called "river rock" regardless of its geologic origin. The largest producing pit for construction aggregate in Wyoming is located in gravel deposits of the Bear River at Evanston (**Figure 1**).

Wyoming contains large resources of sand in active and inactive dune fields, especially common in an area that extends from northwest of Rock Springs through Lamont, Ferris, Casper, and Douglas, to Torrington. Other sand dunes exist in most areas of Wyoming.

Wyoming also contains large reserves of limestone and granitic rocks, some basalt, and other rocks suitable for the production of crushed aggregate.

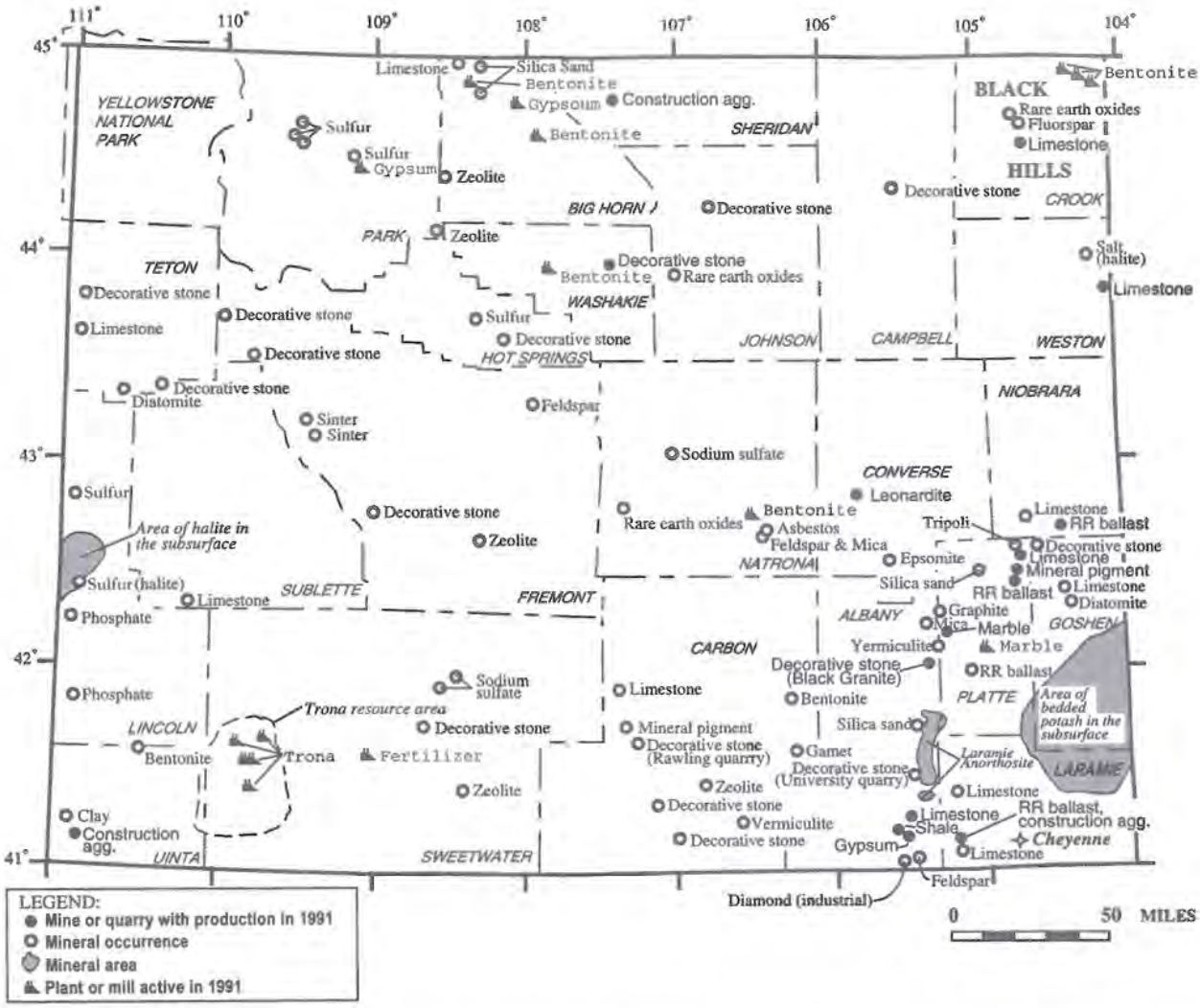

Figure 1. Index map of Wyoming showing selected industrial mineral occurrences, mines and quarries, and refineries or mills. (RR = railroad; agg = aggregate). County names are shown in all capital letters in italic type.

Table 2. Industrial minerals found in Wyoming, but not discussed in this paper.

Commodity	Best available reference
Alum minerals	Harris and King (1986d)
Alunite	Harris and King(1986d)
Cordierite	Osterwald and others (1966)
Corundum	Hausel (this volume)
Kyanite and related minerals	Osterwald and others (1966)
Peat	Sturges (1968)
Pumice and pumicite	Harris and King (1986b)
Rutile	Harris (1990b)
Staurolite	Osterwald and others (1966)
Wollastonite	Osterwald and others (1966)

Crushed aggregate is preferred over river rock where the material must be uniform. Limestone and granite are the most commonly used rock types. Rocks used for crushed aggregate must meet durability specifications and must contain no deleterious minerals such as sulfide minerals or chert that can react with binder materials. Large limestone aggregate quarries are located near Sundance in Crook County, east of Newcastle in Weston County, and near Guernsey in Platte County (see *Wyoming geologic highway map*, **map pocket** for location of cities and towns). The granite ballast

quarry west of Cheyenne also sells granite for construction aggregate (**Figure 1**).

Railroad ballast

Railroad ballast is a type of construction aggregate with special properties used to weight and secure ties and track on rail lines. Since ballast should consist of unequidimensional pieces, the better rock sources are often gneissic granites. Railroad ballast sources must be located near rail lines. Three localities in Wyoming—Granite, west of Cheyenne; Bald Butte, south of Lusk; and Guernsey Stone, near Guernsey (**Figure 1**)—have produced large amounts of ballast in recent years. Other localities in Wyoming contain suitable rock and may be future sources (Harris, 1987a).

Decorative aggregate

Decorative aggregate is used as aggregate in concrete to produce colored concrete products for buildings and other structures, in landscaping, on roofs, and in similar applications. In Wyoming, Georgia Marble operates a quarry for white marble west of Wheatland and a processing plant at Wheatland (**Figure 1**), producing sized, crushed, white marble used primarily for roofing granules, but also sold for landscaping, pigments, and other uses. Small amounts of red granite and other rocks have been shipped from Wyoming in the past. The variety and accessibility of colored granite, quartzite, marble, and other rock in Wyoming could provide the basis for a flourishing industry in the state (Harris, 1991).

Anorthosite

Anorthosite is a plutonic igneous rock composed almost entirely of plagioclase feldspar (Thrush, 1968). Anorthosite became widely known to the public in the 1960s because it was the first type of rock brought from the moon. The only anorthosite body in Wyoming is one of the largest in North America. The Laramie anorthosite is found in the central Laramie Mountains from the latitude of Laramie north almost to the Laramie River (**Figure 1**).

Anorthosite is both an industrial rock and a potential source of aluminum. The Laramie anorthosite is of interest for its aluminum content (Brown and others, 1947; Rocky Mountain Energy, 1985; Grubbs and Moose, 1981; and Harrer, 1954). If bauxite resources are depleted, anorthosite will probably become the most economical source of aluminum. The Laramie anorthosite could have great potential. Magnetic iron and titanium resources are also found within the anorthosite body (see Frost and others, this volume; Hausel; 1990, and Hausel, this volume). Locally, gem-quality labradorite is found in the anorthosite, and some varieties are quarriable as decorative stone (Harris, 1991).

As an industrial material, anorthosite is also a source of feldspar used in ceramics and glass, and as a fluxing agent in metal smelting (Potter, 1993a). The mafic- and sulfide-free phases may be useful as decorative stone. The Laramie anorthosite can potentially be developed for these uses. The Laramie anorthosite has also been used as construction aggregate (Harris, 1990a).

Asbestos

Asbestos is a group of minerals characterized by their fibrous nature. The primary asbestos mineral is chrysotile, a variety of serpentine, but fibrous amphiboles were often used in asbestos products. Recently, asbestos fibers have been suspected as causing various forms of silicosis and as a carcinogen. As a result, the demand for asbestos is very small, though asbestos products including roofing materials, friction products (such as brake linings), asbestos-cement pipe, packing and gaskets, and certain other products are still being made (Virta, 1993). A few asbestos deposits in Wyoming produced small amounts of this mineral before 1940 (Beckwith, 1939). Most of these are in the northern Laramie Mountains, although there are asbestos deposits in the Wind River and Teton ranges (Osterwald and others, 1966). Apart from a mineralogical curiosity, it is not likely that there will be a demand for Wyoming asbestos in the near future.

Bentonite

Bentonite is a clay deposit produced by the diagenetic alteration of volcanic ash. It is used for its physical properties (expansion when wet, high viscosity, cation exchange capacity, and others). Bentonite-bearing rocks (primarily found in the Upper Cretaceous Mowry and Frontier formations) are found at many locations in Wyoming, except for the southeastern corner (**Figure 2**). Wyoming produces

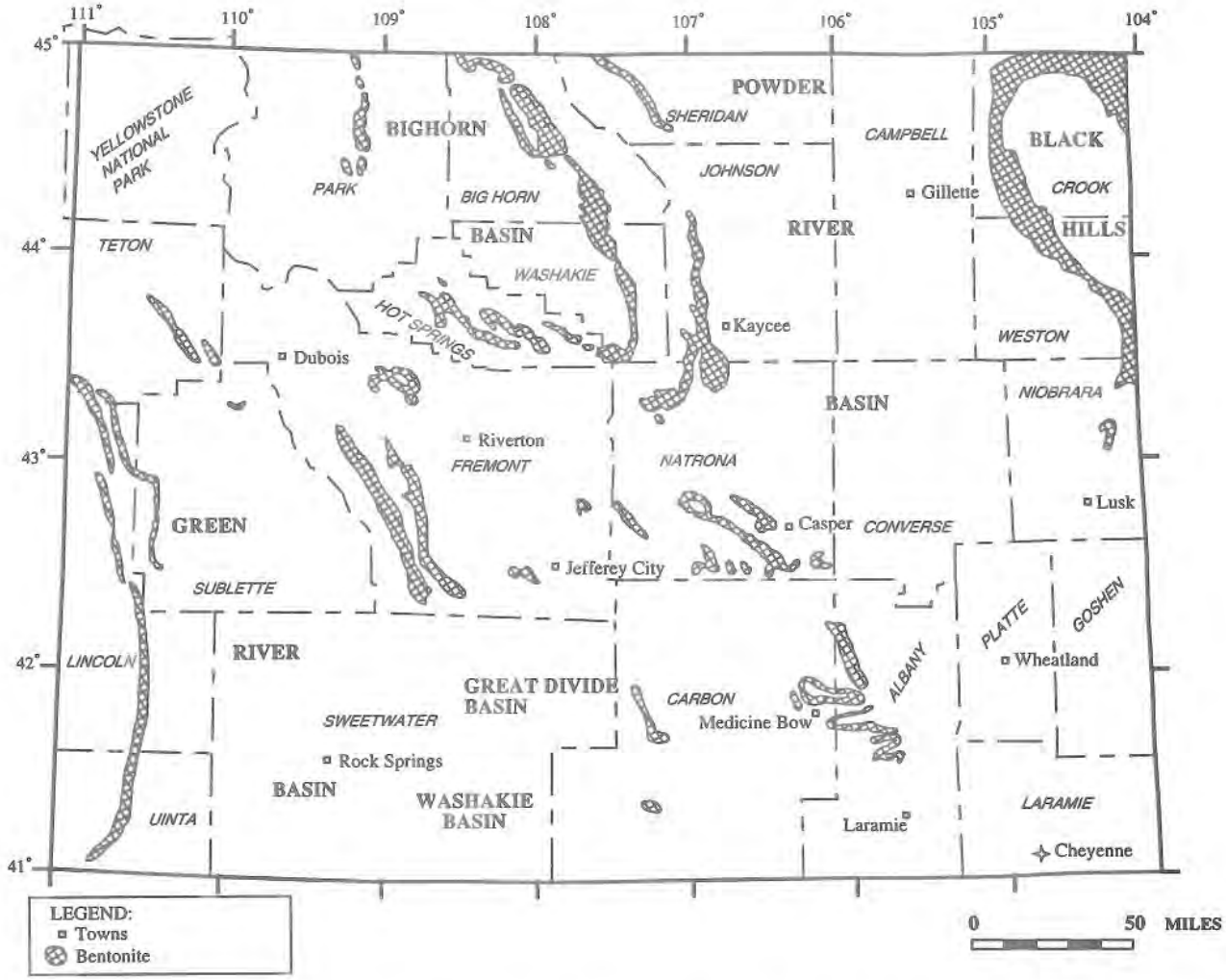

Figure 2. Index map showing outcrop of bentonite-bearing strata in Wyoming. County names are shown in all capital letters in italic type.

more bentonite than any other state, and bentonite was the second most important industrial mineral (in terms of the value of production) produced in Wyoming in 1991. Bentonite is produced in the Black Hills, the Bighorn Basin, and near Kaycee in the western Powder River Basin. In the past, bentonite was produced near Casper, Medicine Bow, and other areas.

Bentonite has many uses and in fact is commonly called "the clay of a thousand uses". Some major uses are as a binder in pelletizing taconite (siliceous iron ore), as a lubricant, sealant, and thickener in drilling fluid, as a sealant in waste-isolation ponds, as a coagulant and cation exchanger in water and waste treatment, and as a mineral filler in many products. Most bentonite is currently sold for use as a binder in taconite pelletizing. Before 1991, most bentonite was used in drilling fluid.

The grade of bentonite varies from place to place, vertically in a bentonite bed, and with the amount of surface alteration (Rath, 1986). Since each of the uses require slightly different properties, bentonite is usually mined from many separate pits, analyzed for quality, and dried and blended in the mill to produce the grade and composition desired.

Clay (common)

Common clay is clay or clay-like material that is sufficiently plastic to permit ready molding (Ampian, 1985). Common clay contains the minerals

illite, smectite, and kaolinite (Patterson and Murray, 1983). Common clay was produced in almost every county in Wyoming during the early years of statehood for bricks, which were used locally (Harris and King, 1987a). At present, common clay is mined near Evanston, in Uinta County (**Figure 1**), and shipped to Utah for brick-making. Occasionally clay pits are opened for an immediate local need. In 1986, clay was mined from a pit near Laramie for use in the construction of an impermeable barrier around a contaminated former industrial site. Small amounts of clay from near Yoder, in Goshen County, have been used for surfacing athletic fields in Wyoming.

Decorative stone

Decorative stone is any rock product exclusive of aggregate that is used for its color or appearance. Natural stone is unprocessed material removed directly from an outcrop. Cut stone is rock cut on at least one side. Color and appearance are criteria in selecting decorative stone and the material must also meet strength, durability, and other tests such as the absence of sulfides or minerals that could weather and stain or discolor the rock. Quarriable granite, marble, quartzite, or other stones must be free of fractures, joints, or other blemishes.

Decorative stone has been produced from several areas in Wyoming. South of Rawlins (**Figure 1**), stone was quarried from an Upper Cretaceous sandstone within the Mesaverde Formation. This stone was used in a number of buildings in Wyoming and the region, including the Wyoming State Capitol and the Union Pacific Railroad Depot in Ogden, Utah. A sandy limestone from a quarry in the Permian-Pennsylvanian Casper Formation 6 miles north of Laramie (**Figure 3**) was used in some of the buildings on the University of Wyoming campus in Laramie. Granite, onyx, sandstone, and marble were quarried from several locations in the Hartville uplift north of Guernsey. This stone was processed into monuments by Jay Em Stone Company in Jay Em, Wyoming. A monument stone quarry developed in a pink granite was reportedly located in Sinks Canyon south of Lander, and a monument stone quarry developed in a gray granite was worked in Teton Canyon, on the west side of the Teton Mountains near the Grand Targhee ski area. Stone was quarried at several locations in Wyoming by the operators of the marble aggregate quarry near Wheatland. Some Precambrian green serpentine was quarried for decorative stone, and a quarry in Precambrian green quartzite was operated near Browns Mountain in the Medicine Bow Mountains west of Centennial (see Harris, 1991, for descriptions of these and other locations). There have probably been other small quarries worked in the past for decorative stone, but many of these were not reported and produced only small amounts of stone for local uses. A stone quarrying and finishing industry in Wyoming may be economically competitive with other areas.

Diamond (industrial)

Industrial-grade diamonds have been found in Wyoming in the State Line district south of Laramie (see Hausel, this volume, for a discussion of the geol-

Figure 3. The University of Wyoming stone quarry 6 miles north of Laramie.

ogy and occurrence of diamonds in Wyoming). The major uses for industrial diamonds are in machinery, mineral services (diamond drilling bits), stone and ceramic processing (cutting and polishing), abrasive sand, contract construction, transportation equipment, and others (Austin, 1993a).

Diatomite

Diatomite, also known as diatomaceous earth or kieselguhr, is a siliceous sedimentary rock composed of the skeletal remains of single-celled aquatic plants (diatoms) (Kadey, 1985; Thrush, 1968). Diatomite is found in geologically young rocks that have not been subjected to metamorphism or destructive diagenesis (Williamson, 1966). Diatomite is used primarily in filter aids and mineral fillers (Davis, 1993a). The material is characteristically cellular silica and can be used, when pure, in untreated form.

In Wyoming, diatomite is found in Yellowstone National Park associated with lacustrine sediments in active and inactive thermal areas, in Pliocene and Miocene rocks in Teton County, and on Casebier Hill in Goshen County (**Figure 1**). No diatomite has been produced in Wyoming (Harris and King, 1986a). Since all current production of diatomite is west of Wyoming, and most of the U.S. diatomite is used in the eastern United States, a deposit in Wyoming would save some transportation costs to eastern markets.

Feldspar

Feldspars of commercial importance occur in large bodies of pure or consistent grade without other mineral impurities and usually free from iron oxides (Rogers and others, 1983). Deposits of commercial-grade feldspar are usually found in pegmatites.

Ninety-nine percent of all feldspar mined is used in ceramics and as an ingredient in glassmaking, where it functions as a flux (Potter, 1993a). The remaining 1% is used for abrasives, in false teeth and related items, and in other minor products.

Feldspar was produced in several localities in Wyoming before the 1960s and again in the early 1980s. Many pegmatites in the southern Laramie Mountains (**Figure 1**) were mined for feldspar. Much of this production went into dental products. Other producing areas included Casper Mountain and north of Bonneville, Wyoming.

Fluorspar

Fluorspar, rarely called florspar (Thrush, 1968), is the mineral fluorite. It is an important source of fluorine and is also used as a flux. Fluorspar is found in several areas in Wyoming, notably in the Black Hills (**Figure 1**). There, fluorspar is found in Tertiary peralkaline and carbonatitic intrusives and veins and in replacement bodies in Mississippian limestones surrounding the intrusives. Fluorspar was produced until recently by the Ozark-Mahoning Company at Kings Canyon, Colorado, 2 miles south of the Wyoming State Line southwest of Laramie. However, there has been no large-scale production from Wyoming (Harris and King, 1988).

Garnet (industrial)

The garnet mineral group is used both as an industrial mineral and as a semiprecious gemstone. As an industrial mineral, its primary use is as an abrasive in the petroleum industry where much of it is used for cleaning the interior of petroleum carrying ships. The remaining uses of garnet are in filtration, transport manufacturing, in sandpaper for wood finishing, in electronic components, and in ceramics and glass (after Austin, 1993b).

There are several garnet occurrences in Wyoming (see Hausel, this volume). Small amounts of garnet have been produced from localities near Garnet Hill in the Hartville uplift. Reserves are large, and garnet may be a future Wyoming industrial mineral product.

Graphite

Graphite was formerly called plumbago (black lead). Graphite occurs naturally and can also be produced synthetically from coke or other carbon residues. It is used by several hundred manufacturing firms in the United States in refractories, brake linings, lubricants, dressings and molds in foundries, and in other minor products (Taylor, 1993). The demand for graphite should increase as a result of its

substitution for asbestos in brake linings and other friction products.

Graphite is found in Wyoming in Precambrian metamorphic rocks. Most graphite occurrences are in the Laramie Mountains and the Hartville uplift (Harris, 1989b). There are no producing graphite mines in Wyoming (1993), though there was some production of graphite from Platte County (*circa* 1900). Moderate to large resources of graphite may be present at some of these occurrences (Harris, 1989b).

Gypsum

Gypsum is used in agriculture as a soil conditioner, as a cement retarder, in industrial building products (especially wallboard), or in plaster (Davis, 1993b). Gypsum is produced in many states.

In Wyoming, gypsum is found in the Pennsylvanian Amsden Formation, the Permian-Triassic Goose Egg and Spearfish formations and equivalents, the Jurassic Gypsum Spring Formation, and locally in the Jurassic Sundance Formation. Postdepositional tectonics have deformed layered gypsum deposits into thick lens-shaped deposits at the hinges of folds in certain areas, particularly along the east side of the Laramie Mountains from south of Douglas to Cheyenne. Quaternary deposits of gypsite are found near outcrops of these units, especially near Laramie, where they were mined for gypsum in past years.

Although Wyoming is not a major gypsum producer, its gypsum deposits are closer to the Pacific Northwest than others, and have the potential to supply that area. Wallboard is manufactured at two plants in the Bighorn Basin (**Figure 1**).

Leonardite

Leonardite is a naturally occurring organic material produced by the oxidizing of lignite or coal (Thrush, 1968). Leonardite is mined north of Glenrock in Converse County (**Figure 1**) and processed in a plant in Casper for use as a soil conditioner. It can also be used as a wood stain and as a well-drilling fluid additive.

Limestone

Chemical grade (high-calcium) limestone is used as an industrial mineral. Most high-calcium limestone is roasted to produce lime (CaO), which is used in refining beet sugar, in cement, in glass, and as a soil conditioner (Boynton and others, 1983; Carr and Rooney, 1983). Chemical-grade limestone is also used as an abrasive, as an industrial chemical in calcining processes, and in many other minor products.

Several rock units in Wyoming contain high-grade limestone. These include the Cambrian Gallatin and Pilgrim limestones (in northwest Wyoming); the Devonian-Mississippian Guernsey Formation; the Mississippian Madison and Pahasapa limestones; the Permian-Pennsylvanian Casper, Hartville, and Minnelusa formations; the Permian Minnekahta Limestone; the Triassic Alcova and Thaynes limestones; and the Cretaceous Niobrara and Greenhorn formations.

Limestone is quarried from the Casper Formation near Laramie for cement. It is also quarried from the Guernsey Formation north of Hartville for use in emissions control in the coal-fired electricity generating plant north of Wheatland. In recent years, limestone was quarried for use in sugar-beet refining from the Guernsey Formation north of Fort Laramie, from the Madison Limestone near Lovell, and from the Madison Limestone on the west slope of the Teton Mountains south of Alta. A lime plant is under construction west of Frannie. The source of limestone for this plant is from the Warren quarry in Montana. However, a limestone quarry in the Madison Limestone is planned for east of Frannie. The limestone from this plant is to be used for power plant emissions control products.

Mica

Muscovite and rarely phlogopite are the only micas that have industrial potential. Sericite is a potentially important variety of fine-grained muscovite characterized by a distorted platy structure (Chapman, 1983). Mica can be split into very thin sheets that are durable and transparent and also have dielectric and insulating capabilities.

Commercial categories of mica include sheet mica (sheets large enough to be cut, punched, or stamped into various shapes and sizes), punch mica (an archaic term for sheet mica cut by a punch), and scrap and flake mica (small flakes that used to be the waste from sheet mica production) (Chapman, 1983). Sheet mica was once used for glazing stove windows, doors, lamp chimneys, and lampshades (Gwinn, 1951). The production of mica declined in the late 1940s and early 1950s as other material substituted for mica for these uses. There has recently been a small increase in the use of mica (all scrap and flake) for pearlescent additives to paint, pigment, and decorative facing material. In the past, the best mica was the most colorless. Now, colored varieties are in demand. Currently, mica is used in joint cement, paint, roofing, oil well drilling fluid, and rubber products (Davis, 1993c).

In Wyoming, possible commercial deposits of mica are most often found in pegmatites. Sericite is found in some Precambrian schists. The principal areas of muscovite-bearing pegmatites are the Medicine Bow Mountains, Sierra Madre, northern Laramie Mountains, and Hartville uplift (Harris, 1989b).

Mineral pigments

Mineral pigments are naturally occurring insoluble minerals used to provide color to selected products (after Thrush, 1968; Hancock, 1983). The most common mineral pigments are iron oxides. These produce colors of brown, red, yellow, or orange. Rutile is used to produce white titanium oxide pigment . In Wyoming, mineral pigments were one of the first mineral products to be used and exported. Archaeological evidence indicates that red hematite pigment from the Sunrise area of Platte County was used by prehistoric Indians for body decoration and carried to other areas for trade (George Frison, Wyoming State Archaeologist, personal communication, 1986).

In modern times, red iron-oxide pigment, occurring as pockets of replacement ore in the Madison Limestone 1 mile north of Rawlins in Carbon County (**Figure 1**), was mined for paint pigment. This product was known as "Rawlins Red", and was a major source of pigment used on railroad cars. Currently, small amounts of iron-oxide fines, waste from past iron mining at Sunrise (**Figure 1**), are being shipped to the eastern United states for pigment in cosmetics (this color is known as "desert dust") and to South America for boxcar paint pigment. Other sources of mineral pigment are found in Wyoming (Harris, 1992).

Phosphate

Phosphate rock is the source for calcined phosphate compounds, 90% of which are used as a major component of fertilizer. The remaining 10% is used to produce industrial chemicals such as elemental phosphorous or phosphoric acid (Morse, 1993).

The Permian Phosphoria Formation is a major source of phosphate rock in the western U.S. Phosphate is found in mineable concentrations in the Meade Peak and Retort Phosphatic Shale Members. Phosphate has not been mined in Wyoming since 1977. Before that time, phosphate was one of the major industrial materials produced in the state, beginning in 1906 with production from near Cokeville (Lloyd, 1970). The largest Wyoming phosphate operation was the mine and calcining plant at Leefe, west of Kemmerer in Lincoln County (**Figure 1**). The mine at this location closed in 1977; the plant closed in 1985 and has since been dismantled.

In 1986, Chevron Chemical Company began producing phosphate fertilizer at a plant near Rock Springs (**Figure 1**). This plant is operated by FS industries (1993). It uses Wyoming sulfur, but receives its phosphate from a mine north of Vernal, Utah. The phosphate is transported to the mine by slurry pipeline over the Uinta Mountains.

Rare earth oxides and yttrium

Rare earth oxides are industrial compounds used in the manufacture of catalysts used in petroleum refining, as ceramic and glass coloring agents, in electrical products, in color phosphors, in laser generating machinery, and in other products. Rare earth metals are used in metallurgical products including pyrophoric alloys and permanent magnets (Hedrick, 1993a). The rare earth minerals are the lanthanide series (**Table 3**). The element yttrium is considered together with the rare earths since it is usually found with the lanthanides. It is used as a

Table 3. Chemical symbols and atomic weights of rare earth elements and yttrium.

Element	Chemical symbol	Atomic number
Yttrium	Y	35
Light rare earth elements		
Lanthanum	La	57
Cerium	Ce	58
Praseodymium	Pr	59
Neodymium	Nd	60
Prometheum	Pm	61
Samarium	Sm	62
Europium	Eu	63
Gadolinium	Gd	64
Heavy rare earth elements		
Terbium	Tb	65
Dysprosium	Dy	66
Holmium	Ho	67
Erbium	Er	68
Thulium	Tm	69
Ytterbium	Yb	70
Lutetium	Lu	71

phosphor in televisions and computer monitors, trichromatic fluorescent lights, temperature detectors, and x-ray screens (Hedrick, 1993b). Rare earth oxides have been used as a group, in part due to the difficulty in separating the individual oxides. Recently, the trend in consumption is towards the use of individual oxides.

Minerals containing rare earth elements are present in alkaline igneous rocks, carbonatites, pegmatites, veins, breccias, and in both fossil and Quaternary placers (King and Harris, 1987). [For a discussion of the geology of rare-earth bearing rocks, see Hausel, this volume.]

Wyoming contains several occurrences of rare-earth-bearing minerals in black sand paleoplacer deposits in Cretaceous rocks, in peralkaline igneous rocks of Tertiary age in the Black Hills and Rattlesnake Hills (**Figure 1**), in veins and pegmatites in Precambrian igneous rocks, in Eocene lacustrine rocks, and in the Permian Phosphoria Formation. Perhaps the most important of these is the Bear Lodge Mountains igneous intrusive complex, northwest of Sundance in Crook County (King and Harris, 1987) (**Figure 1**). Rare earth minerals, especially the heavy rare earth minerals, are in demand. The price of heavy rare earth oxides is usually much greater than precious metals.

Saline minerals (exclusive of trona)

Saline minerals are found in several areas of Wyoming as bedded deposits in sedimentary rocks or as evaporite deposits in modern playas. Halite occurs in several areas and potash occurs at depth in east-central Wyoming. Sodium carbonate minerals and epsomite (hydrous magnesium sulfate) are found in Quaternary playa lake deposits.

Epsomite (epsom salt) has been used in relatively small quantities in the past for industrial chemicals and medical products. In the early years of this century, at the Rock Creek Lakes, in Albany County, and at Poison Lake, in Converse County, small plants were constructed to produce epsomite. Small resources of epsomite are present in Wyoming at these and other sites (Harris, 1987b).

Halite (table salt) is important as a preservative. Some salt springs in Wyoming were known by the Native Americans and early pioneers. Notable among these was the salt spring north of Newcastle in Weston County (Harris, 1988a), and the salt spring on the Salt River north of Cokeville, in Lincoln County (Harris, 1987c) (**Figure 1**). Salt is presently used by the chemical industry, for highway deicing, and in other products including soil conditioners, food, and water treatment (Kostick, 1993a).

In Wyoming, halite deposits are found at the surface in a few localities associated with brine springs. Halite occurs mixed with trona in the Green River Basin trona resource area (Culbertson, 1986). A sizable occurrence of halite is present in the Jurassic Preuss Formation, in far west-central Wyoming (Peterson, 1972).

Potash is used almost exclusively in agriculture as a soil conditioner or as a primary ingredient in fertilizer. It has not been produced in Wyoming in the past (Searls, 1993). Evaporite beds of potash are present in the subsurface in Goose Egg equivalent rocks (Triassic) in eastern Wyoming (Rascoe and Baars, 1972). Oil wells have penetrated this section, and a few cores of potash-rich rock have been recovered (J. D. Love, personal communication, 1984).

These beds may be an economically viable resource of potash.

Sodium sulfate is an industrial chemical used for soap and detergents, in pulp and paper treatment, in glass, and in many minor products (Kostick, 1993c). Pure sodium sulfate is found in nature as the minerals thenardite (anhydrous) and mirabilite (hydrous). Mirabilite is produced in Wyoming at the Pratt sodium sulfate deposit near Natrona, in Natrona County. The large wooden barn near Highway 26 is the drying and storage facility associated with this relatively small operation. The sodium sulfate minerals are recovered from an alkali lake north of the shed, stored, and shipped in closed hopper cars to a purchaser in Chicago. Other sodium sulfate-rich lakes are also found in Wyoming (Harris and others, 1985).

Shale

Shale is an industrial mineral used as an additive in cement and as construction aggregate, when durable. Siliceous shale is being mined for this purpose from the Cretaceous Mowry Shale near Laramie (**Figure 1**). In the past, shale was mined from the Cretaceous Niobrara Formation near Laramie and expanded by heating into lightweight aggregate.

Silica raw materials

Quartz is the most common silica mineral. The primary sources of silica are ancient and recent quartzose sand or sandstone deposits and pegmatite quartz.

Silica is the primary ingredient for the manufacture of glass, ceramics, and related products. Silicon metal, produced from silica by an expensive, energy-consuming process, is used in electronics and in solar cells and other applications. Industrial sand is a classification of sand based on both physical and chemical properties. Silica sand is classified as a type of industrial sand. Industrial sand is used for foundry sand, abrasives, traction sand, hydraulic fracturing sand (frac sand), and related products.

Wyoming contains numerous sand or sandstone deposits of 90% SiO_2 or better. These silica sources are found in the Cambrian Flathead Sandstone, Permian-Pennsylvanian Casper and Tensleep formations, Jurassic Morrison Formation, Cretaceous Cloverly Formation, and Quaternary eolian sand dune deposits (Harris, 1988b; Harris, 1988c; Harris and Warchola, 1992). In the late 1800s and early 1900s, many Wyoming communities had small glass plants that served local needs. The source of silica was usually any sand, and glass produced in these places was usually colored and used primarily for containers.

Soda ash, lime, and feldspar are also major ingredients in glass manufacture. All of these ingredients are found in Wyoming. Ninety percent of all soda ash produced in the United States comes from mined trona west of Green River (see Trona).

Sulfur

Sulfur is an important industrial mineral used in fertilizer, organic and inorganic chemicals (particularly sulfuric acid), petroleum refining, metal refining, and numerous other application (Ober, 1993). In the United States, sulfur is mined by the Frasch process, in which hot water is pumped down a well to melt elemental sulfur in-situ; the melted sulfur is pumped to the surface, where it is refined. Sulfur is also produced from the refining of sour natural gas, in which sulfur is recovered from hydrogen sulfide, the undesirable component in sour gas.

Wyoming contains natural sulfur deposits. Sulfur was mined from bedded replacement deposits in the Phosphoria Formation west of Thermopolis, and large reserves may still be present in this area. Sulfur deposits associated with recent hot spring or fumarolic activity are also found in Wyoming (Harris and King, 1985), for example in Sunlight Basin and at Auburn Hot Springs in northern Lincoln County (**Figure 1**).

In Wyoming, all current sulfur production is by natural gas refiners. Some of this sulfur is used to produce fertilizer in FS Industries' fertilizer plant near Rock Springs (**Figure 1**).

Tripoli

Tripoli, also called tripolite, is an industrial term for a rock composed of soft and friable microcrystal-

line quartz. Tripoli probably forms by leaching of calcium carbonate from limestones containing abundant finely dispersed chert. The particle size in tripoli ranges from 0.1 to 10 microns (Bradbury and Ehrlinger, 1983). Tripoli has been reported to occur in Wyoming (Harris, 1989a), but no commercial deposits have been identified.

Tripoli is used in many industrial products including abrasives (buffing, scouring, and polishing compounds; toothpaste; and industrial cleaners and soaps); as mineral fillers in paint, plastic, and rubber, and in electrical plastics, since tripoli adds dielectric properties (Rheams and Richter, 1988, Bradbury and Ehrlinger, 1983). Other uses include refractory glasses and ceramics, carriers in insecticides, and fillers in adhesives, wallboard and plastic wood (Metcalf, 1946).

Trona

Trona (natural sodium carbonate-bicarbonate) is the most important industrial mineral produced in Wyoming in terms of value and employment. Presently, trona is being mined west of Green River and refined to soda ash and other sodium products at five plants (**Figure 1**). Soda ash is used in the manufacture of glass, sodium chemicals (especially sodium cyanide, used in recovering gold from its ore), and baking soda and related products. It is also used in flue gas desulfurization, soap and detergents, and water treatment (after Kostick, 1993b).

A resource of 134.4 billion tons of minable trona and mixed trona and halite is present in the Green River Basin of Wyoming (**Figure 1**) (Culbertson, 1986). This resource occurs in the Wilkins Peak Member of the Eocene Green River Formation, where 25 of 42 known individual beds of trona are of sufficient thickness to be considered minable (Culbertson, 1986). Trona is an evaporite mineral apparently deposited in a closed basin during periods in which Eocene Lake Gosiute evaporated to dryness or near-dryness. Leigh (1991), Bradley and Eugster (1969), and Surdam and Wolfbauer (1974) discuss the geochemical conditions necessary to produce trona.

Sodium carbonate was known and produced from brines from the Wilkins Peak Member near the town of Green River in 1896 (Schultz, 1909). However, trona deposits were not identified until just after World War II, when a core from an oil well was sent to the U. S. Geological Survey for identification of unusual minerals found in the Wilkins Peak Member (Lindeman, 1954; Fahey, 1962). Westvaco Chlorine Products Company began mine construction in 1947 in the area of the oil well in which trona was first identified and limited soda ash production began in 1948 (Arundale and Barsigian, 1948). Since that time, soda ash production has more or less steadily increased. Most of this increase has been due to a replacement of soda ash produced synthetically by soda ash produced from mined trona.

Trona should continue to be a valuable industry in Wyoming. New uses for soda ash are being developed, exports of soda ash and other sodium products are expected to increase, and Wyoming has enough minable trona to supply the world's demand for soda ash for a very long time.

Sinter (including travertine)

Sinter is a chemically precipitated sedimentary rock deposited from mineralized waters. Calcareous sinter is composed of calcium carbonate and is commonly known as travertine. Siliceous sinter is composed of silica. Sinter is used primarily for decorative stone. It is cut and polished for building interiors and façades, monument stone, counter and table tops, and other decorative products. Calcareous sinter is also used in agriculture as an easily soluble form of calcium carbonate.

Most sinter deposits in Wyoming are located in the northwestern quarter, although a few are present along the western edge of the state (Harris and King 1986c). Sinter has been mined in Wyoming near Cody, Thermopolis, and Dubois for local uses, often for agricultural applications such as soil conditioners. No sinter is currently mined in Wyoming.

Vermiculite

Vermiculite is the name for a group of hydrated aluminosilicate minerals that have the capacity to expand when heated (Stewart, 1983). The expanded product is also called vermiculite. It is used as an

insulating material, in construction as a lightweight aggregate, in agriculture and horticulture as a soil conditioner, and in other materials (Potter, 1993b).

Vermiculite forms by weathering or hydrothermal alteration of biotite and by the hydrothermal alteration of basic igneous or metamorphic rocks, usually at or near the contact of intrusive silicic igneous rocks (Hagner, 1944; Bothner, 1967; Meisinger, 1985).

Vermiculite occurs in Wyoming in several areas in biotite schist, hornblende schist, diorite and metadiorite, hornblendite, and serpentinite at or near a contact with granite, granite gneiss, granite pegmatite, or vein quartz. Vermiculite was produced in the past in Wyoming from deposits near Encampment, west of Casper, and in the central Laramie Mountains (Harris, 1990c).

Zeolites

Zeolites are a group of chemical compounds characterized by a ring-silicate structure and a high cation-exchange capacity. Natural zeolite minerals and synthetic zeolites have a porous structure that permits small molecules and ions to enter and leave the zeolite. This characteristic adsorption and desorption gives rise to the description "molecular sieve", and is the property that makes zeolites economically valuable as an industrial mineral. Natural zeolites are found in a variety of igneous rocks and in sedimentary rocks containing a high percentage of volcanic glass. They form during devitrification and diagenetic alteration of glass and aluminosilicate minerals. Technical reviews on the origin of zeolites are given in Hay (1978), Surdam and Sheppard (1978), Boles and Surdam (1979), and Iijima (1980).

The naturally-occurring zeolites and their chemical formulas are listed in **Table 4**. The chemical formulas for some zeolite minerals are not precisely defined; the formulas shown on **Table 4** are those that are generally accepted.

Several factors control the properties of individual zeolites. The narrowest portion of the structure controls the size of the ion or molecule that can be adsorped or desorped. Synthetic zeolites usually have larger apertures, which makes them more suitable for petroleum refining. The natural zeolites chabazite, erionite, and mordenite have relatively large apertures. Natural erionite and mordenite have acicular to fibrous habits with aspect ratios equivalent to cleavage fragments of amphiboles. They do not have the aspect ratios of asbestos fibers. Only rare wooly erionite, known from one site in Nevada has an aspect ratio similar to asbestos (Shedd and others, 1982).

Table 4. Selected zeolite minerals and their chemical formulas (modified from Deer and others, 1966; Barrer, 1982).

Name	Chemical formula
Analcite (analcime)*	$Na[AlSi_2O_6]\bullet H_2O$
Chabazite*	$(Ca,Na_2)_2[Al_4Si_8O_{24}]\bullet 13H_2O$
Clinoptilolite*	$(Na_2,K_2,Ca)[Al_3Si_{10}O_{24}]\bullet 8H_20$
Dachiardite	$(Ca,Na_2,K_2)_5[Al_{10}Si_{38}O_{96}\bullet 24H_20$
Epistilbite	$Ca_3[Al_6Si_{18}O_{48}]\bullet 16H_2O$
Erionite*	$(Na_2,K_2,Ca)_{4.5}[Al_9Si_{27}O_{72}]\bullet 27H_2O$
Faujasite	$(Ca,Na_2)[Al_2Si_4O_{12}]\bullet 8H_2O$
Ferrierite	$(K,Na)_2(Mg)[Al_3Si_{15}O_{36}](OH)\bullet 9H_2O$
Gismondite (gismodine)	$(Ca,Na_2,K_2)[Al_2Si_2O_8]\bullet 4H_2O$
Gonnardite	$Na_2Ca[(Al,Si)_5O_{10}]_2\bullet 7H_2O$
Harmotome	$Ba[Al_2Si_6O_{16}]\bullet 6H_2O$
Heulandite*	$(Ca,Na_2)[Al_2Si_7O_{18}]\bullet 6H_20$
Laumontite*	$Ca[Al_2Si_4O_{12}]\bullet 4H_2O$
Mordenite (ptilolite)*	$(Na_2,K_2,Ca)[Al_2Si_{10}O_{24}]\bullet 6H_2O$
Natrolite	$Na_2[Al_2Si_3O_{10}]\bullet 4H_2O$
Phillipsite*	$(K_2,Na_2,Ca)_{2.5}[Al_5Si_{11}O_{32}]\bullet 10H_2O$
Scolecite	$Ca[Al_2Si_3O_{10}]\bullet 3H_2O$
Stilbite	$Ca_2Na[Al_5Si_{13}O_{36}]\bullet 16H_2O$
Thomsonite	$Ca_2Na[(Al,Si)_5O_{20}]\bullet 6H_2O$
Wairakite	$Ca[Al_2Si_4O_{12}]\bullet 2H_2O$
Yugawaralite	$Ca[Al_2Si_5O_{14}]\bullet 4H_2O$

(* indicates common natural zeolites).

Because of the molecular sieve properties of zeolites, they can be used to remove selected molecules and ions from the environment. Uses range from kitty litter and barnlot deodorizers to toxic-element adsorpers in heavy-metal waste control in environmental cleanup operations. Zeolites can be used in many other industrial applications (**Table 5**) and new uses for zeolites are constantly being developed. In the latter part of the 1980s, a demand for zeolites was developed for sewage treatment, for heavy-metal and radioactive-element isolation, and as a filler and whitening agent in paper. In Wyoming, the

Table 5. Uses of natural zeolites (after Mumpton, 1978; Flanigen, 1980; Minato, 1988; Tsitsishvili, 1988).

Application	Status
Gas purification	
oxygen separation	used in Japan
nitrogen separation	used in Japan
natural gas purification(acid resistant CO_2, SO_2, H_2O, H_2S removal)	used in United States and Europe
Pollution abatement	
ammonia removal	used in Japan and United States
pet litter	used in United States
non-phosphate detergent	used in Japan and Europe
radioactive element isolation	experimental use worldwide
heavy-metal scavenging	experimental use worldwide
water softening	experimental use in United States
water filtering	experimental use in Europe
flue-stack gas clean-up (SO_2, nitrous oxides, hydrocarbons)	experimental use in Japan and Europe
oil spill cleanup	potential
Agricultural products, including aquaculture	
soil conditioner	number 1 use in Japan
dietary supplement	used worldwide
ammonia abatement	used worldwide
fertilizer enhancer	used in Japan and Europe
fungicide, pesticide and herbicide carrier	experimental use in Japan and Europe
Desiccant and decaking agent	minor use worldwide
Filler and extender	
paper	used in Japan and Canada
rubber	experimental use in Europe
polymers	experimental use in Europe
paint	potential
Construction materials	
dimension stone	used worldwide, but uncommon
pozzolanic (high silica cement)	used in Europe
lightweight aggregate	experimental use in Europe
Energy storage	
methane storage in a solid	experimental
hydration-dehydration of zeolite	experimental
Catalysis	experimental
Feedstock for synthetic zeolite production	experimental

gas-purification properties of natural zeolites may be used in coal gasification to provide an oxygen-enriched combustion gas and to clean the gas produced during this combustion. Zeolites could also be used to clean coalbed methane before it is introduced into natural gas pipelines (Harris and King, 1990).

Wyoming contains several large and potentially minable deposits of natural zeolites (**Figure 4**), and small amounts have been mined in recent years for deodorizers. These came from the robins-egg blue tuff in the Eocene Washakie Formation near historic Fort LaClede southeast of Bitter Creek, the light-colored sand shown in black and white in **Figure 5**. Other potentially minable deposits of zeolites have been identified in the Washakie Formation in the Washakie Basin and at Beaver Divide (**Figure 4**).

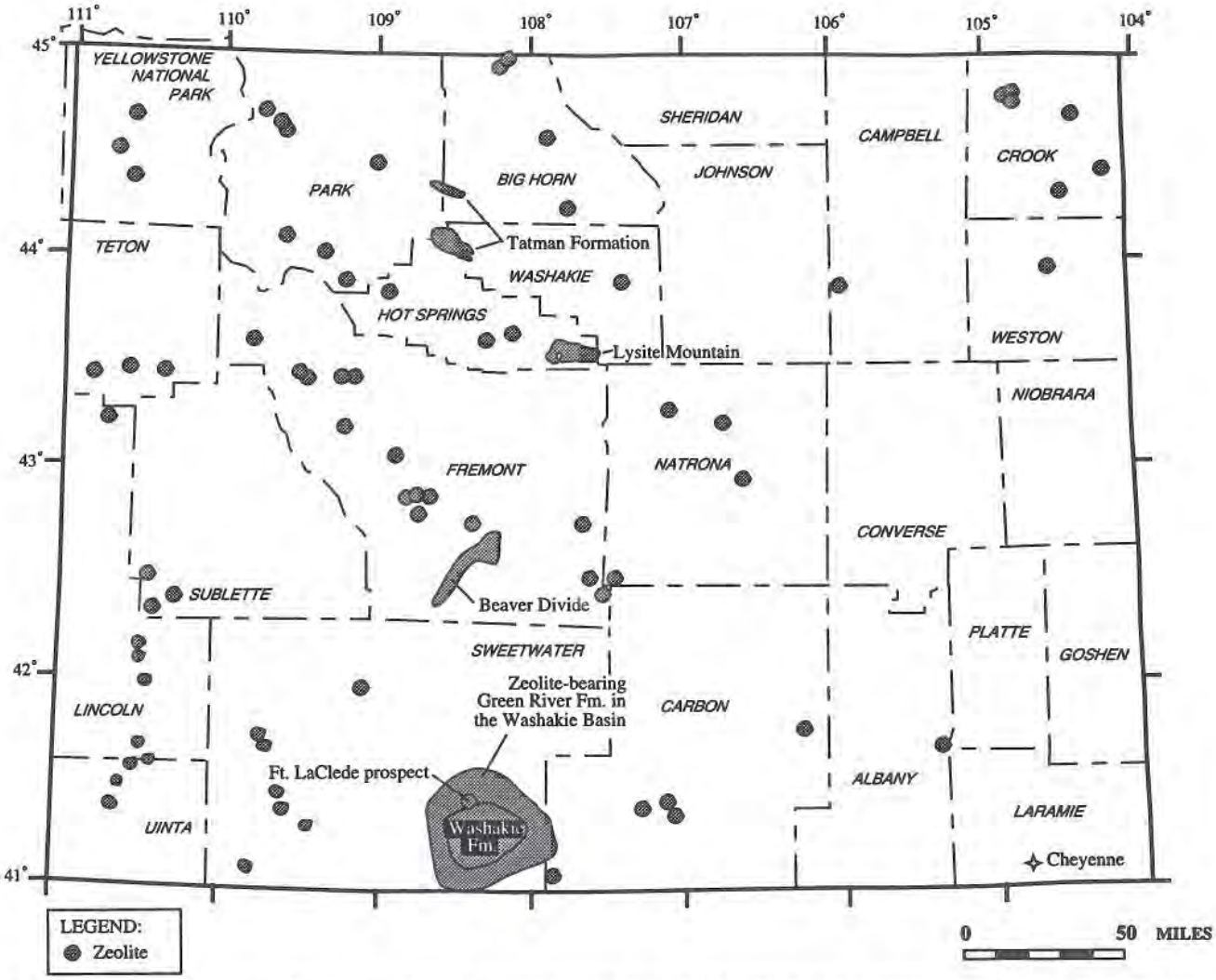

Figure 4. Map of Wyoming showing zeolite occurrences and outcrops of zeolite-bearing strata (after Harris and King, 1990). County names are shown in all capital letters in italic type.

Figure 5. Quarry in robins-egg blue zeolitic tuff, Fort LaClede area, Washakie Basin.

Summary

Industrial minerals have been a part of the economy of Wyoming since the first Native Americans found sources of salt within the present borders of Wyoming, as well as sources of flint and chert for arrowheads and iron for paint. Wyoming presently (1993) leads the nation in the production of trona and bentonite and is an important producer of gypsum, cement, and other materials. Unexploited industrial minerals such as silica, limestone, zeolites, and others could be developed to create a more diversified mineral economy for the state. The development of new technologies should create new uses of industrial mineral products.

References cited

Ampian, S.G., 1985, Clays, *in* Mineral facts and problems, 1985 edition: U.S. Bureau of Mines Bulletin 675, p. 157-169.

Arundale, J.C., and Barsigian, F. M., 1948, Salines—miscellaneous: U.S. Bureau of Mines Minerals Yearbook 1948, p. 1068-1074.

Austin, G.T., 1993a, Diamond, industrial: U.S. Bureau of Mines Mineral Commodity Summaries 1993, p. 56-57.

_____ 1993b, Garnet, industrial: U.S. Bureau of Mines Mineral Commodity Summaries 1993, p. 66-67.

Barrer, R.M., 1982, Hydrothermal chemistry of zeolites: Academic Press, New York, p. 5, 18-19.

Beckwith, R.H., 1939, Asbestos and chromite deposits of Wyoming: Economic Geology, v. 34, p. 812-843.

Boles, J.R., and Surdam, R.C., 1979, Diagenesis of volcanogenic sediments in a Tertiary saline lake, Wagon Bed Formation, Wyoming: American Journal of Science, v. 279, p. 832-853.

Bothner, W.A., Jr., 1967, Petrology, structural geometry, and economic geology of the Cooney Hills, Platte County, Wyoming [Ph.D. dissertation]: Laramie, University of Wyoming, 68 p.

Boynton, R.S., Gutschick, K.A., Freas, R.C., and Thompson, J.L., 1983, Lime, *in* LeFond, S.J., editor, Industrial minerals and rocks, 5th edition: American Institute of Mining, Metallurgical and Petroleum Engineers, Inc., New York, p. 809-831.

Bradbury, J.C., and Ehrlinger, H.P., III, 1983, Tripoli, *in* LeFond, S.J., editor, Industrial minerals and rocks, 5th edition: American Institute of Mining. Metallurgical and Petroleum Engineers, Inc., New York, p. 1363-1374.

Bradley, W.H., and Eugster, H.P., 1969, Geochemistry and paleolimnology of the trona deposits and associated authigenic minerals of the Green River Formation of Wyoming: U.S. Geological Survey Professional Paper 496B, 71 p.

Brown, R.A., Cservenyak, F.J., Anderberg, R.G., Kandiner, H.J., and Frattali, F.J., 1947, Recovery of alumina from Wyoming anorthosite by the lime-soda-sinter process: U.S. Bureau of Mines Report of Investigations 4132, 127 p.

Carr, D.D., and Rooney, L.F., 1983, Limestone and dolomite *in* LeFond, S.J., editor, Industrial minerals and rocks, 5th edition: American Institute of Mining, Metallurgical and Petroleum Engineers, Inc., New York, p. 833-868.

Chapman, G.P., 1983, Mica, *in* LeFond, S.J., editor, Industrial minerals and rocks, 5th edition: American Institute of Mining, Metallurgical and Petroleum Engineers, Inc., New York, p. 915-929.

Culbertson, W.C., 1986, Genesis and distribution of trona deposits in southwest Wyoming, *in* Roberts, S., editor, Metallic and nometallic deposits of Wyoming and adjacent areas, 1983 conference proceedings: Geological Survey of Wyoming Public Information Circular 25, p. 94.

Davis, L.L., 1993a, Diatomite: U.S. Bureau of Mines Mineral Commodity Summaries 1993, p. 58-59.

_____ 1993b, Gypsum: U.S. Bureau of Mines Mineral Commodity Summaries 1993, p. 76-77.

_____ 1993c, Mica: U.S. Bureau of Mines Mineral Commodity Summaries 1993, p. 112-113.

Deer, W.A., Howie, R.A., and Zussman, J., 1966, An introduction to the rock-forming minerals: John Wiley and Sons, Inc., New York, p. 511-513.

Fahey, J.J., 1962, Saline minerals of the Green River Formation: U.S. Geological Survey Professional Paper 405, 50 p.

Flanigen, E.M., 1980, Molecular sieve zeolite technology—the first twenty-five years *in* Rees, L. V. C., editor, Proceedings of the fifth international conference on zeolites: Heyden, London, p. 760-780.

Grubbs, D.K., and Moose, A.B., 1981, Oklahoma and Wyoming anorthosite; potential domestic sources of alumina: Society of Mining Engineers, AIME Transactions, v. 270, p. 1932-1935.

Gwinn, G.R., 1951, Domestic mica: U.S. Bureau of Mines Information Circular 7617, 37 p.

Hagner, A.F., 1944, Wyoming vermiculite deposits: Geological Survey of Wyoming Bulletin 34, 47 p.

Hancock, K.R., 1983, Mineral pigments, *in* LeFond, S.J., editor, Industrial minerals and rocks, 5th edition: American Institute of Mining, Metallurgical and Petroleum Engineers, Inc., New York, p. 349-372.

Harrer, C.M., 1954, Wyoming anorthosite and related resources as a basis for an alumina industry: U.S. Bureau of Mines Preliminary Report 92, 30 p.

Harris, R.E., 1987a, Ballast in Wyoming: Geological Survey of Wyoming Open File Report 87-22, 22 p.

_____ 1987b, Epsomite (magnesium sulfate) in Wyoming: Geological Survey of Wyoming Open File Report 87-2, 7 p.

_____ 1987c, Industrial minerals of western Wyoming: Wyoming Geological Association 38th Annual Field Conference Guidebook, p. 329-335.

_____ 1988a, Industrial minerals in northeastern Wyoming: Wyoming Geological Association 39th Annual Field Conference Guidebook, p. 315-321.

_____ 1988b, The Plumbago Creek silica sand deposit, Albany County, Wyoming: Geological Survey of Wyoming Report of Investigations 40, 31 p.

_____ 1988c, The Cassa silica rock deposit, Platte County, Wyoming: Geological Survey of Wyoming Report of Investigations 42, 38 p.

_____ 1989a, Tripoli (tripolite) in Wyoming: Geological Survey of Wyoming Open File Report 89-3, 22 p., 2 sheets.

_____ 1989b, Graphite in Wyoming: Geological Survey of Wyoming Open File Report 89-11, 11 p.

_____ 1990a, Anorthosite in Wyoming: Geological Survey of Wyoming Open File Report 90-1, 7 p.

_____ 1990b, Rutile in Wyoming: Geological Survey of Wyoming Open File Report 90-2, 6 p.

_____ 1990c, Vermiculite in Wyoming: Geological Survey of Wyoming Open File Report 90-3, 11 p.

_____ 1991, Decorative stones of Wyoming: Geological Survey of Wyoming Public Information Circular 31, 27 p.

_____ 1992, Mineral pigment in Wyoming: Geological Survey of Wyoming Open File Report 92-6, 8 p.

Harris, R.E., and King, J.K., 1985, Sulfur deposits in Wyoming: Geological Survey of Wyoming Open File Report 85-15, 15 p.

_____ 1986a, Diatomite (diatomaceous earth) in Wyoming: Geological Survey of Wyoming Open File Report 86-16, 7 p.

_____ 1986b, Pumice, scoria, and pumicite in Wyoming: Geological Survey of Wyoming Open File Report 86-17, 20 p.

_____ 1986c, Sinter (including travertine) resources of Wyoming: Geological Survey of Wyoming Open File Report 86-20, 15 p.

_____ 1986d, Alum minerals in Wyoming (including alunite): Geological Survey of Wyoming Open File Report 86-24, 9 p.

_____ 1987a, Clay resources of Wyoming (excluding bentonite and fuller's earth): Geological Survey of Wyoming Open File Report 87-3, 26 p.

_____ 1987b, Columbium (niobium) and tantalum in Wyoming: Geological Survey of Wyoming Open File Report 87-6, 21 p.

_____ 1988, Fluorite in Wyoming: Geological Survey of Wyoming Open File Report 88-10, 26 p.

_____ 1990, Natural zeolites in Wyoming: Geological Survey of Wyoming Open File Report 90-4, 51 p.

Harris, R.E., and Warchola, R.J., 1992, The John Blue Canyon silica sand deposit: Geological Survey of Wyoming Open File Report 92-3, 26 p.

Harris, R.E., Hausel, W.D., and Meyer, J.E., 1985, Metallic and industrial mineral resources map of Wyoming: Geological Survey of Wyoming Map Series 14, scale 1:500,000.

Hausel, W.D., 1990, Strategic mineral resources in Wyoming—titanium: Geological Survey of Wyoming Open File Report 90-7, 18 p.

Hay, R.L., 1978, Geologic occurrences of zeolites, *in* Sand, L.B., and Mumpton, F.A., editors, Natural zeolites—occurrence, properties, use: Pergamon Press, New York, p. 135-143.

Hedrick, J.B., 1993a, Rare earths: U.S. Bureau of Mines Mineral Commodity Summaries 1993, p. 138-139.

_____ 1993b, Yttrium: U.S. Bureau of Mines Mineral Commodity Summaries 1993, p. 192-193.

Iijima, A., 1980, Geology of natural zeolites and zeolitic rocks, *in* Rees, L.V.C., editor, Proceedings of the fifth international conference on zeolites: Heyden, London, p. 103-118.

Kadey, F.L., 1985, Diatomite, *in* LeFond, S.J., editor, Industrial minerals and rocks, 5th edition: American Institute of Mining, Metallurgical, and Petroleum Engineers, Inc., New York, p. 605-635.

King, J.K., and Harris, R.E., 1987, Rare earth elements and yttrium in Wyoming: Geological Survey of Wyoming Open File Report 87-8, 43 p.

Kostick, D.S., 1993a, Salt: U.S. Bureau of Mines Mineral Commodity Summaries 1993, p. 146-147.

_____ 1993b, Sodium carbonate (soda ash): U.S. Bureau of Mines Mineral Commodity Summaries 1993, p. 148-149.

_____ 1993c, Sodium sulfate: U.S. Bureau of Mines Mineral Commodity Summaries 1993, p. 162-163.

Leigh, R.T., 1991, Wyoming trona—an overview of the geology and economic utilization: Wyoming Geological Association 42nd Annual Field Conference Guidebook, p. 103-120.

Lindeman, H.B., 1954, Sodium carbonate brine and trona deposits in Sweetwater County, Wyoming: U.S. Geological Survey Circular 235, 10 p.

Lloyd, J.E., 1970, The history of Cokeville [M.S. thesis]: Logan, Utah State University, 160 p.

Meisinger, A.C., 1985, Vermiculite, *in* Mineral facts and problems 1985 edition: U.S. Bureau of Mines, p. 917-922.

Metcalf, R.W., 1946, Tripoli: U.S. Bureau of Mines Information Circular 7371, 25 p.

Minato, H., 1988, Occurrence and application of natural zeolites in Japan, *in* Kallo, D., and Sherry, H.S., editors, Occurrence, properties and utilization of

natural zeolites: Akademiai Kiado, Budapest, p. 395-418.

Morse, D.E., 1993, Phosphate rock: U.S. Bureau of Mines Mineral Commodity Summaries 1993, p. 128-129.

Mumpton, F.A., 1978, Natural zeolites—a new mineral commodity, *in* Sand, L.B., and Mumpton, F.A., editors, Natural zeolites—occurrence, properties, use: Pergamon Press, New York, p. 3-27.

Ober, J.A., 1993, Sulfur: U.S. Bureau of Mines Mineral Commodity Summaries 1993, p. 170-171.

Osterwald, F.W., Osterwald, D.B., Long, J.S., Jr., and Wilson, W.H. (revised by W.H. Wilson), 1966, Mineral resources of Wyoming: Geological Survey of Wyoming Bulletin 50, 287 p.

Patterson, S.H., and Murray, H.H., (revised by H.H. Murray), 1983, Clays, *in* LeFond, S.J., editor, Industrial minerals and rocks, 5th edition: American Institute of Mining, Metallurgical and Petroleum Engineers, Inc., New York, p. 585-651.

Peterson, J.A., 1972, Jurassic system, *in* Geologic atlas of the Rocky Mountain region: Rocky Mountain Association of Geologists, Denver, Colorado, p. 177-189.

Potter, M.J., 1993a, Feldspar: U.S. Bureau of Mines Mineral Commodity Summaries 1993, p. 60-61.

_____ 1993b, Vermiculite: U.S. Bureau of Mines Mineral Commodity Summaries 1993, p. 190-191.

Rascoe, B., Jr., and Baars, D.L., 1972, Permian system, *in* Geologic atlas of the Rocky Mountain region: Rocky Mountain Association of Geologists, Denver, Colorado, p. 143-165.

Rath, D.L., 1986, Origin and characteristics of Wyoming bentonite deposits *in* Roberts, S., editor, Metallic and nonmetallic deposits of Wyoming and adjacent areas, 1983 conference proceedings: Geological Survey of Wyoming Public Information Circular 25, p. 84-90.

Rheams, K.F., and Richter, K.E., 1988, Tripoli deposits in northern Alabama—a preliminary investigation: Geological Survey of Alabama Circular 135, 54 p.

Rocky Mountain Energy, 1985, Anorthosite resources, Albany County, Wyoming: Rocky Mountain Energy Company Report, Geological Survey of Wyoming Files (unpublished), 12 p.

Rogers, C.P., Neal, J.P., and Teague, K.H., 1983, Feldspars, *in* LeFond, S.J., editor, Industrial minerals and rocks, 5th edition: American Institute of Mining, Metallurgical, and Petroleum Engineers, Inc., New York, p. 1375-1381.

Schultz, A.R., 1909, Deposits of sodium salts in Wyoming: U.S. Geological Survey Bulletin 430, p. 570-589.

Searls, J.P., 1993, Potash: U.S. Bureau of Mines Mineral Commodity Summaries 1993, p. 132-133.

Shedd, K.B., Virta, R.L., and Wylie, A.G., 1982, Size and shape characterization of fibrous zeolites by electron microscopy: U.S. Bureau of Mines Report of Investigations 8674, 20 p.

Stewart, O.F. (original by P.R. Strand). 1983, Vermiculite, *in* LeFond, S.J., editor, Industrial minerals and rocks, 5th edition: American Institute of Mining, Metallurgical, and Petroleum Engineers, Inc., New York, p. 1375-1381.

Sturges, D.L., 1968, Hydrologic properties of peat from a Wyoming mountain bog: Soil Science, v. 106, no. 4, p. 262-264.

Surdam, R.C., and Sheppard, R.A., 1978, Zeolites in saline, alkaline lake deposits, *in* Sand, L.B., and Mumpton, F.A, editors, Natural zeolites—occurrence, properties, use: Pergamon Press, New York, p. 145-174.

Surdam, R.C., and Wolfbauer, C.A., 1974, Green River Formation, Wyoming—a playa lake complex: Geological Society of America Bulletin, v. 86, p. 335-345.

Taylor, H.A., Jr., 1993, Graphite (natural): U.S. Bureau of Mines Mineral Commodity Summaries 1993, p. 74-75.

Thrush, P.W., 1968, A dictionary of mining, mineral, and related terms: U.S. Bureau of Mines, 1269 p.

Tsitsishvili, G.V., 1988, Perspectives of natural zeolite applications, *in* Kallo, D., and Sherry, H.S., editors, Occurrence, properties and utilization of natural zeolites: Akademiai Kiado, Budapest, p. 367-393.

Virta, R.L., 1993, Asbestos: U.S. Bureau of Mines Mineral Commodity Summaries, 1993, p. 26-27.

Williamson, D.R., 1966, Exploration for diatomites: Colorado School of Mines Mineral Industries Bulletin, v. 9, no. 3, p. 1-14.

ISBN 1-884589-01-4

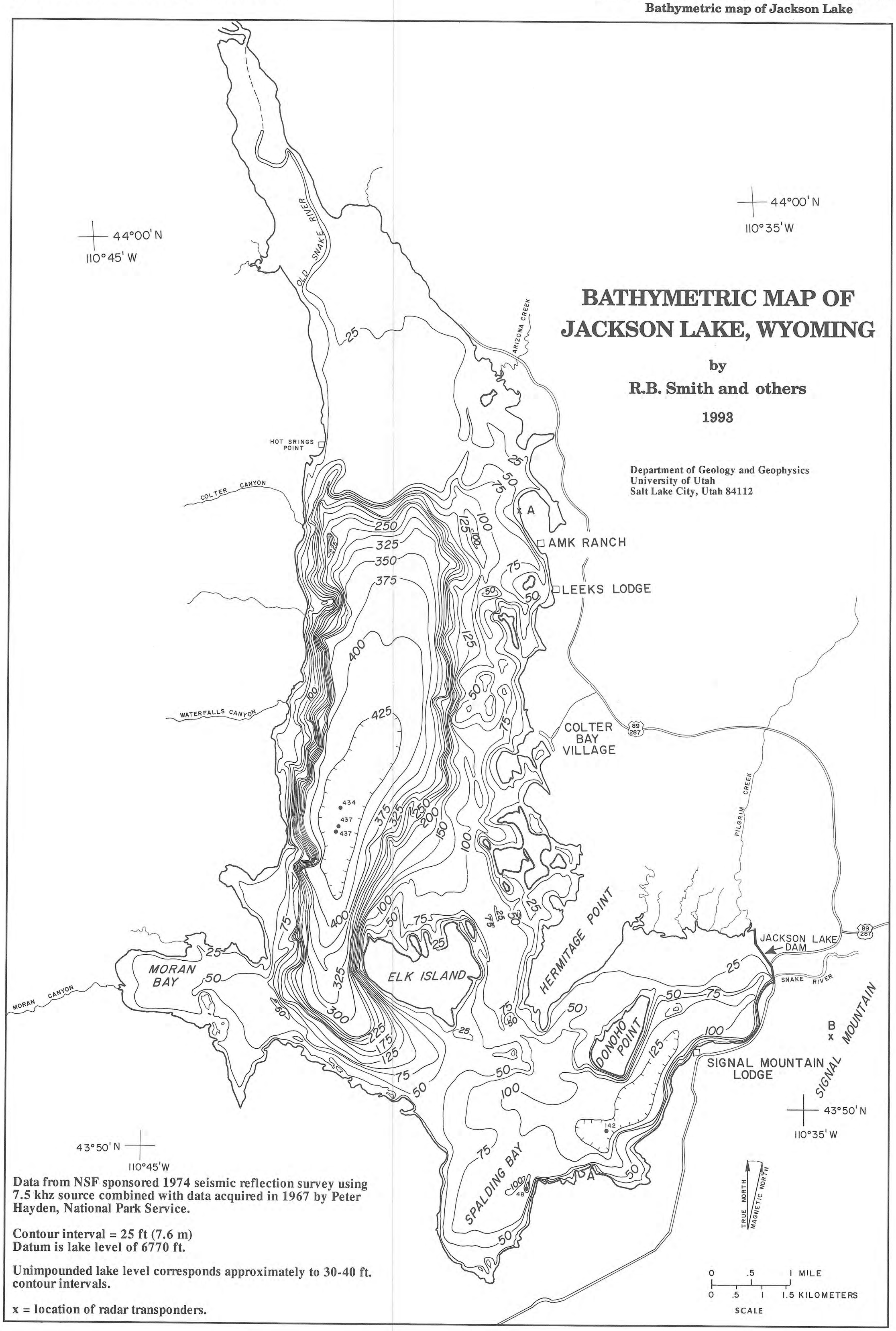

Data from NSF sponsored 1974 seismic reflection survey using 7.5 khz source combined with data acquired in 1967 by Peter Hayden, National Park Service.

Contour interval = 25 ft (7.6 m)
Datum is lake level of 6770 ft.

Unimpounded lake level corresponds approximately to 30-40 ft. contour intervals.

x = location of radar transponders.

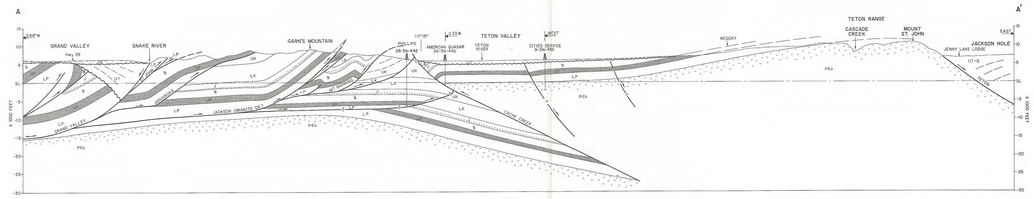

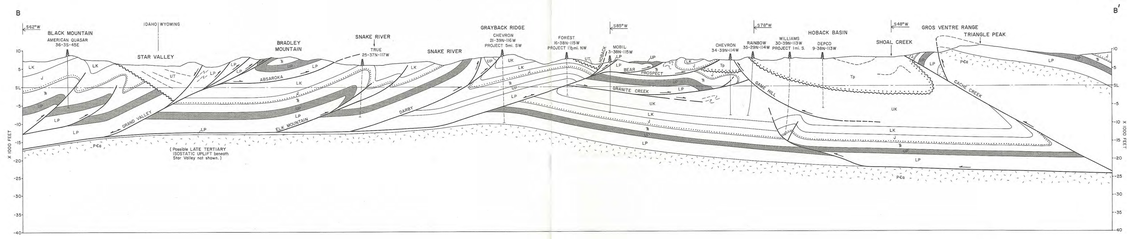

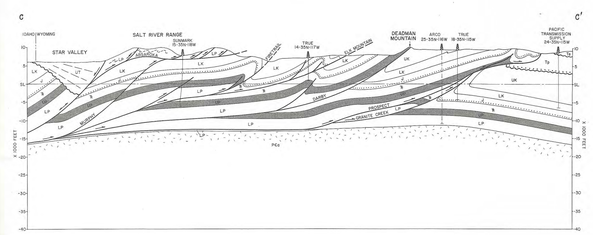

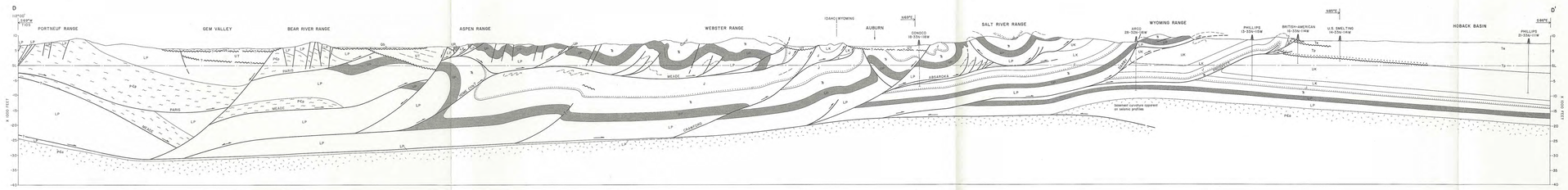

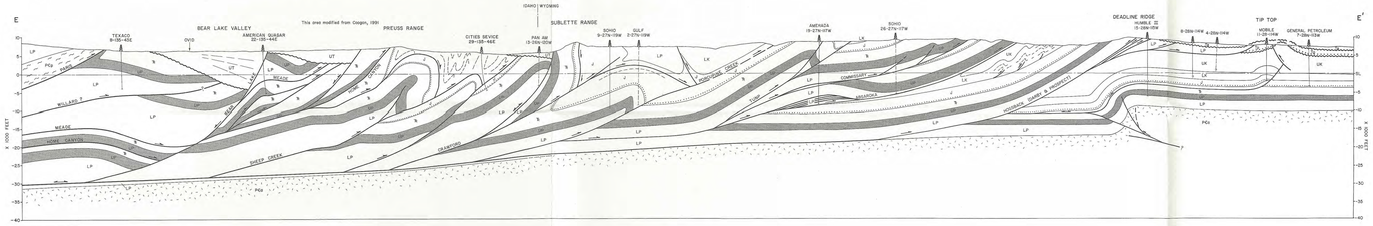

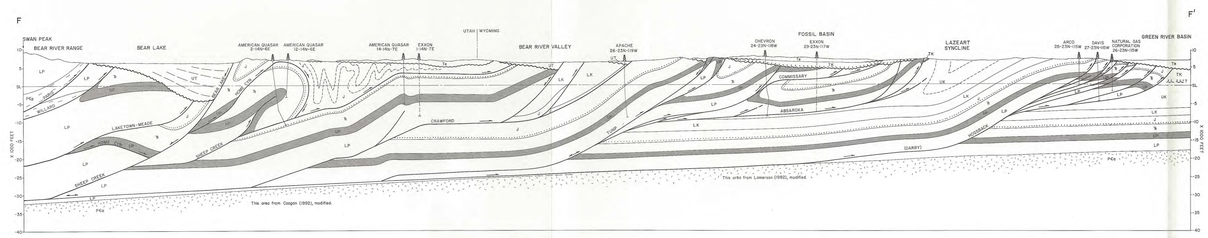

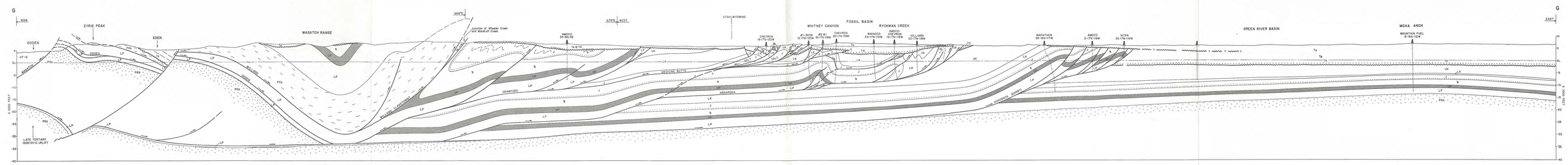

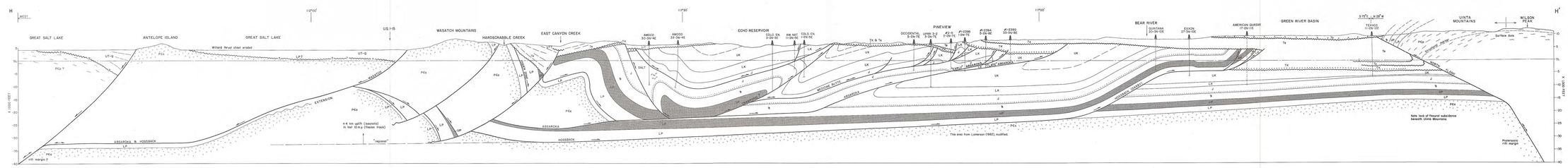

EXPLANATION

UT = Upper Tertiary

Te = Eocene

Tp = Paleocene

TK = Paleocene and Maastrichtian

UK = Upper Cretaceous

LK = Lower Cretaceous

J = Jurassic

Ꞧ = Triassic

UP = Upper Paleozoic (shaded)

LP = Lower Paleozoic

P€p = Proterozoic

P€a = Archean

Stippled pattern = Nugget Sandstone
Dashed well bores are projected into line of section
Basal decollement lies above basal Cambrian sandstone

EIGHT REGIONAL STRUCTURAL CROSS SECTIONS IN THE WYOMING-UTAH-IDAHO THRUST BELT

(see Figure 1 for locations)

by
Frank Royse, Jr.

1993

0 5,000 10,000 15,000 20,000 25,000 FEET
0 1 2 3 4 5 6 7 KILOMETERS

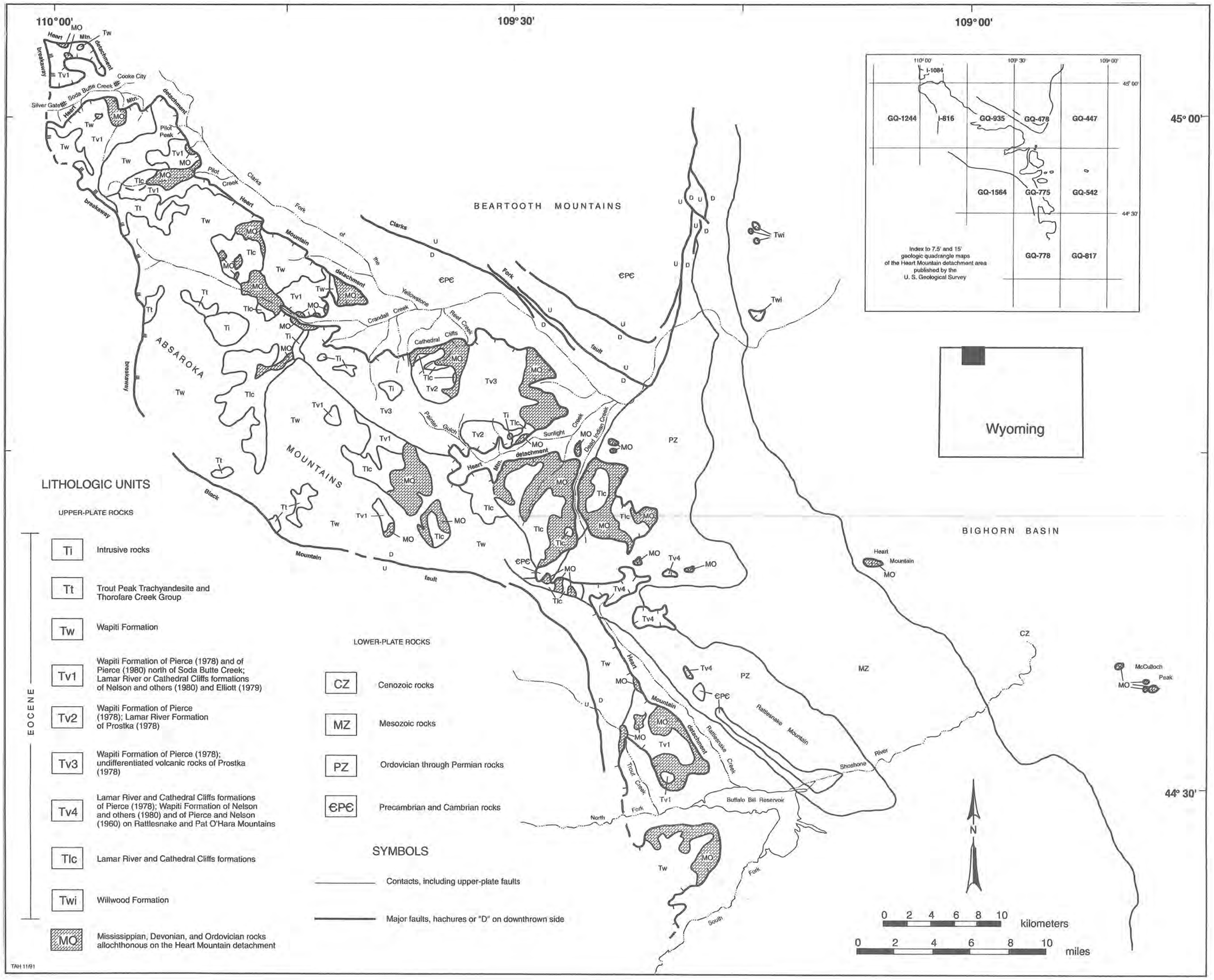

GENERALIZED GEOLOGIC MAP OF THE HEART MOUNTAIN DETACHMENT, NORTHWESTERN WYOMING

by

Thomas A. Hauge

1993

EXPLANATION

Archean and Proterozoic dike swarms

Early and Middle Proterozoic felsic intrusions (~2,000–1,400 Ma)

Early and Middle Proterozoic mafic intrusions and Laramie Anorthosite Complex (~1,800–1,500 Ma)

Early Proterozoic immature metasedimentary and metavolcanic rocks (~1,700–1,900 Ma)

Early Proterozoic mature metasedimentary rocks (~1,900–2,000 Ma)

Late Archean felsic intrusions (2,500–2,700 Ma)

Late Archean mafic intrusions (~2,700 Ma)

Late Archean metasedimentary and metavolcanic rocks (≧2,700 Ma)

Late Archean granitic gneiss and intrusions (~2,800 Ma)

Middle(?) and Late Archean metasedimentary and metavolcanic rocks (>2,800 Ma)

Middle(?) and Late Archean orthogneiss and paragneiss (≦2,900 Ma)

Middle Archean felsic intrusions (≧3,000 Ma)

Middle Archean metasedimentary and metavolcanic rocks (>3,000 Ma)

Middle Archean orthogneiss and paragneiss (>3,000 Ma)

Limit of exposed Archean rocks of Wyoming Province

Rocks least affected by 1,800–1,400 Ma metamorphism (inside hachures)

2,880 ± 130 Ma

Age and lithology of drill-core sample (Peterman, 1981)

Shear zone

Fault

Mesozoic thrust fault, sawteeth on upper plate

Trend of foliation

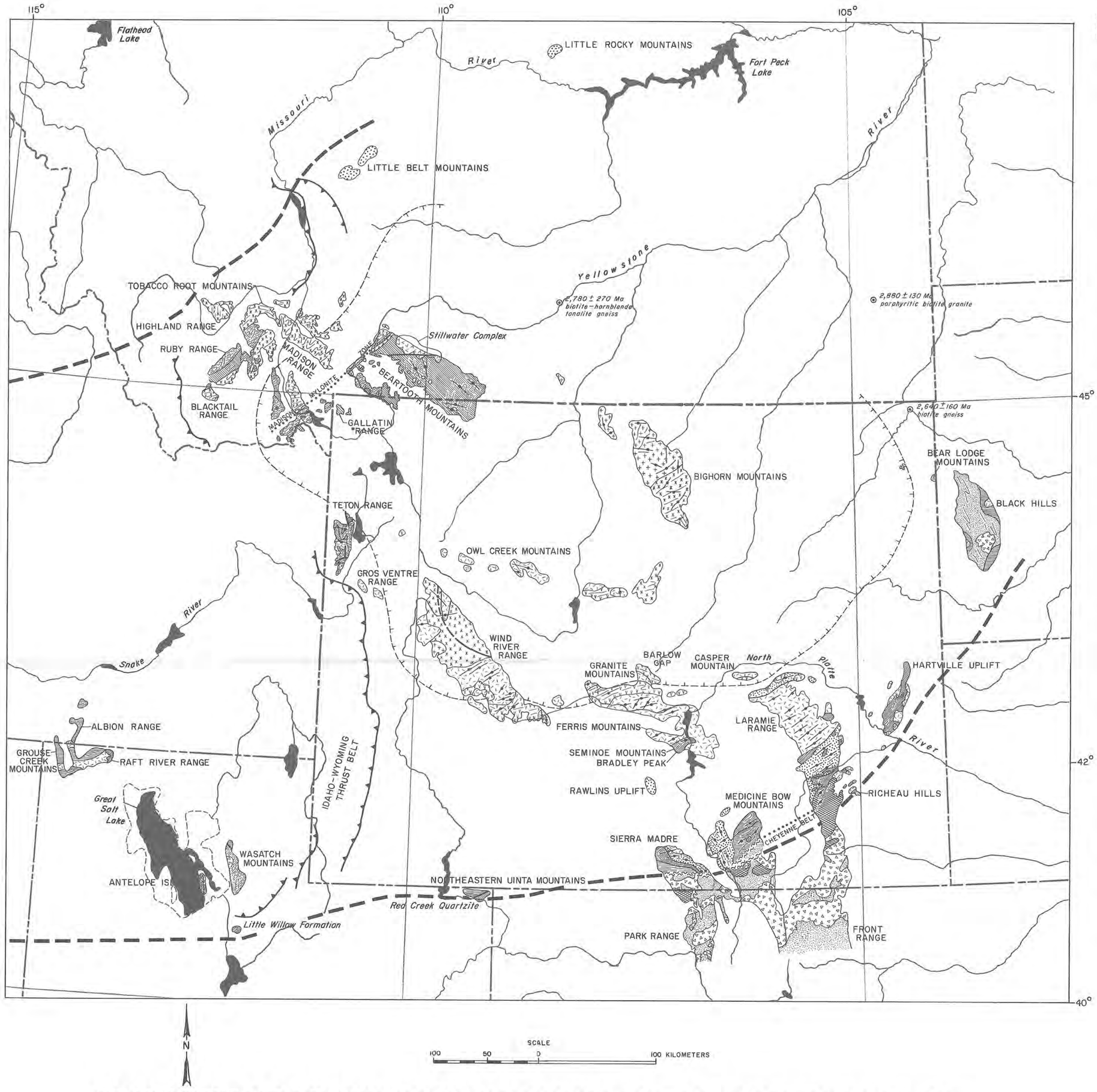

GEOLOGIC MAP OF PRECAMBRIAN ROCKS OF THE WYOMING PROVINCE

by

Robert S. Houston

1993

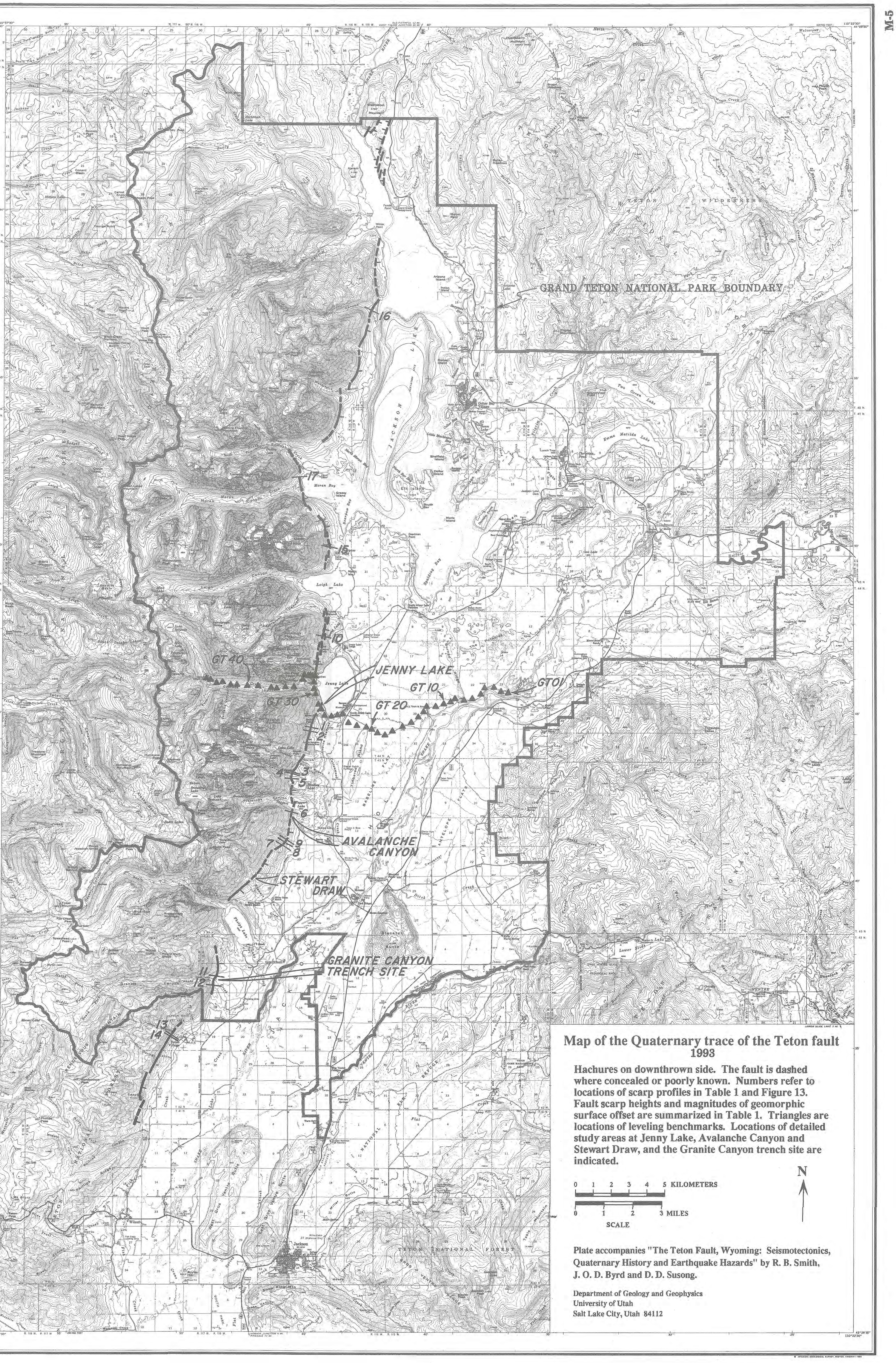

Map of the Quaternary trace of the Teton fault
1993

Hachures on downthrown side. The fault is dashed where concealed or poorly known. Numbers refer to locations of scarp profiles in Table 1 and Figure 13. Fault scarp heights and magnitudes of geomorphic surface offset are summarized in Table 1. Triangles are locations of leveling benchmarks. Locations of detailed study areas at Jenny Lake, Avalanche Canyon and Stewart Draw, and the Granite Canyon trench site are indicated.

0 1 2 3 4 5 KILOMETERS

0 1 2 3 MILES

SCALE

N

Plate accompanies "The Teton Fault, Wyoming: Seismotectonics, Quaternary History and Earthquake Hazards" by R. B. Smith, J. O. D. Byrd and D. D. Susong.

Department of Geology and Geophysics
University of Utah
Salt Lake City, Utah 84112

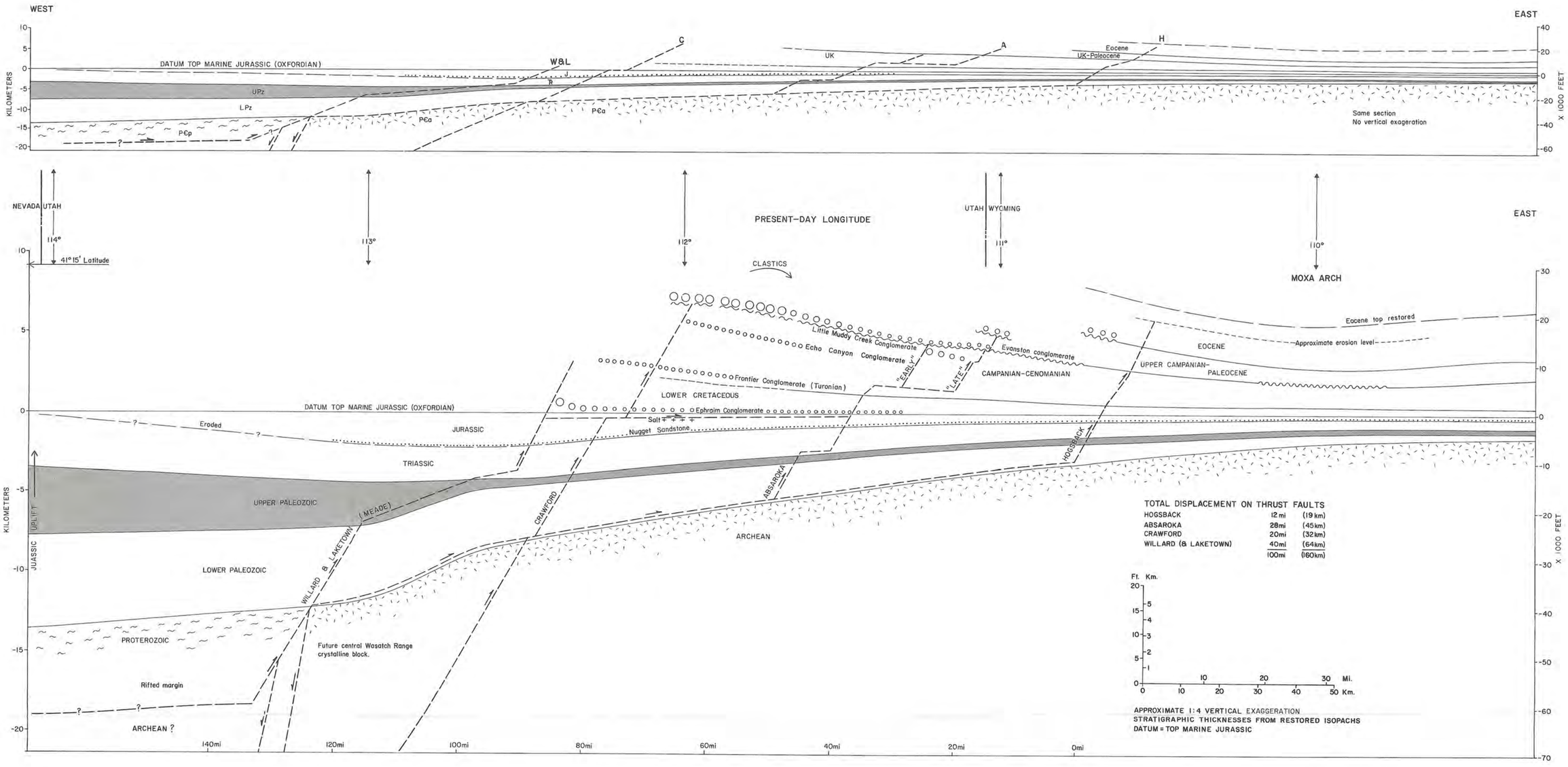

RESTORED STRUCTURAL CROSS SECTION ALONG LATITUDE 41°15' WYOMING-UTAH THRUST BELT

(see text for explanation).

by

Frank Royse, Jr.

1993

Reflections were traced from large-scale seismograms. Units A-D described in text.

A. East-West profiles (locations on Figure 4a).

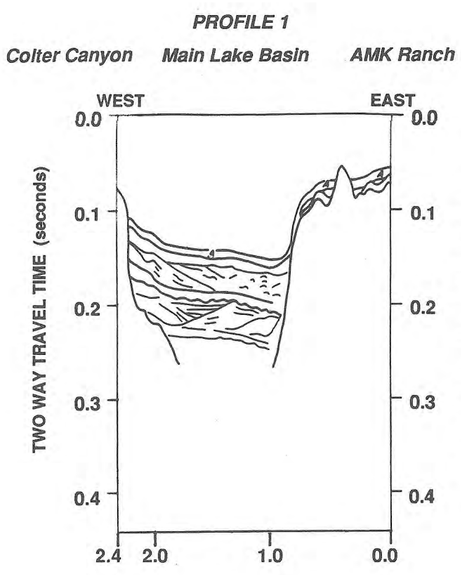

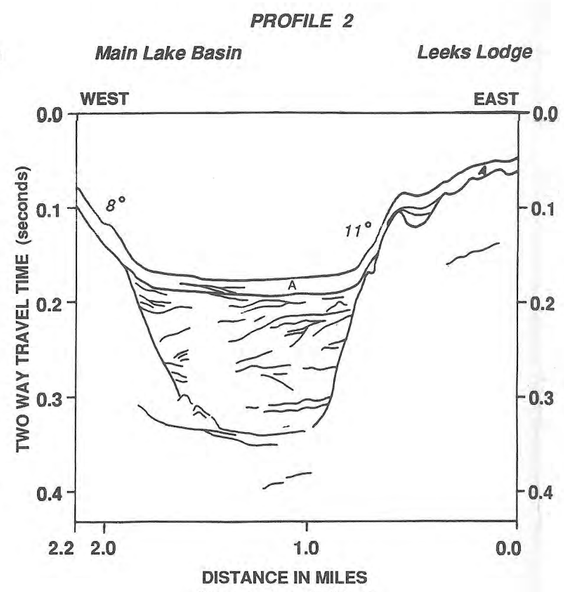

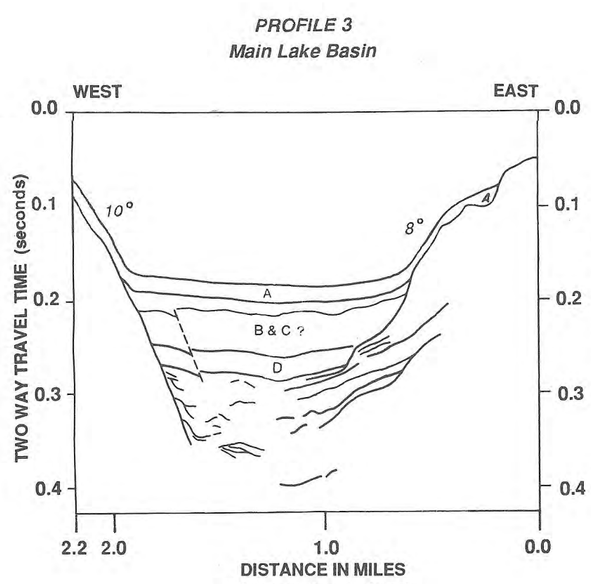

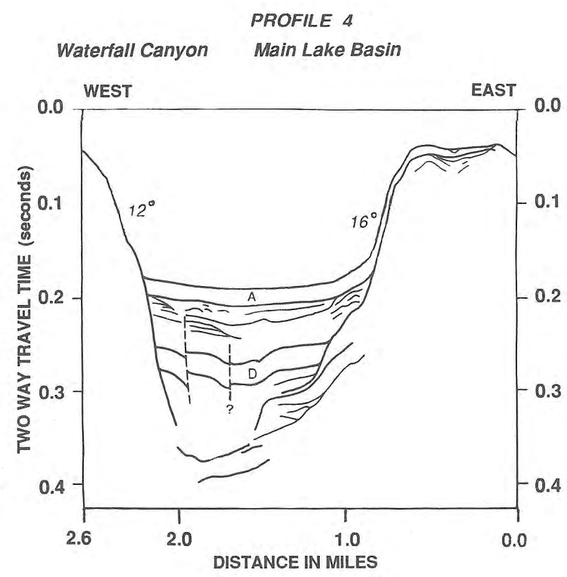

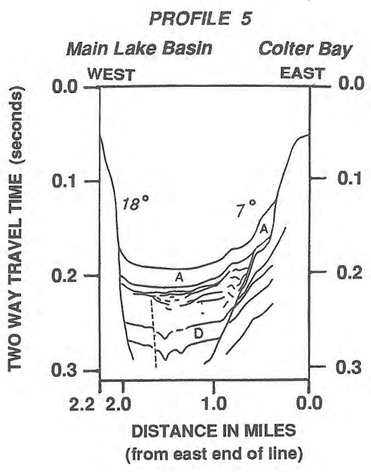

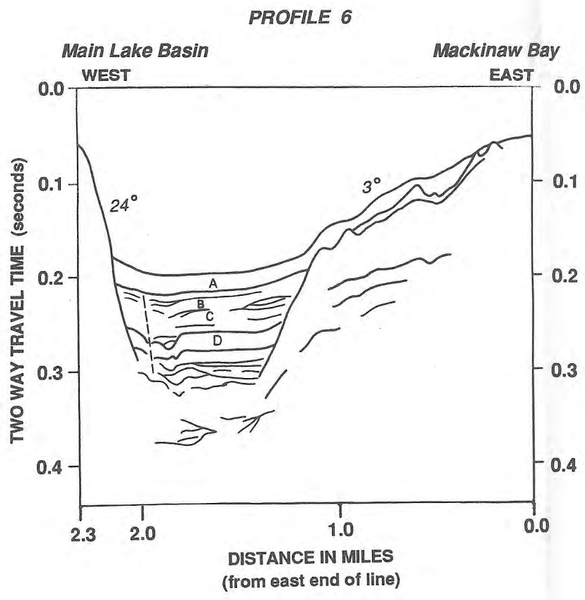

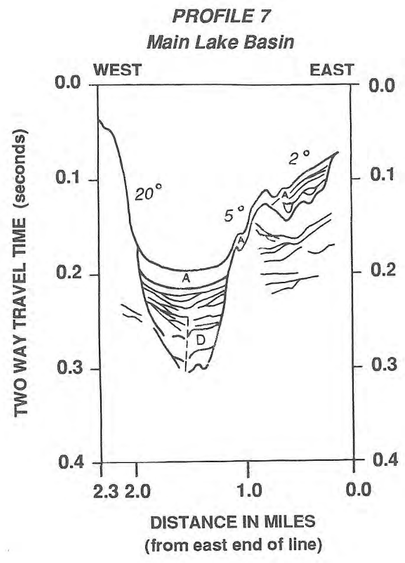

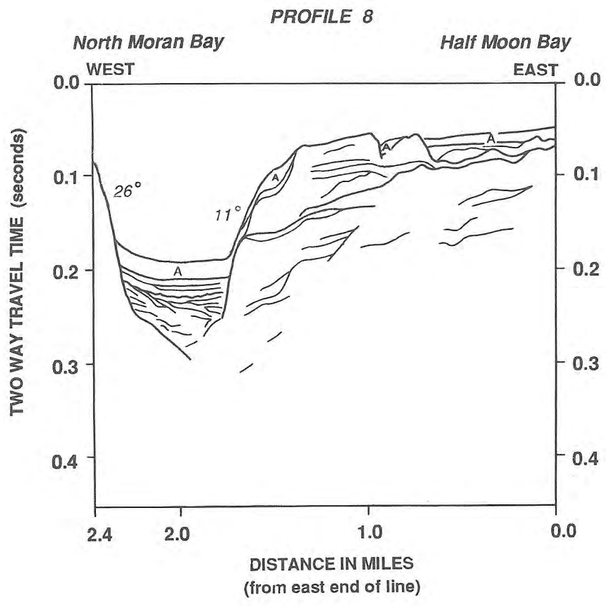

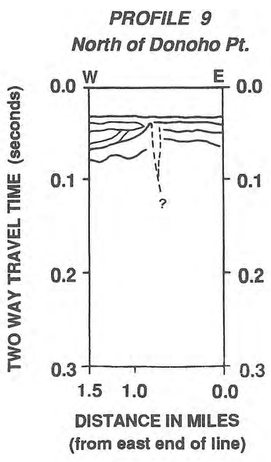

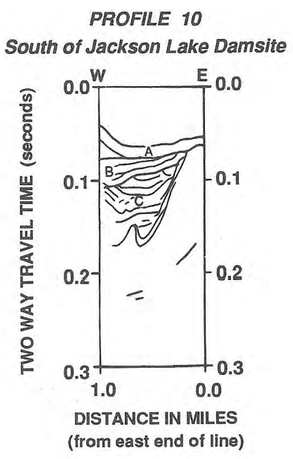

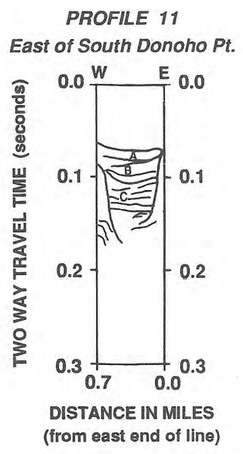

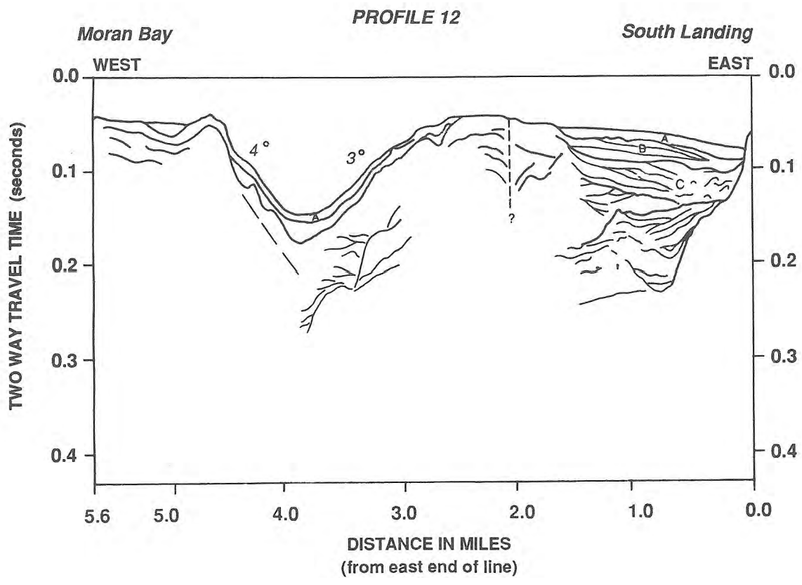

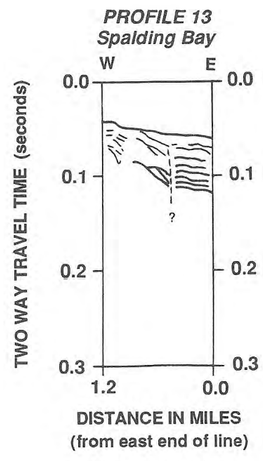

B. North-South profiles (locations on Figure 4b).

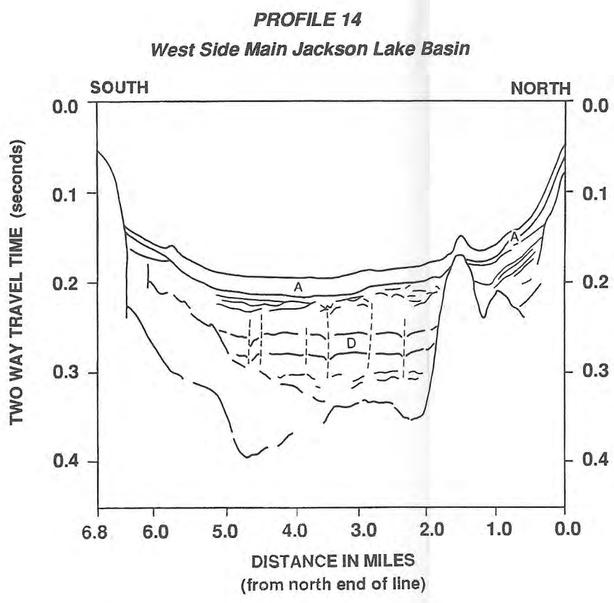

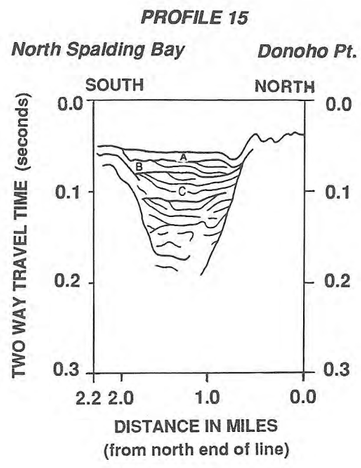

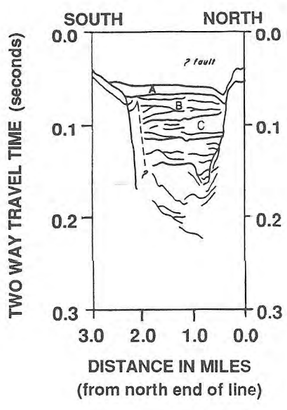

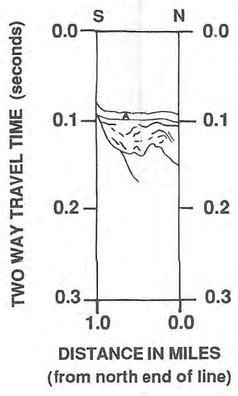

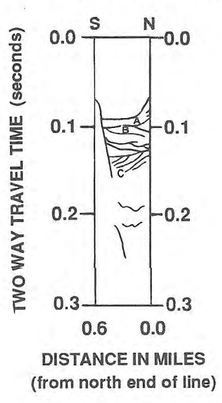

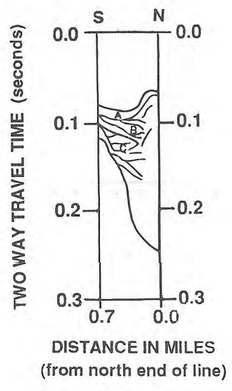

Department of Geology and Geophysics
University of Utah
Salt Lake City, Utah 84112

SEISMIC REFLECTION PROFILES OF JACKSON LAKE

by

R.B. Smith and Others

1993